SHORT PAPERS

ISSN 1679-3684

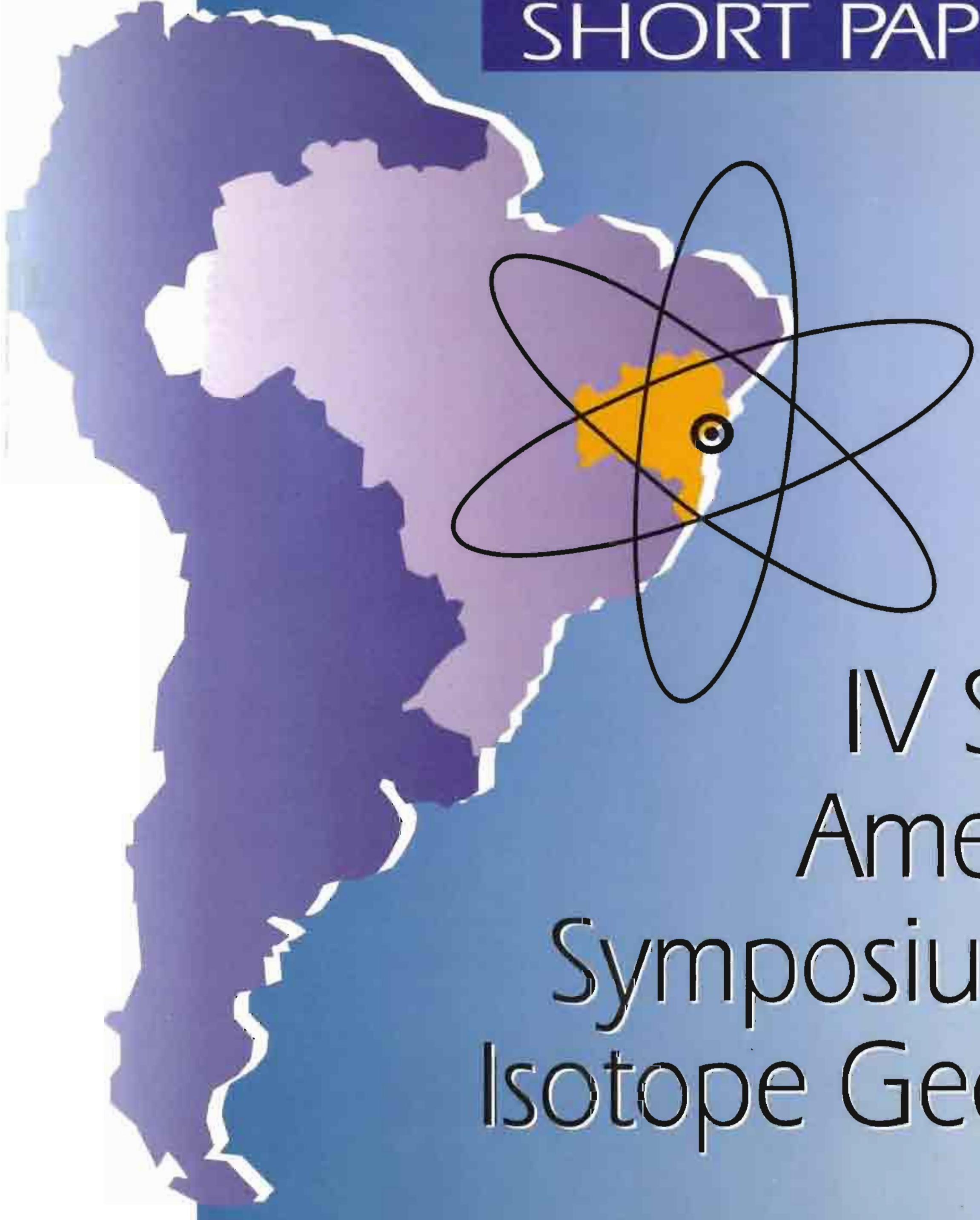

IV South American Symposium on Isotope Geology

SALVADOR-BA, BRAZIL AUGUST 24th - 27th, 2003

- VOLUME I -

30 anos companhia baiana de pesquisa mineral

IV SSAGI
Brazil - 2003

IRD
Institut de recherche pour le développement

SHORT PAPERS

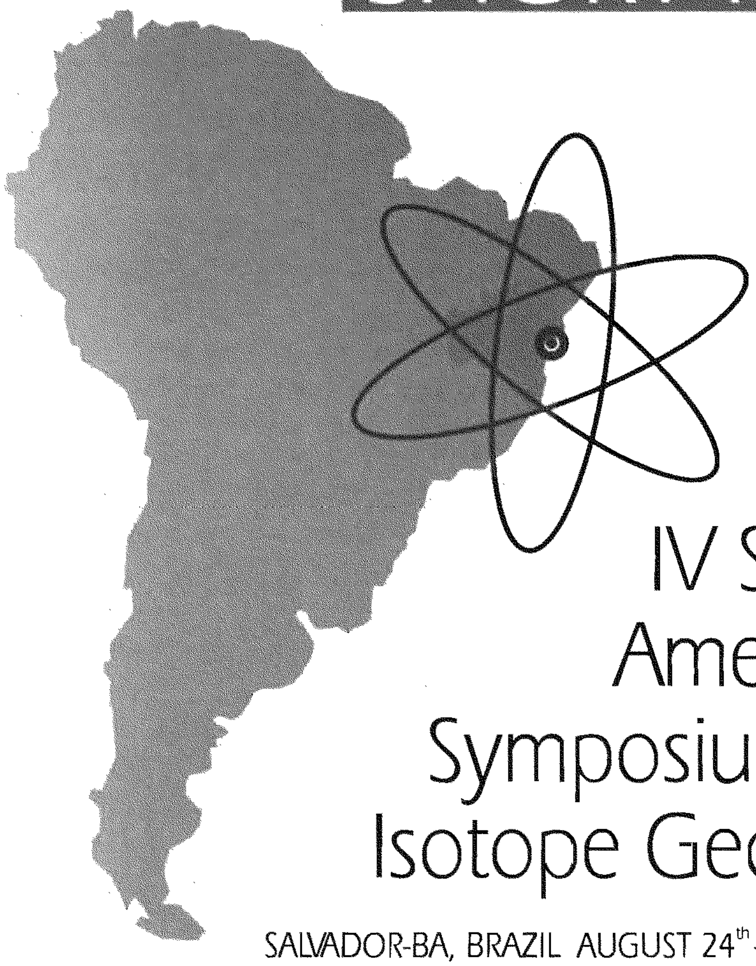

IV South American Symposium on Isotope Geology

SALVADOR-BA, BRAZIL AUGUST 24th - 27th, 2003

Organizers

Maria de Lourdes da Silva Rosa
Débora Correia Rios
Marília Kosin
Marilda Santos Pinto Miedema

companhia baiana de pesquisa mineral

IV SSAGI
Brazil - 2003

IRD
Institut de recherche pour le développement

South American Symposium on Isotope Geology. (4.: 2003: Salvador)
Short Papers of the IV South American Symposium on Isotope Geology – IV SSAGI, Salvador, August 24th - 27th ; Maria de Lourdes da Silva Rosa et al. (Organizers). – Salvador : CBPM; IRD, 2003.
ii-xxii - 789p. : il.

Reference.

1. Isotope Geology. 2. Geology – South America. 3. Geology – International Meeting. 4. Symposium. I. Rios, Débora Correia. II. Kosin, Marília. III. Santos Pinto, Marilda. IV. Title.

CDD 551.701
CDU 550.42

ORGANIZING COMMITTEE

President
Ruy Fernandes da Fonseca Lima (CBPM)

Vice President
Moacyr Moura Marinho (CBPM)

Scientific Coordinators
Alcides N. Sial (UFPE)
Aroldo Misi (UFBA)
Herbet Conceição (UFBA)
Pierre Sabaté (IRD)

General Secretary
Hélio A. Azevedo (CBPM)

Associate Secretary
Maria de Lourdes da Silva Rosa (UFBA)

Deputy Secretaries
Débora Correia Rios (UFBA)
Johildo F. S. Barbosa (UFBA)
Marilda Santos Pinto Miedema (UEFS)
Marília Kosin (CPRM)

Publications
Hermes A.V. Inda (CBPM)
Valderez P. Ferreira (UFPE)

Coordinator of Finances
Herbet Conceição (UFBA)
Maria José dos Santos Rêgo (UFBA)

Coordinator of Excursions
Marília Kosin (CPRM)

Digital Support
Basílio Elesbão da Cruz Filho (UFBA)
Rita Cunha Leal Menezes (UFBA)

REGIONAL COORDINATORS

Claudio Gaucher (Uruguay)
Enrique Linares (Argentina)
Francisco Munizaga (Chile)
Miguel Parada (Chile)
Olga Rey (Venezuela)
Umberto G. Cordani (Brazil)

SCIENTIFIC ADVISORS

Antônio Expedito Azevedo (UFBA)
Colombo C. G. Tassinari (USP)
Ênio Soliani (UFRS)
Jean M. Lafon (UFPA)
Koji Kawashita (UFRS)
Luiz Carlos Ruiz Pessenda (CENA)
Miguel A.S. Basei (USP)
René Rodrigues (PETROBRAS)
Roberto M. Argollo (UFBA)
Wilson Teixeira (USP)

SPONSORS

Governo do Estado da Bahia
Companhia Baiana de Pesquisa Mineral (CBPM)
Sociedade Brasileira de Geologia (SBG)
Serviço Geológico do Brasil (CPRM)
Universidade Federal da Bahia (UFBA)
Institut de Recherche pour le Développment (IRD)
Conselho Nacional de Desenvolvimento Científico e Tecnológico (CNPq)
Coordenação de Aperfeiçoamento de Pessoal de Nível Superior (CAPES)
Fundação de Amparo à Pesquisa do Estado da Bahia (FAPESB)
Petróleo Brasileiro S.A. (PETROBRAS)
Geologia e Sondagens Ltda (Geosol)
Academia Brasileira de Ciências
Sinc do Brasil – Micromass
ThermoFinnigan

FOREWORD

In the last three decades, many geologists in South America have turned their attention to isotopic geology as a tool in the wider context of the Earth Sciences. As a result, it has been proposed that a series of symposia on the South American Isotope Geology (SSAGI), organized every two years, would provide the appropriate forum for discussion of methods and applications of stable and radiogenic isotopes in the Earth Sciences. In these symposia, progress made in this field in South America would be assessed, encouraging scientific interaction at both national and international levels.

We are very pleased the IV SSAGI has met very good interest from the national and international community reflected by 212 scientific contributions from 15 countries. They were selected for oral and poster sessions and distributed in seven thematic sessions: (i) Methodology and Application of Isotope Geology; (ii) Crustal Evolution of South America; (iii) Temporal Isotopic Variation and Chemostratigraphy; (iv) Environmental Geology and Water Resources; (v) Genesis and Evolution of Igneous and Metamorphic Rocks; (vi) Metallogenesis and Mineral Exploration; and (vii) Oil Exploration. These contributions, with the seven invited lectures on selected themes, compose these Short Papers volumes.

To prepare the volumes the organizers utilize the original files sent in by the authors. However, some modifications have been suggested by the Editorial Board in order to improve the text. Most of the papers were not returned to the authors and modifications have been performed by the organizers of the volumes looking for standardization. All figures and references were not edited. The final quality of figures, photos and tables presented here reflect the quality of the originals forwarded by the authors.

The Organizing Committee gratefully acknowledges the financial support from the Government of the State of Bahia, the major sponsor of this Meeting, that has deemed timely to provide the site and sponsorship, reasserting with the *Companhia Baiana de Pesquisa Mineral* (CBPM) its longstanding practice of fruitful interaction with the Earth Sciences community. Thanks are also due to the *Sociedade Brasileira de Geologia (SBG-Núcleo Bahia-Sergipe),* Brazilian Council for Scientific and Technological Development (CNPq), CAPES and also to CPRM (Brazilian Geological Survey), Sinc do Brasil (Micromass), Finnigan and *Geologia e Sondagens* (GEOSOL) for their financial support. We thank the *Institut de Recherche pour le Développment* (IRD), for publishing these volumes, and to Dr. Augusto Pedreira for a final review. We also recognize the efforts of Dr. Alcides Sial from the Stable Isotope Laboratory (LABISE) at Federal University of Pernambuco to have the IV SSAGI at the Northeastern Brazil.

The Organizing Committee wishes to welcome all participants and that all of them have a enriching and a pleasant stay in Salvador. The success of the meeting is due to both inovating ideas and very productive discussions among the participants. The high quality of the papers presented in these issues provide a good guarantee that in forthcoming years new SSAGI will prolong the dynamics of this field.

IV SSAGI Organizing Committee

- VOLUME I -

- VOLUME II -

CONTENTS

CONFERENCES

METHODOLOGY AND APPLICATION OF ISOTOPE GEOLOGY

CRUSTAL EVOLUTION OF SOUTH AMERICA

TEMPORAL ISOTOPIC VARIATION AND CHEMOSTRATIGRAPHY

ENVIRONMENTAL GEOLOGY AND WATER RESOURCES

GENESIS AND EVOLUTION OF IGNEOUS AND METAMORPHIC ROCKS

METALLOGENESIS AND MINERAL EXPLORATION

OIL EXPLORATION

SPONSORS NOTES

Conferences

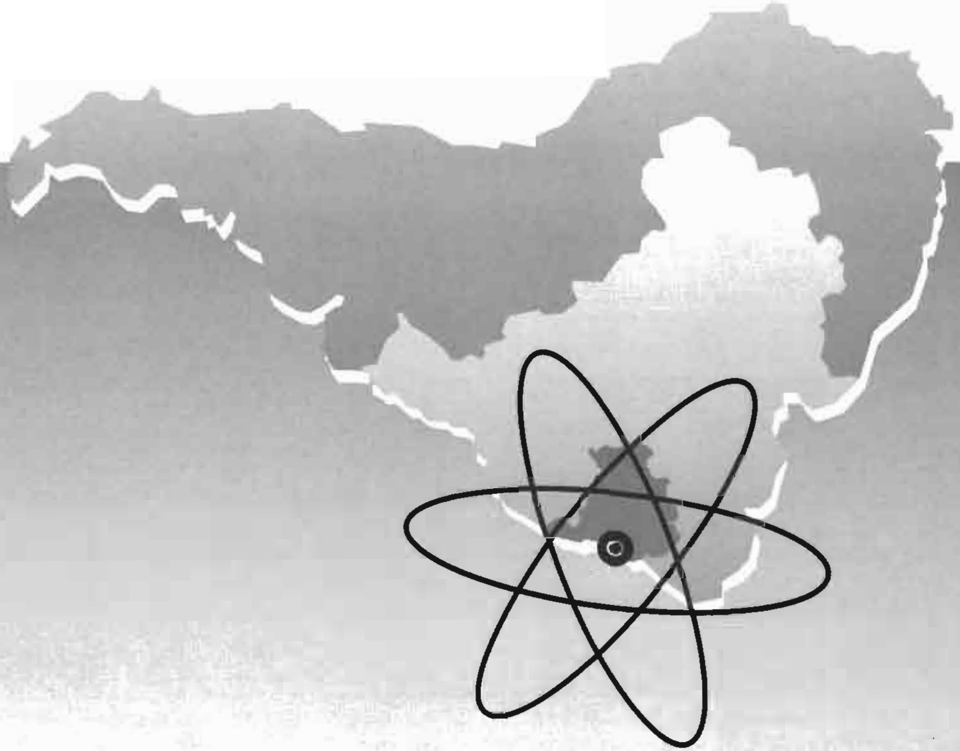

THE SMALLER THE SAMPLE, THE BIGGER THE STORY? DEVELOPMENTS AND TRENDS IN ISOTOPE ANALYSIS

Armstrong, R.A.

Research School of Earth Sciences, the Australian National University, Mills Road, Acton, Canberra, A.C.T., Australia.
richard.armstrong@anu.edu.au

Keywords: Geochronology, isotope analysis, zircons, SHRIMP

There is virtually no part of geology that is not critically dependant on high-quality and high precision isotope analysis and geochronology. Time is the essential parameter in deciphering how Earth and it's solar system have evolved. To understand this evolution requires high quality age determinations and isotopic analyses to calibrate geological processes and rates of change. The measurements of absolute time may be on a very small scale, such as the lifespan of a magma chamber, or the rate of diffusion of an element in a crystal, to the larger continental-scale phenomena associated with plate tectonic processes.

Geochronology has seen great advances in the past few decades, made possible by improvements in established techniques and by the introduction of new technological developments and methodologies. This talk will review some of these advances and trends in isotope analysis and geochronology highlighting problems we currently face and how future developments might address these.

There is no doubt that whatever the analytical technique, the major recent advances in geochronology have been due to the recognition that geological materials are heterogeneous on all scales, and that there is a need to analyse smaller and smaller samples or domains. To be able to translate what is observed in petrographic detail to, for example, the establishment of a P-T-t path for a metamorphic terrane, is now possible through microsampling and analysis. These advances in micro-analytical techniques have been achieved either by improving existing methodologies (e.g. the "Krogh" technique of zircons analysis); by the development of new technologies which allow *in situ* analysis, such as the SHRIMP (**S**ensitive **H**igh **R**esolution **I**on **M**icro**P**robe) and the LA-ICP-MS (laser ablation ICP mass spectrometry); or by innovative use of established technology – such as CHIME method of dating of monazites using the electron microprobe.

In geochronology there have been major improvements in the application of all "traditional" methods (Rb-Sr, Sm-Nd, Pb-Pb and K-Ar) plus the application of relatively new techniques, such as Re-Os method. But there has been no development more dramatic than the advance in the application of the U-Pb dating technique to zircons and other U-bearing accessory minerals. Given the unique advantages of the double ^{238}U – ^{206}Pb and ^{235}U – ^{207}Pb decay schemes and the relative certainty of their decay constants, the U-Pb method is undoubtedly the premier geochronometer currently available and the natural benchmark to compare against other techniques.

There have been two major parallel developments in U-Pb geochronology that have allowed geologists to work on rocks spanning the whole time-scale of the Earth with unprecedented precision and accuracy. One of these was the development of low-blank ID-TIMS methods by Tom Krogh and colleagues at the Royal Ontario Museum that enabled geochronologists to get high-precision dates from very small samples (single grains or parts of grains) of zircon. This, combined with developments in abrasion and leaching techniques has allowed geochronologists to largely overcome the problem of discordance in U-Pb zircon analyses. Zircon is a remarkably resilient mineral, but this feature is both its strength and its weakness. On the positive side, the ability of zircon to retain its isotopic integrity and to thereby record original age information even through high temperature metamorphism or anatexis, or to survive the rigours of erosion, transportation and sedimentation, makes it unique. The negative side is that zircons can be preserved, either as inherited cores (Fig. 1), or caught up as xenocrysts in a magma, potentially giving spurious or mixed ages even on a single grain sample size.

The second major development grew from the need to do analyses *in situ* to avoid these problems and to decipher the commonly complex geological history of a zircon population. This was the development of the SHRIMP at the Australian National University, the first ion microprobe built specifically for the analysis of geological samples. Although unable to obtain the high precisions possible using ID-TIMS techniques, SHRIMP U-Pb dating of zircons and other accessory minerals has had a remarkable impact on both our understanding of the behaviour of these minerals under various geological conditions and on U-Pb geochronology in general. Advantages of SHRIMP U-Pb dating include its ability to accurately date very small (<30μm) areas within grains. Thus it is possible to determine multiple ages within a zircon population which might have inheritance or rims of metamorphic zircon. Some rocks have been shown to preserve as many as four different generations of zircon growth, each recording a specific event in the history of the host rock (e.g. Black et al., 1986). It is also a virtually nondestructive method, allowing *in situ* age measurements to be made of different generations of minerals in thin or polished sections. Thus the analyst can relate recorded ages to observed petrographic relationships. The routine use of cathodoluminescence

(CL) has added integrity to zircon dating. A number of studies (e.g. Hanchar & Millar, 1993; Varvra, 1994; Varvra et al., 1996; Rubatto & Gebauer, 2000) have shown how this imaging technique can reveal detailed internal structures, and CL has become an essential and routine part of the pre-analysis preparation. Clearly it should not only be applied to the SHRIMP technique, but to any U-Pb zircon analysis. Unfortunately this is not always the case.

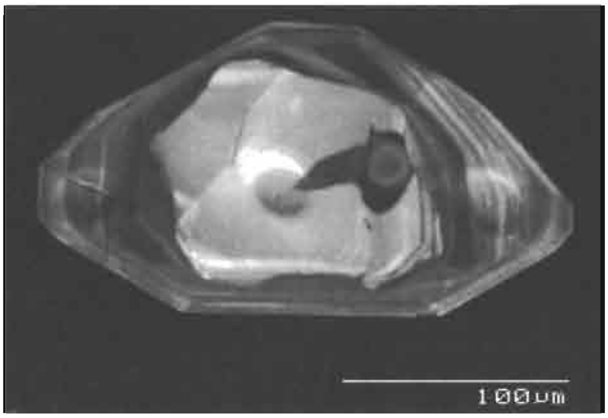

Figure 1. Cathodoluminescence image of a zircon from the Seapoint Granite (Cape Town) showing the 542 Ma zoned magmatic zircon enclosing an inherited core.

Inheritance and other internal complexities are not unique to the mineral zircon. Nevertheless, it is only recently that SEM imaging techniques have also been applied to the other U-bearing minerals commonly used in geochronology. Backscatter electron imaging of titanites and monazites also show both inheritance and multi-generational growth (Fig. 2). Titanite ages can be combined with major-element chemistry and backscatter imaging to trace multiple episodes of growth, not always recorded in the coexisting zircons (e.g. Aleinikoff et al., 2002).

The increasing use and relevance of monazite as a means of dating metamorphic rocks has led to the greater usage of the total Pb or CHIME method of dating, originally developed by Suzuki et al. (1991). This is a potentially useful technique that has been enthusiastically adopted by some laboratories and can be useful for determining high spatial resolution *in situ* ages in monazites, xenotime, zircon and thorianite (e.g. Asami et al., 2002), with obvious applications to metamorphic petrology or to the understanding of the closure of the U-Th-Pb system in monazite (e.g. Cocherie et al., 1998). Unfortunately the statistical reporting of some published CHIME data sets has been far too optimistic and the rigorous assessments of the ages applied to other techniques needs to be applied to this method too.

One of the more recent exciting applications of the U-Pb technique has been the dating of authigenic xenotime in sediments (McNaughton et al., 1999). This requires very high spatial resolution (commonly <15µm) and is only realistically possible using the SHRIMP (or electron microprobe for CHIME dating) on well-characterised samples.

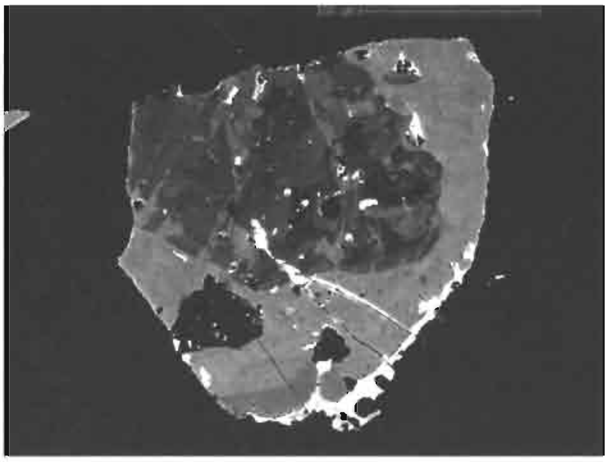

Figure 2. Backscattered SEM image of a titanite grain from a phonolite at the Cripple Creek gold deposit, USA, showing a ~1350 Ma inherited core (dark, mottled titanite) overgrown by ~29 Ma magmatic titanite.

This requires very high spatial resolution (commonly <15µm) and is only realistically possible using the SHRIMP (or electron microprobe for CHIME dating) on well-characterised samples. The xenotime occurs as tiny overgrowths on detrital zircon and is thought to develop very early in diagenesis, thus providing a potentially accurate (minimum) estimate of the age of sedimentation.

U-Pb dating of detrital zircons (or monazite, rutile) and ^{40}Ar/^{39}Ar dating of muscovites are becoming increasingly relevant in tectonic reconstruction studies, stratigraphic correlations, and in the establishment of maximum age constraints on sediments. This is a very powerful tool useful for the study of sedimentary sequences that were previously unsuitable for analysis by the other more conventional techniques.

The development of LA-ICP and it's application to U-Pb geochronology is rapidly finding favour in laboratories which don't have the specialist clean laboratory facilities required for ID-TIMS analysis or expensive SHRIMP instrumentation. This provides a relatively inexpensive method of dating zircons, and once such problems as resolving high interferences on the ^{204}Pb are solved this will be an increasingly popular technique which will find it's own niche in isotope analysis and geochronology.

Stable isotope geochemistry has its own special analytical requirements, but as with the study of radiogenic isotopes, sample size and the resolution of small-scale heterogeneity is important. The ability to assess and quantify these heterogeneities for sulphur isotope studies has long been recognised (Eldridge et al., 1987), and more recent studies on oxygen isotopes have convincingly demonstrated the importance of these studies on such diverse targets as speleothems (Yehoshua et al., 2003) or ancient detrital zircon grains (Mojzsis et al., 2001; Wilde et al., 2001).

Future developments in isotope geochemistry will undoubtedly see more emphasis placed on the inter-relationship between petrography (textures), petrology and geochronology. This will require new instrumentation developments and innovations. Unique experiments aimed at obtaining invaluable extra-terrestrial samples will soon set new challenges for analytical geochemists. The recognition of the importance of the scale of sample heterogeneity and the relevance of the information contained therein, plus the physical limitations on some sample sizes (e.g. extraterrestrial material) will set new goals. Some new and potential developments in this regard will be discussed. In any event, it is clear that the way forward in the future is to develop and use techniques that allow the fine-scale heterogeneities observed in geological samples to be measured with accuracy and precision.

REFERENCES

Aleinikoff, J.N.; Wintsch, R.P.; Fanning, C.M.; Drais, M.J. 2002. U-Pb geochronology of zircon and polygenetic titanite from the Glastonbury Complex, Connecticut, USA: and integrated SEM, EMPA, TIMS, and SHRIMP study. Chemical Geology, 188, 125-147.

Asami, M.; Suzuki, K.; Grew, E.S. 2002. Chemical Th-U-total Pb dating by electron microprobe analysis of monazite, xenotime and zircon from the Archean Napier Complex, East Antarctica: evidence for ultra-high temperature metamorphism at 2400 ma. Precambrian Research, 114, 249-275.

Black, L.P.; Williams, I.S.; Compston, W. 1986. Four zircon ages from one rock: the history of a 3,930 Ma-old granulite from Mount Scones, Enderby Land, Antarctica. Contributions to Mineralogy and Petrology, 94, 427-437.

Cocherie, A.; Legendre, O.; Peucat, J.J.; Pouamelan, A.N. 1998. Geochronology of polygenetic monazites constrained by in situ electron microprobe Th-U-total Pb determinations: implications for Pb behaviour in monazite. Geochimica Cosmochimica Acta, 62, 2475-2497.

Eldridge, C.S.; Compston, W.; Williams, I.S.; Walshe, J.L. 1987. In situ microanalysis for $^{34}S/^{32}S$ ratios using the ion microprobe SHRIMP. International Journal of Mass Spectrometry and Ion Processes, 76, 65-83.

Hanchar, J.M. & Millar, C.F. 1993. Zircon zonation patterns as revealed by cathodoluminescence and backscattered electron images: Implications for interpretation of complex crustal histories. Chemical Geology, 112, 1-13.

McNaughton, N.J.; Rasmussen, B.; Fletcher, I.R. 1999. SHRIMP Uranium-lead dating of diagenetic xenotime in siliciclastic sedimentary rocks. Science. 285, 78-80.

Mojzsis, S.J.; Harrison, T.M.; Pidgeon, R.T. 2001. Oxygen isotope evidence from ancient zircons for liquid water at the Earth;s surface 4,300 Myr ago. Nature, 409, 178-181.

Rubatto, D. & Gebaüer, D. 2000. Use of cathodoluminescence for U-Pb zircon dating by ion microprobe: some examples from the Western Alps. In: Cathodoluminescence in Geosciences (eds. Pagel, M.; Barbin, V.; Blanc, P.; Ohnenstetter, D.), Springer-Ver;ag, 373-400.

Suzuki, K.; Adachi, M.; Tanaka, T. 1991. Middle precambrian provenance of jurassic sandstone in the Mino Terrane, central Japan: Th-U-total Pb evidence from an electron microprobe monazite study. Sedimentary Geology, 75, 141-147.

Varvra, G. 1994. Systematics of internal zircon morphology in major Varicsan granitoid types. Contributions to Mineralogy and Petrology, 117, 331-344.

Varvra, G.; Gebaüer, D.; Schmid, R.; Compston, W. 1996. Multiple zircon growth and recrystallisation during polyphase Late Carboniferous to Triassic metamorphism in granulites of the Ivrea Zone (Southern Alps); an ion microprobe (SHRIMP) study. Contributions to Mineralogy and Petrology, 122, 337-358.

Wilde, S.A.; Valley, J.W.; Peck, W.H.; Graham, C.M. 2001. Evidence from detrital zircons for the existence of continental crust and oceans on the Earth 4.4 Gyr ago. Nature, 409, 175-178.

Yehoshua, K.; Bar-Matthews, M.; Ayalon, A.; McKeegan, K.D. 2003. A high spatial resolution $\delta^{18}O$ profile of a speleothem using an ion-microprobe. Chemical Geology, 197, 21-28.

APPLICATION OF THE Pt-Re-Os ISOTOPIC SYSTEMS IN IGNEOUS GEOCHEMISTRY AND GEOCHRONOLOGY

Carlson, R.W.

Carnegie Institution of Washington, Department of Terrestrial Magnetism, 5241 Broad Branch Road, NW, Washington, DC 20015, USA. carlson@dtm.ciw.edu

Keywords: Osmium isotopes, lithospheric mantle, geochronology, igneous petrogenesis

INTRODUCTION

Two radiometric systems, involving the same daughter element, that have seen recent dramatic expansion of their use involve isotopic variations in ^{186}Os and ^{187}Os generated, respectively, by the decay of ^{187}Re (half life = 41.6 Gyr) and ^{190}Pt (half life = 449 Gyr) (Shirey & Walker, 1998). Primarily responsible for the accelerating use of this system was the application of negative thermal ionization mass spectrometry (Creaser et al. 1991; Volkening et al., 1991) that improved Os ionization efficiency by at least 2 orders of magnitude and allows the precise isotopic analysis of Os sample sizes extending into the sub-picogram level. Of similar significance were developments in the chemistry laboratory that slowly migrated Os separation techniques from cumbersome, and dirty, distillation methods to clean and reproducible extraction techniques that can be performed with inexpensive apparatus available to most isotope geology laboratories (Reisberg & Meisel, 2002).

Re-Os ABUNDANCE VARIATION

High-sensitivity, low blank, analysis procedures are critical for Os isotopic work because the abundance of Os in most natural materials is a factor of 10^3 to 10^6 lower than more familiar trace elements, for example Nd (Fig. 1). Fortunately, variations in Re/Os ratio also are some 2 to 3 orders of magnitude larger than the variability in Sm/Nd ratios (Fig. 1) with the result that Os isotopic compositions are reported in percent deviations relative to estimates of bulk-earth evolution:
(γ_{Os} = (((^{187}Os/^{188}Os$_{sample}$/^{187}Os/^{188}Os$_{bulk-earth}$) - 1)*100) (Walker et al., 1989) rather than in parts in 10000 as used for Sr, Nd and Hf. During melting, Os is compatible, but Re is mildly incompatible. In essentially all other radiometric systems, both parent and daughter element are incompatible during melting. Very high degree mantle melts, such as komatiites (Walker et al., 1988, 1991a), will have Re/Os ratios ranging from close to the mantle source to as much as a factor of 20 higher, whereas lower degree melts, such as basalts, can have ^{187}Re/^{188}Os ratios approaching 1000 compared to a mantle ratio of 0.43 (Meisel et al., 1996). During fractional crystallization of a mafic magma, the Re/Os ratio will increase until oxide phases such as magnetite crystallize and begin removing significant Re from the magma (Righter et al., 1998). Consequently, Re/Os ratios peak in evolved basaltic compositions, but remain much higher than mantle values in more evolved magmas ranging from andesite through granite. Mantle residues of melting have low Re/Os, in some cases approaching zero, but high Os contents (Fig. 1).

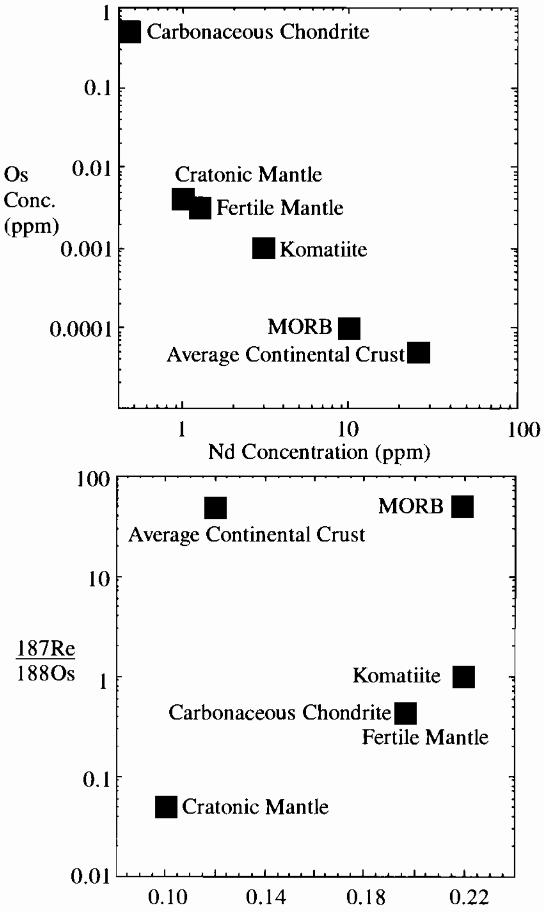

Figure 1. Re and Os concentration variation in a variety of terrestrial materials in comparison to a lithophile trace element like Nd.

DATING MANTLE LITHOSPHERE FORMATION

Because of the high Os concentrations of peridotites, and the low Os concentrations of most melts, the Os isotopic composition of mantle peridotite is less sensitive than other radiometric systems to the metasomatism that commonly affects mantle samples. With care, Os measurements can be used to date the time of melt extraction responsible for the formation of the Ca, Al and southern Africa compared to those erupted from three Fe depleted peridotites that are found beneath most old continental terrains (Fig. 2). Studies of mantle xenoliths

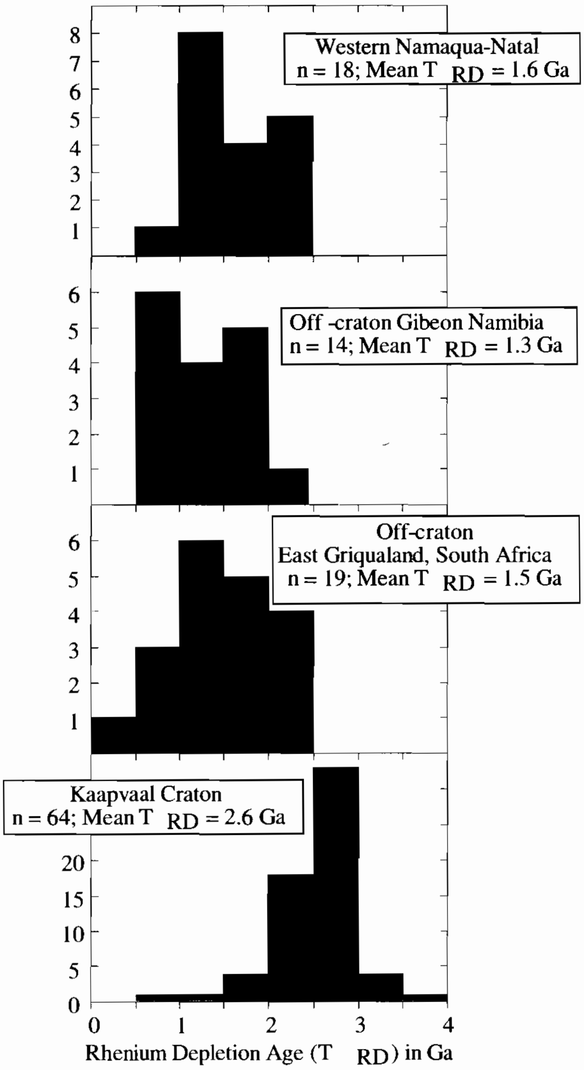

Figure 2. Re-depletion ages for peridotite xenoliths from kimberlites that erupt through the Archean Kaapvaal Craton of kimberlite groups erupted through the surrounding Proterozoic mobile belts.

and tectonic peridotites commonly provide Re-Os ages indicative of ancient melt depletion showing that stable lithospheric mantle keels can persist beneath old crustal sections (Walker et al., 1989; Pearson et al., 1995; Reisberg & Lorand, 1995; Handler et al., 1997; Carlson et al., 1999; Peslier et al., 2000; Hanghoj et al., 2001; Irvine et al., 2003), but at least some cratons, notably China (Gao et al., 2002) and the Wyoming (Carlson & Irving, 1994) cratons appear to have had their keels removed by sufficiently intense tectonic events. Recently, techniques have been developed that allow in-situ analysis of high Os content sulfides found in mantle rocks (Pearson et al., 2002). These detailed analyses confirm much of the previous whole rock results (Pearson et al., 1995; Griffin et al., 2002), but also show the complexity of mantle processes by being particularly sensitive to sampling the metasomatic history of the mantle (Alard et al., 2002). Single-grain Re-Os studies also have been carried out on sulfide grains extracted from diamonds (Pearson et al., 1998a, b, 1999; Pearson & Shirey, 1999; Shirey et al., 2001) revealing new chronological information on the formation of diamonds including the connection of diamond-forming events with circumcratonic subduction (Richardson et al., 2001; Shirey et al., 2002).

DEFINING MAGMA SOURCE COMPOSITIONS

Because of the dramatic distinction between peridotite and melt Re/Os ratios, the Os isotopic system is a very sensitive tracer of the presence of mafic materials in the mantle sources of magmas. Os isotopic studies show that some Na-rich mafic alkalic magmas have very radiogenic Os indicative of a mafic source; other potassic magmas with unradiogenic Os appear to derive from phlogopite-metasomatized peridotitic sources (Carlson et al., 1996; Araujo et al., 2001; Carlson & Nowell, 2001). This approach also has been applied to the study of ocean island basalts (OIB). Certain groups of OIB, particularly the HIMU islands, have radiogenic Os isotopic compositions possibly indicative of recycled subducted oceanic crust in their mantle source regions (Pegram & Allegre, 1992; Hauri & Hart, 1993; Reisberg et al., 1993). The alternative explanation to recycled crust to explain the elevated Os isotopic composition of some OIB is that their sources include a small contribution from the outer core (Walker et al., 1995). Based on iron meteorite analogs, crystallization of the inner core should result in increasing Re/Os and Pt/Os in the outer core with the consequent increases in radiogenic ^{187}Os and ^{186}Os. If even a very small amount (<0.5%) of outer core were entrained in the plumes that may be supplying these OIBs, then the resultant magmas could have the radiogenic Os signatures observed in places like Hawaii (Brandon et al., 1999) and the Siberian flood basalts (Horan et al., 1995).

ORE GEOCHRONOLOGY

Another important distinction of the Re-Os isotope system is that the abundances of Re and Os during partial melting and fractional crystallization are controlled primarily by sulfides, chromites and PGE alloys rather than the silicate phases that determine lithophile element partitioning. As a result, the Re-Os system has proven particularly useful for: 1) defining the conditions of chromite crystallization in ophiolites (Walker et al., 2002), alpine peridotites (Becker et al., 2001) and layered mafic intrusions (Lambert et al., 1994; Marques et al., 2003); 2) determining whether the platinum-group elements in PGE (McCandless & Ruiz, 1991) and Ni (Walker et al., 1991b, 1994; Foster et al., 1996) ore deposits derive from crustal or mantle sources; and 3) dating a variety of ore deposits ranging from PGE (McCandless & Ruiz, 1991) to gold (Frei et al., 1998; Kirk et al., 2002). Molybdenite, in particular, has proven to be a particularly good chronometer since it contains high Re concentrations but almost no Os, except that produced by the decay of Re (Luck & Allegre, 1982; McCandless et al., 1993; Stein et al., 2001).

The Pt-Re-Os isotopic systems thus form an important complement to other radiometric systems by providing a radiometric tracer for the chemical evolution of the non-lithophile element component of the Earth. With the continually improving ease of Re-Os measurement techniques, this system likely will be incorporated as a staple of isotope geochemistry.

REFERENCES

Alard, O.; Griffin, W.L.; Pearson, N.J.; Lorand, J.-P.; O'Reilly, S.Y. 2002. New insights into the Re-Os systematics of sub-continental lithospheric mantle from in-situ analysis of sulphides. Earth and Planetary Science Letters 203, 651-663.

Araujo, A.L.N.; Carlson, R.W.; Gaspar, J.C.; Bizzi, L.A. 2001. Petrology of kamafugites and kimberlites from the Alto Paranaiba Alkaline Province, Minas Gerais, Brazil. Contributions to Mineralogy and Petrology 142, 163-177.

Becker, H.; Shirey, S.B.; Carlson, R.W. 2001. Effect of melt percolation on the Re-Os systematics of peridotites from a Paleozoic convergent plate margin. Earth and Planetary Science Letters 188, 107-121.

Brandon, A.D.; Norman. M.D.; Walker, R.J.; Morgan, J.W. 1999. 186Os-187Os systematics of Hawaiian picrites. Earth and Planetary Science Letters 174, 25-42.

Carlson, R.W. & Irving, A.J. 1994. Depletion and enrichment history of subcontinental lithospheric mantle: an Os, Sr, Nd and Pb isotopic study of ultramafic xenoliths from the northwestern Wyoming Craton. Earth and Planetary Science Letters 126, 457-472.

Carlson, R.W. & Nowell, G.M. 2001. Os and Hf Isotopic Evidence for a Mafic Source Component for Potassic Volcanism on the Colorado Plateau. G3 2000GC000128.

Carlson, R.W.; Esperanca, S.; Svisero, D.P. 1996. Chemical and Os isotopic study of Cretaceous potassic rocks from southern Brazil. Contributions to Mineralogy and Petrology 125, 393-405.

Carlson, R.W.; Pearson, D.G.; Boyd, F.R.; Shirey, S.B.; Irvine, G.; Menzies, A.H.; Gurney. J.J. 1999. Re-Os systematics of lithospheric peridotites: implications for lithosphere formation and preservation. Proc. 7th Int. Kimberlite Conf., 99-108.

Creaser, R.A.; Papanastassiou, D.A.; Wasserburg, G.J. 1991. Negative thermal ion mass spectrometry of osmium, rhenium, and iridium. Geochimica et Cosmochimica Acta 55, 397-401.

Foster, J.G.; Lambert, D.D.; Frick, L.R., Maas, R. 1996. Re-Os isotopic evidence for genesis of Archaean nickel ores from uncontaminated komatiites. Nature 382, 703-706.

Frei, R.; Nagler, T.F.; Schonberg, R.; Kramers, J.D. 1998. Re-Os, Sm-Nd, U-Pb, and stepwise lead leaching isotope systematics in shear-zone hosted gold mineralization: genetic tracing and age constraints of crustal hydrothermal activity. Geochimica et Cosmochimica Acta 62, 1925-1936.

Gao, S.; Rudnick, R.L.; Carlson, R.W.; McDonough, W.F.; Liu, Y.-S. 2002. Re-Os evidence for replacement of ancient mantle lithosphere beneath the North China craton. Earth and Planetary Science Letters 198, 307-322.

Griffin, W.L.; Spetsius, Z.V.; Pearson, N.J.; O'Reilly, S.Y. 2002. In-situ Re-Os analysis of sulfide inclusions in kimberlitic olivine: new constraints on depletion events in the Siberian lithospheric mantle. Geochemisty, Geophysics, Geosystems 1069.

Handler, M.R.; Bennett, V.C.; Esat, T.M. 1997. The persistence of off-cratonic lithospheric mantle: Os isotopic systematics of variably metasomatised southeast Australian xenoliths. Earth and Planetary Science Letters 151, 61-75.

Hanghoj, K.; Kelemen, P.; Bernstein, S.; Blusztajn, J.; Frei, R. 2001. Osmium isotopes in the Wiedemann Fjord mantle xenoliths; a unique record of cratonic mantle formation by melt depletion in the Archaean. Geochemisty, Geophysics, Geosystems, 2000GC000085.

Hauri, E.H. & Hart, S.R. 1993. Re-Os isotope systematics of HIMU and EMII oceanic island basalts from the south Pacific Ocean. Earth and Planetary Science Letters 114, 353-371.

Horan, M.F.; Walker, R.J.; Fedorenko, V.A.; Czamanske, G.K. 1995. Osmium and neodymium isotopic constraints on the temporal and spatial evolution of Siberian flood basalt sources. Geochimica et Cosmochimica Acta 59, 5159-5168.

Irvine, G.J.; Pearson, D.G.; Kjarsgaard, B.A.; Carlson, R.W.; Kopylova, M.G.; Dreibus, G. 2003. Evolution of the lithospheric mantle beneath Northern Canada: A Re-Os isotope and PGE study of peridotite xenoliths from Somerset Island kimberlites and a comparison to Slave craton lithospheric mantle. Lithos in press.

Kirk, J.; Ruiz, J.; Chesley, J.; Walshe, J.; England, G. 2002. A major Archean, gold- and crust-forming event in the Kaapvaal Craton, South Africa. Science 297, 1856-1858.

Lambert, D.D.; Walker, R.J.; Morgan, J.W.; Shirey, S.B.; Carlson, R.W.; Zientek, M.L.; Lipin, B.R.; Koski, M.S.; Cooper, R.L. 1994. Re-Os and Sm-Nd isotopic evidence for the petrogenesis of the Stillwater Complex, Montana. Journal of Petrology in press.

Luck, J.-M. & Allegre, C.J. 1982. The study of molybdenites through the 187Re - 187Os chronometer. Earth and Planetary Science Letters 61, 291-296.

Marques, J.C.; Filho, C.F.F.; Carlson, R.W.; Pimentel, M.M. 2003. Re-Os and Sm-Nd isotope systematics and trace element geochemistry setting constraints in the chromite deposits of Ipueira-Medrado Sill, Bahia, Brazil. Journal of Petrology in press.

McCandless, T.E. & Ruiz, J. 1991. Osmium isotopes and crustal sources for platium-group mineralization in the Bushveld Complex, South Africa. Geology 19, 1225-1228.

McCandless, T.E.; Ruiz, J.; Campbell, A.R. 1993. Rhenium behavior in molybdenite in hypogene and near-surface environments: implications for Re-Os geochronometry. Geochimica et Cosmochimica Acta 57, 889-905.

Meisel, T.; Walker, R.J.; Morgan, J.W. 1996. The osmium isotopic composition of the Earth's primitive upper mantle. Nature 383, 517-520.

Pearson, D.G. & Shirey, S.B. 1999. Isotopic dating of diamonds. In Applications of radiogenic isotopes to ore deposit research and exploration (ed. D. Lambert and J. Ruiz), pp. 143-171. Society of Economic Geologists.

Pearson, D.G.; Shirey, S.B.; Carlson, R.W.; Boyd, F.R.; Pokhilenko, N.P.; Shimizu, N. 1995. Re-Os, Sm-Nd and Rb-Sr isotope evidence for thick Archaean lithospheric mantle beneath the Siberian craton modified by multistage metasomatism. Geochimica et Cosmochimica Acta 59, 959-977.

Pearson, D.G.; Shirey, S.B.; Bulanova, G.P.; Carlson, R.W.; Milledge, H.J. 1998a. Re-Os isotope measurements of single sulfide inclusions in a Siberian diamond and its nitrogen aggregation systematics. Geochimica et Cosmochimica Acta 63, 703-711.

Pearson, D.G.; Shirey, S.B.; Harris, J.W.; Carlson, R.W. 1998b. Sulfide inclusions in diamonds from the Koffiefontein kimberlite, S. Africa: Constraints on diamond ages and mantle Re-Os systematics. Earth and Planetary Science Letters 160, 311-326.

Pearson, D.G.; Shirey, S.B.; Bulanova, G.P.; Carlson, R.W.; Milledge, H.J. 1999. Dating and paragenetic distinction of diamonds using the Re-Os isotope system: application to some Siberian diamonds. Proceedings of the 7th International Kimberlite Conference, 637-643.

Pearson, N.J.; Alard, O.; Griffin, W.L.; Jackson, S.E.; O'Reilly, S.Y. 2002. In-situ measurement of Re-Os isotopes in mantle sulfides by laser ablation multi-collector inductively coupled mass spectrometry: analytical methods and preliminary results. Geochimica et Cosmochimica Acta 66, 1037-1050.

Pegram, W.J. & Allegre, C.J. 1992. Osmium isotopic compositions from oceanic basalts. Earth and Planetary Science Letters 111, 59-68.

Peslier, A.H.; Reisberg, L.; Ludden, J.; Francis, D. 2000. Re-Os constraints on harzburgite and lherzolite formation in the lithospheric mantle; a study of northern Canadian Cordillera xenoliths. Geochimica et Cosmochimica Acta 64, 3061-3071.

Reisberg, L. & Meisel, T. 2002. The Re-Os isotopic system: A review of analytical techniques. Geostandards Newsletter 26, 249-267.

Reisberg, L.; Zindler, A.; Marcantonio, F.; White, W.; Wyman, D.; Weaver, B. 1993. Os isotope systematics in ocean island basalts. Earth and Planetary Science Letters 120, 149-167.

Reisberg, L.C. & Lorand, J.-P. 1995. Longevity of sub-continental mantle lithosphere from osmium isotope systematics in orogenic peridotite massifs. Nature 376, 159-162.

Richardson, S.H.; Shirey, S.B.; Harrism J.W.; Carlson, R.W. 2001. Archean subduction recorded by Re-Os isotopes in eclogitic sulfide inclusions in Kimberley diamonds. Earth and Planetary Science Letters 191, 257-266.

Righter, K.; Chesley, J.T.; Geist, D.; Ruiz, J. 1998. Behavior of Re during magma fractionation; an example from Volcan Alcedo, Galapagos. Journal of Petrology 39, 785-795.

Shirey, S.B. & Walker, R.J. 1998. The Re-Os isotope system in cosmochemistry and high-temperature geochemistry. Annual Reviews of Earth and Planetary Science 26, 423-500.

Shirey, S.B.; Richardson, S.H.; Menzies, A.; Pearson, D.G.; Harris, J.W.; Carlson, R.W.; Wiechert, U.; Gurney, J.J. 2001. Archean emplacement of eclogitic components into the lithospheric mantle during formation of the Kaapvaal craton. Geophysical Research Letters 28, 2509-2512.

Shirey, S.B.; Harris, J.W.; Richardson, S.H.; Fouch, M.J.; James, D.E.; Cartigny, P.; Deines, P.; Viljoen, F. 2002. Diamond genesis, seismic structure, and evolution of the Kaapvaal-Zimbabwe craton. Science 297, 1683-1686.

Stein, H.; Markey, R.J.; Morgan, J.W.; Hannah, J.L.; Schersten, A. 2001. The remarkable Re-Os chronometer in molybdenite: how and why it works. Terra Nova 13, 479-486.

Volkening, J.; Walczyk, T.; Heumann, K.G. 1991. Osmium isotope ratio determinations by negative thermal ionization mass spectrometry. International Journal of Mass Spectrometry and Ion Processes 105, 147-159.

Walker, R.; Morgan, J.; Horan, M. 1995. Osmium-187 enrichments in some plumes: evidence for core-mantle interaction? Science 269, 819-822.

Walker, R.J.; Shirey, S.B.; Stecher, O. 1988. Comparative Re-Os, Sm-Nd and Rb-Sr isotope and trace element systematics for Archean komatiite flows from Munro Township, Abitibi Belt, Ontario. Earth and Planetary Science Letters 87, 1-12.

Walker, R.J., Carlson, R.W.; Shirey, S.B.; Boyd, F.R. 1989. Os, Sr, Nd, and Pb isotope systematics of southern African peridotite xenoliths: Implications for the chemical evolution of subcontinental mantle. Geochimica et Cosmochimica Acta 53, 1583-1595.

Walker, R.J.; Echeverria, L.M.; Shirey, S.B.; Horan, M.F. 1991a. Re-Os isotopic constraints on the origin of volcanic rocks, Gorgona Island, Colombia: Os isotopic evidence for ancient heterogeneities in the mantle. Contributions to Mineralogy and Petrology 107, 150-162.

Walker, R.J.; Morgan, J.W.; Naldrett, A.J.; Li, C.; Fassett, J.D. 1991b. Re-Os isotope systematics of Ni-Cu sulfide ores, Sudbury igneous complex, Ontario; evidence for a major crustal component. Earth and Planetary Science Letters 105, 416-429.

Walker, R.J.; Morgan, J.W.; Horan, M.F.; Czamanske, G.K.; Krogstad, E.J.; Likhachev, A.P.; Kunilov, V.E. 1994. Re-Os isotopic evidence for an enriched mantle source for the Noril'sk-type ore-bearing intrusions, Siberia. Geochimica et Cosmochimica Acta 58, 4179-4197.

Walker, R.J.; Prichard, H.M.; Ishiwatari, A.; Pimentel, M. 2002. The osmium isotopic composition of the convecting upper mantle deduced from ophiolite chromitites. Geochimica et Cosmochimica Acta 66, 329-345.

GROWTH OF THE ARCHAEAN SUPERIOR CRATON AS REVEALED BY U-Pb GEOCHRONOLOGY AND Hf ISOTOPES IN ZIRCON

Davis, D.W.

Earth Sciences Department, Royal Ontario Museum, 100 Queen's Park, Toronto ON, Canada M5S 2C6. dond@rom.on.ca

Keywords: Superior, Archean, zircon, U-Pb, geochronology

The Superior province (Fig. 1) is Earth's largest preserved fragment of Archean crust and has been an important area for testing theories of early crustal development (Card, 1990). Its formation around 2.7 Ga occurred during a unique period in Earth's history when the bulk of juvenile continental crust may have been extracted from the mantle. The same style of orogeny is seen in early Proterozoic orogenies such as the 2.1 Ga Transamazonian and Eburnean of South America and Africa. This period may represent the transition from an early small-scale permobile plate tectonic regime to one dominated by large scale interaction of rigid plates. Zircon has played a preponderant role in understanding the Superior province because of its unique characteristics as an effective U-Pb geochronometer as well as its capacity to preserved primary petrogenetic information through Hf and O isotopes.

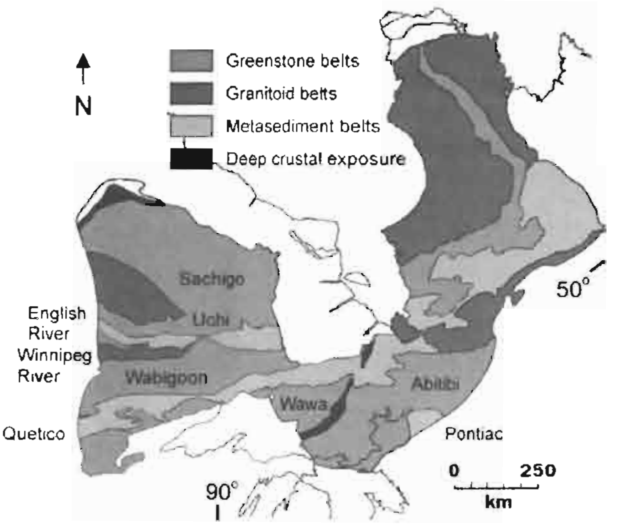

Figure 1. Generalized map of Superior province showing major subprovinces from Card & Ciesielski (1986).

The oldest rocks known in the Superior province extend back to 3.8 Ga (Bohm et al., 2000) and are found near the northern edge of the craton. Zircon dating shows an uneven but near continuous record of magmatism from about 3.1 Ga to 2.65 Ga (Fig. 2). Areas older than 2.8 Ga often contain komatiite – quartz arenite sequences and associated basement plutons. These form thin but widespread units in the northern half of the province (Thurston & Chivers, 1990). Detrital zircons from quartz arenites often show uniform ages similar to the underlying basement. These sedimentary rocks likely resulted from intense weathering of an early continental platform while the komatiites may be products of Mesoarchean plumes.

A resurgence of magmatism in the period 2750-2650 Ma generated the bulk of exposed rocks and also reworked older terrains. Events during this period show a bimodal age distribution. The first peak largely comprises arc-related volcanics and associated tonalite plutons. Arc volcanism ended at about 2700 Ma and was replaced by large scale melting of crust and metasomatized mantle, giving the younger age peak. Regional deformation, thickening and uplift during this period resulted in the rapid deposition of large volumes of orogenic sandstones now preserved in the major metasedimentary subprovinces such as English River, Quetico and Pontiac (Fig. 1). Events that formed individual greenstone belts and basins are often compressed into a few 10's of m.y. or less. The rapidity of major orogenic processes presented a significant challenge to geochronology from the beginning and was the main impetus for developing methods of high precision, high sensitivity U-Pb dating.

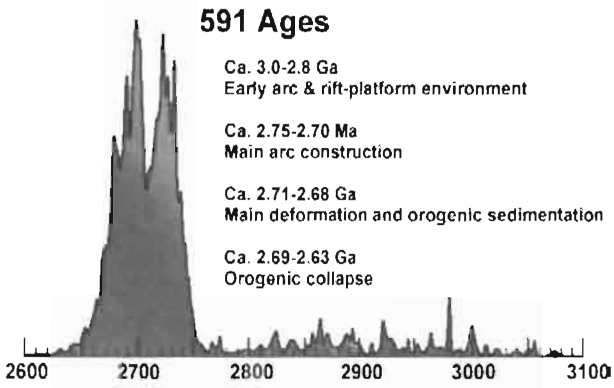

Figure 2. Compilation of U-Pb zircon ages from the Superior province made by summing gaussian error curves.

Superior province consists of lithologically and metamorphically distinct terrains. Its southern half shows a large-scale east-west trending belt structure defined by alternating granite-greenstone and metasedimentary dominated subprovinces (Fig. 1). Two decades ago, it was commonly believed that greenstone belts in the Superior province formed by eruption and collapse of large volcanic edifices and that modern-style plate tectonics did not play a major role. The discovery that older rocks are restricted to the more northerly parts of the province led to the first suggestions of that it formed by accretionary processes (Langford & Morin, 1976).

Later work showed that ages of magmatic rocks are quite variable but the ability to precisely date single detrital zircons in sandstones furnished decisive evidence in support of the accretionary model. Because uplift and erosion occurred during widespread magmatism, detrital zircons in metasandstones and cross-cutting intrusions often tightly constrain ages of deposition. They also give important information on provenance. Systematic dating of detrital zircons in different subprovinces has shown a generally consistent younging of deposition from north to south over the narrow time span 2.71-2.67 Ga, synchronous with diachronous onset of regional deformation (Fig. 3). This is clearly evident for the metaturbidite-dominated subprovinces. Metasedimentary rocks within greenstone belts usually form thin, fault-bounded units that sometimes mark age reversals within the volcanic sequences, suggesting that thrust tectonics played a role in their emplacement (Davis et al., 1988, 1989). These orogenic sandstones appear to represent foreland basins formed in front of an advancing thrust complex during assembly of the craton (Davis, 1998, 2002).

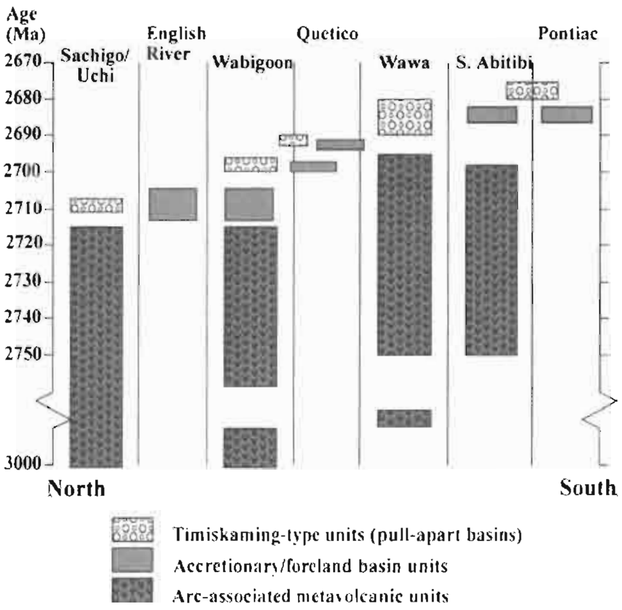

Figure 3. Southward progression of ages for late orogenic sedimentation across the Superior province.

The later structural regime was one of dextral transpression that led to formation of large E-W trending strike-slip faults. Alluvial conglomerates and alkaline volcanic rocks are often localized along these faults and are known as Timiskaming-type sequences. These are thought to have formed in wrench basins associated with transcurrent fault movement and are an important host for gold mineralization.

Another unique rock type associated with this period is the sanukitoid magmatic suite. This consists of plutons that vary from gabbro to quartz monzonite but show enrichment in both compatible and incompatible elements. They are suggested to have formed by partial melting and differentiation of metasomatized mantle (Shirey & Hanson, 1984). Sanukitoid magmas intruded during regional deformation, often into dilatent structures such as the hinge zones of large folds where they show a cresentic shape. The oxygen isotopic signature of zircons from the sanukitoid plutonic suite is slightly but distinctly higher than that from other arc-related plutons (King et al., 1998) indicating a crustal component. Such studies have shown that zircon is often the only common mineral to preserve its primary oxygen isotopic signature through Archean metamorphism. Primary sanukitoid magmas may have been produced by an influx of hot aesthenosphere into previously metasomatized supra-subduction zone mantle following slab breakoff or delamination. Varying degrees of fractionation and crustal assimilation generated the magmatic suite. The final magmatic events involved emplacement of I and S-type crustal melts, which form extensive plutons within the granitoid and metasedimentary belts. Rare exposures of the deep crust, discussed below, record high grade metamorphism and orogenic collapse during his period.

Hf isotopes in zircon as well as age inheritance and Nd whole rock isotopic data show that the granite-greenstone belts consist of terranes formed in at least three distinct environments that were juxtaposed during assembly of the craton (Corfu & Stott, 1993, 1996; Corfu & Noble, 1992; Davis et al., 2000; Henry et al., 2000). The Sachigo subprovince consists partly of an older juvenile 3.0 Ga terrane, the North Caribou block, which may have acted as a protocontinental nucleus. This terrane was reworked sporadically over a 300 m.y. period in what is suggested to have been an Andean-type active margin now preserved as the Uchi subprovince (Stott & Corfu, 1991). The Winnipeg River subprovince to the south contains a deep level exposure of a still older terrain containing gneisses at least 3.3 Ga old with mantle extraction ages that extend to 3.5 Ga. Younger rocks within this terrane record the earliest phases of Neoarchean accretion at 2715 Ma. This age may correspond to collision of a continental fragment with the North Caribou block. It is coincident with deposition of the earliest orogenic sandstones within greenstones of the adjacent western Wabigoon subprovince. Periods of deformation in both terrains are coeval. The Wabigoon subprovince as a whole is a complex amalgamation of terranes. It contains juvenile Neoarchean greenstone belts in the west, rocks that are isotopically similar to the Winnipeg River subprovince in the north and a terrane similar to the North Caribou block in its south-central part (Tomlinson et al., 2003). The Wawa and Abitibi subprovinces on the exposed southern margin of the craton consist mostly of juvenile 2.73-2.66 Ga rocks. They may in part represent a once continuous 2.72 Ga arc that collided with the accretionary margin shortly after 2700 Ma along with fragments of younger arc and back-arc systems.

Hf isotopic analysis of single detrital zircons, along with U-Pb dating, is a powerful method for tracing provenance. Detrital zircons in the Quetico subprovince, deposited at about 2700 Ma, show evidence for sources in the Winnipeg River terrane, indicating that early rocks within this terrane must have been exposed to erosion at this time and may have been deposited onto juvenile arc rocks accreting from the south.

Seismic reflection profiles, acquired from the eastern and western Superior province as part of the Lithoprobe program show generally north dipping reflectivity beneath what are thought to be accreted terranes. There is some evidence for mantle reflectors that could represent fossil subduction zones. Reflectivity changes to south-dipping beneath the contact between the accretionary complex and the supposed Mesoarchean protocontinental nucleus to the north. Seismic reflectivity in lower crustal regions of the Superior province crust is largely subhorizontal in contrast to common steeply dipping structures in mid-upper crust.

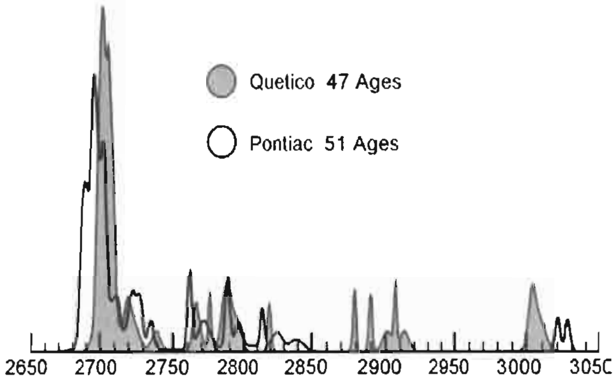

Figure 4. Normalized detrital zircon age distributions for the Quetico and the Pontiac subprovinces.

Areas of Proterozoic uplift, such as the Kapuskasing structural zone between the Abitibi and Wawa subprovinces, provide a window into the Archean lower crust. Zircon dating in the Kapuskasing structure has shown that steep fabrics were cross-cut by subhorizontal fabric at about 2670 Ma (Moser et al., 1996). This age corresponds to emplacement of late crustal melts and may reflect deep crustal extension during collapse of the orogen possibly associated with delamination. Some of the lower crustal sequences consist of alternating layers of metasedimentary rock and mafic granulites. Detailed dating of different generations of metamorphic zircon in mafic granulites suggests that the crust was constructed at least partly by successive under thrusting of mafic slabs followed by metamorphism (Krogh, 1993). Fluid released during metamorphism apparently re-hydrated earlier granulites at higher crustal paleo-level, growing a new generation of metamorphic zircon around earlier metamorphic cores. Such fluids may represent one source for late Archean lode gold deposits. The underthrusting scenario is supported by the presence of conglomerate in the lower crust whose clasts give ages that are younger than the youngest supracrustal rocks preserved in the upper crust.

The existence of the belt structure in the southern half of the Superior province has often been considered a primary effect of accretion, the different granite-greenstone belts representing accreted terranes and subprovince boundaries in some cases representing suture zones. In detail, however, this simple picture breaks down. Some subprovinces contain a variety of distinct terranes while in other cases areas that could belong to a single terrane are found in different subprovinces. The Winnipeg River subprovince represents a deep level exposure of an old terrane that likely extends well into the Wabigoon subprovince. The south-central part of the Wabigoon subprovince may represent a thin fragment of the 3.0 Ga North Caribou terrane that was thrust southward over the accretionary margin. The Wabigoon subprovince contains volcanic assemblages that are similar in age and magmatic provenance to those found in most other terranes.

Although volcanic sequences may be locally conformable, there has apparently been significant lateral transport and interleaving of crust during diachronous formation of an extensive foreland basin. The metasedimentary Pontiac subprovince is the southernmost exposed terrane and was deposited at close to 2685 Ma. Except for the youngest detrital components, its provenance is similar to that of the Quetico subprovince, found between the Wabigoon and Wawa subprovinces which was deposited 10-15 m.y. earlier (Fig. 4). Seismic evidence indicates that these metasedimentary rocks dip beneath adjacent greenstone belts, suggesting that the metasedimentary subprovinces represent exposed parts of a linked foreland basin over which late-Archean arc volcanic assemblages that now form the Wawa, Abitibi and perhaps parts of the Wabigoon subprovinces were thrust. If so, the present map pattern of subprovinces may represent the effect of late differential uplift of a complexly layered accretionary complex, rather than that of early collisional processes (Davis, 1998). In this case the search for suture zones at surface may be futile, the important problems being to identify fragments of collided terranes and to determine how they were assembled to form the crust. Without access to precise geochronology and isotope geochemistry from zircon we would have little hope of solving these problems.

REFERENCES

Bohm, C.O.; Heaman, L.M.; Creaser, R.A.; and Corkery, M.T. 2000. Discovery of pre-3.5 Gs exotic crust at the northwest Superior Province margin, Manitoba. Geology 28: 75-78.

Card, K.D. 1990. A review of the Superior province of the Canadian shield, a product of Archean accretion. Precambrian Research 48: 99-156.

Card, K.D. & Ciesielski, A. 1986. DNAG #1. Subdivisions of the Superior province of the Canadian shield. Geoscience Canada, 13: 5-13.

Corfu, F. 1987. Inverse age stratification in the Archean crust of the Superior Province: evidence for infra- and subcrustal accretion from high resolution U-Pb zircon and monazite ages. Precambrian Research 36: 259-275.

Corfu, F. & Noble, S.R. 1992. Genesis of the southern Abitibi greenstone belt, Superior province, Canada: evidence from zircon Hf isotopic analyses using a single filament technique. Geochim. Cosmochim. Acta 56: 2081-97.

Corfu, F. & Stott, G. 1993. Age and petrogenesis of two late Archean magmatic suites, northwestern Superior province, Canada: Zircon U-Pb and Lu-Hf isotopic relations. Jour. Petrol. 34: 817-838.

Corfu, F. & Stott, G. 1996. Hf isotopic composition and age constraints on the evolution of the Archean central Uchi subprovince, Ontario, Canada. Precambrian Research 78: 53-63

Davis, D.W. 1998. Speculations on the formation and crustal structure of the Superior province from U-Pb geochronology. Western Superior Lithoprobe Transect Fourth Annual Workshop, Lithoprobe Report 65: 21-28.

Davis, D.W. 2002. U-Pb geochronology of Archean metasediments in the Pontiac and Abitibi subprovinces, Quebec, constraints on timing, provenance and regional tectonics. Precambrian Research, 115: 97-117.

Davis, D.W.; Sutcliffe, R.H.; Trowell, N.F. 1988. Geochronological constraints on the tectonic evolution of a late Archean greenstone belt, Wabigoon Subprovince, northwest Ontario, Canada. Precambrian Research 39: 171-191.

Davis, D.W.; Poulsen, K.H.; Kamo, S.L. 1989. New insights into Archean crustal development from geochronology in the Rainy Lake area, Superior Province, Canada. The Journal of Geology 97: 379-398.

Davis, D.W.; Amelin, Y.; Nowell, G.M.; Parrish, R.R. 2000. Constraints on crustal development in the Western Superior Lithoprobe Transect from Hf isotopes in zircons. Western Superior Lithoprobe Transect Sixth Annual Workshop. Lithoprobe Report 77: 38-44.

Henry, P.; Stevensen, R.K.; Larbi, Y.; Gariepy, C. 2000. Nd isotopic evidence for early to late Archean (3.4-2.7 Ga) crustal growth in the western Superior province (Ontario, Canada). Tectonophysics 322, 135-151.

King, E.M.; Valley, J.W.; Davis, D.W.; Edwards, G.R. 1998. Oxygen isotope ratios of Archean plutonic zircons from granite-greenstone belts of the Superior province: indicator of magmatic source. Precambrian Research 92: 365-387.

Krogh, T.E. 1993. High precision U-Pb ages for granulite metamorphism and deformation in the Archean Kapuskasing Structural Zone, Ontario: Implications for structure and development of the lower crust. Earth and Planetary Science Letters 119: 1-18.

Langford, F.F. & Morin, J.A. 1976. The development of the Superior province of northwestern Ontario by merging island arcs. American Journal of Science 276: 1023-1034.

Moser, D.E.; Heaman, L.M.; Krogh, T.E.; Hanes, J.A. 1996. Intracrustal extension of an Archean orogen revealed using single-grain U-Pb zircon geochronology. Tectonics 15: 1093-1109.

Shirey, S.B. & Hanson, G.N. 1984. Mantle-derived Archean monzodiorites and trachyandesites. Nature, 310: 222-224.

Stott, G.M. & Corfu, F. 1991. Uchi Subprovince. In Geology of Ontario. Edited by P.C. Thurston, H.R. Williams, R.H. Sutcliffe, and G.M. Stott. Ontario Geological Survey Special Volume 4: 145-236.

Thurston, P.C. & Chivers, K.M. 1990. Secular variation in greenstone sequence development emphasising Superior Province, Canada. Precambrian Research, 46: 21-58.

Tomlinson, K.Y.; Davis, D.W.; Stone, D.; Hart, T.R. 2003. U-Pb age and Nd isotopic evidence for crustal recycling and Archean terrane development in the south-central Wabigoon subprovince, Canada. Contributions to Mineralogy and Petrology, 144: 684-702.

TOWARDS A COMPOSITE CARBON ISOTOPIC SECTION FOR THE NEOPROTEROZOIC

Halverson, G.P.[1,2]; Hoffman, P.F.[1]; Maloof, A.C.[1] and Rice, A.H.N.[3]

1. Harvard University, Dept. of EPS, 20 Oxford St.; Cambridge, MA 02138. hoffman@eps.harvard.edu, maloof@eps.harvard.edu
2. Geological Survey of Namibia, PO Box 2168, Windhoek Namibia and University of Namibia, PO Box 1331, Windhoek, Namibia. halvers@eps.harvard.edu
3. Institute for Geology, University of Vienna, Althanstrasse 14, A-1090 Vienna, Austria. Alexander.Hugh.Rice@univie.ac.at

Keywords: Neoproterozoic, carbon isotopes, glaciation, stratigraphy, cap carbonate

INTRODUCTION

The Neoproterozoic (~1000 - 543 Ma) experienced the most widespread and severe glaciations in Earth's history. The occurrence of extensive cap carbonates directly atop the glacial deposits and paleomagnetic evidence (e.g. Sohl et al., 1999) that ice sheets breached the tropics present the climatic paradox that distinguishes these glaciations from those of the Phanerozoic. The coincidence of extreme variation in the ^{13}C-composition of marine carbonates with these glaciations attests to an intimate link between the global carbon cycle and climate. The snowball Earth hypothesis, as rearticulated by Hoffman et al. (1998), has been challenged from many sideses, but remains the only comprehensive explanation for the various characteristics of the low-latitude glaciations.

A lingering challenge to testing the snowball hypothesis and, more generally, to reconstructing Neoproterozoic Earth history, is the paucity of useful radiometric ages and biostratigraphy for this time period (Knoll, 2000). The fragmented geochronology has made it difficult to correlate glacial deposits and other strata globally, establish time scales for the glaciations and δ^{13}C anomalies, and answer the fundamental question of how many ice ages occurred during the Neoproterozoic. Chemostratigraphy has long held promise as a tool that might help cinch up the chronology, but has not solved this question. Here, we propose a new correlation scheme for the Neoproterozoic that is based in large part on recognition of globally consistent and distinct stratigraphic and isotopic boundary conditions to the Sturtian- and Marinoan-aged glaciations. Correlations between Svalbard, northern Namibia, and northern Norway lead to the conclusion that there were three distinct glaciations after ~750 Ma, the youngest hereafter to referred to as the Gaskiers events. The connection between the Svalbard and Namibian successions is the basis for a new, high-resolution δ^{13}C record that spans over half of the Neoproterozoic. Additional data is tacked onto the record to extend it to the Precambrian-Cambrian boundary.

THE SVALBARD-NAMIBIA CONNECTION

Previous δ^{13}C compilations for the Neoproterozoic (e.g. Hayes et al., 1999) have consisted of data from various successions joined together on the basis of poorly constrained correlations. The strength of the δ^{13}C composite presented here is that it principally consists of data from just two stratigraphic successions: the Otavi Group in northern Namibia and the Akademikerbreen and Polarisbreen groups in northeastern Svalbard. The overlap between the two successions is adventitious insofar as it results in nearly 4 km of almost continuous carbonates (barring glacial periods), likely spanning over 200 m.y.

The Otavi Group of northern Namibia contains the glacigenic Chuos and Ghaub formations, which separate the carbonates of the Ombombo, Abenab, and Tsumeb subgroups. The older (Sturtian) Chuos Formation is commonly the thicker and more widespread of the two diamictites on the Otavi platform. It is overlain by the Rasthof cap carbonate sequence, which exhibits a sharp rise in δ^{13}C from ~ -4‰ at its base to > +5‰. The younger and presumably Marinoan-aged Ghaub diamictite (Kennedy et al., 1998; Hoffman & Schrag, 2002) is only patchily preserved on the platform, but is ubiquitous in slope settings. The Ghaub glaciation was presaged by a large (>10‰) but gradual decline in δ^{13}C in the upper Ombaatjie Formation (Halverson et al., 2002) and was followed by deposition of the Maieberg cap carbonate sequence. The basal dolostone of the cap carbonate (Keilberg Member) exhibits a slight decrease in δ^{13}C upsection from -3 to -4‰ and contains unusual accretionary oscillation megaripple (AOM) and tube-like structures (Hoffman & Schrag, 2002). The dolostone is bound above by a flooding surface, which corresponds to a sharp decline in δ^{13}C of 1 to 2‰, coincident with a shift from dolomite to calcite. Locally, build-ups of seafloor aragonite cements occur just above the flooding surface (Hoffman & Schrag, 2002). The isotopic trends and sedimentology of the lower Maieberg Formation are characteristic of inferred Marinoan cap carbonates globally.

Whereas most Marinoan cap dolostones are overlain by shales, carbonates persist for >1400 m (Tsumeb Group) above the glacial interval in Otavi platform sections and provide a rare glimpse of the post-Marinoan carbon-isotopic evolution of seawater. Significantly, following a recovery to highly ^{13}C-enriched compositions in the upper half of the section, δ^{13}C declines again to negative values just beneath a major unconformity marking the contact with the overlying Mulden Group siliciclastics.

The upper Hecla Hoek Succession of northeastern Svalbard contains two distinct glacigenic intervals. The Petrovbreen Member and Wilsonbreen Formation diamictites are separated by over 200 m of strata and occur within the middle of the mixed carbonate-siliciclastic Polarisbreen Group. Like the Ghaub diamictite in Namibia, the older Petrovbreen is presaged by a large negative $\delta^{13}C$ anomaly (Halverson et al., 2003), rests atop an erosional disconformity, consists predominantly of clasts from the immediately subjacent strata, and is thin to patchily preserved. The Petrovbreen lacks a transgressive cap carbonate and is instead overlain by a thick (200 m) stack of very finely laminated olive-green to black rhythmites (Macdonaldryggen Member). The younger Wilsonbreen Formation is not associated with a large erosional surface. It is much thicker (~100 m on average), contains abundant extrabasinal clasts, and is overlain by the Dracoisen cap dolostone. The 5-15 m-thick, yellow weathering dolostone contains distinctive peloids and AOM structures. $\delta^{13}C$ through the Dracoisen cap dolostone is consistently -3 to -4‰. The dolostone is transgressed by red then green and black shales, and its overal resemblance to Marinoan cap dolostones is striking (Halverson et al., 2003).

Correlation of 1) the $\delta^{13}C$ anomalies beneath the Petrovbreen and Ghaub diamictites and 2) the Dracoisen and lower Maieberg cap dolostones indicates that both Polarisbreen diamictites are Marinoan in age. Indeed, the two diamictites and intervening strata may provide a window into the evolution of a snowball Earth (Halverson et al., 2003). This hypothesis, which implies sedimentation, including deposition from dynamic, wet-based glaciers, persisted through the snowball, is supported by recent ice-sheet modeling by Donnadieu et al. (2003).

If both Polarisbreen diamictites are Marinoan in age, then it follows that the Sturtian glaciation or proxy thereof should occur in the underlying stratigraphy in Svalbard (Knoll, 2000). No glacial deposits have been found either in Svalbard or in the correlative succession (Eleanor Bay and Tillite groups) in East Greeland. However, we suggest that the equivalent of the Sturtian cap carbonate occurs at the base of the Polarisbreen Group (lower Russøya Member). Though the negative $\delta^{13}C$ anomaly has not been found in Svalbard, a sharp rise in $\delta^{13}C$ is preserved in this organic-rich sequence that bears similarities to Sturtian cap carbonate sequences elsewhere. Furthermore, a negative anomaly occurs in the equivalent interval in East Greenland (Fairchild et al., 2001).

Beneath the Polarisbreen Group, the Akademikerbreen Group provides a nearly continuous record of $\delta^{13}C$ evolution through 2 km of marine carbonates. This interval is typically ^{13}C-enriched, but the trend is interrupted by a major negative anomaly in the upper Grusdievbreen and lower Svanbergfjellet formations (Fig. 1). The implication of the above correlation that this anomaly predates and is not related to Sturtian glaciation is supported by strong similarities in carbon and strontium isotopic profiles between the lower Akademikerbreen Group and the Bitter Springs Formation (Hill et al., 2000) in central Australia, which is unambiguously pre-Sturtian in age.

THE NORTHERN NORWAY LINK

The Neoproterozoic Vestertana Group in Finnmark, northern Norway contains two distinct, well-studied glacigenic formations separated by hundreds of meters of sandstone and shale. The Smalfjord and Mortensnes diamictites are commonly correlated with the diamictite pairs in Svalbard and East Greenland (e.g. Hambrey, 1983). However, both sedimentological evidence and recent isotopic data argue against this correlation. The older Smalfjord Formation is preceded by a negative $\delta^{13}C$ anomaly (upper Grasdal Formation) and overlain by a distinctive cap dolostone (basal Nyborg Formation), with $\delta^{13}C$ of -2 to -4‰. The simplest conclusion is that the Smalfjord Formation records the Marinoan glaciation and the Mortensnes diamictite a younger glacial episode. The Mortensnes diamictite is preceded by $\delta^{13}C$ values < -8‰ and lacks a cap carbonate.

THREE NEOPROTEROZOIC GLACIATIONS

Correlation of diamictites in northern Namibia, northeastern Svalbard, and northern Norway supports recent speculation (Knoll, 2000; Hoffman & Schrag, 2002) that there were three distinct glaciations during the latter half of the Neoproterozoic. This conclusion differs from Kennedy et al. (1998) who proposed that there were only two glaciations, though we do agree with these authors that the two older glaciations (Sturtian and Marinoan) may be distinguished in some successions by the sedimentological and isotopic characteristics of their respective cap carbonates. In our correlation scheme, we further consider pre-glacial isotopic and stratigraphic features to distinguish between the three glaciations. Because the glacial deposits are highly variable and often absent, they do not prove as useful in establishing correlations.

Available data suggest that the Sturtian glaciation was preceded by a positive carbon isotopic trend. The cap carbonate to the Sturtian glaciation is commonly organic- and/or sulfide-rich, shows evidence of syn-depositional slumping, contains abundant microbilites, and is isotopically negative at its base (Kennedy et al., 1998). When compared to the Marinoan cap carbonate, the Sturtian cap appears bottom-truncated (Hoffman and Schrag, 2002); in some sections, the negative anomaly is absent altogether. Thus, isotopically, it may be best distinguished by a sharp rise in $\delta^{13}C$ to > 5‰ in the lower part of the sequence.

Notable and unequivocally Sturtian glacial deposits occur in northwest Canada, Australia, and Namibia, but are absent in the present day north Atlantic region. The Sturtian glaciation is constrained to post-date 746±2 Ma in Namibia from an U-Pb zircon age on volcanics 700 m beneath the Chuos Formation (Hoffman et al., 1996). Brasier et al. (2000) produced an age of 723 +16/-10 Ma from a purported ash bed within Sturtian glacial deposits in Oman. No undisputed radiometric age tightly constrains the end of the Sturtian glaciation.

Glacial deposits of Marinoan age appear to be the most widespread of the three glaciations, but are highly variable and frequently absent in continental shelf settings. It is proposed here that diamictite pairs in Svalbard, East Greenland, and Death Valley (Kingston Peak Formation) jointly belong to the Marinoan. The glaciation is preceded by an impressive but gradual decline in $\delta^{13}C$ of > 10‰ (Halverson et al., 2002) that is best documented in northern Namibia (Halverson et al., 2002), but is also found in Svalbard (Halverson et al., 2003), northern Norway (Rice & Halverson, unpublished data), South Australia (McKirdy et al., 2001), northwestern Canada (Hoffman & Schrag, 2002), and Scotland (Brasier & Shields, 2000). Halverson et al. (2002) argued that the anomaly is best explained by a protracted release of methane from marine clathrate reservoirs.

The thick cap carbonate sequence to the Marinoan glaciation includes a basal 5 to 15 m-thick cap dolostone with $\delta^{13}C$ invariably -2 to -4‰. The typically yellow or cream-colored dolostone is distinguished by peloids, AOM, and less commonly, tube structures and isopachous cements (Hoffman & Schrag, 2002). The dolostone commonly passes upward into finely laminated limestone or shale, but in some locations also contians barite and/or aragonite seafloor cements.

The age of the Marinoan glaciation is constrained to be younger than ~650 Ma from detrital zircons in the Enorama Formation (Ireland et al., 1998), which occurs below the Elatina Formation in South Australia. Assuming the Port Askaig Tillite in Scotland is Marinoan (contra Brasier & Shields, 2000), then this glaciation is older than the 601±4 Ma Tayvallich Volcanics (Dempster et al., 2002).

The youngest Neoproterozoic glaciation is named after the glacigenic Gaskiers Formation in eastern Newfoundland, which is constrained to lie between 595 Ma (assuming correlation with the Squantum diamictite in the Boston Bay Group to the south; Thompson & Bowring, 2000) and 565 Ma (Benus, 1988). Other inferred Gaskiers-aged glacial deposits include the Mortensnes diamicite in northern Norway, the Loch na Cille Boulder Bed in Scotland, and the Hankalchough in western China. However, as the Gaskiers glacial deposits lack appear to lack proper cap carbonates, it cannot be concluded that this glaciation ended synchronously. Indeed, given the drift of the continents to the high southerly latitudes late in the Neoproterozoic (Torsvik et al., 1995), it is reasonable to surmise that this ice age was not global, but rather diachronous, analogous to the Permo-Carboniferous glaciation.

Several latest Proterozoic successions contain deep paleovalley incisions, which may record the glacioeustatic response to the growth of vast polar ice sheets. Significantly, paleovalleys in the Wonoka Formation in South Australia (Calver, 2000) and the Johnnie Formation in Death Valley (Corsetti & Kaufman, 2003) are at least temporally associated with the most extreme negative $\delta^{13}C$ anomaly in the Neoproterozoic. The "Wonoka" anomaly, also well-documented in Oman (Burns & Matter, 1993) spans several hundred meters of section and features $\delta^{13}C$ values < -10‰ (Calver, 2000). Correlation with the highly ^{13}C-depleted carbonate beneath the Mortensnes diamictite and the occurrence of the $\delta^{13}C$ minimum beneath the oldest Wonoka canyon (Calver, 2000) suggest that like the Marinoan, the Gaskiers glaciation may have followed a massive release of methane.

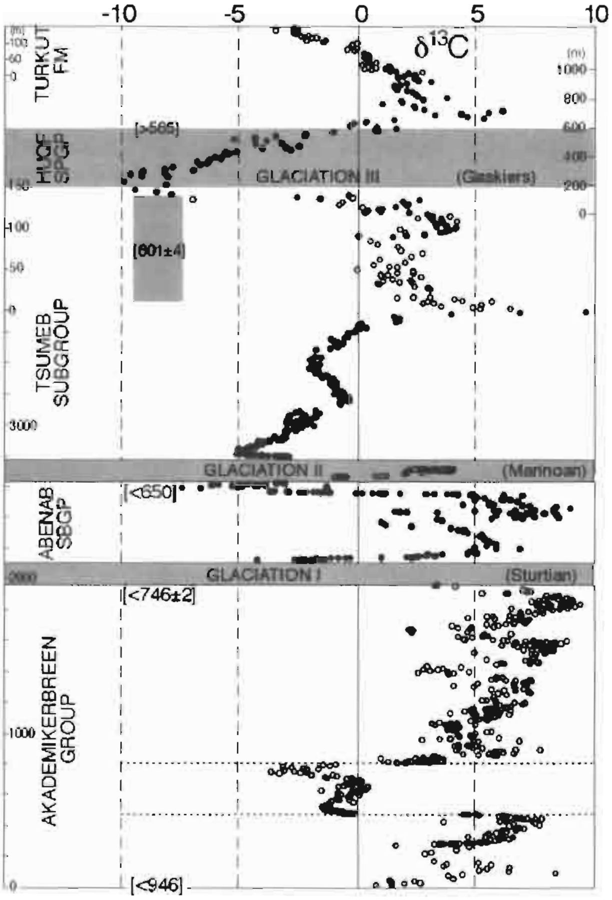

Figure 1. Composite $\delta^{13}C$ section for the Neoproterozoic. Bracketed numbers are radiometric age constraints discussed in text.

A COMPOSITE $\delta^{13}C$ SECTION

Figure 1 presents a new composite $\delta^{13}C$ section that spans much of the Neoproterozoic. The lower part of the record is derived from the Akademikerbreen Group, which is only constrained to be less than 946 Ma from the age of basement granites (Gee et al., 1995). The data between the Sturtian and Marinoan glaciations are from the Abenab Group in Namibia, while presumed syn-Marinoan data are from the inter-diamictite strata in Svalbard (Halverson et al., 2003). No single record links the Marinoan and Gaskiers glaciations. However, it is postulated here that the decline in the upper Tsumeb Subgroup in Namibia marks the onset of the Wonoka anomaly, and thus that the trend joins with a detailed profile from the Huqf Supergroup in Oman (Burns & Matter, 1993) that spans the anomaly. The Terminal Proterozoic profile has been established by previous authors; here, we use data from northeastern Siberia (Pellachaty, 1998) to extend the composite section to the Precambrian-Cambrian boundary.

CONCLUSIONS

A new correlation scheme proposed here supports recent suggestions (Knoll, 2000; Hoffman & Schrag, 2002) that there were three Neoprotertozoic ice ages after ~750 Ma. The correlations are consistent with available radiometric, Sr-isotopic, and biostratigraphic data. Whereas all three events appear to be related to major perturbations in the global carbon cycle, the magnitude and timing of the related negative $\delta^{13}C$ anomalies is different for each glaciation. The largest (Wonoka) anomaly coincides with the youngest (Gaskiers) glaciation, which appears to lack a cap carbonate and may have been diachronous.

The correlation scheme is the basis for a $\delta^{13}C$ composite section for the Neoproterozoic. The strength of this compilation is that the data are derived almost entirely from just two successions (Namibia and Svalbard) correlated along multiple tie points. The record is not complete as it does not cover the earliest Neoproterozoic, and it is as yet poorly calibrated. Nonetheless, this new $\delta^{13}C$ chronology helps put into perspective not only the three Neoproterozoic glaciations, but also impressive biogeochemical perturbations that occurred earlier in the era.

REFERENCES

Benus, A.P. 1988. Sedimentological context of a deep-water Ediacaran fauna (Mistaken Point Formation, Avalon zone, eastern Newfoundland). In E. Landing, G.M. Narbonne, and P.M. Myrow (Eds.), Trace Fossils, Small Shelly Fossils, and the Precambrian-Cambrian Boundary. Bull. N.Y. St. Mus. 463, 8-9.

Brasier, M.; McCarron, G.; Tucker, R.; Leather, J.; Allen, P.; Shields, G. 2000. New U-Pb zircon dates for the Neoproterozoic Ghubrah glaciation and for the top of the Huqf Supergroup, Oman. Geology 28, 175-178.

Brasier, M.D. & Shields, G. 2000. Neoproterozoic chemostratigraphy and correlation of the Port Askaig glaciation, Dalradian Supergroup of Scotland. J. Geol. Soc. Lon. 157, 909-914.

Burns, S.J. & Matter, A. 1993. Carbon isotopic record of the latest Proterozoic form Oman. Eclog. Geol. Helv.; 86, 595-607.

Calver, C.R. 2000. Isotope stratigraphy of the Ediacarian (Neoproterozoic III) of the Adelaide Rift Complex, Australia, and the overprint of water column stratification. Precambrian Res. 100, 121-150.

Corsetti, F.A. & Kaufman, A.J. *in press*, Stratigraphic investigations of carbon isotope anomalies and Neoproterozoic ice ages in Death Valley, California. Geol.Soc. Am. Bull.

Dempster, T.J. et al. 2002. Timing of deposition, orogenesis and glaciation within the Dalradian rocks of Scotland: constraints from U-Pb zircon ages. Journal of the Geological Society, London, 159: 83-94.

Donnadieu, Y.; Fluteau, F.; Ramstein, G.; Ritz, C.; Besse, J. 2003. Is there a conflict between Neoproterozoic glacial deposits and the snowball Earth interpretation: an improved understanding with numerical modeling. Earth Plan. Sci. Let. 208, 101-112.

Fairchild, I.J.; Spiro, B.; Herrington, P.M. and Song, T.; 2000. Controls on Sr and C isotope compositions of Neoproterozoic Sr-rich limestones of East Greenland and North China. In: J.P. Grotzinger and N.P. James (Eds.), Carbonate Sedimentation in the Evolving Precambrian World. SEPM Spec. Pub. 67, Tulsa, pp. 297-313.

Gee, D.G. et al. 1995. Grenvillian basement and a major unconformity within the Caledonides of Nordaustlandet, Svalbard. Precam. Research 70, 215-234.

Halverson, G.P.; Hoffman, P.F.; Schrag, D.P.; Kaufman, A.J. 2002. A major perturbation of the carbon cycle before the Ghaub glaciation (Neoproterozoic) in Namibia: prelude to snowball Earth? Geochem.; Geophys.; Geosys. 3, 10.1029/2001GC000244.

Halverson, G.P.; Maloof, A.C.; Hoffman, P.F. 2003. Stratigraphic and geochemical boundary conditions to Neoproterozoic glaciation in Svalbard. to be submitted to Precambrian Res.

Hambrey, M.J. 1983. Correlation of late Proterozoic tillites in the North Atlantic region and Europe. Geol. Mag. 120, 290-320.

Hayes, J.M.; Strauss, H.; Kaufman, A.J. 1999. The abundance of ^{13}C in marine organic matter and isotopic fractionation in the global beogeochemical cycle of carbon during the past 800 Ma. Chem. Geol. 161, 103-126.

Hill, A.C.; Arouri, K.; Gorjan, P.; Walter, M.R. 2000a. Geochemistry of marine and nonmarine environments of a Neoproterozoic cratonic carbonate/evaporite: the Bitter Springs Formation, Central Australia. In: J.P. Grotzinger & N.P. James (Eds.), Carbonate Sedimentation and Diagenesis in an Evolving Precambrian World, SEPM Spec. Pub. 67, Tulsa, pp. 327-344.

Hoffman, P. & Schrag, D.P.; 2002. The snowball Earth hypothesis: testing the limits of global change. Ter. Nova 14, 129-155.

Hoffman, P.F.; Hawkins, D.P.; Isachsen, C.E.; Bowring, S.A. 1996. Precise U-Pb zircon ages for early Damaran magmatism in the Summas Mountains and Welwitschia Inlier, northern Damara belt, Namibia. Com. Geol. Surv. Namibia 11, 47-52.

Hoffman, P.F.; Kaufman, A.J.; Halverson, G.P.; Schrag, D.P. 1998. A Neoproterozoic snowball Earth. Science 281, 1342-1346.

Ireland, T.R.; Flöttmann, T.; Fanning, C.M.; Gibson, G.M.; Preiss, W.V. 1998. Development of the early Paleozoic Pacific margin of Gonddwana from detrital-zircon ages across the Delamerian orogen. Geology 26, 243-246.

Kennedy, M.J.; Runnegar, B.; Prave, A.R.; Hoffman, K.H.; Arthur, M. 1998. Two or four Neoproterozoic glaciations? Geology 26, 1059-1063.

Knoll, A.H. 2000. Learning to tell Neoproterozoic time. Precambrian Res. 100, 3-20.

McKirdy, D. M. et al. 2001. A chemostratigraphic overview of the late Cryogenian interglacial sequence in the Adelaide Fold-Thrust Belt, South Australia. Precambrian Res. 106, 149-186.

Pelachaty, S.M. 1998. Integrated chronostratigraphy of the Vendian System of Siberia: implications for a global stratigraphy. J. Geol. Soc. Lon. 155, 957-973.

Sohl, L.E.; Christie-Blick, N.; Kent, D.V. 1999. Paleomagnetic polarity reversals in Marinoan (ca. 600 Ma) glacial deposits of Australia: implications for the duration of low-latitude glaciations in Neoproterozoic time. Geol. Soc. Am. Bull. 111, 1120-1139.

Thompson, M.D. & Bowring, S.A. 2000. Age of the Squantum 'tillite', Boston basin, Massachusetts: U-Pb zircon constraints on terminal Neoproterozoic glaciation. Am. J. Sci. 300, 630-655.

Torsvik, T.H.; Lohman, K.C.; Sturt, B.A. 1995. Vendian glaciations and their relation to the disperal of Rodinia: Paleomagnetic constraints. Geology 23, 727-730.

GOLD EXTRACTION OF THE MANTLE THROUGH TIME BASED ON Re-Os ISOTOPES

Ruiz, J.

Department of Geosciences, University of Arizona, Tucson, Arizona 85721. jruiz@pop.geo.arizona.edu

Keywords: Re-Os isotopes, gold, mantle

Geologists have long recognized that Gold deposits, excluding placers, are found in environments where there is material transfer from the mantle to the crust, such as island arcs. An evaluation of deposits in the geologic record clearly has shown that orogens where there is little addition of mantle material, such those produced by the Grenville Orogeny do not contain significant gold. Environments where there is significant juvenile material, such as those of Alaska and the circum-pacific, in general, contain much gold. Another observation is that gold deposits also have a close spatial relation with thick sequences of shale. The two observations suggest that gold deposits can be formed from gold transferred from the mantle directly in arcs but can also be form when gold is recycled and concentrated in shales. What has not been evaluated before, however, is whether there is a variation in time as to the type of source for the gold. In other words, the question is whether the gold in the Proterozoic is typically juvenile, and typically recycled in the Phanerozoic, or whether there is no difference. Understanding this issue can constrain the models for the extraction of gold from the mantle and can also help exploration models for gold in a very broad sense.

In the past, answering the question posed above was not possible since gold could not be traced in the geologic environment by isotopic methods as other elements and minerals. This was because all the isotopic systems used where typically lithophillic and not concentrated in gold. However, now that Re and Os and their isotopic ratios can be measured accurately even in very low concentrations, it is possible to examine the sources of gold assuming that Re and Os behave similarly to gold in the geologic environment. This seems like a reasonable assumption since gold and platidoids, such as Os have similar chemical behavior.

Gold contains measurable amounts of Re and Os that vary according to its environment of deposition. The isotopic ratio of Os can be used to trace its source and therefore may constrain the extraction rates of gold from the mantle through time.

Our data show that gold from systems that are strictly hydrothermal and associated with igneous rocks , such as many base metal porphyry copper deposits, have Os concentrations between 7 and 30 ppt, and Re between 200 ppt to 10 ppb. If the hydrothermal systems also involve shale-rich sedimentary sequences, then Re and Os concentrations can be much higher

Here I will describe the Re-Os isotope systematics from the Witwatersrand Supergroup (WSG) of South Africa and the Grasberg deposit in Papua New Guinea. In these deposits Os clearly shows that gold can be extracted from different geologic reservoirs and still be concentrated to form giant gold deposits.

The Witwatersrand basin has been the focal point of studies devoted to the evolution of the atmosphere and gold mineralization because of the large accumulation of gold and the presence of uraninite and sulfides in the sediments of this Archean basin. Understanding if the gold, uranium and sulfides are detrital or were introduced to the basin by hydrothermal fluids has been at the center of debates for ~100 years (see recent reviews by Frimmel & Minter, 2002; Phillips & Law, 2000). As recently as at the last Geological Society of America, Holland (2003), discussed the importance of the age of sulfide sedimentation of the Witwatersrand basin to constrain the question of whether the early Archean atmosphere was more reduced than that of the present atmosphere. Simply put, sulfides and uranium minerals require a more reduced atmosphere than we have at present for them to survive as detrital minerals during weathering and transport. Regarding the gold mineralization, detrital gold concentrations require exploration models that are based on sedimentology, while exploration based on hydrothermal models focus on possible structural controls and patterns of hydrothermal alteration. In order to constrain these models, we dated the gold and sulfides of the Witwatersrand basin using Re-Os isotopes.

The Witwatersrand basin in South Africa hosts the largest concentration of gold on Earth, is an Archean system that contains gold and rounded pyrite. The gold contains much higher concentrations of Re and Os, mostly in the high ppb to ppm range, suggesting an entirely different mechanism for the formation of this gold from that of Grasberg. Samples from the Vaal Reef conglomerate of the WSG, yield a Re-Os isochron age of 3.03 ± 0.02 Ga and an initial ^{187}Os/^{188}Os ratio of 0.1079 ± 0.0001. Ages of gold and rounded pyrite are older than the 2.89-2.71 Ga conglomerates that host them, indicating that the gold is mostly detrital (Kirk et al., 2002). A possible source would be the Murchison Greenstone belt, which is 3.03 Ga old, and occurs just north of the Witwatersrand basin. Other younger Proterozoic paleoplacer deposits in Brazil and show that gold was not entirely juvenile. The Re-Os data on all the gold deposits analyzed suggest that large quantities of gold was extracted early and recycled in the crust and that based on the Re and Os systematics the gold in the Witwatersrand could have been nagnatic at 3.0 Ga.

In contrast to the Witwatersrand, the Grasberg in the South Pacific is distinguished from similar base metal porphyry deposits by its high gold content.

The Ertsberg district consists of both stockwork and contact controlled mineralization, porphyry copper type deposits, related to the Grasberg and Ertsberg intrusion centers. High-grade gold skarn mineralization exists on the periphery of each of the ore bodies (Kucing Liar, the massive sulfide on the periphery of the Grasberg Intrusive Complex (GIC), and the Dom, DOZ/IOZ/GBT surrounding the Ertsberg Intrusive System (EIS)). In order to resolve the genetic and geochronologic links of the peripheral sediment-hosted ore bodies and the intrusion-hosted ore bodies we examined the Re-Os isotopes of the ores and certain sub adjacent Precambrian to Tertiary crust. Molybdenite geochronology was used to resolve the age relationships of the ore bodies. The Grasberg and Kucing Liar deposits have roughly similar molybdenite mineralization ages of 2.88 ± 0.01 Ma and 2.97 ± 0.01 Ma, respectively; whereas the Ertsberg molybdenite has an age of 2.54 ± 0.01 Ma. These data are in accord with Ar chronologies (Pollard & Taylor, 2000) of the alteration associated with mineralization, and also indicate that mineralization of the Grasberg and Kucing Liar molybdenites are closely similar, and older than the that of the EIS.

An isochron plot of the low Re-Os concentration sulfides and oxides (pyrite, chalcopyrite, and magnetite) for the stockwork, intrusion-hosted, mineralization from the Ertsberg provides an errorchron (MSWD 6.06) age of 1.8 ± 0.7 Ma with an initial $^{187}Os/^{188}Os$ ratio of 0.41± 0.04. None of the samples from the peripheral ore deposits plot on the isochron developed for the EIS or GIC (Mathur et al., 2000), rather they form a distinct mixing trend. The initial $^{187}Os/^{188}Os$ of the peripheral ores range from 0.69 to 1.2. Data from the Kucing Liar deposit (a skarn) and the massive sulfide (sulfide ores close to the intrusion and wall rock of the Grasberg ore deposit) form a mixing trend with the Grasberg stockwork mineralization. This relationship implies a link between the mineralizing fluids for these different types of mineralization associated with emplacement and cooling of the Grasberg intrusive complex. The Os initial ratios of the stockwork mineralization of the Ertsberg and skarn mineralization of Dom lie off of the mixing trend of the Grasberg, indicating a significant genetic difference between the Grasberg and Ertsberg ores. Thus, geochronologic and genetic evidence indicates that mineralization in these two proximal porphyries are not related to one system at a shallow depth, rather these adjacent hydrothermal systems evolved independently during a short interval.

The initial $^{187}Os/^{188}Os$ ratios of all ores of the district are highly radiogenic and indicate a significant crustal source for Os and by inference the other base metals. The mixing diagrams reveal that the mineralizing fluid acquired Os from a higher concentration (>500ppt), and more radiogenic source than the stockwork. In order to resolve the source of this end member, we analyzed sedimentary rocks from seven formations of Proterozoic through Jurassic-Cretaceous age that the porphyries intruded. The units vary lithologically from black shale to sandstone to carbonate. The rocks contain Os concentrations that range from 5 to 452 ppt, and measured $^{187}Os/^{188}Os$ of 0.52 to 3.81. Concentrations of gold in the sedimentary rocks ranged from 5 (average continental crust) to 151 ppb. The presence of relatively higher concentrations of Au in some of the sedimentary rocks and the radiogenic/ concentrated Os signatures in these rocks provide strong evidence for two different crustal sources for metals in the district. The data suggests a model in which the continental crust may have supplied a major portion of the metals during both the magma genesis in the lower crust and another source in surrounding sedimentary rocks.

In summary, it has been known from previous work that gold resources are typically related to orogenic systems and that gold mineralization has been episodic throughout geologic time (e.g. Goldfarb et al., 2001). The main periods for gold mineralization based on the age dating of the deposits were 3400-3100, 2800-2555 Ga, 2100-1800 Ga and then continuously from 0.6 Ga. The Re-Os data supports this general model bu clearly shows that about 40% of the known gold resources were extracted from the mantle at about 3Ga related to the formation of the Kaapval craton. The Phanerozoic deposits, even if they are in orogenic belts contain significant gold that has been recycled in the crust.

REFERENCES

Frimmel, H.E. & Minter, W.E.L. 2002. Recent Developments Concerning the Geological History and Genesis of the Witwatersrand Gold Deposits, South Africa: Society of Economic Geologists Special Publication, v. 9, p. 17–45.

Goldfarb R.J.; Groves D.I.; Gardoll S. 2001. Orogenic gold and geologic time: a global synthesis. Ore Geology Reviews 18, 1-75.

Kirk, J.; Ruiz, J.; Chesley, J.; Walshe, J.; England, G. 2002. A Major Archean, Gold- and Crust-Forming Event in the Kaapvaal Craton, South Africa: Science, v. 297, p. 1856-1858.

Phillips, G.N. & Law, D.M. 1994. Metamorphism of the Witwatersrand gold fields: a review: Ore Geology Reviews, v. 9, p. 1-31.

Mathur R.; Ruiz J.; Titley S.; Gibbins S.; Martogomo W. 2000. Different crustal sources for Au-rich and Au-poor ores of the Grasberg Cu-Au porphyry deposit. Earth Planetary Science Letters 183, 7-14.

MAGMAS THROUGH TIME: OXYGEN ISOTOPE GEOCHEMISTRY OF ZIRCON

Valley, J.W.[1]; Basei, M.A.S.[2]; Bindeman, I.N.[1]; Ferreira, V.P.[3]; King, E.M.[4]; Lackey, J.S.[1]; Peck, W.H.[5]; Sial, A.N.[3] and Spicuzza, M.J.[1]

1. Dept. of Geology, Univ. of Wisconsin, Madison, WI, 53706, USA. valley@geology.wisc.edu, inbindem@geology.wisc.edu, jadestar@geology.wisc.edu, spicuzza@geology.wisc.edu
2. Dept. de Mineralogia Geotectonica, Univ. Sao Paulo, Brazil. baseimas@usp.br
3. NEG-LABISE, Dept. of Geology, Federal Univ. of Pernambuco, Recife, PE 50732-970, Brazil. valderez@ufpe.br, ans@ufpe.br
4. Dept. of Geology, Illinois State Univ., Normal, IL 61790, USA. emking@ilstu.edu
5. Dept. of Geology, Colgate Univ., Hamilton, N.Y.13346, USA. wpeck@mail.colgate.edu

Keywords: Zircon, igneous, oxygen isotopes, age, evolution of crust

Zircon is a common accessory mineral in intermediate to felsic igneous rocks and also occurs in some mafic rocks. Analysis of zircon provides the most reliable record of magmatic $\delta^{18}O$ as well as U-Pb age (see Valley, 2003). High temperatures of mineral stability and melting, slow diffusion rates for cations and anions, chemical inertness, hardness, and small crystal size all combine to create a robust and retentive geochemical record if attention is paid to avoid excessive radiation damage. Zoned magmatic zircons serve as time capsules, preserving isotopic, trace element and mineral/melt inclusion evidence of evolving magmatic conditions. No other mineral permits $\delta^{18}O$ (magma) to be confidently determined and coupled to age of crystallization.

The interpretation of $\delta^{18}O$ values for magmatic zircon is aided by recent determinations of the diffusion rate of oxygen in zircon (Watson & Cherniak, 1997; Peck et al., 2003) and the fractionation of oxygen isotopes between zircon and rock forming minerals (Valley, 2003; Valley et al., 2003). At magmatic temperatures, $\Delta^{18}O$ (whole rock-zircon) ~ 1 to 2‰ for intermediate to felsic compositions, respectively.

Magmatic zircons of known age (3600 to 0.2 Ma) have been analyzed for $\delta^{18}O$ by laser fluorination at the University of Wisconsin from over 700 rocks worldwide to test the generality that Archean magmas had values of $\delta^{18}O$ similar to the mantle while younger magmas were more variable (King et al., 1998; Peck et al., 2000). In addition to laser analyses of zircon concentrates (1-3 mg), single detrital zircons (4400 to 3000 Ma) from the Jack Hills, Western Australia were analyzed *in situ* (30 µm spot, ~2 ng) by ion microprobe (Fig. 1).

The range and variability of $\delta^{18}O$ in all Archean samples is subdued ($\delta^{18}O$(Zrc) = 5 to 7.5‰). Most samples at ~2.7 Ga are from the Superior Province of Canada and average $\delta^{18}O$ is consistent with high temperature equilibrium with zircon from the mantle (5.3±0.3‰, Valley et al., 1998). Only sanukitoids have slightly evolved, higher values (Fig. 2; King et al., 2000). No magmatic zircons have been analyzed from the Archean with $\delta^{18}O$ above 8‰. This includes samples analyzed by laser fluorination from the Lewisian of Scotland. (2.7 Ga), Slave Province (2.7 Ga), and Barberton (3.5 to 2.7 Ga). Samples analyzed by ion microprobe from the Jack Hills are indistinguishable within uncertainty. The oldest zircon shows the same range of $\delta^{18}O$ values with the mildly evolved, higher value (7.4‰) interpreted to result from exchange of magmatic protolith with surface water (Peck et al., 2001).

Values of $\delta^{18}O$ are significantly more variable from the Proterozoic and Phanerozoic. Many values are above 8‰ suggesting that magmas with $\delta^{18}O$ (WR) > 9-10‰ became common after 2.5 Ga. Such high $\delta^{18}O$ magmas can only form through remobilization of high-$\delta^{18}O$ crustal rocks. Values of $\delta^{18}O$ (Zrc) > 10 have been found in a small group of plutons in the Grenville Province (Peck et al., 2003), but are not common elsewhere. Likewise, samples with $\delta^{18}O$ < 5 ‰ are over represented in Figure 1 due to intense study of low $\delta^{18}O$ sub-volcanic granites from the British Tertiary Igneous Province (Gilliam & Valley, 1997; Monani & Valley, 2001) and low-$\delta^{18}O$ rhyolites from Yellowstone (Bindeman & Valley, 2001).

The Archean-Proterozoic boundary approximately coincides with a first order increase in the variability of the oxygen isotope ratios of intermediate to felsic magmas. Since fractionation of oxygen isotopes to values higher or lower than the mantle requires lower temperatures where fractionation is large, the greater variability in $\delta^{18}O$ must reflect recycling of supracrustal lithologies. The dominant sources of high-$\delta^{18}O$ are sediments, and rocks weathered or altered at low temperatures. Low values of $\delta^{18}O$ come largely from rocks that have exchanged with heated meteoric or seawater. Clearly such protoliths have increasingly been involved in magma genesis for younger rocks.The nature and exact timing of the Archean-Proterozoic transition in $\delta^{18}O$ is not yet known due to limited data between 2.5 and 2.0 Ga. This may be a sharp transition at the end of the Archean or at some time within the next 500 Ma, or it may be a gradual change. In either case, one would expect many samples to have a mantle-like $\delta^{18}O$ value and more samples must be analyzed to determine if higher $\delta^{18}O$ magmas existed in this period. Possible causes of the transition to higher $\delta^{18}O$ in younger magmas include: changes in the composition and abundance of sediments available for recycling due to increased sedimentary environments at the end of the Archean; the onset or acceleration of subduction at the end of the Archean; or differences in weathering as the atmosphere became more oxygen rich.

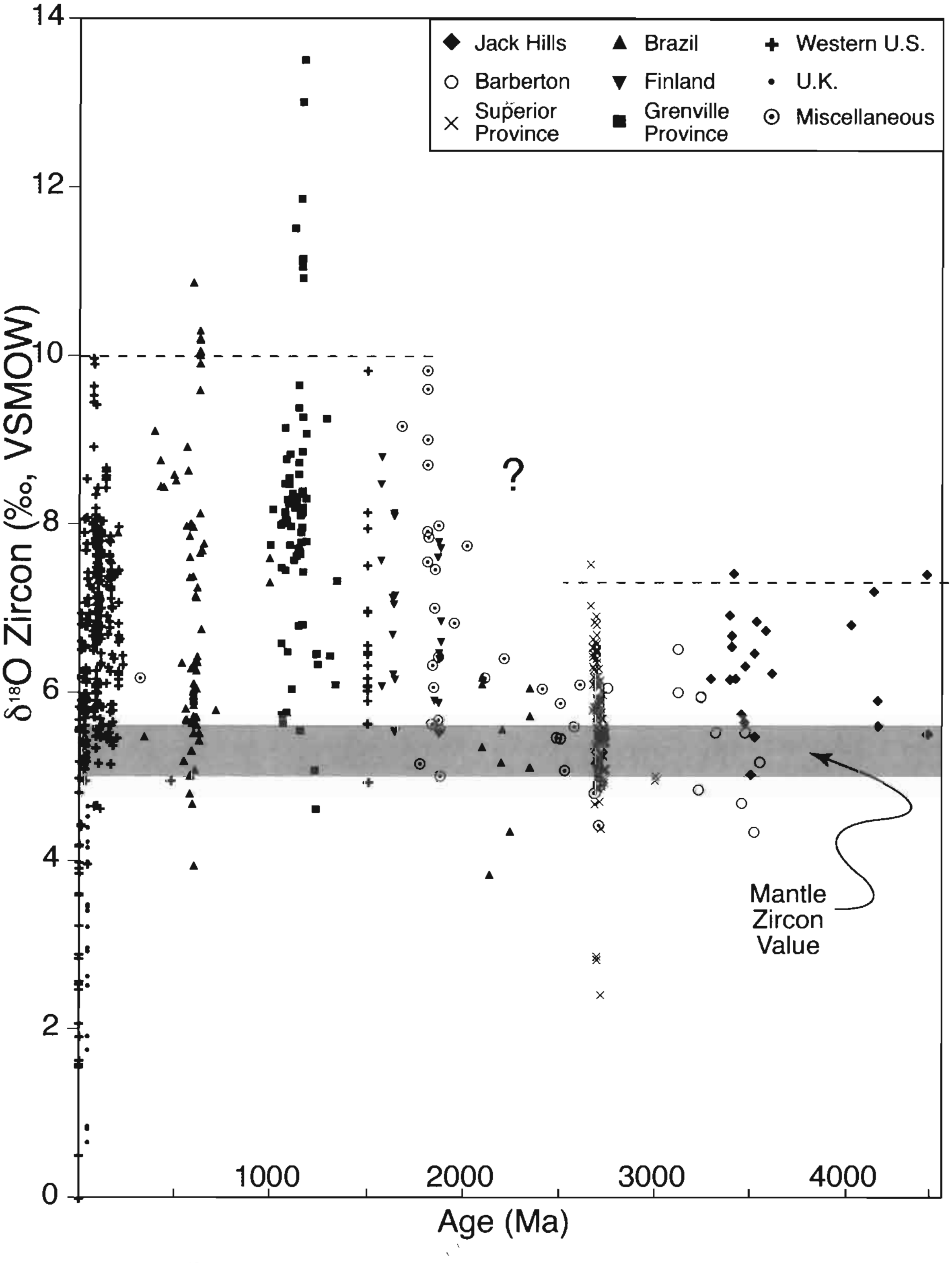

Figure 1. Compilation of $\delta^{18}O(Zrc)$ vs. age for zircons from over 700 rocks with published age. Oxygen isotope ratios were analyzed by laser fluorination at the University of Wisconsin (most samples) or in situ by ion microprobe at the University of Edinburgh (Jack Hills zircons). Samples range in age from 4400 to 0.2 Ma and come from many terranes on seven continents. A remarkable uniformity is seen in the Archean, values cluster near the mantle ($\delta^{18}O(Zc) = 5.3 \pm 0.3‰$) with some values as high as 7.5 due to recycling of supracrustal material. High $\delta^{18}O$, above 8‰ becomes common until after 2 Ga, reflecting recycling of high $\delta^{18}O$ sediment and maturation of the crust. Oxygen isotope data are from referenced sources.

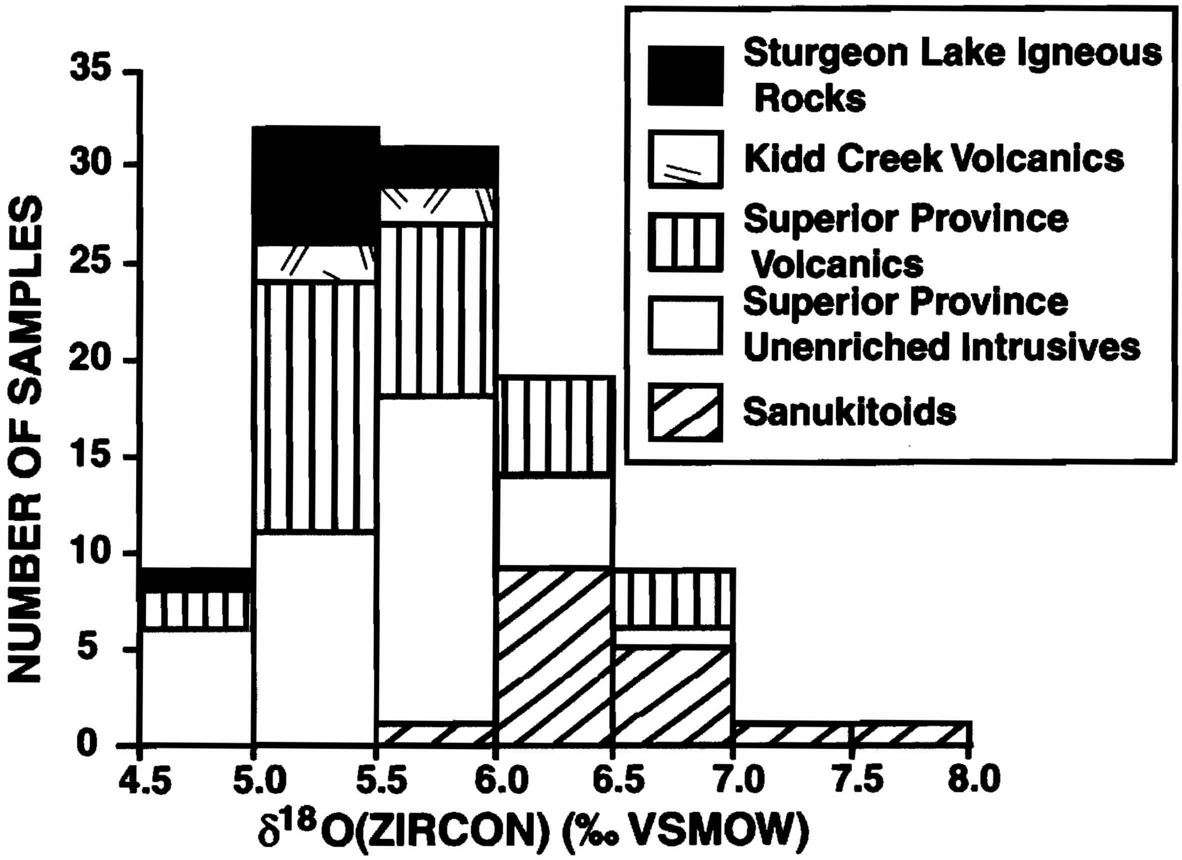

Figure 2. Histogram of $\delta^{18}O$ for magmatic zircons from 110 volcanic and plutonic rocks (3.0 – 2.7 Ga) of the Superior Province (from King et al., 2000).

REFERENCES

Bindeman, I.N. & Valley, J.W. 2001. Low $\delta^{18}O$ rhyolites from Yellowstone: magmatic evolution based on analysis of zircons and individual phenocrysts. Journal of Petrology 42:1491-1517

Bindeman, I.N. & Valley, J.W. 2003. Rapid generation of both high and low-$\delta^{18}O$, large volume silicic magmas at Timber Mountain/Oasis Valley caldera complex, Nevada. Geological Society of America Bulletin 115: in press

Ferreira, V.P.; Valley, J.W.; Sial, A.N.; Spicuzza, M.J. 2003. Oxygen isotope compositions and magmatic epidote from two contrasting metaluminous granitoids, NE Brazil. Contributions to Mineralogy and Petrology, in press

Gilliam, C.E. & Valley, J.W. 1997. Low $\delta^{18}O$ magma, Isle of Skye, Scotland: Evidence from Zircons. Geochimica et Cosmochimica Acta 61: 4975-4981

King, E.M.; Valley, J.W.; Davis, D.W.; Edwards, G.R. 1998. Oxygen isotope ratios of Archean plutonic zircons from granite-greenstone belts of the Superior Province; Indicator of magmatic source. Precambrian Research 92: 47-67

King, E.M.; Valley, J.W.; Davis, D.W. 2000. Oxygen isotope evolution of volcanic rocks at the Sturgeon Lake volcanic complex, Ontario. Canadian Journal of Earth Science 37: 39-50

King, E.M.; Valley, J.W.; Stockli, D.F.; Wright, J.E. 2003. Oxygen isotope trends of granitic magmatism in the Great Basin. In review

Lackey, J.S.; Hinke, H.J.; Valley, J.W. 2002. Tracking contamination in felsic magma chambers with $\delta^{18}O$ of magmatic garnet and zircon. Goldschmidt Conf: extended abstracts, Geochimica et Cosmochimica Acta 66, Supplement 1:428

Lackey, J.S.; Valley, J.W.; Saleeby, J.B. 2003. Evidence from zircon for high $\delta^{18}O$ contamination of magmas in the deep Sierra Nevada Batholith, California. Geology in review

Monani, S. & Valley, J.W. 2001. Oxygen isotope ratio of zircon: magma genesis of low $\delta^{18}O$ granites from the British Tertiary Igneous Province, western Scotland. Earth and Planetary Science Letters 184: 377-392

Peck, W.H.; King, E.M.; Valley, J.W. 2000. Oxygen isotope perspective on Precambrian crustal growth and maturation. Geology 28: 363-366

Peck, W.H.; Valley, J.W.; Wilde, S.A.; Graham, C.M. 2001. Oxygen isotope ratios and rare earth elements in 3.3 to 4.4 Ga zircons: Ion microprobe evidence for high $\delta^{18}O$ continental crust and oceans in the Early Archean. Geochimica et Cosmochimica Acta 65: 4215-4229

Peck, W.H.; Valley, J.W.; Graham, C.M. 2003. Slow oxygen diffusion rates in igneous zircons from metamorphic rocks. American Mineralogist, in press

Peck, W.H.; Valley, J.W.; Corriveau, L.; Davidson, A.; McLelland, J.; Farber, D. 2003. Mapping terrane boundaries in the deep crust of the Grenville Province using oxygen isotope ratios of zircon from anorthosite-suite granitoids. In: Geological Society of America Memoir, Proterozoic Evolution of the Grenville Orogen in North America, accepted

Valley, J.W. 2003. Oxygen isotopes in zircon. In: Zircon, J. Hanchar and P. Hoskins (eds) Reviews in Mineralogy and Geochemistry 53, in press

Valley, J.W.; Chiarenzelli, J.; McLelland, J.M. 1994. Oxygen Isotope Geochemistry of Zircon. Earth and Planetary Science Letters 126: 187-206

Valley, J.W.; Graham, C.M.; Harte, B.; Kinny, P.; Eiler, J.M. 1998a. Ion microprobe analysis of oxygen, carbon, and hydrogen isotope ratios. In: McKibben MA, et al. (eds), Society of Economic Geology Reviews in Economic Geology 7: 73-98

Valley, J.W.; Kinny, P.D.; Schulze, D.J.; Spicuzza, M.J. 1998b. Zircon Megacrysts from Kimberlite: Oxygen isotope heterogeneity among mantle melts. Contr. Min. Petrol., 133, 1-11.

Valley, J.W.; Bindeman, I.N.; Peck, W.H. 2003. Empirical calibration of oxygen isotope fractionation in zircon. Geochimica et Cosmochimica Acta 67: in press

Watson, E.B. & Cherniak, D.J. 1997. Oxygen diffusion in zircon. Earth and Planetary Science Letters 144:527-544

Wei, C.S.; Zheng, Y.F.; Zhao, Z.F.; Valley, J.W. 2002. Oxygen and neodymium isotope evidence for recycling of juvenile crust in Northeast China. Geology 30: 375-37.

NOBLE GAS GEOCHRONOLOGY AND GEOCHEMISTRY IN SURFICIAL PROCESSES

Vasconcelos, P.M.

Department of Earth Sciences, The University of Queensland; Brisbane Qld 4072, Australia. paulo@earth.uq.edu.au

Keywords: Weathering, erosion, $^{40}Ar/^{39}Ar$ geochronology, (U-Th)/He geochronology, cosmogenic ^{3}He

INTRODUCTION

Quantifying rates of surficial processes, weathering and erosion, is a current and challenging area for isotope geochemistry and geochronology. The open system nature of the surficial environment, the superposition of processes, and the lack of experience of the geochronological community in applying radiogenic isotopic techniques to mineral species present in the surficial environment (oxides, clays, sulfates, etc.) have prevented or delayed advances in this research area. However, despite the odds, progress during that past decade has been considerable.

One of the most encouraging areas is the application of noble gas geochemistry to the study of surficial processes. Expansion on the application of $^{40}Ar/^{39}Ar$ geochronology of supergene manganese oxides and sulfates has provided important insights on the longevity of weathering profiles, on rates of weathering and erosion, and on mechanisms shaping the Earth's surface. These studies have also provided new means for testing models of landscape evolution. Recent advances in (U-Th)/He dating of hematite and goethite provides a new tool for understanding the formation of weathering profiles. When this approach is coupled with exposure dating by measuring cosmogenic ^{3}He generated on iron oxides, it creates a powerful tool that combines weathering geochronology and erosion rate measurements in the same mineral phase. I will present below results from some of these applications and discuss new developments.

GEOCHRONOLOGICAL TOOLS IN SURFICIAL STUDIES

K-Ar AND $^{40}Ar/^{39}Ar$

Weathering geochronology by the K-Ar method has been available for several decades (Chukhrov et al., 1969; Gustafson & Hunt, 1975; Ashley & Silberman, 1976; Varentsov & Golovin, 1987; Alpers & Brimhall; 1988; Bird et al., 1990). However, high-resolution laser-heating $^{40}Ar/^{39}Ar$ dating of single crystals of alunite, jarosite, and clusters of K-Mn-oxides has provided the technological edge necessary to enable weathering geochronology to develop as a significant research area (Vasconcelos et al., 1992, 1994a, b, 1995; Ruffet et al., 1996; Vasconcelos, 1998, 1999a, b; Dammer et al., 1996, 1999; Hénocque et al., 1998; Hautmann & Lippolt, 2000; Mote et al., 2001). This single-crystal or single-grain approach, possible due to the high spatial resolution and low blanks inherent to laser extraction systems, allows the study of weathering profiles where K-bearing supergene minerals occur as minor phases. The incremental heating $^{40}Ar/^{39}Ar$ method also provides information on the Ar and K retention history of the mineral analyzed, an important determination in weathering profiles where minerals are continuously exposed to weathering solution fluxes. Finally, the full automation in modern $^{40}Ar/^{39}Ar$ systems enables rapid analysis of several samples from each site, providing a comprehensive database.

(U-Th)/He

Similarly, in theory, (U-Th)/He geochronology of supergene Fe oxides is not new (Strutt, 1910), and it has been recently revived by Wernicke & Lippolt (1993), Bahr et al. (1994) and Lippolt et al. (1998), who demonstrated that hematite and goethite contain significant U and He and can be dated by the (U-Th)/He method. In practice, however, a major limitation of (U-Th)/He dating of supergene oxides is the lack of appropriate He retentivity information and uncertainties about the sites where U resides in these phases. Recent incremental-heating experiments on supergene goethite and cryptomelane provide quantitative information on the He retentivity of goethite and cryptomelane (Shuster et al., 2000). Moreover, recent experimental investigation on uranium co-precipitation with Fe oxides provides compelling evidence that U is incorporated into oxide structures and is not simply adsorbed onto mineral surfaces, rendering (U-Th)/He dating results more reliable (Duff et al., 2002).

Preliminary studies support the reliability of weathering ages obtained by the (U-Th)/He method in goethite (Shuster et al., 2000). Supergene cryptomelane and goethite from the Igarapé Bahia profile, PA, Brazil, and weathered pegmatites in eastern Brazil, contain significant U (1-400 ppm) and radiogenic He (5-400 $ncc.mg^{-1}$). Goethite samples from the Igarapé Bahia profile yield internally consistent (U-Th)/He ages (Shuster et al., 2000). The internal consistency of the (U-Th)/He ages and the stratigraphic consistency between (U-Th)/He and $^{40}Ar/^{39}Ar$ ages suggest that goethite may yield reliable (U-Th)/He results. Using natural ^{4}He and proton induced ^{3}He, diffusion experiments on distinct fragments of goethite (one BAH-F124-111.2m and two BAH-F124-114m grains) yield reproducible results and roughly linear on Arrhenius plots, suggesting nearly quantitative ^{4}He retentivity for goethite.

COSMOGENIC ^{3}He ON IRON OXIDES

Stable cosmogenic ^{3}He produced in olivine, pyroxene, and plagioclase has been used to measure exposure history and erosion rates (Gosse & Phillips, 2001). However, these minerals are not resistant in the weathering environment. Thus, developments on the application of stable cosmogenic ^{3}He measurements on supergene minerals, such as hematite and goethite, may provide a useful combination of a geochronometer (U-Th/He) and an exposure history chronometer. Iron oxides exposed to cosmic ray neutrons undergo production of measurable amounts of spallogenic ^{3}He (Shuster et al., 2002). Further development in quantifying the He retentivity of iron oxides, combined with improved quantification of the ^{3}He production rates on iron oxides, will permit widespread application of these minerals in weathering geochronology and exposure history studies.

UNDERSTANDING LANDSCAPE EVOLUTION THROUGH WEATHERING GEOCHRONOLOGY

Laser-heating ^{40}Ar/^{39}Ar dating of weathering profiles in Australia and Brazil demonstrates that weathering geochronology permits the numerical correlation of land surfaces on a local, regional, and possibly cratonic scale (Vasconcelos, 1998; Vasconcelos & Conroy, 2003). More complex and ancient weathering profiles are found at higher topographic levels (table and ridge tops), while nearby lower elevation profiles preserve only post-Miocene supergene minerals. The results demonstrate that stepped landscapes, such as those found in Australia and the Carajás region, Brazil, preserve a complex history of weathering, partial dissection, and reweathering. The results also show that older weathering profiles are preserved in areas of greater tectonic stability (e.g., the centre of the Mount Isa block, Australia; the Carajás Plateau and the Qudrilatero Ferrífero Regions, Brazil), while more tectonically active areas (e.g., the Charters Towers, Canarvon Gorge, SE Queensland, etc.) only preserve a more recent record (Feng & Vasconcelos, 2001, in press; Li & Vasconcelos, 2002; Carmo & Vasconcelos, this symposium).

The combination of weathering geochronology by the ^{40}Ar/^{39}Ar method with erosion rate measurements using cosmogenic isotope studies (^{10}Be, ^{26}Al, and ^{36}Cl) also reveals that, in ancient stepped landscapes in Australia, rates of erosion are small (<3 m.Ma^{-1}) in the high-elevation sites containing the most ancient weathering profiles, while low-elevation sites containing more recently formed weathering profiles are characterized by relatively large erosion rates (5-20 m.Ma^{-1}) (Stone & Vasconcelos, 2000).

INSIGHT INTO PALEOCLIMATES FROM WEATHERING GEOCHRONOLOGY

Independent studies reveal episodicity in the history of supergene mineral precipitation (Vasconcelos et al., 1994a; Dammer et al., 1996, 1999; Ruffet et al., 1996; Hénocque et al., 1998; Hautmann & Lippolt, 2000). However, there is disagreement on the factors controlling weathering and the episodic precipitation of minerals during weathering. We interpret this intermittent precipitation of supergene minerals as evidence for paleoclimatic control on weathering. Since the amount of rainfall, ambient temperature, and the abundance and type of vegetation changes with climate, weathering rates should also vary with climate. The volume of newly formed minerals in a weathering profile should be large during warm humid climates, when conditions of high fluid/rock ratio and reactive organic-rich solutions prevail, and relatively small during unfavorable arid conditions. Comparisons between the frequency of mineral ages and independent climatic records (oceanic δ^{18}O, fossil record, etc.) show good correlation between peaks of mineral precipitation and other climatic indicators (Feng & Vasconcelos, 2001, in press; Li & Vasconcelos, 2002; Carmo & Vasconcelos, in press). Other researchers, however, propose that the intermittent precipitation of minerals in the weathering record primarily reflects tectonic controls and the enhanced physical and chemical weathering associated with mountain building processes (Hautmann & Lippolt, 2000).

The debate on whether climate or tectonics provides the ultimate control on rates of chemical weathering is crucial to establish the effect of varying pCO$_2$ on global climates. Any feedback control on the accumulation of greenhouse gases in the atmosphere depends on a direct link between climate and weathering (Berner, 1994). This link is difficult to establish by studying current weathering processes. Studies on the solution chemistry of modern rivers often leads to inconclusive or controversial results (White & Blum, 1995; Edmond et al., 1995; Berner & Berner, 1997; Edmond & Huh, 1997; Gaillardet et al., 1999; White et al., 1999). Attempts to use the marine ^{87}Sr/^{86}Sr and the ^{187}Os/^{186}Os oceanic record as paleoclimatic indicators also lead to inconclusive results (Raymo & Ruddiman, 1992; Richter et al., 1992; Peucker-Ehrenbrink et al., 1995; Sharma et al., 1999).

Some of the discrepancies resulting from the use of ^{87}Sr/^{86}Sr and ^{187}Os/^{186}Os isotopic composition of oceanic sediments as proxies for the intensity of chemical weathering in the past may result from the fact that the increase in these isotopes on oceanic basins result from chemical erosion, which is not necessarily coupled with chemical weathering. In some cases, weathering profiles may in fact behave as reservoirs for mobile species. Highly mobile cationic species such as Ca, Mg, and Sr maybe released from primary silicates during weathering, but may be retained in weathering profiles as supergene carbonates, phosphates, sulfates, and clay minerals for considerable periods of time. This behavior is well established in the case of supergene ore systems, where desirable metals such as Cu, Mn, Mg, Fe, Ni, and Al are stored in weathering profiles as supergene enrichment zones. Supergene Cu systems, for example, exhibit thick Cu-carbonates (malachite/azurite) horizons. Similarly, supergene Mg-carbonate and Ni-silicates are common in weathered ultramafic rocks. Decoupling between chemical weathering and chemical erosion may complicate or even prevent the use of the oceanic record as a direct indicator of active continental weathering rates. Weathering geochronology, where the timing of precipitation of the products of silicate weathering are measured and quantified, provides an independent and more direct way to determine the variation of weathering rates in the past. This information, coupled with paleo CO_2 concentration estimations (Pearson & Palmer, 2000; Kump et al., 2000), may thus provide a more reliable test linking the accumulation of greenhouse gases in the atmosphere and increased silicate weathering.

To address the problems above, a detailed and comprehensive chronology of formation of weathering profiles is necessary. Despite advances in understanding the continental weathering history in some parts of Australia, South America, and Africa, many continents still remain to be studied in detail. A summary of weathering geochronology studies in weathering profiles from around the globe will be presented and the current and future developments will be discussed.

REFERENCES

Alpers, C.N.: Brimhall, G.H. 1988. Middle Miocene climatic change in the Atacama Desert, northern Chile: Evidence from supergene mineralization at La Escondida. Geol. Soc. Am. Bull. 100:1640-56

Berner, R.A. 1994. Geocarb II: A revised model of atmospheric CO_2 over Phanerozoic time. Am. J. Sci. 294:56-91

Berner, R.A. & Berner, E.K. 1997. Silicate weathering and climate. In Tectonic uplift and climate change. (ed. W. Ruddiman), pp. 353-365. Plenum Press.

Bird, M.; Chivas, A.R.; McDougall, I. 1990. An isotopic study of surficial alunite in Australia: 2. Potassium-argon geochronology. Chem. Geol. 80, 133-145.

Carmo, I.O. & Vasconcelos, P. 2003. Geochronological evidence for pervasive Miocene weathering, Minas Gerais, Brazil. Earth Surface Processes and Landforms, in press

Chukhrov, F.V.; Yermilova, L.P.; Shanin, L.L. 1969. Age of alunite from certain deposits. Trans. Acad. Sci. USSR, Dokl., Earth-Sci. Sect. 185:49-51

Dammer, D.; Chivas, A.R.; McDougall, I. 1996. Isotopic dating of supergene Mn oxides from the Groote Eylandt Deposit, Northern Territory, Australia, Econ. Geol. 91, 386-401.

Dammer, D.; McDougall, I.; Chivas, A. 1999. Timing of weathering-induced alteration of manganese deposits in Western Australia; evidence from K/Ar and ^{40}Ar/^{39}Ar dating. Econ. Geol. 94, 87-108.

Duff, M.C.; Coughlin, J.U.; Hunter, D.B. 2002. Uranium co-precipitation with iron oxide minerals. Geochim. Cosmochim. Acta 66(20), 3533-3547

Edmond, J.M. & Huh, Y. 1997. Chemical weathering yields from basement and orogenic terrains in hot and cold climates. In Tectonic uplift and climate change. (ed. W. Ruddiman), pp. 329-351. Plenum Press.

Edmond, J.M.; Palmer, M.R.; Measures, C.I.; Grant, B.; Stallard, R.F. 1995. The fluvial geochemistry and denudation rate of the Guiana Shield in Venezuela, Colombia, and Brazil. Geochim. Cosmochim. Acta 59(16), 3301-3325.

Feng, Y.X. & Vasconcelos, P.M. 2001. Quaternary Continental Weathering Geochronology by Laser-Heating ^{40}Ar/^{39}Ar Analysis of Supergene Cryptomelane. Geology, 29(7):635-638.

Feng, Y. & Vasconcelos, P. 2003. Paleoclimatic and erosional controls on timing of supergene enrichment of Upper Kandanga Mn-deposit, Mary Valley, Australia. Earth Planet. Sci. Lett., in press

Gaillardet, J.; Dupre, B.; Louvat, P.; Allegre, C.J. 1999b. Global silicate weathering and CO_2 consumption rates deduced from the chemistry of large rivers. Chem. Geol. 159(1-4), 3-30.

Gosse, J.C. & Phillips, F.M. 2001. Terrestrial in situ cosmogenic nuclides: theory and application. Quat. Sci. Rev., 20: 1475-1560.

Guftafson, L.B; Hunt, J.P. 1975. The porphyry copper deposit at El Salvador, Chile. Econ. Geol. 70: 857-912

Hautmann, S.; Lippolt, H. 2000. ^{40}Ar/^{39}Ar dating of central European K-Mn oxides; chronological framework of supergene alteration processes during the Neogene. Chem. Geol. 179, 37-80.

Hénocque, O.; Ruffet, G.; Colin, F.; Feraud, G. 1998. ^{40}Ar-^{9}Ar dating of West African lateritic cryptomelanes. Geochim. Cosmochim. Acta 62(16), 2739-2756.

Kump, L.; Brantley, S.; Arthur, M. 2000. Chemical Weathering, Atmospheric CO2, and Climate. Annu. Rev. Earth Planet. Sci. 28:611-667.

Li, J.W. & Vasconcelos, P. 2002. Cenozoic continental weathering and its implications for paleoclimatic: evidence from ^{40}Ar/^{39}Ar geochronology of supergene K-Mn oxides in Mt. Tabor, central Queensland, Australia. Earth Planet. Sci. Lett., 200: 223-239.

Lippolt, H.J.; Brander, T.; Mankopf, N.R. 1998. An attempt to determine formation ages of goethites and limonites by (U+Th)-He-4 dating. Neues Jahrbuch Fur Mineralogie-Monatchefte, 11: p. 505-528.

Mote, T.; Becker, T.; Renne, P.; Brimhall, G. 2001. Chronology of Exotic Mineralization at El Salvador, Chile, by ^{40}Ar/^{39}Ar Dating of Copper Wad and Supergene Alunite. Econ. Geol. 96, 351-366.

Pearson, P.N. & Palmer, M.R. 2000. Atmospheric carbon dioxide concentrations over the past 60 million years. Nature 406, 695-699.

Peucker-Ehrenbrink, B.; Ravizza, G.; Hofmann, A.W. 1995. The marine ^{187}Os/^{186}Os record of the past 80 million years. Earth Planet. Sci. Lett. 130(1-4), 155-167.

Raymo, M.E. & Ruddiman, W.F. 1992. Tectonic forcing of late Cenozoic climate. Nature 359(10), 117-122.

Richter, F.M.; Rowley, D.B.; DePaolo, D.J. 1992. Sr isotope evolution of seawater; the role of tectonics. Earth Planet. Sci. Lett. 109(1-2), 11-23.

Ruffet, G.; Innocent, C.; Michard, A.; Feraud, G.; Beauvais, A.; Nahon, D.; Hamelin, B. 1996. A geochronological ^{40}Ar/^{39}Ar and ^{87}Rb/^{87}Sr study of K-Mn oxides from the weathering sequence of Azul, Brazil." Geochim. Cosmochim. Acta 60(12): 2219-2232.

Sharma, M.; Wasserburg, G.J.; Hofmann, A.W.; Chakrapani, G.P. 1999. Himalayan uplift and osmium isotopes in oceans and rivers. Geochim. Cosmochim. Acta 63(23/24), 4005-4012.

Shuster, D. & Farley, K.A. 2003. ^{4}He/^{3}He thermochronometry. Earth Planet. Sci. Lett., in press.

Shuster, D.; Farley, K.A.; Vasconcelos, P.M. 2000. Geochronology of Weathering Processes by (U-Th)/He analysis of supergene goethite and cryptomelane. Eos Abstracts, 2000. 81(48): p. 1263.

Shuster, D.; Farley, K.A.; Vasconcelos, P.M. 2002. Cosmogenic 3He in goethite. Goldschmidt 2002, A713.

Stone, J. & Vasconcelos, P. 2000. Studies of geomorphic rates and processes with cosmogenic isotopes - examples from Australia. Goldschmidt 2000, 961

Strutt, R.J. 1910. The accumulation of helium in geological time III. Proceedings of the Royal Society. A83:p. 96-99.

Varentsov, I.M. & Golovin, D.I. 1987. Manganese beds of Groote Eylandt, northern Australia; K/Ar dating of cryptomelane minerals and genetic aspects. Doklady, Earth-Sciences Section 294, 149-153.

Vasconcelos, P.M. 1998. Geochronology of weathering in the Mt Isa and Charters Towers regions, northern Queensland. Restricted Report 68R/E&M Rep. 452R, Pert, Australia, CRC LEME.

Vasconcelos, P.M. 1999. K-Ar and $^{40}Ar/^{39}Ar$ Geochronology of Weathering Processes. Annu. Rev. Earth Planet. Sci. 27:183-229.

Vasconcelos, P.M, & Conroy, M. 2003. Geochronology of weathering and landscape evolution, Dugald River, NW Queensland, Australia. Geochim. Cosmochim. Acta, in press.

Vasconcelos, P.M.; Becker, T.A.; Renne ,P.R.; Brimhall, G.H. 1992. Age and duration of weathering by K-Ar and $^{40}Ar/^{39}Ar$ analysis of K-Mn Oxides. Science 258, 451-455.

Vasconcelos, P.M.; Becker, T.A.; Renne, P.R.; Brimhall, G.H. 1994a. Direct dating of weathering phenomena by K-Ar and $^{40}Ar/^{39}Ar$ analysis of supergene K-Mn oxides. Geochim. Cosmochim. Acta, 58, 1635-1665.

Vasconcelos, P.M.; Brimhall, G.H.; Becker, T.A.; Renne, P.R. 1994b. $^{40}Ar/^{39}Ar$ analysis of supergene jarosite and alunite: Implications to the paleo weathering history of western US and West Africa. Geochim. Cosmochim. Acta, 58, 401-420.

Vasconcelos, P.M.; Wenk, H.-R.; Echer, C. 1994c In situ study of the thermal behavior of cryptomelane by high voltage and analytical electron microscopy. Am. Mineral., 79, 80-90.

Vasconcelos, P.M.; Renne, P.R.; Becker, T.A.; Wenk, H.-R. 1995. Mechanisms and kinetics of atmospheric, radiogenic, and nucleogenic argon release from cryptomelane during $^{40}Ar/^{39}Ar$ analysis. Geochim. Cosmochim. Acta, 59, 2057-207.

White, A.F. & Blum, A.E. 1995. Effects of climate on chemical weathering in watersheds. Geochim. Cosmochim. Acta 59(9), 1729-1747.

White, A.F.; Blum, A.E.; Bullen, T.D.; Vivit, D.V.; Schulz, M. Fitzpatrick, J. 1999. The effect of temperature on experimental and natural chemical weathering rates of granitoid rocks. Geochim. Cosmochim. Acta 63(19-20), 3277-3291.

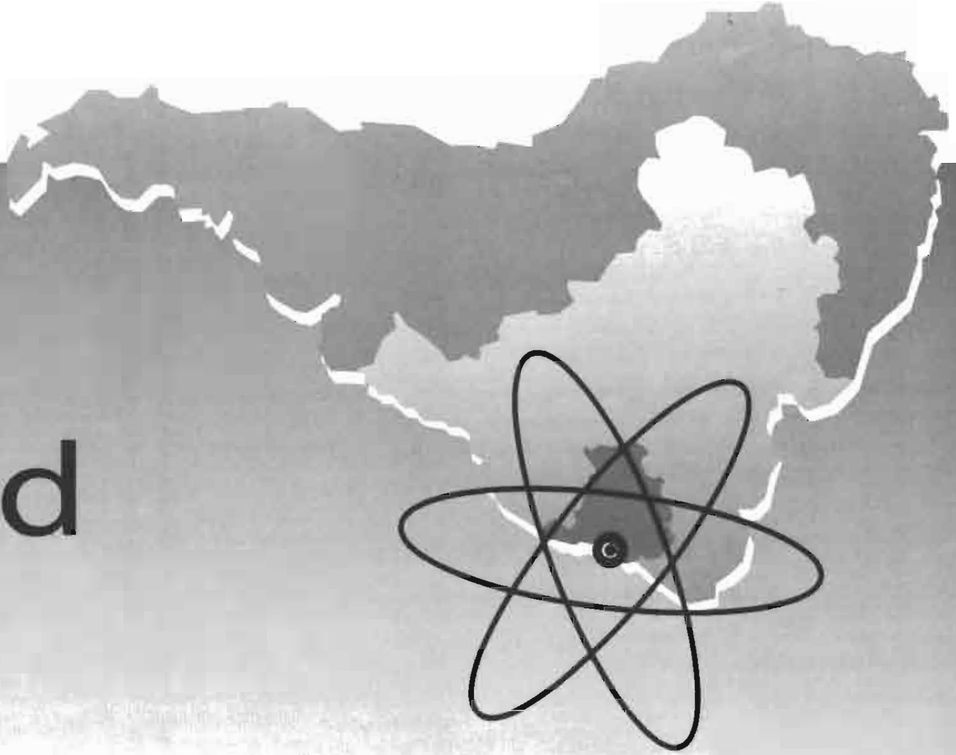

Methodology and Application of Isotope Geology

STUDY OF THE APPLICATION OF INDUCTIVELY COUPLED PLASMA QUADRUPOLE MASS SPECTROMETRY FOR THE DETERMINATION OF MONAZITE AGES BY LEAD ISOTOPE RATIOS

Aronne, C.C.[1]; Godoy, J.M.[1, 2] and Godoy, M.L.D.P.[1]

1. Departamento de Química, Pontifícia Universidade Católica do Rio de Janeiro (PUC-Rio), Rua Marquês de São Vicente 225, 22453-900, Rio de Janeiro, Brazil. jmgodoy@rdc.puc-rio.br
2. Instituto de Radioproteção e Dosimetria (IRD), Caixa Postal 37750, Barra da Tijuca, 22642-970, Rio de Janeiro, Brazil

Keywords: Inductively coupled plasma mass spectrometry (ICP-MS), lead dating, isotope ratio, monazite

INTRODUCTION

Considering the four stable isotopes of lead, only ^{204}Pb is non-radiogenic. Since the other three, ^{206}Pb, ^{207}Pb and ^{208}Pb, are end-members of the ^{232}Th (^{208}Pb), ^{235}U (^{207}Pb) and ^{238}U (^{206}Pb) radioactive decay chains, different minerals show different isotopic compositions according to their age and the initial Th and U contents of the source rock (Jager & Hunziker, 1979). Monazite has been proposed for dating since it is more resistant to physical and chemical change than zircon and offers the advantage of generally higher U and Th content (Machado & Gauthier, 1996).

For the purpose of lead dating, thermal ionization mass spectrometry (TIMS) using a magnetic sector mass analyzer has been the conventional method for high precision isotopic analysis with relative standard deviations (RSD) lower than 0.05% when applied to reference materials (Hoven et al., 1999; Thirwall, 2000). However, the precision values obtained for real samples are in the range of 0.1-0.3% (Pomies et al., 1998; Halicz et al., 1996; Weiss et al., 2000). Moreover, the relatively high cost of TIMS instrumentation and the (necessary) extensive chemical pre-treatment of the sample prior to analysis have imposed serious limitations on the routine use of TIMS techniques in geochemical exploration applications (Towsend et al., 1998; Wannemacker et al., 2000).

Although the quadrupole inductively coupled plasma mass spectrometry (ICP-MS) shows an inferior precision in comparison with TIMS, it has some important advantages, such as (i) simple sample pre-treatment, (ii) high sample throughput and simple sample introduction and (iii) widespread availability (Prohaska et al., 2000).

Quadrupole based ICP-MS instruments have been used in many studies to measure Pb isotope ratios. The precisions measured in reference materials are typically 0.1- 0.3% RSD (Heumann et al., 1998; Platzner et al., 1999; Becker & Dietze, 2000; Begley & Sharp, 1997), whereas for real samples, a precision in the range of 0.2 – 0.5% RSD (Halicz et al., 1996; Weiss et al., 2000; Barbaste et al., 2001; May et al., 1999) is usually obtained. Despite of the fact that quadrupole based instruments may offer a precision 100 times worse than that obtained with TIMS for reference materials, the precision values obtained for real samples are similar in comparison with that determined by TIMS (Pomies et al., 1998; Halicz et al., 1996; Weiss et al., 2000). Several factors may be responsible for this variability, but the most important factors affecting the precision are those regarding sample matrix effects and chemical steps associated with the method other than with the instrumental technique itself (Pomies et al., 1998; Halicz et al., 1996; Weiss et al., 2000).

In the present work, the application of quadrupole ICP-MS for the determination of lead isotope ratios has been evaluated aiming its application on dating of monazites, using U-Pb, Th-Pb and Pb-Pb methods.

EXPERIMENTAL

INSTRUMENTATION

A Perkin-Elmer SCIEX ELAN 6000 ICP-MS was used for the Pb isotopic measurement equipped with the original cross flow nebulizer. A peristaltic pump performed the solution aspiration. The ICP-MS instrumental operating conditions were automatically optimized by the instrument using the SIMPLEX method and were in agreement with the conditions proposed by Halicz et al. (1996). They are summarized in Table 1.

Table 1. Perkin-Elmer SCIEX ELAN 6000 ICP-MS operation conditions.

RF Power	1050W
Plasma gas flow rate	17 L min^{-1}
Auxiliary gas flow rate	1.2 L min^{-1}
Nebulizer gas flow rate	0.9 L min^{-1}
Sample uptake rate	1.0 mL min^{-1}
Scan mode	Peak hopping
Lens scanning	Enabled
Detector mode	Dual – Pulse and Analog

REAGENTS AND STANDARD SOLUTIONS

All reagents used were of analytical-reagent grade or higher purity and de-ionized water was further purified using a Millipore Milli-Q water purification system. Certified lead isotopic standard materials (SRM 981) and (SRM 982) were purchased from the National Institute of Standards and Technology (NIST, USA).

MONAZITE SAMPLES

Buena monazite sample: A pure monazite concentrate sample from Buena (São Francisco de Assis county), in the north of the Rio de Janeiro State (Brazil), was obtained from INB (Indústrias Nucleares Brasileiras).

Sugar Loaf Hill and Black Sand Beach samples: In both locations (Urca beach, Rio de Janeiro/RJ and Black Sand beach, Guarapari/ES), the area with the highest radioactivity was localized with a cintilometer and circa 5 kg sand samples taken. The monazite fraction was separated as described by Barling et al. (2000).

SAMPLE DISSOLUTION AND ANALYSIS

Three 25 mg aliquots, for each sample, were weighed, transferred to a 10 mL platinum crucible, 500 μL of phosphoric acid added and heated to the red for a few minutes applying a Meker burner. A clear solution was observed after that and it was diluted, with 7.2M nitric acid, to 10 mL. One milliliter was taken and diluted to 50 mL with 2% nitric acid.

Using this solution, lead, uranium and thorium content were determined by ICP-MS. Lead and thorium results were also confirmed by Inductively coupled plasma atomic emission spectrometry (ICP-AES). Based on the lead content, the sample solution dilution was calculated in order to obtain a lead concentration around 20 μg L^{-1}.

RESULTS AND DISCUSSION

ISOTOPE RATIO DETERMINATIONS

Many factors directly control the signal acquisition process on the ELAN 6000 ICP-MS. However, several ones are automatically optimized through the Simplex method. Others can be manually set-up, among them, the dwell time, the number of sweeps/replicate and the number of replicates/analysis. These three parameters were selected in this study in order to determine the best operation condition. Initially, the default operation conditions were applied and a high RSD was obtained. Considering the different isotope ratios involved, better results were achieved applying different dwell time for each isotope, higher for ^{204}Pb, the least abundant, and lower for ^{208}Pb, the most abundant, according Platzner et al. (1999).

Based on the ELAN 6000 operation manual (1997), the dwell time for each isotope was calculated in order to obtain 10^6 counts/replicate, using 200 sweeps/replicate. Also based on that, it was chosen ten replicates/analyses. As the sample volume required and the time expended for each sample were too high, the same calculation was performed for 500.000 counts and 6 replicates/analyses. It was also included ^{202}Hg, because of a potential isobaric interference of ^{204}Hg, a dwell time equal to that of ^{204}Pb was chosen.

A 100 mg L^{-1} stock solution was prepared starting from the NIST SRM 981 and diluted to 1.5, 7.5, 15, 30 and 45 μg L^{-1}. Initially, the isotope ratio was determined without a mass bias correction. Similarly, the same procedure was performed using the results of the 10 μg L^{-1} standard solution to correct mass discrimination. The results shown in Figure 1 demonstrate the efficiency of this procedure. Nevertheless, lead concentration cannot be higher than 20 μg L^{-1} in order to avoid dead time effects as can be observed. It can be seen that, as ^{208}Pb is the most abundant lead stable isotope, it is more subjected by dead time effects.

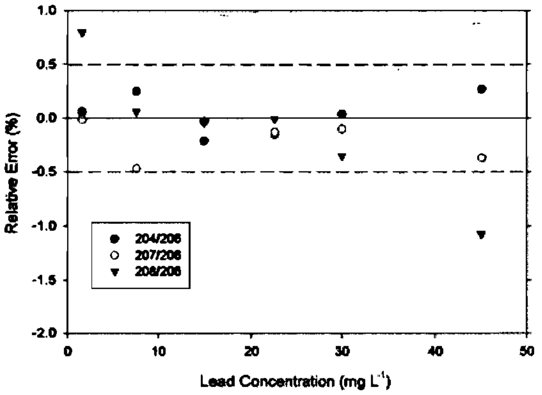

Figure 1. Relative error for Pb isotope ratios measurements after mass bias correction.

According to Platzner et al. (1999), it is possible to reduce RSD in isotope composition determinations using a quadrupole ICP-MS by consecutive measurements. This procedure of multiple determinations was performed employing a solution of 10 μg L^{-1} of SRM 981 to nine sequential determinations. For a sample containing 10 μg L^{-1} of lead, a sample volume around 20 mL is necessary If nine measurements should be carried out, it would be necessary circa 200 mL of sample solution. It means that, dealing with real samples, in the future, the aliquot taken should contain 2 μg Pb. The results obtained with the SRM 981 solution are shown in Table 2 and demonstrate that a relative error of the mean lower than 0.1% is obtained in all three-isotope ratios.

The previous procedure was repeated after calibrating the equipment regarding mass discrimination with a solution of 10 μg L^{-1} SRM 981 and using 10 μg L^{-1} SRM 982 as "unknown", which has an isotope composition similar to the expecting isotope compositions, low Pb-204 (non-radiogenic) and Pb-206/Pb-204, Pb-207/Pb-204 and Pb-208/Pb-204 ratios similar to the expected compositions. The results obtained are demonstrated in Table 3 and show that precision better than 0.1% as well as accuracy in the range of 0.1 to 1% can be achieved.

Table 2. Reproducibility observed for a 10μg L^{-1} SRM 981 solution.

	204/206	207/206	208/206
Reference value	0.059042	0.91464	2.1681
Mean value (n=9)	0.058761	0.913525	2.188593
RSD (%)	0.25	0.18	0.33
Relative error of the mean (%)	0.08	0.06	0.11
Relative bias (%)	-0.47	-0.13	0.95

Table 3. Reproducibility observed for a 10µg L^{-1} SRM 982 solution.

	204/206	207/206	208/206
Reference value	0.027219	0.46707	1.00016
Mean value (n=9)	0.027782	0.46550	0.997151
RSD (%)	0.39	0.12	0.19
Relative error of the mean (%)	0.13	0.04	0.06
Relative bias (%)	2.1	-0.34	-0.30

REAL SAMPLES

The lead, uranium and thorium contents of the three analyzed monazite samples are shown in Table 4 and the observed lead isotope ratio in Table 5. The observed elevate RSD, for the lead isotope ratios and for the elemental concentrations, reflect much more the sample inhomogeneity than the analytical techniques themselves. The monazite ages were calculated applying the U-Pb, Th-Pb and Pb-Pb methods and the obtained values are shown in Table 6. The agreement between the individual results for each dating method as well as among the dating methods is very good. Moreover, the obtained ages are in agreement with Brasiliano orogeny (Babinski et al., 1999; Söllner & Trouw, 1997; Leite et al., 2000). The obtained Sugar Loaf Hill U-Pb age is in agreement with the 560 My value announced during the 31st International Geological Congress (2000) using the SHRIMP method.

Table 4. Mean lead, uranium and thorium content of the analyzed monazite samples (values in g kg^{-1}).

Sample	Lead	Uranium	Thorium
Buena	1.23 (1.7%)	1.72 (0.3%)	45.2 (1.7%)
Sugar Loaf Hill*	1.45	1.83	47.4
Black Sand Beach	2.31 (3.4%)	1.20 (7.3%)	58.9 (5.4%)

*Only two aliquot analyzed

Table 5. Mean observed lead isotope ratio.

Sample	204/206	207/206	208/206
Buena	0.00264 (8.0%)	0.09786 (3.1%)	7.9320 (0.41%)
Sugar Loaf Hill	0.00420 (3.6%)	0.12072 (2.0%)	8.3067 (0.23%)
Black Sand Beach	0.000624 (29%)	0.06592 (5.8%)	15.5244 (1.9%)

Table 6. Obtained monazite ages (values in Ma).

Sample	U/Pb	Th/Pb	Pb/Pb	Mean age
Buena	(542±2)	(532±1)	(544±3)	(539±6)
Sugar Loaf Hill	(560±7)	(593±7)	(601±37)	(585±22)
Black Sand Beach	(535±13)	(544±19)	(527±50)	(535±9)

Each Black Sand beach sample aliquot was analyzed only once whereas the aliquots of the two other samples were analyzed three times, and consequently, better isotope ratio precisions were obtained. Also, the association of a higher thorium content with a lower uranium concentration lead to a low ^{207}Pb signal and to a large standard deviation related to the Pb-Pb age.

Since the lead, uranium and thorium contents are different; REE compositions were determined in order to clarify the genetic origins. The chondrite-normalized REE content is shown in Figure 2. All monazite samples have patterns with negative europium anomalies and with similar light REE compositions. The HREE are divergent, the largest difference being found for the heaviest elements.

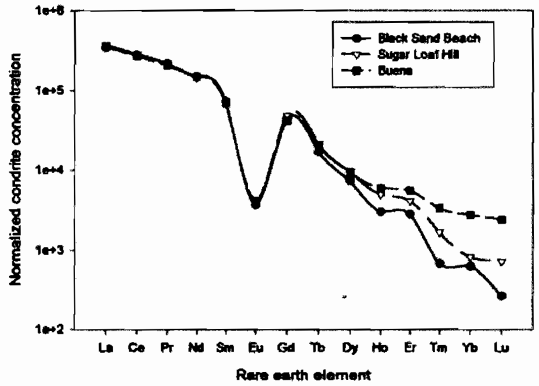

Figure 2. Rare-earth elements concentration, normalized to the Chondrites, in the studied monazite samples. Chondrite values are taken from Anders & Grevesse (1989).

Finally, the method was tested with older samples. A thorianite sample from Amapá was obtained from the Brazilian Nuclear Energy Commission. Three 10 mg aliquots were taken, after total dissolution with HNO_3-HF-$HClO_4$, they were analyzed in the same way as the monazite samples. The Th-Pb, U-Pb and Pb-Pb ages obtained were 2152 ± 53 My, 2032 ± 11 My, 2044 ± 6 My respectively, with a mean value of 2076 ± 66 My. This value is coherent with the 2.08 ± 0.02 Gy age of the Bacuri complex, Amapá, reported by Pimentel et al. (2002).

CONCLUSIONS

The present study showed that, it is possible to obtain useful monazite dating regarding precision and accuracy when the acquisition setting parameters of the ICP-MS Perkin Elmer-Sciex ELAN 6000 are optimized. Moreover, the use of monazite allows the direct determination of lead isotope ratios without the need of a chemical separation.

ACKNOWLEDGEMENT

The present work was supported by FINEP (Financiadora de Estudos e Projetos) and CAPES (Coordenação de Aperfeiçoamento de Pessoal de Ensino Superior). The authors wish to express their gratitude to Claudio Valeriano (UERJ) and Marcio Pimentel (UnB) for their help during different phases of the present work.

REFERENCES

Anders, E. & Grevesse, N., 1989. Abundances of the elements: Meteoritic and solar. Geochimica Cosmochimica Acta e3, 197-214.

Babinski, M.; Van Schmus, W.R.; Chemale Jr., F., 1999. Pb-Pb dating and Pb isotope geochemistry of neoproterozoic carbonate rocks from São Francisco basin, Brazil. Chemical Geology 160, 175-199.

Barbaste, M.; Halicz, M.; Galy, A.; Medina, B.; Emterborg, H.; Adams, F.; Lobinski, R., 2001. Evaluation of the accuracy of the determination of lead isotope ratios in wine by ICP-MS using quadrupole, multicollector magnetic sector and time-of-flight analysers. Talanta 54, 307-317.

Barling, J.; Weis, D.; Demaiffe, D., 2000. A Sr, Nd and Pb isotopic investigation of the transition between two megacyclic units of the Bjerkrein-Sokndal layered intrusion, south Norway. Chemical Geology 165, 47-65.

Becker, J.S. & Dietze, H.J., 2000. Precise and accurate isotope ratio measurements by ICP-MS. Fresenius Journal of Analytical Chemistry 368, 23-30.

Begley, I. & Sharp, B., 1997. Characterisation and correction of instrumental bias in ICP-QMS for accurate measurement of lead isopote ratios. Journal of Analytical Atomic Spectrometry 12, 395-402.

Halicz, L.; Erel, Y.; Veron, A., 1996. Lead isotope ratio measurements by ICP-MS: accuracy, precision and long-term drift. Atomic Spectroscopy 17, 186-189.

Heumann, K.G.; Gallus, S.M.; Radlibger, G.; Vogl, J., 1998. Precision and accuracy in isotope ratio measurements by plasma source mass spectrometry. Journal of Analytical Atomic Spectrometry 13, 1001.

Hoven, H.; Gaudette, H.; Short, F., 1999. Isotope ratios of ^{206}Pb/^{207}Pb em eelgrass, Zostera Marina. Marine Environmental Research 48, 377–387.

Jager, E. & Hunziker, J., 1979. Lectures in Isotope Geology, Springer Verlag, New York.

Leite, J.A.D., Hartmann, L.A.; Fernandes, L.A.D.; McNaughton, N.J.; Soliani Jr., E.; Koester, E.; Santos, J.O.S., Vasconcellos, M.A.Z., 2000. Zircon U-Pb SHRIMP dating of gneissic basement of the Dom Feliciano Belt, southernmost Brazil. Journal of South American Earth Sciences 13, 739-750.

Machado, N. & Gauthier, G., 1996. Determination of ^{207}Pb/^{206}Pb ages on zircon and monazite by laser ablation ICP-MS and application to a study of sedimentary provenance and metamorphism in southeastern Brazil, Geochimica et Cosmochimica Acta 60, 5063-5073.

May, T.; Wiedmeyer, R.; Brown, L.; Casteel, S., 1999. A lead isotope distribution study in swine tissue using ICP-MS. Atomic Spectroscopy 20, 199-211.

PERKIN-ELMER, 1997. Inductively Coupled Plasma Mass Spectrometer ELAN 6000, software guide, PERKIN-ELMER SCIEX Instruments, Canada.

Pimentel, M.M.; Spier, C.A.; Ferreira Filho, C.F., 2002. Estudo Sm-Nd do complexo máfico-ultramáfico Bacuri, Amapá: Idade da intrusão, metamorfismo e natureza do magma original. Revista Brasileira de Geociências 32(3), 1-6.

Platzner, I.; Becjer, J.; Dietze, H., 1999. Stability study of isotope ratio measurements for uranium and thorium by ICP-QMS. Atomic Spectroscopy 20, 6-12.

Pomies, C.; Cocheire, A.; Guerrot, C.; Marcoux, E.; Lancelot, J., 1998. Assessment of the precision and accuracy of lead isotope ratios measured by TIMS for geochemical applications. Chemical Geology 144, 137-149.

Prohaska, T.; Latkoczy, C.; Wenzel, W.; Stingeder, G., 2000. Lead isotope ratio analysis by ICO-SMS in soil digests of a depth profile. Journal of Analytical Atomic Spectrometry 15, 365-369.

Söllner, J. & Trouw, R.A.J., 1997. The Andrelândia depositional cycle (Minas Gerais/Brazil), a post-transamazonic sequence south of the São Francisco craton: Evidence from U-Pb dating on zircon of a metasediment. Journal of South American Earth Sciences 10, 21-28.

Thirwall, M., 2000. Inter-laboratory and other errors in Pb isotope analyses investigated using a ^{207}Pb/^{204}Pb double spike. Chemical Geology 163, 299-322.

Towsend, A.; Yu, Z.; Mcgoldrick, P.; Hutton, H., 1998. Precise lead isotope ratios in Australian galena samples by resolution ICP-MS. Journal of Analytical Atomic Spectrometry 13, 809-813.

Wannemacker, G.; Vanhaecke, F.; Moens, L.; Mele, A.; Thoen, H., 2000. Lead isotopic and elemental analysis of copper alloy statuettes by double focusing sector field ICP-MS. Journal of Analytical Atomic Spectrometry 17, 323-327.

Weiss, D.; Boyle, E.; Chavagnac, V.; Herwegh, M.; Wu, J., 2000. Determination of lead isopope ratios in seawater by ICP-QMS after Mg(OHO$_2$ co-precipitation Spectrochimica Acta Part B 55, 363-374.

MESOZOIC TO CENOZOIC THERMO-TECTONIC EVOLUTION OF THE SOUTHERN PRECORDILLERA, NW-ARGENTINA: PRELIMINARY RESULTS FROM APATITE FISSION TRACK THERMOCHRONOLOGY

Ávila, J.N.[1]; **Chemale Jr., F.**[2]; **Borba, A.W.**[1] **and Vignol-Lelarge, M.L.M.**[2]

1. Programa de Pós-graduação em Geociências, IG, UFRGS, Brazil. janaina.avila@ufrgs.br, awborba.voy@terra.com.br
2. Laboratório de Geologia Isotópica, IG, UFRGS, Brazil. farid.chemale@ufrgs.br, lidia.vignol@ufrgs.br

Keywords: Fission track dating, apatite, thermochronology, precordillera, Argentina

INTRODUCTION

Apatite fission-track thermochronology (AFTT) is a temperature-sensitive technique applied to the understanding of burial and exhumation of basement rocks and sedimentary basins (e.g. Naeser et al., 1989; Foster & Raza, 2002). This study describes the application of AFTT to the southern Precordillera of Argentina (Fig. 1), near the town of Potrerillos (Mendoza Province), in order to constrain the thermal and tectonic evolution of this area. Rock units developed in diverse tectonic settings from the Paleozoic to the Cenozoic crop out, limited by structures generated by Andean tectonics (Ramos, 1999).

METHODOLOGY AND SAMPLING

Apatite fission track thermocronology (AFTT) is a powerful tool for constraining the low-temperature history of rocks over a range of 3-5 km (Raab et al., 2002). Thus, AFTT can reconstruct the cooling history of rocks as they approached the surface in response to erosion and tectonic processes, and represent an ideal method for studying the morphotectonic effects of deformation.

AFTT is based on the spontaneous decaying of ^{238}U by nuclear fission, process that causes linear damage tracks (the fission tracks) in the U-bearing mineral (in this case, apatite). The number and density (number/area) of spontaneous fission tracks is proportional to the ^{238}U content of the apatite sample. This is compared to the ^{235}U content, which can be achieved by irradiating the sample in a nuclear reactor and inducing its fission and the appearing of new tracks (induced tracks). This isotopic relationship provides the fission-track (FT) age of the studied sample.

We collected nine samples of different ages for AFTT. They are Permian igneous rocks (granodiorites, syenogranites and breccia volcanic), Triassic volcano-sedimentary rocks of the Cuyo Basin and Miocene sedimentary rocks (Fig. 2).

The Fission Track analyses have been carried out at the Laboratório de Geologia Isotópica of the Universidade Ferderal do Rio Grande do Sul. Apatites were separated using conventional heavy liquid and magnetic techniques, mounted in epoxy resin and etched for 30s at 20°C in 0,5N HNO_3. Neutron irradiation was carried out in the IPEN-CNEN Reactor, in São Paulo, Brazil. Ages were measured using the external detector method (Naeser & McKee, 1970) with Kapton® detectors to record induced track densities. Thermal neutron fluxes were monitored by measuring the track density in muscovite mica attached to CN-1 and SRM 612 standard glasses. Track counting was perfomed in transmitted light at a total magnification of 1000 x (oil immersion). Ages were calculated using the zeta calibration method, and are expressed as central ages (Galbraith & Laslett, 1993). The lengths of spontaneous, fully etched, confined, horizontal fission tracks were measured in four samples. The FT ages and track lengths were used to model thermal histories by using the Monte Trax program (Gallagher & Sambridge, 1994). This program applies the relationship between FT length shortening and FT density reduction, as a function of time/temperature conditions, based on the annealing model obtained by Laslett et al. (1987) for the Durango fluorapatite (0.4% wt of Cl).

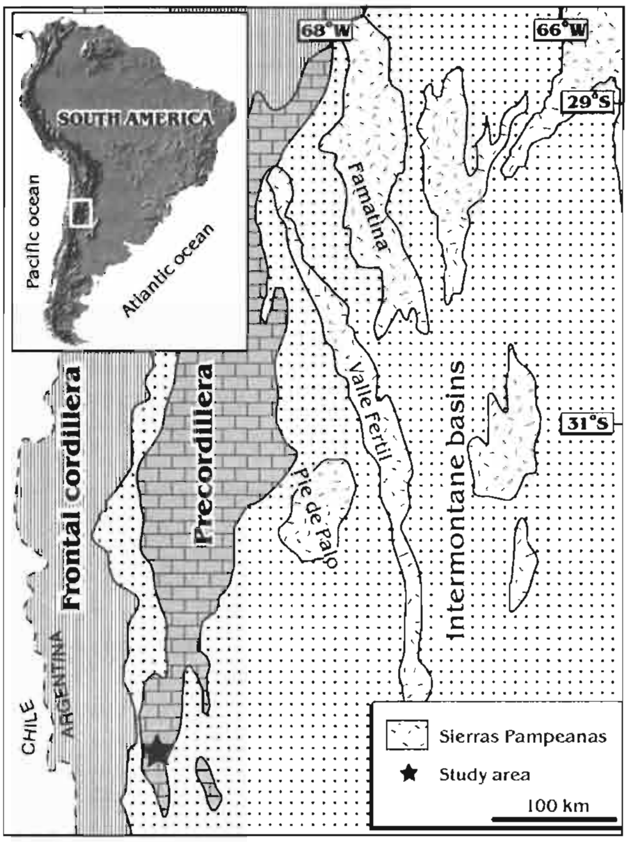

Figure 1. Morphotectonic units of the western Argentina and location of the studied area.

RESULTS AND DISCUSSION

The obtained results (Fig. 2) demonstrate that the central block (Permian basement samples Cuy-1, Cuy-59, and Triassic Cuyo basin volcano-sedimentary samples Cuy-3, Cuy-6 and Cuy-7), bounded by thrust (northwest) and inverse (southeast) faults, contain the older central ages (between 179 and 133 Ma). On the other hand, the basement samples situated in the northwestern and southeastern blocks (granitic bodies) yielded FT ages of 23 and 17 Ma, respectively. All these samples display FT ages younger than their stratigraphic ages, representing cooling (uplifting or denudation) events. Sample Cuy-17 consists of andesitic clasts from the framework of conglomerates deposited at around 15.7 – 15.4 Ma (Irigoyen et al., 2002). Its FT age (64.9 ± 7.6 Ma) is older than the depositional age, probably representing a provenance age (FT age of the source rocks).

The results suggest that the central block (older FT ages), composed of volcanic and sedimentary units, and passed through the partial annealing zone (PAZ) before the lateral blocks, where granitoids crop out. The juxtaposition of rocks of different crustal levels would have occurred during the compressive Andean tectonics, in the Tertiary.

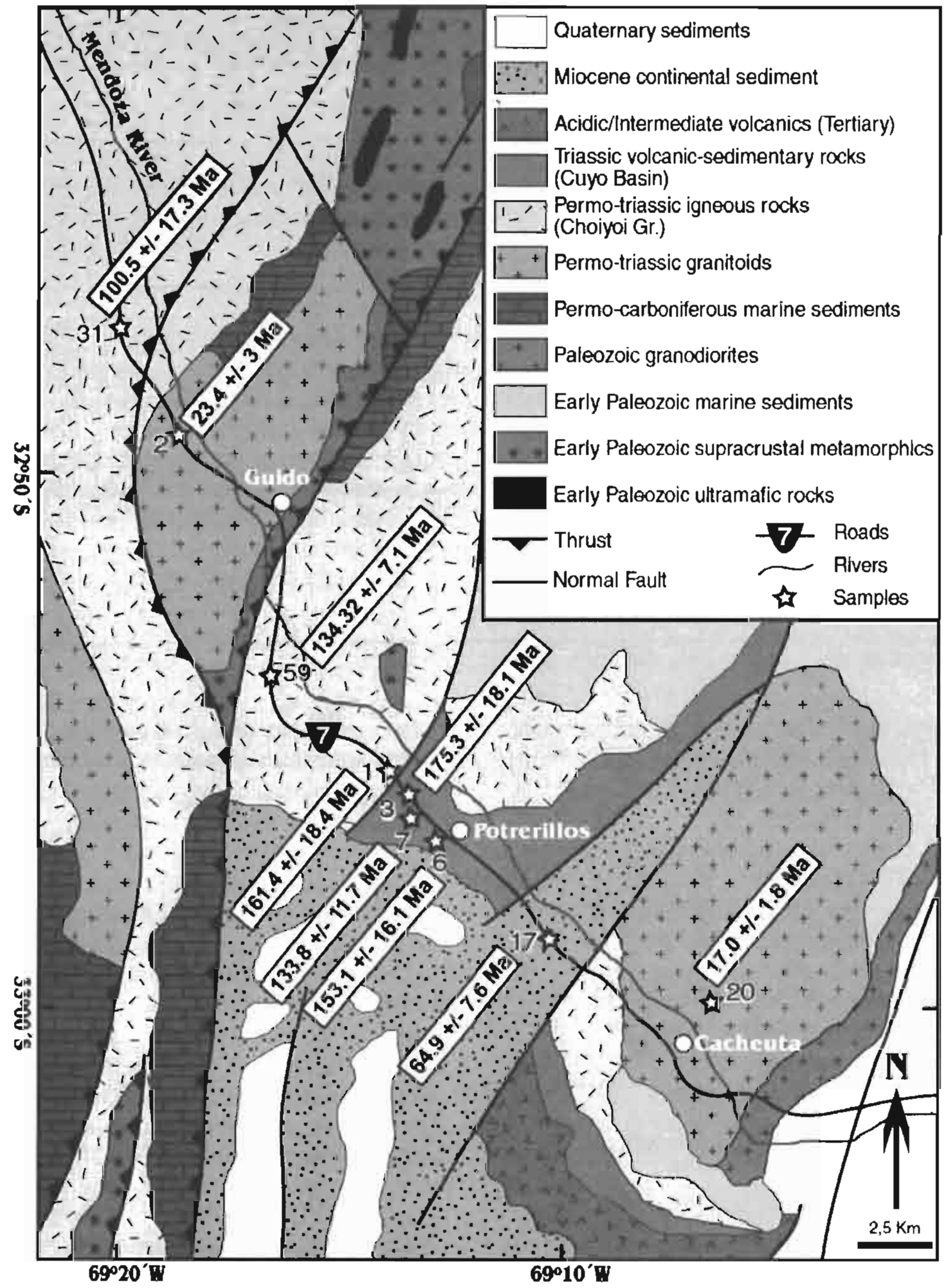

Figure 2. Geological map of the Potrerillos region, located in the southern Precordillera of Argentina, showing the rock units (Early Paleozoic to Cenozoic), the location of the analyzed samples and the fission-track ages obtained in the present work.

The application of the annealing models (Fig. 3) through the integration of FT ages and confined lengths suggest four different evolutionary phases for the volcano-sedimentary and basement rocks of the Potrerillos region:

PHASE I: during the Triassic, the thermal history of the Cuyo Basin volcano-sedimentary samples shows a progressive heating until they reached the PAZ (Early Triassic). Synchronous uplifting of rift shoulders is marked by a cooling trend obtained for the basement samples.

PHASE II: the Jurassic is characterized by processes of isostatic compensation between the rift shoulders (where temperature increases) and depositional areas (where a cooling trend is observed). The shifting of both trends is related to the geostatic load balance between basin and source areas.

PHASE III: from Cretaceous to Early Cenozoic, the studied region apparently passed through a stabilization phase, without significant tectonic and thermal modifications. A slight increase of the temperature may be related to changes in geothermal gradient.

PHASE IV: in the Miocene, an important change in the evolution of the Potrerillos region can be inferred. This period is marked by the transition from extensional to compressive conditions, associated with the change in the subduction angle of the Nazca plate beneath the South American continent. This is well constrained in the thermal history modellings, which show a progressive temperature decrease, possibly related to the differential uplift of crustal blocks bounded by thrust and inverse faults. During this time, there was probably the juxtaposition of rock units formed in different crustal levels, reflected in the difference between FT ages (17 and 23 Ma for granitoids and between 175 and 100 Ma for volcano-sedimentary rocks) in contrasting blocks.

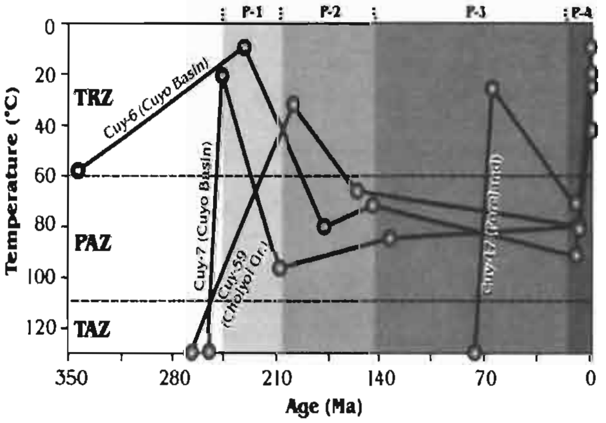

Figure 3. Fission-track data modelling obtained from Monte Trax program for the Cuy-7, Cuy-6, Cuy-59 and Cuy-17 samples: best-fitting thermal history curves showing the four different evolutionary phases for this samples. TRZ = total retention zone; PAZ = partial annealing zone; TAZ = total annealing zone. P1 – P4 correspond to the phases cited in text.

CONCLUDING REMARKS

Apatite fission track thermochronology data provided an important base for the characterization of the main subsidence and uplift phases of igneous and sedimentary rocks of the Argentine Southern Precordillera during Mesozoic and Cenozoic times. During the Triassic, thermochronological data refer to the evolution of the Cuyo Basin, with subsidence and burial of volcano-sedimentary units and concomitant uplift of rift shoulders. This phase was followed by isostatic compensation (Jurassic) and a long period of tectonic quiescence (Cretaceous to Early Cenozoic). A significant uplift occurred during the upper Miocene that may be related with changing from extensional to compressive tectonic regimes. A differential uplift of blocks was also distinguished, where a central block characterized by volcanic and sedimentary rocks was juxtaposed with basement blocks situated to northwest and southeast.

REFERENCES

Foster, D.A & Raza, A. 2002. Low-temperature thermocronological record of exhumation of the Bitterroot metamorphic core complex, northern Cordilleran Orogen. Tectonophysics, v. 349, n. 1-4, p. 23-36.

Galbraith, R.F. & Laslett, G.M. 1993. Statistical Models for Mixed Fission Track Ages. Nuclear Tracks and Radiation Measurements, v. 21, n. 4, p. 459 -470.

Gallagher, K. & Sambridge, M. 1994. Genetic Algorithms: a powerfull method for large-scale non-linear optimization problems. Computer & Geosciences, v.20, p. 1229-1236.

Irigoyen, M.V; Buchan, K.L; Villeneuve, M.E.; Brown, R.L. 2002. Cronología y significado tectónico de los estratos sinorogénicos neógenos aflorantes en la región de Cacheuta-Tupungato, Provincia de Mendoza. Revista de la Asociación Geológica Argentina, v. 57, n.1, p. 3-18.

Laslett, G.M.; Green, P.F.; Duddy, I.R. & Gleadow, A.J.W. 1987. Thermal annaaling of fission tracks in apatite 2. A quantitative analysis. Chemical Geology, v.65, p. 1-13.

Naeser, N.D. & Mckee, E.H. 1970. Fission-track and K-Ar Ages of Tertiary Ash-Flow Tuffs, North-Central Nevada. Geological Society of America Bulletin, v.81, p. 3375-3384.

Naeser, N.D; Naeser, C.W. & McCulloh, T. H. 1989. The applications of fission-track to the depositional and thermal history of rocks. In: Thermal History of Sedimentary Basins - Methods and Case Histories, N.D. Naeser e T.H. McCulloh (eds). Springer-Verlag. p. 157 -180.

Raab, M.J.; Brown, R.W.; Gallagher, K.; Carter, A.; Weber, K. 2002. Late Cretaceous reactivation of major crustal shear zones in northern Namibia: constrains from apatite fission track analysis. Tectonophysics, v. 349, n. 1-4, p. 75-92.

Ramos, V.A. 1999. Evolucion tectonica de la Argentina. In: Rasgos Estructurales del Território Argentino, Instituto de Geologia y Recursos Minerales, Anais 29 (24), p. 715-751.

CARBON AND OXYGEN ISOTOPE COMPOSITION OF CARBONATE CEMENTS OF BEACHROCKS AT THE LAGOINHA AND URUAU BEACHES, STATE OF CEARÁ, NORTHEASTERN BRAZIL

Barros, S.D.S.[1]; Sial, A.N.[2] and Cunha, I.S.[3]

1. LABISE, PPGeoc, Federal University of Pernambuco, CP 7852, Recife, Brazil, 50732-970. sbarros@ufpe.br
2. NEG-LABISE, Dept. of Geology, CP 7852, Federal University of Pernambuco, Recife, Brazil, 50732-970. ans@ufpe.br
3. LGPSR, Dept. of Geology, Federal University of Ceará, Fortaleza, Brazil. x7hmp@ufc.br

Keywords: Carbon-oxygen isotopes, beachrocks, sea level fluctuation

INTRODUCTION

In the last decades, beachrock deposits have been investigated in coastal zones around the world. Usually, these deposits are identified in the coastline or near to river mouths in the tropical to subtropical littoral region and are indicators of paleo-coastline markers. In the global scenario, several researchers (e. g. Craig, 1961; Stoddart & Cann, 1965; Alexanderson, 1972; Hudson, 1977; Suhayda et al., 1977; Holail & Rashed 1992; Bezerra et al. 1998; Chaves, 2000) have discussed the mechanisms governing their formation and significance in recent littoral environment. Beachrocks are regarded as the most common Holocenic feature and their relative distribution in relation to the coastline attests to sea level fluctuations during the Quaternary. Ground penetrating radar helps investigating the architecture of outcrops that are partially or totally buried. Carbon and oxygen isotopes are used to estimate precipitation and post-depositional conditions and allow correlating these deposits with sea level variation.

Several beachrock strings are known in northeastern Brazil (e.g. Bahia, Pernambuco and Rio Grande do Norte). Barros & Sial (2001) described systematic discontinuous beachrock alignments concordant with the coastline configuration in the Ceará littoral zone and investigated carbon and oxygen isotope composition of the beachrock carbonate cement. The outcrops are exposed in a narrow intertidal zone, near river mouths or as buried paleochannels. Generally, they constitute tabular bodies with gentle seaward dips, variable grain size, and variable widths and lengths.

This study aims at investigating the isotope behavior of carbonate cements of beachrocks located at Lagoinha and Uruau beaches, State of Ceará. Comparison of features observed in both localities may inform the temporal distribution and processes of beachrock cementation on regional scale.

COASTAL GEOLOGICAL SCENARIO

Some morphological features of the Ceará littoral zone have been strongly dissected by internal and external agents. The Lagoinha and Uruau beaches are part of the scenario (Fig. 1). The geological units are similar in these sites and are composed by Barreiras Fm (Tertiary) and some quaternary deposits (marine terraces, fixed and mobile coastal dunes and beachrocks).

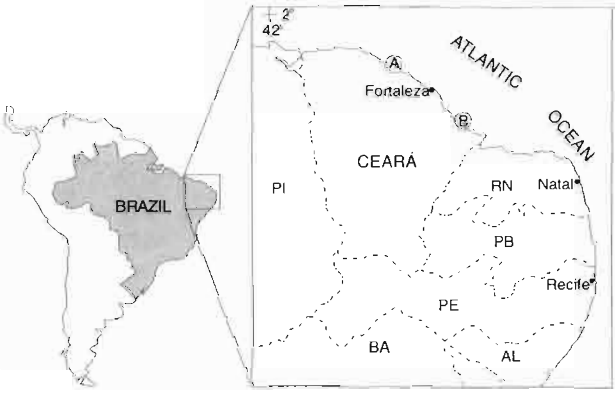

Figure 1. Lagoinha (A) and Uruau (B) beachrock outcrops, State of Ceará.

The tertiary Barreiras Fm. comprises uncon-solidated, coalescing alluvial fans that form gently seaward-dipping surfaces. In some places, these deposits reach the coastline, forming active cliffs that extend by several meters. Massive detrital material composed of quartz and angular feldspar grains in ferruginous matrix form paleochannels in depressions in Barreiras Fm, which represents an episodic sedimentation during the principal deposition in littoral zone.

Quaternary marine terraces are composed by very fine to coarse-grained, unconsolidated sandy sediments and shell fragments. The aeolian deposits are formed by active or fixed sand dunes which normally cover more ancient sedimentary units and are composed by fine to medium-grain size quartz sands; white in the recent dunes and yellowish to orange in paleodunes. The fixed dunes were installed as strandline shore over the cliffs on the Barreiras Fm. sediments. The fixation of the dunes of older generation is responsible for pedogenic processes and vegetation. The younger unit (beachrock deposit) presents some different features in these sites.

The sandstone beachrocks are composed of terrigenous detritus sediments (e.g. quartz, feldspar, heavy minerals), with medium to coarse-grain size, as well as biogenic fragments (e.g. molluscs, algae, corals) whereas beachrock cement may vary from aragonite to Mg-calcite (Stoddart & Cann, 1965; Alexanderson, 1972).

At the Lagoinha beach, two beachrock lines are present. The outer line between the lower foreshore and the upper shoreface zone is formed by tabular beds, and is composed of medium to coarse sandstone, sometimes conglomeratic, weakly cemented. The inner line is partially buried by an aeolian strandline. Castro et al. (2001), using ground penetration radar (GPR), mapped two buried layers, one at 1.5 and other at 4 meters below unconsolidated quaternary sediments. The buried outcrops have been truncated along the frontal boundary, a feature that resulting from recent extensional movements.

In Uruau beach, the outcrops form a 1.5km-long body, parallel to coastline, exhibit subhorizontal bedding, and are sometimes, covered by unconsolidated sediments. A 1.5m thickness is exposed at ebbtide, and the body is 50m wide in backshore zone.

The uppermost surface of the outcrops has an irregular shape due to erosion by tidal oscillations, wind action and biochemical agents. Potholes and cracks are the most common erosional features. Elongate potholes are shallow structures that reflect the action of differential erosion sometimes filled with rock or shell fragments and beach sediments. Cracks are disposed in two preferential directions, one perpendicular to the length of the outcrop and another parallel to the coastline. The onset of these structures could be associated to the mechanical action of the waves, or to tectonic reactivation of the Meso-cenozoic coastal basins of the eastern portion of northeastern Brazil. Some cracks are filled with lithified sediments that suggest a late cementation, evidencing two sedimentation events. Conglomerate layers composed by rock and shell fragments occur intercalated in the sandstone. Sedimentary structures include plane-parallel lamination and mesoscale cross-bedding structures, associated to tidal environment.

CARBON AND OXYGEN ISOTOPE DATA

Lagoinha and Uruau beachrock outcrops were studied and sampled. Stable isotopes were analyzed in beachrock cements of a total of 29 samples from the two studied localities. The samples were carefully prepared and analyzed due to small quantity cement enclosing the grains or filling void.

Samples were split into two populations, grains cement and shells. To avoid the influence of carbon from shells, samples contain shell fragments were discarded.

Normally, 20 to 50mg of powdered carbonate cement samples were reacted with a 100% orthophosphoric acid at 25°C overnight and the released CO_2 gas, after cryogenically cleaned, was analyzed in a SIRA II mass spectrometer at the Stable Isotopes Laboratory-(LABISE, Federal University of Pernambuco) at Recife, Brazil.

OXYGEN AND CARBON RESULTS

Temperature and salinity are parameters to lead the carbon-oxygen isotopic behavior in the seawater, than Climatic and environmental changes will be monitories through beachrock carbonate cement studies. The oxygen isotopic behavior reflects climatic changes, while carbon isotopic behavior is associated to environmental conditions during cement precipitation.

At the Lagoinha beach (Fig 2), $\delta^{13}C$ ranges from +1.9 to +3.1‰$_{PDB}$, whereas in Uruau beach, $\delta^{13}C$ values from +0.5 to +3.4 ‰$_{PDB}$ were obtained. All $\delta^{13}C$ values are positive, confirming precipitation from a ^{13}C-enriched seawater. At the Lagoinha beach, these data reflect a precipitation in shallow warm seawater whereas, a carbon isotope values at Uruau beach show a broader range, that will be signifying a freshwater influx caused alteration in the carbonate cement associated to exposure after coastline regression or uplift correlated to quaternary tectonic activity.

It has been proposed that positive $\delta^{13}C$ values for marine deposits are possibly related to transgression periods whereas negative values are correlated to regression periods. The C-isotope systematic may be proves to be a valuable tool in tracking sea level variation during the quaternary.

Sedimentary structures observed in these outcrops, such as mesoscale cross-bedding and plane-parallel lamination are diagnostic of partially-submerged beach under low tide conditions, and under high tide, respectively. Sedimentary structures in this study as well as $\delta^{13}C$ values, support the assumption that carbonate cement precipitated a transgressive marine environment.

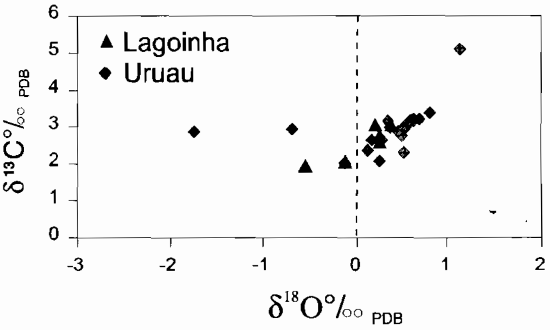

Figure 2. $\delta^{13}C$ and $\delta^{18}O$ behavior in carbonate cement in the two studied beachrock localities.

The results for carbonate cement in Lagoinha beach present $\delta^{18}O$ values from –0.5 to +0.4‰$_{PDB}$, whilst in the Uruau outcrops, $\delta^{18}O$ ranges from -1.8 to +1.2‰$_{PDB}$ (Fig. 2). In both localities, oxygen isotope values vary from positive to negative.

Applying the thermometric equation by Epstein at al (1963) to estimate paleotemperature (T°C), temperatures in the Lagoinha beach range from 15° to 19°C, while at Uruau, temperatures vary from 14° to 24°C (Fig. 3). Larger variation in Uruau beach may reflect one or more successive phases of carbonate cement precipitation, whilst in the Lagoinha beachrock, a progressive temperature range was observed.

Although beachrocks at both localities were formed in intertidal environment, the carbon and oxygen isotope data reveal differences between the carbonate cements of the two localities. It is likely that at Uruau, C and O isotope data have undergone some post-depositional modification.

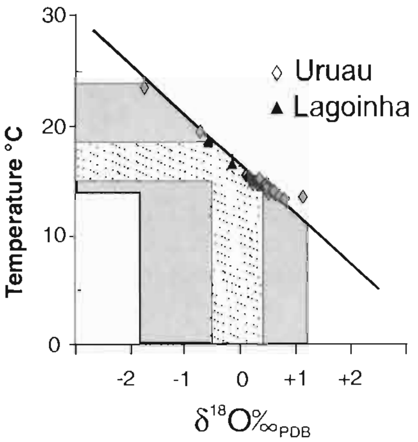

Figure 3. Plot of variation of $\delta^{18}O$ with temperature in both localities.

ACKNOWLEDGMENTS

SDSB wishes to thank the National Council for Scientific and Technological Development (CNPq) for a scholarship and the LGPSR of the Federal University of Ceará for logistical support during the fieldwork. Thanks are also due to Gilsa Maria Santana and Vilma Sobral for help with the isotopic analyses; David Castro and Loreci Lehugeur the help during the fieldtrips. This is the contribution n. 216 of the NEG-LABISE.

REFERENCES

Alexanderson, T., 1972. Mediterranean beach-rock cementation: Marine precipitation of Mg calcite, in Stanley, D. J., ed, Part 5. Coastal and shallow water sedimentation: Carbonate sediments: p. 203-233.

Barros, S.D.S & Sial, A.N. 2001. $\delta^{13}C$ and $\delta^{18}O$ in beachrocks of the state of Ceará, Northeastern Brazil. III South American Symposium on Isotope Geology, Pucon-Chile, expanded abstract, digital.

Bezerra, F.H.R; Lima Filho, F.P.; Amaral, R.F.; Caldas, L.H.O.; Costa-Neto, L.X. 1998. Holocene coastal tectonics in NE Brazil, in Stewart, I.S. & Vita Finzi, C. eds., Coastal Tectonics, Geological Society, London, Special Publications, 146:279-293.

Castro, D.L.; Barros, S.D.S.; Castelo Branco, R.M.G.; Sial, A.N.; Guimarães Júnior, A.; Baptista Filho, R.M. 2001. Uso do GPR na caracterização interna de feições geológicas cenozoicas no litoral centro-oeste do Ceará, Brasil. VII International Congress of Geophysics da SBGf, Salvador-Br, expanded abstract, digital.

Chaves, N.S., 2000. Mecanismo de cimentação em sedimentos marinhos recntes, exemplo beachrocks do litoral de pernambuco., tese ., Univ. Estadual de São Paulo, Rio Claro, 194p.

Craig, H., 1961. The measurements of oxygen isotope paleotemperatures, in Tongiorgi, E., ed., Stable isotopes in oceanographic studies and paleotemperatures: Pisa, CNR, 1-24.

Epstein, S; Buchsbaum, R; Lowenstam. H.A.; Urei, H.C., 1963. Revised carbonate-water isotopic temperature scale. Bulletin of the Geological Society of America, 64:1315-1326.

Holail, H. & Rashed, M., 1992. Stable isotopic composition of carbonate-cemented recent beachrock along the Mediterranean and Red Sea coasts of Egypt: Marine Geology, 106:141-148.

Hudson J.D., 1977. Stable isotopes limestone of lithification. J. Geol. Soc. London, 133:637-660.

Stoddart, D.R. & Cann, J.R., 1965. Nature and origin of beach rocks: Jour. Sediment. Petrol., v.35, p. 43 - 273.

Suhayda, J.N.; Hsu, S.A.; Robert, H.H.; Short, A.D., 1977. Documentation and analysis of coastal process, northeast coast of Brazil: Baton Rouge, LA: Coastal Studies Institute, Louisiana State University, Tech. Rep. n°. 23, 98p.

TIMING OF HIGH-GRADE METAMORPHISM: EARLY PALEOZOIC U-Pb FORMATION AGES OF TITANITE INDICATE LONG-STANDING HIGH-T CONDITIONS IN THE SOUTHERN PUNA AND WESTERN SIERRAS PAMPEANAS (ARGENTINA, 26 - 29°S)

Becchio, R.[1, 2] **and Lucassen, F.**[3, 4]

1. Universidad Nacional de Salta, Buenos Aires 177, 4400 Salta, Argentina. tato@unsa.edu.ar
2. Technische Universität Berlin, Inst. f. angewandte Geowissenschaften, FG Petrologie, Str. d. 17. Juni 135, 10653 Berlin, Germany
3. GeoForschungsZentrum Potsdam, Telegrafenberg, 14473 Potsdam, Germany. Lucassen@gfz-potsdam.de
4. Freie Universität Berlin, FB Geowissenschaften, Malteserstr. 74-100, 12249 Berlin, Germany

Keywords: Titanite, U-Pb dating, metamorphic rocks, Puna, Sierras Pampeanas

INTRODUCTION

Isotopic dating of metamorphism in areas with polymetamorphism and/or polyphase deformation at high-T and moderate pressure is still a challenge in geochronology. The construction of internal (mineral) isochrons, e.g. in the Sm-Nd or Rb-Sr isotope systems, requires three or more minerals with sufficient spread in their Sm/Nd or Rb/Sr ratios in the peak-metamorphic mineral assemblage to demonstrate isotopic equilibrium, i.e. that the minerals of the peak assemblage remained a closed systems during slow cooling from high-T or multiple heating. Zircon is generally suitable for dating of high-T processes in the U-Pb system due to the insignificant diffusion of Pb at most geologically relevant temperatures (e.g. Mezger & Krogstad, 1997). However, new growth of zircon in metasedimentary and metaigneous rocks frequently occurs as overgrowths on cores of inherited zircon, and dating of whole grains using conventional U-Pb methods gives discordant results. In situ U-Pb age determination by high resolution SIMS technology partially overcomes this problem, but resetting of the U-Pb system in overgrowth patterns may be incomplete if processes such as leaching or solid-state recrystallization have taken place (Mezger & Krogstad, 1997; Hoskin & Black, 2000) and calculated concordant U-Pb ages from such overgrowth pattern are difficult to interpret.

Titanite is a common metamorphic mineral in calcsilicate rocks, which has long been recognised as suitable for U-Pb dating. Having a closure temperature > 650 °C (review in Frost et al., 2000), titanite is suitable for dating events up to upper amphibolite facies. This case study from western Argentina presents U-Pb ages of metamorphic titanite mainly from calc-silicate rocks that occur within uniform upper amphibolite to granulite facies rocks. The sampling strategy was aimed at providing a regional documentation of the timing of peak metamorphism over a wide area (c. 400 x 100 km; Fig. 1). Four to eight fractions of euhedral titanite from each sample were analysed to evaluate the reproducibility of the U-Pb ages, to check for the influence of accidental inhomogeneity of the sample, different types of titanite in the same sample, and analytical bias. The new age data in combination with the interpretation of titanite chemistry and observation of the mineral assemblage and metamorphic fabric show that: (1) titanite retained its chemical composition and U-Pb signature once acquired even under long-standing high-T conditions; (2) the driving force for reequilibration of the U-Pb system in the titanite was recrystallization during localized deformation and not Pb – loss by diffusion in most samples; (3) geodynamic interpretation of a small number of ages may be misleading in long-standing high–T regimes with multiple thermal peaks and/or deformations, e.g. in the mid-crust of continental magmatic arcs.

GEOLOGICAL FRAMEWORK AND PETROLOGY

The western margin of Proterozoic Gondwana has been substantially reworked by metamorphism and magmatism in an Early Palaeozoic mobile belt (ca 18° - 32°S) active from Cambrian to Silurian times (Fig.1; recent summaries for the area c. 30° - 32°S, Pankhurst & Rapela, 1998; and for c. 18 - 27°S, Lucassen et al., 2000). The metamorphism with widespread anatexis and extended crust-derived magmatism indicates high temperatures at a midcrustal level. High pressure rocks typical of collisional tectonic regimes are unknown. The mobile belt north of ca 28°S and the area east of the Argentine Precordillera and south of ca 28°S formed part of Gondwana throughout its thermo-tectonic evolution, whereas the Argentine Precordillera is considered as an exotic terrane (Fig. 1) with a possible Early Ordovician docking age (e.g. Casquet et al., 2001). Published ages of high-T metamorphism are *c.* 510 Ma in the southern Puna (Fig. 1) and *c.* 470 - 460 Ma, with a possible continuation of the high-*T* metamorphism into the Silurian - Devonian (Fig. 1; Lucassen et al., 2000). Similar Late Cambrian and Mid-Ordovician ages of metamorphism are reported from the eastern Sierras Pampeanas south of c. 30°S (Pankhurst & Rapela, 1998).

In the southern Puna and in the western Sierras Pampeanas the bulk of the high-grade metamorphic rocks have silici-clastic protoliths and form monotonous gneiss - migmatite areas with little lithological variation. The mineral paragenesis of the gneiss-migmatite is quartz - plagioclase - biotite - minor garnet with increasing modes of potassic feldspar, alumino-silicate and cordierite in the more pelitic compositions. Marbles, calcsilicate rocks and amphibolites occur locally within this unit, and are common in a belt from the southern Puna stretching into western Sierras Pampeanas. Their thickness varies between dm and tens to hundreds of meters.

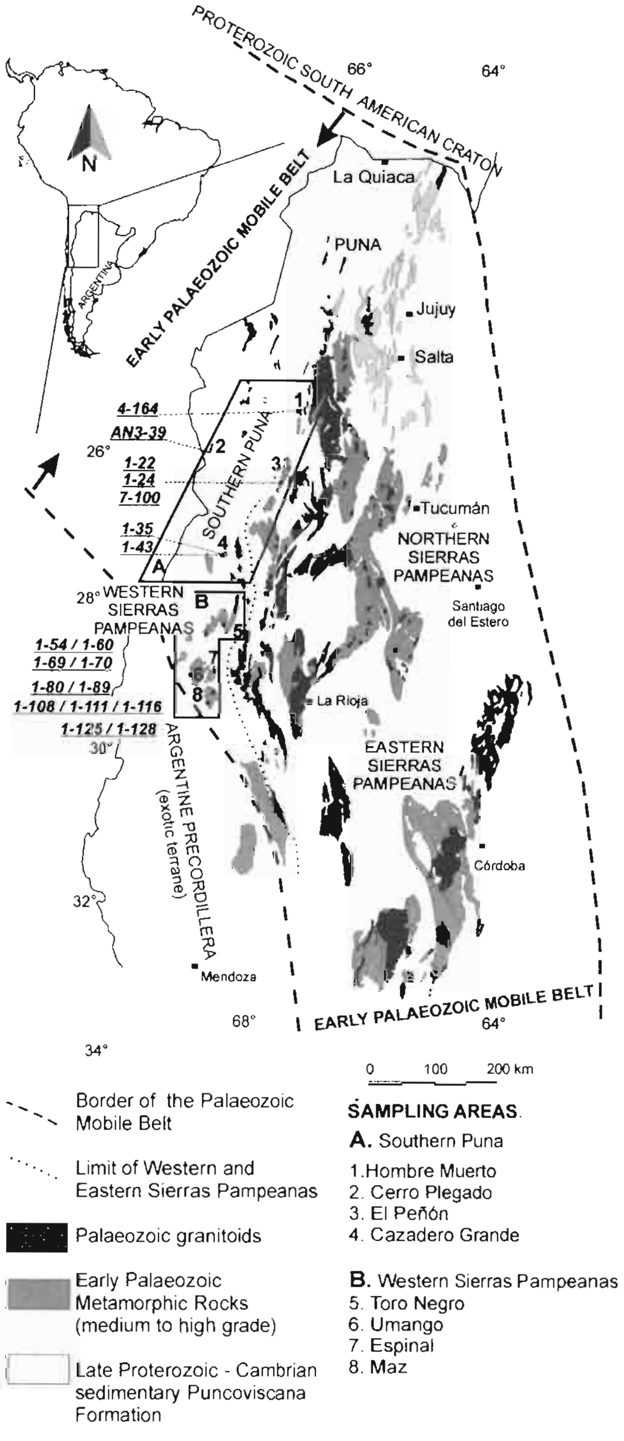

Figure 1. Geological map, sample locations and sample numbers. For titanite U-Pb ages see Table 1.

The typical mineral paragenesis of the calcsilicate rocks is calcite -uartz - plagioclase - clinopyroxene - garnet and accessory titanite with epidote, scapolite and amphibole in some samples. The temperature of metamorphism at all sample locations was above the wet granite solidus as indicated by widespread anatexis of pelitic compositions. The peak metamorphic paragenesis is commonly preserved without thorough retrogression. Deformation occurs at T close to peak-metamorphic conditions in all sample areas with subsequent high temperature recovery of the microfabric. Subsequent deformation is located in shear zones (cm - km scale) and overprints the annealed fabrics at high T and with no change of the mineral paragenesis.

U-Pb DATING

TITANITE CHARACTERISTICS

Euhedral titanite forms part of the stable mineral paragenesis in the calcsilicate rocks. Optical zoning is absent. Major element patterns from electron microprobe analysis indicate no overgrowths, inherited cores, or gradual core-rim diffusion zoning. We conclude from the textural position of the titanite and from its compositional pattern that it formed close to upper amphibolite facies conditions and has not been altered during retrogression. Thorough deformation at high temperature in shear zones is observed in the field and in the development of microfabrics. Dynamic recrystallization of the metamorphic mineral assemblage during deformation at high-T leaves the stable mineral assemblage unchanged but may reset the U-Pb isotope system in the titanite.

U-Pb AGES

The average values of $^{206}Pb/^{238}U$ and $^{207}Pb/^{235}U$ ages of five to eight different titanite fractions from each sample are listed in Table 1. The titanite shows a high content of radiogenic ^{206}Pb ($^{206}Pb/^{204}Pb$ > ca. 200 - 700) in most calcsilicate rocks. Therefore, the uncertainties in the common lead correction are minor. Most samples and fractions plot on or very close to the U-Pb concordia and only one sample is clearly discordant. Different size fractions of euhedral titanite from one sample yield identical ages and no influence of the cooling history or possible reheating is seen in their U-Pb systematics. In addition, the chemical homogeneity of the titanites and their appearance in the metamorphic fabric without reaction textures largely exclude a multistage development of titanite. The following discussion is based on the assumption that the U-Pb ages present the age of formation of the titanite.

DISCUSSION

Reliable age data of high grade metamorphic rocks from Sierras Pampeanas and the Puna Plateau are scarce and only recently few U-Pb and Sm-Nd ages using metamorphic minerals became available (northern Sierras de Pampeanas; Büttner et al., in revision; 21-27°S; Lucassen et al., 2000; ca 30-32°S; southern Sierras Pampeanas and Argentine Precordillera: in Pankhurst and Rapela, 1998). The Neoproterozoic - Cambrian Pampean orogeny and the Ordovician - Silurian Famatinian orogeny have been previously constrained by the ages of two distinct magmatic - sedimentary cycles (def. by Aceñolaza and Toselli, 1976; see also Rapela et al., 1998). Pampean (530 - 510) and Famatinian ages (470-420) are now well established in the high temperature metamorphic rocks in the southern Puna and western Sierras Pampeanas (Fig. 1; Table 1). Famatinian ages have been also found in high grade metamorphic rocks of the Chilean Precordillera at ca 21°S (ca 470 - 420 Ma, U-Pb ages on titanite; unpublished data of F. Lucassen).

Table 1. Titanite average U-Pb ages of the samples in Figure 1. Sample AN-25 is a granite from the Archibarca intrusion / Salar de Antofalla. Errors are 2 σ.

Location/Sample	Rock Type	$^{206}Pb/^{238}U$	$^{207}Pb/^{235}U$
Southern Puna		(Ma)	(Ma)
Hombre Muerto / 4-164	calcsilicate	515±2	514±2
El Peñon / 01-22	calcsilicate	528±3	525±3
01-24	calcsilicate	520±8	523±7
7-100	calcsilicate	517±6	515±6
Salar Antofalla / AN-25	granite	454±4	452±10
Cerro Plegado / AN-3-39	migmatite	463±3	464±6
Cazadero Grande / 01-35	calcsilicate	451±4	449±5
01-43	calcsilicate	444±3	446±3
Western Sierras Pampeanas			
Sierra Toro Negro / 01-54	calcsilicate	454±3	451±2
01-60	calcsilicate	432±2	433±5
Sierra Espinales / 01-69	calcsilicate	465±1	465±1
01-70	calcsilicate	466±1	465±1
Sierra Umango / 01-80	calcsilicate	425±4	424±5
01-89	calcsilicate	422±5	421±5
Sierra De Maz / 01-108	amphibolite	401±18	426±17
01-111	calcsilicate	443±3	443±2
01-116	calcsilicate	535±4	539±4
01-125	Intercepts at 432 ± 15 & 1208 ± 38 Ma		
01-128	calcsilicate	428±6	431±3

Proterozoic ages of metamorphism seem to be absent in the whole area. The age gap of ca 40 Ma between Pampean and Famatinian metamorphism might be an artefact of the still scarce data. The ages of Famatinian crust-derived magmatism of Sierras Pampeanas and south-eastern Puna (ca 495 - 460 Ma; e.g. Pankhurst et al., 2000) suggest a continuation of the Cambrian high T conditions in the crust during the Early Ordovician.

IS IT POSSIBLE TO DERIVE A GEOTECTONIC SCENARIO?

Age data of metamorphic rocks have been used to support petrological evidence in the controversy concerning the Laurentian origin and early Palaeozoic accretion history of the Argentine Precordillera terrane (Fig. 1; e.g Casquet et al., 2001). The new ages of metamorphic rocks from Sierras de Maz, Umango, Espinal, and Toro Negro (Fig. 1) show the complexity of age relations: concordant U-Pb ages of *c.* 530, 460, 440, 430, 420 Ma and lower and upper intercept ages of *c.* 430 and 1200 Ma from strongly discordant titanite document polymetamorphism and/or polyphase deformation. Provided the proposed eastern boundary of the Precordillera terrane is correct, the Sierras de Maz, Umango, Espinal, and Toro Negro formed part of the western leading edge of Gondwana (Fig. 1). Metamorphism occurred in Sierra de Maz at *c.* 530 Ma, before docking of the Precordillera terrane, and contemporaneous and at similar high-T and moderate-P as in the Pampean orogen of the eastern Sierras Pampeanas, southern Puna, and N Chile. Given that the docking age of the Precordillera was >460 Ma (Casquet et al., 2001), high-T metamorphism and deformation occurred after the possible collision of the Precordillera at *c.* 460, 440, 430 and 420 Ma and possibly in the Early Devonian, contemporaneous with metamorphism of the Famatinian orogeny in the Sierras Pampeanas, the southern Puna, and N Chile. Pampean and Famatinian metamorphism and magmatism formed a large mobile belt with more than 1400 km N-S extension of high-T metamorphic rocks and mainly crustal-derived magmatic rocks at the western edge of Gondwana. The observed age patterns of metamorphic rocks imply that the inferred accretion of the old and cold continental crust of the Precordillera had no traceable effect on the thermal regime and the focus of the magmatic arc at the former leading edge. Further, inherited Laurentian 'Grenville' ages are indistinguishable from inherited 'Sunsas' ages of the Brazilian Shield and cannot be used to distinguish between a Laurentia or Gondwana origin of the Precordillera metamorphic rocks. The absence of Neoproterozoic or Cambrian ages in the U-Pb overgrowth pattern (*c.* 460 Ma) of 'Grenvillian' 1.1 Ga zircons from a Precordillera migmatite is considered typical for Laurentian Palaeozoic metamorphic rocks (Casquet et al., 2001). These ages can be also interpreted as autochthonous South American 'Sunsas' which has not recorded any second thermo-tectonic event before 460 Ma (or 430 Ma in the case of sample 00-125). Terrane accretion cannot be proven by the available petrological data and would introduce additional complications to the interpretation of the observed continuity of the thermal regime.

The ages of metamorphism and crustal-derived magmatism indicate high temperature in the crust over a time span of at least 50 Ma in Ordovician and Silurian, possibly 110 Ma from the Cambrian onwards. The best here for the general geotectonic setting is a continental magmatic arc, which provides the heat for metamorphism and crust-derived magmatism along the considerable N-S extent of the early Palaeozoic mobile belt (e.g. Rapela et al., 1998; Lucassen et al., 2000). In the Ordovician – Silurian, the observed age differences between the samples are small but well defined and are interpreted to represent different events of titanite crystallization. Age differences (10 - 20 Myr) occur even at outcrop scale (Sierra Torro Negro; Sierra de Maz) in the same rock unit. Variations in the metamorphic grade are small and mineral compositions represent peak-metamorphic conditions without complex compositional zoning and little or no influence of retrogression. Metamorphic conditions and fabrics show no variation with the different ages. Spatially varying thermal peaks within the magmatic arc could explain the different ages of metamorphism between the distant outcrops. At the outcrop scale, this explanation is less convincing because relict minerals and textures of a previous stage of metamorphism are absent. A commonly observed feature is, however, the gradual transition of migmatite texture into gneiss by deformation without changing the metamorphic mineral paragenesis. A feasible process to create age differences at the outcrop scale would be recrystallization of titanite during repeated local deformation at distinct times but under similar P-T conditions leaving the stable mineral assemblage unchanged. The presence of rigid matrix minerals such as epidote, plagioclase, hornblende and clinopyroxene makes recrystallization of the accessory titanite during deformation possible. Preferred orientation of titanite in the metamorphic fabric is present in many samples. A second important prerequisite for validity of this process of local dynamic recrystallization at similar P-T conditions but at different times is the absence of important volume diffusion in titanite at temperatures of the upper amphibolite to granulite facies and the absence of unconstrained, inherited initial lead. Substantial volume diffusion or significant heterogeneity of the initial Pb can be excluded in most of our titanite samples. Repeated deformation is common in high-grade shear zones in all sample areas and described in detail in the northern Sierras Pampeanas (Büttner et al., in revision) and southeastern Puna. Polyphase deformation is also present in the Neoproterozoic to Cambrian sedimentary rocks and their low to medium grade metamorphic equivalents from Sierras Pampeanas (Willner et al., 1987).

REFERENCES

Aceñolaza F.G. & Toselli, A.J., 1976. Consideraciones estratigráficas y tectónicas sobre el Palozoico inferior del Noroeste Argentino. Mem. II Congreso Latinoamaricano de Geologia 1976, 2, 755-764, Caracas.

Büttner, S., Glodny, J., Lucassen, F., Wemmer, K., Handler, R., Franz, G., (in revision). Ordovician mid-crustal extension in the Northern Sierras Pampeanas (NW Argentina) and its relation to sediment basin formation: Constraints from the P-T-d-t evolution of the Puncoviscana formation. Journal of Petrology.

Casquet, C., Baldo, E., Pankhurst, R.J., Rapela, C.W., Galindo, C., Fanning, C.M., Saavreda, J., 2001. Involvement of the Argentine Precordillera terrane in the Famatinian mobile belt: U-Pb SHRIMP and metamorphic evidence from the Sierra de Pie de Palo. Geology 29, 703-706.

Frost, B.R., Chamberlain, K.R., Schumacher, J.C., 2000. Sphene (titanite): phase relations and role as a geochronometer. Chemical Geology 172, 131-148.

Hoskin, P.W.O. & Black, L.P., 2000. Metamorphic zircon formation by solid-state recrystallization of protolith igneous zircon. Journal of Metamorphic Geology 18, 423-439.

Lucassen F., Becchio, R., Wilke, H.G., Thirlwall, M.F., Viramonte, J., Franz, G., Wemmer, K., 2000. Proterozoic-Paleozoic development of the basement of the Central Andes (18-26°S)- a mobile belt of the South American craton. Journal of South American Earth Sciences 13, 697-715.

Mezger, K. & Krogstad, E.J., 1997. Interpretation of discordant U-Pb zircon ages: an evaluation. . Journal of Metamorphic Geology 15, 127-140.

Pankhurst R.J. & Rapela C.W. (eds) 1998. The Proto-Andean Margin of Gondwana. Geological Society of London Special Publication 142, London.

Pankhurst, R.J., Rapela, C.W.. Fanning, C.M., 2000. Age and origin of coeval TTG, I- and S-type granites in the Famatinian belt of NW Argentina. Trans Royal Soc Edinburgh Earth Sciences 91, 151-168.

Rapela, C. W., Pankhurst, R. J., Casquet, C., Baldo, E., Saavedra, J., Galindo, C., 1998b. Early evolution of the Proto-Andean margin of South America. Geology 26, 707-710.

Willner, A.P., Lottner, U.S., Miller, H., 1987. Early Palaeozoic structural development in the NW Argentine basement of the Andes and its implications for geodynamic reconstructions. In: McKenzie, G.D. (ed.) Gondwana six: Structure, tectonics and geophysics; Geophysical Monograph 40, 229-239; Washington D.C.

Sr-Nd ISOTOPE SIGNATURE AND THE PROVENANCE OF FLUVIAL DEPOSITS OF THE GUARITAS FORMATION (ORDOVICIAN), CAMAQUÃ GROUP, SOUTHERN BRAZIL

Borba, A.W.[1]; Mizusaki, A.M.P.[2]; Koester, E.[2]; Conceição, R.V.[2] and Silva, D.R.A.[2]

1. Universidade Federal do Rio Grande do Sul (UFRGS), Laboratório de Geologia Isotópica. awborba.voy@terra.com.br
2. Universidade Federal do Rio Grande do Sul (UFRGS), Laboratório de Geologia Isotópica

Keywords: Provenance, Sr-Nd isotopes, Guaritas Formation, southern Brazil

INTRODUCTION

The Guaritas Formation (Robertson, 1966) crops out in south-central Rio Grande do Sul State, near the town of Santana da Boa Vista (Fig. 1). This unit comprises red-colored, arkosic, immature conglomerates, sandstones and siltstones deposited under continental semi-arid climate (De Ros et al., 1994) in the latest stages of the Brasiliano/Pan-african Cycle (900-500 Ma). The sedimentation was accompanied by alkaline basaltic magmatism, represented by the Rodeio Velho Member (470 ± 19 Ma, Hartmann et al., 1998).

The Guaritas sedimentary rocks were deposited by fluvial, fan-deltaic, lacustrine and eolian systems in a NE-trending, strike-slip or extensional basin (the Guaritas Hemi-Graben, Paim et al., 2000). Stratigraphically, the Guaritas Formation shows, at the base, alluvial and fluvial deposits interlayered with the Rodeio Velho basalts. Two desertic sequences (corresponding to the Pedra Pintada Alloformation of Paim et al., 2000), with predominant eolian dune and wet interdune deposits, unconformably overlie the basal section. Laterally, the eolian deposits are interfingered with lacustrine, fan-deltaic and fluvial facies associations. At the top of the sedimentary succession, an erosively unconformable fluvial sequence (corresponding to the Varzinha Alloformation) records inversion of paleocurrents and the definitive outfilling of the basin.

Integrated provenance analysis of conglomerates (clast-counting in outcrops), sandstones and siltstones (petrography and isotopic analysis) would make it possible to draw a model concerning the available (and active) sediment source areas during the different stages of deposition of the Guaritas Formation. Preliminary Sr and Nd analyses were performed in 8 (eight) samples corresponding to one interval located near the base of the first desertic sequence, near the present-day eastern limit of outcrop, near Santana da Boa Vista (see Fig. 1). The sampled rock is a 5cm-thick bed of a very indurated, reddish siltstone (with grayish to greenish portions), which caps red-colored sandstones of fluvial origin. The results shown here indicate the appropriateness of applying these isotopic systems to provenance studies in the Early Paleozoic basins of southern Brazil.

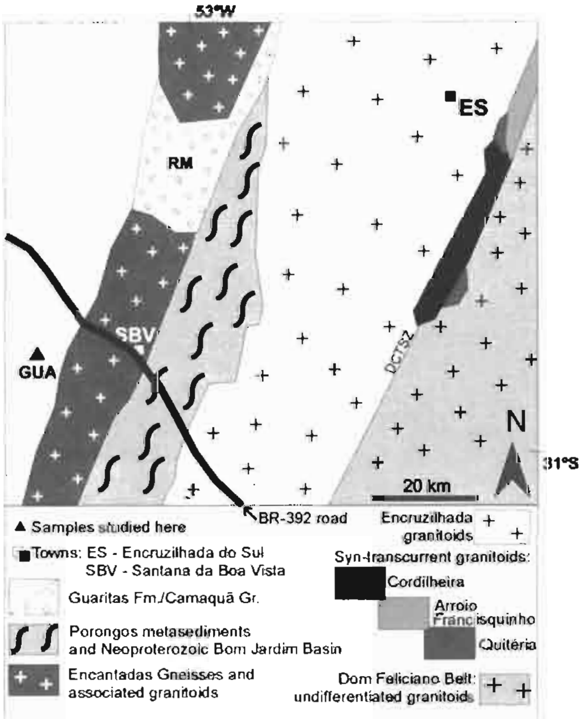

Figure 1. Gelogical map of the Encruzilhada do Sul – Santana da Boa Vista region, showing the basement units, the eastern portion of the Guaritas Formation, and the location of samples (modified after Caravaca, 1998); RM – Rincão dos Mouras region.

METHODS AND PRELIMINARY RESULTS

The Sm-Nd isotopic system has been succesfully applied to provenance studies of sedimentary rocks since the early work of Nelson & DePaolo (1988). Different terranes or crustal blocks show distinct $^{143}Nd/^{144}Nd$ ratios, εNd parameters and T_{DM} model ages. When mechanically disaggregated by weathering processes, the resulting sedimentary load preserves the Nd isotopic signature of the source rocks, allowing the recognition of the provenance of detritus (e.g. McLennan et al., 1990). On the other hand, the behavior of the Rb-Sr system is more complex during surface processes. For sedimentary rocks with low content of clastic detritus, high percentage of newly-formed minerals (humid climate at the source area) and deposited under the influence of halmirolysis and low depositional ratios, the Rb-Sr analysis can provide the depositional age of these rocks (e.g. Thomaz Filho, 1976; Mizusaki, 1992). The prevailing conditions during the deposition of the Guaritas Formation are exactly opposite: semi-arid climate, dominance of physical weathering, absence of vegetation and soil profiles, long-lived dry periods and short-lived rainstorms (flash-flood dominated depositional processes), and high subsidence and burial rates. Associated with that, the fine-grained rocks are, in fact, siltstones and not shales, and their content of newly-formed (authigenic) minerals is very low. These characteristics favor the application of strontium contents and $^{87}Sr/^{86}Sr$ ratios (integrated with petrography and Nd analyses) to the determination of the provenance signal of the sedimentary rocks of the Guaritas Formation.

All the procedures of sample preparation and analysis were carried out at the Laboratório de Geologia Isotópica (LGI) of the Universidade Federal do Rio Grande do Sul (Porto Alegre, RS). The samples show a high Rb content (226 to 245 ppm) if compared to Sr (70 to 83 ppm), with very high $^{87}Sr/^{86}Sr$ measured ratios, which range from 0.777791 to 0.793590. The Sm content ranges from 6 to 14 ppm, and the Nd varies between 39 and 85 ppm. The $^{143}Nd/^{144}Nd$ ratios spread from 0.511936 to 0.512028, the εNd(0) is about –13 and the εNd(t=480Ma) concentrates around –7, with T_{DM} ages of 1.4 to 1.5 Ga.

DISCUSSION AND CONCLUSIONS

The obtained results for the Guaritas samples (plotted in Figs. 2, 3) suggest a potassic source for these sediments (high Rb/Sr ratios). This is coherent with the dominance of K-feldspar (original average 13%) over plagioclase (5%) in Guaritas sandstones pointed out by De Ros et al. (1994). The very high $^{87}Sr/^{86}Sr$ ratios and the absolute Rb and Sr contents (in ppm) find correspondence mainly in the easternmost segment of the Sul-rio-grandense Shield, the Dom Feliciano Belt (Chemale Jr., 2000).

The syn-transcurrent (meta-)granitoids of the Dorsal de Canguçu Transcurrent Shear Zone (DCTSZ in Fig. 1) (Quitéria, Arroio Francisquinho and Cordilheira), studied by Koester et al. (1997), display similar Rb-Sr data (Fig. 2). The same rocks have Nd parameters ($^{143}Nd/^{144}Nd$ and εNd values, Frantz et al., 1999) compatible with the data obtained here (Fig. 3), despite the older T_{DM} ages of the Quitéria granitoids (around 2.0 Ga). The contribution of these syn-transcurrent granitoids to the framework of the Camaquã Group conglomerates (in the Rincão dos Mouras region, Fig. 1) was suggested by Caravaca (1998), who stated that these rocks comprise 51% (34% turmaline-granitoids and 17% muscovite-granitoids) of the counted clasts.

The volcanic samples of the Acampamento Velho Formation upper felsic association (see Almeida et al., 2002 and this symposium), which are presently poorly exposed in the focused region, also have Sr and Nd data that fit very well with the Guaritas samples (Figs. 2 and 3). This includes T_{DM} ages of 1.3 to 1.6 Ga. In fact, the presence of rhyolitic fragments in the sandstone framework of the Guaritas Formation (maximum 11.8%) was cited by De Ros et al. (1994).

Some samples of the Encruzilhada do Sul granitoids, the results of which were presented by Cordani et al. (1974) and Teixeira (1982), show similar Sr values and are plotted in Fig. 2. One sample of the Encruzilhada do Sul granitoids (a syenogranite) was analyzed for Sm and Nd and yielded a lower $^{143}Nd/^{144}Nd$ ratio (0.511449) and an older T_{DM} age of 2.08 Ga (Babinski et al., 1997). The contribution of some granitic facies of the Encruzilhada do Sul granitoids, however, is not discarded, since this unit shows a very wide compositional and textural variation (Vasquez, 1997), which could be reflected in isotopic diversity (?). In terms of Nd parameters, samples from the Pinheiro Machado Intrusive Suite, also studied by Babinski et al. (1997), have values that fit with the Guaritas samples (including T_{DM} ages of 1.37, 1.41 and 1.69 Ga).

By considering the obtained isotopic Sr and Nd preliminary results for the Guaritas Formation, a sedimentary influx provenant from an eastern outcrop belt located near the Dorsal de Canguçu Transcurrent Shear Zone is suggested. This sediment catchment area would certainly not be composed by a single source rock, but by variable lithologies and units. The predominant sources would be the syn-transcurrent granitoids (Quitéria, Arroio Francisquinho and Cordilheira), volcanic felsic rocks (Acampamento Velho Fm.), and subordinated collisional (Pinheiro Machado) and post-collisional (Encruzilhada do Sul) granitoids (Fig. 4). Other presently exposed units in the focused region, such as the Encantadas Gneisses (more mafic and older) and the Porongos Group (few data), should have been buried or not available to be eroded during the deposition of the studied interval of the Guaritas Formation.

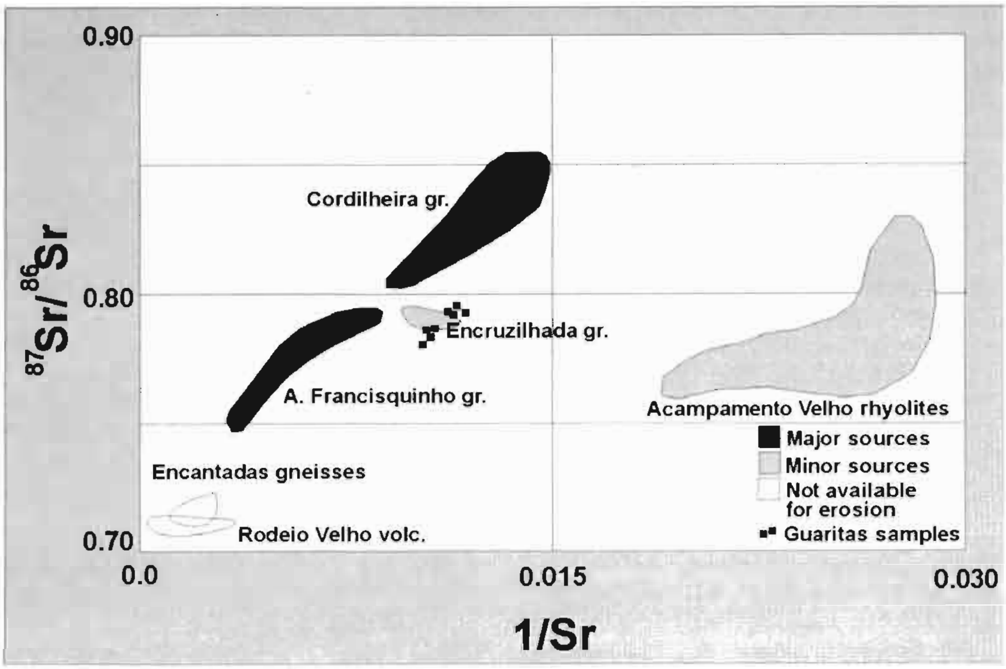

Figure 2. $^{87}Sr/^{86}Sr$ vs. 1/Sr plot showing the major and minor sources for the Guaritas sedimentary rocks, and the units which were not available for erosion at the time of deposition.

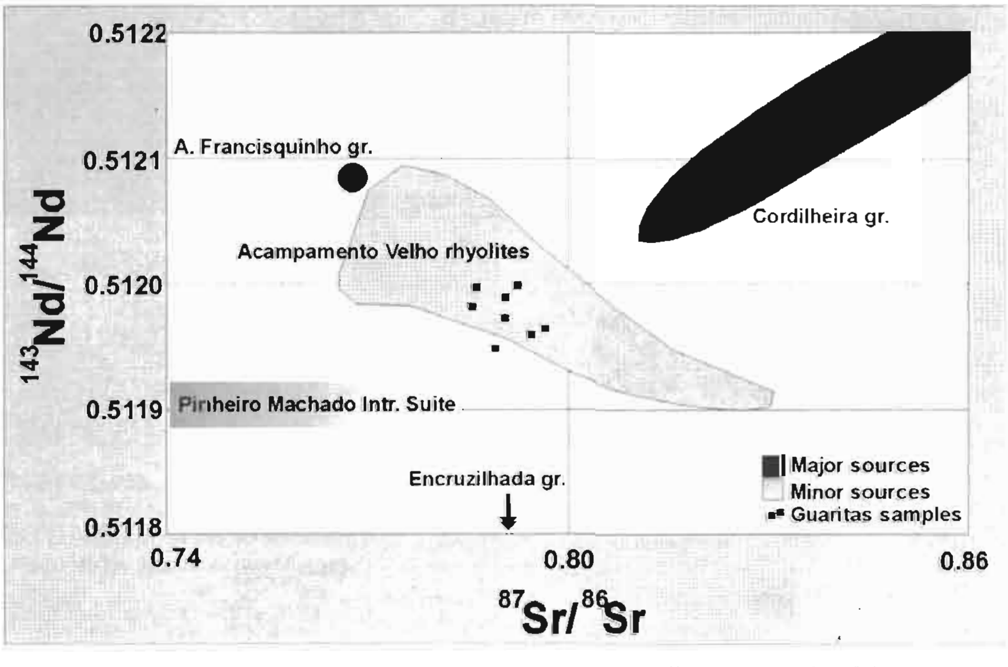

Figure 3. Plot of Nd vs. Sr measured ratios for the Guaritas Samples and the possible source rocks of the eastern region of Sul-rio-grandense Shield; Encantadas gneisses and Rodeio Velho volcanics have too low Sr ratios and are not shown in plot.

REFERENCES

Almeida, D.P.M.; Zerfass, H.; Basei, M.A.S.; Petry, K.; Gomes, C.H. 2002. The Acampamento Velho Formation, a Lower Cambrian bimodal volcanic package: geochemical and stratigraphic studies from the Cerro do Bugio, Perau and Serra de Santa Bárbara (Caçapava do Sul, Rio Grande do Sul – RS, Brazil). Gondwana Research, vol. 5 (3): 721-733.

Babinski, M.; Chemale Jr, F.; Van Schmus, W.R.; Hartmann, L.A.; Silva, L.C. 1997. U-Pb and Sm-Nd Geochronology of the Neoproterozoic Granitic-Gneissic Dom Feliciano Belt, southern Brazil. Journal of South American Earth Sciences, vol. 10 (3-4): 263-274.

Caravaca, G. 1998. Estratigrafia, faciologia e proveniência dos Alogrupos Bom Jardim e Santa Bárbara na região de Encruzilhada do Sul, RS: uma contribuição à análise da Bacia do Camaquã. M.Sc. Dissertation, PPGGeo/UFRGS, 139p.

Chemale Jr., F. 2000. Evolução Geológica do Escudo Sul-rio-grandense. In: Holz, M. & De Ros, L.F. (eds.) 2000. Geologia do Rio Grande do Sul, CIGO/UFRGS, pp. 13-52.

Cordani, U.G.; Halpern, M.; Berenholc, M. 1974. Comentários sobre as determinações da Folha de Porto Alegre. In: DNPM, Carta Geológica do Brasil ao Milionésimo, texto explicativo da Folha de Porto Alegre e Lagoa Mirim, pp. 70-84.

De Ros, L.F.; Morad, S.; Paim, P.S.G. 1994. The role of detrital composition and climate on the diagenetic evolution of continental molasses: evidence from the Cambro-Ordovician Guaritas Sequence, southern Brazil. Sedimentary Geology, vol. 92: 197-228.

Frantz, J.C.; Botelho, N.F.; Pimentel, M.M.; Potrel, A., Koester, E.; Teixeira, R.S. 1999. Relações isotópicas Rb-Sr e Sm-Nd e idades do magmatismo granítico Brasiliano da região leste do Cinturão Dom Feliciano no Rio Grande do Sul: evidências de retrabalhamento de crosta continental Paleoproterozóica. Revista Brasileira de Geociências, vol. 29(2): 227-232.

Hartmann, L.A.; Silva, L.C.; Remus, M.V.D.; Leite, J.A.D.; Philipp, R.P. 1998. Evolução geotectônica do Sul do Brasil e Uruguai entre 3,3 Ga e 470 Ma. In: Congreso Uruguayo de Geología, 2, Punta del Este, pp.277-284.

Koester, E.; Soliani Jr.; E., Fernandes, L.A.D.; Kraemer, G.; Tommasi, A. 1997. Geocronologia Rb/Sr e K/Ar dos granitóides sintectônicos à Zona de Cisalhamento Transcorrente Dorsal de Canguçu na região de Encruzilhada do Sul (RS). Pesquisas, vol. 24 (1/2): 67-77.

McLennan, S.M.; Taylor, S.R.; McCulloch, M.T.; Maynard, J.B. 1990. Geochemical and Nd-Sr isotopic composition of deep-sea turbidites: crustal evolution and plate tectonic associations. Geochimica et Cosmochimica Acta, vol. 54: 2015-2050.

Mizusaki, A.M.P. 1992. Comportamento do Rb e do Sr em sedimentos recentes – implicação na datação radiométrica de rochas sedimentares. Ph.D. Thesis, IG/USP, 140p.

Nelson, B.K. & DePaolo, D.J. 1988. Application of Sm-Nd and Rb-Sr isotope systematics to studies of provenance and basin analysis. Journal of Sedimentary Petrology, vol. 58: 348-357.

Paim, P.S.G.; Chemale Jr., F.; Lopes, R.C. 2000. A Bacia do Camaquã. In: Holz, M., De Ros, L.F. (eds.) 2000. Geologia do Rio Grande do Sul, CIGO/UFRGS, pp. 231-274.

Robertson, J.F. 1966. Revision of the stratigraphy and nomenclature of rock units in Caçapava – Lavras region, State of Rio Grande do Sul, Brazil. Notas e Estudos, IG/UFRGS, vol 1(2): 41-54.

Teixeira, W. 1982. Folhas SH.22 – Porto Alegre, SI.22 – Lagoa Mirim e SH.21 – Uruguaiana. Interpretação dos dados radiométricos e evolução geocronológica. Projeto RADAMBRASIL.

Thomaz-Filho, A. 1976. Potencialidades do método Rb/Sr para datação de rochas sedimentares. Ph.D. Thesis, IG/USP, 124p.

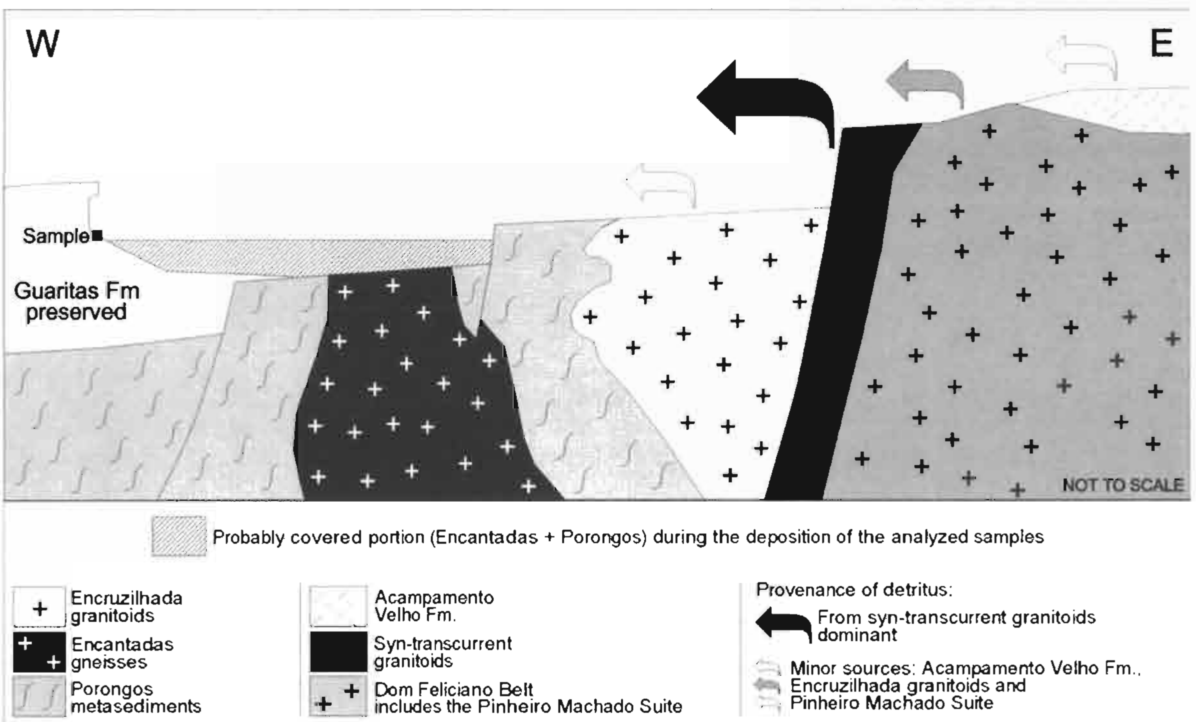

Figure 4. Sketch showing the suggested provenance of the east-derived fluvial siltstones of the Guaritas Formation by integrating petrography, conglomerate clast data and Sr – Nd isotopic analyses.

$^{40}Ar/^{39}Ar$ GEOCHRONOLOGY OF WEATHERING PROFILES IN SOUTHEASTERN BRAZIL

Carmo, I.O.[1] and Vasconcelos. P.M.[2]

1. CNPq Felowship (CNPq 141169/00-1 and CNPq 200642/01-4); Depto. Geologia/Universidade Federal do Rio de Janeiro, Av. Brigadeiro Trompowski, Prédio CCMN, Ilha do Fundão, 21949-900 Rio de Janeiro, RJ, Brazil. icarmo@connection.com.br
2. Dept. Earth Sciences/University of Queensland, Steele Building, 4072 Brisbane, QLD, Australia. paulo@sol.earth.uq.edu.au

Keywords: $^{40}Ar/^{39}Ar$ geochronology, weathering, Cenozoic, SE Brazil

INTRODUCTION

The depth and stratigraphy of weathering profiles in SE Brazil vary systematically from the interior towards the coast. Along a 400 Km traverse, from Belo Horizonte (Quadrilátero Ferrífero region) to Rio de Janeiro (Fig. 1), weathering profiles vary from deep (200 m on average, and up to 400 m) and complete lateritic profiles in the interior to shallow and incipient profiles at the coast. The transition zone (Brazilian Atlantic Plateau) between those two extreme profile types hosts truncated weathering profiles with 40-80 m average depths, characterized by deep saprolites capped or not by detrital cover, usually composed of transported fragments of duricrust and other weathered and unconsolidated materials.

Since time is one of the factors controlling the formation of weathering profiles, we raise the hypothesis that the variation in weathering profile depth may be related to their ages. If this hypothesis is correct, older weathering profiles should be preserved in the Quadrilátero Ferrífero (QF) region, intermediate age profiles should occur along the Brazilian Atlantic Plateau, and weathering profiles along the coast should be the youngest. To test this hypothesis, we dated, by $^{40}Ar/^{39}Ar$ method, 146 grains of K-bearing manganese oxides from 9 different weathering profiles from three distinct geomorphological zones.

SAMPLING AND ANALYTICAL PROCEDURES

We selected 40 hand specimens from 9 weathering profiles from 3 distinct weathering zones: (i) 4 lateritic profiles in the QF region, (ii) 3 deep saprolites devoid of hardcaps or sedimentary cover in the Brazilian Atlantic Plateau, and (iii) 2 saprolites in the Paraíba do Sul Valley (Fig. 1).

Some samples were divided into 2 or more sub-samples, according to the presence of distinct generations or growth bands of Mn-oxides in the same hand specimen. A total of 54 samples (samples or sub-samples) were analyzed. All the samples were crushed, and washed in ultrasonic bath (ca. 1 hour) with absolute ethanol. For each sample, approximately 20-30 grains (0.5-3 mm) of suitable Mn-oxides were hand-picked under a binocular microscope. Optical and electron microscopy on polished thin sections provided information on the mineralogy and paragenesis of Mn-oxides, and the possible presence of contaminants mixed with the datable phases. After the scanning electron microscope (SEM/EDS) analysis, representative grains underwent spot electron microprobe analysis to quantify the potassium content of the grain population selected for argon geochronology. We used the facilities of the Centre for Microscopy and Microanalysis at the University of Queensland (CMM-UQ) for the mineralogical studies (Scanning Electron Microscope Phillips XL30 and Electron microprobe JEOL 8800L).

After petrographic and mineralogical analyses, 0.5-2 mm grains from the samples determined to be K-rich and devoid of primary contaminants were picked for $^{40}Ar/^{39}Ar$ laser heating geochronology. These grains were mounted in a 21-pit aluminum disk together with Fish Canyon sanidine neutron fluency monitors, as shown in Vasconcelos et al. (2002). Some of the disks (containing 38 samples/sub-samples) were irradiated for 30 hours at the IPEN/CNEN IEA-R1 nuclear reactor (at The University of São Paulo – USP) and analyzed at the CPGeo-USP Argon Laboratory. A second set of disks (containing 16 samples/sub-samples) were irradiated for 14 hours at the Oregon State University Triga Reactor (OSU – CLICIT Facility) and analyzed by the laser incremental heating $^{40}Ar/^{39}Ar$ method at The University of Queensland Argon Geochronology in Earth Sciences (UQ-AGES) Laboratory. A total of 146 grains were analyzed with 2-3 grains from each sample or sub-sample. The analytical procedures followed those given by Vasconcelos (1999) and Vasconcelos et al. (2002). Correction factors for samples irradiated at the IPEN reactor are provided by Vasconcelos et al. (2002). We also analyzed a series of international K-Ar and $^{40}Ar/^{39}Ar$ standards: Alder Creek sanidine – 1.194 ± 0.007 Ma, GA-1550 biotite – 98.79 ± 0.54 Ma (Renne et al., 1998), and HB3gr hornblende – 1072 ± 11 Ma or 1079 ± 1 Ma (McDougall & Harrison, 1999). All standards analyzed as unknowns yield results within error from the internationally accepted values.

RESULTS

Most of the grains analyzed are cryptomelane or hollandite, yielding reliable geochronological results. Space constraints do not permit showing results for all grains analyzed. Representative data from each site are illustrated in Fig. 2. The results we obtained from the three distinct weathering zones (Quadrilátero Ferrífero, Brazilian Atlantic Plateau, and Paraíba do Sul Valley) support the proposed hypothesis that older weathering profiles are found inland, whereas weathering profile ages decrease towards the coast.

In the QF region (Fig. 1), we sampled three different sites along Serra da Moeda and one site at Sapecado Mine (MBR Co.), located at the western and eastern flanks of the Moeda Syncline, respectively. Surface samples 40-60 m below the top of the Serra da Moeda (Varanda de Pilatos and Moeda Road sites, 1440 m and 1480 m elevation, respectively) yield plateau ages ranging from 55.1 ± 0.7 Ma to 34.3 ± 1.3 Ma (Fig. 2.1a). Samples from 100 m below the top of the plateau (Serra da Moeda Mine, southern part of Serra da Moeda) yield results ranging from 24.5 ± 1.1 to 13 ± 4 Ma (Fig. 2.1b). Surface samples from the Sapecado Mine (1400 m elevation) yield plateau or forced plateau ages between 67 ± 3 and 59.1 ± 0.5 Ma (Fig. 2.1c). These results range from terminal Cretaceous to Miocene, suggesting a protracted history of weathering for the Quadrilátero Ferrífero profiles.

Three distinct sites (Barbacena, São João del Rei, and Dom Silvério; Fig. 1), in the Brazilian Atlantic Plateau, distant up to 200 Km from each other, yield younger results than those obtained for the Quadrilátero Ferrífero region. Incremental-heating ^{40}Ar/^{39}Ar analyses for grains of Mn-oxides yield dates ranging from 9.97 ± 0.16 to 8.28 ± 0.05 Ma for the Barbacena profile (Fig. 2.2a), 12.74 ± 0.05 to 5.18 ± 0.08 Ma for the São João del Rei profile (Fig. 2.2b), and 10.31 ± 0.04 to 9.8 ± 0.3 Ma for the Dom Silvério profile (Fig. 2.2c). All three profiles studied in this region yield compatible results, indicating that the profiles preserved in the region contain supergene minerals precipitated from the Miocene to Pliocene.

Two different sites, also approximately 200 Km apart, were sampled at the Paraíba do Sul Valley - Volta Grande region and Resende Basin (Fig. 1). Manganese oxide plateau ages from Volta Grande range from 4.2 ± 0.2 to 1.5 ± 0.7 Ma (Fig. 2.3a). One sample from the Resende Basin yields a plateau age of 1.45 ± 0.04 Ma (Fig. 2.3b). Despite the smaller number of samples analyzed for this region, the results obtained are consistently younger than the results obtained for the Quadrilátero Ferrífero and the Brazilian Atlantic Plateau.

CONCLUSION

The ages obtained for all 146 grains so far analyzed confirm the proposed hypothesis that weathering profiles in southeastern Brazil increase in age from the coast towards the interior. The results also indicate that the depth and complexity of weathering profiles reflect the longevity of their exposure to weathering conditions. Stratified lateritic weathering profiles composed of indurated hardcap, a mottle zone, and deep saprolites are older than 40 Ma. Deep saprolites (40-80 m), devoid of major hardcap horizons have formed in the past 13 Ma, and shallow weathering profiles, exposed at the saprolite stage, are younger than 5 Ma.

The underlying mechanisms controlling the variation in weathering profile ages are not yet determined. A possible explanation for the trends observed is that erosion rates are lower in the Quadrilátero Ferrífero, intermediate at the Brazilian Atlantic Plateau, and higher at the Paraíba do Sul valley. Further studies, using techniques suitable to the measurement of erosion rates (apatite fission track thermochronology, cosmogenic isotopes, etc.), are necessary to test this hypothesis.

REFERENCES

McDougall, I. & Harrison, T. M. 1999. Geochronology and thermochronology by the ^{40}Ar/^{39}Ar method. Oxford Univ. Press. 269 p.

Vasconcelos, P. M., 1999. ^{40}Ar/^{39}Ar geochronology of supergene processes in ore deposits. Economic Geology 12, 73-113.

Vasconcelos, P. M.; Onoe, A. T.; Kawashita, K.; Soares, A. J.; Teixeira, W. 2002. ^{40}Ar/^{39}Ar Geochronology at the Instituto de Geociências, USP: Instrumentation, Analytical Procedures, and Calibration. Anais da Academia Brasileira de Ciências, 74(2), 297-342.

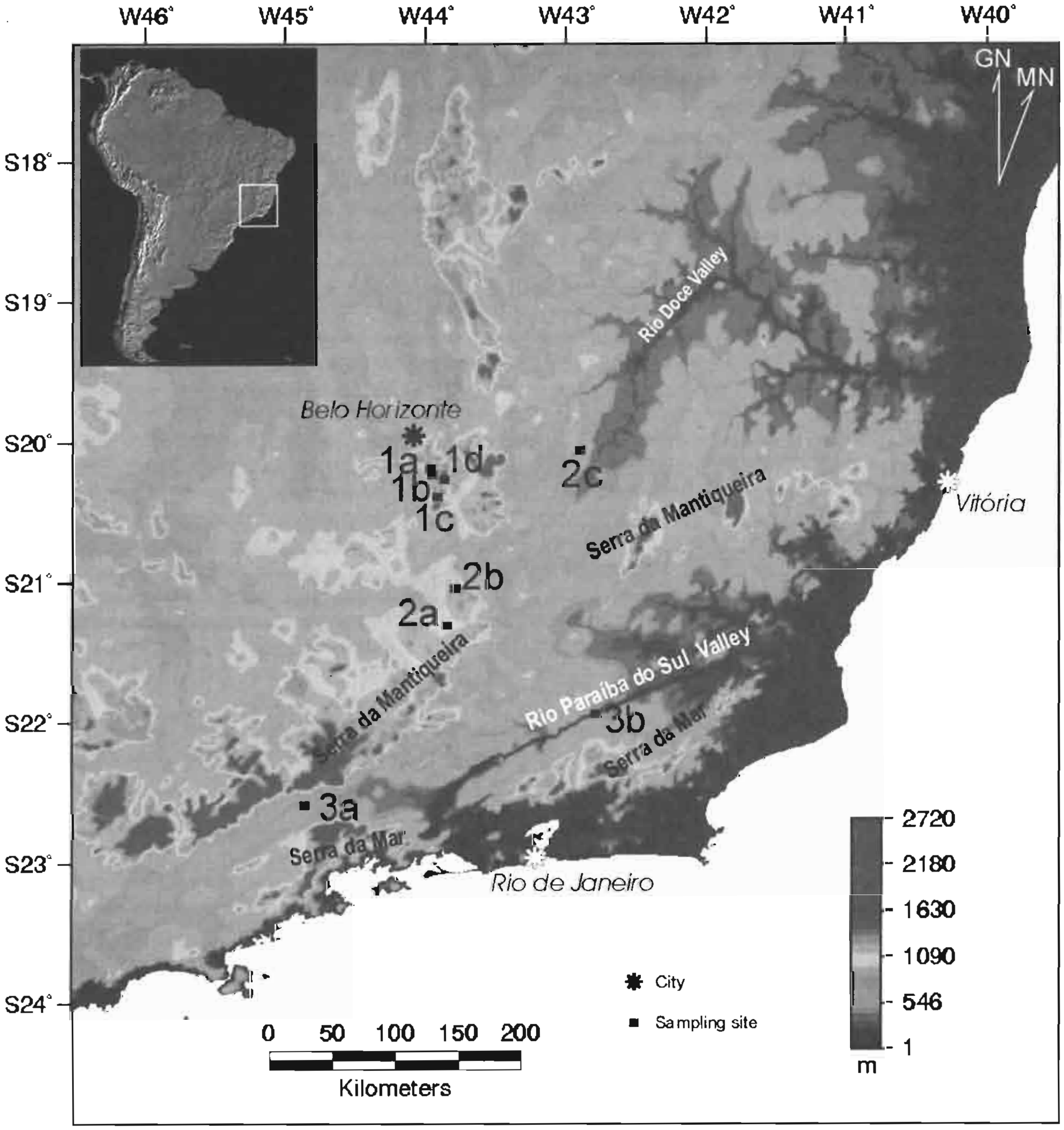

Figure 1. A regional digital elevation model for southeastern Brazil (source: TOPO30, USGS/EROS Data Center) provides an overview of the three weathering zones sampled in this study (black squares): Quadrilátero Ferrífero region – 1a- Varanda de Pilatos, 1b- Moeda Road, 1c- Serra da Moeda Mine, 1d- Sapecado Mine; Brazilian Atlantic Plateau – 2a- Barbacena, 2b- São João del Rei, 2c- Dom Silvério; Paraíba do Sul Valley – 3a- Volta Grande, 3b- Resende Basin.

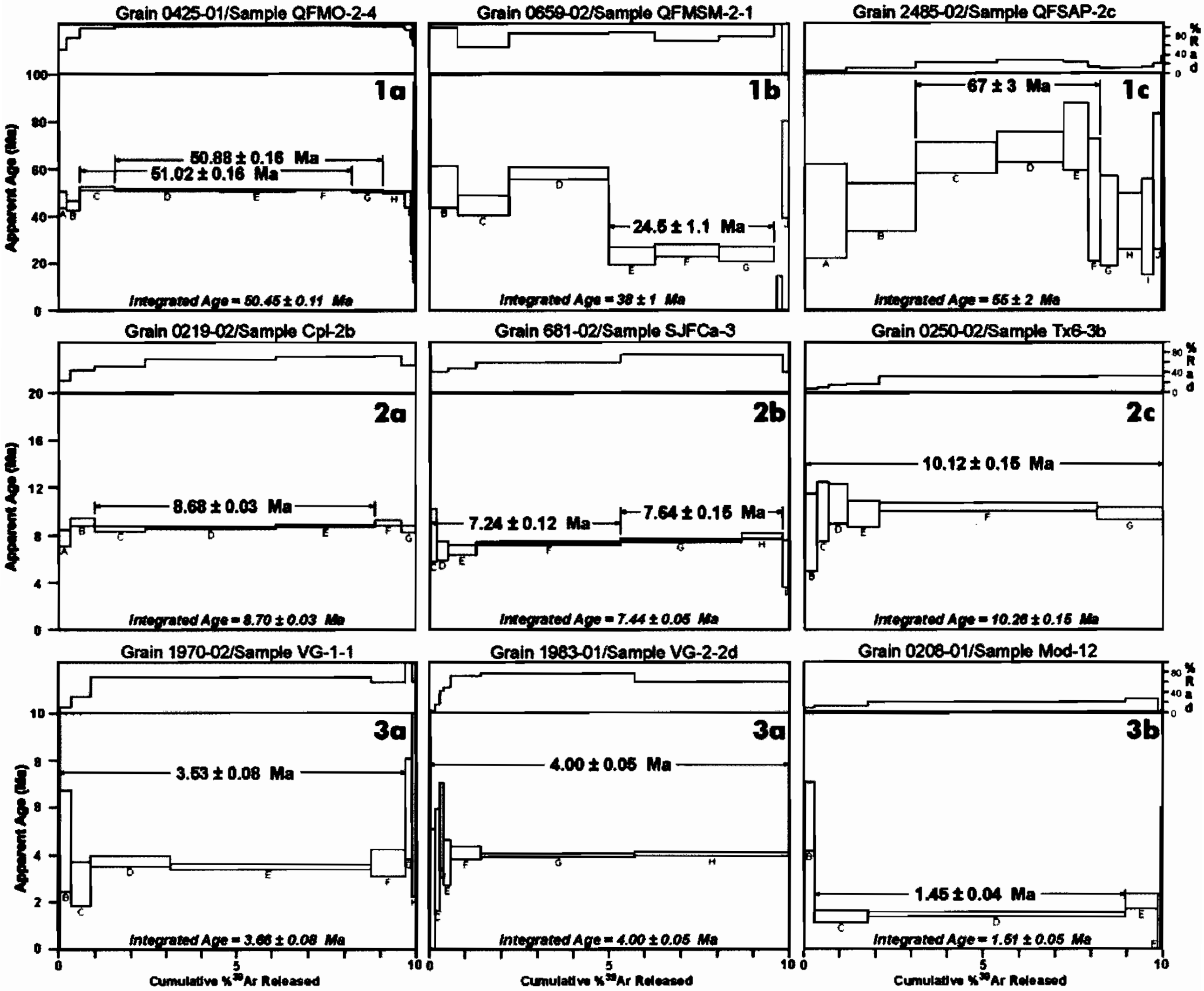

Figure 2. Incremental-heating spectra for representative samples from the nine weathering profiles selected for this study: 1a- Moeda Road, 1b- Serra da Moeda Mine, 1c- Sapecado Mine; 2a- Barbacena, 2b- São João del Rei, 2c- Dom Silvério; 3a- Volta Grande, 3b- Resende Basin.

ISOTOPIC CONSTRAINTS ON EARLY EVOLUTION OF THE EARTH: EVIDENCE FOR PRISCOAN CRUST AND THE EMERGENCE OF THE BIOSPHERE IN THE NORTH ATLANTIC CRATON

Collerson, K.D. and Kamber, B.S.

Advanced Centre for Queensland University Isotope Research Excellence (ACQUIRE), University of Queensland, Brisbane, Q, 4072 Australia. k.collerson@acquirelab.uq.edu.au

Keywords: Priscoan crust, core formation, biosphere, tungsten isotopes, lead isotopes

INTRODUCTION

Time between accretion of the Earth (4.56 Ga) and the first extensive rock record (~3.8 to 4.0 Ga) is known as the Priscoan. This >600 Ma period witnessed some of the most important events in the planet's evolution, including accretion and formation of the core, initiation of the magnetic field, the mega-impact that formed the moon, the loss of the proto-atmosphere and stabilization of the hydrosphere. These events had a major influence on the subsequent geological evolution of the planet and on development of the biosphere.

Unfortunately, the record of Earth's early Archaean crustal growth is cryptic and incomplete. Evidence from achondritic meteorites indicates that growth of protocrust and core formation on planetesimals occurred essentially contemporaneously, within <35 Ma of the formation of the solar system (Schoenberg et al., 2002a). Although detrital zircons of up to 4.4 Ga occur in much younger Archean sedimentary rocks in the Jack Hills of the Yilgarn craton (Nelson et al., 2000; Wilde et al., 2001), the only direct record of existence of rocks older than 4 Ga are granodioritic Acasta gneisses from the Slave craton, Canada (Stern & Bleeker, 1998; Bowring & Williams, 1999).

The age of the oldest terrestrial rocks is not an issue of rock formation, but one of preservation given that Earth's Priscoan surface environment would have been extremely dynamic due to meteorite impacts (Greive, 1980; Abe, 1993). As a result, it is likely that (basaltic?) protocrust would have been efficiently recycled into the mantle with the onset of subduction. Thus the oldest crustal rocks must have formed in an environment that promoted preservation. This most likely relates to the formation and stabilizing effect of sub-continental lithospheric mantle that acts a mechanical and thermal boundary layer, preserving crust from recycling into the mantle. As a result, preservation of the oldest terrestrial rocks must be related to the dynamics of Priscoan and post-Priscoan magmatic and tectonic processes.

Discoveries that have provided information regarding the character of Priscoan crust include:

- ~ 4.0 Ga zircons in granodioritic gneisses in the Acasta Gneiss Complex in the Slave craton, Canada (Stern & Bleeker, 1998; Bowring & Williams, 1999);
- Extremely ancient zircon grains (up to 4.4 Ga) in quartzites and conglomerates from Western Australia (Wilde et al., 2001). In addition to preserving a Pb-isotope record of periodic thermal reworking (Nelson et al., 2000) these ancient zircons also show O-isotope compositions interpreted to indicate involvement of low-T fluids in melt generation (Peck et al., 2001). Importantly, many of these >4 Ga zircons contain inclusions of quartz and monazite (Maas et al., 1992) which indicates presence of silicic lithologies on the Priscoan Earth;
- The recent revised ^{176}Lu decay constant (Scherer et al., 2001) requires reinterpretation of Hf-isotope data for terrestrial crust via remelting of Priscoan crust with relatively low Lu/Hf (Kramers, 2001);
- ^{142}Nd isotope anomalies in clastic metasediments from the Isua Greenstone Belt (Harper & Jacobsen, 1992) require the Priscoan mantle reservoir to have had an elevated Sm/Nd ratio. This ultra-depleted reservoir had been identified previously with Nd isotopic data for early Archaean ultramafic rocks from the North Atlantic Craton (Collerson et al., 1991; McCulloch & Bennett, 1994);
- Pb-isotope composition of galena (Frei & Rosing, 2001), metasediments and > 3.8 Ga tonalite gneisses (Kamber et al., 2003) from SW Greenland and Northern Labrador requires coexistence of melt sources with U/Pb different to the contemporary mantle. These Pb isotopic compositions are interpreted to reflect existence of a moderately high □ mantle source as well as remelting of high U/Pb Priscoan crust, possibly older than 4.3 Ga;
- Existence of negative ^{182}W isotope anomalies in metasediments from the North Atlantic Craton (Schoenberg et al., 2002b) are the only direct evidence of the lunar late heavy meteorite bombardment on Earth (cf., Tera et al., 1974). This discovery requires weathering of Priscoan crust and supports the evidence provided by anomalous ^{142}Nd-isotope ratios in Isua sediments;
- Nb/Th and Nb/U ratios clearly indicate fluid-enhanced element transport into the supra-subduction zone source of the oldest TTG gneisses by ~3.75 to 3.8 Ga (Collerson & Kamber, 1999, Kamber et al., 2002). They contrast with the plume-like geochemistry of ~3.9 Ga Fe-rich Nanok orthogneisses from Northern Labrador.

The cryptic record of the oldest rock suggests that during initiation of subduction, terrestrial protocrust was largely recycled into the mantle, because of the lack of a stabilising mantle lithosphere. Prior to subduction, the rigid protocrust formed a single plate without a deep lithospheric mantle root (Collerson & Kamber, 1999). The essential requirement for preservation of all ≥3.8 Ga terrestrial crustal material was the intrusion of voluminous TTG granitoids. These arc generated magmas formed via subduction of hydrated oceanic lithosphere and in the process induced creation of a lithospheric keel from the buoyant depleted mantle wedge that represents the residue of melt extraction (Frankland et al., 1998).

THE NORTH ATLANTIC CRATON

Although gneisses in the North Atlantic Craton (Fig. 1) experienced a complex igneous and tectonothermal history between ~4. and ~ 1.8 Ga, regional mapping has shown existence of low strain domains where protolith relationships and relative stratigraphies can be inferred (e.g., Collerson et al., 1976; Myers, 2001). These domains preserve some of the most important sequences for establishing processes of early Earth evolution (e.g. Nutman & Collerson, 1991; Collerson et al., 1991; McCulloch & Bennett, 1994; Frei & Rosing, 2001; Kamber et al., 2003; Schoenberg et al., 2002b; Nutman et al., 1999; Rosing 1999). Although > 3.8 Ga gneisses in West Greenland have yielded important information about the early Earth the potential of similar age sequences in Northern Labrador has largely been ignored, due mainly to logistics of field work in the area.

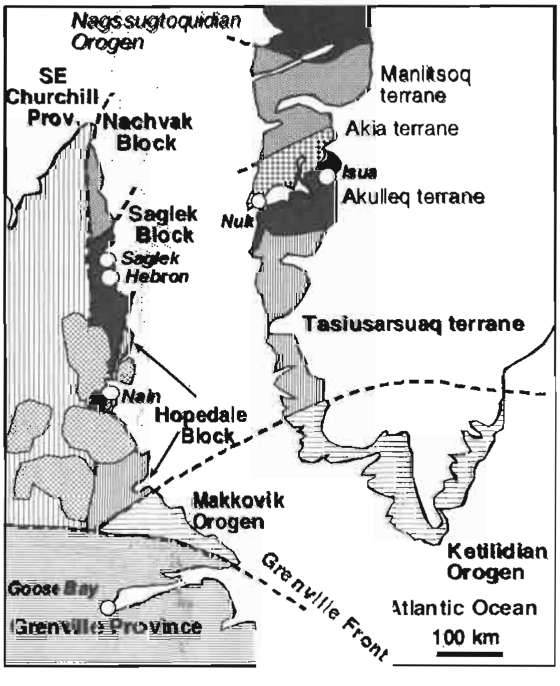

Figure 1. Pre-drift reconstruction of the North Atlantic Craton. Early Archean crust occurs in the Saglek Block in Labrador, and in the Akulleq and Maniitsoq terranes in West Greenland The craton is surrounded by Paleoproterozoic and Mesoproterozoic orogens. (After James et al., 2002).

LABRADOR RELATIVE CHRONOLOGY

Deciphering the crustal history of the gneiss complex has been based on a relative chronology, established using intrusive relationships between protoliths and on the occurrence of a distinctive suite of feldspar-phyric mafic dykes which were emplaced at ~ 3.2 Ga (Collerson et al., 1984). These Saglek and Amerilik dykes are ubiquitous in crust dominated by early Archean gneisses in the Saglek Block and the Akelluq terrane in Labrador and Greenland respectively (Fig. 1). The relative chronology of events in the evolution of early Archean crust established in coastal exposures of the Saglek Block between Saglek and Hebron is given in Table 1.

Table 1. Relative Pre-Saglek Chronology in Northern Labrador

(8) Emplacement of protoliths of Uivak 11 gneiss (~3.4 Ga).
(7) Thermotectonism and intercalation of supracrustals and orthogneisses (3.5 - 3.6 Ga).
(6) TTG protoliths of Uivak 1 gneiss (~3.7 Ga).
(5) Emplacement of mafic dykes.
(4) Thermotectonism and intercalation of supracrustals and orthogneisses (3.8 Ga).
(3) Intrusion of Mentzel igneous suite - *gabbro & anorthosite.*
(2) Erosion of Priscoan crust and deposition of protoliths of supracrustals (pre-3.80 Ga) *clastic, BIF, chemical, biogenic sediments & eruption of komatiite and basalt.*
(1) Emplacement of Fe-rich *monzo-dioritic protoliths* of pre-3.95 Ga Nanok gneisses (Collerson, 1983) into pre-existing Priscoan crust.

This chronology forms the basis for continuing research on aspects of Earth's early evolution in the gneiss complex of Saglek-Hebron of the North Atlantic Craton. Several highlights of this research are summarized below.

W ISOTOPIC EVIDENCE OF DEBRIS FROM THE LATE HEAVY METEORITE BOMBARDMENT

Extensive early Archean TTG gneisses in SW Greenland and Northern Labrador potentially preserve enclaves of Priscoan crust, or its erosion products. This possibility was suggested by Harper & Jacobsen (1992) and Caro et al., (2002) using existence of anomalous $^{142}Nd/^{144}Nd$ [caused by the decay of short-lived ^{146}Sm ($T_{1/2}$=103 Ma)] in sediments from Isua. It was recently confirmed by Schoenberg et al., (2002b) who reported anomalous ^{182}W isotopic compositions [reflecting decay of ^{182}Hf ($T_{1/2}$=9 Ma)] in pre 3.75 Ga clastic and chemical metasediments from Northern Labrador and Greenland. Sediments containing these isotopic anomalies were not derived from the supracrustal units, but have a source component derived from Priscoan protocrust that contained meteorite-derived debris (Fig. 2).

Basins in which these sediments were deposited contained Priscoan zircons in reworked quartzites (Nutman and Collerson 1991). These metasediments thus hold clues to the nature of the weathered and eroded pre-3.8-4.0 Ga crust.

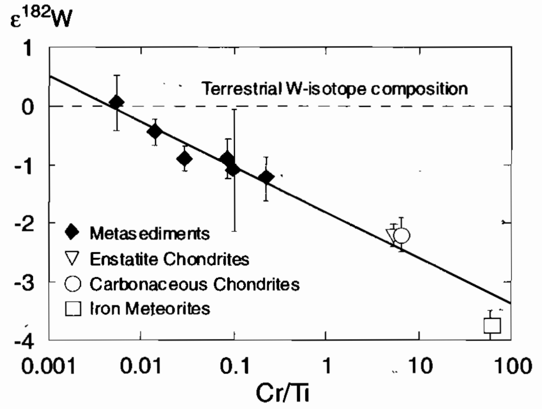

Figure 2. Covariation between □W and Cr/Ti. Sediments define a log fit (r2=0.92) passing through the compositions of carbonaceous and enstatite chondrites.

Pb ISOTOPIC EVIDENCE FOR PRISCOAN CRUST

Comparison of initial Pb-isotope signatures of several early Archaean (3.65-3.82 Ga) lithologies (orthogneisses and metasediments) and minerals (feldspar: Kamber et al., 2003; and galena: Frei and Rosing, 2001) implies the existence of substantial isotopic heterogeneity in the early Archean, particularly in the $^{207}Pb/^{204}Pb$ ratio. A high μ_1 source is evident from the secondary feldspar isochrons obtained for >3.8 Ga Nanok and Itsaq gneisses (Fig. 3).

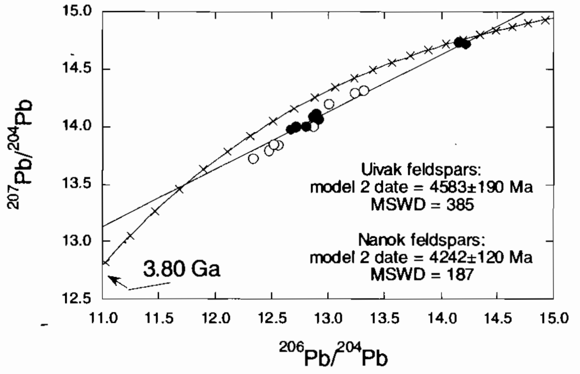

Figure 3. Secondary Pb-isotope regression lines for Nanok (grey solid circles) and Uivak gneiss (open circles) feldspars. Regression line shown is for Nanok feldspars.

Although the slope of such 'isochrons' has no direct age significance (being the result of Pb-isotope rehomogenisation at ca. 1.85 Ga), the important observation is that the Nanok regression line does not intersect the mantle evolution curve near the protolith age, but at a much younger mantle model age. This indicates derivation from a high μ source, as discussed by Kamber et al. (2003). The magnitude of isotopic variability at 3.82-3.65 Ga requires source separation between 4.3 and 4.1 Ga, depending on the extent of U/Pb fractionation possible in the early Earth. If U/Pb fractionation was similar to that experienced by lunar rocks, the minimum age of Priscoan crust is ca. 4.1 Ga, if it was less severe, crust-mantle separation must have occurred between 4.3 and 4.4 Ga. The isotopic heterogeneity probably reflects separation of a terrestrial protocrust with a $^{238}U/^{204}Pb$ (μ) that was ca. 20-30% higher than coeval mantle. The high-μ signature is most evident in metasediments (that formed at the Earth's surface). The Pb-isotope evidence for a long-lived protocrust complements similar Hf-isotope data from the Earth's oldest zircons, which also require an origin from an enriched (low Lu/Hf) environment.

With the initiation of terrestrial subduction at ca. 3.75 Ga, most of the ≥ 3.8 Ga basaltic shell (and its differentiation products) was recycled into the mantle, because of the lack of a thick stabilising mantle lithosphere. The key event responsible for preservation of all ≥3.8 Ga terrestrial crust was intrusion of voluminous granitoids following initiation of global subduction, with preservation possible because of complementary creation of a lithospheric keel.

THE EARLY BIOSPHERE

Figure 4 shows that laminated calcsilicates from pre-3.8 Ga supracrustal sequences from Northern Labrador, that contain anomalous W isotopic compositions, have identical REE patterns to those described from Palaeozoic Proterozoic and Late Archean carbonates by Kamber and Webb (2001. There is close resemblance and a strong indication that the >3.6 Ga sample has preserved its chemical integrity. It is an approximation to the REE chemistry of very ancient seawater (with positive La, Eu, Gd and Y anomalies). This exciting finding must be corroborated with further samples from outcrops with carefully described relative age relationships. These REE signatures are an excellent proxy for seawater providing valuable information about the chemistry of the early hydrosphere and the antiquity of the biosphere.

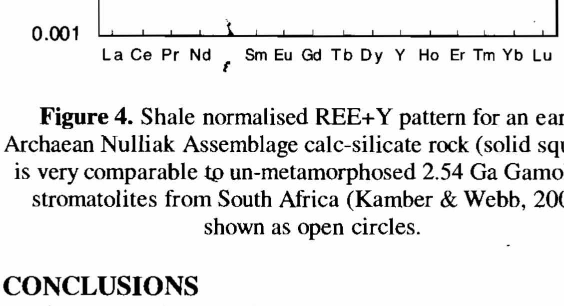

Figure 4. Shale normalised REE+Y pattern for an early Archaean Nulliak Assemblage calc-silicate rock (solid squares) is very comparable to un-metamorphosed 2.54 Ga Gamohaan stromatolites from South Africa (Kamber & Webb, 2001) shown as open circles.

CONCLUSIONS

Cryptic evidence for Priscoan crust in the North Atlantic Craton yields information regarding: (1) the nature of pre-subduction zone igneous rocks that hosted the oldest terrestrial minerals (zircon); (2) the surface environment during late heavy meteorite bombardment; (3) the nature of the early hydrosphere and biosphere. These observations are clearly important for models of

Earth's early evolution. Results clearly have implications in the search in other cratons for remnants of Priscoan crust. They also provide useful information relevant to planetary comparison.

REFERENCES

Abe Y. 1993. Physical state of the very early Earth, Lithos, 30: 223-235.

Bowring, S.A. & Williams, IS. 1999. Priscoan (4.00-4.03 Ga) orthogneisses from northwestern Canada. Contr. Mineral. Petrol., 134, 3-16.

Caro, G.; Bourdon, B.; Birck, J.L.; Moorbath, S. 2002. Nd-142/Nd-144 precise determination in early Archaean rocks. Geochim. Cosmochim. Acta, 66: A-120 Suppl. 1.

Collerson, K.D. 1983. Ion probe zircon geochronology of the Uivak gneisses: implications for the evolution of the early terrestrial crust in the North Atlantic craton. In: L.D. Ashwal & K.D. Card (Editors), Workshop of a Cross Section of Archaean Crust. LPI Technical Report, pp. 28-33.

Collerson, K.D. & Kamber, B.S. 1999. Evolution of the continents and the atmosphere inferred from Th-U-Nb systematics of the depleted mantle. Science, 283: 1519-1522.

Collerson, K.D.; Jesseau, C.W.; Bridgawter, D. 1976. Crustal development of the Archaean gneiss complex: Eastern Labrador. In: Windley, B.F. (Editor) The Early History of the Earth, Wiley, London, 237-253.

Collerson, K.D.; McCulloch, M.T.; Bridgwater, D. 1984. Nd and Sr isotopic crustal contamination patterns in an Archaean meta-basic dyke from northern Labrador. Geochim. Cosmochim. Acta, 48: 71-83.

Collerson, K.D.; Campbell, L.M.; Weaver, B.L.; Zenon, A.P. 1991. Evidence for extreme mantle fractionation in early Archaean ultramafic rocks from northern Labrador. Nature, 349: 209-214.

Frankland, R.A.; Collerson, K.D.; Ewart, A.; Niu, Y.; Kepezhinskas, P.; Defant, M.J. 1998. Modelling the formation of sub-continental lithosphere. Geol. Soc. Aust. Abstracts 42, 153.

Frei, R. & Rosing, M.T. 2001. The least radiogenic terrestrial leads: implications for the early Archaean crustal evolution and hydrothermal-metasomatic processes in the Isua Supracrustal Belt (West Greenland). Chem. Geol., 181: 47-66.

Grieve, R.A.F. 1980. Impact bombardment and its role in protocontinental growth on the early Earth. Precambrian Res. 10, 217-248.

Harper, C.L. & Jacobsen, S.B. 1992. Evidence from coupled 147Sm-143Nd and 146Sm-142Nd systematics for very early (4.5 Ga) differentiation of the Earth's mantle. Nature, 360: 728-732.

James, D.T.; Kamo, S. & Krogh, T. 2002. Evolution of 3.1 and 3.0 Ga volcanic belts and a new thermotectonic model for the Hopedale Block, North Atlantic Craton (Canada). Can. J. Earth Sci. 39: 687-710.

Kamber, B.S. & Webb, G.E. 2001. The geochemistry of late Archaean microbial carbonate: Implications for ocean chemistry and continental erosion history. Geochim. Cosmochim. Acta. 65, 2509-2525.

Kamber, B.S.; Ewart, A.; Collerson, K.D.; Bruce, M.C.; McDonald, G.D. 2002. Fluid-mobile trace element constraints on the role of slab melting and implications for Archaean crustal growth models. Contrib. Mineral. Petrol., 144: 38-56.

Kamber, B.S.; Collerson, K.D.; Moorbath, S.; Whitehouse, M.J. 2003. Long-lived high ^{238}U/^{204}Pb source of the most ancient TTG gneisses and the nature of the Earth's oldest crust. Contrib. Mineral. Petrol., 145. 25-46.

Kramers, J.D., 2001. The smile of the Cheshire cat. Science, 293: 619-620.

Maas, R., Kinny, P.D., Williams, I.S., Froude, D.O. and Compston, W., 1992. The Earth's oldest known crust: A geochronological and geochemical study of 3900-4200 Ma old detrital zircons from Mt. Narryer and Jack Hills, Western Australia. Geochim. Cosmochim. Acta, 56: 1281-1300.

McCulloch, M.T. and Bennett, V.C., 1994. Progressive growth of the Earth's continental crust and depleted mantle: Geochemical constraints. Geochim. Cosmochim. Acta, 58: 4717-4738.

Myers, J.S. 2001. Protoliths of the 3.8-3.7 Ga Isua greenstone belt, West Greenland. Precambrian Res., 105(2-4): 129-141.

Nelson, D.R.; Robinson, B.W.; Myers, J.S. 2000. Complex geological histories extending for ≥4.0 Ga deciphered from xenocryst zircon microstructures. Earth Planet Sci. Lett., 181: 89-102.

Nutman, A.P. & Collerson, K.D.,1991. Very early Archaean crustal-accretion complexes preserved in the North Atlantic craton. Geology, 19: 791-794.

Nutman, A.P.; Bennett, V.C.; Friend, C.R.L.; Norman, M.D. 1999. Meta-igneous (non-gneissic) tonalites and quartz-diorites from an extensive ca. 3800 Ma terrain south of the Isua supracrustal belt, southern West Greenland: constraints on early crust formation. Contrib. Mineral. Petrol., 137(4): 364-388.

Peck, W.H.; Valley, J.W.; Wilde, S.A.; Graham, C.M. 2001. Oxygen isotope ratios and rare earth elements in 3.3 to 4.4 Ga zircons: Ion microprobe evidence for high □^{18}O continental crust and oceans in the Early Archaean. Geochim. Cosmochim. Acta, 65: 4215-4229.

Regelous, M. & Collerson, M.D. 1996. ^{147}Sm-^{143}Nd, ^{146}Sm-^{142}Nd systematics of early Archaean rocks and implications for crust-mantle evolution. Geochim. Cosmochim. Acta, 60: 3513-3520.

Rosing, M.T. 1999. C-13-depleted carbon microparticles in > 3700-Ma sea-floor sedimentary rocks from west Greenland. Science, 283: 674-676.

Scherer, E.; Münker, C.; Mezger, K. 2001. Calibration of the lutetium-hafnium clock. Science, 293: 683-687.

Schiøtte, L.; Compston, W.; Bridgwater, D. 1989. Ion probe U-Th-Pb zircon dating of polymetamorphic orthogneisses from northern Labrador. Can. J. Earth Sci., 26: 1533-1556.

Schoenberg, R.; Kamber, B.S.; Collerson, K.D.; Eugster, O. 2002a. New W-isotope evidence for rapid terrestrial accretion and very early core formation. Geochim. Cosmochim. Acta, 66: 3151-3160.

Schoenberg, R.; Kamber, B.S.; Collerson, K.D.; Moorbath, S. 2002b. Tungsten isotope evidence from ~3.8-Gyr metamorphosed sediments for early meteorite bombardment of the Earth. Nature, 418: 403-405.

Stern, R.A. & Bleeker, W. 1998. Age of the world's oldest rocks redefined using Canada's SHRIMP: The Acasta gneiss complex, Northwest Territories, Canada. Geosci. Can. 25: 27-31.

Tera, F.; Papanastassiou, D.A.; Wasserburg, G.J. 1974. Isotopic evidence for a terminal lunar cataclysm. Earth Planet Sci. Lett., 22: 1-21.

Wilde, S.A.; Valley, J.W.; Peck, W.H.; Graham, C.M. 2001. Evidence from detrital zircons for the existence of continental crust and oceans on the Earth 4.4 Gyr ago. Nature, 409: 175-178.

Nd PROVENANCE OF LOCAL CENOZOIC SEDIMENTARY DEPOSITS IN CONTINENTAL SOUTHEASTERN BRAZIL: EVIDENCE FOR LIMITED MIXING OF SEDIMENT SOURCES DURING EROSION, TRANSPORT AND DEPOSITION

Fetter, A.H.[1]; Hackspacher, P.C.[1]; Dantas, E.L.[2]; Saad, A.R.L.[3]; Bistrichi, C.A.[3] and Ávila, C.A.[4]

1. Instituto de Geociências e Ciências Exatas, Universidade Estadual Paulista,
Av. 24 A, nº 1515, 13506-900, Rio Claro, SP, Brazil. fetter@ms.rc.unesp.br
2. Instituto de Geociências, Universidade Federal de Brasília, 70910-900, Brasília-DF
3. Universidade de Guarulhos, UnG, 07023-070 Guarulhos-SP, Brasil
4. Departamento de Geologia e Paleontologia, Museu Nacional - UFRJ, Rio de Janeiro-RJ, 20940-040

Keywords: Southeast Brazil, Nd provenance, cenozoic deposits

INTRODUCTION

Cenozoic continental basin deposits of southeastern Brazil contain sediments that were derived primarily from the Precambrian crystalline basement during several pulses of uplift, subsidence and erosion during the Phanerozoic. The crystalline rocks that make up the basement in this region represent a mosaic of different crustal blocks that were amalgamated and tectonized during the Brasiliano Orgeny at the end of the Neoproterozoic. Because the different crustal blocks within this region are quite heterogeneous in terms of their Nd isotopic signatures, we decided to study the relationship between basement rocks and Cenozoic deposits using Sm-Nd studies in order to understand sediment provenance and to evaluate the degree of intermixing between different sources during erosion, transport and deposition. In this study we present Nd data obtained from crystalline basement rocks, Cretaceous alkaline intrusions and minor Cenozoic continental deposits in southeast Brazil and discuss the significance of these findings.

PRECAMBRIAN BASEMENT

The rocks that make up the Precambrian crystalline basement in southeast Brazil include Archean to Paleoproterozoic orthogneisses and paragneisses, Paleoproterozoic to Neoproterozoic supracrustal rocks and Neoproterozoic plutons generated during Brasiliano orogenesis. Our Nd data obtained from these different rocks display a wide range of isotopic signatures and are in line with other Nd studies of the regional crustal architecture (e.g. Sato, 1998; Cordani et al., 2000; Dantas et al., 2000). Archean and Paleoproterozoic gneisses yield T(DM) model ages between 3.28 and 2.25 Ga, with epsilon Nd (t=0) values from -42.9 to -19.5, respectively. Supracrustal rocks and brasiliano granitoids display T(DM) model ages between 2.28 and 1.30 Ga and epsilon Nd (t=0) values from -23,8 to -7.2 (Table 1). The granitoids and supracrustal rocks with older Nd signatures indicate the influence of older crust in their formation, while younger values indicate asthenospheric mantle contributions (in the case of granitoids), or sediments derived from juvenile Neoproterozoic island arcs.

CRETACEOUS ALKALINE INTRUSIONS

A series of late Cretaceous alkaline bodies intrude the basement along the 125° A/Z lineament running from Poços de Caldas, MG to Rio de Janeiro, RJ. Although the emplacement ages and sizes of these intrusions are variable, Nd analyses of nine different samples along this lineament show a remarkable consistency in their isotopic signatures. T(DM) model ages occupy an interval between 0.90 and 0.75 Ga (with most model of the ages between 0.80 and 0.84 Ga; see Table 1) and the epsilon Nd (t=0)values range from -7.1 to -4.6. In addition to their relatively homogenous isotopic signatures of these bodies, they are also distinctly different from the Nd values of the Precambrian basement. The uniqueness of these younger signatures makes them useful in that their eroded remains should be easily identifiable in younger Cenozoic deposits. We attribute the homogeneous signatures of these alkaline intrusions their derivation from a homogenous mantle source, probably the Trinidade plume, and their rapid emplacement, hence minimal interaction with the surrounding country rocks.

CENOZOIC DEPOSITS

In this study, we sampled and performed Nd analyses on Cenozoic sediments from the Tanque Basin and other local continental deposits in the region (see Table 1). The results obtained thus far show the local deposits to have a relatively high degree of isotopic heterogeneity. On an outcrop scale, it is possible to observe large differences in Nd signatures from one layer to the next. The most notable example is seen in sample outcrop SB-36 of the Santa Isabel-Igaratá deposit (table 1) where two distinct layers, A and B, yield T(DM) model ages of 3.07 and 1.67 Ga and epsilon Nd (t=0) values of -39.5 e -18.9, respectively. In principle, layer A would have been derived from an Archean source, while layer B probably reflects derivation from a brasiliano granitoid. Other examples of the variable isotopic signatures in these deposits can be seen in Table 1. These alternating sources suggest that the infilling of these smaller basins involved pulses of deposition in which clastic material came from various individual sources, being eroded and transported during discrete events in local hydrographic basins.

Table 1. Sm/Nd results from crystalline basement and Cenozoic deposits in southeast Brazil.

Sample	Litology	Locale/ Basin	Nd ppm	Sm ppm	$\frac{^{147}Sm}{^{144}Nd}$	$\frac{^{143}Nd}{^{144}Nd}$	ε Nd (0 Ma)	$T_{(DM)}$ Ga
Precambrian crystalline rocks - Archean and Paleoproterozoic gneisses (some examples)								
H540	ortogneiss	Faixa Alto Rio Grande	46.7	8.1	0.10460	0.511428	-23.6	2.26
H543	ortogneiss	Faixa Alto Rio Grande	8.4	1.7	0.11850	0.511641	-19.5	2.25
H587A	ortogneiss	Faixa Alto Rio Grande	20.9	4.3	0.12320	0.511129	-29.4	3.28
H601	ortogneiss	Faixa Alto Rio Grande	38.9	6.0	0.09352	0.510692	-38.0	3.02
H607A	ortogneiss	Faixa Alto Rio Grande	34.9	5.2	0.09077	0.510438	-42.9	3.28
H620	ortogneiss	Faixa Alto Rio Grande	7.7	1.5	0.11710	0.511594	-20.4	2.30
H684	ortogneiss	Faixa Alto Rio Grande	139.2	26.6	0.11540	0.511553	-21.2	2.29
Precambrian crystalline rocks - Brasiliano granitoids and supracrustal rocks (some examples)								
H360	granitoid	Piedade-SP	184.6	25.1	0.08224	0.511420	-23.8	1.88
H514	granitoid	Ibiuna-SP	239.8	36.1	0.09105	0.511507	-22.0	1.91
H535	granitoid	Inconfidentes-MG	10.3	1.7	0.10060	0.511941	-13.6	1.48
H597	granitoid	Igarata-SP	43.0	6.1	0.08624	0.511459	-23.0	1.90
H687A	schist	Cambuqueira-MG	20.0	4.1	0.12420	0.512271	-7.2	1.30
H511A	metapelite	Sao Roque-SP	35.9	6.5	0.11030	0.511500	-22.2	2.28
Cretaceous alkaline intrusions (some examples)								
H696	alkaline	Pocos de Caldas-MG	44.6	7.0	0.09530	0.512404	-4.6	0.82
ATF 5	alkaline	Passa Quatro-MG	243.0	31.2	0.07760	0.512338	-5.9	0.80
ATF 6	alkaline	Passa Quatro-MG	87.1	11.3	0.07870	0.512313	-6.4	0.83
ATF 7	alkaline	Passa Quatro-MG	101.3	13.0	0.07730	0.512300	-6.6	0.84
ATF 8	alkaline	Passa Quatro-MG	144.7	18.8	0.07860	0.512382	-5.0	0.75
HE 987	alkaline	Itatiaia-RJ	239.0	32.6	0.09060	0.512359	-5.4	0.80
CAA1B	alkaline	Itauna-RJ	86.2	11.1	0.07800	0.512338	-5.9	0.80
CAA2	alkaline	Marapicu-RJ	24.1	3.2	0.81200	0.512276	-7.1	0.88
CAA3	alkaline	Morro dos Gatos- RJ	1055.6	174.2	0.09970	0.512370	-5.2	0.90
Cenozoic sediments (Tanque basin and local desposits)								
SB02A	sediment	Tanque	8.4	54.0	0.09350	0.511606	-20.1	1.81
SB04	sediment	Tanque	101.1	16.1	0.09650	0.511595	-20.4	1.87
SB07	sediment	Vargem	104.6	13.4	0.07730	0.511751	-17.3	1.44
SB13	sediment	B.J. dos Perdoes	26.1	3.5	0.08090	0.511622	-19.8	1.63
SB14	sediment	B.J. dos Perdoes	38.4	6.3	0.09890	0.510456	-42.6	3.46
SB15	sediment	Dom Pedro-Jarinu	46.8	4.6	0.05980	0.511356	-25.0	1.67
SB19	sediment	B.J. dos Perdoes	14.0	2.3	0.10040	0.511884	-14.7	1.56
SB20	sediment	Santa Isabel-Igarata	224.1	35.0	0.09450	0.511429	-23.6	2.06
SB21	sediment	Santa Isabel-Igarata	44.9	7.2	0.09730	0.511626	-19.7	1.85
SB2A	sediment	Santa Isabel-Igarata	54.0	8.4	0.09350	0.511606	-20.1	1.82
SB36A	sediment	Santa Isabel-Igarata	39.5	6.1	0.09320	0.510615	-39.5	3.11
SB36B	sediment	Santa Isabel-Igarata	54.7	8.0	0.08842	0.511671	-18.9	1.67
SB41B	sediment	Santa Isabel-Igarata	33.1	4.8	0.08847	0.511719	-17.9	1.61
SB41C	sediment	Santa Isabel-Igarata	42.3	6.3	0.09063	0.51165	-19.3	1.73
SB43C	sediment	Santa Isabel-Igarata	29.4	4.2	0.08635	0.511782	-16.7	1.51
SB45	sediment	Atiabaia-Jarinu	33.0	5.3	0.09747	0.511648	-19.3	1.83
SB50	sediment	Batatuba	41.9	6.8	0.09740	0.511522	-21.8	1.99
SB51	sediment	Batatuba	14.2	1.9	0.07940	0.511464	-22.9	1.79
SB53	sediment	Santa Isabel-Igarata	31.5	5.1	0.09780	0.511479	-22.6	2.06
SB59	sediment	Pinhalzinho	51.8	8.3	0.09730	0.511784	-16.7	1.65
SB63	sediment	Pedra Bela	55.5	8.6	0.09360	0.511484	-22.5	1.98
SB64	sediment	Pinhalzinho	40.9	5.4	0.07970	0.511699	-18.3	1.53
SB65	sediment	Rio Jaguari	114.1	18.5	0.09790	0.511648	-19.3	1.84
SB71	sediment	Jarinu	38.4	5.8	0.09190	0.511546	-21.3	1.87
SB72	sediment	Jarinu	11.7	2.0	0.10130	0.511768	-17.0	1.73
SBJ 01	sediment	Jundiai	42.9	8.1	0.11390	0.511739	-17.5	1.99
SBJ 02	sediment	Jundiai	26.3	4.1	0.09331	0.511516	-21.9	1.94
SBJ 03	sediment	Jundiai	18.8	2.9	0.09418	0.511633	-19.6	1.80
SBJ 04	sediment	Jundiai	27.9	4.7	0.10060	0.511541	-21.4	2.03

In contrast, transport via a major fluvial system, or mixing in a large lacustrine setting, would have the tendency to homogenize sediments from various sources, resulting in more uniform isotopic signatures in the deposits. This homogenizing phenomena is seen to a fair extent in the sediments of the Taubaté basin (Sant'Anna et al., this symposium) where many sediments in the central part of the basin display T(DM) model ages between 2.2 and 1.8 Ga.

ACKNOWLEDGEMENTS

The authors wish to thank FAPESP (Proc. 00/03960-5) and CNPq (Proc. 464175/00-0) for their financial support for this study.

REFERENCES

Cordani, U.G.; Sato, K.; Teixeira, W.; Tassinari, W.; Tassinari, C.C.G.; Basei, M.A.S., 2000. Crustal evolution of the South American platform. In: Tectonic Evolution of South America. Cordani, U.G.; Milani, E.J.; Thomaz Filho, A.; Campos, D.A. (Eds.), p. 19-40, Rio de Janeiro, Brazil.

Dantas, E.L.; Hackspacher, P.C.; Ebert, H.D. 2000. Sm/Nd Isotopic Patterns of the Guaxupé, Alto Rio Grande and Socorro Domains, South of the São Francisco Craton, Brazil. 31st International Geological Congress, Rio de Janeiro, Brazil.

Sato, K., 1998. Evolução crustal da Plataforma Sul Americana, com base na geoqúimica isotópica Sm-Nd. Doctoral Thesis, Institute of Geosciences, University of São Paulo.

$^{13}CO_2$, $^{14}CO_2$ AND ORGANIC CARBON ISOTOPES MEASUREMENTS IN TWO TROPICAL AND A SUB-TROPICAL SOIL IN BRAZIL

Freitas H.A.[1]; Pessenda L.C.R.[2] and Leite, A.Z.[3]

1. Center for Nuclear Energy in Agriculture (CENA). hfreitas@cena.usp.br
2. Center for Nuclear Energy in Agriculture (CENA). pessenda@cena.usp.br
3. Center for Nuclear Energy in Agriculture (CENA)

Keywords: Carbon-13, carbon-14, soil organic matter, soil respiration

INTRODUCTION

Carbon isotopes (^{12}C, ^{13}C, ^{14}C) provide a powerful tool to elucidate carbon dynamics in soil and are widely used to understand ecosystem carbon budgets (e.g. Camargo et al., 1999; Trumbore et al., 1993, 1995), gas flux from soil (e.g. Davidson, 1995; Dörr & Münnich, 1980, 1986), decomposition of organic matter (e.g. Balesdent et al., 1993; Martin et al., 1990; Wedin et al., 1995) and paleovegetation dynamics (e.g. Freitas et al., 2001; Pessenda et al., 2001).

Carbon dioxide is produced in soil through biological processes (organic matter decomposition and root respiration) and it is transported to the overlying atmosphere via molecular diffusion. Research has focused on both the isotopic composition of respirated CO_2 (CO_2 that diffuses across the soil-atmosphere interface) and soil CO_2 (CO_2 that exists at any given soil depth). While much remains to be learned about the natural variations in the isotopic composition of soil and respired CO_2, interest in this topic will increase due to the magnitude of soil respiration on a global scale, and its role in the process controlling the isotopic composition of atmospheric CO_2 (Amundson et al., 1998).

The carbon isotope ratios in soil CO_2 are determined by the mixture of CO_2 derived from three sources: inward diffusion from the overlying atmosphere, respiration of live roots and the oxidation of soil organic matter (SOM) by soil microorganisms (Nordt et al., 1996). It is recognized that most soils at quasi-steady state, have the same C isotopic composition of respired CO_2 as that of biological sources in the soil, although carbon isotopes ratios in the plant-derived component of soil CO_2 can change during decomposition. This change is mediated by the isotopic composition of the chemical constituents of SOM as well as discrimination during decomposition by soil microorganisms (Boutton, 1996). In addition, the diffusion coefficients for $^{12}CO_2$ and $^{13}CO_2$ in soil, differ, producing at least a 4.4 ‰ or greater enrichment in ^{13}C to soil CO_2, relative to soil-respired CO_2 (Davidson, 1995; Dörr & Münnich, 1980; Cerling et al., 1991). However, studies have shown that enrichment in ^{13}C to soil CO_2 can be considerably less than 4.4 ‰ if the difference between the $\delta^{13}C$ of atmospheric CO_2 and soil-respired CO_2 is small, or greater than 4.4 ‰ for soils where the $\delta^{13}C$ of organic matter is less than about –12.5 ‰ (Davidson, 1995).

The magnitude and timing of the response of the soil carbon reservoir to changes in land use or climate is a large source of uncertainty in global carbon cycle models (Trumbore, 1993) and, presently, there is no adequate model describing the $^{14}CO_2$ distribution in soils. Therefore, a better understanding of $^{14}CO_2$ distribution in soils would have very important implications in the study of organic carbon cycling in soils and other knowledge (Nepstad et al., 1994; Trumbore, 1993; Wang et al., 1993, 1994).

Here we show some data of soil CO_2 and organic matter isotopic composition ($\delta^{13}CO_2$ and $^{14}CO_2$). The results are part of an on going research whose main aim is to characterize ($\delta^{13}CO_2$, $\Delta^{14}CO_2$ and flux of CO_2 and CH_4) the carbon cycle soil gases in two tropical and a sub –tropical soil in Brazil. These soils have different vegetations and land uses (Table 1). Samples were all collected in 2001 and 2002.

Table 1. Sites, vegetation types and geographic coordinates of CO_2 sampling.

Site	Vegetation	Geographic coordinates
Porto Velho	Tropical forest/savanna	8°11' S/63°49' W
Pontes e Lacerda	Tropical forest/pasture	15°19' S/59°13' W
Piracicaba	Sub-tropical forest/sugar-cane	22°42' S/47°39' W

In order to collect soil CO_2 from the soil surface we used a metal chamber (39-cm diameter and 20-cm high) with appropriate connections (Fig. 1). To limit direct contact with the outside atmosphere, the chamber was usually hammered ca. 7 cm into the uppermost layer of the soil. The air was pumped from the chamber, circulated through a system with two traps (1 L each) filled with drying agent (silica gel) and a trap (1 L) filled with synthetic sodium aluminosilicate zeolite (Type 13 X, beads 12-mesh, Aldrich Chemical Company, Milwaukee, USA). To obtain information about the isotopic composition of soil CO_2 from different depths (1-m and 2-m), the soil air was pumped through the same system, but instead of using a chamber, the air was pumped from the desired depth through a pipe inserted into the soil. In both situations the air was pumped at specified intervals using a diaphragm pump for ca. 10 days. Experimental set-up used is shown in Fig. 1.

Each trap (cartridge) of molecular sieve was activated to eliminate any adsorbed H_2O, CO_2 and organic contaminants present, by evacuating the cartridge in a furnace to 550 °C and vacuum (10^{-1} atm) for at least 3 h.

After each collection, the CO_2 was recovered from the molecular sieve by placing a cartridge in the furnace and connecting it to the vacuum line. The CO_2 was condensed in liquid-nitrogen-cooled CO_2 traps. Before heating and condensing the CO_2, the cartridge and the liquid-nitrogen-cooled CO_2 traps were pumped (10^{-1} atm) at room temperature. The $\delta^{13}CO_2$ was determined by mass spectrometry and the $^{14}CO_2$ by liquid scintillation or accelerator mass spectrometry (AMS), depending on the amount of CO_2 available. The $^{13}CO_2$ results were expressed as δ_{PDB} (‰) and analytical precision ± 0.2 ‰. $^{14}CO_2$ results were expressed as pmc (percent of modern carbon, with respect to oxalic acid standard) and normalized to a $\delta^{13}C$ value of -25‰.

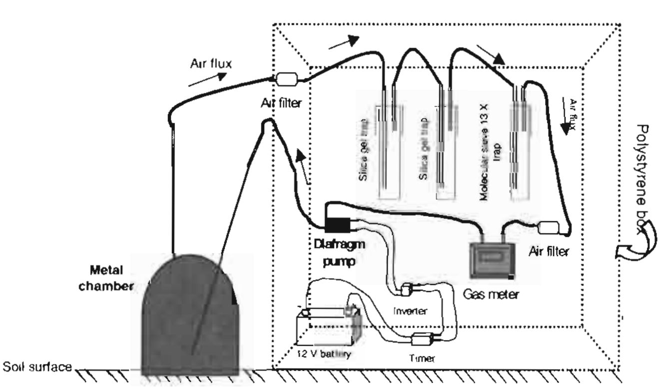

Figure 1. Sampling system used for flux and isotopic composition of soil CO_2 from soil surface. To obtain CO_2 at deeper layers a pipe inserted into the soil replaced the chamber.

RESULTS AND DISCUSSION

The SOM and CO_2 isotopic composition, as well as soil organic carbon content results are presented in the Table 2 and Figs. 2a, b, 3a, b.

Table 2. Results of $^{14}CO_2$ and $\delta^{13}CO_2$ of the soils under forest and sugar-cane at Piracicaba.

	Sugar-cane soil ($^{14}CO_2/\delta^{13}CO_2$) (pcm/‰)	Forest soil ($^{14}CO_2/\delta^{13}CO_2$) (pcm/‰)	^{14}C / $\delta^{13}C$ of SOM under forest (pcm/‰)
Soil surface	102.3 ± 0.8/ -12.8	102.1 ± 0.5/ -22.6	107.3 ± 0.8/ -25.7
1 m deep	111.0 ± 0.8/ -10.7	109.1 ± 0.8/ -22.8	68.8 ± 0.7/ -17.2
2 m deep	109.1 ± 0.8/ -10.3	112.2 ± 0.8/ -	63.7 ± 0.6/ -16.0

The total organic carbon content data of the studied soils show a general decrease with depth, similar to other studies (e.g. Freitas et al., 2001; Pessenda et al., 2001). Values ranged from 2.37 % in the uppermost strata to 0.06 % in the deepest sampled levels.

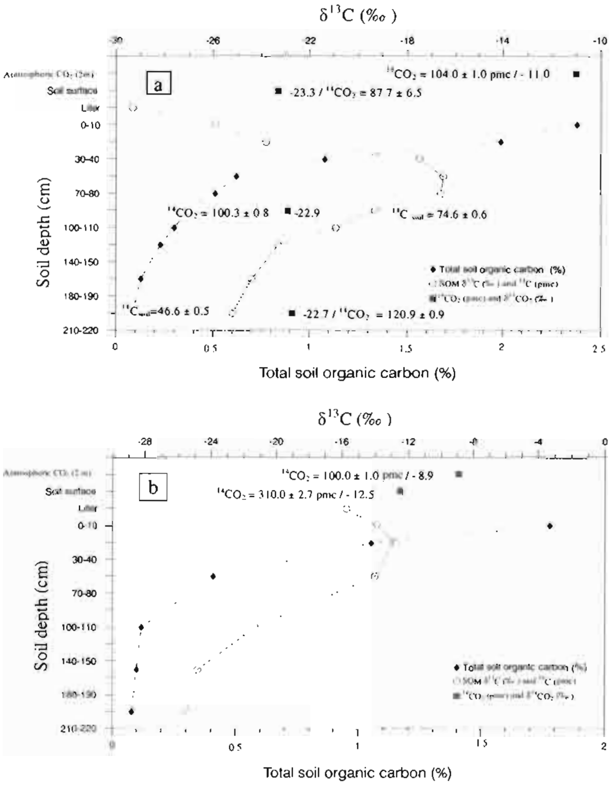

Figure 2. The $\delta^{13}C$ of SOM, $\delta^{13}CO_2$, total organic carbon and $^{14}CO_2$ variation with depth at (a) forest and (b) savanna soils, in Porto Velho.

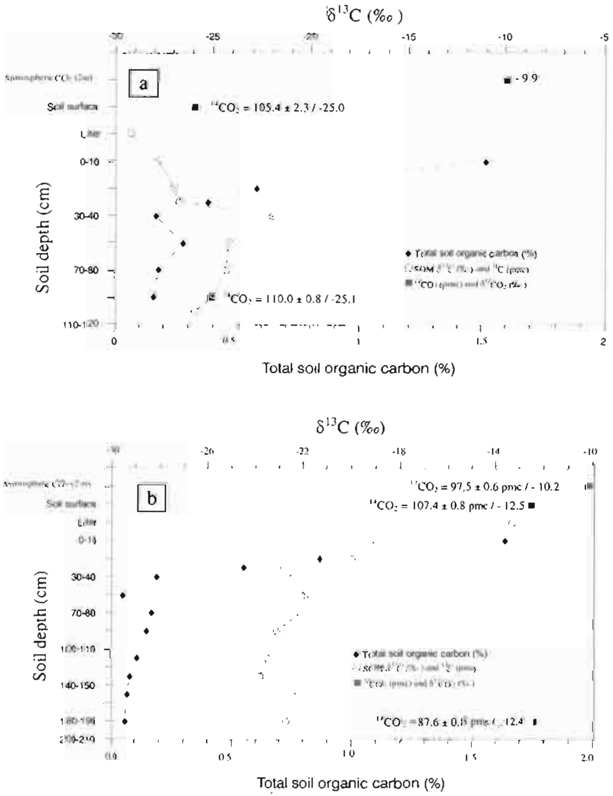

Figure 3. The ^{13}C of SOM, $\delta^{13}CO_2$, total organic carbon and $^{14}CO_2$ variation with depth at (a) forest and (b) pasture, in Pontes e Lacerda.

The atmospheric CO_2 measured 2 m above ground (Figs. 2a, b, 3a, b), showed the influence of tropospheric CO_2 ($\approx$ -8 ‰) and respired CO_2 (which depends on the SOM been decomposed and vegetation isotopic composition). It is in good agreement with other studies (e.g. Buchmann et al., 1997). The $\delta^{13}CO_2$ values ranged from -11.0 to -8.9 ‰ at forest and savanna, respectively, in Porto Velho. The value 100.0 pmc for the $^{14}CO_2$ at savanna in Porto Velho is expected to be the closest to the actual atmospheric $^{14}CO_2$ in this region.

The soil surface $^{14}CO_2$ data show very similar values for the soils in Piracicaba (Table 2) and Pontes e Lacerda (Figs. 3a, b), ranging from 102.1 pmc (forest in Piracicaba) to 107.4 pmc (pasture in Pontes e Lacerda). These values indicate that the most important CO_2 source, at these places, is the decomposition of recently fixed C (which includes root respiration, rapid decomposition of root exudates and labile organic matter) (Dörr & Münnich, 1986; Trumbore et al., 1995). The 310.0 pmc $^{14}CO_2$ (Fig. 2b, savanna in Porto Velho) is an unexpected value. This result will be interpreted after additional soil ^{14}C and $^{14}CO_2$ data of the profile. The $^{14}CO_2$ values were usually a little enriched with depth but contrasting with the SOM ^{14}C which were depleted in ^{14}C (Table 2, Fig. 2a), indicating that the bulk organic matter did not contributed significantly to soil CO_2 composition. The soil $^{14}CO_2$ values at depth are higher than the obtained for the atmospheric CO_2, indicating that decomposition of organic matter, which was fixed by plants several years to decades ago when atmospheric $^{14}CO_2$ was higher, contributes significantly to CO_2 fluxes (Trumbore et al., 1995).

All $\delta^{13}CO_2$ values on the surface were more enriched than the $\delta^{13}C$ liter fraction. The difference ranged from + 6.2 (forest in Porto Velho) to +0.8 ‰ (pasture in Pontes e Lacerda). Camargo et al. (1999) observed larger differences in pasture soils. In addition, the isotopic composition of soil CO_2 reflected the $\delta^{13}C$ of the present vegetation (C_3 – forest – or C_4 – savanna, pasture or sugar-cane). These results reinforce the hypothesis that, on the soil surface, the main source of CO_2 is the decomposition of recently fixed organic matter. For deeper soil layers, no variation was observed in $^{13}CO_2$, even at the pasture in Pontes e Lacerda (Fig. 3b), in spite of the enriched SOM $\delta^{13}C$ value, which was -19 ‰ in the uppermost stratum (0-10) and -22.7 at 200 cm depth, indicating that old C_3 derived carbon decomposition was not an important CO_2 source at this depth.

Our preliminary conclusions are: although the origin of the organic matter being decomposed may differ between C_3 and C_4 plants, the ^{14}C content of the material being decomposed were usually similar; the isotopic compositions ($\delta^{13}C$) of CO_2 in soil profiles up to a depth of 2-m were similar but heavier compared to that of the vegetation above ground.

REFERENCES

Amundson, R.; Stern, L.; Baisden, T.; Wang, Y., 1998. The isotopic composition of soil and soil-respired CO_2. Geoderma 82, 83-114.

Balesdent, J.; Girardin, C.; Mariotti, A., 1993. Site-related $\delta^{13}C$ of tree leaves and soil organic matter in a temperate forest. Ecology 74, 1713-1721.

Boutton, T.W. 1996. Stable carbon isotope ratios of soil organic matter and their use as indicators of vegetation and climate change. In: Boutton, T.W. & Yamasaki, S. (Ed.). Mass spectrometry of soils. New York: Marcel Dekker,. pp.47-82.

Buchmann, N.; Guehl, J.M.; Barigah, T.S.; Ehleringer, J.R., 1997. Interseasonal comparison of CO_2 concentrations, isotopic composition, and carbon dynamics in an Amazonian rainforest (French Guiana). Oecologia 110, 120-131.

Camargo, P.B.; Trumbore, S.E.; Martinelli, L.A.; Davidson, E.A.; Nepstad, D.C. et al., 1999. Soil carbon dynamis in regrowing Forest of eastern Amazônia. Global Change Biology 5, 693-702.

Cerling, T.E.; Solomon, D.K.; Quade, J.; Bowman, J.R., 1991. On the isotopic composition of carbon in soil carbon dioxide. Geochimica et Cosmochimica Acta 55, 3403-3405.

Davidson, G.R., 1995. The isotopic composition and measurement of carbon in soil. Geochimica et Cosmochimica Acta 59, 2485-2489.

Dörr, H. & Münnich, K.O., 1980. Carbon-14 and carbon-13 in soil CO_2, Radiocarbon 22, 909-918.

Dörr, H. & Münnich, K.O., 1986. Annual variations of the ^{14}C content of soil CO_2. Radiocarbon 28, 338-345.

Freitas, H.A.; Pessenda, L.C.R.; Aravena, R.; Gouveia, S.E.M.; Ribeiro, A.S.; Boulet, R., 2001. Late Quaternary vegetation dynamic record in southern Amazon inferred from carbon isotopes in soil organic matter. Quaternary Research 55, 39-46.

Martin, A.; Mariotti, A.; Balesdent, J.; Lavelle, P.; Vuattoux, R., 1990. Estimate of organic matter turnover rate in a savanna soil by ^{13}C natural abundance measurements. Soil Biology and Biochemistry 22, 517-523.

Nordt, L.C.; Wilding, L.P.; Hallmark, C.T., 1996. Stable carbon isotope composition of pedogenic carbonates and their use in studying pedogenesis. In: Boutton, T.W. & Yamasaki, S. (Ed.). Mass spectrometry of soils. New York: Marcel Dekker, pp. 133-154.

Pessenda, L.C.R.; Boulet, R.; Aravena, R.; Rosolen, V.; Gouveia, S.E.M. et al., 2001. Origin and dynamics of soil organic matter and vegetation changes during the Holocene in a forest-savanna transition zone, Brazilian Amazon region. The Holocene 11, 283-287.

Trumbore, S.E., 1993. Comparison of carbon dynamics in tropical and temperate soils using radiocarbon measurements. Global Biogeochemical Cycles, 7, 275-290.

Trumbore, S.E.; Davidson, E.A.; Camargo, P.B.; Nepstad, D.C.; Martinelli, L.A., 1995. Belowground cycling of carbon in forests and pastures of eastern Amazonia. Global Biogeochemical Cycles 9, 515-528.

Wang, Y.; Amundson, R.; Trumbore, S., 1993. Processes controlling the ^{14}C content of soil carbon dioxide: model development. Chemical Geology 107, 225-226.

Wedin, D.A.; Tieszen, L.L.; Dewey, B.; Pastor, J., 1995. Carbon isotope dynamics during grass decomposition and soil organic matter formation. Ecology 76, 1383-1392.

NEW U-Pb AGES FOR HOST ROCKS, MINERALIZATION AND ALTERATION OF IRON OXIDE (Cu-Au) DEPOSITS IN THE COASTAL CORDILLERA OF NORTHERN CHILE

Gelcich, S.H.[1]; Davis, D.W.[2] and Spooner, E.T.C.[3]

1. SERNAGEOMIN (Chile) - University of Toronto, Ontario, Canada. gelcich@geology.utoronto.ca
2. Earth Science Department, Royal Ontario Museum, Toronto, Ontario, Canada
3. Department of Geology, University of Toronto, Ontario, Canada

Keywords: Iron oxide deposits, U-Pb dating, Coastal Cordillera Northern Chile, Manto Verde, Carmen

INTRODUCTION

The Coastal Cordillera of northern Chile is a very fertile province in terms of Fe-oxide deposits, including Kiruna type and hydrothermal systems rich in Fe, Cu and Au. One of the main metallogenic features of the Coastal Cordillera in northern Chile is the Chilean Iron Belt (CIB), a 600 km N/S belt that includes ~ 50 iron deposits (Nystrom & Henríquez, 1994). These deposits are of massive magnetite–apatite type; they occur as veins, irregular and pseudo stratiform bodies and are always hosted in volcanic and/or plutonic suites that record magmatic activity in the early Andean Stages (Jurassic-Early Cretaceous). A number of hydrothermal iron oxide Cu-Au deposits are spatially related to the pure iron deposits; e.g. Manto Verde (Vila et al., 1996; Zamora & Castillo, 2001). The age of the mineralization and related alteration is poorly constrained.

The Coastal Cordillera in the area of Chañaral (Fig. 1) has been the subject of recent studies including: regional geology (Godoy & Lara, 1998: Lara & Godoy, 1998); geochronology (Dallmeyer et al., 1996; Gelcich et al., 2002); structural geology and batholith architecture (Brown et al., 1993: Grocott & Taylor, 2002). This work presents new preliminary U-Pb ages of intrusive rocks and related mineralization in two areas in the Coastal Cordillera of Chañaral: Manto Verde and Carmen (Fig.1).

METHODS

U-Pb analyses were carried out at the Royal Ontario Museum. Zircons were dissolved in teflon bombs according to methods described in Krogh (1973, 1982). Apatites and titanites were dissolved in Savillex vials. U and Pb were separated using HCl for zircon analysis Krogh (1973) and HBr for titanite and apatite (Corfu, 1988). Precise ages on Mesozoic minerals must rely on the $^{206}Pb/^{238}U$-decay system. All errors are given at 2 sigma levels. Current Pb blank levels of less than 1 picogram permit precise analyses of fractions consisting of one (zircons) or several grains (titanite and apatites). The isotopic composition of initial Pb was estimated using the model of Stacey & Kramers (1975). Titanite and apatite ages are especially sensitive to the inferred initial Pb isotopic composition. Further analyses are required on low U/Pb coexisting mineral phases in order to get a better estimation of the common lead component.

RESULTS AND DISCUSSION

New ages have been obtained in the Manto Verde (Cu-Au) and Carmen (Fe) areas. The new record includes U-Pb zircon ages for spatially associated plutons and minor stocks and U-Pb mineralization ages from titanite (Manto Verde) and apatite (Carmen).

CARMEN MINE

Carmen is an irregular magnetite body elongated in a west-east direction, with a length of about 550 m, a width of between 30 and 50 m and a depth greater than 250 m (Henríquez et al., 1991). It is hosted by volcanic rocks of the La Negra Formation affected by contact metamorphism related to the intrusion of the early Cretaceous Sierra Aspera pluton (131.3 ± 0.4 Ma (Fig. 2a); Gelcich et al., 2002). Mineralization in Carmen consists of magnetite with variable contents of apatite and actinolite. This mineral suite forms massive and breccia type bodies (Henríquez et al, 1991). Apatite from a distal magnetite-apatite dyke located 500 m south of the main pit in Carmen was dated at 129.8 ± 3.0 Ma (Fig. 2b); this is the first reported dating of apatite associated with massive magnetite ore in the CIB. The 3-m wide dyke is subvertical and has a general NS strike. It shows some banded intergrowth textures of magnetite and wedge-shaped apatites. The dyke has fine grained borders, and magnetite stockworks developed as halos in the volcanic host rock. Zircon from a mineralized quartz diorite stock, in the northern pit of Carmen Mine was dated at 130.6 ± 0.3 Ma (Fig. 2c). These two new ages are in the range of zircon U-Pb ages in the Sierra Aspera pluton (Gelcich et al., 2002).

MANTO VERDE

Manto Verde is the largest and the main economic deposit in the area of Chañaral. Cu mineralization is present mainly as oxides, products of oxidation of original Cu sulphide hypogene mineralization in specularite-rich hydrothermal breccias. At deeper levels the main iron oxide in association with Cu sulphide mineralization is magnetite (Zamora & Castillo, 2001). Cornejo et al. (2000) inferred a series of metasomatic-hydrothermal stages for the hydrothermal alteration assemblages at Manto Verde, starting with potassic metasomatism, followed by hydrothermal magnetite-sulphide, hematite-sulphide stages, and a later carbonate phase. The host rock in Manto Verde is mainly composed of andesitic lavas of the La Negra Formation that are intruded by a number of small dykes. These rocks define a structural block limited by the central and eastern branches of the Atacama Fault System. The Manto Verde structural Block is bounded on the west by the Las Tazas North Pluton (134.1 ± 0.4 Ma; Gelcich et al., 2002) and on the east by the Sierra Dieciocho Pluton (129.6 ± 0.3 Ma, Fig. 2d; Gelcich et al., 2002). A primary zircon U-Pb crystallization age of 128.9 ± 0.6 Ma (Fig. 2e) was obtained for a quartz monzodioritic to granodioritic dyke (felsic intrusive or "pseudo aplite" in the terminology of Zamora & Castillo, 2001).

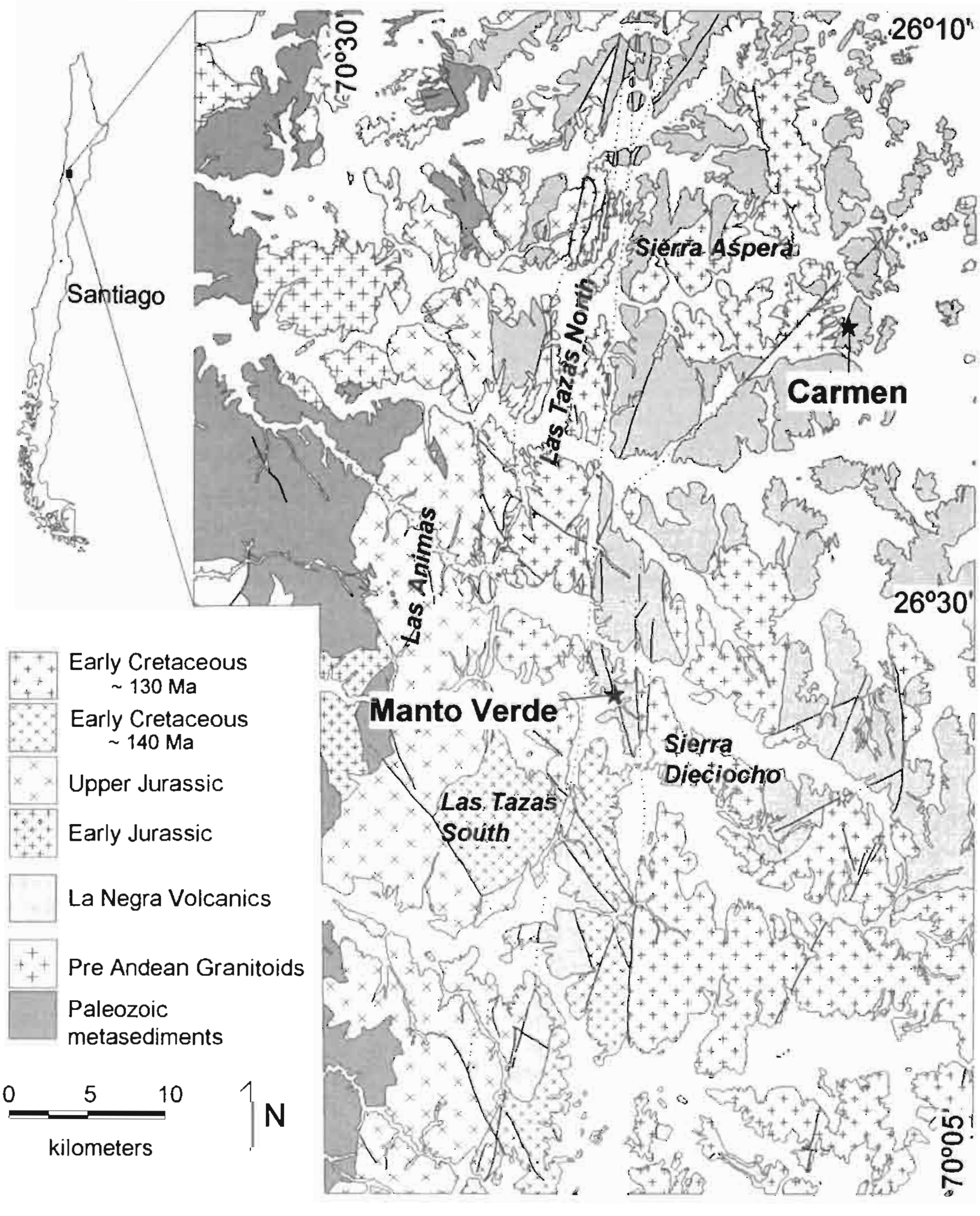

Figure 1. Geological map of the Coastal Cordillera of Chañaral, with the location of Manto Verde and Carmen. The main plutons are labeled. From Godoy & Lara, 1998; Lara & Godoy, 1998.

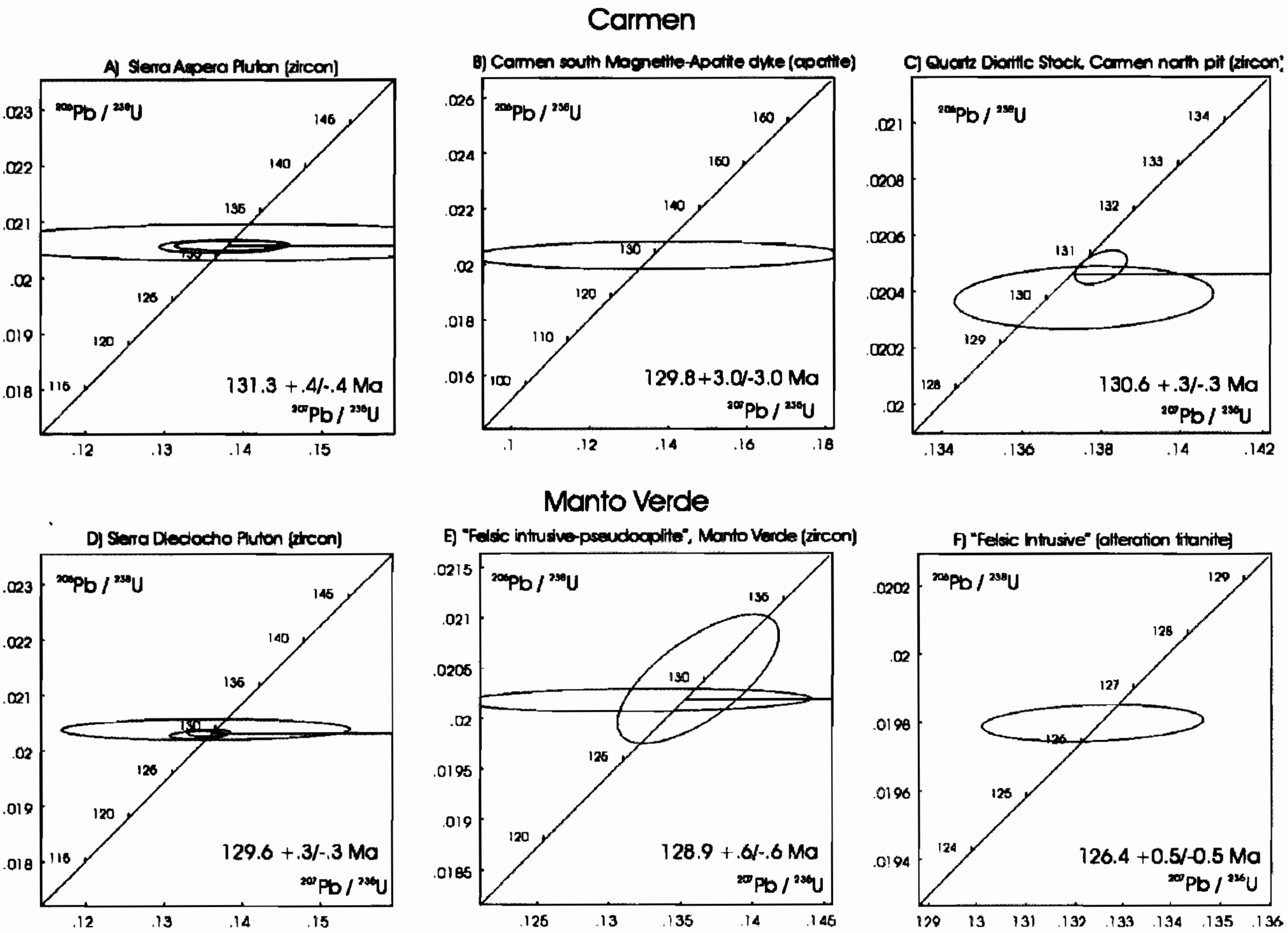

Figure 2. U-Pb concordia diagrams. Carmen ages: A) zircon age of the Sierra Aspera pluton (Gelcich et al., 2002); B) apatite age from magnetite-apatite south dyke; c) quartz dioritic host rock in Carmen north pit. Manto Verde ages. D) zircon age of Sierra Dieciocho Pluton (Gelcich et al., 2002); E) zircon age of the "Felsic Intrusive"; F) titanites associated with potassic alteration of the "Felsic intrusive". Apatite and titanite ages should be considered preliminary, see text for discussion.

This unit shows pervasive potassic alteration (Stage I in the Cornejo et al., 2000, model), including titanite as a major phase. According to Cornejo et al. (2000) titanite represents the alteration product of primary ulvöspinel, with a consequent liberation of Fe to the hydrothermal fluids, which finally precipitated as iron oxides accompanying the main sulphide mineralization. Titanites were dated giving a concordant age of 126.4 ± 0.5 Ma (Fig. 2f). U-Pb data from this area define a closely spaced succession of thermal events. They indicate that mineralization in Manto Verde is most probably related to the cooling and differentiation of the Sierra Dieciocho pluton.

Both massive magnetite-apatite (Carmen) and Hydrothermal Fe-Cu-Au (Manto Verde) deposits show clear temporal relationships to stocks or dykes that intruded volcanic cover sequences. These later intrusive units represent more differentiated phases that can be temporally and compositional related to the main plutonic units in the area. Thus, Fe oxide mineralization in the coastal Cordillera can be genetically related to the extensive Jurassic to Early Cretaceous plutonism of the Coastal cordillera.

ACKNOWLEDGEMENTS

We acknowledge Richard Zamora and Boris Castillo for access to samples from Manto Verde, and Sernageomin for their field logistics. Special thanks to Mr. Bob McRae for his essential financial support.

REFERENCES

Brown, M.; Diaz, F.; Grocott, J. 1993. Displacement history of the Atacama fault system, 26°00'S-27°00'S, northern Chile. Geological Society America Bulletin, 105, p. 1165-1174.

Corfu, F. 1988. Differential response of U-Pb systems in coexisting accessory minerals, Winnipeg River Subprovince, Canadian Shield; implications for Archean crustal growth and stabilization. Contributions to Mineralogy and Petrology, vol.98, no.3, p.312-325.

Cornejo, P.; Matthews, S.; Orrego, M.; Robles, W. 2000. Etapas de minerlizacion asociadas a alteracion potasica en un sistema de Fe-Cu-Au: Yacimiento Manto Verde, III Region de Atacama, Chile. In: IX Congreso Geologico Chileno, Actas Vol.2 p. 97-101.

Dallmeyer, R.D.; Brown, M.; Grocott, J.; Graeme, K.T.; Treolar, P. 1996. Mesozoic magmatic and tectonic events within the Andean plate boundary zone, 26°-27°30'S, north Chile: constraints from 40Ar/39Ar mineral ages. The Journal of Geology, 104, p. 19-40.

Gelcich, S.; Davis, D.; Spooner, E.T.C. 2002. U-Pb dating with sub-million year precision of early Andean plutonic rocks in the coastal cordillera of Chañaral, Northern Chile. In V International Symposium on Andean Geodynamics, Toulouse, p. 239-242.

Godoy, E. & Lara, L. 1998. Hojas Chañaral y Diego de Almagro, region de Atacama. Servicio Nacional de Geologia y Mineria. Mapas Geologicos No 4. 1 map scale 1:100.000, Santiago.

Grocott, J. & Taylor, G.K. 2002. Magmatic arc fault systems, deformation partitioning and emplacement of granitic complexes in the Coastal Cordillera, north Chilean Andes (25 degrees 30'S to 27 degrees 00'S). Journal of the Geological Society of London, vol.159, Part 4, p.425-442.

Henriquez, F.; Dobbs, M.; Nystrom, J. 1991. Caracterizacion geoquimica de magnetita, apatita y anfibola del yacimiento de hierro Carmen, Region de Atacama, Chile. In: Congreso Geológico Chileno Nº 6, Viña del Mar , Actas, p. 159-161.

Krogh T. E. 1973. A low-contamination method for hydrothermal decomposition of zircon and extraction of U and Pb for isotope age determinations. Geochim. Cosmochim Acta, 37, p. 485–494.

Krogh T. E. 1982. Improved accuracy of U-Pb zircon ages using an air abrasion technique. Geochim. Cosmochim Acta 46, 637–649.

Lara, L. & Godoy, E. 1998. Hoja Quebrada Salitrosa, Region de Atacama. Servicio Nacional de Geologia y Mineria. Mapas Geologicos No 3. 1 map scale 1:100.000, Santiago.

Nystrom, J. & Henriquez, F. 1994. Magmatic Features of iron ores of the Kiruna type in Chile and Sweden; ore textures and magnetite geochemistry. Economic Geology Vol. 89, p. 820-839.

Stacey, J.S. & Kramers, J.D. 1975 Approximation of terrestrial lead isotope evolution by a two-stage model. Earth and Planetary Science Letters, vol. 26, no.2, p. 207-221

Vila, T.; Lindsay, N.; Zamora, R. 1996. Geology of the Manto Verde Deposit, northern Chile: A specularite-rich breccia related to the Atacama Fault Zone. In: Andean Copper Deposits: New discoveries, mineralization, styles and metallogeny. Society of Economic Geologists, Special Publication Nº5, Camus, F., Sillitoe, R.H., Peterson, R. eds., p. 157-170.

Zamora, R. & Castillo, B. 2001. Mineralización de Fe-Cu-Au en el Distrito Manto Verde, Cordillera de la Costa, III Región de Atacama, Chile. In: II Congreso Internacional de Prospectores y Exploradores, ProEXPLO 2001 Lima, Peru, 13 p.

CONTINOUS DIFFUSION Pb LOSS IN IGNEOUS ZIRCON: A BSE, ID-TIMS AND RAMAN STUDY ON A MESOPROTEROZOIC GRANITE FROM SW AMAZONIAN CRATON

Geraldes, M.C.[1]; Silva, D.[2]; Valeriano, C.M.[1] and Nogueira, J.R.[1]

1. Tektos Research Group-Faculty of Geology, State University of Rio de Janeiro (UERJ), Rua São Francisco Xavier 524, 20559-900 Rio de Janeiro-RJ, Brazil. geraldes@uerj.br
2. Department of Metalogenesis and Geochemistry, Institute of Geosciences-State University of Campinas (UNICAMP) P.O. Box 6152, 13081-970 Campinas-SP, Brazil

Keywords: Diffusion, Pb-loss, Mesoproterozoic, Amazonian Craton

INTRODUCTION

The metamictization of zircon has been the subject of extensive research (Nasdala et al., 1999; Wopenka et al., 1996; Hartmann et al., 1997; Poller et al., 1997; Balan et al., 2001). Understanding how the zircon structure responds to radiation damage is important for both the storage of high-level radioactive waste (Ewing et al., 1995) and the use of U-Th-Pb isotopic systematics. In the latter case, the fracturing due to volume expansion that accompanies metamictization may lead to diffuse loss or heterogeneous redistribution of radiogenic Pb (Pidgeon, 1992).

The metamictization of zircon can be characterized by Raman spectroscopy (Knittle & Willians, 1993; Jolliff et al., 1995). This method of analysis has the advantage that little or no sample preparations is necessary, and analysis can be done in a reasonable time. Particularly important is the ability of Raman spectroscopy to determine the crystallinity of micro-areas, allowing information by profiling across zircon grains (Jolliff et al., 1995) to be obtained. In addition, BSE images give complete information about internal structures of zircon grains (Poller et al., 1997). As earlier investigations have shown (Harchar & Miller, 1993), the parallel use of BSE pre-investigating method allow to distinguish inherited cores, desorbed areas and magmatic zonation. Thus, BSE is an important tool to solve the main problem for the successful zircon dating: Selection of appropriate grains.

We present results of a detailed investigation of zircons from a Mesoproterozoic granite from SW Amazonian craton, using a combination of back scattered electron (BSE) imaging, thermal ionization mass spectrometry (TIMS) and Raman spectroscopy. The objective of this work is to study the correlation between metamictization and U-Pb isotopic discordance of zircon.

PROCEDURES

For the U-Pb analyses, separation of zircon was done using standard procedures of the Isotope Geochemistry Laboratory (IGL), Department of Geology, University of Kansas (USA). Procedure details are found in Geraldes et al. (2001). Decay constants used were 0.155125 x 10^{-9} year^{-1} for ^{238}U and 0.98485 x 10 $^{-9}$ year^{-1} for ^{235}U (Steiger & Jäger, 1977). Zircon data were regressed using the ISOPLOT program of Ludwig (1998). Uncertainties in concordia intercept ages are given at the 2 sigma (σ) level. The zircons grains from the same sample were analyzed in a CCD T64000 Jobin-Yvon laser-Raman microprobe in the Fluid Inclusion Laboratory of the Institute of Geosciences of the State University of Campinas (Brazil). The laser Ar$^+$ wavelength was 5145 (green). The theoretical diffraction-limited focal spot diameter at the sample surface is about 1 µm for the Olympus 80x long distance objective. The laser power at the sample surface is 10 mW, which is typically nondestructive to samples of geologic interest. For BSE the 180° backscattered light was detected with a 1 in., 1024 element optical diode-array detector.

ID-TIMS DATING

U-Pb (single grain) zircon geochronology was undertaken on a granitic sample. The analyzed zircon grains were clear, slightly caramel with rounded ends and short prismatic lateral faces. The grains present multiple sizes with large, medium and small grains. Six zircons were analyzed and the results when plotted in the concordia diagram yielded an upper intercept age of 1423.0 ± 3.8 Ma (Fig. 1a), which may be interpreted as crystallization age of the rock, as discussed below. Each one of the analyzed zircon grains presented different weight and when the analytical results were plotted in the concordia diagram the heaviest zircon grain (0.018 mg) was the more concordant (99%). With the purpose of better understanding the isotopic patterns of the zircons grains, a second diagram was made (Fig. 1b) using Grain Weight (mg) *versus* ^{205}Pb/^{235}U Age Concordance (%). The results when plotted in such diagram indicate that U-Pb isotopes are volume-dependent in the studied zircon grains.

BSE IMAGING

BSE reveals contrasts in average atomic number of regions of a phase: the higher the number, the more electrons will reflect and the brighter it will appear. BSE imaging is used for a variety of geologic studies and is recognized as a powerful tool for studying zonation in accessory minerals (Hanchar & Miller, 1993). In zircons, Hf is the main element responsible for the variation in BSE intensity, with U having a secondary effect. Both elements have much higher atomic number than the principal constituents of zircon (Zr, Si and O), so the substitution of Zr by U and Hf results in increased brightness.

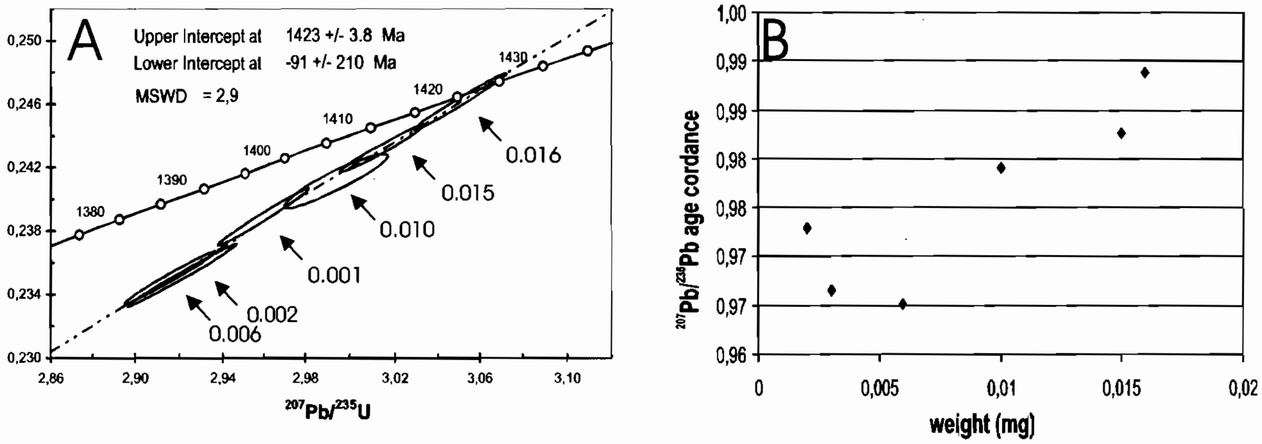

Figure 1. a) U-Pb isotopic results plotted in the concordia diagram. b) Grain Weight (mg) *versus* ^{205}Pb/^{235}U Age Concordance (%). Weight values are in mg. Concordance was calculated with respect to the upper intercept age (1423 ± 3.6 Ma).

Different observations can be made on the scanning electron microscopy (SEM), but to geochronologic purposes the most important one is BSE imaging of each single zircon. Figure 2 illustrates BSE images of zircons grains from the granite sample used in this study. The zircons have a euhedral external shape and fine-scale euhedral oscillatory zoning. Purely magmatic zoned zircons were found, indicating that the granitic sample did not suffer metamorphic heating or any other process forming new phases. Another noteworthy point about zoning observed under BSE is the lack of evidence of discordant zoning and color-zoned areas, which corroborates the hypothesis that zircons grew during one episode, according to Pidgeon (1992) and Vavra (1993). In addition BSE images can give further information, especially in the case of inclusions. Such inclusions are frequently apparent in the sampled zircons and might cause problems to U-Pb dating and to Raman analysis.

RAMAN MONITORING

Raman spectrum of zircon is sensitive to its degree of metamictization. With decreasing crystallinity, the Raman bands become less intense (peak half-width variation), increasingly broadened (peak area variation), and show lowered frequencies (wavelength shift). In synthetic single crystal of zircon there are 36 modes first-order Raman-active modes and they can be subdivided into internal and external vibrations. External vibrations are related to complex massive silicate rotatory and translatory motions; and internal vibrations involve silicon-oxigen and metal-silicate bonds and sites. We analyzed the degree of metamictization using half-width of the Raman bands calculated in three different (modes) peaks: (E_g) 360 cm^{-1}, ($A1_g$) 978 cm^{-1} and (B_{1g}) 1012 cm^{-1}. The objective was to identify the best or the Raman parameter most sensitive to metamictization.

Conventional Raman spectroscopy in zircon analyses are concerned with the peak shift, half-width and peak area. In this study we used, from the Raman spectra, a plot of the intensity of the inelastically scattered radiation (measured in photons per second) as a function of the half-width in each analysed spot. The mechanical configuration of the high-resolution monochromator in combination with the argon ion laser as excitation source makes it possible to monitor the Raman shift within the scale of the profile at the zircon surface.

In this way, Raman technique had the objective to obtain vibrational spectroscopic characteristics from the zircon lattice correlative to punctual structural variations. The individual measurement spots are shown in the backscattered electron images (Fig. 2). Three zircon grains were analysed with profiles through the zoning areas of the zircon surface. The results (Fig. 3) indicate that the increasing width of the internal (B_{1g} mode) vibration (antisymmetric strenching of SiO_4 tetrahedra) is sensitive enough to determine the increasing degree of metamictization. Furthermore, evidence for metamictization is given in Figure 3. The results display a marked heterogeneity of half-width values of the represented three peaks comprised of a decreasing trending from center to the border in the three analyzed grains.

DISCUSSION AND CONCLUSIONS

We reported results of a combined ID-TIMS and Raman microprobe study of the correlation between metamictization and U-Pb isotopic discordance of zircon. The spatial resolution of the Raman probe allows a direct comparison of U-Pb isotopic discordance and metamictization of zoned areas within zircon crystal. The combination of the two measurements also gives informations on the Pb loss. We found that the degree of U-Pb isotopic discordance correlates closely with the volume of the zircon grain. The data, in addition to the lateral degree of metamictization detected by the Raman technique, indicate that the loss of radiogenic Pb may be linked to continuous diffusion of this element.

The correlation of U-Pb discordance and metamictization makes Raman spectroscopy analysis of zircon prior dating a helpful tool for geochronologists. Since discordant isotopic ratios may give ambiguous ages, it is advantageous to select zircons with well ordered lattices for age determinations measurements. The investigation here reported also suggests that linear array of data points on the concordia diagram is not only linked to the magnetic suscepbility of the zircon grains, but that the Pb loss, in response to metamictization, is found to be inversely proportional to grain volume (as pointed out by Krogh, 1973).

Oscillatory zoning is a common feature in zircon from acid igneous rock and is believed to form during crystallization of zircon from magma. The ID-TIMS and Raman here presented indicate that Pb diffusivity in slightly damaged zircon is not negligible and Pb loss is not restricted to zircons that have experienced episodic Pb loss (U-Pb mineral systems opened during a secondary event) or a protracted low-temperature (annealing) history. The data points lying on a discordia here reported corroborates the hyphothesis in which the radiogenic lead was lost by continuous diffusion and the upper intercept age closely approaches the age of formation of the rock.

REFERENCES

Balan, E.; Neuville, D.R.; Trocellier, P.; Fritsch, E.; Muller, J-P.; Calas, G.; 2001. Metamictization and chemical durability of detrital zircon. American Mineralogist, 86:1025-1033.

Ewing, R.C.; Lutze, W.; Weber, .J.; 1995. Zircon: A host-phase for the disposal of weapons plutonium. Journal of Materials Research 10:243-246.

Geraldes, M.C.; Van Schmus, W.R.; Condie, K.C.; Bell, S.; Teixeira, W.; Babinski, M., 2001. Proterozoic Geologic Evolution of the SW Part of the Amazonian Craton in Mato Grosso State, Brazil. Precambrian Research. 111:91-128.

Harchar, J.M. & Miller, C.F., 1993. Zircon zonation patterns as revealed by cathodoluminescense and backscattered electron images: Implications for interpretation of complex crustal histories. Chemical Geology 110:1-13.

Hartmann, L.A.; Takehara, L.; Leite, J.A.D.; McNaughton, N.J.; Vasconcellos, M.A.Z., 1997. Fracture sealing in zircon as evaluated by electron microprobe analyses and back-scattered electron imaging. Chemical Geology 141:67-72.

Jolliff, B.L.; Wopenka, B.; Zinner, E.; Kresner, D.T., 1995. A zoned lunar zircon in a quartz-monzodiorite breccia from Apollo 14: U, Th, other trace elements, and Raman spectral parametrers. Lunar and Planetary Science, XXVI, 695-696.

Knittle, E. & Willians, Q., 1993. High-pressure Raman spectroscopy of $ZrSiO_4$: Observation of the zircon to scheelite transition at 300 K. American Mineralogist 78:245-252.

Krogh, T.E., 1973. A low contamination method for hydrothermal decomposition of zircon and extraction of U and Pb for isotopic age determinations. Geochimica et Cosmochimica Acta 37:485-494.

Ludwig, K.L., 1998. Using Isoplot/Excel, version 1.00b, A geochronological toolkit for Microsoft Excel. Berkely Geochronology Center Spec. Pub. n°. 1: 43p.

McLaren, A.C.; FitzGerald, J.D.; Willians, I.S., 1994. The micro-structure of zircon and its influence on the age determination from Pb/U isotopic ratios measured by ion microprobe. Geochimica et Cosmochimica Acta 58:993-1005.

Nasdala, L.; Enzel, T.; Pidgeon, R.T.; Kronz, A., 1999. Internal structures and dating of complex zircons from Meissen Massif monzonites, Saxony. Chemical Geology 156:331-341.

Pidgeon, R.T., 1992. recrystallization of oscillatory zoned zircon: some geochronological and petrological implications. Contribution to Mineralogy and Petrology 110:463-472.

Poller, U.; Liebetrau, V.; Todt, G., 1997. U-Pb single-zircon dating under cathodoluminescence control (CLC-method): application to polymetamorphic orthognaisses. Chemical Geology 139:287-297.

Steiger, R.H. & Jäger, E., 1977. Subcommission on Geochronology-convention and use of decay constants in geochronology and cosmochronology. Earth and Planetary Science Letters 36:359-362.

Vavra, G., 1993. A guide to quantitative morphology of accessory zircon. Chemical Geology. 110:15-28.

Wopenka, B.; Jolliff, B.L.; Zinner, E.; Kremser, R., 1996. Trace element zoning and incipient metamictization in a lunar zircon: Application of three microsprobe techniques. American Mineralogist 81:902-912.

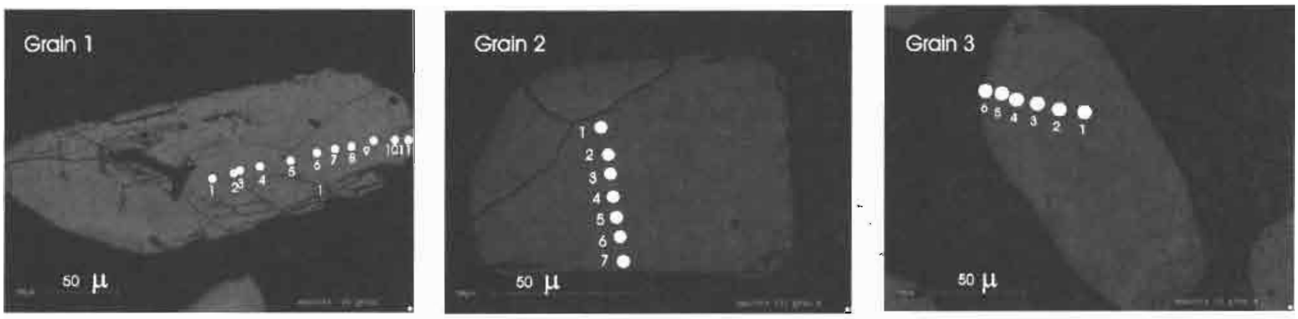

Figure 2. Backscattered images of zircon grains. Raman analyses were taken in the cross section showed on the grains. The zircons have a euhedral external shape and fine-scale euhedral oscillatory zoning indicates igneous origin.

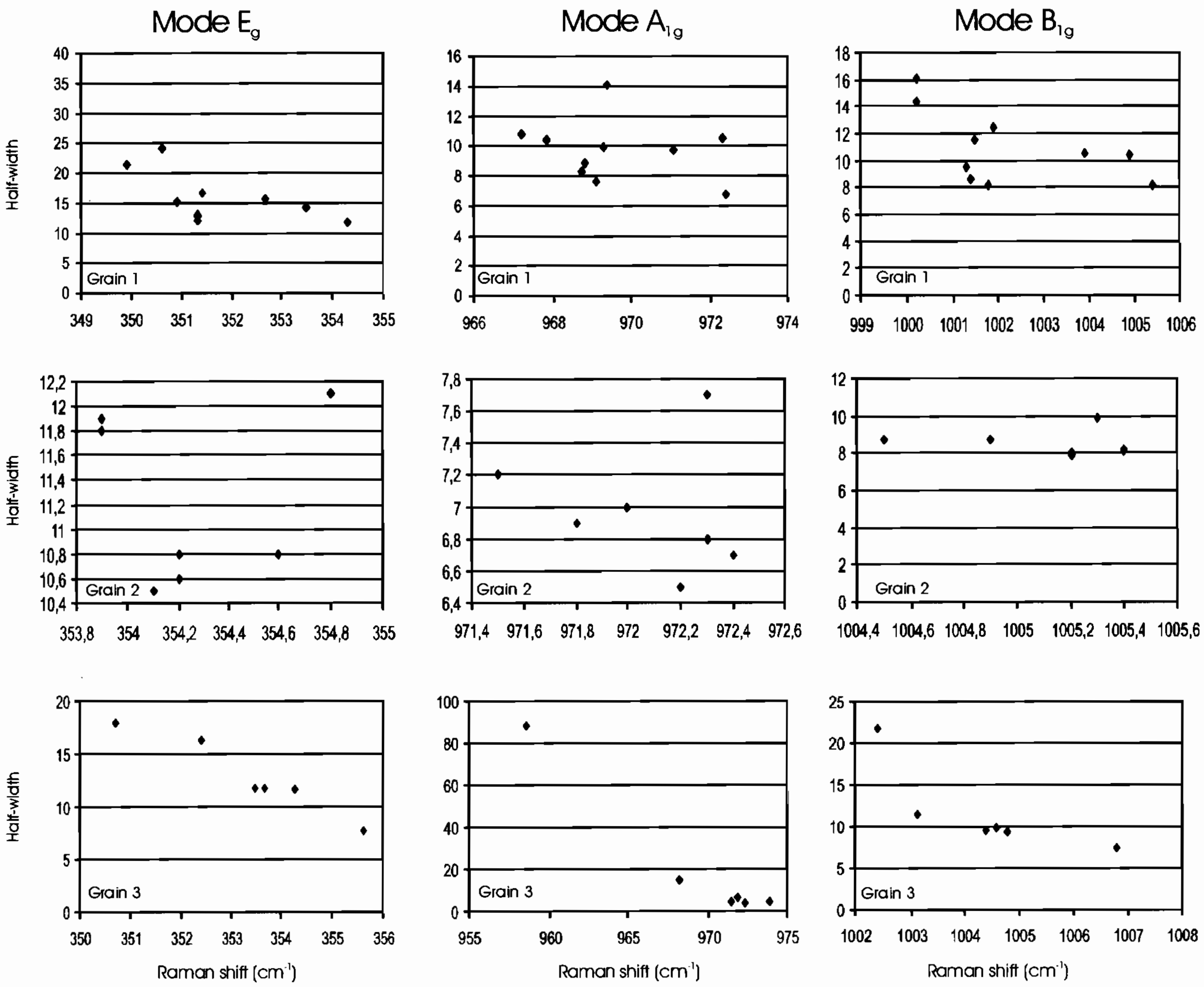

Figure 3. Raman results for three zircon grains profiles (shown in Figure 2). Three peaks were studied ($360\ cm^{-1}$, $978\ cm^{-1}$ and $1012\ cm^{-1}$) using half-width as parameter. Evidence for metamictization is given by a marked heterogeneity of half-width values.

FISSION-TRACK DATING OF JANKOV MOLDAVITE USING U AND Th THIN FILM NEUTRON DOSIMETRY

Guedes, S.[1]; Iunes, P.J.[1]; Bigazzi, G.[2]; Hadler Neto, J.C.[1]; Laurenzi, M.A.[2]; Balestrieri, M.L.[2]; Norelli, P.[2]; Osorio, A.M.A.[3]; Tello, C.A.S.[1,5] and Paulo, S.R.[4]

1. Instituto de Fisica Gleb Wataghin, Universidade Estadual de Campinas, UNICAMP, 13083-970,
Campinas – SP, Brazil. guedes@ifi.unicamp.br
2. Istituto di Geoscienze e Georisorse, C.N.R., Area della Ricerca di Pisa, Via G. Moruzzi 1, 56124 Pisa, Italy
3. Departamento de Física, Química e Biologia, Universidade do Estado de São Paulo, 19060-900 Presidente Prudente – SP, Brazil
4. Instituto de Ciências Exatas e da Terra, Universidade Federal do Mato Grosso, UFMT, 78070-900 Cuiabá – MT, Brazil
5. Departamento de Física, Química e Biologia, Universidade do Estado de São Paulo,
UNESP, 19060-900 Presidente Prudente – SP, Brazil

Keywords: Fission-track dating, neutron dosimetry, U thin film, Th thin film, moldavite

INTRODUCTION

During the last decade most fission-track (FT) age determinations were performed using the zeta calibration (Hurford & Green, 1983). The use of the zeta calibration is a way of overcoming difficulties related with i) uncertainties on the fundamentals (such as the value of the ^{238}U spontaneous fission decay constant or the approach to be adopted for an adequate neutron dosimetry) as well as on parameters related to some experimental procedures (such as the external detector method). However, the zeta calibration makes the FT method dependent on the other isotopic techniques used for dating the age standards used for the determination of the zeta factor. For this reason research on procedures devoted to enable FT dating to be an independent system with an absolute calibration was encouraged (see, for instance, Hurford, 1998).

One of the crucial points in obtaining an absolute system calibration is the neutron dosimetry. Bigazzi et al. (1999) have shown that the use of natural U and Th thin films can be an efficient alternative for a correct neutron dosimetry. In addition, it has been shown that U and Th thin films make it possible to apply the FT method also when only low thermalization irradiation facilities are available, such as in many research nuclear reactors. The International Union of Geological Sciences (I.U.G.S.) had discouraged the use of such facilities (Hurford, 1990), because of the difficulties related to the determination of the contribution of the U and Th fissions induced by epithermal and fast neutrons to the induced track density.

Recently neutron dosimetry based on U and Th thin films was adopted for dating Durango apatite (Iunes et al., 2002), one of the age standards recommended by the I.U.G.S. Subcommission on Geochronology (Hurford, 1990). Our result, 29.7 ± 1.1, was consistent with the reference age, 31.4 ± 0.5, recommended based on other dating methods.

In the present work, the neutron dosimetry based on U and Th thin films was used for dating Moldavite, the central European tektite also recommended as an age standard for glass (Hurford, 1990).

EXPERIMENTAL

Neutron irradiations were performed in three nuclear reactors: IPEN/CNEN – São Paulo, Brazil (irradiation I27MD and I32MD), LENA – Pavia, Italy (irradiation P4MD) and IPEN – Lima, Peru (irradiation L19MD). The sample-set present in these irradiations was made up by Th thin films, natural U doped glasses (Cornig glass CN1 in irradiations I32MD and P4MD, and Cornig glasses CN2 and CN5 in irradiations I27MD and L19MD, respectively) and two Moldavites (MJ1 and MJ2) from the Middle Miocene deposit of Jankov, southern Bohemia (Bouška, 1994). Moldavite MJ1 and MJ2 were included in irradiation I32MD, only MJ1 was included in the other irradiations. Only in case of irradiation I32MD Moldavite samples were pre-heated for 10h at 560°C in order to erase spontaneous tracks.

Ages were computed using the following equation:

$$T = \frac{1}{\lambda}\ln\left[\frac{\left(\dfrac{\rho_S}{\rho_I}\right)\lambda R_M}{C_{238}\lambda_F}+1\right] \qquad (1)$$

where, $$R_M = R_U + \left(\frac{N_{Th}}{N_U}\right)R_{Th} \qquad (2)$$

where, $$R_U = C_{235}A_{235} + C_{238}A_{238}\,, \qquad (3)$$

where, $$R_{Th} = A_{232} \qquad (4)$$

where λ is the ^{238}U α-decay constant; ρ_S/ρ_I is the spontaneous to induced track areal density ratio; C_{235} (C_{238}) is the ^{235}U (^{238}U) abundance in natural U; λ_F is the ^{238}U spontaneous fission decay constant; N_{Th}/N_U is the Th/U ratio of the sample; A_{235}, A_{238} and A_{232} are the number of fissions per ^{235}U, ^{238}U and ^{232}Th target nucleus, respectively. The following values for the constants of equation 1 were adopted: $\lambda = 1.55125 \times 10^{-10}\ a^{-1}$, $C_{238} = 0.99275$ and $\lambda_F = 8.46 \times 10^{-17}\ a^{-1}$. This λ_F value is in close agreement with a mean of five determinations carried out using a neutron dosimetry based on natural U thin films, $(8.35 \pm 0.24) \times 10^{-17}$ a^{-1} (Guedes et al., 2000).

The R_M values used in the present work were computed from the determinations of R_U and R_{Th}, using in equation 2 a Th/U ratio of 4.41 for Jankov Moldavite (Bouška, 1994).

The R_U values were obtained through natural U doped glasses present in the irradiations quoted above. The calibration of these glasses was carried out irradiating them together with natural U thin films (Bigazzi et al., 1999), which played the role of primary calibrators.

The R_{Th} values were obtained through Th thin films, also present in the irradiations (Bigazzi et al., 1999).

RESULTS AND DISCUSSION

Results of age determinations of Moldavites MJ1 and MJ2 from the Jankov deposit are shown in Table 1. These samples showed a certain degree of reduction of the spontaneous track size in comparison with the induced ones ($D_S/D_I < 1$). Reduced track sizes indicate that the glass suffered a certain amount of partial annealing of spontaneous tracks. In this work the Plateau Method introduced by Storzer & Poupeau (1973) was used for correcting thermally lowered ages. For applying this age correction technique, two splits from each sample – one for spontaneous track counting and the irradiated one – were heated for 24h at 350°C. This heating step produced a significant reduction of track densities. The attainment of the plateau condition – an equal revelation efficiency for spontaneous and induced tracks – is proved by the D_S/D_I ratio value that became close to 1.

Considering only the plateau age determinations of irradiation I32MD, the weighted mean of the ρ_S/ρ_I ratios is 0.422 ± 0.019. Using this value and the R_M value of Table 1, a mean plateau age of 13.31 ± 0.83 Ma is computed through equation 1.

For irradiation P4MD two thermal treatments were imposed for the plateau age determinations – 4h and 24 h at 350°C, respectively. In both cases the plateau condition was attained ($D_S/D_I \sim 1$). The weighted mean of the ρ_S/ρ_I ratios is 0.688 ± 0.043, and the corresponding mean plateau age is 14.2 ± 1.1 Ma.

Considering the mean ages of irradiations I32MD and P4MD and the ages determined through irradiations L19MD and I27MD as independent determinations, the weighted mean of these four plateau ages is 13.98 ± 0.58 Ma, with a λ^2 of 2.2 for three degrees of freedom ($p(\lambda^2) \sim 0.50$). In other words, the four independent determinations agree within experimental errors.

The mean value of the plateau FT ages of the Jankov Moldavites studied in this work agree with the mean value of 17 determinations made using the K/Ar and $^{40}Ar/^{39}Ar$ methods before 1995 (14.82 ± 0.32 Ma; Storzer et al., 1995) and with a recent datum based on several determinations on Moldavites from different sediments, including the Jankov deposit (14.37 ± 0.37 Ma, $^{40}Ar/^{39}Ar$ method; Laurenzi et al., 2001).

CONCLUSIONS

The age of the Moldavite from the Middle Pliocene deposit of Jankov determined in this work is in close agreement with the more recent independent $^{40}Ar/^{39}Ar$ determination made on Moldavites. The results of this work confirm those previously obtained through the analysis of another age standard - Durango apatite - and indicate that a neutron dosimetry based on natural U and Th thin films turns to be a reliable tool to be used for an absolute approach in FT dating.

ACKNOWLEDGEMENTS

The authors are grateful to State of São Paulo Research Foundation, FAPESP, for financial support (Proc. 00/0960-5) and the fellowships of S.G. (Proc. 01/02805-9), P.J.I. (Proc. 00/07195-1) and C.A.T.S. (Proc. 01/07937-0).

REFERENCES

Bigazzi, G.; Guedes, S.; Hadler N., J.C.; Iunes, P. J.; Oddone, M., Osorio A., A.M., Paulo, S.R.; Zúñiga, A. 1999. Potentialities and practical limitations of an absolute neutron dosimetry using thin films of uranium and thorium applied to the Fission Track Method. Radiat. Meas. 31, 651-656.

Bouška, V. 1994. Moldavites. The Czech tektites. Stylizace, Prague.

Guedes S.; Hadler N., J.C.; Iunes, P. J.; Paulo, S.R.; Zúñiga, G. A. 2000. Measurement of the spontaneous fission decay constant of ^{238}U using thin films of natural uranium as neutron dosimeters. J. Radioanal. Nucl. Chem. Letters 245, 441-442.

Hurford, A. J. 1990. Standardization of fission track dating calibration: recommendation by the Fission Track Working Group of the I.U.G.S. Subcommission on Geocronology. Chem. Geology (Isot. Geosci. Section) 80, 171-178.

Hurford, A. J. 1998. Zeta: The ultimate solution or just an interim measure? In: Advances in Fission-Track Geochronology (eds Van den Haute, P. & De Corte, F.), pp. 19-32. Kluwer Academic Publishers, Dordrecht.

Hurford, A.J. & Green, P.F. 1983. The Zeta age calibration of fission track dating. Chem. Geology (Isot. Geosci. Section) 1, 285-317.

Iunes P.J., Hadler N., J.C.; Bigazzi, G.; Tello S., C.; Guedes, O. S.; Paulo. S.R. 2002. Durango apatite fission-track dating using length-based age corretions and neutron fluence measurements by thorium thin films and natural U-doped glasses calibrated through natural uranium thin films.Chem. Geology (Isot. Geosci. Sect.),187, 201-211.

Laurenzi, M.; Bigazzi, G.; Balestrieri, M.L. 2001. $^{40}Ar/^{39}Ar$ chronology of central Europe tektites (Moldavites). Abstracts for the 64th Annual Meeting of the Meteoritical Society, Rome, 10-14 Sept. 2001. Meteoritics & Planet. Sci. 36 Supl., A109.

Storzer, D. & Poupeau, G. 1973. Ages-plateaux de minéraux et verres par la méthode des traçes de fission. Comp. Rend, Acad. Sci. Paris 276 D, 137-139.

Storzer, D.; Jessberger, E.K.; Kunz, J.; Lange, J.-M. 1995. Synopsis von Spaltspuren- und Kalium-Argon-Datierungen an Ries-Impaktgläsern und Moldaviten. Exkurs. f. u. Veröfftl. GGW 195, 79-80.

Table 1. Fission-track dating of Moldavites from the Middle Miocene deposit of Jankov. R_M is the value computed through equation (2); Heating is the thermal treatment imposed for the plateau age determination; N_S (N_I) and n_S (n_I) are the number of spontaneous (induced) counted tracks and the corresponding number of observed fields of view; P(χ^2) is the probability of obtaining λ^2 value testing induced track counts against a Poisson distribution; ρ_S (ρ_I) is the spontaneous (induced) track density; D_S / D_I is the σ[I.
* Values refer to ρ_{S+I} measurements.

Irradiation	R_M (x 10^{-9})	Sample (Heating)	N_S n_S	P(χ^2)	ρ_S (x 10^4 cm^{-2})	N_I n_I	P(χ^2)	ρ_I (x 10^4 cm^{-2})	D_S / D_I	T (Ma)
I32MD	2.65 (±4.2%)	MJ1 (no heating)	342 80	0.30	1.145 (±5.4%)	577 56	0.50	2.76 (±4.2%)	0.901 (±3.1%)	13.1±1.0 (±8.0%)
		MJ1 (24h350°C)	515 200	0.20	0.689 (±4.4%)	505 76	0.50	1.788 (±4.4%)	0.991 (±3.0%)	12.23±0.92 (±7.5%)
		MJ2 (no heating)	950 195	0.50	1.304 (±5.1%)	788 70	0.40	3.01 (±3.6%)	0.876 (±3.3%)	13.66±0.87 (±6.4%)
		MJ2 (24h350°C)	537 150	0.60	0.959 (±4.3%)	452 60	0.60	2.017 (±4.7%)	0.985 (±3.5%)	15.0±1.2 (±7.7%)
P4MD	1.733 (±4.6%)	MJ1 (4h350°C)	322 98	0.40	0.880 (±5.6%)	538* 66*	0.75*	1.30 (±8.2%)	0.985 (±3.2%)	14.0±1.5 (±10.9%)
		MJ1 (24h350°C)	497 177	0.60	0.752 (±4.5%)	835* 122*	0.75*	1.081 (±6.7%)	1.061 (±3.1%)	14.4±1.3 (±9.3%)
L19MD	0.949 (±5.2%)	MJ1 (24h350°C)	540 193	0.90	0.750 (±4.3%)	627* 133*	0.10*	0.512 (±11.5%)	1.021 (±2.5%)	16.5±2.2 (±13.4%)
I27MD	1.591 (±5.3%)	MJ1 (24h350°C)	352 127	0.40	0.742 (±5.3%)	923* 145*	0.60*	0.962 (±7.1%)	0.957 (±3.4%)	14.6±1.5 (±10.4%)

COOLING HISTORY OF THE SOUTH AMERICAN PLATFORM IN THE MANTIQUEIRA PROVINCE, SOUTHEASTERN BRAZIL: ISOTOPIC AND APATITE FISSION TRACK METHODOLOGIES

Hackspacher, P.C.[1]; Ribeiro, L.F.B.[1]; Fetter, A.H.[1]; Dantas, E.L.[2]; Hadler Neto, J.C.[3]; Tello, C.A.S.[3]; Ribeiro, M.C.S.[1]; Franco, A.O.[1] and Maia, A.O.[1]

1. Instituto de Geociências e Ciências Exatas, Unesp, P.O. Box 178, 13506-900 Rio Claro- SP, Brazil. phack@rc.unesp.br
2. Instituto de Geociências, UnB, Brasília-DF, Brazil. elton@unb.br
3. Instituto de Física, Unicamp, P.O. Box 6152, 13081-970 Campinas- SP, Brazil. hadler@ifi.unicamp.br

Keywords: Tectonothermal evolution, South American Platform

Agglutination and break–up of West-Gondwana has to be understood considering different tectonic and stabilization stages that occurred at the end of the Proterozoic and during the Phanerozoic. For that purpose parts of the South American Platform in southeastern Brazil were studied concerning the exhumation and denudation histories in the last 650 million years. This was done by obtaining thermal, tectonic and denudation histories of the Precambrian basement in three transects crossing different regions of the Ribeira and Brasília belts (Fig. 1). Geocronological and thermal data (U/Pb, Sm/Nd, K/Ar, Ar/Ar and corrected Apatite Fission Track ages) (Table 1) were used for that purpose. According the literature, available data and field observations a pre-collisional history can be considered starting at 650 Ma for the region (Hackspacher et al., 2003). Collision and lateral escape tectonics (630 and 610 Ma), associated with granithogenesis, succeed the geological evolution of the region (Hackspacher & Godoy, 1999).

U-Pb zircon and monazite ages between 610 and 595 Ma (Fig. 2) were obtained in igneous bodies associated with transpressional tectonics. The rapid exhumation was related to huge vertical displacement along shear zones (Hackspacher & Godoy, 1999) in the brittle-ductile transition zone, under greenschist grade conditions (ca. 450 to 300 °C). K-Ar ages on biotite and hornblende between 600 and 580 Ma, are also confirmed by a Sm-Nd mineral isochron.

Figure 2 shows that a regional exhumation process between 610 and 580 Ma yields cooling rates of ca. 12°C/Ma, related to collisional and escape tectonics of the Brasiliano Orogeny throughout the Mantiqueira Province, in the Ribeira and Brasília belts (Hackspacher et al., 2003). The intrusion of the Itu Granite marks the post-tectonic history. ^{40}Ar/^{39}Ar biotite ages between 560-550 Ma obtained on muscovite in paragneiss mark the end of the Neoproterozoic with the West-Gondwana agglutination and exhumation processes.

Up to that time a long stabilization phase started, with low exhumation, and cooling rate around 0.25°C/Ma. Apatite Fission Track analysis of a sample collected near Jundiaí, at the Itu-Jundiuvira Shear Zone, shows a corrected Fission Track Age of 477 Ma, and the region is interpreted as a stabilized area not affected by later denudation processes. The stabilization finished in the Mesozoic with the opening of the South Atlantic Ocean.

The three transects registered the Mesozoic Rifting Phase at 120 Ma (Tello et al., 2003) The Rifting Phase accelerated the cooling process with strong uplift of the Mantiqueira Mountain System reflecting an intense exhumation.

At the Lower Tertiary, at 65 Ma, an acceleration of the uplift and denudation affected the entire region, with reworking of the South American Surface with cooling rate of 1.5°C/Ma (Fig. 2).

The studied profiles all registered the later uplift. Corrected Fission Track ages younger than 65 Ma were registered at the Serra do Mar Mountain range with ages around 40 Ma and younger (Hackspacher et al., 2003), interpreted as the age of the origin of that mountain range, associated with lateral erosional processes causing long-term scarp retreat (Almeida & Carneiro, 1998), combined with an intense progressive denudation towards the continent of about 3 km.

The time-temperature models for the South American Platform at the Mantiqueira Province shows a similar cooling history. The assembly and break-up of the West-Gondwana are confirmed through the isotopic and corrected fission track data. Local, Phanerozoic magmatic and tectonic activities [illegible]d to be studied in detail.

ACKNOWLEDGEMENTS

This study was made possible by grants awarded by FAPESP (grant numbers 96/4403-5, 97/06544-8, 97/1397-7, 93/4550-0, 01/04420-7, 99/00358-3 and 00/03960-5) and CNPq (grant numbers 52.2388/95-7, 400490/94-3, 522386/95-4).

REFERENCES

Almeida, F.F.M. & Carneiro, C.D.R., 1998. Origem e evolução da Serra do Mar. Revista Brasileira de Geociências, v. 28 (2), pp. 135-150.

Hackspacher, P.C. & Godoy, A.M., 1999. Vertical displacement during late–collisional escape tectonics (Brasiliano Orogeny) in Ribeira Belt, São Paulo State, Brazil. Journal of African Earth Sciences, v. 29, pp. 25-32.

Hackspacher, P.C.; Fetter, A.H.; Ebert, H.D.; Janasi, V.A.; Dantas, E.L.; Oliveira, M.A.F.; Braga, I., 2003. Magmatismo cálcio-alcalino a ca 660-640 Ma no Domínio Socorro: Registros de convergência pré-colisional na aglutinação do Gondwana Ocidental Revista IG/USP. Prelo.

Hackspacher, P.C.; Ribeiro, L. F.B.; Ribeiro, M.C.S.; Fetter, A.H.; Hadler Neto, J.C.; Tello, C.E. S.; Dantas, E.L., 2003. Consolidation and breakup of the South American Platform in Southeastern Brazil: tectonothermal and Denudation Histories. Gondwana Research. Prelo.

Tello, C.A.S.; Guedes, S.; Hackspacher, P.C.; Hadler Neto, J.C.; Iunes, P.J.; Paulo, S.R.; Ribeiro, L.F.B.; 2003. Recognition of Cretaceous, Paleocene and Neogene Activities, through AFTA, in Precambrian areas of the Southeast Brazil: Association with the South Atlantic Ocean Opening. Journal S.A.E.S. 15: 765-774.

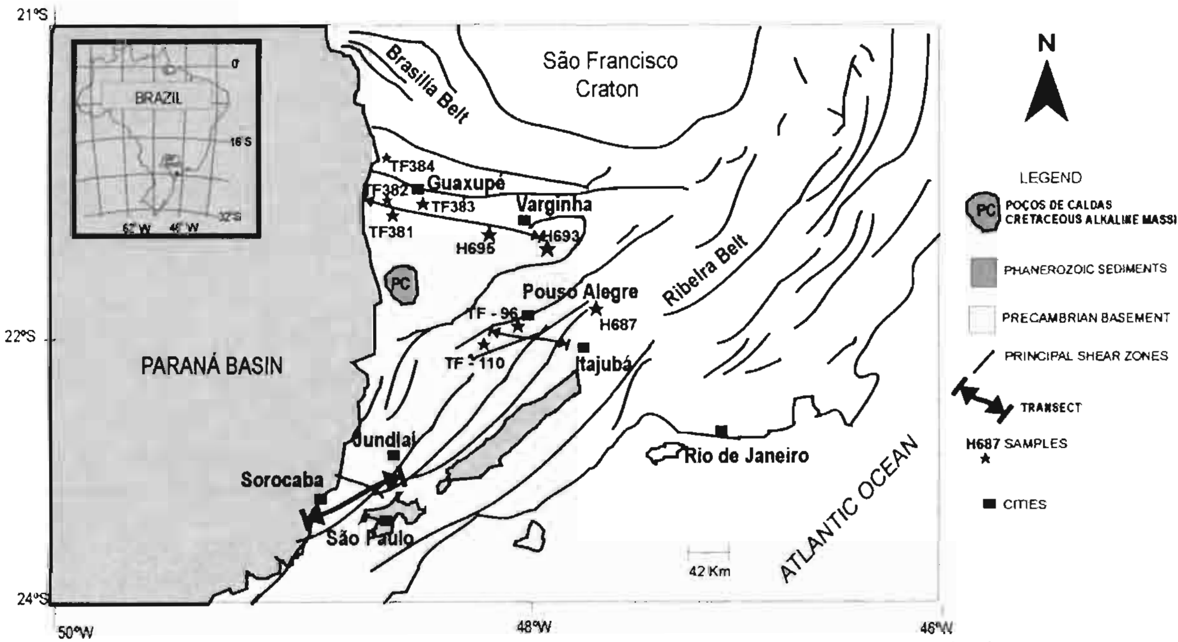

Figure 1. Sketch map of the central part of the Mantiqueira Province with location of the three transects.

Table 1. U-Pb Monazite and corrected Apatite Fission Track Data of paragneiss from the Ribeira and Brasília belts, SE Brazil.

	Samples	U/Pb monazite	Sm/Nd minerals	Ar/Ar muscovite	Ar/Ar biotite	Corrected Apatite Fission Track ages
GUAXUPÉ - VARGINHA TRANSECT	H692		590±2 Ma			
	H693a	614±6Ma				
	H693c	613±8Ma				
	H695	634±3Ma				
	TF – 381					115±10Ma
	TF – 382					93±21Ma
	TF – 383					69±14Ma
	TF - 384					118±15Ma
POUSO ALEGRE - ITAJUBÁ TRANSECT	H687b	598±7Ma		568±8Ma	523±9 Ma	
	TF –110					37±5Ma
	TF -96					86±15Ma

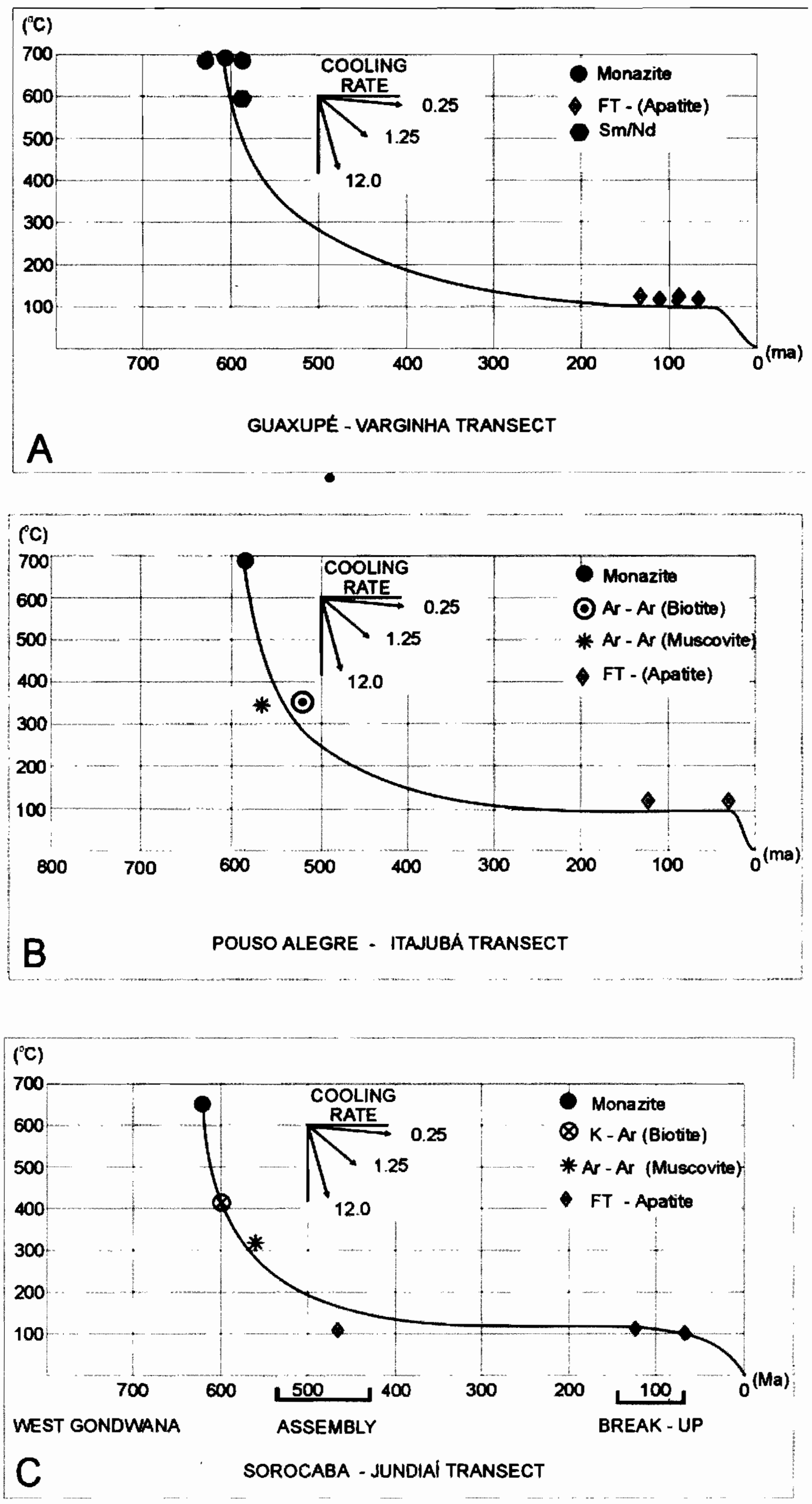

Figure 2. Temperature - time correlation diagrams of three different transects on the South American Platform using geochronological data and corrected Apatite Fission Track ages of Precambrian igneous and metamorphic rocks.

DATING BY FISSION TRACK METHOD SUBSTITUTING THE NUCLEAR REACTOR BY AN ICPMS

Hadler Neto, J.C.[1]; Iunes, P.J.[1]; Kawashita, K.[2]; Guedes, S.[1]; Tello, C.A.S.[1,4] and Paulo, S.R.[3]

1. Instituto de Fisica Gleb Wataghin, Universidade Estadual de Campinas, UNICAMP, 13083-970, Campinas – SP, Brazil. hadler@ifi.unicamp.br
2. Instituto de Geociências, UFRGS, 91509-900, Porto Alegre, RS, Brazil
3. Instituto de Ciências Exatas e da Terra, Universidade Federal do Mato Grosso, UFMT, 78070-900 Cuiabá – MT, Brazil
4. Departamento de Ciências Ambientais, Universidade do Estado de São Paulo, 19060-900 Presidente Prudente – SP, Brazil

Keywords: Fission-track dating, ICPMS

INTRODUCTION

In general, minerals contain several ppm of uranium as impurity. The most abundant of its isotopes, ^{238}U, decays by spontaneous fission. The energy of this process (~180 MeV) goes mainly to two fragments which produce a disarranged zone - the latent track - in the crystalline structure of the mineral. Latent tracks are continuously produced inside minerals. But action of temperature can lead to reconstruction of the crystalline structure near the latent tracks; this process is called annealing of the fission tracks.

If the mineral is submitted to a suitable chemical etching, latent tracks are amplified so that they can be observed at the optical microscope. By analyzing the density and lengths of the tracks it is possible to infer the "age" when tracks began to be recorded by the mineral. This age might represent the time of mineral formation, or of an event which caused annealing that erased all the fission tracks prior to it.

The spontaneous track length distribution gives information about the thermal history of minerals that is important for some geological applications. For instance, due to the fact that condition for hydrocarbons can be transformed in petroleum (temperature between ~60 to 120°C for several tens of Ma) is roughly the same as fission tracks in apatite suffer decrease in amount and length that can be easily measured, this mineral largely studied during the last two decades (Gleadow et al., 1983). Our research group has been worked in this area (Amaral et al., 1995; 1997; Bigazzi et al., 2000; Guedes et al., 1999; 2000; Hadler et al., 1993; 1995; 2001; Tello et al., 2003). Our approach is based in the methodology of the Australian School (Laslett et al., 1987) with some modifications, i. e. laboratory annealing data, software, and the grouping of samples with similar geological features.

The usual methodology of dating by FTM requires the use of a nuclear reactor where the neutron irradiation role is to determine the product of ^{238}U amount and fission track observation efficiency for the mineral. Then, in the cases where an ICPMS can determine with great precision the amount of ^{238}U a new FTM approach is possible, if the fission track observation efficiency is know.

This idea was born inside our group in the end of 2000. It is important to mention that other researchers had a similar insight independently (Cox et al., 2000; Hasebe et al., 2002; Barry Khon, personal communication). However this fact does not fade the originality and opportunity of our approach since our methodology involve the direct determination of the track observation efficiency, through neutron dosimetry by thin films of uranium and thorium.

METHODOLOGIES NOWADAYS EMPLOYED IN FTM DATING

The number of spontaneous tracks per unit area, ρ_s, depends on the age of the mineral as follows:

$$\rho_S = N_U C_{238} \frac{\lambda_F}{\lambda}\left[e^{\lambda t} - 1\right]\varepsilon_{238} \qquad [1]$$

Where: N_U is the number of uranium atoms per unit volume, C_{238} is the isotope concentration of ^{238}U in natural uranium, λ_f is the ^{238}U spontaneous fission decay constant and ε_{238} is the detection efficiency, representing the ratio between the number of spontaneous fission tracks observed in a unit surface of the mineral and the number of spontaneous fission which took place in unit volume.

To avoid the determinations of N_U and ε_{238}, the mineral is irradiated with a fluence ϕ_o of thermal neutrons. This irradiation induces fission of ^{235}U. The induced fission per unit area, ρ_I, is given by:

$$\rho_I = N_U C_{235} \sigma_0 \phi_0 \varepsilon_{235} \qquad [2]$$

where C_{235} and ε_{235} refer to ^{235}U but are analogous to C_{238} and ε_{238} defined above and σ_o is the cross section for ^{235}U fission induced by neutrons.

Assuming no annealing, spontaneous and induced efficiencies can be put equal, i. e. $\varepsilon_{238} = \varepsilon_{235}$. In this way, the age of the mineral can be obtained from equations 1 and 2:

$$t = \frac{1}{\lambda}\ln\left(1 + \frac{\lambda\sigma_0\phi_0}{\lambda_f \eta}\frac{\rho_S}{\rho_I}\right) \qquad [3]$$

Where $\eta = C_{238}/C_{238}$.

What was summarized up to here resulted from the pioneering work of Fleischer, Price and Wlaker in the beginning of the sixties (Price & Walker, 1962 a-d; 1963; Fleisher & Price 1963).

To avoid the explicit use of ϕ_o and λ_f, considered in the eighties the main source of systematic error of FTM, the majority of the researchers prefer to adopt a neutron fluence determination called Zeta calibration (Hurford & Green, 1983). In this case the neutron dosimeter is an uranium doped glass calibrated through a mineral of known age. However several fission track groups employ different approach to determine neutron dosimetry (Van den Haute et al., 1988; Iunes et al., 2002a)

PROPOSITION OF A METHODOLOGY TO SUBSTITUTE THE NUCLEAR REACTOR BY A ICPMS

It was shown above that the nuclear reactor is employed in the FTM to avoid the determinations of N_U and ε_{238}. However, the mineral age can be obtained using only the equation 1. Taking into account that $N_U C_{238}$ is the number of ^{238}U atoms per unity volume, N_{U238}, and that $\varepsilon_{235} = \varepsilon_{238}$, the mineral fission-track age can be written as

$$t = \frac{1}{\lambda}\ln\left(1+\frac{\lambda}{\lambda_f N_{U238}\,\varepsilon_{235}}\rho_S\right) \qquad [4]$$

Below, the procedures that make possible the determination of N_{U238} and ε_{235} and the age correction in case of $\varepsilon_{235} \neq \varepsilon_{238}$ are described.

DETERMINATION OF N_{U238}

In the scope of FTM, the most suitable equipment to the direct determination of N_{U238} is the laser ablation ICPMS. In this case, the measurement precision and accuracy are very high compared with other methods.

Normally, the samples to be dated through the FTM, are presented as extensive surfaces (in this case, natural glasses are the most dated) or as grains (for instance, zircon, epidote and apatite). In the case of grains, the laser ablation ICPMS makes possible the determination of N_{U238} even in grains as thick as some tens of microns (the hole in the sample is about a few microns thick).Therefore, this equipment allows the determination of ages grain-by-grain

DETERMINATION OF ε_{235}

In the equation 2, only the ^{235}U fission due to thermal neutrons were considered. However, besides uranium, the thorium can be also found as accessory in rocks. In addition, at most irradiation positions, the ^{235}U fission induced by epithermal and rapid neutrons cannot be ignored (Iunes et al., 2002).

Considering also the not well thermalized, equation 2 can be generalized to give (Iunes et al., 2002):

$$\rho_I = \xi_{235} N_U R_M \qquad [5]$$

where

$$R_M = R_U + \left(\frac{N_{Th}}{N_U}\right)R_{Th} \qquad [6]$$

where,

$$R_U = C_{235} A_{235} + C_{238} A_{238} \qquad [7]$$

and

$$R_{Th} = A_{Th} \qquad [8]$$

where R_M represents the number of fissions per uranium target nucleus in the mineral, taking also into account its thorium content ($N_U R_M$ is the total number of fission per volume unit occurred in the mineral due to the neutron irradiation), R_U represents the number of fissions per target nucleus in natural uranium, considering $^{238}U$and ^{235}U isotopic concentrations, R_{Th} is the number of fissions per target nucleus of Th-232 ($R_{Th} = A_{Th}$ because Th-232 is the only isotope of thorium), A_{235} (A_{238}) is the number of fissions per target nucleus of ^{238}U (^{235}U) that took place due to the neutron irradiation and N_{Th} / N_U is the thorium-uranium ratio in the mineral

Through equation 5, ε_{235} can be obtained if ρ_I is measured and R_M and N_U are known. N_U can be obtained from direct determinations of N_{U238}, N_{U235} and N_{U234} using an ICPMS or measuring N_{U238} via ICPMS and using the isotope concentration of ^{238}U in natural uranium as constant.

R_M can be obtained from direct determinations of R_U and R_{Th}, if the Th/U ratio of the mineral is knonw. This ratio can be found using an ICPMS and R_U and R_{Th} through thin films of uranium and thorium (Bigazzi et al., 1993; 1995; 1999).

AGE CORRECTION WHEN $\varepsilon_{235} \neq \varepsilon_{238}$

It is usual to find in nature minerals whose fossil track lengths were shortened due to their thermal history, i. e. $\varepsilon_{235} \neq \varepsilon_{238}$. In these cases their age can be corrected, in principle, using methods developed to this purpose (for instance, Bigazzi, 1967; Storzer & Wagner, 1969; Storzer & Poupeau, 1973).

In the case of apatite, it is intended to employ the size correction method via the correction curve presented in Tello (1998). Another approach that can be adopted for this mineral is based in the data set for track densities also presented Tello (1998).

CONCLUSIONS

This new methodology can represent independence of the use of nuclear reactor and, besides, it will bring an increase of the age accuracy, since the statistical errors related with neutron dosimetry and induced track count will not be propagated into the age equation.

The advantages from the practical point of view are many. For instance, concerning the quickness of this new approach, age and thermal history of a petroleum well can be obtained almost simultaneously to its drilling.

ACKNOWLEDGEMENTS

The authors are grateful to State of São Paulo Research Foundation, FAPESP, for financial support (Proc. 00/0960-5) and the fellowships of S.G. (Proc. 01/02805-9), P.J.I. (Proc. 00/07195-1) and C.A.T.S. (Proc. 01/07937-0).

REFERENCES

Amaral, G.; Born, H.; Hadler N., J. C.; Iunes, P. J.; Kawashita, K.; Machado Jr., D. L.; Oliveira, E. P.; Paulo, S. R.; Tello S., C. A. 1995. Fission track analysis of some Brazilian apatites. Radiation Measurements. 25, p. 499-502.

Amaral, G.; Born, H.; Hadler N., J. C.; Iunes, P. J.; Kawashita, K.; Machado Jr., D. L.; Oliveira, E. P.; Paulo, S. R.; Tello S., C. A. 1997. Fission track analysis from São Francisco craton and mesozoic alcaline - carbonatite complexes from central southeastern Brazil. Journal of South American Earth Science. 25, pg. 285-294.

Bigazzi, G. 1967. Length of fission tracks and age of muscovite samples. Earth and Planetary Science Letters, 3, 434 – 438.

Bigazzi, G., J.C.Hadler N., P.J.Iunes e S.R. Paulo, 1993. Mineral dating by Fission Track Method: Neutron dosimetry by thin film of natural uranium. Revista de Fisica Aplicada e Instrumentação, 8 , 13-23.

Bigazzi, G., J.C.Hadler N., P.J.Iunes, T.C.W.P. Mello, L.M.S. Navia,S.R. Paulo; A.R.Zuniga G., 1995. Employment of thim thorium films in fission track neutron dosimetry. Brazilian Journal of Physics, 25 ,246-251.

Bigazzi, G.; Guedes, O.S.; J.C.Hadler N., P.J.Iunes, M.Oddone, A.M. Osorio A., S.R.Paulo e A.Zúñiga G., 1999. Potentialities and practical limitations of na absolute neutron dosimetry using thin films of uranium and thorium applied to the fission track method. Radiation Measurements, 31, 651-656.

Bigazzi, G.; Guedes, S.; Hadler N., J. C.; Iunes, P. J.; Paulo, S. R.; Tello S., C. A., 2000. Application of neutron dosimetry by natural Uranium an Thorium thin films in fission track dating. 9th International Conference on Fission Track Dating and Thermochronology. pg. 33-35.

Cox, R.; Kosler Jan, Sylvester, P.; Hodych J. 2000. Apatite Fission-Track (FT) Dating by LAM-IO-MS Analysis. Journal of Conference Abstracts, Goldschmidt 2000, An International Conference for Geochemistry. Cambbridge Publications. Volume 5(2), 322.

Fleischer, R. L.; Price, P. B. 1963. Charged particle tracks in glass. J. Appl. Phys., 34, 2903-2904.

Gleadow, A. J. W.; Duddy, I. R.; Lovering; J. F. 1983. Fission track analysis: a new tool for the evaluation of thermal histories and hydrocabon potential. Austral. Petrol. Expl. Ass. J., 23, 93-102 .

Guedes, S.; Hackspacher, P.; Hadler N., J. C.;Iunes, P. J.; Machado, D. L.; Paulo, S. R.; Ribeiro, L. F. B.; Tello S., C. A. 1999. Thermal history by fission track analysis of Serra Negra, Salitre, Catalão II and Tapira carbonatite complexes, Brazil: methodological study. First Latin American Symposium on Nuclear Tracks and its Aplications in Physics, Health, Enviromental Studies and Industry., Caracas, Venezuela, pg. 9.

Guedes, S.; Hadler N., J. C.; Iunes, P. J.; Paulo, S. R.; Zuñiga, A. 2000. The spontaneous fission decay constant of ^{238}U using SSNTD. Journal of Radioanalytical and Nuclear Chemistry, 245: 441-442.

Hadler N., J. C.; Iunes, P.J.; Oliveira, E.P.; Osorio A., A.M.; Paulo, S.R.; Tello S. C.A. 1993. Thermal History of Copper- Bearing Rocks from the Caraiba Mine, Brazil: Preliminary Results from Fission Track Analysis. 3rd. International Congress of the Brazilian Geophysical Society, Rio de Janeiro (Brazil), 7-11 Nov. Expanded abstracts, Vol. 2, 845-850.

Hadler N., J. C.; Iunes, P. J.; Paulo, S. R.; Tello S., C. A. 1995. Obtainment of thermal histories for sets of geologically compatible localities by using apatite fission track analysis. Revista de Física Aplicada e Instrumentação. 10: 1-10.

Hadler N., J. C.; Paulo, S. R.; Iunes, P. J.; Tello S., C. A.; Balestrieri, M. L.; Bigazzi, G.; Curvo, E. A. C.; Hackspacher, P. 2001. A PC compatible Brazilian software for obtaining thermal histories using apatite fission track analysis. Radiation Measurements. 34: 149-154.

Hasebe, N.; Barbarand, J.; Jarvis, K.; Carter, A.; Hurford, T. 2002. Can FT ages be derived using LA-ICP-MS?. Geochimica et Cosmochimica Acta, Journal of the Geochimical Society, Special Suplement, Abstracts of the 12th Annual V.M. Goldschmidt Conference, Davos, Switzerland.

Hurford, A. J.; P. F. Green., 1983. The zeta age calibration of fission track dating. Chemical Geology (Isotope Geoscience Section), 1, 285-317.

Iunes, P. J.; Hadler N., J. C.; Bigazzi, G.; Tello S., C. A.; Guedes O, S.; Paulo, S. R. 2002. Durango apatite fission-track dating using length-based age corrections and neutron fluence measurements by natural thorium thin films and natural U-doped glasses calibrated through natural uranium thin films. Chemical Geology, 187: 201-211.

Laslett, G. M.; Green, P. F.; Duddy, I. R.; Gleadow, A. J. W. 1987. Thermal annealing of fission tracks in apatite: 2. A quantitative analysis. Chem. Geol. (Isot. Geosci. Sect.), 65: 1-13.

Price, P. B.; Walker, R. M. 1962a. A new detector for heavy particle studies. Phys. Lett., 3: 113-115 .

Price, P. B.; Walker, R. M. 1962b. Observations of charged-particle tracks in solids. J. Appl. Phys, 33: 3400-3406.

Price, P. B.; Walker, R. M. 1962c. Chemical etching of charged-particle tracks in solids. J. Appl. Phys, 33: 3407-3412.

Price, P. B.; Walker, R. M. 1962d. Observation of fossil particle tracks in natural micas. Nature, 196: 732-734.

Price, P. B.; Walker, R. M. 1963. Fossil tracks of charged particles in mica and the age of minerals. J. Geophys. Res., 68: 4847-4862.

Storzer, D., G. A. Wagner, 1969. Correction of thermaly lowered fission tracks ages of tektites. Earth and Planetary Science Letters, 5 , 463-468.

Storzer, D., G. Poupeau, 1973. Ages-plateaux de minéraux et verres par la méthode des traçes de fission. Comp. Rend. Acad. Sci. Paris, 276 D, 137-139.

Tello S., C.A. 1998. Estudo do annealing de traços de fissão em apatitas, tanto em seções basais como em seções sem orientação preferencial, a partir do comprimento e da densidade de traços de fissão. Tese de doutorado, Universidade Estadual de Campinas. Campinas-SP, Brasil., 93 pp.

Tello S., C.A., P. Hackspacher, J.C. Hadler N., P.J. Iunes, S. Guedes O., S.R. Paulo and L.F. Ribeiro B. 2003. Recognition of Cretaceus, Paleocene and Neogene Tectonic Reactivation, through Apatite Fission-Track Analysis, in Precambrian areas of the Southeast Brazil: Association with the South Atlantic Ocean Opening. Journal of South American Earth Science, 15, 765-774.

Van den haute, P., R. Jonckheere e F. De Corte, 1988. Thermal neutron dosimetry for fission track dating with metal activation monitors: A reinvestigation. Chemical Geology (Isotope Geoscience Section), 731, 233-244.

Pb ISOTOPIC COMPOSITION IN WEATHERING PROFILES FROM BASIC ROCKS, SOUTHERN BRAZIL

Koester E.[1]; Oliveira L. D.[2]; Conceição R.V.[1,3]; Schenato F.[4]; Trevisan L.F.[5]; Gollmann K.[5] and Kawashita K.[1]

1. Laboratório de Geologia Isotópica, IG, UFRGS, Brazil. koester@ufrgs.br
2. Programa de Pós-Graduação em Geociências , CAPES, IG, UFRGS, Brazil. leondres.oliveira@ufrgs.br
3. Departamento de Geologia, IG, UFRGS, Brazil. rommulo.conceicao@ufrgs.br
4. Universidade Luterana do Brasil, ULBRA, Brazil
5. Programa de Bolsa de Iniciação Científica - CNPq, Universidade Federal do Rio Grande do Sul, Brazil

Keywords: Soil, lead, Pb isotopes, weathering, basic rocks

INTRODUCTION

The isotopic geology has been used as the main tool in the study of pedogenetic process (e.g. soil generation rates), as well as age of different mechanisms in earth crust. Researches utilising Pb isotopic composition changes in natural soil have focused on tracing anthropogenic Pb (Erel et al., 1997; Semlali et al., 2000, 2001), as well as estimaties of soil ages (Erel et al., 1994; Harlavan et al., 1997).

The main purpose of this paper is to present a preliminary study of Pb isotopic ratios in soil profile from basalt and gabbro rocks. Weathering of basalt and gabbro in northern Rio Grande do Sul, Brazil results in the formation of well-developed soils. The basalt is typical of the basic rocks of the Serra Geral Formation, and the gabbro is related to Lomba Grande Basic Complex. Both are Mesozoic magmatic components of the Paraná Basin. In order to study the changes of the Pb isotopic composition, three profiles were selected and different horizons were analysed.

The Parana Basin is located at the centre and south of South America. An extensive volcanic pile named Serra Geral Formation covers around 75% of the Devonian-Triassic sedimentary rocks. The mean thickness of the volcanics over the whole basin is about 350 m, and about 1,000 m are present in the sampled area. The Serra Geral Formation is represented by different rock-types, i.e. tholeiitic basalts, tholeiitic andesites, rhyodacites-rhyolites (Melfi et al., 1988). These basaltic flows are covered by, or intercalated with acids flows, and have an age around 130 Ma (Renne et al., 1992; Ernesto et al., 1999). Geochemical characteristics define three main groups according to their TiO_2 content (high and intermediate $\geq$ 2% TiO_2 and low $\leq$ 2% TiO_2) (Montovani et al., 1988). There is an intrusive magmatism related to the flood volcanism of the Paraná basin, essentially basaltic in composition. These intrusions occur in the pre-volcanic sediments and have thickness ranging from few to hundred meters. They also are contemporaneously to volcanic activity.

The studied weathering profiles correspond to three sampling station located in two distinct regions. The first region, in which two sampling station were described (A and B), is located in Gravataí District, and is represented by olivine-gabbro of Lomba Grande Basic Complex. The olivine-gabbro is characterised by aphanitic groundmass and olivine + clinopyroxene mega-crystals. According Viero & Roisenberg (1992), it has high MgO, Cr, Ni, and Co concentrations and low K, Rb, Ba, Zr, REE concentrations. The REE pattern is similar to the P-MORB and the K-Ar ages are 160 Ma, interpreted as crystallisation age. The second region is located in Três Forquilhas River valley, a volcanic sequence of Serra Geral Formation. The volcanic rocks are basics in its base end acids in its top (Jesus, 2002). The studied volcanic sequence is constituted of microporphyritic basalts with zeolites as amigdales, plagioclase, olivine and pyroxene. The soils are composed of carbonate and silicate minerals (kaolinite-smectite clays, quartz, plagioclase, pyroxene and olivine) oxide and organic matter.

ANALYTICAL METHODS AND RESULTS

At the sampling stations A and B three soil samples were taken from different depths, as well as, respective rock samples. At the sampling station C it were taken five soil samples beyond four rock samples. The soil of A and B stations consist of well-developed “Argissolo” profiles, moreover the C station consist of “Cambissolo” profile, according Soil Map of Rio Grande do Sul (Streck et al., 2002).

In station A and B, one sample was taken from A-Horizon, B-Horizon, and C-Horizon. At the station A and B the uppermost leached part of the soil, the A-Horizon, is generally c.a. 10 cm thick, characterised by organic matter enrichment. The B-Horizon is characterised by red colour and more fine texture, and was c.a. 40-60 cm thick. The C-Horizon is undisturbed original soil characterized by red colour and unconsolidated material, and was c.a. 40-70 cm thick.

At the station C, the A-Horizon, rich in organic matter, is generally c.a. 10 cm thick, the E-horizont has sand texture and was c.a. 40-50 cm. B-Horizon is characterised by red colour and clay texture, and has c.a. 60-70 cm thick. The C-Horizon is undisturbed original soil characterized by red colour and is c.a. 80-120 cm thick. In station C, one sample was taken from the A-Horizon, E-Horizon, B-Horizon, B-C-Horizon limit, C-Horizon, two samples of weathered rock, one of fresh-basalt and one of fresh-basalt with amigdales.

The soil samples were dried, hand desegregated and quarted. A fraction of this material was used for analyses as whole-soil (W.S). Other fraction was sieved in order to obtain a material with particle size < 2 µm (A.F.). X-Ray diffraction analyses were performed in all material. The rock samples were milled to powder. The Pb isotopic compositions were measured using a multi-collector VG SECTOR 54 mass spectrometer at the LGI, Universidade Federal do Rio Grande do Sul. Samples were completely digested in a combination of HNO_3, HCl, and HF, and Pb was separated using anion exchange columns and HBr 0,6N. Lead isotopic rations were corrected for mass fractionation using Pb/Pb = 0.01%.

Soil, rock and clay fraction (A.F), isotopic data analysed in this study are shown in Table 1. The ^{206}Pb/^{204}Pb and ^{208}Pb/^{204}Pb of whole soils and rocks of A, B and C stations *versus* the horizon code, (1 = A-Horizon, 2 = E-Horizon, 3 = B-Horizon, 4 = B+C-Horizon, 5 = C-Horizon, 6 = Weathered Rock, and 7 = Unweathered Rock) are shown in the Figure 1. The Figure 2 shows the ^{206}Pb/^{204}Pb and ^{208}Pb/^{204}Pb of fration clay *versus* horizons code. The Table 2 shows the mineralogical composition of the samples, by X-Ray diffraction analysis, with qualitative results.

The whole soil of A-station shows Pb isotopic ratios enrichment with decreasing depth (Fig. 1), which probably reflects the increasing of weathering. This linear behaviour is indicative of exogenous Pb incorporation in the horizons, decreasing with soil depth. Semlali et al. (2000), studying of lead isotopes in soils, attributed this behaviour to the incorporation of exogenous Pb. The Pb isotopic ratios of the whole soil and rocks of B station remain constant throughout the profile (Fig. 1), from the rock (the parent material), to the upper horizon. Harlavan et al. (1998), studying soils from glacial granitic terrains, attributed the isotopic constancy to the parent material.

Despite of the same lithologic composition of the rock that generated the weathering profile, the different isotopic behaviour in the A and B stations can be explained through the different levels of weathering that is higher in A station and lower in the B station. This is shown in the mineralogical composition (Table 2) of C-Horizons that reflects the stronger parental material in B station compared to A station.

In the isotopic data of < 2 µm fration (Table 1, Fig. 2), the behaviour is similar between A and B profile, which show the decreasing of the isotopic ratios of C-Horizons to B-Horizons and enrichment from rock to B horizon. This behaviour is related to the Fe-oxide and clay mineral concentration in this fraction however there is not connection between isotopic ratios and Fe-oxide and clay mineral ratios. The finest fraction of A and B station, that containg more secundary constituints, exhibit the highest isotopic values than whole soil.

The isotopic variation in the whole-soil fraction of C station is shown in Figure 1. There is an enrichment of Pb ratios from rock (7) to weathered rock 2 (6), following a smoth enrichment to C, C+B, and B horizons. This enrichment is related to the formation of clay minerals and quartz concentration. The decreasing of Pb ratio from B-Horizon to E-Horizon and increasing to A-Horizon can be explain by increasing plagioclase in E-horizon and decreasing of claymineral related to eluvion process in this horizon.

Table 1. Isotopic composition of lead in whole soil (W.S.), fraction < 2µm (A-F), and rock samples of three station. (W.R. Weathered Rock, Unc. uncertainties).

	Deph m.	Code	^{206}Pb/^{204}Pb	Unc.(±)	^{208}Pb/^{204}Pb	Unc.(±)
Station A						
WS- A	0.40	1	18.642	0.062	38.749	0.126
WS- B	1.40	3	18.510	0.003	38.527	0.005
WS C	2.70	5	18.272	0.004	38.201	0.008
AF- A	0.40	1	18.588	0.015	38.757	0.034
AF- B	1.40	3	18.452	0.004	38.560	0.007
AF- C	2.70	5	18.883	0.004	38.738	0.008
Gabbro	3.20	7	18.220	0.003	38.251	0.006
Station B						
WS- A	0.35	1	18.367	0.003	38.354	0.007
WS- B	1.60	3	18.385	0.004	38.373	0.008
WS C	2.40	5	18.362	0.011	38.408	0.024
AF- A	0.35	1	18.625	0.003	38.820	0.007
AF- B	1.60	3	18.639	0.003	38.826	0.007
AF- C	2.40	5	18.681	0.003	38.984	0.007
Gabbro	3.00	7	18.380	0.010	38.443	0.020
Station C						
WS- A	0.05	1	18.748	0.007	39.064	0.022
WS- E	0.40	2	18.604	0.005	38.872	0.011
WS- B	0.90	3	18.694	0.003	38.896	0.007
WS- B+C	1.30	4	18.646	0.003	38.842	0.005
WS C	1.90	5	18.635	0.006	38.803	0.013
W. R. 1	2.20	6	18.322	0.004	38.324	0.008
W. R. 2	2.30	6	18.621	0.004	38.823	0.009
AF- A	0.05	1	18.463	0.006	38.560	0.012
AF- E	0.40	2	18.411	0.003	38.456	0.007
AF- B	0.90	3	18.370	0.005	38.329	0.011
AF- B+C	1.30	4	18.497	0.004	38.536	0.008
AF- C	1.90	5	18.547	0.008	38.845	0.017
AF- W.R. 1	2.20	6	18.169	0.003	38.181	0.006
AF- W.R. 2	2.30	6	17.906	0.003	37.806	0.007
Basalt	2.50	7	18.508	0.004	38.771	0.009
Amigdales	2.50	7	18.506	0.003	38.179	0.006

The amigdales ^{208}Pb/^{204}Pb isotopic composition is smaller than basalt composition, which shows that there was an interation of different isotopic composition fluids during the amigdales generation process.

The enrichment of Pb ratios from weathered rock 2 to weathered rock 1 at the C station (Table 1) probably can be explained by the decresing of quartz concentration.

The < 2 µm fraction isotopic data of C station (Fig. 2; Table 1) show a similar behaviour to A and B stations. A sequence of increasing-decreasing-increasing isotopic ratio is observed from rock to C-Horizon, C- to B-Horizons, and B to A-Horizons. This behaviour is also related to the Fe-oxide and claymineral concentration present in this fraction.

The results of this preliminary study show that Pb ratio is usefull tool to determinate same weathering process.

REFERENCES:

Erel, Y., 1997. Tracing the transport of antropogênic lead in the atmosphere and in soils using isotopic rations.

Ernesto, M.; Raposo, M.I.B.; Marques, L.S.; Renne, P.R.; Diogo, L.A.; De Min, A., 1999. Paleomagnetism, geochemistry and 40Ar/39Ar dating of the north-eastern Paraná Magmatic Province: tectonic implications. J. Geodyn. 28:321–340.

Harlavan, Y.; Erel, Y.; Blum, J.D., 1998. Systematic changes in lead isotopic composition with soil age in glacial terrains. Geochimica et Cosmochimica Acta, 62(1): 33-46. Jesus, C.M. 2002. Os Derrames Basálticos do Vale do Rio Três Forquilhas. Trabalho de Conclusão do Curso de Geologia. Instituto de Geociências, UFRGS. Porto Alegre, 129 p.

Melfi, A.J.; Piccirillo, E.M.; Nardy, A.J.R., 1998. Geological and magmatic aspects of the Paraná Basin – an introduction. In: The Mesosoic flood volcanism of the Paraná Basin: petrogenetic and geophysical aspects. Ed. E. M. Piccirilo and A.J. Melfi. São Paulo, Universidade de São Paulo, 600p.

Montovani, M.S.M.; Peate, D.W.; Hawkesworth, C.J., 1998. Geochemical stratigraphy of Paraná Continental Flood Basalts: 'A contribution from borehole samples. In: The Mesosoic flood volcanism of the Paraná Basin: petrogenetic and geophysical aspects. Ed. E. M. Piccirilo and A.J. Melfi. São Paulo, Universidade de São Paulo, 600p.

Renne, P.R.; Ernesto, M.; Pacca, I.G.; Coe, R.S.; Gler, J.M.; Prévot, M.; Perrin, M., 1992. The age of Parana flood volcanism, rifting of Gondwanaland, and the Jurassic–Cretaceous boundary. Science 258, 975–979.

Semlali, R.M; Van Oort, F.; Loubet, M.; Denaix, L., 2000. La composition isotopique du plomb: un outil privilégié pour l'estimation de la distribution du plomb anthropique et naturel dans les sols. Sciences de la Terre et des planétes, 331: 595-600.

Semlali, R.M; Van Oort, F.; Denaix, L.; Loubet, M., 2001. Estimating Distributions of Endogenous and Exogenous Pb in Soils by using Pb Isotopic Ratios. Environment Scienci Technology, 35: 4180-4188.

Streck E.V.; Kämpf, N.; Dalmolin, R.S.D.; Klamt, E.; Nascimento, P.C.; Schneider, P., 2002. Solos do Rio Grande do Sul. Porto Alegre, EMATER/RS, Editora da UFRGS. 107 p.

Viero, A.P. & Roisemberg, A., 1992. Petrologia e Geoquimica do Complexo Básico de Lomba grande, RS. Pesquisas, 19(1): 41-52.

Table 2. Mineralogical composition (%) in whole soil (W.S.), fraction < 2µm (A-F), and rock samples of three station. (We. Weathered, Unc. Uncertainties, Plg = plagioclase, Olv = olivine, Prx = pyroxene, Ghot = ghoethite, Qtz = quartz, Mag = magnetite, Sme = smectite, Zeol = zeolite, Calc = calcite).

	Depth (m)	Code	Plg.	Olv.	Prx	Ghot.	Hemt.	Caul.	Qtz	Mag.	Sme.	Zeol.	Calc.
Station A													
WS- A	0.40	1	0	0	0	0	12	24	64	0	0	0	0
WS- B	1.40	3	0	0	0	45	22	33	0	0	0	0	0
WS C	2.70	5	43	0	0	0	0	57	0	0	0	0	0
AF- A	0.40	1	0	0	0	26	20	54	0	0	0	0	0
AF- B	1.40	3	0	0	0	0	15	85	0	0	0	0	0
AF- C	2.70	5	0	0	0	35	0	65	0	0	0	0	0
Gabbro	3.20	7	60	16	24	0	0	0	0	0	0	0	0
Station B													
WS- A	0.35	1	0	0	0	29	0	22	38	11	0	0	0
WS- B	1.60	3	0	0	0	40	0	24	0	0	36	0	0
WS C	2.40	5	24	29	19	0	0	12	0	0	16	0	0
AF- A	0.35	1	0	0	0	35	0	29	0	0	0	0	0
AF- B	1.60	3	0	0	0	48	0	52	0	0	0	0	0
AF- C	2.40	5	0	0	0	29	0	47	0	0	24	0	0
Gabbro	3.00	7	53	23	19	0	0	5	0	0	0	0	0
Station C													
WS- A	0.05	1	20	0	0	0	9	10	41	0	20	0	0
WS- E	0.40	2	43	0	0	0	8	16	14	0	19	0	0
WS- B	0.90	3	34	0	0	0	8	23	15	0	20	0	0
WS- B+C	1.30	4	32	0	0	0	0	21	16	0	31	0	0
WS C	1.90	5	18	0	0	0	0	24	39	0	19	0	0
W. R. 1	2.20	6	34	0	22	0	0	14	0	0	19	11	0
W. R. 2	2.30	6	33	0	0	0	0	28	0	0	39	0	0
AF- A	0.05	1	20	0	0	0	8	11	47	0	14	0	0
AF- E	0.40	2	9	0	0	0	0	23	55	0	13	0	0
AF- B	0.90	3	0	0	0	0	0	26	38	0	36	0	0
AF- B+C	1.30	4	0	0	0	0	0	35	25	0	40	0	0
AF- C	1.90	5	0	0	0	0	0	46	0	0	54	0	0
AF- W.R. 1	2.20	6	0	0	0	0	0	42	0	0	58	0	0
AF- W.R. 2	2.30	6	0	0	0	0	0	25	21	0	54	0	0
Basalt	2.50	7	49	0	33	0	0	0	0	0	11	7	0
Amigdales	2.50	7	0	0	8	0	0	0	32	0	0	51	9

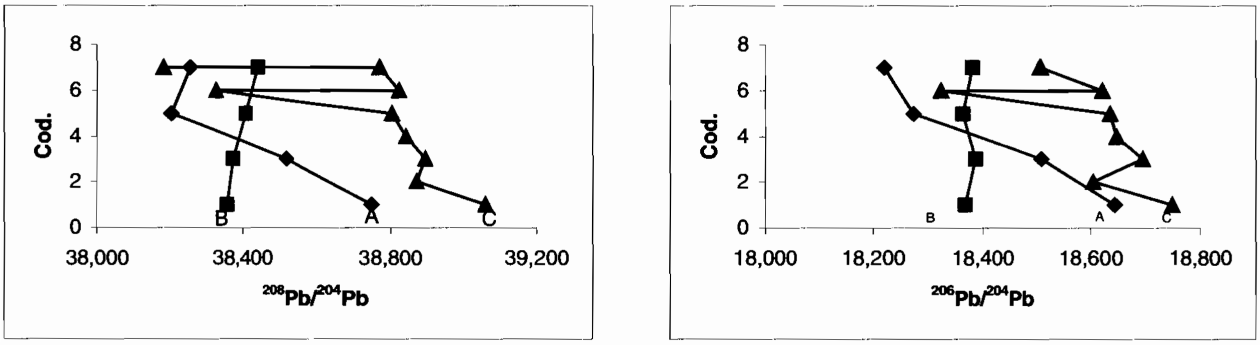

Figure 1. Isotopic composition of ^{206}Pb/^{204}Pb and ^{208}Pb/^{204}Pb, in the profile soil and rocks from three station (the diamonds are A station, the rectangle is B station, and the triangle is C station).

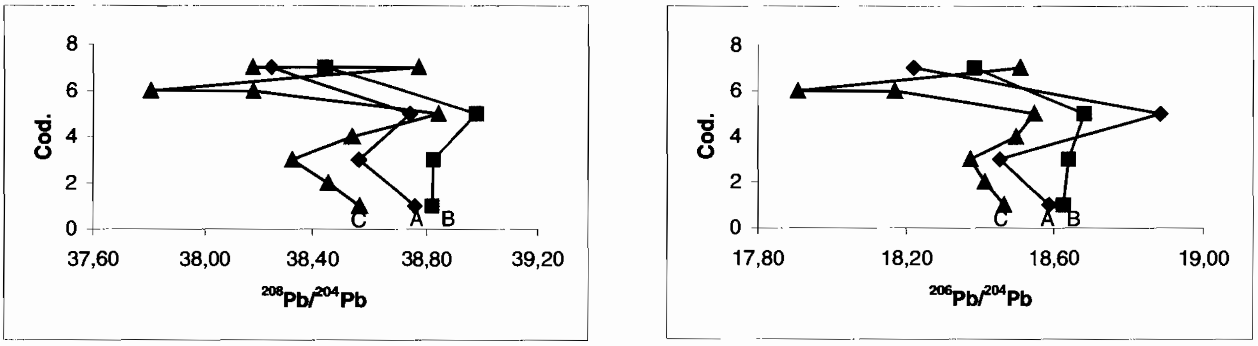

Figure 2. Isotopic composition of ^{206}Pb/^{204}Pb and ^{208}Pb/^{204}Pb, in fraction < 2μm from three station (the diamonds is A station, the rectangle is B station, and the triangle is C station).

URANIUM – LEAD TECHNIQUE ON APATITE AND RUTILE AT THE LABORATORY OF ISOTOPE GEOLOGY - PARÁ-ISO, BELÉM: APPLICATION TO KIMBERLITE DATING

Krymsky, R.S.[1]; Lafon J.M.[1]; Delor, C.[2] and Milési J.P.[2]

1. Universidade Federal do Pará, CG, Laboratório Pará-Iso, Av. Augusto Corrêa, 01, Belém 66075-900, Brazil. krymski@ufpa.br
2. Bureau de Recherche Géologiuqes et Minières, BP 6009, 45060, Orléans, France

Keywords: U-Pb, kimberlite, apatite, rutile

INTRODUCTION

We describe the experimental procedure in use at the Laboratory of Isotope Geology (Pará-Iso) of the Federal University of Pará, at Belém for the U-Pb dating of accessory minerals like apatite and rutile, based on methods developed such as Parrish et al. (1987) and Tera & Wasserburg (1975), respectively and adapted to our laboratory conditions. Examples of application of U-Pb dating on apatites and rutiles from the kimberlites are also presented.

ANALYTICAL TECHNIQUE

DIGESTION AND SPIKING

The selected single grains of apatite and rutile and multigrain fractions of rutile, after being previously photographed, were transferred to small PTFE Teflon beakers. The apatite grains were washed in bi-distilled methanol in an ultrasonic bath (20 min) and rinsed 3 times with pure water. The rutile grains were cleaned in bi-distilled methanol (20 min), followed by hot (70°C) 3N HCl (20 min), both in the ultrasonic bath, and rinsed 3 times with pure water. After drying, the samples were weighed in aluminum foil boats using microbalance and loaded in PFA Teflon Savillex microcapsules.

For analysis of 0.05 – 0.5 mg of rutile we added to each microcapsule and weighed on the same microbalance 2–5 µl of ^{235}U-^{205}Pb spike from the geochronological laboratory of the University of Brasília. For apatite analysis, 0.07-0.23 mg of sample were mixed with 1 µl of "IPGG" ^{235}U-^{208}Pb spike after apatite dissolution and aliquoting. The ^{235}U-^{208}Pb spike was used for apatite analyses because ^{235}U-^{205}Pb spike was not available at that time

Rutile digestion was performed in Ludwig design microcapsules with 30 µl of hydrofluoric acid. A set of 12 microcapsules was arranged in a 120-ml PTFE Teflon bomb enclosed in a stainless steel jacket Model 4748, Parr Instrument, following the method outlined by Parrish (1987). 5 ml of HF was added into the PTFE liner and the whole assembly was closed and heated during 24 h in an oven at 240–245°C. The complete dissolution of the rutile was checked under a binocular microscope and the sample solutions evaporated to dryness. Then the fluoride salts were digested overnight at 200°C with 3 N HCl, 30-60 µl in the capsules and 5 ml in the liner.

For apatite digestion we used Parrish design PFA Teflon Savillex microcapsules filled with 60 µl of a mixture of 6N HCl + 14N HNO_3 during 6 hours on a hot plate at 100°C.

LEAD AND URANIUM SEPARATION

For analyses of single crystals of apatite and rutile we used a miniaturized and modified procedure after the method of Parrish et al. (1987), which is based on classical technique by Krogh (1973). We used hand-made shrinkable Teflon micro-columns with an internal diameter of 1.8 mm and 11 mm height, with reservoir for 1.5 ml (diameter = 6 mm). The columns were filled with 40 µl of previously washed Dowex® AG1x8 200-400 mesh resin. When new, the columns with resin were washed 20-40 times with 6N HCl and H_2O, alternately. Between each sample separation, columns were washed 8-10 times with 6N HCl and H_2O. For counting the volume of acid, we used 30 ml Nalgene™ drop-dispensers for which one drop corresponds to about 30 µl. The sequence of element separation with micro-column is the following: a) Resin media equilibration: 2x3 drops of 3N HCl; b) Loading 3N HCl sample solution; c) Sample washing: 1+2+2 drops of 3N HCl; d) Pb Elution: 10 drops of 6N HCl (collection in PFA Teflon 3 ml beaker); e) U Elution: 10 drops of H_2O (collection in the same beaker as Pb); f) Addition of 5 µl of a silica gel + H_3PO_4 mixture in beaker and evaporation.

For analyses of 0.1– 2 mg of multigrain fraction of rutile, we used the technique proposed by Terra and Wasserburg (1975), with modification. The chloride solution was evaporated, 10 µl of concentrated HBr were added and evaporated again. After addition of 3-5 drops of 0.6N HBr, the HBr solution was heated in closed microcapsule on hot plate at 100°C, passed 20 min in ultrasonic bath and centrifuged.

The separation sequence for Pb was the following: a) Resin media equilibration: 2x3 drops of 0.6 N HBr; b) Loading 0.6 N HBr sample solution / collecting solution 1; c) Sample washing with 2+2+2+10 drops of 0.6N HBr / collecting solution 1; d) Elution of Pb with 10 drops of 6N HCl (collection in PFA Teflon 3 ml beaker); e) Addition of 5 µl of a silica gel – H_3PO_4 mixture in beaker with Pb and evaporation.

Uranium can be separated from solution 1 by the same method as mentioned for apatite separation in HCl and H_2O or by the following HNO_3 technique: a) Evaporation of the solution 1, conversion to nitrate by 2 drops 14N HNO_3, evaporation; b) Addition of 5 drops of 7N HNO_3, transfer to microcapsule, heating during 30 min at 100°C, centrifugation; c) Washing of the column 3 times with H_2O and 6N HCl; d) Resin equilibration with 3x5 drops of 7N HNO_3; e) Loading 7N HNO_3 sample solution; f) Sample washing with 2+2+2+4 drops of 7N

HNO_3; g) Elution of U: 15 drops of 0.25N HNO_3 (collection in PFA Teflon 3 ml beaker); h) Addition of 3 μl of silica gel – H_3PO_4 mixture in beaker with U and evaporation.

MASS SPECTROMETRY

Isotopic compositions of Pb and U are measured on a Finnigan MAT 262 variable multicollector mass spectrometer equipped with 7 Faraday cups and 1 ion counter (IC). The lead-uranium fraction mixed with the silica gel – phosphoric acid solution is loaded in HEPA air environment to a single degassed rhenium filament. For sample transference to the filament it 1 μl of pure water is used. Then the filament is heated slowly from 0.7 to 2.2 A until it glows pink.

The Pb analyses were carried out in static mode on Faraday cups (^{206}Pb, ^{207}Pb ^{208}Pb) and IC (^{204}Pb). In case of low signal of Pb, the measurements by IC are run in peak jumping mode. The filament with sample is heated during 10 min and analyzed at a temperature interval of 1400 - 1500°C with maximum of signal at 1470°C. The total time required for collection of 5 blocks of data is about 30 min. The mass fractionation correction for lead is 0.12 ± 0.01 % a.m.u.$^{-1}$ calculated from 25 analyses of NBS 982 standard.

The U was analyzed as UO_2 just after lead measurement from the same filament. Depending on the signal level, UO_2 was analyzed either in static mode on Faraday cups or in peak jumping mode on IC. The initial temperature for UO_2 measurement is 1500 - 1530°C and maximum temperature is 1570°C. The acquisition time for 3 blocks is about 15 min. The mass fractionation correction for UO_2 was not applied because of its insignificant small value (~ 0.002 - 0.03 % a.m.u.$^{-1}$) determined from NBS-500 analyses.

DATA PROCESSING

The initial statistical data reduction is performed by the custom made laboratory software "Finres2" by Dr Thomas Scheller. This program calculates the measured isotope ratios and their 2σ errors. The data is entered to a PbDat-compatible format file. After that the data set is processed by the PbDat (version 1.24) program (Ludwig, 1993), which produced Pb/U and Pb/Pb isotope ratios corrected for blanks and common lead. Finally the data are processed by the Isoplot for Excel program (Isoplot/Ex version 2.49e - Ludwig, 2001) and plotted in the Concordia diagram.

The common lead correction for apatite samples was made by taking initial $^{206}Pb/^{204}Pb$ and $^{207}Pb/^{204}Pb$ ratios from U-Pb isochrons. The common Pb correction for rutile samples was carried out with using Stacey-Kramers (1987) model for t = 0 Ma.

BLANKS

The total blanks (digestion, U-Pb separation and loading) for $HCl-H_2O$ chemistry are 20-30 pg for Pb and 0.1-0.5 pg for U. For $HBr-HCl-HNO_3$, chemistry total blanks are 60 pg (Pb) and 0.1 pg (U). The blanks of filament loading procedure are 2 pg for Pb and < 0.1 pg for U.

APPLICATION TO KIMBERLITE GEOCHRONOLOGY

The U-Pb systematic of zircon is widely considered as the best method for dating the emplacement of magmatic rocks. However, dating of kimberlitic eruptions using zircon is a challenge for geochronologist because of the presence of zircon xenocrysts from the wall-rocks and crystals derived from the mantle. Due to its high closure temperature, estimated to be at least 900 – 1000 °C (Lee et al., 1997; Cherniack & Watson, 2000), the U-Pb zircon chronometer furnish ages which may be unrelated to the kimberlite emplacement. Apatite and rutile, when present in the kimberlitic paragenesis, can be considered as magmatic and U-Pb dating of theses minerals can be a reliable tool for the determination of the age of kimberlite emplacement. As their closure temperatures are significantly lower than those of zircons (apatite: 400–500°C, Cherniack et al., 1989; rutile: 380-430°C, Metzger et al., 1991) problems of inheritance are drastically minimized when compared to U-Pb system of kimberlitic zircons. Taking into account that cooling of kimberlites occurs very quickly after emplacement, apatite or rutile U-Pb ages can be considered as crystallization ages despite their low closure temperature.

In West Africa, several generations of kimberlite with different ages have been identified. In southeastern Guinea, Liberia and Sierra Leone a cretaceous age has been admitted while in Ivory Coast and Mali, the emplacement ages are supposed to be in the 1100 - 1400 Ma range (Bardet, 1966). Contrasting with these field evidences of dyke emplacement, the numerous diamonds, found in alluvionary sediments covering Paleoproterozoic (Birimian) sequences in Ivory Coast and Ghana, as well as in Birimian "detrital sequences", have been hitherto considered as indirect arguments for the existence of Paleoproterozoic or Archean primary host-rocks.

In order to determine the age of eruption of the two generations of kimberlite, two samples have been selected for U-Pb dating on apatite and rutile. Sample ZW-52 come from a kimberlite located in the Bir Amrane prospect (Mauritania) own by Rex Mining Company. The kimberlite is intensively recrystallized (calcretization) but the silicified and carbonatic paragenesis also contains relics of phlogopite, Cr-pyrope and Mg-ilmenite.

Sample 02GH8 was collected from a tufficic dyke at the Beduara prospect in the Akwatia region (southern Ghana) which represents the biggest diamondiferous alluvionary prospect in Western Africa with 100 million carats produced so far. These dykes correspond to suprakimberlitic facies and are oriented in NE-SW direction, according to the main Paleoproterozoic regional structural pattern. They constitute an anastomosed network, which crosscuts Birimian sediments formed between 2.2 Ga and 2.1 Ga (Milesi et al., 1989). The dykes include some clasts of these sediments. Excepting diopside, no typical mineral of kimberlite paragenesis has been identified in the matrix that mainly consists of quartz, feldspar, micas and rutile. The latter was selected for U-Pb geochronology.

U-Pb analyses have been performed on five single grains of apatite from the ZW-52 sample of Bir Amarane kimberlite. In the Concordia diagram (Fig. 1) analytical points are fitting on a straight line which defined a lower intercept of 154.3 ± 5.8 Ma (2σ) and a upper intercept age of 2278 ± 570 Ma (2σ) (mswd = 1.19). Four of the five grains are concordant and one point is slightly discordant. Concentrations range between 1.07 ppm and 3.29 ppm for U and from 0.69 ppm to 1.90 ppm for total Pb. $^{206}Pb/^{204}Pb$ are very low ($21.97 < {}^{206}Pb/^{204}Pb < 197.49$)

The age of 154.3 Ma is considered as the age of emplacement of the kimberlite while the age of 2.28 Ga corresponds to a minimum age for an inherited lead component incorporated by apatite during crystallization. This age of 154.3 Ma confirms a Mesozoic age of the Bir Amrane kimberlite but it is significantly older than the previous Cretaceous ages obtained on kimberlite from the West African Craton (Bardet, 1966) and indicates that kimberlitic activity began at the limit between middle and upper Jurassic.

Seven single grain and multi-grain fractions of rutile from dyke GH8 have been analyzed (fig.2). As for apatites, U and total Pb concentrations are low (U: 1.39–1.97ppm; Pb_{tot}: 0.77-9.81ppm) as well as $^{206}Pb/^{204}Pb$ ratios ($25.45 < {}^{206}Pb/^{204}Pb < 48.15$). Six of the analytical points defined a linear array which crosscuts the Concordia curve at 2029 ± 22 Ma (mswd = 1.5). The seventh point furnished a younger age at about 1.81 Ga. Most of the points display a very elongated error ellipse which account for the uncertainty of the U/Pb value of blank used for common lead correction. The age of 2029 Ma is interpreted as the age of emplacement of the dyke in good agreement with structural features and relationships of the dyke with Birimian country rock, which favored a late-birimian age.

Concluding, despite the low $^{206}Pb/^{204}Pb$ ratios related to significant amount of common lead, apatite and rutile can provide confident and precise U-Pb ages and constitute useful geochronological tools for dating emplacement of kimberlites and related dykes.

ACKNOWLEDGEMENTS

We are grateful to Dr M.M. Pimentel from University of Brasília which gave the $^{235}U/^{205}Pb$ spike. UFPA authors (RK and JML) thank CNPq for grants and financial support while BRGM authors (CD and JPM) thank BRGM scientific Direction through the funding of "Projet Afrique" and of a specific "Matuta research grant" on West African diamond sources. Further, we wish to thank Luc Rombouts (Rex Mining) for ceding the samples and to James Lemaire (Ghana Consolidated Diamonds Limited) for logistic support and kind hospitality during our May 2002 field sampling in Akwatia. Both companies are thanked for permitting publication of the results.

REFERENCES

Bardet M.G. & Vachette M., 1966. Détermination d'âges de kimberlites de l'Ouest Africain et essai d'interptétation des datations des différentes venues diamantifères dans le monde. 3° Coll.Geol.Afri., Tervuren, BRGM, Paris

Cherniak, D.J. & Watson, E.B. 2000. Pb diffusion in zircon. Chem. Geology, 172, 5-24.

Cherniak, D.J.; Lanford, W.A.; Ryerson F.J., 1991. Lead diffusion in apatite and zircon using ion implantation and Rutherford Backscattering techniques. Geochim. Cosmochim. Acta 55, 1663-1673.

Krogh, T.E., 1973. A low contamination method for hydrothermal decomposition of zircon and extraction of U and Pb for isotopic age determination. Geochim. Cosmochim. Acta 37, 485–494.

Lee, J.K.W.; Williams, I.S.; Ellis, D.J., 1997. Pb, U and Th diffusion in natural zircon. Nature 390, 159–162.

Ludwig, K.R., 1993. PBDAT. A computer program for processing Pb-U-Th isotope data. Version 1.24. USGS Open-file report 88-542. 34 p.

Ludwig, K.R., 2001. User's manual for Isoplot Ex Version 2.49. A geochronological toolkit for Microsoft Excel. Berkeley Geochronology Center, Berkeley, CA, USA, Spec. Pub. no.1a, 59 p.

Mezger, K.; Nanson, G.N.; Bohlen, S.R., 1989. High precision U-Pb ages of metamorphic rutile: application of high grade terrane, Earth Planet. Sci. Lett. 96, 106-118.

Milesi, J.P.; Feybesse, J.L.; Ledru, P.; Dommanget, A.; Ouedraogo, M.F.; Marcoux, E.; Prost, A.; Vinchon, C.; Sylvain, J.P.; Johan, V.; Tegyey, M.; Calvez, J.Y.; Lagny, Ph., 1989. Les minéralisations aurifères de l'Afrique de l'Ouest. Leur évolution lithostructurale au Protérozoïque inférieur. Notice et Carte à 1/2 000 000. Chronique de la Recherche Minière, Fr., n° 497, 3-98.

Parrish, R.R., 1987. An improved micro-capsule for zircon dissolution in U–Pb geochronology. Chem. Geol. 66, 99–102.

Parrish, R.R., Roddik J.C., Loveridge, W.D.; Sullian, R.W. 1987. Uranium-lead analytical techniques at the geochronology laboratory, Geological Survey of Canada. in: Radiogenic age and isotopic studies: Report 1, Geological Survey of Canada, Paper 87-2, 3-7.

Tera, F., Wasserburg, G.J., 1975. Precise isotopic analysis of lead in picomole and subpicomole quantities. Anal. Chem. 47 (13), 2214–2220.

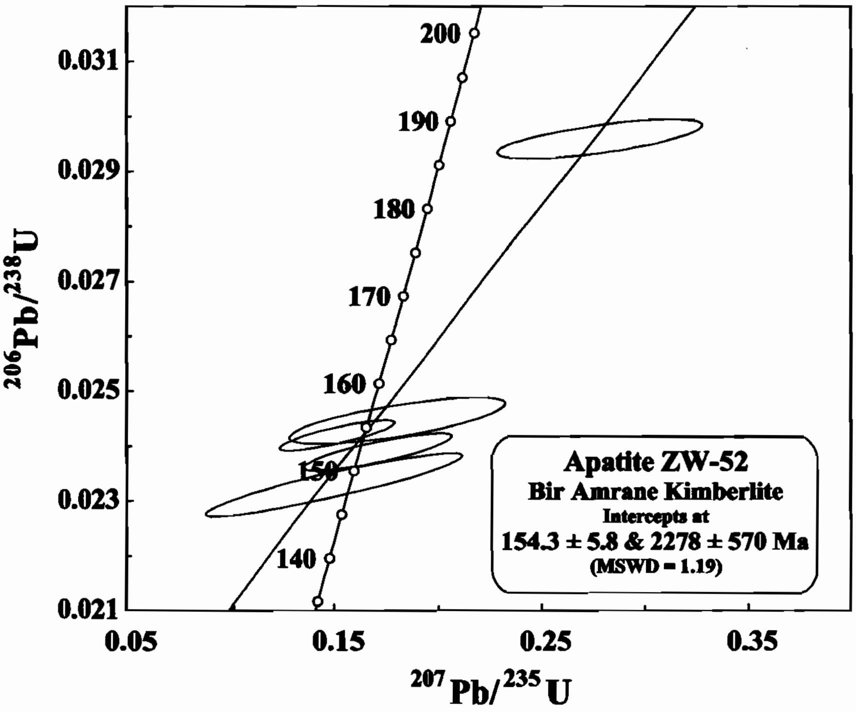

Figure 1: Concordia diagram for U-Pb analyses obtained on apatites ZW-52

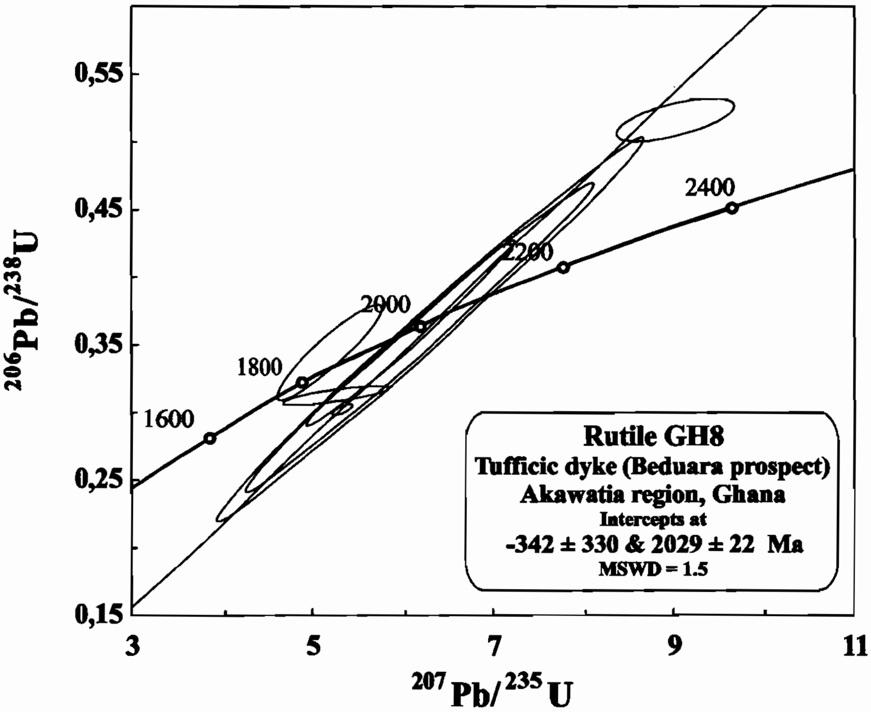

Figure 2: Concordia diagram for U-Pb analyses obtained on rutiles GH8

IN SITU ^{10}Be PRODUCED FROM A STONE-LINE OF THE JARDIM RIVER BASIN - DF, BRAZIL

Lima, C.V.[1]; Braucher, R.[2]; Gaspar, J.C.[3] and Bourlès, D.[4]

1. Instituto de Estudos Sócio-Ambientais, Universidade Federal de Goiás, Goiânia - GO. claudia@iesa.ufg.br
2. Centre Europèen de Recherche et d'Enseignement de Gèosciences de l'environnement, France. braucher@cerege.fr
3. Instituto de Geociências, Universidade de Brasília, Brasília - DF. gasp@unb.br
4. Centre Europèen de Recherche et d'Enseignement de Gèosciences de l'environnement, France. bourles@cerege.fr

Keywords: Cosmogenic nuclides, erosion, stone-line, creeping rate

INTRODUCTION

Cosmogenic nuclides are produced by nuclear reactions induced by cosmic rays. In the atmosphere ^{10}Be ($T_{1/2}$ = 1.5 Ma) is produced by interactions of primary cosmic rays (protons and α particles) and secondary particles (neutrons and muons) with atmospheric nuclei of ^{14}N and ^{16}O. Although most of the cosmic energy dissipates in the atmosphere, ^{10}Be may also occur in the lithosphere as a result of spallation reactions of ^{16}O, ^{27}Al, ^{28}Si and ^{56}Fe (Lal & Peters, 1967; Nishiizumi et al.; 1989; Raisbeck & Yiou, 1984; Lal, 1988, 1991a).

^{10}Be (and also ^{26}Al) has been used to quantify erosive processes, denudation rates and burial processes. It is useful to elucidate mechanisms involving evolution of the landscape and formation of soils. The application of the *in-situ* produced cosmogenic nuclides to quantify geomorphological processes is based on the fact that the production rates are extremely depth dependent (Lal et al., 1996; Brown et al., 1995; Cerling & Craig 1994; Braucher et al., 2000a, b; Siame et al., 2001). ^{10}Be can also be used as a parameter to distinguish autochthonous from allochthonous processes during soil formation (Brown et al., 1994).

The production rates of ^{10}Be and ^{26}Al have been estimated at 10 and 37 atom/g/SiO_2/year, respectively (Nishiizumi et al., 1986, 1989; Bierman, 1994). However, production rates for any latitude and altitude can be calculated using a third degree polynom deduced experimentally from glacial polished surfaces (Lal, 1991a).

A cosmogenic nuclide concentration increases with its exposure time until a steady-state, a balance between production and losses due to the erosion and radioactive decline is achieved. This dynamic allows us to determine the minimum exposure age of a surface or to calculate the maximum erosion rate (Fig. 1).

Erosion processes induce a loss of ^{10}Be or ^{26}Al. Braucher et al. (1998a, b, 2000a) used cosmogenic nuclides in quartz veins and stone-lines to calculate erosion rates and the formation dynamics of lateritic profiles in tropical environment. The evolution of the cosmogenic nuclides concentration considering a certain surface submitted to an erosion rate, during a time interval, at a depth can be expressed as follows (Braucher et al., 2000a):

$$C(x,t) = p_n.P_0.e^{(-x/\Lambda_n)} / (\varepsilon/\Lambda_n + \lambda)\ x\ [1 - e^{(-t(\varepsilon/\Lambda_n + \lambda))}] + $$
$$+\ p_\mu .P_0.e^{(-x/\Lambda_\mu)} / (\varepsilon/\Lambda_\mu + \lambda)\ x\ [1 - e^{(-t(\varepsilon/\Lambda_\mu + \lambda))}] + C_0e^{(-\lambda t)}$$

where Λ_n (150 g/cm^2) and $\Lambda\mu$ (1300 g/cm^2) represent the characteristic attenuation for neutrons and muons (Brown et al., 1995); pn and pμ refer to the neutrons and muons contribution for the total production of the cosmogenic nuclide (pn + pμ = 100%); C_0 is the number of atoms in the beginning of the exposure and P_0 represents the production rate of the cosmogenic nuclide in the surface.

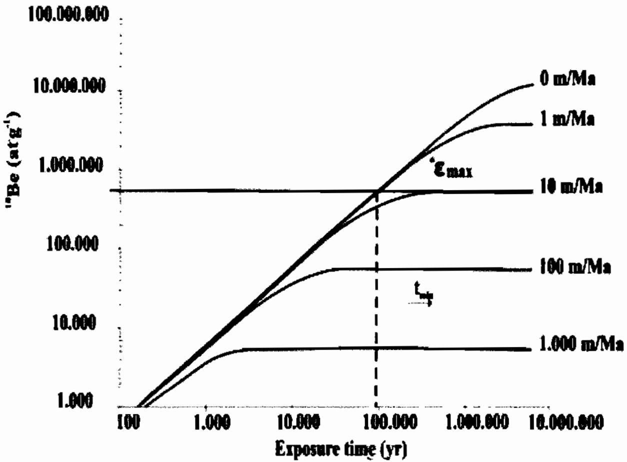

Figure 1. Theoretical ^{10}Be concentration evolution with exposure time for different erosion rates (Braucher, 1998).

In this study we have used ^{10}Be data in quartz from a stone-line of the Jardim river basin (Federal District, Brazil) to determinate rate production values and evolution of profile alteration. Quartz is the ubiquitous mineral for analysis because it is constituted by the main target of ^{10}Be production, and is resistant to erosion (Lal & Arnold, 1985; Lal, 1991b; Siame et al., 2000).

The Jardim river basin is located to the southeast of Federal District, Brazil between latitude 15°40' and 16°02' S, and longitude 47°20' and 47°40' W. The geology of the area is represented by terrains of the Paranoá, Canastra and Bambuí Groups.

The samples were collected in a quartz vein and a stone-line exposed in a road cut (15°51'68"S, 47^{0}28'42"W) where slates belonging to the Bambui Group predominate (Fig.2). ^{10}Be analyses were performed by accelerator mass spectrometry (AMS) at the Tandétron AMS Facility at Gif-sur-Yvette, France. Analitical incertainties of 5% were assumed based on counting statistics, as well as 15% incertainities related to rate production values (Lal, 1991a).

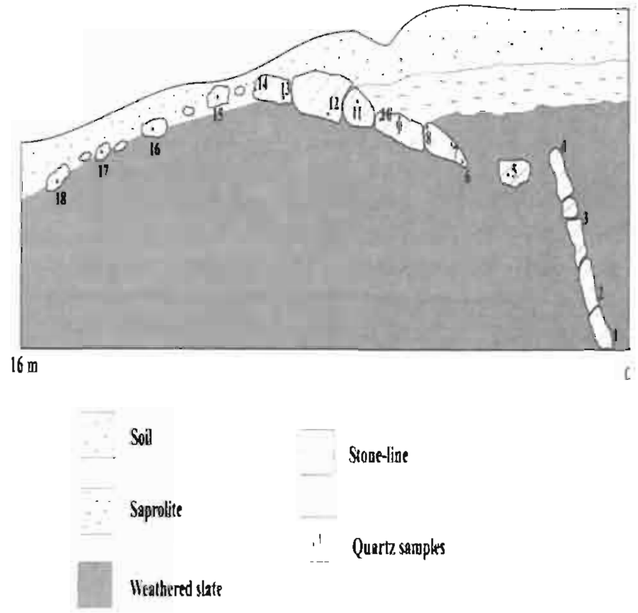

Figure 2. Sample distribuition at Jardim River.

RESULTS AND DISCUSSION

In the studied area the ^{10}Be production rate is 7 atoms/g/year (based on Lal polynom; Lal, 1991a) and the mean erosion rate is 5 m/Ma (using the surface samples).

^{10}Be concentrations (Table 1) measured along the quartz vein show a decrease as a function of depth (Fig. 3). According to Brown et al. (1995) and Lal (1991a) this behaviour indicates an *in situ* development resulting from the reduction of the cosmic radiation.

^{10}Be concentrations along the stone line allow an estimation of the displacement velocity of quartz cobbles from their original position (Fig. 4). The systematic increase in the ^{10}Be content as a function of the distance from the quartz vein suggests that the quartz samples in the stone line quartz have accumulated ^{10}Be continually during their migration. Such data can be used to evaluate the rate of lateral creeping, assuming that the samples of the stone-line resulted from the breaking down of the top of the quartz vein and that the production rate was constant during the migration of the quartz cobbles (Braucher et al., 1998a, b). In this case, the difference in the ^{10}Be concentration comparing two successive samples represents the maximum exposure time to cover the downslope interval between those samples. Considering the muon contributions to the ^{10}Be production rate, the displacement is 53 m/My. If muons are discounted, the displacement is 50 m/My (Fig. 5). Samples CV-16, 17 and 18 were excluded from the displacement calculation because they are located on the plateau area. Such samples present similar ^{10}Be concentrations suggesting that the area reached a steady state.

Cosmogenic nuclides produced *in situ* constitute an important tool to quantify surficial processes. ^{10}Be concentrations of the surficial samples indicate that the area reached the steady state and the average erosion rate is 5 m/My. The systematic increase in ^{10}Be concentration observed in the quartz from the stone line in function of the distance of the quartz vein indicates a continuous ^{10}Be accumulation during their migration from their original location. This indicates an autochthonous process for the development of the stone-line with a creeping rate of approximately 50 m/My.

Table 1. Concentrations of in situ-produced ^{10}Be along the Jardim River stone-line and a quartz vein.

Sample	Depth (cm)	Distance from Quartz vein (m)	Density (g/cm^{3})	^{10}Be (10^{4} at/g)
CL-01	220	0	1.8	0.56 ± 0.10
CL-02	200	0	1.8	0.73 ± 0.10
CL-03	180	0	1.8	0.88 ± 0.10
CL-04	160	0	1.8	0.93 ± 0.12
CL-05	180	1.3	1.8	0.93 ± 0.25
CL-06	180	2.0	1.8	1.02 ± 0.14
CL-07	160	2.2	1.8	1.09 ± 0.16
CL-08	160	2.3	1.8	1.27 ± 0.14
CL-09	160	2.5	1.8	1.16 ± 0.10
CL-10	140	2.8	1.8	1.63 ± 0.19
CL-11	150	3.0	1.8	1.23 ± 0.10
CL-12	110	3.2	1.8	1.70 ± 0.15
CL-13	70	3.6	1.8	1.96 ± 0.20
CL-14	50	4.0	1.8	2.95 ± 0.28
CL-15	50	7.2	1.8	3.93 ± 0.37
CL-16	30	11.0	1.8	8.54 ± 0.56
CL-17	30	13.2	1.8	9.17 ± 0.64
CL-18	15	15.2	1.8	9.74 ± 0.87

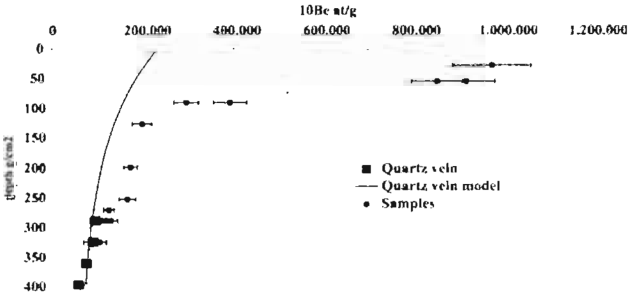

Figure 3. In situ-produced ^{10}Be concentrations as a function of depth along the quartz vein and a stone line from the Jardim River basin.

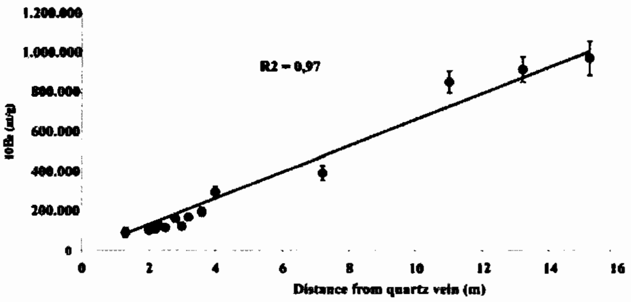

Figure 4. In situ-produced ^{10}Be concentrations as a function of the distance from the quartz vein from the Jardim River basin.

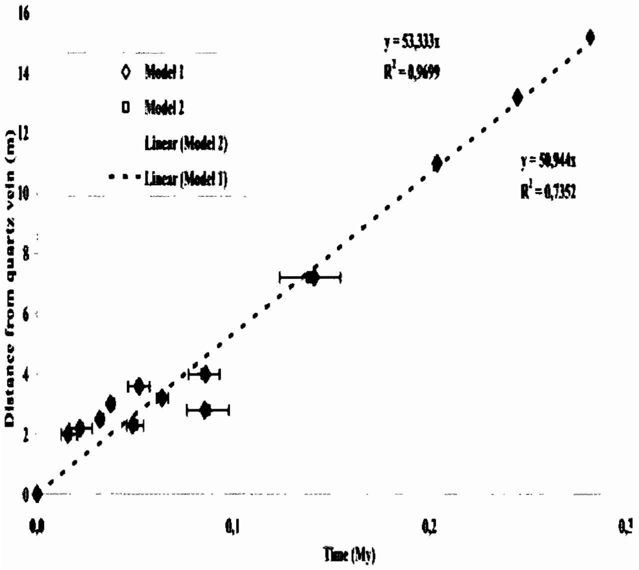

Figure 5. Estimation of lateral displacement at Jardim River basin. Model 1 consider the muons contribution to the ^{10}Be production rate. Model 2 does not consider the muons contribution to the ^{10}Be production rate.

REFERENCES

Bierman, P.R., 1994. Using in situ produced cosmogenic isotopes to estimate rates of landscape evolution: a review from the geomorphic perspective. Journal of Geophysical Research, 99(B7):13855-13896.

Braucher, R.; Bourlès, D.; Colin, F.; Brown, E.T.; Boulangé, B., 1998a. Brazilian laterite dynamics using in situ-produced ^{10}Be. Earth and Planetary Science Letters, 163:197-205

Braucher, R.; Colin, F.; Brown, E.T.; Bourlès, D.; Bamba, O.; Raisbeck, G.M.; Yiou, F.; Koud, J.M., 1998b. African laterite dynamics using in situ-produced ^{10}Be. Geochimica et Cosmochimica Acta, 62(9):1501-1507

Braucher, R.; Bourlès, D.; Brown, E.T.; Colin, F.; Muller, J.P.; Braun, J.J.; Delaune, M.; Minko, A.E.; Lescouet, C.; Raisbeck, G.M.; Yiou, F., 2000a. Application of in situ-produced cosmogenic ^{10}Be e ^{26}Al to the study of lateritic soil development in tropical forest: theory and examples from Cameroon and Gabon. Chemical Geology, 170:95-111

Braucher, R.; Siame, L.; Bourlès, D.; Colin, F., 2000b. Utilisation du ^{10}Be cosmogénique produit in-situ pour l'étude de la dynamique et de l'évolution des sols en milieux latéritiques. Bull. Soc. Géol. France, 171(5):511-520

Brown, E.T.; Stallard, R.F.; Mattew, C.L.; Raisbeck, G.M.; Yiou, F., 1995. Denudation rates determined from the accumulation of in situ-produced ^{10}Be in the Luquillo Experimental Forest, Puerto Rico. Earth and Planetary Science Letters, 129:193-202.

Cerling, T.E. & Craig, H., 1994. Geomorphology and in-situ cosmogenic isotopes. Annu.Rev.Earth Planet. Sci. 22:273-317.

Lal, D., 1988. In situ-produced cosmogenic isotopes in terrestrial rocks. Ann. Rev. Earth Planet. Sci., 16:355-388

Lal, D., 1991a. Cosmic ray labeling of erosion surfaces: in situ nuclide production rates and erosion models. Earth and Planetary Science Letters, 104:424-439.

Lal, D., 1991b. The present scope of the field of terrestrial cosmogenic nuclides. Current Science. 61(11): 744-751.

Lal, D. & Arnold, J.R., 1985. Tracing quartz through the environment. Proc. Indian Acad. Sci. (Earth Planet. Sci.), 94(1):1-5.

Lal, D.; Pavich, M.; Gu, Z.Y.; Jull, A.J.T.; Caffee, M.; Finkel, R.; Southon, J., 1996. Recent erosional history of a soil profile based on cosmogenic in-situ radionuclides ^{14}C and ^{10}Be. In: Earth Processes Reading the Isotopic Code. Asish Basu & Stan Hart (eds). Geophysical Monograph 95. American Geophysical Union, Washington.

Lal. L. & Peters, B., 1967. Cosmic Ray Produced Radioactivity on the Earth. In: Flugge, S. (ed.), Handbook of Physics. Springer-Verlag, pp.551-612.

Nishiizumi, K.; Lal, D.; Klein, J.; Middleton, L.; Arnold, J.R., 1986. Production of ^{10}Be e ^{26}Al by cosmic rays in terrestrial quartz and implications for erosion rates. Nature, 319:134-136

Nishiizumi, K.; Winterer, E.L.; Kohl, C.P.; Klein, J.; Middleton, R.; Lal, D.; Arnold, J.R., 1989. Cosmic ray production rates of ^{10}Be and ^{26}Al in quartz from glacially polished rocks. Journal of Geophysical Research, 94(B12):17907-17915.

Raisbeck, G.M. & Yiou, F., 1984. Production of long-lived cosmogenic nuclei and their applications. Nuclear Instruments and Methods in Physics Research. B5:91-99.

Siame, L.L.; Braucher, R.; Bourlès, D.; Bellier, O.; Sébrier, M., 2001. Datation de surfaces surfaces géomorphologiques repères par le ^{10}Be produit in-situ: implications tectoniques et climatiques. Bull. Soc. Géol. France, 172 (2): 223-236.

COOLING HISTORY OF THE CORONEL JOÃO SÁ PLUTON, BAHIA, BRAZIL

Long, L.E.[1]; Castellana, C.H.[2] and Sial, A.N.[3]

1. Department of Geological Sciences, University of Texas, Austin, TX 78712-0254, U.S.A. leonlong@mail.utexas.edu
2. Weston Solutions, Inc., 14724 Ventura Boulevard, Suite 1000, Sherman Oaks, CA, 91403-3501.
C.Castellana@westonsolutions.com
3. NEG-LABISE, Dept. Geología, Universidade Federal de Pernambuco, C. P. 7582, 50670-000, Recife-PE, Brazil. ans@ufpe.br

Keywords: Rb-Sr, U-Pb, diffusion, closure temperature, cooling rate

INTRODUCTION

A Rb-Sr mineral isochron from a plutonic rock commonly exhibits poor alignment of data points; a large MSWD indicates that the data points scatter about the best-fit regression line more than analytical error alone can account for. This is the case even for rocks lacking any evidence of later geochemical disturbance.

While a deeply buried pluton is yet at high temperature, all of the minerals are above their respective closure temperatures for retention of Sr. Rapid diffusion continually "levels" the value of $^{87}Sr/^{86}Sr$ amongst the mineral species that are in grain-to-grain contact. As cooling proceeds, diffusion eventually ceases in the mineral species with the highest closure temperature. It becomes an isolated chemical system, in which the rate of further growth of radiogenic Sr is proportional to Rb/Sr in that mineral, not in the whole rock, which was the situation before closure. Meanwhile, rapid diffusion of Sr prevails throughout the "residual whole rock"—all of the remaining mineral species having lower closure temperatures.

The process continues as each mineral species becomes a closed system in succession. Finally, after the residual whole rock has been reduced to only two participating minerals, communication ceases when the mineral with the higher closure temperature becomes closed, regardless of the intrinsic diffusion properties of the other mineral.

Giletti (1991) postulated this process of cooling and closure. The isochron concept assumes that all mineral species became closed at the same moment whereas for a plutonic rock, closure had occurred incrementally over a prolonged interval of slow cooling. This more complex history is reflected in a poor alignment of data points on an isochron diagram.

THEORETICAL BASIS

Dodson (1973) developed a mathematical relationship of the closure temperature to the diffusion coefficient, activation energy, effective diffusion radius for the crystal, and rate of cooling (closure temperature being higher if cooling is more rapid). Giletti (1991), Giletti and Casserly (1994), Cherniak and Watson (1994) and other workers have determined the diffusion characteristics of common silicate minerals as a function of temperature: the empirical data that are applied to the Dodson formulation.

Figures 1a-d show the increase of $^{87}Sr/^{86}Sr$ from the time that a whole rock becomes a closed isotopic system, until the present day. Consider a hypothetical rock that consists of three minerals. It contains titanite (ti), which closes first, at highest temperature. K feldspar (Kf) closes next, and finally biotite (bio). Rb/Sr in titanite is approximately zero; Rb/Sr in K feldspar is "low," and Rb/Sr in biotite is "high." To clarify details of the process, the diagrams assume that each mineral is a large Rb-Sr reservoir, such that closure to diffusion induces a substantial change in Rb/Sr in the residual whole rock.

Figure 1a is simple: $^{87}Sr/^{86}Sr$ in the whole rock increases monotonically until the present day at a rate proportional to Rb/Sr. Titanite (Fig. 1b) experiences the whole-rock rate of increase until it closes, after which there is no further increase of $^{87}Sr/^{86}Sr$. Because the closure of titanite has removed Sr, but not Rb from the budget of the residual whole rock, $^{87}Sr/^{86}Sr$ subsequently grows at a faster rate until K feldspar closes (Fig. 1c). Following closure, $^{87}Sr/^{86}Sr$ continues to increase in K feldspar according to its Rb/Sr. Biotite (Fig. 1d) is forced to close at the same time as K feldspar because diffusion exchange cannot occur unless a co-existing mineral is also diffusionally active.

The whole rock consists of a set of mineral Rb-Sr "reservoirs" whose sizes depend upon elemental and isotopic concentrations and modal abundances. When a reservoir cools to its closure temperature it ceases to communicate. We calculate the proportional sizes of the remaining reservoirs, which continue to communicate until the next one drops out, and so on. Our objective is to devise a cooling history that accommodates all of the data, which are: the age of the whole rock (determined by an independent method such as U-Pb on zircon), Rb and Sr concentrations and $^{87}Rb/^{86}Sr$ and $^{87}Sr/^{86}Sr$ in the whole rock and each mineral, mineral modal abundances, and for each mineral species the diffusion coefficient, activation energy, and effective diffusion radius estimated from crystal size. Interactive spreadsheet calculations simulate a pathway of Rb-Sr development—the steps illustrated generically in figures 1a-d.

If cooling is sufficiently slow, each mineral becomes closed at a significantly different time and temperature. The variables are the temperature at which the whole rock became a closed system, and the rate of cooling. The cooling rate influences the Dodson (calculated) closure temperature, and also the intervals among mineral closure

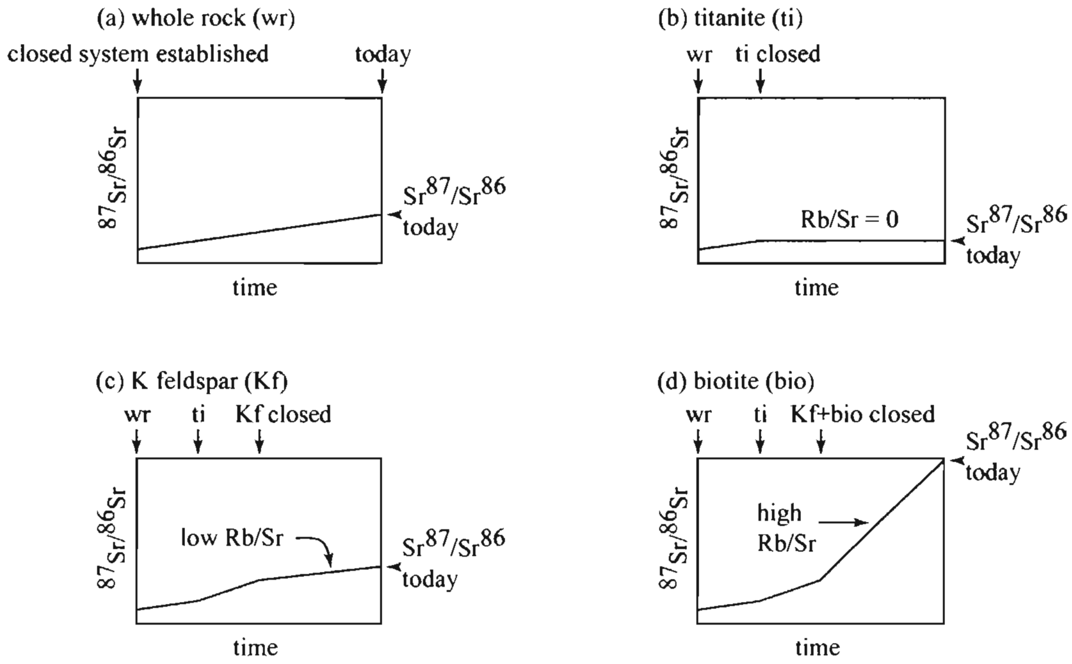

Figure 1. Rb-Sr isotopic closure of whole rock and mineral species during slow cooling.

ages. The starting temperature determines how far the temperature must drop (i.e., how much time passes) before the first mineral closes; its value adjusts this range of closure ages up or down in an absolute sense. With correct choices of the fixed data (isotopic concentrations, modal abundances, diffusion parameters) and of starting temperature and rate of cooling, the calculated Rb-Sr data can be made to match the scattered, non-linear data plotted in an isochron diagram.

APPLICATION TO CJS PLUTON

The unfoliated, post-tectonic Coronel João Sá (CJS) granodiorite pluton, Bahia, is emplaced into host schist of the Macururé domain of the Sergipano Foldbelt (Fig. 2). We collected a fresh sample from a centrally located active quarry for isotopic analyses of whole rock and the chief mineral reservoirs of Rb and Sr, which are titanite, plagioclase, K feldspar, apatite, and biotite. U-Pb analysis of zircon provides a concordant 625 ± 2 Ma age of emplacement. U-Pb ages of titanite are younger and slightly discordant, approximating 621 Ma.

Unfortunately, the calculations are compatible with a range, not a single unique combination of cooling parameters. Largely this is because the growth of $^{87}Sr/^{86}Sr$ in titanite, apatite, and plagioclase (low Rb/Sr minerals) is so insensitive to the passage of time that the data fit various cooling scenarios almost equally well. Further constraint is provided by U-Pb data from zircon ($T_{closure} \approx 800°C$ at 625 Ma) and titanite ($T_{closure} \approx$ 660-700°C at 621 Ma). The U-Pb and Rb-Sr data, taken together, give an excellent match (Table 1) to a beginning temperature of 840°C, and a cooling rate of 36°C/million years. Qualitative estimates of paleo-pressure are on the order of 4-5 kbar (12-15 km paleodepth), roughly consistent with a cooling rate of 36°C/million years.

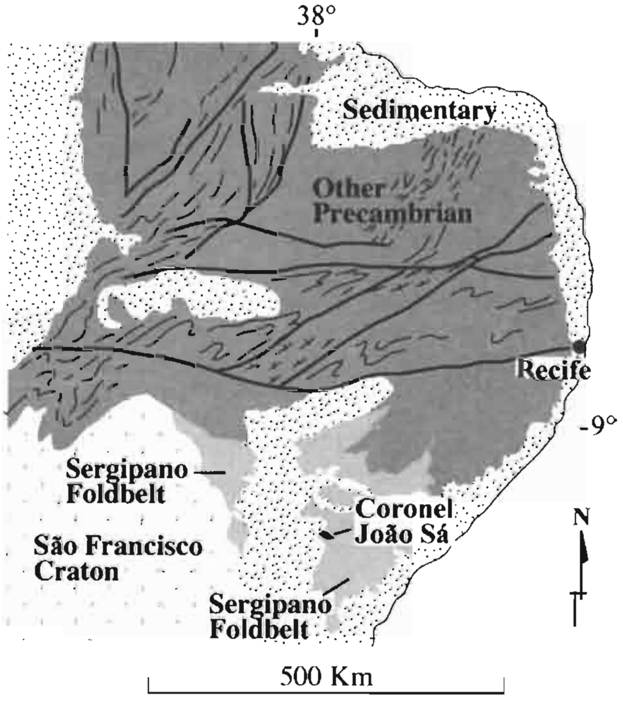

Figure 2. Location of Coronel João Sá pluton.

The calculated initial temperature (840°C) is surprisingly high, and in fact, experiments by Naney (1983) on artificial granodiorite melts indicate that the Coronel João Sá rock would have been partially molten at that temperature. However, the Giletti procedure for calculating successive closure temperatures does not require that the whole rock be entirely solid, but only that it be a closed system. Minerals that closed late during cooling may not even have existed when early-crystallized minerals became closed.

Table 1. Optimum calculated Rb-Sr cooling history of Coronel João Sá sample CJS 20.

	Closure Age (Ma)	T_C (°C)	$^{87}Sr/^{86}Sr$ Today	
			Measured	Calculated
Whole rock	625	840	0.7126	—
Titanite	622	737	0.7083	0.7082
Plagioclase	617	561	0.7082	0.7082
K-feldspar	614	449	0.7116	0.7116
Apatite	609	249	0.7082	0.7084
Biotite	609	249	1.9129	1.9129

REFERENCES

Cherniak, D. J. and Watson, E. B., 1994. A study of strontium diffusion in plagioclase using Rutherford backscattering spectroscopy: Geochimica et Cosmochimica Acta 58, 5179-5190.

Dodson, M. H., 1973. Closure temperature in cooling geochronological and petrological systems: Contributions to Mineralogy and Petrology 40, 259-274.

Giletti, B. J., 1991. Rb and Sr diffusion in alkali feldspars, with implications for cooling histories of rocks: Geochimica et Cosmochimica Acta 55, 1331-1343.

Giletti, B. J. and Casserly, J. E. D., 1994. Strontium diffusion kinetics in plagioclase feldspars: Geochimica et Cosmochimica Acta 58, 3785-3793.

Naney, M. T., 1983. Phase equilibria of rock-forming ferromagnesian silicates in granitic systems: American Journal of Science 283, 883-1033.

PHANEROZOIC THERMO-TECTONIC EVOLUTION OF NW NAMIBIA AND IMPLICATIONS ON WALVIS BASIN

Luft, F.F.; Chemale Jr., F.; Lelarge, M.L.M.V. and Luft Jr., J.L.

Universidade Federal do Rio Grande do Sul, Av. Bento Gonçalves, 9500. Instituto de Geociências,
Programa de Pós Graduação. fernanda.fernandes@ufrgs.br, farid.chemale@ufrgs.br, lidia.vignol@ufrgs.br, joao.luft@ufrgs.br

Keywords: Tectonic reactivations, Apatite Fission Track Thermochronogy, Purros Mylonitic Zone, Walvis Basin

INTRODUCTION

The Namibian continental margin records tectonic activity from the Proterozoic to the present. The collision of Congo and Rio de la Plata plates during the Pan-African/Brasiliano Cycle (Neoproterozoic to Early Paleozoic) gave rise to NNW-trending crustal discontinuities in the Kaoko Belt, Namibia. These pre-existing structures were active during the Phanerozoic, playing a very important role in the tectonic evolution of the Namibian continental margin and of the passive margin Walvis Basin.

In order to study the different uplift and erosion events in the Namibian continental margin Apatite Fission Track Thermochronology was applied to granitic and gneissic rocks from the central part of the Kaoko Belt.

GEOLOGICAL SETTING

The studied area is located in the NW portion of Namibia, central zone of Kaoko Belt, in the vicinity of Purros Mylonitic Zone (PMZ) – a sub-vertical shear zone of crustal scale (Fig. 1). PMZ has a NNW trend parallel to the Namibian passive margin with a approximately 500 Km of length. Based on field geology we recognize that this shear zone underwent Phanerozoic tectonic reactivation, which is characterized by the direct contact between the Proterozoic basement and Etendeka Basalt, and the occurrence of remylonitization processes in the vicinity of this lineament.

The SW Africa offshore margin is composed by four passive marginal basins called, from south to north: Orange, Lüderitz, Walvis and Namibe. In this context the Phanerozoic reactivations are also manifested in the Walvis marginal Basin through unconformities along the deposicional sequences.

The continental basement area studied here is adjacent to the Walvis Basin which is marked by Paleozoic to Cenozoic sedimentation formed essentialy by Syn-Rift (Permian to Early Triassic), Early Drift (Aptian to Cenomanian) and Late Drift (Turonian to Recent) Sequences (Fig. 2). The Walvis Basin is a typical post-rift wedge shaped basin, with the geometry of a passive margin and water depths of 150–3000 m, which is an unexplored basin. Recent drilling results prove elements of aviable petroleum system (Bray et al., 1998).

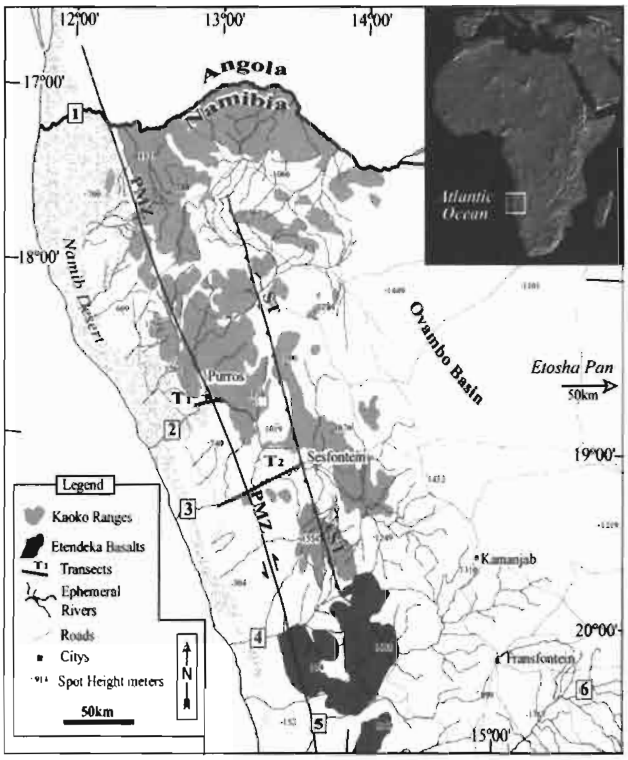

Figure 1. Map showing the studied area with the transects where were collected the fission track samples. 1. Cunene River; 2. Hoarusib River; 3. Hoanib River; 4. Uniab River; 5. Huab River and 6. Ugab River. PMZ: Purros Mylonitic Zone and ST: Sesfontein Thrust.

METHODOLOGY AND SAMPLING

Apatite Fission Track Thermochronology is a powerful tool over a temperature range between 60°-110°C which characterizes the upper few kilometers of the Earth´s crust (Raab et al., 2002). This technique is based on fission track (FT) dating method that compares the densities (FT number/area) of spontaneous track (generated by the fission of ^{238}U) with induced tracks (produced by irradiation the samples with thermal neutrons in nuclear reactor). The FT ages are generally younger than the stratigraphic age expected for the samples which is explained by the low stability of the FTs in minerals when exposed to increasing temperature during a significant geological time span (Bigazzi, 1967).

The reduction of track length, density and FT age is called thermal annealing that is the disordering of the ordered structure of the mineral that was affected by the passage of the heavy particles originated in the uranium fission (Borba et al., 2002).

We collected seven outcrop samples of Proterozoic granites and gneisses through two transects along the Hoanib and Horusib valleys.

The Fission Track analyses have been carried out at the Laboratório de Geologia Isotópica of the Universidade Federal do Rio Grande do Sul. The apatites grains were concentrated by conventional magnetic, heavy liquid, and hand-picking techniques and mounted in a epoxy resin. After, the minerals were polished and etched in 0.5% HNO_3 at 22°C for 45s to reveal the spontaneous FTs. The apatite mounts were covered with Kapton® (polyethylene-glycol) sheets to obtain FT ages using external detector method (Gleadow, 1981). Neutron irradiation was carried out in a poorly-thermalised M 23 position of the IPEN-CNEN reactor (Instituto de Pesquisa em Energia Nuclear – Centro Nacional de Energia Nuclear – São Paulo, Brasil). Thermal neutron fluencies were monitored by measuring the track density of the mica attached to CN_1 and CN_2 standard glasses. After this, the Kapton® detectors were etched in a NaOCl (14%) + NaCl (12%) solution for 8 minutes at a boiling temperature to reveal the induced FTs. Fission tracks were counted in transmitted light using a 100 x oil-immersion objective at a magnification of 1000 x on a Olympus BX40 microscope. As a rule, 50 individual crystals were analysed by sample and a set of 50-130 confined tracks were measured. Fission track ages were calculated using the zeta calibration method and expressed as central and pooled ages with percent variation (Galbraith & Laslett, 1993). The calculated values of the zeta factor (ζ) is 89.04 ± 6.82 and 159.07 ± 10.5 to the CN_1 and CN_2 standard glasses respectively. Track lengths were measured in each samples, as recomended by Gleadow et al. (1986), only the fully etched, horizontal, confined tracks in prismatic sections were measured using a digitizing table. The thermal histories were modeled using the Monte Trax program (Gallagher, 1993). The fission track analysis were performed in Fission Track Laboratory of the Universidade Federal do Rio Grande do Sul.

FISSION TRACK RESULTS AND DISCUSSION

The FT data showed apparent FT ages ranging from 34.8 ± 3.3 to 133.6 ± 9.6 Ma with a decreasing in direction to the Purros Mylonitic Zone. The tracks lengths ranged from 12.47 ± 2.51 to 10.50 ± 2.31 µm with a standard deviation between 2.08 and 2.83 µm. The track length distribution and the apparent FT ages are quite important to understand the thermal histories underwent by the samples. Thermal histories were modeled using the Monte Carlo and Genetic Algorithm probabilistic simulations proposed by Gallagher & Sambridge (1994) and after assembled in Monte Trax program (Gallagher, 1993).

Based on fission track thermal history modeling (Fig. 3) five main events have been recognized in the studied area, which occurred in Permian, Neocomian, Turonian, Eocene-Oligocene, and Miocene, respectively. These events are well correlated with the main stratigraphic discontinuities in the Walvis Basin (Fig. 2). Special attention is given to the Miocene Event because it has not yet recorded in the earlier studies in the Namibian margin.

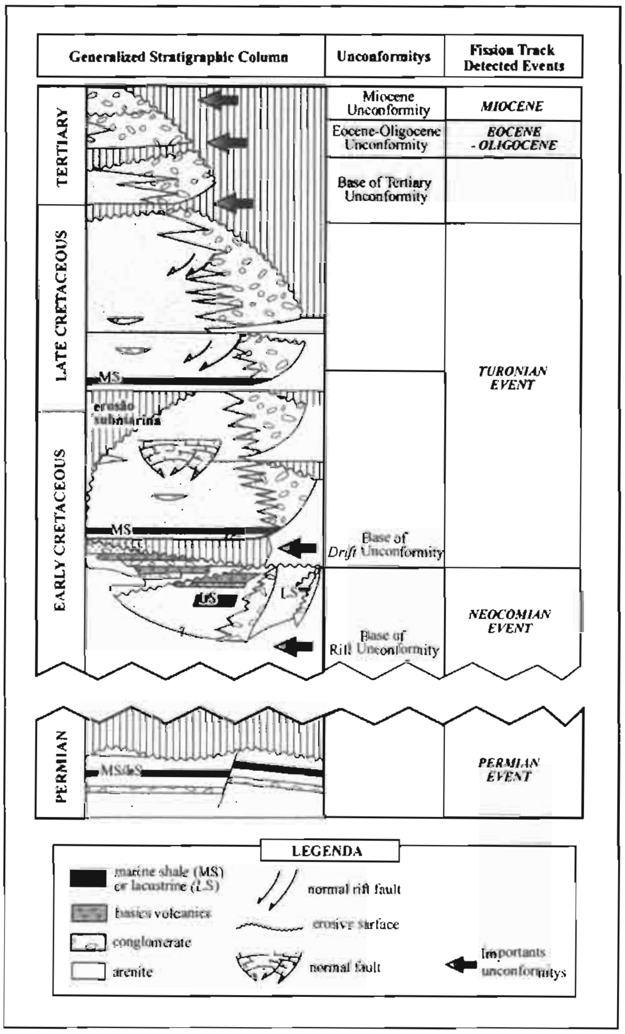

Figure 2: General stratigraphic column of Walvis Basin showing the correlation between the main unconformities of the sedimentary register with the main events detected by apatite fission track thermochronology analysis (Modified from Bray el al., 1998).

The Permian Event is an important regional tectonic mark detected in the Precambrian continental basement as well as basement rocks for the Walvis Basin units (Fig. 2). The FT data suggest here the Neo-Paleozoic Samfrau Orogeny influence above the Kaoko Belt basement generating half-graben structures. This Orogeny is also registered in Walvis Basin through Pre-Rift Sequence marked by continental sedimentation with marine and lacustrine oil-prone.

The Neocomian Event has also regional magnitude detected in the continental basement and in the Walvis Basin through unconformity presence in the base of the Syn-Rift Sequence. This event is associated with the South Atlantic opening through generation of a strong crustal uplift and than basic magmatism widely observed in South America (Serra Geral) and SW Africa (Etendeka).

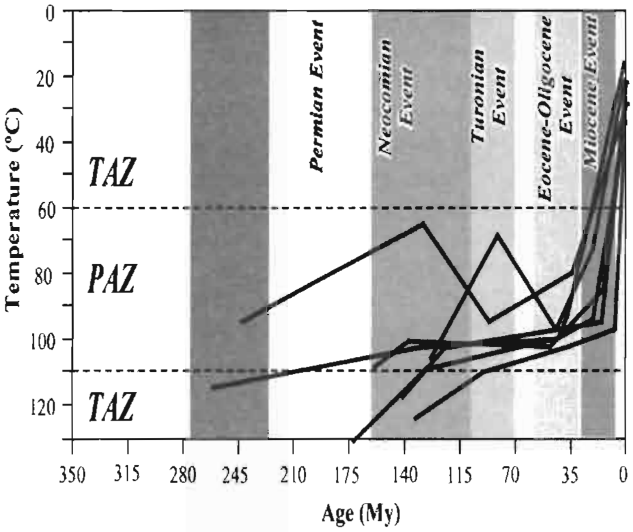

Figure 3: Thermal histories modelaments of the samples analysed by apatite fission track thermochronology showing the main events detected.

The Turonian Event was marked by a regional tectonic quiescence where the important thermal events were restricted to the passive marginal basins and adjacent continental areas. At this time a resurgent basic magmatism occurred in northern portion of Walvis Basin called Walvis Igneous Centre which may have caused the heating of adjacent continental basement.

The Eocene-Oligocene Event is an important local scale event that marked a crustal cooling period ranging from 30 to 50 Ma which is interpreted a result of gentle uplift of the continental margin and a decrease on the amount of denudation. This event is manifested in the Walvis Basin through the presence of an important Tertiary unconformity in the sedimentary record.

After a long period of gradual cooling occurred an accelerated period of crustal cooling here called Miocene Event. This event has influenced also the sedimentary record in the Walvis Basin with the generation of a regional unconformity of Miocene age and further deposition of thick sedimentary section (at least 1000 meter thick). Therefore it may have contributed to generation of oil reservoirs.

ACKNOWLEDGEMENTS

We thank the Agência Nacional do Petróleo (ANP) for the financial support and the Geological Survey of Namibia (GSN) for logistic support during the field work in Namibia.

REFERENCES

Bigazzi, G. 1967. Length of fission tracks and age of muscovite samples. Earth and Planetary Science Letters, 3: 434-438.

Borba, A.W.; Lelarge, M.L.M.V.; Mizusaki, A.M.P. 2002. Uplift and denudation of the Caçapava do Sul granitoids (southern Brazil) during Late Paleozoic and Mesozoic: constraints from apatite fission track data. Journal of South American Earth Sciences, 15:683-692.

Bray, R.; Lawrence, S.; Swart, R. 1998. Source rock, maturity data indicate potencial off Namibia. Oil & Gas Journal, 1: 1-10.

Galbraith, G.F. & Lasllet, G.M. 1993. Statistical models for mixed fission tracks ages. Nuclear Tracks and Radiation Measurements, 21: 459-470.

Gallagher, K. 1993. Monte Trax: A Fission Track Thermal History Modeling Program for the Macintosh, Department of Earth Sciences, The Open University, London.

Gallagher, K. & Sambridge, M. 1994. Genetic algorithms: a powerful method for large scale non linear optimization problems. Computer Geosciences, 20: 1229-1236.

Gleadow, A.J.W. 1981. Fission track dating methods: what are the real alternatives? Nuclear Tracks and Radiation Measurements, 5: 3-14.

Gleadow, A.J.W.; Duddy, I.R.; Green, P.F.; Lovering, J.F. 1986. Confined tracks lenghts in apatite: a diagnostic tool for thermal history analysis. Contributions to Mineralogy Petrology, 94: 405-415.

Raab, M.J.; Brown, R.W.; Gallagher, K.; Carter, A.; Weber, K. 2002. Late Cretaceous reactivation of a major crustal shear zones in northern Namibia: constraints from apatite fission track analysis. Tectonophysics, 349: 75-92.

OPTICAL CATHODOLUMINESCENCE FOR THE STUDY OF INTERNAL TEXTURES OF ZIRCON

McReath, I.[1] and Vicente, L.C.[2]

1. Departamento de Mineralogia e Geotectônica, Instituto de Geociências, USP. ianmcr@usp.br
2. Scientific Initiation Scholar, PIBIC-USP/CNPq Program (2002)

Keywords: Cathodoluminescence, zircon, internal textures

In recent years the importance of a through investigation of the internal textures and (where possible) the distribution of minor elements in zircon crystals used for U-Th-Pb or Pb-Pb dating has become very clear. Cathodoluminescence (CL) represents one of the means for texture investigations. We present here our experience of the use of the Luminoscope, a simple and robust accessory easily mounted on conventional optical microscopes, for this type of study. We examined about 75 zircon concentrates each containing from around 10 to more than 30 grains, about 20 large single crystals, as well as numerous uncovered or polished thin sections and rock slabs. The second author contributed to the study of about 30 of the grain concentrates.

The grain concentrates were usually prepared by magnetic separation of heavy mineral frations, hand-piced according to shape, colour and extent of fracturing. Heavily metamict zircon grains are usually excluded during the hand-picking process, so we have had no opportunity to study the effects of metamictization on CL patterns, and the possibility that U/Th act as activators for CL.

The rock samples include medium- to high-grade, polymetamorphic gneisses and granulites of Archaean and Proterozoic ages, and a few mainly Neoproterozoic, mostly granitic plutonic rocks. A few of the results have already been published (McReath et al., 2002) or otherwise communicated, and others are presented in detail in other communications to this symposium.

CL is excited when an electron beam is directed onto suitably activated crystals. The light usually originates from the top 2-3μm layer, and may be observed visually and recorded by conventional or digital cameras, or analyzed by a spectrometer. We use a Luminoscope ELM-3R made by the Nuclide Corporation, which operates stably with electron beams generated by excitation at ≤15kV and ≤1mA, producing focused elliptical spots with diameters between a few mm and a few cm. Although rustic, with totally manual operation of potentiometer controls and selector switches, with meter readouts of operating conditions of the power supply, and only simple controls for X-Y adjustment of the sample position ion the vacuum chamber, the equipment is easily serviced since the electronic circuits are simple and contain components which have equivalents easily found in Brazil, and the vacuum chamber has very simple mechanics easily maintained by machine shop technician.

Sample grains are mounted in epoxy resin discs. The resin burns under higher power loads, so most CL images are obtained at 7.5kV/0.4ma using a defocussed beam with diameter around 1 cm. Under certain conditions (see later), the resin appears to be reflective/refractive, but is sufficiently clear to permit examination of the grains in transmitted light.

Microscopes used for visual/photographic observation include a zoom stereomicroscope for large crystals up to about 1 cm, and a binocular research or a simple monocular microscope for other imaging or spectrometric work. For the latter, best results are obtained with large aperture objective lenses and high transmission "straight through" optical systems with the minimum of lenses or prisms between the objective and the eyepiece. We find the Olympus UMPlanFl 5x objective with an effective aperture of 0.15 to be adequate, but the Gamma Scientific 700-10 -4A 2.9x objective with adjustable effective aperture up to 0.36 is better when the emitted CL is weak. The necessary combinations of effective aperture, working distance between ojective and sample, and the geometry of the Lumionoscope vacuum chamber severely restirct the choice of objectives. So far we have found only one 25x objective which is satisfactory for imaging purposes, but not for spectrometry since its effective aperture is very low.

The spectrometer is a dual grating ARC SpectraPro 150, connecected to the microscope using a special ocular with a collecting fibre which transmits the light to the spectrometer via glass fibre. The sampled area is between about 50μm and 150μm, depending on the ocular magnification and the fibre diameter. The digital camera is a ~0.3 megapixel Media Cybernetics Pro-Series 3 chip color camera with appropriate capture kit which allows realtime visualization of the field-of-view, which is about 0.92x0.68mm with a 5x objective and a 3.3x camera eyepiece, while that for the 2.9x objective with a 10x eyepiece is 1.4x1.0 mm. With an adequately prepared resin mount, these fields-of-view allow the simultaneous observation of number of zircon grains. Maximizing the optical and digital magnifications up to the limit in which pixels appear allows the enlargment of an image of a 200μm long crystal to around 20 cm.

A lack of CL in zircon is often observed, at least in parts of, if not in the whole crystal. Pale or intense blue, deep to medium violet, yellow, yellow-orange and green CL colours have all been reported (Marshall, 1988) although the identification of the activator elements is sometimes far from unanimous. In contrast, images obtained with most CL attachments for microprobes or SEM are only false color, usually rendered in black and white. Zoning is also a common feature. Repeated fine- to medium-scale concentric zoning around a euhedral core is common in zircon crystals in igneous rocks, and is frequently preserved with slight modification in the form of zone broadening after medium- to high-grade metamorphism. The latter feature has also been recorded by Connelly (2000). Most of the samples with these features which have also been analysed for the U/Pb system are slightly to strongly discordant. The repeated CL zoning may mimic color zoning in transmitted light. Variations in the widths of dark and light bands are common, ranging from a type with broad dark bands and very thin bright bands to another with broad bright and dark bands have been observed. Repetitions of zoning patterns vary from abundant to rare. In cases where few repetitions are present, the zoning may appear to be restricted to parallel bands, though this pattern could also be a consequence of grain fragmentation. All these features have been discribed by Hoskin (2000) in his systematic study of the evolution of zoning patterns in zircon from a zoned pluton. At present, we have had no opportunity to perform a similar study. Sector zoning including the hourglass type is also common in zircon from kimberlites, and hourglass zoning is sometimes seen in other igneous and in metamorphic rocks. In a few of these cases, the colour zoning in transmitted light repeats the CL pattern.

Various special situations affect the validity of zircon geochronology: (i) the presence of inherited cores older than the crystallization age of an igneous rock; (ii) the presence of overgrowths younger than crystallization or metamorphic ages; and (iii) redsitribution of material by leaching along fractures or other mobilization processes. Exactly what consitutes an inherited core is not always obvious, but we believe that a few unequivocal cases with different characteristics have been observed. Examples of elliptical nuclei without CL have been seen for which the long axes do not coincide with the axes of the repeatedly zoned external part. Cracked nuclei with brighter CL and zoning patterns different from those in the overgrowths are sometimes observed. In transmitted light these nuclei are darker and apparently more metamict than the zoned part.

The identification of overgrowths is made difficult when the preparation of the grain mount is imperfect. Ideally, the grains should be ground down to "waist level" so that the conacts between grains and resin are vertical. Where "waist level" is not reached the contacts are inclined and produce shadows over the unexposed portions of the crystals which are usually seen in transmitted light images, while the edges of the resin may apprear as thin, bright and continuous CL lines symmetrical with the crystal outlines. This might be confused with a thin overgrowth. For this reason, each grain mount should contain only fractions of similar grain size, and the preparation should include grinding and polishing in stages, with checks on the adequacy of the mount after each grinding stage until a satisfactory finish is achieved. What we believe to be overgrowths frequently do not completely surround the rest of the grain, and may be brighter or darker than the edge of the main mass of the grain. The outline of the main overgrown grain may or may not be rounded at the apexes. Another consequence of not attaining an adequate depth of cutting is that the working face may be dominated by a single exposed igneous zone and due to the shallow depth of origin the CL image will appear to be rather uniform.

Fractures are often accompanied by the interruption of repeated CL zoning. They may be darker or lighter than the underlyingCL pattern. Patches of darker or lighter material may sprout from the fractures. These features may sometimes de seen in the transmitted light images.

Ideally, the CL studies should be complemented by the obtention of back-scattered electron images and, where possible, by secondary X-ray maps of the grains for elements such as Hf, U, Th etc. In the few cases that we have been able to study in detail, it is clear that zoning of other elements does not necessarily follow the zoning of CL activator elements. Fractures may be accompanied by local loss or gain of one or all of the other analysed elements, and the anomalous patches representing either deficiencies or concentrations of the element are also present. It has not yet been possible to check whether these features are also accompanied by changes in U/Pb ages, or in the degree of concordance.

Although monocrystal Pb-Pb evaporation or U-Pb geochronology using grains selected by optical CL will obviously not substitute SHRIMP or other point analysis methods, the combination offers a useful alternative for dating of zircon grains which do not present registers of complex evolution.

ACKNOWLEDGEMENTS

The Foundation for the Support of Research in the State of São Paulo (FAPESP) financed the equipment up-grading through contract no. 1997/10818-6. I. McReath thanks the National Research Council (CNPq) for a Research Scholarship. Don Marshall gave much technical support.

REFERENCES

Connely, J. N., 2000. Degree of preservation of igneous zonation in zircon as a signpost for concordancy in U/'b geochronology. Chemical Geology, 172: 25-39

Hoskin, P. W. O., 2000. Patterns of chaos: Fractal statistics and the oscillatory chemistry of zircon. Geochim. Cosmochim. Acta, 64: 1905-1923

Marshall, D. J., 1988. Cathodoluminescence of geological materials. Unwin Hyman, Boston. 146 pp.

COMPARISON OF CARBON ISOTOPE VARIATIONS ON HAIR OF TWO INCA MUMMIES FROM CHUSCHA AND ACONCAGUA MOUNTS, ARGENTINA

Panarello, H.O.[1]; Valencio, S.A.[1] and Schobinger, J.[2]

1. Instituto de Geocronología y Geología Isotópica. Pabellón INGEIS, Ciudad Universitaria, C. A. de Buenos Aires. C1428EHA, Argentina. hector@ingeis.uba.ar, susana@ingeis.uba.ar
2. Universidad Nacional de Cuyo. Mendoza, Argentina. jschobinger@hotmail.com

Keywords: Inka, mummy, palaeodiet, carbon isotopes, Argentina

INTRODUCTION

In past decades it was established the existence of two metabolic pathways for higher plants. The most common one fix atmospheric CO_2 in the form of intermediate compounds of 3 carbon atoms, following the well-known Calvin Benson cycle. This process introduces a large fractionation in carbon isotopes, leading to highly depleted values in the synthesized organic matter in comparison with the source, atmospheric CO_2. As a general rule, if we assume a value of $\delta^{13}C^1 = -8$ ‰ *vs.* V-PDB (see footnote) for CO_2 in the atmosphere, these plants (called C_3) reach values normally distributed around $\delta^{13}C = -26$‰ *vs.* V-PDB, and constitute most of the trees and plants all over the world. More recently, a second group of plants with a different photosynthetic pathway has been described. They are adapted to arid environments and strong sunshine and present a characteristic foliar anatomy in the form of a "crown" (Kranz in German). They follow the metabolic pathway described by Hatch-Slack and receive the name of Kranz or C_4 plants, since they fix CO_2 in the form of intermediate compounds of 4 carbon atoms. Their organic matter is less depleted in ^{13}C than in C_3 plants, having $\delta^{13}C$ values between -14 and -9 ‰ *vs* V-PDB. In this group we find maize, sugar cane, sorghum, etc. There is also a third group called C.A.M. (Crassulean Acid Metabolism) represented by cactus and orchids, that present values whether of C_3 or C_4 plants or intermediates.

Hairs of animals reflect closely the isotopic composition of the diet during its growing period. Seasonal and also monthly variations in the composition of diet are registered in every centimetre of hair. The isotopic enrichment factor relative to diet, which is slightly over 5 ‰ in collagen, decreases to 1‰ in hair (Minson et al., 1975; DeNiro & Epstein, 1978; Jones et al., 1981; Tieszen et al., 1983). In the case of natural feeding, fractionation is greater, around 1.3‰ and 3.4‰ (Nakamura et al., 1982; Schoeller et al., 1986; Katzenberg & Krouse, 1989; White, 1993; Fernández et al., 1999, Panarello & Fernández, in press).

This work compares $^{13}C/^{12}C$ ratios on hair of two Inka mummies found in the Aconcagua and Chuscha mounts, Argentina and makes a preliminary interpretation of why it occurred in this way.

THE INCA MUMMY OF MOUNT CHUSCHA

In recent years a new speciality, the "high mountain Archaeology", has investigated the so called "high altitude sanctuaries" that are sites located at more than 5000 m high, found between southern Perú and central Chile and Argentina. Up to the moment, about 140 of these sites have been found, 15 of them bearing mummies. They belong to the Inca expansion period, 1475-1532, thus their age round 500y bp. The rather good preservation of these bodies, allows obtaining valuable biological information that is not possible in other kind of human remains. The same happens with textiles and cultural elements found together.

The mummy of Mount Chuscha was encountered by local people in the time span comprised between 1920-1922, towards the top of the Nevado de Chuscha at about 5200 m a. s. level. The city of Cafayate, in the south of the Salta province, is the nearest locality to this site (Fig. 1). Mummy consists of a dried dead body of a girl (*ca.* 8 years old) dressed with an "unco" (an Andean tee-shirt) and accompanied of some adorns and ritual elements.

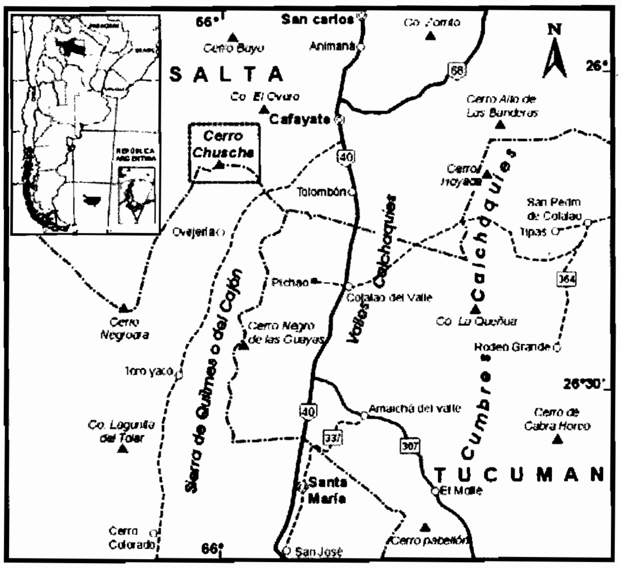

Figure 1. Location map showing the site where Chuscha mummy remains have been encountered.

---

[1]
$$\delta^{13}C = 1000\ \frac{[^{13}C/^{12}C]_S - [^{13}C/^{12}C]_R}{[^{13}C/^{12}C]_R}\ ‰$$

Where:

$\delta^{13}C$ isotopic deviation in per mil, ‰
$^{13}C/^{12}C$ isotope ratio
S = sample
R = reference standard

As in the case of the mummy of Mount Aconcagua (Fernández et al., 1999) and other similar cases, it is interpreted as a human sacrifice, an atavism called "capacocha". In this ceremony, children between 6 and 15 years old were offered to the deities presided by the sun, the imperial god.

MATERIALS AND METHODS

In order to study the relative proportion of C_3 and C_4 plants in the Chuscha's mummy diet, a thread of hair was washed with petroleum ether to remove rests of eggs of insects and fat. The thread was then cut in 15mm sections and combusted in accordance to the technique of Panarello (1987). $^{13}C/^{12}C$ ratios in each section were contrasted in a Finnigan Delta-S, McKinney type, and triple collector mass spectrometer with the internal reference INGEIS-1, Carrara Marble and are expressed as δ‰ against V-PDB standard (Table 1).

Table 1. Isotopic values of the samples of Chuscha mummy.

Laboratory #	Distance to head [mm]	$\delta^{13}C$
AIE 12316	0-15	-12.1
AIE 12317	15-30	-10.8
AIE 12318	30-45	-10.8
AIE 12319	45-60	-13.0
AIE 12320	60-75	-15.2
AIE 12321	75-90	-15.8
AIE 12322	90-105	-17.1
AIE 12323	105-120	-18.9
AIE 12324	120-135	-19.1
AIE 12325	135-150	-20.0
AIE 12326	150-160	-21.7

DISCUSSION

Figure 3 shows the variations in the isotopic composition of carbon starting in the head and going away in 15 mm interval towards the tip.

Starting at the length of 160 mm, the oldest hair shows a value of -21.7 ‰ corresponding to a diet composed mainly of C_3 plants (*ca* 80%). As we approximate to the head the values become more and more positives, reaching the value -10.8 ‰ at 15 mm, corresponding to a pure C_4 diet. It is interpreted in the sense that from a determined moment, perhaps at the beginning of her trip to the sacrifice site, the mummy was fed with corn and derivates beverages till any signal of C_3 plants disappears.

Fernández et al. (1999) used carbon, nitrogen and sulfur isotopes in order to decode the ethnic origin of the Mummy of the Mount Aconcagua. Particularly, $\delta^{13}C$ on hair presented cyclical variations that could be interpreted as alternating between C_4 (corn) (and marine food?) and C_3 plants derived aliments, perhaps due to the non-possibility of store grains out of the season of harvest. Fig. 2, modified from Fernández et al. (1999), shows those results.

Observed differences found in $\delta^{13}C$ of hair from the two mummies may be due to the provenance of individuals. In the case of the Aconcagua mummy, it seems that it was living near the site of sacrifice, thus she ate cultivated corn during the months following the harvest. If the culture had not storing possibilities, when corn was over, mainly C_3 plants were consumed and thus the hair isotope composition became more depleted. The final segment of the curve shows an increase in ^{13}C, which in this case may be due to continuation of the cycle or to the special diet given to the "messengers of deities".

The Chuscha mummy has probably been taken from a distant region, where corn was not significant for its diet (other ethnical origin?) and the journey to the sacrifice point started earlier. Since that moment, C_4 diet *i.e.* corn and derivate beverages, is responsible of the ^{13}C increase. Although, it is not possible to discard foods of marine origin.

CONCLUSIONS

^{13}C content of hair in well-preserved mummies is an excellent tool to trace the palaeodiet of the so-called messengers of deities *i.e.* children sacrificed in order to calm the anger of gods.

Different behaviors are found in the diet of the Chuscha and the Aconcagua mummies. The former shows a barely descendent pattern, while the latter exhibits a cyclical one.

One probable explanation is the different place where mummies originally lived: near the sanctuary of sacrifice that of the mount Aconcagua and the Chuscha one in a distant zone. The discussion about the ethnical origin of individuals continues.

Taking into account that ^{13}C of C_4 plants can be indistinguishable from that of certain marine foods; futures studies involving $\delta^{15}N$ and $\delta^{34}S$ will help to determine the relative contribution of every sources of alimentation.

AKNOWLEDGEMENTS

Authors are indebted to the staff of the Stable Isotopes Laboratory of INGEIS who perform $\delta^{13}C$ analyses, and the present owner of the Mummy Mr Mateo Goretti who provided the body and funds for this study.

REFERENCES

DeNiro, M.J. & Epstein, S., 1978. Influence of diet on the distribution of carbon isotope in animals. Geochimica et Cosmochimica Acta 42: 495-506.

Fernández C., J.; Panarello, H.O.; Schöbinger, J. 1999. The Inka mummy from Mount Aconcagua: Decoding the geographic origin of the "Messenger to the Deities" by means of stable carbon, nitrogen and sulphur isotope analyses. Geoarchaeology 14 Nº 1: 24-46.

Jones, R.J.; Ludlow, M.M.; Troughton, J.H.; Blunt, C.D., 1981. Changes in the natural carbon isotope ratios of the hair from steers feed diets of C_4, C_3 and C_4 species in sequence. Search 12 (3-4): 85-87.

Katzenberg, N.M. & Krouse, H.R., 1989. Application of stable isotope variation in human tissues to problems of identification. Canadian Society for Forensic Sciences Journal 22: 7-19.

Minson, D.J.; Ludlow, M.M.; Troughton, J.H., 1975. Differences in natural carbon isotope ratios of milk and hair from cattle grazing tropical and temperate pastures. Nature 256: 602.

Nakamura, K.; Schoeller, D.A.; Winkler, F.J.; Schmidt. H. L., 1982. Geographical variation in the carbon isotope composition of the diet and hair in contemporary man. Biomedical Mass Spectrometry 9: 390-394.

Panarello, H.O., 1987. Relaciones entre concentraciones de isótopos livianos utilizados como indicadores ambientales y de paleotemperaturas. Doctoral Tesis, Universidad de Buenos Aires. 103pp.

Panarello, H.O. & Fernández C., J., in press. Stable Carbon Isotope Measurements on Hair from Wild Animals from Altiplanic Environments of Jujuy, Argentina. Radiocarbon.

Schoeller, D.A.; Minigawa, M.; Slater, R.; Kaplan, I.R., 1986. Stable isotopes of carbon, nitrogen and hydrogen in the contemporary North America food web. Ecology of food and nutrition, 18: 159-170.

Tieszen, L.L.; Boutton, T. W.; Tesdahl, K. G.; Slade N.A., 1983. Fractionation and turnover of stable carbon isotopes in animal tissues, implications for ^{13}C analysis of diet. Oecologia 57: 32-37.

White, C.D., 1993. Isotopic determination of seasonality in diet and death from Nubian mummy hair. Journal of Archaeological Science 20: 657-666.

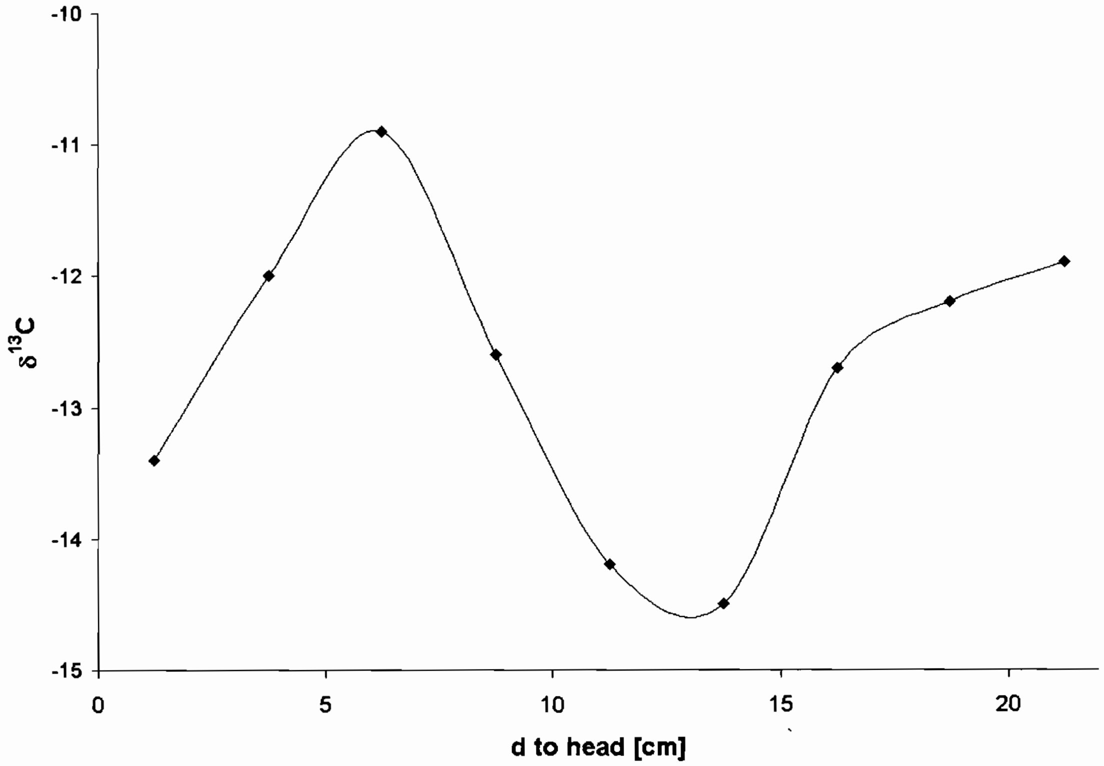

Figure 2. ^{13}C variations in the Mummy of Mount Aconcagua (after Fernández C. et al., 1999). Note the cyclical sequence.

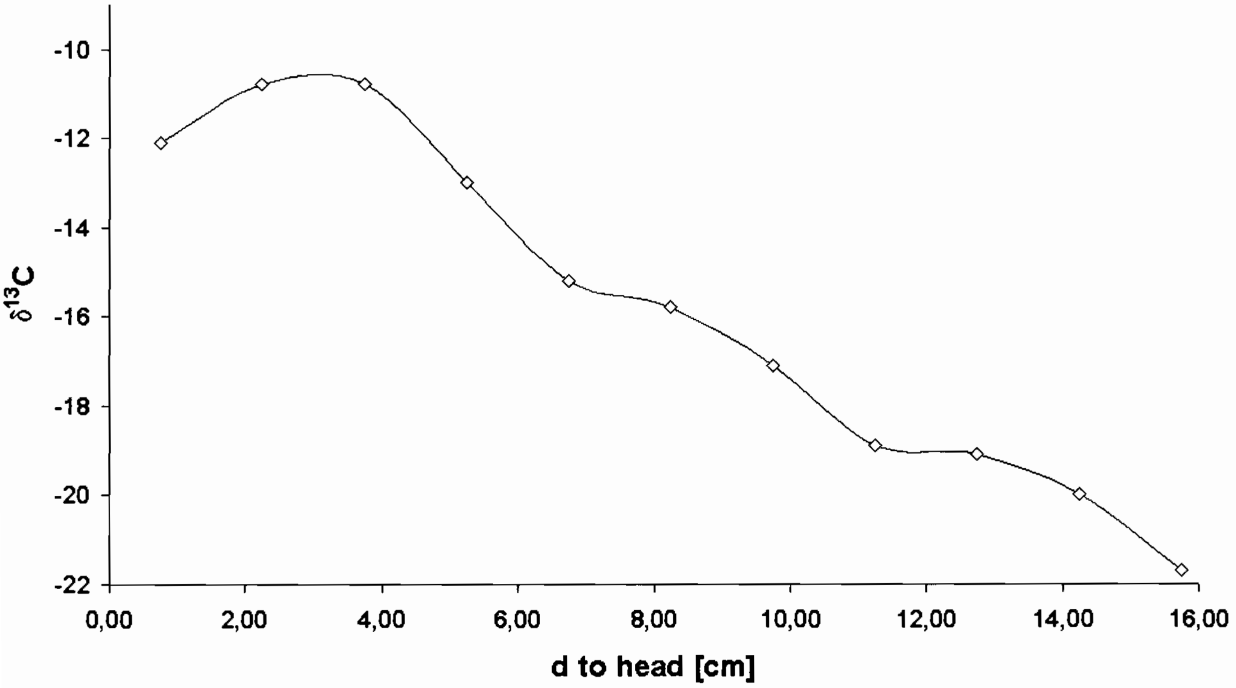

Figure 3. δ^{13}C variations along the hair of the Chuscha mummy from the head to the tip.

PALAEOVEGETATION AND PALAEOCLIMATE CHANGES DURING THE LATE QUATERNARY IN THE NORTHEASTERN BRAZIL, BASED ON CARBON ISOTOPES IN SOIL ORGANIC MATTER

Pessenda L.C.R.[1]; Ribeiro, A.S.[2]; Gouveia, S.E.M.[1]; Aravena, R.[3]; Boulet, R.[4] and Bendassolli, J.A.[1]

1. Center for Nuclear Energy in Agriculture (CENA), Box 96, 13400-000, Piracicaba-SP, Brazil. pessenda@cena.usp.br, susyeli@cena.usp.br; jab@cena.usp.br
2. Federal University of Sergipe - Department of Biology – Aracaju-SE, Brazil. asr@ufse.br
3. Department of Earth Sciences, University of Waterloo, Waterloo, Ontario N2L3G1, Canada. roaraven@sciborg.uwaterloo.ca
4. IRD, Geoscience Institute/University of São Paulo, 05508-900, São Paulo-SP, Brazil

Keywords: Carbon isotopes, soil organic matter, palaeovegetation, palaeoclimate, late Quaternary

INTRODUCTION

Most of the studies on palaeoenvironmental reconstruction during the late Quaternary and the Holocene have been based on pollen record obtained from lacustrine sediments.The regions investigated include, the Amazon (Absy & Van der Hammen, 1976; Van der Hammen & Absy, 1994), central (Ledru, 1993; Salgado-Laboriau et al., 1998) and southeastern and south regions (Roth & Lorscheitter, 1993; Behling, 1995, 1997a, b). Carbon isotopes technique in soil organic matter have also been applied to reconstruct palaeovegetation changes in south, southeastern (Pessenda et al., 1993, 1996a), central (Gouveia et al., 2002) and northern region of Brazil (Gouveia et al., 1997; Freitas et al., 2001).

Few palaeoclimate studies have been developed in the northeastern region, probably due to the difficult to find stable and perennial lakes. One of these studies carried out in the Icatu river valley located in the semi-arid region of Bahia state, documented vegetation and climate changes during the last 11,000 years BP (De Oliveira et al., 1999), with a humid and cold period during the late Pleistocene and drier climate during the early to mid Holocene. Other studies based on pollen data collected at Lagoa do Caçó, Maranhão state, show higher frequencies of *Podocarpus* at the end of the Pleistocene than today, suggesting a late-glacial increase of moist and cool climatic conditions (Ledru et al., 2001). From the early to mid Holocene (ca 6000 yrs BP) the Caçó lake level rose gradually (Sifeddine et al., in press) and the presence of microscopic charcoal fragments (Ledru et al., 2001), indicated that the humid phase was interrupted by dry phases.

In this paper we present the first comprehensive carbon isotope record of vegetation dynamics in the northeastern region of Brazil, covering the late Pleistocene and Holocene. This study is part of a major research program carried out at the Centre for Nuclear Energy in Agriculture (CENA), whose aim is to evaluate vegetation dynamics during the last 20,000 years in Brazil using carbon isotopes (Pessenda et al., 1996a, 1998a, b, c, 2001a; Gouveia et al., 2002; Freitas et al., 2001).

STUDY AREA

A mean annual temperature of around 26°C and a mean annual precipitation of around 1400-1500 mm characterize the climate of the region. The study area is located at an altitude between 100 and 120 m.

Soil samples were collected from eight points on a 78-km transect including Forest (F) and Cerrado (C) vegetations (woody savanna), along the road between the cities of Barreirinhas (referenced as km zero) and Urbano Santos (Fig.1). The sites are denominated F15 (the numbers represent km), F16 (transition), C16 (transition), C17, C20, C25, F46, C54 and F78.

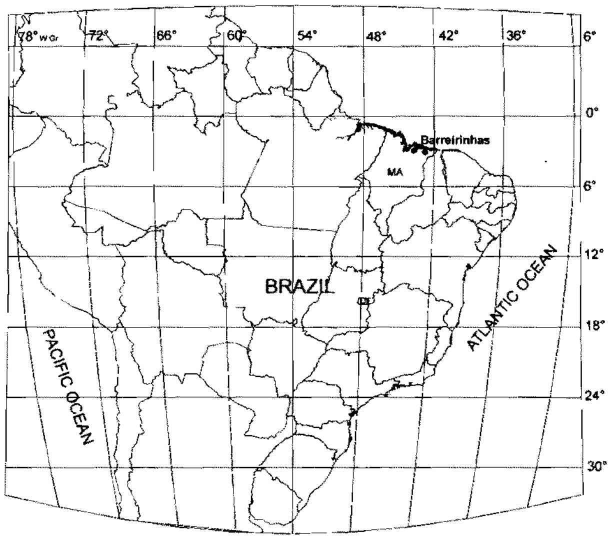

Figure 1. Map of Brazil showing the study site.

The study transect is located between the coordinates 2°52'S/45°55'W, corresponding to km 15 covered by "Restinga", the steppe vegetation along Brazil's coast which is dominate by *Manikara* sp, *Capaifera martii*, *Platonia insignis* and *Dimorphandra gardneriana* in the arboreal extract and 3°11'S/43°22'W in the km 78, covered by a Cerradão - semi deciduous forest (Pessenda et al., 1998). The sandy "Cerrado" savanna vegetation is located between the km 16 in an ecotone with Restinga vegetation and km 54, and is characterized by short trees (< 10 m) as *Curatella americana*, *Byrsonima* *verbascifolia*, *Annona coriacea* Mart. and grasses as *Andropogan bicornis* L., *Aristida longfolia* Trin, *Panicum* sp and *Paspalum* sp. Soil samples and buried charcoal fragments were also collected in a semi deciduous forest located 200 m (F200) from Caçó lake (2°58'S/43°25'W), and approximately 10 km northwestern from the ecosystem transect of 78 km.

METHODS

The soil of the study sites was classified as sandy soil (Typic Quartzipsament) over eolian sand. Soil samples were collected from trenches or with a hand-auger

From trenches, up to 5 kg of material were collected in 10 cm increments to a maximum depth of 300 cm. For $\delta^{13}C$ analysis, about 0.5 kg of soil and about 0.2 kg in case of samples collected by a hand auger was sieved (5 mm), dried at 50°C to a constant weight and root fragments were discarded by hand picking. The dry samples were sieved again (210 μm) and any remaining debris was removed by flotation in hydrochloric acid 0.01 M and wet sieved (210 μm). For ^{14}C analysis, the buried charcoal fragments in the soil received the conventional acid-alkaline-acid treatment (Pessenda et al., 1996a) and dried to a constant weight.

The grain size analyzes were carried out at the Soil Science Department of the Escola Superior de Agricultura "Luiz de Queiroz", Piracicaba, Brazil, on sieved through a 2 mm samples of dry soils. The results are expressed in percentage (%).

The carbon analyzes on soils ($\delta^{13}C$, total C) were carried out at the Stable Isotope Laboratory of CENA. Results are expressed as $\delta^{13}C$ with respect to PDB standard using the conventional δ (‰) notations:

$$\delta^{13}C\,(‰) = \frac{R_{sample} - R_{s\tan dard}}{R_{s\tan dard}} \times 1000$$

where, R_{sample} and $R_{standard}$ are the $^{12}C/^{13}C$ ratio of the sample and standard, respectively. Analytical precision is ± 0.2‰.

The ^{14}C analyzes on charcoal fragments collected at site F 200 were carried out by AMS at Isotrace Laboratory, University of Toronto, Canada. Radiocarbon ages are expressed in years B.P, normalized to a $\delta^{13}C$ of -25‰ PDB.

RESULTS

SOIL PROPERTIES AND TOTAL ORGANIC CARBON CONTENT

The grain-size analyses showed that the clay content was low (around 6 to 14%) in the six locations, with exception to km 46 (forest) that presented up to 28% of clay. The carbon content data show a general decrease with depth, similar to that observed in other studies in distinct regions of Brazil (Pessenda et al., 1998a, b, c). Values range from 1.42% in the shallow part of the soil to 0.04% in the deepest sample levels (Pessenda et al., 2001b).

CHARCOAL CHRONOLOGY AND SOM $\delta^{13}C$

These data are presented in Fig. 2. The radiocarbon dates range from about 1890 yrs BP (30-40 cm) to about 9000 yrs BP at 230-240 cm soil depth. Significant carbon isotopic variations were observed in some points of the study transects. The $\delta^{13}C$ values of soil surface characterized very well the distinct vegetation cover. $\delta^{13}C$ values of -27‰ to -25‰ represent the predominance of C_3 forest vegetation (F15, F16, C16). The $\delta^{13}C$ values of -21.4 to -17.7‰ showed the contribution of C_4 plants (C20, C25, C54), and soil under cerradão vegetation (C78) characterized by a $\delta\ ^{13}C$ value of -25.3‰. Litter samples from each location presented more depleted $\delta^{13}C$ values up to 0.9‰ (C54) and 3.5‰ (C78) compared to the shallow soils.

The cerrado sites (C17, C20, C25 and C54) show a wide range in isotopic composition that varies between -26.1‰ and -16.9‰. The forest sites (F15, F46 and F78) also show a wide range, with more depleted values, from -29.6 to -21.9‰. The soil at transition sites (F16 and C16) show more enriched values (-22.1 to -20.2‰) at the lower section (100-90 to 80-70 cm) than in shallow depth.

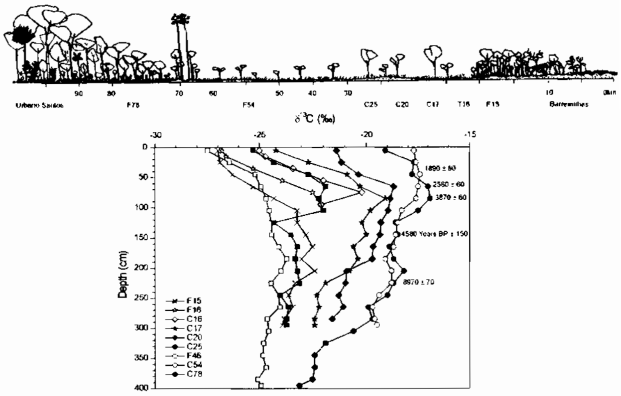

Figure 2. $\delta^{13}C$ variation of SOM of ecosystem transect and ^{14}C age of charcoal fragments.

DISCUSSION

CHARCOAL CHRONOLOGY AND $\delta^{13}C$ VARIATIONS

Based on extrapolation of the radiocarbon dates obtained with the charcoal fragments, it is possible to postulate that the carbon isotope record represents the last 15,000 yrs BP.

It was observed that since 330-320 cm (approximately between 12,000-11,000 yrs BP) up to approximately 70-60 cm (around 3000 yrs BP), there was a tendency of isotopic enrichment in several points of the soil transect. This is clearly observed in the locations of more dense cerrados in the km 17, 20 and 25 (-26.1 ‰ up to -16.9‰) and in the open cerrado in the km 54. The enrichment trend (-28.9‰ up to -21.9‰) in case of in km 78 is observed from approximately 4600 yrs BP until approximately 3000 yrs BP. The exceptions occurred in the forest in the km 15 and the forest LCF46, located around 10 km southeast of cerrado site km 54.

The results also indicated that mainly from 250-240 cm (approximately 9000 yrs BP) up to 70-60 cm (around 3000 yrs BP) the $\delta^{13}C$ values were clearly more enriched (up to -17‰), indicative of the presence of C_4 plants in several points of transect, aspect that can be associated with a drier climate in the region.

It is interesting to emphasize that the value of -19.5‰ at 300 cm for C54, probably characterize the presence of an open vegetation from late Pleistocene/ early Holocene. The isotopic enrichment up to -17.4‰ at 50 cm soil depth (around 2500 yrs BP) followed the general tendency and reinforces the presence of a paleocerrado in that location.

In terms of vegetation dynamics it was verified that approximately since the late Pleistocene up to the early Holocene, arboreal vegetation probably related to forest, covered most of the ecosystem transect of 78 km constituted of forest-cerrado-restinga ecotone on the Barreirinhas region. Afterwards, since approximately 8000 yrs BP until around 3000 yrs BP the cerrado expanded, probably related to the presence of a drier climate. From 3000 yrs BP to the present, more depleted $\delta^{13}C$ of SOM in several points of soil transect were interpreted as a forest expansion over the cerrado, due to the return to a humid climate and probably similar to the present.

The paleoclimatic interpretations for this study is in agreement with the article of De Oliveira et al. (1999), where a probable dry period dominated the north region of Bahia from the early Holocene (around 9000 yrs BP) up to mid-Holocene (4000-3000 yrs BP), following a more humid period and probable similar to the present.

In Carajás (PA), central Amazon region, around 1400 km west from Barreirinhas region, Sifeddine et al. (1994) verified through pollen analysis em lacustrine sediment, a dry period between approximately 7000 yrs BP and 4000 yrs BP, reinforcing the interpretations.

Other studies based on used carbon isotopes of SOM in an ecosystem transect of a ecotone forest-savanna in the Humaitá region, southern part of Amazonas State, approximately 3000 km west from Barreirinhas) verified that in the period of 17,000 yrs BP to 9000 yrs BP the transect was covered by forest vegetation (Gouveia et al., 1997; Pessenda et al., 1998a, c, 2001a; Freitas et al., 2001). From about 9000-8000 yrs BP up to approximately 3000 yrs BP, several locations in the study transect were substituted by savanna vegetation (C_4 grasses), probably due to the presence of dry climate. Since approximately 3000 yrs BP up to the present, the isotopic data indicated the predominance of C_3 plants, related with the presence of a humid climate. Similar palaeovegetation and palaeoclimatic reconstruction were documented by Pessenda et al. (1998d) in the southeastern part of Rondônia State, south Amazon region.

It is important to high light different palaoevegetation and palaeclimatic signals were observed in the southeast and south regions of Brazil, in the late Pleistocene/early Holocene.

Isotopic data of Salitre, western region of Minas Gerais State (Pessenda et al., 1996a, 1998d), Piracicaba, São Paulo State and Londrina, Paraná State (south) (Pessenda et al., 1996b, 1998d) and Jaguariúna, São Paulo State (Gouveia et al., 1999, 2002) indicated the significant presence of C_4 grasses since approximately 11,000 yrs BP till about 4000 yrs BP, that was associated to the presence of a dry climate. Palinological data from lake sediments also indicated a dry climate in similar period in sites located in the south of Brazil (Ledru et al., 1996; Behling, 1997a, 1998).

A hypothesis for the occurrence of these climate changes could be related with the position of Intertropical Convergence Zone (ITCZ) between 12,400 and 8800 calendar yrs, which correspond to approximately 10,500 yrs BP and 7300 yrs BP. According with Martin et al. (1993), the present precipitation over the South America continent is amply controlled by seasonal movements of ITCZ. During the summer, the ITCZ moves to the south due to the heating of continent. In the period 12,400 yrs and 8800 yrs, the east part of the Amazon received substantial humidity, while in the Bolivian Altiplano (located more in the south and to the east) was arid. The authors suggested this pattern was related to the ITCZ position more in the north during the summer, in relation to the present days. In similar form in the mentioned period, the northeastern and Amazon regions presented higher precipitations than the south region, occurring situations of more humid climate in the north and drier in the south, between approximately 10,500 yrs BP and 7300 yrs BP.

REFERENCES

Absy, M.L. & Van der Hammen, T., 1976. Some paleoecological data from Rondônia, Southern part of Amazon Basin. Acta Amazônica, v.6, n.3, p.283-299.

Behling, H., 1995. A high resolution Holocene pollen record from Lago do Pires, SE Brazil: vegetation, climate and fire history. Journal of Paleolimnology, v.14, n.3, p.253-268.

Behling, H., 1997a. Late Quaternary vegetation, climate and fire history from the tropical mountain region of Morro de Itapeva, SE Brazil. Palaeogeography, Palaeoclimatology, Palaeoecology, v.129, p.407-422.

Behling, H., 1997b. Late Quaternary vegetation, climate and fire history of the Araucaria forest and campos region from Serra Campos Gerais, Paraná State (South Brazil). Review of Palaeobotany and Palynology, v.97, p.109-121.

Behling, H., 1998. Late Quaternary vegetational and climatic changes in Brazil. Review of Palaeobotany and Palynology, v.99, p.143-156.

De Oliveira, P.E.; Barreto, A.M.F.; Suguio, K., 1999. Late Pleistocene/Holocene climatic and vegetacional history of the Brazilian caatinga: the fossil dunes of the middle São Francisco River. Paleogeography, Paleoclimatology, Palaeoecology, v.152, p.319-337.

Freitas, H.A.; Pessenda, L.C.R.; Aravena, R.; Gouveia, S.E.M.; Ribeiro, A.S.; Boulet, R., 2001. Late Quaternary vegetation dynamics in the Southern Amazon Basin inferred from carbon isotopes in soil organic matter. Quaternary Research, v.55, p.39-46.

Gouveia, S.E.M.; Pessenda, L.C.R.; Aravena, R.; Boulet, R.; Roveratti, R.; Gomes, B.M., 1997. Dinâmica das vegetações durante o Quaternário Recente no sul do Amazonas indicada pelos isótopos do carbono (^{12}C, ^{13}C, ^{14}C) do solo. Geochimica Brasiliensis, v.11, n.3, p.355-367.

Gouveia, S.E.M.; Pessenda, L.C.R.; Aravena, R., 1999. Datação da fração humina da matéria orgânica do solo e sua comparação com idades ^{14}C de carvões fósseis. Química Nova, v.22, n.6, p.810-814.

Gouveia, S.E.M.; Pessenda, L.C.R.; Arvena, R.; Boulet, R.; Scheel-Ybert, R.; Bendassoli, J.A.; Ribeiro, A.S.; Freitas, H.A., 2002. Carbon isotopes in charcoal and soils in studies of paleovegetation and climate changes during the late Pleistocene and the Holocene in the southeast and centerwest regions of Brazil. Global and Planetary Change, v.33, p.95-106.

Ledru, M.-P., 1993. Late Quaternary and climatic changes in Central Brazil. Quaternary Research, v.39, p.90-98.

Ledru, M.-P.; Braga, P.I.S.; Soubiès, F.; Fournier, M.; Martin, L.; Suguio, K.; Turcq, B., 1996. The last 50,000 years in the Neotropics (Southern Brazil): evolution of vegetation and climate. Palaeogeography, Palaeoclimatology, Palaeoecology, v.123, p.239-257.

Ledru, M.-P.; Cordeiro, R.C.; Dominguez, J.M.L.; Martin, L.; Mourguiart, P.; Sifeddine, A.; Turcq, B., 2001. Late-glacial cooling in Amazonia inferred from pollen at Lagoa do Caçó, Northern Brazil. Quaternary Research, v.55, p.47-56.

Martin, L.; Fournier, M.; Mourguiart, P.; Sifeddine, A.; Turcq, B., 1993. Southern oscillation signal in South American palaeoclimatic data of the last 7.000 years. Quaternary Research, v.39, p.338-346.

Pessenda, L.C.R.; Camargo, P.B.; Cruz, M.V.L.; Lisi, C.S.; Valencia, E.P.E., 1993. Laboratório de radiocarbono do CENA/USP no programa internacional de intercomparação laboratorial de resultados. Química Nova, v.16, n.3, p.221-223.

Pessenda, L.C.R.; Aravena, R.; Melfi, A.J.; Telles, E.C.C.; Boulet, R.; Valencia, E.P.E.; Tomazello, M., 1996a. The use of carbon isotopes (C-13, C-14) in soil to evaluate vegetation changes during the Holocene in Central Brazil. Radiocarbon, v.38, n.2, p.191-201.

Pessenda, L.C.R.; Valencia, E.P.E.; Camargo, P.B.; Telles, E.C.C.; Martinelli, L.A.; Cerri, C.C.; Aravena, R.; Rozanski, K., 1996b. Natural radiocarbon measurements in brazilian soils developed on basic rocks. Radiocarbon, v.38, n.2, p.203-208.

Pessenda, L.C.R.; Valencia, E.P.E.; Aravena, R.; Telles, E.C.C.; Boulet, R., 1998a. Paleoclimate studies in Brazil using carbon isotopes in soils. In: Wasserman, J.C.; Silva-Filho, E.; Villas-Boas, R. (Ed.) Environmental geochemistry in the tropics. Berlin: Springer-Verlag, p.7-16.

Pessenda, L.C.R.; Gouveia, S.E.M.; Gomes, B.M.; Aravena, R.; Boulet, R.; Ribeiro, A.S., 1998b. Studies of palaeovegetation changes in the central Amazon by carbon isotopes (^{12}C, ^{13}C, ^{14}C) of soil organic matter. In: International Symposium on Isotope Techniques in the Study of Past and Current Environmental Changes in the Hydrosphere and the Atmosphere, Vienna, 1998. Proceedings..., Vienna: IAEA, p.645-652. (IAEA-SM, 349/46)

Pessenda, L.C.R.; Gouveia, S.E.M.; Aravena, R.; Gomes, B.M.; Boulet, R.; Ribeiro, A.S., 1998c. ^{14}C dating and stable carbon isotopes of soil organic matter in forest-savanna boundary areas in the southern Brazilian Amazon region. Radiocarbon, v.40, n.2, p.1013-1022.

Pessenda, L.C.R.; Gomes, B.M.; Aravena. R.; Ribeiro, A.S.; Boulet, R.; Gouveia, S.E.M., 1998d. The carbon isotope record in soils along a forest-cerrado ecosystem transect: implications for vegetation changes in the Rondonia state, Southwestern Brazilian Amazon region. The Holocene, v.8, n.5, p.631-635.

Pessenda, L.C.R.; Boulet, R.; Aravena, R.; Rosolen, V.; Gouveia, S.E.M.; Ribeiro, A.S.; Lamotte, M., 2001a. Origin and dynamics of soil organic matter and vegetation changes during the Holocene in a forest-savanna transition zone, Brazilian Amazon region. The Holocene, v.11, n.2, p.250-254.

Pessenda, L.C.R.; Ribeiro, A.S.; Gouveia, S.E.M.; Bendassoli, J.A.; Boulet, R.; Pellegrinotti, T.C.; Silva, V.F. 2001b. Dinâmica do ecótono cerrado-floresta desde o Pleistoceno tardio na região de Barreirinhas, estado do Maranhão, empregando os isótopos do carbono do solo. In: Congresso da ABEQua, 8., Imbé, 2001. Boletim de Resumos..., Imbé: UFRGS; CECO; ABEQUA, p.344-345.

Roth, L. & Lorscheitter, M.L., 1993. Palynology of a bog in Parque Nacional de Aparados da Serra, East Plateau of Rio Grande do Sul, Brazil. Quaternary of South America and Antartic Peninsula, v.8, p.39-69.

Salgado-Labouriau, M.L.; Barberi, M.; Ferraz-Vicentini, K.R.; Parizzi, M.G., 1998. A dry climatic event during the late Quaternary of tropical, Brazil. Review of Palaeobotany and Palynology, v.99, p.115-129.

Sifeddine, A.; Fröhlich, F.; Fournier, M.; Martin. L.; Servant, M.; Soubiès, F.; Turcq, B.; Suguio, K.; Volkmer-Ribeiro, C. 1994. La sédimentation lacustre indicateur de changements des paléoenvironnements au cous des 30000 dernières années (Carajas, Amazonie, Brésil). Compte Rendus de l'Academie des Sciences. Série 2, v.318, p.1645-1652.

Sifeddine, A.; Albuquerque, A.L.S.; Ledru, M.-P.; Turcq, B.; Knoppers, B.; Martin, L.; Mello, W.Z.; Passenau, H.; Dominguez, J.M.L.; Cordeiro, R.C.; Abrão, J.A.; Bittencourt, A.C.S.P., in press. Paleogeography, Paleoclimatology, Paleoecology.

Van der Hammen, T. & Absy, M.L., 1994. Amazonia during the last glacial. Palaeogeography, Palaeoclimatology, Palaeoecology, v.109, p.247-261.

U-Pb SPOT DATING BY LA/ICP-MS OF SINGLE DETRITAL ZIRCON GRAINS COLLECTED AT THE MOUTH OF THE AMAZON RIVER: CONTINENTAL CRUSTAL GROWTH HISTORY OF THE AMAZON RIVER BASIN

Rino, S.[1]; Motoki, A.[2]; Hirata, T.[1] and Maruyama, S.[1]

1. Tokyo Institute of Technology, Japan, Tokyo, Japan. 2-12-1, O-okayama, Meguro-ku, Tokyo, Japan. rsyuji@geo.titech.ac.jp, hrtl@geo.titech.ac.jp, smaruyam@geo.titech.ac.jp
2. Universidade do Estado do Rio de Janeiro, Rio de Janeiro, Brazil. Rua São Francisco Xavier 524, Sala A4023, Maracanã, Rio de Janeiro, 20550-990, Brasil. motoki@uerj.br

Keywords: Continental growth, U-Pb, LA/ICP-MS, detrital zircon, Amazon

Alluvial sand of the mouth of large rivers is composed of the mineral grains originated from various areas within the fluvial basin, forming a general mixture of the region. They are constituted predominantly by quartz, but contain also small amount of heavy minerals, such as ilmenite, magnetite, zircon, rutile, monazite, tourmaline, and rarely microdiamond. Among them, zircon is a highly stable one against chemical and physical weathering during fluvial transportation. In this sense, detrital zircon of river outlet represents that of whole continental crust rocks of the fluvial basin.

In case of a very large river of continental extension, such as the Amazon, the La Plata, the Mississippi, and the Macknzie, river mouth detrital zircon represents a huge area, corresponding sometimes to entire craton or a half of the continent. Therefore, the geochronological studies of detrital river mouth zircon of main continental scale rivers of the world can reveal continental crust growth history of the Earth. This paper presents partial results of this worldwide research project, applied to Amazon River.

In general, orogenic belts of the late Proterozoic and the Phanerozoic occupy about 50% of continental area. In case of South American Continent, the Pan-African orogenic belts (about 600 Ma) constitute a well-developed network, surrounding old continental crust massif, so-called craton or terrain. These old continental platforms are made up of granite and orthogneiss, showing two important tectonic cycles: the Trans-Amazonian (2000-2200 Ma) and the Jequié (about 2700 Ma). However, recent studies revealed that the ages of the cratonic rocks are much more complex (e.g. Tassinari et al., 2000).

On the other hand, the orogenic belts of the Phanerozoic and the late Proterozoic are composed dominantly, more than 90%, of sedimentary or meta-sedimentary rocks. The zircon grains present in these rocks were derived from older granitic rocks of the source area. In this sense, either in the regions in which granitic rocks are directly exposed at the surface, or in the areas covered by sedimentary or meta-sedimentary formations, the river mouth zircon grains contain geochronological information related to their primary continental crust formation event of the fluvial basin.

During metamorphic events, original igneous zircon overgrows on the surface of the grains (Fig. 1). By means of multiple metamorphic experiences, multiple-zoning structure can be formed. In order to get the age of juvenile continental crust formation age and to elaborate continental crust growth history, the U-Pb or Pb-Pb spot (pinpoint) dating must be realised at the core domain of the zircon grains. This purpose can be performed by means of SHRIMP or LAICPMS.

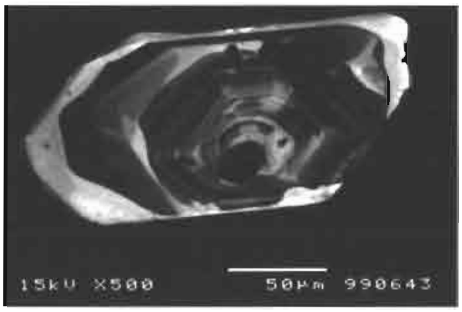

Figure 1. Cathode-luminescence image of a zircon grain collected from the mouth of Amazon River, showing zonal structure formed by overgrowth.

Goldstein et al. (1997) presented a pioneer study based on above-mentioned conception, dating 49 detrital zircon grains collected from Orinoco River sand with help of SHRIMP. In spite of small number of grains analysed, the U-Pb spot ages showed a sharp and clear fingerprint of the tectonic history of the continental crust basement of Orinoco River fluvial basin. The age histogram affirmed prominent age populations of 2800 Ma (Alto Guyana Imataca event), 2000-2200 Ma (Trans-Amazonian one), and 1000-1200 Ma (Grenvillean one).

However, in order to establish highly reliable tectonic fingerprint of a very large area, such as Amazon River fluvial basin, a much larger number of detrital zircon dating is required. Although SHRIMP is high precision U-Pb dating equipment, it takes too much time for spot dating of hundreds of zircon grains. Therefore, a rapid U-Pb spot dating is desired.

To achieve the purpose, the authors adopted LA/ICP-MS installed at Tokyo Institute of Technology. The mass spectrometer is a ThermoElemental VG PlasmaQuad 2 quadrupole based-ICP-MS equipped with S-option interface (Hirata & Nesbitt, 1995, 1997). With application of the chicane ion lens, the elemental sensitivity is enhanced by factors of 3 to 4, and the instrument has count rates about 2 x 108 cps/μg g^{-1} for U (Hirata, 2002), while the background counts was significantly minimized. Typical background counts for mid-mass range (80-150 amu) is about 5 cps, and for high mass range (220 Dalton) is 2~5 cps. The slightly higher background in mid-mass range is mainly due to detection of scattered Ar-related polyatomic ions. Moreover, the chicane ion lens has the added advantage of minimizing the oxide formation.

The laser ablation system is of MicroLas production (Gottingen, Germany) GeoLas 200CQ. This system utilizes Lambda Physik (Gottingen, Germany) COMPex 102 ArF excimer laser as a 193 nm DUV (deep ultraviolet) light source. The instrumental sensitivities achieved by the present LA/ICP-MS are 1.5 x 104 cps/μg g-1 for Pb and U on NIST 610 SRM from a diameter of 20 μm pit size ablated by 5 Hz repetition rate with source pulse energy of 140 mJ.

All measurements are carried out in peak jump acquisition mode. For U-Pb age determinations, the peaks ^{202}Hg, ^{204}Pb (^{204}Hg), ^{206}Pb, ^{207}Pb, and ^{238}U are monitored. A major problem associated with the analysis of ^{204}Pb using the LA/ICP-MS is ^{204}Hg isobaric interference. It is recognized that Hg is mainly originating from Ar gas, since the Hg signals have long duration and does not decay away with time. Twenty-two ^{204}Hg are corrected for by measuring ^{202}Hg (which can reach 800 cps) and subtracted an appropriate number of counts from total signal intensity at 204 Dalton. Typical bulk error for the standard of about 1000 Ma is less than 3%. No statistic correction to improve apparent dating precision is applied.

The detrital zircon of Amazon River has been collected at Santana Island, about 30km west south west of Macapá, State of Amapá. In total, 20kgs' natural river sand has been collected. The heavy minerals have been concentrated up to 20 times by means of in place panning. In laboratory, zircon grains are extracted using the ZR-2001 zircon separation system, which is installed at Tokyo Institute of Technology.

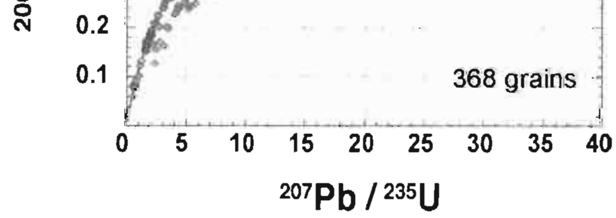

Figure 2. Concordia plot diagram of U-Pb spot dating with help of LAICPMS for 368 grains of detrital zircon collected from the mouth of Amazon River. The error bar corresponds to 1σ.

More than 70% of Amazon fluvial basin belong the Amazon Craton. Pan-African continental collision zone, Tocantins belt of about 600Ma, is present in southeastern part of the fluvial basin, and Phanerozoic one, Andes orogenic belt, takes place along the western margin.

In the Central Amazonian region, mid-downstream of Amazon fluvial basin, the oldest rocks of the Amazon Craton, 2300 to 3100 Ma, are distributed. To the west, the radiometric ages of basement rocks tend to become gradually younger: in Maroni-Itacaiúna region, midstream, 1950 to 2200 Ma; in Ventuari Tapajós region, mid-upstream, 1800 to 1950 Ma; Rio Negro region, upstream, 1550 to 1800 Ma; Rondonian - San Ignácio, south-west upstream, 1300 to 1500 Ma; Sunsas, south-west end of the Amazon Craton, 1000 to 1250 Ma. The last group is correlated to the Grenvillean cycle (Teixeira et al., 1989; Tassinari, 1999; Tassinari et al., 2000).

In total, 369 spots of detrital zircon grains are dated. More than a half of the data falls close to the concordia curve. However, but some of them fall significantly to the right (Fig. 2) due probably to Pb loss during the tectonic events after igneous formation of these zircon grains. In order to solve above-mentioned problem, ^{207}Pb-^{206}Pb age histogram also has been elaborated.

The U-Pb age histogram shows existence of three prominent age populations (Fig. 3a). The highest peak, that occupies 34% of all data, is of 1800-2200 Ma. This event is correlated to the Trans-Amazonian cycle and the rocks are found in Maroni-Itacaiúna region, of the midstream. The second highest one, 22%, is of 2400-2700 Ma, of Central Amazon region. The third one, 7%, is of 900-1100 Ma, of the Sunsas region of the Grenvillean event. Also observed two plateaux, of 1300-1800 Ma and of 2700 to 3200 Ma, which correspond respectively to of the Rio Negro - San Ignácio regains of the upstream and Central Amazon region of the mid-downstream. Only four grains show an age little older than the Pan-African event. The oldest ^{238}U-^{206}Pb age is 3401±54 Ma.

The ^{206}Pb-^{207}Pb age histogram shows a similar pattern of the U-Pb one, but presents more clearly tectonic fingerprint with higher and narrower age population peaks and lower background (Fig. 3b). The highest one, 37% of all data, is of 2000 to 2300 Ma of the Trans-Amazonian cycle, the second one, 29%, is of 2500-2800 Ma of the Central Amazon event, and the third one, 6%, is of 1000-1200 Ma of the Grenvillean. These peaks are slightly older than those of the U-Pb histogram, with difference of about 100 million years. A low plateau of 2700-3400 Ma, takes place, however the plateau of the Rio Negro - San Ignácio, 1300-1800 Ma, is not clearly observed. No Pan-African like peak is detected. It is worth noting that three grains older than 3500 Ma are present, and the oldest ^{207}Pb-^{206}Pb age is 3523 ± 41 Ma. This is one of the oldest radiometric ages of South America Continent.

In case of Orinoco River, the U-Pb dating of detrital zircon showed sharp age histogram in comparison with other method of radiometric dating (Goldstein et al., 1997). In case of Amazon River, the age histogram of detrital zircon, especially that of ^{207}Pb/^{206}Pb method, also shows very sharp age population peaks, indicating clearly continental crust formation events in comparison with the studies based on Sr (Cordani et al., 1988) and Nd (Cordani & Sato, 1999; Cordani et al., 2000) isotopes. It is noted that almost no Pan-African ages are detected in both the U-Pb and the Pb-Pb histograms, and the Rio Negro - San Ignácio age plateau in the Pb-Pb histogram. The fact suggests that the spot ages of zircon core,especially of Pb-Pb ones, are stable and maintained even in later metamorphic event. Therefore, the U-Pb dating by means of LAICPMS of detrital zircon grains of, continental size large rivers is useful for the purpose of continental growth history study.

A. U-Pb age histogram

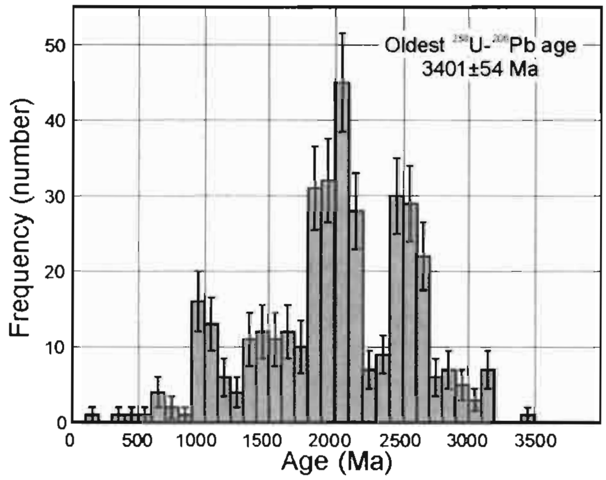

B. Pb-Pb age histogram

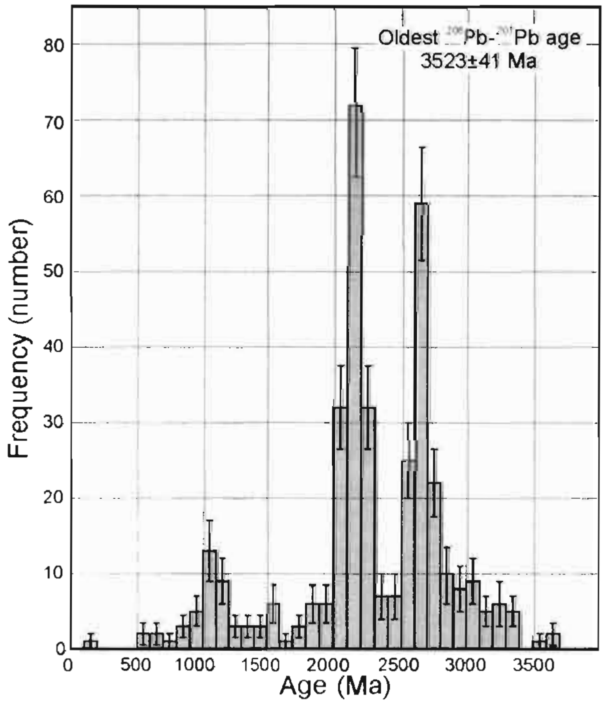

Fig. 3. Histograms for U-Pb ages (A) and Pb-Pb ages for 369 grains of detrital zircon collected from the mouth of Amazon River outlet. The error bar correspond to 1σ.

REFERENCE

Cordani, U.G. & Sato, K.. 1999. Crustal evolution of the South American Platform based on Nd isotope systematics on granithoid rocks. Episodes, 22-3, 167-173.

Cordani, U.G.; Teixeira, W.; Tassinari, C.C.G.; Kawashita, K.; Sato, K. 1988. The growth of the Brazilian shield. Episodes, 11-3, 163-167.

Cordani, U.G.; Sato, K.; Teixeira, W.; Tassinari, C.C.G.; Basei, M.A.S., 2000. Crustal evolution of the South American Platform. The Amazonian Craton. In U.G. Cordani, E.J. Milani, A. Thomáz Filho, and D.A. Campos. Tectonic evolution of South America, 19-40.

Goldstein, S.L.; Arndt, N.T.; Stallard, R.F., 1997. The history of continent form age of U-Pb zircon from Orinoco River sand and Sm-Nd isotopes in Orinoco Basin. Chemical Geology, 139, 271-286.

Hirata, T. 2002. In-situ precise isotopic analysis of tungsten using laser ablation-multiple collector-inductively coupled plasma mass spectrometry (LA-MC-ICPMS) with time resolved data acquisition technique, J. Anal. Atom. Spectrom., 17, 204-210.

Hirata, T. & Nesbitt, R.W., 1995. U-Pb isotope geochemistry of zircon: Evaluation of laser prove-inductively coupled prasma mass spectrometer technique. Geochim. Consmochim. Acta, 59, 2491-2500.

Hirata, T. & Nesbitt, R.W., 1997. Distribution of platinum group elements and rhenium between metallic phases of iron meteorites. Earth and Planet. Sci. Lett. 147, 11-24.

Tassinari, C.C.G., 1999. Geochronologica Province of the Amazonian Craton. Episodes, 22-3, 174-182.

Tassinari, C.C.G.; Bittencourt, J.S.; Geraldes, M.C.; Macambira, M.J.B.; Lafon, J.M., 2000. The Amazonian Craton. In U.G. Cordani, E.J. Milani, A. Thomáz Filho, D.A. Campos. Tectonic evolution of South America, 41-95.

Teixeira, W.; Tassinari, C.C.G.; Cordani, U.G.; Kawashita, K., 1989. A review of the geochronology of the Amazonian Craton: tectonic implications. Precambrian Research, 42, 213-227.

LEACHING TECHNIQUE AND PARTIAL DIGESTION USING MICROWAVE OVEN: TREATMENT PROCEDURES FOR U-Pb DATING OF METAMICTIC AND OVERGROWN ZIRCONS

Sato, K.[1]; Siga Jr., O.[1]; Basei, M.A.S.[1]; Nutman, A.P.[2] and Sproesser, W.[1]

1. Geoscience Institute of São Paulo University-SP-Brazil, CEP05422. keisato@usp.br
2. RSES - Australian National University – Canberra – Act 0200, Australia

Keywords: SHRIMP, TIMS, leaching, high uranium, microwave

THE ANALYTIC METHOD

The leaching technique was used to treat metamict zircons showing overgrowth rims and high uranium concentration. Petrographic studies using cathodeluminescence (CL) and transmitted light (TL) was carried out in order to evaluate the method efficiency. Crystals (around 10) of the same typology were photographed. These crystals, previously washed with HNO3, were then put in a savillex cup and attacked by an with 600µl of concentrated HF. The savillex cup was placed inside a microwave oven at temperatures not higher than 130 °C and 4 cycles of 90 minutes of heating and 10 minutes in stand-by (oven turned off) were applied in order not to overload or damage the microwave. After 360 minutes of heating, less than 5% of the acid solution evaporated from the savillex cup. With a micropipette the acid solution containing Pb and U leached from zircon rims was carefully separated from the remaining crystals and transported to another clean savillex cup, to which ^{205}Pb spike and H_3PO_4 were added. HF was completely evaporated on a hot plate, remaining only H_3PO_4 and leached material at the bottom of the cup.

To the first savillex containing partially leached zircons a reload of acid solution containing 600 µl of concentrated HF was again added and the whole procedure was repeated for 4 times (I, II, III and IV).

Before the final chemical attack, the grains were recounted and photographed. The dissolution using HF and HNO_3 took place in a digestion bomb with a special stainless steel protector placed inside a resistive oven kept at 180 °C during 3 days for a complete chemical digestion of the zircons. Pb and U were purified using the ion exchange column. The resulting H_3PO_4 solution containing Pb and U was loaded with silicagel on the Re filament and the isotopes ratio were measured by Finnigan MAT 262 Thermal Ionization Mass Spectrometer (TIMS).

DESCRIPTION OF THE SAMPLES

For the proposed experiment, 3 zircon fractions were selected from the two different zircon typologies observed in the leucosome veins present in the Atuba migmatites from Atuba quarry (north of Curitiba). These rocks are located in the Atuba Complex - SE Brazil.

- Group I: coarse-grained zircons, of average sizes between 200 and 400 µm x 130 µm, prismatic habit, relatively homogeneous, soft brown in reflective light and dark in transmitted light.
- Group II: Similar to group I in habit and in size but with intense metamictization. The grains are dark brown and inhomogeneous in reflective light and opaque in transmitted light

Figure 1 illustrates the above-mentioned characteristics using cathodeluminescence images (CL). The CL images show grains generally homogeneous, but locally with hints of oscillatory zoning parallel to the grain boundaries. There are some recrystallisation domains which appear bright and homogeneous in the images. All SHRIMP analyses show high U content (3000 – 7000 ppm, Sato et al., 2003), with variable and generally high common Pb content. The Fig. 2 show TeraWasserburg concordia diagram from SHRIMP analysis. One zircon yielded the oldest $^{207}Pb/^{206}Pb$ date of 795 ± 15 Ma. A group of four analysis yielded a weighted mean $^{207}Pb/^{206}Pb$ date of 573 ± 55 Ma with 96.5% confidence and MSWD of 0.4.

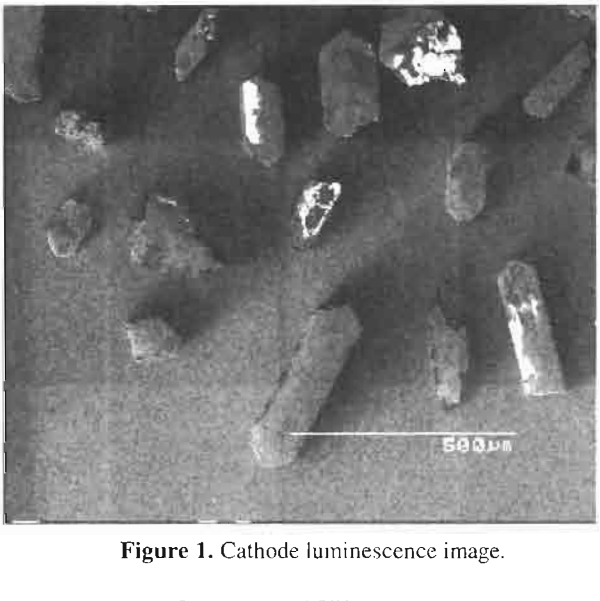

Figure 1. Cathode luminescence image.

DISCUSSION OF THE RESULTS

The grains were completely destroyed after 2 leaching phases of 6 hour cycles for each phase (Fig. 3).

It is possible to see in the Fig. 4a that U content goes down in the exponential form. These results may to indicate a preferential U leaching or of a possible higher U concentration in the zircon rim. The total amount of Pb and U extracted for the 4 leaching stages exceed 85% for Pb (Fig 4b). The values of $^{207}Pb/^{206}$ x $^{238}U/^{206}Pb$ ratios of the 3 initial phases plot on a straight line that intercepts

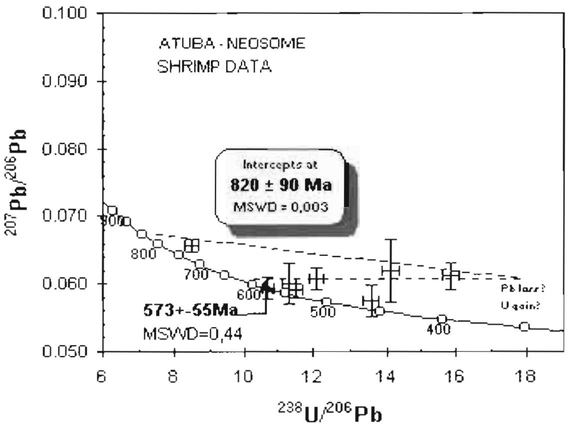

Figure 2. TeraWasserburg diagram. SHRIMP zircon analyses.

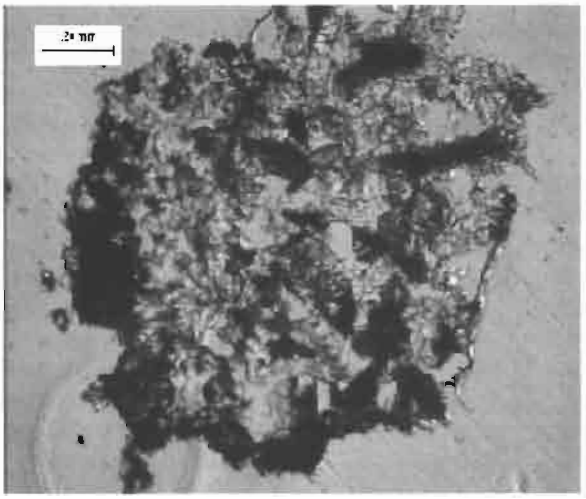

Figure 3. Leach residue after IV step. The zircons are completely destroyed in very small fragments.

the concordia curve between 700 and 800 Ma (Figs 5 a, b, c, d, e, f). This value is very close to the zircon age obtained by SHRIMP (Fig. 2, $^{207}Pb/^{206}Pb$ age of 795 ± 15 Ma). The large age variation are due: very large amounts of common Pb, intense metamictization, continuous lead loss and also mixture age between inherited zircon (around 1700 Ma, Fig. 6) and the Neoproterozoic overgrowths around 570 Ma (SHRIMP ages; Sato et al., 2003). In addition for each leaching step it also is possible to see high U for step I (normal discordance) and decreasing to low U content for step IV (reverse discordance).

The final leaching fractions (attack in the bomb) yielded the U/Pb age (upper intercept) of 1635 ± 25 Ma (Fig. 6). These values registered in the residue material may reflect a mixed age with major contribution from inherited Paleoproteozoic material.

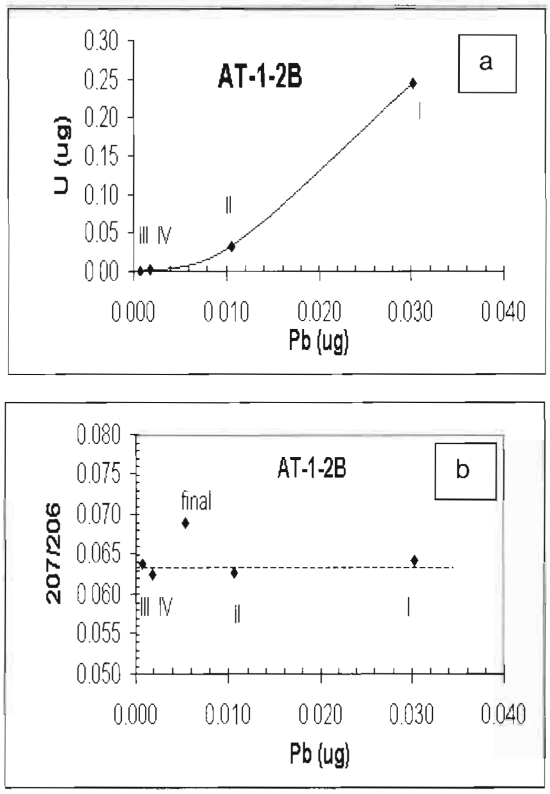

Figure 4. a) The U content decrease relative to Pb in the exponential mode from leach step I to IV; b) The fig. 3b shows the ratio $^{207}Pb/^{206}Pb$, with Neoproterozoic age, no change to 4 initial phases but the final residue data indicate Paleoproterozoic inherited component.

FINAL CONSIDERATIONS

The partial chemical attack using HF and HNO_3 was done in savillex cup and microwave oven. Normally the dissolution occur only in the zircon rim due low temperature (< 130 °C), but highly metamictic zircons the chemical digestion was very strong (>85%). The initial leaching fractions indicate Neoproterozoic ages (~ 750 Ma). These ages are probable a mixture between the Neoproterozoic recrystallized grain and the Paleoproterozoic inherited material that was evidenced in the final residues after the dissolution in the bomb.

REFERENCE

Sato, K; Siga Jr., O; Nutman, A. P.; Basei, M.A.S.; McReath, I.; Kaulfuss, G., 2003. The Atuba Complex. Southern South American Platform: Archean Components and Paleoproterozoic to Neoproterozoic Tectonothermal Events. Gondwana Research, 6 (2):.251-263.

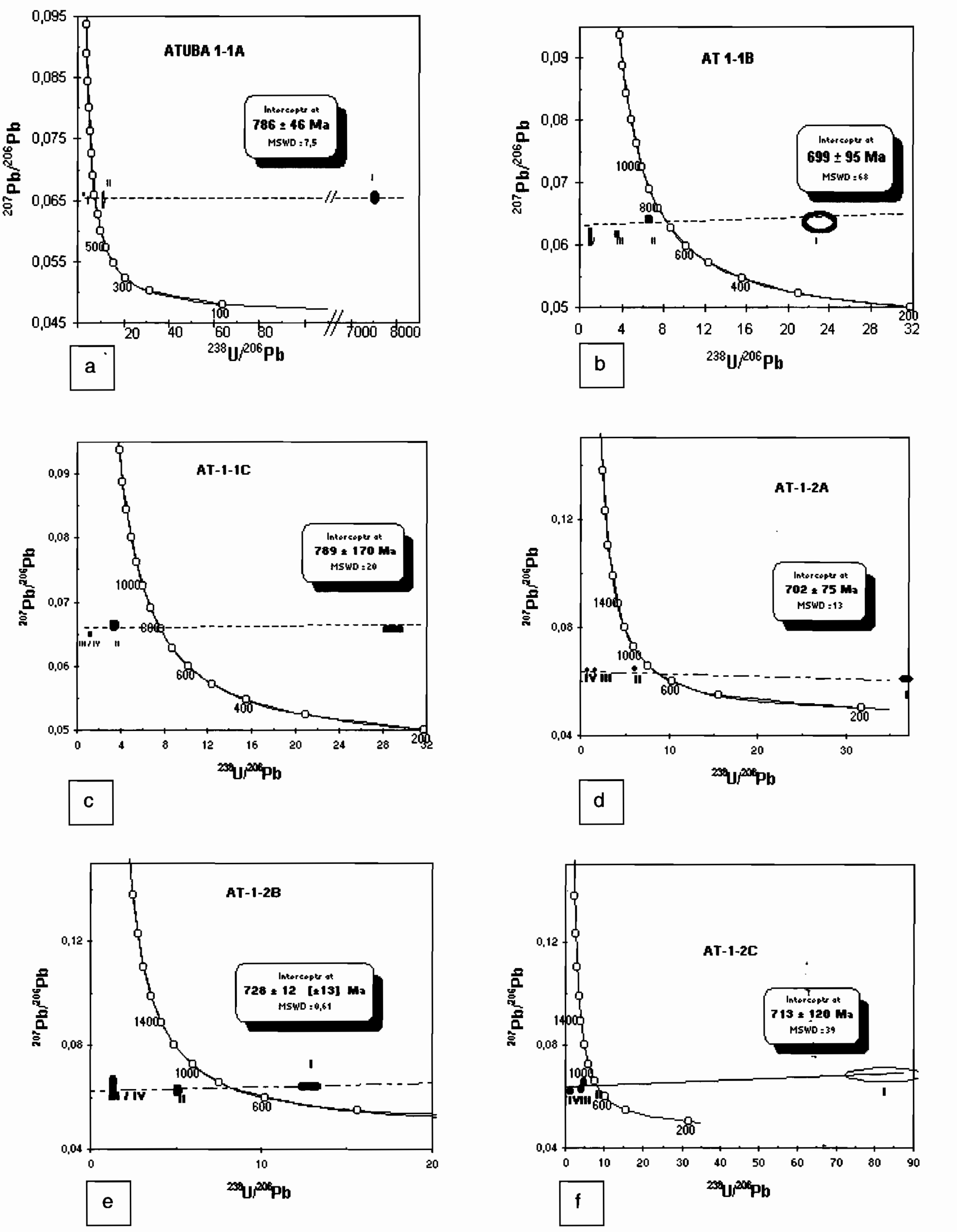

Figure 5. TeraWasserburg diagram. The group I correspond for diagrams a, b and c and group II correspond to diagrams d, e and f. The Pb-Pb ages for the first four leach steps, varied between 700 and 790 Ma for different fractions,but is relatively constant for the leaches into same fraction.

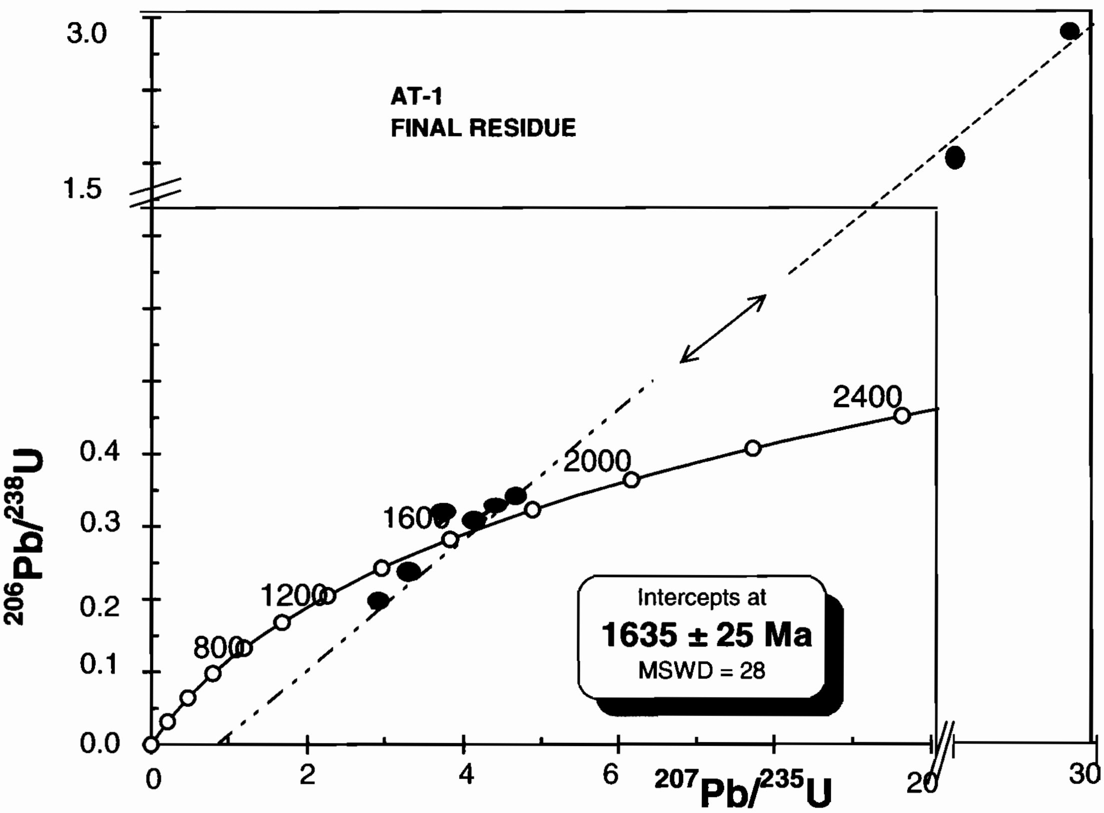

Figure 6. Concordia diagram for final residue. The upper intercept indicate 1635 ± 25 Ma. Some groups indicates reverse discordance that may be due preferential U removing during the first leach step or due a possibility of the migration these element from core to rim during zircon recrystallization during Neoproterozoic thermal event.

THE BRAZILIAN NATIONAL GEOCHRONOLOGICAL DATABASE: CHRONOBANK

Silva, L.C.[1]; Rodrigues, J.B.[2]; Silveira, L.M.C.[2] and Pimentel, M.M.[3]

1. Serviço Geológico do Brasil – CPRM, Pesquisador Associado IG-UnB. luizcar@unb.br
2. Serviço Geológico do Brasil - CPRM
3. Instituto de Geociências, Universidade de Brasília, Brasília-DF, 70910-900. marcio@unb.br

Keywords: Database, geochronology, GIS, Brazil

INTRODUCTION

Geochronological and isotopic data represent important tools to help unraveling the geological and metalogenetic evolution of large areas of the continental crust. Good quality isotopic data has been progressively more used as a fundamental piece of information for scientific research as well as for mineral exploration programs and the existence of easy-to-use and up-to-date geochronological databanks have been demanded by both the academic and mining sectors.

The absence of a national geological database in Brazil, including the isotopic record, led several institutions, geochronology laboratories and private exploration companies to produce isolated, non-relational and incomplete geochronological databanks. The most comprehensive of them was that produced by the CPGEO/Universidade de São Paulo (Mellito et al., 1997). However, since the early 90's these efforts did not respond to the growing necessity and demand of the academic and industrial sectors for a complete and up-to-date isotopic data bank. In 2001, a larger initiative carried out by the Geological Survey of Brazil - CPRM, in association with the universities of Brasília, São Paulo and Pará, and some private mining companies started the setting up the first national geochronological database in the country. The major difficulties in building such a large database are: i) the size of the country; ii) the lack of precision on the location of the data produced before the introduction of GPS tool; iii) the very large amount of available data, by far the largest isotopic databank in Latin America, and, iv) the lack of a national management group allowing permanent feeding of the database and development routines. The recent accomplishment of the "Geological, Tectonic and Mineral Resources Map of Brazil, Scale 1:2,500,000" and the "Geological Chart of Brazil, 1:1,000,000" on a GIS basis by the Geological Survey of Brazil (CPRM), highlighted the necessity of organizing the Brazilian gechronological data, fragmented between several individual databanks. As a consequence, a group of researchers are presently modelling the first national GIS-based geochronological database (CHRONOBANK), which represents a specialized module of the CPRM's national geological databank (GEOBANK). The work is supported by an agreement between the Ministry of Science and Technology (MCT/FINEP), the isotopic laboratories from the universities of São Paulo (USP), Pará (UFPA), Brasília (UnB), the Agency for the Development of the Brazilian Mineral Industry (ADIMB) and CPRM.

ORGANIZING THE NATIONAL GEOCHRONOLOGIC DATABASE, ON A GIS: THE PROBLEM OF ASSESSING PRECISE SAMPLE LOCATION

The major problem that had to be tackled during the initial data collecting phase was the scarcity of precise sample location data. To make the compiling process faster, the availability of precise location information was used as a criterion for quality control of the data. The analyses were divided into three classes: a) those located by means of a GPS; b) those which had been plotted on accurate location maps and; c) those plotted on inaccurate maps or for which no location information was provided (Table 1). The procedure to include samples from group 'b' consisted in scanning and geo-referencing the available map, using the ArcView tool to extract the approximate coordinates. In the present stage only samples with relatively precise location (groups 'a' and 'b', Tab.1) were included into the CHRONOBANK (Tab.1). Samples from the last group (group 'c', Tab.1) were catalogued but their inclusion in the bank depends on a posterior attempt to obtain more precise location data trough direct contact with the authors and/or laboratories.

Table 1 shows the number of registered data in each situation.

Table 1: Total stored data in the initial phase of the project: (a) samples with field-measured coordinates (GPS) or located in ArcView georeferenced maps, (b) samples with maps to be georeferenced; (c) samples with no precise location. The GEOBANK/CHRONOBANK system was developed with three-layer architecture: &#61623: Client – interface with user in the internet, &#61623: Applying – definition and development of the applying of interface with user – Oracle 91AS, &#61623: Data Storage – Data Bank Oracle 91.

Group	(a)	(b)	(c)
Ar-Ar Pooled Age	51	10	22
U-Pb (TIMS) Pooled Age	150	144	78
U-Pb (SHRIMP) Pooled Age	157	133	114
Sm-Nd (isochronic)	15	39	5
Sm-Nd (T_{DM})	570	258	182
Pb-Pb (evaporation)	10	78	19
Pb-Pb (Laser ablation)	10	6	12
Total stored analyses	733	401	303

MAIN CHARACTERISTICS OF THE BANK

The basic focus of the modelling is on the relational nature of the bank, based on the inter-linking of several key-data columns and on the portability of the bank, in order to permit its insertion in any platform. Other main characteristic of the bank is its easy-to-use nature being accessible in multiple media, including the internet, permitting even easy raw data reprocessing. Owing to the very large amount of information to be joined and analyzed, this initial modelling phase priorized the conventional U-Pb, SHRIMP U-Pb, Sm-Nd, evaporation and laser ablation Pb-Pb data produced in the last decade (Table 1).

In the present modelling phase the bank was fed by the data available in the literature, primary data from the isotopic laboratories or even, unpublished data, when authorized by the researchers. In this experimental phase the bank was submitted to multiple modelling tests under distinct situations and analytical peculiarities. In order to become useful to a wide universe of users, with different needs, a complete list of general, isotopic and equipment analytical information is provided. The information is stored in sixteen normalized linked tables, separated into three groups of entrance data. The first group contains general information common to all the analyzed samples: identification of the sample according to the GEOBANK sample/outcrop code, geographic location (coordinates) geologic and stratigraphic data and source references. When available, original geological and location maps, outcrop photos, etc, are also stored. The second group of entrance data contains analytical data with information on the age calculation, uncertainty, value of statistical parameters indicating the quality of the data, etc. The third group of entrance data includes the measured contents of the elements, isotopic ratios, images of the analyzed minerals and concentrates, diagrams (isochrones, concordias, etc).

To make the feeding process easier and more homogeneous, lists of options were created for the fields: “Geological Unity”, " Pooled Age", "Interpretation of the Age: crystallization, metamorphism, Inheritance, hydrothermal alteration, source, etc”, “Position of the Spot”, “Statistical Parameters”, “Standards Parameters”, “Laboratory”, “Analyzed Material” and “Reduction Program”. All ages are recorded and registered in Ma, even in the case of the model ages.

The access to the stored data will be available to all internet users as soon as the operational routine for the bank is established. Insertion of new data, as well as updating of the stored data will also be available in the internet to authorized users, as soon as the system starts working in routine. Any interested user will have access to a specific electronic storage form created for this purpose. The user interaction control will be made through selective password getting in touch with CPRM/UnB/USP/UFPA scientific administrators of the bank (Drs. Luiz Carlos da Silva: luizcar@unb. br; Márcio Martins Pimentel: marcio@unb.br; Celso Colombo Gaeta Tassinari: ccgtassi@usp.br; Michel Lafon: lafon@ufpa.br).

REFERENCE

Mellito, K.M.; Rodrigues, L.V.; Tassinari, C.C.G.; Sonoki, I.K., 1997. The Geochronological Database of Brazil. I SSAGI, pp. 197-198.

THE COOLING HISTORY OF THE BASEMENT COMPLEX OF THE SIERRA DE SAN LUIS (EASTERN SIERRAS PAMPEANAS/ARGENTINA) AND ITS IMPLICATION FOR FAMATINIAN VS. ACHALIAN EVENTS BASED ON K-Ar-GEOCHRONOLOGY

Steenken, A.[1,2]; Wemmer, K.[1]; López de Luchi, M.G.[2] and Siegesmund, S.[1]

1. Geowissenschaftliches Zentrum der Universität Göttingen (GZG), Goldschmidtstr. 1-3, 37077 Göttingen, Germany. asteenk@gwdg.de, kwemmer@gwdg.de, ssieges@gwdg.de
2. Instituto de Geocronologia y Geologia Isotópica (INGEIS), Pabellón INGEIS, Ciudad Universitaria, C1428EHA, Buenos Aires, Argentina. deluchi@ingeis.uba.ar

Keywords: Sierra de San Luis, K-Ar mica dating, cooling history, Famatinian orogeny, Achalian orogeny

INTRODUCTION

The application of the K-Ar-dating method on muscovites and biotites of medium to high-grade metamorphic basement rocks is used to characterise the post-metamorphic cooling history of orogenic processes. However, in polyphase deformed basement rocks the method may be handicapped by subsequent deformational events combined with either a regional reheating of the basement or disturbance of isotopic systems by regional scale ductile shearing. Those processes may partly or entirely reset the isotopic system. Therefore, the interpretation of cooling ages could be established only with a profound knowledge of the regional structural evolution as well as microstructural studies of the dated sample material.

We will present an outline of our research on the structural and thermal evolution of the Sierras de San Luis (Steenken et al., in prep). The presented isotopic data is part of a huge data collection of more than 71 biotite and muscovite K-Ar cooling ages. The basement complex was subjected to the K-Ar dating method in order to unravel differences in the cooling history of the different domains. Although it appears that the whole basement complex suffers a common post-Famatinian cooling history a vast spread of biotite and muscovite K-Ar ages have to be explained in a sound geological framework.

GEOLOGICAL SETTING

The Sierras Pampeanas generally forms north-south striking mountain ranges representing a metamorphic basement complex that is partly overlain by Carboniferous to Permian terrigenous sedimentary rocks outcropping within the Cenozoic sedimentary cover of central and northwestern Argentina. The tectono-metamorphic and magmatic history of the complex documents the polyphase accretion of cratonic fragments and terranes along the active continental margin of southwestern Gondwana during Proterozoic and Early Paleozoic times (Ramos, 1988, 1991). Different models were proposed for the collisional history along the southwestern margin of Gondwana (i.e. Dalla Salda et al., 1998; Quenardelle & Ramos, 1999; Stuart-Smith et al., 1999; Rapela et al., 2000). They share the accretion of the Pampean Terrane that was followed by the Famatinian orogeny, i.e. the collision of the Precordillera (Cuyania) Terrane. The lack of detailed time constraints on those events is the main deficiency of those models. Collisional activity ceased after the Achalian orogeny during the Devonian with the accretion of the Chilenia Terrane (Stuart-Smith et al., 1999; Siegesmund et al., in review).

The present paper is focused on the basement rocks of the Sierra de San Luis that forms the southernmost tip of the Eastern Sierras Pampeanas. This basement block comprises three variable NNE-SSW striking basement domains of medium to high-grade metamorphic gneisses, schists and migmatites. Namely from west to east the Nogolí, Pringles and Conlara metamorphic complexes (Sims et al., 1998). Those are largely separated by an assemblage of lithic wacke sandstones and phyllites (San Luis formation of von Gosen & Prozzi, 1996) where P-T-conditions never exceed lower greenschist facies conditions. The whole basement complex was invaded by numerous magmatic intrusions of (ultra-)mafic to granitic composition during at least two distinguishable events of Ordovician and Devonian age (López de Luchi et al., in prep.).

Hauzenberger et al. (2001) suggested a back-arc setting for the sedimentation of the high-grade metamorphic rocks of the Pringles complex and the lower grade equivalents of the San Luis formation. The timing of sedimentation is still a matter of discussion. Sims et al. (1998) deduced from SHRIMP analyses of zircon cores of a migmatitic rock of the Pringles complex a maximum age for the sedimentation of about 530 Ma. A similar sedimentation age was reported by Söllner et al. (2000) on the basis of U-Pb zircon dating for the low-grade metamorphic volcanic rocks within phyllites. Prior to peak metamorphism under granulite facies conditions at about 460 Ma (Sims et al., 1998 – SHRIMP monazite dating) the sedimentary pile underwent a deformational event that led to the development of a penetrative S_1 foliation. This was followed by the emplacement of mafic to ultra-mafic rocks as well as granitoid and pegmatoid intrusions that are widespread within the Pringles complex. Hauzenberger et al. (2001) concluded on the basis of geothermo-barometric results that those mafics intruded an environment already in amphibolite facies conditions. Granulite facies conditions with a near isobaric P-T slope could be the result of the emplaced

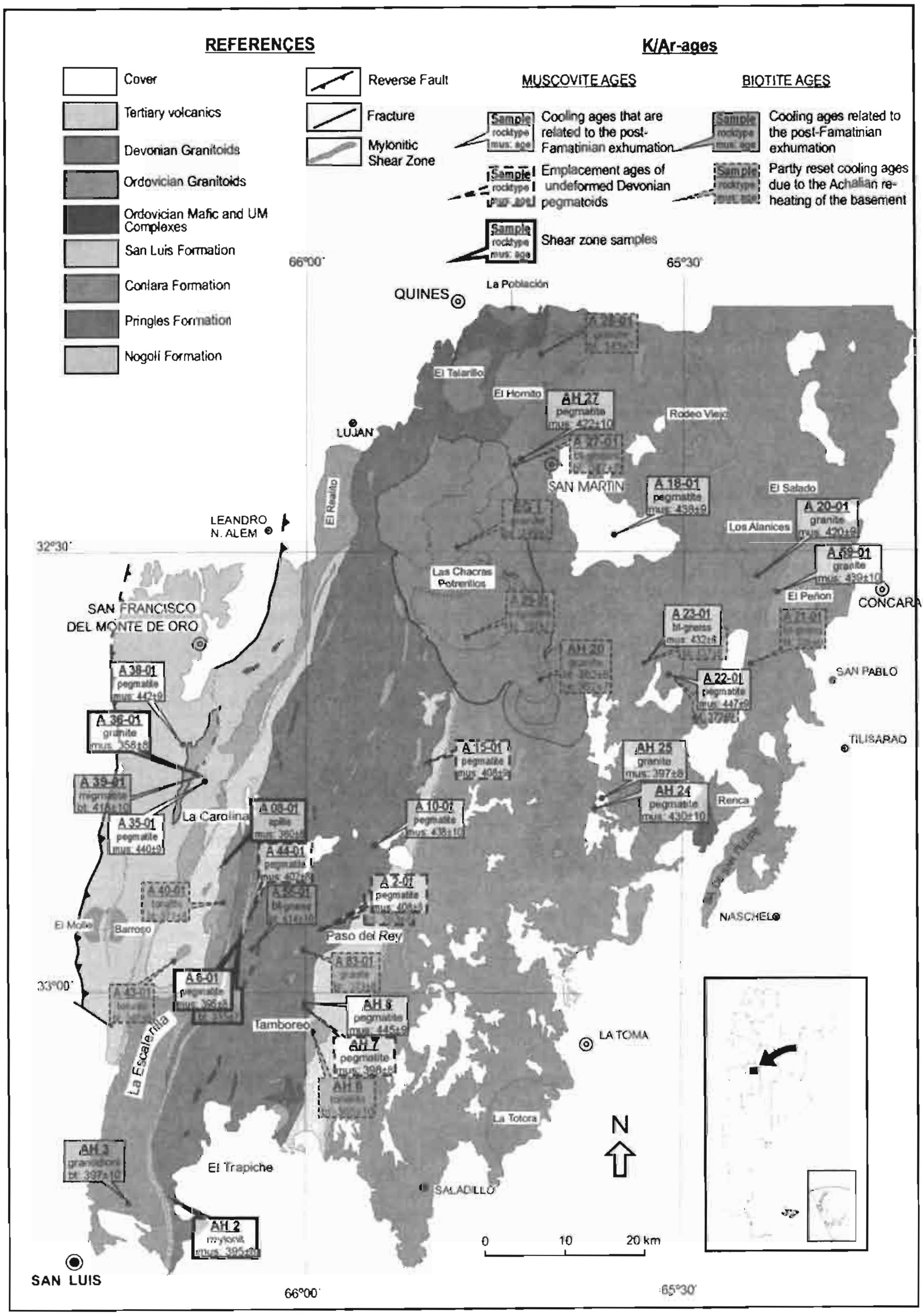

Figure 1. Schematic map of the Sierra de San Luis Proterozoic to Palaeozoic units (based on López de Luchi, 1993; von Gosen & Prozzi, 1998; Sims et. al., 1998 and references therein). Presented is a selection of new muscovite (white boxes) and biotite (brownish boxes) K/Ar-cooling ages. The different frames of the boxes denote to the significance of cooling ages concerning the post-Famatinian history (see inserted references).

mafic rocks. Subsequently the whole basement complex underwent a second deformational (D_2) event, that results in small scale and up to 10m to 100m wide tight to isoclinal folds that partly merge into sheath-fold geometry (von Gosen, 1998). The newly developed pervasive S_2 foliation generally strikes NNE-SSW. Late-stage tectonics are recorded by crustal scale ductile shear zones.

ANALYTICAL RESULTS

K-Ar age dating was performed in the Geowissenschaftliches Zentrum of the University in Göttingen. For analytical precision and standards the reader is referred to Wemmer (1991). In general the obtained K-Ar muscovite ages (n=26) of all rock samples show a wide spread ranging from 345 Ma to 447 Ma, while K-Ar biotite ages (n=23) cover a somewhat younger spectrum from 319 Ma to 418 Ma. However, all data can be explained together with other isotope data in their geological context.

A first survey of K-Ar muscovite ages allows the separation into three groups of a different cooling history. The oldest group (n=13) exhibits cooling ages in the range from 417±9 Ma to 447±9 Ma (Fig. 1). This group is largely represented by huge pegmatoids and solid-state deformed granites that are present in all the basement domains, except for the San Luis Formation. The western areas of the Pringles complex seem to lack K-Ar ages of the oldest group (Fig. 1). Cooling ages for the gneissic country rocks are difficult to establish, since the high-grade metamorphic paragenesis lacks muscovite. Furthermore, lower-grade metamorphic rocks exhibit a widespread post-deformational overgrowth of muscovite plates that is probably related to the Devonian intrusive activity. Ages are generally slightly younger than those of the neighbouring pegmatoids but overlap within error. It is assumed that the archived ages are mixed ages due to a partial resetting during the Devonian. Younger K-Ar muscovite ages (n=8) are restricted to the western areas of the Pringles complex. Pegmatoid ages range from 395±8 Ma to 408±9 Ma (Fig. 1). Even younger ages down to 358 Ma are obtained from mylonitic shear zone samples (n=4).

K-Ar-biotite ages show a high spatial and temporal variation. The lower limit of the age spectra of about 315 Ma correlates with K-Ar ages obtained on fine mica fractions of the two phyllitic belts (Wemmer et al., in prep). The highest ages of about 415 Ma were archived by two migmatite samples of the Pringles and Nogolí complexes. Intermediate ages ranging from 335 Ma to 383 Ma were obtained for the Ordovician tonalitic intrusions as well as for the gneissic country rocks. Again, huge biotite crystals of pegmatoids yield higher ages than the adjacent host.

DISCUSSION AND CONCLUSION

The clear-cut separation in to three groups based on the K/Ar muscovite data is not straight forwarded by structural observations. Young pegmatoids show a high variability of contact relationships with their host. Highly deformed and partly mylonitic bodies are concordant to the S_2-foliation, whereas narrow undeformed pegmatitic dikes cross-cut the penetrative foliation. For the latter it appears reasonable to relate the cooling age with their time of intrusion. Those pegmatoids might be in connection with the Devonian emplacement of large granitoids like the La Escalerilla batholith (Sims et al., 1998).

A characterisation of the older group of pegmatoids concerning their state of deformation is not easy to establish since the invading pegmatoids exhibit an enormous dimension. During deformation they behave as rigid bodies within the host and bear a marginal deformation, only. However, their age scatter in between 420 Ma to 445 Ma might be related to the regional cooling of the basement. This is supported by few muscovite cooling ages on the metamorphic country rocks that overlap within analytical error those pegmatoid cooling ages.

In contrast, part of the younger pegmatoid group has a pervasive high temperature solid-state deformation. Those will probably not retain any information concerning their intrusion time. Mylonitisation in connection with the recrystallisation of plagioclase requires a minimum temperature of at least 450 °C (Tullis & Yund, 1992). Time constraints for this deformation are difficult to establish, since the impact of the Achalian deformation on the basement complex is so far poorly understood. It is assumed that the first deformation took place subsequent to the granulite facies metamorphism during the Famatinian orogeny. Therefore, the closure of the K-Ar isotopic system for large 'muscovite-books' at 395 Ma will approximate the cooling below the 350±50 °C isotherm of the basement domain in this area. Though, Late Devonian to Early Carboniferous K/Ar muscovite ages of the mylonitic shear zones along the eastern margin of the Pringles complex have to be related to the Achalian accretion of the Chilenia Terrane (see also Sims et al., 1998). Therefore, it is indicated that Famatinian shear zones were reactivated during the Achalian event.

Additionally, the young K-Ar muscovite cooling age of 395 Ma for the high temperature solid-state deformed pegmatoids might point to a differential exhumation of this basement domain. Even though the amount of a probable resetting of this age is unknown, since adjacent biotite cooling ages are slightly older (see below). This hypothesis is in accordance with the continuity of the structural cross-section in the eastern part of the Pringles complex (Steenken et al., 2002). Furthermore, the transition from the lower-grade country rocks in the east of the La Escalerilla pluton towards the granulite facies rocks of the Pringles complex is controlled by a number of wide mylonitic belts with a prominent E-side up shear indication. As it turns out, the outcropping rocks of the Pringles complex could be regarded as a crustal cross section from the lower-crust to the mid upper-crust. Additionally, the hypothesis of basement tilting is supported by the spatial distribution of mafic and higher fractionated granitoids within the complex (Fig. 1).

K-Ar biotite ages usually document the cooling history below 300±50 °C. Unfortunately the analysed samples exhibit a variable degree of resetting. The highest ages archived by migmatites of the Pringles and Nogolí complexes are about 25 Ma younger than adjacent muscovite cooling ages. Those are regarded to represent cooling below the 300±50 °C isotherm after the Famatinian orogeny. The lower limit of obtained K-Ar-biotite ages marks the end of Achalian shear zone activity. However, the range of ages in between cannot be explained by local shearing or by a differential exhumation of the basement block. Huge pegmatoid biotite crystals generally yield higher ages than those of their host rocks that range about 340 Ma. Furthermore, cooling ages of tonalitic and granodioritic intrusions in the range between 361 Ma and 383 Ma cannot be related to their emplacement since U-Pb SHRIMP zircon data (Sims et al., 1998) point to an emplacement during the Ordovician. Consequently, intrusive rocks may suffer a common cooling history with the basement. It is strongly suggested that those intermediate ages are the result of a partial resetting during the Devonian. Though, regarding the highest pegmatoid K-Ar biotite ages of the Conlara complex as closest approximation to the basement cooling below 300±50 °C, the whole complex had to be differentially exhumed. However, the high variability in biotite ages has to be addressed to the differences in grain size of the analysed minerals and the resulting thermodynamic properties (Villa 1998). However, the variability in resetting indicates that during the Achalian deformation the whole basement suffered an additional major temperature input apart from local shearing.

REFERENCES

Dalla Salda, L.H.; López de Luchi, M.G.; Cingolani, C.; Varela, R., 1998. Laurentia-Gondwana collision: the origin of the Famatinian-Appalachians Orogenic Belt. In: Pankhurst, R.J. and Rapela, C.W.(eds): The Proto-Andean Margin of Gondwana. Geol. Soc. Lond. Spec. Public 142: 219-234.

Gosen, W. von, 1998. Transpressive deformation in the southwestern part of the Sierra de San Luis (Sierras Pampeanas, Argentina). J. South. Amer. Earth. Sciences 11(3): 233-264.

Gosen, W. von & Prozzi, C.R., 1996. Geology, Structure and metamorphism in the area south of La Carolina. Actas 12° Congreso Geologico Argentino y 3° Congreso de Exploracion de Hidrocarburos 2:301-314, Buenos Aires

Gosen, W. von & Prozzi, C., 1998. Structural evolution of the Sierra de San Luis (Eastern Sierras Pampeanas, Argentina): implications for the Proto-Andean Margin of Gondwana. In: Pankhurst, R.J. and Rapela, C.W. (eds.) The Proto-Andean Margin of Gondwana. Geol. Soc. Lond. Spec. Public 142: 235-258.

Hauzenberger, Ch.; Mogessie, A.; Hoinkes, G.; Felfernig, A.; Bjerg, E.; Kostadinoff, J.; Delpino, S.; Dimieri, L., 2001. Metamorphic evolution of the Sierras de San Luis, Argentina: granulite facies metamorphism related to mafic intrusions. Mineralogy and Petrology, 71(1/2): 95-126.

López de Luchi, M.G., 1993. Caracterización geológica y emplazamiento del Batolito de Renca. Actas 12° Congreso Geológico Argentino y 2° Congreso de Exploración de Hidrocarburos 4:42-53

Quenardelle, S. & Ramos, V.A., 1999. Ordovician western Sierras Pampeanas magmatic belt: record of Precordillera accretion in Argentina. In Ramos, V,A. and Keppie, J.D. (eds). Laurentia Gondwana connections before Pangea. Geol. Soc. Amer. Special Paper 336: 63-86., Boulder Colorado

Ramos, V.A., 1988. Late Proterozoic - early Pataeozoic of South America - a collisional history. Episodes 11, 168-174.

Ramos, V.A., 1991. Terrane history of southern South America. Revista de Comunicaciones, 42: 184-185.

Rapela, C.W., 2000. The Sierras Pampeanas of Argentina: Paleozoic Building of the Southern Proto-Andes. In: Cordani, U.G., Milani, E.J., Thomaz-Filho, A. and Campos, D.A. (Eds.) "Tectonic Evolution of South America", 31st International Geological Congress, Río de Janeiro, Brazil: 381-387.

Siegesmund S.; Steenken, A.; López De Luchi, M.G.; Wemmer, K.; Hoffmann, A.; Mosch, S., in review. The Las Chacras-Potrerillos Batholith: Structural evidences on its emplacement and timing of the intrusion. Int. J. Earth. Sci. (Geol. Rundsch.)

Sims, J.P.; Ireland, T.R.; Camacho, A.; Lyons, P.; Pieters, P.E.; Skirrow, R.G.; Stuart-Smith, P.G.; Miró, R., 1998. U-Pb, Th-Pb and Ar-Ar geochronology from the southern Sierras Pampeanas, Argentina: implications for the Paleozoic evolution of the western Gondwana margin. In: Pankhurst, J.R., Rapela, C.W. (eds). The Proto-Andean Margin of Gondwana. Geol. Soc. Lond. Spec. Public 142:259-281

Söllner, F.; Brodtkorb, M.K.; Miller, H.; Pezzutti, N.; Fernández, R.R., 1998. Early Cambrian effussion of metavolcanic rocks from the Sierra de San Luis, Argentina: evidence from U-Pb age determinations on zircons. Actas 10° Congreso Latinoamericano de Geología y 6° Congreso Argentino de Geología Económica, 2: 387., Buenos Aires, Argentina

Steenken, A.; López de Luchi, M.G.; Siegesmund, S.; Wemmer, K., 2002. An insight into the structural evolution of the Sierra de San Luis (southeastern Sierras Pampeanas, Argentina); a progress report. In: Cabaleri, N., Linares, E., López de Luchi, M. G., Ostera, H y Panarello, H. (eds). Actas 15 Congreso Geológico Argentino, CD Edition, 6 ges.

Stuart-Smith, P.G.; Camacho, A.; Sims, J.P.; Skirrow, R.G.; Lyons, P.; Pieters, P.E.; Black, L.P., 1999. Uranium lead dating of felsic magmatic cycles in the southern Sierras Pampeanas, Argentina: Implications for the tectonic development of the Proto-Andean Gondwana margin. In Ramos, V,A. and Keppie, J.D. (eds). Laurentia Gondwana connections before Pangea. Geol. Soc. Amer. Special Paper 336: 87-114., Boulder Colorado

Tullis, J. & Yund, R.A., 1992. The brittle-ductile transition in feldspar aggregates: an experimental study. In: Evans B. and Wong, T.F. (eds.) Fault Mechanics and Transport Properties of Rocks. Academic Press, NY, 89-118.

Villa, I.M., 1998. Isotopic Closure. Terra Nova, 10: 42-47.

Wemmer, K. 1991. K/Ar-Altersdatierungsmöglichkeiten für retrograde Deformationsprozesse im spröden und duktilen Bereich - Beispiele aus der KTB-Vorbohrung (Oberpfalz) und dem Bereich der Insubrischen Linie (N-Italien). - Göttinger Arbeiten zur Geologie und Paläontologie. 51, 1-61. Göttingen.

THERMOCHRONOLOGICAL HISTORY OF THE IMATACA COMPLEX, NW AMAZONIAN CRATON

Tassinari, C.C.G.[1]; Munhá, J.M.U.[2];Teixeira, W.[1]; Nutman, A.[3]; Palácios, T.[2]; Sosa, S.C.[4] and Calado, B.O.[5]

1. Centro de Pesquisas Geocronológicas, Instituto de Geociências da Universidade de São Paulo
2. Centro-Departamento de Geologia da Faculdade de Ciências da Universidade de Lisboa
3. Research School of Earth Sciences, Australian National University
4. Ministério de Minas de Venezuela
5. Centro de Pesquisas Geocronológicas, Instituto de Geociências da Universidade de São Paulo-PIBIC

Keywords: Imataca Complex, thermochrological history

INTRODUCTION AND GEOLOGICAL SETTING

Archean and Proterozoic events have played an important role on the geodynamic evolution of the Amazonian craton, whose tectonic stability took place at the end of the Late Mesoproterozoic (Cordani & Brito Neves, 1982).

The Archean Imataca Complex (IC) occurs in the Venezuelan NW corner of the Amazonian Craton and forms a ENE-trending, fault-bounded block adjacent to the Palaeoproterozoic Maroni-Itacaiúnas Belt. IC rocks are intensely deformed, by folding, thrusting and shearing. Transcurrent faults (like the Guri Fault) are important. along the southeastern edge of the IC. Imataca Complex (IC) comprises mostly medium- to high-grade facies quartz-feldspathic paragneisses (e.g. Sidder & Mendoza, 1995); granitoids and calc-alkaline gray gneisses of igneous derivation are also present, as well as dolomitic marbles, mafic/intermediate granulites and BIFs that constitute huge iron ore deposits of Algoma type. Several quartz-monzonite sills and granitoid plutons (e.g., Encrucijada granite) were emplaced into the IC during the Transamazonian orogeny, between 2.2 and 2.0 Ga, (e.g. Gibbs & Barron, 1983; Onstott et al., 1989).

Geophysical and isotopic evidence, coupled with the recognized polyphase tectonic framework of the Archean crust, indicate that the IC is an allochthonous block which was juxtaposed to the Maroni-Itacaiunas belt during Late Paleoproterozoic times (Onstott & Hargraves, 1981; Tassinari & Macambira, 1999). Therefore, Transamazonian events play an essential role on the development of major petrologic and tectonic features of IC. Accordingly, this study starts by characterizing Transamazonian granulitic metamorphism in the San Felix - Upata area. New petrological and isotopic data will be used to discuss the age/nature of protoliths and, particularly, their thermochronologic evolution during the Transamazonian event. In this respect our new data complements and updates previoius studies by Onstott et. al. (1989) and Swapp & Onstott (1989) on Imataca Complex.

METAMORPHISM

Rocks from the Imataca Complex of Venezuela record high temperature regional re-crystallization at granulite facies peak metamorphism during the Trans-Amazonian Orogeny (Dougan, 1974; Swapp & Onstott, 1989).

Within the collecting area, the general strike of metamorphic foliation is close to E-W (steeply the dipping to S) and predates the development of NE-SW left-lateral shearing, representing local expressions of the main Guri and El Pao regional fault zones. Four samples were selected for detailed petrological and isotopic analysis, because they contain convenient assemblages for geothermobarometric and thermochronological determinations, and/or reflect structural relations that constraint relative timing of metamorphism and deformation. Of the four selected samples, two (63A, 63B) are garnet + orthopyroxene + plagioclase + Kfeldspar + biotite bearing granulites, 65A is a two-pyroxene + plagioclase + Kfeldspar + hornblende + biotite + quartz granulite, and 65-1 is a felsic "blastomylonite" collected from a (metric) shear zone that cuts across previous metamorphic structures.

Sample 65-1 is composed of quartz + plagioclase + Kfeldspar + biotite ± muscovite. It has a distinctive planar fabric defined by aligned biotite and ribbons of quartz; feldspars have experienced grain size reduction and some grains have been deformed into sigmoid-shaped crystals. Shearing was associated with retrograde development of (secondary) muscovite, contrasting with the observations of Swapp & Onstott (1989) at El Pao mine.

Two pyroxene granulite 65A has typical granuloblastic texture and relatively homogeneous mineral compositions.

Garnet granulites have granoblastic texture, particularly well equilibrated in sample 63A. Sample 63B has higher modal amounts of garnet and displays gneissic structure due to alternating garnet + biotite- and feldspar-richer layers. Orthopyroxene and (particularly) garnet contain abundant biotite inclusions (especially, in sample 63B) and larger orthopyroxene crystals surround (earlier) garnet, separating it from plagioclase; these features, coupled with complex plagioclase + K-feldspar intergrowths, suggest that the decompression P-T path followed by these rocks may have reached conditions that were close to those of biotite dehydration melting (biotite + quartz $\rightarrow$ orthpyroxene + K-feldspar + liquid).

THERMOBAROMETRY: PEAK METAMORPHIC CONDITIONS AND P-T PATH

Previous estimates of Trans-Amazonian peak metamorphic conditions in the Imataca Complex have been reviewed by Swapp & Onstott (1989), who suggested T and P in the range of 750 - 800 °C and 8 - 8.5 kbar for granulites at El Pao mine.

Overall geothermobarometric data indicates that San Felix granulites reached similar peak metamorphic conditions at 750 - 800 °C, 6 - 8 kbar, followed by decompression and cooling.

Petrographic evidence to constraint the prograde P-T evolution of San Felix granulites has been mostly erased by subsequent reactions. However, our data is consistent with that of Swapp & Onstott (1989) and both suggest a clockwise P-T path involving decompression and heating to peak conditions; the general absence of early kyanite in Imataca rocks (Dougan, 1974; Swapp & Onstott, 1989) limits the amount of decompression to < 2 kbar. A constraint on the retrograde P-T path comes from noting that 3qz + gr + 2alm = 6fs + 3an equilibrium has an almost constant slope for the investigated compositions. Thus, the retrograde path was defined as to follow that line down to about 600 °C, at ~ 15 bars/degree °C. Regardless of the actual meaning of the estimated retrograde P-T path, it is worth noting that the San Felix granulites must have remained at relatively high temperatures for long enough to allow the observed retrograde re-equilibration.

ISOTOPE GEOLOGY

GEOCHRONOLOGY

Several radiometric studies were performed in the Imataca Complex (IC) (Hurley et. al., 1976, Montgomery, 1979, Montgomery et al., 1977, Onstott et al., 1989; Tassinari et. al.. 2001). The geochronological pattern indicates that the IC comprises na Late Archean (~ 2.8 Ga) reactivated during the Transamazonian orogeny (2.2 - 2.0 Ga)

^{40}Ar/^{39}Ar data (Onstott et al., 1989) on El Pao mine (IC) high-grade gneisses range from 1.97 to 1.76 Ga, recording the warning stages of the Transamazonian orogeny (uplift and cooling.), whereas 1.4 - 1.1 Ga dates indicate further reactivation during the Mesoproterozoic.

During this study new SHRIMP zircon U-Pb age determinations were undertaken on banded granulitic rocks from San Felix-Upata area. Dominant oscillatory zoned, prismatic, zircons from a quartzo-feldspathic segregation vein yielded a core ^{207}Pb/^{206}Pb date of 3229 ± 39 Ma (MSWD = 5. 2), pointing towards an Archean age for the granulite igneous protolith.

Sm-Nd whole rock analysis indicates extensive isotope homogenization during Transamazonian granulite metamorphism; an average model age for this crustal segment is about 3 Ga, suggesting that the mantle-differentiation episode occurred shortly before the rock-forming event.

THERMOCHRONOLOGY

- Petrological cooling rates:

The theory and methods that use chemical zoning in minerals to infer cooling rates (referred to here as "petrological cooling rates" according to Spear & Parrish, 1996) have been discussed at length by a large number of workers and they will not be repeated here.

The method adopted in this study follows the technique developed by Spear & Parrish (1996) that uses diffusion modeling of Fe-Mg exchange between host garnet and biotite inclusions to assess cooling rates of their respective host rocks. As it should be expected, the results indicate that there is a broad correlation between inclusion biotite size and garnet-botite closure temperatures (550 - 720 C°). Using a slight modification of the technique proposed by Spear & Parrish (1996), regression of the data and comparison with controlled diffusion modeling experiments suggest that San Felix granulites cooled at a rate approaching 50 - 100 °C/Ma over the first 150 °C (800 - 650 °C), followed by much slower cooling.

- Geochronological Cooling Rates:

Previous thermochronological studies in the IC (Onstott et al., 1989) used Ar/Ar dating on metamorphic hornblende, biotite and Kfeldspar and adressed the lower temperature range of the retrograde Transamazonian metamorphic path. In this study we used a multi-isotope system (U/Pb, Sm/Nd and Rb/Sr) aproach in order to assess higher-T conditions, complementing the existing data.

The age of peak metamorphism is still not precisely defined. New SHRIMP spot analysis in zoned zircons yielded a ^{207}Pb/^{206}Pb age range from 2.63 - 2.82 Ga on core areas to 2.21 - 2.05 Ga on metamorphic overgrowths. The younger age is consistent with both whole rock Rb-Sr at 2.02 Ga (Montgomery and Hurley, 1978) and new WR-CPX Sm-Nd at 1.98 Ga, all indicating that peak metamorphic conditions may have lasted until 2 Ga (however, the available data does not put any constraints on its duration). Gt-WR Sm-Nd also cluster at 1.90 - 2.00 Ga , whereas biotite Rb-Sr ages from the same samples range from 1.77 to 1.72 Ga. Coupled with Onstott et al. (1989) Ar-Ar hornblende ages at 1.95 - 1.97 Ga, and considering typical closure temperatures for the respective isotope-mineral systems, the data requires that the San Felix granulites cooled very rapidly during the initial 200 °C (800 - 600 °C), followed by a drastic decrease in cooling rates to about 1 °C/Ma down to 350 °C. Geochronological and petrological cooling rate results are therefore consistent; in this respect, it is worth noting that congruence between the two thermochronological techniques, which are based on independent and quite distinct experimental data, strongly support the general reliability of both methods.

On this study we have also attempted to assess the age of the main shearing (mylonitic) event in the area.

Towards this aim, Rb-Sr isotope analysis have been performed on biotite - feldspar - WR from mylonitic sample 65-1, which was collected on discrete shear zone from the same outcrop as the granulites discussed above. Results indicate that shearing has promoted complete Sr isotope resetting at 1.39 Ga. This result suggests that the Ar-Ar biotite ages (1.45 - 1.25 Ga; as well as the 1.3 - 1.1 Ga Kfeldspar ages) attributed by Onstott et al. (1989) to the so-called Nickerie Orogeny, could instead represent local repeated reactivation related to the main Guri transcurrent fault system. Indeed, (except for specific igneous bodies) all the available radiometric data on the Guyana Shield within this time span has been attributed to dynamic overprinting (Berrangé, 1977; Gibbs & Barron, 1983), which we interpret as a consequence of late (Greenvillian; Sadowski & Bettencourt, 1996) collision between Laurentia and Amazonian Craton.

REFERENCES

Cordani, U.G. & Brito Neves, B.B., 1982. The geologic evolution of South America during the Archean and Early Proterozoic. Rev. Bras. Geoc., v.12, p. 78-88.

Dougan , T.W., 1977. The Imataca Complex, near Cerro Bolivar, Venezuela - A Calc-Alkaline Archean protolith., Precambrian research, 4, p. 237-268.

Gibbs, A.K. & Barron C., 1983. The Guyana Shield reviewed. Episodes, 2, p. 7-14

Hurley, P.M., Fairbairn, H.W., Gaudette, H.E., 1976. Progress report on early Archean rocks in Liberia, Sierra Leone, and Guayana, and their general stratigraphic setting. In: The Early History of the Earth (B.F. Windley, ed.) Chichester: Wiley, p. 511-521.

Montgomery, C.W., 1979. Uranium – Lead Geochronology of the archean Imataca series. Venezuelan Guayana Shield. Contrib. Mineral. Petrol. , 69, 167-176

Montgomery, C.W. & Hurley, P.M., 1978. Total-Rock U-Pb Systematics in the Imataca Series, Guayana Shield, Venezuela. Earth Plan. Sci. Letters, 39:281-290.

Onstott, T. & Hargraves, R.B., 1981, Proterozoic transcurrent tectonics: palaeomagnetic evidence from Venezuela and Africa. Nature, v. 289, p. 131-136.

Onstott, T.C.; Hall, C.M.; York, D., 1989. 40Ar/39Ar Thermochronometry of the Imataca Complex, Venezuela. Precambrian Res., 42:255-291.

Sadowski, G.R. & Bettencourt, J.S., 1996. Mesoproterozoic tectonic correlations between eastern Laurentia and the western border of the Amazonian Craton. Precambrian Research, V. 76, p. 213-227.

Sidder G.B. & Mendoza, V., 1995. Geology of the Venezuelan Guayana Shield and its relation to the Geology of the entire Guayana Shield. U. S. Geological Survey Bulletin, v. 2124, n. B, p. 1-33.

Spear, F.S. & Parrish, R.R., 1997. Petrology and cooling rates of the Valhalla Complex, British Columbia, Canada, J. Petrology, v.37, p. 733-765.

Swapp, S. M. & Onsttot, T. C., 1989. P-T-time characterization of the Transamazonian orogeny in the Imataca Complex, Venezuela. Precambrian Research, v. 42, p. 293-314.

Tassinari, C.C.G. & Macambira, M.B., 1999. Geochronological provinces of the Amazonian Craton. Episodes v. 22, n. 3, p. 174-182.

THERMOCHRONOLOGY OF THE SOUTH AMERICAN PLATFORM IN THE STATE OF SÃO PAULO, THROUGH APATITE FISSION TRACKS

Tello, C.A.S.[1,4]; Hadler Neto, J.C.[1]; Iunes, P.J.[1]; Guedes, S.[1]; Hackspacher, P.C.[2]; Ribeiro, L.F.B.[2]; Paulo, S.R.[3] and Osório, A.M.A.[4]

1. Instituto de Física "Gleb Wataghin", Universidade Estadual de Campinas, UNICAMP, 13083-970 Campinas-SP, Brazil. saenz@ifi.unicamp.br
2. Instituto de Geociências e Ciências Exatas, Universidade Estadual Paulista, UNESP, 13506-900, Rio Claro-SP, Brazil
3. Instituto de Ciências Exatas e da Terra, Universidade Federal de Mato Grosso, UFMT, 78060-900, Cuiabá-MT, Brazil
4. Departamento de Física, Química e Biologia, Universidade do Estado de São Paulo, UNESP, 19060-900, Presidente Prudente-SP, Brazil

Keywords: Fission-track analysis, thermochronology, thermal histories, apatite, Southeast Brazil

INTRODUCTION

The fission-track method, MTF, in apatite, was applied to samples collected in the Serra da Mantiqueira (Mantiqueira mountain range), in the Serra do Mar (Mar mountain range), in regions next to these mountain ranges and in the coastal region between Ubatuba and Santos in the State of São Paulo, Brazil, to study the thermochronology of the South American Platform in Southeast Brazil and its influence on Santos and Campos basins.

In order to obtain ages through the MTF, it was utilized a neutron dosimetry via natural uranium and thorium thin films (Iunes et al., 2002), along with a value of λ_f (^{238}U spontaneous fission decay constant) determined using fission-track techniques (Guedes et al., 2003). This allows the age computation in a direct fashion without the need of utilizing a standard sample as in the case of Zeta Calibration. (Hurford & Green, 1983).

The methodology of fission-track annealing (shortening of tracks as a function of temperature) in apatite was utilized to determine a thermal history through the model developed by Laslett et al. (1987) and the socalled inverse model from Lutz & Omar (1991) with some modifications. These modifications, carried out by our research group, are based on the hypothesis that samples presenting similar geological features should have experienced, in principle, the same thermal history (Amaral et al., 1997; Guedes et al., 2000; Hadler et al., 2001; Tello et al., 2003). I.e., it is analyzed a group of samples collected in regions geologically compatible. Thus, it is intended to reach the same results as those obtained when a large number of samples are individually analyzed.

RESULTS AND DISCUSSIONS

In Table 1, the results of the apparent, T_{ap}, and corrected ages, T_{corr} (in which the annealing effect is taken into account), obtained in each region where samples were collected, are shown. The ages were computed using the equation 10 from Iunes et al. (2002) (see also Tello et al., 2003) and a value of $\lambda_f = (8.35 \pm 0.24)\ x10^{-17}\ a^{-1}$ (Guedes et al., 2003). In Table 2, the weighted means and the results of the χ^2 test for each sample group are shown. These groups were determined taking into account geological constraints (same type of rock, tectonic data, geomorphologic data and compatible ages) among the samples. The values of χ^2_v and P (χ^2_v) for each region indicate that these groups have statistically compatible ages. The geological constraints together with these results allow the sample treatment in groups in which a common thermal history can be found for each group. A comprehensive description of the thermal history methodology can be found in Tello et al. (2003). In Figure 1, the thermal histories of each studied region are shown.

The weighted mean of the corrected ages from high Mantiqueira, (121 ± 6) Ma, coincide with the South Atlantic opening. The fact that the thermal history shown in Fig. 1a starts at a relatively low temperature (~ 80 ° C), suggests that the age of ~ 120 Ma would be the formation age of Serra da Mantiqueira due to a rapid pulse, in which tracks had no time to be retained at the closure temperature, that is ~ 120 °C. This hypothesis is strengthened by the age and thermal history results (not shown in this work) of the region of Jundiaí. After this, the thermal history indicates a small heating from ~ 80 to ~ 90 °C in the time interval of 120-60 Ma, followed by a linear cooling until the present days. It is worth noting that the Low Mantiqueira starts its history at ~ 60 Ma (Fig. 1b). In this Figure, it can be observed that the low Mantiqueira experiences a cooling from ~ 100 to ~ 85 °C in the time interval of 60-20 Ma followed by a faster cooling in the last 20 Ma.

The Serra do Mar presents a more complicate thermal history (Fig. 1c) with several reactivations indicated by the changes in the slope of the cooling curve. In this case, also the fact that the Serra do Mar thermal history starts at a relatively low temperature, ~ 70 °C, suggests that its corrected age of ~ 80 Ma, is its formation age. In addition, this age coincides with a discordance observed in Santos basin, reflecting an uplift correlated with the formation of the Serra do Mar (Almeida & Carneiro, 1998). Soon after this, the thermal history indicates a cooling from ~ 70 to ~ 60 °C in the time interval of 80-45 Ma followed by a heating from ~ 60 to ~ 90 °C in the time interval of 45-25 Ma and, finally, a linear cooling in the last 25 Ma. Note that the changes in the slope of the thermal history coincide with discordances observed in stratigraphic profile of Santos basin (Pereira & Feijó, 1994). On the other hand, in the coastal line between

Ubatuba and Santos, it can be observed (Table 1) ages varying between 10 and 80 Ma indicating the complexity of the Serra do Mar thermotectonics. The samples from Ilha Bela present thermal histories (not shown in this work) compatible with those from Serra do Mar.

The ages and thermal histories from Pouso Alegre and Socorro (not shown) can be related with a heavy erosion occurred in this region, which originated the Japi surface (Almeida & Carneiro, 1998).

ACKNOWLEDGMENTS

The authors are grateful to State of São Paulo Research Foundation, FAPESP, for financial support (Proc. 00/0960-5 and 95/4417-3) and the fellowships of Carlos A. Tello Saenz (Proc. 01/07937-0) and Sandro Guedes (Proc. 01/02805-9).

REFERENCES

Almeida, F.F.M. & Carneiro, C.D.R., 1998. Origem e evolução da Serra do Mar. Revista Brasileira de Geociências, 28, 135-150.

Amaral G.; Born H.; Hadler N., J.C.; Iunes P.J.; Kawashita, K.; Machado Jr., D.L.; Oliveira, E.P.; Paulo R., S; Tello S., C.A., 1997. Fission track analisys of apatites from São Francisco craton and mesozoic alcaline-carbonatite complexes from central and southeastern Brazil. Journal of South American Earth Science, 10, 285-294.

Guedes O., S.; Hadler N., J.C.; Iunes P.J.; Zuñiga G., A.; Tello S., C.A.; Paulo R., S., 2003. The use of the U(n,f) reaction dosimetry in the determination of the λ_f value through fission-track techniques. Nuclear Instruments and Methods in Physics Reseach A, 496, 215-221.

Guedes, S.; Hackspacher, P.; Hadler N., J.C.; Iunes, P.J.; Paulo R., S.; Ribeiro B., L.F.; Tello S., C.A., 2000. Constraints on the evolution and thermal history of the continental plataform of southeast Brazil, São Paulo state, using Fission Track Analyses (AFTA). Revista Brasileira de Geociências, 30, 107-109.

Hadler N., J.C.; Paulo R., S.; Iunes, P. J.; Tello S., C.A.; Balestrieri, M. L.; Bigazzi, G.; Curvo C., E. A.; Hackspacher, P., 2001. A PC compatible Brazilian software for obtaining thermal histories using apatite fission track analysis. Radiation Measurements, 34, 149-154.

Hurford, A.J.; Green, P.F., 1983. The zeta age calibration of fission track dating. Chem. Geol., Isot. Geosci. Sect. 1, 285-317.

Iunes P.J.; Hadler N., J.C.; Bigazzi, G.; Tello S., C.A.; Guedes O., S.; Paulo R., S., 2002. Durango apatite fission-track dating using length-based age corrections and neutron fluence measurements by thorium thin films and natural U-doped glasses calibrated through natural uranium thin films. Chemical Geology,187, 201-211.

Laslett, G.M.; Green, P.F.; Duddy, I.R.; Gleadow A., J.W., 1987. Thermal annealing of fission tracks in apatite 2. The quantitative analysis. Chemical Geology (Isot. Geosci. Sect.) 65, 1-13.

Lutz, T.M. & Omar, G., 1991. An inverse method of modeling thermal histories from apatite fission-track dates. Earth and Planetary Science Letters 104, 181-195.

Pereira, M.J. & Feijó, F.J., 1994. Bacia de Santos. Boletim de Geociências Petrobrás 8, 219-234.

Tello S., C.A.; Hackspacher, P.; Hadler N., J.C.; Iunes, P.J., Guedes O., S., Paulo R., S.; Ribeiro B., L.F., 2003. Recognition of Cretaceus, Paleocene and Neogene Tectonic Reactivation, through Apatite Fission-Track Analysis, in Precambrian areas of the Southeast Brazil: Association with the South Atlantic Ocean Opening. Journal of South American Earth Science, 15, 765-774.

Table 1. Results of ages obtained in each studied region.

Area	Sample	R_U x10^{-9}	L_S/L_I	$\varepsilon_{238}/\varepsilon$	ρ_S/ρ_I	Tap (Ma)	Tcorr (Ma)
High Serra da Mantiqueira (> 1000m)	TF-1	3.371 (± 4%)	0.79 (± 1.6%)	0.74 (± 10%)	1.97 (± 9.7%)	79.6 (± 11%)	107 (± 15%)
	TF-9	3.371 (± 4%)	0.76 (± 1.6%)	0.70 (± 10%)	1.99 (± 10%)	80.4 (± 11%)	115 (± 15%)
	TF-10	3.371 (± 4%)	0.76 (± 1.8%)	0.70 (± 10%)	2.20 (± 7%)	88.9 (± 8%)	126 (± 13%)
	TF-11	3.371 (± 4%)	0.75 (± 1.6%)	0.67 (± 10%)	2.65 (± 12.5%)	106.9 (±13%)	159 (± 16%)
	CT-1	6.958 (± 4%)	0.74 (± 1.6%)	0.67 (± 10%)	1.28 (± 13%)	107 (± 14%)	160 (± 17%)
	CT-2	6.958 (± 4%)	0.71 (± 1.6%)	0.64 (± 10%)	0.86 (± 9%)	72 (± 10%)	113 (± 14%)
	CT-3	6.958 (± 4%)	0.72 (± 1.8%)	0.64 (± 10%)	1.30 (± 11%)	83 (± 13%)	130 (± 16%)
	CT-5	6.958 (± 4%)	0.75 (± 1.6%)	0.70 (± 10%)	2.65 (± 12%)	86 (±13%)	123 (± 16%)
	CT-6	6.958 (± 4%)	0.69 (± 1.4%)	0.63 (± 10%)	0.80 (± 11%)	67 (± 12%)	106 (± 16%)
Low Serra da Mantiqueira (<1000m)	TF-4	3.371 (± 4%)	0.85 (± 1.3%)	0.80 (± 10%)	1.329 (± 8.0%)	53.8 (± 9.4%)	67.2 (± 14%)
	TF-5	3.371 (± 4%)	0.82 (± 1.4%)	0.77 (± 10%)	1.05 (± 7.5%)	42.5 (± 8.9%)	55.1 (± 13%)
	TF-12	3.371 (± 4%)	0.82 (± 1.2%)	0.77 (± 10%)	1.12 (± 7.5%)	45.4 (± 9%)	58.9 (± 13%)
	TF-13	3.371 (± 4%)	0.78 (± 1.4%)	0.72 (± 10%)	1.22 (± 12.5%)	49.4 (±13%)	68.5 (± 16%)
	CT-4	6.958 (± 4%)	0.74 (± 1.3%)	0.67 (± 10%)	0.463 (± 8 %)	39 (± 10%)	58 (± 14%)
Serra do Mar	TF-17	3.844 (± 3.5%)	0.74 (± 1.8%)	0.65 (± 10%)	1.54 (± 12.9%)	71.0 (± 14%)	108.9 (± 17%)
	TF-22	3.844 (± 3.5%)	0.78 (± 1.4%)	0.72 (± 10%)	1.23 (± 8.8%)	56.8 (± 9.9%)	78.7 (± 14%)
	TF-29	3.844 (± 3.5%)	0.76 (± 1.6%)	0.70 (± 10%)	1.34 (± 12.3%)	61.8 (± 13%)	88.2 (± 16%)
	TF-30	3.844 (± 3.5%)	0.80 (± 1.4%)	0.74 (± 10%)	1.14 (± 11.3%)	52.6 (±12.1%)	71.0 (± 16%)
	TF-31	2.251 (± 4%)	0.83 (± 1.0%)	0.77 (± 10%)	2.73 (± 13%)	74 (± 14%)	96 (± 17 %)
	TF-32	2.251 (± 4%)	0.82 (± 1.1%)	0.77 (± 10%)	2.25 (± 9.3%)	61 (±10 %)	79 (± 14%)
	TF-33	2.251 (± 4%)	0.82 (± 1.5%)	0.77 (± 10%)	2.36 (± 10%)	64 (± 11%)	83 (± 15%)
	TF-34	2.251 (± 4%)	0.81 (± 1.2%)	0.74 (± 10%)	1.61 (± 11%)	44 (± 12%)	59 (± 16 %)
	TF-35	2.251 (± 4%)	0.82 (± 1.2%)	0.77 (± 10%)	1.89 (± 15%)	51 (± 18%)	66 (± 21%)
	TF-39	2.251 (± 4%)	0.81 (± 1.0%)	0.74 (± 10%)	1.83 (± 9.7%)	50 (± 10%)	67 (± 14%)
	CT-9	2.323 (± 4.5 %)	0.77 (± 1.6%)	0.70 (± 4%)	1.48 (± 11%)	41 (± 13%)	59 (± 14%)
Coastal line	TF-20	3.844 (± 3.5%)	0.76 (± 2.6%)	0.70 (± 10%)	0.15 (± 7.9%)	6.95 (±9.1%)	9.9 (± 13%)

Table 1. Continuation

Coastal line	TF-21	3.844 (± 4%)	0.76 (± 1.6%)	0.70 (± 10%)	0.87 (± 8.9 %)	40.2 (± 10%)	57.4 (± 14%)
	TF-45	2.251 (± 4%)	0.77 (± 1.2%)	0.70 (± 10%)	2.26 (± 10%)	61 (± 11%)	87 (± 15%)
	CT-7	6.958 (± 4%)	0.68 (± 1.8%)	0.60 (± 10%)	0.53 (± 13%)	45 (± 14%)	66 (± 17%)
	CT-8	6.958 (± 4%)	0.72 (± 1.4%)	0.64 (± 10%)	0.68 (± 9%)	57 (± 10%)	89 (± 14%)
Ilha Bela	TF-42 A	2.251 (± 4%)	0.81 (± 1.1%)	0.74 (± 10%)	1.45 (± 7.0%)	39 (± 9%)	53 (± 13%)
	TF-42 B	2.251 (± 4%)	0.80 (± 1.4%)	0.74 (± 10%)	0.63 (± 10%)	17 (± 11%)	23 (± 15%)
Pouso Alegre	TF-51	5.382 (± 3%)	0.78 (± 1.5%)	0.72 (± 10%)	0.96 (± 10.5%)	62 (±11%)	89 (± 15%)
Jundiaí	TF-24	3.790 (± 3.5%)	0.74 (± 1.7%)	0.65 (± 10%)	2.20 (± 11%)	100 (±12%)	142 (± 16%)
	TF-25	3.790 (± 3.5%)	0.74 (± 1.4%)	0.65 (± 10%)	4.05 (± 8.7%)	183 (± 10%)	259 (± 13%)
	TF-52	5.281 (± 3%)	0.74 (± 1.8%)	0.65 (± 10%)	4.07 (± 7%)	254 (± 8%)	387 (± 13%)
	TF-53	5.281 (± 3%)	0.75 (± 1.7%)	0.67 (± 10%)	1.21 (± 10.7%)	77 (± 11%)	114 (± 15%)
Itú-SP	TF-54	5.281 (± 3%)	0.72 (± 3.7%)	0.64 (± 10%)	0.87 (± 24%)	55 (± 25%)	86 (± 27%)
Socorro	TF-55	5.281 (± 3%)	0.73 (± 1.6%)	0.64 (± 10%)	0.39 (± 13.6%)	25 (±14 %)	39 (± 17%)
	TF-56	5.382 (± 3%)	0.75 (± 1.4%)	0.67 (± 10%)	0.33 (± 10.3%)	22 (± 11%)	32 (± 15 %)

Table 2. Results of the weighted mean values of the χ^2 test in the studied regions.

Area	Valores médios		Teste do χ^2			
	$T_{ap} \pm 1\sigma$ (Ma)	$T_{corr} \pm 1\sigma$ (Ma)	Idade aparente (T_{ap})		Idade corrigida (T_{corr})	
			χ^2_v	$P(\chi^2_v)$	χ^2_v	$P(\chi^2_v)$
Serra da Mantiq. alta	75 ± 3	121 ± 6	1.485 ($v = 8$)	≈ 0.20	0.826 ($v = 8$)	≈ 0.60
Serra da Mant. Baixa	45 ± 2	61 ± 4	1.546 ($v = 4$)	≈ 0.20	0.734 ($v = 4$)	≈ 0.55
Serra do Mar	53 ± 2	72 ± 3	2.310 ($v = 10$)	≈ 0.01	1.196 ($v = 10$)	≈ 0.30

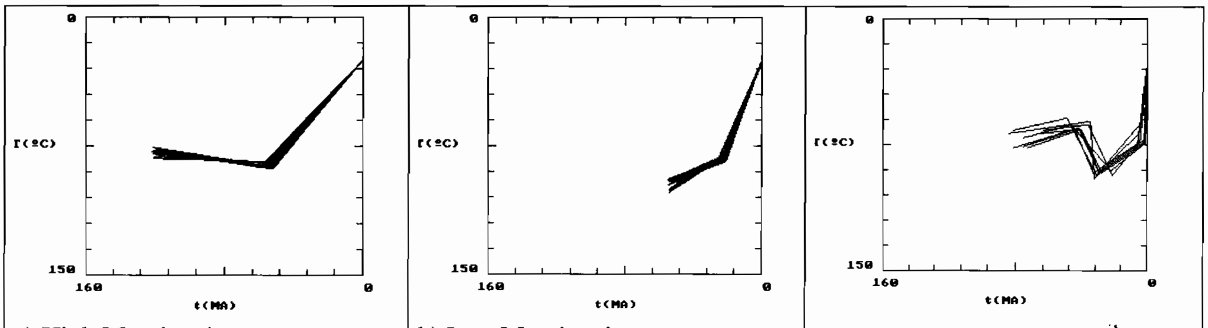

a) High Mantiqueira

b) Low Mantiqueira

c) Serra do Mar

Figure 1. Thermal history of the studied regions.

MONITORING ^{13}C IN CO_2 SOIL GAS FROM A LANDFILL: FIRST RESULTS FROM A CASE STUDY

Valencio, S.A.[1]; Ostera, H.A.[1,2] and Panarello, H.O.[1]

1. Instituto de Geocronología y Geología Isotópica. Pabellón INGEIS. Ciudad Universitaria, 1428, Buenos Aires, Argentina. susana@ingeis.uba.ar, hector@ingeis.uba.ar
2. Facultad de Ciencias Exactas y Naturales (UBA). Pabellón 2 Ciudad Universitaria, 1428, Buenos Aires, Argentina. ostera@ingeis.uba.ar

Keywords: CO_2, ^{13}C, landfill

INTRODUCTION

The majority of municipal solid waste, composed of paper and paperboard products, yard trimmings, glass, metals, plastics, wood, and food wastes still ends up in landfills. Prior to the adoption of good practices, municipal landfills commonly accepted a wide variety of hazardous and industrial wastes. As a result of such non-discriminatory waste disposal practices, municipal solid waste landfills are repositories of large amounts of toxic and hazardous waste.

Once waste is deposited in a landfill, biological and chemical processes act to change its structure and characteristics in a natural process. The time frame for waste decomposition varies greatly depending upon the nature of the waste (its physical and chemical composition) as well as the conditions present in the landfill. The process of waste degradation produces byproducts that can endanger the health of humans and the environment. Naturally occurring microorganisms such as bacteria biologically break down some waste components, emitting methane, other gases and chemical byproducts in the process. Modern landfills are built in cells at a time over years period, with each typical cell containing the amount of waste deposited in one day. Since the waste in some cells was placed in the landfill years or even decades before the waste in newer cells, different parts of the same landfill may undergo different stages of decomposition simultaneously, making the leachates and gas quality differ greatly between old and new cells.

For many of the microbial byproducts, there are large differences in the isotopic compositions of compounds produced from bacterial degradation of hydrocarbons and those produced from other substrates, such as soil organic matter (Conrad et al., 1996, 1997; Whiticar et al., 1986; Suchomel et al., 1990). In several studies, changes in the stable isotope ratios of soil gas CO_2 have been cited as evidence of intrinsic biodegradation of hydrocarbons (Landmeyer et al., 1996).

We present the first results from a soil-CO_2 survey using ^{13}C isotopes in soil-gas CO2, focussed in a Municipal landfill as part of a multidisciplinary approach (Orgeira et al., 2003) for understanding the evolution, processes and decomposition stage of the landfill.

LOCATION AND GEOLOGICAL SETTING

The landfill is located at Gualeguaychú, Entre Ríos Province (Fig. 1), and is operated by a Municipal service. We analyzed a three years old landfill, without references on classification of waste and presence of hazardous ones.

Holocene outcrops belonging to Punta Gorda Group (Pampean Loess) are exposed and are the substratum for the landfill. A geophysical survey (Figs. 2, 3) detected the inactive cells and the presence of leachates.

Water table levels, sampling topography and background reference samples were also taken.

METHODOLOGY

A soil gas probe (emplaced to depths of approximately 25 cm), coupled with a manual vacuum pump and also a battery pump was used for sampling the soil CO_2. Before sampling, three volumes of gas were purged from the sampling tube. After purging, 7.5 L of gas was collected at a flow rate of 100 mL/minute. The CO_2 reacted in a 1 N NaOH and was converted to $BaCO_3$ and dried. To perform carbon isotopic analyses, samples were reacted in 100% H_3PO_4 acid at 60°C for two hours. The carbon isotopic ratios of evolved CO_2 gas were determined in a Delta S Finnigan Mat triple collector mass spectrometer, at INGEIS. The isotopic composition is reported as deviation per mil (δ‰) relative to the V-PDB standard. Analytical uncertainty is 0.1‰ (±2σ) for $\delta^{13}C$.

RESULTS

The first results are shown in Table 1 and Fig. 3. The values range from -34‰ to -13‰. The areal distribution is shown in Fig. 3, overlapped with the water table level and the magnetometric survey.

Table 1. Location of samples and analytical data.

X	Y	$\delta^{13}C$	$HCO_3^-(w)$
5636883	6342812	-13.5	1159
5636114	6342748	-34.7	3294
5636907	6342688	-22.0	1189
5636777	6342671	-27.4	1433
5636974	6342668	-30.6	
5636805	6342841	-20.6	

DISCUSSION

The heterogeneity of values suggests different sources for soil CO_2, associated with three variables that we consider closely associated. The spatial distribution of $\delta^{13}C$ values reflects an inverse relationship with bicarbonate concentration of water (lowest values of $\delta^{13}C$, higher values of bicarbonate).

The bicarbonate concentrations are at least twice the values present in neighboring wells, marking an essential alteration of groundwater geochemistry by the landfill. The inverse correlation seems to be related with CO_2 generation by CH_4 oxidation in anaerobic conditions (Conrad et al., 1999). The CO_2 generated in this process is retained in water, and the resulting CO_2 is depleted. On the other hand, $\delta^{13}C$ of CO_2 is enriched to the north, as a consequence of oil gas CO_2 controlled by carbonate dissolution ($\cong$ 8 per mil) by leachates. We suggest that acid leachates are being neutralized by the soil carbonate. Resistivity models (Fig. 2) also suggest a limited amount of acid leachates that are buffered by the soil-.substrate response. Further research is in progress to monitor gas concentrations and isotopic variations during the year.

CONCLUSIONS

The first results of $\delta^{13}C$ on soil gas CO_2 in the Gualeguaychú landfill reflects heterogeneity and mixing of sources. The enrichment in $\delta^{13}C$ values coupled with higher concentrations of bicarbonate in groundwater could be explained by methane oxidation under anaerobic conditions. Enriched values can be associated with carbonate dissolution by acid leachates, responding to a natural attenuation process.

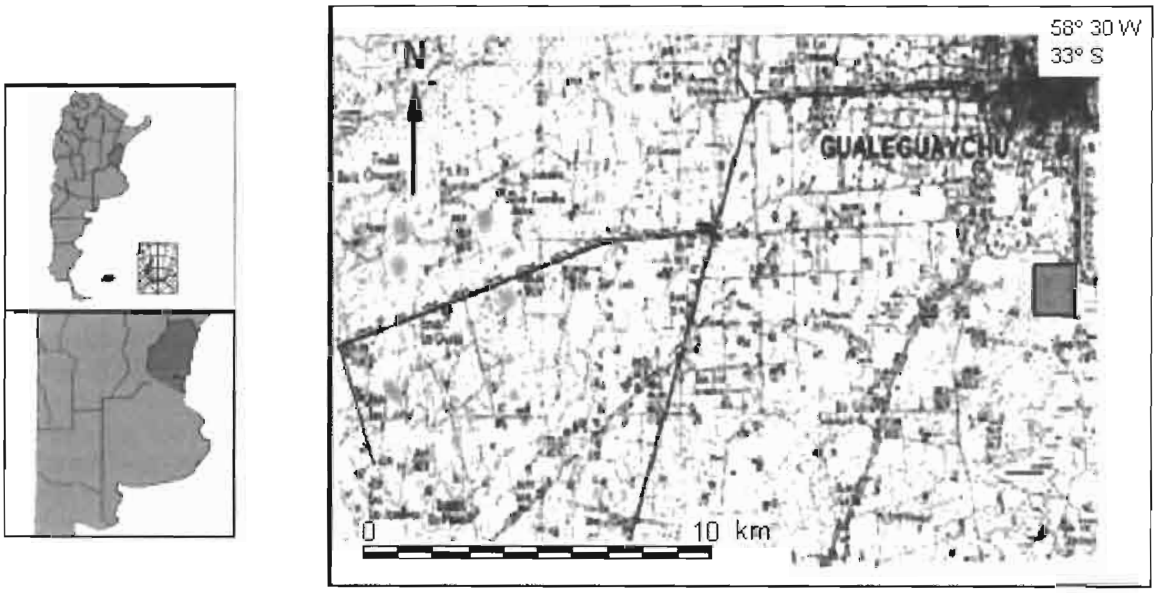

Figure 1. Location map

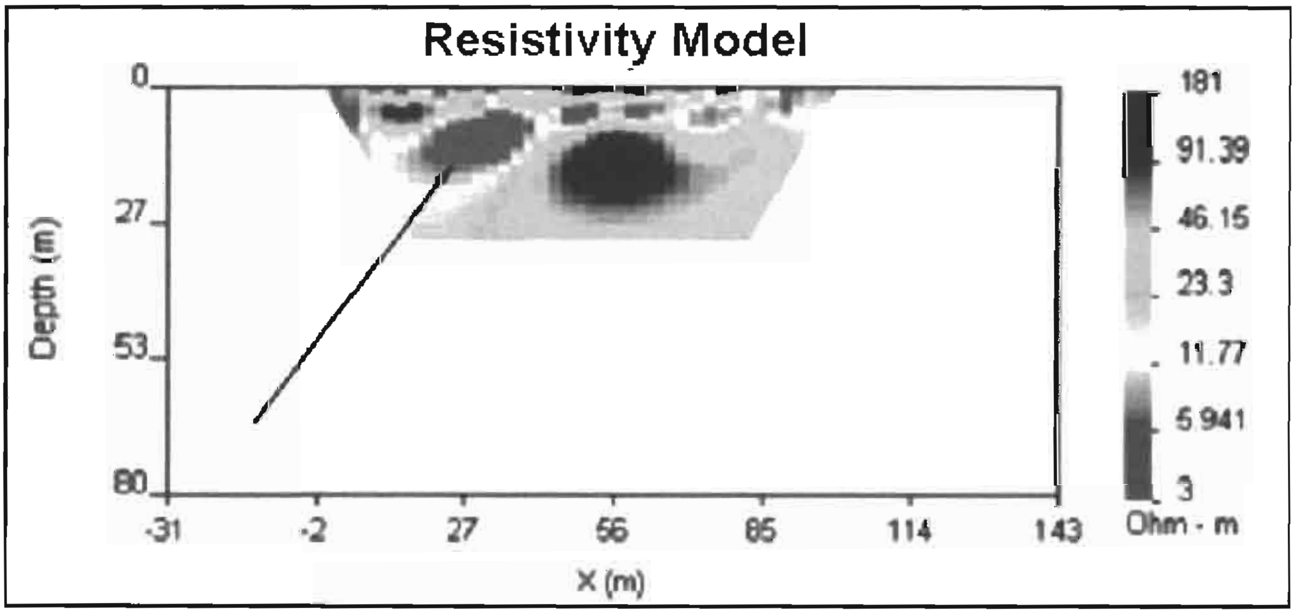

Figure 2. Resistivity model. Arrow: detected leachates.

REFERENCES

Conrad, M.E.; Templeton, A.S.; Daley, P.F.; Alvarez-Cohen, L., 1996. Coupled methanogenesis and methane oxidation of petroleum hydrocarbons. Geological Society of America, Abstracts with Program 28 (7), A132.

Conrad, M.E.; Daley, P.F.; Fischer, M.F.; Buchanan, B.B.; Leighton, T.; Kashgarian, M., 1997. Combined ^{14}C and $\delta^{13}C$ monitoring of in situ biodegradation of petroleum hydrocarbons. Environmental Science and Technology 31, 1463-1469.

Conrad, M.; Templeton, A.; Daley, P.; Alvarez-Cohen, L., 1999. Isotopic evidence for biological controls on migration of petroleum hydrocarbons. Organic Geochemistry 30: 843-859.

Landmeyer, J.E.; Vroblesky, D.A.; Chapelle, F.H., 1996. Stable carbon isotope evidence of biodegradation zonation in a shallow jet-fuel contaminated aquifer. Environmental Science and Technology 30, 1120-1128.

Orgeira, M.J.; Vásquez, C.A.; Ostera H.A., 2003. Relevamiento magnetométrico terrestre de rellenos sanitarios: estudio piloto en Gualeguaychú, Entre Ríos. Revista Asociación Geológica Argentina (submited).

Suchomel, K.H., Kreamer, D.K.; Long, A., 1990. Production and transport of carbon dioxide in a contaminated vadose zone: a stable and radioactive carbon isotope study. Environmental Science and Technology 24, 1824-1831.

Whiticar, M.J.; Faber, E.; Schoell, M., 1986. Biogenic methane formation in marine and freshwater environments: CO_2 reduction vs. acetate fermentation - Isotope evidence. Geochimica et Cosmochimica Acta 50, 693-709.

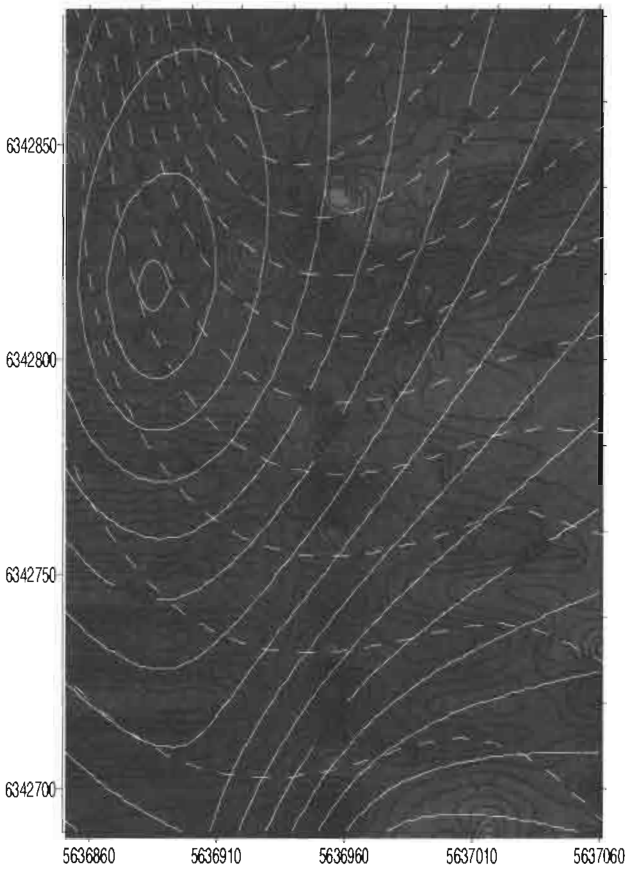

Figure 3. $\delta^{13}C$ curves, piezometric surface overlapped to magnetometric survey.

A NEW TIMS LABORATORY UNDER CONSTRUCTION IN RIO DE JANEIRO, BRAZIL

Valeriano, C.M.; Ragatky, D.; Geraldes, M.C.; Heilbron, M.; Valladares, C.S.; Schmitt, R.; Tupinambá, M.; Palermo, N.; Almeida, J.C.H.; Duarte, B.P.; Martins Jr., E.C. and Nogueira, J.R.

TEKTOS – Geotectonics Study Group, Faculdade de Geologia, Universidade do Estado do Rio de Janeiro,
Rua São Francisco Xavier 524/4006-A, Rio de Janeiro-RJ, 20559-900, Brazil. cmval@uerj.br

Keywords: Laboratory, TIMS, mass spectrometry, isotope geochronology, isotope geochemistry

INTRODUCTION

Several geochronology laboratories in Brazil have been built in the last decades. The first mass spectrometer (AMS-2) was installed at the IPEN (Instituto de Pesquisas Energéticas e Nucleares) in 1958. The first geochronology laboratory was built at the Universidade de São Paulo in 1962, when a Reynolds mass spectrometer started to run K-Ar analyses. In 1973 the second mass spectrometer (STH-5) was installed to run Rb-Sr analyses. In the Universidade Federal de Pará (Belem) was installed the next isotope laboratory specifically for geologic materials, equipped with a VG mass spectrometer in 1981. During the 90's four Finnigan mass spectrometers were installed (including two new isotope laboratories): at the Universidade Nacional de Brasilia (Brasilia), the Universidade Federal do Rio Grande do Sul (Porto Alegre), the Universidade Federal do Para and the Universidade de São Paulo.

This contribution has the objective to describe a new geochronology laboratory under construction at the Universidade do Estado do Rio de Janeiro (UERJ).

Thermal ionization mass spectrometry (TIMS) is a powerful method to measure very small concentrations of radio nuclides in different materials. However, the isotopic measurement of elements in low concentration is only possible by eliminating the natural contamination during the preparation and analysis procedures. Therefore, special construction standards for so-called clean laboratories have been developed in the last decades and presently there exist several facilities around the world which are specifically dedicated to isotopic analyses. In addition, low laboratory blanks are better obtained by using small amounts of high-purity reagents and miniaturized vials, beakers and ion exchange columns.

The architectural outline, mass spectrometer configuration and the operational facilities of the Laboratory of Geochronology and Isotope Geochemistry (LGIG), the fifth TIMS laboratory in Brazil, are briefly described.

ARCHITECTURAL OUTLINE

The LGIG is located on the forth floor of the Faculdade de Geologia, Universidade do Estado do Rio de Janeiro. The LGIG has external dimensions of 31m x 6m and comprises following compartments (Fig. 1): entrance room, clean room 1, clean room 2, two weighting rooms, sample-loading room and mass spectrometer room (Fig. 1).

The entrance room is to be used for changing clothes and also houses an oven and a refrigerator. The clean room 1 is equipped with three laminar flow hoods, one exhaustion hood and water distillation units. The clean room 2 contains an exhaustion hood and acid distillators. One of the two weighting rooms is dedicated to whole rock and the other one to grain samples. The sample-loading room is equipped with a small horizontal laminar flow hood. The mass spectrometer room also houses a computer and the degassing unit. In this room, the beads and filaments are also prepared.

In order to maintain a positive air pressure, refrigerated and filtered air is pumped into all the rooms. Three separate pre-filtering and refrigerating systems work for the clean rooms, spectrometer room and the entrance aisle respectively, collecting 100% of the air from the external environment. The cooler system is characterized by fan-coils that perform heat transfer with cold water ducts distributed from the central cooling unit of the University building.

In the clean rooms, the air undergoes a second filtering process with HEPA (high efficiency particulate air) type filters.

The combination of air inflow with the exhaustion system, which withdraws air from near-floor levels, is designed to result in a positive pressure of 2.5 mmCA, automatically controlled with pressure sensors.

MASS SPECTROMETER CONFIGURATION

The Triton TI is a magnetic sector thermal ionization mass spectrometer from Finnigan MAT^{TM}. This model incorporates some new characteristics, such as automated vacuum system, zoom optics featuring two quadrupoles and sample turret with 21 positions. The collector array (Table 1) consists of a fixed ion counting device (SEM) in the axial position, with a piggy-back Faraday cup and eight movable collectors. Three Faraday cups are placed on the high-mass side and four on the low-mass side. The lowest mass position is equipped with two MIC channels placed in tandem.

This configuration is suitable for measurement of isotopic composition of the most common elements used in geology research (Nd, Ca, Hf, Pb, U, Th, Sr).

Further software and hardware features and model innovations are available from the manufacturers.

Table 1. Collector array of the Finnigan Triton TI mass spectrometer and possible mass configurations for the most common applications in radiogenic isotope geology.

	L5		L4	L3	L2	L1	Axial	H1	H2	H3
Faraday cup			F	F	F	F	F	F	F	F
Ion counting							SEM			
MIC channel	MIC	MIC								
Var/fixed	var		var	var	var	fixed	var	var	var	var
Nd			142	143	144	145	146	147	148	150
Nd				142	143	144	145	146	147	150
Ca						42		43		44
Hf				174		176	177	178	179	180
Pb	204	205	206	207	208					
U	233	234	235	236	238					
Th							230		232	
Sr						84	85	86	87	88

ISOTOPE SYSTEMATICS AND POTENTIAL APPLICATIONS

The LGIG is designed to run, in the first moment, the U-Pb, Sm-Nd, Pb-Pb and Rb-Sr systematics. Equipment and lay-out were planned to run these four procedures, but other methods (e.g. Re-Os, U-Th series, etc.) may be developed in the future.

The LGIG is backed by another laboratory (Geologic Laboratory of Sample Processing- LGPA), which is in routine work at UERJ. Facilities include rock crushing, milling (disk- and ball-mills), sieving and gravimetric (panning and Wilfley table) and magnetic (Franz) separation. In addition, mineral grain hand-picking under binoculars is performed in the LGPA. All the above procedures are carried out in compliance with the requirements of minimized inter-sample contamination.

The laboratory incorporates recent improvements that minimize environmental contamination, such as sub-boiling distillation of water and acids, the use of Teflon bombs for sample dissolution in HF (oven or microwave) and the use of micro-columns in the chemistry procedures. Laminar flow hoods with HEPA filters also provide local particle-free environments for sample manipulation.

These systematics allow the LGIG facilities to a broad range of applications, such as igneous, metamorphic and sedimentary petrology. Research in metallogenesis, environmental sciences, hydrogeology and petroleum geology are potential fields of applications.

ACKNOWLEDGEMENTS

The construction of the laboratory was made possible with funding from: FINEP/CT-INFRA (0921/01) for the mass spectrometer; the Universidade do Estado do Rio de Janeiro for the facility construction; FAPERJ (Proc. E-26/170-684/00, Proc. E-26/170-523/00 and Cientistas do Nosso Estado- Proc. E-26/151.915/2000) and CNPQ (Proc. 46817/2000-0) for the chemistry laboratory equipments and supplies.

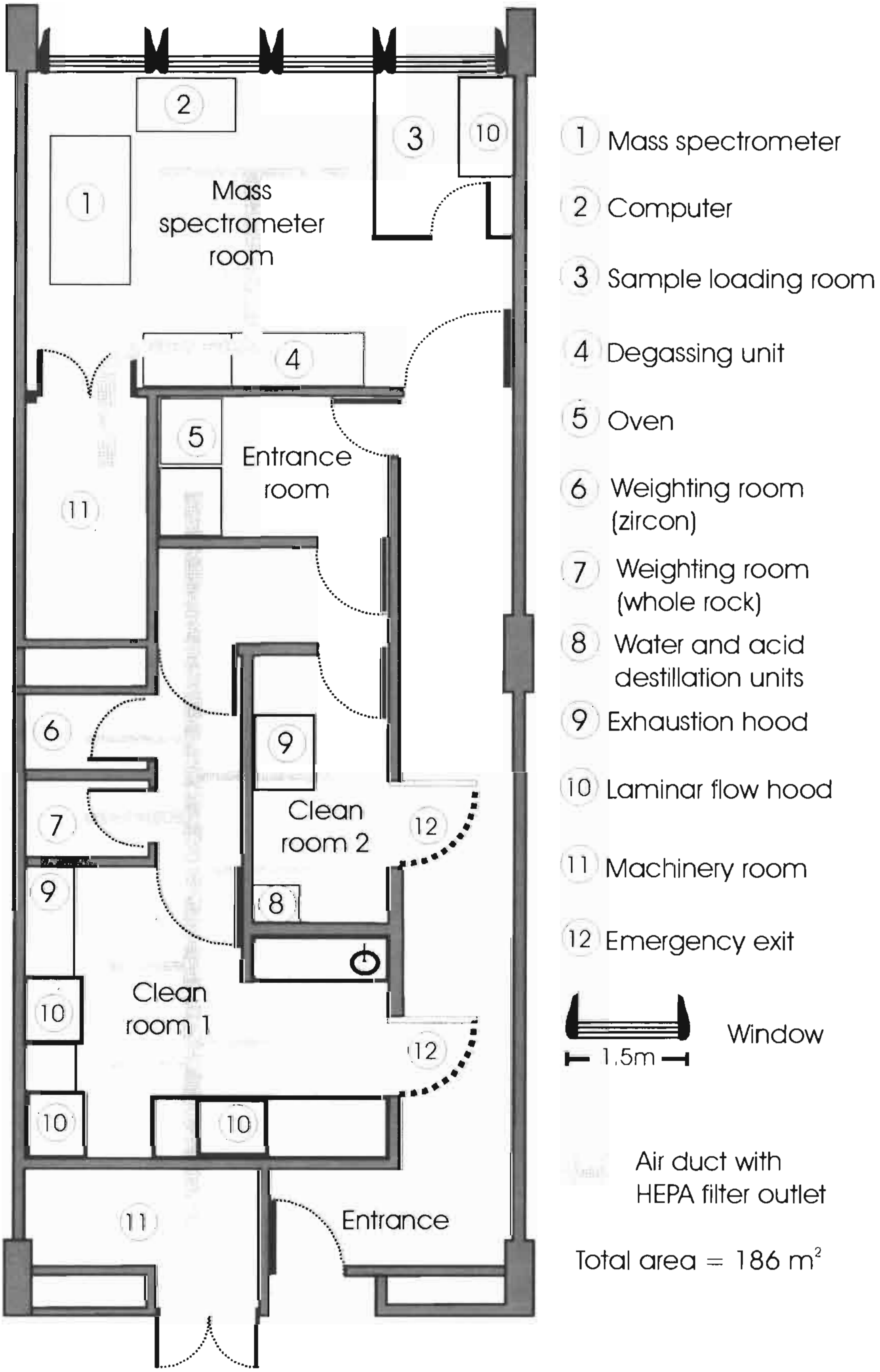

Figure 1. Architectural outline of the Laboratory of Geochronology and Isotope Geochemistry at UERJ.

INTEGRATED GEOCHRONOLOGICAL AND STRUCTURAL EVALUATION OF THE SIGNIFICANCE OF DETRITAL ZIRCON CRYSTALS FROM THE PORONGOS COMPLEX, SOUTHERN BRAZILIAN SHIELD

Vasconcellos, M.A.Z.[1]; Giuriatti, G.[1]; Hartmann, L.A.[2]; Liu, D.[3] and Philipp, R.P.[2]

1. Instituto de Física, Universidade Federal do Rio Grande do Sul, Avenida Bento Gonçalves, 9500; 91500-000, Porto Alegre, Rio Grande do Sul, Brazil. marcos@if.ufrgs.br
2. Instituto de Geociências, Universidade Federal do Rio Grande do Sul, Avenida Bento Gonçalves, 9500; 91500-000, Porto Alegre, Rio Grande do Sul, Brazil. leo.hartmann@ufrgs.br
3. Chinese Academy of Geological Sciences, 26 Baiwanzhuang Road, Beijing 100037, P. R. China. liudunyi@public.bta.net.cn.vcf

Keywords: U-Pb zircon SHRIMP, Raman spectroscopy, Porongos Complex, Paleoproterozoic

INTRODUCTION

We integrated four analytical techniques to understand the geochronological and structural evolution of detrital zircon crystals from the Porongos Complex, southern Brazilian Shield – sensitive high resolution ion microprobe (Beijing SHRIMP II), cathodoluminescence, photoluminescence and Raman spectroscopy.

The Porongos Complex is a major geological unit and has been variably interpreted as cratonic cover (Jost & Bitencourt, 1981) or back-arc association (Fernandes et al., 1992; Fragoso-Cesar, 1991) of the Brasiliano Cycle. It is made up mostly of metapelites and quartzites, intensely recrystallized in the greenschist and low amphibolite facies. Deformation is intense and affected both this clastic unit and its gneissic basement (Encantadas Complex). Provenance determination of the quartzites is of major significance for the understanding of the relationship of the unit with the Neoproterozoic Brasiliano Cycle (0.90-0.55 Ga) and the Paleoproterozoic Trans-Amazonian Cycle (2.26-2.00 Ga).

The geochronology of zircon is more reliable when based on the observation of the internal structure of the analyzed crystal (Vavra et al., 1999; Hartmann et al., 2000). Cathodoluminescence images show the internal structure in fine detail.

The cathodoluminescence and optical images can be used for the precise location of a laser beam, so the micro-Raman spectroscopic characteristics of zircon can be evaluated. Because the incidence of an ion beam (SHRIMP II) does not modify significantly the structural properties of the crystal, the laser beam can be located near the ion probe spot for the integrated evaluation of the structural and isotopic characteristics.

Our objective is to characterize the provenance of the detrital zircon crystals and the relationship between internal structure and isotopic composition of the crystals.

RESULTS AND INTERPRETATION

The SHRIMP II isotopic results (Fig. 3) of the zircon crystals (six rock samples) are remarkably confined to Paleoproterozoic ages (one Archean age). This implies the presence of a continent of this age in the region and that the Porongos Complex sediments were deposited on a stable platform.

The cathodoluminescence images show a variable light emission behaviour from fine euhedral zonning to no zonning and strong light emission to very weak light emission. Figure 2a shows an example of a grain (Grain 5-1) with fine euhedral zonning and portions with broad bands with no defined zonning distribution. Figure 2b show another example of a grain (Grain 5-7) with very weak light emission and a remaining euhedral zonning

The micro-Raman spectroscopy results of the points indicated in Figure 2 of the zircon crystals are shown in Fig. 4. Predicted Raman lines located at 202, 214, 225, 355, 439, 975 and 1008 cm^{-1} (Zhang, 2000) were observed in the grain 5-1. The same lines are also observed in grain 5-7, but with very low intensity and line-broadening at the position 975 and 1008 cm^{-1} in the spectra of different points.

The low intensity of Raman lines located at 975 and 1008 cm^{-1}, the decreasing in the frequency when compared to theorectical prediction (975 to 964 cm^{-1} and 1008 to 997 cm^{-1} in grain 5-7) and the observed line-broadening are all indicative of some degree of radiation damage induced on the structure of the zircon by the α-decay process.

Photoluminescence spectra for grains 5-1 (point 3) and 5-7 (point 1) are shown in Figures 5a and 5b, respectively. Lines are indicative of the occurrence of Er, Dy and Pr rare earth elements (Dieke, 1968) in variable amounts.

The integrated use of four analytical techniques for the investigation of zircon crystals from the Porongos Complex led to the determination of the Paleoproterozoic ages of the geological unit and the description of the internal structure of the crystals. The damage degree and the identification of REE of the whole set of SHRIMP dated grains is under evaluation. This is a fertile methodology for the study of complex crystals and geological terrains.

REFERENCES

Dieke, G. H.; 1968. Spectra and Energy Levels of Rare Earth Ions in Crystals. New York: Interscience Publishers.

Fernandes, L.A.D.; Tommasi, A.; Porcher, C.C.; 1992a. Deformation patterns in the southern Brazilian branch of the Pan-African Dom Feliciano Belt. Journal of South America Earth Sciences 5, 77-76.

Fragoso-César, A.R.S., 1991. Tectônica de placas no Ciclo Brasiliano: as orogenias dos Cinturões Dom Feliciano e Ribeira no Rio Grande do Sul. Universidade de São Paulo. Doctoral Thesis, 367 p.

Hartmann, L.A.; Leite, J.A.D.; Silva, L.C.; Remus, M.V.D.; McNaughton, N. J.; Groves, D. I.; Fletcher, I. R.; Santos, J.O.S.; Vasconcellos, M.A.Z., 2000. Advances in SHRIMP geochronology and their impact on understanding the tectonic and metallogenic evolution of southern Brazil. Australian Journal of Earth Sciences 47 829-844.

Zhang, M.; Salje, E.K.H.; Farnan, I.; Graeme-Barbet, A.; Daniel, P.; Ewing, R.C.; Clark, A.M.; Leroux, H., 2000. J.Phys:Condens.Matter 12: 1915-1925.

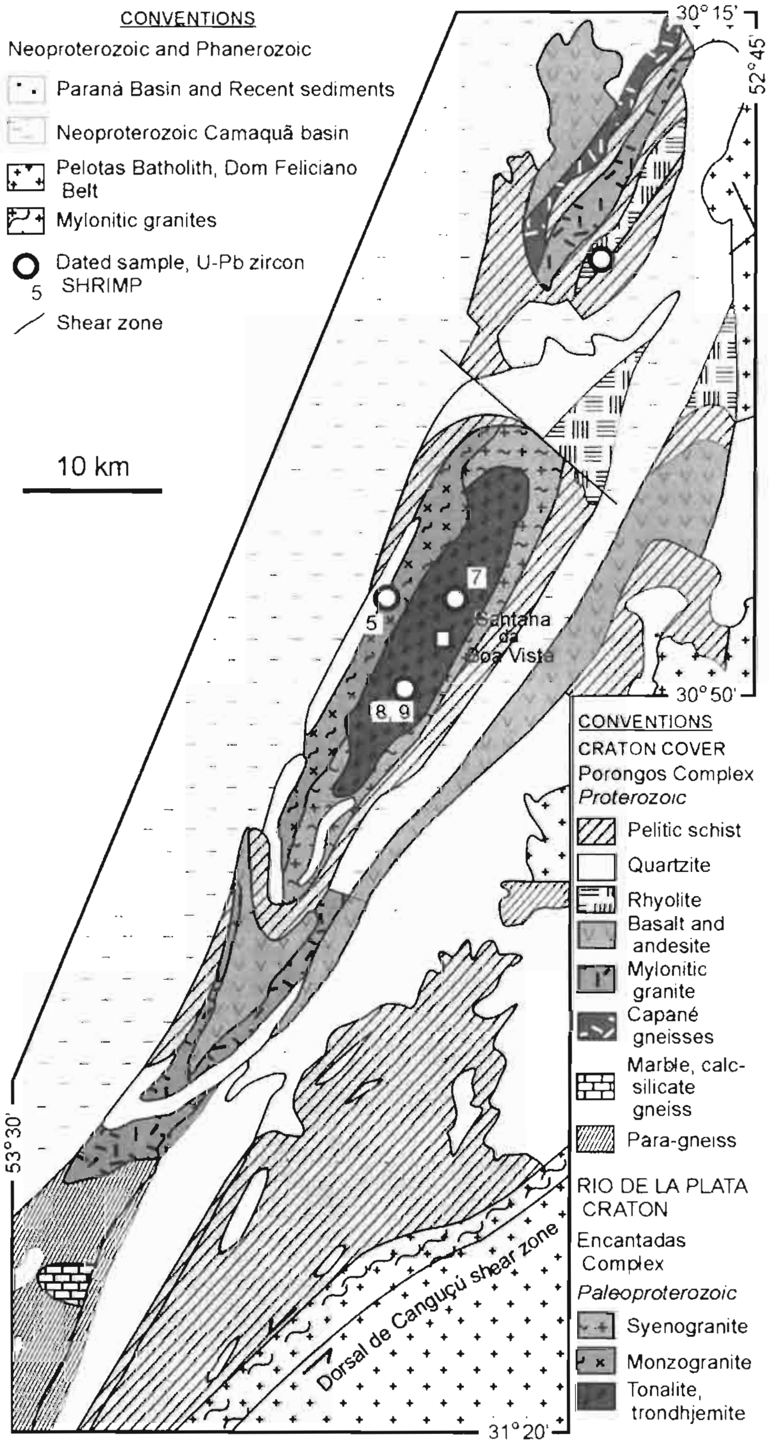

Figure 1. Geological map of Tijucas Belt, southern Brazilian Shield, showing distribution of the Porongos Complex and the location of studied quartzite samples.

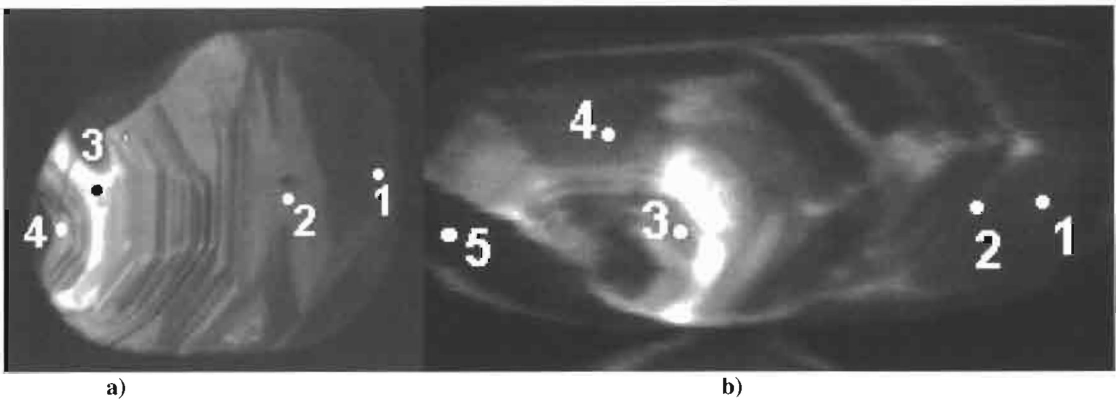

Figure 2. Cathodoluminescence images of zircon crystals from the Porongos Complex quartzites dated by U-Pb SHRIMP and investigated with Raman spectroscopy. Spots analyzed by Raman spectroscopy are shown as small white circles. Sample 5 of a) grain 5-1 and b) grain 5-7.

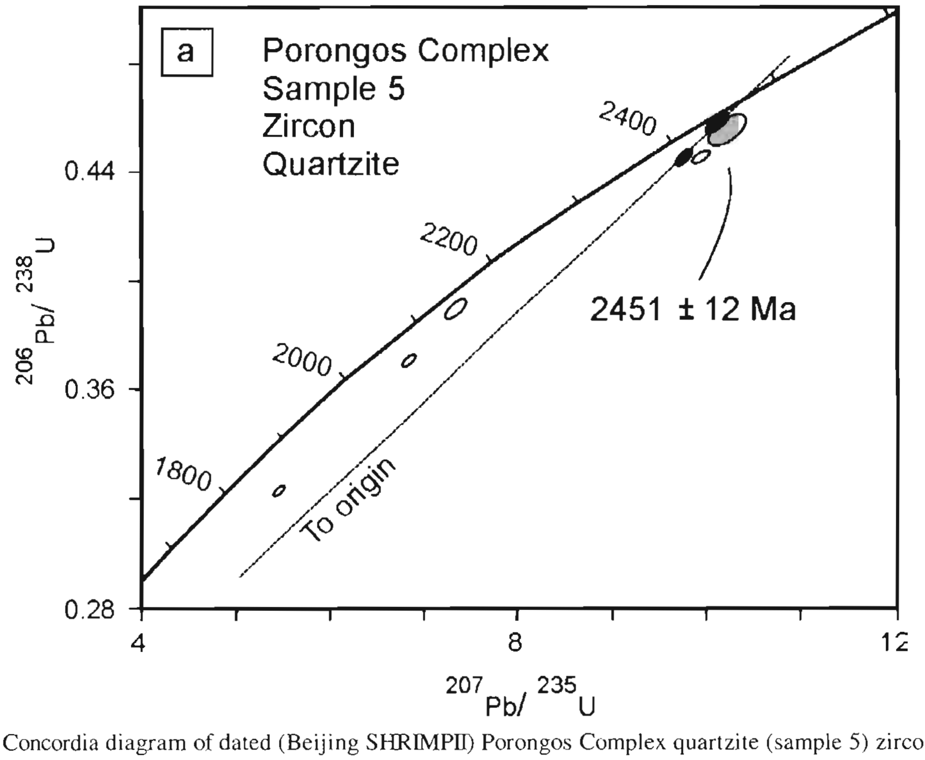

Figure 3. Concordia diagram of dated (Beijing SHRIMPII) Porongos Complex quartzite (sample 5) zircon crystals.

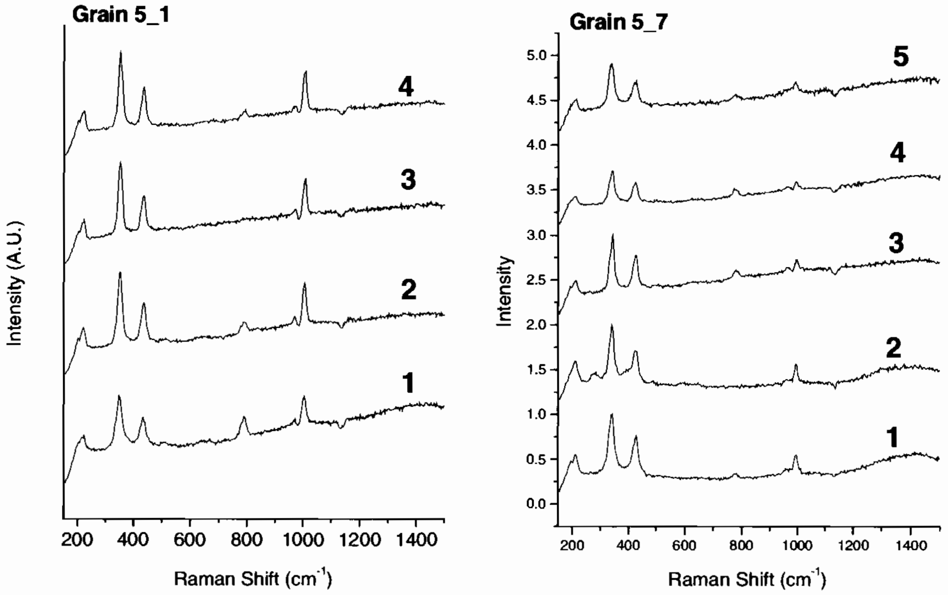

a) b)

Figure 4. Raman spectra of dated (Beijing SHRIMPII) Porongos Complex quartzite zircon crystals. Sample 5 of a) grain 5-1 and b) grain 5-7.

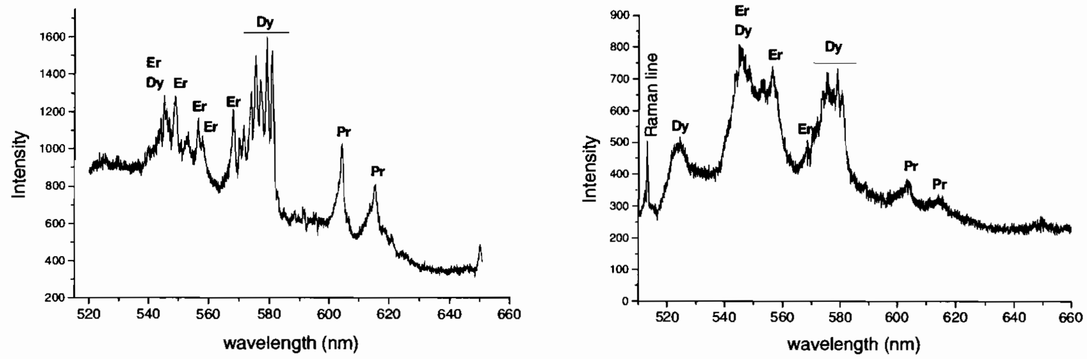

a) b)

Figure 5. Photoluminescence spectra of dated (Beijing SHRIMPII) Porongos Complex quartzite zircon crystals. Sample 5 of a) point 3 of grain 5-1 and b) point 1 of grain 5-7.

APPLICATION OF THE ^{40}Ar/^{39}Ar METHODOLOGY IN THE STUDY OF TECTONIC REACTIVATIONS OF SHEAR ZONES: ROMERAL FAULT SYSTEM IN THE CENTRAL CORDILLERA OF COLOMBIA

Vinasco C.J.[1]**; Cordani U.G.**[1] **and Vasconcelos P.**[1,2]

1. Institute of Geosciences, University of São Paulo - Rua do Lago, 562, Cidade Universitária, 05508-080, São Paulo, Brazil. cesarj@usp.br
2. University of Queensland, Department of Earth Sciences, Brisbane, Qld, 4072, Australia. paulo@earth.uq.edu.au

Keywords: ^{40}Ar/^{39}Ar, fine micas, mylonitic rocks, deformational events, Northern Andes

INTRODUCTION

The ^{40}Ar/^{39}Ar methodology is an applicable tool to a wide spectrum of geological problems (McDougall & Harrison, 1999; Renne, 2000). In the case of thermocronology of shear zones (Goodwin & Renne, 1991; Dunlap, 1997) and mylonitic dating (West & Lux, 1993; Freeman et al., 1998; Kligfield, et al., 1986) important results were obtained.

The main goal of the present work is to verify the feasibility of the ^{40}Ar/^{39}Ar methodology in the study of tectonic reactivations of shear zones using the new installed Ar-Ar equipment in the Centro de Pesquisas Geocronológicas in the Institute of Geosciences at the University of São Paulo, Brazil. To reach the proposed objectives, deformed, neo-formed and recrystallized minerals were used from igneous and metamorphic rocks of the Romeral fault system in the northern part of the Central Cordillera of Colombia. Fine muscovites and biotites found in mylonitic rocks and in hydrothermal alteration areas generated during the main tectono-magmatic episodes supplied the main keys for obtaining deformational ages. K-Ar analyses in mylonitic, volcanic and hydrothermalized rocks were carried out to yield complementary results.

The main advantage of the method consists on the possibility of obtaining reliable results with little amount of material, such as individual crystals or small mineral concentrates of fine micas carefully selected by handpicking.

DATING MYLONITIC ROCKS

The knowledge of the deformational textures and the role of the different mineral species in the deformational fabric becomes necessary in order to determine which minerals can supply results with geological meaning. In addition, the understanding of the deformational mechanisms and temperatures reached during the process is necessary to establish that such results represent deformational and not cooling ages. Because of their good Ar retentivity, analyses of pure concentrate of neo-formed potassium micas have a potentiality to yield deformational ages in greenschist facies conditions.

Neo-crystallization of micas during deformation is a widely recognized phenomenon and is the most important process in the Ar-Ar dating, because usually these crystals should not contain ^{40}Ar in relevant amount at the moment of deformation (Reddy & Potts, 1999). Micas offer a considerable potential to date crustal deformations because of their stability in a wide spectrum of metamorphic conditions. Therefore, from a practical point of view, the most important limitation to meaningful results is the appropriate concentration of the mineral of interest, so much for the amount of sample available as for its grain size, because the amount of gas to be obtained in the ar extractions should be well above the level of blank of the extraction system.

In this work, strongly deformed and mylonitized rocks with generation of neo-formed potassium micas are key samples to obtain deformational ages. Intensely altered rocks, products of fluid activity, are a second objective for complementary results.

SAMPLING AND EXPERIMENTAL METHODS

The sampling area for this study is located WSW of Medellin, Colombia within the Romeral fault system. Four metamorphic rocks, six mylonitic rocks and two igneous rock samples were crushed, ultrasonicated in ethanol, and dried. Ten to fifteen single crystals of biotite or muscovite from each sample were picked with metal tweezers, placed in wells in Al-irradiation disks, and irradiated, together with Fish Canyon sanidine fluence monitors, in the IEA-R1 nuclear reactor at IPEN, São Paulo, Brazil. After 2-3 weeks, three grains from each sample or concentrates of 10-15 grains for fine micas were analyzed by the laser incremental heating ^{40}Ar/^{39}Ar method at the CPGeo-USP laboratory. Irradiation, analysis, and interpretation procedures follow the methodology presented in Vasconcelos et al. (2001). Additionally, K-Ar whole rock analysis for six mylonitic rocks and three hydrotermalized volcanic rocks for comparison purposes were carried out (Table 1).

The final selection of samples for Ar-Ar analysis was defined during a detailed petrographic study supported by X ray and SEM studies, especially for the finest grained rocks.

THE PROBLEM OF GRAIN SIZE AND ANALYTICAL ASSESSMENT

Sample size requested for analysis ^{40}Ar/^{39}Ar is one of the main advantages of the method, because in deformational areas neo-formed micas are usually very fine, about 25 to 50 µm. The amount and size of the mineral of interest in mylonitic rocks frequently prevent the concentration of enough material for analysis.

The amount of sample necessary for Ar-Ar analysis depends fundamentally of the amount of radiogenic ^{40}Ar* that allows the measurement of the ^{40}Ar/^{39}Ar age spectrum with appropriate resolution. The most important factors that rule the generation of enough gas are the age and the concentration of K in the sample.

For the analyses made in this work, the argon extraction line in the ^{40}Ar/^{39}Ar equipment at CPGeo-USP reached blank values in the order of 10^{-16} moles of ^{40}Ar, varying between 1.73×10^{-16} and 1.40×10^{-15} moles, with an average value of 2.79×10^{-16} moles of ^{40}Ar. Individual grains with size among 0.5-1.0 mm and weight between of 10^{-3} and 10^{-5} gm, yielded values between 1.99×10^{-12} and 5.46×10^{-14} moles of ^{40}Ar for biotite, 1.31×10^{-12} and 2.97×10^{-13} for muscovite, and 1.21×10^{-13} and 2.01×10^{-15} for amphiboles. Biotite and muscovite crystals yielded levels of released ^{40}Ar up to two magnitude orders higher than blanks.

Concentrates of about 10-15 grains of fine micas from deformed and mylonitic rocks with approximate total weights of 1×10^{-5} gm, corresponding to individual grain sizes among 25 to 50 μm, yielded values between 1×10^{-14} and 1×10^{-16} moles of ^{40}Ar. Such amount of gas is at the limit of the analytical possibilities of the equipment, and the obtained spectra varied greatly in quality. Some samples could not release gas above blank values. However, most of them yielded enough gas in the initial steps, and the age spectra could be considered geologically meaningful.

The curves of figure 1 represent acceptable minimum values in terms of amount of sample vs. age according to the obtained experimental results. About 50 times the amount of gas in moles of ^{40}Ar above the blank of the system was considered acceptable for appropriate determinations. Analyses with slightly lower amounts of gas released didn't yield good quality step heating spectra. Additionally to the minimum values suggested in this work for appropriate analyses, other difficulties related to the size of the material to be analyzed and to the amount of atmospheric argon present in the sample were found. An additional problem is the difficult manipulation of very small grains and the risk of contamination during the operation at the nuclear reactor and in the handling of samples in the holder.

From the results, were confident that a concentrate of 15 to 20 grains of fine micas (25-50 μm.), with an average percentage of K of 7% and older than 10 Ma could yield a reliable age (Fig. 1).

DEFORMATIONAL AND RESETTING AGES

Mylonitic rocks are direct representatives of activation episodes of fault systems in ductile intermediate crustal levels. Very good spectrums were obtained from mylonitic rocks in neo-formed fine mica concentrates, yielding in most cases concordant plateau ages for different samples and similar K-Ar ages (Table 1). Mineral concentrates were analyzed instead of individual grains because of the fine grain size and the necessity of obtaining enough gas for reliable measurements.

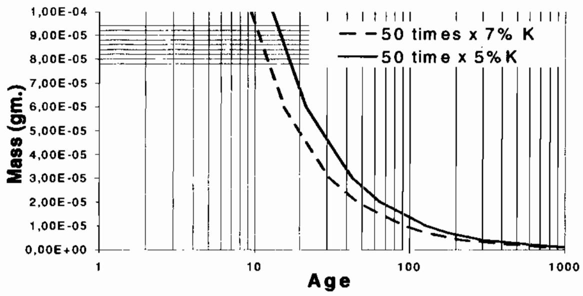

Figure 1. Curves representing the acceptable minimun values for appropiate Ar-Ar analysis in terms of amount of sample vs. Age according to the obtained experimental results. Values of 40Ar released 50 times the blank of the system for 7 and 5% K are represented.

Samples collected from the basic volcanic Quebradagrande Fm., correspond to centimetric mylonitic bands within the sequence, presenting variable degree of deformation.

A tuffaceous mylonitic rock of intermediate composition yields a well defined plateau age in sericite above 90% of the total gas released of 74 ± 2 Ma, interpreted as a deformational age because the temperatures reached are probably below 450° C. This age is close to a whole rock K-Ar apparent age of 69 ± 2 Ma for the same sample. Similar results were obtained from a phyllonite with fine grained sericite generation. In spite of the little quantity of gas released, it was possible to obtain an amount of gas critically above the blank value in the first two steps of the degasification process. One of the concentrates yields a plateau age of 72 ± 4 Ma for 80% of gas released, considered as a reliable value, because is concordant to a whole rock K-Ar analysis of 65 ± 3 Ma (Table 1) for the same sample. This age value is interpreted as directly related to the activity of the fault system, indicating a time of deformation. The reached temperatures would be in the interval corresponding to the greenschist facies, given the presence of neoformed chlorite and sericite and formation of ribbons textures in quartz with appreciable recovery, confirming a temperature for deformation compatible with metamorphism of medium to high greenschist grade (Simpson, 1985). The integrated ages around 34 Ma are considered as due of the heterogeneity of the spectrum, without geological significance.

A basic mylonitic rock within the same Quebradagrande formation was analyzed using a concentrate of graphite-bearing sericite grains, given the reduced size of the sericites. The amount of gas obtained was very low, with generation of gas just above blanks value for the initial steps. The obtained spectrum is of low analytical quality and the integrated age of 84 ± 4 Ma and the K-Ar whole rock age of 66 ± 3 Ma (Table 1) barely reflect the deformational episode of the upper Cretaceous, recorded for some others regional samples. A sample of more mafic composition in the same volcanic rocks shows a high homogeneity for 80% of gas released and yields biotite plateau ages of 89.8 ± 1 Ma and 87.8 ± 0.7 Ma, considered as cooling ages of an Albian-Cenomanian

Table 1. Ar-Ar and K-Ar results of deformed and hydrothermalized rocks.

Unit	Mineral	Integrated Age (Ma)	Plateau Age (Ma)
Tuffaceous mylonitic rocks of Quebradagrande formation	Ser	86±2	74±2
		84.9±1.3	81±5
	Bi	96.6±1.1	89.8±1.1
		83.2±0.7	87.8±0.7
	Ser	93±14	
		89±5	
Sabaletas schist	Ser	102±3	
		115.9±1.6	127.5±2.0
Phylonite of Quebradagrande formation	Ser	32±5	72±4
		34±15	
Mylonite basic rock of Quebradagrande formation	Ser	84±4	
		70±30	
Santa Barbara metagabbro	Amp	119±5	
		141±7	
Sabanalarga batholith	Amp	152.7±0.7	
		145.9±0.5	
	Amp	145.1±0.7	
		90±20	89.9±0.6
	Amp	92±3	92±2
		108±4	106±3 / 95±4
Palmitas gneiss	Bi	67.95±0.11	68.13±0.12
		68.09±0.14	
Amphibolite of the Arquia group	Bi	4.5±0.4	5.6±0.4
		0.3±1.1	4.5±1.1

Unit	Material	%K	%^{40}Ar Atm	Age (Ma)
Gabbro Quebradagrande formation	WR	0.20	56.45	102±7
	WR	0.94	34.19	64.7±3
Tuffaceous mylonitic rocks of Quebradagrande formation	WR	1.73	19.66	73±2
	WR	4.04	12.49	62±1
	WR	1.95	18.19	69±2
Basic pyroclastic rock of Quebradagrande formation	WR	0.31	58.58	68±5
Mylonite básic rock of Quebradagrande formation	WR	1.08	39.82	66±3
Phylonite of Quebradagrande formation	WR	0.59	47.67	65±3
Mylonitic band bordering metric unaltered lenses of Triassic quartzodioritic material of the Cambumbia stock	WR	0.59	42.66	86±16

rock deformation episode. However, a whole K-Ar age of 62 ± 1 Ma was obtained for the same sample, clearly discordant in relation to the previous results, suggesting that this age is not well constrained. To complete the picture, a tuffaceous mylonitic rock of felsic composition collected in the same outcrop yields a very heterogeneous spectrum. The amount of gas obtained for this sample was critical, and it was possible to obtain an amount of gas above blank levels only in the first stages of fusion.

The ages obtained when about the 90% of the gas was released, are considered as hardly reflecting a not well constrained regional deformational episode about 100 Ma. Integrated ages of and 89 ± 5 Ma are considered as a reasonable approach for this deformational episode, and they agree within experimental errors with values registered for other samples in the same area. However, were obtained K-Ar whole rock discordant results of 73 ± 2 Ma suggesting again that the age is not very well constrained.

One sample from the Sabaletas quartz micaceous polymetamorphic schist yielded a sericite plateau age of 127.5 ± 2.0 Ma registered when the largest amount of gas was released. This age coincides in general with values obtained for the concentrate of a second analyzed mineral of the same sample. A precise age was not obtained, and the plateau age is here considered to be close of the deformational metamorphic event that formed the sericites.

Analyses for the Palmitas gneiss show very well defined plateaus, indicative of a complete resetting of the system because the complete recrystallization of biotite. The plateau age obtained of 68.13 ± 0.12 Ma may reflects the intrusion of the Antioquian batholith and or the upper cretaceous well constrained deformational event.

A deformed amphibolite of the Arquia Group, relatively altered, yields very low amount of gas and spectra with high associated error and complex geometries. However, one of the analyzed grains yielded a plateau age in biotite for 50% of released gas of 5.6±0.4 Ma, interpreted as a reflex of the deformation that would have recrystallized the biotites, being coincident with the intrusion ages of neo-Tertiary bodies in the proximities.

CONCLUSIONS

The most important advantages of the use of the $^{40}Ar/^{39}Ar$ methodology in dating deformational episodes are: (1) the possibility to work with potassium micas, which commonly define deformational fabrics; (2) the use of a small amount of sample and (3) the possibility to interpret adequately the spectrum obtained.

In order to obtain satisfactory results we shall observe: (1) the usefulness of working with highly deformed and highly hydrothermalized rocks with neoformed potassium micas and (2) the need to carefully isolate micas from the most deformed segments of the hand sample. Finally, complementary K-Ar whole rock analyses in the case of fine grained, hydrothermalized and mylonitic rocks may yield important information.

An amount of 50 times of ^{40}Ar moles above the system blank was considered acceptable as a lower limit for reliable analysis, provided that the amount of atmospheric argon in the extraction system be sufficiently low.

Concentrates with 15 to 20 grains of fine micas with K concentration of 7% and grainsize between 25 to 50 µm, may yield significant results for samples older than 10 Ma.

For fine micas from mylonitic rocks, with grain size between 25 to 50 µm, between $1x10^{-14}$ e $1x10^{-16}$ moles of ^{40}Ar were obtained at the limit of the analytical possibilities of the equipment. Most samples yielded enough gas for analysis in the initial steps of the fusion process, where it was possible obtain geologically meaningful results.

The strong concordance observed between K-Ar whole rock ages and mineral Ar-Ar results from the same samples, and samples of the same area, indicate that the results obtained have geological meaning and show that Ar-Ar analysis for small concentrates of potassium micas yield good results.

Lower Cretaceous deformational events were recorded in a quarzo-sericite schist, hydrothermal ages of the Sabanalarga batholith and amphiboles from a metagrabbro.

On the basic volcanic sequences of Quebradagrande formation of lower Cretaceous age, a K-Ar total rock age of 102 ± 7 Ma in a cataclastic gabbro was interpreted as hydrothermal alteration age indicative of the fault system activity in Albian – Cenomanian times. $^{40}Ar/^{39}Ar$ analyses from the same sequence yielded biotite and sericite plateaus ages between 87 and 90 Ma of poor interpretative value.

In the same volcanic sequence were obtained apparent Ar-Ar plateau ages about 72 Ma very well constrained with whole rock K-Ar results, being this the better recorded deformational event. Another whole rock K-Ar ages between 66 and 73 Ma confirm the lower cretaceous deformational event. $^{40}Ar/^{39}Ar$ biotite plateau ages of 5.6±0.4 Ma obtained for an amphibolite, recorded the last important activation episode of the Fault System.

ACKNOWLEDGEMENTS

This research was supported by FAPESP process 01/05304-0 and PRONEX/FINEP No 41.96.0899.00. The field work was executed with the cooperation of INGEOMINAS, Colombia.

REFERENCES

Dunlap, W.J., 1997. Neocrystallization or cooling? $^{40}Ar/^{39}Ar$ ages of white micas from low grade mylonites. Chemical Geology. 143. p. 181-203.

Freeman, S.; Butler, R.; Cliff, R.A., 1998. Direct dating of mylonite evolution: a multi-disciplinary geochronological study from the Moine thrust zone, NW Scotlaand. In: Journal of the Geological Society, London, Vol 155. 1998. p. 745-758.

Goodwin, L. &; Renne, P. 1991. Effects of progressive mylonitization on Ar retention in biotites from the Santa Rosa mylonite zone, California, and thermochronologic implications. Contributions to Mineralogy and Petrology. 108 283-297.

Kligfield, R.; Hunziker, J.; Dall, R.; Meyer, 1986. Dating of deformation phases using K-Ar and Ar/Ar techniques: results from the Northern Apennines. in: Journal of Structural Geology Vol 8, No 7. 791-798.

McDougall, I. & Harrison, T., 1999. Geochronology and Thermocronology by the 40Ar-39Ar method. Oxford University Press. New York. 269.

Reddy, S. & Potts, G., 1998. Constraining absolute deformation ages: the relationship between deformation mechanisms and isotope systematics. in: Journal of Structural Geology Vol 2 1. 1999 1255-1265.

Renne, P., 2000. K-Ar and ^{40}Ar-^{39}Ar dating. In: J.S Noller, J.M Sowers, W.M. Lettis. (eds.) Quaternary Geochronology: Methods and applications. American Geophysical Union. p. 77-100.

Simpson, C., 1985. Deformation of granitic rocks across the brittle-ductile transition. in: Journal of Structural Geology Vol 7, No 5. 503-511.

Vasconcelos, P.; Onoe, A.; Kawashita, K.; Soares, A.; Teixeira, W., 2001. $^{40}Ar/^{39}Ar$ Geochronology at the Instituto de Geociências, USP: Instrumentation, Analytical procedures and calibration. Anais da Academia Brasileira de Ciências.

Vinasco, C.J., Cordani, U.G., Vasconcelos, P., 2001. $^{40}Ar/^{39}Ar$ dates in the central cordillera of Colombia: Evidence for an upper triassic regional tectonomagmatic event. Ext. Abstracts. III SSAGI. Pucón, Chile.

West Jr, D. & Lux, D., 1993. Dating mylonitic deformation by the Ar/Ar method: An example from Norumbega Fault zone, Maine. in: Earth and Planetary Science Letters 120. 1993 221-237.

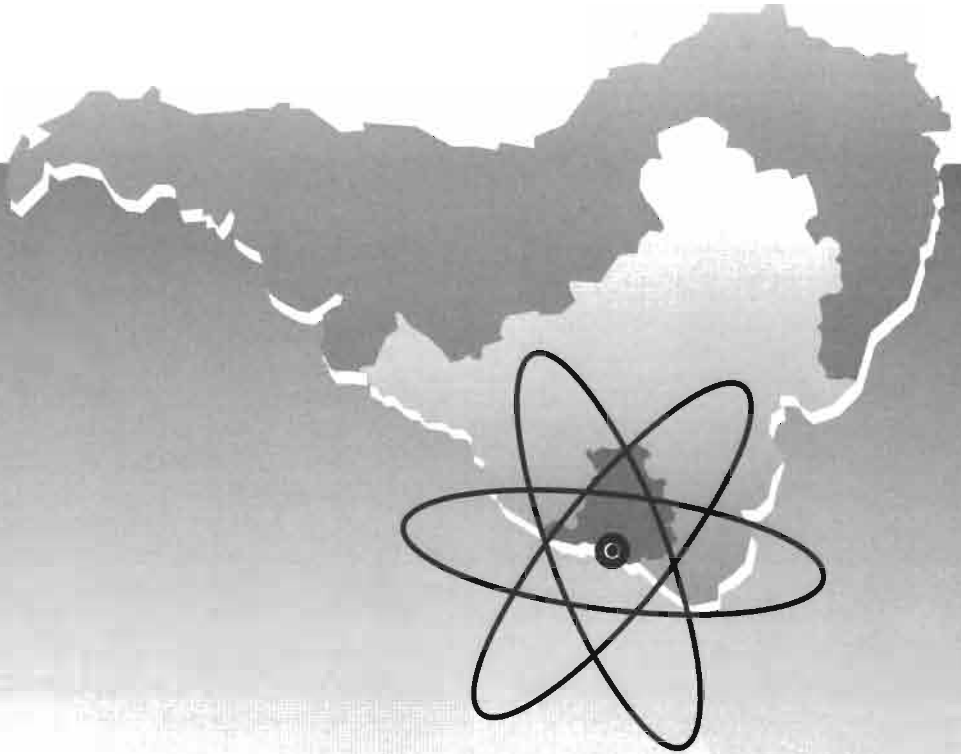

Crustal Evolution of South America

SYN-TECTONIC GRANITE EMPLACEMENT IN AN EARLY NEOPROTEROZOIC CRUST (ESPERANÇA PLUTON, NE BRAZIL): RESULTS FROM AMS AND ISOTOPIC (U-Pb, Sm-Nd) DATA

Archanjo, C.J.[1] **and Fetter, A.H.**[2]

1. Universidade de São Paulo, IG. archan@usp.br
2. Universidade Estadual Paulista, Rio Claro, IGCE. fetter@ms.rc.unesp.br

Keywords: Granite, AMS, isotope geochemistry, shear zones, regional tectonics

Anisotropy of magnetic susceptibility (AMS) and isotopic data (U-Pb, Sm-Nd) were combined to study the emplacement and tectonic setting of the Esperança pluton in the Borborema Province (NE Brazil). It is included in the high-K metaluminous calc-alkaline plutons (Guimarães et al., 1998) that usually occur emplaced near the major shear zones that run cross the province. The Esperança pluton is intrusive into Early Neoproterozoic rocks of the Alto Pajeú "terrane" that, approaching the Atlantic coast, occurs between Paleoproterozoic gneisses (Brito Neves et al., 2001). The limit of these chronologically different rock sequences is marked by regional-scale lineaments, such as the Patos shear zone that juxtaposes the Alto Pajeú belt against the São José de Campestre gneisses and migmatites to the north.

The Esperança pluton is formed by sheet-like granitoids that, along with its host rocks, dip moderately (~ 40°) to the SE. These tilted sheets allow the internal architecture of the pluton to be observed. It consists, from the top to the bottom, of coarse porphyritic granite, leucogranite, equigranular syenogranite and tonalite. Biotite and hornblende are the main mafic minerals. The AMS was determined in 136 sites distributed within the central and western part of the pluton. Sampling was avoided to the northeast due to deep alteration of the regional rocks. The granitic sheets normally have susceptibility lower than 0.35×10^{-3} SI, indicating that Fe-silicates control the AMS. The orientation of the magnetic fabric is very uniform in the upper sheets. In the coarse porphyritic granite and leucogranite the foliation dips moderately while the lineation strikes NE-SW parallel to the pluton elongation. In the lower sheets the foliation dips uniformly to the south. The lineation of the syenogranite and tonalite forms an anticlockwise trajectory, rotating progressively from SSE to E as it approaches the dextral Campina Grande shear zone. The fabric pattern of the lower sheets is consistent with a transtensional tectonic setting, which probably made room for pluton emplacement.

Wall rocks beneath the pluton floor near Pocinhos consist of variably migmatized orthogneisses. $T_{(DM)}$ model ages of the gneissic paleosomes range between 2.1 and 2.4 Ga with εNd (t=0) values around -22 (Table 1). Similar isotopic data are found in the Paleoproterozoic São José de Campestre block situated at north of the Patos shear zone (Dantas et al., 1998). The gneisses above the pluton roof gave U-Pb zircon ages between925 and 940 Ma (Brito Neves et al., 2001). The corresponding $T_{(DM)}$ model ages range between 1.4 and 1.8 Ga with εNd (t=0) values around -16 (Table 1). Preliminary U-Pb zircon data from the syenogranite yield a nearly concordant age of 585 Ma, attributed to the timing magmatic crystallization. In the leucogranite, Guimarães et al., (1998) obtained an U-Pb zircon age of 581 Ma. The pluton shows εNd (t=0) values normally higher than -15 and T(DM) model ages in the range of 1.6 and 1.4 Ga for the tonalite and syenogranite, and of 1.6 up to 1.9 Ga for the coarse porphyritic and leucogranite. Similar isotopic results were documented to the southeast in the Campina Grande pluton (Almeida et al., 2002).

These combined results indicate that the regional structures of the eastern Alto Pajeú belt were formed in a tectono-thermal event in the Brasiliano, around 580 Ma, and that includes the low angle regional foliations and folds and the strike-slip shear zone system. The high-K calc-alkalic syn-kinematic plutons of Esperança and Campina Grande seem to have emplaced occupying principally the contact zone between the Paleoproterozoic and Early Neoproterozoic rocks. $T_{(DM)}$ model ages and εNd values indicate that these granitoids were contaminated during their emplacement by partial melting of the regional host rocks. The entire rock sequence forms a stacked sheet pile dipping to the southeast, with the Alto Pajeú belt sandwiched between the older Paleoproterozoic basement.

REFERENCES

Almeida, C.N.; Guimarães I.P.; Silva Filho A.F., 2002. Petrogênese de rochas plutônicas fésicas e máficas na Provincia Borborema, NE do Brasil: o complexo cálcio-alcalino de alto-K de Campina Grande. Rev. Bras. Geoc., 32: 205-216.

Brito Neves, B.B.; Campos Neto, M.C.; Van Schmus, W.R.; Santos, E.J., 2001. O sistema Pajeú-Paraíba e o maciço São José de Campestre no Leste da Borborema. Rev. Bras. Geoc., 31: 173-184.

Dantas, E.L.; Hackspacher, P.C.; Van Schmus, W.R.; Brito Neves, B.B., 1998. Archean accretion in the São José de Campestre Massif, Borborema Province, Northeast Brazil. Rev. Bras. Geoc., 28: 221-228.

Guimarães I.P.; Silva Filho, A.F.; Almeida, C.N.; Melo, E.B.; Araújo, J.M.M.; Sales A., 1998. Sm-Nd isotope geochemistry and U/Pb zircon ages of he Brasiliano granitoids from the Pajeú-Paraíba terrain, Borborema Province, Northeastern Brazil. South Am. Symp. Isotope Geology, 2, Córdoba, Anais, 300-301

Table 1. Sm-Nd data of the Esperança pluton and its host rocks. 1. This work, 2. Brito Neves et al. (2001).

Rock	**Sm^{147}/Nd^{144}**	**Nd^{143}/Nd^{144}**	$\varepsilon_{Nd(0)}$	**T_{DM} (Ma)**	**ref**
Esperança pluton					
tonalite	0.1187	0.512047	-11.53	1.595	1
syenogranite	0.0830	0.511891	-14.57	1.344	1
porphyritic granite	0.1299	0.512127	-9.97	1.662	2
Nortthern host rock					
bi gneiss	0.0936	0.511397	-24.21	2.092	1
augen gneiss	0.1136	0.511497	-22.26	2.363	1
Southern host rock					
mus. bi gneiss	0.1283	0.512252	-7.53	1.406	2
augen gneiss	0.1310	0.512079	-2.92	1.774	2

Sm-Nd ISOTOPIC SIGNATURE AND U-Pb SHRIMP ZIRCON DATING OF THE CACHEUTA SUB-BASIN, CUYO BASIN, NW-ARGENTINA

Ávila, J.N.[1]; Chemale Jr., F.[2]; Kawashita, K.[3]; Armstrong, R.[4] and Cingolani, C.A.[5]

1. Programa de Pós-graduação em Geociências, IG, UFRGS, Brazil. janaina.avila@ufrgs.br
2. Laboratório de Geologia Isotópica, IG, UFRGS, Brazil. farid.chemale@ufrgs.br
3. Laboratório de Geologia Isotópica. labiso@ufrgs.br
4. Research School of Earth Sciences, ANU, Australia. richard.armstrong@anu.edu.au
5. Universidad Nacional de La Plata, Argentina. ccingola@museu.edu.unlp

Keywords: Sm-Nd isotopes, U-Pb SHRIMP, Cuyo Basin, rift-basin, provenance

INTRODUCTION

The Cuyo Basin rift is located in the northwestern Mendoza Province (NW-Argentina), as part of the Argentine Precordillera. It is a Triassic basin which has a very dynamic evolution controlled by climatic and tectonic events during the geological time. Such events influenced directly the basin inception, geometry and depositional evolution, leading to correlation between strata in different regions to be a very difficult task.

The Cacheuta sub-basin consists in one of the most important depocenters of the Cuyo Basin, especially due to its economic potential in hydrocarbon exploration (Chebli et al., 2001). The Cuyo Basin displays a general NW-SE trend, mostly controlled by pre-existing structures (Ramos, 1992) (Fig. 1). The eastern limit of this basin coincides with an important suture generated in the Silurian through the amalgamation of the Cuyania Terrane to the southwestern margin of Gondwana. On the other hand, the western border is a structure that represents the Devonian accretion zone of the Chilenia and Cuyania terranes (Ramos & Kay, 1991) (Fig. 1).

According to Mpodozis & Kay (1990) the extensional tectonic setting of the southwestern Gondwana at the Permian/Triassic boundary is related to processes of crustal thinning, which occurred after the end of the Paleozoic collisional phenomena, as already mentioned. This extensional event was accompanied by an extensive acidic-intermediate volcanism, characterized by andesites, rhyolites, and breccias (Choiyoi Group of Rolleri & Criado Roqué, 1968). The inception of the Cuyo basin, whose sediments were unconformably deposited upon Choiyoi volcanics and Paleozoic sediments, is also result of this generalized extensional setting (Ramos & Kay, 1991).

The aim of this study is to characterize the depositional history of the sedimentary and volcaniclastic deposits related to the active faulted margin of the Cacheuta sub-basin, Cuyo Basin, located near the town of Potrerillos. This work deals with (i) the sequence stratigraphic arrangement of the depositional systems; (ii) the geochronology of the volcaniclastic rocks that occur interlayered with the sedimentary deposits; and (iii) investigation of sediment provenance using Sm-Nd isotopes.

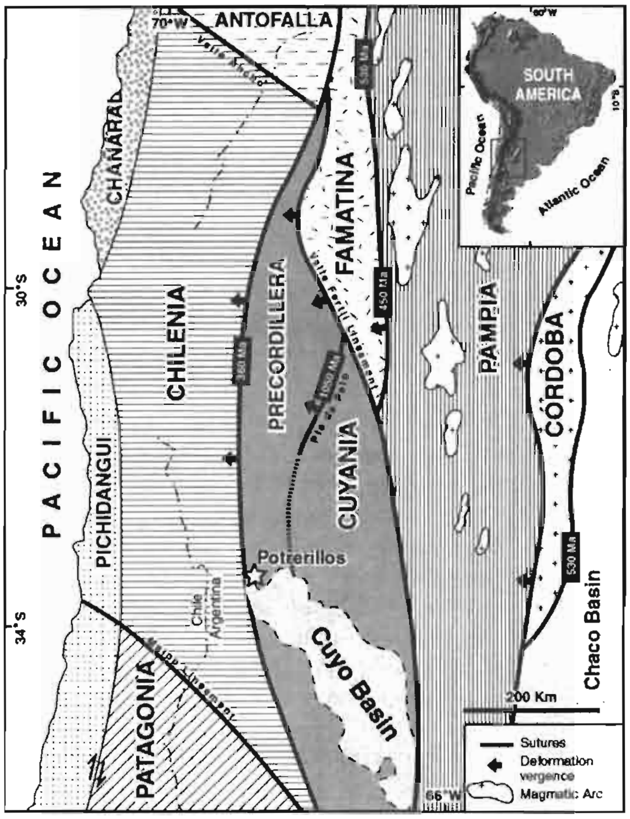

Figure 1. Main exotic terranes and sutures of NW Argentina and location of the subsurface portion of Cuyo Basin. The numbers indicate the approximate ages of the sutures (Ramos, 1995). Star designates the study area.

DEPOSITIONAL SEQUENCES

The composite stratigraphic profile was performed in the Potrerillos section, which comprises the coarse-grained deposits related to the active faulted margin of the Cacheuta sub-basin. The depositional stages correspond to the lowstand, trangressive, and highstand systems tracts of a second-order depositional sequence (the whole record of the Cuyo Basin).

During the initial stages (lowstand systems tract – LST), the active margin of the Cacheuta sub-basin was controlled by tectonic processes that influenced directly in the subsidence rate and quantity and type of material from source areas. The LST encompasses thick conglomerate succession associated with coarse-grained alluvial fans (sheetflood and debris-flow deposits) and pyroclastic flow deposits unconformably deposited upon pyroclastic rocks of the Choiyoi Group. Reddish-brown colored, poorly sorted, crudely stratified or massive, clast- and matrix-supported conglomerates, and interlayered conglomeratic sandstones comprise this basal section, which corresponds in the lithostratigraphy to the Rio Mendoza Formation as described by Borrello (1962). The conglomerate clasts are dominantly of volcanic origin (andesites, rhyolites, pyroclastic rocks), and reach up to 30 cm in diameter (mean diameter around 5 cm). The matrix is coarse sand-sized, and composed also of volcanic fragments. Interlayered with these deposits are rhyolitic, pumice-rich pyroclastic rocks. Expressive action of sheetflood- and debris-flow-dominated alluvial fans was responsible for the initial phase of the deposition in the Cacheuta sub-basin. Tectonics, basin-related volcanism, climate, and source area material were the primary controls on the active faulted margin sedimentation.

The transgressive surface is clearly delineated upon the lowstand deposits. The transgressive systems tract (TST) is composed of at least four parasequence sets which display an overall retrogradational trend. Clast-supported, massive and cross-bedded conglomerates and conglomeratic sandstones dominate the base of the package, while fine-grained sandstones and siltstones with horizontal and climbing ripple laminations are more common towards the top. The volcaniclastic contribution in the TST is very expressive, in the matrix and framework of the conglomerates and sandstones. Shards and pumice are present also in the finer-grained rocks. The TST corresponds, in the lithostratigraphy, to the Cerro de Las Cabras (Frenguelli, 1944) and Potrerillos (Truempy & Lhez, 1937) formations.

The maximum flooding surface was traced on lacustrine black shales of the Cacheuta Formation (Truempy & Lhez, 1937). These rocks have high content of organic matter and constitute the principal source rock for the hydrocarbon accumulations in this basin (Chebli et al., 2001).

The transition from black (Cacheuta Formation) to reddish (Rio Blanco Formation, Fossa-Mancini, 1937) siltstones and shales marked the onset of a progradational trend that characterizes the highstand systems tract. This prograding section begun with the establishment of oxidizing conditions, and continued with the progressively increased sedimentary influx to the basin depocenters by means of lacustrine deltas, which deposited sigmoidal- and cross-bedded sandstones associated with finer-grained rocks. The trend culminated with the deposition of a high-sinuosity, sandy, fluvial facies association, when the sedimentary influx overcame the creation of accommodation space. This phase is associated with thermal subsidence, corresponding to a "sag" basin (Kokogian et al., 1993), and the volcanic contribution in this portion of the succession is subordinated.

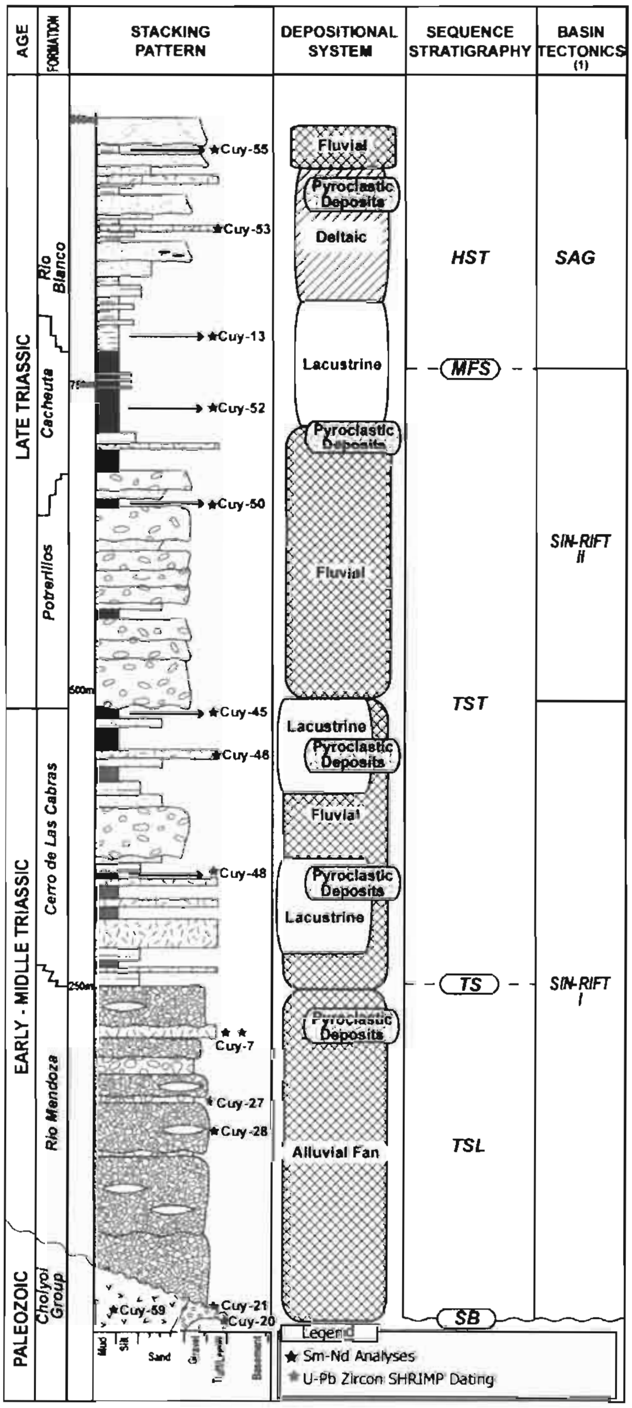

Figure 2. Sequence stratigraphic division chart of the Cacheuta sub-basin faulted margin, showing the stacking pattern, depositional characteristics and the sample location. (1) Kokogian et al., 1993.

U-Pb SHRIMP ZIRCON DATING

The selected sample for the application of U-Pb SHRIMP (Sensitive High-resolution Ion Microprobe) zircon dating is a pumice-rich, lithoclast-free, acidic ignimbrite (pyroclastic flow deposit) interlayered with the basal alluvial fan facies association (lowstand systems tract). The sample was crushed, milled, sieved, and the zircon crystals were separated by conventional magnetic and heavy liquid methods. Zircons were mounted in an epoxy disk with SL-3 and FC-1 standards and studied using petrographic microscopy, BSE and CL images. The U-Pb SHRIMP Zircon analyses were carried out at the Research School of Earth Sciences, Australian National University.

The analyzed zircons are euhedral and inclusion-free crystals, and they are interpreted as having a juvenile magmatic origin. Seven spot analyses in six zircon crystals yielded a 243 ± 4.7 Ma age (Fig. 3), positioning the lowstand deposits of the Cacheuta sub-basin (the Rio Mendoza Formation) in the Early to Middle Triassic.

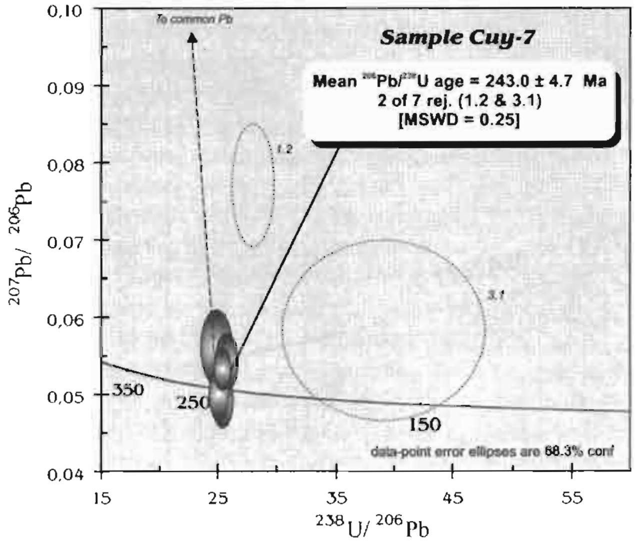

Figure 3. U-Pb SHRIMP zircon Concordia diagram for ignimbrite interlayered with the basal alluvial fan facies association of the Cacheuta sub-basin.

Sm-Nd ISOTOPES

Samples selected for the application of the whole-rock Sm-Nd isotopic analyses comprise: three basement rocks of the Cacheuta sub-basin (Silurian and Permian) and eleven samples of volcano-sedimentary rocks distributed through the sedimentary package (Fig. 2).

Rock powders for Sm-Nd analysis were spiked with mixed ^{149}Sm-^{150}Nd spike and dissolved using an HF-HNO_3 mixture and 6N HCL in teflon vials, warmed in hot plate until complete dissolution. The REE were extracted using a standard AG-50W cation resin; Sm and Nd were extracted using HDEHP-coated Teflon powder. Isotopic compositions were measured with a VG Sector multicollector mass spectrometer at the Laboratório de Geologia Isotópica of Universidade Federal do Rio Grande do Sul. Sm was loaded on Ta filament and Nd on external Ta triple filament (Ta-Re-Ta) with 0.25N H_3PO_4. All analyses are adjusted for variations instrumental bias due to periodic adjustment of collector positions as monitored by measurements of our internal standard; on this basis our analyses of La Jolla Nd average 0.511859 ± 0.000010. During the course of the analyses Nd and Sm blanks were lesser than 750 and 150 pg, respectively.

Sm-Nd data are illustrated in figure 4. Three basement samples of different ages were analyzed. A Sm-Nd model age (T_{DM}) of 1159 Ma and $\varepsilon_{Nd(t)}$ value of -2.1 were obtained for a granodiorite of Silurian age (t = 417 Ma, Cingolani, pers. comm.), exposed in the SE of Potrerillos town. A volcanic breccia of the Choiyoi Group (t = 260 Ma), exposed in the NW of Potrerillos town yielded a Sm-Nd model age of 990 Ma and $\varepsilon_{Nd\,(t)}$ value of -3.1. A model age (T_{DM}) of 867 Ma and an $\varepsilon_{Nd\,(t)}$ of -1.27 were obtained for a Permian syenogranite intrusive in the Silurian granodiorite.

The volcano-sedimentary samples of the Cacheuta sub-basin, black shales, sandstones and tuffs, yield Sm-Nd model ages ranging from 0.90 to 1.34 Ga and ε_{Ndt} values from -5.03 to -0.61.

CONCLUDING REMARKS

U-Pb SHRIMP zircon dating of a lithoclast-free ignimbrite interlayered with basal alluvial fan facies of Cuyo Basin yielded a magmatic age of 243 ± 4.7 Ma, and positioned these lowstand deposits in the Eotriassic to Mesotriassic boundary.

Sm-Nd model ages (T_{DM}) of 0.87 to 1.16 Ga and negative $\varepsilon_{Nd\,(t)}$ values (-3.1 to -1.27) obtained from samples of basement rocks indicate that they are derived from reworked Mesoproterozoic crust (Grenvillian rocks). The volcano-sedimentary samples of the Cacheuta sub-basin show T_{DM} model ages ranging from 0.90 to 1.34 Ga and $\varepsilon_{Nd\,(t)}$ values from -5.03 to -0.61, which are similar to the basement samples and, consequently, indicates that the sediment source areas for the Cacheuta sub-basin were located on igneous rocks from reworking of the Cuyania Terrane.

ACKNOWLEDGMENTS

This work was funding by Programa de Especialização em Geologia do ANP/UFRGS and CNPq (Project 520019-96-2).

REFERENCES

Borrello, A.V. 1962. Fanglomerado Río Mendoza (Triássico – Provincia de Mendoza). Comisión de Investigaciones Científicas, Notas 1, n. 3, p. 3-9.

Chebli, G.A.; Ploszkiewicz, J.V; Azpiroz, G.M. 2001. El sistema Triássico y los hidrocarburos. In: Artabe, A.E.; Morel, E.M.; Zamuner, A.B. (eds.), El sistema Triássico en la Argentina, Fundación Museo de La Plata “Francisco Pascasio Moreno”, p. 283-315.

De Paolo, D.J. 1981. Neodymium isotopes in the Colorado Front Range and implications for crust formation and mantle evolution in the Proterozoic. Nature, v. 291, p. 193-197.

Fossa-Mancini, E. 1937. Las investigaciones geológicas de Y.P.F. en la provincia de Mendoza y algunos problemas de estratigrafía regional. Boletín de Informaciones Petroleras, v. 14, n. 154, p. 51-118.

Kokogian, D. A.; Fernández Seveso, F.; Mosquera, A. 1993. Las seqüências sedimentarias triásicas. In: Ramos, V. A. (ed.) Geología y Recursos Naturales de Mendoza, Congreso Geológico Argentino, 12, Mendoza, Relatório 2, n. 13, p. 65-78.

Mpodozis, C. & Kay, S.M. 1990. Provincias magmáticas ácidas y evolución tectónica de Gondwana: Andes Chilenos (28° - 31°S). Revista Geológica de Chile, v. 17, n. 2, p. 153-180.

Ramos, V.A. 1992. Control Geotectónico de las cuencas triásicas de Cuyo. Boletín de Informaciones Petroleras, 3ra. Época, v. 9, n. 31, p. 2-9.

Ramos, V.A. 1995. Sudamérica: um mosaico de continentes y oceanos. Ciência Hoy, Buenos Aires, v. 6, p. 24-29.

Ramos, V.A. & Kay, S.M. 1991. Triassic rifting and associated basalts in the Cuyo Basin, central Argentina. In: HARMON, R.S., RAPELA, C.W. (eds.). Andean magmatism and its tectonic setting. Geological Society of America Special Paper, v. 265, p. 79-91.

Rolleri, E.O. & Criado Roqué, P. 1968. La cuenca triásica del norte de Mendoza. 3ª Jornadas Geológicas Argentinas, Actas 1, p. 1-76.

Truempy, E. & Lhez, R. 1937. División estratigráfica de los terrenos aflorantes en la región comprendida entre Luján de Cuyo, Potrerillos y Tupungato. Boletín de Informaciones Petroleras, v. 14, n. 152, p. 39-56.

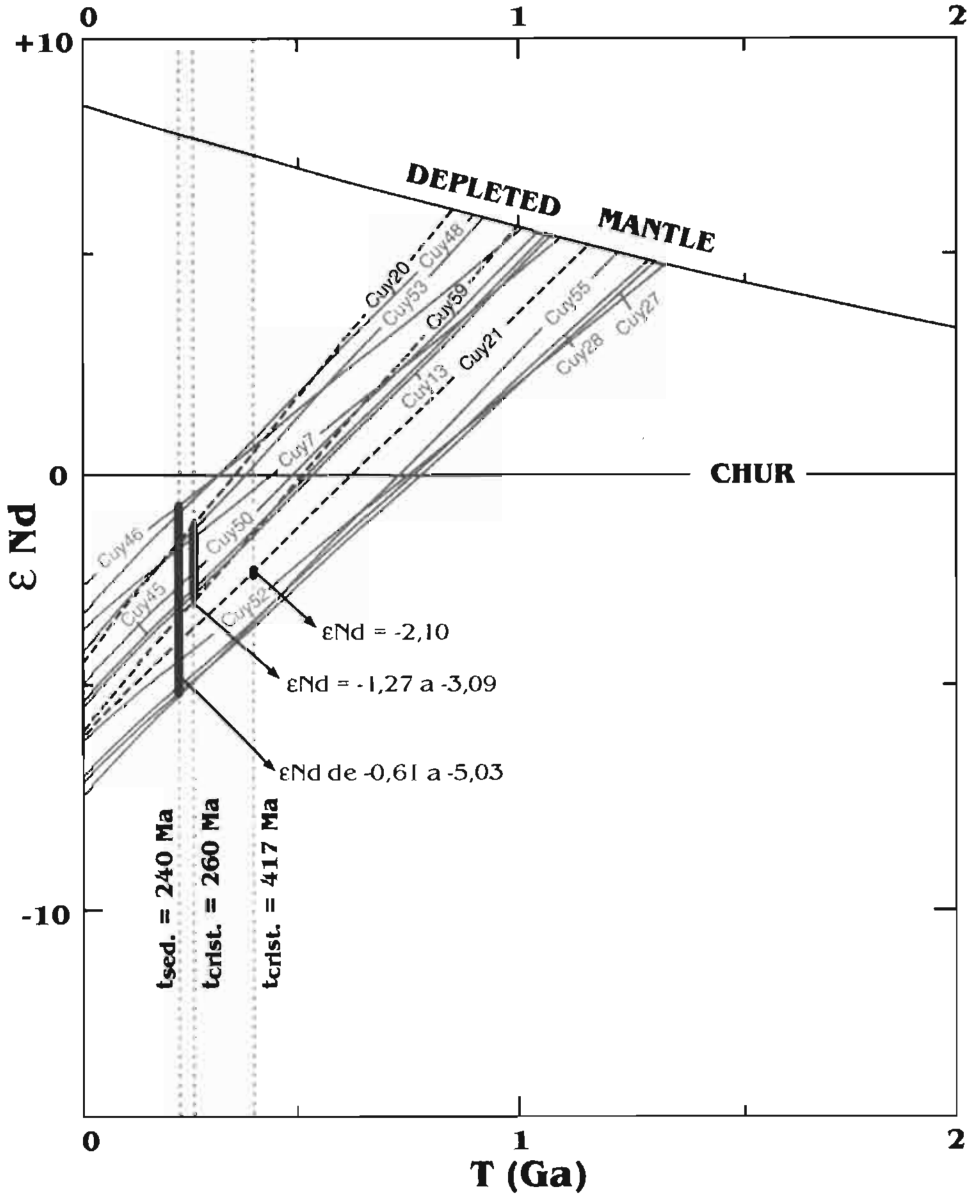

Figure 4. Plot showing εNd for igneous and sedimentary rocks of Argentine Southern Precordillera. Continuous lines correspond to Triassic volcano-sedimentary rocks of the Cuyo Basin, and dashed lines represent igneous basement rocks.

THE FOUR ARCHEAN CRUSTAL SEGMENTS OF THE SÃO FRANCISCO CRATON, BAHIA, BRAZIL AND THEIR PALEOPROTEROZOIC COLLISION

Barbosa, J.S.F.[1] **and Sabaté, P.**[2]

1. CPGG - Centro de Pesquisa em Geofísica e Geologia/UFBA. johildo@cpgg.ufba.br
2. IRD/ORSTOM, Laboratoire de Tectonophysique. pierre@dstu.montp2.fr

Keywords: Archean, Paleoproterozoic, collision, São Francisco Craton, Bahia, Brazil

THE ARCHEAN BLOCKS

Each aforementioned segment is well discriminated by Sm-Nd model ages as well as the distribution in the ε_{Nd} x ε_{Sr} diagram, supporting their distinct origin, evolution and metallogenetic characteristics.

In the Gavião Block two groups of TTG rocks constituted the early continental crust into the amphibolite facies. The first with age varying between 3.4-3.2 Ga has been considered, as originated from the melting of tholeiitic basalts. The second with age of 3.2-3.1 Ga, had similar origin but with some crustal contamination (Martin et al., 1991; Santos Pinto, 1996; Cunha et al., 1996; Bastos Leal, 1998). The greenstone belts in the greenschist facies (Contendas Mirante, Umburanas, Mundo Novo) (Marinho, 1991; Mascarenhas and Silva, 1994; Cunha et al., 1996), have been formed in intracratonic basins of the early TTG crust, with basal komatiites, pyroclastic rocks, chemical exhalative sediments and tholeiitic basalts with pillow-lava (3.1 Ga). The 2.8-2.7 Ga granitic-granodioritic-migmatitic crust, metamorphosed under amphibolite facies conditions is interpreted as products of partial melting of the TTG (Santos Pinto, 1996) during the closing of these basins. Calc-alkaline volcanics (2.6 Ga), granite intrusions (2.5 Ga) and mafic-ultramafic intrusions (2.4 Ga), besides phyllites and grawackes occur associated with the Archean greenstone belts (Marinho, 1991).

The Itabuna-Salvador-Curaçá Belt is composed by at least three tonalite/trondhjemites groups with 2.7-2.6 Ga (Silva et al., 1997). These rocks are interpreted, by the REE geochemistry, as result of the tholeiitic oceanic crust melting. Reequilibrated in the granulite facies, also include charnockite bodies, stripes of intercalated metasediments (quartzites with garnet, Al-Mg gneisses with sapphirine, graphitites and manganesiferous formations) and ocean-floor/back-arc gabbros and basalts. These latter ones are originated from mantle sources (Teixeira, 1997). 2.4 Ga old, shoshonitic monzonites occur in this belt as important intrusive bodies (Ledru et al., 1994). The island-arcs, back-arc basins and subduction zones were the dominant environments during the construction of this belt (Barbosa, 1990, 1997).

The Jequié Block is characterized by migmatites with supracrustal bodies (the oldest component, with 3.0-2.8 Ga) and granodiorític–granitic intrusions (the youngest component, with 2.8-2.7 Ga). The oldest component is mainly constituted of granitic rocks that form the basement of the rift-type intracratonic basins, where basalts and andesitic basalts, cherts, banded iron formation, graphitites and kinzigites were accumulated. The youngest component is constituted of multiple intrusions of granodiorites and granites of high to low Ti that eventually contain megaenclaves of the oldest component.

In the NE, occurs the Serrinha Block with c.a. 2.9 Ga old orthogneisses and migmatites, which represent the basement of the Paleoproterozoic greenstone belts. This orthogneisses and migmatites are granitic to granodioritic composition, with gabbroic enclaves, metamorphosed under amphibolite facies conditions.

THE PALEOPROTEROZOIC COLLISION

During the Paleoproterozoic (c.a. 2.3-2.0 Ga) (Barbosa & Dominguez, 1996), these four crustal segments collided resulting in the formation of an important mountain belt. The evidences of this collision are found not only through the structural elements, but also in the pre- and syn-tectonic Paleoproterozoic rocks that are present in the above mentioned crustal segments.

In the Gavião Block it was identified: (i) the Jacobina Group (foreland basin) formed by schists, banded iron formations, manganesiferous formations, quartzites and metaconglomerates with intrusions of mafic-ultramafic rocks (Mascarenhas et al., 1992), where the siliciclastic metassediments contain detrital zircons with ages 2.1 Ga and (ii) the Areião Formation constituted of arkoses and sands containing also detrital zircons dated 2.1-2.2 Ga.

In the Itabuna-Salvador-Curaçá Belt, the most important paleoproterozoic lithologies are: (i) tonalites and trondhjemites, with zircons dated approximately 2.1 Ga (Sabaté et al., 1994, Silva et al., 1997); (ii) Caraiba norites and Medrado gabbros, both with ages slightly older than 2.0 Ga (Oliveira and Lafon, 1995); and (iii) syntectonic granites dated about 2.1 Ga (Sabaté et al., 1990).

In the Serrinha Block occurs the Greenstone Belts Rio Itapicuru and Capim, formed from back-arc basins (Silva, 1992; Winge, 1984) where: (i) the lower unit of basaltic lava (2.2 Ga) is constituted by tholeiitic basalts and maffic tuffs, associated with banded iron formation, cherts, and graphitic phyllites; (ii) the intermediate unit is formed mainly by felsic rocks (2.1 Ga), with its composition varying from andesites to calcalkaline dacites; and (iii) the upper unit is composed by thick packages of psefites, psamites and pelites. These paleoproterozoic greenstone belts are essentially different from the Archean greenstone belts of the Gavião Block mainly because they lack significant proportion of komatiitic volcanic rocks.

The Paleoproterozoic collision occurred with the movement of the four blocks in the NW-SE sense, identified by the presence of large thrusts and transcurrence zones, in general sinistral, as the kinematics of the late ductile shear zones demonstrate (Figs. 1, 2).

The Paleoproterozoic high grade metamorphism has average pressures of 7 kbar and temperatures of about 850 °C, with its peak occuring at about 2.0 Ga (Barbosa, 1990, 1997). It is interpreted as originated from the crust thickening related to the tectonic superposition of blocks during the collision. Along the Itabuna-Salvador-Curaçá Belt, this metamorphism reached the granulite grade and the obduction of the Itabuna-Salvador-Curaçá Belt over the Jequié Block transformed the Jequié rocks, from amphibolite to granulite facies. The presence of coronitic reactions with destruction of garnet-quartz or garnet-cordierite, producing simplectites of orthopyroxene-plagioclase, are observed in the high degree gneisses, both in the SSE, SSW, and NE. They have been interpreted as suggestion of pressure release. This fact reinforces the presence of these collision processes and of great thrusts, that brought blocks of rocks from deep zones to the more surficial parts of the crust. PTt diagrams elaborated for these metamorphites show a trajectory of the metamorphism of the clockwise type, confirming the collision context (Barbosa, 1990, 1997).

It is also worth while to observe the late charnockitic and granitic intrusions that crossed the segment of rocks stacked by the tectonic. Charnockitic bodies with ages of about 2.1 Ga intruded the northern part of the Jequié Block, in all the other blocks, granitic bodies, in general with peraluminose characteristics (Sabaté et al., 1990). With a major concentration in the NE of Bahia, these granites exhibit, in general, ages of about 2.0 Ga and can be assumed to have origin from the melt of hydrated rocks of the amphibolite facies, tectonically placed under rocks of the granulite facies as aforementioned.

Late deformations have formed retrograde shear zones in the Archean blocks under consideration. It is assumed that alkaline syenitic bodies, with minimum ages of 1.9 Ga, have been emplaced in these shear zones (Conceição, 1993). The syenites intruded the granulites after these rocks reached the amphibolite facies crustal environment.

REFERENCES

Barbosa, J.S.F. 1990. The granulites of the Jequié Complex and Atlantic Mobile Belt, Southern Bahia, Brazil - An expression of Archaean Proterozoic Plate Convergence. Granulites and Crustal Evolution. In: Vielzeuf D., Vidal P. (Eds.), Springer-Verlag Proc. of ARW, Clermont Ferrand (France), pp. 195-221.

Barbosa, J.S.F. 1997. Síntese do conhecimento sobre a evolução geotectônica das rochas metamórficas Arqueanas e Paleoproterozoicas do embasamento do Craton do S. Francisco na Bahia. Rev. Bras. Geoc. 27(3):241-256.

Barbosa, J.S.F., Dominguez, J.M.L., 1996. Texto Explicativo para o Mapa Geológico ao Milionésimo. SICM/ SGM, Salvador, (Edição Especial), 400 p.

Bastos Leal, L.R. 1998. Geocronologia U/Pb (SHRIMP), ^{207}Pb/^{206}Pb, Rb/Sr, Sm/Nd e K/Ar dos Terrenos Granito-Greenstone do Bloco do Gavião: Implicações para a Evolução Arqueana e Paleoproterozoica do Craton do São Francisco, Brasil. PhD Thesis. São Paulo Univ. 178pp.

Conceição, H. 1993. Sienitos do Estado da Bahia: Um Epítome do Tema e Interpretação à Luz do Conhecimento Atual. In: Dominguez, J.M.L. & Misi, A. (Eds.) O Craton do São Francisco, SBG/SGM/CNPq, Salvador, 52-55.

Cunha, J.C.; Bastos Leal, L.R.; Fróes, R.J.B.; Teixeira, W.; Macambira, M.J.B. 1996. Idade dos Greenstone Belts e dos Terrenos TTGs Associados da Região do Cráton do São Francisco (Salvador, Bahia, Brasil). In: Congr. Bras. Geol., 29, Soc. Bras. Geol. Abstr. 1: 62-65,

Ledru, P.; Cocherie, A.; Barbosa, J.S.F.; Johan, V.; Onstott, T. 1994. Âge du Métamorphisme Granulitique dans le Craton du São Francisco (Brésil). Implications sur la Nature de l'Orogène Transmazonien. C.R. Acad. Sci. Paris. 211:120-125.

Marinho, M.M. 1991. La Séquence Volcano-Sedimentaire de Contendas-Mirante et la Bordure Occidentale du Bloc Jequié (Cráton du São Francisco-Brésil): Un exemple de Transition Archéean-Protérozoique. PhD Thesis. Blaise Pascal Univ., Clermont Ferrand, França. 388pp.

Martin, H., Peucat, J.J., Sabaté, P., Cunha, J.C., 1991. Crustal evolution in the early Archaean of South America: example of the Sete Voltas Massif, Bahia State, Brazil. Precambrian Research 82, 35-62.

Mascarenhas, J. de F.; Conceição Filho, V.M.; Griffon, J.C. 1992. Contribuição à Geologia do Grupo Jacobina na Região Jacobina/ Pindobaçu. In: Congr. Bras. Geol., 37. Ext. Abstr.. Soc. Bras. Geol, 2, 141-142.

Mascarenhas, J de F. & Alves da Silva, E.F. 1994. Greenstone Belt de Mundo Novo (Bahia): Caracterização e Implicações Metalogenéticas no Cráton do São Francisco. CBPM. Final Rapport., 32 pp.

Oliveira, E.P. & Lafon, J.M. 1995. Age of ore-rich Caraíba and Medrado. Bahia, Brazil. In: Congr. Bras. Geoq. CD-ROM.

Sabaté, P.; Marinho, M.M.; Vidal, P.;Vachette, M.C. 1990. The 2-Ga Peraluminous Magmatism of the Jacobina-Contendas Mirante Belts (Bahia-Brazil): Geologic and Isotopic Constraints on the Sources. Chem. Geol., 83:325-338.

Sabaté, P.; Peucat, J.J.; Melo, R.C.; Pereira, L.H.M. 1994. Datação por Pb evaporação de monozircão em ortognaisse do Complexo Caraiba. Expressão do Acrescimento Crustal Transamazônico do Cinturão Salvador-Curaçá (Craton do São Francisco-Bahia, Brasil). In: Congr. Bras. Geol., 38. So Paulo, Brazil. Soc. Bras. Geol. Ext. Abstr. 1, 219-220.

Santos Pinto, M.A., 1996. Le recyclage de la croûte continentale archéene: Exemple du bloc du Gavião - Bahia, Brésil. PhD Thesis, unpublished. University of Rennes I, 193p.

Silva, M.G., 1992. Evidências Isotópicas e Geocronológicas de um Fenômeno de Acrescimento Crustal Transamazônico no Cráton do São Francisco, Estado da Bahia. In: Congr. Bras. Geol., 37 São Paulo, Brazil. Soc. Bras. Geol. 2, 181-182,

Silva, L.C. da; McNaughton; R.C.deMelo;Fletcher, I.R. 1997. U-Pb SHRIMP ages in the Itabuna-Caraiba TTG hight-grade Complex: the first window beyond the Paleoproterozoic overprint of the eastern Jequié Craton, NE Brazil. In: Intern. Symp on Granites and Assoc. Mineral. ISGAM, Salvador, Bahia, Brazil. Abstr. 282-283.

Teixeira, L.R. 1997. O Complexo Caraíba e a Suite São José do Jacuipe no Cinturão Salvador-Curaçá (Bahia-Brasil): Petrologia, Geoquímica e Potencial Metalogenético. PhD Thesis. Federal da Bahia Univ., 201pp.

Winge, M. 1984. A Sequencia Vulcanossedimentar do Grupo Rio Capim, Bahia. In: P.V. da S. Viveiro Sá & F.B. Duarte (Eds.) Geologia e Recursos Minerais do Estado da Bahia, , Salvador, Brazil, SME/CPM., Spec. Publ. 5, 43-103.

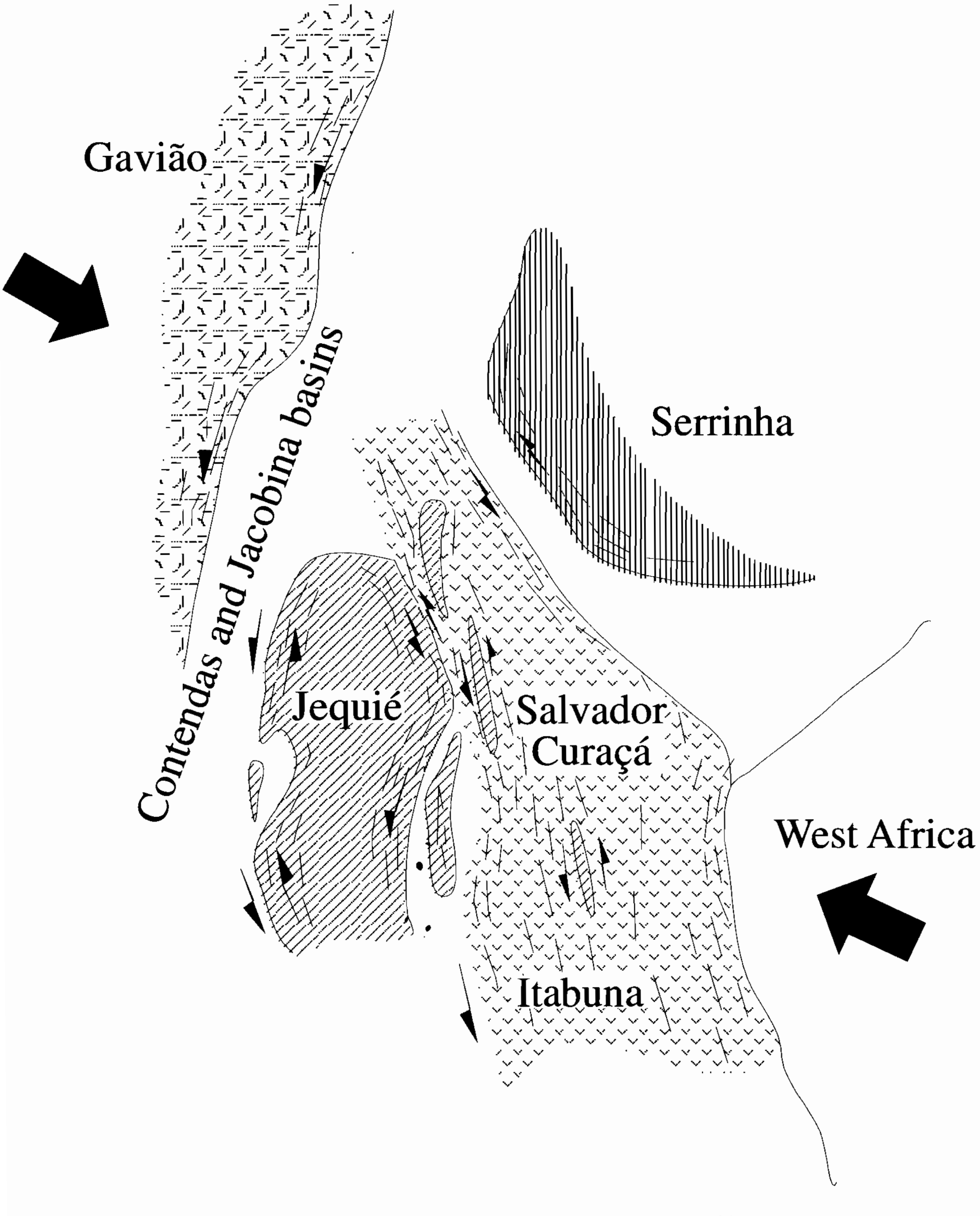

Figure 1. Postulated position of the archean blocks prior to collision.

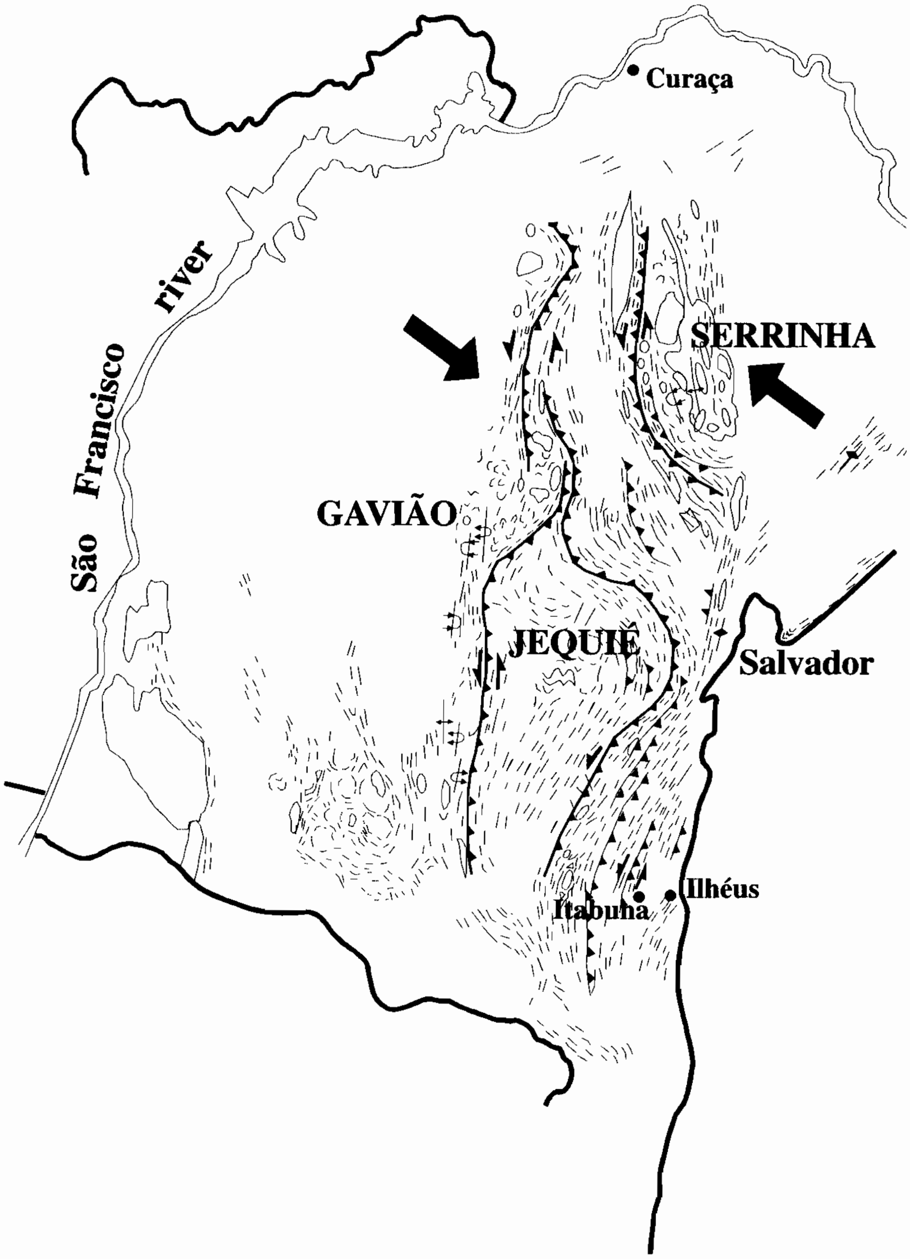

Figure 2. Display of the Archean blocks after collision during the Paleoproterozoic Transamazonian Cycle.

GEOLOGY, GEOCHEMISTRY AND GEOCHRONOLOGY (Rb-Sr, U-Pb, Sm-Nd AND Ar-Ar) OF THE ORTHOGNEISSES FROM THE ALTO PAJEÚ TERRANE

Brito Neves, B.B.[1]; Guimarães, I.P.[2]; Santos, E.J.[2]; Van Schmus, W.R.[3] and Campos Neto, M.C.[1]

1. Instituto de Geociências da Universidade de São Paulo. bbleybn@usp.br, camposnt@usp.br
2. Departamento de Geologia, Centro de Tecnologia e Geociências, UFPE. ignez@npd.ufpe.br, ediltonjsantos@terra.com.br
3. Department of Geology, University of Kansas, Lawrence, Kansas, USA. rvschmus@ku.edu

Keywords: Cariris Velhos, Alto Pajeú, Borborema Province, orogenic system, Brasiliano

GENERAL GEOLOGICAL FEATURES

In the central domain of the Borborema Province, from the Pernambuco/Piauí boundary (to the SSW) up to the coastal area, north of João Pessoa (to the ENE, Mari municipality) occurs a fold belt of ca. 700 km long (over 100 km wide, at some places), with a WSW-ENE general trend, Early Neoproterozoic in age. This fold belt/terrane called Alto Pajeú is mostly composed of volcanic-sedimentary and immature sedimentary supracrustal assemblages ("Complexo São Caetano do Navio") which are pierced by dozens sheets and small bodies of orthogneisses (so-called "Cariris Velhos Orthogneisses").

This orogenic system was developed in the early beginnings of the Neoproterozoic time (990-930 Ma), which includes all their evolutionary stages, since the complex system of paleogeographic realms (small ocean basins??) up to the main deformational events (contracional deformation was rather important). Later on, during the Neoproterozoic III and Cambrian times, this belt was submitted to important overprint of the Brasiliano collage and their related extrusional events (Brito Neves et al., 2000).

There are some recent signs of occurrences of additional branches of the Alto Pajeú belt to the south of the central domain ("Zona Transversal") of the Borborema, in the Pernambuco-Alagoas massif as well as in the northern part of the Sergipano Belt ("Southern Domain"). These possibilities are being matter of geological investigations in the present moment by researchers of the UNICAMP. To the north of the Zona Transversal ("Rio Grande do Norte Terrane"or "Northern Domain" of the Borborema Province), no indication for these orogenic development has up to now been noticed.

The main area of occurrence of this orogenic system is bounded by important shear zones, as Serra do Caboclo and Patos (to the northwest and north) and Afogados do Ingazeira (partially) and Congo shear zones (to the south and southeast).

Even though the structures of this orogenic systme are diagonally reaching the shore line and the continental shelf, the continuity of this development (to the Cameroon?) in the African territory has not been recorded. Actually, it is necessary to state that geologic analogues for the Alto Pajeú Belt (ages and composition) were not pointed out in the South America continent, so far.

The supracrustal assemblages ("São Caetano do Navio") are mostly banded rocks, with biotite and muscovite (+ garnet) schists and metagraywackes predominating, with intercalations of metadacites (some metabasalts), metarhyolites (metafelsites) and some local metacarbonates, under amphibolite facies of metamorphism. Migmatites have broadly been generated in many places (like Guarabira and north Floresta areas), so increasing the banded features of these rocks. Many small bodies, sheet-like bodies of othogneisses occur somehow crosscutting these supracrustal assemblages. These are (usually) rocks with high SiO_2 and K_2O contents and high Rb/Sr ratios, with biotite and muscovite (+ sillimanite) as common minerals for orthogneisses (so-called "Ambó", "Recanto" etc. leuco-orthogneisses), which use to present modal composition of syenogranites, granites, monzogranites and (minor) granodiorites. In spite of the few amounts of supracrustals xenoliths in these gneisses, in many places their structural relationships as younger intrusive bodies seem to be clear.

From the point of view of the regional structural geology, these rock assemblages were involved in a very important contractional event (what is confirmed by the geochemical data of the orthogneisses), probably as result of a collisional event. Such event (D_{n+1}) and the predominating foliation (S_{n+1}) then generated were clearly produced by a second (superposed) generation of tectonic movements. Such tangential deformation, with kinematics indicators towards NW and NNW is pervasive along important part of the "Transversal Zone", particularly to the southeastern and central-eastern part of the Paraíba State, and to the central-north and southwest part of Pernambuco State (Brito Neves et al., 2001). This tangential framework occurs affecting both the Paleoproterozoic basement rocks and the Early Neoproterozoic assemblages, and it was later or involved in the Brasiliano phases of deformation

A preliminary interpretation for this framework sugestes an outstanding collisional process, between the Alto Moxotó terrane (Paleoproterozoic, to the south) and the Rio Grande do Norte terrane (to the north) in the aftermaths of a period of B subduction ("Pedras Pretas magmatism"/ ophiolitic remnants?, accretionary calc-alkaline volcanism of "Lagoa das Contendas" etc., described by Santos, 1995). Part of the the Cariris Velhos orthogneisses are probalble to be generated by fusion of the supracrustal assemblages during that collisional process, what is a conclusion placed in advance, but that will partially be reiterated by the lithogeochemical data.

The structural patterns obtained by the collisional events were widely affected by the tectogenic (taphrogeneses and orogeneses, magmatism) processes of the superposed Brasiliano Cycle. Several ways of Brasiliano overprint (two up to three phases of deformation) may be observed, from discontinuous or local processes of folding up to huge events of shearing and strucutural transposition. The Brasiliano heating processes used to be widespread, as it will be later on discussed, therefore making difficult to point out absolutely unaffected Cariris Velhos domains. Many Brasiliano processes of lateral and vertical accretion are well known (many references available, see Brito Neves et al., 2000) for the Borborema Province as a whole, being specially relevant the events associated to the final extrusional phases (shearing and granitogenesis s.l.) that gave the final geometric-geologic outlines of the Province as a whole. Brasiliano tectonic-magmatic episodes have been recorded the beginnings of the Cryogenian period (taphrogeneses and magmatism) up to the early-Ordovician (extrusional shearing and cooling processes).

Thus, the (Early Neoproterozoic) Alto Pajeú terrane is actually only part of a fold belt that could be discriminated in the complex basement of the Brasiliano Borborema Province (Middle Neoproterozoic - Early Ordovician development)

The compositions of the Cariris Velhos orthogneisses varies - most of all - from syenogranites, monzogranites and granodiorites. Muscovite and muscovite-biotite (+ garnet) are common. Garnet, apatite, turmaline and zircon occur as accessory minerals (monazite is particularly rare as accessory). These orthogneisses use to crop aout as small bodies (stocks) and sheet-like bodies, these latter positioned in structural concordance with the contractional tectonic that characterize most of the Cariris Velhos terrane. Mostly in the southeast of Pernambuco (Floresta area) and northeast of Paraíba (Guarabira area) there are widespread occurrences of migmatized facies of these rocks. Banding from compositional features as well as due to some migmatizations processes are rather usual for these rock assemblages.

PRELIMINARY GEOCHEMICAL DATA

The geochemical analyses of the orthogneisses display high contents of SiO_2 (> 7%), Al_2O_3 (> 13%) and Na_2O (5,3%), and the Ba contents are variables (from 100 up to 1100 ppm). These and other characteristics may point out these rocks either for the group II of Harris et al. (1986) or the MPG group (between MPG and the CPG group) of Barbarin (1999). In both cases, the small amounts of monazite (as above mentioned) and the frequency of sphene were not expected, but they are understandable when the large possibilities/variety of sources are took into account.

These rocks are positioned in the metaluminous (most of them) to peraluminous and sub-alkalines fields. In the spidergrams normalized for primitive mantle, the final results obtained for these leuco-orthogneisses is coherent with those of Santos (1995, in Floresta-PE area), i. e., exhibiting typical depletions in Ba, Nb, Sr and Ti, and so presenting general geochemical data and characteristics of collisional granites, according to Thompson et al (1984), so reiterating the previous petrographic assumptions according to Barbarin (1999, MPG group). Even some sheet-like bodies of orthogneisses (that use to occur circumscribing the main batholiths, resembling ring complexes) keep these same general pattern of geochemical data.

The use of discrimination diagrams present some controvertial features. The distribution of points falls in different fields (Pearce et al., 1984), from volcanic arc (+ syn- Colg) up to anorogenic granites, with major concentration of points in the "within plate" field. The use of the diagram of Pearce et al. (1986), most of the granites fall in the "post-Colg" field. In recent thesis, Kozuch (2003, unpublished) made analyses of many Cariris Velhos orthogneisses (different samples) and she got geochemical results very similar to these granites of Andean and Japan arcs, using the same discrimination diagram. So, without discarding the problem existence, it is necessary to consider that there are many aspects to be faced: the nature and paradigms of the diagrams, the present (still small) critical mass of data, the overprint of metamorphism (Cariris Velhos and Brasiliano), and of other still unsuspected processes.

GEOCHRONOLOGICAL DATA

The orthogneisses of the Alto Pajeú display coherent set of Rb-Sr isochronic diagrams. Different parts of the terrane have been sampled and presented ages values 915 Ma, 954 Ma and 966 Ma. Particularly the isochrons with age values over 950 Ma are more frequent and with better analytical quality (high Rb/Sr ratios). Even regarding the general nature and characteristics of this method, these values are significant because of their consistency (and the correspondence with U-Pb data), and because they were preserved in spite of the widespread overprint of the Brasiliano processes

The results obtained with U-Pb method in the Alto Pajeu terrane- both from conventional method and from SHRIMP analyzes are still deserving a refining in their knowledge and interpretation. Age values have been obtained since from 920 Ma (large errors involved) up to 995 Ma (small amount of errors), with the most important set of ages around 950 Ma (sheets of othogneisses enclosed by metagraywackes). So doing, these age values are repeating those obtained by Rb-Sr methodology. It is necessary to emphasize the importance of these data which support the existence of an Early Neoproterozoic orogenic event in the Borborema Province, but the origin, number and sucession of events still remain as open questions.

Sm-Nd data for both the Cariris Velhos orthogneisses and for their enclosing metagraywackes and schists ("S. Caetano do Navio Complex") display similar behavior. For the cases of metragraywackes de $T_{(DM)}$ values varies from 1300 up to 2500 Ma, but in the majority of the cases this upper limit is below 2000 Ma. The εNd values use to be positive between (+1) and (+2) for the cases with the lowest values of $T_{(DM)}$, and they are moderately negative, between (-7) and (-10), for the cases with highest values of $T_{(DM)}$. So, the admittance of some cases of juvenile sources for the formation of theses rocks seems to be reasonable. Otherwise, there are some few particular cases of very high values of $T_{(DM)}$ (between 2500 and 3600 Ma), and negative values of εNd indicating sparse contribution of older source rocks, even from far Archean domains.

For the orthgneisses themselves the range of values for $T_{(DM)}$ is mostly between 1300 and 1900 Ma, with some rare cases of values over 2000 Ma. The values for εNd use to show remarkable regularity, with the lowest values between (-0.12) up to (+2.0), i.e. near zero, for the cases of lowest values of $T_{(DM)}$, and the negative values around (-3.0) and (-5.0) for the case of high $T_{(DM)}$ values, over 1700 Ma. According to these data it is possible to assume important juvenile contribution in the formation of part of the Cariris Velhos orthogneisses.

Just some few Ar-Ar data were run in samples of these rock assemblages, in order to evaluate the behavior of the Alto Pajeu Terrane (Fold Belt Pajeú-Paraíba) during the subsequent events of the Brasiliano Collage. The choosen samples were collected from areas where (apparently) the events of the Brasiliano were of lesser importance, far from Neoproterozoic intrusives and shearing domains. The results from amphibole (S. José do Egito, amphibolite), 623 ± 15 Ma; muscovites (S. José do Egito, metagraywacke and Lagoa do Meio metadacite), 512 ± 3 Ma; and rhyolite, whole rock (Serra do Machado rhyolite, intrusive in Cariris Velhos orthogneiss) give an idea of widespread occurrence of the Brasiliano events and different times of cooling, as well as they are clearly showing the difficulty to state some unaffected areas, preserved of the thermal events of the superposed Brasiliano Cycle.

REFERENCES

Brito Neves, B.B.; Santos, E.J.; Van Schmus, W.R. 2000. Tectonic History of the Borborema Province. In: U.G. Cordani; E.J. Milani; A. Thomaz Filho; D.A. Campos (eds.) Tectonic Evolution of South America.Rio de Janeiro, 31th International Geological Congress, 151-182.

Barbarin, B. 1999. A review of the realtionships between granitoid types, their origin and their geodynamic environment.Lithos, 46:605-626.

Harris, N.B.W.; Pearce, J.A.; Tindle, A.G. 1986. Geochemical characteristics of collision aonde magmatism. In: M.P. Coward & A.C. Ries (eds.) Collision Tectonics.London, Geological Society Special Publication, 19: 67-81

Pearce, J.A. 1996. Sources and settings of granitic rocks. Episodes, 19:126-133

Pearce, J.A.; Harris, N.B.W.; Tindle, A.C. 1984. Trace elements discrimination diagrams for the tectonic interprettion of granitic rocks. Journal of Petrology, 25:956-983.

Rollinson, H. 1994. Using geochemical data: evaluation, presentation, interpretation. New York, Longman Scientifphic and Technical, 352 p.

Santos, E.J. 1995. O Complexo Granítico Lagoa das pedras. Floresta (Pernambuco): acresção e colisão na Província Borborema, Nordeste do Brasil. Tese de Doutoramento, Instituto de Geociências da Universidade de São paulo, 219p.

Thompson, R.N.; Morrison, M.A.; Hendry, G. L.; Parry, S.J. Na assessment of the relative roles of crust and mantle in magma genesis. Phil. Trans. Royal Society of London, A 310:549-590.

Van Schmus, W.R.; Brito Neves, B.B.; Hackspacher, P.C.; Babinski, M. 1995. U/Pb and Sm/Nd studies of the eastern Borborema Province, Northeast Brazil: initial conclusions.Journal of south American Earth Sciences, 8:267-288.

U-Pb ZIRCON AGES OF SOME CLASSIC GRANITES OF THE BORBOREMA PROVINCE

Brito Neves, B.B.[1]; Passarelli, C.R.[2]; Basei, M.A.S.[1] and Santos, E.J.[3]

1. GMG- Instituto de Geociências – Universidade de São Paulo. bbleybn@usp.br, baseimas@usp.br
2. CPGeo – Instituto de Geociências - Universidade de São Paulo. crpass@usp.br
3. Centro de Tecnologia e Geociências - Universidade Federal de Pernambuco. ediltonjsantos@terra.com.br

Keywords: Borborema Province, granitic plutonism, "Conceição"- type granites, "Itaporanga"-type granites

INTRODUCTION

The Borborema Structural Province, in Eastern Northeast of the South American Platform, is a branching system of orogens which evolution was developed during the Neoproterozoic among different descendents of the Rodinia supercontinent (such as "Parnaíba Block", São Luis-West Africa and São Francisco-Congo-Angola Craton). Its extension in the African continent (Pan African Systems) has been recognized - by many different authors - in the area between Togo and Gabon.

First of all, some main characteristics may be mentioned to this province: (i) the participation of the reworked Paleoproterozoic basement (basement inliers, with different sizes and roles in the geotectonic evolution), (ii) different types of fold belts (in terms of different tectonic behavior and lithostratigraphic assemblages), and (iii) the remarkable granitic plutonism. A recent synthesis for the evolution of this province may be found in Brito Neves et al. (2000).

About 35 years ago a previous and classical paper by Almeida et al. (1967) had preliminarily discriminated a series of granitic typologies, as "Conceição" type, "Itaporanga" type and so on, mostly based upon general geological features and petrographic grounds. A numerous and outstanding group of scientific articles has since then been developed on these granites up to present, with remarkable enrichment of new petrological, isotopic and geochemical data. Additionally, many new granites occurrences have been reported in that structural province, where that preliminary classification has somehow been preserved. The papers of Sial (1986), Ferreira et al. (1998), Santos & Medeiros (1999) and Brito Neves et al. (2000), may be suggested as good syntheses on this subject, among a very rich and proliferating bibliography. It is necessary to remark the special emphasis on this subject given by the group of petrologists (NEG-LABISE) of the Department of Geology of Universidade Federal de Pernambuco, with remarkable bibliographic documentation available (e.g. Almeida et al., 2002; Guimarães et al., 1998; Guimarães & Almeida, 2001).

THE GRANITIC PLUTONISM

The granitic plutonism of the Borborema Province is rather important and widespread in terms of occurrence. Many granitic occurrences intrude supracrustal belts of Eo-Neoproterozoic (Cariris Velhos Orogeny) and Mid and late Neoproterozoic (Brasiliano collage). Other granitic occurrences are intrusives in the basement inliers of Paleoproterozoic, sometimes forming large batholiths. Some other granites are clearly related to the linear shear belts, which gave the final geometric-geologic shape to the Borborema Province. Even, in the distal reworked marginal zones of the cratonic nuclei of São Francisco ("Sobradinho Massif", to the south) and São Luis ("Granja Massif", to the north) granitic occurrences has been recorded. This remarkable granitic plutonism has been matter of outstanding number of bibliographic references, so including many Master dissertations and PhD theses, as well as it has been subject of scientific articles of important national and international symposia (e.g. ISGAN I and II; Hutton symposium).

GEOCHRONOLOGICAL DATA

Samples of these classical types of granites, collected in their typical localities, were submitted to geochronological determinations by U-Pb method, in order to fulfill a demand of the geological community, because most of the previous determinations were run with methods of lower accuracy. These new obtained data were now reunited with some preexisting U-Pb data from other granitic bodies (most of them run during the last decade), in order to try to make possible to recognize the main stages of granitic plutonism of the Borborema province as a whole.

With all data assembled – and having the geological development of the province in mind – it was possible to distinguish three major stages of granitic plutonism (Table 1): 650-625 Ma, 580-560 Ma and 540-520 Ma. The first two groups of ages use to assemble those granites that have many times been related to arc plutonism, while the latter time interval assembles those granites in close association to the events of escape tectonics of the Brasiliano-Pan African collage (Jardim de Sá et al., 1999), which has preceded the assembly of a supercontinental landmass (Western Gondwana). Actually, these span of time of these intervals are far from the wishable table, but this is the result that can be stated at the present moment of geochronological knowledge (at reconnaissance scale). The idea was to draw this preliminary and realistic approach, in order to establish a first basis that could step by step be improved with the advent of further data.

REFERENCES

Almeida, F. F. M.; Leonardos Jr., O .H.; Valença, J. 1967. Granitic rocks of Northeast South America. International Union of Geological Sciences/SUDENE, Special Review prep. to IUGS/UNESCO Symposium in Recife-SUDENE, 37pp.

Almeida, N. C.; Guimarães, I. P.; Silva Filho, A. F. 2002. A-Type post-collisional granites in the Borborema Province – NE Brazil – The Queimadas pluton. Gondwana Research, 5 (3): 667-681.

Brito Neves, B. B.; Santos, E. J.; Van Schmus, W. R. 2000. Tectonic History of the Borborema Province. In: Cordani, U. G.; Milani, E. J.; Thomaz Filho, A.; Campos, D. A. (eds.) Tectonic Evolution of South-America. Rio de Janeiro, 31th International Geological Congress, p. 151-182.

Ferreira, V. P.; Sial, A. N.; Jardim de Sá, E. F. 1998. Geochemical and isotopic signatures of Proterozoic Granitoids in terranes of the Borborema structural province, northeast Brazil. Journal of south American Earth Sciences, 11 (5): 438-455.

Guimarães, I. P.; Silva Filho, A. F.; Almeida, C. N.; Araújo, J. M. M.; Sales, A.; Melo, S.C. 1998. The Brasiliano granitoids from the Pajeú-Paraíba belt and Teixeira High: Sm-Nd isotope geochemistry and U-Pb in zircon ages. In: Congresso Brasileiro de Geologia, 40, Belo Horizonte-MG, 1998. Anais. Belo Horizonte, SBG, p. 48.

Guimarães, I. P.; Almeida, C. N. 2001. The Calk-alkaline Brasiliano granitoids in the Pajeú-Paraiba belt, Northeast Brazil: the Timbaúba Complex. In: Simpósio de geologia do Nordeste, 19, Natal. Resumos. Natal, SBG (Bol. 17), p. 232-233.

Jardim De Sá, E. F.; Trindade, R. I. F.; Hollanda, M. H. B. M.; Araújo, J. M . M.; Galindo, A. C.; Amaro, V.; Souza, Z.; Vigneresse, J. L.; Lardeaux, J. M. 1999. Brasiliano syntectonic alkaline granites emplaced on a strike-slip/extensional setting. Anais da Academia Brasileira de Ciências, 71 (1): 17-28.

Santos, E. J. & Medeiros, W. C. 1999. Constraints from granitic plutonism on Proterozoic crustal growth of the Transverse Zone, Borborema Province, NE Brazil. Revista Brasileira de Geociências 29 (1): 73-84.

Sial, A.N. 1986. Granite-types in Northeast Brazil: current knowledge. Revista Brasileira de Geociências, 16 (1):54-72.

Table 1. Main geochronological determinations (Ma) of granitic rocks of Borborema Province (U-Pb and Pb-Pb).
* Rb-Sr age ** Sm-Nd age; # of these work

	NORTHERN DOMAIN			TRANSVERSAL ZONE	SOUTHERN DOMAIN
	NW CEARÁ	CENTRAL CEARÁ	R. G. NORTE		
LATE BRASILIANO	507 ± 36 (Meruoca)			505 ± 4 (Palmeira)	
				517 ± 18 (Jati/Bodocó)	
	532 ± 4		530 ± 54 * (S.Algodão)		528 ± 4 (Águas Belas)
	532 ± 6 (548 ± 24 *) (Mucambo)			540-520 (Diversos)	
			557 ± 13 * D. Inês	551 (Tuparetama)	555 ± 20 * (Rajada)
	563 ± 17 (Tucunduba)			570 ± 10 (S. João) 570 ± 24 (Queimadas) 572 ± 20 (S. Branca) 573 ± 45 # (**Catingueira**)	
		574 ± 32 (NW S.Quitéria)		574 ± 54 (Solidão)	
			576 ± 24 (Caraúbas) 578 ± 14 ** (Caxexa) 579-555 (Acari) 579 ± 7 (S. Rafael) 580 ± 4 (Tourão)	580 ± 4 # (**Itaporanga**)	
				581 ± 2 (C. Grande)	
				583-591 (Brejo M. Deus)	
		585 ± 5 (Quixadá) 587 ± 19 (Anil)		585 ± 2 588 ± 12 (Faz. Nova)	
	591 ± 10 (Chaval)				
			593 ± 5 (Umarizal)	592 ± 7 (B. Jardim)	593 ± 5 (Correntes)
EARLY BRASILIANO		599 ± 16 (Poço Verde)			
				612 ± 9 * (Tabira)	613 ± 8 (S. Catú) 614 ± 18 (C. João Sá) 616 ± 4 (Caiçara) 624 ± 5 (A. Branca)
		614 ± 2 (Central Ceará) 622 ± 4 (Sul Fortaleza)		621 ± 14 (Tabira)	
			628 ±11 (Macaiba)	> 620 (Teixeira) 635 ± 9 # (**Conceição**) 638 ± 5 (Brejinho) 644 ± 5 (Timbaúba) 651 ± 15 # (**Tavares**) 750 ± 20 (Riacho Icó)	
	630 ± 18 (NW Ceará)				
		660± 15 (S. Quitéria) 665± 40 (W Ceará)			

Nd DATA FROM CENTRAL CEARÁ DOMAIN: ARCHEAN RELICTS, PALEOPROTEROZOIC RECORD AND NEOPROTEROZOIC CRUSTAL REWORKING

Castro, N.A.[1]; Basei, M.A.S.[1] and Sato, K.[2]

1. Universidade de São Paulo, Instituto de Geociências, Dep. Geoquímica e Geotectônica.
neivaldoac@hotmail.com, baseimas@usp.br
2. Universidade de São Paulo, Instituto de Geociências, CEPEGEO (Centro de Pesquisas Geocronológicas)

Keywords: Nd, juvenile, Borborema, Archean, Paleoproterozoic, Neoproterozoic

New geological interpretations based on Nd isotopic results for rocks situated south-southeast of the Transbrasiliano Sobral-Pedro Segundo Lineament and north-northwest of the Senador Pompeu Lineament (Central Ceará Domain of Brito Neves et al., 2000 or subprovince 2 of Van Schmus et al., 1998) are here presented. The Central Ceará Domain (CCD) is situated in the northwestern portion of Almeida's et al. (1981) Borborema Province, being its counterpart in the African side the Nigerian Province Precambrian rocks (Fig. 1). In CCD, isotopic studies by Fetter (1999) indicated the existence of an Archean nucleus (Tróia-Pedra Branca-Mombaça, with zircon U-Pb ages between 2.69-2.83 Ga and Nd T_{DM} between 2.69-3.04 Ga) surrounded by rocks of ages varying between Paleo and Neoproterozoic. Caby and Arthaud (1986) and Ar-Ar studies carried out in the State of Ceará by Monié et al. (1994) stressed out the importance of the Neoproterozoic orogeny. Martins (2000), studying the Quixadá western region (Algodões-Choró Metamorphic Suite), found new informations that proved the existence of Paleoproterozoic rocks, apparently formed in an island arc environment. Fetter et al. (2003) considered the Santa Quitéria Complex as the record of a Neoproterozoic magmatic arc, and the Martinópolis Group supracrustal rocks, located north-northwestwards, as deposited under a fore-arc regime around 0.77 Ga (U-Pb in zircons from probable meta-rhyolites). In this context, the supracrustal rocks situated south-southeast of the Santa Quitéria Complex must have deposited under a back-arc regime (zircon U-Pb age of ~0.77 Ga of a probable meta-rhyolite from the Independência region). Sm-Nd data confirm such model, with the majority of T_{DM} ages yielding values intermediate to those found for the Paleoproterozoic basement and the oldest Neoproterozoic zircon U-Pb ages for granitoids identified within the Santa Quitéria Complex.

In this work a set of new Sm-Nd data is presented, expressed in the form of T_{DM} ages and ε_{Nd}. This data set encompasses Paleoproterozoic rocks (situated west of the region studied by Martins, 2000), here named Madalena-Algodões-Choró Complex (MACHC); supracrustal rocks found west of MACHC, here named Rio Curú-Itataia-Independência supracrustal rocks (RCIISC), and a small volume of rocks representing the eastern margin of the Santa Quitéria Granitic-Migmatitic Complex (SQGMC). Figure 1 presents the spatial distribution of the different lithotectonic units. Table 1 contains the results of the analyses available. These data will be in the future complemented by U-Pb (zircons and monazites) and Ar-Ar dating of micas and amphiboles.

The Archean T_{DM} ages correspond to biotite and hornblende-bearing migmatitic nuclei exposed within RCIISC and MACHC supracrustal rocks. In the first case a T_{DM} age of 2.73 Ga, with corresponding $\varepsilon_{Nd(0)}$ of -22.4, was found. For the migmatitic nucleus present in the MACHC sediment-derived association the T_{DM} interval falls in the 2.6-2.8 Ga interval, with $\varepsilon_{Nd(0)}$ from -19.1 to -15.2.

MACHC encompasses two distinct lithologic associations, one of them sediment-derived, mainly constituted by garnet-bearing biotite gneisses, hornblende-biotite gneisses and smaller volumes of muscovite-biotite gneisses, quartzites, occasional gondites, and contribution of basic volcanics (amphibolites). The second association is represented by orthogneisses of quartz-dioritic to tonalitic composition, with variable hornblende and biotite proportions, here considered as intrusive in the sediment-derived association. For the sediment-derived association, the interval of T_{DM} model ages ranged from 2.41 to 2.36 Ga, with $\varepsilon_{Nd(0)}$ values between -25.8 and -21.7. In the sediment-derived association, two determinations made in muscovite/biotite gneisses yielded T_{DM} ages in the 2.38 to 2.23 Ga interval, with $\varepsilon_{Nd(0)}$ between -19.7 and -18.3.

The predominant RCIISC lithotypes (~ 60% in volume) are locally migmatized biotite gneisses, with variable amounts of muscovite, garnet, sillimanite and kyanite. The other ~40% are (pure, or muscovite- or feldspar-bearing) quartzites, calc-silicate rocks and gray to whitish marbles and usually garnet-rich amphibolites. T_{DM} values found for the gneisses/migmatites fall in the 1.1-2.4 Ga interval, with less negative $\varepsilon_{Nd(0)}$ values being associated with younger ages (-5.48 and -6.55). Conversely, more negative $\varepsilon_{Nd(0)}$ values are associated with older T_{DM} ages (-19.5 and -23.8). It is worth pointing out that out of three analyses, which correspond to amphibolites considered representative of syn-depositional magmatism, two samples yielded positive $\varepsilon_{Nd(0)}$ values, respectively +3.18 and +5.16.

The study region includes only the eastern margin of the Santa Quitéria Batholith studied by Fetter (1999) and Fetter et al. (2003), and in this context, part of the granitoids and migmatites analyzed for the present work could have originated from protoliths with important participation of RCIISC. Remains of calc-silicate rocks and sillimanite gneisses found in the center of SQGMC, seem to reinforce this hypothesis. In the study region, SQGMC is preferentially composed of migmatites that usually contain biotite and less frequently hornblende, with mesosomes of granodioritic to monzogranitic compositions. In the more diatexitic portions that grade to nebulitic granitoids, monzo to syenogranites are found. West of Taperuaba, an approximately circular isotropic biotite granite stock is polyphase, with concentric phases of monzo- to syeno-granitic composition. These are the SQGMC post-orogenic granitoids, apparently correlated with the Serra da Barriga stock. It is also worth pointing out the occurrence of isotropic to weakly foliated leucogranitoids (Fazenda Memória and Serrote de São Paulo) within SQGMC, which certainly represent partial melting conditions and/or protoliths distinct from those present in the genesis of other SQGMC granitoids. The available Nd isotopic information indicate three distinct groups, compatible with the petrographic characteristics and mode of occurrence in the field: a) rocks of the metatexite-diatexite transition, with T_{DM} in the 1.68-1.74 Ga interval and $\varepsilon_{Nd(0)}$ varying between -16.9 and -6.1; b) characteristically diatexitic rocks - T_{DM} in the 1.18-1.38 Ga interval, with $\varepsilon_{Nd(0)}$ varying between -15 and -11.6; c) post-orogenic granitoids, corresponding to the Serrote São Paulo leucogranitoid, situated north of Santa Quitéria city, with T_{DM} model age of 2.2 Ga (double-stage calculation) and $\varepsilon_{Nd(0)}$ of -4.05.

Resulting from the analysis of Nd data, five main points can be listed: a) for the gneissic-migmatitic nuclei that occur within the supracrustal rocks, Archean T_{DM} ages were found, indicating that these rocks may be correlated with the Archean nucleus located *ca.* 50 km south of the studied region (Tróia-Pedra Branca-Mombaça Complex); b) the Paleoproterozoic (Nd, Sr and U-Pb) results obtained for MACHC rocks, including Martins' (2000) data and airbone geophysical, enable to extend it to the Madalena region and to consider a juvenile Paleoproterozoic origin for MACHC; c) the T_{DM} age interval found for SCRCII evidences a conspicuous participation of the Paleoproterozoic basement in the genesis of the supracrustal rocks in question, opposite to what happens in the region situated north-northwest of SQGMC (Martinópolis Group), considered by Fetter et al. (2003) the record of SQGMC fore-arc; d) two major groups of T_{DM} ages (1.74 to 1.68 and 1.38 to 1.18) were found for SQGMC. Both intervals, also identified by Fetter et al. (2003), are interpreted, by now, as indicative of mixing, respectively involving less and more amounts of juvenile material in the generation of the magmatic arc in question during the Neoproterozoic orogeny.

REFERENCES

Brito Neves, B.B.; Santos, E.J.; Van Schmus, W.R. 2000. Tectonic history of the Borborema Province, northeast Brazil. In Cordani, U.G.; Milani, E.J.; Thomaz Filho, A.; Campos, D.A. (eds.). Ed. Esp. XXXI International Geological Congress, SBG, Rio de Janeiro, Brasil, p.151-182.

Caby, R. & Arthaud, M.H. 1986. Major Precambrian nappes of the Brazilian belt, Ceara, northeast Brazil. Geology, 14: 871-874.

Castro, N.A.; Basei, M.A.S.; Brito Neves, B.B. 2002. Considerações tectono-estratigráficas sobre as principais unidades proterozóicas do Ceará Central (Folhas Itatira e Taperuaba). Anais do XLI Congresso Brasileiro de Geologia, João Pessoa-PB, p.298.

DePaolo, D.J. 1981. A neodymium and strontium isotopic study of the Mesozoic calc-alkaline granitic batholiths of the Sierra Nevada and Peninsular Ranges, California. Journal Geophysical Research, v.86, pp. 10470-10488.

Fetter, A.H. 1999. U-Pb and Sm-Nd geochronological constraints on the crustal framework and geological history of Ceara state, NW Borborema Province, NE Brasil: implications for the assembly of Gondwana. Ph. D. Thesis, Departament of Geology, Kansas University, Lawrence, KS-USA, 164p.

Fetter, A.H; dos Santos, T.J.S.; Van Schmus, W.R.; Hackspacher, P.C.; Brito Neves, B.B.; Arthaud, M.; Nogueira Neto, J.A.; Wernick, E. 2003. Evidence for Neoproterozoic continental arc magmatism in the Santa Quiteria Batholith of Ceará State, NW Borborema Province, NE Brasil: Implications for the assembly of west Gondwana. Gondwana Research, V. 6, nº 2, pp. 265-273

Martins, G. 2000. Litogeoquímica e controles geocronológicos da Suíte Metamórfica Algodões-Choró. Doctoral Thesis, IG-UNICAMP, inédito, 218p.

Monié, P.; Caby, R.; Arthaud, M.H. 1997. The Neoproterozoic Brasiliano orogeny in northeast Brazil: ^{40}Ar/^{39}Ar and petrostructural data from Ceará. Precambrian Research, 81: 241-264.

Sato, K. 1998. Evolução crustal da Plataforma sul Americana com base na geoquímica isotópica Sm-Nd. Doctoral Thesis, Institute of Geosciences, University of São Paulo, Brasil. 301p.

Van Schmus, W.R.; Brito Neves, B.B.; Hackpascher, P.C.; Fetter, A.; Kozuch, M.; Dantas, E.L.; Babinski, M. 1998. The Borborema Province: A collage of polyciclic domains in northeast Brazil. International Conference on Precambrian Craton Tectonics, Ouro Preto-MG, p. 80-83.

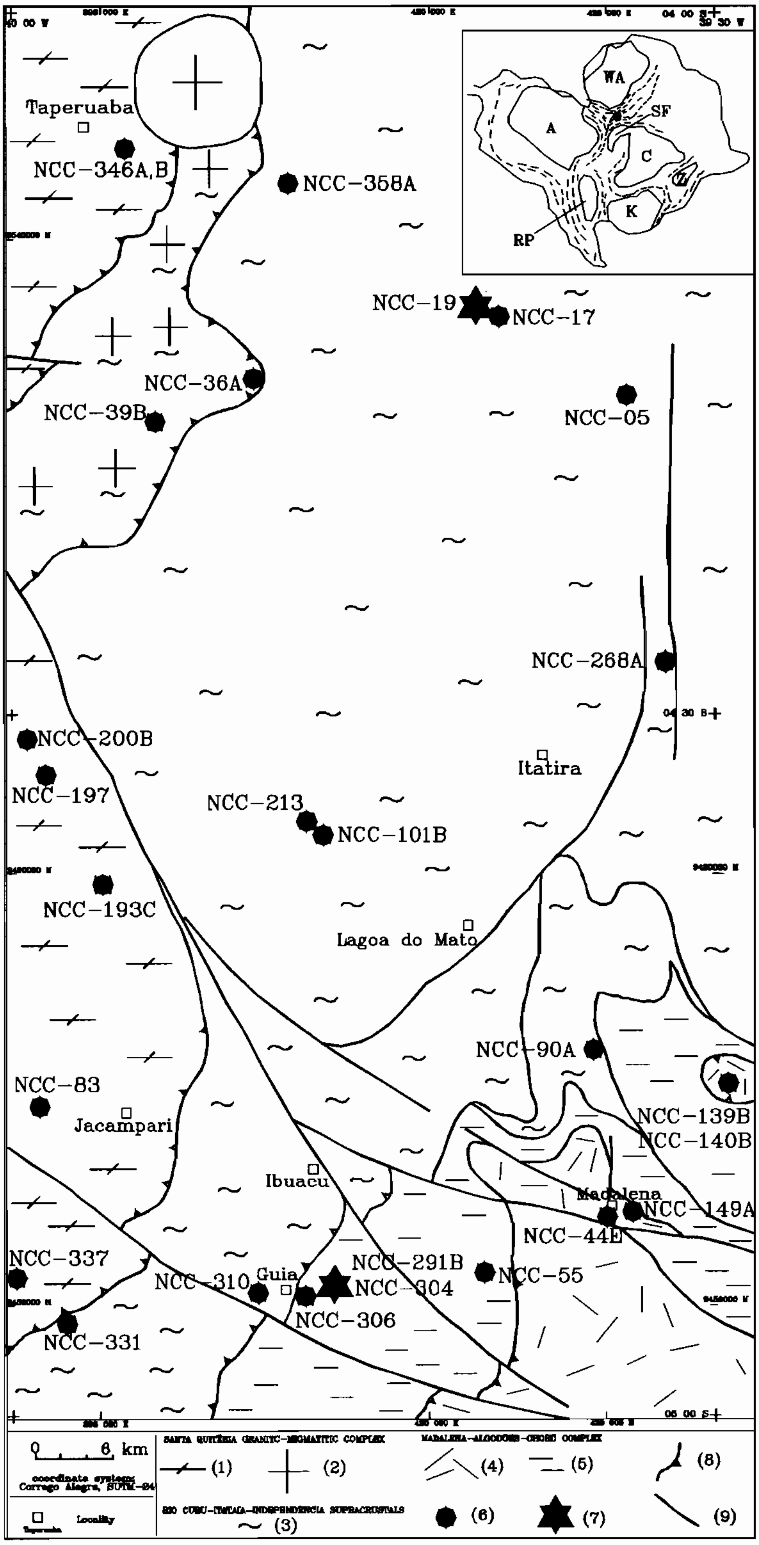

Figure 1. Geological simplified map of the Central Ceará Domain in the region cover by the Taperuaba and Itatira 1:100 000 maps. (1) Santa Quitéria Granitic-migmatitic Complex (SQGMC), (2) SQGMC pos-orogenic granitoids, (3) Rio Curú-Itataia-Independência Supracrustals (RCIISC), (4) Madalena-Algodões-Choró Complex (MACHC), intrusive quartz-dioritic to tonalite gneiss, (5) MACHC, paraderived association with anphibolites and gondites, (6) Nd analysis, (7) Nd analysis, Archean, (8) pos-nappes thrusts and (9) faults and contacts. Minnor figure on the upper right corner: study area (black filled circle) on the West-Gondwana context, with Major Neoproterozoic cratonic areas: A (Amazonas), WA (West-Africa), SF (São Francisco), C (Congo), RP (Rio de La Plata), K (Kalahari), Z (Zimbabwe).

Table 1. Sm-Nd whole rock analysis from Central Ceará Domain (northeast Brazil, Borborema Province), region cover by the Taperuaba and Itatira 1: 100 000 maps. For sample location, see map on the Figure 1. $\varepsilon_{Nd(0)}$ calculated with $^{143}Nd/^{144}Nd$ today=0.512638, with data normalized to $^{146}Nd/^{144}Nd$=0.72190. CHUR (DePaolo, 1981). T_{DM} (DePaolo, 1981). DS (double stage of Sato, 1998).

GEOLOGICAL MARK / SAMPLE	**Rock**	**T_{DM} (Ga)**	**ε_{Nd} (0)**
NEOPROTEROZOIC "REWORK"			
SANTA QUITÉRIA GRANITIC-MIGMATITIC COMPLEX			
pos-orogenic granitoid			
NCC-392	(biotite)-muscovite-granite	2.2 (DS, 0.53Ga)	-4.05
diatexites			
NCC-39B	biotite-gneiss with garnet	1.10	0.1
NCC-200B	biotite-granite foliated	1.38	-15.09
NCC-36A	biotite-gneiss/foliated granite	1.18	-11.89
NCC-197	biotite-granite foliated	1.24	-11.63
Metatexite to diatexite			
NCC-193C	hornblende-biotite-gneiss	1.74	-13.90
NCC-346A	biotite-horblende-gneiss	1.70	-6.15
NCC-346B	biotite-gneiss/foliated granite	1.73	-8.77
NCC-337	(hornblende)-biotite-gneiss	1.70	-14.27
NCC-83	biotite-gneiss	1.68	-16.19
RIO CURÚ-ITATAIA-INDEPENDÊNCIA SUPRA-CRUSTALS			
metasediments			
NCC-05A	garnet-biotite-muscovite feldspar schist/gneiss	1.97	-15.00
NCC-17	muscovite-biotite-gneiss	2.45	-23.87
NCC-213	sillimanite-biotite-gneiss	2.26	-19.25
NCC-310	sillimanite-muscovite-biotite-gneiss	2.12	-18.94
NCC-358A	garnet-sillimanite-biotite-gneiss	1.6 (DS, 0.65Ga)	-6.55
NCC-90A	biotite-gneiss	1.12	-5.48
metabasic rocks			
NCC-268A	garnet-hornblende-anphibolite	0.55 (DS, 0.65Ga)	5.16
NCC-331	garnet-hornblende-anphibolite gneiss	1.25	3.18
NCC-101B	garnet-hornblende-anphibolite	1.8 (DS, 0.65Ga)	-8.49
PALEOPROTEROZOIC RECORD			
MADALENA-ALGODÕES CHORÓ COMPLEX			
Quartz-dioriteic to tonalitic gneiss			
NCC-149A	biotite-hornblende-gneiss	2.38	-22.73
NCC-44E	hornblende-biotite-gneiss	2.36	-24.40
NCC-140B	hornblende-biotite-gneiss	2.36	-21.75
NCC-139B	hornblende-biotite-gneiss	2.41	-25.85
supra crustal rocks			
NCC-55	biotite-gneiss (meta-riolite?)	2.22	-18.37
NCC-306	biotite-muscovite-gneiss	2.38 (DS, 0.65Ga)	-19.75
ARCHEAN RECORD (basement inliers)			
NCC-304	hornblende-biotite-gneiss/migmatite	2.60	-19.10
NCC-291B	biotite-hornblende-gneiss	2.80	-15.29
NCC-19	biotite-gneiss/diatexite	2.73	-22.45

Sr ISOTOPIC COMPOSITION AND Pb-Pb AGE OF NEOPROTEROZOIC-LOWER PALEOZOIC CARBONATE SEQUENCES AT SALINAS HILL AND PIE DE PALO RANGE, WESTERN ARGENTINA

Cingolani, C.A.[1]; Kawashita, K.[2]; Naipauer, M.[1]; Varela, R.[1] and Chemale Jr., F.[2]

1. Centro de Investigaciones Geológicas-Departamento Geología, Universidad Nacional de La Plata, calle 1 n. 644, 1900, La Plata, Argentina, ccingola@cig.museo.unlp.edu.ar
2. Laboratório de Geologia Isotópica, Universidade Federal do Rio Grande do Sul, Av. Bento Gonçalves 9500, Porto Alegre, Brasil

Keywords: Carbonate rocks, Sr isotopes, Pb-Pb dating, Precordillera Terrane, Neoproterozoic-Lower Paleozoic

INTRODUCTION

It is well known that isotope stratigraphy is one of the most powerful tools in Upper Precambrian to Lower Paleozoic chronostratigraphy. The Sr isotope composition of seawater for this age interval is characterized by a continuous increase of $^{87}Sr/^{86}Sr$ that is interrupted, by sharp rises, which represent important changes in the Earth history. During Late Cambrian to Early Ordovician time the $^{87}Sr/^{86}Sr$ seawater ratio is high and close to the modern value of 0.70907 (Kaufman et al., 1993; Veizer et al., 1997; Jacobsen & Kaufman, 1999; Montañez et al., 2000). The Pb-Pb isotopic dating technique have been refined and successfully applied to a variety of geological problems (Jahn & Cuvellier, 1994, Babinski et al., 1999). We examine in this paper carbonate sequences from the Precordillera or Cuyania Terrane that are located at the Salinas Hill and Pie de Palo Range (Fig. 1), as a part of the "Angaco Belt" (Vujovich & Ramos, 1994). Also for comparison, we use two samples from the fossiliferous Lower to Middle Cambrian carbonates in the Eastern Precordillera (La Laja Fm.). We have studied their $^{87}Sr/^{86}Sr$ composition and compare it to global Sr isotope secular variation curves and we present new Pb-Pb isotope analyses on carbonate samples from Salinas Hill. The aims of the study were to constrain the timing of deposition/diagenesis and of subsequent metamorphism/deformation of the carbonate levels from the Caucete Group.

GEOLOGICAL SETTING AND PREVIOUS ISOTOPIC DATA

The study area encompasses the eastern side of the Precordillera from San Juan and the western foothills of the Western Pampean Ranges (Fig. 1) as a part of the Precordillera or Cuyania composite Terrane. Lower Cambrian-Ordovician platform limestones characterize eastern Precordillera. The western sector of Pampean Ranges at Pie de Palo area has a low to high metamorphic basement with two different sequences: the Pie de Palo Complex that consists of an ophiolitic assemblage, schists and gneisses of Grenvillian-age and the low grade metamorphic rocks "Angaco Belt" represented by the Caucete Group, that is characterized by platform clastic to carbonate sequence of uncertain age between Neoproterozoic to Lower Paleozoic (Ramos & Vujovich, 2000). The contact between both units is tectonic. Pioneer work on this region was produced by Schiller (1912) who mentioned the limestone rocks as a Lower Paleozoic belt. The Caucete Group (Puntilla Blanca, Angaco, Pie de Palo and El Quemado Fms.) was defined by Borrello (1969) as an 'Infracambrian' sequence. Linares et al. (1982) using statistical methods on C and O data found a similar isotopic composition that suggests a same depositional environment for the precordilleran "Zonda Limestones" and "Pie de Palo Limestones". Dalla Salda and Varela (1984) mentioned these carbonates as a Vendian age rocks. The "Angaco Belt" outcrops are extended from western Pie de Palo Range to Salinas Hill towards the South, where were defined by Vujovich and Ramos (1994). Ramos & Vujovich (2000) mapped part of the Pie de Palo Range, and discussed the possibility that the Caucete Group could be Neoproterozoic to Lower Paleozoic in age. Bordonaro et al. (1992) on the basis of trace fossils suggest a Neoproterozoic-Cambrian age for the Angaco Fm. Sial et al. (2001) studied C and Sr isotopic composition on some carbonate rocks of the Caucete Group and suggest a Vendian to Cambrian time of deposition. Finally, SHRIMP U-Pb detrital zircon ages comprise two populations that fall between c. 1.2 and c. 0.67 Ga, from El Quemado quartzites, were obtained by van Staal et al. (2002).

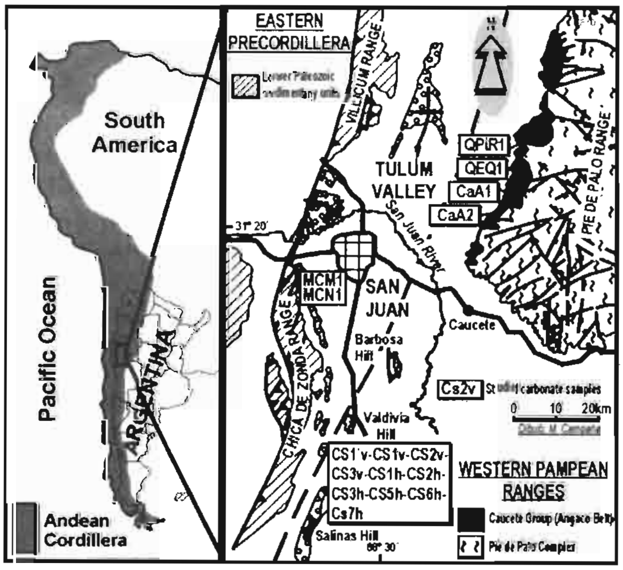

Figure 1. Regional geological map showing the sample locations.

ANALYTICAL PROCEDURES

Sr sample preparations were carried out at the Centro de Investigaciones Geológicas (CIG), University of La Plata. All whole-rock carbonate samples were crushed and dissolved in HCl 0.5N for no more than 5'. After that the Sr was concentrated in cationic exchange columns. The mass spectrometer measurements and Pb/Pb analyses were carried out at Laboratório de Geologia Isotópica, UFRGS, Porto Alegre, Brazil. For Pb-Pb method, nearly 1 gr of sample were weighed and leached with HCl 0.1N. The residue was leached again with HCl 1.0 N and 5 ml of the leached solution were used to determine the Pb/Pb isotopic ratios. Pb was separated with AG1X8 anion exchange column with 0.6 HBr and extracted with 6M HCl. Isotopic analyses were carried out with a multicollector VG Mass spectrometer at UFRGS. The Pb isotopic composition ratios were corrected to a fractionation factor based on successive determinations of NBS 981 Standard. Isochron regressions were done using the ISOPLOT program of Ludwig (1990).

RESULTS

Sr ISOTOPIC DATA

Major and trace element distribution and XRD analyses are used to identify carbonates that are most likely to have retained the original seawater ^{87}Sr/^{86}Sr (Denison et al., 1994, Jacobsen & Kaufman, 1999). The accurate definition of the ^{87}Sr/^{86}Sr in seawater with time depends on three major factors: analytical accuracy, retention of the original ratio and the precision of the biostratigraphic assignment. Diagenetic or metamorphic alteration is clearly a major cause of scatter and this increase with time. Twenty two carbonate samples from Angaco Fm. outcropped in the western side of Pie de Palo Range were stratigraphically collected (in vertical and horizontal profiles) from La Petaca, El Gato, El Quemado and Pirquitas creeks and twenty carbonate samples from the Salinas Hill as a southern end of the Angaco Fm. (Fig. 1). Based on the Fe, Sr, Mn contents (Table 1) determined by XRF in compacted powdered samples using international reference standards (INGEIS, University of Buenos Aires) and excluded samples with high dolomitic contents detected by XRD (CIG, La Plata), we finally selected four samples from Pie de Palo (CaA1, CaA2, QEQ1 and Qpir1), and ten from Salinas Hill (CS'1v, CS1v, CS2v, CS3v, CS1h, CS2h, CS3h, CS5h, CS6h, CS7h). For comparison two carbonate samples from La Laja Fm. at the Zonda Creek classical eastern Precordillera Lower to Middle Cambrian outcrop (MCM1, MCN1) has been studied. As we can see on the Fe/Sr vs. Mn/Sr diagram (Fig.2) only two samples (CaA2, QEQ1) both from Pie de Palo Range, are far from the recommended values for primary isotopic studies (Jacobsen & Kaufman, 1999). As shown in Table 1 the ^{87}Sr/^{86}Sr ratios of the Angaco Fm. outcropped at Pie de Palo area, range from 0.7089 to 0.7091, only the QEQ1 sample with high Mn and Fe content goes up to 0.7094. At the Salinas Hill the southern end of the Angaco Fm. yield ratios from 0.7091 to 0.7099. For comparison, the two samples from the unmetamorphosed Cambrian fossiliferous La Laja Fm. (Precordillera) range in between 0.7088-0.7089, in agreement with seawater curve (Veizer et al., 1997).

The values of ^{87}Sr/^{86}Sr were plotted versus Mn/Sr ratio according to the fluid-rock interaction models proposed by Jacobsen & Kaufman (1999). It is shown (Fig. 3) that the samples are outside of the primary sector and in coincidence with diagenetic open system.

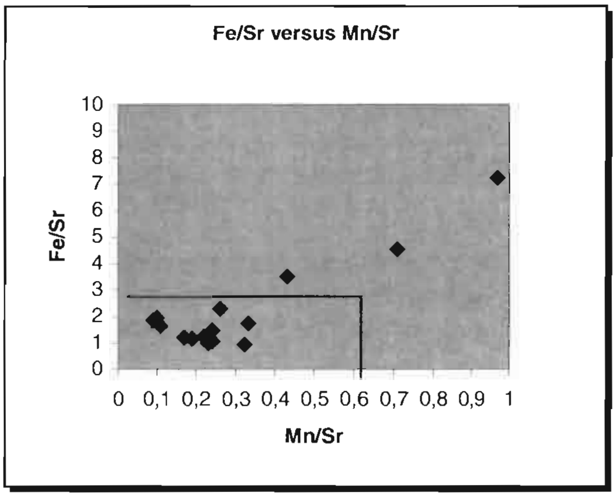

Figure 2. Fe/Sr vs. Mn/Sr diagram.

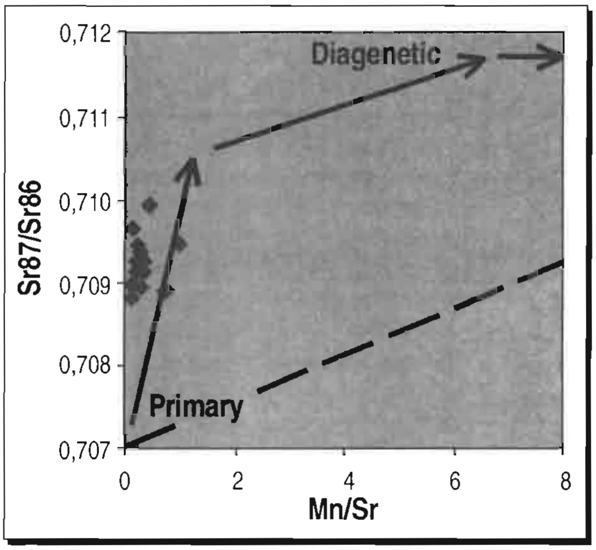

Figure 3. Sr^{87}/Sr^{86} vs. Mn/Sr diagram. Arrows indicate the trends between Primary and Diagenetic end-members (Jacobsen & Kaufman, 1999).

Table 1. Some major element ratios and Sr isotopic data.

Field N°	Fe2O3 (%)	MnO (%)	Fe (ppm)	Mn (ppm)	Sr (ppm)	Mn/Sr	Fe/Sr	($^{87}Sr/^{86}Sr)_n$*	*Error (%)*
			ANGACO Formation (Pie de Palo Range)						
Ca A 1	0.040	0.006	280	46	193	0.24	1.45	0.709112	0.0013
Ca A 2	0.134	0.019	937	147	207	0.71	4.53	0.708919	0.0022
QEQ 1	0.486	0.059	3399	457	471	0.97	7.22	0.709471	0.0020
Qpir 1	0.112	0.005	783	39	428	0.09	1.83	0.708986	0.0018
			ANGACO Formation (Salinas Hill)						
CS' 1 v	0.046	0.006	322	46	272	0.17	1.18	0.709247	0.0021
CS 1 v	0.037	0.006	259	46	212	0.22	1.22	0.709448	0.0015
CS 2 v	0.046	0.008	322	62	187	0.33	1.72	0.709294	0.0019
CS 3 v	0.133	0.015	930	116	267	0.43	3.48	0.709929	0.0012
CS 1 h	0.047	0.003	329	23	202	0.11	1.63	0.709661	0.0022
CS 2 h	0.025	0.008	175	62	191	0.32	0.92	0.709163	0.0018
CS 3 h	0.043	0.009	301	70	287	0.24	1.05	0.709376	0.0017
CS 5 h	0.028	0.006	196	46	202	0.23	0.97	0.709213	0.0020
CS 6 h	0.035	0.006	245	46	204	0.23	1.2	0.709280	0.0013
CS 7 h	0.033	0.005	231	39	201	0.19	1.15	0.709150	0.0016
			LA LAJA Formation (Precordillera)						
MCN 1	0.234	0.006	1637	46	719	0.26	2.28	0.708958	0.002
MCM 1	0.177	0.008	1238	62	639	0.1	1.94	0.708837	0.002

Mean of ±100 isotopic ratios, static mode, 1.0 V ionic intensity and multicollector, with 86 in axial collector.

*Normalized from 86Sr/87Sr: 0.1194 and adjusted for bias.

$SrCO_3$ NBS-987 assumed ($^{87}Sr/^{86}Sr$) n=0.71025.

Pb-Pb ISOTOPIC AGE

The Pb-Pb isochron method has provided a useful technique for determining ages on carbonate rocks and to obtain ages of sedimentation or metamorphic activity (Jahn et al., 1990). Ten analyses from Angaco Fm. at Salinas Hill outcrop, define a good linear trend in the $^{207}Pb/^{204}Pb$ vs. $^{206}Pb/^{204}Pb$ diagram (Fig. 4) that corresponds to an age of 546±74 Ma (MSWD=11,8). The isotopic data of Pb-Pb analyses of Angaco Fm. are presented on Table 2. $^{206}Pb/^{204}Pb$ values have a range between 20 to 31. If we consider the isochron error range, the age could be from Upper Neoproterozoic to Lower Ordovician time.

Table 2. Pb/Pb isotopic data.

Field N°	$^{206}Pb/^{204}Pb$	error (%)	$^{207}Pb/^{204}Pb$	error (%)	$^{208}Pb/^{204}Pb$	error (%)
			Angaco Formation (Salinas Hill)			
CS1'v	20.064	0.019	15.689	0.019	38.106	0.019
CS1 v	21.300	0.023	15.772	0.023	38.173	0.024
CS2 v	30.824	0.018	16.308	0.018	38.130	0.019
CS3 v	27.145	0.023	16.119	0.024	38.321	0.025
CS1 h	21.412	0.016	15.779	0.016	38.191	0.016
CS2 h	20.119	0.026	15.693	0.026	38.071	0.026
CS3 h	20.742	0.017	15.717	0.018	38.102	0.017
CS5 h	19.926	0.019	15.687	0.019	38.073	0.019
CS6 h	19.697	0.017	15.663	0.018	38.147	0.017
CS7 h	20.670	0.018	15.725	0.018	37.959	0.018
	1.002		1.003		1.004	
NBS981·	16.877	0.008	15.421	0.008	36.498	0.008
NBS981·	16.937		15.491		36.721	

NBS 981- 0,001% /u.m.a.

Average of more than 50 isotopic ratios, ionic intensity 0.5 V for ^{206}Pb multicollector with 206 axial collector.

·= LGI/UFRGS. ·· = International

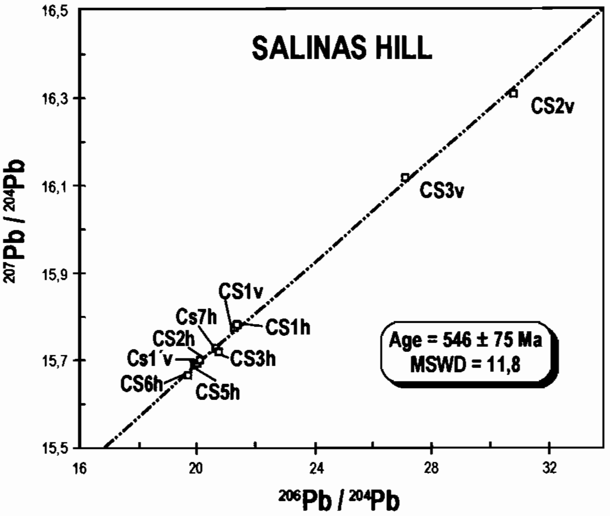

Figure 4. Pb-Pb isochron diagram for Salinas Hill rocks.

DISCUSSION

Many authors have suggested a sedimentation age for the Angaco Fm. as a range in between the Neoproterozoic to the Lower Paleozoic time. The lack of accurate fossils from the Caucete Group, with the exception of trace fossils, was an important stratigraphic limitation. Our $^{87}Sr/^{86}Sr$ isotopic ratios from 0.7089 to 0.7099 are in coincidence with data obtained by Sial et at. (2001) in Pie de Palo Range. Those ratios are rather high for the best-known Neoproterozoic seawater curve but are close to Middle and Late Cambrian $^{87}Sr/^{86}Sr$ values that rose to a maximum 0.7091. However we interpret these high values as a result of secondary alteration (diagenetic or metamorphic events) as we shown in the fluid-rock interaction models, or influence of continent sedimentation in the seawater during the carbonate deposition. The good aligneament on Pb-Pb isochron of c. 546 Ma determined from carbonates is interpreted as a last diagenetic/metamorphic event affecting the Angaco Fm. at Salinas Hill area. This suggests that the depositional age of this unit could be older, and range the Neoproterozoic time. If we consider the c. 670 Ma U-Pb detrital zircon age obtained by van Staal et al. (2002) in the El Quemado siliciclastic rocks, the deposition age of the Angaco Fm. could be constrained in between 670 and 546 Ma.

ACKNOWLEDGMENTS

This study was supported partially by CONICET and CNPq. We are recognized to Lic. A. Ramos for XRF determinations at INGEIS (University of Buenos Aires). This is a Contribution to IGCP N° 478 "Neoproterozoic-Early Palaeozoic Events in SW-Gondwana".

REFERENCES

Babinski, M.; Van Schmus, W.R.; Chemale Jr., F., 1999. Pb-Pb dating and Pb isotope geochemistry of Neoproterozoic carbonate rocks from the São Francisco basin, Brazil: implications for the mobility of Pb isotopes during tectonism and metamorphism. Chemical Geology 160:175-199.

Bordonaro, O.; Aceñolaza, G.; Pereyra, C., 1992. Primeras trazas fósiles de la sierra de Pie de Palo, San Juan, Argentina. Ciencias 1 (1): 7 – 14, San Juan.

Borrello, A. V., 1969. Los Geosinclinales de la Argentina. Dirección Nacional de Geología y Minería, Anales 14: 1-136, Buenos Aires.

Dalla Salda, L. & Varela, R., 1984. El metamorfismo en el tercio sur de la sierra de Pie de Palo, San Juan. Revista de la Asociación Geológica Argentina, 39(1-2): 68-93, Buenos Aires.

Denison, R.E.; Koepnick, R.B.; Burke, W.H.; Hetherington, E.A., 1998. Construction of the Cambrian and Ordovician seawater 87Sr/86Sr curve. Chemical Geology 152:325-340.

Jacobsen, S.B. & Kaufman, A.J., 1999. The Sr, C and O isotopic evolution of Neoproterozoic seawater. Chemical Geology 161:37-57.

Jahn, B.M. & Cuvellier, H., 1994. Pb-Pb and U-Pb Geochronology of carbonate rocks: an assessment. Chemical Geology, 115: 125-151.

Jahn, B.M.; Bertrand-Sarfati, J.; Morin, N.; Mace, J., 1990. Direct dating of stromatolic carbonates from the Schmidtsdrif Formation (Transvaal Dolomite), South Africa, with implications of the age of Ventersdorp Supergroup. Geology 18:1211-1214.

Kauffman, A.J.; Jacobsen, S.B.; Knoll, A.H.; 1993. The Vendian record of Sr and C isotopic variations in seawater: implications for tectonics and paleoclimate. Earth Planet. Sc. Letters, 120:409-430.

Linares, E.; Panarello, H.O.; Valencio, S. A.; Garcia, C. M., 1982. Isótopos del Carbono y Oxígeno y el origen de las calizas de la sierra Chicas de Zonda y de Pie de Palo, provincia de San Juan. Revista de la Asociación Geológica Argentina, 37(1): 80-90, Buenos Aires.

Ludwig, K.R., 1990. Isoplot: a plotting and regression program for radiogenic-isotope data, for IBM-PC compatible computers. Version 2.02. USGS Open-File rep. 88-557.

Montañez, I.P.; Banner, J.L.; Osleger, D.A.; Borg, L.E.; Bosserman, P.J., 1996. Integrated Sr isotope variations and sealevel history of the Middle and Upper Cambrian platform carbonates: implications for the evolution of Cambrian seawater $^{87}Sr/^{86}Sr$. Geology 24:917-920.

Ramos, V. & Vujovich, G. 2000. Hoja Geológica 3169-VI, San Juan, Servicio Geológico Minero Argentino, Boletín 243: 1-82, Buenos Aires.

Schiller, W., 1912. La alta cordillera de San Juan y Mendoza y parte de la provincia de San Juan. Ministerio de Agricultura de La Nación, Sección Geología, mineralogía y Minería., Anales 7(5): 1-68, Buenos Aires.

Sial, A.N.; Ferreira, V.P.; Toselli, A.J.; Aceñolaza, F.G.; Pimentel, M.M.; Parada, M.A.; Alonso, R.N. 2001. C and Sr isotopic composition of probable Vendian-Tommotian carbonate sequences in NW Argentina. III Symposium on Isotope Geology, Pucón, Chile. CD Rom version.

Van Staal, C.; Vujovich, G.I.; Davis, B., 2002. Tectonostratigraphic relationships and structural evolution of the western margin of the Sierra de Pie de Palo, Cuyania (Precordillera) Terrane, Argentina. Geological Society of America, Meeting, Denver, Co.n. 223-7. Abstract.

Veizer, J.;Buhl, D.; Diener, A.; Ebneth, S.; Podlaha, O.G.; Bruckschen, P.; Jasper, T.; Korte, Ch.; Schaaf, M.; Ala, D.; Azmy, K., 1997. Strontioum isotope stratigraphy: potential resolution and event correlation. Palaeogeography, Palaeoclimatology, Palaeoecology 132: 65-77.

Vujovich, G. I. & Ramos, V.A., 1994. La faja de Angaco y su relación con las Sierras Pampeanas Occidentales. Actas 7° Congreso Geológico Chileno, 1: 215-219, Concepción.

Nd ISOTOPES FROM THE ARAÉS METAVOLCANO-SEDIMENTARY SEQUENCE IN THE PARAGUAY BELT, NOVA XAVANTINA, MATO GROSSO, CENTRAL BRAZIL

Dantas, E.L. and Martinelli, C.D.

Instituto de Geociências - Universidade de Brasília, 70910-900. elton@unb.br

Keywords: Paraguay Belt, Nd isotopes, provenance ages

INTRODUCTION

The Paraguay Belt in Central Brazil is a large fold belt surrounding the SE border of the Amazon Craton. The Cuiabá Group is the most extensive lithostratigraphic unit of the belt and consists mainly of low grade metasedimentary rocks including phylites, quartzite, carbonate and glacial sediments, interpreted as deposited in a passive margin enviroment (Alvarenga & Trompette, 1999, 2002). Since the 1960´s, the stratigraphy of the Cuiabá Group has been described (Almeida, 1968), metavolcanic rocks are rare and poorly known, occurring only in the Nova Xavantina region, where they are individualize as the Araés metavolcano-sedimentary sequence (Pinho, 1990; Martinelli, 1998). Several authors consider this sequence as an extension of the Cuiabá Group, while others consider as an independent basal unit of the Paraguay Belt. Contact relationships are poorly constrained and their stratigraphic position is still a matter of debate and is controversial.

Ediacara-like fauna present in the Paraguay Belt suggests an Upper Vendian age for this unit (590-545 Ma) (Zaine & Fairchild, 1985; Alvarenga & Trompette, 1992). This fossil record is in agreement with the few geochronological data available for these rocks (Hasui & Almeida, 1970; Tassinari, 1981), allowing considering a Neoproterozoic age at around 549 Ma, as related to the main metamorphic event occurring in the region. The Cuiabá Group is intruded by ca. 503 Ma São Vicente granite. The absolute age of the Paraguay Belt rocks is still an open question.

The aim of this paper is to present news Nd isotopic data from the Araés metavolcano-sedimentary rocks and discuss their significance in terms of geotectonic evolution of the Paraguay Belt.

GEOLOGICAL FRAMEWORK OF THE NOVA XAVANTINA REGION

A detailed geologic mapping in the Araés gold deposit (Nova Xavantina region) revealed the presence of well-preserved metasedimentary and metavolcanic sequence (Martinelli, 1998).

The basal unit is composed of metabasalt and by basic metatuffs, lappili tuff, meta-andesites and quartz-sericite chlorite schists. The basic rocks occur as thick layers intercalated in phyllite and are the host rocks of the gold deposit. A clastic-chemical sequence is formed by layers of banded iron formations (BIFs), dark carbonaceous rocks, phylites and metacherts, occurring mainly associated with the metavolcanic rocks, which is estimated in average thickness of 250 m (Martinelli, 1998). An upper clastic unit formed of dominantly psamitic rocks (including metarenites and quartzites) and pelitic rocks (phyllites and metargillites).

Cenozoic colluvial and alluvial sediments largely lateritized cover the metamorphic rocks, inhibiting the continuity of its exposition.

Several authors have proposed a correlation between the Araés or Nova Xavantina sequence and the Cuiabá Group (Pinho, 1990; Alvarenga et al., 2002) however the lithological components found in this region are atypical when compared to those described in other exposures of the Cuiabá Group. Also, contact relationships between the metavolcanic association and other metasedimentary rocks are not well constrains to elucidate this relationship.

RESULTS AND DISCUSSION

Nd isotopic data from the Araés metavolcano-sedimentary sequence in the Nova Xavantina region are shown in Table 1. Rocks from the entire stratigraphic column of the area were sampled.

Rocks from the clastic unit present T_{DM} model ages varying between 1.7 and 2.3 Ga, suggesting a dominantly paleoproterozoic source area. Possible sources are in the Amazon Craton exposed to the northwest of the study area. Similar T_{DM} model ages were obtained in chemical sediments. However, the highly fractionated $^{147}Sm/^{143}Nd$ ratios in these rocks, suggests that their isotopic system has been open by fluids interaction.

T_{DM} model ages in the metavolcanic rocks range from 1.5 to 2.4 Ga, suggesting a more complex Nd isotopic evolution than the metasedimentary rocks. A mixing of Paleoproterozoic and younger sources is required to explain this variation. Also, some kind of continental contamination for an older crust is necessary to explain the highly εNd negative values recorded on the more basic volcanic rocks. A poorly constrained Sm-Nd isocron age of ca. 570 Ma was obtained on the samples of metabasic rocks and tuffs. Despite the fact that this age shows a large error, it is a reasonable estimation for the chrystallization time of these rocks.

Our results demonstrate that the rocks from the Araés metavocano-sedimentary sequence have a dominant Paleoproterozoic source and, although our data are preliminary, it is Neoproterozoic in age. The available data do not allow concluding wheter these rocks are part of the Cuiabá Group or an independent unit, even considering that they have similar provenance sources. The source area for the Cuiabá Group determined by Dantas et al. (2002) point the Amazon Craton as the main supplier of detritus to fill up the Paraguay basin.

REFERENCES

Almeida, F. F. M., 1968. Evolução tectônica do centro-oeste brasileiro no Proterozóico Superior. Rio de Janeiro, Brasil. Anais da Academia Brasileira de Ciências, 40, 285-293.

Alvarenga, C. J. S & Trompette, R., 1992. Glacial influenced turbidite sedimentation in the uppermost Proterozoic and Lower Cambrian of the Paraguay Belt (MT, Brazil).Paleogeography, Paleoclymatology and Paleoecology, 92, 85-105.

Dantas, E. L; Alvarenga, C. J. S., Ventura, R. S.; Pimentel, M M., 2002, Proveniênica de sedimentos glaciogênicos e carbonáticos na Faixa Paraguai baseados em isótopos de Nd. XLI Congr. Brasileiro de Geologia, João Pessoa. 303.

Gioia, S. M. C. L. & Pimentel, M. M., 2000. The Sm-Nd method in the Geochornology Laboratory of the University of Brasília. An. Acad. Brás. Cienc., 72 (2): 219-245.

Hasui, Y & Almeida, F. F. M., 1970. Geocronologia do centro-oeste brasileiro. Boletim da Sociedade Brasileira de Geologia., São Paulo, 19 (1): 5-26.

Martinelli, C . A, 1998.Petrografia, estrutural e fluidos da mineralização aurífera dos Araés-Nova Xavantina-MT. Doutorado. Instituto de Geociências, UNESP, 183p.

Pinho, F. E. C., 1990. Estudo das rochas encaixantes e veios mineralizados a ouro do Grupo Cuiabá, na região denominada Garimpo do Araés, Nova Xavantina, MT. Msc. Thesis, Instituto de Geociências, UFGRS, 114p.

Tassinari, C. C. G., 1981. Panorama geocronológico da folha SD22 Goiás e suas implicações geotectônicas. Goiânia, Projeto Radambrasil, 58p.

Zaine, M. F & Fairchild, T. R., 1987. Novas considerações sobre os fósseis da formação Tamengo, Grupo Corumbá, SW do Brasil. Anais Cong. Brasileiro de Paleontologia, Rio de Janeiro, Brazil, 2, 797-806.

Table 1. Nd isotopes results from the Araés Metavolcano-sedimentary sequence.

Sample	Rock Type	Sm (ppm)	Nd (ppm)	$^{147}Sm/^{144}Nd$	$^{143}Nd/^{144}Nd$ (±1σ)	$\varepsilon_{Nd(0)}$	T_{DM} (Ma)
Metavolcanic Unit							
NX 1	Metabasic rock	6.76	36.29	0.1124	0.511439 (28)	-23.4	2.40
NX 2	Tuff	7.02	33.5	0.1267	0.511790 (12)	-16.54	2.18
NX 3	Metabasic rock	3.5	9.77	0.2166	0.512053 (26)	-11.41	--
NX 6	Metabasic rock	1.41	4.71	0.1815	0.511942 (30)	-13.58	--
NX 15	Metabasic rock	3.03	8.5	0.2156	0.512063 (16)	-11.23	--
NX 16	Tuff	8.18	46.4	0.1067	0.511928 (17)	-13.86	1.57
NX 16^{a}	Tuff	7.05	37.45	0.1138	0.511824 (17)	-15.87	1.84
NX 17	Tuff	3.5	17.24	0.1228	0.512037 (06)	-11.73	1.67
NX 18	Tuff	7.0	36.46	0.1175	0.511705 (06)	-18.2	2.10
NX 19	Tuff	7.9	44.96	0.1063	0.511433 (16)	-23.51	2.27
NX 30	Lapilli tuff	2.9	12.79	0.1375	0.511746 (09)	-17.4	2.59
Clastic-chemical Unit							
NX 4	BIF	4.67	23.02	0.1226	0.511791 (21)	-16.51	2.08
NX 8	Jasper	3.52	14.91	0.1431	0.511581 (15)	-20.63	3.19
NX 9	BIF	3.53	10.94	0.1959	0.512024 (16)	-11.98	--
NX 20	Carbonate rocks	0.12	6.33	0.1264	0.511852 (10)	-15.33	2.06
Clastic Unit							
NX 7	Psamitic rock	2.21	11.07	0.1208	0.511988(06)	-12.67	1.71
NX 10	Pelite rock	7.28	38.96	0.1129	0.511649 (06)	-19.3	2.09
NX 11	Pelite rock	16.63	99.24	0.1013	0.511761 (17)	-17.11	1.72
NX 12	Ardose	14.25	74.77	0.1152	0.511779 (12)	-16.76	1.94
NX 13	Metarenite	10.23	47.33	0.1308	0.511772 (13)	-16.89	2.32

PRELIMINARY ^{39}Ar/^{40}Ar AGES FROM THE SOCORRO-GUAXUPÉ NAPPE COMPLEX IN SOUTHEASTERN BRAZIL: TIME-CONSTRAINTS ON THE FINAL COOLING OF THE SOUTHERN TOCANTINS OROGENIC SYSTEM AND THE SUPERPOSITION OF THE TRANSPRESSIVE RIO PARAÍBA DO SUL SHEAR BELT

Fetter, A.H.[1]; Hackspacher, P.C.[1]; Ebert, H.D.[1]; Dantas, E.L.[2] and Teixeira, W.[3]

1. Instituto de Geociências e Ciências Exatas, Universidade Estadual Paulista, Av. 24 A, nº 1515, 13506-900, Rio Claro-SP, Brazil. fetter@ms.rc.unesp.br
2. Instituto de Geociências, Universidade Federal de Brasília, 70910-900, Brasília-DF, Brazil
3. Centro de Pesquisas Geocronológicas, Instituto de Geociências, Universidade de São Paulo, Rua do Lago, 562, São Paulo-SP, 05508-080, Brazil

Keywords: Tocantins Orogenic System, Guaxupé-Socorro Nappe, Ribeira Belt, Ar-Ar dating

INTRODUCTION

In southeastern Brazil there is an important juncture between two major West Gondwana orogenic systems, the Southern Tocantins Orogenic System (Brasília Fold Belt) and the Mantiqueira Orogenic system (Ribeira Fold Belt). The Tocantins Orogenic System is related to the closure of the Goianides Ocean along the western-southwestern margin of the São Francisco Craton, whereas the Mantiqueira Orogenic system is associated with the closure of the Adamastor Ocean to the east-southeast of the craton (Campos Neto, 2000). The interaction between these two orogenic systems during the assembly of West Gondwana generated a vexing array of structural features, which have led to the development of different tectonic models to explain them (e.g. Hasui, 1982; Campos Neto et al. 1984; Ebert & Hasui, 1998, Hackspacher & Godoy, 1999; Campos Neto & Caby, 1999). In this paper we present new preliminary Ar-Ar data from the Socorro-Guaxupé/Três Pontas-Varginha nappe system that shed new light on the chronology of the late tectonic evolution of this part of southeastern Brazil during the assembly of West Gondwana.

GEOLOGIC SETTING

The southern part of the Tocantins Orogenic system consists of a series of flat-lying packages of nappes, displaced to the ENE, collectively known as the Socorro-Guaxupé/Três Pontas-Varginha nappe system (Campos Neto & Caby, 1999). To the southeast of this nappe system is the Central Ribeira Belt, a mosaic of different crustal domains that are separated and crosscut by a series of NE-SW trending transcurrent shear zones, first described by Braun (1975) as the Rio Paraíba do Sul Zone, that developed during a transpressional tectonic regime (Ebert & Hasui, 1998; Hackspacher & Godoy, 1999). A number of U-Pb geochronological studies have shown that the closure of the respective oceanic domains in both orogens was both diachronous and complex, and involved various episodes of precollisional magmatism (e.g. Machado et al., 1996; Ebert et al., 1996; Janasi, 1999; Schmidt et al., 1999; Pimental et al., 2000; Hackspacher et al., 2000; Janasi et al., 2001; Cordani et al., 2002; Heilbron & Machado, 2002; Negri, 2002). Nonetheless, is has been recognized that the main orogenic period in the Ribeira Belt is younger than that observed in the Southern Tocantins Province (Campos Neto & Figueiredo, 1995, Trouw et al. 2000). Specifically, peak metamorphism and collisional magmatism, followed by post orogenic uplift and magmatism occurred in the Socorro-Guaxupé/Três Pontas-Varginha nappe system between 630 – 620 Ma (Töpfner, 1996; Janasi, 1999) and 610 - 590 Ma (Vlach et al., 1990; Janasi, 1993; Töpfner, 1996; Wernick, 1998), respectively. In contrast, the Ribeira Belt is marked by several main pulses of orogenic magmatism and metamorphism along its length. From the Central Ribeira Belt (São Paulo State) southwestward, 610 – 600 Ma peak orogenic magmatism is dominant (Janasi et al., 2001), whereas two major pulses between 590 – 565 Ma and 535 – 520 Ma are recognized to the east and northeast in the belt (Machado et al., 1996, Schmidt et al., 1999). Post orogenic uplift and magmatism from the Central Ribeira Belt northwards has been documented between around 520 and 480 Ma (Wiedemann, 1993; Heilbron & Machado 2002).

While precise U-Pb (zircon and monazite) geochronology done in recent years has helped to resolve the timing of major tectonothermal events in southeastern Brazil, the formation of some key structural features in the orogen have not been not been well determined. Specifically, ages of strike slip shear zones and transpressional structures in the southern part of the Socorro-Guaxupé/Três Pontas-Varginha nappe system are lacking. Consequently, it has remained unclear whether these structures were generated during the emplacement of the nappe system, as suggested by Campos Neto & Caby (1999), or if they were the result of the transpressional tectonic regime of the Ribeira Belt, as proposed by Ebert et al. (1996), Ebert & Hasui (1998) and Hackspacher & Godoy (1999). New preliminary ^{39}Ar-^{40}Ar data obtained from biotite schists and paragneisses from the Socorro-Guaxupé/Três Pontas-Varginha nappe system now provide age constraints on both the primary cooling of the complex through the 350 °C isotherm and on the development of transpressional features in its southern portion.

SAMPLING AND Ar-Ar DATA

For this study we collected 19 samples of paragneisses and schists throughout the Socorro-Guaxupé/Três Pontas-Varginha nappe system for ^{39}Ar-^{40}Ar analyses of biotite and muscovite. Samples were collected from a variety of outcrops, some where the rocks are imprinted solely with a low-angle tectonic fabric related to amphibolite facies metamorphism, while other sample locations show transpressional features as well. Following initial separation and handpicking of mineral separates, biotite and muscovite fractions were irradiated at USP's research nuclear reactor and analyzed via gas mass spectrometer in the Institute of Geosciences at USP. Although analyses of all 19 samples have yet to be realized, 9 initial analyses (uncorrected ideogram ages; Table 1) done so far permit us to draw some preliminary conclusions regarding the late tectonic evolution of the studied region.

Samples from the northern part of the nappe system (Fig. 1; Table 1) yield a fairly tight cluster of cooling ages, from 594 to 580 Ma. These data indicate that the exhumation of the northern part of the nappe system through the 350°C isotherm was, by and large, a synchronous event. These data are also in line with conclusions summarized by Janasi et al. (2001), stating that post orogenic uplift and magmatism affected this region between ca. 610 and 590 Ma. As expected, the ^{39}Ar-^{40}Ar ages are somewhat younger than the magmatic zircon ages in the region.

In the southern portion of the nappe system (from the Senador Bento shear zone southward), the ^{39}Ar-^{40}Ar data show a different story. The oldest uncorrected ideogram ages obtained in this region are somewhat younger, around 571 to 559 Ma (Table 1, Fig. 1). In addition, samples associated with transpressional structures yield ideogram ages from 518 to 489 Ma (Table 1, Fig. 1). The two samples with ages of 518 and 517 Ma are associated with NE-SW trending strike slip shear zones within the interior of the nappe system, whereas the sample with the age of 489 Ma is located adjacent to a major shear zone (the Pinheiros-Rio Preto Lineament) along the southeastern margin of the nappe system. The ages along strike-slip shear zones from the interior of the southern nappe system suggest that they are related to the later transpressional tectonic regime in the Ribeira Belt, not the initial emplacement of the nappe package. We attribute the youngest age of 489 Ma to its proximity a major Ribeira Belt shear zone, which probably took longer to cool than subordinate related structures. The older ages of 571 and 559 Ma, which are younger than those to the north, may reflect either a later initial cooling than the northern region or partial resetting during the transpressional tectonic regime. As we acquire additional ^{39}Ar-^{40}Ar data from this region, we will be able to evaluate this question more thoroughly.

ACKNOWLEDGEMENTS

The authors are grateful for support provided by FAPESP (process numbers 99/00358-3 and 00/03960-5) to make this research possible, and to Artur Takashi Onoe of the Institute of Geosciences at USP for the careful effort he made to analyze the samples for this study.

REFERENCES

Braun, O.P.G. 1975. The coastal orogenic-belt structure of south-eastern Brazil. International Symposium on Continental Margins of Atlantic Type, São Paulo, 21 p.

Campos Neto, M.C., 2000. Orogenic systems from southwestern Gondwana. An approach to Brasiliano-Pan African cycle and collage in southeastern Brazil. In Cordani, U.G, Milani, E.J., Thomaz Filho, A. and Campos D.A (Eds.): Tectonic evolution of South America. Rio de Janeiro, 31st International Geological Congress, p. 335-365.

Campos Neto M.C. & Figueiredo, M. 1995. The Rio Doce Orogeny, southeastern Brazil. Journal South America Earth Science, v 8, p. 143-162.

Campos Neto M.C. & Caby, R. 1999. Neoproterozoic high-pressure metamorphism and tectonic constraints from the nappe system south of the São Francisco Craton, southeast Brazil. Precambrian Research, v 97, p. 3-26.

Campos Neto, M.C., Basei, M.A.S., Alves, F.R., Vasconcellos, A.C.B. de, 1984. A Nappe de Cavalgamento Socorro (SP-MG). Anais do 33° Congresso Brasileiro de Geologia, Rio de Janeiro. SBG, v. 4, 1809-1822.

Cordani, U. G., Coutinho, J.M.V., Nutman A.P., 2002. Geochronological constraints on the evolution of the Embu Complex, São Paulo, Brazil. Journal of South American Earth Sciences, v. 14, p. 903-910.

Table 1. Preliminary ^{39}Ar/^{40}Ar data from the Socorro-Guaxupé/Três Pontas-Varginha nappe system.

Sample	Location (see Fig. 1)	Material	Lab #	Integrated Age 01 (Ma)	Integrated Age 02 (Ma)	Integrated Age 03 (Ma)	Ideogram Age (Ma)
Samples unassociated with transpressional structural features							
H-693C	Varginha Quarry	Biotite	1485	576±1	580±1	585±1	580±3
HE-465	Três Pontas	Biotite	1489	586±1	593±1	583±2	589±2
HE-559	São Bento do Abade	Muscovite	1491	592±2	591±2	586±1	588±4
HFT-349	Sapucaí Mirim	Biotite	1494	572±1	570±1	575±4	571±2
HFT-351	Paraisópolis	Biotite	1495	565±1	573±1	543±1	559±8
HFT-359	15 km E of Caldas	Biotite	1512	594±1	592±1	594±2	594±8
Samples associated with transpressional structural features							
H-681	Silvianópolis	Biotite	1499	522±1	522±1	515±1	518±5
HE-109	Cruzeiro	Biotite	1488	488±1	485±1	487±1	489±3
HE-751	São Bento Sapucaí	Biotite	1492	517±1	512±1	522±1	517±6

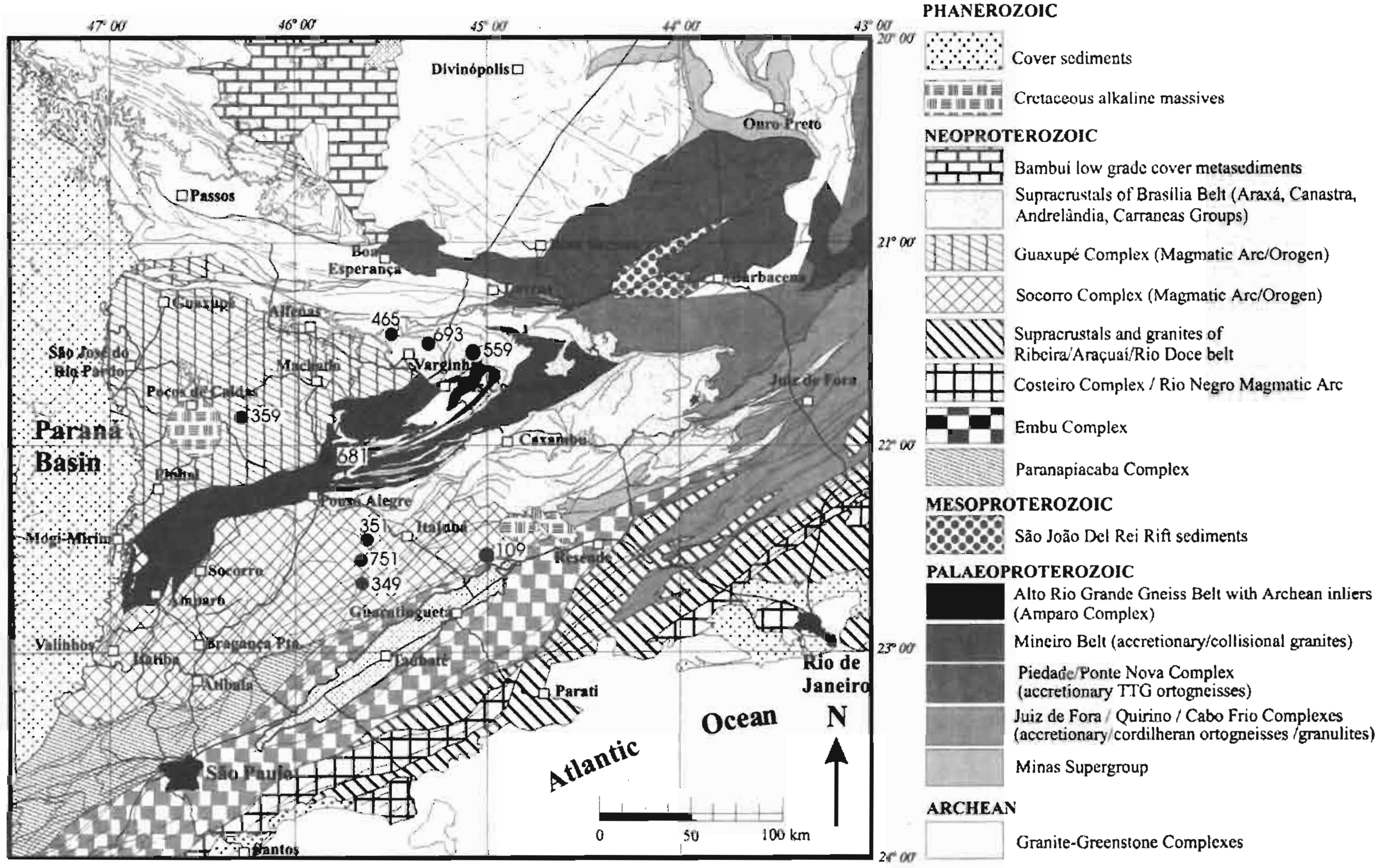

Figure 1. Geologic Map of SE Brazil (modified after CPRM, 2002) showing ^{39}Ar/^{40}Ar sample locations.

Ebert, H.D. & Hasui, Y., 1998. Transpressional tectonics and strain partitioning during oblique collision between three plates in the Precambrian of southeast Brazil, In: Holdsworth, R.E.; Strachan, R.A.; Dewey. J.F. Continental Transpressional/Transtensional Tectonics, Geological Society, London, Special Publications, 135, p. 231-252.

Ebert, H.D.; Chemale, Jr., F., Babinski, M., Artur, A.C., Van Schmus, W.R., 1996. Tectonic setting and U/Pb zircon dating of the plutonic Socorro Complex in the Transpressive Rio Paraíba do Sul Shear Belt, SE Brazil. Tectonics, AGU-American Geophysical Union, v. 15, n. 3, p.688-699.

Hackspacher P.C. & Godoy A.M. 1999. Vertical displacement during late-collisional escape tectonics (Brasiliano Orogeny) in the Ribeira Belt, São Paulo State, Brazil. Journal of African Earth Sciences, v. 29, p. 25-32.

Hackspacher, P.C., Dantas, E.L., Spoladore, A., Fetter, A.H. and Oliveira, M.A.F. 2000. Evidence For Neoproterozoic Backarc Basin Development in the Central Ribeira Belt, Southeastern Brazil: New Geochronological and Geochemical Constraints from the São Roque - Açungui Groups. Revista Brasileira de Geociências, v. 30 (1), p. 110-114.

Hasui, Y. 1983. Aspectos geológicos essenciais da seção Caconde-Caraguatatuba e suas implicações na reconstituição da organização e evolução do Pré-Cambriano do leste paulista. Atas 1ª Jornada sobre a Carta Geológica do Estado de São Paulo em 1:50.000. 227-252,

Hasui, Y.; Carneiro, C.D.: Coimbra, A.M. 1975. The Ribeira Folded belt. Revista Brasileira de Geociências, 5, 257-266.

Heilbron, M. & Machado, N.M., 2002. Geochronologia U/Pb do Terreno Oriental: Implicações para a Colagem Brasiliana no Segmento Central na Faixa Ribeira. XLI Congresso Brasileiro de Geociências, Jõa Pessoa, Anais, p. 311

Janasi V.A. 1999. Petrogênese de granitos crustais na Nappe de Empurrão Socorro-Guaxupé (SP-MG): uma contribuição da geoquímica elemental e isotópica. 304 p. (Livre Docência Thesis,. IG/USP).

Janasi, V.A., Vlach, S.R.F., Ulbrich, H.H.G.J., 1993. Enriched-mantle contributions to the Itu granitoid belt, southeastern Brazil: evidence form K-rich diorites and syenites. In: A.N. Sial and V.P. Ferreira (Eds): Proceedings of the workshop MAGMA. Anais da academia Brasileira de Ciências, v. 65 (1), p. 107-118.

Janasi, V.A., Leite, R.J.; Van Schmus, W.R., 2001. U-Pb chronostratigraphy of the granitic magmatism in the Agudos Grandes Batholith (West of São Paulo, Brazil) – implications for the evolution of the Ribeira Belt. Journal of South American Earth Sciences, v. 14, p. 363-376.

Machado N., Valladares C.S., Heilbron M., Valeriano C.M. 1996. U-Pb geochronology of the central Ribeira belt (Brazil) and implications for the evolution of the Brazilian Orogeny. Precambrian Research, v. 79, p. 347-361.

Negri, F.A., 2002. Petrologia das rochas charnockito-graníticas e encaixantes de alto grau associadas na região de São Francisco Xavier, SP. Tese de Doutorado IGCE/UNESP, 404 pp.

Pimentel, M.M, Fuck, R.A., Jost, H., Ferreira Filho, C.F., Araújo, S.M. 2000. The basement of the Brasília Fold Belt and the Goiás Magmatic Arc. In Cordani, U.G, Milani, E.J., Thomaz Filho, A. and Campos D.A (Eds.): Tectonic evolution of South America. Rio de Janeiro, 31st International Geological Congress, p. 195-230

Töpfner, C., 1996. Brasiliano-Granitoide in den Bundesstaaten São Paulo und Minas Gerais, Brasilien – Eine Vergleichende Studie. Münchner Geologische Hefte A17, 258p.

Trouw, R.A.J., Heilbron, M., Ribeiro, A., Paciullo, F., Valeriano, C.M., Almeida, J.C.H., Tupinambá, M., Andreis, R.R., 2000. The central segment of Ribeira Belt. In Cordani, U.G, Milani, E.J., Thomaz Filho, A. and Campos D.A (Eds.): Tectonic evolution of South America. Rio de Janeiro, 31st International Geological Congress, p. 287-310.

Schmidt, R. S., Trouw, R.J., Van Schmus, W.R., 1999. The characterization of a Cambrian (520 Ma) tectonometamorphic event in the coastal domain of the Ribeira Belt (SE Brazil) using U/Pb in syntectonic veins. II South American Symposium on Isotope Geology (Córdoba, Argentina), Actas, p. 363-366.

Vlach, S.R.F., 2001. Microprobe monazite constraints for an early (ca. 790 Ma) Brasiliano Orogeny: The Embu Terrane, Southeastern Brazil. III SAGGI, Comunicaciones, v. 52, p. 72.

Wernick, W., 1998. The pluriserial Ribeira magmatic system 590, SE/S Brazil and Uraguay. Revista Brasileira de Geociências, v. 28, no. 4, p. 533-542.

Wiedemann, C., 1993. The evolution of the early Paleozoic , late to post-collisional magmatic arc of the coastal mobile belt, in the state of Espírito Santo, eastern Brazl. Anais da Academia Brasileira de Ciências, v. 65, p. 162-181.

SHRIMP U-Pb ZIRCON AGES OF GRANITOIDS FROM SOUTHERNMOST BRAZIL: CONSTRAINTS ON THE TEMPORAL EVOLUTION OF THE DORSAL DE CANGUÇU TRANSCURRENT SHEAR ZONE AND THE EASTERN DOM FELICIANO BELT

Frantz, J.C.[1]; McNaughton, N.J.[2]; Marques, J.C.[1]; Hartmann, L.A.[1]; Botelho, N.F.[3] and Caravaca, G.[1]

1. Instituto de Geociências - Universidade Federal do Rio Grande do Sul - Brazil. jose.frantz@ufrgs.br, juliana.marques@ufrgs.br, jose.frantz@ufrgs.br, gcar@portoweb.com.br
2. Centre for Global Metallogeny-University of Western Australia - Australia. nmcnaught@geol.uwa.edu.au
3. Instituto de Geociências-Universidade de Brasília - Brazil. nilsonfb@unb.br

Keywords: U-Pb geochronology, granitoids, shear zones, Dorsal de Canguçu, Dom Feliciano Belt

INTRODUCTION

The Eastern Dom Feliciano Belt (Frantz & Botelho, 2000) is formed by granitic rocks and supracrustal rocks evolved during Neoproterozoic ages. This belt was built in the southermost part of Brazil during the Brasiliano Cycle.

The main geological associations in the Eastern Dom Feliciano Belt developed during a continental collision about 800 Ma (Frantz & Botelho, 2000) and during an intracontinental transpressive period between 658 Ma and 625 Ma that resulted in the building of the Dorsal de Canguçu Transcurrent Shear Zone (DCTSZ). The transcurrent shear zone was active until around 600 Ma as a transtractive environment.

The present paper discusses the U-Pb SHRIMP zircon ages from granitic magmatism associated with the temporal evolution of the DCTSZ in the Eastern Dom Feliciano Belt.

The granitic rocks associated with the transpressive/transtractive periods are separated in two units: Arroio Moinho Intrusive Suite and Cordilheira Intrusive Suite.

The main structures generated during the transpressive period are a steep dipping foliation and a sub-horizontal stretching lineation associated with heterogeneous deformation in the DCTSZ. During the transtractive period the structures evolved to brittle conditions, quartz stretching and mica orientation.

U-Pb isotopic analyses were performed using the SHRIMP II at the Curtin University of Technology, Australia. The procedures used were similar to those detailed by Compston et al. (1992). Common Pb was corrected and composition determined following the model proposed by Cumming & Richards (1975). Errors presented in ages were quoted at ± 2σ. Decay constants used were those suggested by Steiger & Jager (1977).

GEOLOGICAL SETTING

The granitic rocks intruded in the DCTSZ are heterogranular, with K-feldspar phenocrysts and scarce plagioclase. Equigranular textures can be subordinated in some granitoids.

The composition can vary from granodiorites to syenogranites, with a high proportion of monzogranites. The granitic rocks can be separated into two groups: the calc-alkaline granitoids of the Arroio Moinho Intrusive Suite and the crustally derived peraluminous two-mica granites of the Cordilheira Intrusive Suite.

CALC-ALKALINE GRANITOIDS

The calc-alkaline granitoids from the Arroio Moinho Intrusive Suite are composed by quartz, K-feldspar, plagioclase, biotite and amphibole with minor titanite, alanite, magnetite, zircon and apatite. Epidote, chlorite and muscovite are associated with low-temperature reequilibration.

Syn-transpressive intrusions were submitted to higher temperature deformation. The main structures and textures resulted from deformational phases. Solid-state deformation has generated textural changes in different degrees, with production of K-feldspar augen, sometimes surrounded by biotite. Mortar and shadow-pressure textures, disrupted grains, ondulatory extinction and sub-grains formation are common in K-feldspar and plagioclase. Also common are recrystallization and size reduction of quartz and feldspars grains, foliation and stretching lineation developed on the entire intrusion. Grain size reduction, segregation of quartz-feldspathic and mica beds and asymmetrical folds are common in the higher strain zones. Quartz occurs as ribbon aggregates or polygonized aggregates, which resulted from recrystallization of recovered grains. Plagioclase has reactive borders in rocks submitted to higher strain deformation. Biotite and amphibole are oriented according to the foliation. Biotite and feldspar phenocrysts can be oriented accord to the magmatic flow. Foliation can evolve laterally to mylonitic zones, owing to the heterogeneous deformation. The textural features indicate P-T conditions in the high greenschist facies, the main characteristic is the change from brittle to ductile deformation in feldspars which occurs about 450^{0}C to 500^{0}C (Tullis, 1982; Ord & Hobbs, 1989).

Late-transpressive to syn-transtractive intrusions were submitted to lower temperature deformation. Quartz is a stretched and ondulatory extinction mineral and sub-grains and new grain formation are common. K-feldspar and plagioclase show mainly brittle fabric. Biotite occurs as oriented grains, or aggregates mainly in the evolved transtractive intrusion.

Magmatic flow structures are defined by the orientation of K-feldspar phenocrysts, amphibole, biotite, dioritic autoliths, and by the increase concentration of phenocrysts and biotite around autoliths and xenoliths. Magmatic flow structures are common in the syn-transpressive intrusions of the calc-alkaline granitoids, similar to the Quiteria Granite. Magmatic flow structures usually evolve to solid-state structures with the same orientation. Late-transpressive and syn-transtrative intrusions are characterized by low concentration of flow structures, probably owing to a progressive decrease of the tensional field during the transcurrence.

PERALUMINOUS GRANITES

The Cordilheira Intrusive Suite (Frantz & Nardi, 1992) is composed by K-feldspar, quartz and plagioclase leucosyenogranites to leucomonzogranites with muscovite, biotite, tourmaline, garnet, apatite and zircon. Chlorite, titanite and hematite result from recrystallization associated to deformation or hydrothermal alteration. Illite and fluorite are hydrothermal only.

The textures are highly variable in each intrusion. Porphyrytic and pegmatitic zones are common and show an increase in the amount of tourmaline, muscovite and magmatic flow structures. These features resulted from local accumulation of a volatile-rich phase.

Syn-transpressive peraluminous granites and higher strain zones show solid-state deformation as recrystallization and reduction of quartz and feldspars grains, ribbon quartz and segregation of mica beds. Quartz aggregates with granoblastic fabric indicate local recrystallization with recover. K-feldspar occurs with ondulatory extinction along grain borders and with patch pertitic exsolution when submitted to recrystallization conditions and grain reduction. Plagioclase has mortar arrangements, rounded grains, and reduction in the grains borders as a consequence of deformation. Muscovite and biotite occur as oriented lamellae along the foliation. Biotite is common in syn-transpressive intrusions whilst muscovite is frequent in more evolved late-transpressive to syn-transtractive intrusions. Muscovite occurs associated here with garnet and quartz, and K-feldspar and tourmaline are more abundant.

Late-transpressive to syn-transtractive peraluminous intrusions show mainly textures with grains indicating brittle fabric. Chlorite and white mica replacing biotite and feldspars are compatible with low greenschist facies P-T conditions for deformation and metamorphism of these granites. Quartz has ondulatory extinction and recrystallization, with sub-grain and grain formation. Magmatic flow structures are common in these intrusions and are defined by orientation of tourmaline, muscovite and K-feldspar. The differentiation in the peraluminous granites occurred associated with an increase in the volatile contents implicating in an increasing volume of muscovite, tourmaline, greisens, tourmalinites and pegmatitic zones.

The extensive formation of segregated mica beds during the mylonitic deformation (Frantz et al., 1984; Frantz & Remus, 1986) on the peraluminous granites of the Cordilheira Intrusive Suite is probably related to their compositional characteristics and higher fluid amount present in these granites (White et al., 1980; Ramsay, 1982).

TEMPORAL EVOLUTION OF THE DCTSZ

The mylonitic deformation generated during the evolution of the transpressive tectonic period can be classified as a heterogeneous deformation. It developed a steep dipping foliation and sub-horizontal stretching lineation, with a NE-SW mass transport, parallel to the elongation of the Dom Feliciano Belt (Frantz et al., 1984; Jost et al., 1984; Fernandes et al., 1989).

The transcurrent tectonic regime (Frantz et al., 1984) was responsible for parallel dislocations along the belt (Jost et al., 1984). This mechanism controlled the calc-alkaline granitoids and the crustal melted granite injections of the Arroio Moinho Intrusive Suite and the Cordilheira Intrusive Suite, and also the intrusions of mafic dykes (Frantz & Remus, 1986). Additionally, geological units of different ages, structural and metamorphic evolution were placed in contact at the same stratigraphic level (Frantz & Botelho, 2000).

Geologic features observed in the mylonitic zones are equivalent to a peak of greenschists facies metamorphic conditions. Development in a large scale of white mica, stable biotite and garnet paragenesis, and the deformational characteristics of the syn-transpressive granitoids are consistent with that P-T condition.

The studied granitoids were intruded during the tectonic evolution of the DCTSZ and represent syn- to late-transpressive intrusions, transitional intrusions and syn-transtractive intrusions. The granitoids that characterize the beginning of the transpressive period are the calc-alkaline intrusions of the Arroio Moinho Intrusive Suite. The granites that are the best examples of the evolutionary history of the transpressive period, transition period and transtractive period up to the end of transcurrent tectonic regime are the crustal melted peraluminous granites from the Cordilheira Intrusive Suite. The intrusions selected to constrain the evolution of the transcurrent shear zones are the Quiteria Granite from the Arroio Moinho Intrusive Suite, and the Francisquinho, the Cordilheira, the Cerro Agudo and the Figueiras granites from the Cordilheira Intrusive Suite.

The beginning of the transpressive period corresponds to the intrusion of the first calc-alkaline granitoid, the Quiteria Granite. The emplacement of this granite occurred during the peak of the deformation. The U-Pb SHRIMP age of 658 ± 4 Ma to the Quiteria granite represents a concordia plot of 13 analytical results (Fig. 1).

The tectonic evolution of the transcurrent shear zones was recorded by the emplacement of the calc-alkaline granitoids from the Arroio Moinho Intrusive Suite until the end of this evolution. However, the crustal melted peraluminous granites from the Cordilheira Intrusive Suite are the best markers for the evolutionary history of the DCTSZ. Biotite-muscovite granites represent the first intrusions. The evolution of the granitic rocks from the Cordilheira Intrusive Suite follow the evolution of the transcurrent tectonic regime with the emplacement of increasingly evolved granitic intrusions showing progressively lower temperature deformation. These granites indicate changes that occurred during the evolution of all transcurrent tectonic activity, from a transpressive deformational condition, through a transitional period and a final evolution of a transtractive period. Muscovite-tourmaline granites are the last intrusions.

The first intrusions of biotite-muscovite granites occurred under transpressive conditions, resembling the Francisquinho Granite. The U-Pb SHRIMP age of 634 ± 6 Ma to the Francisquinho Granite represents a concordia plot of 10 analytical results (Fig. 2).

The transition from transpressive period to transtractive period was defined by the attenuation of the ductile deformation with a progressive development of brittle features (Frantz & Fernandes, 1994). The emplacement of the Cordilheira Granite represents the beginning of the transition from the transpressive period to the transtractive period. The evolution of this change is characterized by the intrusion of the Cerro Agudo Granite. The U-Pb SHRIMP age of 625±6 Ma to the Cordilheira Granite represents a concordia plot of 12 analytical results (Fig. 3). The U-Pb SHRIMP age of 617±8 Ma to the Cerro Agudo Granite represents a concordia plot of 12 analytical results (Fig. 4). These two granitic intrusions represent a transition about 8 Ma from a transpressive to a transtractive period in the DCTSZ evolution.

The clearly transtractive period defined in the DCTSZ evolution is characterized by the emplacement of the Figueiras Granite. Its structural and textural aspect exemplifies a typical brittle deformation. The U-Pb SHRIMP age of 605±8 Ma to the Figueiras Granite represents a concordia plot of 12 analytical results (Fig. 5).

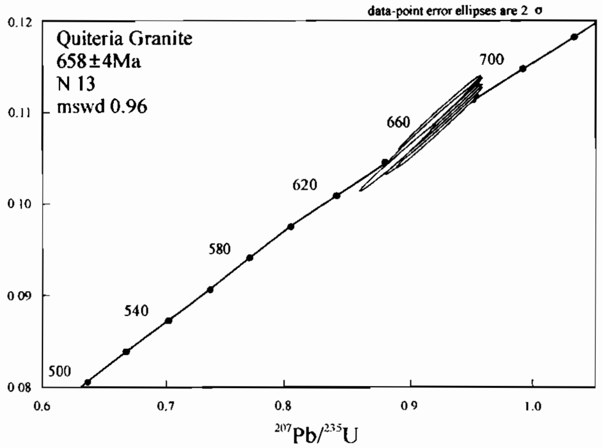

Figure 1. Quiteria Granite Concordia plot representing the highest strain under transpressive conditions and the first syn-transpressive granitic intrusion in the DCTSZ.

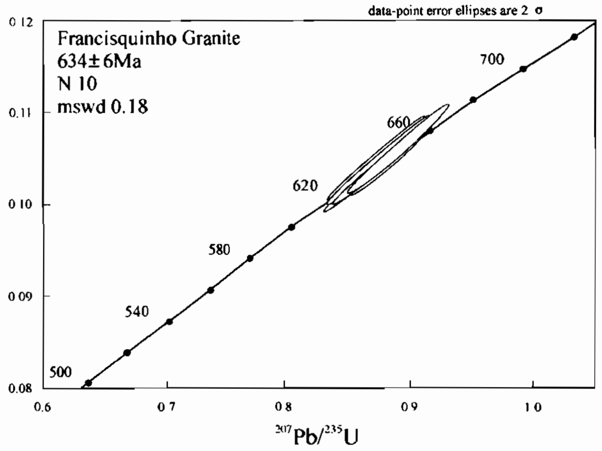

Figure 2. Francisquinho Granite Concordia plot represents the first syn-transpressive peraluminous crustal melted intrusion in the DCTSZ under transpressive conditions.

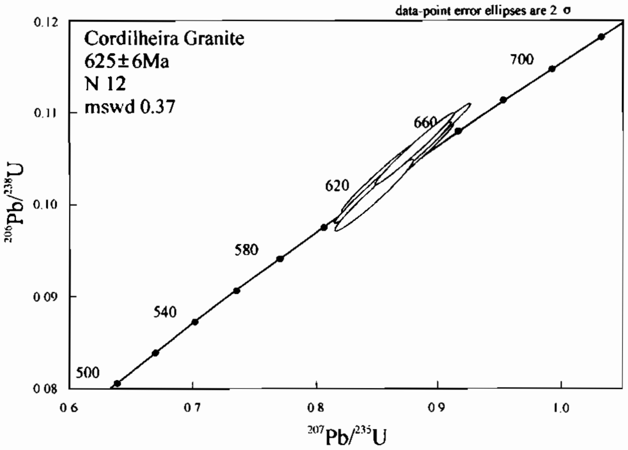

Figure 3. Cordilheira Granite Concordia plot representing the first register of the transition from transpressive to transtractive conditions in the DCTSZ.

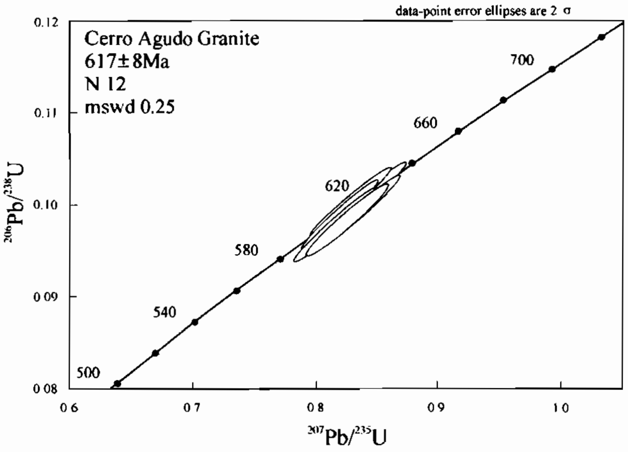

Figure 4: Cerro Agudo Granite Concordia plot representing the evolution of the transition from transpressive to transtractive conditions in the DCTSZ.

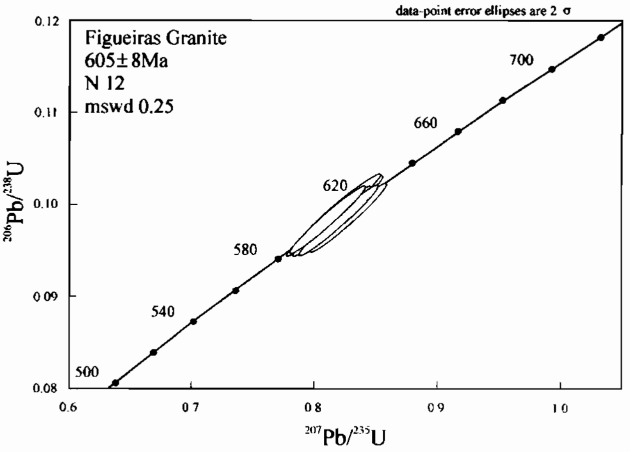

Figure 5. Figueiras Granite Concordia plot represents a transtractive condition to the DCTSZ.

CONCLUSIONS

The geochronological relationships between a variety of granitic intrusions, with emplacement controlled by the action of transpressive and transtractive periods in the DCTSZ evolution, have some implications that must be considered in any evolutionary or tectonic model for the Brasiliano Cycle in southernmost Brazil, particularly, for the Eastern Dom Feliciano Belt.

The U-Pb SHRIMP data for the granitic intrusions related with the DCTSZ denote the existence of an intracontinental trascurrent tectonic activity from 658 to 605 Ma. This tectonic activity was active over 50 m.y. and does not comprise the continental collision that preceded the transcurrence.

The processes involved in the generation of the crustal melted peraluminous granites were active during the last 30 m.y. of the transcurrent tectonic regime, from 634 to 605 Ma.

The first record of the crustal melted granites occurred 20 m.y. after the beginning of the transpressive period. The reasons for that can be related with the necessity of additional thermal gradients. It occurred only after a significant volume of calc-alkaline granitoids had been intruded in the transcurrent shear zones.

Moreover, the crustal melted granites had their main volume intruded during the tectonic mitigation phase in the DCTSZ. It can be perceptible by the end of the transpressive period and by the transition to the transtactive period. During that transition, the decreasing of pressure represented the most important mechanism that controlled the crustal melting. It can be confirmed by the deformational history (changes in type and intensity) correlated with the ages of the Cordilheira, the Cerro Agudo and the Figueiras granites.

ACKNOWLEDGMENTS

Supported by the Fundação de Amparo à Pesquisa do Estado do Rio Grande do Sul through research grant 01/07510.

REFERENCES

Compston, W.; Williams, I. S.; Kirschvink, J. L.; Zhang, Z. C.; Ma, G. G. 1992. Zircon U-Pb ages for the Early Cambrian time scale. J.Geol.Soc. (London) 149: 171-184.

Cumming, G. L. & Richards, J. R. 1975. Ore lead isotope rations in a continuously changing Earth. Earth Planet. Sci. Lett. 28: 155-171.

Fernandes, L. A. D.; Tommasi, A.; Porcher, C. C.; Marques-Toigo, M.; Guerra-Sommer, M.; Piccoli, A. E. M. 1989. Mapa Geológico de Parte das Folhas de Quitéria e Várzea do Capivarita-RS. Porto Alegre, IG/UFRGS. (Série Mapas).

Fernandes, L. A. D.; Tommasi, A.; Porcher, C. C. 1990. Esboço Estrutural de Parte do Batólito Pelotas - Região de Quitéria-Capivarita. Estudos Tecnológicos, v. XIII. Acta Geol. Leopold., 30: 117-138.

Frantz, J. C. & Remus, M. V. D. 1986. Geologia da Região de Canguçu - Torrinhas, RS - Caracterização Petrográfica, Estrutural e Estratigráfica. In: Cong. Bras. Geol., 34. Goiânia, 1986. Anais..., Goiânia, S.B.G. v. 2, p. 931-948.

Frantz, J. C. & Nardi, L. V. S. 1992. O Magmatismo Granítico da Região Oriental do Escudo Sul-rio-grandense. Uma Revisão. Pesquisas, 19(2): 183-189.

Frantz, J. C. & Fernandes, L. A. D. 1994. Os Granitóides Tardi a Pós-Orogênicos do Ciclo Brasiliano no Cinturão Dom Feliciano-RS. In: Cong. Bras. Geol., 38. Camboriu, 1994. Boletim de Resumos Expandidos..., Camboriu, S.B.G. v. 1, p. 150-152.

Frantz, J. C. & Botelho, N. F. 2000. Neoproterozoic Granitic Magmatism and Evolution of the Eastern Dom Feliciano Belt in Southernmost Brazil: A Tectonic Model. Godwana Research, 3(1): 7-19.

Frantz, J. C.; Lima, E. F.; Pinheiro-Machado, R.; Naumann, M. P. 1984. Contribuição à geologia da região de Encruzilhada do Sul, RS. In: Cong. Bras. Geol., 33. Rio de Janeiro, 1984. Anais..., Rio de Janeiro, S.B.G. v. 5, p. 2407-2416.

Jost, H.; Frantz, J. C.; Brod, J. A. 1984. Revisão da Tipologia, Cronologia e Significado Geotectônico dos Falhamentos do Escudo Sul-rio-grandense. In: Cong. Bras. Geol., 33. Rio de Janeiro, 1984. Anais..., Rio de Janeiro, S.B.G. v. 3, p. 1707-1720.

Ord, A. & Hobbs, B. E. 1989. The strength of the continental crust, detachment zones and the development of plastic instabilities. Tectonophysics, 158: 269-289.

Ramsay, J. G. 1982. Rock ductility and its influence on the development of tectonic structures in mountain belts. In: Hsu, K. J. ed. Mountain Building Processes. London, Academic Press. p.111-127.

Steiger, R. H. & Jager, E. 1977. Subcommission on geochronology: convention on the use of decay constants in geo- and cosmochronology. Earth Planet. Sci. Lett. 36: 359-362.

Tullis, J. 1982. Deformation of feldspars. In: Ribbe, P.H. ed. Feldspars Mineralogy. Mineralogical Society of America. p. 297-325.

White, S. H.; Burrows, S. E.; Carreras, J.; Shaw, N. D.; Humphreys, F. J. 1980. On mylonites in ductile shear zones. Jour. Struct. Geol., 2: 175-187.

OCEANIC PLATEAU ACCRETION AT 705 Ma IN THE SOUTHERN BRAZILIAN SHIELD

Hartmann, L.A.[1]; Lopes, A.P.[1]; Wang, Y.[2]; Liu, D.[2] and Vasconcellos, M.A.Z.[3]

1. Instituto de Geociências, Universidade Federal do Rio Grande do Sul, Avenida Bento Gonçalves, 9500; 91500-000 Porto Alegre, Rio Grande do Sul, Brazil. leo.hartmann@ufrgs.br
2. Chinese Academy of Geological Sciences, 26 Baiwanzhuang Road, Beijing 100037, P. R. China. liudunyi@public.bta.net.cn.vcf
3. Instituto de Física, Universidade Federal do Rio Grande do Sul, Avenida Bento Gonçalves, 9500; 91500-000 Porto Alegre, Rio Grande do Sul, Brazil. marcos@if.ufrgs.br

Keywords: U-Pb zircon SHRIMP, oceanic plateau, Mina da Palma, southern Brazilian Shield

The difficulty of dating oceanic plateaus accreted to old continents is overcome in this investigation by the use of the sensitive high resolution ion microprobe (Beijing SHRIMP II) for the U-Pb isotopic analyses of zircon crystals from associated chert. We dated two zircon crystals (four analyses) previously separated from 3 kg of chert from the Mina da Palma basalt-limestone-chert association (Strieder et al., 2000). The rocks are part of the juvenile Neoproterozoic Vila Nova Belt (Babinski et al., 1996; Hartmann et al., 2000) in the southern Brazilian Shield (Figs. 1 - 2), and share many geological and geochemical characteristics (e.g., Kent et al., 1996; Kerr et al., 2000; Condie et al., 2002; Kerr, 2003) with oceanic plateaus such as the Kerguelen (Figs. 3, 4), including rock association, juvenile arc setting, incompatible trace element contents of basalts between oceanic island and mid-ocean ridge, lack of Nb anomaly and $La_N/Nb_N < 1.1$ (Lopes & Hartmann, 2003). The association is also comparable to the Neoproterozoic (900 Ma) oceanic plateau described by Stein & Goldstein (1996) in the Arabian-Nubian Shield.

The concordia age of three SHRIMP analyses (Figs. 5 - 6) is 705 ± 2 Ma, and the two analyzed zircon crystals have Th/U ratios = 0.9, Hf = 1.0 wt% and Y = 0.06 wt% (12 electron microprobe analyses). We interpret the data as the age of deposition of chert and consequently of oceanic plateau formation, because the high Th/U ratios and low Hf and Y contents are typical of basaltic or tonalitic zircon. We thus specify the age of the newly discovered Mina da Palma oceanic plateau, a remnant basalt-limestone-chert association in the Neoproterozoic juvenile environment of an old Paleoproterozoic/Archean continent, and demonstrate a procedure for dating old oceanic crust.

REFERENCES

Babinski, M., Chemale, F., Hartmann, L. A., Van Schmus, W. R., Silva, L.C., 1996. Juvenile accretion at 750-700 Ma in southern Brazil. Geology 24, 439-442.

Condie, K. C., 1993. Mantle plumes and their record in earth history. Cambridge University Press, Oxford, UK, 306 p.

Condie, K. C., Frey, B. A., Kerrich, R., 2002. The 1.75-Ga Iron King Volcanics in west-central Arizona: a remnant of an accreted oceanic plateau derived from a mantle plume with a deep depleted component. Lithos 64, 49-62.

Hartmann, L. A., Leite, J. A. D., Silva, L. C., Remus, M. V. D., McNaughton, N. J., Groves, D. I., Fletcher, I. R., Santos, J. O. S., Vasconcellos, M. A. Z., 2000. Advances in SHRIMP geochronology and their impact on understanding the tectonic and metallogenic evolution of southern Brazil. Australian Journal of Earth Sciences 47 829-844.

Kent, R. W., Hardarson, B. S., Saunders, A. D., Storey, M., 1996. Plateaux ancient and modern: Geochemical and sedimentological perspectives on Archaean oceanic magmatism. Lithos 37, 129-142.

Kerr, A. C., 2003. Oceanic Plateaus. Treatise on Geochemistry: Volume 3: Geochemistry of the Earth's Crust (in press).

Kerr, A. C., White, R. V., Saunders, A. D., 2000. LIP reading: Recognizing oceanic plateaux in the geological record. Journal of Petrology 41, 1041-1056.

Lopes, A. P. & Hartmann, L. A., 2003. O platô oceânico Mina da Palma no Cinturão Vila Nova, Bloco São Gabriel, Escudo Sul-riograndense. Pesquisas em Geociências (UFRGS). (Submitted).

Stein, M. & Goldstein, S. L. 1996. From plume head to continental lithosphere in the Arabian-Nubian shield. Nature 382, 773-778.

Strieder, A. J., Roldão, D. G., Hartmann, L. A., 2000. The Palma Volcano-Sedimentary Supersuite, Precambrian Sul-Riograndense Shield, Brazil. International Geology Review 42, 984-999.

Sun, S. S. & McDonough, W. F., 1989. Chemical and isotopic systematics of oceanic basalts: implications for mantle composition and processes. Geological Socity of London Special Publication 42, 313-345.

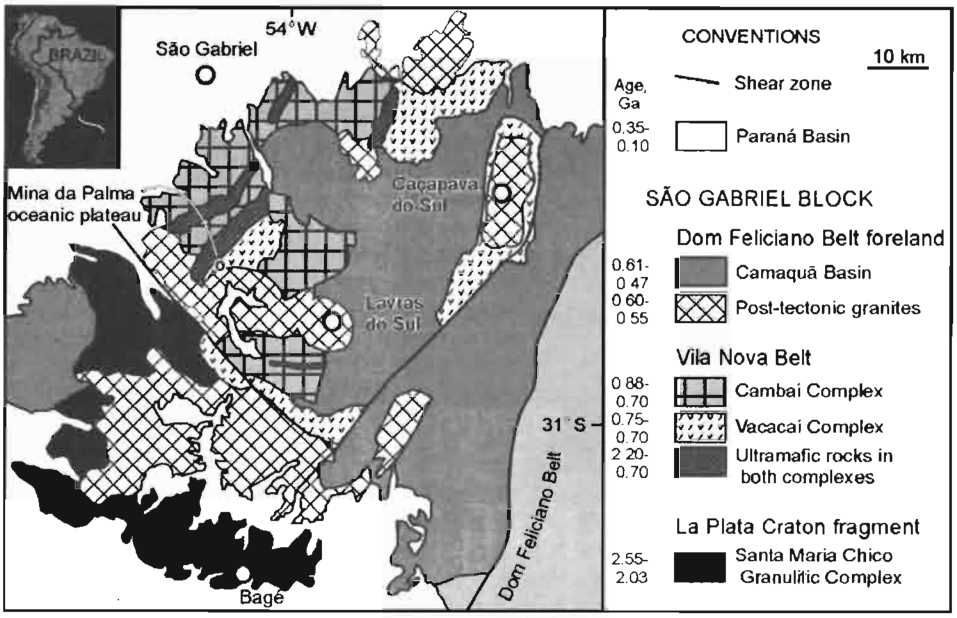

Figure 1. Geological map of the São Gabriel Block, southern Brazilian Shield, showing location of Mina da Palma.

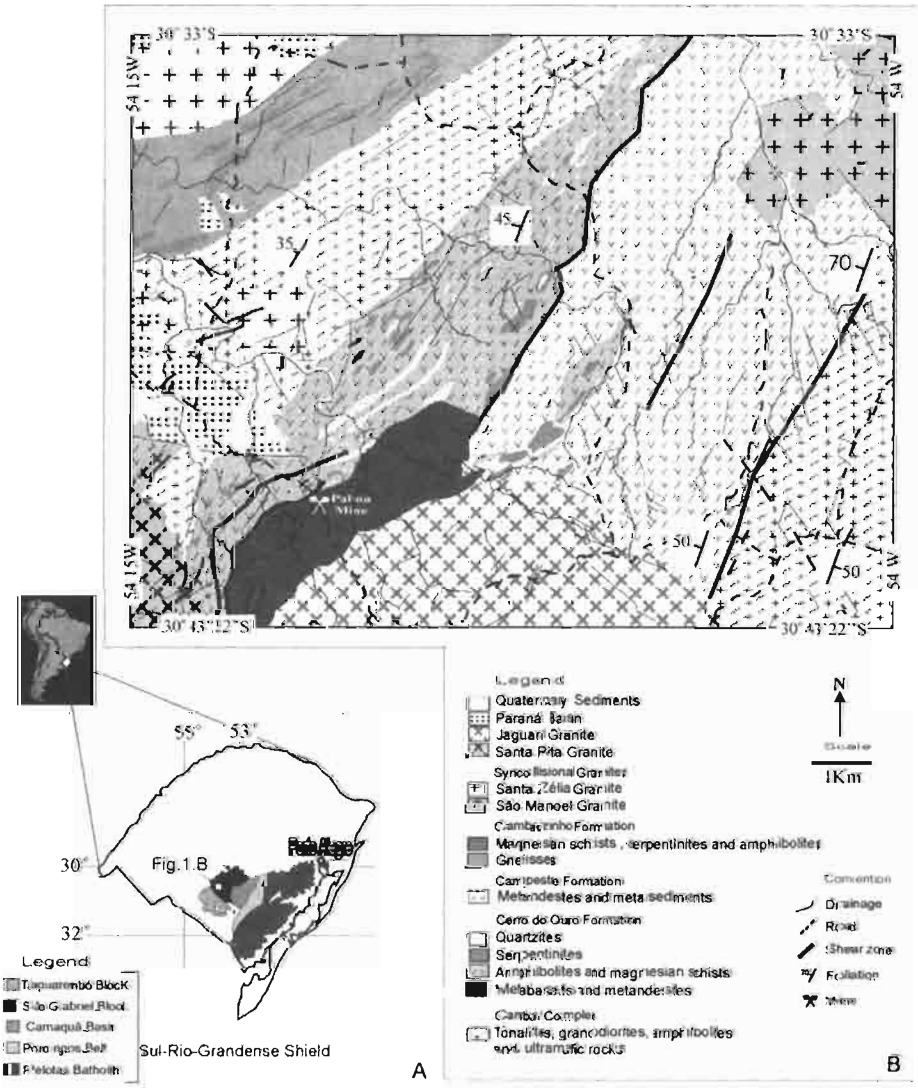

Figure 2. Geological map of Palma Complex, indicating location of Mina da Palma.

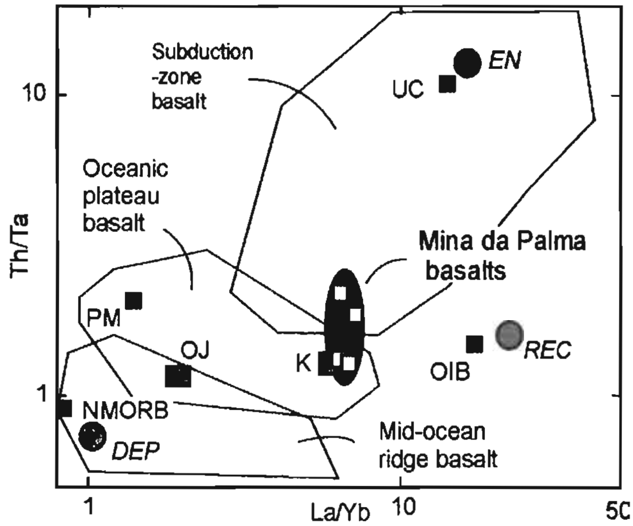

Figure 3. La/Yb x Th/Ta diagram (Condie et al., 2002) of selected, least-altered basalts from the Palma Mine, compared with some other basalt associations. Average compositions shown: subduction zone basalt (SZB); oceanic island basalt (OIB); N-type mid-ocean ridge basalt (NMORB); primitive mantle (PM, Sun & McDonough, 1989); upper crust (UC, Condie, 1993). Hypothetical compositions (Condie et al., 2002): depleted mantle (DEP); recycled slab component (REC); enriched mantle component (EN). Average compositions of oceanic plateaux (Condie et al., 2002): Ontong Java (OJ); Kerguelen (K).

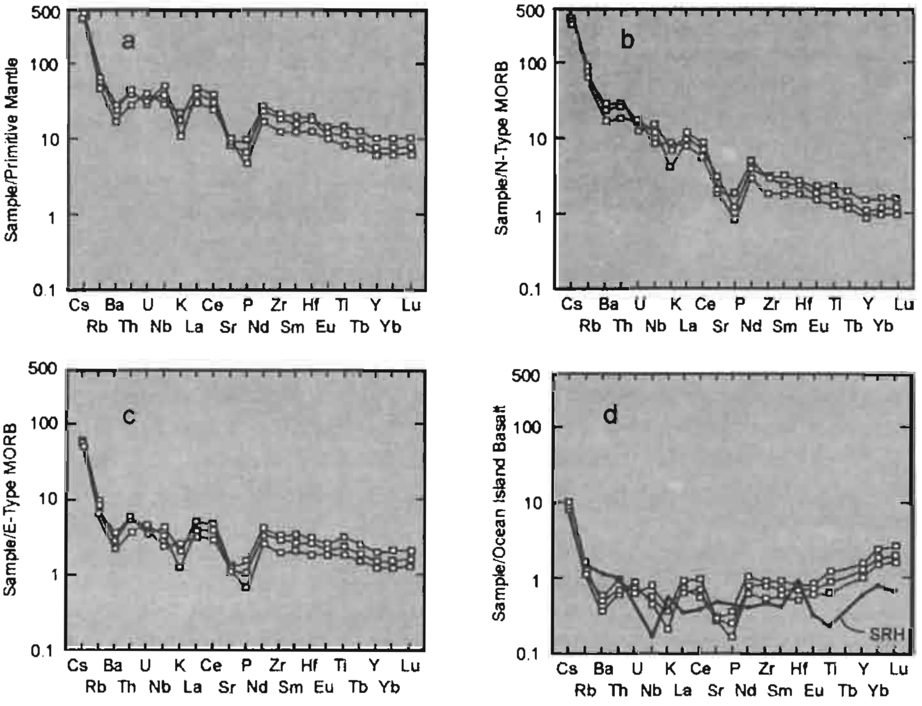

Figure 4. Normalized incompatible element plots of selected, least-altered Palma Mine metabasalts. Normalization values from Sun and McDonough (1989). (a) normalization to primitive mantle; (b) normalization to N-type mid-ocean ridge basalt N(MORB); (c) normalization to E-type mid-ocean ridge basalt (EMORB); (d) normalization to oceanic-island basalt (OIB). In (d), SRH = Strieder, Roldão, Hartmann average of three analyses (Strieder et al., 2000).

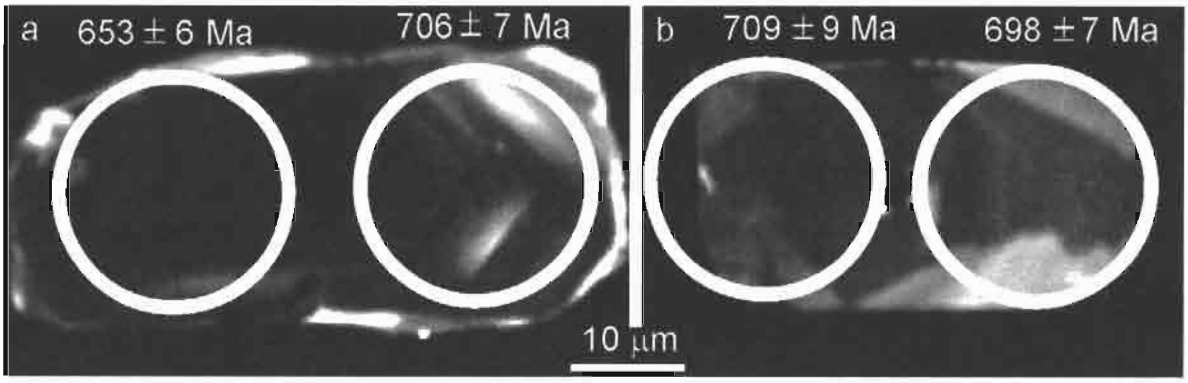

Figure 5. Two zircon crystals from the Mina da Palma chert dated by U-Pb SHRIMP. Four analyzed spots shown as white circles. $^{206}Pb/^{238}U$ ages also indicated.

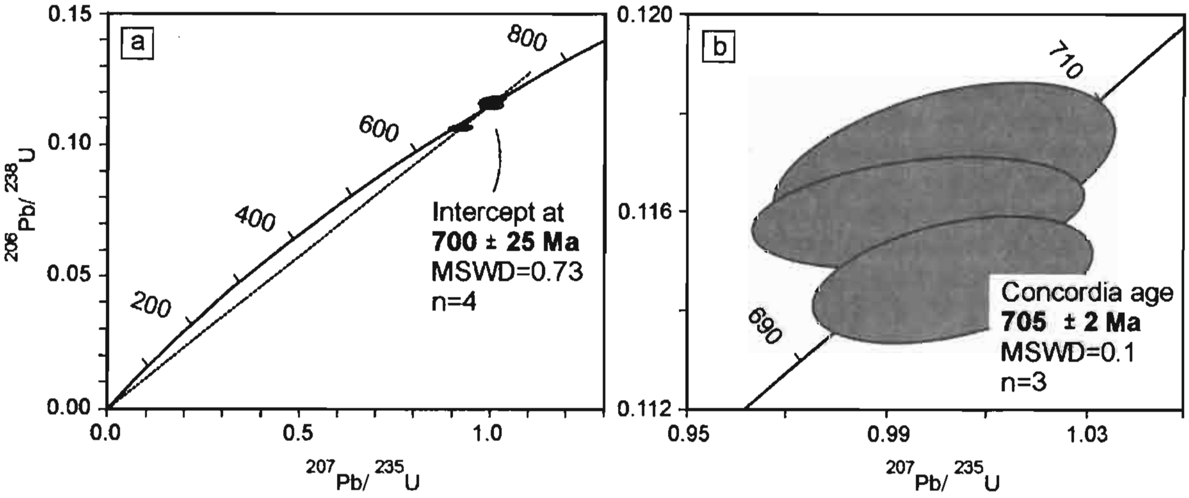

Figure 6. Concordia diagrams of dated Mina da Palma chert zircon crystals.

TIMING OF TERRANE ACCRETION IN THE NEOPROTEROZOIC-EOPALEOZOIC RIBEIRA OROGEN (SE BRAZIL)

Heilbron, M.[1] and Machado, N.[2]

1. Departamento de Geologia Regional e Geotectônica, Faculdade de Geologia,
Universidade do Estado do Rio de Janeiro (UERJ). heilbron@uerj.br
2. Centre de Recherche en Géochimie et Géodynamique – GEOTOP-UQAM-McGill and Départment des Sciences de la Terre et de l'Atmosphère, Université du Québec à Montreal. machado.nuno@uqam.ca

Keywords: Western Gondwana, Ribeira belt, U-Pb

TECTONIC SETTING AND OBJECTIVES

The Ribeira belt of southeastern Brazil occupies a central position in Western Gondwana and is one of the key units for reconstructing the history of this supercontinent. Recent geological data for the central Ribeira belt reveal a complex history with the accretion of a cordilleran arc and the collision of at least two terranes onto the eastern margin of the São Francisco plate (Heilbron et al., 2000; Trouw et al., 2000; Brito Neves et al., 1999). The Oriental terrane is the firstly accreted one and is the locus of the cordilleran magmatic arc (Tupinambá et al., 2000) that collided with the São Francisco Plate at ca. 580 Ma. Compared to the other tectonic terranes of the belt, very few geological and geochronological data have been reported for the Oriental Terrane, especially concerning the region of the Rio de Janeiro State. This contribution presents new ID-TIMS U-Pb isotopic data, which combined with detailed geological data support the proposed tectonic evolution of the central segment of the Ribeira belt. Finally, a comparison with the other terranes of the belt and the role of this terrane within the Western Gondwana amalgamation are discussed.

TECTONIC ORGANIZATION OF THE ORIENTAL TERRANE

The Oriental terrane can be subdivided into three tectonic domains: the Cambuci domain, the Costeiro domain and the Italva klippe (Fig 1). The Cambuci domain represents the basal thrust sheet of the Oriental terrane at the Northern portion of the Rio de Janeiro State. The Costeiro domain overrides the Cambuci domain and the Occidental terrane. The Italva klippe represents the uppermost thrust slice of the Oriental terrane and overrides the Costeiro domain

LITHOLOGICAL UNITS

The lithological associations of the three structural domains of the Oriental terrane are presented on Table 1. Analyzed samples are also pointed with bold letters on this table.

Table 1. Lithological associations of the Oriental Terrane.

	Major lithological associations of the Oriental terrane		
Rock type	**Cambuci domain**	**Costeiro domain**	**Italva klippe**
Non-foliated granitoids	Leucogranites	Dikes of Favela granite (**g**) Pedra Branca granite (**f**) and similar granites	Leucogranites
Late-collisional slightly foliated granitoids		Serra dos Órgãos granodiorite Bela Joana and Ilha Grande charnockites and charno-enderbites	
Syn-collisional foliated granitoids	Leucosomatic veins and diatexites (**e**)	"Facoidal" augen gneiss (**d**) Leucogneiss	Leucosomatic veins
Foliated granitoids of unknown stratigraphic position	Tonalites, charnockites, porphyritic granites and leucogranites	Angelim hornblende biotite tonalite	Italva hornblende biotite gneiss
Pre-collisional foliated granitoids	---------------------	Rio Negro tonalitic to dioritic ortho-gneisses (**b, c**)	
Metasedimentary Successions	Sill-garnet-biotite banded gneisses with marble, gondite and calcsilicate layers	Biotite gneiss and kinzigitic gneiss (**i**) with quartzitic and calcsilicatic layers	Biotite gneisses, marbles interlayered with amphibolites (**a**)

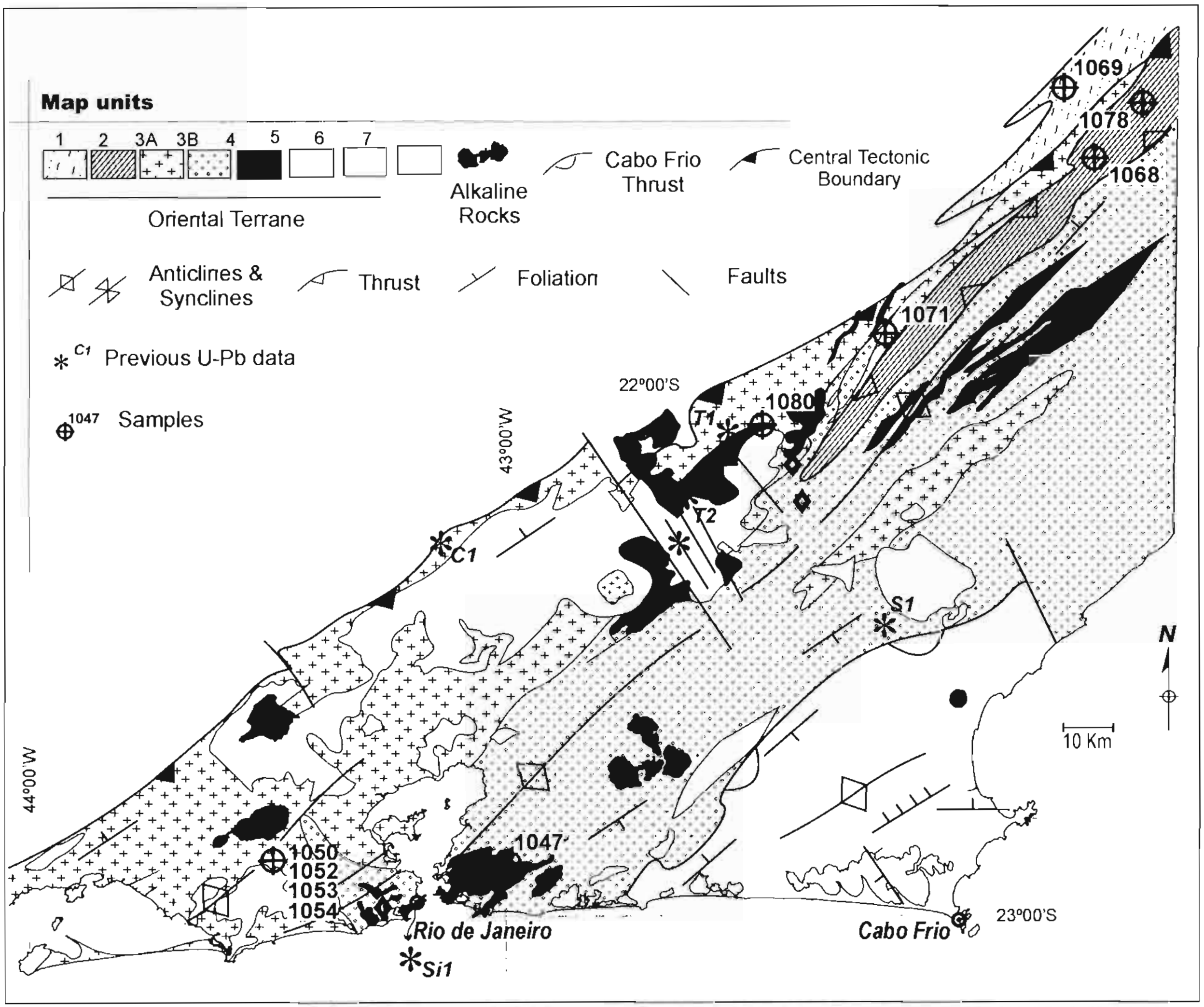

Figure 1. Tectonic Map of the Oriental Terrane, subdivided in the Cambuci, Costeiro and Italva domain. Sample locations are represented by numbered dots. Asterisks with lettered symbols present previous U-Pb data, T-Tupinambá, 1999; S-Schmitt, 2000; Si- Silva et al., 2000. 1- Metasediments of the Cambuci klippe; 2 Metasediments and amphibolites of the Italva klippe; 3a- arc-related granitoids and 3b-Metasediments and (Rio Negro complex) of the Costeiro domain 4- Syn-collisional granitoids related to the 590-550 Ma orogeny; 5- Late-Syn-collisional granitoids related to the 530- 490 Búzios Orogeny; 6- 490-480 Ma late-tectonic granitoids; 7- Cabo Frio Terrane.

ANALYTICAL TECHNIQUES

Samples were crushed and pulverized with standard equipment under clean conditions and the heavy minerals concentrated by panning at the Laboratório de Preparação de Amostras (LOPAG) of the Ouro Preto Federal University, Minas Gerais. The heavy mineral concentrates were passed through a Frantz magnetic separator to extract monazite, sphene and zircon. Zircon was further separated into four magnetic and two diamagnetic fractions, the latter being preferred for hand picking. Following the procedure of Krogh (1982), most of the analyzed zircon fractions were abraded between ~72 h and 120 h. Mineral dissolution, chemical extraction of U and Pb, and mass spectrometric analyses were carried out following the procedures described in Machado et al. (1996). Total procedural blanks average were 10 pg for Pb and 2 pg for U for zircon analyses and 15 pg for Pb and 5 pg for U for sphene and monazite analyses. The uncertainties in isotopic ratios were calculated with an error propagation program that takes into consideration the analytical precision of the measured isotopic ratio. Regressions were calculated and concordia diagrams plotted using the Isoplot-Ex Version 2 (Ludwig, 2000). Errors are represented at the 1σ level but all ages are quoted at the 95% confidence interval.

RESULTS

We selected to analyses the most important magmatic episodes, as well as some of the metasedimentary units. The complete data set is to be found in Heilbron & Machado (2003, in press). The results are summarized below.

BASIC MAGMATISM

a) Three zircon fractions of an amphibolite layer within the carbonatic rocks of the Italva domain yelded a discordia with an upper intercept (UI) at 848 ± 11 Ma, and a lower intercept (LI) at 500 ± 7 Ma. One zircon fraction analysis is concordant (CA) at 501 ± 7 Ma.

PRE-COLLISIONAL MAGMATISM AND METAMORPHIC OVERPRINT

b) Five fractions, including one single and one monazite of a tonalitic gneiss of the Rio Negro Complex, located at Rio de Janeiro city, resulted in a discordia with an UI of 792 ± 12 Ma and a LI 493 +6/-5 Ma. One zircon and monazite grain yelded concordant analysis at, respectively, 792 ± 2 Ma and 494 +6/-5 Ma. Two other discordant zircon fractions gave 207Pb/206Pb minimum ages of 808 Ma and 733 Ma.

c) Three zircon fractions of another tonalitic gneiss located nearby the Cantagalo town yelded a discordia with an UI of 633 ± 5 Ma. One fraction of large prismatic zircons is discordant, with a ^{207}Pb/^{206}Pb age of 845 Ma, similar to the age of the amphibolite of the Italva association.

OROGENIC MAGMATIC EPISODES

Syn-collision I magmatism:

d) Several analyses of the Facoidal augen gneiss result on a discordia with UI of 578 ± 19 Ma. Other fraction is discordant and indicates inheritance components (^{207}Pb/^{206}Pb ages of 600, 634, 643, 702 and 967 Ma). A single monazite grain is concordant at 552 ± 2 Ma, indicating the metamorphic overprint.

e) A Leucogneiss lense within the tonalites of the Rio Negro Complex resulted in a discordia with an UI of 576 ± 2. One monazite grain is concordant at 571 +14/-15 Ma, and another zircon is concordant at 612 ± 15 Ma, suggesting inheritance from arc rocks.

Post-collision I and syn-collision 2 magmatism:

f) The Pedra Branca leucogranite yielded a discordia with an UI of 513 ± 5 Ma. Discordant zircons yelded ^{207}Pb/^{206}Pb minimum ages of 524 and 579 Ma, also suggesting some degree of crustal contamination.

Post-collision 2 Magmatism:

g) A granitic dike of the Favela suite, in the Costeiro domain, yelded two concordant fractions at 484 +9/-11 Ma and 480 +8/-7 Ma, (482 ± 6 Ma mean)

METAMORPHIC AGES OF THE METASEDIMENTARY SEQUENCES

h) A leucosomatic vein of the high-grade pelitic gneisses of Cambuci Domain resulted in a discordia with an UI of 623 ± 5 Ma, probably reflecting an inheritance component from the Rio Negro arc.

i) The garnet gneiss of Costeiro domain resulted on a discordia with UI of 576 +20/-21 Ma, with a concordant analysis of 573 +21/-20 Ma. Contrasting with the other granitoid rocks of the Oriental terrane, discordant fractions gave ^{207}Pb/^{206}Pb minimum ages of 665 and 1906 Ma, suggesting the participation of a Paleoproterozoic crust. The obtained results are consistent with unpublished ^{207}Pb/^{206}Pb laser-ablation ICPMS data for detrital zircons of quartzites interlayered with the pelitic gneiss.

DISCUSSIONS

The data presented in this work, together with previous field, structural, geochemical and other geochronological data (Heilbron, et al. 1995, 2000; Machado et al., 1996; Schmitt, 2000; Tupinambá et al., 2000) suggest that the Ribeira belt may have evolved through the following stages (Fig 2)

1) Although no ocean floor has been recognized in the central sector of the belt, the occurrence of MORB-type magmatism as the oldest magmatic event is compatible with the existence of an ocean between the São Francisco margin and the Oriental Terrane at ca. 848 Ma. This age is similar to the 816 ± 72 Ma Sm-Nd isochron age for a unit interpreted to represent ocean floor in the Araçuaí Belt (Pedrosa-Soares et al., 1998). Thus, break-up of a former supercontinent, generally admitted to have occurred at ca. 900 Ma based in part on the age of mafic dikes of the São Francisco craton (e.g. Machado et al., 1989), was followed by the generation of ocean floor between the craton and a continental landmass to the east between ca. 848 Ma and ca. 790 Ma, the age of the oldest arc rocks.

2) Convergence between the eastern continent (Oriental terrane) and the São Francisco craton led to eastward subduction and the formation of one or more arc complexes starting at ca. 790 Ma. The main Rio Negro arc complex would have been generated in the 640-620 Ma interval and possibly lasted until ca. 590 Ma when collision with the São Francisco margin was initiated.

3) Collision of the Oriental terrane with the São Francisco margin led to the reactivation of the basement associated with north-westward thrusting of foreland crustal blocks, and to the generation of granitoids and of the main structures (the main foliation and large-scale D2 recumbent folds) in the Oriental terrane, between 590 Ma and 550 Ma.

4) Continued convergence led to the first Cambrian event represented in the central Ribeira belt: the development of major dextral transcurrent faults and associated metamorphism in the foreland thrust complexes at 540-520 Ma. Partially overlapping in time, the collision of the Cabo Frio terrane with the already accreted Oriental terrane occurred during the Cambrian-Ordovician at 530-490 Ma and generated granitoids as young as Lower Silurian (Schmitt, 2000).

5) East-vergent late deformational and post-collisional granitoids may represent the collapse of the orogenic building (ages < 510 Ma).

ACKNOWLEDGEMENTS

Field work was financed through Faperj, Cnpq, and CT-PETRO/FINEP grants to M. Heilbron, who also acknowledges a Post-doctoral grant (1032/99-2) from CAPES (Brazilian Ministry of Education) to support her stay in Canada. A Natural Sciences and Engineering Research Council of Canada research grant to N. Machado financed the analytical work at UQAM. FCAR

(Québec) and NSERC (Canada) support the UQAM geochronology facility. We also acknowledge the technical support of R. Lapointe whose steadfast dedication made this work possible. The authors are also indebted to the TEKTOS group of the Universidade Estadual do Rio de Janeiro (M. Tupinambá; B. Duarte, C. Valeriano, C. Valladares, C. D. Ragatky, J. Almeida, L. G. Eirado Silva and J. R. Nogueira) for the last ten years of hard field work, scientific cooperation and stimulating discussions.

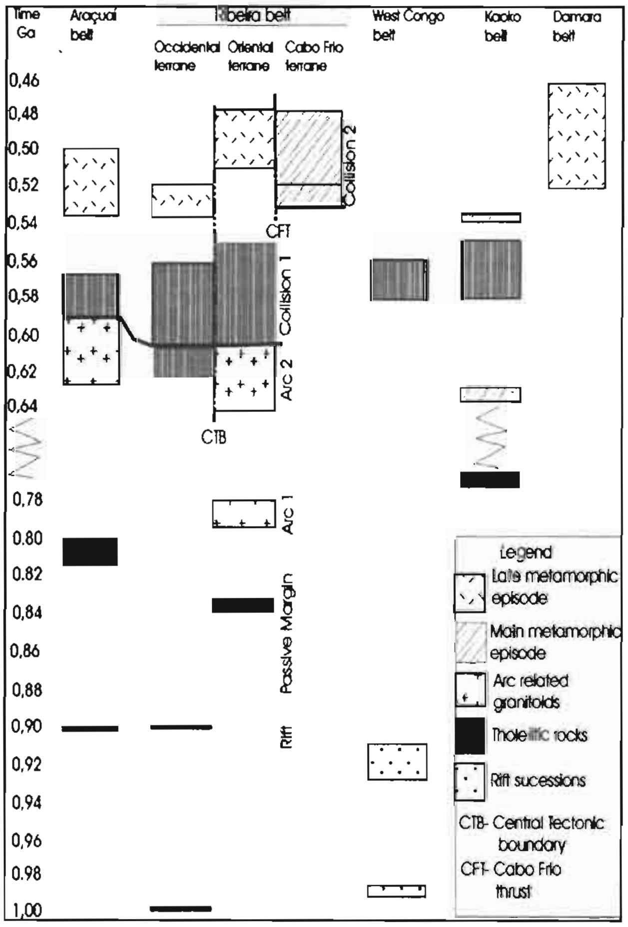

Figure 2. Schematic time-space diagram with the major events recorded at the different terranes of the Ribeira belt. Only U-Pb data were compiled and combined with the data presented in this work. Data from West Congo and Kaoko belts are shown for comparison. Data from: Cordani et al., 1973; Machado et al., 1996; Seth et al., 1998; Solner et al.1991; Tupinambá 1999; Luck Tack et al., 2000; Pedrosa Soares et al., 2000; Schmit, 2000; and this paper).

REFERENCES

Almeida, F.F.M. et al. 2000. The origin and evolution of the South American Platform Earth-Science Reviews 50, 77-111.

Brito-Neves, B.B., Campos-Neto, M.D., Fuck, R.A., 1999. From Rodinia to Western Gondwana: An approach to the Brasiliano-Pan African Cycle and orogenic collage. Episodes 22(3): 155-166.

Cordani, U.G., Delhal, J., Ledent, D., 1973 Orogenéses Superposées dans Le Precambrien du Brésil Sud-Oriental (États de Rio de Janeiro et de Minas Gerais). Revista Brasileira de Geociências, 3: 1-22

Heilbron, M. & Machado, N. 2003 (in press) Timing of terrane accretion in the Neoproterozoic-Eopaleozoic Ribeira orogen (SE Brazil). Precambrian Research.

Heilbron, M. et al., 2000 From Collision to Extension: The Roots of the Southeastern Continental Margin of Brazil. IN: Atlantic Rifts and Continental Margins, Talwani & Mohriak eds. , 354ps. Geophysical Monograph Series, V 115, p:

Krogh, T.E., 1982 Improved accracy of U-Pb zircon dating by selection of more concordant systems using a hugh gradient magnetic separation technique. Geochemica and Cosmochemica Acta, 46: 631-635.

Ludwig, K.L., 2000. Users manual for Isoplot/Ex v. 2.3. A geochronological toolkit for Microsoft Excel. Berkeley Geochronology Center Special Publication No. 1a. Berkeley, California.

Machado, N., Valladares, C.S.; Heilbron, M., Valeriano, C.M., 1996. U-Pb Geochronology of Central Ribeira belt, Prec. Res., 79, 347-361.

Pedrosa Soares, A.C.; Vidal, P.; Leonardos, O.H.; Brito-Neves, B.B., 1998. Neoproterozoic oceanic remnants in eastern Brazil: further evidence and refutation of an exclusively ensialic evolution for the Araçuaí-West Congo orogen. Geology 26(6):519-522

Schmitt, R.S. et al. 1999. The characterization of a Cambrian (~ 520 Ma) tectono metamorphic event in the Costeiro domain of the Ribeira belt, using U/Pb in syn-tectonic veins. Boletim Geologico Minero Argentino 34, 363-366.

Seth, B.; Kröner, A.; Mezger, K.; Nemchin, A.A.; Pidgeon, R.T.; Okrusch, M, 1998. Archaean to Neoproterozoic magmatic events in the Kaoko belt of NW Namibia and their geodynamic significance. Precambrian Res. 92:341-363

Tack, L.; Wiggate, M.D.T.; Liégeois, J.P.; Fernadez-Alonso, M.; Deblond, A, 2001. Early Neoproterozoic magmatism (1000-901 Ma) of the Zadinian and Maymbian Groups (Bas Congo): onset of Rodinia rifting at the western edge of the Congo craton. Precambrian Research 110 (1-4):1-23.

Trouw, R.A. J. et al. 2000. The central segment of the Ribeira belt, in: U.G. Cordani, E.J. et al. (Eds), Tectonic Evolution of South America, 854 p. 31st International Geological Congress, Rio de Janeiro, 287-310.

Tupinambá, M. et al. 2000. Neoproterozoic Western Gondwana assembly and subduction-related plutonism: the role of the Rio Negro Complex in the Ribeira Belt, Southeastern Brazil. Revista Brasileira de Geociências 30, 7-11.

A PALEOPROTEROZOIC OROGEN REWORKED WITHIN THE NEOPROTEROZOIC RIBEIRA BELT, SOUTHEASTERN BRAZIL

Heilbron, M.[1]; Machado, N.[2,3]; Simonetti, A.[2] and Duarte, B.P.[1]

1. TEKTOS–Geotectonics Study Group, Universidade do Estado do Rio de Janeiro, Rua São Francisco Xavier 524/4006-A, Rio de Janeiro, RJ, 20559-900, Brazil. Tel/Fax: ++55-21-2254-6675. heilbron@uerj.br, biapasc@uerj.br
2. Centre de Recherche en Géochimie et Géodynamique (GEOTOP-UQAM-McGill), Université du Québec à Montréal. simonetti.antonio@uqam.ca
3. Département des Sciences de la Terre et de l'Atmosphère, Université du Québec à Montréal, CP 8888, Succ. Centre-Ville, Montréal, QC, H3C 3P8, Canada. machado.nuno@uqam.ca

Keywords: Paleoproterozoic, basement, ICPMS-Laser ablation, ID-TIMS U-Pb data

INTRODUCTION AND TECTONIC SETING

The external portion of the Paleoproterozoic Orogen is well constrained at eastern border of the São Francisco craton (Machado et al., 1996; Alkmin & Marshak, 1998; Teixeira et al., 2000). The Paleoproterozoic belt is also called the Mineiro belt and was built during the Transamazonian Cycle (ca. 2.2-1.9 Ga). As previously described, the orogen is characterized by a passive margin sequence (Minas Supergroup) that began deposition at ca. 2.5 Ga along the Archaean continental margin. Both sequences were deformed as a thrust and fold belt vergent to northwest between 2.125-2.0 Ga. Pre-collisional rocks have ca. 2.2 Ga and late granitoids ca. 1.9 Ga. Dome-and-keel structures have been described as the effects of the orogenic collapse at 2.095 Ga, at the Iron Quadrangle region (Alkmin & Marshak, 1998). A molasse succession (Sabara formation) overlays the passive margin sequence and is supposed to be deposited within a foreland tectonic setting, with contribution of the orogen at that time (Machado et al., 1996).

The internal domain of the Paleoproterozoic (Tranzamazonian) belt is exposed futher north, at the northeastern segment of the São Francisco craton, at Bahia state (Teixeira et al., 2000) and as tectonic slices disrupted and reworked during the Neoproterozoic tectonic episodes of the central Ribeira belt (Heibron et al., 2000, 2003).

In spite of the high metamorphic grade and deformation, the combination of detailed geological mapping and geochronology allow the distinction between basement and cover within the high grade gneisses and granulites that outcrop within the central Ribeira belt (Heilbron et al., 2000). This paper reports new LA-ICPMS and ID-TIMS from pre-1.8 Ga basement associations of the Occidental terrane and combined the data with the available geochemical and geological data. The discussion of the data addresses to important questions related to the internal portions of the Transamazonian orogen, that now are hidden within the Ribeira belt.

CENTRAL RIBEIRA BELT: TECTONIC ORGANIZATION

The TEKTOS/UERJ research group has recently reviewed the proposed structural organization of the central segment of the Ribeira belt (Heilbron et al., 2000; Trouw et al., 2000) within four different tectono-stratigraphic terranes progressively accreted to the São Francisco margin. From NW to SE, these terranes are: a) the reworked margin of the SFC, defined as the Occidental Terrane; b) The Paraíba do Sul Klippe that overthrusts the Occidental Terrane c) the Oriental (Costeiro or Serra do Mar) Terrane that probably includes another cratonic block or microplate (Campos Neto & Figueiredo, 199) and is the locus of the Ribeira magmatic arc (Tupinambá et al., 2000); and d) The Cabo Frio Terrane lately (ca. 520 Ma) accreted to the belt (Schmit et al., 1999). The contact between the Occidental and Oriental terranes is given by a conspicuous NW-dipping shear zone that can be traced continuously for at least 200 km from the coast of São Paulo state to the Serra dos Orgãos region at the Rio de Janeiro state (Central Tectonic Boundary).

BASEMENT ASSOCIATIONS OF THE OCCIDENTAL TERRANE

AUTOCHTHONOUS DOMAIN

The Autochthonous domain borders the southern portion of the São Francisco craton and comprises Archaean and Paleoproterozoic basement complexes overlain by metasedimentary successions in greeschist to amphibolite facies. The basement includes Archaean granite-greenstone belt associations (Barbacena Complex and Rio das Velhas Supergroup), orthogneisses, migmatites and granulites of unknown age but presumed to be Archean (Piedade, Mantiqueira complexes) and Paleoproterozoic granitoids generated during the Transamazonian Cycle (2.2-1.86 Ga; Machado et al., 1992; Machado & Carneiro, 1992; Teixeira et al., 2000). The lower metasedimentary sequence is represented by the São João del Rei rift sucession, and is followed upwards by a carbonatic sequence (Carandaí) and by the Andrelândia passive margin succession (Ribeiro et al., 1995; Trouw et al., 2000). The ages of the youngest detrital zircons limit the maximum age for the deposition of the lower sequence at 1.81 Ga and at 1.0-1.1 Ga for the Andrelândia sequence (Valladares et al., 2001).

ANDRELÂNDIA DOMAIN

The Andrelândia Domain composes the basal allochthonous thrust sheet of the central Ribeira belt and comprises the Mantiqueira basement complex and the

Andrelândia passive margin successions both in amphibolite facies. Map-scale folds of the basement-cover contact, two phases of isoclinal to tight folds related to the developmemnt of the main schistosity and two phases of open to tight subvertical folds are the main structural features of this domain. Detailed structural investigation indicates that the basement association has a more complex tectonic evolution, with at least one older deformational phase.

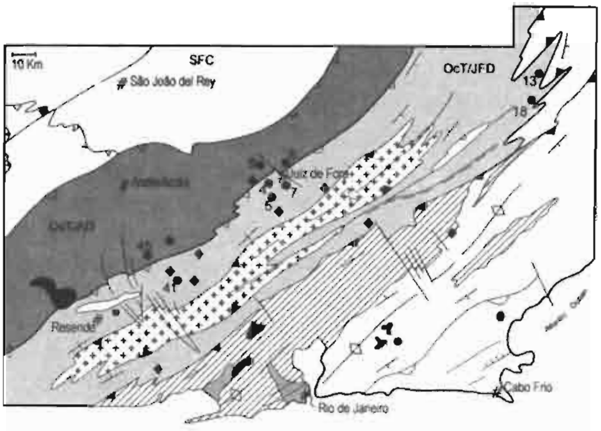

Figure 1. Tectonic map of central Ribeira belt, modified from Heilbron & Machado (2003). Dark gray- Andrelândia domain, Pale gray- Juiz de Fora domain. Filled circles- U-Pb analyses from the basement associations, Filled diamonds- U-Pb data of detrital zircons from the cover rocks.

The Mantiqueira Complex is a very heterogenous unit that comprises calc-alkaline gneiss-migmatitic suites with amphibolitic layers, intruded by granitic plutons and by younger felsic and mafic dykes. Alkaline felsic plutons also intrude the gneisses. Available Rb-Sr data indicate Paleoproterozoic ages and suggest derivation from older Archaean protoliths (Teixeira et al., 2000). The Sm/Nd model ages reported by Fischel et al. (1998), Ragatky et al. (1999) and Bruekner et al. (2000) also suggest reworking of an older Archaean crust (Table 1).

Based on detailed geological and geochemical investigation carried out at the Juiz de Fora region, Duarte (1999) proposed the subdivison of the Mantiqueira complex within four calc-alkaline groups and one very heterogeneous tholeiitic group, listed from the older to the youngest unit: a) tonalitic to granodioritic banded orthogneisses with amphibolites; b) tonalitic to granodioritic weakly foliated orthogneisses; c) tabular sheets and dikes of amphibolite; d) intrusive leucogneisses; and e) augen gneisses of granitic composition clearly intrusive in all above mentioned units. All of the four groups of calc-alkaline orthogneisses are compatible with continental-arc and collisional settings of active tectonic margins. The basic rocks comprise E-MORB ($[La/Yb]_N$ ca. 1.0 – 3.0) and intraplate continental basalts subdivided in the tholeiitic group with lower ($[La/Yb]_N$ ratios ca. 3.5 – 5.0, and an alkaline group with higher $[La/Yb]_N$ ratios ca. 13-18).

JUIZ DE FORA DOMAIN

The Juiz de Fora Domain is defined as an intensely imbricated thrust system that overthrusts the Andrelândia Domain. It is considered a crustal scale duplex (Heilbron et al., 2000). The basement complex is termed the Juiz de Fora Complex and the metasedimentary cover succession is correlated with the Andrelândia passive margin sequence. Both are in upper amphibolite to granulite metamorphic facies.

The Juiz de Fora Complex comprises orthogranulites of a wide compositional range, with a predominance of enderbites and charno-enderbites over charnockites and basic rocks.

The felsic granulites comprise two distinct calc-alkaline geochemical groups (Heilbron et al., 1988). One is a medium-K group that comprises a wide range composition, from diorites to granodiorites; and the other is a high-K group (K_2O up to 4.1%) represented only by acid rocks (granites and subordinated granodiorites). The field relationships indicate that the charnockitic group is younger than the other one. The chemical composition of both groups also indicates convergent tectonic settings with the suggestion of a progressive chemical maturity, as observed in modern magmatic arcs, with enrichment in Alk and in the total LILE from medium to high-K calcalkaline groups.

The most abundant basic rocks of the Juiz de Fora Complex are low-TiO_2-P_2O_5 tholeiitic basic rocks. The second basic group comprises alkaline to transitional basic rocks enriched in TiO_2 > 3.3%; K_2O 1.1-1.7%; FeO* > 10%; P_2O_5 > 0.58% and in all incompatible elements. The chemical signature is consistent with an intracontinental tectonic setting.

ANALITICAL PROCEDURES

New U-Pb analyses were carried out at the Centre de Recherche en Géochimie et Géodynamique (GEOTOP-UQAM-McGill), Université du Québec à Montréal, Canada. We selected samples from geochemical groups of rocks of the Mantiqueira and Juiz de Fora complexes. Both Isotope Dilution Thermal Ionization Mass Spectrometry (ID-TIMS) and Laser Ablation Multi Collection Inductively Coupled Plasma Mass Spectrometry (LA-MC-ICPMS) methodologies were applied.

For the LA-MC-ICPMS the selected grains together with fragments of in-house standard zircon (UQ-Z8) were mounted on epoxy known to be devoid of Pb and U from previous analyses and manually polished on alumina (Al_2O_3) lapping film. Due to the poor precision of the measured $^{207}Pb/^{235}U$ values obtained for the youngest zircons (< 1 Ga) ablated in an Ar atmosphere, the results are presented on $^{238}U/^{206}Pb$ vs. $^{207}Pb/^{206}Pb$ concordia diagrams.

For the TIMS-ID methodology, and following the procedure of Krogh (1982), most of the analyzed zircon fractions were abraded between ~72h and 120h. Mineral dissolution, chemical extraction of U and Pb, and mass spectrometric analyses were carried out following the procedures described in Machado et al. (1996).

Age calculations and plotting were done with Isoplot-Ex Version 2 (Ludwig, 2000). The precision of the isotopic ratios is reported and plotted as standard error of the mean at the 1 sigma level but all ages are quoted at the 95% confidence interval.

SAMPLED UNITS AND RESULTS

We select to analyze different rock types of the Mantiqueira and the Juiz de Fora complexes. They represent, respectively, the basement associations of the Andrelândia and Juiz de Fora domains of the Occidental terrane. The description of the rock type and the obtained results are reported in Table 1, togheter with other available U-Pb data from Machado et al. (1996), Cordani et al. (1973) and Sm-Nd data from Ragatky et al. (1999), Fischel et al. (1999) and Brueckner et al. (2000).

DISCUSSIONS

The integration of the new U-Pb data with the previously reported geochronological data support the following conclusions:

a) The Mantiqueira association includes calc-alkaline arc-related banded gneisses (c.a 2.2 Ga) and collisonal granitoids (ca. 2.15 Ga). Isotopic data indicate an Archaean crustal component suggesting a cordilleran tectonic setting. A metamorphic episode at ca. 2.04 Ga is also detected. Both units are cut by bimodal composite dikes still undated.

b) To the east and outcroping at the Juiz de Fora Domain, the Juiz de Fora Complex is represented by ortho-granulites with a wide range of compositions. The major lithological units are two arc-related calc-alkaline suites (ca .2.1) with juvenile isotopic signature and minor tholeiitic basic rocks (ca. 2.4 Ga) with both ocean floor and island arc geochemical signature. The data suggest a juvenile terrane accreted to the Tranzamazonian belt.

c) The Juiz de Fora association is also intruded by alkaline basic rocks (ca. 1.7 Ga) related to subsequent rifting of the São Francisco paleocontinent that resulted in the development of the São João del Rei and Espinhaço rift basins.

d) The Neoproterozoic orogenic overprint is characterized by amphibolite facies metamorphism and by several folding phases identified at the Mantiqueira Complex at ca. 590 Ma. Granulite facies metamorphism and a pervasive mylonitic foliation indicate relatively more intense Neoproterozoic reworking of the Juiz de Fora complex that is located at the internal segment of the Neoproterozoic Ribeira orogen.

The new data suggest that the basement exposed at the Occidental terrane of Ribeira belt represents the extension of the São Francisco paleocontinent amalgamated in the end of the Tranzamazonian Cycle. The Mantiqueira Complex represents the reworked margin of the Archaean paleocontinent in a cordilleran tectonic setting, while the arc(s)-ocean floor (plateau??) associations of the Juiz de Fora complex indicate juvenile component and were probably developed within an oceanic setting. At this time and to the west on the cratonic foreland, the deformation of the Minas passive margin and the development of the Sabará basin were in course (Alkmin & Marshak, 1998; Machado et al., 1996). The Juiz de Fora Complex was probably accreted to the the active margin of the paleocontinent during the latest stages of the Transamazonian Orogeny around ca. 2.05 Ga resulting on the deformation and metamorphism of the Mantiqueira Complex.

After the Transamazonian Orogeny, the basement associations were intruded by alkaline and basic rocks related with the distinct extensional phases that result on the opening of the intracratonic Paleo and Mesoproterozoic basins at ca. 1.7 and 1.3 Ga, and at ca. 1.0-0.9 Ga related with the development of the Neoproterozoic Andrelândia passive margin. As suggested before by Heilbron et al. (2000), the Transamazonian suture located between the Mantiqueira and Juiz de Fora Paleoproterozoic terranes could have controlled the Neoproterozoic passive margin tectonics and the development of a major thrust during the Neoproterozoic/Cambrian Brasiliano convergence.

Although less precise than ID-TIMS data, these results also illustrate the applicability of the LA-MC-ICP-MS method to unravel the history of polyphasic metamorphic terrains.

REFERENCES

Alkmin, F. F. & Marshak, S. 1998. Trasamazonian Orogeny in the Southern São Francisco Craton Region, Minas Gerais State, Brazil: Evidence for Paleoproterozoic collision and collapse in the Quadrilátero Ferrífero. Precambrian Research 90: 29-58

Brueckner, H.K.; Cunningham, D.; Alkmin, F.F.; Marshal, S. 2000. Tectonic implications of Precambrian Sm-Nd dates from Araçuaí and Ribeira belts, Brazil. Pracambrian Research 99, p.255-269

Cordani, U. G.; Delhal, L. ; Ledent, O. 1973. Orogéneses Superposées dans le Precambrien du Brésil Sud-Oriental (États de Rio de Janeiro et de Minas Gerais). Rev. Bras. Geoc. 3(1):1-22.

Fischel, D.P.; Pimentel, M.; Fuck, R.A.; Costa, A.G.; Rosiere, C.A. 1998. Geology an Sm-Nd isotopic data for the Mantiqueira and Juiz de For a complexes (Ribeira belt) in the Abre Campo-Manhuaçu region, Minas Gerais, Brazil. IN 14th International Conference on Basement tectonics, Ouro Preto, Brazil, Proceedings, p.21-23

Heilbron, M.; Mohriak, W.; Valeriano, C.M.; Milani, E.; Almeida, J.C.H.; Tupinambá, M. 2000. From Collision to Extension: The Roots of the South-eastern Continental Margin of Brazil. In: Atlantic Rifts and Continental Margin, Talwani and Mohriak editors. AGU Geophysical Monograph Series 115, 354p., p. 1-32.

Heilbron, M. & Machado, N. 2003 (in press) Timing of terrane accretion in the Neoproterozoic-Eopaleozoic Ribeira orogen (SE Brazil). Precambrian Research.

Krogh, T.E. 1982 Improved accuracy of U-Pb zircon dating by selection of more concordant systems using an air abrasion technique. Geochemical and Cosmochemica Acta, 46: 637-649.

Ludwig, K.L. 2000. Users manual for Isoplot/Ex v. 2.3. A geochronological toolkit for Microsoft Excel. Berkeley Geochronology Center Special Publication No. 1a. Berkeley, California.

Machado, N. & Carneiro, M.A. 1992. A major Archean tectonothermal event in the São Francisco shield, Brazil: U-

Pb evidence from the Quadrilátero Ferrífero, Minas Gerais. Canadian Journal of Earth Sciences 29, 2341-2346

Machado, N., Valladares, C.S.; Heilbron, M.; Valeriano, C.M. 1996. U-Pb Geochronology of Central Ribeira belt, Prec. Res., 79, 347-361.

Machado, N.; Noce, C.M.; Ladeira, E.A.; Belo de Oliveira, O. 1992. U-Pb geochronology of Archean magmatism and Proterozoic metamorphism in the Quadrilátero Ferrífero, southern São Francisco craton, Brazil. Geological Society of America Bulletin 104, 1221-1227.

Ragatky, D.; Tupinambá, M.; Heilbron, M; Duarte, B.P.; Valladares, C.S. 1999. New Sm/Nd Isotopic Data From Pre-1.8 Ga. Basement Rocks of Central Ribeira Belt, SE Brazil. In: South-American Symposium On Isotope Geology, 2, Córdoba, 1999. Actas..., p. 346-348.

Schmitt, R.S. et al. 1999. The characterization of a Cambrian (~ 520 Ma) tectono-metamorphic event in the Costeiro domain of the Ribeira belt, using U/Pb in syn-tectonic veins. Boletim Geologico Minero Argentino 34, 363-366.

Teixeira, W.; Sabaté, P.; Barbosa, J.; Noce, C.M.; Carneiro, M.A. 2000. Archean and Paleoproterozoic tectonic evolution of the São Francisco craton, Brazil. In Tectonic Evolution of South America, U.G. Cordani, E.J. Milani, A. Thomaz Filho, and D.A. Campos editors, 854 p. 31st International Geological Congress, Rio de Janeiro, 101-137.

Trouw, R.A.J.; Heilbron, M.; Ribeiro, A.; Paciullo, F.V.P.; Valeriano, C.M.; Almeida, J.C.H.; Tupinambá, M.; Andreis, R.R. 2000. The central segment of the Ribeira belt, in U.G. Cordani, E.J. Milani, A. Thomaz Filho, D.A. Campos (Eds), Tectonic Evolution of South America, 854 p. 31st International Geological Congress, Rio de Janeiro, 287-310.

Tupinambá, M. et al. 2000. Neoproterozoic Western Gondwana assembly and subduction-related plutonism: the role of the Rio Negro Complex in the Ribeira Belt, Southeastern Brazil. Revista Brasileira de Geociências 30, 7-11

Valladares, C.; Machado, N.; Ribeiro, A.; Paciullo, F.V.P.; Heilbron, M., Gauthier, G. 2001. Ages of detrital zircon from siliciclastic sucessions of the Brasília belt, southern border of São Francisco craton: implications for the evolution of Proterozoic basins. Revista Comunicaciones, 52, p. 71.

Table 1. Geochronological data from the basement complexes of the Occidental terrane, central Ribeira belt. New data is from this work. Compiled data from: 1-Machado et al. (1996), 2- Cordani et al (1973), 3- Brueckner et al. (2000), 4- Fischel et al. (1998) and 5- Ragatky et al (1999).

Unit and tectonic domain	Lithology	U-Pb method.	Results	T_{DM} (2.1-2.0) and reference
Andrelandia domain Mantiqueira Complex	Tonalitic banded gneiss with amphibolite lenses and leucosomatic veins	LA-ICPMS	Population1-Discordia with 2206± 17 Ma and 734±93 Ma intercepts Population2- Concordant zircons at 2041±8 Ma Population3- ^{207}Pb/^{206}Pb ages of 2781 Ma	2.8-2.7 Ga (3) 3.3-3.0 Ga (4)
	Granodioritc gneiss with dioritic lenses	LA-ICPMS ID-TIMS	Population1 Discordia with 2101 Ma Population2 ^{207}Pb/^{206}Pb ages of 2.3 Ga. Titanites: 569 Ma (8% discordant), 565 Ma (3% discordant) and 604±4 Ma (1)	2.6 Ga (5)
	Granitic augen gneiss		Discordia with UI of 2170 Ma	2.5 Ga (5)
Juiz de Fora domain Juiz de Fora complex	Tholeiitic basic granulite mylonitic	ID-TIMS	Discordia with intercepts at 2427±9 Ma and 654±12 Ma	
	Enderbitic granulite mylonitic	ID-TIMS	Discordia with intercepts at 2070±70 and 600 Ma (2)	
	Charnockitic granulite mylonitic	ID-TIMS	Discordia with intercepts at 2134 and 579 Ma (1)	
	Charnockitic granulite granoblastic	LA-ICPMS	Concordant age of 2138±47 Ma	
	Alkaline basic granulite mylonitic	LA-ICPMS	Discordia with intercepts at 1707+/-36 Ma and 619±21 Ma One concordant analysis at 599±2 Ma.	2.2 Ga (5)

SHRIMP U-Pb AND FT PLIOCENE AGES OF NEAR-TRENCH GRANITES IN TAITAO PENINSULA, SOUTHERN CHILE

Hervé, F.[1]; Fanning, M.C.[2]; Thomson, S.N.[3]; Pankhurst, R.J.[4]; Anma, R.[5]; Veloso, A.[5] and Herrera, C.[1]

1. Departamento de Geología, Universidad de Chile, Casilla 13518, Correo 21, Santiago, Chile. fherve@cec.uchile.cl
2. Research School of Earth Sciences, The Australian National University, Canberra ACT 0200, Australia. mark.fanning@anu.edu.au.
3. Institut für Geologie, Mineralogie & Geophysik, Ruhr-Universität Bochum, D-44780 Bochum, Germany. stuart.thomson@rub.de (from 01.05.03: Dept. of Geology and Geophysics, Yale University, P.O. Box 208109, New Haven, CT, USA).
4. NERC Isotope Geosciences Laboratory, British Geological Survey, Keyworth, Nottingham NG12 5GG, United Kingdom. r.pankhurst@bas.ac.uk.
5. School of Life and Environmental Sciences, University of Tsukuba, Tsukuba, Ibaraki, Japan

Keywords: Pliocene granites, U-Pb SHRIMP zircon ages, zircon and apatite FT ages, Taitao ophiolite, Chile

INTRODUCTION

The Taitao Peninsula of the continental margin of southern Chile (46° 15' S) is located 40 km south of the present day Chile Triple Junction (CTJ) of the Nazca, Antarctic and South America plates. South of this triple point, the active oceanic ridge has been progressively subducted below South America, starting at the southern tip of the continent at 14 Ma (Cande & Leslie, 1986). The peninsula is characterized by the presence of the Taitao ophiolite (Forsythe & Nelson, 1985; Bourgois et al., 1992), a unique occurrence of this rock association along the Pacific margin of Chile. The ophiolite was emplaced in a segment of the continental margin where fossil accretionary complexes of Late Paleozoic to Early Mesozoic age predominate.

In Taitao Peninsula there are several small (< 10 km^2) granitoid plutons, considered to have adakitic affinities (Lagabrielle et al., 2000; Veloso, 2001) (Fig.1). Some of these have been previously dated as Late Cenozoic by the K-Ar method (Mpodozis et al., 1985; Bourgois et al., 1992, 1993; Guivel et al., 1996).

As the exact geological significance of these ages is unclear, zircons from two samples of the Cabo Raper pluton, which intrudes the Taitao ophiolite, were dated by the SHRIMP U-Pb method on zircon to establish their crystallization ages. The thermochronological history of three of the plutons was further investigated by fission track dating of zircon and apatite. The dating of the crystallization and the cooling history of these intrusive rocks will help to constrain the tectonic evolution of the continental margin in this region.

GEOLOGY

The Taitao Ophiolite has been interpreted as emplaced as part of the collision processes between the Chile Rise and the Andean margin (*e.g.* Forsythe et al., 1986; Nelson et al., 1993; Lagabrielle et al., 1994, 2000; Veloso, 2001). During the last 14 Ma the Chile Triple Junction (CTJ) has migrated northwards from the extreme south of the continent (Cande & Leslie, 1986), and is located at present 40 km north of the Taitao Peninsula at 46° 05' S. Since the Pliocene, this area has experienced successive subduction, with partial overlap, of three short segments of the Chile Rise that are separated by oceanic fracture zones (Cande & Leslie, 1986). The subduction-collision process has exposed the following units in the continental margin:

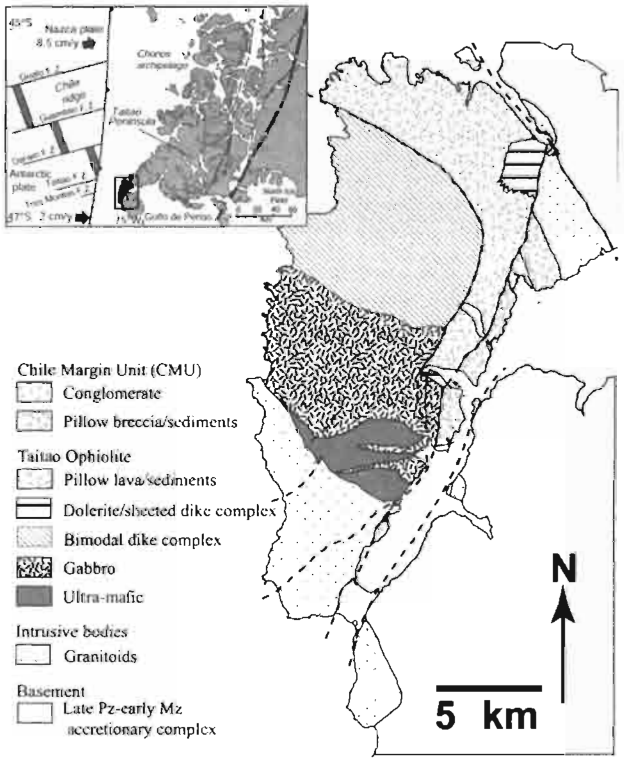

Figure1. Geological map of the Taitao Peninsula.

(1) The Taitao ophiolite: a succession of partly serpentinized peridotites (ultramafic tectonites), gabbros, and bimodal sheeted dyke complex and volcanic products (Main Volcanic Unit (MVU), Bourgois et al., 1993; Lagabrielle et al., 1994) intercalated with marine sediments of Miocene to Pliocene age (Forsythe et al., 1985; Forsythe & Nelson, 1985).

(2) A series of calcalkaline plutons with TTG affinities (Veloso, 2001), the Cabo Raper, Central, Seno Hoppner, Barrientos and Estero Cono plutons, which intrude the ophiolite or its immediate surrounding rocks.

(3) The Chile Margin Unit (CMU) (Bourgois et al., 1993) of Late Pliocene to Pleistocene age, Contrary to

previous interpretations, these authors consider this unit to be unrelated to the effusive products of the ophiolite (MVU), based on outcrop and geochemical differences.

Forsythe & Nelson (1985) showed that the ophiolite is limited to the north by low grade metamorphic rocks belonging to the Chonos Metamorphic Complex, which is of Late Triassic depositional age (Hervé & Fanning, 2000). The ophiolite is intruded by the Cabo Raper granodiorite pluton and by the Central Pluton, while the Estero Cono granodiorite pluton, the Bahia Barrientos and the Seno Hoppner plutons intrude the basement rocks in the immediate vicinity of the ophiolite (Mpodozis et al., 1985), and perhaps the ophiolite itself in inaccessible internal areas of the peninsula.

The generation and emplacement ages of the ophiolite are not well established. A Late Miocene K-Ar age in a coarse amphibole vein cutting the gabbro section of the ophiolite (Bourgois et al., 1992) indicates a Late Miocene minimum age for its generation. The age of the cross-cutting Raper pluton constrains the emplacement of the ophiolite on the continental margin. Emplacement took place either by localized obduction from the otherwise normally subducting oceanic crust or by in situ generation in an extensional environment in the continental margin (Nelson & Forsythe, 1985; Nelson et al., 1993, Bourgois et al., 1993). The ophiolite was affected by brittle deformation after emplacement (Veloso, 2001).

PETROGRAPHY OF THE ANALYSED SAMPLES.

The Cabo Raper Pluton crops out in the southwestern part of the Taitao Peninsula, and covers an area of ca. 30 km^2. It intrudes the peridotite and gabbro facies of the ophiolite (contacts not seen). Grain size varies from 0.5 to 6.0 mm, with granular to porphyritic texture. It corresponds to a granodiorite. It is composed of plagioclase (35%), alkali feldspar (10%), quartz (25%), biotite (20%) and hornblende (10%). Zircon and apatite are accessory minerals. Secondary minerals are white mica, chlorite, smectite and epidote.

The Estero Cono pluton covers approximately 6 km^2 at the northern end of the ophiolite and, where it intrudes the basement rocks. It is a tonalite, with granular and porphyritic texture, similar to the Cabo Raper granodiorite, but poorer in alkali feldspar.

GEOCHRONOLOGY

Previous radiometric datings of rocks of the area, all by the K-Ar method, are presented in Table 1 and Fig. 2.

Results obtained during the present investigation are presented in Table 2 and Figs 3 and 4.

SHRIMP U-Pb zircon ages were obtained at the Australian National University in Canberra, and FT ages by ST at the Ruhr-University in Bochum, Germany. Methodologies at these two centres were the same as presented in Williams (1998) and Thomson et al. (2001), respectively.

The U-Pb SHRIMP zircon ages obtained on clear tips of euhedral crystals are 3.84 ± 0.09 Ma (TPO 127) and 3.97 ± 0.14 Ma (TPO 128b). The first sample has inherited zircon components of ca. 5, 105 and 295 Ma, though other such inheritance was not specifically targeted during the analytical session.

The FT ages are in consistent with the U-Pb ages, with the FT zircon ages being slightly younger, and the apatite ages further so.

DISCUSSION

Subduction processes in the area of the Taitao peninsula have been very complex in the last 6 Ma. The Chile Rise is segmented by fracture zones, which are oblique to the margin. Thus events in which fracture zones are subducted, with the CTJ migrating slowly southwards, alternate with others in which segments of spreading ridge are subducted and the CTJ migrates rapidly northwards. The timing of these events has been established by Cande and Leslie (1986), and we examine below the possible correlation between the crystallization and cooling of the studied plutons with these different subduction events.

The U-Pb SHRIMP age determinations in zircons indicate that the Cabo Raper pluton crystallized at 3.9 Ma during the Early Pliocene, in the Zanclean stage according to the IUGS Time Scale (IUGS, 2000). This age is: (a) younger than two of the previous K-Ar ages on the Cabo Raper pluton (Guivel et al., 1996), (b) within the large errors of four other previous determinations (Mpodozis et al., 1985), and (c) older than the three others, two of which do not have reported errors. Thus, the relationship between the K-Ar and U-Pb ages is not systematic. The Seno Hoppner pluton, not dated in this study, has older K-Ar ages of 6.8 ± 0.2 and 5.2 ± 0.3 Ma, but the geological significance of these are not precisely established. The crystallization ages of the plutons are similar, within error, to five of the eight K-Ar ages of the volcanic rocks of the CMU, suggesting that they represent closely related events and that the emplacement of the CMU continued after the intrusions had crystallized.

One of the zircon FT ages of Cabo Raper is concordant within error with the U-Pb SHRIMP crystallization age, and the other (TPO 128b) is only 0.06 to 0.53 Ma younger than the crystallization age. The data point to a very rapid cooling to below ca. 250°C after crystallization of these plutons. The apatite FT age for both Cabo Raper and Estero Cono are significantly younger than the crystallization ages, but the other apatite FT age is within error of the obtained crystallization ages. These data indicate that cooling of the plutons in the Taitao Peninsula area from crystallization temperatures (ca. 650°C) to below 60°C occurred in an interval no longer than 2 Ma, during which the volcanic rocks of the CMU were emplaced.

Samples TPO 137 (Seno Barrientos pluton) and TPO 173 (Estero Cono pluton) yield similar FT zircon ages, and though no SHRIMP U-Pb ages have been obtained in these samples, they very probably have similar crystallization ages to the Cabo Raper pluton.

Table 1. Previous age determinations of rock units in the Taitao Peninsula. (1) Bourgois et al., 1992 (2) Munizaga, 1970, (3) Mpodozis et al., 1985 (4) Guivel et al., 1996, (5) Bourgois et al., 1993, (6) Lemoigne, 1994, (*) nannofossil age.

Unit	Age (Ma)	Error (2 σ)
Gabbro (1)	13.8	2.6
C Raper(2)	3.2	-
C Raper(2)	3.0	-
C Raper(3)	4.1	2.4
C Raper(3)	3.6	0.6
C Raper(3)	3.4	0.8
C Raper(3)	3.3	0.3
C Raper(3)	3.2	1.2
C Raper(4)	5.0	1.0
C Raper(4)	4.8	0.3
S.Hoppner(3)	5.5	0.4
S Hoppner(3)	5.2	0.3
S Hoppner(4)	5.9	0.5
S Hoppner(4)	6.8	0.2
CMU(5)	2.3(*)	1.3
CMU(3)	4.6	1.0
CMU(3)	4.4	1.0
CMU(3)	4.4	0.6
CMU(3)	3.7	0.6
CMU(3)	3.0	0.8
CMU(3)	3.0	1.4
CMU(3)	2.9	0.8
CMU(3)	2.5	0.3
CMU(6)	6.0	0.0

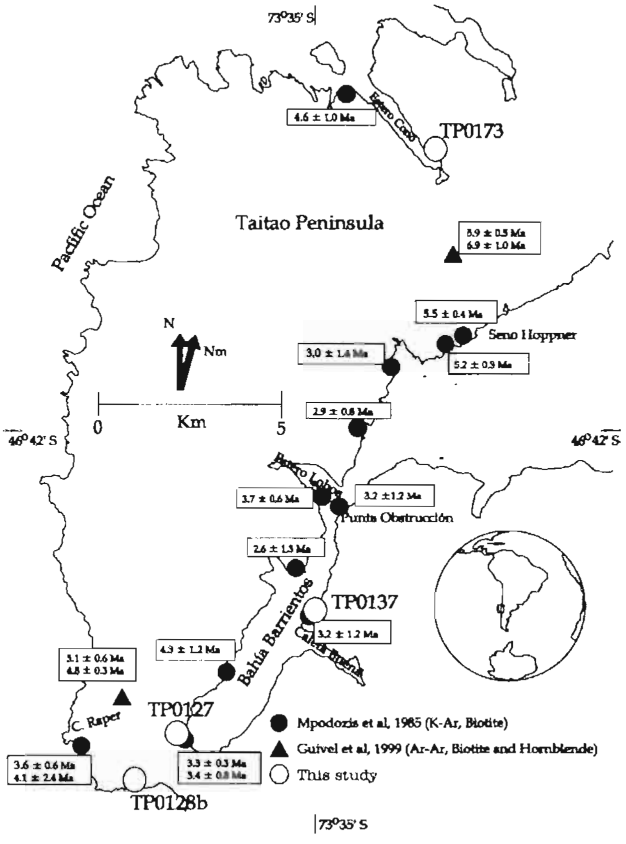

Figure2. Radiometric ages in Taitao Peninsula.

Table 2. New (U-Pb SHRIMP and FT) age determinations on theTaitao Peninsula plutons.

Sample	Unit	U-Pb zircon (Ma ± 2σ)	FT zircon (Ma ± 1σ)	FT apatite (Ma ± 1σ)
TPO 127	Cabo Raper	3.84 ± 0.09	4.05 ± 0.29	1.85 ± 0.56
TPO 128b	Cabo Raper	3.97 ± 0.14	3.51 ± 0.26	2.88 ± 0.76
TPO 137	Seno Barriento	-	3.47 ± 0.22	3.14 ± 1.30
TPO 173	Estero Cono	-	3.49 ± 0.27	-

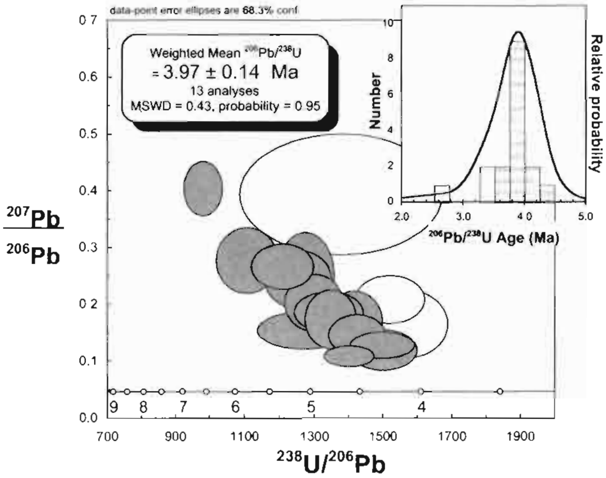

Figure 3. Tera & Wasserburg Concordia plot of SHRIMP U-Pb zircon data for sample TP01-28B (calibrated, total ratios plotted as 1σ error ellipses). Inset is a relative probability plot with stacked histogram.

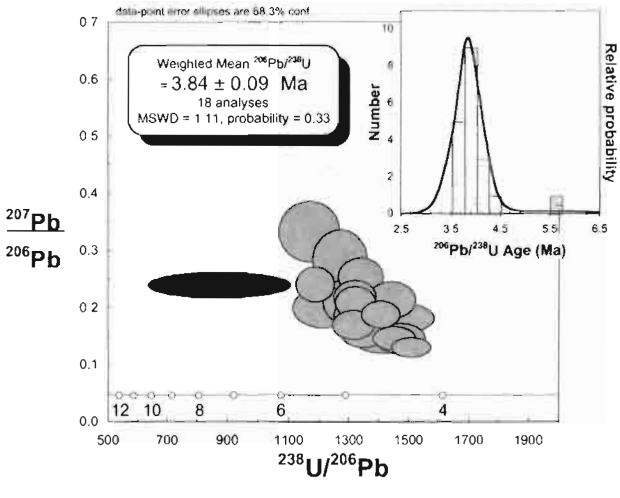

Figure 4. Tera & Wasserburg Concordia plot of SHRIMP U-Pb zircon data for sample TP0127 (calibrated, total ratios plotted as 1σ error ellipses). Inset is a relative probability plot with stacked histogram.

According to Cande & Leslie (1986) the Tres Montes Fracture Zone was being subducted in the interval between 5-6 and 3 Ma, when the Cabo Raper pluton was emplaced, and very probably also the Estero Cono and Seno Barrientos plutons. This apparently triggered the intrusion of the granitoid bodies. The LIL-depleted adakitic characteristics of these granites are probably related to this scenario. Defant & Drummond (1990) advocate genesis of adakite by melting of young subducted oceanic crust, whereas Petford & Atherton (1996) suggest melting of lower crustal underplate beneath a thickened volcanic arc. Either possibility would be compatible with the rise of excess heat or hot fluids along the fracture zone as it was subducted to the partial melting zone. When the later subduction of a short segment of the Chile Rise occurred (3 to 2.8 Ma), the granitoid bodies had already cooled to below 250°C. This cooling was probably induced by associated rapid uplift and erosion of the continental margin, which is known to be produced by subduction of a spreading ridge (Cande & Leslie, 1986).

Similar very young (7 to 2 Ma) FT ages on apatite have been obtained by Thomson (2002) near to the southern termination of the Liquiñe-Ofqui fault zone (shown by dashed lines in Fig.1) which implies that the ridge collision was a major force driving late Cenozoic transpression in the area.

ACKNOWLEDGEMENTS

Field work by RA, EV and CH was carried out under the “Superplume project” of Tsukuba University, Tokyo University and the Museum of Natural Sciences, Tokyo, Japan, provided the analysed samples. Fondecyt project 1010412 to FH financed the SHRIMP analyses. The work of SNT was supported by DFG Stipendium Th 573/2-1.

REFERENCES

Bourgois, J., Lagabrielle, Y., Maury, R., Le Moigne, J., Vidal, P., Cantagrel, J., Urbina, O., 1992. Geology of the Taitao Peninsula (Chile margin triple junction area, 46°-47°S): Miocene to Pleistocene obduction of the Bahía Barrientos Ophiolite. EOS, 73, 43, 592.

Bourgois, J., Lagabrielle, Y., Le Moigne, J., Urbina, O., Janin, M-Ch., Beuzart, P., 1993. Prelimanary results of a field study of the Taitao ophilithe (Southern Chile): Implications for the evolution of the Chile Triple Junction. Ofioliti, 18(2), 113 - 129.

Bourgois, J., Martin, H., Lagabrielle, Y., Le Moigne, J., Frutos Jara, J., 1996. Subduction erosion releated to spreading-ridge subduction: Taitao peninsula (Chile margin triple junction area). Geology, 24 (8), 723 – 726.

Cande, S. & Leslie, R. 1986. Late Cenozoic tectonics of the southern Chile trench. Journal of Geophysical Research, Vol. 91, N° B1, 471-496.

Defant, M. J. & Drummond, M.S. 1990. Subducted lithosphere-derived andesitic and dacitic rocks in young volcanic arc setting, Nature, 347, 662–665,.

Forsythe, R., Olsson, R., Johnson, C., Nelson, E., 1985. Stratigraphic and micropleontological observations from the Golfo de Penas-Taitao basin, southern Chile. Revista. Geologica de Chile, N° 25-26, 3-12.

Forsythe, R. & Nelson, E., 1985. Geological manifestations of the ridge collision: Evidence from the Golfo de Penas-Taitao basin, southern Chile. Tectonics, Vol. 4, N° 5, 477 – 495.

Forsythe, R., Nelson, E., Carr, M., Keading, M., Hervé, M., Mpodozis, C., Soffia, J., Harambour, S., 1986. Pliocene near-trench magmatism in southern Chile: A possible manifestation of the ridge collision. Geology, 14, 23 – 27.

Guivel, C., Lagabrielle, Y., Bourgois, J., Maury, R., Martin, H., Arnaud, N., Cotten, J., 1996. Magmatic responses to active spreading ridge subuction: Multiple magma sources in the Taitao peninsula region (46° - 47°S, Chile Triple Junction). Third International Symposium on Andean Geodynamics ISAG, St. Malo (France), 575 – 578.

Thomson, S.N., Hervé, F., Brix, M., Stöckhert, B., 2001. The Mesozoic-Cenozoic denudation history of the southern Chilean Andes and its correlation to different subduction processes. Tectonics, vol. 20, n°5, 693-711.

Lagabrielle, Y., Le Moigne, J., Maury, R., Cotten, J., Bourgois, J., 1994. Volcanic record of the subduction of an active spreading ridge, Taitao Peninsula (southern Chile). Geology, Vol. 22, 515 – 518.

Lagabrielle, Y., Guivel, C., Maury, R., Bourgois, J., Fourcade, S., Martin, H., 2000. Magmatic-tectonics effects of high thermal regime at the site of active ridge subduction: the Chile Triple Junction Model. Tectonophysics 326, 255 – 268.

Mpodozis, C., Hervé, M., Nasi, C., Soffia, J., Forsythe, R., Nelson, E., 1985. El magmatismo plioceno de la península Tres Montes y su relación con la evolución del punto triple de Chile austral. Revista Geológica de Chile , N° 25-26, 13-28.

Munizaga, F., 1970. Informe preliminar sobre las edades radiométricas en la provincia de Aysén. Instituto de Investigaciones Geológicas (Chile), Unpublished Report, 14 p.

Nelson, E., Forsythe, R., Diemer, J., Allen, M., Urbina, O., 1993. Taitao Ophiolite: a ridge collision ophiolite in the forearc of southern Chile (46°S). Revista Geológica de Chile, 20, 137 – 166.

Nelson, E., Forsythe, R., Arit, I., 1994. Ridge collision tectonics in terrane development. Journal of South American Earth Sciences, vol. 7, N° 3-4, 271 – 278.

Petford, N. & Atherton, M. 1996. Na-rich partial melts from newly un-derplated basaltic crust: The Cordillera Blanca batholith, Peru, Journal of Petrology, 17, 1491–1521.

Thomson, S.N. 2002. Late Cenozoic geomorphic and tectonic evolution of the Patagonian Andes between latitudes 42°S and 46°S: an appraisal based on fission-track results from the transpressional intra-arc Liquiñe-Ofqui fault zone. Geological Society of America, Bulletin, Vol.114, no 9, 1159 – 1173.

Thomson, S.N., Hervé, F., Stöckhert, B., 2001. The Mesozoic-Cenozoic denudation history of the southern Chilean Andes and its correlation to different subduction processes. Tectonics, vol. 20, n°5, 693-711.

Veloso, E., 2001. Condiciones de emplazamiento y deformacion fragil de la ofiolita Taitao (46°42'S, 73°35'W), Peninsula de Taitao, Region de Aysen, Chile. Graduation Thesis, Departamento de Geología, Universidad de Chile, 100 p.

Williams, I.S., 1998. U-Th-Pb Geochronology by Ion Microprobe. In Applications of Microanalytical Techniques to Understanding Mineralizing Processes. McKibben, M.A., Shanks III, W.C. & Ridley, W.I. (Eds). Reviews in Economic Geology. Vol. 7, 1-35.

ISOTOPIC AND GEOCHRONOLOGICAL CONSTRAINTS FOR THE ORIGIN OF SYN- TO POST-BRASILIANO MAFIC MAGMATISM AND CRUSTAL RE-MELTING IN THE BRASÍLIA BELT (CENTRAL BRAZIL)

Hollanda, M.H.B.M.[1]**; Pimentel, M.M.**[2] **and Armstrong, R.**[3]

1. Centro de Pesquisas Geocronológicas, Instituto de Geociências – Universidade de São Paulo, Rua do Lago 562, Cidade Universitária, 05508-080, São Paulo-SP, Brasil
2. Instituto de Geociências – Universidade de Brasília, Campus Universitário Darcy Ribeiro, 70910-900, Brasília-DF, Brasil
3. Research School of Earth Sciences, Australian National University, Canberra, ACT 0200, Australia

Keywords: Brasília Belt, mafic magmatism, U-Pb SHRIMP, Sr-Nd isotopes, Brasiliano orogeny

INTRODUCTION

The syn- to post-orogenic stages of the Brasiliano orogeny in central Brazil were characterized by the emplacement of numerous mafic intrusions that occur either associated with larger volumes of K-rich granitic intrusions, within the Neoproterozoic Goiás Magmatic Arc or as individual mafic-ultramafic layered intrusions within the arc and in the so-called Anápolis-Itauçu high-grade Complex, to the east. Until recently, very few geochronological constraints existed for the emplacement ages of these mafic intrusions, and they were mainly indirect ages based on Rb-Sr data for the associated granites (Pimentel et al., 1996). Recent U-Pb zircon and Sm-Nd isotopic data, allied with previous regional geological knowledge, indicate that the Neoproterozoic mafic magmatism played an important role in the Brasiliano tectonic evolution in Central Brazil, and was probably closely related to the heating, crustal re-melting and high temperature metamorphism in both Goiás Magmatic Arc and Anápolis-Itauçu Complex.

REGIONAL GEOLOGY

The Brasília Belt is a large Neoproterozoic orogenic belt developed along the western margin of the São Francisco Craton, Central Brazil. It is composed of four main tectonic segments: (i) a thick Meso-Neoproterozoic metasedimentary/sedimentary pile comprising typical passive margin (Paranoá and Canastra groups) and back-arc (e.g., Araxá and Ibiá groups) sucessions, and a younger unit (Bambuí Group) probably representing a post-inversion, foreland sequence; (ii) a large Neoproterozoic juvenile arc in its western portion (Goiás Magmatic Arc); (iii) a micro-continent (or allochthonous sialic terrain) formed mainly by Archaean rock units (the Crixás-Goiás granite-greenstones) and Paleo- to Mesoproterozoic mafic-ultramafic high-grade complexes (Barro Alto, Niquelândia and Canabrava complexes), and (iv) a metamorphic core complex comprising felsic granulites and sillimanite-garnet and hypersthene-bearing gneisses and intrusive peraluminous granite, known as the Anápolis-Itauçu Complex, in the central part of the belt.

Two distinct high-grade metamorphic events are constrained in the southern (Anápolis-Itauçu Complex) and northern parts of the Brasília Belt. While high-grade metamorphism in the northern complexes occurred between ca. 740-780 Ma (Ferreira Filho et al., 1994; Suita et al., 1994; Correa et al., 1997), granulites in the Anápolis-Itauçu Complex are younger and metamorphic recrystallization took place at ca. 650 Ma (Fischel et al., 1998; Piuzana et al., 2002). Sm-Nd isotopic signature and SHRIMP U-Pb metamorphic ages of the Araxá metasediments and the Anápolis-Itauçu granulites and its intrusive granites (650-640 Ma) are all very similar (Pimentel et al., 1999a; Fischel et al., 1999a, b; Seer, 1999), suggesting that the granulites might represent high-grade equivalents of the Araxá metasedimentary rocks and that at least some of the intrusive peraluminous granites are partial melt products of this metasedimentary protolith (Pimentel et al., 1999a; Fischel et al., 1999a). Mineral assemblage containing sapphirine and quartz in garnet-orthopyroxene-sillimanite granulites of that complex indicates metamorphism at ultra-high temperatures (ca. 1050°C at 10 Kbar) (Moraes et al., 2001), compatible with extensive re-melting of the crust. These new geochronological and isotopic data, therefore, suggest that the Anápolis-Itauçu complex may be now considered to be the metamorphic core complex of the Brasília Belt and not the sialic basement of the Araxá Group (Piuzana et al., 2002). Mafic-ultramafic bodies remained, however, undated, and their tectonic significance, uncertain.

The Goiás Magmatic Arc, in the westernmost part of the Brasília Belt, consists of a large Neoproterozoic juvenile terrane formed by arc-type volcano-sedimentary rocks and tonalite/granodiorite gneisses. It comprises two main magmatic terranes - the Arenópolis and Mara Rosa arcs, located in western and northern Goiás, respectively (Pimentel & Fuck, 1992; Fuck et al., 1994; Pimentel et al., 1997, 2000a, b). In both areas, geological evolution started at ca. 900-860 Ma with the crystallization of very primitive calc-alkaline volcanics and associated tonalites/granodiorites (ε_{Nd} values between ca. +3 and +6, and T_{DM} values mostly between ca. 0.8 and 1.1 Ga; Pimentel et al., 1991, 1997, 2000; Pimentel & Fuck, 1992). Geochemical and isotopic data from suggest that the original magmas were formed in an intraoceanic multi-arc system (Pimentel, 1991, Pimentel et al., 1997). Calc-alkaline igneous activity lasted until ca. 640 Ma, and the main deformational-metamorphic episode occurred at ca. 620 Ma, as indicated by U-Pb titanite and Sm-Nd garnet ages (for a review, see Pimentel et al., 2000).

During the waning stages or immediately after the last Brasiliano deformation, a number of small mafic-ultramafic layered complexes, gabbro-dioritic intrusions, and large granite plutons were emplaced into the Goiás Magmatic Arc (Pimentel et al., 1996). In the Arenópolis region, Rb-Sr and U-Pb data suggest that the Brasiliano granite magmatism took place in two distinct episodes: (i) an older event between ca. 590 and 560 Ma, and (ii) a young event dated between ca. 508 and 485 Ma (Pimentel et al., 1996).

THE MAFIC-ULTRAMAFIC INTRUSIONS IN THE ANÁPOLIS-ITAUÇU COMPLEX

Layered, mafic-ultramafic intrusions in the Anápolis-Itauçu Complex form NW-SE elongated bodies, parallel to the regional deformational fabrics of the granulitic country-rocks. Examples of mafic-ultramafic bodies are (i) the Goianira-Trindade Complex, which is made up of pyroxenite, garnet-hypersthene pyroxenite, metagabbro, amphibole schist, and is associated with supracrustal calc-silicate rocks (Nilson & Motta, 1969) and the (ii) Taquaral zoned intrusion comprising gabbros and peridotites marginal to main pyroxenitic and gabbroic units, positioned in tectonic contact with granulite gneissic rocks (Silva, 1997). They frequently display well developed foliation and mylonitic fabrics, however, relict features such as cumulate textures and igneous layering are found in most of the intrusions, attesting to their original layered character (Silva, 1991, 1997).

SYN- TO POST-OROGENIC MAFIC AND ULTRAMAFIC INTRUSIONS IN THE GOIÁS MAGMATIC ARC

In a broad regional scale, the syn- to post-orogenic igneous activity in the Goiás Magmatic Arc is typically bimodal, including large bodies of K-rich calc-alkaline granites (e.g., Serra Negra, Serra do Iran, Caiapó, Iporá, Sanclerlândia and Serra do Impertinente granites) associated with minor gabbo-dioritic end-members. Small mafic-ultramafic layered complexes (e.g., Americano do Brasil and Córrego Lageado complexes) occur as individual bodies. The gabbro-dioritic intrusions and mafic-ultramafic layered complexes are either only slightly deformed or completely free of any pervasive deformational fabric. The gabbro-diorites have typical arc geochemical signature and commonly display magma mixing features with gabbro "globules" enclosed in granitic rocks.

ANALYTICAL PROCEDURES

U-Pb analysis were carried out using SHRIMP I and II at the Research School of Earth Sciences, Australian National University, Canberra. Data were collected and reduced as described by Williams & Claesson (1987) and Compston et al. (1992). Uncertainties are given at 1 σ level, and final age was quoted at 95% confidence level. Reduction of raw data was carried out using Squid 1.02 (Ludwig, 2001a). U/Pb ratios were referenced to the RSES standard zircon FC1 (1099 Ma, ^{*206}Pb/^{238}U=0.1859). U and Th concentrations were determined relative to those measured in the RSES standard SL13.

Sm-Nd isotopic analyses followed the method described by Gioia & Pimentel (2000) and were carried out at the Geochronology Laboratory of the University of Brasília. Sm and Nd samples were loaded on Re evaporation filaments of double filament assemblies and the isotopic measurements were carried out on a multi-collector Finnigan MAT 262 mass spectrometer in static mode. Uncertainties for Sm/Nd and ^{143}Nd/^{144}Nd ratios are better than ± 0.4 % (1σ) and ± 0.005% (1σ) respectively, based on repeated analyses of international rock standards BHVO-1 and BCR-1. ^{143}Nd/^{144}Nd ratios were normalized to ^{146}Nd/^{144}Nd of 0.7219 and the decay constant (λ) used was 6.54 x 10^{-12}. Isochron ages and parameters were calculated using Isoplot/Ex 2.47 (Ludwig, 2001b).

SHRIMP AND CONVENTIONAL U-Pb RESULTS

Samples from four mafic intrusions - Rio Caiapó gabbro and Serra do Iran diorite, and the Córrego Lageado and Americano do Brasil complexes were selected for U-Pb analyses.

RIO CAIAPÓ GABBRO

Zircon grains from this gabbro are pink, euhedral to subhedral and show strong concentric compositional zoning. Cathodoluminescence imagens reveal oscilatory zoning and cores of possibly inherited zircon. Only the zoned rims and crystals were analysed. Six analysis have produced a discordia indicating the upper intercept age of 589±19 Ma (MSWD =0.9).

SERRA DO IRAN DIORITE

Zircon form pink, prismatic stubby crystals. Cathodoluminescence imaging shows thick magmatic concentric compositional zoning. Core might be present, but these were not analysed. Ten spot analysis defined a discordia with an upper intercept age of 623±16 Ma, which agrees with previous Rb-Sr data indicating the isochron age of ca. 622 Ma (Pimentel et al., 1996).

CÓRREGO LAGEADO COMPLEX

Zircon grains are colourless to light pink forming very clear, fracture- and inclusion-free crystals. Cathodoluminescence imaging shows well-developed sector and subordinate concentric compositional zoning. Fourteen analysis yielded concordant results which indicate a concordia age of 672±6 Ma.

AMERICANO DO BRASIL COMPLEX

Most of the grains are long and tabular displaying thick zoning typical of crystals formed in mafic magmas. Cathodoluminescence images show no obvious inherited cores. Magmatic cores are surrounded and embayed by thin and very bright rim, which certainly have low U and Th, and might represent late stage crystallization from the mafic magma.

Eight spot analysis yielded a concordia age of 631±6 Ma. Sm/Nd analysis of mafic and ultramafic rocks from this complex define an isochron (MSWD = 0.9) indicating the age of 616±81 Ma (2σ), with ε_{Nd} (T) of +2.4. The large uncertainty in Sm-Nd isochron age is caused by the limited spread in Sm/Nd ratio of the samples used.

GOIANIRA-TRINDADE COMPLEX

Zircon grains separated from one leucogabbro sample of this complex were analysed by ID-TIMS. Three concordant analysis yielded the concordia age of 626±2 Ma which is interpreted here as the best estimate for the crystallisation age of the complex.

Sm-Nd ISOTOPIC RESULTS

Sr and Nd isotopic analyses were carried out on thirteen representative samples of the mafic magmatism in Goiás Magmatic Arc, seven of them from the syn- to late-orogenic gabbros and diorites (Rio Caiapó, Serra do Iran, Iporá, Israelândia), and six from the Córrego Lageado and Americano do Brasil mafic-ultramafic complexes. These samples exhibit a relatively narrow range of initial $^{87}Sr/^{86}Sr$ ratios from 0.70262 to 0.70363, excluding one sample from the Serra do Iran gabbro with $^{87}Sr/^{86}Sr$ ratios of 0.7056. ε_{Nd} values calculated for their respective U-Pb crystallization ages vary from slightly negative (-0.75 to -0.32) to positive (+2.1 to +5.5). The Iporá diorite presents moderately negative ε_{Nd} value of –2.14, calculated for ca. 500 Ma crystallization age determined for a contemporaneous and spatially associated granite. $^{147}Sm/^{144}Nd$ ratios ranging from 0.11 to 0.153 combined with higher than 0.5118 $^{143}Nd/^{144}Nd$ ratios provide T_{DM} ages between ca. 1.1 and 0.88 Ga, closely coeval with the rocks from the Neoproterozoic juvenile Goiás Magmatic Arc. T_{DM} ages higher than 1.1 Ga for the Iporá, Serra do Iran and Israelândia diorites seem to indicate some incipient contamination with older crustal rocks.

Sm-Nd isotopic analysis were also carried out in samples from the Goianira-Trindade mafic-ultramafic Complex. These are metamorphosed into amphibolite to granulite facies, however samples used in this study are from outcrops in which igneous textures and structures such as compositional layering and cumulate textures are preserved. Seven samples define an "errorchron" (MSWD = 6.1) with age of ca. 621 Ma. The ε_{Nd} (T) value is close to zero (-0.3), suggesting some degree of crustal contamination of the original magma.

CONCLUSIONS

The SHRIMP U-Pb zircon ages for mafic rocks within the Goiás Magmatic Arc and the Anápolis-Itauçu granulite Complex presented in this study represent the first geochronological constraint for the emplacement age of these rocks. The data suggest that mafic magmatism was important between ca. 670 and 590 Ma, and probably played an important role during the final stages of the Neoproterozoic evolution of this orogen.

Within the Goiás Magmatic Arc, mafic rocks associated with the Serra do Iran, Rio Caiapó and Iporá granite intrusions and both Córrego Lageado and Americano do Brasil complexes indicate that mafic magmatism was important mainly during late- to post-orogenic stages. Nd isotopic data for these rocks reveal mostly positive $\varepsilon_{Nd}(T)$ values between ca. +5.5 and +2.1, indicating the depleted nature of the mantle source and little contamination with older continental crust.

All ages presented in this study overlap with U-Pb titanite and Sm-Nd garnet (between ca. 600 and 630 Ma) ages for metamorphic rocks of the Goiás Magmatic Arc (Pimentel et al., 2000) and with SHRIMP U-Pb ages for granite emplacement and high-grade metamorphism in the Anápolis area (Piuzana et al., 2002). This suggests that final metamorphism and mafic magmatism took place roughly within the same time interval, and were coeval or shortly followed by uplift, extension and erosion of the orogen (Pimentel et al., 1996, 2003). Uplift was probably more pronounced in the Anápolis-Itauçu Complex allowing exposure of high grade rocks, and also of a larger amount of mafic intrusions, when compared with the Goiás Magmatic Arc.

It is likely that the late Neoproterozoic mafic magmatism have underplated important fractions of the central and western parts of the Brasília Belt continental crust, and may have been responsible for the development of ultra-high temperature metamorphic mineral assemblages, observed in the Anápolis-Itauçu Complex.

REFERENCES

Compston, W., Williams, I.S., Kirschvink, J.L., Zhang, Z., Guogan, M.A., 1992. Zircon U-Pb ages for the Early Cambrian time-scale. Jour. Geolog. Soc. London, 149: 171-184

Correia, C.T., Girardi, V.A.V., Lambert, D.D., Kinny, P.D., Reeves, S.J., 1997. 2 Ga U-Pb (SHRIMP-II) and Re-Os ages for the Niquelândia Basic-Ultrabasic Layered Intrusion, Central Goiás, Brazil. In: 39 Congresso Brasileiro Geologia, 6, SBG, Salvador-BA, 187-189.

Ferreira Filho, C.F., Kamo, S., Fuck, R.A., Krogh, T.E., Naldrett, A.J,. 1994. Zircon and rutile geochronology of the Niquelândia layered mafic and ultramafic intrusion, Brazil: constraints for the timing of magmatism and high grade metamorphism. Precambrian Research, 68: 241-255.

Fischel, D.P., Pimentel, M.M., Fuck, R.A., 1998. Idade de metamorfismo de alto grau no Complexo Anápolis-Itauçu, determinada pelo método Sm-Nd. Revista Brasileira de Geociências, 28 (4): 543-544.

Fischel, D.P., Pimentel, M.M., Fuck, R.A., 1999. Preliminar Sm-Nd isotopic study of the Anápolis-Itauçu Complex, Araxá Group and associated granite intrusions, Central Brazil: implications for the evolution of the Brasília Belt. In: 2 Simposio Sudamericano de Geologia Isotopica, Cordoba-Argentina, 302-305.

Fuck, R.A., Pimentel, M.M., D'el-Rey Silva, L.J.H., 1994. Compartimentação tectônica da porção oriental da Província Tocantins. In: 38 Congresso Brasileiro Geologia, 1, SBG, Balneário Camboriú-SC, 215-216.

Gioia, S.M.C.L. & Pimentel, M.M., 2000. The Sm-Nd isotopic method in the Geochronology Laboratory of the University of Brasília. Anais Acad. Bras. Ciênc., 72: 1125-1140.

Ludwig, K.R., 2001a. Squid 1.02. A user's manual. BGC Special Publ. 2., Berkeley, 19p.

Ludwig, K.R., 2001b. User's manual for Isoplot/Ex v. 2.47. A geochronological toolkit for Microsoft Excel. BGC Special Publ. 1a, Berkeley, 55p.

Moraes, R., Brown, M., Fuck, R.A., Camargo, M.A., Lima, T.M., 2001. The evolution of melt-bearing UHT metamorphic mineral assemblages and construction of P-T paths: an example from Central Brazil. Journ. of Metam. Geology, 43(9): 1673-1705.

Nilson, A.A. & Motta, J., 1969. Geologia da área Goianira-Trindade, Goiás. Rio de Janeiro, DNPM/DFPM, (Boletim 133), 108 pp.

Pimentel, M.M. & Fuck, R.A., 1992. Neoproterozoic crustal accreation in Central Brazil. Geology 20, 375-379.

Pimentel, M.M., Fuck, R.A., Alvarenga, C.J.S., 1996. Post-Brasiliano (Pan-African) high-K granitic magmatism in Central Brazil: Late Precambrian/Early Paleozoic extension. Precambrian Research, 80: 217-238.

Pimentel, M.M., Fuck, R.A., Botelho, N.F., 1999. Granites and the geodynamic history of the Neoproterozoic Brasília Belt, Central Brazil: a review. Lithos, 46: 463-483.

Pimentel, M.M., Fuck, R.A., Gioia, S.M.C.L., 2000a. The Neoproterozoic Goiás Magmatic Arc, Central Brazil: a review and new Sm-Nd isotopic data. Revista Brasileira de Geociências, 30(1): 35-39.

Pimentel, M.M.; Fuck, R.A.; Jost, H.; Ferreira Filho, C.F., Araújo, S.M., 2000b. The basement of the Brasília Fold Belt and the Goiás Magmatic Arc. In: Cordani, U.G.; Milani, E.J.; Thomaz Filho, A., Campos, D.A. (eds). Tectonic Evolution of South America: 190-229.

Pimentel, M.M., Hollanda, M.H.B.M., Laux, J.H., Gioia, S.M.C.L., 2003. The Brasília Belt as a "hot orogen": new SHRIMP and conventional U-Pb data and Sm-Nd isotopic constraints from terminal mafic magmatism in central-western Goiás. In: Simp. Nac. Estudos Tectônicos, SNET, in press.

Piuzana, D., Pimentel, M.M., Armstrong, R., Fuck, R.A., 2002. SRHIMP U-Pb and Sm-Nd geochronology of the Anápolis-Itauçu Complex and associated granites: Neoproterozoic magmatism and high grade metamorphism in the Brasília Belt, Central Brazil. Precambrian Research, in press.

Silva, F.O., 1991. Geologia, estrutura, petrologia e mineralizações Fe-Ti-V associadas ao Complexo gabro-anortosítico de Santa Bárbara (Goiás). Msc Dissertation, Universidade de Brasília, 101 pp.

Silva, F.O., 1997. Geologia e petrologia do extremo noroeste do Complexo Máfico-Ultramáfico de Taquaral, GO. PhD Thesis. Universidade de Brasília, 171 pp.

Suita, M.T.F., Kamo, S.L., Krogh, T.E., Fyfe, W.S., Hartmman, L.A., 1994. U-Pb ages from the high-grade Barro Alto mafic-ultramafic complex (Goiás, Central Brazil): Middle Proterozoic continental magmatism and Upper Proterozoic continental collision. In: International Conference on Geochronology and Isotope Geology, 8., Abstracts, USGS, Berkeley, p. 309.

Williams, I.S. & Claesson, S., 1987. Isotopic evidence for the provenance and Caledonian metamorphism of high grade paragneisses from the Seve Nappes, Scandinavian Caledonides: ion microprobe zircon U-Th-Pb. Contrib. Mineral. Petrol., 97: 205-217.

NEW ID-TIMS U-Pb AGES IN THE WESTERN PORTION OF THE MARA ROSA ARC: TWO HUNDRED MILLION YEARS OF ARC BUILDING

Junges, S.L.; Pimentel, M.M.; Dantas, E.L. and Laux, J.H.

Instituto de Geociências, Universidade de Brasília. sjunges@yahoo.com, marcio@unb.br, elton@unb.br, slauxjh@unb.br

Keywords: Neoproterozoic, Brasilia Belt, Mara Rosa Arc, Pan-African/Brasiliano Cycle

INTRODUCTION

The Goiás Magmatic Arc was formed by accretion of island arc systems to the western margin of the São Francisco Craton during ca. 280 Ma; since ca. 890 Ma until ca. 610 Ma (Pimentel & Fuck, 1992, Pimentel et al., 2000). Particularly in the Mara Rosa area, in the northern section of the arc, the earlier magmatic activity has been dated at approximately 860 Ma, and is represented by juvenile rocks with island arc signature (Pimentel et al., 1997). The younger ages, at approximately 560 Ma, refer to post-tectonic granites. Peraluminous, syntectonic granites, as well as one diorite intrusion are in the age interval between ca. 640-615 Ma. Sm-Nd garnet ages and titanite U-Pb ages at 610, 600, 630 and 760 Ma are indicative of the main metamorphic events (Junges et al., 2002a, b). In this study we report new U-Pb zircon ages indicating a very young episode of juvenile magmatism at ca. 600-640 Ma in the western part of the Mara Rosa arc, leading to new considerations about the Goiás Magmatic arc evolution in Mara Rosa, mainly regarding the timing of tonalitic magmatism and arc building episodes.

GEOLOGICAL SETTING

The Goiás Magmatic Arc in the Mara Rosa area is characterized by three NE-SW trending belts of supracrustal rocks separated from each other by tonalitic terrains (Fig. 1, Arantes et al., 1991). All rocks units are metamorphosed under amphibolite facies conditions but have kept major geochemical and isotopic features indicating the juvenile, mantle-derived nature of the igneous protoliths (Pimentel et al., 1997; Junges, 1998; Junges et al., 2002). The supracrustal belts include mainly amphibolite and feldspar schist. Mylonitic and peraluminous granites are associated with ductile shear zones. Late to post-tectonic gabbroic and dioritic intrusions intrude into the supracrustal rocks.

The very primitive chemical nature of the amphibolites suggests that the protoliths were calc-alkaline basalt and andesite. Also, subalkaline tholeiitic basalt has been identified in the area (Kuyumjian, 1994; Palermo, 1996; Junges, 1998). The tonalitic rocks show volcanic arc chemical characteristics and positive ε_{Nd} values, pointing to a depleted mantle component. T_{DM} model ages for the arc rocks range from 900 to 1200 Ma, with isotopic signatures typical of rocks generated in an island arc enviroment (Kuyumjian, 1989; Viana & Pimentel, 1994; Junges et al., 2002a).

The oldest U-Pb zircon ages in the arc are about 860 Ma and refer to a tonalitic gneiss and one mylonitic granite, in the eastern belt (Pimentel et al., 1997). Mylonitic granites and a syn-tectonic diorite, in the western belt, show ages of 645 Ma and 630 Ma. Two main metamorphic events are recorded in theses rocks, with approximate ages at ca. 760 and 630 Ma (Table 1).

RESULTS AND DISCUSSION

Two amphibolite samples were dated, one from an elongated body at the west limit of the arc (MR-150) and another from the western supracrustal belt (MR-144) (see Figure 1 for sample location). Both amphibolite samples show coarse grain size, indicating the intrusive nature of the protoliths. Three tonalitic orthogneiss units (MR-143, MR-128, MR-135; Fig. 1) in the vicinities of the western belt of the arc were also investigated.

Zircons grains from MR-144 sample are very clear, prismatic and form short to medium prisms. They yielded a concordia age of 638 +/-2 Ma (Fig. 2a). Zircon grains from MR-150 are dark pink to brown, prismatic and medium to long in size. They indicated an upper intercept age of 603 +/-6 Ma (Fig. 2b). Zircon crystals from the tonalite rocks are mainly light pink, prismatic and short to medium. MR-135 has a concordia age of 807 +/-5Ma (Fig. 2c); MR-143 crystallized 629 +/-5 Ma ago (Fig. 2d) and MR-128, in a Tera-Wasserburg diagram shows an age of 622 +/-3 Ma, (Figs. 2e and 2f).

The identification of metaigenous rocks, with island arc signature in the west portion of the Mara Rosa arc, which are ca. 250 Ma younger than the rocks from the eastern portion, raises some new hypothesis about the evolution of the Goiás Magmatic Arc in this region:

1) The two sets of ages point to island arc rocks formed in two distinct episodes; one generated at ca. 860 Ma at the east and the other formed at approximately 630 Ma in the western part of the arc;

2) Rocks with ages at about 640 Ma to 600 Ma seem have a more significant role in the arc evolution in terms of magma volume and possibly heat flow;

3) The Goiás Magmatic Arc is a very expressive tectonic unit in Central Brasil. In the Mara Rosa region, magmatic activity started at ca. 860 Ma and ended at ca. 560 Ma, with an apparently important peak at ca. 630 Ma.

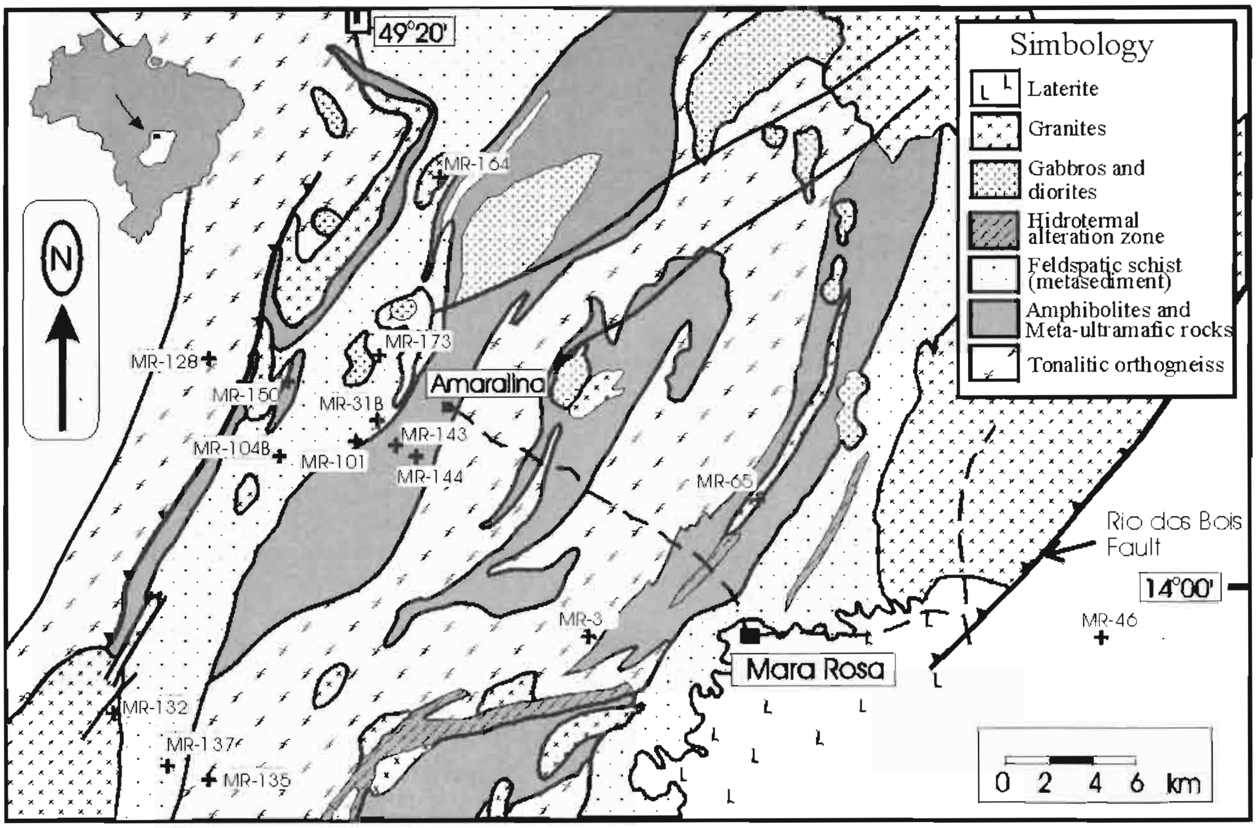

Figure 1. Mara Rosa geologic map (after Arantes et al., 1991).

Table 1. Main, ***and new,*** Mara Rosa region ages.

Sample	**Rock**	**Age** (Ma)	**Method**
MR-46	Pau de Mel granite, eaest of the arc	2,176+12/-9	U-Pb in zircon
MR-65	millonitic granite, Posse mine	862+/-8 632+/-4	U-Pb in zircon U-Pb in titanite
MR-3	tonalitic orthogneiss	856+13/-7	U-Pb in zircon
MR-135 New	***tonalitic orthogneiss***	***807+/-5***	***U-Pb in zircon***
MR-137B	fine feldspathic schist	765+/-75	Sm-Nd mineral isochron
MR-137A	coarse feldspathic schist	760+/-75	Sm-Nd mineral isochron
MR-164	millonitic granite	645+/-9 and 2,249+/-32	U-Pb in zircon
MR-144 New	***coarse amphibolite***	***638+/-2***	***U-Pb in zircon***
MR-104B	millonitic granite vein	635+/-12	U-Pb in zircon
MR-31B	subvulcanic diorite	630+/-3	U-Pb in zircon
MR-128 New	***tonalitic orthogneiss***	***623+/-2***	***U-Pb in zircon***
MR-143 New	***tonalitic orthogneiss***	***629+/-7***	***U-Pb in zircon***
MR-101A	feldspathic schist	610+/-52	Sm-Nd mineral isochron
MR-173	feldspathic schist	604+/-66	Sm-Nd mineral isochron
MR-150 New	***coarse amphibolite***	***603+/-3***	***U-Pb in zircon***
MR-132	Faina postectonic granite	576+/-6,4	U-Pb in zircon

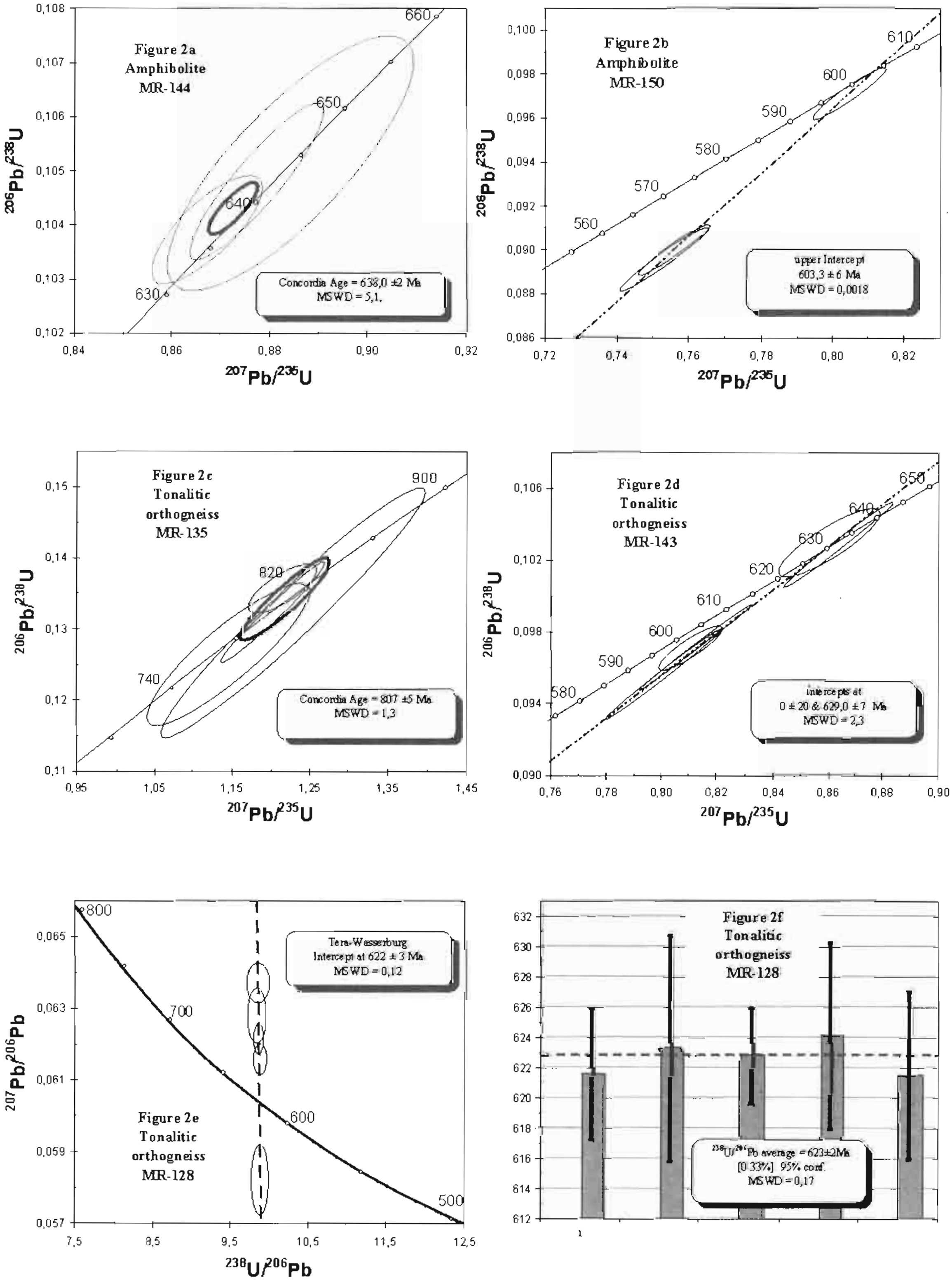

Figure 2. U-Pb data.

REFERENCES

Arantes D.; Osborne, G. A.; Buck, P. S.; Porto, C. G. 1991. The Mara Rosa Volcano-sedimentary Sequence and associated gold mineralization. Brazil Gold'91, E. A. Ladeira (ed.). Balkena. p221-229.

Kuyumjian, R. M. 1989. The Geochemistry and Tectonic Ssignificance from the Chapada Sequence, Central Brazil. D.Phil. Thesis, Royal School of Mines, Imperial College of Science and Technology, University of London, 289p.

Kuyumjian, R. M. 1994. Geologia da seqüência Mara Rosa na região de chapada, Goiás. IV Simpósio de Geologia do Centro-Oeste, anais p142-144.

Junges, S. L., 1998. Caracterização Geoquímica e Isotópica da Faixa Oeste da Seqüência Vulcanossedimentar de Mara Rosa. 'MSc dissertation. Univ. de Brasília, 120p, (unpublished).

Junges, S. L.; Pimentel, M. M.; Moraes, R., 2002a. Nd isotopic study of the Neoproterozoic Mara Rosa Arc, central Brazil: implications for the evolution of the Brasilia Belt. Precambrian Research 117, p101-118.

Junges, S. L., Pimentel, M. M., Dantas, E. L. & Laux, J.H., 2002b. Idades U-Pb de granitos sin- a tardi-tectônicos do Arco de Mara Rosa, Goiás. Anais do XLI Congresso Brasileiro de Geologia.

Palermo, N., 1996. Le Gissement aurifère précambrien de Posse (Goiás, Bresil) dans sou cache géologique. These de doctorat, ENSPM, Paris, 175p + annexes.

Pimentel, M. M. & Fuck, R. A. 1992. Neoproterozoic crustal accretion in central Brazil. Geology, 20:375-359.

Pimentel, M. M.; Whitehouse, M. J., Viana, M. G., Fuck, R. A., Machado, N., 1997. The Mara Rosa Arc in The Tocantins Province: further evidence for Neoproterozoic crustal acreation in Central Brazil. Precambrian Res. 81, 299-310.

Pimentel, M. M.; Fuck, R.A.; Jost, H.; Ferreira Filho, C. F.; Araújo, S.M. 2000. Geology of the central part of the Tocantins Province: Implications for the geodynamic history of the Brasília belt. In: Cordani, U.G. (Editor), Tectonic Evolution of South America p.195-229.

Viana, M. G. & Pimentel, M. M. 1993. Dados geoquímicos e isotópicos Sm-Nd preliminares para rochas metavulcânicas e metaplutônicas da região de Mara Rosa. IV Simpósio de Geologia do Centro-Oeste. SBG, Brasília, anais, p148-151.

PROBING THE CRUST FROM THE NE BRAZIL THROUGH THE ISOTOPIC GEOLOGY FROM THE PROTEROZOIC ÁGUAS BELAS-CANINDÉ GRANITIC BATHOLITH, PERNAMBUCO-ALAGOAS TERRANE, BORBOREMA PROVINCE

Lyra de Brito, M.F.[1]; Silva Filho, A.F.[2]; Guimarães, I.P.[2] and Santos, E.J.[2]

1. CPRM-RE, Av. Sul, 2291, Afogados Recife-PE, 50770-011-Brasil. geremipe@fisepe.pe.gov.br
2. DGEO-UFPE, Recife-PE , 50740-530 Brasil. afsf@ufpe.br

Keywords: Isotope geology, geology of granites, crustal evolution, geotectonic

INTRODUCTION

The Pernambuco-Alagoas Terrane (PAT) was proposed by Santos (1995) to the unit previously defined by Neves (1975) as the Pernambuco-Alagoas Massif. This unit is limited to the north by the Rio Capibaribe, Alto Moxotó and Alto Pajeú Terranes and to the south by the Sergipano System and the São Francisco Craton. Silva Filho et al. (2002) characterized several batholiths of the PAT where the Águas Belas-Canindé Batholith (ABCB) is the larger one, located into the Água Branca Crustal Domain.

The ABCB occupies an area of ca. 5,000 sq. km, showing a NE-SW trending axis. It makes making contact to the south and to the east with the Sergipano Fold System, through low-angle faults, and to the west and to the north with the metassediments of the Cabrobó Complex, through the Ouro Branco low-angle fault. The contacts with the Cabrobó Complex are sharp and marked by the Tanquinho Granitic Complex. Geochemical signature showed by various granitic plutons from the ABCB suggests the same evolved during two processes, subduction and a later collisional process, respectively. Same fault was later reactivated as a transcurrent one. This work evaluates the significance of the Águas Belas-Canindé Batholith during the Brasiliano and the pre-Brasiliano orogenies which might have occurred in the area, based on field and isotopic geology.

GEOLOGIC SETTING AND PETROGRAPHY

Geologic mapping 1:100.000 have recently been done, supported by remote sensing imagery and petrographic studies. It reveals the existence of dozens of granitic plutons and stocks, mainly late tectonic, intruded into tonalitic to syenogranitic diatexites. Some have been dated (Silva Filho et al., 2002), yielding Neoproterozoic ages. The diatexites form nucleus around Fazenda Nova Village, to the SE of Dois Riachos town and around Poço das Trincheiras town, totaling ca. 200 km^2. Metatexites occur to the south of Inhapi, along the contact with the Cabrobó Complex, grading into diatexites and forming a complex of ca. 200 km^2. Orthogneisses of metaluminous composition occur only in the Fazenda Nova village.

Preliminar petrographical and field work data show the granites, together with previous works, are either peraluminous and metaluminous. The peraluminous super-suite is represented by medium to high-K and high-K granites. The medium to high-K, peraluminous plutons are represented by Serra do Boqueirão, Carneiros (one of the largest plutons of the batholith), Lagoa do Correio, Ouricuri, Fazenda Ribeira de Baixo, Serra da Capela, Rui Palmeira, Dois Riachos, São José da Tapera, Serra do Poço, Serra do Macaco, Serra do Almeida, Lagoa do Tanque and Manuel da Costa. The syn-tectonic plutons show NE-SW trends. They are mainly quartz-diorites to quartzmonzonites, biotite quartzmonzodiorites to granodiorites, tonalites, biotite monzogranites, biotite granodiorites, syenogranites and monzogranites. The mineralogy is comprised by biotite, ± muscovite, plagioclase, quartz, zircon, ± apatite, microcline and ± opaques. No one shows either garnet or alumino-silicates. The high-K, peraluminous plutons are the Serra das Lagoas pluton and Fazenda Gameleira stock. They are biotite quartzmonzonites and quartzsyenites, and syenogranites in composition, respectively.

The metaluminous super-suite is represented by medium to high-K plutons and stocks, high-K plutons, shoshonitic affinity plutons (ex: the Serra do Catu Complex). The medium to high-K series is represented by the Lagoa do Correio pluton and the Fazenda Supapo stock. They are quartzdiorite, quartzmonzodiorite, quartzmonzonite, granodiorite, tonalite, and monzogranite in the composition. The texture ranges from equigranular to inequigranular. When porphyritic, they show phenocrystals ranging from 1 to 5cm long. The main minerals are plagioclase, alkali feldspar and quartz. The accessories are amphibole, biotite, titanite, opaques, apatite, zircon, ± epidote, ± leucoxene, ± allanite, ± sericite, ± carbonate, ± rutile and ± muscovite. The high-K suite is represented by the Tanquinho Complex (Serra Negra, São Raimundo, Serra dos Bois and Maravilha plutons), Moita stock and the syn-tectonic stock of Santana do Ipanema. The Tanquinho Complex occupies ca. 600 km^2 of area, being among the major one in the Borborema Province. It is comprised by four plutons of quartz-monzonitic, granodioritic, monzogranitic and syenogranitic composition. They have medium to coarse inequigranular texture, with phenocrystals ranging from 2 to 5 cm long. Some plutons show dioritic enclaves. The main minerals are quartz, plagioclase and alkali feldspar. The accessories are amphibole, pyroxene, titanite, apatite, zircon, opaques, magmatic epidote, allanite, chlorite, carbonate, rutile and leucoxene. Rapakivi texture is common. The shoshonitic affinity suite is represented by the Serra do Catu Complex, Serra da Caiçara and Fazenda Branquinha stocks, Santana do Ipanema dykes and Ribeira do Capiá megadykes. The Serra do Catu

Complex is comprised by porphyritic to inequigranular quartz-monzonites, syenites and quartz-syenites. They commonly show mafic enclaves. The main minerals are alkali feldspars, quartz and plagioclase. The accessories are calcic amphibole, alkali amphibole, clinopyroxenes, opaque, sphene, allanite, apatite, secondary epidote and zircon. The Serra da Caiçara stock is comprised by porphyritic syenogranites. The megadykes are comprised by porphyritic syenogranites, quartzsyenites and syenites. The mineralogy of the Serra da Caiçara and of the megadykes are similar to that showed by the Serra do Catu Complex. They fill a NE-SW fracture system.

ISOTOPIC GEOLOGY

Twenty five samples of granites and three of migmatites from the Águas Belas-Canindé Batholith have been analysed in the Isotope Geochemistry Laboratory of the University of Kansas, following the procedures of Patchet & Ruiz (1987). The results show the granites from the batholith groups three-fold; (1) Metaluminous and peraluminous granites with T_{DM} ranging from 0.90Ga to 1.23 Ga. and ε_{Nd} (t=0.6 Ga.) ranging from –2.0 to +3.0; (2) Metaluminous and shoshonitic granites showing T_{DM} ca. 1.40 Ga and ε_{Nd} ca. –6.0 (t=0.6 Ga.). (3) Metaluminous and peraluminous granites with T_{DM} ranging from 1.90 Ga to 2.10 Ga and ε_{Nd} (t=0.6Ga.) ranging from –8.0 to –12.0. The analyzed migmatites are diatexites with metaluminous amphibole bearing non-restitic mafic phase. They show T_{DM} age ranging from 1.16 Ga. to 1.33 Ga. and ε_{Nd} (t=0.6 Ga.) ranging from –0.7 to –2.8. The mineralogy and preliminary whole-rock geochemistry of the Group 1 plutons favors the hypothesis that their protoliths were mainly igneous rocks, either volcanic or plutonic. These data, associated with the Sm-Nd isotopic geochemistry, suggest that the best candidate for their protolith are: (1) mixture of juvenile material associated with the Cariris Velhos cycle and a small amount of older (Paleoproterozoic) crust, or (2) juvenile material of Neoproterozoic age, mixed with Paleoproterozoic or Cariris Velhos crust, giving rise to magmas which evolved through an AFC process. The syenogranites to monzogranites represents the most differentiated members. Amphibole ± biotite granitoids (metaluminous) with composition ranging from diorites to granodiorites of Group 1 granitoids show Nd signatures and tectonic setting similar to the peraluminous intrusions. Thus, different crustal compositions with similar Nd isotope signature were involved in the protolith of the ABCB, suggesting a vertically zoned crust in the area. The tectonic setting suggests the ascent of a primitive magma occurred through an existing shear zone system, reactivated during a Brasiliano transtensional event. Suites similar to the Tanquinho complex have been identified in others batholiths from the PAT, attesting the similarities between the batholiths and the importance of underplating magmas during the Brasiliano cycle. Plutons from Group 2 granites show high-K to shoshonitic composition (Serra do Catu, Serra da Caiçara and the megadykes) and T_{DM} ages around 1.40 Ga. The correlation between their Nd isotopes, geologic setting and geochemistry (Silva Filho et al., 1995, 1996) suggest the possibility of similar protoliths. An enriched lithospheric mantle is the best candidate for the protolith of the high-K calc-alkaline to shoshonitic magmas. The similarities between their isotopic signatures and related migmatitic country rocks suggest they came from same lithospheric layer. The plutons that comprise Group 3, require a variation to the previous described model. These plutons show different Nd isotope and trace element geochemical signatures with T_{DM} around 2.14 Ga. and ε_{Nd} (t=0.6 Ga.) around –12.4, which reflects a small degree of partial melting of a mafic Paleoproterozoic crust.

DISCUSSION AND CONCLUSIONS

The geochemical, geological and isotopic data from Group 1 granites suggest mafic underplating during the late Meso and Neoproterozoic in the PAT. These granites show volcanic arc signature (Silva Filho et al., 2000). Nd isotope associated with the arc signature suggests that the mafic magma may have been a mixture from a subducting oceanic slab (1.0 Ga.?) and older lithospheric mantle. The mafic magmas differentiated to yield a zoned lower crust, explaining the geochemical differences among the granitoid magmas subsequently derived from it.

The Group 2 granites show a narrow range of ε_{Nd} (t=0.6 Ga.) data, suggesting they came from a homogeneous source. They show as well similar isotopic signature to their migmatitic country rocks. The best hypothesis so far identified for generating process of these granites, based on Nd x Sr isotopic data, is melting of mafic rocks derived from enriched mantle, incorporated into the lower crust during the Brasiliano cycle. These mafic rocks might have been originated from a mantle enriched by the subduction of a 1.5 Ga., or even older crust.

The Nd isotopic signatures of Group 3 granites are associated with high LILE contents (Silva Filho et al., 1996). They show inherited zircons and high and restricted SiO_2 values. Evidence of mantle metasomatism during the Trans-Amazonian Orogeny within the Borborema Province has been reported by various authors. Thus the best candidate for the protolith of these granitoids is a mantle material, enriched in incompatible elements during the Trans-Amazonian Orogeny. They might have incorporated (with some assimilation) into the crust during the Brasiliano cycle, or during the later stages of the Trans-Amazonian Orogeny.

REFERENCES

Neves, B.B.B., 1975. Regionalização geotectônica do Precambriano nordestino. Tese doutoramento, USP/Inst. Geoc., 198p. (inédito)

Santos, E.J., 1995. O complexo granítico Lagoas das Pedras: Acresção e colisão na região de Floresta, PE Província Borborema. Doctoral Dissert., USP, São Paulo, 220p.

Silva Filho, A F. Guimarães, I.P., Torres, V.M., 1995. The Shoshonitic Serra do Catu complex, NE Brazil. Anais do 5° Congresso Brasileiro de Geoquímica, Niterói, extended abstract (in CD-ROM).

Silva Filho, A F. Mariano, G. Guimarães, I.P., Luna, E.B.A , 1996. Caracterização do complexo granítico tarditectônico de Santana do Ipanema, AL, Borda sul do maciço PEAL. Anais do 39 Congresso Brasileiro de Geologia, Salvador, V.6, pp. 315-317.

Silva Filho, A.F. & Guimarães, I.P., 2000. Sm/Nd isotopic data and U-Pb geochrology of collisional/post collisional high-K to shoshonitic granitoids from the PE-AL terrane, Borborema province, NE Brazil. Proc. Int. Geological Congress, Rio de Janeiro, abstract in CD-ROM.

Silva Filho, A.F., Guimarães, I.P., Van Schmus, W.R., 2002. Crustal evolution of the Pernambuco –Alagoas Complex, Borborema Province, NE Brazil: Nd isotopic Data from Neoproterozoic granitoids. Gondwana Research, V.5, n. 2, pp. 409-422.

NEW ISOTOPE EVIDENCES CONFIRMING THE EXISTENCE OF A PALEOPROTEROZOIC TERRAIN IN THE REGION AT THE NORTH OF THE CARAJAS MINERAL PROVINCE

Macambira, M.J.B.[1]; Silva, D.C.C.[2]; Barros, C.E.M.[3] and Scheller, T.[1]

1. Laboratório Para-Iso/Universidade Federal do Pará. moamac@ufpa.br
2. Curso de Geologia/Universidade Federal do Pará. danikris@bol.com.br
3. Grupo de Petrologia de Granitóides/Universidade Federal do Pará. cadu@ufpa.br

Keywords: Amazonian Craton, geochronological provinces, Nd isotopes, zircon dating

INTRODUCTION

The geotectonic model of evolution for the Amazonian craton admitting a sequence of Proterozoic provinces surrounding an Archean nucleus was first proposed in the seventies (Cordani et al., 1979), and has been established as the best appropriated model to explain the main geological features of the craton. Since then, this model has been updated and followed, but it is not yet a consensus (e. g. Lima, 1984; Teixeira et al., 1989; Tassinari & Macambira, 1999; Santos et al., 2000; Dall´Agnol et al., 2000).

The limits of these provinces encompass important changes in timing, tectonic regime and products, and are key-regions for the understanding of the evolution of the craton as a whole. However, generally, the geology of these regions is poorly known, specially the nature and geographical location of the boundaries. One of these regions is the boundary between the Archean Carajás Mineral Province and the Paleoproterozoic domain to the north (Maroni-Itacaiunas or Transamazonian Province). Cordani et al. (1984), based on K-Ar and Rb-Sr data, suggested that it is located nearby the 5° S parallel. Further mappings, as those improved by CPRM (Oliveira et al., 1994), show that in this region, the rocks are similar to those of the Carajás Province, and are, probably, Archean. Tassinari et al. (2000) keep this limit but they have introduced some incertitude about its geographical location. On the other hand, some Archean ages obtained on granulites and granitoids from the basement of the Amapá State, as well as on detrital zircons from a quartzite of the French Guyana (e. g. Lafon et al., 1998) induced Santos et al. (2000) to propose the boundary of the Archean domain as located at the central Amapá. For these last authors, the central-southern part of the Amapá State and the Carajás region make part of a single province (Carajás-Imataca), encompassing the Imataca region, in Venezuela.

This work presents new isotope data for the rocks outcropping in the region at the north of the Carajás Mineral Province, Pará State, in order to characterize the nature of these rocks and provide addicional information for the establishment of boundary between the Archean and Paleoproterozoic domains of the southeastern part of the Amazonian craton.

GEOLOGICAL SETTING

The study region represents a 250 km NW band linking the Novo Repartimento and Belo Monte (Xingu river margin) towns, crossed by the Transamazonian route. The rocks of the region are mainly composed by granitoids covered, to the north and east, by sedimentary sequences of the Phanerozoic Amazon and Parnaíba basins, respectively. To the west, the granitoids seem to be associated with a set of metamorphic rocks yielding Rb-Sr ages between 1.9 and 2.0 Ga, and covered by the volcanic rocks and crosscut by the plutonic rocks of the Uatumã Supergroup (Santos et al., 1988). As noted above, the Archean rocks of the Carajás Province occur to the south, but the location of the limit and the nature of the relationships between these two domains are not yet established.

The geology of the study region is relatively monotonous and composed by granitoids previously reported by Reis et al. (1974). They are mainly medium-grained, pink to grey, and monzogranitic to granodioritc in composition. Locally they show heterogranular and porphyritic textures, and aplitic veins. Macambira et al. (2001) reported additional descriptions and propose a syntectonic regime for the emplacement of these granitoids based on their structural and textural features. These authors also reported an age obtained by zircon evaporation method of 2076 ± 6 Ma (2 sigmas), for a gray granodiorite sampled 9 km west from Novo Repartimento town.

ZIRCON GEOCRONOLOGY

Two additional samples of granitoids were analyzed by the zircon evaporation method in the Para-Iso Laboratory of the Federal University of Para (Belém, Brazil) using a Finnigan MAT 262 mass spectrometer. The first one was a pink monzogranite collected 6 km west from Novo Repartimento town. Three zircon grains yielded a confident age of 2075 ± 3 Ma (2 sigmas), confirming the previous age reported by Macambira et al. (2001). As pointed out by these authors, this age is correlated with that of the Transamazonian Cycle, which is supported by the syntectonic signature of the granitoids. The other sample was collected in the extreme west of the region. It represents a pink banded granitoid outcropping on the Xingu river margin. Five crystals from this sample yielded an age of 2154 ± 4 Ma (2 sigmas) and probably express another moment of the Transamazonian Cycle.

Nd ISOTOPES

Four granitoids, including the three dated samples mentioned above, were selected to a Sm-Nd study in the Para-Iso Laboratory using a Finnigan MAT 262 mass spectrometer. The fourth sample is a monzogranite collected similarly nearby Novo Repartimento town. This sample showed higher Sm and Nd contents (25 and 171 ppm, respectively) than the other samples (average of 3 and 25 ppm, respectively). The Nd model ages are comprised between 2.25 and 2.35 Ga, while the $\varepsilon Nd_{(t)}$ values range from +0.83 to -0.6, except the fourth sample, which yielded a model age of 2.57 Ga and an $\varepsilon Nd_{(t)}$ value of -4.12. The behavior of the fourth sample is not well understood, but is probably related to the more evolved character of this sample. In spite of its $^{147}Sm/^{144}Nd$ (0.08903) similar to those of other samples, the model age of this sample (2.57 Ga) is quite different and it was neglected in these preliminary considerations.

DISCUSSION AND CONCLUSIONS

Taking into account our field survey, the study rocks express a domain of coeval granitoids emplaced in a syntectonic regime probably related to the Transamazonian Cycle, 2.07 B.y. ago. The sample from the Xingu river is somewhat older (2.15 Ga), but it could represent an early magmatism in the same cycle. The Nd isotopes indicate that these rocks were extracted from the mantle just before their emplacement and are mainly composed by material with restricted crustal contribution.

The comparison of the rocks from the study region with similar rocks occurring in the Maroni-Itacaiunas or Transamazonian provinces, in French Guyana, suggests a similar evolution in both regions. It could include crustal shortening, anatexis and emplacement of granitic plutons along shear zones, as the modern orogenies, such as proposed by Vanderhaeghe et al. (1998) for the Guyana shield. For the study region, it lacks petrological and structural investigations to propose a more consistent model. Anyway, the volume of rocks is expressive and this region certainly represents a distinct tectonic domain from those of Carajás Province and central-southern part of the Amapá State, as previously proposed by others (e. g. Tassinari & Macambira, 1999). Alternatively, it could represent a magmatic arc which had blended the Archean domains occurring to the north and south.

ACKNOWLEDGMENTS

We are greathful to M. A. Galarza and R. Florença for the isotope analyses at the Para-Iso laboratory. This work is a Núcleo PRONEX/UFPA contribution.

REFERENCES

Cordani U.G., Tassinari C.C.G., Teixeira W., Basei M.A.S., Kawashita, K.1979. Evolução tectônica da Amazônia com base nos dados geocronológicos. In: Cong. Geol. Chileno, 2, Arica, Actas, 4:137-148.

Cordani U.G., Tassinari C.C.G., Kawashita, K.1984. A Serra dos Carajás como região limítrofe entre províncias tectônicas. Ciências da Terra, 9:6-11.

Dall'Agnol, R., Lafon, J.M., Fraga, L.M., Scandolara, J.E., Barros, C.E.M. 2000. The Precambrian evolution of the Amazonian Craton. In: Intern. Geol. Cong., 31, Rio de Janeiro, CD-Rom.

Lafon, J.M., Rossi, P.H., Delor, C., Avelar, V.G., Faraco M.T.L. 1998. Novos testemunhos de relíquias arqueanas na crosta continental paleoproterozóica da Província Maroni-Itacaiunas (sudeste do Escudo da Guianas). In: Cong. Bras. Geol., 40, B. Horizonte, Anais, p.64.

Lima, M.I.C. 1984. Províncias geológicas do Cráton Amazônico em território brasileiro. In: Symp. Amaz. , 2, Manaus, Anais, p. 9-23.

Macambira, M.J.B., Barros, C.E.M., Silva, D.C.C., Santos, M.C.C. 2001. Novos dados geocronológicos para a região ao norte da Província de Carajás: evidências para o estabelecimento do limite arqueano-paleoproterozóico no sudeste do Cráton Amazônico. In: Simp. Geol. Amaz., 7, Belém, CD-Rom.

Oliveira, J.R., Silva Neto, C.S., Costa, E.J.S. 1994. Programa Levantamentos Geológicos Básicos do Brasil. Programa Grande Carajás. Folha SB.22-X-C Serra Pelada. Belém, CPRM .

Reis R.M., Silva G.H., Lobato, T.A.M. 1974. Projeto Transamazônica; trecho Estreito-Itaituba. Belém, MME/CPRM. Relatório Final. 106p.

Santos, J.O.S., Hartmann, L.A., Gaudette, H.E., Groves, D.I., McNaughton, N.J., Fletcher, I.R. 2000. A new understanding of the provinces of the Amazon Craton based on integration of field mapping and U-Pb and Sm-Nd geochronology. Gondwaana Res., 3:453-488.

Santos M.V., Tassinari C.C.G. Souza Filho E.E., Teixeira W., Ribeiro A.C.O., Payolla B.L., Vasconi A.V. 1988. Litoestratigrafia da rochas pré-cambrianas na bacia do médio rio Xingu – Altamira - PA. In: Cong. Latino-Amer. de Geol., 7, Belém, Anais, p.363-377.

Tassinari,C.C.G. & Macambira, M.J.B. 1999. Geochronological provinces of the Amazonian Craton. Episodes, 22:174-182.

Tassinari, C.C.G., Bettencourt, J.S. Geraldes, M.C. Macambira, M.J.B. Lafon, J.M. 2000. The Amazonian Craton. In: Cordani, U.G., Milani, E.J., Thomaz Filho, A., Campos, D.A. (eds.) 2000. Tectonic Evolution of South America. Ac. Bras. Cienc. etc. Rio de Janeiro. p.41-96.

Teixeira, W., Tassinari C.C.G., Cordani U.G., Kawashita, K. 1989. A review of geochronology of the Amazonian Craton; tectonic implications. Precambrian Res., 42:213-227.

Vanderhaeghe, O., Ledru, P., Thiéblemont., Egal, E., Cocherie, A., Tegyey., M., Milési, J.P. 1998. Contrasting mechanism of crustal growth: geodynamic evolution of the Paleoproterozoic granite-greenstone belts of French Guiana. Precambrian Res., 92:165-193.

Sm-Nd AND U-Pb SHRIMP ZIRCON STUDIES OF THE NICO PÉREZ TERRANE, REWORKED RIO DE LA PLATA CRATON, URUGUAY

Mallmann, G.[1]; Chemale Jr., F.[2]; Armstrong, R.[3] and Kawashita, K.[2]

1. Programa de Pós-graduação em Geociências, IG-UFRGS-CNPq, Brazil. guilherme.mallmann@ufrgs.br
2. Laboratório de Geologia Isotópica, IG-UFRGS, Brazil. farid.chemale@ufrgs.br
3. Research School of Earth Sciences, ANU, Australia. richard.armstrong@anu.edu.au

Keywords: Rio de La Plata craton, cratonic margin, Proterozoic, tectonic evolution, supracrustal belt, geochronology

INTRODUCTION

The Precambrian basement rocks of the Uruguay can be grouped in three main tectonic units: Piedra Alta Terrane (PAT), Nico Pérez Terrane (NPT) and Dom Feliciano Belt (DFB). These units are separated by crustal scale transcurrent shear zones named Sarandi del Yi Lineament and Sierra Ballena Shear Zone (Fig. 1).

Piedra Alta and Nico Pérez terranes make up together the Rio de La Plata Craton in the Uruguay, whereas the PAT represent the unreworked cratonic nuclei and the NPT the cratonic margin reworked at Neoproterozoic by Brasiliano/Pan-African cycle. PAT has lithotectonic units with ages ranging from 2.2 to 2.0 Ga and NPT from 3.4 to 0.5 Ga. The eastern Dom Feliciano Belt is the southernmost extension of Brasiliano (0.65 to 0.5 Ga) granitic-gneissic rocks from Brazil (Chemale Jr., 2000) and includes a 0.9 to 1.1 Ga Mesoproterozoic terrane named Punta del Este (Preciozzi et al., 1999).

This work focuses on the southern NPT (Fig. 2), providing a new U-Pb SHRIMP zircon data for mylonitic granite from the Carapé Complex, a Sm-Nd whole-rock isochronic age for Lavalleja basic volcanic-derived rocks and Sm-Nd analyses for some key-units.

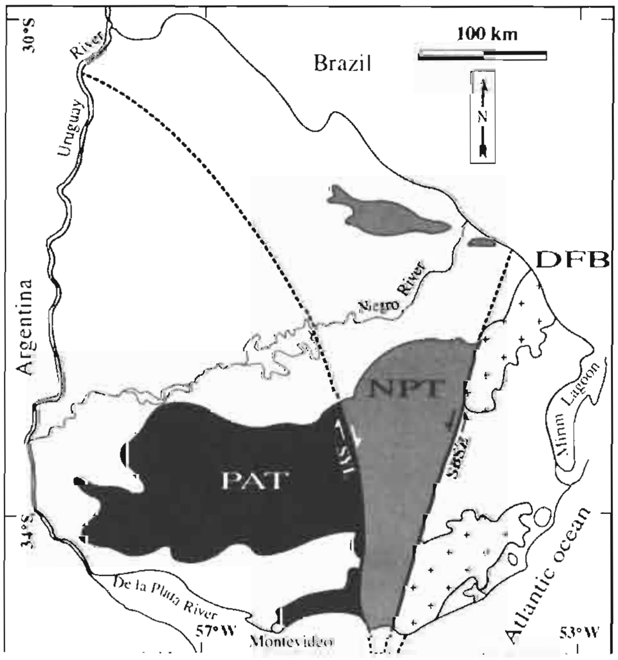

Figure 1. Main tectonic units of the Uruguay (After Bossi et al., 1998). PAT – Piedra Alta Terrane, NPT – Nico Pérez Terrane, DFB – Dom Feliciano Belt. SYL – Sarandi del Yi Lineament, SBSZ – Sierra Ballena Shear Zone.

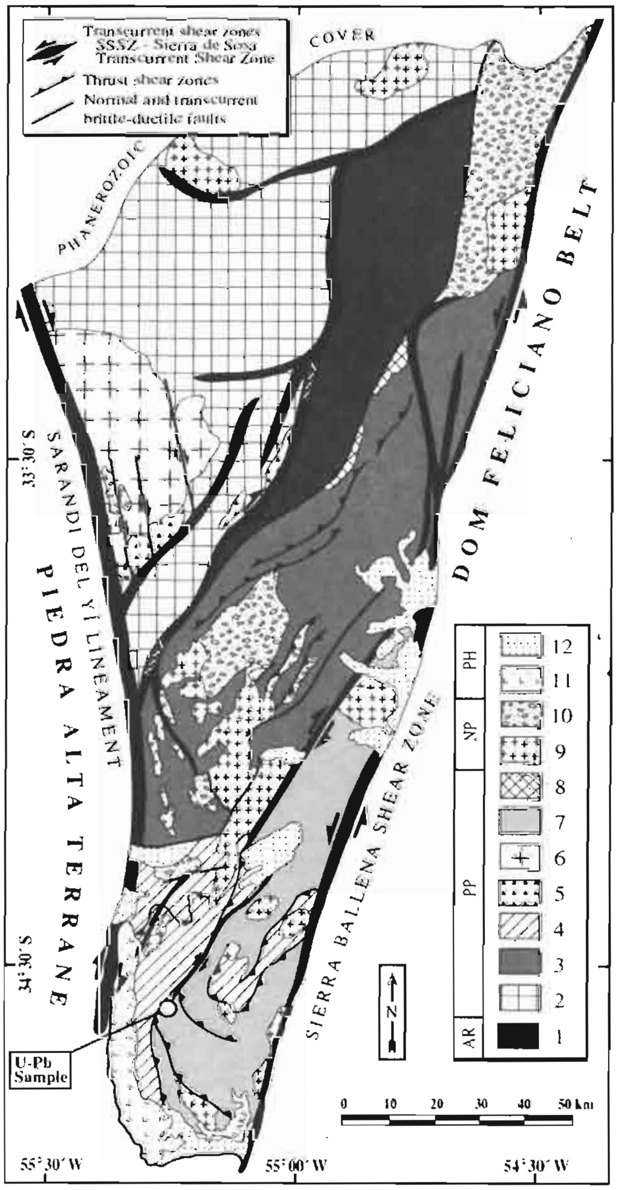

Figure 2. Geologic map of the Nico Pérez Terrane (modified after Bossi et al., 1998). 1- La China Complex, 2- Valentines Granulitic Complex, 3- Las Tetas Complex, 4- Lavalleja Metamorphic Complex, 5-Undivided diorites, 6- Illescas Batholith, 7- Carapé Complex, 8-Undivided granites, 9- Brasiliano granites, 10- Arroyo Del Soldado Group, 11- Las Animas Complex, 12- Phanerozoic cover.

Sm-Nd GEOCRHONOLOGY OF THE LAVALLEJA METAMORPHIC COMPLEX

Lavalleja Metamorphic Complex is a meta-volcano sedimentary sequence exposed along NE-SW-trending belt in the southwestern Nico Pérez Terrane (Fig. 2). It comprises basic metavolcanic rocks and few occurrences of metagabbros and acid volcanic rocks interlayered with chemical and clastic meta-sedimentary rocks (Sánchez Bettucci et al., 2001).

Eigth whole-rock samples of basic volcanic and subvolcanic-derived rocks from this unit were analyzed by Sm-Nd method at the Laboratório de Geologia Isotópica, Universidade Federal do Rio Grande do Sul, using a thermal ionization VG Sector 54 mass spectrometry after isotope dilution procedures. The data plotted in a Sm-Nd isochron yields an age of 1812 ± 360 with MSWD of 1.10 (Fig. 3). In spite of the large error data, this age is here interpreted as an estimated age of magmatic activity of this basin, and can be corroborated by Sm-Nd model ages (see Sm-Nd discussion), positioning the formation of Lavalleja basin in the Paleoproterozoic.

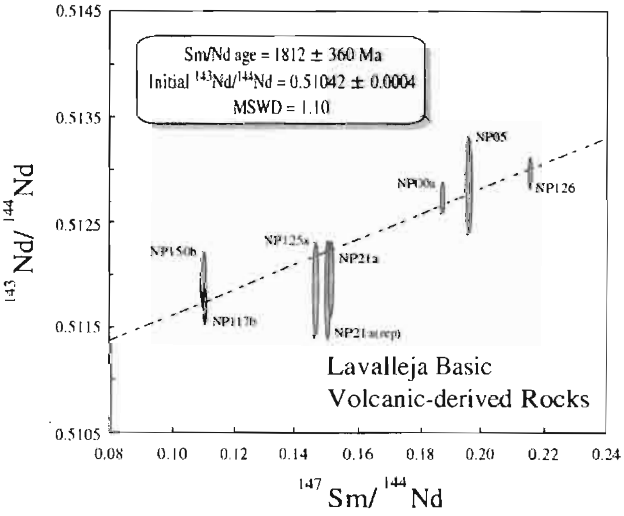

Figure 3. Sm-Nd isochronic age of Lavalleja basic volcanic-derived rocks.

U-Pb SHRIMP ZIRCON GEOCHRONOLOGY OF THE CARAPÉ COMPLEX

Carapé Complex constitutes a granitic-gneissic unit exposed along NE-SW trending belt in the southeastern Nico Pérez Terrane (Fig. 2). It comprises several generations of granitic rocks deformed mainly at Neoproterozoic. Carapé Complex is intruded by sin- to late Brasiliano granites (Sanchez Bettucci et al., 2003) and thrusted over Lavalleja Metamorphic Complex.

A flat-lying mylonitic, gray-colored, fine-grained biotite-muscovite sienogranite was collected along Ruta 60 (10 km south of Ruta 81 crossing point, Fig. 2). Zircons were separated after crushing, milling and conventional heavy liquids and magnetic procedures, and mounted in an epoxy disk to cathodoluminescence and BSE observations. U-Pb zircon SHRIMP analyses were carried out in the Research School of Earth Sciences, Australian National University, and procedures are similar to those described in Armstrong and Wilson, 2000.

Zircon crystals are prismatic, has 200 μm mean length and 2x1 axes relations. No metamorphic recrystallized rims are present. Twelve SHRIMP spots in 9 zircon crystals (central portions) provides a ^{207}Pb/^{206}Pb isochronic age of 1754 ± 6.8 Ma with MSDW of 0.72, interpreted as the magmatic crystallization age of the rock (Fig. 4).

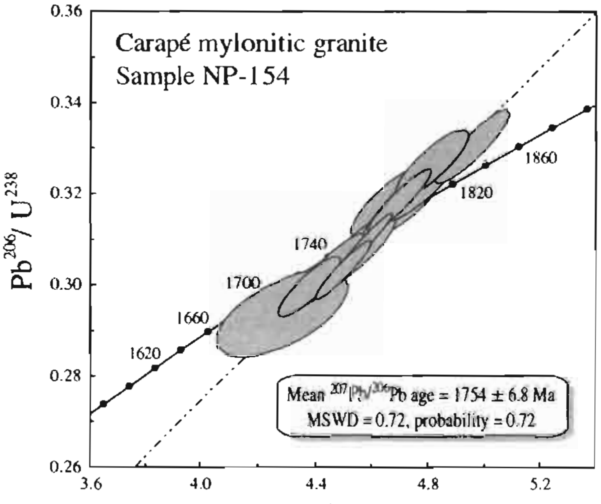

Figure 4. U-Pb SHRIMP isochronic age for Carapé mylonitic granite.

Sm-Nd ISOTOPE GEOCHEMISTRY

Sm-Nd T_{DM} model ages, calculated using De Paolo (1981) model, for some igneous- and sedimentary-derived whole-rock samples of the Nico Pérez Terrane (Fig. 5) presenting a bimodal distribution, with a Paleoproterozoic (1.6 to 1.9 Ga) and an Archean (2.6 to 3.1 Ga) group.

For the central Nico Pérez Terrane, except the Zapican diorite which yield a T_{DM} model age of 1.8 Ga, the other units yield model ages between 2.6 and 3.1 Ga (metatonalite of La China Complex, undivided metagranite and meta-arenite of Las Tetas Complex) (Fig. 5).

For the southern Nico Pérez Terrane, a Carapé Complex metagranite (the same of SHRIMP data) yield an Archean T_{DM} model age with strong negative εNd(t) value, and an intrusive Brasiliano granite in the Carapé Complex yield a Paleoproterozoic model age (sample NP75b). Two T_{DM} model ages populations were recognized for Lavalleja igneous-derived rocks: an Archean and the other Paleoproterozoic (Fig. 5). Estimated εNd(t) values for Archean model ages of the Lavalleja Metamorphic Complex are slight negative, and probably indicates crustal contamination. In contrast, Paleoproterozoic population show estimated εNd(t) values close to the CHUR or slight positive, with two different fractionation paths (more and less flat). So, this model age population probably represents the less modified mantle source for basic magmatism, and can provide an estimated age of volcanic activity. Coarse-grained meta-sediments from Lavalleja Metamorphic Complex show T_{DM} model ages close to the Paleoproterozoic, whilst fine-grained meta-sediments show mixing model ages between Archean and Paleoproterozoic source areas.

CONCLUDING REMARKS

We have the following conclusions:

1. The Sm-Nd isochronic age around 1.8 Ga obtained for volcanic-derived rocks of the Lavalleja Metamorphic Complex and the Sm-Nd T_{DM} model ages close to this value for some samples with juvenile characteristics, point to the time of basin formation during the late Paleoproterozoic.
2. The U-Pb SHRIMP zircon age of 1754±6.8 Ma obtained for a mylonitic granite from the Carapé Complex extends the Rio de La Plata Craton in the Uruguay up to the Sierra Ballena Shear Zone.
3. Bimodal distribution of Sm-Nd T_{DM} model ages in the Nico Pérez Terrane could be distinguish two principal periods of crust generation in the Uruguay: the Archean and the Paleoproterozoic.
4. The Sm-Nd T_{DM} model ages suggest that Lavalleja basin was formed over a composed Archean/Paleoproterozoic crust, and present different degrees of crustal contamination and juvenile contribution (εNd t values close to the CHUR line). And, Carapé Complex was formed as result of a reworked Archean crust.
6. The NPT presents a complex structural framework characterized by thrust stacked units with different ages and tectonic settings. We are interpreting these structures as a consequence of the interaction between the Rio de La Plata and Kalahari cratons during the Brasiliano/Pan-African collage. So, these rocks represent a reworked margin of the Rio de La Plata during the Neoproterozoic.

ACKNOWLEDGMENTS

This work had finnancial support by CNPq (520019-96-2). We thank to Nestor Campal, Jorge Bossi and Ricardo Ayup Zouain for introduction to the area and fruitfully discussions and to Janaina N. Avila, Edinei Koester and Rommulo Conceição for laboratory helps.

REFERENCES

Armstrong, R. & Wilson, A.H., 2000. A SHRIMP U-Pb study of zircons from the layered sequence of the Great Dike, Zimbabwe, and a granitoid anatetic dike: Earth and Planetary Science Letters 180: 1-12.

Bossi, J., Ferrando, L., Montaña, J., Campal, N., Morales, H., Gancio, F., Schipilov, A., Piñeyro, D., Sprechmann, P., 1998. Carta geológica del Uruguay, escala 1:500.000. GEOEDITORES, Montevideo, Uruguay.

Chemale Jr., F., 2000. Evolução geológica do Escudo Sul-rio-grandense. In: M. Holz & L.F. De Ros (Eds.). Geologia do Rio Grande do Sul. CIGO – UFRGS, pp. 13-52.

De Paolo, D., 1981. Neodymium isotopes in the Colorado Front Range and crust-mantle evolution in the Proterozoic: Nature 291: 193-196.

Preciozzi, F., Masquelin, H., Basei, M.A.S., 1999. The Namaqua/Grenville Terrane of eastern Uruguay: 2nd South American Symposium on Isotope Geology, Argentina, pp. 338-340.

Sánchez Bettucci, L., Cosarinsky, M., Ramos, V.A., 2001. Tectonic setting of the late Proterozoic Lavalleja Group (Dom Feliciano Belt) Uruguay: Gondwana Research 4: 395-407

Sánchez Bettucci, L., Oyhantçabal, P., Page, S., Ramos, V.A., 2003. Petrography and geochemistry of the Carapé Granitic Complex (southeastern Uruguay): Gondwana Research 6: 89-105.

Teixeira, W., Renne, P., Bossi, J., Campal, N., Dagrella Filho, M., 1999. Ar^{40}/Ar^{39} and Rb/Sr geochronology of the Uruguay Dike Swarm, Rio de La Plata Craton: Precambrian Research 93: 153-180.

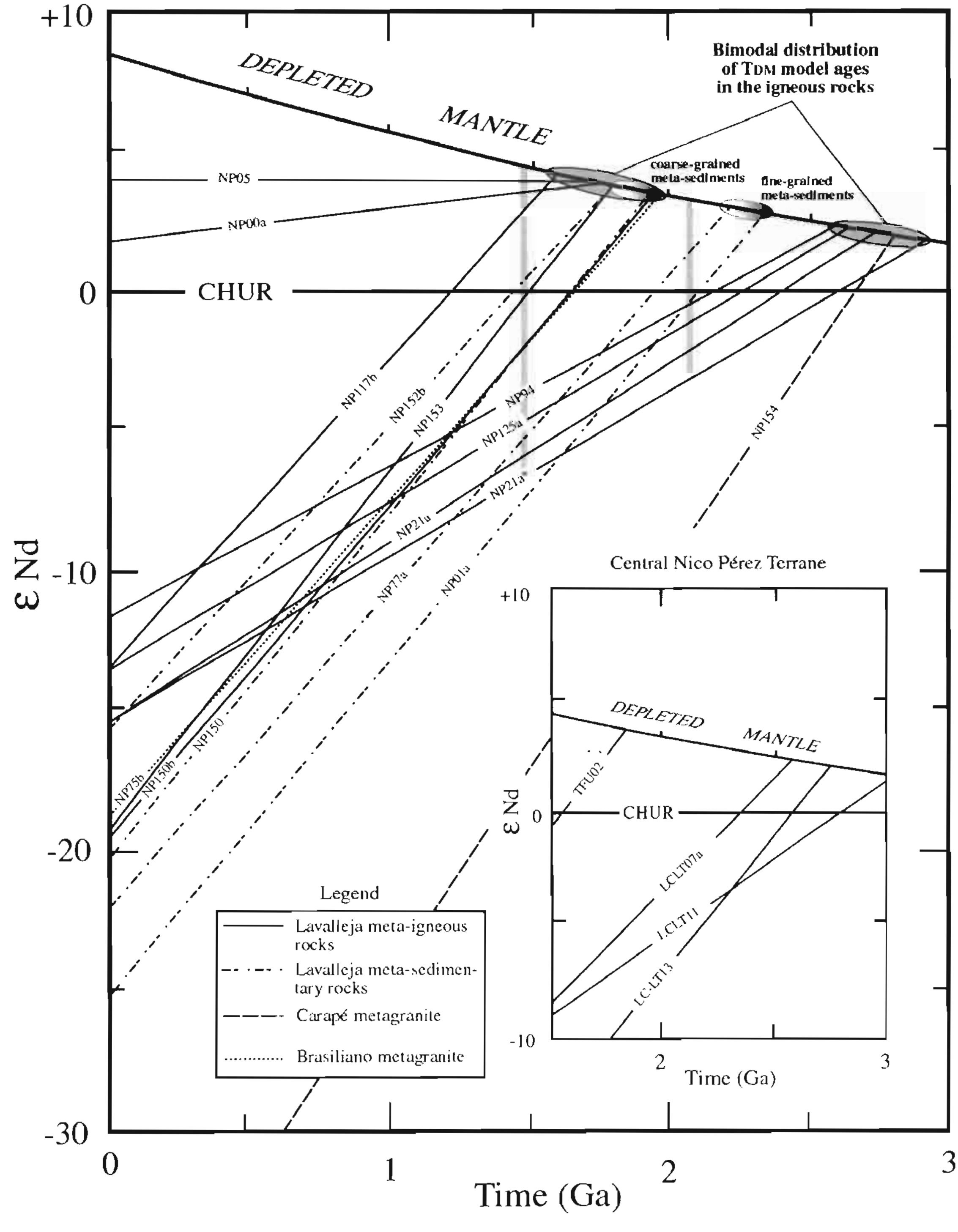

Figure 5. ε_{Nd} diagram (De Paolo, 1981) for units from southern (main box) and central NPT (right box). Samples of the right box represents: LC-LT11 - La China meta-tonalite, LC-LT13 – Las Tetas quartzite, LC-LT07a – undivided metagranite, TFU02 – Zapican diorite. Age of the Lavalleja basin deposition limited by vertical gray lines.

THE ALGODÕES AMPHIBOLITES, CENTRAL CEARÁ DOMAIN: GEOCHRONOLOGIC AND TRACE ELEMENT EVIDENCE FOR ACCRETION OF PALAEOPROTEROZOIC OCEANIC PLATEAU BASALTS IN THE BORBOREMA PROVINCE, BRAZIL

Martins, G.[1] **and Oliveira, E.P.**[2]

1. Departamento de Geologia, UFC, 60455-760 Fortaleza, Brazil. guttenberg-martins@mailcity.com
2. Instituto de Geociências, Unicamp, 13083-970 Campinas, Brazil. elson@ige.unicamp.br

Keywords: Proterozoic oceanic plateau basalt, Sm-Nd geochronology, geochemistry, Borborema Province

INTRODUCTION

The obduction of oceanic plateaux and their preservation in orogenic belts throughout the Earth's evolution is the subject of current international debate (Polat et al., 1998; Puchtel et al., 1998; Kerr et al., 2000; Condie, 1999, 2001; Condie et al. 2002). Because of their thickness well in excess of 10 km oceanic plateaux are less buoyant than normal oceanic crust and tend to subduct. However, if they are younger than 20 Ma, and still hot, they become more buoyant than oceanic crust and are thus prone to obduction (e.g. Nur & Ben-Avraham, 1982; Closs, 1993). Although Condie (1999) argued that accreted oceanic plateaux are relatively uncommon in the geological record, several descriptions of oceanic plateau basalts worldwide (see Table 2 of Kerr et al., 2000) suggest that they may be more common than previously thought. A complete section of an oceanic plateau is not known, and most of the information about its architecture derives from ocean drilling projects and tectonically uplift margins of the Caribbean-Colombian Oceanic Plateau (Kerr et al., 1998) and Ontong-Java Plateau (Neal et al., 1997). The identification of oceanic plateau basalts in ancient terranes is not straightforward. According to Kerr et al. (2000) the salient features are: predominance of massive lavas, low abundances of volcaniclastic deposits, deep to shallow marine sediments may be associated, occurrence of high-MgO lavas, chemically homogeneous basalts with relatively flat chondrite-normalized REE patterns and primitive mantle-normalized low La/Nb ratios.

In this paper we report geochemical and isotopic data for the recently discovered Algodões Amphibolites, Central Ceará domain, which have the potential to be the first remnants of a Palaeoproterozoic oceanic plateau in the Borborema Province, Northeastern Brazil.

GEOLOGIC FRAMEWORK

The studied area is situated in the eastern portion of Central Ceará Domain (CCD), a typical sector of the Borborema Province situated between the Transbrasiliano Lineament and the Senador Pompeu shear zone. The CCD is composed mainly of the minor fragment of reactived Archaean crust named the Troia Massif, which is partially overlain by quartzite-pelite-carbonate units of the Ceara Group. Neoproterozoic-Early Palaeozoic units are represented by syn- to late tectonic calc-alkaline batholiths (e.g., Quixada-Quixeramobim, Itapage, Tamboril granite complexes) and post-tectonic alkaline to peralkaline stocks (Barriga, Serra Aguda, São Paulo e Morrinhos bodies). Martins et al. (1998) and Fetter et al. (2000) reported orthogneisses with 2.1-2.2 Ga in the central and northwestern parts of this domain.

CCD lies in contact to the east with the Rio Grande do Norte terrane (RNT) and to the west with the Médio Coreau Domain (MCD). The RNT comprises a Neoproterozoic plataformal sequence (Seridó Belt), the 1.8 Ga rift suite (Orós belt), 2.1-2.0 Ga high-grade gneiss of basement complexes, minor and isolated Archaean nuclei and voluminous Brasiliano/Pan-African granitic bodies (Sá et al., 1991; Van Schmus et al., 1995; Souza et al., 1993). The MCD crops out beyond the Transbrasiliano Lineament and comprises a Neoproterozoic plataformal sequence (Martinopole Group), 2.4-2.3 Ga high-grade orthogneisses of the basement complexes, early Palaeozoic molassic basins (Ubajara and Jaibaras Groups), minor syn- to late-tectonic calc-alkaline granites and post-tectonic granites.

A sequence of amphibolite-paragneiss and associated orthogneisses has been mapped in the eastern part of CCD. It is referred to here as the Algodões Sequence and is the main interest of this study. This sequence comprises the following lithological units: Algodões Amphibolite – a thick pile of massive, fine-grained amphibolite layers with occasional horizons of garnetiferous amphibolite and lenses of coarse grained hornblendite; Choró paragneisses – fine grained, massive to banded gneisses with minor layers of mica-schists, calc-silicate rocks, quartzites and metaconglomerates; Cipó orthogneisses – tonalite-granodiorite-granite gneisses occurring as stocks and dykes intrusive into the previous units.

The Algodões amphibolite generally crops out surrounding the Cipó orthogneisses or as concordant layers interleaved in the Choró paragneisses. The best sections of amphibolites are found along riverbeds on the western hillside of the Serra do Estevão. Here the amphibolites crop out continuously for several kilometres, and the whole sequence may rich up to 2-3 km in thickness. Field relationships suggest that the Algodões amphibolites may be a thick pile of basaltic lavas, tuffs and sills, such as the common intercalation of garnet-bearing and garnet-free amphibolites (lavas of different composition), lenses of cumulate hornblendite, and occasional occurrences of variolitic structures.

The Choró paragneisses are composed of cream-coloured types enriched in feldspars, grey types enriched in biotite and biotite-hornblende banded gneisses. The Cipó tonalite gneisses contain amphibolite enclaves and are cut by felsic dykes of trondhjemite composition. The granite gneisses occur as elliptical bodies partially migmatised and crosscut by amphibolite to felsic dykes. The Cipó gneisses suite also comprises kilometre-long sheets of granites that crosscut the Choró paragneisses.

ANALYTICAL TECHNIQUES

Major and trace element data were obtained on a XRF spectrometer at the Geosciences Institute of State University of Campinas (Unicamp). Th, Nb, Ta and the rare earth elements were analysed on the ICP-MS laboratory of São Paulo University (USP). Analytical data for Sm and Nd isotopes along with U-Pb data for zircons of a tonalite orthogneiss intrusive in the amphibolites were obtained on a VG mass-spectrometer at the Isotope Geochemistry Laboratory (IGL), Department of Geology of Kansas University.

GEOCHRONOLOGY

Sm-Nd ISOCHRON OF ALGODÕES AMPHIBOLITES

Six samples were analyzed. A four point isochron (samples GM-19A, GM-31-A, GM-58-A and GM-59-A) yielded the age 2,236 ± 55 Ma (Fig.1). Because the rocks are metamorphic this age is interpreted as a minimum age for the crystallization of the igneous protoliths. The depleted mantle Nd-model ages fall in the time span 2.26-2.57 Ga and εNd(t=2.24Ga) values range from +1.65 to +2.90.

ZIRCON AGE AND Sm-Nd OF THE CIPÓ TONALITE ORTHOGNEISS

Three fractions of a single zircon population of sample GM-16 give a concordant upper intercept age of 2,131 ± 11 Ma (cf. Martins et al., 1998). Depleted mantle Nd model ages for this unit range from 2.23 Ga to 2.25 Ga, with εNd(t) values between +1.63 and +1.89.

TRACE ELEMENT GEOCHEMISTRY

Generally, the Algodões amphibolites have MgO contents between 5.5% and 7.5%, Nb/Zr from 0.05 to 0.09, Nb/Y between 0.1 and 0.25, and Zr/Y in the range 1.5-3.8, a characteristic of oceanic plateau basalts. Their mantle-normalised multi-element diagrams (including the rare earth elements) are predominantly flat, with $(La/Nb)_N < 1$. In this aspect they are very akin to basalts of the Ontong-Java plateau (Fig. 2). Similarly, on the La/Yb vs. Zr/Th diagram (Fig. 3) they fall mostly in the field of ocean plateau tholeiites.

DISCUSSION AND CONCLUSIONS

The Algodões amphibolites have several similarities with Phanerozoic oceanic plateau basalts. They are fine-grained, massive metabasalts with occasional variolitic structure. Locally, they have chemical sediments (BIF) and coarse-grained gabbroic lenses associated. Most diagnostic is their flat patterns on mantle-normalised multi-element plots, as well as their low La/Yb and high Zr/Th ratios. The whole-rock Sm-Nd isochron of the Algodões amphibolites indicate a Palaeoproterozoic age (ca. 2.4 Ga), which we interpret as a minimum age for the igneous protolith. This age estimate is consistent with the observed field relationships between amphibolites and the 2.13 Ga-old calc-alkaline tonalites of the Cipó unit, the latter clearly intrusive into the former. The Nd-model ages of the Cipó orthogneisses (2.23-2.25 Ga) and their positive εNd(t) values are also compatible with an origin by partial melting of mafic crust or mantle wedge in an island arc tectonic setting, as suggested by Martins et al. (1998). The identification, for the first time, of remnants of accreted oceanic plateau basalts in the Borborema Province opens a new perspective for understanding the evolution of Palaeoproterozoic orogenic belts in South America with implications for mineral deposits exploration and the reconstruction of the the Atlantica supercontinent (cf. Rogers 1994).

ACKNOWLEDGMENTS

Randy van Schmus is greatly thanked for laboratory facilities at the University of Kansas during a post-doctoral leave of EPO. Professor Valdecir Janasi and Mrs. Sandra Andrade assisted EPO with the ICP-MS analyses at University of São Paulo. The São Paulo State Foundation for Research Support (FAPESP) and the Brazilian National Research Council (CNPq) provided research grants for this project (FAPESP 96/08792-6; CNPq 300.845/91-0 and 142423/1996-3).

REFERENCES

Closs, M., 1993. Lithospheric buoyancy and collisional orogenesis: subduction of oceanic plateaus, continental margins, island arcs, spreading ridges, and seamounts. Geol. Soc. America Bulletin, 105: 715-737.

Condie, K.C., 1999. Mafic crustal xenoliths and the origin of the lower continental crust. Lithos, 46: 95-102.

Condie, K.C., 2001. Mantle plumes and their record in earth history. Cambridge Univ. Press, Oxford, UK.

Condie, K.C., Frey, B.A., Kerrich, R., 2002. The 1.75 Ga Iron King Volcanics in west-central Arizona: a remnant of an accreted oceanic plateau derived from a mantle plume with a deep depleted component. Lithos, 64: 49-62.

Fetter, A.H., van Schmus, W R., Santos, T.J.S., Nogueira Neto, J.A., Arthaud, M.H., 2000. U-Pb and Sm-Nd geochronological constraints on the crustal evolution and basement architeture of Ceara State, NW Borborema Province, NE Brazil: Implications for the existence of the Paleoproterozoic supercontinent "Atlantic". Revista Brasileira de Geologia, 30:102-106.

Kerr, A.C., Tarney, J., Nivia, A., Marriner, G.F., Saunders, A.D., 1998. The internal structure of oceanic plateaus: inferences from obducted Cretaceaous terranes in western Colombi and the Carribbean. Tectonophysics, 292: 173-188.

Kerr, A.C., White, R.V., Saunders, A.D., 2000. LIP reading: Recognizing oceanic plateaux in the geological record. J. Petrology, 41: 1041-1056.

Mahoney, J.J., Storey, M., Duncan, R.A., Spencer, K.J., Pringle, M., 1993. Geochemistry and geochronology of Leg 130 basement lavas: nature and origin of the Ontong Java Plateau. In: Berger, W.H., Kroenke, L.W., Mayer, L.A. (eds) Proceedings of the Ocean Drilling Program, Scientific Results 130. College Station, TX: Ocean Drilling Program, pp. 3-22.

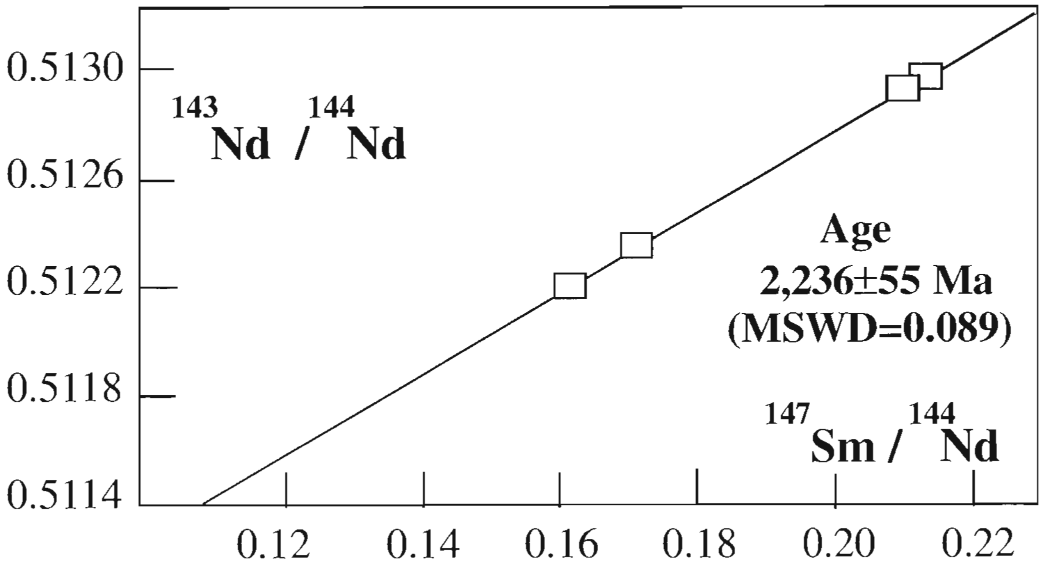

Figure 1. Sm-Nd whole-rock isochron for the Algodões amphibolites.

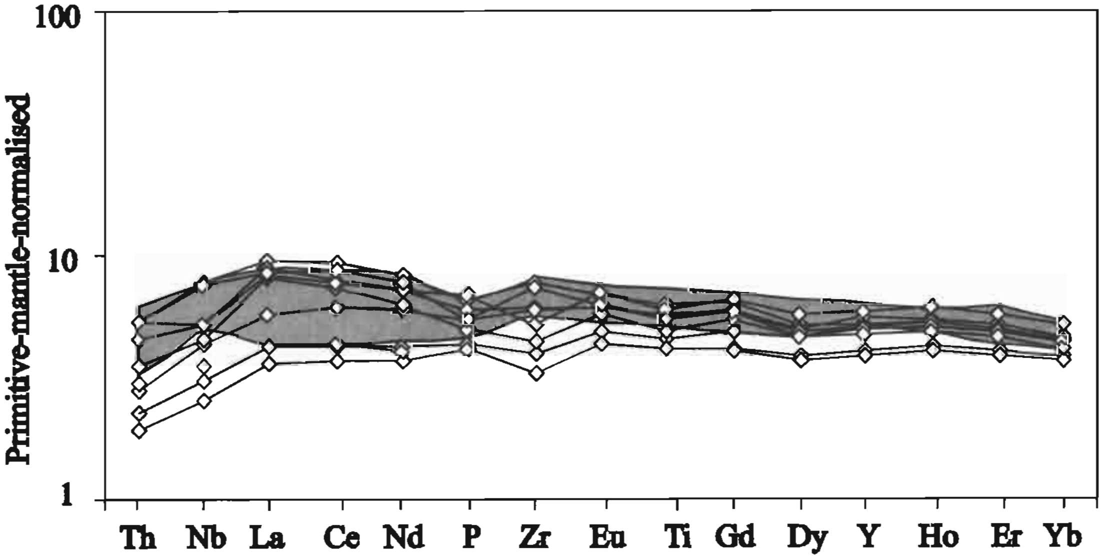

Figure 2. Primitive mantle-normalised multi-element plot (normalising values from Sun and McDonough (1989) showing the Algodões amphibolites and the Ontong-Java plateau basalts (after Mahoney et al., 1993; ornamented field).

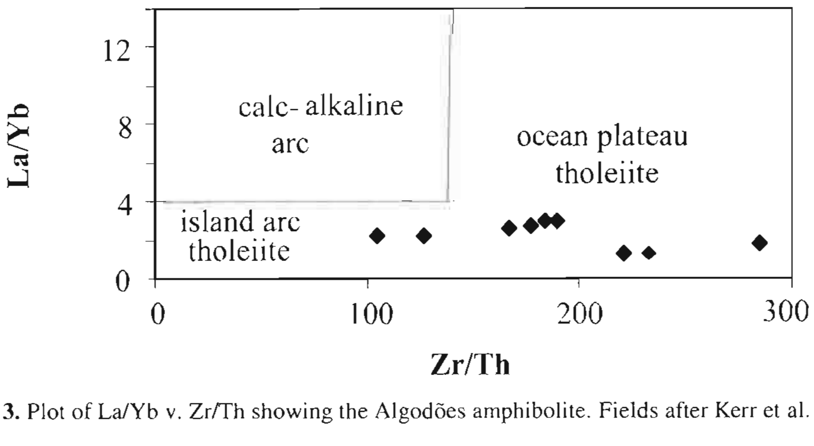

Figure 3. Plot of La/Yb v. Zr/Th showing the Algodões amphibolite. Fields after Kerr et al. (2002).

Martins, G., Oliveira, E.P., De Souza, C.R., Lafon, J-M., 1998. Geochemistry and geochronology of The Algodoes sequence, Ceara, NE Brazil: A Paleoproterozoic magmatic arc in the central Ceara Domain of the Borborema Province? Anais XL Congresso Brasileiro de Geologia, SBG, p. 28.

Neal, C.R., Mahoney, J.J., Kroenke, L.W., Duncan, R.A., Petterson, M.G., 1997. The Ontong-Java Plateau. In: Mahoney, J.J., Coffin, M. (eds). Large Igneous Provinces: continental, oceanic and planetary flood volcanism. Geophysical Monograph, American Geophysical Union 100: 183-216.

Nur, A. & Ben-Avraham, Z., 1982. Oceanic plateaus, the fragmentation of continents, and mountain building. J. Geophysical Res., 87: 3644-3661.

Polat, A., Kerrich, R., Wyman, D.A., 1998. The late Archean Schreiber-Hemlo and White River Dayohessarah greenstone belts, Superior Province: collages of oceanic plateaus, oceanic arcs, and subduction-accretion complexes. Tectonophysics, 289: 295-326.

Puchtel, I.S., Hofmann, A.W., Mezger, K., Jochum, K.P., Shchipansky, A.A., Samsonov, A.V., 1998. Oceanic plateau model for continental crustal growth in the Archaean, a case study from the Kostomuksha greenstone belt, NW Baltic Shield. Earth and Planetary Science Letters, 155: 57-74.

Rogers, J.J.W., 1996. A history of the continents in the past three billion years. Journal of Geology, 104: 1405-1412.

Sá, J. M.; Bertrand, J.M & Leterrier, J., 1991. Geodynamic evolution and Geochronology (U-Pb, Rb-Sr and K-Ar) of the Oros belt, NE Brazil. C. R. Acad. Sci. Paris III, t. 313: 231-237.

Souza, Z.S., Martin, H., Macedo, M.H.F., Peucat, J.J., Jardim de Sá, E.F., 1993. Un segment de croûte continentale juvénile d'âge proterozoique inférieur: Le complex de Caicó (Rio Grande do Norte, NE-Brésil). C. R. Acad. Sci. Paris III, t. 316: 201-208.

Sun, S.-S. & McDonough, W.F., 1989. Chemical and isotope systematics of oceanic basalts: implications for mantle composition and processes. In: Saunders, A.D., Norry, M.J. (eds) Magmatism in the Ocean Basins. Geological Society, London, Special Publication 42: 313-345.

Van Schmus, W.R., Neves, B.B.B., Hackspacher, P., Babinski, M., 1995. U/Pb and Sm/Nd Geochronological studies of the Eastern Borborema Province, Northeastern Brazil – Initial Conclusions. Journal of South American Earth Sciences, 8: 267-288.

ISOTOPE CONSTRAINTS AND RADIOCARBON AGE APPLIED TO LATE HOLOCENE LANDSCAPE EVOLUTION DUE TO SAN MARCOS FAULT ACTIVITY, CORDOBA, ARGENTINA

Massabie, A.[1]; Panarello, H.[2]; Cegarra, M.[1]; Cordero, R.[2]; Lo Forte, G.[1]; Sanguinetti, A.[1] and Valencio, S.[2]

1.Universidad de Buenos Aires. Facultad de Ciencias Exactas y Naturales. Departamento de Cs. Geológicas. Pabellón II.
Ciudad Universitaria. Ciudad Autónoma de Bs. As. C1428EHA.
armando@gl.fcen.uba.ar, marcega@gl.fcen.uba.ar, asan@gl.fcen.uba.ar, galof@gl.fcen.uba.ar
2. INGEIS-CONICET. Pabellón INGEIS. Ciudad Universitaria. Ciudad Autónoma de Bs. As. C1428EHA.
hector@ingeis.uba.ar, 221059@ingeis.uba.ar, susana@ingeis.uba.ar

Keywords: Isotope, radiocarbon age, landscape, neotectonics, Sierras Pampeanas

INTRODUCTION

The San Marcos fault area is located in Sierras Pampeanas Orientales (also named as Eastern Pampean Ranges in English literature), Central Argentina, more than 700 km far from the tectonically active west Andean border of Southern South America (Fig.1), coinciding with 28°S-33°S South Central Andes flat slab subducted segment (Barazangi and Isacks, 1976). Eastern ward, this mountain chain defined the west morphostructural boundary of the extended Chaco-Paraná Basin plains.

In the Province of Córdoba, the Sierras Pampeanas Orientales concentrates an important number of well known fault segments with neotectonic activity, as mentioned in previous works (Massabie et al., 2000; Massabie and Szlafsztein, 1991, among others). Although initial studies (Schlagintweit, 1954; Lencinas and Timonieri, 1968; Massabie, 1976, 1987, among others) postulated a broad span of Late Cenozoic ages for the youngest faults movements, recent works afford evidences about a more restricted and modern activity for the latest neotectonic faulting at Sierras Pampeanas Orientales during Late Holocene times (Massabie et al., 2001; 2002). Assessment of modifications on fluvial channel pattern and landscape modifications associated with neotectonic faulting have a special value in present steps of these studies, but at the same time emphasize the tight correlation of Quaternary landscape evolution with neotectonic faulting in the area.

The classic geologic methods used to determine the age of a structure and its rate of formation are of limited use in this case because of the short time span involved in neotectonic movements. As a result, a whole new set of techniques could be devised to augment the traditional methods.

The aim of this work is focused on isotope constrains and radiocarbon dating applied to the relationships between Holocene neotectonic faulting and associated landscape changes at San Marcos Sierra foothills area. These studies are supported by isotope data evaluation and radiocarbon ages obtained for two selected places situated along Sierra Baja de San Marcos fault scarp (Fig. 1).

GEOLOGY OF SAMPLED SITES

The oldest basement rocks cropping out in the area are represented by Precambrian to Early Paleozoic granites, granodiorites and tonalities with common cataclastic to milonitic textures, which were assigned to the San Marcos Formation (Massabie, 1982). These rocks are overlaying by mainly fluvial sediments of Quaternary age which comprised three ancient agradation levels named Level I, Level II and Level III (Fig. 1). In the southern sector, local eolian deposits overlaying pond sediments in the tectonic damming up area of the River Quilpo were described by Massabie and Limarino (1996) and Massabie et al. (2001). The San Marcos oblique fault (SMF) (Fig. 1), a master fault which extends with northwest strike along the area, was tectonically characterized as a transpressive Andean fault (Massabie, 1982; Massabie et al., 2000).

The sites that were sampled for radiocarbon age and isotope analysis are located along SMF, and are separated by 8,8 km. At Site 1, located in the southern region (Fig.1), limnic gastropod shells, assigned to *Odontostomus (Spixia) columeraris* Parodiz; *Odontostomus (Plagiodontes) dentatus* (Wood); *Lymnaea* cf. *L. beatrix* d'Orbigny; *Bulimulus (Bulimulus) apodemetes* d'Orbigny and *Odontostomus (Scalarinella)?*, were sampled for palaeontologic and isotopic studies in palaeolacustrine deposits. A ^{14}C age of 2560 ± 120 bp was obtained from the shells (Massabie et al.,2001). The dating deposits are located in the footwall block of the SMF and lack later deformation evidences.

The other locality, Site 2, is placed near the northwestern end of SMF (Fig.1). Here, a cross trench was caved in order to investigated the fault continuity in this place and, as a result, the tip of the propagating fault was localized in Quaternary terraces (Level III of Massabie et al., 2002). Both trench sides shown that SMF cuts basement rocks and Quaternary alluvial terrace deposits, but is covered by a dark brown organic soil without any tectonic deformation. Fault zone, about 15 m thick, is composed of crush breccia derived from light grey tonalitic San Marcos Formation sheared rocks. Red clay seams filling interlaced small minor faults and fissures are also present.

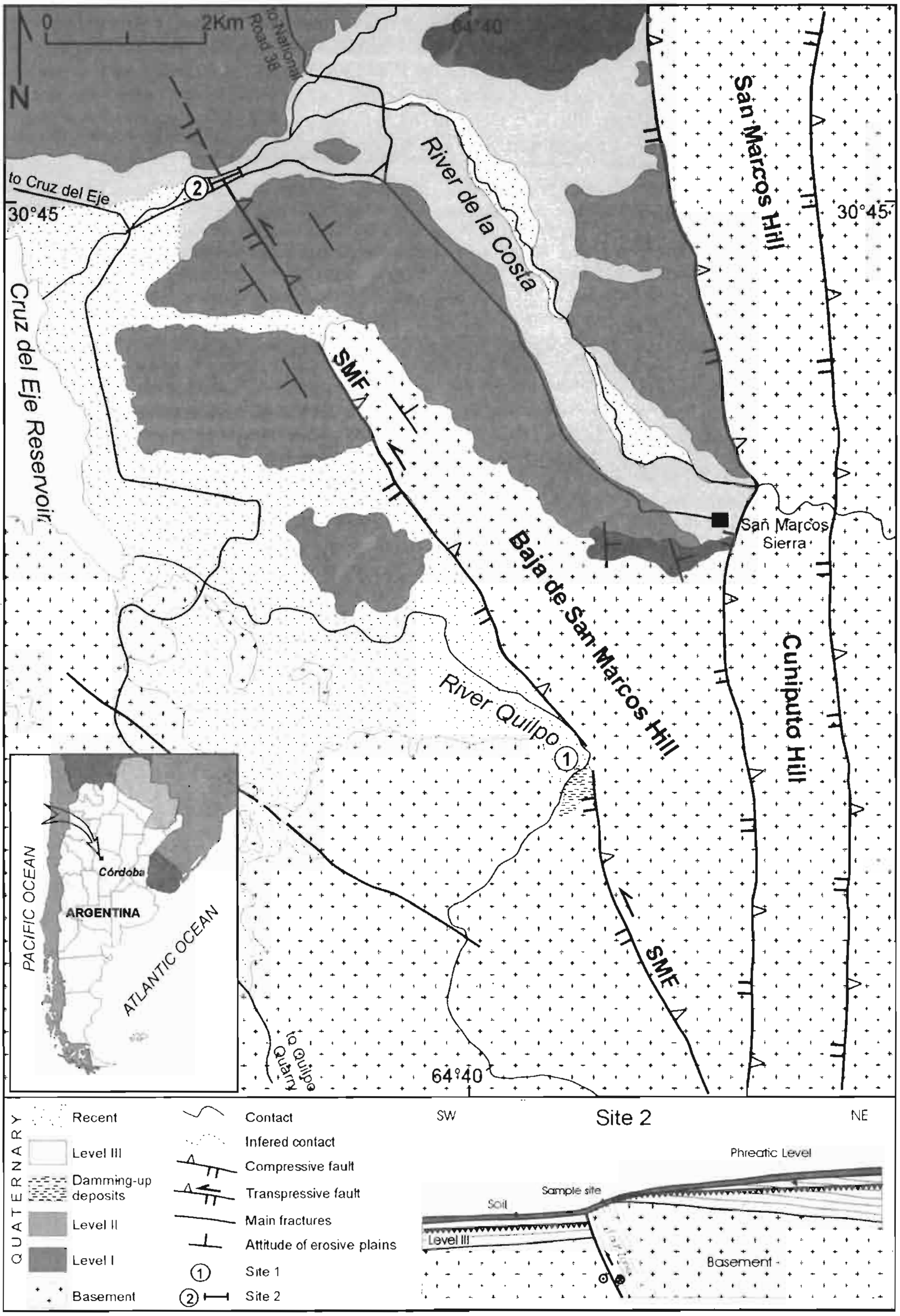

Figure 1. Geologic map with the location of sampled sites for radiocarbon ages and isotope analysis along San Marcos Fault (SMF)

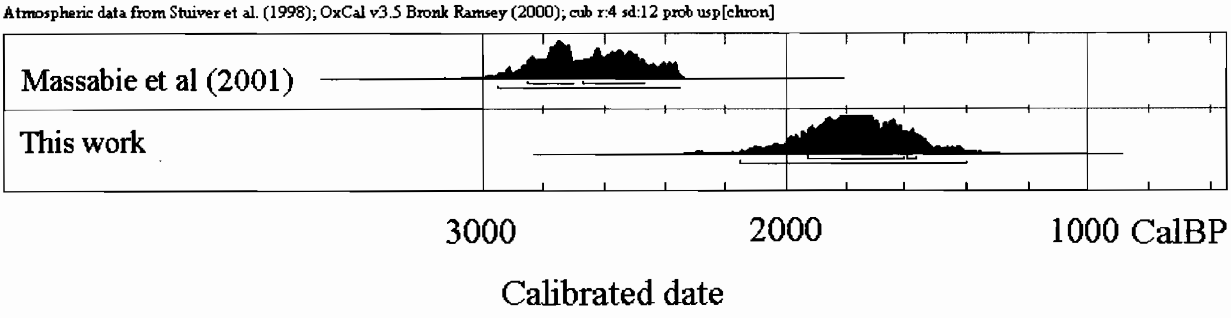

Figure 2. Calibrated ^{14}C ages of the soil sample taken in this work and that presented in Massabie et al., 2001. Calibration data are for the North Hemisphere, 40 year offset for the South Hemisphere has been added.

The thick fault zone (70°, 50°) is a transverse impervious barrier for the phreatic ground water flowing from east and southeast into Levels II and III of alluvium terraces lying over fractured basement in the hanging wall of SMF (Fig. 1). As a consequence, phreatic surface elevates in the back slope just behind the fault and reaches topographic surface forming local springs named "mallines". Here, dissolved salts were concentrated due to direct evaporation. Because this process, the conglomerates with sandy matrix of Level III were cemented by carbonate (named "tosca") precipitated from over-saturated phreatic water. Samples containing detritic diagenetic carbonate ("tosca") precipitated from phreatic water, were taken from the organic soil standing over the fault zone and Level III without any deformation. Isotope analysis over carbonates of these samples gives a final corrected ^{14}C age of 1800±140 bp.

LANDSCAPE CHANGES ASSOCIATED WITH NEOTECTONIC SMF ACTIVITY

In the San Marcos Sierra foothills area of northwest Córdoba Hills, the Holocene activity of the SMF is associated with two main landscape modifications. In a first step its activity originated the elevation of the basement in SMF which give rise to a natural dam over the River Quilpo and, as a consequence, a transitory pond extended over the foot wall block around the sharp curve of the water channel (Site 1, Fig. 1).

If we broadly assumed an elapse time of 500 to 1500 years for the accumulation of fluvial and lacustrine deposits laying between bedrock and ^{14}C dated bed (2560±120bp), (2850-2480) bp (1σ), (Fig. 2), the neotectonic activity of SMF could be placed around 4000 to 3000 bp.

Later on, repeated movements in SMF displaced the tip point to the northwest, modifying the flow path of phreatic water in Level III mainly over the hanging wall block, partially confining it, and causing massive diagenetic carbonate cement formation in the sandy gravel terrace. Basement core of Sierra Baja de San Marcos, which extend beneath Level II and Level III Quaternary terraces, defines a transverse local watershed over River de la Costa banks to the northwest. The river itself crosses it in a narrow gorge where faulted basement of SMF crops out (Fig. 1).

The 1800±140 bp radiocarbon age, correponding to a calibrated (1920-1550) bp (1σ), (Fig. 2) obtained from carbonate in present organic soil laying over SMF zone (Site 2, Fig. 1) short after this final Late Holocene landscape modification due to SMF activity in the area, could be placed around 2000 bp for a one meter thick cemented bed of Level III sandy gravels with 20% efective porosity.

AGE AND ISOTOPIC METHODS

^{14}C analyses on the biogenic carbonate were made at INGEIS by liquid scintillation counting on benzene obtained from the samples, normalized to δ^{11}C=-25‰ content and corrected using the Oxcal 2.5 programme, Bronk Ramsay (2000), (Fig. 2). ^{13}C and ^{18}O were determined also at the INGEIS laboratories barely following the technique of Panarello et al. (1980) *i.e.* reacting the carbonate material with 100% phosphoric acid under, but at a temperature of 60°C; previously, thermal treatment (350°C, under vacuum) was made to eliminate organic matter interferences that could reduce the accuracy of measurements. The obtained CO_2 was then contrasted with CO_2 from Carrara marble in a FINNIGAN Delta-S, triple collector, multiport inlet system, mass spectrometer. Isotopic enrichments are expressed as usual in δ (‰) vs. the V-PDB for ^{13}C and V-SMOW for ^{18}O standards. The overall error is ± 0.1 ‰.

RESULTS AND DISCUSSION

In a previous work Massabie et al. (2001) obtained 2560±120 bp ^{14}C age for damming up of River Quilpo (Site 1) due to SMF Holocene first step of activity and δ^{18}O= +0.4‰. This result was influenced by high evaporation rates in a marshy pond leading the isotopic composition to more enriched values.

The obtained δ^{18}O value on the 1800±140 bp soil carbonate (Site 2) here presented (25,5‰) reflects the equilibrium with water of about -5.4 ‰ in the V-SMOW scale (Gonfiantini, 1978; Hut, 1987). δ^{18}O average on rain is *ca* –5.5‰ for this region in present days (INGEIS - National Network for Isotopes in Precipitation, included in the GNIP database: http://isohis.iaea.org)) therefore, if the climatic conditions have not significantly changed, this could be the value for meteoric water in the phreatic layer when the carbonate was deposited. No evidences of stagnant water as in the 2850-2480 bp (1σ), (Massabie et al., 2001) are reflected by this value. This fact reinforces the hypothesis of free water circulation.

$\delta^{13}C$= -3.2‰ value reflects equilibrium between circulating water and atmosphere in open system conditions. Since it is not probable the presence of ancient ^{14}C -free limestone input, the initial activity of the CO_2 forming the diagenetic carbonate would correspond to the 100% of modern carbon for that moment, thus making reliable the calculated age.

CONCLUSIONS

Validity of 1800±140 bp radiocarbon age of the carbonate in the organic soil laying on SMF is supported by $\delta^{13}C$= -3.2‰ and $\delta^{18}O$= -5.4 ‰ values in equilibrium with circulating water and atmosphere in open system conditions.

Late Holocene activity of SMF determined direct landscape modifications due to its barrier effect over surface and under surface water flow in the San Marcos Sierra foothills area of Córdoba, Central Argentina.

Based on radiocarbon ages, isotope analyses and morphostructural control of Late Quaternary fluvial and phreatic deposits, two final neotectonic activity steps of SMF are placed between 4000 – 2000 bp.

The first step could be constraint between 4,000 – 3,000 bp. It controled the avulsion of River Quilpo associated with a (2560±120 bp) transitory lacustrine paleoenvironment due to neotectonic damming up in the foot wall block of SMF.

The second SMF neotectonic step around 2000 bp, lengthend to the northwest a transverse local watershed over River de la Costa banks introducing an aditional modification of Late Holocene fluvial lanscape around San Marcos Sierra foothills of Cordoba.

Two direct paleoenvironmental evidences of the last SMF tip point displacement to the northwest have been detected: firstly the tectonicaly controled attitude of erosive planes on both sides of fault scarp, and secondly the flow path changes of phreatic water in Level III over SMF hanging wall block which caused massive carbonate precipitation (1800±140 bp) due to groundwater evaporation in the atmosphere.

AKNOWLEDGEMENTS

The authors wish to thank INGEIS-CONICET for ^{14}C age and isotope analyses; Facultad de Ciencias Exactas y Naturales – Universidad de Buenos Aires (EX048 project) for financial support and CONAE for provide satellite images.

REFERENCES

Barazangi, M. and Isacks, B., 1976. Spatial distribution of earthquakes and subduction of the Nazca plate beneath South America. Geology, v. 4: 686-692.

Bronk Ramsey, C. 1995. Radiocarbon Calibration and Analysis of Stratigraphy: The OxCal Program. Radiocarbon, 37(2): 425-430.

Gonfiantini, R., 1978. Standards for stable isotope measurements in natural compounds. Nature, 271: 534.

Hut, G., 1987. Consultants' Group Meeting on Stable Isotope reference samples for geochemical and hydrologycal investigations. IAEA, Vienna, 16-18 September 1985. Report to the Director General, IAEA, Vienna, 42pp.

Lencinas, A. and Timonieri, A., 1968. Algunas características estructurales del valle de Punilla, Córdoba. III Jornadas Geológicas Argentinas, v. I: 195-208.

Massabie, A., 1976. Estructura tectónica cenozoica entre Charbonier y Cosquín, provincia de Córdoba. VI Congreso Geológico Argentino, v. I: 109-123.

Massabie, A., 1982. Geología de los alrededores de Capilla del Monte y San Marcos, provincia de Córdoba. Revista de la Asociación Geológica Argentina, v. XXXVII nº 2: 153-173.

Massabie, A., 1987. Neotectónica y Sismicidad en la región de las Sierras Pampeanas Orientales, Sierras de Córdoba, Argentina. X Congreso Geológico Argentino, v. I: 271-274.

Massabie, A. and Szlafsztein, C., 1991. Condiciones geomecánicas y edad del fallamiento neotectónico en las Sierras Pampeanas Orientales, Córdoba, Argentina. Revista de la Asociación Argentina de Geología Aplicada a la Ingeniería, v. VI: 154-168.

Massabie, A. and Limarino, C., 1996. Facies de endicamiento en el Río Pintos y su relación con la evolución neotectónica de la Sierra de San Marcos, Córdoba. VI Reunión Argentina de Sedimentología, v. I: 237-241.

Massabie, A., Cegarra, M., Idoyaga, M., Mutti, D., Nestiero, O. and Sanguinetti, A., 2000. Neotectonic faulting zoning in the Eastern Sierras Pampeanas, central Argentina. 8th Congress of the International Association of Engineering Geology and the Environment, D. P. Moore and O. Hungr editors,v. VI: 4135-4140, A.A. Balkema.

Massabie, A., Limarino, C., Panarello, H., Cordero, R. and Bertels, A., 2001. Late Holocene tectonic damming in the Eastern Sierras Pampeanas, Córdoba, Argentina. III South American Simposium on Isotope Geology. Actas Simposium en CD-ROM, 4pp; Abbreviated Abstracts: Revista Comunicaciones Universidad de Chile, Facultad de Ciencias Físicas y Matemáticas, Departamento de Geología, nº 52: 108.

Massabie, A., Cegarra, M., Sanguinetti, A. and Lo Forte, G., 2002. Actividad neotectónica del fallamiento andino en la región pedemontana de San Marcos Sierra, Córdoba, Argentina. En: Cabaleri, N., Cingolani, C., Linares, E., López de Luchi, M., Ostera, H. and Panarello, H. (eds.). Actas del XV Congreso Geológico Argentino CD-ROM. Artículo Nº 106, 6pp.

Panarello, H.O., Garcia, C.M., Valencio S.A. y Linares E., 1980. Determinación de la composición isotópica del carbono en carbonatos, su utilización en Hidrogeología y Geología. Revista de la Asociación Geológica Argentina. v. XXXV,4, 460-466.

Schlagintweit, O., 1954. Una interesante dislocación en Potrero de Garay (Valle de Calamuchita), Sierra Chica y Grande de la Provincia de Córdoba. Revista de la Asociación Geológica Argentina, v. IX nº 3: 135-154.

Stuiver, M., Reimer, P.J., Braziunas, T.F., 1998. High-precision radiocarbon age calibration for terrestrial and marine samples. Radiocarbon 40(3): 1127-1151.

Wayne, W., 1999. The Alemanía rockfall dam: A record of a mid-holocene earthquake and catastrophic flood in northwest Argentina. Geomorphology, 27: 295-306.

U-PB DATING FOR SINGLE GRAIN ZIRCON USING LASER ABLATION ICP MASS SPECTROMETER AND FISSION TRACK AGES OF ZIRCON FOR BACK-ARC ADAKITIC BODIES, THE CERRO PAMPA AND THE PUESTO NUEVO, ARGENTINE PATAGONIA

Motoki, A.[1]**; Orihashi, Y.**[2]**; Hirata, D.**[3]**; Haller, M.J.**[4]**; Ramos, V.A.**[5]**; Schilling, M.**[6]**; Iwano, H.**[7]**; Cario, F.D.**[8] **and Anma, R.**[9]

1. Universidade do Estado do Rio de Janeiro, Rio de Janeiro. Rua São Francisco Xavier 524, Sala A4023, Maracanã, Rio de Janeiro, 20550-990, Brasil. motoki@uerj.br
2. The University of Tokyo, Tokyo, Japan. oripach@eri.u-tokyo.ac.jp
3. Kanagawa Prefecture Museum of Natural Science, Odawara, Japan. daiji@yk.rim.or.jp
4. Centro Nacional Patagónico-UNPSJB, Puerto Madrin, Argentina. haller@cenpat.edu.ar
5. Universidad de Buenos Aires, Buenos Aires, Argentina. andes@gl.fcen.uba.ar
6. Universidad de Chile, San Tiago, Chile.
7. Kyoto Fission Track Co. Ltd., Kyoto, Japan. kyoto-ft@mb.neweb.ne.jp
8. Universidade Federal Fulminase, Niterói, Brazil. fdcario@yahoo.com
9. Tsukuba University, Tsukuba, Japan. anma@arsia.geo.tsukuba.ac.jp

Keywords: Adakite, Cerro Pampa, Puesto Nuevo, LAICPMS, fission track

The Patagonian adakitic volcanoes take place in the arc region of the southern end of South America Continent, forming the Austral Volcanic Zone, and are attributed to slab melting caused by on-going active Chile Ridge subduction below South America continental plate (Stern & Killian, 1996). On the other hand, in the back-arc region, two small dacitic adakite bodies, the Cerro Pampa (Ramos et al., 1991; Kay et al, 1993) and the Puesto Nuevo (Ramos et al, 1994) are exposed (Fig. 1). Their peculiar occurrences are of a great interest to understand the tectonic setting of adakitic magma generation.

The previous works show that the K-Ar radiometric age for the Cerro Pampa (Ramos, et al., 1991; Kay, et al, 1993) and the Puesto Nuevo (Ramos, et al, 1994) were widely different. The Cerro Pampa body has Middle Miocene age (12.1 ± 0.7Ma and 12.0±0.7Ma, whole rock), obtained by the Sernageomin, Chile (Ramos, et al., 1991). The Puesto Nuevo body has late Cretaceous ages (84.5 ± 6 Ma and 76.7 ± 5Ma Ma, in hornblende) obtained in the late seventies in the Cambridge University, UK. Because of these Mesozoic ages, the Puesto Nuevo adakitic body was attributed to possible existence of an old ridge subduction, and interpreted to have no relation to on-going Chile ridge subduction.

The authors performed U-Pb dating from spot (pinpoint) analyses of single zircon crystal grains for both adakitic bodies with help of laser ablation-ICP Mass Spectrometry at the Earthquake Research Institute of the University of Tokyo. The laser ablation system utilises a frequency-quadrupled Nd-YAG UV laser (266 nm wavelength) and produces an ablation pit size of 30-35 μm. Detail of the analytical procedure is described by Orihashi & Hirata (2003). No statistic correction to improve apparent dating precision is applied.

It has been dated 25 spots in 21 zircon grains of the Cerro Pampa adakitic body. Among them, 23 spots are plotted close to the concordia curve (Fig. 2). Only two spots have higher $^{206}Pb/^{238}U$ ratio than the Concordia curve due to Pb loss and/or common Pb contamination. All of the 23 ^{206}Pb-^{207}Pb ages are significantly older than the above-mentioned K-Ar age (Fig. 3A), and therefore, they are considered to be recycled zircon grains originated from the country rocks. These ages are subdivided into the following six groups:

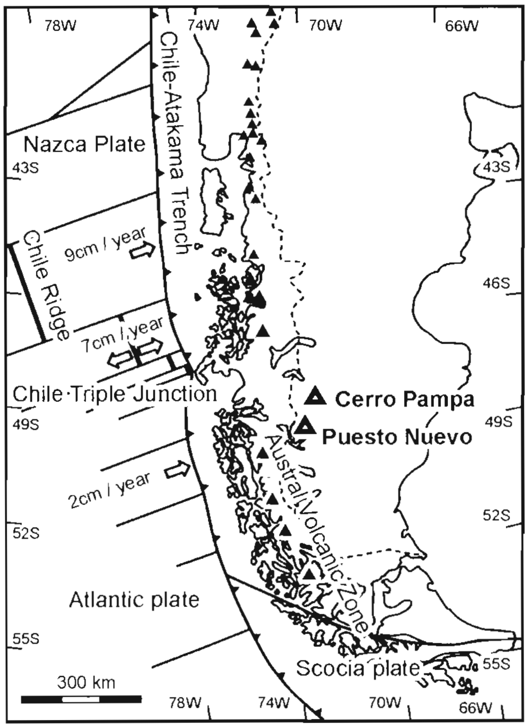

Figure 1. Locality map of the Cerro Pampa and the Puesto Nuevo adakitic rock bodies.

A) 123-129 Ma (3 spots), common age in the adjacent Patagonian Batholith;

B) 139-168 Ma (12 spots), these most abundant zircons between 139 and 168 Ma represent an important period of arc magmatism and crustal melting related to the andesitic and rhyolitic rocks of the Jurassic to early Cretaceous El Quemado Complex that underlies the Puesto Nuevo adakite;

C) 187-188 Ma (2 spots) of unknown sources in the region;
D) 227-263 Ma (2 spots), the age of the late Paleozoic granitic rocks that are emplaced during the metamorphic basement;
E) 714Ma (1 spot) a possible detrital zircon derived from the Deseado Massif
F) 1410-1766Ma (3 spots), zircons of middle Proterozoic age, derived from the continental crust basement, which should be present below the Paleozoic basement.

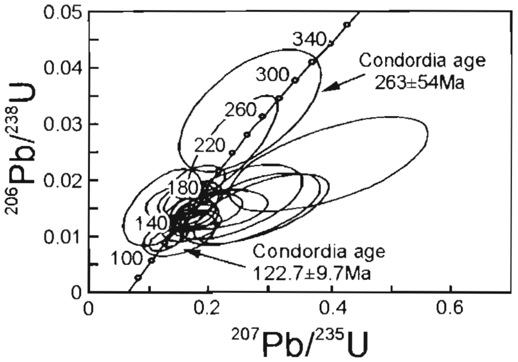

Figure 2. Concordia plot diagram of U-Pb spot analyses with help of LAICPMS for zircon grains extracted from the Cerro Pampa adakitic rock body.

The last group, of the Middle Proterozoic, is interpreted to be of the continental crust basement, which should exist below the sedimentary formations.

From the Puesto Nuevo body, 21 spots in 21 zircon grains have been extracted and dated, in which eight spots indicate concordia age. They are Cretaceous (1 spot), early Miocene (1 spot), and Middle Miocene (6 spots). The middle Miocene concordia ages range from 11.3 to 15.3Ma, with average of 13.3 ± 1.3Ma (1σ). The datings that are not on the concordia curve are due to common Pb contamination, and therefore, the $^{206}Pb/^{238}U$ ages are considered to be near equal to the concordia.

The $^{238}U/^{206}Pb$ ages are of Cretaceous (1 spot), Oligocene (2 spots), and Middle Miocene (10 spots). The Middle Miocene ^{238}U-^{206}Pb ages range from 11.6 to 18.2Ma, with the average of 14.1 ± 3.6Ma (1σ). The high concentration of the Middle Miocene zircon grains on U-Pb age suggests that the intrusive age of the Puesto Nuevo adakitic rock body is at Middle Miocene, and not Cretaceous (Fig. 3B). The grain of oldest spot age, e.g. 109±13Ma (2σ) of the concordia, is interpreted to be recycled zircon originated from the basement country rocks. In order to fix above-mentioned age contradiction, the authors performed fission track dating of zircon grains for both rock bodies, with help of the facility of Kyoto Fission Track Co. Ltd. Either magmatic *in-situ* zircon grains or recycled ones, fission track may indicate age of magma cooling. The result for the Cerro Pampa body is 11.9 ± 0.6Ma (1σ), being close to the K-Ar age of Kay, et al (1993), 12.1 ± 0.7Ma and 12.0 ± 0.7 Ma. This fission track age confirms that the Cerro Pampa adakitic rock body is of Middle Miocene, and that the adakitic magma was generated about 12 million years before the ridge collision at 10 Ma.

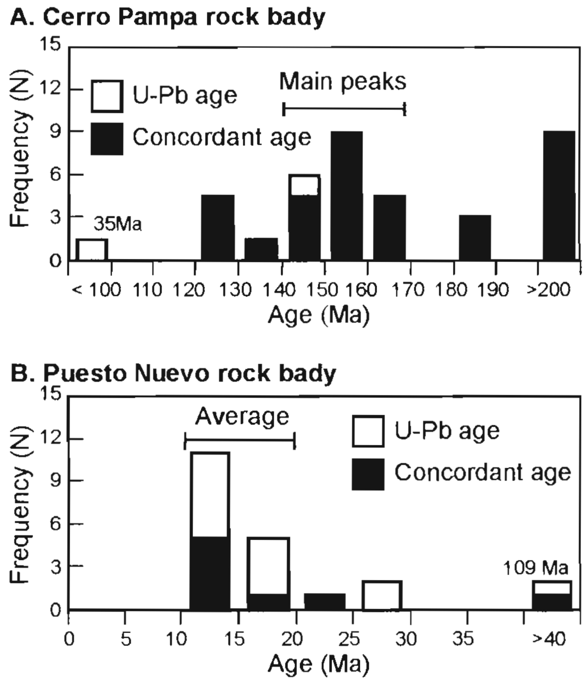

Figure 3. Age histogram of single zircon U-Pb spot dating for the Cerro Pampa (A) and Puesto Nuevo (B) adakitic rock bodies.

It should be also pointed out that the fission track dating for the Puesto Nuevo body indicates 15.9±0.6Ma (1σ), that is, of the Middle Miocene. This age is close to the ^{238}U-^{206}Pb age of *in-situ* zircon grains, 14.1±3.6Ma, suggesting strongly that the Puesto Nuevo adakitic body is also of the Middle Miocene. Considering the sill occurrence of the Puesto Nuevo adakitic body, an excess argon effect could lead to the Late Cretaceous age reported in previous paper.

It is interpreted that the Puesto Nuevo adakitic body is also related to on-going Chile Ridge subduction event, and the adakitic magma generation occurred about 14 tp 16 million years before the ridge collision.

REFERENCE

Kay, S.M.; Ramos, V.A.; Marquez, M., 1993. Evidence in Cerro Pampa volcanic rocks for slab-melting prior to ridge-trench collision in Southern South America. J. Geol. 101, 703-714.

Orihashi, Y.; Hirata, T.; Tani, K.; Yoshida, H., 2003. Rapid and simultaneous multi-elements and U-Pb age determinations of zircon crystal using UV laser ablation ICP-MS. Journal of Mineralogical and Petrological Science, press.

Ramos, V.A.; Kay, S.M.; Márquez, M., 1991. La Dacita Cerro Pampa (Mioceno - provincia de Santa Cruz): evidencias de la colisión de una dorsal oceánica. 4° Congreso Geológico Chileno, Acta 1, 747-751.

Ramos, V.A.; Kay, S.M.; Sacomani, L. 1994. La dacita Puesto Nuevo y otras rocas magmáticas: colisión de una dorsal oceánica cretácica. 7° Congreso Geológico Chileno, Acta 2, 1172-1176.

Stern, C. & Killian, R. 1996. Role of the sbducted slab, mantle wedge and continental crust in the generation of adakite from the Andean Austral Volcanic Zone. Contrib. Mineral. Petrol. 123, 263-281.

U-Pb AGES, Sm-Nd ISOTOPES AND STRUCTURAL ANALYSIS OF THE MOIPORÁ-NOVO BRASIL SHEAR ZONE SYSTEM: THE LIMITS BETWEEN NEOPROTEROZOIC GOIÁS MAGMATIC ARC AND THE ARCHEAN UVÁ COMPLEX, TOCANTINS PROVINCE, CENTRAL BRAZIL

Motta-Araújo, J.G. and Pimentel, M.M.

Instituto de Geociências da Universidade de Brasília. joao@unb.br, marcio@unb.br

Keywords: Goiás Magmatic Arc, Neoproterozoic, shear Zone, U-Pb, T_{DM} Model Ages

INTRODUCTION

The Tocantins Province, in central Brazil, is a large orogenic system formed during the assemblage of the São Francisco, Amazon and Paranapanema cratons (Pimentel & Fuck, 1992) (Fig 1). In the central-southern part of the province, in the vicinities of the towns of São Luis de Montes Belos, Jussara and Mossâmedes, Neoproterozoic orthogneisses of the Goiás Magmatic Arc are in faulted contact with Archean gneisses of the Uvá Complex, along sub-vertical mylonitic zone, known as the Moiporá-Novo Brazil shear zone. This is, in fact, a set of extensive lineaments very clearly marked in radar images for more than 250 km in the NS orientation. Another expressive lineament branch out to NNE in the form of open arc, concave to the SE.

Along the Moiporá-Novo Brasil shear zone, mylonitic gneisses with Neoproterozoic model ages are tectonically interleaved with rocks displaying Paleoproterozoic and Archean model ages (Pimentel et al., 1996; Gioia, 1997; Rodrigues et al., 1999). The nature, kynematics and tectonic significance of this contact is still poorly understood.

The main objective of this work is to investigate the tectonic significance of these lineaments through a detailed structural analysis and geochronological study in order to understand their significance in the tectonic evolution of the southern part of the Tocantins Province. In this paper preliminary field and U-Pb and Sm-Nd isotopic results are presented and discussed.

REGIONAL SETTING

The major tectonic constituents of the Tocantins Province are: Archean and Paleoproterozoic gneissic basement rocks, Neoproterozoics supracrustal fold belts such as the Araguaia, Paraguai and Brasília belts, and Goiás Magmatic Arc (Almeida et al., 1977; Pimentel et al., 1991, 1992; Fuck et al., 1994).

TTG and granite gneiss rocks together with greenstone belt sequences comprise the Archean rock units in the Uvá Complex. The Goiás Magmatic Arc is characterized by metaplutonic rocks, including tonalite and granodiorite association with volcano-sedimentary sequences formed in an oceanic island arc system during the Neoproterozoic (Pimentel & Fuck, 1992, Pimentel et al., 1996).

The metamorphic rocks of the Goiás Magmatic Arc are intruded by a number of K-rich granitic and gabbro-dioritic intrusions, forming a typical late- to post-orogenic bimodal magmatic suite.

LOCAL GEOLOGY

Between São Luís de Montes Belos, Jussara and Mossâmedes, four distinct tectonic blocks are recognized: 1 - Orthogneisses of the Goiás Magmatic Arc; 2 - TTG gneisses of Uvá Complex; 3 - Fazenda Nova-type mylonitic gneisses; 4 - Hornblende gneisses type Sanclerlândia of the Goiás Magmatic Arc.

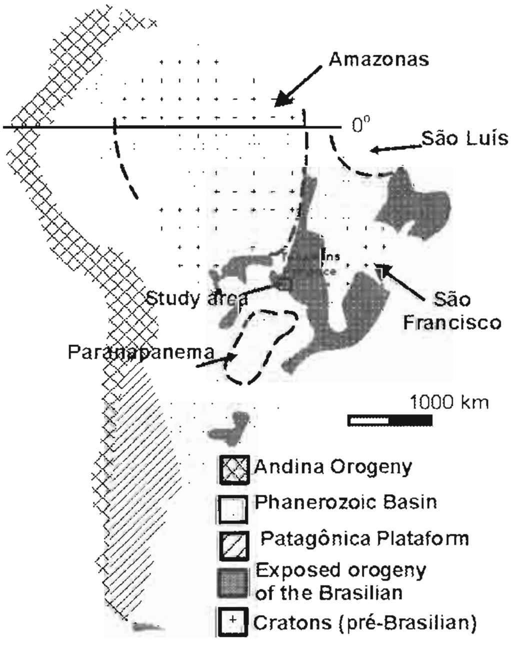

Figure 1 - Tectonic Map of the South Américan. Modificad the Almeida *et al.* (1981)

The contact between the Uvá Complex and Sanclerlândia gneiss is covered by quartzites and muscovite quartz schists of the Serra Dourada and Mossâmedes sequences. Garnet-schists are interlayered with quartzites, along the NE direction, parallel to the Serra Dourada ridge. These rocks were correlated with the Araxá Group and Araí Group (Dardenne, 2000).

Three groups of intrusive igneous rocks are identified in the region. Calc-alkaline to alkali-rich granite magmatism is represented by the large Serra do Impertinente and Israelândia intrusions. These post-orogenic bodies are exposed west of the Moiporá-Jussara lineament. Late- to post-orogenic granites to the east of the Moiporá-Jussara lineation form small intrusions such as the Córrego do Ouro, Novo Brasil, Messianópolis, Itapirapuã and Fazenda Nova granites. Pre to syn-tectonic granite intrusions are recognized in the Sanclerlândia region and are known as the Buriti de Goiás, São Mateus and Mossâmedes granites. The first two are elongated in the NE direction and the Mossâmedes granite is stretched in the EW orientation. Mafic-ultramafic magmatism is intrusive into the Sanclerlândia gneisses. Two of these bodies are associated with the São Luís de Montes Belos lineament. Alkaline magmatism is represented by Cretaceous and Tertiary volcanic e sub-volcanic rocks.

STRUCTURAL ANALYSIS

The Moiporá-Novo Brasil shear system is formed by five large lineaments. The São Luis de Montes Belos-Sanclerlândia lineament forms a narrow ridge in the NS direction. The Córrego do Ouro Lineament is marked by the alignment of quartz-garnet schists and mylonitic quartzite of the Serra Dourada and Mossâmedes sequences, along the NE direction. The Moiporá-Jussara Lineament, in the NNW direction, is formed by mica schist layers. In the NS Cachoeira de Goiás-Itapirapuã shear zone quartzite beds are exposed along the Serra do Facão ridge, and between the towns of Fazenda Nova and Itapirapuã, it represents the contact between gneissic rocks of different nature. The NE-trending strike-slip Faina Fault displays dextral movement.

The kynematics and structural analysis of those lineaments carried out using conventional movement indicators and interpretation of satelite images in association with radiometric ages, suggest an oblique collision between the Sanclerlândia and Uvá blocks, with vergence from south to north causing the rotation of the Sanclerlândia block.

U-Pb AND Sm-Nd ANALYSIS

Samples were analyzed at the Geochronology Laboratory of the University of Brasília.

T_{DM} model ages for the Sanclerlândia hornblende gneisses show values between 0.98 to 1.1 Ga, whereas orthogneisses of the Goiás Magmatic Arc, west of Sanclerlândia, have model ages between 1.13 and 1.29 Ga. Rocks from the Uva Complex have T_{DM} model ages in the interval between 2.85 and 3.28 Ga. The Fazenda Nova Gneisses have T_{DM} model ages between 2.25 and 2.33 Ga.

T_{DM} models ages for syn- to post-orogenic granites fall in three groups: 0.97 to 1.49 Ga, 1.91 to 2.25 Ga and 2.53 to 2.61 Ga.

Two samples of ultramafic rocks present T_{DM} ages of 1.97 and 2.83 Ga and two mafic rocks have model ages of 0.95 and 1.18 Ga.

Fine-grained orthogneisses to the NW of São Luis de Montes Belos, wall rock of mafic-ultramafic complex, have T_{DM} models age of ca. 1.28 Ga.

Metassedimentary rocks present model ages of 0.95 and 2.68 Ga, indicating provenance from both Neoproterozoic and Archean sources.

SHRIMP U-Pb age for the pos-tectonic Messianópolis granite yield a crystallization age of 540 Ma and conventional U-Pb data for the Sanclerlândia hornblende-gneiss yield a crystallization age of 820 Ma.

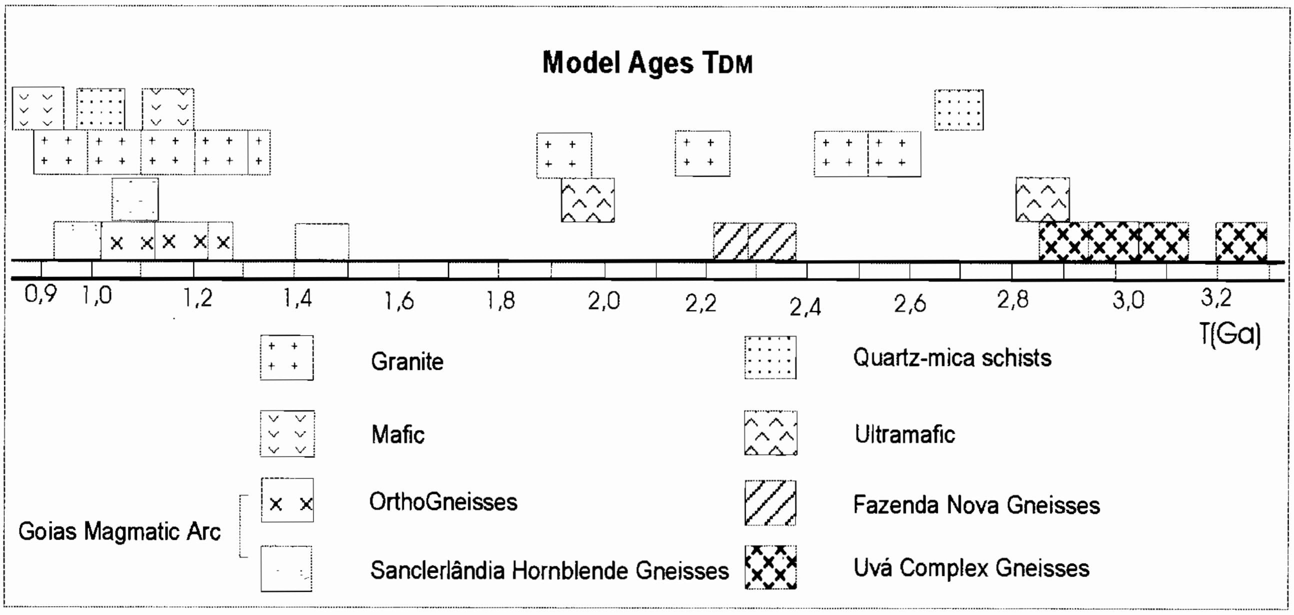

Figure 2. Histogram models age T_{DM} values for rocks in the São L. M. Belos-Jussura-Mossâmedes, region southwestern Goiás.

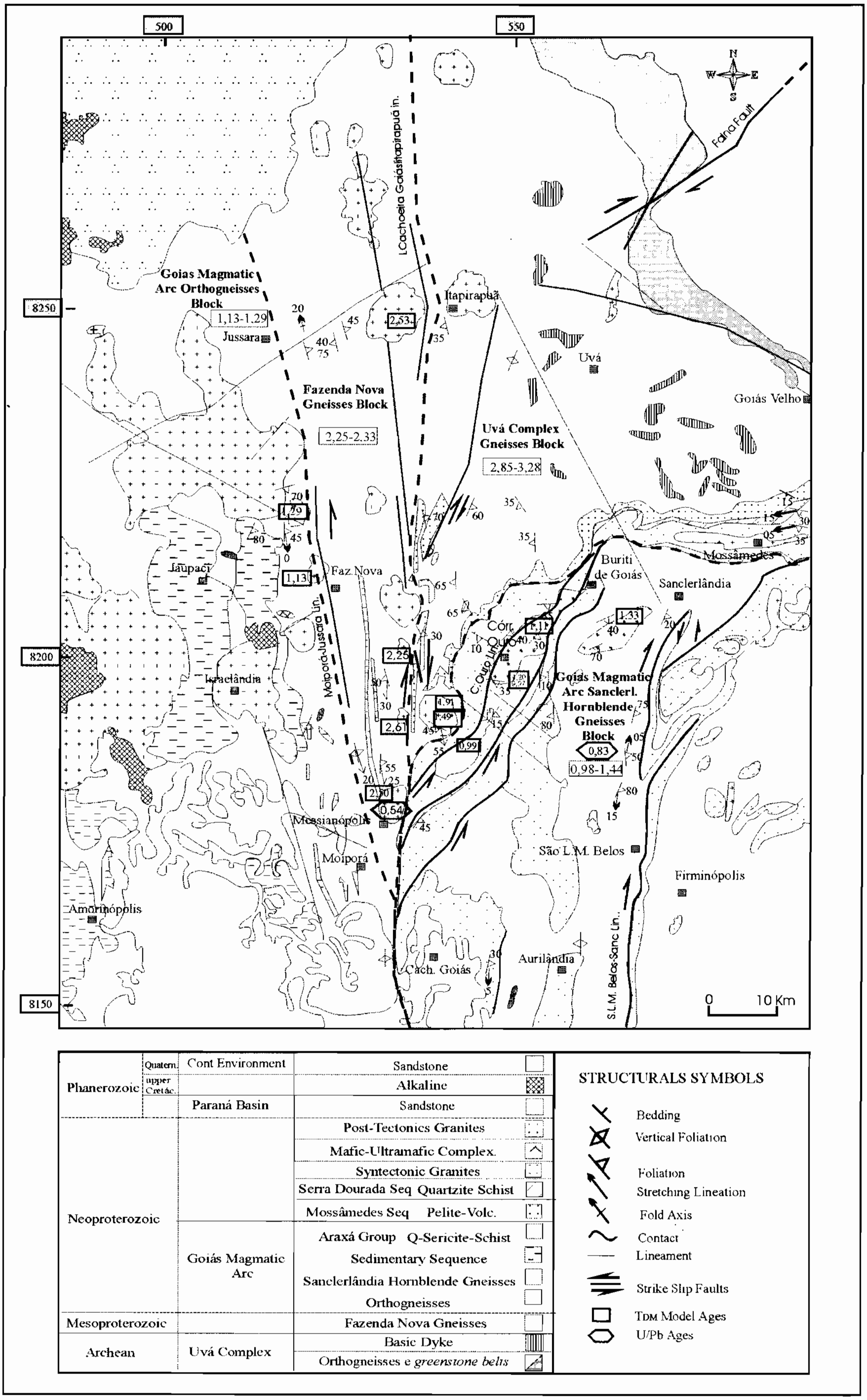

Figure 3 - Geologic-Geocronologic Map from Goias Magmatic Arc and Archean Terrane in region of São Luis de Montes Belos-Jussara-Mossâmedes, modif. SIG-GO 2002

CONCLUSIONS

Preliminary structural and isotopic data for the rocks in the region of the Moiporá-Novo Brasil shear zone allows a better understanding of the geological evolution of this important lineament system. Our results indicate the presence of rocks belonging to the Goiás Magmatic Arc in this region. Different crustal blocks have been recognized in the area, representing several main events of mantle differentiation to produce the continental crust in this region.

The SHRIMP U-Pb age of 542.3 ± 4.4 Ma for the late to post-tectonic Messianópolis granite, characterizes the last displacement of the Moiporá-Novo Brasil shear zone system and represents the upper limit for the Brasiliano event in the region.

The Moiporá-Novo Brasil shear system may represent a very important descontinuity within the Neoproterozoic Goiás Magmatic Arc and also between the arc and older terranes. Addtional studies are necessary to understand the detailed structural evolution of this strucuture. The main question is to address whether this structure represents the limit between crustal blocks, a suture zone or simply limits of terranes, with possible tectonic reactivations during the Phanerozoic.

ACKNOWLEDGEMENTS

This work was supported by grants from CNPq (Process 140306 / 2001-3).

REFERENCES

Almeida, F.F.M., 1977. O cráton do São Francisco. Revista Brasileira de Geociências, 7, 349-364.

Almeida, F.F.M., Hasui, Y., Neves, B.B.B., Fuck, R.A., 1981. Brasilian structural provinces: an introducion. Earth Sciences Review, 17,1-29.

Dardene, M.A., 2000. The Brasília Fold Belt. In: Cordani, U.G., Milani, E.J., Thomaz Filho, Campos, D.A. (eds), Tectonic Evolution of South America p.231-263.

Fuck, R.A., Pimentel, M.M., Silva, L.J.H.D., 1994. Compartimentação tectônica da porção oriental da Província Tocantins. Actas, 38 Congresso Brasileiro de Geologia, Balneário Camboriú-SC, 1, pp. 215-216.

Gioia, S.M.G., 1997. Preparação da metodologia Sm/Nd para datação de amostras geológicas e sua aplicação em rochas das áreas de Firminóplis, Fazenda Nova e Americano do Brasil. Dissertação de Mestrado, Universidade de Brasília, Brasília, 121 p.

Pimentel, M.M. & Fuck, R.A., 1992. Neoproterozoic crustal accretion in central Brazil. Geology. 20: 375-379.

Pimentel, M.M., Fuck. R.A., Silva, L.J.H.D., 1996. Dados Rb-Sr e Sm-Nd da região de Jussara-Goiás-Mossâmedes (GO), e o limite entre terrenos antigos do Maciço de Goiás e o Arco Magmático de Goiás. Revista Brasileira de Geociências, 26(2): 61-70.

Pimentel, M.M., Heaman, L., Fuck, R.A., 1991. Zircon and sphene Pb-U geochronology of Upper Proterozoic volcanic-arc rock units from southwestern Goiás, central Brazil. Journal of South American Earth Science, 4: 329-339.

Rodrigues, J.B., Gioia, S.M.L.C., Pimentel, M.M., 1999. Geocronologia e geoquímica de ortognaisses da região entre Iporá e Firminópolis: Implicações para a evolução do Arco Magmático de Goiás. Revista Brasileira de Geociências, 29(2): 207-216.

GEOCHRONOLOGY OF THE SÃO LUIS CRATON AND THE GURUPI BELT, BRAZIL

Moura, C.A.V.[1]; Abreu, F.A.M.[2]; Klein, E.L.[3,4]; Palheta, E.S.M.[4] and Pinheiro, B.L.S.[4]

1. Universidade Federal do Pará, Centro de Geociências,.Laboratório de Geologia Isotópica (Pará-Iso). C.P. 1611, 66.075-900, Belém-PA, Brazil. c_moura@ufpa.br
2. Universidade Federal do Pará, Centro de Geociências. C.P. 1611, 66.075-900, Belém-PA, Brazil. famatos@ufpa.br
3. CPRM/Serviço Geológico do Brasil - Av. Dr. Freitas, 3645, Belém-PA, Brasil, 66095-110. eklein@amazon.com.br
4. Universidade Federal do Pará, Centro de Geociências, Curso de Pós-Graduação em Geologia e Geoquímica, C.P. 1611, 66.075-900, Belém-PA, Brazil

Keywords: Geochronology, Paleoproterozoic, São Luís Craton, Gurupi Belt, Brazil

INTRODUCTION

Since the early Rb-Sr and K-Ar geochronological studies of Hurley et al. (1967), Almeida et al. (1968) and Cordani et al. (1968) the regions of NE-Pará and NW-Maranhão states, in northern Brazil, has been divided in two geotectonic units: the São Luis Craton and the Gurupi Belt. The former has been considered a small Paleoproterozoic fragment of the West African Craton and the latter a surrounding Pan-African/Brasiliano belt. Recent systematic single zircon Pb-evaporation dating (Pb-Pb zircon) and Sm-Nd isotope investigation, mainly in the granitic rock, and some additional Rb-Sr geochronology, suggest a more complex geologic evolution where the Gurupi Belt may be a paleoproterozoic unit reworked in the Brasiliano (Klein & Moura, 2001; Palheta, 2001; Klein & Moura, in press). These geochronological data are reviewed in this paper and their implications for the lithostratigraphic framework and geologic evolution are discussed.

REGIONAL GEOLOGY

The main lithostratigraphic units recognized in the São Luís Craton and Gurupi Belt are shown in the figure 1. The Tentugal Shear Zone would mark the limit between the cratonic and mobile regions. In the São Luís Craton occur metavolcano-sedimentary rocks of the Aurizona Group, calc-alkaline granitic rocks with TTG affinity grouped in the Tromai Intrusive Suite, and S-type granites of the Tracuateua Intrusive Suite (Lowell, 1985; Pastana, 1995). The metavolcano-sedimentary rocks of the Gurupi Group compose the main lithostratigraphic unit of the Gurupi belt. Orthogneisses of TTG affinity and associated paragneisses and migmatites are grouped in the Maracaçumé Complex. Mylonitic leucogranite (with minor andaluzite) named Maria Suprema Granite is associated with this complex. The Itamoari Tonalite is a strongly deformed rock nearby the Tentugal Shear Zone. The Cantão Granite is a biotite monzogranite intrusive in the rocks of the Gurupi Group rocks. A number of two mica granites occur along the Gurupi belt. Some are of Paleoproterozoic age (Ourém, Jonasa and Japiim) and one is Neoproterozoic (Ney Peixoto Granite). A nepheline syenite is also associated with the Gurupi Belt (Boca Nova Syenitic Gneiss). Precambrian and/or Eopaleozoic molassic cover (Vizeu, Igarapé de Areia and Piriá formations) complete the rock units associated with the evolution of the São Luís Craton and Gurupi Belt.

GEOCHRONOLOGY AND ISOTOPE GEOLOGY

ANALYTICAL TECHNIQUES

Pb-Pb zircon analysis were performed in the Pará-Iso (CG-UFPA) using a Finnigan MAT 262 mass spectrometer, following procedure described in Costi et al. (2000). Sm-Nd analyses were also performed in the same instrument following the analytical procedure described in Palheta (2001). Model ages were calculated based on DePaolo (1988) and the Pb-Pb zircon ages were used to compute the values of $\varepsilon Nd_{(t)}$. Rb-Sr analyses were performed in the single collector VG-54E mass spectrometer of the Pará-Iso.

Pb-Pb ZIRCON AGES

In the domain of the São Luís Craton there are three units of distinct ages. The AzGp whose metapyroclastic rock gave zircon ages of 2240 ± 5 Ma; the TmISt whose magmatism took place between 2150 and 2165 Ma; and, finally, the S-Type granites of the TcISt emplaced around 2080-2090 Ma (Table 1).

Table 1. Pb-Pb zircon ages. Uncertainties are given in 2 σ. Abbreviations of the geologic units are in figure 1. Zr#: number of zircons used in the age calculation. 1- Klein & Moura (2001), 2- Klein & Moura (in press), 3- Palheta (2001).

Units	Rock type	Zr#	Age (Ma)	Ref.
AzGp	metapyroclatic	5	2240 ± 5	1
TmISt	trondhjemite	5	2165 ± 2	1
TmISt	monzogranite	5	2163 ± 3	1
TmISt	tonalite	4	2149 ± 5	1
TmISt	monzogranite	1	2152 ± 3	2
TmISt	syenogranite	4	2149 ± 4	2
TcISt	monzogranite	4	2080 ± 2	3
TcISt	foliat. monzogranite	6	2091± 5	3
ItTn	foliated tonalite	5	2148 ± 4	1
GuGp	felsic metavolcanic	4	2148 ± 1	1
GuGp	metadacite	5	2160 ± 3	1
MaCx	tonalitic gneiss	1	2135 ± 4	2
MaCx	leucogranite	1	2128 ± 16	2
CnGr	monzogranite	1	2163 ± 4	3
JoGr	foliat. granodiorito	2	2073 ± 4	3
JaGr	granodiorite	4	2084 ± 5	3
NPGr	monzogranite	7	549 ± 4	3

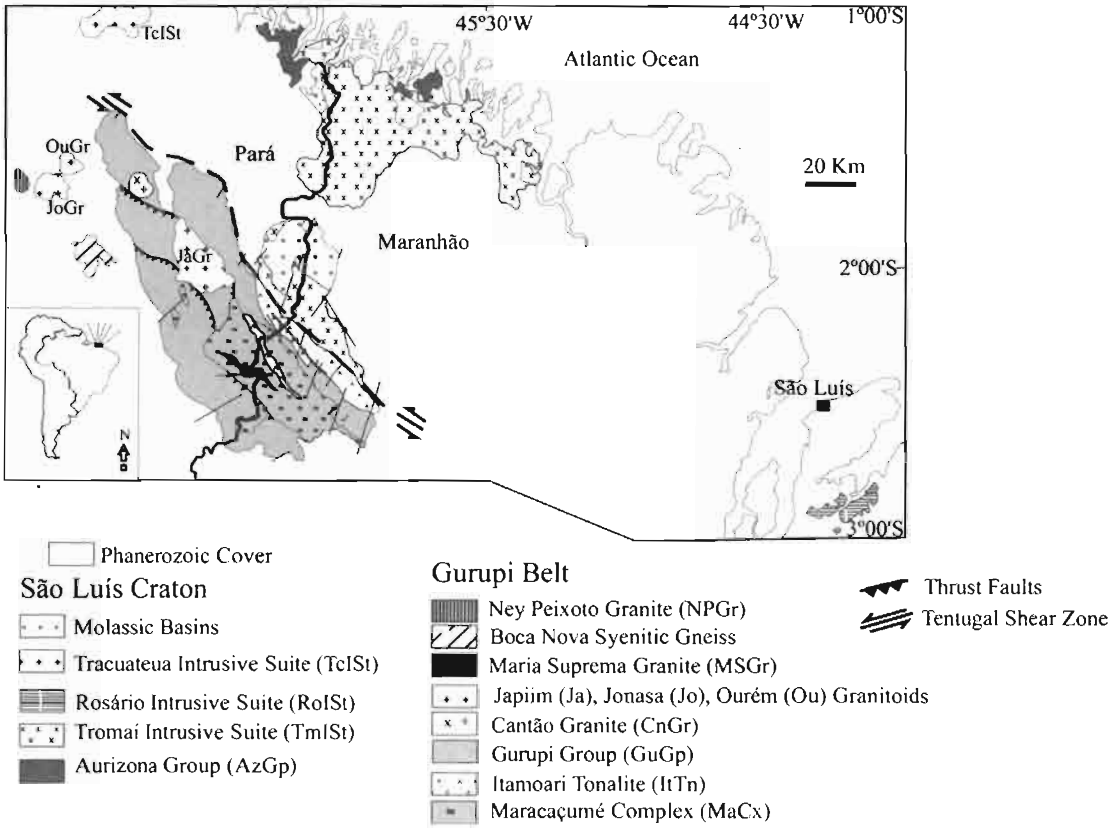

Figure 1. Simplified geologic map of the São Luís Craton and Gurupi Belt based on Hasui et al. (1984), Rodrigues et al. (1994) Pastana (1995) and Klein and Moura (2001).

In the domain of the Gurupi Belt three groups of ages have been recognized. The oldest one includes the ItTn, GuGp, CnGr and the MaCx.The deformed tonalite (ItTn). gave an age around 2150 Ma, and it may be coeval with the TTG rocks of the TmISt. The metavolcanic rocks of the GuGp yielded zircon ages of 2148 ± 1 Ma and 2160 ± 3 Ma, strongly suggesting that this volcanism and the TTG plutonic event may be contemporary. A small granitic pluton intrusive in the GuGp is also part of this older magmatic event (CnGr = 2163 ± 4 Ma). The gneissic rocks of the MaCx (2135 ± 4 Ma) and an associated leucogranitic mobilizate (2128 ± 16 Ma), whose zircons probable yielded minimum ages complete this first group of units. The ages of the two-mica granites JaGr (2084 ± 5 Ma) and JoGr (2073 ± 4 Ma) are similar to those of the S-type granites of the TclSt in the São Luís Craton. The zircon ages of the OuGr, although not well defined, are situated around 2.0 Ga suggesting that it may be part of this magmatic event. Finally, the NPGr with an age of 549 ± 4 Ma is the only Brasiliano age granitic pluton identified, so far, in this belt.

Inherited zircon crystals were found in the MaCx (2607 ± 11, 2509 ± 5 Ma and 2580 ± 4 Ma); JoGr (2325 ± 10 Ma, 2374 ± 6 Ma, 2387 ± 5, 2446 ± 7 Ma); JaGr (2351 ± 12 Ma) and OuGr (2459 ± 16 Ma). Detrital zircon grains of the Vizeu Formation gave ages between 2.0 and 2.1 Ga, while the zircon ages of the Igarapé de Areia Formation grouped in two populations. The older grains gave minimum ages around 2.0 Ga. The younger ones, the most abundant, provide ages mainly between 600 and 650 Ma permitting to constraint the maximum age for the deposition of the Igarapé de Areia Formation.

Sm-Nd ISOTOPE DATA

T_{DM} ages of the TclSt suggest a Paleoproterozoic crustal formation age for this region. However, the slightly positive or negative $\varepsilon Nd_{(t)}$ values of these granitic rocks may indicate some contribution of older crust. The Sm-Nd isotope data for the Paleoproterozoic granites in the Gurupi Belt also permit similar interpretation (Table 2). The contribution of older crust is confirmed by the presence of inherited zircon crystals in these granites, but its age is undefined. It may be an older Paleoproterozoic crust (≈ 2.4 Ga based on the inherited zircon ages) or even Archean.

The Neoproterozoic NPGr, have high negative $\varepsilon Nd_{(t)}$ values indicating a previous crustal history for its protolith (Table 1). The surrounding Paleoproterozoic crust is the natural candidate for source of this pluton, however, Sm-Nd fractionation, or some contribution of juvenile Neoproterozoic (?) sources, has to be argued to account for the younger T_{DM} ages (1.7-1.6 Ga).

Rb-Sr ISOTOPE DATA.

Rb-Sr whole rock isochron for the CnGr gave age of 2051 ± 165 Ma (MSWD = 0.69), with $^{87}Sr/^{86}Sr$ initial ratio of 0.70213 (191), confirming the Paleoproterozoic age of this rock. Rb-Sr internal isochron (rock + feldspar + muscovite) calculated for the JoGr yielded age of 523 ± 21 Ma (MSWD = 9.16) indicating the effect of Brasiliano age thermo-tectonic events in this rock unit. Similar approach was used for the MSGr (Fig. 1), a leucogranite formed by partial melt of the rocks of the MaCx during the formation of the Gurupi Belt (Pastana 1995). Rb-Sr age (rock + feldspar + muscovite) of 1710 ± 32 Ma (MSWD = 0.02) was obtained, suggesting that the Brasiliano event did not play an important role in the generation of this rock unit.

Table 2. Sm-Nd model ages $\varepsilon Nd_{(t)}$ for granitic rocks of the São Luís Craton and Gurupi Belt ater Palheta (2001).

Unit	Rock type	T_{DM} (Ga)	$\varepsilon Nd_{(t)}$
TcISt	Monzogranite	2.46	0.19
TcISt	Monzogranite	2.50	-1.33
TcISt	foliat. Monzogranite	2.32	0.97
TcISt	foliat. Monzogranite	2.31	1.15
JoGr	foliat. Granodiorite	2.40	-1.15
JoGr	foliat. Granodiorite	2.09	3.17
JaGr	Granodiorite	2.22	1.89
CnGr	Monzogranite	2.48	-0.93
CnGr	Monzogranite	2.21	2.68
NPGr	Monzogranite	1.78	-8.50
NPGr	Monzogranite	1.60	-7.83

DISCUSSIONS AND CONCLUSIONS

LITOSTRATIGRAPHIC IMPLICATIONS

The isotope data presented here contributes to understand the litostratigraphic framework of the São Luís Craton and Gurupi Belt and to constraint the ages of the studied geologic units. Although there are some inherited Neoarchean zircon crystals in the rocks of the MaCx, the Paleoproterozoic age of this complex is stressed by the zircon ages. Thus, the suggested Archean age for this unit is not confirmed. The granitic rocks of the TmISt (São Luís Craton) and of the ItTn, CnGr (Gurupi Belt), as well as the volcanic rocks of the GuGp seem to be coeval since their ages are in the same range (2150-2160 Ma). Thus, the relationship among these different magmatic events must be investigated. The ItTn, for instance, may represent a deformed portion of the TmISt. A widespread peraluminous granitic magmatism took place in this region around 2080 Ma generating a number of intrusive plutons, presently exposed in both cratonic and belt domains (TcISt, JaGr, JoGr and OuGr). As a result of the Brasiliano deformation, that reworked the rocks of the Gurupi belt, a small granitc pluton (NPGr) intruded the paleoproterozoic rocks. The detrital zircon ages of the Igarapé de Areia Formation, mainly between 600 and 650 Ma, constraint to the Neoproterozoic (Vendian) the maximum age for the deposition of the molassic cover occurring nearby the Gurupi Belt. The Vizeu Formation, which occurs near the AzGr (Fig. 1), may be contemporary cratonic cover, however, an older age cannot be ruled out since the detrital zircon ages of their rocks concentrated in the Paleoproterozoic.

GEOLOGIC EVOLUTION

The rock of the São Luís Craton and Gurupi Belt seem to share a common Paleoproterozoic evolution. By analogy with the Paleoproterozoic domains of the West African Craton this crustal segment is a result of amalgamation of oceanic plateau and island arc (and the associated back-arc basins) to the pre-existent Archean crust (Libéria, South Pará and Amapá for example). This evolution may have begun around 2.3 Ga, as suggested by some inherited zircon crystals. The older age of the metapyroclastic rocks of the AzGp (2.24 Ga) also suggests an older history, but the main period of rock formation is around 2.16 Ga. This Paleoproterozoic collage resulted in metamorphism and deformation of the metavolcano-sedimentary sequences (GuGp for example), in addition to the partial melt forming peraluminous granitic magmas, that intruded these sequences around 2.08 Ga. Subsequent stabilization was achieved until the assemblage of Gondwana has started. However, an incipient intracratonic fragmentation may have occured prior to this event to account for the presence of the nepheline syenite of Boca Nova (Fig.1) with a minimum Rb-Sr age of 720 Ma (Villas, 1982). The amalgamation of Gondwana resulted in the formation of a number of Pan-African/Brasiliano belts, sometimes involving both the accretion of new crust and reworked crustal segment. The exhumed portion of the Gurupi Belt is a Paleoproterozoic crust reworked during the Brasiliano by transcurrent shear zones (Tentugal Shear Zone) that accommodate mass displacement during Gondwana assemblage. The rock deformation and metamorphism associated with this shear zone reset, in some places, the Rb-Sr and K-Ar mineral system and led to localized partial melt forming granitic magmas (NPGr). Since the Gurupi Belt is covered by phanerozoic sediments to the south, it is not known if it is associated with younger rocks. However, the presence of detrital zircon grains of Brasiliano age in the molassic cratonic cover (Igarapé de Areia Formation) nearby the Gurupi Belt, requires the presence of younger (Brasiliano age) rocks in the neighborhood of the belt.

REFERENCES

Almeida, F. F. M.; Melcher, G. C.; Cordani, U. G.; Kawashita, K.; Vandoros, P., 1968. Radiometric age determinations from northern Brazil: Boletim da Sociedade Brasileira de Geologia, 17:3-14.

Cordani, U. G.; Melcher, G. C.; Almeida, F. F. M., 1968. Outline of the Precambrian geochronology of South America. Canadian Journal of Earth Sciences, 5:629-632.

Costi, H.T.; Dall'Agnol, R.; Moura, C.A.V., 2000. Geology and Pb-Pb geochronology of Paleoproterozoic Volcanic and Granitic rocks of the Pitinga Province, Amazonian craton, northern Brazil. International Geology Review. 42(9): 832-849.

DePaolo, D. J., 1988. Nedymium isotope geochemistry. An introduction. Berlim, Springer-Verlag. 187p.

Hurley, P. M.; Almeida, F. F. M.; Melcher, G. C.; Cordani, U. G.; Rand, J. R.; Kawashita, K.; Vandoros, P.; Pinson, W. H.; Fairbairn, H. W., 1967. Test of continental drift by comparison of radiometric ages. Science, 157:495-500.

Hasui, Y.; Abreu, F. A. M.; Villas, R. N. N., 1984. Província Parnaíba. In: F F M Almeida & Y Hasui. O Pré-Cambriano no Brasil. São Paulo, Edgard Blücher, p. 36-45

Klein, E. L. & Moura, C. A. V., 2001. Age constraints on granitoids and metavolcanic rocks of the São Luís Craton and Gurupi Belt, northern Brazil: implications for lithoestratigraphy and geological evolution. International Geology Review, 43: 237-253.

Klein, E. L. & Moura, C. A. V., in press. Síntese geológica e geocronológica do Cráton São Luís e do Cinturão Gurupi na região do rio Gurupi (NE-Pará/NW-Maranhão) Revista Geologia –USP Série Científica, v.2.

Lowell, G. R., 1985. Petrology of the Bragança batholith. São Luís Craton, Brazil. In: The crust – the significance of granites-gneisses in the lithosphere. Theophrastus Pub., Athens, p. 13-34.

Palheta, E. S. M., 2001. Evolução geológica da região nordeste do Estado do Pará com base em estudos estruturais e isotópicos de granitóides. Tese de Mestrado, Centro de Geociências, UFPA, Belém, 144 p.

Pastana, J. M. N., 1995. Programa Levantamentos Geológicos Básicos do Brasil. Programa Grande Carajás. Turiaçu/Pinheiro, folhas SA.23-V-D/SA.23-Y-B. Estados do Pará e Maranhão. Brasília, CPRM, 205p.

Rodrigues, T. L. N.; Araújo, C. C.; Camozzatto, E.; Ramgrab, G. E., 1994. Programa Levantamentos Geológicos Básicos do Brasil. São Luís, Folha SA.23-Z-A. Cururupu, Folha SA.23-X-C, Estado do Maranhão. Escala 1:250.000. Brasília, CPRM, 185p.

Villas, R. N. N., 1982. Geocronologia das intrusões ígneas na bacia do rio Guamá, nordeste do Estado do Pará. In: Anais do 2° Simpósio de Geologia da Amazônia, Belém, v. 1, p. 233-247.

Nd AND Pb ISOTOPE CONSTRAINTS ON SEDIMENT PROVENANCE IN THE CANINDÉ DOMAIN, SERGIPE OROGENIC BELT (NE BRAZIL)

Nascimento, R.S.[1]; Oliveira, E.P.[1] and Babinski, M.[2]

1. Instituto de Geociências, Universidade Estadual de Campinas, Campinas-SP, Caixa Postal 6152. rosemery@ige.unicamp.br, elson@ige.unicamp.br
2. Instituto de Geociências, Universidade de São Paulo, Rua do Lago, 562, São Paulo-SP, 05508-080. babinski@usp.br

Keywords: Sergipe Belt, Canindé Domain, metasedimentary rocks, Sm-Nd and Pb-Pb geochronology

INTRODUCTION

Neodimium isotope data for clastic sediments of orogenic belts may provide important insights into the potential sources from which they derived. Of particular interest are fine-grained clastic sediments that are generally assumed to represent the mean composition of a large continental segment (e.g. Allegre & Rousseau, 1984; Jahn & Condie, 1995). The similarity of REE patterns in several clastic sedimentary rocks has been taken to imply that little fractionation of Sm-Nd accompanies the generation of clastic sedimentary rocks from their precursors. Consequently, model ages calculated from Sm-Nd data for sedimentary rocks may be expected to reflect the average residence age of the crust feeding sedimentary basins (McCulloch & Wasserburg, 1978). Conversely, the Nd model age of a sedimentary rock is a maximum estimate for its deposition.

The Canindé Domain is one of the seven tectonic domains that make up the Sergipe orogenic belt. It consists of a metavolcano-sedimentary sequence crosscut by a gabbroic complex and granites. The genesis of the mafic rocks of the Canindé Domain has been a matter of intense debate. They have been interpreted as an ophiolite sequence (Silva Filho, 1976), continental-type magmatism (Oliveira & Tarney, 1990), and intra-oceanic arc sequence (Bezerra, 1992; Silva Filho, 1998). However, little has been commented on the sedimentary rocks, their diversity and provenance.

In this paper we report a Pb-Pb isochron for marble samples and Nd isotope data for associated metasedimentary rocks. In order to discuss sediment provenance we present additional Nd isotope data for island arc-type granites and amphibolites of the Canindé Domain, and gneisses from the adjacent Poço Redondo Domain and Pernambuco-Alagoas Massif.

GEOLOGICAL UNITS

The Sergipe orogenic belt trends ESE-WNW and is thought to have originated by the collision between the Pernambuco-Alagoas Massif to the north and the São Francisco craton to the south during the Pan African-Brasiliano Orogeny (Brito Neves et al., 1977; Davison & Santos, 1989; D'el-Rey Silva, 1995). It represents the Brazilian continuation of the Neoproterozoic Oubanguides Fold Belt in Africa (Trompette, 1994), and comprises seven fault-bounded lithotectonic domains: Sul-Alagoas, Canindé, Poço Redondo, Marancó, Macururé, Vaza Barris e Estância (Santos & Souza, 1988; Davison & Santos, 1989; Silva Filho et al., 1997).

The Canindé Domain is made up of volcano-sedimentary rocks of the Novo Gosto and Gentileza units. The latter is crosscut by enclave-rich granodiorite of the Lajedinho Granite, porphyritic granodiorites and rapakivi-like granites. These units are crosscut by the Canindé layered Gabbroic Suite, the Xingó, Boa Esperança and Serrota leucogranites and other minor granite types. To the south the Canindé domain lies in contact with migmatites, gneisses and granites of the Poço Redondo Domain along a high-angle shear zone. To the north it is in contact with rocks of the Pernambuco-Alagoas massif.

The Novo Gosto unit is made up of fine-grained amphibolites intercalated with metapelites, metasiltites, metacherts, graphite schists, calc-silicate rocks and marbles. These rocks are crosscut by mafic and felsic dykes, and by Fe-Ti-rich gabbroic bodies. Field relationships along riverbeds show that the amphibolites are interleaved with marble lenses and fine-grained metagreywacke and metasiltites. They are tightly folded with axial plane foliation dipping 40°NE. Granites of the Gentileza Unit and gabbros of the Canindé Suite crosscut this sequence.

The Gentileza Unit is mainly formed by amphibolites and dolerite dykes, with minor gabbroic bodies and offshoots of porphyritic granodiorite and stocks of the Xingó and Serrota leucogranite.

The Canindé Suite trends E-W and is composed of massive and layered gabbroic rocks with igneous layering dipping 55°SE. They range in composition from peridotite through olivine-gabbronorite, norite, gabbro, pegmatitic gabbro to leucotroctolite and anorthosite. These rocks display nicely preserved intergranular and cumulate textures.

Three additional types of granitic bodies are also known in the Canindé Domain. They are the Serrota, Lajedinho and Boa Esperança granites. Amongst them, the Boa Esperança granite is the most abundant; it is a weakly to non-deformed fine- to medium-grained leucomonzogranite that usually crops out in close association with basic rocks of the Novo Gosto and Gentileza units. The Serrota Granite differs from the Boa Esperança in both structure and composition. It consists of deformed granodiorite, often with gneissic structure and porfiroclastic texture. The Lajedinho Granite crops out close to the Xingó dam and corresponds to a porphyritic monzogranite to granodiorite with superb flow structure defined by mafic enclaves; these features render comparisons with island-arc granitoids.

ANALYTICAL PROCEDURES

Whole-rock Sm-Nd isotope analyses were done at the Laboratory of Geochronology of the University of Brasília following the analytical procedures of Gióia & Pimentel (2000). Depleted-mantle Nd model ages (T_{DM}) were calculated using the model of DePaolo (1981). Pb isotope data were obtained on marble samples from a single outcrop; Analyses were carried out at the Geochronological Research Center of the University of São Paulo following the analytical procedures described in Babinski et al. (1999).

RESULTS

The Pb-Pb isochron (Fig. 1) of four marble samples from the Novo Gosto unit yields the age 963 ± 20 Ma (1σ). Because deformation and metamorphism can affect the Pb isotope system (Babinski et al., 1999), this age must be interpreted as the time of metamorphic recrystallization of the marble protolith.

Sm-Nd isotope data for metasediments, amphibolite and granitic rocks of the Canindé domain are presented in Figure 2. Data for a migmatite from the Poço Redondo Domain (Silva Filho et al., 1997) and representative samples from the Pernambuco-Alagoas Massif (Silva Filho et al., 2002) are also shown for comparison, as these two regions are potential sources for sediments of the Canindé Domain. The depleted-mantle Nd-model ages (T_{DM}) for metasediments of the Novo Gosto Unit cluster in two groups, namely around 1.1 Ga and between 1.3 Ga and 1.5 Ga. The amphibolite to which several marble lenses are associated present Nd-model age of 1.12 Ga, whereas the Lajedinho Granite yields the age 1.22 Ga. If we consider the 960 Ma age as the minimum age for the deposition of the marbles, then the recalculated $\varepsilon_{Nd(t=0.96Ga)}$ value of the amphibolite is +4.2, suggesting a primitive, mantle-derived origin for this rock

DISCUSSION

The isotope data presented here have several implications for the geologic evolution of the Canindé Domain.

Firstly, the Pb-isochron age (ca. 960 Ma) found for a marble lens indicates that the geological evolution of the Canindé Domain must have started at least in the Mesoproterozoic. It is also a minimum estimate for the associated amphibolites, because field relationships between amphibolite and marble on the Riacho dos Porcos suggest that both rock types may be coeval. This is particularly likely because the marble occurs as several narrow lenses (up to 30 cm thick) interleaved with fine-grained amphibolites, and no structural repetition of these rocks by folding or thrusting is observed. On these grounds, we suggest that the amphibolite protoliths were basalt flows separated from each other by deposition of limestones. Initial ICP-MS trace element data for these amphibolites and comparable rocks elsewhere in the Canindé Domain, combined with their positive $\varepsilon_{Nd(t=0.96Ga)}$ values point to a complex and diverse evolution for this domain, with basalts similar to oceanic plateaus, MORBs and island arc tholeiites all occurring in a single tectonic domain. The most likely tectonic setting for the close association of these distinct basalt types is the accretionary wedge of an island-arc system. The occurrence of graphite schists sandwiched in clastic sediments of the Canindé Domain may be an additional evidence for such tectonic setting, because they could well be the metamorphosed equivalent of modern methane hydrate found in accretionary complexes (Hyndman, 1992; Windley, 1995).

Secondly, the bimodal distribution of Nd model ages observed on the Novo Gosto metasediments, i.e. ca. 1.1 Ga and 1.3-1.5 Ga, indicates contribution of at least two main sources for their protoliths. In general, each metasediment Nd model age is interpreted as source mixtures. For the metasediments that present TDM close to 1.1 Ga a likely source is the Novo Gosto amphibolites (T_{DM}=1.12 Ga), which could also have acted as basement for sediment deposition. The Nd model ages for the second group, on the other hand, must be explained by mixing of two or more sources, one old and another young. Amphibolites of the Novo Gosto or of the arc-like Lajedinho Granite (T_{DM}=1.22 Ga) are potential candidates for the young source, whereas the Poço Redondo migmatites (T_{DM}=1.75 Ga; Silva Filho et al., 1997) and gneiss (T_{DM}=1.67; our data), or migmatites and gneisses of the Pernambuco-Alagoas Massif (T_{DM}=1.55-2.51 Ga; Silva Filho et al., 2002) are the most likely old components. Whether these two latter areas have actually contributed sediments to the Canindé domain basin is an open question because the original geographic position of this domain is uncertain. Many modern orogenic belts are composed of exotic terranes that may have travelled several thousands of kilometers from their site of origin.

In summary, our initial findings suggest that the Canindé Domain of the Sergipe orogenic belt is a Mesoproterozoic destructive plate margin sequence, possibly similar to that of western North- and South America or Southeast Asia. During its subsequent collision with the Poço Redondo and/or Pernambuco-Alagoas microcontinents syntectonic granites were emplaced. Later extension made room available for emplacement of the Canindé gabbroic complex and minor rapakivi-like granitoids.

ACKNOWLEDGMENTS

The São Paulo State Foundation for Research Support (FAPESP) and the Brazilian National Research Council (CNPq) provided research grants for this project (FAPESP 02/03085-2, 00/12941-4; CNPq 300.845/91-0).

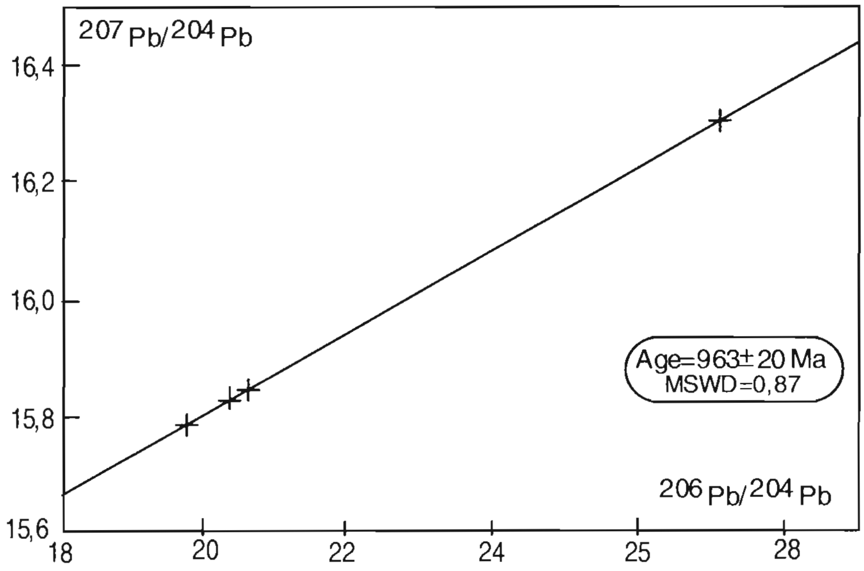

Figure 1. Pb-Pb isochron for marbles of the Novo Gosto Unit.

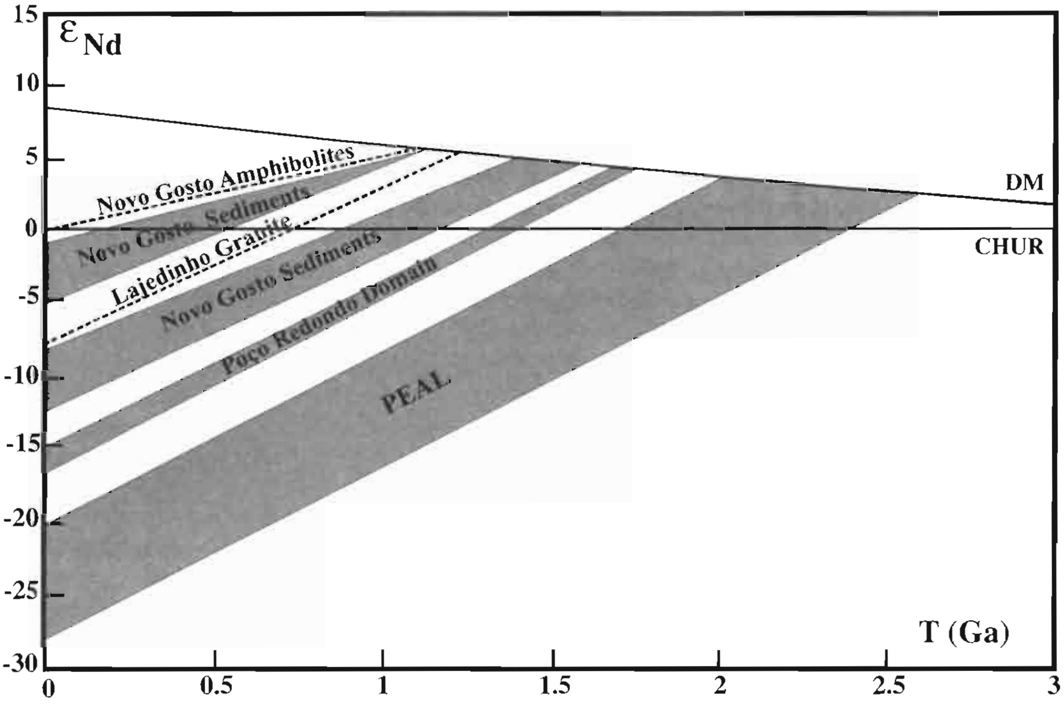

Figure 2. Nd evolution diagram for metasediments of the Novo Gosto Unit and their possible sources.

REFERENCES

Allegre, C.J. & Rosseau, D., 1984. The growth of the continent through geological time studied by Nd isotope analysis of shales. Earth and Planetary Science Letters, 67: 19-34.

Babinski, M., Van Schmus, W.R., Chemale Jr., F., 1999. Pb-Pb dating and Pb isotope geochemistry of Neoproterozoic carbonate rocks from the São Francisco Basin, Brazil: implications for the mobility of Pb isotopes during tectonism and metamorphism. Chemical Geology, 160 : 175-199.

Bezerra, F.H.R., 1992. Geologia e evolução petrológica do Complexo gabróico Canindé do São Francisco e rochas adjacentes (Sergipe e Alagoas). Dissertação de Mestrado, Universidade de Brasília, Instituto de Geociências, 220 p.

Brito Neves, B.B., Sial, A.N., Albuquerque, J.P.T., 1977. Vergência centrífuga residual do Sistema de Dobramentos Sergipe. Revista Brasileira de Geociências, 7 (2): 102-114.

D'el-Rey Silva, L.J.H., 1995. Tectonic evolution of the Sergipe Belt, NE Brazil. Revista Brasileira de Geociências, 25: 315-332.

Davison, I. & Santos, R.A., 1989. Tectonic evolution of the Sergipe Fold Belt, NE Brazil, during the Brasiliano Orogeny. Precambrian Res., 45: 319-342.

De Paolo, D.J., 1981. A neodymium and strontium isotopic study of the Mesozoic calc-alkaline granitic batholithys of the Sierra Nevada and Peninsular Ranges, California. Journal of Geophysical Research, 86:10470-10488.

Gióia, S.M.C.L. & Pimentel, M.M., 2000. The Sm-Nd isotopic method in the Geochronology Laboratory of the University of Brasília. Anais da Academia Brasileira de Ciências, 72:219-245.

Hyndman, R.D. 1992. 'Ice' beneath the deep sea: studies of methane hydrate layers beneath the continental slope off Vancouver Island. Geoscience Canada, 19: 21-26.

Jahn, B.M. & Condie, K.C., 1995. Evolution of the Kaapvaal craton as viewed from geochemical and Sm-Nd isotopic analyses of intracratonic pelites. Geochimica Cosmochimica Acta, 59: 2239-2258.

McCulloch, M.T. & Wasserburg, G.J., 1978. Sm-Nd and Rb-Sr chronology of continental crust formation. Science 200: 1003.

Oliveira, E.P. & Tarney, J., 1990. Petrogenesis of the Canindé do São Francisco complex: a major late Proterozoic gabbroic body in the Sergipe fold belt, NE Brazil. J. South Am. Earth Sci., 3: 125-140.

Santos, R. A. & Souza, J. D., 1988. Programa de levantamentos geológicos Básicos do Brasil; carta metalogenética/ previsional – escala 1:100.000 (Folha CS.24-X-C-VI Piranhas) DNPM/CPRM, 154. p.2.

Silva Filho, A.F., Guimarães, I.P., Lyra de Brito, M.F., Pimentel, M.M., 1997. Geochemical signatures of the main Neoproterozoic late tectonic granitoids from the Proterozoic Sergipe fold belt, NE Brazil and its significance for the Brasiliano orogeny. International Geology Review, 39: 639-659.

Silva Filho, A.F., Guimarães, I.P., Van Schmus, W.R., 2002. Crustal evolution of the Pernambuco-Alagoas Complex, Borborema Province, NE Brazil: Nd isotopic data from neoproterozoic granitoids. Gondwana Research. vol. 5, p.409-422.

Silva Filho, M.A., 1976. A suíte ofiolítica da Geossinclinal de Propriá. In: XXIX Congresso Brasileiro de Geologia. Anais... SBG. vol. 4, p.51-58.

^{40}Ar/^{39}Ar AGES OF THE ALUMINIO (SERRA DO ITABERABA GROUP) AND HERMIDA (ITAPIRA GROUP) AMPHIBOLITE, CENTRAL PORTION OF THE RIBEIRA BELT, BRAZIL: PRELIMINARY INFERENCES

Oliveira, M.A.F.[1]; Souza, S.C.A.[1]; Teixeira, W.[2] and Vasconcelos, P.M.[3]

1. Instituto de Geociências e Ciências Exatas - UNESP - C.P. 178, 13506-900, Rio Claro-SP, Brazil. maurelio@rc.unesp.br
2. Centro de Pesquisas Geocronológicas, Instituto de Geociências, USP, São Paulo-SP, Brazil. wteixeir@.usp.br
3. University of Queensland, Department of Earth Science, Brisbane, Qld, 4072 Australia. paulo@sol.earthsciences.uq.edu.au

Keywords: Amphibolite, São Roque and Itapira Group, Neoproterozoic metamorphism, Ribeira belt

INTRODUCTION

Metabasic rocks and amphibolite are commonly associated with metasediments of São Roque, Serra do Itaberaba and Itapira Groups, in the central east portion of São Paulo State, Ribeira Belt, Brazil. Geochemical studies of these mafic rocks (Souza, 2001) show their igneous nature and tholeiitic E-MORB basalt affinity suggesting their relationship with a back-arc type basin. New ^{40}Ar/^{39}Ar analyses of metabasic rocks and amphibolites that crop out near Alumínio and Hermida, in the vicinities of Sorocaba and Jundiaí are now presented and discussed in order to contribute to the geological history of the Ribeira belt. The analyses were performed at the Geochronological Research Center (CPGeo) of University of São Paulo, Brazil, following Vasconcelos et al., 2002.

GEOLOGICAL SETTING

The Itapira Group, in the central-east part of the State of São Paulo, is tectonically juxtaposed with the São Roque and Serra do Itaberaba Groups - by means of the Jundiuvira shear zone. In the vicinity of Jundiaí, amphibolite crops out in the region of Hermida, associated with quartzite, schist and migmatite and intruded by granitic rocks (Hasui et al., 1978; Oliveira et al., 1987; Souza, 1997; 2001). A K-Ar analysis for one of these amphibolite yields an age of 1046 ± 45 Ma (Hasui & Hama, 1972). In addition, U-Pb determinations (zircon and monazite) of a granitic intrusion, that represents a tangential transpressive tectonic event, yield ages of 625 and 610 Ma, respectively. These ages constrain the time of metamorphism and tectonism in the central part of the Ribeira belt (Hackspacher et al., submitted).

The metamorphic units of São Roque and Serra do Itaberaba Groups crop out along the southern portion of the Jundiuvira shear zone, within the São Roque tectonic domain, limited to the south by the Taxaquara shear zone (Hasui et al., 1969; Hasui et al., 1970; Hasui, 1975). The Serra do Itaberaba Group makes up the basal section of the São Roque Group and include schist units with abundant amphibolite intercalation (Juliani et al., 1986; Juliani & Beljavski, 1995). The São Roque Group consists of phyllite, quartzite, metaconglomerate and metabasic rocks intruded by granitic plutons (Hasui, 1975; Oliveira et al., 1998; Souza, 2001). Only a few isotopic determinations are available for these area: i) two metamorphic events at 1.4 and 0.8-0.7 Ma (Rb-Sr and Pb-Pb) for the São Roque metassedimentary sequence are described by Tassinari et al., 1988; ii) a mafic metavolcanic from Pirapora do Bom Jesus Formation (São Roque Group) has a U-Pb monazite age of 628 ± 8 Ma which is interpreted as the crystallization age (Hackspacher et al., 2000); iii) the deposition time of the Serra do Itaberaba Group is constrained by U-Pb zircon age of 1395 ± 10 for a metandesite (Juliani et al., 2000).

The Hermida amphibolite (Itapira Group) comprises three small lenticular bodies oriented parallel to the regional foliation, composed essentially of andesine and hornblende, with diopside, garnet, quartz and opaque minerals. The metamorphic equilibrium corresponding to this association indicates temperatures between 700 and 830°C and pressures of 6-7 kbar, in coherence with amphibolite facies (Souza, 1997, 2001).

The Alumínio amphibolite is part of the Serra do Itaberaba Group. This body is cross cut by transcurrent faults, whilst its W-NW portion is intruded by the São Francisco granitic massif, emplaced between 0.7 and 0.55 Ga (Tassinari et al., 1988). It shows varied petrographic types such as hornblende amphibolite, hornblende-actinolite amphibolite, actinolite amphibolite, and olivine amphibolite. Two metamorphic peaks are recorded in this rock: one with temperatures between 450 and 550 °C and pressures between 2 and 4 kb (greenschist facies), whereas the other has temperatures in the interval of 550 and 700 °C and pressure between 5 and 7 kbar (amphibolite facies; Souza, 2001).

RESULTS AND DISCUSSION

The Hermida amphibole (hornblende - SH-1B) yields Ar-Ar plateau ages of 614 ± 8, 579 ± 5 and 582 ± 6 Ma, and a mean age of 591 ± 19 Ma (Fig. 1). This mean age constrains the minimum age of metamorphism, which is roughly consistent with the time of transpressive tectonics and metamorphism affecting the Ribeira belt at between 620-610 Ma ago (Hackspacher et al., submitted). In addition, this new Ar-Ar age implies that a previous reported K-Ar age for the Hermida amphibolite (Hasui & Hama, 1972) is probably meanless, due to excess argon.

Two Ar-Ar analyses were performed in the Alumínio amphibolite, but yielded discordant apparent age patterns. SA-81 sample exhibits a Ar-Ar plateu age (one analysis) of 1312 ± 6 Ma, but the other two step heating analyses showed varied isotopic disturbance, which is a common feature of analyses in actinolite (Fig. 2). Particularly the plateau age may be considered as the minimum age for the regional metamorphism - in agreement with the idea that deposition of the Serra do Itaberaba Group started at ca. 1395 Ma ago (Juliani et al., 2000).

Sample SA-142 (hornblende-actinolite) yields much younger ages – a plateau age of 780 ± 10 Ma, and two comparable integrated ages of 799 ± 6 and 852 ± 7 Ma, with a mean age of 800 ± 20 Ma (Fig. 3). Tassinari et al. (1988) describe for the São Roque meta-volcanossedimentary sequence two metamorphic superimposed events at 1.4 and 0.8-0.7 Ma, based on Rb-Sr and Pb-Pb determinations. Recently an age of 811 ± 13 Ma is reported for the Ribeira belt rocks (Embu Complex), by Cordani et al. (2002) and interpreted as the age of crystallization of granodiotitic-tonalitic gneiss, cropping near São Lourenço da Serra, 50 Km SE of Alumínio. The meaning of this age is considered by the authors as related to a magmatic arc activity and later allochthonous terrane assembly, during closure of the Adamastor ocean. So the ages of 1312 ± 6 and 800 ± 20 Ma now obtained may represent minimum ages for two metamorphic events occurred in this area.

ACKNOWLEDGEMENTS

To FAPESP (Project 99/05137-5) for financial support and to Artur T. Onoe for his dedication to the analyses.

REFERENCES

Cordani, U. G.; Coutinho, J. M. V.; Nutman, A. P., 2002. Geochronological constraints on the evolution of the Embu Complex, São Paulo, Brazil. Journal of South American Earth Science, 14: 903-910.

Hackspacher, P. C.; Dantas, E. L.; Spoladore, A.; Fetter, A. H.; Oliveira, M. A. F., 2000. Evidence for Neoproterozoic back arc basin development in the Central Ribeira Belt, southeastern Brazil: new geochronological and geochemical constraints from the São Roque-Açungui Groups. Revista Brasileira de Geociências, 30(1): 110-114.

Hackspacher, P. C.; Ribeiro, L. F. B.; Ribeiro, M. C. S.; Fetter, A. H.; Hadler Neto, J. C.; Tello, C. S.; Dantas, E. L., submitted. Consolidation and break-up of the South American Platform in southeastern Brazil: tectonothermal and denudation histories. Gondwana Research,

Hasui, Y., 1975. Geologia da folha São Roque. Boletim IG-USP, 6: 157-183.

Hasui, Y. & Hama, M., 1972. Geocronologia do Grupo são Roque pelo método potássio-argônio. Revista Brasileira de Geociências, 2: 18-24.

Hasui, Y.; Penalva, F.; Hennies W. T., 1969. Geologia do Grupo São Roque. In: XXIII Congresso Brasileiro de Geologia, Anais, Salvador, 101-135.

Hasui, Y.; Tognon, A. A.; Soares, L., 1978. Geologia e tectônica da Serra do Japi. Boletim IG. Instituto de Geociências, USP, 9: 17-24.

Juliani, C. & Beljavskis, P., 1995. Revisão da litoestratigrafia da faixa São Roque-Serra do Itaberaba, SP. Revista Instituto Geológico, 16(1/2): 33-58.

Juliani, C.; Beljavskis, P. Schorscher, H. D., 1986. Petrogênese do vulcanismo e aspectos metalogenéticos associados: Grupo Serra do Itaberaba na região de São Roque, SP. In: XXXIV Congresso Brasileiro de Geologia, Anais, Goiânia, 2: 730-747.

Juliano, C.; Hackspacher, P. C.; Dantas, E. L.; Fetter, A. H., 2000. The Mesoproterozoic volcano-sedimentary Serra do Itaberaba Group of the central Ribeira Belt, São Paulo, Brazil: implications for the age of the overlying São Roque group. Revista Brasileira de Geociências, 30(1): 82-86.

Oliveira, M. A. F. de; Batista, J. J.; Morales, N., 1987. Caracterização geoquímica de rochas anfibolíticas do Grupo Itapira nas folhas de Atibais e Jundiaí (SP). In: VI Simpósio Regional de Geologia, Anais, São Paulo, 1: 23-32.

Oliveira, M. A. F. de; Godoy, A. M.; Hackspacher, P. C.; Morales, N., 1998. Geologia da folha São Roque (SP) em 1:50000. Geociências, 17(2): 371-398.

Souza, S. C. A., 1997. Anfibolitos ortoderivados do Complexo Itapira e do Bloco São Roque nas folhas Cabreúva, Sorocaba, Itu e São Roque (SP): petrografia, litoquímica, química mineral e termobarometria. Instituto de Geociências e Ciências Exatas, Universidade Estadual Paulista, Dissertação de Mestrado, 137pp

Souza, S. C. A., 2001. Petrologia dos corpos anfibolíticos de Hermida, Alumínio e Pirapora do Bom Jesus, SP. Instituto de Geociências e Ciências Exatas, Universidade Estadual Paulista, Tese de Doutorado, 178pp.

Tassinari, C. C. G.; Kawashita, K.; Van Schmuss, R.; Taylor, P. N., 1988. As idades das rochas e dos eventos metamórficos da região sudeste do estado de São Paulo. In: XXXV Congresso Brasileiro de Geologia, Anais, Belem, 6: 2840-2853.

Vasconcelos, P. M.; Onoe, A. T.; Kawashita, K.; Soares, A. J.; Teixeira, W., 2002. $^{40}Ar/^{39}Ar$ geochronology at the Instituto de Geociências, USP: instrumentation, analytical procedures, and calibration. An. Acad. Bras. Ci., 74(2): 297-342.

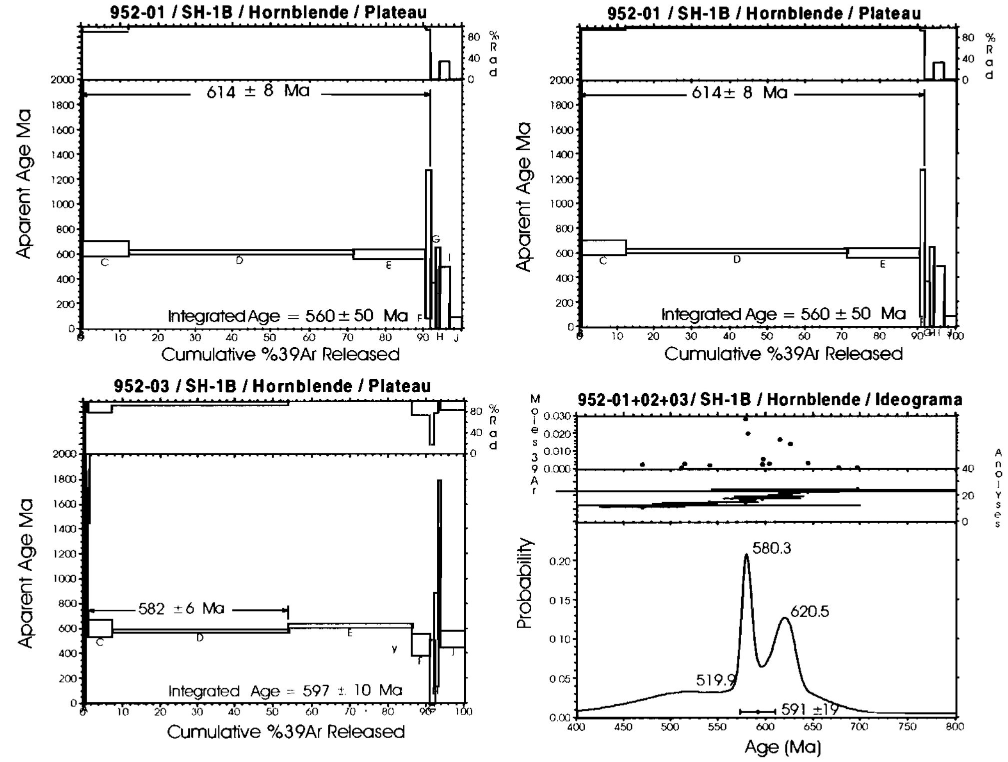

Figure 1. Incremental heating analyses of hornblende of the Hermida amphibolite (Sample SH-1B).

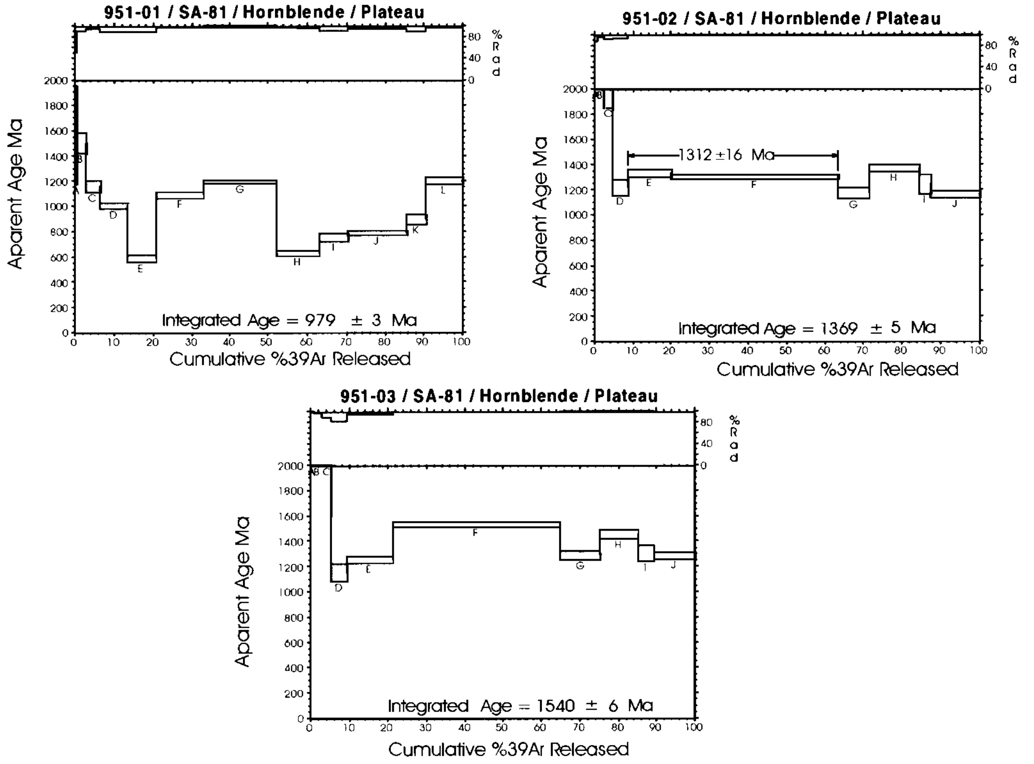

Figure 2. Incremental heating analyses of hornblende of the Aluminio amphibolite (Sample SA-81).

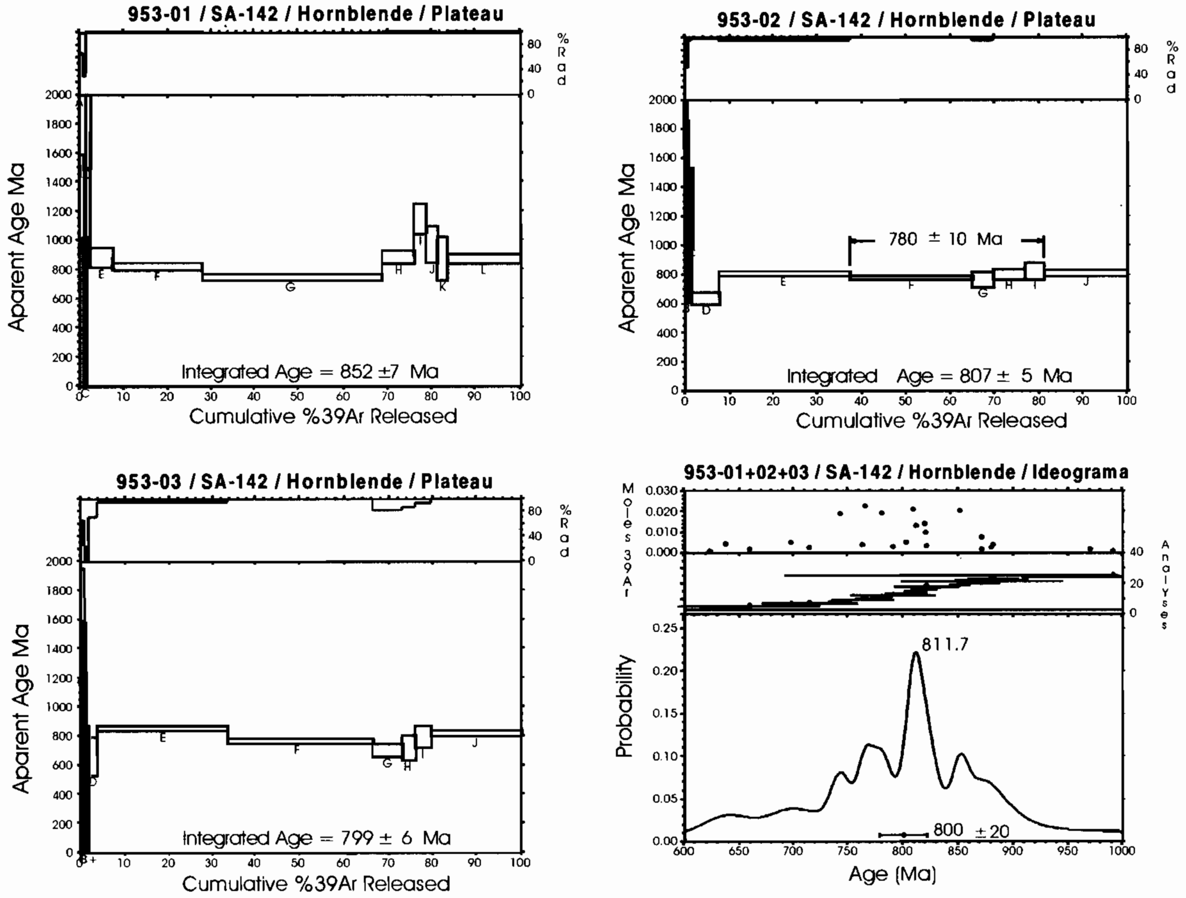

Figure 3. Incremental heating analyses of hornblende of the Aluminio amphibole (Sample SA-142).

ISOTOPIC GEOLOGY OF THE CENTRAL PART OF THE PERNAMBUCO-ALAGOAS COMPLEX AND IMPLICATIONS FOR MESOPROTEROZOIC MAGMATISM WITHIN THE SOUTHERN DOMAIN OF THE BORBOREMA PROVINCE, NE BRAZIL

Osako, L.S.[1]; Silva Filho, A.F.[2]; Guimarães, I.P.[2] and Castro, N.A.[3]

1. Universidade Federal de Pernambuco, Departamento de Geologia. lilianaso@hotmail.com
2. Universidade Federal de Pernambuco, Departamento de Geologia. afsf@ufpe.br, ignez@ufpe.br
3. Universidade de São Paulo, Departamento de Mineralogia e Geotectônica. neivaldoc@bol.com.br

Keywords: Borborema Province, Pernambuco-Alagoas Complex, Nd Model ages (T_{DM}), crustal evolution

INTRODUCTION

The Borborema Province (Almeida et al., 1977) is located in the NE Brazil, comprising an area of aproximately 450,000 sq km. It corresponds to the western part of a great Pan-African-Brasiliano fold belt formed at 600Ma, through the convergence of the cratons São Luís, West Africa, São Francisco and Congo-Kasai. The convergence and aglutination of these cratonic masses during the Neoproterozoic formed the supercontinent Western Gondwana (De Witt et al., 1988). The subsequent break-up of Western Gondwana during the Mesozoic occurred due to the South Atlantic opening. The Borborema Province evolution is closely related to its African counterpart, namely provinces Hoggar, Nigerian, Central Africa and the Pharusian belt (Van Schmus et al., 1995). Geochronological studies have confirmed the occurrence of the orogenies Transamazonian/Eburnean (Paleoproterozoic) and Brasiliano/Pan-African (Neoproterozoic) in both continents. New concepts on the evolution of the Borborema Province during pre-Brasiliano times and correlations with the African counterpart have recently been drawn, together with possible connections between the evolution of the Rodinia supercontinent and the Cariris Velhos event. New Nd isotopic data of metamorphic rocks have been produced in order to better understand the crustal evolution of the Pernambuco-Alagoas Complex (Silva Filho et al., 2002) during pre- and syn-Brasiliano times.

GEOLOGICAL SETTING

The Pernambuco-Alagoas Complex (Silva Filho et al., 2002) belongs to the Southern Tectonic Domain of the Borborema Province (Brito Neves et al., 2000) (Fig. 1). It is limited to the north by the Pernambuco shear zone and to the south and to the southwest by the Sergipano and Riacho do Pontal fold belts. It is comprised by high-grade ortho- and para-derived metamorphic complexes, of possible Mesoproterozoic age (Santos, 1995; Medeiros and Santos, 1998), intruded by Neoproterozoic granites (Silva Filho et al., 2002). The Pernambuco-Alagoas Complex have been divided into two crustal domains namely Garanhuns and Águas Belas, with T_{DM} model ages ranging respectively from 2.40 to 1.80 Ga and from 2.1 to 0.9 Ga. (Silva Filho et al., 2002). Pessoa et al. (1978) obtained a Rb-Sr reference isochron yielding age of 1.45 Ga. on metatexites in contact with garnet-gneisses (Cabrobó Complex) located 30Km to the NE end of the area. Cross sections done recently show the metatexites in contact with the metassediments. The study area is located on the limit between the crustal domains Água Branca and Garanhuns.

FIELD RELATIONS AND PETROGRAPHY

Geological mapping in the scale 1:100,000 of a ca. 2,000 sq km area have been done, aiming to characterize the metamorphic complexes, plutonic and metaplutonic rocks and their stratigraphic relations. The mapping revealed a metassedimentary sequence, a migmatitic-granitic complex and various syn- to late-tectonic plutons of granitic composition.

1. The metassedimentary sequence corresponds to the Cabrobó Complex (CC), recently defined for the eastern part of the Pernambuco-Alagoas Complex by Medeiros and Santos (1998). This complex, in the approached area, is the main unit. It is comprised by garnet-biotite-gneisses locally migmatized, muscovite-biotite-gneisses, quartzites, garnet-calc-silicates, and lenses of amphibolite and metabasic rocks. The sequence is divided into two parts by a migmatitic-granitic complex, described below (Fig. 2). The contacts between the migmatitic-granitic complex and the metassedimentary sequence are sharp and partially marked by a transcurrent shear zone. One deformation phase is characterized by recumbent and isoclinal folds, with vergence towards NW. The sequence is cut by various syn- to late-tectonic granitic plutons, mainly garnet bearing, of tonalitic to granodioritic compositions. Some of them show dioritic enclaves and cuspate contacts between them and their host facies, suggesting that magma mixing process acted during their genesis. The sequence is cut by bodies of syn-tectonic and migmatizes diorites.
2. The Migmatitic - Granitic Complex (MGC) crosses NE-SW the whole area, sectioning the metasediments, following a late transcurrent shear zone. It is mainly comprised by (1) Metatexites with dioritic and amphibole bearing mesossome, and tonalitic to granodioritic leucossome (Fig. 2); (2) Metatexite to diatexite, of leucossome of sienogranitic composition. The later facies is cut by syn-tectonic bodies of diorites, apparently controlled by high-angle shear zone. They grade to the high-K sienogranite leucossome, which can evolve to hundred meters stock. Few granitic plutons and stocks cut

this complex. They show granodioritic to monzogranitic composition, without garnet.

ISOTOPIC DATA

Nd isotopic data were obtained in the Isotope Geochemistry Laboratory, University of Kansas. The table 1 shows the new data from samples from the approached area. Other data are from Silva Filho et al. (2002). There are available 3 samples of garnet-biotite-gneisses from the Cabrobó Complex, located within and close to the study area. They show T_{DM} ages ranging from 2.12 Ga up to 2.60 Ga, and ε_{Nd} ranging from -17.08 to -20.9 (T=0.6 Ga). It was analysed 2 samples which belong to the MGC. They show T_{DM} ages with values 1.41 and 1.34 Ga, and ε_{Nd} (T=0.6Ga.) respectively -13.2 (ortho-gneiss) and -1.84 (metatexite). There are available 3 Nd isotopic data from granites intruded into the Cabrobó Complex (SCB-1, AB-3', and AB-8), and located within and around the study area. The Serra da Caatinga Branca pluton (SCB-1) cuts the Cabrobó Complex, shows tonalitic to granodioritic composition and is garnet bearing. Furthermore, its isotopic signature is close to that showed by the metassediment, sample VENT-6. The Águas Belas granite is intruded in contact with the Cabrobó Complex, showing T_{DM} age of 2.14 Ga and ε_{Nd} (T=0.6 Ga) of -12.4, suggesting hybrid nature. The Curral Novo pluton (AB-3') show even more contrasting result, with T_{DM} age of 1.15 Ga and ε_{Nd} (t=0.6 Ga.) of -2.0.

CONCLUSIONS

1.The CC metassediments Nd isotopic signature suggests a heterogeneous source for it. Their ε_{Nd} (T=0.6 Ga.) suggest a major Paleoproterozoic protolith for them, with minor or none Meso/Neoproterozoic crustal contribution for them. The Serra da Caatinga Branca pluton shows a similar Nd isotopic signature to the metassediments, evidencing that its protolith is mainly crustal and that middle to high crust partial melting process was very significant in the central to the northern part of the Pernambuco-Alagoas Complex. It is expected that similar process acted during the genesis of the others granitic and garnet-bearing plutons intruded into the Cabrobó Complex.

2.The MGC analysed rocks are ortho-derived ones and their T_{DM} ages should represent (1) Mixture of Mesoproterozoic juvenile magma which interacted with a Paleoproterozoic crust, or (2) Mesoproterozoic juvenile magmatism with minor crustal interactions and extracted from an enriched lithospheric mantle. The possible age of ca. 1.45 Ga for the Cabrobó Complex suggests that the MCG should represent a pre- to syn-tectonic juvenile magmatism of similar age.

3. The MGC shows T_{DM} much younger, and much higher ε_{Nd} (T=0.6 Ga) than that showed by the Cabrobó Complex, evidencing that it can not be underlying it. Both ε_{Nd} (T=0.6 Ga) showed by the analysed samples are evidence that different proportions of lower mafic crust and mantle protolith interacted, producing a dioritic batholith, later intruded into the CC and migmatized during regional metamorphism. The migmatization is syn-transposition. Later extraction of magma, with producing of tonalitic stocks has been observed.

4.The MGC records a calc-alkaline magmatism of intermediate composition, typical of active continental margin, possibly of Mesoproterozoic age.

REFERENCES

Almeida, F.F.M.; Hasui, Y.; Brito Neves, B.B.; Fuck, R.A. 1997. Províncias estruturais brasileiras. Atas 8^0 Simpósio de Geologia do Nordeste, Brazil. Campina Grande, v.8, pp.363-391.

Brito Neves, B.B.; Santos, E.J.; Van Schmus, W.R. 2000. Tectonic history of the Borborema Province. In: Cordani et al. Tectonic Evolution of South America. 31st International Geological Congress, p. 151 – 182.

De Wit, M.; Jeffrey, M.; Bergh, H.; Nicolaysen, L. 1988. Geological map of sectors of Gondwana reconstructed to their disposition ca. 150Ma. AAPG, Tulsa, 2 sheets.

Medeiros, V.C., Santos, E.J. 1998. Folha Garanhuns (SC.24-X-B, escala 1:250.000). Integração Geológica (Relatório Interno), CPRM. Recife-PE, 22p.

Pessoa, R.R., Pessoa, D.R., Brito Neves, B.B. and Kawashita, K.. 1978. Magmatismo tardi-tectônico Brasiliano no Maciço Pernambuco-Alagoas: o quartzo sienito de Cachoeirinha-PE. In: Anais do 30^0 Congr. Bras. de Geologia, Recife, 3:1279-1287.

Santos, E.J. 1995. O Complexo Granítico Lagoa das Pedras: Acresção e colisão na região de Floresta (Pernambuco), Província Borborema. PhD. Thesis, IG/USP, Brazil, 219p.

Silva Filho, A.F.; Guimarães, I.P.; Van Schmus, W.R. 2002. Crustal evolution of the Pernambuco-Alagoas Complex, Borborema Province, NE Brazil: Nd isotopic data from Neoproterozoic granitoids. Godwana Research, v.5, n.2, pp. 409-422.

Van Schmus, W.R.; Brito Neves, B.B.; Hackspacher, P.C.; Babinsky, M. 1995. U/Pb and Sm/Nd geochronologic studies of the eastern Borborema Province, NE Brazil. J. South Amer. Earth Sci., v.8, p.267-288.

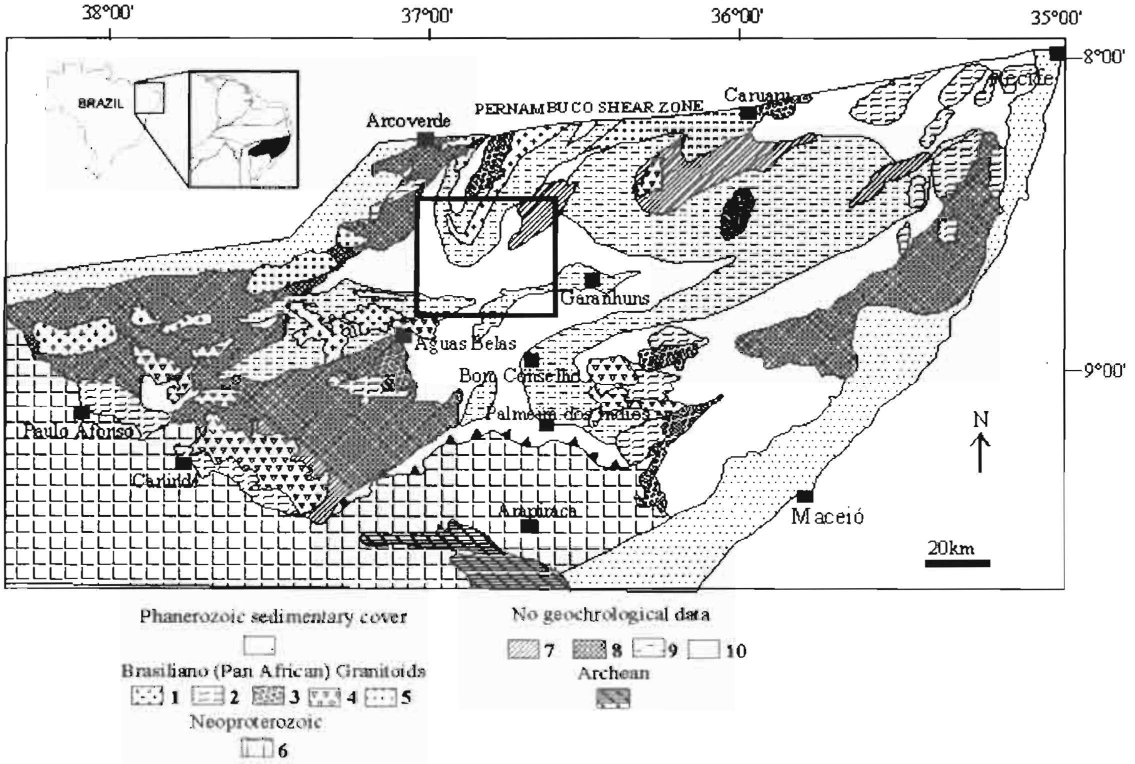

Figure 1. Simplified geologic map of the Pernambuco-Alagoas Complex (Silva Filho et al. 2002). 1. High-K calc-alkaline garnet bearing granites; 2. High-K calc-alkaline peraluminous monzogranites; 3. High-K calc-alkaline metaluminous porphyritic granodiorites; 4. Shoshonitic affinity granitoids; 5. Undifferentiated granites; 6. Sergipano fold belt rocks; 7. Ortho-gneisses; 8. Granitic-migmatitic complexes; 9. Paragneisses and para derived migmatites; 10. Ortho derived migmatites and tonalitic granites; 11. Archean basement.

Table 1 . Nd isotopic data of representative rocks of the Pernambuco-Alagoas Complex. * Denotes new isotopic data and ** denotes isotopic data compiled of Silva Filho et al. (2002).

Sample	Litology	Nd (ppm)	Sm (ppm)	^{147}Sm/ ^{144}Nd	^{147}Nd/ ^{144}Nd	±2σ	ε_{Nd} (today)	ε_{Nd} (0.6 Ga)	T_{DM} (Ga)
Metasedimentary sequence									
95-266	Garnet-biotite-gneiss	54,67	9,54	0,10549	0,51121	9	-27,8	-20,9	2,60**
VENT-6	Garnet-biotite-gneiss	72,59	11,86	0,09876	0,511379	19	-24,56	-17,08	2,20*
VENT-9	Garnet-biotite-gneiss	34,65	4,84	0,08439	0,511234	55	-27,39	-18,8	2,12*
Granites									
SCB-1	Garnet-bearing granite	65,96	8,76	0,08031	0,51122	9	-27,6	-18,7	2,08**
95-268	Diatexite	8,05	1,43	0,10734	0,51159	9	-20,5	-13,7	2,09**
AB-8	Sienogranite	21,26	4,12	0,11710	0,51169	9	-18,5	-12,4	2,14**
AB-3'	Granodiorite	22,83	3,44	0,09107	0,51212	9	-10,1	-2,0	1,15**
Migmatitic-Granitic Complex									
VENT-8	Garnet-bearing gneiss	37,89	1,5	0,02388	0,511283	51	-26,4	-13,2	1,41*
BUQ-6	Metatexite with hornblende dioritic mesosome	35,81	7,46	0,12594	0,512265	41	-7,27	-1,84	1,34*

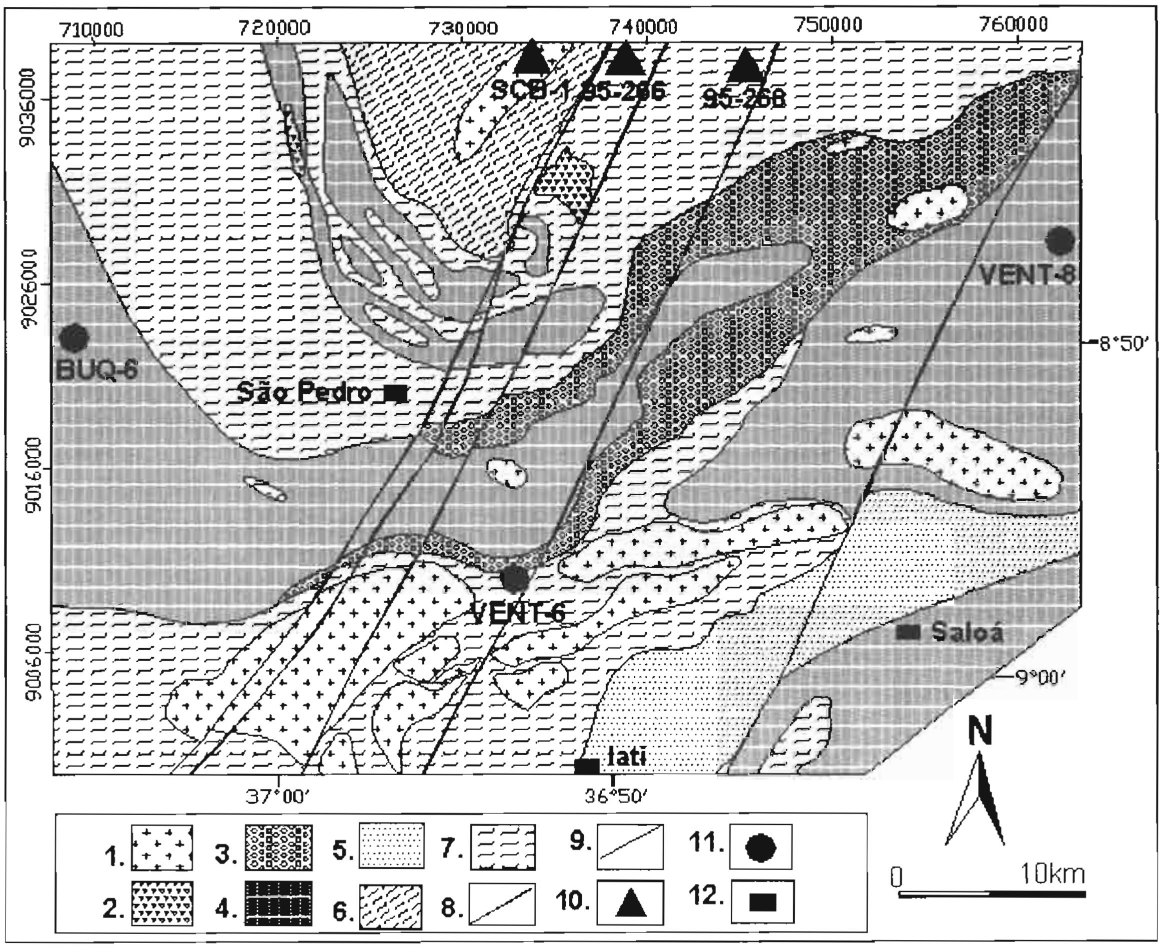

Figure 2. Simplified geologic map of the central part Pernambuco-Alagoas Complex, showing the location of samples analysed by Sm-Nd system. 1. Tonalitic to monzogranitic granites, 2. Biotite-hornblende-gneisses, 3. Migmatites metatexite to diatexite of leucosome of sienogranitic composition, 4. Migmatites metatexite and diatexite with dioritic and hornblende-bearing mesosome and tonalitic to granodioritic leucosome, 5. Quartzites, 6. Muscovite-biotite-gneisses, 7. Garnet-biotite-gneisses, 8. Faults, 9. Geologic contacts, 10. Nd isotopic data compiled of Silva Filho et al. (2002), 11. New Nd isotopic data, 12. Village and town.

SOURCE CONTRIBUTIONS TO ARC MAGMATISM AT CALLE DEL YESO DYKE COMPLEX (PARAMILLOS ALTOS), SOUTHERN MENDOZA, ARGENTINA

Ostera, H.A.[1]; Cagnoni, M.C.[1]; Ramos, A.[1]; Haller, M.[2]; Linares, E.[1] and Joensen, V.

1. Instituto de Geocronología y Geología Isotópica (INGEIS). Pabellón INGEIS. Ciudad Universitaria. Ciudad Autónoma de Buenos Aires. Argentina. ostera@ingeis.uba.ar; mariana@ingeis.uba.ar; adriana@ingeis.uba.ar; linares@ingeis.uba.ar
2. UNPSJB - Centro Regional Patagónico (CENPAT). Puerto Madryn. Chubut. Argentina. haller@cenpat.edu.ar

Keywords: Arc magmatism, Paramillos Altos, Mendoza

INTRODUCTION

Paramillos Altos Intrusive Belt (PAIB) (Ostera, 1996) is located in the thick skinned folded-thrust belt of Malargüe, southwestern Mendoza, Argentina (Fig. 1). Geochemical, geochronologic and isotopic studies were carried out (Ostera, 1996, 1997; Ostera et al., 1999, 2000, 2001) and in this work we present new isotope and geochemical evidences to identify the contribution of the different reservoirs to the arc magmatism.

GEOCHEMISTRY

The study of magma sources at convergent margins presents several difficulties, since geochemical variations acquired during the later evolution obscured primeval characteristics. In this study we focused the characterization of the reservoirs that contribute to the magmatism of Lower Miocene Calle del Yeso Dyke Complex (CYDC, Ostera et al., 1999; Joensen, 2001).

CYDC is composed of Lower Miocene sills and dykes intruding Cenozoic sedimentary sequences of the Neuquen Basin, in the southeastern border of Paramillos Altos Intrusive Belt (PAIB). The rocks are principally basaltic andesites, andesites, trachyandesites, dacites and minor rhyolites associated. They are calc-alkaline rocks, metaaluminous to slightly peraluminous (Ostera et al., 2000). Mafic enclaves (gabbro-amphibolite) have been identified. Complete chemical analyses are presented in Joensen (2001). Major and trace elements variation diagrams show coherent correlations trends. The rocks follow a calc-alkaline trend in an AFM diagram and they are classified as medium to high K andesites. The REE chondrite - normalized plots (Fig. 2) present a LREE enrichment. The trace element MORB-normalized diagram (Fig. 3) shows enrichment in LILE and depletions in HFSE (troughs in Nb-Ta) related to other incompatible elements.

Sr, Nd AND Pb ISOTOPES

Sr, Nd and Pb isotope ratios are presented in Table 1. Sr isotopes show a wide range of values (0.704120-0.706359). We can distinguish two groups, one characterized by the lowest isotopic ratios and correlation with the lowest strontium abundances (Group I) and other with higher $^{87}Sr/^{86}Sr$ ratios and the highest strontium contents (Group II) (Fig. 4).

Nd-isotope ratios varies between 0.512465 and 0.512862, with εNd values ranging from -3.37 to +4.36. The Sr-Nd correlation diagram, shows that most of the samples lie in the high strontium-high neodymium field (Fig. 6). Nd T_{DM} model ages range between 500-700 Ma with a maximum value of 1084 Ma for the sample with the highest $^{87}Sr/^{86}Sr$, probably indicating intracrustal processes that could involve older crustal components.

Lead isotopes show a restricted variation (less than 1%) from 18.7 to 18.588 for $^{206}Pb/^{204}Pb$, 15.65 to 15.626 for $^{207}Pb/^{204}Pb$ and 38.651 to 38.588 for $^{208}Pb/^{204}Pb$ ratios (Table 1). $^{206}Pb/^{204}Pb$ shows almost no variation with $^{87}Sr/^{86}Sr$ and $^{143}Nd/^{144}Nd$ (Figs. 7, 8).

SOURCES

The complex contributions to the arc magmatism are not easily solved by simple models. Although the mantle wedge remains the main control of primary compositions, The crust role and the possibility of interaction with fluid/melts derived from the hydrothermally altered oceanic crust and slab sediments must be considered.

The distribution of the samples in the $^{87}Sr/^{86}Sr$ *vs* $^{143}Nd/^{144}Nd$ diagram (Fig. 6) points out to possible different source compositions. Added to a modified mantle composition (I), some samples (II) show a shift towards higher strontium and neodymium isotopic ratios (except one evolved sample which has lower neodymium ratios). The wide range in $^{87}Sr/^{86}Sr$ ratios could indicate mixing of a modified mantle derived-magma with lower crust components enriched in Sr and depleted in Nd contents. An isotopic modeling, adjusted to the observed values (Joensen, 2001), indicates that the lower crustal component should have an isotopic composition for Sr of 0.7062 and 0.51267 for Nd ratios. A lower crust with such characteristics could have been produced by the extraction of partial melts during the extensive Permian-Triassic magmatism of the area. Additional geochemical data reinforce the lower crust influence, like the REE lower crust-normalized diagram, which shows a smooth pattern with values close to the unit (Fig. 5).

Pb-isotopic values show a limited variation and exhibit shifts to high values $^{207}Pb/^{204}Pb$ and $^{208}Pb/^{204}Pb$ relative to MORB-type Pb and Nazca Plate sediments (Hildreth & Moorbath, 1988). In accordance with this, the reservoir dominating the Pb-isotope signal is likely to be the continental crust.

All these evidence point out to at least three components, with different degrees of involvement in the petrogenesis of the unit: a modified mantle, a lower-crust and the upper crust. In this case, the main contributors seem to be the lower crust and the modified mantle, whereas the influence of the upper crust is limited to the most evolved samples (Figs. 5, 6). However, we cannot discard the input of fluids and partial melts from the subducted slab, responsible of the mantle modification. Other geochemical evidences, on less evolved samples, are in evaluation and the present data are not definitive to elucidate undoubtedly the question.

CONCLUSIONS

Chemical and isotopic evidences suggest that the sources at Calle del Yeso Dyke Complex are mainly represented by a mixture of a modified mantle and lower crustal melts, that controls the early stages of evolution of Paramillos Altos Intrusive Belt. Upper crust inputs seem to be a minor and restricted source for Calle del Yeso Dyke Complex.

REFERENCES

Hildreth, W. & Moorbath, S., 1988. Crustal contributions to arc magmatism in the Andes of Central Chile. Contributions to Mineralogy and Petrology, 98: 455-489.

Joensen, V., 2001. Geología, caracterización geoquímica-isotópica y geocronología K-Ar del Complejo de Diques Calle del Yeso, Malargüe, Provincia de Mendoza. Trabajo Final de Licenciatura. Facultad de Ciencias Exactas y Naturales. Universidad de Buenos Aires. (Unpublished).

Kay, S.M.; C. Mpodozis, V.A.; Ramos; F. Munizaga., 1991. Magma source variation for Mid to Late Tertiaty volcanic rocks erupted over the shallowing subduction zone and through a thickening crust in the Main Andean Cordillera (28-33°). In: Andean Magmatism and its tectonic setting. R.S. Harmon & C. Rapela (Eds.). Geological Society of America, Special Paper 265: 113-137. Boulder, Colorado, USA.

Ostera, H.A., 1996. Geología, Geocronología y Caracterización Geoquímico-Isotópica del Magmatismo Terciario en el área del cerro Serrucho, Departamento Malargue, Mendoza, Argentina. Tesis Doctoral. Departamento de Ciencias Geológicas, Facultad de Ciencias Exactas y Naturales, Universidad de Buenos Aires. (Unpublished.). Buenos Aires, Argentina.

Ostera, H.A. 1997. Síntesis sobre el Magmatismo Terciario en el área del cerro Serrucho, Cordillera Principal, Malargue, Mendoza, Argentina. Simposio Final "Evolución Litosférica de los Andes".Actas VIII Congreso Geológico Chileno ,1: 1418-1423.

Ostera, H.A., Dristas, J.C., Panarello, H.O., Frisicare, C., Valencio, S.A. 1999 .Hydrogen isotopes and fluid inclusions studies at arroyo Serrucho stock, Southern Mendoza, Argentina: Preliminary Report. Actas II South American Symposium on Isotope Geology.:252-255.

Ostera, H.A.; Linares, E.; Haller, M.J., 1999. Paramillos Altos Intrusive Belt, Southern Mendoza, Argentina. Ages, Chemical and Isotopic Constraints. Actas II South American Symposium on Isotope Geology.: 256-260.

Ostera, H.A., Haller, M. J., Linares, E., Joensen, V., 2000. Geochemical evidences and implicancies on contrasting magma sources at Paramillos Altos Intrusive belt, Southern Mendoza, Argentina. IX Congreso Geológico Chileno, Actas, Vol. I: 669-673.

Ostera, H.A., Linares, E., Haller, M.J., Cagnoni, M.C., 2001.The Crust Role At Paramillos Altos Intrusive Belt: Sr and Pb Isotopes Evidence. III South American Symposium on Isotope Geology. CD-ROM Edition, Sociedad Geológica de Chile, pp.329-332.

Tormey, D.R., Hickey-Vargas, R., Frey, F.A.,López Escobar, L., 1991. Recent lavas from the Andean Volcanic Front (33° to 42°S); Interpretation of along-arc compositional variations. In: Andean Magmatism and Its Tectonic Setting. R.S. Harmon & C.W. Rapela (Eds.). Geological Society of America Special Paper 265: 57-78 . Boulder, Colorado, USA.

Table 1. Analytical data. Samples analyzed at Pará-Iso, Brazil.

Sample	^{87}Sr/^{86}Sr	σ	^{143}Nd/^{144}Nd	σ	^{206}Pb/^{204}Pb	σ	^{207}Pb/^{204}Pb	σ	^{208}/^{204}Pb	σ
2	0.70412	0.000006	0.512748	0.000065	18.678	0.015	15.646	0.016	38.627	0.05
4	0.704742	0.000036	0.512727	0.00005	18.63	0.012	15.641	0.015	38.567	0.049
6	0.705938	0.000053	0.512802	0.000052	18.615	0.014	15.65	0.016	38.648	0.051
16	0.705606	0.000066	0.51284	0.000049	18.634	0.013	15.648	0.015	38.635	0.048
25	0.704917	0.000032	0.512771	0.000048	18.671	0.014	15.63	0.016	38.558	0.05
26	0.706359	0.000072	0.512749	0.000053	18.588	0.014	15.645	0.016	38.624	0.05
27	0.706282	0.000031	0.512862	0.000067	18.622	0.012	15.641	0.015	38.627	0.048
34	0.706356	0.000053	0.512465	0.000032	18.61	0.012	15.626	0.015	38.605	0.048
39	0.70473	0.000057	0.512656	0.000082	18.7	0.013	15.634	0.015	38.651	0.049

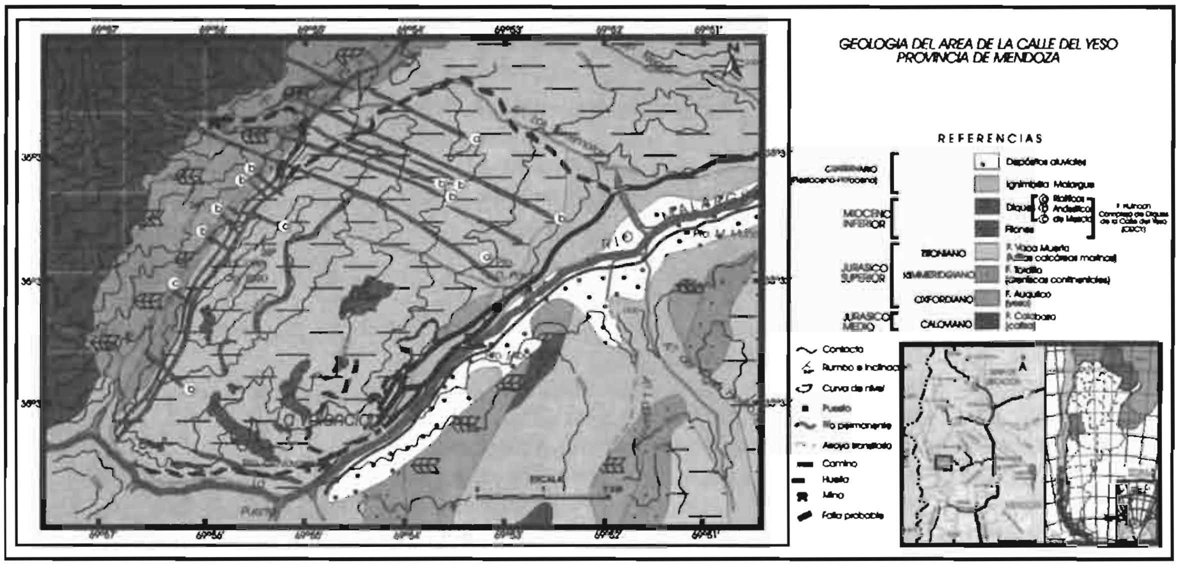

Figure 1. Geological map (Joensen, 2001).

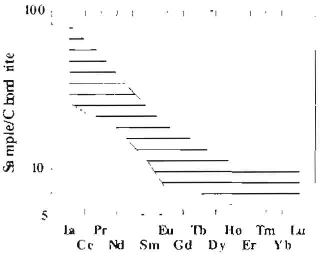

Figure 2.

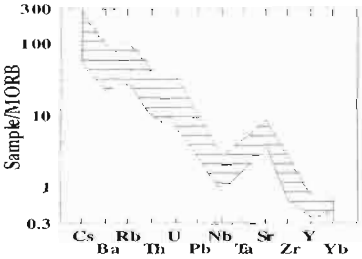

Figure 3.

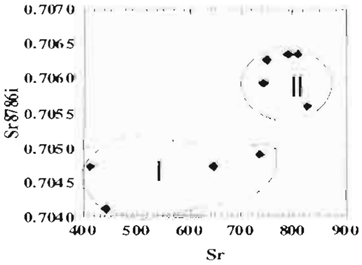

Figure 4.

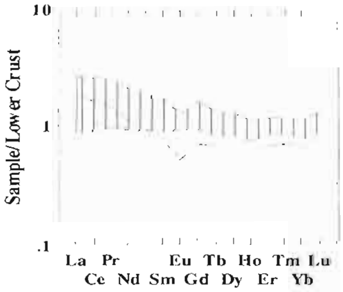

Figure 5.

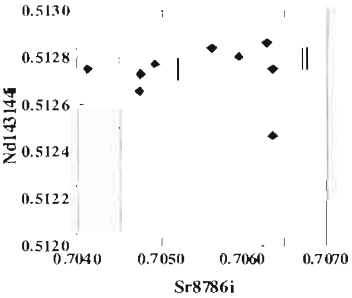

Figure 6.

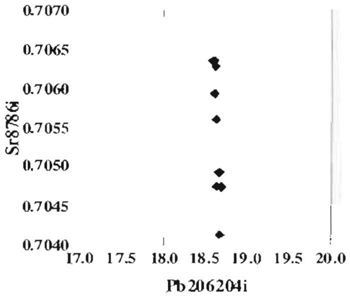

Figure 7.

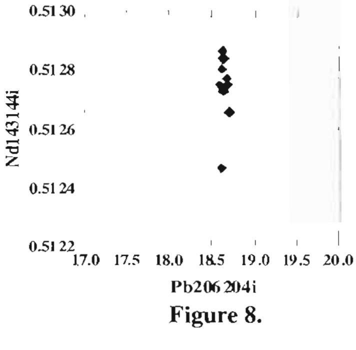

Figure 8.

Figure References

Figure 2. Sample/ Chondrite normalized diagram

Figure 3. Sample/ MORB normalized diagram

Figure 4. Sr isotope ratios vs. Sr abundances

Figure 5. Sample/ Lower Crust normalized diagram

Figure 6. Nd vs. Sr ratios

Figure 7. Sr ratios vs. ^{206}Pb/^{204}Pb ratios

Figure 8. Nd ratios vs. ^{206}Pb/^{204}Pb ratios

U-Pb MONAZITE AGES FROM PELITIC PARAGNEISSES IN NE RONDÔNIA, SW AMAZONIAN CRATON: EVIDENCE FOR 1.54 Ga METAMORPHISM

Payolla, B.L.[1]; Fetter, A.H.[2]; Bettencourt, J.S.[3] and Leite Jr., W.B.[4]

1. Centrais Elétricas do Norte do Brasil S/A – ELETRONORTE, SQN 408, Bloco L, Apartamento 202, 70856-120, Brasília, DF, Brazil. bruno@eln.gov.br
2. Instituto de Geociências e Ciências Exatas, Universidade Estadual Paulista-UNESP, Av. 24 A, nº 1515, 13506-900, Rio Claro, SP, Brazil. fetter@ms.rc.unesp.br
3. Instituto de Geociências, Universidade de São Paulo-USP, Rua do Lago, nº 562, Cidade Universitária, São Paulo, SP, Brazil. jsbetten@usp.br
4. Instituto de Geociências e Ciências Exatas, Universidade Estadual Paulista-UNESP, Av. 24 A, nº 1515, 13506-900, Rio Claro, SP, Brazil. wleite@rc.unesp.br

Keywords: Rondônia, monazite, paragneisses, metamorphism, magmatism

INTRODUCTION

Although recognized as part of the metamorphic basement in the NE Rondônia (Scandolara et al., 1999), only recently the paragneisses has been unambiguously identified as a distinct lithologic unit (Payolla et al., 2002). Within the studied area, the paragneisses are exposed as a distinct NW belt across the Machadinho river basin, intruded by granitoids, mangerites, charnockites and mafic rocks of the Serra da Providência Intrusive Suite (1.60-1.53 Ga; Bettencourt et al., 1999) and granitoids of the Santa Clara Intrusive Suite (1.08-1.07 Ga; Bettencourt et al., 1999). Further west, they occur as minor thin layers and lenses in deformed granitoids and charnockites of the Serra da Providência Intrusive Suite and fine-grained granitic gneiss and charnockitic granulite (1.43-1.42 Ga; Payolla et al., 2002). U-Pb zircon and monazite, Sm-Nd whole-rock-garnet and hornblende $^{40}Ar/^{39}Ar$ ages demonstrate that at least two high-grade tectonometamorphic episodes affected this region at 1.33-1.30 Ga (Tassinari et al., 1999; Payolla et al., 2002; Santos et al., 2002) and 1.20-1.10 Ga (Tohver et al., 2001).

Conventional and SHRIMP-RG U-Pb zircon ages bracket the deposition of the paragneiss protolith between 1660 and 1590 Ma (Payolla et al., 2002, this symposium). As such, the paragneisses probably do not represent high-grade metamorphic equivalents of the 1740-1700 Ma volcano-sedimentary Beneficente and Roosevelt groups (Santos et al., 2000) exposed just to the southeast, but a younger sedimentary sequence deposited after the Juruena Orogeny (1750 Ma; Santos et al., 2001).

Monazite, which is a common mineral in anatectic metapelites, is a powerful tool for the precise dating of anatectic processes and high-grade metamorphism because it is often devoid of any inherited Pb and commonly shows concordant behavior in U-Pb systems (Foster et al., 2000). This study presents U-Pb monazite isotopic data from two high-grade migmatitic paragneisses separated by about 50 km, to place additional constraints on the high-grade metamorphism that affected these rocks. The 1.54 Ga monazite ages obtained for the paragneisses are interpreted as the time of monazite formation under peak metamorphic conditions, spatially and temporally related to the emplacement of plutons of the Serra da Providência Intrusive Suite.

ANALYTICAL TECHNIQUES AND RESULTS

Initial preparation of monazite minerals for isotopic analysis was done at the Universidade Estadual Paulista - Departamento de Petrologia e Metalogenia in Rio Claro, São Paulo. Single monazite crystals, spiked with a ^{205}Pb-^{235}U tracer solution, were dissolved using a solution of concentrated ultrapure H_2SO_4 (5 uL), 6M HCl (40 uL) and 7M HNO_3 (40 uL). Samples were then conditioned with 3.1 M HCl prior to microcolumn chromatography modified from Krogh (1973). Isotopic ratios were measured using the Finnigan MAT-262 multi-collector mass spectrometer at the Geochronology Laboratory of the University of Brasília. Both Pb and U isotopic compositions were analyzed on single Re filaments and corrected for average mass discrimination of 0.12 ± 0.05% per mass unit for multi-collector analyses (based on replicate analyses of common Pb standard SRM 981). Uranium fractionation was monitored by replicate analyses of SRM U-500. Uncertainties in U/Pb ratios due to uncertainties in fractionation and mass spectrometry were around ± 0.5%. Radiogenic Pb isotopes were calculated by correcting for modern blank Pb and for original nonradiogenic original Pb corresponding to Stacey & Kramers (1975) model Pb for the approximate age of the sample. Uncertainties in radiogenic Pb ratios are typically ± 0.1%. Decay constants and isotopic ratios used in the age calculations are those listed by Steiger & Jäger (1977). The U-Pb monazite data were regressed using the ISOPLOT/EX program of Ludwig (1999). For both samples, forced Model 1 regressions were performed as the analytical points were either concordant or nearly concordant with little spread in the data. Uncertainties in concordia intercept ages are given at the 2-sigma level.

Sample WB-152 (Fig. 1) is from a banded high-grade metapelitic migmatite which consists of black or gray 1- to 10 mm wide layers of variable amounts of sillimanite, garnet, biotite, cordierite, orthopyroxene, hercynite and Fe-Ti oxides aluminous melanosome and 5- to 50 mm wide layers and irregular patches of pink K-feldspar, plagioclase, quartz and garnet leucosome. Monazite occurs in both melanosome and neosome domains. Individual monazite grains are clear, pale yellow, subhedral to euhedral and unzoned. Grain sizes range from approximately 50 to 150 µm. Three monazite grain analyzed are high in U (4214 – 10,150 ppm) and plot in the concordia, suggesting little disturbance to the U-Pb isotopic system (Fig. 2). These data define an upper intercept of 1545 ± 4 Ma, and is considered to be the formation age of the monazites in the paragneiss.

Sample WB-140 (Fig. 1) is from a migmatitic metapelite that crops out up near the margin of a granitic pluton of the Santa Clara Intrusive Suite. The migmatite consists of gray mesosome layers of sillimanite, cordierite, garnet, biotite, plagioclase, quartz and K-feldspar and pink to gray irregular patches of plagioclase, quartz, K-feldspar and garnet neosome. Monazite occurs in the mesosome as subhedral, 20 to 100 µm grains. The U-Pb system of monazites from this sample is disturbed and the two grains analyzed are discordant (Fig. 3). The discordia regression intercepts concordia at 1542 ± 4 Ma.

DISCUSSION AND CONCLUSIONS

The monazite ages from both paragneiss samples are mutually indistinguishable and, as a result, records a well-defined monazite growth episode at 1545 Ma, under high-grade metamorphic conditions. In the sample WB-152, three generations of low-Th/U metamorphic overgrowths on the zircon give ages at 1590, 1545 and 1524 Ma (Payolla et al., this symposium). The monazite formation age is the same as the intermediate generation of zircon overgrowth. The zircon overgrowths and monazite ages of the paragneisses agree well with the interval of age emplacements of the intrusive within-plate granitoids, the charnockites and basic rocks of the Serra da Providência Intrusive Suite (1.60–1.53 Ga). This suggests a temporal and spatial relation between 1.60-1.53 Ga magmatism and high-temperature metamorphism and anatexis in NE Rondônia. The discordance shown by monazites from sample WB-140 may be associated with the subsequent 1140 Ma tectonometamorphic event, on the basis of a garnet-whole rock Sm-Nd isochron age for the same rock.

REFERENCES

Bettencourt, J.S., Tosdal, R.M., Leite Jr, W.B., Payolla, B.L., 1999. Mesoproterozoic rapakivi granites of Rondônia Tin Province, southwestern border of the Amazonian craton, Brazil - I. Reconnaissance U-Pb geochronology and regional implications. Precambrian Res., 95: 41-67.

Foster, G., Kinny, P., Vance, D., Prince, C., Harris, N., 2000. The significance of monazite U-Th-Pb age data in metamorphic assemblages; a combined study of maonazite and garnet chronometry. Earth Planet. Sci. Lett., 181: 327-340.

Krogh, T.E., 1973. A low contamination method for hydrothermal decomposition of zircon and extraction of U and Pb for isotopic age determinations. Geochim. Cosmochim. Acta, 37: 485-494.

Ludwig, K.R., 1999. ISOPLOT/EX (A plotting and regression program for radiogenic-isotope data) version 2.05. Berkley Geochronological Center, Special Publication 1A, 51 p.

Payolla, B.L.; Bettencourt, J.S.; Kozuch, M.; Leite Jr, W.B.; Fetter, A.H.; Van Schmus, W.R., 2002. Geological evolution of the basement rocks in the east-central part of the Rondônia Tin Province, SW Amazonian craton, Brazil: U-Pb and Sm-Nd isotopic constraints. Precambrian Res., 119: 141-169.

Payolla, B.L., Bettencourt, J.S., Tosdal, R.M., Wooden, J.L., Leite Jr., W.B., 2003. SHRIMP-RG U-Pb zircon geochronology of high-grade paragneisses from NE Rondônia, SW Amazonian craton, Brazil: constraints on provenance and metamorphism. (this symposium).

Santos, J.O.S.; Hartmann, L.A.; Gaudette, H.E.; Groves, D.I.; McNaughton, N.J.; Fletcher, I.R.; 2000. A new understanding of the provinces of Amazon craton based on integration of field mapping and U-Pb and Sm-Nd geochronology. Gondwana Res., 3: 489-506.

Santos, J.O.S.; Rizzotto, G.A.; Potter, P.E.; Hartmann, L.A.; Easton, R.M.; McNaughton, N.J., 2002. The Sunsas Orogenic Cycle in western Amazon craton, South America and correlation to the Grenville Cycle of Laurentia, based on U-Pb isotopic study of detrital and igneous zircons. XLI CBG. Anais, João Pessoa, Brazil, SBG, pp. 335.

Stacey, J.S. & Kramers, J.D., 1975. Approximation of terrestrial lead isotope evolution by a two-stage model. Earth Planet. Sci. Lett., 26: 207-221.

Steiger, R.H. & Jäger, E., 1977, Subcomission on Geochronology: Convention on the use of decay constants in geo- and cosmochronology. Earth Planet. Sci. Lett., 36: 359-362.

Tassinari, C.C.G.; Cordani, U.G.; Correia, C.T.; Nutman, A. P.; Kinny, P.; Dias Neto, C., 1999. Dating granulites by SHRIMP U-Pb systematics in Brazil: constraints for the age of the metamorphism of Proterozoic Orogenies. II SSAGI. Actas, Cordoba, Argentina, IGRM-SGMA, pp. 234-238.

Tohver, E., Van der Pluijm, B.A., Scandolara, J.E., Rizzotto, G.J., 2001. A reassessment of the tectonics and paleogeography of the Grenville-aged Sunsas-Aguapei belt, SW Amazon craton: new paleomagnetic and ^{40}Ar/^{39}Ar data. In: Bettencourt, J.S., Teixeira, W., Pacca, I.G., Geraldes, M.C., Sparrenberger, I. (Eds.), Geology of the SW Amazonian craton: State-of-the-Art. Workshop Extended Abstracts, São Paulo, Brazil, University of São Paulo, pp. 96-99.

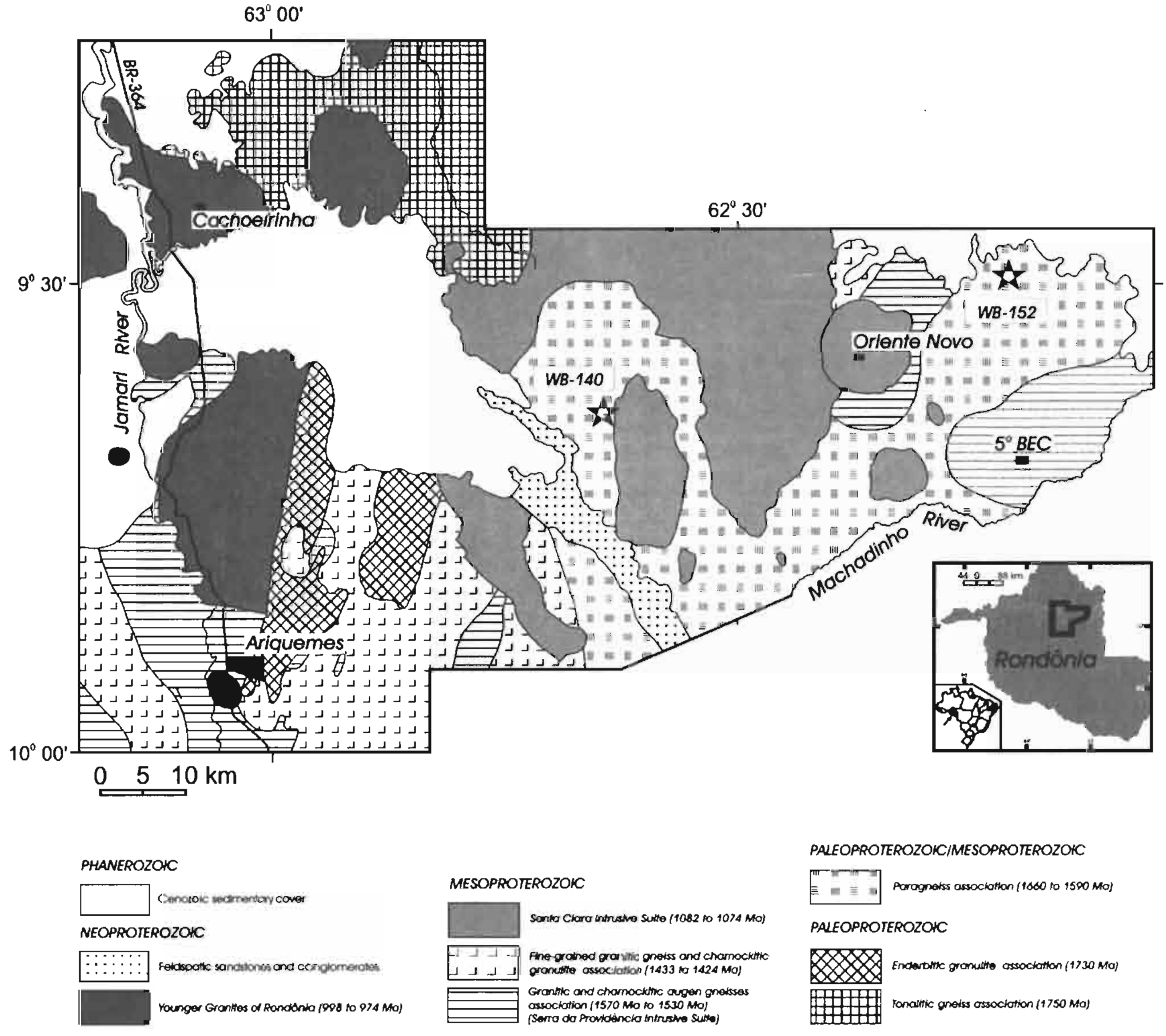

Figure 1. Map of the northeastern part of Rondônia State showing lithological associations and location of sampling sites (modified after Payolla et al., 2002).

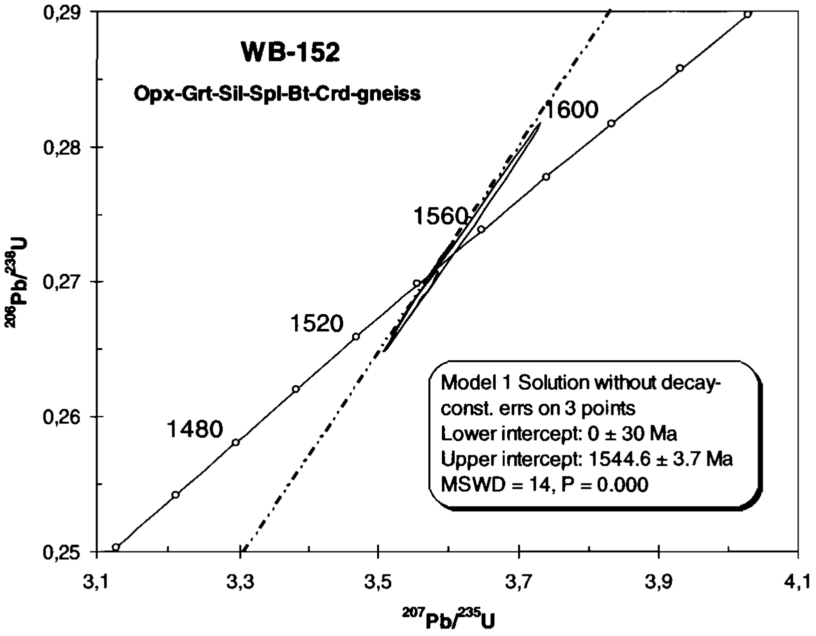

Figure 2. Concordia plot of monazite analyses from paragneiss WB-152. Analytical uncertainties are depicted as 2σ.

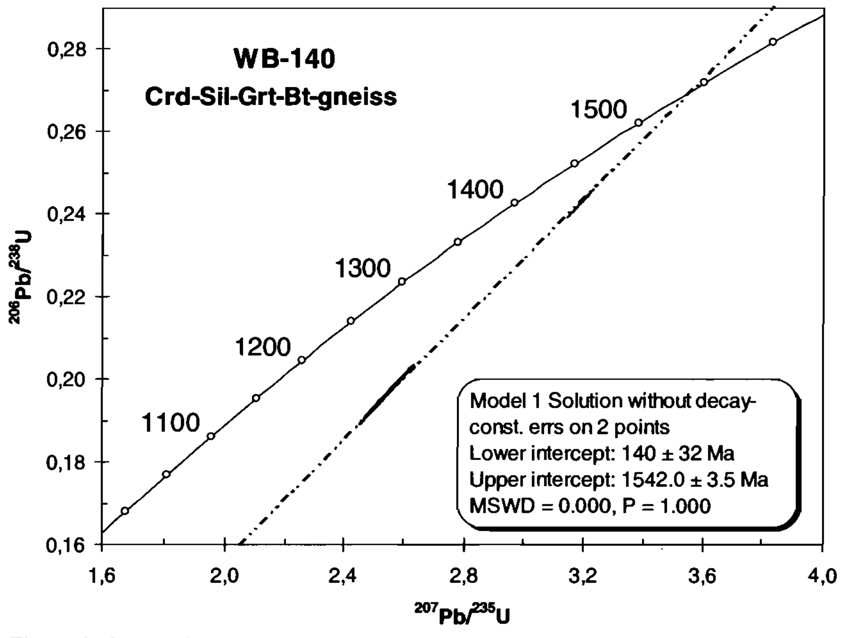

Figure 3. Concordia plot of monazite analyses from paragneiss WB-140.Analytical uncertainties are depicted as 2σ. Note the significative normal discordance.

SHRIMP-RG U-Pb ZIRCON GEOCHRONOLOGY OF HIGH-GRADE PARAGNEISSES FROM NE RONDÔNIA, SW AMAZONIAN CRATON, BRAZIL: CONSTRAINTS ON PROVENANCE AND METAMORPHISM

Payolla, B.L.[1]; Bettencourt, J.S.[2]; Tosdal, R.M.[3]; Wooden, J.L.[4] and Leite Jr., W.B.[5]

1. Centrais Elétricas do Norte do Brasil S/A – Eletronorte, SQN 408, Bloco L, Apartamento 202, 70856-120, Brasília-DF, Brazil. bruno@eln.gov.br
2. Instituto de Geociências, Universidade de São Paulo-USP, Rua do Lago nº 562, Cidade Universitária, São Paulo-SP, Brazil. jsbetten@usp.br
3. Mineral Deposit Reserach Unit, Department of Earth and Ocean Sciences, University of British Columbia, 6339 Stores Road, Vancouver, BC, Canada. rtosdal@eos.ubc.ca
4. USGS-SUMAC, Rm. 89, Íon Probe Lab., Green Building, 367 Panama Street, Stanford University, Stanford, CA 94305-2220, USA. jwooden@usgs.gov
5. Instituto de Geociências e Ciências Exatas, Universidade Estadual Paulista-UNESP, Av. 24 A, nº 1515, 13506-900, Rio Claro-SP, Brazil. wleite@rc.unesp.br

Keywords: Rondônia, zircon, paragneisses, provenance, metamorphism

INTRODUCTION

The SW Amazonian craton is a multi-orogenic region characterized by successive episodes of magmatism, metamorphism, and deformation between 1.80 and 0.97 Ga (Tassinari et al., 2000; Payolla et al., 2002). The age and stratigraphy of the metavolcano-sedimentary units in this region were only partially established by Tassinari et al. (2000) and Santos et al. (2000), though in Rondônia state they have been divided into the Beneficente and Nova Brazilândia groups, both related to the Juruena Orogenic Cycle (1.76-1.72 Ga) and Sunsas Orogenic Cycle (1.20-1.10 Ga), respectively (Santos et al., 2001).

Meanwhile, the high-grade paragneisses previously considered as part of the metamorphic basement remain poorly investigated. Only recently they have been unambiguously identified as a distinct lithologic unit in the NE part of Rondônia (Payolla et al., 2002). They extend across the Preto and Machadinho rivers region, but minor discontinuous zones are observed to the west (Fig. 1). The paragneisses were intruded by granitoids of the Serra da Providência (1.60-1.53 Ga), Rio Crespo (1.43-1.42 Ga) and Santa Clara (1.08-1.07 Ga) intrusive suites (Bettencourt et al., 1999; Payolla et al., 2002), and affected by at least two high-grade tectonometamorphic events at 1.33-1.30 Ga and 1.20-1.10 Ga (Tohver et al., 2001; Payolla et al., 2002). Conventional U-Pb detrital zircon ages and an intrusive granitoid bracket the deposition of paragneiss protoliths between 1.67 and 1.57 Ga (Payolla et al., 2002).

In this paper we report and discuss SHRIMP-RG U-Th-Pb analyses of zircons from two high-grade paragneiss samples (WB-152 and JWB-24/A) from NE Rondônia state (sample WB-152 was also previously studied by Payolla et al., 2002). We show that in both parageneiss samples there was new zircon growth or recrystallization during the early Mesoproterozoic, and that the paragneisses contain distinct Paleoproterozoic components, but none older than ~1940 Ma.

ANALYTICAL TECHNIQUES

Zircon U-Pb geochronology was carried out on the SHRIMP-RG (sensitive high-resolution ion microprobe-reverse geometry) ion microprobe at the Stanford University. The SHRIMP-RG employs magnetic analysis of the secondary ion beam before electrostatic analysis to achieve greater mass resolution compared with previous SHRIMP designs (Clement & Compston, 1994). The ~8 nA primary beam of $^{16}O_2^-$ ions primary beam produced ~30 μm diameter, ~1 μm deep, flat-bottomed analytical pit. Concentration data were standardized against Sri Lanka zircon standard SL-13 and Duluth Gabbro zircon standard AS57, and isotope ratios were calibrated against AS57, with an assumed age of 1099 Ma.

RESULTS

Sample WB-152 is from a banded, high-grade metapelitic migmatite collected 20 km NE from Oriente Novo (Fig. 1), which consists of black or gray 1- to 10-mm-wide layers of Sil, Grt, Bt, Crd, Ilm, Mag, Spl and Opx melanosome and 5- to 50-mm-wide layers of creamy-pink Ksp, Qtz, Pl and Grt leucosome.

The zircon grains from this sample are 70-200 μm in length and generally have the rounded external forms common in zircon from high-grade rocks (Williams & Claesson, 1987). The SEM-CL (scanning electron microscope cathodoluminescence) imaging shows that the zircon crystals contain a main core characterized by euhedral oscillatory zoning and a homogeneous, weakly luminescent overgrowth of variable thickness (<10-30 μm). Some cores are homogeneous and highly luminescent. The core-overgrowth interface is commonly sharp, and displays embayments that truncate the internal core zone structure.

Twenty-six analyses of cores are very heterogeneous, U contents ranging from 53 to 776 ppm, most being between 140 and 377 ppm, and Th/U ranging from 0.30 to 1.32. In the probability distribution diagram (Fig. 3)

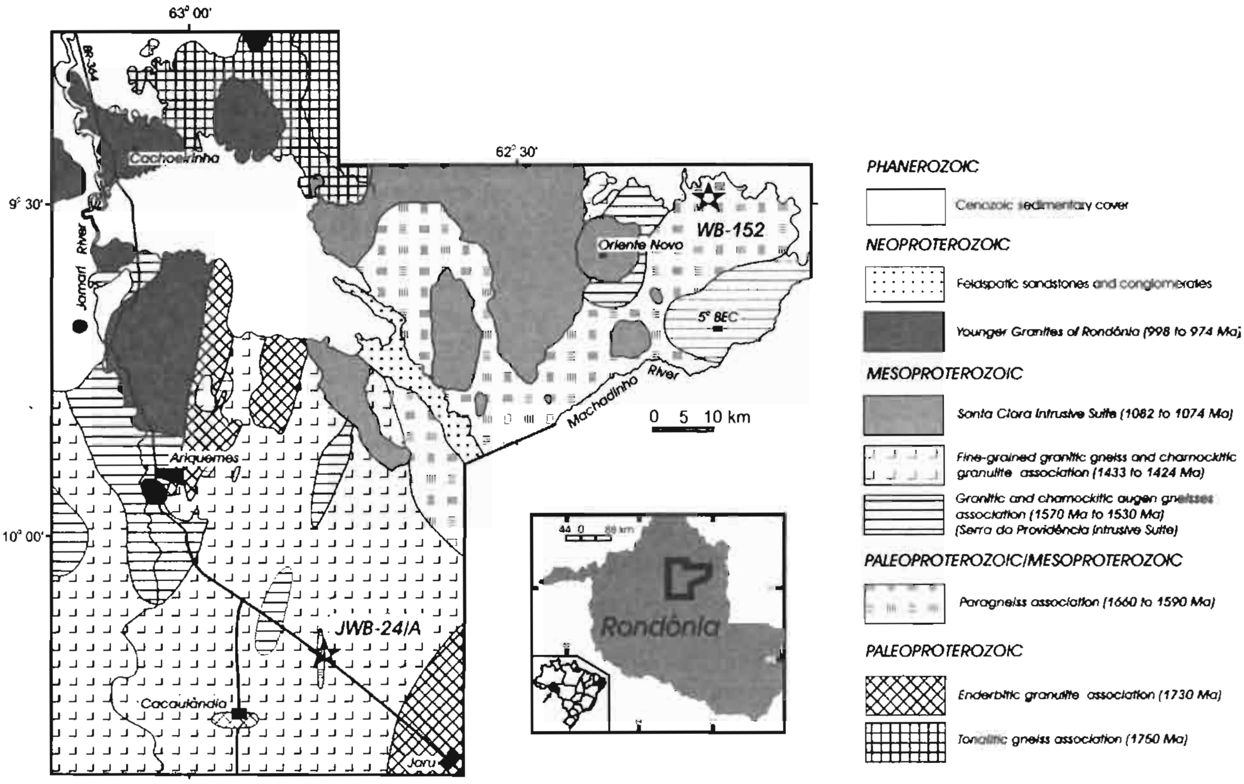

Figure 1. Map of the NE Rondônia State showing lithological associations and location of sampling sites (modified after Payolla et al., 2002).

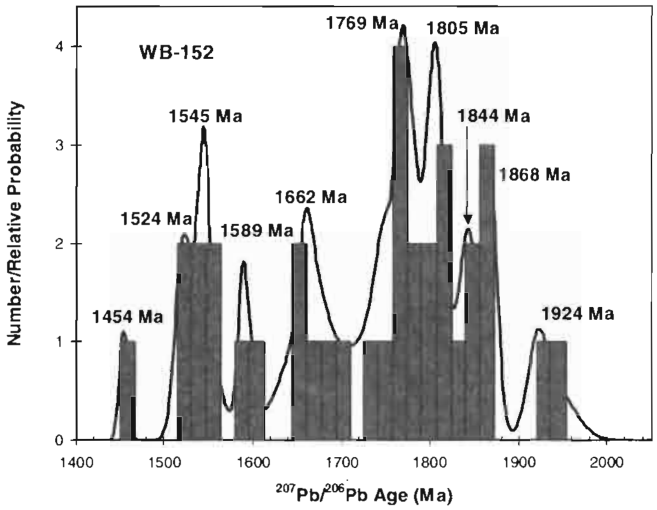

Figure 2. Cumulative probability histogram for all analyses from sample WB-152, illustrating the main age peaks.

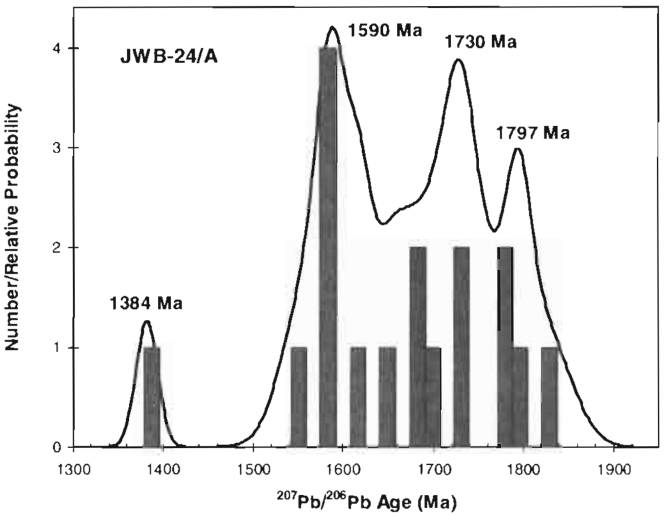

Figure 3. Cumulative probability histogram for all analyses from sample JWB-24/A, illustrating the main age peaks.

the $^{207}Pb/^{206}Pb$ ages range from 1940 to 1644 Ma, and yield distinct concentration of ages at 1924 Ma, 1868 Ma, 1844 Ma, 1805 Ma, 1769 Ma and 1662 Ma. The analyses that define the two main concentrations yield weighted mean $^{207}Pb/^{206}Pb$ ages of 1772 ± 6 Ma (n=6; MSWD=0.70) and 1805 ± 8 Ma (n=5; MSWD=0.29).

In only a few grains were the overgrowths wide enough (~30 μm) to permit SHRIMP analysis. Of the nine spots done, the overgrowths show moderate to high U (360-1340 ppm) and low Th/U (≤ 0.06). The data obtained yield $^{207}Pb/^{206}Pb$ ages in the range 1595-1519 Ma, apart from one point that yielded ca. 1454 Ma (Fig. 3). Four analyses yield a weighted mean $^{207}Pb/^{206}Pb$ age of 1545 ± 8 Ma (MSWD=0.16), but the other ones produce minor concentrations at ca. 1589 Ma and 1524 Ma (Fig. 2).

Sample JWB-24/A was collected from an outcrop of pelitic migmatite along the BR-364 highway, 37 km NW from Jaru (Fig. 1). In this site, the migmatite occurs as a metric-sized band within fine-grained granitic gneiss and charnockitic granulite (1.43-1.42 Ga) and granitic and charnockitic augengneiss (1.60-1.53 Ga). The migmatite contain bands of leucosome composed of coarse-grained, garnet-bearing quartz-feldspatic pegmatite and fine-grained leucogranite. The investigated sample was separated from a homogeneous dark gray mesosome portion consisting of Bt, Sil, Grt, Pl, Qtz and Ksp.

The zircon grains from this sample are 100-300 μm in length. Most grains have rounded external forms, but many preserve an overall prismatic shape. The SEM-CL images show that most zircons are similar to those of sample WB-152 and have CL-dark overgrowths surrounding cores with oscillatory and linear zoning.

The analyses of nine cores yield U contents that range between 148 and 498 ppm, and Th/U ratios varying from 0.25 to 0.75. In the probability distribution diagram (Fig. 3) the $^{207}Pb/^{206}Pb$ ages range from 1829 to 1686 Ma, and yield distinct concentration ages at 1797 Ma and 1730 Ma.

The overgrowth data (n=8) have high U (670-1140 ppm) and low Th/U (≤ 0.09). The data points are concordant to normally discordant and yield $^{207}Pb/^{206}Pb$ ages between 1648-1551 Ma, apart from one analysis that yielded ca. 1382 Ma (Fig. 4). Four $^{207}Pb/^{206}Pb$ ages clustered near 1590 Ma (Fig. 5) yield a weighted mean $^{207}Pb/^{206}Pb$ age of 1589 ± 19 Ma (MSWD=0).

DISCUSSION

Most of the zircons in each paragneiss consist of a Paleoproterozoic cores surrounded by early Mesoproterozoic overgrowths. The core ages show a significant range from 1644 Ma to 1940 Ma. The oscillatory zoning, U contents and Th/U ratios of the cores are diagnostic of a felsic igneous origin (Hanchar & Miller, 1993). The zircon overgrowths have very low Th/U values (<0.1), a feature commonly associated with zircons crystallized at high metamorphic grade (Williams & Claesson, 1987). The overgrowth ages also show a significant range from 1619 Ma to 1382 Ma, but most analyses are between 1590 and 1520 Ma.

Our geochronological data constrained the timing of deposition of sedimentary protoliths between ~1660 Ma and 1590 Ma, well in agreement with Payolla et al. (2002). The maximum age of about 1660 Ma is based on the youngest component identified in the core age spectra. The zircons that characterized this age component show oscillatory zoning interpreted as igneous in origin. The minimum age of 1590 Ma were obtained from the oldest analyzed metamorphic zircon overgrowth.

Age of source components is studied using the core age spectra. The number of analyzed grains in paragneiss WB-152 (n=26) is considered sufficient to yield a reasonable approach of all possible age components. However, this is not valid for the sample JWB-24/A (n=10). Although the spectrum of core ages obtained in both samples of paragneiss (Figs. 2, 4) is exclusively Paleoproterozoic (1940-1644 Ma), each paragneiss shows distinct age components. This suggested that there were different components in each paragneiss protolith or that this distinction reflects the insufficient number of core analyses in sample JWB-24/A. The former implies in a more local and restricted source area for JWB-24/A protolith (ca. 1730 and 1800 Ma) compared with that of paragneiss WB-152 (ca. 1930, 1870, 1840, 1800, 1770 and 1660 Ma).

Our age component data suggest that the detrital zircons in the paragneisses were derived from erosion of a Ventuari-Tapajós (1950-1800 Ma; Tassinari et al., 2000; Santos et al., 2000) and Juruena (1800 to 1700 Ma; Santos et al., 2000) type basement, exposed just to the northeast and east. On the other hand, the source for the ~1660 Ma detrital zircons in this region remains unclear. The tonalitic and enderbitic gneisses of the studied area (1750 Ma and 1730 Ma, respectively; Payolla et al., 2002) contributed with small amount of zircon to paragneiss WB-152, but the latter were a main component in paragneiss JWB-24/A.

As such, the paragneisses do not represent high-grade metamorphic equivalents of the volcano-sedimentary Beneficente Group exposed just to the southeast, but a younger sedimentary sequence deposited after the Juruena Orogeny (1.75 Ga; Santos et al., 2001).

The zircon population in the paragneiss WB-152 records, at least, three periods of zircon overgrowth at ca. 1590, 1545 and 1524 Ma. Single monazite grains in the same rock have U-Pb age of 1545 Ma (Payolla et al., this symposium). In the sample JWB-24/A only one period of zircon overgrowth at ca. 1590 Ma was recorded. These ages match the interval of age emplacement of the within-plate granitoids, mangerites, charnockites and basic rocks of the Serra da Providência Intrusive Suite (1.60-1.53 Ga; Bettencourt et al., 1999). The timing of the early Mesoproterozoic metamorphism and magmatism in the NE Rondônia supports the conclusion that the paragneiss protoliths were metamorphosed and partially melted at extremely high temperatures during the 1.60-1.53 Ga Serra da Providência magmatism. The different overgrowth phases are, either associated to at least three discrete metamorphic events referred to distinct intrusive episodes, or a quasi-continuous magmatic-thermal anomaly which affected the paragneisses during the span of time of emplacement of the Serra da Providência Intrusive Suite.

ACKNOWLEDGMENTS

Financial support: FAPESP Proc. 2.000/08033-5 and FINEP/PADCTII 64.99.027.00.

REFERENCES

Bettencourt, J.S., Tosdal, R.M., Leite Jr, W.B., Payolla, B.L., 1999. Mesoproterozoic rapakivi granites of Rondônia Tin Province, southwestern border of the Amazonian craton, Brazil - I. Reconnaissance U-Pb geochronology and regional implications. Precambrian Research, 95: 41-67.

Clement, S.W.J. & Compston, W., 1994. Ion probe parameters for very high resolution without loss of sensitivity. U. S. Geological Survey Circular 1107: 62 p.

Hanchar, J.M. & Miller, C.F., 1993. Zircon zonation patterns revealed by cathodoluminescence and backscattered electron images: Implications for interpretation of complex crustal histories. Chemical Geology, 110: 1-13.

Payolla, B.L., Bettencourt, J.S., Kozuch, M., Leite Jr, W.B., Fetter, A.H., Van Schmus, W.R., 2002. Geological evolution of the basement rocks in the east-central part of the Rondônia Tin Province, SW Amazonian craton, Brazil: U-Pb and Sm-Nd isotopic constraints. Precambrian Research, 119: 141-169.

Payolla, B.L., Fetter, A .H., Bettencourt, B.L., Leite Jr., W.B., 2003. U-Pb monazite ages of pelitic paragnaiesses in NE Rondônia, SW Amazonian craton: evidence for 1.54 Ga metamorphism. (this symposium).

Santos, J.O.S., Hartmann, L.A., Gaudette, H.E., Groves, D.I., McNaughton, N.J., Fletcher, I.R., 2000. A new understanding of the provinces of Amazon craton based on integration of field mapping and U-Pb and Sm-Nd geochronology. Gondwana Research, 3: 489-506.

Santos, J.O.S., Rizzotto, G.A., Hartmann, L.A., McNaughton, N.J., Fletcher, I.R., 2001. Ages of sedimentary basins related to the Sunsas and Juruena Orogenies, Southwest Amazon craton, established by zircon U-Pb geochronology. In: Bettencourt, J.S., Teixeira, W., Pacca, I.G., Geraldes, M.C., Sparrenberger, I. (Eds.), Geology of the SW Amazonian craton: State-of-the-Art. Workshop Extended Abstracts, São Paulo, Brazil, University of São Paulo, pp. 114-118.

Tassinari, C.C.G., Bettencourt, J.S., Geraldes, M.C., Macambira, M.J.B., Lafon, J.M., 2000. The Amazonian craton. In: Cordani, U.G., Milani, E.J., Thomaz Filho, A., Campos, D.A. (Eds.), Tectonic Evolution of South America. The 31st International Geological Congress, Rio de Janeiro, Brazil, pp. 41-95.

Tohver, E., Van der Pluijm, B.A., Scandolara, J.E., Rizzotto, G.J., 2001. A reassessment of the tectonics and paleogeography of the Grenville-aged Sunsas-Aguapei belt, SW Amazon craton: new paleomagnetic and ^{40}Ar/^{39}Ar data. In: Bettencourt, J.S., Teixeira, W., Pacca, I.G., Geraldes, M.C., Sparrenberger, I. (Eds.), Geology of the SW Amazonian craton: State-of-the-Art. Workshop Extended Abstracts, São Paulo, Brazil, University of São Paulo, pp. 96-99.

Williams, I.S. & Claessom, S., 1987. Isotopic evidence for the provenance and Caledonian metamorphism of high grade paragneisses from the Seve Nappes, Scandinavian Caledonides. II. Ion microprobe zircon U-Th-Pb. Contributions to Mineralogy and Petrology, 94: 289-303.

SHRIMP U-Pb ZIRCON AGES UP TO 3.4 – 3.5 GA IN ARCHAEAN AND PALEOPROTEROZOIC GRANITOIDS OF THE GAVIÃO BLOCK, SÃO FRANCISCO CRATON, BAHIA, BRAZIL

Peucat, J.J.[1]; Santos-Pinto, M.[2]; Martin, H.[3]; Barbosa, J.S.[4] and Fanning, M.C.[5]

1. Géosciences-Rennes, UPR 4661 CNRS, Université de Rennes I, 35042 Rennes, Cedex, France. peucat@univ-rennes1.fr
2. UEFS-Dep. Ciências Exatas, Km 03, BR116, 44031-460, Feira de Santana, BA, Brazil. marilda@uefs.br, mspinto@cpunet.com.br
3. UMR 6524-CNRS, Université Blaise Pascal, 5 rue Kessler, 63038 Clermont-Fd., Cedex France. martin@opgcf5.univ-bpclermont.fr
4. Curso de Pós-graduação de Geologia-IGEO-UFBa, Rua Caetano Moura s/n, Salvador, BA, Brazil. johildo@cpgg.ufba.br
5. Research School of Earth Sciences, ANU, Canberra, Australia. Mark.Fanning@anu.edu.au

Keywords: SHRIMP zircon ages, Gavião Block, TTG, granites

INTRODUCTION

The Gavião block, in the São Francisco craton, is one of the oldest register of the continental crust in South America Plataform with crustal history recorded at 3.4-3.1 Ga (Martin et al., 1991; Nutman & Cordani, 1993; Santos Pinto, 1996; Martin et al., 1997; Bastos Leal et al., 1998; Santos Pinto et al., 1998), 2.9-2.8 (Nutman & Cordani, 1993; Marinho, 1991; Bastos Leal et al., 1998) and 2.0-1.8 Ga (Santos Pinto, 1996; Santos Pinto et al., 1998; Bastos Leal et al., 2000). The aim of this paper is to present new SHRIMP U-Pb zircon age determinations and contribute to the knowledge of the geochronological evolution of this region.

GEOLOGICAL SETTING

The basement of São Francisco Craton is almost completely exposed in Bahia State, Northeast of Brazil. It is made up of two Archaean crustal blocks (Jequié block and Gavião block) separated by a 600Km long, N-S linear, Palaeoproterozoic trending Jacobina - Contendas Mirante belt (Cuney et al., 1990; Sabaté et al., 1990, 1992).

The Gavião block crops out to the west of Paleoproterozoic belt. It is composed of medium-grade supracrustal gneiss-leptinite-amphibole associations, Archaean plutonic tonalite-trondhjemite-granodiorite (TTG) gneisses and Palaeoproterozoic (Transamazonian) granites with some remnants of supracrustal rocks as is the Umburanas greenstone belt (Cunha & Fróes, 1994). Most of these rocks suffered important migmatization.

In the southern part of the Gavião block, Santos Pinto (1996) and Santos Pinto et al. (1998) distinguished three domains on the basis of zircon and monazite $^{207}Pb/^{206}Pb$ ages, Sr-Nd isotopic data and major and trace element geochemical modelling:

1- An Archaean juvenile domain made up of TTG (Bernada Massif) emplaced at a minimum age of 3.33 Ga. These rocks are assumed to be generated through partial melting of an Archaean tholeiite transformed into garnet-bearing amphibolite or eclogite.

2- A mixed Archaean domain partly juvenile and partly recycled. It consists in trondhjemitic grey gneisses (Aracatu Massif) and K-rich calc-alkaline granitic gneisses (Mariana and Eixo Massifs). Their $^{207}Pb/^{206}Pb$ minimum zircon ages are respectively 3.24, 3.26 and 3.16 Ga while model ages range between 3.5 and 3.3 Ga. They probably had a juvenile origin by the melting of an Archaean tholeiite transformed into garnet-bearing amphibolite or eclogite (Serra do Eixo and Aracatu Massifs). However, Nd isotopic compositions may indicate an enriched mantle source or, more probable, crustal contamination processes. In some cases, data are also consistent with the melting of the young juvenile crust ($\varepsilon_{Nd} \approx 0$) (Eixo and Mariana Massifs) as proposed for the Sete Voltas Massif (Martin et al., 1991). The Eixo Massif has been intruded by an alkaline granite of a minimum age of ca.2.6 Ga. It is interpreted as derived from the partial melting of the type I Eixo REE-rich gneisses.

3- A Palaeoproterozoic recycled domain. It consists mainly of the Umburanas peraluminous granite which yielded inherited zircons ages ranging from 3.13 to 2.57 Ga whereas the monazite age is 2.05 Ga. The Aracatu and Mariana Massifs were intruded by K-rich calc-alkaline granites at 2.03 and 1.94 Ga, respectively. The Serra da Franga Massif yielded a 2.04 Ga zircon age. This large scale crustal melting and granitogenesis is result of the Transamazonian collision between the Jequié and Gavião blocks, leading to crustal thickenning.

The occurrence of younger events is indicated by Rb-Sr biotite-whole rock ages on the Serra do Eixo Massif (533 ± 11 Ma) and Aracatu Massif (508 ± 10 Ma) both marking the Brazilian orogeny thermal influence.

PETROGRAPHIC, GEOCHEMICAL AND GEOCHRONOLOGICAL CHARACTERIZATION

In order to better understand the crustal evolution of Gavião block, we perfomed new U-Pb zircon ages using SHRIMP at Australian National University (ANU Camberra), in samples of the Bernada Massif (Archaean juvenile domain), Aracatu grey gneisses (mixed Archaean domain), alkaline granite Serra do Eixo (ca 2.6 Ga) and Aracatu granite (Palaeoproterozoic recycled domain). All new ages are $^{207}Pb/^{206}Pb$ weighted averages, quoted at 2 sigma, using the Isoplot 2.49 calculation program (Ludwig, 2001).

Bernada grey gneisses form a group of three massifs that intrude the heterogeneous metatexites (Sabaté et al., 1988). They are TTG made up of plagioclase (An_{24-32}), quartz, K feldspar, biotite, apatite, opaque minerals, sphene and zircon. Secondary minerals are epidote, sericite and carbonate. They also contain biotite-bearing mafic enclaves of monzogabbroic composition. Zircons from sample BER-120.1 were S25 high temperature zircon type of Pupin (1980). Five sub-concordant zircons define an age at 3378 ± 6 Ma but two grains are slightly older at 3404 ± 10 Ga (Fig.1).

The Aracatu grey gneisses, with a mineralogy similar to that observed for Bernada grey gneisses, are strongly foliated and intensively migmatized. They have a trondhjemitic composition, REE patterns display high LREE contents (La_N= 80 to 170), low HREE contents (Yb_N= 1 to 4) and a weak negative Eu anomalies (Eu*/Eu= 0.57 - 0.70). They are very similar to the Sete Voltas grey gneiss (Martin et al., 1991, 1997) except that they are more HREE depleted. Zircons from sample ARA-78.1 are of the S9, S13 and S18 types of Pupin (1980). Cores and rim complex structures are observed. One set of zoned magmatic zircons defined a sub-concordant age at 3325 ± 10 Ma, a set of cores exhibits an age of 3371 ± 14 Ma and one slightly discordant core defines an age of 3500 ± 9 Ma while an overgrowth defines a younger age of 2506 ± 10 Ma (Fig. 1).

The Late Archaean alkaline granitic gneiss Serra do Eixo is a K-feldspar augen gneiss, LREE rich (La_N= 114 – 263), with low HREE (Yb_N= 1.8 - 6), $La/Yb_{(N)}$ = 10 and with pronounced negatives Eu anomalies (Eu/Eu* = 0.40 to 0.55). Zircons from sample GA-299 are typical of high temperature types (S24 and S25) of Pupin (1980). On Fig. 1, excepting grain spots 9.1, with high discordance, and 14.1, which indicates an age ca 2.6 Ga, all the others analyses defines a weighted mean $^{207}Pb/^{206}Pb$ age of 2695 ± 10 Ma.

Aracatu granite is intrusive into the southern part of the Aracatu grey gneisses and it is composed of plagioclase (An_{25-29}), quartz, microcline, biotite, opaque minerals, sphene, apatite, zircon, secondary muscovite, epidote and carbonate. It contains migmatitic and gneiss enclaves and schliriens. With a calc-alkaline composition, the REE patterns show La_N= 47 - 61, Yb_N= 2.3 - 10, $(La/Yb)_N$= 4.7 - 21.7 and negatives Eu anomalies (Eu/Eu*= 0.64 - 0.73). Zircons from sample ARA-170 are brown, partially metamitic, of S4, S5 and S9 type of Pupin (1980). Despite careful choosing analyses sites, 3 grains have high common lead content but grain 1 has a slightly discordant core with a $^{207}Pb/^{206}Pb$ age of 3245 ± 25 Ma. Grain 2 is an overgrowth with a $^{207}Pb/^{206}Pb$ age of 2061 ± 9 Ma (Fig. 1).

DISCUSSION

As expected in such metamorphic rocks, SHRIMP zircon ages obtained during this work are generally older than those performed with the single zircon evaporation method however the range of age is broadly respected. This work also allowed to recognize older inherited cores, witness of the occurrence of an earlier continental crust ca 3.4 and 3.5 Ga.

Results obtained for Bernarda and Aracatu grey gneisses indicate magmatic stages at 3370 and 3325 Ma which can be correlated to the TTG massifs of Sete Voltas (Martin et al., 1997) and Boa Vista/Mata Verde (3353 ± 5 Ma) (Nutman & Cordani, 1993) which occur as tectonic slices within the supracrustal sequences of the Contendas-Mirante belt and are the oldest rocks recognized in the Gavião block (Martin et al., 1991, 1997; Sabaté et al., 1990, 1992; Nutman & Cordani, 1993). The age of 3325 Ma may be also correlated to the age 3300 ± 45 Ma found by Bastos Leal et al. (1998) to the TTG gneisses with incipient migmatization in Block Gavião by evaporation analyses on single zircon. The occurrence of inherited cores indicates some crustal contamination processes in the genesis of these rocks and the occurrence of old precursors up to 3.40 and 3.50 Ga old. The 3.40 Ga age is similar to that of 3403 ± 5 Ma found by Nutman & Cordani (1993) for the tonalites of Sete Voltas. These authors also recorded the occurrence of a 3345±10 Ma overgrowth in a zircon with an inherited core of 3473 ± 8 Ma in the same sample. The single zircon evaporation yielded younger ages (2284 to 3240) than the ion probe method in sample ARA-78.1. They were interpreted as lead loss from magmatic zircon grains related to Palaeoproterozoic partial melting processes. The 2506 ± 10 Ma SHRIMP zircon age suggest recristallisation at that time which could be related to metamorphic event not yet recognized.

The alkaline granitic gneiss of Serra do Eixo is emplaced at 2695 ± 10 Ma and it is a good evidence of crustal reworking processes ca 2.7 Ga (Nd model ages ca 3.3 Ga) in the Gavião Block, in agreement with previous Rb-Sr ages of gneisses and associated granites (Marinho et al., 1979; Cordani et al., 1985).

The Palaeoproterozoic Aracatu granite resulted of partial melting of Archean precursor (Nd model ages ca. 3.5 Ga). The age of a core at 3245 ± 25 Ma is in the range of age obtained for the surrounding Aracatu grey gneisses (sample ARA 78-1) and the age of 2061 ± 9 Ma is related to the partial melting event which is in agreement with the monazite age of 2049 ± 6 Ma obtained on similar granites (Santos Pinto, 1996; Santos Pinto et al., 1998). On the other hand, REE elements petrogenetic modelling indicates that a liquid with the composition of sample ARA-170 could be produced by 50% of melting of a grey gneiss with the ARA-78.1 sample composition with a residue of 68.00 % plagioclase, 29.31% quartz, 2.06% magnetite, 0.34% sphene, 0.14% biotite and 0.15% of allanite (Santos Pinto, 1996). In summary, this study allowed to precisely determine Archaean magmatic stages in the Gavião Block at 3378 ± 6 Ma, 3371 ± 14 Ma and 3325 ± 10 Ma with the evidence of inheritage ca 3.40 and 3.50 Ga. A late Archaean alkaline granitic stage was emplaced at 2695 ± 10 Ma. All these rocks were partially metamorphosed and melted at ca 2061 ± 9 Ma as indicated by anatectic granites.

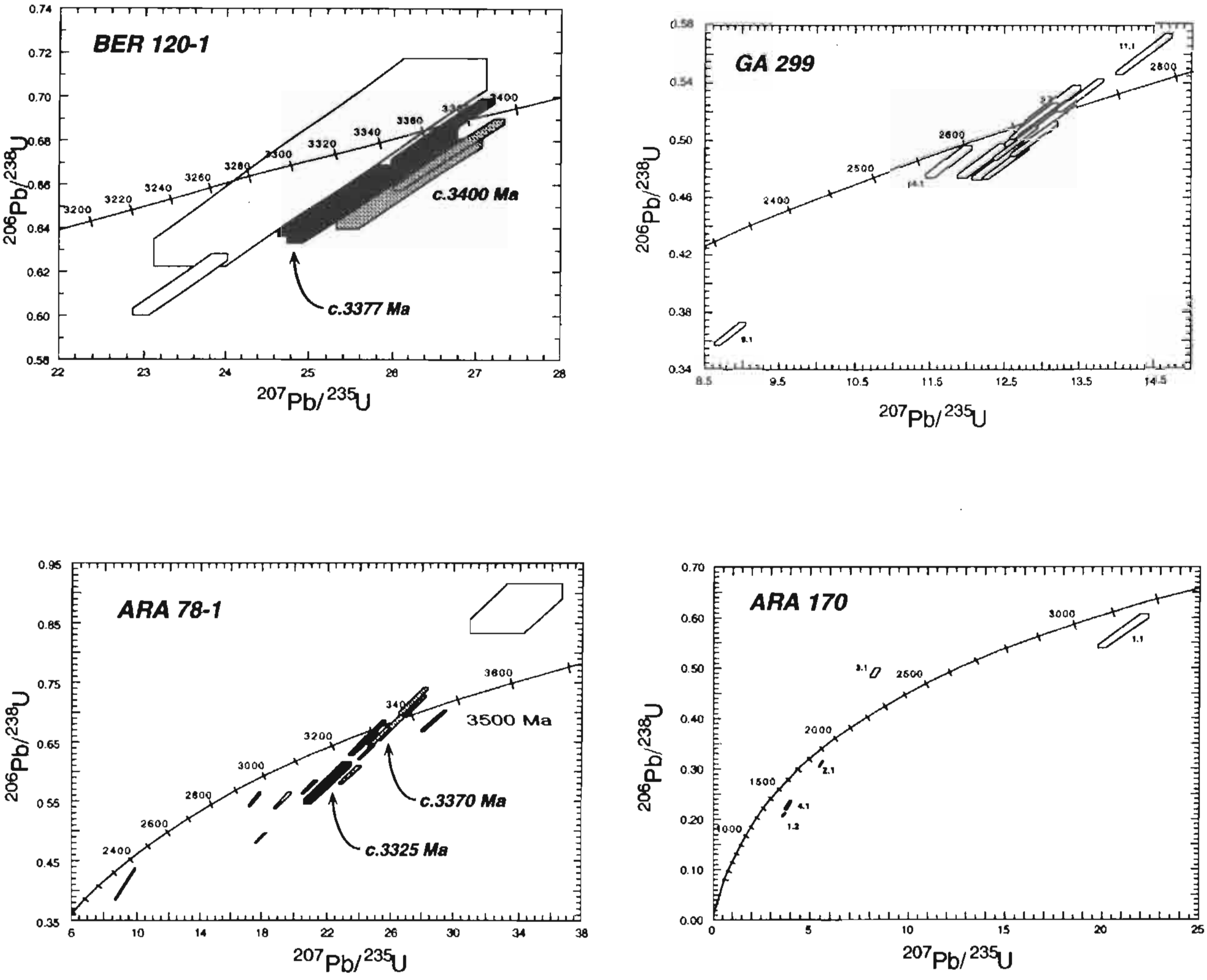

Figure 1. SHRIMP U-Pb concordia diagram for the grey gneisses of Bernada (BER 120-1) and Aracatu (ARA 78-1), alkaline granite of Serra do Eixo (GA 299) and Aracatu granite (ARA 170).

REFERENCES

Bastos Leal, L.R.; Teixeira, W.; Cunha, J.C.; Macambira, M.J.B., 1998. Archaean tonalitic-trondhjemitic and granitic plutonism in the Gavião Block, Sao Francisco Craton, Bahia, Brazil: geochemical and geochronological characteristics. Revista Brasileira de Geociências, 28(2):209-220.

Bastos Leal, L.R.; Teixeira, W.; Cunha, J.C.; Menezes Leal, A.B.; Macambira, M.J.B.; Rosa M.L.S., 2000. Isotopic signatures of Paleoproterozoic granitoids of the Gavião block and implications for the evolution of the São Francisco craton, Bahia, Brazil. Revista Brasileira de Geociências, 30(1):66-69

Cordani, U. G., Sato, K.; Marinho, M.M., 1985. The geologic evolution of the ancient granite-greenstone terrane of central-southern Bahia-Brazil. Precambrian Research, 27: 187-213.

Cuney, M.;. Sabaté, P.;. Vidal, P.; Marinho, M.M.; Conceicão, H., 1990. The 2 Ga peraluminous magmatism of the Jacobina-Contendas Mirante belt (Bahia - Brazil): Major and trace element geochemistry and metallogenic potential, Journal of Volcanology and Geothermal Research, 44: 123-141.

Cunha, J.C. & Froés, R.J.B., 1994. Komatiitos com textura spinifex do Greenstone belt de Umburanas, Bahia. Série Arquivos abertos, vol. 7, CBPM, Salvador, 29p.

Ludwig K.R., 2001. Isoplot/Ex rev. 2,49. A geochronological toolkit for Microsoft Excel. Berkeley Geochronology Center. Special publication n°1a.53p.

Marinho, M.M., 1991. La Sequence Vulcano-Sedimentaire de Contendas-Mirante et la Bordure Occidentale du Bloc de Jequié (Craton du São Francisco, Brésil): Un exemple de transition archeen-proterozoique. Unplublished Ph.D. thesis, University of Clermont-Ferrand, France

Marinho, M.M.; Costa, P.H.; Silva, E.F.A.; Torquato, J.R. 1979. Evolução geotectônica do Pré-cambriano no Estado da Bahia. In: H.A.V. Inda, eds., Geologia e recursos minerais do Estado da Bahia; textos básicos. SME/CPM, Salvador, p. 57-157.

Martin, H.; Sabaté, P.; Peucat, J.J.; Cunha, J.C., 1991. Un segment de croûte continentale d'âge archéen ancien (3,4 milliards d'années): le massif de Sete Voltas (Bahia, Brésil). Cahiers de Recherche de l' Academie des Sciences de Paris, t.313: 531-538.

Martin, H.; Peucat, J.J.; Sabaté, P.; Cunha, J.C., 1997. Crustal evolution in the Early Archaean of South America: example of the Sete Voltas massif, Bahia State, Brazil, Precambrian Research, 82: 35-62

Nutman, A.P. & Cordani, U.G., 1993. SHRIMP U-Pb zircon geochronology of Archaean granitoids from the Contendas-Mirante area of the Sao Francisco Craton, Bahia, Brazil, Precambrian Research , 63: 179-188.

Pupin, J.P., 1980. Zircon and granite petrology. Contribution to Mineralogy and Petrology, 73: 207-220.

Sabaté, P.; Marinho, M.M.; Vidal, P.; Caen-Vachette, M., 1990. The 2-Ga peraluminous magmatism of the Jacobina-Contendas Mirante belts (Bahia, Brazil): Geologic and isotopic constraints on the sources, Chemical Geology , 83: 325-338.

Sabaté, P.; Marinho, M.M.; Barbosa, J.S.F., 1992. The São Francisco craton: a short outline. In: Petrologic and geochronologic evolution of the oldest segments of the Sao Francisco Craton, Brazil. Field guide book for IGCP 280 "The oldest rocks on the Earth". CBPM, Salvador, 29-55

Santos Pinto, M.A., 1996. Le recyclage de la croûte continentale archéenne: exemple du Bloc du Gavião (Bahia - Brésil). Mémoires Géosciences Rennes, vol.75, Géosciences Rennes, 193p.

Santos Pinto, M.A.; Peucat, J.J.; Martin, H.; Sabaté, P., 1998. Recycling of the Archaean continental crust: the case study of the Gavião Block, Bahia, Brazil. Journal of South American Earth Science, 11(5): 487-498.

GEOCHEMICAL AND ISOTOPIC CHARACTERISTICS OF THE MORRO DO PÃO GRANITOID, SOUTHERN BRAZIL

Ragatky, D.[1]; Duarte, B.[1] and Tassinari, C.[2]

1. TEKTOS - UERJ Geotectonic Research Group - Rio de Janeiro State University. dragatky@uerj.br, biapasch@uerj.br
2. Geosciences Institute - São Paulo University. cccgtassi@usp.br

Keywords: Granites, geochemistry, isotopic geology, geochronology, Ribeira belt

INTRODUCTION

The Ribeira belt (Almeida et al., 1973), on the coast of Brazil, extends for 1400 km from the south of Bahia, in the north, to Paraná state, in the south (Fig. 1). It constitutes a Neoproterozoic to Early Paleozoic orogenic belt developed along the southern and southeastern borders of the São Francisco craton during the Brasiliano-Pan-African collage (700 – 450 Ma). This is the result of the collision between three plates or microplates: São Francisco, Serra do Mar and another inferred block presently underlying the Paleozoic sequences of the Paraná basin (Brito Neves & Cordani, 1991; Campos Neto & Figueiredo, 1995; Heibron et al., 2000).

The studied region is located near São Paulo city, in the homonymous state. It consists of Brasiliano orthogneisses and granitoids intruding several metavolcanosedimentary sequences such as the Piracaia Complex, the São Roque and Serra do Itaberaba groups and the Embu Complex (Hasui et al., 1981; Campos Neto & Basei, 1983; Juliani et al., 1986). These granitoids have sizes varying from batolithic to relatively small (stocks) bodies, showing distinct deformation degrees and geochemical and isotopic signatures from different tectonic environments (Janasi & Ulbrich, 1991).

LOCAL GEOLOGY

In São Paulo state, the Ribeira belt is characterized by the presence of terrains of different lithostructural features, limited by high angle shear zones of predominantly northeastern direction (Fig. 1). From northwest to southeast, the Jundiaí, São Roque and Embú domains can be identified.

At the eastern São Paulo state, the Roque domain (Fig. 2) is constituted by rocks of the homonymous metavolcanosedimentary sequence and the underlying Serra do Itaberaba Group. The former displays greenschist metamorphism while the latter underwent amphibolite facies metamorphism (Juliani et al., 1986). Hackpacher et al. (2000) interpreted the lithological, metamorphic and deformational features of the São Roque Group as characterizing a retro-arc basin developed during the collisional phase of the Brasiliano Orogenesis (628-605 Ma). In the focused region, the basement rocks of metavolcano-sedimentary sequences are unknown. Several brasiliano granitoids are intrusive in these rocks

The Morro do Pão granitoid (MPG), target of the present work, is located near Igaratá city. It is a NW elongated body that crosscuts the metavolcano-sedimentary sequence of the São Roque Group. Campos Neto et al. (1983) characterized this body as a syntectonic one.

The more mafic facies is coarse-grained and characterized by the presence of naked eyes visible clots of hornblende crystals. In this facies, elongated crystals of hornblende and biotite defined a weak foliation. Hornblende crystals enclose plagioclase and quartz. Plagioclase occurs as anhedral grains. Fine grained quartz, biotite and plagioclase are minor components of this facies.

The felsic facies shows plagioclase and microcline as anhedral crystals and biotite as the only mafic mineral.

The main accessory minerals, common to both facies, include abundant titanite as euhedral and anhedral crystals, apatite, allanite, zircon, epidote and opaque phases. The Morro Azul granitoid (MAG) and the Machado granitoid (MG), near the MPG, show mafic enclaves similar to the MPG mafic facies.

RESULTS AND DISCUSSION

LITHOGEOCHEMISTRY

Eight samples from the MPG and two samples from the MAG and MG enclaves were analyzed for major and trace elements, including rare earth elements (REE). The analysis were made in the ACTLABS laboratories (Canada).

The composition of the MPG vary from monzonite to granite (Fig. 3). The silica values from the MPG vary between 50.5% and 65.4%, with a gap of about 56% - 63%. They are metaluminous (A/CNK from 0.65 to 0.95), sub-alkaline rocks of calc-alkaline character (Fig. 4). K_2O values range from 2.2%, in the more mafic terms, to 4.4%, in the more felsic ones, while CaO values decrease from 8.36% to 3.0%, Fe_2O_3 values from 9.5 to 5.0 %, and MgO values from 7.9 to 1.6 %. Two samples display relatively high concentrations of TiO_2 (about 2.2%) and P_2O_5 (about 1.0%).

Based on the major elements and the REE patterns (normalized by chondritic values of Boynton, 1984) three groups of rocks were defined: 1) La_N/Yb_N between 8.5 to 27.6; 2) La_N/Yb_N from 48.7 to 70; and 3) the two samples of high Ti and P, with La_N/Yb_N of 44.2 and 46.6.

Plotted in tectonic discriminant diagram (Fig. 5) the majority of the samples fall into the volcanic arc granites field with a trend to the intra-plate granites field.

The enclaves samples of MG and MAG are geochemically undistinguishable from those of the MPG (Figs. 2, 3, 4).

AGE OF THE MORRO DO PÃO GRANITOID: RELATIVE GEOCHRONOLOGY

The crystallization age of the MPG is not available. However, the field observations described above allows us to make some inferences. The presence of mafic enclaves in the MAG and the MG of similar aspect and geochemical features as the MPG suggest that the last could be older than the other two granitoid bodies. The MAG have an age of 532 ± 20 Ma. Another closeby granitic body, the Imbiruçu Granite (IG) displays an age of 598 ± 21 Ma (Rb-Sr whole rock isochronic age, Ragatky et al., in press). The latter displays geochemical features of volcanic arc granites while the former shows transitional geochemical characteristics from volcanic arc to within-plate granites (Ragatky et al., in press). Based on these observations, the age of the MPG could be of *ca.* 532 Ma or older. Considering that some facies of the MPG have chemical characteristics of volcanic arc granites, similar to that of the IG, it is possible that both granites are contemporaneous.

ISOTOPIC DATA

Three samples of the MPG and one sample of the mafic enclave from the MAG were analyzed for Sr and Nd isotopes. The analyses were performed at the Geochronological Research Center of São Paulo University (CPGeo – USP). The three samples of the MPG display depleted mantle model Sm-Nd age (T_{DM}) of 1.4 – 1.5 Ga. The values of ε_{Nd} for 598 Ma are -5.4, -7.5 and -8.1. The initial $^{87}Sr/^{86}Sr$ ratios vary from 0.70620 to 0.70836. The enclave of the MAG displays a T_{DM} age of 1.65, a $\varepsilon_{Nd(0.58)}$ value of -9 and a $^{87}Sr/^{86}Sr$ ratio of 0.70860 (Fig. 6).

The T_{DM} values of the MPG are considerably lower than those of most granitoids of this area, which display T_{DM} values between 2.1 and 1.8 Ga (Ragatky, 1998). The T_{DM} values of the MPG suggest that the parental magma was generated by a mixture with a greater proportion of juvenile neoproterozoic materials. Additionally, the T_{DM} values of the MPG are similar to that obtained for the IG (Ragatky et al, in press).

Indeed, the identified facies of the MPG present the same T_{DM} values which it suggests that the magmatic differentiation occurred from a homogeneous parental magma without the participation of crustal contamination processes.

CONCLUSIVE REMARKS

At the studied region no spatial zoning magmatism is observed. However, as pointed out by Barbarin (1997), in some areas the succession of different granitoid types is not spatially controlled, as in the Andes, but is temporal controlled. The present data suggest that the intrusion of the MPG preceds the emplacement of the MAG and the MG. The isotopic characteristics, together with its geochemical signature, are consistent with a greater participation of the mantle source on the generation of the magma rather than only the involvement of basement rock sources of about 1.4-1.5 Ga as described by Juliani et al. (1998).

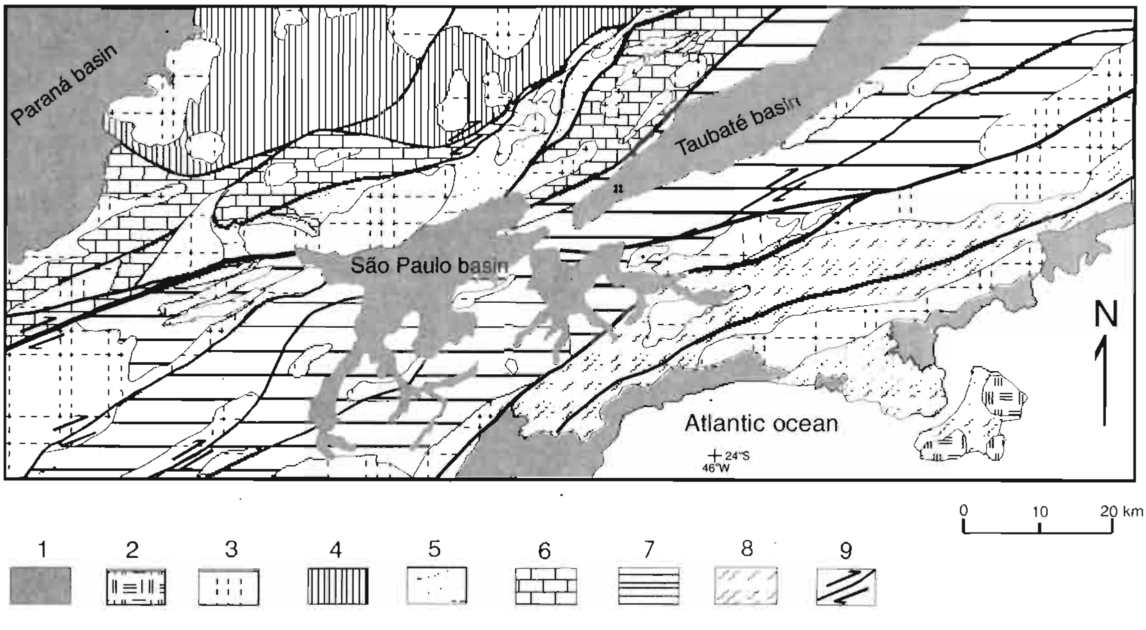

Figure 1. Simplified geological map of the east of São Paulo state (modified after Campos Neto, 2000) Symbols: 1- Phanerozoic cover; 2- Mesozoic alkaline intrusions; 3- Brasiliano granitoids; 4- Piracaia Complex; 5- Serra do Itaberaba Group; 6- São Roque Group; 7- Embú Complex; 8- Costeiro Complex; 9- Shear zones.

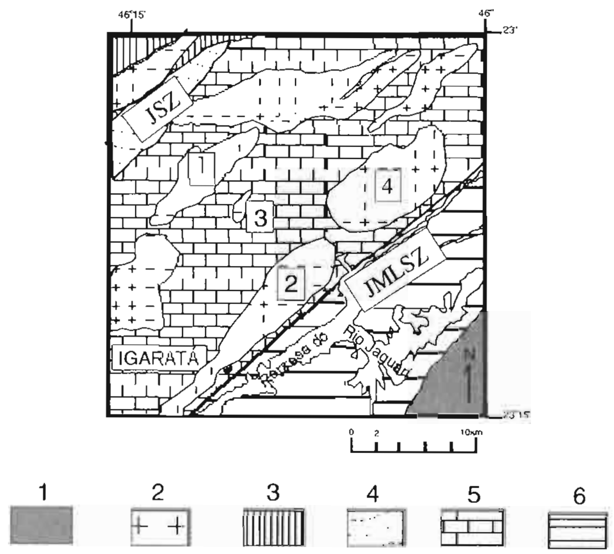

Figure 2: Simplified geologic map of Igaratá region, São Paulo state, with the location of the studied granites (Modified after Campos Neto and Basei, 1983). Symbos: 1- Phanerozoic cover; 2- Brasiliano granitoids; 3- Piracaia complex; 4- Serra do Itaberaba Group; 5- São Roque Group; 6- Embú Complex. JSZ - Jundiuvira shear zone; JMLSZ- Jaguarí-Monteiro Lobatoshear zone
Granitoids: 1- Morro do Pão; 2- Morro Azul; 3- Machado; 4- Imbiruçu.

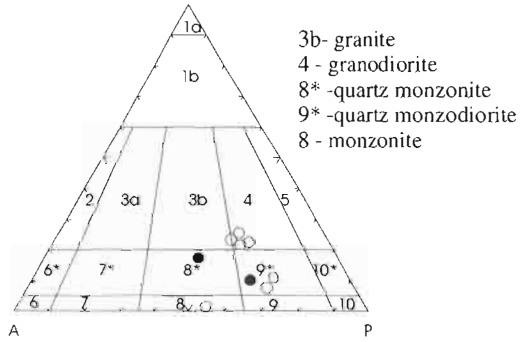

Figure 3. Plots of the samples from the Morro do Pão granitoid (open circles) and the Morro Azul and the Machado granitoids enclaves (filled circles) in the QAP normative diagram (Le Maitre, 1989).

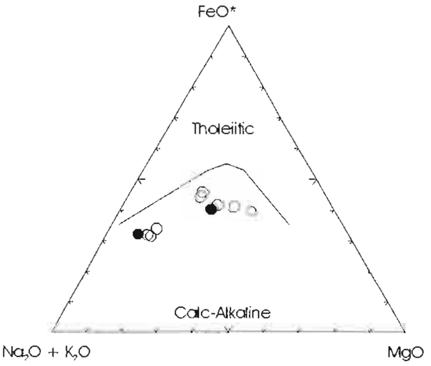

Figure 4. Plots of the Morro do Pão granitoid samples and the Morro Azul and the Machado granitoids enclaves samples in the AFM diagram (Irvine and Baragar, 1971). Symbols as in Figure 3.

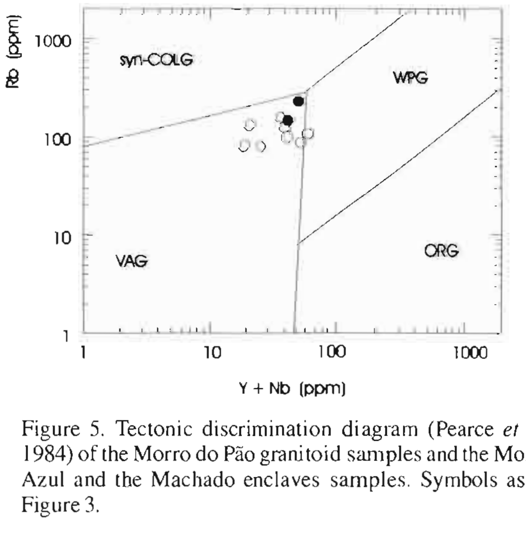

Figure 5. Tectonic discrimination diagram (Pearce *et al*, 1984) of the Morro do Pão granitoid samples and the Morro Azul and the Machado enclaves samples. Symbols as in Figure 3.

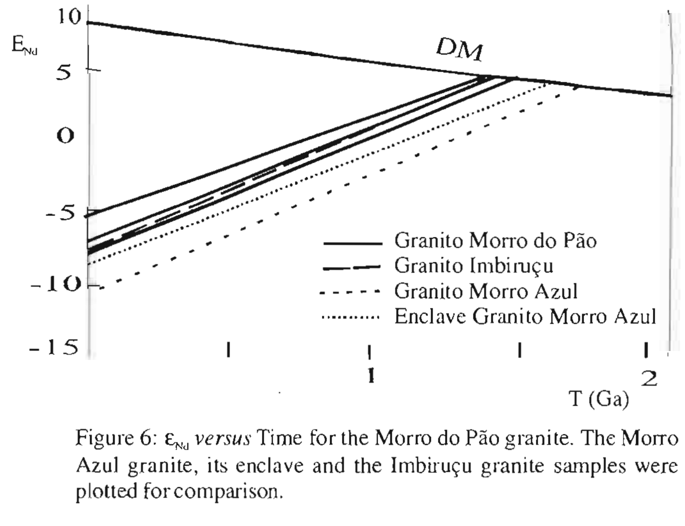

Figure 6: ε_{Nd} *versus* Time for the Morro do Pão granite. The Morro Azul granite, its enclave and the Imbiruçu granite samples were plotted for comparison.

ACKNOWLEDGEMENT

The authors thank FAPESP (grant 96/5017-1 e 96/1409-2) for the financial support given to fieldwork, lithogeochemical and isotopic analyses. D. Ragatky also thanks CNPq and FAPESP for a doctoral grant and B. P. Duarte thanks CNPq for a researcher grant.

REFERENCES

Almeida, F.F.M.; Amaral, G.; Cordani, U.G.; Kawashita, K., 1973. Precambrian evolution of the South American cratonic margin south of Amazon River. In: The Ocean Basins and Margins. E.M. Nairn & F.G. Stheli (eds). New York, Plenun., v. 1, cap. 11, p. 411-446.

Barbarin, B., 1997. From the mineralogical composition of granitoids to their origins and tectonic settings. International Symposium on Granites and Associated mineralizations. Extended abstract. p 95-97.

Bergmann, M., 1988. Caracterização estratigráfica e estrutural da seqüência vulcano-sedimentar do Grupo São Roque na região de Pirapora do Bom Jesus, Estado de São Paulo. Dissertação de Mestrado. Universidade de São Paulo, São Paulo, SP, Brasil. 155 p.

Boynton, W.V., 1984. Cosmochemistry of the rare elements: meteorite studies. In: Developments in geochemistry, 2: Rare Earth Element Geochemistry. Henderson, P. (ed.). Netherlands, Elsevier, p. 63-114.

Brito Neves, B.B. & Cordani, U.G. 1991. Tectonic evolution of South America during the Late Proterozoic Precambrian Research 54: 23-40

Campos Neto, M.C., 2000. Orogenic system from southwestern Gondwana. An approach to Brasiliano-Pan African cycle and orogenic collage in southeastern Brazil. In: Tectonic Evolution of South America. Cordani, U.G.; Milani, E.J.; Thomaz Filho, A.; Campos D.A. (eds). Rio de Janeiro, RJ, Brazil. p. 335-365.

Campos Neto, M.C. & Basei, M.A.S., 1983. Evolução estrutural brasiliana do nordeste de São Paulo: dobramentos superpostos e esboço estratigráfico e tectônico. In: Simpósio Regional de Geologia, 4. São Paulo, 1983. Anais. São Paulo, SBG. p. 61-78.

Campos Neto, M.C., Basei, M.A.S., Artur, A.C., Machado, R., Dias Neto, C.M., Fragoso Cesar, R., Souza, A., 1983. Geologia das folhas Piracaia e Igaratá. In: Jornada sobre a carta geológica do Estado de São Paulo em 1:50.000. 1, São Paulo, 1983, Atas..São Paulo, Secretaria da Indústria, Comércio e Tecnologia, SP, Pró-Minério. IPT. p 61-78.

Campos Neto, M.C. & Figueiredo, M.C.H., 1995. The Rio Doce Orogeny., southeastern Brazil. Journal of South America Earth Science, 8, 143-162.

Haspacker, P.C., Dantas, E.L., Spoladore, A. Fetter, H., Faria de Oliveira, M., 2000. Evidence of Neoproterozoic basin development in the central Ribeira belt, southeastern Brazil: new geochronological and geochemical constraints from the São Roque – Açungui groups. Revista Brasileira de Geociências. 30(1): 110-114.

Hasui, Y., Dantas, A.S.L., Carneiro, C.D.R., Bistrichi, C., 1981. Mapa geológico do Estado de São Paulo. Escala 1:50.000. Almeida, F.F.M., Hasui, Y., Ponçano, W.L., Dantas, A.S.L., Carneiro, C.D.R., Melo, M.S., Bistrichi, C.A (eds). São Paulo. P. 12-45.

Irvine, T.N. & Baragar, W.R., 1971. A guide to the chemical classification of the common volcanic rocks. Canadian Journal of Earth Sciences, 8: 523-548.

Janasi, V.A. & Ulbrich, H.G.J., 1991. Late Proterozoic granitoid magmatism in the state of São Paulo, Brazil. Precambrian Research. 51: 351-374.

Juliani, C., Beljavskis, P., Schorscher, H.D. 1986. Petrogênese do vulcanismo e aspectos metogenéticos associados: Grupo Serra do Itaberaba na região de São Roque. 34 Congresso Brasileiro de Geologia, Goiânia. Anais. V. 2. p. 730-743.

Juliani, C., Martin, M.A.B., McReath, I., Perez-Aguilar, A., Clarimundo, S.J., Chiarini, A.P., Fernandes, F., 1998. A evolução dos grupos Serra do Itaberaba e São Roque a nordeste e noroeste da cidade de São Paulo (SP). 40 Congresso Brasileiro de Geologia, Belo Horizonte. Anais. p. 87.

Le Maitre, R.W. 1989. A classification of igneous rocks and glossary of terms. Blackwell, Oxford. 193 p.

Pearce, J.A, Harris, N.B.W., Tindle, A.G., 1984. Trace elements discrimination diagrams for the tectonic interpretation of granitic rocks. Journal of Petrology. 25: 956-983.

Ragatky, D., 1998. Contribuição à geoquímica e geocronologia do Domínio São Roque e da Nappe Socorro-Guaxupé na região de Igaratá e Piracaia, Sp. Tese de doutoramento. Universidade de São Paulo, SP, Brasil. 130 p.

Ragatky, D., Duarte, B.P., Tassinari, C., Caracterização geoquímica e isotópica de granitóides do domínio São Roque, Faixa Ribeira, São Paulo. Revista da Universidade Federal Rural do Rio de Janeiro. Série Ciências Exatas e da Terra. In press.

ISOTOPIC DATA (Sr AND Nd) FROM THE PARAÍBA DO SUL GROUP ORTHOAMPHIBOLITES

Ragatky, D.; Tupinambá, M.; Heilbron, M. and Santos Marins, G.

TEKTOS - UERJ Geotectonic Research Group - Rio de Janeiro State University.
dragatky@uerj.br, tupi@uerj.br, heilbron@uerj.br, gloriamarins@rj.ibama.gov.br

Keywords: Orthoamphibolites, isotopic geochemistry, Neoproterozoic, Paraíba do Sul Group, Ribeira belt

INTRODUCTION

The geochemical and isotopic composition of metavolcanic rocks is a relevant tool to identify tectonic environments in areas where tectonic and metamorphic events have obliterated the primary features of volcanosedimentary sequences.

In this way, Sr and Nd isotopes of metavolcanic basic rocks provide an important insight into the origin of magmatism and its environment of extrusion. The Rb-Sr method allows an additional parameter to constrain the age of volcanism through its initial $^{87}Sr/^{86}Sr$ ratio.

This work presents the first isotopic results of the metabasic rocks from a long-term project about the lithogeochemical and isotopic characteristics of the metavolcanosedimentary covers from the central segment of the Ribeira belt. The paper focuses on the orthoamphibolites hosted in the metasedimentary rocks of the Paraíba do Sul Group, in the homonymous domain.

TECTONIC SETTING

The Ribeira belt (Almeida et al., 1973) is a Brasiliano/Pan-African belt that resulted from the agglutination of the Gondwana supercontinent (750-500 Ma). Its central segment comprises several tectonic domains, most of them presenting pre-1.8 Ga basement rocks and distinct Proterozoic siliciclastic covers. During the Neoproterozoic, both basement and cover were intruded by granitic plutons.

The major tectonic organization of the central segment of the Ribeira belt is defined by four tectono-stratigraphic terranes (Heilbron et al., 1998, 2000) a) the Occidental terrane represents the passive margin of the São Francisco paleoplate; b) the Paraíba do Sul klippe is the uppermost thrust slice; c) the Oriental terrane is the locus of the Ribeira magmatic arc (Tupinambá, 1998), which intruded a passive margin sedimentary cover; d) the Cabo Frio terrane presents an ordovician magmatism and metamorphism and is the youngest tectonic terrane (Scmitt, 2001). The contact between the Occidental and Oriental terranes is given by a conspicuous NW dipping shear zone, the central tectonic boundary (Almeida et al., 1998).

THE PARAÍBA DO SUL KLIPPE

The pre-1.8 Ga rocks of the Paraíba do Sul klippe comprise granitic to granodioritic orthognaisses with basic and calc-silicatic enclaves (Quirino Complex) of Paleoproterozic age. The overlying metasedimentary rocks belong to the Paraíba do Sul Group. In the southern segment of Rio de Janeiro State, a subdivision of this group was proposed by Almeida et al. (1993) into three units: basal psammites with calc-silicatic rocks, marble and pelitic intercalations; intermediate pelites; and a stratified top unit with psammitic and pelitic layers with abundant marble, calc-silicatic and Mn-rich rocks. Both basement and metasedimentary rocks are intruded by Brasiliano granitoids.

The amphibolites occur as centimetric irregular lenses, layers and boudins and as decametric to metric tabular bodies. They are interpreted as metamorphosed dykes and sills (dos Santos Marins & Duarte, 2000).

Based on geochemical data and comparing with modern environments, dos Santos Marins (2000) and dos Santos Marins & Duarte (2000) identified two groups of amphibolites: a) a major group constituted by tholeiitic continental flood basalts; and b) E-MORB type basalts.

The stratigraphic relationship between pre-1.8 Ga rocks of the Quirino Complex and the cover is not clear and the time interval of sedimentation of the Paraíba do Sul basin is unknown. But the presence of metasedimentary hosted rocks with depleted mantle model Nd age (T_{DM}) of 1.7 Ga (Ragatky et al., 2000) and the intrusive granites with 0.53 Ga (Machado et al., 1996) restrict the sedimentation to this interval (1.7 - 0.53 Ga). Additional data about the metasedimentary rocks of the Paraíba do Sul Group were provided by Valladares et al. (1999) through laser-ablation Pb-Pb determinations in detrital zircons. The provenance ages obtained fit into two classes: between 2.0 - 2.2 Ga and 2.5 - 2.7 Ga intervals.

Recent paleogeographical reconstructions (Heilbron et al. 2000, Tupinambá & Heilbron, 2002) relate the Paraíba do Sul basin to the passive margin of Oriental terrane associated to the Rodinia supercontinent break-up. Also they correlate the Paraíba do Sul basin with the Italva basin at the Oriental Terrane. U-Pb zircon isotopic data yielded a 840 Ma crystallization age for an amphibolite from the Italva Group (Heilbron et al., in press).

RESULTS AND DISCUSSION

Eigth representative samples of amphibolites were selected for Rb-Sr and Sm-Nd isotopic studies. The analyses were performed at the Geochronological Research Center – São Paulo University (CPGeo-USP).

As argued above, the initial $^{87}Sr/^{86}Sr$ ratio imposes a constraint to the age of orthoamphibolites since these values cannot be lower than the evolution line defined by the BABI (Basalt Achondrite Best Initial) value, that is, 0.698990 ± 0.000047 (Papanastassiu and Wasserburg,

1969) and the mantle value at the time of their magma generation.

With the exception of two samples, consistent values of the initial $^{87}Sr/^{86}Sr$ ratios for the 840 Ma (age of the amphibolites of the Italva Group) were obtained. They vary from 0.70669 to 0.71169. The other two samples present coherent results of initial $^{87}Sr/^{86}Sr$ ratios for more recent ages.

The values of initial $^{143}Nd/^{144}Nd$ ratios for the same age show a wide range varying from 0.51176 to 0.51126, corresponding to ε_{Nd} values of 4.2 to –5.5, respectively. These variations are observed in the diagram of Figure 2. The data of the two samples of the Quirino Complex basement rocks (Ragatky et al., 2000 and unpublished data) are plotted in the same diagram.

In general terms, the location of the samples in the $^{143}Nd/^{144}Nd$ versus $^{87}Sr/^{86}Sr$ diagram (Fig. 2) correlates with the groups defined by Marins (2000) and Marins & Duarte (2000). According to the description of Faure (1986) related to this diagram, the following observations could be made:

1. the data show large variations in the isotopic compositions;
2. one sample plots in quadrant I, which displays higher Sm/Nd ratios than CHUR and lower Rb/Sr values than UR. These features correspond to the depleted mantle characteristics;
3. two samples plot in quadrant II, defined by $^{143}Nd/^{144}Nd$ and $^{87}Sr/^{86}Sr$ ratios greater than their values in CHUR and UR, respectively. These relations are contrary to the geochemical behavior of these elements (Faure, 1986). The relatively high $^{87}Sr/^{86}Sr$ values could be due to incorporation of Sr by sea water.
4. three samples plot in quadrant IV, characterized by relatively high $^{87}Sr/^{86}Sr$ and low $^{143}Nd/^{144}Nd$ ratios.

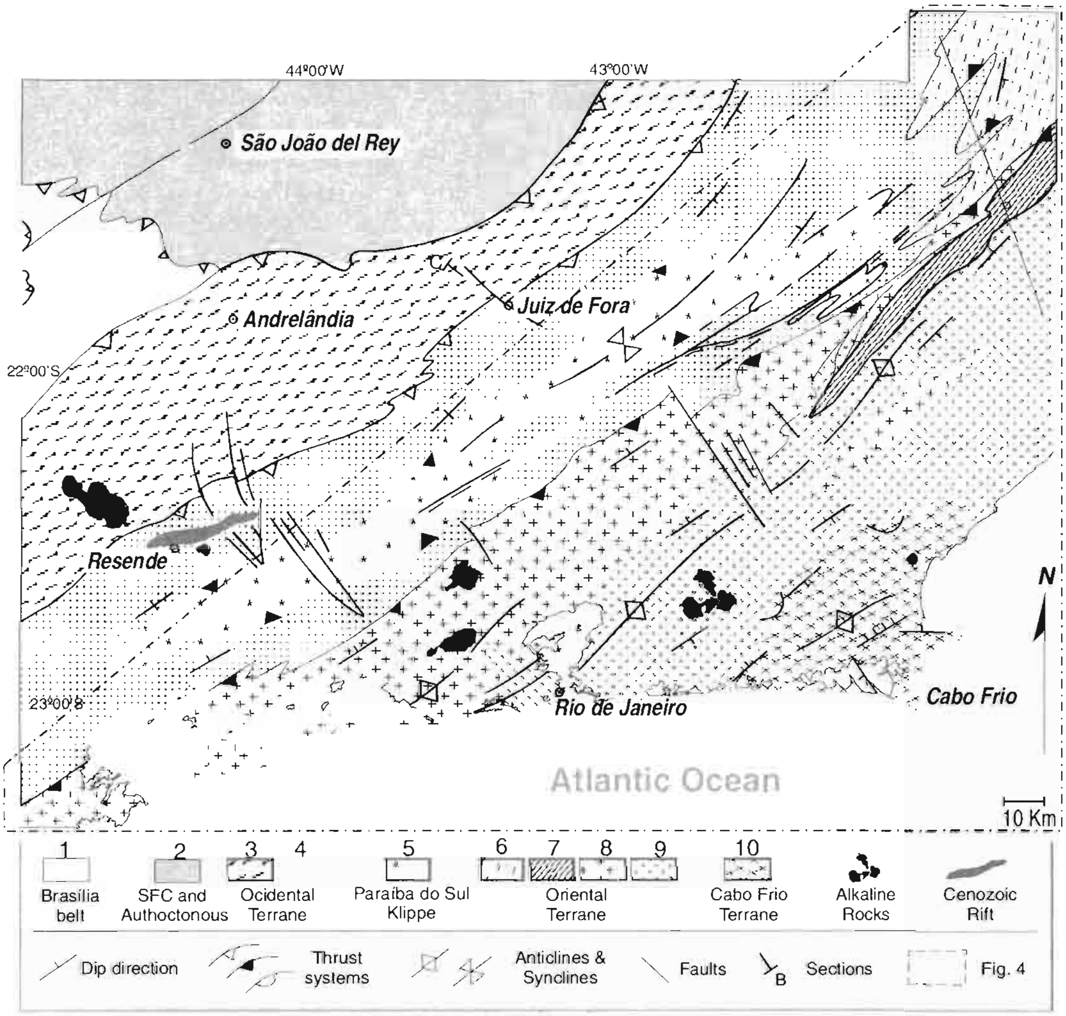

Figure 1. Tectonic map of the central segment of Ribeira belt (Heilbron & Machado, 2003).

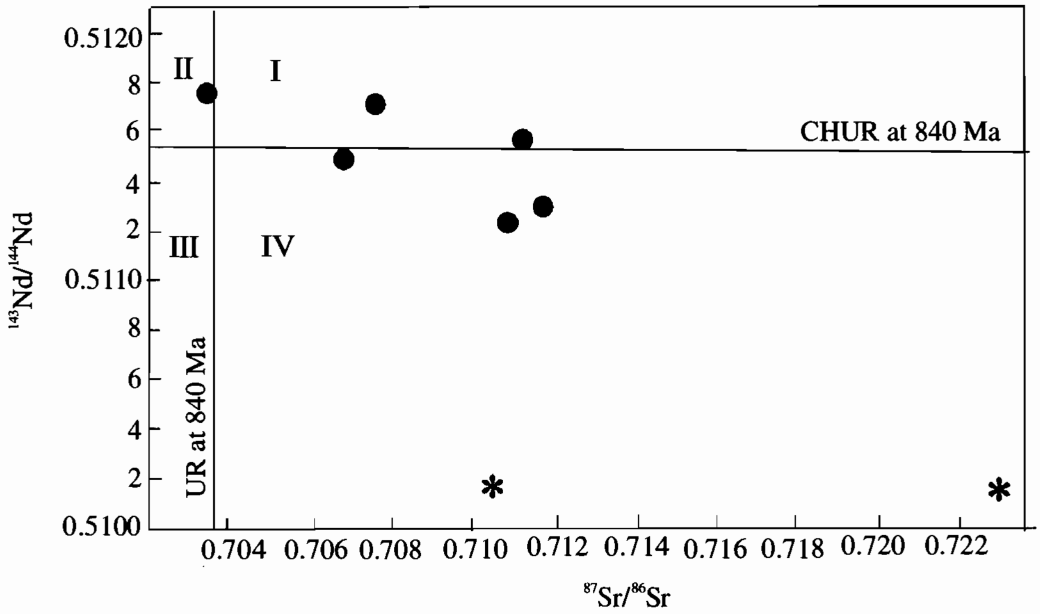

Figure 2: Correlation of ^{143}Nd/^{144}Nd and ^{87}Sr/^{86}Sr ratios of amphibolites from the Paraíba do Sul Group (circles) and orthogneisses of the Quirino Complex (asterisks). The values of CHUR (Chondritic Uniform Reservoir) and UR (Uniform Reservoir) at 840 Ma were calculated from the following parameters at the present time, respectively: ^{143}Nd/^{144}Nd = 0.512638; ^{147}Sm/^{144}Nd=0.1967; ^{87}Sr/^{86}Sr=0.7045; ^{87}Rb/^{86}Sr = 0.0816.

CONCLUSIVE REMARKS

The opening and the closure of the Paraíba do Sul basin are limited by the 1.7 Ga (given by the T_{DM} age of metassedimentary rocks, Ragatky et al., 2000) and 530 Ma (age of granitic intrusion in the Paraíba do Sul Group rocks, Machado et al., 1996). The initial ^{87}Sr/^{86}Sr ratios from the amphibolites yield some clues for a more precise time interval. As the Italva and Paraíba do Sul basins can be correlated as back-arc and fore-arc basins, respectively (Tupinambá & Heilbron, 2002), the obtained results of the present work are consistent with the previously determined age of 840 Ma for the Italva basin (U-Pb in zircon of amphibolite, Heilbron et al., In press).

The location of the Quirino Complex basement rocks samples in quadrant IV (Fig. 2) suggests that they could be the contaminant of the magma derived from residual solid in quadrant II. Another possible contaminant, to be investigated, could be the metasedimentary hosted rocks.

ACKNOWLEDGEMENT

The authors would like to thank FAPERJ (grant number E-26/170.317/2001 - APQ1.) for the financial support given to fieldwork, lithogeochemical and isotopic analyses.

REFERENCES

Almeida, F.F.M. de, Amaral, G., Cordani, U.G. , Kawashita, K., 1973. The Precambrian evolution of the South American Cratonic Margin South of Amazonas River. In: The ocean basin and margins. Nairn & Stille, (eds) 1:411-446, Plenum, New York.

Almeida, J.C.H., Tupinambá, M.A., Heilbron, M., Trouw, R., 1998. Geometric and kinematic analysis at the Central Tectonic Boundary of the Ribeira Belt, southeastern Brazil. In: SBG, Congresso Brasileiro de Geologia, Belo Horizonte, 1998, Anais, p. 32.

Faure, G. 1986. Principles of isotope geology. Jhon Wiley and Sons (Ed). 589 p.

Heilbron, M & Machado, N., 2003. Timing of terrane accretion in the Neoproterozoic-Eopaleozoic Ribeira orogen (SE Brazil). Precambrian Research. In press.

Heilbron, M., Mohriak, W.V., Valeriano, C.M., Milani, E.J., Almeida, J., Tupinambá, M., 2000. From collision to extension: the roots of the southeastern continental margin of Brazil. In: Geology and geophysics of continental margin. W.V. Mohriak and Talwani., M, Eds. Geophysical Monograph 115, American Geophyssical Union: 1-31.

Heilbron, M., Tupinambá, M., Almeida, J.C.H., Valeriano, C.M., Valladares, C.S., Duarte, B.P., 1998. New constraints on the tectonic organization and structural styles related to the Brasiliano Collage of the central segment of Ribeira Belt, SE Brazil. 14th Intern. Conference on Basement Tectonics. Ouro Preto, MG, Brazil. Abstracts. p. 15-17.

Machado, N., Valladares, C., Heibron, M., Valeriano, C., 1996. U-Pb geochronology of the central Ribeira Belt (Brazil) and implications for the evolution of the Brazilian Orogeny. Precambrian Research. 79: 347-361.

Papanastassiou, D. & Wasserburg, G. J., 1969.Initial strontium isotopic abundances and the resolution of small time differences in the formation of planetary objets. Earth Planetary Science Letters, 5: 361-376.

Ragatky, D., Tupinambá, M., Heilbron, M., Paschoal Duarte, B., Valladares, C., 1999. New Sm/Nd isotopic data from pré-1.8 basement rocks of central Ribeira belt, SE Brazil. II South American Symposiun on Isotope Geology. Córdoba, Argentina. p. 346-348.

Ragatky, D., Tupinambá, M., Paschoal Duarte, B., 2000. Sm/Nd data of metasedimentary rocks from the central segment of Ribeira belt, southeastern Brazil. Revista Brasileira de Geologia. 30 (1): 165-168.

Santos Marins, G & Duarte, B.P., 2000. Petrografia, geoquímica e ambientes tectônicos dos anfibolitos da Klippe Paraíba do Sul, setor central da Faixa Ribeira. Congresso Brasileiro de Geoquímica. Curitiba. CD room.

Santos Marins, G. 2000. Petrologia dos anfibolitos do Domínio Juiz de Fora e da Klippe Paraíba do Sul, setor central da Faixa Ribeira. Dissertação de Mestrado. Universidade do Estado do Rio de Janeiro. 136 p.

Schmitt, R. S., 2001. A orogenia Búzios: um evento tectono-metamórfico cambro-ordoviciano caracterizado no Dominio Tectonico de Cabo Frio, Faixa Ribeira, sudeste do Brasil. Universidade Federal do Rio de Janeiro. Tese de doutoramento Rio de Janeiro. 273 p.

Tupinambá, M. & Heilbron, M., 2002. Reconstituição da fase pré-colisional neoproterozóica da Faixa Ribeira: o arco magmático e as bacias de ante-arco e retro-arco do Terreno Oriental. XLI Congresso Brasileiro de Geologia. P. 345.

Tupinambá, M., Teixeira, W., Heilbron, M., Basei, M., 1998. The Pan-African/Brasiliano arc-related magmatism at the Costeiro domain of the Ribeira Belt, southeastern Brazil: new geochronological and litogeochemical data. 14th International Conference on Basement Tectonics. Ouro Preto, MG. P. 12-14.

Valladares, C., Machado, N., Heibron, M. Tupinambá, M. Duarte, B., Giles, G., Noronha, M., 1999. Ages of detrital zircon from central Ribeira belt (Brazil) using laser-abation-ICPMS. II South American Symposiun on Isotope Geology. Córdoba, Argentina. p 145-147.

A NEW PROPOSAL FOR THE SUBDIVISION OF GRANITIC ROCKS AT SERRINHA NUCLEUS, BAHIA, BRAZIL, BASED ON U-Pb AND Pb-Pb GEOCHRONOLOGICAL AND LITHOGEOCHEMICAL DATA

Rios, D.C.[1]; Conceição, H.[1]; Davis, D.W.[2]; Rosa, M.L.S.[1]; Macambira, M.J.B.[3] and Dickin, A.P.[4]

1. Federal University of Bahia. R. Barão de Geremoabo s/n, IGEO/UFBA, room 208A, Salvador-BA, Brazil. debora@cpgg.ufba.br, herbet@cpgg.ufba.br, lourdes@cpgg.ufba.br
2. Royal Ontario Museum. 100 Queen's Park, Toronto-ON, Canada. dond@rom.on.ca
3. Isotopic Laboratory of Pará, Federal University of Pará, IGEO/UFPA, Belém-PA, Brazil. moamac@ufpa.br
4. McMaster University, Hamilton-ON, Canada. dickin@mcmaster.ca

Keywords: Precambrian, alkaline, Archaean, Paleoproterozoic, zircon

INTRODUCTION

The Precambrian terrains of São Francisco Craton basement in the Bahia State consist of three ancient nuclei: (i) the Serrinha Nucleus, in the east; (ii) the Remanso Nucleus, in the central area; and (iii) the Guanambi Nucleus, in the west. The "Serrinha Nucleus" (SerN) is a wedge-shaped terrain about 300 km long and up to 70 km wide, that comprises an Archaean gneissic-migmatitic basement, covered by volcano-sedimentary rocks of the Rio Itapicuru Greenstone Belt (IRGB) and Capim Group. It is intruded by numerous granitic rocks. The principal aim of this work is to present a new stratigraphical proposal for these granitic rocks based on U-Pb and Pb-Pb studies on single zircon crystals, lithogeochemical analyses and Nd-Sr isotopic data.

Granitoid rocks are the principal component of continental crust and at SerN the term "granites" can include not only the most common magmatic rocks types (granites and TTGs) but also the high- to medium-metamorphic grade terrains of the basement, which are represented by migmatites and gneisses. In the past years, diverse studies have revealed the diversity of SerN granites and resulted in a number of proposals for their geological subdivision. Matos & Conceição (1993) were the first, presenting a proposal based on field mapping and few geochemical data. They subdivided these rocks into five types (G1 to G5) according to textural and structural differences observed. This terminology was also adopted by Alves da Silva (1994) and Rios et al. (1998), who also subdivided them into two main groups: Pre- to Syn-tectonics and Post- to Tardi-tectonics one.

THE NEW PROPOSAL

New geochronological, lithogeochemical and isotopic data (Rios, 2002) require a review of these proposals. Table 1 summarizes the principal geochemical and isotopic characteristics of the granitic rocks from SerN and emphasizes their separation based on these criteria.

In the SerN Rios (2002) found evidence of a cryptic Paleoarchaean crust, which is represented by xenocrystic zircon crystals aged > 3.6 Ga, which represent the oldest zircon ages found from magmatic rocks of the South America continent. Most granitic rocks in this area range from Mesoarchaean (3.15 Ga) to Paleoproterozoic (> 2.07 Ga). Two distinct lithologic groups can be identified: (i) the Archaean rocks, including the gneissic-migmatic basement and transitional TTG/calc-alkaline Archaean granites; and (ii) Paleoproterozoic granites, which are represented by TTG/calc-alkaline, shoshonites and potassic-ultrapotassic bodies.

ARCHAEAN MAGMATISM

Well studied Archaean cratons worldwide usually show a classical lithologic trilogy: gneisses/TTGs, greenstones belts and post-tectonic potassic granites (Windley, 1995; Moyen et al., 2001). This typical association had still not been identified in the SerN, probable due to the scarcity of data from its Archaean rocks and the destructive effects of tectonism at 2.7 and 2.2 Ga.

Basement rocks are still poorly characterized, but the first results show an interesting pattern:

(i) Amphibolitic rocks identified in the SerN basement are chemically similar to tholeiitic basalts of Capim Group and IRGB. These less differentiated rocks have igneous protoliths and occur intercalated with calc-alkaline phases in the basement. The lithogeochemical data and ages available for the volcano-sedimentary rocks from Capim Group (2793 a 2519 Ma; Oliveira et al., 1999) allow us to correlate them to this magmatism and now to those amphibolites and the "mafic dykes of Uauá-Capim Group rocks" which have been interpreted as possible mafic relicts of Archaean greenstones.

(ii) The studied Archaean granitic plutons (ArchG) – Araci, Ambrósio and Requeijão – are characteristically highly foliated bodies with calc-alkaline to TTG signature. There is evidence for at least two granitic magmatic episodes during the Archaean in the SerN: the first one occurred from 3.09 to 3.07 Ga and the second, at about 2.9 Ga. Zircon xenocrysts (3.17 Ga) are evidence of the involvement of an older Archaean crust in their generation, probably the present gneissic basement. These granitic magmas are chemically similar to the gneisses and migmatites of the basement (Rios, 2002). They are similar to the TTG suites from East Finland, although SerN rocks are more aluminous. They are LILE enriched in relation to HFSE and show prominent anomalies of Nb and Ti as well as highly fractionated REE patterns, which are usually taken as evidence of subduction related magmatism. Some previously unclassified plutons and almost all of the granites previously designated as G1 and G2 can be grouped here.

The 3.6 Ga zircon xenocrysts and similar model ages found by Martin et al. (1997) in the Remanso Nucleus, suggest the existence of an Early Archaean crust into which the 3.15-2.80 Ga Mesoarchaean granites were emplaced. A Paleoarchaean episode of continental crust formation is also indicated in some areas of West Africa (Kroner et al., 2001 and references therein). Sr and Nd isotopes from the Mesoarchaean granites (Table 1) give close to depleted mantle values at the time of their emplacement, suggesting that Paleoarchaean rocks made only à limited contribution, if any, to their genesis. The Transamazonian event produced zircon overgrowths and metamorphic zircons in the age range 2.09-2.07 Ga in some of these rocks (Table 1).

PALEOPROTEROZOIC MAGMATISM

Since the Paleoproterozoic, SerN has been a relatively well-preserved part of the São Francisco Craton, which is why it is easier to identify the magmatic sucession during this period. At least three distinct magmatic events are identified:

(i) Calc-alkaline Paleoproterozoic Granites (CaG): These rocks are chemically similar to the Archaean plutons (calc-alkaline and TTG associations) although they were emplaced almost 1 Ga later. Eight massifs have been studied: Eficéas, Quijingue, Lagoa dos Bois, Cipó, Teofilândia, Barrocas, Nordestina and Trilhado. The geochronological and isotopic data available for the group (Table 1) show that this magmatic episode was active for almost 30 m.y (2.16-2.13 Ga). Their lithogeochemical features indicate they are related to a collisional event (Rios et al., 1998) suggesting that these rocks could have formed during closure of a back arc basin, that is partly preserved as the IRGB (2.1 to 2.2 Ga; Silva, 1992). If so, they can be considered as plutonic equivalents of the felsic volcanic rocks in IRGB. 2.15 Ga most likely marks the end of extensional magmatism responsible for the generation of the Itapicuru basin and the beginning of its closure. Xenocrysts aged 3.6 Ga and 2.9 Ga are found in rocks of this group and indicate that Archaean crust was involved in their generation (Table 1). Two groups of model ages (T_{DM}) have been found: 2.2 to 2.3 Ga and 3.3 Ga. Most of the rocks from this group show Paleoproterozoic T_{DM} ages (epsilon Nd +1.64 to +2.45) as well as low and variable initial Sr ratios [$^{87}Sr/^{86}Sr$ = 0.7017-0.7025]. These data indicate magmatic generation from a depleted mantle with only small contributions from older crust. Archaean T_{DM} ages were observed only in the Quijingue Massif, the same area where the 3.6 Ga xenocrysts have been identified, showing higher initial Sr ratio (0.7051) and negative epsilon Nd (-11.6), and suggesting an origin where older crustal material predominated. Ring-shaped overgrowths and a younger zircon population (2.09 to 2.05 Ga) indicate a Transamazonian thermal event, strong and intense enough to recrystallize zircons. This event is also registered in the Archaean granites as metamorphic zircon overgrowths (2.07-2.08 Ga) and new zircon grains and may be related to the heat flux that accompanied emplacement of Transamazonian alkaline magmas.

(ii) The Alkaline Magmas (SyG, ShMG and ShKG): In the SerN, silica saturated, potassic alkaline magmas were emplaced over the time span 2105-2070 Ma. These massifs intrude all the older granitic types. Three distinct sub-groups have been observed: syenite (SyG), shoshonitic monzonite (ShMG) and shoshonitic K-rich peraluminous granite (ShKG).

The syenitic massifs Morro do Afonso, Morro das Agulhas-Bananas and Serra do Pintado have crystallization ages ranging from 2.08 to 2.10 Ga. These are small plutons (12-30 km^2) in the southwestern part of SerN, distributed along the 38° coordinate. They are composed of porphyritic alkali-feldspar syenite that shows magmatic flow patterns. The presence of orthocumulates suggests that their evolution involved fractional crystallization processes. Plagioclases are absent and together with lamprophyric dykes (minettes and voguesites) this feature is interpreted as a lamproitic signature. Mixing between felsic and mafic magmas is also thought to be an important process in the evolution of these rocks. The syenites are LILE enriched, and have low contents of HFSE, Nb, Ti and moderate values of Al_2O_3. These features are common in magmas from orogenic environments, where partial melting of subducted crust occurs in the garnet stability zone. The variable and low to moderate initial Sr ratios (0.7022 to 0.7042), as well as negative epsilon Nd values (-2.36 to -4.17) suggest a high-Nd enriched mantle source and storage over a long period in the sub-continental lithosphere. Their model ages (2.58 to 2.69 Ga; T_{DM}) are older than those observed for the CaG, and this may indicate that a subducted slab different from the one related to IRGB generation was associated with the generation of the potassic magmas. Zircon xenocrysts aged 2.6 Ga have been observed and are interpreted as a residue of the magmatic source. Lithogeochemical features indicating a significant interaction with continental crust were not observed.

Shoshonitic magmatism at SerN is represented by metaluminous monzonites (ShMG) and peraluminous K-rich granites (ShKG). These magmas were emplaced over the age range 2106-2071 Ma, and are temporally and spatially associated with the syenitic magmas.

Four monzonitic massifs (ShMG) have been investigated: Euclides, Araras, Cansanção and Itareru. At Araras and Euclides massifs, both located at the Eastern SerN, borders are foliated but the cores are isotropic. The monzonitic rocks from western SerN are less differentiated and occur as separate oval-shaped stocks. These rocks are distinguished from the syenites by the presence of plagioclase crystals. They have similar geochemical characteristics, but are distinct due to their low amounts of alkalis and lower K_2O/Na_2O ratios. Their LILE enrichment (more prominent in the less evolved rocks), high and variable contents of Rb, Sr, Ba, Zr, Nb, Th, Pb, LREE and Y, together with high values for volatile elements suggest that these monzonites could have formed from the same ultrapotassic alkaline magmas that generated the syenites, but with different degrees of assimilation of silica-rich crust. The presence of zircon xenocrysts aged 3.6 Ga (Euclides Massif) and 2.16 Ga (Itareru Massif) also indicates crustal contamination of the shoshonitic magmas. These rocks show variable negative values of epsilon Nd (-2 to -8) and moderate to high initial Sr ratios (0.7030 to 0.7058), which supports the idea of differential assimilation of older material. Their model ages (T_{DM} = 2.55 to 2.96) are a somewhat older than the ones found in the syenitic rocks (Table 1), also suggesting a shallow origin for shoshonitic magmas.

The shoshonitic peraluminous K-rich granites (ShKG) are the last expression of granitic magmatism in the SerN. They were emplaced over a short time span (2.07-2.08 Ga) as numerous small circular or oval shaped stocks and dykes that intrude all other lithologies described above at SerN. The six massifs studied - Marmota, Alto Bonito, Fazenda das Bananas, Maravilha, Barroquinhas and Pedra Vermelha – have post-collisional nature and arc signatures, indicating a strong influence of AFC processes in their evolution (Peixoto, 2000). These are highly fractionated rocks (SiO_2 > 69%) with a fine-texture in which biotite is the predominant mafic mineral. They show variable enrichment in REE, Th, Sr and Zr, as well as negative anomalies of P, Nb and Ti, with smaller amounts of Rb and Sr than the monzonitic rocks. The ShKG show rather low initial Sr ratios (0.7029) but negative epsilon Nd (-4.07 and –10.54), with Archaean model ages (T_{DM} = 2.7 and 3.1 Ga) older than the ones observed in the monzonitic and syenitic rocks of SerN (Table 1).

FINAL REMARKS

Granitic rocks of SerN can be divided into two groups as a function of their ages: (I) Archaean (ArchG) and (II) Paleoproterozoic (CaG, ShMG, SyG, ShKG).

Archaean granitic rocks (ArchG: 3.1-2.8 Ga, with xenocrysts as old as 3.6 Ga) show calc-alkaline and subordinate TTG signatures. They are represented by most of the so called G1-G2 granites and granitic gneisses and migmatites from SerN basement.

Paleoproterozoic rocks are more diverse. They were formed during two episodes. The first was a calc-alkaline/TTG event (CaG - 2.16 to 2.13 Ga for most of the previously called G3 granites), which is probably associated with the closure of the IRGB basin. This was followed by an alkaline event (2.11-2.07 Ga for all of the previously called G4 and G5 bodies) which is preserved as potassic/ultrapotassic (SyG), shoshonitic-monzonitic (ShMG), and shoshonitic peraluminous K-rich (ShKG) granitic plutons.

The SerN was formed during a Paleoproterozoic orogenic cycle that involved reworking of an Archean terrane with an extensive history as well as accretion of juvenile crust. The character of its magmatism at any given time is probably a function of crustal thickness, thermal structure and proximity to active subduction.

ACKNOWLEDGMENTS

This work was supported by CAPES (Process: 1332/98-8), the Royal Ontario Museum, and Companhia Baiana de Pesquisa Mineral. This is contribution number 145 of GPA-CPGG-UFBA.

REFERENCES

Alves da Silva, F.C., 1994. Étude Structural do Greenstone Belt Paleoproterozoique du Rio Itapicuru (Bahia, Brésil). Tese de Doutorado. Université d'Orleans. França. 307p.

Bastos Leal., L.R; Teixeira, W.; Piccirrilo, E.M.; Leal, A.B.M.; Girardi, V.A.V., 1994. Geocronologia Rb-Sr e K-Ar do enxame de diques máficos de Uauá, Bahia, Brasil: Geochim. Brasil., 8: 99-114.

Kroner, A., Ekwueme, B.N. & Pidgeon, R.T. 2001. The oldest rocks in West Africa: SHRIMP zircon age for early Archean migmatitic orthogneiss at Kaduna, northern Nigeria. Journal of Geology, 109: 399-406.

Martin, H.; Sabaté, P.; Peucat, J-J.; Cunha, J.C., 1997. Crustal Evolution in Early Archean of South America: Example of the Sete Voltas Massif, Bahia state, Brazil. Precambrian Research, 82: 35-62.

Matos, F.M.V. & Conceição, H., 1993. Granitogênese associada à parte oeste do Cráton Serrinha e o Greenstone Belt do Rio Itapicuru: Geologia e Tipologia. II Simp. Cráton do São Francisco. SBG/SGM/CNPq, Núcleo Bahia-Sergipe. Salvador -BA. Anais: 60-62.

Mello, E.F., 2000. Estudos isotópicos do Greenstone Belt do Rio Itapicuru, BA: Evolução crustal e metalogenia do ouro. Unpub. Tese de Doutorado, UNICAMP, SP. 162p.

Moyen, J-F.; Martin, H.; Jayananda, M., 2001. Multi-element geochemical modelling of crust-mantle interactions during late-archaean crustal growth: the Closepet granite (South India). Prec. Res., 112: 87-105.

Oliveira, E.P.; Souza, Z.S.; Correia Gomes, L.C., 1999. U-Pb dating of deformed mafic dyke and host gneiss (Uauá Block, NE Sao Francisco Craton, Brazil): Implications for understanding reworking process in Archaean terranes. Proceedings of First International Symposium on Tectonics of the Brazilian Geological Society, Lençois-BA. Abstract-volume.

Peixoto, A.A., 2000. Petrografia, litogeoquímica e idade do magmatismo alcalino metaluminoso a peraluminoso tardio da parte sudoeste do Núcleo Serrinha (Bahia): Granitos Tipo Morro do Lopes. Dissert. Mestrado. CPG em Geologia. Univ. Federal da Bahia. 135p.

Rios, D.C., 2002. Granitogênese no Núcleo Serrinha, Bahia, Brasil: Geocronologia e Litogeoquímica. Tese Doutorado. CPG em Geologia. Univ. Federal da Bahia. 238p.

Rios, D.C.; Conceição, H.; Macambira, M.J.B.; Burgos, C.M.G.; Peixoto, A.A.; Cruz Filho, B.E.; Oliveira, L.L.; Lisboa, M.P., 1998. Granitogênese da parte meridional-oriental do Núcleo Serrinha: idade, petrografia e geoquímica. Pub. Esp. SBG, Núcleo BA-SE. 5:91-113.

Sabaté, P.; Caen-Vachette, M.; Marinho, M.M.; Soares, C.P., 1990. Dados isotópicos Rb-Sr e Sm-Nd da intrusão monzonítica a 2.0 Ga de Cansanção (Bahia-Brasil). XXXVI CBG. Bol. Resumos. Natal-RN. 4: 163.

Silva, M.G., 1992. Evidências isotópicas e geocronológicas de um fenômeno de acrescimento crustal transamazônico no Cráton do São Francisco, Estado da Bahia. XXXVII Cong. Bras. Geol., São Paulo-SP, Bol. Res. Exp, 2: 181-182.

Windley, B.F., 1995. The evolving continents. 3rd. Ed. Chester. John Wiley. 526p.

Table 1. Summary of isotopic data now available for SerN and the new subdivision of its granites.

Present	Former	Massif	Crystallization - Single Zircon Ages (Ma)			T_{DM} (Ga)	ε_{Nd}	Sr_i	U-Pb Ages Data from Single Zircon (Ma)		
			U-Pb	Pb-Pb	SHRIMP				Lower Intercept	Overgrowth	X
ARCHAEAN MAGMATISM											
Basement		Gneiss	3102±5			3.28 [c]	- 0.57	0.7010 [e]	1763	2093	
		Diorite	2793 [c]			2.75	+ 2.89	0.6994		2078	
ArchG	G1	Araci	~ 3070			3.12	+ 0.93	0.6302	310		
	G2	Ambrósio	3088±6						557	2077 [a]	3169
	G2	Pedra Alta				3.17	+ 0.23	0.7000			
	G1	Requeijão	~ 2870						570		
PALEOPROTEROZOIC MAGMATISM											
CaG	G5	Cipó	2164 ± 2	2165 ± 3					886	2088	
	G3	Eficéas	2163 ± 5			2.33	+ 1.64		443		
	G1	Quijingue	2155 ± 3			3.27	- 11.6	0.7051	300		3614 to 3620 and 2891
	?	Trilhado			2155 ± 9	2.22 [a]	+2.41[a]	0.702[a]			
	G1	Teofilândia			2130 ± 7	2.18 [a]	+ 2.45[a]	0.703[a]			
	G1	Barrocas		2127 ± 5 [b]							
	G3	Nordestina		2088 ± 24							
	G3	Lagoa dos Bois	2067 ± 142						315		
ShMG	?	Itareru	2106 ± 2								2162
	G3	Cansanção		2105 ± 2		2.55 [d]	- 2.01	0.703[d]			
	G1	Euclides	2097 ± 8			2.87	- 6.64	0.6940	864		3654
	?	Araras	2076 ± 2			2.96	- 8.12	0.7052	525		
SyG	?	Serra do Pintado	2097 ± 2			2.69	- 4.17	0.7022			
	G4	Morro do Afonso		2098 ± 4 2081 ± 13		2.56 2.58	- 2.36 - 2.80	0.7039 0.7042			2641
	G4	Agulhas/Bananas		2086 ± 9							
ShKG	G1	Pedra Vermelha	2080 ± 7						452		
	G5	Alto Bonito	2076 ± 6						470		
	?	Barroquinhas	2073 ± 1			3.13	- 10.54	0.6882			
	G5	Faz.Bananas (GML)	2072 ± 1						410		
	?	Maravilha	2071 ± 1			2.67	- 4.07	0.7029			2098 and 2087
	G5	Marmota (GML)		2003 ± 2							3002

Now = Nomenclature related to this Actual Stratigraphical Proposal for SerN Granites; Before = Nomenclature proposed by Matos & Conceição (1993) and Rios et al. (1998); ArchG = Archaean Granites; CaG = Calc-alkaline Granites; ShMG = Shoshonitic Granites; SyG = Syenitic Granites, ShKG – Shoshonitic peraluminous K-rich Granites

a = Mello (2000);
b = Alves da Silva (1994);
c = Oliveira et al. (1999)
d = Sabaté et al. (1990);
e = Bastos Leal et al. (1994)

ARCHEAN CRUST FORMATION IN INAJÁ RANGE AREA, SSE OF AMAZONIAN CRATON, BRAZIL, BASED ON ZIRCON AGES AND Nd ISOTOPES

Rolando, A.P. and Macambira, M.J.B.

Laboratório de Geologia Isotópica – Pará-Iso – UFPA, Belém, Pará, Brazil. rolando@ufpa.br, moamac@ufpa.br

Keywords: Amazonian craton, Inajá Range, Archean, granite-greenstone terrain, Pb and Nd isotopes

INTRODUTION

During the past ten years, several authors using U, Pb and Nd isotope data considered the Carajás Metalogenic Province (CMP) the result of successive events of crustal growth from 3.10 Ga to the end of Archean. The southern part of the CMP is formed by Rio Maria, Gradaús and Inajá ranges areas. According to Rolando & Macambira (2002), the Rio Maria and Inajá Range regions could have one similar evolution during the Archean, based on geochronology of granitoids. In the Inajá Range area, there is not clear field relationship, and the geochronological studies are only based in Rb-Sr and Pb-Pb results on whole rocks and minerals (Barbosa & Lafon, 1996).

In this study, we define seven new ages for granitoids and one for meta-basalt using Pb-Pb and U-Pb on zircon and the Sm-Nd on whole rock from granite-greenstones of the Inajá Range area.

GEOLOGICAL SETTING

The Archean terrain of the Inajá Range area (Fig. 1) consists of tonalites-trondhjemite (Arco Verde Tonalite), greenstone sequence (Serra of Inajá Group) and calc-alkaline granitoids (Mata Surrão Monzogranite and Rio Maria Granodiorite). Evidence of pre-3.0 Ga crust was not reported in the Inajá Range, but in Rio Maria area is attested by inherited zircon in magmatic rocks (Machado et al., 1991) and detritical zircons (Macambira & Lancelot, 1991).

The Arco Verde Tonalite is a typical tonalite-trondhjemite suite with an emplacement age of 2.95 Ga in the Inajá Range region (Rolando & Macambira, 2002). These rocks have isotropic igneous to strongly foliated textures. The greenstone belt sequence (Serra of Inajá Group) is composed by meta-ultramafic, metamafic (basalts and gabbros) rocks, and BIF (Neves & Vale, 1999). The stratigraphic position of these volcano-sedimentary sequences is correlated with that of the Rio Maria area, where the age was established between 2.90 and 3.00 Ga (Pimentel & Machado, 1994; Macambira & Lancelot, 1996; Souza et al., 2001). Using Nd isotope composition, Souza et al. (2001) showed that partial melting of depleted mantle produced the rocks of the greenstone belt in the Rio Maria region.

The Rio Maria Granodiorite is weakly foliated and mainly predominantly granodioritic in composition. A Pb-Pb zircon age of 2.87 Ga has been determined for a granodiorite sample from the northern part of the Inajá Range (Rolando & Macambira, 2002). The other Archean granitoid that crops out in the study area is Mata Surrão Monzogranite which is a medium-grained equigranular pink and weakly deformed. This was dated by Pb-Pb zircon method, in the northern part of the Inajá Range, at 2.85 Ga (Rolando & Macambira, 2002). Other lithostratigraphic units reported in the region correspond to Paleoproterozoic clastic sedimentary cover (Rio Fresco Group) and 1.8 Ga anarogenic granite plutons (Neves & Vale, 1999).

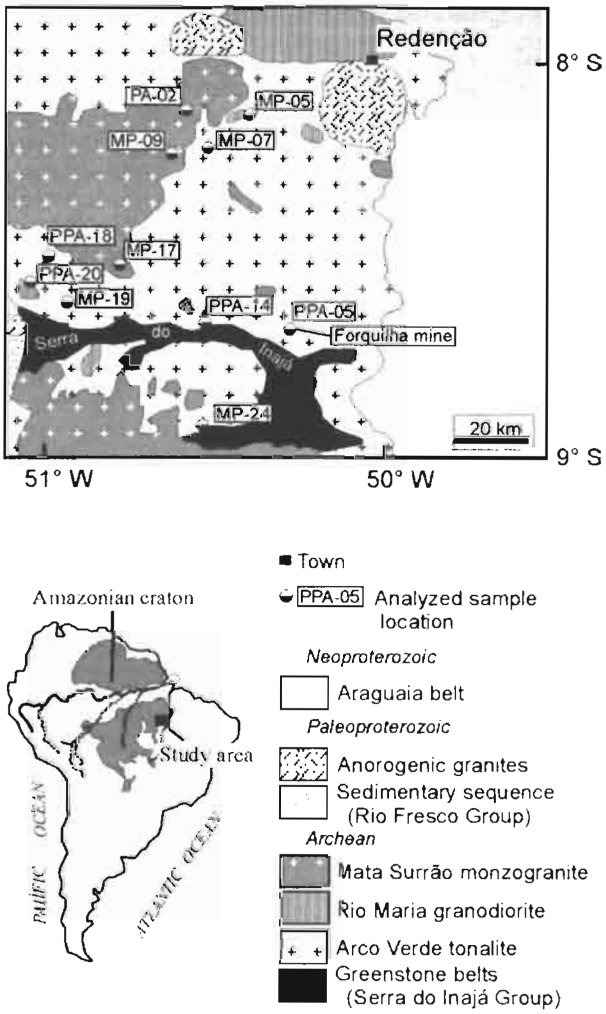

Figure 1. Schematic geological map of the Inajá Range area, southeasthern Amazonian Craton (after Neves & Vale, 1999).

ANALYTICAL METHODS

Analyses of Pb-Pb on zircon, and U-Pb and Sm-Nd on whole rock (Table 1) were carried out at the Pará-Iso Laboratory of the Federal University of Pará, Brazil. Isotopic ratios were determined using a multicolector Finnigan MAT 262 mass spectrometer.

RESULTS

Pb-Pb AND U-Pb RESULTS

A mafic metavolcanic rock from the Serra of Inajá Group (MP-24, see sample localization on Fig. 1) was analyzed by U-Pb zircon method. Granites of Mata Surrão type out crop nearby this metavolcanic rock and provocated an amphibolite metamorphism. The sample is poor in zircon and only five crystals were analyzed. Four grains are discordant on a concordia diagram, except one concordant crystal that yielding an age of 2.988 ± 4 Ma.

Four samples of the Arco Verde Tonalite yielded age of 2.948 ± 7, 2.981 ± 8, 2.965 ± 1 and 2.988 ± 5 Ma, and established a period of ca. 30 and 50 m.y. to this granite genesis.

Two samples of the Mata Surrão Monzogranite, located at northern of the Inajá Range yielded ages of 2875 ± 11 Ma and 2881 ± 2 Ma. The presence of the xenocrystals yielding ages between 2.90-2.98 Ga in these samples indicate the interaction of the magma with older rocks, possibility the Arco Verde Tonalite.

The samples MP-05, PA-02, PPA-20 and PPA-05 from the Rio Maria Granodiorite yielded ages of 2877 ± 6 Ma, 2880 ± 4 Ma, 2881 ± 8 Ma and 2875 ± 7 Ma, respectively. The PPA-05 sample was collected from a pit in the Fourquilha gold mine (Fig. 1), where the contact with greenstone host rock is unknown. The zircon from this rock shows a variety of form and size, and usually composed of rim and nucleus. These crystals presented at the highest temperature of evaporation the ages up to 3.10 Ga. The crystals that defined the age of crystallization of the granodiorite (2.88 Ga) seem to not have nucleus.

Sm-Nd RESULTS

The samples of the greenstone volcanic rocks present ^{143}Nd/^{144}Nd ratios between 0.5117 and 0.5130, and ^{147}Sm/^{144}Nd ratios between 0.1486 and 0.2036. The $\varepsilon_{ND(t)}$ values calculated to 2.99 Ga are positive between 1.67 and 5.78. It was only possible to calculate the T_{DM} for the sample PPA-03 (3.02 Ga) due to for the high ^{143}Nd/^{144}Nd ratios. It was not possible to calculate an isochron with the samples from the greenstones because the lack of the correlation.

Table 1. Pb-Pb, and U-Pb on zircon and Sm-Nd on whole-rock isotopic data for granitoids, metabasalts and metagabbros from the granites-greenstone terrain of the Inajá Range region, southeastern Amazonian Craton. Zr: zircon; [1] age of xenocrystal.

Sample	Rock type	Method	Age (Ma)	^{147}Sm/^{144}Nd	^{143}Nd/^{144}Nd	$\varepsilon_{ND(t)}$	T_{DM}
Greenstone belt (Serra do Inajá Group)							
MP-21B	Metabasalts			0.20359	0.513029	5.02	-
MP-24	Metabasalts	U-Pb (Zr)	2.988 ± 4	0.17866	0.512577	5.78	-
PA-04	Metagabbro			0.19673	0.512783	2.84	-
PPA-03	Metagabbro			0.14863	0.511777	1.67	3.02
Arco Verde Tonalite							
MP-07	Tonalite	Pb-Pb (Zr)	2.948 ± 7	0.06553	0.510136	1.56	3.02
PPA-18	Tonalite	Pb-Pb (Zr)	2.981 ± 8	0.09800	0.510783	1.72	3.01
PPA-14	Saprolite	Pb-Pb (Zr)	2.965 ± 1				
MP-19	Tonalite	Pb-Pb (Zr)	2.988 ± 5				
Mata Surrão Monzogranite							
MP-09	Monzogranite	Pb-Pb (Zr)	2.881 ± 2				
			2930-2960 [1]	0.06062	0.510156	1.89	2.90
MP-17	Monzogranite	Pb-Pb (Zr)	2.875 ± 11				
			2900-2980 [1]	0.13699	0.511535	0.56	3.05
Rio Maria Granodiorite							
MP-05	Granodiorite	Pb-Pb (Zr)	2.877 ± 6	0.09616	0.510706	-0.53	3.07
PA-02	Diorite	Pb-Pb (Zr)	2.880 ± 4				
PPA-20	Granodiorite	Pb-Pb (Zr)	2.881 ± 8				
			3070 ± 6 [1]	0.08484	0.510556	0.74	2.97
PPA-05	Tonalite	Pb-Pb (Zr)	2.875 ± 7				
			2970-3100[1]				
MP-22	Granodiorite			0.09768	0.510731	-0.61	3.07

The Archean granitoids of the Inajá Range region show model ages concentrate between 2.90 and 3.07 Ga (Table 1). Two samples from the Arco Verde Tonalite show $^{143}Nd/^{144}Nd$ ratios between 0.5107 and 0.5110, $\varepsilon_{ND(t)}$ between +1.56 and +1.72, and model ages (T_{DM}) between 3.01 and 3.02 Ga. The $^{143}Nd/^{144}Nd$ ratios of the Rio Maria Granodiorite and Mata Surrão Monzogranite are between 0.5101 and 0.5115, $\varepsilon_{ND(t)}$ between -0.61 and +1.89, and model ages (T_{DM}) between 2.90 and 3.07 Ga.

DISCUSSION

The Nd isotopic compositions obtained for the Arco Verde Tonalite and mafic rocks from the greenstone belt of the Inajá Range show that these rocks derived mainly from the mantle. The $\varepsilon Nd_{(t)}$ values confirm a depleted mantle source for their protoliths.

Rocks older than 3.00 Ga were not reported in this region of the Amazonian Craton, but xenocrystals and zircon with nucleus up to 3.10 Ga are observed in two samples (PPA-20 and PPA-05) from the Rio Maria Granodiorite. The model age (T_{DM}) of the analyzed granitoids show that the extraction from the mantle was in the period between 2.97 and 3.07 Ga.

According to preliminary data, the age of 2988 ± 4 Ma (U-Pb on zircon) for mafic metavulcanic of the Serra of Inajá Group indicated that these rocks are coeval with those of the Andorinhas Super-Group of the Rio Maria region (Pimental and Machado, 1994). The intervals for the formation of the Arco Verde Tonalite, between 2.40 and 2.99 Ga, overlap that proposed to the emplacement of volcanic and sedimentary rocks that conform the greesntone belt of the Inajá Range.

The Sm-Nd model ages and the Pb-Pb zircon ages of the samples of the Arco Verde Tonalite are coherent and demonstrate that the magma was extracted from the mantle ca. 3.00 b.y. ago closed its emplaced into the crust (2.94-2.99 Ga). The Rio Maria Granodiorite and Mata Surrão Monzogranite rock source was separated from mantle at 2.90-3.07 Ga and was finally emplaced at 2.87-2.88 b.y. ago. The Rio Maria Granodiorite shows evidences of crustal contamination as some T_{DM} values lightly negative (-0.6), and the presence of xenocrystals.

Finally, the obtained zircon ages and the Sm-Nd data for the Archean Inajá Range granite-greenstone terrain confirm the similarity between this region and Rio Maria regions.

ACKNOWLEDGEMENTS

Fieldwork was supported by PROINT/UFPA and CNPq projects. The authors are especially grateful to Pablo Monteiro for his help in the fieldwork, and Robert Krymsky and Marco T. Galarza for assistances in U-Pb and Sm-Nd analytical work. The first author thanks the CNPq for his DCR (Desenvolvimento Científico Regional) fellowship. This work is a PRONEX/UFPA Project contribution.

REFERENCES

Barbosa, A.A. & Lafon, J.M., 1996. Geocronologia Pb-Pb e Rb-Sr de granitóides Arqueanos da região de Redenção – sul do Pará. Revista Brasileira de Geociências, 26 (4): 255-264.

Macambira, M.J.B. & Lancelot, J.R., 1991. Em busca do embasamento arqueno da região de Rio Maria, sudeste do estado do Pará. III Simpósio Geológico Amazônico, Belém, SBC, 49-58.

Macambira, M.J.B. & Lancelot, J.R. 1996. Time Constraints for the Formation of the Archean Rio Maria Crust, Southeastern Amazonian Craton, Brazil. International Geology Review, 38: 1134-1142.

Machado, N., Lindenmeyer, Z., Krogh, T.E., Lindenmeyer, D., 1991. U-Pb geochronology of Archaean magmatism and masement reactivation in the Carajás area. Amazon shield, Brazil. Precambrian Researche 49, 329-354.

Neves, A.P. & Vale, A.G., 1999. Programa Levantamentos Geológicos Básicos do Brasil. Folha SC.22-X-A Redenção. Estado do Pará e Tocantins. Escala 1:250.000 – CPRM, Brasilia.

Pimentel, M.M. & Machado, N., 1994. Geocronologia U-Pb dos terrenos granito-greenstone de Rio Maria, Pará. Congresso Brasileiro de Geologia, Camboriú, 2: 390-391.

Rolando, A.P. & Macambira, M.J.B. 2002., Geocronologia dos granitóides arqueanos da região da Serra do Inajá: novas evidencias sobre a formação da crosta continental no sudeste do cráton amazônico, SSE Pará. XLI Congresso Brasileiro de Geologia, 525.

Souza, Z.S., Potrel, A., Lafon, J.M., Althoff, F.J., Pimentel, M.M., Dall'Agnol, R., Oliveira, C.G., 2001. Nd, Pb and Sr isotopes in the Identidade Belt, an Archaean greenstone belt of the Rio Maria region (Carajás Province, Brazil): implications for the Archaean geodynamic evolution of the Amazonian Craton. Precambrian Research, 109:293-315.

PROVENANCE OF DETRITAL CLAY MINERALS OF THE CONTINENTAL RIFT OF SOUTHEASTERN BRAZIL: MINERALOGICAL AND Sm-Nd DATA

Sant'anna, L.G.[1]; Riccomini, C.[2]; Dantas, E.[3]; Fetter, A.H.[4]; Roig, H.L.[5,3] and Hackspacher, P.C.[6]

1. Post-Doctoral fellow of FAPESP-GSA/IGUSP, Rua do Lago 562, 05508-080, São Paulo-SP, Brazil. lsantann@hotmail.com
2. GSA/IGUSP – Research fellow of CNPq. riccomin@usp.br
3. IG – UnB, ICC-Centro, Campus Universitário Darcy Ribeiro Asa Norte, 70910-900 Brasilia-DF, Brazil. elton@unb.br
4. Post-Doctoral fellow of FAPESP-IGCE/UNESP, 13506-900, Rio Claro-SP, Brazil. fetter@ms.rc.unesp.br
5. DGA-FGEL/UERJ. roig@unb.br
6. DPM/IGCE/UNESP - Research fellow of CNPq. phack@ms.rc.unesp.br

Keywords: Paleogene, clay minerals, provenance, Nd isotopes, Brazil

INTRODUCTION

Following the global changes occurred at the K/T boundary, the Paleogene was marked by worldwide paleogeographic reorganizations (Pomerol, 1982; Berggren et al., 1985). At this time, the opening of the South Atlantic Ocean was still in progress, resulting in the generation of several sedimentary basins along the Brazilian coast. The sedimentary rocks of the Continental Rift of Southeastern Brazil (CRSB) are the most complete record of the geological events developed in the onshore area during this period. The provenance of these sedimentary deposits was studied, with emphasis placed on the mineralogy of the clay minerals and recognition of their possible source areas based on Nd isotopic signatures of whole rock and clay (finer than 2 microns) fraction from the central segment of the CRSB.

GEOLOGICAL SETTING

The Continental Rift of Southeastern Brazil (CRSB) (Riccomini, 1989), of Cenozoic age, is an ENE-trending, elongate, narrow trough, about 1000 km long, that stretches from Curitiba (Paraná) in the WSW to Barra de São João (Rio de Janeiro) in the ENE (Fig. 1). The CRSB was formed as a result of late processes related to the break-up of Gondwana, separation of South America from Africa and the opening of the South Atlantic Ocean. In the early Tertiary, NNW-SSE regional extension, related to thermomechanical tilting of the adjoining offshore Santos basin, reactivated ENE shear zones within the Precambrian basement leading to the generation of continental half-grabens.

The sedimentary filling, syn-tectonic to the NNW-SSE extension, is mainly represented by Eocene-Oligocene alluvial siliciclastic rocks (conglomerates, sandstones and mudstones) deposited in an alluvial fan system. Oligocene lacustrine claystones and shales are interfingered with the alluvial sediments in the central portion of the CRSB.

MATERIALS AND METHODS

The studied samples were collected in several outcrops in the central segment of the CRSB (Taubaté and Resende basins) and in a core drilled in the central part of the Taubaté Basin (Fig. 1).

Mineralogical analyses, including petrographic studies, X-ray diffraction and scanning electron microscopy, were developed in the laboratories of the IGUSP. All Nd isotopic analyses were carried out in the Geochronology Laboratory of the UnB, after sample dissolution in the laboratories of the IGCE/UNESP.

MINERALOGICAL AND GEOCHEMICAL RESULTS

Mudstones and claystones in the CRSB are massive and made up essentially of detrital smectite and interstratified illite-smectite (I/S). Mica and kaolinite occur in variable proportions and quartz and feldspar are the main sand-grained clasts in these rocks. The smectite and I/S are platy and relatively coarse-grained (plates coarser than 5 microns in diameter), with slightly undulated boundaries (Sant´Anna, 1999).

T_{DM} model ages obtained for whole rock mudstones and claystones of the central segment of the CRSB vary between ca. 1.8 and 2.2 Ga (Table 1). These values indicate the Precambrian basement as the main source area, for which Proterozoic to Archean T_{DM} model ages were already recorded (e.g. Sato & Campos Neto, 1996; Tassinari & Sato, 1996; Cordani & Sato, 1999). The analyzed clay fraction of lacustrine claystone also displays Proterozoic model age (ca. 1.9 Ga). Younger model age of ca. 1.3 Ga was obtained only for whole rock of alluvial mudstone probably derived from mixed source areas, the Precambrian rocks and Late Cretaceous alkaline massifs (which have T_{DM} model ages around 0.8 Ga).

DISCUSSIONS AND CONCLUSIONS

At the end of the Late Cretaceous and beginning of the Paleogene the relief was low due to the development of the South American Planation Surface (King, 1956). In this geomorphologic context, the origin of the detrital smectite and I/S is attributed to chemical weathering processes forming paleosols by the alteration of the Precambrian basement rocks of CRSB probably during the Early Tertiary. Late Cretaceous alkaline massifs may have contributed only locally. The smectitic paleosols were transported into the continental half-grabens by mudflows in an alluvial fan system during the Eocene-Oligocene, passing laterally and upwards to lacustrine conditions, in the Oligocene (Riccomini et al., 1996; Sant´Anna, 1999).

Eocene sediments of the offshore basins, São Paulo Plateau and Rio Grande Rise are abundant in detrital smectite, considered as supplied from emerged South American continent (Robert, 1987). Geological, mineralogical and geochemical data obtained for the smectitic clay minerals of the CRSB indicate that landmasses in southeastern Brazil probably acted as a major source area to the detrital clay sedimentation in western South Atlantic during this time.

ACKNOWLEDGMENTS

Thanks are due to FAPESP, grants 02/00811-4, 97/12091-6, 99/00358-3, 00/03960-5).

REFERENCES

Berggren, W.A.; Kent, D.V.; Flynn, J.J., 1985. Jurassic to Paleogene: Part2. Paleogene geochronology and chronostratigraphy. In: Snelling, N.J. (ed) 1985. The Chronology of the Geological Record. Geological Society Memoir 10, p.141-186.

Codani, U.G. & Sato, K., 1999. Crustal evolution of the South American Platform, based on Nd isotopic systematics on granitoid rocks. Episodes, 22:167-173.

King, L.C., 1956. A geomorfologia do Brasil oriental. Revista Brasileira de Geociências, 18:147-265.

Pomerol, C., 1982. The Cenozoic Era. Tertiary and Quaternary. Chichester, Ellis Horwood, 272p.

Riccomini, C., 1989. O Rift Continental do Sudeste do Brasil. São Paulo, 256p. (Tese de doutoramento apresentada ao Instituto de Geociências da Universidade de São Paulo).

Riccomini, C.; Coimbra, A.M.; Sant'Anna, L.G.; Brandt Neto, M.; Valarelli, J.V., 1996. Argilominerais do paleolago Tremembé e sistemas deposicionais relacionados (Paleógeno, Rift Continental do Sudeste do Brasil). Revista Brasileira de Geociências, 26:167-180.

Robert, C., 1987. Clay mineral associations and structural evolution of the South Atlantic: Jurassic-to- Eocene. Palaeogeography, Palaeoclimatology, Palaeoecology, 58:87-108.

Sant´Anna, L.G., 1999. Geologia, mineralogia e gênese das esmectitas dos depósitos paleogênicos do Rift Continental do Sudeste do Brasil. São Paulo, 293p. (Tese de doutoramento apresentada ao Instituto de Geociências da Universidade de São Paulo).

Sato, K. & Campos Neto, M.C., 1996. Dados dos principais eventos de acreção manto-crosta continental no sudeste brasileiro, baseado em idades modelo Sm-Nd. In: Congresso Brasileiro de Geologia, 39, Salvador, BA. Anais. Salvador, SBG/BA, v.6, p.528-530.

Tassinari, C.C.G. & Sato, K., 1996. Idades de formação decrosta continental na parte sudeste do Estado de São Paulo, com base em dados Sm-Nd. In: Congresso Brasileiro de Geologia, 39, Salvador, BA. Anais. Salvador, SBG/BA, v.6, p.489-492.

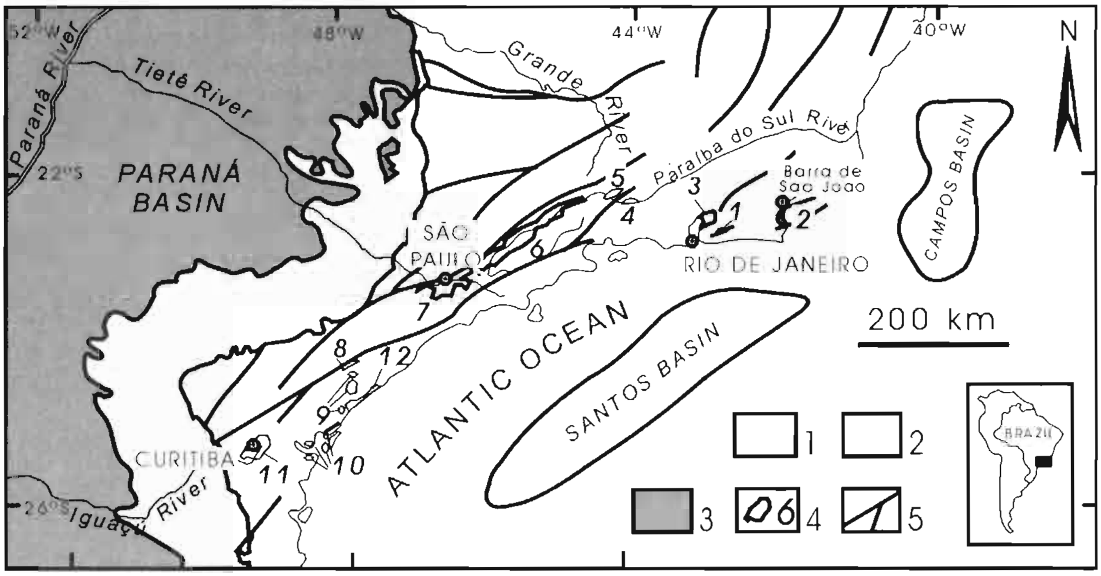

Figure 1. Regional context of the CRSB (Riccomini et al., 1996): 1) Precambrian basement; 2) Paleozoic and Mesozoic sedimentary deposits of Paraná basin; 3) Mesozoic flood basalts, Serra Geral Formation; 4) Tertiary basins and associated deposits of the CRSB (1- Itaboraí basin, 2- Barra de São João graben, 3- Macacu basin, 4- Volta Redonda basin, 5- Resende basin, 6- Taubaté basin, 7- São Paulo basin, 8- Sete Barras graben, 9- Pariqüera-Açú Formation, 10- Alexandra Formation, 11- Curitiba basin, 12- Guaraqueçaba graben); 5) Precambrian shear zones, partially reactivated in the Mesozoic and Cenozoic.

Table 1. Sm-Nd data of sedimentary rocks from the Taubaté and Resende basins.

Sample n°.	Basin	Sm(ppm)	Nd(ppm)	^{147}Sm/^{144}Nd	^{143}Nd/^{144}Nd (± 2SE)	ε(o)	T_{DM} (Ga)
TB50C	Taubaté	11,11	57,89	0,1160	0,511800±32	-16,34	1924
CNP96	Taubaté	7,998	42,752	0,1131	0,511771±13	-16,91	1913
TB534RA	Taubaté	6,632	36,345	0,1103	0,11767±22	-16,99	1867
TB534RA (< 2μm)	Taubaté	6,724	37,043	0,1097	0,511738±10	-17,56	1900
QZ18	Taubaté	56,088	378,44	0,0896	0,511975±21	-12,93	1304
CNP 270	Taubaté	6,772	37,223	0,1100	0,511743±06	-17,46	1897
CNP 314	Taubaté	6,699	36,968	0,1095	0,511727±09	-17,77	1912
CNP 688	Taubaté	3,965	23,054	0,1040	0,511731±09	-17,69	1809
CNP 711	Taubaté	6,691	36,03	0,1123	0,511730±06	-17,71	1959
CNP 738	Taubaté	11,315	65,818	0,1039	0,511728±07	-17,74	1812
CNP 763	Taubaté	5,90	34,16	0,1044	0,511752±06	-17,28	1786
CNP 806	Taubaté	5,34	34,10	0,0946	0,511717±25	-17,96	1685
CNP 818	Taubaté	9,76	55,45	0,1064	0,511693±07	-18,44	1904
RE 10A	Resende	13,072	82,43	0,0959	0,512010±07	-12,26	1328
CNP 33	Taubaté	4,418	25,502	0,1047	0,511703±08	-18,23	1860
CNP 46	Taubaté	6,116	35,44	0,1043	0,511727±06	-17,77	1821
CNP 148	Taubaté	5,743	32,49	0,1068	0,511675±32	-18,78	1937
CNP 289	Taubaté	5,123	28,71	0,1079	0,511725±07	-17,81	1884
RE 14	Resende	5,508	32,85	0,1013	0,511536±06	-21,50	2032
RE 16	Resende	24,274	122,325	0,1200	0,511707±06	-18,16	2160

U-Pb SHRIMP AGES OF THE SERTÂNIA COMPLEX: IMPLICATIONS ON TECTONIC FRAMEWORK OF THE TRANSVERSAL SUBPROVINCE, NORTHEAST BRAZIL

Santos, E.J.[1]; **Nutman, A.P.**[2] **and Brito Neves, B.B.**[3]

1. Geology Departament, Center of Technology and Geoscience, Federal University of Pernambuco
2. Research School of Earth Sciences, Australian National University
3. Mineralogy and Geotectonic Department, Geoscience Department, São Paulo University

Keywords: Geochronology, basement tectonics, Brasiliano province, Borborema Province, Northeast Brazil

INTRODUCTION

Concepts recently developed in the Borborema Province, Northeast Brazil, has envisaged a complex evolution in which terranes of different ages were amalgamated by several events culminating in two successive orogenies in the Late Precambrian. Around three major subprovinces are recognized (Van Schmus et al. 1995; Brito Neves et al. 2000), each one of them comprising terranes of different tectonic patterns and ages (Santos 1996). The Northern subprovince is greatly an wide basement composite terrane involving Archean and Paleoproterozoic blocks and Neoproterozoic linear belts. The Transversal subprovince is made up mainly by Stenian to Tonian terranes placed tectonically side by side to Brasiliano belts, which surround Paleoproterozoic inliers. The Southern subprovince corresponds to the external marginal domain relative to the São Francisco cratonic area in the south, including foreland and hinterland monocyclic belts. The Transversal subprovince includes several supracrustal belts mainly of Cariris Velhos (around 1,0 Ga) and Brasiliano (ca. 0,6 Ga) ages (Brito Neves et al., 1995) but high grade terranes contains also a sedimentary component of unknown age. One of these paragneisses is referred as Sertânia Complex, described originally in the region of the Rio Moxotó valley, state of Pernambuco (Santos, 1977). The Sertânia Complex is formed essentially by high grade migmatitic supacrustals that are typical of the Alto Moxotó terrane (figure 1), although some questions about the relationships with the São Caetano Complex of the Cariris Velhos age yet remain in some areas. This paper presents the first geochronologic data of the Sertânia Complex, in order to aid the tectonostratigraphic comprehension of this important lithotectonic domain of the Borborema Province.

LITHOSTRATIGRAPHIC PATTERNS

The Sertânia Complex is a sedimentary sequence including a subordinate volcanic component, metamorphosed in upper amphibolite conditions, occurring in the Alto Moxotó terrane, Transversal Subprovince of the Borborema Province (figure 3). In the type area environs of the Sertânia town, the complex is formed essentially by migmatites of metapelitic protholith, including sillimanite-in or sillimanite-out garnet-biotite schists, in places carrying a volcanoclastic component, interlayered with marble, minor quartzite, calc-silicate rock and amphibolite (figure 1). In the Sumé (PB) region, the garnet-biotite schists contain abundant lenses of marble and they are lesser migmatized. In the westernmost the supracrustals grade to quartzite-rich facies, and includes also BIF´s and mafic metavolcanics. According to Santos et al (2002), the Sertânia Complex was intruded by tonalitic and trondhjemitic sheets, in places described as Camalaú suite. One sample of alkali-feldspar granitic orthogneiss and two ones of migmatitic metagraywacke and schist of were collected at the region of Aroeiras (PB) (figure 3) for geochronologic purposes. The sample of the São Luís farm (SPP-GN-FSL) is a garnet-biotite-plagioclase schist with disperse quartz porphyroblasts, besides titanite, apatite, zircon and opaque minerals. The zircon of this sample shows well crystallized crystals largely with an oscillatory zoning parallel to margin of crystals (figure 2) suggesting a magmatic or volcanoclastic origin (probably dacitic to quartz andesitic tuffs). Another sample of the same region (SPP-GN-BXS) is a plagioclase-rich gneiss, including also quartz and Ti-rich biotite and occasional sillimanite with a similar composition. The sample SPP-GN-PER is a microcline-rich migmatite with a dominant leucosome matrix and relict of a garnet-plagioclase-quartz schist mesosome, typically of sedimentary origin.

ANALYTICAL PROCEDURES

SHRIMP operating calibrations of data, analytical errors and calculation of dates Zircon U-Pb isotopic data were obtained from the Australian National University (ANU) SHRIMP I instrument using a ca. 25 µm spot with a mass-filtered 02-primary íon beam. A mass resolution of 5,500 to 6,000 (at 1% peak height) was used for analysis. Details of the analytical procedure are presented by Stern (1998) and Williams (1998). Due to effects such as the differential yield of metal and oxide species between elements during sputtering, inter-elements ratios are calibrated with a standard, where the ratios are known by isotope dilution thermal ionisation mass spectrometry (IDITMS). This calibration method is explained fully by Stern (1998) and Williams (1998). Thus ^{206}Pb/^{238}U ratios have an error component (typically 1.5 to 2.0%) from calibration of the measurements using the standard zircons. U abundance was calibrated against 238 ppm U (<±10%) fragments of the single crystal SL13 standard and Pb/U was calibrated against the multicrystal standard AS57 of 1,100 Ma; Paces and Miller 1993). All errors take into account non-linear fluctuations in ion counting rates beyond that expected from counting statistics (e.g.

Stern 1998). The decay constants and present-day $^{238}U/^{235}U$ value given by Steiger & Jäger (1977) were used to calculate dates. For suites Neoproterozoic zircons of lower U (≤1,500 ppm), the most reliable dates considered to be those derived from $^{206}Pb/^{238}U$ ratios, following correction for common Pb by the ^{207}Pb method (Compston et al 1984) and use of the Cummings & Richards (1975) model Pb composition for the likely age of the zircons. For Neoproterozoic higher U zircons suites, where matrix contrasts with the standard zircons can make the calibration of U/Pb unreliable, most confidence is placed in $^{207}Pb/^{206}Pb$ dates, following correction for common Pb based on measured ^{204}Pb. For assessment of dates on older zircons, most reliance is placed on $^{207}Pb/^{206}Pb$ dates on sites with close to concordant dates, following correction for common Pb based on measured ^{204}Pb. Pooled dates calculated in this paper are weighted means (analysis inverse-variance weighted, 95% confidence and rounded to the nearest million year), basing on grouping of sites interpreted from CL (cathodoluminescence) images to belong to one generation of zircon. The dates were calculated using the program Isoplot/Ex of Ludwig (1998). U abundances and Th/U of analyzed sites are only discussed when considered important for interpretation of isotopic data. Data are presented as $^{238}U/^{206}Pb$ versus $^{207}Pb/^{206}Pb$ "Tera-Wasserburg" plots.

GEOCHRONOLOGIC DATA

It were analyzed zircon populations of the SPP-GN-FSL and SPP-GN-PER. The SPP-GN-FSL sample yielded mostly prismatic zircons, up to 200μm long. In CL images many of these display oscillatory zoning subconcordant to the exterior of the grains (figure 2). They commonly have thin partial overgrowths, which appear bright and homogeneous in CL images. A minority of the grains show oscillatory zoning strongly truncated at grain boundaries. Nine analyses are undertaken on 9 grains. All 6 analyses of oscillatory zoned zircons yielded a $^{207}Pb/^{206}Pb$ weighted mean date of 2,126±26 Ma (95% confidence, MSWD=0.14) (figure 3). One analysis of a bright homogeneous rim yielded dates within error of this, whilst analyses of two other grains also of bright rims yielded younger discordant dates. The sample is clearly dominated by Paleoproterozoic zircons of igneous origin and restricted age, which were affected by subsequent metamorphism and disturbance, probably in the Neoproterozoic. The sample SPP-GN-PER contained oval to somewhat rounded prismatic zircons, up to ~250μm long (figure 2). In CL images many grains display oscillatory zoning. This is generally subconcordant with the exterior of the grains, but in some cases it has been truncated. Some grains have overgrowths, which appear homogeneous to weakly oscillatory-zoned in CL images. Sixteen analyses were undertaken on 15 grains. Most sites on oscillatory zoned zircon yielded close to concordant dates, with $^{207}Pb/^{206}Pb$ dates between ~2,200 and 1,950 Ma (figure 3). These grains are interpreted as derived from a Paleoproterozoic terrane dominated by rocks formed in a short period. Given the apparent lack of abrasion of these grains, they were probably not transported far in a sedimentary system. Two analyses of overgrowths yielded much younger dates. Although these not define a precise date, they clearly indicate zircon overgrowth during metamorphism in the Neoproterozoic. The SSP-GN-BJL sample (orthogneiss) data (8 analyses) all produce a model 1 regression of 2,016±27 Ma, 393±150 Ma intercepts, MSWD=0.6 (figure 3). Alternatively, the 4 closest to concordant analyses give a weighted mean $^{207}Pb/^{206}Pb$ date of 2,008±21 Ma, 95% confidence, MSWD=0.8. The ca. 2,000 Ma dates are alternative calculations on the age of igneous zircons in this sample. The 393±150 Ma lower intercept in the regression is an indication of early Palaeozoic to Late Neoproterozoic disturbance. The behavior of Nd isotopic data of both orthogneisses and supracrustals of the Alto Moxotó terrane is also similar. The Aroeira and Sertânia samples show model ages Nd T_{DM} of 2,4 Ga, however samples of other localities exhibit ages around 2,6 Ga, all with negative εNd parameter, clearly indicating an Archean source yet not known in this terrane. The most of Rb-Sr data of the Alto Moxotó rocks plots on reference isochron of 2,190 Ma (Brito Neves et al 2001), supporting the influence of the Transamazonian event in this terrane.

DISCUSSION AND CONCLUSIONS

The ages obtained for orthogneisses and supracrustals of the Alto Moxotó terrane confirm this tectonic segment represent a distinct domain within the Transversal subprovince framework, which is dominated by Cariris Velhos and Brasiliano belts. However recent chemostratigraphic and Pb-Pb ages obtained in marbles of the Alto Pajeú and Alto Moxotó terranes have suggested a Cariris Velhos age for sedimentation and metamorphism of the supracrustals of both terranes (V.H. Santos et al 2002). We believe these more new ages resulted of metamorphic disturbances operating in O and C systems under influence of the Cariris Velhos and/or Brasiliano events acting on both domains.

REFERENCES

Brito Neves, B.B.; Van Schmus, W.R.; Santos, E.J.; Campos Neto, M.C.; Kozuch, M. 1995. O evento Cariris Velhos na Província Borborema. Rev. Bras. Geoc. 25:279-296.

Brito Neves, B.B.; Santos, E.J.; Van Schmus, W.R. 2000 Tectonic history of the Borborema Province. In: Cordani, U.G. et al (Eds.) 2000 Tectonic evolution of the South American Platform. 31st Internat. Geol. Congress, p.151-182.

Brito Neves, B.B.; Campos Neto, M.C.; Van Schmus, W.R.; Fernandes, T.M.G.; Souza, S.L. 2001. O terreno Alto Moxotó no leste da Paraíba ("Maciço Caldas Brandão"). Rev. Bras. Geoc. 31(2):185-194.

Compston, W.; Williams, I.S.; Myer, C. 1984. U-Pb geochronology of zircons from lunar breccia 73217 using a sensitive high mass-resolution ion microprobe. Journ. Geophys. Research 89B:525-534.

Cumming, G.L.; Richards, J.R. 1975. Ore lead ratios in a continuously changing Earth. Earth Planetary Science Letters 28:155-171.

Ludwig, K.R. 1998. Isoplot/Ex. Berkeley Geochronology Center Special Publication 1.

Paces, J.B.; Miller, J.D.Jr. 1993. Precise U-Pb ages of Duluth Complex and related mafic intrusions, northeastern Minnesota: Geochronological insights to physical, petrogenetic, paleomagnetic, and tectonomagmatic processes associated with the 1.1 Ga midcontinent rift system. Journal Geophysical Research 98:13997-14013.

Santos, E.J. 1977 Síntese da geologia precambriana da folha Arcoverde, Pernambuco. Simp. Geol. Nordeste 8, Atas p.225-245.

Santos, E.J. 1996. Ensaio preliminar sobre terrenos e tectônica acrescionária na Província Borborema. Cong. Bras. Geol. 39, Anais 6:47-50.

Santos, E.J.; Ferreira, C.A.; Silva Jr., J.M. 2002. Geologia e recursos minerais do estado da Paraíba. Secretaria de Minas e Metalurgia/PB & CPRM-Serviço Geológico do Brasil, Prog. Levant. Geol. Básicos do Brasil, 142p.

Santos, V.H.; Ferreira, V.P.; Sial, A.N.; Babinski, M.; Pimentel, M.M. 2002 C, Pb and Sr isotopic chemostratigraphy in Proterozoic carbonate sequences in the eastern Transversal domain of the Borborema Province, Northeast Brazil. Congresso Brasileiro de Geologia 41, Anais, p. 509.

Steiger, R.H.; Jäger, E. 1993. Subcommission on geochronology: Convention on the use of decay constants in geo- and chosmochronology. Earth Planet Science Letters 36:359-362.

Stern, R.A. 1998. High resolution SIMS determination of radiogenic trace isotope ratios in minerals. In: L.J. Cabri and D.J. Vaughan (editors). Modern approaches to ore and environmental mineralogy. Mineralogical Association of Canada Short Course Series 27:241-268.

Van Schmus, W.R.; Brito Neves, B.B.; Hackspacher, P.; Babinski, M. 1995 U/Pb and Sm/Nd geochronological studies of eastern Borborema Province, northeastern Brazil: initial conclusions. J. S. Am. Earth Sci., 8:267-288.

(a) (b) (c)

Figure 1. Stromatic and folded migmatites of the Sertânia Complex from the type area: (a) general view of the folded migmatite; (b) preserved piece of metavolcanoclastics in migmatized garnet-biotite schist developing a pegmatitic leucosome along the contact between both two lithologies; (c) amphibolite relict in folded mimatite with metapelitic mesosome.

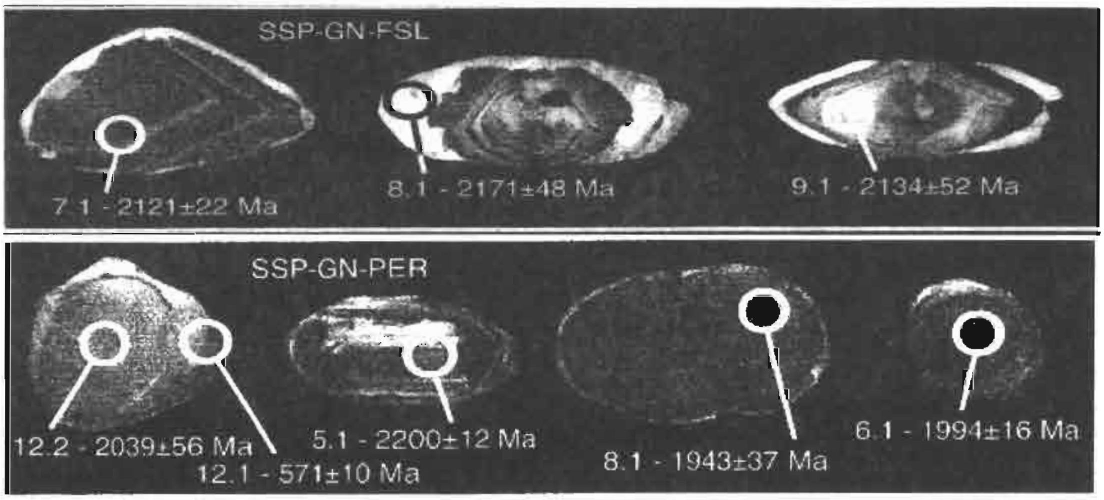

Figure 2. Cathodoluminescence images of zircons of the supracrustals of the Sertânia Complex. Sample SPP-GN-FSL volcanoclastic schist of the São Luís farm; SPP-GN-PER garnet-biotite schist of the Pereiro farm.

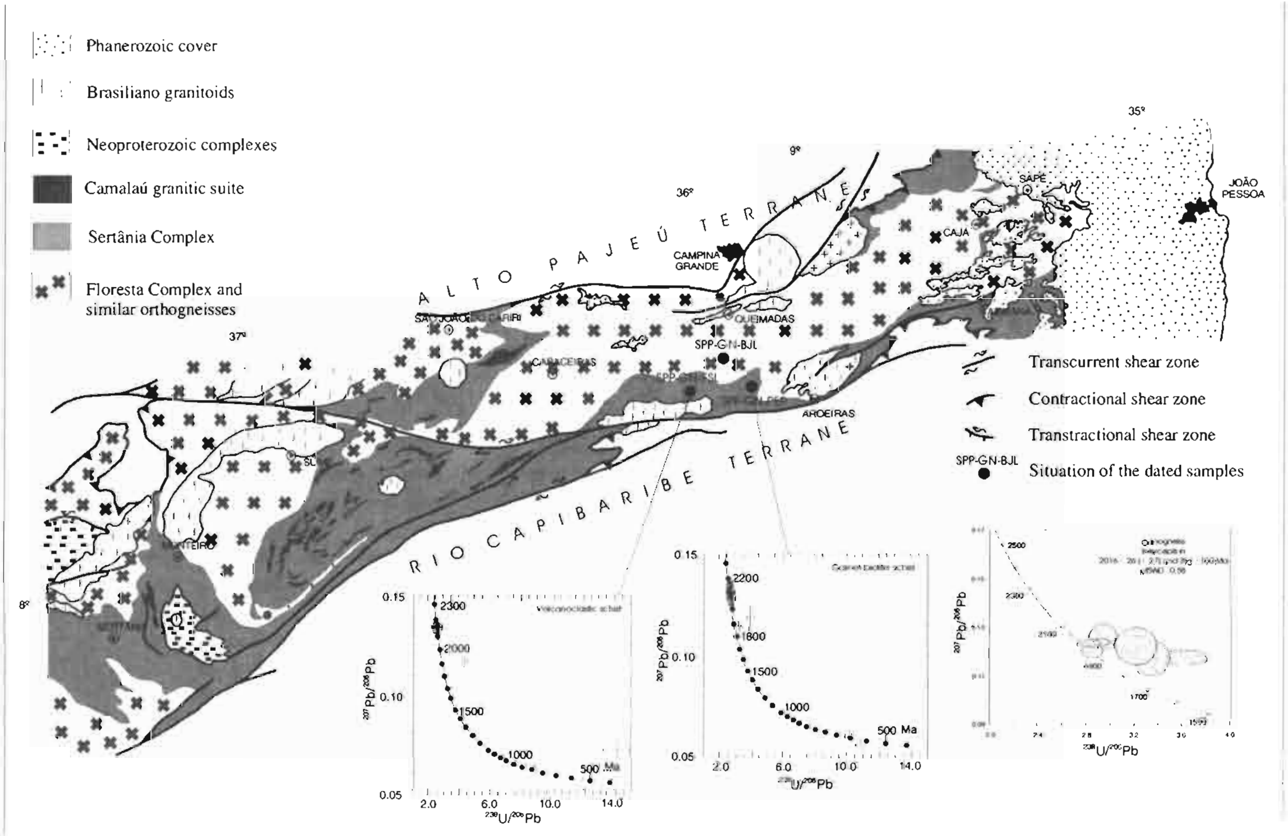

Figure 3. Simplified geological map of the Alto Moxotó terrane, showing the distribution of the Sertânia Complex and the situation of the dated samples (geology according Santos et al., 2002).

PALEOPROTEROZOIC EVOLUTION OF NORTHWESTERN RORAIMA STATE – ABSENCE OF ARCHEAN CRUST, BASED ON U-Pb AND Sm-Nd ISOTOPIC EVIDENCE.

Santos, J.O.S.[1]; Reis, N.J.[2]; Chemale, F.[3]; Hartmann, L.A.[3]; Pinheiro, S.S.[2] and McNaughton, N.J.[4]

1. Companhia de Pesquisa de Recursos Minerais, Rua Banco da Província 105, Porto Alegre-RS. orestes1@uol.com.br
2. Companhia de Pesquisa de Recursos Minerais, Av. André Araújo 2160, Manaus-AM
3. IG/Universidade Federal do Rio Grande do Sul, Av. Bento Gonçalves 9500, Agronomia, Porto Alegre-RS
4. Centre for Global Metallogeny, Crawley 9007, Western Australia, Australia

Keywords: U-Pb geochronology, detrital zircon, Amazon Craton, Roraima State, Tracajá orogeny

INTRODUCTION

The northwestern Roraima region – the Parima Mountains – is one of the least known regions in the world. Reconnaissance studies identified two main units in the Parima region basement: The Urariqüera Complex (Pinheiro et al., 1981; CPRM, 2002) and the Parima Group (Arantes & Mandetta, 1970). Parima Group is an association of green schist facies volcano-sedimentary rocks and amphibolite facies paragneisses. The Urariqüera Complex is an amphibolite facies orthogneiss unit including amphibolites and granitoid. Based on reconnaissance field data, the Parima Group was interpreted as a greenstone belt of Archean (Pinheiro et al., 1981) or Paleoproterozoic (Reis et al., 1994; Gaudette et al., 1996) age. Some authors (Tassinari & Macambira, 1999; Tassinari et al., 2000) propose the existence of a large Archean block in northern Roraima and southeastern Venezuela (the Roraima block), while others include the Parima Group in the Trans-Amazonian Orogeny (Reis et al., 1994; Gaudette et al., 1996). To investigate the question of the basement age in northwestern Roraima region (Archean or Trans-Amazonian) we dated two zircon samples of the Parima Group by U-Pb SHRIMP and seven whole rock samples of the Urariqüera Complex and two samples of the Parima Group using Sm-Nd isotopes.

This abstract reports the results of the U-Pb and Sm-Nd dating and provides a new interpretation for the Parima Group as well as for the Amazon Craton evolution.

REGIONAL GEOLOGY

The Parima Group crops out in the basins of the following rivers: Parima, Auaris, and Mucajaí, Catrimâni and Urariqüera headwaters (Fig. 1). The unit is geographically associated to the Urariqüera Complex composed by orthogneiss, metabasalt and granitoid. Both units are cut by Mesoproterozoic rapakivi granites (Surucucus suite) and mafic-ultramafic bodies (Tapuruquara magmatism) and covered by Mesoproterozoic sedimentary outliers (Serra Surucucus Formation; Santos et al., 2003a). Field and remote sensing data indicate dominant NW-SE to E-W lineaments and sinistral transcurrent movements (Reis & Fraga, 2000). The rocks present at the type-area (lower course of Parima River) are green schist facies meta-andesite, meta-rhyodacite and meta-pyroclastic rocks (Arantes and Mandetta, 1970). Amphibolite facies rocks are present in Couto Magalhães, Parima, and Uatatás rivers headwaters (mostly sillimanite-cordierite paragneisses; Nunes, 1992). The stratigraphic relationship between Parima Group and Urariqüera Complex is unknown and both units show the same style of deformation. The orthogneisses are referred to the complex and the paragneisses are associated to the group.

Uatatás quartzite sample is from Uatatás River headwater (Fig. 1) and was collected in a green schist facies meta-sedimentary sequence compose by orthoclase quartzite, quartz-biotite phyllite, and carbonate quartzite, light to dark grey and fine grained. This sequence is well laminated and interpreted as turbiditic (Reis et al., 1994). Prainha meta-andesite comes from Prainha Creek, a Mucajaí River tributary (Fig. 1). It displays an E-W nematolitic foliation is has actinolite-andesine assemblage (green schist facies).

METHODS

We dated zircon from two samples and integrate the results will all available U-Pb data of the region (Table 1). The two selected samples for U-Pb study are a meta-andesite from Prainha Creek (JO2) and a low grade metamorphosed fine sandstone (LM6). Zircon analyses were carried out on the SHRIMP II at the Curtin University of Technology following standard procedures (Smith et al., 1998; Santos et al., 2000). Reference standard was CZ3 zircon (564 Ma; $^{206}Pb/^{238}U=0.0914$). All presented U-Pb ages are $^{207}Pb/^{206}Pb$ ages. Sm-Nd analyses (Table 2) were done on the Isotopic Geology Laboratory at the Federal University of Rio Grande do Sul. Decay constants used are those recommended by Steiger and Jägger (1977).

RESULTS AND DISCUSSION

The Prainha meta-andesite (JO2) zircons are clear prisms without evidence of older cores. They compose a single population and 13 of 14 analyses are concordant and group at the $^{207}Pb/^{206}Pb$ age of 1946 ± 7 Ma (MSWD=1.6; Fig. 2). This age is about 20-10 m.y. younger than the ages of the rocks formed during the Creporizão orogeny (Santos et al., 2003b), such as the Surumu Group and the Pedra Pintada suite (Orocaima volcano-plutonism, Reis et al., 2000). It is comparable to the ages of several rocks from eastern Roraima State (Rio Urubu Complex, this paper), such as the Tracajá Granodiorite (1941 ± 4 Ma; recalculated from Gaudette et al., 1996) and two metamorphic rocks: the Mucajaí

Gneiss (1938 ± 8 Ma; J.O.S. Santos, unpublished data), the Barauana anatexite (1943 ± 7 Ma; J.O.S. Santos, unpublished data), and the Vilhena mylonite (1937 ± 7 Ma; J.O.S. Santos, unpublished data).

Nineteen zircon crystals from the Uatatás quartzite (LM6) yield concordant to sub-concordant results and two grains are Archean (2869 ± 7 Ma and 2795 ± 9 Ma). Disregarding the eventual removal of large areas of the Amazon Craton since the Archean, the only possible source for those two grains is the Imataca Belt of Venezuela, located about 650 km to the north-northeast. The remaining 17 analyses form four populations with ages from 2203 to 1968 Ma (Fig. 3). Three age groups of 2203 ± 6 Ma (n=5), 2141 ± 5 Ma (n=2), and 2097 ± 14 Ma (n=5) are probably derived from the Trans-Amazonian belt to the north-northeast. The younger group is clearly post-Trans-Amazonian in age (1968 ± 7 Ma) considering the duration of that orogen as 2.26-2.01 Ga (Santos et al., 2003b). This age constrains the maximum possible age for the Uatatás quartzite and the Parima Group. There are two possible main sources for this population. One possibility is the volcano-plutonic rocks cropping out to the east and northeast of the Parima Group Basin, such as the Pedra Pintada Suite and the Surumu Group (1966 Ma; Schobbenhaus et al., 1994). Another possibility is the metamorphic rocks from the Cauarane Group such as the Taiano gneiss molten at 1969 ± 4 Ma (J.O.S. Santos, unpublished data). The ages near 1968 Ma (Surumu, Pedra Pintada, Uatatás) are correlative to the rocks formed during the Creporizão orogeny of the Tapajós domain. Distinctly from the Tapajós domain, the Creporizão orogeny in Roraima is formed not only by volcano-plutonic rocks in a continental arc environment, but it encloses metassedimentary rocks produced in a collisional setting (Uatatás quartzite), Which may be correlative to the Muruwa (Guyana) and Los Caribes (Venezuela) Formations (Gibbs & Barron, 1993; Reis et al., 2000).

The Sm-Nd data for the Urariqüera Complex (Table 2) suggest a derivation from Trans-Amazonian rocks (T_{DM} model ages of 2178-2022 Ma) and a short crustal residence interval (ε_{Nd} greater than zero). The T_{DM} model ages of two Parima Group paragneisses correspond to one Late Neoarchean age (2502 Ma) and one Early Siderian age (2485 Ma), Table 2. These paragneisses may have several sedimentary sources, as shown in the Uatatás quartzite and the two model ages of 2502 and 2485 Ma probably have no geological meaning being the result of a mixture of Nd isotopes of several sources, Archean and Paleoproterozoic.

CONCLUSIONS

The isotopic results indicate that the Parima and Urariqüera units are not Archean nor Rhyacian (Trans-Amazonian) in age, but much younger, Orosirian (ages between 1.97-1.94 Ga). This fact has important implications for the interpretation of the Amazon Craton evolution and for the absence of a large Archean block named the Roraima Block (extension of the Central Amazon Province) in northern Roraima-southeastern Venezuela region (Tassinari et al., 2000). There are two main possibilities for the Archean Roraima Block: a) the rocks older than 2.3 Ga form very small bodies undetected by the regional mappings or b) Archean rocks are totally absent and the Roraima Block crust was formed after ca. 2.1 Ga.

The interpreted sources to the Uatatás quartzite deposition were Trans-Amazonian and Archean rocks located far to the north-northeast (about 650 km) and Orosirian rocks located relatively close (300-150 km) from the Creporizão orogeny to the east and northeast. The maximum age of 1968 Ma precludes any correlation of the Parima Group to Archean or Trans-Amazonian rocks as stated in the past. The absence of detrital zircon crystals having similar ages to the neighboring Prainha meta-andesite (JO2) may suggest that the Uatatás quartzite was deposited before 1940 Ma during the 1968-1940 Ma period. The age of the youngest population (1968 ± 7 Ma) of detrital zircon and the ages of the Orocaima volcano-plutonism (Reis et al., 2000) are typical ages of the Creporizão orogeny of the Tapajós domain, which is dominated by a continental arc environment. The data here presented suggest an extension of that orogeny to the Parima domain.

The Prainha andesitic volcanism at 1946 ± 7 Ma is synchronous with both magmatic (Tracajá and Rio Urubu) and metamorphic (Taiano, Barauana, and Vilhena) events to the east of Roraima State. These events are post-Creporizão in age and no equivalents have been found in the Tapajós Domain. They represent another orogeny in the Tapajós-Parima Orogeny between the Crepozizão (1970-1960 Ma) and Tropas (1900-1890 Ma) orogenies. This orogeny has an important collisional component and is here named the Tracajá orogeny.

REFERENCES

Almeida, M.E., Fraga, L.M.B., and Macambira, M.J.B., 1997a. New geochronological data of calc-alkaline granitoids of Roraima State, Brazil. In: South-American Symposium on Isotope Geology, Campos do Jordão, 1997. Resumo, p. 34-37.

Almeida M.E., Ferreira A.L., Pinheiro S.S., 2001. Principais Associações Graníticas do Oeste do Estado de Roraima. In: Sociedade Brasileira de Geologia-Núcleo Norte, Simpósio de Geologia da Amazônia, 7, Belém, Pará. Sessão Workshop II, 4 p.

Arantes J.L. & Mandetta P., 1970. Reconhecimento geológico dos rios Urariqüera, Aracaçá, Parima e Uauaris, Território federal de Roraima. Departamento Nacional da Produção Mineral, Relatório Inédito 6012, Manaus, 10 p.

Companhia de Pesquisa de Recursos Minerais, 2002. Geologia e Recursos Minerais da Amazônia Brasileira: Sistema de Informações Geográficas - SIG e Mapa na escala 1:1.750.000. In: Luiz Augusto Bizzi, Carlos Schobbenhaus, João Henrique Gonçalves, Franciscus Jacobus Baars, Inácio de Medeiros Delgado, Maísa Bastos Abram, Reginaldo Leão Neto, Gerson Manoel Muniz de Matos, João Orestes Schneider Santos (ed.), Brasília: 1 CD-Rom

Fraga L.M., & Reis N.J., 2002. The Calc-Alkaline Volcano-Plutonism in the Northern Roraima State, Guiana Shield: Implications for the Uatumã Event Concept and Geotectonic Significance. In: Simpósio sobre Vulcanismo e Ambientes Associados, 2, Belém, PA, Anais: 15.

Gaudette, H.E., Olszewski Jr., W.J., and Santos, J.O.S., 1996. Geochronology of Precambrian rocks from the northem part of Guiana Shield, State of Roraima, Brazil. Journal of South American Earth Sciences, 9 (3/4): 183-195.

Gibbs, A.K. & Barron, C.N., 1993. The Guiana Shield reviewed. Episodes, 1983 2:7-14.

Nunes, N.S.V., 1992. Reavaliação petrográfica das amostras coletadas por Arantes & Mandetta (1970) ao longo dos rios Parima, Auaris, Urariqüera e Aracaçá. Porção Oeste do Estado de Roraima. Companhia de Pesquisa de Recursos Minerais, Superintendência Regional de Manaus. Relatório Interno R-111a, 11 p.

Pinheiro, S.S., Nunes, A.C.B., Costi, H.T., Yamaguti, H.S., Faraco, M.T.L., Reis, N.J., Menezes, R.G., Riker, S.R.L., Wildner, W., 1981. Projeto Catrimâni-Urariqüera: Relatório de Progresso. Manaus, Departamento Nacional da Produção Mineral/Companhia de Pesquisa de Recursos Minerais, v.II-B: p.399-401.

Reis, N.J., Fraga, L.M.B., Pinheiro, S.S., 1994. Reconhecimento Geológico da Região do rio Uatatás - setor oeste do Estado de Roraima. In: Sociedade Brasileira de Geologia-Núcleo Norte, Simpósio de Geologia da Amazônia, 4, Belém, Pará. Anais: 33-36

Reis N.J., Faria M.S.G., Fraga L.M.B., Haddad R.C. 2000. Orosirian Calc-Alkaline volcanism and the Orocaima Event in the northern Amazonian Craton, Eastern Roraima State, Brazil. Revista Brasileira de Geociências, 30 (3): 380-383.

Santos, J.O.S, Hartmann, L.A., Gaudette, H.E., Groves, D.I., McNaughton, N.J., Fletcher, I.R., 2000. A new understanding of the provinces of the Amazon Craton based on integration of field mapping and U-Pb and Sm-Nd geochronology. Gondwana Research, 3(4): 453-488.

Santos, J.O.S., Rizzotto, G., Easton, M.R., Potter, P.E., Hartmann, L.A., McNaughton, N.J., 2002. The Sunsás Orogen in Western Amazon Craton, South America and correlation with the Grenville Orogen of Laurentia, based on U-Pb isotopic study of detrital and igneous zircons. In: Geological Society of America, 2002 Denver Annual Meeting (October 27-30, 2002), Precambrian Geology, paper 122-8.

Santos, J.O.S., Potter, P.E., Reis, N.J., Hartmann, L.A., Fletcher, I.R., McNaughton, N.J., 2003a. Age, source and regional stratigraphy of the Roraima Supergroup and Roraima-like outliers in northern South America based on U-Pb geochronology. Geological Society of America Bulletin 115 (3): 331–348.

Santos, J.O.S, Hartmann, L.A., Bossi, J., McNaughton, N.J. Fletcher, I.R., 2003b. Duration of the Trans-Amazon Cycle in South America based on U-Pb SHRIMP geochronology of La Plata Craton, Uruguay. International Geology Review 45 (1): (in press).

Tassinari, C.C.G. and Macambira, M.J.B., 1999. Geochronological Provinces of the Amazonian Craton. Episodes, 22 (3): 174-182.

Tassinari, C.C.G., Bettencourt, J.S., Geraldes, M.J.B., Macambira, M.J.B., Lafon, J.M., 2000. The Amazonian Craton. In: U.G.Cordani, E.J.Milani, A.Thomaz Filho, D.A Campos (eds) Tectonic Evolution of South America. In: International Geological Congress, 31, Rio de Janeiro, p. 41-95.

Table 1. Ages and data of rocks discussed along text.

Sample	Rock	Unit	U-Pb age	MSWD	zircon type	Event	Reference
JO2	Meta-andesite	Parima group	1946 ± 7	1.60	igneous	Tracajá	This work
JO1	Granodiorite	Tracajá	1941 ± 4*	0.25	igneous	Tracajá	Gaudette et al. (1996)
SR6	Anatexite	Barauana	1943 ± 7	1.90	igneous	Tracajá	J.O.S. Santos, unpublished
CA47	Mylonite	Vilhena	1937 ± 7	2.60	igneous	Tracajá	J.O.S. Santos, unpublished
MF6	Gneiss	Mucajaí	1941 ± 5	1.40	igneous	Tracajá	J.O.S. Santos, unpublished
LM6	Quartzite	Parima	1968 ± 7	1.50	detrital	Orocaima	This work
SUR1	Rhyodacite	Surumu	1965 ± 4*	2.40	igneous	Orocaima	Schobbenhaus et al. (1994)
JOSP1b	Paragneiss	Taiano	1969 ± 4	0.13	metamorphic	Orocaima	J.O.S. Santos, unpublished
SR109	Gneiss	Rio Urubu	1966 ± 37	-	igneous	Orocaima	Fraga et al. (1997)**
NR17	Monzogranite	Igarapé Azul	1960 ± 21	-	igneous	Orocaima	Almeida et al. (1997)**
JO180	Monzogranite	Creporizão	1957 ± 6	1.46	igneous	Creporizão	Santos et al. (2001)

Location of most samples shown in Figure 1. MSWD=Mean Standard Weighted Deviation; (*) recalculated age; (**) Pb-Pb data

Table 2. Sm-Nd data of Urariqüera Complex and Parima Group

Sample	Rock	Unit	Latitude	Longitude	T_{DM} model ages	ε_{Nd}
EC-130B	meta-tonalite	Urariqüera	2.76275	-62.07874	2022	+ 2.04
GM-116	Gneiss	Urariqüera	4.07650	-64.35228	2116	+ 0.73
EC-118	meta-tonalite	Urariqüera	2.77987	-61.99956	2090	+ 1.47
WW-111	Gneiss	Urariqüera	3.98505	-64.41337	2096	+ 0.63
SP-34A	meta-diorite	Urariqüera	3.56576	-63.17108	2136	+ 0.79
NR-49B	meta-tonalite	Urariqüera	3.06571	-62.57815	2172	+ 0.01
EC-26	Gneiss	Urariqüera	2.79648	-63.11364	2178	+ 0.82
WW-125	two mica gneiss	Parima	3.98075	-64.27467	2485	- 4.37
AB-47	cord-sill gneiss	Parima	3.85390	-63.74418	2502	- 4.86

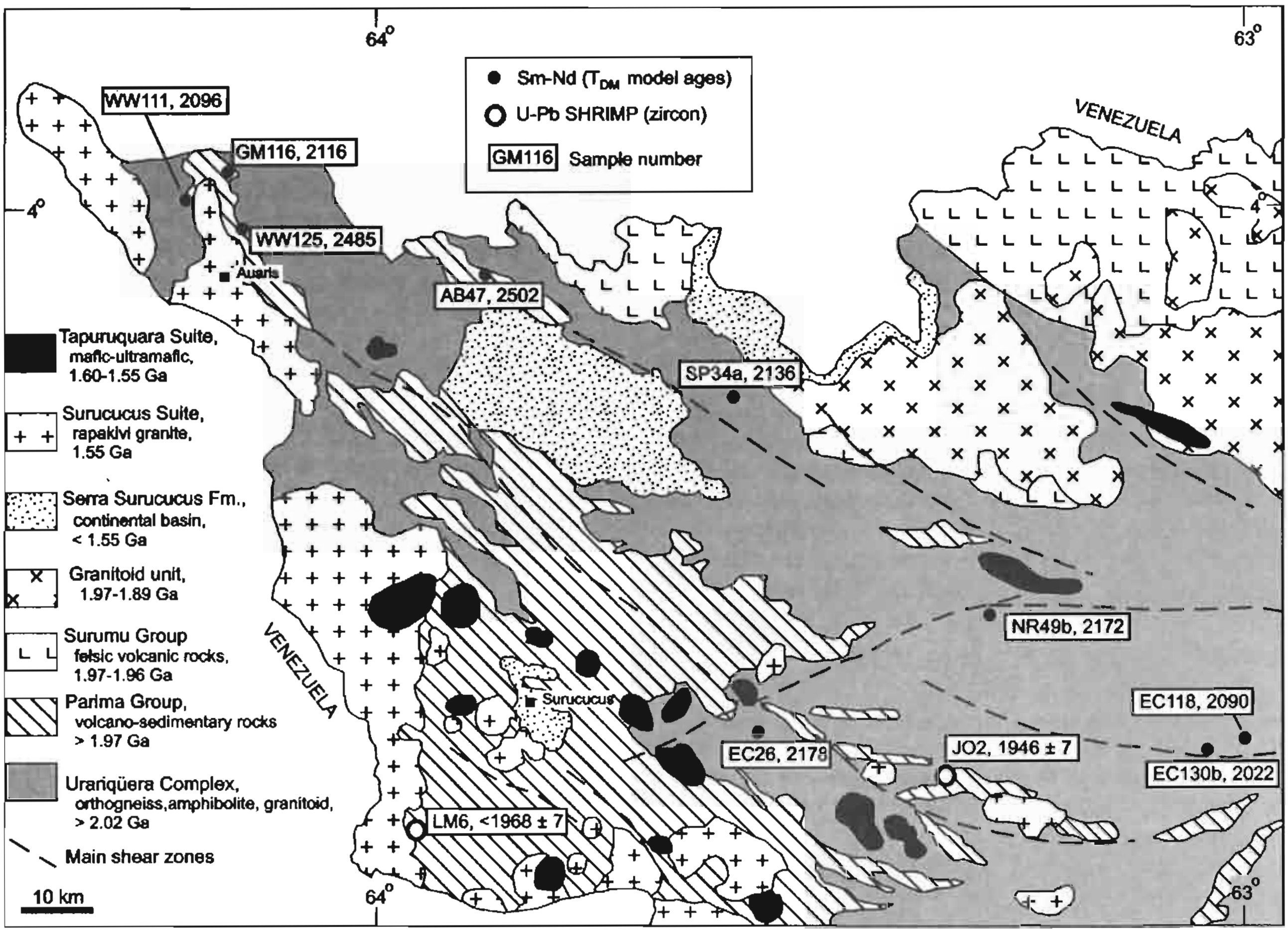

Figure 1. Geological map of northwestern Roraima State showing location of dated samples (ages in Ma).

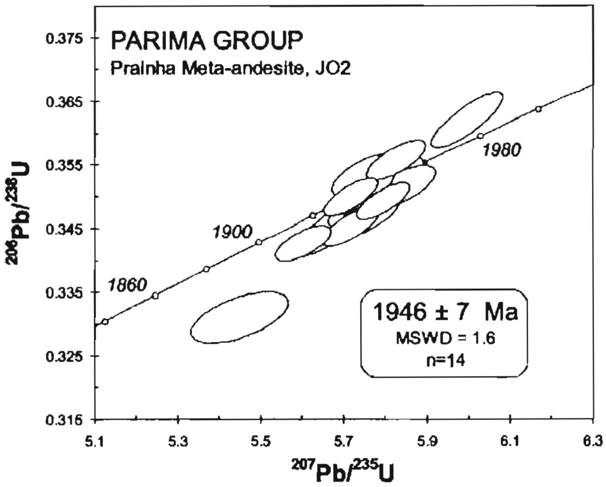

Figure 2. U-Pb concordia diagram for zircon from the Prainha Meta-andesite (JO2), Parima Group.

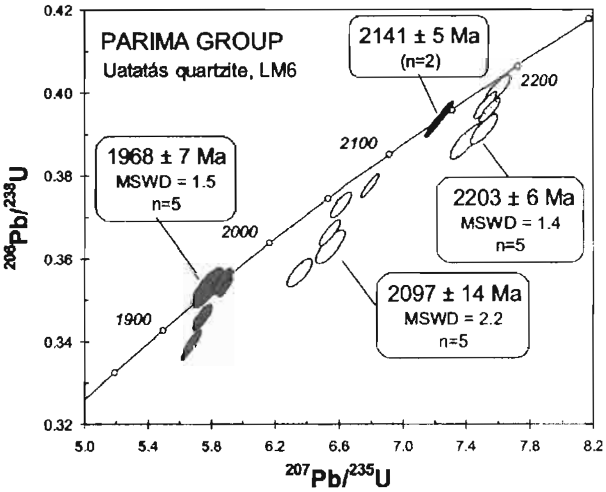

Figure 3. U-Pb concordia diagram for detrital zircon from the Uatatás quartzite (LM6), Parima Group. Two Archean ages are not shown here.

THREE DISTINCTIVE COLLISIONAL OROGENIES IN THE SOUTHWESTERN AMAZON CRATON: CONSTRAINTS FROM U-Pb GEOCHRONOLOGY

Santos, J.O.S.[1]; Rizzotto, G.J.[2]; Chemale, F.[3]; Hartmann, L.A.[3]; Quadros, M.L.E.S.[2] and McNaughton, N.J.[4]

1. Companhia de Pesquisa de Recursos Minerais, Rua Banco da Província 105, Porto Alegre-RS, 90110-150. orestes1@.uol.com.br
2. Companhia de Pesquisa de Recursos Minerais, Rua Lauro Sodré 2561, 78904-300, Porto Velho-RO
3. Instituto de Geociências, Universidade Federal do Rio Grande do Sul, Av. Bento Gonçalves 9500, 91501-970, Porto Alegre, Rio Grande do Sul, Brazil
4. Centre for Global Metallogeny, Crawley 9007, Western Australia, Australia

Keywords: Zircon, U-Pb geochronology, SW Amazon Craton, Collisional orogeny

INTRODUCTION

The characterization of major orogenies in the SW Amazon Craton is an issue of major importance for the evolution of the craton and Amazonia continent. The Southwestern Amazonian Craton contains the Rondônia-Juruena (1850-1540 Ma) and Sunsás (1450-980 Ma) provinces (Santos et al., 2000), which include both orogenic and post-orogenic rock associations. Two domains compose the Rondonia-Juruena Province: the Jamari Domain to the west and the Roosevelt-Juruena Domain to the east (Fig. 1). The Jamari Domain is formed by two main units: the orogenic Jamari Complex (1.76-1.75 Ga; Tassinari et al., 1996; Santos et al., 2000) and the post-orogenic Serra da Providência Intrusive Suite (1.58-1.53 Ga; Tassinari et al., 1996; Santos et al., 2000; Bettencourt et al., 2001; Payolla et al., 2002). The Serra da Providência Suite includes rapakivi-like granites and charnockitoids, which are not discriminated in the geological maps. The Jamari Complex has two main groups of rocks formed in two distinct environments: a tonalite-quartz diorite association possibly related to an island arc environment and an assemblage of high metamorphic grade metassedimentary rocks, such as kingzigite and paragneiss suggestive of a collisional orogenic environment. Both Serra da Providência and Jamari units are strongly affected by a much younger collisional event of the Sunsás Orogen producing mylonite gneisses and augen gneisses and making difficult the discrimination between the orogenic and post-orogenic rocks. This paper investigates the Jamari Complex to establish: a) the timing of the older collision, which formed the kinzigite-paragneiss association, and b) the timing of the younger collision affecting both Serra da Providência and Jamari units.

METHODS

We present the results of zircon geochronology of five rock samples and integrate the results with all available U-Pb isotopic data in the region (Table 1). The five rock samples selected for this investigation are three samples from Jamari Complex (JL78, GR59 and GR35); one sample from Serra da Providência (GR333), and one sample from the Sunsás belt (JS39). We used BSE images to select zircon for U-Pb analyses, picking grains showing evidence of possible metamorphic rims. Zircon analyses were carried out on the SHRIMP II at the Curtin University of Technology following standard procedures (Smith et al., 1998; Santos et al., 2000). Reference standard was CZ3 zircon (564 Ma; $^{206}Pb/^{238}U=0.0914$). We present here only $^{207}Pb/^{206}Pb$ ages. Sm-Nd isotopes were analyzed in the Laboratório de Geologia Isotópica, Universidade Federal do Rio Grande do Sul, Porto Alegre. Decay constants used are those recommended by Steiger & Jägger (1977).

RESULTS AND DISCUSSION

The Jamari Complex zircon crystals have the following magmatic ages (Table 1): 1752 ± 14 Ma (JL78), 1755 ± 9 Ma (GR59), and 1761 ± 3 Ma (GR35). The Sm-Nd model ages are slightly older: 1957, 1838, and 1947 Ma and indicate a short crustal residence (Table 2). The magmatic ages correlate to the age of 1752 ± 2 Ma determined by Tassinari et al. (1996) on zircon from tonalitic gneiss (A338a). Sample A338a, however, has a much older Sm-Nd T_{DM} model age (2200 Ma) than the results presently reported. Sample GR35 has one metamorphic rim formed at 1632 ± 6 Ma (grain d2; Th/U=0.01; Fig. 2) and sample GR59 has another population of magmatic zircon formed at 1677 ± 12 Ma (Fig. 3). These two ages are about 80 to 120 m.y. younger than the age of the Jamari Complex and are similar to several ages recently determined in the Jamari Domain: Ouro Preto Paragneiss (1675 ± 12 Ma; Santos et al., 2000), Machadinho Paragneiss (1677 ± 5 Ma; Payolla et al., 2002), Paraíso Farm granulitic gneiss (1655 ± 11 Ma; Bettencourt et al., 2001), and Presidente Médici garnet gneiss (1634 ± 8 Ma; Bettencourt et al., 2001). Sample JL78 (1752 ± 14 Ma, Fig. 4) was affected by high-grade metamorphism identified in zircon metamorphic rims (Th/U=0.09; Fig. 5) at 1335 ± 2 Ma (Fig. 4). This age is typical of the Candeias Orogeny of Sunsás Orogen (Santos et al., 2002) and is equivalent to the age of Ariquemes kinzigite (1331 ± 8; Tassinari et al., 1999).

Zircon crystals from Serra da Providência Granite (GR333) were formed at 1547 ± 13 Ma and recrystallized by metamorphism at 1349 ± 8 Ma (Th/U=0.009-0.015; Fig. 6), associated to the Candeias Orogeny. Santos et al. (2002) identified four main orogenies in the Sunsás Orogen based on detrital zircon geochronology. The Candeias Orogeny is the second orogeny of the Sunsás

Orogen and developed during the 1370-1320 Ma range according to the ages of populations of detrital zircon grains from the following sedimentary units: Pacaás-Novos (1368 Ma), Nova Brasilândia (1351 Ma), Palmeiral (1330 Ma), and Iata (1320 Ma). Another example of the Candeias metamorphism is the metamorphic age of 1326 Ma determined in monazite from 1526 Ma old WB44 augen gneiss (Payolla et al., 2002).

The Ariquemes Granite (1333 ± 8 Ma old; Santos et al., 2000) and other granites are correlated to the Alto Candeias Batholith (1330 ± 12 Ma; Bettencourt et al., 1999) in Central Rondônia State. Another sample (JS39) from that batholith was investigated to determine its U-Pb age. It has a single igneous zircon population formed at 1339 ± 7 Ma (Fig. 7). This age is within error of the previous age determined for the Ariquemes Granite (Santos et al., 2000), and correlates with the age of metamorphism affecting both Serra da Providência Suite (1349 Ma, sample GR333) and Jamari Complex (1336 Ma, sample JL78).

CONCLUSIONS

The Jamari Complex includes two main groups of rocks: a) an older tonalite-quartz diorite association generated in a juvenile environment at 1.76-1.75 Ga with minor contamination from continental crust (T_{DM} Nd model ages of 1.95-1.84 Ga); and b) a younger (1.67-1.63 Ga) association of high metamorphic grade metassedimentary rocks derived from crustal reworking (T_{DM} Nd model ages of 2.20 Ma and 2.13 Ga) representing a collisional event. The collisional rocks can be separated from the Jamari Complex and included in younger units such as Machadinho and Ouro Preto. The Machadinho-Ouro Preto collision is a regional orogeny affecting the Rondônia-Juruena Province because it is identified not only in the Jamari Domain (western zone), but also in its central and eastern zones. In the eastern Juruena region, metamorphic rims on Monte Verde Amphibolite zircon are 1653 ± 42 Ma old (Márcio Pimentel, 2003, personal communication), and in the Aripuanã River region (Colniza-Mureru area, Fig. 1), Pinho et al. (2003) identify a metamorphic granodiorite (P18) with an age of 1669 ± 13 Ma.

The Candeias Orogeny of the Sunsás Orogen was developed during 1370-1320 Ma and it is compose by two groups of rocks: a) collisional rocks, such as local kinzigite, such as RO8 (Tassinari et al., 1999) and mylonites and gneisses generated by high-grade metamorphism over previous rocks, mostly from Jamari Complex and Serra da Providência Suite; and b) monzo- to syenogranite batholiths probably generated in a continental arc environment; the Candeias Batholith and the Ariquemes Granite are the best examples.

We identify in southwestern Amazonian Craton three main collisional orogenies: The Ouro Preto orogeny (1670-1630 Ma) in the Rondônia-Juruena Province; and the Candeias (1370-1320 Ma) and Nova Brasilândia (1100 Ma; Rizzotto et al., 1999) orogenies related to the Sunsás Orogen (1450-1100 Ma; Santos et al., 2002).

REFERENCES

Bettencourt, J.S., Tosdal, R.M., Leite, W.B., Payolla, B.L., 1999. Mesoproterozoic rapakivi granites of the Rondônia Tin Province, southwestern border of the Amazon Craton, Brazil: I-reconnaissance U-Pb geochronology and regional implications. Precambrian Research, 95: 41-67.

Bettencourt, J.S., Basei, M.A.S., Payolla, B.L., Leite, W.B., 2001. New evidences of recurring convergent margin magmatism in the eastern central Rondônia, Brazil. In: Geology of the SW Amazonian Craton: State of the art, IGCP project 426, University of São Paulo, Extended Abstracts, pp. 48-52.

Payolla, B.L., Bettencourt, J.S., Kozuch, M., Leite Jr., W.B., Fetter, A., Van Schmus, W.R., 2002. Geological evolution of the basement rocks in the east-central part of the Rondônia Tin Province, SW Amazonian Craton, Brazil: U-Pb and Sm-Nd isotopic constraints. Precambrian Research, 119: 141-169.

Pinho, M.A.S.B., 2002. Geoquímica e geocronologia da seqüência vulcano-plutônica Teles Pires, norte de Mato Grosso. In: Sociedade Brasiliera de Geologia, Congresso Brasileiro de Geologia, 41, João Pessoa, Anais, p. 465.

Pinho, M.A.S.B., Chemale Júnior, F., Van Schmus, R.W., Pinho, F.E.C., 2003. U-Pb and Sm-Nd evidence fot 1.77 to 1.76 Ga magmatism in the Mureru region, Maro Grosso, Brazil: Implications for province boundaries in the SW Amazon Craton. Precambrian Research (submitted).

Rizzotto, G.J., 1999. Petrologia e Ambiente Tectônico do Grupo Nova Brasilândia-RO. Dissertação de Mestrado, Universidade Federal do Rio Grande do Sul, Porto Alegre, 136 p.

Santos, J.O.S, Hartmann, L.A., Gaudette, H.E., Groves, D.I., McNaughton, N.J., Fletcher, I.R., 2000. A new understanding of the provinces of the Amazon Craton based on integration of field mapping and U-Pb and Sm-Nd geochronology. Gondwana Research, 3(4):453-488.

Santos, J.O.S., Rizzotto, G., Easton, M.R., Potter, P.E., Hartmann, L.A., McNaughton, N.J., 2002. The Sunsás Orogen in Western Amazon Craton, South America and Correlation With the Grenville Orogen of Laurentia, Based on U-Pb Isotopic Study of Detrital And Igneous Zircons. In: Geological Society of America, 2002 Denver Annual Meeting (October 27-30, 2002), Precambrian Geology, paper 122-8.

Tassinari, C.C.G., Cordani, U.G., Nutman, A.P., Schmus, W.R.V., Bettencourt, J.S., Taylor, P.N., 1996. Geochronological Systematics on Basement Rocks from the Rio Negro–Juruena Province (Amazon Craton) and Tectonic Implications International Geology Review, 38:161-175.

Tassinari, C.C.G., Cordani, U.G., Correia, C.T., Nutman, A., Kinny, P., Marins, C., Dias Neto, C.M., 1999. Dating of granulites by SHRIMP U-Pb systematics in Brazil: Constraints for the age of the metamorphism of Proterozoic orogenies. In: Actas, South American Symposium on Isotope Geology, 2, Cordoba, Argentina, 371-374.

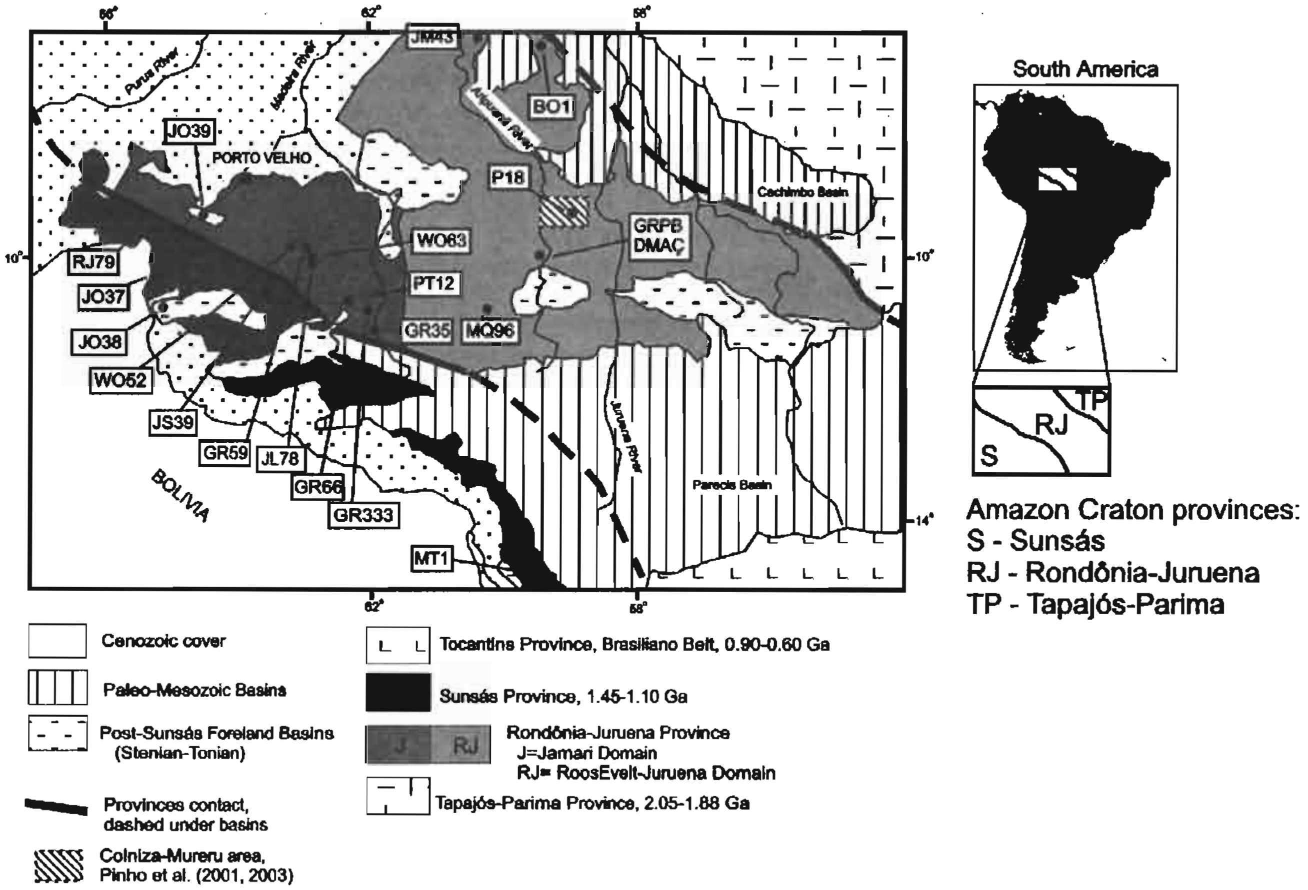

Figure 1. Geological map of southwestern Amazonian Craton showing provinces, domains, and location of samples with U-Pb data.

Table 1. List of rocks dated by U-Pb (this and previous work).

Sample	Rock	Unit	U-Pb age	n^1	n^2	σ	MSWD	zircon type	$T_{DM\,(t)}$	ε_{Nd}	Reference
WB44A	Augen gneiss	Jaru	1326 ± 2	4	1	2	-	metamorphic	1840	+0.50	Payolla et al. (2002)
RO8	Kinzigite	Candeias	1331 ± 8	4	4	2	n.a.	metamorphic			Tassinari et al. (1999)
JL78	Tonalite	Jamari	1336 ± 7	4	4	2	2.10	metamorphic	1947	+1.04	This work
JS39	Granite	Alto Candeias	1339 ± 7	7	6	2	1.70	magmatic			This work
GR333	Meta-granite	S. Providência	1349 ± 8	2	2	2	-	metamorphic	1990	-0.69	This work
P18	Meta-granodiorite	Colniza	1669 ± 13	4	3	1	5.00	metamorphic	2160	-0.30	Pinho et al. (2003)
GR59	Tonalite	Jamari	1677 ± 12	2	2	2	-	magmatic	1838	+2.33	This work
WB152	Paragneiss	Machadinho	1677 ± 5*	3	3	1	1.70	metamorphic	2129	-1.19	Payolla et al. (2002)
PT12	Paragneiss	Ouro Preto	1675 ± 12	4	3	2	0.41	metamorphic			Santos et al. (2000)
JWB10	Granulitic gneiss	Ouro Preto	1655 ± 11	4	4	2	33.00	metamorphic			Bettencourt et al. (2001)
PS171	Amphibolite	Monte Verde	1653 ± 42	4	4	2	n.a.	metamorphic	2001	+0.16	Márcio Pimentel (pers. comm.)
JWB3a	Garnet gneiss	Ouro Preto	1634 ± 8	4	4	2	14.00	metamorphic			Bettencourt et al. (2001)
GR35	Quartz diorite	Jamari	1632 ± 6	1	1	2	-	metamorphic	1957	+1.89	This work
JL78	Tonalite	Jamari	1752 ± 14	4	4	1	1.40	magmatic	1947	+1.04	This work
A338a	Tonalitic gneiss	Jamari	1752 ± 2*	4	4	2	0.02	magmatic	2200	-1.50	Tassinari et al. (1996)
GR66	Quartzite	N.Brasilândia	1753 ± 18	2	2	2	-	detrital	-	-	Santos et al. (2000)
GR59	Tonalite	Jamari	1755 ± 9	3	2	2	1.19	magmatic	1838	+2.33	This work
GR35	Quartz diorite	Jamari	1761 ± 3	9	8	1	0.32	magmatic	1957	+1.89	This work
WB152	Paragneiss	Machadinho	1762 ± 4	1	1	2	-	inherited	2129	-1.19	Payolla et al. (2002)

Table 2. Sm-Nd data of dated samples.

Sample	rock	Unit	Sm (ppm)	Nd (ppm)	$^{147}Sm/^{144}Nd$	$^{143}Nd/^{144}Nd$	T(Ma)	ε_{Nd}	T_{DM}
GR35	quartz-diorite	Jamari	2.0510	8.8010	0.13455	0.512016	1761	+1.89	1957
GR59	tonalite	Jamari	8.4093	45.3861	0.10736	0.511725	1755	+2.33	1838
GR333	meta-granite	Providência	7.4800	35.2100	0.128	0.511916	1547	-0.69	1990
JL78	tonalite	Jamari	8.5100	48.1500	0.10690	0.511669	1752	+1.04	1947

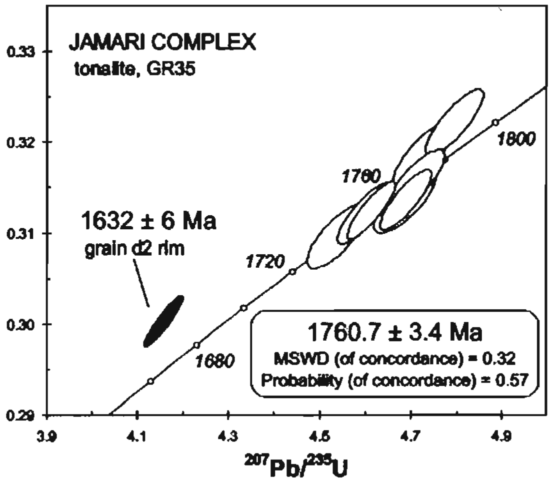

Figure 2. U-Pb concordia diagram for zircon from Jamari Complex quartz diorite (GR35).

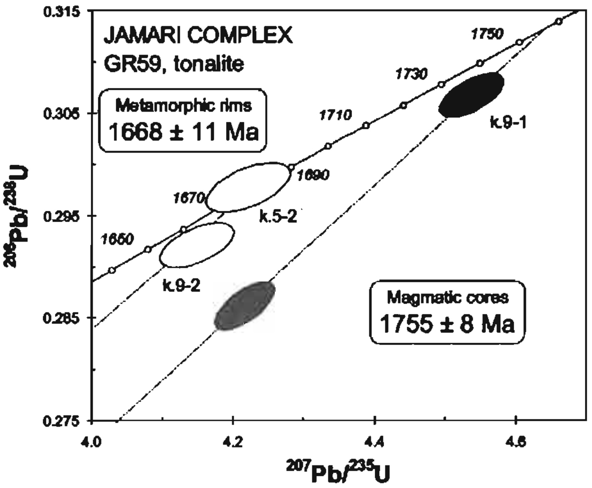

Figure 3. U-Pb concordia diagram for zircon from Jamari Complex tonalite (GR59).

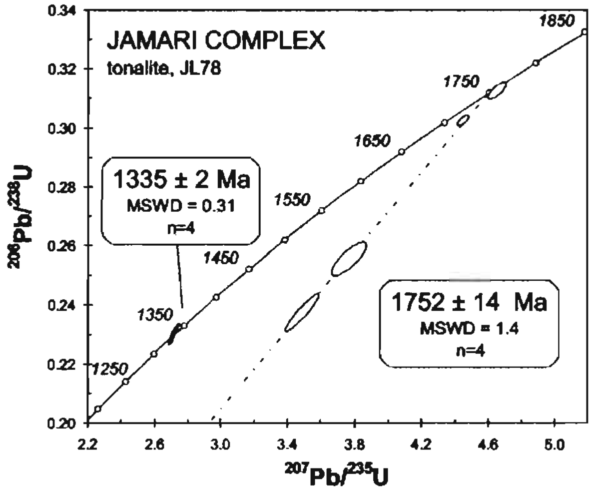

Figure 4. Concordia plot of two populations of zircon data: cores ages grouped at 1752 ± 14 Ma and rim ages at 1335 ± 2 Ma.

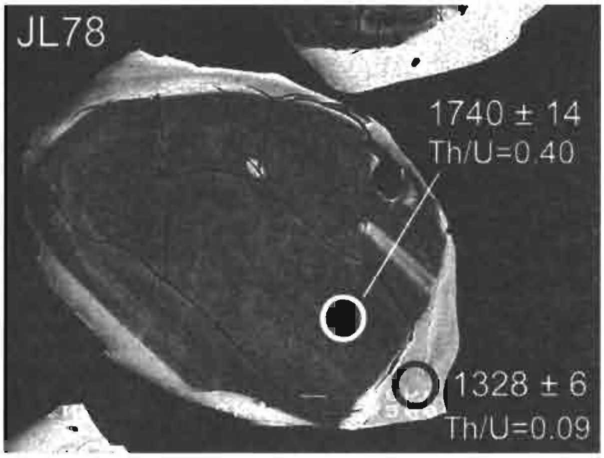

Figure 5. Back-scattered image of zircon h2 of JL78 tonalite, showing metamorphic rim (1328 Ma; Th/U=0.09) and igneous core (1740 Ma, Th/U=0.40).

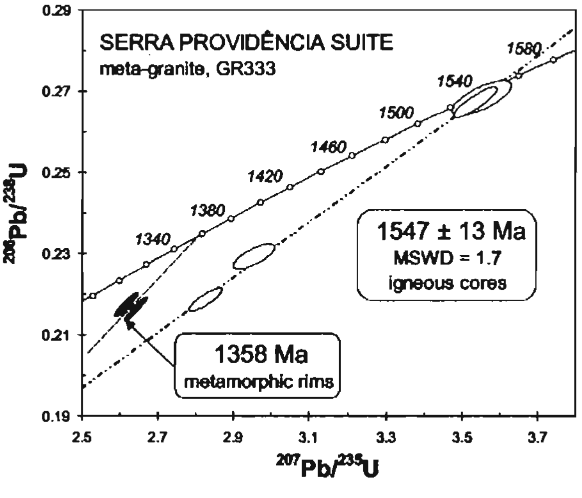

Figure 6. U-Pb concordia plot for zircon cores and rims from Serra Providência Suite meta-granite.

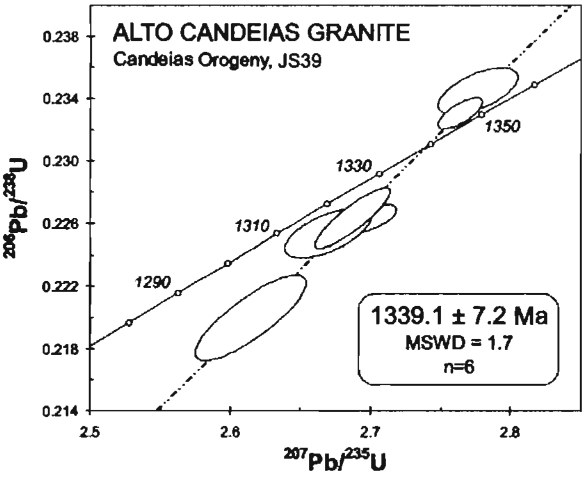

Figure 7. U-Pb concordia plot for igneous zircon from Alto Candeias Batholith (JS39).

Nd ISOTOPES AND THE PROVENANCE OF METASSEDIMENTS OF THE ITATAIA GROUP, NORTHWEST BORBOREMA PROVINCE, NE BRAZIL

Santos, T.J.S.[1]; Santos, A. A.[2]; Dantas, E.L.[3]; Fuck, R.A.[3] and Parente, C.V.[2]

1. Instituto de Geociências, Universidade Estadual de Campinas, P.Box 6152, 13081-970, Campinas-SP, Brazil. ticiano@ige.unicamp.br
2. Departamento de Geologia, Universidade Federal do Ceará, campus do Pici, 60455-760, Fortaleza-CE, Brazil
3. Instituto de Geociências, Universidade de Brasília, 70910-900, Brasília-DF, Brazil

Keywords: Itataia Group, Santa Quitéria arc magmatic, Borborema Province, Ceará Central domain

INTRODUCTION

The Borborema Province (BP) of northeast Brazil (Almeida et al., 1981) represents the western part of a major Brasiliano/Pan-African orogenic belt that can be traced into Central Africa based on pre-drift reconstructions (Caby, 1989; Trompette, 1994). The Borborema Province comprises a number of distinctive crustal domains, ranging from Archean to Neoproterozoic in age, that were deformed during the convergence of the West African-São Luis, Amazonian, and São Francisco-Congo cratons around 600 Ma (Brito Neves & Cordani, 1991). In the northern half of the BP, north of the Patos lineament (Fig. 1a), the basement architecture is dominated by middle Paleoproterozoic gneisses that contain several smaller inliers of Archean crustal fragments (Dantas et al., 1998). Overlying these basement gneisses is a number of supracrustal sequences ranging from Paleoproterozoic to Neoproterozoic in age. Neoproterozoic to Cambrian granitoids (622 to 532 Ma) intrude both basement and supracrustal rocks that were generated during Brasiliano orogenesis (Fetter, 1999).

Three major crustal blocks form the north portion of the Borborema Province, Rio Grande do Norte Terrane, Ceará Central and Médio Coreaú Domain. These areas are correlated with the Dahomey Province, in the southern part of West Africa.

The Rio Grande do Norte Terrain is situated between the Patos Lineament to the south and the Senador Pompeu Lineament to the west. This terrain encloses Archean and Paleoproterozoic basement and Neoproterozoic supracrustal rocks (Seridó Fold Belt) (Dantas et al., 1998). Additionally, in Ceará there is the north-south Orós fold belt, a late Paleoproterozoic volcano-sedimentary sequence (ca. 1.8 Ga, Sá et al., 1995).

The Ceará Central Domain is situated between the Senador Pompeu Lineament and Transbrasiliano Lineament and is represented by Paleoproterozoic gneissic basement with the inclusion of an Archean nucleus (Tróia-Tauá Massif). Based on field investigation and geochronological studies Fetter et al. (2003) have recognized a Neoproterozoic continental magmatic arc inthis domain, the Santa Quitéria Complex, which is the result of southeastward subduction of an oceanic realm during convergence between the West African-São Luis craton and NW Ceará. Felsic volcanic rocks located to the southeast and northwest of the arc are interpreted as fore-arc (Martinópole Group) and back-arc (Independência Group) sequences, respectively. In both sequences the U-Pb zircon crystallization age is ca. 777 Ma, while the granodiorite, diorite, migmatite and metarhyolites from the Santa Quitéria Batholith present ages between 665 and 614 Ma (Fetter et al., 2003). In addition, Nd model ages of the batholith and related metasediments show values between 2.33 and 0.87 Ga (Fetter et al. 2003). These authors suggest that the age disparity between the oldest magmatism yet identified in the Santa Quitéria Batholith and the Martinópole and Independência volcanism maybe a reflection of the limited geochonological study in the batholith.

The Itataia Group corresponds to a metassedimentary sequence located between the Santa Quitéria Batholith and São José da Macaoca Paleoproterozoic basement. This group was highly deformed and metamorphosed during the Brasiliano/Panafrican orogeny.

The aim of this paper is to present Nd isotopic data of the rocks of the Itataia Group and adjacent gneiss terrains. We have studied the provenance source of this unit and its importance for the tectonic evolution of the Ceará Central Domain.

GEOLOGICAL SETTING

The Médio Coreaú Domain is composed of early Paleoproterozoic gneisses, migmatites and granulites, and overlain by volcano-sedimentary sequences, with ages from late Paleoproterozoic (Saquinho Sequence) to Neoproterozoic (Martinópole Group). These rocks were intruded by granitoids emplaced during the Brasiliano/ Panafrican orogeny.

The Ceará Central Domain, which contains the Itataia Group, includes Archean basement, large Paleoproterozoic accretionary terrains, Santa Quitéria terrain and Neoproterozoic supracrustal rocks (Fetter, 1999). Metabasalt, mafic–ultramafic sills, schist and quartzite compose the Archean basement, with U-Pb zircon ages of 2.77 - 3.04 Ga and Nd model ages of 2.81 – 2.92 Ga with εNd between +2,1 and –0.2 (Fetter, 1999). The Paleoproterozoic terrain yields U-Pb zircon age of 2.10 to 2.14 Ga and Nd model ages of 2.22 to 2.44 Ga (Fetter, 1999). The São José da Macaoca basement is composed of tonalite and granodiorite that present crystallization zircon ages of ca. 2.13 Ga and Nd model ages of 2.36 to 2.44 Ga (Fetter, 1999).

The Santa Quitéria Batholith (Fetter et al., 2003), an adaptation from the term "Santa Quitéria Massif" (Santos & Brito Neves, 1984), is a Neoproterozoic continental magmatic arc composed of several granitoid types.

The Itataia Group occurs in a block delimited by two strike-slip faults: the Rio Groairas dextral fault to the west separating it from the Santa Quitéria Batholith and the Itatira sinistral fault to the east, which separates it from the São José da Macaoca Paleproterozóic basement (Fig. 1). The metasediments of this group are of medium to high metamorphic grade (with sillimanite, staurolite, kyanite). It is subdivided in four formations: from base to top, Serra do Céu (gneiss and migmatite); Laranjeira (sillimanite quartzite and muscovite quartzite); Barriga (garnet gneiss and migmatite) and Alcantil (marble with uranium minerallization).

The main tectonic features of the Itataia Group resulted from a southeastward to southward convergent regime that developed a flat-lying foliation, thrust fault with top to south and a stretching lineation that rotates gradually from NW-SE to NE-SW (Fig. 1). A second deformation event, progressive, is responsible for a northward movement of extensional nature. Associated with the deformation there is a high-grade metamorphism with crystallization of sillimanite, kyanite, garnet and amphibole.

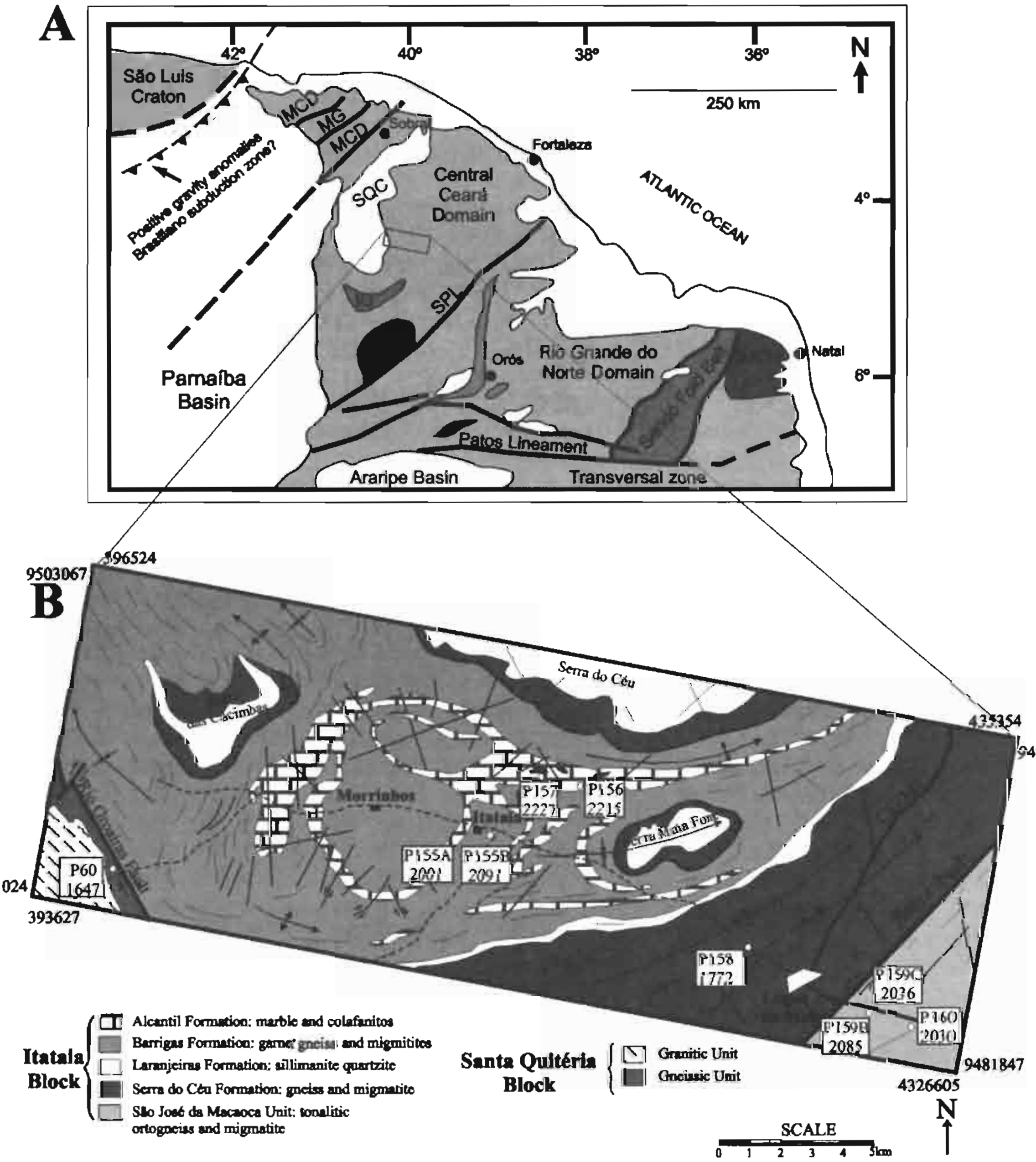

Figure 1. Simplified geological map of the Itataia region (A). Geological map of the Itataia block with location of analyzed samples (B). Lower number in box corresponds to T_{DM} whereas upper number to sample numbers.

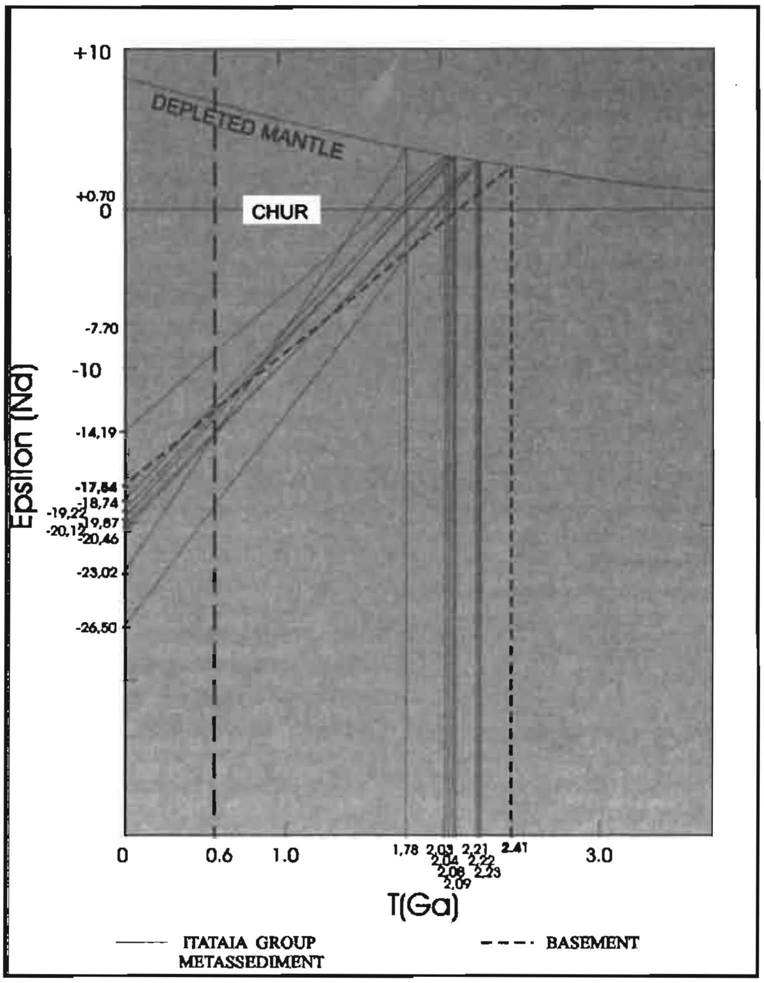

Figure 2. Nd evolution diagram of the rocks Itataia Group.

Table 1. Sm-Nd isotopic data for Itataia region, Ceará Central Domain, Borborema Province.

Sample	Unit	Sm (ppm)	Nd (ppm)	$^{147}Sm/^{144}Nd$	$^{143}Nd/^{144}Nd$	E_{ND} (0)	T_{DM} (Ga)	Rock	Coordinate UTM
P-159c	São José Macaoca	9.50	51.19	0.1121	0.511677±28	-18.74	2.04	Tonalite gneiss	0428469 9484226
P-160	São José Macaoca	6.09	28.49	0.1293	0.511911±26	-14.19	2.03	Paragneiss	0430048 9483772
P-159b	São José Macaoca.	4.51	24.74	0.1103	0.511619±11	-19.87	2.09	Paragneiss	0428469 9484226
P-60	Santa Quitéria block	9.53	52.97	0.1087	0.511900±13	-14.4	1.65	Amphibole gneiss	0396535 9491174
P-158	Itataia Group –Serra do Céu Fm.	8.81	67.71	0.0789	0.511458±10	-23.02	1.78	Gneiss	0422746 9487722
P-155a	Itataia Group – Barriga Fm	11.08	68.61	0.0976	0.511510±17	-22,01	2.00	Migmatite	0411831 9494186
P-155b	Itataia Group – .Barriga Fm	3.74	20.00	0.1130	0.511653±09	-19.22	2.09	Gneiss	0411831 9494186
P-156	Itataia Group – Alcantil Fm.	2.95	15.59	0.1142	0.511589±22	-20.46	2.22	Marble	0415192 9495458
P-157	Itataia Group – Alcantil Fm.	5.57	29.05	0.1159	0.511606±22	-20.12	2.23	Marble	0414627 9495790

Nd ISOTOPIC DATA AND CONCLUSIONS

The Nd isotopic analyses were carried out in the Geochronology Laboratory of Universidade de Brasília, following Gioia & Pimentel (2000).

We present new Sm-Nd isotopic data of nine rock samples from the Itataia Group, from neighboring basement gneiss and from the Santa Quitéria region (Table 1).

The oldest T_{DM} model age was obtained from an orthogneiss from São José da Macaoca basement, which yields a value of 2.04 Ga that characterize a Paleoproterozoic source for these rocks. This value is younger than those obtained in the region by Fetter (1999), which ranged between 2.24 and 2.44 Ga. Thus, this rock may have a more juvenile source than the other basement analyzed until now.

The amphibolite gneiss from Santa Quitéria shows T_{DM} model age of 1.65 Ga, suggesting a hybrid mixture between Neoproterozoic and Paleoproterozoic sources.

All analyzed samples of the Itataia Group present T_{DM} model ages between 1.77 and 2.23 Ga. A dominantly Paleoproterozoic source is evident. This indicates that, the rocks of the southern part of Itataia Group were not derived from the erosion of the Neoproterozoic Santa Quitéria arc (Fig. 2), unlike those of the group analyzed farther to the north (Fetter et al., 2003) A possible source of the original sediments of the southern Itataia Group is the São José da Macaoca basement and similar gneisses of Ceará Central Domain.

The presence of material derived from the Santa Quitéria Arc in the Itataia Group is not likely, meanwhile the delimitation this Group at northward is uncertain, principally because there is T_{DM} in that region with 900 Ma (Fetter et al., 2003) and that certainly evidence a contribution of Neoproterozoic material. In the west side, however, the Rio Groaíras fault corresponds to an important crustal boundary between the Itataia block and Santa Quitéria Arc.

A poorly constrained Sm-Nd isochron age (621±160 Ma) of sample garnet paragneiss from the Barriga Formation (whole rock and garnet results) is interpreted to mark the timing of metamorphism of the Itataia Group. Additional studies using more precise methods, such as Ar-Ar biotite and U-Pb monazite methods should yield better constrains on the timing of Brasiliano metamorphism.

ACKNOWLEGMENTS

The authors thanks CAPES-PROCAD UNB-UFC for financial support.

REFERENCES

Almeida, F.F.M.; Hasui, Y.; Brito Neves, B.B.; Fuck, R.A., 1981. Brazilian structural provinces: an Introduction. Earth Sci. Rev., v. 17, pp. 1-29.

Brito Neves, B.B.; Cordani, U.G., 1991. Tectonic evolution of South America during the Late Protrusion. In: Stern R.J. and Van Schmus W.R., (Eds.), Crustal evolution in the late Proterozoic. Precambrian Research., 53:23-40.

Brito Neves, B.B. & Santos, E.J., 1984. Província borborema. In. O Pré-Cambriano do Brasil. Coord. Fernando Flávio de Marques e Yociteru Hasui. Ed. Edgard Blücher Ltda. P. 123-186.

Caby, R., 1989. Precambrian terrane of Benin-Nigeria and northeast Brazil and late Proterozoic Atlantic fit. - Geol. Soc. Am. Sp. Paper, 230, 145-158

Dantas, E.L.; Hackspacher, P.C.; Van Schmus, W.R.; Brito Neves, B.B., 1998. Archean accretion in the São José de Campestre Massif, Borborema Province, Northeast Brazil. Revista Brasileira de Geociências 28(2): 221-228

Fetter, A.H. 1999. U/Pb and Sm/Nd Geochronological constraints on the crustal framework and geological history of Ceará State, NW Borborema Province, NE Brazil: Implications goes the assembly of Gondwana. University of Kansas, Ph.D Thesis, 164 pp.

Fetter, A.H.; Santos, T.J.S.; Van Schmus, W.R.; Hackspacher, P.C; Brito Neves, B.B.; Arthaud, M.H.; Nogueira Neto, J.A.; Wernick, E., 2003. Evidence for Neoproterozoic Continental Arc Magmatism in the Santa Quitéria Batholith of Ceará State, NW Borborema Province, NE Brazil: Implications for the Assembly of West Gondwana. Gondwana Research, 6(2): 265-273.

Gioia, S.M.C.L. & Pimentel, M.M., 2000. The Sm-Nd method in the geochronology laboratory of the University of Brasília. Anais da Academia Brasileira de Ciência, 72 (2), 219-245

Trompette, R., 1994. Geology of Western Gondwana, Pan-African - Brasiliano aggregation of South America and Africa. A.A. Balkema, Rotterdam, Brookfield, 350p.

THE FAMATINIAN GRANITOIDS OF SOUTHWESTERN SIERRA DE SAN LUIS, ARGENTINA

Sato, A.M.[1]; González, P.D.[1]; Basei, M.A.[2]; Passarelli, C.R.[2]; Tickyj, H.[3] and Ponce, J.M.[4]

1. Centro de Investigaciones Geológicas – Universidad Nacional de La Plata. Calle 1 N° 644, 1900 – La Plata, Argentina. sato@cig.museo.unlp.edu.ar, gonzapab@cig.museo.unlp.edu.ar
2. Centro de Pesquisas Geocronológicas, Universidade de São Paulo, CP 11348, São Paulo-SP 05422-970, Brazil. baseimas@usp.br, crpass@usp.br
3. Universidad Nacional de La Pampa, Av. Uruguay 151, Santa Rosa, La Pampa 6300, Argentina. htickyj@yahoo.com
4. LEMIT. P.O. Box 128, 1900 – La Plata, Argentina

Keywords: Sierras Pampeanas, Famatinian orogeny, granitoids

INTRODUCTION

The Sierra de San Luis is located in the southern part of the Eastern Sierras Pampeanas. The most conspicuous orogenic events (arc magmatism, deformation and metamorphism) took place during the Lower Paleozoic Famatinian orogeny, overprinting the metamorphic and sedimentary rocks already delineated by the previous Pampean orogeny (Proterozoic? to Early Cambrian).

The granitoids were classified into pre-, syn- and post-orogenic plutons on the basis of their structural relationship with the penetrative NNE-SSW trending Ordovician structures, attributed to the main Famatinian phase (Ortiz Suarez et al., 1992; Llambías et al., 1998). Available data constrain the low- to high-grade regional metamorphism associated with the deformation mainly within the Early to Middle Ordovician (see synthesis in Sato et al., 2002).

In this contribution we offer new U-Pb ages obtained from granitoid plutons of the southwestern part of the Sierra de San Luis. The new ages together with the already existing data, allow us to understand the magmatic evolution of the Famatinian orogen in relation to the structural and metamorphic events.

GEOLOGICAL OUTLINE OF THE SOUTHWESTERN SIERRA DE SAN LUIS

The southwestern part of the Sierra de San Luis (Fig. 1) is dominated by the Nogoli Metamorphic Complex (Sims et al., 1998). It comprises micaschists, metaquartzites, paragneisses and migmatites, with minor orthoamphibolites, komatiites to high-Fe tholeiitic basalts, marbles, calcsilicates and banded iron formation (Ortiz Suárez, 1999; González, 2000; González et al., 2002). Although the conspicuous NNE-SSW trending structures are related to the Ordovician deformation and metamorphism, remnant NW-SE trending foliations, attributed to pre-Famatinian deformations, are preserved in a few places. The Early Mesoproterozoic Sm-Nd isochron age of *c.*1500 Ma (Sato et al., 2001a) obtained from amphibolites and komatiites might represent either the age of their original crystallization or that of the crust-mantle differentiation, but it has not been confirmed by other isotopic methods. The high-grade metamorphism associated with the penetrative deformation of this region was constrained by Ar-Ar plateau ages (476 and 457 Ma) and a Sm-Nd isochron (445 ± 21 Ma) for amphibolites, as well as conventional U-Pb age (458 ± 3 Ma) and electron microprobe age (470 ± 15 Ma) on monazites from a sillimanite paragneiss (González et al., 2002). This Ordovician regional metamorphism was followed by ductile shear zone deformations that acted until Early Carboniferous times. Broad mylonite zones are particularly conspicuous in this western part of the Sierra (e.g. Rio de los Bayos and Funes shear zones).

The newly dated Famatinian granitoids (Fig. 1) show different structural relationships. The Pantanos Negros Granodiorite is an elongated pluton that intruded cutting the old NW-SE structures of the Nogolí Metamorphic Complex. It is heterogeneously affected by the NNE-SSW foliation and by parallel shear zones. The composition is mainly leucogranodioritic, with minor tonalitic facies. For this pre-orogenic pluton we have no previous dating.

The El Molle pluton forms a circular post-orogenic intrusion together with the Barroso pluton (González & Sato, 2000). They cut the NNE-SSW foliation of the country rock, and produce a concentric aureole foliation parallel to the magmatic foliation of the border zones. Monzonitic series dominate over granitic series in their composition. Although their emplacement postdates the Ordovician penetrative deformation and metamorphism, the plutons affect and are also affected by the ductile shear zones developed in the late stages of the Famatinian orogeny. Previous isotopic dating for these plutons include Rb-Sr whole rock isochron (378 ± 48 Ma), Sm-Nd mineral and whole rock isochron (348 ± 35 Ma), and K-Ar date on biotite (380 ± 7 Ma) (Sato et al., 2001b).

U-Pb RESULTS AND MAGMATIC EVOLUTION

Four zircon fractions (elongated prisms) from the Pantanos Negros Granodiorite align on a discordia line with an upper intercept at 477 ± 3 (± 5) Ma (MSWD = 3.2) (Fig. 2). This date is interpreted as representing the magmatic crystallization age of the pluton.

Five prismatic zircon fractions from the El Molle Monzonite define another discordia line with upper intercept at 417 ± 6 (±7) Ma (MSWD = 3.3). The two most concordant fractions were subjected to air ablation. We consider this age as that of the crystallization of the pluton.

The crystallization age obtained for the Pantanos Negros Granodiorite is well within the range of the remaining pre-orogenic granitoids of the Sierra de San Luis, and it shares the same structural and compositional

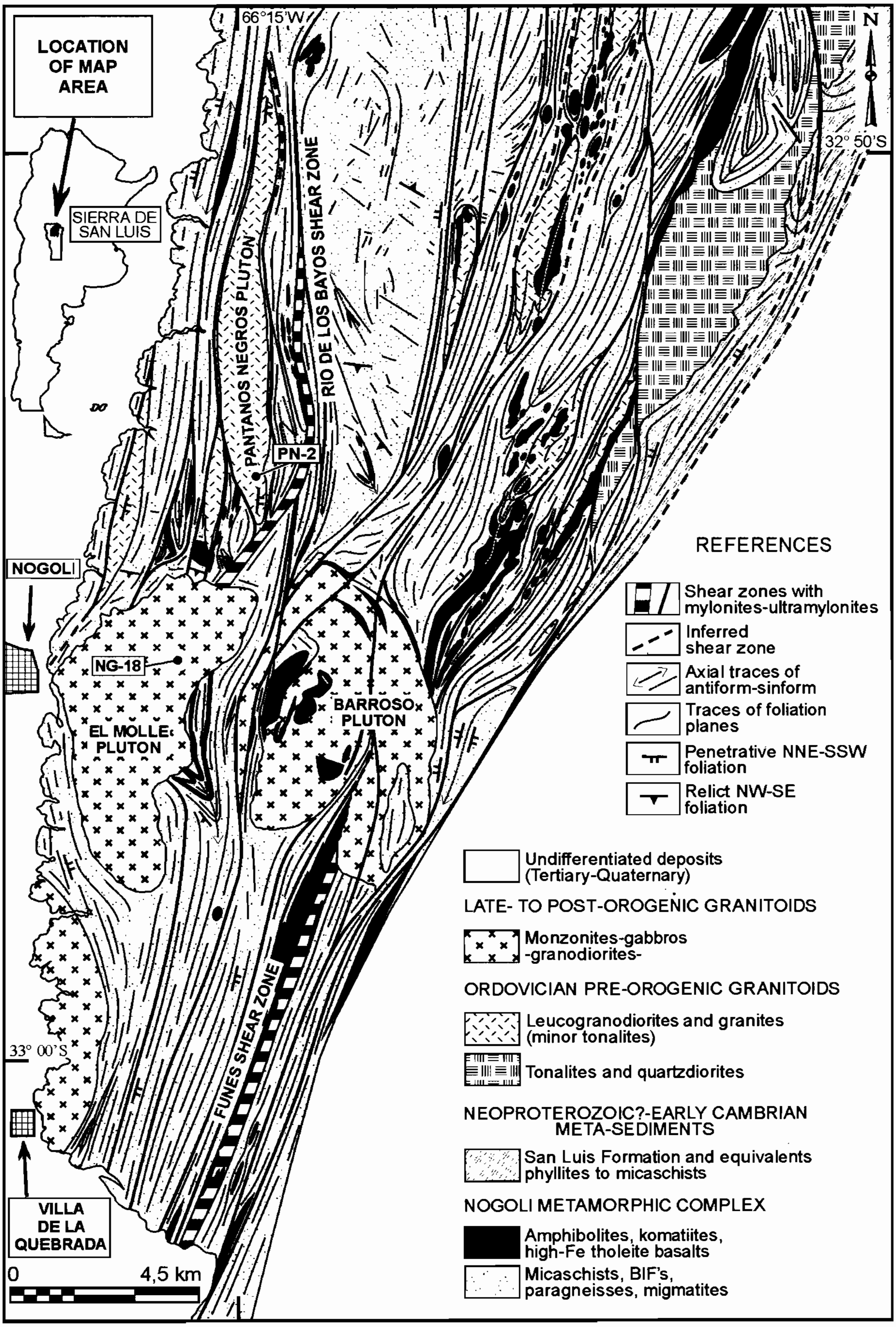

Figure 1. Geological map of the Southwestern Sierra de San Luis, with location of the Pantanos Negros Granodiorite and El Molle Monzonite.

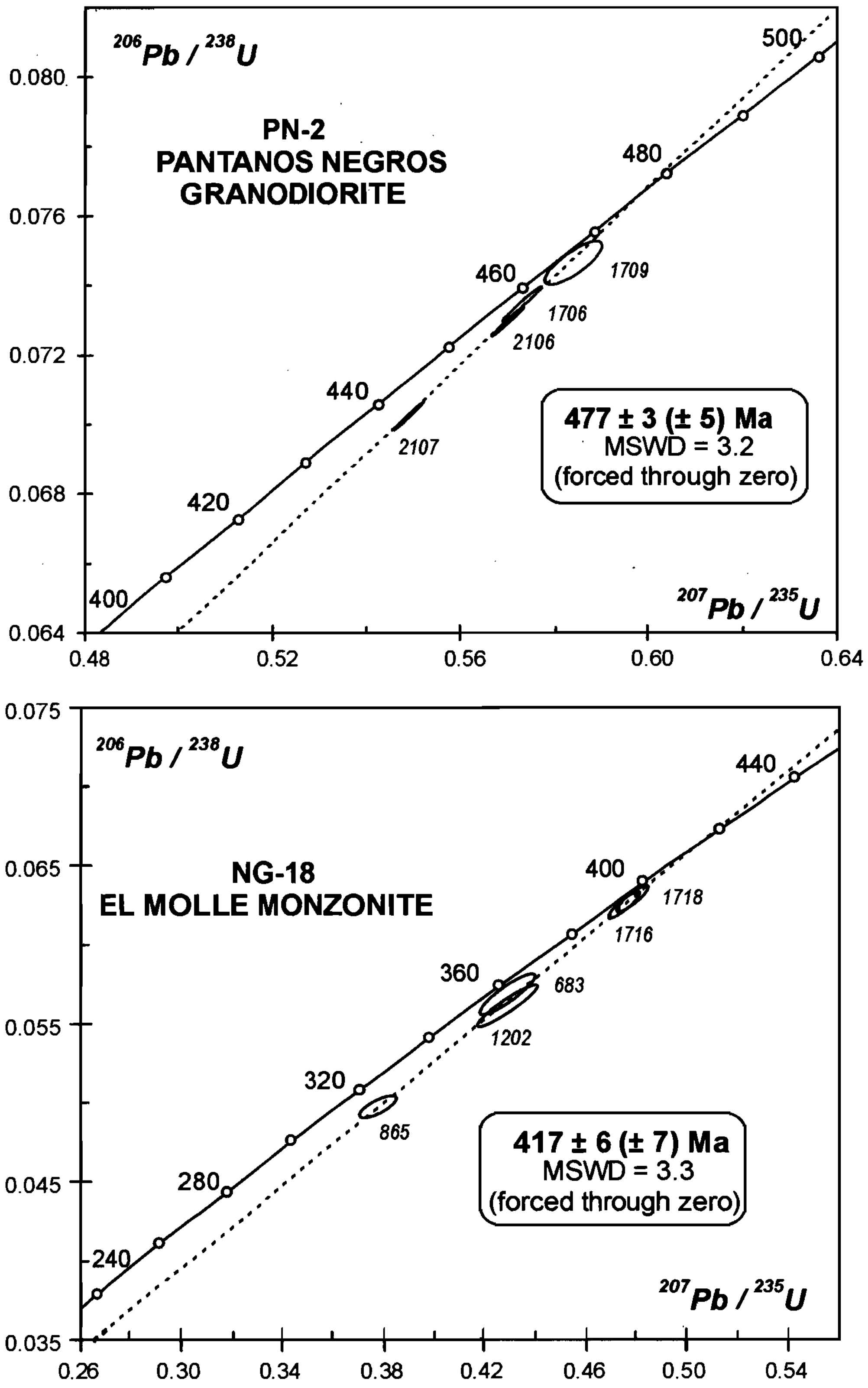

Figure 2. Concordia diagrams (Isoplot/Ex version 2.49)

features. Regionally, the pre-orogenic granitoids are located mainly in the central and western parts of the Sierra and their Rb-Sr and U-Pb dates cover a time span of 512 to 468 Ma, being the Early to Middle Ordovician the most important interval of emplacement. Tonalitic and granitic compositions are the major ones, and when both are exposed together, the granitic plutons intrude the tonalitic ones. They belong to typical calcalkaline series and are affected by the penetrative foliation.

Associated with the Ordovician peak metamorphism, small and numerous anatectic plutons were emplaced following the penetrative structures of the higher grade complexes. They were mostly studied in the central region of the Sierra, and dates around Middle Ordovician predominate for their emplacement (Llambías et al., 1991, 1996, 1998; von Gosen et al., 2002; López de Luchi, 1987; López de Luchi & Cerredo, 2001).

All these peak orogenic processes (arc magmatism, regional metamorphism and penetrative deformation) have been related to a collisional history (collisional Famatinian orogen), in which the Sierra de San Luis is considered as part of the Gondwana autochthon.

Regional metamorphism is no more registered in the post-Ordovician evolution of the Sierra de San Luis, and only ductile shear zones accompany the outlasting compression of the region, producing local metamorphism. The crust thickened in this way favored the production of late to post-orogenic granitoids, which form large anular plutons and batholiths. The monzonitic El Molle pluton is one example of this magmatism, and the crystallization age of 417 ± 6 (± 7) Ma (Late Silurian) places it as one of the earliest late-orogenic plutons of the Sierra de San Luis, whereas the remaining plutons are mainly Devonian to Early Carboniferous. The structural relationship with the shear zones also is in accordance with this early stage emplacement. The Middle to Late Devonian K-Ar, Rb-Sr and Sm-Nd dates of the same pluton suggest the local metamorphism associated with the ductile shear zones. This final stage of the Famatinian orogeny was also referred to as the "Achalian orogeny" (Sims et al., 1998), but based on the lack of regional metamorphism (only local metamorphism related to shear zones) and the lack of arc magmatism (only transitional to anorogenic granitoids), we consider more appropriate to define it as a Famatinian post-orogenic stage.

REFERENCES

González, P.D., 2000. Banded Iron Formation del basamento Pre-Famatiniano de San Luis: primer registro en Argentina. In: Mineralogía y Metalogenia 2000 (Schalamuk, I., M. K. de Brodtkorb and R. Etcheverry, Eds.). INREMI, Publicación N° 6: 191-198. La Plata, Buenos Aires.

González, P.D. & Sato, A.M., 2000. Los plutones monzoníticos cizallados El Molle y Barroso: dos nuevos intrusivos pos-orogénicos en el oeste de las sierras de San Luis, Argentina. 9° Congreso Geológico Chileno, 1 (sesión temática 4): 621-625. Puerto Varas.

González, P.D., Sato, A.M., Basei, M.A.S., Vlach, S.R.F., Llambías, E.J., 2002. Structure, metamorphism and age of the Pampean-Famatinian Orogenies in the Western Sierra de San Luis. XV Congreso Geológico Argentino, Actas, II: 51-56, Calafate.

Llambías, E.J., Cingolani, C.A., Varela, R., Prozzi, C., Ortiz Suárez, A., Caminos, R., Toselli, A., Saavedra, J., 1991. Leucogranodioritas sin-cinemáticas ordovícicas en la Sierra de San Luis. 6° Congreso Geológico Chileno, Resúmenes Expandidos, 187-191, Viña del Mar.

Llambías, E.J., Quenardelle, S., Ortiz Suárez, A., Prozzi, C., 1996. Granitoides sincinemáticos de la Sierra Central de San Luis. XIII Congreso Geológico Argentino y 3° Congreso de Exploración de Hidrocarburos, 3: 487-496. Buenos Aires.

Llambías, E.J., Sato, A.M., Ortiz Suárez, A., Prozzi, C., 1998. The granitoids of the Sierra de San Luis. In: The Proto-Andean Margin of Gondwana (Pankhurst, R. and Rapela, C., eds.). Geological Society of London, Special Publications, 142: 325-341.

López de Luchi, M., 1987. Caracterización geológica y geoquímica del plutón La Tapera y el Batolito de Renca, provincia de San Luis. X Congreso Geológico Argentino, Actas 4: 84-87. Tucumán.

López de Luchi, M. & Cerredo, M.E., 2001. Submagmatic and solid-state microstructures in La Tapera pluton. San Luis. Argentina. Asociación Geológica Argentina, Serie D: Publicación Especial N° 5: 121-125.

Ortiz Suárez, A., 1999. Geología y petrología del área de San Francisco del Monte de Oro, San Luis. Tesis Doctoral, Facultad de Ciencias Físico - Matemáticas y Naturales. Universidad Nacional de San Luis. 259 pp, inédito.

Ortiz Suárez, A., Prozzi, C., Llambías, E.J., 1992. Geología de la parte sur de la Sierra de San Luis y granitoides asociados, Argentina. Estudios Geológicos, 48: 269-277. Madrid.

Sato, A.M., González, P.D., Sato, K., 2001a. First indication of Mesoproterozoic age from the western basement of Sierra de San Luis, Argentina. III South American Symposium on Isotope Geology, Extended Abstract Volume (CD), 620-623, Sociedad Geológica de Chile, Santiago, Chile.

Sato, A.M., González, P.D., Petronilho, L.A., Llambías, E.J., Varela, R., Basei, M.A.S., 2001b. Sm-Nd, Rb-Sr and K-Ar age constraints of the El Molle and Barroso plutons, western Sierra de San Luis, Argentina. III South American Symposium on Isotope Geology, Extended Abstract Volume (CD), 241-244, Sociedad Geológica de Chile, Santiago, Chile.

Sato, A.M., González, P.D., Llambías, E.J., 2002. The Ordovician of Sierra de San Luis: Famatinian magmatic arc and low to high-grade metamorphism. In: Aspects on the Ordovician System of Argentina (F.G. Aceñolaza, Ed.) Serie Correlación Geológica 16: 327-346, Instituto Superior de Correlación Geológica, Tucumán, Argentina.

Sims, J., Ireland, T., Camacho, A., Lyons, P., Pieters, P., Skirrow, R., Stuart Smith, P., Miró, R., 1998. U-Pb, Th-Pb and Ar-Ar geocronology from the southern Sierras Pampeanas, Argentina: implications for the Paleozoic tectonic evolution of the western Gondwana margin. . In: The Proto-Andean Margin of Gondwana (Pankhurst, R. and Rapela, C., eds). Geological Society of London, Special Publications, 142: 259-281.

von Gosen, W., Loske, W., Prozzi, C., 2002. New isotopic dating of intrusive rocks in the Sierra de San Luis (Argentina): implications for the geodynamic history of the Eastern Sierras Pampeanas. Journal of South American Earth Sciences 15: 237-250.

MARINE SEDIMENTATION RELATED TO THE LATEST STAGES OF GONDWANA ASSEMBLY IN THE RIBEIRA BELT: NEW U-Pb DATA

Schmitt, R.S.[1]; Pimentel, M.M.[2]; Van Schmus, W.R.[3]; Trouw, R.A.J.[4] and Armstrong, R.A.[5]

1. TEKTOS - Departamento de Geologia Regional e Geotectônica – FGEL/UERJ, Rua São Francisco Xavier, 524/4006-A, Maracanã Rio de Janeiro-RJ, 20559-900 – Brasil. renataschmitt@uol.com.br
2. Instituto de Geociências – UnB, Brasília-DF, 70910-000 – Brasil. marcio@unb.br
3. Department of Geology, University of Kansas, 120 Lindley Hall, Lawrence-KS, 66045 – USA. rvschmus@ku.edu
4. Departamento de Geologia - IGEO- UFRJ, CCMN, Cidade Universitária, Ilha do Fundão, Rio de Janeiro-RJ, 21949-900 – Brasil. rajtrouw@hotmail.com
5. Research School of Earth Sciences, Australian National University, Canberra ACT 0200, Australia. richard.armstrong@anu.edu.au

Keywords: Cambrian orogeny, provenance ages, Gondwana, Ribeira belt, SHRIMP U-Pb analysis

INTRODUCTION

A Cambrian collisional event, the Búzios Orogeny, was recently recognized in the Cabo Frio Tectonic Domain (CFTD), southeastern part of the Ribeira Belt, in Rio de Janeiro State, Brazil (Schmitt et al., 1999a, Schmitt, 2001, Schmitt et al., submitted) (Fig. 1). This event took place between 525 and 480 Ma, according to U-Pb ages of zircon, monazite, titanite and rutile from high-grade orthogneisses and paragneisses. New SHRIMP U-Pb data presented here reveals that the sedimentation of the paragneisses occurred after 620 Ma. Therefore not only the tectonic events from the CFTD are younger than Neoproterozoic events in Brazil, but also the deposition of the original detrital sediments.

The CFTD paragneisses constitute the Supracrustal Unit, divided in three compositional groups corresponding to the original sedimentary facies (quartz-feldspathic, aluminous with kyanite/sillimanite and calcsilcate rocks), interleaved with amphibolite bodies. The contact with the basement units (Paleoproterozoic orthogneisses) is always strongly tectonized due to the Cambrian deformation. The supracrustals constitute successions of at least 500 meters thick. The compositional layering of these gneisses is interpreted to reflect the original bedding; therefore these rocks were subdivided in two main sedimentary successions based on the frequency of the interbedded lithotypes.

The Búzios Succession is a thick aluminous metasediment package (sillimanite-kyanite-garnet-biotite gneiss) with numerous calc-silicatic and amphibolitic intercalation. The Palmital Succession is constituted mainly of quartz-feldspathic metasediments (paragneiss), more than 300 meters thick, presenting some aluminous intercalations, as well as a few calc-silicatic and feldspathic quartzite layers. The paragneiss shows a regular compositional layering varying from 5 to 30 cm, determined by felsic layers and biotite-rich layers with kyanite and sillimanite.

The two successions are interpreted to have been deposited in the same basin (Búzios-Palmital basin). Minor layers of garnet-quartz gneiss and feldspathic quartzite within both successions may represent interdigitations of chert-like deposits. Based mainly on facies descriptions, the lithotypes are thought to be derived from turbiditic hemipelagic to pelagic sediments of submarine fans. The quartz-feldspathic dominated Palmital Succession may represent deposits of the medium portion of the fan, and the pelitic Búzios Succession may correspond to the pelagic distal facies. The calcsilicate layers might represent chemical deposits from precipitation due to water conditions and volcanic events. The amphibolites, interpreted as mafic subvolcanic intrusions and/or lava flows, are restricted to the pelagic environment of the Búzios Succession.

ISOTOPE GEOCHEMISTRY

T_{DM} model ages for metapelites samples of the Búzios Succession range from 1.7 to 1.4 Ga (Fonseca, 1993; Schmitt, 2001). Sm-Nd data from whole-rock samples of the amphibolites within the Búzios Succession indicated T_{DM} model ages of 1.0 Ga, interpreted as maximum ages for the basin formation (Schmitt et al., 1999b).

Conventional ID-TIMS U-Pb analyses were developed at the Isotope Geochemistry Laboratory (University of Kansas/USA), in a thermal ionization mass spectrometer (TIMS) (VG-Sector multicolector), following the U-Pb standard technique (Krogh, 1973, 1982; Parrish, 1987). The detailed procedure is described in Geraldes et al. (2001).

Four detrital zircon single grains analyses, from a paragneiss sample of the Palmital Succession (BUZ-20-01; location at Fig. 1), indicate $^{207}Pb/^{206}Pb$ ages between 950 and 700 Ma (Fig. 2a). Although discordant, some fractions plot very close to the concordia, suggesting that these could be derived from neoproterozoic source areas.

One monazite crystal from the same sample is clearly detrital, with a $^{207}Pb/^{206}Pb$ age of 1471 ± 50 Ma. Metamorphic monazites grains from this same sample are concordant at 505 and 497 Ma.

The more accurate data came from SHRIMP U-Pb analyses on the same paragneiss sample (BUZ-20-01). Ion microprobe analyses were carried out using SHRIMP RG at the Research School of Earth Sciences, Australian National University, Canberra, Australia. Zircon grains were mounted in epoxy resin and polished. Transmitted and reflected light microscopy, as well as scanning electron microscope cathodoluminescence imagery was used to investigate the internal structures of the zircon crystals prior to spot analysis. Data were collected and reduced as described by Williams & Claesson (1987) and

Compston et al. (1992). Uncertainties are given at 1 σ level, and final age is quoted at 95% confidence level. Reduction of raw data was carried out using Squid 1.02 (Ludwig, 2001a), and final ages and concordia plots were calculated using Isoplot-Ex (Ludwig, 2001b). U/Pb ratios were referenced to the RSES standard zircon FC1 (1099 Ma, $^{*206}Pb/^{238}U=0.1859$). U and Th concentrations were determined relative to those measured in the RSES standard SL13.

The cores of the detrital zircons yielded at least four age groups related to the source rocks: 2.5 Ga; ~2.0 Ga; ~1.0 Ga and a younger and most abundant population with ages ranging from 800 to 620 Ma (Fig. 2b, c). The metamorphic overgrowth is normally very thin and allowed only four spot analyses giving an upper intercept age of 511 ± 31 Ma (Fig. 2d). Although the large uncertainty, the age is coherent with those for metamorphic monazites, indicating the age of the metamorphic peak of the Búzios Orogeny.

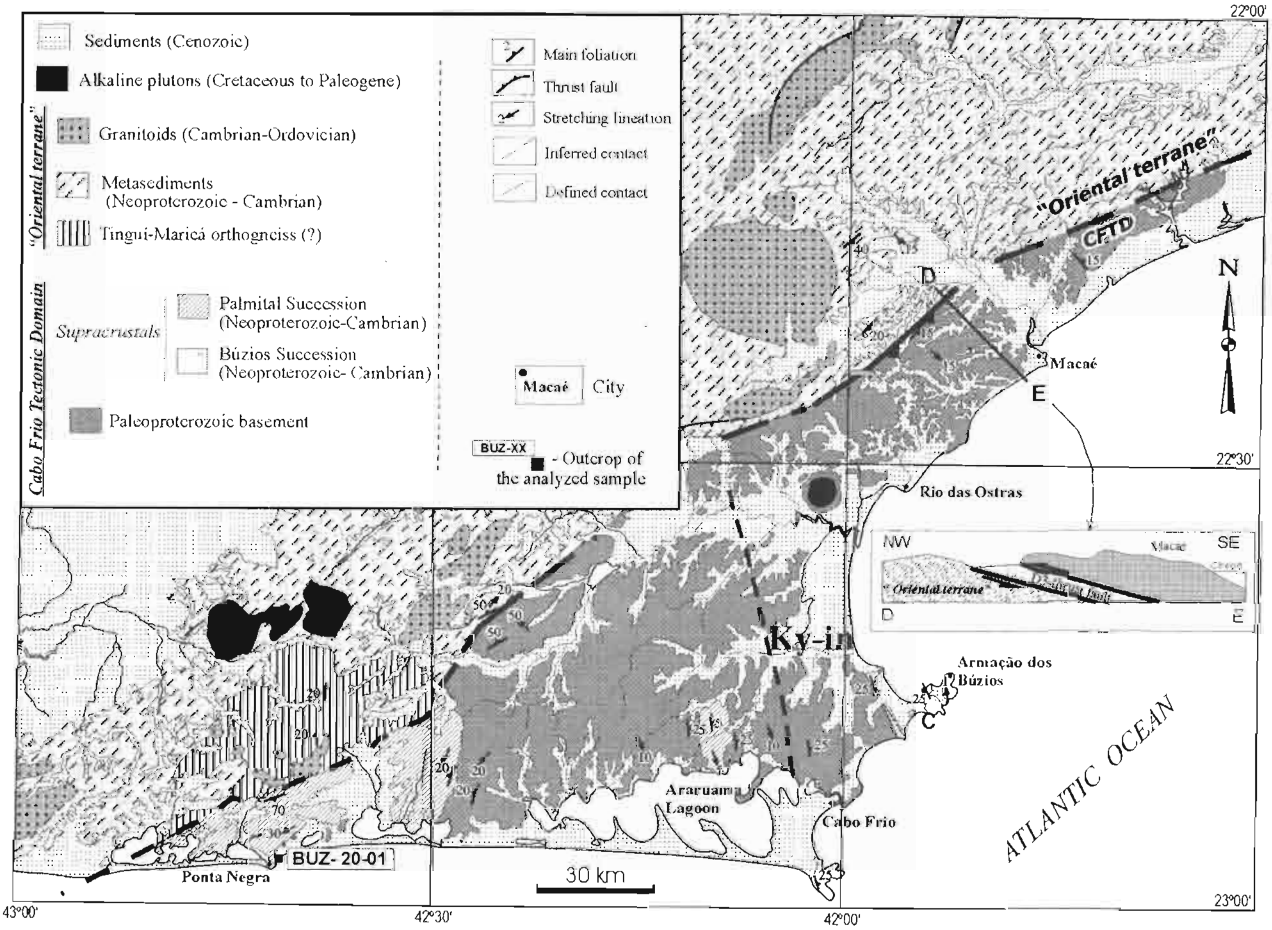

Figure 1. Geological map of southeastern portion of the central segment of the Ribeira belt. The Cabo Frio Tectonic Domain (CFTD) is located at east and part of the *"Oriental terrane"* is located at the west.

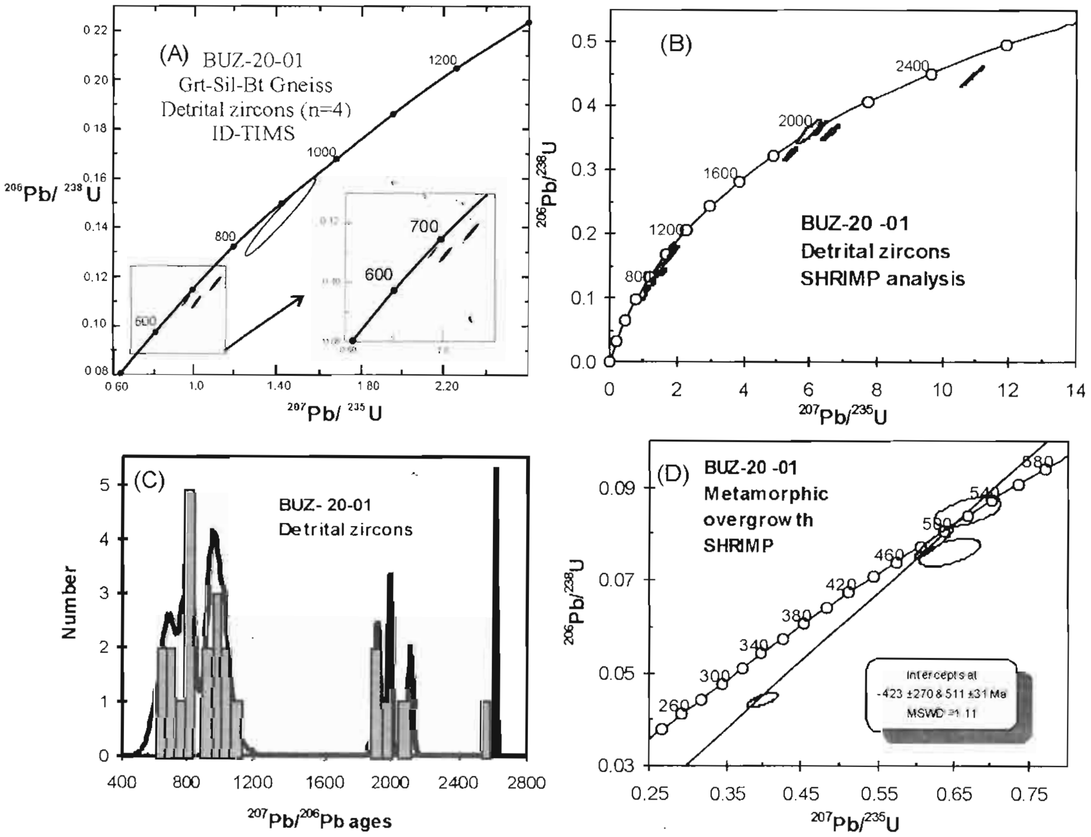

Figure 2. SHRIMP and ID-TIMS data for detrital zircons from a paragneiss of Palmital Succession (Sample BUZ- 20-01). (A) U-Pb conventional ID-TIMS analysis (n = number of fractions analysed); (B) U-Pb analysis from detrital zircon cores - SHRIMP; (C) Plot between number of SHRIMP analysis and age indicating at least 4 sources for the zircons ; (D) SHRIMP analysis in metamorphic overgrowth in detrital zircons.

DISCUSSION

This new SHRIMP U-Pb data indicate that there are several different Neoproterozoic detrital zircon populations in the Palmital paragneiss. These pink crystals present mainly acicular to cat-eye shapes. The metamorphic zircons from the CFTD exhibit very distinct morphology, they are rounded, pristine and small, yielding concordant ages close to 520 Ma. These granulitic zircons occur only in the kyanite metamorphic zone. The sample analyzed here is from the kyanite-out zone, and presents no metamorphic zircons.

In the Oriental terrane, a NE-SW oriented tectonic domain, located to the west of the CFTD (Fig. 1), detrital zircons from supracrustals analyzed with laser ablation-ICPMS show ages distributed between 2.9 Ga and 600 Ma (Valladares et al., 1999). The youngest neoproterozoic Pb-Pb ages were ascribed to partial resetting of the U-Pb system by Brasiliano metamorphism (Valladares et al., 1999).

Considering the discrimination between detrital and metamorphic zircons in the CFTD, it is possible that some Pb-Pb neoproterozoic ages from the Oriental terrane could represent the source area.

The main conclusion from the SHRIMP data is that the sedimentation in the Búzios-Palmital basin occurred at least in part after 620 Ma. Therefore, the neoproterozoic evolution of the CFTD started with the deposition (sediments) and crystallization (volcanics) of the supracrustals in a marine sedimentary basin after 620 Ma (Pb-Pb age in the core of detrital zircons) and before 525 Ma (Búzios Orogeny).

A candidate to represent the source area of the Palmital Succession sediments may be the Rio Negro magmatic arc (part of the Oriental terrane). This arc was generated at ca. 620 Ma as a result of eastward subduction of the passive margin of the São Francisco Craton (Tupinambá et al., 2000; Heilbron et al., 2000). The sedimentation in the Búzios-Palmital basin postdated the arc activity. Actually it was approximately simultaneous with the collision between the Rio Negro arc (within the Oriental terrane) and the Occidental terrane to the west at ca. 590 Ma (Heilbron et al., 2000).

Consequently the Búzios-Palmital basin developed close to an active continental margin. A continental crust was the source area for the sediments of the turbiditic submarine immature fans (Pamital Succession). Whether this basin was a fore-arc basin, an accretionary prism or some other similar basin, is uncertain.

The existence of this basin corroborates with the younger tectonic evolution of the CFTD, where the Cambrian Búzios orogeny was characterized (Schmitt, 2001; Schmitt et al., submitted). Nevertheless, the most striking conclusion is that at the transition from the Neoproterozoic to the Cambrian, there was still an active marine basin located in a region that would become the central part of West Gondwana. The agglutination of this supercontinent was only finished at the end of the Cambrian, resulting from the amalgamation of several continental blocks and subsequent closure of neoproterozoic-cambrian oceans/seas.

REFERENCES

Compston, W., Williams, I.S., Kirschvink, J.L., Zhang, Z., Guogan, M.A., 1992. Zircon U-Pb ages for the Early Cambrian time-scale. Jour. Geolog. Soc. London, 149:171-184

Fonseca, A.C., 1993. Esboço geocronológico da região de Cabo Frio, Estado do Rio de Janeiro. PhD thesis. IG/University of São Paulo. 186 p.

Geraldes, M.C.; Van Schmus, W.R.; Condie, K.C.; Bell, S.; Teixeira, W.; Babinsky, M., 2001. Proterozoic geologic evolution of the SW part of the Amazonian Craton in Mato Grosso state, Brazil. Precambrian Research, 111: 91-128.

Heilbron, M.; Mohriak, W.U.; Valeriano, C.M.; Milani, E.J.; Almeida, J.; Tupinambá, M., 2000. From collision to extension: The roots of the southeastern continental margin of Brazil. In: W.U.Mohriak & M.Talwani (Eds), Atlantic Rifts and continental margins – Geophysical Monograph 115. American Geophysical Union. p. 1-32.

Krogh, T.E., 1973. A low contamination method hydrothermal decomposition of zircon and extraction of U and Pb for isotopic age determinations. Geochemica et Cosmochemica Acta, 37:485-494.

Krogh, T.E., 1982. Improved accuracy of U-Pb zircon ages by the creation of more concordant systems using an air abrasion technique. Geochimica et Cosmochimica Acta, 46: 637-649.

Ludwig, K.R., 2001a. Squid 1.02. A user's manual. BGC Special Publ. 2., Berkeley, 19p.

Ludwig, K.R., 2001b. User's manual for Isoplot/Ex v. 2.47. A geochronological toolkit for Microsoft Excel. BGC Special Publ. 1a, Berkeley, 55p.

Parrish, R.R., 1987. An improved micro-capsule for zircon dissolution in U-Pb geochronology. Isotope Geoscience, 66:99-102.

Schmitt, R.S., 2001. The Búzios Orogeny – a cambrian-ordovician tectonometamorphic event in the Ribeira Belt – southeastern Brazil. Phd Thesis. Federal University of Rio de Janeiro/ University of Kansas. 273 p.

Schmitt, R.S.; Trouw, R.A.J.; Van Schmus, W.R., 1999. The characterization of a Cambrian (~520 Ma) tectonometamorphic event in the coastal domain of the Ribeira Belt (SE Brazil) – using U/Pb in syntectonic veins. Boletín Geologico y Minero Argentino, XXXIV: 363-366.

Schmitt, R.S.; Trouw, R.A.J.; Van Schmus, W.R., 1999b. Discussão sobre a origem dos anfibolitos do Bloco Cabo Frio: dados isotópicos e de terras raras – implicações na evolução tectônica da Faixa Ribeira. In: SBG, Simpósio Geol. Sudeste, 6, São Pedro (SP). Boletim de Resumos... p.13.

Schmitt, R.S.; Trouw, R.A.J.; Van Schmus, W.R.; Pimentel, M.M., The late amalgamation in the center of west Gondwana the characterization of a Cambrian collisional orogeny in the Ribeira Belt (SE Brazil) – new geochronological data. Precambrian Research (submitted to).

Tupinambá, M.; Teixeira, W.; Heilbron, M., 2000. Neoproterozoic western Gondwana assembly and subduction-related plutonism: the role of the Rio Negro Complex in the Ribeira Belt. Revista Brasileira de Geociências, 30 (1): 7-11.

Valladares, C.; Machado, N.; Heilbron, M.; Tupinambá, M.; Duarte, B.; Gauthier, G.; Noronha, M., 1999. Ages of detrital zircon from central Ribeira belt (Brazil) using laser-ablation-ICPMS. Boletín Geologico y Minero Argentino, XXXIV:145-147.

Williams, I.S. & Claesson, S., 1987. Isotopic evidence for the provenance and Caledonian metamorphism of high grade paragneisses from the Seve Nappes, Scandinavian Caledonides: ion microprobe zircon U-Th-Pb. Contrib. Mineral. Petrol. 97:205-217.

MESOPROTEROZOIC BIMODAL MAGMATISM IN THE SOUTHEASTERN PART OF RONDONIA, SW AMAZONIAN CRATON: ^{40}Ar/^{39}Ar GEOCHRONOLOGY AND TECTONIC IMPLICATIONS

Teixeira, W.[1]; Bettencourt, J.S.[1]; Vasconcelos, P.M.P.[2]; Rizzotto, G.J. [3]; Pacca, I.G.I.[1] and D'Agrella Filho, M.S.[1]

1. University of São Paulo, Brazil - Institute of Geosciences. Rua do Lago 562 – Butantã, 05508-080, São Paulo-SP, Brazil. Fone: +55 (11) 3091-4274. Fax: +55 (11) 3091 4295. wteixeir@usp.br
2. University of Queensland, Australia; University of Queensland – Dept. of Earth Sciences. Fone: +61 (7) 3365-2297, Brisbane, Qld 4072. Austrália. paulo@sol.earthsciences.uq.edu.au
3. Brazilian Geological Survey. Av. Lauro Sodré, 256, 78904-300, Porto Velho-RO, Brazil. Fone: +55(69) 223-3544. Fax: +55(69) 221-5435. cprmrepo@enter-net.com.br

Keywords: Amazonian Craton, geochronology, tectonics, Mesoproterozoic

^{40}Ar/^{39}Ar analyses, coupled with U-Pb and Rb-Sr radiometric data were performed on basic rocks, granites and gneisses that occur along a 1000 km transverse (Fig. 1), in the Southeastern part of the State of Rondonia. This area embraces parts of the Rio Negro-Juruena (1.75 - 1.55 Ga), Rondonian (1.48 - 1.41 Ga) and Sunsás (1.36 - 0.97 Ga) provinces – SW sector of Amazonian Craton. This is a key-area for understanding the tectonic and magmatic processes related to the agglutination of Rodinia (1.20 - 1.00 Ga), as well as for global correlation of late Mesoproterozoic intraplate features, widely reported within the broad Greenville province, such as: recurrent bimodal magmatism of AMCG suites, supracrustal sequences, intracontinental shear zones, and rift-basins. Nevertheless, despite the remarkable increase of the geologic knowledge in the SW Amazonian Craton during the last decade there are many open questions regarding the crustal evolution: i) the age and nature of the primary crust, and ii) the number of crustal/ juvenile accretion events that took place in this area during the Mesoproterozoic – among others.

The new ^{40}Ar/^{39}Ar radiometric data, combined with the geochronologic background and geologic setting, are used to constrain the timing of significant processes of extension tectonics and associated bimodal magmatism, and crustal reworking during the Mesoproterozoic, particularly associated with the Rondonian and Sunsás provinces. In addition, such a framework is used for global implications by means of the Eastern Laurentia/ Baltica - SW Amazonia connection.

Mafic and felsic plutonic rocks, located in the northern part of the area, yield ^{40}Ar/^{39}Ar ages in the range of 1.51 – 1.58 Ga, correlatable with the ages of the Serra da Providência Intrusive Suite. The interpretation of the new data is credit to an intraplate episode that originated the oldest phase of MCG magmatism, intrusive into the Rio Negro-Juruena province.

In the southeastern sector of the Rondonian province, the new ^{40}Ar/^{39}Ar ages of amphibolites, paragneisses and granites range from 1.36 to 1.30 Ga. Such rocks comprise the Colorado Metamorphic Suite (CMS), which is older than the evolution of the Nova Brasilândia Group (1.12 - 1.00 Ga). The latter sequence fills one of the rift-basins ascribed to be related to the Sunsás orogen. Undeformed metagabbros of the CMS, as well as the neighbouring gneissic rocks yield U-Pb and Rb-Sr ages of 1.35 and 1.36 Ga, respectively. These data are therefore indicative of a tectonomagmatic event (juvenile accretion and metamorphism) in the SW Amazonian craton. This interpretation is also supported by comparable SHRIMP U-Pb zircon ages that have been reported for the peak of regional granulitic metamorphism in north-central Rondônia, as well as for the time of emplacement of some of the intrusive plutons.

A third group of ^{40}Ar/^{39}Ar ages for mafic and felsic rocks of the Nova Brasilândia sequence (western portion of the rift-basin) yielded plateau ages (horblende and biotite) between 1125 - 980 Ma. Some of these ages (i.e., 1110 – 1000 Ma) probably reflect the tectonic closure of this basin, and the timing of associated shearing and hydrotermal episodes, resulted from the tectonic overprint of the Sunsás events. The youngest ^{40}Ar/^{39}Ar ages (980 Ma) also agree with the time of emplacement of the "Younger Granites" of Rondônia.

Finally, some scattered amphibolites yield constrasting ^{40}Ar/^{39}Ar ages: 1.08 Ga; 1.13 - 1.15 Ga; 1.16 - 1.17 Ga and 1.25 Ga. These apparent ages compare well with the range of K/Ar and Rb-Sr ages available for country rocks in Central Rondônia (Rondônia-San Ignacio province), which have been reworked due to the Sunsás orogen. Nevertheless, some of these ages may have somewhat been influenced either by emplacement of the Alto Candeias Intrusive (1.34 - 1.33 Ga) and Santa Clara (1.08 - 1.07 Ga) plutonic suites, or by the evolution of the Ji-Paraná shear zone (1.08 - 1.05 Ga) – an important tectonic feature of the Rondonian-San Ignacio province, representing a strike-slip motion accompanied by thrust and granite emplacement associated with the Sunsás tectonic overprint.

As a whole, the geochronologic and geologic scenario is consistent with the proposed link between Eastern Laurentia/ Baltica and SW Amazonian Craton during the Mesoproterozoic, signed by the Grenville-Sunsás collage. This assessment has implications for establishing the paleocontinental margin during the final agglutination of Rodinia (1.2 - 1.0 Ga), mirrored by the investigated MCG magmatism, tectonic basins and shear zones.

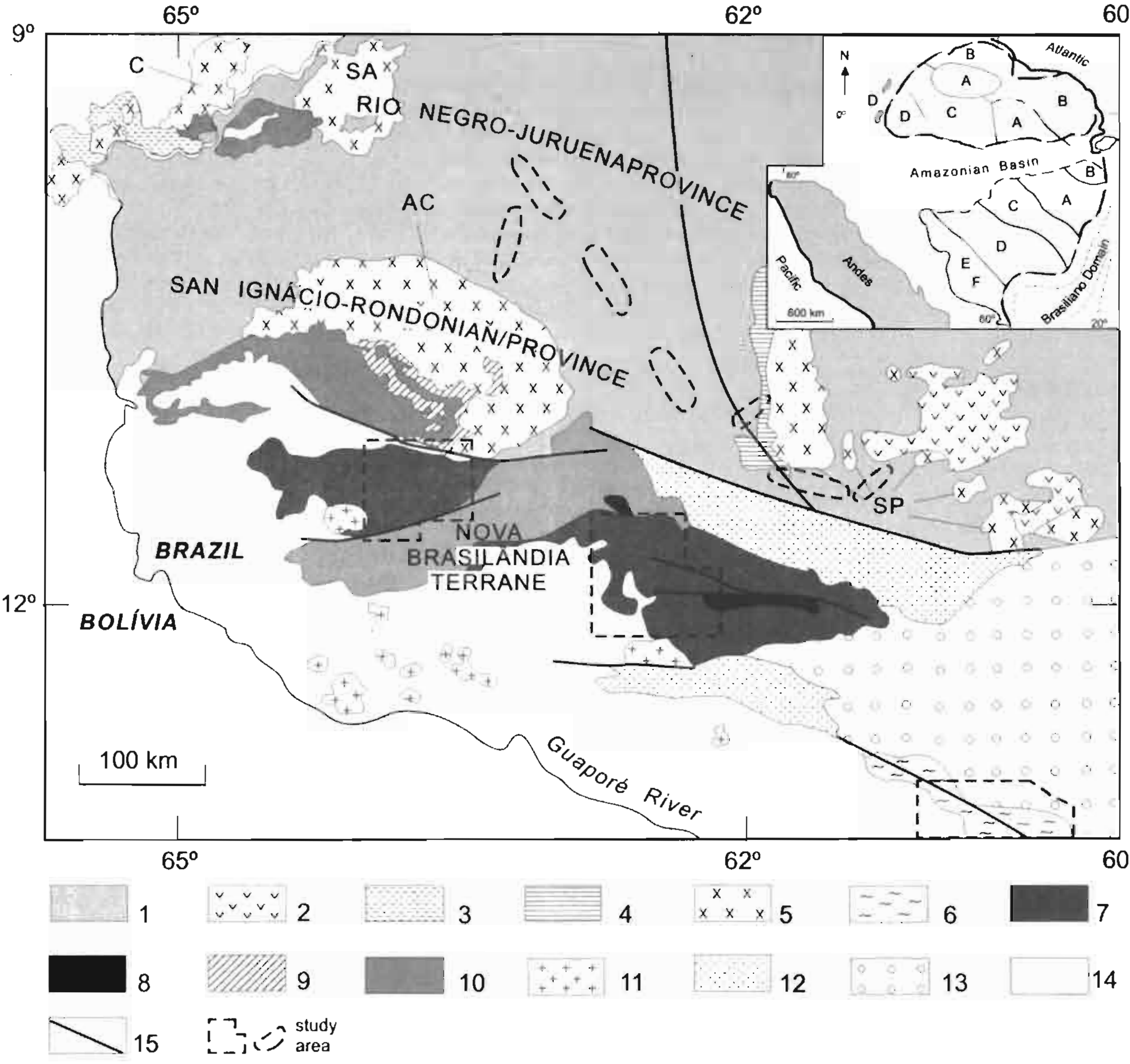

Figure 1. Geological sketch map of part of the SW sector of the Amazonian Craton, showing the study area. 1) Polycyclic basement; 2) Roosevelt volcano-sedimentary sequence; 3) Mutum Paraná metavolcano-sedimentary sequence; 4) Beneficiente Group; 5) Intrusive granitoid suites; 6) Colorado metamorphic suite; 7) Nova Brasilândia Group; 8) Nova Brasilândia Group mafic rocks; 9) Mafic rocks of the Nova Floresta Formation; 10) Supracrustal sequences of the Sunsás/Aguapeí orogeny; 11) Post-tectonic granitoids of the Sunsás/Aguapeí orogeny; 12) Paleozoic cover; 13) Mesozoic cover; 14) Recent; 15) Main tectonic structures. Inset: Main provinces of the Craton: A) Central Amazônia; B) Maroni-Itacaiunas; B) Ventuari-Tapajós; D) Rio Negro - Juruena; E) San Ignácio-Rondonian; F) Sunsás-Aguapeí.

U-Pb PROVENANCE AGES OF DETRITAL ZIRCONS FROM PROTEROZOIC METASEDIMENTARY UNITS ADJACENT TO SOUTHWESTERN AND SOUTHERN SÃO FRANCISCO CRATON

Valeriano, C.M.[1]; Machado, N.[2,3]; Simonetti, A.[2]; Valladares C.S.[1]; Seer, H.J.[4] and Simões, L.S.A.[5]

1. TEKTOS–Geotectonics Study Group, Faculdade de Geologia, Universidade do Estado do Rio de Janeiro, Rua São Francisco Xavier 524/4006-A, Rio de Janeiro-RJ, 20559-900, Brazil. cmval@uerj.br, vallada@uerj.br
2. Centre de recherche en géochimie et géodynamique (GEOTOP-UQAM-McGill), Université du Québec à Montréal. simonetti.antonio@uqam.ca
3. Département des Sciences de la Terre et de l'Atmosphère, Université du Québec à Montréal, CP 8888, Succ. Centre-Ville, Montréal, QC, H3C 3P8, Canada. machado.nuno@uqam.ca
4. Centro Federal de Educação Tecnológica de Minas Gerais, Av. Amazonas 807, Araxá-MG, Brazil. hildor@araxa.cefetmg.br
5. DPM-IGCE, Universidade Estadual Paulista, CP 178, 13506-900, Rio Claro-SP, Brazil. lsimoes@rc.unesp.br

Keywords: Detrital zircon, ID-TIMS, LA-MC-ICPMS, São Francisco Craton, Neoproterozoic

INTRODUCTION

The purpose of this work is to contribute to better understand the development of the passive margin of the São Francisco Paleocontinent by studying detrital zircons of metasedimentary units in the southern Brasília belt and foreland zone south of the São Francisco craton (Fig 1). New U-Pb data were both obtained with Isotope Dilution-Thermal Ionization Mass Spectrometry (ID-TIMS) and Laser Ablation Multi Collection Inductively Coupled Plasma Mass Spectrometry (LA-MC-ICPMS).

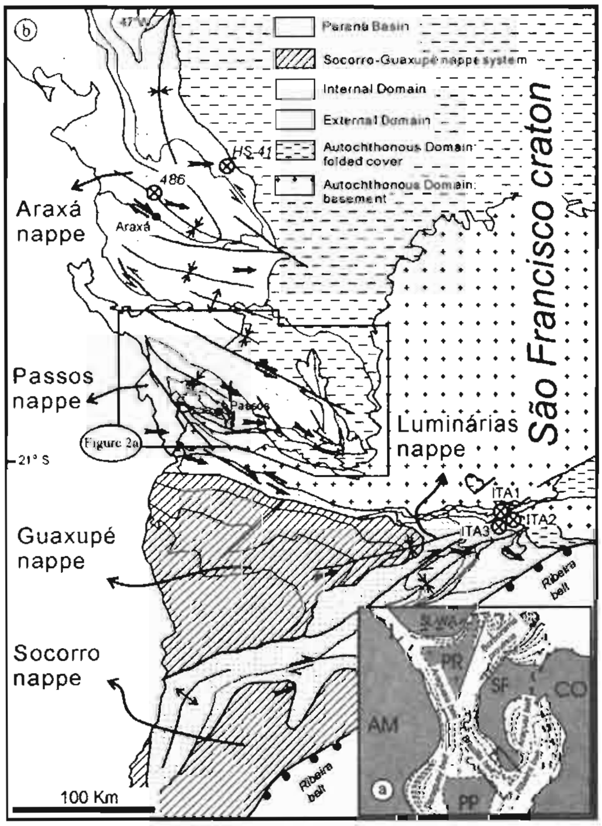

Figure 1. a) Tectonic domains mentioned in this work and sample location (in part). Black arrows: direction of tectonic transport; RB: Ribeira Belt. Adapted from Valeriano et al. (2000). b) The southern Brasília belt in the context of West Gondwana. Adapted from Almeida et al. (2000).

The results yield a Neoproterozoic age for the sedimentation of the Araxá, Canastra and Andrelândia Groups. The data also reveal an unexpected variety of Mesoproterozoic sources, still undetected in the southern São Francisco Craton.

SOUTHERN BRASILIA BELT

The Southwestern portion of the São Francisco craton comprises an Archean-Paleoproterozoic basement, which is mostly covered by autochthonous and para-autochthonous pelitic-carbonatic rocks of the Neoproterozoic Bambuí Group and older metasedimentary successions. In the adjacent orogenic belts (Brasilia and Ribeira) an External Domain is composed of thrust systems of thick low-grade passive margin successions (Canastra, Ibiá and Paranoá, proximal Andrelândia Groups) and subordinate basement slivers. This domain is tectonically thrusted by the metamorphic nappes of the Internal Domain (e.g. Araxá, Passos, Luminárias nappes) composed of distal passive margin and slope sedimentary deposits (Araxá and Andrelândia Groups).

PASSOS NAPPE

Samples from the Araxá Group in this nappe were collected from the lower to the upper structural levels (named units A to I). The lower level was affected by greenschist facies metamorphism whilst the intermediate and the upper levels are at amphibolite and granulite facies, respectively. Results are presented from the lower to the upper levels of the nappe.

UNIT B – FURNAS QUARTZITE

The Furnas Quartzite occurs along the basal levels of the Passos Nappe. It is a 50 m thick layer of white, fine-grained, laminated and micaceous metarenite. Except for subordinate small euhedral grains, detrital zircons from this sample are well rounded and pitted and are devoid of metamorphic overgrowth. A total of 24 detrital grains were analyzed, 8 by ID-TIMS and 16 by LA-MC-ICPMS.

Six of the zircons dated by ID-TIMS yielded ages between 2144 Ma and 1919 Ma and are most likely derived from rocks formed or metamorphosed during the Transamazonian Orogeny. Another one yielded an age of 2480 Ma. The largest of the euhedral zircons yielded a concordant age of 1335 Ma but with relatively large uncertainties in the $^{207}Pb/^{206}Pb$ value. Therefore, the 1336+6/-7 Ma $^{206}Pb/^{238}U$ age is more reliable.

A rounded and pitted detrital monazite grain yielded a $^{207}Pb/^{206}Pb$ age of 2117 Ma (-1.8% discordant). This result indicates that low grade metamorphism did not disturb the U-Pb system of detrital monazite. Thirteen of the zircons dated by LA-MC-ICPMS cluster in the 2.2-2.0 Ga interval, probably derived from units related to the Transamazonian Orogeny. One zircon yielded a minimum age of 2388 Ma and two others yielded minimum ages of 3362 Ma and 3381 Ma. These Archean zircons are older than the oldest documented rock in the southern São Francisco craton, an anorthositic layer in a layered intrusion in the Piumhi greenstone belt (3116 +10/-7 Ma; Machado & Schrank, 1989) but are coeval to others found in detrital rocks of the Rio das Velhas Supergroup and the Minas Supergroup (Quadrilátero Ferrífero area; Machado et al., 1996). Therefore, although rock exposures older than 3.1 Ga are not known in the presently exposed sectors of the São Francisco craton, detrital zircons indicate their occurrence.

UNIT E – MICACEOUS QUARTZITE

Sample 1040 was collected from a coarse-grained garnet-biotite-muscovite quartzite at amphibolite facies, in the intermediate portion of the Passos Nappe.

The zircons are rounded and pitted and display incipient pyramidal outgrowths. This is the lowest level of the Passos nappe where zircon overgrowths are observed. Those features indicate that the metamorphic conditions affecting the quartzite were compatible with the generation of new zircon population.

Seven detrital zircons were analysed by ID-TIMS. One yielded a concordant age of 2916 +21/-20 Ma, the large uncertainty probably related to high common Pb. The other six grains yielded ages between 1323 +8/-9 Ma and 1160 Ma, one of which is concordant at 1296 +6/-5 Ma.

Twenty one zircons were analysed by LA-MC-ICPMS indicating $^{207}Pb/^{206}Pb$ ages between 2463 Ma and 907 Ma. Nine are concordant at 1924 ±11, 1806 ±6, 1794 ±11, 1756 ±11, 1756 ±9, 1565 ±5, 1506 ±8, 1224 ±9 and 907 +69/-72 Ma.

Some of the zircons are derived from known sources: those dated between 2053 Ma and 1863 Ma are inferred to be from Transamazonian rocks, and those dated at ca. 1750 Ma are most likely derived from igneous rocks related to Statherian rifting events documented in the São Francisco Craton (Espinhaço rift). The sources of zircons with Mesoproterozoic ages ranging from 1565 Ma to 1224 Ma are intriguing since no rocks of these ages are known in the São Francisco craton or in the surrounding areas. However, these ages are significant because they indicate for the first time the presence of Mesoproterozoic magmatism, possibly of anorogenic character. Although it could be argued that some of these zircons are older and were affected by Neoproterozoic metamorphism, the fact that some grains are concordant (e.g. 1565, 1506 and 1223 Ma) supports the inference that they are derived from rocks of these ages. The youngest concordant zircon, dated at ca. 907 Ma provides the first reliable maximum age of sedimentation for the Araxá Group.

Sample 1041 is from a quartz-schist intercalation within the predominant metapelitic schists of Unit E, in the intermediate portion of the nappe. Zircon grains are also typically detrital - rounded and pitted with incipient pyramidal outgrowths. A colorless, small zircon was analyzed by ID-TIMS and yielded a minimum age of 2152 Ma (3.2% discordant). Most of the twenty grains analyzed by LA-MC-ICPMS yielded ages clustering in the 2259 Ma to 2041 Ma interval, probably derived from rocks formed or metamorphosed during the Transamazonian Orogeny. The youngest grain yielded a minimum age of 1039 Ma (6.7% discordant).

UNIT H – ORTHOQUARTZITE

Sample 1042 is from a well recrystallized orthoquartzite intercalation within paragneisses of Unit H, in the upper portions of the nappe, with metamorphic grade at the amphibolite-granulite facies transition. The predominant zircon morphology is represented by grains with well preserved rounded, presumably detrital cores and distinct euhedral overgrowths. Small equant, euhedral, multifaceted and colorless crystals typical of granulite facies rocks are less abundant. Grains containing two or three cores surrounded by new zircon (synneusis) are also observed.

Five small equant grains were selected for ID-TIMS analysis. In spite of extended abrasion, all five analyses are discordant (12% to 44%) and yield minimum ages between 2057 Ma and 1697 Ma. Cores were not observed when selecting these crystals under a binocular microscope. However, cathodoluminescence imaging of several crystals of this type carried out after the isotopic analysis, revealed the presence of cores and explains the discordance pattern. The three most concordant analyses define a reliable discordia with intercepts of 2123 ±7 and 658 ±21 Ma, indicating that the cores are derived from rocks of Transamazonian age and underwent Neoproterozoic metamorphism.

The detrital cores of thirty-one zircons were analyzed by LA-MC-ICPMS and, with the exception of an Archean grain, they scatter along a discordia band between ca. 2.2 and 0.6 Ga, indicating derivation from a Paleoproterozoic source and strong Pb loss due to Neoproterozoic high-grade metamorphism.

EXTERNAL DOMAIN - ARAXÁ SEGMENT

A fine-grained orthoquartzite of greenschist facies was collected from the upper portion of the Canastra Group (sample HS41), in the classical region where this unit was originally defined (Barbosa, 1954). Colorless to dark pink-purple zircon grains are sub-rounded to well rounded, pitted and devoid of metamorphic overgrowth. The ages of twenty grains analyzed by LA-MC-ICPMS fall into three main groups: Archean (2875 ±3, 2583 and 2581 Ma), Paleoproterozoic (2237-1743 Ma) and Mesoproterozoic (1536-1180 Ma). The youngest grain yielded a $^{207}Pb/^{206}Pb$ age of 1226 ±8 Ma. Archean and Paleoproterozoic sources have already been referred to above for the Araxá Group metasediments. The 1536-1180 Ma ages are similar to those found in the Araxá Group and confirm the previous inference for the occurrence of Mesoproterozoic sources in the São Francisco craton. The youngest zircon (ca. 1226 Ma) provides an upper limit for the sedimentation of the Canastra Group.

EXTERNAL DOMAIN – FURNAS SEGMENT

The External Domain, to the east of the Passos nappe, consists of an imbricated thrust system (Ilicínea-Piumhi thrust system, Valeriano et al., 1995) comprising from bottom to top sheets of felsic metavolcanic rocks (Costas schist), metasedimentary sequences (Serra da Boa Esperança sequence; Valeriano, 1992), Archean granite-greenstone basement slivers (Piumhi greenstone belt, Schrank, 1982) and chromitite-bearing serpentinites, which are overlain by an upward-coarsening metasedimentary sequence (Serra da Mamona unit). All rock units are in the chlorite zone of the greenschist facies. Results are presented from the lower to the upper structural levels.

SERRA DA BOA ESPERANÇA SEQUENCE

The basal thrust sheet of this sequence comprises gray, coarse-grained micaceous metarenite from which two samples were collected (1044 and 1046). Zircons extracted from the first sample are colorless or exhibit different shades of pink and display typically detrital morphological features. Two analyses by ID-TIMS yielded minimum ages of 2081 Ma and 1946 Ma (both 2% discordant), a third one is concordant at 1445 ±2 Ma. Twenty four analyses by LA-MC-ICPMS cluster in the following age groups: one Archean ($^{207}Pb/^{206}Pb$ ages of 2768-2694 Ma); three Paleoproterozoic (2324-2278 Ma and 2012-1841 Ma and a concordant analysis at 1728 ±28 Ma); one Mesoproterozoic with six grains between 1397 Ma and 1331 Ma and one Neoproterozoic, with the two most concordant grains yielding $^{207}Pb/^{206}Pb$ ages of 1072 Ma and 989 Ma. Detrital zircons from sample 1046, pink and colorless rounded, were analyzed by ID-TIMS and yielded minimum ages of 1948 Ma and 1396 Ma.

Sample 1128 is a meta-arkose that formed along the sole thrust of the External Domain (near the locality of Santo Hilário). The results of two single-grain analyses by ID-TIMS and of twenty five by LA-MC-ICPMS plot in the same age groups as defined by the previous samples. One of the grains is concordant at 1234 ±7 Ma and the youngest age obtained is 1086 Ma (8.7% discordant).

The Archean and Paleoproterozoic provenance ages are similar to those found for the Araxá Group and can be attributed to the sources previously mentioned. It is worth noting that the 1.2-1.4 Ga old zircons were also found in the Araxá Group, reinforcing the occurrence of a magmatic (or metamorphic) event in that age range. The 1086 Ma and 989 Ma old zircons bracket the upper limit for the sedimentation of the Serra da Boa Esperança sequence.

SERRA DA MAMONA UNIT

The uppermost thrust-sheet of the External Domain is represented by the upward-coarsening Serra da Mamona unit (Valeriano, 1992). Basal BIF intercalations within carbonaceous metapelite grade into metarenite and overlying quartzitic metaconglomerate. This thrust-sheet rests on a tectonic lens composed of chromitite-bearing serpentinites and talc-schists. Detrital zircons extracted from a metaconglomerate layer (sample 1084) are typically pink-colored, rounded and pitted. Two ID-TIMS analyses yielded minimum ages of 2976 Ma (15% discordant) and 2817 Ma (2.2% discordant). The ages of 24 zircons dated by LA-MC-ICPMS are between 3060 ±7 Ma and 2685 Ma, including another concordant zircon at 2906 ±2 Ma. The exception is a grain with a minimum age of 2197 Ma (20% discordant) with a probable age between 2.2 Ga and 2.3 Ga indicating that the deposition of the Serra da Mamona unit is Paleoproterozoic or younger.

EXTERNAL DOMAIN SOUTH OF SFC

This area constitutes a transition zone between the autochthonous southernmost São Francisco craton and the external allochthons. It is composed by both autochthonous and allochthonous units of the predominantly metasedimentary Andrelândia Group and its Archean-Paleoproterozoic basement. These allochthons may have been affected by the development of both Brasilia and (younger) Ribeira belts.

The age of sedimentation of the Andrelândia Group is limited by the Paleoproterozoic age of its basement and by metamorphic age given by a ca. 567 Ma discordia lower intercept (Söllner & Trouw, 1997). Samples ITA-2 and ITA-3 are from a thin thrust sheet of the Andrelândia Group whilst ITA-1 is from the underlying intensely folded but autochthonous Andrelândia Group. The three samples are orthoquartzites representing typical units of this group at lower amphibolite facies. Zircons extracted from these samples are typically detrital. Thirty zircon analyses by LA-MC-ICPMS (sample ITA-1), yielded ages clustering in the same Archean and Paleoproterozoic groups already mentioned. A series of concordant zircons in the 1484-1246 Ma range was also found. Given that the unit sampled is in the Autochthonous domain and that zircons show no overgrowth, these ages certainly document the presence of Mesoproterozoic sources in the São Francisco craton. In addition, zircons with ages in the 1.0-1.1 Ga range, including a concordant one at 1011 +39/-40 Ma, are the best estimate for the upper limit for the sedimentation of the Andrelândia Group.

Zircons from sample ITA-3, also from the allochthonous portion of the Andrelândia Group, analyzed by the same method, yielded a similar pattern of ages. Two rounded monazite grains with rough surface were analyzed from the same klippe of Andrelândia Group quartzites. One yielded a minimum age of 588 Ma (1.7% discordant, ITA3-2) and the other 2027 Ma (16%

discordant, ITA2-1). A discordia line constructed with the two grains yields an upper intercept at 2104 Ma and indicates that the latter is probably detrital and was affected by Neoproterozoic metamorphism. It is noted that in spite of the growth of new monazite in sample ITA3, the detrital zircons analyzed do not show Pb loss related to the Neoproterozoic metamorphism. The data for this sample thus bracket the sedimentation of the Andrelândia Group in the Neoproterozoic between the age of the youngest detrital zircon - ca. 1011 Ma - and the age of metamorphism at ca. 588 M.

DISCUSSION

The Araxá, Canastra and Andrelândia Groups are consensually interpreted as part of the sedimentary succession of the Neoproterozoic passive margin bordering the western and southern parts of the São Francisco craton. A common feature of the clastic rocks from these units is the similarity of zircon provenance ages. The Archean and Paleoproterozoic ages are compatible with erosion of the São Francisco craton. Particularly interesting are the Mesoproterozoic provenance ages between ca. 1.2 Ga and 1.6 Ga, with a cluster at ca. 1.3 Ga (Fig 2).

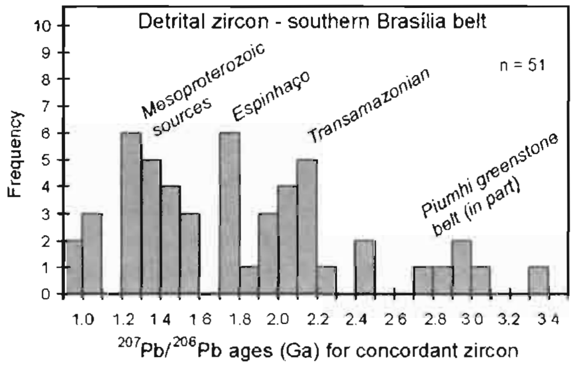

Figure 2. Provenance of passive margin units around SW and S São Francisco craton, given by U-Pb ages of concordant detrital zircons.

Several zircons with ages in this range are concordant to sub-concordant, indicating that these ages are not due to the effect of Neoproterozoic metamorphism on Archean-Paleoproterozoic grains. Therefore, one of the main conclusions of this work is that Mesoproterozoic sources must be present in the São Francisco craton but its exposures have yet to be identified. These sources may be located underneath the Bambuí Group, which covers most of the southern São Francisco craton, or at the western margin of the São Francisco Paleocontinent, which is presently overridden by the external and internal allochthons. The latter hypothesis would imply that the locus of the Neoproterozoic continental break-up occurred preferentially along Mesoproterozoic rift systems. The ages of the youngest detrital zircons from the Araxá, and Andrelândia Groups and the Serra da Boa Esperança Sequence lie between 1.0 Ga and 0.9 Ga and provide the upper limit for the sedimentation age. The lower limits are the metamorphic ages of ca. 630 Ma for the Araxá Group and of 588 Ma for the Andrelândia Group. Because of the lack of sedimentation age constraints and of reasonable stratigraphic correlation, the Serra da Boa Esperança sequence was individualized (Valeriano et al., 2000). However, a Neoproterozoic age for the Serra da Boa Esperança sequence supports the inclusion of this unit amongst the proximal successions around the São Francisco craton. The age limits for the sedimentation of the Canastra Group remain poorly defined and it can only be stated that it must be younger than the youngest zircon dated at 1266 Ma.

ACKNOWLEDGEMENTS

C. Valeriano acknowledges financial support from CNPq (proc. 471931/01-2), UERJ/SR-1 and a post-doctoral grant (CAPES BEX-1032/99-2). The Micromass Isoprobe instrument and the Lambda Physik-Merchantek-New Wave laser system installed at the UQAM were financed through NSERC-Canada and contributions from FCAR (Québec) and Foundation UQAM. The laboratory is maintained in part with a NSERC MFA grant. A NSERC grant to N. Machado partly financed this work. Laboratory support from R. Lapointe is thankfully acknowledged. Suggestions from Renata Schmitt helped to improve this manuscript.

REFERENCES

Almeida, F.F.M., Brito Neves, B.B., Carneiro, C.D.R., 2000. The origin and evolution of the South American Platform. Earth-Science Reviews 50, 77-111.

Barbosa, O., 1954. Évolution du geosynclinal Espinhaço. In: Congres Geol. Intern. 19, Alger, 1952. Compt. Rend.,.Sect. 13, fasc. 14. Alger, 1954, 17-36.

Machado, N. & Schrank, A., 1989. Geocronologia U-Pb no maciço de Piumhi – resultados preliminares. In: Simposio de Geologia de Minas Gerais 5, Belo Horizonte. Anais... SBG-MG, Bol. 10, 45-49.

Pimentel, M.M., Dardenne, M.A., Fuck, R.A., Viana, M.G., Junges, S.L., Fischel, D.P., Seer, H.J., Dantas, E.L., 2001. Nd isotopes and the provenance of detrital sediments of the Neoproterozoic Brasília belt, central Brazil. J. South Am. Earth Sci. 14, 571-585.

Schrank, A., 1982. Petrologie des komatiites et des roches associées de la ceintures verte du Massif Précambrien de Piumhi (Minas Gerais - Brazil). Thèse 3ème Cycle, Univ. Paris-Sud, Orsay, 270 p.

Söllner, F. & Trouw, R.A.J., 1997. The Andrelândia depositional cycle (Minas Gerais, Brazil), a post-Transamazonic sequence south of the São Francisco craton: evidence from U-Pb dating on zircons of a metasediment. J. South Am. Earth Sci. 10, 21-28.

Valeriano, C.M., 1992. Evolução tectônica da extremidade meridional da Faixa Brasília, região da Represa de Furnas, Sudoeste de Minas Gerais. PhD Thesis, Univ. São Paulo-IG, 192 p.

Valeriano, C.M., Almeida, J.C.H., Simões, L.S.A., Duarte, B.P., Heilbron, M., 1995. Evolução estrutural do domínio externo da Faixa Brasília no sudoeste de Minas Gerais: registros de uma tectônica pré-brasiliana. Rev. Bras. de Geociências 25, 221-234.

Valeriano, C.M., Simões, L.S.A., Teixeira, W., Heilbron, M.,. 2000. Southern Brasilia belt (SE Brazil): tectonic discontinuities, K-Ar data and evolution during the Neoproterozoic Brasiliano orogeny. Rev. Brasileira de Geociências 30, 195-199.

GRENVILLIAN BASEMENT AND FAMATINIAN EVENTS OF THE SIERRA DE UMANGO (29ºS): A REVIEW AND NEW GEOCHRONOLOGICAL DATA

Varela, R.[1]**; Basei, M.A.S.**[2]**; Sato, A.M.**[1]**; González, P.D.**[1]**; Siga Jr., O.**[2]**;**
Campos Neto, M.C.[2] **and Cingolani, C.A.**[1]

1. Centro de Investigaciones Geológicas, Universidad Nacional de La Plata y Consejo Nacional de Investigaciones Científicas y Técnicas. Calle 1 Nº 644, 1900 La Plata, Argentina. varela@cig.museo.unlp.edu.ar, sato@cig.museo.unlp.edu.ar, gonzapab@cig.museo.unlp.edu.ar, ccingola@cig.museo.unlp.edu.ar
2. Instituto de Geociências, Universidade de São Paulo. Rua do Lago 562, 05508-900 São Paulo-SP, Brasil. baseimas@usp.br, siga@usp.br, camposnt@usp.br

Keywords: Grenvillian basement, Middle Proterozoic, Lower Paleozoic, geochronology

INTRODUCTION

The Sierra de Umango (29º00'S-68º40'W) was interpreted as part of a northernmost Grenvillian-age rocks of Laurentian-derived terrane, accreted to the southwestern margin of Gondwana. The most important tectono-metamorphic and magmatic processes related to this collision occurred along the N-S trending Famatinian orogen since the Ordovician to Devonian (e.g. Dalla Salda et al., 1992, 1998; Ramos et al., 1998; Astini, 1998; Casquet et al., 2001), overprinting the magmatic and metamorphic rocks already affected by previous Grenvillian history.

In this paper we present new U-Pb ages that extends the outcrops of Grenvillian rocks to the north of the well known localities with Mesoproterozoic rocks, and also constrain the age of the subsequent overprinting events. The new ages together with the already existing data, allow us to understand the geological evolution of the Sierra de Umango in relation to the Lower Paleozoic Famatinian Orogeny.

GEOLOGICAL OUTLINE OF THE SIERRA DE UMANGO

The Sierra de Umango (Fig. 1) is located in the northern part of the Western Sierras Pampeanas (Caminos, 1979) and the Grenvillian basement rocks are composed of medium to high grade orthogneisses of basic to acid composition (Juchi Orthogneiss of Varela et al., 1996). The conventional U-Pb data (granitic orthogneiss) of 1108±13 Ma was interpreted as magmatic crystallization age (Varela et al., in press) as well as Rb-Sr whole rock isochron of 1030±30 Ma from the same rock was related to overprinting amphibolite-granulite facies metamorphic event (Varela et al., 1996). A garnetiferous orthoamphibolite has given a K-Ar hornblende age of 539±14 Ma and 442±15 Ma, consistent with post-intrusion amphibolite facies metamorphic event (Varela et al., in press).

The Grenvillian basement rocks are separated by shear zones from medium to high grade siliciclastic and calcareous sequence (Tambillo Metamorphites), composed mainly of schists and marbles with orthoamphibolites and minor gneisses and pegmatites. This sequence was interpreted as a platform covering the Mesoproterozoic cratonic basement (Varela et al., 2001). The initial ratio $^{87}Sr/^{86}Sr$ and $\delta^{13}C$ from marbles suggest a sedimentation age in the range 640-580 Ma (Varela et al., 2001). The Rb-Sr whole rock+minerals isochrons of 379±41 Ma and 373±7 Ma from two foliated pegmatites were interpreted as the age of the latest metamorphism and ductile deformation event (Varela et al., 2002). The Sm-Nd whole rock+minerals isochron of 392±50 Ma from an amphibolite intercalated in the sequence, also confirm the tectonothermal event at Middle to Late Devonian times.

The El Peñón Granite intruded the Tambillo Metamorphites of possible Neoproterozoic sedimentation age, and is composed of foliated granodiorites and granites. The conventional U-Pb zircon crystallization age of 473±17 Ma (Varela et al., in press) from El Peñón Granite was overprinted at least by two metamorphic events, at ~469 Ma (Rb-Sr whole rock isochron; Varela et al., 2000) and 409-381 Ma (K-Ar, muscovite; Varela et al., in press). The Early Ordovician metamorphism age was confirmed with the new U-Pb results (see below) and the Early to Middle Devonian ages partly overlap the time span of 392-373 Ma from the pegmatites and amphibolite.

NEW U-Pb RESULTS AND DISCUSSION

New conventional U-Pb data (zircon) from two tonalitic orthogneisses yielded ages of 1090±35 Ma -MSWD 0.038- and 1216+29/-16 Ma -MSWD 1.9- (Fig. 1, Table 1). These Mesoproterozoic datums are interpreted as representing the magmatic crystallization age of the igneous protolith of the Juchi Orthogneiss, and are also consistent with previous geochronological data.

Five zircon fractions from a biotitic paragneiss define a discordia line with upper intercept at 1139±82 Ma – MSWD 40- and lower intercept at 447±36 Ma (Fig. 1, Table 1). We consider the Mesoproterozoic data as that of the heritage age of the Tambillo Metamorphites (related to Grenvillian basement) and we interpret the Late Ordovician data as the metamorphic overprint related to Famatinian Orogeny.

Three monazite fractions from a mylonitic paragneiss define an ^{238}U-^{206}Pb age of 452±6 Ma, -MSWD 0.47- (Fig 1, Table 1). This data is interpreted as representing the same Late Ordovician metamorphic event of biotitic paragneiss.

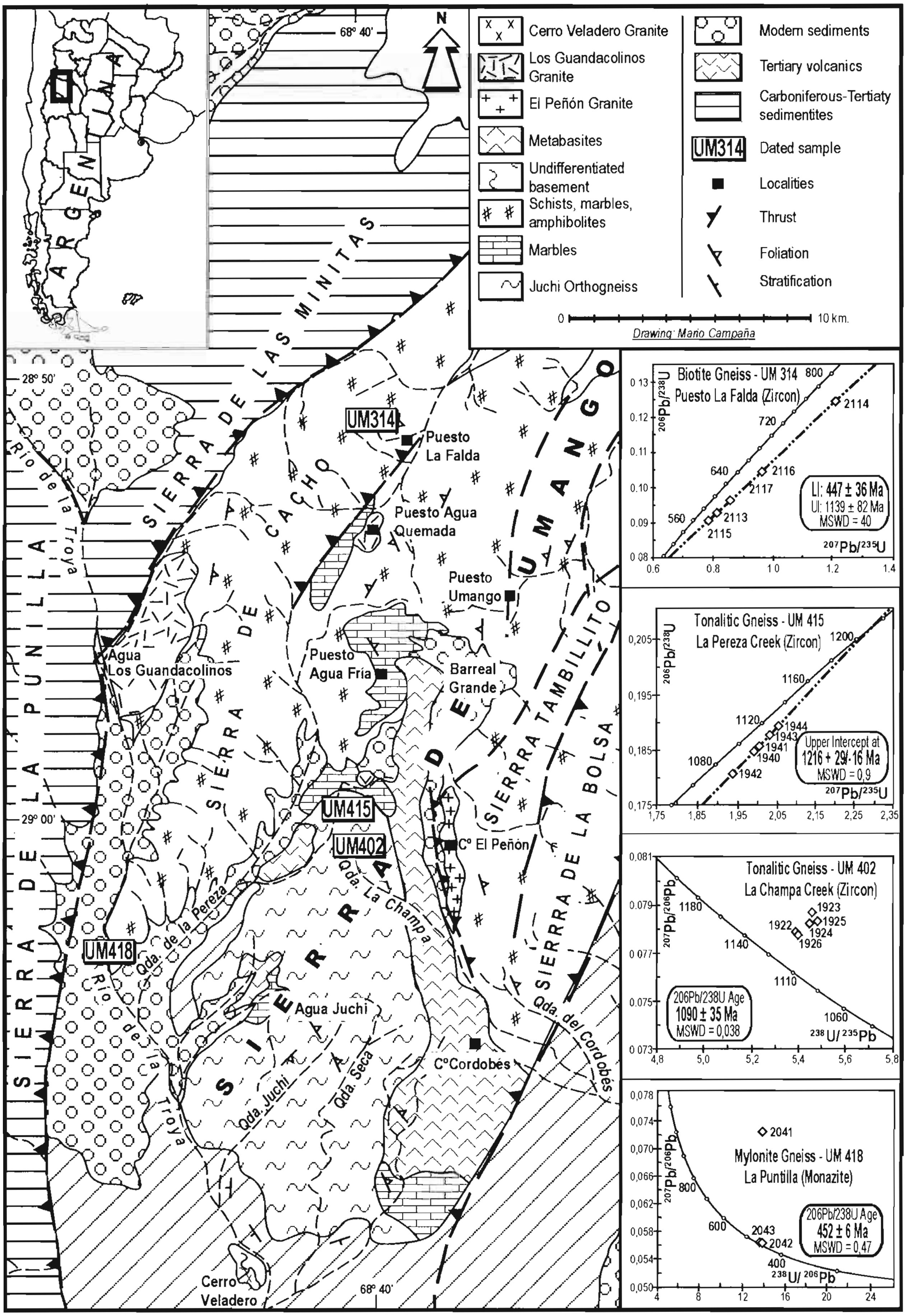

Figure 1. Geological map and diagrams of new U-Pb ages.

The new conventional U-Pb ages from the Juchi Orthogneiss confirm the Mesoproterozoic Grenvillian age previously reported, and also extends the outcrops of the orthogneisses to the north of Agua de Juchi section. Early to Late Ordovician regional metamorphism and deformation were interpreted as the orogenic event that affected the Mesoproterozoic basement during the collisional history of the Famatinian orogen. The Middle to Late Devonian ages were also interpreted as shear zone metamorphism (Varela et al., 2002).

All these Early Paleozoic orogenic processes (metamorphism and deformation) have been related to the collisional history of Famatinian Orogeny, in wich the Sierra de Umango is considered as part of the Laurentian-derived allochton. Further south to the Sierra de Umango at Sierra de Pie de Palo, Casquet et al. (2001) delineated a comparable tectono-metamorphic history related to the Early Paleozoic Famatinian events that overprinted the allochton basement of Grenvillian-age.

ACKNOWLEDGEMENTS

This contribution was supported by funding provided by Consejo Nacional de Investigaciones Científicas y Técnicas (CONICET, Argentina) and Conselho Nacional de Desenvolvimento Científico e Tecnológico (CNPq, Brasil). The Comisión Nacional de Actividades Espaciales (CONAE, Argentina) also provided the satellite images within the project "Investigaciones Geológicas en el Centro-Oeste de Argentina". This paper is a contribution to IGCP 436 "Pacific Gondwana Margin".

REFERENCES

Astini, R.A., 1998. Stratigraphical evidence supporting the rifting, drifting and collision of the Laurentian Precordillera terrane of western Argentina. In PankhurstR.J. and Rapela,C.W.(eds.) The Proto-Andean Margin of Gondwana. Geological Society, Special Publications, 142: 11-33.

Caminos, R., 1979. Sierras Pampeanas Noroccidentales. In Segundo Simposio de Geología Regional Argentina, Academia Nacional de Ciencias de Córdoba, Argentina, 1: 225-291.

Casquet, C., Baldo, E., Pankhurst, R., Rapela, C., Galindo, C., Fanning, C., Saavedra, J., 2001. Involvement of the Argentine Precordillera terrane in the Famatinian mobile belt: U-Pb SHRIMP and metamorphic evidence from the Sierra de Pie de Palo. Geology, 29 (8): 703-706.

Dalla Salda, L., Cingolani, C., Varela, R., 1992. Early Paleozoic orogenic belt of the Andes in southwestern South America: Result of Laurentia-Gondwana collision?. Geology, 20: 617-620.

Dalla Salda, L., López de Luchi, M.G., Cingolani, C.A., Varela, R., 1998. Laurentia-Gondwana collision: the origin of the Famatinian-Appalachian orogenic belt (a review). In PankhurstR.J. and Rapela,C.W.(eds.) The Proto-Andean Margin of Gondwana. Geological Society, Special Publications, 142: 219-234.

Ramos, V.A., Dallmeyer, R.D., Vujovich, G.I., 1998. Time constraints on the Early Palaeozoic docking of the Precordillera, central Argentina. In PankhurstR.J. and Rapela,C.W.(eds.) The Proto-Andean Margin of Gondwana. Geological Society, Special Publications, 142: 143-158.

Varela, R., López de Luchi, M., Cingolani, C., Dalla Salda,,L., 1996. Geocronología de gneises y granitoides de la sierra de Umango, La Rioja. Implicancias tectónicas. XIII Congreso Geológico Argentino y III Congreso de Exploración de Hidrocarburos (Buenos Aires, Argentina), III: 519-527.

Varela, R., Roverano, D., Sato, A.M., 2000. Granito El Peñón, sierra de Umango: descripción, edad Rb/Sr e implicancias geotectónicas. Revista de la Asociación Geológica Argentina, 55,4: 407-413.

Varela, R., Valencio, S., Ramos, A., Sato, K., González, P., Panarello, H., Roverano, D., 2001. Isotopic Strontium, Carbon and Oxygen stydy on Neoproterozoic marbles from sierra de Umango, Andean Foreland, Argentina. III South American Symposium on Isotope Geology (Pucón, Chile). Abbreviated Abstract in Revista Comunicaciones, 52: 121. Extended Abstract in CD-R Servicio Nacional de Geología y Minería: 450-453.

Varela, R., Sato, A.M., González, P.D., 2002. Metamorfismo y deformación Devónicos en la Sierra de Umango, Sierras Pampeanas Occidentales, La Rioja, Argentina. XV Congreso Geológico Argentino (El Calafate), 2: 57-63.

Varela, R., Sato, A.M., Basei, M.A.S., Siga Jr., O., in press. Proterozoico medio y Paleozoico inferior de la Sierra de Umango, Antepaís Andino (29° S), Argentina. Edades U/Pb y caracterizaciones isotópicas. Revista Geológica de Chile. Santiago.

Table 1. New U-Pb zircon and monazite ages from Sierra de Umango.

Geologic unit	Locality	Dated rock type	Dated process	Method - Material	Age (Ma)
Orthogneiss Juchi	La Champa creek	tonalitic orthogneiss	magmatic crystallization	U-Pb - zircon in magnetic fractions	1090 ± 35
Orthogneiss Juchi	La Pereza creek	tonalitic orthogneiss	magmatic crystallization	U-Pb - zircon in magnetic fractions	1216 +29 / -16
Tambillo Metamorphites	Puesto La Falda	biotitic paragneiss	metamorphism and heritage age	U-Pb - zircon in magnetic fractions	lower int.: 447 ± 36 & upper int.: 1139 ± 82
Tambillo Metamorphites	La Troya river	mylonitic paragneiss	metamorphism	U-Pb - monazite	452 ± 6

CONTACT METAMORPHISM IN METAPELITES FROM THE NOVA LIMA GROUP, RIO DAS VELHAS SUPERGROUP, QUADRILÁTERO FERRÍFERO: A MONAZITE Th-U-Pb_T DATING BY THE ELECTRON-PROBE MICROANALYSER

Vlach, S.R.F.[1]; Campos Neto, M.C.[1]; Caby, R.[2] and Basei, M.A.S.[1]

1. Instituto de Geociências, Universidade de São Paulo, São Paulo, Brazil. srfvlach@usp.br
2. Université de Montpellier II, France. caby@babouin.dstu.univ-montp2.fr

Keywords: Th-U-Pb_T dating, electron-probe microanalyser, monazite, metapelites, Quadrilátero Ferrífero

INTRODUCTION

Th-U-Pb_T dating of monazite by high spatial resolution techniques as the electron-probe microanalyser (EPMA) is a valuable tool for understanding the geochronological patterns of metamorphic events within the continental crust (*e.g.*, Vlach and Del Lama, 2002) and, in connection with textural and chemical data for equilibrated metamorpic minerals, can also provide useful constraints on P-T-t paths.

We present chemical and dating results of monazite from an amphibolite-grade aureole metamorphism over the regional metapelites of the Nova Lima Group, Rio das Velhas Supergroup, Quadrilátero Ferrífero (MG), due to a strong thermal imprint caused by Paleoproterozoic regional granite intrusions.

GEOLOGICAL SETTING AND SAMPLING

The last deformation and metamorphism events in the Quadrilátero Ferrífero rocks were controlled by the Brasiliano front of the Araçuaí Orogen. Fold-and-thrust belt deformation presents a decreasing polarity towards W and is associated with white mica, kyanite, and pyrophyllite linear growth.

The granite-gneissic rocks of the Quadrilátero Ferrrífero Archaean basement (Figure 1) are roughly coeval with the Rio das Velhas Super Group metavulcanosedimentary sequence, with ages in the 2.6-2.8 Ga range (Teixeira et al., 2000; Machado et al., 1992). The sedimentation of the basal units of the Minas Supergroup appears to have occurred in the Siderian Paleoproterozoic (*ca.* 2.4 Ga, Babinski et al., 1995). The metasediments of the Sabará Group, discordantly overlying these sequences, and the uppermost Itacolomi Group, present detritic zircon dated at 2.1 and 2.0 Ga, respectively (Machado et al., 1996).

Local contact aureole metamorphism dated at about 2.06 Ga (internal Sm/Nd isochron) occurs in the Sabará Group rocks (CHUR model Sm/Nd ages about 2.2 Ga) near the Belo Horizonte granite-gneissic dome (Brueckner et al., 2000). Similar contact aureoles are widely distributed in the Nova Lima Group.

The structural relationships between the Nova Lima Group and the Moeda Formation of the Minas Supergourp are well exposed at the northern downhill side of the Serra de Ouro Preto (Dorr, 1976). Along the Vitoria-Minas railroad, near the Funil Station, white mica crystallization defines a fine schistosity concordant with the compositional banding in the first layer of the Moeda quartzites. These quartzites clearly overlay the chlorite-muscovite-biotite schists of the Nova Lima Group. It is worth noting that the later rocks contain fibrous white mica after sillimanite. Several muscovite leucogranites are concordand with the main Nova Lima schistosity.

These schists show a high metamorphic gradient towards the Bação granite-gneiss complex and, after about *ca.* 200 m., the mineral paragenesis reaches up to amphibolite facies, with peak P-T conditions of about 650° C and 8 kbar (TEEWQU, Berman, 1991). The typical rocks are quartz-poor schist displaying fresh cm-sized garnet and prismatic sillimanite in a groundmass containing cordierite (?), andalusite, red biotite and andesine. Rutile, graphite, ilmenite, monazite, and relict of prograde staurolite preserved both in plagioclase and sillimanite, are the accessory minerals. This mineral assemblage is syn-kinematic; kyanite appears as post-kynematic porphyroblasts. Monazite forms xeno- and idioblastic crystals, appearing as inclusions in the main minerals and as isolated crystals in the matrix.

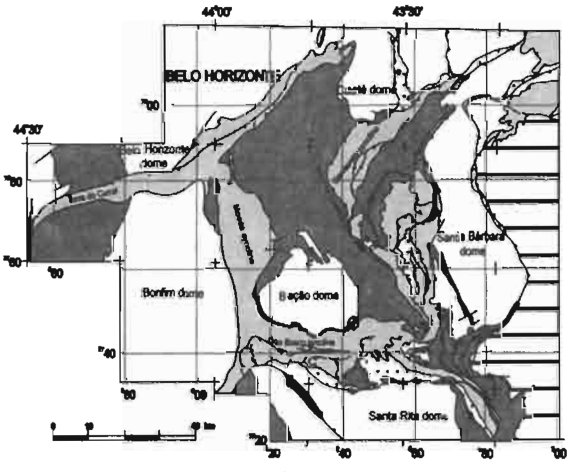

Figure 1: GEOLOGIC MAP OF SE- SÃO FRANCISCO CRATON, MG, BRAZIL.
Modified from Dorr (1969).

NEOPROTEROZOIC BELT

⊟ MANTIQUEIRA GNEISSES: Paleoproterozoic reworked ortogneisses and migmatites

ARCHAEAN / PALEOPROTEOZOIC

⊡ ITACOLOMI GROUP: coarse and cross-stratified sandstones and polymitic conglomerate

☐ MINAS SUPERGROUP: Moeda and Batatal Fms (sandstones and metapelites), Cauê and Gandarela Fms (BIF and carbonates) and Piracicaba and Sabará Grs (metapelites, sandstones, metavolcaniclastic rocks, conglomerates).

■ RIO DAS VELHAS SUPERGROUP: Archaean (2.7 Ga) basalt, komatiite and ryolitic lavas intercaleted with sedimentary units

☐ SOUTHEASTERN SÃO FRANCISCO CRATON GNEISSES: gneiss/migmatite complex, calc-alkaline granitoid plutons and Espinhaço-related syenite and alkaline-like granite-gneisses

● Sample

ANALITYCAL AND DATING METHODS

Monazite EPMA analyses were made in conventional carbon-coated polished thin-sections at the microprobe lab at the Instituto de Geociências, Universidade de São Paulo, with a 5-WDS spectrometer JEOL JXA-8600 machine, following general procedures and instrumental settings described by Vlach and Gualda (2000). The WDS analyses were made after BSE imaging of grains selected under the microscope by textural criteria.

Almost complete monazite analyses were obtained for 35 spots along single traverses and over high-contrast BSE areas in 5 crystals, representing garnet and plagioclase inclusions and isolated grains. Spectral lines for the age determining elements were Mα for Th and Pb and Mβ for U; detection limits were close to 130, 90, and 110 ppm, respectively. Th and Y (on Pb) and Th (on U0 interferences were corrected on-line. Synthetic $ThSiO_4$, UO_2, and $PbCrO_4$ were used as elemental standards. Two homogeneous monazite crystals from high-grade metapelites, with 625 Ma (conventional monazite U/Pb) and 790 Ma (zircon SHRIMP age), respectivley, were used as age-reference standards. Total deviations for these elements were taken as counting deviations, adding 2% to account for other errors. Matrix effects were corrected with a PROZA program.

Chemical (Th^*-Pb_T) isochrons were computed with the IsoPlot software (Ludwig, 1998). Our results are reported on the basis of a 95 % confidence level.

CHEMICAL AND DATING RESULTS

Representative WDS analytical monazite results, molecular proportions of the main components, Th, U, and Pb contents and spot ages are presented in Table 1. BSE imaging of monazite grains reveals contrasted zoning patterns (Figure 2): the inclusions in garnet and feldspar show typical dissolution-recrystallization features, while the isolated crystals present a more normal zoning, Th and U contents step-increasing towards crystal rims.

The studied monazite is a Ce-rich variety with variable amounts of the huttonite, xenotime, and brabantite molecules, depending on textural setting. So, the grains included in garnet and the cores of grains included in feldspars are typically richer in monazite and xenotime and poorer in huttonite and brabantite than the isolated crystals or the rims of grains included in feldspars.

These chemical variations are well correlated with the calculated spot ages and the analytical spots with higher xenotime contents give also older ages (Figure 3). The higher xenotime contents correspond mainly to grains included in garnet and the cores of the grains included in feldspar. The apparent ages suggest to some extent a bimodal data distribution (Figure 4). A chemical cationic isochron (Th^* - the measured Th added to the equivalent in Th from the measured U content - vs Pb_T), considering all analytical data yelds a mean age of about 2.06 (± 0.02) Ga, with a good MSWD value.

If we consider, however, a bimodal age distribution, well supported by our chemical data, the isochron computations give an age of about 2.08 (± 0.02 Ga, grains included in garnet and cores of grains included in feldspar) and another one of about 2.04 (± 0.02 Ga, rims of inclusions in feldspar and isolated crystals). The statistical fit parameters (probability of fit and MSWD) will be significantly better (Table 2).

Table 1. Representative WDS data and apparent spot ages of monazite from the studied prophyroblastic schist (c = core, r = rim, b.d. = below detection limit).

	Inclusion in Grt		Isolated crystal	
Grain	2, c	2, r	1, c	5, r
SiO_2	0.08	0.13	0.34	0.52
ThO_2	2.55	4.74	6.79	10.59
UO_2	1.49	0.70	0.73	0.44
La_2O_3	13.91	14.63	12.80	10.28
Ce_2O_3	27.84	28.64	28.29	25.70
Pr_2O_3	3.03	3.20	3.16	3.31
Nd_2O_3	11.11	11.95	12.55	13.36
Sm_2O_3	2.06	1.99	1.95	2.40
Gd_2O_3	1.79	1.40	0.90	0.85
Dy_2O_3	0.81	0.11	bd	0.10
Yb_2O_3	0.05	bd	bd	bd
Y_2O_3	2.44	0.11	0.03	0.04
FeO	0.22	0.18	0.11	0.05
CaO	0.97	1.21	1.41	2.07
PbO	0.77	0.68	0.86	1.10
P_2O_5	30.86	30.50	30.05	29.55
Total	99.99	100.16	99.97	100.35
Molecular proportions				
Huttonite	0.03	0.05	1.4	2.1
Monazite	83.0	87.0	85.0	78.9
Xenotime	8.5	2.2	1.2	1.3
Brabantite	8.2	10.2	12.4	17.8
Age determining elements and deviations (ppm)				
Th	22370	41690	59630	93070
2σ	508	893	1255	1930
U	13173	6151	6435	3891
2σ	298	172	176	143
Pb	7157	6344	8021	10178
2σ	187	175	206	247
Spot age (Ma) and deviations				
Age	2108	2086	2046	2024
2σ	53	59	56	57

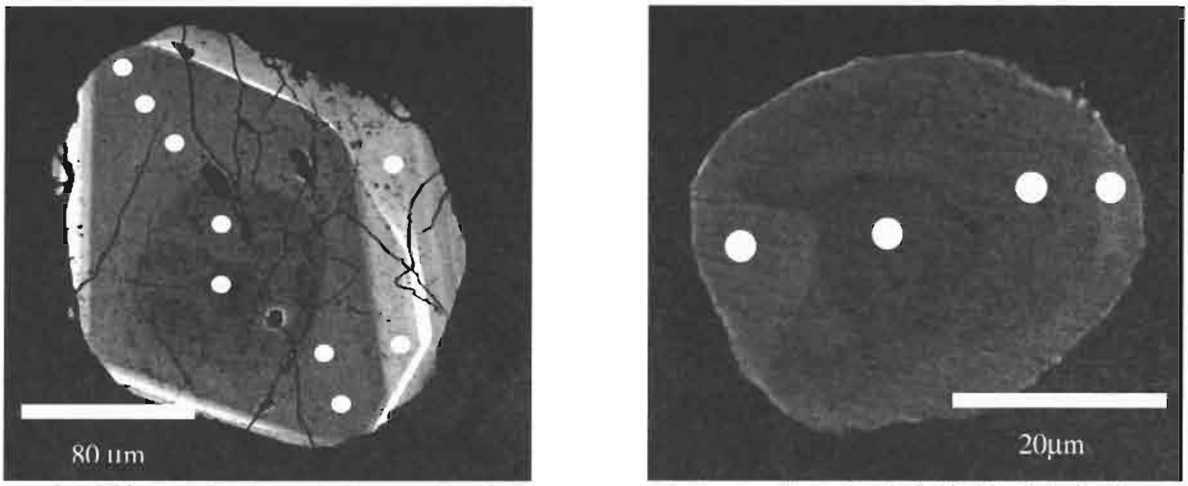

Figure 2. BSE images showing typical compositional zoning patterns of two monazite grains. Left: idioblastic isolated crystal with regular pattern (Th and U step-increase towards crystal rims). Right: rounded inclusion in garnet, showing a complex irregular pattern, suggesting dissolution-recrystallization mechanisms; darker areas are more xenotime-rich than the clearer ones. White circles are WDS spot locations (not to scale).

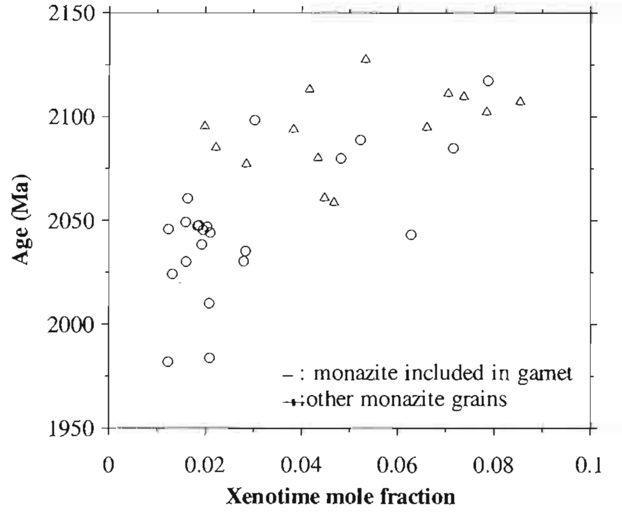

Figure 3. Apparent individual spot aged plotted against the xenotime mole fracion in monazite from the Nova Lima schists. See text for discussion.

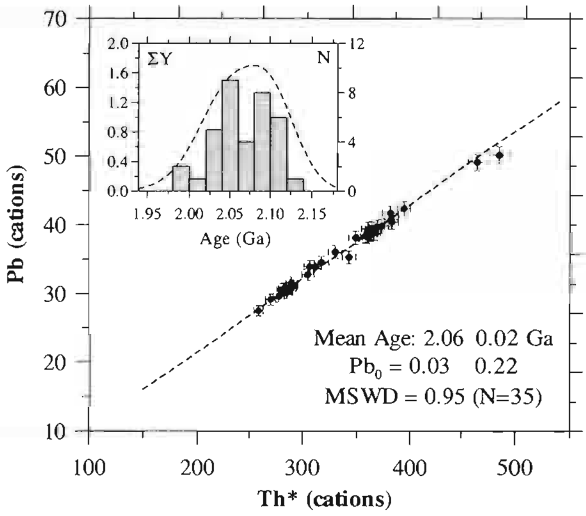

Figure 4. Cationic isochron diagram for all monazite data; computations after Ludwig (1998), fitting through the origin. Inset: apparent spot age distribution. ΣY is the sum of density of probability functions of each spot.

Table 2. Isochron results for monazite from the Nova Lima Schist. Computations after Ludwig (1998), drawing the fit trough origin. Errors are quoted to the 95 % confidence level.

Sampled spots	All data	High xenotime contents (inclusions in garnet and some cores from inclusions in felspars)	Low xenotime contents (isolated grains and rims from inclusions in feldspar)
Age (Ga)	2.06 ± 0.02	2.08 ± 0.02	2.04 ± 0.02
MSWD	0.95	0.40	0.57
Prob. fit	0.55	0.99	0.90
N	35	19	16

DISCUSSION

The mean monazite chemical age of the aureole metamorphism over the Nova Lima Group herein reported is identical to the internal Sm/Nd isochron age obtained by Brueckner et al. (2000) for aureole metamorphism in the Sabará Group. On the other hand, our data bring some additional geochronological constraints to this event.

The chemical EPMA dating results support a bimodal age distribution for the metamorphic event, a point strongly reinforced by both micro-structural and chemical contrasted features of monazite grains occurring included in garnet, in plagioclase, and as idioblastic isolated crystals. A better statistical fit for the bimodal case gives additional support to this interpretation. If both textural monazite generations were formed during an almost continuous contact metamorphic event, we should conclude that such thermal imprint lasted during a time interval up to 40-60 Ma. This metamorphic event is distributed overall the Quadrilátero Ferrífero.

ACKNOWLEDGEMENTS

We thank Fundação da Amparo à Pesquisa do Estado de São Paulo for continuous microprobe laboratory support at the Instituto de Geociências da Universidade de São Paulo.

REFERENCES

Berman, R.G., 1991. Thermobarometry With Estimation of Equilibrium state (TWEEQU). Versões 1.2 e 2.02 (software).

Brueckner, H.K., Cunningham, D., Alkmim, F.F. and Marshak, S., 2000. Tectonic implications of Precambrian Sm-Nd dates from the southern São Francisico craton and adjacent Araçuaí and Ribeira belts, Brazil. Precambrian Research, 99: 255-269.

Dorr, J.V.N.II, 1969. Physiographic, stratigraphic and structural developent of the Quadrilátero Ferrífero, Minas Gerais, Brazil. U.S. Geological Survey, Prof. Paper 1119, B1-B19.

Ludwig, K.R., 1998. Isoplot/Ex: a geochronological toolkit for Microsoft Excel. Berkeley Geochronological Center, Special Publication No. 1. 43 p.

Machado, N., Noce, C.M., Ladeira, E.A. and Oliveira, O.A.B., 1992. U-Pb Geochronology of Archaean magmatism and Proterozoic metamorphism in the Quadrilátero Ferrífero, southern São Francisco craton, Brazil. Geological Society of America Bulletin, 104, 1221-1227.

Machado, N., Schrank, A., Noce, C.M. and Gauthier, G., 1996. Ages of detrital zircon from Archaean-Paleoproterozoic sequences: implications for Greenstone Belt setting and evolution of a Transamazonian foreland basin in Quadrilátero Ferrífero, southeast Brazil. Earth and Planetary Science Letters, 141, 259-276.

Teixeira, W., Sabaté, P. Barbosa, J. and Carneiro, M.A., 2000. Archaean and Paleoproterozoic tectonic evolution of the São Francisco Craton, Brazil. In: U.G. Cordani, E.J. Milani, A. Thomaz Filho and Campos, D.A., editors, Tectonic Evolution of South America. 31ST International Geological Congress, Rio de Janeiro, Brazil: 101-137.

Vlach, S.R.F. and Del Lama, E.A., 2002. Idades Th-U-PbT de monazita e geotermobarometria de rochas metapelíticas de alto grau do Sistema Orogênico Itabuna-Salvador-Curaçá, BA, Brasil: um estudo em microssonda eletrônica. Revista do Instituto de Geociências (Série Científica), 2:9-22.

Vlach, S.R.F. and Gualda, G.A.R., 2000, Microprobe monazite dating and the ages of some granitic and metamorphic rocks from Southeastern Brazil. Revista Brasileira de Geociências, 30:214-218.

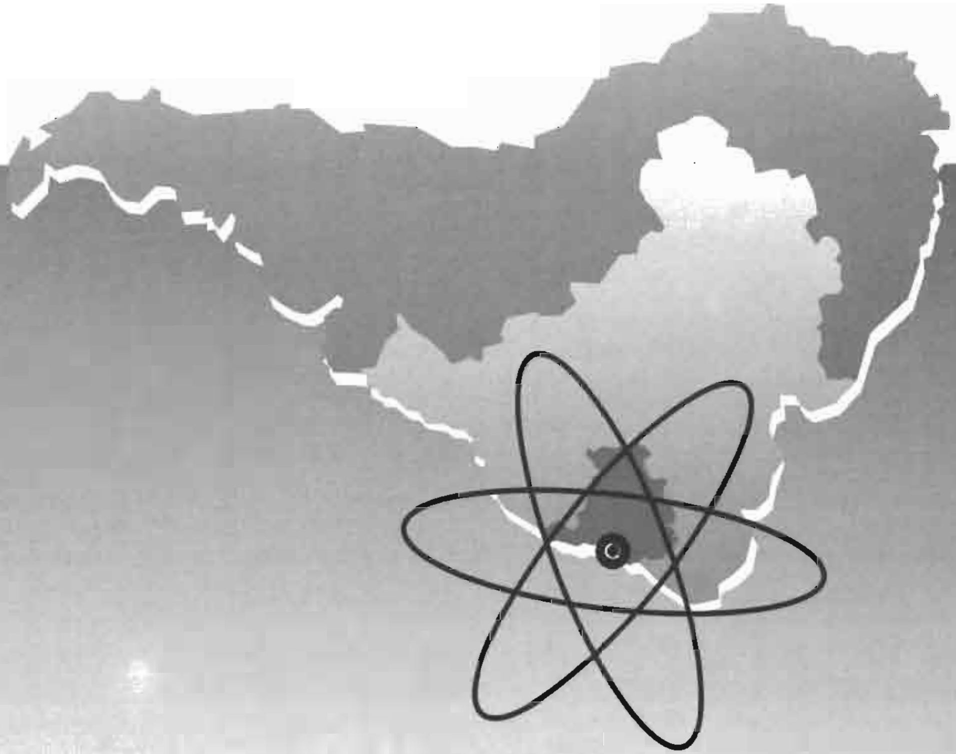

Temporal Isotopic Variation and Chemostratigraphy

C, O AND Sr ISOTOPE IN THE CAP CARBONATE SEQUENCE OVERLYING STURTIAN-RAPITAN AND VARANGER-MARINOAN GLACIAL EVENTS IN BRAZIL

Alvarenga, C.J.S.; Santos, R.V; Dantas, E.L.; Brod, E.R. and Gioia, S.M.C.L.

Instituto de Geociências, Universidade de Brasília, Campus Universitário, ICC-Centro, 70910-900, Brasília-DF.
alva1@unb.br, rventura@unb.br, elton@unb.br, manubrod@yahoo.com.br, sgioia@unb.br

Keywords: Neoproterozoic, carbon isotope, strontium, Araras Formation, Bambuí Group

INTRODUCTION

Glacial events are well documented during the Sturtian-Rapitan (from ~760-700 Ma) and, the Varanger or Marinoan (from ~620-580 Ma) periods around the world (Hoffman et al., 1998; Kennedy et al., 1998). Both glacial events, appear to have reached very low latitudes (Hoffman et al., 1998; Kennedy et al. 1998; Hyde et al., 2000; Jacobsen, 2001; Kennedy et al. 2001), have been widely identified in central Brazil, where they are always overlain by cap carbonate sequence.

The older cap carbonate sequence covers large areas of the São Francisco Craton and of the surrounding Neoproterozoic folded belts (Rio Preto, Araçuaí, Ribeira and Brasília). This cap carbonate comprises the basal part of the Bambuí and Una groups, which overlie glacial diamictites of the Jequitaí and Bebedouro formations, respectively, as well as the Macaúbas Group (Dardenne, 1978; Misi & Veizer 1998; Uhlein et al., 1999; Santos et al., 2000). These diamictites are considered to be ca. 700-800 Ma old (Misi & Veizer, 1998, Santos et al., 2000) and were, therefore, correlated with the "Sturtian" event.

Another carbonate sequence is recognized in the Paraguay Belt and presents Ediacaran-like fauna with *Corumbella werneri* and *Cloudina Lucianoi* (Tamengo Formation) (Hahn et al., 1982; Zaine & Fairchild, 1985) suggesting an upper-Vendian (590-545 My) age (Zaine & Fairchild, 1985; Alvarenga & Trompette, 1992). It overlies late Neoproterozoic Varanger-Marinoan glacial sediments (Alvarenga & Trompette, 1992).

Carbon-isotope and $^{87}Sr/^{86}Sr$ stratigraphy have been widely used to correlate cap carbonate strata overlying Sturtian and Varanger-Marinoan glaciogenic rocks worldwide (Kennedy et al., 1998). Isotope stratigraphy in South America Neoproterozoic limestone are available for rocks of the São Francisco Basin (Bambuí and Una groups) overlying Sturtian glacial diamictites (Iyer et al., 1995; Misi & Veizer, 1998; Martins, 1999; Santos et al., 2000), and for the Paraguay Belt rocks (Boggiani et al., 1997; Alvarenga et al. submitted).

In this study, we present new C-O and Sr-isotope data for samples collected systematically along continuous limestone profiles of the Bambuí Group on the border of the São Francisco Craton (Bambuí Group rocks) and of the Araras Formation on the border of the Amazon Craton and in the Paraguay Belt (Fig. 1). The main objective is to correlate the isotopic signature for these rocks with isotopic record available for similar sequences around the world.

RESULTS

The $\delta^{13}C_{PDB}$ values of Araras carbonates vary between -10.5‰ and -2.7‰ within a short stratigraphic interval of cap dolomite (12 m), near the border of the basin (Fig. 2). The isotopic profile across the basal 200 m of laminated microcrystalline limestone and clay-limestone, overlying glacial diamictites and interpreted as being deposited in a deep shelf environment, is also characterized by negative $\delta^{13}C_{PDB}$ (-5.3‰ and +0.6‰). In contrast with the lower portion of the carbonate sequence, thick shallow-water dolostone covering this horizon present uniform and positive $\delta^{13}C_{PDB}$ values (+1.9‰ to +2.4‰) for more than 800 m. Dolostone and sand-bearing dolostone from the upper parts of the Araras Formation have high $\delta^{13}C_{PDB}$ values (+4.1‰ to +9.6‰). This is followed by an abrupt decrease in $\delta^{13}C$ values, down to –1.0‰. The carbonates of the Araras Formation are characterized by $^{87}Sr/^{86}Sr$ ratios ranging from 0.70753 to 0.70960, comparable to cap carbonates overlying Varanger-Marinoan glacial deposits in other neoproterozoic sequences.

In the Bambuí Group, negative $\delta^{13}C_{PDB}$ values are found only within the lowermost meters of the sequence, which are immediately followed by positive values (+0.9‰ to +3.3‰) within the lowermost portion of the Sete Lagoas Formation (Fig. 3). The upper carbonates of the Bambuí Group (upper portion of the Sete Lagoas and Lagoa do Jacaré Formations) present an extensive positive carbon isotope excursion (values ranging from +6.9‰ to +16.0‰). $^{87}Sr/^{86}Sr$ ratios in limestone of the Bambuí Formation range from 0.70580 to 0.70760 and are comparable with data present in other studies (Misi & Veizer, 1998).

DISCUSSION AND CONCLUSIONS

The carbon isotope profile of the Paraguay Belt (Araras Formation) is very different from that of the Bambuí Group carbonates, although both carbonate sequences overlie glacial sediments. The $\delta^{13}C_{PDB}$ profile observed across the Araras Formation exhibits an approximately 200 m thick section of carbonates with low $\delta^{13}C_{PDB}$ values while in the Bambuí Group the negative values are not frequently present in the cap carbonates.

Strontium isotopes evolution curves for neoproterozoic carbonates show that post Sturtian sediments present strontium ratios ranging between 0.7063 and 0.7074, whereas post Varanger/Marionan carbonates present strontium ratios ranging from 0.7068 to 0.7087 (Jacobsen & Kaufman, 1999). Our isotopic data support the hypothesis that diamictites underlying the Bambuí basin are related to the Sturtian glacial event, whereas diamictites of the Araras Formation are related to the worldwide Varangian/Marionan glaciation.

The data presented here indicate that two distinct glacial events are present in Central Brazil. In terms of geodynamic implications to supercontinent reconstruction models, the Varanger/Marionan glaciation was preserved only in the southeastern border of Amazon Craton. Evidence of this event was probably eroded from higher latitude regions, such as the border of the São Francisco Craton, where is preserved only the Sturtian glaciation event.

REFERENCES

Alvarenga, C.J.S., Trompette, R., 1992. Glacial influenced turbidite sedimentation in the uppermost Proterozoic and Lower Cambrian of the Paraguay Belt (Mato Grosso, Brazil). Palaeogeogr., Palaeoclimatol., Palaeoeçol., 92, 85-105.

Boggiani P.C., Sial, A.N., Coimbra, A. M., Ferreira; V P., 1997. The carbon and oxygen isotope record of Neoproterozoic carbonate rocks of the Paraguay fold belt (central South America). South American Symposium on Isotope Geology, 1, Extended Abstracts, Campos do Jordão, Brazil, Brazil, pp. 57-59.

Dardenne, M.A., 1978. Síntese sobre a estratigrafia do Grupo Bambuí no Brasil Central. In: Congresso Brasileiro de Geologia, 30, Anais, Recife, Brazil, SBG, Vol. 2, pp. 597-610.

Hahn, G., Hahn, R., Leonardos, O.H. , Pflug, H.D., Walde, D.H.G., 1982. Körperlich erhaltene Scyphozoen - Reste aus dem Jungprakambrium Brasiliens. Geologica et Palaeontologica, 16, 1-18.

Hoffman, P.F., Kaufman, A.J., Halverson, G.P., Schrag, D.P., 1998. A Neoproterozoic snowball earth. Science, 281: 1342-1346

Hyde, W.T., Crowley, T.J., Baum, S.K., Peltier, W.R., 2000. Neoproterozoic ' snowball Earth' simulations with a coupled climate/ice-sheet model. Nature, 405 (6785): 425-429.

Iyer, S.S., Babinski, M., Krouse, H.R., Chemale, Jr. F., 1995. Highly (super 13) C-enriched carbonate and organic matter in the Neoproterozoic sediments of the Bambuí Group, Brazil. Precambrian Res., 73: 271-282.

Jacobsen, S.B., 2001. Gas hydrates and deglaciations. Nature, 412: 691-693.

Jacobsen, S.B, Kaufman, A.J. 1999. The Sr, C and O isotope evolution of Neoproterozoic seawater. Chem. Geology, 161: 37-57

Kennedy, M.J., Christie-Blick, N., Sohl, L. E., 2001. Are Proterozoic cap carbonates and isotopic excursions a record of gas hydrate destabilization following Earth's coldest intervals? Geology, 29: 443-446.

Kennedy, M.J, Runnegar, B., Prave, A. R., Hoffmann, K.-H., Arthur, M. A., 1998. Two or four Neoproterozoic glaciations?. Geology, 26: 1059-1063.

Martins, M. 1999. Análise estratigráfica das seqüências mesoproterozóicas (borda oeste e neoproterozóicas da Bacia do São Francisco. Máster Universidade Federal do Rio Grande do Sul, Porto Alegre, Brazil, 214p.

Misi, A., Veizer, J. 1998. Neoproterozoic carbonate sequence of the Una Group, Irecê Basin: chemostratigraphy, age and correlations. Precambrian Res., 89: 87-100.

Santos, R.V., Alvarenga, C.J.S., Dardenne, M.A., Sial, A.N., Ferreira, V.P., 2000. Carbon and oxygen isotope profiles across Meso-Neoproterozoic limestones from central Brazil: Bambuí and Paranoá groups. Precambrian Research, 104: 107-122.

Uhlein, A., Trompette, R., Alvarenga, C.J.S., 1999. Neoproterozoic glacial and gravitational sedimentation on a continental rifted margin: The Jequitaí – Macaúbas sequence (Minas Gerais, Brazil). J. South Am. Earth Sci., 12: 435-451.

Zaine, M.F., Fairchild T.R., 1985. Comparaison of Aulophycus Lucianoi BEURLEN and Sommer from Ladario (MS) and the geans Cloudina Germs, Ediacaran of Namibia . An. Acad. Brasileira Cienc. , Rio de Janeiro, v. 57, p.180.

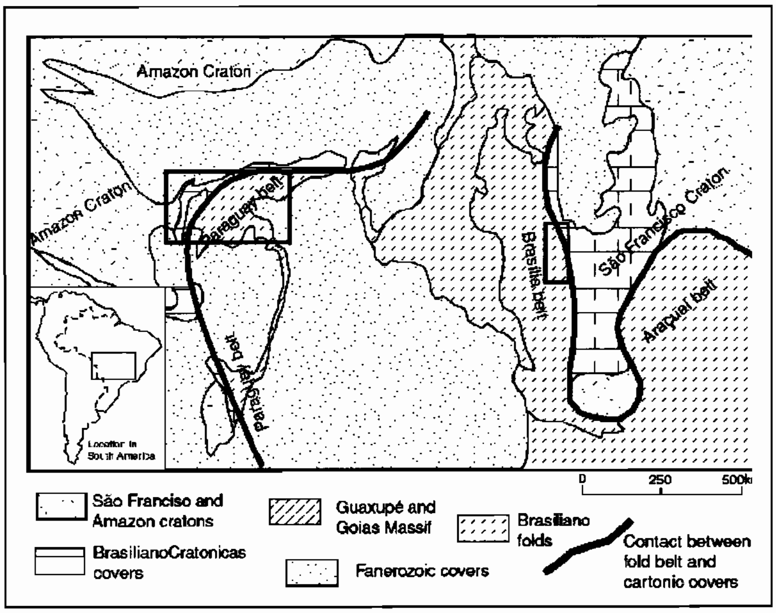

Figure 1. Map of the Paraguay Belt along the border of the Amazon Craton and of the Brasília belts along the border of the São Francisco Craton. Squares indicate the locations of samples of this study.

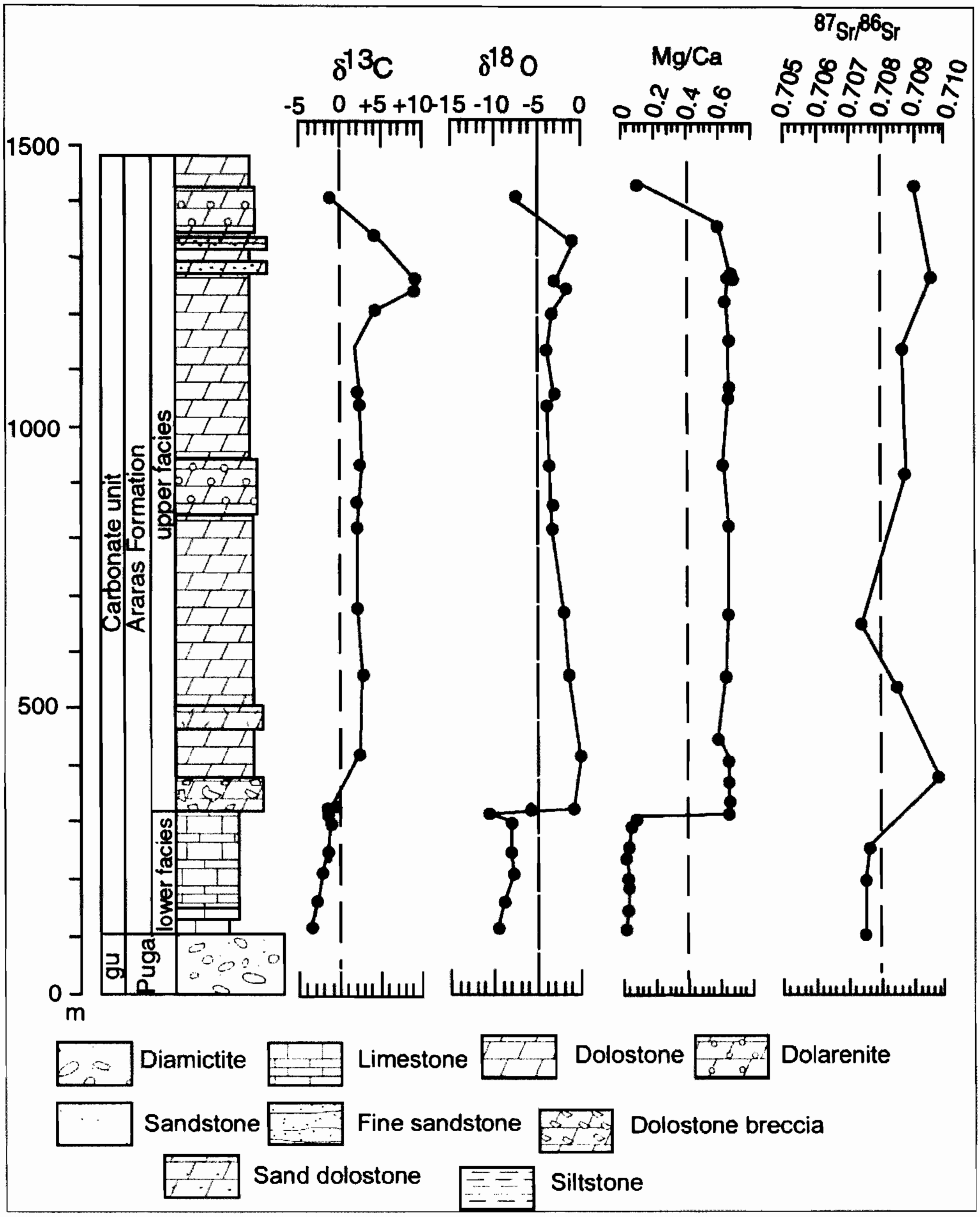

Figure 2. Stratigraphic section of carbonates of the Araras Formation showing the variation of $\delta^{13}C_{PDB}$, $\delta^{18}O_{PDB}$, Mg/Ca and $^{87}Sr/^{86}Sr$.

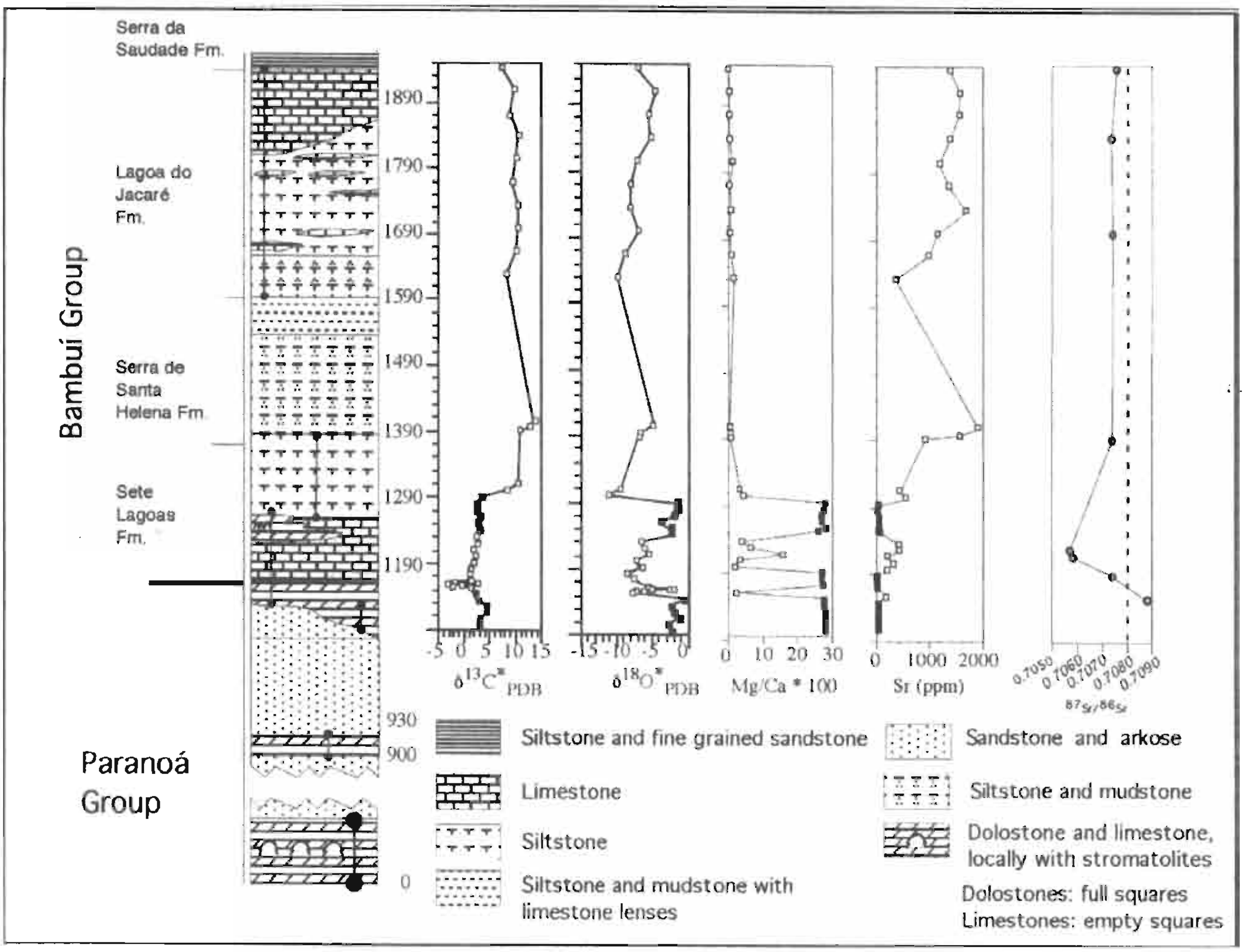

Figure 3. Stratigraphic section of the Bambuí Group showing variation of $\delta^{13}C_{PDB}$, $\delta^{18}O_{PDB}$, Mg/Ca and $^{87}Sr/^{86}Sr$.

GEOCHRONOLOGY AND ISOTOPE GEOCHEMISTRY OF THE MAFIC DIKES FROM THE VAZANTE GROUP, BRAZIL: IMPLICATIONS FOR THE TIMING OF THE Zn-(Pb) MINERALIZATION

Babinski, M.[1]; Fetter, A.H.[2]; Monteiro, L.V.S.[3]; Bettencourt, J.S.[1] and Oliveira, T.F.[4]

1. Centro de Pesquisas Geocronológicas, Instituto de Geociências, Universidade de São Paulo, Rua do Lago, 562, São Paulo-SP, 05508-080, Brazil. babinski@usp.br, jsbetten@usp.br
2. Instituto de Geociências e Ciências Exatas, Universidade Estadual Paulista - UNESP, Av. 24 A, nº 1515, CEP 13506-900, Rio Claro, SP, Brazil. fetter@ms.rc.unesp.br
3. Instituto de Geociências, Universidade Estadual de Campinas - UNICAMP, R. João Pandiá Calógeras, 51, 13083-970, Campinas-SP, Brazil - Fax 19 32891097. lenavsm@zipmail.com.br
4. Companhia Mineira de Metais Vazante, Caixa Postal 03, 38780-000, Vazante-MG. flavio@vz.cmm.com.br

Keywords: Vazante Group, ore deposits, geochronology, stable isotopes

INTRODUCTION

The Vazante Group (Dardenne et al., 1998), which occurs in the northwest part of Minas Gerais State, hosts the most important zinc non-sulfide (Vazante) and sulfide (Morro Agudo) deposits known in Brazil. This group represents one of the metasedimentary units of the southern segment of the Brasília Fold Belt, which extends for more than 1000 km over a width of 300 Km along the western margin of the São Francisco Craton (Fig. 1).

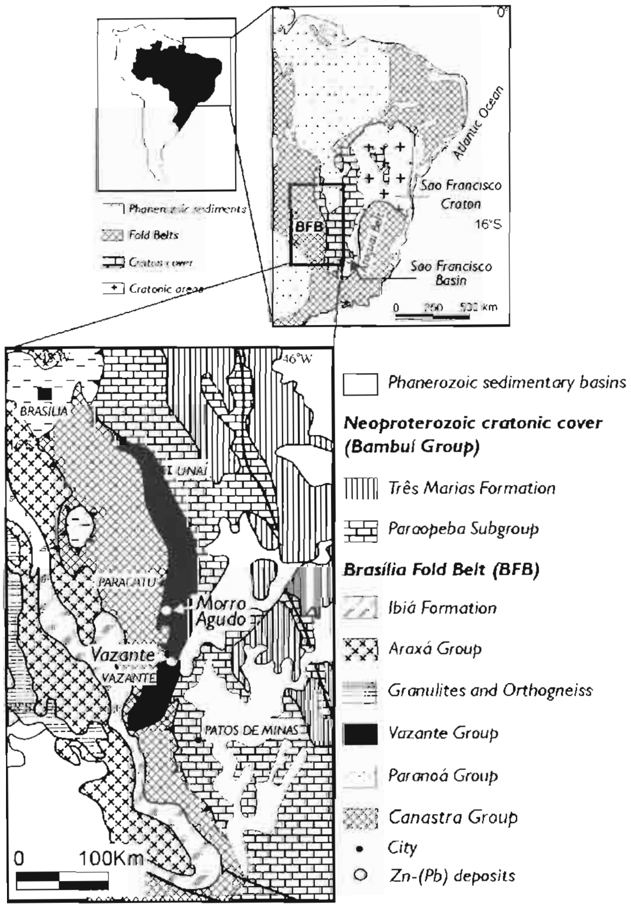

Figure 1. Geological map of the southern part of the Brasília Fold Belt (Dardenne, 2000).

The tectonic setting of this unit, however, is controversial. Recent studies indicate that the Vazante Group could represent the sedimentation in a rapidly subsiding zone forming a depression in the Brasília Fold Belt initial thrust fronts (Dardenne, 2000), in a similar setting to that of the Bambuí Group, or might correspond to top of the meso/neoproterozoic passive margin sequence, represented mainly by the Paranoá Group (Pimentel et al., 2001).

The Vazante Group is composed by a thick sedimentary sequence and its depositional age is still disputable. The available geochronological data do not give reliable constraints on the depositional age of the sequence, but indicate that it was metamorphosed during the Brasiliano Orogeny (Amaral & Kawashita, 1967). Recently, however, metamorphosed basic dikes cutting the sedimentary sequence were found and their geologic relationship showed promise for constraining the minimum depositional age of the sediments and timing of the mineralization event. Here we present U-Pb, Pb-Pb, and Sm-Nd isotopic data obtained from these mafic dikes, along with petrological, geochemical and C, O and Sr isotopic studies.

GEOLOGICAL SETTING

The Vazante Group is composed, from base to top, of metapelitic units with phosphorite occurrences (Retiro and Rocinha Formations), metapsamo-pelitic units and stromatolitic bioherm facies (Lagamar Formation), gray slates (Serra do Garrote Formation), dolomite, slates, sericite phyllite and marls (Serra do Poço Verde Formation), stromatolitic bioherm facies (Morro do Calcário Formation), carbonaceous slate, phyllite, dolomite and quartzite lenses (Lapa Formation) (Dardenne, 2000).

Minor magmatism associated with the Vazante Group is represented by small bodies of metabasic rocks, identified mainly at the Vazante zinc mine (Fig. 2). In this deposit, the metabasic rocks (Fig. 2) occur, within the Vazante Shear Zone, tectonically imbricated with hydraulic breccias, hydrothermally altered rocks, and with zinc ore, composed mainly of willemite (Zn_2SiO_4).

This lithotype was described initially as diabase dikes of Cretaceous age (Rigobello et al., 1988). However, the presence of a metamorphic mineral assemblage (described below), and mylonitic fabric, which is not recognized in the Brazilian cretaceous rocks, are features that indicate that this unit was affected by the regional Brasiliano deformation event (Monteiro, 1997).

The metabasites and ore bodies are off-set by normal and reverse faults and also cut by late hydrothermal veins, which are likely to have caused complex relationships between ore bodies and the host sequence.

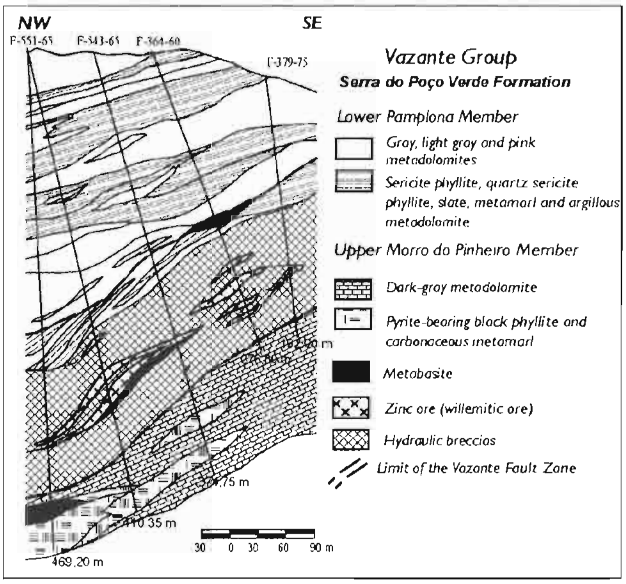

Figure 2. Cross – section of the Vazante ore zone showing the spatial relationship between metabasites, host sequence and the Vazante Fault Zone (simplified from Monteiro, 2002).

The metabasic rock exhibits relicts of sub-ophitic igneous texture and remnants of igneous minerals, such as plagioclase, pyroxene and ilmenite, which are replaced by a typical low greenschist facies assemblage. Sericite, clinozoizite, chlorite and carbonates replace plagioclase. Pyroxene exhibits strong chloritization, whereas ilmenite, initially zoned, is replaced by leucoxene, rutile and titanite (Fig. 3). Biotite remnants indicate early potassification, possibly preceding the mylonitization of this rock.

HYDROTHERMAL ALTERATION

Besides the low greenschist facies metamorphism, mylonitization and hydrothermal activity related to fluid flow within the Vazante Shear Zone also affected the metabasic rock. Chlorite (penninite), chrysotile and apatite formation, related to S-C structures, overprints the potassification. Late dolomitization associated with the formation of titanite, leucoxene, rutile and hematite, within brittle structures, accompany the total destruction of igneous textures and minerals.

Mass balance calculations (Monteiro, 1997) indicate that the mylonitized metabasite displays slightly mass increase (3%) relative to least-mylonitized metabasite. This mass increase is related mainly with MgO (~ 60%), CO_2 (~ 60%), Pb (~ 174%) e Zn (~ 212%) enrichments. Relative loss of Fe_2O_3 (~ 33%), Ba and Sr (~ 60%) are also observed.

The zinc ore, in tectonic contact with metabasic rocks, shows a different mineral association characterized by the Zn-rich chlorite, hematite, talc, and apatite.

Along the contact with metabasite, the dolomites are bleached and metasomatically altered and display also great differences in the isotopic compositions ($\delta^{18}O_{VSMOW}$= +21.4 to +16.7‰ and $\delta^{13}C$= -0.2 to -1.5‰) relative to unaltered dolomites ($\delta^{18}O_{VSMOW}$= +26.2 to +27.2‰ and $\delta^{13}C$ = -1.0 to +2.7‰).

The $^{87}Sr/^{86}Sr$ ratios of these bleached rocks ($^{87}Sr/^{86}Sr$= 0.732660) are also more radiogenic than the unaltered dolomites ($^{87}Sr/^{86}Sr$= 0.709239 to 0.709764) and the altered dolomites ($^{87}Sr/^{86}Sr$= 0.712948 to 0.715980) (Monteiro, 2002).

The calcite of this bleached metadolomite has the most distinct $\delta^{13}C$ value (-10.3‰), in relation to the hydrothermal carbonates within the fault zone ($\delta^{13}C$= -5.9 to +1.7‰) (Monteiro et al., 1999).

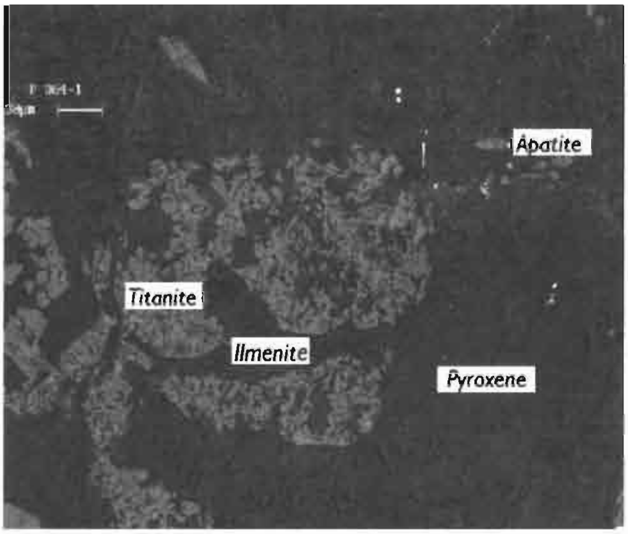

Figura 3. Back-scattered SEM image, showing the formation of titanite, which replaces igneous euhedral ilmenite.

RELATIONSHIPS BETWEEN THE METABASITE AND ZINC ORE

The metabasic rocks occur mainly within the Vazante Shear Zone, juxtaposed to dolomites and slates of the Vazante Group. This makes the recognition of the relationship between this metabasite and the host sequence difficult. However, there is evidence that this rock was affected by hydrothermal processes similar to those responsible by the zinc ore formation, which is coeval with the Vazante Shear Zone development (Monteiro, 1997; Monteiro et al., 1999).

Mass balance calculations and stable isotopic studies (Monteiro, 1997; Monteiro et al., 1999) indicate that the Zn- and Pb-rich fluids affected the metabasic rocks. Metasomatic processes affected metabasite, dolomites and zinc ore, indicating also strong fluid-rock interaction along the tectonic contact zones.

GEOCHRONOLOGY

Samples of the metamorphosed mafic dikes were recovered from drill cores. Three whole rock samples were powdered and Sm-Nd isotopic analyses were carried out. The T_{DM} model ages are between 1.16 to 1.21 Ga, and the $E_{Nd(0)}$ varies from +0.16 to –0.41. Because the Sm/Nd ratios are very fractionated (0.16) these T_{DM} ages are overestimated and represent the maximum crystallization age of the dikes. In addition, crustal contamination during magma ascent, which could increase the T_{DM} ages, cannot be ruled out.

Zircon and titanite grains were separated from two different cores.

The samples were crushed, sieved, and the <100 mesh heavy mineral fraction was concentrated. Sample VZ-1 yielded a reasonable quantity of small pink clear zircons. Another sample (VZ-2) had very low yield of zircons (also small pink clear ones); however a great amount of titanite was recovered from this sample.

The titanite grains are creamy brown in color, have a sugary texture, and are opaque (due to their microcrystalline texture).

Five small zircon fractions with different morphologies (from euhedral to rounded grains) of sample VZ-1 were analyzed, and all of them are discordant (Fig. 4). The zircons yielded $^{207}Pb/^{206}Pb$ minimum ages ranging from 2096 to 2398 Ma; the oldest age was determined on euhedral acicular zircons. A single fraction of euhedral zircons was recovered from sample VZ-2 and it yielded a $^{207}Pb/^{206}Pb$ minimum age of 2092 Ma with a very large error. However, this age is similar to ages obtained from two fractions of sample VZ-1 (Fig. 4). The U-Pb ages determined on zircons recovered from the mafic dikes are too old and indicate that the zircons were assimilated by the magma from the basement rocks. Although the results show some scatter on the U-Pb diagram, some fractions define a discordia that yields an upper intercept age of 2100 ± 25 Ma indicating the presence of a Paleoproterozoic basement for the Vazante Group. Furthermore, because of the older $^{207}Pb/^{206}Pb$ ages determined on some fractions, we can suggest that either the magma passed through crust composed of magmatic rocks older than 2.1 Ga or that metassedimentary rocks containing zircons from different sources are part of the basement in the area.

Seven single-crystal fractions of titanite were analyzed. Surprisinly, all the samples contained only common non-radiogenic Pb. The isotopic ratios are uniform and do not present a large variation. The $^{206}Pb/^{204}Pb$ values range from 17.68 to 17.92, $^{207}Pb/^{204}Pb$ from 15.60 to 15.70, and $^{208}Pb/^{204}Pb$ from 36.90 to 37.19, and most of them have large errors. The obtained results are in agreement with Pb isotopic ratios reported for galenas from the Pb-Zn deposits of Morro Agudo, Vazante, Ambrósia e Fagundes (Cunha et al., 2002; 2003) indicating that hydrothermal fluids responsible for the mineralizations might have affected the metabasic rocks. In addition, the presence of common Pb in the titanite, which typically has high U/Pb ratio, confirms the petrographic observations that this mineral is hydrothermal and it is coeval with the timing of Pb-rich fluid percolation.

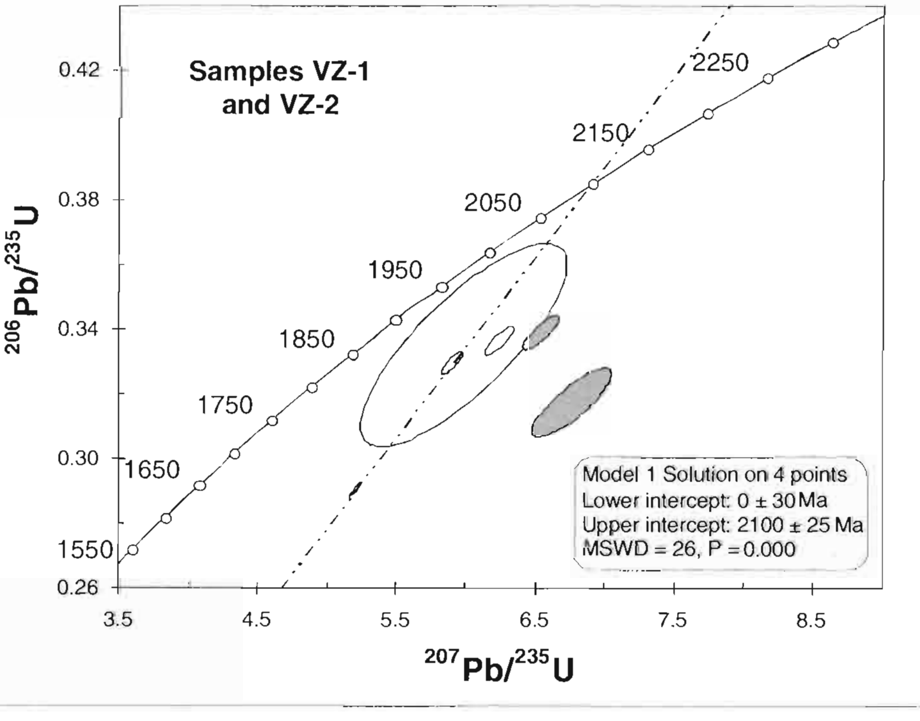

Figure 4. U-Pb concordia diagram of zircons from metabasites from the Vazante Formation. The analyses represented by filled ellipses were not used for regression. The analysis with higher error is from sample VZ-2; all the other points were obtained from zircon fractions separated from sample VZ-1.

CONCLUSIONS

The metabasite was affected by epigenetic-hydrothermal processes similar to those responsible for the Vazante zinc non-sulfide mineralization, which is closely linked to the Vazante Shear Zone development. The similar Pb isotopic composition of hydrothermal titanite from this metabasite and galena from the others zinc sulfide deposits hosted by the Vazante Group, could reinforce the importance of epigenetic-hydrothermal processes associated with the late Brasiliano event for the genesis of the zinc deposits in the Vazante-Paracatu Zn – (Pb) district.

ACKNOWLEDGMENTS

We are grateful to Companhia Mineira de Metais for continuous support and hospitality at the mine. This research was partially supported by PRONEX funds (Project 167/96), and FAPESP grants (Proc. 98/0412-3 and 95/4652-2).

REFERENCES

Amaral, G. & Kawashita, K., 1967. Determinação da idade do Grupo Bambuí pelo método Rb/Sr. In: Congr. Bras. Geol., 21., Anais, SBG, p.214-217.

Cunha, I.A., Babinski, M, and Misi, A., 2002. Isótopos de Pb em galenas dos depósitos de Pb-Zn da região de Vazante-Paracatu: Dados preliminares. In: Congr. Bras. Geol., 41, Anais, SBG, p. 492

Cunha, I.A., Babinski, M, and Misi, A., 2003. Lead isotope study of galenas from the Vazante Group, Minas Gerais, Brazil. This volume.

Dardenne, M.A., 2000. The Brasília Fold Belt. In: Cordani, U.G.; Thomaz Filho, A.; Campos, D.A. (eds) Tectonic evolution of South America, Rio de Janeiro, Intern. Geol. Congr., 31st, p. 231-263.

Dardenne, M.A.; Freitas-Silva, F.H.; Souza, J.C.F.; Campos, J.E.G., 1998. Evolução tectono-sedimentar do Grupo Vazante no contexto da Faixa de Dobramentos Brasília. In: Congr. Bras. Geol., 40., Belo Horizonte, 1998., Resumos, SBG, p. 26.

Monteiro, L.V.S., 1997. Contribuição à gênese das mineralizações de zinco da Mina de Vazante, MG. Master Thesis, IGc-USP, 159 p.il.

Monteiro, L.V.S. 2002. Modelamento metalogenético dos depósitos de zinco de Vazante, Fagundes e Ambrósia, associados ao Grupo Vazante, Minas Gerais. Doctorate Thesis, IGc-USP, 317 p. il.

Monteiro, L.V.S.; Bettencourt, J.S.; Spiro, B; Graça, R.; Oliveira, T.F., 1999. The Vazante Zinc Mine, MG, Brazil: Constraints on Fluid Evolution and Willemitic Mineralization. Explor. Mining Geol., 8: 21-42.

Pimentel, M.M.; Dardenne, M.A;, Fuck, R.A.; Viana, M.G.; Junges, S.L; Fischel, D.P.; Seer, H.J.; Dantas, E.L., 2001. Nd isotopes and the provenance of detrital sediments of the Neoproterozoic Brasília Belt, central Brazil. J. South Am. Earth Sci., 14: 571 – 585.

Rigobello, A.E.; Branquinho, J.A.; Dantas, M.G. da S.; Oliveira, T.F.; Neves Filho, W., 1988. Mina de Zinco de Vazante. In: Schobbenhaus, C. & Coelho, C. E.S. (coords). Principais depósitos minerais do Brasil. DNPM, v.3, p. 101-110.

FIRST DIRECT DATING OF A NEOPROTEROZOIC POST-GLACIAL CAP CARBONATE

Babinski, M.[1] **and Kaufman, A.J**[2]

1. Centro de Pesquisas Geocronológicas, Instituto de Geociências, Universidade de São Paulo, Rua do Lago, 562, São Paulo-SP, 05508-080, Brazil. babinski@usp.br
2. Geology Department, University of Maryland, College Park, MD 20742, USA. jkaufman@geol.umd.edu;

Keywords: Sturtian Glaciation, Cap carbonates, Bambuí Group, São Francisco Basin, Pb-Pb geochronology

INTRODUCTION

The dawn of the Phanerozoic Eon (~544 Ma) was marked by the rapid development of animal phyla, termed the "Cambrian Explosion," which must somehow relate to vast changes in Earth's surface climate in the preceding Neoproterozoic Era. Clues to the environmental perturbations of the "Cryogenian" and terminal "Neoproterozoic III" (Knoll & Walter, 1992) are recorded in the widespread deposition of glacial rocks in some cases down to equatorial latitudes systematically overlain by enigmatic dolomite and limestone deposits, known as the "cap carbonates (e.g. Kennedy, 1996)," as well as strong temporal anomalies in $\delta^{13}C$ and $^{87}Sr/^{86}Sr$ of seawater proxies (Kaufman et al., 1997).

Several models have been developed to explain the pre-Phanerozoic ice ages along with the cap carbonates and associated biogeochemical anomalies, including the "snowball Earth" hypothesis (Kirschvink, 1992; Hoffmann et al., 1998; Hoffman & Schrag, 2002), which advocates that the planet was completely entombed in ice resulting in extreme albedo; recovery from the frozen Earth required the multi-million year buildup of volcanic CO_2, and must have happen at least twice in the interval between 750 Ma and the Precambrian-Cambrian boundary. Existing radiometric data constrain the older glacial epoch, called the Sturtian and best represented by iron-rich deposits in Australia, Namibia, and arctic Canada, to have occurred between 760-700 Ma (e.g. Hoffman et al., 1996). The younger glacial epoch is called the Marinoan in the southern hemisphere or Varanger in the peri-North Atlantic region and is temporally poorly constrained, but is likely to have occurred between ~625 and 585 Ma (Saylor et al., 1998; Thompson and Bowring, 2000). Tests of the snowball scenario demand stricter controls on the relative and absolute timing of the ice ages. While the former may be provided by chemical stratigraphy (Kaufman et al., 1997), precise ages of the diamictites are rare (Brasier, 2000; Thompson & Bowring, 2000; Gorokhov et al., 2001), and the caps, non-existent.

In Brazil and surrounding countries lithologic records of both Sturtian and Varangian ice ages are preserved, including distinctive cap carbonates with extreme biogeochemical anomalies. In this paper we present the first direct dating of a cap carbonate from the Bambuí Group in southern Brazil on the São Francisco Craton, which is texturally and isotopically indistinguishable from the Maieberg Formation cap in the Otavi Group on the Congo Craton. Our Pb-Pb isochon age for these caps supports the view that the Sturtian epoch included at least two discrete ice ages. Application of this geochronometer to well-preserved cap carbonates throughout the Neoproterozoic should pave the way toward a better understanding of the tempo of Neoproterozoic climatic cycles, as well as the evolution of metazoan life.

GEOLOGICAL SETTING

The São Francisco basin is some 200-350 km wide and 800 km long and contains an extensive sedimentary cover of Neoproterozoic clastic and carbonate sedimentary rocks of the São Francisco Supergroup. The supergroup is divided into two groups, the Macaúbas and the overlying Bambuí. The older Macaúbas Group includes widespread glacial diamictites (Dardenne, 1978; Karfunkel & Hoppe, 1988), shales, and quartzites. The younger Bambuí Group consists of two main sequences: a lower slope to platform interval of marine strata and an upper succession of shallow-water to alluvial strata. The lower sequence is divided into four formations: Sete Lagoas, Serra de Santa Helena, Lagoa do Jacaré, and Serra da Saudade, which correspond to cycles of carbonate and pelitic-psamitic sedimentation. The Sete Lagoas Formation contains well preserved stromatolites and seafloor cements. In the Lagoa do Jacaré Formation beds of, oolitic and pisolitic carbonates occur. Pelitic to psamitic sediments of the Serra de Santa Helena and Serra da Saudade formations represent clastic cycles within this sequence. Overlying the lower sequence is a clastic shallow-marine to alluvial unit, the Três Marias Formation, which was deposited in a foreland basin associated with the ca. 600 Ma Brasiliano Orogeny (Marshak & Alkmim, 1989; Brito Neves & Cordani, 1991).

Deformation in the São Francisco Supergroup increases progressively towards the Brasília and Araçuaí fold belts on the west and east, respectively (Chemale et al., 1993). Metamorphism reaches greenschist facies at the eastern border of the basin but decreases rapidly towards the center where two undeformed regions (C_1 and C_2 sub-zones) are recognized (Alkmim et al., 1989). These regions are probably related to pre-Brasiliano topographic highs that played an important role during the deposition and inversion of sediments in the São Francisco basin (Chemale et al., 1993).

Studied limestone samples from the Sete Lagoas Formation (Pedro Leopoldo facies) were collected at Sambra quarry about 60 km northwest of Belo Horizonte in the C_2 sub-zone. The contact of this facies with the lower Sete Lagoas beds is unclear; some authors suggest that the area represents a structural high point in the basin

(Chemale Jr. et al., 1993) and the carbonates were deposited directly over Archean basement. From the base of the exposure, the Sambra carbonates consist of cm-scale layers of gray-to-black acicular seafloor cements draped by red-to-cream colored microsparite (Peryt et al., 1990) that continue for about 8 meters. The irregularly crosscut cements are composed of feathery precursor crystal bundles with squared-off growth zones; ghosts of an original fibrous material, hexagonal in cross-section, is observed. The thickness of individual layers of these seafloor cements range from 3 to 98 mm, but most are between 10 and 35 mm. Based on morphologic characteristics and Sr abundances, Peryt et al. (1990) suggested that these inorganic seafloor precipitates were originally composed of aragonite. Similar carbonate fabrics are described in the Maieberg Formation cap carbonate atop the Ghaub diamicitite in the Otavi Group of northern Namibia (Halverson et al., 1999; Hoffman & Schrag, 2002). In the lower Sambra quarry, the precipitate interval is overlain by ~20 m of ribbon laminated and massive beds of limestone and dolomite. A second upper quarry, which exposes another 40 m of massive and evaporitic grey to green carbonates, lies stratigraphically above the lower exposure. For this study we collected samples of precipitate and microspar couplets from the banded portion of the lower quarry, as well as massive carbonates from the upper quarry.

ANALYTICAL PROCEDURES

The Pb isotope analyses were carried out at the Geochronological Research Center, at the University of São Paulo, following the analytical procedures of Babinski et al. (1999). Pb isotopic compositions were corrected for a mass fractionation factor of 0.12% amu^{-1} determined based on analyses of common Pb standard NBS 981. Pb blanks were 30-50 pg and have negligible effect on the Pb measured isotopic compositions. Pb-Pb isochron ages were determined using the Model 1 regression of Isoplot (Ludwig, 1999). Errors are reported at 95% confidence level.

Stable carbon and oxygen isotopic compositions of carbonates were determined with a Micromass Isoprime mass spectrometer coupled with a MultiPrep inlet system for on-line acidification and transfer of sample gases at the University of Maryland. Uncertainties of sample measurements based on the analysis of multiple standard materials are better than 0.1‰ (2σ) for both C and O isotopes.

Strontium was isolated from carbonate samples by repeated leaches with 0.2M ammonium acetate prior to sample dissolution in 0.5M acetic acid; solutions were then passed through Sr-SPEC resin and the Sr collected for mass spectrometric analysis. The Sr was loaded with TaO_2 on a Re filament and analyzed between 1400-1600° C with a VG Sector-54 thermal ionization mass spectrometer at the University of Maryland. Repeated measurements of NBS-987 during the period of sample analysis had an average $^{87}Sr/^{86}Sr$ of 0.710240 ± 0.000008 (2σ).

RESULTS AND DISCUSSION

The isotope results determined on the carbonate rocks from Sambra Quarry show $\delta^{13}C$ excursion from the base at -4 to near 0‰ some 8 meters higher on the sequence (*cf.* Peryt et al., 1990; Iyer et al., 1995); carbonate carbon isotope values remain relatively constant above this transition zone, in a succession that shows evidence for some shallowing and an upsection increase of siliciclastic detritus. In the lower part of the quarry insoluble residues compose less than 5% of the rock, which increase to 10% above the transition zone. Over the same interval, $\delta^{18}O$ values appear to co-vary with carbonate ^{13}C abundance; from the base of the exposure to the 8-meter mark, oxygen isotope values rise from ca. -10 to -6‰, and then again remain constant to the top of the exposure. Organic matter is anomalously enriched in the ^{13}C near the base, with remarkably constant values of ca. 18 to 20‰, resulting in strongly reduced carbon isotope fractionations ($\Delta\delta$) between inorganic and organic phases, ranging from 12 to 14‰ (Kaufman, 2000; Kaufman et al., 2001).

Elemental abundances and ratios (i.e. Mn/Sr) determined on the carbonates suggest that the best-preserved samples correspond with precipitate textures in the lower reaches of the quarry. These samples contain Sr concentrations up to 3000 ppm, and the Mn/Sr close to zero. Above this level in dolomitic samples, Sr concentrations are < 300 ppm and Mn/Sr increases up to 1-2. The $^{87}Sr/^{86}Sr$ ratios from the best-preserved limestone samples show constant values of 0.7074.

Based on the negative $\delta^{13}C$ compositions at the base of the exposure, Iyer et al. (1995) suggested that the Pedro Leopoldo facies accumulated in a locally evaporitic environment unrelated to post-glacial transgression, insofar as diamictite has not been found beneath the carbonate in the Belo Horizonte area. In contrast, we suggest that the negative $\delta^{13}C$ values in the Sambra sea floor precipitates are consistent with other cap carbonates deposited during deglaciation. Furthermore, the $^{87}Sr/^{86}Sr$ of 0.7074 measured on the Sambra carbonates are in close agreement values determined in similarly textured and Sr-rich limestone rhythmites from the Maieberg Formation cap carbonate (atop Ghaub Formation diamictite) in Namibia (Schrag et al., 1999), suggesting that these deposits were contemporaneous.

Eight carbonate samples were selected for the geochronology study; six from the lower quarry and two from the upper quarry. Four of the lower quarry samples contained both precipitate and microspar components; these were analyzed separately. All other samples were composed of homogeneous microspar. Samples from the lower quarry yielded variably radiogenic Pb isotopic compositions with $^{206}Pb/^{204}Pb$ ratios ranging from 19.1 to 32.8, $^{207}Pb/^{204}Pb$ from 15.68 to 16.56, and $^{208}Pb/^{204}Pb$ from 38.1 to 39.0. The fibrous precipitates presented the most radiogenic Pb ratios. Samples from the upper quarry revealed uniform and non-radiogenic Pb ratios ($^{206}Pb/^{204}Pb = 18.8$; $^{207}Pb/^{204}Pb = 15.65$), and the results of these two samples were not used for regression. In the Pb-Pb diagram the Pb ratios obtained from the samples from the lower part of the sequence defined a straight line, which yielded a very precise Pb-Pb isochron age of 740 ± 22 Ma (95% confidence level). Because the rocks of this outcrop are extremely well preserved and undeformed, suggesting that the Pb isotopic system was not disturbed by later events, we interpret this as a depositional age for this cap carbonate. If the correlation of the Sete Lagoas cap carbonate from the Sambra Quarry with the Maieberg is correct, the Pb-Pb age from Brazil constrains two discrete ice ages in Gondwanaland (represented by the Ghaub and Chuos diamictites in the Otavi Group of Namibia and equivalents) to between about 760 and 720 Ma. This supports the view that the Sturtian glacial epoch includes multiple and distinct ice ages (Kennedy et al., 1998).

REFERENCES

Alkmim, F.F., Chemale, F., Bacellar, L.A.P., Oliveira, J. and Magalhães, P.M., 1989. Arcabouço estrutural da porção sul da Bacia do São Francisco. In: Simp. Geol. Núcleo Minas Gerais, 5; Simp. Geol. Núcleo Brasília, 1, Belo Horizonte. Anais, SBG, p. 289-293.

Babinski, M., Van Schmus, W.R. and Chemale, F., 1999. Pb-Pb dating and Pb isotope geochemistry of Neoproterozoic carbonate rocks from the São Francisco basin, Brazil: implications for the mobility of Pb isotopes during tectonism and metamorphism. Chem. Geol., 160:175-199.

Brito Neves, B.B. and Cordani, U.G., 1991. Tectonic evolution of South America during the Late Proterozoic. Precambrian Res., 53:23-40.

Brasier, M.D., McCarron, G., Tucker, R., Leather, J., Allen, P. and Shields, G., 2000. New U-Pb zircon dates for the Neoproterozoic Ghubrah glaciation and for the top of the Huqf Supergroup, Oman. Geology, 28: 175-178.

Chemale, F., Alkmim, F.F. and Endo, I., 1993. Late Proterozoic tectonism in the interior of the São Francisco craton. In: R.H. Findley et al. (Eds.), Gondwana Eight-Assembly, Evolution and Dispersal, Balkema, pp. 29-42.

Dardenne, M.A., 1978. Síntese sobre a estratigrafia do Grupo Bambuí no Brasil Central. In: Congr. Bras. Geol., 30, Recife. Anais, SBG, v. 2, p. 597-610.

Gorokhov, I.M., Siedlecka, A. Roberts, D., Melnikov, N.N. and Turchenko, T.L., 2001. Rb-Sr dating of diagenetic illite in Neoproterozoic shales, Varanger Peninsula, northern Norway. Geol. Mag., 138: 541-562.

Halverson, G.P., Kaufman, A.J., Hoffman, P.F. and Soffer, G., 1999. Stratigraphy and carbon isotopic record through the Neoproterozoic Rasthof Formation cap carbonate, Otavi Group, Northwest Namibia. Geol. Soc. Am, Abstract with Programs, 31:486.

Hoffman, P.F. and Schrag, D.P., 2002. The Snowball Earth Hypothesis: testing the limits of global change. Terra Nova, 14:129-155.

Hoffman, P.F., Hawkins, D.P., Isachsen, S.E. and Bowring, S.A., 1996. Precise U-Pb zircons ages for early Damaran magmatism in the Summas Mountains and Welwitschia inlier, northern Damara belt, Namibia. Geol. Surv. Namibia Comm., v. 11, p. 47-52.

Hoffman, P.F., Kaufman, A.J., Halverson, G.P. and Schrag, D.P., 1998. A Neoproterozoic snowball Earth. Science, 281:1342-1346.

Iyer, S.S., Babinski, M., Krouse, H.R. and Chemale Jr., F., 1995. Highly ^{13}C-enriched carbonate and organic matter in the Neoproterozoic sediments of the Bambuí Group, Brazil. Precambrian Res. 73, 271-282.

Karfunkel, J. and Hoppe, A., 1988. Late Proterozoic glaciation in central-eastern Brazil: synthesis and model. Palaeogeog., Palaeoclimat., Palaeoecol. 65:1-21.

Kaufman, A.J., Knoll, A.H. and Narbonne, G.M., 1997. Isotopes, ice ages, and terminal Proterozoic Earth history. Proceedings of the National Academy of Sciences, 94:6600-6605.

Kaufman, A.J., 2000. The biogeochemical aftermath of Snowball Earth conditions. In: Int. Geol. Congress, 31st , Rio de Janeiro, Brazil. CD Abstracts.

Kaufman, A.J., Varni, M.A., Misi, A. and Brito Neves, B.B., 2001. Anomalous δ^{34}S signatures in trace sulfate from a potencial cap carbonate in the Neoproterozoic Bambuí Group. In: IGCP 450 Meeting, Proceedings, Belo Horizonte, Brazil, p. 62-65.

Kirschvink, J.L., 1992. Late Proterozoic low-latitude global glaciation: the snowball Earth. In: The Proterozoic Biosphere (Eds. Schopf, J.W. and Klein, C.), pp. 51-52. Cambridge University Press, Cambrigde.

Kennedy, M.J., 1996. Stratigraphy, sedimentology, and isotopic geochemistry of Australian Neoproterozoic postglacial cap dolostones; Deglaciation, δ^{13}C excursions, and carbonate precipitation. Journal of sedimentary Research, 66:1050-1064.

Kennedy, M.J., Runnegar, B., Prave, A.R., Hoffmann, K.-H. and Arthur, M.A., 1998. Two or four Neoproterozoic glaciations? Geology, 26:1059-1063.

Knoll, A.H. and Walter, M.R., 1992. Latest Proterozoic stratigraphy and Earth history. Nature, 356:673-678.

Ludwig, K.R., 1999. User's manual for Isoplot/Ex Version 2. A geochronological toolkit for Microsoft Excel. Berkeley Geochronological Center Spec. Publ. 1a, 47p., Berkeley, CA. USA.

Marshak, S. and Alkmim, F.F., 1989. Proterozoic contraction/extension tectonics of the southern São Francisco region, Minas Gerais, Brazil. Tectonics, 8:555-571.

Peryt, T.M., Hoppe, A., Bechstädt, T., Köster, J., Pierre, C. and Richter, D.K., 1990. Late Proterozoic aragonitic cement crusts, Bambuí Group, Minas Gerais, Brazil. Sedimentology, 37:279-286.

Saylor, B.Z., Kaufman, A.J., Grotzinger, J.P. and Urban, F., 1998. A composite reference section for terminal Proterozoic strata of Southern Namibia. J. Sedim. Res., 68(6):1223-1235.

Schrag, D.P., Hoffman, P.F. and Bowring, S.A., 1999. Geochemical and isotopic implications of the snowball Earth hypothesis. Geol. Soc. Am. Program with Abstracts, v. 31, p. 372.

Thompson, M.D. and Bowring, S.A., 2000. Age of Squantum "tillite', Boston Basin, Massachusetts: U-Pb zircon constraints on terminal Neoproterozoic glaciation. Am. J. Sci., 300: 630-655.

THE CAP CARBONATE OF THE PUGA HILL (CENTRAL SOUTH AMERICA) IN THE CONTEXT OF THE POST-VARANGER GLACIATION

Boggiani, P.C.[1]; Ferreira, V.P.[2]; Sial, A.N.[2]; Babinski, M.[3]; Trindade, R.I.F.[4]; Aceñolaza, G.[5]; Toselli, A.J.[5] and Parada, M.A.[6]

1. IG-USP - Instituto de Geociências – USP, Rua do Lago, 562, 05508-080, São Paulo-SP, Brasil boggiani@usp.br
2. NEG-LABISE – UFPE - Dept. Geology C.P. 7852, 50670-000 Recife-PE, Brasil. valderez@npd.ufpe.br, ans@mail.ufpe.br
3. IG-USP - Instituto de Geociências – USP, Rua do Lago, 562, 005508-080, São Paulo-SP, Brasil. babinski@usp.br
4. Departamento de Geofísica, Instituto de Astronomia, Geofísica e Ciências Atmosféricas, USP, Rua do Matão, 1226, 055508-090, São Paulo-SP, Brasil. rtrindad@iag.usp.br
5. INSUGEO – S. M. De Tucuman, Miguel Lillo, 205, Argentina, 4000
6. Univ. Chile – Santiago, Chile

Keywords: Cap carbonate, Corumbá Group, Varanger Glaciation, stable isotopes, Brazil

INTRODUCTION

The cap carbonates are thin, laterally persistent carbonate layers that usually cover the Neoproterozoic glacial deposits, without significant hiatus. These deposits typically have $\delta^{13}C_{PDB}$ values in the range of 0 to –5‰, and exhibits anomalous sedimentary structures (Kaufman et al., 1993, 1997; Kennedy et al., 2001; Hoffman & Schrag, 2002). These ubiquitous negative anomalies in C isotopes together with the low-latitude of glacial deposits derived from paleomagnetic data, and the anomalous occurrence of banded iron formations (BIFs) associated with these rocks are the main evidence in support to the Snowball Earth hypothesis put forward by Kirschvink (1992) and Hoffman et al. (1998).

If the Neoproterozoic glaciations have attained tropical latitudes over millions of years, as suggested by the paleomagnetic results from Elatina Formation in Australia (Sohl et al., 1999), then the global oceanic circulation would be inhibited resulting in a stratified ocean. The build up of atmospheric CO_2 along this time span would trigger a strong greenhouse event, rapidly melting the ice cover. Recovering of the oceanic global circulation would promote the deposition of iron in BIFs; the increase in ocean alkalinity associated to the strong weathering of the Earth surface would promote the precipitation of mostly inorganic, and thus ^{12}C depleted, cap carbonates.

In central South America, all these key features (glacial deposits, BIFs and cap carbonates) are present within the Neoproterozoic-Cambrian Corumbá basin context. Here we present preliminary results of an isotope, paleomagnetic and sedimentological study on the Puga Hill region, where Vendian glacial deposits of the Puga Formation are covered by carbonate rocks of the Corumbá Group (Boggiani, 1998; Gaucher et al., 2003). Also discussed are the implications of these results to the Snowball Earth debate.

STRATIGRAPHY

The Corumbá Basin (500-km-long and NNW oriented) was developed along the eastern border of the Rio Apa Block (Amazonian Craton). It comprises Varanger glaciomarine sediments of the Puga Formation (Alvarenga & Trompette, 1992), and the terrigenous and carbonate sediments of the Corumbá Group (Almeida, 1965). The lower units of the Corumbá Group (Cadiueus and Cerradinho Formations) were deposited in a fault-limited, confined basin. The shallow-water dolomitic and phosphatic rocks of the overlying unit (Bocaina Formation) have spread along a larger area, covering the other units and also the granitic-gneissic basement. Subsequent regression eroded part of these sediments and re-deposited them as slope breccia. Carbonaceous limestones and shales of the Tamengo formation, with *Cloudina* and *Corumbella*, cover these deposits (Fairchild & Zaine, 1987). They have positive $\delta^{13}C_{PDB}$ of +5‰. These limestones are covered by shales of Guaicurus Formation, under unconfined oceanic conditions. In this context, the Corumbá Basin is interpreted as associated to the contemporaneous Iapetus opening (Cawood et al., 2001). It has closed/inverted as a result of the Brasiliano collision.

THE PUGA HILL CAP CARBONATE

The carbonates of the Puga Hill are located at the right margin of Paraguay River (19°37'20''S, 57°31'40''W), where the underlying glacial deposits of the Puga Formation were first described by Maciel (1959). These diamictites contain abundant carbonate clasts and the presence of these could be a cause of a high matrix carbonate content, considering the relative softness of carbonate minerals.

The studied section is a ca. 12 m thick section located in the northen sector of the Puga Hill (Fig. 1). It consists of alternating pinkish and grey, laminated limestone (rhythmite), alternating peloidal and microcrystaline carbonate.

Since, the Puga Hill is isolated from other carbonate occurrences, its stratigraphic position within the Bocaina Formation (Corumbá Group) is a matter of discussion. The Bocaina Formation (Almeida, 1965; Boggiani 1998) is a 30 to 80 m thick dolomitic carbonate unit, at the base of the carbonate succession of the Corumbá Group. These sediments were deposited shallow-water, under warm-water conditions. They comprise stromatolitic path reef, shoal and lagoonal ooides, and phosphorite rocks formed by the arrival of upwelling fluxes (Boggiani et al., 1993). In contrast, the Puga Hill carbonates were probably deposited at deep-water conditions. They have distinct isotopic signature; the cap carbonates of the Puga Hill showing homogeneous values of $\delta^{13}C_{PDB}$ near -5‰, while the dolomites of the Bocaina formation exhibit values near zero ($\delta^{13}C$ between -1.0 and +0.6‰).

RESULTS AND DISCUSSION

We collected a 12-m thick series of samples from the entire rhythmite unit, with sampling spacing of 1 to 2 m (Fig. 2). Distribution of $\delta^{13}C_{PDB}$ values in the section is homogeneous and close to -5‰ (Fig. 2). Paleomagnetic samples were collected at only two layers. Negative inclinations between 10° and 25° obtained for one of these sites suggest low paleolatitudes for deposition of these sequences.

These results are in agreement with those obtained for the Mirassol d'Oeste quarry, located 600 km northwards along the margin of the Amazonian Craton. In the Mirassol d'Oeste region, cap carbonates of the Araras Group cover diamictites of the Puga Formation (Nogueira et al., 2003). The contact between the diamictite and the carbonate was plastically deformed, implying a short time between the end of glaciation and the deposition of platform carbonates. Previous work by Boggiani et al. (1997) has interpreted the Araras carbonate facies as related to a sedimentation in a restricted sea, without communication with neoproterozoic global ocean according to their C and O isotope signature. The Araras and Corumbá succession have contrasting lithological palaeontological record; the metazoan fossils being exclusively found in the Corumbá Group.

The negative values of $\delta^{13}C_{PDB}$ observed on the Puga Hill cap carbonate and on several other Varanger-type cap-carbonates are similar to the isotopic composition of the mantle-derived carbon ($\delta^{13}C_{PDB} = -6 \pm 1‰$). Strongly negative $\delta^{13}C_{PDB}$ values would be generated by the following processes (or more probably the combination of them): (a) millions of years of low organic productivity during snowball events; (b) high rates of carbonate sedimentation due to the intensive silicate weathering in the ultra-greenhouse aftermath; (c) Rayleigh distillation of atmospheric carbon source as the large CO_2 reservoir is transferred rapidly to the ocean; (d) ocean overturn,; (e) enhanced organic weathering, and (e) massive methane burst (Hoffman et. al.1998; Kennedy et al. 2001; Higgins & Schrag, 2003).

Prave et al. (2001) have examined in detail the Varanger and Sturtian cap carbonates on three cratons (southeastern Congo, northwestern Kalahari and southwestern Laurentia) in terms of their isotopic record. They have found a great variability in $\delta^{13}C_{PDB}$ trends of as much as ±10‰); the isotopic signatures showing strong differences for different sedimentary succession and palaeogeographic settings (shelf, slope, basinal). If cap carbonate deposition was synchronous worldwide then wide variability in $\delta^{13}C$ trends indicates that Earth's oceans in the immediate aftermath of Neoproterozoic glaciations were not sterile, -5‰ realms, but rather a richly isotopically varied world whose local diversity was captured in the rapidly precipitating cap carbonates. In contrast to Prave's findings, the isotopic record derived from different facies of the Puga Hill and the correlative Mirassol d'Oeste indicate that the isotopic composition of the ocean's water was rather constant and similar to the -5‰ mantle-carbon values. These results are consistent with a 3-box model recently run by Higgins and Schrag (2003). Increased alkalinity was derived from the extreme surface water, but also by oceanic overturn. In the Puga Hill, the association of glacial sediments with BIF's of Jacadigo Group (Urucum Massif), and the occurrence of phosphatic rocks in the top of the Bocaina Formation suggest the influence of oceanic overturn in increasing alkalinity. In this scenario, the ocean re-oxygenate and dissolved Fe oxidizes to form iron formation.

The inconsistencies in the isotopic record found by Prave and co-authors may lay in the lack of a complete sedimentological and stratigraphic characterization of carbonates topping glacials around the world. Different isotopic values may arise if not true cap carbonates are compared to true ones, as occurs on most of the Bocaina Formation outcrops, where upper carbonates overlie diamictites; only the Puga Hill occurrence, described consists of a true post-glacial cap carbonate.

CONCLUSION

The values of $\delta^{13}C$ observed in the Puga Hills, close to -5‰, are against the Prave et al. (2001) conclusion, that find a strong variability in $\delta^{13}C_{PDB}$ trends in different caps carbonates, and favor a global-scale homogeneity of the C isotopes in these carbonates.

ACKNOWLEDGMENTS

This project has been partially financed by VITAE (B-11487/10B00). IGCP (UNESCO) 478 "Neoproterozoic - Early Palaeozoic Events in SW – Gondwana".

REFERENCES

Almeida, F.F.M. 1965. Geologia da Serra da Bodoquena (Mato Grosso), Brasil. Boletim da Divisão de Geologia e Mineralogia, DNPM, 219:1-96.

Alvarenga, C.J.S. de & Trompette, R. 1992. Glacially influenced sedimentation in the later Proterozoic of the Paraguay Belt (Mato Grosso, Brazil). Palaeogeography, Palaeoclimatology, Palaeoecology, 92:85-105.

Boggiani, P.C. 1998. Análise Estratigráfica da Bacia Corumbá (Neoproterozóico) – Mato Grosso do Sul. Tese de Doutorado, Inst. de Geociências – USP, São Paulo, 181 p.

Boggiani, P.C.; Fairchild, T.R.; Coimbra, A.M. 1993. O Grupo Corumbá (Neoproterozóico-Cambriano) na região Central da Serra da Bodoquena, Mato Grosso do Sul (Faixa Paraguai). Rev. Brasileira de Geociências, 23(3):301-305.

Boggiani, P.C.; Sial, A.N.; Coimbra, A.M.; Ferreira, V.P. 1997. The carbon and oxygen isotope record of Neoproterozoic carbonate rocks of the Paraguay Fold Belt (Central South America). In Simpósio Sulamericano de Geologia Isotópica, Campos do Jordão, 1997. Extended Abstracts , CEPEGEO-IGUSP, p.57-59.

Cawood, P.A., McCausland, P.J.A. and Dunning, G.R., 2001. Opening Iapetus: Constraints from the Laurentia margin in Newfoundland, Geol Soc. Am. Bull., 113: 443-453.

Fairchild, T.R. & Zaine, M.F. 1987. Novas considerações sobre os fósseis da Formação Tamengo, Grupo Corumbá, SW, Brasil. In: Congresso Brasileiro de Paleontologia, 10, Anais..., 2:797-807.

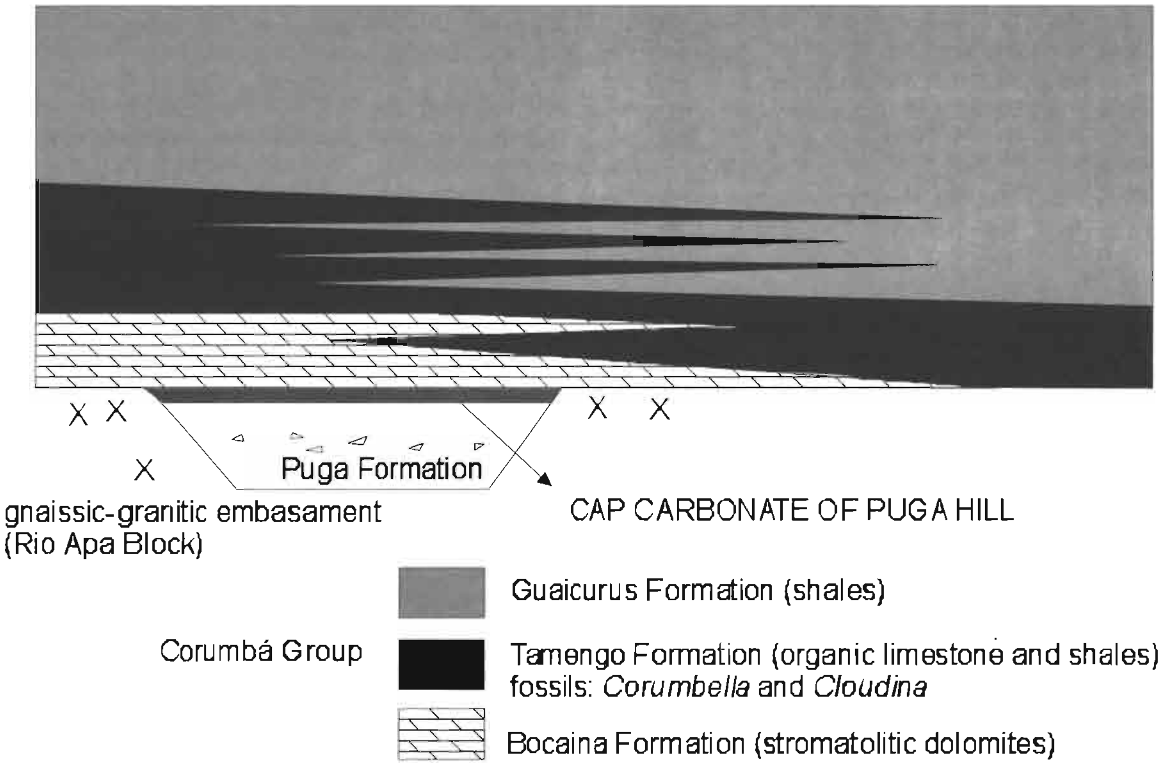

Figure 1. Geological sketch of the Puga Hill cap carbonate occurrence.

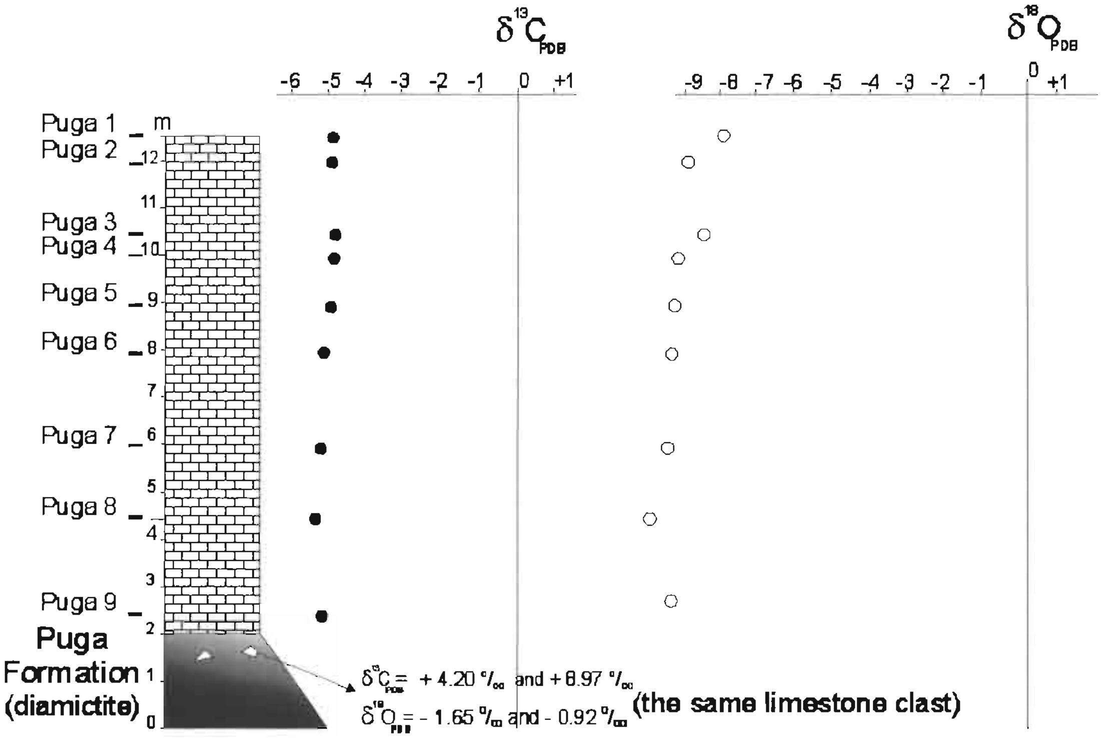

Figure 2. Isotopic record of Puga Hill Cap Carbonate.

Gaucher, C.; Boggiani ,P.C.; Sprechmann, P.; Sial, A. N.; Fairchild, T.R. 2003. Integrated correlation of Vendian to Cambrin Arroyo del Soldado and Corumbá Groups (Uruguay and Brazil): palaeogeographic, palaeoclimatic and palaeobiologic implactions. Precambrian Research 120(3-4):241-278.

Higgins, J.A. and Schrag, D.P. 2003. Aftermath of a snowball Earth. Geochem., Geophys, Geosyst., 4: art. no. 1028

Hoffman, P.F. & Schrag, D.P. 2002. The snowball Earth hypothesis: testing the limits of global change. Terra Nova, 14:129-155.

Hoffman, P.F.; Kauffman, A.J.; Halverson, G.P. and Shrag, D.P. 1998. A Neoproterozoic snowball Earth. Science, 281:1342-1346

Kaufman, A.J.; Jacobsen, S.B.; Knoll, A.H. 1993. The Vendian record of Sr- and C- isotopic variations in sea-water: implications for tectonics and paleoclimate. Earth Planet. Science Letters. 120:409-430.

Kaufman A.J., Knoll, A.H. and Narbonne, G.M. (1997) Isotopes, ice ages, and terminal Proterozoic earth history. Proceedings of the National Academy of Sciences 94: 6600-6605.

Kirchvink, J.L. 1992. Late Proterozoic low-latitude global glaciation: the snow-ball earth. In: The Proterozoic Biosphere (J.W. Schopf and C. Klein, ed.), Cambridge Universit Press, Cambridge.

Kennedy, M.J.N., Christie-Blick, N.; Prave, A.R. 2001. Carbon isotopic composition of Neoproterozoic glacial carbonates as a test of paleoceanographic models for snowball Earth phenomena. Geology, 29:1135-1138.

Maciel, P. 1959. Tilito Cambriano (?) no Estado de Mato Grosso. Boletim da Sociedade Brasileira de Geologia, 8(1): 31-40.

Nogueira, A. C., Riccomini, C., Sial, A. N., Moura, C., Fairchild, T.2003. Soft-sediment deformation at the base of the Neoproterozoic Puga cap carbonate (southwestern Amazon Craton, Brazil): Confirmation of rapid icehouse-greenhouse transition in snowball earth. Geology., (in press).

Prave, A.R, Fallick, A.E., Hoffmann, K. H., Benn, D. & Condon, D.J. 2001. The aftermath of Neoproterozoic glaciations. Geological Society of America & Geological Society of London, Earth System Processes - Global Meeting, Edinburgh.

Sohl, L.E., Christie-Blick, N., and Kent, D.V. 1999. Paleomagnetic polarity reversals in Marinoan (ca. 600 Ma) glacial deposits of Australia: Implications for the duration of low-latitude glaciation in Neoproterozoic time. Geological Society of America Bulletin, v. 111, p. 1120-1139.

MIDDLE MIOCENE TEMPERATURE CHANGES IN THE CENTRAL PARATETHYS: RELATIONS WITH THE EAST ANTARCTICA ICE SHEET DEVELOPMENT

Bojar, A.V.[1]; Hiden, H.[1]; Fenninger, A.[1] and Neubauer, F.[2]

1. Institute of Geology and Paleontology, Karl-Franzens University, Heinrichstrasse 26, A-8010 Graz, Austria,
fax: ++43 (316) 380-9871. ana-voica.bojar@kfunigraz.ac.at, alois.fenninger@kfunigraz.ac.at
2. Institute of Geology and Paleontology, Paris-Lodron University, Hellbrunnerstrasse 32, A-5020, Salzburg, Austria.
franz.neubauer@sbg.ac.at

Keywords*:* Styrian basin, Miocene, cooling, stable isotopes

INTRODUCTION

An important interval in the global climatic and cryospheric development of the Cenozoic was the early to middle Miocene, from 17 to 12 Ma. The climatic optimum near the early/middle Miocene was followed by global cooling at around 14 Ma, the latter being concomitant with the expansion of the east Antarctica ice sheet (Savin et al., 1985; Billups & Schrag, 2002). Thus the middle Miocene is characterized by climatic changes, which resulted in a rapid shift from relative high-latitude warmth to high-latitude refrigeration.

In this study molluscs and brachiopod shells have been used to evaluate palaeoclimatic parameters for a shelf environment during the middle Miocene times. The studied outcrop, which is stratigraphically well documented, belongs to the Miocene of the Styrian basin. This basin was part of the Central Paratethys realm, a land-locked remnant sea which formed subsequent to the collision of Europe and Africa-derived microplates.

GEOLOGICAL POSITION

There are several published studies concerning the stratigraphy, lithology and palaeogeography of the Styrian basin deposits (Ebner & Sachsenhofer, 1991; Rögl, 2001). The sedimentation started in Ottnangian times (Early Miocene); the preserved thickness of the deposits reaches c. 4 km.

The "Retznei Zementwerk" quarry is situated not far away from the border to Slovenia. The lithology and faunal assemblage have been described by Friebe (1990, 1991) and Fritz & Hiden (2001) and are of Badenian age (for the Paratethys timescale, see Rögl (1996)). From bottom to top the following lithofacies were found: 1) Sands and silts with marl boulders of Karpathian and/or Badenian age with *Gastrochaena* and *Lithophaga*. For this facies, Friebe (1991) assumed deposition in a sub- to intertidal environment; 2) and 3) Coral carpets (with *Porites, Tarbellastraea, Acanthastraea, Montastraea,* Sparidae, Balistidae and shark teeth) with intercalations of sand with crustaceans; and 4) Algal debris. According to Friebe (1991), lithofacies 2, 3 and 4 were deposited at a depth above the fair weather-wave base; 5) Bioclastic rhodolith limestones with various fossils e.g. scallops, oysters, red algae; 6) Marly limestone; 7) Sands and silts with molluscs and crabs.

At the base of lithofacies 7, a discontinuous tuff intercalation was described. The tuff contains unaltered phenocrysts of feldspars and fresh biotites, and was deposited during an eruption of one of the volcanic centers situated farther to the east (e.g. Ebner & Sachsenhofer, 1995 (cum. lit)). The lithofacies levels 5, 6 and 7 were deposited at depths less than the storm waves base. For lithofacies 7, a Ichnofauna (Ophiomorpha, Scolithos and Planolites) was described by Hiden, 1995. This fauna is characteristic for the transition from nearshore to shoreface, and indicates depths around 10 m (Dodd & Stanton, 1990). Facies 1 to 6 are characterized by the occurrence of various coral fauna. In contrast, this coral fauna is not found in the facies 7, but echinoids (*Schizaster*), crustaceans (*Calianassa, Portunus*) were found. This change is interpreted as indicating a transition from a subtropical to a temperate faunal assemblage.

METHODS AND MATERIAL STUDIED

In this study we analyzed large calcitic shells of benthic organisms as *Macrochlamys* sp., *Flabellipecten* sp. and an indeterminate terebratulid collected from different horizons of the outcrop. The scallop shells consist of an external foliated layer, an intermediate fine crystalline layer and an internal foliated layer. Study of thin sections under polarized light shows preservation of the internal structure of the scallop shells. Microbeam analyses indicate that all measured shells consist entirely of low-magnesium calcite, implying that the primary mineralogical composition has been preserved. Cathodoluminescence may also serve as an indicator of eventual alteration because the manganese content, the common activator of luminescence in calcite, increases as skeletal carbonates are diagenetically altered (Brand &Veizer, 1980). Thin sections of the studied shells show no luminescence. For these reasons we consider that the effect of diagenesis was minimal and the data can be used for palaeoclimatic reconstructions.

Samples of powdered shell of *Macrochlamys* sp., *Flabellipecten* sp. and the terebratulid were analyzed for $\delta^{18}O$ and $\delta^{13}C$. A total of c. 270 analyses were performed. The shells were sequentially sampled along the dorso-ventral axis (average sample separation 1.5-2 mm) using a 0.5 mm drill bit. Isotopic analyses were performed using an automatic Kiel II preparation line and a Finnigan MAT Delta Plus Mass Spectrometer. NBS-19 and an internal laboratory standard were analyzed continuously for accuracy control. Standard deviation was 0.1‰ for both $\delta^{18}O$ and $\delta^{13}C$. All isotopic results are reported in per mil, relative to the Pedee belemnite standard (PDB). The $^{40}Ar/^{39}Ar$ laser-ablation technique was applied to several fresh grains of biotite phenocrysts from the tuff level (sample AVB-2). The technique is described in detailed by Liu et al. (2001). The biotite concentrate of sample AVB-2 records a plateau age of 14.2 +/- 0.1 Ma. Neither extraneous argon nor disturbance of the age pattern were detected. The age is, therefore, considered to be geologically significant, recording the age of the volcanic eruption.

RESULTS

The resulting $\delta^{18}O$ and $\delta^{13}C$ values are plotted on the y-axis against shell length from the origin of growth. The $\delta^{18}O$ values of *Macrochlamys* species show cyclical patterns ranging between approximately –3.5 to 0‰. The $\delta^{13}C$ values in the shells range between 0 to 2.2‰. For *Flabellipecten* and the terebratulid, the $\delta^{18}O$ values range from –1 to 0%, and $\delta^{13}C$ values from 0.5 to 2.2‰.

DISCUSSION AND CONCLUSIONS

Previous studies have shown that scallops grown in various climatic settings, such as tropical and subtropical (Jones & Allmon, 1995; Hickson et al., 2000), temperate (Krantz et al., 1987; Hickson et al., 1999) and Antarctic (Barrera et al., 1994), precipitate their shells in equilibrium with the seawater. Moreover scallops as well as brachiopods populate only environments with little salinity variation. Consequently, when their shells are not diagenetically altered, the $\delta^{18}O$ values of calcite can be interpreted in terms of seasonal changes in water temperatures, with lower values calcite representing summer and higher values representing winter.

Palaeotemperatures were calculated using the equation of O`Neil et al. (1969) for water-calcite system. Taking into account that at that time, Paratethys was related to the oceanic domain, and that within the Styrian realm there was no massive fresh water input, we assume a typically interglacial value of 0‰ for the $\delta^{18}O$ value of water. For *Macrochlamys* the calculated temperatures range between approximately 17° and 30° C and indicate a subtropical environment with strong seasonal variations. Previous studies have shown that for temperate regions, growth cessations, marked by prominent rings on the shell surface, occur during the cold season (Hickson et al., 2000). The studied *Macrochlamys* shells show that growth began during the warm season, and that growth interruptions on the external surface were associated with the next warm season. The growth interruptions are likely related to the warm season because during these periods the scallops used their energy for the growth and maturation of gonads (Amler et al., 2000; Mandic, personal communication). If the cycle in oxygen isotopes reflects growth rate, then the scallop shells analyzed in this study reached their preserved length within approximately 1-2 years.

At about 14 Ma, a significant change in the $\delta^{18}O$ of the ocean occurred due to a major widespread of the Antarctic ice sheet. Thus, for calculating temperature distribution within F1 and B1, we assumed a 0.8‰ value of water. In this case, the temperatures calculated from the $\delta^{18}O$ isotopic profiles across both F1 and B1 show much lower values, between 17 and 23°C. When the $\delta^{18}O$ value of water is kept at 0‰, the temperatures calculated for F1 and B1 are between 15 and 21°C. The data indicate change in annual temperature distributions across, below and above the tuff level.

Radiogenic dating of the tuff layer situated in the uppermost part of the marly limestone layer make it possible to correlate this climatic shift with the world-wide palaeoceanographic events at that time. $^{39}Ar/^{40}Ar$ dating of the fresh biotites gives a plateau age of 14.2 ± 0.1 Ma. The position of this sample is within the clastic deposits, just below the sand layers where the *Flabellipecten* sp. and the terebratulid come from. The radiogenic data fit well with the beginning of the widespread of the Antarctic ice sheet, for which an age of c. 14 Ma has been assumed (Shackleton & Kennett, 1975; Savin, 1985; Billups & Schrag, 2002). Thus, we consider that the shift from a subtropical climate to much cooler annual temperatures, as well as the shift from biogenic carbonates to the dominantly clastic deposits, are related to the widespread of the East Antarctica ice sheet. This event constituted one of the major palaeoceanographic events of the Miocene times.

The $\delta^{13}C$ values of brachiopods and molluscs are usually similar to those of ambient dissolved inorganic carbon (DIC), but cases of $\delta^{13}C$ depletions also occur (Epstein et al., 1952; Mook, 1971). These depletions, due to skeletal incorporation of respired CO_2 into the shell skeleton, are related to metabolic activities (Aharon, 1991; Wefer & Berger, 1991; Tanaka et al., 1986; Krantz et al., 1987). More recent studies (McConnaughey et al., 1997; Hickson et al., 1999) have shown that aquatic invertebrates using respiration incorporate little respired CO_2 into their shells. However, this issue is still under discussion (Owen et al., 2002). Thus, for this group of organisms, the $\delta^{13}C$ values of the shells are primarily controlled by the $\delta^{13}C$ of dissolved inorganic carbon (DIC), and secondary by the metabolic rates.

For marine waters, the main inorganic dissolved carbon species is HCO_3^-, the occurrence of dissolved CO_2 being subordinate. Thus the $\delta^{13}C$ values of shells will reflect the $\delta^{13}C$ composition of dissolved HCO_3^-. The calcite-bicarbonate fractionation is not temperature dependent for carbon (Romanek et al., 1992), but the isotope fractionation between dissolved HCO_3^- and air CO_2 is temperature dependent (Mook, 1974). For the analyzed shells, the amplitude of temperature dependent $\Delta HCO_3^--CO_2$ values fit the amplitude of $\delta^{13}C$ values measured in calcite. Moreover, some of the $\delta^{13}C$ profiles show cyclicity, in phase with the $\delta^{18}O$. Therefore for temperatures calculated using the calcite thermometer, we have statistically tested the presence of the correlation between the calculated $\Delta HCO_3^--CO_2$ and the measured $\delta^{13}C$ values along the shells, using both the Pearson and Spearman tests. The data indicate that for some of the measured shells there is a correlation between the two data sets. In this case the cyclical fluctuation of $\delta^{13}C$ values of calcite may be explained considering the temperature dependent fractionation between dissolved HCO_3^- and air CO_2. Relatively low water depths and a favorable mixing of waters may have also favored the seasonal equilibration between CO2 and HCO3–. For two of the measured shells the correlation between the two data sets is poor, most probably due to local, seasonal events which can be poorly documented.

ACKNOWLEDGEMENT

Financial support was provided by FWF Project 13029-Geo.

REFERENCES

Aharon, P., 1991. Recorders of reef environment histories: Stable isotopes on corals, giant clams, and calcareous algae. Coral Reefs 10, 71–90.

Amler, M., Fischer, R., Rogalla, N. S., 2000. Muscheln. Akademischer Verlag, Stuttgart, 214 p.

Billups, K., Schrag, D. P., 2002. Palaeotemperatures and ice volume of the past 27 Myr revisited with paired Mg/Ca and $^{18}O/^{16}O$ measurements on benthic foraminifera. Paleoceanography 17, 1–11.

Brand, U., Veizer, J., 1980. Chemical diagenesis of a multicomponent carbonate system: Trace elements. J. Sediment. Petrol. 50, 1219–1236.

Ebner, F., Sachsenhofer, R.F., 1991. Die Entwicklungsgeschichte des Steirischen Tertiärbeckens. Mitteilungen der Abteilung für Geologie und Paläontologie des Landesmuseum Joanneum 49, 96 p.

Ebner, F., Sachsenhofer, R.F., 1995. Palaeogeography, subsidence and thermal history of the Neogene Styrian basin (Pannonioan basin system, Austria). Tectonophysics 242, 133–150.

Epstein, S., Buchsbaum, R., Lowenstam, H.A., Urey, H.C., 1952. Revised carbonate-water isotopic temperature scale. Bull. Geol. Soc. Amer. 64, 1315–1326.

Friebe, J., 1990. Lithostratigraphische Neugliederung und Sedimentologie der Ablagerungen des Badenium (Miozän) um die Mittelsteirische Schwelle. Jahrbuch der Geologischen Bundesanstalt Wien 133/2, 223–257.

Friebe, J., 1991. Neotektonik an der Mittelsteirischen Schwelle (Österreich): Die "Steirische Phase". Zentralblatt für Geologie und Paläontologie I, 41–54.

Fritz, I., Hiden, H., 2001. Fossilgrabung im Steinbruch Retznei (Südsteiermark), Projektmappe für Schulen, Graz, 40pp.

Hickson, J.A., Johnson, A.L.A., Heaton, T.H.E., Balson, P.S., 1999. The shell of the Queen Scallop *Aequipecten opercularis* (L.) as a promising tool for palaeoenvironmental reconstruction: evidence and reasons for equilibrium stable-isotope incorporation. Palaeogeogr., Palaeoclimatol., Palaeoecol. 154, 325–337.

Hickson, J.A., Johnson, A.L.A., Heaton, T.H.E., Balson, P.S., 2000. Late Holocene environment from the Southern North Sea from the Stable isotopic composition of Queen Scallop Shells. Palaeontologia Electronica 3, 3–11.

Hiden H.R., 1995. *Sepia vindobonensis* (Cephalopoda, Coleoida aus dem Mittel-Miozän von Retznei (Steiermark, Österreich). Mitt. Abt. Geol. und Paläont. Landesmuseum Joanneum 52/53, 111-124.

Jones, D.S., Allmon, W.D., 1995. Records of upwelling, seasonality and growth in stable-isotope profiles of Pliocene mollusc shells from Florida. Lethaia 28, 27–74.

Krantz, D.E., Williams, D.F., Jones, D.S., 1987. Ecological and paleoenvironmental information using stable isotopes from living and fossil molluscs. Palaeogeogr., Palaeoclimatol., Palaeoecol. 58, 249–335.

McConnaughey, T.A., Burdett, J., Whelan, J.F., Paull, C.K., 1997. Carbon isotopes in biological carbonates: Respiration and photosynthesis. Geochim. Cosmochim Acta 61/3, 611–622.

Mook, W.G., 1971. Palaeotemperatures and chlorinities from stable carbon and oxygen isotopes in shell carbonate. Palaeogeogr. Palaeoclimat. Palaeoecol. 9, 245–264.

Mook, K.A., 1974. Carbon isotope fractionation between dissolved bicarbonate and gaseous carbon dioxide. Earth and Planet. Sci. Lett. 22, 169–176.

O`Neil, J.R., Clayton, R.N., Mayeda, T.K., 1969. Oxygen isotope fractionation in divalent metal carbonates. Journal of Chemical Physics 51, 5547–5548.

Owen, R., Kennedy, H., Richardson, C., 2002. Experimental investigation into partitioning of the stable isotopes between scallop (Pecten maximus) shell calcite and sea water. Palaeogeogr. Palaeoclimat. Palaeoecol. 185, 163-174.

Romanek, C.S., Grossman, E.L., Morse, J.W., 1992. Carbon isotopic fractionation in synthetic aragonite and calcite: effects of temperature and precipitation rate. Geochim. Cosmochim. Acta 56, 419–430.

Rögl, F., 2001. Mid-Miocene Circum Mediterranean Palaeogeography. EEDEN Environmental and Ecosystem Dynamics of the Eurasian Neogene, Stratigraphy and Palaeogeography, Workshop. Berichte des Institutes für Geologie und Paläontologie der Karl-Franzens Universität Graz, Österreich, 49–59.

Savin, S.M., Abel, L., Barrera, E., Hodell, D., Keller G., Kennett, J.P., Killingley, J., Murphy, M., Vincent, E., 1985. The evolution of Miocene surface and near-surface marine temperature: oxygen isotopic evidence. In: Kennett (Ed.), The Miocene Ocean: Paleocenography and Biogeography. Mem. Geol. Soc. of Am., 163, 49–82.

Shackleton, N.J., Kennett, J.P., 1975. Palaeotemperature history of the Cenozoic and the initiation of Antarctic glaciation: oxygen and carbon analyses in DSDP Sites 277, 279, 281. In: Kennett, J.P., et al. (Eds.), Initial reports of the Deep Sea Drilling Project 29, Washington D.C., 743–755.

Tanaka, N., Monaghan, M.C., Rye, D.M., 1986. Contribution of metabolic carbon to mollusc and barnacle shell carbonate. Nature 320, 520–523.

Wefer, G., Berger, W.H., 1991. Isotope paleontology: growth and composition of extant calcareous species. Marine Geology 100, 207–248.

$\delta^{13}C$ AND $\delta^{18}O$ IN LATE APTIAN LIMESTONES OF QUINDIO, COLOMBIAN CENTRAL CORDILLERA

Correa, A.M.[1]; Sial, A.N.[2]; Mojica, J.[3] and Arévalo, O.J.[3]

1. Instituto de Geociências, Universidade de Brasília, Brasília-DF, 70910900, Brazil. anamacor@unb.br
2. Dept. de Geologia, Universidade Federal de Pernambuco, Recife-PE, 50732-970, Brazil. ans@npd.ufpe.br
3. Dept. de Geología, Universidad Nacional de Colombia, Apartado 14490, Bogotá, Colombia. jmojica@ciencias.unal.edu.co

Keywords: C isotopes, O isotopes, limestones, Late Aptian, Colombia

INTRODUCTION

Stable isotope studies of $\delta^{13}C$ and $\delta^{18}O$ secular variations in Cretaceous pelagic, hemipelagic, shallow-water carbonates and fossils from different latitudes have been usually used to monitoring paleoambiental changes. $\delta^{18}O$ values have been used to investigate oceanic paleotemperatures and to assess Cretaceous climatic trends (Norris and Wilson, 1998; Clarke and Jenkyns, 1999). $\delta^{13}C$ fluctuations are ascribed to primary variations in the carbon isotope composition of sea water during Cretaceous time and are thus related to paleo-oceanographic events (Scholle and Arthur, 1980; Vahrenkamp, 1996). Carbon isotope composition is more and more accepted as a valuable tool to improve stratigraphic resolution in Cretaceous marine carbonates and to establish correlation among marine basins (Scholle and Arthur, 1980, Grötsch et al., 1998).

This paper presents isotopic $\delta^{13}C$ and $\delta^{18}O$ data for Cretaceous pelagic carbonates of Colombian Central Cordillera, specifically from limestones of Rio Lejos sedimentary sequence. This study was geared to assess the behaviour of carbon and oxygen isotope in some Late Aptian carbonates of Colombia. This study aimed also to compare the $\delta^{13}C$ and $\delta^{18}O$ values from Colombia with those from other locations in the world for this time span.

GEOLOGICAL SETTING

Rio Lejos sedimentary sequence occurs in the western side of Colombian Central Cordillera in the Quindio Department to the southwest of Pijao town (Fig. 1). The sequence crops out as tectonic slices in a faulted contact with igneous and metamorphic rocks. This sequence was interpreted as a segment of a major discontinuous volcano-sedimentary belt known as Quebradagrande Complex, which exhibits oceanic affinity and it was formed during Early Cretaceous (Mojica et al., 2001).

Rio Lejos sequence is composed of three units: clay-sandstone, pyroclastic-clay and carbonate successions. The biostratigraphy has shown to be Late Aptian after the identification of the fossil *Riedelites obliquum* (Mojica et al., 2001). The petrographic and palaeontologic evidences indicate that sedimentation occurred in an oxygen-poor deep-marine water environment, which was affected by the influence of turbiditic currents. Mojica et al. (2001) pointed out that sedimentation was contemporaneous with sea-floor vulcanism.

The studied area corresponds to a carbonate pile, which comprises recrystallized micritic limestones, lithoclastic limestones and pellet-limestones. Some of these sediment horizons were affected by thermal metamorphism whereas most of all have underwent dynamic metamorfism. The recrystallization of limestones may be due to diagenetic effects or dynamic metamorphism.

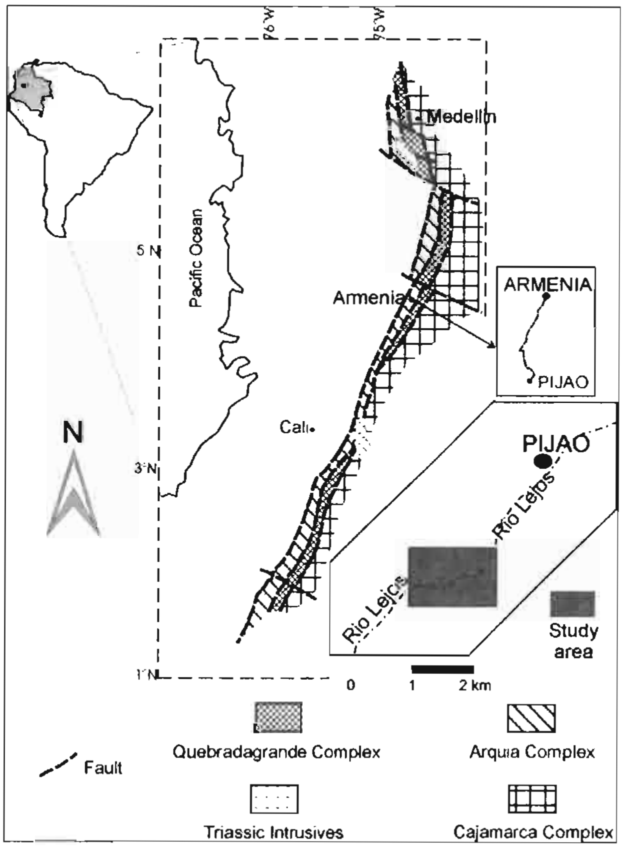

Figure 1. Generalized geologic map of the Colombian Central Cordillera showing location of Rio Lejos area. Modified from Nivia et al. (1996) and Mojica et al. (2001).

SAMPLES AND METHODS

Due to the structural complexity of the studied area only a limited number of carbonate samples was possible to sample.

A total of twenty bulk-rock samples were assayed for their $\delta^{13}C$ e $\delta^{18}O$ isotopic composition. Thirteen limestone samples were stratigraphically collected in the Puente Nuevo Section and seven samples in the Puente Tabla Section. C and O isotope analyses were performed at LABISE - Stable Isotope Laboratory, Federal Univ. of

Pernambuco, at Recife, Brazil. CO_2 gas was extracted from powdered carbonates in a high vacuum line after reaction with 100% phosphoric acid at 25^0C for one day. The CO_2 released, after cryogenic cleaning, was analysed in a double inlet, triple collector mass spectrometer. Results are reported in the δ notation (‰, PDB).

C AND O ISOTOPE COMPOSITION

Three packages of carbonates occur in the Puente Nuevo Section, which exhibit $\delta^{13}C$ values from –2.1‰ to +3.2‰$_{PDB}$ and $\delta^{18}O$ values from –15.3‰ to –13.0‰$_{PDB}$ (Fig. 2).

The first bed located 5m from bottom is made up of pellet and recrystallized micritic limestones. A pellet limestone sample shows $\delta^{13}C$ and $\delta^{18}O$ values of +2.3‰ and –14.8‰$_{PDB}$ respectively. The next carbonate portion begins 17m from the bottom of the profile. It consists of recrystallized micritic limestones, with minor lithoclastic limestones, pellet-limestones beds and a 1 meter thick marble layer, at the base, where carbonates are in the intrusive contact with gabbroic rocks. In this bed, a $\delta^{13}C$ and $\delta^{18}O$ continuous curve was obtained from a 30m-tick carbonates package (Fig. 2), which displays $\delta^{13}C$ variation from –0.9‰ to +3.2 ‰$_{PDB}$ and $\delta^{18}O$ variation –15.1‰ to –14.3‰$_{PDB}$. The third limestone occurrence in Puente Nuevo Section consists of fragments enclosed within shales bed in a shear zone, located 53m from base of the column. A sample of limestone fragment in this package yields $\delta^{13}C$ and $\delta^{18}O$ values of –2.1‰ and –15.3‰$_{PDB}$ respectively.

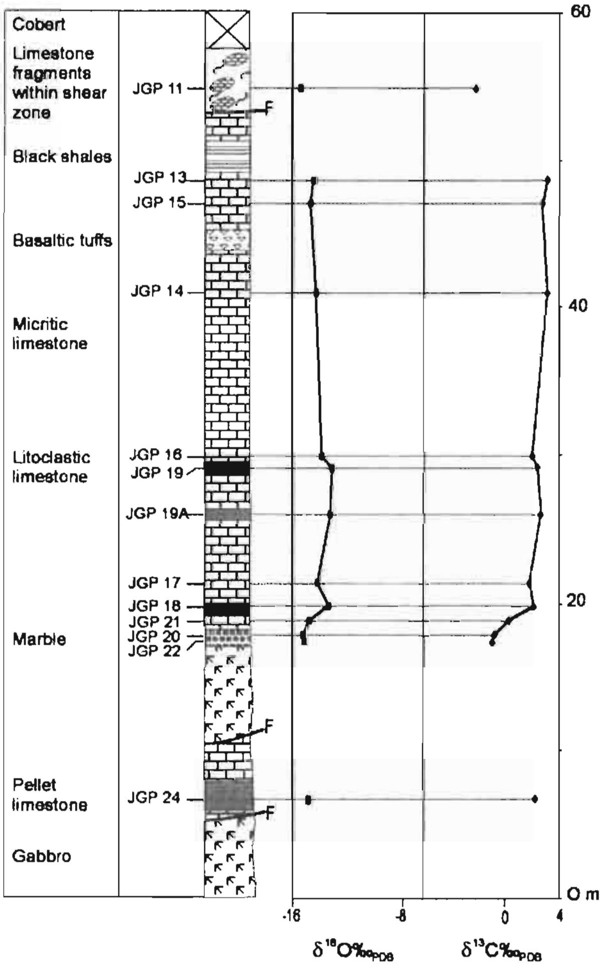

Figure 2. $\delta^{13}C$ and $\delta^{18}O$ (‰ PDB) in carbonates rocks along the stratigraphic column of Puente Nuevo Section.

Carbonates in Puente Tabla Section occur as fragments associated to shales layers and as continuous limestones packages. Examples of the first are observed about 85m and 93m from base of column (Fig. 3). These samples yielded $\delta^{13}C$ negative values between -2.9‰ and -2.1‰$_{PDB}$ and $\delta^{18}O$ values between -14.7‰ and -14.4‰$_{PDB}$. The other carbonate occurrence is about 128m from the base of the section. This portion is characterised by 50m-thick recrystillized micritic limestones. Pellet limestones and tuffs are eventually intercalated. Isotopic data obtained here display $\delta^{13}C$ variation from +0.05‰ to +2.7‰$_{PDB}$ and $\delta^{18}O$ variation from -14.8‰ to -13.6‰$_{PDB}$ (Fig. 3).

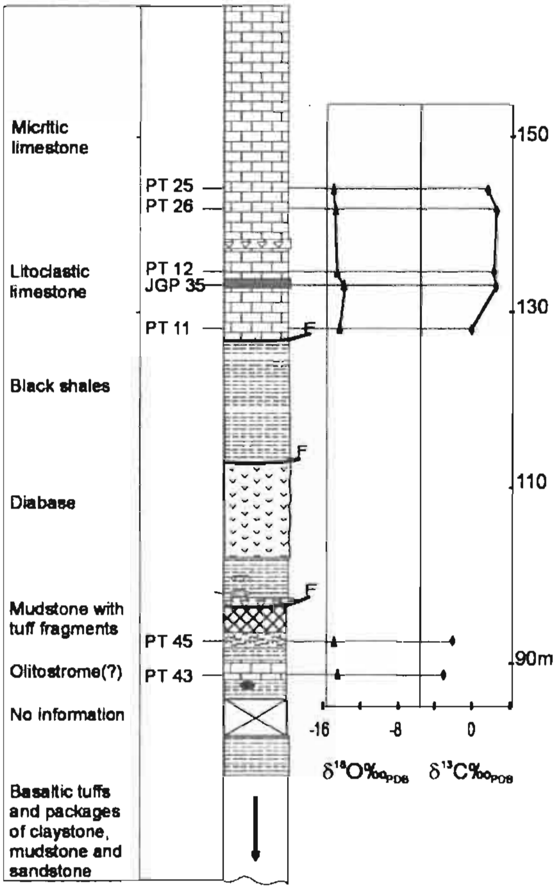

Figure 3. $\delta^{13}C$ and $\delta^{18}O$ (‰ PDB) in carbonates rocks along the stratigraphic column of Puente Tabla Section.

DISCUSSION

Aptian and Albian carbonates carbon and oxygen isotope data available in the literature have consistently shown positive $\delta^{13}C$ values, which range from +0.5‰ to +4.0‰$_{PDB}$ and are generally higher than +2‰$_{PDB}$ (Scholle and Arthur, 1980; Grötsch et al., 1998). $\delta^{18}O$ values range from -4.0‰ to -6.0‰$_{PDB}$ in pelagic carbonates from low-latitudes (Scholle and Arthur, 1980). Pelagic and hemipelagic carbonates from high-latitudes usually exhibit $\delta^{18}O$ ranging from +0.5‰ to -1.5‰$_{PDB}$ in (Clarke and Jenkyns, 1999).

Figure 4 presents the $\delta^{13}C$ and $\delta^{18}O$ cross plot, which shows that most $\delta^{13}C$ values are clustered within the range for Aptian-Albian as mentioned above and that all $\delta^{18}O$ values lie outside the range for the same time span. This suggests that oxygen isotopic system in all analysed carbonates was opened and that they have undergone isotopic alteration. In the case of $\delta^{13}C$, values ranging from +1.6‰ to +3.2‰$_{PDB}$ should represent primary $\delta^{13}C$ signatures, whereas those samples with the least positive values and yet negative indicate disturbance in their primary carbon isotopic composition.

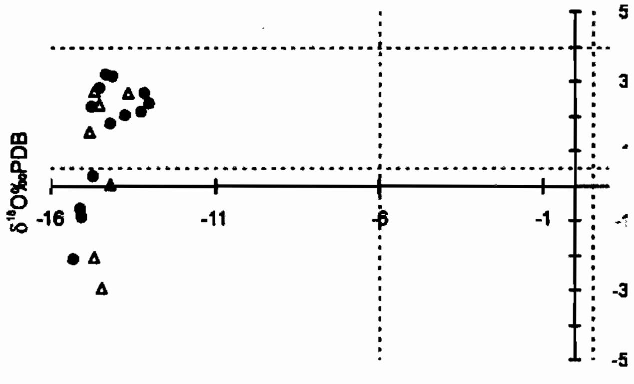

Figure 4. Cross plot of $\delta^{18}O$ *vs* $\delta^{13}C$ (‰ PDB) for carbonates from Puente Tabla (triangular) and Puente Nuevo (full circle) Sections. Vertical and horizontal stippled lines: range of $\delta^{18}O$ and $\delta^{13}C$ values respectively for Albian-Aptian limestones in the world.

Crossplot of $\delta^{13}C$ and $\delta^{18}O$ for Puente Nuevo section show that there is a positive correlation for some samples (JGP-22, JGP-20, JGP-21 e JGP-11), which indicate secondary overprint of the O and C isotope values. In the case of the first three samples (JGP-22, JGP-20, JGP-21) it is possible to explain low $\delta^{13}C$ and $\delta^{18}O$ values (Fig. 2) through decarbonation processes, as they are believed to be formed by contact metamorphism.

Shieh and Taylor (1969) concluded that contact metamorphic decarbonation reactions produce a net lowering of O^{18}/O^{16} in the rocks of a contact aureole. They also pointed out that the contact metamorphic marbles that are low in O^{18}/O^{16} also tend to be low in C^{13}/C^{12}, indicating that the CO_2 liberated during metamorphic decarbonation reactions is enriched in both O^{18} and C^{13} relative to the carbonates. These types of marbles are generally associated with calc-silicate minerals (Shieh and Taylor, 1969).

The marbles from Puente Nuevo section exhibit low $\delta^{13}C$ and $\delta^{18}O$ values and also tremolite that is the likely result of thermal metamorphism. A possible contact metamorphic decarbonation reaction in these samples would be:

$$\underset{\text{dolomite}}{5CaMg(CO_3)_2} + \underset{\text{quartz}}{8SiO_2} + H_2O = \underset{\text{tremolite}}{Ca_2Mg_5Si_8O_{22}(OH)_2} + \underset{\text{calcite}}{3CaCO_3} + 7CO_2$$

An explanation of the $\delta^{13}C$ and $\delta^{18}O$ values of JGP-11 sample is that its original isotopic composition was probably affected by interaction with isotopically "light" fluids within a shear zone.

In the Puente Tabla Section the $\delta^{13}C$ of four samples may represent primary values, whereas the other three samples may have undergone disturbance of its carbon isotope composition. The PT-11 sample has a low $\delta^{13}C$ positive value possibly by reaction with fluids circulating in shear zone. The $\delta^{13}C$ values for the PT-43 and PT-45 samples could be interpreted as primary or secondary. The $\delta^{13}C$ values could be primary because these limestones are closely associated to shales and so the isotopic characteristics could reflect different depositional conditions to those of the others limestones. The $\delta^{13}C$ values would be secondary due to the proximity of these samples to shear zones and also by the fact that they possibly belong to olitostromes, where it is possible to occur the interaction with fluids of distinct isotopic composition.

CONCLUSIONS

The carbon stable isotope studies reported here indicate that most of $\delta^{13}C$ values obtained in Rio Lejos sequence limestones apparently reflect original isotopic composition, as they are similar to those reported from others Albian-Aptian limestones of low-latitude in the world. On the other hand the low $\delta^{13}C$ values in some Puente Nuevo carbonates can be ascribed to decarbonation processes during thermal metamorphism. $\delta^{18}O$ values of all analysed limestones of both sections indicate that their oxygen isotopic systems were disturbed by post-depositional processes.

REFERENCES

Clarke, L.J. and Jenkyns, H.C., 1999. New oxygen isotope evidence for long-term Cretaceous climatic change in the Southern Hemisphere. Geology, 27 (8): 699-702

Grötsch, J., Billing, I. And Vahrenkamp, V., 1998. Carbon-isotope stratigraphy in shallow-water carbonates: implications for Cretaceous black-shale deposition. Sedimentology, 45: 623-634

Mojica, J., Patarroyo, P., Camargo, G. and Arévalo, O.J., 2001. Sedimentitas del Aptiano Tardío en el Flanco Occidental de la Cordillera Central, Río Lejos, Pijao, Quindío- Colombia. In: Congreso Colombiano de Geología, Memorias in CD.

Nivia, A., Gizelle M. and Andrew, K., 1996. El Complejo Quebradagrande una posible cuenca marginal intracratónica del Cretáceo Inferior en la cordillera Central de los Andes Colombianos. In: VII Congreso Colombiano de Geología, Memorias I: 54-67

Norris, R.D. and Wilson, P.A., 1998. Low-latitude sea-surface temperatures for the mid-Cretaceous and the evolution of planktic foraminifera. Geology, 26: 823-826

Scholle, P.A. and Arthur, M.A., 1980. Carbon Isotope Fluctuations in Cretaceous Pelagic Limestones: Potencial Stratigraphic and Petroleum Exploration Tool. Am. Assoc. Pet. Geol. Bull., 64: 67-87

Shieh, Y.N. and Taylor, JR., 1969. Oxygen and Carbon Isotope Studies of Contact Metamorphism of Carbonate Rocks, Journal of Petrology, 10(2): 307-331

OXYGEN ISOTOPIC COMPOSITION OF BENTHIC FORAMINIFERA: CORE-TOP CALIBRATION

Costa, K.B.[1]; Toledo, F.A.L.[2]; Chemale Jr., F.[1] and Moura, C.A.V.[3]

1. Laboratório de Geologia Isotópica, IG, UFRGS – Laboratório de Geologia Isotópica, C.P. 15001, Porto Alegre, RS, Brazil. karen.costa@ufrgs.br, farid.chemale@ufrgs.br
2. Centro de Estudos Costeiros e Oceânicos, CECO, UFRGS, Brazil. felipe.toledo@ufrgs.br
3. Laboratório de Geologia Isotópica, CG-UFPA (Pará-Iso), Brazil. c_moura@ufpa.br

Keywords: Oxygen isotopes, benthic foraminifera, paleoceanography

INTRODUCTION

The oxygen isotopic analysis of tests of microfossils plays a major role in studies of paleoceanography and paleoclimatology. The isotopic and elemental studies of benthic foraminifera species are very important to the knowledge of the circulation and chemistry of the oceans in the past, and are used to reconstruct variations in the models of circulation of the deep waters and its intensity in terms of glacial-interglacial variations. An assumption implicit in all paleoceanographic isotopic studies is that the oxygen isotopic composition of the microfossil accurately reflects the temperature and oxygen isotopic composition of the sea water in which it grew. Thus, the precise calibration of variations in $\delta^{18}O$ of Recent samples with modern oceanographic conditions is a necessary precondition for the quantitative interpretation of down-core isotopic record.

The $\delta^{18}O$ in foraminifera has been thought as a "paleothermometer" because the $\delta^{18}O$ of calcite ($\delta^{18}O_c$) increases as calcification temperatures decrease (Emiliani, 1955). Glacial-interglacial fluctuations of foraminifera $\delta^{18}O$ combine signals of changing temperature and changing $\delta^{18}O$ of seawater ($\delta^{18}O_w$). This is because the $\delta^{18}O_c$ also reflects the $\delta^{18}O$ of the water in which the foraminifera grew. To solve for temperature, we must choose among available isotopic equilibrium equations. The fractionation between calcite precipitated inorganically and the water which it forms increase by 0.2‰ for every 1°C decrease in temperature (O'Neil, 1969; Kim & O'Neil, 1997). In general, the isotopic composition of benthic foraminifera precipitated in seawater shows this relationship with temperature as well (Shackleton, 1974; Herguera *et al.*, 1992), but the absolute value of $\delta^{18}O_c$ may be shifted from predicted inorganic value depending on the species analyzed (Lynch-Stieglitz et al., 1999). The exact $\delta^{18}O$ value of equilibrium calcite precipitation ($\delta^{18}O_{eq}$) depends on the choice of equilibrium equation.

Previously, benthic foraminifera genus *Cibicidoides* were believed to not precipitate its tests in equilibrium with $\delta^{18}O_w$. The $\delta^{18}O$ of *Cibicidoides* appeared to have consistent "vital effect" offset of 0.64‰ (Shackleton & Opdyke, 1973) or 0.83‰ (Herguera et al., 1992) from $\delta^{18}O_{eq}$ calculated using equations as the one from O'Neil (1969). Similarly, for many years the benthic foraminifera genus *Uvigerina* was widely believed to precipited its test in oxygen isotopic equilibrium with ambient water (Shackleton, 1974). However, core-top *Uvigerina* from NW-Pacific (Keigwin, 1998) are more depleted in ^{18}O than is predicted by Shackleton's equation, and recent evaluation of the problem indicates that *Uvigerina* are not in equilibrium (Bemis et al.,1998). Recent studies (Lynch-Stieglitz et al.,1999) concluded that *Cibicidoides* species do precipited their tests near equilibrium.

Analysis of core-top samples of benthic foraminifera is the most straightforward approach to evaluating the paleoclimatic and paleoceanographic utility of isotopic measurements in foraminifera. This sort of studies have been made progress toward calibrating benthic foraminifera isotopic measurements with modern oceanographic conditions in Pacific (Keigwin, 1998), Indian (McCorkle et al., 1998) and North Atlantic (Lynch-Stieglitz et al., 1999) core-top samples. However little attention is paid to South Atlantic.

Our approach in this study has been to test one isotopic equilibrium equation (Kim & O'Neil, 1997) using South Atlantic core-tops and water column data to determine oxygen isotope fractionation in the foraminifera genus *Cibicidoides* and *Uvigerina* as function of temperature. Therefore, the relationship of isotopic variation in benthic foraminifera in this data set with modern physical oceanographic parameters (*e.g.* temperature and salinity) can provide a realistic framework within which down-core isotopic records can be interpreted.

METHODS

We have analyzed the isotopic composition of two genus of benthic foraminifera picked in the top centimeter of four cores of Brazilian Continental Margin, and used three additional core-tops to comparison (Tab. 1). The core-top calibration studies are based on comparison of foraminiferal data and modern physical oceanographic parameters from similar water depths at nearby Geochemical Ocean Sections Study (GEOSECS) stations (Bainbridge,1981).

The core-top samples were disaggregated in distilled water at room temperature and dry-sieved on a 0.150µm sieve. Oxygen isotope analysis was performed at the Pará-Iso (CG-UFPA) using a Finnigan MAT 252 mass spectrometer. CO_2 extraction of single foraminifera tests was done using an on line KIEL-III system coupled to the instrument. Isotope rations are reported relative to PDB, based on analysis of NBS-19 carbonate standard which was reacted with each set of samples. Results are reported in the standard δ (‰) notation relative to Chicago PDB standard. The precision of these foraminiferal isotopic analyses is better than 0.08%, based on replicated analysis of carbonate standard.

Table 1. Core locations and water depths.

core	Latitude	Longitude	depth (m)
MP-01	21°08' 18"S	40°10'21"W	900
MP-02	21°08'24"S	40°10"13"W	1000
MP-03	21°08'18"S	40°10'16"W	1100
MP-04	22°20'04"'S	41°26'04"W	1200
CMU-14	14°24'S	38°49'W	965
PAR-40	07°29'S	34°20'W	1261
PAR-36	08°22'S	34°27'W	1315
GEOSECS 54	15°2'S	29° 32'W	
GEOSECS 56	21° 0'S	33°0'W	

DATA

Prior to estimating the $\delta^{18}O_{eq}$ for the South Atlantic, the regional $\delta^{18}O_w$-salinity relationship should the established. The $\delta^{18}O_w$ of sea water primarily reflects patterns of evaporation and fresh water influx to the surface of the oceans. Because salinity also reflects these. same process, salinity and $\delta^{18}O_w$ are often well correlated in the ocean. Although the exact correlation varies in different areas of the surface ocean (Paul et al.,1999), the vast majority of the surface and subsurface water warmer than 5°C fall along the surface water trend. The linear relationship between $\delta^{18}O_w$ and salinity was estimated here using GEOSECS data station 54 and 56 (Fig. 1), and the equation resulting from linear regression of observed $\delta^{18}O_w$ and observed salinity in the South Atlantic may be written relative to the SMOW standard as follows:

$$\delta^{18}O_{w(SMOW)} = (0.460 \times \text{salinity}) - 15.884 \qquad (1)$$

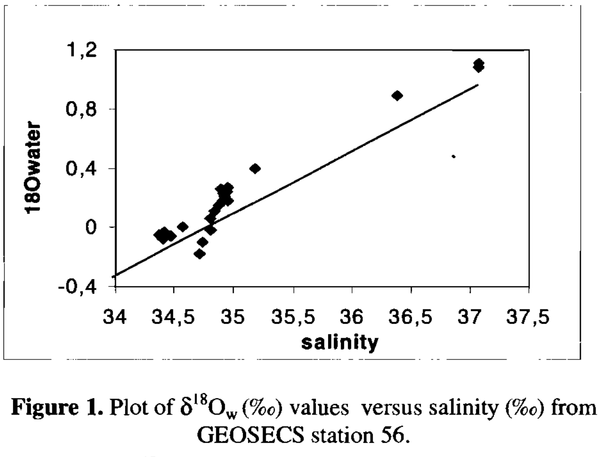

Figure 1. Plot of $\delta^{18}O_w$ (‰) values versus salinity (‰) from GEOSECS station 56.

Using $\delta^{18}O_w$ values calculated from equation.1, expected isotopic values for calcite precipitated in equilibrium with surface conditions at each core-top location have been calculated using the Kim and O'Neil (1997) paleotemperature equation that is function of temperature T(°C) and $\delta^{18}O_{w(SMOW)}$ converted to PDB scale by subtracting 0.27‰:

$$\delta^{18}O_{eq(PDB)} = \delta^{18}O_{w(SMOW)} - 0.27 + 3.25 - (0.2 \times T) \quad (2)$$

The oxygen isotopic variation observed in benthic foraminifera and the expected isotopic values for calcite precipitated in equilibrium with surface conditions calculated from equation.2 are presented in table 2 and figure 2.

Table 2. Observed and calculated oxygen isotopic values for foraminifera by core-top and $\delta^{18}O_{eq}$ by water depth.

Core	genus	$\delta^{18}O$ (‰)	$\delta^{18}O_{eq}$ (‰)
MP-01	*Cibicidoides*	2.3	2.22
MP-02	*Cibicidoides*	2.21	2.26
MP-03	*Cibicidoides*	2.19	2.27
MP-04	*Cibicidoides*	2.48	2.29
MP-01	*Uvigerina*	2.9	2.22
MP-02	*Uvigerina*	2.94	2.26
MP-03	*Uvigerina*	2.88	2.27
CMU-14	*Cibicidoides*	2.36	2.23
PAR-40	*Cibicidoides*	2.35	2.29
PAR-36	*Cibicidoides*	2.26	2.32

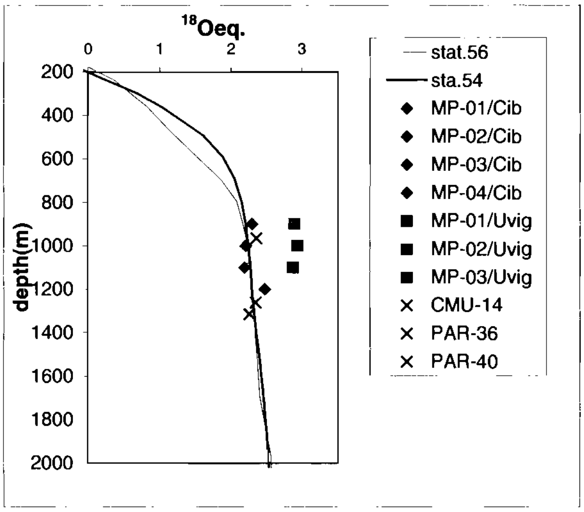

Figure 2. A comparison of $\delta^{18}O$(‰) values from core-top benthic foraminifera *Cibicidoides* (diamonds) and *Uvigerina* (squares) with $\delta^{18}O$ predicted values calculated using equation 2.

DISCUSSION

It is apparent from figure 2 that the observed $\delta^{18}O$ values for *Cibicidoides* generally fall within 0.07‰ of calculated equilibrium values. We consider this a relatively small deviation and conclude that these foraminifera species precipitated their tests close to oxygen isotopic equilibrium with sea water. In contrast, the $\delta^{18}O$ values observed for *Uvigerina* are ~0.66‰ higher than $\delta^{18}O_{eq}$ calculated.

The scatter within data is probably easily accommodated by foraminifera calcification, imperfection of our $\delta^{18}O_w$–salinity relationship and post-depositional physical or chemical alterations. The enrichment of *Uvigerina* tests relative to *Cibicidoides* would be consistent with the habitats differences of the genus. For instance, *Uvigerina* is infaunal and experiences low pH and decreased CO^{2-}_3 concentration in pore waters, whereas *Cibicidoides* inhabits the sediment surface where bottom water pH and CO^{2-}_3 concentration are higher (McCorkle & Keigwin, 1990). In such scenario the isotopic offset between the foraminifera genus should partially reflect of CO^{2-}_3 concentration gradient in the sediments.

Our conclusions about equilibrium foraminifera test precipitation in South Atlantic, using Kim and O'Neil (1997) paleotemperature equation, are substantially in agreement with other studies of oxygen isotopic variations of benthic foraminifera (McCorkle & Keigwin, 1990; Keigwin, 1998; Lynch-Stieglitz et al., 1999).

CONCLUSIONS

We have developed a new relationship between $\delta^{18}O_w$ and salinity for South Atlantic mid-latitude using GEOSECS data. After, we were able to estimating the $\delta^{18}O_{eq}$ using Kim & O'Neil (1997) paleotemperature equation for the waters covering Brazilian Continental Margin - South Atlantic.

Given the agreement between foraminiferal *Cibicidoides* oxygen isotopic data and predicted equilibrium isotopic values, the linear equation applied here is the most accurate for estimate predicted isotopic values in this region of South Atlantic Ocean. In addition this agreement suggest that this genus precipites its tests near oxygen isotopic equilibrium, whereas *Uvigerina* tests are relativelly enriched in ^{18}O.

The results presented here in core-top samples have the potential to improve paleoceanographic interpretations from foraminiferal $\delta^{18}O$ values.

REFERENCES

Bainbridge, A.E. (1981) GEOSECS Atlantic Expedition. In: GEOSECS, Hydrographic Data (1972-1973), 1 (Ed. by A. E. Bainbridge), pp. 121. U.S. Government Printing Office, Washington, D.C.

Bemis, B.E., Spero, H.J., Bijma, J., Lea, D.W. (1998) Reevaluation of the oxygen isotopic composition of planktonic foraminifera: experimental results and revised paleotemperature equations. Paleoceanography, 13(2), 150-160.

Emiliani, C. (1955) Pleistocene Temperatures. Journal of Geology, 63, 538-578.

Herguera, J.C., Jansen, E., Berger, W.H. (1992) Evidence for a Bathyal front at 2000-m depth in the glacial Pacific, based on a depth transect on Ontong Java Plateau. Paleoceanography, 7(3), 273-288.

Keigwin, L.D. (1998) Glacial-age hydrography of the northwest Pacific Ocean. Paleoceanography, 13(4), 323-339.

Kim, S.-T. & O'Neil, J.R. (1997) Equilibrium and nonequilibrium oxygen isotope effects in synthetic carbonates. Geochim. Cosmochim. Acta, 61, 3461-3475.

Lynch-Stieglitz, J.C., Curry, W.B., Slowey, N.C. (1999) A geostrophic transport estimate for the Florida Current from the oxygen isotopic composition of benthic foraminifera. Paleoceanography, 14(3), 360-373.

McCorkle, D.C., Heggie, D.T. e Veeh, H.H. (1998) Glacial and Holocene stable isotope distributions in the southeastern Indian Ocean. Paleoceanography, 13(1), 20-34.

McCorkle, D.C., Keigwin, L.D., Corliss, B.H., Emerson, S.R. (1990) The influence of microhabitats on the carbon isotopic composition of deepsea benthic foraminifera. Paleoceanography, 5, 161-185.

O'Neil, J.R., Clayton, R.N., Mayeda, T.K. (1969) Oxygen isotope fractionation in divalent metal carbonates. Journ. Chem. Phys., 51, 5547-5558.

Paul, A., Mulitza, S., Pätzold, J., Wolff, T. (1999) Simulation of oxygen isotopes in global ocean model. In: Use of proxies in paleoceanography: examples from the South Atlantic (Ed. by G. Fisher, Wefer,G.), pp. 655-686. Springer-Verlag, Berlin Heidelberg.

Shackleton, N.J. (1974) Attainment of isotopic equilibrium between ocean water and benthonic foraminifera genus Uvigerina : Isotopic changes in the ocean during the last glacial. Colloque Int. CNRS, 219, 203-209.

Shackleton, N.J. & Opdyke, N.D. (1973) Oxygen Isotope and Palaeomagnetic Stratigraphy of Equatorial Pacific Core V28-238: Oxygen Isotope Temperatures and Ice Volumes on a 10^5 Year and 10^6 Year Scale. Quaternary Research, 3, 39-55.

CARBON AND OXYGEN ISOTOPE DATA FROM CENOMANIAN – TURONIAN BOUNDARY IN THE LARANJEIRA AREA, SERGIPE–ALAGOAS BASIN, BRAZIL

Dias, A.E.S.; Pereira, E. and Rodrigues, R.

FGEL -Universidade do Estado do Rio de Janeiro - Rua São Francisco Xavier, 524/2020 A, Maracanã, Rio de Janeiro - RJ, Brazil
annaeliz@bol.com.br, egberto@uerj.br; rene@uerj.br

Keywords: Cenomanian-Turonian boundary, stable isotopes, Sergipe-Alagoas Basin

INTRODUCTION

The Sergipe Basin, southern half of the Sergipe/Alagoas Basin (Fig. 1), contains one of the most extensive Late Cretaceous marine carbonate successions of all the South Atlantic basins (Viviers et al., 2000). However, the exact location of the Cenomanian-Turonian (C-T) Boundary at this basin still remains uncertain.

The C-T sedimentary succession in the Sergipe Basin is found within the Cotinguiba Formation (Sapucari Member), which is formed mainly by limestone/marlstones couplets that have been related to orbital-climatic driven cycles (Cunha & Koutsoukos, 2001).

The C-T boundary is known worldwide as a prominent oceanic anoxic event of the Cretaceous, with sedimentary records in all the ocean basins (PPG report, 1998). This event is related to sharp changes in marine and terrestrial biota marked by pronounced turnovers of calcareous nannoplankton, radiolaria, planktonic foraminifera, benthic foraminifera, ammonites, bivalves and even angiosperms (PPG report, 1998). Such extinctions are considered associated to abrupt modifications in the distribution of carbon isotope related to the above anoxic event (with carbon isotopic variations of 2-2.5 °/₀₀).

According to Takaki & Rodrigues (1993), the co-variation of the carbon isotope data of the organic matter of the pelagic sediments and the corresponding shallow carbonate facies points to closely related phenomena, caused by global oceanic anoxic events. Isotopic variations occur in relatively short time span. Therefore, $\delta^{13}C$ and $\delta^{18}O$ distributions constitute good markers being widely used in stratigraphic correlations of Cretaceous geologic sections.

The $\delta^{13}C$ curves for the whole C-T interval generically show a pre-excursion background, a build-up $\delta^{13}C$ values, a recovery phase and a new post-excursion background thereafter. In addition, the more negative $\delta^{18}O$ for the same stratigraphic interval suggests that the anoxic event took place under mild climatic conditions, associated with a relatively higher water temperature. These carbon isotope fluctuations, turning gradually less positive in the Turonian and earlier sequences, might reflect a decrease in organic productivity of the ocean, probably linked to the progressive cooling (greater $\delta^{18}O$) of oceanic waters towards to the end of Cretaceous (e.g. Takaki & Rodrigues, 1993).

The study area of this research is an onshore portion of the Sergipe Basin, at the Laranjeiras region (SE), about 18 km north of Aracaju (Fig. 2), where the Sapucarí Member crops out.

Tupinambá (2000) and Tupinambá et al. (2002) caracterized sedimementary cycles and deposicional systems of three sedimentological profiles using detailed stratigraphic description and geochemical data (total organic carbon/TOC and insoluble residue/IR) for the same area. According to these authors, the sediments were deposited under the influence of turbidity flows. These flows are related to the sea level variation, which is controlled by the Milankovitch cycles (Tupinambá et al., 2002). The Cohab quarry is one of the referred profiles (thickness of 12 m). It presents a well marked limit defined by the contact among a set of marlstone, that dominates the base of the studied section, and limestone/marlstone couplets, which predominate at intermediate and the top levels. In this limit, C-T age ammonites are found.

OBJECTIVE

The purpose of this paper is to link geochemical changes that took place at the scale of global cycles, such as those expressed in the typical excursions in stable isotope curves ($\delta^{13}C$ e $\delta^{18}O$), to bio- and lithostratigraphic data in order to refine global correlation of the C-T boundary in the Sergipe Basin.

BIOSTRATIGRAPHY

The microfossil assemblage in Cohab quarry suggests an external neritic environment explaining the absence of keeled planktonic foraminiferal, which need a deeper water to develop its complete cycle of life (written information, Oscar Strohschoen Jr, 2003).

The biochronostratigraphy of the quarry has been established on the basis of ammonites (Tupinambá, 2000; Tupinambá et al., 2002) and planktonic foraminiferal. The identified association of the foraminiferal *Whiteinella aprica, Guembelitria cenomana and Heterohelix sp.*, is characteristic of the uppermost Cenomanian/middle Turonian interval.

Furthermore, the section yields planktonic foraminifera of the W. *archeocretacea – Heterohelix reussi* Zone, assigned to the uppermost Cenomanian/lowermost Turonian (e.g. Koutsoukos & Bengston, 1993), at 6 meters in the profile.

CARBON AND OXYGEN ISOTOPES

The isotopic analyses were carried out by mass spectrometry, using samples spaced 20 cm.

The $\delta^{13}C$ values (whole rock) shows a continuous C^{13} decrease towards the top of the Cohab section. In detail it was observed two sharp isotopic increases at 3.0 and 6.0 meters, respectively. The first one coincides with those observed in the TOC and IR curves, as well as the described facies change (Fig. 3). This shift is considered a chemostratigraphic marker, and it was interpreted as a limit of 4th order sequences by Tupinambá et al. (2002). The second one occurs close to the suggested top of the *W. Archeocretacea-H. reussi* Zone.

The $\delta^{18}O$ values turning gradually less positive to the top section (Fig. 3) are linked to the progressive cooling (greater $\delta^{18}O$ values) of oceanic waters towards to the end of Cretaceous.

Compared to isotope curves for entire Cretaceous sequence (e.g. Jenkyns et al., 1994) , the observed $\delta^{13}C$ and $\delta^{18}O$ excursions correspond to the recovery phase of the C-T Boundary event (Figs. 4, 5).

STATISTICAL TREATMENT OF THE DATA

The spectral analysis is considered as an appropriate tool to identify ciclicity patterns in stratigraphic sections (Tupinambá et al., 2002; Cunha & Koutsoukos, 2001).

At the periodogram of $\delta^{13}C$ spectral analyses for Cohab quarry, the most significant frequencies found are related to the periods of 4.13; 2.81 and 2.21.

Accumulation rates have been calculated on the basis of the frequencies associating the isotope patterns to the Milankovitch astronomical cycles. Assuming these hypoteses, the period of 4.13 would be related to the precession cycle of 19 Ma and the period of 2.81 to the cycle of 11.52 Ma cycle (half precession cycle).

The following formula was applied:

$(4.13X20)/19.00 = 4.35$ cm/ka

$(2.81X20)/11.52 = 4.89$ cm/ka

An average accumulation rate (4.62 cm/ka) corroborates those found by Tupinambá et al. (2002) and Chaves et al. (2002) for the TOC values of the same quarry.

CENOMANIAN-TURONIAN BOUNDARY

Based on the integration of isotope results with available biostratigraphy and faciological data, the C-T boundary may be placed between 3.0 and 6.0 meters in the studied section.

CONCLUSIONS

A correlation of isotope data to TOC and IR values confirms the existence of a chemostratigraphic marker at the base of the Cohab quarry section.

In spite of low values (°/₀₀), the $\delta^{13}C$ and $\delta^{18}O$ statistical study confirms the periodicity of the sedimentation cycles, related to Milankovitch precession cycles, and the accumulation rates previously found by Tupinambá et al. (2002) and Chaves et al. (2002).

The terminal phase of the recorded event is show by the carbon isotope distribution with a recovery phase of the C-T interval positive excursion.

Finally, the association of the stable isotope results with biostratigraphic data allows the proposition of a global stratotype for the C-T boundary in the Sergipe-Alagoas Basin.

ACKNOWLEDGEMENTS

We are grateful for the logistic support in the isotope analyses provided by PETROBRAS-CENPES. Oscar Strohschoen Jr. (PETROBRÁS-CENPES) is thanked for helping with the biostratigraphy. A.E.S. Dias and E. Pereira also thank Conselho Nacional de Desenvolvimento Científico e Tecnológico (CNPQ).

REFERENCES

Chaves, H. A. F., Tupinambá, L. R., Pombo, E. R. and Pereira, E., 2002. Sedimentary cycles in the Cenomanian Turonian transition in the Sergipe Basin, Brazil. 8th Annual Conference of the International Association for Mathematical Geology (2002). Bulletin of Expanded Abstract, p. 233-238.

Cunha, A. A. S. and Koutsoukos, E. A. M., 2001. Orbital Cyclicity in a Turonian sequence, Sergipe Basin, NE Brazil. Cretaceous Resarche (2001) 22, p. 529-548.

Jenkyns, H. C., Gale, A. S. and Corfield, R. M., 1994. Carbon- and Oxygen isotope stratigraphy of the English chalk and Italian scaglia and its paleoclimate significance. Geological Magazine, v. 131, p. 1-34.

Koutsoukos, E.A.M. and Bengston, P., 1993. Towards an integrated biostratigraphy of the upper Albian-Maastrichtian of the Sergipe Basin, Brazil. In Gayet, M., ed., Round table Europeenne: Documents des Laboratoires de Geologie, Lyon 125: Lyon, Universite Claude Bernard, Departement des Science de la Terre, p. 241-262.

Mendes, J. M. C., Eiras, J. F. and Rangel, H. D., 1988. Cenário geológico nas bacias sedimentares no Brasil. In Schlumberger Searchig For Oil and Gas in the Land of Giants, Search: Edição Especial Sobre o Brasil, p. 16-22.

PPG Report, 1998. Report from "extreme climates" Setembro, 1998. Edinburgo. Available online at: http://joides.rsmas.miami.edu\files\ec__report_9_98.pdf, Visited in 11/01/2002.

Rodrigues, R., Abreu, V.S. and Takaki, T., 1989. Utilização de Isótopos de carbono, Oxigênio e Estrôncio em Correlações Estratigráficas. I Seminário de Interpretação Exploratória – Petrobrás – Departamento de Exploração (Maio/1999), p. 317-325.

Takaki, T. and Rodrigues, R., 1993. Isotopic evidence of de Cenomanian-Turonian anoxic event in the Sergipe-Alagoas Basin, Brazil. Third Latin American Congress on Organic Geochemistry. Bulletin of Expanded abstract, p. 141-143.

Tupinambá, L.R., 2000. Estratigrafia de Alta Resolução Aplicada à Geometria e Qualidade de Reservatórios Carbonáticos do Cenomaniano - Turoniano da Bacia SE/AL, na região de Laranjeiras (SE). Monografia Final de Graduação, Faculdade de Geologia, UERJ, 55 p.

Tupinambá, L. R., Pombo, E. R. and Pereira, E., 2002. Análise estratigráfica do intervalo Cenomaniano/Turoniano da Bacia de Sergipe/Alagoas, na região de Laranjeiras (SE). 6° Simpósio sobre o Cretáceo do Brasil. Boletim de Resumos Expandidos, p. 285-290.

Viviers, M.C., Koutsoukos, E.A.M., Silva, A.C., Bengston, P., 2000. Stratigraphy and biogeographic affinities of the late Aptian-Campanian ostracods of the Potiguar and Sergipe basins in northeastnern Brazil. Cretaceous Research (2000) 21, p. 407-455.

Figure 1. Location of the Sergipe/Alagoas Basin (Mendes, 1988).

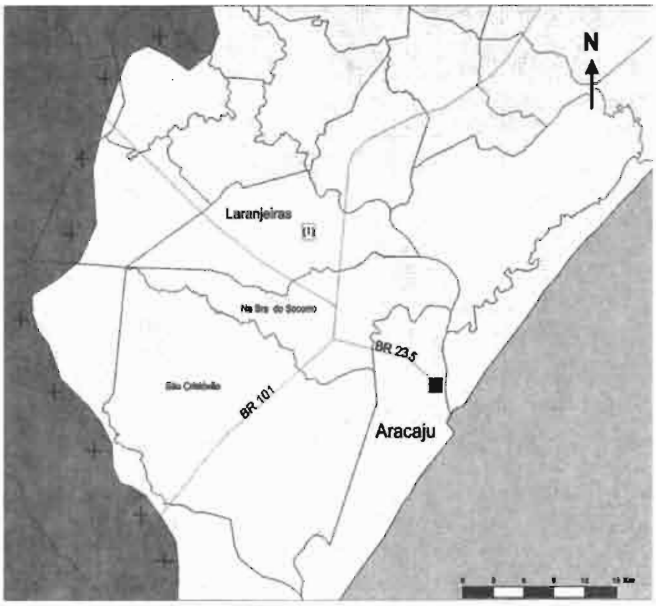

Figure 2. Location of the study area (1) (24L 0701339/ 805316 UTM).

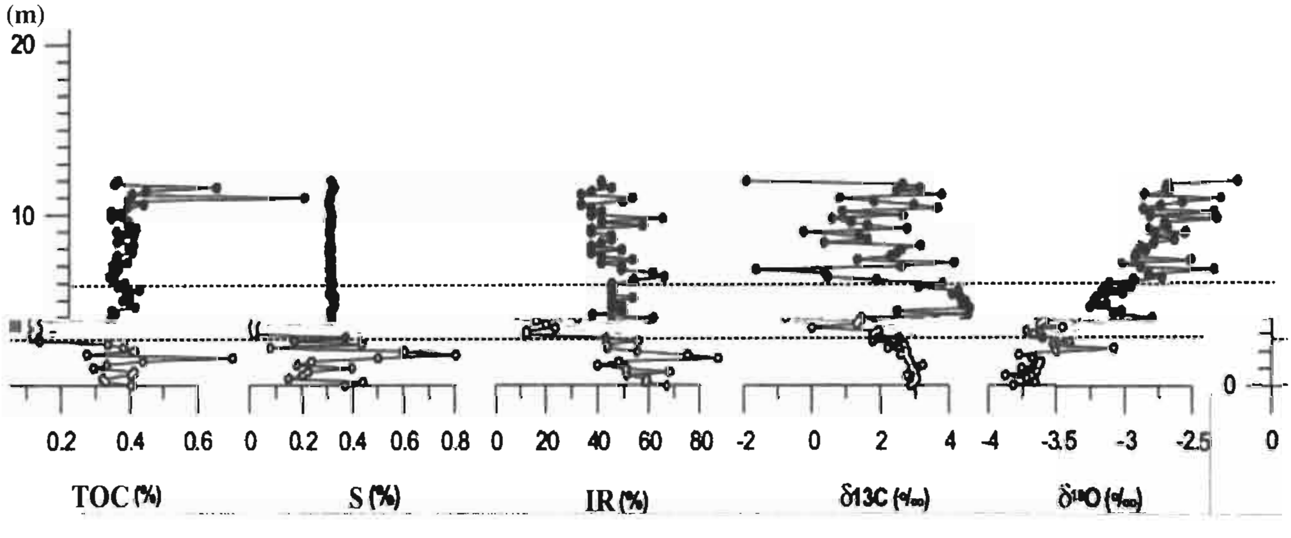

Figure 3. Chemostratighraphic curves of the Cohab quarry (TOC, S, IR, $\delta^{13}C$ and $\delta^{18}O$). The hatched straight lines mark the carbon isotope shifts referred in this paper.

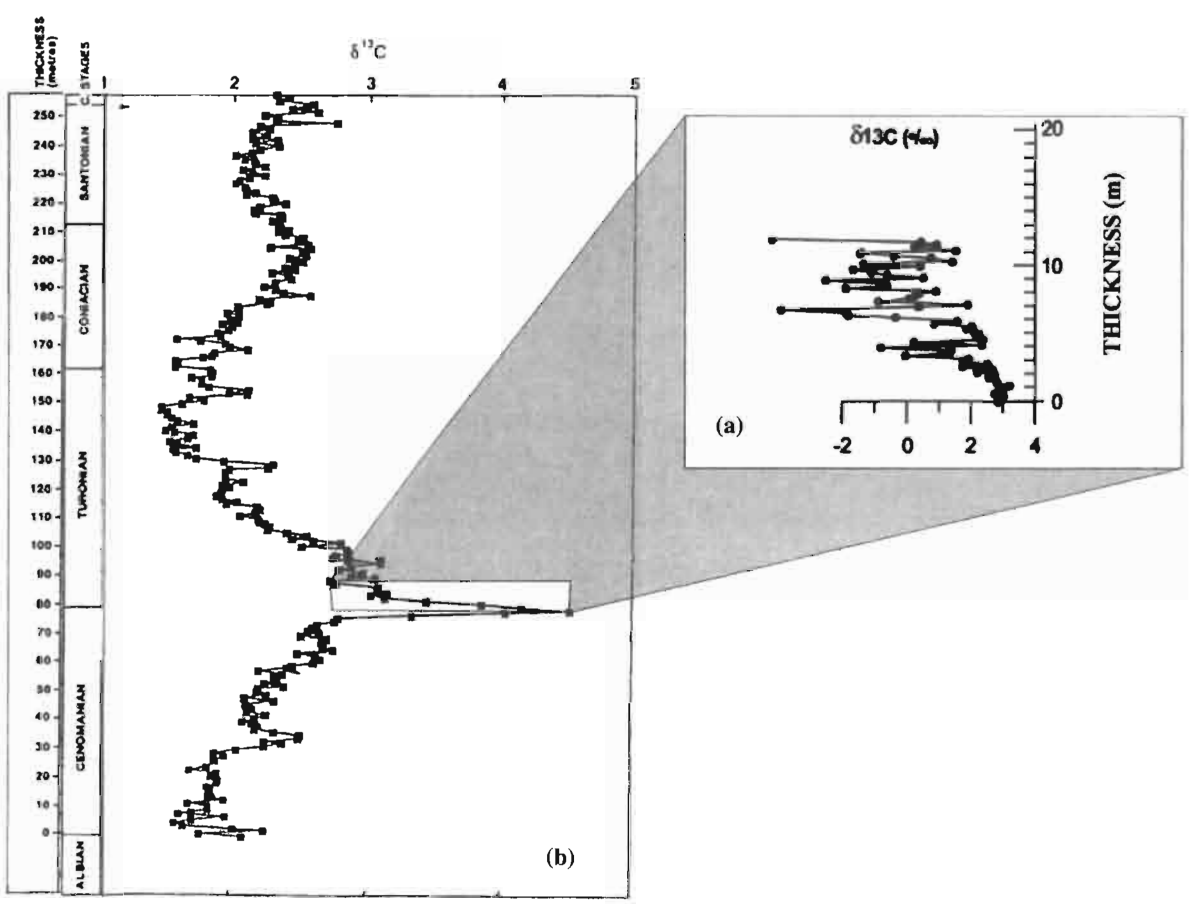

Figure 4. $\delta^{13}C$ excursion at the studied section (a) compared to Jenkyns et al. (1994) carbon isotope curve (b) for Cretaceous sequence.

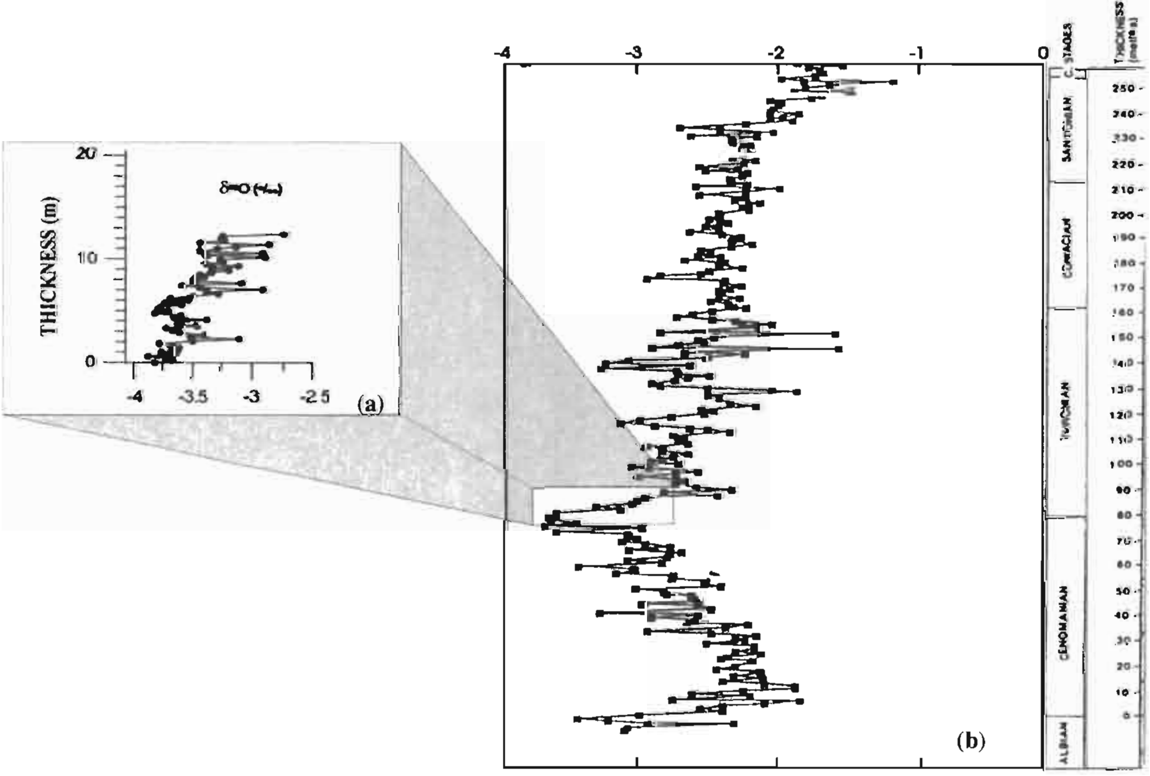

Figure 5. The studied section $\delta^{18}O$ curve (a) compared to Jenkyns et al. (1994) oxygen excursion (b) for Cretaceous sequence.

CARBON STABLE ISOTOPE ANALYSIS AS A SEQUENCE STRATIGRAPHY TOOL: CASE STUDY FROM LOWER JURASSIC MARLY LIMESTONES OF PORTUGAL

Duarte, L.V.[1]; Rodrigues, R.[2] and Dino, R.[2,3]

1. Dep. Ciências da Terra, Centro Geociências, F.C.T. Universidade de Coimbra, 3000-272 Coimbra, Portugal. lduarte@ci.uc.pt
2. Universidade do Estado do Rio de Janeiro, Faculdade de Geologia, 20559-900, Rio de Janeiro, Brazil. rene@uerj.br
3. Petrobrás-Cenpes - Cidade Universitária, Ilha do Fundão, 21949-900, Rio de Janeiro, Brazil. dino@cenpes.petrobras.com.br

Keywords: Sequence stratigraphy, Carbon stable isotopes, Toarcian, Lusitanian Basin, Portugal

INTRODUCTION

In Portugal, the Lower Jurassic sediments crop out in two different geo-structural settings, both bounded by the Iberian Hercynian Massif: the Algarve Basin, in the south of Portugal and in the Lusitanian Basin (west-central Portugal). In this last basin, the Lower Jurassic corresponds to a thick carbonate succession (dolomites, limestones and marly limestones), can reach more than 500 m. In this context, the Upper Liassic (Toarcian) is continuous and well exposed in several points of the basin (Duarte, 1997). Generally it is dominated by marl/marly limestone and limestone alternations, usually characterised by a rich and diverse necktonic (ammonites and belemnites) and benthic (mainly brachiopods, bivalves, crinoids and siliceous sponges) macrofauna (Duarte, 1995, 1997; Duarte et al., 2001).

The hemipelagic nature (marl/limestone alternations) of the Portuguese Toarcian sediments, supported by an accurate ammonite biostratigraphic chart, constitute a good context for carbon an oxygen stable isotope studies. In this kind of sediments, particularly in pelagic environments, these isotopes have been widely used as an important stratigraphic tool or as an important palaeoceanographic/palaeoclimatic indicator (Scholle & Arthur, 1980; Shacleton & Hall, 1984; Weissert 1989; Follmi et al., 1994; Weissert et al., 1998; Jenkyns et al., 2002). The interesting record of carbon stable isotope signal in the Toarcian sediments of the Lusitanian Basin proves this parameter as a useful tool in sequence stratigraphy analysis.

STRATIGRAPHIC CHART

In the Lusitanian Basin, the Toarcian successions are very rich in ammonites and calcareous nannofossils that allow a good biostratigraphic control of the series (Elmi et al., 1989; Rocha et al., 1996; Perilli & Duarte, 2003). The studied succession crops out in northern part of the basin (Coimbra area), where the Toarcian is more thick and hemipelagic (Duarte, 1997). It belongs to the S. Gião Formation (Duarte & Soares, 2002), ranging in age from the Early Toarcian (Polymorphum Zone) up to Late Toarcian (Meneghinni Zone). Based on the vertical facies arrangement and the stratigraphical distribution of the macrofauna, this unit can be subdivided into five members (Fig. 1), easily recognizable across a large area of the Lusitanian Basin. Only the first following four units were analyzed in the present study: Marly limestones with Leptaena facies Member (MLLF), Thin Nodular Limestones Member (TNL), Marls and marly limestones with Hildaites and Hildoceras Member (MMLHH), Marls and marly limestones with sponge bioconstructions Member (MMLSB).

These units are organised into three third-order depositional sequences (ST1 to ST3), bounded by four (DT1 to DT4) isochronous regional discontinuities (Polymorphum Zone, Polymorphum/Levisoni Zone boundary, intra-Bifrons Zone and around Bonarelli/ Speciosum Zone boundary). The ST1-ST3 sequences have been deposited in the differentiated context of a homoclinal carbonate ramp system dipping towards the northwest (Duarte, 1997).

CARBON STABLE ISOTOPES

METHODS

To investigate $\delta^{13}C$ stable isotopes, 38 samples of bulk-rock micritic carbonate sediments from calcareous levels belonging to the several Toarcian units were analysed. The total carbonate content of each sample was analysed through the Bernard calcimeter. The final isotopic composition of carbon (and also oxygen) was obtained using a Finnigan MAT 252 mass spectrometer at Petrobras Research Center (Cenpes, Brazil), following the traditional procedures (McCrea 1950). All the values are reported in parts per mil (‰) notation (δ) relative to the PDB (Pee Dee Belemnite) international standard (Craig, 1957). Carbon-isotope ratios of Lower to lowermost Middle Toarcian series are plotted along the stratigraphic section in figure 1.

RESULTS

The carbon stable isotope values range between -0.24‰ and +3.93‰. Despite the low number of analysis, significant oscillations are observed within and between each member or depositional sequence. The isotopic variation curve of $\delta^{13}C$ roughly agrees with the trends observed in other sections of the Lusitanian Basin, as pointed out by Duarte (1995, 1998); the achieved results also support the $\delta^{13}C$ as a good stratigraphic tool.

As outlined in figure 1, the lower part of the succession is characterized by two positive trends observed within the MLLF (0.56 to 2.6‰) and between TNL and the base of MMLHH Member (-0.24 to 3.93‰), both separated by a minimum values found in the TNL Member (base of Levisoni Zone). Besides, the greatest Toarcian change occurs at the boundary between those first units (from 2.6 to - 0.24‰).

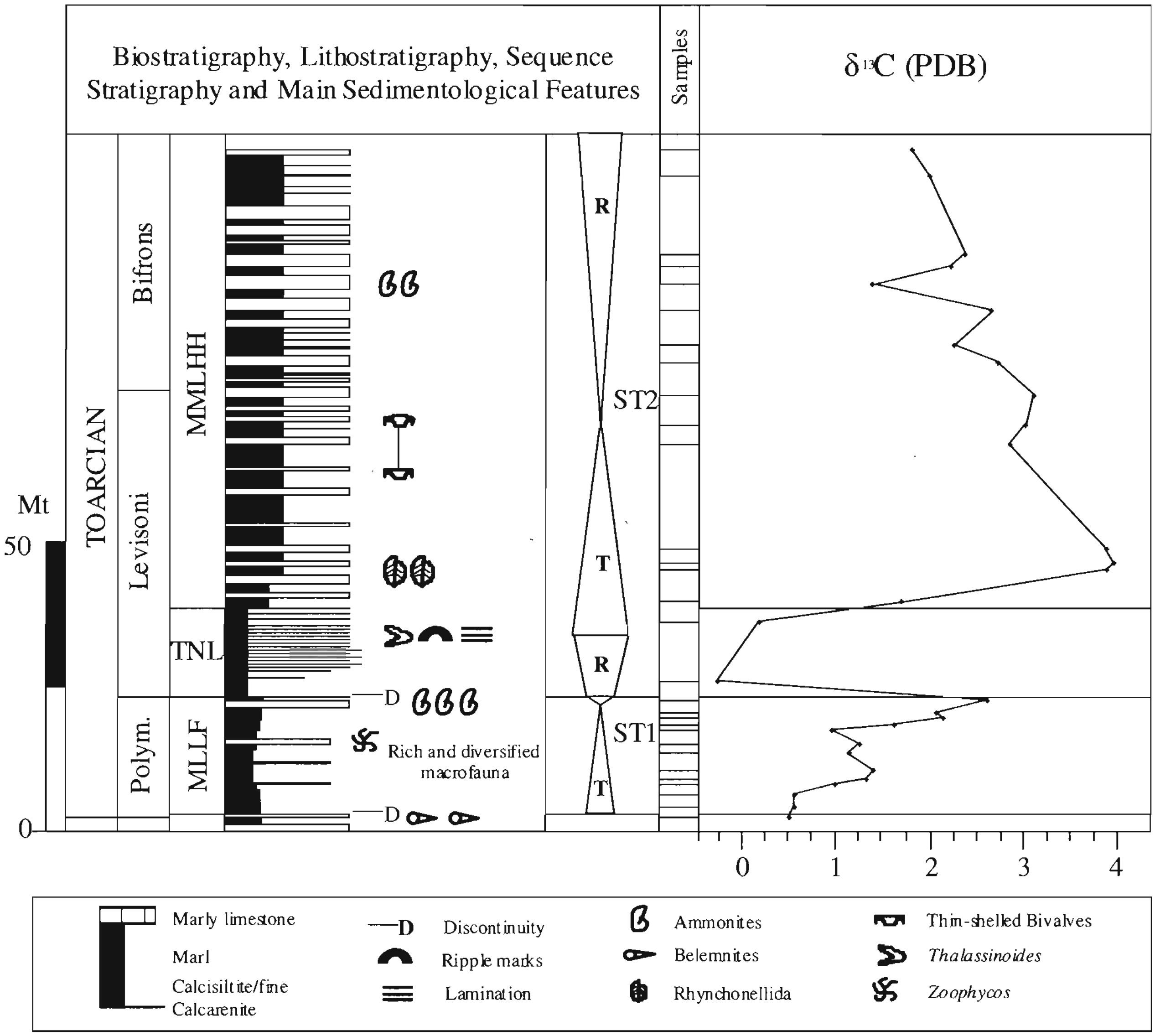

Figure 1. Synthetic stratigraphic and sedimentological chart for the Lower and base of Middle Toarcian of the Lusitanian Basin northern sector (Coimbra region). Sequence stratigraphy, transgressive-regressive cycles and carbon-isotopic record. MLLF – Marly limestones with Leptaena facies; TNL – Thin nodular limestones; MMLHH – Marls and marly limestones with *Hildaites* and *Hildoceras*. T – Transgressive phase; R – Regressive phase.

In the other side, the highest $\delta^{13}C$ occurs in the middle part of the Levisoni Zone (base of MMLHH Member), with values around 3.90%o. Fluctuations in $\delta^{13}C$ are generally negative in the upper part of the MMLHH Member (Bifrons Zone; from 3.1 to 1.79%o) and throughout the MMLSB Member (uppermost Bifrons Zone to Bonarellii Zone; 1.89 to 0.48%o).

$\delta^{13}C$ AND SEQUENCE STRATIGRAPHY INTERPRETATION

Facies analysis and stable isotopes, in particular, are useful tools to identify the major transgressive-regressive cycles and sequence evolution, mainly based on the recognition of the main discontinuities (sequence boundaries) and flooding surfaces (Duarte et al., 2003; Fig. 1).

ST1: this sequence corresponds to the MLLF Member, and is the most argillaceous unit of the entire Toarcian succession. This sequence is very asymmetric, and a large part of it is interpreted as a transgressive system tract (Duarte et al., 2002). This transgressive trend is well documented by the $\delta^{13}C$ evolution values. The maximum excursion (2.6%o) is interpreted as the maximum flooding surface, also well documented by a condensed Dactylioceratid-rich horizon (Duarte et al., 2003). Besides, the small trends observed within the MLLF Member seem to be related with fourth-order depositional sequences.

ST2: this sequence begins with brownish clays and marls that characterize the base of TNL Member. Upwards, this sequence grades into thin silty to sandy limestone alternations with marly clay interbeds that corresponds to the typical TNL Member in whole the basin. These facies show tempestitic-turbiditic features, observed in the other sections of the Lusitanian Basin, and related to tectonic trigger mechanisms (Duarte, 1997). The carbon-isotope evolution in these levels shows an abrupt decrease, which support the lowstand system tract interpretation, through the increase of lighter continental ^{12}C in the depositional system.

The overlying part of ST2, coincident with the MMLHH Member, is composed of a thick (around 90m) marl/limestone decimetric to metric alternations. The base of this unit is interpreted as a transgressive event (transgressive system tract), shown by an increase in marly deposits and a positive carbon-isotope excursion (values above 3.00 ‰) (Fig. 1). This event ends with some evidences of pelagic deposition (top of the Levisoni Zone). In fact, the maximum flooding surface is shown by thin-shelled bivalve-rich (*Bositra* sp.) horizons (Fig. 1). The transgressive system tract is overlain by a thick agrading/prograding package. The series become progressively more calcareous and the vertical facies association, compared with the evolution recognized in other points of the basin (Duarte, 1997), illustrate a shallowing-upward evolution (highstand system tract). This trend is corroborated by the $\delta^{13}C$ record, showing a negative excursion (from 3.1 to 1.79‰), interpreted as the result of an increase in continental ^{12}C than a decrease in marine productivity.

ST3: this unit is correlatable with the MMLSB Member. The increase of bioclastic remains at the top of this sequence, easily recognizable in the southeastern (proximal) part of the basin (Duarte, 1997), suggests an important regressive phase (highstand system tract). In ST3 of Coimbra section, the regressive trend is correlative of a slight negative trend in the $\delta^{13}C$ record (from 1.89 to 0.48‰).

DISCUSSION AND CONCLUSIVE REMARKS

The carbon-isotope ($\delta^{13}C$) record shown herein confirms the trends illustrated in Duarte (1998), for other regions of the Lusitanian Basin. The first main conclusion of the observed variations is that the link with the sequence analysis previously established, should indicate a mechanism of a primary nature. The isotopic variation curve clearly shows remarkable changes at the boundaries between the several depositional sequences. The large positive fluctuations correspond to transgressive periods. With the exception of ST1, which is truncated at the top (erosional surface), the uppermost part of ST2 and ST3 shows gradual negative shifts, associated with regressive phases. As demonstrated in previous work (Duarte, 1998), the good correlation between the sequence development and the carbon-isotope variation can be explained by the interplay of ^{12}C of continental origin. In fact, the increase of lighter carbon-isotope in the carbonate sediments confirms the continental influence on deposition and consequently a regressive phase. A good example can be seen at the base of ST2 (TNL Member), where the lowest values of $\delta^{13}C$ are observed (Fig. 1). As demonstrated above, the detrital facies and other features present in the TNL Member indicate lowstand deposition.

With these results the $\delta^{13}C$ is confirmed as an important tool in sequence stratigraphic interpretation of Toarcian marl/limestone alternations of Portugal. Besides, some of these events (positive and negative excursions) are also recognized in some other European basins (Jenkyns & Clayton, 1986; Jenkyns et al., 1994, 2002; Jiménez et al., 1996; Hesselbo et al., 2000; Beerling et al., 2002).

REFERENCES

Beerling, D. J.; Lomas, M. R. & Gröcke, D. R., 2002. On the nature of methane gas-hydrate dissociation during the Toarcian and Aptian Oceanic Anoxic events. American Journal of Science, 302: 28-49, New Haven.

Craig, H., 1957. Isotopic standards for carbon and oxygen and correction factors for mass-spectrometric analysis of carbonate dioxide. Geochim. Cosmochim. Acta, 12: 133, Oxford.

Duarte, L. V., 1995. O Toarciano da Bacia Lusitaniana. Estratigrafia e Evolução Sedimentogenética. Unpublished PhD, Centro de Geociências, Departamento de Ciências da Terra, Universidade de Coimbra, 349p.,14 pl.., Coimbra.

Duarte, L. V., 1997. Facies analysis and sequential evolution of the Toarcian-Lower Aalenian series in the Lusitanian Basin (Portugal). Com. Inst. Geol. e Mineiro, 83: 65-94, Lisboa.

Duarte, L. V., 1998. Clay minerals and geochemical evolution in the Toarcian Lower Aalenian of the Lusitanian Basin. Cuad. Geol. Iberica, 24: 69-98. Madrid.

Duarte, L. V. & Soares, A F., 2002. Litostratigrafia das séries margo-calcárias do Jurássico inferior da Bacia Lusitânica (Portugal). Com. Inst. Geol. Mineiro, 89: 115-134, Lisboa.

Duarte, L. V.; Krautter, M. & Soares, A. F., 2001. Bioconstructions à spongiaires siliceux dans le Lias terminal du Bassin lusitanien (Portugal): stratigraphie, sédimentologie et signification paléogéographique. Bull. Soc. Géol. France, 172 (5): 637-646, Paris.

Duarte, L. V.; Perilli, N.; Dino, R.; Rodrigues, R. & Paredes, R., 2003. Lower to Middle Toarcian from the Coimbra region (Lusitanian Basin, Portugal): Sequence stratigraphy, calcareous nannofossils and stable-isotope evolution. Proceedings of 6th International Symposium on the Jurassic System. *Rivista Italiana di Paleontologia e Stratigrafia*, Special Number (in press), Milano.

Elmi, S.; Goy, A.; Mouterde, R.; Rivas, P. & Rocha, R., 1989. Correlaciones biœstratigraficas en el Toarciense de la Peninsula Iberica. Cuad. Geol. Iberica, 13: 265-277, Madrid.

Föllmi, K.; Weissert, H.; Bisping, M. & Funk, H., 1994. Phosphogenesis, carbon-isotope stratigraphy and carbonate-platform evolution along the Lower Cretaceous northern Tethyan margin. Geol. Soc. Amer. Bull., 106: 729-746, San Antonio.

Hesselbo, S. P.; Gröcke, D. R.; Jenkyns H. C.; Bjerrum C. J.; Farrimond, P.; Morgans, B. H. & Green, O., 2000. Massive dissociation of gas hydrate during a Jurassic Oceanic Anoxic Event. Nature, 406: 392-395, London.

Jenkyns, H. C. & Clayton, C. J., 1986. Black shales and carbon isotopes in pelagic sediments from the Tethyan Lower Jurassic. Sedimentology, 33: 87-106, Oxford.

Jenkyns, H. C.; Gale, A. S. & Corfield, R. M., 1994. Carbon- and oxygen-isotope stratigraphy of the English Chalk and Italian Scaglia and its palaeoclimatic significance. Geol. Mag., 131 (1): 1-34, Cambridge.

Jenkyns, H. C.; Jones, C. E.; Gröcke D. R.; Hesselbo S. P. & Parkinson D. N., 2002. Chemostratigraphy of the Jurassic System: applications, limitations and implications for palaeoceanography. J. Geol. Soc. London, 159: 351-378, London.

Jiménez, A. P.; Cisneros, C. J.; Rivas P. & Vera J. A., 1996. The Early Toarcian anoxic event in the westernmost Tethys (Subbetic): Paleogeographic and paleobiogeographic significance. J. Geol., 104: 399-416, Chicago.

McCrea, J. M., 1950. On the isotopic chemistry of carbonates and a paleotemperature scale. J. Chem. Phys., 18 (6): 849-857, Amsterdam.

Perilli, N. & Duarte, L. V., 2003. Dating of the Toarcian succession from the Lusitanian Basin based on calcareous nannofossils. Abstract Volume of VI Congresso Nacional de Geologia, 4p., Lisboa.

Rocha (General Coordinator), 1996. The 1st and 2nd rifting phases of the Lusitanian Basin: stratigraphy, sequence analysis and sedimentary evolution. Final report, CEC, Project MILUPOBAS, Contract no JOU-2-CT94-0348, 4 vols, Lisboa.

Scholle, P. & Arthur, M. A., 1980. Carbon isotopic fluctuations in pelagic limestones: potential stratigraphic and petroleum exploration tool. AAPG Bull., 64: 67-87, Tulsa.

Shackleton, N. J. & Hall, A., 1984, Carbon isotope data from Leg 74 sediments. In: Moore, T. C. et al. (eds.) - I, Init. Report D.S.D.P., U.S. Gov. Printing Office, Washington, 74: 613-644.

Weissert, H., 1989. C-Isotope stratigraphy, a monitor of paleoenvironmental change: a case study from the Early Cretaceous. Surveys in Geophysics, 10: 1-61, Dordrecht.

Weissert, H.; Lini, A.; Follmi, K. B. & Kuhn, O., 1998. Correlation of Early Cretaceous carbon isotope stratigraphy and platform drowning events: a possible link. Palaeogeog., Palaeoclim., Palaeoecol., 137: 189-203, Amsterdam.

δ^{13}C MINIMUM IN THE LATE CRETACEOUS-PALEOCENE YACORAITE CARBONATE SEQUENCE, NW ARGENTINA

Ferreira, V.P.[1]; Sial, A.N.[1]; Alonso, R.N.[2]; Toselli, A.J.[3]; Acenolaza, F.G.[3]; Parada, M.A.[4] and Rossi de Toselli, J.[3]

1. NEG-LABISE, Dept. of Geology, UFPE, C.P. 7852, Recife-PE, Brazil, 50670-000. ans@ufpe.br, valderez@ufpe.br
2. Dept. of Geology, Nat. Univ. of Salta, Argentina, 4400. rnalonso@sinectis.com.ar
3. INSUGEO, Nat. Univ. of Tucuman, Argentina, 4000. atoselli@cpsarg.com
4. Dept. of Geology, Univ. of Chile, Santiago, Chile. maparada@cec.uchile.cl

Keywords: C isotopes, O isotopes, Late Cretaceous, Paleocene, South America

INTRODUCTION

Carbon and oxygen isotopes are important sensors for climatic changes and constitute important tools in the study of geologic time boundaries. Important environmental changes have been observed in many basins `at most geological boundaries, among them the Cretaceous-Tertiary (K-T) transition, a time of very important worldwide massive faunal extinction. One of the characteristics of this boundary is negative excursion in the δ^{13}C values right before the transition, followed by a positive excursion suggesting an important cooling at the K-T transition. Important environmental changes have been detected in many basins where the K-T transition has been investigated using C and O isotopes. This transition was recorded by carbonates only in few places in South America. Among these localities are Pernambuco-Paraíba coastal basin, NE Brazil, the Yacoraite and Neuquen basins, Argentina, and Navidad, Algarrobo and Magellan basins, Chile. Carbon and oxygen isotope data for carbonates from the K-T transition are available for the Pernambuco-Paraíba coastal basin (Albertão & Kotsoukos, 1994, Albertão et al., 1994, Ferreira et al., 1994), and for the basins in Chile (Sial et al., 2001a). Preliminary C and O isotope data were reported by Sial et al (2001a, b) for one section of the Yacoraite Fm near Cabra Corral, Argentina. They found positive δ^{13}C values up to +2‰ PDB and a shift to negative values down to ~ -5‰$_{PDB}$ followed by a gradual increase, in the contact with a red sandstone, believed to mark the beginning of the Paleocene.

We examine here the behavior of C and O isotopes and chemistry (Si, Mg, Ca, Sr, Fe and Mn) in another section of the Yacoraite Fm carbonates, not studied before, and compare these data with the data previously reported by Sial et al. (2001a) and with the C e O isotope patterns from elsewhere in the world.

GEOLOGICAL SETTING

The K-T transition has been recorded in NW Argentina by sediments of the Salta Group represented by the Yacoraite (Maastrichtian)-Olmedo and Mealla (Paleocene) Fms. (Fig. 1) that extend into Bolivia and Paraguay. This Group has a long evolutionary history (Lower Cretaceous-Middle Paleogene) and comprises a great variety of sedimentary environments whose deposits reach a total thickness of more than 5,000m (Marquillas et al., 1999). The Salta Group encompasses the Balbuena (older) and the Santa Barbara (younger) Subgroups. Salfity et al. (1998) regarded the Yacoraite Fm. as part of the Balbuena Subgroup, overlying the Lecho Fm. and overlain, in turn, by the Tunal Fm., which is the base of the Santa Barbara Subgroup. The deposition of the Salta Group from the Neocomian to the Campanian was controlled by rift environment, while the post-rift environment was marked by a deep Maastrichtian marine ingression (Marquillas et al., 1999) that marked the termination of the arid environment and installed a carbonate system, which persisted until the Early Paleocene. Presence of some foraminifer and fish species in the Yacoraite Fm. implies a marine influence, a likely assumption if taken into account sea level rise during the Late Cretaceous and that these marine faunistic elements could have undergone adaptation to continental conditions. Excellent exposures of limestones of the Yacoraite Fm. can be observed at Cabra Corral dam, 70 km south of Salta, where the K-T transition is recorded. A few kilometers east from this outcrop, down the Juramento river, late Maastrichtian dinosaur tracks are found in the yellow limestone (Alonso, in preparation).

THE CABRA CORRAL SECTION

Carbonates of the Yacoraite Fm were sampled along a well exposed road cut next to the Cabra Corral dam, in a section parallel to the one described by Sial et al (2001a). The section in this locality is characterized by repetition of strata due to faults associated with topography, position of the road cut, and erosion. The most continuous, thicker (over 80m) and best exposed section was sampled for this study. It encompasses about 20 m of yellow limestones that pass into greenish marls. The contact between these two major lithologies is marked by red impure sandstone whose top shows bioturbation that constitute an excellent layer guide in the Cabra Corral zone, and is believed to mark the Cretaceous-Paleocene transition. Above this layer shales are intercalated with fossiliferous limestones, which locally show hammock and oolitic structures.

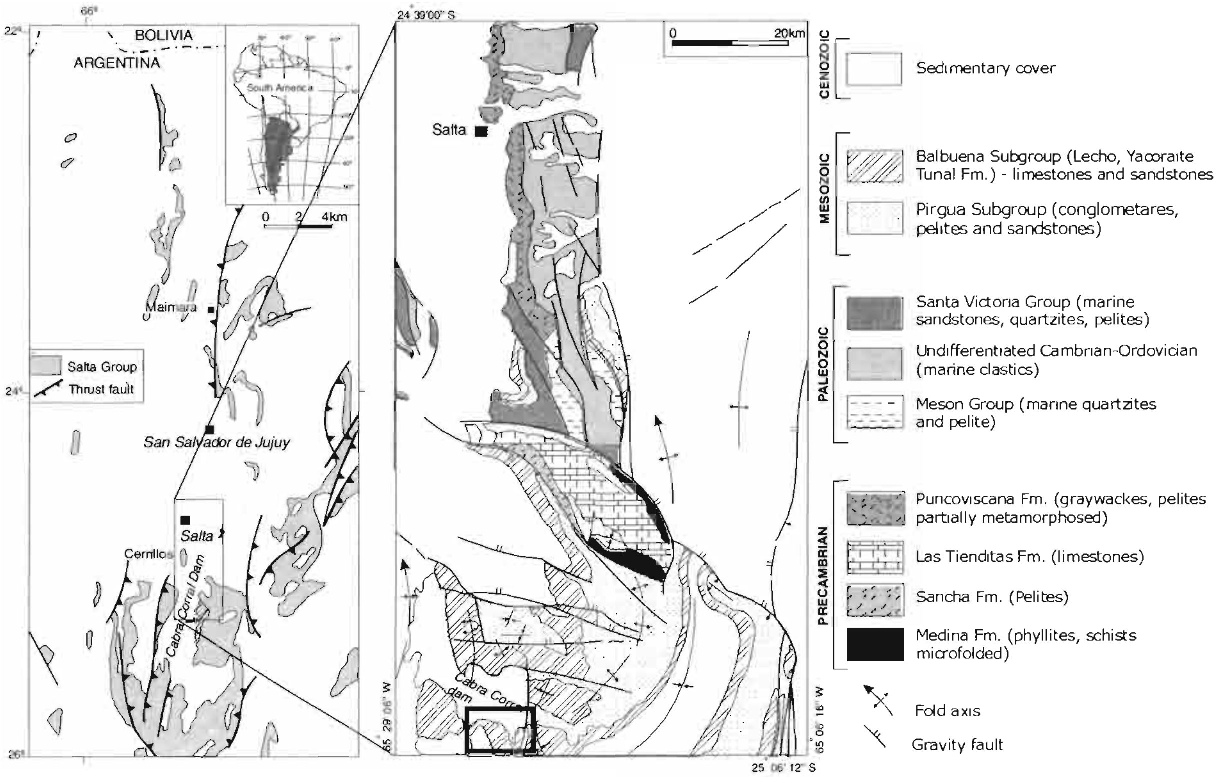

Figure 1. (A) Sites of occurrence of the Yacorite and El Tunal Formations in Jujuy and Salta Provinces, NW Argentina. (B) Geologic map of the Cabra Corral area, south of the town of Salta (after Salfity et al., 1998).

METHODOLOGY AND EVALUATION OF SAMPLE QUALITY

Around sixty carbonate samples were stratigraphically collected along the road cut with distances between samples varying from 0.2 to 3.3 m (most samples spaced between 1 and 2 m). Samples were collected from the Yacoraite Fm up to the red sandstone (total thickness of 20m in this section) through the top of the section (total thickness around 60 m). These samples were cut and powered for whole rock chemical analyses. Major and trace elements analyses were determined at the Department of Geology, Federal University of Pernambuco (UFPE) by X-ray fluorescence in a Rigaku RIX 3000 unit, using fused beads prepared with Li tetraborate. Carbon and oxygen isotope analyses were done at the Stable Isotope Laboratory, Department of Geology, UFPE. Powders for these analyses were obtained by microdrilling of samples with no apparent veins, recrystallization or silicification. CO_2 gas was extracted on a conventional high vacuum line after reaction with 100% orthophosphoric acid at 25°C, following the method described by McCrea (1950). The CO_2 released, after cryogenic cleaning, was analyzed in a double inlet, triple collector mass spectrometer. Results are in the δ notation (‰, PDB).

Post-deposition alterations such as diagenesis and metamorphism can alter the original isotopic composition and before interpreting the isotopic variations these data must be evaluated to assure the values are primary. There is no correlation between $\delta^{13}C$ and Mn/Sr as well as between $\delta^{18}O$ and Mn/Sr (Fig. 2), as expected for samples not affected by meteoric alteration that tends to increase Mn contents while decreasing Sr contents. There is no correlation between $\delta^{13}C$ and $\delta^{18}O$ values, although an apparent trend of positive correlation seems to occur, suggesting a secondary overprint of the O isotope values. Mn/Sr ratios for these samples, however, are << 10 (0.09 to 2.56), an indication of little secondary alteration.

GEOCHEMICAL AND ISOTOPIC DATA

All studied samples are limestones with low dolomite contents. Samples have highly variable Mn (153-1808 ppm), Sr (360-2000 ppm), and Fe (2803-46116 ppm) contents. Mg/Ca ratios (which reflect the dolomite content) are cyclic at the lower part of the studied section, and above the red sandstone layer there is a predominance of calcitic carbonates. Oxygen isotope values are highly variable ($\delta^{18}O$ from -8.7 to +6.0‰$_{PDB}$) as well as $\delta^{13}C$ values (from –3.7 to +2.2 ‰$_{PDB}$), but most samples have negative $\delta^{13}C$ values. From the base of the studied section to the top, both oxygen and carbon isotope values are positive and gradually decrease to the top of the yellow limestones reaching a mininum at the red sandstone layer. At this layer $\delta^{13}C$ reachs its lowest value (-3.7‰) after which values are all negative and oscillate for about 32 m until the middle part of the greenish marls, when they shift to positive values for ca. 20 m, and shift again to negative values. The shif to the most negative $\delta^{13}C$ value at the red sandstone layer is accompanied by important shifts in Si, Ca, Mg, Sr, Mn and Fe (Fig. 3). Considering these values as primary, they suggest cooling followed by an important temperature increase right after the transition.

DISCUSSION AND CONCLUSIONS

Negative carbon isotope excursions in marine carbonates are usually interpreted as indicating low relative burial of organic matter and decrease in the organic production. The negative $\delta^{13}C$ values for the studied carbonate suggest incorporation of considerable C of organic origin, and the most negative values at, and right above the red sandstone layer, which is believed to represent the K-T boundary, are compatible with the pattern observed elswhere in the world in the K-T boundary. These negative carbon isotope excursions have been interpreted as indicative of climatic changes as a consequence of either intense volcanism or to the impact of a meteorite that led to the formation of a huge dust cloud leading to sun block and greenhouse effect, affecting the biogeochemical cycling of carbon.

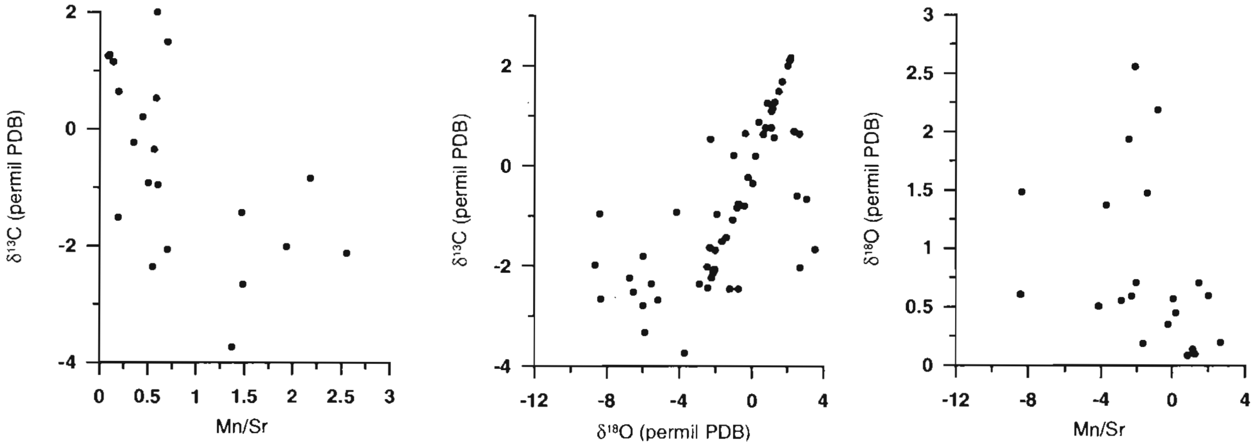

Figure 2. $\delta^{13}C$, $\delta^{18}O$ and Mn/Sr variations in carbonates of the Yacoraite Formation, at the Cobra Corral section, NW Argentina.

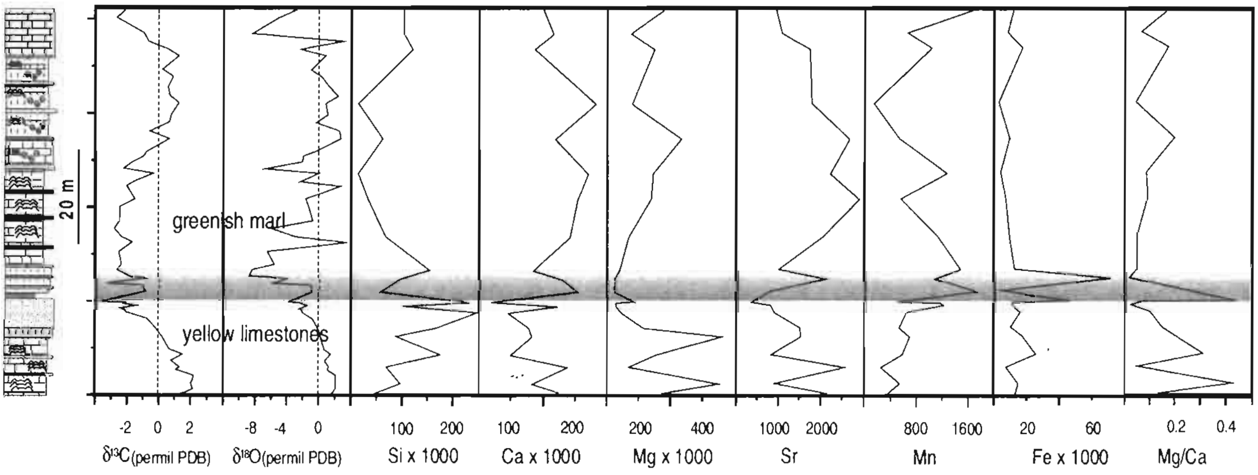

Figure 3. C and O isotope, and element stratigraphic variations for the Yacoraite Formation at Cabra Corral section, NW Argentina.

ACKNOWLEDGEMENTS

This project has been financed by VITAE (B-11487/10B00). This is the NEG-LABISE contribution n. 210.

REFERENCES

Albertão, G.A. and Koutsoukos, E.A.M., 1994, The Cretaceous-Tertiary boundary in Pernambuco, northeastern Brazil. 14th Intern. Sediment. Congr., Recife. Field Guide to the Poty quarry section, p. 1-14.

Albertão, G.A. Koutsoukos, E.A.M., Regali, M.S.P., Attrep, M., Martins, P.P. Jr., 1994, The Cretaceous-Tertiary boundary in southern low-latitude regions: preliminary study in Pernambuco, northeastern Brazil. Terra Nova, 6:366-375.

Ferreira, V.P., Sial, A.N., Menor, E.A. (1996) Carbon and oxygen isotopes in offshore and continental Mesozoic and Tertiary limestones, NE Brazil: the K-T boundary and Tertiary climatic variations. Acta Geologica Hungarica, 39, Suppl.:43-46.

Hsu, K.J. and Wissert, H.J. (1980) South Atlantic Paleoceanography. Cambridge Univ. Press, pp. 230-234.

Huber, B.T., Hodell, D., Hamilton, C.P. (1995) Middle-Late Cretaceous climate of the southern high latitudes: stable isotopic evidence for minimal equator-to-pole thermal gradient. GSA Bulletin, October, v. 107 (10): 1164-1191.

Magaritz, M. (1989) ^{13}C minima follow extinction event: a clue to faunal radiation. Geology 17: 337-340.

Marquillas, R.A., Del Papa, C.E., Sabino, I.F. (1999). Environmental variations during the Cretaceous-{Paleogene: Salta Group Basin, northwest Argentina). Extended Abstract.

Salfity, J.A., Monaldi, C.R., Guidi, F., Sales, R.J. (1998). Mapa geológico de la Província de Salta: Buenos Aires, Secretaría de Industria, Comercio y Minería, Serv. Geol. Argentino, scale 1:500,000.

Sial, A.N., Ferreira, V.P., Alonso, R.N., Toselli, A.J., Acenolaza, G.F., Pimentel, M.M., 2001a, The Late Cretaceous-Paleocene carbonate sequences in Argentina: a carbon and oxygen isotope view. III Simp. Geologia Isotopica America do Sul. Pucon Chile, Extended abstract (em CD).

Sial, A.N., Ferreira, V.P., Toselli, A.J., Parada, M.A., Acenolaza, F.G., Pimentel, M.M., Alonso, R.N., 2001b, Carbon and oxygen isotope compositions of some Upper Cretaceous-Paleocene sequences in Argentina and Chile. Intern. Geol. Rev., 43:

THE PRECAMBRIAN-CAMBRIAN BOUNDARY IN URUGUAY: CHEMOSTRATIGRAPHY OF THE CERRO VICTORIA FORMATION, UPPER ARROYO DEL SOLDADO GROUP

Gaucher, C.[1]; Sial, A.N.[2]; Ferreira,V.P.[2]; Chiglino, L.[1] and Sprechmann, P.[1]

1. Instituto de Geología y Paleontologia, Facultad de Ciencias, Iguá, 4225, 11400, Montevideo, Uruguay
2. NEG-LABISE, Departamento de Geologia, UFPE, C.P. 7852, Recife-PE, 50670-000, Brasil

Keywords: Chemostratigraphy, Cambrian, Vendian, Uruguay

INTRODUCTION

The Arroyo del Soldado Group (ASG) is a 5 km-thick platform succession unconformably overlying a mainly Archean to Mesoproterozoic basement (Nico Pérez Terrane), occurring in central-eastern Uruguay (Gaucher et al., 1996, 1998; Gaucher, 2000). The group is characterized by an alternance of mainly siliciclastic (Yerbal, Cerro Espuelitas, Barriga Negra and Cerros San Francisco Formations) and carbonatic units (Polanco and Cerro Victoria Formations, Fig. 1). Volcanic, volcaniclastic and pyroclastic rocks are completely absent. Carbonatic units represent pericontinental, storm-dominated carbonate ramps. Siliciclastic units were deposited in a basin with gentle palaeoslope, sandstones being texturally and mineralogically mature quartzarenites or subarkoses (Gaucher, 2000). Alltogether, these facts strongly indicate a stable, Atlantic-type continental platform as the geotectonic setting of the Arroyo del Soldado basin (Gaucher, 2000).

The ASG is notable for its extensive and very thick carbonate deposits, namely (a) the Polanco Formation, more than 900 m in maximum thickness, (b) the Cerro Victoria Formation (CVFm), composed of up to 400 m of stromatolitic, oolitic and micritic limestones, and (c) various isolated dolostone and limestone strata in the lower Cerro Espuelitas Formation and upper Yerbal Formation (Fig. 1). Carbon and oxygen isotopic data from carbonates of the ASG have been previously reported by Boggiani (1998), Kawashita et al. (1999), Gaucher (2000) and Gaucher et al. (2002, 2003). Kawashita el al. (1999) present four Sr-isotopic determinations from the lowermost Polanco Formation. We report here the results of a series of 32 C- and O-isotopic determinations on carbonates of the CVFm, which imply that the Precambrian/Cambrian boundary is located in the upper ASG.

CERRO VICTORIA FORMATION

Montaña & Sprechmann (1993) were the first to recognize the existence of stromatolitic communities in Uruguay, which were grouped into the Cerro Victoria Member. Gaucher et al. (1996) give this unit the rank of a formation and include it in the Arroyo del Soldado Group. The main outcrop area is located approximately 8 km NW of the town of Illescas, in the Florida Department. The contact of the CVFm with the underlying Cerros San Francisco Formation is transitional (Figs. 1, 2), and is characterized by the occurrence of mature, medium-grained quartz-arenites, followed by sandstone interbedded with centimetric limestone beds and stromatolites, which sometimes exceed 1,5 m in diameter. Up section, ca. 150 m of planar and LLH-S stromatolites interbedded with micritic, gray limestones occur. Sheet-like bioherms up to 4 m in height occur, alternating with deeper water ramp muds. The middle part of the unit presents mainly planar, but also domic and columnar stromatolites interbedded with subordinate oolitic calcarenites and micritic limestones. Domic stromatolites reach maximum diameters of 0.75 m. The upper 150 m are formed by almost pure stromatolitic limestones. Stromatolites in growth position and up to 1 m in diameter predominate, including microdigitate forms, and are often partially silicified. Broken fragments and stromatolitic breccias also occur. Micritic limestones are rare, as well as black cherts containing abundant organic mater. Trace fossils occur in this part, burrows reaching large diameters of 4 - 7 cm by diagenetic growth, representing concretions formed by replacement of the micrites by fine-grained flint. Finally, in the uppermost 30-50 m, micritic limestones become again more abundant and are interbedded with planar stromatolites.

Colour of carbonates is mainly pale red to purple at the base, reddish gray to medium gray in the middle and light gray at the top (Fig. 2). Micritic limestones are common at the base of the CVFm, becoming rarer up section. Montaña and Sprechmann (1993) interpreted the CVFm as a shallowing-upward sequence, but there seems to be more than one superimposed cycle. The unit records shallow subtidal to supratidal conditions. Palaeobathymetry is remarkably stable throughout the unit, with a tendency to slightly shallower environments towards the top. This fact indicates that sedimentation rate matched subsidence in the latest Arroyo del Soldado basin. Occurrence of evaporites (halite and possibly gypsum), oolites and common dessiccation (tepee) structures indicate a tropical climate for the CVFm.

AGE OF THE ASG

Age of the ASG is geochronologically constrained by: (a) a maximum U-Pb SHRIMP II age of 633 ± 12 Ma for the Puntas del Santa Lucía pluton (Bossi et al., 2001), which is overlain with erosional unconformity by the ASG; and (b) a minimum Rb-Sr isochron age for the Guazunambí Granite of 532 ± 11 Ma (Ro=0.70624: Kawashita et al., 1999), which intrudes into the ASG causing contact-metamorphism. Biostratigraphic data also point to an upper Vendian age for the lower-middle ASG, and a lowermost Cambrian age for the CVFm (Fig. 1). An assemblage of skeletal fossils containing *Cloudina riemkeae* Germs, *Titanotheca coimbrae* Gaucher and Sprechmann (1999) and at least five other genera- and species occurs in the uppermost Yerbal Formation of the ASG (Gaucher and Sprechmann, 1999; Gaucher, 2000; Fig. 1). *Cloudina* is recognized as an index-fossil of the upper Vendian (Grant, 1990), and has a global distribution in rocks of that age. A low-diversity, high-abundance assemblage of organic-walled microfossils is preserved in the ASG as well (Gaucher et al., 1996, 1998; Gaucher, 2000). The genera *Bavlinella* and *Soldadophycus* are dominant in the siliciclastic units (Gaucher, 2000), while in the Polanco Formation a slightly more diverse assemblage (*Leiosphaeridia-Lophosphaeridium* assemblage) occurs. These data are in accordance with an upper Vendian age for the lower-middle ASG, specially considering the absence of large sphaeromorphs and acantomorphs (Knoll, 2000).

The CVFm has been placed in the lowermost Cambrian using following criteria:
(a) Large ichnofossils with complex burrow systems, classified by Sprechmann et al. (submitted) as *Thalassinoides* igen, occur . This behavioural pattern is absent in the Proterozoic (Crimes, 1992), and indicates a maximum Cambrian age for the CVFm. They are associated to other ichnofossils whose ichnofabrics follow the characteristic lowermost Cambrian pattern (Droser et al., 2002); (b) absence of *Conophyton*, a characteristic stromatolite morphogroup of the Proterozoic, which disappears in the Cambrian (Altermann, 1999); (c) the low-diversity stromatolite community, formed by non-branched morphogroups, is typical for Upper Vendian and Phanerozoic communities (Altermann, 1999; Pratt et al., 2001); (d) thrombolites occur, which were rare in the Proterozoic but abundant in the early Paleozoic (Pratt et al., 2001); and (e) tropical climate reported for the CVFm (Montaña and Sprechmann, 1993) correlates better with the Lower Cambrian global warming.
Deposition of the CVFm must, therefore, have taken place in the Nemakit-Daldyn stage. Chemostratigrapic data presented below confirm this age assignment.

CHEMOSTRATIGRAPHY

We sampled continuous sections of the CVFm at its stratotype, located along the Arroyo de la Pedrera. A negative $\delta^{13}C$ excursion (-0.5 ‰ PDB) is recorded at the Cerros San Francisco-Cerro Victoria contact (Fig. 2). Up section, values become more negative, reaching a plateau around -1.0 to -1.3 ‰ PDB. After ca. 110 m of carbonates yielding negative $\delta^{13}C$ values, a transition to positive values around +0.3 ‰ PDB is recorded. This positive excursion shows fairly constant values for ca. 180 m of mainly stromatolitic carbonates (Fig. 2). Peak values occur 300 m above the base of the CVFm, yielding +0.64 ‰ PDB. Up section, low-amplitude oscillations are recorded in trace fossil-bearing limestones. Finally, negative values of up to -1.1 ‰ PDB characterize uppermost carbonates of the CVFm, concomitant to an increase in the frequency and thickness of intercalated micritic limestone beds.

$\delta^{18}O$ values show no direct relationship with $\delta^{13}C$ in the section studied (Fig. 2), implying that $\delta^{13}C$ values in most of the analyses reported here represent primary or near-primary isotopic ratios.

DISCUSSION

The $\delta^{13}C$ curve obtained for the CVFm is remarkable for the low amplitude of the oscillations observed, around 2 ‰ PDB. This situation contrasts with values obtained for the lower and middle Arroyo del Soldado Group, in which a series of impressive, large amplitude $\delta^{13}C$ excursions (up to 9 ‰ PDB) occur (Fig. 1). In fact, $\delta^{13}C$ oscillations show a persistent tendency towards smaller amplitudes towards the top. Falling amplitudes of $\delta^{13}C$ excursions characterize Vendian to Lower Cambrian successions worldwide (Derry et al., 1994; Knoll, 2000; Walter et al., 2000). A Vendian age for the Yerbal, Polanco and Cerro Espuelitas Formations is further indicated by biostratigraphic data (see above) and $^{87}Sr/^{86}Sr$ determinations (Kawashita et al., 1999). Gaucher et al. (2002) interpreted $\delta^{13}C$ data of the lower ASG as consistent with the global $\delta^{13}C$ curve for the late Vendian. The data presented here for the CVFm strongly resemble $\delta^{13}C$ curves of lowermost Cambrian (Nemakit-Daldyn) carbonates in Siberia (Yudoma Formation: Derry et al., 1994), Mongolia (Brasier et al., 1996) and Argentina (lower La Laja Formation: Sial et al., 2003). According to the detailed $\delta^{13}C$ curve presented by Derry et al. (1994: fig. 5) for carbonates from the Siberian craton, the CVFm spans the interval 540-533 Ma. Geochronologic constraints of the mentioned curve rely on many U-Pb zircon dating coupled with detailed biostratigraphic data (Bowring et al, 1993; Brasier, 1996).

Given the above interpretation of the negative $\delta^{13}C$-excursion of the basal CVFm as representing the upper part of the negative W anomaly of Brasier and Lindsay (2001), the Precambrian/Cambrian boundary might be, therefore, preserved in the upper-middle Cerros San Francisco Formation. Absence of carbonates in the unit prevent the precise location of the boundary with chemostratigraphic tools, but micropalaeontology might, however, enable determination of its position. These results are encouraging, because they imply that the boundary is actually preserved in the ASG, contrary to previous suggestions that located it at the basal erosional unconformity of the Cerros San Francisco Formation, as known from many succesions elsewhere (Brasier and Lindsay, 2001).

CONCLUSIONS

C- and O-isotopic data for the Cerro Victoria Formation are discussed in the framework of previously reported C-, O- and Sr-isotopic data for the lower-middle ASG. $\delta^{13}C$ values are interpreted to represent primary or near-primary seawater composition. Falling amplitudes of $\delta^{13}C$ fluctuations recorded in these carbonates are in accordance with the trend observed in Vendian-Lower Cambrian successions worldwide. The curve obtained for

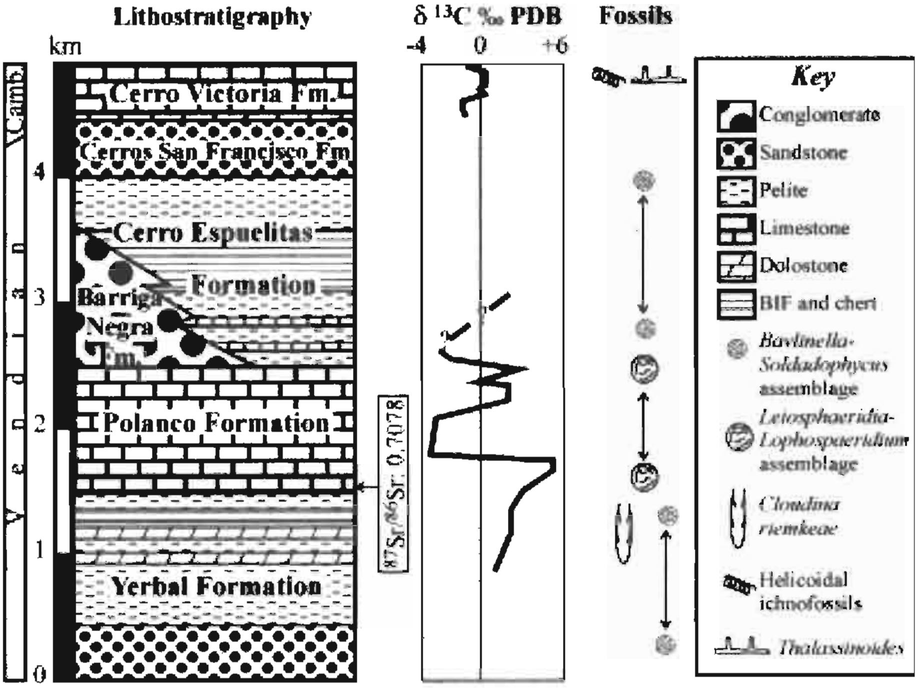

Figure 1. Litho, bio and chemostratigraphy of the Arroio del Soldado Group.

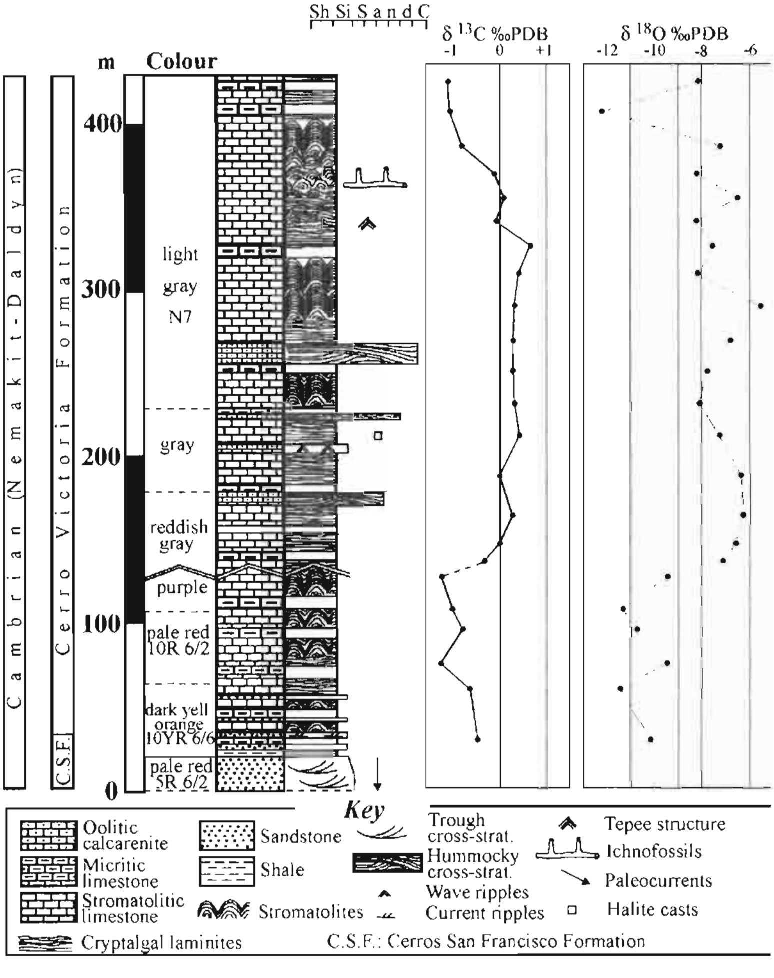

Figure 2. Stratigraphy collumn of the Cerro Victoria Formation, showing C- and O- isotopic data.

the Cerro Victoria Formation parallels curves reported for the Nemakit-Daldyn stage of the Lower Cambrian. Considering the detailed carbon isotopic data from Lower Cambrian carbonates of Siberia (Derry et al., 1994; Brasier and Lindsay, 2001), the Cerro Victoria Formation was entirely deposited in the lower-middle Nemakit-Daldyn stage, between 540-533 Ma. In South America, carbonates of the lowermost La Laja Formation (Argentine Precordillera) show similar $\delta^{13}C$ values. On the basis of the above mentioned data, we suggest that the Precambrian/Cambrian boundary is located in the upper-middle Cerros San Francisco Formation of the ASG. This implies that the ASG is one of the few units worldwide, where this important boundary is preserved. More biostratigraphic and Sr-isotopic data are required, however, to precisely locate this important event.

ACKNOWLEDGEMENTS

This study is part of project AC-38/2002, financed by PROSUL/CNPq, involving researchers from Brazil, Argentina, Chile and Uruguay. Further funding by research project CONICYT 6007 to C.G. is gratefully acknowledged. This is a contribution to Project IGCP 478 "Neoproterozoic-Early Palaeozoic Events in SW-Gondwana".

REFERENCES

Altermann, W. (1999) Die Sedimente der Transvaal Supergruppe, Kaapvaal Kraton, Südafrika: Stromatolithenfazies, Beckenanalyse und regionale Entwicklung im Neoarchaikum und Paläoproterozoikum. Münchner Geol. Hefte, A 25: 1-140.

Boggiani, P. C. (1998) Análise estratigráfica da Bacia Corumbá (Neoproterozoico)- Mato Grosso do Sul.- Unpublished Ph. D. thesis, Universidade de São Paulo, Brazil.

Bossi, J., Campal, N., Hartmann, L.A. and Schipilov, A. (2001) Predevoniano en el Uruguay: terrenos y SHRIMP II.- XI Congreso Latinoamericano y III Congreso Uruguayo de Geología, Actas (CD-ROM), Montevideo, Nr. 94.

Bowring, S.A., Grotzinger, J.P., Isachsen, C.E., Knoll, A.H., Pelechaty, S.A. and Kolosov, P. (1993) Calibrating rates of Early Cambrian evolution. Science, 261: 1293-1298.

Brasier, M.D. (1996) U/Pb dates for the base of the terminal Proterozoic and Cambrian. Episodes, 19 (3).

Brasier, M.D., Dorjnamjaa, D., and Lindsay, J.F. (1996) The Neoproterozoic to early Cambrian in southwest Mongolia: an introduction. Geol. Mag., 133: 365-369.

Brasier, M.D., and Lindsay, J.F. (2001) Did supercontinental amalgamation trigger the "Cambrian Explosion" ? In: Zhuravlev, A.Yu. and Riding, R. (Eds.), The Ecology of Cambrian Radiation. Columbia Univ. Press, New York, pp. 69-89.

Crimes, P.T. (1992) The record of trace fossils across the Proterozoic-Cambrian boundary. In: Lipps, J.H. and Signor, P.W. (Eds.), Origin and early evolution of the Metazoa. Plenum Press, pp. 177-202.

Derry, L.A., Brasier, M.D., Corfield, R.M., Rozanov, A.Yu., and Zhuravlev, A.Yu. (1994) Sr and C isotopes in Lower Cambrian carbonates from the Siberian craton: A paleoenvironmental record during the "Cambrian explosion". Earth Planet. Sci. Lett., 128:671-681.

Droser, M. L., Jensen, S., Gehling, J.G., Myrow, P.M. and Narbonne, G.M. (2002) Lowermost Cambrian Ichnofabrics from the Chapel Island Formatiion, Newfoundland: Implications for Cambrian Substrates. Palaios, 17: 3-15.

Gaucher, C. (2000) Sedimentology, palaeontology and stratigraphy of the Arroyo del Soldado Group (Vendian to Cambrian, Uruguay).-Beringeria, 26: 1-120.

Gaucher, C.; Sprechmann, P. and Schipilov, A. (1996) Upper and Middle Proterozoic fossiliferous sedimentary sequences of the Nico Pérez Terrane of Uruguay: Lithostratigraphic units, paleontology, depositional environments and correlations.- Neues Jahrbuch für Geologie und Paläontologie, Abhandlungen, 199: 339- 367.

Gaucher, C.; Sprechmann, P. and Montaña, J. (1998) New advances on the geology and paleontology of the Vendian to Cambrian Arroyo del Soldado Group of the Nico Pérez Terrane of Uruguay.- Neues Jahrbuch für Geologie und Paläontologie, Monatshefte, 1998: 106- 118.

Gaucher, C.; Sprechmann, P. (1999) Upper Vendian skeletal fauna of the Arroyo del Soldado Group, Uruguay.- Beringeria, 23: 55-91.

Gaucher, C.; Sial, A.N.; Blanco, G. and Sprechmann, P. (2002) Chemostratigraphy of the lower Arroyo del Soldado Group (Vendian, Uruguay): a potential reference section for W-Gondwana and its implications. In: Gaucher, C. (Ed.), II International Colloquium Vendian-Cambrian of W-Gondwana, Extended Abstracts, Facultad de Ciencias-UNESCO, Montevideo, pp. 21-24.

Gaucher, C., Boggiani, P.C., Sprechmann, P., Sial, A.N. and Fairchild, T.R. (2003): Integrated correlation of the Vendian to Cambrian Arroyo del Soldado and Corumbá Groups (Uruguay and Brazil): palaeogeographic, palaeoclimatic and palaeobiologic implications.-Prec. Res., 120: 241-278 .

Grant, S.W.F. (1990) Shell structure and distribution of *Cloudina*, a potential index fossil for the terminal Proterozoic.-Am. Jour. Sci., v. 290-A, pp. 261-294.

Kawashita, K.; Gaucher, C.; Sprechmann, P.; Teixeira, W. and Victória, R. (1999) Preliminary chemostratigraphic insights on carbonate rocks from Nico Pérez Terrane (Uruguay).- Actas II South American Symposium on Isotope Geology, 399-402; Córdoba (Argentina)..

Knoll, A.H. (2000) Learning to tell Neoproterozoic time.- Precamb. Res., 100: 3-20.

Montaña, J. and Sprechmann, P. (1993) Calizas estromatolíticas y oolíticas y definición de la Formación Arroyo de la Pedrera (?Vendiano, Uruguay). Rev. Bras. de Geoc., 23: 306-312.

Pratt, B.R., Spincer, B.R., Wood, R.A. and Zhuravlev, A.Yu. (2001) Ecology and Evolution of Cambrian Reefs. In: Zhuravlev, A.Yu. and Riding, R. (Eds.), The Ecology of Cambrian Radiation. Columbia Univ. Press, New York, pp. 254-274.

Sial, A.N., Peralta, S., Ferreira,V.P., Toselli, A.J., Aceñolaza, F.G., Parada, M.A., Gaucher, C., Alonso, R.N., and Pimentel, M.M. (2003) C-, O- and Sr-isotope chemostratigraphy of Cambrian carbonate sequences, Precordillera, western Argentina. IV SSAGI, Salvador (this volume).

Sprechmann, P., Gaucher, C, Blanco, G. and Montaña, J. (submitted) Stromatolitic and Trace Fossils Community of the Cerro Victoria Formation, Arroyo del Soldado Group (lowermost Cambrian, Uruguay). Gondwana Research.

Walter, M.R.; Veevers, J.J.; Calver, C.R.; Gorjan, P. and Hill, A.C. (2000) Dating the 840-544 Ma Neoproterozoic interval by isotopes of strontium, carbon and sulfur in seawater, and some interpretative models.- Prec. Res., 100:371-433.

ISOTOPIC AND DIAGENETIC CONSTRAINTS OF THE NEOPROTEROZOIC VILLA MONICA AND LOMA NEGRA FORMATIONS, TANDILIA SYSTEM, ARGENTINA – FIRST RESULTS

Gómez Peral, L.[1,2]**; Poiré, D.G.**[1]**; Strauss, H.**[3] **and Zimmermann, U.**[2]

1. Centro de Investigaciones Geológicas, CONICET-UNLP,1 N° 644, 1900 La Plata, Argentina. poire@cig.museo.unlp.edu.ar
2. Department of Geology, RAU University, Auckland Park 2006, Johannesburg, South Africa. uz@na.rau.ac.za
3. Geologisch-paläontologisches Institut, Westfälische-Wilhelms-Universitäti Münster, Corrensstrasse 24, 48149 Münster, Germany

Keywords: Carbonate rocks, stable isotopes, diagenesis, Upper Precambrian, Tandilia system

INTRODUCTION

The objective of this case study in Argentine Neoproterozoic successions is twofold. On one hand we want to add stable isotope data combined embedded in a diagenetic study to correlate these outcrops with similar lithologies of the Neoproterozoic world-wide.

The Tandilia System is a 350 km long, northwest-southeast orientated orographic belt, located in the Province of Buenos Aires (Fig. 1), which is comprised by an igneous metamorphic basement and a Neoproterozoic to Lower Palaeozoic sedimentary cover. In the Olavarría area, this Neoproterozoic sedimentary succession is composed of the Villa Mónica, Cerro Largo and Loma Negra formations (Sierras Bayas Group) and the Cerro Negro Formation (Poiré, 1993; see Fig. 2). These lithostratigraphic units were grouped into four depositional sequences: Tofoletti (I), Malegni (II) Villa Fortabat (III) and La Providencia (IV) sequences (Spalletti and Poiré, 2000).

The Neoproterozoic rocks are not affected by metamorphism, nearly undeformed and overlying unconformably basement rocks.

The oldest depositional sequence (Tofoletti, 52 m thick; Fig. 2) is equivalent to the Villa Mónica Formation, and shows two sedimentary facies associations: (a) quartz-arkosic arenites at the base and (b) dolomites including shallow marine stromatolitic dolomites and shales at the top. The dolomites and shales facies association (36 m thick), is composed by laminated stromatolitic dolomites, interdolomitic green shales and supradolomitic red shales with associated mudstones. Eight sedimentary facies have been recognized along these vertical sections. The dolostones of the Villa Mónica Formation support a very good assemblage of stromatolites, which is composed of *Colonella* fm., *Conophyton ?resotti*, *Conophyton* fm., *Cryptozoon* fm., *Gongylina* fm., *Gymnosolem* fm., *Inzeria* fm., *Jacutophyton* fm., *Jurusonia nisvensis*, *Katavia* fm., *Kotuikania* fm., *Kussiella* fm., *Minjaria* fm., *Parmites* fm., *Parmites* cf. *cocrescens* and *Stratifera* fm. (Poiré, 1993). An 800-900 Ma age for the stromatolite assemblage of Villa Mónica Formation has been suggested by Poiré (1987, 1989, 1993), based on world-wide stromatolite biostratigraphy (e.g. Semikhatov, 1986).

The 793 ± 32 Ma radiometric age (Cingolani and Bonhomme, 1988), for the diagenesis of Villa Mónica Formation coincide with the proposed age of the stromatolites by Poiré (1993).

The second depositional sequence (Malegni, 75 m thick; Fig. 2) consists of a basal succession composed of chert breccia, fine-laminated glauconitic shales, and fine-grained sandstones, followed by cross-bedded quartz arenites which are in turn covered by siltstones and claystones. This sequence represents a shallowing upward succession from subtidal nearshore to intertidal flat deposits. A depositional age of older than 730 Ma has been interpreted by Rb-Sr analyses on whole rock samples (e.g. Kawashita et al., 1999).

The youngest pre-Vendian depositional sequence (Villa Fortabat; Fig.2) is a 40 m thick unit composed almost exclusively of brownish (lower section) and black (upper) micritic limestones, originated by suspension fall-out in open marine ramp and lagoonal environments.

On top of the Sierras Bayas Group a regional unconformity is recognised (Barrio et al., 1991). This surface has been related to a eustatic movements. Meteoric dissolution of the carbonatic sediments is interpreted as a karstic surface on which residual clays and brecciated chert have been accumulated.

The Vendian Cerro Negro Formation (La Providencia depositional sequence; Fig. 2) appears on top of the above described unconformity. It is a more than 100 m thick unit characterised by claystones and heterolithic fine-grained sandstone-claystone intercalations, mainly formed in upper to lower intertidal flats. The lower part is composed by marls and mudstones (Fig. 2). Through radiometric dating on whole rock samples with Rb-Sr a depositional age older than 730 Ma could be established (Kawashita et al., 1999).

DIAGENESIS AND C-O ISOTOPES

The dolomites of the Villa Mónica Formation show a complex diagenetic history. The early diagenetic dolomite mosaic has grown from primitive LMC (protonuclei), placing them in the field of secondary dolomites. Later, different cements filled voids and fractures, and could be differentiated in three principal stages:

(1) Dolomitic cement constituted by macrosparitic rombohedral crystals of dolomite, partly with an iron-rich nuclei, and sizes between 200 to 750 µm, coating the pore walls.

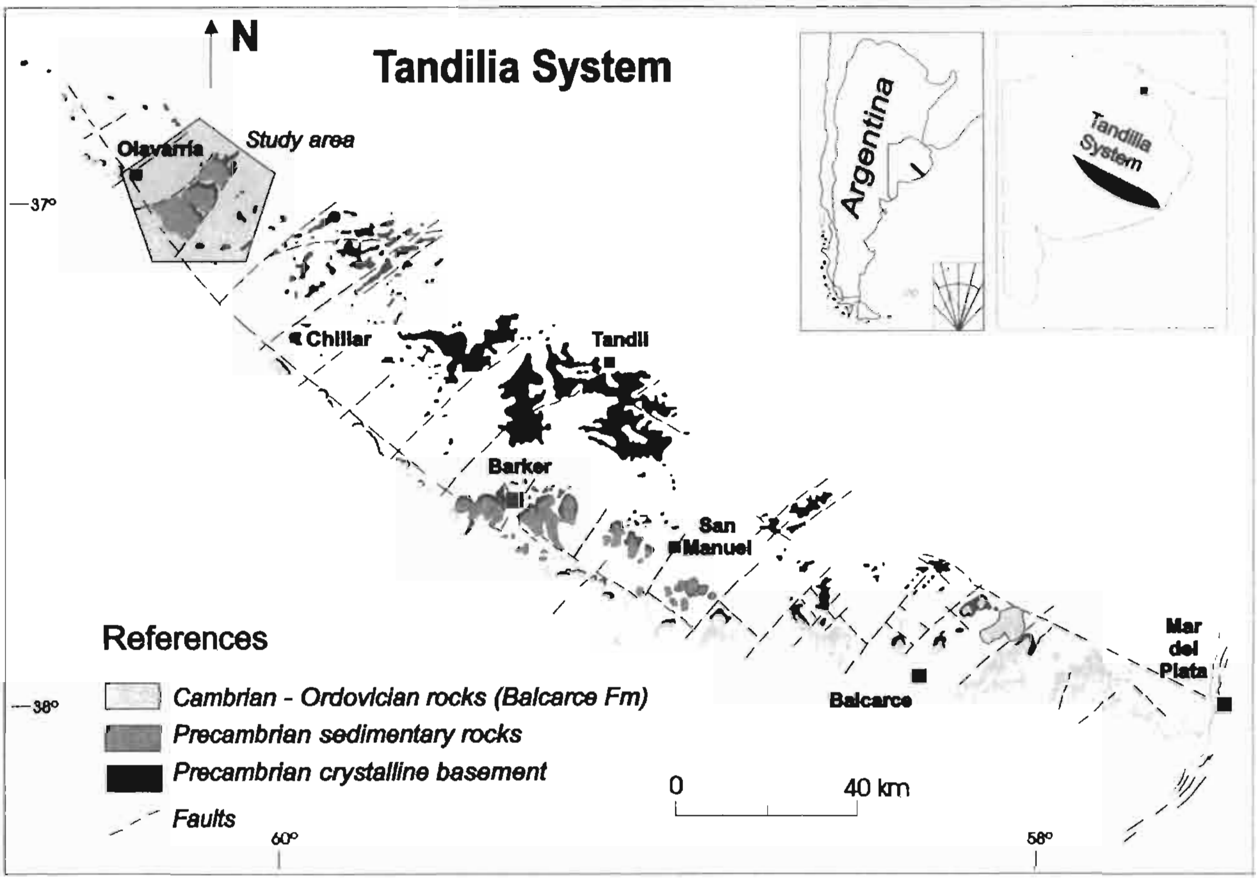

Figure 1. Location map (after Poiré et al., 2003).

(2) Silica cement which covers the porewalls in a geode form, closing partly or completely the pore space.

(3) High-Mg-calcite cement grew as anhedral to euhedral macrosparitic crystals.

These cements are filling voids and fractures up to 15 cm in diameter, and their origin have not been determined yet.

The limestones show homogeneous micritic to sub-sparitic calcite with a xenotopic texture. Microprobe analysis shows that crosscutting veins are filled by sparitic to sub-sparitic calcite and very fine-grained chert. While, irregular stylolites are filled by illite, chlorite and different Fe-oxides. The following diagenetic processes are interpreted:

(1) Chemical dissolution that generates veins and cavities.

(2) Cementation of voids and cavities by calcite cements.

(3) Pressure solution which produces the irregular stylolites and their mineralogical components.

(4) Silicification by the precipitation of silica gels along the veins and as replacement of carbonate crystals.

However, the silicification processes have affected more intensively the upper section (black micritic limestone) than the lower section (brownish micritic limestone).

Using CL two different classes of veins could be classified. One generation (< 250µm wide) shows a very low orange luminescent calcite, and a second generation (±30 µm wide), which crosscuts the first, and contains bright yellow luminescent calcite. The veins are mostly vertical to the stratification and could reflect extensional conditions probably caused by diagenesis.

The carbonate rocks of the Loma Negra Formation (Fig. 2) contain a TOC (total organic carbon) value between -0.15% and 0.35%, TIC (total inorganic carbon) between 8.41% and 11.30%, TC between 8.42% and 11.58%. $\delta^{13}C_{Carb}$ between +2.77 and +4.54‰, and $\delta^{18}O_{Carb}$ between -14.13 and -7‰. These data are only slightly different from preliminary values measured by Valencio (1985). The $\delta^{13}C_{org}$ lies constantly between -27.1 and -28.1‰.

The dolomites of the Villa Mónica Formation show TOC value between 0.37% and %1.22, TIC between 3.97% and 11.89%, and TC between 4.34% and 12.79%.

In a $\delta^{13}C_{Carb}$ - $\delta^{18}O_{Carb}$ diagram (Fig. 3) from Loma Negra Formation it is possible to distinguish three fields, according to the kind of rock analyzed: brownish micritic limestones, ii) black micritic limestones, and iii) red marls.

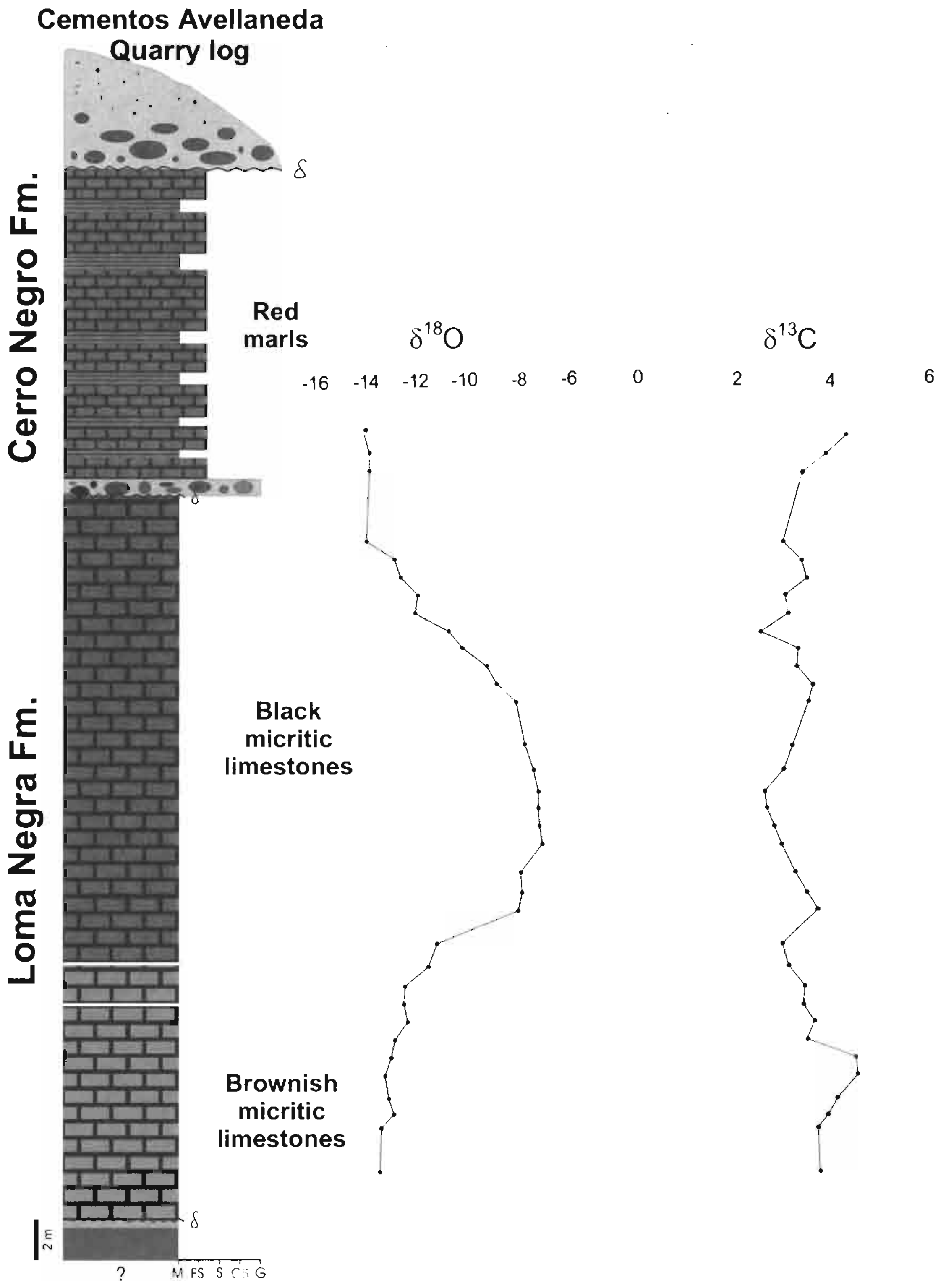

Figure 2. Stratigraphic framework and $\delta^{13}C_{Carb}$ - $\delta^{18}O_{Carb}$ (°/oo PDB) isotope curves from the Cementos Avellaneda quarry, Olavarría.

DISCUSSION

In figure 2, the C-O isotopic values are correlated with the stratigraphic framework: Loma Negra Formation and its transition to Cerro Negro Formation.

First, preliminary stable isotope data from the upper cycle (Loma Negra Formation) shows that the $\delta^{18}O_{carb}$ (‰) values are all negatives but in the middle part of the profile the curve shows a less negative excursion. The curve of $\delta^{13}C$ show very low fluctuations, however, it is possible to observe an increase (peak) in the brownish micritic limestones and two negative peaks in the black micritic limestones.

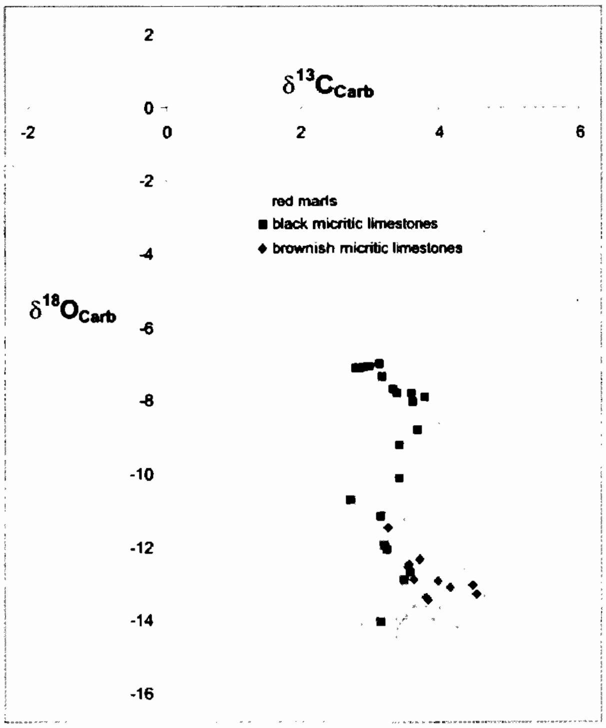

Figure 3. $\delta^{13}C_{Carb}$ versus $\delta^{18}O_{Carb}$ (°/₀₀ PDB) plot of samples from Loma Negra Formation and its transition to Cerro Negro Formation.

These $\delta^{13}C_{Carb}$ - $\delta^{18}O_{Carb}$ values are quite similar to those from Sete Lagoas Formation, Bambuí Group, Brazil (Santos et al., 2000), Polanco Formation, Arroyo del Soldado Group, Uruguay (Kawashita et al., 1999) and the Upper Proterozoic successions in Namibia (Kaufman, 1999), which were part of the South-western Gondwana margin during the Upper Proterozoic.

Further investigation on C-O isotopes of the lower cycle (Villa Mónica Formation) and the major and trace element geochemistry of the carbonates and the siliciclastic sedimentary record as well as detailed microprobe analysis on single grains will give more insight in the complex diagenetic history and the source areas for the clastic rocks. C-O-S data for the whole group and combined with a provenance analysis of the clastic record will complete this study in the near future to correlate the section with those in Brazil, Uruguay and southern Africa.

REFERENCES

Barrio C.A., Poiré D.G. y Iñiguez M.A., 1991. El contacto entre la Formación Loma Negra (Grupo Sierras Bayas) y la Formación Cerro Negro, un ejemplo de paleokarst, Olavarría, prov. de Bs. As. Revista de la Asociación Geológica Argentina XLVI(1-2): 69-76.

Cingolani, C. and Bonhomme, M.G., 1988. Resultados geocronológicos en niveles pelíticos intercalados en las dolomías de Sierras Bayas (Grupo La Tinta), provincia de Buenos Aires. Actas Segundas Jornadas Geológicas Bonaerences :283-289.

Kaufman, A.J., Hayes, J.M., Knoll, A.H. and Germs, G.J.B., 1991. Isotopic compositions of carbonates and organic carbon from Upper Proterozoic successions in Namibia: stratigraphic variations and the effects of diagenesis and metamorphism. Precambrian Research 49: 301-327.

Kawashita, K., Gaucher, C., Sprechman, P., Teixeira, W. And Victória, R., 1999. Preliminary chemostratigraphic insights on carbonate rocks from Nico Pérez terrane (Uruguay). Actas II South American Symposium on Isotope Geology :399-402.

Kawashita, K., Varela R., Cingolani C., Solían E., Linares, E., Valencio, S. A., Ramos, A. V. and Do Campo, M. 1999. Geochronology and Chemostratigraphy of "La Tinta" Neoproterozoic Sedimentary rocks, Buenos Aires Province, Argentina. Actas II South American Symposium on Isotope Geology :403-407.

Poiré D. G., 1987. Mineralogía y sedimentología de la Formación Sierras Bayas en el Núcleo Septentrional de las sierras homónimas, partido de Olavarría, provincia de Buenos Aires. Facultad de Ciencias Naturales y Museo, Universidad Nacional de La Plata, Tesis Doctoral 494 (unpublished).

Poiré D. G., 1989. Stromatolites of the Sierras Bayas Group, Upper Proterozoic of Olavarría, Sierras Septentrionales, Argentina. Stromatolite Newsletter XIV:58-61.

Poiré, D.G., 1993. Estratigrafía del Precámbrico sedimentario de Olavaria, Sierras Bayas, Provincia de Buenos Aires, Argentina. Actas XII Congreso Geológico Argentino y II Congreso de Exploración de Hidrocarburos II: 1-11.

Poiré, D.G., Spalletti, L.A.and Del Valle, A,.2003. The Cambrian-Ordovician siliciclastic platform of the Balcarce Formation (Tandilia System, Argentina): facies, trace fossils, palaeoenvironments and sequence stratigraphy. Geologica Acta 38(1): 41-60.

Santos, R. V., Alvarenga C. J. S., Dardenne M. A., Sial A. N., Ferreira V. P. 2000. Carbon and oxygen isotope profiles across Meso-Neoproterozoic limestones from Central Brazil: Bambuí and Paranuá groups. Precambrian Research 104: 107-122

Semikhatov, M.A. 1976. Experiences in stromatolite studies in the USSR. In M.R. Walter (Ed.), Stromatolites. Elsevier :337-357, Amsterdam.

Spalletti, L. A., Poiré, D. G., 2000. Secuencias silicoclásticas y carbonáticas del Precámbrico y Paleozoico inferior del Sistema de Tandilia, Argentina. II Congreso Latinoamericano de Sedimentología y VIII Reunión Argentina de Sedimentología, Guía de Campo, 39 pp.

Valencio S., Linares, E. and Panarello, H. O., 1985. Composición isotópica del carbono y oxígeno de rocas carbonáticas de las Sierras Septentrionales de la Provincia de Buenos Aires. Evidencias de cambios post-deposicionales. . (Tandil). Comisión de Investigaciones Científicas, Actas I Jornadas Geológicas Bonaerenses I: 51-67. La Plata.

DIAGENETIC MODEL FOR BEACHROCKS OF THE ALAGOAS STATE, NORTHEASTERN BRAZIL: ISOTOPIC AND PETROGRAPHIC EVIDENCE

Guerra, N.C.[1] **and Sial, A.N.**[2]

[1] Bolsista RD-CNPq, Stable Isotope Laboratory (LABISE), Depto. Geologia, UFPE, Recife-PE, Brazil, 50732-970.
nschaves@ufpe.br
[2] NEG-LABISE, Depto. Geologia, UFPE, C.P. 7852, Recife-PE, Brazil, 50732-970

Keywords: Beachrocks, diagenesis, C – O stable isotopes, Brazilian littoral, Quaternary rocks

INTRODUCTION

Beachrocks have been widely recognized in the Brazilian littoral. A number of theories have been invoked to explain the origin of the beachrock cement, including precipitation at the water table, precipitation from mixed meteoric and marine waters, and precipitation directly from seawater. A detailed petrographic and isotopic analysis of beachrock was conducted to determine the origin of these deposits and to identify processes responsible for their early diagenetic alteration.

The littoral of the state of Alagoas (Fig. 1), likewise the littoral of Pernambuco, is limited by a relative shallow shelf, which supports a wide variety of carbonate-producing organic communities. Coastal landforms range from cliffs of sandy beaches between rocky headlands.

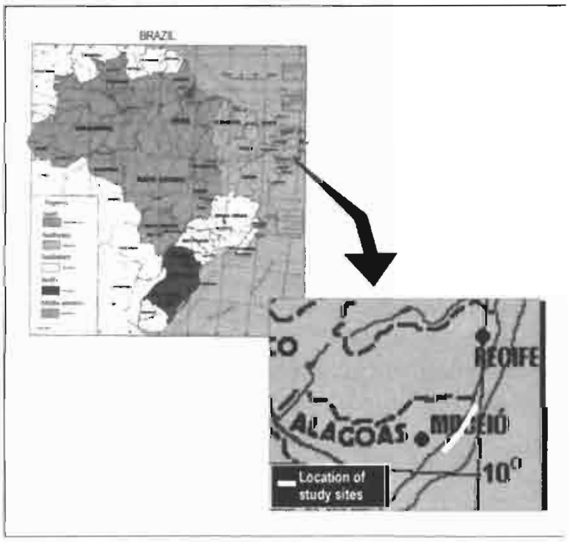

Figure 1. Location map.

Many of these beaches favor beachrock increase. Younger beachrock units are forming in the intertidal zone. These comprise 40-50 cm thick, indurated slabs of beach sand, jointed normal and parallel to the shoreline, which slope 5° to 10° seaward. Exposures begin at the high-tide level and may extend a few meters seaward of low-tide level. Beachrock surfaces grade from yellow in the lower-intertidal zone to brown in the upper-intertidal zone, a color zonation that has been attributed to the types of algae that colonize the beachrock. These surfaces are commonly pitted from the grazing of gastropods that feed upon algae. Larger pits (up to 50 cm in diameter) are probably erosion features. These are commonly filled with debris such as broken glass and bits of steel which are cemented to the bottoms of the pits. Sediment grains in beachrock are identical to those of adjacent, unlithified beach sands, consisting of foraminifers, bivalve, gastropod, red and green algal, coral fragments, as well as lithoclasts. Grain sizes range from fine to very coarse sand. Large slabs of beachrock and other rock types may also be cemented onto the beachrock surface, forming an intertidal conglomerate.

High temperatures and rates of evaporation on the beach evidently create ideal environments for inorganic carbonate precipitation just below the sediment/water interface. The conditions for precipitation may be augmented further by daily metabolic activity of endolithic algae or other microorganisms known to colonize carbonate sediments once they have been stabilized by early cementation.

DIAGENETIC FACIES

Petrographic and isotopic analyses of cements and other early diagenetic features furnish a basis for the classification of the beachrocks of Alagoas. These features reflect the age and diagenetic history of the beachrocks.

Beachrock of the Alagoas littoral are nearly identical in outcrop appearance. Petrographically, this beachrock is characterized by high-calcite cement, micritized grains, and micritic envelopes, all of which are products of marine-phreatic diagenesis. Carbon and oxygen isotopic compositions of beachrock and uncemented sand are nearly identical; $\delta^{13}C$ is approximately +3.0‰$_{PDB}$, and $\delta^{18}O$ is approximately –0.1‰$_{PDB}$ (Table 1).

Table 1. $\delta^{13}C$ and $\delta^{18}O$ values are given as ‰ vs. the PDB standard.

Sample Location	$\delta^{18}O_{PDB}$	$\delta^{13}C_{PDB}$
Pontal 1	-0.37	+2.55
Pontal 2	+0.04	+2.59
Pontal 3	-0.24	+2.92
Pontal 4	-0.08	+2.52
Bitingui	-0.48	+1.90
Japaratinga	-5.69	-8.10
Marceneiro	-0.07	+2.14
São Bento	-0.19	+3.24

Many beachrock allochems are partially to completely micritized. Micritization of grains is most extensive at, and in some cases limited lo, grain boundaries, and results in development of a micritic rim or envelope around each grain.

Evidence of endolithic activity is extensive in beachrock. Small pits are apparent in thin sections. In addition, algal filaments are common in intertidal beachrock. In some cases, these occupy microborings.

The exclusive presence of high-calcite cement in the beachrock suggests that lithification of beach sediments is predominantly a marine process. There is no petrographic evidence of meteoric groundwater influence in the precipitation of these beachrock cements and, therefore, no need to invoke seawater/groundwater mixing models to explain the cementation process. The isotopic composition of cement also indicates precipitation from normal seawater. The rapid growth of calcite crystals in beach sediments is readily accounted for in terms of seawater supersaturation and enhancement of conditions for precipitation by elevated temperature, evaporation, and perhaps by fluctuations of pH and P_{CO_2} due lo photosynthesis by algae living in and on the sediment grains.

The algae are also responsible for micritization. The formation of micritic cement has long been attributed to the filling of algal borings with minute crystals of secondary calcium carbonate. In some beachrocks, micrite suggest two separate phases of endolithic activity followed by growth of calcite cement.

DIAGENETIC MODEL

The diagenetic cements of intertidal beachrock indicate sediment alteration in a variety of diagenetic environments. Relict micritic rims, although rare, indicate early diagenesis in a marine-phreatic environment. Blocky spar cements are characteristic of meteoric-phreatic diagenesis. This environment must have developed after early diagenesis in the marine-phreatic zone, because neomorphic calcite replaces aragonite needles. The isotopic composition of the vadose features (random needle-fiber calcite, micritic networks, and calcified algae filaments) indicates that they were not precipitated from the same water as the spar cement, and, therefore, the precipitation of spar cement was not contemporaneous with formation of the vadose features.

The following model for a progressive, diagenetic sequence is proposed for beachrocks that pass through a cycle of eustatic sea-level changes (Fig.2).

Stage 1 is typified by rocks like that of the Holocene beachrock facies. Calcite cement is evidence that marine-phreatic processes are dominant in the intertidal zone and that lithification occurs in this zone. The even coaling of calcite cement on sediment grains indicates that these crystals precipitated from pores filled with normal seawater. Colonization by endolithic algae and subsequent micritization of grains and cement alter the newly lithified beachrock and result in the formation of well-defined micritic rims around each grain.

Stage	Schematic representation	Diagenetic features	Isotopic values (PDB)	Diagenetic environment
1	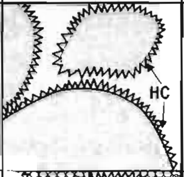	HC: High-Mg Calcite needle cement	$\delta^{13}C = +3.0‰_{PDB}$ $\delta^{18}O = -0.1‰_{PDB}$	Marine phreatic intertidal zone
2	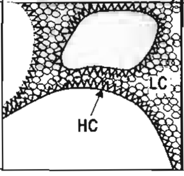	LC: Low-Mg Calcite cement	$\delta^{13}C = -2.5‰_{PDB}$ $\delta^{18}O = -5.0‰_{PDB}$	Meteoric phreatic interstitial zone

Figure 2. Schematic sequence of diagenetic events for beachrocks during eustatic fall and rise of sea level.

As long as the beachrock occupies the intertidal zone, growth of calcite cement and endolithic activity will continue. New sand, cobbles of older limestone, corals, and other debris are cemented onto the beachrock surface. In this earliest stage of diagenesis, beachrock surfaces are commonly eroded by grazing intertidal organisms.

In stage 2, a lowering of sea level moves the shoreline seaward, leaving beachrock deposits in a more landward situation relative to that of their deposition. During this interval, the sediment is in contact with meteoric interstitial water. This meteoric water was probably contained in a micro-phreatic environment within the vadose zone, rather than an extensive groundwater lens, as evidenced by the discontinuous distribution of the spar cements. The most important process in stage 2 is, probably, neomorphic replacement of early calcitic cement by larger crystals of low-Mg calcite, and precipitation of low-Mg calcite in pores. Reduction of porosity is greatest in stage 2 because low-Mg calcite completely fills some pores.

With further lowering of sea level, the beachrock deposits are left even farther inland. In this environment, and erosion processes act during this third stage. In this stage, numerous organic filaments become encrusted with microcrystalline calcite and thus become preserved within interstitial pores. These calcified filaments are thought to be related to the formation of the micrite networks which are seen in thin section. Random needle-fiber calcite also occurs in association with micritic networks. $\delta^{13}C$ values indicate that all of these features form as a result of vadose diagenesis in areas where organic-rich environments also form. The presence of enlarged pores indicates that leaching also occurs in this stage -of diagenesis.

ACKNOWLEDGEMENTS

This study is part of Project n.. 300656/00-9, granted to NCG by the National Council for Scientific and Technological Development (CNPq). This the NEG-LABISE contribution n. 217.

CARBON ISOTOPIC EVIDENCE FOR NEOPROTEROZOIC GLACIAL CYCLES DRIVEN BY IRON- AND PHOSPHOROUS-STIMULATED PRODUCTIVTY

Kaufman, A.J.[1]; Varni, M. A.[1]; Hebert, C.L.[1]; Wing, B.[1]; Misi, A.[2]; Babinski, M.[3]; Halverson, G.P.[4] and Corsetti, F.A.[5]

1. University of Maryland, Geology Department, College Park, MD 20742-4211, USA. kaufman@geol.umd.edu
2. Instituto de Geociências, Universidade Federal da Bahia, Salvador, Brazil. misi@ufba.br
3. Instituto de Geociências, Universidade de São Paulo, São Paulo, Brazil. babinski@usp.br
4. Department of Earth and Planetary Sciences, Harvard University, Cambridge, MA 02138, USA. halvers@fas.harvard.edu
5. Department of Earth Sciences, University of Southern California, Los Angeles, CA 90089, USA. fcorsett@usc.edu

Keywords: Carbon isotope, fractionation, productivity, Neoproterozoic, glaciation

Carbon isotopic evidence for sustained blooms in primary productivity before and after Neoproterozoic ice ages suggest that climate cycles were likely modulated by iron and phosphorus availability in the ancient oceans. The productivity spikes are noted in equivalent organic-rich, pre-glacial, carbonates with extreme positive $\delta^{13}C$ compositions (up to +16‰, V-PDB) in northern Namibia and Brazil (Fig. 1), and in post-glacial organic-rich cap carbonates in northern Namibia (Fig. 2), Brazil (Fig. 3), and the United States that record profound reductions in the biological fractionation of carbon isotopes.

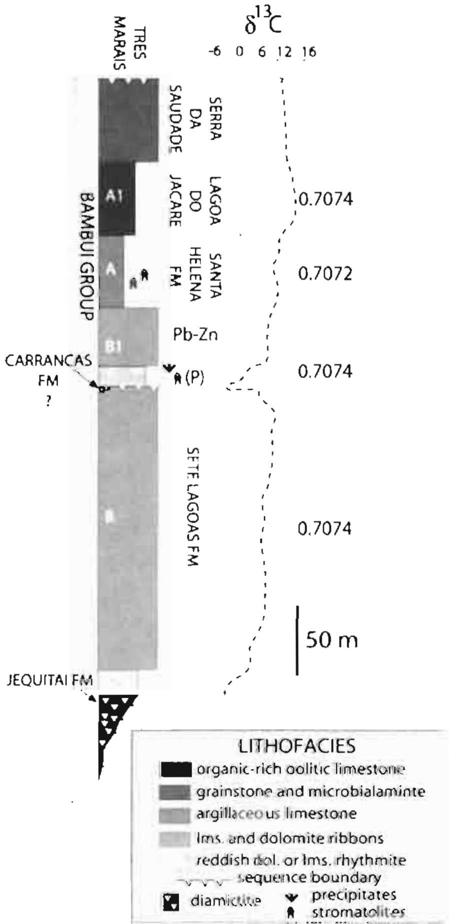

Figure 1. Litho- and chemostratigraphy of the organic- and limestone-rich Neoproterozoic Bambuí Group in Brazil.

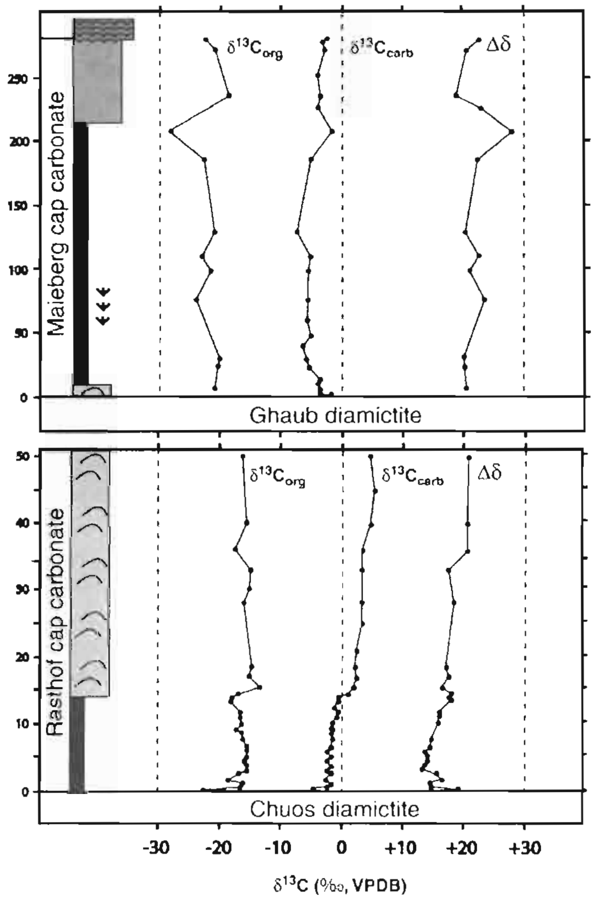

Figure 2. Carbon isotopic compositions of carbonate and co-existing organic matter in the Rasthof and Maieberg cap carbonates from the Otavi Group in Namibia. The notable ^{13}C enrichment of the organic C results in anomalously low $\Delta\delta$ values, which are interpreted to reflect extreme growth rates and carbon limitation in nutrient-rich post-glacial oceans.

It is suspected that high primary productivity, sustained throughout most of the Neoproterozoic by the hydrothermal delivery of reductants to the deep ocean, stimulated glaciation by pumping CO_2 out of the atmosphere and into sediments. The ^{13}C enrichment of organic matter in these caps are unlikely to be metamorphic or diagenetic artifacts, but may be caused by carbon limitation initiated by rapid iron and phosphorous stimulated growth of photoautotrophs (cf. Bidigare et al., 1999) in the immediate aftermath of Neoproterozoic glaciation.

By increasing the flow of energy in the biogeochemical carbon cycle, the sustained productivity events would also stimulate heterotrophic communities that could overprint Rubisco based fractionations by the further metabolic redistribution of carbon. Under conditions of high seawater alkalinity the rise in temperatures and the photosynthetic uptake of CO_2 during blooms allowed for the rapid deposition of cap carbonate lithofacies. Through the same stimulated process O_2 would be released to the oceans and atmosphere, as recorded in our study areas as iron-rich sediments, terrestrial red beds, and oxidized paleosols. Iron enrichment in the Neoproterozoic oceans is linked to the hydrothermal dominance of seawater chemistry (as evidenced by mantle related $^{87}Sr/^{86}Sr$ values in marine carbonates, during discrete rifting events that fragmented Rodinia, and mass extinction of photoautotrophs, which lowered primary O_2 fluxes, thus spreading oceanic anoxia.

REFERENCES

Bidigare, R.R., Hanson, K.L., Buesseler, K.O., Wakeham, S.G., Freeman, K.H. Pancost, R.D. Millero, F.J., Steinberg, P., Popp, B.N., Latasa, M., Landry, M.R., and Laws, E.A., 1999. Iron-stimulated changes in ^{13}C fractionation and export by Equatorial Pacific phytoplankton; toward a paleogrowth rate proxy: Paleoceanography, v. 14, 589-595.

Jacobsen, S.B. and Kaufman, A.J. 1999. The Sr, C and O isotopic evolution of Neoproterozoic seawater. Chemical Geology 161: 37-57.

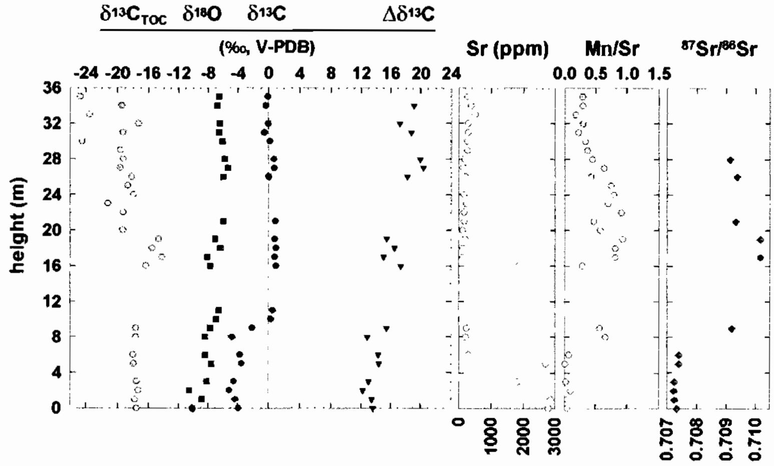

Figure 3. Elemental and stable isotopic variations in the Pedro Leopoldo facies at the top of the Sete Lagoas Formation at Sambra Quarry. Again, the notable ^{13}C enrichment of the organic C results in anomalously low Δδ values, which is particularly noticeable in the ex-aragonite precipitates occurring at the base of the exposure. The $^{87}Sr/^{86}Sr$ values of high Sr precipitates are an exact match with precipitates in the Maieberg Formation in Namibia.

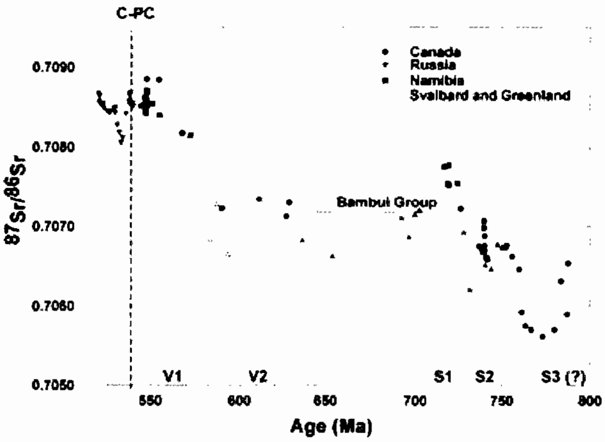

Figure 4. Secular variations in $^{87}Sr/^{86}Sr$ through the glaciogenic Neoproterozoic Era (after Jacobsen & Kaufman, 1999).

SULFUR ISOTOPES IN EVAPORITES OF THE NEUQUEN BASIN, SOUTHERN MENDOZA, ARGENTINA

Linares, E.[1]; Armella, C.[1]; Cabaleri, N.[1]; Ostera H.A.[1]; Haller, M.J.[2] and Iglesias, V.H.[1]

1. Instituto de Geocronología y Geología Isotópica (INGEIS). Pabellón INGEIS, Ciudad Universitaria, 1428
Ciudad Autónoma de Buenos Aires, Argentina. linares@ingeis.uba.ar, armella@ingeis.uba.ar,
cabaleri@ingeis.uba.ar, ostera@ingeis.uba.ar, iglesias@ingeis.uba.ar
2. Universidad Nacional de la Patagonia- Centro Regional Patagónico (CENPAT), Puerto Madryn, Chubut, Argentina.
haller@cenpat.edu.ar

Keywords: Sulfur isotopes, Neuquen Basin, evaporites

INTRODUCTION

Upper Jurassic to Cretaceous evaporitic sequences of the Neuquén Basin in the central western Argentina and eastern Chile, between 34° and 41° S.L. have a wide distribution in southern Mendoza Province. These evaporites include: a- the Río Blanco Formation (Triassic); b- the Tabanos Formation (Callovian) and the Auquilco Formation (Oxfordian) of Jurassic age, the last one deposited during an episode of limited marine connection; and c- the Huitrin and Rayoso Formations of the Middle Cretaceous.

Some authors (i.e. Groeber, 1947; Groeber et al., 1953; Stipanicic, 1969), have linked the huge amounts of gypsum deposited in these formations with a possibility of a magmatic/volcanic source rather than a primary origin due to an evaporitic origin. Recent papers by Brodtkorb et al. (1999), Brodtkorb and Danieli (1999) and Del Blanco and Barbieri (1999), had focussed the research in the sulfur and strontium isotopes studies of the baritine, celestine and gypsum deposits of the Basin. In these papers, the cited authors proposed that the celestine and gypsum deposits are of evaporitic origin, and that the baritine ones were probably formed, due to the very low content of barium in the sea waters, by some volcanogenic sources related to the volcanic rocks erupted in these areas in the interval Triassic to Cretaceous.

The aim of this paper is to present the first data obtained in evaporites principally gypsum, from the Auquilco Formation at the Malargüe fold and thrust belt, whose stratigraphic position is well known and documented, as a part of a project that includes the elucidation of the genesis of these massive evaporite sequence.

ANALYTICAL TECHNIQUES AND METHODOLOGY

Detailed profiles from a 200 m thick outcrop located at arroyo Negro, near Malargüe city, southern Mendoza (Fig. 1) were taken. The main sequence in arroyo Negro is composed of gypsum levels of variable thickness, overlaying basal carbonate-evaporite meteorized beds. Lower thin levels (5 mm to 10 cm) of milky gypsum increase their thickness at the top, forming massive and homogeneous beds up to 3 m, showing contraction-dissecation evidences. They are composed by well crystallized and fine-grained gypsum and crop in jointed and fractured layers. Fine laminated beds of probably biogenic origin (5 mm) are interstratified within the massive horizons. Conspicuous grey to dark grey amorphous silica concretion with quartz nucleous are interbedded.

Careful separation and X-ray diffraction was done on selected samples collected on several outcrops of the Auquilco Formation of the area. Sulfate samples were converted first to AgS and then to sulfur dioxide according with the techniques described in Panarello and Dapeña (1986) and analyzed using a VG-602D and Finningan-delta S mass spectrometers, and CTA for standard geochemical analysis. Delta values are referred to CDT in the common usual expression:

$$\delta^{34}S = \left[\frac{\left(^{34}S/^{32}S\right)_S - \left(^{34}S/^{32}S\right)_{St}}{\left(^{34}S/^{32}S\right)_{St}} \right] x1.000$$

RESULTS

The results obtained during the present research are presented in the Table 1.

Table 1. $\delta^{34}S$ ‰ of the samples analyzed.

Sample N°	δ ‰ $^{34}S_{(corr.)}$ ‰
A1	15.6 ± 1
A2	15.7 ± 1
A3	15.2 ± 1
A4	14.9 ± 1
A5	15.2 ± 1
Mean	15.3 ± 1

DISCUSSION AND PRELIMINARY CONCLUSIONS

Sample results agree well with the previous reported values for the Jurassic-Lower Cretaceous sequences (Claypool et al. 1980; Strauss, 1997). Also, the main value obtained in this research is similar to those obtained by Del Blanco and Barbieri (1999) for gypsum deposits outcropping in the same basin in Neuquén and to the south of Malargüe in the Sierra Azul.

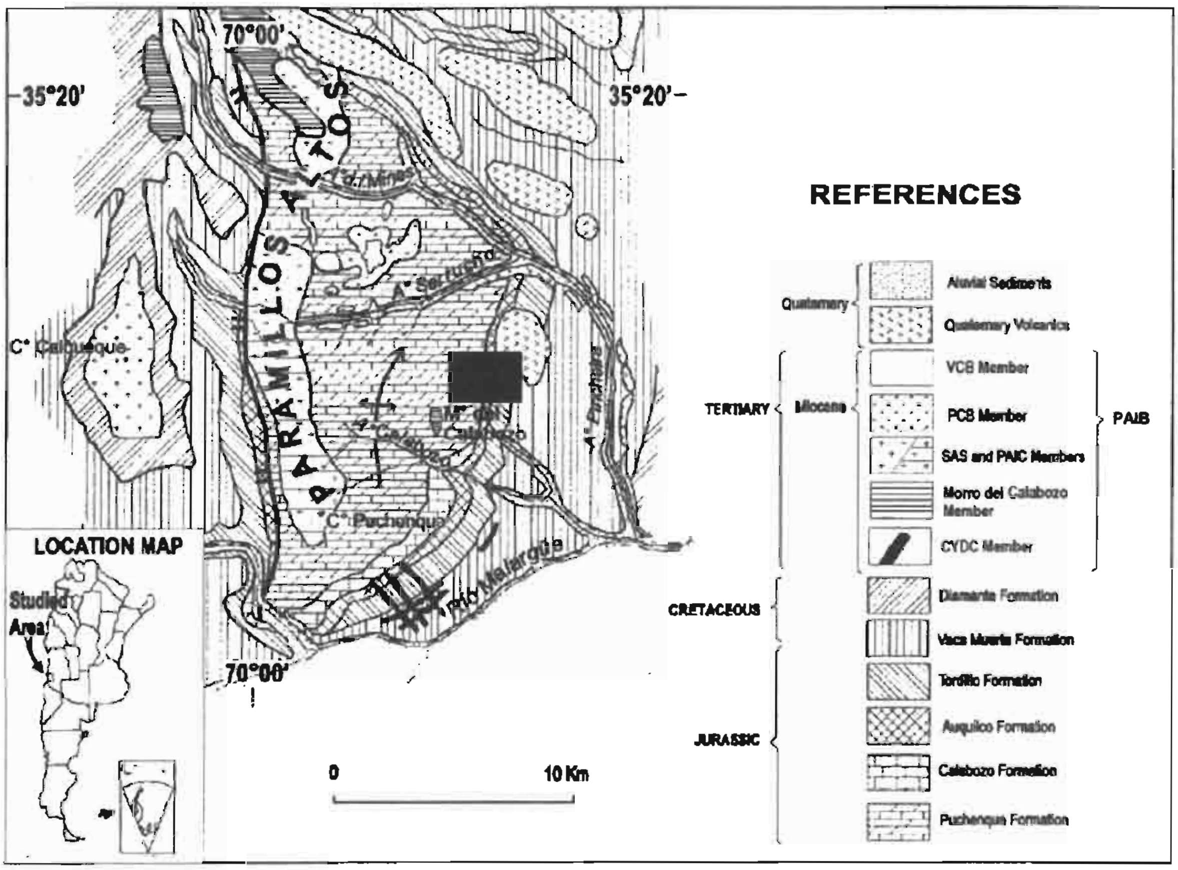

Figure 1. Geological map and location.

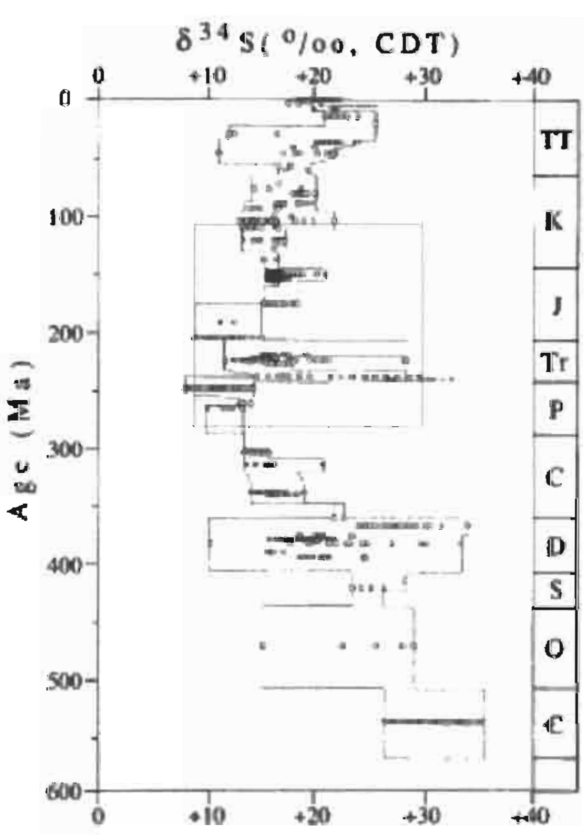

Figure 2. Sulfur isotopic composition of seawater in Phanerozoic times (from Strauss, 1997). Black quadrangle: samples.

There were not detected vertical variations in the delta ^{34}S values, suggesting that during the evaporite deposition, the sulfate source was constant in composition. These values agree with a sedimentary-evaporitic origin, owing to the relationships with the global marine sulfate curve for the Oxfordian times. Although an additional data processing is in progress, there is no isotopic evidences at this point for a magmatic/volcanic source for the sulfur of the evaporite sequence of the Auquilco Formation at the Malargüe fold and thrust belt. These results confirm a depositional pattern of hypersaline marine conditions for the Auquilco Formation and the basin restriction in the Late Oxfordian.

REFERENCES

Brodtkorb, M.K. de,R.E.. de Barrio, M. del Blanco y R.O. Etcheverry. 1999. Geología de los depósitos de baritina, celestina, yeso y halita de la Cuenca Neuquina. En E.O. Zappettini (ed.): Recursos Minerales de la República Argentina. II: 1041-1046. SEGEMAR, Anales 35. Buenos Aires.

Brodtkorb, M.K. de & J.C. Danieli. 1999. El depósito de baritina Arroyo Nuevo, Neuquén. En E.O. ZAPPETTTINI (ed.): Recursos Minerales de la República Argentina. II: 1047-1049. SEGEMAR, Anales 35. Buenos Aires.

Cclaypool, G.E., W.T. Holser, I.R. Kaplan, H. Sakai, and I. Zak. 1980. The age curve of sulfur and oxygen isotopes in marine sulfates and their mutual interpretation. Chemical Geology. 28: 190-260. Elsevier, Amsterdam, Holanda.

Del Blanco, M.A. y M.A. Barbieri. 1999. Depósitos de baritina y celestina relacionados a las Formaciones La Manga y Auquilco, Mendoza y Neuquén. En E.O. ZAPPETTINI (ed.): Recursos Minerales de la República Argentina. II: 1057-1069. SEGEMAR, Anales 35. Buenos Aires.

Groeber, P. 1947. Observaciones geológicas a lo largo del meridiano 70. 4. Hojas Bardas Blancas y Los Molles. Revista Asociación Geológica Argentina. 2(4): 409-433. Buenos Aires.

Groeber, P., P.N. Stipanicic y A. Mingramm. 1953. Jurásico. En: Geografía de la República Argentina. Sociedad Argentina de Estudios Geográficos (GAEA). II(I): 143-347. Buenos Aires.

Panarello, H.O. y C. Dapeña. 1986. Isótopos del azufre. Su determinación en materiales naturales y aplicaciones a la Geología. Revista Asociación Geológica Argentina. 41(1-2): 210-215. Buenos Aires.

Stipanicic, P.N. 1969. El avance en los conocimientos del jurásico argentino a partir del esquema de Groeber. Revista Asociación Geológica Argentina. 24(1-4): 367-388. Buenos Aires.

Strauss, H. 1997. The isotopic composition of sedimentary sulfur through time. Palaeogeography, Palaeoclimatology, Palaeocology. 132: 97-118. Elsevier, Amsterdam, Holanda.

LOMAGUNDI PHENOMENON IN PALEOPROTEROZOIC CARBONATES OF BRAZIL AND INDIA

Maheshwari, A.[1]; Sial, A.N.[2]; Ferreira, V.P.[2] and Romano, A.W.[3]

1. Department of Geology, University of Rajasthan, Jaipur, 302004, India. anilm@datainfosys.net
2. NEG-LABISE, Dept. of Geology, UFPE, C.P. 7852, Recife-PE, 50670-000, Brazil. ans@ufpe.br; valderez@ufpe.br
3. Institute of Geosciences, UFMG, Belo Horizonte-MG, Brazil, 30430-120. romanoaw@dedalus.lcc.ufmg.br

Keywords: Lomagundi, C isotopes, Minas Gerais, Aravalli, Gondwana

INTRODUCTION

The positive $\delta^{13}C$ anomaly in Paleoproterozoic carbonate sequences in continents that once were part of Gondwanaland demonstrates that the "Lomagundi phenomenon" was recorded in every continent which was once part of this supercontinent. Among the successions that recorded this event, besides the Lomagundi belt carbonates in Zimbabwe, one finds the Pretoria Group and Transvaal Succession, South Africa (Buick et al., 1998; Bekker et al., 2001), Francevillian province, Gabon, of west Africa (Gauthier-Lafaye and Weber, 1989) and Western Australia basins (Lindsay and Brasier, 2002).

The Paleoproterozoic $\delta^{13}C$carb positive excursion has a global character, but no occurrence in South America and India had been thus far registered until recently. Maheshwari et al. (1999) and Sial et al. (2000) reported the presence of Paleoproterozoic $\delta^{13}C$carb positive excursion for the first time in India and Brazil subcontinents. Sreenivas et al. (2001) also provided C-isotope data for Paleoproterozoic carbonates from Aravalli Supergroup, India. This study discusses the C isotope anomaly in early paleoproterozoic shallow-water, marine carbonates of India and Brazil.

C-ISOTOPE STRATIGRAPHY

EVALUATING DATA QUALITY

In regional meta-morphic terrains, $\delta^{18}O$ and $\delta^{13}C$ depletions are generally less pronounced (Rye et al., 1976; Valley, 1986) and the cause and timings of the isotopic depletions are less clear. In the Adirondacks, granulite facies marble has oxygen and carbon isotopic compositions that are similar to those of unmetamorphosed Grenville-age limestones (Valley and O'Neil, 1984). In contrast, metamorphosed carbonates in other regional metamorphic terranes are variably depleted in $\delta^{18}O$ as a result of synmetamorphic fluid infiltration (Wickham and Taylor, 1987; Cartwright et al., 1995); premetamorphic magmatism (Buick and Cartwright, 1996), premetamorphic diagenesis (Rumble et al., 1991), or a combination of these processes. $\delta^{13}C$ is much more difficult to change than $\delta^{18}O$ in a rock system-the relative masses of C in rock vs diagenetic fluids is typically such that $\delta^{13}C$ compositions will be buffered to rock values (Banner and Hanson, 1990). As such, oxygen isotopic compositions of the carbonate will be altered upon diagenesis at a much quicker rate than carbon isotopic compositions.

There is no correlation between $\delta^{13}C$ and Mn/Sr as well as between $\delta^{18}O$ and Mn/Sr for all studied samples, as expected for samples not affected by meteoric alteration that tends to increase Mn contents while decreasing Sr contents.

BRAZIL

The Minas Supergroup, Brazil, encompasses, from bottom to top the Caraça, Itabira and Piracicaba Groups. The $\delta^{13}C$ stratigraphy of carbonate sequences from Minas Supergroup examined in this study includes the Gandarela Formation (top of the Itabira Gr.), the Cercadinho Fm (base of the Piracicaba Gr.) and the overlain Fecho do Funil Fm. The 2.42Ga-old Gandarela Fm consists of red carbonate BIF at the base of the sequence, gradually replaced upwards by buff dolomites, and limestones, locally stromatolitic, in light and dark-gray alternating bands. Carbonates display $\delta^{13}C$carb from -1.6 to +0.4‰$_{PDB}$ (n=58), the most negative values found in red dolomites in contact with the underlying, finely laminated, Cauê banded iron formations. Gandarela carbonates from the Heargraves quarry yielded $\delta^{13}C$carb from -1.4 to -0.6‰$_{PDB}$ (n=28). In the Cercadinho Fm., $\delta^{13}C$carb varies from +3.3 to +4.2 ‰$_{PDB}$ (n=10), and values decrease erratically with depth (Fig. 1a).

The Fecho do Funil dolomites (2.11 ± 0.11Ga, deformation/metamorphic age) were probably deposited within the time span for the Lomagundi positive excursion age of the Kaapval craton, Africa. The sampled section of this Formation consists, at the base, by fine-grained, stromatolite-rich white and pink dolostones, and then by fine-grained white marble. Stratigraphically collected samples show positive and remarkably homogeneous $\delta^{13}C$carb values (+6.0 to +6.5‰$_{PDB}$, n=47) (Fig. 1b). Oxygen isotopes are also fairly constant (-9.7 to -10.8‰$_{PDB}$) and show a trend that is rather antipathetic to the variation in C isotopes. These high $\delta^{13}C$carb carbonates show little scatter, relatively shallow trend on $\delta^{13}C$carb vs $\delta^{18}O$ diagram, consistent with low-grade metamorphic decarbonation. The elevated C-isotope values were least reset and probably reflect their protolith composition, rather than subsequent diagenetic or metamorphic processes. Carbonates from the Fecho do Funil and Cercadinho formations are a proxy, in South America, for the global Lomagundi phenomenon.

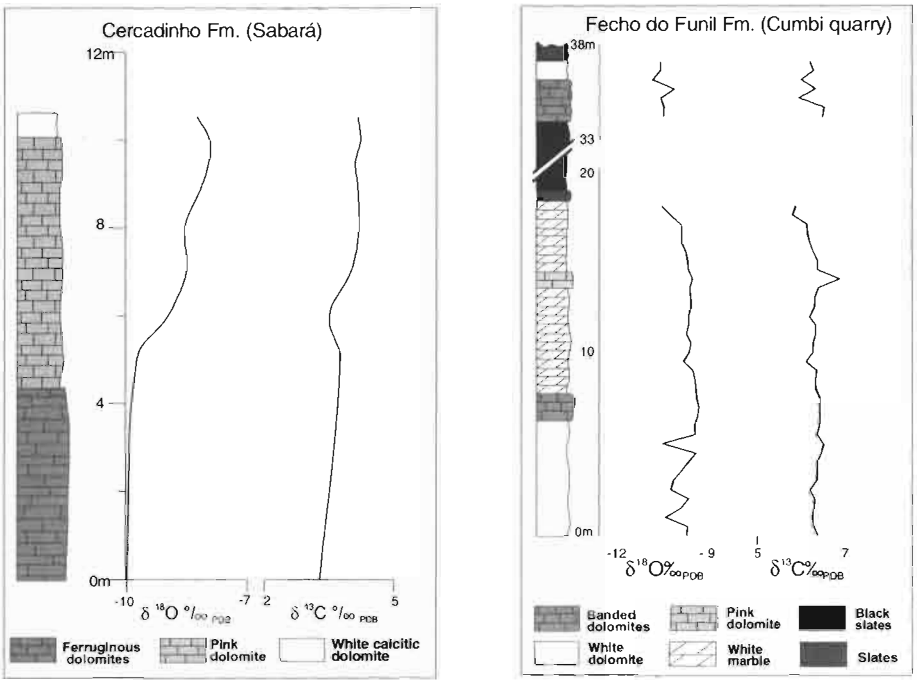

(a) (b)

Figure 1. C- and O-isotope chemostratigraphic curves for the Cercadinho Fm (Fig. 1a) and Fecho do Funil (Fig. 1b) Fm., Minas Gerais, Brazil.

INDIA

Carbon-isotope measurements have been carried out on nearly 150 carbonate samples from different localities of the early Proterozoic Aravalli craton, western India (Fig. 2). Although Aravalli Supergroup carbonates are dolomitic in composition, dolomite is generally considered as a diagenetic mineral. Nonetheless, there is growing evidence that precipitation of dolomite in the Precambrian was either coeval with calcite or that dolomitization was an early diagenetic phenomenon caused by waters isotopically comparable to that of seawater (e.g. Veizer and Hoefs, 1976; Veizer et al., 1992; Kah, 2000).

The Aravalli rocks of study areas have suffered low to very low grade of regional metamorphism to greenschist facies (Sharma, 1988). Oxygen isotopic compositions preserved in Aravalli Group carbonates are fairly consistent with "least altered" isotopic compositions from many other Precambrian carbonate successions and suggest that the rocks have undergone relatively little post-depositional exchange. Therefore, it is unlikely that the carbon isotopic compositions have changed much from their primary depositional compositions.

Carbonate rocks from Bari Talab are characterized by δ^{13}C values up to 4.4‰$_{PDB}$. Although δ^{18}O values of Bari Talab carbonates are quite low (-12.6 to -16.4‰$_{PDB}$), these values may be attributed to their intimate association with Delwara volcanic rocks as contact-metamorphosed carbonate rocks commonly exhibit large depletions in δ^{18}O (Valley, 1986). Iswal dolomites show δ^{13}C values up to 11.2‰$_{PDB}$ with an average δ^{13}C of + 9.1‰ with δ^{13}C values ranging between +8 and +10‰$_{PDB}$. δ^{18}O in Iswal dolomites ranges from -12.4 to -8.1‰$_{PDB}$. The carbonates from Babarmal have relatively high δ^{18}O values (-7.0 to -12.1‰, averaging -8.0‰$_{PDB}$) and δ^{13}C values between + 0.05 and +3.2‰$_{PDB}$.

The C-isotopic values from Babarmal (up to +3.2‰$_{PDB}$) and Bari Talab (up to +4.4‰ $_{PDB}$) are significantly lighter than values recorded in Iswal strata (+11.2‰$_{PDB}$). The difference in C-isotopic values of carbonates from different study areas are most likely attributed to their different stratigraphic position within the Jhamarkotra Formation of Aravalli Supergroup. Carbonates strata from the study areas do not occur as a continuous sequence. In the absence of age constraints, the stratigraphic position of these carbonates has been deciphered mainly from field observations. The Iswal dolostones, however have been assigned an age of 2.1 Ga (Sreenivas et al., 1999). On the basis of lithological setting, the Bari Talab carbonates are interpreted as stratigraphically lower than Iswal carbonates, and the Babarmal carbonates are interpreted to be youngest strata among study areas. This stratigraphic observation also gets support from the fact that the carbon isotopic compositions of Bari Talab carbonates are clearly enriched with respect to the Babarmal region. The overall trend of the carbon-isotopic profile along three studied stratigraphic sections shown in figure 2 indicates that the carbon isotopic compositions in Jhamarkotra Formation of Aravalli Supergroup varies from ~3‰ to >9‰ within a short stratigraphic interval.

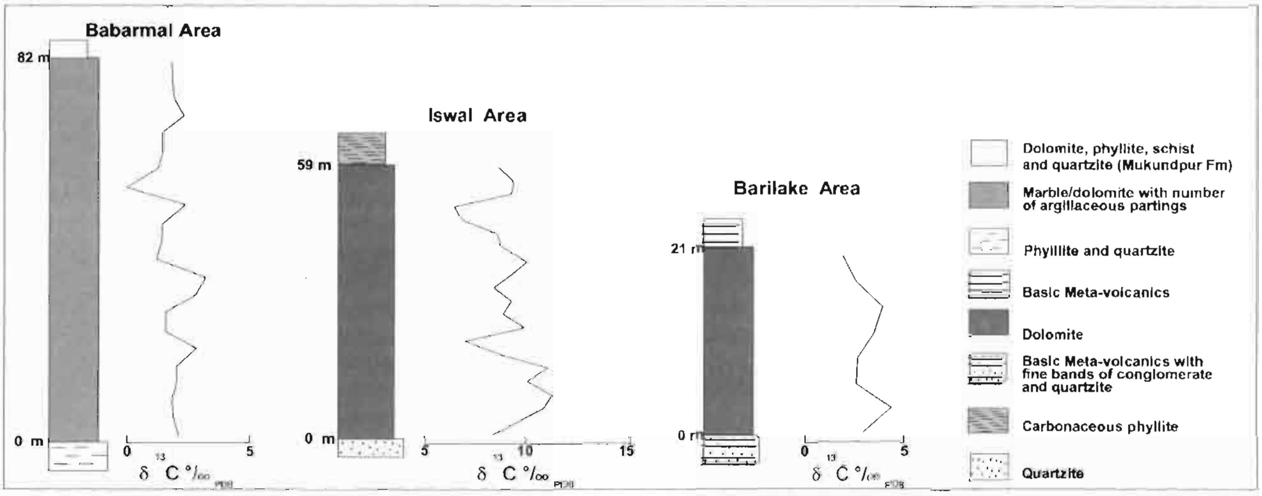

Figure 2. C-isotope chemostratigraphic curves for Paleoproterozoic Fms., Aravalli craton, India.

DISCUSSION

Instead of being primary depositional feature, elevated $\delta^{13}C$ values could be due to diagenesis. However, burial and meteoric diagenesis typically results in shifts toward lower $\delta^{13}C$ values (Marshall, 1992; Saltzman et al., 1998). Moreover, studies of Paleoproterozoic carbonates suggest that diagenetic shifts in $\delta^{13}C$ are typically markedly smaller (< 1‰) than in Phanerozoic equivalents (Strauss et al., 1992). Similarly, dolomitization of ~2 Ga Proterozoic mixed dolomite-calcite carbonates elsewhere appears to be associated with very slight lowering of $\delta^{13}C$ values (~1‰; Schidlowski et al., 1976) and, therefore, are unlikely to have resulted in the elevated $\delta^{13}C$ values observed in this study.

The high positive $\delta^{13}C$ values up to +11.2‰$_{PDB}$, from the early Proterozoic Aravalli Craton, western India, coincide with the appearance of stromatolites and the development of 'red beds'. These observations support global paleoenvironment change during the Paleoproterozoic, as reported from other parts of Gondwana-land.

One possible interpretation for this positive $\delta^{13}C$ anomaly in the Indian carbonates is that it is a consequence of a large-scale sequestration and/or burial of organic ^{12}C in the lower compartment of a stratified ocean that progressively increased the heavy complement in the surface waters (Schidlowski and Todt, 1998). Melezhik et al.(1999) presented a detailed overview on the record and characteristics of the Lomagundi phenomenon and pointed that there is a close association of ^{13}C-rich carbonates with abundant stromatolites, and that it corresponds with substantial increase in the level of atmospheric O_2.

No clear evidence was found for the triad early paleoproterozoic glacial events of the (2.45 -2.22Ga interval) recognized in North America. C-isotope patterns for carbonates of the Minas Supergroup suggest that the Gandarela Fm. was deposited around 2.4Ga; the moderate C-positive anomaly of the Cercadinho carbonates suggests deposition around 2.3 and the Fecho do Funil carbonates were deposited probably around 2.2 Ga.

The carbon isotopic compositions of Paleoproterozoic carbonates of the Aravalli craton and Fecho do Funil and Cercadinho Formations of Brazil and their similarities with Paleoproterozoic strata from other continents strongly support current hypotheses suggesting significant global paleoenvironmental change during the Paleoproterozoic. The new C and O isotopic data generated under the present study contribute to the knowledge of the geochemistry of the global ocean during the Paleoproterozoic.

ACKNOWLEDGEMENTS

We are indebted to Gilsa M. Santana and V. S. Bezerra for assistance with the stable isotope analyses at the LABISE, UFPE, Brazil. We also thank S. Diene Barros for drafting the figures. This is the NEG-LABISE contribution n. 215.

REFERENCES

Banner, J.L., and Hanson, G.N., 1990. Calculation of simultaneous isotopic and trace element variations during water-rock interaction with applications to carbonate diagenesis. Geochim. Cosmochim. Acta 54: 3123-3137.

Bekker, A., Kaufman, A.J., Karhu, J.A., Beukes, N.J., Swart, Q.D., Coetzee, L.L., Eriksson, K.A., 2001. Chemostratigraphy of the Paleoproterozoic Duitscland Formation, South Africa: implications for coupled climate change and carbon cycling. Amer. Jour. Sci., 301: 261-285.

Buick, I.S., and Cartwright, I., 1996. Fluid-rock interaction during low-pressure polymetamorphism of the Reynolds Range Group, central Australia. Jour. of Petrology 37: 1097-1124.

Buick, I.S., Uken, R., Gibson, R.L., Wallmach, T., 1998. High $\delta^{13}C$ Paleoproterozoic carbonates from the Transvaal Supergroup, South Africa. Geology 26, no.10: 875-878.

Cartwright, I., Vry, J., and Sandiford, M., 1995. Changes in stable isotope ratios of metapelites and marbles during regional metamorphism, Mount Lofty ranges, South Australia: Implications for crustal scale fluid flow. Contrib. Mineral. and Petrol. 120: 292-310.

Gauthier-Lafaye, F. and Weber, F., 1989. The Francevillian (Lower Proterozoic) uranium ore deposits of Gabon. Econ. Geoloy, 84: 2267-2285.

Kah, L.C., 2000. Depositional $\delta^{18}O$ signatures in Proterozoic dolostones: Constraints on seawater chemistry and early diagenesis. Carbonate sedimentation and diagenesis in the evolving Precambrian world, SEPM Special Publication 67, 345-360.

Lindsay,J.F. and Brasier, M. D., 2002. Did global tectonics drive early biosphere evolution? Carbon isotope record from 2.6 to 1.9 Ga carboantes of Western Australian basins. Prec. Research 114: 1-34.

Maheshwari, A., Sial, A.N. & Chittora, V.K. (1999) High-$\delta^{13}C$ Paleoproterozoic carbonates from the Aravalli Supergroup, Western India. Intern. Geol. Review 41: 949-954.

Marshall, J.D., 1992. Climatic and oceanographic isotopic signals from the carbonate record and their preservation. Geol. Magazine 129: 143-160.

Melezhik, V.A, Fallick, A.E., Medvedev, P.V. and Marakarikhin, V.V., 1999, Extreme ^{13}Ccarb enrichment in ca.2.0Ga magnesite-stromatolit-dolomite-'red beds' association in a global context: a case for thr world-wide signal enhanced by a local environment. Earth-Sci. Reviews, 48: 71-120.

Rumble, D., III, Oliver, N.H.S., Ferry, J.M., and Hoering, T.C., 1991. Carbon and oxygen isotope geochemistry of chlorite-zone rocks of the Waterville limestone, Maine, U.S.A. Am. Mineralogist 76: 857-866.

Rye, R.O., Schuiling R.D., Rye, D.M., and Hansen, J.B., 1976. Carbon, hydrogen and oxygen isotope studies of the regional metamorphic complex at Naxos, Greece. Geochim. et Cosmochim. Acta 40: 1031-1049.

Saltzman, M.R., Runnegar, B., Lohmann, K.C., 1998. Carbon isotope stratigraphy of upper Cambrian (Steptoean Stage) sequences of the eastern Great Basins: Record of a global oceanographic event. GSA Bulletin 110: 285-297.

Schidlowski, M., Eichmann, R., Junge, C.E., 1976. Carbon isotope geochemistry of the Precambrian Lomagundi carbonate province, Rhodesia. Geochim. Cosmochim. Acta 40, 449-455.

Schidlowski, M, and Todt, W., 1998. The Proterozoic Lomagundi carbonate Province as paragon of a ^{13}C-enriched carbonate facies: Geology, Radiometric Age and Geochemical Significance. ICOG-9, Chinese Science Bulletin, 43, Supp. August, Beijing, China: 114.

Sharma, R.S., 1988. Patterns of metamorphism in the Precambrian rocks of the Aravalli mountain belt. In: A. B. Roy (ed.): Precambrian of the Aravalli Mountain, Rajasthan, India. Memoir Geol. Soc. of India 7: 33-76.

Sial, A.N., Ferreira, V.P., Almeida De, A.R., Romano, A.W., Parente, C.V., Costa, M.L., and Santos, V.H., 2000. Carbon isotope fluctuations in Precambrian carbonate sequences of several localities in Brazil. An. Acad. Bras. Ci. 72(4):539-558.

Sreenivas, B., Das Sharma, S., Kumar, B., Patil, D.J., Roy, A.B., Srinivasan, R., 2001. Positive $\delta^{13}C$ excursion in carbonate and organic fractions from the Paleo-proterozoic Aravalli Supergroup, Northwestern India. Prec. Research 106, pp. 277-290.

Sreenivas, B., Srinivasan, R., and Roy, A.B., 1999. Geochemical changes across the Archaen-Proterozoic boundary- as study from the Udaipur area of Aravalli mountain belt, Rajasthan, India: Geology of Rajasthan, Status and prospective P.Kataria (ed.): 57-86.

Strauss, H., Des Marais, D.J., Hayes, J.M., Summons, R.E., 1992. The carbon-isotopic record, in Schopf, J.W., and Klein, C., eds., The Proterozoic biosphere, a multidisciplinary study: New York, Cambridge University Press, 117-128.

Valley, J.W., 1986. Stable isotope geochemistry of metamorphic rocks, in Valley, J.W., Taylor, H.P., and O'Neil, J.R., eds., Stable isotopes in high temperature geological processes: MSA Rer. in Mineraloly 16: 445-490.

Valley, J.W., and O'Neil, J.R., 1984. Fluid heterogeneity during granulite facies metamorphism in the Adirondacks: Stable isotope evidence. Contrib. Mineral. Petrol. 85: 158-173.

Veizer, J., Clayton, R.N., Hinton, R.W., 1992. Geochemistry of Precambrian carbonates: IV, Early Paleoproterozoic (2.25 + 0.25 Ga) seawater. Geochim. Cosmochim. Acta 56:875-885.

Veizer, J., Hoefs, J., 1976. The nature of $^{18}O/^{16}O$ and $^{13}C/^{12}C$ secular trends in sedimentary carbonate rocks. Geochim. Cosmochim. Acta 40: 1387-1395.

Wickham, S.M., and Taylor, H.P., Jr., 1987. Stable isotope constraints on the origin and depth of penetration of hydrothermal fluids associated with Hercynian regional metamorphism and crustal anatexis in the Pyrenees. Contrib. Mineral. Petrol. 95: 255-268.

CHEMOSTRATIGRAPHIC CORRELATION OF THE NEOPROTEROZOIC SEQUENCES FROM SOUTH AMERICA

Misi, A.[1]; Teixeira, J.B.G.[1]; Gaucher, C.[2]; Remus, M.V.D.[3]; Boggiani, P.C.[4] and Iyer, S.S.S.[5]

1. Grupo de Metalogênese, Centro de Pesquisa em Geofísica e Geologia, UFBA, Salvador, Bahia, Brazil. misi@ufba.br
2. Facultad de Ciencias, Departamento de Paleontologia, Montevideo, Uruguay
3. Instituto de Geociências, Universidade Federal do Rio Grande do Sul, Brazil
4. Instituto de Geociências, Universidade de São Paulo, Brazil
5. Department of Physics and Astronomy, University of Calgary, Canada

Keywords: Chemostratigraphy, Neoproterozoic Basins, correlation, South America

GEOTECTONIC SETTING

The deposition of the Neoproterozoic sedimentary sequences in South America, some of which are hosting base metal deposits, took place as a consequence of extensional events that occurred during the fragmentation of the Rodinia supercontinent between 900 and 600 Ma. Although associated with the closure of the Pan-African-Brasiliano rift system (~900 to 500 Ma, Porada, 1989), the Neoproterozoic basins were essentially formed by extensional processes. In this sense, Condie (2002) suggested that the overall processes that led to the Rodinia formation and breakup, along with the subsequent assembly of Gondwana may be considered a unique cycle, although overlaps between each stage did occur. The diachronic history of the Pan African-Brazilian orogeny in South America was pointed out by Brito Neves et al. (1999).

The Neoproterozoic sedimentary basins are shown in Figure 1. The sequences are distributed in the following geotectonic settings:

1. Carbonatic and siliciclastic sequences deposited on tectonically stable terranes (cratonic areas): (a) on the São Francisco Craton (Brazil): Bambuí and Una groups (São Francisco, Irecê and Una-Utinga Basins) and Rio Pardo Group (Rio Pardo Basin); (b) on the Amazonas Craton: Alto Paraguay, Corumbá, Murciélago, Itapucumi, Tucuvaca, Jacadigo, Boqui groups and Araras and Puga Formations, in the marginal basins of the Paraguay Belt; (c) on the Rio de La Plata cratonic area: Arroyo del Soldado, Puncoviscana and La Tinta or Sierras Bayas groups.
2. Intensely deformed siliciclastic and carbonatic sequences in passive margin basins surrounding the cratonic areas: Cuiabá Group (Paraguay Belt), Ibiá and Vazante groups (Brasília Fold Belt), Miaba, Canudos and Vasa Barris groups (Sergipe Fold Belt), Açungui Group (Ribeira Fold Belt), Macaúbas Group (Araçuaí Fold Belt), and Porongos Group (Dom Feliciano Belt).
3. Siliciclastic + volcanic-volcanoclastic infills in basins associated with fold belts in tectonically active settings: Bom Jardim, Camaquã, Fuente del Pluma groups (Dom Feliciano Belt).

AGE CONSTRAINTS

The most significant age constraints available for the Neoproterozoic sediments are the following:

- U-Pb SHRIMP age of 950 Ma obtained in detrital zircons extracted from basal diamictite of glacio-marine origin within the Araçuaí fold belt may be considered the upper age limit of the glaciation. Pedrosa Soares et al. (2000) attributed this value to a magmatic episode during a rifting event.
- Based on Rb-Sr age determination Macedo (1982) and Macedo and Bonhomme (1984) suggested a time interval of 667 ± 30 to 932 ± 30 Ma for the glaciogenic basal sediments of the Una Group (Bebedouro Fm.).
- From the Rb-Sr isotopic dating of pelitic sediments the same authors suggested a time interval of 560 to 770 Ma for the sedimentation of the carbonate sequence above the glaciogenic units of the Una Group.
- Babinski et al. (2002) obtained a Pb-Pb isochron age from well-preserved carbonates of the Bambuí Group of 740 ± 22 Ma. (MSDW = 0.66), and interpreted it as the depositional age.
- The lower age limits are represented by Vendian fossils of the genus *Cloudina* and *Corumbella* (580 to 543 Ma.) reported in the Corumbá and Arroyo del Soldado groups by Zaine (1991), Boggiani (1998) and Gaucher et al. (2003), among others.

CHEMOSTRATIGRAPHIC CORRELATION

High resolution isotope stratigraphy may be a powerful tool for solving important controversies of the Neoproterozoic successions, specially related to regional and global stratigraphic correlations, and to the age of sedimentation. Adequate use of chemostratigraphic data depends on the existence of high quality stratigraphic sections and of detailed petrographic and geochemical investigation, allowing for accurate interpretation of diagenetic processes and extent of sample alteration. In this study we have used samples with clear indication of good preservation, on the basis of trace element determination. Only samples retaining the lowest Mn/Sr ratios (<1) and/or the highest Sr concentration (>500ppm) were selected, specially in consideration of their $^{87}Sr/^{86}Sr$ ratios. The preservation of the carbon isotope signal is possible, even in conditions not favorable for $^{87}Sr/^{86}Sr$ preservation. On the other side, for the oxygen isotopes, the signal is reseted during recrystallization.

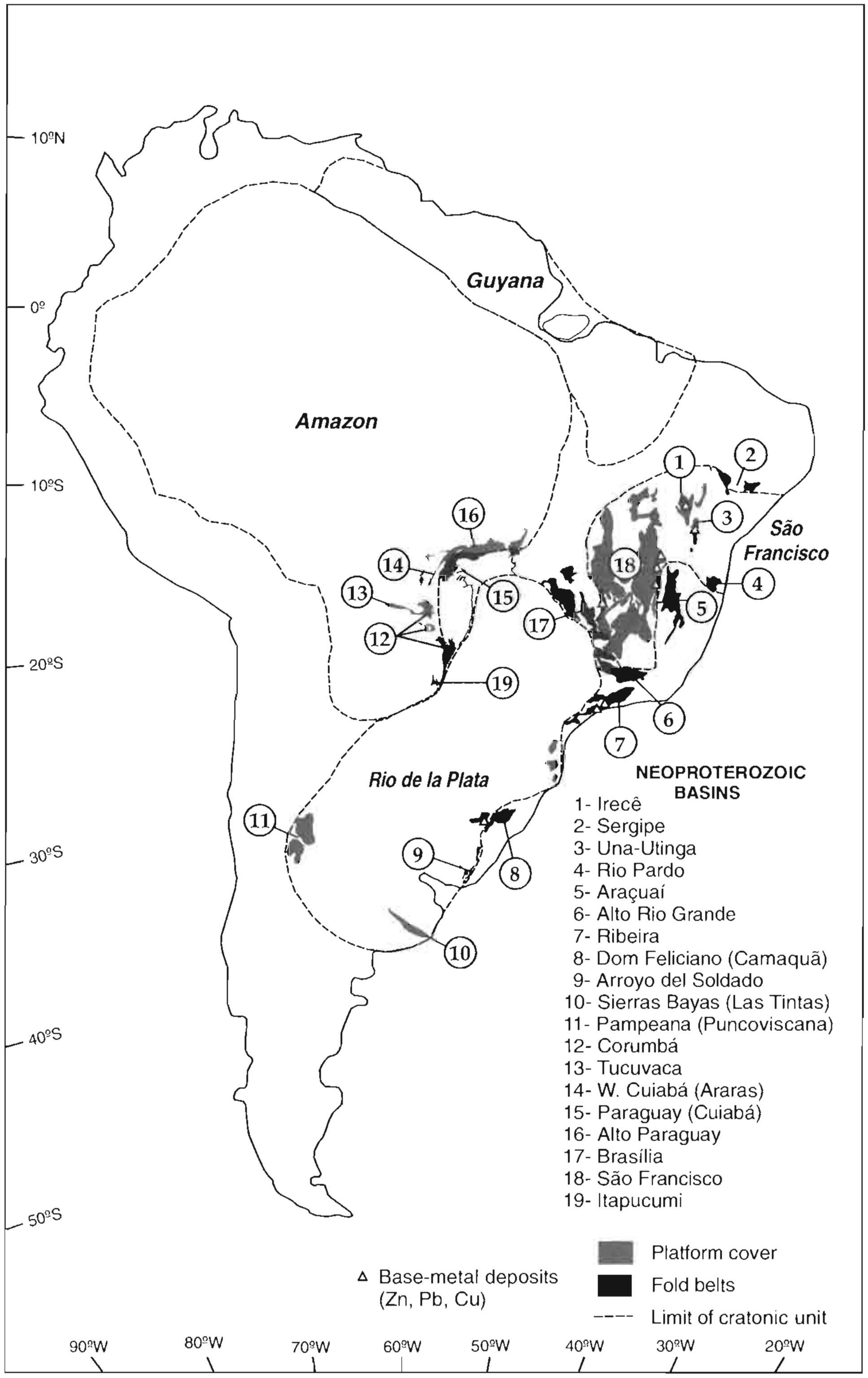

Figure 1. The Neoproterozoic Basins of South America.

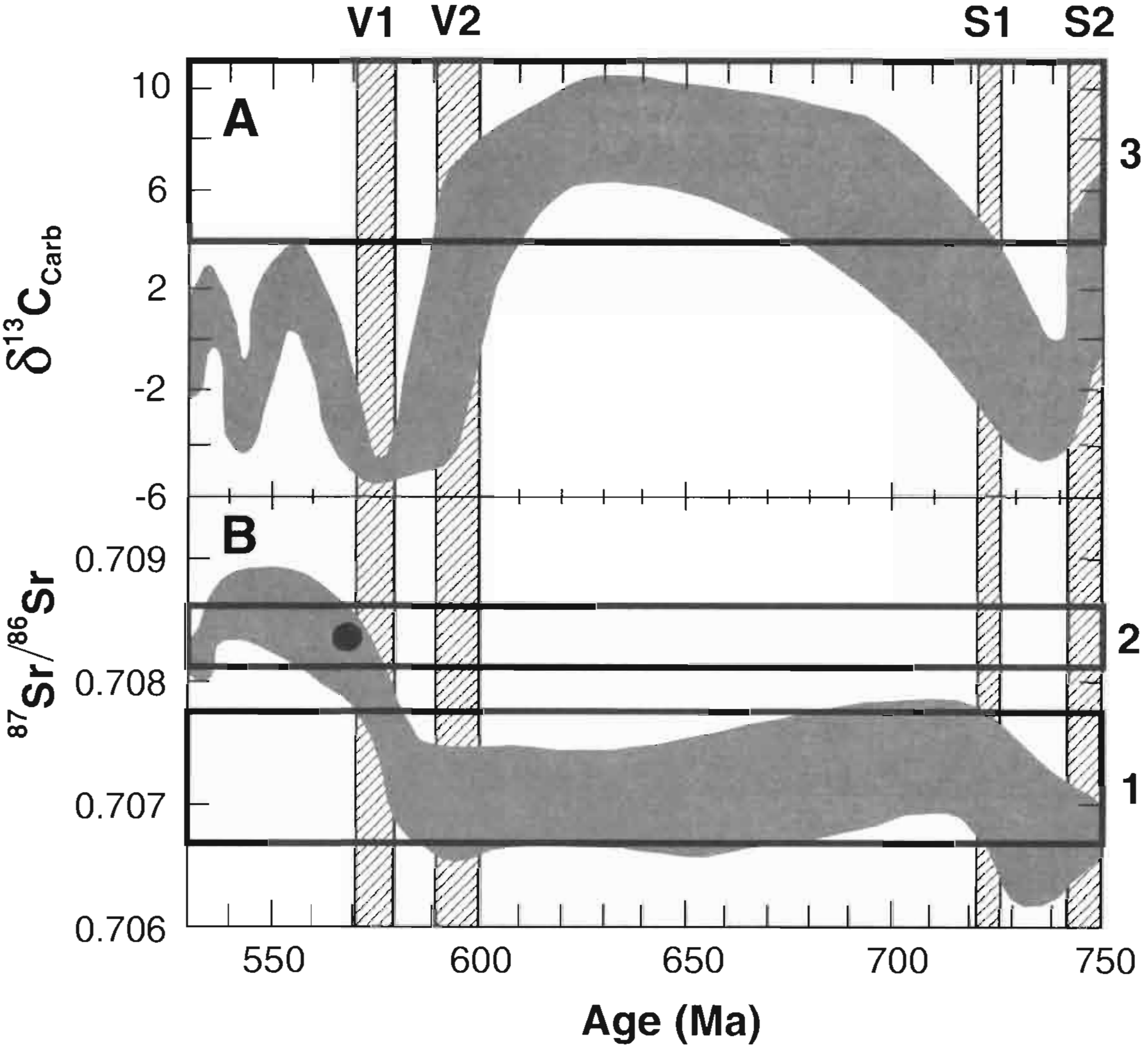

Figure 2. $\delta^{13}C$ and $^{87}Sr/^{86}Sr$ evolution of Neoproterozoic seawater according to Jacobsen and Kaufman (1999). V1, V2: upper and lower Vendian glaciations; S1, S2: upper and lower Sturtian glaciations. **1** – Range of $^{87}Sr/^{86}Sr$ least radiogenic values in the following groups: Arroyo del Soldado (Yerbal Fm.), Cuiabá (Araras Fm.), Vazante, Bambuí and Una. **2** – Least radiogenic values of $^{87}Sr/^{86}Sr$ in the Corumbá Group. **3** – Range of $\delta^{13}C$ positive excursions in the Groups: Vazante (Upper Pamplona Fm.), Bambuí (Lagoa do Jacaré Fm.) and Una (A1 Unit). The black dot, indicates the only samples with unequivocal geochronological markers (Vendian fossils) from the Corumbá Group.

Three mega-stratigraphic sequences are represented in the cratonic as well as in the passive margin basins (1 and 2 above) by the following respective mega-sequences: The Glaciogenic Sequence, the Carbonate/Siliciclastic Sequence and the Molassic-Type Sequence. They are separated by unconformities, and within each mega-unit there are other secondary boundaries that may be useful for regional correlation purposes (Misi, 2001).

At least two transgressive-regressive marine cycles appear to have occurred during the evolution of the Carbonate/Siliciclastic Sequence above a glaciogenic diamictite (Sturtian glaciation?). They are represented by two shallowing-upward sub-sequences. The first sub-unit initiated with cap dolomites and laminated limestone and terminated by an extensive sub-aerial exposure with the occurrence of dolostone with tepee structures. The zinc-lead deposits of the Vazante, Bambuí and Una groups are associated to the end of this first cycle (Misi et al., 1999). The second sub-sequence is represented by marl and shale followed by black oolitic and pisolitic limestone. A glaciogenic diamictite is present in the Corumbá Group at a stratigraphic position probably situated at the end of the first sub-sequence, but there is no direct evidence of this second glaciation (Varengerian?) in the other sections, except for the negative $\delta^{13}C$ values in the Upper Pamplona Fm. (Vazante Gr.) and in the B1 Unit of the Una Group.

$^{87}Sr/^{86}Sr$ determinations of well preserved carbonate samples permit a better correlation. Excepting for the Corumbá Basin, the $^{87}Sr/^{86}Sr$ least radiogenic set of data range from 0.70684 to 0.70780 suggesting that the age of sedimentation are between the Sturtian (~750 Ma) and the Varanger ice age of *ca.* 600 Ma ago, or have been deposited immediately after the first Varanger glaciation (Jacobsen and Kaufman, 1999) (Fig. 2 B). In the Corumbá Basin, the best preserved carbonates of the Polanco and Tamengo Formations (Corumbá Group) show ratios around 0.70850 (Boggiani, 1998), suggesting that the sequences are younger (Fig. 2 B). This is confirmed by the presence of Vendian fossils (Boggiani, 1998; Gaucher et al., 2003).

$\delta^{13}C$ and $\delta^{18}O$ studies in the same sequences revealed some remarkable excursions that may also be used for stratigraphic correlation:

a. $\delta^{13}C$ negative excursion with values ranging from -2 to -6‰ PDB in different sections, present in the cap carbonates at the base of the Vazante, Bambuí and Una groups. These negative excursions are normally observed in post-glacial Neoproterozoic carbonates worldwide. Another negative carbon isotope excursion appear to occur in dolostone at the top of the first sub-sequence, suggesting the existence of a second glaciation at the end of the first transgressive-regressive cycle. This could be represented by the diamictites of the Puga Formation (Corumbá), but the only possible indication in the other sequences are the negative $\delta^{13}C$ excursions in the Vazante and Una groups.

b. $\delta^{13}C$ positive excursion ranging from +4 to +14‰ PDB in different sections, immediately above dolostone with teepee structures in the second cycle, present in the Vazante, Bambuí and Una groups (Fig. 2 A).

c. Increase in the $\delta^{18}O$ positive values observed in the shallow water dolomite at the top of the first sub-sequence, confirming the evaporative nature of the sedimentary environment due to sub-aerial exposure.

The $\delta^{34}S$ data obtained from sulfate minerals and trace sulfates of carbonate samples from most of the sequences – varying from +15 to + 46‰ CDT – are consistent with known Neoproterozoic changes.

REFERENCES

Babinski, M., Kaufman, A.J. and Varni, M.A., 2002, New evidence for Sturtian glaciation in Brazil based on Pb isotopes. Gondwana 11 Correlations and Conections. Christchurch, New Zealand. Program and Abstracts.

Boggiani, P.C., 1998, Análise Estratigráfica da Bacia Corumbá (Neoproterozóico) – Mato Grosso do Sul. Doctoral Thesis, Instituto de Geociências da Universidade de São Paulo, 181 p.

Brito Neves, B. B., Campos Neto, M.C. and Fuck, R.A., 2000, From Rodinia to Western Gondwana: na approach to the Brasiliano-Pan African cycle and orogenic collage. Episodes, 22 (3): 155-166.

Condie, K. C., 2002, The supercontinent cycle: are there two patterns of cyclicity? Jour. African Earth Sci., 35:179-183.

Gaucher, C., Boggiani, P.C., Sprechmann, P., Sial, A. N., and Fairchild, T., 2003, Integrated correlation of the Vendian to Cambrian Arroyo del Soldado and Corumbá Groups (Uruguay and Brazil): paleogeographic, paleoclimatic and paleobiologic implications. Precambrian Research, 120: 241-278.

Jacobsen, S. B., Kaufman, A. J., 1999, The Sr, C and O isotopic evolution of Neoproterozoic seawater. Chemical Geology, 161: 37-57.

Macedo, M. H. F., Bonhome, M. G., 1984, Contribuição à croestratigrafia das Formações Caboclo, Bebedouro e Salitre na Chapada Diamantina (BA) pelos métodos Rb-Sr e K-Ar. Revista Brasileira de Geocências, 14: 153-163.

Macedo, M. H. F., 1982, Les Systhèmes Isotopiques Rb-Sr et K-Ar dans les argiles extraités de sédiments carbonatés. Application à la datation du Protérozoique sédimentaire du Brésil dans les États de Bahia et Santa Catarina. Doctoral Thesis, Université Louis Pasteur, Strasbourg, France, 119 p.

Misi, A., 2001, Estratigrafia Isotópica das Seqüências do Supergrupo São Francisco, Coberturas Neoproterozóicas do Cráton do São Francisco. Idade e Correlações. In, C. P. Pinto & M. A. Martins-Neto, Bacia do São Francisco: Geologia e Recursos Naturais, Soc. Bras. Geologia, Núcleo de Minas Gerais, p. 67-92.

Misi, A., Iyer, S.S., Tassinari, C.C.G., Coelho, C.E.S., Franca-Rocha, W.J.S., Gomes, A.S.R., Cunha, I.A. and Carvalho, I.G., 1999, Geological and isotopic constraints on the metallogenic evolution of the Proterozoic sediment-hosted Pb-Zn (Ag) deposits of Brazil, Gondwana Research, 2 (1999), 47-65.

Pedrosa Soares, A. C., Cordani, U.G., and Nutman, A., 2000, Constraining the age of Neoproterozoic glaciation in Eastern Brazil: first U-Pb (SHRIMP) data for detrital zircons. Revista Brasileira de Geociências, 30: 58-61.

Porada, H., 1998, Pan-African rifting and orogenesis in Southern to Equatorial Africa and Eastern Brazil. Precambrian Research, 44: 103-136.

Zaine, M., 1991, Análise dos fósseis de parte da Faixa Paraguai (MS, MT) e seu contexto temporal e ambiental. Doctoral Thesis, Instituto de Geociências da Universidade de São Paulo.

$\delta^{13}C$ AND $\delta^{18}O$ DISTRIBUTIONS IN THE CERRO PAMPA SECTION (SANTA MARÍA-HUALFÍN BASIN, CATAMARCA, ARGENTINA) AND THEIR PALEOGEOGRAPHIC IMPLICATIONS

Muruaga, C.M.[1]; Sial, A.N.[2] and Bossi, G.E.[1]

1. IESGLO, UNT, Miguel Lillo 205, (4000) Tucumán, Argentina
2. NEG-LABISE, Dept. Geology, Federal University of Pernambuco, C.P. 7852, Recife-PE, 50.670-000, Brasil

Keywords: Stable isotopes, chemostratigraphy, Neogene Continental Basin, climatic evolution

INTRODUCTION

The Neogene successions of the Santa María-Hualfín Basin, Argentina (Fig. 1) have yielded consistent evidences of $\delta^{13}C$ and $\delta\ ^{18}O$ paths that could be used to adjust correlation between stratigraphic sections (Fig. 2a). Isotopic changes at 9-3 Ma interval were assigned to moisture stress responsible for C3 to C4 vegetation transition (Latorre et al., 1997) that was assumed to be global for the Neogene times. Kleinert and Strecker (2001) analyzed the Santa María Valley data (a composed 12-3 Ma section 180 km to the NNE of the study area), and concluded that the observed changes in the C and O isotope composition are related to the uplift during the Andean Orogeny that induced a climate shift toward aridity. They also accepted the possibility that a vegetation change from C3 to C4 occurred into the 9 to 3 Ma interval. The paleogeographic evolution of the basin from an extensional regime (shallow hemigraben style of basin filling) to a tectonic inversion around 4.5-5 Ma elevated the eastern border mountain ranges (Bossi et al., 2001). This uplift reduced progressively the influence of the southeastern humid winds coming from the Atlantic Ocean, which is the main supply of rain for NW Argentina in the present time climate. The moisture stress induced the vegetation shift from grasses (C3) to a scarce cover of spiny bushes, trees and shrubs (C4) or a mixture of C3/C4 components (Quade et al., 1993). Through 9 to 4 Ma interval, the basin was defined as savannah plain (Marshall and Patterson, 1981) with dense cover of grasses and tree patches being the main support of the rich vertebrate fauna of the Santa María and Puerta de Corral Quemado sections. The fauna was assigned to Huayquerian mammal age. The fauna persisted up into younger times (4 Ma) and became mostly relictic after 6 Ma. Probably the tectonic inversion located in 5-4 Ma time showed in paleogeographic modification leading up to progressive aridification. Many changes operated in vegetation population, rivers′ regime and relief lead to a decline and final extinctions of the fauna.

Table 1: Stable isotope composition of calcretes, carbonate rhyzoconcretion and nodules from Cerro Pampa section.

Sample	Stratigraphic Units (Formations)	Profile height (m)	$\delta^{18}O$ PDB (‰)	$\delta^{13}C$ PDB (‰)
C-36	Hualfín	21.46	-7.43	-4.50
C-34	Hualfín	53.36	-11.52	-5.94
C-37	Hualfín	70.86	-11.00	-6.05
C-38	Hualfín	105.04	-9.82	-6.60
C-35	Hualfín	134.14	-10.56	-8.06
C-32	Hualfín	231.39	-9.81	-8.33
C-31	Hualfín	318.16	-9.05	-7.67
C-30	Las Arcas	341.10	-11.97	-8.09
C-29	Las Arcas	431.89	-10.83	-6.83
C-28	Las Arcas	441.09	-9.88	-7.53
C-27	Las Arcas	481.47	-10.42	-7.10
C-41	Las Arcas	524.67	-9.07	-7.16
C-42	Las Arcas	581.65	-9.04	-7.74
C-43	Chiquimil	691.62	-7.66	-7.44
C-13	Chiquimil	732.91	-6.56	-9.89
C-44	Chiquimil	743.34	-7.91	-9.44
C-45	Chiquimil	746.71	-6.88	-10.31
C-14	Chiquimil	814.06	-8.81	-11.51
C-15	Andalhuala	888.31	-9.56	-5.84
C-16	Andalhuala	912.11	-7.83	-9.28
C-17	Andalhuala	941.51	-7.43	-8.68
C-20	Andalhuala	1079.16	-7.09	-7.50
C-22	Andalhuala	1216.68	-6.27	-7.29
C-25	Andalhuala	1340.10	-5.62	-7.27
C-26	Andalhuala	1350.60	-4.78	-7.65
C 5-2	Andalhuala	1359.34	-5.95	-7.70
C-3	Andalhuala	1359.49	-12.51	-8.15
C-23	Andalhuala	1361.96	-5.57	-8.30
C 39-6	Andalhuala	1388.05	-5.42	-7.09
C 65-7	Andalhuala	1411.92	-6.05	-7.17
C 80-8	Andalhuala	1426.42	-5.29	-6.87
C 95-9	Andalhuala	1442.10	-5.51	-8.34

METHODS

Samples were taken in the field as carbonate nodules, calcretes (normally sandy irregular bodies) and rhyzoconcretion (sandy to massive carbonate with gross cylindrical shapes). Many fine sandstone and siltstones of floodplain deposits present pedogenic carbonates. Most of them are also associated with root clayish fillings and/or mottled massive sediments.

The isotope analysis (A.N.S. at the NEG-LABISE, UFPE, Recife, Brazil) started with 10-20 mg of powdered sample reacted with 100%-ortophosphoric acid by 2 hours. The liberated CO_2 was collected through a vacuum extraction line and the $\delta^{13}C$ and $\delta^{18}O$ values analyzed with a mass spectrometer SIRA II (VG-ISOTECH). Data are reported in the δ notation in ‰ relative to PDB, and presented in Table 1 and also as curves (smoothing of three points) with individual points in figure 2b.

THE CERRO PAMPA SECTION

The Cerro Pampa section (Fig. 1) is a Tertiary stratigraphic succession (Fig. 2a). The reduced stratigraphic thickness (1,600 m) and the disconformities that punctuated the succession indicate a position on the ramp of a hemigraben, developed to the west, which has its maximum thickness around the town of Puerta de Corral Quemado (located around 20 km to the WNW). The section (Fig. 2a) could be correlated with the Puerta de Corral Quemado (and Villavil) successions using several stratigraphic similarities and three prominent stratigraphic markers (Fig. 2 a,b). (1) The contact (and disconformity) at the base of Las Arcas Formation (red fine sandstone and shale), located at 10.7 Ma (Kleinert y Strecker, 2001); (2) The contact (or disconformity) between the Chiquimil Formation and the Andalhuala Formation (known also as the yellow line) that define the final decline of the andesite intrabasinal volcanism. The age of the limit is marked by the proximity of the 7.14 Ma tephra (Latorre et al., 1997). (3) The disconformity, (an angular unconformity at Cerro Pampa area) at the base of the Corral Quemado Formation, defined by the massive entrance of conglomerates derived from Crystalline Basement. This limit was located around 3.5 Ma in Villavil-Corral Quemado area (Muruaga, 1998, 2001) and at 3 Ma by Kleinert and Strecker (2001) at Santa María Valley. Many other regional and stratigraphic considerations support also those contact ages.

The Cerro Pampa section shows many primary sedimentary features in their facies that indicate a progressive aridity toward the upper units. The $\delta^{13}C$ and $\delta^{18}O$ data, taken from calcretes, rhyzoconcretions and soil nodules along the section, produced a clear signature that is consistent with the Puerta de Corral Quemado path (Latorre et al., 1997). In Latorre et al. section, there are also some age inconsistencies that arose with the actual location of the 7.14 Ma tephra. According to the magnetostratigraphy of Butler et al. (1985), it should be located in a long reverse interval around 7 Ma (GMTS of Cande and Kent, 1992, 1995) but it was positioned in front of a thick normal interval placed well below the normal 7 Ma interval of the CK92 scale.

Comparison between the isotope curves of Puerta de Corral Quemado, Valle de Santa María and Cerro Pampa sections were made using equal interval distance for the stratigraphic markers (disconformities and/or low angle angular unconformities in the Cerro Pampa section) mentioned above. The allostratigraphic correlation produced two positive effects: a) equalized the three sections to be compared, and b) produced a reasonable event time scale for the 9-3 Ma interval not complicated by individual age extrapolation for every soil carbonate sample.

Figure 2b presents the $\delta^{13}C$ and $\delta^{18}O$ smoothed paths of the compared three sections and confirmed the correlation potential of the C and O isotope data. Latorre et al. (1997) located the C3-C4 vegetation transition at $\delta^{13}C = -8.0‰$ limit value. Such a transition is also present in the Cerro Pampa data, but is a minor detail considering other variation features of curves as a whole (Fig. 2b). First, there is a strong correlation between pebble composition of the Cerro Pampa section and the stable isotope paths (Figure 2b). The curves have three important negative excursions both for C and O isotopes around the correlation stratigraphic markers, being peak of marker (2) the most prominent (Fig. 2b). The correlation is particularly strongly positive with the volcanic pebble composition. Associated with this peak, there is a higher dispersion of individual data, a feature repeated in the three considered sections (Cerro Pampa, Puerta de Corral Quemado and Santa María Valley). The peak of marker (2) represents also the massive onset of clastic material from volcanic sources.

The isotope path of lower units below 9 Ma is poorly correlated probably because ages are coming from indirect evidences and regional correlations and need to be adjusted.

The isotope curves of the two complete sections (Cerro Pampa and Santa María Valley) present a very complex pattern which explanation goes far than a simple shift between the C3 and C4 vegetation types and moisture stress. This factor could explain only the behavior of the upper third of the curves. The data dispersion of the lower two third should be related with the contributions of relief (affecting in turn the climate and moisture levels), changes of volume, texture, chemical and mineralogical compositions of the source materials.

It is important to remark the vicinity of the Puerta de Corral Quemado and the Cerro Pampa sections to the huge volcanic center known as Farallón Negro Complex. The volcanic centre was active during the 11 to 6 Ma interval (Caelles et al., 1971). The Villavil section (Muruaga, 1998, 2001), located 20 km north of Puerta de Corral Quemado, presents a very similar pebble composition with Cerro Pampa succession. The Puerta de Corral Quemado section is located between the two of them.

It is obvious that the intrabasinal volcanism is in part responsible for the observed isotope paths. The strong volcanism could induce part of the climatic and soil modifications that affected the $\delta^{13}C$ and $\delta^{18}O$ paths in carbonates around 9 Ma. After the tectonic inversion started (5-4 Ma, Bossi et al., 2001), the $\delta^{13}C$ and $\delta^{18}O$ paths should be related to uplift and climatic changes by emplacement of mountain barriers.

Finally we confirmed the power of defined allostratigraphic markers combined with stable isotope data as a tool to refine stratigraphic correlations.

REFERENCES

Bossi, G.E.; Georgieff, S.M,; Gavriloff, I.J.C.; Ibañez, L.M & Muruaga, C.M., 2001. Cenozoic Evolution of the intramontane Santa María basin, Pampean Ranges, northwestern Argentina. J. S. Am. Earth Sciences, 14:725-734.

Butler, R.I.; Marshall, I.G.; Drake, R.E. & Curtis, G.H., 1985. Magnetic polarity stratigraphy and 40K-40Ar dating of late Miocene and early Pliocene continental deposits. Catamarca Province, NW Argentina. J. Geol., 92: 623-636.

Caelles, J.C.; Clark, A.H.; Farrar, E.; McBride, S.L. & Quirt, S., 1971. Potassium-Argon ages of porphyry cooper deposits and associated rocks in the Farallón Negro Capillita district. Catamarca. Argentina. Economic Geology, 66: 961-964.

Cande, S.C. & Kent, D.V., 1992. A new geomagnetic polarity time scale for the late Cretaceous and Cenozoic. J. Geophys.Res., 97(B10): 13,917-13,951.

Cande, S.C. & Kent, D.V., 1995. Revised calibration of the geomagnetic polarity time scale for late Cretaceous and Cenozoic. J. Geophys.Res., 100(B4): 6,093-6,095.

Cerling, T.E.; Wang, Y. & Quade, J., 1993. Expansion of C4 ecosystem as an indicator of global ecological change in the late Miocene. Nature, 361: 344-345.

Kleinert, K. & Strecker, M.R., (2001) Climate change in response to orographic barrier uplift: Paleosol and stable isotope evidence from the late Neogene Santa María basin, northwestern Argentina. GSA Bull., 113(6):728-742.

Latorre, C., Quade, J. & McIntosh, W.C., 1997. The expansion of C4 grasses and global change in the late Miocene: Stable isotope evidence from the Americas. Earth & Planetary Science Letters, 146:83-96.

Marshall, L.G. & Patterson B., 1981. Geology and Geochronology of the mammal-bearing Tertiary of the Valle de Santa María and Río Corral Quemado, Catamarca province, Argentina. Fieldiana Geology, 9:1-80.

Muruaga, C.M., 1998. Estratigrafía y Sedimentología del Terciario Superior de la Sierra de Hualfín, entre las localidades de Villavil y San Fernando, Prov. de Catamarca. Doctoral Dissertation, Library of the Facultad de Ciencias Naturales e I.M.L., UNT, Tucumán, Argentina : 269.

Muruaga, C.M., 2001. Estratigrafía y desarrollo tectosedimentario de sedimentos terciarios en los alrededores de la Sierra de Hualfín, borde suroriental de la Puna, Catamarca, Argentina. Revista de la Asociación Argentina de Sedimentología. vol. 8 (1): 27-50.

Sasso, A., 1997. Geological Evolution and Metallogenic Relationships of the Farallón Negro Volcanic Complex, NW Argentina. Vol 1, Ph.D. Queens University, Kingston Ontario,Canada.

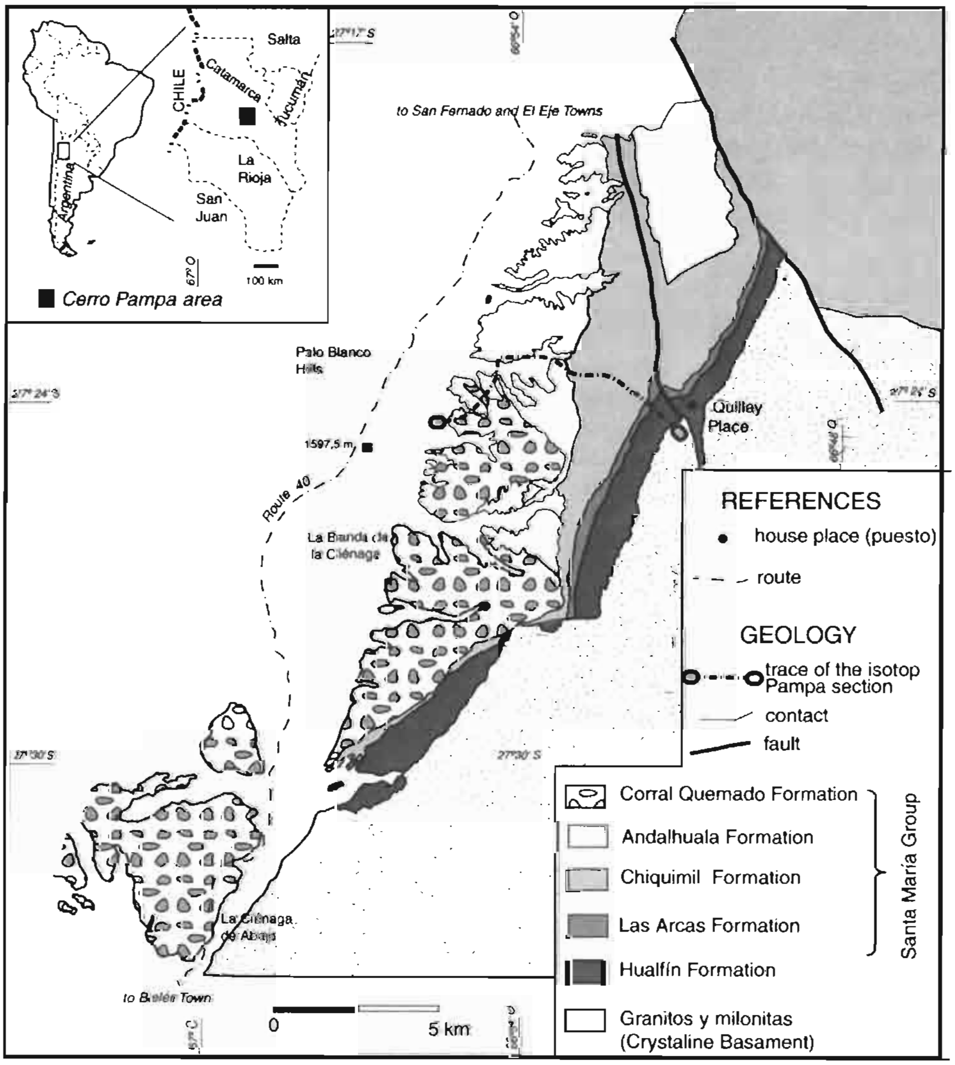

Figure 1. Location and geological map of the Cerro Pampa area.

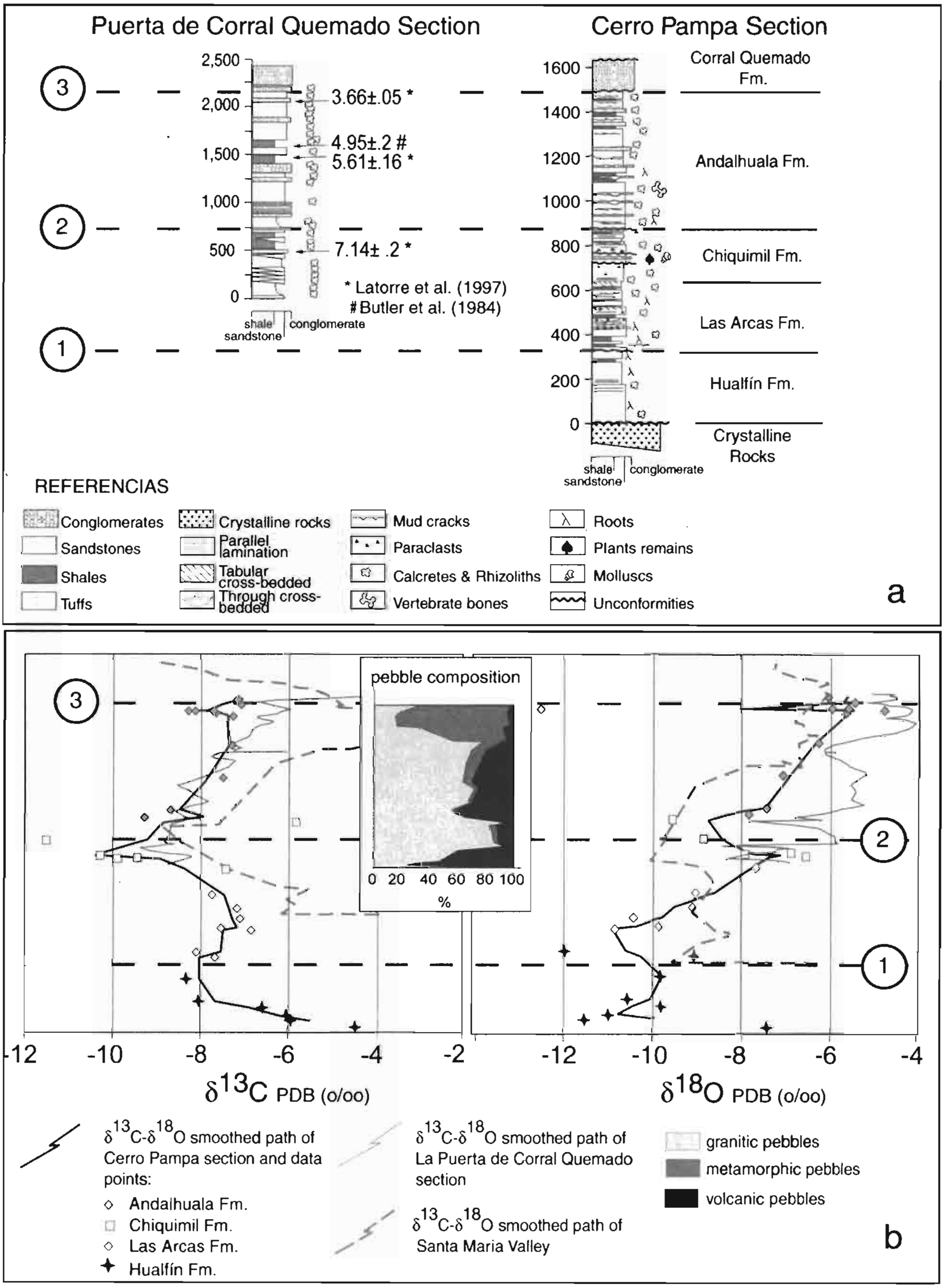

Figure 2. a. Stratigraphic sections from Puerta de Corral Quemado and Cerro Pampa correlated by allostratigraphic levels; b. Stable isotope paths of the three considered sections (Puerta de Corral Quemado, Latorre et al., 1997, Santa María Valley, Kleinert & Strecker, 2001 and Cerro Pampa, this paper).

C AND Sr-ISOTOPE BEHAVIOR AND THE AGE OF MARBLES OF THE SERIDÓ FOLD BELT, NORTHEASTERN BRAZIL

Nascimento, R.S.C.[1]; Sial, A. N.[2] and Pimentel, M.M.[3]

1. NEG-LABISE, Dept. of Geology, Federal University of Pernambuco;. current address: Institute of Geosciences, University of Brasilia, 70910-900. Brasília-DF, Brazil. rielva@unb.br
2. NEG-LABISE, Dept. of Geology, Federal University of Pernambuco, C.P. 7852, 50670-000, Brazil. ans@ufpe.br
3. Institute of Geosciences, University of Brasilia, Brasilia,. 70910-900. Brasília-DF, Brazil. marcio@unb.br

Keywords: C-isotopes, northeastern Brazil, Seridó Belt, marble, Neoproterozoic age

INTRODUCTION

The reconstruction of the original stratigraphy of Precambrian sequences, whose sedimentary structures and original relationships of their strata have been masked or obliterated by metamorphism and deformation, is very complex. Lack of fossil record is an additional complication and precludes dating of the sedimentation as well as, inter- and intra-basinal stratigraphic correlation. Petrographical, geochemical and structural studies are, sometimes, tools to minimize these problems, allowing inferring, beyond deformation and metamorphism, the nature of protoliths and their original relationships. C and Sr chemostratigraphic studies applied to Precambrian marbles have helped to establish stratigraphic correlation between strata and also to estimate the age of sedimentation (Melezhki et al., 2001). Radiogenic dating methods applied to sedimentary carbonate rocks that have undergone thermal events, generally yield the age of the last thermal event. The combined use of C and Sr isotopic composition of carbonatic rocks, instead represent an additional tool that can be used to estimate depositional ages. Ages of deposition of marine carbonates, submitted to metamorphism at variable degree, have been estimated by comparing their C and or Sr isotope chemostratigraphic curves with the global, secular C and Sr variation curves for seawater (e.g. Melezhki et al., 2001).

GEOLOGICAL SETTING

The Seridó Belt, localized in the northeastern part of the Borborema Province in northeastern Brazil (Fig. 1), has been the target of several studies in the last two decades. This Belt encompasses a vulcanosedimentary sequence that was deposited on a Paleoproterozoic basement. It was subsequently affected by strong transpressional deformation, intrusion of voluminous granitic magmatism and reworking by transcurrent structures that imparted a N-NE trend to the Belt (Fig. 1). Intense deformation poses some difficulty in the reconaissance of original stratigraphic relationships and has led to divergent interpretation of the age of sedimentation, stratigraphy and evolution of the supracrustal rocks.

The stratigraphic column proposed for this Belt (Jardim de Sá and Salim, 1980) includes all metasedimentary rocks in the Seridó Group, subvided in three formations, from base to top (Fig. 1): (a) the Jucurutu Fm. (gneisses with intercalations of marble, quartzite, micaschist, calc-silicate rocks, iron formations, metavolcanic rocks and basal conglomerate); (b) the Equador Fm. (quartzite with meta-conglomerate lenses, calc-silicate rocks and paragneisses) and finally, (c) the Seridó Fm. (feldspathic or aluminous micaschists, with subordinate marble, calc-silicate rocks, paragneiss, basic metavolcanic rocks, quartzite and meta-conglomerate).

The association of marble, iron formation, and the calcitic-quartzitic tendency of the paragneisses of the Jucurutu Fm. (quartzite-pelite-carbonate association) point to deposition in a shallow marine environment. The Equador Fm. represents the terrigenous component of this shallow marine association (still in the quartzite-pelite-carbonate association), perhaps deposited under stable condition, whereas micaschists of the Seridó Fm. represent a thick package of turbiditic, flyschoid deposits (graywacke-greenstone association with predominance the sedimentary component) marking the inversion of the basin (Jardim de Sá, 1994).

The age of the Seridó Group rocks has been investigated in several studies. Sm-Nd isochron data for basic metavolcanic rocks of the Jucurutu and Seridó Fms yielded extremely old ages (3.027 ± 0.525 Ma and 1.399 ± 0.110 Ga, respectively - Jardim de Sá, 1994). Indirect dating of supracrustal rocks was obtained from granitic orthogneisses, regarded as intrusive into the Seridó Group with ages between 2.0 and 1.9 Ga (Rb-Sr and U-Pb). However, the relationships between these intrusions and their metasedimentary hosts are far from unequivocal because contacts are usually marked by shear zones (Archanjo and Legrand, 1997). Detrital zircon ages for Seridó micaschists indicate contribution from sources as younger as 650 Ma (Van Schmus et al. 2000), and establish a late Neoproterozoic maximum age for the deposition of the original sediments.

Considering the difficulty in establishing a chronological sequence of events in the Seridó Belt based on radiogenic methods, we suggest that Sr and C-isotope chemostratigraphy applied to the Seridó marbles may contribute to address this problem and help establishing the age of sedimentation.

PETROGRAPHY OF THE SERIDÓ BELT

Lenses of marble are largely distributed within the Seridó Belt. In the Jucurutu Fm., marble lenses are abundant and occur in two or three stratigraphic levels, one of which near the base of the sequence (Jardim de Sá, 1994). In the Seridó Fm., due to the tectonic nature of the original basin, considered to be an inversion sequence, marble lenses are scarcer and are found only near the base of the sequence.

Marbles of the Jucurutu Fm. occur as metric to decametric lenses of predominantly massive, in places compositionally banded (white and gray bands in a zebra-like pattern) rocks. In the seven marble lenses sampled for this study (Jucurutu, São Rafael, Caicó-Jardim do Seridó, Várzea-São João do Sabugi, Ipueira, Messias Targino and Almino Afonso lenses; Fig. 1) the silicate minerals are observed and are more abundant close to contacts wich pelitic metasedimentary rock. Amphibole is the most abundant among the silicate minerals and varies from tremolite to Mg-hornblende and edenite. Pyroxene is usually represented by diopside, and wollastonite was found in lenses near granitic plutons, and in marbles with intercalations of calc-silicate rocks and pegmatite dikes. Phlogopite, clinozoisite and forsterite were found in some lenses as rare accessory phases.

In the Seridó Fm., only two marble lenses have been sampled: São Mamede and Serra do Cruzeiro da Maniçoba (Fig. 1). The São Mamede is compositionally banded, and has been tightly and asymmetrically folded. It is constituted by calcite marbles with tremolite and sillimanite, the latter disposed according to the fold axial planes, in the contact zone with schists. The Serra do Cruzeiro da Maniçoba marble lens consist of pure marbles, essentially calcitic, with some quartz and opaques as rare accessory phases.

C- ISOTOPE GEOCHEMISTRY

Three stratigraphically distinct levels of carbonate lenses can be recognized in the Jucurutu Fm. based on their $\delta^{13}C$ values. The first one is observed in the Jucurutu, Caicó-Jardim do Seridó, Ipueira and Várzea-São João do Sabugi marble lenses, with $\delta^{13}C$ values between +2.8 and +11.8‰ PDB and $\delta^{18}O$ between -20.3 and -5.6‰ PDB. Silicate minerals are more common in marbles near their contact with pelitic metasedimentary rocks. Comparing the C-isotope and mineralogical compositions of the marbles, there is a close relationship between the amount of silicate and the depletion in ^{13}C. If altered samples are discarded ($\delta^{13}C$ <7.8‰ PDB) the first carbonate sedimentation level of the Jucurutu Fm. displays $\delta^{13}C$ between +8.3 and +11.8‰ PDB (Fig. 2).

The Almino Afonso marble lens represents the second level of carbonate sedimentation. $\delta^{13}C$ in this lens varies from -1.1 to +8.7‰ PDB and $\delta^{18}O$ from –19,1 to -5.7‰ PDB. The negative values are found at the base of the section, in marbles with wollastonite and pegmatitic veins and calc-silicate nodules. The mineralogical constitution of the samples more depleted in ^{13}C (sample with wollastonite and calc-silicate nodules), demonstrates a large amount of fluid infiltration. This fluid allowed, by means of decarbonation reactions, the formation of wollastonite and subordinate Mg-olivine, resulting in the modification of the original $\delta^{13}C$ and $\delta^{18}O$ isotope signatures. In samples consisting of essentially by calcite, $\delta^{13}C$ values vary from +7.6 to +8.7‰ PDB (Fig. 2) and $\delta^{18}O$ from -10,9 to -5.7‰ PDB.

The São Rafael and Messias Targino marble lenses define the third level of carbonate sedimentation. The Messias Targino marbles present a very homogeneous isotope composition with $\delta^{13}C$ values from +2.3 to 3.7‰ PDB that apparently were not affected by modification of the isotopic composition (Fig. 2). The São Rafael marbles, on the other hand, are characterized by strong variation of their C and O isotopic compositions. The $\delta^{13}C$ varies from -8.9 to +3.8‰ PDB and $\delta^{18}O$ from -10,3 to -2.8‰PDB. Excluding the altered samples, $\delta^{13}C$ and $\delta^{18}O$ values for the São Rafael marbles, are between +0.7 and +3.8‰PDB (Fig 2) and -10.3 to -5,5‰ PDB respectively.

In the Seridó Fm., the two lenses sampled gave distinct $\delta^{13}C$ composition. The São Mamede lens has $\delta^{13}C$ values between +4.4 and +10.7‰ PDB and $\delta^{18}O$ from -9,4 to -6.9‰ PDB, with lowest values located near the contact with the host schist. In these samples, the silicate mineralogy is represented by tremolite, phlogopite and sillimanite in the more ^{13}C-depleted samples. If altered samples were discarded, $\delta^{13}C$ would be in the interval between +8.9 and +10.7‰ PDB (Fig. 2) and $\delta^{18}O$ between –9.4 to -6.9‰ PDB.

The samples from the Serra do Cruzeiro da Maniçoba lens have negative $\delta^{13}C$. The $\delta^{13}C$ values are very homogeneous, varying from -4.0 to -4.6‰ PDB (Fig. 2) and $\delta^{18}O$ from -16.4 to -15.2‰ PDB. Silicate minerals are absent in these marbles.

Sr-ISOTOPE GEOCHEMISTRY

The $^{87}Sr/^{86}Sr$ ratios have been determined for the Jucurutu and Messias Targino lenses, intercalated in the Jucurutu Fm., and São Mamede and Serra do Cruzeiro da Maniçoba lenses, intercalated in the Seridó Fm..

The Jucurutu and Messias Targino lenses, although display variable $\delta^{13}C$ compositions, and gave similar Sr isotopic ratios ($^{87}Sr/^{86}Sr$ ratio between 0.7074 and 0.7075; Fig. 2). The São Mamede marble lens, although intercalated in the Seridó Fm., yielded Sr isotope composition similar to the stratigrafically older marble lenses of the Jucurutu Fm. ($^{87}Sr/^{86}Sr$ ratios between 0.7041 and 0.7056). In the section of the Serra do Cruzeiro da Maniçoba, $^{87}Sr/^{86}Sr$ is higher and more variable, with values between 0.7077 and 0.7094 (Fig. 2).

In the Serra do Cruzeiro da Maniçoba lens section, the gradational increase in $^{87}Sr/^{86}Sr$ indicates different degrees of isotopic exchange. When compared to those of the remaining chemostratigraphic sections it, leads us to conclude that the isotope exchange was rather limited in samples with $^{87}Sr/^{86}Sr$ <0.7080, and by comparison with the composition of samples in the São Mamede lens section, samples with $^{87}Sr/^{86}Sr$ <0.7080 from the Serra do Cruzeiro da Maniçoba section, have not been discarded from the chemostratigraphic studies (Fig. 2).

AGE OF SEDIMENTATION OF THE SERIDÓ CARBONATES INFERRED FROM C AND Sr-ISOTOPE STRATIGRAPHY

The majority of $\delta^{13}C$ values for the Jucurutu Fm. lenses are between +8.3 and +11.8‰ PDB, despite their distinct geographic locations and the compositional-mineralogical variations. This suggests that the carbonate sedimentation was spatially and temporally homogeneous in the Seridó Belt. The characterization of three compositional plateaus of $\delta^{13}C$, characterize more than one stratigraphic level of carbonate rocks deposition in the Jucurutu Fm., as already suggested by Jardim de Sá (1994). The correlation with stratigraphic profiles proposed by Jardim de Sá (1994), in the region of São José do Sabugi and Ipueira, allows inferring that the Ipueira marble lens is the oldest, and it is probably equivalent to the Caicó-Jardim do Seridó, Jucurutu and Várzea-São João do Sabugi marble lenses, as they exhibit similar C-isotope compositions.

According to the secular C-isotope variation curve (Hoffman et al. 1998), continuous and vigorous oscillation in $\delta^{13}C$ values, from +11.8 to -4.6‰ PDB, is restricted to the Neoproterozoic. These are also the extreme $\delta^{13}C$ values found in the marbles of the Seridó Group. A zoom in the Neoproterozoic is seen in the Fig.10A, with vertical areas illustrating the composition interval of the marble lenses studied. Taking into account the plateau between +8.3 and +11.8‰ PDB as the lowest depositional level of the carbonate sedimentation in the Seridó Belt, a comparison with Hoffman *et al* (1998) C-isotope variation curve, suggests that the Almino Afonso lens represents the intermediate stratigraphic level ($\delta^{13}C$ between 7.6 and 8.7‰ PDB) and the São Rafael lens forms the upper stratigraphic level ($\delta^{13}C$ between 0.7 and 3.8‰ PDB) of the Jucurutu Fm..

In the Seridó Fm., the intervals of variation of $\delta^{13}C$ also demonstrate the existence of more than one depositional level. Likewise the Jucurutu Fm., the gradational decrease of $\delta^{13}C$ values towards the top, suggests that São Mamede lens ($\delta^{13}C$ = +8.9 to +10.7‰ PDB) represents the base of the Seridó Fm. and the Serra do Cruzeiro da Maniçoba marble lens ($\delta^{13}C$ = -4 to -4.6‰ PDB) represents an upper depositional level (Fig. 3A).

The age estimate for the original carbonate sedimentation of the Seridó Belt, obtained from the $\delta^{13}C$ fluctuations in marble lenses compared with the C-isotope secular variation curve (Hoffman et al., 1998), suggests that the carbonate sedimentation of the Seridó Group ocurred in the late Sturtian to early Vendian (640 to 570 Ma, Fig. 3A). However, regarding the general tendency for a decrease of ^{13}C upsection in all of the studied Seridó Group marbles, the age interval for deposition of these carbonates most probably lies within the early Vendian (590 to 570 Ma, Fig. 3A-$I_{mín}$).

Sr-isotope composition also supports a Neoproterozoic age for the Seridó Belt marbles. $^{87}Sr/^{86}Sr$ values of 0.7074 to 0.7079, in Precambrian sedimentary carbonates are typical for the Neoproterozoic. In figure 3B, ages estimated by $\delta^{13}C$ and by $^{87}Sr/^{86}Sr$ for the Jucurutu and Messias Targino marble lenses (Jucurutu Fm.) and São Mamede and Serra do Cruzeiro da Maniçoba (Seridó Fm) are compared.

The $^{87}Sr/^{86}Sr$ ratios suggest a shorter age interval, between 610 and 590 Ma according to the trend of Melezhik et al. (2001) and 580 to 570Ma according to the global trend of Azmy et al. (2001) (Fig. 3B). In both cases, the ages estimated lie within the maximum age interval estimated from C-isotope stratigraphy.

The slight difference in the ages observed for carbonate deposition in the Seridó Belt obtained from the C chemostratigraphy, could result from the difference in residence time of Sr and C in the oceans. The residence time for Sr is estimated to be around 4 Ma (Kaufman and Knoll, 1995), while for C it is around 10^5 years (Kump and Arthur, 1999).

CONCLUSIONS

The progressive decrease of $\delta^{13}C$ values towards the top, suggests a continuous sedimentation for the Seridó Group and synchronism during a certain time interval between the sedimentation of upper carbonate levels of the Jucurutu Fm. and the sedimentation of the basal levels of the Seridó Fm.. The age interval (590 to 570 Ma) for the deposition of the Seridó Group is in agreement with U-Pb ages obtained for detrital zircons from the Seridó Fm. (650 Ma; Van Schmus et al., 2000). These data also are in agreement with $^{40}Ar/^{39}Ar$ studies of mica and amphibole by Figueiredo et al. (1992) in supracrustal rocks that indicate two metamorphic events, the earlier of high temperature with 544±3 Ma a later event of low temperature with minimum age of 505-500 Ma.

ACKNOWLEDGMENTS

We would like to thank E. F. Jardim de Sá for valuable suggestions and geological information about the Seridó Belt during the development of this study. This is the contribution n. 206 of the NEG-LABISE, Dept. of Geology, Federal University of Pernanbuco, Brazil

REFERENCES

Archanjo, C.J. and Legrand, J.M. 1997. Pre-Brasiliano orogenic evolution in the Seridó Belt, NE Brazil: conflicting gechronological and structural data. Rev. Bras. Geociências 27: 309-314.

Azmy, K., Veizer, J., Misi, A., Oliveira, T.F., Sanches, A.L., Dardenne, M.A. 2001 Dolomitization and isotope stratigraphy of the Vazante Formation, São Francisco Basin, Brazil. Precambrian Research, 112: 303-329.

Figueiredo, L.L.; Feraud, G.; Caby, R.; Corsini, M.; Arthaud, M.; Archanjo, C.J.; Jardim de Sá, E.F.; Egydio da Silva, M. (1992) O sincronismo termo-tectônico polifásico brasiliano dos sistemas cisalhantes Patos-Seridó e Campina Grande (Província Borborema) à luz de datações 40Ar/39Ar de monocristais com sonda laser. 37o Congr. Bras. Geol., Bol. Res. Exp., 2: 378-379.

Hoffman, P.F., Kaufman, A.J., Halverson, G.P. 1998. Comings and goings of Global glaciations on a Neoproterozoic Tropical Platform in Namibia. GSA Today, 8 (5), 1-10.

Jardim de Sá, E.F. 1994. A FSe (Província Borborema, NE do Brasil) e o seu significado geodinâmico na cadeia Brasiliana/Pan-Africana. Inst. de Geociências, Universidade de Brasília, Tese de Doutoramento, 803p

Jardim de Sá, E.F. and Salim, J. 1980. Reavaliação dos conceitos estratigráficos na região do Seridó (RN-PB). Miner. Metal., 80(421): 16-28.

Kaufman, A. J. and Knoll, A. H. 1995. Neoproterozoic variations in the carbon isotopic composition of seawater: stratigraphic and biogeochemical implications. Precambrian Res., 73: 27-49.

Kump, L.R. and Arthur, M.A. 1999. Interpreting carbon-isotope excursions: carbonates and organic matter. Chem. Geology, 161:181-198.

Melezhik, V. A., Gorokhov, I.M., Fallick, A.E., Gjelle, S. 2001. Strontion and carbon isotope geochemistry applied to dating of carbonate sedimentation: an example from high-grade rocks of the Norwegian Caledonites. Precambrian Res., 108: 267-292.

Van Schmus, W.R., Neves, B.B.B., Hackspacher,P.C., Wiliiams, I.S., and Fetter, A.H., 2000. The Seridó Group, NE Brazil: a Late Neoproterozoic (650 Ma) a pre-collisional, Brasiliano flysch basin? 31st IGC, Rio de Janeiro, Brazil (CD-ROM).

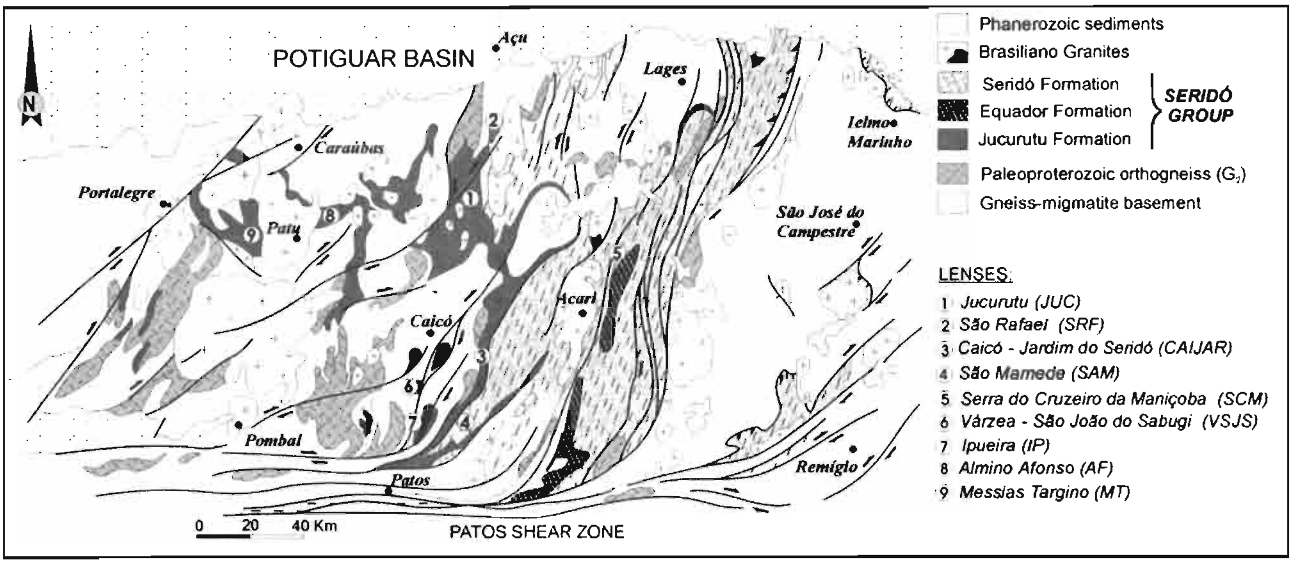

Figure 1. Simplified geological map of the Seridó Belt, showing the geographic and geological location of marbles in the present study. Modified from Jardim de Sá (1994).

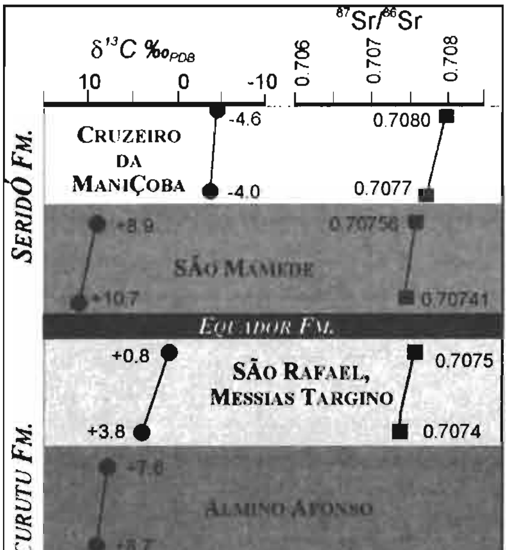

Figure 2. C and Sr compositions of marbles in the Seridó Belt.

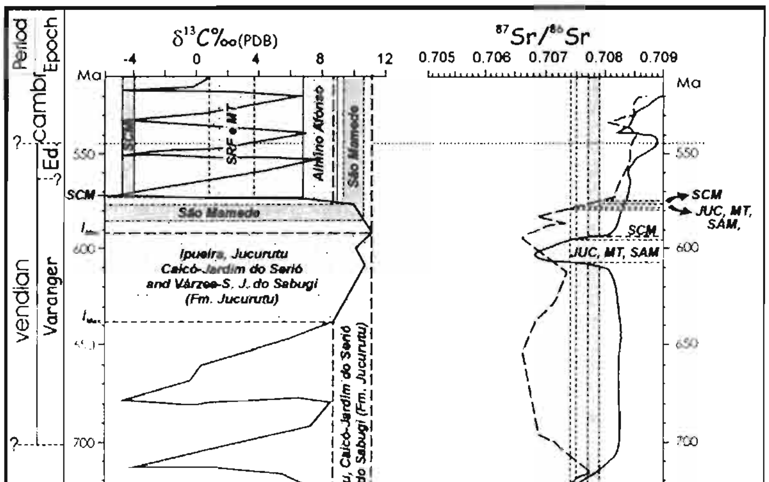

Figure 3. Global trends of C isotope variation (A) and Sr (B) for the Neoproterozoic, according to Hoffman et al. (1998) in (A), Azmy et al. (2001) and Melezhik et al (2001) in (B), dashed and solid lines, respectively. I_{max} and I_{min}, maximum and minimum ages, respectively for the sedimentation of carbonate rocks of the Seridó Belt.

C AND Sr ISOTOPE VARIATIONS AND PALEOCEANOGRAPHIC CHANGES AS RECORDED IN THE LATE NEOPROTEROZOIC ARARAS CARBONATE PLATFORM, AMAZON CRATON, BRAZIL

Nogueira, A.C.R.[1]; Riccomini, C.[2]; Sial, A.N.[3]; Moura, C.A.V.[4] and Trindade, R.I.F.[5]

1. Departamento de Geociências, Universidade Federal do Amazonas, Manaus, AM, and Programa de Pós-Graduação em Geologia Sedimentar, Departamento de Geologia Sedimentar e Ambiental, Instituto de Geociências, Universidade de São Paulo, Rua do Lago, 562, 05508-000, São Paulo-SP, Brazil. anogueira@ufam.edu.br
2. Departamento de Geologia Sedimentar e Ambiental, Instituto de Geociências, Universidade de São Paulo, São Paulo-SP, Brazil. riccomin@usp.br
3. NEG-LABISE, Departamento de Geologia, Universidade Federal de Pernambuco, CP 7852, 50732-970, Recife-PE, Brazil. ans@npd.ufpe.br
4. Laboratório de Geologia Isotópica-Pará-Iso, Instituto de Geociências, Universidade Federal do Pará, CP 1611, 66.075-900, Belém-PA, Brazil. c_moura@ufpa.br
5. Departamento de Geofísica, Instituto de Astronomia, Geofísica e Ciências Atmosféricas, Universidade de São Paulo, Rua do Matão, 1226, 05508-900, São Paulo-SP, Brazil. rtrindad@iag.usp.br

Keyword: C isotopes, Amazon craton, Araras Group, Varanger/Marinoan glaciation

Isotopic variations of seawater have been used as paleoenvironmental markers in the chemostratigraphy of Neoproterozoic successions and for correlation among cratonic regions worldwide (Knoll et al. 1986, Derry et al. 1992, Narbonne et al. 1994, Kaufman et al. 1997, Saylor et al. 1998, Walter et al. 2000). In this paper, we present carbon ($\delta^{13}C$) and strontium ($^{87}Sr/^{86}Sr$) isotopic data for the carbonate rocks of the late Neoproterozoic Araras Group, exposed on the southern border of the Amazon craton and within the North Paraguay Belt. The Araras Group (Almeida 1964) is more than 600m thick, and overlies the diamictites of the Puga Formation (Fig.1). It consists of four formations (Mirassol d'Oeste, Guia, Serra do Quilombo and Nobres) summarized in a composite section representative of deep to shallow platform deposits that crop out around Mirassol d´Oeste and Cáceres, Mato Grosso, Brazil (Fig. 1).

The $\delta^{13}C$ values along the Araras carbonate succession are interpreted as representatives of the original ocean water chemistry ($\delta^{13}O$ > -8‰$_{PDB}$). It exhibits a monotonic trend with strongly depleted $\delta^{13}C$ values at the base and enriched compositions towards the top of the succession (Fig. 2). The deep platform deposits constitute two units of cap carbonate, the cap dolomite (Mirassol d´Oeste Formation) and cap limestone cementstone (Lower Guia Formation) that show depleted $\delta^{13}C$ values around -5‰$_{PDB}$ (Nogueira *et al.* 2003). The anoxic deep platform limestone succession (Guia Formation) that covers the cap succession presents a homogeneous behavior of ^{13}C isotopic curve, with values around -2.50 to -1‰. The overlying platform dolomitic succession (lower Serra do Quilombo Formation) shows slightly positive values (+0,14 to +0,26‰$_{PDB}$) in the shoreface to shallow platform deposits (uppermost part of the Serra do Quilombo Formation), and oscillates to slightly negative values in the peritidal facies (Nobres Formation). The $^{87}Sr/^{86}Sr$ follows the general trend of C isotopes, with values increasing upsection (Fig. 2).

Although the values reach 0.7082 at the base of the succession (Mirassol d'Oeste Formation), a clear increasing is verified upwards, reaching 0.7081 in the Guia and Serra do Quilombo formations, and 0.7088 in the Nobres Formation. Anomalous $\delta^{13}C$ values around -9‰ or higher, and the striking shifts in $^{87}Sr/^{86}Sr$ up to 0.7113 are observed close to discontinuity surfaces (Fig.2).

$^{87}Sr/^{86}Sr$ values above 0.7081 far from any key surface at well preserved cap carbonate rocks suggest that the Puga glaciation correlates to the younger event of the Varanger/Marinoan glaciation (~575-570 Ma). The increasing of the $^{87}Sr/^{86}Sr$ values upsection, as observed in the Araras Group, is similar to others Neoproterozoic successions in Namíbia and Canada, generally interpreted as post-glacial continental influx to the oceans related to the Brasilian-Pan-African orogeny (*e.g.* Hoffman et al. 1998, Jacobsen & Kauffman 1999).

Each strong negative isotope excursion is associated with a sequence boundary and/or a marine flooding surface and may provide an independent tool for estimating ancient eustatic sea-levels. The correlation $\delta^{13}C$ and the relative sea-level curves reinforces the idea of a close association between the paleoceanographic changes and the paleoenvironmental evolution of the Araras carbonate platform. Sharp shifts in the isotopic values record changes in the carbon cycle as well as of upwelling of deep water masses depleted in $\delta^{13}C$ at times of rapidly changing sea-level caused by post-Varanger/Marinoan deglaciation. The composite C and Sr isotope stratigraphy of the late Neoproterozoic Araras carbonate platform records the dramatic paleoceanographic changes that preceeded the irradiation of metazoans in Cambrian times.

ACKNOWLEDGEMENTS

We thanks to FAPESP by financial support (grant to C.R., number 00/02903-8).

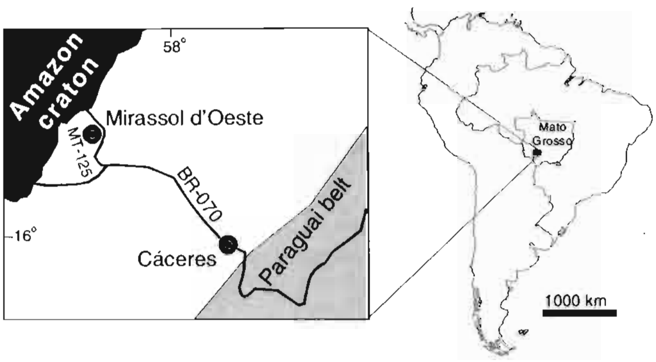

Figure 1. Location and geologic map.

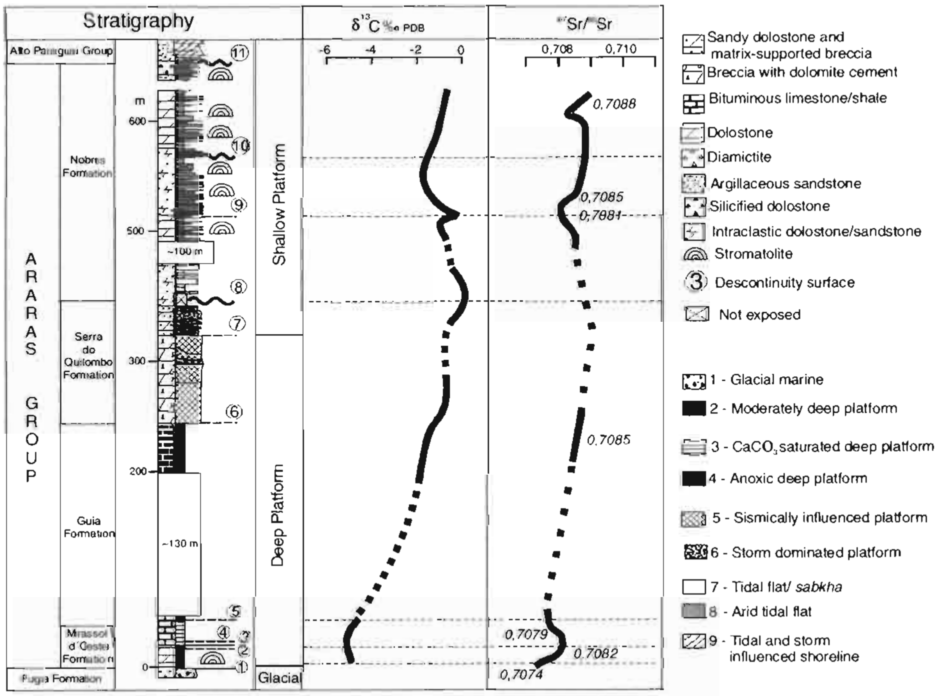

Figure 2. Lithostratigraphy, paleoenvironments and chemostratigraphy of Araras Group. The carbonate succession overly Varanger/Marinoan Puga diamictites. The values of $\delta^{13}C$ and $^{87}Sr/^{86}Sr$ are considered primary and representative of the Post-Varanger/Marinoan seawater.

REFERENCES

Almeida, F.F.M. 1964a. Geologia do Centro-Oeste Matogrossense. Boletim da Divisão de Geologia e Mineralogia-DNPM, 219, p. 1-53.

Derry, L.A.; Kaufman, A.J.; Jacobson, S.B. 1992. Sedimentary cycling and environmental change in the Late Proterozoic: evidence from stable and radiogenic isotopes. Geochim. Cosmochim. Acta, 56:1317-1329.

Hoffman, P.F.; Kaufman, A.J.; Halverson, G.P.; Schrag, D.P. 1998a. A Neoproterozoic Snowball Earth. Science, 281:1342-1346.

Jacobsen, S.B., & Kaufman, A.J. 1999. The Sr, C and O isotopic evolution of Neoproterozoic seawater. Chem. Geol., 161:37-57.

Kaufman, A.J.; KnolL. A.H.; NarbonnE, G.M. 1997. Isotopes, ice ages and terminal proterozoic stratigraphy – An example from the Olenek Uplift, northeastern Siberia. Precamb. Res., 73:251-270.

Knoll, A.H.; Hayes, J.M.; Kaufman, A.J.; Swett, K.; Lamert, I.B. 1986. Secular variation in carbon isotope ratios from Upper Proterozoic successions of Svalbard and Eats Greenland. Nature, 321: 832-838.

Narbonne, G.M., Kaufman, A.J., Knoll, A.H. 1994. Integrated chemostratigraphy and bioestratigraphy of the upper Windermere Supergroup (Neoproterozoic), northwestern Canada: Implications for Neoproterozoic correlations and the early evolution of animals. Geol. Soc. Am. Bull., 106:1281-1292.

Nogueira, A.C.R.; Riccomini, C.; Sial, A.N.; Moura, C.A.V.; Fairchild, T.R. 2003b. Soft-sediment deformation at the Neoproterozoic Puga cap carbonate (southwestern Amazon Craton, Brazil): conformation of rapid icehouse to greenhouse transition in snowball Earth. Geology, 31:613-616.

Saylor, B.Z.; Kaufman, A.J.; Grotzinger, J.P.; Urban, F. 1998 A composite reference section for terminal Proterozoic strata of southern Namibia: J. Sediment. Res., 68(6): 1223-1235.

Walter, M.R.; Veevers, J.J; Calver, C.R.; Gorjan, P.; Hill, A.C. 2000. Dating the 840-544 Ma Neoproterozoic interval by isotopes of strontium, carbon, and sulfur in seawater, and some interpretative models. Precamb. Res., 100:371-433.

THE GONDWANAN ORIGIN OF THE CUYANIA TERRANE, WESTERN ARGENTINA, BASED ON EARLY PALEOZOIC U-Pb GEOCHRONOLOGY AND CHEMOSTRATIGRAPHY

Peralta, S.[1]; Finney, S.C.[2]; Gehrels, G.[3]; Gleason, J.[4] and Aceñolaza, G.F.[5]

1. Instituto de Geología, Universidad Nacional de San Juan-CONICET, Argentina, 5400. speralta@unsj.cuim.edu.ar
2. Department of Geology, California State University, Long Beach, CA 90840, USA. scfinney@csulb.edu
3. Department of Geosciences, University of Arizona, Tucson, AZ 85721, USA. ggehrels@geo.arizona.edu
4. Department of Geological Sciences, University of Michigan, Ann Arbor, MI 48109, USA. jdgleaso@unmich.edu
5. INSUGEO, Miguel Lillo 205, S.M. Tucuman, Argentina, 4000. insugeo@unt.edu.ar

Keywords: U-Pb Geochronology, Graptolites, Early Paleozoic, Cuyania Terrane, Argentina

INTRODUCTION

In this paper geochronology and graptolite biostratigraphy of the Early Paleozoic from Cuyania Terrane, are used to address its geotectonic and paleogeographic evolution. The Cuyania Terrane (Ramos et al., 1986) is a tectono-stratigraphic unit placed in the central-western part of Argentina, which includes the Precordillera of La Rioja, San Juan and Mendoza Provinces (Furque & Cuerda, 1979), the Sanrafaelino-Pampean geological Province (Criado Roque & Ibáñez, 1979), including the San Rafael and Las Mahuídas Blocks, and the Angaco Belt (Vujovich & Ramos, 1994), as part of the western Sierras Pampeanas. This terrane has special significance in the Early Paleozoic geotectonic evolution of Western Gondwana (Ramos et al., 1984, 1986; Astini et al., 1996). In this scenery, the widely accepted model of the Cuyania (=Precordillera) terrane as an exotic Laurentia-derived fragment, is mainly based on stratigraphic and paleobiologic similarities of their correlative cambrian until early ordovician carbonate bank (Astini et al., 1995; Thomas & Astini, 1996; Astini et al., 1996), besides its basement, though as Grenvillian type (Kay et al., 1996), also it is considered as argument to support the Laurentian connection of Precordillera. Since the Penrose Conference held in 1995 at San Juan, many workers have provided additional geological evidence in order to support such model, known as the "funeral ship" model. Other alternative models to explain the allochtonous character of Precordillera were suggested by Dalziel (1997) and Dalla Salda et al. (1992). On the other hand, formerly Baldis et al. (1989) suggested a para-autochthonous model for the Precordillera, as a displaced terrane from Gondwana. Additional data were provided by Aceñolaza et al. (1999, 2002) to support this para-autochthonous model.

Chemostratigraphic data combining neodymium isotope studies and graptolite stratigraphy from Middle-Upper Ordovician from Precordillera at San Juan province (Gleasson et al., 2001) provided some evidence about the connection of Precordillera with western Gondwana on that time. Recently, new geochronologic data from U-Pb age obtained from individual detrital zircons (Finney et al., 2002, 2003), from Cambrian and Upper Ordovician rocks, and paleobiologic study of Upper Ordovician graptolite fauna from Precordillera and San Rafael Block (Peralta and Finney, in press), have provided strong evidences to support Gondwanan affinities for the Cuyania Terrane, challenging the widely accepted Laurentian origin. U-Pb ages (Finney et al., 2003) were acquired from quartz sandstone beds of the Early Cambrian Cerro Totora Fm., and Late Ordovician Las Vacas Fm. in the Argentine Precordillera, at La Rioja Province, and from the lowest Ordovician La Cébila Fm., in the Sierra de Ambato, northwestern Sierra Pampeanas, at Catamarca Province.

Paleobiologic data were obtained by mean of the study of graptolite faunas of several Upper Ordovician (Caradocian), lithostratigraphic units of Precordillera and San Rafael Block. The analyzed graptolite faunas belong to *N. gracilis* and *C. bicornis* Zone showing a warm Pacific province signature, like that of the Laurentia continent. In this case, sampled sandstones for U-Pb age data are associated with one other of these faunas. In this paper, geochronological data are from Finney et al. (2003), Nd isotope data from Gleason et al. (2001) and graptolite biostratigraphy from Peralta & Finney (in press).

GEOLOGICAL SETTING

The geological province of Precordillera includes three morpho-structural units: the Eastern Precordillera, characterized by westward vergence, like Western Sierras Pampeanas; the Central Precordillera, showing eastward vergence, and the Western Precordillera with eastward vergence (Baldis et al., 1982). U-Pb age came from sandstone beds of the Cerro Totora and Las Vacas Formations in the Central Precordillera, at La Rioja Province (Fig. 1A). Graptolite biostratigraphy is considered to La Cantera Formation in the Eastern Precordillera, and Los Azules and Las Chacritas Formations in the central Precordillera, besides the Portezuelo del Tontal Formation in western Precordillera, all of them placed in San Juan province . Additional graptolite data were taken from the Las Vacas Fm. and Las Aguaditas Fm., at central Precordillera, and from the Yerba Loca Fm., at western Precordillera, besides the Empozada Fm. in the eastern belt of the Mendoza Precordillera, though as an extension towards south of the Central Precordillera of San Juan Province (Baldis and Peralta, 1999). In the northwestern Sierras Pampeanas, a sample was colleted from the La Cébila Fm, placed at the southern end of the Sierra de Ambato, at Catamarca Province (Fig. 1A).

U-Pb GEOCHRONOLOGY AND CHEMO-STRATIGRAPHY

In accordance with Finney et al. (2002, 2003), in the northern part of the central Precordillera a sandstone bed from the upper part of the Cerro Totora Fm., sampled for U-Pb age in zircon detrital grains indicates a Brasiliano/Pan-African age (0.55-0.80 Ga), but the most abundant population of zircons is Early Proterozoic, Transamazoninan – Birimian - Eburnian provenance, between 2.00 and 2.25 Ga. This sample also includes a substantial population of Archean grains (2.40-2.80 and 2.67-2.75 Ga). These data indicate clearly lack of any Laurentian signature, raising serious questions regarding the affinity of the Precordillera basement. It is noteworthy that the detrital zircon age population of the Cerro Totora Formation, is remarkably similar to that of exotic early Paleozoic sedimentary rocks in the Florida basement (Suwannee basin, Fig. 1B).

The quartz-sandstone sample collected from the Las Vacas Formation is interbedded with conglomerate deposit in the upper member of the unit of Early Caradocian age (*C. bicornis* Zone). The acquired age-zircons are concentrated between 1.0 and 1.5 Ga, with peaks at 1.19, 1.30 and 1.45 Ga. A large population of Grenvillian-age zircons are similar to that of the La Cébila Fm., and different of the Grenvillian zircons population from the Ordovician of Ouachita orogen and Appalachian region. It is noteworthy the absence of detrital zircons less than 520 Ma (Fig. 1B) which suggests that the Precordillera terrane was not at its present location close to the Sierra de Famatina during Early Caradocian. On the other hand, detrital zircon age and regional comparisons, for the Cerro Totora Formation, indicate a Gondwanan provenance besides a Gondwanan affinity for the Precordillera basement, in accordance with Finney et al. (2002, 2003).

An other additional sample was taken from the La Cébila Formation, outcropping in Sierra de Ambato, to the east of the Famatinan System, at Northwestern Sierras Pampeana. This unit is composed mainly by interbedde metasandstones and metapelites d, deposited in shelf environment. Zircon-age from the sampled sandstone fall into three broad groups indicating the following sources: 0.48-0,72 Ga likely derived from intrusions of the Pampean Orogeny, reworked from Puncoviscana Formation, and possibly sediment derived from Brasiliano-Pan-African orogenic belts; 1.05-1.48 Ga grains indicating provenance from Sunsas orogenic belt of the Amazonian craton or the Kibaran belts of the Congo and Kalahari cratons; and 1.90-2.30 Ga, grains likely derived from older Transamazonian/Birimian age terranes. The age distribution of detrital zircons from La Cébila Formation presented here, indicates a Lowest Ordovician (<480) age, and it might correlate, at least in part, with other Gondwanan units, such as Balcarce Fm. in the Tandilia terrane and Jagüelito Fm. in the North-Patagonian massif.

Additional U-Pb zircon-age were obtained recently (Finney et al., in progress) from both Caradocian La Cantera Formation (*Nemagraptus gracilis* time), in the eastern Precordillera at San Juan Province, and the Empozada Formation (*Climacograptus bicornis* time), in the Eastern Belt of the Mendoza Precordillera. The data set support a Gondwanan provenance for these units which are consistent with the zircon age previously given for Cerro Totora, Las Vacas and La Cébila Fm.

In accordance with Gleason et al. (2001), Nd-graptolite stratigraphy of ordovician shales from Gualcamayo, La Cantera and Don Braulio Formations, at Don Braulio creek, eastern Precordillera, and from Gualcamayo and Los Azules Formations at cerro La Chilca, in Central Precordillera, at San Juan Province, are remarkably homogeneous in composition (ε_{Nd} =-11± 0.5 present; -6.5±0.5 initial), which would appear to favor an orogenic sourge (e.g., Famatina Range) rather than localized sources. In contrast, late Middle and Late Ordovician graptolites shales (*N. gracilis* and younger) of the Yerba Loca and Alcaparosa Formations (n=4), at western Precordillera, San Juan Province, show greater variation ((ε_{Nd} =-8 to -12 present; -4 to -8 initial), indicating that less well-mixed material was entering the western basin (trench fore-deep assemblage?) (Gleason et al., 2001). This material does no represent distal deposits of the orogenic sources supplying sediment to the eastern part of the Precordillera, nor does it match the more homogeneous composition of late Middle and Late Ordovician shales of the Laurentian margin. The most likely source was an approaching arc of continental affinity (Famatinian orogen?).

On the other hand, Peralta and Finney (in press) suggested that Caradocian graptolite faunas from Precordillera geological province and San Rafael block, show strong affinities which that from Ordovician Alabama basin at Ouachita region, indicating that both terranes were in close proximity at low latitude (Fig. 1C). This means combining geochronological and paleobiological data, that Precordillera stated at low latitude close Laurentia, at least up to Caradocian (*N. gracilis* and *C. bicornis* Zone). Current-controlled this way, faunal similarities might be explained by oceanic migration as suggested by Aceñolaza et al. (2002) and Finney et al. (2003).

DISCUSSION

It is clear that the stratigraphic, faunal and paleomagnetic data used to support an allochthonous model for Precordillera as a Laurentian-derived fragment can be also used , in fact, to explain these phenomena as a result of close paleogeographic proximity, such as suggested by Finney and Peralta (2000) and Finney et al. (2003). The strong affinity of graptolite fauna with the Caradocian Laurentian Pacific realm (Peralta and Finney, in press) is not consistent with the suggested collision in the late Early Ordovician (Astini et al., 1995; Thomas and Astini, 1996). In agreement with regional considerations, likely Precordillera reached its present position on post-Ordovician (Silurian or Devonian) time, in agreement with Keller (1999). In this scenery, early Late (Caradocian) Ordovician basins of the Cuyania terrane could be though as transtensive, pull-apart basins, as a

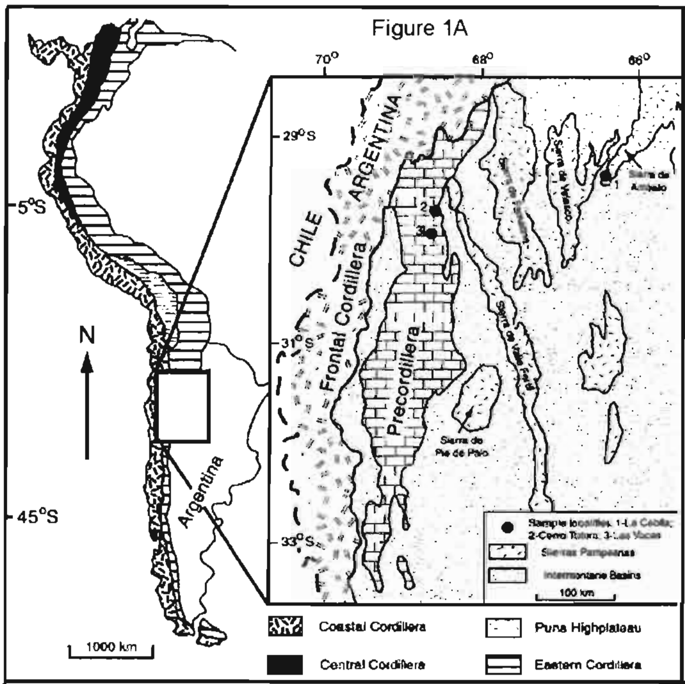

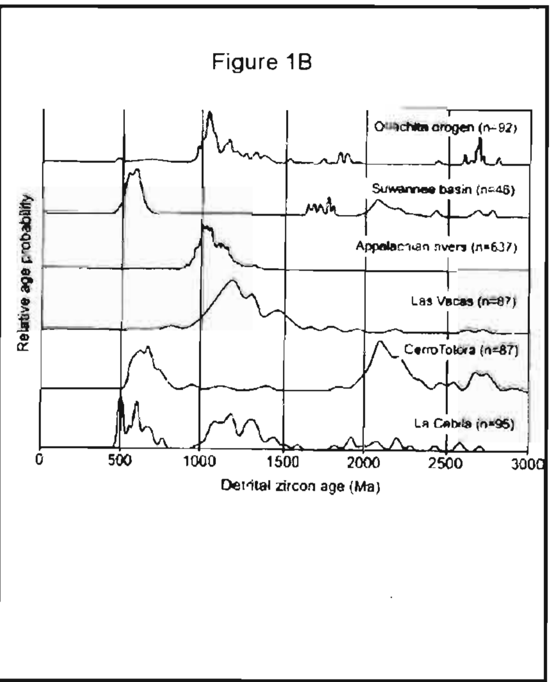

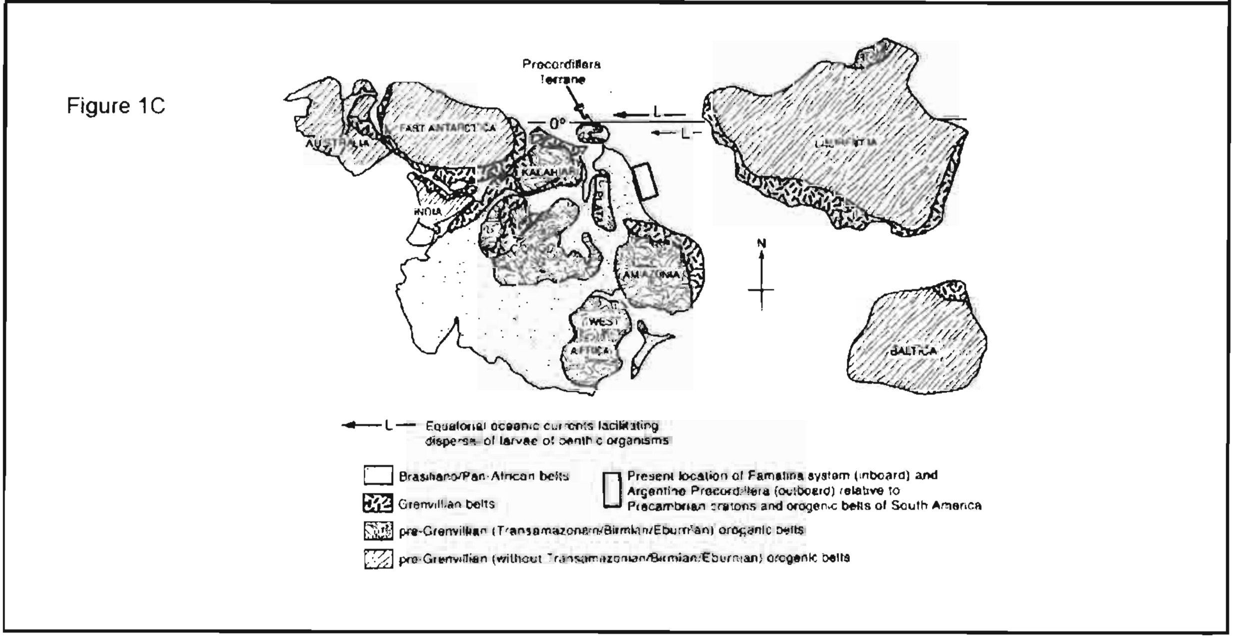

Figures 1A, B, C, taken from Finney et al. (2003)

Figure 1 A: Index map the location of La Cébila, Cerro Totora, and Las Vacas samples in Sierras Pampeanas and Precordillera of norweest Argentina.

Figure 1B: Relative age-probality curves showing U-Pb individual detrial zircon age spectra for La Cébila Fm. (Upper Cambrian? To Lower Ordovician), and Las Vacas Formation (lower Upper Ordovician). Shown for comparison are U-Pb individual detrial zircon age data for US modern Appalachian rivers, Quachita orogen Paleozoic sandstone of Gondwanan affinity from the Florida subsurface Suwannee basin. Number of grains analyzed in each sample is shown in parentheses. In this figure, each curve incorporates the age and analytical uncertainty for each grain as a normal probality disrtibution. Each curve is then normalized to the number of grains analyzed resulting in curves of equal area.

Figure 1C: Early Cambrian (~ 500 Ma) paleogeographic reconstruction,showing the Gondwanan model for the Precordillera terrane,and the present position (rectangle)of Famatina System and Precordillera relative to Precambrian cratons and orogenic belts of South America. (See Finney et al., 2003, for references).

result of distensional or transcurrent tectonic regime, according to Baldis et al. (1989), Aceñolaza and Toselli (1999), and Aceñolaza et al. (2002). This model explains accurately the latitudinal movement of the Cuyania terrane, from low (Pacific realm) to high latitude (Atlantic Realm), from Early Cambrian until Silurian or Devonian time. It is noteworthy that Porcher et al. (2003) on the basis of the presence of T_{DM} ages in the 2.6-2.0 Ga, acquired from metamorphic Maz Complex, point out this interval is not typical of the Grenvillean rocks of Laurentia being similar to the ones reported by Finney et al. (2003) for rocks of Gondwana. On the other hand, recently sedimentologic and biostratigraphic data obtained from the Late Ordovician of the western Precordillera, at Sierra del Tontal, discard previous interpretation of continental margin emplacement on the western border of Precordillera, taking into account that such deposits have evolved on a shelf environment (Basilici et al, 2003). These data set suggests a clear Gondwanan affinity for the Cuyania terrane, and a close paleogeographic proximity to Laurentia until Caradocian.

REFERENCES

Aceñolaza, F. G. and Toselli, A., 1999. Argentine Precordillera: allochthonous or autochthonous Gondwanic? Zbl. Geol. Paläontol. Teil. I, 7/8: 743-756.

Aceñolaza, F.G., Miller, H. and Toselli, A., 2002. Proterozoic-Early Paleozoic evolution in western South America – a discussion. Tectonophysics . 354, 121-137. Elsevier.

Astini, R. A., Benedetto, J. L. and Vaccari, N. E., 1995. The Early Paleozoic evolution of the Argentine Precordillera as a Laurentian rifted, drifted, and collided terrane: A geodynamic model. Geological Society of America, Bulletin, v. 107, pp. 253-273.

Astini, R. A., Ramos, V. A., Benedetto, J. L., Vaccari, N. E. y Cañas, F. L., 1996. La Precordillera: Un terreno exótico a Gondwana. Actas XIII Congreso Geológico Argentino y III Congreso de Exploración de Hidrocarburos, v. 5, pp. 293-324. Buenos Aires.

Baldis, B. A. and Peralta, S. H., 1999. Silúrico y Devónico de la Precordillera de Cuyo y Bloque de San Rafael. In: Geología Argentina, Instituto de Geología y Recursos Minerales, Anales 29(10): 215-238. Buenos Aires.

Baldis, B. A., Beresi, M. S., Bordonaro, O. L. & Vaca, A., 1982. Síntesis evolutiva de la Precordillera Argentina. V Congreso Latinoamericano de Geología, Actas, v. 4: 399-445. Buenos Aires.

Baldis, B. A., Peralta, S. H. y Villegas, C. R., 1989. Esquematizaciones de una posible transcurrencia del Terrane de Precordillera como fragmento continental procedente de áreas Pampeano-Bonaerenses. Serie Correlación Geológica, INSUGEO-UNT, v. 5, pp. 81-100. San Miguel de Tucumán.

Basilici, G., Peralta, S. H. and Finney, S. C., 2003. The Portezuelo del Tontal Formation: A widespread storm-dominated siliciclastic shelf of the Lower Caradocian, Western Precordillera, San Juan Province, Argentina. Latinoamerican Congress of Sedimentology (Abstract), Belem Do Para, Brasil.

Criado Roque, P. and Ibáñez, G., 1979. Provincia Geológica Sanrafaelino-Pampeana. In: II Simposio de Geología Regional Argentina, V. I: 837-869. Academia Nacional de Ciencias. Córdoba

Dalla Salda, L., Cingolani, C. A. & Varela, R., 1992. Early Paleozoic belt of the Andes and Southwestern South America: Result of Laurentia-Gondwana collision? Geology, v. 20, pp. 617-620.

Dalziel, I. W. D., 1997. Neoproterozoic-Paleozoic geography and tectonics: review, hypothesis, environmental speculation. Geological Association of America, Bulletin 109:16-42.

Finney, S. C., Gleason, J. D., Gehrels, G. G and Peralta, S. H., 2002. Early Gondwanian affinity of the Argentine Precordillera: evidences from U-Pb geochronology of detrital zircon population from Cambrian and Ordovician sandstones. Geological Society of America, Annual Meeting, with Program, Paper # 245-13. Denver, Colorado.

Finney, S. C., Gleason, J. D., Gehrels, G. G., Peralta, S. H., and Aceñolaza, G. F., 2003. Early Gondwanan Connection for the Argentine Precordillera Terrane. Earth and Planetary Science, Letters, 205: 349-359. Elsevier.

Finney, S.C. & Peralta, S. H., 2000. Paleogeographic implications of the Early-Middle Ordovician graptolite faunas from North America and South America. 31th International Geological Congress, Abstract. Rio de Janeiro.

Furque, G. and Cuerda, A. J., 1979. La Precordillera de La Rioja, San Juan y Mendoza. In: II Simposio de Geología Regional Argentina, V. I: 455-522. Academia Nacional de Ciencias. Córdoba

Gleason, J. D., Finney, S. C. and Peralta, S. H., 2001. Neodymium-graptolite stratigraphy of Ordovician shales from the Precordillera Terrane, Argentina: Laurentian or Gondwanan source? Geological Society of America, Annual Meeting, Paper # 19774.

Kay, S. M., Orrell, S. and Abbruzzi, J. M., 1996. Zircon and whole rock Nd-Pb isotopic evidence for a Grenville age and Laurentian origin for the basement of the Precordillera terrane in Argentina. J. Geol. 104: 637-648.

Keller, M., 1999, Argentine Precordillera. GSA Special Publication 341: 140.

Penrose Conference Report, 1996. The Argentine Precordillera: A Laurentian terrane. GSA Today (February): 16-18. Boulder.

Peralta, S. H. and Finney, S. C., in press. Upper Ordovician graptolite faunas of the Cuyania Terrane: Their paleogeographic and geodynamic significance in the western margin of Gondwana. In: Aspects of the Ordovician System of Argentina, Aceñolaza, F. G. (ed.), Serie Correlación Geológica N°16 (2003), INSUGEO. Tucumán.

Porcher, C. C., Fernández, L. A. D. and Vujovich, G. I., 2003. Sm/Nd ages thermobarometry and metamorphic evolution of the NW Sierras Pampeanas, Argentina. Simposio International: Acresção do microcontinente Cuyania a proto-margem do Gondwana, Abstracts, p. 11, Porto Alegre

Ramos, V.A., Jordan, T. E., Allmendiger, R. W., Kay, S., Cortés, J. M., and Palma, M. A., 1984. Chilenia: un terreno alóctono en la evolución paleozoica de los Andes Centrales. In Actas, IX Congreso Geológico Argentino, v. 2, pp. 84-106. San Carlos de Bariloche.

Ramos, V.A., Jordan, T. E., Allmendiger, R. W., Mpodozis, C., Kay, S., Cortés, J. M., and Palma, M. A., 1986. Paleozoic terranes of the Central Argentine-Chilean Andes. Tectonics, v. 5, pp. 855-880.

Thomas, W. A. and Astini, R. A., 1996. The Argentine Precordillera: a traveler from the Ouachita embayment of North American Laurentia. Science, 273: 752-757.

Vujovich, G. and Ramos, V. A., 1994. La Faja de Angaco y su relación con las sierras Pampeanas Occidentales, Argentina. VII Congreso Geológico Chileno, Actas I: 215-219. Concepción.

CONTRIBUTION TO THE NEOPROTEROZOIC C- AND O-ISOTOPIC RECORD: CARBONATE ROCKS FROM THE PARAGUAY BELT, MATO GROSSO, BRAZIL

Pinho, F.E.C.[1]; Sial, A.N.[2] and Figueiredo, M.F.[3]

1. Departamento de Recursos Minerais – UFMT. aguapeí@yahoo.com
2. Departamento de Geologia – UFPE, CP. 7852, Recife-PE
3. Curso de Geologia UFMT, Bolsista PIBIC-CNPq

Keywords: Paraguay belt, C and O isotopic composition, carbonate rocks, Araras Formation and Cuiabá Group

INTRODUCTION

Here, we present preliminary results on an ongoing investigation of the Paraguay Belt. This paper focuses on C- and O-isotopic composition of carbonates from the Cuiabá Group and Araras Fm..

The purpose of this paper is to contribute to the records of isotopic data from the Neoproterozoic carbonatic units and to locate the carbonate rocks of the Paraguay Belt on the Neoproterozoic secular variation curves of Carbon.

GEOLOGIC SETTING

The Paraguay belt has been defined in two main structural domains, the Metamorphic Brazilides and the Non-metamorphic Brazilides (Almeida, 1984). It is an approximately 1500 km long arc, located on the southeastern margin of the Amazonian Craton, and eastern limit of the Rio Apa cratonic block. The studied part of the belt is located in the Mato Grosso state (Fig. 1).

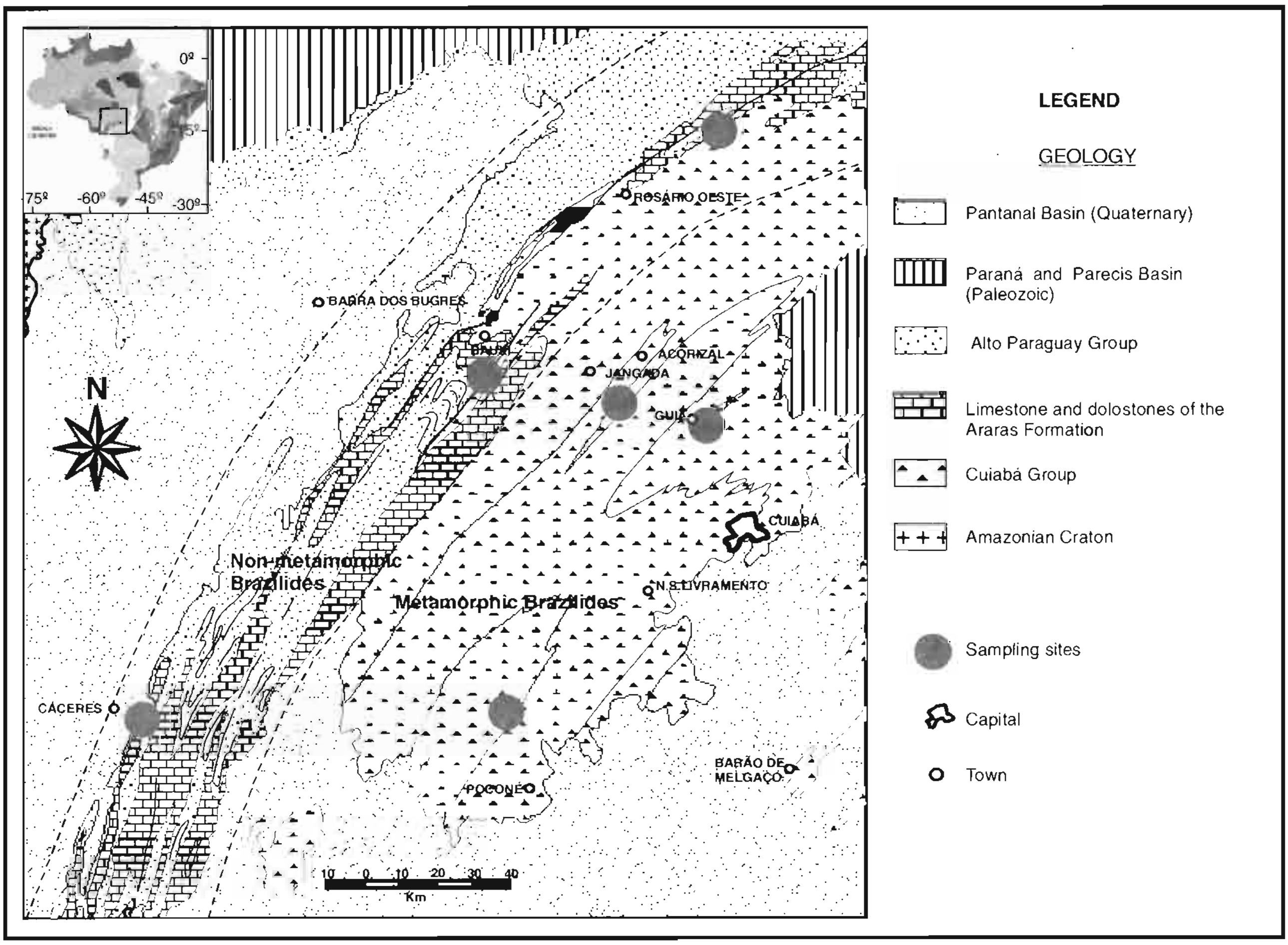

Figure 1. Paraguay Belt in the Mato Grosso state, Brazil, with carbonate rocks and location of the sampling sites (modified after Alvarenga, 1990).

The Metamorphic Brazilides is represented by the Cuiabá Group to the E of the belt, that is considered to start to be deposited during the Vendian (~610-570Ma) (Pimentel et al. 1996). The boundary with the Non-metamorphic Brazilides has been described as a gradation to the glacial and glaciomarine sediments of the Puga Formation.

The Non-metamorphic Brazilides includes the Puga Fm., a carbonate marine sedimentation with alternation of siliciclastic sediments to the top, wich overlies conformably the Cuiabá Group and the Puga Fm.. The carbonate sequence is named Guia Fm. when in the Metamorphic Brazilides Domain, and Araras Formation in the Non-metamorphic Brazilides Domain. A siliciclastic sedimentation known as Alto Paraguay Group (Raizama and Diamantino Fms.), represents the top sequence of the Paraguay Belt.

Basei and Brito Neves (1992) defined the Paraguay Orogeny (540 to 490 Ma), when the Paraguay Belt rocks were deformed and metamorphosed. The Cuiabá Group has been intruded by post-tectonic granites during the Cambrian and by alkaline complexes and granites during the Cretaceous. The São Vicente granite that yielded K/Ar in biotite age of 504 ±12 Ma (Almeida and Mantovani, 1975), is an example of these intrusions. Volcanic sequences have been described in Nova Xavantina, northeastern portion of the Paraguay Belt (Pinho and Pinho, 1990).

The Araras and Guia formations are the main subject of the present work. Luz and Abreu Filho (1978) estimated that the Araras Fm. has approximately 1200m thick of limestones and dolostones. In most part of the belt this unit is represented by a basal portion is composed of limestones that grades to dolostones to the top. Limestones are up to ~250m thick, grey to black in color and finely laminated. Dolostones show hundreds meters thick, mainly clear gray and present no clear stratification. To the top, siliciclastic sediments and black cherts are common. In some areas, as in Mirassol D'Oeste, the sequence starts with a pink dolostone overlying the Puga Fm.

STABLE ISOTOPE RESULTS

We present in this paper 90 (ninety) $\delta^{13}C$ and $\delta^{18}O$ determinations for carbonate rock samples from six different sites of the Metamorphic Brazilides and of the Non-metamorphic Brazilides domains (Table 1).

Carbon and oxygen isotopic compositions of the carbonate rock samples were obtained in the NEG-LABISE, and the results are show in the Table 2.

When samples from the Table 2 are plotted on a $\delta^{13}C$ vs. $\delta^{18}O$ diagram in Figure 2, three major fields named A, B and C are identified.

- Field A: represents dolostone samples of the Araras Fm. and some samples of the Guia Fm. Part of this field is overlaying the Field B. These samples define the range +21.9‰ to +30.2‰ ($\delta^{18}O$ - SMOW) and –1.1‰ to +2.7‰ ($\delta^{13}C$ – PDB).
- Field B: represents limestones samples of the Araras and Guia Fms. These samples define a narrow range +20.3‰ to +25.2‰ ($\delta^{18}O$ - SMOW) and -2.8‰ to -0.4‰ ($\delta^{13}C$ – PDB).
- Field C: represents samples of the Metamorphic Brazilides carbonate rocks (Guia, Jangada and Poconé). These samples define a wide range +17.9‰ to +25.2‰ ($\delta^{18}O$ - SMOW) and –6.9‰ to +5.7‰ ($\delta^{13}C$ – PDB).

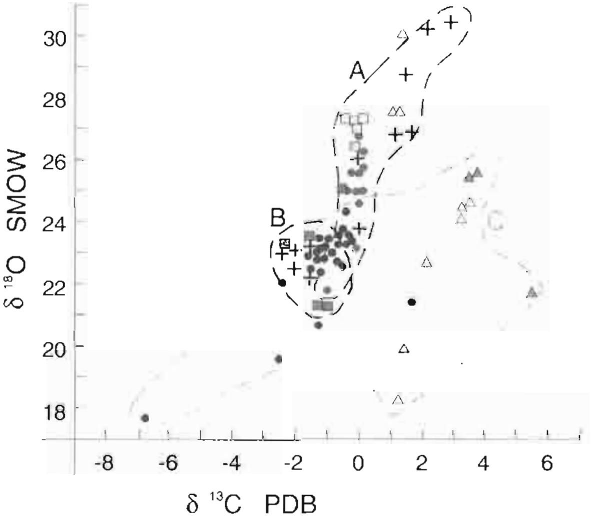

Figure 2. δ. ^{13}C vs. $\delta^{18}O$ diagram for 90 carbonate rock samples of the Paraguay Belt. Field A=dolostones of the Araras Fm. and Guia, Field B=limestones of the Araras Fm. and Guia, and Field C=carbonate rocks from Jangada, Poconé and Guia, representing the Metamorphic Brazilides.

DISCUSSIONS

Apart from the Guia Formation samples the dolostones carbonate rock samples of the Metamorphic Brazilides, show a large $\delta^{13}C$ – PDB range that is expressed by the field C (Fig. 2). This variation can be caused by metamorphic processes. The C-isotopic composition of a carbonate rock sample can be altered by re-equilibration with fluids of different isotopic composition during neomorphism or recrystallization, by the addition of isotopically distinct carbonate to the rock, or by decarbonation reactions in the presence of siliciclastic rocks (Shieh and Taylor, 1969). Most of the samples from Jangada and Poconé appear to have $\delta^{13}C$ altered by recrystallization, that is an intense process affecting them. However, for the most parth of the samples from Guia, $\delta^{13}C$ – PDB values remain close to –1‰.

Samples of the Araras Fm. show $\delta^{13}C$ – PDB values close to zero, with some incursions of limestones for negative values and some incursions of dolostones for positive values.

Gaucher et al. (2003) described negative $\delta^{13}C$ – PDB peaks for the Tamengo and Corumbá formations in the southwestern portion of the Paraguay Belt and related this fact to the negative peak that is globally associated with the first occurrence of relatively diverse Ediacaran fossils and *Claudina* (Narbonne et al. 1994 and Saylor et al. 1998).

Positive $\delta^{13}C$ – PDB values are only related to dolostones in the analyzed samples, and can be caused during dolomitization process. Sheppard and Schwarcz (1970) stated that dolomite in isotopic equilibrium with calcite will be enriched in ^{13}C by about 2%.

For the 90 analyzed samples, 70% presented $\delta^{13}C$ – PDB values ranging from -2 to 0 ‰. These values plotted on the diagram of secular variations in $\delta^{13}C$ – PDB in the Neoproterozoic to basal Cambrian carbonates (~850 to 530 Ma) (Fig. 3), related Paraguay Belt carbonate rock samples to the Post-Varanger terminal Proterozoic interval (~590 to 550 Ma), as was confirmed before (e.g. Boggiani 1998; Alvarenga et al., 2002; Nogueira et al., 2002; Gaucher et al., 2003).

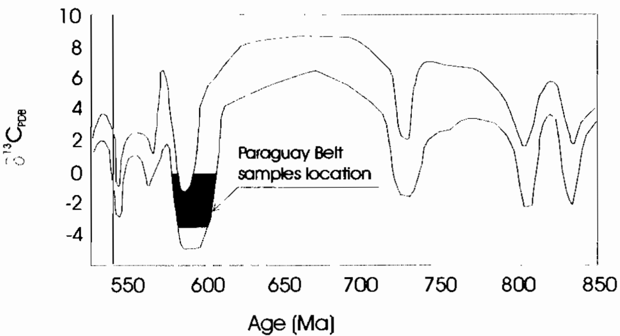

Figure 3. Diagram of secular variations in $\delta^{13}C$ – PDB in the Neoproterozoic to basal Cambrian carbonates (~850 to 530 Ma), plotted samples from the Paraguay Belt (modified after Kaufman and Knaoll, 1995).

Table 1. Samples distribution in the Paraguay Belt.

Site	Remarks	# Samples
Camil	Cáceres-MT. Araras Fm. Low angle limestones grading to dolostones.	Limestone 10 Dolostone 12
Copacel	Nobres-MT. Araras Fm. Grey to black limestones, Serragem river. Dolostones from Copacel-Nobres	Limestone 10 Dolostone 12
Império	Rosário D'Oeste-MT. Araras Fm. A dolomitic breccia.	Dolostone 8
Guia	Guia (Cuiabá-MT). Metamorphic Brazilides.	Limestone 19 Dolostone 7
Poconé	Poconé-MT. Metamorphic Brazilides. Sillicified carbonate rocks, overlying sulfide rich black shales.	General 4
Jangada	Jangada-MT. Metamorphic Brazildes. Breccia with fragments of carbonate rocks.	General 8

REFERENCES

Almeida, F. F. M., 1984. Província Tocantins, setor sudoeste. In: O Pré-Cambriano do Brasil (Almeida, F. F. M. e Hasui, Y., coord.). São Paulo, Edgard Blucher. p.265-281.

Almeida, F.F.M. de & Mantovani, M.S.M. 1975. Geologia e geocronologia do granito de São Vicente, Mato Grosso. Anais da Academia Brasileira de Ciências 47:451-458.

Alvarenga, C. J. S., 1990. Phenomenes sedimentaires, structuraux et circulation de fluides developpes a la transition chaine-craton. Exemple de la Chaine Paraguai d'age Proterozoique Superieur, Mato Grosso, Bresil. Docteur These. Universite de Droit, D'Economie et des Sciences D'Aix-Marseille. 177p.

Alvarenga, C. J. S. de, Santos, R. V. e Dantas, E. L., 2002. estratigrafia de isótopos estáveis em carbonatos que recobrem os diamictitos da Glaciação Varangiana, na Faixa Paraguai, Brasil. XLI Cong. Brás. Geol. João Pessoa-PB. P. 486.

Basei, M. A. S., Brito Neves, B. B. de, 1992. Características geológicas da transição Proterozóico-Fanerozóico no Brasil. In: Gutiérrez Marco, J. G., Saavedra, J., Rábano, I. (Eds), Paleozóico Inferior de Iberoamérica. Universidad de Extremadura, Mérida, pp. 331-342.

Boggiani, P. C., 1998. Análise estratigráfica da Bacia Corumbá (Neoproterozóico) – Mato Grosso do Sul. Tese de Doutorado USP. 181p.

Gaucher, C., Boggiani, P. C. Sprechmann, P, Sial, A. N., and Fairchild, T., 2003. Integrated correlation of the Vendian to Cambrian Arroyo del Soldado and Corumbá Group (Uruguay and Brazil): palaeogeographic, palaeoclimatic and palaebiologic implications. Precambrian Research 120:241-278.

Kaufman, A. J. and Knoll, A. H. 1995. Neoproterozoic variation in the C isotopic composition of seawater: stratigraphic and biogeochemical implications. Precambrian Research 73: 27-49.

Luz, J. da S. and Abreu Filho, W. 1978. Aspectos Geológicos-econômicos da Formação Araras do Grupo Alto Paraguai-MT. XXX Congresso Brasileiro de Geologia. Recife-PE. SBG, v. 4. p 1816-1826.

Narbone, G.M., Kaufman, A.J. and Knoll, A.H. 1994. Integrated chemostratigraphy and biostratigraphy of the upper Windermere Supergroup (Neoproterozoic). Mackenzie Mountains, northwestern Canada. Geol. Soc. Am. Bull, 106:1281-1291.

Nogueira, A.F.R., Riccomini, C., Sial, A.N e Moura, C.A.V. 2002. Capa Carbonatica Neoproterozóica no Sudeste do Craton Amazônico. XLI Cong. Bras. de Geologia. João Pessoa-PB. SBG. P 323.

Pimentel, M.M., Fuck, R.A. and Alvarenga, C.J.S. 1996. Post-Brasiliano (Pan-African) high-K granitic magmatism in Central Brasil: the Role of Late Precambrian-early Paleozoic extension. Precambrian Research, 80:217-238.

Pinho, F. E. C., e Pinho, M. A. S. B., 1990. Geoquímica do depósito de ouro de Nova Xavantina-Leste do Estado de Mato Grosso. XXXVI Cong. Bras. de Geol. Natal-RN. Anais Vol. 3:1316-1330.

Saylor, B.Z., Kaufman, A.J., Grotzinger, J.P. and Urban, F. 1998. A composite reference section for terminal Proterozoic strata of southern Namibia. Journal of Sedimentary Research 68:1223-1235.

Sleeppard, S.M.F. and Schwarcs, H.P. 1970. Fractionation of carbon and oxygen isotopes and magnesium between coexisting metamorphic calcite and dolomite. Contrib. Mineral. Petrol. 26:161-198.

Shieh, Y.N. and Taylor, H.P. 1969. Oxygen and Carbon isotopes studies of contect metamorphism carbonate rocks. J. Petrol, 10: 307-331.

Table 2. Carbon and Oxygen isotopic data of carbonates rocks samples of the Paraguay Belt.

Sample	$\delta^{18}O$ SMOW	$\delta^{18}O$ PDB	$\delta^{13}C$ PDB
IMP 1	+26,7	-4,0	+1,0
IMP 2	+26,9	-3,7	+1,6
IMP 3	+27,2	-3,5	-0,0
IMP 4	+25,9	-4,7	-0,0
IMP 5	+23,9	-6,6	-0,0
IMP 6	+29,8	-0,9	+2,2
IMP 7	+28,6	-2,1	+1,7
IMP 8	+30,2	-0,6	+2,7
CAMIL C1	+22,9	-7,6	-2,4
CAMIL C2	+23,0	-7,5	-2,3
CAMIL C3	+22,3	-8,2	-2,1
CAMIL C4	+23,1	-7,4	-1,7
CAMIL C5	+23,0	-7,6	-1,6
CAMIL C6	+22,4	-8,1	-1,6
CAMIL C7	+22,2	-8,3	-1,5
CAMIL C8	+23,5	-7,0	-1,2
CAMIL C9	+22,1	-8,4	-1,3
CAMIL C10	+23,2	-7,3	-1,7
CAMIL D1A	+26,5	-4,2	-0,0
CAMIL D1B	+25,6	-5,0	+0,0
CAMIL D1C	+25,8	-4,8	-0,0
CAMIL D2A	+26,3	-4,4	+0,0
CAMIL D2B	+24,3	-6,2	+0,0
CAMIL D2C	+25,1	-5,4	+0,2
CAMIL D3A	+25,1	-5,5	-0,4
CAMIL D3B	+25,0	-4,6	+0,0
CAMIL D3C	+24,7	-5,9	+0,0
CAMIL D4A	+25,0	-5,6	-0,8
CAMIL D4B	+21,9	-8,6	-1,1
CAMIL D4C	+23,6	-6,9	-0,2
COP C1	+23,1	-7,4	-2,4
COP C2	+21,2	9,2	-1,2
COP C3	+22,3	-8,2	-1,3
COP C4	+23,4	-7,1	-2,7
COP C5	+21,3	-9,1	-1,0
COP C6	+22,8	-7,7	-1,3
COP C7	+20,8	-9,7	-1,3
COP C8	+23,1	-7,4	-2,4
COP C9	+22,4	-8,1	-1,1
COP C10	+25,2	-5,4	-0,6
COP D1A	+27,2	-3,5	-0,2
COP D1B	+26,5	-4,2	+0,1
COP D1C	+27,1	-3,5	+0,3
COP D2A	+27,2	-3,4	-0,0
COP D2B	+26,4	-4,2	-0,1
COP D2C	+26,8	-3,8	-0,1
COP D3A	+27,5	-3,2	+0,4
COP D3B	+27,5	-3,2	-0,0
COP D3C	+27,3	-3,3	+0,0
COP D4A	+27,2	-3,5	+0,4
COP D4B	+26,4	-4,2	-0,0
COP D4C	+27,0	-3,6	+0,5
MTG 1	+17,9	-12,9	-6,9
MTG 2	+22,2	-8,3	-2,4
MTG 3	+23,0	-7,5	-1,6
MTG 5	+22,6	-7,7	-1,4
MTG 6	+23,0	-7,5	-1,2
MTG 7	+23,3	-7,3	-1,6
MTG 8	+23,5	-7,0	-1,3
MTG 9	+23,7	-6,9	-1,1
MTG 10	+22,9	-7,6	-1,9
MTG 11	+23,4	-7,2	-1,0
MTG 12	+23,6	-7,0	-0,8
MTG 13	+22,7	-7,8	-1,5
MTG 14	+24,3	-6,2	-0,4
MTG 15	+23,9	-6,7	-0,8
MTG 16	+22,4	-8,1	-1,7
MTG 17	+23,6	-6,9	-0,2
MTG 18	+22,9	-7,6	-1,5
MTG 19	+23,9	-6,7	-0,5
MTG 20	+23,7	-6,8	-0,8
MTG 21	+23,1	-7,5	-0,5
MTG 22	+23,2	-8,3	-0,2
MTG 24	+22,5	-8,0	-0,8
MTG 26	+20,3	-10,1	-1,4
MTG 27	+21,2	-9,2	+1,8
MTG 29	+19,8	-10,6	-2,8
MTG 30	+22,1	-8,4	-0,5
9BEC 1	+26,5	-4,2	+2,3
9BEC 2	+27,6	-3,1	+1,2
9BEC 3	+18,2	-12,2	+1,1
9BEC 4	+24,0	-6,6	+3,2
9BEC 5	+24,7	-5,9	+3,5
9BEC 6	+29,0	-1,7	+1,3
9BEC 7	+27,9	-2,8	+1,4
9BEC 8	+24,4	-6,2	+3,5
POC C1	+21,3	-9,219	+5,7
POC C2	+20,5	-9,984	+1,5
POC C3	+22,2	-5,436	+3,5
POC C4	+25,5	-5,107	+3,6

C-, O- AND Sr-ISOTOPE CHEMOSTRATIGRAPHY OF CAMBRIAN CARBONATE SEQUENCES, PRECORDILLERA, WESTERN ARGENTINA

Sial, A.N.[1]; Peralta, S.[2]; Ferreira, V.P.[1]; Toselli, A.J.[3]; Aceñolaza, F.G.[3]; Parada, M.A.[4]; Gaucher, C.[5]; Alonso, R.N.[6] and Pimentel, M.M.[7]

1. NEG-LABISE, Dep. Geologia, UFPE, C.P. 7852, Recife-PE, 50670-000, Brasil. ans@ufpe.br; valderez@ufpe.br
2. Instituto de Geología, Universidad Nacional de San Juan-CONICET, Argentina, 5400. speralta@unsj.cuim.edu.ar
3. INSUGEO, Miguel Lillo 205, S.M. Tucuman, Argentina, 4000. atoselli@cpsarg.com
4. Departamento de Geología, Universidad de Chile, Santiago, Chile. maparada@cec.uchile.cl
5. Departamento de Paleontologia, Facultad de Ciencias, Iguá, 4225, 11400 Montevideo, Uruguay. gaucher@chasque.apc.org
6. Departamento. de Geología, Universidad Nacional de Salta, Argentina. rnalonso@sinectis.com.ar
7. Instituto de Geociências, Universidade de Brasilia, Brasília-DF. 70.910-900, Brasil. marcio@unb.br

Keywords: C and Sr isotopes, Cambrian, Argentina, Precordillera, chemostratigraphy

INTRODUCTION

The highly oscillatory C-isotope record of the Late Neoproterozoic coincides with major glacial to interglacial fluctuations. Except for a glaciation at the Vendian/Cambrian boundary coincident with a large ^{13}C negative excursion (Bertrand-Sarfati et al., 1995), in the Cambrian period "greenhouse" conditions seem to have predominated (Tucker, 1992). In addition, the widespread occurrence of phosphorites in the Early Cambrian suggest vigorous oceanic circulation and upwelling (Cook and Shergold, 1984). The falling amplitude of C-isotopic values between 750 and 500Ma may be related, somehow, to the change from glacial "icehouse" conditions in the Cryogenian to "greenhouse" conditions in the Middle Cambrian. C-isotope oscillations in the Early Cambrian result, probably, from climatic oscillations either than from glaciations that have not been proved to have occurred (Brasier and Sukhov, 1998).

A large and global positive excursion in $\delta^{13}C$ of Late Cambrian (Steptoean) carbonates has been reported from North America, Kazakstan, South China and Australia that begins at a worldwide extinction of trilobites (Saltzman et al, 2000). This Steptoean positive C-isotope excursion ($+5‰_{PDB}$), baptized as SPICE (Saltzman et al., 1998) represents a major perturbation of the Cambrian carbon cycle ~500Ma and, as a peculiarity, a mass extinction coincides with the onset of the positive shift, rather with the rising limb of the excursion. The peak of faunal diversity (Saltzman et al. (2000), correlates in North America with the peak of the SPICE excursion. The Cambrian-Ordovician boundary is characterized by synchronous change in sea-level, conodont biozones and $\delta^{13}C$ of marine inorganic carbon (Ripperdan et al., 1992).

The Sr-isotope composition of the seawater in the Cambrian interval is characterized by a continuous increase of $^{87}Sr/^{86}Sr$ that is interrupted, several times, by sharp rises representing important changes in the Earth history (Montañez et al., 2000). The shape of the Sr secular variation curve allows, in many cases, estimating the depositional age of Cambrian carbonates.

We examine here, cambrian carbonate-dominated sequences at Sierra Chica de Zonda (Early to Middle Cambrian), San Juan province, and at Cerro La Silla and Quebrada de La Flecha (Late Cambrian) in the Precordillera, proxies for cambrian geological evolution in the southern edge of the South America continent. We have studied the C- and Sr-isotope stratigraphies of representative sections, examining: (a) the paleoenvironmental conditions under which carbonates were deposited; and (b) searching for the Steptoean positive C-isotope excursion in western Argentina.

GEOLOGIC SETTING

(a) Early to Middle Cambrian: The Precordillera is an elongated geological province, located between the Andean belt to the west and the Pampean Ranges to the east. In the Precordillera basin, San Juan province, a continuous sequence of carbonates with regressive characteristics developed from the Early Cambrian (Ollenelus zone) to the base of the Ordovician, at which point a transgressive stage started (Baldis et al., 1984).

La Laja Fm. is the oldest unit of the carbonate platformal succession and consists of several large-scale sedimentary sequences which have two main components, a siliciclastic interval and a calcareous one (Keller,1999). The lower boundary of this Formation is poorly known due to tectonic disturbance. The upper boundary is drawn at the transition between limestones and dolomites of the Zonda Fm. (Bordonaro, 1980). Siliciclastic intervals have been used by Bordonaro (1980) as marker horizons to define the members of this Formation. These cycles were formed in an open, shallow platform, with clean and warm water with free circulation, by fluctuation of the sea level, which suffered an important lowering during the deposition of the upper portion of the La Laja Fm.. (Baldis and Bordonaro, 1982). Four members are recognized in the La Laja Fm. with a total thickness of about 1400m: Early Cambrian- De La Roza (black lutites and limestones), Soldano (marls and mudstones); Bernadino Rivadavia (homogeneous set of black limestones) and Juan Pobre (oolitic limestones and black limestones). The De La Roza member lower boundary is unknown due to faulting, and no fossil has been found.

(b) Late Cambrian: Cerro La Silla represents a significant outcrop of Cambrian rocks in the northern Precordillera (150 km north of San Juan town, central Precordillera). The Cerro La Silla section includes a thick

Late Cambrian to Early Ordovician carbonate sequence, dipping westward and comprises Zonda, La Flecha, La Silla and San Juan Fms, the last one overlain by siliciclastic Silurian deposits.

La Flecha Fm. is almost totally composed of small-scale, shallowing upward cycles (1-5m) and exhibits a great variety of stromatolites, and cryptalgal laminites together with subtidal to supratidal lithologic types (Keller et al., 1999). A high amount of chert and chalcedony replaces, sometimes, the biogenic structures (assigned to *Thalassinoides isp.* This ichnogenera is referred to feeding structures of living decapod crustacea, and representative of intertidal to upper part of subtidal zone in marine environment) as well as oolite beds. The shallowing upward cycles are peritidal in origin and conform small-scale, stacked successions (Peralta, 2000).

The Cerro La Silla is the type locality for the Silla Fm. where it shows a thickness of 350m. This Formation is predominantly calcareous with dolomites mainly in sparse biolaminated horizons. The succession is composed of an alternation of peloidal grainstones, intraclast grainstones and mudstones with abundant bioturbation. Distribution of facies seems to be random and no cycle or sedimentary rhythm could be demonstrated to date (Peralta, 2000).The San Juan Fm. of Late Tremadoc and Early Arenig, has a thickness of ~350m limestones and its lower boundary being characterized by an open marine fauna (Peralta, 2000).

CHEMOSTRATIGRAPHY

We examined and strati-graphically sampled continuous sections at Quebrada de Zonda and Quebrada de La Flecha in Chica de Zonda Range (Eastern Precordillera) and at Cerro La Silla locality (central Percodillera). Samples were collected along traverses, perpendicular to the strike of the carbonate strata, at a metric scale.

Knowledge on the behavior of Rb, Sr, Mn and Fe helps selecting samples that have undergone little or no alteration (Kaufman and Knoll, 1995; and Kha et al.,1999). Among all the parameters used to make such an evaluation, it seems that the simplest and one of the most effective is the Mn/Sr ratio. Limestones or dolostones with Mn/Sr<10 commonly retain near primary $\delta^{13}C$ abundances according to these authors. Mn/Sr ratios for carbonate rocks from La Laja, Zonda, Flecha and Silla Fms. carbonates are much lower than 10 (usually <0.5). In the $\delta^{13}C$ and $\delta^{18}O$ crossplots for both Formations, apparent scatter rather than co-variance seems to predominate. These observations imply in that the $\delta^{13}C$ values in most of the analyses reported here are primary values.

(a) Quebrada de Zonda Section. Thirty-five samples have been stratigraphically collected (~700m) from carbonates of the La Laja Fm. along the Quebrada de Zonda section (El Estero, Soldano, Bernardino Rivadavia and Juan Pobre Members), west of San Juan town and 8 samples for 15m at the Cerro de Marquesado, in the northern portion of the Chica de Zonda Range (from El Estero Member). Carbonate rocks in this section are characterized by dark limestones with intercalation of layers of less than one-meter thick, fine-grained sandstones, in the Soldano member (for ~120m). This situation is followed by ~100m of pure limestones (SiO_2 content decreases while CaO increases towards the top). The next 200m are characterized by marly limestones (distal facies) which are followed in the upper-most portion of this section by 160m-thick fossiliferous (with bioturbation) buff dolomitic limestones, deposited in open sea. In some portions of this section, rocks show well-developed cleavage caused by pervasive faults and mesoscale drag folds whose axes dip almost vertically. As the structural pertubations make the precise stratigraphic position of samples difficult, sampling from these portions has been omitted to avoid ambiguities.

The chemostratigraphic section at Chica de Zonda Range (not shown) displays an overall $\delta^{13}C$ variation from -2 to + 1‰$_{PDB}$. The C-isotope curve for the lowermost portion of the profile (limestones/sandstones intercalations) shows much stronger oscillations, with values varying from +1 to -2‰$_{PDB}$. For the next 100m upsection, this C-isotope chemostratigraphic proflile is characterized by progressively more negative $\delta^{13}C$, reaching a minimum of about -2 at approximately 250m from the base of the section. For the next 350 m upsection, $\delta^{13}C$ values are around -0.5.

At Cerro de Marquesado, $\delta^{13}C$ values vary from -1 to -3 ‰$_{PDB}$ is observed. The C-isotope profile for the La Laja Fm., when compared to that for the Vendian-Tommotian transition elsewhere (e.g. Magaritz 1989; Magaritz et al. 1991; Brasier et al. 1994), suggests that El Estero (De La Rosa facies) carbonates of La Laja Fm. may have recorded this transition (a value of -3‰$_{PDB}$ was recorded at one of the lowermost samples in this section).

Apparently, in the uppermost portion of this section, dolomitic limestones do not show any substantial change in the C-isotopic composition in relation to the underlying marly limestones.

Eight samples from the lower 350m of this carbonate section were also analyzed for Sr isotopes and $^{87}Sr/^{86}Sr$ values vary from 0.70926 to 0.70950 with the exception of one sample (>0.7100). The higher $^{87}Sr/^{86}Sr$ value is recorded at the basal portion of the section which coincides with sandstone intercalations. In the lowermost 80m of the section, Sr isotope ratios drop from an initial value slightly higher than 0.71000 to 0.70926 and, thereafter, it rises to 0.70985. Such differences in the carbonate Sr isotopic signatures between the lowermost and upper portions of the section indicate a significant variation in the depositional environment and can be correlated with possible Precambrian-Cambrian transition that the La Laja Fm. carbonates, at the basal portion of the Formation, may have recorded.

(b) Cerro La Silla. Fifty samples from Cerro La Silla were analyzed for C and O isotopes, including carbonates from Zonda, Flecha, Silla and San Juan Fms..

The C- and O-isotope profiles display clear differences in the isotopic behavior of these two formations.

According to Ramos et al. (1999), La Flecha Fm. was deposited in a shallow environment of low-energy conditions, with water of restricted circulation and periodical subaerial exposure, with only little or no terrigenous sediment input. Such characteristics imply, in principle, that these carbonates should display some ^{13}C- and ^{18}O-enrichment, when compared with isotopic signatures of coeval marine carbonates.

All $\delta^{13}C$ values obtained in the entire section in the present study are negative, except one (very close to $0‰_{PDB}$). In this $\delta^{13}C$ stratigraphic profile, 5 small positive excursions are observed (labelled from I through V in Fig. 1a).

The $\delta^{18}O$ values are slightly higher (mostly ~ $-5‰_{PDB}$, with few exceptions, defining two groups, ~ -7 and $-8‰_{PDB}$; Fig. 1a) than those observed in La Silla Fm.

Such well-defined trends suggest that most $\delta^{18}O$ values are primary and imply that environments in which these two Formations were deposited differed from each other, La Flecha Fm. environment being more restricted, of hypersaline tendency, approaching a sabkha.

Five samples from La Flecha carbonates and four from La Silla, were analyzed for Sr isotopes and $^{87}Sr/^{86}Sr$ va-lues vary from 0.70710 to 0.70980 with just one exception (0.71011). The highest value was found in La Flecha carbonates by the transition between these two Formations. Flecha Fm. carbonates exhibit values from 0.70914 to 0.71011, with one exception (0.70710) while La Silla Fm. displays values from 0.70898 to 0.70980. Values for la Silla Fm., except one, are more in consonance with globally reported Late Cambrian seawater $^{87}Sr/^{86}Sr$ and, therefore, were little affected by secondary alteration.

(c) **Quebrada de la Flecha.** Eighty samples were collected from the carbonates at this locality. At this section, the lower boundary is characterized by stromatolites (LLH and SH types) and thrombolites and the upper boundary is drawn where the content of stromatolites decreases and dolomites predominate. Likewise in the Cerro la Silla, the $\delta^{13}C$ stratigraphic profile revealed 5 discrete positive excursions (labelled I through V in Fig. 1b) with the uppermost one in the dolomites of the top of this Formation (SPICE anomaly?). The cyclicity of this Fm. is well reflected in the C-isotope profile (Fig. 1b).

The behavior of $\delta^{18}O$ is less uniform than at Cerro La Silla. An important drop in the $\delta^{18}O$ values are well recorded towards the top of this Formation.

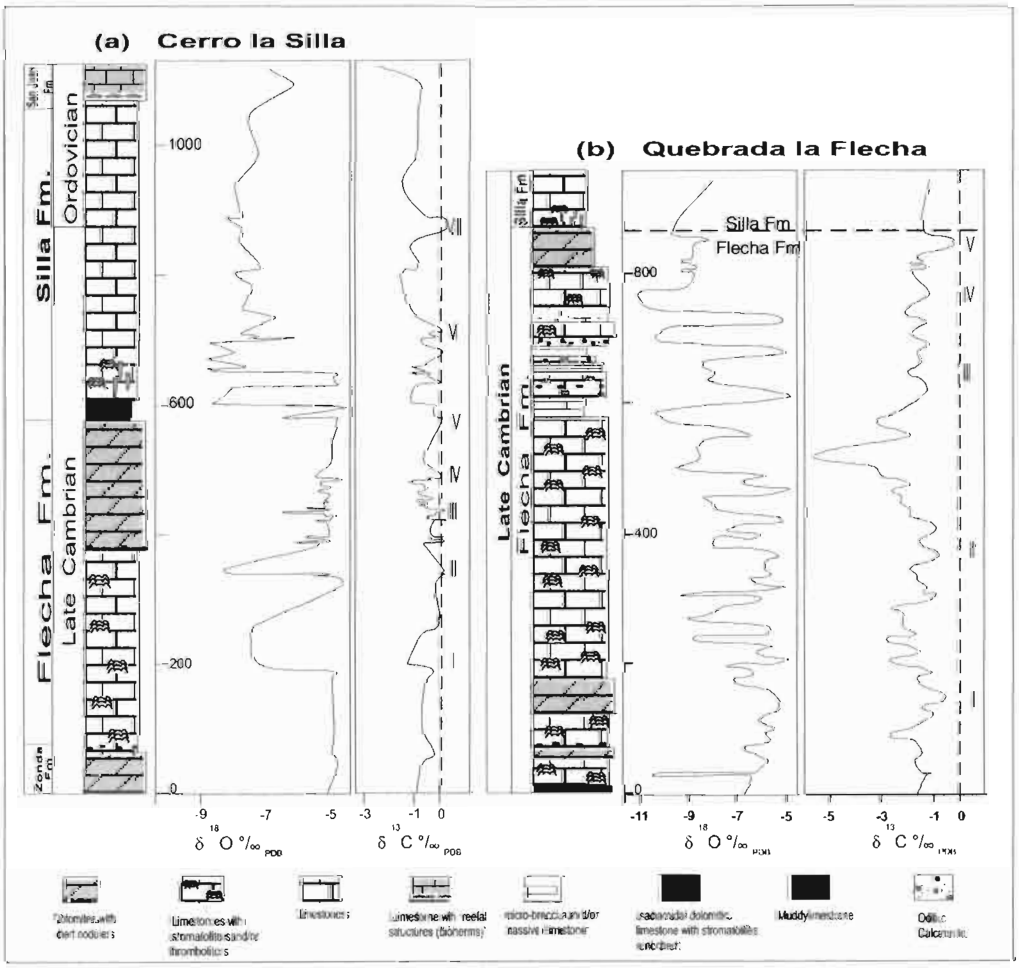

Figure 1. Lithostratigraphic profile and C- and O- variations for the Cerro la Silla (a) and Quebrada la Flecha (b) carbonate sequences, Precordillera, western Argentina. See text for explanations on the I through VII roman letters.

CONCLUSIONS

The combined C-, O- and Sr-isotope data for Chica de Zonda, Cerro La Silla and Quebrada La Flecha allow an insight of the isotopic record of most of the Cambrian history in the Precordillera of western Argentina.

The $\delta^{18}O$ variation curve at Cerro La Silla, shows an average difference of about 2‰$_{PDB}$ between La Silla and La Flecha Fms. carbonates. This divergence simply reflects the variation in the Mg/Ca composition of the corresponding carbonates, which in turn may reflect different depositional environments. La Flecha carbonates are more dolomitic, $\delta^{18}O$ averaging -5‰$_{PDB}$ and representing hypersaline, restricted, sabkha environments, while in La Silla Fm., $\delta^{18}O$ averages -7‰$_{PDB}$, representing open marine conditions.

The $\delta^{13}C$ in the entire Cambrian section analyzed is slightly negative without large fluctuations, except in La Flecha Fm where more pronounced excursion is observed. Carbonates in the De la Rosa facies (El Estero Member) display values as low as -3‰$_{PDB}$ and the top of the La Flecha Fm. delineates a positive excursion, here interpreted as probably the time when the SPICE anomaly was globally developed. $\delta^{13}C$ at Quebrada de La Flecha ranges mostly from –2.7 to –0.6‰$_{PDB}$. At Cerro La Silla, about 200km to the north, $\delta^{13}C$ shows less negative values, ranging from –1.4 to +0.1‰$_{PDB}$. At Guandacol, La Rioja, about 150km further north, La Flecha Fm. may have recorded more positive $\delta^{13}C$ values and the SPICE anomaly might be unambiguously represented.

ACKNOWLEDGEMENTS

This study is part of project financed by PROSUL/CNPq (project # AC-38/2002) envolving researchers from Brazil, Argentina, Chile and Uruguay. Universidad Nacional de San Juan provided field vehicles. This is the contribution n. 208 of the NEG-LABISE.

REFERENCES

Baldis, B., A.J. and Bordonaro, O., 1982. Comparación entre El Cámbrico de la "Great basin" norteamericana y la Precordillera de San Juan, Argentina, su implicación intercontinental. Actas V Cong. Latinoamericano de Geol. Buenos Aires, Argentina, 1: 97-108.

Baldis, B., Beresi, M., Bordonaro, O. and Vaca, A., 1984. The Argentine Precordillera as a key to the Andean structure. Episodes, 17, p.14-19.

Bertrand-Sarfati, J., Moussine-Pouchkine, A., Amard, B. And Ait Kaci Ahmed, A. 1995 First Ediacaran fauna found in western Africa and evidence for an Early Cambrian glaciation. Geology, 23 (2): 133-136.

Bordonaro, P., 1980. El Cámbrico en la Quebrada de Zonda. Revista. de la Asociación Geol. Argentina, 35: 26-40.

Brasier, M.D. and Sukhov, S.S., 1998. The falling amplitude of carbon isotopic oscillations through the Lower to Middle Cambrian: northern Siberia data. Can. J. Earth Sci., 35: 353-373.

Brasier, M.D., Rozanov, A.Y., Zhuravlev, A. Y., Corfield, R.M.,Derry, L.A., 1994. A carbon isotope reference scale for the Lower Cambrian succession in Siberia: report of IGCP Project 303. Geol. Mag. 131: 767-783.

Cook, P.J. and Shergold, J.H., 1984. Phosphorus, phosphorites and skeletal evolution at the Precambrian-Cambrian boundary. Nature, 308: 231-136.

Kaufman, A.J. and Knoll, A.H., 1995, Neoproterozoic variations in the C-isotopic composition of seawater: Stratigraphic and biogeochemical implications. Precamb. Res. 73: 27-49.

Kha, L. C., Sherman, A.G., Narbonne, G.M., Knoll, A.H., and Kaufman, A. J., 1999. $\delta^{13}C$ stratigraphy of the Proterozoic Bylot Supergroup, Baffin Island, Canada: implications for regional lithostratigraphic correlations: Can. Jour. Earth Sci., 36: 313-332.

Keller, M., 1999, Argentine Precordillera. GSA Special Publication 341: 140.

Magaritz, M., 1989, $\delta^{13}C$ minima follow extinction events: A clue to faunal radiation. Geology, 17, p. 337-340.

Magaritz, M., Kirschvink, J., Latham, A.J. , Zhuravlev, A.Yu. and Rozanov, A.Yu., 1991, Precambrian/ Cambrian boundary problem: carbon isotope corre-lations for Vendian and Tommotian time between Siberia and Morocco. Geology, 19: 847-850

Montañez, I.P., Osleger, D. A., Banner, J. , Mack, L.E. and Musgrove, M., 2000, Evolution of the Sr and C isotope Composition of Cambrian Oceans. GSA Today, 10, 1-7.

Peralta, S. H., 2000. Cerro la Silla Field Trip: Cambrian and Lower Ordovician carbonate deposits of the Cer-ro la Silla Section, northern Precordilera, Province of San Juan. Stratigraphy and faunas (conodonts and trilobites). Aceñolaza, G. and Peralta, S. (eds), Cambrian from, the southern edge, Inst. Superior de Correlación Geológica, Miscelánea 6: 39-45

Ramos, A., Valencio, S., Panarello, H., Armella, C. and Cabareli, N., 1999. Isotope and trace element evidence of post-depostional changes in carbonates of La Flecha Formation, San Juan, Argentina.Actas II South American Symposium on Isotope Geology, Vila Carlos Paz, Argentina: 437-440.

Ripperdan, R.L., Magaritz, M., Nicoll, R.S., Shergold, J.H., 1992. Simultaneous changes in carbon , sea level, and conodont biozones within reg Cambrian-Ordovi-cian boundary interval at Black Mountain, Australia. Geology, 20: 1039-1042.

Saltzman, M.R., Ripperdan, R.L., Brasier, M.D., Lohmann, K.G., Robison, R.A., Chang W.T., Pemf. S., Ergaliev, E.K. and Runnegar, B., 2000. A global carbon isotope excursion (SPICE) during the Late Cambrian: relation to trilobite extinctions, organic-matter burial and sea level. Palaeogeography, Pa-laeoclimatology, Palaeoecology 162.: 211-223.

Saltzman, M.R., Runnegar, B. and Lohmann, K.C., 1998. Carbon isotope stratigraphy of the Upper Cambrian (Steptoean Stage) sequence of the eastern Gretab basin: record of a global oceanographic event. GSA Bulletin, 110: 285-297.

Tucker, M.E., 1992. The Precambrian-Cambrian bounda-ry: seawater chemistry, ocean circulation and nutrient supply in metazoan evolution, extinction and biomineralization. Journal of the Geological Society, 149: 655-668.

C-, O- AND Sr-ISOTOPE STRATIGRAPHY OF THE STURTIAN JACOCA AND OLHO D'AGUA FORMATIONS, STATE OF SERGIPE, NORTHEASTERN BRAZIL

Sial, A.N.[1]; Ferreira, V.P.[1]; Moura, C.V.A.[2] and Santos, V.H.[1]

1. NEG-LABISE, Dep. Geologia-UFPE, C.P. 7852, Recife-PE, 50670-000, Brasil. ans@ufpe.br; valderez@ufpe.br petrovic@ufpe.br
2. Laboratório de Geologia Isotópica (Pará-Iso), UFPA, C.P. 1611, Belém-PA, 66.075-900, Brasil. c_moura@ufpa.br

Keywords: C isotopes, Sr isotopes, Sturtian, Sergipe, Brazil

INTRODUCTION

The Neoproterozoic, poly-deformed and poly-metamorphosed, Sergipano belt is located at the southern border of the Borborema Province. Around the south-central part of this belt and its interface with the northern margin of the São Francisco craton, sedimentation took place at a passive continental margin (D'el Rey da Silva, 1999). Two cycles of sedimentation were recognized in this area, both with a continental to shallow marine, basal siliciclastic megasequence, overlain by a carbonate sequence.

The lower siliciclastic megasequence is represented by the Juetê (arkosic sandstone, conglomerate lenses, diamictites), Itabaiana (conglomerates, quartzites, metasiltites) and Ribeirópolis Fms. (silty phyllites, metagreywa-ckes, pebbly phyllites, diamictites) and the lower carbo-nate megasequence, by the Acauã and Jacoca Fms. These two megasequences form the Estância-Miaba Group. The upper siliciclastic megasequence (Simão Dias Group) is represented by the Lagarto-Palmares, the Jacaré and the Frei Paulo Fms.. This megasequence is overlain by meta-sediments of the Vaza Barris Group that comprises dia-mictites of the Palestina Fm. and the upper carbonate me-gasequence (Olhos D'Agua Fm.).

THE LOWER CARBONATE MEGASEQUENCE

The Acauã Fm. conformably overlies the Juetê Fm. and unconformably the basement gneiss (D'el Rey da Silva, 1999). It consists of basal limestone, dolomite, calci-argillite with lime-stone lenses and layers of limestone and dolomites with intercalations of cross-bedded red sandstone and green argillite.

The Jacoca Fm. overlies the pebbly phyllites/ conglomerates of the Ribeiropolis Formation and comprises two lithofacies: metacarbonates and a mixed lithofacies of metasiliciclastics and metacarbonates (D'el Rey da Silva, 1995). The metasedimentary carbonates are <300m thick around the Itabaiana dome with the best exposures, in the Capitão Farm, along the Salgado and Vaza Barris rivers, southwest of Macambira village. A typical section of the Jacoca Fm., as described in the Capitão Farm by D'el Rey da Silva (1995), starts with a thick layer of laminated white to gray, 1-3cm thick beds of dolomites containing pyrite and chalcopyrite. This is followed upsection by a 15m thick layer of laminated dolomites, and dark gray to black phyllites and about 10m thick of massive dolo-mites. This unit is overlain by a 40m thick sequence of gray limestones, calcarenites and dark gray to black phyllites. Finally, a sequence of gray metadolomites, 200m thick, is observed.

All of these rocks spread continuously across the craton margin into the Sergipano belt where they occur around the Itabaiana and Simão Dias basement domes and are overlain by a metadiamictite formation and a metacarbonate formation of the upper megasequence. According to D'el Rey da Silva (1999), basement and cover underwent the same Neoproterozoic compressive deformation under sub-greenschist facies.

UPPER CARBONATE MEGASEQUENCE

The upper silicilastic megasequence (Simão Dias Group) is represented by mudstones, siltstones, sandstones and lithic wackes (Lagarto-Palmares Fm.), metasiltites to meta-sandstones (Jacaré Fm.) and silty phyllites with intercalations of metasandstones, metacarbonates and wackes (Frei Paulo Fm.). Metasediments of the Vaza Barris Group (diamictites of the Palestina Fm. and the upper carbonate megasequence) overlie the upper siliciclastic megasequence.

The thick Olho D'Agua Fm. is composed of a sequence of marbles and interbedded green, calcareous chlorite-schists and silty phyllites of the Vaza Barris Group and overlies the thick diamictites, pebbly metagreywackes of the Palestina Formation. Marble beds are interbedded with blue to black, fine-grained metalimestone and gray metadolomite. Individual marble beds vary from one to 40m thick in the lower part of the Formation with only local one meter-thick beds in the upper part. Thicker and more abundant carbonate beds are observed in the south limb of the Pinhão anticline. The thick carbonates around the Simão Dias dome pass upward into supertidal-intertidal facies with oolites, and wave-reworked structures indicating a near shore environment (D'el Rey da Silva, 1995).

C-AND O-ISOTOPE STRATIGRAPHY

Thirty-one samples of Jacoca carbonates were stratigraphically sampled from a section along the Vaza Barris River (Capitão Farm) for almost 70m. C and O isotopes were analyzed at the stable isotope Laboratory (LABISE), Recife, Brazil, using a conventional high vacuum extraction line and a SIRA II mass spectrometer.

$\delta^{13}C$ varies from -6.4 to $-8‰_{PDB}$, with majority of values ~ $-4‰_{PDB}$. $\delta^{18}O$ values are mostly ~ $-8‰_{PDB}$ (Fig. 1). C- and O-isotope oscillations are more intense at the first 5 to 10m from the base of this section. Strong oscillations are also observed in Mg/Ca, Si, Fe, Mn and Rb in this portion of this profile. Mn/Sr is <0.5 which suggest that it is very possible that the C- and O-isotope record examined is rather primary. Very high Sr values (above 1000ppm in some cases) suggest that aragonite was formed and later converted to calcite.

The $\delta^{13}C$ for twenty-one carbonate samples from the Acauã Fm. (not shown) stratigraphically collected at Brejinho Farm, 10 km southeast from Lagarto village, tend also to group ~ -4‰$_{PDB}$ and $\delta^{18}O$ spreads within the same range as for Jacoca carbonates, with stronger oscillation of values upsection. Mn/Sr ratios are always <7 and, therefore, there is a possibility that these isotope values are primary. The C-isotope behavior of the Acauã and Jacoca sequences confirms the assumption made by Del Rey (1995) that these carbonates of the Acauã and Jacoca Fms. were deposited simultaneously. If the O- and C-isotope variations are compared to the temporal $\delta^{13}C$ and $\delta^{18}O$ variation curves of Jacobsen and Kaufman (1999), they point to probable depositional age ~740Ma.

Five samples from a 10m-thick (meta) marl to marly carbonate lens intercalated in phyllites of the Frei Paulo Fm., which underlies Palestina diamictites were collected north of the Pinhão village. The $\delta^{13}C$ varies from +3 to +8‰$_{PDB}$ and $\delta^{18}O$, from -9 to -6 ‰$_{PDB}$. This isotope behavior suggests a carbonate deposition between the lower (740-750Ma) and upper (720Ma) Sturtian glacial events, probably ~730Ma.

The Olho D'Agua Fm. is formed by marbles and interbedded calcareous chlorite-schists and silty phyllites of the Vaza Barris Group and overlies the diamictites, pebbly metagreywackes of the Palestina Fm.. About 120 samples of Olho D'Água carbonates were collected, starting from the contact with the Palestina diamictite/pebbly metagreywackes (Fig. 2). Basal marly and dolomitic carbonates, near the contact with Palestina diamictites (first 50m of the section), display strong oscillations of $\delta^{13}C$ with values as low as -4.7‰$_{PDB}$, increasing up-section (0 to 1‰$_{PDB}$). Towards the top of the sequence, $\delta^{13}C$ changes dramatically to values around + 8‰$_{PDB}$ (values as high as +10‰$_{PDB}$ are occasionally found). This vigorous isotope fluctuation suggests that environmental conditions during deposition at the base of this sequence were in contrast to those for carbonates at the top, allowing for an enormous C-isotope oscillation. This $\delta^{13}C$ trend, in which negative values are abruptly replaced by strong positive excursion is typical of Sturtian post-glacial cap carbonates (Kennedy, 1996, Hoffman and Schrag, 2002), suggests that Palestina diamictites are correlatable to Upper Sturtian glacial episode (720-725Ma). $\delta^{18}O$ values vary from -7 to -10 ‰$_{PDB}$, a range typical for carbonates deposited in this Sturtian interval.

Three minor negative excursions (I, II and III in Fig. 2) in the top portion of this section are, perhaps, the result sea-level oscillation.

Sr ISOTOPES

Three carbonate samples from the Jacoca Fm. and three from the Olho D'Água Fm. were analyzed for Sr isotopes at the Federal University of Pará, Belem, Brazil.

These two Formations display similar Sr-isotope (Table 1) ratios, Jacoca averaging 0.707974 and Olho D'Água, 0.707922. A temporal variation of $^{87}Sr/^{86}Sr$ in Neoproterozoic carbonates compiled by Jacobsen and Kaufman (1999) using screened database (Siberian Canada, Namibia, Svalbard and Greenland) from best preserved marine limestone samples, improved the $^{87}Sr/^{86}Sr$ record for the late Neoproterozoic to Early Cambrian.

If one compares the average $^{87}Sr/^{86}Sr$ for the Olho D'Água Fm. carbonates with the $^{87}Sr/^{86}Sr$ temporal variation curve by Jacobsen and Kaufman (1999), it is in very good agreement with values reported for seawater at ca. 720Ma supporting what was deduced from C isotopes.

The average $^{87}Sr/^{86}Sr$ for the Jacoca carbonates, however, it is a bit too high for the seawater at ca. 740Ma, age inferred from the C-isotope signatures, discussed above. In the compilation made by Jacobsen and Kaufman (1999), one observes that the curve for $^{87}Sr/^{86}Sr$ around 740Ma is not so well constrained.

Table 1. $^{87}Sr/^{86}Sr$ (1 sigma) for Olho D'Água and Jacoca carbonates.

Formation	Sample	$^{87}Sr/^{86}Sr$
Olho D' Agua	3OD-1	0.70798 (03)
	3OD-4	0.70799 (04)
	3OD-6	0.70778 (04)
Jacoca	JACCA P22	0.70811 (05)
	JACCA P25	0.70810 (03)
	JACCA P20	0.70769 (02)

CONCLUSIONS

C isotopes suggest that Jacoca-Acauã Fms. were deposited ~740Ma, on top of diamictites (Ribeiropolis, Jacarecica Fms.) correlatable, perhaps, to the lower Sturtian glaciation episode. Values of $\delta^{13}C$ ~ -4‰$_{PDB}$ are observed in both Fms. and no positive $\delta^{13}C$ value was recorded, although only about 70m of carbonates of this Formation were examined. Metacarbonate lenses of the Frei Paulo Fm. show positive $\delta^{13}C$ (average +5‰$_{PDB}$) and, based on the temporal $\delta^{13}C$ variation curve compiled by Jacobsen and Kaufman (1999) a depositional age of ~720-725Ma may be inferred. Olho D'Agua carbonates seem to have been deposited after the Upper Sturtian glaciation, between 700 and 720 Ma.

The depositional and temporal picture deduced from Jacoca, Acauã, Frei Paulo and Olho D'Água carbonates in this central portion of the Sergipano belt needs a confirmation from the western extension of the belt (west of the Tucano basin), in the state of Bahia, where a large amount of carbonates equivalent to Jacoca and Olho D' Água are known since long ago (Jordan, 1971).

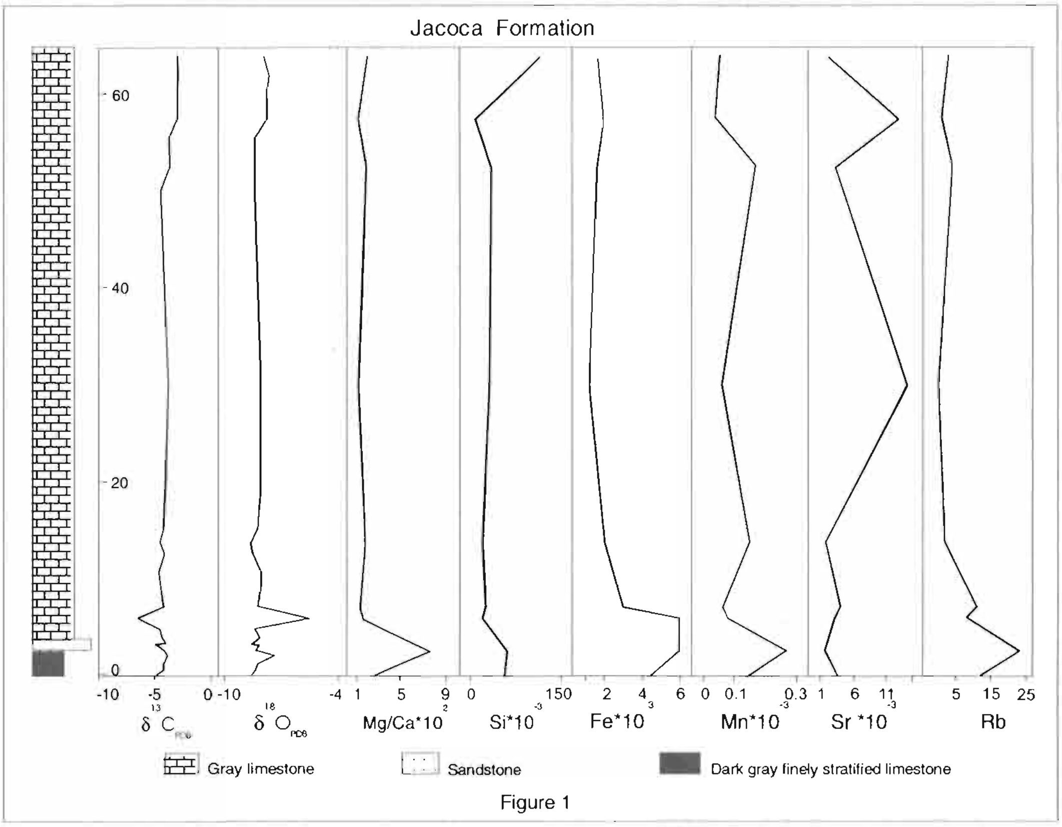

Figure 1. Chemostratigraphic profiles ($\delta^{13}C$, $\delta^{18}O$, Mg/Ca, Si, Fe, Mn, Sr and Rb) for the Jacoca Formation carbonate sequence, northeastern Brazil.

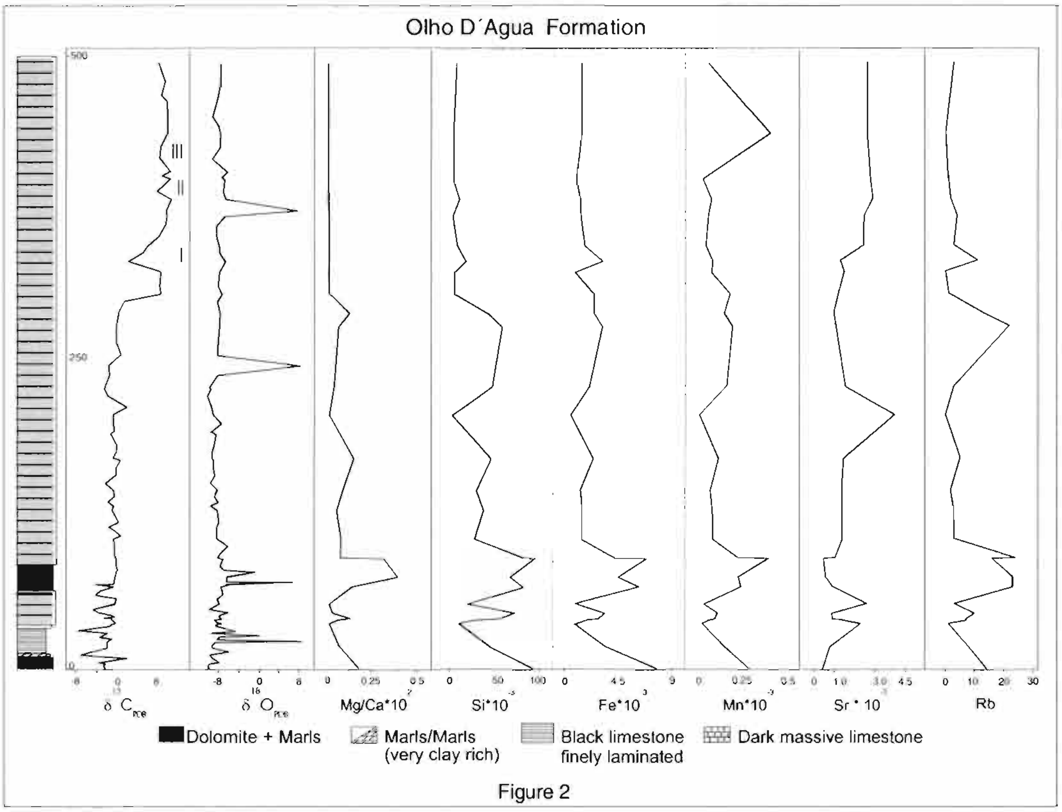

Figure 2. Chemostratigraphic profiles ($\delta^{13}C$, $\delta^{18}O$, Mg/Ca, Si, Fe, Mn, Sr and Rb) for the Olho D´Água Formation carbonate sequence, northeastern Brazil.

ACKNOWLEDGEMENTS

Authors are indebted to Silvana D.S. Barros for drafting the Figures in this paper. This is the contribution n. 209 of the NEG-LABISE.

REFERENCES

D'el Rey Silva, L.J.H. (1995) The evolution of basement gneiss domes of the Sergipano fold belt (NE Brazil) and its importance for the analysis of Proterozoic basins. Journal South American earth Sciences, 8 , 3/4: 325-340.

D'el Rey Silva, L.J.H. (1999). Basin in-filling in the southern-central part of the Sergipano Belt (NE Brazil) and implications for the evolution of Pan-African/Brasiliano cratons and Neoproterozoic sedimentary cover. Journal of South American Earth Sciences, 4-5 (2): 1-18.

Hoffman, P.F. and Schrag, D.P., 2002. The snowball Earth hypothesis: testing the limits of global change. Terra Nova, 14: 129-155.

Jacobsen, S.B. and Kaufman, A.J., 1999. The Sr, C and O isotopic evolution of Neoproterozoic seawater. Chemical Geology 161: 37-57.

Jordan, H., 1971. The late Precambrian Synclinorium of Curaçá (Brazil). Geol. Jb. 88: 617-628.

Kennedy, M.J., 1996. Stratigraphy, sedimentology, and isotopic geochemistry of Australian cap dolostones: deglaciation, $\delta^{13}C$ excursions, and carbonate precipitation. Jour. Sed. Research 6: 1050-1064.

AN ISOTOPIC INSIGHT OF THE SERGIPANO BELT STRATIGRAPHY: RADIOGENIC AND CARBON ISOTOPES

Silva Filho, M.A.[1]; Sial, A.N.[2]; Ferreira V.P.[2] and Silva, J.C.[2]

1. CPRM/NEG-LABISE, Department of Geology, Federal University of Pernambuco, CP 7852, Recife-PE, 50670-000. masf@br. inter. net
2. NEG-LABISE, Dep. Geologia-UFPE, C.P. 7852, Recife-PE, 50670-000, Brasil. ans@ufpe.br, valderez@ufpe.br

Keywords: C-isotopes, Meso-Neoproterozoic, Sergipano Belt, Brazil

INTRODUCTION

The aim of this work is to constrain the depositional time interval of some stratigraphic units that belong to the Sergipano fold belt (SFB), northeastern Brazil. Based on a review of the existing radiogenic and stable isotope data, as well as on field stratigraphic considerations, a new startigraphic position for the Macururé (MA) and Araticum (AT) groups is proposed as well as their relationship with other stratigraphic units.

The SFB belongs to the Borborema Geotectonic Province and is located in the northern margin of the São Francisco Craton (SFC) (Fig. 1). A generalized stratigraphic division of this belt was proposed by Humphrey & Allard (1962, 1969), in which they identified that the Miaba (MI) and Vaza Barris (VB) groups are located in the SFB itself and that the Estância (ES) Group is located overlying the (SFC). North of this area, the same authors also identified biotite-garnet schists surrounding some granitic stocks, and considered them as hornfelses. On the other hand, Barbosa (1970) characterized the Canudos (CA) Group, west of the Tucano basin, which is equivalent to the MI and VB. Additionally, this author characterized the MA, which is composed by siliciclastic metasediments and is correlative with the hornfelses of Humphrey and Allard (1969). According to Silva Filho & Torres (2002) the Araticum complex comprises the Araticum, Timbaúba e Batalha units from Silva Filho et al. (1981) and is correlatable with the hornfelses from Humphrey and Allard (1969), which then were characterized as pellitic (Traipú) and quartz-feldspar (Jaramataia) hornfelses. Additionally, Silva Filho & Torres (2002) separated the AT from the MA and proposed different age and depositional environments for them, based on the presence of amphibolites (MORB metabasalts) and some BIF in the AT that are not present in the MA.

D'el-Rey Silva (1995), modified the stratigraphic division from Humphrey & Allard (1969) and a new stratigraphy was proposed for the SFB. Nevertheless, Davison & Santos (1989) came up with another subdivision in which the Estância Domain and its respective foreland basin (ES); the Vaza Barris Domain including the MI and VB; the Macururé Domain including the MA; the Poço Redondo Domain; Marancó Domain and the Canindé Domain were proposed based on tectono-stratigraphic considerations.

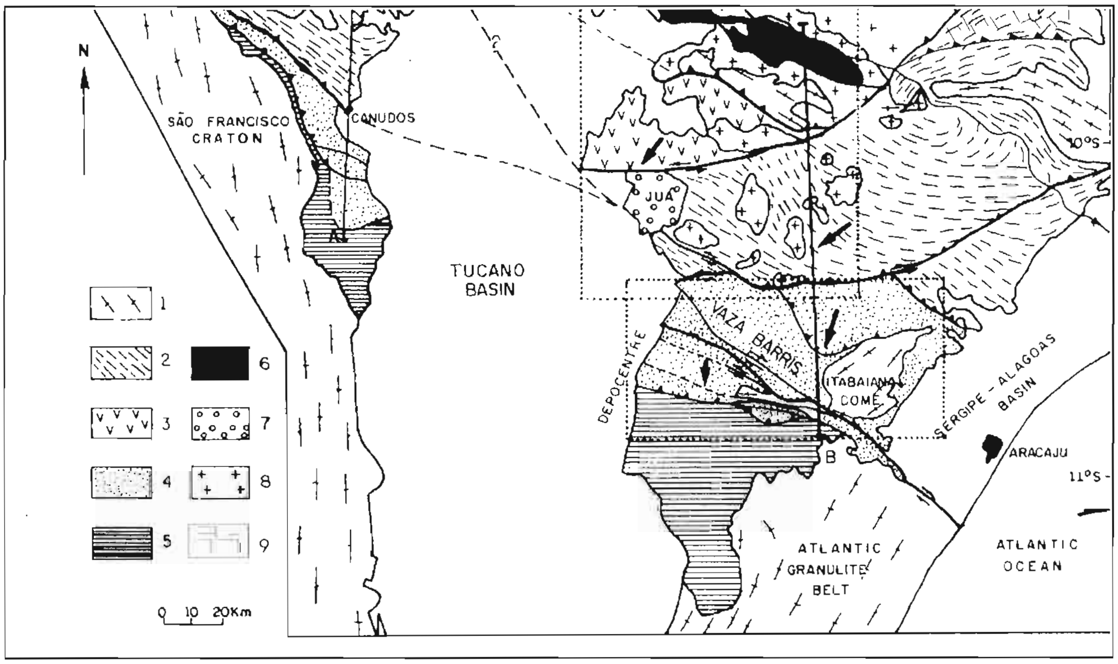

Figure 1. Simplified geologic map of the Sergipano fold belt and its basement. 1- High-grade gneiss; 2- Macururé; 3- Marancó; 4- Vaza Barris; 5- Estância; 6- Canindé; 7- Juá graben; 8- Granites; 9- Rio Coruripe Domains.

Silva Filho & Torres (2002), recognized the above mentioned domains, as well as the Rio Coruripe (RC) Domain, including the AT and the Pernambuco-Alagoas (PE-AL) Domain, which comprise Meso-Neoproterozoic metaplutonic and metasedimentary rocks and Neoproterozoic granitoids. These authors also stated that the VB, MA and RC belong to an ensialic fold belt (SFB) and that the others to an oceanic fold belt, known as the Sul-Alagoano fold belt respectively, which amalgamated along the Jeremoabo-Belo Monte shear zone.

PROBLEM CHARACTERIZATION

Based on geochronologic data in some granites which show ages around 0.6 Ga, the SFB has been considered as part of a group of fold belt affected by the Brasiliano orogeny (Brito Neves et al., 1978; Santos et al., 1998). However, some 1.04 and 1.0 Ga (U/Pb) ages were obtained in felsic metavolcanic rocks from the MA and other of 0,98 Ga from some orthogneiss that intrude the Cabrobó Complex (CC) in the PE-AL (Van Schmus, et al., 1995; Silva Filho et al., 1997) .

The time span of deposition of the MA and AT sequences is a topic of continuous debate. The existing discrepancies are based on the lack of fossils and radiogenic data. For instance, the MA was considered older than the CA by Barbosa (1970), while Silva Filho et al. (1978) and Santos et al., (1998) considered it as the coeval deep water equivalent of the VB and MI and proposed a Neoproterozoic age. Silva Filho & Torres (2002) considered the MA as correlative of the MI, both of Mesoproterozic age. Davison & Santos (1989) proposed a Neoproterozoic age for the previously mentioned domains, but without following any stratigraphic consideration. The AT was separated from the MA, but was considered as correlative of the CC, assigning a Meso-Neoproterozoic age (Silva Filho and Torres, 2002).

STABLE vs. RADIOGENIC ISOTOPES

Sial et al., (2000), analyzed several carbonate sequences located in the SFB using C and O stable isotopes and compared the resulting C-isotope data with preexisting C-isotope secular variation curves (Hoffman et al.,1998 ; Kha et al. , 1999). These authors collected 25 samples in a 80m thick marble sequence in the Batalha city (Al) region and obtained fluctuating positive $\delta\ ^{13}C$ values between + 3 a + 4 $^{o}/_{oo\ PDB}$ and two slight shifts to values as low as 0 $^{o}/_{oo}$ (Fig. 2). According to Silva Filho and Torres (2002) these marbles belong to the AT and therefore the secular variation curve proposed by Sial et al (2000) might represents Meso-Neoproterozoic ages instead of solely representing Neoproterozoic ages. On the other hand, Silva and Sial (2003) found similar $\delta\ ^{13}C$ pathways in marbles from the São Caetano Complex whose age range between 1.1 and 0.98 Ga.

Sial et al. (2000) also sampled the Acauã Formation of the ES, the Jacoca Formation of the MI, and the Olhos D'Água Formation of the VB. In the Acauã Formation 21 samples were collected by these authors and $\delta^{13}C$ values arround -4 $^{o}/_{oo}$, as well as some small shift in the top, were found (Fig. 3a). In the Jacoca Formation a 300m thick carbonate sequence was studied and 31 samples collected. The $\delta^{13}C$ values vary between -6,4 and -2,8 $^{o}/_{oo\ PDB}$ with a mean of -4 $^{o}/_{oo\ PDB}$ (Fig. 3b). The $\delta^{13}C$ record of the Acauã and Jacoca formations confirm the contemporaneous age proposed by Silva Filho et al. (1978). The Frei Paulo Formation, is currently considered as the result of facies lateral variation of the Jacoca Formation and present carbonates stratigraphically overlaying the latter formation. The $\delta^{13}C$ values obtained by Sial et al. (2000) vary from +3 to +8$^{o}/_{oo\ PDB}$ and from -9 to -6$^{o}/_{oo\ PDB}$, suggesting that they are postglacial cap carbonates.

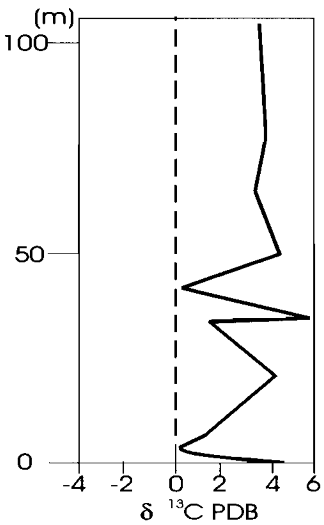

Figure 2. C-Isotope chemostratigraphic profile of the Meso-Neoproterozoic Araticum complex. (Isotopic data after Sial et al., 2000).

The Olhos d'Água Formation is overlaying diamictite sediments of the Palestina Formation. 130 samples were collected by Sial et al. (2000) in discontinuous marble outcrops, covering the whole sequence from the contact with the diamictite to the Pinhão anticline. The $\delta^{13}C$ values oscillate between -7$^{o}/_{oo}$ and -1$^{o}/_{oo\ PDB}$, at the base, and shift to values around 0 and -1$^{o}/_{oo\ PDB}$, and then shift to values as high as 10$^{o}/_{oo\ PDB}$ at the top (Fig. 3c). These $\delta^{13}C$ characteristics as well as the underlying diamictite led Sial et al. (2000) to propose a post glacial origin (cap carbonates).

The composition of the $\delta^{13}C$ values obtained in the AT (Fig. 2) with the general C-isotope secular variation curve proposed by Kah et al. (1999) (Fig. 4a), suggests that the AT deposition time interval spans from the late Mesoproterozoic to early Neoproterozóico. According to Silva Filho and Torres (2002) this sequence deposited in a rift-like basin and its chronostratigraphic correlation with the CC is plausible given that the latter is intruded by Cariris Velhos orthogneiss (0.98 Ga).

Given that the MA is not intruded by the Cariris Velhos orthogneiss (0.98 Ga) but by some leucogranites of 0.76 Ga age (Rb-Sr) (Amorim, 1995) the age for the deposition of this complex can be restricted between 0.98 and 0,76 Ga. The presence of the 0.76 Ga leucogranites characterizes the first NW trending deformation event that affected this group. (Dextro et al., 1993; Silva Filho, et al., 2002).

Figures 3b and 3c show the $\delta^{13}C$ curve for the Jacoca and Olhos d´Água formations. Comparing these curves with the curve in figure 4, Sial et al. (2002) proposed the ages 0.74 and 0.72 Ga respectively for these groups, and that they registered the Sturtian glaciation in the brasilian shield. The age of the Canindé Complex (0.748 Ga – K-Ar) (Bezerra et al., 1992}, as well as the anorogenic environment assigned by Oliveira & Tarney (1990) allow to the statement that there probably were some extensional movements coeval with the deposition of the Ribeirópolis Formation. Figure 4b shows the strong correlation between the stratigraphy of the Otavi Group in Namíbia (Hoffman et al., 1998a,b) and the stratigraphic units in the SFB.

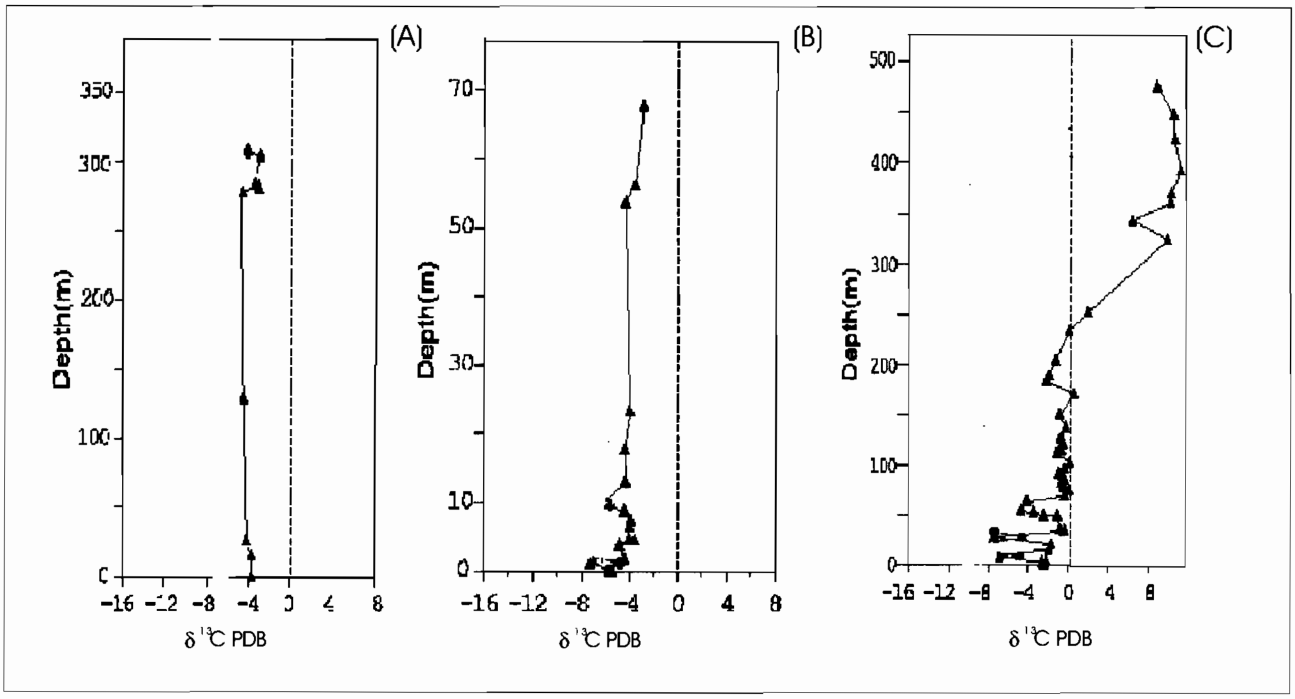

Figure 3. C-Isotope chemostratigraphic profiles of some Neoproterozoic sequences in the Sergipano Belt. (a) Acauã (b) Jacoca (c) Olhos D´Água. (Sial et al., 2000).

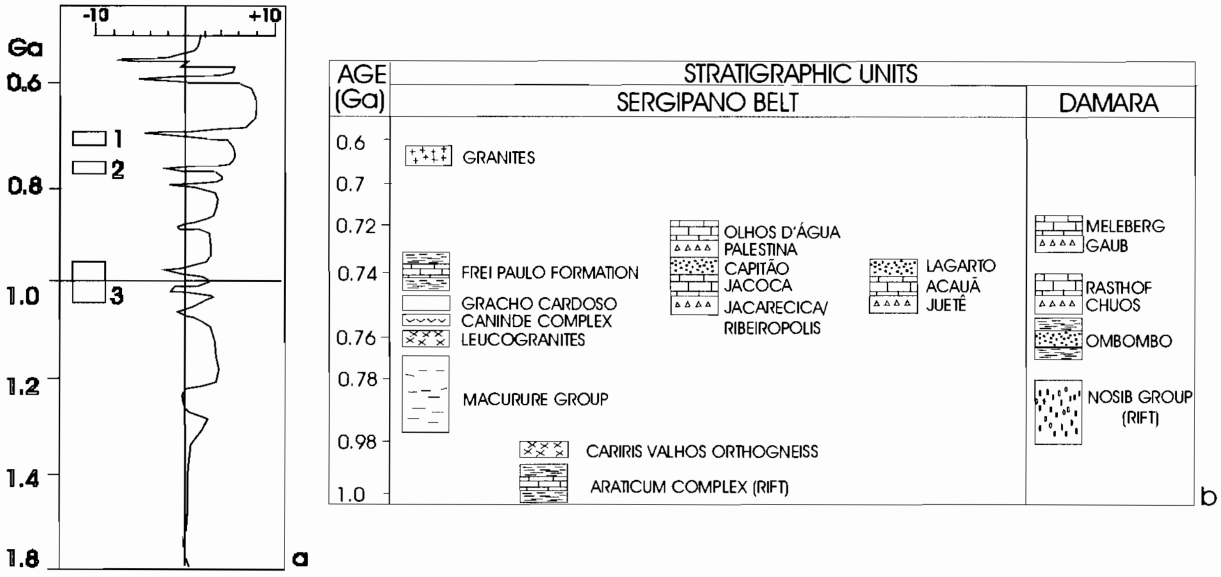

Figure 4. (a) Meso-Neoproterozoic C-isotope secular curve (After Kah et al., 1999) 1. Olhos D´Água 2. Jacoca 3. Araticum. (b) Stratigraphic framework for the studied sequences (Sergipano belt) and other coeval sequences (Damara belt).

CONCLUSIONS

The C-isotope data of carbonate (limestone/marble) sequences are useful for the delimitation of depositional intervals. Based on the data published by Sial et al (2000) and other published radiogenic data, it was possible to propose a stratigraphic framework for some units located in the Sergipano fold belt as follow:

a- The Araticum Complex not only represents Neoproterozoic ages but late Mesoproterozoic to early Neoproterozoic ages.

b- The Jacoca and Olhos d´Água formations were deposited at 0.74 and 0.72 Ga, respectively.

c- It is suggested that the Jacarecica diamictites were diacronic with some expreading movements (an-orogenic) registered in the Canindé Domain, which are represented by the stratified gabbroic Canindé Complex.

d- It is proposed that in the Macururé Domain not only exist present metasedimentary rocks from the Macururé Group (0.98 and 0.76 Ga), but also metasedimentary rocks from the Ribeirópolis Formation.

REFERENCES

Amorim, J. L. 1995. Programa de Levantamentos Geológicos Básicos do Brasil, Arapiraca, Folha SC.24-X-D-V. Estado de Alagoas, Escala 1:100000. Brasília; CPRM , 1995 p. 100

Barbosa, O. 1970. Geologia de parte da região do médio São Francisco, NE do Brasil. Rio de Janeiro: DNPM: DFPM, 1970. 98 p. (Boletim 140)

Bezerra, F. H. R,; Jardim de Sá, E.F.: Nilson, A. A. et al. 1992. O ambiente tectônico do Complexo Canindé do São Francisco e rochas encaixantes – Faixa Sergipana, NE do Brasil. Simpósio Regional de Geologia, 1., Salvador, SBG, Anais, p.117 – 120.

D´el-Rey Silva, L.J.H. 1995. The evolution of basement gneiss domes of the Sergipano fold belt (NE Brazil) and its importance for analysis of Proterozoic basins .Journal of South American Earth Sciences, v. 8, n.3/4, p.325-340,1995

Davison, I.; Santos, R. S. 1989. Tectonic evolution of the Sergipano belt, NE do Brasil, during the brasiliano orogeny. Precambrian Research, v.45, p, 319-342, 1989.

Dextro, N,; Magnavita, L.P.; Aragão, M. A. N. F. 1993. Faixa de dobramentos do Baixo São Francisco: individualização tectônica do segmento norte da Faixa Sergipana. Simpósio do Cráton São Francisco, 2 Salvador, Anais, SBG. P.312-314. 1993

Hoffman, P. F.; Kaufman, A J.; Halverson, G. P. 1998a. Comings and goings of global glaciations on a tropical platform Neoproterozoic in Namibia. GSA Today 8 (5): 1-10.

Hoffman, P. F.; Kaufman. A.J.; Halverson, G.P.; Schrag, D.P. 1998b. A Neoproterozoic Snowball Earth. Science 281: p.1342-1346

Humphrey, F ; Allard, G. O. 1962. Reconnaissance of the geology of Pre-Cretaceous rocks in state of Sergipe. Salvador: Petrobrás,1962. 37p. Relatório1625

Humphrey, F.; Allard, G. O. 1969. Geologia do Domo de Itabaiana (Sergipe) e sua relação com a geologia da Geossinclinal de Própria, um elemento tectônico recém reconhecido do escudo brasileiro. Rio de Janeiro: Petrobrás/CENPES,1969.104p.

Kha, L. C.; Sherman, A.G.; Narbonne,G.M.; Knoll, A. H.; Kaufman, A.J. 1999. δ 13 C stratigraphy of the Proterozoic Bylot Supergroup, Baffin Islands, Canada: implications for regional lithostratigraphy correlations. Can. Journ Earth Sci 36: p.313-332.

Oliveira, E. P.; Tarney, J. 1990. Petrogenesis of the Canindé de São Francisco Complex: a major late Proterozoic gabbroic body in the Sergipe fold belt, northeastern Brazil. J. South Amer. Earth Sci., v.3 .p. 125- 140,1990.

Santos, R. A.; Martins, A. A. M.; Neves, J. P.; Leal, R. A. 1998. Geologia e Recursos Minerais do Estado de Sergipe. Brasília; CPRM, 1998, p. 156

Sial, A. N.; Ferreira, V. P.; Almeida, A. 2000. Carbon isotope fluctuations in the Precambrian carbonate sequences of several localities in Brazil. An. Acad. Bras. Cien.Anais 72(4) : 539 – 558.

Sial, A.N., Ferreira, V.P and Santos, V.H. 2002. C and O isotopes of the Jacoca and Olhos D'Água cap carbonates sequences, Sergipe, Northeastern Brazil. João Pessoa; XLI CBG. SBG . Anais. Pp. 509

Silva Filho, A . F.; Guimarães, I. P.; Lyra de Brito, M. F.; Pimentel, M.M. 1997. Geochemical signatures of main Neoproterozoic late-tectonic granitoids from the Proterozoic Sergipano fold belt, Brazil: significance for the Brasiliano orogeny. Int.Geol. Rev. v. 39, p. 639-659.

Silva Filho, M, A.; Torres, H.H. F.; Brito. R. S. C. 2002. Mapa Geológico de Alagoas. Brasília ; CPRM, 2002, Escala : 1: 250 000

Silva Filho, M. A. ; Bomfim, L. F. C.; Santos, R. A. 1978. A geossinclinal Sergipana: estratigrafia , estrutura e evolução. CBG, 30, 1978, Recife. Anais, v 6 , p. 2464 –2477.

Silva Filho, M. A.; Torres, H. H. F. 2002. A new interpretation on the Sergipano belt domains. An. Acad. Bras. Cienc. Anais 74 (3) : p. 556-557.

Silva Filho, M.A.; Bomfim, L.F.C.; Santos, R. A. et al. 1981. Geologia das áreas dos estados de Alagoas, Sergipe e Bahia: Projeto Canindé do São Francisco. Brasília : DNPM/CPRM, 1981, p. 118 (Série Geologia, 19. Seção Geologia Básica, 14)

Silva, J. C. and Sial, A.N. 2003. C-isotope stratigraphy as a tool for correlating global events: a case from northeastern Brazil. IX Colombian geological congress. Medellin, Colombia. CD.

Van-Schmus, W. R.; Brito Neves, B. B.; Hackspacker, P. et al. 1995. U/Pb and Sm/Nd geocronologic studies of the eastern Borborema Province, Northeastern Brazil; initial conclusions. Journ. South American Earth Sciences, v.8, n 3/4 p.267-285

THE MESO-NEOPROTEROZOIC TRANSITION IN THE BORBOREMA PROVINCE, NORTHEASTERN BRAZIL: THE SÃO CAETANO COMPLEX C-ISOTOPE CHEMOSTRATIGRAPHY

Silva, J.C.; Sial, A.N. and Ferreira, V.P.

NEG-LABISE, Department of Geology, Federal University of Pernambuco, C.P. 7852, Recife-PE, Brazil, 50670-000.
juancst@ufpe.br, ans@ufpe.br, valderez@ufpe.br

Keywords: C Isotopes, Meso-Neoproterozoic, chemostratigraphy, Borborema Province, Brazil

CARBON ISOTOPES AND THE NEO-MESOPROTEROZOIC TRANSITION

The C-isotope composition of ancient oceans has been a topic of continuous debate among the geoscientific community. Biological evolution, atmospheric oxygenation levels, tectonic events and, to some extent, unusual global climate episodes have been regarded as factors controlling the primary composition of this stage of earth's hydrosphere. Throughout the Precambrian, the C-isotope composition of ocean water was shaped mostly by the above-mentioned factors. From this, new perspectives for the complex paleotectonic, paleoclimatic and paleobiological conditions that have dominated our planet during that time have been pursued.

Well-constrained C-isotope data have been used to construct a secular variation curve (Fig. 1). Nevertheless, for the Mesoproterozoic this curve is less well-constrained. It is well known that this Era was characterized by biochemical ecstasies and high tectonic activity.

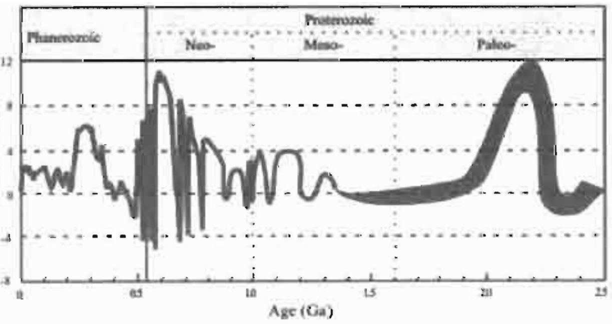

Figure. 1 Conjugated secular C variation curve based on Hoffman et al. (1998) and Kha et al. (1999) chemostratigraphic curves. In (Sial et al. , 2000).

Few studies have supplied reliable C-isotope chemostratigraphic information for this period (e.g Bartley et al., 2001; Kah et al., 1999, 2001; Knoll et al., 1995).Carbonate sequences from Australia, United States, China and Siberia (Bartley et al., 2001 and references therein) have demonstrated that Early to Middle Mesoproterozoic (1.6-1.3 Ga) is characterized by a narrow variation of $\delta^{13}C$ values which jumps around 0‰$_{PDB}$. This behavior is replaced in the Late Mesoproterozoic-Early Neoproterozoic transition by a new pathway characterized by slightly stronger C-isotope fluctuations, which roughly coincide with the onset of the Grenville orogeny. The chemostratigraphic pathways observed for this interval (1.2-0.85Ga) display $\delta^{13}C$ values averaging 3.5±0.5‰$_{PDB}$, with pulses between -2.7‰ $_{PDB}$ and +4‰$_{PDB}$ (Fig. 2a).) (e.g. Knoll et al., 1995; Kah et al., 1999; Kah et al., 2001; Bartley et al., 2001; among others).

Bartley et al. (2001) supplemented the C-isotope data reported by Kah et al. (1999) with data from carbonate sequences from Canada and a well-constrained C-isotope secular variation curve was, then, compiled for the Meso-Neoproterozoic transition (Fig. 2b). These authors, as well as Knoll et al. (1995), studied the Middle to Late Riphean transition and two trends with important $\delta^{13}C$ fluctuations were identified. These trends encompass values in the -2 and 0‰ range for the Middle Riphean, and between -2.4‰ and 3‰ for the upper Middle-Late Riphean, which are separated by an autonomous increase, from 0‰$_{PDB}$ to nearly 2.5‰$_{PDB}$, that characterizes the Meso-Neoproterozoic boundary (Knoll at al., 1995; Bartley et al., 2001). According to Kah et al. (1999) these trends are related to the agglutination and break-up of Rodinia (1.2-0.85 Ga) which caused an increase in the Corg burial rates and high ocean-water oxygenation levels, leading to the diversification of life and $\delta^{13}C$ increase.

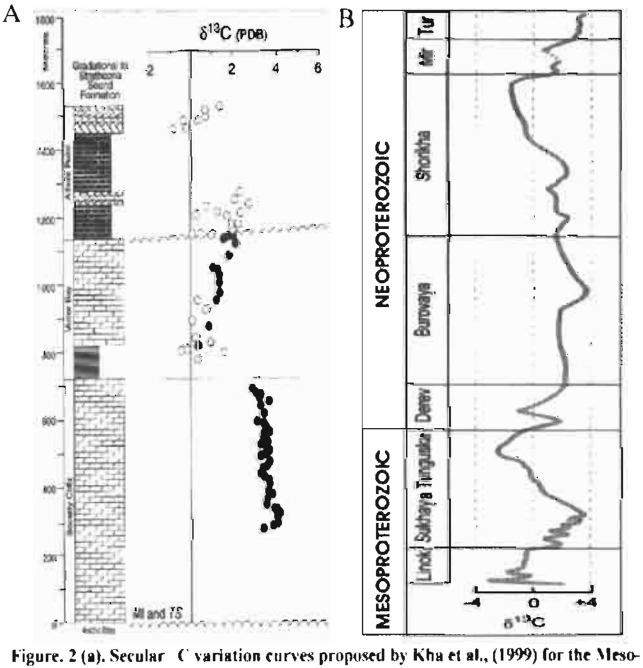

Figure. 2 (a). Secular C variation curves proposed by Kha et al., (1999) for the Meso-Neoproterozoic transition in Canada(b). C-isotopes chemostratigraphic curve found in Siberia by Bartley et al., (2001).

GEOLOGICAL SETTING AND CHEMOSTRATIGRAPHY

The São Caetano Complex (SCC) is a volcano-sedimentary sequence characterized by the presence of garnet-biotite paragneiss, quarzite, marble, metagraywacke, metadacite, metarhyolite, metapelite and metabasalt, metamorphosed under the amphibolite-facies conditions during the Brasiliano orogeny (0.75-0.5 Ga.) (Brito Neves et al., 2002). The SCC is located in the Alto Pageú terrane (APT), and makes part of the Cariris Velhos belt (CVO) developed between 1.1 and 0.95 Ga in the Borborema Province. Regionally, it is associated to some metavolcanic sequences as well as to some MORB mafic and ultramafic suites (e.g Riacho-Gravata belt and Serrote das Pedras Pretas) that have been interpreted as part of a mid-oceanic rift sequence developed ~ 1.0 Ga.(Brito Neves et al., 2002 and references therein). The SCC is also intruded by various Neoproterozoic plutonic and orthoderived suites and associated to some metamorphic Paleo-Mesoproterozoic belts (Brito Neves et al., 2002). The older age assigned to the SCC is quite uncertain and is inferred from some sedimentary zircons of Archean to Late Mesoproterozoic age. The younger age obtained for the SCC is 0.96 Ga (U-Pb) from a Cariris Velhos granodioritic-biotite orthogneiss that intruded the SSC to the north of the study area (Britto Neves et al., 2002).

Five continuous marble stratigraphic sections near the Flores Town (Pedra de Cal, Santa Rosa, Rodiador, Malutagem) and Sitio dos Nunes town, Pernambuco, were examined and 120 samples were analyzed for C-isotopes. δ^{13}C chemostratigraphic pathways were obtained and used to correlate the five stratigraphic sections and to construct a composed C-isotope variation curve (compound stratigraphic section ~250m) for the studied marbles (Fig. 3). The thicker and most complete stratigraphic section (Pedra de Cal locality) consists of 44 samples that correspond to nearly 110 m. The sequence starts with very oscillating δ^{13}C values, which vary from 2‰$_{PDB}$ to 3.6‰$_{PDB}$ and present some depletions to values around 1‰$_{PDB}$ (I). Those values remain constant, averaging 2.3‰$_{PDB}$, then decrease to values as low as -2.2‰$_{PDB}$ and finally establish around -1.5 ‰$_{PDB}$ (II). However, some positive shifts of no more than 0.5‰$_{PDB}$ are also noticeable. A sole enrichment, from 0 to near 1.8‰$_{PDB}$ (III) characterizes the upper part of the section just before falling to values around 0 and -1‰$_{PDB}$ (IV).

The Malutagem (2) and Sitio dos Nunes (3) sections (Fig. 3) present predominant negative δ^{13}C values. Both sections start with oscillating values in which shift from near -2.6‰$_{PDB}$ to near 1‰$_{PDB}$ are identified (II). This pathway is interrupted by a very pronounced enrichment from -1.5 to 2.5‰$_{PDB}$ (III), which then is followed by a decrease to values near -2‰$_{PDB}$ (IV)

The Santa Rosa (4) and Rodiador (5) sections (Fig. 3) provided the most positive δ^{13}C values of this study and comprise the uppermost part of the composite stratigraphic section. Both sections start with negative δ^{13}C values, varying between -1.8‰$_{PDB}$ and 1.5‰$_{PDB}$ (IV), which then increase up-section to values as high as 3.7‰$_{PDB}$ (V). In the Rodiador sections those positive values sporadically decrease to values near -1.8‰$_{PDB}$ (VI, VII), whereas in the Santa Rosa section, those positive values (2.7‰$_{PDB}$) are preserved and present not negative shifts (VII).

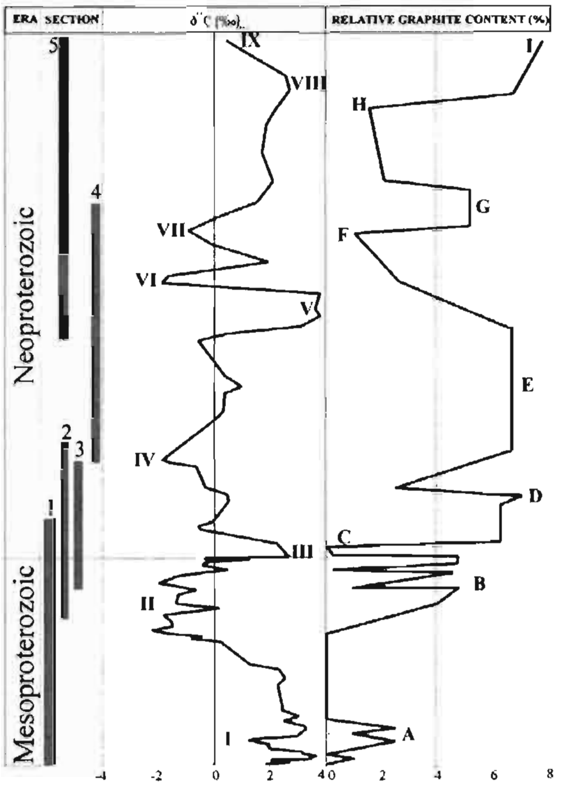

Figure 3. Composite δ^{13}C chemostratigraphyc section and variations in the relative graphite content of the São Caetano Complex. Numbers represent stratigraphic sections. (1) Pedra de cal; (2) Malutagem;(3) Sitio dos Nunes: (4)Santa Rosa;(5)Rodiador.

Since the C-isotope composition of carbonate sequences can be tied to changes in the global Corg burial during sedimentation (Bartley, et al., 2001 and references therein), variations in the δ^{13}C values were contrasted with variations in the relative content of graphite (Fig. 3). Large amounts of graphite were observed in the analyzed samples. In the Piedra de cal locality, graphite contents range from 0% to 4.7% (A) but some shifts to near 2% are also common (B). The Malutagem and Sitio dos Nunes sections present more fluctuating patterns with graphite contents shifting from 0 to 7% (C,D) and, in some cases, from 0 to 4% (B). The Santa Rosa and Rodiador sections start with high contents of graphite (~7%) (E), that decrease up section to values near 1.5% (F,H) to finally increase to values near 8.5% (I) .

After comparing C-isotope and graphite content variation curves, an opposite behavior can be noted. For instance in the lower part of the stratigraphic section, increases in the content of graphite (A, B) coincide with decreases in the δ^{13}C values (I, II); whereas in the upper part of the section large enrichment in the graphite content (D, E, G, I) coincide with depletions in the δ^{13}C values (IV, VI, VII, IX) and viceversa (G,VIII). Likewise, in the middle part of the stratigraphic section a negative shift in the graphite content (C) coincides with an increase in the $\delta^{13}C$ values (III).

δ^{13}C SECULAR VARIATIONS: REGIONAL AND GLOBAL IMPLICATIONS.

The general Mesoproterozoic $\delta^{13}C$ secular variation curve presents an almost invariant pathway, with values near 0 and 1‰$_{PDB}$; resulting from a period of relative stable tectonics in which the ocean-water geochemical composition remained in a widespread steady state (Fig. 1) (Lindsay and Brasier, 2002; Bekker et al., 2003). Nevertheless, by the Meso-Neoproterozoic transition, that steady state seems to have changed and a more varying pathway should have resulted from biological ecstasies during a period of high tectonics associated to the agglutination of the supercontinent Rodinia (Fig. 2a,b) (Bartley et al., 2001).

The $\delta^{13}C$ secular variation pathways encountered in the SCC (Fig. 3) seems to match with those encountered in Meso-Neoproterozoic carbonate sections from Canada and Siberia (Figs. 2a,b). Nevertheless, some short term variations are identified in the former due to the high resolution method adopted during sampling in this work (sample collection spacing~1m in average). Two different $\delta^{13}C$ values trends were found in the SCC marbles, one decreasing from 4‰$_{PDB}$ to -2.2‰$_{PDB}$ (I-II) and another increasing from nearly -2‰$_{PDB}$ to 3.7‰$_{PDB}$. (IV-IX), which are separated by a slightly positive anomaly with values as high as 2.7‰$_{PDB}$ (III). The same secular variation was found in carbonate sequences located in the Uchur-Maya and Turukhansk regions (Siberia) (Fig 2b) in which both the decrease and later increase in $\delta^{13}C$ are separated by slightly positive anomaly (~2.4‰$_{PDB}$). Meanwhile, in carbonate sequences from the Bylot Supergroup, Canada, those different $\delta^{13}C$ trends are separated by a positive anomaly with values near 2.7‰$_{PDB}$ (Kah et al., 1999) According to Bartley et al. (2001) that anomaly marks the Meso-Neoproterozoic passage and can be considered as having occurred some time between 1.035 and 1.03 Ga., based on well constrained U-Pb and Sm-Nd geochronological data found in some mafic sills intruding those stratigraphic sections. These similarities were thus taken in to account to (1) propose a contemporary sedimentation for these two sequences, spanning from 1.3 to 0.95 Ga, and (2) state that the Meso-Neoproterozoic passage was registered by the SCC original carbonate sequence.

Highly fluctuating $\delta^{13}C$ values in carbonate sequences are expected during periods of ocean rifting and high tectonic activity (Des Marais et al., 1992, 1994). For instance, enriched $\delta^{13}C$ values have been attributed to periods of high tectonic activity during which Corg burial cause high levels of ocean oxygenation and high biologic diversification (Des Marais 1994). These kinds of values are also expected in periods of high Corg sequestration during widespread subduction and oceanic closure (Lindsay and Brasier, 2002, Bekker et al., 2003). Oppositely, low $\delta^{13}C$ values are associated to periods of stable tectonics; in which low Corg burial contribute to the oxidation and incorporation of the available ^{12}C rich organic matter into the ocean system (Des Marais, 1994; Kah et al., 1999; Bartley et al., 2001). Moreover, depleted $\delta^{13}C$ values can be also expected during periods of oceanic rifting and spreading, as well as to superplume events, in which depleted volcanic CO_2 is released into the ocean water (Lindsay and Brasier, 2002)

As it was mentioned previously, secular variations in the Meso-Neoproterozoic $\delta^{13}C$ has been considered as the result of an enhanced Corg matter burial that occurred during the agglutination and later break-up of Rodinia (Kah et al., 1999; Bartley et al., 2001). According with these authors, that enhancement in the Corg burial should have prevented the oxidation of large amounts of ^{12}C rich organic matter and incorporation of the available ^{12}C into the ocean water. This should have generated high ocean water oxygenation levels that led to an increase in life diversification, which in turn, contributed to that general $\delta^{13}C$ increase due to high ^{12}C biological consumption.

Augments in the content of graphite in the São Caetano Complex marbles, which might represent increases of Corg burial in a marine carbonate platform, coincide with depletions in the $\delta^{13}C$ values (Fig. 3b compared with 3a). This characteristic is not in agreement with the generalized assumption of Bartley et al. (2001) in which high organic matter burial was related to decreases in the $\delta^{13}C$, and viceversa. Therefore, other variables such as carbon tectonic sequestration, changes in sea level, ocean spreading and closure and/or local seawater stratification should be regarded as alternative factors controlling the SCC $\delta^{13}C$ paths.

Oscillatory $\delta^{13}C$ pathways encountered in the carbonate sequences world-wide have been attributed, in the long term, to high tectonic activity during which inputs and outputs of available ^{12}C strongly changed as consequences of Corg burial and sequestration (Lindsay and Brasier, 2002; Bekker et al., 2003). Likewise, short term phenomena such as upwelling, relative sea level changes, ocean water stratiphication, among other; can also generate fluctuating $\delta^{13}C$ paths by locally controlling the C-cycle as proposed by Mitchell et al. (1996) in Phanerozoic sections

CONCLUSIONS.

An alternative sequence of events is, thus, proposed to explain the oscillating trend of SCC $\delta^{13}C$ secular variation curve, which can be subdivided into four stages as follows:

(1) A combination of global Corg burial and sequestration during uplift and widespread development of subduction zones. These processes generate $\delta^{13}C$ positive excursions as those found in the lower most part of the SCC sequence (I). The positive excursion can be related to the onset of the Grenville orogeny (~1.3-1.1 Ga.) elsewhere, in which widespread large orogenic belts and subduction zones development have been amply identified.

(2) Addition of large amounts of volcanic ^{12}C enriched CO_2. General rifting event have been related to the separation of the San Francisco,

Congo, São Luiz Craton, just before Rodinia agglutination. (~1.1-1.0 Ga.) This process should have added large amounts of ^{12}C enriched CO_2 through degassing and generated a general depletion in the $\delta^{13}C$ of ocean water. This event was probably registered by the lower part of the SCC (II).

(3) Rapid Corg matter sequestration through subduction. This phenomenon should have been associated to the CVO in the Borborema Province, north of the São Francisco craton, and generated the rapid and sharply positive excursion registered during the Meso-Neoproterozoic transition (~1.0 Ga.) in the SCC (III). This subduction event is supported by the existence of eclogites associated to the SCC. (Brito Neves et al., 2002 and references therein). Nevertheless, the onset of the CVO should have also generated high Corg burial due to high continental erosion rates during rapid uplift.

(4) ^{12}C rich organic matter sequestration during subduction and posterior ocean closure (1.0 and 0.96 Ga.). After the Meso-Neoproterozoic passage, the SCC carbonates sequences should have registered an oceanic basin closure during the accretion of the Riacho Gravata complex to the Paleproterozoic supracrustal blocks of the B.P. (from 1.0 to 0.96 Ga.), which was accompanied by subduction (Brito Neves et al., 2002). This closure led to a pronounced increase in the $\delta^{13}C$ values due to Corg sequestration (IV-IX). Nonetheless, fluctuating and slightly positive $\delta^{13}C$ values (V-VII) are also encountered and can be interpreted as the result of oceanic stratification, associated to relative sea level changes and ocean closure, that might have also controlled the C-cycle.

From this panorama, it can be stated that the $\delta^{13}C$ secular variation curve for the SCC and, in general, the Late Mezoproterozoic- Early Neoproterozoic C-isotope curve; seem to have been controlled by tectonic events such as Grenville orogeny (I-II) and CVO (III). However, local changes in the ocean geochemistry such as oceanic water stratiphication and relative sea level changes (IV-VII) should have shaped the C-cycle during the SCC deposition by sequestering and adding the organic and inorganic carbon present in the ocean system.

Nevertheless, some differences between this curve (IV, VI and VII) and the curve from Bartley et al. (2001), above the proposed Meso-Neoproterozoic transition, can be partially related to the presence of silicates in some protions of the marble sequence. Those silicates could have generated depletion patterns in the $\delta^{13}C$ due to the release of depleted CO_2 during the amphibolite facies metamorphism.

Finally, there is a clear coincidence between the time span comprising the sedimentation of the SCC and the assumed age for the agglutination of supercontinent Rodinia (1.0 Ga.). If the data obtained in the SCC represent the above-mentioned conditions and time span, the agglutination of Rodinia would had not involved some ancient continental blocks belonging to the surrounding Transversal Zone.

ACKNOWLEDGEMENTS.

We want to thank Gilsa M. Santana, who helped with the C-isotope analyses. J.C.S. whishes to express his gratitude to COLFUTURO for providing full-tuition scholarship. This is the NEG-LABISE contribution N° 211.

REFERENCES

Bartley,J., Semikhatov,M., Kaufman,A., Knoll,A., Pope,M., Jacobsen,S. 2001. Global events across the Meso-Neoproterozoic boundary: C and Sr Isotopic evidence from Siberia. Precam. Res. 111: 165-202

Bekker,A., Karhu,J., Eriksson,K., Kauman,A. 2003. Chemostratigraphy of the Paleoproterozoic carbonate successions of the Wyoming Craton: Tectonic forcing of biochemical change? Precam. Res. 120: 279-325

Brito Neves, B., Santos, E., Van Schmus, W. 2002. Roteiro de excursão Dominio Central (zona Transversal) da Província Borborema e o sistema orogênico Cariris Velhos. XLI Congreso Brasileiro de Geologia.

Des Marais,D., Strauss,H., Summons,R., Hayes,J. 1992Carbon isotope evidence for the step-wise oxidation of the Proterozoic environment. Nature. 359: 605-609

Des Marais, D. 1994. Tectonic control of the crustal organic carbon reservoir during the Precambrian. Chem. Geol. 114: 303-314.

Hoffman,P., Kaufman,A., Halverson, S. 1998. Comings and goings of global glaciations on a Neoproterozoic tropical platform in Namibia. GSA Today 8 (5): 1-10.

Kah,l., Sherman,A., Narbonne,G., Kaufman,A., Knoll,A., James,N. 1999. Isotope stratigraphy of the Mesoproterozoic Bylot supergroup, Northern Baffin Island: Implication for regional lithostratigraphic correlation. Can. J. Earth Sci. 36:313-332.

Kah,L., Lyons,T., Chesley,J. 2001. Geochemestry of a 1.2 Ga carbonate-evaporite succession, northern Baffin and Bylot Island: Implications for Mesoproterozoic marine evolution. Prec. Res. 111: 203-236.

Knoll,A., Kaufman,A., Semikhatov,M. 1995. The carbon isotopic composition of Proterozoic carbonates: Riphean succesions from nortwestern Siberia (Andabar Massif, Turukhansk uplift) Am. J. Sci. 295: 823-850.

Lindsay,J., Brasier,M., 2002. Did global tectonics drive early biosphere evolution? Carbon isotope record from 2.6 to 1.9 Ga carbonates of western Australian basins. Prec. Res. 114: 1-34.

Mitchell,S., Paul,C., Gale,A. 1996, Carbon isotopes and sequence stratigraphy. In Howell,J and Aitken,J. (eds) High resolution sequence stratigraphy: innovations and applications. Geol. Soci. Spec. Publ.. 104: 11-24.

Sial,A.N., Ferreira,V., De Almeida, A., Romano,A., Parente,C., Dacosta,M., Santos,V. 2000. Carbon isotope fluctuations in the Precambrian carbonate sequences of several localities in Brazil. An. Acad. Bras. Cien. 72 (4): 539-558.

NEOPROTEROZOIC – EARLY CAMBRIAN ISOTOPIC VARIATION AND CHEMOSTRATIGRAPHY OF THE LESSER HIMALAYA, INDIA IN EASTERN GONDWANA

Tewari, V.C.[1] and Sial, A.N.[2]

1. Wadia Institute of Himalayan Geology, 33, General Mahadev Singh Road, Dehra Dun- 248001, Uttaranchal, India. vctewari@rediffmail.com
2. NEG-LABISE, Dep. Geologia-UFPE, C.P. 7852, Recife-PE, 50670-000, Brasil. ans@mail.ufpe.br

Keywords: Neoproterozoic, chemostratigraphy, Lesser Himalaya, India, C-isotope

The Rodinia supercontinent was broken around 750Ma and the East Gondwana (India, Australia and Antarctica) separated from West Laurentia (Powell et al., 1993). The Baltika, Africa and South America occupied the other side of the Rodinia. The Neoproterozoic rifting, breakup of Rodinia and fragmentation of the Gondwanaland, low latitude glaciation and global warming events have been recorded from the Lesser Himalaya of India (Tewari, 2002). The Carbon and Oxygen isotopic variation and chemostratigraphy of the Lesser Himalayan carbonate formations reflect global palaeoclimatic and palaeobiological events (Tewari, 2001). The Neoproterozoic – early Cambrian chemostratigraphy of the Blaini – Krol – Tal succession strongly supports the Precambrian – Cambrian transition lies in the Lower Tal Formation ($\delta^{13}C = -4‰$ PDB). The Krol belt in the Lesser Himalaya is characterised by positive $\delta^{13}C$ value (+1 to 6‰ PDB). The emergence of multicellular Ediacaran life in the Upper Krol is consistent with an increase in atmospheric oxygen ($\delta^{18}O=+30‰$ SMOW). The oxygen isotope supports that oxygen played a major role in metazoan evolution and Cambrian explosion. The base of the Terminal Proterozoic System in the Lesser Himalaya is established in the Blaini Formation (Tewari, 2001). The pink cap carbonate of the Blaini Formation shows negative $\delta^{13}C$ value (-3‰ PDB) and correlated with Varanger glacial event. A comparison of the available carbon and oxygen isotope curves from other regions of the Eastern Gondwanaland and South China, parts of Siberia and North Africa suggest that the Neoproterozoic – early Cambrian chemostratigraphy is consistent in the isotopic variation. There is carbon isotopic similarity between Neoproterozoic Bambui Group in Central Brazil, South America and the Krol Formation of the Lesser Himalaya India.

Consistency in the C-isotopic composition during the geological past has been observed in the critical sections world widely. Schidlowski et al. (1976) developed a well constrained carbon isotopic evolution curve. The concept of C-isotope chemostratigraphy is based upon the assumption that C-isotopic ratios fluctuate with time, largely in response to the changes in net rate of organic burial and climatic variations (availability of atmospheric oxygen).

In the NE Lesser Himalaya, India Neoproterozoic sedimentary succession shows well developed carbonate sequence – the Buxa (Menga) Dolomite (Fig.1). The recent discovery of microbialites and organic walled microfossils (Tewari, 2002; photo 1 and 2) confirm Terminal Neoproterozoic age for the Buxa Dolomite. The C-isotope chemostratigraphy of the Buxa (Menga) Dolomite is shown in figure 2. The C-isotopic ratios are significantly positive and quite consistent with the $\delta^{13}C$ (carbonate carbon) values ranging from + 3.7 to + 5.4‰ (PDB) in the Buxa Dolomite. The 0-isotopic data also shows remarkable consistency with the $\delta^{18}O$ values fluctuating within a narrow range between -8.9 and -7.2‰ (PDB). The significantly positive C-isotopic results correspond to the Terminal Proterozoic C-isotopic evolution, followed by oscillations during the Precambrian – Cambrian transition in the Lesser Himalaya.

Terminal Proterozoic glaciogenic deposits have been recorded from all the continents. They were formed by breakup of Rodinia supercontinent. Recent carbon isotopic studies of Phanerozoic and Terminal Proterozoic glaciogenic deposits in general has suggested that palaeoclimate changes on Earth over the last 650 Ma is directly related to atmospheric CO_2 fluctuations (Jacobson, 2001; Tewari, 2001, 2003). The snowball Earth model suggests that during global glaciation there may be a short lived change in the carbon isotopic ratios of the ocean because of elimination of marine life. Hence the $\delta^{13}C$ in marine carbonates will drastically decrease to -6 ± 1‰ (PDB) (Jacobsen, 2001). The deglaciation event is also well recorded in the carbon isotope variation from pink cap carbonate indicating end of the Terminal Proterozoic glaciation (Tewari, 2001, 2003). Kaufman et al. (1997) have observed that $\delta^{13}C$ values in cap carbonates globally range from 0 to -5‰ (PDB). The $\delta^{13}C$ values of the pink Blaini Limestone also range from 0 to -3‰ (PDB) confirming the global event. The major palaeoclimatic changes, carbon isotopic fluctuations, biotic extinction-evolutionary events, and sea level changes recorded from the Lesser Himalaya, India has been discussed in the present paper in detail.

REFERENCES

Jacobson, Stein, B., 2001. Gas hydrates and deglaciations. Nature, 412 : 691-693.

Kaufman, A.J., Knoll, A.H. and Narbonne, G.M., 1997. Isotopes, ice ages and Terminal Proterozoic earth History. Proc. Nat. Acad. Sci. 94 : 6600-6605.

Powell, C.M., Li, ZX., M.C. Elhinny, M.W., Meert, J.G. and Park, J.K., 1993. Palaeomagnetic constraints on timing of the Neoproterozoic breakup of Rodinia and the Cambrian formation of Gondwanaland Geology, V. 21, 889-892.

Schidlowski, M., Eichmann, R., Junge, C.E., 1976. Carbon isotope geochemistry of the Precambrian Lomagundi carbonate province. Geochem. Cosmochim Acta, V. 40, 449-455.

Tewari, V.C., 2001. Neoproterozoic glaciation in the Uttaranchal Lesser Himalaya and the global palaeoclimatic change. Nat. Symp. Role of E.Sci. in Integrated Development and related Societal Issues GSI Spl.Publ. No.65, (III), 49-56.

Tewari, V.C., 2002. Lesser Himalayan stratigraphy, sedimentation and correlation from Uttaranchal to Arunachal. Gyanodaya Prakashan, Nainital, India, 63-88.

Tewari, V.C., 2003. Snowball Earth and global palaeoclimate change : evidences from the Lesser Himalaya. Quaternary International (in press).

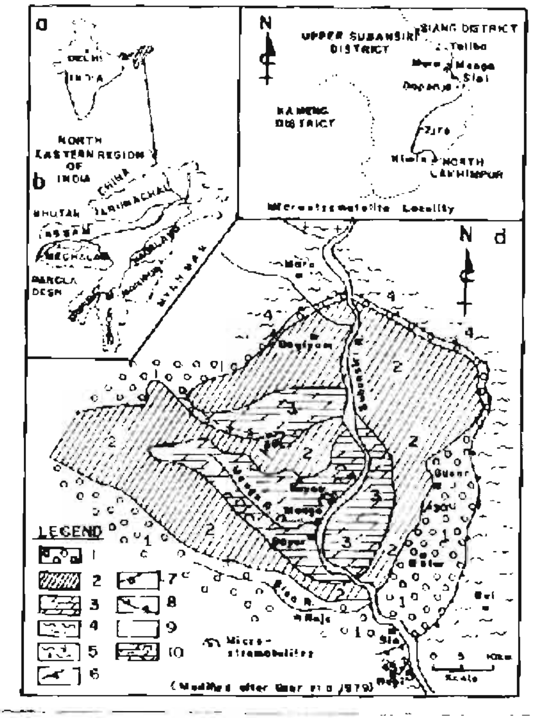

Figure 1. Gelogical map of the Menga area eastern Himalaya.

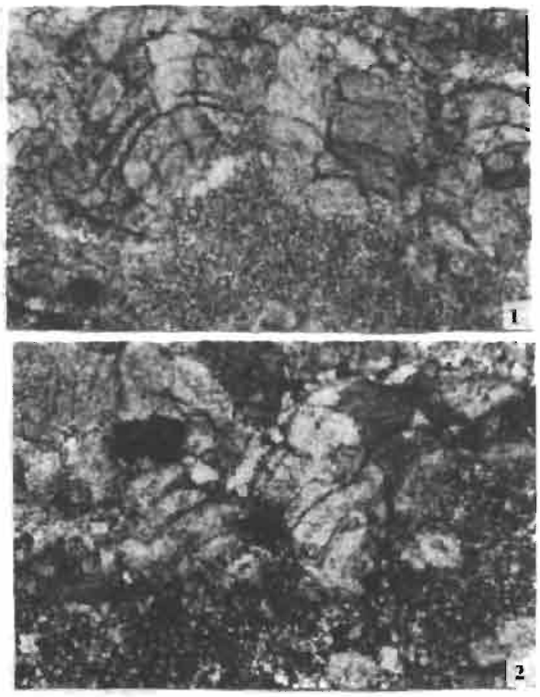

Photos. Microphotograph of microstromatolite and organic walled micro-fossiles.

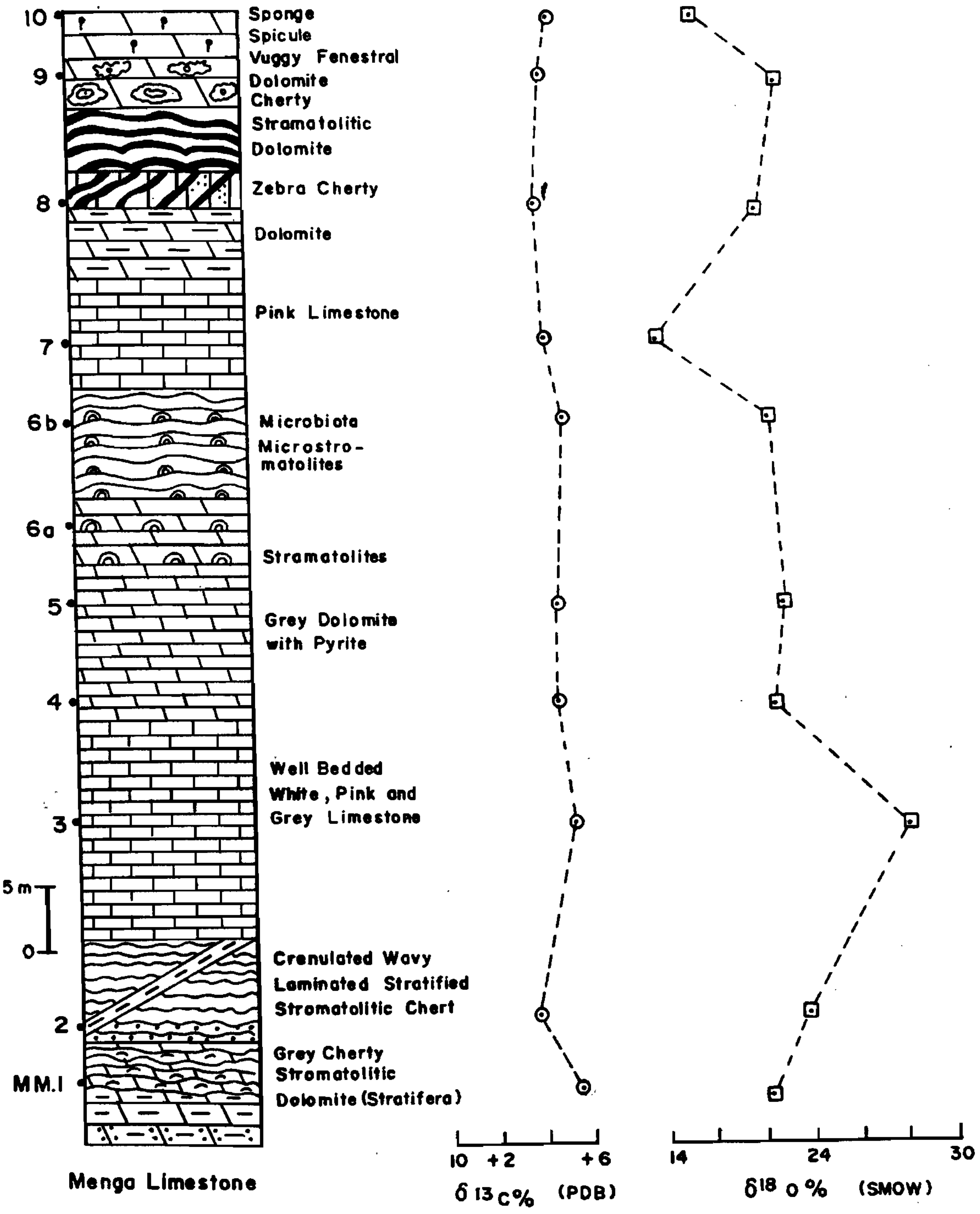

Figure 2. Carbon and oxigen isotope chemostratigraphy of the Menga (Buxa) Dolomite, eastern Himalaya.

ISOTOPE SIGNAL OF THE MIDDLE JURASSIC CARBONATE RAMP OF CALABOZO FORMATION, AT ARROYO EL PLOMO, MENDOZA, ARGENTINA

Valencio, S.A.[1]; Ramos, A.M.[1]; Cagnoni, M.C.[1]; Panarello, H.O.[1]; Cabaleri, N.G.[1,2] and Armella, C.[1]

1. Instituto de Geocronología y Geología Isotópica. Pabellón INGEIS, Ciudad Universitaria, C1428EHA, C.A. de Buenos Aires, Argentina. susana@ingeis.uba.ar, adriana@ingeis.uba.ar, mariana@ingeis.uba.ar, armella@ingeis.uba.ar
2. Departamento de Ciencias Geológicas, Universidad de Buenos Aires. Pabellón 2, Ciudad Universitaria, C1428EHA, C.A. de Buenos Aires, Argentina. cabaleri@ingeis.uba.ar

Keywords: Limestones, isotope geochemistry, Jurassic, Neuquina basin, Argentina

INTRODUCTION

This study is a new contribution to the facial/ microfacial and geochemical characterization (Cabaleri et al., 2001, in press) of the marine jurassic carbonates of Calabozo Formation. This unit, of Early Callovian age, crops out in the Neuquina basin of southwestern Mendoza province, Argentina. It is exposed from Salado River in the north to the Bardas Blancas region in the south. This work deals with chemical, ^{13}C and ^{18}O analyses in order to reconstruct the palaeoenvironment and post-depositional history of Calabozo Formation at arroyo El Plomo (Fig.1). Also, isotope strontium determinations were done to compare the chemostratigraphic age given by the global jurassic seawater curve with the Early Callovian biostratigraphic age of the succession.

GEOLOGICAL SETTING

Sedimentological analyses in El Plomo creek sections (Fig. 2) indicate that limestones of Calabozo Formation were deposited on an extended shallow-water ramp. Facies associations are indicative of mid and inner ramp subenvironments (Cabaleri et al., in press). Carbonate facies were deposited on a delta plain (Lajas Formation). On this substrate, during the Callovian transgression, began the sedimentation of Calabozo Formation with a basal floatstone. Afterwards, prograding parasequences were developed producing subtidal facies characteristic of a mid-ramp subenvironment. Three shallowing-upward cycles are identified: the lower and the middle ones are typically mid-ramp, whereas the upper cycle finishes with a characteristic facies association of an inner ramp. The mid-ramp facies is composed by wackestones, packstones, packstone with channels and floatstones, while the inner ramp is characterized by grainstones and boundstones. Restriction of the basin becomes more evident towards the upper levels of the Calabozo Formation with the deposition of restricted circulation facies, on top of which the evaporitic succession of Tábanos Formation is developed.

ANALYTICAL TECHNIQUES

Limestones were collected in two profiles (Fig. 2). Samples are composed principally by calcite with small quantities of magnesium calcite and dolomite crystals with calcite nucleus, suggesting more than a process of re-crystallization under different conditions. Isotopic and chemical analyses were performed on bulk rock samples, since it was not possible to carry out the separation of the different carbonate components.

The trace elements were determined by wavelength dispersive X-ray fluorescence using standard techniques on bulk rock compacted powder. XRF analyses were done at INGEIS with a Philips PW 1410 spectrometer. International standards NBS-1b, NIST-1c, NIST- 88b, JLs-1 and JDo-1 were used as reference materials. Analytical uncertainties are: ± 2% for Sr, ± 7% for Fe_2O_3 T, ± 12% for MnO.

Carbon and oxygen isotopic analyses were carried out by the usual techniques. Isotopic ratios were determined in a Delta S Finnigan Mat triple collector mass spectrometer, at INGEIS. The isotopic composition is reported as deviation per mil (δ ‰) relative to the V-PDB standard. The analytical error is 0.1‰ (±2σ) for both $\delta^{13}C$ and $\delta^{18}O$.

Strontium isotopes were analyzed at the Centro de Geociencias, UFPA, Brazil. $^{87}Sr/^{86}Sr$ ratios were determined with a thermo-ionization multicollector mass spectrometer Finnigan Mat 262. Results were normalized to the standards Eimer & Amed: 0.70800 and NBS-987: 0.710250.

RESULTS AND DISCUSSION

Trace element contents of this sequence do not present high variations (Table 1). Their concentrations keep a pattern of variation within each sedimentological cycle in agreement with depositional conditions. Contents reflect syn-depositional fluctuations in the best preserved carbonate rocks of profile 1. They also evidence superposed post-depositional modifications related to pore fluids during burial and late diagenetic fluids. The latter have been more active in the high energy levels containing reworked biogenic materials. According to Brand and Veizer (1980), Mn/Sr ratio is used as a geochemical tracer. The more marked modifications are indicated by a rise in Mn/Sr ratios and a weak increase in Fe contents as is observed towards the end of the middle cycle and at the beginning of the upper one. In these levels more evaporative conditions begin to prevail under sub-superficial environment.

The isotopic composition through the carbonate succession in profile 1 (Fig. 2), do not show a high span: $\delta^{13}C$ values vary between 0.8‰ and 2.0‰ and $\delta^{18}O$ ones between -11.3‰ and -9.9‰ (Table 1). The latter

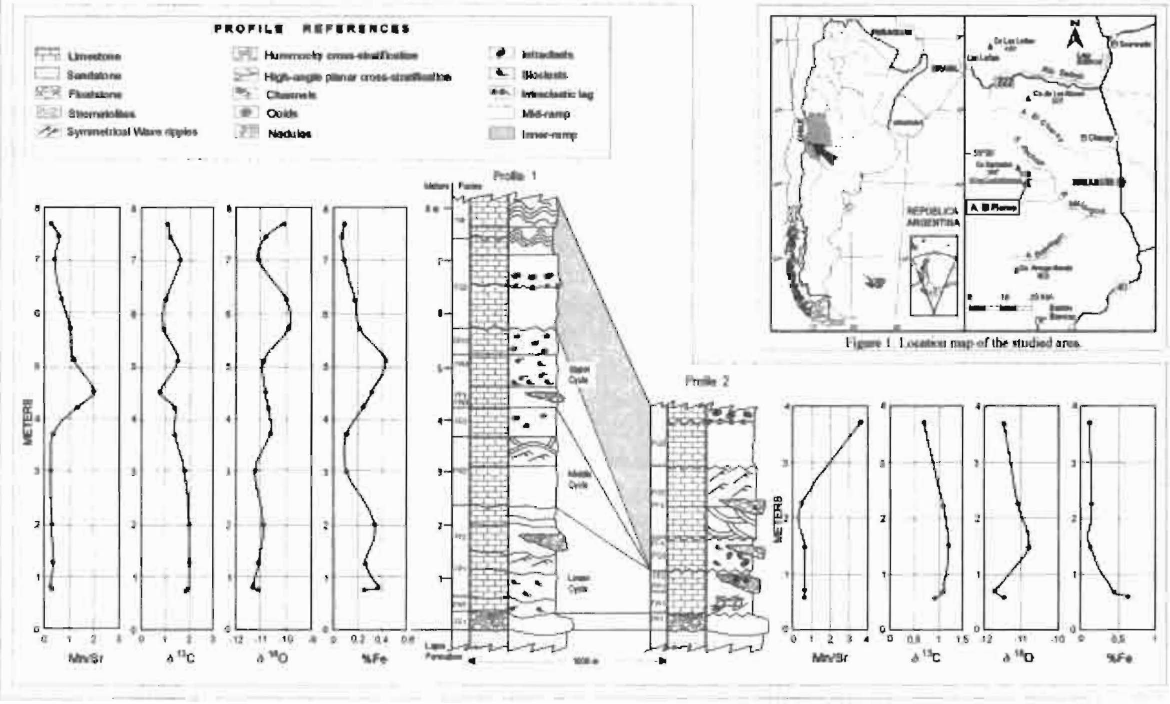

Figure 1. Location map of the studied area.

Figure 2. Correlation between facial/microfacial and geochemical data of limestones at arroyo El Plomo.

parameters are quite depleted in comparison with those of the coeval unaltered marine carbonates (Veizer et al., 1999). This indicates episodes of post-depositional interaction with very depleted fluids (Popp et al., 1986), like water coming from high altitude in the Andes range, similar to Mendoza and Tunuyán rivers (Panarello and Dapeña, 1996). Despite this diagenetic overprint, $\delta^{18}O$ values still keep a variation pattern that reflects the environmental conditions prevailing during deposition. Otherwise, $\delta^{13}C$ proved to be less or not sensitive to diagenesis under the same water/rock interactions.

Carbonate sedimentation in the basin deepest areas is represented by the facies association of the lower cycle in the mid-ramp. Limestones are well preserved according to the geochemical parameters (Table 1) and their carbon-13 composition is almost constant (1.9‰ to 2.0‰) and within the highest frequency (2‰ - 4‰) in the estimated range for Callovian unaltered marine carbonates (Anderson et al., 1994; Veizer et al., 1999). Oxygen-18 values (-11.3‰ to -10.9‰) show a very small shift to a more positive value at the top of the cycle, in concordance with its shallowing-upward tendency.

	Cycle	Sample Nº	$\delta^{13}C$	$\delta^{18}O$	$^{87}Sr/^{86}Sr$	Error (2σ)	Sr ppm	Mn ppm	Mn/Sr	Fe %
PERFIL 1	LOWER	CAP 4	1,9	-11,1	0.707005	0.000036	540	163	0.30	0.247
		CAP 5	2,0	-11.3			440	116	0.26	0.365
		CAP 6	2,0	-11,1			514	178	0.35	0.266
		CAP 8	2,0	-10.9			379	108	0.28	0.343
	MIDDLE	CAP 9	1,8	-11.2	0.706994	0.000031	549	124	0.23	0.110
		CAP 10	1,4	-10.6			374	124	0.33	0.110
		CAP 11	1,4	-10.7			366	480	1.31	0.245
	UPPER	CAP 12	0,8	-10,8			298	588	1.97	0.309
		CAP 13	1,4	-11.1			387	441	1.14	0.423
		CAP 14	0,9	-9.9			423	434	1.03	0.209
		CAP 15	1,0	-10.0			352	248	0.70	0.171
		CAP 17	1,6	-11,1	0.706943	0.000030	398	147	0.37	0.084
		CAP 18	1,2	-10,8			505	286	0.57	0.064
		CAP 19	1,1	-10.1	0.707083	0.000037	377	85	0.23	0.086
PERFIL 2	LOWER	CAP 21b	1,1	-11.7			341	194	0.57	0.473
		CAP 21a	0,9	-11.5			252	163	0.65	0.631
	UPPER	CAP 23	1,2	-10,8			360	224	0.62	0.120
		CAP 24	1,1	-11,1	0.707011	0.000030	408	170	0.42	0.158
		CAP 25	0,7	-11.5			268	968	3.61	0.121

Table 1. Chemical and isotopic data of limestones in profile 1 and 2 at arroyo El Plomo.

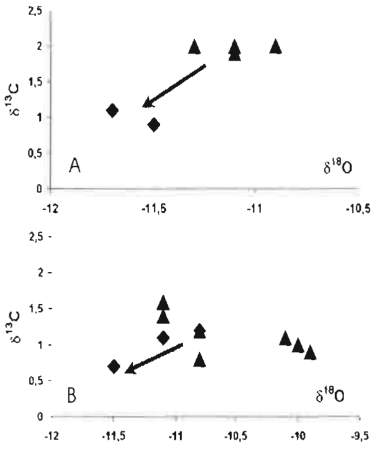

Figure 3. $\delta^{13}C$ *vs* $\delta^{18}O$ of samples of profile 1 and 2 showing the diagenetic trend. A. Lower cycle. B. Upper cycle.

In the middle cycle, also characteristic of the mid-ramp, $\delta^{13}C$ values range upward from 1.8‰ to 1.4‰, probably due to the incorporation of small amounts of isotopically light carbon derived from the oxidation of organic matter (Kaufman et al., 1992). On the other hand, $\delta^{18}O$ values become enriched (-11.2‰ to -10,6‰) towards the top of the cycle, indicating more intense evaporative conditions. The shifts observed in both isotopes evidence once more, the shallowing-upward tendency of each cycle after a new transgression in the basin and the establishment of more conspicuous shallow water conditions.

In the upper cycle, developed in the mid and in the inner ramp, more variation in the values of both isotopes is observed ($\delta\ ^{13}C$: 0.8‰ to 1.6‰; $\delta^{18}O$: -9.9‰ to -11,1‰). At the beginning of the cycle (CAP 12), the $^{13}C/^{12}C$ ratio becomes lighter in 0.6‰ compared to the signal of the limestones at the top of the middle cycle. This sample shows the highest evidence of post-depositional changes (Mn/Sr: 1.97) that might justify this variation. The high organic productivity and the organic matter oxidation in this level, should have produced a reducing media and waters depleted in oxygen content. Under these conditions, Mn divalent is more probably concentrated in the early diagenetic phases (Jenkins et al., 2002) . The ^{13}C depletion is not accompanied by the oxygen-18 composition, that remains almost in the same value that at the top of the above cycle. Going up in the stratigraphic succession, carbon-13 of CAP 13 returns to almost the same signal registered at the end of the middle cycle, indicating the beginning of a new transgression. From there, $^{18}O/^{16}O$ ratios become heavier while $^{13}C/^{12}C$ ratios more depleted, remarking the shallowing trend of the carbonatic sequence, that produce an increase in the evaporative conditions (Frank et al., 1997) and in the biological productivity with the further oxidation of the organic matter. There are petrographic evidences of subaereal exposure in CAP 14, pointed isotopically by the incorporation of soil gas CO_2 and the lost of ^{16}O due to evaporation. This is remarked by the shifts to more positive $\delta\ ^{13}C$ and more negative $\delta^{18}O$ for samples below it (Allan and Matthews, 1982). The same pattern is observed at the upper levels of the profile in the inner ramp, where stromatolitic mats grew in the shallower areas and the circulation of water was locally restricted. These areas underwent recurrent episodes of subaereal exposure and evaporation (Cabaleri et al., in press).

Petrographic and geochemical tracers indicate that limestones in profile 2 show higher evidences of post-depositional changes than those in profile 1. The $\delta^{13}C$ *vs* $\delta^{18}O$ cross-plots (Figs. 3A,B) for samples of the lower and upper cycle in both profiles, show a positive correlation that mark the general diagenetic trend followed by carbonate sediments in profile 2.

Table 1 shows the strontium isotope data for the Calabozo Formation. As it was not possible to carry out determinations in all samples, analyses were performed on the best preserved ones of each cycle according to the geochemical tracers. Two samples of the upper levels were also processed in both profiles. The values are slightly scattered and the most divergent ratios are those of samples CAP 19 (profile 1) and CAP 24 (profile 2) that correspond to the upper levels of the successions and therefore present evidence of subaereal exposure.

The level of resolution of the Jurassic strontium isotope record varies from the Early to the Middle/Late Jurassic. The Early Jurassic seawater curve is well constrained and shows a minima in the Pliensbachian-Toarcian boundary associated with an Ocean Anoxic Event (OAE) (Jones et al., 1994, 2001). The isotope data for the Middle/Late Jurassic do not define a clearly curve because the values are scarce and divergent. Consequently, the stratigraphic resolution for this section of the Jurassic seawater curve is reduced. Jones et al. (2001) present a minima in the interval Callovian-Oxfordian but, as it lasts a long period of time (30 My) and does not return to the pre-excursion isotope ratio, they do not consider it as a short term event.

The strontium isotope values for the Calabozo Formation correspond, within the analytical errors, to the Late Bathonian-Early Callovian boundary (Jones et al., 1994, 2001).

CONCLUSIONS

A good agreement between the facial/microfacial (Cabaleri et al., in press) and the chemical and isotopic data is observed in the reconstruction of the palaeoenvironment during deposition of the carbonatic succession of Calabozo Formation, at El Plomo creek. Although these carbonates undergone more than a post-depositional process, petrographic and geochemical determinations indicate that they did not highly affected these rocks. Oxygen isotope system, the most sensitive indicator of diagenesis, show O-18 compositions quite depleted, indicating they are obliterated by later post-depositional events. Despite of this, $\delta^{18}O$ still maintain a variation pattern that reflects the environmental conditions prevailing during deposition. A shift to enriched values is observed towards the upper levels of each shallowing-upward cycle, indicating the establishment of more intense evaporative conditions and the progressive restriction in the water circulation, with the consequent loss of ^{16}O. On the other hand, carbon isotope system retained best the primary isotopic characteristics. Limestones deposited in the deepest areas of the basin (lower cycle), are the best preserved and their ^{13}C signature is in concordance with the Callovian unaltered marine carbonates. A grow to isotopically lighter carbon is observed through the shallowing-upward levels of the middle and upper cycles, remarking the input of organically derived carbon and episodes of subaereal exposure.

Within the grade of resolution of the Bathonian-Callovian seawater curve, chemostratigraphic age of Calabozo Formation is similar to the biostratigraphic one. Taking into account the resolution of this section of the curve, we can not affirm if the little variations in the $^{87}Sr/^{86}Sr$ ratios reflect diagenetic alteration or represent real isotope fluctuations.

ACKNOWLEDGEMENTS

This work was funded by CONICET, PIP N°4517 and ANPCyT, PICT N°1661.

REFERENCES

Allan, J.R. and Matthews, R.K., 1982. Isotope signatures associated with early meteoric diagenesis. Sedimentology, 29: 797-817.

Anderson, T.F., Popp, B.N., Williams, A.C., Ho, L.Z. and Hudson, J.D., 1994. The stable isotopic records of fossils from the Peterborough Member, Oxford Clay Formation (Jurassic), UK: palaeoenvironmental implications. Journal of the Geological Society, London, Vol. 151: 125-138.

Brand, U. and Veizer, J., 1980. Chemical diagenesis of a multicomponent carbonate system-1: Trace elements. Journal of Sedimentary Petrology, Vol.50, N°4: 1219-1236.

Cabaleri, N.G., Valencio, S.A., Cagnoni, M.C., Ramos, A.M., Armella, C., Panarello, H.O. and Riccardi, A.C., 2001. Facies and carbon/ oxygen isotopes of the Calabozo Formation (Middle Jurassic), arroyo La Vaina, Mendoza, Argentina. Sociedad Geológica de Chile. III South American Symposium on Isotope Geology. Extended Abstracts Volume: 363-366.

Cabaleri, N.G., Armella, C., Cagnoni, M., Ramos, A.M. and Valencio, S.A., in press. Ramp facies at the Calabozo Formation (Middle Jurassic), Mendoza, Argentina. Revista Geológica de Chile. Servicio Nacional de Geología y Minería.

Frank, T.D., Lyons, T.W. and Lohmann, K.C., 1997. Isotopic evidence for the paleoenvironmental evolution of the Mesoproterozoic Helena Formation, Belt Supergroup, Montana, USA. Geochimica et Cosmochimica Acta, 61: 5023-5041.

Jenkyns,H.C., Jones,C.E., Gröcke,D.R., Hesselbo,S.P. and Parkinson,D.N., 2002. Chemostratigraphy of the Jurassic System: applications, limitations and implications for palaeoceanography. Journal of the Geological Society, 159 (4): 351-378.

Jones, C.E., Jenkyns, H.C., Coe, A.L. and Hesselbo, S.P., 1994. Strontium isotopic variations in Jurassic and Cretaceous seawater. Geoch. et Cosmochimica Acta, 58 (14): 3061-3074.

Jones, C.E. and Jenkyns, H.C., 2001. Seawater strontium isotopes, oceanic anoxic events, and seafloor hydrothermal activity in the Jurassic and Cretaceous. American Journal of Science, 301: 112-149.

Kaufman, A.J. and Knoll, A.H., 1995. Neoproterozoic variations in the C-isotopic composition of seawater: stratigraphic and biogeochemical implications. Precambrian Research, 73: 27-49.

Panarello, H.O. and Dapeña, C., 1996. Mecanismos de recarga y salinización en las cuencas de los ríos Mendoza y Tunuyán, Mendoza, Rep. Argentina: evidenciados por isótopos ambientales. Memorias XII Congreso Geológico de Bolivia: 531-543.

Popp, B.N., Anderson, T.F. and Sandberg, P.A., 1986. Brachiopods as indicators of original isotopic compositions in some Paleozoic limestones. Geological Society of America Bulletin, 97: 1262-1269.

Veizer, J., Ala, D., Azmy, K., Bruckschen, P., Buhl, D., Bruhn, F., Carden, G., Diener, A., Ebneth, S., Godderis, Y., Jasper, T., Korte, C., Pawellek, F., Podlaha, O. and Strauss, H., 1999. $^{87}Sr/^{86}Sr$, $\delta^{13}C$ and $\delta^{18}O$ evolution of Phanerozoic seawater. Chemical Geology, 161: 59-88.

AUTHORS INDEX

GOVERNO DA BAHIA
SECRETARIA DA INDÚSTRIA,
COMÉRCIO E MINERAÇÃO

30 anos
companhia baiana de pesquisa mineral
Descobrindo as riquezas da Bahia

IRD
Institut de recherche
pour le développement

CNPq
Conselho Nacional de Desenvolvimento
Científico e Tecnológico

VIRTUTE SPIRITUS
UNIVERSIDADE FEDERAL
DA BAHIA - UFBA
Grupo de Petrologia Aplicada
a Pesquisa Mineral

C A P E S

fapesb
Fundação de Amparo
à Pesquisa do Estado da Bahia

BR
PETROBRAS

CPRM
Serviço Geológico do Brasil

Thermo Finnigan

SCIENTIFIC INSTRUMENTS CO.
SINC DO BRASIL
INSTRUMENTAÇÃO CIENTÍFICA LTDA.

micromass
The Mass Spectrometry People

MCMXVI

SOCIEDADE BRASILEIRA DE GEOLOGIA
DESDE 1946
Núcleo Bahia-Sergipe

GEOSOL

SHORT PAPERS

ISSN 1679-3684

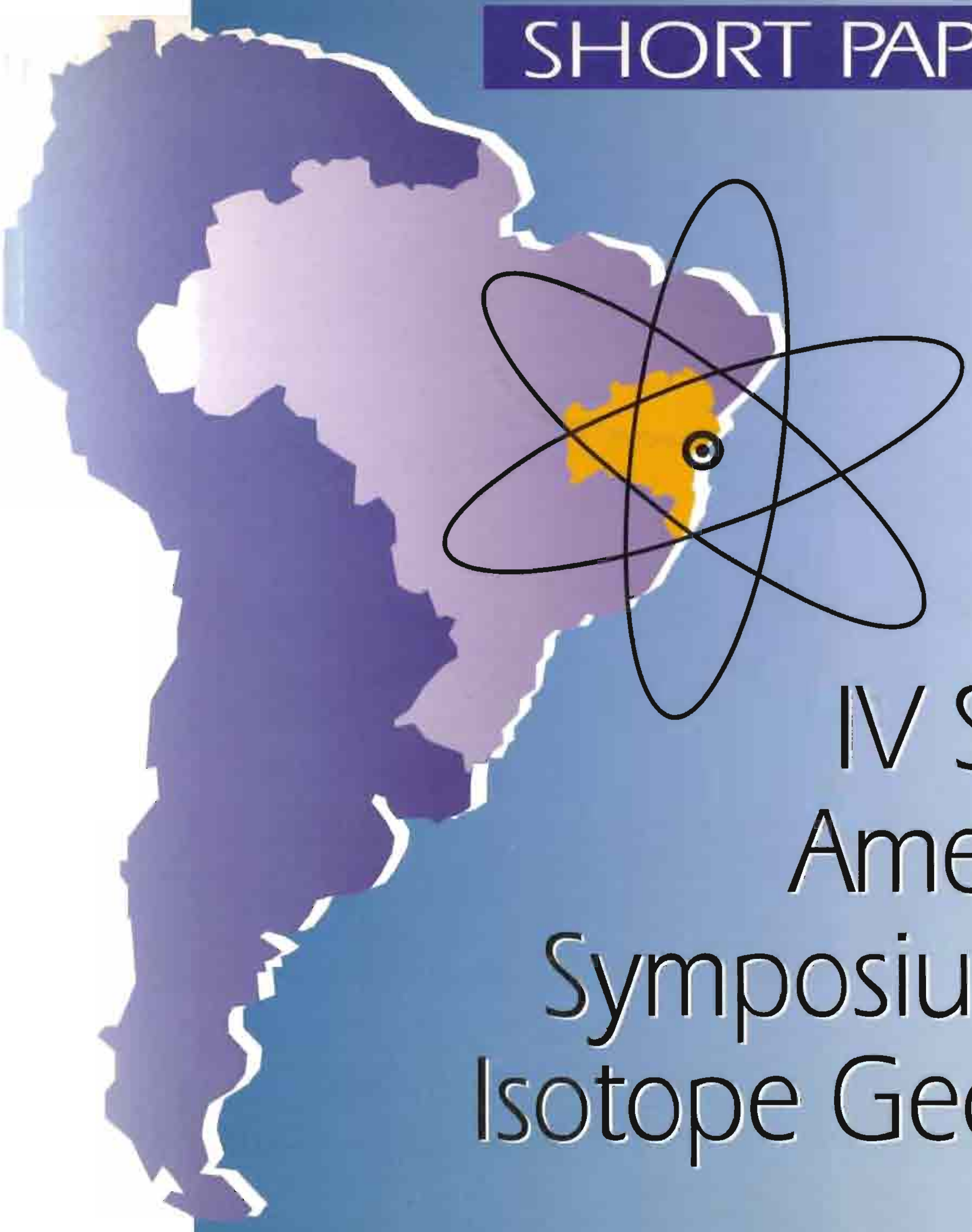

IV South American Symposium on Isotope Geology

SALVADOR-BA, BRAZIL AUGUST 24th - 27th, 2003

- VOLUME II -

30 anos companhia baiana de pesquisa mineral
Desenvolvendo as riquezas da Bahia

IV SSAGI
Brazil - 2003

IRD
Institut de recherche pour le développement

SHORT PAPERS

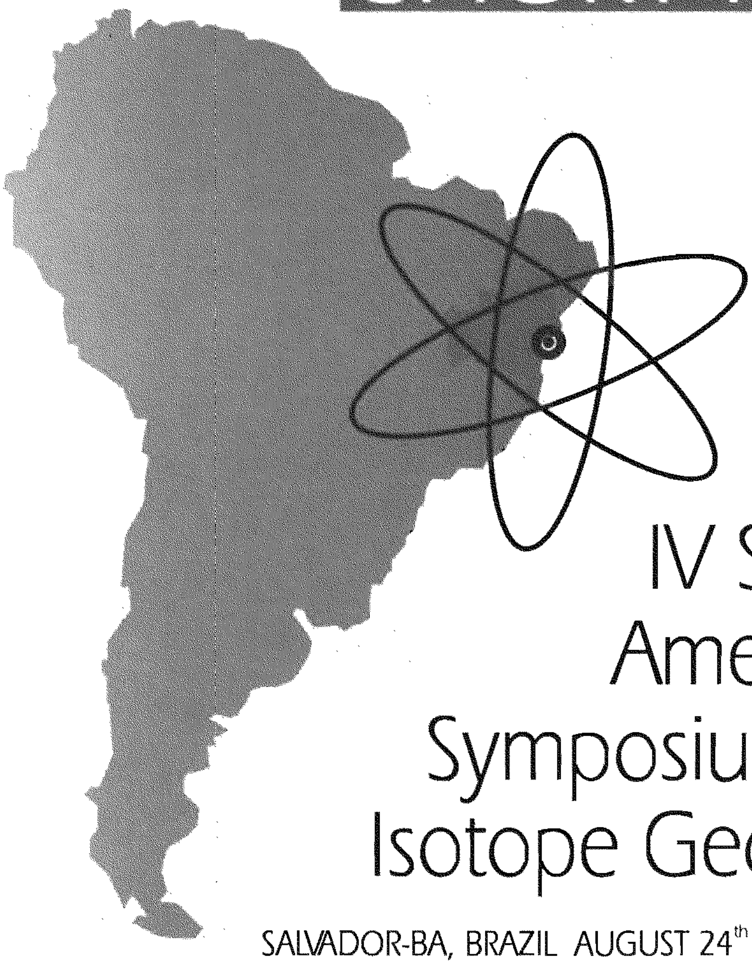

IV South American Symposium on Isotope Geology

SALVADOR-BA, BRAZIL AUGUST 24th - 27th, 2003

Organizers

Maria de Lourdes da Silva Rosa
Débora Correia Rios
Marília Kosin
Marilda Santos Pinto Miedema

companhia baiana de pesquisa mineral

IV SSAGI
Brazil - 2003

IRD
Institut de recherche pour le développement

South American Symposium on Isotope Geology. (4.: 2003: Salvador)
Short Papers of the IV South American Symposium on Isotope Geology – IV SSAGI, Salvador, August 24th - 27th ; Maria de Lourdes da Silva Rosa et al. (Organizers). – Salvador : CBPM; IRD, 2003.
ii-xxii - 789p. : il.

Reference.

1. Isotope Geology. 2. Geology – South America. 3. Geology – International Meeting. 4. Symposium. I. Rios, Débora Correia. II. Kosin, Marília. III. Santos Pinto, Marilda. IV. Title.

CDD 551.701
CDU 550.42

ORGANIZING COMMITTEE

President

Ruy Fernandes da Fonseca Lima (CBPM)

Vice President

Moacyr Moura Marinho (CBPM)

Scientific Coordinators

Alcides N. Sial (UFPE)
Aroldo Misi (UFBA)
Herbet Conceição (UFBA)
Pierre Sabaté (IRD)

General Secretary

Hélio A. Azevedo (CBPM)

Associate Secretary

Maria de Lourdes da Silva Rosa (UFBA)

Deputy Secretaries

Débora Correia Rios (UFBA)
Johildo F. S. Barbosa (UFBA)
Marilda Santos Pinto Miedema (UEFS)
Marília Kosin (CPRM)

Publications

Hermes A.V. Inda (CBPM)
Valderez P. Ferreira (UFPE)

Coordinator of Finances

Herbet Conceição (UFBA)
Maria José dos Santos Rêgo (UFBA)

Coordinator of Excursions

Marília Kosin (CPRM)

Digital Support

Basílio Elesbão da Cruz Filho (UFBA)
Rita Cunha Leal Menezes (UFBA)

REGIONAL COORDINATORS

Claudio Gaucher (Uruguay)
Enrique Linares (Argentina)
Francisco Munizaga (Chile)
Miguel Parada (Chile)
Olga Rey (Venezuela)
Umberto G. Cordani (Brazil)

SCIENTIFIC ADVISORS

Antônio Expedito Azevedo (UFBA)
Colombo C. G. Tassinari (USP)
Ênio Soliani (UFRS)
Jean M. Lafon (UFPA)
Koji Kawashita (UFRS)
Luiz Carlos Ruiz Pessenda (CENA)
Miguel A.S. Basei (USP)
René Rodrigues (PETROBRAS)
Roberto M. Argollo (UFBA)
Wilson Teixeira (USP)

SPONSORS

Governo do Estado da Bahia
Companhia Baiana de Pesquisa Mineral (CBPM)
Sociedade Brasileira de Geologia (SBG)
Serviço Geológico do Brasil (CPRM)
Universidade Federal da Bahia (UFBA)
Institut de Recherche pour le Développment (IRD)
Conselho Nacional de Desenvolvimento Científico e Tecnológico (CNPq)
Coordenação de Aperfeiçoamento de Pessoal de Nível Superior (CAPES)
Fundação de Amparo à Pesquisa do Estado da Bahia (FAPESB)
Petróleo Brasileiro S.A. (PETROBRAS)
Geologia e Sondagens Ltda (Geosol)
Academia Brasileira de Ciências
Sinc do Brasil – Micromass
ThermoFinnigan

FOREWORD

In the last three decades, many geologists in South America have turned their attention to isotopic geology as a tool in the wider context of the Earth Sciences. As a result, it has been proposed that a series of symposia on the South American Isotope Geology (SSAGI), organized every two years, would provide the appropriate forum for discussion of methods and applications of stable and radiogenic isotopes in the Earth Sciences. In these symposia, progress made in this field in South America would be assessed, encouraging scientific interaction at both national and international levels.

We are very pleased the IV SSAGI has met very good interest from the national and international community reflected by 212 scientific contributions from 15 countries. They were selected for oral and poster sessions and distributed in seven thematic sessions: (i) Methodology and Application of Isotope Geology; (ii) Crustal Evolution of South America; (iii) Temporal Isotopic Variation and Chemostratigraphy; (iv) Environmental Geology and Water Resources; (v) Genesis and Evolution of Igneous and Metamorphic Rocks; (vi) Metallogenesis and Mineral Exploration; and (vii) Oil Exploration. These contributions, with the seven invited lectures on selected themes, compose these Short Papers volumes.

To prepare the volumes the organizers utilize the original files sent in by the authors. However, some modifications have been suggested by the Editorial Board in order to improve the text. Most of the papers were not returned to the authors and modifications have been performed by the organizers of the volumes looking for standardization. All figures and references were not edited. The final quality of figures, photos and tables presented here reflect the quality of the originals forwarded by the authors.

The Organizing Committee gratefully acknowledges the financial support from the Government of the State of Bahia, the major sponsor of this Meeting, that has deemed timely to provide the site and sponsorship, reasserting with the *Companhia Baiana de Pesquisa Mineral* (CBPM) its longstanding practice of fruitful interaction with the Earth Sciences community. Thanks are also due to the *Sociedade Brasileira de Geologia (SBG-Núcleo Bahia-Sergipe),* Brazilian Council for Scientific and Technological Development (CNPq), CAPES and also to CPRM (Brazilian Geological Survey), Sinc do Brasil (Micromass), Finnigan and *Geologia e Sondagens* (GEOSOL) for their financial support. We thank the *Institut de Recherche pour le Développment* (IRD), for publishing these volumes, and to Dr. Augusto Pedreira for a final review. We also recognize the efforts of Dr. Alcides Sial from the Stable Isotope Laboratory (LABISE) at Federal University of Pernambuco to have the IV SSAGI at the Northeastern Brazil.

The Organizing Committee wishes to welcome all participants and that all of them have a enriching and a pleasant stay in Salvador. The success of the meeting is due to both inovating ideas and very productive discussions among the participants. The high quality of the papers presented in these issues provide a good guarantee that in forthcoming years new SSAGI will prolong the dynamics of this field.

IV SSAGI Organizing Committee

- VOLUME I -

- VOLUME II -

CONTENTS

CONFERENCES

METHODOLOGY AND APPLICATION OF ISOTOPE GEOLOGY

CRUSTAL EVOLUTION OF SOUTH AMERICA

TEMPORAL ISOTOPIC VARIATION AND CHEMOSTRATIGRAPHY

ENVIRONMENTAL GEOLOGY AND WATER RESOURCES

GENESIS AND EVOLUTION OF IGNEOUS AND METAMORPHIC ROCKS

METALLOGENESIS AND MINERAL EXPLORATION

OIL EXPLORATION

SPONSORS NOTES

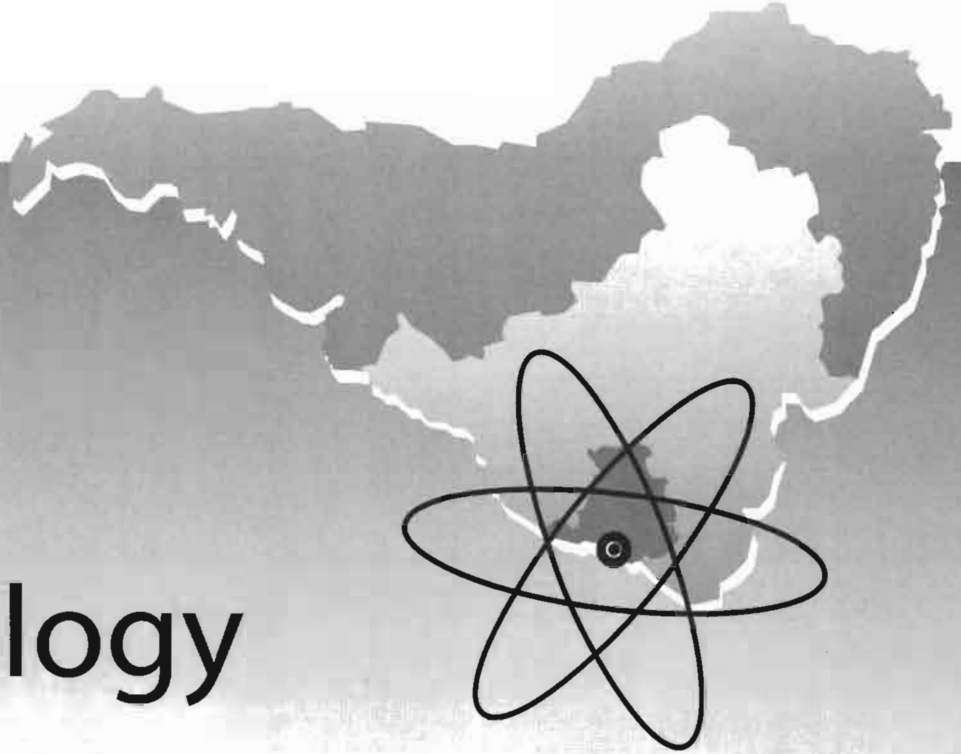

Environmental Geology
And Water Resources

RADIOMETRIC CHARACTERIZATION OF SEDIMENTARY ROCKS AT CORUMBATAÍ RIVER BASIN, SÃO PAULO STATE, BRAZIL

Conceicão, F.T. and Bonotto, D.M.

Instituto de Geociências e Ciências Exatas (IGCE)/ UNESP/ Rio Claro. Avenida 24-A nº 1515, C. P. 178,
13506-900, Rio Claro-SP, Brazil. rstein@claretianas.com.br, dbonotto@rc.unesp.br

Keywords: Radionuclides, Corumbataí River basin, exposure rate

INTRODUCTION

This study was realized at Corumbataí River basin, São Paulo State (Brazil), comprising most of the stratigraphic units from the giant Paraná sedimentary basin (Palaeozoic-Caenozoic), which covered 70% of the whole São Paulo State. This state produces much of the Brazilian sugar cane, and, consequently, a large quantity of fertilizers is involved in the agricultural activities. Applications of chemical fertilizers increase the phosphate and uranium concentrations in soils, resulting in impacts on natural systems, such as increasing nutrient and uranium concentration in surface waters, soils and sediments. In order to evaluate the natural "background" of radionuclides, it is important to measure their maximum natural concentrations in rocks located in this area, which is intensively utilized by sugar cane crops. Thus, the objective of this work was to evaluate the concentration and variability of ^{238}U, ^{234}U, ^{226}Ra, ^{232}Th and ^{40}K in different sedimentary rocks from Corumbataí River basin. The results obtained were discussed in terms of the spatial representativity of the various formations present in the area. Moreover, some indexes some contamination index have been applied to provide a basis for comparison of potential radionuclide hazards.

PHYSIOGRAPHIC FEATURES

The Corumbataí River basin extends over an area of about 1,710 km^2 in the middle-east part of the São Paulo State (Fig. 1). The Corumbataí River flows from the cuestas zone to the confluence with the Piracicaba River. Rio Claro city is the most important municipality in the basin, with 170,000 inhabitants. The tropical climate of the region is characterized by a wet summer (October through March) and dry winter (April through September).

The Corumbataí River basin is a sub-basin of the giant Paraná sedimentary basin, that extends over an area of 1,700,000 km^2 (1,000,000 km^2 in Brazilian surface). Several stratigraphic units of the Paraná basin (Palaeozoic - Caenozoic) crop out in it (IPT, 1981): the Tubarão Group comprising the Itararé Subgroup (sandstones, conglomerates, diamictites, tillites, siltstones, shales and rythmites) and Tatuí Formation (siltstones, shales, silex and sandstones with local concretions); the Passa Dois Group comprising the Irati Formation (siltstones, mudstones, black betuminous shales and limestones) and Corumbataí Formation (mudstones, shales and siltstones); the São Bento Group comprising the Pirambóia Formation (sandstones, shales and muddy sandstones), Botucatu Formation (sandstones and muddy sandstones), Serra Geral Formation (basalts and diabases) and related basic intrusives; different types of Caenozoic covers such as the recent deposits, terrace sediments, and the Rio Claro Formation (sandstones, conglomerate sandstones and muddy sandstones).

SAMPLING AND METHODS

Rock samples (20 samples) were collected throughout the whole basin, taking into account the geological context, the rock types and their abundance or spatial representativity. Uranium concentration and isotopic composition of all samples were determined using standard alpha spectrometric technique. The ^{238}U concentration was calculated by isotope dilution from the counting rates of ^{238}U and ^{232}U peaks, and ^{234}U/^{238}U AR was calculated from the counting rates of ^{238}U and ^{234}U peaks. The gamma spectrometry was utilized to measure the ^{226}Ra, ^{232}Th and ^{40}K activities concentrations for all samples. The ^{226}Ra activity was evaluated through 1.76 MeV gamma ray emission of its daughter ^{214}Bi; ^{232}Th was determined through the ^{228}Ac gamma ray line at 2.62 MeV; ^{40}K was directly measured from the 1.46 MeV peak energy. The Ra_{eq} is related to the external gamma dose and the internal dose due to radon and its daughters, representing a single quantity that takes into account the radiation hazards. The Ra_{eq} assumes that 370 Bq ^{226}Ra/kg, 259 Bq ^{232}Th/kg and 4810 Bq ^{40}K/kg produce the same gamma dose. The Ra_{eq} of a sample is defined as (Berekta & Mathew, 1985):

$$Ra_{eq} = A_{Ra} + 1.43A_{Th} + 0.077A_K,$$

where: A_{Ra}, A_{Th} and A_K are the specific activities of ^{226}Ra, ^{232}Th and ^{40}K (Bq/kg), respectively.

RESULTS AND DISCUSSIONS

The activities concentrations of ^{238}U, ^{234}U, ^{226}Ra, ^{232}Th, ^{40}K and ^{238}U/^{234}U and ^{226}Ra/^{238}U activity ratios in these sedimentary rocks are represented in Table 1. Table 2 presents weighted mean activities concentration, Ra_{eq} and exposure rates of all formations.

The weighted mean activities concentrations of ^{238}U in sedimentary rocks from Corumbataí River basin is 109 Bq/kg. The highest activity concentration was obtained for sample FM-7 (398 ± 49 Bq/kg), representing a siltstone from Corumbataí Formation, and the smallest activity concentration was found for sample FM–12 (19 ± 4 Bq/kg), referring to a sandstone from Pirambóia Formation. The samples FM-7 and FM-9 (upper portion from Corumbataí Formation) present an elevated ^{238}U activity concentration when compared with samples FM-8 and FM-10 (lower portion from Corumbataí Formation). Despite all samples have been deposited in superficial marine environment, the different oxidizing and reducing conditions controlled the behavior of ^{238}U during the deposition of these sedimentary rocks.

Wedepohl (1969) and Gabelman (1977) report that normally the uranium concentration is greater in siltstones and claystones than in sandstones, being this fact related with the grain size of these sedimentary rocks and the differential behavior of ^{238}U into their minerals. The ^{238}U activity concentration in the analyzed sedimentary rocks is dependant of the lithology, so that siltstones and claystones (Corumbataí, Tatuí and Irati Formations) have higher uranium concentration than sandstones (Pirambóia and Botucatu Formations). Such is reinforced when the two samples from Itararé Subgroup Itararé are considered, i. e. the sample FM-1 (diamictite) and FM-2 (sandstone) whose ^{238}U activity concentration corresponds to 140 ± 17 Bq/kg and 49 ± 7 Bq/kg, respectively. Wedepohl (1969) and Gabelman (1977) also considered that limestones should have ^{238}U activity concentration lower than 24.66 Bq/kg (or 2.00 µg/g), but this fact is not verified for limestone from Irati Formation (^{238}U activity concentration = 191 ± 36 Bq/kg). This higher ^{238}U activity concentration must be associated with the limestones composition, i. e. limestones layers (superficial marine environment) intercalated by black betuminous shales (basin restrictions), rocks that are normally more enriched in ^{238}U than other sedimentary rocks. Some similarities and differences exist for ^{232}Th e ^{40}K in relation to ^{238}U activity concentration.

The weighted mean $^{238}U/^{234}U$ AR is 1.08, indicating near secular equilibrium between ^{238}U and ^{234}U isotopes at least over the last 1 million years. The weighted mean $^{226}Ra/^{238}U$ AR is lower than 1.00, suggesting a higher solubility and mobility of ^{226}Ra in relation to ^{238}U in these rocks.

If we considered the average annual effective dose from natural sources as 2.4 mSv per year (UNSCEAR, 1993), then, the maximum Ra_{eq} would be 544 Bq/kg. All formations found at Corumbataí River basin show Ra_{eq} activity concentration lower than allowed, indicating low radioactivity level in these sedimentary rocks. Exposure rate is the radiation effect in the air above 1 m of the area, estimated using dose-rate conversion factors (DRCF) adopted by UNSCEAR (1993). The weighted mean value of 36 $nGyh^{-1}$ represents 65% of the world average outdoor exposure due to terrestrial gamma radiation (55 $nGyh^{-1}$, according to UNSCEAR, 1993). Thus, the radioactive impact and the additional external radiation exposure for population due to sedimentary rocks are negligible and, consequently, the possible increase of a) radon flux from the soil; b) uptake by plants; c) natural alpha activity of food products must be minimal.

If we know the geology of the area and the exposure rate for all formations found at Corumbataí River basin, it is possible to obtain the map of exposure rate in air 1 m above the area of Corumbataí River basin (Fig. 1). The south-east portion of the area has higher exposure rate due to the occurrence of sedimentary rocks from Corumbataí, Irati, Tatuí and Itararé formations. Rio Claro city is located in this portion and, consequently, its inhabitants are subjected to exposure rates higher than that of others municipalities at Corumbataí River basin. The lower exposure rates are mainly related to the presence of sandstones and muddy sandstones from Pirambóia and Botucatu formations, as well diabases from Serra Geral Formation.

ACKNOWLEDGEMENTS

This investigation was performed under a scholarship from FAPESP-Brazil (Process N°. 98/02217-5 and 00/03136-0). The authors specially thank Dr. Jairo Roberto Jimenez-Rueda and Dr. Jorge Luis Nepomuceno de Lima for their general help during its development.

REFERENCES

Berekta, J.; Mathew, P. J., 1985. Natural radioactivity of Australian building materials waste and by-products. Health Physics, 48:87.

Gabelman, J., 1977. Migration of U and Th exploration significance. Study in geology N° 3. AAPG.

UNSCEAR, 1993. Sources and effects of ionizing radiation. United Nations Scientific Committee on the Effects of Atomic Radiation. United Nations, New York.

Wedepohl, K. H., 1969. Handbook of geochemistry. New York.

Table 1. Activities concentrations of radionuclides and ^{234}U/^{238}U and ^{226}Ra/^{238}U activity ratios in sedimentary rocks from Corumbataí River basin, São Paulo State, Brazil.

Amostra	^{238}U (Bq/kg)	^{234}U (Bq/kg)	^{226}Ra (Bq/kg)	^{232}Th (Bq/kg)	^{40}K (Bq/kg)	^{234}U/^{238}U	^{226}Ra/^{238}U
FM - 1	140	170	44	58	395	1.22	0.31
FM - 2	49	45	9	21	169	0.91	0.18
FM - 3	138	112	34	16	143	0.81	0.25
FM - 4	181	132	63	25	113	0.73	0.35
FM - 5	85	102	21	38	169	1.20	0.25
FM - 6	191	210	51	<4	<5	1.10	0.27
FM - 7	398	573	93	122	369	1.44	0.24
FM - 8	75	67	7	23	395	0.90	0.10
FM - 9	244	288	63	51	339	1.18	0.26
FM - 10	87	83	8	25	256	0.95	0.10
FM - 11	70	80	7	16	199	1.14	0.10
FM - 12	19	18	2	5	56	0.94	0.11
FM - 13	76	80	9	15	113	1.05	0.12
FM - 14	34	36	4	9	169	1.05	0.12
FM - 15	23	28	8	5	113	1.22	0.35
FM - 16	43	46	11	10	226	1.07	0.26
FM - 17	47	53	6	36	169	1.12	0.13
FM - 18	35	38	5	22	143	1.10	0.14
FM - 19	55	62	8	12	<5	1.13	0.15
FM - 20	123	144	19	31	<5	1.17	0.16

Table 2. Weighted mean of activities concentrations of radionuclides, Ra_{eq}, exposure rates and ^{234}U/^{238}U and ^{226}Ra/^{238}U activity ratios of all formations at Corumbataí River basin, São Paulo State, Brazil.

Formation	% of area	^{238}U (Bq/kg)	^{226}Ra (Bq/kg)	^{232}Th (Bq/kg)	^{40}K (Bq/kg)	Ra_{eq} (Bq/kg)	Exposure rate* (nGyh^{-1})	^{234}U/^{238}U	^{226}Ra/^{234}U
Itararé	5	95	27	40	282	105	48	1.07	0.25
Tatuí	4,5	156	49	21	128	89	40	0.77	0.30
Irati	3,5	138	36	21	85	73	33	1.15	0.26
Corumbataí	30,5	201	43	55	340	148	60	1.12	0.18
Pirambóia	31,5	50	6	11	134	17	16	1.05	0.11
Botucatu	6,5	33	10	8	113	30	14	1.14	0.31
Serra Geral	8	41	6	29	156	59	27	1.11	0.14
Rio Claro	9,5	89	14	22	<5	44	20	1.15	0.16
Grupo Bauru	1	---	---	---	---	---	---	---	---
Weighted mean		**109**	**22**	**29**	**191**	**78**	**36**	**1.08**	**0.17**

* Estimated using DRCF = 0.0414, 0.623 and 0.461 nGyh^{-1} per Bq/kg of ^{40}K, ^{232}Th and ^{226}Ra, respectively (UNSCEAR, 1993).

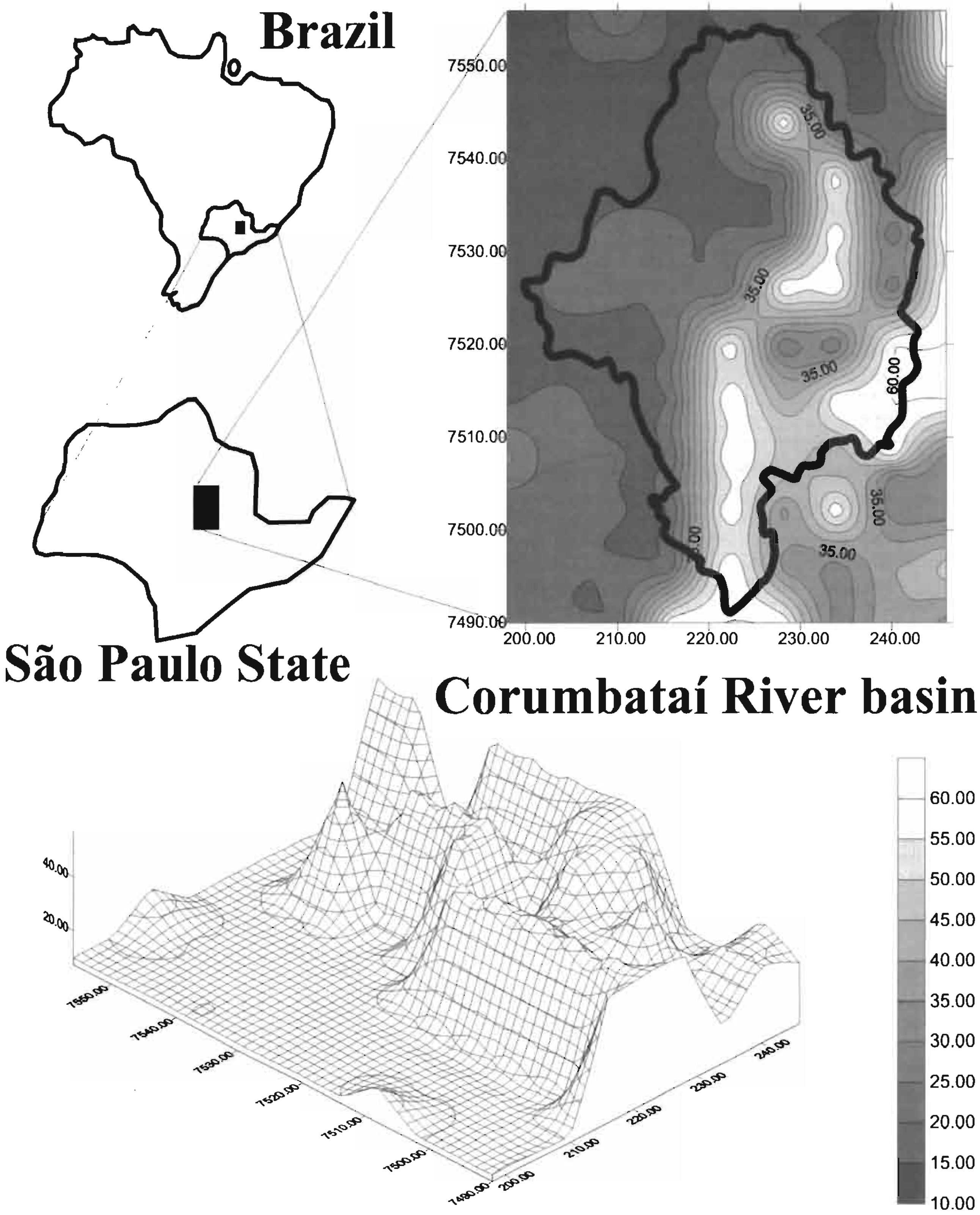

Figure 1. Map of exposure rate (nGyh^{-1}) in air 1 m above the area of Corumbataí River basin.

RADIOLOGICAL INCIDENCE AT TAPIRA AND CATALÃO PHOSPHATE ROCKS, THEIR (BY) PRODUCTS, PHOSPHATE FERTILIZERS AND AMENDMENTS

Conceicão, F.T. and Bonotto, D.M.

Instituto de Geociências e Ciências Exatas (IGCE)/ UNESP/ Rio Claro. Avenida 24-A n° 1515, C. P. 178, 13506-900,
Rio Claro-SP, Brazil. rstein@claretianas.com.br, dbonotto@rc.unesp.br

Keywords: Radionuclides, phosphate rocks, industrials products, phosphate fertilizers and amendments

INTRODUCTION

The phosphate rocks used as raw material for fertilizers production is enriched in uranium, thorium and their daughters, which were deposited as calcium phosphate minerals during their formation. The principal phenomenon is the isomorphic substitution, where the natural uranium can be substituted for calcium in the phosphate rocks structure. The apatite on the phosphate rocks concentrated is destroyed by action of sulfuric acid during the production of superphosphate, concentrating the radionuclides in final phases. This industrial process can disrupt the radioactive equilibrium found in the phosphatic rocks, taking their redistribution and fractioning in the industrialized products. The use of phosphate fertilizers and their by-products can redistribute and elevate the radionuclides concentration throughout in environmental systems, constituting an additional source of radiation exposure for workers and members of the public when applied in agricultural soils. Thus, the objective of this work was to evaluate the concentration and variability of ^{238}U, ^{234}U, ^{226}Ra, ^{232}Th and ^{40}K in different samples of phosphate rocks until the final products (MAP - monoammonium phosphate, DAP - diammonium phosphate, SSP - simple superphosphate, TSP - triple superphosphate), their by-products (phosphogypsum, H_3PO_4 and H_2SiF_6), and in phosphate fertilizers and amendments (carbonate failings, KCl and phosphogypsum) utilized in the sugar cane crops at São Paulo State, Brazil. Moreover, some contamination indexes have been applied to provide a basis for comparison of potential radionuclides hazards.

SAMPLING AND METHODS

Samples of phosphate rocks were collected from two bigger Brazilian mines located at Catalão city (southeast of Goiás State) and at Tapira city (west of Minas Gerais State). Sampling was also performed represented all production process, since the phosphate rocks, passing to the phosphate concentrated and reject, until the final products MAP, DAP, SSP, TSP, H_3PO_4, H_2SiF_6 and phosphogypsum. The phosphate fertilizers (NPK type or 5% of N, 25% of P and 25% of N), limestone, KCl and phosphogypsum utilized in the sugar cane crops were collected in a sugar cane mill at Piracicaba city, São Paulo State.

Uranium concentration and isotopic composition of all samples were determined using standard alpha spectrometric technique. The ^{238}U concentration was calculated by isotope dilution from the counting rates of ^{238}U and ^{232}U peaks, and ^{234}U/^{238}U AR was calculated from the counting rates of ^{238}U and ^{234}U peaks. The gamma spectrometry was utilized to measure the ^{226}Ra, ^{232}Th and ^{40}K activities concentrations for all samples. The ^{226}Ra activity was evaluated through 1.76 MeV gamma ray emission of its daughter ^{214}Bi; ^{232}Th was determined through the ^{228}Ac gamma ray line at 2.62 MeV; ^{40}K was directly measured from the 1.46 MeV peak energy. The Ra_{eq} is related to the external gamma dose and the internal dose due to radon and its daughters, representing a single quantity that takes into account the radiation hazards. The Ra_{eq} assumes that 370 Bq ^{226}Ra/kg, 259 Bq ^{232}Th/kg and 4810 Bq ^{40}K/kg produce the same gamma dose. The Ra_{eq} of a sample is defined as (Beretka & Mathew, 1985):

$$Ra_{eq} = A_{Ra} + 1.43A_{Th} + 0.077A_K,$$

where: A_{Ra}, A_{Th} and A_K are the specific activities of ^{226}Ra, ^{232}Th and ^{40}K (Bq/kg), respectively.

RESULTS AND DISCUSSION

PHOSPHATE ROCKS AND THEIR (BY) PRODUCTS

The activities concentrations of ^{238}U, ^{234}U, ^{226}Ra, ^{232}Th, ^{40}K and Ra_{eq} in the Catalão and Tapira phosphate rocks and their industrial products are represented in Tables 1, 2 and 3. The phosphate rock samples show ^{238}U and ^{226}Ra activities concentration within the world range (Pfister et al., 1976), whereas ^{232}Th and ^{40}K activities concentration are higher (Menzel, 1968). The ^{232}Th abundance, probably, may be explained due to its enrichment during weathering processes.

The ^{234}U/^{238}U activity ratio in Tapira phosphate rocks is lower than 1 (0.87) due to the preferential leaching of ^{234}U relative to ^{238}U, a typical result for weathered rocks. For the Catalão phosphate rocks, the ^{234}U/^{238}U activity ratio is practically 1 (1.03), suggesting secular radioactivity equilibrium. The ^{226}Ra/^{238}U activity ratios lower than 1 indicate a higher solubility and mobility of ^{226}Ra in relation to ^{238}U during weathering processes.

The radium-equivalent activity of the Catalão and Tapira phosphate rocks indicates that these deposits have high radioactivity content, mainly due to high ^{232}Th activities concentration accumulated by weathering processes. Exposure rate is the radiation effect in the air above 1 m of the area, being estimated using dose-rate conversion factors adopted by UNSCEAR (1993) (DRCF = 0.0414, 0.623 and 0.461 nGyh^{-1} per Bq/kg to ^{40}K, ^{232}Th and ^{226}Ra, respectively). Exposure rates corresponding to 2184 and 874 nGyh^{-1} can be estimated for Tapira and Catalão area, respectively, considering the obtained mean radionuclides activities concentration for phosphate rocks (Tables 1, 2). Thus, these areas may be considered as high background areas, because of their external gamma radiation greater than 230 nGyh^{-1} (UNSCEAR, 1993).

The first step to obtain the industrialized products derived from Tapira and Catalão phosphate rocks is the flotation-separation process, where the apatites are concentrated. The apatite is destroyed by action of H_2SO_4 during the production of SSP and H_3PO_4, originating H_2SiF_6 and phosphogypsum as by-products. The TSP is obtained with the phosphate concentrated being attacked by H_3PO_4 and the MAP and DAP by H_3PO_4 mixed with ammonium. The radionuclides activities concentrations in the industrialized products are within the values range obtained around the world (Pfister et al. 1976; Sam et al., 1999). The ^{238}U is concentrated in SSP, TSP, MAP and DAP in relation to phosphogypsum, whereas ^{226}Ra tends to be incorporated preferentially in the phosphogypsum. The H_3PO_4 and H_2SiF_6 produced get rich in ^{238}U, ^{232}Th and deficient in ^{226}Ra in relation to concentrated, as reinforces the ^{226}Ra/^{238}U AR (Tables 1, 2, 3).

PHOSPHATE FERTILIZERS AND AMENDMENTS UTILIZED AT SÃO PAULO STATE

Table 4 and figure 1 show the activities concentrations of ^{238}U, ^{234}U, ^{226}Ra, ^{232}Th, ^{40}K and Ra_{eq} in phosphate fertilizers (NPK) and amendments (carbonate failings, KCl and phosphogypsum) used in sugar cane crops.

The phosphate fertilizers (NPK) and amendments contribute with different inputs of radionuclides to the soils. The ^{40}K activities concentration in phosphate fertilizers NPK used in sugar cane crops are higher than in phosphate rocks due to KCl incorporation in the final formula. If we consider the average annual effective dose from natural sources to 2.4 mSv per year (UNSCEAR, 1993), then, the maximum Ra_{eq} would be 544 Bq/kg. Phosphate fertilizer NPK and KCl possess Ra_{eq} higher than this maximum due to ^{40}K included in KCl.

The dominant agricultural production at São Paulo State is the sugar cane, where are applied 500 to 600 kg/hec (24,400 m^2) of phosphate fertilizers NPK, 2 ton/hec of limestones, 200 kg/hec of KCl and 1,5 ton/hec of phosphogypsum per year (João Américo Beltrame, personal communication). Under this figure, it is possible to deduce that an average of 26, 11, 10 and 359 Bqm^{-2} of ^{238}U, ^{226}Ra, ^{232}Th and ^{40}K, respectively, will be distributed per unit arable land. These values are lower than in many parts of the world such as Marroco, Florida (USA), Taiba-Togo, Bu-Craa (Western Sahara), Kola (URSS), Uro and Kurun (Sudan), where untreated ground phosphate rocks have been used as plant fertilizers, being the ^{40}K the exception (Pfister et al., 1976; Sam et al., 1999). Considering these annual inputs of ^{238}U, ^{226}Ra, ^{232}Th and ^{40}K, and since these radionuclides are homogeneously distributed in the upper 10 cm of the soil with an apparent density of 1.5 g/cm^3 (Bolívar et al., 1995), an increase in about 0.17, 0.07, 0.07 and 2.39 Bq/kg of soil is estimated to ^{238}U, ^{226}Ra, ^{232}Th and ^{40}K, respectively. The added amount of ^{238}U does not reach 0.68% of the normal content of ^{238}U in an undisturbed soil (world average of 25 Bq/kg). For the estimation of external radiation exposure caused by phosphate fertilizers NPK and amendments used in sugar cane crops at São Paulo State, a value of 0.17 nGyh^{-1} at 1 m above the ground level (DRCF = 0.0414, 0.623 and 0.461 Gyh^{-1} per Bq/kg to ^{40}K, ^{232}Th and ^{226}Ra, respectively, adopted by UNSCEAR, 1993) would generated, just representing 0.31% of the world average outdoor exposure due to terrestrial gamma radiation (55 nGyh^{-1}, according to UNSCEAR, 1993). Thus, the radioactive impact and the additional external radiation exposure for population due to phosphate fertilizers NPK and amendments are negligible and, consequently, the possible increase of a) radon flux from the soil, b) uptake by plants and c) natural alpha activity of food products must be minimal. These concerns are very important in agricultural systems traditionally having a "clean" image, like Brazil, where low agrichemical inputs of these radionuclides by phosphate fertilizers NPK and amendments are used in the sugar cane crops at São Paulo State, Brazil.

ACKNOWLEDGEMENTS

This investigation was performed under a scholarship from FAPESP-Brazil (Process N$_{o.}$ 00/03136-0). The authors specially thank Dr. Jairo Roberto Jimenez-Rueda, Dr. Gilberto José Garcia, Carlos Cordeiro Ribeiro, Robson Santos Aglisnkas, Luis Antonio Fonseca de Barros and João Américo Beltrame for their general help during its development.

REFERENCES

Berekta, J., Mathew, P. J. 1985. Natural radioactivity of Australian building materials waste and by-products. Health Physics, 48:87.

Bolívar, J. P.; García-Tenorio, R.; García-Leon M. 1995. Fluxes and distribution of natural radionuclides in the production and use of fertilizers. Appl. Radiat. Isot. 46:717-718.

Menzel, R. G. 1968. Uranium, radium and thorium content in phosphate rocks and their possible radiation hazard. J. Agr. Food Chem., 16:231-284.

Pfister, R. J.; Philipp, G., Pauly, H. 1976. Population dose from natural radionuclides in phosphate fertilizers. Radiation and Environmental Biophysics, 13:247-261.

Sam, A. K.; Ahamed, M. M. O.; Khangi, F. A. El; Nigumi, Y. O. El; Holm, E. 1999. Radiological and chemical assessment of Uro and Kurun rock phosphate. Journal of Environmental Radioactivity, 42:66-75.

UNSCEAR 1993. Sources and effects of ionizing radiation. United Nations Scientific Committee on the Effects of Atomic Radiation. United Nations, New York.

Table 1. Activities concentration of radionuclides (Bq/kg), Ra$_{eq}$ (Bq/kg) and activities ratios of ^{234}U/^{238}U and ^{226}Ra/^{238}U in industrial products and by-products from Tapira, Minas Gerais State, Brazil.

Sample	^{238}U	^{234}U	^{226}Ra	^{232}Th	^{40}K	Ra$_{eq}$	^{234}U/^{238}U	^{226}Ra/^{238}U
Phosphate rock	1270	1105	295	3344	1303	5177	0.87	0.24
Phosphate rock	1356	1166	217	3131	1100	4779	0.86	0.17
Reject	274	284	195	579	504	1061	1.04	0.71
Reject	353	339	214	631	532	1157	0.96	0.60
Concentrated	394	394	140	588	132	991	1.00	0.35
Concentrated	577	583	189	557	140	996	1.01	0.33
SSP	1007	997	304	286	<5	713	0.99	0.30
SSP	690	690	262	272	<5	651	1.00	0.37
TSP	857	848	7	408	<5	590	0.99	<0.01
TSP	538	527	9	311	<5	454	0.98	0.02
MAP	613	607	<1	200	<5	286	0.99	<0.01
MAP	1159	1124	<1	221	<5	316	0.97	<0.01
Phosphogypsum	210	210	180	206	60	479	1.00	0.86
Phosphogypsum	178	178	169	185	63	438	1.00	0.95

Table 2. Activities concentration of radionuclides (Bq/kg), Ra$_{eq}$ (Bq/kg) and activities ratios of ^{234}U/^{238}U and ^{226}Ra/^{238}U in industrial products and by-products from Catalão, Goiás State, Brazil.

Sample	^{238}U	^{234}U	^{226}Ra	^{232}Th	^{40}K	Ra$_{eq}$	^{234}U/^{238}U	^{226}Ra/^{238}U
Phosphate rock	872	898	342	1232	282	2125	1.03	0.40
Phosphate rock	863	889	289	1070	291	1841	1.03	0.34
Reject	801	785	364	989	276	1799	0.98	0.45
Reject	624	636	297	1081	255	1862	1.02	0.47
Concentrated	392	396	327	385	143	888	1.01	0.83
Concentrated	606	612	514	520	134	1268	1.01	0.85
MAP	1849	1849	11	65	<5	104	1.00	<0.01
MAP	1615	1615	11	41	<5	70	1.00	<0.01
DAP	953	924	11	42	<5	70	0.97	<0.01
DAP	1398	1440	11	34	<5	60	1.03	<0.01
Phosphogypsum	321	321	292	172	53	542	1.00	0.91
Phosphogypsum	234	229	213	151	48	433	0.98	0.91

Table 3. Activities concentration of radionuclides (Bq/L) and activities ratios of ^{234}U/^{238}U and ^{226}Ra/^{238}U in H_3PO_4 and H_2SiF_6 derived from Tapira and Catalão.

Sample	^{238}U (Bq/L)	^{238}U (ppm)	^{232}Th (Bq/L)	^{232}Th (ppm)	^{226}Ra (Bq/L)	^{40}K (Bq/L)	^{234}U/^{238}U	^{226}Ra/^{238}U
H_3PO_4[1]	157	12,757	158	38,566	12	<5	1.02	0.08
H_3PO_4[2]	375	30,387	458	111,829	26	<5	1.01	0.07
H_2SiF_6[2]	0.5	41	2.5	625	<1	<5	1.01	<0.01

1 – Catalão, 2 - Tapira

Table 4. Activities concentration of radionuclides (Bq/kg), Ra$_{eq}$ (Bq/kg) and activities ratios of ^{234}U/^{238}U and ^{226}Ra/^{238}U in phosphate fertilizers and amendments utilized in sugar cane crops at São Paulo State.

Sample	^{238}U	^{234}U	^{226}Ra	^{232}Th	^{40}K	Ra$_{eq}$	^{234}U/^{238}U	^{226}Ra/^{238}U
NPK	587	587	13	20	8915	728	1.00	0.02
NPK	588	588	14	31	8936	746	1.00	0.02
KCl	<0.1	<0.1	<1	<1	19341	1489		
KCl	<0.1	<0.1	<1	<1	20204	1558		
Carbonate failings	191	210	69	<1	56	73	1.10	0.36
Carbonate failings	10	9.8	7	<1	62	12	0.98	0.70
Carbonate failings	11	11.3	8	<1	45	11	1.03	0.73
Phosphogyspum	126	126	106	183	199	383	1.00	0.84
Phosphogyspum	155	155	137	147	169	360	1.00	0.88

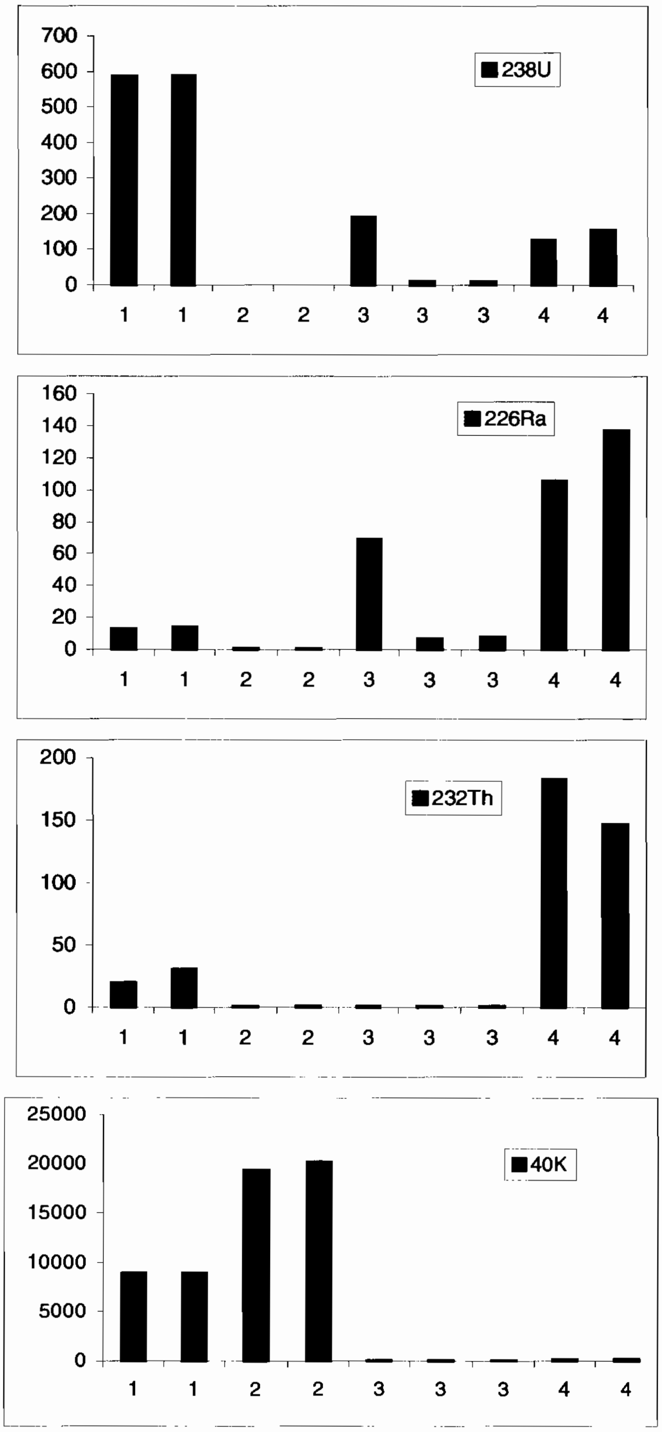

Figure 1. Activity concentration of ^{238}U, ^{226}Ra, ^{232}Th and ^{40}K (Bq/kg) in phosphate fertilizers and amendments utilized at São Paulo State. 1 = NPK, 2 = KCl, 3 = Carbonate failings, 4 = Phosphogypsum.

ENVIRONMENTAL ISOTOPES OF PAMPA DE GAN GAN, NORTH PATAGONIAN MASSIF, CHUBUT

Dapeña, C.[1,2]; Parica, C.A.[1,3]; Bechis, F.[1] and Remesal, M.B.[1,3]

1. Departamento de Ciencias Geológicas, Facultad de Ciencias Exactas y Naturales, Universidad de Buenos Aires, Pabellón II, Ciudad Universitaria, 1428 Buenos Aires, Argentina. paricac@gl.fcen.uba.ar, remesal@gl.fcen.uba.ar, florbechis@yahoo.com
2. Instituto de Geocronología y Geología Isotópica (INGEIS-CONICET), Pabellón INGEIS, Ciudad Universitaria, 1428 Buenos Aires, Argentina. dapenna@ingeis.uba.ar
3. Consejo Nacional de Investigaciones Científicas (CONICET)

Keywords: Environmental isotopes, water, Patagonia

INTRODUCTION

The area is located in the centre north of the Patagonian Massif. The studies presented in this paper are part of the University of Buenos Aires projects UBACYT X 164 and X 628. The aim of these investigations is to gain a better comprehension of the hydrological system in the area of the Pampa de Gan Gan and the surrounding ranges using environmental stable isotopes (^2H and ^{18}O), and to make a first approach to the origin of natural Chubut province, Argentina (42°00'-42°30' S; 69°00'-67°15' W) (Fig. 1).

The region is formed by several elevated ranges and displays a typically broken morphology, dissected by ephemeral streams and creeks ("arroyos"). The surface waters formed temporary and permanent lakes. The highest points are Sierra de Chacays (1400 m), Sierra de Talagapa (1600 m) and Sierra Pire Mahuida (close to 2000 m) (Fig. 1). Gan Gan town is located over an old depressed plain surrounding by those highest ranges. The water circulation from the higher to lower altitudes flows through the fractures in hard rocks and alluvial fans close to the border of the ranges. Spring waters generally flow along the surface or subsurface before they infiltrate through the detrital sediments or basalt flows. Small alluvial deposits cover depressed areas.

Gan Gan town has a phreatic well drilled in alluvial sediments, which provides drinkable water.

The equilibrium of the system is very fragile; the hydrologic balance is usually negative so the evaporation predominates over the inputs (precipitation, stream flow, infiltration and surface runoff). Occasionally, some recuperation of the water lake level is observed during higher rainy years. Infiltration is high due to volcanic rocks fissures and soil characteristics. The insufficient number of water wells reduces the groundwater interpretation of the global area.

The region has a cold arid climate with a dry cold season. Although the region cannot be considered to be homogeneous , the lack of available information allow us to use the few meteorological data which are assumed to be representative for the whole area. However, it is known that a snow cover is common during the winter season. The mean annual precipitation (rain and snow) is frequent below 200 mm, but the distribution is heterogeneous. Precipitation is higher in winter and snow remains until November. Summer is warm and very dry. The mean annual temperature is 13°C, January being the warmest month (20°C) and July the coldest (< 5°C). The region is very windy, predominantly from the West.

The precipitation-evaporation balance is usually negative in summer promoting an increase in the water content of dissolved solids and enrichment in the isotope stable composition.

Precipitation (snow and rain) is the variable contribution to the whole system and local infiltration the only recharge process.

GEOLOGICAL REGIONAL SETTING

The area is emplaced in the Somuncura Massif (Ramos, 1999), Extra Andean Chubut (Fig. 1). On regional scale, the basement consists of metamorphic and igneous rocks of Paleozoic age, and a Mesozoic sequence integrated by volcanic and sedimentary rocks. The marine deposits of the Upper Cretaceous - Lower Tertiary are represented by the Chubut Group and Colonia Formation. The Tertiary magmatic sequence includes in the lower level the basic intrusive bodies of the El Buitre Formation (Ardolino and Franchi, 1993; Ardolino et al., 1995) of Paleocene-Eocene age and olivine basaltic flows with a possible link in age with the intrusive bodies (Bechis, 2003).

The Quiñelaf Super Unit (Oligocene-Miocene) represents the main structure of the range (Franchi et al., 2001). This unit is integrated by basic and mesosilicic lava flows and hipabisal rocks.

The lava flow of the Plan Luan volcano outcrops overlying the deposits of the Colhue Huapense (Sarmiento Group, Simpson, 1941). The volcanic rocks of Plan Luan are Miocene according to Corbella and Barbieri (1989).

Sandstones and conglomerates deposits of Miocene-Pliocene? age (Ardolino, 1987) compose the Pampa Sastre Formation (out of the map).

Alluvial, colluvial, lake deposits and gravity slumps represents the Quaternary stratigraphy.

MATERIALS AND METHODS

During April, 2000, seven water samples were collected from springs, surficial water and groundwater.

Temperature, electric conductivity (CEE) and pH were determined in field by means of a portable conductivimeter, pH meter and the positioning of samples with GPS technology (datum WGS84).

Isotopic analyses were done at INGEIS Laboratories. ^2H in water samples was measured by Coleman et al. (1982) procedure and for the measurement of ^{18}O was used the methodology described in Panarello and Parica (1984). Isotope ratios were measured with a multicollector McKinney type mass spectrometer, Finnigan MAT Delta S.

The results are expressed like δ‰ defined as:

$$\delta = 1000 \frac{R_S - R_P}{R_P} ‰$$

δ: isotopic deviation in ‰
S: sample P: international standard
R: isotopic ratio ($^2H/^1H$; $^{18o}/^{16o}$).

The standard is Vienna Standard Mean Ocean Water (V-SMOW) (Gonfiantini, 1978). The analytical errors were ±0.1‰ and ±1.0‰ for $\delta\,^{18}O$ and $\delta\,^2H$ respectively.

RESULTS AND DISCUSSION

The spring waters (M4, M7), small streams ("arroyos") M2 and M5, phreatic water from Gan Gan well, Verde (M3) and Gan Gan (M1) lakes were sampled to perform isotope analyses (^{18}O, ^2H) (Fig. 1).

The pH shows slightly variations, from 7 to 7.5, only M3 is strongly alkaline, probably related to presence of carbonates. Conductivity ranges from 700 to 1700µS/cm, indicative of low to medium salinity. The water temperature is very cold (Table 1) showing good correlation with the ambient temperature.

Table 1 shows the isotopic values for $\delta^{18}O$, δ^2H, conductivity and water temperature of the analyzed samples. In addition, Figure 2 exhibits a scatter plot $\delta^{18}O$ *vs* δ^2H of samples, global meteoric water line (MWL), $\delta^2H = 8*\delta^{18}O + 10‰$ (Craig, 1961) and some individual precipitation from Comodoro Rivadavia city. During 1985 some rain samples were collected at this city (Levin et al., 1988). Southwards, the precipitation collector station Los Altares has a very short isotope record, with some $\delta^{18}O$ values (-13.6 to -1.8‰). It belongs to the National Network of Isotopes in Precipitation (RNC) of Argentina and the Global Network for Isotopes in Precipitation (GNIP) (Dapeña and Panarello, 1999; IAEA/WMO, 2002). Today, it is out of service.

Springs, streams and phreatic water show very depleted isotopic values (Table 1; Fig. 2).

The depletion of the heavy isotope content of precipitation as a function of altitude and latitude, designate "Altitude effect" and "Latitude Effect" were defined by Dansgaard (1964) and has been most usefully applied in hydrologic research (Gat and Reitti-Shati, 1999) .

The spring M4 shows the most depleted values ($\delta^{18}O$= -12,9‰, δ^2H= -109‰) indicating probably higher altitude. M5 and M2 have values also depleted ($\delta\,^{18}O$= -11,1‰, -10,5‰) but lower than M4 probably showing different altitude recharge or a selective precipitation. The Gan Gan well has $\delta\,^{18}O$= -12,4‰ and reflects the mixing from waters coming from the surrounding ranges.

The lake waters have the most enriched isotope values indicating high evaporation. They fit on an evaporation line: δ^2H=5,4; $\delta^{18}O$= -31,5.

These evidences support the idea that meteoric waters are the main source of recharge for surficial waters and groundwater. Local meteoric rainwater could play a minor role by direct infiltration through fractured volcanic rocks. In addition, the snow cover represents an important water source.

CONCLUSIONS

We propose that the main sources of recharge are related of the phreatic level in Gan Gan are related to meteoric waters, which isotopic composition represents the mixing of snowfall or rainfall in the higher levels of the surrounding ranges. The different values obtained for different points of the hydrological system are closely related to "Altitude Effect" and "Latitude Effect". Evaporation is mainly represented in lakes by large isotopic enrichment.

REFERENCES

Ardolino, A. A., 1987. Descripción geológica de la Hoja 42f, Sierra de Apas. Provincia de Chubut. Dirección Nacional de Minería y Geología Boletín 203.

Ardolino, A. A. & Franchi, M., 1993. El vulcanismo cenozoico de la meseta de Somún Curá, provincias de Río Negro y Chubut. Actas del XIII Congreso Geológico Argentino y II Congreso de Exploración de Hidrocarburos, IV: 225- 235.

Ardolino, A. A.; Busteros, R.; Cucchi, M.; Franchi, H.; Lema; Remesal, M., 1995. Cuerpos alcalinos básicos paleógenos del sur de Somún Curá (Argentina) y su marco estratigráfico. Ameghiniana, Asociación Paleontológica Argentina, Publicación Especial No. 3: 7-22. Buenos Aires.

Bechis, F., 2003. Estratigrafía y petrografía del área central de la Sierra de los Chacays. Patagonia Extraandina. Chubut. Argentina. Informe Beca Estímulo, Ubacyt. Inédito.

Coleman, M. L.; Sheperd, T. J.; Durham, J. J.; Rouse, J. E.; Moore, F.R., 1982. A rapid and precise technique for reduction of water with Zinc for Hydrogen isotope analysis. Analytical Chemistry. 54: 993-995.

Corbella, H. & Barbieri, M., 1989. Sierra de los Chacays, Extraandean Patagonia, Chubut, Argentina. $^{87}Sr/^{86}Sr$ Isotopic ratios of the alkaline rocks and age of the potassic volcanics of Mt. Plan Luan. Revista de la Asociación Geológica Argentina, XLIV (1-4): 133-140.

Craig, H., 1961. Isotopic variations in Meteoric waters. Science 133: 1702-1703.

Dansgaard, W., 1964. Stable Isotopes in precipitation. Tellus, 16: 436-468.

Dapeña, C. & Panarello, H. O., 1999. Development of the National Network for Isotopes in Precipitation of Argentina. II South American Symposium on Isotope Geology, 503-508.

Franchi, M.; Ardolino, A.; Remesal, M., 2001. Descripción geológica de la Hoja 4166-III, Cona Niyeu, provincia de Río Negro. SEGEMAR, IGRM. Buenos Aires.

Gat, J. R. & Rietti-Shati, M., 1999.The meteorological *vs* the hydrological altitude effect on the isotopic composition of meteoric waters. In: Isotope techniques in water resources development and management. Proc. Symposium, Vienna.IAEA. 5p.

Gonfiantini, R., 1978. Standards for stable isotope measurements in natural compounds. Nature 271: 534

IAEA/WMO, 2002. Global Network for Isotopes in Precipitation. The GNIP Database. http://isohis.iaea.org

Levin, M.; Panarello, H. O.; Albero, M. C.; Castrillo, E.; Grizinik, M.; Amoroso, A., 1988. Groundwater and subsurface flor in the Comodoro ivadavia Area, Chubut province, Argentina. Isotopic and chemical study. In: Simmers, I. (Ed). Estimation of Natural Groundwater Recharge: 377-393.

Panarello, H. O. & Parica, C. A., 1984. Isótopos del oxígeno en hidrogeología e hidrología. Primeros valores en aguas de lluvia de Buenos Aires. Asociación GeológicaArgentina, Revista XXXIX (1-2): 3-11.

Ramos, V. A., 1999. Las Provincias Geológicas del Territorio Argentino. En Geología Argentina. Caminos, R. (Ed.). Anales 29 (3): 41-96. Buenos Aires.

Simpson, G. G., 1941. The Eogene of Patagonia. Amer. Mus. Novitates, 1120: 1-15. New York.

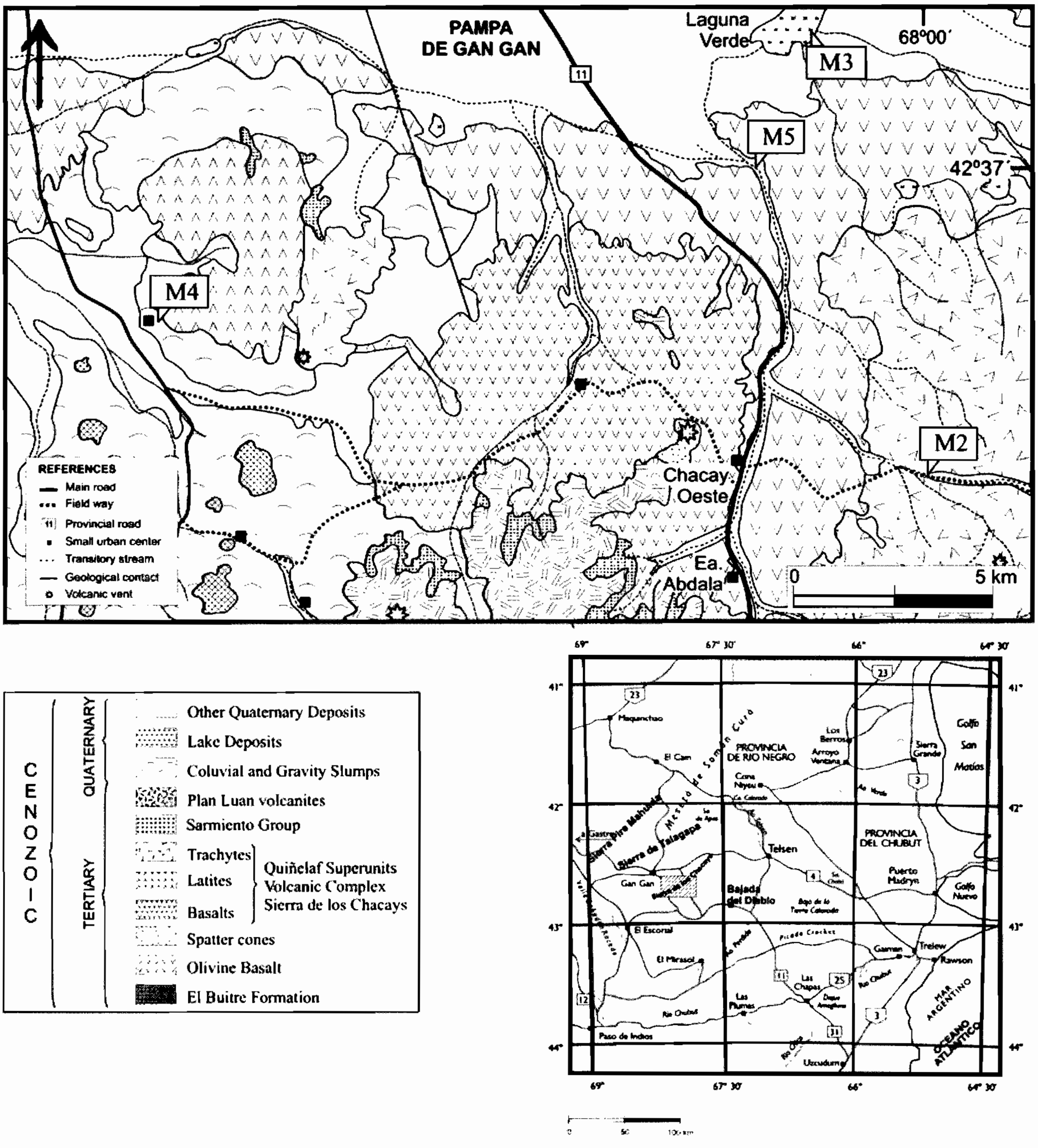

Figure 1. Location area (dashed) and geological map (adapted from Bechis, 2003).

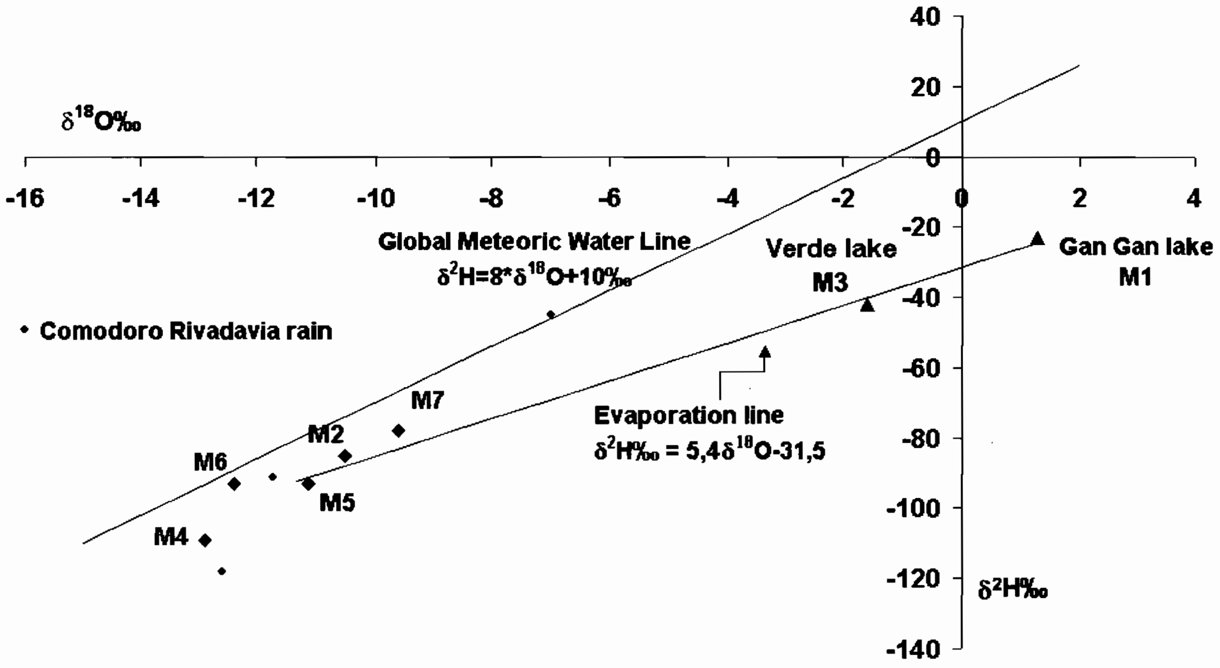

Figure 2. Scatter plot $\delta^{18}O$ *vs* $\delta^{2}H$.

Table 1. Location, water temperature, conductivity, isotope values.

# Lab	Sample	Latitude	Longitude	$\delta^{18}O \pm 0.1‰$	$\delta^{2}H \pm 1‰$	T °C	CEE µS/cm
11531	M1	42°31'15"	68°16'45"	1.3	-23	7.0	700
11532	M2	42°40'44"	68°00'30"	-10.5	-85	9.1	700
11533	M3	42°30'35"	67°58'22"	-1.6	-42	5.9	1700
11534	M4	42°39'05"	68°14'08"	-12.9	-109	8.7	600
11535	M5	42°37'21"	68°03'20"	-11.1	-93	7.6	1300
11536	M6	42°21'52"	68°17'18"	-12.4	-93	9.6	700
11537	M7	42°53'16"	67°29'17"	-9.6	-78	7.2	1200

C AND O ISOTOPES AND THERMAL STRESS IN CORALS FROM NORTHEASTERN BRAZIL

Fisner, M.[1]; Maÿal, E.M.[1]; Pinheiro, B.R.[1]; Ferreira, V.P.[2] and Sial, A.N.[2]

1. NEC-LACE, Departamento de Zoologia, CCB, UFPE, 50670-420, Recife-PE, Brasil. mara_fisner@zipmail.com.br
2. LABISE, Departamento de Geologia, CTG, UFPE, 50670-000, Recife-PE, Brasil. valderez@ufpe.br, ans@ufpe.br

Keywords: Thermal stress, coral, C and O isotopes, bleaching, northeastern Brazil

INTRODUCTION

The behavior of C and O isotopes in coral skeleton was investigated by the first time by Keith and Weber (1965). In addition, Fairbanks and Dodge (1979) established that temperature variations could be estimated in coral skeletons by examining O-isotope ratios. The variation of $\delta^{13}C$ in coral skeletons is directly related to the zooxanthellar density and/or productivity, in such a way that the denser the algae, the heavier the $\delta^{13}C$ in the skeletons. The hermatypic corals, however, appear to have a limit to this value indicating a connection between the zooxanthellar activity and the C- and O-isotope fractionation.

The $\delta^{18}O$ of the biogenic calcium carbonate precipitated in isotopic equilibrium with seawater, decreases in about 0.22‰ for each 1°C increase in temperature of the seawater. Corals that suffer thermal stress start to segregate skeletons depleted in ^{13}C. Therefore, negative $\delta^{13}C$ anomalies in corals are due to the physiologic stress and bleaching. This implies that the distribution of $\delta^{13}C$ in skeletons of scleractinia depends on the contents of CO_2 derived from breathing during dinoflagellata photosynthesis in the seawater used in skeletonization (Swart, 1983). An assessment of the exchange between the biota and the environment depends on our knowledge of the climatic variation patterns, and corals give such information.

METHODOLOGY

Coral samples were sliced, microdrilled and collected powders were placed in reaction vessels and were left to react overnight with 100% orthophosphoric acid. Next day, reaction vessels were placed in a high vacuum extraction line and the CO_2 released from each sample, after cryogenically cleaned, was analyzed in a dual inlet, triple collector mass spectrometer (SIRA II) in stable isotope laboratory (LABISE) at Recife. C- and O-isotope ratios are reported on the PDB scale.

Assuming isotopic equilibrium between aragonite and seawater, temperature for each coral sample was estimated using the Horibe and Oba (1986) equation and $\delta^{18}O‰_{PDB}$.

RESULTS AND DISCUSSION

In this study, is regarded as anomalous any estimated temperature equal or above 30°C. Temperature estimates are found in Table 1. We analyzed O isotopes in specimens of *F. gravida.* specie, along the skeletons of the specimens. Results indicate that skeletons developed, in the majority of the analyzed specimens, above anomalously high temperatures.

Table 1. C and O isotope ratios (‰$_{PDB}$) and temperature estimated from Horibe and Oba (1986) equation.

Year	Locality	$\delta^{13}C$	$\delta^{18}O$	T°C	Specimen
1993	Tamandaré (Pernambuco)	-0.2	-4.4	34.6	1
		-0.0	+4.2	33.6	2
1995		-0.8	-4.1	33.1	1
		-0.8	-3.8	31.7	2
		-1.2	-4.4	34.6	3
		-2.3	-4.1	33.6	4
		-0.9	-4.2	33.6	5
2000	Maracajaú (Rio Grande do Norte)	-1.9	-4.1	33.1	1
		-0.8	-4.1	33.1	2
		-1.6	-4.3	34.1	3
		+0.1	+3.9	32.2	4
		-1.3	-3.8	31.7	5
		-0.7	-4.0	32.6	6
		-1.3	-4.1	33.1	7
		-1.3	-3.6	30.7	8

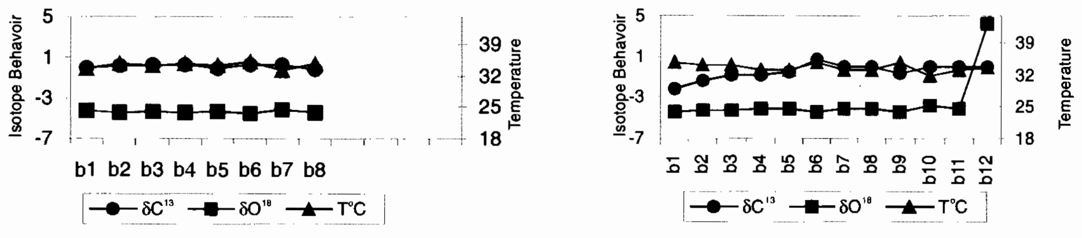

Specimen 1

Specimen 2

Figure 1. Specimens collected in Tamandaré beach, state of Pernambuco (1993).

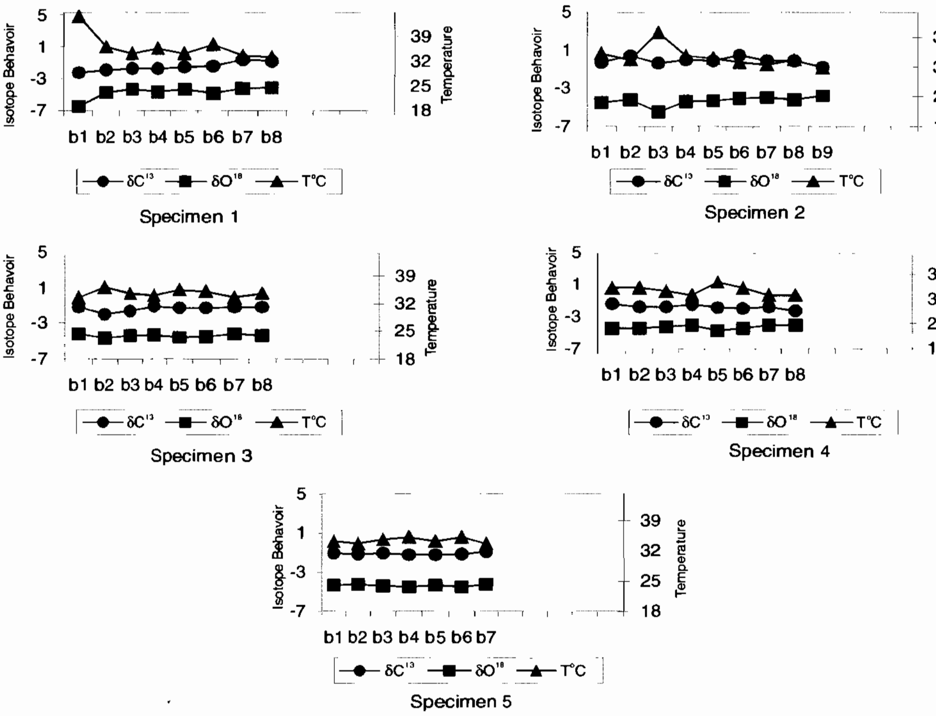

Figure 2. Specimens collected during 1995 at Tamandaré beach, state of Pernambuco.

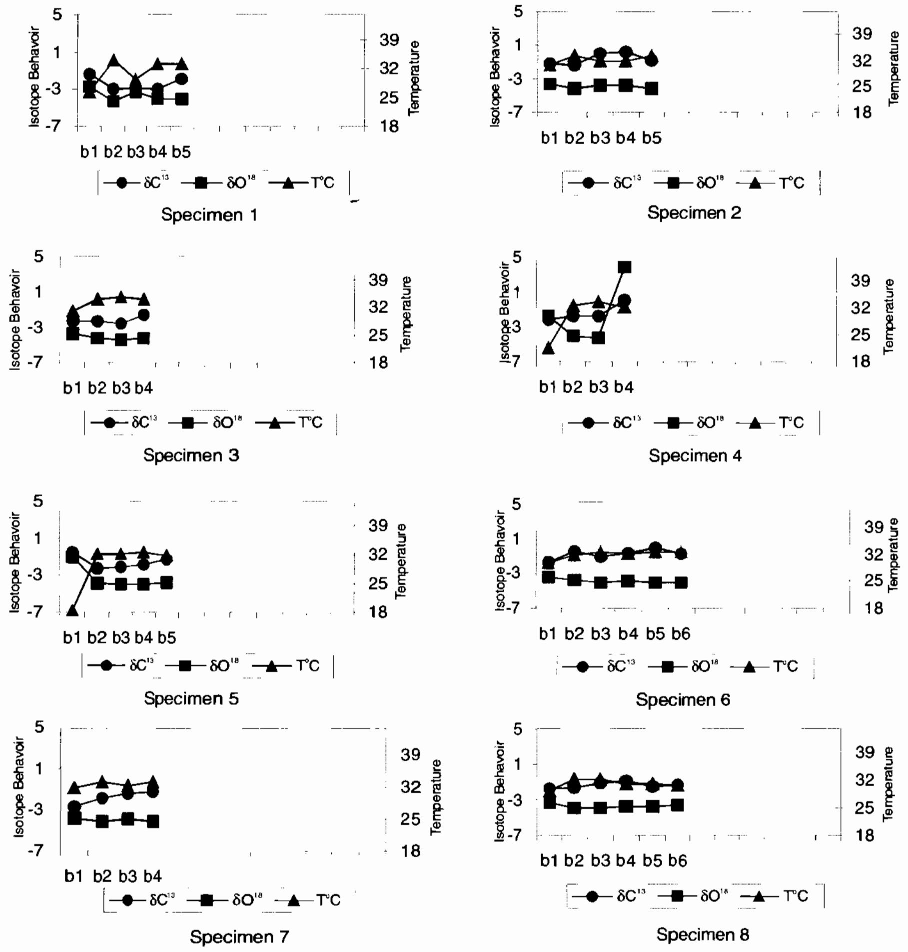

Figure 3. Specimens collected during 2000 at Maracajaú beach, state of Rio Grande do Norte.

CONCLUSIONS

Corals are excellent temperature bioindicators and can be used to monitor climatic changes. Some coral species appear to provide more reliable results than others, when O isotopes are analyzed in their skeletons used for thermometric determinations. C isotopes attest to zooxantellar activity, high δC^{13} values found whenever zooxantellar activity is high. The *F. gravida* species appears to be sensitive to temperature variations and records thermal stress.

ACKNOWLEDGEMENTS

Mara Fisner expresses her gratitude to the LABISE for the analytical support and to the CNPq for a PIBIC scholarship. (This is the contribution n° 212 of NEG-LABISE).

REFERENCES

Fairbanks, R.G. & Dodge, R.E., 1979. Annual periodocy of the $^{18}O/^{16}O$ and $^{13}C/^{12}C$ ratios in the coral *Montastrea annularis*. Geochim. Cosmochim. ACTA, 43:1009-1020.

Horibe, Y. & Oba, T., 1986. Temperature scale of aragonite – water and calcite – water systems (in Japanese) Fossils, p. 23-24, 69-79, 1972 In: Faure, G., Principles of Isotopy Geology. John Wiley & Sons 589p.

Keith, M.L. & Weber, J.N., 1965. Vital effect on the carbonate isotopic composition of reef communities. Proc. Spoleto Conf. Paleotemp. Isotope Oceanogr.,: 267-283.

Swart, P.K., 1983. Carbon and oxygen isotope fractionation in scleractinian corals: a review. Earth-Science Rec. 19:51-80.

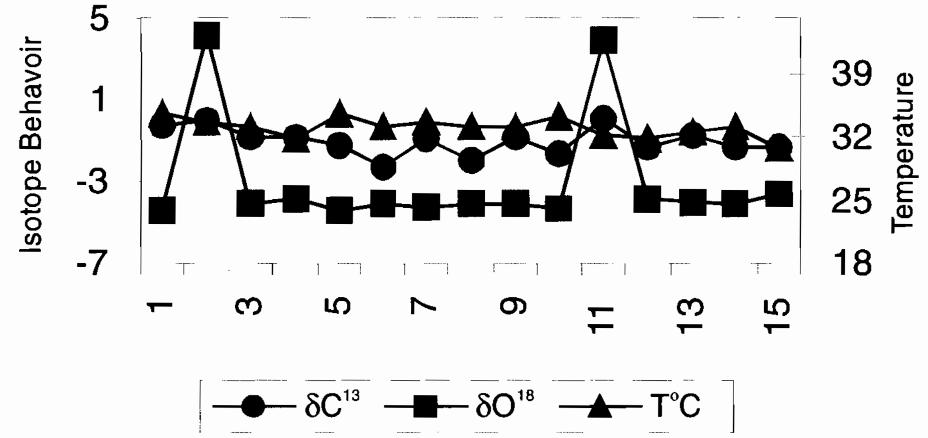

Figure 4. The last analysis in each specimen in year of collect
(1-2: Tamandaré beach – 1993; 3-7: Tamandaré beach – 1995 and 8-15: Maracajaú beach – 2000).

HISTORY OF ISOTOPIC COMPOSITION OF ATMOSPHERIC LEAD EMISSIONS RECORDED BETWEEN 5,280 AND 164 YR. BP IN LAGOA FEIA - CENTRAL BRAZIL

Gioia, S.M.C.L.[1]; Pimentel, M.M.[1] and Salgado-Labouriau, M.L.[2]

1. Laboratório de Geocronologia, Instituto de Geociências, Universidade de Brasília, 70910-900, Brasília-DF.
sgioia@unb.br, marcio@unb.br
2. Laboratório de Micropaleontologia, Instituto de Geociências, Universidade de Brasília, 70910-900, Brasília-DF.
mlea@unb.br

Keywords: Inter-hemispheric exchange, Brazilian Lake, Pb isotopes, charcoal particles

INTRODUCTION

Natural fires probably started on the surface of Earth since the times when terrestrial plants became abundant enough to accumulate fuel for fire propagation (between 400-350 Myr ago, Andreae, 1991). The onset of natural fires depends on appropriate climatic conditions (duration and intensity of the dry seasons) as well as on ignition sources, such as lightning. These factors are, in general, of short duration (Goldammer, 1991). Reconstruction of fire history may be carried out with the quantitative determination of charcoal particles in the sediments, combined with palynological analysis.

This study uses the geochronological and palynological background available for the Lagoa Feia sediments to reconstruct the atmospheric Pb isotopic composition in Central Brazil during the last 6,000 yr. In special, the relationships between atmospheric Pb isotopic composition and the occurrence of natural fires are considered.

Pb ISOTOPES, ENVIRONMENT POLLUTION AND CORRELATION WITH FIRE

Large amounts of Pb were added to the atmosphere by coal burning during and after the industrial revolution. Before this period, several anthropogenic and natural pre-industrial sources were available. Natural sources include windblown dust, plant exudates, volcanic eruptions, forests fire; meteorite impact, radioactive decay and steams of seawater (Faure 1986). Anthropogenic sources are represented by mining and foundry of lead as far as 4,500 yr. BP in Asia. Romans produced strong Pb contamination between 2,100-1,800 yr. BP. They used Pb in domestic utensils, cosmetics and mainly in the production of "sapa", the base of Pb acetate, which was added to sweeten and to avoid deterioration of wine (Lessler, 1988). Hong et al. (1994, 1996) found lead contamination during 2,500 and 1,600 yr. BP and Rosman et al. (1997) showed that the Spanish mines were the principal source of Pb, also in that period under Roman occupation.

Pb pollution is recorded in several environments especially in the polar ice (Murozumi et al., 1969; Hong et al., 1994, 1996). These authors demonstrated the increase of Pb concentration associated with the decrease of the $^{206}Pb/^{207}Pb$ ratio between 600 BC. and 300 AC. As well as the ice, lake sediments have been used as records of the history of the pre-industrial atmospheric pollution (Renberg et al., 1994). Atmospheric Pb pollution from 12,000 yr. BP was investigated in a Swiss mountain peat bog (Shotyk et al., 1998) and 6,000 yr. BP in marshes from SW France (Alfonso et al., 2001).

Lake sediments serve as a natural record of anthropogenic Pb contribution along time, varying in the stratigraphical column, as the history of regional pollution (Kober et al., 1999). The anthropogenic lead in sediments corresponds to Pb adsorbed by grains, which may be extracted by acid leaching in the laboratory. The natural composition will probably correspond to the Pb isotopic composition in the rocks exposed in the areas adjacent to the lake (Kober et al., 1999). In the case of paleosediments, adsorbed Pb might be significant if the amount of lead added to the atmosphere by pollution is expressive, and therefore the paleosediment record will work as the historical record of the atmospheric Pb contamination during a certain period of time.

In this study we investigate paleosediments of Lagoa Feia, deposited in the period between 164 and 5,280 yr. BP. The geochronological record, as well as the variations in Pb isotopic composition and concentration was compared with the amount of coal particles, whose palynological record has been described by Ferraz-Vicentini (1999). This study is relevant to investigate the behaviour of Pb with respect to natural fires which are very frequent in the Distrito Federal area, and to look for correlation between isotopic and palynological data that could be used in future studies.

SAMPLE LOCATION AND LOCAL GEOLOGY

The Lagoa Feia is located near Formosa, 60 km east of Brasília, 831m above sea level. It is a 5km long lake elongated in the NE-SW direction. It represents a rainwater collector, without a feeder stream. The natural vegetation is an open arboreal savannah (*"cerrado"*).

The main rock associations exposed in the vicinities of Formosa are the Meso-neoproterozoic Carbonatic Psamo-pelitic unit of the Neo-Mesoproterozoic Paranoá Group, the Neoproterozoic Paraopeba Subgroup of the Bambuí Group, and Tertiary-Quaternary lateritic cover sediments and sediments.

RESULTS AND DISCUSSION

The combined use of lead isotopic composition and charcoal fragment data for 15 sediment samples of the Lagoa Feia – GO (Fig. 1) shows evidences of changes in isotopic composition in association with fire events in the "*cerrado*".

The isotopic record found in the profile, between 164 and 5,280 ^{14}C yr. BP, shows a positive correlation (Fig. 1) between $^{206}Pb/^{207}Pb$ ratio and the charcoal particle number (million/cm^3). The results allow to distinguish between natural from anthropogenic periods.

THE NATURAL PERIOD

The background corresponds to the period with high $^{206}Pb/^{207}Pb$ ratios between 5,280 and 2,774 ^{14}C yr. BP. The $^{206}Pb/^{207}Pb$ values are between 1.222 and 1.196, similar to isotopic composition of other sediment samples from the Northern Hemisphere (Fig. 2) (Alfonso et al., 2001; Shotyk et al., 2001; Hong et al., 1994). Some isotopic variations can be explained by the degree of efficiency of lead extraction during sample digestion step and by variations in relative proportions of organic and detrital material (Alfonso et al., 2001). During this period the soil dust and vegetation fires were probably the main sources of lead.

High values of the isotopic ratio are coincident with the high charcoal fragment counts, indicating the accretion of natural Pb in the sediments during the fire, around 5,000 yr. BP in central Brazil. $^{206}Pb/^{207}Pb$ values for pre-industrial sediments of Lagoa Feia are very similar, but slightly more radiogenic than, those found in the Northern Hemisphere. For example, in two cores of the coastal marshes of France, the mean ratio measured as background value is approximately 1.1903-1.198, and in a Switzerland peat bog (Shotyk et al., 2001) this period is marked by $^{206}Pb/^{207}Pb$ between 1.193 and 1.179. Similar ratios in a Saharan Holocene loess (1.199) correspond to a natural lead source in the Northern Hemisphere. The corresponding composition for the Southern Hemisphere remains unknown, although one can assume that the main natural source is probably represented by a combination of contributions from volcanic emissions and from crustal rock and soil dust. We can admit a natural contribution similar in composition to Holocene sediments, since their isotopic composition roughly coincide with our results (Fig. 3), except for the anomalous points as discussed below.

ANTHROPOGENIC PERIOD

The expressive decrease in the $^{206}Pb/^{207}Pb$ ratio observed at 2,222 yr. BP. is indicative of some lead pollution accretion (Fig. 2).

Available sources in South America are unknown for this period, but this decrease in good agreement with well marked anthropogenic events in the Northern Hemisphere. The lowest ratios were observed in a Greenland ice core between 2,600 and 1,700 BP., with 206/207 around 1,201 for the background and 1,183 at 2,000 yr. BP (Rosman et al., 1997). Similar variations were recorded in environments like marshes (Alfonso et al., 2001), lake sediments (Brännvall et al., 1997) and peat bogs (Shotyk et al., 1998). These studies suggested the influence of another source in the Southern Hemisphere at that time: Roman mining.

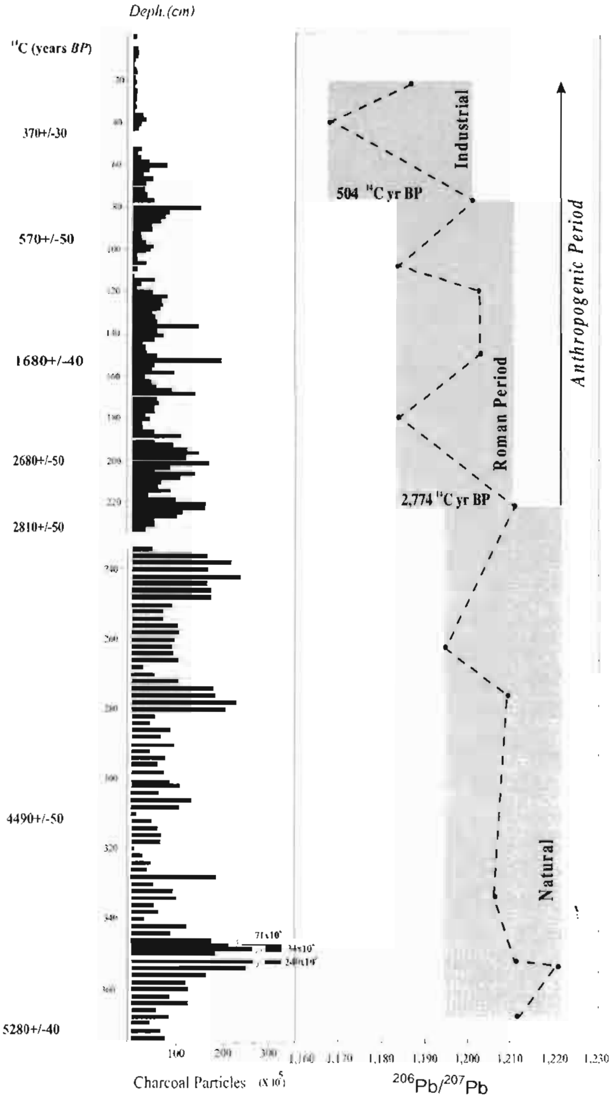

Figure 1. Variation in ($^{206}Pb/^{207}Pb$) with age (^{14}C) and charcoal particles counting (Ferraz-Vicentini 1999) for profile samples from Lagoa Feia.

During the Inca Empire very rarely lead and mercury were used. Only native copper, gold, silver, and tin were alloyed to form bronze (Mason, 1991). Consequently, in the absence of another source in the Southern Hemisphere at that time, one can suggest the transport of aerosol from the Northern Hemisphere.

Between 1,597-1,025, the Pb isotopic composition tend to became more radiogenic, equivalent to the period of time corresponding to the decline of the Roman Empire and consequent decrease in lead production (Settle & Patterson, 1980). At 1,025-829 BP., another decrease in $^{206}Pb/^{207}Pb$ value is observed corresponding to the medieval period. In fact, silver production from Europe lead mines started around 1,000 yr. BP (Alfonso et al., 2001).

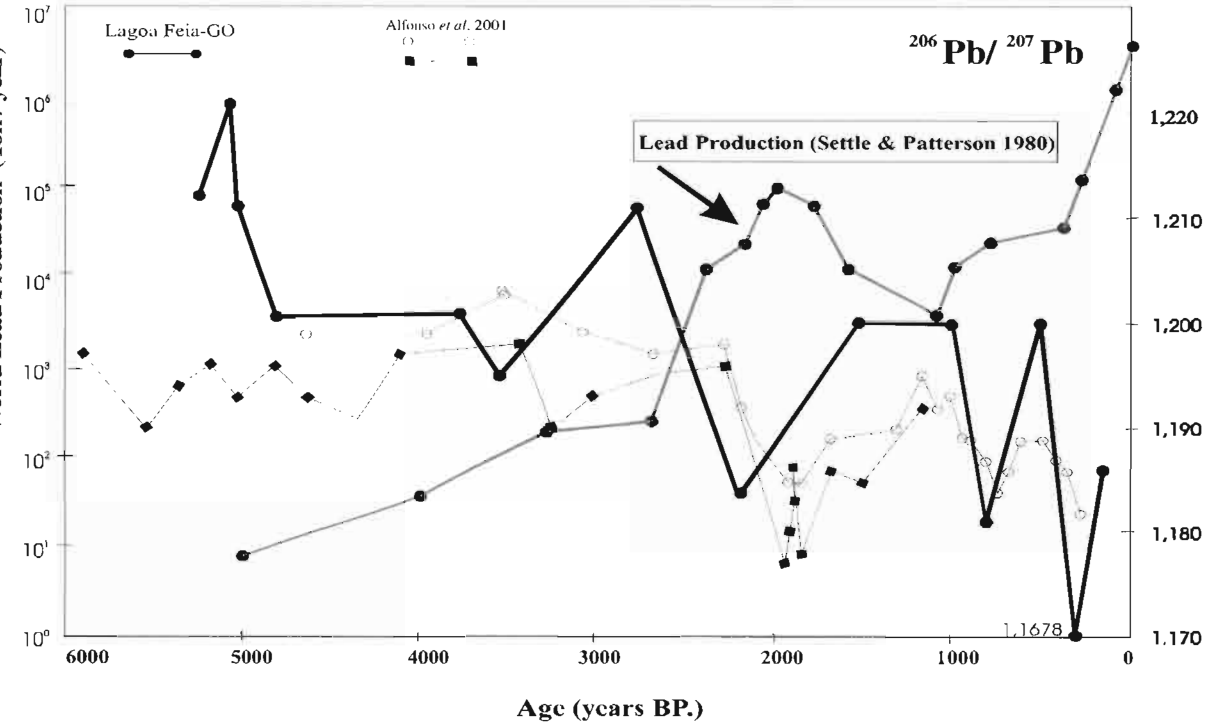

Figure 2. Lead isotopic composition evolution (^{206}Pb/^{207}Pb) of Lagoa Feia correlated with the world Pb production during the last 5,000 yrs reconstructed by Settle & Patterson (1980) and the lead composition of two cores in coastal marshes-SW France (Alfonso et al., 2001).

At 326 BP, the lowest charcoal particles counts per cm^3 and ^{206}Pb/^{207}Pb values are observed (Fig. 1), similarly to the period between 3,000-2,000 BP., suggesting addiction of lead to the atmosphere by an anthropogenic source. At approximately 164 BP, this unknown source disappeared or was reduced in the environment. A second hypothesis would be soil dust contribution with a high flux sedimentation, with lead radiogenic isotopic composition, as reported by Turcq et al., (2002).

Comparing with similar studies, the analyses of sediments attacked by leaching are more effective to extract lead adsorbed by sediments (Fig. 3), although the results are not too different from the bulk attack, used in Shotyk et al. (2001) and Alfonso et al. (2001). The combined use of lead isotopes and charcoal particles counts indicates (Fig. 1) that the presence charcoal particles coincide with result of more radiogenic ^{206}Pb/^{207}Pb values. By normalising the isotopic ratios by the number of charcoal particles we can identify more clearly the major anthropogenic events and the background composition for the Lagoa Feia sediments (Fig. 4).

The similarity between this results with other found in the Northern Hemisphere suggest important Inter-hemispheric exchange, traditionally considered to be an unlikely process (Bollhöfer & Rosman, 2000), because of the air barrier formation ITCZ (*Inter-Tropical Convergence Zone*) and the short residence time of Pb aerosols in the troposphere (< 14 days) (Turekian et al., 1977). In this case, the interchange can be explained by the hypothesis of North Hemisphere contribution during summer, when the ITCZ limit moves towards the north (Alfonso et al., 2001).

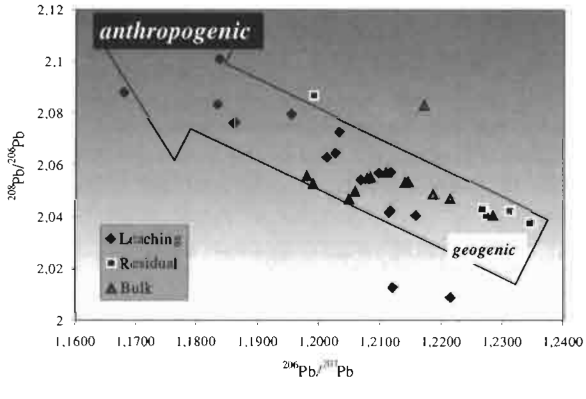

Figure 3. Lead isotopic composition (^{206}Pb/^{207}Pb) and (^{208}Pb/^{206}Pb).

CONCLUSIONS

In this study, the temporal evolution of lead isotopic composition in a sediment profile from the Lagoa Feia-GO, between 5,280 and 164 BP, was established. The results can be divided into two groups: (i) Pre-anthropogenic (> 2,774 yr. BP.) with high charcoal and ^{206}Pb/^{207}Pb between 1.196 and 1.222; (ii) anthropogenic (beginning in 2,222 until 164 yr. BP) with low quantity of charcoal and ^{206}Pb/^{207}Pb between 1.182, and 1.204 during the Roman period and 1.170-1.201 during the industrial period.

Further studies to assess the mass-air exchange between the hemispheres are required. Our understanding of this process will certainly benefit in the future from the study of other sediment profiles in the Southern Hemisphere.

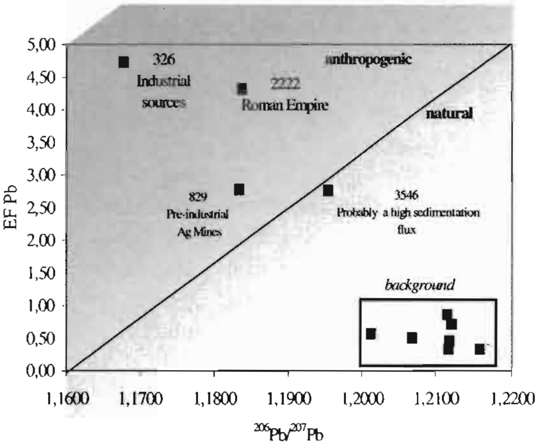

Figure 4. Plot of measured lead isotopic composition ($^{206}Pb/^{207}Pb$) vs. lead concentration (ppm)/number of charcoal particles (EF).

REFERENCES

Alfonso, S., Grousset, F. Massé, L., Tastet, J.-P., 2001. A European lead isotope signal recorded from 6000 to 300 yrs BP in coastal marshes (SW France). Atmospheric Environment. 35:3595-3605.

Andreae, M.O., 1991. Biomass burning: its history, use, and distribution and its impact on environment quality and global climate. In: Global biomass burning. Levine, J.S. (ed.). MIT Press Cambridge, London, 569pp.

Bollhöfer, A, & Rosman, K.J.R., 2000. Isotopic source signatures for atmospheric lead in the southern hemisphere. Geochimica et Cosmochimica Acta. 64(19)1: 3251-3262.

Brännvall, M.-L., Bindler, R., Emteryd, O., Nilsson, M., Renberg, I., 1997. Stable isotope and concentration records of atmospheric lead pollution in peat and lake sediments in Sweden. Water, Air, and Soil Pollution. 100:243-252.

Faure G., 1986. Principles of Isotope Geology. Prentice Hall. 2ª. ed.

Ferraz-Vicentini, K., 1999. História do Fogo no Cerrado. Instituto de Geociências, Universidade de Brasília, Brasília, Dissertação de Mestrado. 157p.

Goldammer, J.G., 1991. Tropical wild-land fires and global changes: prehistoric evidence, present fire regimes, and future trends. In: Global Biomass Burning. J.S. Levine (ed.). MIT Press Cambridge, London, 10:83-91.

Hong, S., Candelone, J.-P., Patterson, C.C., Bourtron, C.F., 1994. Greenland ice evidence of hemispheric lead pollution during Roman and Medieval Times recorded in Greenland ice. Science. 265:1841-184.

Hong, S., Candelone, J.-P., Patterson, C.C., Bourtron, C.F., 1996. History of ancient copper smelting poluttion during Roman and Medieval Times recorded in Greenland Ice. Science. 272:246-249.

Kober B., Wessels, M., Bollhöfer, A., & Mangini, A., 1999. Pb isotopes in sediments of Lake Constance, central Europe constrain the heavy metal pathways and the pollution history of the catchment, the lake and the regional atmosphere. Geochimica et Cosmochimica Acta. 63(9):1293-1303.

Lesser, M.A., 1988. Lead migration in forest soils: Response to changing atmospheric inputs. Environment Science Technology. 28:662-669.

Mason, J.A., 1991. The ancient civilizations of Peru. Penguin Books, London, pp.335.

Murozumi, M., Chow, T., Patterson, C., 1969. Chemical concentrations of pollutant aerosols, terrestrial dusts and sea salts in Greenland and Antarctic snow strata. Geochimica et cosmochimica Acta. 33: 1247-1294.

Renberg, I., Persson, M., Emtcryd, O., 1994. Pre-industrial atmospheric lead contamination detected in Swedish lake sediments. Nature. 368:323-326.

Rosman, K., Chisholm, W., Hong, S., Candelone, J.-P., Bourtron, C.F., 1997. Lead from Carthaginian and Roman Spanish mines isotopically identified in Greenland ice dated from 600 a.c. a 300 d.c. Environmental Science and Technology. 31:3413-3416.

Settle, D., & Patterson, C.C., 1980. Lead in albacore: guide to lead pollution in Americans. Science. 207:1167-1176.

Shotyk, W., Weiss, D., Appleby, P., Checurkin, A., Frei, R., Gloor, M., Kramers, J., Reese, S., Van Der Knaap, W., 1998. History of atmospheric lead deposition since 12.370 14C yr. bp from a peat bog, Jura Mountains, Switzerland. Science. 281:1635-1640.

Turcq, B., Albuquerque, A.L.S., Cordeiro, R.C., Sifeddine, A, Simões Filho, F.F.L., Souza, AG., Abrão, J.J., Oliveira, F.B.L., Silva, AO, Capitâneo, J., 2002. Accumulation of organic carbon in five Brazilian lakes during the Holocene. Sedimentary Geology. 148:319-342.

Turekian, K.K., Nozaki, Y., Benninger, L.K., 1977. Geochemistry of atmospheric radon and radon products. Annal Review of Earth Planetary Science. 5:227-255.

ATMOSPHERIC DEPOSITION AND SOURCES OF ANTHROPOGENIC LEAD IN SEDIMENTS FROM A RECENT LAKE IN BRASILIA-CENTRAL BRAZIL

Gioia, S.M.C.L.[1]; Pimentel, M.M.[1]; Guimarães, E.M[2]; Campos, J.E.G.[3]; Dantas, E.L.[1] and Maruoka, M.T.S.[1]

1. Laboratório de Geocronologia, Instituto de Geociências, Universidade de Brasília, 70910-900, Brasília-DF.
sgioia@unb.br, marcio@unb.br, elton@unb.br
2. Laboratório de Raios-X, Instituto de Geociências, Universidade de Brasília, 70910-900, Brasília-DF.
rxedi@unb.br

Keywords: Brazilian Lake, Pb isotopes, urban lake sediments, atmospheric deposition, X-ray diffraction

INTRODUCTION

The Paranoá Lake, in Brasília, is a forty year-old artificial reservoir. The pollutant sources in Brasilia are limited and the major causes of sediment pollution are: (i) inadequately treated domestic sewage, (ii) location of the sewage treatment plants (from Water and Sewage Company of Brasilia - ET south, ET north - CAESB) in the branches of the lake, (iii) high urban density in the catchments area and (iv) sewage and other contamination transport from tributaries (Altafin et al. 1995). It is necessary to distinguish between anthropogenic and natural inputs, and lead represents an ideal pollution indicator. It is easy to analyse, and is reasonably immobile in environmental sinks (e.g., lake sediments). Although Pb concentrations provide useful information, Pb isotopes have the potential to distinguish between Pb originated from natural sources (rocks, soil) and that from pollution sources (e.g., fuel combustion, sewage, atmospheric deposition).

The primary objectives of the present study are to characterize the different potential sources that will input different lead isotopic compositions into the lake, especially atmospheric deposition, and to elucidate the origin of Pb in sediments of the Lago Paranoá.

Lead concentrations and isotopic compositions were determined on bulk sediments and residues, in order to identify the sources (geogenic or anthropogenic) and to quantify the different Pb inputs.

SAMPLE LOCATION AND LOCAL GEOLOGY

The Lago Paranoá (38 km^2 surface area, 498 x 10^6 m^3 volume, 13m and 40m mean and maximum depths, respectively) is a lake located in the central Brazil, surrounded by the city of Brasilia (15° 48'S and 47° 50'W), at an approximate altitude of 1,000m. Its climate has two well-defined periods: a dry winter (May-September), and rainy summer (October-April). Its main tributaries are the Ribeirão Bananal and the Ribeirão do Torto, to the north, and the Ribeirão do Gama, Riacho Fundo and Cabeça do Veado Creek, to the south (Fig. 1). It has been divided into five compartments (Fig. 1): branch A (Riacho Fundo), branch B (Gama), branch C (Cent zone), branch D (Torto) and branch E (Bananal).

The geological environment consists of low grade metamorphic rocks, comprising pelitic, psammitic and carbonate metasediments. The Meso and Neoproterozoic rocks belong to the Canastra, Paranoá, Araxá and Bambuí groups. The Paranoá Group is the major group exposed in the area, and consists of six units, named from base to top: S- clay-rich metasiltstone, A-slate, R3- sandy metarhythmite, Q3- quartzite (q2- quartzite), R4- clay-rich metarhythmite and PPC- carbonate psammo-pelitic (Fig 2). These are covered by extensive lateritic soil.

RESULTS AND DISCUSSION

X-RAY DIFFRACTION

Clay minerals, together with other fine-grained particles, are released into the bottom sediments during transport. This allows one to trace back the sediment pathway from the depositional area to the source area. It Fourteen sediment samples (depth of 2cm) and one sediment profile from the Torto branch were investigated in this study (Fig. 1)

X-ray diffractometry results for superficial sediment (silt+clay), reveals the presence of quartz, kaolinite, ilite, gibbsite, hematite, rutile, diaspore and anatase.

In compartments C and D quartz is the main mineral, indicating contribution from R3 and Q3 units of the Paranoá Group. Gama and Riacho Fundo branches (compartments B and A, respectively) are richer in illite. At the Bananal branch (E compartment) gibbsite was observed in important proportions compared with the other branches. The influence of soils from the Slate Unit of the Paranoá Group is evident in E compartment, which is confirmed by the increasing abundance of iron rich minerals, such as hematite and goethite.

The core profile from the Torto branch (D compartment) was found like mainly silt-clay fraction quartz, illite, kaolinite and hematite, goethite, rutile and diaspore. Quartz enrichment is observed with depth, and two sections can be distinguished: one between 0 - 29cm and a second between 29-40cm, the latter being the quartz-rich part of the core. The boundary between them probably reflects the moment of creation of the lake in 1959 (Fig. 1).

LEAD ISOTOPES

The samples analyzed represent the upper 2 cm of the sedimentary pile at the bottom of the lake (Fig. 1), Pb isotopic composition and concentration were determined in 14 samples. Pb concentrations isotopic compositions found in the leachates (weakly acid) are presented in figure 1. Pb concentrations found, in general, may be considered normal for sediments, but are distinctively higher in the collection points near the Sewage Stations. Important isotopic differences, however, are observed between the compartments. Pb isotopic composition tends to be more radiogenic (high $^{206}Pb/^{207}Pb$ ratio) in compartments D and B. In branch E, upstream of the ET north plant, $^{206}Pb/^{207}Pb$ ratio is between 1.1869-1.1893, but near the plant it is much lower (1.1526), and some way downstream the composition becomes more radiogenic again. This indicates a simple binary mixing of geogenic with anthropogenic Pb, considering low human activity along tributaries.

A similar behaviour was observed for branch A, but with stronger isotopic contrasts, indicating more than two anthropogenic sources and Pb isotopic composition which is more radiogenic than in branch E ($^{206}Pb/^{207}Pb$ ratio between 1.1932-1.1827. It is likely, therefore, that either the input from the Sewage Tratament Plant in the south is more radiogenic or the sediment flux from tributaries is higher, diluting the anthropogenic effect, with Pb isotopic composition $^{206}Pb/^{207}Pb$ in sediment of 1.2028, upstream the ET south.

Near the Yacht Club, another area of anthropogenic contribution has been detected, with $^{206}Pb/^{207}Pb$ value as low as 1.1700.

D and B compartments are distinguishable from the others by their more radiogenic isotopic compositions (1.1971 and 1.1899, respectively), and lower Pb concentrations. This area suffered a smaller impact and the observed compositions may be closer to the geogenic background (residual phase from the Lago Paranoá sediment samples).

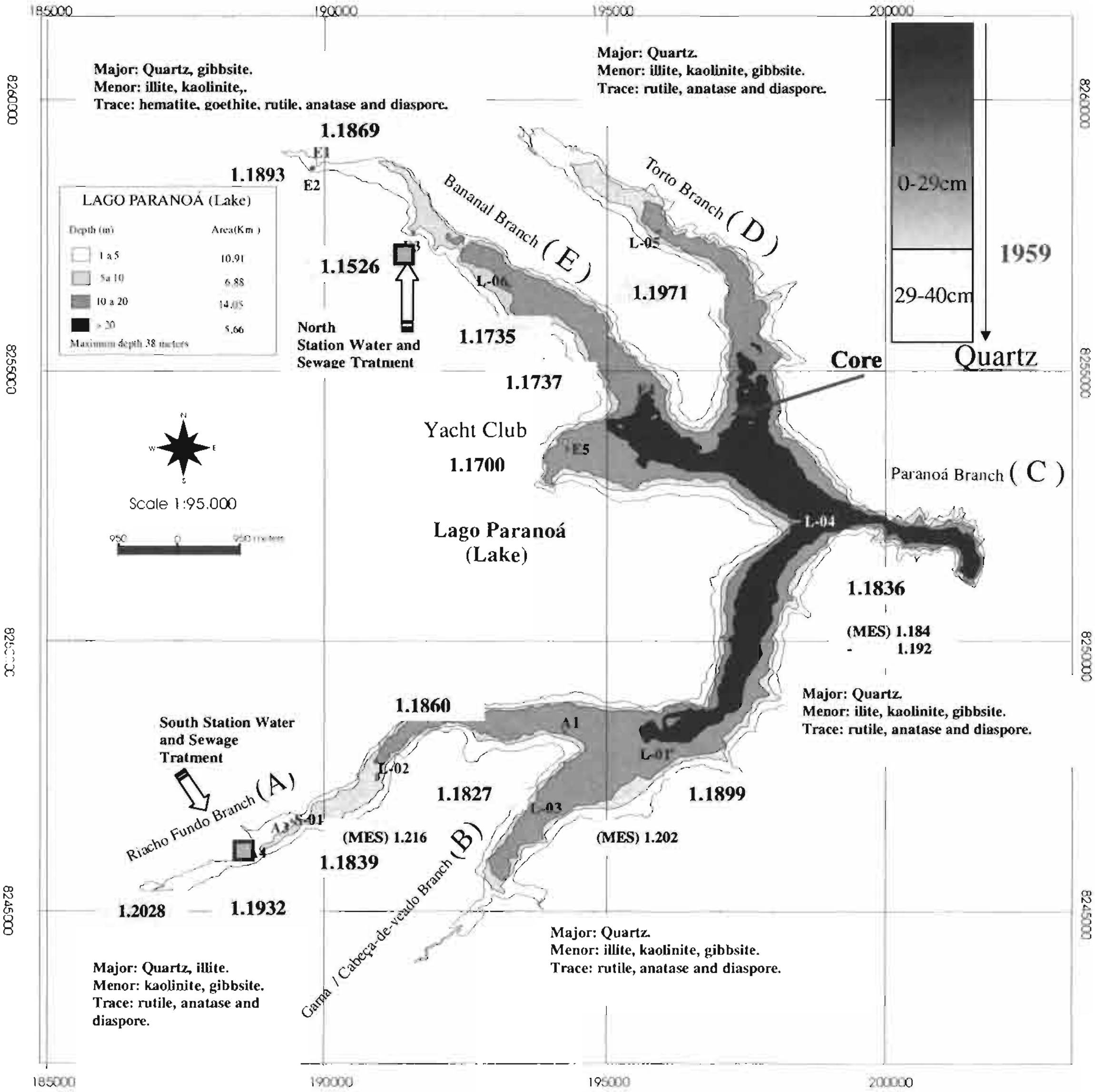

Figure 1. Lago Paranoá showing sample location with respective Pb isotopic composition $^{206}Pb/^{207}Pb$ and mineralogical composition for the branches of the Lago Paranoá. Also the profile (with quartz behaviour) and the depth of lake floor are showed.

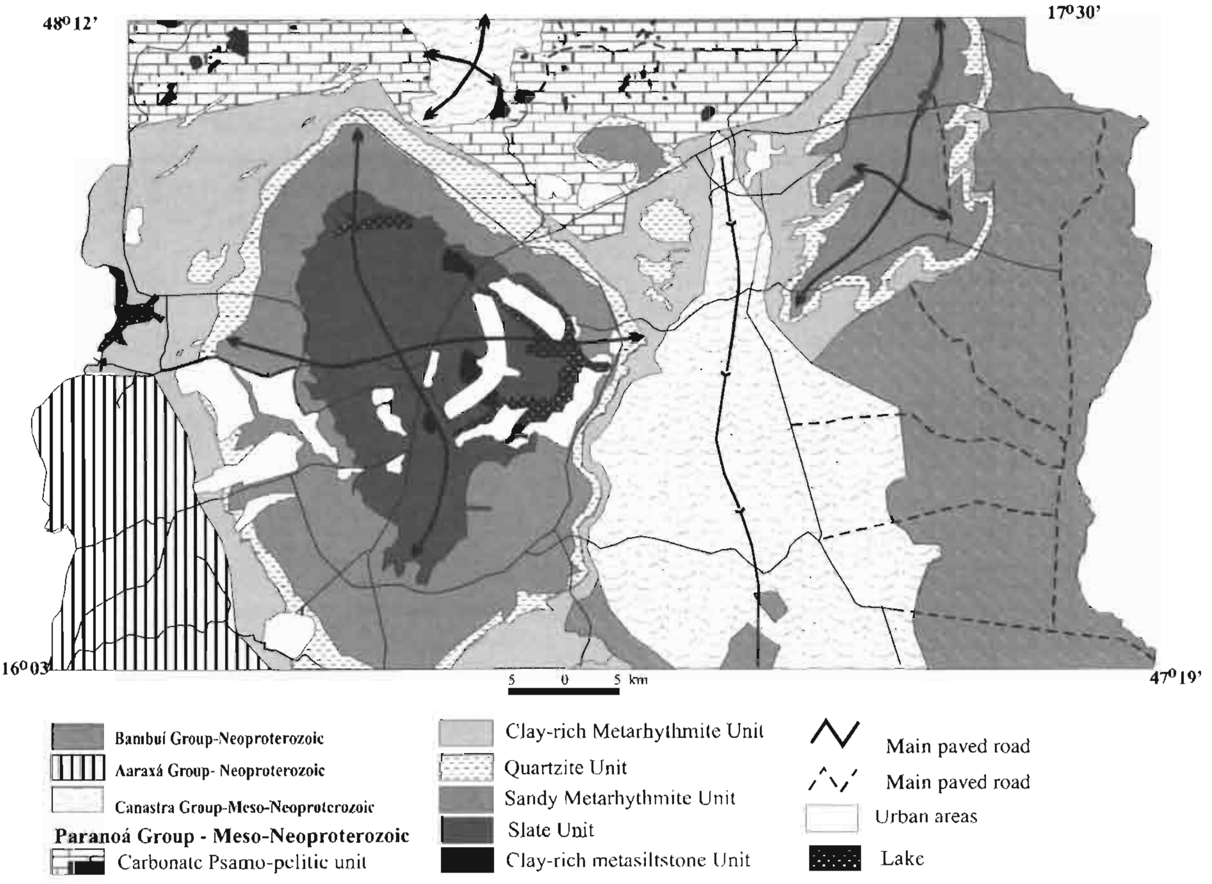

Figure 2. Geologic sketch map of the Distrito Federal (Freitas-Silva & Campos, 1998).

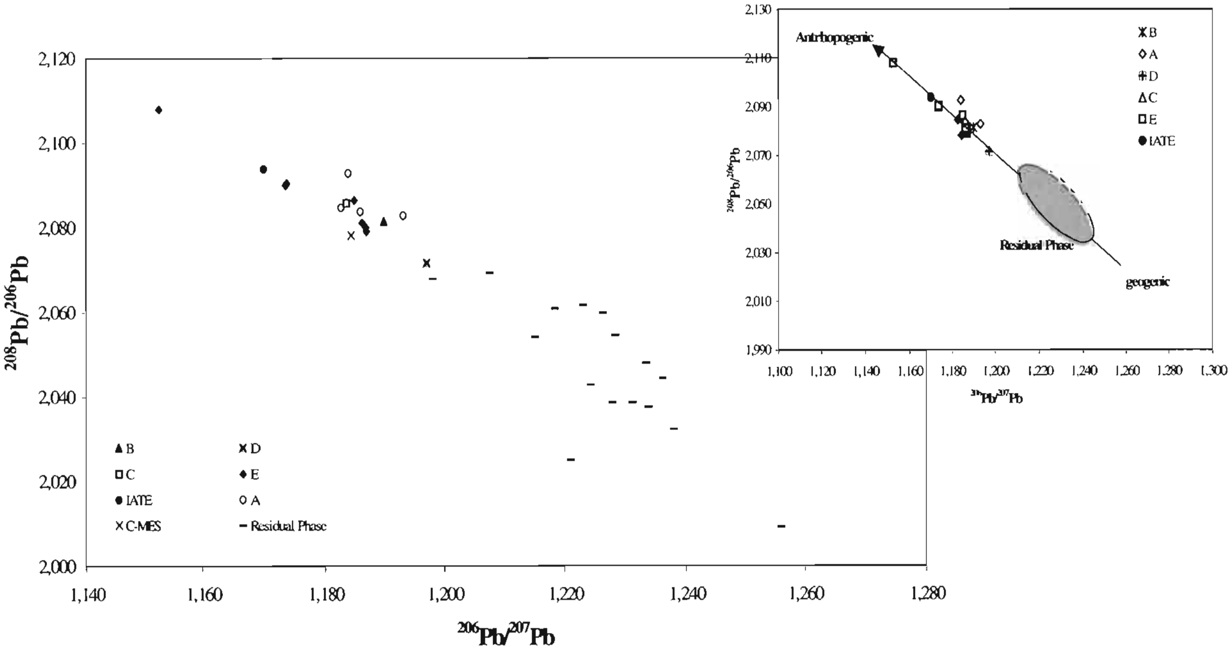

Figure 3. The relationship between $^{206}Pb/^{207}Pb$ and $^{208}Pb/^{206}Pb$ ratios of Lago Paranoá sediments in the branches and in a point near a club and the residual phase for respectively branch and suspend sediment in branch C. The linear data array (inset) compatible with simple binary mixing of geogenic with anthropogenic Pb.

C compartment, that receives sediments from the others branches, presents $^{206}Pb/^{207}Pb$ between the extreme ratios from branches B (radiogenic), and E (anthropogenic ratio). It is evident that Pb isotopic composition in branch C corresponds to a mixture of sediments from the other branches, with the anthropogenic component coming from branches E and A and the natural composition coming from branches D and B.

The geogenic contribution from units R4, R3 and Q3 of the Paranoá Group into the lake, as well as the similarity between the compositions of fuels and the anthropogenic component are clear from Figure 4. In the aerosols in Brasília there is a major input from this anthropogenic source, whose isotopic composition tend to be less radiogenic ($^{206}Pb/^{207}Pb=1.1673-1.1735$) than that found in the lake sediments ($^{206}Pb/^{207}Pb=1.1526-1.1971$). In some cases, however, the aerosols present compositions, which are more radiogenic ($^{206}Pb/^{207}Pb=1.1962-1.2075$) and less thorogenic ($^{208}Pb/^{206}Pb=2.0444-2.0279$), indicating larger contribution from rocks of the Paranoá Group, principally from altered samples. These preliminary values obtained for aerosols collected in Brasilia (UnB) are in close agreement with those from São Paulo-USP (Aily, 2001) and from general work in Brazil (Bollhöfer & Rosman, 2000).

CONCLUSIONS

The present study demonstrates that leachable Pb in sediments of the Lago Paranoá discriminated two possible anthropogenic sources: the proximity with the Sewage Tratament Stations and the atmospheric deposition corresponding mainly to the release of automobile emissions. The Paranoá Group rocks and corresponding soils represent the main geogenic source.

Pb isotopic distributions in the Lago Paranoá are essential for the interpretation of the pollution trends and to distinguish natural and anthropogenic sources.

ACKNOWLEDGEMENTS

The authors thanks the professor Dermeval do Carmo (UnB), geologist Alan Armele and Brasília Water and Sewage Company (CAESB) for help during sample collection in the Lago Paranoá. The authors also thank Shell engineer Adair Narazeth Santos Júnior for fuel samples.

REFERENCES

Aily, C., 2001. Caracterização Isotópica de Pb na atmosfera: um exemplo da cidade de São Paulo. Dissertação de Mestrado. USP. p. 76

Altafin, I.G., Mattos, S.P., Cavalcanti, C.G.B. & Estuqui, V.R., 1995. Paranoá Lake – Limnology and recovery Program. Limnology in Brazil: 325-349.

Bollhöfer, A, & Rosman, K.J.R. 2000. Isotopic source signatures for atmospheric lead in the southern hemisphere. Geochimica et Cosmochimica Acta. 64(19)1: 3251-3262.

Freitas-Silva, F..H. & Campos, J.E.G., 1998. Geologia do distrito Federal. In: Inventário Hidrogeológico e dos recursos hídricos superficiais do Distrito Federal. Vol I. IEMA/UnB.

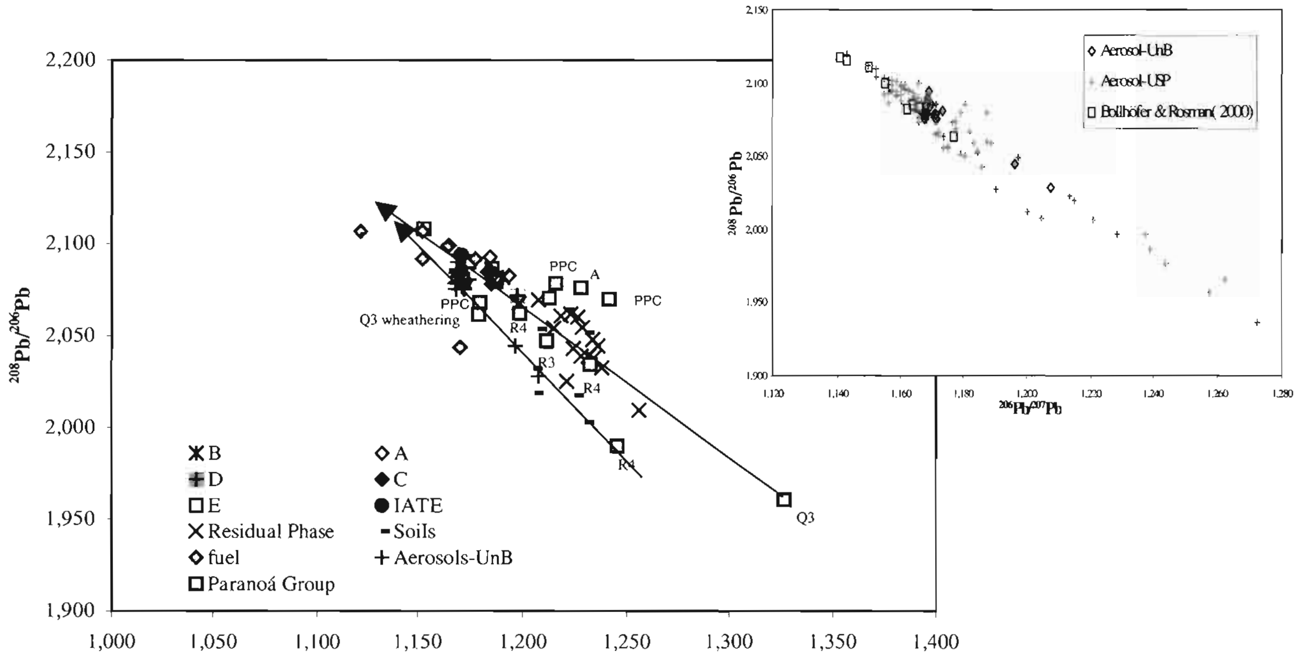

Figure 4. The relationship between $^{206}Pb/^{207}Pb$ and $^{208}Pb/^{206}Pb$ ratios of Lago Paranoá sedments, antrhopogenic and natural sources, and atmospheric deposition in Brasilia-UnB. The linear data array (inset) indicates the similarity between the Pb isotopic compositions to atmospheric deposition in this study with other studies.

ISOTOPIC EVIDENCE FOR BIODEGRADATION IN A SULFATE-RICH BTEX-CONTAMINATED AQUIFER

Knöller, K.[1]; Weise, S.M.[1]; Vieth, A.[2]; Gödecke, S.[3]; Weiss, H.[3] and Schirmer, M.[4]

1. Isotope Hydrology Group, UFZ Centre for Environmental Research, Theodor-Lieser-Str. 4,
D-06120 Halle/Saale, Germany. knoeller@halle.ufz.de
2. Department of Remediation research, UFZ Centre for Environmental Research,
Permoser Str. 15, D-04318 Leipzig, Germany
3. Interdisciplinary Department of Industrial and Mining Landscapes, UFZ Centre for Environmental Research,
Permoser Str. 15, D-04318 Leipzig, Germany
4. Department of Hydrogeology, UFZ Centre for Environmental Research, Theodor-Lieser-Str. 4, D-06120 Halle/Saale, Germany

Keywords: Groundwater, BTEX-contamination, sulfate reduction, stable isotopes, tritium

INTRODUCTION

The mineralization of organic contaminants to carbon dioxide and water by naturally occurring in-situ biodegradation is the basic concept of the natural attenuation of polluted aquifers. Numerous laboratory and field studies have shown that natural attenuation has the capacity to reduce the contaminant concentrations to acceptable levels (e.g. Hinchee et al., 1995; Alleman and Leeson, 1997; Anderson and Lovley, 2000; Fetzner, 1998). One method to assess the in-situ biodegradation is the monitoring of the temporal decrease in concentration of the contaminants. However, such a decrease of contaminant concentrations in a plume can be caused by different processes. Of these processes, only biodegradation leads to a sustainable contaminant reduction. Other processes like dilution or sorption only temporally or locally displace the actual contamination problem.

One possibility to distinguish between real biodegradation and other concentration effects is the assessment of biochemical processes that control the biodegradation at the contaminated site. Sulfate reducing bacteria can contribute extensively to the degradation of organic contaminants and hence dissimilatory sulfate reduction may be a very important process for the long-term natural attenuation of polluted aquifers (e.g. Chapelle et al., 1996; Reinhard et al., 1997; Vroblesky et al., 1996, Davis et al., 1999; Spence et al., 2001).

During the dissimilatory reduction of sulfate, the microorganisms produce hydrogen sulfide to obtain energy for the oxidation of organic carbon provided by the organic contaminants. The preferential utilization of the lighter isotopes by bacteria usually results in the enrichment of the lighter isotope in the produced sulfide and of the heavier isotope in the remaining sulfate (e.g. Kaplan and Rittenberg, 1964; Canfield, 2001). This isotope discrimination enables the detection and quantification of the reduction process by stable isotope measurements.

In this study different isotope methods have been used to characterize the hydrodynamics and to evaluate the potential and extent of bacterial sulfate reduction in an aquifer sequence partly polluted with various BTEX-species.

STUDY SITE

The area of investigation is located on the site of a former hydrogenation plant in the town of Zeitz (Saxonia-Anhalt, Germany, Fig. 1). The plant was set up in 1938 to produce gasoline and lubricants for the German war industry. In 1944 and 1945 severe bombing resulted in the spilling of about 250 m^3 hydrocarbons into the soil. In 1946 the plant was rebuilt and at the beginning of the 1960's part of the plant was upgraded for the production of benzene. Between 1963 and 1990 the plant produced more than 750,000 t of benzene with a maximum production rate in 1979 (79,000 t per year). During the time of operation numerous production accidents and leaks contributed to the BTEX-contamination of the groundwater.

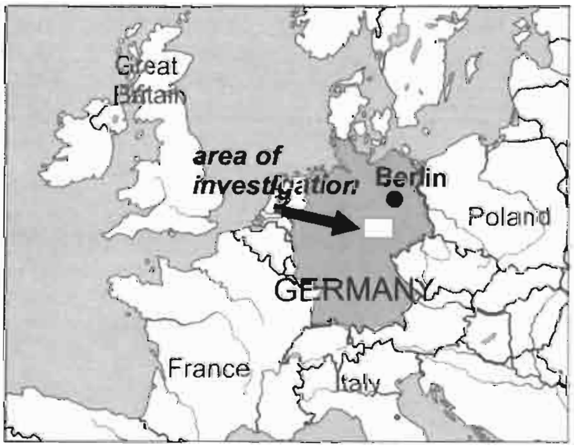

Figure 1. Location of the study area in Central Europe

The aquifer sequence comprises two different aquifers that are separated by silt, clay, and parts of a lignite seam of Tertiary age. The BTEX-contaminations are present in both aquifers. The upper (Quaternary) aquifer (I) mainly consists of sandy and clayey deposits from the Pleistocene Elster-glacial and has a thickness of 5-10m. The lower (Tertiary) aquifer (II) is composed of gravel deposited by an Eocene river. The prevailing contaminants of the upper aquifer are BTEX, dominated by high benzene concentrations up to 850 mg L^{-1}. Toluene concentrations are much lower reaching maximum values of 50 mg L^{-1}. Ethylbenzene and xylene are present in concentrations of a few mg L^{-1} only. Benzene is the dominant pollutant in the lower aquifer as well. . However, total BTEX-concentrations are considerably lower (100 mg L^{-1}) than in the upper aquifer.

Almost 200 groundwater samples have been analyzed for $\delta^{34}S$-SO_4, $\delta^{18}O$-SO_4, $\delta^{18}O$-water, and δD-water. At three sampling locations, groundwater samples for tritium and ^3He analyses were taken from both aquifers trying to match beginning, centre, and end of the contamination plume. Furthermore, isotopic analyses were conducted on the dissolved inorganic carbon in groundwater samples from the immediate area of the contamination plume.

RESULTS

ISOTOPIC COMPOSITION OF THE GROUNDWATER

While most samples exhibit tritium contents of about 10 TU, the groundwater from deepest well has a tritium content of 11.7 TU. Tritiugenic ^3He contents in the upper aquifer ranged from 0 to 3.3 $TU_{equivalent}$ (1 $TU_{equivalent}$ is the ^3He content yielded by the decay of 1 TU tritium) corresponding to ^3He/tritium ratios of 0.31 or less. In the lower aquifer tritiugenic ^3He contents between 19 and 37 $TU_{equivalent}$ were measured and the ^3He/tritium ratio varies in flow direction from 2.0 to 3.1. In terms of apparent groundwater ages these contents correspond to 3 – 5 years in the upper and 10 – 25 years in the lower aquifer (Fig. 2). The samples from the lower aquifer might suggest increasing apparent ages in flow direction.

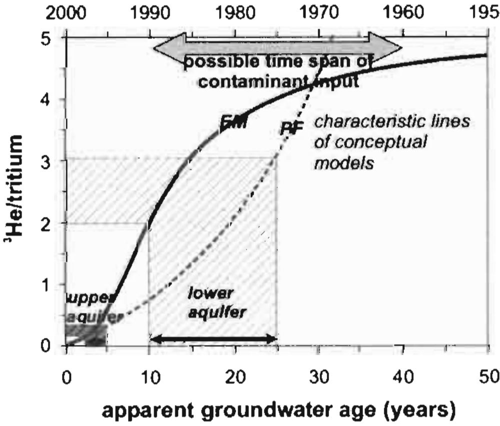

Figure 2. ^3He/tritium ratios of groundwater samples and correlated apparent groundwater ages. The extreme situations piston flow (PF) and exponential mixing (EM) were assumed as flow conditions

The hydrological differences between the upper and the lower aquifer are also expressed by the stable oxygen and hydrogen isotope data of the groundwater samples. While in the upper aquifer the $\delta^{18}O$ values varied between -8.8 and -8.0 ‰ (VSMOW), a much smaller variation between -9.0 and -8.7 ‰ was measured in the lower aquifer. The same differences in the data variability were observed for δD. In general, the stable isotopic composition of the groundwater is in good agreement with the average isotopic composition of the local precipitation. This agreement and the apparent groundwater ages support the assumption that the recharge of the groundwater that is now contaminated occurred within the past 30 years.

ISOTOPIC COMPOSITION OF THE DISSOLVED GROUNDWATER SULFATE

The isotopic composition of the dissolved groundwater sulfate showed a very heterogeneous regional distribution that cannot be explained by a simple mixing pattern. Generally, $\delta^{34}S$-sulfate values ranged from -1 to +48‰ (VCDT). A similar heterogeneity was detected for sulfate concentrations (2 to 1350 mg/L). Smaller variations (+1 to 16‰ VSMOW) were observed for $\delta^{18}O$-sulfate.

Sulfur from historic atmospheric deposition appears to be the predominant sulfate source for the regional groundwater in the upper aquifer. The combustion of sulfur rich lignite in power plants that are located in the closer vicinity of the study site is responsible for a heavy atmospheric sulfate deposition over many decades of the last century. The deposited sulfate was stored in the sediment matrix of the unsaturated zone in the form of different soil sulfur species. Even though the atmospheric deposition decreased by one order of magnitude in the last decade, the stored soil sulfur is still being mobilized by different processes and transported as sulfate into the aquifer.

Some sulfate may derive from the oxidation of pyrite that is present in variable amounts in lignite seams locally occurring in the investigation area. In contrast to the mostly negative $\delta^{34}S$ values of sedimentary pyrites in Tertiary sediments of Germany, the lignite seams also contain pyrite with positive $\delta^{34}S$ values similar to those of the atmospheric deposition. Hence, sulfate from pyrite oxidation cannot be positively recognized by its sulfur isotope signature. Due to the oxidation mechanism and the incorporation of isotopically light water-derived oxygen into the sulfate molecule, however, sulfate from pyrite oxidation can be identified by its characteristically low $\delta^{18}O$ values compared to the sulfate from atmospheric deposition.

Increasing $\delta^{34}S$ values and simultaneously decreasing sulfate concentrations along the groundwater flow path in the northern outflow of the contaminant plume indicate the occurrence of bacterial sulfate reduction (Fig. 3). While sulfate concentration drop from over 300 to less than 20mg/L, $\delta^{34}S$ values increase up to +45‰ (VCDT). Using a Rayleigh model for the reduction process, an isotope enrichment factor (ε) of ca. -12‰ was obtained. This value appears to be relatively low compared to fractionation factors for sulfur observed in laboratory experiments with toluene degrading bacteria (Bolliger et al., 2001) or in not contaminated aquifers (e.g. Foulliac et al., 1990; Bottrell et al., 1991; Asmussen and Strauch, 1998; Bottrell et al., 2000) but is consistent with recently reported data from similar case studies (Knöller et al. 2003, Spence et al., 2001). In contrast to the enrichment of ^{34}S, no enrichment of ^{18}O in the remaining sulfate was observed (Fig. 3). This is probably due to the specific reaction mechanism that results from the high concentration of organic carbon and the relatively low sulfate concentrations. This mechanism inhibits the oxygen isotope exchange between sulfate and water during the reduction process and hence disables the ^{18}O enrichment in the remaining sulfate. A similar behavior of the oxygen isotopes in the dissolved sulfate was reported by Spence et al. (2001) for bacterial sulfate reduction in a phenol contaminated aquifer.

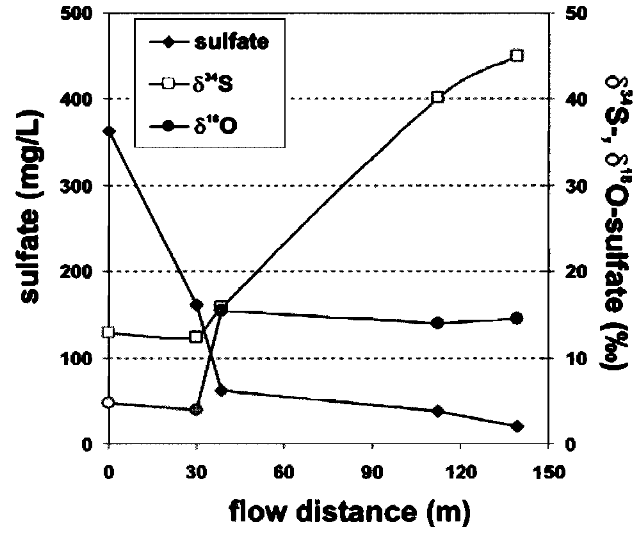

Figure 3. Sulfate concentrations and isotopic sulfate composition of groundwater samples from the northern outflow of the contamination plume.

The $\delta^{13}C$ values of the dissolved inorganic carbon (DIC) decrease slightly in flow direction in the contamination plume from -22.4 ‰ to -23.7 ‰ (VPDB). One product of the bacterial sulfate reduction is isotopically light carbon dioxide. When this CO_2 is added to the DIC pool in the groundwater, a negative isotopic shift of the isotopic DIC composition, as observed in the examined samples, occurs.

CONCLUSIONS

The isotopic investigation of water and solutes in two aquifers at the BTEX contaminated site Zeitz (Germany) revealed that the decrease of BTEX concentrations is due to biodegradation leading to a sustainable contaminant reduction. To a large extent the biodegradation is controlled by bacterial sulfate reduction. Even though part of the contamination is almost 45 years old, no water older than 30 years seems to be affected by the contaminants. This suggests that the present biodegradation rate inhibits a widespread distribution of the pollutants in the flow direction of the aquifer.

REFERENCES

Alleman, B.C. and Leeson, A. (eds.), 1997. In situ and on-site bioremediation. Vol. 1, Battelle Press, Columbus, OH

Anderson R.T. and Lovley, D.R., 2000. Anaerobic bioremediation of benzene under sulfate-reducing conditions in a petroleum contaminated aquifer. Environ. Sci. Technol. 34, 2261-2266

Asmussen, G. and Strauch, G., 1998. Sulfate reduction in a lake and the groundwater of a former lignite mining area studied by stable sulfur and carbon isotopes. Water, Air, and Soil Pollution 108, 271-284

Bottrell, S.H., Moncaster, S.M., Tellam. J.H., Lloyd, J.W., Fisher, Q.J. and Newton, R.J., 2000. Controls on bacterial sulphate reduction in a dual porosity aquifer system: the Lincoln Limestone aquifer, England. Chemical Geology 169, 461-470

Bottrell, S.H., Smart, P.I., Whitaker, F., and Raiswell, R., 1991. Geochemistry and isotope systematic of sulfur in the mixing zone of Bahamian blue holes. Applied Geochemistry 6, 97-103

Canfield, D.E., 2001. Isotope fractionation by natural populations of sulfate-reducing bacteria. Geochim. Cosmochim. Acta 65, 1117-1124

Chapelle, F.H., Bradley, P.M., Lovley, D.R. and Vroblesky, D.A., 1996. Measuring rates of biodegradation in a contaminated aquifer using field and laboratory methods. Ground Water 34, 691-698

Davis, G.B., Barber, C., Power, T.R., Thierrin, J., Patterson, B.M., Payner, J.L. and Qinglong Wu, 1999. The variability and intrinsic remediation of a BTEX plume in anaerobic sulphate-rich groundwater. Journ. Contam. Hydrol. 36, 265-290

Fetzner, S., 1998. Bacterial degradation of pyridine, indole, quinoline, and their derivates under different redox conditions. Appl. Microbiol. Biotechol. 49, 237-250

Foulliac, C., Foulliac, A.M. and Criaud, A., 1990. Sulphur and oxygen isotopes of dissolved sulfur species in formation waters from the Dogger geothermal aquifer, Paris, France. Applied Geochemistry 5, 415-429

Hinchee, R.E., Wilson, J.T. and Downey, D.C. (eds.), 1995. Intrinsic bioremediation. Battelle Press, Columbus, OH

Kaplan, I.R. and Rittenberg, S.C., 1964. Microbiological fractionation of sulphur isotopes. Journal Gen. Microbiology 34, 195-212

Knöller, K., Fauville, A., Mayer, B., Strauch, G., Friese, K. and Veizer, J., 2003. Sulfur cycling in an acid mining lake and its vicinity in Lusatia, Germany. Chemical Geology, in press

Reinhard, M., Shang, S., Kitanidis, P.K., Orwin, E., Hopkins, G.D. and Lebron, C.A., 1997. In situ BTEX biotransformations under enhanced nitrate- and sulfate-recucing conditions. Environ. Sci. Technol. 31, 28-36

Spence, M.J., Bottrell, S.H., Thornton, S.F. and Lerner, D.N., 2001. Isotopic modeling of the significance of bacterial sulphate reduction for phenol attenuation in a contaminated aquifer. Journal of Contaminant Hydrology 53, 285-304

Vroblesky, D.A., Bradley, P.M. and Chapelle, F.H., 1996. Influence of electron donor on the minimum sulfate concentration required for sulfate reduction in a petroleum hydrocarbon-contaminated aquifer. Environ. Sci. Technol. 30, 1377-1381.

APPLICATION OF STABLE ISOTOPE TRACERS TO EVALUATE THE SULFUR CYCLE IN MINING LANDSCAPES OF EASTERN GERMANY

Knöller, K.[1]; Strauch, G.[2]; Trettin, R.[1] and Mayer, B.[3]

1. Isotope Hydrology Group, UFZ Centre for Environmental Research, Theodor-Lieser-Str. 4, D-06120 Halle/Saale, Germany. knoeller@halle.ufz.de
2. Department of Hydrogeology, UFZ Centre for Environmental Research, Theodor-Lieser-Str. 4, D-06120 Halle/Saale, Germany
3. Departments of Geology & Geophysics and Physics & Astronomy, University of Calgary, 2500 University Drive NW, Calgary, Alberta, Canada, T2N 1N4

Keywords: Groundwater, lignite mining lake, sulfide oxidation, sulfate reduction, stable isotopes

INTRODUCTION

Throughout the 20th century, extensive open pit mining of lignite in the Tertiary lignite districts of Eastern Germany resulted in dramatic changes of landscape and of the hydrologic system. The hydrogeological rehabilitation in these mining areas by flooding of the abandoned mining pits or groundwater rise causes long term changes of the groundwater quality. One result of this process is the formation of numerous mining lakes, of which a large number has pH values of less than 4. Oxidation of sulfide minerals in aerated zones of the mine dumps generates dilute sulfuric acid, which is often transported with the groundwater into the mining lakes. This continuous formation of dilute sulfuric acid often resulted in sustained acid conditions of the lakes long after cessation of mining operations. The Tertiary sediments surrounding the established or forming mining lakes contain variable quantities of sedimentary sulfides (pyrite/marcasite). Consequently, the sedimentary and dissolved sulfur species, and their transformations, play a key role in the hydrochemical development of the lake and of the local groundwater. Oxidation of reduced inorganic sulfur compounds generates acidity, which might reach the groundwater and/or the lake. This process is known as the strongest naturally occurring acidification reaction (2 mol H^+ for each mol FeS_2) (Singer and Stumm, 1970) and well studied in the huge literature of acid mine drainage formation (e.g. Alpers and Blowes, 1994). In contrast, bacterial (dissimilatory) sulfate reduction produces alkalinity, if the formed H_2S is fixed in sedimentary sulfide minerals, and hence may facilitate the neutralization of lake water and groundwater (Schindler et al., 1980; Brown, 1985; Rudd et al., 1986; Spratt et al., 1987; Spratt and Morgan, 1990; Vile and Wieder, 1993; Blodau et al., 1998). Effective remediation measures for acid mining lakes and their surroundings in the lignite districts of Eastern Germany must therefore take into account the relative importance of these two processes, sulfide oxidation and bacterial (dissimilatory) sulfate reduction. Stable isotope studies could serve as a tool to separate both processes, identify sources and describe pathways and rates of transformations (e.g. Harrison and Thode, 1958; Kaplan and Rittenberg, 1964; Toran and Harris, 1989; Taylor and Wheeler, 1994; Knöller and Strauch, 1999; Knöller, 2000; Mandernack et al., 2000; Knöller and Strauch, 2002). Quantification of sulfur sources and transformations is essential if we are to understand the current hydrochemical status of lignite mining areas and propose successful remediation strategies. In this study, we utilize stable isotope ($\delta^{34}S_{sulfate}$, $\delta^{18}O_{sulfate}$, $\delta^{34}S_{dissolved\ sulfide}$, $\delta^{18}O_{water}$) and hydrochemical data of lake and groundwater samples as well as the concentrations and isotope ratios of various sedimentary sulfur compounds (acid soluble sulfate, acid volatile sulfur, chromium reducible sulfur) in aquifer and lake sediments, for assessing the biogeochemical sulfur cycle in lignite mining areas of the lignite districts in Eastern Germany.

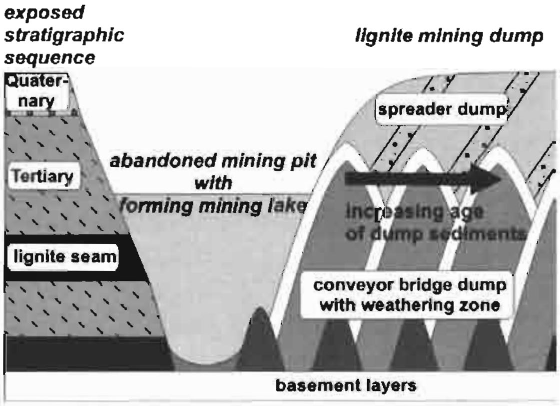

Figure 1. Schematic cross section of a typical lignite mining landscape.

STUDY SITES

If carried out by the conveyor bridge technology, open pit lignite mining produces typical landscapes that comprise three basic structural elements. These elements are the undisturbed sediments that are exposed to the atmosphere, the mining void that results from the removal of sediment material and lignite and that later becomes the mining lake, and the mining dump where the sediments that overlaid the lignite seam are deposited as a heterogeneous mixture (Fig. 1). The mining dump itself can be vertically divided into two genetically different sections, the conveyor bridge dump (CBD) with its typical rib structure that is caused by the movements of the conveyor bridge and the spreader dump (SD) on top of the CBD. While the CBD is dominated by material from Tertiary sediments, the SD mainly consists of

Quaternary material. Usually, the SD is deposited 5 to 10 years later than the CBD leaving the surface of the sulfide containing CBD exposed to atmospheric oxygen for a long time. During that exposure time, sulfide oxidation occurs in the uppermost layers of the CBD. The oxidation products are stored in the sediment matrix, in a so-called weathering zone.

Between the three structural elements intense hydrochemical and geochemical interactions take place that strongly influence the quality development of the lake water and groundwater. These interactions were studied at three different abandoned lignite mining sites in the Central German and the Lusatian Lignite District (Fig. 2).

Figure 2. Location of the study areas in Central Europe.

THE GOITSCHE AREA

The lignite mining area Goitsche had been exploited from 1949 to 1991. Since the flooding is not yet completed it represents the hydrogeologically most instable system of the three investigated areas. The lignite deposits present in the study area can be referred to the epirogenetic formation type. Underneath the exploited lower Miocene Bitterfelder lignite seam with a thickness of about 5 to 11 m lie the Bitterfelder mica sands of Tertiary age. These sediments contain variable amounts of sedimentary sulfides. The Quaternary sediments in the Bitterfeld region can be divided into a lower and an upper Weichselian gravel terrace. The mining process produced four residual mining voids. The future water surface of the whole mining lake including all four subbasins will cover an area of about 13 km^2. The main flooding sequence was started in May 1999 by river water from the nearby river Mulde. Prior to the start of the flooding, precursor lakes were formed in three subbasins by rising groundwater. Since the river water shows a relatively low mineralization and the groundwater flow comes from undisturbed sediments that are not significantly affected by sulfide oxidation, only a minor impact of the mining activities on the lake water quality is expected at the Goitsche site.

THE COSPUDEN AREA

In the larger mining area of Cospuden, located at the southern border of the city of Leipzig within the Central German Lignite District, lignite from the Tertiary lignite seams (Bornaer Hauptflöz) has been mined since 1950. The investigated Cospuden mine was closed in 1990 after only ten years of operation. During active mining the groundwater level was lowered to 80m below ground. After the cessation of mining operations, the Cospuden mine was filled by rising groundwater from the Early Weichsel glacial terrace aquifer (about 90%) and from the dump site located south of the lake (10%). From 1996 to 2000 the Cospuden open pit was re-planted and additionally flooded by river water from the nearby river Weisse Elster and by processing water from other active mining areas in the region. The flooding which was completed in 2000 resulted in a lake that covers a surface area of 4 km^2. Despite the completion of the flooding, no stable hydrogeological conditions have been established in the surrounding of the lake yet.

THE PLESSA AREA

Lignite exploitation in the Plessa open pit mine, which encompasses mining lake ML111, ceased in the late 1950's and the residual depressions were flooded by the ascending groundwater. The flooding was completed in 1969. Comparison of hydrochemical results from the 1970's with the more recent data suggests that the lake has undergone only minor changes in its hydrochemical conditions since the completion of the flooding.

The mining lake is 900m long and a maximum of 140m wide, with the surface area of 110,000m^2. The lake consists of three basins of comparable size separated by narrow zones of shallow water. The western shore of the ML 111 is formed by undisturbed Tertiary sediments, estuarine carbonaceous sulfide- and mica-containing silts and sands with small lignite seams (Schreck and Gläßer, 1998). The eastern, northern, and southern shores of the lake are flanked by dump sediments composed mainly of mixtures of Tertiary sediments re-deposited by mining activities. Quaternary sediments were almost completely removed from the immediate mining area and re-deposited some hundred meters west of the lake. ML111 receives groundwater influx from two sources, the western aquifer on the southwestern shore and the dump aquifer south of the lake. The water balance of lake, calculated by Knöller and Strauch (2002), suggests an annual groundwater influx of 23,700m^3, with 13,000m^3 coming from the southern dump aquifer and 10,700m^3 from the southwestern part of the western aquifer.

RESULTS

THE GOITSCHE AREA

The dominating process of the sulfur cycle of the mining lake is the mixing of sulfate from flooding water from the Mulde River ($\delta^{34}S$: +4‰ VCDT) with an initial sulfate type ($\delta^{34}S$: -10‰) that itself represents a mixture of sulfate from sulfide oxidation ($\delta^{34}S$: ca. -20‰) and from groundwater that is not affected by sulfide oxidation ($\delta^{34}S$: ca. 0‰). In the initial stage of the flooding, the separate basin Döbern showed different characteristics that are related to the influence of the local groundwater. The disastrous 2002 flood caused a change of $\delta^{34}S$ towards the river water signature as well as the accidental establishment of the final flooding level. Therefore, further hydrochemical changes are only defined by lake water - groundwater interactions. Isotopic evidence for the occurrence of bacterial sulfate reduction was not observed in the Goitsche area.

THE COSPUDEN AREA

Since the lake water mineralization of Lake Cospuden is relatively moderate, the investigations in the Cospuden area were focused on the hydrochemical development of the mining dump. Due to the interactions between dump and mining lake this development can have a significant effect on the future water quality of the lake especially with respect to its utilization as a recreation area.

In the spreader dump, the sulfate concentration and the $\delta^{34}S$ correlate with the age of the mining dump in a way characteristic for sulfate reduction (Fig. 3). The annual degradation rate of sulfate by bacterial reduction has been calculated to 0.6mmol $l^{-1}a^{-1}$ using initial values for $\delta^{34}S$ of the dissolved sulfate of -13.5‰ and for SO_4^{2-} concentrations of 1,900mg L^{-1}. The degradation of sulfate was also confirmed by the $\delta^{18}O$ values of sulfate in correlation with the sulfate content and $\delta^{34}S$. Exceptions from the general trend are possibly caused by the isotopic variability of the local sulfur source and/or by a different extent of sulfate reduction due to variable hydrochemical conditions. From the correlation of $\delta^{18}O$-SO_4^{2-} with the sulfate concentration an enrichment factor ε for ^{18}O of -7‰ was calculated using the modified Rayleigh equation.

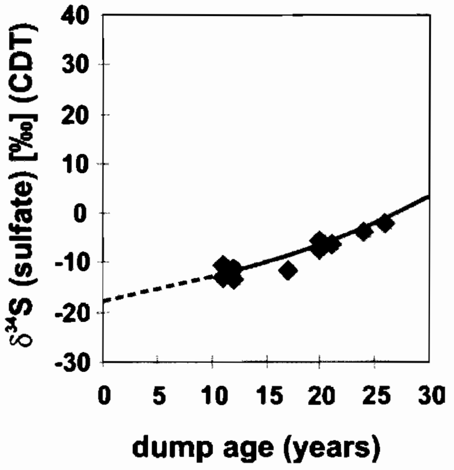

Figure 3. Correlation between dump age and $\delta^{34}S$-sulfate (spreader dump, Cospuden area).

In contrast to the clear reduction trend in the SD, the $\delta^{34}S$ and the concentration of dissolved sulfate do not correlate with the age structure of the conveyor bridge dump. This fact was again related to the heterogeneity of the conveyor bridge dump resulting in variable initial sulfate concentrations, to possible influences of the weathering zone on top of the CBD, and to a variable sulfate reduction rate. However, the significant enrichment of the heavy sulfur and oxygen isotopes up to 0‰ (VCDT) and +3‰ (VSMOW) at some sampling locations (compared to initial values of -22‰ and -2‰) proves the local occurrence of dissimilatory sulfate reduction in the CBD.

THE PLESSA AREA

Sulfate concentrations in the Quaternary/Tertiary aquifers varied between 40 and 700 mg/l, whereas sulfate concentrations of up to 4300 mg/l were observed in dump water. Sulfur isotope ratios of dissolved sulfate in groundwater from Tertiary and Quaternary aquifers ranged from -9.9 to +23.1 ‰. Dissolved sulfate in the dump water showed generally positive $\delta^{34}S$ values ranging from +7 to +32 ‰. Increasing $\delta^{34}S$ and $\delta^{18}O$ (SO_4) values and simultaneously decreasing sulfate concentrations (Fig. 4) indicate that bacterial (dissimilatory) sulfate reduction is an important process for the natural attenuation of the mining induced acidification in groundwater in the northern part of the study area.

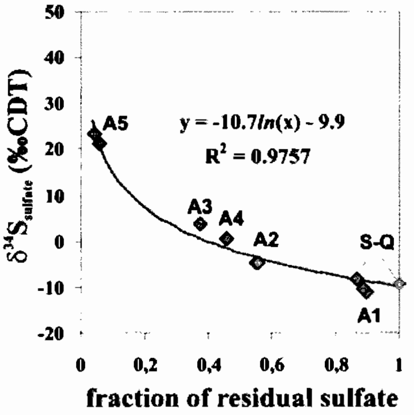

Figure 4: Correlation between fraction of residual sulfate and $\delta^{34}S$-sulfate (aquifer, Plessa area).

Several lines of evidence suggest that ML 111 receives groundwater influx from two sources, the Quaternary/Tertiary aquifers on the southwestern shore and from the dump site to the south of the lake. The average concentrations and $\delta^{34}S$ values of sulfate in the inflow from the aquifers were 700 mg/l and -9.9 ‰, respectively. Groundwater inflow from the dump had an average sulfate content of 2200 mg/l and a mean $\delta^{34}S$ value of +7‰. This resulted in sulfate concentrations between 1000 and 1900 mg/l and $\delta^{34}S$ values of lake water sulfate between +3.0 and +5.5 ‰. Concentrations and $\delta^{34}S$ values of lake water sulfate increased with depth indicating that influx of groundwater from the dump, and not bacterial (dissimilatory) sulfate reduction in the lake was responsible for the increasing $\delta^{34}S$ values.

Lake sediments were obtained from a site in 7m depth and from the deepest location in the lake (10m). Contents and isotope ratios of acid soluble sulfate (ASS), acid volatile sulfur (AVS), and chromium reducible sulfur (CRS) were determined. Sediments from 7m depth were representative for most of the lake. Their sulfur contents ranged from 30 mg g^{-1} near the water/sediment interface to less than 5 mg g^{-1} below 20 cm depth. Sulfur was found almost exclusively in form of sulfate with $\delta^{34}S$ values similar to those of lake water sulfate. At the deepest location of the lake, sedimentary S contents varied between 1 and 15 mg g^{-1}. Sulfate comprised typically more than 50% of total sedimentary S and had sulfur isotope ratios similar to that of lake water sulfate. In the uppermost 20 cm of the core, there were also significant amounts of inorganic reduced sulfur (AVS and CRS) with $\delta^{34}S$ values varying between -20 and -40 ‰. The occurrence of acid volatile sulfur with $\delta^{34}S$ values between -30 and -40 ‰ was interpreted as evidence for bacterial (dissimilatory) sulfate reduction in the shallow sediments at the deepest location of the lake, but this process was found to be not of major importance for sulfur fluxes in the entire lake ML 111.

CONCLUSIONS

The example from the Goitsche area shows that lignite mining not necessarily leads to an acidification and to high loads of sulfate. The rapid flooding of the mining lakes by river water suppresses the effects of sulfide oxidation. In those cases, sulfur transformations are limited to mixing of dissolved sulfate from different sources especially due to the water exchange between lake and aquifer. The results from the Cospuden area illustrate that, even though the lake water quality is good, surrounding sediments and the water therein can be extensively polluted. If the flooding is performed by rising groundwater and the sediments have a low buffer capacity (as in the Plessa area) then sustained acidic conditions in lake and groundwater can form.

Bacterial sulfate reduction seems to be the only relevant process that enables a long-term auto-regeneration of the water quality. The occurrence and the extent of sulfate reduction in lignite mining areas are strongly controlled by the present environmental conditions. Ongoing transport of oxygen into dump sediments, the subsequent oxidation of pyrite, and the mobilization of stored oxidation products inhibit the formation of sustained reducing conditions and hence limit the effect of the bacterial sulfate reduction on the water quality improvement.

REFERENCES

Alpers, C.N. and Blowes, D.W., 1994. Environmental geochemistry of sulfide oxidation. ACS Book Series, Washington.

Blodau, C., Hoffmann, S., Peine, A. and Peiffer, S., 1998. Iron and sulfate reduction in the sediments of acidic mine lake 116 (Brandenburg, Germany): Rates and geochemical evaluation. Water, Air and Soil Pollution 108, 249-270.

Brown, K.A., 1985. Sulphur distribution and metabolism in water-logged peat. Soil Biology and Biochemistry 17, 39-45.

Harrison, A.G. and Thode, H.G., 1958. Mechanism of the bacterial reduction of sulphate from isotope fractionation studies. Transactions of the Faraday Society 54, 84-92.

Kaplan, I.R. and Rittenberg, S.C., 1964. Microbiological fractionation of sulphur isotopes. Journal Gen. Microbiology 34, 195-212.

Knöller, K., 2000. Anwendung stabiler Umweltisotope zur Bewertung hydrochemischer Zustände und Prozesse in Folgelandschaften des Braunkohlebergbaus. Ph.D. Thesis, University of Leipzig, UFZ-Report Nr. 33/2000, ISSN 0948-9452, 153 pp.

Knöller, K. and Strauch, G., 1999. Assessment of the flow dynamic of a mining lake by stable isotope investigations. Isotopes in Environmental and Health Studies 35, 75-83.

Knöller, K., Strauch, G., 2002. The application of stable isotopes for assessing the hydrological, sulfur, and iron balances of acidic mining lake ML111 (Lusatia, Germany) as a basis for biotechnological remediation. Water, Air and Soil Pollution: Focus 2, 3-14.

Mandernack, K.W., Lynch, L., Krouse, H.R. and Morgan, M.D., 2000. Sulfur cycling in wetland peat of the New Jersey Pinelands and its effect on stream water chemistry. Geochimica et Cosmochimica Acta 64, 3949-3964.

Rudd, J.W.M., Kelly, C.A., St. Louis, V, Hesslein, R.H., Furutani, A. and Holoka, M.H., 1986. The role of sulfate reduction in long term accumulation of organic and inorganic sulfur in lake sediments. Limnology and Oceanography 31, 1281-1291.

Schindler, D.W., Wagemann, R., Cook, R.B., Ruszczynski, T. and Prokopowich, J., 1980. Experimental acidification of Lake 223, experimental lake area: background data and the first three years of acidification. Canadian Journal of Fishery and Aquatic Sciences 37, 342-354.

Schreck, P. and Gläßer, W., 1998. Regional geology of the lignite mining districts in Eastern Germany. In Geller, W., Klapper, H. and Salomons, W. (eds.), Acidic mining lakes, Springer, Berlin, Heidelberg, New York, 15-24.

Singer, P.C. and Stumm, W., 1970. Acidic mine drainage: the rate determining step. Science 167, 1121-1123.

Spratt, H.G. and Morgan, M.D., 1990. Sulfur cycling in a cedar-dominated, freshwater wetland. Limnology and Oceanography 35, 1586-1593.

Spratt, H.G., Morgan, M.D. and Good, R.E., 1987. Sulfate reduction in peat from a New Jersey Pinelands cedar swamp. Applied Environmental Microbiology 53, 1406-1411.

Taylor, B.E. and Wheeler, M.C., 1994. Sulfur- and oxygen isotope geochemistry of acid mine drainage in the Western United States. In: Alpers, C.N. and Blowes, D.W. (eds.), Environmental geochemistry of sulfide oxidation, American Chemical Society Symposium Series 550, Washington D.C., 481-514.

Toran, L. and Harris, R.F., 1989. Interpretation of sulfur and oxygen isotopes in biological and abiological sulfide oxidation. Geochimica et Cosmochimica Acta 53, 2341-2348.

Vile, M.A. and Wieder, R.K., 1993. Alkalinity generation by Fe(III) reduction versus sulfate reduction in wetlands constructed for acid mine drainage treatment. Water, Air and Soil Pollution 69, 425-441.

ENVIRONMENTAL ISOTOPES AND THE ANALYSIS OF THE ORIGIN OF GROUNDWATER SALINITY IN THE CABO AQUIFER IN RECIFE COASTAL PLAIN, PERNAMBUCO, BRAZIL

Lima, E.S.[1]; Montenegro, S.M.G.[2] and Montenegro, A.A.[3]

1. Geology Department, Federal University of Pernambuco. delima@ufpe.br.
2. Civil Engineering Department, Federal University of Pernambuco. suzanam@ufpe.br
Av. Acad. Hélio Ramos, s/n. Cidade Universitária. Recife-PE, Brazil, 50.740-530
3. Federal Rural University of Pernambuco

Keyworks: Environmental isotopes, salinization, coastal aquifer, groundwater, seawater intrusion

INTRODUCTION

The over-exploitation of groundwater and the difficulties in recharging the aquifers in the highly urbanized areas of Recife Metropolitan Region (RMR) has severely depleted the potenciometric levels of the aquifers in the last 20 years and increased their vulnerability to seawater intrusion. Many wells have been abandoned as a consequence of high salinity content in the groundwater. A monitoring program has been established to assess the groundwater salinity in the most extensively exploited area in Recife coastal plain. This paper presents the results of part of the monitoring program and analyses the causes for the high salinity levels in some points, based on environment isotope analysis.

GEOLOGY

The aquifers in the RMR are classified as: 1) fractured aquifer (Basement rocks plain) and 2) porous aquifer (Northern Sedimentary and Recife Coastal plains). The Recife Coastal plain occupies an area of 112 km^{2}in the southern part of RMR and includes two interstitial aquifers: Cabo and Boa Viagem. The Cabo aquifer comprises sandstones, siltstones and mudstones, with average thickness of 90 m. The Boa Viagem aquifer, an unconfined formation comprises sand, silt and clay, with an average thickness of 40 m. The Beberibe aquifer occurs in the Northern Sedimentary plain, with average thickness of 100 m of sandstones with intercalations of mudstone. Both Beberibe and Cabo aquifers are semi-confined formations. Although the Beberibe aquifer is the most important formation in terms of water storage, the Cabo aquifer is the most exploited. The Boa Viagem aquifer overlies both the Beberibe and Cabo aquifer and is the most vulnerable formation in terms of water quality, as a consequence of strong leakage from many septic tanks and some sewers since the public sewage system in the RMR is very deficient; and due to connection to mangroves and rivers estuaries. Since the area is highly urbanized, recharge from rainfall is decreasing throughout the years.

GROUNDWATER EXPLOITATION

Population growth and deficiencies in the public water supply system have led to an intensively exploitation of groundwater. The use of groundwater without control, mainly in the Cabo aquifer, has led to an over-exploitation situation. The number of production wells has increased dramatically with the urbanization process. The majority of the active wells are private. This over-exploitation has changed potentiometric gradients between the upper and the lower aquifers, and between the sea and the lower aquifer. Now, in some places, head gradients produce flow from the sea towards the continent, with high risk of seawater intrusion and in some places from upper to lower aquifer (Costa et al., 1998). This makes the Cabo aquifer vulnerable to diffuse contamination.

Recently, Government agencies started controlling the drilling and exploitation of groundwater by private wells. However, the technical information about the wells is, in general, not satisfactory. An information system software was developed and implemented (Cabral et al., 2000) to compile all the available data on the active wells.

A recent study funded by the Canadian International Development Research Center (IDRC) (Costa et al., 1998) has showed that the massive exploitation of the aquifers in the coastal plain has deteriorated the system both in terms of groundwater quality and quantity. During this period, piezometric levels were lowered up to 70 m in some areas (Costa et al., 1998). One of the major problems related to the groundwater quality in this system is the high salinity level observed in some wells. Seawater intrusion and hydraulic interconnection to mangroves and estuarine areas have been pointed out as the main causes for the increasing salinity in this intensively exploited coastal aquifer system. The main contribution of the reported study was the proposal of a groundwater management plan for the Cabo aquifer. According to this plan, all the new-drilled wells should encompass devices to allow evaluation of groundwater level and discharge rate. It also established control zones, each of which with a maximum extraction rate per single well. In one of these zones, drilling would no longer be permitted. At that time, the management plan was not implemented due to a severe water supply shortage (up to seven days without by one day with running water) caused by a drought that occurred in the Northeast Brazil in 1998 and 1999, when the annual rainfall volume was less than 65% the annual historic mean. As a consequence, an excessive and disorganized exploitation of the coastal aquifers has occurred in order to overcome surface water supply shortage problems. It has been estimated that the number of private operating deep wells has increased from 2,000 to 4,000 during that period, while the total extraction rate increased from 1.6 to 4.0 m^3/sec (Costa, 2000). The estimated deficit, considering the balance inflow and outflow in Recife Coastal Plain, is around 37,8x10^6 m^3/year (Costa and Costa Filho, 2001)

The rainy season in the year 2000 has changed this scenario. The annual rainfall volume was, on the average, 50% higher than the historic annual mean. As a consequence, the Pernambuco State Secretary for Water Resources attempted to implement the proposed management plan. However, the groundwater management plan has not yet been fully implemented because building constructers have claimed the need to construct new wells in the restricted zones since they had sold apartment buildings promising groundwater supply. This overexploitation may increase the Cabo Aquifer vulnerability to salt water intrusion and contamination from the upper aquifer. Also, the inadequate land occupation and the wells drilled without the appropriated technical support increase the aquifer degradation risk.

STABLE ISOTOPE DATA

Costa Filho et al. (1998b) were the first to apply oxygen stable isotope to try to explain the groundwater salinization in the RMR aquifer system (Boa Viagem, Cabo and Beberibe aquifers). Based on the $\delta^{18}O$ they concluded that in the three aquifers recharge processes were similar and the origin of groundwater salinization was not from marine intrusion. Costa Filho et al. (1998a) using $\delta^{18}O$ and $\delta^{2}H$ ratios concluded that isotopic signature of the groundwater in the aquifer system in RMR represents evaporated waters and the salinization process is probably related to dissolution of salts and contamination from paleo-mangroove waters.

Stable oxygen and hydrogen isotope analyses for the groundwater from the Cabo and Boa Viagem aquifers were analyzed by mass spectrometry (Finnigan Delta E) at the Stable Isotope Laboratory, *Centro de Energia Nuclear na Agricultura* (CENA). Oxygen was analyzed using a modified version of Epstein and Mayeda (1953) method proposed by Matsui (1980). Deuterium was analyzed using the method proposed by Coleman *et al.* (1982). The ^{18}O and ^{2}H are reported in per mil ($^0/_{00}$) units and relative do Vienna Standard Mean Ocean Water (VSMOW). The data for the analyzed wells are shown in Table 1.

The range of $\delta^{18}O$ is $-1.5^0/_{00}$ to $-0.86\ ^0/_{00}$ and of $\delta^{2}H$ is $0.2^0/_{00}$ to $2.94^0/_{00}$. Figure 1 shows a plot of $\delta^{18}O$ against $\delta^{2}H$ for the wells which data on both isotopes were measured. It also shows the data for local rainwater along with the Global Meteoric Water Line (Craig, 1961). The regression equation for the data, including local rainwater data, is:

$$\delta^2H = 7.1\delta^{18}O + 7.11 \ (r=0.878) \qquad (1)$$

The equation indicates a slope similar to the Global Meteoric Water Line (GMWL) and most of the samples analyzed during the monitoring program plot close to the GMWL. Three samples plot away from this line and very close to the *y-axis* ($\delta^2H=0$). One sample (deep well) plots on the GMWL midway between rainwater and the majority of groundwater samples. All samples show an isotopic enrichment relative to present-day local meteoric water, however much less enriched than the data presented by Costa Filho et al. (1998a).

DISCUSSION

Electrical conductivity in the monitored wells does not show a regular pattern suggesting that there would be different causes for the salt concentration in the groundwater in the aquifer system in RMR. The magnesium to calcium ionic ratio (rMg/rNa) indicates values in the range of those proposed for continental waters but also presents values in the range, or even higher than those of oceanic waters (Montenegro *et al.*, 2002; 2003).

The stable isotope data also show a pattern that is not explained by a simple groundwater/seawater mixing relationship as pointed out by Costa Filho et al. (1998a). The distribution of the samples in the $\delta^{18}O$ against δ^2H diagram shows three distinct situations. The majority of the analyzed samples plots along the GMWL, but enriched in $\delta^{18}O$ and δ^2H relative to local rainwater. Another group of samples plots away from the GMWL but close to the *y-axis* ($\delta^2H=0$), and one sample plots along the GMWL but less enriched than the first group.

The data suggest that isotopic signature reflects a strong influence of evaporative process in the groundwater in the aquifer system in the RMR, when comparing to present day rainwater. This could be a consequence of evaporation of rainwater during recharge processes. The data also suggests that a mixing between fresh groundwater with saline waters is occurring in some wells in the studied area. So far it is not possible to precise what type of saline water is mixing with fresh groundwater. It could be an effect of seawater intrusion, a mixing with brackish water (estuarine and mangrove waters) through hydraulic interconnection or a mixing with paleo saline waters. This is observed in deep and also in shallow wells confirming salinization processes in both aquifer systems.

The isotope data also show that the lower (Cabo) and upper (Boa Viagem) groundwater have the same isotopic signature no matter they present high salinity concentration or not. This implies a homogeneous mixing between both aquifers, which would confirm that deficiencies in well construction would cause a hydraulic interconnection. However, this is not occurring in the whole system as can be seen in two wells (a deep and a shallow) located in the same apartment building in which the deep well shows an isotopic signature completely distinct and the shallow well show the same signature as the other deep and shallow wells.

Permeability also plays a role in the isotopic signature of groundwater. This is observed through the data presented by Costa et al. (1998) in which the Cabo aquifer shows $\delta^{18}O$ higher than the Boa Viagem and Beberibe aquifers. The higher permeability (Boa Viagem and Beberibe) would help recharge flow and a mixing of new groundwater, whereas the lower permeability would help equilibrium with older, and probably, isotopically heavier waters.

FINAL CONSIDERATIONS

The isotopic data presented in this study support the hypothesis of hydraulic interconnection between the Boa Viagem and Cabo aquifers proposed by Costa et al. (1998) as a consequence of deficiencies in well construction practice. Even though this could be the case for some wells, the seawater intrusion could not be ruled out entirely as a cause for aquifer salinization.

Montenegro et al. (2002, 2003) has shown that even where the salinity is high, the occurrence of seawater intrusion was not clearly identified, due to the absence of a general pattern among the monitoring wells. In some cases, the salinity increased during the monitoring period, whereas in others, the salinity decreased or remained stable. There are some areas where the salinity is high for a large number of wells. In other cases, highly saline wells are close located to others with very good quality water.

Stable isotope data helped in understanding the behavior of groundwater recharge and mixing, but it is still not conclusive regarding the origin of salinization of the aquifer system in RMR. From the isotopic signature it can be said that the groundwater in the aquifer system has a three-fold component: fresh groundwater recharge component, old evaporated groundwater and saline waters. Therefore, detailed studies including $\delta^{18}O$ and $\delta^{2}D$ ratios in surface, estuarine and sea-waters are necessary in order to better understand the recharge and mixing mechanism of groundwater in the RMR aquifer system.

ACKNOWLEDGMENTS

This financial support from PADCT/FINEP (Brazil); CT-HIDRO/CNPq; CNPq and FACEPE (Brazil) is greatly acknowledged. The authors also acknowledge the contribution from CPRH (Pernambuco State Environmental Company), through Mr. Veronilton Farias and Dr. Mario T. Kato for reviewing the final text.

REFERENCES

Cabral, J. J. S. P.; dos Santos, S. M.; Montenegro, S. M. G. L., 2000. "Groundwater information system for Recife Metropolitan Region.". In: Brebbia C.A. and Pascolo P.(eds.) Management Informations Systems, GIS and Remore Sensing. WIT Press, UK.: 489- 498.

Coleman, M.L.; Shepherd, T.J.; Durham, J.J.; Rouse, J.E.; Moore, G.R., 1982. Reduction of water with zinc for hydrogen isotope analysis. Anal. Chem., 54, 993-995.

Costa Filho, W.D.; Santiago, M.F.; Costa, W.D; Mendes Filho, J., 1998^{a}. Isótopos estáveis e a qualidade das águas subterrâneas na planície do Recife. In: Proc. X Congresso Brasileiro de Águas Subterrâneas, São Paulo, Brazil, CD-ROM, 1-9.

Costa Filho, W.D.; Santiago, M.F.; Mendes Filho, J.; Costa, W.D., 1998b. Concentração salina das águas subterrâneas na planície do Recife. In: Proc. III Simpósio de Hidrogeologia do Nordeste, Recife, PE:124-131.

Costa, W. D. and Costa Filho, W. D., 2001. Recarga artificial dos Aqüíferos da Planície do Recife. In: Proc. IV Simpósio de Hidrogeologia do Nordeste, Recife, PE: 543-554.

Costa, W. D., 2000. Riscos potenciais e reais decorrentes da super-explotação de águas subterrâneas no Recife-PE. In: Proc. 1st Joint World Congress on Groundwater. Ceará, Brazil (CD-rom).

Costa, W.D., 1998. Estudo Hidrogeológico da Região Metropolitana do Recife, Report HIDROREC Project", IDRC – UFPE/FADE, Recife, Brazil.

Costa, W.D.; Manoel Filho, J.; Santos, A.C.; Costa Filho, W.D.; Monteiro, A.B.; Sousa, F.J.A.de; Lopes, A.V.G.; Santos, A.J.C.; Silva Filho, M.M.C.; Silva, M.M.J. da., 1998. Hydrogeological study of Recife Metropolitan Region.(Project Report). UFPE, Recife, Brazil

CPRM/FIDEM, 1994. Sistema de informações para Gestão Territorial da Região do Recife, Companhia de Pesquisa de Recursos Minerais, Recife-PE, Brazil

Craig, H., 1961. Isotopic variations in meteroric waters. Science 133:1702-1703.

Custódio, E. and Llamas, M.R., 1975. Hidrología Subterránea, Barcelona: Editorial Omega, 2 vol., pp. 1-2350.

Epstein, S. and Mayeda, T., 1953. Variations in ^{18}O content of water from natural sources. Geochimica Cosmochimica Acta, 27, 213-224.

Matsui, E., 1980. A simple method using a disposable syringe to prepare samples for delta^{18}O measurements in water samples. Analytica Chimica Acta, 120, 423-425.

Monteiro, A.B., 2000. Modelagem de Fluxo subterrâneo nos aqüíferos da planície do Recife seus encaixes, M. Sc. Dissertation, UFPE, Brazil.

Montenegro, S.M.G.; Costa, W.D.; Cabral, J.J.S.P; Montenegro, A.A.; Lima, E.S. de; Manoel Filho, J.; Demétrio, J.G.A., 2003. Monitoring time and spatial changes in groundwater salinity in Recife Coastal plain. Proceedings of the Second International Conference on Salt Water Intrusion and Coastal Aquifers (SWIACA), Merida, Mexico. CD-ROM.

Montenegro, S.M.G.; Montenegro, A.A.; Cabral, J.J.S.P; Demétrio, J.G.A.; Manoel Filho, J.; Lima, E.S. de; Oliveira, E.M.; Paiva, A.L.R., 2002. Groundwater salinity in the Cabo aquifer in Recife Coastal Plain, Pernambuco, Brazil. Proceedins of the XXXII IAH & VI ALHSUD Congress-Groundwater and Human Development, p.1-10, Mar del Plata, Argentina.

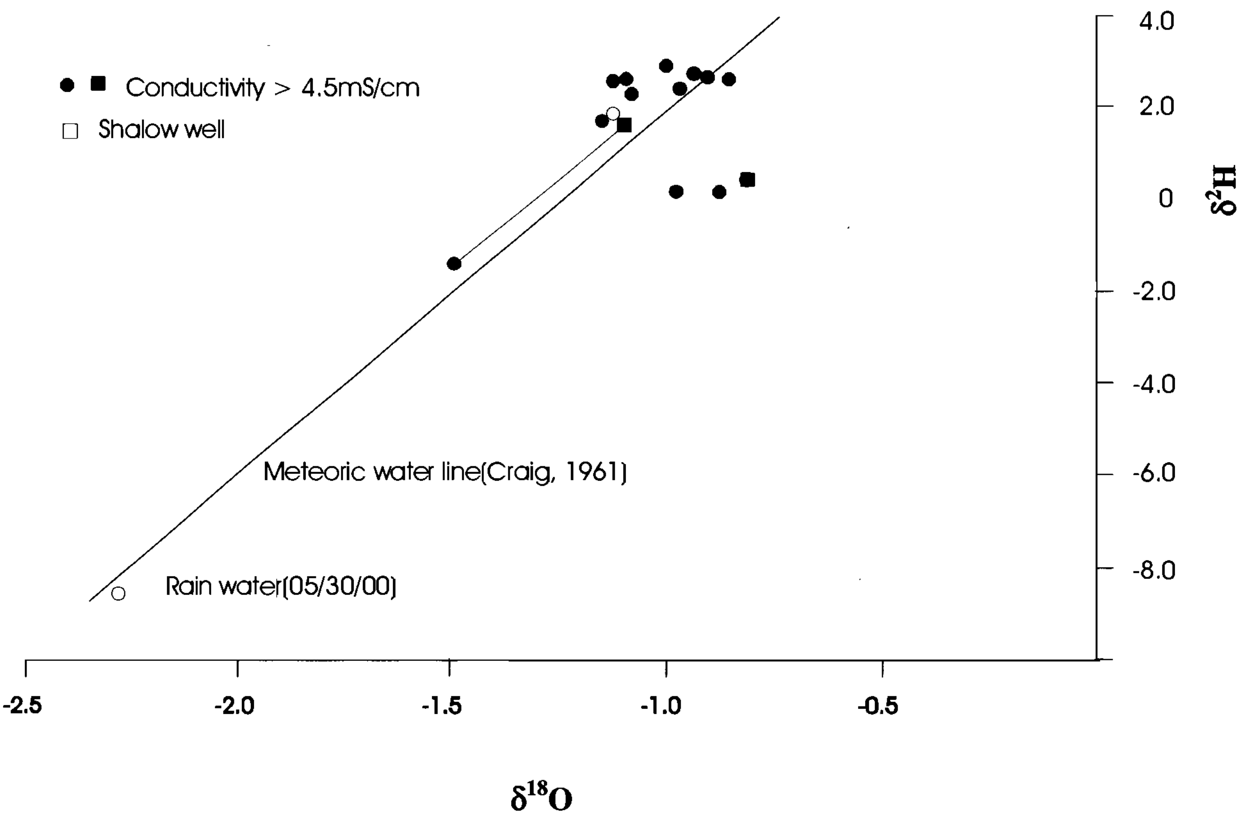

Figure 1. Stable isotope relationship between groundwater for the aquifer system in the Recife Metropolitan Area. The regression line for the data (including local rainwater) is $\delta^2H=7.1\delta^{18}O + 7.11$ permil VSMOW.

Table 1. Stable isotope data for selected wells in Recife coastal plain aquifer system. EC=Electrical Conductivity.

Well	**$\delta^{18}O$**	**δD**	**EC(dS/m)**	**Depth(m)**
Funchal	-1.08	2.30	0.39	134
Príncipe Navarro	-1.13	1.79	0.64	134
Ana Virginia (Dec/99)	-0.98	0.20	6.36	9
Ana Virginia (Feb/00)	-0.82	0.44	6.36	9
Flora Rubin	-0.91	2.63	1.13	160
Encanta Moça	-1.15	1.73	0.54	150
Studio Everest	-0.96	2.45	3.90	154
Alfamar	-1.00	2.94	1.50	152
Maria Yolanda	-1.10	2.55	0.55	150
Nápoles	-0.88	0.17	4.93	50
Monte Sagrado	-0.86	2.61	6.29	180
Marante Plaza Hotel	-0.94	2.70	4.50	171
Ilha de Tasso	-1.12	2.58	0.41	154
Montifiori	-1.50	-1.44	0.60	135
Montifiori	-1.10	1.59	2.45	25
Rain water	-2.28	-8.54	-	-

USE OF ^{210}Pb GEOCHRONOLOGY TO EXPLORE THE CENTURY-SCALE MERCURY CONTAMINATION HISTORY AND THE IMPORTANCE OF FLOODPLAIN ACCUMULATION IN ANDEAN TRIBUTARIES OF THE AMAZON RIVER

Maurice-Bourgoin, L.[1]**; Aalto, R.**[2]**; Rhéault, I.**[3] **and Guyot, J.L.**[4]

1. IRD, HyBAm Program, CP 7091 Lago Sul, 71619-970, Brasília-DF, Brazil. lmaurice@unb.br
2. Quaternary Research Center and Department of Earth and Space Sciences, University of Washington, Seattle, WA 98195-1310, USA. aalto@u.washington.edu
3. University of Québec in Montréal, UQAM-GEOTOP, CP8888, Montréal, Québec H3C 3P8, Canada
4. IRD–UMR LMTG, Université Paul Sabatier, 38 rue des 36 ponts, 31000-Toulouse, France. guyot@cict.fr

Keywords: ^{210}Pb geochronology, Amazon basin, mercury, floodplain, sediment

INTRODUCTION

Mercury pollution of water and fish in the Amazon basin is a significant hazard for riparian populations, especially for people whose primary protein source is contaminated fish (Lebel et al., 1999; Maurice-Bourgoin et al., 2000; Roulet & Maury-Brachet, 2001); irreversible Hg damage has been implicated for the nervous and immune systems (Lebel et al., 1998). In the Bolivian Andes, at the headwaters of the Beni river, erosion of contaminated soils and weathering of mercury-bearing rocks during the rainy season can increase the water concentration of Hg by 50 fold (Maurice Bourgoin et al., 2001). These soils may have become contaminated through natural crustal degasification and dissolution of Hg, and also by centuries of extensive Hg use during both the colonial and post-colonial extraction of massive quantities of gold and silver (Nriagu et al., 1992). More recently, a new gold-mining boom starting in the 1970s has introduced an estimated 0.25 to 0.5 tonnes/year of Hg into the Beni River basin (Maurice-Bourgoin et al., 2000). The mercury used can be released directly into the river itself or indirectly through the atmosphere by open-air burning of the amalgam (Malm et al., 1990; Maurice-Bourgoin et al., 1999). But the major environmental impact of these mining activities is the deforestation of the exploited areas and the release of millions of tonnes of Hg-contaminated sediments and soils to affected rivers, rather than the direct release of Hg used during the last stages of the gold extraction (Maurice-Bourgoin, 2001). Numerous studies have documented the distribution of Hg in water, fish, and people throughout the Amazon basin (Akagi et al., 1995; Malm et al., 1995; Barbosa et al., 1997; Roulet et al., 1999; Silva-Forsberg et al., 1999; Maurice-Bourgoin et al., 2000), but the important link between Hg and sediment transport had not been fully explored. To investigate the sources, transport and storage mechanics, and contamination history of Hg for the Madeira River, one of the most important tributary to the Amazon in terms of sediment input, we analysed the Hg concentration and relevant geochemistry of floodplain and river sediments.

STUDY AREA

The Bolivian Amazon basin represents the Andean headwaters of the Madeira River, one of the most important tributaries of the Amazon River. In Bolivia, its drainage basin is 0,9 x 10^6 km^2, with 25% in the Andes, 27% on the Brazilian shield and 48% in the plain. The Beni and the Mamore Rivers, the largest sediment suppliers of the Madeira river (Guyot, 1993), constitute the focus of our study. Andean tributaries of these rivers drain both semi-arid areas of high altitude and areas of tropical humid forest of the sub-Andes. Heights above sea level range from 6400 m at the highest headwaters to 115 m at the Brazilian border. The Beni and Mamore Rivers (Fig. 1) transport sediments from the rapidly eroding Bolivian Andes across the floodplains of a large foreland basin. Floodplains and channels are essentially pristine, without artificial levees, dams, dredging, numerous roads, or other anthropogenic complications. At the edge of the sub-Andes, the drainage area of the Beni River at the edge of the piedmont, is 67,500 km^2 and the mean annual discharge during the sampling period, 1998-1999, averaged 2300 m^3 s^{-1}. The Beni River collects numerous Andean tributaries, half of which is exploited for their alluvial gold since the 1960s (Fig. 1). The adjacent Mamore drains a 600,000 km^2 basin, much of which is floodplain. These basins are representative of the vast expanse of Andean-Amazonian foreland basins to the north.

MATERIAL AND METHODS

One sampling survey was conducted along the entire Beni river in August-September, 1999 and another along the Mamore River in September, 2000. Water samples were collected using Teflon bottles and all procedures were performed using 'ultra-clean' techniques (Nolting and De Jong, 1994; Gaudet et al., 1995). Sediment cores were sampled 1.3 meters deep into the floodplain at different locations along these rivers (Fig. 1); they were frozen on the field and subsequently dried and processed in the laboratory. The T-Hg was determined by Atomic Fluorescence Spectrometry after reduction with Sn(II); the detection limit was 2 ng g^{-1}. The accuracy and reproducibilty of the method were calibrated by the analysis of a reference standard; the mean T-Hg concentration obtained was 92 ± 4 ng g^{-1} (dw) for a recommanded value of 92 ± 9 ng g^{-1} (dw). The concentrations of T-Hg, organic carbon and nitrogen, iron (Fe$_{cdb}$) and aluminium (Al$_{cdb}$) substituted into oxy-hydroxydes, as associated with the granulometry and

^{210}Pb activity within the same sediment cores, were used to characterise the main geochemical processes controlling the deposition of Hg within the floodplain.

A new model has been developed for ^{210}Pb geochronology on river floodplains, termed Constant Initial Reach Clay Activity and Unknown Sedimentation rate (CIRCAUS) and has been applied to more than two hundred locations throughout the Beni and Mamore systems (Aalto, 2002). The approach employs discrete down-core, clay-normalised measurements of ^{210}Pb activity and is coupled with a geomorphic model of the input concentration of ^{210}Pb in sediment during large floods. The numerical modelling approach is supplemented with an empirical determination of the supported ^{210}Pb activity, the meteoric input of ^{210}Pb, and the clay-normalized ^{210}Pb activity in fresh sediment for that reach of river. The sediment age is determined from the "decay" age of any activity plateaus (zones of uniform activity found in most cores), as well as independently calculated from the excess "meteoric cap" ^{210}Pb activity grown in above the activity of the plateau.

RESULTS AND DISCUSSION

EFFLUX OF SEDIMENTS AND ASSOCIATED MERCURY TO THE BENI FLOODPLAIN

The T-Hg concentrations in the Beni river range from 19 ng l^{-1} during the dry season to 460 ng l^{-1} at peak flood stage. The Hg associated with the particles represents 59 and 98% of the T-Hg, respectively. In this Andean tributary, the importance of soil erosion during the rainy season in controlling the mercury concentrations of freshwater has been previously demonstrated (Maurice-Bourgoin et al., 2001). For the 1999 water year, from surface water samples, we estimated a total suspended particulate matter (SPM) fflux in the Beni R. of 302 10^{6} tonnes; 97% of this material was transported during the first four months of high water and about 40% is later deposited in the Amazonian floodplain, as shown in a previous study (Guyot, 1993). The total Hg (T-Hg) flux associated with sediment reached 33 tonnes, 96% of which was particulate Hg (P-Hg). During the wet season, from November to March, Hg-contaminated particles are transported from the Andean sub-basins characterised by steep slopes and by an accelerated erosion rate driven by recent agriculture practices and the ongoing construction of a major road. Due to the high adsorption capacity of mercury on fine particles (clays) in the white water rivers (in contrast to organic-rich "black waters"), most of the mercury is transported on SPM. In the Beni river basin, a depth-integrated average of 35% of the deposited sediment collected in the floodplain is composed of clays, and these contains most of the sediment-born mercury.

CENTURY-SCALE CONTAMINATION HISTORY AND IMPORTANCE OF SEDIMENT TRANSPORT AND FLOODPLAIN ACCUMULATION

For the 180 sediment samples analyzed we observe (Fig. 2) a strong correlation between T-Hg and clays content ($r^2 = 0.80$), Al_{tot} ($r^2 = 0.65$), Fe_{tot} ($r^2 = 0.64$) and with Fe incorporated in clay minerals, Fe_{Si}, ($r^2 = 0.53$) concentrations. This confirms that clays and Al and Fe oxy-hydroxides in sediments may serve as the primary carrier and facilitate the transport and storage of Hg within the Beni and Mamore river-floodplain systems.

By utilising results from a detailed model for the transport and deposition of river sediment (including clays) along the Beni river floodplain system (Aalto, 2002), we estimate, using the observed Hg-Clay relationship (Fig. 2), an annual exchange of clay-affiliated Hg between the floodplain and the channel of 2.1 tonnes Hg, primarily due to channel migration. This exchange has been estimated by subtracting the net Hg deposition of 2.4 tonnes year^{-1}, primarily lost into the distal floodplain, from the total deposition of 4.5 tonnes year^{-1}.

In many of our cores, we observe an increase of the T-Hg concentrations in sediments with depth. Applying the CIRCAUS model to date the sediment within our floodplain cores, we find that the ratio of observed Hg concentration to expected Hg concentration (as derived from measured clay abundance or from measured Al incorporated in clay minerals, Al_{Si}) is approximately 1 from 1900 to 1965 and then increases starting in the 70s (Fig. 3). This increase is most evident for the clay-normalized Hg content where we observed a best correlation between these two elements. This suggests that the clay, and in a less extend Al-normalized Hg concentration in sediment is constant from 1900-1965, and then shows an increase over the past 30 years, mostly likely due to a new input of Hg in the Andean drainage basins. This influx of Hg can be attributed to accelerated erosion of Hg enriched soils, due increased gold-mining activities, recent colonisation, and new agriculture practices (e.g. burning after deforestation), road construction, and other human activities. A substantial increase in the price of gold during the 70s, with a maximum in 1980, sparked a new gold boom in various tropical countries, and especially in Latin America (Cleary, 2000).

CONCLUSION

The substantial increase of clay-normalised Hg concentration in the sediments of an important tributary of the Amazon during the last 30 years might be explained by a recent gold mining boom and also by increased deforestation of steep hillsides and the resulting erosion of soils. This study represents the first geochronological determination of heavy metal pollution history from floodplain sediments. These results underscore the importance of river sediment as a carrier of Hg, and the key role of channel-floodplain sediment interchange in regulating the transport and accumulation of any sediment-associated pollution.

ACKNOWLEDGEMENTS

This research was funded by the HyBAm Program of IRD, French Research Institute for the Development, and by the University of Washington with the supports of NSF and NASA.

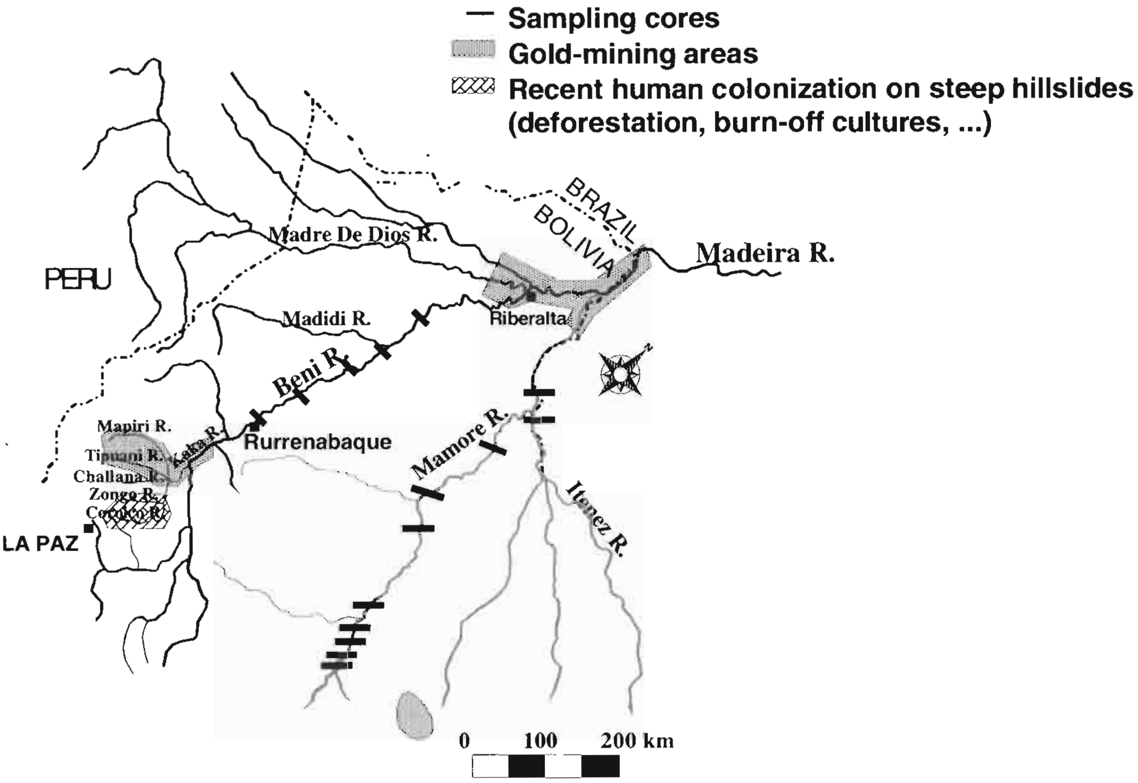

Figure 1. Location of the sampling cores and distribution of the recent anthropogenic disturbance (deforestation, mining, road construction) on the hydrological map of the Madeira tributaries.

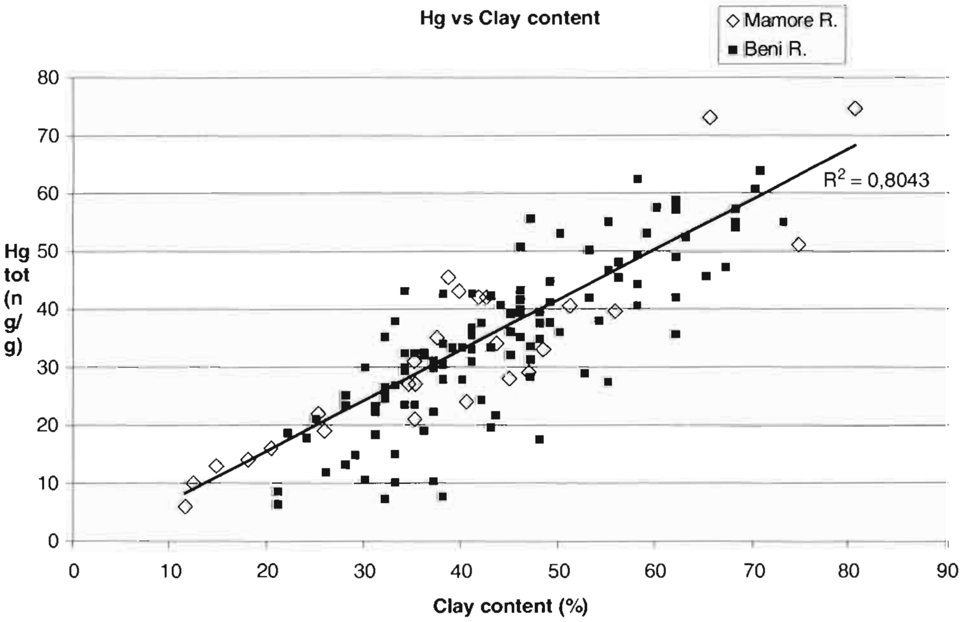

Figure 2. Correlation between total Hg concentrations and clay content in sediment samples from the beni and Mamore Rivers

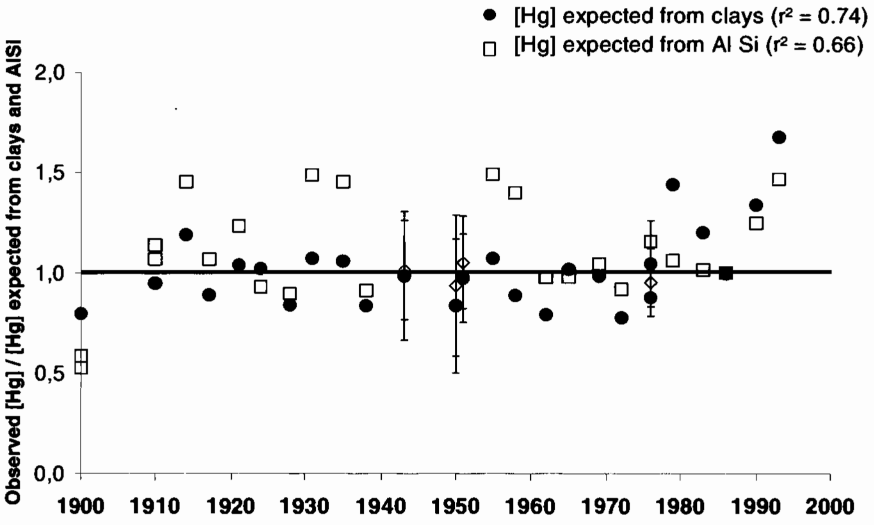

Figure 3. Observed Hg concentration / expected Hg ratio from measured clay abundance (circles), and Al incorporated in clay minerals (open diamonds), in the Beni river sediments, over the last century.

REFERENCES

Aalto, R., 2002. Geomorphic Form and Process of Sediment Flux within an Active Orogen: Denudation of the Bolivian Andes and Sediment Conveyance across the Beni Foreland, Ph.D. Dissertation, University of Washington, Seattle. 365p.

Akagi H., Malm O., Branches F. J. P., Kinjo Y., Kashima Y., Guimaraes J. R. D., Oliveira R. B., Haraguchi K., Pfeiffer W. C., Takizawa Y. & Kato H., 1995. Human exposure to mercury due to goldmining in the Tapajós River basin, Amazon, Brazil: speciation of mercury in human hair, blood and urine. Water, Air and Soil Pollution, 80, 85-94.

Barbosa, A.C., Garcia, A.M., & de Souza J., 1997. Mercury contamination in hair of riverine populations of Apiacas Reserve in the Brazilian Amazon. Water, Air and Soil Pollut. 97, 1-8.

Cleary D., 2000. Small scale gold-mining in Brazilian Amazonia. In: Amazonia at the crossroads (ed. by Hall A.), London, Institute of Latin America studies : 58-72.

Gaudet, C., Lingard, S., Cureton, P., Keenleyside, K., Smith, S. & Raju, G., 1995. Canadian environmental quality guidelines for mercury. Water, Air and Soil Pollut. 80, 1149-1159.

Guyot J.L., Filizola N., Quintanilla J., Cortez J., 1996. Dissolved solids and suspended sediment yields in the Rio Madeira basin, from the Bolivian Andes to the Amazon, 55-63. In Erosion and Sediment yield : Global and Regional Perspectives, Exeter, July 1996. IAHS Publ. 236.

Guyot, J.L., 1993. Hydrogeoquemistry of the Bolivian Amazonian Rivers. Ph.D. dissertation. ORSTOM France (eds.), 261 pp.

Lebel, J., Mergler, D., Branches, F., Lucotte, M., Amorim, M., Larribe, F. & Dolbec, J., 1998. Neurotoxic effects of low-level mercury contamination in the Amazonian basin. Environment. Res. A79, 20-32.

Lebel, J., Roulet, M., Mergler, D., Lucotte, M., & Larribe, F., 1999. Fish diet and mercury exposure in a riparian Amazonian population. Water, Air and Soil Pollut. 97, 31-44.

Malm O., Branches F.J.P., Akagi H., Castro M.B., Pfeiffer W. C., Harada M., Bastos W.R., & Kato H., 1995. Mercury and methylmercury in fish and human hair from the Tapajós river basin, Brazil. Sci. Total Environ. 175, 141-150.

Malm, O., Pfeiffer, W.C., Souza, C.M.M. and Reuther, R., 1990. Mercury pollution due to gold mining in the Madeira river basin, Brazil. AMBIO 19(1), 11-15.

Maurice-Bourgoin L., 2001. Le mercure dans les eaux de surface du bassin amazonien – Transfert du mercure des sols aux milieux aquatiques – Spéciation, transport et sédimentation dans les rivières et plaines d'inondation. In : Le mercure en Amazonie : Rôle de l'homme et de l'environnement, (Carmouze J.P., Lucotte M. and Boudou A., Eds.) IRD Publications (Expertise Collégiale), pp : 167-200.

Maurice-Bourgoin L., Quiroga I., Chincherros J. & Courau P., 2000. Mercury distribution in waters and fishes of the Upper Madeira rivers and mercury exposure in riparian Amazonian populations. The Science of the Total Environment, 260: 73-86.

Maurice-Bourgoin L., Quiroga I., Guyot J.L. & Malm O., 1999. Mercury pollution in the upper Beni River basin, Bolivia. AMBIO, 28(4): 302-306.

Nolting, R.F. & de Jong, J.T.M., 1994. Sampling and analytical methods for the determination of trace metals in surface seawaters. Intern. J. Environ. Anal. Chem. 57, 189-196.

Nriagu, J.O., Pfeiffer, W.C., Malm, O., Souza, C.M.M. & Mierle, G., 1992. Mercury pollution in Brazil. Nature (London), 356-389.

Roulet, M. & Maury-Brachet, R., 2001. Le mercure dans les organismes aquatiques amazoniens. In : Le mercure en Amazonie : Rôle de l'homme et de l'environnement, (Carmouze J.P., Lucotte M. and Boudou A., Eds.) IRD Publications (Expertise Collégiale), pp : 203-271.

Roulet, M., Lucotte, M., Farella, N., Serique, G., Coelho, H., Sousa Passos, C.J., De Jesus da Silva, E., Scavone de Andrade, P., Mergler, D., Guimaraes, J.RD., and Armorim, M., 1999. Effects of recent human colonization on the presence of mercury in Amazonian ecosystems. Water, Air and Soil Pollut. 112, 297-313.

Silva Forsberg, M.C., Forsberg, B. R., & Zeidemann, V. K., 1999. Mercury contamination in humans linked to river chemistry in the Amazon basin. AMBIO 28(6): 519-521.

ISOTOPE TRACING OF THE HYDROLOGICAL DYNAMICS OF AN AMAZONIAN FLOODPLAIN

Maurice-Bourgoin, L.[1]; Kosuth, P.[2]; Chaffaut, I.[3]; Martinelli, L.A.[4] and Ometto, J.P.[4]

1. IRD, Institut de Recherche pour le Développement, CP 7091, 71619-970 Brasilia-DF, Brasil. lmaurice@unb.br
2. Cemagref, 500 rue Jean-François Breton, 34093 Montpellier Cedex 05, France. pascal.kosuth@teledetection.fr
3. 1020 rue des Ecoles, 34270 Saint Mathieu de Tréviers, France. chaffaut.isabelle@wanadoo.fr
4. Centro de Energia Nuclear na Agricultura – Av.Centenário 303, Piracicaba-SP, 13416-000, Brazil. zebu@cena.usp.br

Keywords: Water isotopes, hydrology, Amazon, floodplains

INTRODUCTION

AMAZON BASIN HYDROLOGY

The Amazon Basin (79.7°W to 50.0°W; 5.4°N to 20.5°S) extends over 6,112,000 km² in both equatorial and subtropical regions. Atmospheric water vapour enters the Basin from the Atlantic Ocean, and moves westward to the Andean Cordillera. The mean annual precipitation over the basin is 2322 mm.y^{-1} (Costa and Foley, 1998). Mean annual water discharge back to the ocean is 209 000 m^3/s (Molinier et al., 1997), which corresponds to about 20% of the total freshwater input from the continents to the oceans. Average discharge (~1079 mm.y^{-1}) corresponds to 50% of the annual rainfall, as a result of an internal recycling precipitation/ evapotranspiration (1243 mm/y/ precipitation).

Due to the size of the Amazon drainage basin, large scale deforestation and land use changes can affect both regional and global climate, while regional climate changes can modify the hydrological dynamics of its rivers (Shukla et al., 1990; Costa and Foley, 1998). All the hydrological models participating in Global Soil Wetness Project showed a strong underestimation and a significant lag in the annual runoff cycle of the Amazon basin (Chapelon et al., 2002). Therefore, a better understanding of the processes that control the Amazon Basin hydrology and climatology is of major interest.

Two of the major research Projects currently in development in the Amazon basin (LBA and HyBAm) are dedicated to improve the understanding of the Amazon hydrology, climatology and biogeochemistry.

AMAZON FLOODPLAINS HYDROLOGY

Floodplains play a major role in the Amazon River hydrology. They store water during the river rising phase and release it when the river level is decreasing. The main consequence on the river annual hydrograph is the smoothing of the river discharge variation: this explains why the maximum discharge at Obidos (280 000 m^3/s) is only 4 times the minimum value (70 000 m^3/s). Floodplains also play an important paper in the sediment dynamics and in the geochemical cycles.

Overall extension of Amazon basin flooded areas (300 000 km², Junk, 1997) is still under investigation. Different remote sensing methods are tested (visible, active radar, passive radar). Sippel et al. (1998) analyzed the SMMR 37GHz polarization difference and estimated a mean annual flooded area of 47 000 km² along the Amazon mainstream (from 70°W to 55.5°W), with a maximum value of 90 000 km² (1953). Radar imagery mosaics (JERS) allowed a finer resolution and gave a 450 000 km² (low river stage) to 750 000 km² (high river stage) estimation for the overall basin (Seyler et al., 2003). The annual volume of river water that passes through floodplains and the contribution of floodplains to the overall river discharge at different phases of the hydrological cycle are still largely unknown.

Few studies are dedicated to detailed hydrological monitoring of specific Amazonian floodplains. Since 1999, the HYBAM Project, has been studying the role of the floodplain lakes ("várzeas") in the hydrological and sedimentological dynamics of the Amazon river, with a particular focus on the Curuai floodplain (Kosuth, 2002; Martinez at al., 2003).

ISOTOPIC GEOCHEMISTRY OF THE AMAZON BASIN WATERS

The isotopic composition of natural waters provides information on both their origin and the processes affecting their cycle, like evaporation, transpiration, condensation, or even mixing (Fritz and Fontes, 1980). Measuring the spatial and temporal isotopic variability of different water bodies (like precipitations, water vapour, surface waters and groundwaters) completes traditional hydrological measurements (rainfalls, discharges, water levels, water conductivity).

Various studies on the isotopic composition of precipitation on the Amazon basin have been published (Gatt and Matsui, 1991; Chaffaut, 1998); some information on the Amazon surface waters is available (Moura dos Reis et al., 1975; Martinelli et al., 1996), explaining their implications on the dynamics of atmospheric circulation and vapour recharge processes. Isotopic composition of Amazonian precipitations and river waters varies along the hydrologic cycle. Precipitations are impoverished during the rainy season due to the mass effect. Surface waters of the Amazon River show an isotopic enrichment during the low river stage (from September to December) and a maximum impoverishment during the high river stage (from April to July), later than the maximum impoverishment observed in the rainfall.

CURUAI FLOODPLAIN : DATA ACQUISITION AND HYDROLOGICAL MODELING

The Lago Grande de Curuai floodplain (Fig. 1) is located on the right margin of the Amazon river, in front of Obidos city (1.9°S, 55.5°W), 900 km upstream from the Ocean. This floodplain is a complex system of more than 30 interconnected lakes, linked to the Amazon river by 8 channels, 2 of them with a permanent flow. Floodplain extension varies from 700 km² to 2300 km² (Martinez et al., 2003). Maximum flood amplitude is 7.0 m at Obidos station (1990-2002).

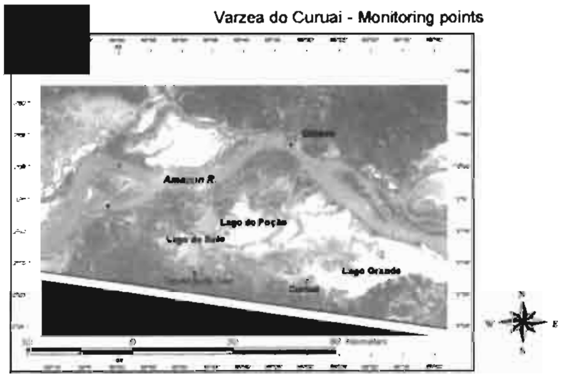

Figure 1. Monitoring points on the Lago Grande de Curuai floodplain.

Floodplain hydrology is controlled by the main river regime depending on the floodplain geometry (lakes, channels), the local climate regime (rainfall and radiations), the watershed hydrology (runoff to the floodplain) and all other related processes (infiltration, runoff, evaporation, channel flow, lake storage, etc...). The hydrology of the Curuai floodplain has been monitored since March, 1999 through daily records of rainfall, and water levels in the main river, in the major lakes and in an evaporation tank. Water samples have been collected every ten days in 10 stations for geochemical and sedimentological analysis. Fifteen field measurement campaigns have been organized at various stages of the hydrological cycle to measure liquid and solid discharges in the channels and to study the spatial heterogeneity of waters geochemical characteristics.

An hydrological-hydrodynamical model of the Amazonian floodplains has been developed and validated on the Curuai floodplain (Kosuth, 2002). Calibration was realised on measured channel discharges and lakes water levels. The model was run over the 1998-2002 period and provided time series of simulated lakes water levels and water flux (channel discharges, watershed runoffs, rainfall and evapotranspiration). Field measurements and hydrological modelling allowed us to estimate and quantify the various water fluxes and the volume of river water entering the floodplain during an hydrological cycle. Anyhow some water fluxes cannot be directly measured (evapotranspiration, watershed runoff, river bank overflow) and indirect methods, such as isotopic geochemistry, are needed to confirm or infirm these first hydrological hypothesis and results.

ISOTOPIC GEOCHEMISTRY OF THE CURUAI FLOODPLAIN WATERS

Temporal changes in the isotopic ratios of lakes waters may provide a sensitive record of water inflows origin and intensity of evaporation, related to water residence time in the lake. The present study has been realized in the framework of the "Isotope tracing of hydrological processes in large river basins" IAEA Programme.

Isotopic monitoring started by August 2001 with systematic sampling of water every ten days at 12 locations. First results for 2001-2002 hydrological cycle are presented in Table 1.

Table 1. Isotopic composition of floodplain main water bodies along the (2001-2002) hydrologic cycle (the river water values are estimated from Moura dos Reis et al, 1975).

	Amazon river Obidos (sim.)		Curuai Rain		Watershed runoff (Tabatinga)		Groundwaters (Curuai Well)		L. Salé (São Nicolau)		L. Poção		L. Grande (Curuai)		L. Grande (downstr. Channel)	
	O18 (°/°°)	D (°/°°)	O18 (°/°°)	D (°/°°)	O18 (°/°°)	D (°/°°)	O18 (°/°°)	D (°/°°)	O18 (°/°°)	D (°/°°)	O18 (°/°°)	D (°/°°)	O18 (°/°°)	D (°/°°)	O18 (°/°°)	D (°/°°)
20/08/2001	-6.2	-39.2			-5.6	-34.7	-6.5	-42.6	-4.4	-30.1		-31.3		-30.3		
30/08/2001	-6.0	-37.8			-5.7	-34.8	-5.6	-42.3	-4.0	-27.7		-29.3		-28.7		
10/09/2001	-5.8	-36.2	-2.3	-11.4	-5.3	-33.5	-1.1	-41.9	-3.9	-26.8		-27.0		-27.8		
20/09/2001	-5.6	-35.0	-0.2	5.7	-5.4	-34.7	-6.8	-42.5	-3.3	-22.8		-24.7		-26.5		
30/09/2001	-5.5	-33.7			-5.6	-36.1	-6.7	-43.0	-2.9	-21.3		-20.5		-24.6		
10/10/2001	-5.3	-32.6			-5.4	-36.4	-6.6	-42.7	-2.1	-17.5		-16.6		-29.2		
20/10/2001	-5.2	-31.7			-5.5	-35.5		-42.0	-2.0	-14.9		-10.3		-27.1		
30/10/2001	-5.0	-30.9	6.8	37.1	-5.6	-35.5		-43.6	-1.0	-8.8		-4.9		-31.7		
10/11/2001	-5.0	-30.4	-11.8	-85.4	-5.5	-35.0		-43.4	-0.4	-6.7		4.7		-32.7		
20/11/2001	-4.9	-30.3			-5.7	-35.5		-43.1	-3.5			11.1		-32.4		
30/11/2001	-4.8	-30.4			-5.8	-35.1		-43.2	0.4	-2.6		16.5		-31.9		
10/12/2001	-4.8	-30.8	-1.6	-3.8	-5.6	-35.5		-41.7	0.4	-2.7		12.7		-17.3		-21.6
20/12/2001	-4.8	-31.1			-5.7	-35.5		-42.8	-1.6	-11.3		-0.5		[illegible]		-28.7
30/12/2001	-4.9	-31.6	-2.0	-7.5	-4.9	-30.9		-43.1	-1.5	-10.9		-17.0		-19.1		-28.7
10/01/2002	-5.0	-32.2	-1.9	-11.6	-5.7	-35.1	-6.7	-43.0	-3.6	-22.1		-22.3		-20.3		-29.1
20/01/2002	-5.1	-32.7	2.2	17.4	-7.8	-32.7		-43.7	-3.5	-22.7		-28.0		-35.6		-29.4
30/01/2002	-5.1	-33.3	-1.3	-1.2				-43.5	-3.3	-22.4		-27.4		-31.6		-34.3
10/02/2002	-5.3	-34.0	-3.0	-18.8	-7.8	-37.1		-43.9	-4.2	-26.5		-23.4		-28.9		-26.1
20/02/2002	-5.4	-34.4	-4.6	-30.4	-6.0	-36.0		-43.8	-4.1	-27.1		-24.1		-25.0		-28.8
28/02/2002	-5.5	-35.0	-3.1	-13.9	-5.1	-30.5		-44.2	-3.7	-25.8		-22.5				-30.5
10/03/2002	-5.6	-35.5			-5.8	-36.7		-43.7	-4.2	-26.6		-2.9		-25.5		-30.8
20/03/2002	-5.8	-36.3	-7.0	-46.8	-5.7	-34.5		-43.3				-20.7		-31.2		
30/03/2002	-5.9	-37.1	-8.1	-52.3	-6.3	-39.6										
10/04/2002	-6.1	-38.0	-9.7	-69.4		-41.7		-43.3				-23.7		-34.4		-34.8
20/04/2002	-6.2	-38.7	-14.2	-106.9	-6.6	-41.2										
30/04/2002	-6.4	-39.3	-6.6	-40.1	-5.7	-38.8										
10/05/2002	-6.5	-40.0	-6.0	-36.8	-5.4	-36.7		-43.3				-37.4		-32.3		-29.7
20/05/2002	-6.6	-40.8	-4.1	-22.3	-5.9	-37.7										
30/05/2002	-6.6	-42.1	-2.9	-11.4	-5.4	-35.4										
10/06/2002	-6.7	-43.3	-4.2	-22.1	-5.3	-35.0		-42.7				-41.9		-36.1		-29.1
20/06/2002	-6.7	-43.6	-5.2	-29.3	-6.9	-33.7										
30/06/2002	-6.7	-43.0			-5.0	-34.7										
10/07/2002	-6.7	-42.3														
20/07/2002	-6.6	-41.6														
30/07/2002	-6.5	-41.0														
10/08/2002	-6.3	-40.1														
20/08/2002	-6.2	-39.1	-1.2	-4.3												
average	-5.8	-36.3	-4.0	-24.6	-5.8	-35.7	-5.7	-43.1	-2.7	-18.9		-16.5		-28.3		-29.4
st. Dev.	0.7	4.3	4.5	32.4	0.7	2.4	2.1	0.6	1.5	8.8		15.7		5.3		3.3

WATER INPUTS TO THE FLOODPLAIN

The different classes of water inputs to the floodplain are (1) the Amazon river, (2) direct rainfalls, (3) surface runoff from the watershed, and (4) groundwater flow. Fig. 2 illustrates the isotopic composition (in Deuterium) of each of these sources for the 2001-2002 period (measurement errors have been filtered).

Isotopic composition of the Amazon River at Obidos is not yet analysed for this period but values have been derived from measurements at the Amazon mouth (Moura dos Reis et al, 1975). Comparison with measured values for the 2001-2002 period is satisfactory. River waters isotopic composition presents limited variations: -5.8 +/- 0.7‰ (^{18}O); -36.3 +/-4.3‰ (D). The river isotopic signature becomes impoverished in phase with increasing discharge.

Local rainfalls show large annual variations (D from +30‰ to –90‰). Weighted averages are –4.5‰ (O^{18}) and –26.8‰ (D). The rainfall isotopic signature is out of phase with the pluviograph (enriched during the dry season, and impoverished during the rainy season).

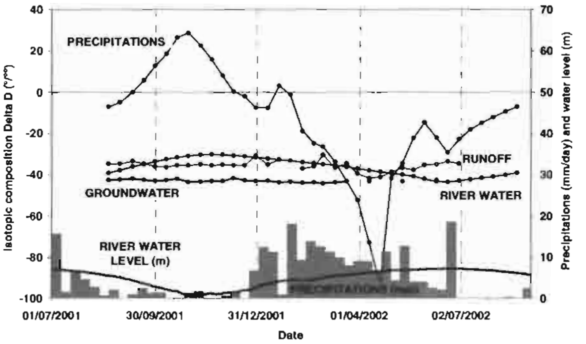

Figure 2. Isotopic composition (deuterium) along the hydrological cycle (2001-2002) of the different main water inputs to the floodplain system.

Groundwater presents a steady isotopic composition of -43.1 +/-0.6‰(D), averaging large rainfalls signature.

Surface runoff from the watershed (stream at Tabatinga do Sale) presents a uniform composition throughout the year (-35.7 +/- 2.4‰), probably due to a dominant contribution by groundwater and the runoff on the forested drainage basin.

FLOODPLAIN LAKES

Figure 3 illustrates the evolution of the isotopic composition (Deuterium) in the main lakes of the várzea along the hydrological cycle.

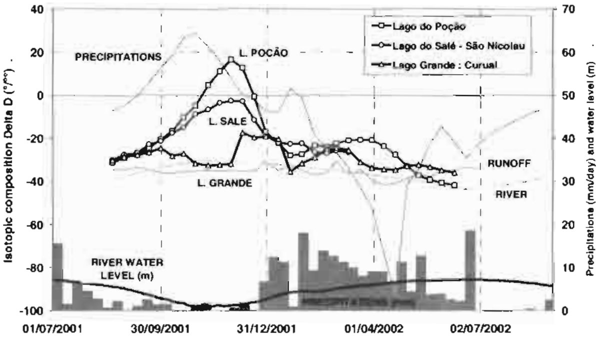

Figure 3. Isotopic composition of the surface waters of the main floodplain lakes of the Curuai várzea (deuterium) during one hydrologic cycle (2001-2002).

Poção and Salé lakes, located in the inner part of the floodplain lakes system, clearly show an isotope enrichment during the river decreasing stage (dry season). This is due to the active evaporation process and the absence of external water inputs (either rainfall or river inflow). Although river starts rising on Nov./10/2002, isotope impoverishment of lakes waters only starts by the first weeks of December 2001, when the river inflow reaches a certain threshold.

Lake Grande isotopic composition shows a more erratic dynamics without dry season enrichment and with relatively high values from Dec., 10th to Jan., 10th. This can be explained by the sampling site (Curuai) location, situated on the southern limit of the lake, under the influence of groundwater and watershed runoff. During the low water stage, groundwater with constant isotope composition flows to the lake. When the river starts rising (in early December), the water inflow coming from the Amazon pushes isotopically enriched lake waters (submitted to high evaporation during the dry season) from the eastern part of the lake towards Curuai. By January, 20th of 2002, low rainfalls and stabilised river level induce renewed groundwater contribution at Curuai.

During the dry season, the maximum enrichment of lakes waters decreases from the Lake Poção (max. +16‰) to the Lake Salé (max. -3‰) and Lake Grande (max. -15‰). During the river rising stage (rainy season), lakes waters show a decreased isotopic composition, tending to the river waters isotopic values. Local temporary enrichments can be observed (Lake Poção, February – March 2002) probably due to the evaporation process when new inputs of water are limited.

WATER OUTPUTS BACK TO THE RIVER

Isotopic composition of waters from the eastern (downstream) channel connecting the floodplain to the river (Boca do Lago from 20/04/2002) show that permanent channel water is in phase with the river water during the rainy season (Fig. 4), but is enriched at the end of the rising stage when water flows back to the mainstream (-30‰ against -40‰).

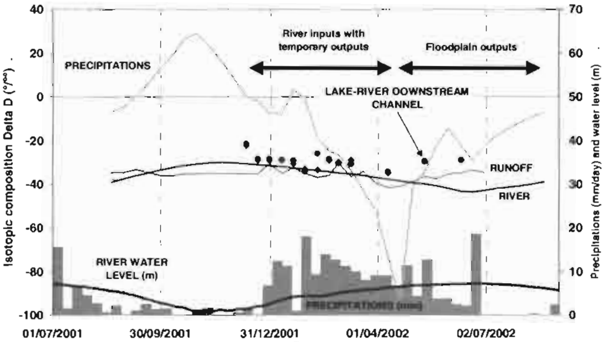

Figure 4. Isotopic composition of waters on downstream connexion canal between lake and floodplain.

ISOTOPIC GEOCHEMISTRY CONTRIBUTION TO THE UNDERSTANDING OF FLOODPLAIN HYDROLOGY

As mentioned above, most part of the floodplain flows cannot be regularly measured (river inflow to the floodplain, bank overflow, watershed runoff to the lakes, intensity of the evaporation process) and related hypothesis on the floodplain hydrological dynamics can hardly be verified. Thanks to the conservativity of the water stable isotopes, isotopic geochemistry can help in evaluating the validity of current assumptions concerning the hydrological dynamics of the system.

ISOTOPIC MODELING OF FLOODPLAIN

We developed a model of isotopic geochemistry dynamics, simulating mixing and fractioning processes, and we coupled it to the hydrological model. Model inputs are time-varying isotopic composition of rainfall, runoff and river waters, and lakes water temperatures that influence equilibrium fractioning during evaporation. Model outputs are the time-varying isotopic compositions of lakes and water fluxes between the lakes and the river. Although the general dynamics of isotopic composition is retrieved, some model discrepancies can be identified:

(1) observed isotopic impoverishment of lakes starts on the first week of December while simulated impoverishment starts one month later. This indicates an overestimation of the channel bottom topography that delays the inflow from the river to the floodplain.

(2) calculated maximum enrichments are underestimated for the Poção and Salé lakes and overestimated for the Grande lake; the isotopic impoverishment during the river rising stage (and rainy season) is slower than observed (Poção, Sale).

This indicates that respective contributions by rainfall, river inflow and lake evaporation are not fully satisfactorily retrieved in the model.

CONTRIBUTION OF FLOODPLAIN OUTPUTS TO THE RIVER DISCHARGE

As shown earlier through measured values (Fig. 4) and simulation results, isotopic composition of floodplain waters flowing back to the river is richer than that of the Amazon River water. At the annual scale, the floodplain dynamics contributes to smoothen the isotopic composition of the water of the Amazon River downstream.

Although further studies are clearly needed, these first results allow estimating the contribution of the floodplain lakes to the isotopic enrichment of the Amazon River during an hydrological cycle.

CONCLUSION

Tracing of stable isotopes in Curuai floodplain proved to be useful to characterize the spatial and temporal variability of floodplain hydrological dynamics.

Measured isotopic compositions of floodplain waters were compared to values calculated by a coupled hydrological-isotopical simulation model. The method allowed to constraint contributions by different water sources (river, rainfall, watershed runoff, groundwater) and control by various physical processes (mixing, fractioning). Above all, isotopic geochemistry provides an indirect method to validate the estimation of some water flux that cannot be directly measured like watershed runoff, river bank overflow, or lake evaporation.

Floodplain waters flowing back to the river are generally enriched in stable isotopes, due to the evaporation of the lakes during the dry season. This suggests a method to quantify floodplains contribution to river discharge and chemical composition along the hydrological cycle.

ACKNOWLEDGMENTS

Authors are grateful to the AEIA (Atomic Energy International Agency) and ANA (Agencia Nacional das Aguas, Brazil) for their support and to all the observers who collected water in the Curuai floodplain.

REFERENCES

Chaffaut I., 1998. Précipitations d'altitude, eaux souterraines et changements climatiques de l'Altiplano nord-chilien. PhD dissertation, Université Paris XI Orsay, France.

Chapelon N., Douville H., Kosuth P., Oki T., 2002. Off-line simulation of the Amazon water balance. in Climate Dynamics vol. 19 , pp 141-154.

Costa M. H., Foley J.A., 1998. Trends in the hydrologic cycle of the Amazon basin. Journal of Geophysical Research, vol. 104, NO.D12, pp 14189-14198.

Fritz P., Fontes Ch., 1980. Handbook of Environmental Isotope Geochemistry, The Terrestrial Environment-A, Elsevier.

Gat, J.R. Matsui, E. 1991. Atmospheric water balance in the amazon basin : an isotopic evapotranspiration model. In : J. Geophys. Res., vol. 96, n° D7, p. 13179-13188.

Junk W.J., 1997. General aspects of the floodplain ecology with special reference to amazonian floodplains, 3-20. In The central Amazon floodplain, Ecology of a pulsing system. Junk W.J. (ed.), Ecological Studies 126, Springer.

Kosuth P., 2002. Hydrological dynamics of the varzea of Lago Grande de Curuai. In 2nd LBA (Large Scale Biosphere Atmosphere) Scientific Conference, Manaus, Brazil.

Martinelli, L.A., Victoria R.L., Sternberg L.S.L., Ribeiro A. and Moreira M.Z., 1996. Using stables isotopes to determine sources of evaporated water to the atmosphere in the Amazon basin. In : Journal of Hydrology 183, pp 191-204.

Martinez J.M., Kosuth P., Cochonneau G., Maurice-Bourgoin L., Seyler F., Bourrel L. and Guyot J.L., 2003. Application of remote sensing data for the quantification of an Amazon floodplain extension, dynamics and water storage. EGS-AGU-EUG Joint Assembly, Nice, April, 2003, France.

Molinier M., Guyot J.L., Callède J., Guimarães V., Oliveira E., Filizola N., 1997. Hydrologie du bassin amazonien, 24-41. In Environnement et développement en Amazonie brésilienne, Théry H. (ed.), Publ. Belin, Paris.

Moura dos Reis C., Tancredi A. C. F. N. S., Matsui E., Salati E., 1975. Caracterização das águas da região de Marajo através de concentrações de O 18 e D. In : A.Amazônica vol.7 n2, 209-222

Seyler F., Martinez J.M., Prigent C., Kosuth P., 2003. Apports de la télédétection à la quantification de la dynamique des zones inondées du bassin amazonien. In Revue de la SFPT (subm.)

Sippel S.J., Hamilton S.K., Melack J.M., Novo E.M.M., 1998. Passive microwave observations of inundation area and the area/stage relation in the Amazon River floodplain. In Int. Journal of Remote Sensing, vol 19, NO 16, pp 3055-3074.

Shukla J, Nobre C, and Sellers P., 1989. Amazon deforestation and climate change. Science 247, 1322-1325.

OXYGEN ISOTOPIC COMPOSITION OF SURFACE AND GROUND-WATERS FROM RIO DAS FÊMEAS SUB-BASIN – URUCUIA AQUIFER – BA, BRAZIL

Nascimento, K.R.F.[1]; Costa, A.B.[2]; Zucchi, M.R.[2]; Matos, C.R.A.[2]; Azevedo, A.E.G.[2] and Pedreira, C.B.[2]

1. Superintendência de Recursos Hídricos - Bahia, CPGG/UFBA. katia@cra.ba.gov.br
2. Laboratório de Física Nuclear Aplicada, Instituto de Física/CPGG/UFBA. abc@ufba.br

Keywords: Isotopes, groundwater, hydrochemistry, $\delta^{18}O$, mass spectrometry

INTRODUCTION

The distribution of isotopes in the water molecules together with the concentration and isotopic composition of the elements dissolved in it have been used increasingly to analyze problems related to the hydrological cycle and the source and dynamic of the groundwater flow. During its flow in the aquifer, the isotopic composition of water is not changed, being related otherwise with the isotopic composition of the precipitations in the recharge areas, usually modified by the evaporation prior infiltration (Nascimento, 1999).

The Rio das Fêmeas sub-basin was selected as a pilot area of the Project of Integrated Management of the Activities Developed in Land in the São Francisco Basin (ANA/GEF/UNEP/OAS), having as main objective to establish guidelines for the integrated management of the superficial and subterranean hydric resources with effective actions executed between March of 2001 and October of 2002, by the Superintendência de Recursos Hídricos – SRH, administrative organ of waters in Bahia State, Brazil (Bahia,2003).

In the present study we report the isotopic characterization of ^{18}O in samples from the main rivers and caption wells in the Rio das Fêmeas Sub-basin, and correlate those data with the hydrochemical analysis, to understand the flow and linkage mechanisms between the superficial and ground waters.

STUDY AREA

The Rio das Fêmeas sub-basin is inserted in the Rio Grande Basin, located in the West of Bahia State, Brazil, this last being a left margin tributary of Middle São Francisco River, with an area of 6,300 km², as shown in Figure 1. The region is characterized by plane relief slightly inclined towards East, sculptured over the Urucuia Formation sandstones, being positioned in height levels between 500 and 900 m, where the most elevated sectors are located in the western border, forming the divisor of waters of the hydrographic basin of São Francisco and Tocantins rivers. The Urucuia sediments are mainly sandstones (Campos, 1996); below them occur the limestones of Bambuí Group, while above emergent aluvionar sandy to clay-sandy deposits of Quaternary. The predominant vegetation in the region is the savannah, whose presence is related to the predominance of latossols (Bahia, 2003).

The meteorological conditions in the region determine two kinds of climates: Humid (B1wA') and Humid to Sub-humid (C2wA'), with a dry season well defined in the winter and rain in the spring/summer. The precipitation regime in the Rio das Fêmeas sub-basin varies between 900 and 1,200 mm/year, varying positively towards West. The average annual temperature is 23.2°C, with the medium temperatures, maxim and minimum, of 32°C and 18°C, respectively. The relative humidity of the air shows annual average of 68%, varying from 45% in August to 79% in March. The annual evaporation rate is about 1,580 mm (Bahia, 2003).

The Rio das Fêmeas sub-basin is one of the biggest aquifers from Bahia State. The annual average discharge is 52.17 m³/s. From the hydrogeological viewpoint, the post-depositional siliceous cementation that is found in the Urucuia Formation in almost the entire area of this study defines two aquifers: a superior with predominant fissural characteristics and other granular on the bottom. This silicified zone obstructs part of the primary porosity of top sediments, giving a character semi confined to the granular aquifer (Bahia, 2003).

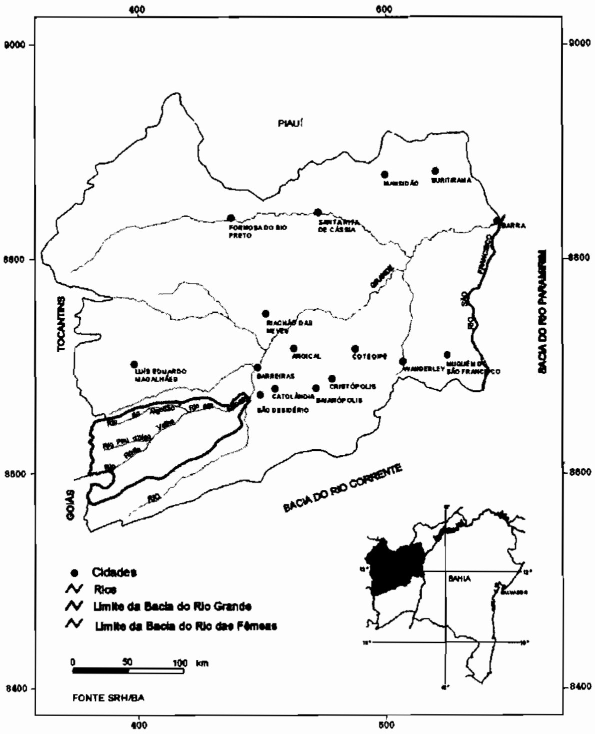

Figure 1. Study Site showing its location in Bahia State, Brazil (Bahia, 2003).

METHODOLOGY

In this study were collected samples of superficial waters (6 points from rivers and dams) and groundwaters (19 points from production wells and open wells), in September of 2001 and June of 2002, for the $\delta^{18}O$ and physical-chemical analysis. The samples were collected in white polyethylene bottles of 1,000 ml and 100 ml to the geochemical and isotopic analysis, respectively. The bottles were washed with the sample of water and filled out completely. After the arrival in the laboratory, they were stored in the dark and under refrigeration (Mazor, 1991).

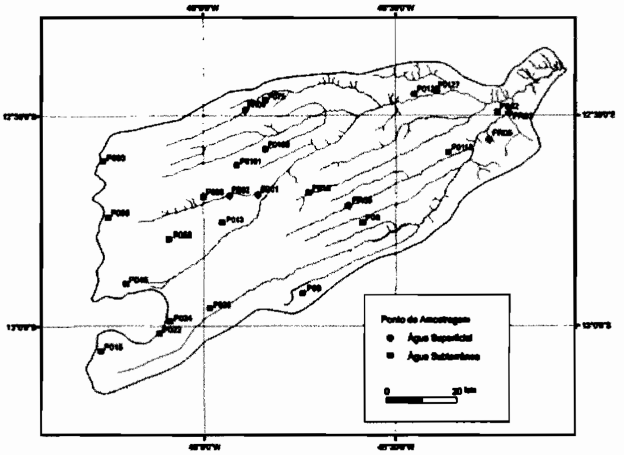

Figure 2. Samples collection points for both campaigns.

LABORATORY MEASUREMENTS

The isotopic analysis of ^{18}O was realized in the Applied Nuclear Physics Laboratory (LFNA) CPGG/UFBA, using a mass spectrometer DELTA PLUS ThermoFinnigan.

The method used for the $\delta^{18}O$ analysis was the equilibration of water with CO_2 , at the temperature of 25,0 ± 0.1 °C, for at least 8 hours (Costa, 1990), and reported as a deviation from the SMOW.

The samples were prepared in duplicate, with 3 ml of water sample introduced in a glass syringe containing one drop of 100% sulphuric acid. After the air is removed of the syringe, 5 ml of CO_2 are addicted to it, with pressure slightly over 1 atm. These syringes are conditioned in a metal box into a thermostatic bath at 25.0 ± 0.1°C during 16h and after that period, the CO_2 resulting from that equilibrium is purified in a high vacuum line and collected in gas canisters. The sample is inserted in the mass spectrometer for the ^{18}O measure. A secondary standard water referenced to SMOW follows each set of samples to be analysed. The data acquisition and the calculations of the $\delta^{18}O$ are done through the ThermoFinnigan software ISODAT. The standard deviation of the secondary standard of a set of samples from the SMOW is calculated and from this result, evaluated the deviation of the samples from the secondary standard that accompanied them and thus, from the SMOW.

The chemical analysis of the waters was realized in EMBASA laboratories and the methodologies utilized in the physical-chemical analysis were based in the manuals Standard Methods for the Examination of Water and Wastewater, 19th Edition (APHA/AWWA/WEF, 1995) and American Society for Testing of Materials (1992).

RESULTS AND DISCUSSION

HYDROCHEMICAL DATA

From the physic-chemical analysis, it was observed that all samples possess few dissolved salts with concentration of main anion and cation values, in most of the samples, being under the detection limit of the method utilized for the analysis.

In the Rio das Fêmeas sub-basin the sodium analysis was made only in the 2002 campaign, when was found an average concentration of 0.03 mg Na^+/L for the 20 points sampled. In both 2001 and 2002 campaigns it was not detected salinity at the sampled points, in the ground as well superficial water, what characterizes a water with low concentrations of salts, that can be utilized for irrigation without risk of soil salinization.

The average concentrations of total dissolved solids (TDS) were 48.39 mg/L and 28.60 mg/L for the 2001 and 2002 samples collection, respectively. These values of TDS characterize the water as good for human consumption (maximum 500 mg/L) as well as for animal consumption (maximum 2,500 mg/L) and for agricultural use.

ISOTOPIC DATA DISCUSSION

The analysis of the data from the first group of samples (end of dry season in the region) showed an isotopic behavior with variation from -5.0‰ to -1.2‰; the most enriched samples were from open and shallow wells (about 10 m of depth), subjected to hard evaporation and without water renovation. For the groundwater data the values had a $\delta^{18}O$ average around –4.4‰, disregarding the open wells. In the superficial water samples an average -3.8‰ $\delta^{18}O$ value was found.

In the second group of samples (beginning of the dry season), the values obtained in the samples analysis had a variation between -5.5‰ and -2.2‰ with an average to superficial waters of -4.2‰ and to groundwaters of -4.7‰, disregarding the open and shalow wells.

Figure 3 shows that there is a slight enrichment in the ^{18}O values of the samples collected in September of 2001 when compared to that collected in June of 2002. That enrichment can be explained by the time that the samples were collected, the first in the end and the last in the beginning of the dry season. At the end of the dry season, the water is more evaporated than at the beginning of the period, that is, it shall occur a higher enrichment in ^{18}O at the end of the dry season, as showed in the data of this study. It also can be observed, specially in the June of 2002 group of samples, that the values obtained for the superficial water are very close to those obtained for the groundwater samples. These data show that there is a connection between both waters in the Rio das Fêmeas sub-basin region, as it was found in the hydrological characterization and the mathematical modeling of the Subproject 3.2 (Bahia,2003).

Table 1. Hydrochemical and isotopic data for the samples collected in September-2001 and June-2002 at Rio das Fêmeas sub-basin. Data values with the symbol "< "were below the detection limit of the methodology used in this study, while an means the samples could not be analysed.

Points	September 2001						June 2002								
	Mg^{++} (mg/l)	Ca^{++} (mg/l)	Cl$^-$ (mg/l)	SO$_4^-$ (mg/l)	Total alkalinity (mg/l)	δ ^{18}O‰	Points	Mg^{++} (mg/l)	Ca^{++} (mg/l)	Cl$^-$ (mg/l)	SO$_4^-$ (mg/l)	K$^+$ (mg/l)	Na$^-$ (mg/l)	Total alkalinity (mg/l)	δ ^{18}O‰
P006	0.12	0.51	na	<1	2.02	-4.58	P008	< 0.30	6.61	< 1.50	< 1.00	< 0.02	0.4	na	-5.13
P009	0.25	1.01	3.43	<1	na	-4.58	P009	< 0.30	< 0.40	2.52	5.1	0.7	1.4	na	-4.75
P012	1.97	13.2	5.14	2.3	na	-1.2	P012	0.3	2.99	4.03	1.7	0.7	6.2	na	-2.23
P015	nd	0.51	na	<1	0.5	-5.05	P015	< 0.30	< 0.40	< 1.50	< 1.00	< 0.02	0.2	na	-5.46
P024	0.12	0.51	na	<1	0.35	-3.93	P024	< 0.30	< 0.40	< 1.50	< 1.00	na	0.3	na	-4.86
P028	0.12	1.52	na	<1	1.56	-4.37	P028	< 0.30	< 0.40	< 1.50	< 1.00	< 0.02	0.3	0.25	-4.93
P042	0.12	0.51	na	<1	0.76	-4.19	P042	< 0.30	< 0.40	< 1.50	1.4	na	0.7	0.25	-4.25
P045	0.49	23.3	na	1.2	na	-4.33	P045	< 0.30	< 0.40	< 1.50	< 1.00	na	0.2	1.26	-4.93
P058	0.25	1.01	na	1.2	1.46	-4.13	P058	< 0.30	0.44	< 1.50	< 1.00	na	0.5	1.51	-4.04
P065	nd	0.51	na	<1	0.4	-4.52	P065	< 0.30	< 0.40	< 1.50	< 1.00	na	0.2	na	-4.88
P075	0.74	1.01	na	2	2.27	-4.19	P075	< 0.30	0.52	< 1.50	< 1.00	< 0.02	0.4	3.03	-4.36
P083	0.49	5.07	na	<1	3.53	-4.81	P083	< 0.30	< 0.40	< 1.50	< 1.00	< 0.02	0.2	na	-5.17
P096	0.37	1.01	na	<1	3.53	-4.4	P096	< 0.30	< 0.40	< 1.50	< 1.00	< 0.02	0.3	na	-4.65
P101	0.25	2.03	na	<1	3.28	-4.47	P101	< 0.30	< 0.40	< 1.50	< 1.00	< 0.02	0.2	2.02	-4.33
P109	0.74	6.09	na	<1	8.72	-4.12	P109	< 0.30	0.52	< 1.50	< 1.00	0.1	1.2	3.53	-4.51
P113	0.25	2.03	na	<1	2.42	-4.3	P113	< 0.30	< 0.40	< 1.50	< 1.00	na	0.4	0.5	-4.42
P118	na	na	na	7.4	na	-4.58	P118	na	na	na	na	na	na	na	-4.75
P127	0.12	0.51	2.94	<1	0.25	-4.93	P127	< 0.30	< 0.40	< 1.50	1.4	0.1	0.8	0.76	-4.97
P128	0.12	0.51	na	<1	0.76	-2.92	P128	na	na	na	na	na	na	na	-3.55
FR02	0.25	1.01	na	1.8	1.51	-4.32	FR02	< 0.30	< 0.40	< 1.50	< 1.00	na	0.3	0.5	-4.36
FR03	na	na	na	2.65	na	-3.91	FR03	< 0.30	< 0.40	< 1.50	2.4	0.1	0.4	0.25	-4.22
FR04	na	na	na	7.4	na	-4.14	FR04	na	na	na	na	na	na	na	-4.59
FR05	na	na	na	1.2	na	-3.94	FR05	na	na	na	na	na	na	na	-4.02
FR06	na	na	na	6	na	-3.57	FR06	na	na	na	na	na	na	na	-4.08
FD07	na	na	na	2.37	na	-2.7	FD07	na	na	na	na	na	na	na	-3.97
FD08	-	-	-	-	-	-	-	< 0.30	< 0.40	< 1.50	< 1.00	< 0.02	0.3	0.25	-

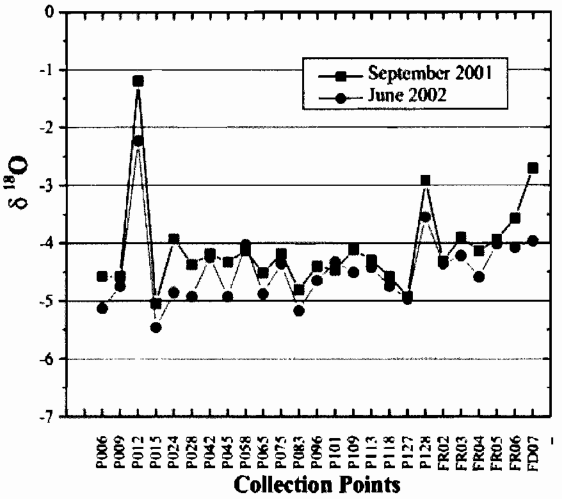

Figure 3. Graphic of the δ ^{18}O values found in the 2001 and 2002 Rio das Fêmeas sub-basin campaigns.

CONCLUSIONS

Through the results obtained by the physical-chemical parameters and ^{18}O isotopic analysis it can be concluded that:

The hydrochemical data presented certain uniformity in their values (the majority having values below the detection limit), being the water quality considered as good for both agricultural and human use.

The isotopic values showed that the superficial and groundwaters have an isotopic composition very similar, indicating that there is a connection between them, what is in accordance with the results found in the hydrological characterization and the mathematical modeling.

ACKNOWLEDGEMENTS

The authors are grateful to Superintendência de Recursos Hídricos – SRH, Agência Nacional de Águas – ANA, Global Environment Facility – GEF, United

Nations Environment Program - UNEP, Organization of American States – OAS and Conselho Nascional de Desenvolvimento Científico e Tecnológico - CNPq.

REFERENCES

APHA/AWWA/WEF, 1995. Standard Methods for Examination of Water and Wastewater. 19th EDITION.

ASTM, 1992. American Society for Testing of Materials.

Bahia, 2003. Subprojeto 3.2- Uso Conjunto da Águas Superficiais e Subterrâneas da Sub-bacia do Rio das Fêmeas - Bahia, parte integrante do Projeto de Gerenciamento Integrado das Atividades Desenvolvidas em Terra na Bacia do Rio São Francisco (ANA/GEF/PNUMA/OEA).

Campos, J. E. G., 1996. Estratigrafia, Sedimentação, Evolução Tectônica e Geologia do Diamante da porção Centro-Norte da Bacia Sanfranciscana. Brasília, Universidade de Brasília. Tese de Doutorado. Instituto de Geociências da Universidade de Brasília. Brasília-DF, 204p.

Costa, I. S., 1990. Hidrologia isotópica de águas subterrâneas na região de Cipó-BA. Salvador, Universidade Federal da Bahia. Dissertação de Mestrado.

Mazor, E., 1991. Applied Chemical and Isotopic Groundwater Hydrology.

Nascimento, K.R.F., 1999. Estudo isotópico e hidroquímico de aqüíferos no Pólo Petroquímico da Bahia. Salvador, Universidade Federal da Bahia, Dezembro de 1999 Dissertação de Mestrado apresentada em Dezembro de 1999, para obtenção do Título de Mestre em Geofísica. Universidade Federal da Bahia, 67 p.

ENVIRONMETAL ISOTOPES AND GEOCHEMISTRY OF BAÑADO CARILAUQUEN, MENDOZA, ARGENTINA

Ostera, H.A.[1,2] and Dapeña, C.[1,2]

1. Instituto de Geocronología y Geología Isotópica (INGEIS-CONICET), Pabellón INGEIS, Ciudad Universitaria, 1428 Buenos Aires, Argentina. ostera@ingeis.uba.ar, dapenna@ingeis.uba.ar
2. Departamento de Ciencias Geológicas, Facultad de Ciencias Exactas y Naturales, Universidad de Buenos Aires, Pabellón II Ciudad Universitaria, 1428 Buenos Aires, Argentina

Keywords: Geochemistry, environmental isotopes

INTRODUCTION

The environmental impact of the industrial activities leads to a great concern about the conservation of natural pristine resources. This objective confronts with a big challenge: How we can determine the original environmental parameters before the anthropic influence?

Moreover, in petroleum fields the base levels of hydrocarbon concentration in waters and soils have natural anomalies related to existence of oil reservoirs themselves.

Consequently, it is very complex to quantify the environmental impact of petroleum exploitation and the influence of possible spills if previous base studies were not made. Since 1930, the Llancanelo oil field, located at Malargüe, Mendoza province, has been exploited and explored. Sulfurous waters and gas manifestations were found near the mouth of the arroyo Carilauquen. The aim of this study is to characterize the natural pristine conditions of the system by means of geochemistry and environmental stable isotopes (^{2}H and ^{18}O) and also, a first approach for the origin and circulation pattern of water.

GEOLOGIC AND HYDROLOGIC SETTING

The Bañado Carilauquen is located at Departamento Malargüe, Mendoza Province and in the hydrogeologic province "Valle Medio de los ríos Atuel, Salado y Malargüe" (Pazos et al., 1993) (Fig.1). It belongs to the Llancanelo Lake close system, where the main flow is the Malargüe river. The term "Bañado" corresponds to a geographic word and means a wetland under arid conditions. Several small streams ("arroyos") named Chacay, Alamo, Mocho, Durazno and springs Los Menucos and Carilauquen form this system.

This region is part of the Neuquén sedimentary basin. The sedimentary sequence, from top to base, begins with sandstones and claystones alternating with basalts of Tertiary age (700/1000 m). Upper Cretaceous beds composed by gypsum, carbonates, marls, claystones and sandy siltstones underlie this section. The stratigraphic column continues with the Neuquén Group integrated by conglomerates and conglomeradic sandstones alternating with silty claystones. The column lies over a volcanic sequence and in some areas outcrops the Lower Cretaceous Mendoza Group. Quaternary basalts intrude and cover all the sedimentary sequences. A detailed description about this basin can be found in Legarreta and Uliana (1999) and Riccardi et al. (1999).

An alluvial sedimentary thickness of 500m was measured by geophysical methods at Malargüe basin. Towards the Llancanelo Lake this thickness increases up to 1000m but the grain size decreases gradually and near the shoreline there are fine sediments and salts.

The Bañado Carilauquen is a geomorphic unit intimate related to the Laguna Llancanelo, covers an area of 70 km^{2} and is drained by a semi permanent course of water (Arroyo Carilauquen). It is a Provincial Reserve, with a wide spectrum of animal and vegetation life.

The equilibrium of the system is very fragile. Evaporation predominates over precipitation, stream flow, infiltration and surface runoff; therefore the hydrologic balance is usually negative. Occasionally, a little recuperation of the water lake level is observed during some hydrological rich years. Infiltration is high due to volcanic rocks fissures and soil characteristics, and the water table is near surface at most places

The insufficient number of water wells reduces the groundwater interpretation of the global area.

The region has an arid climate and very dry. The mean annual precipitation (rain and snow) is about 241 mm, but their distribution is heterogeneous. There are higher from May to October (snow) but during summer there are short and intense rains. The mean annual temperature is 12,5°C (January: 21,3°C and July: 3,6°C).

The precipitation-evaporation balance is usually negative in summer promoting an increase in the water content of dissolved solids and enrichment in the isotope stable composition.

Precipitation (snow and rain) is the variable contribution to the whole system and local infiltration the only recharge process.

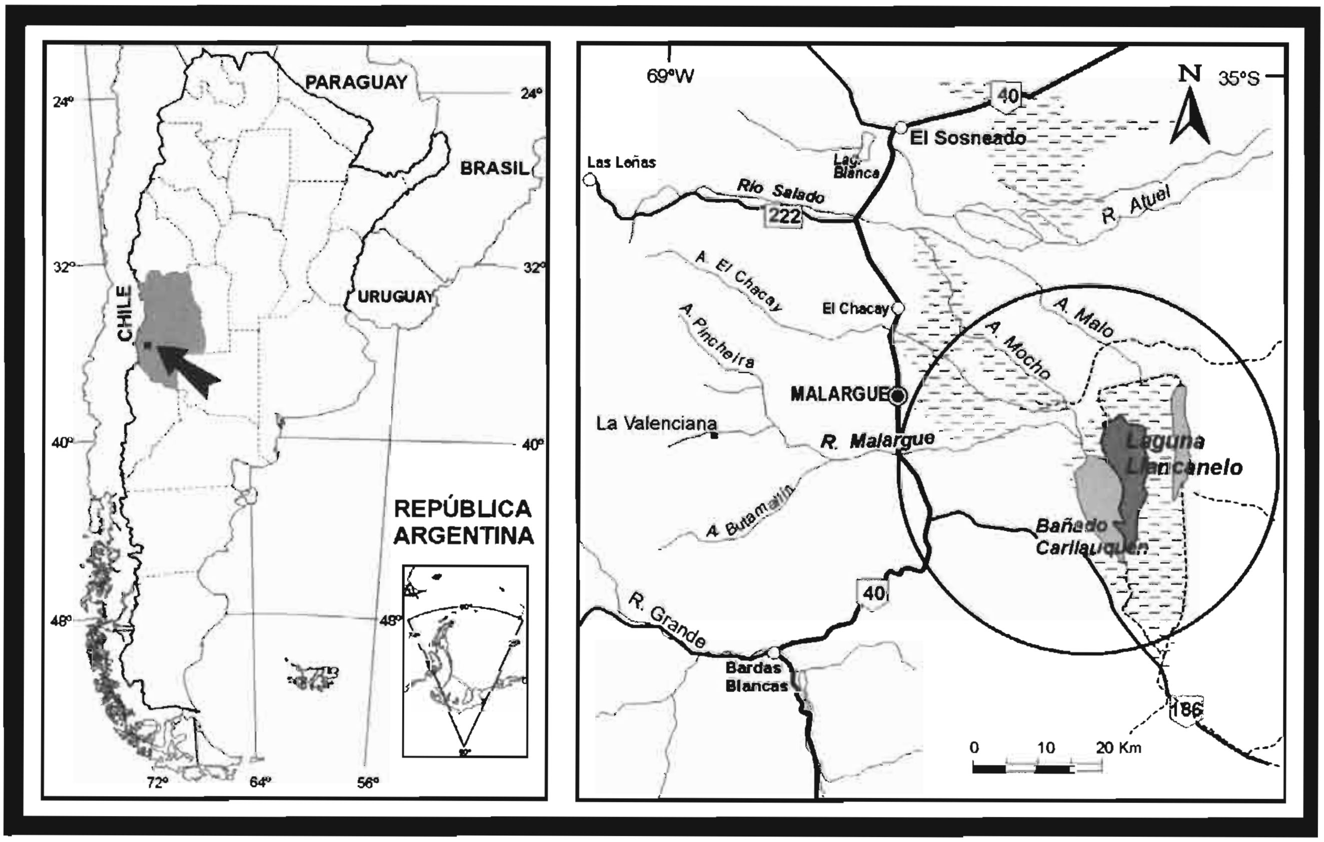

Figure 1. Location map.

MATERIALS AND METHODS

During February, 2001, water samples were collected from the Bañado Carilauquen water, springs, and Malargüe river. Groundwater was sampled from 3 phreatic wells used by rural population for cattle, small crops and consumption.

Temperature and pH were determined in the field by means of a portable pH meter and titration. Major ions were determined by conventional methods and by Inductively Coupled Plasma Spectrometry (ICP, BAIRD 2070). Total dissolved solids (TDS) were calculated as the sum of the above ion concentrations. Hydrocarbon concentrations were measured by infrared spectrometry. Chemical and isotopic analyses were done at INGEIS Laboratories.

^2H in water samples was measured by Coleman et al. (1982) procedure and for the measurement of ^{18}O was used the methodology described by Epstein and Mayeda (1953) and Roether (1970) and modified by Panarello and Parica (1984) at INGEIS' Laboratory. Isotope ratios were measured with a multicollector McKinney type mass spectrometer, Finnigan MAT Delta S.

The results are expressed like δ(‰) defined as:

$$\delta = 1000 \frac{R_S - R_P}{R_P} ‰$$

δ: isotopic deviation in ‰ ; S: sample; P: international standard; R: isotopic ratio ($^2H/^1H$; $^{18}O/^{16}O$).

The standard is Vienna Standard Mean Ocean Water (V-SMOW) (Gonfiantini, 1978). The analytical errors were ±0,1‰ and ±1,0‰ for $\delta\,^{18}O$ and $\delta\,^2H$ respectively.

RESULTS AND DISCUSSION

A summary of percentage ionic composition is shown in a Piper diagram (Fig.2). Schoeller graphic point up the relationships between the different types of samples, where water of similar composition plot as near-parallel lines. In this case the Bañado Carilauquen water follows the Malargüe river type, while the Llancanelo lake samples have another pattern (Fig.3). The groundwater are between both types. Field water temperature varies from 15,6°C to 31,6°C and pH values range between 7,5 and 8,1.

Bañado Carilauquen and springs samples were 100 % strongly calcium (> 75 % meq/L Ca^{++}), 75 % strongly sulfated (> 75 % meq/L SO_4^-) and 25% sulfated (> 50 % meq/L SO_4^-). Total dissolved solids varies from 878 to 1168 mg/L. Piper diagram shows that Bañado Carilauquen and springs samples, Malargüe river water and phreatic wells are sulfate-chloride-calcium type while the Llancanelo lake waters and South Well phreatic water are chloride-sulfate-sodium type (Fig.2).

Sulfate contents exceed drinking water regulations suggested by OMS. Nitrate concentrations are very low, most of the samples were below the detection limit (maximum value: 3 mg/L). Ostera (2001) indicates the existence of a mixing of 2% between the South Well and the Llancanelo lake waters. This is probably a consequence of the overexploitation and reveals the possibility of a saline wedge.

Hydrocarbons were not detected in all the cases.

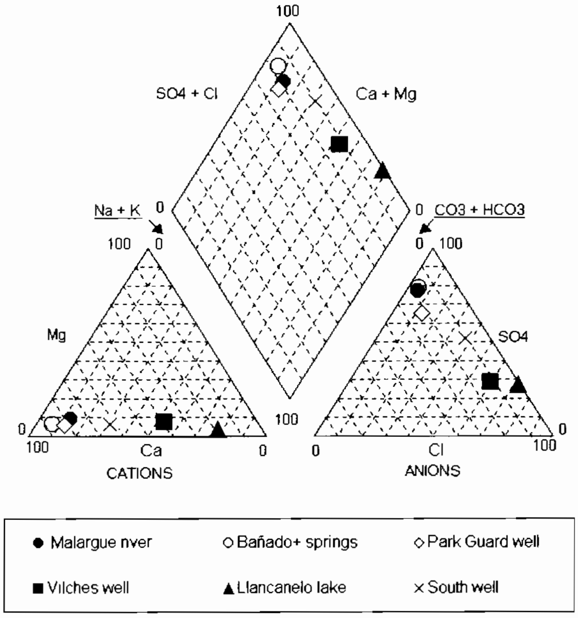

Figure 2. Piper diagram.

The Bañado Carilauquen and springs water, the arroyo Serrucho (headwaters of Malargüe river, altitude: 3000m), groundwater from South Well, Park Guard Well, Vilches Well and the Llancanelo lake were sampled to perform isotope analyses (^{18}O, ^{2}H). Figure 4 exhibits a scatter plot $\delta^{18}O$ *versus* ^{2}H of the analyzed samples, the global meteoric water line (MWL), $\delta^{2}H=8*\delta^{18}O$ +10‰ (Craig, 1961) and some individual precipitation from Bardas Blancas station. This station, next to the study area, has a short isotope record. It belongs to the National Network of Isotopes in Precipitation (RNC) of Argentina and the Global Network for Isotopes in Precipitation (GNIP) (Dapeña and Panarello, 2001; IAEA/WMO, 2002). At present, it is out of service.

The Arroyo Serrucho shows the most depleted values ($\delta\ ^{18}O$=-16,5‰) indicating recharge at high altitude. The depletion of the heavy isotope content of precipitation as a function of altitude, denoted "Altitude effect" was defined by Dansgaard (1964) and has been most usefully applied in hydrologic research (Gat and Reitti-Shati, 1999). The Malargüe river, Bañado and springs Carilauquen have values also depleted ($\delta\ ^{18}O$=-14,9 to –14,4‰) but lower than Serrucho and higher than local precipitation, showing different altitude recharge. The phreatic waters from Park Guard and South wells have the same values of Bañado waters but the Vilches well is slightly enriched ($\delta\ ^{18}O$=-13,9‰). The lake waters have the maximum enrichment isotope values indicating high evaporation. They fit on an evaporation line: $\delta^{2}H=5,3\delta^{18}O-30,7$.

These evidences support the idea that the Malargüe River infiltration westwards is the main source of recharge for surficial waters and groundwater. Local meteoric rainwater could play a minor role by direct infiltration through fractured volcanic rocks northwards, as suggested by geochemistry and isotope content.

The chemical mixing observed at South well by hydrochemical modeling, is poorly detected by isotopes, probably due to the mixing proportions that mask the isotopic response.

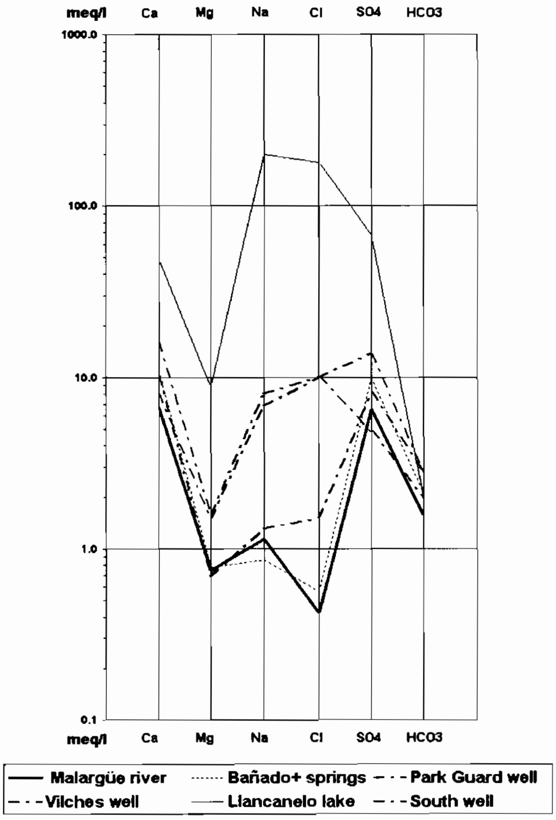

Figure 3. Schoeller diagram.

CONCLUSIONS

Geochemistry and isotope baseline study of Bañado Carilauquen indicate that there are two main types of water in the area: sulfate-chloride-calcium type and subordinate chloride-sulfate-sodium type. The sulfate contents are higher than limits proposed by OMS.

Hydrocarbon pollution was not detected.

The main sources of recharge for Carilauquen springs could be related to the Malargüe River infiltration westwards owing the similarities on isotope composition.

However, it cannot discard some local meteoric recharge detected in groundwater. Mixing processes due overexploitation are detected by geochemical modeling, but are masked in the isotope signal. Lake waters show a marked isotope enrichment, linked with evaporation processes. These environmental parameters establish the natural geochemical and isotope background of this area, which fragile equilibrium could be endangered by human activities.

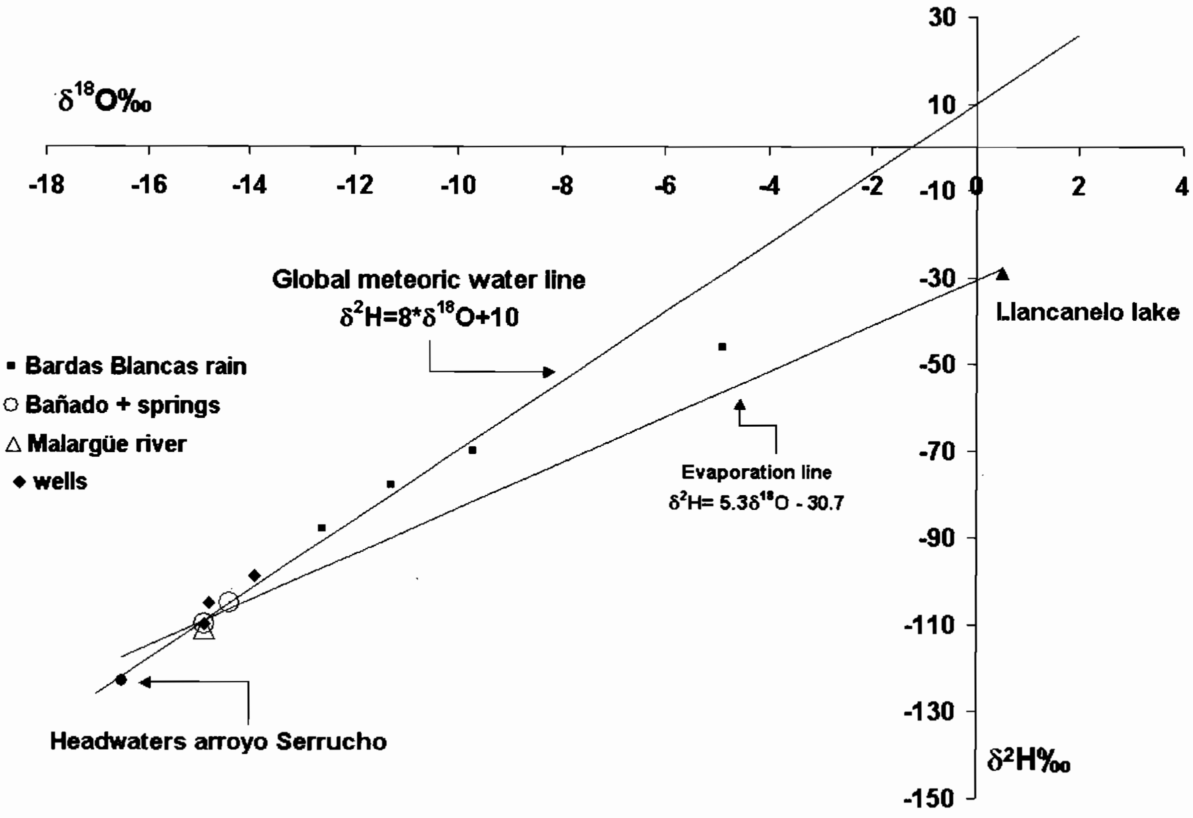

Figure 4. Scatter plot $\delta^{18}O$ *versus* $\delta^{2}H$.

REFERENCES

Coleman M.L., Sheperd, T.J., Durham, J.J., Rouse, J.E. and Moore, F.R., 1982. A rapid and precise technique for reduction of water with Zinc for Hydrogen isotope analysis. Analytical Chemistry. 54: 993-995.

Craig, H., 1961. Isotopic variations in Meteoric waters. Science 133: 1702-1703.

Dansgaard, W., 1964. Stable Isotopes in precipitation. Tellus, 16: 436-468.

Dapeña, C., Panarello, H.O., 1999. Development of the National Network for Isotopes in Precipitation of Argentina. II South American Symposium on Isotope Geology, 503-508.

Epstein, S. and Mayeda, T., 1953. Variation of $\delta^{18}O$ content of water from natural sources. Geochimica and Cosmochimica Acta 4: 213-224.

Gat, J.R. and Rietti-Shati, M., 1999.The meteorological vs the hydrological altitude effect on the isotopic composition of meteoric waters. In: Isotope techniques in water resources development and management. Proc. Symposium, Vienna.IAEA. 5p.

Gonfiantini, R. 1978. Standards for stable isotope measurements in natural compounds. Nature 271: 534

IAEA/WMO, 2002. Global Network for Isotopes in Precipitation. The GNIP Database. http://isohis.iaea.org

Legarreta, L and Uliana, M.A., 1999. El Jurásico y Cretácico de La Cordillera Principal y La Cuenca Neuquina. 1. Facies Sedimentarias. Geología Argentina. Caminos, R. (Editor). Anales N° 29. Servicio Geológico y Minero Argentino; 399-416. Buenos Aires, Argentina.

Ostera, H.A. 2001. Estudio geoquímico base. Bañado Carilauquen, Departamento Malargue, Provincia de Mendoza. Informe inédito. Fundación CRICYT. Mendoza

Panarello, H.O. and Parica, C.A., 1984. Isótopos del oxí-geno en hidrogeología e hidrología. Primeros valores enaguas de lluvia de Buenos Aires. Asociación Geológica Argentina, Revista XXXIX (1-2): 3-11.

Pazos J.A. , Bessone, J.L., Vivas, J.A., Vaca, A., Wetten, C.y Valero, C.E. , 1993. Recursos hídricos subterráneos y aguas termales. Capítulo V-1. XII Congreso Geológico Argentino. Geología y Rrecursos Naturales de Mendoza. V,A, Ramos (ed) Relatorio V (1): 551-599.

Riccardi, A., Damborenea, S., Manceñido, M.and Ballent, S., 1999. El Jurásico y Cretácico de la Cordillera Principal y la Cuenca Neuquina.3. Bioestratigrafía. Geología Argentina. Caminos, R. (Ed.) N.°29.Servicio Geológico Minero Argentino, 419-432.BuenosAires, Argentina.

Roether, W., 1970. Water CO_2 exchange set-up for the routine oxygeen-18 assay of natural water. International Journal Applied Rad. Isotopes, 21: 379-387.

HOLOCENE Pb ISOTOPE CHRONOLOGICAL STANDARD CURVE: A REVIEW OF THE RECORD OF THE ANTHROPOGENIC ACTIVITY IN THE LAST 6,000 YEARS

Paula, A.H. and Geraldes, M.C.

Tektos Research Group-Faculty of Geology, State University of Rio de Janeiro (UERJ),
Rua São Francisco Xavier 524, 20559-900 Rio de Janeiro-RJ, Brazil

Keywords: Isotope, anthropogenic, standard curve

INTRODUCTION

Over the last 6,000 years, anthropogenic Pb has been introduced into the global environment through atmosphere transport. Prior to the industrial revolution, anthropogenic lead was emitted solely as a by-product of mining and smelting of lead, silver and copper ores. By the mid-18th century, combustion of Pb-containing coal became the primary source of industrial lead emissions to the atmosphere. Since the 1920s, automobile exhaust, with Pb-containing gasoline additives (alkyllead), has overwhelmed all others sources of anthropogenic Pb emitted into the environment. Actually, more than 95% of lead deposited in the environment is of anthropogenic origin (Marcantonio et al., 2002).

Attempts to identify pollution sources have included the use of elemental ratios, but total Pb concentrations alone may be insufficient for separating pollution from natural background. This is because the background Pb concentration is often highly variable due to natural processes (Helland et al., 2002). In contrast, Pb isotope abundances are not affected to any measurable extent by physical or chemical processes in terrestrial environments. Given the significant isotopic differences in Pb emissions, researchers have been able to use historical records of anthropogenic Pb isotope variations to trace the changing sources of pollutant Pb in continental environment through the time.

Pb is one of the high priority contaminants in surface water and occurs naturally as four stables isotopes. Pb is known to adsorb strongly to particles and typically follows organic particles draining out of the soil. In the last decades Pb isotopic analysis has been used with great success to trace elements in recent sediments back to their source, distinguishing between sources, tracing elements along their route from source to burial, and assessing the effect of remedial actions taken to reduce emissions from a specific polluter. In addition, establishing references sites is a critical factor in determining the baseline of ecosystems and the information on contaminant background concentrations subsidizes the remediation of impacted landscapes. Thus, it would be important the construction of a Pb isotope chronological standard curve applicable to these environment over the last millennia. This contribution aims to make a tentative Holocene Pb isotope curve (using reported data) and also intends to encourage future research on Holocene deposits with the objective to obtain the Pb isotopes curve for the South America continent.

Pb ISOTOPES IN AEROSOL, WATER, SEDIMENTS, ICE AND SOIL

The anthropogenic Pb is distributed through the atmosphere and subsequently enters the terrestrial and marine environments by wet and dry deposition. The history of anthropogenic Pb emissions has been investigated by analyzing the isotope composition of Pb in suspended particulate matter (aerosols), sediments, water, ice and soil. The time of residence of Pb isotopes in the atmosphere is about 2 weeks (Verón et al., 1992); the residence time of Pb in deep water is about 50 to 200 years. Further, the geographic distribution of Pb isotopes in sedimentary deposits worldwide is not simple response to local sources.

Studies of airborne particulates have show that atmospheric Pb is dominated by long-range, transported anthropogenic Pb. The sources of the anthropogenic Pb differs between regions, as example the northern Canadian and Greenland High Artic (Outridge et al. 2002), US and part of Canadian territory (Sturges and Barrie, 1989), and Europe (Luck and Othman, 2002). About 85% of the global industrial emissions are introduced into the atmosphere in the Northern Hemisphere. It has been shown, however, that the characteristic time for the inter-hemisphere exchange is about one year. Since the mean residence time of Pb rich aerosols in the atmosphere is ~two weeks, thus Northern Hemisphere emissions are taken to have a negligible influence on the Southern Hemisphere.

Pb isotope vertical profiles in recent sediment cores have been used for various purposes, such as stratigraphic interpretation of paleoenvironment and recent pollution history. There has been an increasing interest in the application of radiogenic isotopic tracers (Nd, Pb and Sr) in marine deposits to oceanographic problems, and to the cycling of these elements in seawater (Hemming and McLennan, 2001). These tracers are largely derived from continental sources and must ultimately enter the ocean by rivers or in the form of wind-blown dusts. In estuarine marshes, such a global atmospheric signal should be recorded, despite local input (industry, shipping and dense human population), which could obscure the atmospheric signal. By contrast, local mantle-derived inputs are evident in hydrothermal Fe-Mn deposits located near active spreading ridges. River and anthropogenic inputs, and biological and geochemical cycling may influence the concentration of metals in estuarine and coastal seawater to a much greater extent than that occurring in open-ocean water and deep-sea turbidites. The mechanism for dispersal of these metals, and their inputs into receiving systems such as sediments, have been the subject of numerous studies and, in such research, it is often necessary to attempt to evaluate the impact of local, point source releases against background levels due to regional or global contamination.

Continental Pb contamination may originate from diffuse sources, such as vehicle exhaust emission, or from point sources, such as metal smelters or mine waste tips. Pb isotope data from natural environmental archives are useful not only for assessing background concentration and temporal trends, but can also potentially be used to identify source regions. Unfortunately, data from many regions are sparse and individual sites are often used to characterize and reconstruct depositional trends over vast areas. On local scale Pb isotope studies have been applied in the investigation of contaminant Pb sources and behavior within specific environments with, for example, applications in the studies of streams and groundwater, soils and rivers. Various investigations have confirmed the advantages of the use of Pb isotopes to probe the anthropogenic inputs *versus* natural origins of this toxic heavy metal in well-preserved snow and ice archives of atmosphere constituents. Most investigations have been devoted to the Greenland icecap, high-altitude alpine regions, and in Antarctic snow (Planchon et al., 2003).

In stratigraphic studies, the most commonly used chronological tool is the down-core oxygen isotope variations measured in foraminifera and calibrated according to the standard SPECMAP curve. In coastal and continental environment, there is no such toll due the lack of foraminifera. A similar approach could be applied using ostracoda, when they are present. Consequently, in such environment, dating is generally obtained by radiochronology (^{14}C, ^{210}Pb, ^{137}Cs, etc). However, ^{14}C measurements provide only discrete data, while ^{137}Cs and ^{210}Pb is best applied in the last century.

PRIOR INDUSTRIAL REVOLUTION Pb RECORD

The history of anthropogenic Pb emission has been investigated by analyzing the isotope composition of Pb in sediments and ice to evaluate the pre-industrial revolution Pb record (Fig. 1A). The natural background corresponds to sections displaying high ^{206}Pb/^{207}Pb between 12,000 and 2,600 years. A continuous atmospheric Pb pollution from 12,000 years has been observed in peat bog (in Swiss) and the average ^{206}Pb/^{207}Pb value is 1.199. Pb isotopic composition has been reported in Holocene estuarine marshes (in France) dated at 6,053 ± 172 years (^{14}C age), with background ^{206}Pb/^{207}Pb values about 1.20–1.19.

During the time of the Roman Empire, due to an intensive mining activity, large quantities of heavy metals were emitted into the atmosphere. Metal pollution dating to ancient times was recorded in various types of environment such as polar ice, ombrotrophic peat bogs and lake sediments (Niagru, 1989). The Pb isotope contamination in Greenland icecap was dated at 2,500 years ago (^{210}Pb age; Hong et al., 1994) and at 2,600 years ago (^{210}Pb age; Renberg et al., 1994) in lake sediments of Sweden. The depression of the ^{206}Pb/^{207}Pb values occurred from the background values of 1.199-1.206 to values from 1.176 to 1.184 and may be explained by the influence of ore Pb signature exploited at that time. The main lead deposit in operation was the Rio Tinto deposit in Spain, which ^{206}Pb/^{207}Pb values from 1.162 to 1.168.

During the Medieval period (1,700-1,200 years ago) ^{206}Pb/^{207}Pb values increased whereas, at the same time, the worldwide Pb production decreased after the fall of Rome, and the values of ^{206}Pb/^{207}Pb recorded in sediments is about 1.176. From 1,200 years ago the ^{206}Pb/^{207}Pb values (about 1.172) can be associated to the increase of the Pb signature related to the production of mining Pb ores in Europe. The more important mining areas during this period were located in Germany (Harz Montains and Rammelsberg mines) and in England (Derbyshire mine), which ^{206}Pb/^{207}Pb values are 1.180, 1.164-1.168, and 1.171-1.187, respectively (Alfonso et al., 2001).

INDUSTRIAL REVOLUTION Pb ISOTOPE RECORD

Pb isotopes have proven to be powerful tracers of the origin and provenance of soils, lake sediments, coasts estuarine sediments and ice in distinguishing the Pb isotope signatures contamination resulted of the industrial revolution (Fig. 1B). Since the economic development occurred in specific periods and with distinct characteristics in countries and continents, the Pb isotopes record of this period of time is geographic- and time-dependent. In this way, the Holocene Pb isotope curve recorded in several continental masses presents different patterns. Actually, it is possible to have this approach in three continental areas: Europe, North America and Antarctica. In general way, the Pb isotope curve to the last 200 years records the initial period of industrialization, when coal was the main source of energy, followed by the Pb-enriched gasoline, and as last period, occurred the fall in the use of gasoline Pb additives.

In Europe, several investigations have confirmed variation of the Pb signatures in the last two centuries. Pb isotopes results of ice and sediments (Rosman et al., 2000; Monna, et al., 2000) show ^{207}Pb/^{206}Pb decreased from 1.18 in the earliest core (200 years B.P.) to 1.17 by the mid twentieth century. The rate of decline then increases significantly until 1969 probably reflecting the increasing Pb emission from automobile exhausts following the introduction of leaded gasoline in the mid 1920s. Deposits from the late 1800s have high ^{206}Pb/^{207}Pb=1.200 interpreted as regional background and inputs of coal and wood burning. The following lowered Pb ratios (1.142-162) indicate an influence of industrial and domestic emissions, and the uppermost sediments record the leaded gasoline ^{206}Pb/^{207}Pb values of 1.069-1.094.

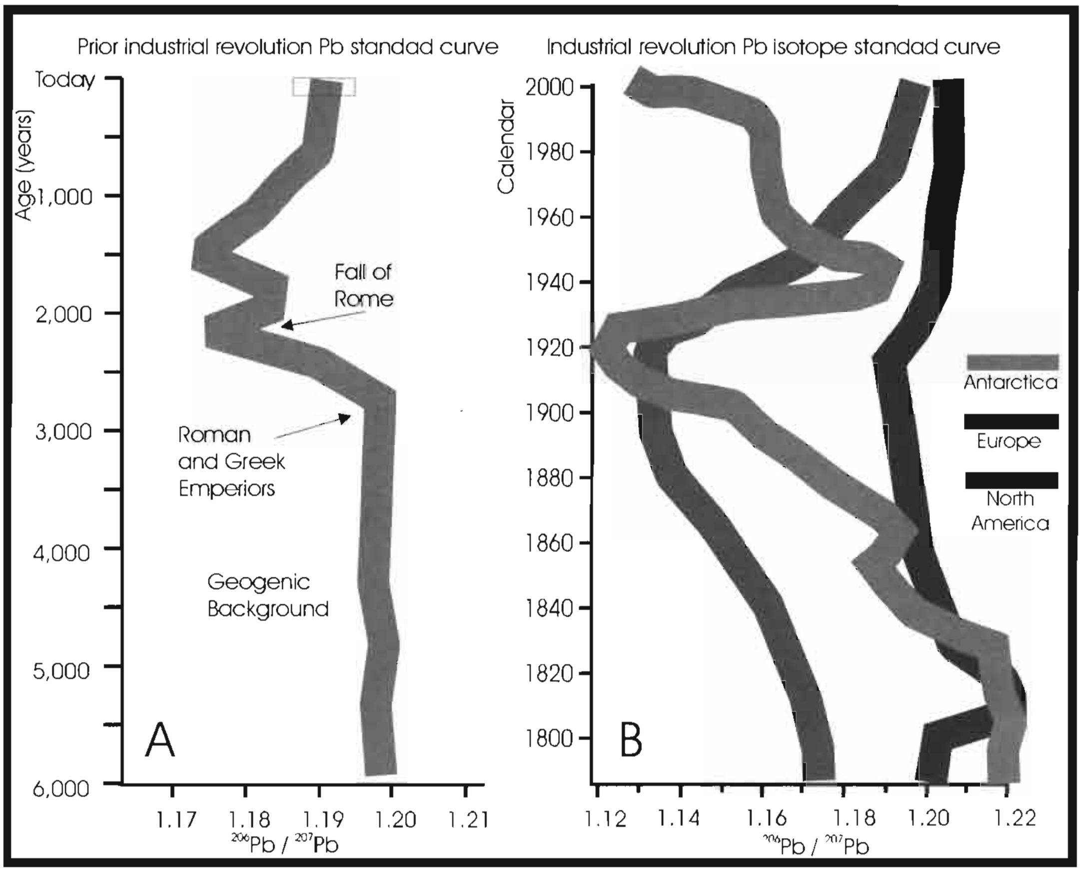

Figure 1. A tentative Holocene Pb isotope standard curve. (A) Prior industrial revolution and (B) during the industrial revolution.

In North America, the history of anthropogenic Pb emission has been investigated by analyzing the isotope composition of Pb in sediments, corals and ice. The Pb isotope recorded in Chesapeake Bay (east of U.S.) demonstrated that the anthropogenic Pb isotope in the bay is derived from regional industrial emissions that vary through time (Marcantonio et al., 2002). Over the past century, there is an excellent temporal agreement between anthropogenic $^{206}Pb/^{207}Pb$ isotope ratios of this bay and those determinate in a dated coral in Bermuda, almost 2000 km away. This correlation is used to argue that these Pb signature contain a regional industrial atmospheric Pb isotope signal that is representative of the mid-Atlantic region of U.S. Anthropogenic Pb is found in sediments deposited as early as approximately 1800 and the background (sediments older than 200 years) is characterized by the $^{206}Pb/^{207}Pb$=1.210-1.205. From about 1880 to 1930, the Pb signal is probably derived from burning of coal ($^{206}Pb/^{207}Pb$=1.125). After this period, and up until about the 1980s, the signal is overwhelmed by the Pb derived from the combustion of leaded gasoline ($^{206}Pb/^{207}Pb$=1.195-1.190).

In Antarctica, initial investigations indicate the $^{206}Pb/^{207}Pb$ value of 1.196 for regional background in ice dated at 22.6 kyr, corresponding to the last glacial maximum. In addition, one hundred fifty-year record of Pb isotopes in Antarctic snow, covering the period between ~1840 and 1990, shows evidence of pollution for this metal as early as 1880s (Rosman et al., 1994). Observed Pb isotope signature at the beginning of the 20th century show $^{206}Pb/^{207}Pb$ values ranging from 1.165 to 1.209. There is a $^{206}Pb/^{207}Pb$ peak (1.174) about 1834 is interpreted as a result of Mount Erebus volcanic contribution. About 1890, the $^{206}Pb/^{207}Pb$ presented a significantly decrease to 1.200, which may be linked to Australian contribution (Pb-contamining aerosols emitted during Pb mining, smelting, or coal combustion), or whaling and sealing activities very significant in the southern ocean at that time. The $^{206}Pb/^{207}Pb$ values from 1.145 to 1.200, during the 1940s and 1950s, suggest that there has been a weakening in anthropogenic inputs of Pb to the remote Antarctica (probably linked to the decrease in ship traffic around the southern tip of South America due to the opening of canal of Panama in 1914). There is a clear decrease from the early 1960s to the early 1980s in $^{206}Pb/^{207}Pb$ values as consequence of the very large rise in the use of leaded gasoline in the Southern Hemisphere continents during that period, combined with the continuous increase in nonferrous metal production in South America, South Africa and Australia.

HOLOCENE Pb ISOTOPES STUDIES IN SOUTH AMERICA

Pb isotope studies in South America on Holocene sediments are rare. Most of the reports are about Pb concentrations in rivers and estuaries. Two studies using Pb isotope signatures of aerosols have been reported: The first study (Bollhöfer and Rosman, 1991) report aerosols Pb signatures from Brazil (9 samples), Argentina (3 samples) and Chile (9 samples) and show $^{206}Pb/^{207}Pb$ values from 1.147 to 1.177. Studies on the Pb isotope composition of the São Paulo (Ayale, 2001) city atmosphere collected daily during fourteen months (August, 1999-September, 2000) indicated $^{206}Pb/^{207}Pb$ values from 1.142 to 1.273. The values are related to contribution of Pb-containing gasoline additives and industrial activities. In addition, investigations on Pb isotopes analysis in mining waste (galena massive vein hosted in Neoproterozoic carbonates), and river channel sediments in a transect downstream from the mine dump, readily identified the mines as a highly pollutant (Moraes, 1997). Ongoing investigations using Pb isotopes in aerosols (Brasilia-Brazil and Santiago-Chile) and Holocene deposits (Rio de Janeiro-Brazil) will contribute to a better understanding on this subject in South America.

REFERENCES

Ayale, C., 2002. Caracterização isotópica de Pb na atmosfera: um exemplo da cidade de São Paulo. Master Dissertation. Instituto de Geociências, USP-São Paulo. 76p.

Alfonso, S., Grousset, F., Massé, L. e Tastet, J-P., 2001. A European lead isotope signal recorded from 6000 to 300 years BP in coastal marshes (SW France). Atmospheric Environment 35:3595-3605.

Bollhöfer, A., Chisholm, W., Rosman, K.J.R., 1999. Sampling aerosols for lead isotopes on a global scale. Analytical Chimica 390:227-235.

Helland, A., Göran, A. e Skei, J., 2002. Source dependent behaviour of lead and organic matter in the Glomma estuary, SE Noway: evidence from isotope ratios. Marine Chemistry 78:149-169.

Hemming, S.R. e McLennan, S.M., 2001. Pb isotope compositions of modern deep sea turbidites. Earth and Planetary Sciences Letters 184:489-503.

Hong, S., Candelone, J.P. e Boutrons, C.F., 1994. Greenland ice evidence of hemisphere scale pollution for lead two millennia ago by Greek and Roman civilizations. Science, 265:1841-1843.

Luck, J.M. e Othman, D.B., 2002. Trace elements and Pb isotope variability during rainy events in the NW Mediterranean: constraints on anthropogenic and natural sources. Chemical Geology 182:443-460.

Marcantonio, F., Zimmerman, A., Xu, Y. e Canuel, E., 2002. A Pb isotope record of mid-Atlantic US atmosphere Pb emissions in Chesapeake Bay sediments. Marine Chemistry 77:123-132.

Monna, F., Clauer, N., Toulkeridis, T. e Lancelot, J.R., 2000. Influence of anthropogenic activity on the lead isotope signature of Thau Lake sediments (southern France): origin and temporal evoltion. Applied Chemistry 15(9):1291-1305.

Moraes, R.P., 1997. Transporte de chumbo e metais pesados no rio Ribeira de Iguape, São paulo, Brasil. Master Dissertation. Instituto de Geociências-UNICAMP, Campinas-SP. 126 p.

Nriagu, J.O., 1989. A global assessment of natural sources of atmospheric trace metal. Nature 338:47-49.

Nriagu, J.O., 1990. The rise and fall of leaded gasoline. The Science of the Total Environment 92:13-28.

Outridge, P.M., Hermanson, M.H. e Lockhart, W.L., 2002. Regional variations in atmospheric deposition and sources of anthropogenic lead in lake sediments across the Canadian Artic. Geochimica et Cosmochimica Acta 66(20):3521-3531.

Planchon, F.A.M., Van der Velde, K., Rosman, J.R., Wolf, E.W., Ferrari, C.P. e Boutron, C.F., 2003. One hundred fifty-years record of the lead isotopes in Antartic snow from Coats Land. Geochimica et Cosmochimica Acta 67(4):693-708.

Renberg, I, Brannvall, M-L., Bindler, R., Emteryd, O., 2000. Atmospheric lead pollution history during four millennia (2000 BC to 2000 AD) in Sweden. Ambio 29(3):150-156.

Rosman, K.J.R., Chisholm, W., Boutron, C.F., Candelone, J.P. e Gorlach, U., 1994. Antropogenic lead isotope in Antartic. Geophysical Research Letters 21(24):2669-2672.

Rosman, R.J.R., Ly, C., Van de Veld, K. e Boutron, C.F., 2000. A two century record of lead isotopes in high altitude Alpine snow and ice. Earth and Planetary Sciences Letters 176:413-424.

Sturges, W.T. e Barrie, L.A., 1989. The use of stable lead 206/207 isotope ratios and elemental composition to discriminate the origins of lead in aerosols at a rural site in eastern Canada. Atmospheric Environment 23(8):1645-1657.

Verón, A., Flament, P., Bertho, M.L., Alleman, L., Flegal., R. e Hamelin, B., 1999. Isotopic evidence of pollutant lead sources in northwestern France. Atmospheric Environment 33(20):3377-3388.

INTEGRATED FACIES AND ISOTOPE ANALYSIS OF THE CODÓ FORMATION (APTIAN, NORTHERN BRAZIL) AS A KEY FOR RECONSTRUCTING LAKE PALEOHYDROLOGY

Paz, J.D.S.[1] and Rossetti, D.F.[2]

1. Universidade Federal do Pará, Av. Perimetral 1901, CPPG/Lab. Institucionais, CP. 399, 66077-530. jackpaz@bol.com.br
2. Museu Paraense Emílio Goeldi, Av.Perimetral 1901, CPPG/Lab. Institucionais, CP. 399, 66077-530. rossetti@museu-goeldi.br

Keywords: Codó Formation, stable isotopes, lake, Aptian

The Late Aptian Codó Formation is a dominant lacustrine unit deposited in a tectonically subsiding basin during the early rifting stages that culminated with the opening of the South Atlantic Ocean along the Equatorial Brazilian Margin (Fig. 1A). Detailed facies analysis based on outcrops exposed in the east and south margins of the São Luís-Grajaú Basin revealed that the Codó Formation records central lake (betuminous shale and evaporite), intermediate lake (green laminated argillite, rhythmite of mudstone and shale, and peloidal mudstone to packstone) and marginal lake (blocky pelite, gypsarenite/calcarenite with evidence of subaerial exposure, ostracodal and oolitic/pisolitic packstone/grainstone, microbial laminite, and nodular chert) depositional environments. The facies associations are arranged into shallowing upward cycles averaging 1 m thick that are superposed on a main prograding cycle associated with a period of expansion and contraction of the lacustrine basin, probably due to tectonism (Paz & Rossetti, 2003).

$\delta^{13}C$ and $\delta^{18}O$ analyses have been used as paleoclimatic and paleohydrologic indicators in lacustrine settings. Although the interpretation of these isotopic parameters might be very complex, there is a general assumption that higher $\delta^{13}C$ values are related to more arid climates, while lower $\delta^{13}C$ values indicate relatively more humid climates (e.g., Talbot & Keltz, 1990; Valero-Garcés et al., 1995). This is because dry climates favor evaporation, increased influence of C4-path vegetation type, lower influx, and lake stratification, which ultimately lead to organic matter preservation with the consequent output of ^{12}C from the lake water. Similarly, low $\delta^{18}O$ values have been related to higher lake levels, while high $\delta^{18}O$ are attributed to lower lake levels (e.g., Lister et al., 1991); these values are also indirectly related to climate. In addition, the behavior of $\delta^{13}C$ relative to $\delta^{18}O$ has been used to determine episodes of lake closure and opening, indicated by direct and indirect covariance, respectively.

$\delta^{13}C$ and $\delta^{18}O$ values were obtained from seventy samples of carbonates of the Codó Formation exposed near the towns of Grajaú (localities G1 and G2) and Codó (localities C1 to C3) (Fig. 1B). The data were analysed in the LABISE/UFPE (Stable Isotope Laboratory of the Universidade Federal de Pernambuco), and include only mudstones and ostracodal packstones with no detectable diagenetic modification under optical microscope. The results, interpreted on the light of detailed facies analysis, provide new insights for the interpretation of $\delta^{13}C$ and $\delta^{18}O$ values of lacustrine environments.

In general, the isotopic values range from –0,57 ‰ to –10,80 ‰$_{(PDB)}$ for $\delta^{18}O$, and –2,27 ‰ to –14,02‰$_{(PDB)}$ for $\delta^{13}C$. The correlation coefficient is equal to 0,09, confirming that diagenetic modification was not significant. The depleted $\delta^{13}C$ values are quite different from the $\delta^{13}C$ marine-bearing Neoaptian carbonates, which range between + 2,0‰ and + 4,0‰$_{(PDB)}$ (cf. Jones & Jenkins, 2001). These values, added to the wide distribution of the $\delta^{13}C$ and $\delta^{18}O$ values, are consistent with a dominant lacustrine interpretation for the Codó Formation in the study area.

In addition, the distribution of the isotopic data throughout the study area revealed an overall direct relationship of the $\delta^{13}C$ relative to the $\delta^{18}O$ in the profiles C2 and C3 (Fig. 1C), with positive correlation coefficients of +0.40 and +0.32. The other profiles show an indirect relationship, with negative correlation coefficients of –0.55, –0.67 and – 0.36. The profiles with direct correlation show $\delta^{13}C$ values averaging –10.59‰(PDB), while in the others this average is –7.74‰ (PDB). These data suggest that the profiles C2 e C3 record prevalence of closed lake phases (i.e., with no outlets). The almost absence in sand grain size even in marginal facies, the stratified nature, and the anoxic water conditions suggested by both the abundance of bituminous shale and high content in chemical deposits (including evaporites), are facies characteristics supporting the prevalence of a hydrologically closed lake system during most of the depositional time of the Codó Formation in the study area. However, there are small-scale changes in both facies and isotopic data within these profiles, which are associated with short-term opening episodes. Similarly, the behavior of profiles G1 and G2 is more likely related with open phases. Therefore, though closed lake conditions seem to have prevailed in the Codó area, there were episodes of lake opening, or even places where the Codó Formation seems to have been deposited in entirely open lake conditions, as it is the case of the Grajaú area.

Furthermore, the analysis of isotope data within individual cycles led to clearly record an enrichment of $\delta^{13}C$ values within the marginal facies. Decyphering the origin of the shallowing upward cycles in the Codó Formation might be the clue to analyse the causes of such variations. Climate change, as generally proposed, might led to decreasing lake level due to increased evaporation,

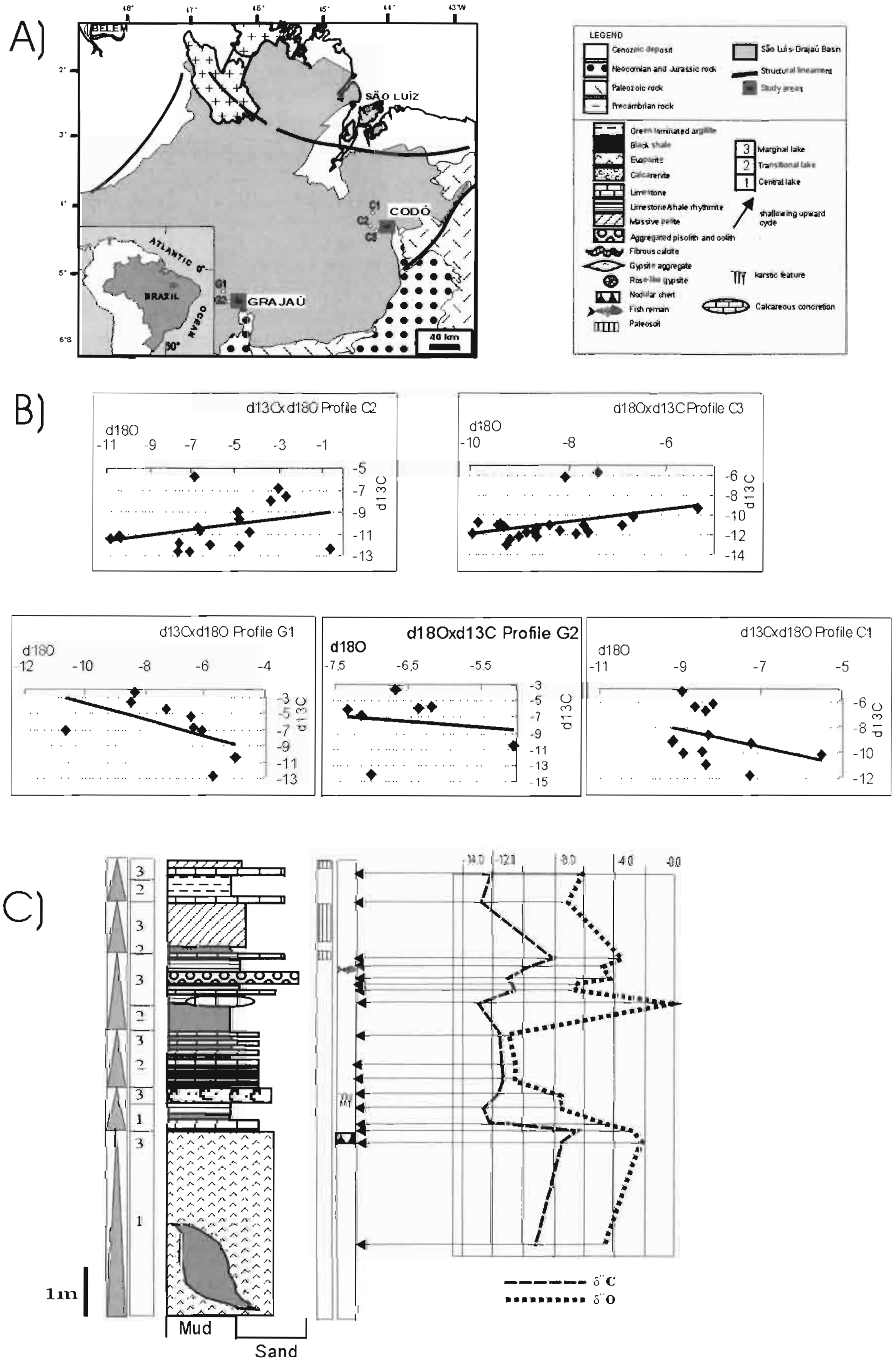

Figure 1. A) Location of the study areas; B) Covariant carbon and oxygen trends from the analyzed profiles; C) Carbon and oxygen isotopic upward trend through Profile C2.

with the consequent enrichment of the $\delta^{13}C$ values. However, these shallowing upward cycles seem to be more likely related to changes in subsidence within the lake basin (Paz & Rossetti, 2003). Hence, phases with lower subsidence would have favored the development of shallower facies, inducing increased evaporation due to a decrease in lake level, and ultimately producing more positive $\delta^{13}C$ values, without a need for any climate variation. This reasoning would be applied for closed lake successions, as dominant in the Codó area, because in open lake systems the introduction of fluvial inflow could result in depletion of the $\delta^{13}C$ in marginal facies.

REFERENCES

Jones, C.E. & Jenkins, H.C., 2001. Seawater strontium isotopes, oceanic anoxic events, and seafloor hydrothermal activity in the Jurassic and Cretaceous. Am. J. Sci., 301: 112-149.

Lister, G.S; Kelts, K; Chen, K.Z.; Yu, J, -Q; Niessen, F., 1991. Lake Qingai, China: closed-lake bain levels and the oxigen isotope record for ostracoda since the latest Pleistocene. Palaeogeogr., Palaeoclimatol., Palaeoecol., 84: 141-162.

Paz, J.D.S. & Rossetti, D.F., 2003. Tectonically-influenced shallowing-upward cycles in the lacustrine Codó Formation (Late Aptian), mid-northern Brazil. In: Latinamerican Congress of Sedimentology, 3, Belém, Livro de Resumos. in press.

Talbot, M.R. & Kelts, K., 1990. Paleolimnological signatures from carbon and oxygen isotopic ratios in carbonates from organic carbon-rich lacustrine sediments. In: B.J. Katz (Ed.) Lacustrine Basin Exploration: Case Studies and Modern Analogs. Tulsa, A.A.P.G., p. 99-112.

Valero-Garcés, B.L.; Kelts, K.; Ito, E., 1995. Oxigen and carbon isotopes trends and sedimentological evolution of a meromictic and saline lacustrine system: the Holocene Medicine Lake basin, north American Great Plains, USA. Palaeogeogr., Palaeoclimatol., Palaeoecol., 177: 253-278.

OXYGEN-ISOTOPE COMPOSITION OF SCLERACTINIAN CORALS FROM OCEANIC ISLANDS OF NORTHEASTERN BRAZIL

Pinheiro, B.R.[1]; Maÿal, E.M.[1]; Sial, A.N.[2] and Ferreira, V.P.[2]

1. Laboratório de Ambientes Coralinos e Estuarinos (LACE), Departamento de Zoologia, CCB, UFPE,
Av. Prof. Moraes Rêgo 1235, 50670-420, Recife-PE. barbara.pinheiro@ufpe.br
2. Laboratório de Isótopos Estáveis (LABISE), Departamento de Geologia, CTG, UFPE,
Av. Prof. Moraes Rêgo 1235, 50670-420, Recife-PE. ans@ufpe.br

Keywords: O-isotopes, scleratinian, termal stress, bleaching

INTRODUCTION

There are two groups of scleractinian corals; the hermatypic or reef-building coral, characterized by the presence of a great number of dinoflagellates in its tissue, and the ahermatypic or non reef-building coral which is less restricted to the reefal environment. The reef-building coral develops well between 25 and 29°C, the maximum temperature being around 36°C. Few of hermatypic corals can live for any time at temperatures of 15°C. Luminosity is important for the development of these animals (Wells, 1956). The evolutive success of the corals is related to the association that cnidarians have with dinoflagellates (known as zooxanthellas). These zooxanthellas live in the coral tissues through photosynthesis and are responsible for recycling and conservation of nutrients such as nitrogen, and actively assist the calcium carbonate deposition that forms the skeleton of their hosts. This can be potentially evaluated through breathing rates, growth and reproduction of the corals. This relationship is also advantageous for the zooxanthellas, as they survive and grow using the metabolic products from the corals, such as CO_2, nitrogen compounds and phosphates. It is believed that these nutritional interactions have a basic importance for the success of the cnidarian-zooxanthella symbiosis in an environment where supplies of zooplancton, bacteria and dissolved organic matter are limited (Davy et al, 1997). Hermatypic corals deposit calcium carbonate faster than the ahermatypic ones, because the zooxanthellas, whose density reaches $10^6/cm^2$, create an adequate chemical environment for the crystallization and precipitation of calcium carbonate (Hoegh-Guldberg, 1999). Investigation on the behavior of stable isotopes in coral skeletons received its first attention from Keith & Weber (1965). However, Fairbanks and Dodge (1979) were responsible for establishing that temperature variations in coral skeletons were recorded by O-isotope fractionation. Their assumption was based on the O-isotope fractionation between aragonite or calcite and seawater under equilibrium conditions. The zooxanthellar activity affects the skeleton growth rate for the CO_2 removal during photosynthesis and favors aragonite precipitation that incorporates diverse chemical tracers (C- and O-isotope ratios, Cd/Ca, Ba/Ca, Mn/Ca, Sr/Ca) used to monitor the variability of oceanic and atmospheric processes. The higher algal densities leading to higher $\delta^{13}C$ values in skeletons. Neither the ahermatypic nor the hermatypic coral precipitate skeletons in isotopic equilibrium with seawater. The hermatypic coral, however, seems to have a much narrower range of values, indicating a connection between the zooxanthellar activity and C- and O-isotope fractionation (Swart, 1983). The $\delta^{18}O$ of biogenic carbonates precipitated in equilibrium with seawater decreases in about 0.22‰ for 1°C temperature incrise in the water.

STUDY AREAS

The Rocas atoll is located at about 144 nautical miles eastern of Natal, northeastern Brazil, and 80 nautical miles west of the Fernando de Noronha Archipelago (between 3° 45` and 3° 56`S and 33° 37` and 33° 56`W). It is built on the western side of the flat top of a seamount within the Fernando de Noronha fracture zone (Kikuchi and Leão, 1997). Saint Paul's Rocks (SPR) are located in the northern hemisphere, on the Mid-Atlantic ridge, (00°56'N and 29°22'W), at about 1100 km from the coast of Rio Grande do Norte, 330 nautical miles from Fernando de Noronha Archipelago and 510 nautical miles from Cabo Calcanhar, Rio Grande do Norte, the closest point on the Brazilian coast.

METHODS

At the Rocas atoll, one specimen of *Siderastrea stellata* and two of *Porites astreoides* were collected in 1998; and in 1999, three specimens of *S.stellata* and three of *P.astreoides* were collected, all in the Anchors' pool. At the SPR, three specimens of *S. stellata* were collected in 1999. Collected specimens were washed with tap water and then immersed in a container with hydrogen peroxide ($15\%H_2O_2$) for 24 - 48 hours for removal of any organic matter. After this stage, they were washed with distilled water and left to dry at room temperature. Next, corals were cut according to growth line. In one of the halves, points 2 mm apart were marked on the skeleton. From each of those points, in each sample, micro-drilll holes were made to remove powder for isotope analyses. Each sample powder from coral skeletons (aragonite) was left to react with 100% orthophosphoric acid (H_3PO_4). Reaction vessels were placed in a water-bath 25°C for approximately 12 hours to release CO_2. Next day, the reaction vessels were conected to a high vacuum extraction line, the CO_2 was extracted from each sample and, after cryogenic cleaning, the gas samples stored in bottles (Craig's method; 1957). The C- and O- isotope ratios were measured in a dual inlet, triple collector SIRA II mass spectrometer, using BSC (Borborema Skarn Calcite) as the reference gas, that is periodically calibrated against NBS-18, NBS-19and NBS 20. Results are expressed in δ‰ in in the PDB scale. The temperature values were estimated from δ^{18}O‰$_{PDB}$ values, assuming isotopic equilibrium with sea water and using the Horibe and Oba (1972) equation.

RESULTS

The specimen of *S.stellata* collected in 1998 at the Rocas atoll, showed values of δ^{13}C -0.6‰$_{PDB}$, δ^{18}O -3.4‰$_{PDB}$ and water temperature of 29.8°C for that year. Along the analysed skeletons profiles, ranges of δ^{13}C were from -0.13 to -0.8‰$_{PDB}$; and for δ^{18}O, from -3.1 to -3.7‰$_{PDB}$ and temperatures between 31.4 and 28.1°C were obtained. This specimen apparently had not been subjected to abnormal seawater temperatures (>30°C) during its growth (Fig 1), even though the year was considered especially hot.

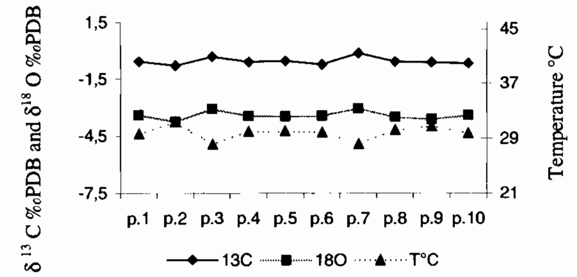

Figure 1. Isotopic and temperature variations obtained from the specimen of *S.stellata* collected at Rocas atoll in 1998.

In this same year, the two specimens of *P.astreoides* displayed variations of δ^{13}C from -0.4 to -0.5 ‰$_{PDB}$ and δ^{18}O from -4.0 to -4.1‰$_{PDB}$, indicating that this species was submitted to anomalous temperatures that oscillated between 32.6 and 33.3°C. This year presented high temperatures due to the vey strong El Niño southern oscillation (ENSO), between mid 1996 and 1999, the highest temperautre being reached in 1998. The temperature record in specimens 1 and 2 showed very little variation, with an average value of 33.2°C (Fig. 2).

The specimens of *S.stellata* collected in 1999 at Rocas atoll recorded variations of δ^{13}C from -0.3 to -1.0‰$_{PDB}$ and δ^{18}O, from -3.4 to 3.6‰$_{PDB}$ (Fig 3). For the *P.astreoides* species collected in 1999 at Rocas atoll the variations were: $\delta\ ^{13}$C -0.6 to -1.4‰$_{PDB}$; $\delta\ ^{18}$O from -4.2 to -4.3‰$_{PDB}$; temperatures between 33.6 and 34.0°C. When analyses along the skeleton profiles are considered, the results show that specimens were under thermal stress for most of the period of development (Fig 4). Three specimens of *S.stellata* collected in the SPR in 1999 presented the isotopic variations: δ^{13}C from -0.4 to 1.0‰$_{PDB}$ and δ^{18}O, from -2.1 to -3.6‰$_{PDB}$ and temperatures between 23.7 and 30.9°C (Fig. 5).

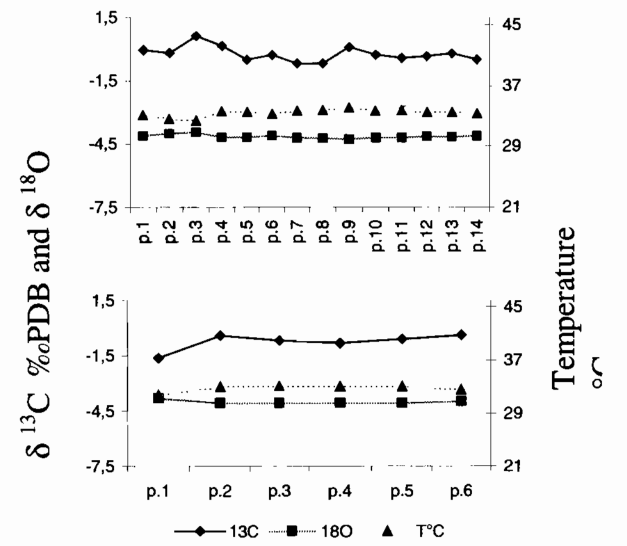

Figure 2. Isotopic and temperature variations from the specimens of *P.astreoides* collected at Rocas atoll in 1998.

DISCUSSION

In 1998, ENSO phenomenon was regarded as the most severe ever registered, with bleaching affecting the reefs of the whole world (Hoegh-Guldberg, 1999). In 1998, the *P.astreoides* and the Brazilian endemic species *S.stellata* from the Rocas atoll were analyzed, both species being from the same locality (Anchors' pool), collection time (July).

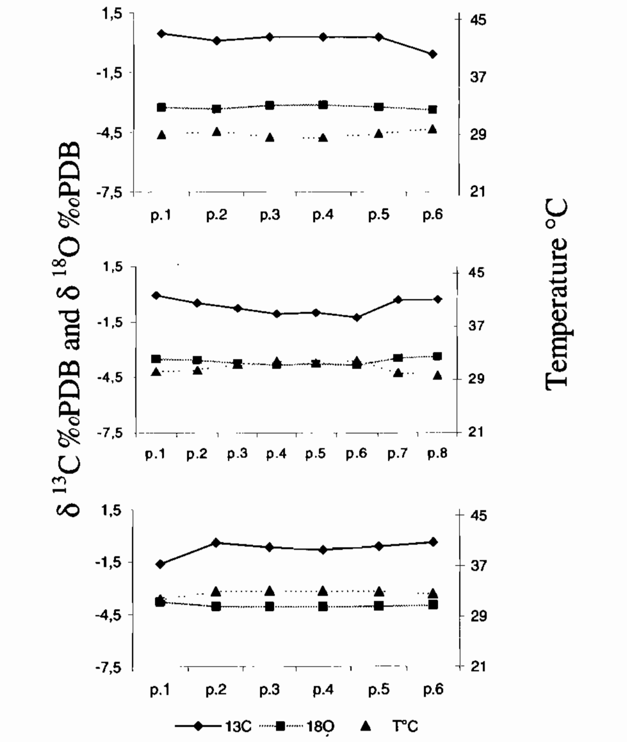

Figure 3. Isotopic and temperature variations for specimens of *S.stellata* collected at the Rocas stoll in 1999.

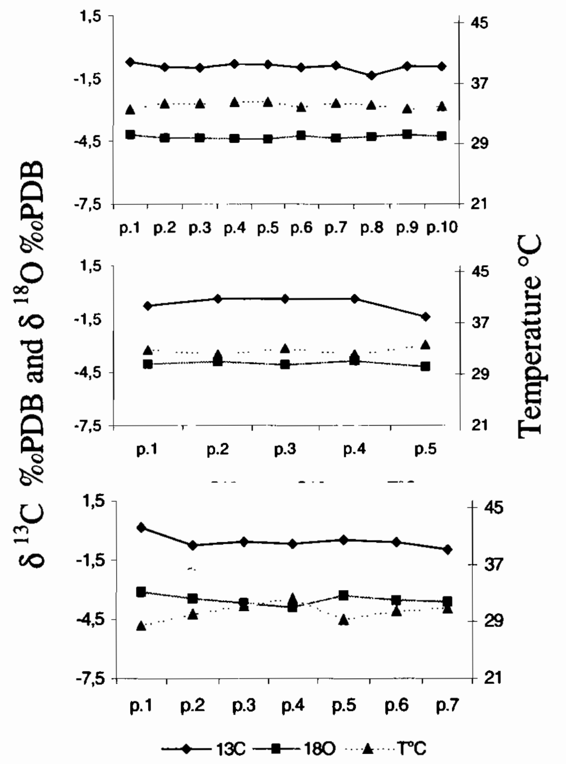

Figure 4. Isotopic and temperature variations from specimens of *P.astreoides* collected at the Rocas atoll in 1999.

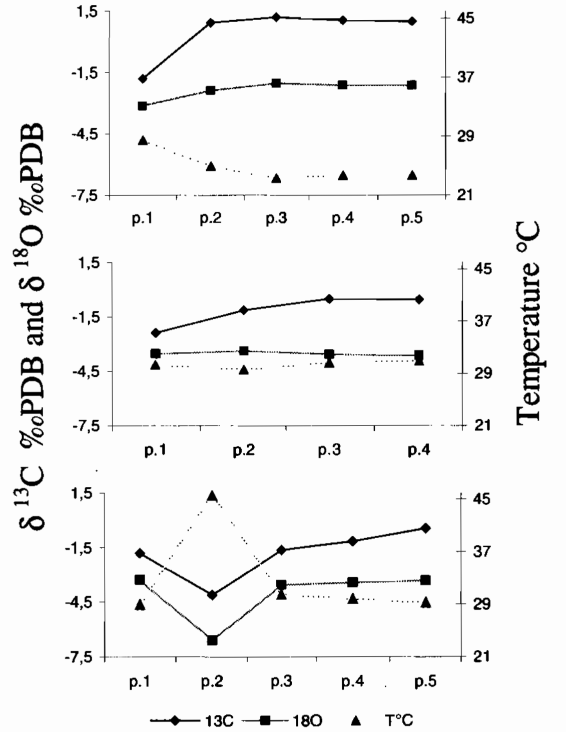

Figure 5. Isotopic and temperature variations from specimens of *S.stellata* at Saint Paul's Rocks Archipelago in 1999.

They displayed different information on the temperature, being the *P.astreoides* species more precise. According to the National Oceanic and Atmospheric Adiministration (NOAA), it was a full period of heating; and the *S.stellata* did not register this, recording temperatures around 29.8°C, while the *P.astreoides* recorded temperatures of 32.6 and 33.3°C. One knows that species in exactly the same locality can register different temperatures, and that specimens of the same species also can yield different variations of temperatures. Besides, bleached specimens do not represent all species. According to Porter et al. (1989) it is not yet clear why some colonies of corals are bleached and others are not, even for a single species thaken from similar depths. It is also necessary to consider the large evaporation during periods of low tide at the atoll, since corals are confined to large pools around the ring. Specimens of *P.astreiodes* collected in 1998 showed, along their skeletons, that anomalous temperatures were frequent in the Atoll, before 1998. This constant temperature, even if not extremely raised, is more harmful than a high, anomalous temperature whose highest heating point does not last for long time. At the Rocas atoll, the situation in that year was deplorable, with more of the half of the corals suffering damages due to bleaching and proliferation of zooxanthellas. In 1999, the *S.stellata* did not show constant anomalous temperatures. In three specimens, temperatures recorded were not so high, but in three specimens of *P.astreoides* from the same place, the O-isotope record from skeletons points to anomalous and relatively constant temperatures, in good agreement with NOAA.

It has been well-established that the O-isotope composition in skeletons of corals is negatively correlated to temperature as a result of a normal equilibrium or kinetic processes. C-isotope composition in skeletons of hermatypic corals, in its turn, often shows an oscillation due to temperature and insolation. δ ^{13}C is controlled mainly by interaction between photosynthesis and breathing of zooxanthellas hosted by coral tissue (Swart et al., 1996). According to Swart et al, (1996), during the period of increased photosynthesis an increase in CO_2 for zooxanthella leads to an isotopic enrichment of ^{13}C in the calcification process. Consequently, in the periods when the photosynthesis rate decreases, there will be little C-isotope fractionation, lowering δ^{13}C values. It is probable that the variations in the photosynthesy/breathing rates of corals through the year are responsible for a cycle in the C-isotope composition in the skeleton of the scleractinians In the SPR, specimens of *S.stellata* were collected at depths of 30.5 and 32 meters, therefore without influence from evaporation in their temperature record. Thermal stress was not observed, in a general way, at this site. Some anomalous, but not constant, temperatures were observed, favoring development of specimens. The only extremely high temperature record (45.6°C) was observed in specimen 3. It is likely that anomalous temperatures in this case had the influence from oceanic currents in the place.

The species *S. stellata*, although more tolerant to salinity, sedimentation and insolation variations, is not regarded here as a reliable thermal stress indicator. Among the studied species, *P. asteroides* appear to be by far the best.

ACKNOWLEDGEMENTS

We want to express our gratitude to Gilsa M. Santana and Vilma Sobral for the assistance with the isotopic analyses at the LABISE. This is the contribution n. 213 of the NEG-LABISE.

REFERENCES

Craig, H., 1957. Isotope Standard for Carbon and Oxygen and Correction factors for Mass Spectometry Analysis of Carbon Dioxide. Geoch. Cosmoch. ACTA 12:133-149

Davy, S. K; Turner, Jr. & Lucas, I.A.N., 1997. The nature of temperate anthozoan- dinoflagellate symbioses. Proc 8th Int Coral Reef Sym 2: 1307-1312

Fairbanks, R. G & Dodge, R. E., 1979 Annual periodicity of the $^{18}O/^{16}O$ and $^{13}C/^{12}C$ ratios in the coral Montastrea annularis. Geochimic et Cosmochimica Acta v.43, p. 1009-1020.

Hoegh-Guldberg O., 1999. Climate change, coral bleaching and the future of the world's coral reefs. Mar Freshwather Res. 50: 839 – 866

Horibe, Y. & Oba, T., 1972. Temperature scale of aragonite – water and calcite – water systems (in japanese) Fossils, 23/24, 69-79 *In*: Faure, G. 1986. Principles of Isotopy Geology. John Wiley & Sons 589p

Keith, M. L. & Weber, J. N., 1965. Vital effect on the carbonate isotopic composition of reef communities. Proc. Spoleto Conf. Paleotemp., Isotop Oceanogr., 267-283pp.

Kikuchi, R. K. P de & Leão, Z. M. A. N., 1997. Rocas (Southwestern equatorial Atlantic Brazil): an atoll built primarily by coraline algal. Proc 8th Int Coral Reef Sym 1:731-736

Porter, J. W.; Fitt, W. K.; Spero, H. J.; Rogers, C. S. & White, M. W., 1989. Bleaching in Reef Corals: Physiological and Stable Isotopic Responses. Proc. Natl. Acad. Sci.86: 9342-9346

Swart, P. K., 1983. Carbon and Oxygen isotope fractionation in Scleractinian Corals: a review. Earth-Science reviews V.19 51-80p.

Swart, P. K., Dodge, R. E. & Hudson, H. J., 1996. A 240-year stable oxygen and carbon isotopic record in a coral from South Florida: Implications for the prediction of precipitation in Southern Florida. Palaios V.11 362-375p.

Wells, J.W., 1956. Scleractinia. In: Treatise of Invertebrate Peleontology (F): Coelenterata – Geol. Soc. Am., F328-F444p.

THE EFFECTS OF WEATHERING PROCESS ON Sm-Nd ISOTOPIC SIGNATURES IN SOIL AND SEDIMENTS IN THE QUELUZ WATERSHED, PARAÍBA DO SUL RIVER SYSTEM, SE BRAZIL

Roig, H.L.[1,2,3]**; Dantas, E.L.**[2] **and Meneses, P.R.**[3]

1. Laboratório de Geoprocessamento - FGEL/Uerj. R. São Francisco Xavier 524, 4006A, Maracanã–RJ. roig@unb.br
2. Laboratório de Geocronologia – IG/UnB. elton@unb.br
3. Laboratório de Sensoriamento Remoto e Análise Ambiental. IG/UnB. pmeneses@unb.br

Keyword: Nd isotopes, provenance, weathering process, soil source, sediments

INTRODUCTION

The Sm-Nd isotopic method has been used to study the provenance of sedimentary rocks and can have a critical role in the assessing of paleogeographic reconstruction and tectonic models in Precambrian orogenic belts (Haughton et al., 1991; Dantas et al., 2000). Also, this method has been used in understanding the dynamics of recent sedimentary process in basin systems (Goldstein et al., 1984; Mearns, 1992; Weldeab et al., 2001; Bayon et al., 2002).

The principle of Sm-Nd method assumes that the isotopic system is closed and has not been fractionated during the erosion, transport and deposition of the sedimentary rocks. Thus, the sediment should show the same isotopic signature of their rock source. (Nohda & Wasserburg, 1986; Goldstein & Jacobsen, 1988; Mearns, 1992). The crustal residence age on T_{DM} of a sedimentary rock is a function of the source rock or rocks from which was derived, hence can be used to help determine the provenance of the sediment. In the infilling of a basin, sediments often come from many sources and can get mixed during erosion, transport and deposition. As such sedimentary units in basin often yield Nd isotopic signatures that represent hybrid or average ages of different source. Nonetheless, if transport is minimal, the original Nd signature can be preserved.

However, the change of Nd isotope composition during weathering process may lead to a modification of the Sm/Nd ratio, suggesting that the isotopic composition of Nd exported from a large basin is controlled by a selective weathering and does not directly reflect the composition of bedrock (Öhlander et al., 2000; Anderson et al., 2001). Consequently, the Nd isotopic composition of the load sediments transported by the river could not necessarily reflect the exactly composition of the source area.

In the present study we demonstrated the behavior of the Nd isotopes during the weathering process in gneiss and sediments that are the main sources of the load sediments present in the Paraíba do Sul River system. This research, is part of a major project of which the main objective is to modeling the erosion and transport of sediments into the Funil Dam in the middle part of Paraíba do Sul Basin (Fig. 1). Also, try to understand how the Nd isotopes changes in the weathering process in warm climates.

STUDY AREA

The Paraíba do Sul Basin comprises a geomorphological domain, an elongate NE-trending, narrow trough, about 600 km long, that is situated principally in the eastern part of São Paulo state and extends to the boundaries of Rio de Janeiro and Minas Gerais states (Fig. 1). The geological framework where the river is developed is characterized by supracrustal Neoproterozoic sequences overlying Archean and Paleoproterozic basement rocks of the Mantiqueira Province (Almeida & Hasui, 1984). These units are intruded by Cretaceous alkaline rocks and covered by Phanerozoic sedimentary deposits (Ricomini et al., 1996).

The samples used in this study were collected in the watershed near Queluz city (São Paulo State). This watershed was selected because the geological substrate is formed only by orthogneisses of the Mantiqueira Complex and sedimentary deposits with a strong influence of alkaline rocks (Fig.1).

SAMPLING STRATEGIES

Three profiles were selected for these studies, whose sample stations are situated in a small watershed of the Paraíba do Sul basin, Brazil (Fig. 1).

The first profile (sample QUE7) is a well-developed *in situ* soil formed on hornblende biotite gneiss of the Matiqueira Complex. From this profile four samples were taken at different depths, representing the different horizons of the weathered host rock – A, B and C (Photo 1A).

The second profile (samples QUE4) represents rocks collected from the contact between a colluvium and a saprolite of the biotite gneiss. This contact showed a stone line (straight layer of quartz and lateritic fragments). In this profile two samples were collected: one in the colluvium and the other in the saprolite, represented by A and B in the Photo 1B.

The third profile shows an erosive contact between a conglomerate and a saprolite of gneiss rocks (samples QUE2). The conglomerate is mainly represented by pebbles of alkaline rocks within an immature matrix. Two samples were collected from this profile: one of a conglomerate and the other of a saprolite, represented by the A and B in the Photo 1C.

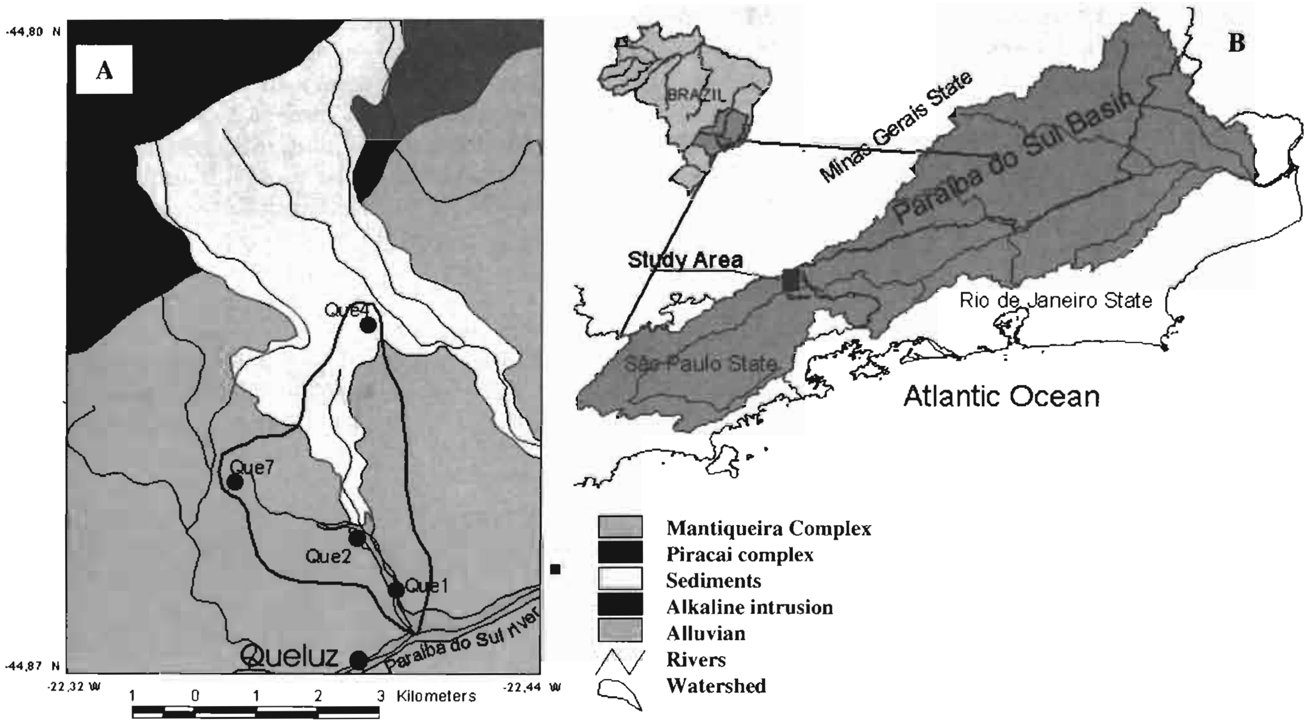

Figure 1. (A) Geologic map showing the location of the samples used in this study - QUE 2, QUE4 and QUE7. (B) Localization of the area near Queluz City (São Paulo state) in the Paraíba do Sul Basin.

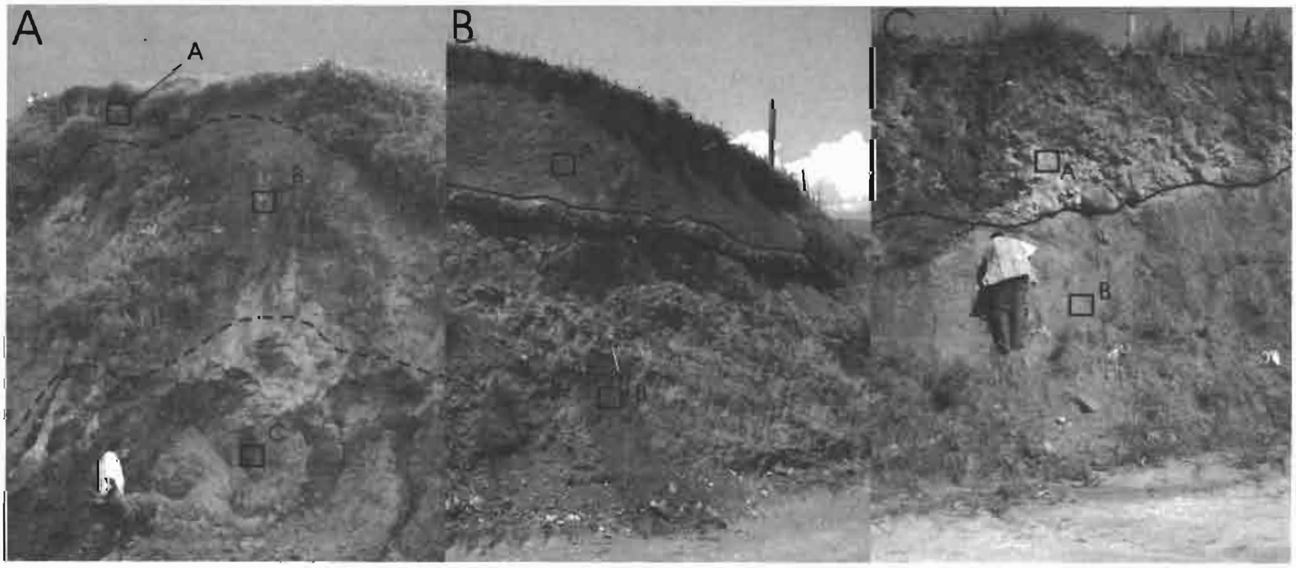

Photo 1. (A) QUE7 - profile of *in situ* soil development over the honblende biotite gneiss. Samples C, B, and A represent the C-horizon, B-horizon and A-horizon respectively. (B) QUE4 - contact between a colluvium and a saprolite of the biotite gneiss. Samples A and B correspond the colluvium and saprolite, respectively. (C) QUE2 - profile shows an erosive contact between a conglomerate (A) and a saprolite of gneiss rocks (B).

ANALYTICAL PROCEDURES

Nd isotopes were carried out at the geochronological laboratory of Universidade de Brasília using the procedures described in Gioia and Pimentel (1999).

RESULTS

Table 1 shows the isotopic composition of samples analyzed in this study. In the Profile 1 (sample QUE7A-C), the ratios Sm/Nd are slightly greater from the C-horizon to the A-horizon (Table 1). However, the concentration of the Sm and Nd increase in the B-horizon and reduces in the A-horizon with relation of C-horizon. The A-horizon sample has lower $^{143}Nd/^{144}Nd$ and more negative $\varepsilon_{Nd(0)}$ value than C-horizon, whereas, in the opposite manner, the B-horizon sample shows higher $^{143}Nd/^{144}Nd$ ratio and less negative $\varepsilon_{Nd(0)}$ value (Table 1). T_{DM} model ages ranges from 2.8 to 2.5 Ga, suggesting an Archean source for the gneiss.

The different trends between the isotopic composition and Nd concentration of the different horizons characterizes the influence of the weathering process in these rocks. Also, is evident the migration of Nd concentration from the B horizon to the A-horizon.

Therefore, our data suggests there's an insignificant loss of the Nd isotopic composition, but the Nd concentration changes during the weathering process, and these changes are caused by the migration of clay minerals into different horizons. Other process acting during the release of the Nd concentration to the B-horizon is the presence of organic material in the A-horizon. It can generate humic acids that destroy the clay minerals and enrich the horizon below.

In the profile 2, the upper layer is characterized by a colluvium showing $\varepsilon_{Nd(0)}$ value of -9.3 and T_{DM} model age of 1.1 Ga. The lower layer represents a C-horizon derived from the biotite-gneiss and shows a T_{DM} of 2.1 and $\varepsilon_{Nd(0)}$ value of -8. This result indicates that the colluvium represents a mixed source derived from alkaline rocks ($\varepsilon_{Nd(0)}$ of -6.1 and T_{DM} of 0.75) with soil formed by orthogneiss ($\varepsilon_{Nd(0)}$ of -20 and T_{DM} of 2.1). In this case, the saprolite and colluvium has similar $\varepsilon_{Nd(0)}$ values, but different T_{DM} model ages.

In profile 3, the conglomerate of the upper layer has T_{DM} model age of 0.85 Ga and $\varepsilon_{Nd(0)}$ of -8. This isotopic composition reflects a strong influential Neoproterozoic signature, which characteristic of cretaceous alkaline rocks in SE Brazil such as the Passa Quatro Intrusion (Fetter et al., in this symposium). The saprolite of the biotite gneiss in the lower layer shows T_{DM} model age of 1.6 Ga and $\varepsilon_{Nd(0)}$ of -16. A possible explanation for the higher Nd concentration (>100 ppm) in the gneiss is a migration of the material released from the matrix of the conglomerate.

DISCUSSION

Our preliminary data indicating that in situ weathering leads to a change in Sm/Nd ratio resulting in an insignificant change of the Nd isotope composition of the altered rocks (Fig. 2A,B).

The variation in the Sm and Nd concentration is interpreted by the migration of the clay minerals from the A-horizon to the B-horizon, typical of this type of soil in this region. However, variation in the Sm/Nd ratio and Nd composition between soils horizons *in situ*, isn't significant enough to cause profound changes in the provenance ages of the studied rocks (Fig. 2A,B).

One the other hand, the strong variation of de Sm/Nd ratio in the superficial material - colluviums and conglomerate – can be explained by the mixing of two contrasting sources, a gneissic rock and an alkaline rock with T_{DM} values of 2.7 – 2.5 Ga. and 0.8 Ga. respectively.

The next step for this study is to continue the sampling of weathering profiles of gneiss rocks and modeling the mass balance of the different sources involved in the supply of material to the Funil Dam in the Paraíba do Sul Basin.

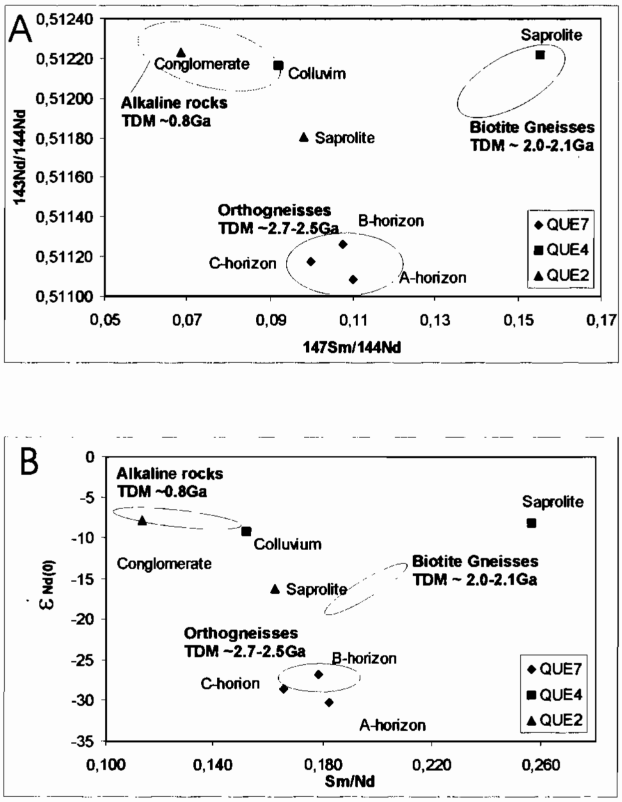

Figura 2. (A) Diagram of the $^{143}Nd/^{144}Nd$ vs. $^{147}Sm/^{144}Nd$ from form the sample from QUE2,QUE4 and QUE7. (B) Diagram εnd(0) vs. Sm/Nd form the sample from QUE2,QUE4 and QUE7. The ellipse represent the area of occurrence of the regional geologic units in the region.

ACKNOWLEGEMENTS

To PICDT/CAPES for the doctoral fellow for the first author. The ANEEL (National Agency of Electric Energy) for financial support for this study. We thank Simone Goia for the technical assistance and discussions for the analytical process, and to Allen Fetter for helping with the enghish.

Table 1. The Sm-Nd concentrations and Nd isotopic composition of the soils and sediments.

Number	Sample	Sm (ppm)	Nd (ppm)	$^{147}Sm/^{144}Nd$	$^{143}Nd/^{144}Nd$ ($\pm 1\sigma$)	$\varepsilon_{Nd(0)}$	T_{DM} (Ga)
QUE 7A	A-horion	2.871	15.755	0.1102	0.511088+/-14	-30.24	2.8
QUE 7B	B-horizon	9.937	55.80	0.1076	0.511264+/-06	-26.81	2.5
QUE 7C	C-horizon	7.553	45.75	0.0998	0.511175+/-07	-28.54	2.5
QUE 2A	Conglomerate	11.216	98.81	0.0686	0.512231+/-06	-7.93	0.8
QUE 2B	Saprolite	20.21	124.62	0.0980	0.511806+/-06	-16.23	1.6
QUE 4A	Colluvium	2.506	16.508	0.0918	0.512163+/-12	-9.27	1.1
QUE 4B	Saprolite	2.016	7.857	0.1551	0.512215+/-11	-8.25	2.1

REFERENCES

Almeida, F.F.M. & Hasui, Y., 1984. O pré-cambriano do Brasil. Edgard Blucher. 378p.

Andersson, S.P.; Dahlqvist, R.; Ingri, J., Gustafsson, O.R., 2001. The isotopic composition of Nd in a boreal river: A reflection of selective weathering and colloidal transport. Geochimica et Cosmochimica Acta, Vol. 65 (4), pp. 521–527.

Bayon, G.; German, C. R.; Boella,;. Milton, J. A R.; Taylor N.; Nesbitt, R. W. An improved method for extracting marine sediment fractions and its application to Sr and Nd isotopic analysis. Chemical Geology, Vol. 187 (3-4), pp 179-199.

Dantas, L.L.; Hackspacher, P.C.; Fetter, A.H.; Sato, K.; Pimentel, M.M.; Godoy, A.M., 2000. Nd isotope systematic related to proterozoic evolution of the Central Ribeira Belt in the state of São Paulo, SE Brazil. Revista Brasileira de Geociências. Vol 30 (1). pp. 140-143.

Goldstein, S. J.; O'Nions, R.K.; Hamilton, P.J. 1984., A Sm.Nd isotopic study of atmospheric dusts and particulates from major river systems. Earth and Planetary Science Letters. Vol.70.

Goldstein, S. J. and Jacobsen S. B., 1988. The Nd and Sr isotopic characteristics of river water dissolved material: Implications for sources of Nd and Sr in seawater. Chemical Geology. 66, pp.245–272.

Gioia, S.M.C.L. & Pimentel, M.M., 2000. The Sm-Nd isotopic method in the Geochronology Laboratory of the University of Brasília. An. Acad. Bras. Cienc. Vol. 72. pp. 219-245.

Haughton, P.D.W.; Todd, S.P.; Morton, A.C., 1991. Sedimentary provenience stydies. In: Morton, A.C.; Todd, S.P.; Haughton, P.D.W. Developments in sedimentary Provenience Studies. London. The Geology Society. pp.1-11

Mearns, E.W., 1992. Samarium-Neodimium isotopic contrains on the provenece of Brent Grup. In: Morton, A.C.; Haszeldine, R.S.; Giles, M.R.; Brown, S. Geology of the Brent Group Geological Society Special Publication. 61,pp 213-255.

Nohda, S. & Wasserburg, G. J., 1986.Trends of Sr and Nd isotopes through time near the Japan Sea in northeastern Japan, Earth and Planetary Science Letters, Vol. 78, Issues 2-3, pp 157-167.

Öhlander, B.; Ingri, J.; Land, M.; Schöberg, H., 2000. Change of Sm-Nd isotope composition during weathering of till. Geochimica et Cosmochimica Acta, Vol. 64, Issue 5, pp 813-820.

Ricommini, C; Coimbra, A.M.; Sant'Anna, l.G.; Brandt Neto, M.; Valarelli, J.V., 1996. Argilominerais do paleolago Tremenbé e sistema continental relacionados (Paleógeno, Rift Continental do Sudeste do Brasil). Revista Brasileira de Geociências. Vol 26, pp 167-180.

Weldeab, S; Emis, K.C.; Hemleben, C.; Siebel, W., 2002. Provenece of lithogenic surface sediments and pathway of riverine suspended matter in the eastern Mediterraneam Sea: evidence from 143/Nd144Nd and 87Sr/86Sr isotope ratios. Chemical Geology, Vol. 186 (1-2), pp. 139-149.

THE USE OF SOIL GAS RADON AS A NATURAL TRACER FOR SOIL CONTAMINATION BY NON-AQUEOUS PHASE-LIQUIDS

Schubert, M.[1]; Freyer, K.[1] and Weiss, H.[2]

1. UFZ Centre for Environmental Research Leipzig–Halle, Department of Analytical Chemistry;
Permoser Str. 15, 04318 Leipzig, Germany. schubert@ana.ufz.de, freyer@ana.ufz.de
2. UFZ Centre for Environmental Research Leipzig–Halle, Interdisciplinary Department of Industrial and Mining Landscapes;
Permoser Str. 15, 04318 Leipzig, Germany. weiss@pro.ufz.de

Keywords: Non-aqueous phase liquids, NAPLs, contamination, soil gas radon, detection method

INTRODUCTION

Ground contamination by non-aqueous phase-liquids (NAPLs) has to be named as one of the major problems concerning the risk assessment at polluted industrial sites. Due to their low solubility in water NAPLs can become long-term sources for ground and groundwater contamination. Thus, risk assessment at such sites is obligatory. Effective risk assessment and remediation planning, however, requires the accurate location and, if possible, quantification of the NAPL contamination in the subsurface previous to the remediation actions. Thus pre-remediation activities usually start with ground or groundwater surveys.

For the localization and characterization of NAPL contamination in the unsaturated zone of the soil a number of conventional methods are in use. They include soil coring, soil gas analysis, and some highly sophisticated cone penetration techniques such as rapid optical screening using laser-induced fluorescence (ROST-LIF) (USEPA, 1995, 1997) or membrane interface probing (MIP) (Nadolishny and Fraser, 2001). For the localization of dense NAPL contamination in the aquifer below the ground water table (DNAPLs) other methods have been developed. Besides conventional ground water analysis tracer test have been applied which use partitioning tracers such as alcohols or inert gases like SF_6. In these approaches DNAPL saturations are achieved from the retardation factors of the tracers (Davies et al, 2002; Semprini et al., 2000). Subject of the method described in this paper is NAPL contamination in the unsaturated zone of the soil.

As mentioned above several conventional methods for the NAPL localization in the unsaturated zone of the soil are in use. All of these methods are based on a direct analysis of the soil or soil gas samples for their NAPL content. However, the local infrastructure or a tight budget often limits the number of bore holes as sampling points quite drastically. That makes a sufficient tracing of a subsurface NAPL contamination usually difficult. To obtain a more precise picture of ground contamination, adequate for remediation planning, a detection method, which allows a larger number of monitoring points, would be desirable.

Radon-222 (hereafter referred to as radon) is a naturally occurring compound of soil gas. Radon has, as a radioactive noble gas, a half-life of $T_{½} = 3.83$ days. It is part of the uranium-238 decay series and is continuously produced in the mineral matrix of the soil via α-decay of its parent nuclide radium-226 ($T_{½} = 1600$ years). The steady-state radon concentration of the soil gas is a function of the radium concentration of the mineral matrix, its emanation coefficient, the bulk density of the soil, and its porosity. Values for the radon concentration of the soil gas are highly variable, ranging normally from approximately 10 kBq/m³ to 100 kBq/m³.

Due to its properties as a radioactive noble gas radon can be determined individually and very precisely. Besides that it exhibits very good solubility in almost all NAPLs (Clever, 1979) In view of these facts it was assumed that if a NAPL contamination of the ground is present, the NAPLs should accumulate and "trap" part of the radon which is available in the soil gas, giving rise to a local reduction of the soil gas radon concentration in the close vicinity of that contamination. Given that this effect was significant, a NAPL contamination could be localized indirectly by carrying out a straightforward radon survey on a suitable sampling grid covering the area of concern.

To verify that thesis numerous experiments have been carried out and several NAPL contaminated sites have been chosen to test the on-site applicability of the method. In the on site experiments the lateral radon distribution patterns achieved were compared to the extent of the NAPL contamination, which had been previously investigated with conventional methods. The research described in this paper demonstrates that subsurface NAPL contamination does give rise to anomalous low soil gas radon concentrations. It could be shown that the lateral soil gas radon distribution pattern at a NAPL contaminated site can be used as an indicator for the extent of NAPL contamination, providing an economic tool supplementary to conventional methods.

THEORETICAL BACKGROUND

The central fact which stands behind the newly developed methodology is that radon is very soluble in a wide range of NAPLs as shown by several authors (Barton, 1991; Prausnitz et al., 1986; Clever, 1979). Thus solubility can be explained with the "Hildebrand Parameter", which represents the cohesive energy density of a liquid phase, i.e. its cohesive energy per unit volume. The Hildebrand Parameter is literally a function of the energy required to vaporize one mole of the liquid substance to its saturated vapor (Barton, 1991). Since the Hildebrand Parameter of a substance can easily be achieved if the molar volume and the molar vaporization enthalpy have been determined at the temperature of concern, the Hildebrand Parameter is easily attainable for most NAPLs.

Since the Hildebrand Parameter is in principle a liquid state property, the situation is different for gases, such as radon. If the Hildebrand Parameters of liquids are to be compared to those of gases, the gases have to be treated as hypothetically liquid solutes at atmospheric pressure. For further reading, see Prausnitz et al. (1986).

The dependence of the mutual solubility of two or more substances on their Hildebrand Parameters can be explained as follows. A substance with a high molar vaporization enthalpy, i.e. with a high Hildebrand Parameter, requires more energy for dispersal than can be gained by mixing it with a substance with a low molar vaporization enthalpy. This finally results in immiscibility of the substances. On the other hand, two substances (gases, liquids or solids) with similar Hildebrand Parameters gain enough energy on mutual dispersion to allow mixing. Figure 1 shows the Hildebrand Parameters of some NAPLs and of water at room temperature (data by Barton, 1991) vs. the respective radon partitioning coefficients $K_{NAPL/air}$ ($K_{w/air}$ for water) (data by Lewis et al., 1987; Clever, 1979). The Hildebrand Parameter of radon amounts to about 18.1 MPa$^{1/2}$ (Prausnitz and Shair, 1961). It can be seen that substances with Hildebrand Parameters that are comparable to that of radon show the best radon solubilities with partitioning coefficients of about $K_{NAPL/air} = 15$. On the other hand, polar liquids such as glycerin and water exhibit much higher Hildebrand Parameters and, thus, values for $K_{NAPL/air}$ of only ca. 0.25.

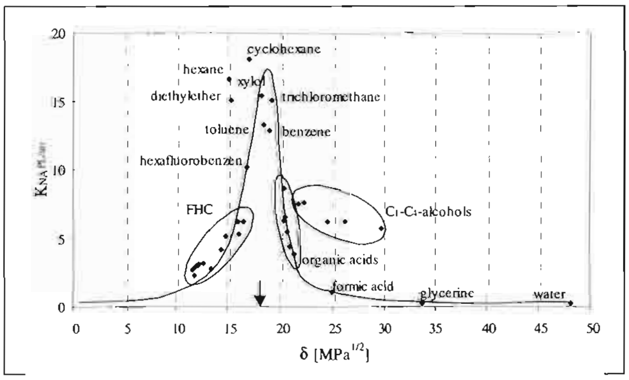

Figure 1. Hildebrand Parameters δ of some NAPLs (and of water) at room temperature vs. the radon partitioning coefficients $K_{NAPL/air}$ ($K_{w/air}$ for water). The δ of radon is 18.1 MPa$^{1/2}$ (arrow). The curve shows the trend of $K_{NAPL/air}$ vs. δ.

Due to the similar Hildebrand Parameters of radon and NAPLs in general, i.e. due to the good solubility of radon in NAPLs, the soil gas radon becomes trapped in the non-aqueous phase if a NAPL contamination is present in the ground. As a result of this accumulation effect the soil gas radon concentration in the contaminated soil volume and in the close vicinity of that contamination is significantly reduced relatively to its geological background concentration (Fig. 2).

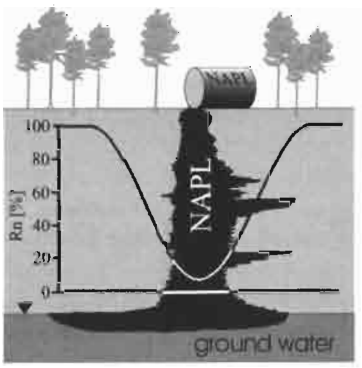

Figure 2. Reduction of the soil-gas radon concentration in a NAPL- contaminated soil volume and in its close vicinity.

EXPERIMENTAL

The efficiency of the newly developed method as a localization tool for NAPL contamination was evaluated in laboratory, lysimeter, and on-site experiments.

Laboratory experiments were carried out to validate the solubility of radon in environmentally relevant NAPLs such as diesel fuel, kerosene, and gasoline. For this purpose, a 1-liter glass bottle was filled with 0.5 liter of tap water, which had previously been enriched in radon, and 0.5 liters of the choser NAPL. To guarantee radon equilibrium between the phases, the bottle was shaken for three hours at room temperature. After shaking, the bottle was kept still for about 90 minutes to allow the water and the NAPL to separate and to establish equilibrium between the radon and its progeny in either phase. Afterwards, the radon activities of the aqueous and the non-aqueous phase were measured and the radon partitioning coefficients between NAPL and water $K_{NAPL/w}$ were determined. The respective partitioning coefficients for $K_{NAPL/air}$ were achieved by using the known value for $K_{w/air}$, which has been published by several authors (Clever, 1979) and which amounts at the given temperature to about 0.25.

Subsequently to the laboratory experiments the method was tested in specially adapted lysimeters or "Gas Migration Simulators" (Schubert et al., 2002). The "GAMS" was designed at the UFZ - Centre for Environmental Research Leipzig-Halle GmbH. Its main body is entirely made of polyethylene and takes the form of a 2 m³ cylindrical box with a surface area of 1 m². The GAMS was filled homogenously with a defined sand with a constant moisture content of about 4%. The sand was represented by the grain size class 0.2 - 0.63 mm. The density of the dry sand was 1.55 g/cm^3. The porosity of the sand, which was determined by measuring the mass increase of a known dry volume due to water saturation was 0.42. The radium activity of the sand was 260 Bq/kg. The effective diffusion coefficient D of the sand column amounted to about 5 x 10^{-6} m^2/s. It had been inferred by fitting the measured radon concentration gradient in the column to a one-dimensional diffusive migration model.

Radon concentration, soil temperature, and soil moisture content in the soil column have continuously been measured using respective probes installed at depths of 5, 30, 70, and 140 cm. Additionally the wind speed, the atmospheric pressure and the air temperature have been recorded with a mobile weather station at distances of 10 m and 1 m above the ground.

Finally the method was tested on several real contaminated sites such as gas stations and air ports. Each of these sites had been investigated previously to the radon survey by conventional means. For the radon surveys, each site was covered with a suitable grid of soil gas sampling points, which was chosen to be densest in those areas where the contamination source was to be expected. To avoid influences of diurnally changing meteorological conditions on the results, the soil gas samples were taken from a depth of 70 cm, a depth which had been proven to be sufficient in previous investigations (Schubert and Schulz, 2002). In addition to the soil-gas radon concentration, the soil moisture content at each of the sampling points was measured with a regular TDR soil moisture probe. Finally, the lateral radon distribution pattern obtained on each of the sites was compared to the respective findings of the earlier research done by conventional means.

Furthermore the method was backed up theoretically by using the relevant equations which govern the radon migration in the soil gas (Schubert et al., 2000). This theoretical investigation included the evaluation of natural parameters that are likely to influence the soil gas migration such as changing meteorological conditions (Schubert and Schulz, 2002).

RESULTS AND DISCUSSION

The laboratory tests proved the very good solubility of radon in environmentally relevant NAPLs. The results of the laboratory experiments are displayed in Table 1. The experiments yielded radon partitioning coefficients between NAPLs and soil gas $K_{NAPL/air}$ ranging between about 10.5 and 13.5. The results correspond to the partitioning coefficients published for pure NAPLs (Clever, 1979) and clearly show the very strong affinity of radon to the NAPL mixtures examined.

Table 1. Radon partitioning coefficients $K_{NAPL/air}$ between NAPLs and air (n = No. of experiments).

NAPL	$K_{NAPL/air}$	N
Gasoline	13.2 ± 1.5	7
Diesel fuel	11.4 ± 1.2	10
Kerosene	10.6 ± 2.1	4

Several lysimeter tests showed that the accumulation of radon in the NAPLs gives rise to significantly reduced soil gas radon concentrations in the contaminated soil volume as well as in the vicinity of the contamination. The results also show that these NAPL-dependent changes in radon concentration are significant compared to the changes that may arise due to meteorological influences. Figure 3 shows the changes in radon concentration at the four probe layers in the GAMS after the injection of 20 liters of gasoline at a depth of 120 cm. It can clearly be seen that the radon concentration of the soil gas in the NAPL contaminated soil volume (probe layer 140 cm) drops from about 170 kBq/m³ to about 50 kBq/m³ immediately after the injection.

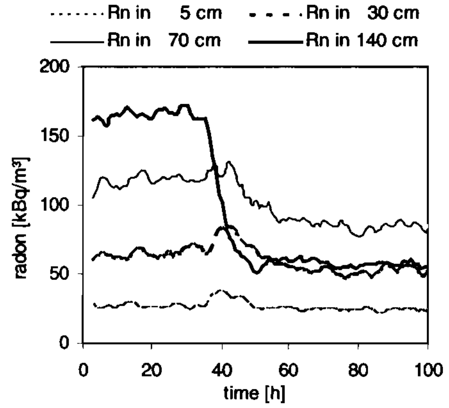

Figure 3. Rn conc. in 5, 30, 70 and 140 cm below ground level after a gasoline injection at t = 35 h and a depth of 120 cm.

That is due to the accumulation of radon in the gasoline. However, not only the soil gas radon concentration in the contaminated zone is influenced. Also the radon concentration in the probe layer 70 cm below the ground level, i.e. 50 cm above the NAPL injection level, drops from ca. 120 kBq/m³ to 80 kBq/m³. That result suggests that an indirect localization of the NAPL plume, using radon as an indicator, is possible.

Several in situ test of the method were carried out. Figure 4 shows the results of the radon survey carried out at an abandoned petrol station along with the shape of the subsurface NAPL contamination, as previously discovered by conventional methods (soil coring). The old storage tanks and the petrol pumps were assumed to be the source of the contamination. It can clearly be seen that the minimum radon concentrations found match the extent of NAPL contamination detected by conventional methods. The results also confirm the tanks to be the source of the contamination.

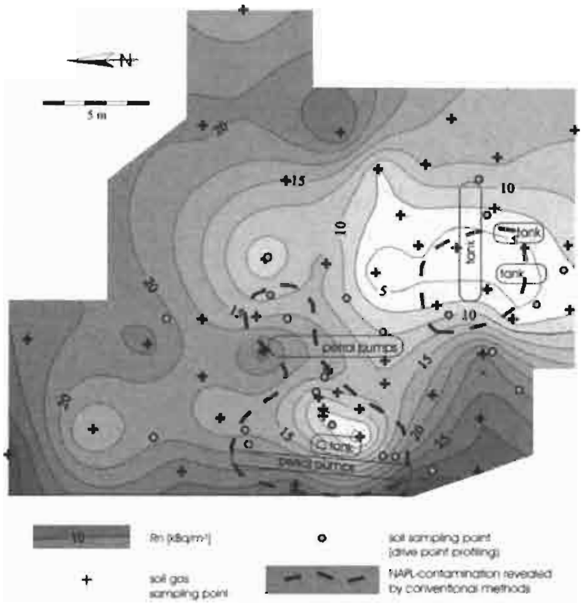

Figure 4. Anomalous low radon concentrations of the soil gas indicating the extent of a NAPL-contaminated soil volume at an abandoned petrol station.

SUMMARY

The investigation showed that a significant depletion of the radon concentration in the soil gas does occur in the presence of subsurface NAPL contamination. The depleted radon concentrations can be used as an indicator for the NAPLs in the ground. The new method, which is described in this paper is based on that effect and uses radon distribution patterns in the soil gas for the localization of the NAPL contaminated zones. These radon distribution patterns can easily be achieved by carrying out straightforward radon surveys. The much larger number of monitoring points available with the new method, compared to conventional methods, and the substantially lower time and energy required, quickly emerged as general technical advantages of the "radon method". Thus, the radon method appears to be an effective tool which should be used supplementary to conventional methods.

Besides the localization of subsurface NAPL-contamination the depletion factors for radon might also be an indicator for the degree of the NAPL saturation of the soil matrix and an indicator of the kind of NAPL the soil is contaminated with. However, these two possible applications demand equilibrium concentrations for radon between soil gas and NAPLs and significantly different partitioning coefficients for different NAPLs respectively and are subject of ongoing investigation.

Comparable investigations concerning the use radon as a partitioning tracer for aquifer contaminations by dense NAPLs (DNAPLs) have been carried out by Hunkeler et al. (1997), Semprini et al. (2000), and others. These studies, however, are focused on the radon concentration in groundwater and its dependence on NAPL contaminations of the aquifer.

REFERENCES

Barton, A.F.M., 1991. Handbook of solubility parameters and other cohesion parameters, 2nd ed.; CRC Press; Boca Raton/USA.

Clever, H.L. (Ed.), 1979. Solubility data series, vol. 2: Krypton, Xenon and Radon; Pergamon; Oxford/UK.

Davis, B.M., Istok, J.D., and Semprini L., 2002. Push–pull partitioning tracer tests using radon-222 to quantify non-aqueous phase liquid contamination, Journal of Contaminant Hydrology 58; 129-146.

Hunkeler, D., Hoehn, E., Hoener, P. and Zeyer, J., 1997. ^{222}Rn as a Partitioning Tracer To Detect Diesel Fuel Contamination in Aquifers: Laboratory Study and Field Observations; Environmental Science and Technology 31,3180-3187.

Lewis, C., Hopke, P.K., and Stukel, J., 1987. Solubility of radon in selected perfluorocarbon compounds and water; Industrial Engineering & Chemical Research 26; 356-359.

Nadolishny, A.N. and Fraser, M.T., 2001. Membrane Interface Probe (MIP) for Expedited DNAPL delineation. International Containment Technology Conference, Orlando/USA, June 13.

Prausnitz, J.M. and Shair, F.H., 1961. A thermodynamic correlation of gas solubilities, American Institute of Chemical Engineering Journal 7; 682-687.

Prausnitz, J.M., Lichtenthaler, R.E., and de Azevedo, E.G., 1986. Molecular thermodynamics of fluid phase equilibria, 2nd ed.; Prentice Hall; Englewood Cliffs/USA.

Schubert, M., Freyer, K., Treutler, H.C., and Weiss, H., 2000. Radon as an indicator of subsurface NAPL contamination. In: Rosbjerg et al. (ed.): Groundwater Research, Balkema, Rotterdam/Holland; 127-128.

Schubert, M., Freyer, K., Monnin, M., Seidel, J.P., Treutler, H.-C., and Weiss, H., 2002. The "Gas-Migration-Simulator" (GAMS) - A new device for the simulation of soil gas migration processes; Geofisica Internacional 41; 429-432.

Schubert, M. and Schulz, H., 2002. Diurnal radon variations in the upper soil layers and at the soil-air interface related to meteorological parameters; Health Physics 83; 91-96.

Semprini, L.M., Hopkins, O.S., and Tasker, B.R., 2000. Laboratory, field and modeling studies of radon-222 as a natural tracer for monitoring NAPL contamination; Transport in Porous Media 38; 223 - 240.

USEPA, 1995. Rapid Optical ScreenTool (ROST), Innovative Technology Evaluation Report; EPA/540/R-95/519.

USEPA, 1997. The Rapid Optical Screening Tool (ROST) Laser-Induced Fluorescence (LIF) System for Screening of Petroleum Hydrocarbons in Subsurface Soils, Innovative Technology Verification Report; EPA/600/R-97/020.

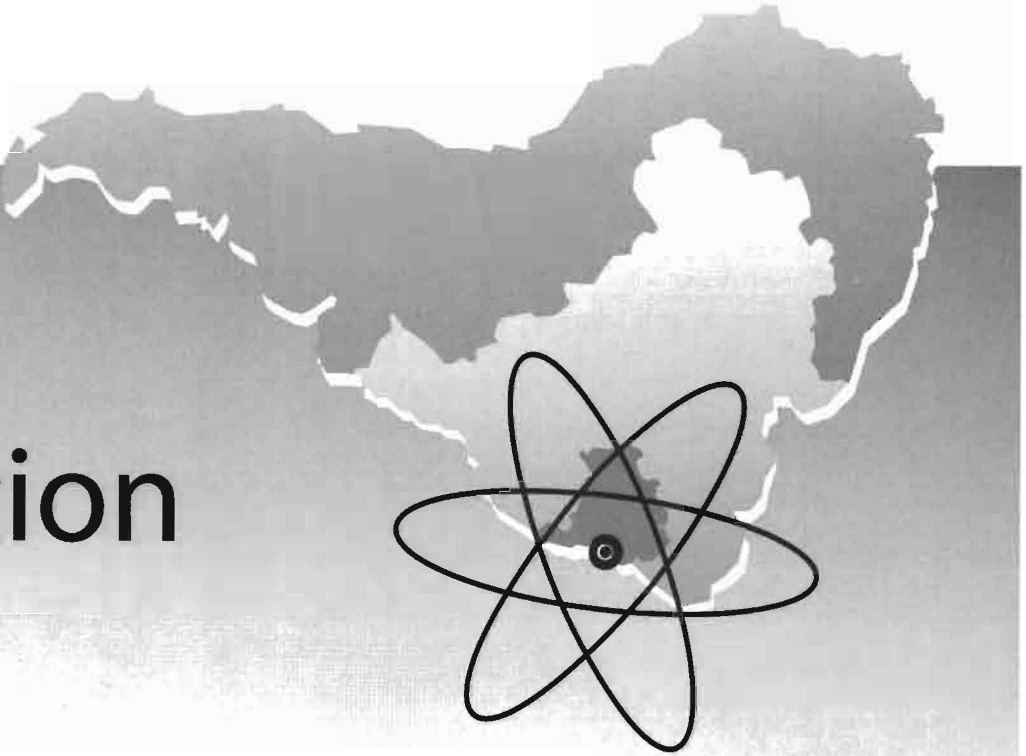

Genesis and Evolution of Igneous and Metamorphic Rocks

THE AGES OF CRYSTALLIZATION AND METAMORPHISM OF THE PASSIRA ANORTHOSITE COMPLEX-BORBOREMA PROVINCE-NORTHESTERN BRAZIL

Accioly, A.C.A.[1]; McReath, I.[2]; Santos, E.J.[3]; Guimarães, I.P.[3] and Santos, A.C.[4]

1. CPRM Geological Survey of Brazil, Recife Branch, Pernambuco. geremipe@fisepe.pe.gov.br
2. Geochemistry and Geotectonic Research Programmer, Geosciences Institute, University of São Paulo, Brazil. ianmcr@usp.br
3. Department of Geology, UFPE - Universidade Federal de Pernambuco, Recife-PE, Brazil. ignez@ufpe.br, edilton@ufpe.br
4. Department of Mines Eng. UFPE - Universidade Federal de Pernambuco, Recife-PE, Brazil. almany@ufpe.br

Keywords: Mineral isochron, massif-anorthosite, proterozoic age, metamorphism, garnet age

THE PASSIRA ANORTHOSITE COMPLEX

The Passira Anorthositic Complex (PAC) is located in Pernambuco State, Northeastern Brazil and crops out around the neighborhood of Passira City. It is situated in the Borborema Province, north of the Pernambuco Lineament and it is nested in Rio Capibaribe terrain. The Paudalho and Limoeiro shear zones are the tectonic limits of this Complex and they are both part of the Pernambuco Lineament (Fig.1).

The local lithostratigraphy is divided into the following units, from top to base: Undifferentiated Granitoids represented by diorites related to the Pernambuco Lineament, Peralkaline Orthogneiss, the metavolcano-sedimentary rocks of the Vertentes Complex, Anorogenic Granitic Orthogneiss associated to the Passira Complex; and high grade metamorphic rocks of the Transamazonian Gneissic-Migmatitic Complex.

The Passira Complex is a batholithic body, which consists of metanorthosites, subordinate metagabbros, metagabbro-norites, and lenses of Fe-Ti oxides-bearing ultramafic rocks, considered as a massif-type anorthosite complex. A dyke complex, made up of apatite-rich metaferrodiorite, encloses the Passira Anorthositic Complex. The PAC is deformed and recrystallized by at least two tectonic-metamorphic events, which have produced two distinct structural elements. The first is a penetrative sub-horizontal foliation denoted by amphibole-rich bands and the second is a sub-vertical to sub-horizontal foliation, which corresponds to the steeply dipping foliation on rocks, mainly near the shear zones. Symplectitic garnet was produced by the tectonic metamorphic event.

This paper presents K-Ar, Sm-Nd and U-Pb geochronology data that together with the mineral chemistry of the metamorphic paragenesis will be used to assess the crystallization and metamorphic age of the complex.

PETROGRAPHIC ASPECTS OF THE PASSIRA ANORTHOSITE COMPLEX

Qualitative studies of mineral relationships were performed in order to determine the peak of the metamorphism. The mineral assemblage in meta-diorites, metagabbros and metanorthosites (metabasites) were compared with some other examples described in literature (Winkler, 1977; Yardley, 1989; Ashwal, 1993, Cotkin, 1997, Emslie, 1985).

The metabasitic rocks of the PAC have the following parageneses:

(1) Primary Association: Plagioclase (andesine, labradorite) + pyroxene (Fe-enstatite metanorthosites; augite metagabbros) ± amphibolies (Metadiorites) + ilmenite. This association may represent the original mineral assemblage that could be represented by plagioclase, pyroxene megacrystals. This paragenesis shares many features with undeformed anorthosites/ gabbros/ diorites described in literature (Ashwal, 1993).

(2) Main metamorphic assemblages: Pyroxene megacrystals (augite recrystallized) + brown greenish amphibole (Mg-hornblende/tschermakite) ± garnet ± plagioclase ± rutile. This assemblage is ascribed the main metamorphism in area and it is mostly observed in garnet-bearing metagabbros, which also contain recrystallized augite, amphibole (tremolite) that replace Fe-enstatite in metanorthosites (Photo 1).

(3) Retrometamorphic-related assemblage: Amphibole (reoriented) + biotite (annite-flogopite) + epidote + chlorite ± garnet (meta-stable). This mineral assemblage was formed during principal metamorphism (Photo 2).

Pyroxene, amphibole and garnet were formed during the peak of metamorphism and they represent a transitional stage between the amphibolite and granulite facies in the garnet zone sequence. Garnet formation in metabasitic rocks in Passira Anorthosite Complex is here explained via two metamorphic reactions:

$$\text{OPX} + \text{PLG} \rightarrow \text{GAR} + \text{CPX} + \text{QTZ} \qquad \text{(I)}$$
$$\text{OPX} + \text{PLG} \rightarrow \text{GAR} + \text{QTZ} \qquad \text{(II)}$$

Evidence for reaction (I) was found in the rare examples of high pressure (>6Kb) granulite facies metagabbros. Reaction (II) was observed in the majority of the metagabbros, and in the metanorthosites of the PAC. Temperatures would have been around 700° C (Yardley, 1989).

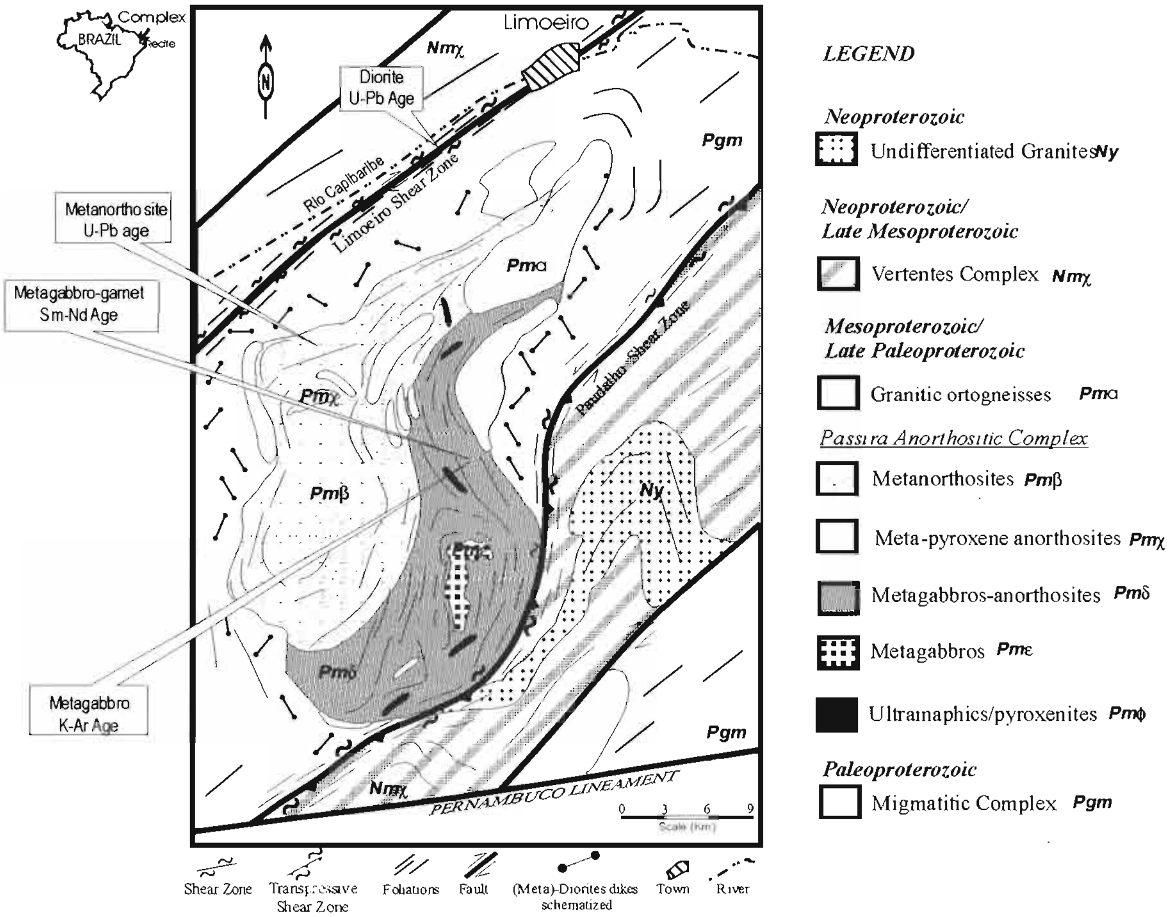

Figure 1. Schematic geological map of the PAC showing the location of the main shear zones, and the location of the analyzed samples.

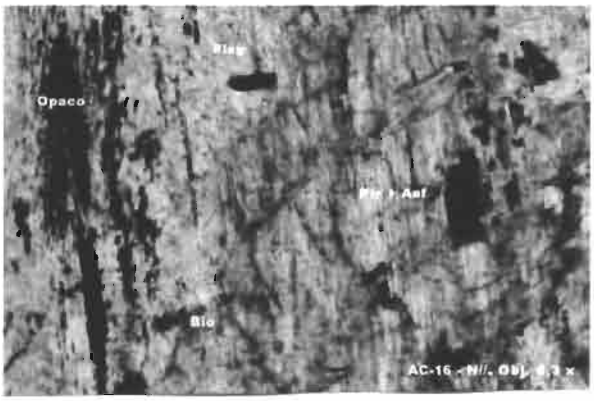

Photo 1. Amphibole (tremolite) replacing pyroxene in metanorthosite. Opaco-opaque minerals. Plag-plagioclase. Pir-pyroxene. Anf-Amphibole. Bio-Biotite.

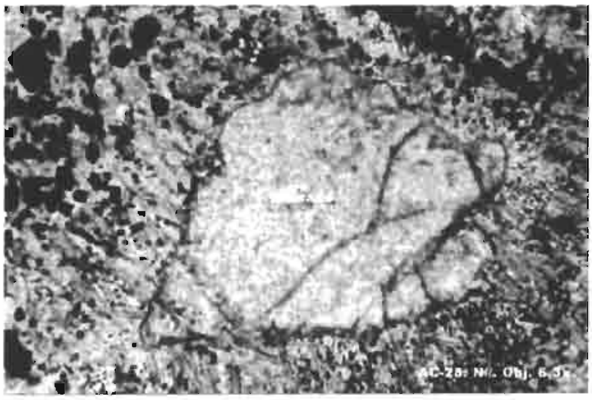

Photo 2. Coronitic-textured meta gabbros exhibiting amphibole, opaque and plagioclase around garnet.

The retrometamorphic effects are represented by: hydrous secondary phases (biotite, epidote, chlorite), garnet and quartz, which might be ascribed to metamorphic destabilization and replacing processes of original paragenesis. These processes are observed in sheared metadiorites, in garnet bearing metagabbros and metanorthosites mostly present in the Paudalho and Limoeiro shear zones.

Reaction coronas around garnet (Photo 2) are diagnostic for the retro metamorphic episodes.

These coronas are formed in greenschist facies (Messiga et al., 1995) and represent symplectitic intergrowth between amphibole and plagioclase around garnet. This association is conformable to stretching lineation and it is mainly observed near the shear zones.

GEOTHERMOMETRY

The application of quantitative geobarometry to the metabasites is difficult since specific calibrations for anorthosites are very scarce. We therefore focus on geothermometry to understand the metamorphic evolution of the PAC, using geobarometers only for the minor components of the intrusion.

P-T conditions were estimated by the semi-quantitative calibrations of TiO2 and Al2O3 contents in amphibole presented by Ernst & Liu (1998). These temperatures around 675°C and pressures of about 13.5 Kb were obtained for metagabbros.

The amphibole–plagioclase geothermometry (Holland & Blundy, 1990) yielded temperatures of about 750°-770°C for metagabbros, 693°-735°C for metanorthosites and 638°-699°C for metadiorites, for an estimate interval pressure of 10-15Kb. A temperature range of 634°-700°C for metagabbros of the PAC has been obtained by the garnet-clinopyroxene geothermometer (Ellis & Green, 1979). A major oxides profile as performed in a single grain garnet by electron microprobe (Fig. 2), which depicts uniform outlines ascribed to temperature higher than 700° C.

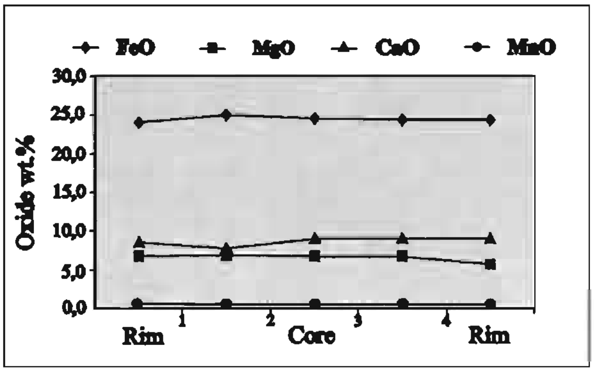

Figure 2. Electron microprobe major oxides profile in a single grain garnet from metagabbro.

Estimates of the crystallization temperatures of anorthosite complexes are in the range from 1140° to 1185°C (Markl et al., 1998). The calculated temperatures presented here are interpreted to represent the conditions of granulite facies metamorphism.

GEOCHRONOLOGY

U-Pb dating of four hand-picked least magnetic multi-crystal zircon fractions separated from pegmatitic anorthosite yielded nearly-concordant points defining an age of 1,718 ± 20 Ma, which is interpreted as the crystallization age of the anorthosite complex (Fig. 3).

The age of metamorphism was investigated via K-Ar system and by preliminary Sm-Nd mineral/whole rock isochron. The results obtained for garnet-amphibole metagabbros has yielded ages that vary from 1,100 to 1,000 Ma, which are correspondent to the Cariris Velhos event (Table 1).

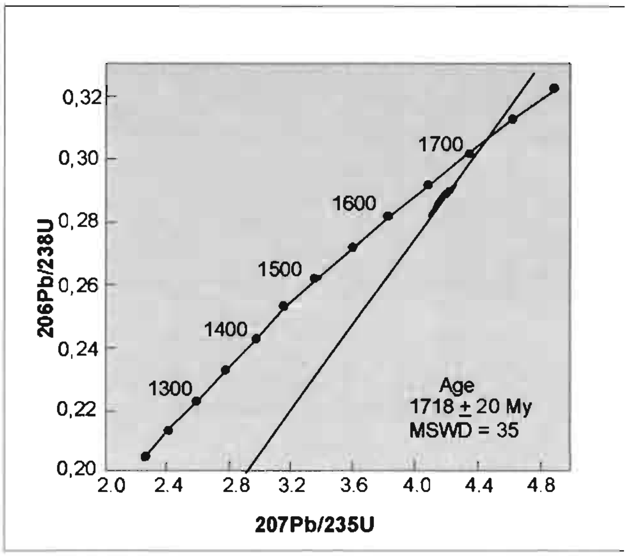

Figure 3. Age of anorthosite using U-Pb method on zircon.

These data are well in accordance with a 1,100 Ma T_{DM} model age obtained by Accioly (2001) for a Neoproterozoic peralkaline orthogneiss body located 8km eastward of the anorthositic complex. This apparently confirms the effects of the Cariris Velhos event in the area, despite that it should be expected amphibole production via metamorphic recrystallization would provoke possible losses of radiogenic Ar. This would eventually reset the isotopic system, which might have produced younger ages for those amphiboles. In meta-igneous rocks, K-Ar ages normally reflect that isotopic resetting which commonly obliterate the crystallization ages during medium to high metamorphism (Faure, 1986).

Table 1. Representative mineral analyses from amphibole from metagabbros.

	K (%)	Error	Ar^{40} (rad)	Ar^{40} (atmos)	T_{MAX} (Ma)	Error (Ma)
AC-23	0.38	0.017	19.7	15.50	1,000	56.7
AC-28	0.33	0.039	21.6	16.78	1,100	78.9

A Sm-Nd internal isochron using garnet and whole rock for metagabros indicates a Brasiliano age (612 ± 50 Ma), interpreted as correspondent to the age of the metamorphic peak in area (Fig. 4).

Sm-Nd and K-Ar results are conflicting and present no firm conclusions on the age(s) of the metamorphic event(s) can be made.

It should be expected that the metamorphic peak would be registered by the amphibole K-Ar method, but nevertheless the age are rather related to the Brasiliano event. The calculated metamorphic temperatures show that some resetting of the K-Ar system in amphibole must be expected, and the K-Ar ages obtained are probable mixed.

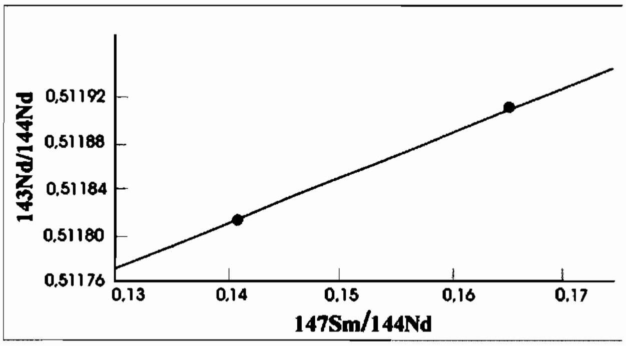

Figure 4. Garnet whole-rock isochron for garnet- metagabbros. Age = 612 ± 150 Ma, Nd^{143}/Nd^{144} = 0.51125 + 0.000014.

CONCLUSIONS

The geochronological data presented here point to the possible effect of the main metamorphic event and its peak in the mineral and whole-rock Sm-Nd systems. This metamorphism could be associated to the Brasiliano Cycle. Accioly (2001) has produced 597 Ma U-Pb age by the multicrystal zircon method of sheared diorites which she assumes that is due to later tectonic thermal retro-metamorphism that produced these shear zones such as the Paudalho and Limoeiro shear zones.

The amphibole + clinopyroxene + garnet + labradorite assemblage generated by the metamorphic peak, with a later re-equilibrium given by the amphibole +biotite +epidote + carbonate association could be related to the following episodes:

(a) Crystallization of the original gabbroic assemblage: (plagioclase ± clino or orto pyroxene) – U-Pb zircon: 1,718 ± 20 Ma.

(b) Paragenesis related to the metamorphic peak: garnet + clino-pyroxene whole-rock (opx + plg → cpx + gar + qtz) Sm-Nd - garnet isochron - 612 ± 150 Ma.

(c) Destabilization of the high or P/T mineral phases and formation of stable plagioclase and amphibole (pirox → anf + plag) possibly around 597 Ma.

Thus, the Passira Anorthositic Complex has crystallized in Upper Paleoproterozoic to Mesoproterozoic and it resembles some analogous features with Proterozoic anorthosites massif-type complexes described in literature. It is also suggested here the possible existence of a post-tectonic thermal event that latter affected the complex. This event is interpreted through the isotopic date of peralkaline orthogneiss (T_{DM} 1,100Ma). The Sm-Nd age of 612 ± 150 Ma suggest that the main metamorphic event was occurred during the Braasiliano event and the retro-metamorphic assemblage is associated to the Paudalho and Limoeiro Shear zones, which represent a later Brasiliano related thermal event.

ACKNOWLEDGEMENTS

This article is part of the Ana C. A. Accioly Doctoral Thesis, which was supported by a National Research Council Research (CNPq) Scholarship and Foundation of Research Support in São Paulo State (FAPESP). The authors wish to acknowledge CPRM-Geological Survey of Brazil for the logistic and financial support for this research project. The authors also wish to thank Dr. Reinaldo S.C. de Brito for the revision of this manuscript.

REFERENCES

Accioly, A.C.A. 2000. Geologia, Geoquímica e Significado Tectônico do Complexo Metanortosítico de Passira – Província Borborema – Nordeste Brasileiro. Unpublished Doctorate Thesis. Instituto de Geociências, Universidade de São Paulo, Brazil. 168p.

Ashwal, L.D. 1993. Anorthosites - Springer-Verlag. Berlim. 422p.

Brito Neves, B.B.; Santos, E.J. Dos; Van Schmus, W.R. 2000. Tectonic history of the Borborema Province, Northeastern Brazil – In Cordani, V.G. Et Al.. Editors – Tectonic Evolution Of South America. Rio de Janeiro. P.151-182.

Cotkin, S.J. 1997. Igneous and metamorphic petrology of the eclogitic Seljeneset Meta-anorthosite and related jotunites, Western Gneiss Region, Norway. Lithos.,40: 1-30.

Ellis, D.J.; Green, E.H. 1979. An experimental study of the effect of Ca upon garnet-clinopyroxene Fe-Mg exchange equilibria. Contrib. Mineral and Petrol., 71: 13-22.

Emslie, R. F.1985. Proterozoic anorthosite massifs. In: Tobi, A C. & Touret, J. L. R. (eds) The Deep Proterozoic Crust in the North Atlantic Provinces. NATO ASI C158. Dordrecht: Kluwer Academic, pp. 39-60.

Ernst, W.G ; Liu, J. 1998. Experimental phase-equilibrium study of Al- and Ti- contents of calcic amphibole in MORB – A semiquantitative thermobarometer. American mineralogist., 83: 952-969.

Faure, G. 1986. Principles of isotope Geology. John Wiley & Sons. 589p

Holland, T. ; Blundy, J. 1994. Non-ideal interactions in calcic amphiboles and their bearing on amphibole-plagioclase thermometry. Contrib. Mineral. Petrol., 116:433-447.

Markl, G.; Frost, B.R.; Bucher, K. 1998. The origin of anorthosites rocks from the Lofoten Islands, Northhern Norway: I. Field relations and Estimation of Intrisic Variables. Journ. Petrol. 39(8): 1425-1452

Messiga, B.; Tribuzio, R.; Bottazzi, P., Ottolini, L. 1995. An ion micrpobre study of trace element compositions of clinopyroxenres from blueschist and eclogitized Fe-Ti-gabbrosv = (Ligurian Alps, Northwestern Italy): some petrologic considerations: Geochimica et cosmochimica Acta.,59:59-75.

Rollinson, H. R. 1993. Using geochemical data: evaluation, presentation, interpretation. New York Wiley. p- 215-265.

Winkler, H. 1977. Petrogênese de Rochas Metamórficas.

Yardley, B.W.D. 1989. An introduction to metamorphic petrology. Ed. Longman Scientific.

ISOTOPIC SIGNATURE OF THE ACAMPAMENTO VELHO AND RODEIO VELHO VOLCANIC SUCCESSIONS FROM THE CAMAQUÃ BASIN, SOUTHERN BRAZIL

Almeida, D.P.M.[1]; Borba, A.W.[2]; Chemale Jr, F.[2]; Koester, E.[2] and Conceição, R.V.[2]

1. Universidade do Vale do Rio dos Sinos (UNISINOS), Departamento de Geologia. pilar@euler.unisinos.br
2. Universidade Federal do Rio Grande do Sul (UFRGS), Laboratório de Geologia Isotópica. awborba.voy@terra.com.br, chemale@ufrgs.br, koester@ufrgs.br, rommulo.conceicao@ufrgs.br

Keywords: Acampamento Velho formation, Rodeio Velho magmatism, Camaquã basin, Sr and Nd isotopes

INTRODUCTION AND GEOLOGICAL SETTING

The latest stages of the Brasiliano/Pan-african Cycle (900-500Ma) (Chemale Jr., 2000) in the Sul-rio-grandense Shield were marked by the inception of a series of fault-bounded basins filled with thick sedimentary and volcanic successions (Paim et al., 2000). The preserved stratigraphic units, which unconformably overlie igneous and metamorphic basement rocks, were considered as "molassic" by Almeida (1969) and named the "Camaquã Basin".

Focusing on the evolution of the Brasiliano Cycle in the studied region, Chemale Jr. (2000) proposed westward subduction from 650 Ma, and positioned the latest deformational events around 540 Ma. The Camaquã Basin would have occupied a retroarc position, with the onset of sedimentation and magmatism at 620 Ma. A different model has been proposed by Basei et al. (2000), who suggested two Neoproterozoic orogenies, the Brasiliano (700-620Ma) and Rio Doce (620-530Ma). The Camaquã Basin should represent the foreland sedimentation related to the Rio Doce orogenic event. Alternatively, Fragoso-César et al. (2001) suggested that the Camaquã Basin deposits would have evolved under intraplate (anorogenic) conditions, by reactivating NE-trending structures inherited from Brasiliano foldbelts.

The Camaquã Basin fill was subdivided by Paim et al. (2000) in five unconformity-bounded units: the Maricá Allogroup, with continental to marine deposits and subordinate volcanic rocks; the Bom Jardim Allogroup, composed by continental sedimentary rocks and a thick volcanic package of basaltic-andesitic composition and shoshonitic affinity; the Cerro do Bugio Allogroup, represented by bimodal alkaline volcanics (the Acampamento Velho Formation) and alluvial conglomerates; the Santa Bárbara Allogroup, entirely composed of fluvio-deltaic red beds; and the Guaritas Allogroup, made up of continental eolian, fluvial and lacustrine deposits and basaltic to andesitic alkaline volcanics (the Rodeio Velho Member) at the base of the succession.

This study focuses on the isotopic signature of the two latest volcanic events preserved in the Camaquã Basin: the Acampamento Velho Formation and the Rodeio Velho Member. Nd and Sr isotopic ratios can provide important information about processes of mantle extraction, generation and eventual crustal contamination of the magmas and about the plate tectonic setting responsible for the extrusive events.

CHARACTERISTICS AND PREVIOUS ISOTOPE DATA OF THE FOCUSED VOLCANIC EVENTS

The Acampamento Velho Formation (Ribeiro & Fantinel, 1978) consists, according to Zerfass et al. (2000) and Almeida et al. (2002a), of a lower mafic and an upper felsic volcanic associations. The lower one consists of gray-colored, porphyritic (plagioclase phenocrysts) andesite/basalt and andesitic massive flows and breccias with a total maximum thickness of 350 meters. Geochemical analyses (Almeida et al., 2002) showed a moderately sodium alkaline character (high La/Yb and Eu/Sm ratios) and absence of significant Eu negative anomaly. There are negative anomalies of P and Ti, and enrichment in Ce, Th and Zr. The upper association comprises rhyolitic rocks, with lapilli-tuffs, tuffs and welded tuffs at the base, and pink-colored, flow-banded lava flows at the top of the volcanic package. These rocks are highly siliceous (av. SiO_2 73.09% for tuffs, 77.2% for rhyolite flows), with variable negative Eu anomalies and markedly alkaline affinity. Nb/Zr and Y/Zr trends show different evolutionary trends for the lower and upper associations, reinforcing the bimodal character of this volcanic event. The first isotopic data focusing on the Acampamento Velho Formation were presented by Cordani et al. (1974) and Soliani Jr. (1986), who presented Rb/Sr isochrons of 525 and 529 ± 4 Ma (R_0=0.706), respectively. Almeida et al. (1996), studying the rhyolitic flows, determined whole-rock Rb-Sr ages of 545.1 ± 12.7 Ma (R_0=0.70932) and 546 ± 12.9 Ma (R_0=0.71454). Chemale Jr. (2000) presented ε_{Nd} (t=570Ma) values of –9.34 and –9.37, Sm-Nd T_{DM} model ages of 1.7 to 1.9 Ga, and a U-Pb zircon age of 573 ± 18 Ma. Almeida et al. (2002b) determined ε_{Nd} values of –8 to –20 for t=570 Ma.

The Rodeio Velho magmatism consists of highly vesicular, andesitic lava flows with aa and pahoehoe structures, which were emplaced as flows, stratified pyroclastic deposits and intrusions, (Almeida et al., 2000). Intrusive rocks were pointed as predominant by Silva Filho et al. (1996), fact that lead Fragoso-César et al. (1999) to redefine this unit as the Rodeio Velho Intrusive Suite. This volcanic event was considered as the precursor of the sedimentation in the intraplate Paraná Basin (an early rift phase) (Lopes et al., 1999). Petrographically. They correspond to andesites, sub-alkaline basalts and trachiandesites, the coherent rocks show plagioclase phenocrysts with glomeroporphyritic texture, opaque and accessory (apatite, zircon) minerals immersed in a pilotaxitic, vitrophyric or ophitic matrix constituted of plagioclase, pyroxene and olivine (Almeida et al., 2000). The mentioned authors presented trace-elements and REE geochemical data coherent with an alkaline character, and related these rocks to the field of intraplate continental basalts of Pearce et al. (1984), proposing that this event corresponds to the latest magmatic manifestation of the Brasiliano/ Pan-African Orogeny, which occurred right after the collision of the Rio de La Plata and Kalahari continental plates. SHRIMP U-Pb dating of one zircon crystal (Hartmann et al., 1998) yielded an Ordovician (470 ± 19 Ma) age for this magmatism, while Sm-Nd data (T_{DM} ages of 1.6 to 1.9 Ga) suggest a modified-mantle origin for these rocks (Chemale Jr., 2000).

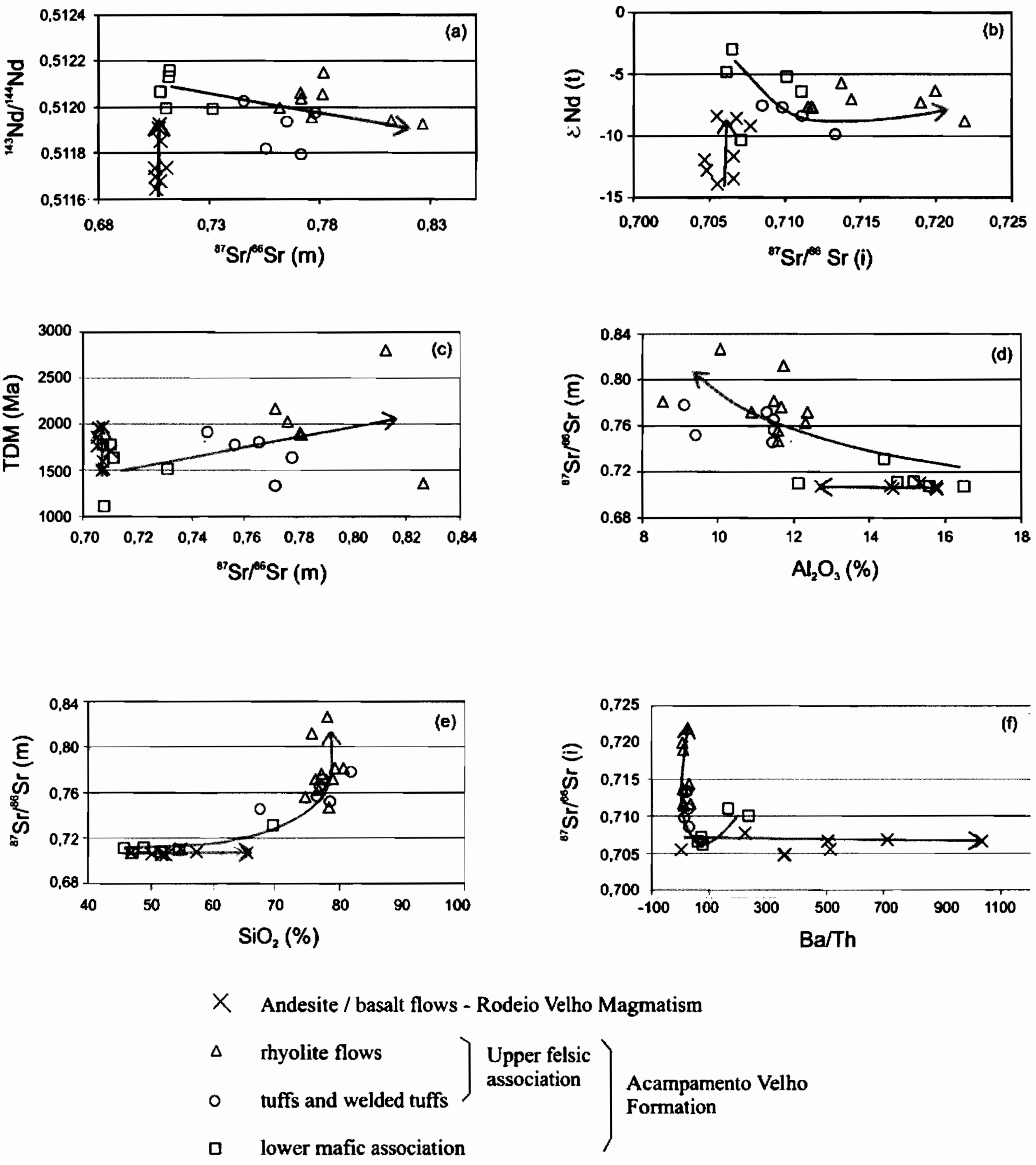

Figure 1. Diagrams for the isotopic data obtained for the volcanic rocks of the Rodeio Velho Magmatism and Acampamento Velho Formation.

OBTAINED ISOTOPIC DATA

For the Acampamento Velho Formation (AVF), six (6) samples of the lower mafic association and fifteen (15) samples of the upper felsic association (tuffs, welded tuffs and lava flows) were analyzed for Rb, Sr, Sm and Nd and isotopic ratios by mass spectrometry (TIMS) in the Laboratório de Geologia Isotópica (Laboratory of Isotope Geology) of the UFRGS. Eight (8) samples representing the Rodeio Velho Member (RVM) were also studied.

The samples of the lower mafic association of AVF show Rb (12.1 to 82.9 ppm) and Sr (23.5 to 703.4 ppm), contents coherent with mean values for andesitic to basaltic rocks. Measured ^{87}Sr/^{86}Sr ratios spread from 0.70755 to 0.73125, while initial ratios are between 0.70616 and 0.71103. The Sm content varies ranges from 5.02 to 13.74 ppm, and the Nd ranges from 22.9 to 78.2 ppm. The measured ^{143}Nd/^{144}Nd ratios concentrate between 0.51199 and 0.51216, with ε_{Nd}(0) from –9.34 to –16.66 and ε_{Nd} (t=550Ma) of –2.97 to –10.31. The T_{DM} model ages give values between 1.11 and 1.78 Ga.

Tuffs and welded tuffs of the upper felsic association have Rb values of 91.6 to 167.0 ppm, and 36.2 to 98.8 ppm for Sr, compatible with acidic (potassic) volcanics. The mesured ^{87}Sr/^{86}Sr ratios are high, spreading between 0.74597 to 0.77196, while the initial values are from 0.7014 to 0.7133. They present low Sm (0.8 to 9.5 ppm) and Nd (4.1 to 43.8 ppm) contents, and ^{143}Nd/^{144}Nd ratios of 0.51180 to 0.51205. The ε_{Nd} (0) concentrates between –11.93 and –16.44, while the ε_{Nd} at the time of cystallization (t=550Ma) spreads from –7.2 to –9.8. The T_{DM} model ages for the particulate fraction of AVF are between 1.33 and 1.92 Ga.

The rhyolitic lava flows of the upper felsic association of AVF show even higher values of Rb (100.3 to 176.7 ppm) compared to Sr (13.1 to 55.6 ppm), with very high measured (0.77186 to 0.93947) and initial (0.7014 to 0.7218) ^{87}Sr/^{86}Sr ratios. The ^{143}Nd/^{144}Nd ratios spread from 0.51181 to 0.51215, corresponding to ε_{Nd} (0) values of –7.14 to –16.25, ε_{Nd} (for t=550Ma) of –5.36 to –9.56 and T_{DM} ages between 1.35 and 2.17 Ga.

For the RVM, the results show low Rb (4.5 to 91.0 ppm) and high Sr (310.1 to 1,203.25 ppm), with low Sr isotopic ratios (0.70526 to 0.71040 for measured, and 0.70467 to 0.70774 for initial ^{87}Sr/^{86}Sr). The ^{143}Nd/^{144}Nd values concentrate between 0.51165 and 0.51193, corresponding to strongly negative ε_{Nd} (0) (–13.89 to –19.36) and ε_{Nd} (t=470Ma) (–8.39 to –13.92) and T_{DM} model ages of 1.50 to 1.96 Ga.

DISCUSSION AND CONCLUSIONS

The isotopic data obtained here were plotted in $^{87/86}$Sr versus $^{143/144}$Nd, ε_{Nd}(t), T_{DM}, SiO_2, Al_2O_3, and Ba/Th diagrams (Fig. 1 a - f). In the ^{87}Sr/^{86}Sr vs. ^{143}Nd/^{144}Nd (Fig. 1a) and ^{87}Sr/^{86}Sr(i) vs. εNd(t) (Fig. 1b) plots, clear crustal contamination trends can be seen for the Acampamento Velho Formation: from the base (lower mafic association) towards the top (rhyolite lavas of upper felsitic association), there is an increase in the Sr measured and initial ratios and a progressive decrease in the Nd ratio and a tendency of more strongly negative ε_{Nd} values (represented by the oblique arrows in both plots). The rhyolite lava flows have also the older T_{DM} values (Fig. 1c), reinforcing the presence of a crustal contaminant. For the Rodeio Velho Member, on the other hand, the lack of more differentiated volcanic facies does not allow the formation of a "trend", and one can see a concentration of values towards lower values of ^{143}Nd/^{144}Nd ratio and more negative ε_{Nd}(t) (indicated by the vertical arrows in the three plots).

Comparing the mafic rocks of the two volcanic units, a clear difference in isotopic behavior can be observed: the original basaltic magmas of the AVF have ^{143}Nd/^{144}Nd ratios higher than 0.51199 and less negative ε_{Nd}(t) values (–2 to –7 predominant), while the RVM samples have lower Nd ratios (reaching values as low as 0.51165) and more negative ε_{Nd}(t) (reaching –13.92). Such differences should suggest that the original magma of AVF was originated in a more "pure" mantle, less modified by metasomatism or subduction-introduced crustal components than the RVM.

When plotted against geochemical parameters such as Al_2O_3 and SiO_2 (Fig. 1d, e), the two volcanic units still display diverse behaviors: while the AVF shows increase in Sr measured ratios with the differentiation (increased SiO_2 and lower Al_2O_3 contents), the RVM does not vary (or varies very slightly, in the case of Al_2O_3), suggesting the absence of significant crustal contamination for the RVM. This is also indicated by the Ba enrichment of RVM, plotted against constant initial Sr ratio values (Fig. 1f): Ba might have been input to the original mantle during metasomatism (or subduction-introduced contamination). On the other hand, for AVF, the lower mafic association shows a proportional Ba/Th and initial Sr increasing, still suggesting a crustal contamination trend (oblique arrow in Fig. 1f), despite the fact that the upper felsic association does not show Ba/Th variations (vertical trend in Fig. 1f).

The isotopic results shown here indicate different evolutions for the original basaltic magmas of the two latest volcanic events of the Camaquã Basin: the Acampamento Velho magmas may have originated from a more undifferentiated mantle, and were progressively contaminated by crustal components; on the other hand, the Rodeio Velho magmas would have been extracted from a more modified mantle (metasomatism or subduction-related contamination) and experienced minor crustal contamination.

ACKNOWLEDGEMENTS

Project supported by FAPERGS # 01/08881.5.

REFERENCES

Almeida, F.F.M. 1969. Diferenciação tectônica da Plataforma Brasileira. In: Congresso Brasileiro de Geologia 23, SBG, Anais, 1: 29-46.

Almeida, D.P.M.; Zerfass, H.; Basei, M.A.S. 1996. Mineralogia, geoquímica e novas idades para o vulcanismo ácido da Bacia do Camaquã. In: Congresso Brasileiro de Geologia 39, SBG, Anais, 2: 19-21.

Almeida, D.P.M.; Lopes, R.C., Lima, L.; Gomes, C.H. 2000. Petrography and geochemistry of the volcanic rocks of the Rodeio Velho Member, Ordovician of the Camaquã Basin (RS – Brazil): preliminary results. Revista Brasileira de Geociências, 30(4): 763-768.

Almeida, D.P.M.; Zerfass, H.; Basei, M.A.S.; Petry, K.; Gomes, C.H. 2002a. The Acampamento Velho Formation, a lower Cambrian bimodal volcanic package: geochemical and stratigraphic studies from the Cerro do Bugio, Perau and Serra de Santa Bárbara (Caçapava do Sul, Rio Grande do Sul, RS – Brazil). Gondwana Research, 5(3): 721-733.

Almeida, D.P.M.; Zerfass, H.; Lopes, R.C.; Basei, M.A.S.; Pertry, K. 2002b. Caracterização e posicionamento do Vulcanismo Acampamento Velho (Neoproterozoixo III) e do Magmatismo Rodeio Velho (Meso-Ordoviciano) na Bacia do Camaquã, RS, Brasil. Simpósio sobre Vulcanismo e Ambientes Associados, 2, Boletim de Resumos, p. 110.

Basei, M.A.S.; Siga Jr., O.; Masquelin, H.; Harara, M.; Reis Neto, J.M.; Preciozzi, P.F. 2000. The Dom Feliciano Belt of Brazil and Uruguay and its foreland domain, the Rio de la Plata Craton. In: Cordani, U.G.; Milani, E.J.; Thomaz Filho, A.; Campos, D.A. (eds.) Tectonic Evolution of South America, pp. 311-334.

Chemale Jr., F. 2000. Evolução Geológica do Escudo Sul-rio-grandense. In: Holz, M.; De Ros, L.F. (eds.) Geologia do Rio Grande do Sul. CIGO/UFRGS, pp. 13-52.

Cordani, U.G.; Halpern, M.; Berenholc, M. 1974. Comentários sobre as determinações geocronológicas da Folha Porto Alegre. In: Carta Geológica do Brasil ao Milionésimo – texto explicativo das Folhas Porto Alegre e Lagoa Mirim, DNPM, pp. 70-84.

Fragoso-César, A.R.S.; Silva Filho, W.F.; Fambrini, G.L.; Machado, R.; Riccomini, C.; Paes de Almeida, R.; Pelosi, A.P.M.R.; Janikian, L. 1999. Significado tectônico do Magmatismo Rodeio Velho no Rift Guaritas (Eopaleozóico do Rio Grande do Sul, Brasil). In: Simpósio sobre vulcanismo e ambientes associados, 1, Boletim de Resumos, p.16.

Fragoso-César, A.R.S.; Fambrini, G.L.; Paes de Almeida, R.; Pelosi, A.P.M.R.; Janikian, L.; Nogueira, A.C.R.; Riccomini, C. 2001. As coberturas do Escudo Gaúcho no Rio Grande do Sul: revisão e síntese. Abstracts, Edición Electrónica del Congreso Latinoamericano de Geología XI y Congreso Uruguayo de Geología III.

Hartmann, L.A.; Silva, L.C.; Remus, M.V.D.; Leite, J.A.D.; Philipp, R.P. 1998. Evolução geotectônica do Sul do Brasil e Uruguai entre 3,3 Ga e 470 Ma. Congreso Uruguayo de Geología II, Actas, pp. 277-284.

Lopes, R.C.; Wildner, W.; Sander, A.; Camozzato, E. 1999. Alogrupo Guaritas: aspectos gerais e considerações sobre o posicionamento do vulcanismo Rodeio Velho (encerramento do Ciclo Brasiliano ou instalação da Bacia do Paraná?). In: Simpósio sobre vulcanismo e ambientes associados, 1, Boletim de Resumos, p. 17.

Paim, P.S.G.; Chemale Jr., F.; Lopes, R.C. 2000. A Bacia do Camaquã. In: Holz, M.; De Ros, L.F. (eds) Geologia do Rio Grande do Sul. CIGO/UFRGS, pp. 231-174.

Pearce, J.A.; Harris, N.B.W.; Tindle, A.G. 1984. Trace element discrimination diagrams for the tectonic interpretation of granitic rocks. Journal of Petrology, 25 (4) : 956-983.

Ribeiro, M.; Fantinel, L.M. 1978. Associações petrotectônicas do Escudo Sul-rio-grandense. Iheringia, Série Geológica, vol. 5, pp. 19-54.

Silva Filho, W.F.; Fragoso-César, A.R.S.; Machado, R.; Sayeg, H.S.; Fambrini, G.L.; Ribeiro de Almeida, T.I. 1996. O magmatismo Rodeio Velho e a Formação Guaritas no Eopaleozóico do Rio Grande do Sul: uma revisão. Congreso Brasileiro de Geologia 39, Anais, 5: 433-435.

Soliani Jr., E. 1986. Os dados geocronológicos do Escudo Sul-rio-grandense e suas implicações de ordem geotectônica. Tese de Doutoramento, IG/USP, inédita, 239p.

Zerfass, H.; Almeida, D.P.M.; Gomes, C.H. 2000. Faciology of the Acampamento Velho Formation volcanic rocks (Camaquã Basin) in the region of Serra de Santa Bárbara, Cerro do Perau and Cerro do Bugio (Municipality of Caçapava do Sul – RS). Revista Brasileira de Geociências, 30(3): 375-379.

ARCHEAN-PALEOPROTEROZOIC CRUSTAL CHARNOCKITIC EVOLUTION OF THE JAGUAQUARA, LAJE, MUTUIPE, BREJÕES AND SANTA INÊS REGION, JEQUIÉ BLOCK, BAHIA, BRAZIL

Barbosa J.S.F.[1]; Martin, H.[2]; Peucat , J.J.[3] and Macedo, E.P.[1]

1. CPGG- Centro de Pesquisa em Geofisica e Geologia/UFBA, Rua Caetano Moura 123, Federação, 40210-350, Salvador, Bahia, Brazil. johildo@pppg.ufba.br
2. Université Blaise Pascal, 5 rue Kessler, 63038 Clermont-Ferrand, France. martin@opgc.univ-bpclermont.fr
3.Géosciences Rennes, UPR CNRS 4661, 35042 Rennes cedex, France. peucat@univ-renes1.fr

Keywords: Archean, Paleoproterozoic, granulites, Bahia, Brazil

Gravitational dome-and-basin structures have been recognized in Archaean terrains of different metamorphism grades and related to diapiric instabilities developped between gneisses and greenstone belts (Choukroune et al., 1997; Bouhallier et al., 1995; Chardon et al., 1998). These structures are interpreted as due to crust reheating by mantle derived thermal materials which induced gravity instabilities caused by the emplacement of high density volcanic traps over a low density protocontinental crust.

In Brazil, similar structures were also reported in the granulitic Jequié Complex (Alves da Silva et al., 1996) of the São Francisco Craton close to Brejões and Santa Inês in the south of the Bahia State. Previous studies (Barbosa, 1986, 1990; Fornari, 1993), demonstrated that these domains are composed of charnockitic domes (CH6) surrounded by charno-enderbites and charnockites (CH1, CH2), heterogeneous granulites (HG) and supracrustal rocks (SP).

Recent investigations show that supracrustal rocks (SP) are enclaves in the heterogeneous granulites (HG), and would represent the oldest rocks found in this area, even if no geochronological data is available. Heterogeneous granulites (HG) exhibit ^{207}Pb/^{206}Pb mono-zircon evaporation minimum ages ca 2.6 Ga and Rb-Sr isochron age at 2.7 Ga (Wilson, 1987). They are considered as contemporaneous to charnockites (CH1, CH2) respectively dated by SHRIMP on zircon at 2.8 and 2.7 Ga (Alibert & Barbosa, 1992; Marinho et al., 1994). Within domes, charnockites (CH6) have complex zircons displaying inherited cores and minimum evaporation ages ca. 2.55 Ga which are similar with that found in other charnockites. All rocks have a restricted range of Nd depleted model ages between 3.0 and 3.2 Ga.

Doming is constrained ca. 2.05-2.03 Ga by monazite dating (cooling <750°C) from the intusive charnockites (CH6) and by monazite from garnet-cordierite bearing charnockitic magmas synchronous of the doming. The age of the granulite facies metamorphism in the Jequié Complex is ca. 2.0 Ga (Wilson, 1987). In southern and northern parts of the Complex, zircon ages respectively of 2086 ± 18 (Ledru et al., 1994) and of 2096 ± 3 Ma (Peucat et al., unpublished) give a more precise timing of high-grade metamorphism. All these data lead to the conclusion that charnockitic doming in Brejões and Santa Inês was contemporaneous (or late) with the regional granulite facies metamorphism. Geothermometry performed on (CH6) indicate temperature ca. 1100°C, higher that these reached during the regional granulite facies metamorphism. Consequently, it is concluded that doming processes have occurred between 2.10 Ga and 2.05-2.03 Ga.

Geochemical modelling based on trace element compatible (i.e. Rb) and incompatible (i.e. Sr) behaviour shows that rocks such as (CH1, CH2) differentiated through fractional crystallization. On the contrary, (CH6) is directly produced by partial melting of a source that was similar to (CH2); a (CH1) -like source being precluded. Computed models indicate that both (CH1, CH2) formed respectively through 30% and 20% fractional crystallization of a plagioclase, hornblende, clinopyroxene and accessories (magnetite, ilmenite, apatite, allanite) cumulate. In addition, $\varepsilon_{Nd\ (T)}$ ranging between 0 and –4 point out a significant crustal input such that these rocks can be interpreted as generated (i) either by melting of a crust contaminated depleted mantle source or (ii) by melting of an enriched mantle source.

REFERENCES

Alibert C., Barbosa, J.S.F., 1992. Ages U-Pb déterminés à la "SHRIMP" sur des zircons du Complexe de Jequié, Craton du São Francisco, Bahia, Brésil. In: 14 Réunion Science de la Terre, Toulouse, Societé Géologique de France, p. 4.

Alves da Silva, F.C., Barbosa, J.S.F., Damanesco, J.A., Rodriguez, Z.R.C., Paim, M., 1996. Estrutura Dômica de Brejões (SE-Bahia): padrão de interferência, produto de anomalia termal ou feição ignea preservada? XXXIX Congresso Brasileiro de Geologia, Salvador (BA), Anais 6, 266-269.

Chardon, D., Choukroune, P., Jayananda, M., 1998. Sinking of the Dharwar basin: implications for Archaean tectonics. Precambrian Research 91, 15-39.

Barbosa, J.S.F. 1990., The granulites of the Jequié Complex and Atlantic Mobile Belt, Southern Bahia, Brazil - An expression of Archaean Proterozoic Plate Convergence. Granulites and Crustal Evolution. In: Vielzeuf D., Vidal P. (Eds.), Springer-Verlag Proc. of ARW, Clermont Ferrand (France), pp. 195-221.

Barbosa J.S.F., Alves da Silva F.C., Silva R.I., Paim M.M., Rodrigues Z.R.C. 1996 - Anais XXXIX Cong. Bras. Geol. Salvador- Bahia, vol.6 : 285-292.

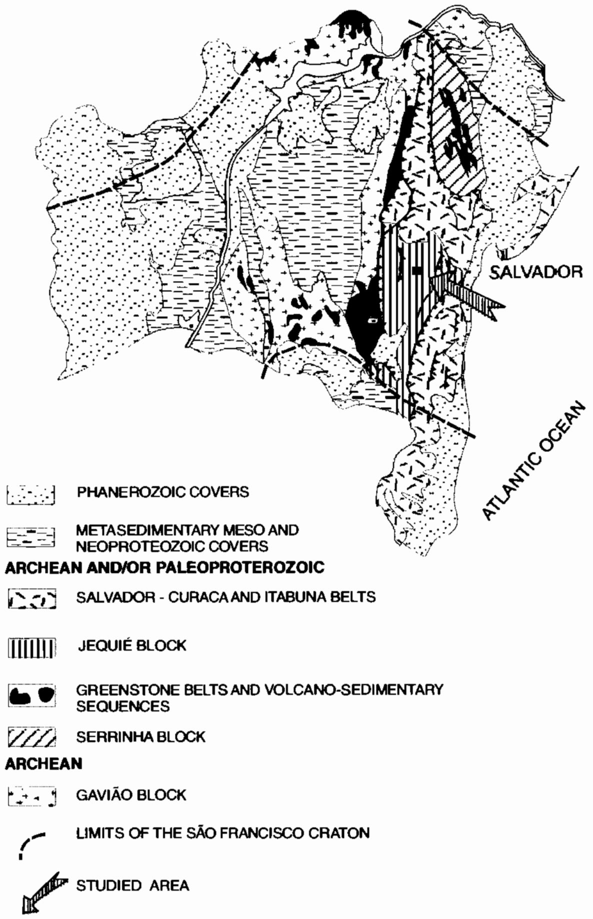

Figure 1. Location of the studied area, of the cratons and of fold belts of the Brazilian cycle (Almeida, 1977) after Schobbenhaus et al. (1984).

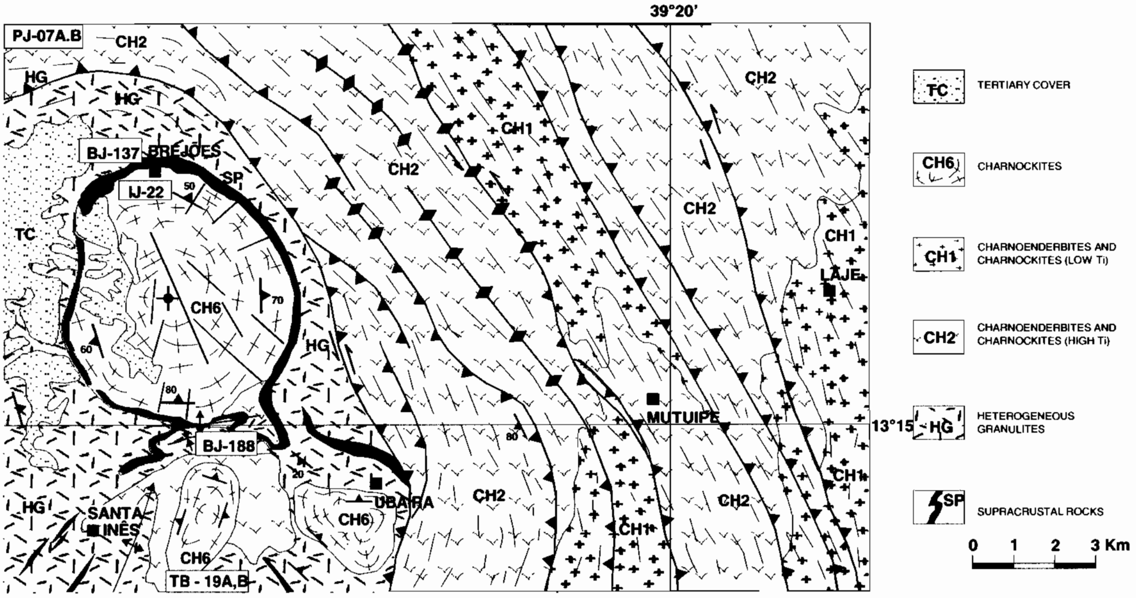

Figure 2. Geologic sketch map of the Laje, Mutuípe, Brejões and Santa Inês regions. Jequié block, Bahia, Brazil. Samples for geochronological study are reported.

Bouhallier, H., Chardon, D., Choukroune, P., 1995. Strain patterns in Archaean dome and basin structures: the Dharwar craton (Karnataka, south India). Earth and Planetary Sciences Letters 135, 57-75.

Chardon, D., Choukroune, P., Jayananda, M., 1998. Sinking of the Dharwar basin: implications for Archaean tectonics. Precambrian Research 91, 15-39.

Choukroune, P., Ludden J.N., Chardon, D., Calvert, A.J., Bouhallier, H., 1997. Archaean crustal growth and tectonic processes: a comparison of the Superior Province, Canada and the Dharwar Craton, India. In: Burg, J.P., Ford, M. (Eds.), Orogeny Through Time, Geological Society Special Publication 121, 63-98.

Fornari, A., 1993. Petrologia, geoquímica e metamorfismo das rochas enderbíticas-charnockíticas da região de Lage e Mutuipe, Bahia. M.Sc. Thesis, unpublished. University of Bahia, Brazil. 143p.

Ledru, P., Cocherie, A., Barbosa, J.S.F., Johan, V., Onstott, T., 1994. Age du métamorphisme granulitique dans le Craton du São Francisco (Brésil). Implications sur la nature de l'orogène transmazonien. C. R. Academie des Sciences de Paris 211, 120-125.

Marinho, M.M., Vidal, P., Alibert, C., Barbosa, J.S.F., Sabaté, P., 1994. Geochronology of the Jequié-Itabuna granulitic belt and of the Contendas-Mirante volcano-sedimentary belt. Boletim de Instituto de Geociências, University of São Paulo, Brazil. Special Publication 17, 73-96.

Wilson, N., 1987. Combined Sm-Nd, Pb/Pb and RbSr geochronology and isotope geochemistry in polymetamorphic precambrian terrains: examples from Brazil and Channel Island, U.K. Master of Science. M.Sc. Thesis, unpublished. Oxford University. U.K. 250p.

Sm-Nd DATA OF THE ESTRELA GRANITE COMPLEX, CARAJÁS METALLOGENETIC PROVINCE, NORTHERN BRAZIL

Barros, C.E.M.[1,2] **and Macambira, M.J.B.**[1,3]

1. Universidade Federal do Pará - Centro de Geociências
2. Grupo de Pesquisa Petrologia de Granitóides, Bolsista do CNPq. cadu@ufpa.br
3. Laboratório de Geologia Isotópica (Pará-Iso). moamac@ufpa.br

Keywords: Sm-Nd, Estrela Granite Complex, Carajás Province, A-type granites

INTRODUCTION

A-type granites are characterized by elevated $(K_2O+Na_2O)/(K_2O+Na_2O+CaO)$ $FeO/(FeO+MgO)$ ratios and high concentrations of incompatible elements (Whalen et al., 1987). Two main petrogenetic models try to explain the origin of these granite magmas: (1) partial melting of crustal rocks (Anderson & Bender, 1989; Patiño-Douce, 1996) and (2) fractionation of mafic magmas (Turner et al., 1992; Whalen et al., 1996). A particular petrogenetic model involving crustal sources invokes the partial melting of granulites (Landerberger & Collins, 1996; Skjerlie & Johnston, 1993). The magmas formed from fractionation of mafic magmas display positive ε_{Nd} values and low $^{87}Sr/^{86}Sr$ initial ratios, mirroring the mantle souce. On the other hand, magmas derived from crustal sources present negative ε_{Nd} values and high initial ratios. However, these ratios may be relatively low in crustal sources that underwent previous granulitic metamorphism. According to Sylvester (1989), mantle-derived A-type magmas are more probably formed in extensional tectonic regimes, whereas alkaline granites formed in compressional setting are normally of crustal origin. The aim of this paper is to discuss the petrogenesis of the Archean A-type Estrela Granite Complex (EGC) on the basis of $^{87}Sr/^{86}Sr$ initial ratio and Sm-Nd data.

TECTONIC SETTING

The Carajás Metallogenetic Province located in the southeastern part of the Amazonian Craton represents an cratonic Archean nuclei with important ore deposits (Docegeo, 1988). The meridional part of this nucleus is made of 3.0 Ga enderbites and mafic granulites (Macambira & Lancelot 1996, Pidgeon et al., 2000), 2.97 Ga greenstone belts, 2.96 Ga calc-alkaline tonalites and 2.87 Ga granodiorites and granites (Docegeo, 1988, Dall'Agnol et al., 1997). According to Pidgeon et al. (2000) the granulite metamorphism occurred 2.85 Ga ago, roughly coeval with the emplacement of large granitoid bodies. To the north of the province, local occurrences of 2.81 Ga metagranitoids, extensive 2.76 Ga metavolcano-sedimentary (Machado et al., 1991) which are crosscut by 2.76-2.74 Ga syntectonic alkaline granitoids (Estrela Granite Complex, Plaquê Suíte, Planalto and Serra do Rabo granites) (Dall'Agnol et al., 1997, Barros et al., 2001a, b), 2.64 Ga mafic dikes sills (Dias et al., 1996) and minor 2.56 Ga granites have been described. Both domains are crosscut by several 1.88 Ga anorogenic granites (Docegeo 1988, Dall'Agnol et al., 1997).

STRUCTURAL GEOLOGY

The EGC crops out to the east of the Carajás Range as a EW elongated elliptical body concordant with the regional structures. Igneous layering (S_0) is subvertical in peripheral zones and in the central domains of plutons. Lying E-W/subvertical Schistosity (S_1) is outlined by the preferred orientation of mafic minerals and by the flattening of quartz grains. Decimeter- to meter-wide mylonite zones (S_{1m}) concordant with the schistosity are described. The S_1 surfaces developed during the non-completely crystallized stage and the S_{1m} developed after complete crystallization. Progressive deformation in decreasing temperature regimes testifies the syntectonic character of the EGC which would have been emplaced and inflated (ballooning) concomitantly to horizontal shortening. A tectono-thermal aureole was produced in the metavolcano-sedimentary envelope due to the thermal metamorphism and lateral expansion stresses of the granite massif (Barros et al., 2001a).

PETROGRAPHY AND GEOCHEMISTRY

Monzogranites are by far the most abundant facies in the complex comparatively to syenogranites, granodiorites and tonalites. Mafic minerals assemblage permit to distinguish different facies among the monzogranites (hbl+cpx, hbl, hbl+biot, biot+hbl e biot). Quartzfeldspahic mobilizates and hornblende megacrysts-bearing pegmatoid veins crosscut the above mentioned granitoids. These rocks display high $[Fe_2O_3/(Fe_2O_3+MgO) = 0.83 - 0.99]$ and $[(K_2O+Na_2O)/(K_2O+Na_2O+CaO) = 0.60 - 0.89]$ ratios, elevated incompatible elements concentrations (Zr = 146 – 640 ppm; Y = 13 – 404 ppm; Ce = 115 – 441 ppm; Nb = 21 – 45 ppm) and high values of earth-rare elements (ΣETR= 275 – 941 ppm), with moderate negative Eu anomalies (Eu/Eu* = 0.25 – 0.65).

WHOLE-ROCK Rb-Sr DATING AND Pb-Pb ZIRCON EVAPORATION

A whole-rock Rb-Sr isochron yielded the age of 2527 ± 34 Ma and low $^{87}Sr/^{86}Sr$ initial ratio (0.7018 ± 0.00197) to the EGC (Barros et al., 1992). Pb-Pb evaporation of zircon dating furnished an age of 2763 ± 7 Ma (Barros et al., 2001b) for hornblende syenogranites. The latter, considered as the crystallization age of the EGC, is very close to the ages obtained in zircons from some metabasalts and ultramafites (Machado et al., 1991). The $^{87}Sr/^{86}Sr$ initial ratio must not be considered the real value since the Pb-Pb zircon evaporation crystallization age is higher than that yielded by Rb-Sr isochron. In this case, the $^{87}Sr/^{86}Sr$ initial ratio must be even lower than that indicated by the Rb-Sr isochron.

Sm-Nd DATA

Sm-Nd data were obtained in the Laboratory of Isotopic Geology (Pará-Iso) of the Federal University of Pará. The selected samples correspond to a hornblende granodiorite (CAP 5), a hornblende monzogranite (PSV-VIII-75) and a biotite monzogranite (PSV-VIII-77). The first two samples belong to the metaluminous group (Al_2O_3 ~ 11.5%) whereas the latter one belong to the weakly peraluminous group (Al_2O_3 ~ 13.5 %) (Barros et al., 1997). The $^{147}Sm/^{144}Nd$ ratios of the EGC samples rouge from 0.1050 to 0.1475 (Tab. 1). The values grow from the biotite monzogranites to the hornblende granodiorite. ε_{Nd} values are between –0.38 and –1.34. The analysed rocks, which Pb-Pb zircon age is 2763 Ma, present $T_{(DM)}$ ages between 2.97 Ga and 3.12 Ga (Fig. 1).

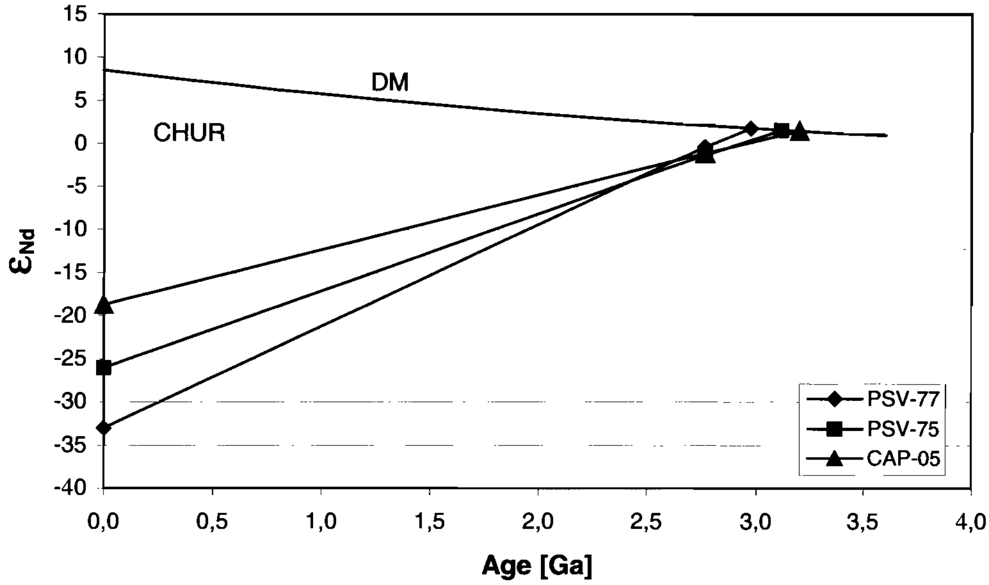

Figure 1. Age (Ga) vs. $\varepsilon_{(Nd)}$ diagram of the Estrela Granite Complex.

Table 1. Sm-Nd analytical data of the Estrela Granite Complex.

Sample	Sm	Nd	$^{147}Sm/^{144}Nd$	1σ	$^{143}Nd/^{144}Nd$	1σ	f (Sm/Nd)	$\varepsilon_{Nd(0)}$	$T_{(DM)}$	$\varepsilon_{Nd(t)}$	$T_{(CHUR)}$
PSV-77	5.85	33.67	0.10503	0.00021	0.510947	0.000008	-0.4660	-32.99	2.97	-0.38	2.79
PSV-75	16.04	76.20	0.12729	0.00072	0.511304	0.000018	-0.3529	-26.02	3.12	-1.34	2.91
CAP05	18.28	74.94	0.14749	0.00037	0.511682	0.000009	-0.2502	-18.65	3.20	-1.15	2.94

PETROLOGIC SIGNIFICANCE

The close time relationship between the mafic-ultramafic sequences and the EGC, in adition to the low initial $^{87}Sr/^{86}Sr$ ratio could suggest the fractionation of mafic magmas to explain the origin of the EGC magmas. However the absence of mafic enclaves and the emplacement of granitoids concomitantly to compressive stresses seem to point to partial melting of crustal rocks as the petrogenetic model to explain the origin of the EGC. The low initial $^{87}Sr/^{86}Sr$ (0.7018 ± 0.00197) ratio and the negatives values of ε_{Nd} (–0.38 and –1.34) should be interpreted as the participation of crustal sources (cf. Patiño-Douce 1996), probably of granulitic nature (cf. Creaser et al., 1991, Landenberger & Collins, 1996), where low initial Sr ratios may be expected. Enderbites (hyperstene tonalites), as those formed at 2.85 Ga ago (cf. Pidgeon et al., 2000), could be potential source rocks. Partial melting of dehydrated tonalitic rocks has been proposed as a probable model to explain the petrogenesis of hot A-type granite magmas (Patiño-Douce, 1997). This model seems to be coherent with the origin of the Estrela Granite Complex.

ACKNOWLEDGEMENTS

We would like to express our gratitude to: Universidade Federal do Pará, Núcleo Pronex (PADCT-FINEP 4/3/87/0911/00 and 6.5.92.0025.00), and CNPq (Edital Universal 476623/2001-4). We are greatful to M.A. Galarza and R. Florenço who carried the analytical procedures.

REFERENCES

Anderson, J.L. and Bender, E. 1989. Nature and origin of Proterozoic A-type granitic magmatism in the southwestern United States of America. Lithos, 23, 19-52.

Barros, C.E.M.; Dall'Agnol, R.; Barbey, P. and Boullier, A.M. 1997. Geochemistry of the Estrela Granite Complex, Carajás Region, Brazil: an example of an Archaean A-type granitoid. Journal of South-American Earth Sciences, 10(3-4):321-330.

Barros, C.E.M.; Barbey, P. and Boullier, A.M. 2001a. Role of magma pressure, tectonic stress and crystallization progress in the emplacement of the syntectonic A-type Estrela Granite Complex (Carajás Mineral Province, Brazil). Tectonophysics, 343, 93-109.

Barros, C.E.M.; Sardinha, A.S.; Barbosa, J.P.O.; Krimsky, R. and Macambira, M.J.B. 2001b. Pb-Pb and U-Pb zircon ages of some Archean syntectonic granites of the Carajás Metalogenetic Province, Northern Brazil. In: Simposio Sul-Americano de Geología Isotópica, 3, Pucón.

Barros, C.E.M.; Dall'Agnol, R.; Lafon, J.M.; Teixeira N.P. and Ribeiro J.W. 1992. Geologia e geocronologia Rb-Sr do Gnaisse Estrela, Curionópolis, PA. Boletim do Museu Paraense Emílio Goeldi, Ciências da Terra, 4:83-102.

Dall'Agnol, R.; Souza, Z.S.; Althoff, F.J.; Barros, C.E.M.; Leite, A.A.S. and Jorge-João, X.S. 1997. General aspects of the granitogenesis of the Carajás Metalogenetic Province. In Ferreira, V.P., Sial, A.N. Excursion guide - II International Symposium of Granites and Associated Mineralizations, SCBPM – SGM, Salvador, 135-161.

Docegeo (Rio Doce Geologia e Mineração), 1988. Revisão litoestratigráfica da província mineral de Carajás. In: 35e Congresso Brasileiro de Geologia, Belém, 1988. Província Mineral de Carajás - Litoestratigrafia e principais depósitos minerais. Anexo aos anais. Belém, CVRD/SBG. 11-59.

Landenberger, B. and Collins, W.J. 1996. Derivation of A-type granites from a dehydrated charnockitic lower crust: Evidence from the Chaelundi Complex, eastern Australia. Journal of Petrology, 37, 145-170.

Macambria, M. J. B. and Lancelot, J. R. 1996. Time constraints for the formation of the Archean Rio Maria crust, southeastern Amazonian Craton, Brazil.. International Geology Review, 38:1134-1142.

Machado, N.; Lindenmayer, Z.; Krogh, T.H. and Lindenmayer, Z.G. 1991. U-Pb geochronology of Archaean magmatism and basement reactivation in the Carajás area, Amazon shield, Brazil. Precambrian Research, 49:329-354.

Patiño-Douce, A.E. 1997. Generation of metaluminous A-type granites by low-pressure melting of calc-alkaline granitoids. Geology, 25, 743-746.

Pidgeon, R.T.; Macambira, M.J.B. and Lafon, J.M. 2000. Th-U-Pb isotopic systems and internal structures of complex zircons from an enderbite from the Pium Complex, Carajás Province, Brazil: evidence for the ages of granulites facies metamorphism and the protolith of the enderbite. Chemical Geology, 166, 159-171.

Skjerlie, K.P. and Johnston, A.D. 1993. Fluid-Absent Melting Behavior of an F-Rich Tonalitic Gneiss at Mid-Crustal Pressures: Implications for the Generation of Anorogenic Granites. Journal of Petrology, 34(4):785-815.

Sylvester, P.J. 1989. Post-collisional alkaline granites. Journal of Geology, 97:261-280.

Turner, S.P.; Foden, J.D. and Morrison, R.S. 1992. Derivation of some A-type magmas by fractionation of basaltic magma: An example from the Padthaway Ridge, South Australia. Lithos, 28:151-179.

Whalen, J.B.; Currie, K.L. and Chappell, B.W., 1987. A-type granites: geochemical characteristics, discrimination and petrogenesis. Contributions to Mineralogy and Petrology, 95:407-419.

Whalen, J.B.; Jenner, G.A.; Longstaffe, F.; Robert, F. and Gariépy, C. 1996. Geochemical and Isotopic (O, Nd, Pb and Sr) Constraints on A-type Granite Petrogenesis Based on the Topsails Igneous Suite, Newfoundland Appalachians. Journal of Petrology, 37(6):1463-1489.

GEOCHRONOLOGY AND ISOTOPE GEOCHEMISTRY OF VOTUVERAVA AND PERAU MESOPROTEROZOIC BASINS, SOUTHERN RIBEIRA BELT, BRAZIL

Basei, M.A.S.[1]; Siga Jr, O.[1]; Kaulfuss, G.A.[1]; Cordeiro, H.[1]; Nutman, A.[2]; Sato, K.[1]; Cury, L.F.[1]; Prazeres Filho, H.J.[1]; Passarelli, C.R.[1]; Harara, O.M.[1]; Reis Neto, J.M.[3]; Weber, W.[1]

1. Instituto de Geociências, Universidade de São Paulo, Brazil. baseimas@usp.br
2. Research School of Earth Sciences, Australian National University. Allen.Nutman@anu.edu.au
3. Departamento de Geologia, Universidade Federal do Paraná. jmreis@setuva.geologia.ufpr.br

Keywords: Amphibolite, zircon, Mesoproterozoic, model ages, crustal evolution

INTRODUCTION

The main problems concerning the majority of the stratigraphic syntheses and tectonic models proposed for the southern portion of the Ribeira Belt (Paraná and São Paulo States) come from the lack of information on the time of sedimentation and metamorphic climax of great part of the metavolcano-sedimentary units that predominate in the region. This fact causes serious problems when correlations are made, and it is possible to find in the geologic literature conflicting proposals, where the same formation can be placed in different stratigraphical position.

Recent works have searched for more reliable isotopic methods, in order to contribute to the solution of countless interpretation problems that still exist. This paper focuses on the evolution of Votuverava and Perau formations, located north of Curitiba, based mainly on new (conventional and SHRIMP) zircon U-Pb ages and whole rock Sm-Nd and Rb-Sr data for the metabasic rocks found in these units.

U-Pb Zircon ages of the order of 1470 Ma are presented for the metabasic rocks associated with the Votuverava and Perau units. It is suggested that both formations be chronocorrelated and their sedimentation age close to the Mesoproterozoic metabasics, emplaced during the extensional phase of the basin. The lithologic differences between the Votuverava and Perau formations are explained as faciologic variations within the same paleobasin.

The basic rocks represent Mesoproterozoic juvenile material extracted from the mantle and quickly emplaced as sills and dykes within the sediments of the Votuverava-Perau paleobasin. Differently, strongly negative Epsilon Nd values and old model ages (T_{DM}) for the Votuverava phyllites, Varginha Granite, and Setuva, Betara and Tigre nuclei suggest a long period of crustal residence for their protoliths.

For the Varginha Granite, late-tectonic in relation to the Brasiliano deformations and intrusive in the Votuverava sediments, a zircon U-Pb age of 603 Ma is pointed out.

GEOLOGICAL SETTING

The Votuverava Formation is a greenschist-facies metavolcano-sedimentary sequence, where the distal lithofacies predominates being characterized by thick pelitic to psammopelitic piles composed of phyllites, usually carbonaceous, metarhythmites and subordinated metasandstones, also including metacalcarenites of turbiditic nature, interfingered with varied metabasites, volcaniclastic rocks and deep-water iron-manganiferous formations (CPRM, 1998). Fiori (1992) considers that the Votuverava Formation was deposited in a backarc basin in relatively calm waters with some glacial contribution.

The Perau Complex is composed of a metavolcano-sedimentary sequence that crops out in the areas of Canoas and Perau Pb-Zn-Ag mines corresponding to the Unit "B" proposed by Daitx (1996). Represents from bottom to top, quartzites, carbonatic rocks and a thick pile of mica schists with amphibolite intercalations. A peculiar characteristic of this group is the large quantity of amphibolite and metabasite bodies.

Regionally, Soares et al. (2000), interpret the evolution of the Apiaí belt as polycyclic. Two major events are important in its geologic history, one Mesoproterozoic, generating the rocks of the Perau-Setuva-Água Clara Complex, and the other Neoproterozoic, related to the formation and metamorphism of the Capiru-Votuverava-Itaiacoca Sequence. The last event was also responsible for the second metamorphic phase of the Mesoproterozoic rocks. Campanha and Sadowski (1999) attribute the name Votuverava Group to the Lajeado (carbonatic platform) and Ribeira (distal turbiditic sequence) subgroups. For these authors, the Ribeira subgroup is further divided in three units, the basal being the Perau Formation.

CHARACTERIZATION OF METABASIC ROCKS

In the Votuverava Formation, several amphibolitic bodies, in general strongly weathered, are found. These amphibolites underwent greenschist facies metamorphism (chlorite/biotite zone), and the metamorphic assemblage is composed of tremolite/actinolite, plagioclase, epidote and chlorite. During metamorphism, the replacement of the primary mineralogy was intense, and in some cases is well marked by the presence of hornblende nuclei surrounded by tremolite/actinolite. Another frequent feature is the presence of tremolite/actinolite crystals clearly oriented according to foliation.

In the Perau region the amphibolites occur preferentially in the western flank of the anticlinal that exposes paleoproterozoic gneissic nuclei of the area of the Perau Pb mine. They are almost always concordant with the host rocks and coherent with the regional structuration. When evident, a foliation given by actinolite trends regionally N20°E, dipping NW. Petrographically they are composed of actinolite (main mineral), hornblende and plagioclase, indicating varying metamorphic grades, from medium to medium-high greenschist. The texture varies from granoblastic to nematoblastic, locally occurring igneous minerals such as hornblende and plagioclase with high anorthite content.

In the region of the Canoas old Pb Mine amphibolite bodies occur concordant with the amphibole schists. These rocks belong to the Perau sequence, intercalated in quartzites and overlying gneissic rocks. Its main constituents are plagioclase, actinolite and hornblende, with subordinated quartz, epidote and microcline. The metabasite protoliths can be interpreted as of transitional composition between monzodiorite and monzogabbro. The metamorphism reached medium to high greenschist facies. The texture is nematoblastic, with incipient actinolite orientation.

LITHOGEOCHEMICAL CHARACTERIZATION

According to Maniese and Oliveira (1999) and Daitx (1996), the majority of the amphibolitic rocks are orthoderived and resultant from basic magmatism, probably intrusive, and genetically related to the evolution of the Açungui and Setuva sedimentation. These amphibolites present oceanic basalt characteristics, and would result from varying partial melting degrees of a mantle source that, from lower to higher partial melting rate evolved from E-MORB, then to OIB (Adrianópolis), T-MORB (Campo Largo and Perau), and to N-MORB (Rio Branco do Sul).

New lithogeochemical analyses indicate that the metabasites and amphibolites have the following characteristics: a) basaltic compositions varying to both picro-basalts and andesitic basalts, according to alkalis x SiO_2 proportions; considering the relation between SiO_2 x Zr/SiO_2 all rocks are of basaltic composition; b) the orthoderived character of the amphibolites in question is attested by the FeO(t) x TiO_2 ratio; c) regarding the alkalinity, the Na_2O+K_2O x SiO_2 diagram shows the presence of sub-alkaline rocks, with only one sample plotting in the alkaline field. Considering the proportion between Na_2O+K_2O x FeO(t) x MgO AFM diagram, these are tholeiitic rocks.

The rare earth distribution pattern is always flat, enriched 3 to 30 times in relation to chondrite (Fig. 1). Incipient negative Eu anomaly occurs for only one sample; for another, it is slightly positive, and for the others it is lacking. The normalization to primitive mantle values tend to diminish considerably the rare earth enrichment, bringing the normalized values close to one. Comparing them with the patterns presented by Wilson (1991), the analyzed metabasites are more similar to T-MORB (transitional between N- and P-MORB); the volcanic-arc basalt characteristics pointed out before must be ruled out, once there is a very weak to null LREE and HREE fractionation.

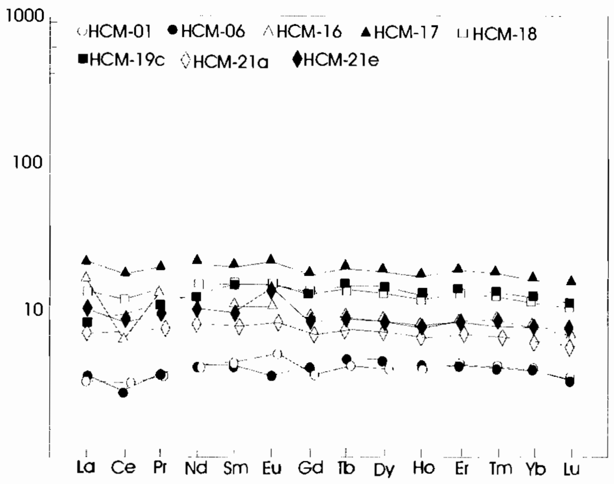

Figure 1. REE pattern (normalized to chodrite) for metabasic rocks from Votuverava and Perau basins.

ISOTOPE DATA

As it happens with the majority of metasedimentary sequences of the Vale do Ribeira, previous geochronological data result a dispersion of ages, predominantly falling between the Meso- and Neoproterozoic. Our geochronologic studies were concentrated on two target areas, one including the Votuverava Formation, and the other the Perau Formation, both situated north of Rio Branco do Sul. Three samples were collected from the Votuverava Formation, two of metabasic rocks (HCM-01 and HCM-16) and one of the regional phyllite (HCM-03) that host the metavolcanic rock. A sample of the Varginha Granite (HCM-13) was also collected for a complementary study of the rocks intrusive in these metavolcano-sedimentary units. An amphibolite sample of the Perau unit (GKM-41) was analyzed by the SHRIMP method.

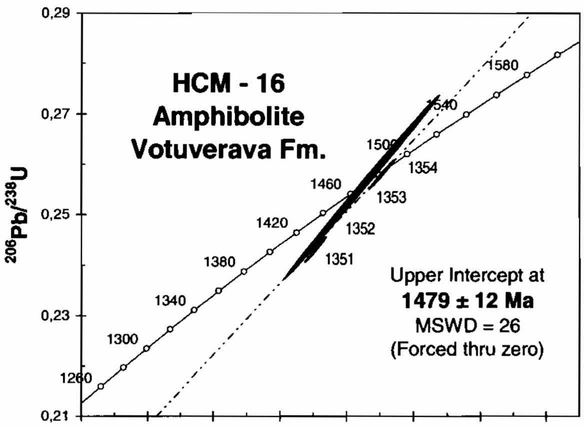

Figure 2. Concordia diagram for sample HCM 16.

The phyllite detrital zircons were grouped in four distinct populations according to their typology: 1)- short prismatic crystals with rounded edges; 2)- clean prismatic crystals; 3)- rounded crystals, and 4)- opaque prismatic crystals. The results obtained indicate a major paleoproterozoic source area for the phyllites (Pb207/Pb206 ages between 1760 and 1941 Ma). This source must have been composed of rocks similar to the gneisses that form the Tigre and Betara basement nuclei (Kalfuss 2001). The fraction constituted by opaque zircon crystals yielded the oldest value, close to 2670 Ma, which is distinct from the others, indicating an archean source.

Two U-Pb results were obtained for the metabasic rocks of the Votuverava Formation. For sample HCM-01, an age of 1451+/-39 Ma was defined by the alignment of three zircon fractions, two of which with high discordance degree. The best analytical results being composed of zircon crystals, clear than those of the other fractions. The age obtained is interpreted as the time of formation and emplacement of the igneous body. The other sample (HCM-16) presented a more reliable geochronologic pattern. The four magnetic fractions analyzed present good concordance, defining the 1479+/-12 Ma age (Fig. 2), equally interpreted as the time of emplacement of this body. Sample GKM 41 (metabasic rock from Perau Fm.) zircon crystals were dated by the SHRIMP method (Fig. 3). Similarly to both previous cases, the age of 1484+/-16 Ma is interpreted as the time of emplacement of the basic body. The mediun-grade neoproterozoic metamorphism superimposed to this rock is not registered in the zircons.

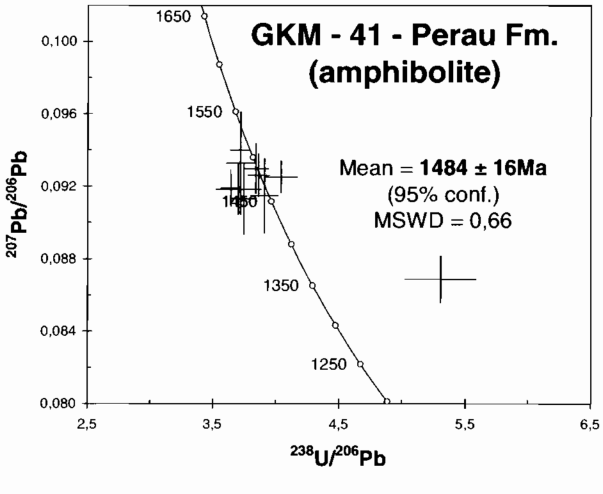

Figure 3. Terra-Wasserburg diagram for the sample GKM 41.

Additionally, a sample of the Varginha Granite, a leucogranitoid intrusive in the metamorphites of the Votuverava Formation, was analyzed (HCM-13). The 603 ± 23 Ma age was obtained from the alignment of five zircon crystal fractions with different magnetic susceptibilities, represented by prismatic typology with some inclusions and fractures. The value obtained mustreflect both the time of emplacement of this igneous body and the youngest age possible for the Brasiliano metamorphism that affected the area.

Nd AND Sr ISOTOPIC GEOCHEMISTRY

A total of 15 samples with available petrographic and geochemical data were analyzed by Rb-Sr and Sm-Nd methods. It is composed of 8 samples of metabasic rocks, 4 of phyllites and 3 of granitic rocks. To complement the study, 5 results available in Kaulfuss (2001) were added, concerning the Setuva, Tigre and Betara gneissic nuclei, possible candidates to "source areas" of the Votuverava and Perau metasedimentary rocks.

In the Epsilon Nd vs. Epsilon Sr diagram set to present values, the metabasic rocks stand out for their positive Epsilon Nd values, which are even more positive for the Votuverava basic rocks, suggesting that these rocks are less evolved than those of the Perau Formation.

It is clear the participation of the crust in the genesis of the other rocks, as indicated by very negative Epsilon Nd values (between -9 and -37) and very high Epsilon Sr values. The points relative to the Votuverava sediments plot between the paleoproterozoic gneisses of the Tigre, Betara and Setuva nuclei and the late-Brasiliano Varginha leucogranite.

Based in the Sr and Nd data, the following petrogenetic and tectonic interpretation can be drawn: 1) - the basic rocks are the only ones to present small differences between U-Pb ages, and Nd model ages, confirming their juvenile nature in the Mesoproterozoic; 2) -the model ages for the old nuclei gneisses are all archean, between 2700 and 3000 Ma, older than the U-Pb paleoproterozoic values around 2100Ma for their igneous constituents, characterizing a long crustal residence of the protoliths; 3) -the metasedimentary rocks, represented by phyllites, show model ages around 2200 Ma and inclination of the evolution line similar to that of the paleoproterozoic gneisses. However, as the two sets do not overlap, the gneisses cannot be the only source for the sediments. If one admits mixing of materials, which is quite possible, one end member may be the Tigre and Betara nuclei gneisses. The other, still undefined, would furnish the younger component of the mixture and equally be sialic material of age between 1760 and 1470 Ma, which would explain the parallel trends for the two sets. Anyway, the participation of basic material in this mixture is ruled out; 4) -as a reflex of the crustal characteristics of the Varginha Granite, implying fractionation of the Sm-Nd ratio, part of the results were calculated assuming a double stage, using the age of its generation (603 Ma) and the $^{147}Sm/^{143}Nd$ ratio of 0.11, representative of the average sialic crust values. The inclination of the epsilon Nd evolution line and the model ages shows that this leucogranite was not generated from direct melting of the metasedimentary host rocks. However, these indicators also suggest that the materials involved in the granite genesis may be the same of the phyllites, but in different proportions, explaining the dislocation and parallelism of both sets (phyllites and granites) in the diagram.

CONCLUSIONS

Mesoproterozoic ages around 1470 Ma characterize the important basic magmatism of the Rio Branco do Sul and Perau regions of the Vale do Ribeira, Paraná State.

The suggested sedimentation interval for the Perau and Votuverava Formations is defined by the age of the basic rocks that crosscut these units (around 1480 Ma), and the youngest values obtained for old nuclei gneissic leucogranites (1750 Ma) such as Tigre and Betara. However, due to field relations that showed a close association between the metasedimentary and the metabasic rocks, it is quite possible that the time of sedimentation is very close to the age of the basic magmatism, implying a Calymminian Votuverava-Perau paleobasin. The reasonable geochemical similarity and the concordant U-Pb ages of the basic magmatism of both units, as well as the spatial relation between their amphibolites and metasediments, reinforce the chronocorrelation between the Perau and Votuverava Formations.

The present distribution of the Perau and Votuverava Formations must be credited to the Brasiliano event, as well as the metamorphism of the supracrustal sequences and the granitic magmatism of the Vale do Ribeira. However, great part of the metasedimentary covers seems to be previous to this cycle, as now documented in the Perau and Votuverava Sequences.

From the tectonic point of view, the present data do not support simplified models that involve solely neoproterozoic subduction and collision to explain the geology of the Vale do Ribeira. Oceanic crust subduction in the Neoproterozoic is documented by the occurrence of calc-alkaline Cunhaporanga, Três Córregos, Agudos Grandes granitic batholiths; however, it is probable that great part of the granitic bodies be intrusive in metamorphic units whose sedimentation took place some 1000 Ma before the intrusions.

It is proposed that around 1480 Ma an important extensional phase must have occurred, associated with the emplacement of mantelic material and consequent continental rupture responsible for the opening of basins and marine sedimentation. The time of closing of these basins it is still uncertain, one possibility being Neoproterozoic or, better yet, the Meso-Neoproterozoic transition. It is quite possible that the Mesoproterozoic events that caused the opening of large sedimentary basins in southern-southeastern Brazil are underestimated. Regional geochronological correlations with the Mesoproterozoic Água Clara Formation (PR-SP) and the Serra do Itaberaba Group (SP) can provide the magnitude of the extensional process associated with the breaking of the preexisting continental masses.

REFERENCES

Campanha, G.A.C.; Sadowski, G.R. 1999. Tectonics of southern portion of the Ribeira Belt (Apiaí Domain). Precambrian Research 98, 31-51.

CPRM 1998. Projeto Folha Curitiba (SG.22-X-D I) Relatório Final. São Paulo, 91p (mapas).

Daitx, E. C. 1996. Origem e evolução dos depósitos sulfetados tipo-Perau (Pb-Zn-Ag), com base nas jazidas Canoas e Perau (Vale do Ribeira,PR). Tese de Doutoramento. IGCE-UNESP, Rio Claro, 435pp.

Fiori, A.P. 1992. Tectônica e Estratigrafia do Grupo Açungui, PR. Bol. IG-USP, Série Científica, 23:55-74

Kaulfuss, G.A. 2001. Geocronologia dos Núcleos de Embasamento Setuva, Betara e Tigre, Norte de Curitiba, Paraná. Dissertação. de Mestrado, IG-USP, S.P, 115p

Maniesi, V.; Oliveira, M.A.F. 1999. Quimismo mineral e metamorfismo dos anfibolitos de Adrianópolis, Rio Branco do Sul e Campo Largo, PR, Anais do V Congresso de Geoquimica dos países de língua Portuguesa & VII Congr. Brasil. de Geoquimica- Bahia -541-543.

Soares, P.C.; Fiori, A.P.; Rostirolla, S.P. 2000. A geotectonic view of the Ribeira and Dom Feliciano belts. Revista Brasileira de Geociências 30 (1): 130-134.

Wilson, M. 1991. Igneous petrogenesis. Harper Collins Academic, 466 p.

K-Ar ON WHOLE-ROCK AND <2μm ILLITE FRACTION AGES FROM TRIASSIC-JURASSIC BASEMENTS: DATING OF VERY LOW-GRADE METAMORPHISM IN COASTAL BELT, CENTRAL ANDES, CHILE

Belmar, M.[1]; Munizaga, F.[1]; Morata, D.[1]; Pérez de Arce, C.[2] and Morales, S.[3]

1. Departamento de Geología, Universidad de Chile, Plaza Ercilla 803, Santiago, Chile. mbelmar@ing.uchile.cl
2. Servicio Nacional de Geologia y Mineria, Santa Maria 0104, Providencia, Santiago, Chile
3. Departamento de Mineralogía y Petrología, Universidad de Granada. Avda. Fuentenueva s/n, Granada, España

Keywords: Illite, K-Ar age, very low-grade metamorphism, Chile

INTRODUCTION

The interpretation of the origin of Andean very low grade metamorphism is a controversial point. The link between the various styles of burial, diastathermal and contact metamorphism with major geodynamic processes represents a complex model of metamorphic history.

Illitic clay minerals have been used in several studies to constrain the geologic timing of hydrothermal episodes in ore deposit, heating event or meteoritic impact, but also in regional overthrusting, faulting, and oil and gas migration. Particularly important is the study of illite in sedimentary basin research because the smectite illitization can be use as a geothermometer of burial subsidence. Both illite and illite/smectite have been shown to be reliable clocks at temperatures below 260± 20° C (Hunziker et al., 1986), a property that makes them potentially attractive tools for reconstructing burial history. Formation of illite fixes potassium during burial diagenesis and illite crystallites retain argon, which allows this system to act as a radiometric clock.

The aim of the present research is to outline the time-temperature relation of regional metamorphism by integrating a multimethodological data result. This can help to distinguish between very low-grade metamorphic burial events to the hydrothermal heating event in connection with contact metamorphism. These distinctions are relevant because the occurrences of intrusion are common in the history of Andean formation, since the Palaeozoic to the less than 1 Ma Miocene magmatism.

GEOLOGICAL SETTING

The studied area is located in the Coast Range in the central part of Chile between 34° 45' and 35° 20' South, ca. 300 km South of Santiago. Late Triassic to Early Jurassic sedimentary and Middle to Late Jurassic volcanic rocks are exposed in the region. The marine sedimentary rocks form part of an almost continuous belt, which is approximately 60 km in length and unconformably overlies the Palaeozoic crystalline basement. Tectonic development during the Triassic was controlled by continuous movements and differential uplift of the Palaeozoic basement and lasted until at least the Jurassic (Thiele & Morel, 1981). The western Palaeozoic areas were exhumed at a faster rate than those to the east, which preserve Mesozoic sedimentary rocks. The regional paleogeographic and tectono-sedimentary evolution during the Triassic–Jurassic resulted in a simple morphology is characterized by basins and high structures. Uplift of the western Palaeozoic basement during the Triassic-Jurassic boundary resulted in the development of two sedimentary basins, known as the Vichuquén-Tilicura basin in the north and the Hualañé-Gualleco basin to the southeast. The principal structures in the sedimentary strata are north-south fold axes and normal faults, which are generally attributed to the rejuvenation of deep-seated structures in the Palaeozoic basement. East-west faulting in the northern part of the Hualañé-Gualleco basin predates the prevailing NW–SE faulting (Thiele & Morel, 1981; Corvalán, 1982). No cleavage is visible in the north, whereas an incipient cleavage has developed in the central and southern part of the Hualañé-Gualleco basin, indicating an increase in deformation towards the south.

In the eastern most part of the studied area, andesitic lava flows, volcanic breccias and minor sedimentary intercalations of Middle and Upper Jurassic are exposed, and reach a maximum thickness of c.a. 3680 m (Altos de Hualmapu formation (Morel, 1981). No isotopic data are available on this unit, however, the upper part of Jurassic marine unit presents volcanic intercalations of lavas and breccias with green sandstone containing a paleontological fauna that demonstrate the Toarcian age for the finishing the marine sedimentation. Corvalán, (1982) suggested this time for the probably fulfil or uplift of the basins. Clearly it is the indication for the Late Toarcian age for the beginning of the volcanic deposition. In the southern part the volcanic unit is intruded by Jurassic granodiorites dated by Gana & Hervé (1983) in 165 ± 5 Ma (biotite) and 175 ± 5 Ma (hornblende) using K-Ar method.

ANALYTICAL METHODS AND SAMPLE PREPARATION

Shales and slates were cleaned from weathering rims with a steel brush, crushed into small pieces with a hammer and c.a. 100 g of sample were ground with a rotary disk mill. Short milling duration was applied to avoid fragmentation of coarse grains. Carbonate was removed by treating with 5% acetic acid and by washing with deionised water. The <2 μm fraction was obtained using settling tubes and Millipore filters with 0.1 μm pore size at room temperature on a perfectly even table. Oriented slides were prepared by pipetting suspension onto glass slides (5 mg cm^2) and allowing to air-dry. Glycolated mounts were prepared in a glycol steam bath at 60 °C overnight.

Powder X-ray diffraction measurements were performed with a Siemens D-5000 diffractometer using the following instrumental settings: Cu Kα radiation, 40 kV, 30 mA; automatic primary and secondary divergence slits; secondary graphite monochromator. The d-spacing was calibrated against quartz occurring in the samples.

K-Ar dating was performed with instruments constructed in the Laboratorio de Geocronología, Servicio Nacional de Geología y Minería (SERNAGEOMIN) in Santiago, Chile. Sample were degassed by high frequency induction heating. The argon was cleaned and purified in Pyrex extraction lines and the radiogenic ^{40}Ar volumes were determined using standard isotopic dilution techniques in a MS10S Mass Spectrometer, with a total accuracy of 1 – 2 %. The potassium analyses were done in triplicate by atomic absorption techniques with an accuracy of 0.7 - 1.3 %, depending on the K content and using internal standard of Li. The inter-laboratory standard GL-0 was used for controlling and the calibration of Ar and K determination. Errors of K-Ar ages are quoted at the two sigma (2σ) level and the decay constants are those suggested by Steiger & Jäger (1977). This includes a 1.5% estimated error for the standard GL-0 and a 1% error for the Ar isotope ratios.

To avoid the disturbing effects of detrital muscovite the K-Ar ages obtained on the 0.1-2μm fractions were used for dating metamorphism following the practice of Hunziker et al. (1986).

METAMORPHIC EVENTS

P-T estimation of diagenesis and very low-grade metamorphism have been determined for Late Triassic to Early Jurassic sedimentary rocks from the Vichuquén-Tilicura and the Hualañé-Gualleco basins in Central Chile using illite crystallinity (Kübler Index, KI; Kübler 1967, 1984), coal rank data, K-white mica *b* cell dimension, characteristic mineral assemblages and fluid inclusion data (Belmar et al 2000, 2002). A burial-related diagenetic to low-grade metamorphic event, which is recorded in both basins, is partially overprinted in the Hualañé-Gualleco basin by contact metamorphism around Jurassic dioritic to granodioritic intrusions. Diagenetic conditions prevailed in the northern Vichuquén-Tilicura basin, whereas in the southern Hualañé-Gualleco basin low-grade metamorphism is observed with an increase in metamorphic grade from north to south. Epizonal conditions are locally reached in the very south of the Hualañé-Gualleco basin. Low-pressure conditions were determined using the K-white mica *b* cell dimension. Evidence of contact metamorphism in the immediate proximity of some Jurassic intrusions includes: (1) hornfels facies assemblages such as ferrosilite (XFe0.6)-magnesiohornblende- ferroactinolite, biotite together with chlorite, plagioclase, stilpnomelane and (2) natural coke and pyrolitic bituminite in some sedimentary samples. Epizonal IC and high coal rank values are probably a result of this locally occurring contact metamorphism (Belmar et al. 2000).

TEMPERATURE AND PRESSURE

The sample selection was based on the multimethodological investigation on low-grade metamorphism in this region by Belmar et al. (2000, 2002). From an universe of 71 samples, mainly shales and slates, was selected 5 of them using a criteria of geological unit, mainly Triassic (deeper samples), illite cristalinity index (KI indicating anchi and epizonal conditions), Mineral index (mainly occurrence of a characteristic and indicative mineral, e.g. paragonite) and clear indication of temperature of metamorphic condition by fluid inclusion or other methods. This selection was summarized in the table 1 and as follow.

The ordering and the percentage of illite in mixed-layer illite/smectite (I/S) were determined in the samples. The occurrence of R1 with 65 to 85 % illite in I/S in the northern part of the Vichuquén-Tilicura basin contrast with to R3 (> 90% illite in I/S) observed in the sample H3-10 localized in the southern part. This transformation probably occurred at a temperature of 170°-180° according to Pollastro (1993), and fit well with other temperature indicators (KI= 0.36 Δ°2θ, Rmax =3.8 %) see table 1.

The appearance of index mineral paragonite on four samples, according to KI and coal rank data, is characteristic of beginning of anchizone until lower epizone. Temperature in one of the samples (H6-18) of the Lower-Jurassic sediments was calculated to be above 187°C as determined by fluid inclusion thermometry. The corresponding fluid pressure determined in the same fluid inclusions is 1.4 kbar corresponding to an overburden of ca. 5.5 km and agrees well with the b_0 parameter determinations which indicate low pressure metamorphism for this region. These results are in agreement with the measured KI = 0.37 Δ°2θ and Rmax= 2.9% values in the same sample, as well as with a sample from the nearby Upper Triassic horizon (H6-19) which gave similar conditions (KI = 0.41 and Rmax= 3.0). High conditions were determined on the sample H1-02 (KI = 0.33 Δ°2θ and Rmax= 3.9%) which contain also paragonite (see table 1).

The H4-02 sample, located south of Gualleco, contain the assemblage chlorite- muscovite- paragonite-quartz. Epizonal condition is inferred from KI value of 0.23 Δ°2θ and coal rank of 5.6 % Rmax.

A contact metamorphism was observed in the immediate proximity of some Jurassic intrusions as evidenced by the pyroxene hornfels facies paragenesis and by the natural coke and pirolitic carbon in sedimentary samples. Pyrolitic carbon of identical form and properties as observed in this study was experimentally produced in the laboratory at temperatures >500°C (Stach et al., 1982).

Table 1. Results of the K-Ar analyses (Ma±2σ) on representative rock samples with illite crystallinity (K.I.), polymorphous type (% of 2M1) and coal rank data (Rmax) (ordering from North to South).

Samples	Age	Size fraction [µm]	K [%]	Ar rad nl/g	Ar atm [%]	Age [Ma±2σ]	polim. type	K.I. Δ°2 Ø	Rmax %
H3-10	Upper Triassic	whole rock	1.564	26.826	4	395 ± 12			
H3-10		<2µm	3.072	26.074	7	206 ± 6	87% 2M1	0.36	3.8
H1-02	Upper Triassic	whole rock	3.384	30.95	3	221 ± 7			
H1-02		<2µm	3.634	26.846	16	181 ± 6	22% 2M1	0.33	3.9
H6-19	Upper Triassic	whole rock	2.606	23.57	6	219 ± 7			
H6-19		<2µm	2.887	21.748	11	184 ± 6	55% 2M1	0.41	3.0
H6-18	Lower Jurassic	whole rock	1.74	44.33	5	559 ± 16			
H6-18		<2µm	5.76	43.272	7	184 ± 4	57% 2M1	0.39	2.9
H4-02	Lower Jurassic	whole rock	2.843	20.136	2	174 ± 5			
H4-02		<2µm	2.985	18.835	21	155 ± 5	90% 2M1	0.23	5.6

The temperatures of the contact metamorphism were calculated based on coexisting plagioclase with An$_{57}$ and magnesiohornblende with Al$_{(VI)}$ = 0.12, Na = 0.94 and Si = 7.3 apfu using the amphibole- plagioclase thermometer of Holland & Blundy (1994). Calculated temperatures of the edenite-tremolite solid solution lie within a range of 655 °C to 691 °C and a pressure of <4 kbar. Due to this increased temperatures, the sedimentary rocks near this sample show a strong increase in coal rank and KI values.

RESULTS

K-Ar ages were determined for the whole rock and <2µm size fraction in five samples (table 1). The whole rock range from 559±16 to 174±5 Ma and the <2µm size fraction from 206±6 to 155±5 Ma. For each sample the K-Ar age presents a considerable decrease in the fine mica fraction. The principal constituents of the clay fraction in the analyzed samples are: illite, illite/smectite, pyrophyllite and/or paragonite (chlorite only in the sample H4-2). All these clay minerals are considered authigenic low-grade metamorphic minerals (Belmar et al., 2002). However the absence of contamination by detrital mica in separated size fraction can never be claimed. Additional to the contamination by detrital minerals another uncertainties remain about ancient radiogenic ^{40}Ar possibly trapped in the illite crystals.

The very low-grade temperatures in the area were not sufficiently high for a complete reset of the K-Ar system. However the sample H4-02, is localized near to the intrusion and the temperature of this around rock was over 600° C. The metamorphism indicators show a Kubler index of this sample high epizone conditions and the coal rank indicate high thermal event. In this case, the K-Ar age in whole rock is 174±5 Ma.

INTERPRETATION OF K-AR AGES ON FINE MICA FRACTION

The K-Ar ages of the anchizonal Triassic-Jurassic shale measured on the <2µm size fraction varies between 206 to 181 Ma, significantly younger ages were obtained in the epizonal Jurassic sample H4-02 which experienced a contact metamorphism, and shows an age of 155±5 Ma indicating a probably an younger newly formed <2µm illite as a product of later hydrothermal activity. Maximum temperature estimations during the very low-grade burial metamorphism in the study area probably did not exceed 190°C with exception of aureole of contact metamorphism (Belmar et al., 2002). According to Hunziker et al. (1986), a totally outgas of ^{40}Ar in case of <2µm size illite grains was produced at temperatures around of 260 ±30° C during 10±5 Ma. This indicates that the temperature of the low anchizonal metamorphism in the study area might be insufficient to reach the total resetting of the Ar system in the newly formed <2µm size illite. Therefore, we consider the K-Ar determination of 181±6, 184±6, and 184±4 Ma correspond to the maximum burial induced heating condition which was consider by Belmar et al. (2002) at 190 ±10° C and ≥1.3 kbar. In sample H3-10, the <2µm size fraction give an intermediate age of 206±6 Ma. This value suggests to be a mixed age and not represent a real geologic event, because this sample shows an anomalous high value of KI parameter, indicating a contamination of detrital high crystalinity phase, same situation with the polymorphism which it with >90% 2M1 polymorph type (table 1).

CONCLUSIONS

Gana & Hervé (1983) published K-Ar ages of 165 ± 5 Ma (biotite) and 175 ± 5 Ma (hornblende) for the Jurassic pluton. The whole rock of a sample from the contact aureole yielded an age of 174 ± 5 Ma. These determinations constrain the age of Altos de Hualmapu fm. which are intruded by the Jurassic granodiorite at late Toarcian (from a paleontological evidence) and maximum Aalenian age (from a isotopic evidence). The small period of deposition for this unit and the great thickness show a high rate of volcanic deposition. The intercalations of marine sediment in the volcanic lower part of this unit indicate a continuous extension period also in the time of lava deposition. All of these previous hypothesis of Belmar et al. (2002) indicate for the thermal maturity model an overburden of 4.8 km and corresponding geothermal gradient to >35° C/km. This overburden is obtained with 2100 m of Triassic Jurassic pile of sediment plus the continuous overlying of volcanic unit, which have at list 3600 m.

The maximum burial was probably simultaneously produced with the deposition of overlie Jurassic volcanic lavas, which was constrain at least Aalenian age, and agree well with the K-Ar age determinations in the <2µm size fraction of the anchizonal Triassic-Jurassic shale, which records ages of 181 to 184 Ma for the metamorphism.

The age of contact metamorphism is 174 to 175 +5 Ma, and the 10 Ma of difference in relation to the timing of metamorphism avoid an hypothetical thermal overprint origin for the regional metamorphism.

ACKNOWLEDGMENTS

We would like to thank the Servicio Nacional de Geología y Minería de Chile for laboratory support in special to Paula Cornejo and Steve Matthews, for their help and information. This study was supported by the MECESUP Grants Nr 0010, and internal project of SERNAGEOMIN-Universidad de Chile, Departamento de Geología,

REFERENCES

Belmar, M.; Schmidt, S.; Frey, M.; Ferreiro-Mählmann, R.; Mullis, J. and Stern, W., 2000. Diagenesis, Low-grade and Thermal Metamorphism in the Triassic–Jurasic Successions, Coast Range, Central Chile (35° S). IX Congreso Geológico Chileno, Actas, Vol. 2, p. 505-509. Puerto Varas, Chile.

Belmar, M., Schmidt, S. Th., Ferreiro-Mählmann, R., Mullis, J., Stern, W. B. and Frey, M; 2002. Diagenesis, low- grade and contact metamorphism in the Triassic–Jurassic of Vichuquén-Tilicura and Hualeñé-Gualleco Basins, Coast Range of Chile. Schweizeriche Mineralogische und Petrographische Mitteilungen. 82, 375-392.

Corvalán, J. (1982): El Límite Triásico-Jurásico en la Cordillera de la Costa de las Provincias de Curicó y Talca. 3, F63–F85. III Congreso Geológico Chileno, Concepcion, Chile.

Gana, P. and Hervé, F. (1983): Geología del Basamento Cristalino en la Cordillera de la Costa entre los ríos Mataquito y Maule, VII Región. Chile. Revista Geológica de Chile 19/20, 37–56.

Holland, T. and Blundy, J. (1994): Non-ideal interactions in calcic amphiboles and their bearing on amphiboles-plagioclase thermometry. Contributions to Mineralogy and Petrology. 116, 433–447.

Hunziker, J.C., Frey, M., Clauer, N., Dallmeyer, R.D., Friedrichsen, H., Flehmig, W., Hochstrasser, K., Roggwiler, P., Schwander, H., 1986 . The evolution of illite to muscovite: mineralogical and isotopic date from the Glarus Alps Switzerland. Contributions to Mineralogy and Petrology 92, 157-180.

Kübler, B., (1967): La Crystallinité de l'illite et les zones tout à fait supérieures du métamorphisme. Étages tectoniques. Colloq. Neuchâtel, 105–122.

Kübler, B., (1984): Les indicateurs des transformations physiques et chimiques dans la diagenèse, temperature et calorimétrie. In: LAGACHE, M. (ed.): Thérmométrie et barométrie géologiques, Société Française. Minéralogie. Cristalographie, Paris, 489–596.

Morel, R. (1981): Geología del sector norte de la hoja Gualleco, entre los 35°„00' y los 35°„10' latitud sur, provincia de Talca, VII Región, Chile. Tesis de Grado, M. Cs., Universidad de Chile, Departamento de Geología, Santiago.

Pollastro, R.M. (1993): Considerations and applications of the illite/smectite geothermometer in hydrocarbon- bearing rocks of Miocene to Mississippian age. Clay and Clay Minerals 41, 119–133.

Stach, E., Mackowsky, M.-T., Teichmüller, M., Tayloer, G.H., Chandra, D. and Teichmüller, R. (1982): Coal Petrology. Gebrüder Bornträger, Berlin- Stuttgart, 535 pp.

Steiger, R.H. & Jäger, E. 1977.Subcommission on geochronology: convention on use of decay constants in geo-and cosmochronology. Earth and Planetary Science Letters 36, pp 359-362.

Thiele, R. and Morel, R. (1981): Tectonica Triásico-Jurásica en la Cordillera de la Costa, al norte y sur del Río Mataquito (34°45' - 35°15' Lat. S), Chile. Revista Geológica de Chile 13/14, 49–61.

Sr-Nd ISOTOPIC COMPOSITION OF HIGH-GRADE METASEDIMENTARY ROCKS, MIGMATITES AND GRANITOIDS AT PUERTO EDÉN (49°S), SOUTHERN CHILE

Calderón, M.[1]; Hervé, F.[1]; Godoy, E.[2]; Pankhurst, R.J.[3]; Tassinari, C.G.[4] and Massonne, H.J.[5]

1. Departamento de Geología, Universidad de Chile, Casilla 13518, Correo 21, Santiago, Chile.
caldera@esfera.cl, fherve@cec.uchile.cl
2. Servicio Nacional de Geología y Minería, Avda. Santa María 0104, Santiago, Chile. egodoy@sernageomin.cl
3. British Geological Survey, Keyworth, Nottingham NG12 5GG, UK
4. Centro de Pesquisas Geocronológicas, Universidade de São Paulo, Brasil
5. Institut für Mineralogie und Kristallchemie, Universität Stuttgart, Azenbergstrasse 18, D-70174, Stuttgart, Germany

Keywords: Metatexite, leucodiatexite, late Jurassic, Patagonia, Sr-Nd isotopes

INTRODUCTION

Migmatites, subdivided into metatexites and diatexites, are the main rocks in which partial melting processes may be studied. Metatexite is defined as a migmatite containing evident pre-migmatization layering, foliation or banding, which survived partial melting (low melt fraction; Brown, 1973). Diatexite is a migmatite in which pre-migmatization structures are destroyed (medium or high melt fraction; Brown, 1973). The melt fraction in migmatites can be increased by: (1) a rise of metamorphic temperature (Brown, 1973); (2) melt injection from elsewhere (Greenfield et al., 1996); or (3) melt redistribution within melting layers (Sawyer, 1998). Migmatites are of special interest because of their inferred role as a link between high grade metamorphic rocks and the generation of larger-scale granitic bodies (e.g. Solar & Brown, 2001). This study examines the isotopic variations within the high-grade metamorphic rocks, migmatites and granitic rocks, with the aim of evaluating the relationship between the anatexis of metasedimentary rocks and the generation of granitic melts in the petrogenesis of the Puerto Edén igneous and metamorphic complex (PEIMC). Mineral abbreviations are according to Kretz (1983).

GEOLOGICAL BACKGROUND

The eastern basement of the southern Patagonian Andes (Fig. 1a; 48°-52°S), refered to as Eastern Andean Metamorphic Complex (EAMC; Hervé, 1993) is mainly composed of a polydeformed assemblage of metagreywackes, metapelites and marbles, as well as of scarce metabasites. The maximum and minimum sedimentation ages of the psammo-pelitic protolith are 374 Ma and 233 Ma, respectively (ca. 48°S; Thomson & Hervé, 2002). This sequence underwent greenschist facies regional metamorphism (e.g. Hervé et al., 1998) at about 300±23 Ma (Thomson et al., 2000). The PEIMC (49°S; Fig. 1b) is composed mainly of amphibolite facies schists and gneisses, migmatites, a biotite schlieren-bearing porphyritic monzogranite, and several leucogranites. It is flanked on both sides by biotite-hornblende-(allanite) granitoid rocks.

Plutonic activity in the South Patagonian Batholith (SPB) ranges from 151 to 16 Ma (e.g. Martin et al., 2001). The oldest plutons occur on the eastern margin (ca. 151-141 Ma), with Early Cretaceous units in the west (ca. 137 Ma), and Late Cretaceous to Tertiary granitoids concentrated near the central axis of the batholith (U-Pb conventional and SHRIMP zircon dating; Martin et al., 2001).

METAMORPHISM AND MIGMATIZATION

The PEIMC lies within the area of most intense nearly isobaric Late Jurassic high T – low P metamorphism of the EAMC with peak metamorphic P-T conditions of ca. 3.5-4.4 kbar and 650-700°C (U-Pb SHRIMP age of overgrowth rims from detrital zircon in a sillimanite gneiss or metatexite; Calderón et al., in prep.). The foliated rocks were described and subdivided into two metamorphic domains by Watters (1964): El Indio schists, consisting of biotite, staurolite, andalusite and sillimanite schists and gneisses, and Edén gneiss, a heterogeneous coarse-grained pale granitic body (Fig. 1b). However, the Edén gneiss, with biotite as the dominant mafic phase defining the foliation within schlieren structures, is interpreted here as a leucodiatexite, because of: (1) the presence of centimetre-long ellipsoidal enclaves of quartz, probably representing relics of quartz veins that survived migmatization; (2) the probable residual origin of the biotite in the schlieren, which shows microscopic similarities to the biotites in the schists and gneisses; and (3) the abundance of stromatic migmatites and leucogranite segregations in the outcrop area. This suggests that anatexis occurred during relatively low temperature conditions (700-800°C; e.g. Patiño Douce & Harris, 1998), in the stability field of biotite + quartz, involving the breakdown of muscovite (e.g. Ms +Pl + Qz = Melt + Ksp + Sil + Bt). As showed by Calderón et al. (in prep.), the breakdown of biotite also played a role in the generation of the garnet-tourmaline leucogranites.

Retrograde metamorphism is characterized by late stage crystallization of muscovite, with biotite and sillimanite as the principal observed reacting phases; it is recorded in gneisses and leucodiatexites. Pinitization of cordierite and andalusite, chloritization of biotite and crystallization of prehnite (in veins and in biotite cleavages) are also characteristic.

ANALYTICAL METHODS

The most representative and the least or not altered samples from the PEIMC were selected for the Sr-Nd isotope analyses: an And-schist (sample DE00-44); a Sil-gneiss or metatexite (sample PE99-32A); a leucodiatexite (sample IC00-09); a porphyritic monzogranite (sample DE00-07); a Bt granite (sample FF99-09A); a Grt-Tur leucogranite or leucosome (sample PE99-32D); a Ms-Grt leucogranite (sample DE00-48A); and a Bt-Hbl-(Aln) monzogranite (sample YEK00-05). For location of samples see Fig. 1b.

Rb-Sr and Sm-Nd isotope analyses were performed in the Centro de Pesquisas Geocronológicas of the Universidade de São Paulo, except sample FF99-09A (NERC Isotope Geosciences Laboratory, Keyworth, U.K.). Rb and Sr contents were determined by X-ray fluorescence spectrometry. $^{87}Sr/^{86}Sr$ ratios were measured by thermal ionization mass-spectrometry, corrected for mass fractionation to $^{86}Sr/^{88}Sr = 0.1194$ normalization. Sm and Nd (and other lanthanides) were chemically separated in HDEHP columns supported by teflon powder. The Sm and Nd concentrations were obtained by isotopic dilution using a mixed ^{149}Sm and ^{150}Nd tracer. The isotopic ratios were calculated relative to $^{146}Nd/^{144}Nd = 0.7219$. All radiogenic isotope analyses were performed using a VG 354 Micromass spectrometer. At the time of the analyses the following standard values were obtained: $^{87}Sr/^{86}Sr = 0.71026 \pm 0.00002$ (2σ) for NBS-987 and $^{143}Nd/^{144}Nd = 0.511847 \pm 0.00002$ (2σ) and 0.512662 ± 0.000027 (2σ) values for La Jolla and BCR-1 respectively.

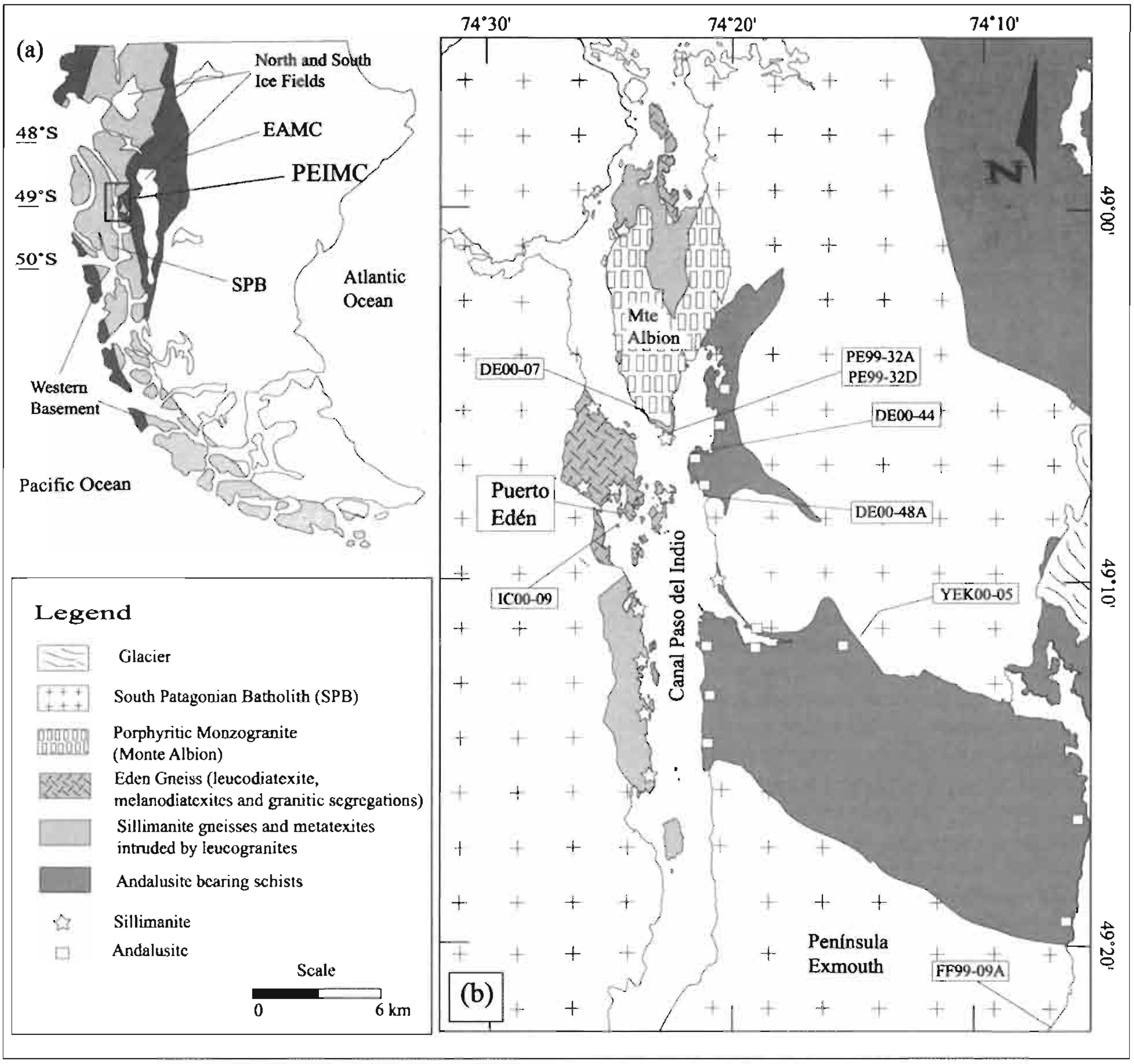

Figure 1. (a) South-western Patagonian geological units. EAMC (Eastern Andean Metamorphic Complex); SPB (South Patagonian Batholith); PEIMC (Puerto Edén Igneous and Metamorphic Complex). (b) Geological map of the PEIMC and surrounded Areas. Extracted from Watters (1964) and this work. Location of analysed samples.

AGES AND Sr-Nd ISOTOPE COMPOSITION

The initial Sr and Nd compositions were calculated at both 150 Ma (age of the high T – low P metamorphism; Calderón et al., in prep.) and 100 Ma (K-Ar biotite and muscovite ages of metamorphic rocks, migmatites and granitoids; Calderón et al., 2001), the presumed times of metamorphic recrystallization or rock formation, depending on the lithology (Fig. 2). The K-Ar age of the Ms-Grt leucogranite and the Bt-Hbl-(Aln) monzogranite were obtained on medium grained muscovite and primary biotite, respectively. The Bt granite (sample FF99-09) which crops out at Fiordo Eyre, has a crystallization age of 151 ± 1 Ma (SHRIMP U-Pb age; Martin et al., 2001)

Both high-grade metamorphic rocks have high $^{87}Sr/^{86}Sr$ ratios related to 150 Ma (Sr_0) of 0.7156 (And-schist) and 0.7134 (Sil-gneiss), and correspondingly low initial εNdt values of –7.6 and –7.1, respectively. At 150 Ma, the leucodiatexite and the Bt granite have slightly less radiogenic Sr and more radiogenic Nd, but they are indistinguishable from each other (Sr_0 of 0.7089, and εNdt values of –4.4 and –4.9, respectively). At 100 Ma, the leucodiatexite has a higher Sr_0 (0.7116) and lower εNdt (-4.9). The Grt-Tur leucogranite, showing a high Rb/Sr ratio of 5.25, is charaterized by isotopic compositions generally comparable to the metasediments, especially related to 150 Ma (Sr_0 = 0.7127 and εNdt = –6.5; Fig. 2). The porphyritic monzogranite, for the relevant age interval, has the lowest Sr_0 in this group (0.7073 – 0.7081) but a Nd isotope relation very similar to the high-grade metasediments (εNdt = –7.6 at 150 Ma, –8.1 at 100 Ma).

There are similarities between the isotope compositions of the Ms-Grt leucogranite and the Bt-Hbl-(Aln) monzogranite. For the leucogranite at 100 Ma the Sr_0 is 0.7067 and the εNdt –1.8. In the case of the Bt-Hbl-(Aln) monzogranite the Sr_0 is 0.7049 and the εNdt –2.6. At 150 Ma lower values for Sr_0 and less negative εNdt were obtained (Fig. 2).

The metamorphic rocks have depleted mantle model ages (T_{DM}) of 1408 (And-schist) to 1358 (Sil-gneiss) Ma. Similar values of 1339 Ma and 1392 Ma are obtained for the Bt granite and porphyritic monzogranite, respectively, but the T_{DM} model age of the leucodiatexite is lower (1169 Ma). The Ms-Grt leucogranite and the Bt-Hbl-(Aln) monzogranite also have a lower T_{DM} of 1206 and 1280 Ma, respectively. The model age of the Grt-Tur leucogranite is unrealistic related to the high $^{147}Sm/^{144}Nd$ ratio in this rock, probably associated to an unrepresentative population of garnets in the analysed material. This problem is overcome in models that incorporate an additional stage of crustal residence after differentiation from the depleted mantle but preceding the formation of the final rock, such as that of DePaolo et al. (1991). These 'crust-derived' model ages show that the high-grade metamorphic rocks and the porphyritic monzogranite share similar initial mantle separation ages of 1520-1560 Ma. The Grt-Tur leucogranite gives a comparable value of 1474 Ma, the leucodiatexite and Bt granite slightly younger values of 1320 - 1360, and the Ms-Grt leucogranite and Bt-Hbl-(Aln) monzogranite the youngest values of 1100-1160 Ma.

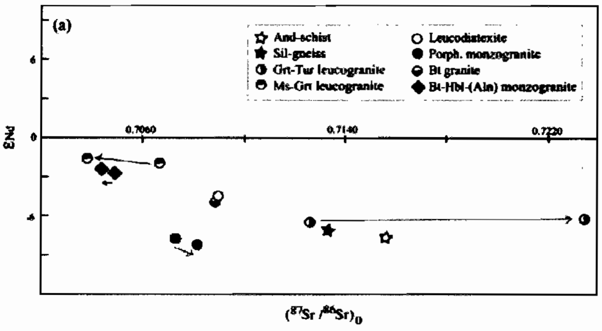

Figure 2. Initial $^{87}Sr/^{86}Sr$ ratio v/s εNd values of the studied samples. Arrows indicate the isotopic signature calculated either for 100 Ma (Grt-Tur leucogranite and porphyritic monzogranite) or 150 Ma (Ms-Grt leucogranite and Bt-Hbl-(Aln) monzogranite).

PETROGENETIC IMPLICATIONS

The sillimanite gneiss has a higher Rb/Sr ratio and lower Sr_0 than the andalusite schist. This difference could be due either to a small compositional difference between the protoliths of both rocks or to the effects high-grade metamorphism resulting in relative enrichment of biotite and depletion of plagioclase in the sillimanite gneiss. The latter supported by the mesosome character of the sillimanite gneiss, i.e. small volumes of granitic melt have been removed from the original rock (see the dehydration melt-producing reaction above). The Sr and Nd isotopic ratios were not significantly affected by the high grade metamorphism, as shown by similar Sr_0 and εNd values of both rocks.

The Grt-Tur leucogranite has a very similar Sr-Nd signature compared to the sillimanite gneiss (at 150 Ma), with which it is closely associated in the field. Since the leucogranite bears almandine-spessartine garnets similar to those in thin leucosomes within other sillimanite gneisses and has a similar isotopic signature, the Grt-Tur leucogranite is considered as an evolved and redistributed partial melt of the sillimanite gneiss. At this point the andalusite schist, sillimanite gneiss, and leucogranite preserve a common Sm-Nd isotopic signatures, whereas the Rb-Sr system was in disequilibrium due to unequilibrated source differences and/or major phase redistribution.

The Sr-Nd isotopic similarities between the leucodiatexite and the Bt granite, imply a common source for these two rocks. The age of metamorphism and that of crystallization of the granite, their Sr_0 (~0.709 related to 150 Ma) and εNdt values (-4.4, -4.9) are lower and higher respectively than those of the sillimanite gneiss, but are still indicative of a significant crustal component. It seems to be probable that the source region of the migmatites, 150 Ma ago, was isotopically more variable than it is shown by the two analysed high-grade metasedimentary rocks, and may have been more akin to the wider range exhibited by the EAMC according to the data of Weaver et al. (1990). Thus, it is reasonable to suppose that the leucodiatexite (Edén gneiss in Fig. 1b) was generated by anatexis during Late Jurassic high T – low P metamorphism recorded in the sillimanite gneiss, and that a similar petrogenesis applies to the Bt granite. The porphyritic monzogranite has an even lower Sr_0 (0.7073) than the leucodiatexite and the Bt granite, but its εNdt value (-7.6 related to 150 Ma) is indistinguishable from those of the high-grade metamorphic rocks. Moreover, the Sm and Nd contents of all three igneous rocks are strikingly similar. The real crystallization age of the porphyritic monzogranite (Monte Albion pluton in Fig. 1b) and its cooling history are not known. However, because it preserves small schlieren of anhedral biotite that crystallizes under low-oxidizing conditions (QFM fo_2 buffer, similar than those in metamorphic rocks; Calderón et al., in prep.) and is delimited to the north and south by leucodiatexite bodies, we postulate a common process for their genesis, and hence assume a Late Jurassic age. The low Sr_0 value implies a higher plagioclase content in the source than in the analysed metasedimentary rocks, which again suggest that the latter are not totally representative of the natural isotopic variation in the migmatite source. The difference in Sm-Nd signature between the porphyritic monzogranite and the leucodiatexite is explained by different degrees of homogenization between the residuum of a heterogeneous source and the melt generated.

The Sr-Nd isotopic signature of the Ms-Grt leucogranite, related to 150 Ma or 100 Ma, suggests a strong mantle-derived component for their petrogenesis. Because the Ms-Grt leucogranite has a similar Sr-Nd isotopic signature to the Bt-Hbl-(Aln) monzogranite, and both rocks could be petrogenetically related, it is suggested that the leucogranite may represent a more evolved marginal phase that was fractionated from the metaluminous magma chamber. This does not discount the possibility that the corresponding magmas were mantle-derived and mixed with partial melts of early contaminated plutons or metasediments, as proposed by Weaver et al. (1990).

ACKNOWLEDGEMENTS

This work was supported by Fondecyt 1010412 grant to F. Hervé, MCT-PRONEX (167/96) grant to C. Tassinari, Conicyt-BMBF (CHL 99/031) grant, the Beca de Apoyo para Realización de Tesis Doctoral (Conicyt) and Beca PG/61/2001 to M. Calderón and a Leverhulme Trust Emeritus Fellowship to R.J. Pankhurst. The authors are grateful to the technicians of the Centro de Pesquisas Geocronológicas (USP) for their help in the isotope analytical work.

REFERENCES

Brown, M., 1973. The definition of metatexis, diatexis and migmatite. Proceedings of the Geologist's Association, 84, 371-382.

Calderón, M., Hervé, F., Godoy, E., Suárez, M. and Watters, W.A., 2001. Middle Cretaceous crustal anatexis associated to constrictional deformation on Edén shear zone. III South American Symposium on Isotope Geology, Pucón, Chile, extended abstracts (CD), pp. 550-553.

Calderón, M., Hervé, F., Godoy, E., Massonne, H.-J., Theye, T. and Fanning, M., (in prep.). Late Jurassic high-T-low-P metamorphism and partial melting of aluminous metagreywackes at Puerto Edén (southern Chile).

DePaolo, D.J., Linn, A.M. and Schubert, G., 1991. The continental crustal age distribution; methods of determining mantle separation ages from Sm-Nd isotopic data and application to the Southwestern United States. Journal of Geophysical Research, B96, 2071-2088.

Greenfield, J.E., Clarke, G.L., Bland, M. and Clarke, D.J., 1996. In-situ migmatite and hybrid diatexite at Mt. Stafford, central Australia. Journal of Metamorphic Geology, 14, 413-426.

Hervé, F., 1993. Paleozoic metamorphic complexes in the Andes of Aysén, southern Chile (west of? Occidentalia). In: Ortega Gutiérrez, F., Coney, P.j., Centeno García, E. and Gomez-Caballero (Eds), Proceedings of the First Circum-Pacific and Circum-Atlantic Terrane Conference, Guanajuato, Mexico, pp. 64-65.

Hervé, F., Aguirre, L., Godoy, E., Massonne, H.-J, Morata, D., Pankhurst, R.J., Ramírez, E., Sepúlveda, V. and Willner, A., 1998. Nuevos antecedentes acerca de la edad y las condiciones P-T de los complejos metamórficos en Aysén, Chile. X Congreso Latinoamericano de Geología y VI Congreso Nacional de Geología Económica, Buenos Aires, Argentina, 2, pp. 134-137.

Kretz, R., 1983. Symbols for rock-forming minerals. American Mineralogist, 68, 277-279.

Martin, M., Pankhurst, R.J., Fanning, C.M., Thomson, S.N., Calderón, M. and Hervé, F., 2001. Age distribution of plutons across the southern Patagonian batholith: New U-Pb data on zircons. III South American Symposium on Isotope Geology, Pucón, Chile, extended abstracts (CD), pp. 585-588.

Patiño Douce, A.E. and Harris, N., 1998. Experimental constraints on Himalayan anatexis. Journal of Petrology, 39, 4, 689-710.

Sawyer, E.W., 1998. Formation and evolution of granite magmas during crustal reworking: the significance of diatexites. Journal of Petrology, 39, 1147-1167.

Solar, G. and Brown, M., 2001. Petrogenesis of migmatites in Maine, USA: possible source of peraluminous leucogranite in plutons? Journal of Petrology 42, 4, 789-823.

Thomson, S.N., Hervé, F. and Fanning, C.M., 2000. Combining fission-track and U-Pb SHRIMP zircon ages to establish stratigraphic and metamorphic ages in basement sedimentary rocks in southern Chile. IX Congreso Geológico Chileno, Puerto Varas, Chile, 2, pp. 769-773.

Thomson, S.N. and Hervé, F., 2002. New time constraints for the age of metamorphism at the ancestral Pacific Gondwana margin of southern Chile (42-52°S). Revista Geológica de Chile, 29, 2, 255-271.

Watters, W.A., 1964. Geological work at Puerto Edén, Wellington island, southern Chile. Transactions of the Royal Society of New Zeland, Geology, 2, 11, 155-168.

Weaver, S.G., Bruce, B., Nelson, E.P., Brueckner, H.K. and LeHuray, A.P., 1990. The Patagonian batholith at 48°S latitud, Chile: geochemical and isotopic variations. In: Harmon, R.S. and Rapela, C.W. (Eds), Andean magmatism and its tectonic setting. Boulder, Colorado, Geological Society of America, Special Paper 241, pp. 33-50.

GEOCHRONOLOGY OF 1.76 TO 1.50 Ga TTD SEQUENCES OF THE HOANIB VALLEY, KAOKO BELT, NAMIBIA

Chemale Jr., F.[1]; Luft Jr., J.L.[2]; Armstrong, R.[3] and Bitencourt, M.F.[4]

1. Laboratório de Geologia Isotópica, IG-UFRGS, Brazil. farid.chemale@ufrgs.br
2. Programa de Pós-graduação em Geociências, IG-UFRGS, Brazil. joao.luft@ufrgs.br
3. Research School of Earth Sciences, ANU, Australia. richard.armstrong@anu.edu.au
4. Departamento de Geologia, IG-UFRGS, Brazil. fatimab@ufrgs.br

Keywords: U-Pb geochronology, Hoanib River, Kaoko Belt, Western Gondwana, 1.7-1.5 Ga TTD sequences

INTRODUCTION

The Kaoko Belt - KB (Miller, 1983), located in the northwestern portion of the Namibian territory, is the result of tectonic interaction between the Rio de la Plata (South America) and Congo (Southwestern Africa) Plates during the Brasiliano/Pan-African Cycle. In general, the KB is characterized by Pan-African NNW-trending ductile to ductile-ruptile structures formed by east-vergent regional anticlinal/synclinal systems of folding with a well-recognized and important thrust zone in the Sesfontein region (Sesfontein Thrust Zone - STZ). The stratigraphy of the KB is largely controlled by these structures which divide the occidental portion of the belt in three zones: Western Kaoko Zone (WKZ), Central Kaoko Zone (CKZ) and Eastern Kaoko Zone (EKZ), each marked by contrasting tectonic and stratigraphic styles (Miller, 1983; Dingeldey et al., 1994) (Fig. 1).

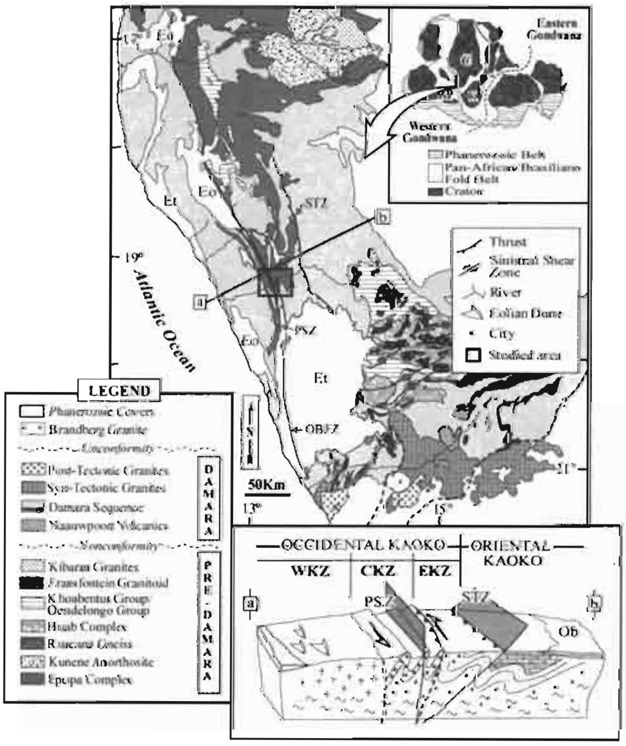

Figure 1. Geological map of the Kaoko Belt with schematic structural section (modified from Geological Map of the South West Africa/Namibia, scale 1:1.000.000).

In this work we discuss a section situated in the region of the Hoanib, Obias, Goreas and Hoarusib rivers, comprising the eastern part of the WKZ, CKZ and the western part of EKZ (Fig. 2).

STRUCTURAL GEOLOGY

Based on the lithostructural mapping of a 640 km^2 area (scale 1: 50,000) we recognized as older tectonic features of basement structures mylonitic foliation and related structures which crop out in the preserved Palaeoproterozoic to Archean blocks. In the reworked Archaean to Mesoproterozoic rocks and Pan-African rocks we recognized at least three deformational phases, which are D1, D2 and D3. Phase D_1 is herein interpreted as those mylonitic structures with roughly vergence to east (as L1 and S1 on Fig. 2). These structures are poorly recorded along the Hoanib area, restricted to low strain areas of D2 deformational phase. They comprise mainly rootless mesoscale isoclinal folds developed in mafic tonalitic gneisses of the basement, transposed by banding and shearing of D_2 phase. On the other side, both D_2 and D_3-phases are widely recorded in the gneissic sequence (ortho- and paragneisses) through NNW-trending banding and mylonitic zones formed during the transpressive collision of the Kaoko Belt (Dürr & Dingeldey, 1996).

Phase D_2 is represented by two intimately related pairs of planar-linear ductile high-temperature structures: gneissic banding (S_2band)/mineral lineation (L_2min) and mylonitic foliation (S_2myl)/stretching lineation (L_2stret) (represented as S2 and L2 on Fig. 2). In the kilometric scale this phase was responsible for the formation of NNW-trending/east-verging tightly and overturned anticlinal and synclinal systems of folds and thrusts, which characterize the tectonic style of the Central Kaoko Zone. Kilometric-spaced and narrow zones of lower temperature shear are described as D_3 deformational phase in the Hoanib Area. This phase, characterized by meter width mylonitic to ultramylonitic bands, deformed all gneissic sequences. They are represented by steeply dipping S3 mylonitic foliation with average orientation around 354°/67°SW and directional stretching lineation 14°/338° to 14°/157° (not represented on Fig. 2)). The kinematic indicators (e.g. asymmetric porphyroclasts) for this phase point to a sinistral top-to-SE sense of movement as equally determined for the D_2-structures.

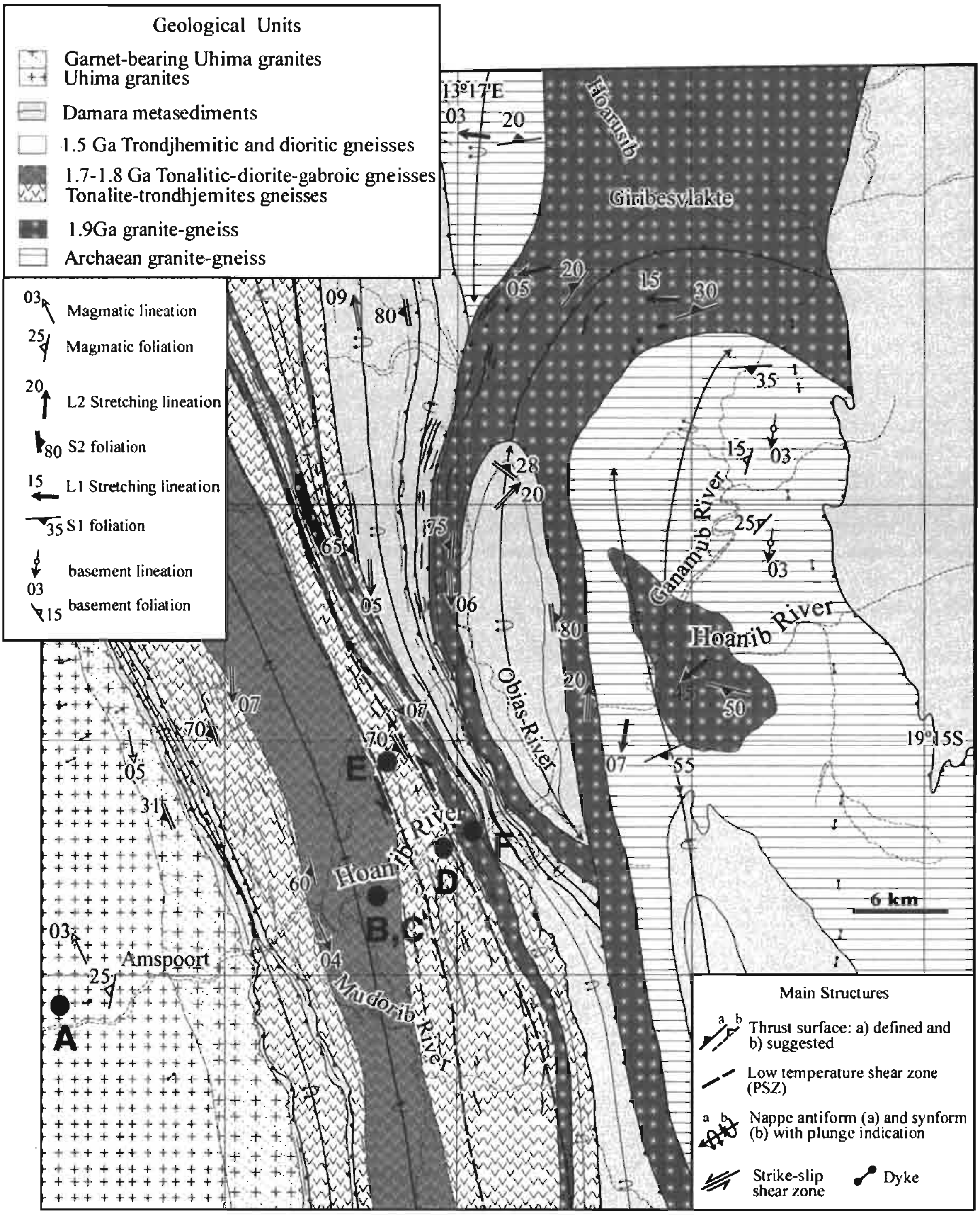

Figure 2. Lithostructural map of Hoanib Valley River region, Kaoko Belt, NW Namibia (Luft, in prep.). A=PZ-01, B=PZ-15-1A, C=PZ-15D, D=PZ-17B, F=PZ-19A e PZ-29C.

GEOLOGY OF HOANIB VALLEY

Based on their rock characteristics, structural style and relative/absolute age relationships (including the ages obtained in this work) we recognize six main units in the Hoanib Valley and adjacents areas Archaean granite-gneiss; 1.9 Ga granite gneiss; 1.7-1.8 Ga tonalitic/trondjhemitic and dioritic/gabbroic gneisses; 1.5 Ga trondhjemitic and dioritic gneisses; Damaran metasediments and granitoids.

The Archaean gneisses correspond to a rigid eastern block (Fig. 2) that represented as the hinterland region for the east-vergent Pan-African agglutination (fold and thrust system). This unit comprises 2.6 Ga old granodiorite gneiss (Seth, 1998) metamorphosed in the greenschist facies.

In the vicinity of Goreas River, 1.9 Ga augen gneiss crops out as NNW-trending gneissic body of six kilometers length and 500 meters wide. It is composed of amphibolite facies monzogranitic gneiss with well preserved porphyritic and cumulate textures in his central portion, and with a pervasive mylonitic foliation along the border. This unit is tectonically juxtaposed to the 1.7-1.8 Ga tonalitic/trondjhemitic gneisses by the Pan-African deformational phases (D_2/D_3 phases).

In the central portion of the studied area, the 1.7-18 Ga sequence is represented by NNW-trending amphibolite facies gneissic association composed by centimeter- to metrical-wide interlayered tonalite/trondjhemite gneisses with minor amount of dioritic gneisses and local xenoliths of garnet-schists and gabbros. This sequence records a very heterogeneous deformation along the central domain of the belt (high and low deformational zones), represented by km to cm-spaced folding, banding and shear zones generated during three deformational phases described above. In the low deformational zones occur igneous textures and primary relationship of the tonalite/trondjhemite gneisses and gabbroic.

The 1.5 Ga trondhjemitic-dioritic gneisse are exposed as m-wide bands intrusive in the 1.7 – 1.8 Ga sequence.

The Damara metasedimentary units are represented by marbles, garnet-bearing quartzites, quartz-schists and metarenites (Kuiseb Formation) and metavolcanics, observed as cm to km layers and/or lenses thrust on the older units (Fig. 2).

The westernmost portion of Hoanib Valley is dominated by a sequence of Pan-African porphyritic biotite-rich monzogranites and granodiorites (Uhima granites) with later injections of felsic garnet-granites. The dominant phase observed is a porphyritic monzogranite with igneous layering and biotite schlieren.

ISOTOPE RESULTS

U-Pb zircon and Sm-Nd WR Isotopic studies have been carried out on rock samples of the region (see location on fig. 2). Zircon ages were obtained at the Research School of Earth Sciences of ANU (SHRIMP method) and Laboratório de Geologia Isotópica of UFRGS (TIMS method).

The TIMS zircon age for augen gneiss is 1968±7 Ma which is similar to those ages obtained by Seth (1998) for the same unit.

Samples of Central Kaoko were dated by SHRIMP which provided two crystallization age groups. Two samples (one dioritic gneiss and one tonalite gneiss) yielded ages of 1731± 8 Ma (sample PZ-29 C) and 1763±10 Ma (PZ-15-1-A), respectively. We collected two samples of younger geisses cutting the dioritic/fonolitic rocks above. They are tonalitic and syeno granitic gneisses, strongly mylonitized, which are 1500±19 Ma and 1503±12 Ma old, respectively. The syenogranitic gneiss has a metamorphic border with a Pan-African age (510 Ma), which we interpret as the result of Pan-African deformation

Sample PZ-15-1-A has been dated by the single crystal TIMS method yielding the age of 1718±81 Ma.

The Pan-African granites have been dated by the TIMS and SHRIMP methods, yielding ages of 568 ± 6 Ma and 557±6 Ma.

Sm-Nd analyses have been carried out at the Laboratório de Geologia Isotópica at UFRGS. The of 1.9 Ga augen-gneiss show $\varepsilon_{Nd}(t = 1.9\ Ga)$ value of -4.6 and T_{DM} of 2.5 Ga. The gneissic rocks crystallized at 1.73 to 1.76 show positive $\varepsilon_{Nd}(t)$ values and T_{DM} ranging from 2.3 to 1.73 Ga, while those rocks crystalyzed at 1.50 Ga have ε_{Nd} values of -2.11 to -5.36 and T_{DM} of 2.03 to 2.34 Ga.

CONCLUSIONS

Based on the lithostructural mapping we recognized six units in the Hoanib Valley which have been described before. However in the Central Zone of the mostly Kaoko Belt two tonalitic-throndjemitic-dioritic sequences which can be divided into a 1.73-176 Ga magmatic arc and a 1.5 dioritic-tonalitic intrusions are recognized.

The older tonalitic-trondhjemitic-dioritic sequence is represented by juvenile material (positive ε_{Nd} values and model ages 2.3 to 1.73 Ga) while the second is characterized by reworked crustal material at 1.5 Ga. It is important to emphasize that these sequences has not yet been described in the Kaoko Belt and are here called the Mudorib Complex.

The metamorphism of the Kaoko Central and Western Zones has been already dated by U-Pb monazite method from gneiss samples which yielded the age of 550 Ma (Franz et al., 1999). Our single data of metamorphic zircon border confirms the Pan-African deformation.

REFERENCES

Dürr, S.B.; Dingeldey, D.P. 1996. The Kaoko belt (Namibia): Part of a late Neoproterozoic continetal-scale strike-slip system. Geology, 24(6), 503-506.

Franz, L.; Romer, R.L.; Dingeldey, D.P. 1999. Diachronous Pan-African granulite-facies metamorphism (650Ma and 550Ma) in the Kaoko belt, NW Namibia. Eur. J. Mineral, 11,167-180.

Geological map of South West Africa, 1:1.000.000. 1963. Gov. Printer, Pretoria.

Luft Jr., J. L. Tectonic Evolution of Hoanib-Hoarusib Valleys, Kaoko Belt. PhD Thesis, UFRGS (in prep.).

Miller, R. McG. 1983. Evolution of the Damara Orogen of South West Africa/Namibia. Inn. Special Pub. N° 11, Geol. Soc. S. Africa (edited by Miller, R. McG), 515p.

ISOTOPE GEOLOGY OF SYNTECTONIC MAGMATISM ALONG THE MAJOR GERCINO SHEAR ZONE, SOUTHERN BRAZIL: IMPLICATIONS FOR THE TIMING OF DEFORMATION EVENTS

Chemale Jr., F.[1,2]; Mallmann, G.[3]; Bitencourt, M.F.[2] and Kawashita, K.[1]

1. Laboratório de Geologia Isotópica, IG-UFRGS, Brazil. farid.chemale@ufrgs.br
2. Programa de Pós-graduação em Geociências, IG-UFRGS-CNPq, Brazil. guilherme.mallmann@ufrgs.br
3. Instituto de Geociências, IG-UFRGS. fatimab@ufrgs.br

Keywords: Neoproterozoic, magmatism, U-Pb, Sm-Nd, Santa Catarina, Southern Brazil

INTRODUCTION

The Dom Feliciano Belt (DFB) is part of a major orogenic system of the Brasiliano-Pan-African Cycle situated at the continental margin of southern Brazil (Fig. 1). From the tectonic point of view these rocks formed as result of an oblique collision that affected both African and Brazilian margins during the Neoproterozoic to Early Paleozoic times. Such tectonic record is well exposed in the Dom Feliciano Belt (Uruguay and southern Brazil), Kaoko Belt and Gariep Belt (southern Africa). The DFB is marked by NE-SW trends, encompassing flat-lying thrusting and strike-slip structures (Fernandes et al., 1992;, Chemale Jr. et al., 1995). It consists of granitic-gneissic-migmatitic terranes with multiple magmatic intrusions, mostly controlled by transcurrent shear zones. One of these structures is the Major Gercino Shear Zone (MGSZ), a NE-SW dextral transcurrent structure located at the northern limit of the Dom Feliciano Belt.

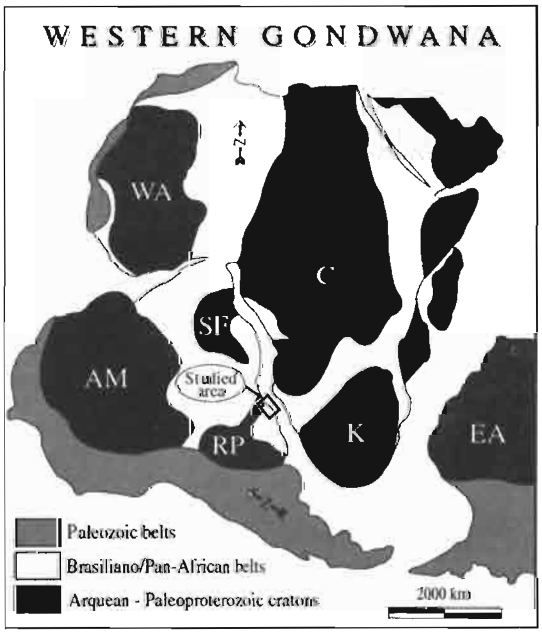

Figure 1. Distribution of the Archean to Paleoproterozoic cratons (WA-West Africa, C-Congo, K-Kalahari, EA-East Africa, AM-Amazônico, SF-São Francisco, RP-Rio de La Plata) and Neoproterozoic to Early-Paleozoic belts of the western Gondwana with location of the studied area.

In order to establish the temporal relationship between magmatism and shearing processes, we carried out U-Pb zircon dating on several intrusions from the Porto Belo region, at the northern extreme of the MGSZ. A better approach on the magmatic evolution is herein presented using Sm-Nd methodology to establish the time of crustal residence and probable sources of granitic magmas within the shear zone and in adjacent units.

GEOLOGICAL SETTING

The Porto Belo-Itapema region is located in the state of Santa Catarina, southern Brazil (Fig. 2). From NW to SE, three major tectonic domains are distinguished according Basei (1985), namely: External (Luis Alves block or craton), Intermediary and Internal (Dom Feliciano belt or Florianópolis Batholith), separated by the Itajaí-Perimbó and Major Gercino shear zones, respectively (Fig. 2a).

In the External Domain the main unit is the Paleoproterozoic Santa Catarina Granulitic Complex, whose primary evolution is Neoarchean. This terrane shows mostly Palaeoproterozoic metamorphism and deformation, but there are some discrete shear zones which cut across the older structures. This domain also includes a Brasiliano (Neoproterozoic to Cambrian) volcano-sedimentary sequence (Itajaí and Campo Alegre basins) that presents some ductile-ruptile oblique thrusting structures.

The Intermediary Domain comprises the Brusque Metamorphic Complex (BMC) and the Camboriú Complex (CC), both deformed in the Brasiliano Cycle. The BMC is a volcano-sedimentary sequence of uncertain age (Paleoproterozoic or Neoproterozoic) metamorphosed under greenschist to amphibolite facies conditions, while the CC consists of Paleoproterozoic granitic-gneissic rocks. Neoproterozoic granitic intrusions are also described in this domain.

The Internal Domain (Dom Feliciano Belt) is a shear belt made up by several granitic intrusions of calc-alkaline to alkaline signatures ranging from undeformed to intensely deformed bodies, and remnants of Palaeoproterozoic gneisses, migmatites and amphibolites. This belt is composed of NE- to NNE-trending shear zones that can be divided into three main groups of structures: (i) the sinistral transcurrent N20E-S20W shear zones, (ii) the dextral transcurrent N45E-S45W shear zones, and (iii) sinistral transcurrent NS-trending shear zones. Based on the available data, these shear zones has been active mainly from 650 to 590 Ma, but crustal reworking in lower greenschist facies is also dated by Ar-Ar on biotite of the Sierra Ballena-Dorsal de Canguçu shear zones at 540 Ma. Flat-lying structures are often cut by one or more transcurrent shear zones which are attributed to earlier thrusting (Fernandes et al., 1992; Chemale Jr. et al., 1995). We interpret such features as resulting from the initial stages of oblique shear zones that evolved to transcurrent ones.

THE MAJOR GERCINO SHEAR ZONE

The MGSZ is a megastructure composed of several anastomosed segments that deform earlier granitic-gneissic rocks and contain successively emplaced syntectonic granitic bodies. In the Porto Belo region, the MGSZ consists of a 5 to 6 km-wide and 14 km-long (total length within the Santa Catarina State is around 80 km) (Fig. 2a-b). According to Bitencourt (1996) this structure results from simple shearing at ductile-brittle conditions (350°C to 480°C and 2 to 5Kb), with dextral shear sense, variable and no symmetric strain from the border to the center.

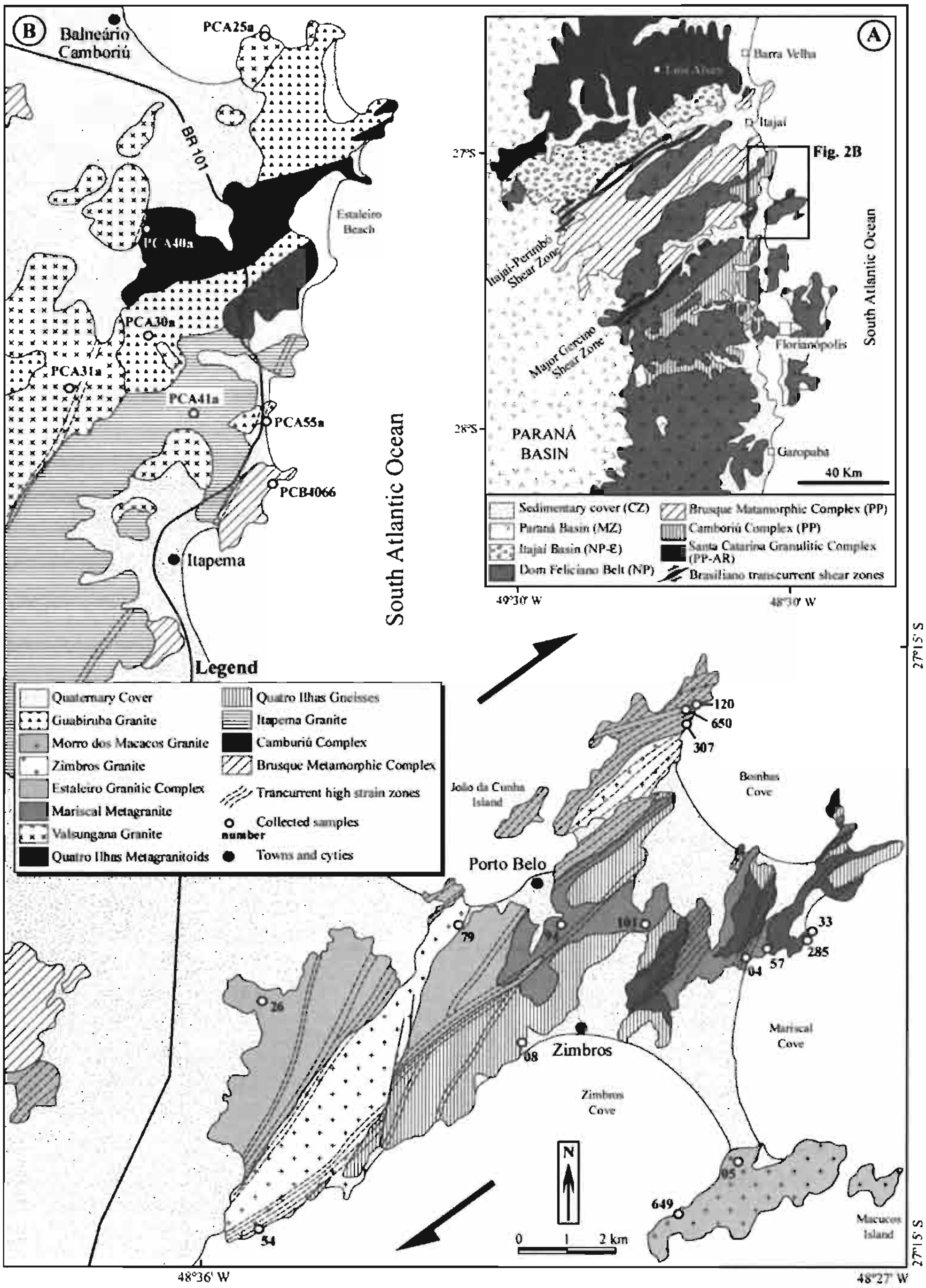

Figure 2. A) Main geotectonic units of the Santa Catarina state, southern Brazil (modified after Chemale Jr. et al., 1995). B) Geologic map of the Porto Belo-Itapema region, Santa Catarina state, Brazil (after Bitencourt, 1996; UFRGS, 2000).

Bitencourt (1996) describes two major rock associations in the region (a) granitic-tonalitic orthogneisses with flat-lying metamorphic foliation, defined as embasement to the Brasiliano rocks, and (b) deformed to undeformed granitic rocks intimately related to the MGSZ evolution. Based on field relations, petrography and geochemistry, Bitencourt and Nardi (1993) divided the shear zone-related granitoids into: (i) High-K, calc-alkaline, early transcurrent Quatro Ilhas Granitoids, (ii) Early transcurrent, peraluminous Mariscal Granite, (iii) Syn-transcurrent, shoshonitic, Estaleiro Granodiorite, (iv) late-transcurrent, metaluminous, mildly alkaline magmatism of the Zimbros Intrusive Suite represented by the Zimbros and Morro dos Macacos granites, rhyolites and mafic rocks, sometimes forming composite dykes. The Morro dos Macacos Granite consists of an isolated, dominantly massive intrusion, interpreted as a batch of magma emplaced outside the shear zone.

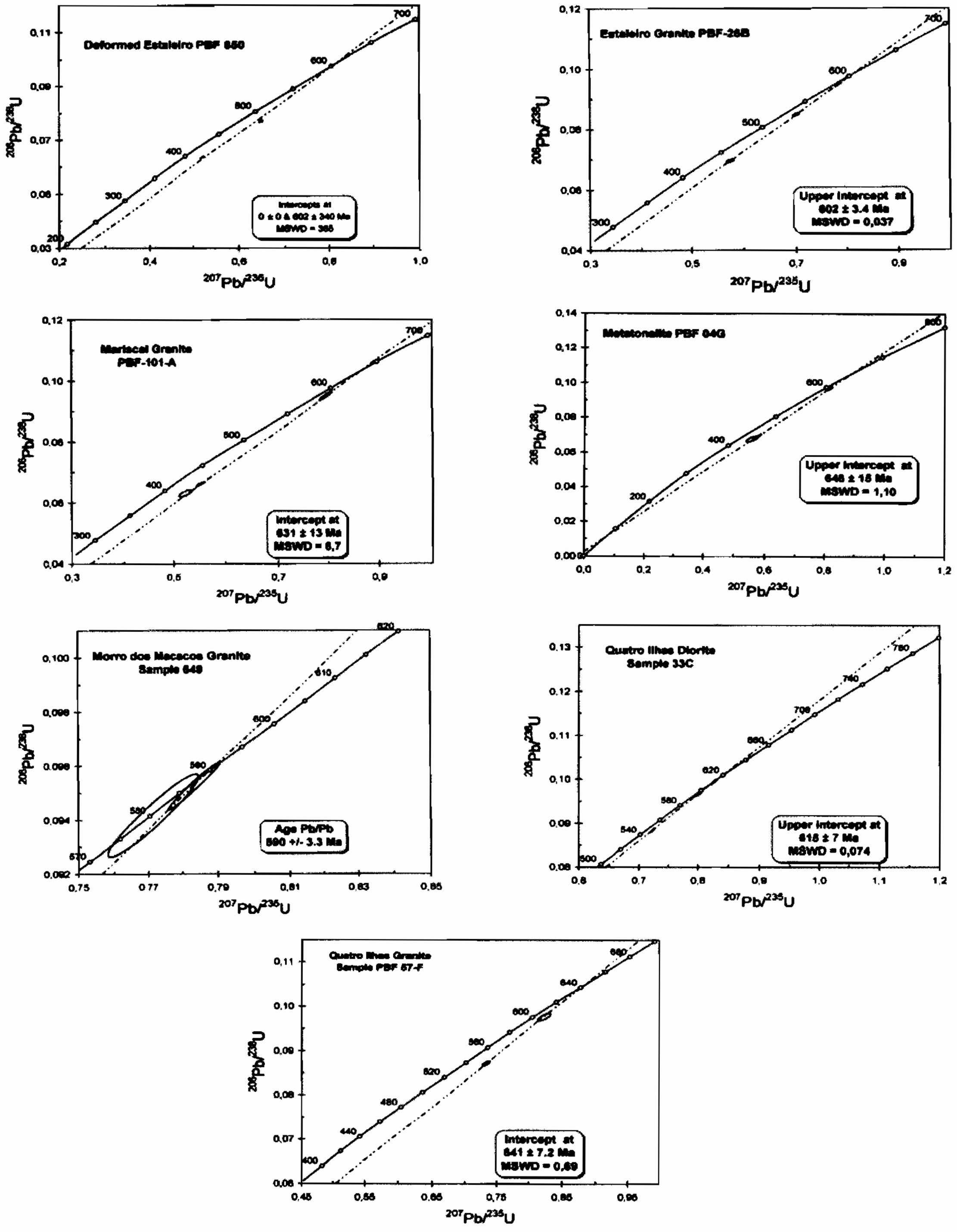

Figure 3. U-Pb zircon ages for the analyzed samples.

U-Pb ZIRCON GEOCHRONOLOGY

Seven samples were collected for U-Pb zircon dating (Fig. 1b). Zircons were separated after crushing, milling and conventional heavy liquids and magnetic procedures. Lesser magnetic zircons were handpicked and fractions of single crystal were dissolved with $^{205}Pb/^{235}U$ spike. The dissolved zircons have been analyzed at the Laboratório de Geologia Isotópica of Universidade Federal do Rio Grande do Sul with a multi-colletor VG Sector 54 Mass Spectrometer and preliminary results are presented in the figure 3.

The oldest U-Pb zircon data have obtained from a tonalitic gneiss (considered as basement for shear-related granites, sample PBF-04G) which yielded an age of 646±15 Ma (Fig. 3). The zircon ages for the granites of the MGSZ range from 641 to 590 Ma. The Quatro Ilhas and the Mariscal granites which are intruded during the earlier stages of transcurrent shearing are 641±7.2 Ma and 631±13 Ma old, respectively. Its important to emphasize that these granites display flat-lying structures. The undeformed sample of syn-trancurrent Estaleiro Granite have been intruded at 602±3.4 Ma while de deformed Estaleiro Granite yielded large uncertanity due to the shearing process that affected this rock. The alkaline magmatism is dated at 590±3.3 Ma (Morro dos Macacos Granite) which are the youngest observed age.

Sm-Nd ISOTOPES

Sm-Nd isotopes of the 18 samples of the MGSZ-related rocks (Internal Domain) and 5 samples of the Intermediary Domain (Fig. 2b) have been carried out at the Laboratório de Geologia Isotópica of UFRGS. Rock powders for Sm-Nd analysis were dissolved in Teflon vial and Sm-Nd extracted using chromatographic procedures. Isotopic compositions were measured with a multi-collector VG Sector 54 Mass Spectrometer.

The granitic rocks of the Internal Domain, which include tonalitic gneisses and granite-related rocks show $\varepsilon Nd_{(t)}$ values from -2.5 to -7.5 (for t=646 to 590 Ma) and T_{DM} model ages (De Paolo, 1981) of 1.35 to 2.05 Ga. The granitic rocks of the Intermediary Domain have usually older model ages. The Paleoproterozoic Itapema Granite (Hartmann et al., 2003) display $\varepsilon Nd_{(t)}$ value of -6.1 (for t=2.0 Ga) and T_{DM} model ages of 2.96 Ga. The Valsungana Granite has $\varepsilon Nd_{(t)}$ values of -14 to -15 (for t=650 Ma) and model ages of 2.04 to 1.77 Ga, while the Guabiruba Granite show $\varepsilon Nd_{(t)}$ values of -22 to -24 (for t= 590 Ma) and Archean model ages (2.9 to 3.0 Ga).

DISCUSSION OF RESULTS

The dating of the metatonalite (sample 04G), which is considered the basement of granites from Porto Belo region, suggests a Brasiliano age for this rock with model age around 1.5 Ga. The set of ages between 641 to 631Ma, obtained for the Quatro Ilhas and Mariscal granites, could be represent an early flat-lying stage of the Major Gercino Shear Zone. The ages between 631 to 590 Ma clearly suggests the timing of the transcurrent process, as defined by Bitencourt (1996). The Sm-Nd data support a clear separation between the internal and intermediary domains magmatism, where the rocks Intermediary Domain presents more negative $\varepsilon Nd_{(t)}$ values for Brasiliano crystallized ages and Archean model ages for most of analyzed samples. The Sm-Nd isotope signature of the Porto Belo region (Internal Domain) display model ages always lesser than 2.05 to 1.35 Ga which are interpreted to be mixing source of reworked Paleoproterozoic crust and juvenile Brasiliano sources.

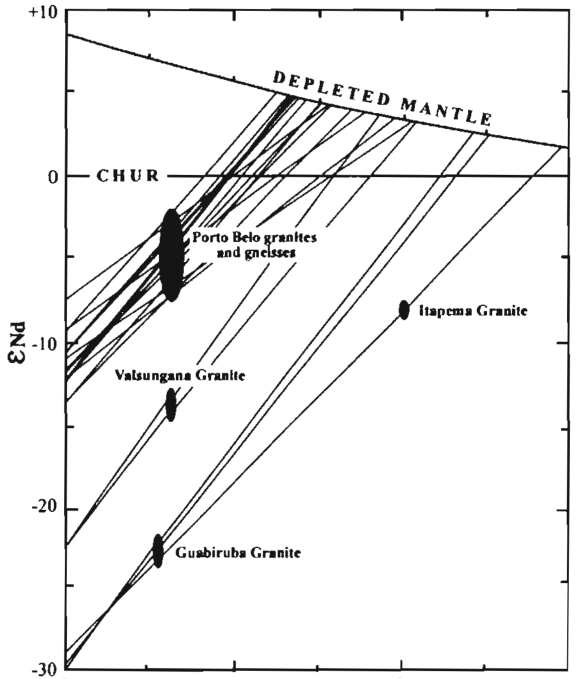

Figure 4. ε_{Nd} versus time diagram (De Paolo, 1981) for the studied samples (see Fig. 2b for reference).

REFERENCES

Basei, M.A.S., 1985. O Cinturão Dom Feliciano em Santa Catarina. PhD Thesis, USP.

Bitencourt, M.F. & Nardi, L.V.S., 1993. Anais da Academia Brasileira de Ciências 65 (Supl.1) 3-16.

Bitencourt, M.F., 1996. Granitóides sintectônicos da Região de Porto Belo, SC. PhD Thesis. (Unpublished).

Chemale Jr. et al., 1995. Communication of Geological Survey Namibia 10: 151-166.

De Paolo, D.J., 1981. Nature 291: 193-197.

Fernandes et al., 1992. Journal of South American Earth Sciences 5: 77-96.

Hartmann et al. 2003. Submitted to Journal of South American Earth Sciences.

CARBONATITES FROM SOUTHEASTERN BRAZIL: Sr-Nd-Pb SYSTEMATICS

Comin-Chiaramonti, P.[1]; Gomes, C.B.[2]; Marques, L.S.[3]; Censi, P.[4]; Ruberti, E.[2] and Antonini, P.[1]

1. Dipartimento di Ingegneria Chimica (DICAMP), Trieste University, Piazzale Europa 1, I-34127 Trieste, Italy. comin@univ.trieste.it, antonini@univ.treste.it
2. Instituto de Geociências, Universidade de São Paulo, Rua do Lago 562, 05508-080, São Paulo-SP. cgomes@usp.br
3. Instituto de Astronomia, Geofísica e Ciências Atmosféricas, Universidade de São Paulo, Rua do Matão 1226, 05508-900, São Paulo-SP. leila@iag.usp.br
4. Dipartimento di Geologia, Università di Catania, Corso Italia 55, I-95129, Catania, Italy. pcensi@mbox.unict.it

Keywords: Carbonatites, Paraná Basin, O-C isotopes, fractionation model

Early and Late Cretaceous carbonatitic complexes from southern Brazil occur along the main tectonic lineaments of the South America platform. A similar situation is recognized for the Angolan and Namibian occurrences in Africa.

Processes of liquid immiscibility are believed to have generated carbonatitic liquids, as evidenced by the field relationships and by the geochemical characteristics.

Calcio-, magnesio- and ferrocarbonatites are widespread even in the same complex (Fig. 1). The remarkable scatter of the incompatible elements is mainly due to (1) the control of accessory phases, e.g. apatite, pyrochlore, fluorcarbonates and fluorite, and (2) the repeated overprinting of hydrothermal over magmatic processes.

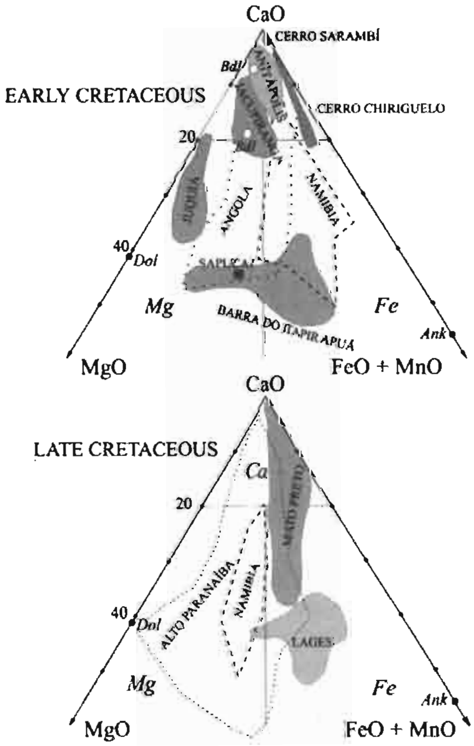

Figure 1. Classification of the carbonatitic associations (after Woolley & Kempe, 1989) in the various complexes and fields from southern Brazil, Angola and Namibia. Data source, Brazil: Morbidelli et al. (1986), Censi et al. (1989), Beccaluva et al. (1992), Meyer et al. (1994), Huang et al. (1995), Toyoda et al. (1995), Ruberti et al. (2002), Comin-Chiaramonti et al. (2001a, 2002) and unpublished data; Angola: Alberti et al. (1999) and therein references; Namibia: Milner & Le Roex (1996), Le Roex & Lanyon (1998), Kurszlaukis et al. (1999).

Sr-Nd-Pb systematics highlight heterogeneous mixtures between HIMU and EMI mantle components, likewise to the associate alkaline rocks and the flood tholeiites of the Paraná-Angola-Namibia Province (Fig. 2).

The areal distribution shows that the time-integrated isotopic enrichment of the carbonatites and alkaline rocks decreases from West (Eastern Paraguay) to East (Angola and Namibia), and it is associated with the age decrease of the alkaline magmatism, i.e. from Early Cretaceous to Tertiary.

As a whole, the data indicate that the alkaline-carbonatitic magmatism originated from a significant but small scale heterogeneous subcontinental mantle. In this scenario, the Walvis Ridge-Rio Grande Rise and Vitória-Trindade hotspot tracks might reflect the accomodation of stresses in the lithosphere during rifting, rather than continuous magmatic activity induced by mantle plumes beneath the moving lithosphere (Fig. 3).

REFERENCES

Alberti, A., Castorina, F., Censi, P., Comin-Chiaramonti, P. and Gomes, C.B., 1999. Geochemical characteristics of Cretaceous carbonatites from Angola. Journal of African Earth Sciences 29, 735-759.

Andrade, F.R.D., Möller, P. and Höhndorf, A., 1999. The effect of hydrothermal alteration on the Sr and Nd isotopic signatures of the Barra do Itapirapuã carbonatite, southern Brazil. Journal of Geology 107, 177-191.

Beccaluva, L., Barbieri, M., Born, H., Brotzu, P., Coltorti, M., Conte, A., Garbarino, C., Gomes, C.B., Macciotta, G., Morbidelli, L., Ruberti, E., Siena, F. and Traversa, G., 1992. Fractional crystallization and liquid immiscibility processes in the alkaline-carbonatite complex of Juquiá (São Paulo, Brazil). Journal of Petrology 33, 1371-1404.

Bell, K. and Tilton, G.R., 2001. Nd, Pb and Sr isotopic compositions of East African carbonatites: evidence for mantle mixing and plume inhomogeneity. Journal of Petrology 42, 1927-1945.

Bellieni, G., Montes-Lauar, C.R., De Min, A., Piccirillo, E.M., Cavazzini, G., Melfi A.J. and Pacca, I.G., 1990. Early and Late Cretaceous magmatism from São Sebastião island (SE-Brazil): geochemistry and petrology. Geochimica Brasiliensis 4, 59-83.

Bennio, L., Brotzu, P., Gomes, C.B., D'Antonio, M., Lustrino, M., Melluso, L., Morbidelli, L. and Ruberti, E., 2002. Petrological, geochemical and Sr-Nd isotopic features of alkaline rocks from the Arraial do Cabo Frio Peninsula (southern Brazil). Periodico di Mineralogia 71, 137-155.

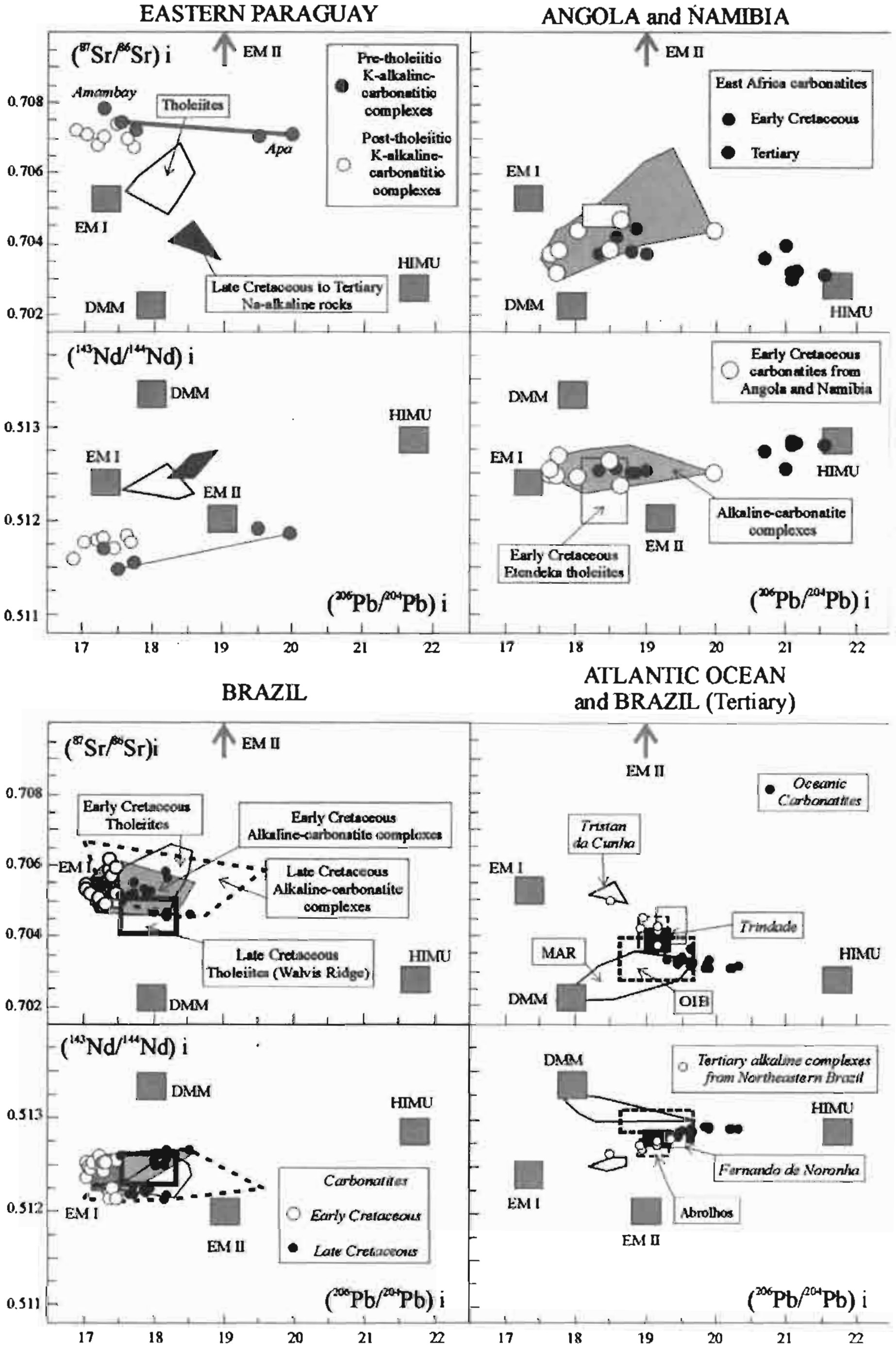

Figure 2. Sr_i and Nd_i vs. $^{206}Pb/^{204}Pb$ (initial ratios). Data source, A, Eastern Paraguay: Comin-Chiaramonti et al. (1991, 1995, 1997, 2001b), Comin-Chiaramonti & Gomes (1996), Castorina et al. (1997), Marques et al. (1999a), Comin-Chiaramonti (unpublished data); B, Angola and Namibia: Milner & Le Roex (1996), Le Roex & Lanyon (1998), Gibson et al. (1999), Harris et al. (1999), Ewart et al. (1998), Cooper & Reid (1998), Smithies & Marsh, 1998, Alberti et al. (1999), Kurzslaukis et al. (1999); East Africa: Bell & Tilton (2001); C, Brazil, Early Cretaceous: Toyoda et al. (1995), Huang et al. (1995), Walter et al. (1995), Garda et al. (1995), Marques et al. (1999a), Gibson et al. (1999), Andrade et al. (1999), Comin-Chiaramonti et al. (2001a, 2002), Ruberti et al. (2002); Uruguay, Early Cretaceous: Kirkstein et al. (2000); Brazil, Late Cretaceous: Bellieni et al. (1990), Bizzi et al. (1994, 1995), Toyoda et al. (1994), Meyer et al. (1994), Gibson et al. (1995, 1997, 1999), Carlson et al. (1996), Thompson et al. (1998); D, Atlantic Ocean: Walvis Ridge, Richardson et al. (1982); Rio Grande Rise, Gamboa & Rabinowitz (1984); Mid Atlantic Ridge (MAR), Hamelin et al. (1984), Ito et al. (1987), Fontignie & Shilling (1997); OIB, Halliday et al. (1988, 1995); Atlantic carbonatites, Hoernle et al. (2002); Tristan da Cunha, Le Roex (1985), Le Roex et al. (1990); Trindade, Marques et al., (1999b), Siebel et al. (2000); Brazil, Tertiary: Serra do Mar, Thompson et al. (1998), Bennio et al. (2002); Abrolhos, Fodor et al. (1989); Northeastern Brazil, Fodor et al. (1998); Fernando de Noronha, Gerlach et al. (1987). DMM, HIMU, EMI and EMII are approximations of mantle end-members taken from Hart et al. (1992). It should be noted that in all the diagrams the Rio Grande Rise basalts (not shown) plot in the same field of the Walvis Ridge samples.

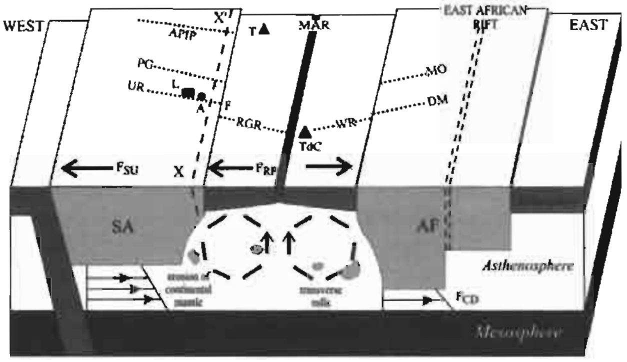

Figure 3. Forces acting on plates in rotational model illustrated for the South Atlantic Ocean (after Smith & Lewis, 1999, modified). Major rifting occurs parallel to X-X' pre-existing suture. Intraplate volcanism follows the second order sutures (e.g. PG-MO: Ponta Grossa-Moçâmedes Arch, UR: Uruguay lineament; DM: Damara belt). SA: South America plate; AF, African plate; RGR: Rio Grande Rise; WR: Walvis Ridge; TdC: Tristan da Cunha; T: Trindade. F_{CD}: continental drag; F_{RP}: ridge push; F_{SU}: trench suction. F, Florianópolis; A, Anitápolis; L, Lages.

Bizzi, L.A., Smith, B.C., De Wit, M.J., MacDonald, I. and Armstrong, R.A., 1994. Isotope characteristics of the lithospheric mantle underlying the SW São Francisco craton margin, Brazil. In: International Symposium on the Physics and Chemistry of the Upper Mantle. Invited Lectures, São Paulo pp. 227-256.

Bizzi, L.A., de Wit, M.J., Smith, C.B., McDonald, I. and Armstrong, R.A., 1995. Heterogeneous enriched mantle materials and Dupal-type magmatism along SW margin of the São Francisco craton, Brazil. Journal of Geodynamics 20, 469-491.

Carlson, R.W., Esperança, S. and Svisero D.P., 1996. Chemical and Os isotopic study of Cretaceous potassic rocks from southern Brazil. Contributions to Mineralogy and Petrology 125, 393-405.

Castorina, F., Censi, P., Comin-Chiaramonti, P.A., Gomes, C.B., Piccirillo, E.M., Alcover Neto, A., Almeida R.T., Speziale, S. and Toledo M.C., 1997. Geochemistry of carbonatites from Eastern Paraguay and genetic relationships with potassicc magmatism: C, O, Sr and Nd isotopes. Mineralogy and Petrology 61, 237-260.

Censi, P., Comin-Chiaramonti, P., Demarchi, G., Longinelli, A. and Orué, D., 1989. Geochemistry and C-O isotopes of the Chiriguelo carbonatite, northeastern Paraguay. Journal of South American Earth Sciences 3, 295-303.

Comin-Chiaramonti, P. and Gomes, C.B., 1996. Alkaline magmatism in Central-Eastern Paraguay. Relationships with coeval magmatism in Brazil. Edusp/Fapesp, São Paulo, 464p.

Comin-Chiaramonti, P., Castorina, F., Cundari, A., Petrini, R. and Gomes C.B. 1995. Dykes and sills from Eastern Paraguay: Sr and Nd isotope systematics. In: Baer, G. & Heimann, A. (eds.) Physics and chemistry of dykes. Balkema, Rotterdam, pp. 267-278.

Comin-Chiaramonti, P., Civetta, L., Petrini, R., Piccirillo, E.M., Bellieni, G., Censi, P., Bitschene, P., Demarchi, G., De Min, A., Gomes, C.B., Castillo, A.M.C. and Velazquez, J.C., 1991. Tertiary nephelinitic magmatism in Eastern Paraguay: petrology, Sr-Nd isotopes and genetic relationships with associated spinel-peridotite xenoliths. European Journal of Mineralogy 3, 507-525.

Comin-Chiaramonti, P., Cundari, A., Piccirillo, E.M., Gomes, C.B., Castorina, F., Censi, P., De Min A., Marzoli, A., Speziale, S. and Velázquez, V.F., 1997. Potassic and sodic igneous rocks from Eastern Paraguay: their origin from the lithospheric mantle and genetic relationships with the associated Paraná flood tholeiites. Journal of Petrology 38, 495-528.

Comin-Chiaramonti, P., Gomes, C.B., Castorina, F., Censi P., Antonini, P., Furtado, S., Ruberti, E. and Scheibe, L.F., 2002. Anitápolis and Lages alkaline-carbonatite complexes, Santa Catarina State, Brazil: geochemistry and geodynamic implications. Revista Brasileira de Geociências 32, 43-58.

Comin-Chiaramonti, P., Gomes, C.B., Ruberti, E., Antonini, P. and Censi, P., 2001a. Mato Preto alkaline-carbonatite complex: geochemistry and isotope (O-C, Sr-Nd) constraints. Geochimica Brasiliensis 15, 23-34.

Comin-Chiaramonti, P., Princivalle, F., Girardi, V.A.A., Gomes, C.B., Laurora, A. and Zanetti F., 2001b. Mantle xenoliths from Ñemby, Eastern Paraguay: O-Sr-Nd isotopes, trace elements and crystal chemistry of hosted clinopyroxenes. Periodico di Mineralogia 70, 205-230.

Cooper, A.F. and Reid, D.L., 1998. Nepheline sövites as parental magmas in carbonatite complexes: evidence from Dicker Willem, soutwest Namibia. Journal of Petrology 39, 2123-2136.

Ewart, A., Milner, S.C., Armstrong, R.A. and Duncan, A.R., 1998. Etendeka volcanism of the Goboboseb Mountains and Messum igneous complex, Namibia. Part I: geochemical evidence of Early Cretaceous Tristan plume melts and the role of crustal contamination in the Paraná-Etendeka CFB. Journal of Petrology 39, 191-225.

Fodor, R.V., Mukasa, S.B., Gomes, C.B. and Cordani, U.G., 1989. Ti-rich Eocene basaltic rock, Abrolhos plattform, offshore Brazil, 18°S: petrology with respect to South Atlantic magmatism. Journal of Petrology 30, 763-786.

Fodor, R.V., Mukasa, S.B. and Sial, A.N., 1998. Isotopic and trace-element indications of lithospheric and asthenospheric components in Tertiary alkalic basalts, northeastern Brazil. Lithos 43, 197-217.

Fontignie, D. and Schilling, J.G., 1996. Mantle heterogeneities beneath the South Atlantic: a Nd-Sr-Pb isotope study along the Mid-Atlantic Ridge (3°S-46°S). Earth Planetary Science Letters 146, 259-272.

Gamboa, L.A.P. and Rabinowitz, P.D., 1984. The evolution of the Rio Grande Rise in Southwest Atlantic. Marine Geology 58, 35-58.

Garda, G.M., Schorscher, H.D., Esperança, S. and Carlson, R.W., 1995. The petrology and geochemistry of coastal dikes from São Paulo State, Brazil: implications for variable lithospheric contributions to alkaline magmas from the western margin of the South Atlantic. Anais da Academia brasileira de Ciências 67, 191-216.

Gerlach, D.C., Stormer, J.C. and Mueller, P.A., 1987. Isotope geochemistry of Fernando de Noronha. Earth and Planetary Science Letters 85, 129-144.

Gibson, S.A., Thompson, R.N., Leonardos, O.H., Dickin, A.P. and Mitchell, J.G., 1995. The Late Cretaceous impact of the Trindade mantle plume; evidence from large-volume, mafic, potassic magmatism in SE Brazil. Journal of Petrology 36, 189-229.

Gibson, S.A., Thompson, R.N., Leonardos, O.H., Dickin, A.P. and Mitchell, J.G., 1999. The limited extent of plume-lithosphere interactions during continental flood-basalt genesis: geochemical evidence from Cretaceous magmatism in southern Brazil. Contributions to Mineralogy and Petrology 137, 147-169.

Gibson, S.A., Thompson, R.N., Weska, R.K., Dickin, A.P. and Leonardos, O.H., 1997. Late-Cretaceous rift-related upwelling and melting of the Trindade starting mantle plume head beneath western Brazil. Contributions to Mineralogy and Petrology 126, 303-314.

Halliday, A.N., Dickin, A.P., Fallick, A.E. and Fitton, J.G., 1988. Mantle dynamics: a Nd, Sr, Pb and O isotopic study of the Cameroon Line volcanic chain. Journal of Petrology 29, 181-211.

Halliday, A.N., Lee, D.C., Tommasini, S., Davies, G.R., Paslick, C.R., Fitton, G.J. and James, D.E., 1995. Incompatible trace elements in OIB and MORB and source enrichment in the sub-oceanic mantle. Earth and Planetary Science Letters 133, 379-395.

Hamelin, B., Dupré, B. and Allègre, C.J., 1984. Lead-strontium isotopic variations alongt the East Pacific Rise and Mid-Atlantic Ridge: a comparative study. Earth and Planetary Science Letters 67, 340-350.

Harris, C., Marsh, J.S. and Milner, S.C., 1999. Petrology of the alkaline core of the Messum igneous complex, Namibia: evidence for the progressively decreasing effect of crustal contamination. Journal of Petrology 40, 1377-1397.

Hart, S.R., Hauri, E.H., Oschmann, L.A. and Whithehead, J.A., 1992. Mantle plumes and entrainement: isotopic evidence. Science 256, 517-520.

Hoernle, K., Tilton, G., Le Bas, M.J., Duggen, S. and Garbe-Schömberg, D., 2002. Geochemistry of oceanic carbonatites compared with continental carbonatites: mantle recycling of oceanic crustal carbonate. Contributions to Mineralogy and Petrology 142, 520-542.

Huang, H-M., Hawkesworth, C.J., Van Calsteren, P. and Mcdermott, F., 1995. Geochemical characteristics and origin of the Jacupiranga carbonatites, Brazil. Chemical Geology 119, 79-99.

Ito, E., White, W.M. and Göpel, C., 1987. The O, Sr, Nd and Pb isotope geochemistry of MORB. Chemical Geology 62, 157-176.

Kirkstein L.A., Peate, D.W., Hawkesworth C.J., Turner, S.P., Harris C. and Mantovani, M.S.M., 2000. Early Cretaceous basaltic and rhyolitic magmatism in southern Uruguay associated with the opening of the South Atlantic. Journal of Petrology 41, 1413-1438.

Kurszlaukis, S., Franz, L. and Brey, G.P., 1999. The Blue Hill intrusive complex in southern Namibia. Relationships between carbonatites and monticellite picrites. Chemical Geology 160, 1-18.

Le Roex, A.P. and Lanyon, R., 1998. Isotope and trace element geochemistry of Cretaceous Damaraland lamprophyres and carbonatites, northwestern Namibia: evidence for plume-lithosphere interaction. Journal of Petrology 39, 1117-1146.

Le Roex, A.P., Cliff, R.A. and Adair, B.J.I., 1990. Tristan da Cunha, south Atlantic: geochemistry and petrogenesis of a basanite-phonolite lava series. Journal of Petrology 31, 779-812.

Marques, L.S., Dupré, B. and Piccirillo, E.M. 1999a. Mantle source compositions of the Paraná magmatic province (southern Brazil): evidence from trace element and Sr-Nd-Pb isotope geochemistry. Journal of Geodynamics 28, 439-458.

Marques, L.S., Ulbrich, M.N.C., Ruberti, E. and Tassinari, C.G., 1999b. Petrology, geochemistry and Sr-Nd isotopes of the Trindade and Martin Vaz volcanic rocks (Southern Atlantic Ocean). Journal of Volcanology and Geothermal Research 93, 191-216.

Meyer, H.O.A., Blaine, L.G., Svisero, D. P. and Craig, B.S., 1994. Alkaline intrusions in western Minas Gerais, Brazil. Proceedings of the Fifth International Kimberlite Conference, Araxá, pp. 140-155.

Milner, S.C. and Le Roex, A.P., 1996. Isotope characteristics of the Okenyenya igneous complex, nortwestern Namibia: constraints on the composition of the early Tristan plume and the origin of the EM1 mantle component. Earth Planetary Science Letters 141, 277-291.

Morbidelli, L., Beccaluva, L., Brotzu, P., Conte, A.G., Garbarino, C., Gomes, C.B., Macciotta, G., Ruberti, E., Scheibe, L.F. and Traversa, G., 1986. Petrological and geochemical studies of alkaline rocks from continental Brazil. 3. Fenitization of jacupirangite by carbonatite magmas from Jacupiranga. Periodico di Mineralogia 55, 261-295.

Richardson, S.H., Erlank, A.J., Duncan, A.R. and Reid, D.L., 1982. Correlated Nd, Sr and Pb isotope variations in Walvis Ridge basalts and implications for the evolution of their mantle source. Earth and Planetary Science Letters 59, 327-342.

Ruberti, E., Castorina, F., Censi, P., Comin-Chiaramonti, P., Gomes, C.B., Antonini P. and Andrade, F.R.D., 2002. The geochemistry of the Barra do Itapirapuã carbonatite (Ponta Grossa Arch, Brazil): a multiple stockwork. Journal of South America Earth Sciences 15, 215-228.

Siebel, W., Becchio, R., Volker, F., Hansen, M.A.F., Viramonte, J., Trumbull, R.B., Haase, G. and Zimmer, M., 2000. Trindade and Martin Vaz islands, South Atlantic: isotopic (Sr, Nd, Pb) and trace element constraints on plume related magmatism. Journal of South American Earth Sciences 13, 79-103.

Smith A.D. and Lewis, C., 1999. The planet beyond the plume hypotesis. Earth-Science Reviews 48, 135-182.

Smithies, R.H. and Marsh, J.S., 1998. The Marinkas Quellen carbonatite complex, southern Namibia; carbonatite magmatism with an uncontaminated depleted mantle signature in a continental setting. Chemical Geology 148, 201-212.

Thompson, R.N., Gibson, S.A., Mitchell, J.G., Dickin, A.P., Leonardos, O.H., Brod, J.A. and Greenwood, J.C., 1998. Migrating Cretaceous-Eocene magmatism in the Serra do Mar alkaline Province, SE Brazil: melts from the deflected Trindade mantle plume? Journal of Petrology 39, 1493-1526.

Toyoda, K., Horiuchi, H. and Tokonami, M., 1995. Dupal anomaly of the Brazilian carbonatites: geochemical correlations with hotspots in the South Atlantic and implications for the mantle source. Earth and Planetary Science Letters 126, 315-331.

Walter, A.V., Flicoteaux, R., Parron, C., Loubet, M. and Nahon, D., 1995. Rare-earth and isotopes (Sr, Nd, O, C) in minerals from the Juquiá carbonatite (Brazil): tracers of a multistage evolution. Chemical Geology 120, 27-44.

Woolley, A.R. and Kempe, D.R.C., 1989. Carbonatites: nomenclature, average chemical compositions, and element distribution. In: Bell, K. (ed.) Carbonatites: genesis and evolution. Unwin Hyman, London, pp. 1-14.

CARBONATITES FROM THE PARANÁ BASIN: C-O ISOTOPE VARIATIONS

Comin-Chiaramonti, P.[1]; Gomes, C.B.[2] and Censi, P.[3]

1. Dipartimento di Ingegneria Chimica (DICAMP), Trieste University, Piazzale Europa 1, I-34127 Trieste, Italy. comin@univ.trieste.it
2. Instituto de Geociências, Universidade de São Paulo, Rua do Lago 562, 05508-080, São Paulo-SP. cgomes@usp.br
3. Dipartimento di Geologia, Università di Catania, Corso Italia 55, I-95129, Catania, Italy. pcensi@mbox.unict.it

Keywords: Carbonatites, Paraná Basin, O-C isotopes, fractionation model

Carbonatitic complexes show large compositional ranges relative to the oxygen and carbon isotopes. The variations are mostly attributable to 1) magmatic processes, 2) hydrothermal processes, 3) crustal contamination, 4) deuteric processes. Determining to what extent the oxygen and carbon isotope variations are "primary" or related to crustal processes has important implications for evaluating the isotopic characteristics of the source regions (Deines, 1989). In order to address some of these questions, a model of isotopic O-C fractionation relative to the carbonatites from the Paraná Basin (Southern Brazil, Fig. 1), has been developed. The oxygen and carbon isotope data are from borehole and surface specimens. The model of isotopic fractionation of $\delta^{18}O$ and $\delta^{13}C$ is consistent with isotope exchange during fractional crystallization of the carbonatite liquid (magmatic processes) and by isotope exchange between carbonatitic rocks and H_2O-CO_2 fluids at different temperatures and with different H_2O/CO_2 ratios in hydrothermal conditions.

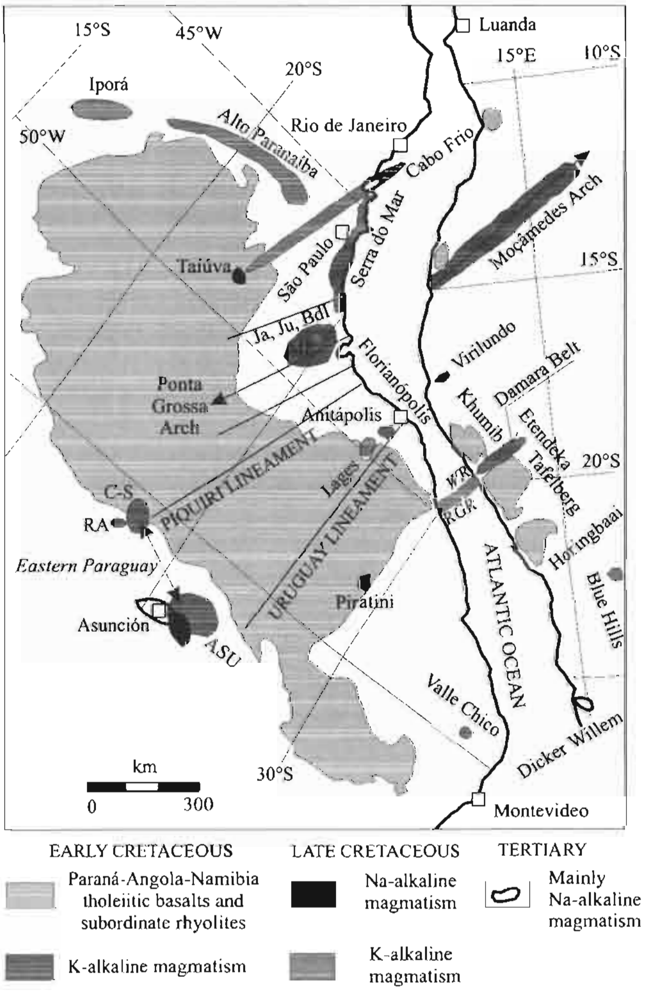

Figure 1. Distribution of the magmatism in the Paraná-Angola-Namibia Province (South American and African plates, Western Gondwana, arranged at about 110 Ma; modified after Comin-Chiaramonti et al., 1997, 1999), and location of the main alkaline-carbonatitic occurrences. Ja, Jacupiranga; Ju, Juquiá; BdI, Barra do Itapirapuã; Mp, Mato Preto; RA, Rio Apa; C-S, Cerros Chiriguelo-Sarambí; ASU, Asunción-Sapucai Province.

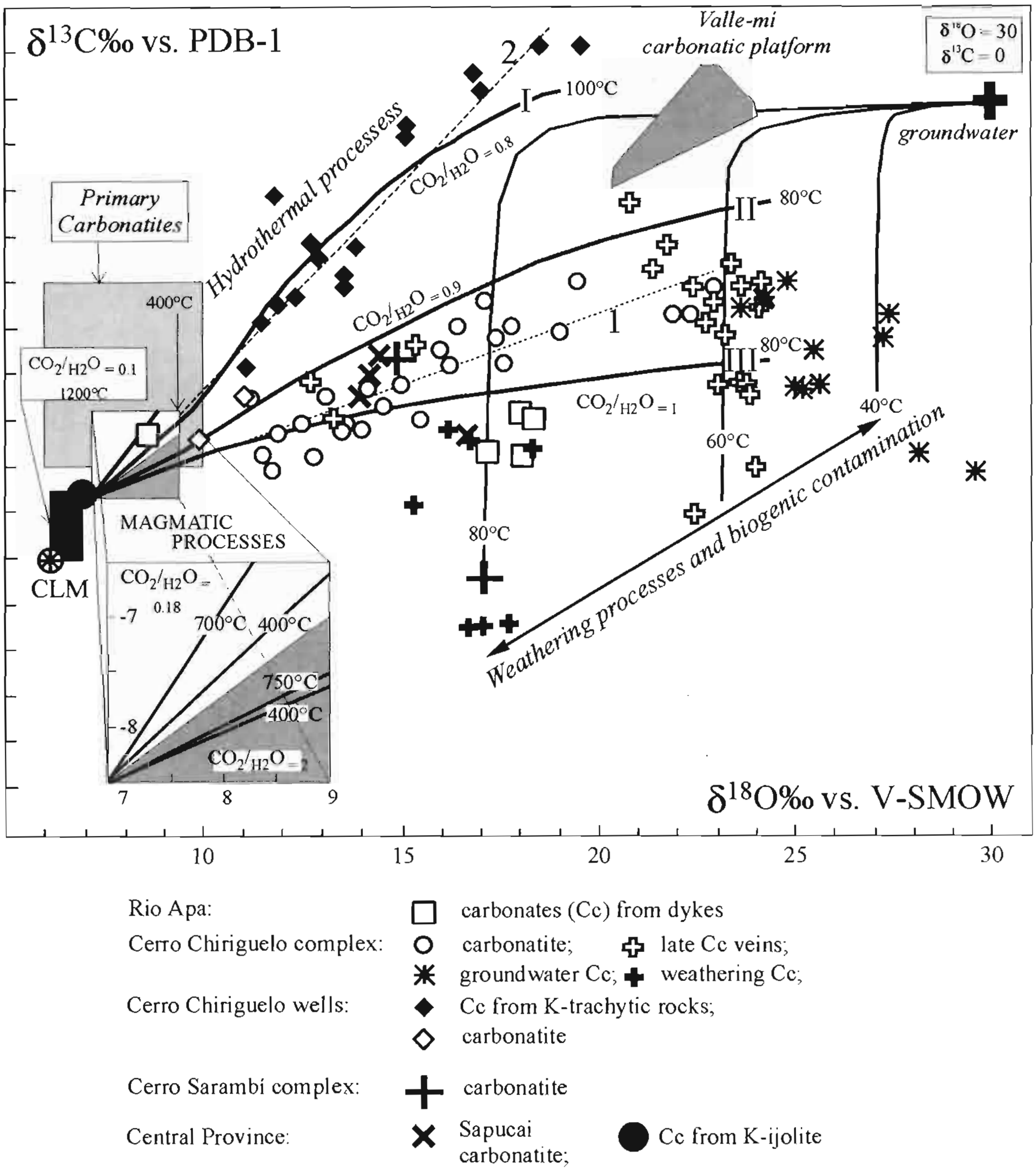

Figure 2. Plot of $\delta^{18}O$ (V-SMOW) vs. $\delta^{13}C$‰ (PDB-1) vs. $\delta^{13}C$ for the primary carbonates and carbonatites from Eastern Paraguay (Early Cretaceous) and evolution of the O-C isotope composition of carbonates (magmatic conditions, i.e. 1200-400°C; hydrothermal environment: I up to 100°C, II and III up to 80°C; low temperature conditions: biogenic component with pH ~ 5 and temperature = 40-80°C). Arbitrary starting compositions: $\delta^{13}O$ = 30‰, $\delta^{18}O$ = 0; cf. Taylor, 1978 and Usdowski, 1982). CLM: continental lithospheric mantle (Kyser, 1990). Cc, carbonates; I and 2: regression lines from field and borehole samples, respectively. Primary carbonatites after Taylor et al. (1967) and Keller & Hoefs (1995). Data source for Valle-mí carbonate platform: Castorina et al. (1996).

The O-C isotope compositions of the carbonatites from the Paraná Basin appear to be in general in agreement with a magmatic origin from hypercrytical fluids with $CO_2/H_2O \sim 0.2$-0.6 molar ratios and temperatures ranging from 700 to 400°C (i.e. "orthomagmatic vs. pegmatitic" environment; cf. Wyllie, 1989). However, significant variations in O-C isotope compositions are noticed in primary carbonates of alkaline rock-types and associated carbonatites and are mainly due to isotope exchange between carbonates and H_2O-CO_2 rich fluids; magmatic processes, i.e. fractional crystallization or liquid immiscibility, probably affect the δ^{18} and δ^{13} values by not more than 2‰. The isotope exchange model implies that the main isotopic variations occurred at low temperatures, in a hydrothermal environment, e.g. in the range 400-80°C, involving fluids with a CO_2/H_2O ratio ranging from 0.8 to 1.

Two main paths of $\delta^{18}O$ and $\delta^{13}C$ fractionation appear to be generated by the emplacement levels (Figs. 2 and 3).

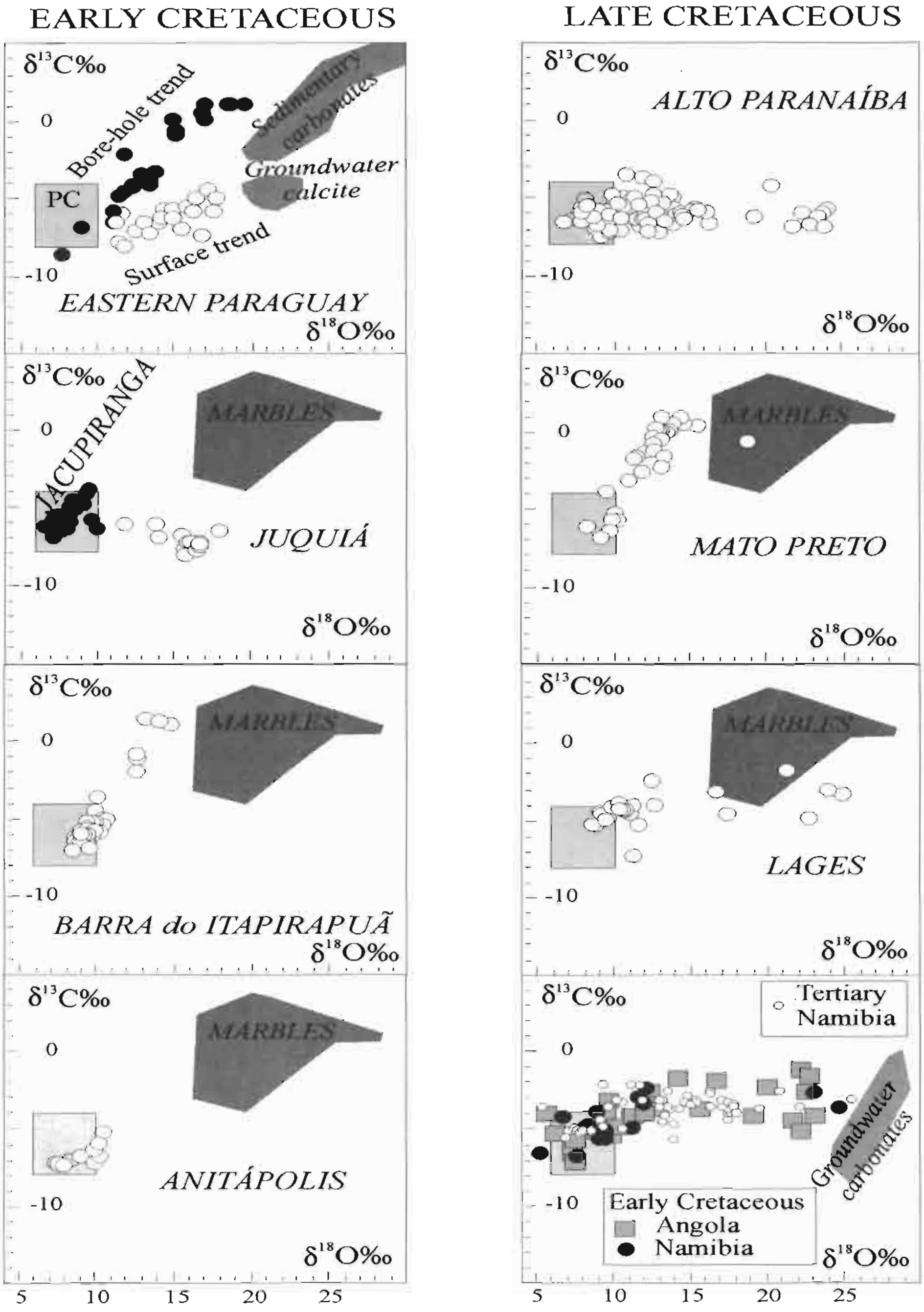

Figure 3. Plot of $\delta^{18}O$‰ (V-SMOW) vs. $\delta^{13}C$‰ (PDB-1) for carbonatites from the PAEP. For comparison the fields relative to sedimentary carbonates, groundwater calcite and marbles are also shown. Data source: Scheibe & Formoso (1982), Censi et al. (1989), Robaina et al. (1991), Reid & Cooper (1992), Castorina et al. (1994, 1997), Huang et al. (1995), Walter et al. (1995), Santos & Clayton (1995), Speziale et al. (1997), Alberti et al. (1999), Ruberti et al. (2002), Comin-Chiaramonti (unpublished data). PC: "primary carbonatite box" (Keller & Hoefs, 1995).

Weathering and groundwater fluids are locally important, as well as meteoric water, which yielded samples strongly enriched in light carbon due to contamination by a biogenic component.

The addition of carbonates from the country rocks to "fresh" and even to "overprinted" carbonatites, as suggested by Santos & Clayton (1995) (e.g. Açunguí Group: $\delta^{18}O = 25.0$ to 24.4 and $\delta^{13}C = 3.5$ to -8.6‰), appears to be unnecessary to explain the considerable enrichment in both heavy oxygen and carbon of some samples. This interpretation is also supported by the initial $^{87}Sr/^{86}Sr$ and $^{143}Nd/^{144}Nd$ isotope ratios of the carbonatites that mantain the same values of the associated alkaline rocks.

REFERENCES

Alberti, A., Castorina, F., Censi, P., Comin-Chiaramonti, P. and Gomes, C.B., 1999. Geochemical characteristics of Cretaceous carbonatites from Angola. Journal of African Earth Sciences 29, 735-759.

Castorina, F., Censi, P., Barbieri, M., Comin-Chiaramonti, P., Cundari, A. and Gomes, C.B., 1994. Carbonatites from the Paraná basin: a 130 Ma transect. International Symposium on the Physics and Chemistry of the Upper Mantle, São Paulo, Extended Abstracts, pp. 52-55.

Castorina, F., Censi, P., Comin-Chiaramonti, P., Gomes, C.B., Piccirillo, E.M., Alcover Neto, A., Almeida R.T., Speziale, S. and Toledo M.C., 1997. Geochemistry of carbonatites from Eastern Paraguay and genetic relationships with potassic magmatism: C, O, Sr and Nd isotopes. Mineralogy and Petrology 61, 237-260.

Censi, P., Comin-Chiaramonti, P., Demarchi, G., Longinelli, A. and Orué, D., 1989. Geochemistry and C-O isotopes of the Chiriguelo carbonatite, northeastern Paraguay. Journal of South American Earth Sciences 3, 295-303.

Comin-Chiaramonti, P., Cundari, A., DeGraff, J.M., Gomes, C.B. and Piccirillo, E.M., 1999. Early Cretaceous-Tertiary magmatism in Eastern Paraguay (western Paraná basin): geological, geophysical and geochemical relationships. Journal of Geodynamics 28, 375-391.

Comin-Chiaramonti, P., Cundari, A., Piccirillo, E.M., Gomes, C.B., Castorina, F., Censi, P., De Min A., Marzoli, A., Speziale, S. and Velázquez, V.F., 1997. Potassic and sodic igneous rocks from Eastern Paraguay: their origin from the lithospheric mantle and genetic relationships with the associated Paraná flood tholeiites. Journal of Petrology 38, 495-528.

Deines, P., 1989. Stable isotope variations in carbonatite. In: Bell, K. (ed.) Carbonatites: genesis and evolution. Unwin Hyman, London, pp. 301-359.

Huang, H-M., Hawkesworth, C.J., Van Calsteren, P. and Mcdermott, F., 1995. Geochemical characteristics and origin of the Jacupiranga carbonatites, Brazil. Chemical Geology 119, 79-99.

Keller, J. and Hoefs, J., 1995. Stable isotope characteristics of recent natrocarbonatites from Oldoinyo Lengai. In: Bell, K. & Keller, J. (eds.) Carbonatite volcanism: Oldoynio Lengai and the petrogenesis of natrocarbonatites. Springer, Berlin, pp. 113-123.

Kyser, T.K., 1990. Stable isotopes in the continental lithospheric mantle. In: Menzies, M.A. (ed.) Continental mantle. Clarendon Press, Oxford, pp. 127-156.

Reid, D.L. and Cooper, A.F., 1992. Oxygen and carbon isotope patterns in the Dicker Willem carbonatite complex, southern Namibia. Chemical Geology 94, 293-305.

Robaina, L.S.S., Formoso, M.L.L. and Spadini, A.R., 1991. Carbonatos reservatório da Formação Macaé, Bacia de Campos, RJ, Brasil. Geochimica Brasiliensis 5, 69-78.

Ruberti, E., Castorina, F., Censi, P., Comin-Chiaramonti, P., Gomes, C.B., Antonini, P. and Andrade, F.R.D., 2002. The geochemistry of the Barra do Itapirapuã carbonatite (Ponta Grossa Arch, Brazil): a multiple stockwork. Journal of South America Earth Sciences 15, 215-228.

Santos, R.V. and Clayton, R.N., 1995. Variations of oxygen and carbon isotopes in carbonatites: a study of Brazilian alkaline complexes. Geoch. et Cosmochimica Acta 59, 1339-1352.

Scheibe, L.F. and Formoso, M.L.L., 1982. Contribuição da geoquímica de terras raras à caracterização dos carbonatitos da Fazenda Varela, Lages, SC. Revista Brasileira de Geociências 12, 553-561.

Speziale, S., Censi, P., Comin-Chiaramonti, P., Ruberti, E. and Gomes, C.B., 1997. Oxygen and Carbon isotopes in the Barra do Itapirapuã and Mato Preto carbonatites (southern Brazil). Mineralogica et Petrographica Acta 40, 1-21.

Taylor, H.P.Jr., Frechen, J. and Degens, E.T., 1967. Oxygen and carbon isotope studies of carbonatites from Laacher See district, West Germany and Alno district, Sweden. Geochimica et Cosmochimica Acta 31, 407-430.

Usdowski, E., 1982. Reaction and equilibria in the system CO_2-H_2O and $CaCO_3$-CO_2-H_2O (0°-50°). A review. Neues Jahrbuch für Mineralogie Abhandlungen 144, 148-171.

Walter A.V., Flicoteaux, R., Parron, C., Loubet, M. and Nahon, D., 1995. Rare-earth elements and isotopes (Sr, Nd, O, C) in minerals from the Juquiá carbonatite (Brazil): tracers of a multistage evolution. Chemical Geology 120, 27-44.

Wyllie, P.J., 1989. Origin of carbonatites: evidence from phase equilibrium studies. In: Bell, K. (ed), Carbonatites: genesis and evolution. Unwin Hyman, London, pp. 500-545.

NEW INSIGHTS ON THE ANDEAN-RELATED SUBCONTINENTAL LITHOSPHERIC MANTLE AND EVIDENCE OF Sr-Nd DECOUPLING

Conceicão, R.V.[1,2]; Koester, E.[2]; Mallmann, G.[3]; Kawashita, K.[2]; Chemale Jr., F.[1,2]; Cingolani, C.[4]; Hervé, F.[5]; Bertotto, G.W.[4]; Schilling, M.[5]; Rodriguez, A.[6]; Weber, M.B.I.[6]; Morata, D.[5] and Espinoza, F.[5]

1. Departamento de Geologia, IG, UFRGS Laboratório de Geologia Isotópica, C.P. 15001, Porto Alegre-RS, Brazil. rommulo.conceicao@ufrgs.br
2. Laboratório de Geologia Isotópica, IG, UFRGS, Brazil. koester@ufrgs.br
3. Programa de Pós-graduação em Geociências, CNPq, IG, UFRGS, Brazil. guilherme.mallmann@ufrgs.br
4. CONICET, Universidad Nacional de La Plata, Argentina. ccingola@cig.museo.unpl.edu.ar, gwbertotto@yahoo.com.ar
5. Universidad de Chile, Chile. mschilling@esfera.cl
6. Universidad Nacional da Colômbia, Colômbia. zafiromerca@hotmail.com, mweber@perseus.unlmed.edu.co

Keywords: Subcontinental lithospheric mantle, South America, isotope geology, Sr-Nd decoupling, mantle xenoliths

INTRODUCTION

The subcontinental lithospheric mantle, assumed to be the portion of the lithosphere below the Mohorovicic discontinuity and above the asthenosphere, can be defined in terms of its chemical, thermal, seismic and/or mechanical properties. Simple petrological and chemical models have been suggested for the bulk composition and mineralogy of the oceanic lithospheric mantle (Ringwood, 1982). However, for the understanding of the subcontinental lithospheric mantle composition and mineralogy, difficulties have arisen due to its long-term evolution and processes responsible for continuous changes of its composition (McDonough, 1990). Some of these processes have been described as metasomatism. Metasomatism is defined as the percolation of fluids or melts through the mantle inducing its compositional, and in some cases mineralogical, modifications. The metasomatic agent has been attributed to products derived either from the asthenosphere underneath or from the subducted crust in compressive regimes. In both cases, and in a simple constrain, the isotopic composition of a lithospheric mantle, initially characterized by depletion of incompatible elements, must change due to incorporation of more radiogenic Sr, but less radiogenic Nd once this mantle undergone es a metasomatic event. This simplistic model assumes that the metasomatic agent will be mixed to the depleted mantle lithosphere by "two-end member simple mixture process" and do not consider chromatographic process that could take place due to the different mineralogy with different partition coefficients related to Sm and Rb. Some authors, however, have been calling attention to this possibility (Navon & Stolpler, 1987; Bedini et al., 1997; Hauri, 1997).

Spinel- and/or garnet-bearing ultrabasic mantle xenoliths brought to the Earth's surface by intraplate alkaline basalts provide direct information on the nature and processes involved in the modifications of the subcontinental mantle lithosphere, such as mantle metasomatism. These xenoliths have been used to identify processes involved in the growth of the continental lithosphere, constrain the tectonic setting of its formation and provide an estimate of the primitive mantle composition. Additionally, geochemical and isotopic studies have been done on these xenoliths in order to provide further insights on the composition of magmas. These studies, however, are based on the hypothesis that some magmas, such as ultrapotassic, kimberlites and some rinds of basalts, could be derived from the lithospheric mantle. This assumes that this part of the mantle is able to melt, in spite of its refractory characteristic, to generate basalts or mantle derived magmas.

Problems in studying mantle xenoliths and processes responsible for the changing of its pristine composition arise from several areas. After the exposition of the xenoliths to the surface, supergenic processes could change its isotopic composition increasing radiogenic Sr and depleting radiogenic Nd. Infiltration of the host material (in general alkali basalts and kimberlitic melt) into the xenoliths will tend to equalize xenoliths isotopic characteristics to the host magma isotopic composition. In general, such evidence has been wrongly used by some authors to argue that the host magma could be generated from a mantle with the same characteristic of the mantle xenoliths included in them. The discrimination of these secondary processes (supergenic and magma infiltration) from the primary processes (depletion event and possible metasomatic events) must be carefully done. The characteristic, origin and how metasomatic agent proceed in the xenoliths must be determined therein.

SOUTH AMERICAN LITHOSPHERIC MANTLE AND THE STUDIED XENOLITHS

The western part of the South American plate is a natural laboratory for petrological investigations of the subcontinental lithosphere due to the complex tectonic arrangement of the Andes. This complexity has its basis on the configuration of an active continental margin in which two oceanic plates (Nazca and Antarctic) with different velocities subduct under a continental margin formed by several events of accretion. Besides that, variation on the subduction angles along the active margin and the presence of seismic and asseismic ridges help to define four distinctive zones of active volcanism (Ramos, 1999): the Northern, Central, Southern and Austral Volcanic Zones (NVZ, CVZ, SVZ and AVZ,

Figure 1. Present geodynamic configuration of the South American continent. Circles indicate localities of studied samples: M – Mercaderes, A – Agua Poca, C – Chile Chico, G – Gobernador Gregores (Lote 17), R – Cerro Redondo. Modified after Ramos, 1999.

respectively, Fig. 1). Flat-slab segments without evidence of volcanism separate these zones, except the SVZ and AVZ that are separated by the subduction of the Chile Seismic Ridge, which comprehend the limit between the Nazca and Antarctic plates. Spinel- and/or garnet-ultrabasic mantle xenoliths are frequently described in all zones associated to alkaline basalts, except in the CVZ where crust appear to be thicker.

This study comprises a synthesis of the observations on 19 ultrabasic mantle xenoliths that came from 5 separate alkaline basalt centers in the Cenozoic to Recent volcanoes from the Andes (infra and back-arc volcanoes in convergent plate areas). Nine of them came from Mercaderes (1° 45' N, 77° 3' E) - Colombia (NVZ), in which 2 samples are spinel-lherzolites and 7 samples are garnet-lherzolites and harburgites. Three samples from Agua Poca (67° 07' W, 37° 01' S), and one sample from Chile Chico (46° 20' S and 71°50' W) came from the SVZ. The other seven samples are spinel-lherzolite and harburgite from the AVZ. They correspond to six samples from Cerro Redondo (70°08' W, 49°07' S), and one sample from Gobernador Gregores (48.5° S, 70.2° W). Fine-grained texture veins filling fractures cutting crystals and matrix indistinctly are ubiquitous in Cerro Redondo xenoliths. Geothermobarometry suggests that these xenoliths crystallized under 1100° to 1200° C and 3 to 4 GPa (grt-peridotites – based on Mercaderes xenolith Weber, 1998) and 815° to 1226°C and 1 to 2 GPa (sp-peridotite - based on data from Cerro Redondo – Schilling, 2002).

Sr AND Nd ISOTOPES

Sr-Nd isotopic data are illustrated in Figure 2a-c. In addition to our results, data from the literature have also been included: basalts and veined- and unveined-, garnet- and/or spinel-xenoliths from Pali Aike (Stern et al., 1990, 1999); basalts and metasomatized (apatite and phlogopite present) xenoliths from Gobernador Gregores (Gorring & Kay, 2000); and anhydrous xenoliths from Mercaderes (Weber, 1998). For comparison, OIB, MORB, BSE and CPB (continental plate basalts) isotopic data are also illustrated.

Tests of basalt contamination into the xenoliths were carried out based on the two-end member mixing (Schilling et al., this symposium). In Figure 2, the samples with evidence of this contamination were drawn with dashed lines. Samples not affected by infiltration of basalts are drawn with solid lines. All xenolith samples contaminated by the host basalts are displaced along the same trend of the mantle-derived magmas from all Andean volcanic zones (Fig. 2a), and in the MORB-OIB-

BSE trend. However, samples not affected by the host basalt plot within or outside these trends. The ones plotted outside the MORB-OIB-BSE trend show enrichment in radiogenic Sr without expressive changes in the Nd isotope ratio (Fig. 2c).

DISCUSSION AND CONCLUDING REMARKS

Our data suggest that isotopic data of mantle xenoliths of the South America plate subcontinental lithosphere plot outside the MORB-OIB-BSE trend. This configuration seems to characterize some kind of mantle process that ends up in enrichment of Sr radiogenic composition, without dramatically changing the Nd isotopic characteristic of the mantle. Such process could be considered as one kind of metasomatic process that involves interaction between a depleted mantle and a metasomatic agent. Carbonatitic melts have been used as a relevant metasomatic agent due to their high Nd/Sr ratios (ranging from 0.01 to 0.18) similar to the ratio observed in some metasomatised xenoliths (around 0.05). However, xenoliths with well-known infiltration of carbonatitic melts from South America are represented in the Figures 2a-c by the xenoliths from Gobernador Gregores and some samples of Pali Aike peridotite. Gobernador Gregores samples usually plot to the left of the MORB-OIB-BSE trend in spite of the carbonatite influence, while one sample from Pali Aike plots to the right side. The Gobernador Gregores sample analyzed in this study does not show any vestiges of modal metasomatism characterized by the crystallization of carbonate. However, it plots far right in the diagram (Fig. 2). This observation demonstrates that the influence of carbonatitic melts as metasomatic agent result in a different isotopic signature of the whole rock peridotite, enriching or not the Sr radiogenic composition and that it could not be considered a general process.

The understanding of the metasomatic process requires more than two-end member mixing processes does. Our data suggest that metasomatism in these peridotites resulted in some kind of Sr and Nd decoupling that occurred possibly due to different Rb and Sm partition coefficients of some minerals present in the xenoliths, such as clinopyroxene, orthopyroxene and garnet. Samples from Eastern China (Tatsumoto et al., 1992) and the North Atlantic region (Ionov et al., 2002) are also displayed on Figure 2c (a and b fields) for comparison. These samples present model metasomatism characterized by phlogopite and/or amphibole crystallization and also plot to the right side of the MORB-OIB-BSE trend. To explain this behavior, several authors as Navon & Stolper (1987), Bedini et al. (1997), and Hauri (1997) also suggest the Nd-Sr decoupling in the course of metasomatism. A better understanding of this process is required in order to constrain it.

ACKNOWLEDGEMENTS

This research was supported by funding from CNPq - PROSUL (project AC-74) and we are grateful to the facilities available in the Laboratório de Geologia Isotópica of Universidade Federal do Rio Grande do Sul.

REFERENCES

Bedini, R.M., Bodinier, J. -L., Dautria, J. -M. and Morten, L. 1997. Evolution of LILE-enriched small melt fractions in the lithospheric mantle: a case study from the East African Rift, 153: 67-83

Gorring, M.L., Kay, S.M. 2000. Carbonatite metassomatized peridotite xenoliths from southern Patagonia: Implications for lithospheric process and Neogene plateau magmatism. Contributions to Mineralogy and Petrology, 140:55-72.

Hauri, E.H. 1997. Melt migration and mantle chromatrography, 1: simplified theory and conditions for chemical and isotopic decoupling. EPSL, 153: 1-19.

Ionov D. A., Mukasa, S.B., Bodinier, J-L 2002. Sr-Nd-Pb isotopic composition of peridotite xenoliths from Spitsbergen: numerical modelling indicates Sr-Nd decoupling in the mantle by melt percolation metasomatism. J. Petrol. 43: 2261-2278.

McDonough, 1990. Constraints on the composition of the continental lithospheric mantle. EPSL, 101:1-18.

Mercier, J.C.C. and Nicolas, A. 1975. textures and fabrics of upper-mantle peridotites as illustrated by xenoliths from basalts. J. Petrol. 16: 454-487.

Navon, O. and Stolper, E. 1987. geochemical consequences of melt percolation: the upper mantle as a chromatographic column. J. Geol. 95: 285-307, 1987,

Ramos, V.A. 1999. Plate tectonic setting of the Andean Cordillera. Episodes 22 (3): 183-190.

Ringwood, A.E. 1982. Phase transformations and differentiation in subducted lithosphere: Implications for the mantle dynamics, basalt petrogenesis, and crustal evolution, J. Geol., 90, 611-643.

Schilling, M. 2002. Estudio petrogáfico y geoquímico de enclaves ultramáficos incluídos en basalto alcalino Plioceno-pleistoceno de Cerro Redondo (49°07'S-70°08'W), en la provincia de Santa Cruz, Patagonia Argentina: Memoria, Universidad de Chile, 84p. (unpublished).

Stern, C.R., Frey, F.A., Kiyoto F., Zartman, R.E., Peng, Z., Kyser, T.K. 1990. Trace element and Sr, Nd, Pb, and O isotopic composition of Pliocene and Quaternary alkaline basalts of the Patagonia Plateau lavas of southernmost South America. Contrib. Mineral. Petrol. 104: 294-308.

Stern, C.R.; Killian, R.; Olker, B.; Hauri, E.H.; Kyser, T.K. 1999. Evidence from mantle evolution for relatively thin (<100 km) contiental lithosphere below the Phanerozoic crust of souhternmost South America. Lithos, 48:217-235.

Tatsumoto M., Basu. A.R. Wankang, H., Junwen, W., Guanghong, X., 1992. Sr, Nd and Pb isotopic of ultramafic xenoliths in volcanic rocks of Eastern China: enriched components EMI and EMII in subcontinental lithosphere. EPSL, 113: 107-128.

Weber, M.B.I. 1998. The Mercaderes-Rio Mayo xenoliths, Colombia: Their bearing on mantle and crustal processes in the Northern Andes. PhD Thesis, University of Leicester, UK, 277p.

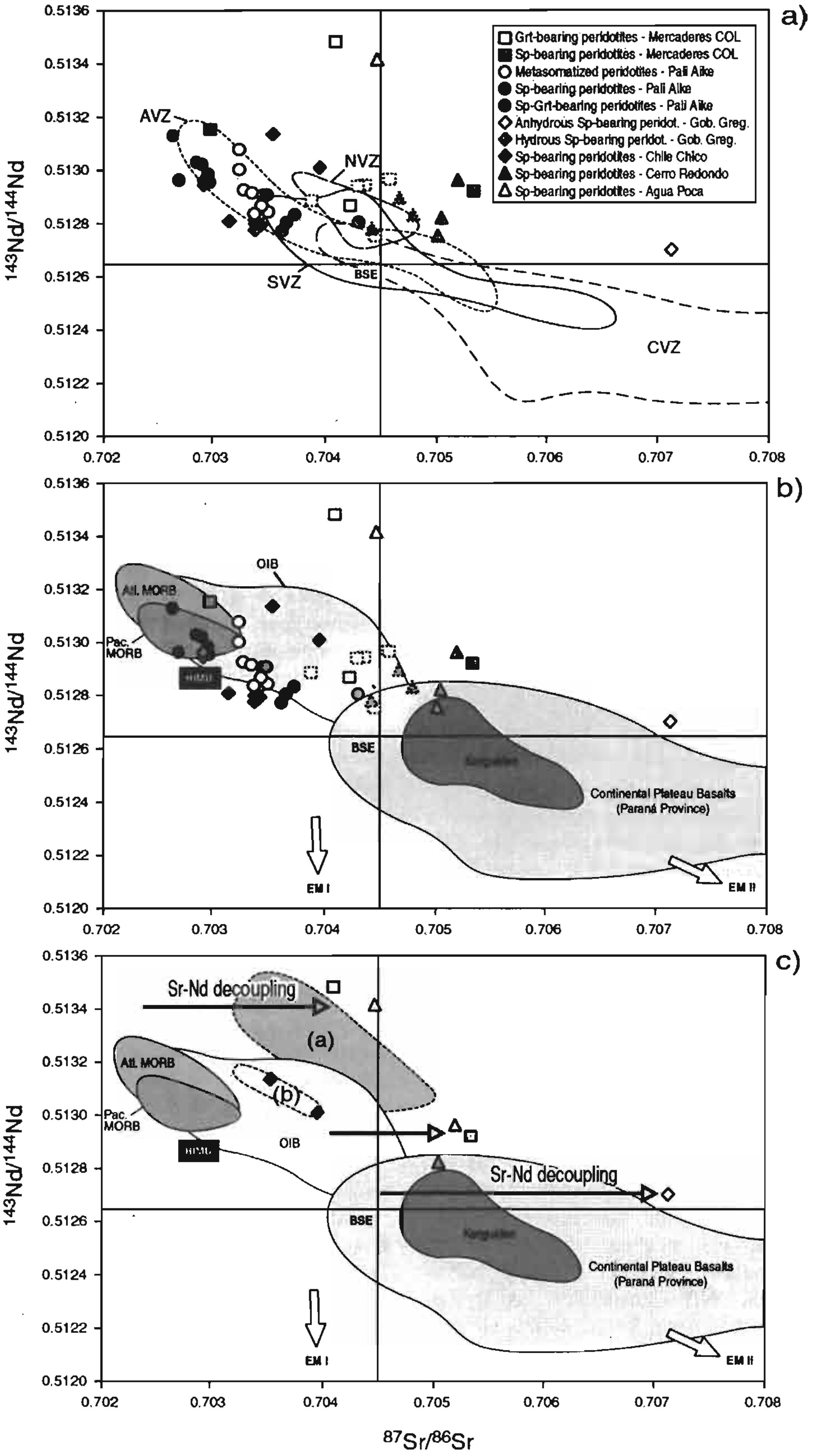

Figure 2. Isotope data (this work and from literature) for South American lithospheric mantle xenoliths. Samples with basalt contamination are drawn with dashed lines. NVZ, CVZ, SVZ and AVZ refer to volcanic areas of South America. Tectonic setting fields are compiled from "http://georoc.mpch-mainz.gwdg.de/". OIB-field draw using Hawaii, La Palma, Azores, St. Helena, Easter and Ascension islands. In figure 2c, fields a and b correspond to Eastern China (Tatsumoto et al., 1992) and North Atlantic (Ionov et al., 2002), respectively. Pali Aike-field drawn from Stern et al. (1999), and Gobernador Gregores-field (hydrous xenoliths) from Gorring & Kay (2000).

NEW Pb-Pb EVAPORATION AGE ON ZIRCON OF NORDESTINA BATHOLITH, NORTHEAST OF BAHIA STATE, BRAZIL

Cruz Filho, B.E.[1,3]; Rosa, M.L.S.[2,3]; Conceição, H.[3]; Macambira, M.J.B.[4]; Scheller, T.[4]; Rios, D.C.[3] and Marinho, M.M.[5,3]

1. Curso de Pós-Graduação em Geologia; IGEO-UFBA. basilio@ufba.br
2. Pesquisadora do CNPq. lourdes@cpgg.ufba.br
3. Grupo de Petrologia Aplicada a Pesquisa Mineral – GPA; CPGG; IGEO-UFBA. herbet@pppg.ufba.br, debora@cpgg.ufba.br
4. Laboratório de Geologia Isotópica (PARÁ-ISO)-UFPA. moamac@ufpa.br
5. Companhia Baiana de Pesquisa Mineral – CBPM. cbpmdt@cbpm.com.br

Keywords: Nordestina, trondhjemite, Paleoproterozoic, zircon, ages

INTRODUCTION

This work presents new single-zircon $^{207}Pb/^{206}Pb$ age determinations for Nordestina Batholith (NB; ~ 720 km^2), which is an intrusion located in the central portion of Serrinha Nucleus (SerN), in northeastern São Francisco Craton, Bahia State, Brazil (Fig. 1A). It intrudes the gneissic-migmatitic Archaean basement and the volcano sedimentary sequences of the Rio Itapicuru Greenstone Belt (RIGB).

GEOLOGICAL FEATURES

The NB shows a north-south elongated shape, associated with concentric magmatic foliation, which becomes more intense towards the border, it is interpreted as the result of syn-tectonic emplacement and correlated with the compressional Transamazonic event responsible for the closure of the Rio Itapicuru Basin. In this trondhjemitic batholith there are two predominant lithologies: (i) medium-grained phaneritic rocks; and (ii) porphyritic rocks, limited to the central portion of the massif. Granitic dykes and dioritic enclaves are subordinate lithotypes of this batholith. It is composed essentially of zoned oligoclase and quartz, with subordinate biotite, microcline and hornblende. Common accessories are titanite, apatite, zircon, and allanite.

The studied trondhjemitic rocks show a narrow range of SiO_2 contents (68-72 wt. %), low FeO, MgO and TiO_2, high Al_2O_3 (15-17 wt. %), fractionated REE patterns, weak and variable Eu anomalies, and La and Yb contents similar to those reported for the Archaean trondhjemites of East Finland. Geochemically, the trondhjemite is low-K calc-alkaline, plotting in the volcanic arc granites field of Pearce et al. (1984). Silva (1991) suggested that NB geochemical data are comparable to those of the coeval 2.1 Ga felsic-volcanic rocks of RIGB.

ANALYTICAL TECHNIQUES

One sample rock (1851) collected in the central portion of the NB was selected for $^{207}Pb/^{206}Pb$ single zircon evaporation analyses. The sample is a biotite-trondhjemite which was prepared using standard techniques of crushing and mineral separation in the laboratories of the UFBA Geochemical Department.

Zircon crystals were hand-picked from the least magnetic fractions and loaded on a canoe-shaped Re filament.

The single zircon Pb-evaporation analyses (Kober, 1986) were carried out at the Isotopic Laboratory of Pará (PARAISO), at the Federal University of Pará (Bélem/Brazil) on a Finnigan MAT 262 thermal ionization mass spectrometer (TIMS) following the routine procedure established at the Pará-Iso. uncertainties on zircon ages are reported as 2σ (±95% of precision).

RESULTS

Sample 1851, selected for Pb-Pb age, is located at the Sítio das Flores Villa in the central part of the NB (Fig.1B). It is a medium to coarse-grained isotropic biotite-trondhjemite displaying a porphyritic texture with plagioclase megacrystrs up to 4 cm. It contains 60% oligoclase, 30% quartz, 4% biotite, 5% microcline and 1% accessory mineral (titanite, apatite and zircon).

The analyzed crystals are prismatic, with length/width ratios varying between 3:1 and 2:1, transparent to translucent, faintly colored in shades of brown. Microfratures or translucent borders indicative of incipient metamictic alteration were observed in a few crystals.

Of the nine zircon crystals analyzed, three did not contain enough Pb for analysis. Only four analyzed crystals presented good analytical results in only one temperature stage, supplying very coherent ages between 2.14 and 2.16 Ga. These four temperature steps corresponding to 106 isotopic ratios were used to calculate a average age of 2155 ± 9 Ma (MSWD = 3.3) what is intermeted as the minimum age of crystallization of the central part of BN (Fig. 2).

The ages obtained by crystals 1851/2 and 1851/3 were discarded because of discrepant results in relation to the ages of the other zircon crystals, associate to this fact the first step of temperature of these crystals supplied high ($^{204}Pb/^{206}Pb$) ratios > 0.012.

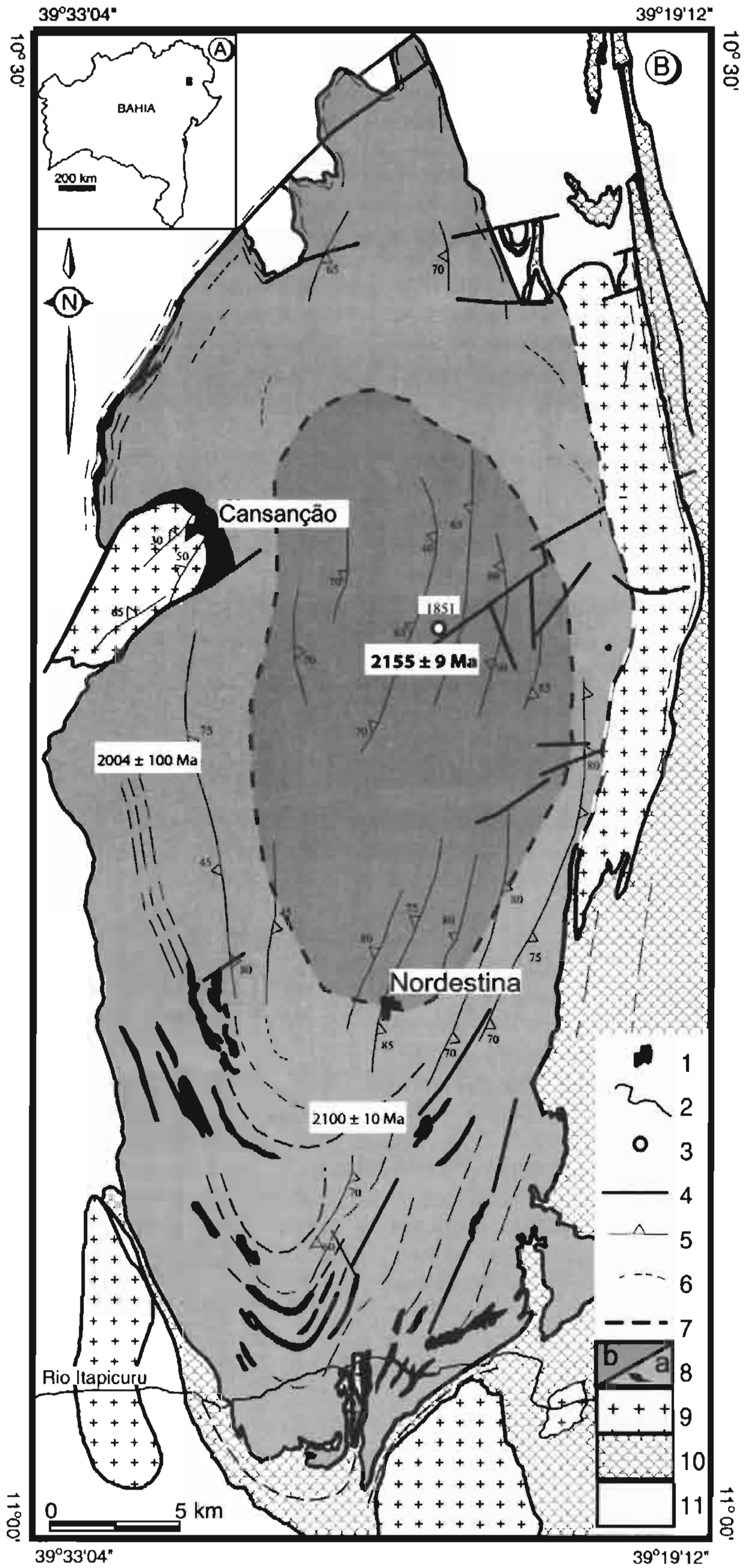

Figure 1. (A) Location of the study area in Bahia State (Brazil). (B) Simplified geological map of the Nordestina Batholith showing sample localities. 1. Cities; 2. River; 3. Sample with isotopic results; 4. Fault and Fractures; 5. Foliations; 6. Inferred foliations; 7. Geological contact; 8. Nordestina Batholith: (a) Medium-grain Facies (FFM), (b) Porphyritic facies (FP); 9. Paleoproterozoic granites; 10. GBRI; 11. Basement.

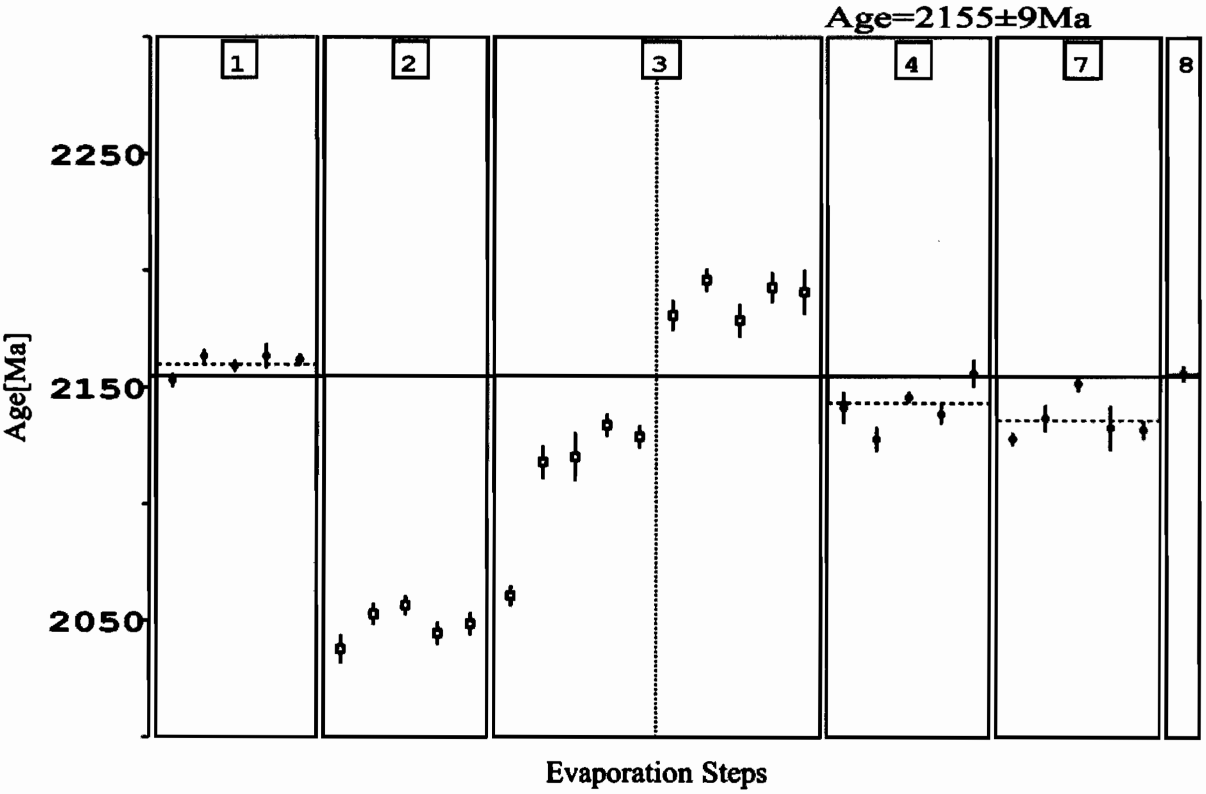

Figure 2. Age *vs.* evaporation steps diagram for zircon crystals from the Nordestina Batholith. Full circle = analyzed zircon grains; square boxes = subjectively eliminated date; bar = 2σ. The zircon´s number are indicated.

CONCLUSIONS

Other $^{207}Pb/^{206}Pb$ ages have also been reported for the NB. Alves da Silva (1994) found an age of 2100 ± 10 (1σ) Ma (Fig. 1B) from a sample located to the south of Nordestina, Rios et al. (1998) measured an age of 2004 ±100 (1σ) for a sample located next to Cansanção town. This latter age show a greater error but overlap within error bars with the former age.

These ages suggest that the central part (2155 ± 9 Ma) is older than the borders (2100 ± 10 Ma), but such a geochronological argument is not consistent with the geochemical model mesented by Cruz Filho (2003) indicating that the former was produced by fractional crystallization of the latter.

ACKNOWLEDGMENTS

This research is supported by the Companhia Baiana de Pesquisa Mineral - CBPM, the Conselho Nacional de Desenvolvimento Científico e Tecnológico (CNPq). This is the contribution number 142-2003 of the Applied Petrology Group (GPA).

REFERENCES

Alves da Silva, F.C., 1994. Étude Structural do "Greenstone Belt" Paleoproterozoïque du Rio Itapicuru (Bahia Brésil). Tese de Doutorado. Université d'Orleans. France. 307 p.

Cruz Filho, B.E.; Conceição, H.; Rios, D.C.; Silva Rosa, M.L.; Marinho, M.M. 2000. Geologia, Petrografia e Litogeoquímica do Batólito Trondhjemítico Nordestina, Núcleo Serrinha, Nordeste da Bahia-Brasil. Revista Brasileira de Geociências (submited).

Köber, B.,1986. Whole-grain evaporation for 207Pb/206Pb age investigation on single zircon using a double filament thermal ion source. Cont. Min. Petrol., 93:482-490.

Pearce, J.A.; Harris, N.B.W.; Tindle, A. D.,1984. Trace elements discrimination diagrams for the tectonic interpretation of rocks. J. Petrol. 25:956-983.

Rios, D.C.; Conceição, H.; Macambira, M.J.B.; Burgos. C.M.G.; Peixoto, A.A.; Cruz Filho, B.E.; Oliveira, L.L.; Lisboa, M.P., 1998. Granitogênese da parte meridional-oriental do Núcleo Serrinha: idade, petrografia e geoquímica. In: Conceição, H; Cruz, M.J.M; Sá, H,J.S.; Sabaté, P. (Eds.) Contribuição ao Estudo dos Granitos e Rochas Correlatas. Pub. Esp. SBG, Núcleo Bahia-Sergipe. 5: 91-113.

Silva, M.G., 1991. Evidências de uma tectônica de colisão-subducção no Proterozóico Inferior do Estado da Bahia. Simp. de Geol. do NE, Recife-PE, SBG, Anais:216-219.

Sm-Nd ISOTOPIC CONSTRAINTS ON THE ORIGIN OF NORDESTINA BATHOLITH, NORTHEAST OF BAHIA STATE, BRAZIL

Cruz Filho, B.E.[1,3]; Rosa, M.L.S.[2,3]; Conceição, H.[3]; Macambira, M.J.B.[4]; Scheller, T.[4]; Rios, D.C.[3] and Marinho, M.M.[5,3]

1. Curso de Pós-Graduação em Geologia; IGEO-UFBA. basilio@ufba.br
2. Pesquisadora do CNPq. lourdes@cpgg.ufba.br
3. Grupo de Petrologia Aplicada a Pesquisa Mineral – GPA; CPGG; IGEO-UFBA. herbet@pppg.ufba.br, debora@cpgg.ufba.br
4. Laboratório de Geologia Isotópica (PARÁ-ISO)-UFPA. moamac@ufpa.br
5. Companhia Baiana de Pesquisa Mineral – CBPM. cbpmdt@cbpm.com.br

Keywords: Batholith, trondhjemite, Paleoproterozoic, zircon, ages

INTRODUCTION

In order to contribute to the understanding of the age and origin of Nordestina Batholith, new zircon Pb–Pb geochronologic data (Cruz Filho et al., in this volume) and whole-rock Nd isotopic characteristics were obtained.

The Nordestina Batholith (NB) is situated in the central part of the Serrinha Nucleus (SerN), a geotectonic unit of the northeastern portion of the São Francisco Craton, northeast Bahia State, Brazil (Fig.1A). The SerN is composed of an Archean gneissic-migmatitic basement, covered by supracrustal belts that are the Paleoproterozoic volcanosedimentary sequences of the Capim Group and Rio Itapicuru Greenstone Belt (IRGB), and intruded by a wide range of granites. Geochemical and geochronological data show that the Paleoproterozoic granites of the SerN include large volumes of calc-alkaline granitoids (2.12-2.10 Ga) and alkaline granitoids (2.10-2.07 Ga) (Rios, 2002).

Although the granites are widespread, representing approximatly one third of the exposed rocks of the SerN, their sources are still not well understood.

GENERAL FEATURES AND AGE

The NB underlies an area of nearly 720 km^2 representing the largest granitic body of the area. It intruded both the IRGB and basement terrains (Fig.1B). It is a hololeucocratic rock that is texturally medium to coarse grain sized and exhibits porphyritic subhedral to anhedral fabric in the central portion. The NB rocks frequently enclose mafic enclaves. The NB has a ^{207}Pb/^{206}Pb minimum zircon age of 2155 ± 9 Ma.

Rocks of the NB have trondhjemitic composition. Zoned oligoclase and quartz are the main minerals, while microcline is absent or occurs only subordinate amounts (< 5%). Biotite (< 10%) is the mafic main whereas hornblende is rare. Accessories are apatite, zircon, and allanite.

In terms of chemical composition the NB rocks show: SiO_2 (68 to 72%), MgO (0.6 to 1.10 %), K_2O (1.1 to 2.3%) and K_2O/ Na_2O (0.2 to 0.4), enrichment in Ba ($\approx$ 451ppm); Zr ($\approx$184 ppm) and Sr ($\approx$ 412 ppm), and they have medium to low contents of Rb ($\approx$ 75 ppm), Nb ($\approx$ 10 ppm) and Y ($\approx$ 8 ppm), fractionated rare earth elements (REE) patterns, weak and variable Eu anomalies, and La and Yb contents similar to those reported for the Archaean trondhjemites of East Finland. They are low potassium calc-alkaline, and show metaluminous to weakly peraluminous character. Geochemical data confirm their volcanic arc signature, as observed in the other trondhjemite (Pearce et al., 1984). Silva (1991) suggested that geochemical data for the Paleoproterozoic calc-alkaline granites are comparable to those coeval 2.1 Ga felsic-volcanic rocks of the IRGB.

ANALYTICAL METHODS

Nd analyses were performed on three representative samples of the NB (Fig. 1B). They were crushed using a hydraulic press and a representative fraction was powered in a tungsten carbide shatterbox in the Laboratories of the UFBA Geochemical Department.

Procedures for dissolution of whole-rock powders, Sm and Nd separation, and mass spectrometric techniques were carried out at the Laboratory of Isotopic Geology of the Federal University of the Pará (Pará-Iso). About 50 mg of sample, mixed with 100 mg spike, was dissolved using HF–HNO_3 (3:1) in PARR bomb dissolution. The sample was then attacked with 6.2N HCl to dissolve remaining residue. Chemical separation of Sm-Nd was done in two steps, first an ion exchange resin was employed for separation of the REE, and then, Sm and Nd were extracted using teflon powder-supported HDEHP. A MAT 262 mass spectrometer was used to determine the Sm and Nd contents as well as the isotopic ratios of the whole-rock samples.

Isotopic ratios ^{143}Nd/^{144}Nd are useful to calculate model ages (T_{DM}), considered as representative of time when crustal materials were segregated depleted upper mantle. The notation of ε_{Nd} was defined as: ε_{Nd} = [(^{143}Nd/^{144}Nd)s / (^{143}Nd/^{144}Nd)$_{CHUR}$ – 1)] x 10000, where s = sample, ^{143}Nd/^{144}Nd)$_{CHUR}$ = 0.512638. Sm–Nd model ages can be calculated in two ways in function of the $f_{Sm/Nd}$ factor {= [((^{147}Sm/^{144}Nd)s / (^{147}Sm/^{144}Nd)$_{CHUR}$) – 1)], where where s = sample, (^{147}Sm/^{144}Nd)$_{CHUR}$ = 0.1967}. The one-stage model age (T_{DM-1}) is calculated when $f_{Sm/Nd}$ is within the -0.45±0.10 interval in granitoid rocks, indicating that there was little or no Sm-Nd fractionation during magma genesis. When $f_{Sm/Nd}$ is out side that interval it is common by assumed that chemical fractionation event of Sm-Nd took place, possibly during partial melting of crustal protholith previously recycled and enriched (e.g. Sato & Siga Junior, 2000). In this case, model ages may be calculated using a double stage model (T_{DM-2}).

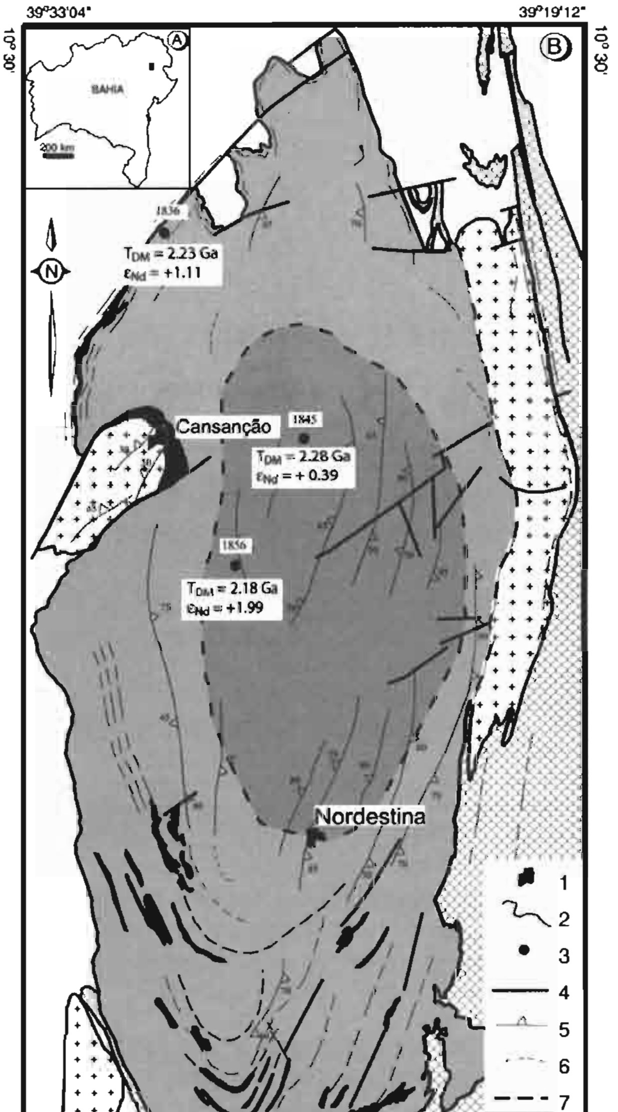

Figure 1. (A) Location of the study area in Bahia State (Brazil). (B) Simplified geological map of the Nordestina Batholith showing sample localities. 1. Cities; 2. River; 3. Sample with isotopic results; 4. Fault and Fractures; 5. Foliations; 6. Inferred foliations; 7. Geological contact; 8. Nordestina Batholith: (a) Medium-grain Facies (FFM), (b) Porphyritic facies (FP); 9. Paleoproterozoic granites; 10. GBRI; 11. Basement.

In this research, $f_{Sm/Nd}$ values are between -0.44 and -0.50 and suggest that significant fractionation did not occur in the Sm–Nd system during the process of formation of the magmas from which the NB crystallized.

Sm-Nd model ages were calculated based on the depleted mantle (T_{DM-1}) assuming a linear Nd isotopic growth. The equation used is:

$$T_{DM} = 1/\lambda \ \{1 + [(^{143}Nd/^{144}Nd)s - 0.513114]/[(^{147}Sm/^{144}Nd)s - 0.222]\}.$$

The decay constant (λ of ^{147}Sm used in age calculations is 0.00654 Ga-1.

RESULTS AND CONCLUSIONS

The NB rocks have εNd (2155 Ma) values between + 0.39 and +1.99, indicating their relatively juvenile, rather than recycled, character. The model ages range between 2.18 to 2.23 Ga.

The difference between Sm-Nd model ages (TDM) - accretion event - and rock formation age T(Pb-Pb in monozircon) range between 0.020 and 0.13 Ga.

In general, the trondhjemitc rocks are assumed to be generated through partial melting of a tholeiite transformed into garnet-bearing amphibolite or eclogite (e.g. Martin, 1987).

The Nd model ages of the NB rocks indicate that the magmas that generated these rocks evolved from Paleoproterozoic mafic protoliths with a short crustal residence time.

ACKNOWLEDGMENTS

This research was support by the Companhia Baiana de Pesquisa Mineral - CBPM, the Conselho Nacional de Desenvolvimento Científico e Tecnológico (CNPq). This is the contribution number 141-2003 of the Applied Petrology Group (GPA).

REFERENCES

Alves da Silva, F.C., 1994. Étude Structural do "Greenstone Belt" Paleoproterozoique du Rio Itapicuru (Bahia Brésil). Tese de Doutorado. Université d'Orleans. France. 307 p.

Martin, H., 1987. Petrogenesis of Archaean trondhjemites, tonalites, and granodiorites from eastern Finland: major and trace element geochemistry. J. Petrol. 28: 921-953.

Pearce, J.A.; Harris, N.B.W.; Tindle, A. D., 1984. Trace elements discrimination diagrams for the tectonic interpretation of rocks. J. Petrol. 25:956-983.

Rios, D.C., 2002. Granitogênese no Núcleo Serrinha, Bahia, Brasil: geocronologia e litogeoquímica. Tese de Doutorado. Universidade Federal da Bahia. 239p.

Sato, K. & Siga Junior, O. 2000. Evidence of the superproduction of the continental crust during paleoproterozoic in south american platform. Implications regarding the interpretative value of the Sm-Nd model ages. Revista Brasileira de Geociências, 30(1):126-129.

Silva, M.G., 1991. Evidências de uma tectônica de colisão-subducção no Proterozóico Inferior do Estado da Bahia. Simp. de Geol. do NE, Recife-PE, SBG, Anais:216-219.

GEOCHRONOLOGY OF CERNE GRANITE (APIAÍ FOLDED BELT, SOUTHEAST BRAZIL) – INTERPRETATION OF DISCORDANT U-Pb ZIRCON AGE

Cury, L.F.; Siga Jr., O.; Sato, K.; Prazeres Filho, H.J.; Basei, M.A.S.; McReath, I. and Onoe, A.T.

Instituto de Geociências – USP. Rua do Lago 562, Cidade Universitária – São Paulo-SP, 05508-080.
leonardocury@ip2.com.br

Keywords: U-Pb (zircon), discordant ages, late to pos-orogenic granites

The Apiaí Folded Belt (as defined by Hasui et al., 1975) configures an extensive NE-SW oriented domain, located in the eastern of Paraná State (Southeastern Brazil). It is constituted by meso to supracrustal rocks, deformed and metamorphosed at greenschist to amphibolite facies, intruded by Paleoproterozoic and Neoproterozoic granitic batholiths and stocks.

The Cerne Granite (Fig. 1) covers an area of approximately 45 km^2, being recognized like one of most expressive granitic intrusions of Apiaí Folded Belt. It is constituted mainly by syenogranites with microcline, quartz, plagioclase An $_{7-10}$, green biotite, Ca-amphibole and opaque (magnetite, ilmenite and pyrite). The accessory phases are represented by sphene, apatite, fluorite, zircon and allanite. Others terms like monzogranites and quartz-syenites are subordinated. Those rocks show a medium to coarse inequigranular texture, characterized by megacrystals of microcline (up to 2cm), with solid to slightly magmatic flow structures. Other feature often recognized in the intrusion is microcrystalline mafic enclaves with syenitic composition, in spherical forms and centimeter sizes. In the granite border areas a restricted deformation is expressed by protomylonitic to mylonitic structures, always in small narrows (metric scale) between the contacts of the intrusion with the surrounding rocks.

According to Prazeres Filho (2000), the Cerne Granite represents an alkaline magmatism phase (shoshonitic character), late to pos-orogenic in relation to the Neoproterozoic Três Córregos-Cunhaporanga magmatic arc.

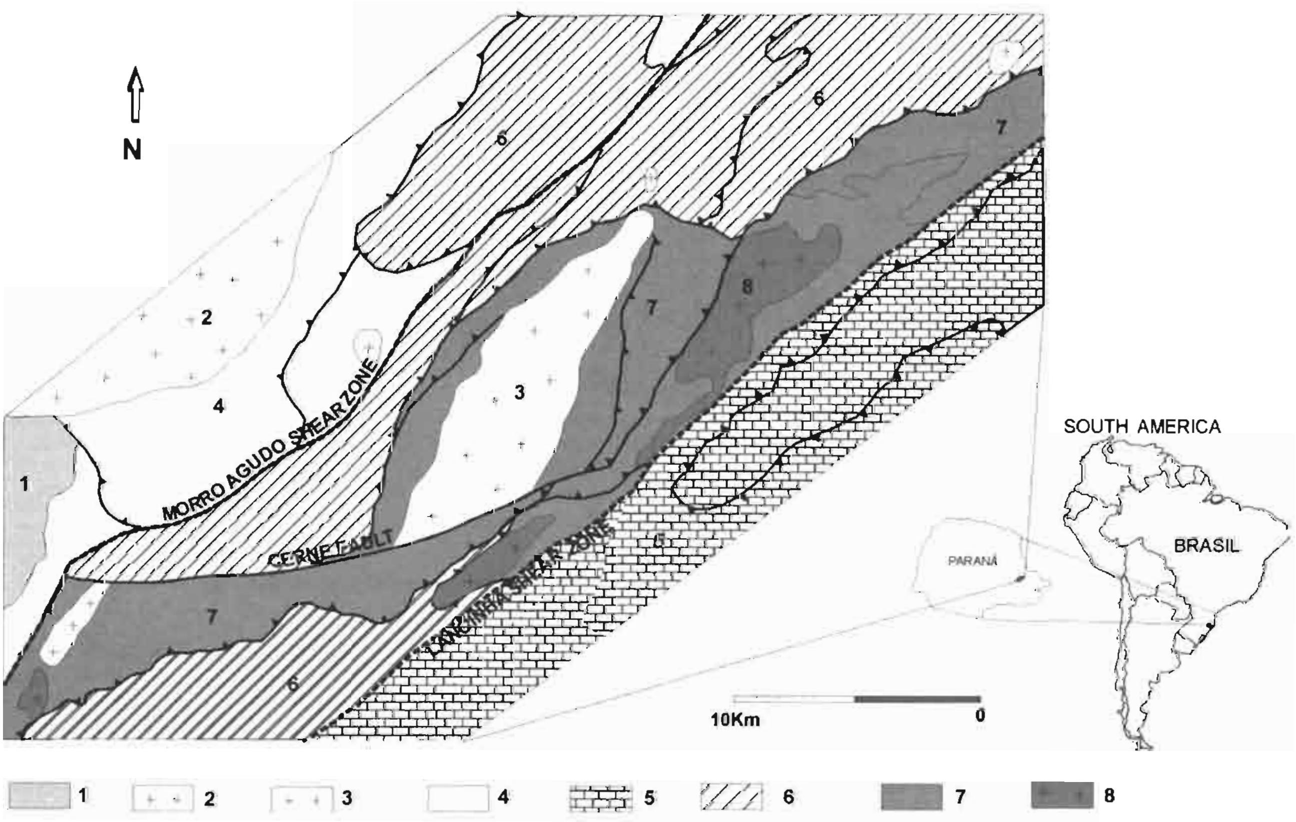

Figure 1. Geological sketch of Apiaí Folded Belt southern portion. (1) Camarinha Formation; (2) Três Córregos Granitic Batholith; (3) Cerne Granite; (4) Água Clara Formation; (5) Capirú Formation; (6) Votuverava Formation; (7) Betara Formation; (8) Alcaline Deformed Granitoids.

The intrusion shows an ellipsoidal form, elongated according to the regional structural trend (NE-SW). The contact areas between granite ad surrounding rocks are often made by high angle shear zones (75-90°) and unusually show evidences of thermal metamorphism. The granitic body is located in antiformal folds originated by the displacement of dextral faults and adjacent shear zones (Lancinha Shear Zone, Morro Agudo Shear Zone and Cerne Fault). Fiori (1990, 1993) suggests that Cerne Grantie was contemporaneous to the development of the shear zones in ductile conditions, through a process of simple shear acquiring the present ellipsoidal form.

We documented geochronological dates of Cerne Granite by integrated U-Pb (zircon) conventional, Pb-Pb (zircon) evaporation, Ar-Ar (biotite) and Sm-Nd (whole rock) methods, accomplished in three samples from the different facies of the intrusion. The samples represent the granite with microcrystalline enclaves (CER-15), the isotropic sienogranite (CER-16) and the monzogranite (CER-23). The three samples seemingly contain the same zircon types. This typology study of the zircons was accomplished with the aid of cathode luminescence images.

The U-Pb (zircon) conventional ages obtained in the Cerne Granite are characterized by the great discordance of zircon fractions and, consequently, by the high error. The Concordia Diagram (Fig. 2) to the three samples of the Cerne Granite defines lower intercept age about of 563±34Ma and upper intercept age about of 2518±150Ma. The lower intercept age is interpreted as Cerne Granite crystallization age, supported by Ar-Ar (biotite) age about of 557±2Ma (CER-16 sample). The upper intercept age seems to be geological meaningless.

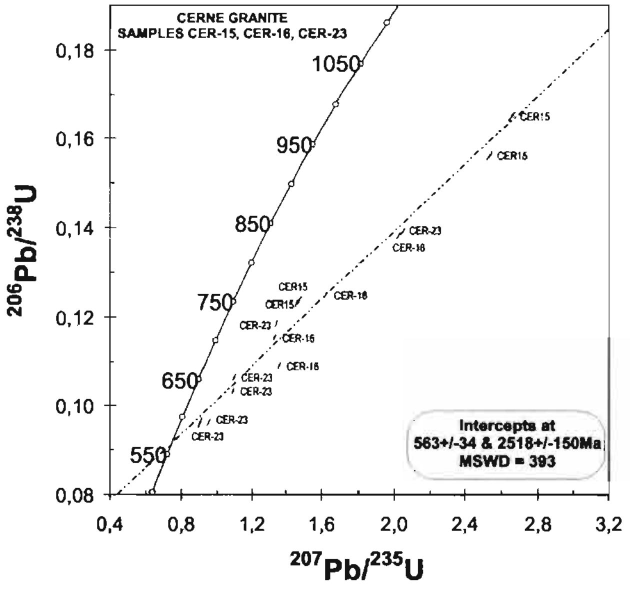

Figure 2. Concordia Diagram for samples of the Cerne Granite.

The most frequent zircons (type 1) are prismatic transparent crystals with few inclusions and weight between 0.1 and 1μg, showing length - width proportion between 2:1 and 4:1 (Fig. 4). The cathode luminescence images (Fig. 3) allow recognized sub-types of this zircon population, showing crystals with igneous zoning, crystals without zoning and some times with presence of rims and cores. The igneous zoning is defined by relatively thick strips or by sector zoning. Some crystals show a metamitic aspect. The presence of cores in some crystals, as well as the radiometric pattern U-Pb, suggest isotopic inheritance.

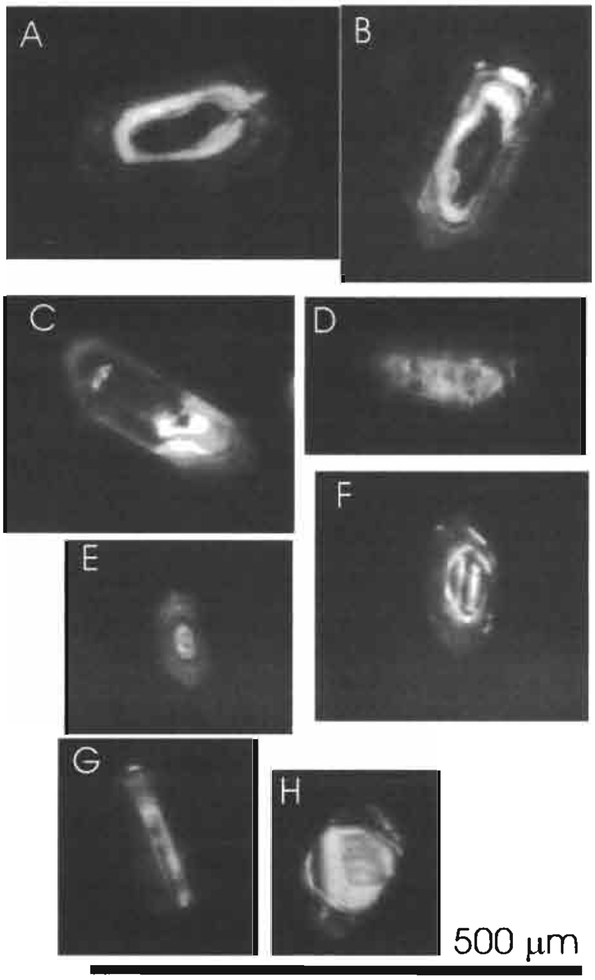

Figure 3. Cathode luminescence images. (A, B) crystals with 'irregular' core; (C, D) zircons perturbed; (E, F) concentric 'regular' cores; (G, H) "igneous" zoning sector.

The second zircon population of in the Cerne Granite samples (type 2) is characterized by larger prismatic translucent crystals (between 1 and 2 μg), balloon form, with length: width rate between 2:1 and 1:1 (Fig. 4).

The two different zircon types mentioned were analyzed by the ^{207}Pb-^{206}Pb by step and heat evaporation method -EVTIMS (Evaporation Thermal Ionisation Mass Spectometry). The two zircon types showed different isotopic rations defining different ages (Fig. 5). The type 1 zircon presents a plateau around 600 Ma, quite imprecise due to low amount of lead, with low detection in the spectrometer ion counter. The type 2 zircon presents a little more accurate plateau around 2.2 Ga, without evidences of Neoproterozoic ages.

Therefore the Cerne Granite zircon is characterized by the presence of crystals formed during Neoproterozoic, as well as crystals with significant Paleoproterozoic inheritance. Such inheritance seems to be associated with possible granite sources. However, part of this population with inheritance can be represent by captured zircons during the emplacement of the body. This idea is supported by Sm-Nd model ages about 2.1 Ga (CER-16 sample) very close, or even younger than ages ^{207}Pb-^{206}Pb of type 2 zircons.

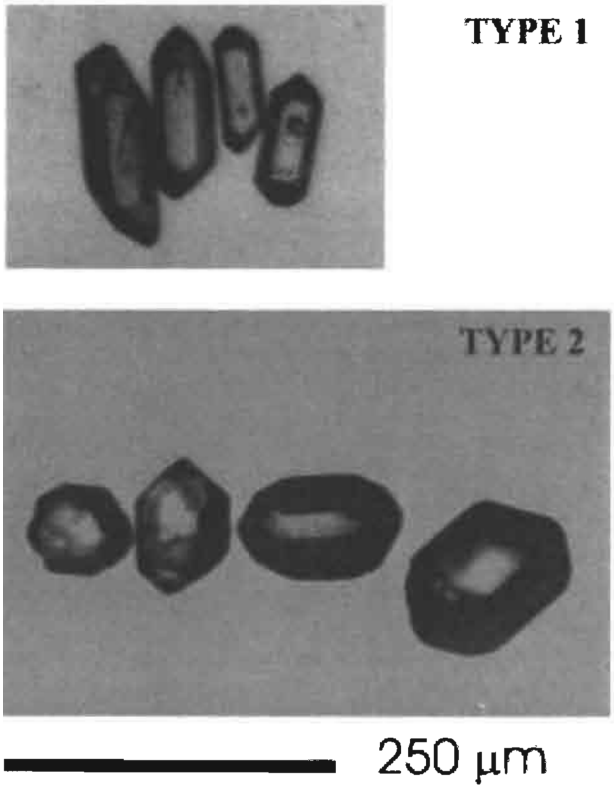

Figure 4. Images of transmitted light of zircon. Crystals from types 1 and 2.

The Cerne Granite geochronological scenario shows a great complexity expressed by discordance of zircon fractions and high error ages, explained here by presence of different zircon types. Techniques of high precision (like SHRIMP and LA-ICPMS) are necessary as well new cathode luminescence studies for a better understanding of the zircon morphology.

The Cerne Granite crystallization age about of 563±34Ma (U-Pb, lower intercept) supported by the granite cooling age about 557±2Ma (Ar-Ar on biotite) is assumid here. Such age is quite similar to ages obtained in the Morro Grande and Serra do Carambeí granites (Prazeres Filho, in the press), which characterizes a latter to pos-orogenic magmatic episode in relation to the Três Córregos – Cunhaporanga magmatic arc.

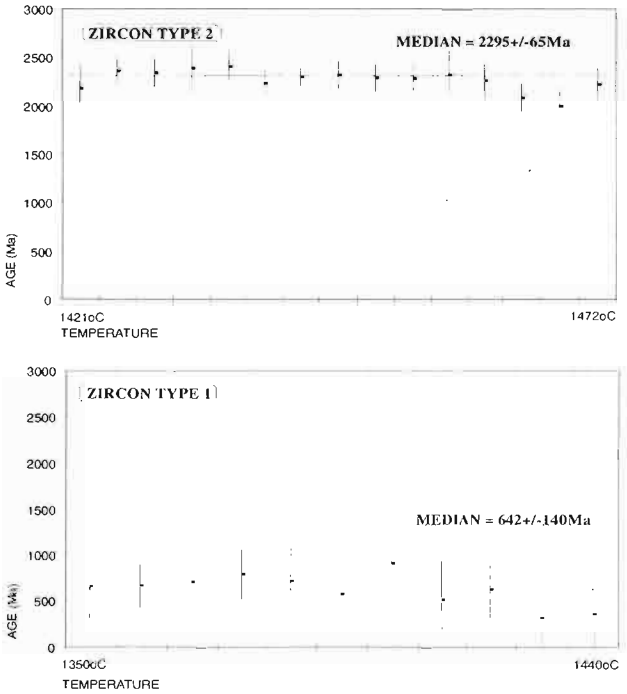

Figure 5. Pb-Pb graphics – evaporation of single grain of the two zircon types.

ACKNOWLEDGMENTS

The authors would like to thank the support from FAPESP (process n°. 01/00961-3) and to CPGeo-IGc-USP that made available the accomplishment of this work.

REFERENCES

Fiori, A.P. 1990. Tectônica e estratigrafia do Grupo Açungui a norte de Curitiba. Inst. de Geociências, Universidade de São Paulo, São Paulo, Tese de Livre Docência, 261p.

Fiori, A.P. 1993. O Sistema de Dobramento Apiaí, Estado do Paraná. Rev. Bras. Geoc., 23(10): 05-17.

Fuck, R.A.; Marini, O.J.; Trein, E. 1967. Contribuição ao estudo ao estudo das rochas graníticas do Estado do Paraná. Boletim Paranaense de Geociências, 23-25:183-221.

Hasui, Y.; Carneiro, C.D.R.; Coimbra, A.M. 1975. The Ribeira Folded Belt. Revista Brasileira de Geociências, 5: 257-266

Prazeres Filho, H.J. 2000. Litogeoquímica, Geocronologia (U-Pb) e Geologia Isotópica dos Complexos Graníticos Cunhaporanga e Três Córregos, Estado do Paraná. Dissertação de Mestrado-IGc-USP, 180p.

ORIGIN OF EARLY JURASSIC CONTINENTAL THOLEIITIC MAGMATISM IN FRENCH GUYANA AND GUINEA, CENTRAL ATLANTIC MAGMATIC PROVINCE (CAMP)

Deckart, K.[1]; Liégeois, J.P.[2] and Bertrand, H.[3]

1. Universidad de Chile, Departamento de Geología, Plaza Ercilla 803, Casilla 13518, Santiago de Chile. kdeckart@cec.uchile.cl
2. Isotope Geology, Africa Museum, B-3080 Tervuren, Belgium. jean-paul.liegeois@africamuseum.be
3. Laboratoire de Géologie, ENS Lyon, 46, Allée d'Italie, F-69364 Lyon Cédex 07, France. Herve.Bertrand@ens-lyon.fr

Keywords: Geochemistry, Nd-Sr isotopes, CAMP, French Guyana, Guinea

French Guyana and Guinea dykes and sills belong to the widespread CAMP magmatism which is related to the break-up of Pangea supercontinent ca. 200 m.y. ago (Deckart et al., 1997; Fig. 1).

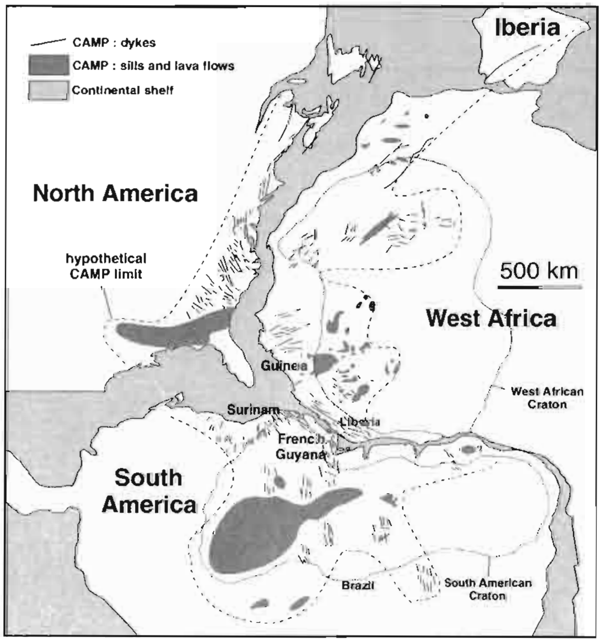

Figure 1. CAMP magmatism around the initial Central Atlantic Ocean (modified from May, 1971; Deckart et al., 1997; Marzoli et al., 1999).

Guyana dykes and sills consist in tholeiitic dolerites and gabbros, and can be considered as liquids characterized by low SiO_2 (48-50 wt.-%), high TiO_2 (1.4-3.7 wt.-%) and FeO (13-16 wt.-%) contents. Their trace elements patterns are slightly enriched in LREE patterns ($(La/Yb)_N$: 1.5-5.1), but are devoid of Ba, K, Rb, Th enrichment and no negative Nb-Ta anomaly is observed. They yield positive ε_{Ndi} values (+4.2 to +5.8) and rather low, although variable, $^{87}Sr/^{86}Sr_i$ ratios (0.70319-0.70509).

In contrast, Guinean sills, dykes and layered intrusion show a wider petrographic diversity (doleritic, gabbroic, dioritic liquids and ultramafic-mafic cumulates). The mafic suite consists of low TiO_2 (<2 wt.-%) and high SiO_2 (>50 wt.-%) tholeiites. They display patterns enriched in LREE ($(La/Yb)_N$: 3.2-6.3) and Ba, K, Rb, Th with slight-to-strong negative Nb-Ta anomalies. Isotopically, Guinean samples differ from Guyanan by their a broader range of isotopic signatures, showing mostly less depleted ε_{Ndi} values (+0.4 to –5.3) and more radiogenic $^{87}Sr/^{86}Sr_i$ ratios (0.70481-0.71072).

The Guyana tholeiites share their chemical features with the nearby high-Ti tholeiites from Liberia and Brazil. The chemical composition of the Guinean tholeiites largely overlaps whit that of other low-Ti CAMP tholeiites, although slightly shifted towards less radiogenic Nd ratios.

In both Nd-Sr diagram and VICE/VICE ratios diagram (very incompatible element ratios reflecting the relative source abundances, if magmas are uncontaminated; after Hofmann & Jochum, 1996), Guyana (and other high-Ti) samples and Guinea (and other low-Ti) samples define two distinct fields. The former display a depleted signature with PREMA-like characteristics, while the latter has an enriched signature, trending towards EMII component (Fig. 2).

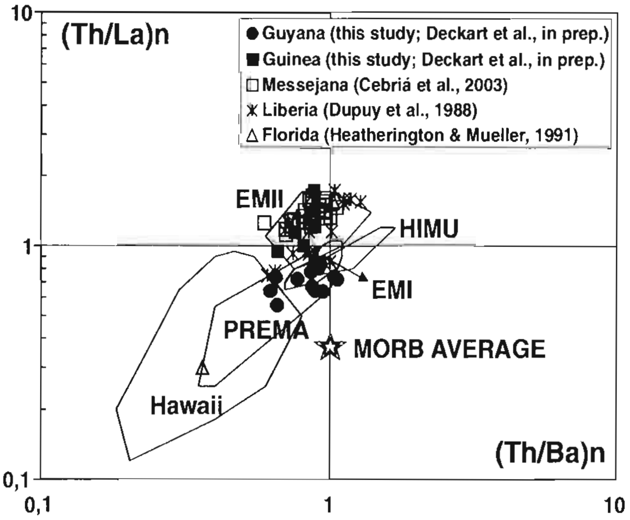

Figure 2. VICE/VICE ratio plot of French Guyana and Guinea mantle melts, compared with other CAMP data. (mantle source fields after Hoffman & Jochum, 1996).

Despite interactions with the continental crust (mostly in Guinea, indicating longer residence time of the magma within the crust), the observed differences between these two groups are believed to reflect primary mantle source heterogeneities. The Guinea magmas (as other low-Ti CAMP magmas) have a predominant previously enriched of lithospheric mantle signature (plausibly by metasomatism or by crustal recycling through subduction), while the Guyana magmas (as other high-Ti magmas) require the additional involvement of a depleted mantle source, probably located in the asthenosphere.

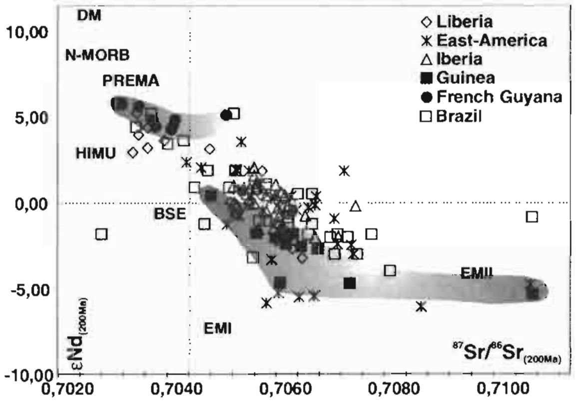

Figure 3. Initial Nd-Sr isotope compositions for Guyana and Guinea compared to other CAMP data. Iberia (Alibert, 1985; Cebriá et al., 2003), East-America (Pegram, 1990; Heatherington & Mueller, 1991), Liberia (Dupuy et al., 1988), Brazil (De Min et al., 2003).

Our data are consistent with a model in which magma generation is the consequence of linear lithospheric delamination along reactivated lithospheric discontinuities (adapted after Black & Liégeois, 1993; Anderson, 1994) followed by asthenospheric upwelling inducing adiabatic melting through pressure release. In such a scenario, the necessity of a thermal incubation (e.g., Wilson, 1997; Courtillot et al., 1999) should be tested.

REFERENCES

Anderson, D.L., 1994. The sublithospheric mantle as the source of subcontinental flood basalts; the case against the continental lithosphere and plume head reservoir. Earth Planet. Sci. Lett. 123, 269-280.

Alibert, C., 1985. A Sr-Nd isotope and REE study of late Triassic dolerites from the Pyrenées (France) and the Messejana Dyke (Spain and Portugal). Earth Planet. Sci. Lett. 73, 81-90.

Black, R., and Liégeois, J.P., 1993. Cratons, mobile belts, alkaline rocks and continental lithospheric mantle: the Pan-African testimony. J. Geol. Soc., London 150, 89-98.

Cebriá, J.M., López-Ruiz, J., Doblas, M., Martins, L.T., and Munha, J., 2003. Geochemistry of the Early Jurassic Messejana-Plasencia dyke (portuga-Spain); Implications on the Origin of the Central Atlantic Magmatic Province. J. Petrol. 44, 547-568.

Courtillot V., Jaupart C., Manighetti I., Tapponnier P. and Besse J., 1999. On causal link between flood basalts and continental breakup. Earth Planet. Sci. Lett. 166, 177-195.

Deckart, K., Féraud, G., and Bertrand, H., 1997. Age of Jurassic continental tholeiites of French Guyana, Surinam and Guinea: Implications for the initial opening of the Central Atlantic Ocean. Earth Planet. Sci. Lett. 150, 205-220.

Deckart K., Bertrand H. and Liegeois J.P. Contrasting mantle sources and processes in French Guyana and Guinea related to the Early jurassic Central Atlantic Magmatic Province (CAMP). In prep.

De Min A., Piccirillo E.M., Marzoli A., Bellieni G., Renne P.R., Ernesto M., and Marques L., 2003. The central Atlantic magmatic province (CAMP) in Brazil: petrology, geochemistry, 40Ar/39Ar ages, paleomagnetism and geodynamic implications. In: The central Atlantic magmatic province: insights from fragments of Pangea. AGU Geophysical Monograph 136, 209- 226.

Dupuy, C., Marsh, J., Dostal, J., Michard, A., and Testa, S., 1988. Asthenospheric and lithospheric sources for Mesozoic dolerites from Liberia (Africa): trace element and isotopic evidence. Earth Planet. Sci. Lett. 87, 100-110.

Heatherington, A.L., and Mueller, P.A., 1991. Geochemical evidence for Triassic rifting in southwestern Florida. Tectonophysics 188, 291-302.

Hofmann, A.W. and Jochum, K.P., 1996. Source characteristics derived from very incompatible trace elements in Mauna Loa and Mauna Kea basalts, Hawaii Scientific Drilling Project. J. Geophys. Res. 101, 11.831-11.839.

Marzoli, A., Renne, P.R., Piccirillo, E.M., Ernesto, M., and De Min, A., 1999. Extensive 200-millon-year-old continental flood basalts of the Central Atlantic Magmatic Province. Science 284,616-618

May, P.R., 1971: Patterns of Triassic Diabase Dikes Around the North Atlantic in the Context of Predrift Position of the Continents. Geol. Soc. Amer. Bull. 82, 1285-1292.

Pegram, W.J., 1990. Development of continental lithospheric mantle as reflected in the chemistry of the Mesozoic Appalachian Tholeiites, U.S.A. Earth Planet. Sci. Lett. 97, 316-331.

Wilson, M., 1997. Thermal evolution of the Central Atlantic passive margins: continental break-up above a Mesozoic super-plume. J. Geol. Soc.London 154, 491-495.

K-Ar GEOCHRONOLOGY AND Sr AND Nd ISOTOPIC COMPOSITION OF THE PATAGONIAN BATHOLITH IN THE MADRE DE DIOS ARCHIPELAGO (50°30' S), SOUTHERN CHILE

Duhart, P.[1,2]; **Muñoz, J.**[1]; **Tassinari, C.**[2] **and Quiroz, D.**[1]

1. Servicio Nacional de Geología y Minería, SERNAGEOMIN-Chile. pduhart@sernageomin.cl, jmunoz@sernageomin.cl, dquiroz@sernageomin.cl
2. Universidade de São Paulo, USP-Brasil. pduhart@usp.br, ccgtassi@usp.br

Keywords: Patagonian magmatism, isotopic geochemistry, southern Chile

INTRODUCTION

Outcrops of plutonic rocks belonging to the PB conform a 40 to 100 km wide continuous belt extending from 40° to 56° S in the main Andean Cordillera (SERNAGEOMIN, 2002). The Andean Cordillera and associated magmatism have been genetically related to subduction of the oceanic plates below the South American plate at least since Jurassic times. Geochronological studies in its southern segment show magmatic pulses during Jurassic, Cretaceous and Miocene (Munizaga et al., 1988). Along the 41° to 44° S segment, Early Cretaceous, Miocene and Pliocene plutonic magmatism are well represented (Pankhurst et al., 1992; Duhart et al., in prep.). Also, rare Upper Cretaceous and Eocene plutons have been reported (Duhart et al., in prep.). In the segment between 44° and 47° S, plutonic magmatism evidences a complex geographic distribution of ages, changing, as follows, from west to east (Pankhurst et al., 1999): Upper Cretaceous, Early Cretaceous, Eocene, Miocene and Early Cretaceous. At 48° S and south of 50° S reported ages range from 146 to 46 Ma (Weaver et al., 1991) and 160 to 12 Ma (Halpern, 1973), respectively. Regionally, PB is tonalitic to granodioritic in composition, with scarce gabbroic, dioritic, granitic and leucogranitic members and locally important K-rich monzogranites.

From 50° to 51° S, Madre de Dios Archipelago is formed by two major islands, Madre de Dios to the north and Duque de York to the south, and a numbers of minor islands such as Tarlton, Ramón, Guarello, Caracciolo and Doñas. These islands show an abrupt relief with altitudes up to 1,000 m and deep canyons and fiords. The western half of the archipelago is formed by semicontinuous belt of Paleozoic-pre-Jurassic rocks representing the basement of the Patagonian Andes (Fig. 1). The eastern half is composed by extensive and continuous outcrops of intrusive rocks belonging to the Mesozoic to Cenozoic PB (Fig.1).

Three main basement units have been described in this region (Forshyte & Mpodozis, 1983). The Tarlton Limestone Unit represents a sequence of massive limestones with Upper Carboniferous-Early Permian fusulinide fossils. The Denaro Complex includes a succession of oceanic pillow basalts with thin layers of metalliferous chert, chert with radiolarian and calcareous sandstones. The Duque de York Complex is represented by a silicic-clastic sequence formed by sandstones and shales in a turbiditic succession and conglomerates. These units have been interpreted as part of an accretionary prism (Forshyte & Mpodozis, 1983). Under this interpretation, oceanic type basalts (Denaro Complex) and exotic terrains (Tarlton Limestones) previously covered by continental detrital deposits (Duque de York Complex) were accreted to the southwestern margin of Gondwana prior to Jurassic times. In this latitude, Early Cretaceous granodioritic rocks of the PB were emplaced in these basement units.

THE PATAGONIAN BATHOLITH IN THE MADRE DE DIOS ARCHIPELAGO

GEOLOGY

In this area, the PB is conformed by a homogeneous granodioritic body with an approximately N-S trending intrusive contact with the basement units to the west. Rocks are medium to coarse grain biotite granodiorites with locally centimetric oriented microdioritic inclusions. Granular felsic W-E oriented metric vertical dykes are spatially associated to the main granodioritic body and they are also emplaced in the basement units. Centimetric vertical basaltic dykes clearly cut both the granodioritic body and the basement units.

PETROGRAPHY AND GEOCHEMISTRY

Granodioritic rocks in thin sections have inequigranular hypidiomorphic to allotriomorphic holocrystalline textures. Main mineralogy includes anhedral quartz (35%), subhedral plagioclase with polysynthetic twins and in cases with strong zonation (30%), subhedral K-spar (20%), subhedral to anhedral biotite (10%), opaque minerals (3%) and accessory tourmaline and zircon (2%). In cases, biotite evidences an incipient chloritization and some plagioclase crystals exhibit a weak sericitation.

Major element compositions of four samples vary as follows: SiO_2, 71.6-73.5 %; K_2O, 1.5-2.1 %; Na_2O, 3.6-4.1 %; CaO, 2.8-3.2 %; Al_2O_3, 13.6-14.6 %; Fe_2O_2, 1.0-1.5 %; and FeO, 1.2-1.4 %. In the AFM diagram rocks plot in the calcalkaline field; in the K_2O versus SiO_2 diagram in the medium potassium field and in the Peacock diagram they show a calcic index. Also, rocks evidence relatively normal Rb (60 ppm), Zr (100 ppm), Sr (200 ppm) and Ba (500 ppm) contents. Chondrite normalized rare earth pattern evidence light REE enrichment, La/Yb ratios close to 10 and two of the analyzed samples show positive Eu anomaly probably as consequence of plagioclase cumulates. Rb versus (Y+Nb) discriminant diagram classifies these rocks as volcanic arc granites.

K-Ar GEOCHRONOLOGY AND Sr AND Nd ISOTOPIC DATA

Four new K-Ar age determinations on biotite, separated from the main granodioritic body, in the range 133-140 Ma have been obtained (Fig.1, Table 1). These ages are slightly older than three ages previously reported by Halpern (1973), in the range 120 to 125 Ma in the same area. Although two of which were obtained by using the Rb-Sr method (125±8 and 120±8 Ma) and only one by using the K-Ar method (122±6 Ma). The new K-Ar ages are interpreted as cooling ages and are considered as minimum ages for the plutonic magmatic event in the Madre de Dios area. Initial Sr isotopic ratios, for the same samples, are in the range 0.7046-0.7050 ($\varepsilon_{Sr} = 4.16\text{-}9.45$, Table 2) and the Nd isotopic ratios are in the range 0.512516 to 0.512584 ($\varepsilon_{Nd} = -1.03$ to -0.04, Table 3).

Table 1. K-Ar ages of granodiorites from the PB, Madre de Dios area.

Sample	Material	%K	Ar rad. (nl/g)	Ar atm. (%)	Age±2σ
UP-0006A	Bt+chlorite	6.447	36.601	5	140 ± 3
UP-0009	Biotite	5.854	31.434	3	133 ± 3
UP-0021	Biotite	7.123	38.391	2	134 ± 3
UP-0024	Biotite	7.155	38.598	2	134 ± 3

Table 2. Sr isotopic composition of granodiorites (PB), Madre de Dios area.

Sample	Rb (ppm)	Sr (ppm)	^{87}Rb/^{86}Sr	^{87}Sr/^{86}Sr	T_I (K-Ar)	ε (TI)	(^{87}Sr/^{86}Sr) initial
UP-0006A	68.56	240.50	0.8250	0.70638	140	5.66	0.7047
UP-0009	70.36	208.43	0.9769	0.70686	133	9.45	0.7050
UP-0021	64.24	271.80	0.6842	0.70594	134	4.16	0.7046
UP-0024	63.13	212.76	0.8586	0.70657	134	8.31	0.7049

Table 3. Nd isotopic composition of granodiorites (PB), Madre de Dios area.

Sample	Sm (ppm)	Nd (ppm)	^{147}Sm/^{144}Nd	^{143}Nd/^{144}Nd	T_{DM} (Ma)	T_I (K-Ar)	$\varepsilon_{(TI)}$
UP-0006A	1.347	7.694	0.1059	0.512550	709	140	-0.09
UP-0009	2.094	10.832	0.1169	0.512516	838	133	-1.03
UP-0021	1.191	5.226	0.1379	0.512579	939	134	-0.15
UP-0024	1.399	6.162	0.1373	0.512584	823	134	-0.04

DISCUSSION

The four new reported K-Ar ages are interpreted as minimum cooling ages. If the closing temperature for biotite is taken as 280 ± 40 °C (Rollinson, 1993), the new ages would represent the time in which the rocks reached this temperature. In this way, plutonic activity in this region would have occurred during the lower Early Cretaceous and in accordance with new geochronological data of Pálfy et al. (2000) in the Berriasiano near the limit with the Upper Jurassic. These new ages are slightly older than those reported by Halpern (1973) and both sets of data could indicate disturbance in the Ar system. Currently in progress step heating Ar-Ar measurements for the same samples will help to clarify the last possibility.

The new K-Ar ages are consistent with ages reported in a similar geological context along the western part of the PB at Los Chonos Archipelago (Pankhurst *et al.*, 1999). The existence of Early Cretaceous and Eocene (?)-Miocene sedimentary units in cases evidencing granitic detrital sedimentary components in the Chonos Archipelago and Continental Chiloé, in both cases intruded by plutons assigned to the PB, suggests that the PB was generated by episodic magmatism and associated to episodic intrusion, exhumation and erosion events.

Major, trace and REE composition of the granodioritic rocks are typical of subduction related magmatism. Initial ε_{Sr} and ε_{Nd} values indicate that the magma sources are located at the base of the continental crust, involving a mixing of different geochemical reservoirs in different proportions, like upper mantle and lower and upper continental crust. Depleted mantle Nd model ages suggest mantle magmas differentiation in the range of 700-900 Ma.

ACKNOWLEDGEMENTS

Carlos Perez de Arce and Felipe Llona, both from the laboratory of SERNAGEOMIN, are respectively akmowledged for the K-Ar ages and geochemical major, trace and REE analyses. The Sr and Nd isotopic analysis were carried out at the Centro de Pesquisas Geocronologicas of the University of São Paulo, Brazil. Special thanks to the French Speleologic Expedition "Ultima Patagonia-2000", in the names of Jean Francoise Pernette and Richard Maire, by the opportunity given to Paul Duhart to be part of the expedition to Madre de Dios Archipelago. This publication is sponsored by the National Subdirection of Geology, SERNAGEOMIN-Chile.

REFERENCES

Duhart, P.; Prian, J.P.; Hervé, F.; Munizaga, F.; Pérez, Y.; Crignola, P.; Pankhurst, R.; Tassinari, C. En prep. Petrografía, geocronología y geoquímica del Batolito Norpatagónico en Chiloé Continental (41°-44°S): evolución Mesozoica-Cenozoica del batolito.

Forsythe, R. and Mpodozis, C. 1983. Geología del Basamento pre-Jurásico Superior en el Archipiélago Madre de Dios, Magallanes, Chile. Servicio Nacional de Geología y Minería, Boletín No. 39, 1 mapa escala 1:137.000, 63 p.

Halpern, M. 1973. Regional geochronology of Chile South of 50° Latitude. Geological Society of America Bulletin, Vol. 84, No. 7, p. 2407-2422.

Munizaga, F.; Hervé, F.; Drake, R.; Pankhurst, R.J.; Brook, M. and Snelling, N. 1988. Geochronology of the Lake Region of south-central Chile (39°-42°S): Preliminary results. Journal of South American Earth Sciences, Vol. 1, No. 3, p. 309-316.

Pálfy, J.; Smith, P.L. and Mortensen, J.K. A U-Pb and $^{40}Ar/^{39}Ar$ time scale for the Jurassic. Canadian Journal of Earth Sciences, Vol. 37, p. 923-944.

Pankhurst, R.J.; Hervé, F.; Rojas, L. and Cembrano, J. 1992. Magmatism and tectonics in continental Chiloé, Chile (42°-42°30' S). Tectonophysics, Vol. 205, p. 283-294.

Pankhurst, R.J.; Weaver, S.D.; Hervé, F. and Larrondo, P. 1999. Mesozoic-Cenozoic evolution of the North Patagonian Batholith in Aysén, Southern Chile. Journal of the Geological Survey, London, Vol. 156, p. 673-694.

SERNAGEOMIN, 2000. Mapa Geológico de Chile, Servicio Nacional de Geología y Minería, Carta Geológica de Chile, Serie Geología Básica No. 75, 1 mapa en 3 hojas, escala 1:1.000.000. Santiago.

Suárez, M. 1977. Notas Geoquímicas preliminares del Batolito Patagónico al sur de Tierra del Fuego, Chile. Revista Geológica de Chile, No. 4, p. 15-33.

Weaver, S.; Bruce, R.; Nelson, E.; Bruckner, H. and Le Huray, A. 1991. The Patagonian Batholith at 48°S, Chile: Geochemical and geochronological variations. Geological Society of America. Special Paper No. 291. p. 33-50.

Rollinson, H. 1993. Using geochemical data (Longman Group, ed.). Reino Unido. 352 p.

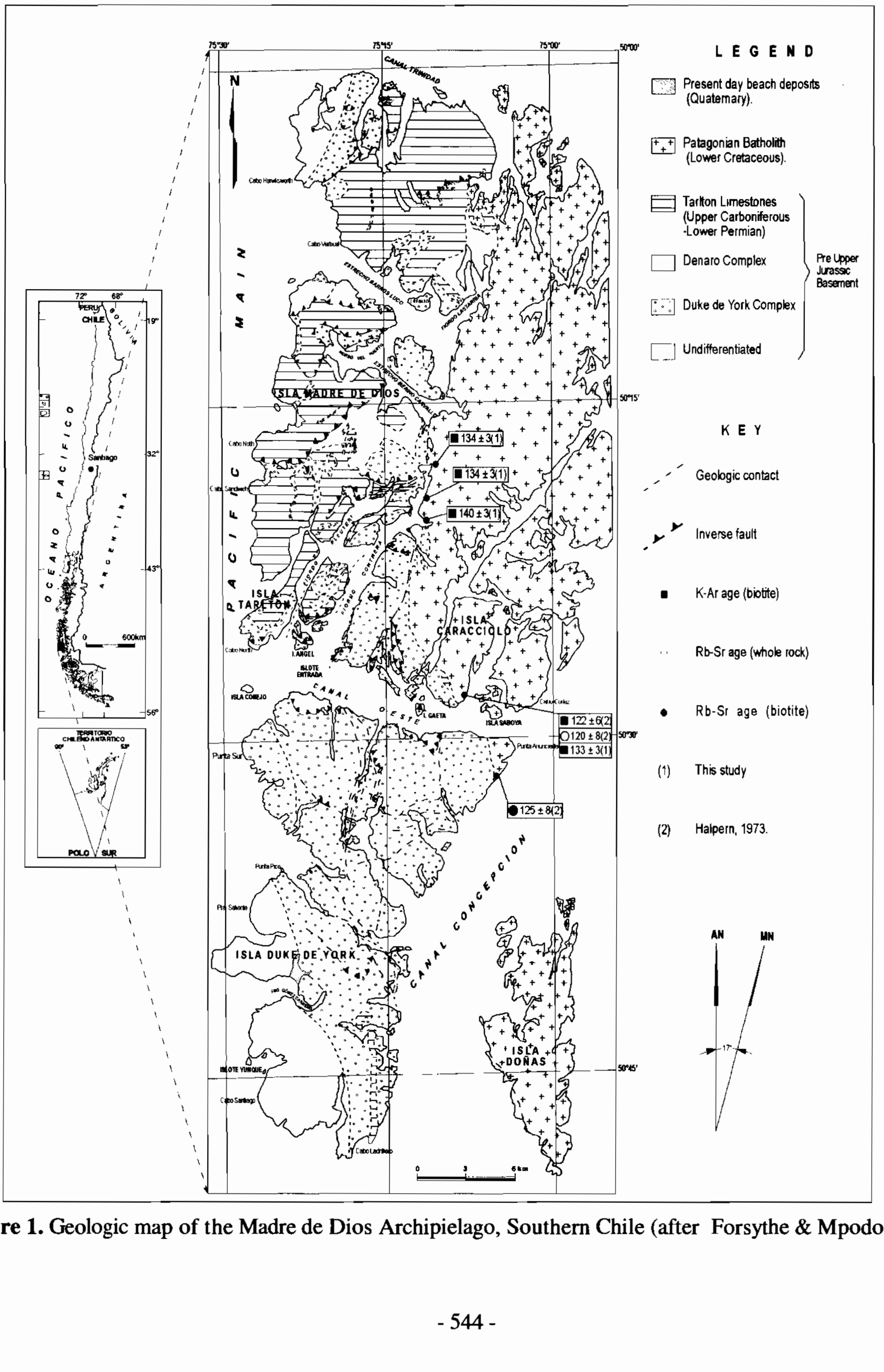

Figure 1. Geologic map of the Madre de Dios Archipielago, Southern Chile (after Forsythe & Mpodozis, 1983).

THE MESETA CHILE CHICO BASALTS, EASTERN CENTRAL PATAGONIAN CORDILLERA: K-Ar GEOCHRONOLOGY AND GEOCHEMISTRY OF A COMPRESSIONAL TO EXTENSIONAL BACK-ARC VOLCANISM

Espinoza, F.[1]; Morata, D.[1]; Suárez, M.[2] and De la Cruz, R.[2]

1. Departamento de Geología, Universidad de Chile, Casilla 13518, Correo 21, Santiago, Chile. feespino@ing.uchile.cl
2. Servicio Nacional de Geología y Minería, Avenida Santa María 0104, Santiago, Chile. msuarez@sernageomin.cl

Keywords: Patagonia, flood basalts, K-Ar ages, long-lived magmatism, slab window

INTRODUCTION

The Meseta Chile Chico basalts (46°35'-46°47' S - 71°46'-72°02' W), located southwest of the village of the same name, belongs to a flood basalt province that extends along the oriental side of the Andean Cordillera, (the Patagonian Plateau Lavas). This Meseta is located on the back-arc of Patagonian Andes (46° S), just above the extrapolation of the last Chile Ridge segment that collided in Pliocene times. The existence of enormous volumes of basalts forming the Meseta (~270 km^3) and some older andesites near Chile Chico indicates a long-lived, although intermittent, volcanic activity in Patagonia since Late Cretaceous.

The aim of this work is to point out the particularity of this Cenozoic volcanism in Patagonia, that evidence significant changes on the tectonic regime along the oriental margin of South America, and remark the influence of the lithospheric plates setting on the volcanic activity at the surface.

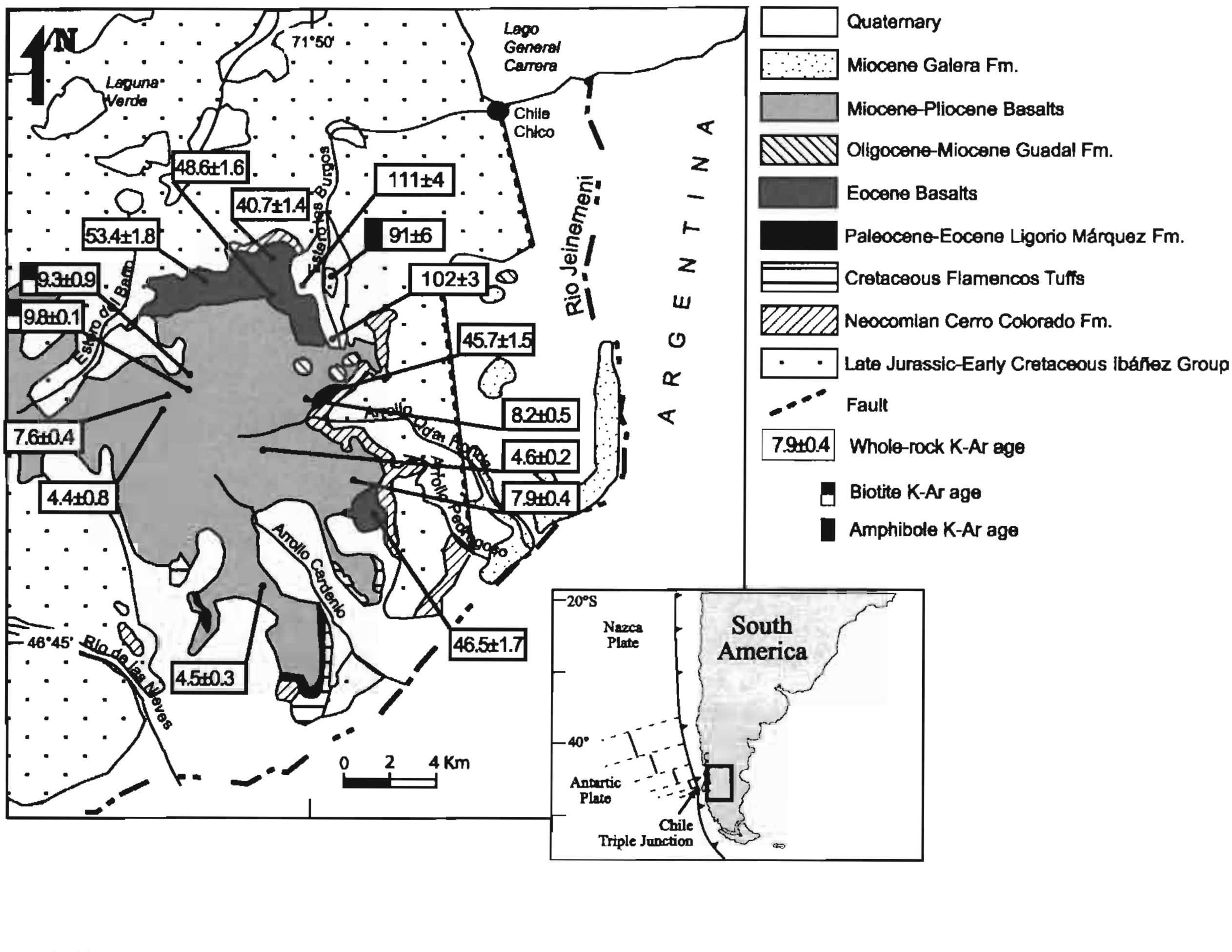

Figure 1. Simplified geological map of the Meseta Chile Chico basalts (46°35'-46°47' S--71°46'-72°02' W), south of Lago General Carrera. Numbers indicate K-Ar ages (error in 2σ). Modified from Suárez and De la Cruz, 2000a.

REGIONAL GEOLOGY

The oldest rocks exposed south of General Carrera Lake, in the Aysén Region, southern Chile, are the volcanic and acid volcaniclastic deposits of the Ibáñez Group, assigned to the Late Jurassic-Earliest Cretaceous. (Suárez & De la Cruz, 2000b; Parada et al., 2001; Fig. 1). This unit unconformably overlies the Eastern Metamorphic Complex (Niemeyer et al., 1984; Hervé et al., 1998), exposed west of the studied area, and is intruded by many large younger andesitic subvolcanic bodies (e.g. Cerro Cuadro). The geochemistry of the Ibáñez Group indicate calc-alkaline affinity that clearly relate with subduction volcanism processes. (Baker et al., 1981; Suárez et al, 1999; Suárez & De la Cruz, 2000b). Over these Mesozoic rocks, sediments associated with a marine transgression were deposited as consequence of a first stage of development of a back-arc basin (Cuenca Austral), along with some volcanics of the Coyhaique Group. In the studied area, this group is represented by the shallow marine facies with continental interbedding of the Neocomian Cerro Colorado Formation, that overlies the tuffs of the Ibáñez Group and appear at the base of the Meseta Chile Chico (Fig. 1). These sedimentary rocks are covered by subaerial volcanism in the Early Cretaceous (Flamencos Tuffs, Barremian, Suárez et al., 2000; Fig. 1). At the studied area, the Tertiary is represented by thick sedimentary sequences and the Meseta Chile Chico flood basalts Upper and Lower sequences (Niemeyer et al., 1984; Espinoza, 2003) (Fig. 2).

The Lower Basaltic Sequence of the Meseta (57-42 Ma, Charrier, 1979; Baker et al., 1981; Petford et al., 1996; De la Cruz & Suárez, unpublished) have an approximated thickness of 500-550 meters, and at the northern side lies discordantly over the Mesozoic Ibáñez Group and, at the south, lies discordantly over the Neocomian Cerro Colorado Formation (Fig. 1). This sequence may be correlated stratigraphic and chronologically to the west with the 57-45 Ma Posadas Basalt (Baker et al., 1981), and to the north with the 42±6 Ma Balmaceda Basalts (Baker et al., 1981; Demant et al., 1996; De la Cruz et al., in press).

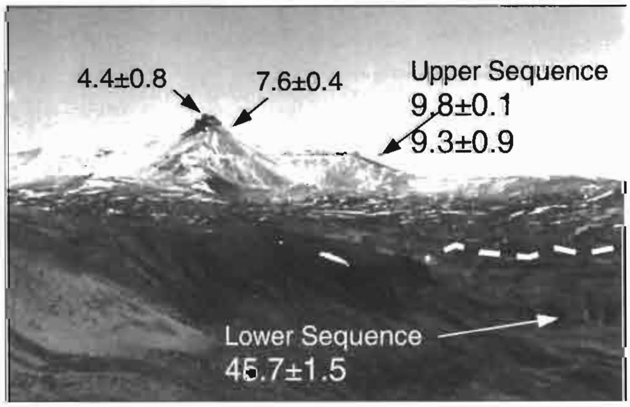

Figure 2. Photography from southeast of Cerro Sombrero hill indicating K-Ar ages (Ma±2σ) of some lava flows of the Lower and Upper Basaltic Sequences.

The Upper Sequence (16-3 Ma; Charrier, 1979) have a thickness of 400 meters covering an area of 300 km^2 that correspond to the actual erosion surface. This Sequence correlates with similar volcanic rocks at the Argentinean side of the Meseta (Meseta Lago Buenos Aires Fm.–Upper Miocene- and El Sello Fm.–Early Pleistocene-, Busteros y Lapido, 1983; Gorring & Kay, 2002). According to Espinoza (2003), this sequence may be chronologically, and probably genetically correlated with the Neogene Patagonian Plateau Lavas (Gorring & Kay, 2001).

Southwest of Lago General Carrera outcrops the Late Paleocene–Early Eocene Ligorio Márquez Formation (Suárez et al., 2000; Fig. 1), formed by tropical to subtropical vegetal fossil-bearing sandstones; the Late Oligocene–Early Miocene Guadal Formation, ("Patagoniano", Frassinetti & Covacevich, 1999; Fig. 1), a marine sequence formed by sandstones and mollusk fossil-bearing beds that overlies with an erosional unconformity the Lower Basaltic Sequence of the Meseta and underlies with an angular unconformity the Upper Basaltic Sequence (Charrier et al., 1979); and the Upper Early Miocene-Middle Miocene Galera Formation ("Santacrucense", Marshall & Salinas, 1990; Flynn et al., 2002), mainly formed by sandstones and fluvial conglomerates. Finally, Pliocene-Pleistocene fluvial gravel and Pleistocene–Recent glacial deposits are recognized in this zone.

GEOCHRONOLOGY AND GEOCHEMISTRY

The geochemical analyses were made by ICP-AES at the Departamento de Geología of the Universidad de Chile. Some selected samples were also analyzed at the Centro de Instrumentación Científica in the Universidad de Granada, España by ICP-MS. All the K-Ar dating was carried out at the Geochronology Laboratory of the Servicio Nacional de Geología y Minería in Santiago, Chile. Sample dating was carried out on whole-rock (13 samples) biotite separates (2 samples) and on an amphibole inclusion separate.

In the studied area of the Meseta Chile Chico andesitic and basaltic lava flows of Cretaceous (111±4 to 102±3 Ma) and numerous outcrops of calc-alkaline subvolcanic bodies intruding the Ibáñez Group, representing a Cretaceous calc-alkaline volcanism identified in other parts of the Patagonian Cordillera (Baño Nuevo Volcanic Complex, Suárez et al., 1996), conform the first group of volcanic rocks defined on this work. One of these subvolcanic bodies, the high-K amphibole-bearing andesite of the Cerro Cuadro was dated at 91±6 Ma (K-Ar age on a amphibole separate from a gabbroic inclusion). This andesite shows a primitive mantle normalized pattern that evidence an arc-like affinity with a marked Nb-Ta negative anomaly, medium to small enrichments of incompatible elements (Fig. 3) and low LREE/HREE ratios ($La/Yb_n=6$).

A second group of volcanic rocks defined in this work is formed by the Lower Basaltic Sequence of the Meseta Chile Chico lava flows together with various volcanic necks genetically related with them (e.g. the lherzolitic xenoliths-bearing basanite of Cerro Lápiz, 40.7±1.4 Ma in figure 1, $(^{87}Sr/^{86}Sr)_o$ = 0.70312 and ε_{Nd} = +9.9). These rocks are mainly olivine alkali basalts with ages ranging from 55 to 40 Ma (Fig. 1). They are characterized by strong enrichments in incompatible elements (Fig. 3), REE patterns showing LREE enrichment with high LREE/HREE ratios (La/Yb_n=8-14), HREE depletion (6-8 x chondrite) and $(^{87}Sr/^{86}Sr)_o$ ratios of 0.70385 and ε_{Nd} values of +5.1.

A third group of volcanic rocks is composed by the Upper Basaltic Sequence of the Meseta which includes two interbedded acid rhyolitic flows. The basalts of this group yield ages between 8 and 4 Ma. Biotite separates from both rhyolites yield ages of 9.8±0.1 Ma and 9.3±0.9 Ma (Fig. 1). Similarly to in the Lower Basaltic Sequence, basic lavas from this sequence are alkali olivine basalts with a similar primitive mantle normalized pattern (enrichments in LILE, HFSE, high LREE/HREE ratios, HREE depletion) and isotopic ratios ($(^{87}Sr/^{86}Sr)_o$ 0.70414; ε_{Nd} +4.7). Nevertheless, a marked Nb-Ta negative anomaly and lower concentrations of Ti with respect to basalts from the lower Sequence (Fig. 3) is observed. The acid rocks are hornblende-biotite rhyolites characterized by high LILE concentrations and positive anomalies of Pb, K and Rb, a marked negative anomalies of Nb-Ta, P and Ti (Fig. 3), and $(^{87}Sr/^{86}Sr)_o$ ratios of 0.70449 and ε_{Nd} values of +0.7.

DISCUSSION AND CONCLUSIONS

The existence of andesitic lavas with Late Cretaceous ages and arc-related affinities (Group 1) suggest that these magmas were generated by common subduction related processes. According to the geochemical signature of these andesites, this volcanism developed during a compressional tectonic regime, active during the Cretaceous, related with the subduction of the Aluk plate (Cande & Leslie, 1986). During the Early Eocene, a new volcanic episode started with the extrusion in the back-arc region of the lower flood basalts of the Meseta Chile Chico, that extended to the Early Late Eocene (Group 2). Their incompatible trace elements characteristics indicate a strong OIB-like signature without any influence of arc and/or crustal components, suggesting an origin by low degrees of partial melting from a primitive OIB-like LREE and Ti-enriched mantle source (Espinoza, 2003). These geochemical features of basalts could be generated in an extensional tectonic regime active in Patagonia during Eocene. This tectonism and subsequent volcanism are probably related with the collision at ~53 Ma at this latitude of one segment of the Ridge between Aluk and Farallon plates (Cande & Leslie, 1986) and the opening of a slab window below the continent (Espinoza, 2003). Finally, a third volcanic episode, that covered the Eocene basalts and reached further to the east, began in the Late Miocene with a bimodal volcanism (Group 3). Trace elements and isotopic characteristics of the basalts from this group indicate an origin from a similar source of than Group 2, but Ti-depleted. The Nb-Ta negative anomaly, high La/Sr and La/Nb ratios and the Pb and Sr positive anomalies reflect the influence of some slab/arc (?) components in the magmatic evolution. This fact could represent a posible remanent of the prior arc-like volcanism or could be the consequence of a major cortical interaction. The isotopic values of rhyolites (ε_{Nd} =+0.7) indicate an origin by crustal melting reflecting the high intensity of the extension during the first stages. The flood basaltic volcanism would continue until Late Miocene-Early Pliocene as long as the slab window opened by the subduction of the Chile Ridge segment collided ~6Ma ago pass below the Lago General Carrera region.

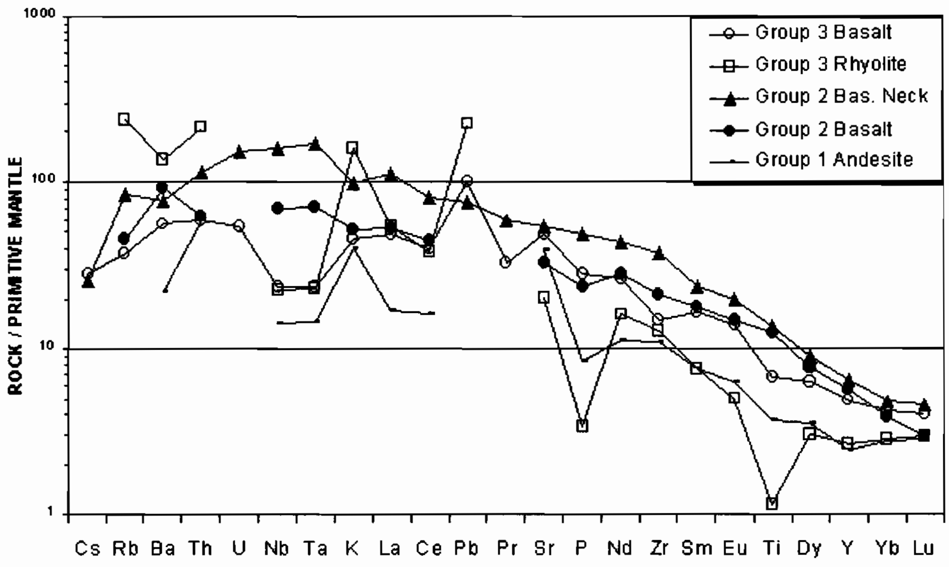

Figure 3. Primitive mantle normalized trace incompatible elements diagram of rocks in the Meseta Chile Chico. Normalization factors from Sun & McDonough (1989).

The data presented here is interpreted as consequence of a long-lived magmatism in Patagonia since Late Cretaceous to Pliocene times. This magmatism may be a consequence of some kind of "temperature and compositional anomaly" under this sector of the continent. The collision of different ridge segments during the Eocene and Miocene might have produced a significant change in the tectonic regime in the continental margin. The opening of slab windows beneath Patagonia would then allow the upwelling of primitive basaltic melts from the subslab asthenosphere.

ACKNOWLEDGEMENTS

Field and analysis support was provided by FONDECYT project number 1000125. This work also forms part of a geologic mapping project of the Servicio Nacional de Geología y Minería in collaboration with the Regional Government of the XI Region. We also wish to thank Mr Leonardo Zuñiga for his field assistance and Mr Jaime Martínez (U. de Chile) for the chemical analyses.

REFERENCES

Baker, P.E.; Rea, W.J.; Skarmeta, J.; Caminos, R.; Rex, D.C. 1981. Igneous history of the Andean Cordillera and Patagonian Plateau around latitude 46°S. Philos. Trans. R. Soc. London, Ser. A, 303, pp. 105-149.

Busteros, A. y Lapido, O. 1983. Rocas básicas en la vertiente noroccidental de la meseta del Lago Buenos Aires, provincia de Santa Cruz. Rev. Asoc. Geo. Arg., 38 (3-4), pp. 427-436.

Cande, S.C. and Leslie, R.B. 1986. Late Cenozoic tectonics of the southern Chile trench. Journal of Geophysical Research, Vol. 91, N° B1, pp. 471-496.

Charrier, R.; Linares, E.; Niemeyer, H. and Skarmeta, J. 1979. K-Ar ages of basalt flows of the Meseta Buenos Aires in southern Chile and their relation to the southeast Pacific triple junction. Geology, Vol. 7, pp. 436-439.

Demant, A.; Hervé, F.; Pankhurst, R. and Suárez, M. 1996. Geochemistry of early tertiary back-arc basalts from Aysén, southern Chile (44-46°S): Geodynamic implications. In Andean Geodynamics, 3rd ISAG, Orstom editions, París, pp. 17-19.

Espinoza, F. 2003. Petrología y Geoquímica de los basaltos cenozoicos de la meseta Chile Chico, 46° 35'-46°47'S - 71°46'-72°02'W, XI Región de Aysén, Chile. M. Sc Tesis. Departamento de Geología, Universidad de Chile, 220 p. (unpublished).

Frassinetti, D. and Covacevich, V. 1999. Fauna de invertebrados fósiles marinos de la Formación Guadal en Pampa Castillo, sur del lago General Carrera, Aysén, Chile. Boletín, 51, Servicio Nacional de Geología y Minería, Chile, 96 p.

Flynn, J. J; Novacek, M.; Dodson, H.; Frassinetti, D.; McKenna, M.; Norell, M.; Sears, K.; Swisher III, C. and Wyss, A. 2002. A new fossil mammal assemblage from the southern Chilean Andes: implications for geology, geochronology, and tectonics. J. South Am. Sci., 15, pp. 285-302.

Gorring, M. and Kay, S. 2001. Mantle processes and sources of Neogene slab window magmas from southern Patagonia, Argentina. Journal of Petrology, 42 (6), pp. 1067-1094.

Hervé, F.; Aguirre, L.; Godoy, E.; Massone, H.; Morata, D.; Pankhurst, R.; Ramirez, E.; Sepúlveda, V. and Willner, A. 1998. Nuevos antecedentes acerca de la edad y las condiciones P-T de los complejos metamórficos en Aysén, Chile. En X Congreso Latinoamericano de Geología y VI Congreso Nacional de Geología Económica, Actas II, 133-137.

Kay, S.; Ramos, V. A. and Gorring, M. L. 2002. Geochemestry of Eocene plateau basalts related to ridge collision in southern patagonia. Actas del XV congreso Geológico Argentino, El Calafate.

Marshall, L. G. and Salinas, P. 1990. Stratigraphy of the Río Frías Formation (Miocene), along the Alto Río Cisnes, Aysén, Chile. Revista Geológica de Chile, 17, 57-88.

Niemeyer, H.; Skarmeta, J.; Fuenzalida, R.; Espinosa, W. 1984. Hojas Península de Taitao y Puerto Aysén, 1:500.000, N° 60-61, Serv. Nac. de Geol. y Min, Chile.

Parada, M. A.; Lahsen, A y Palacios, C. 2001. Ages and geochemistry of Mesozoic-Eocene back-arc volcanic rocks in the Aysén region of the Patagonian Andes, Chile. Rev. Geo. Chile, v. 28, n° 1, pp. 25-46.

Petford, N.; Cheadle, M.; Brewer, T.; Barreiro, B. 1996. Age and origin of southern Patagonian flood basalts, Chile Chico Region (46°45'S). In Andean Geodynamics, 3rd ISAG, Orstom editions, París, pp. 629-632.

Suárez, M., De la Cruz, R. and Bell, M. 1996. Estratigrafía de la región de Coyhaique (latitud 45°-46°S); Cordillera Patagónica, Chile. XII Congreso Geológico Argentino y III Congreso de Exploración de Hidrocarburos I, pp. 575-590.

Suárez, M., Demant, A. and De la Cruz. 1999. Volcanismo calcoalcalino en W Provincia Chon Aike: Grupo Ibáñez, Jurásico Superior-Cretácico Inferior temprano, Cordillera Patagónica de Aysén, Chile (45°30'-46°30' S). Actas IV congreso Geológico Argentino, Salta II, pp. 186-189.

Suárez, M. and De la Cruz, R. 2000a. Tectonics in the eastern central Patagonian Cordillera (45°30'-47°30'S). Journal of the Geological Society of London, v. 157, pp. 995-1001

Suárez, M. and De la Cruz, R. 2000b. Geología de la zona del lago General Carrera, Región de Aysén, Chile. En IX Congreso Geológico Chileno. Actas II, pp. 264-268.

Suárez, M.; De la Cruz, R. and Troncoso, A. 2000. Tropical/Subtropical Upper Paleocene-Lower Eocene fluvial deposits in eastern central Patagonia, Chile (46°45'). Journal of South American Earth Science, 13 (6), pp. 527-536.

Sun, S. and McDonough, W.F. 1989. Chemical and isotopic systematics of oceanic basalts; implications for mantle composition and processes. En: Saunders, A.D & Norry, J.M. (edit) Magmatism in the Ocean Basins. Geological Society, London, Special Publications 42, pp. 313-345.

UNRAVELLING COMPLEX SHRIMP U-Pb ZIRCON AGES FOR PALAEOZOIC AND MESOZOIC MAGMATIC ROCKS: FACT OR ARTEFACT

Fanning, M.C.[1]; Pankhurst, R.J.[2]; Rapela, C.W.[3] and Hervé, F.[4]

1. Research School of Earth Sciences, The Australian National University, Mills Road, Canberra, ACT 0200, Australia. Mark.Fanning@anu.edu.au
2. NERC Isotope Geosciences Laboratory, British Geological Survey, Keyworth, Nottingham NG12 5GG, United Kingdom. rjpt@bas.ac.uk
3. Centro de Investigaciones Geológicas, Universidad Nacional de La Plata, 644 Calle N° 1, 1900 La Plata, Argentina. CONICET. crapela@cig.museo.unlp.edu.ar
4. Departamento de Geología, Universidad de Chile, Casilla 13518, Correo 21, Santiago, Chile. fherve@cec.uchile.cl

Keywords: Geochronology, magmatic rocks, zircon, SHRIMP U-Pb analyses, age dispersions

INTRODUCTION

U-Pb zircon geochronology is one of the most widely used tools to determine the crystallization ages of magmatic rocks and the timing of high grade metamorphism. The mineral zircon is particularly robust and retains information about crustal history even through melting events. There are now a variety of analytical methods available to determine U-Pb ages, and the more widely used methods are: (1) conventional wet chemistry, isotope dilution thermal ionisation mass spectrometry (IDTIMS), (2) Sensitive High Resolution Ion Microprobe (SHRIMP) and (3) laser ablation ICP MS (LAM-ICP). Each method has it particular strengths, and weaknesses, but it is our contention that the particular complexities to be discussed in this paper are a consequence of geological processes resulting in multiple generations of zircon crystallisation over relatively short periods of time.

The significant advance in U-Pb geochronology over the past decade is the ability to consistently analyse tiny portions or fragments of zircon grains, in particular the ability to sample a volume ~20 µm diameter by ~1 µm depth (see Williams, 1998). Perhaps the most far-reaching advance has been the application of cathodoluminescence (CL) SEM images (Hanchar & Millar, 1993; Vavra, 1994; Vavra et al., 1996; Rubatto & Gebauer, 2000) to decipher the internal structure of sectioned zircon grains.

From the considerable SHRIMP U-Pb zircon data set that we have gathered, we often see complex, bimodal or skewed age distributions particularly in the ^{206}Pb/^{238}U ages of Palaeozoic and younger magmatic rocks. In general such dispersions cannot be correlated with obvious internal complexity as evidenced by CL images (for example a structurally discordant core and rim) and it is the nature of this complexity that this presentation will address.

To highlight and examine the problem of bimodal U-Pb zircon ages, two examples are shown from a study of the magmatic history of the pre-Permian basement of the Deseado massif in the Dos Hermanos area, Argentina (Pankhurst et al., in press). We will also draw on an example from a late Cenozoic magmatic rock in the Southern Patagonian Batholith, Chile (Fanning et al., 2001).

EXAMPLES OF BIMODAL AGE DISTRIBUTIONS

Two samples of granitic cobbles from a Permian conglomerate in the Deseado massif of Argentina have elongate euhedral zircon that is clearly magmatic in origin (Fig. 1). Inherited centres to grains are observed but they are not the focus of this discussion (see Fig. 4). Such complexity is clearly evident and can be deciphered from the CL images.

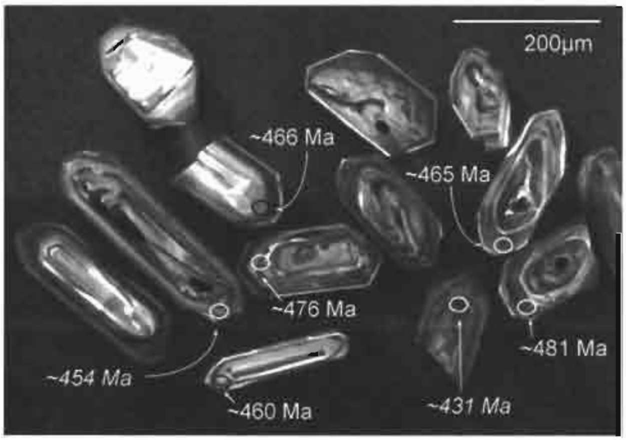

Figure 1. CL image of sectioned zircons grains from sample GOL-6 showing the dominant simple zoned magmatic structure, with some inherited low U centres. Areas analysed by SHRIMP are shown as ellipses, labelled with the ^{206}Pb/^{238}U ages.

Analyses of the simple zoned rims or tips to grains, that is, the latest magmatic components, yield SHRIMP U-Pb data that show dispersion on the Tera and Wasserburg concordia plot of the calibrated ^{238}U/^{206}Pb ratios versus the total ^{207}Pb/^{206}Pb (no correction for common Pb has been made to the data normally shown on this concordia diagram; Fig. 2). The dispersed, or bimodal age distribution for the data for sample GOL-6 is highlighted on a relative probability plot of the radiogenic ^{206}Pb/^{238}U ages. There appear to be two closely spaced, partially overlapping peaks. The analysis with an age of ~430 Ma can be reasonably excluded as a single analysis of an area of zircon that has lost radiogenic Pb. For the remainder of the data, one interpretation is to assume that the slightly older peak at ~480 Ma represents the magmatic crystallization age and that the slightly younger peak at ~465 Ma is due to radiogenic Pb loss. Equally plausible is the interpretation that the younger peak reflects the magmatic event and that the older peak is a consequence of inheritance from a slightly older magmatic crystallisation event.

Interpretation of the data for a second granite cobble (GOL-2) is perhaps more, or less difficult. The U-Pb SHRIMP zircon data shows some dispersion on the Tera-Wasserburg plot (Fig. 5); the relative probability plot appears as essentially a single peak that is skewed towards the older end of the age spectrum (Fig. 6).

KEY POINTS OF NOTE

These complex age distributions are apparent despite:

- The analyses are of areas that show relatively simple, continuous zoning with no apparent internal structures evident in the CL imaging to indicate different periods of zircon growth; that is, areas that are interpreted as simple and continuous magmatic zonation.
- There is no correlation between spot location within a particular grain (or type of zoning) and apparent age.
- The data for both samples were collected during a single extended SHRIMP analytical session, with a single calibration for the U/Pb ratio of the reference zircon.
- From our experience, often within such extended analytical sessions other samples analysed will show a simple, unimodal age distribution (that is a simple bell curve on the relative probability plot) indicating one period of zircon crystallization, implying stable instrument operating conditions.
- The dispersion is not a consequence of the analytical uncertainties; that is the 1σ SHRIMP errors are about 1-1.5% per spot analysis and so at about 500 Ma this is of the order of ±5 to 7 Ma per spot analysis. Any dispersion would be more apparent if individual spot uncertainties were ±0.5%, and conversely the dispersion would not be apparent if the individual spot uncertainties were ±3%.
- There is no simple correlation between apparent age and either U or Th concentration, nor Th/U ratio.

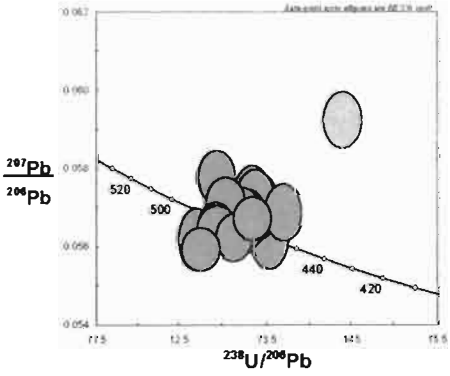

Figure 2. Tera & Wasserburg concordia plot of SHRIMP U-Pb zircon data for sample GOL-6. Analyses plotted uncorrected for common Pb as 1σ error ellipses.

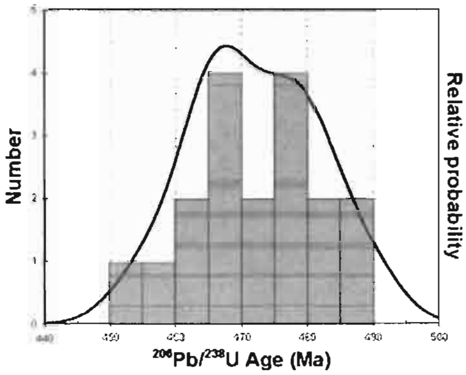

Figure 3. Relative Probability plot, with stacked histogram, of the ^{206}Pb/^{238}U ages for sample GOL-6. The bimodal nature of the age distribution is clearly evident.

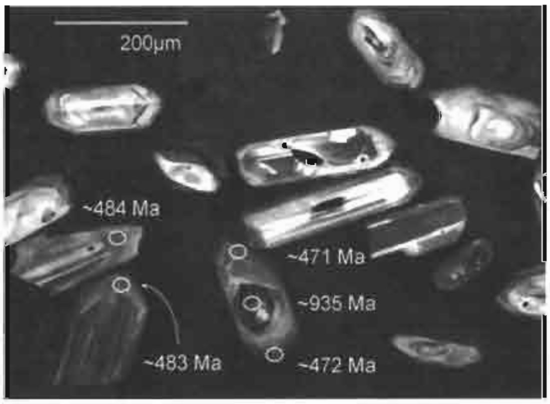

Figure 4. CL image of sectioned zircons grains from sample GOL-2 showing the dominant simple zoned magmatic structure and the clearly inherited centre to one grain. Areas analysed by SHRIMP are shown, labelled with the ^{206}Pb/^{238}U ages.

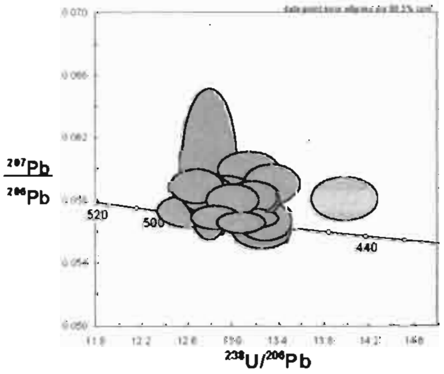

Figure 5. Tera & Wasserburg concordia plot of SHRIMP U-Pb zircon data for sample GOL-2. Analyses plotted uncorrected for common Pb as 1σ error ellipses.

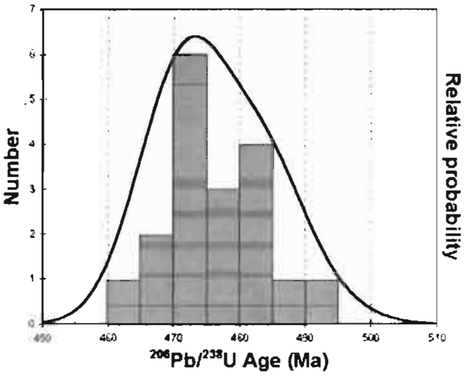

Figure 6. Relative Probability plot, with stacked histogram, of the ^{206}Pb/^{238}U ages for sample GOL-2. The relative probability curve is skewed.

OTHER U-Pb ZIRCON METHODS

The dispersed age distributions noted above (and seen in numerous SHRIMP studies) may be an artefact of the SHRIMP analytical technique and so, from publications of IDTIMS U-Pb zircon data, a number of possible similar dispersed age patterns can be used to discount this possibility. Unfortunately many IDTIMS studies involve multi-grain zircon analyses and so any such bulk analyses would necessarily be complicated by the averaging of a large and often complex zircon sample. There are a number of IDTIMS examples, mainly dealing with resolution of the Permian-Triassic Time Scale whereby dispersed age patterns are evident and interpretation of the true magmatic crystallization age is clouded. Such studies are of tuffaceous rocks and so the possibility of geological contamination by transport or inclusions is a further complexity (see for example Mundil et al. 2001; Bowring et al. 1998 & data supplement; Ludwig & Mundil, 2002).

A more relevant and crucial example is from a detailed study of the Tuolumne Intrusive Suite, Yosemite National Park, USA (Coleman et al., 2002; Glazner et al., 2002). High precision IDTIMS U-Pb zircon analyses document the sequence of successive intrusive phases over a period of 2.5 Ma, between 93.1 ± 0.1 Ma (tonalite of Glen Aulin) and 90.6 ± 0.5 Ma (bottom of the Half Dome Granodiorite). Inclusion of the 88.1 ± 0.2 Ma for the Cathedral Peak Granodiorite, at the slightly distal Tuolumne Meadows, means that this large intrusive complex was emplaced over a period of 5 Ma.

More significantly, within this date-set one can see that the younger phases record zircon inheritance presumably from the slightly older intrusive events. Although this inheritance complicates the age interpretation, by using the concordant youngest age groupings a consistent and coherent age sequence is obtained (Coleman et al., 2002). The inheritance documents complex and bimodal age distributions by IDTIMS, analogous to those seen with the SHRIMP data presented herein, and as seen in numerous other magmatic zircon suites.

FURTHER SHRIMP EXAMPLES

In the Cambrian and Ordovician, at 95% confidence limits, a pooled weighted mean SHRIMP ^{206}Pb/^{238}U age uncertainty is normally ±1% (or ±~5 Ma). This uncertainty is of the order of the total age range reported for the Tuolumne Intrusive Suite. Thus it would not be possible using SHRIMP to resolve the age sequence similar to the 5 Ma total range for the Tuolumne Intrusive Suite in Ordovician or Cambrian magmatic suites.

However, the ±1% SHRIMP U-Pb uncertainty is the long-term external uncertainty that is reproduced through out the Palaeozoic and Cenozoic. Thus it should be possible to resolve such 5 Ma age differences using the SHRIMP for zircons of the order of 5-10 Ma. One such example is a columnar jointed, hornblende dacite from Fiordos Calvo and Peel, southern Patagonia (Fanning et al., 2001). The analyses of the dominantly simple zoned magmatic zircons reveal central zones that are ~10 Ma with outer magmatic zones of ~5 Ma, the interpreted crystallization age for the dacite. At this age range SHRIMP can clearly resolve the 5 Ma difference between the magmatic cores and magmatic rims. In fact at ~5 Ma, the SHRIMP uncertainties enable one to resolve 4.88 ± 0.10 Ma from 5.42 ± 0.10 Ma components within the interpreted magmatic "rim" components to the same zircon population. This latter age resolution of ~0.5 Ma is at the generally considered maximum time limits for magma residence within the upper crust; that is maximum time for crystallization of a single magmatic body.

DISCUSSION

Returning to the data for GOL-6 and GOL-2 in the light of the above examples, it is possible for apparently simply zoned magmatic zircons to contain inherited components that cannot be deciphered even with a detailed study of CL images. Inherited zoned magmatic zircon say 0.5 to 5 Ma or older than the magmatic crystallisation age from within a generally coherent series of magmatic intrusive (or eruptive) events would appear under CL and under morphological criteria to be similar if not identical to the latest crystallizing zircon. Thus resultant, apparently dispersed ages are not an artefact of the SHRIMP analytical technique but a consequence of successive zircon crystallization in an evolving magmatic system.

For the bimodal distribution observed from GOL-6, the favoured crystallisation age would be 465 ± 5 Ma (the younger and slightly more dominant peak). The older subordinate peak at 480 ± 5 Ma peak is thus interpreted to reflect zircon crystallization in an earlier phase of a perhaps related magmatic process.

For the skewed age distribution recorded in sample GOL-2, the interpreted magmatic age is 473 ± 5 Ma for the dominant age grouping. The skew is interpreted to result from incorporation of an older component of magmatic zircon at 483 ± 6 Ma.

These results represent a statistically significant revision to the ages of 472 ± 5 Ma and 476 ± 5 Ma, respectively for these two samples, published by

Pankhurst et al. (in press) without attempting to resolve these internal variations. The revision does not however significantly affect the geological implications based on the data by these authors, who recognized the boulders as being derived from a nearby Famatinian magmatic arc. Famatinian magmatism dated by U-Pb zircon methods ranges from ca. 460 Ma to ca. 490 Ma (Pankhurst et al. 1998).

REFERENCES

Bowring S.A., Erwin D.H., Jin Y. G., Martin M.W., Davidek K. & Wang W. (1998) U/Pb Zircon Geochronology and Tempo of the End-Permian Mass Extinction. Sci., 280:1039-1045.

Coleman D.S., Gray W. & Glazner A.F. (2002) U-Pb geochronologic evidence of the incremental filling of the Tuolumne Intrusive Suite magma chamber. Geological Society of America Abstracts with programs. 34(6):121-5.

Fanning C.M., Hervé F., Pankhurst R.J., Thomson S. and Faúndez V. (2001) Late Cenozoic magmatism in the South Patagonian Batholith. SHRIMP U-Pb zircon age evidence. III South American Symposium on Isotope Geology, Pucon, Chile.

Glazner A.F., Taylor R.Z., Bartley J.M. & Gray W. (2002) Dike assembly of the Tuolumne Intrusive Suite, Yosemite National Park, California. Geological Society of America Abstracts with programs. v.34 n.6; 121-4.

Hanchar J.M & Millar C.F. (1993) Zircon zonation patterns as revealed by cathodoluminescence and backscattered electron images: Implications for interpretation of complex crustal histories. Chemical Geology 112: 1-13.

Ludwig KR, and Mundil R. (2002) Extracting reliable U-Pb ages and errors from complex populations of zircons from Phanerozoic tuffs. J. Conf. Abstr. 12th Goldschmidt Conf.

Mundil R., Metcalfe I., Ludwig K.R., Renne P.R., Oberli F, Nicoll R.S. (2001) Timing of the Permian-Triassic biotic crisis : implications from new zircon U/Pb age data (and their limitations). Earth & Planetary Science Letters v.187: 131-145.

Pankhurst R.J., Rapela C.W., Saavedra J., Baldo E., Dahlquist J., Pascua I. & Fanning C.M. (1998). The Famatinian magmatic arc in the southern Sierras Pampeanas. In: The Proto-Andean Margin of Gondwana (eds. Pankhurst, R.J. & Rapela , C.W.), Special Publication of the Geological Society, London, No. 142, 343-367.

Pankhurst, R.J., Rapela, C.W., Loske, W.P., Fanning, C.M. & Márquez, M. (in press). Geochronological study of the pre-Permian basement rocks of southern Patagonia. Journal of South American Earth Sciences (accepted 6 January 2003).

Rubatto D and Gebaüer D (2000) Use of cathodoluminescence for U-Pb zircon dating by ion microprobe: some examples from the Western Alps. In: Cathodoluminescence in Geosciences (eds. Pagel M, Barbin V, Blanc P and Ohnenstetter D) Springer Verlag, 373–400.

Varvra G (1994) Systematics of internal zircon morphology in major Variscan granitoid types. Contributions to Mineralogy & Petrology 117: 331-344.

Varvra G, Gebauer D, Schmid R and Compston W (1996) Multiple zircon growth and recrystallisation during polyphase Late Carboniferous to Triassic metamorphism in granulites of the lvrea Zone (Southern Alps); an ion microprobe (SHRIMP) study. Contributions to Mineralogy and Petrology 122: 337–358.

Williams I.S. (1998) U-Th-Pb Geochronology by Ion Microprobe. In: McKibben, M.A., Shanks III, W.C. and Ridley, W.I. (eds), Applications of microanalytical techniques to understanding mineralizing processes, Reviews in Economic Geology, 7: 1-35.

OXYGEN ISOTOPE SYSTEMATICS AND THE ORIGIN OF A HIGH-K CALC-ALKALIC GRANITIC PLUTON FROM THE BORBOREMA PROVINCE, NORTHEASTERN BRAZIL

Ferreira, V.P.[1]; Valley, J.W.[2]; Sial, A.N.[1]; Pessôa, R.J.R.[1] and Spicuzza, M.[2]

1. NEG-LABISE, Department of Geology, UFPE, C.P. 7852 Recife-PE, 50670-000, Brazil
2. Department of Geology and Geophysics, University of Wisconsin, 1215 W. Dayton St., Madison, WI, 53706, USA

Keywords: Oxygen isotopes, high-K calc alkalic, magmatic epidote, zircon

INTRODUCTION

Oxygen isotopes are important tools for petrogenetic processes as they are good indicators of granite source materials, providing also valuable information about cooling history and sub-solidus fluid interaction processes. The objective of this work is to present $\delta^{18}O$ values of a granitic pluton and characterize possible protoliths.

The Tavares pluton is one of the best exposed Neoproterozoic undeformed magmatic epidote-bearing granitoid in the Alto Pajeú terrane, Borborema province, northeastern Brazil. This batholith (200 km^2 in area) intruded the 1.0 Ga Ambó gneiss of the Alto Pajeú terrane and schists of the Cachoeirinha terrane, being bounded by shear zones along its northern (Juru shear zone) and southern margins (Lagoa da Cruz shear zone).

PETROGRAPHY AND FIELD RELATIONS

The Tavares pluton is a NE-SW elongate 165 km^2 pluton intrusive into Mesoproterozoic orthogneisses and minor paragneisses, parallel to the regional foliation. It encompasses porphyritic quartz syenite, quartz monzonite, monzogranite and syenitogranite, in which K-feldspar crystals up to 6cm long and plagioclase are the main megacrystic phases. Hastingsite, biotite, titanite, magmatic epidote, allanite, zircon and apatite, and rare opaque minerals are accessory phases. Magmatic epidote occurs as euhedral to subhedral, zoned or twinned crystals, enclosed or partially enclosed by biotite, sometimes showing allanite cores. The main mafic phases are typical of granitoids with igneous (I-type) rock source.

Linearly distributed tonalitic to quartz dioritic enclaves are common and are interpreted as disrupted synplutonic dikes. These structures attest to coexistence of mafic and felsic magmas in this pluton. In the central portion of the pluton, pillow-like structures are observed, as well as some angular shaped, up to 10m-long, layered (amphibolite alternates with epidote-rich layers) megaxenoliths. The pluton exhibits diverse magmatic structures, encompassing, besides magmatic foliation, ladder dikes, snail, mushroom shaped-structures, K-feldspar dikes, blebs and concentric rings.

GEOCHEMISTRY

The porphyritic granitoids as well as the quartz diorite and tonalite syn-magmatic enclaves are high-K calc-alkalic in composition. The mafic enclaves are metaluminous while the porphyritic granitoids are metaluminous to peraluminous, characterized by relatively low SiO_2 contents ($\approx$ 65 – 72wt%), moderate MgO and CaO ($\approx$ 0.8 – 2wt% and $\approx$ 2 – 3.3 wt%, respectively), and high Cr (up to 789 ppm) and Ni (up to 1690 ppm) in some samples, especially those near the largest and more numerous expositions of mafic enclaves and a mega (10m long) ortho-amphibolite xenolith.

A six-point whole rock Rb-Sr isochron yields an age of 590 ± 36 Ma, with initial $^{87}Sr/^{86}Sr$ of 0.71017, and attests to a Neoproterozoic age for this pluton, intrusive during the Brasiliano orogenic cycle. Values of ε_{Nd} calculated at 600 Ma range from -3.6 to -3.2 and T_{DM} varies from 1.3 to 1.4 Ga (Pessôa, 2001).

METHODOLOGY

Oxygen isotope ratios have been determined in four whole rock powders (including a mafic enclave) and thirty six mineral separates, including zircon, quartz, titanite, epidote, and feldspar, among which titanite, quartz and epidote are from a mafic enclave, and from an amphibolite mega xenolith sample. Mineral separates were analyzed for oxygen isotope ratios by CO_2-laser fluorination at the University of Wisconsin, using BrF_5 as reagent, following the methodology described by Valley et al. (1995). Quartz was analyzed using the rapid heating and defocused laser beam technique as described by Spicuzza et al. (1998). All results are reported in the δ standard notation, in permil relative to Vienna Standard Mean Ocean Water (VSMOW).

WHOLE-ROCK AND MINERAL SEPARATE OXYGEN ISOTOPE DATA

Values of $\delta^{18}O$ (whole rock) are homogeneous, varying from 10.58‰ to 10.93‰, with average of 10.78‰ ± 0.15‰. A mafic enclave has $\delta^{18}O$ = 10.59‰, i.e. close to the lower limit of the host rock $\delta^{18}O$ (whole rock). Values of $\delta^{18}O$ of mineral separates show the expected order of ^{18}O-enrichment in the different analyzed samples, i.e. $\delta^{18}O$ quartz (average 13.10‰ ± 0.15‰) > feldspar (average 10.92‰ ± 0.07‰) > zircon (average 9.13‰ ± 0.09‰) > epidote (average 8.04‰ ± 0.10‰) > titanite (average 7.90‰ ± 0.16‰), although $\delta^{18}O$ values of epidote and titanite are the same (differences in the second decimal) in three out of eight analyzed samples. Values of $\delta^{18}O$ for different minerals are quite different but variations within each mineral are limited.

Oxygen isotope fractionations among minerals are significantly higher than those expected in equilibrium at magmatic (800°-700°C) temperatures, and mineral pairs do not preserve a common equilibrium temperature. As expected, coexisting zircon-titanite fractionations show a more limited range (average Δ(Zir-Ttn) = 1.24 ± 0.19‰; Fig. 1), representing a higher temperature (T = 644°C, calculated after King et al., 2001) than do other mineral pairs. The values of $\delta^{18}O$ for quartz coexisting with zircon (average Δ (Qtz-Zir) = 3.97 ± 0.17‰), and titanite (Δ (Qtz-Ttn) = 5.20 ± 0.17‰) (Figs. 2, 3) indicate apparent temperatures of 514°C (Qtz-Zir; calculated after Valley et al., 2003), and 556°C (Qtz-Ttn, calculated after King et al., 2001). Oxygen isotope fractionations among minerals are compatible with closed system conditions, and likely reflect their different closure temperatures.

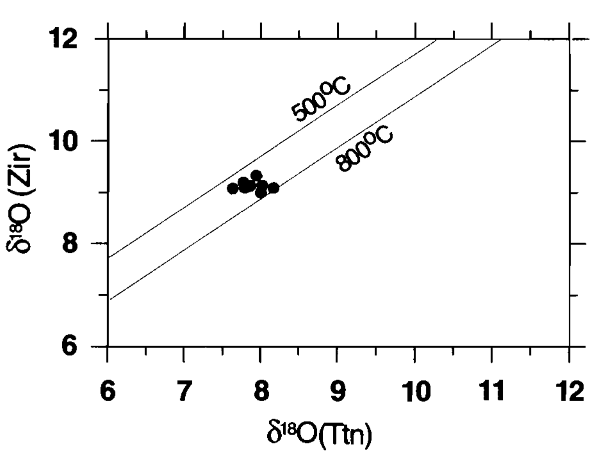

Figure 1. $\delta^{18}O$ for titanite coexisting with zircon in the Tavares pluton. Isotherms calculated after King et al. (2001).

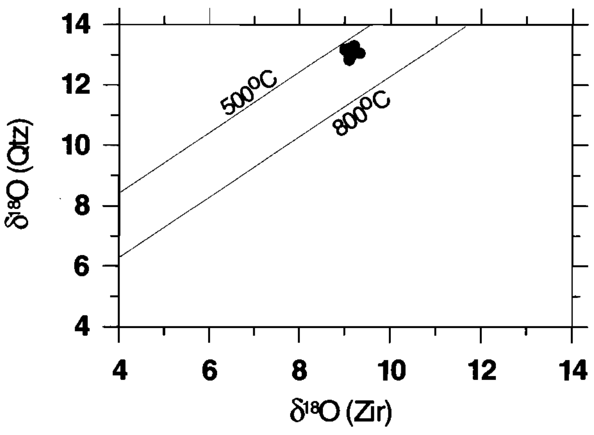

Figure 2. $\delta^{18}O$ for zircon coexisting with quartz in the Tavares pluton. Isotherms calculated after Valley et al. (2003).

Values of $\delta^{18}O$ of epidote for one mafic enclave (12.94‰) and one orthoamphibolite sample (12.66‰) are higher than the average observed for epidote from the host porphyritic granitoid (8.03‰), while the value for titanite in the mafic enclave (7.89‰) is close to the average value (7.90‰) in the granitoid.

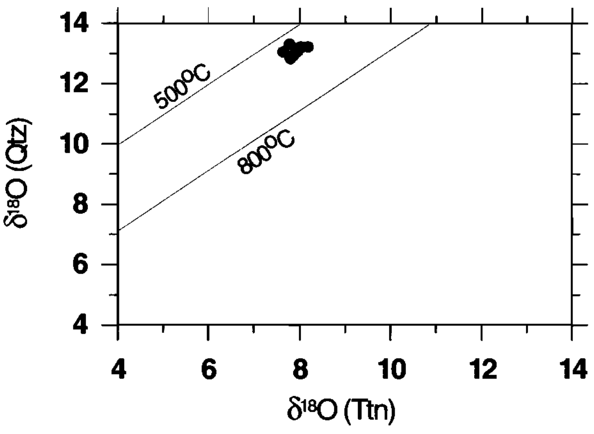

Figure 3. $\delta^{18}O$ for titanite coexisting with quartz in the Tavares pluton. Isotherms calculated after King et al. (2001).

Magmatic whole-rock oxygen isotope ratios for the Tavares pluton vary from 10.79 to 11.09‰, as calculated using the values of $\delta^{18}O$(zircon) (9.00-9.33‰) and whole-rock SiO_2 contents (65.5-69.9wt%) (Valley et al., 1994, 2003). Assuming a closed system, the estimated $\delta^{18}O$(whole rock) should be close to the $\delta^{18}O$ of the original magma. The average of $\delta^{18}O$ calculated magma values (10.90‰) is very close to the average $\delta^{18}O$ determined whole rock (10.78‰), indicating that the system has been closed for oxygen isotope exchange after solidification. The estimated low apparent temperature for quartz-mineral would most likely be due to oxygen isotope exchange with feldspar within the system.

DISCUSSION

Many features observed in the Tavares pluton indicate that the porphyritic granitoids have been in contact with a more mafic magma during the magmatic stage, and that there was convection during the formation of the magma chamber due to intermittent heat from external sources. This is indicated by the presence of quartz-dioritic syn-plutonic dikes and other magmatic structures such as ladder dikes, up to 1 m long snail and elliptical or circular concentric structures, in which mafic-rich layers alternate with felsic layers in the latter ones. In many of these structures K-feldspar megacrysts are in the nucleous. These structures are common in a single outcrop, although of random distribution within the pluton. These features are interpreted as to be due to convective currents originated by underplating of a mafic magma (Weinberg et al., 2001), implying in contrast of temperatures within the magma chamber at short distances. The concentric structures represent magma flow in conduits and a frozen snapshot of thermal plume.

One tectonic setting in which high-K calc-alkalic magmas can be generated is postcollisional setting where melting of the source rocks occurs as a consequence of decompression following crustal thickening. This would allow mantle upwelling and underplating of the lower crust by mafic magmas and would provide extra heat necessary for partial melting (Roberts & Clemens, 1993). High-K calc-alkalic I-type granitoids are generated through partial melting of metaigneous rocks in the lower crust and data on the experimental partial melting of common crustal rocks suggest that they can be derived from the partial melting of hydrous calc-alkalic metamafic to intermediate igneous rocks (Roberts & Clemens, 1993).

These tectonic and petrogenetic models are consistent with the tectonic setting for the emplacement and with field observations at the Tavares pluton and with the oxygen isotope ratios. The magmatic oxygen isotope values for the porphyritic granitoid are high for an I-type granitoid (up to 10‰), but very uniform, and oxygen isotope fractionation among minerals is very consistent. These values coupled with high $^{87}Sr/^{86}Sr$ ratios and mantle-like ε_{Nd} values, are compatible with a crustal protolith contaminated at the source with a mantle-derived material. The Nd model age is close to the interval when a large input of mantle material has been added to the continental crust, during the Grenville event, although no orogenic event of this age interval has been described in this part of Brazil.

An alternative possible source rock for the porphyritic granitoid is amphibolite, whose melting can generate magmas of this composition. The mega amphibolite xenolith found in the pluton would be a possible source on the basis of its oxygen isotope values, which are very close to that for the host granitoid. However, the origin for the high $\delta^{18}O$ values for these mafic rocks would remain with no explanation in light of the present data.

ACKNOWLEDGMENTS

VPF and ANS are grateful to CAPES for post-doctoral and senior post-doctoral scholarships that allowed them to perform the oxygen isotope analyses at the University of Wisconsin. This is the contribution n. 214 of NEG-LABISE.

REFERENCES

Ferreira, V.P., Valley, J.W., Sial, A.N., Spicuzza, M. (2003) Oxygen isotope compositions and magmatic epidote from two contrasting metaluminous granitoids, NE Brazil. Contrb. Mineral. Petrol. (in press).

King, E.M., Valley, J.W., Davis, D.W. and Kowallis, B.J. (2001). Empirical determination of oxygen isotope fractionation factors for titanite with respect to zircon and quartz. Geochim. Cosmochim. Acta, 65(18):3165-3175.

Pessôa, R.J. (2001). Mecanismos de alojamento e construção do batólito granítico Neoproterozóico de Tavares, Estado da Paraíba, nordeste do Brasil. Doctoral dissertation, Federal University of Pernambuco, Recife, 218p.

Roberts, M.P. and Clemens, J.D. (1993). Origin of high-potassium, calc-alkaline, I-type granitoids. Geology, 21:825-828.

Spicuzza, M.J., Valley, J.W., Kohn, M.J., Girard, J.P. and Fouillac, A.M. (1998). The rapid heating, defocused beam technique: a CO_2-laser-based method for highly precise and accurate determination of $\delta^{18}O$ values of quartz. Chem. Geol. 144:195-203.

Valley, J.W., Chiarenzelli, J.R., McLelland, J.M. (1994). Oxygen isotope geochemistry of zircon. Earth Plan. Sci. Lett. 126:187-206

Valley, J.W., Kitchen, N., Kohn, M.J., Niendorf, C.R. and Spicuzza, M.J. (1995). UWG-2 a garnet standard for oxygen isotope ratios: strategies for high precision and accuracy with laser heating. Geochim. Cosmochim. Acta 59:5223-5231.

Valley, J.W., Bindeman, I.N. and Peck, W.H. (2003). Empirical calibration of oxygen isotope fractionation in zircon. Geochim. Cosmochim. Acta, 67(11) (in press).

Weinberg, R., Sial, A.N. and Pessôa, R.J.R. (2001). Magma flow within the Tavares pluton, northeastern Brazil: compositional and thermal convection. Geol. Soc. Amer. Bull., 113(4):508-520.

Sr AND Nd ISOTOPE SIGNATURES OF A-TYPE ALKALINE SYENITES, GRANITES AND ASSOCIATED DIORITES AND HYBRID ROCKS FROM THE CORUPÁ MASSIF (SC), SERRA DO MAR PROVINCE, S BRAZIL

Garin,Y.[1,2]; Vlach, S.R.F.[1] and Tassinari,C.G.C.[1]

(1) Instituto de Geociências, Universidade de São Paulo, São Paulo-SP, Brazil. srfvlach@usp.br
(2) Faculdade de Geologia, Universidade Estadual do Rio de Janeiro-RJ. ygarin@netscape.net

Keywords: A-type syenites and granites, diorites and hybrid rocks, Sr and Nd isotopes, Serra do Mar Province

INTRODUCTION

One of the most important Neoproterozoic (*ca.* 590 Ma) A-type granite province in Southern Brazil is the so-called Serra do Mar Province. This province presents both alkaline and aluminous petrographic associations of A-type syenites and granites forming about a dozen high-level intrusive massifs with some related mafic and felsic volcanics cropping out in the states of São Paulo, Paraná and Santa Catarina, with a general NNE structural trend.

The Corupá Massif is the most meridional massif of that province, cropping out in the SW limit of the Campo Alegre vulcano-sedimentary basin, in Santa Catarina State. It was emplaced in to older granulites and migmatites of the Luis Alves cratonic fragment and is one of the few A-type massifs from that province entirely made of rocks belonging to the alkaline association.

We present in this report representative Sr and Nd isotope data for selected samples of the main syenites, granites, and hybrid rocks, emphasizing the contrasting syenite-granite vs diorite-hybrid rock associations.

PETROGRAPHY AND GEOCHEMISTRY

The Corupá Massif (formely *Corupá Granite*, *e.g.*, Albuquerque et al., 1971) is a relatively small massif (*ca.* 50 km^2) with a semi-ring structure (Garin, 2002). Most of the outcrop areas are covered with dense forest and the access is very difficult, turning field mapping and *in situ* sample collection a very difficult task.

The main petrographic facies are coarse- and medium-grained dark green or rose-colored syenites with a massive or a somewhat oriented structure. They comprise hypidiomorphic-textured *hypersolvus* alkali-feldspar syenites and quartz syenites (Fig. 1). The typical mafic minerals are hedenbergite, calcic- and calcic-sodic amphiboles and fayalite olivine. In the more felsic rock varieties, olivine tends to disappear and both pyroxene and amphibole becomes richer in Na (for instance, egirine-augite and Fe-richterite). Magnetite (in most mafic types), ilmenite, chevkinite, zircon, apatite and some titanite are common accessories. A local mela-syenite (M up to 65) associated with coarse-grained green syenites has a typical cumulatic texture with abundant olivine, pyroxene, magnetite, ilmenite and apatite as cumulus phases with intercumulus alkali-feldspar and some biotite. The alkali-feldspar granites are subordinated and appear as minor irregular (?) bodies within the main syenites. The characteristic mafic mineral is calcic-sodic and sodic (riebeckite, predominant) amphibole. Zircon, apatite, ilmenite, chevkinite, and some sphalerite are accessory minerals. The primary mineralogy indicates that the main rocks crystallized close to the QFM buffer.

The coarse-grained syenites and the granites present a typical late, intersticial, hydrothermal mineralogy. High Si/Al, Fe-rich biotite, among other phylossilicates, and Fe-actinolite are typical in the syenites, while Fe-rich allanite, epidote, and zircon are more common in the granites. Albite, hematite, sulphides, and some unidentified phases are common to both.

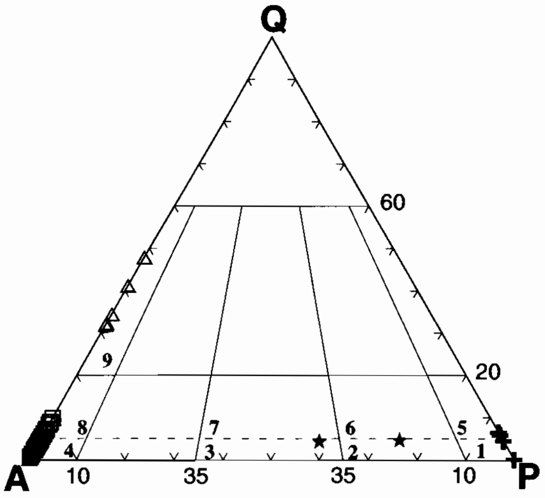

Figure 1. QAP modal diagram for rocks from the Corupá Massif. Symbols: alkali-feldspar syenites and quartz-syenites: open squares; alkali-feldspar granites: open triangles; diorites and quartz-diorites: crosses; hybrid monzonites and monzodiorites: stars.

K-rich diorites, monzodiorites and monzonites appear as syn-plutonic dikes and several centimetric- to decimetric-sized hybrid enclaves closely associated with the more evolved medium-grained syenites. The diorites are made up mainly of oligoclase, diopside, biotite, quartz and some calcic-amphibole. Magnetite, ilmenite and apatite are accessories. With the exception of the alkali-feldspar, the mineralogy of the hybrid rocks is similar. These rocks preserve some mixing-related textures (*e.g.*, mantled feldspars). Epidote, prehnite, chlorite, and opaque minerals grow during a post-magmatic stage. The hybrid enclaves were seen only near the main dioritic bodies, suggesting that the mixing phenomena took place close to the emplacement levels.

The main geochemical features of the Corupá rocks do not depart from the typical patterns observed elsewhere in A-type syenites and associated granites from post-collisional tectonic settings (Garin & Vlach, 2002, see also Figs. 2, 3). Syenites and diorites are metaluminous rocks with mg# numbers ranging from 0.03 to 0.26 and 0.35 to 0.40 respectively, while the granites are peralkaline, with 0.05 ≤ mg# ≤ 0.02. The hybrid enclaves are metaluminous and present intermediate mg# values. REE patterns are highly fractionated for the syenites with a slighly positive (cumulatic coarse rocks) to negative (medium differentiated rocks) Eu anomaly, flattening in the peralkaline granites, with a strong negative Eu anomaly. The diorites and the hybrid rocks present fracionated REE patterns without significant or with a slightly negative Eu anomaly.

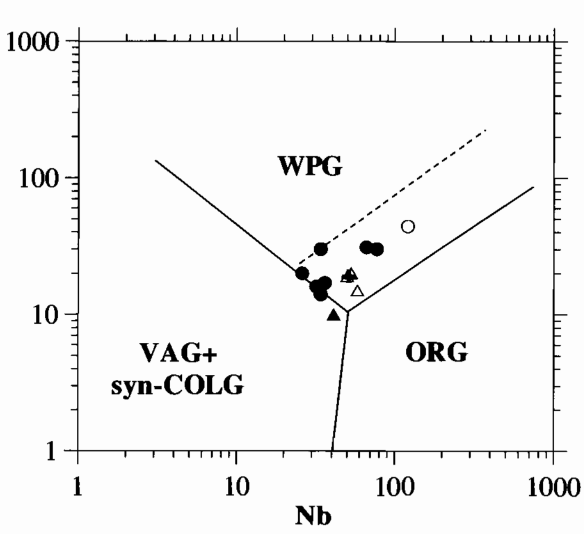

Figure 2. Nb-Y discrimination diagram for the Corupá samples (after Pearce et al., 1984). Symbols: open circles: granites; full circles: syenites; cross: melasyenite; full triangle: diorite; open triangle: hybrid monzodiorites and monzonites.

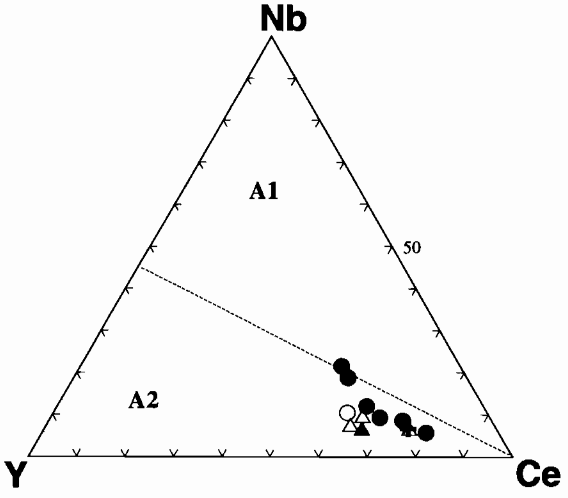

Figure 3. Y-Nb-Ce plot for Corupá samples. A1 and A2 compositional fields after Eby (1992). Symbols as in Figure 2.

Conventional zircon U-Pb dating results for the Corupá "granite" and related massifs from the Serra do Mar Province point to crystallization ages close to *ca.* 590 Ma (*e.g.*, Siga Jr. et al., 1997).

ISOTOPE DATA

Six samples collected in the massif were selected for isotopic Rb-Sr and Sm-Nd analyses. They are representative of the melasyenites (1) syenites (2), granites (1) diorites (1) and hybrid monzonitic enclaves (1). Isotopic analyses were carried out the Centro de Pesquisas Geocronológicas of the University of São Paulo, following conventional analytical procedures (Sato et al., 1995).

The whole rock Rb-Sr system was significantly disturbed in most of the Corupá samples due to late hydrothermal imprint, an effect most pronounced in the more felsic samples. The present day $^{87}Sr/^{86}Sr$ vs $^{87}Rb/^{86}Sr$ ratios obtained in this work and those presented by Siga Jr. (1995) and Siga Jr. et al. (1997) are plotted in Figure 4 with the 590 Ma reference isochron. With the exception of three samples, the melasyenite and the less differentiated syenites with $^{87}Rb/^{86}Sr$ up to about 4 align on a 7-point reference isochron (Model 3 of Ludwig, 1998) of 575 ± 50 Ma (MSWD = 3) with a $(^{87}Sr/^{86}Sr)_0$ initial ratio of about 0.7057. Considering the well constrained 590 Ma age, the best initial ratio will be close to 0.7051, a value very similar to the initial ratio of the melasyenite at 590 Ma, the sample presenting no evidence of significant hidrothermal effects. All other samples with higher $^{87}Rb/^{86}Sr$ (differentiated syenites and granites) plot well below the 590 reference line (see Fig. 4 inset) and give apparent isochron ages down to 530-550 Ma. For instance, the analyzed granite yields a very low, anomalous $(^{87}Sr/^{86}Sr)_{590}$ value of about 0.687±0.002.

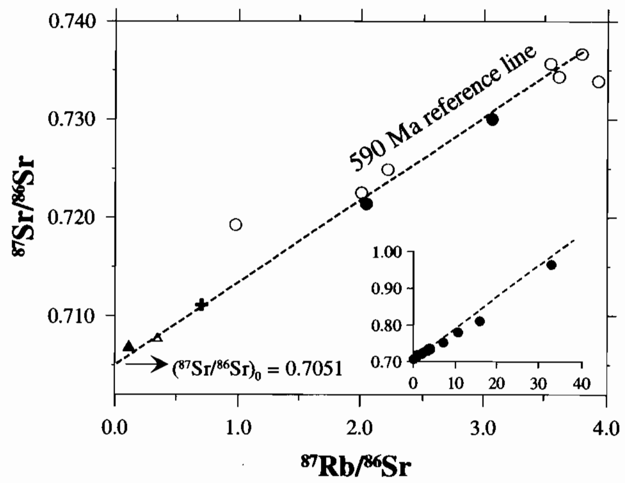

Figure 4. $^{87}Sr/^{86}Sr$ vs $^{87}Rb/^{86}Sr$ diagrams for the Corupá Massif. Main diagram symbols: less differentiated alkali-feldspar syenites (open circles, previous literature data; full circles, this work), alkali-feldspar melasyenite (cross), diorite (full triangle), hybrid monzonite (open triangle). Inset: All data, including differentiated alkali-feldspar syenites and granites.

The $(^{143}Nd/^{144}Nd)_{590}$ ratios (Fig. 5) are between 0.51117 and 0.51122 (syenites, 0.5122 for the melasyenite), 0.51126 (alkali-feldspar granite), 0.51134 (diorite), and 0.51122 (monzonitic enclave). With the exception of the diorite with the highest, and the medium grained syenite with the lowest initial ratios, the other samples present similar values within 2σ errors. Sm/Nd ratios are in the range 0.17-0.22. The granite sample presents the most contrasted and highest Sm/Nd value, due to significant removal of chevkinite - a typical REE-rich titanossilicate accessory, with Sm/Nd between 0.076 and 0.084 - from the original syenitic melts (Vlach, 1998).

The T_{DM} model ages (DePaolo, 1981; see Fig. 6) are 2.05-2.15 for the main syenites, 2.20 for the melasyenite, 2.02 (diorite), 1.98 (monzonite). The granite sample present a higher model age (*ca.* 2.43 Ga), as chevkinite removal leads to a decrease in the $f_{Sm/Nd}$ parameter.

The isotope Nd-Sr correlation diagram (Fig. 7) shows that the Corupá rocks present relatively evolved Nd, and to a lesser extent Sr isotope compositions compared to the Bulk Earth (at 590 Ma). It also points to the contrasting signatures of syenites and granites on the one hand and the diorites on the other. The latter have more primitive and evolved Nd and Sr isotope ratios than syenites and granites. Within syenite rocks, the medium grained sample has somewhat lower Nd isotope ratio. The monzonite plots close to a diorite - medium-grained syenite tie-line, supporting a mixing hypothesis for its origin.

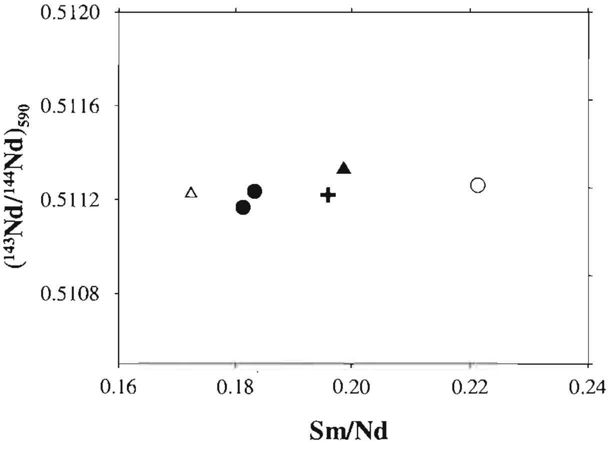

Figure 5. $(^{143}Nd/^{144}Nd)_{590}$ vs Sm/Nd plot for the Corupá alkali-feldspar syenites and granite, diorite and monzonite. Sample symbols as in Figure 2.

FINAL REMARKS

The isotope Sr-Nd data presented for the Corupá Massif (see also Siga Jr. et al., 1997) reveals its evolved isotope compositions, with special reference for the Nd initial ratios, suggesting an enriched mantle source for the parental magmas. These results, in connection with geochemical data, indicate a "crustal" component in their sources as suggested also by trace element behavior (Garin & Vlach, 2002, see also Fig. 3). We interpret this component as older materials carried into the mantle through a subduction zone, rather than incorporated during magma ascent and evolution though the crust.

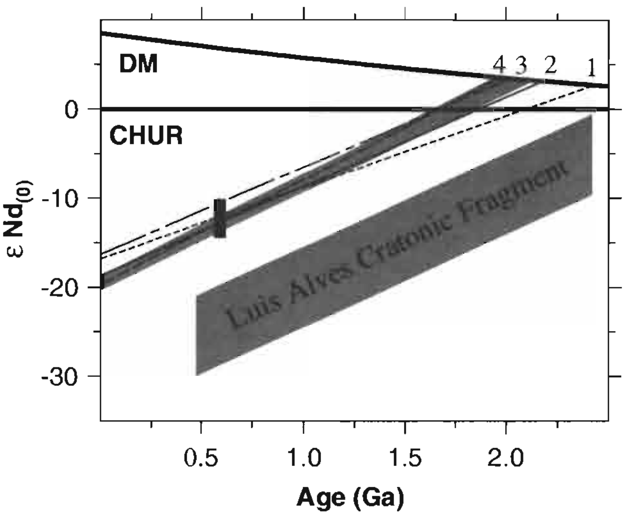

Figure 6. Evolution of ε_{Nd} against time for the sampled Corupá rocks. Main alkali-feldspar syenites, hatched area; alkali-feldspar granite, 1; melasyenite, 2; monzonite enclave, 3; diorite, 4. The hatched field of Luis Alves Cratonic Fragment is based on data from M.A.S. Basei (pers. comm.)

The Sr-Nd isotopic signatures and the depleted mantle ages of about 2.0 Ga of the Corupá Massif are very similar to those representative of the aluminous A-type granites and associated K-diorites from the Itu Province to the Northeast (*e.g.*, Vlach et al., 1996). We suspect that quite similar mantle enrichment mechanisms could have operated in both provinces.

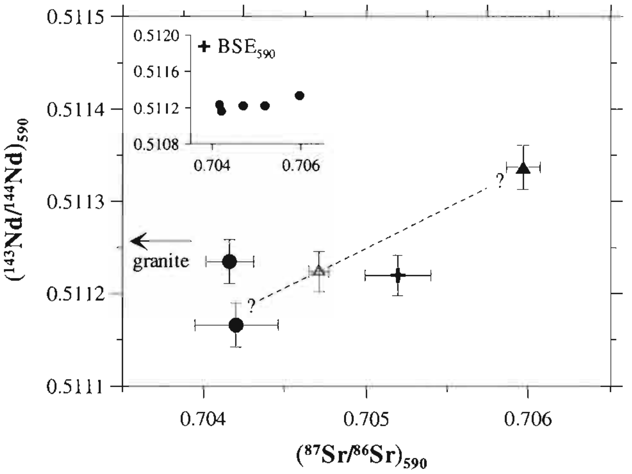

Figure 7. Sr-Nd isotope correlation diagram for the Corupá Massif rocks. The inset compares their isotope compositions with the Bulk Earth at 590 Ma. Symbols in the main figure as in Figure 4.

The isotope data also support petrographic and geochemical information, suggesting that syenites - apart from the medium-grained sample with unexpected low Nd initial ratios - and granites were most likely comagmatic, the latter being evolved residual melts extracted from the crystallizing syenites, through a filter-pressing process (Garin & Vlach, 2002). The diorites, on the other hand, were originated from a diffentent, but also enriched mantle source. The more basic parental magmas (?), which may have originated syenite melts by crystal fractionation, are not observed at the present day erosion levels.

The monzodiorites and monzonites represent more probably local syenite-diorite mixing phenomena, occurring near the emplacement levels, rather than discrete magma batches.

ACKNOWLEDGEMENTS

We thank the Centro de Pesquisas Geocronológicas at the University of São Paulo for analytical facilities. YG thanks CAPES for a Ms. studentship.

REFERENCES

Albuquerque, L.F.F.; Arioli, E.E.; Dias, A.A. and Kirchner, C.A., 1971. Geologia das quadrículas de Blumenau e Santa Catarina. Relatório de arquivo técnico, DGM, 1768. DNPM/CPRM, Porto Alegre. 121 p.

Garin, Y., 2002. Mineralogia e petrologia da associação de sienitos e granitos de tipo-A do Maciço Corupá (SC). Dissertação de Mestrado. Inédita. IGc-USP. 168 p.

Garin, Y. and Vlach, S.R.F., 2002. Geologia e petrologia da associação alcalina de granitos de tipo-A na Província Serra do Mar, Sul do Brasil: O Maciço Corupá (SC). Anais do XLI Congresso Brasileiro de Geologia, João Pessoa. SBG. p. 447.

Ludwig, K.R., 1998. Isoplot/Ex: a geochronological toolkit for Microsoft Excel. Berkeley Geochronological Center, Special Publication No. 1. 43 p.

Eby, W.A., 1992. Chemical subsivion of the A-type granitoids: petrogenetic and tectonic implications. Geology, 20:641-644.

Pearce, J.A.; Harris, N.B.W. and Tindle, A.G., 1984. Trace element discrimination diagrams for the tectonic interpretation of granitic rocks. Journal of Petrology, 25:956-983.

Sato, K., Tassinari, C. C. G.; Kawashita, K. and Petronilho, L., 1995. O método geocronológico Sm/Nd no IG/USP e suas aplicações. Anais da Academia Brasileira de Ciências, 67:313-336.

Siga Jr., O., 1995. Domínios tectônicos do sudeste do Paraná e nordeste de Danta Catarina: geocronologia e evolução crustal. Tese de Doutoramento. Inédita. IGc-USP. 164 p.

Siga Jr., O.; Basei, M.A.S.; Reis Neto, J.M.; Harara, O.M.; Passareli, C.R.; Prazeres, H.; Weber, W. And Machiavelli, A., 1997. Ages and tectonic setting of alkaline-peralkaline granitoids of Paraná ans Santa Catarina States, southern Brazil. I South American Symposium on Isotope Geology, Campos de Jordão. Extended Abstracts, 301-303.

Vlach, S.R.F., 1998. Ocorrência e variações composicionais de chevkinita-Ce e allanita(-Fe) em quartzo sienitos do Maciço Corupá (SC), Província Serra do Mar. Anais do V Congresso dos Países de Lingua Portuguesa, SBGq. P. 627-630.

Vlach, S.R.F.; Janasi, V.A. and Ulbrich, H.H.G.J., 1996. Ages and typology of the Brasiliano granitic magmatism close to the Proterozoic-Phanerozoic boundary, States of São Paulo and Paraná, SE Brazil. Anais da Academia Brasileira de Ciências, 68:597-598.

Sm-Nd ISOTOPIC COMPOSITIONS AS A PROXY FOR MAGMATIC PROCESS DURING THE NEOPROTEROZOIC OF THE SOUTHERN BRAZILIAN SHIELD

Gastal, M.C.P.[1]; Lafon, J.M.[2]; Hartmann, L.A.[1] and Koester, E.[3]

1. Centro de Estudos em Petrologia e Geoquímica, Instituto de Geociências, UFRGS, CP 15 001, Porto Alegre-RS, 91501-970, Brazil. maria.gastal@ufgrs.br, leo.hartmann@ufrgs.br
2. Laboratório de Geologia Isotópica, Centro de Geoc., UFPA, CP 1611, Belém-PA, 66 075-900, Brazil. lafonjm@ufpa.br
3. Laboratório de Geologia Isotópica, IGEO, UFRGS, CP 15001, Porto Alegre-RS, 91501-970, Brazil. koester@ufrgs.br

Keywords: Nd isotopes, subcontinental lithosphere, southernmost Brazilian shield, Brasiliano Cycle

INTRODUCTION

A large database of Sm-Nd isotopic analyses of igneous rocks from southernmost Brazilian shield is reviewed to evaluate their sources. The data are combined with previous petrologic interpretations to assess the role and importance of mantle and crust components in the Neoproterozoic magmatic events. Two major periods of tectono-magmatic activity are well characterized in the Brasiliano Cycle of the region (Hartmann et al., 2000). These are the Early (900-700 Ma) – São Gabriel Orogeny, and Late (670-550 Ma) – Dom Feliciano Orogeny, responsible respectively for the generation of the São Gabriel Arc (northwestern part of the shield), and the Dom Feliciano collisional belt (eastern part) (Fig. 1A). Fragments of the Rio de la Plata Craton (mostly 2.26-2 Ga) are present in both belts. According to existing geotectonic models, Neoproterozoic magmatic events represent more than one arc, or else arc and back-arc environments developed at different ages. The collisional belt has been interpreted as an active continental arc evolving up to continent-continent collision. It started at *ca.* 800 Ma, and the Late Brasiliano event is mainly related to a general northeastern migration of the belt along NE-SW megashear zones (Fernandes et al., in prep.). This second Brasiliano orogenic phase was driven by one or several collisional events placed to the east or north, and related to the amalgamation of west Gondwana. Such context characterizes a post-collisional setting for the emplacement of the granitic associations during the Late Brasiliano event, in both the Dom Feliciano Belt and the western Neoproterozoic foreland - São Gabriel Arc and Taquarembó Block (Fig. 1A).

Lithospheric mantle components are discussed in a comparative study of Sm-Nd isotopic data from Precambrian and Mesozoic basic-to-intermediate igneous rocks. Cretaceous (130 - 100 Ma) continental tholeiites and subcoeval alkalic rocks (Fig. 1B) provide a fundamental approach for the lithospheric mantle at the end of the Neoproterozoic. These rocks and the Late Brasiliano intrusions represent the two major magmatic events in the region, related respectively to the break up and amalgamation of the west Gondwana. In a similar comparative study of tholeiites from the South American Platform, Iacumin et al. (2003) show that both Mesozoic and Precambrian LTi and HTi (low and high Ti) tholeiites exhibit similar geochemical and Sr-Nd isotopic signatures, particularly those from the same craton. In the region, the correspondence of Nd isotopic ratios between the two groups of rocks (Precambrian and Cretaceous) supports previous models for mantle sources of the Paraná Magmatic Province, which envisage a heterogeneous and stratified subcontinental lithosphere variously modified during early tectono-thermal events (Marques et al., 1999). The simplified sketch of the subcontinental lithosphere proposed by Garland et al. (1996) is adapted for magma producing events during the Late Brasiliano event in southernmost Brazilian Shield. The older Paleoproterozoic subcontinetal lithosphere, hydrous and refractory at shallower depths gives way to younger Neoproterozoic lithospheric mantle, fertile and anhydrous at depth. The influence of the Transamazonian subduction was more prominent in the Paleoproterozoic lithosphere, while the young lithosphere, less modified by such event, would be differently affected by OIB-like metasomatizing agents. Subcontinental lithosphere modified during the São Gabriel Orogeny seems to be more localized.

Recent studies have established that significant and, at times, considerable fractionation of Sm/Nd ratio is very common during crustal processes (anatexis, fractional crystallization, etc.). Despite this, the ε_{Nd}-growth paths for the Late Brasiliano granitic suites reveal important differences in magmagenesis for the two regions: the Pelotas Batholith and the western foreland. Although a subcontinental lithosphere produced at old events is widely implied, it is possible to conclude that both, mantle and crust components were somewhat distinct in the two regions.

CRUST SEGMENTS

In southernmost Brazilian Shield, at least, three juvenile crust segments formed in arc setting at distinct ages are recognized (Fig. 2). These suites show T_{DM} (Nd) ages close to the respective crystallization age, positive ε_{Nd}(t)-values (+1 to +7), and typically crustal values of $f_{Sm/Nd}$ (-0.38 to -0.44), but they have distinct geochemical and Sr-isotopic signatures. They are: (1) the oldest primitive tholeiitic arc suite - Santa Maria Chico granulitic complex (magmatism at 2.55 Ga, and metamorphism at 2.02 Ga), which has unradiogenic I_{Sr} (~0.702) and is interpreted as equivalent to the lower crust within the cratonic segments (LC; Fig. 2); (2) the Paleoproterozoic continental arc suite- Arroio dos Ratos gneiss complex (ca. 2.1 Ga), which was recycled by new input of mantle-derived magmas during the São Gabriel

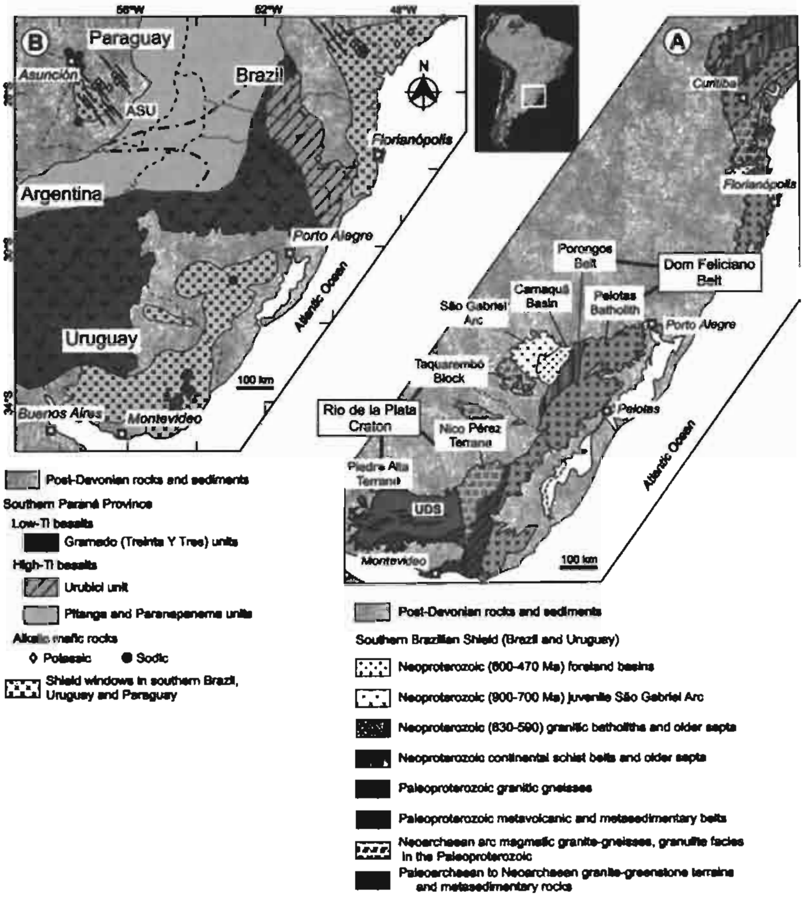

Figure 1. Geological map of southernmost Brazilian and Uruguayan shields (A) and Cretaceous Paraná Province (B). A - Geotectonic units from Hartmann et al. (2000); UDS - Uruguayan dyke swarm; B - Occurence of tholeiites and subcoeval alkalic mafic rocks, showing the distribution of chemical types and regional units (Peate et al., 1992; Comin-Chiaramonti et al., 1997). Acid volcanics and sedimentary units above basalts are not shown; dot-dashed line for the LTi Esmeralda basalts, and ASU - Asunción-Sapucaí Graben (Eastern Paraguay Alkalic Province). Fine-dashed and dotted lines for international and state limits respectively.

Orogeny - Pinheiro Machado Suíte (*ca.* 0.8 Ga). They are medium- to high-K calc-alkaline compositions with a more radiogenic I_{Sr} (> 0.707), and represent the crust segments in the collisional belt (CC; Fig. 2); and (3) the São Gabriel Arc including more than one arc sequences formed during a period of *ca.* 180 Ma (879–704 Ma). It is a primitive continental margin and comprises low- to medium-K calc-alkaline suites with low I_{Sr} (~0.703) – the plutonic Cambaí Complex and the supracrustal Vacacaí Group (CV; Fig. 2).

EARLY BRASILIANO LITHOSPHERE

Components of the lithosphere formed during the subduction event of the São Gabriel Orogeny are simplified in figure 2: CV-juvenile crust, IAB - island arc basalts, and W - subarc mantle wedge. The last two are less fractionated (Sm/Nd of 0.22-0.28), but show Sr-Nd signature similar to other CV-rocks. Amphibolites from the Cerro Mantiqueiras Ophiolite–CMO, taken as representative of an IAB, were derived from a mantle wedge contaminated with subducted sediments. This is supported by the lower value of $\varepsilon_{Nd}(t)$ and the more radiogenic Sr-Pb initial ratios than DMM. For CMO-harzburgites, the geochemistry shows a residual mantle, but variable values of Sm/Nd (0.17–0.27) and Rb/Sr (0.02–0.26) suggest some IE (incompatible elements)-enrichment. Contamination with both old components and subducting slab-derived fluids is suggested to explain Nd isotopic ratios and older T_{DM} (Nd) ages. So they are taken as representative of a residual mantle wedge containing old recycled components (W).

CONSTRAINTS ON THE LITHOSPHERIC MANTLE

Two groups of basic-to-intermediate rocks are recognized based on ε_{Nd}-evolutionary patterns (Fig. 2). Those derived from a subcontinental lithosphere produced during the Transamazonian, or older orogenies, have εNd(0) lower than –9 and T_{DM}(Nd) ages older than 1.4 Ga (mostly > 1.6 Ga). They include the Paleoproterozoic Uruguayan dyke swarm – UDS, the Ordovician Rodeio Velho volcanics, and the Cretaceous potassic rocks from the Asunción-Sapucaí graben – ASU. The other group has diversified origins and is characterized by εNd(0)-values higher than –7 and T_{DM}(Nd) ages varying from 0.6 to 2.4 Ga (mostly < 1.7 Ga). It includes rocks produced during the Early Brasiliano subduction, those with a mixing origin involving IE-depleted components and older IE-enriched mantle end-members (Paraná basalts), and also those with an OIB signature (ASU-sodic suites). Minette dykes from the Lavras do Sul Intrusive Complex - LSIC show an intermediate ε_{Nd}-evolution path, implying a more complex origin. All but ASU-sodic rocks show negative Nb-Ta anomalies indicating mantle sources modified in subduction events, or its contamination with ancient, recycled crust.

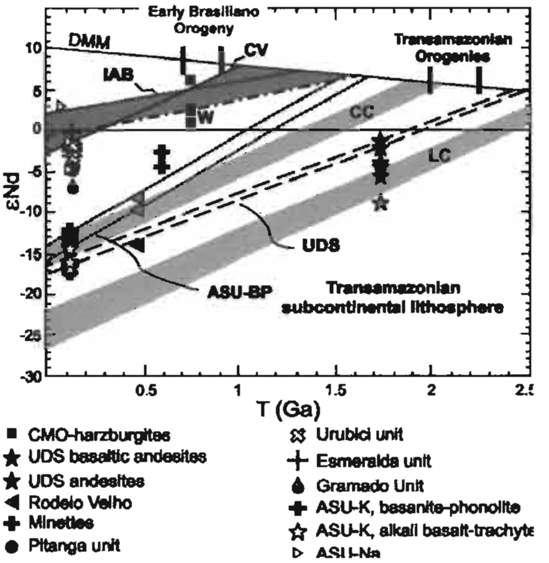

Figure 2. ε_{Nd} – t evolutionary diagram for mantle-derived rocks highlighting the main crust and mantle components. CMO – Cerro Mantiqueiras Ophiolite; UDS and ASU as in figure 1; see text for details.

SUITES WITH A TRANSAMAZONIAN SIGNATURE

Two extreme compositions can be identified, suggesting at least two end-members for the subcontinental lithosphere modified in old events. One has a strong IE-signature of the Transamazonian subduction (ε_{Nd}-growth paths – UDS in Fig. 2), and shows high $^{147}Sm/^{144}Nd$ ratios (~0.12) and low Nd concentrations (~50 ppm). This end-member is best represented by the less evolved UDS-basaltic andesites, which have I_{Sr} of 0.705 but high Rb/Sr (~0.21-0.29). It includes also some potassic rocks of the alkali basalt-trachyte suite from ASU, characterized by older T_{DM} (Nd) ages (~2.3 Ga), I_{Sr} of 0.707, low values of REE, TiO_2, P_2O_5 and Ti/Y, and high Rb/Sr. The less evolved potassic rocks of the basanite-phonolite suite from ASU (εNd-growth paths – ASU-BP in Fig. 2) represent the other IE-enriched end-member, characterized by younger T_{DM} (Nd) ages (1.5-1.7 Ga), lower $^{147}Sm/^{144}Nd$ ratios (~0.09), higher Nd (~100 ppm), and similar I_{Sr} (0.706-0.707). LSIC-minettes show similar Sm-Nd composition and IE-pattern. These rocks (ASU-BP and minettes) have also higher values of TiO_2, P_2O_5, REE and Ti/Y, and less pronounced P-Ti negative anomalies than the other suites. Such compositional variation, between the two end-members, can be attributed to distinct degrees of re-enrichment of a mantle source already modified during the Transamazonian subduction. This new event of metasomatism may have occurred during the latest Transamazonian collisions (~2 Ga) or later. For LSIC-minettes, a subduction-effect of the São Gabriel Orogeny is suggested (Gastal et al. this symposium).

SUITES WITH YOUNGER SIGNATURE

HTi Paraná basalts (Pitanga and Urubici; Fig. 2) have primitive Sr-Nd-Pb isotopic signature with T_{DM} (Nd) ages varying from 0.9 to 1.5 Ga, and low Rb/Sr, I_{Sr} and $^{206}Pb/^{204}Pb_i$. They are fractionated compositions (Sm/Nd of 0.16-0.23), and their genesis has been attributed to mixing of an IE-depleted DMM-like source and an IE-enriched mantle end-member (EM I), thought to be linked in some way with the less subduction-affected Brasiliano lithosphere (Garland et al., 1996; Peate et al., 1999). LTi southern Paraná basalts (Gramado and Esmeralda units, Fig. 2) have more Sr-Nd-Pb radiogenic and less fractionated (Sm/Nd of 0.21-0.29) compositions. They exhibit also older T_{DM} (Nd) ages (1.3 to 2.4 Ga) and more pronounced Nb-P-Ti negative anomalies, so that the participation of an older subduction-modified mantle is implied (Marques et al., 1999). On $\varepsilon_{Nd}(0)$ *vs.* $^{147}Sm/^{144}Nd$ or 1/Nd diagrams (not shown), the two LTi units plot along a mixing line between the Early Brasiliano IAB and the ASU-BP-like IE-enriched mantle end-member.

LATE BRASILIANO (670–550 Ma) IGNEOUS SUITES

These suites occur in two regions of the southernmost Brazilian Shield differently placed relative to the Dom Feliciano collisional front, and already transformed by previous sucduction-collisional events: the Pelotas Batholith and the western Neoproterozoic foreland. They have T_{DM} (Nd) ages and $f_{Sm/Nd}$ within the same range of values, respectively 1.3 to 2.7 Ga and –0.14 to –0.57, but show constrasting $\varepsilon_{Nd}(t)$-values (Fig. 3). The Pelotas Batholith (670 – 580 Ma) is characterized by a more homogeneous group of granitoids, displaying Nd isotopic ratios akin those of the Early Brasiliano-Paleoproterozic crust (CC in Fig. 3A) and high I_{Sr} (0.706 to 0.740). In the western foreland, two groups of rocks with distinct Nd-Pb-Sr isotopic compositions are well defined. They correspond to the two major period of magma production in the region, respectively the early - 605–581 Ma, and the late - 575–550 Ma events (Fig. 3B).

PELOTAS BATHOLITH

The Pelotas Batholith includes syn to post-transcurrent granitic suites, mainly high-K and highly evolved, calc-alkaline compositions and subordinate peraluminous, and alkaline metaluminous. All but the alkaline granitoids (Encruzilhada do Sul intrusive suite – ESIS), show $\varepsilon_{Nd}(t)$-values in more restricted range (–3.7 to –7.8), but large variations of $f_{Sm/Nd}$ (Fig. 3). This is particularly valid for peraluminous and highly evolved calc-alkaline suites, in which anomalous values of T_{DM} (Nd) and/or $f_{Sm/Nd}$ indicate isotopic disequilibrium. The genesis of the Pelotas Batholith suites, except ESIS, involved an intimate mixture of a Paleoproterozoic crust and an IE-enriched ASU-type old mantle, with the increasing participation in time of a more primitive mantle source (DMM or IAB-like). The alkaline suite (ESIS) is in the northwestern extreme of the batholith, to the west of the Dorsal de Canguçu shear zone. It exhibits low values of εNd(t) (< -10) and $f_{Sm/Nd}$ (~0.51), and T_{DM} (Nd) ages of *ca.* 2.1 Ga. It is thus comparable to analogous western alkaline granites for which the participation of the Neoarchaean lower crust (LC), and IE-enriched ASU-BP-like old mantle components are implied (Figs. 3B and C).

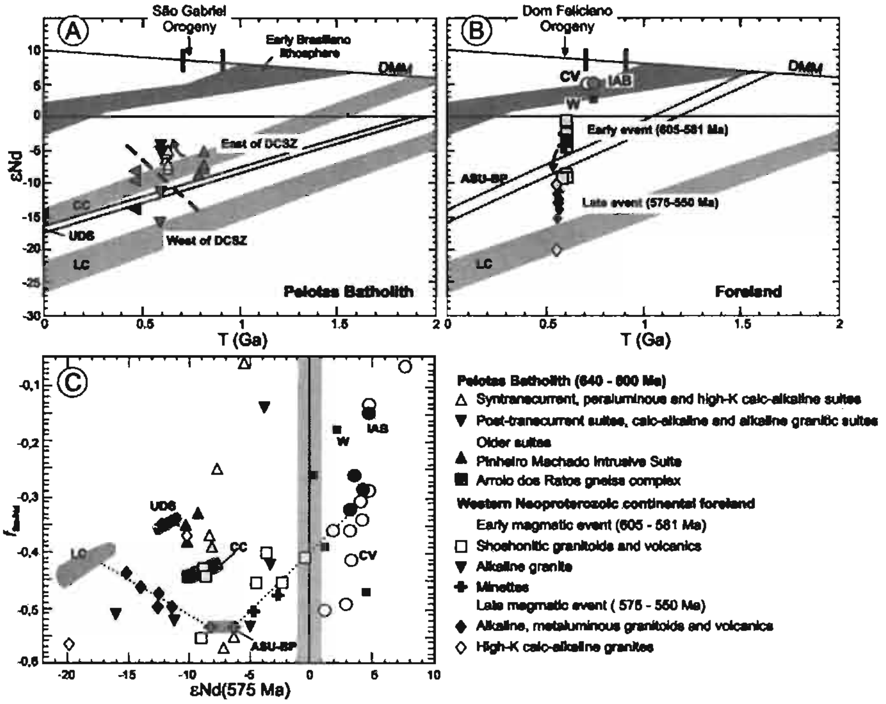

Figure 3. Sm-Nd isotopic ratios for Late Brasiliano igneous suites from the southernmost Brazilian shield. A and B - ε_{Nd} - t, and C - $f_{Sm/Nd}$ *vs.* ε_{Nd} (575Ma) diagram. The main crust and mantle segments, identified in figure 2, are shown; arrows in A indicated the evolution in time; dotted line in B for mixing among lithospheric components; DCSZ – Dorsal de Canguçu Shear Zone.

WESTERN NEOPROTEROZOIC CONTINENTAL FORELAND

Although formed at distinct periods, the two groups of igneous suites in the foreland of the Dom Feliciano Orogeny shared the same IE-enriched ASU-BP-like old mantle component as suggested in figure 3C. Then, the differences in the Nd-Pb-Sr isotopes reflect the progressive change of the other end-member of a mixture of source materials, from an IAB-like mantle to the Neoarchaean-Paleoproterozoic lower crust (Fig. 3C). The early magmatic event includes shoshonitic, post-tectonic volcano-plutonic suites, and subordinate alkaline granites. Their generation can be associated with the subduction-related hydrous mantle wedge produced at the São Gabriel Orogeny, containing segments of an old IE-enriched subcontinental lithosphere (Gastal *et al.*, this symposium). This is particularly valid for the Lavras do Sul Intrusive Complex (600-590 Ma), whereas other coeval volcanics and younger intrusions (~583 Ma) require the participation of the lower crust (ε_{Nd}(t) of –9). The youngest magmatic event includes apparently three distinct associations separated into two ages group: 575-570 Ma – post-tectonic volcano-plutonic, silica over-saturated alkaline suite; and 570-550 Ma – post-tectonic, alkaline metaluminous and syntectonic, high-K calc-alkaline granites. For these rocks, the contribution of the lower crust (LC) is well characterized by low values of ε_{Nd}(t) (< -10) and Pb common initial ratios.

ACKNOWLEDGEMENTS

This study was financially supported by FAPERGS (n° 00/1368.8; 00/2366.3), PROPESQ/UFRGS and PRONEX/CNPq.

REFERENCES

Comin-Chiaramonti, P.; Cundari, A.; Piccirillo, E.M.; Gomes, Castorina, F.; Censi, P.; De Min, A.; Marzoli, A.; Speziale, S.; Velázquez, V.F. 1997. Potassic and sodic igneous rocks from eastern Paraguay; their origin from the lithospheric mantle and genetic relationships with the associated Paraná flood tholeiites. J. Petrol., 38:495-528.

Garland, F.; Turner, S.; Hawkesworth, C. 1996. Shifts in the source of the Paraná basalts through time. Lithos, 37:223-244.

Hartmann, L.A.; Leite, J.A.D.; Silva, L.C. da; Remus, M.V.D.; McNaughton, N.J.; Groves, D.I.; Fletcher, I.R.; Santos, J.O.S.; Vasconcellos, M.A.Z. 2000. Advances in SHRIMP geochronology and their mpact on understanding the tectonic and metallogenic evolution of southern Brazil. Australian J. Earth Sci, 47: 829-844.

Iacumin, M.; De Min, A.; Piccirillo, E..M.; Bellieni, G. , 2003. Source mantle heterogenity and its role in the genesis of Late Arcahean-proterozoic (2.7-1.0 Ga) and Mesozoic (200 and 130 Ma) tholeiitic magmatism in the South American Plataform. Earth Sci. Rev., 1:1-33 (in press).

Marques, L.S.; Dupré, B.; Piccirillo, E.M. 1999. mantle source compositions of the Paraná Magmatic Province (southern Brazil): evidence from trace element and Sr-Nd-Pb isotope geochemistry. J. Geodynamics, 28:439-458.

Peate, D.W.; Hawkesworth, C.J.; Mantovani, M.S.M. 1992. Chemical stratigraphy of the Paraná lavas (South America): classification of magma types and their spatial distribution. Bull. Volcanol., 55:119-139.

Peate, D.W.; Hawkesworth, C.J.; Mantovani, M.S.M.; Rogers, N.W.; Turner, S.P. 1999. Petrogenesis and stratigraphy of the high-Ti/Y Urubici magma type in the Paraná flood basalt Province and implications for the nature of "Dupal"-type mantle in the south atlantic region. J. Petrol., 40:451-474.

Sr-Nd-Pb ISOTOPES FOR MINETTES AND GRANITOIDS FROM THE LAVRAS DO SUL INTRUSIVE COMPLEX, RS

Gastal, M.C.P.[1]**; Lafon, J.M.**[2] **and Koester, E.**[3]

1. Centro de Estudos em Petrol. e Geoq., IGEO, UFRGS, CP 15 001, Porto Alegre-RS, 91501-970, Brazil. maria.gastal@ufgrs.br
2. Laboratório de Geologia Isotópica, Centro de Geoc., UFPA, CP 1611, Belém-PA, 66 075-900, Brazil. lafonjm@ufpa.br
3. Laboratório de Geologia Isotópica, IGEO, UFRGS, CP 15001, Porto Alegre-RS, 91501-970, Brazil. koester@ufrgs.br

Keywords: Sr-Nd-Pb isotopic geochemistry, Lavras do Sul Intrusive Complex, minettes, shoshonitic, alkaline granites

INTRODUCTION

Models on the petrogenesis and the crystallization interval of different petrographic facies of the Lavras do Sul Intrusive Complex – LSIC are improved by new isotopic data for granitoids and minette dykes. The relationship of the LSIC-magmatic events with the genesis of both, the gold-ore occurrences and the Jaguari Granite are also discussed. The intrusive complex and coeval volcanics (Hilário Formation) occur in the foreland of Dom Feliciano collisional orogen (660–550 Ma). They are situated in the western portion of the Sul-Riograndense Shield, in a region formed by the São Gabriel magmatic arc (900-700 Ma). U-Pb and ^{207}Pb/^{206}Pb ages, listed in table 1, reveal that most of LSIC-granitoids were formed during a period of ca. 10 Ma (601–594 Ma). This is valid either for shoshonite (granodiorite, monzonite and monzodiorite) and for alkaline granitoids (perthite granite and syenogranite), though a younger U-Pb age of ca. 583 Ma has been registered in one sample of the perthite granite located in the south of LSIC (Leite et al., 1998). The contemporaneity and the multiplicity of magma production events with distinct geochemical affinities – shoshonitic and alkaline, both are features reinforced in this study for the formation of the intrusive complex.

Minette and olivine minette occur as dykes in the central portion of LSIC, intruding shoshonitic monzogranites. They are enriched in REE, LILE and HFSE, and have negative Nb anomalies (La/Nb of 2-3; Gastal & Lafon, 2002). They show also an enriched isotopic signature, with I_{Sr} of ca. 0.705, low ^{143}Nd/^{144}Nd (ε_{Nd} of –2.6 to –4.5), high ^{207}Pb/^{204}Pb$_i$ (15.47-15.56), and variable ^{208}Pb/^{204}Pb$_i$ (36.8-38.16) and ^{206}Pb/^{204}Pb$_i$ (16.61-17.52) (Tables 1, 3). They are derived by small-degree of partial melting from an IE (incompatible element)-enriched subcontinental lithosphere. The olivine minette has ^{206}Pb/^{204}Pb$_i$ similar to those of amphibolites from the Cerro Mantiqueiras Ophiolite (CMO), but it shows higher ^{207}Pb/^{204}Pb$_i$, ^{208}Pb/^{204}Pb$_i$ (Fig. 1) and I_{Sr}, and lower ^{143}Nd/^{144}Nd. The CMO-amphibolites represent an IAB (island arc basalt) formed during the São Gabriel accretionary orogeny (900-700 Ma; Leite, 1997), so the olivine minette can be derived from a phlogopite-bearing asthenospheric wedge modified by slab-derived fluids during this subduction event. Nevertheless, an IE-enriched mantle component with a long residence time would be also required to explain the minette magma, which has lower ^{206}Pb/^{204}Pb$_i$ (Fig. 1) and higher I_{Sr}. The Rb-Sr age of 581 ± 29 Ma (1σ) obtained on minerals and whole rock for one sample of minette is concordant with the ca. 580 Ma age of the hydrothermal event registered in the alterated granites associated with gold-ore occurrences (Bongiolo et al., 2002; Mexias, 2000). Such results suggest a later magmatic event in the formation of LSIC, responsible also by the latest ore-related hydrothermal episodes, which postdated by 10 Ma the main period of magmatic activity.

Sr-Nd isotopic compositions of LSIC-granitoids are in the same range of values observed minettes, as shown by I_{Sr} of 0.704-0.705, $\varepsilon_{Nd}(t)$ of –0.3 to –4.5 and T_{DM}(Nd) ages of 1.3 to 1.6 Ga (Tables 1, 2). Some samples of the coeval volcanic sequence (trachyandesites from the Hilário Formation) have a similar isotopic signature, so that a common mantle source is implied. On the Sr-Nd isotopic correlation diagram (not shown), LSIC-granitoids, minettes and some trachyandesites initial ratios fit along a linear array deviated from the mantle array, indicating at least two types of mantle sources. One is depleted in IE component, and has a high Sm/Nd ratio and a DM-signature. It had been generated during the Early Brasiliano subduction (900 – 700 Ma). The other one is IE enriched, with low Sm/Nd ratio and long residence time. For other coeval volcanics, the contamination of mantle-derived melts with lower crust components is also required to explain the isotopic data. Most of granitoids and volcanics have ^{206}Pb/^{204}Pb$_i$ (17.6-17.4) and ^{207}Pb/^{204}Pb$_i$ (15.5) ratios comparable to those of olivine minette, but at lower values of ^{208}Pb/^{204}Pb$_i$ (37.3-37.5). They plot between olivine minette and the Early Brasiliano IAB (Cerro Mantiqueiras amphibolites) on ^{206}Pb/^{204}Pb vs. ^{207}Pb/^{204}Pb and ^{208}Pb/^{204}Pb diagrams (Fig. 1). Sr-Nd-Pb isotopes for LSIC-granitoids, minettes and coeval volcanics allow to indicate their derivation by "vein plus wall-rock" melting processes (Foley, 1992; O'Brien et al., 1995), involving mantle components with diversified origins. Their generation can be related to the uprise of a subduction-related hydrous mantle wedge produced at the São Gabriel Orogeny, containing segments of an old subcontinental lithosphere.

The alkaline, metaluminous Jaguari granite is intrusive in to the northwestern portion of the LSIC. Compared with the LSIC-alkaline granites classified as A1 types (Eby, 1992), it shows distinct geochemistry. Jaguari Granite has a high-silica composition and is an A2-type granite, as argued by Gastal & Lafon (1998). A younger ^{207}Pb/^{206}Pb age of 567 ± 4 Ma (2σ) is confirmed for this granite, indicating that it represents the latest Neoproterozoic magmatic event in the region. Extremely low ^{143}Nd/^{144}Nd ratios (ε_{Nd} of ~ –13), at

Table 1. U-Pb, Pb-Pb, Rb-Sr and Nd isotopic data for granitoids and minettes from Lavras do Sul Intrusive Complex and Jaguari Granite. 1. Gastal & Lafon (1998); 2. Remus et al. (2000); 3. Leite et al. (1998); 4. Gastal & Lafon (2001); 5. Babinski et al. (1996); 6. Chemale Jr. et al. in prep.; **a.** t = time of crystallization of the granites; **b.** DM Nd model ages calculated according to Goldstein et al. (1984, in Rollinson 1993). Bold highlights the geochronological results presented in this paper.

	Ages (Ma)					
	U/Pb	$^{207}Pb/^{206}Pb$	Rb/Sr	I_{Sr}	εNd(t)[a]	T_{DM} (Ga)[b]
Lavras do Sul Intrusive Complex						
Alkaline granites			556 ± 34 (2σ)[1]	0.70489 ± 0.00208 (2σ)	-3.1[5]	1.5
Perthite granite – north	594 ± 4 (2σ)[2]					
Perthite granite – south	583 ± 11 (2σ)[3]	with Pb inheritance of 610 ± 10				
Syenogranite - south		**598 ± 3 (2σ)**				
Shoshonitic granites			608 ± 54 (2σ)[1]	0.70415 ± 0.00058 (2σ)	-0.28[5]	1.3
Granodiorite	594 ± 5 (2σ)[2]					
Northern portion						
Monzonite		601 ± 5 (2σ)[4]				
Arroio do Jacques Monzodiorite			606 ± 56 (1σ)[1]	0.70534 ± 0.00031 (1σ)	-3.5 to -4.3[4]	1.6
Monzodiorite		599 ± 7 (2σ)[4]				
Minette dykes					-2.6 to -4.5	1.4 to 1.5
Kl 647E - mineral isochron			**581 ± 29 (1σ)**	0.70538 ± 0.00023 (1σ)		
Jaguari Granite			537 ± 10 (2σ)[1]	0.70551 ± 0.0007 (2σ)	-12.6[6]	2.1
Monzogranite		**567 ± 4 (2σ)**				

Table 2. Pb isotopic results of feldspars for granitoids from Lavras do Sul Intrusive Complex.

Sample	$^{206}Pb/^{204}Pb$	1σ	$^{207}Pb/^{204}Pb$	1σ	$^{208}Pb/^{204}Pb$	1σ
KL109 – Perthite granite	17.605	0.011	15.527	0.014	37.493	0.045
KL405 - Alkaline syenogranite	17.459	0.010	15.508	0.014	37.348	0.044
KL159 - Monzonite	17.558	0.010	15.542	0.014	37.486	0.045
KL97 - Monzodiorite	17.512	0.013	15.548	0.016	37.509	0.046

Table 3. Pb isotope composition and concentrations of U, Th and Pb for minettes from Lavras do Sul Intrusive Complex. 1σ uncertainties are denoted in parenthesis. Initial Pb isotope compositions are age-corrected assuming a crystallization age of 581 Ma. Th and U concentrations determined by ICP-MS, and Pb by ICP-AES.

	Measured (1σ)			ppm			Initial		
Sample	$^{206}Pb/^{204}Pb$	$^{207}Pb/^{204}Pb$	$^{208}Pb/^{204}Pb$	U	Th	Pb	$^{206}Pb/^{204}Pb$	$^{207}Pb/^{204}Pb$	$^{208}Pb/^{204}Pb$
647E-1 Minette	20.80 (1)	15.72 (1)	42.53 (5)	7.7	33	12	16.61	15.47	36.80
647A- Olivine minette	19.28 (1)	15.67 (1)	39.95 (5)	3.7	11.8	13	17.52	15.56	38.16

similar I_{Sr} (0.705), indicate the participation of lower crust components in its source. However, the involvement of an IE-enriched old mantle component, like that of the minette, is suggested by the Pb common initial ratios (Fig. 1).

The U-Pb, Pb-Pb and Rb-Sr dating indicate thus that at least three magmatic episodes marked the post-collisional period of the Dom Feliciano Orogeny in the region. The two older are responsible for the formation of the Lavras do Sul Intrusive Complex and the associated gold ore occurrences (600–580 Ma), and the other episode is younger and related with the Jaguari Granite (567 Ma). The Sr-Nd-Pb isotopic results reveal strong mantle in put for the first two, and a major contribution of lower crust components for the latter.

Pb-Pb ZIRCON AGES

Pb-Pb single zircon evaporation ages were obtained for one sample of the alkaline syenogranites from the Lavras do Sul intrusive complex, and for another sample of monzogranitic facies from the Jaguari granite. For both samples, the zircon crystals are nonmagnetic, prismatic and subhedral. The $^{207}Pb/^{206}Pb$ ages are presented at 2σ error in table 1, which lists the main geochronological data for granitoids and minettes in the region. In this study, the $^{207}Pb/^{206}Pb$ age of 565 ± 55 (2σ), previously obtained for the same sample of the Jaguari granite (Gastal & Lafon, 1998), is confirmed and improved. The analyses were performed on a Finnigan MAT 262 multicollector mass

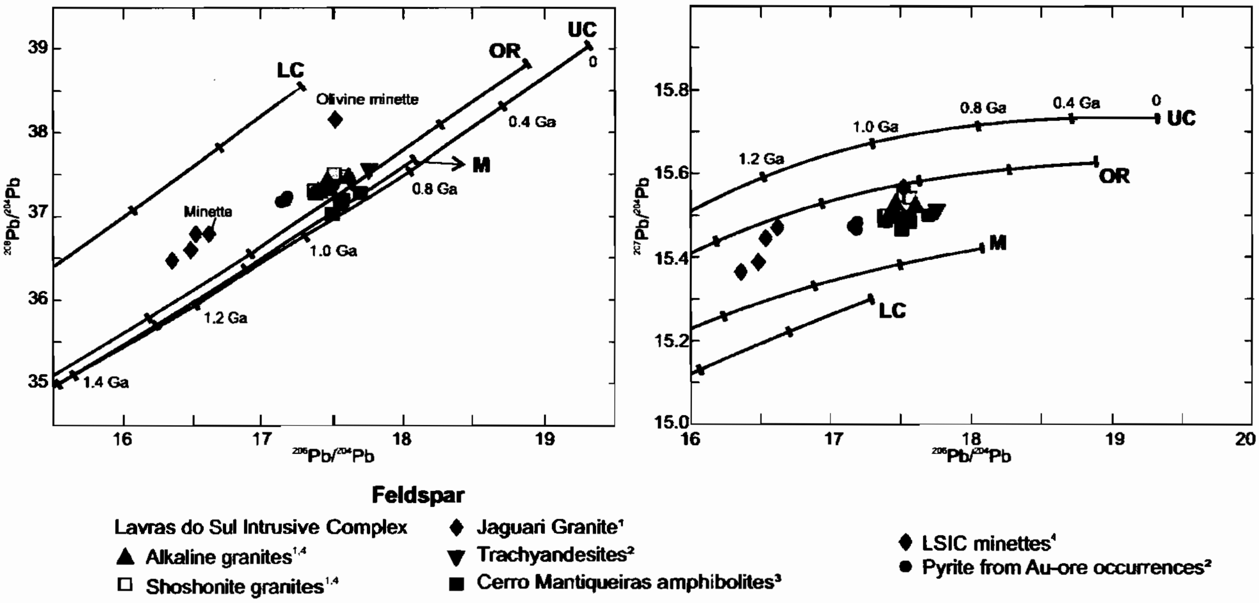

Figure 1. Pb isotopic evolution - Plumbotectonics version I (Doe & Zartmann, 1979) showing the composition of feldspars from: granitoids of the Lavras do Sul Intrusive Complex, trachyandesites of the Hilário Formation, Jaguari Granite and amphibolites of the Cerro Mantiqueiras Ophiolite. It is also shown the calculated Pb common initial ratios of minettes and isotopic Pb ratios of pyrites from the gold-ore occurrences in the intrusive complex and coeval volcanics. Pb evolution curves for the main source reservoirs are shown (ticks at 0.4 Ga intervals): LC. lower crust; UP. upper crust; OR. Orogen; M. Mantle; 1. Gastal & Lafon (1998); 2. Remus et al. (2000); 3. Leite (1997); 4. this study.

spectrometer at the laboratory of isotope geology – Pará-Iso / UFPA, following the procedures of Kober (1986; 1987). For each sample, sixteen chemically untreated crystals of zircon have their isotopic ratios analyzed using a Re double-filament arrangement, in dynamic mode. Following Kober (1986), the method involves repeated cycles of evaporation-deposition-ionization of the Pb isotopes, at increasing temperatures. The temperature range for Pb evaporation is of 1450-1550°C, and of 1050°-1150°C for ionization. At each step, the isotopic ratios were measured on five blocks of 10 cycles each. The $^{207}Pb/^{206}Pb$ ratios are corrected using a mass discrimination factor of 0.12% ± 0.03 per a.m.u., determined by repeated analyses of NBS 982 standard. Common Pb correction is calculated using the model of Stacey & Kramers (1975) at the age of the analysed crystal. The statistical treatment is described by Gaudette et al. (1998). For excluding errors caused by inaccurate common lead correction, data blocks with a $^{204}Pb/^{206}Pb$ ratio higher than 0.0004 are eliminated. For each step, the mean age and the standard error are calculated, and the age of the zircon crystal is the weighted average of ages. The age of the sample is determined by the mean of the ages obtained on at least five crystals.

Rb-Sr WHOLE-ROCK AGES

Rb-Sr isotopic data for minerals (diopside, phlogopite and feldspars groundmass) and whole rock were obtained for one minette sample. Four analytical points define a isochron with a MSWD of 1.07, which yields an age of 581 ± 29 Ma (1σ) and I_{Sr} of 0.70538 ± 0.00023 (1σ) (Table 1). This age is considered to be a good approximation for the crystallization age of the minette dykes, discarding they are related to the Ordovician or younger magmatic events in the region. Rb-Sr isotopic analyses were performed at the Laboratório de Geologia Isotópica, Instituto de Geociências/ UFRGS, on a VG Sector 54 mass spectrometer operating in static mode. After acid dissolution of the sample and Rb and Sr separations on ion-exchange resin (DOWEX AG 50X8), Sr isotopic compositions were measured on Ta single filament. The total procedural blank for Rb and Sr was lower than 150 pg. The reproducibility of Sr standard (NBS 987) is $^{87}Sr/^{86}Sr$ of 0.71026 ± 0.00011 (1σ on the mean), and the fractionation was corrected to $^{86}Sr/^{88}Sr$ of 0.1194. Rb and Sr concentrations were obtained by isotope dilution using $^{87}Rb/^{84}Sr$ spike. For $^{87}Sr/^{86}Sr$ and $^{87}Rb/^{86}Sr$, typical analytical errors are equal or better than 0.02% and 0.9%, respectively (1σ). The Rb-Sr age was calculated following Ludwig (2001).

Pb ISOTOPES

Common Pb isotopic ratios of feldspars are obtained for diverse samples from LSIC-granitoids, and of whole rock for the two samples from dykes (minette and olivine minette). The Pb common isotopic ratios of LSIC-granitoids and minettes are shown in tables 2 and 3, respectively. Pb isotopic analyses were carried out on a VG-ISOMASS 54E mass spectrometer with a mono-collector at the Pará-Iso laboratory. The sample dissolution and Pb separation were performed using the technique developed by Manhes (1982), adapted for LGI/UFPA (Rodrigues, 1992). Before dissolution, feldspar separates were pretreated by leaching with hot HCl (6 N) and HF (1N). Lead was purified by repeating two times the separation procedure in ion-exchange chromatographic columns, using DOWEX AG

1X8 resin. The Pb was loaded on Re single filaments following the H_3PO_4-silica gel method. All samples were corrected for mass fractionation by a factor of 0.12% ± 0.03 per a.m.u. The total Pb blanks were about 1ng. Initial Pb isotope compositions for minettes, shown in table 3, are age-corrected assuming a crystallization age of 581 Ma and taken the Th, U and Pb concentrations determined by ICP-MS and ICP-AES (ACME Analytical Laboratories Ltda).

Nd ISOTOPES

For Sm-Nd whole rock isotope analyses were carried out. The routine procedures at Pará-Iso/UFPA followed Oliveira et al. (2001). Sm and Nd Isotopic compositions were determined on a Finnigan MAT 262 multicollector mass spectrometer. $^{143}Nd/^{144}Nd$ ratios were normalized to $^{146}Nd/^{147}Nd$ = 0,7219. Nd model ages were calculated according Goldstein et al. (1984 in Rollinson, 1993), using $^{147}Sm/^{144}Nd$ of 0.2137 and $^{143}Nd/^{144}Nd$ of 0.51316. The present day $^{143}Nd/^{144}Nd$ and $^{147}Sm/^{144}Nd$ ratios for the CHUR (Chondritic Uniform Reservoir) are also from Goldstein et al. (1984 in Rollinson, 1993). εNd notation is the deviation in part per 10^4 from the chondritic growth curve. The decay constants used for ^{87}Rb, ^{147}Sm, ^{238}U, ^{235}U, and ^{232}Th were those recommended by Steiger & Jäger (1977) and Wasserburg et al. (1981).

ACKNOWLEDGEMENTS

This study was financially supported by FAPERGS (nº 00/1368.8; 00/2366.3), PROPESQ/UFRGS and PRONEX/CNPq. Thanks are due to the staff of the Laboratório de Geologia Isotópica at the Centro de Geociências/UFPA, for the help and assistance with analytical work. We thank the assistance of João F. H. Appollo preparing the minerals concentrated.

REFERENCES

Babisnki, M.; Chemale Jr., F.; Hartmann, LA., Van Schmus, W.R.; Silva, L.C., 1996. Juvenile accretion at 759-700 Ma in Southern Brazil. Geology, 24(5): 439-442.

Bongiolo, E.M.; Mexias, A.S.; Gomes, M.E.B.; Formoso, M.L.L. 2002. Características das mineralizações e química de minerais hidrotermais na região de Lavras do Sul – RS. In: Cong. Bras. Geol., 41, João Pessoa, SBG... Anais, p. 435.

Doe, B.R.; Zartman, R.E., 1979. Plumbotectonics I, The Phanerozoic. In: Barnes, H.L. (Ed.). Geochemistry of Hydrothermal Ore Deposits, 2ª ed., Wiley Intersc., p.22-70.

Eby, G.N., 1990. The A-type granitoids: A review of their occurrence and chemical characteristics and speculations on their petrogeneis. Lithos, 26(1/2):115-134.

Foley, S., 1992. Vein-plus-wall-rock melting mechanisms in the lithosphere and the origin of potassic alkaline magmas. Lithos, 28:435-453.

Gastal, M.C.; Lafon, J.M., 1998.Gênese e evolução dos granitóides metaluminosos de afinidade alcalina da porção oeste do Escudo Sul-Riograndense: geoquímica e isótopos de Rb-Sr e Pb-Pb. Rev. Brasil. Geoc., 28(1):11-28.

Gastal, M.C.P.; Lafon, J.M. 2001. Novas idades $^{207}Pb/^{206}Pb$ e geoquímica Nd-Sr para granitóides shoshoníticos e alcalinos das regiões de Lavras do Sul e Taquarembó, RS. In: Cong. Bras. Geoq., 7, Curitiba...SBGP Anais CD-Room, nº 094, 7p.

Gastal, M.C.P.; Lafon, J.M. 2002. Geoquímica isotópica Sr-Nd-Pb e química mineral de minete e olivina minete do Complexo Intrusivas Lavras do Sul, RS: registros do manto litosférico metassomatizado. In: Simp. Vulcanismo e ambientes associados, 2, Belém, SBG. Bol. Resumos, p. 80.

Gaudette, H.E.; Lafon, J.M.; Macambira, M.J.B.; Moura, C.A.V.; Scheller, T., 1998. Comparison of single filament Pb evaporation/ionization zircon ages with conventional U-Pb results: examples from the Precambrian of Brazil. J. South Amer. Earth Sci., 11(4):351-363.

Kober, B., 1986. Whole-grain evaporation for $^{207}Pb/^{206}Pb$-age-investigations on single zircons using a double-filament thermal ion source. Contrib. Mineral. Petrol., 93:482-490.

Kober, B., 1987. Single-zircon evaporation combined with Pb^+ emitter bedding for $^{207}Pb/^{206}Pb$-age investigations using thermal ion mass spectrometry, and implications to zirconology. Contrib. Mineral. Petrol., 96:63-71.

Leite, J.A.D., 1997. A origem dos harzburgitos da Seqüência Cerro Mantiqueiras e implicações tectônica para o desenvolvimento do Neoproterozóico no sul do Brasil (Tese de Doutoramento, Instituto de Geociências, UFRGS), 243p.

Leite, J.A.D.; Hartmann, L.A.; McNaughton, N.J.; Chemale Jr. 1998. SHRIMP U/Pb zircon geochronology of Neoproterozoic juvenile and crustal-reworked terranes in southernmost Brazil. Intern. Geol. Rev., 40:683-705.

Ludwig, K.R. 2001. Isoplot/Ex rev. 2.49 – A geochronological toolkit for Microsoft Excel. Berkeley Geochronology Center – Special Publication No 1a, 55 p.

Manhes, G., 1982. Développement de L'ensemble Chronomêtrique U-Th-Pb. Contribution à la Chronologie Initiale du Système Solaire. (Thèse de doctorat d'état, Université de Paris VII), 294p.

Mexias, A. S., 2000. Alteração hidrotermal associada ao Distrito Aurífero de Lavras do Sul, RS – A área do Bloco Butiá (Tese de Doutoramento, Instituto de Geociências, UFRGS), 360p.

O'Brien, H.E.; Irving, A.J.; McCallum, I.S.; Thirlwall, M.F.,1995. Strontium, neodymium, and lead isotopic evidence for the interaction of post-subduction asthenospheric potassic mafic magmas of the Highwood Mountains, Montana, USA, with ancient Wyoming craton lithospheric mantle. Geochim. Cosmochim. Acta, 59(21): 4539-4556.

Oliveira, E.C.; Lafon, J.M.; Gioia, S.M.L.; Pimentel, M.M. 2002. Implantação do método Sm-Nd para minerais metamórficos e sua aplicação em rochas da região central do Amapá, Sudeste do Escudo das Guianas. In: Congresso Brasileiro de Geologia, 41. João Pessoa, SBG... Anais de resumos, p. 502.

Remus, M.V.D.; Hartmann, L.A.; McNaugton, N.J.; Groves, D.I.; Reischl, J.L.2000. Distal magmatic-hydrothermal origin for the Camaquã Cu (Au-Ag) and Santa Maria Pb, Zn (Cu-Ag) deposits, southern Brazil. Gondwana Res., 3(2):155-174.

Rodrigues, E. M. S. 1992. Implantação do método de datação Pb-Pb em rochas totais. Exemplos de aplicação em rochas da Província Mineral de Carajás. (Diss. Mestrado, UFPA), 128p.

Rollinson, H.R., 1993. Using Geochemical Data: Evaluation, Presentation, Interpretation. Ed. Longman, New York, 352p.

Stacey, J.S. and Kramers, J.D., 1975. Approximation of terrestrial lead isotope evolution by a two-stage model. Earth Planet. Sci. Lett., 26:207-221.

Steiger, R.H. & Jäger E, 1977. Subcommission on geochronology: convention on the use of decay constants in geo- and cosmochronology. Earth Planet. Sci. Lett. 36:359-362

Wasserburg, G.J.; Jacobsen, S.B.; DePaolo, D.J.; McCulloch, M.T.; Wen, T. 1981. Precise determination os Sm/Nd ratios, Sm and Nd isotopic abundances in standard solutions. Geochim. Cosmochim. Acta, 45: 2311-2323.

DATING HIGH-GRADE METAMORPHISM BY U-Pb, Sm-Nd AND K-Ar ISOTOPIC SYSTEMS: PALEOPROTEROZOIC I-TYPE GRANULITES FROM THE NORTHERN BORDER OF THE LUIS ALVES GNEISS-GRANULITE TERRANE, SOUTHERN BRAZIL

Harara, O.M.M.; Basei, M.A.S.; Siga Jr., O.; Campos Neto, M.C. and Prazeres Filho, H.J.

Universidade de São Paulo, Instituto de Geociências, Rua do Lago, 562, CEP:05508-080, São Paulo, Brazil.
osmmh@ig.com.br

Keywords: U-Pb, zircon, Paleoproterozoic, Sm-Nd, granulite, Luis Alves Terrane

The two principal Neo-Archean(?)/ Paleoproterozoic basement terranes exposed in southern Brazil are the Luis Alves Gneiss Granulite Terrane (GGT) and Atuba Gneiss-Migmatite Terrane which are surrounded by Neoproterozoic granite and metasedimentary belts (Figs. 1a, b): Piên Mafic-Ultramafic Suite and Piên-Mandirituba Granite Belt to the north, Dom Feliciano Belt to the south and Paranaguá-São Francisco do Sul Granite Belt to the east. The central and northern portion of the GGT and the southern border of the GMT are intruded by the Neoproterozoic Serra do Mar Plutonic-Volcanic Suite that is composed by alkaline-peralkaline granite and volcanic rocks. The northern border of the GGT and the whole GMT are affected by tectonic, magmatic and metamorphic processes of the Brasiliano/Pan-African orogenesis.

Regionally, the Luis Alves Gneiss-Granulite Terrane (GGT) is constituted by mafic, intermediate and felsic layered orthogranulites, pyroxene-free biotitic and amphibolitic gneisses, deformed calc-alkaline and alkaline granitoids and lenses of mafic and ultramafic rocks such as amphibolites, gabbros, pyroxenites and peridotites (Siga Jr., 1995; Basei et al., 1998, 1999; Fornari, 1998; Harara 2001). The granulites of sedimentary origin are rare and include garnet and rutile-bearing quartzites, cordierite-bearing kinzigitic gneisses and banded iron formations. The available U-Pb (conventional and SHRIMP) geochronological data (Siga Jr., 1995; Basei et al., 1998, 1999; Hartmann et al., 2000; Harara, 2001) on prismatic, rounded and elliptical zircons of the granulites, gneisses and deformed granitoids suggest the following ages for the high-grade metamorphism and synchronic magmatic periods: rare 2700 Ma, occasional 2400 and 2300 Ma and, frequent 2200 Ma, 2100 Ma and 2060 Ma. The U-Pb zircon ages of 2700 Ma and between 2400 and 2300 Ma are characteristic of the central and southern portions of the GGT while the ages between 2200 and 2060 Ma are characteristic of the northern portion of the GGT. The main geochronological data register the Paleoproterozoic metamorphic and magmatic events of the Trans-Amazonian orogenesis (Almeida et al., 2000). The K-Ar (biotite, amphibole) geochronological investigations (Siga Jr., 1995; Harara, 2001) carried out in the granulites and gneisses indicate ages around 1800 Ma and interpreted as the ages of the cooling and tectonic stability of the GGT.

Sm-Nd isotopic data (Siga Jr., 1995; Harara, 2001) revealed depleted mantle model ages (T_{DM}) between 2800 and 2500 Ma (Neo-Archean-Paleoproterozoic) for the granulites, biotitic and amphibolitic gneisses and deformed granitoids. These model ages indicate the time of the mantle differentiation of the GGT protholites.

The part of the northern border of the GGT, in the Rio Negro region (Fig. 1c), is constituted by LILE-depleted layered mafic, intermediate and felsic orthogranulites (norites, quartz norites, enderbites, rare charno-enderbites) and pyroxene-free biotitic and amphibolitic gneisses with compositions that include shoshonitic diorites/monzodiorites, quartz diorites and tonalites (Fig. 2). Lenses of biotite and amphibole-rich layered mafic orthogranulites and garnet-rich layered mafic and felsic orthogranulites occur within the mafic and felsic orthogranulites.

The mafic and felsic granulites are composed of quartz, plagioclase (oligoclase/andesine to labradorite), orthopyroxene, clinopyroxene, and minor amphibole, biotite, and interstitial microcline. The accessories minerals in both granulites are apatite, zircon, rutile and magnetite. The mafic and felsic granulites exhibit granoblastic, deformed granoblastic and lepido-granoblastic textures. The pyroxene-free biotitic and amphibolitic gneisses are composed of plagioclase, quartz, biotite, amphibole and epidote, minor K-Feldspar and rare orthopyroxene relicts. The accessories minerals are apatite, allanite, titanite, zircon and magnetite.

New U-Pb (conventional), Sm-Nd and K-Ar geochronological investigations carried out on biotite and amphibole-free mafic and felsic granulites, biotite and amphibole-rich mafic charnockites (isotropic appearance) and garnet-rich mafic granulites.

In the mafic granulites, elliptical (potato-type) and rounded (spherical-type) high re-crystallized metamorphic zircons, from the same rock, fall in the same discordia line and yielded similar upper intercept age of 2062 ± 65 Ma and one zircon concordant age of 2059 ± 6.6 Ma (Fig. 3).

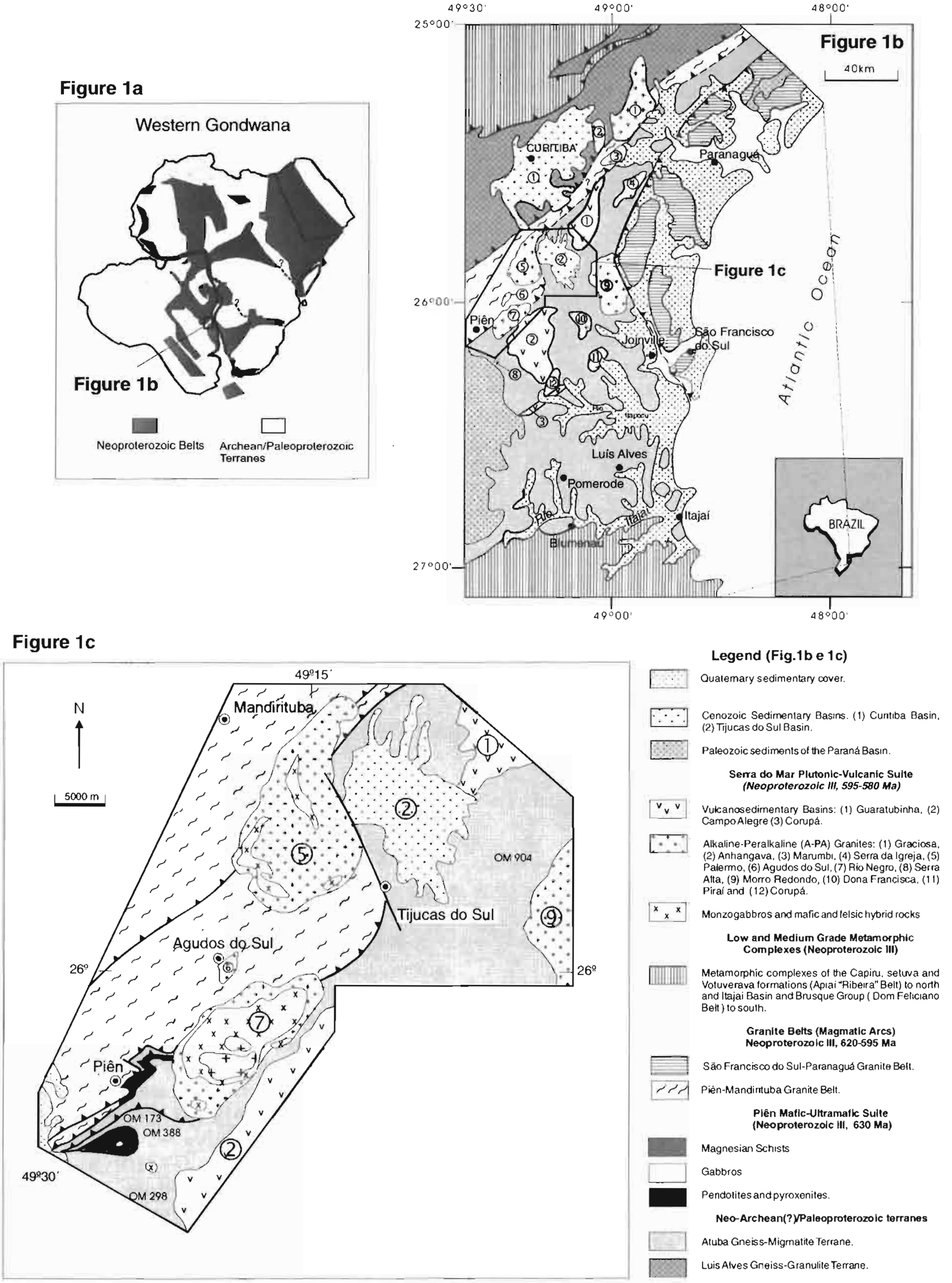

Figure 1. a) Sketch map of Archean/Paleoproterozoic Cratons and Neoproterozoic Belts of western Gondwana. Source: Modified from Unrug (1996). b) Geological map of south-eastern Paraná and north-eastern Santa Catarina states. Source: Siga Jr. (1995) and Harara (2001). c) Geological map of the Upper Rio Negro Region (PR-SC). Source: Harara (2001). The Samples dated by U-Pb and Sm-Nd methods, are indicated in the map.

In the felsic granulites, the elliptical zircons yielded an age of 2115 ± 31 Ma and the rounded (metamorphic) zircons, from the same rock, yielded upper intercept age of 2.060 ± 19 Ma (Fig. 4). The ages around 2060 Ma of the rounded metamorphic zircons, in both mafic and felsic granulites, and the concordant rounded zircon age of 2059 ± 6.6 Ma from the mafic granulites are interpreted as the ages of high-grade metamorphism of the northern border of the GGT.

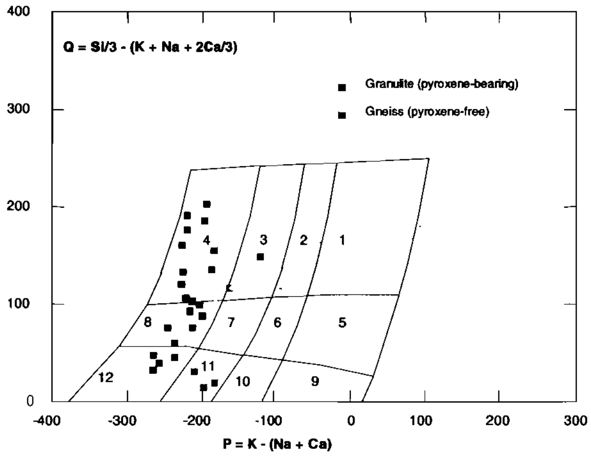

Figure 2. P-Q diagram (Debon & Lefort, 1983) for classification of igneous rocks applied to GGT rocks. Classification based on whole-rock chemical data (Harara 2001). 3. Granodiorites (Charno-enderbites), 4. Tonalites/Trondhjemites (Enderbites), 8. Quartz Diorites/QuartzNorites, 11. Monzodiorites/ Monzogabbros, 12. Diorites/Gabbros/Norites.

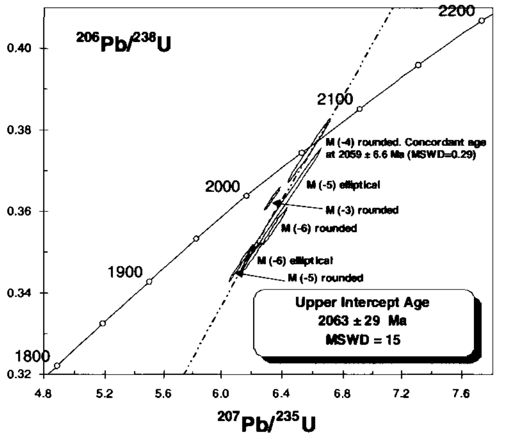

Figure 3. U-Pb Concordia diagram for elliptical and rounded zircons from mafic granulites. Sample OM 298.

The prismatic and long prismatic (acicular) zircons extracted from the biotite and amphibole-rich mafic charnockites fall on the same discordia line and yielded similar upper intercept ages of 2200 ± 7.3 Ma (Fig. 5). Based on the mineralogy, textures and typology of the zircon populations of these rocks, we interpret the age of 2200 Ma as the age of the igneous protholites of the granulite rocks from the northern border of the GGT.

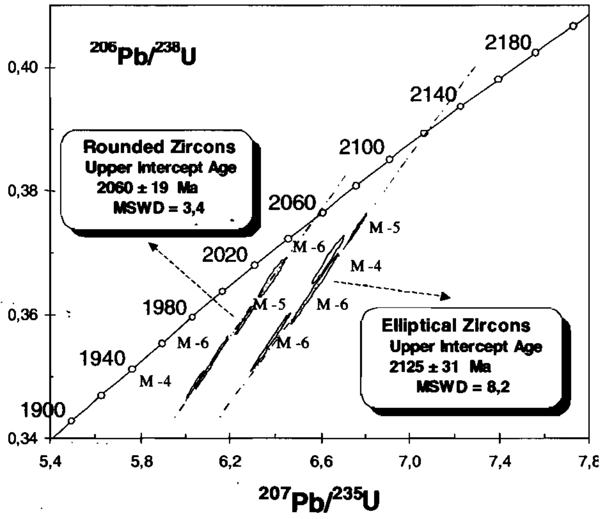

Figure 4. U-Pb Concordia diagram for elliptical and rounded zircons from felsic granulites Sample 388.

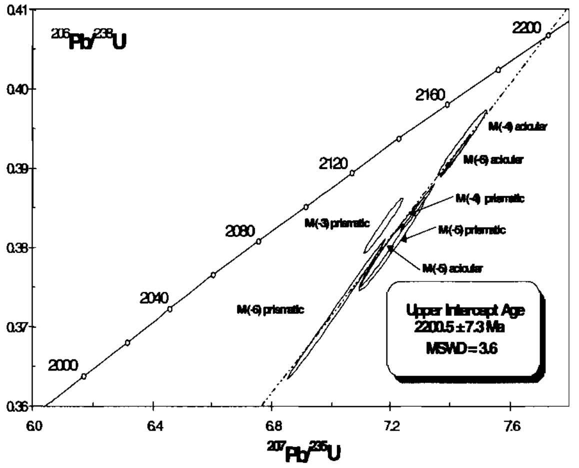

Figure 5. U-Pb Concordia diagram for prismatic and long prismatic (acicular) zircons of a biotite and amphibole-rich mafic charnockite. Sample OM 904.

Sm-Nd (whole rock, plagioclase and garnet) dating of garnet-rich mafic granulites yielded isochronic age of 1831 ± 17 Ma (Fig. 6). This age is similar to the K-Ar (biotite and amphibole) cooling ages, around 1800 Ma (Siga Jr., 1995; Harara, 2001) obtained in granulites and gneisses and interpreted as the cooling age of these rocks.

The time gap between K-Ar and Sm-Nd isochronic cooling ages of 1800 Ma and the U-Pb high-grade metamorphic ages of 2060 Ma suggest a slow cooling path for the GGT.

The GGT remained tectonically stable and cold until Neoproterozoic period, between 630 and 585 Ma, when its northern border was heated and affected by the adjacent Neoproterozoic subduction, collision and post-collision processes. These Neoproterozoic tectonic and metamorphic reactivations of the northern border of the GGT are suggested by pyroxene replacement by amphiboles, formation of epidote in the granulites, re-crystallization of biotite in the gneisses, parallelism of the tectonic foliations in the GGT with the tectonic foliations in the Piên Mafic-Ultramafic Suite and Piên-Mandirituba Granite Belt and resetting of the Paleoproterozoic K-Ar ages around 1800 Ma to Neoproterozoic ages between 650 Ma (amphibole) and 620 Ma (biotite).

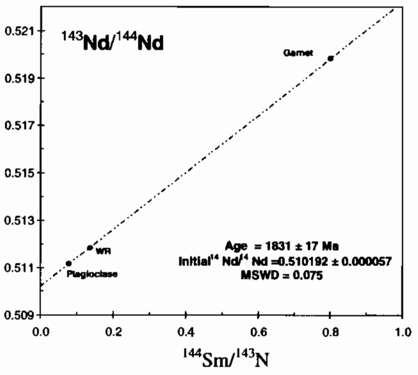

Figure 6. Sm-Nd isochron diagram for the garnet-rich mafic granulites.

ACKNOWLEDGMENTS

To FAPESP (Grants: 97/10964-2 and 02/01014-0) and Universidade de São Paulo.

REFERENCES

Almeida, F.F.M, Brito Neves, B.B. & Carneiro, C.D.R. (2000) The origin and evolution of the South American Platform. Earth Science Reviews, 50, 77-111.

Basei, M.A.S., McReath, I., Siga Jr. O. (1998) The Santa Catarina Granulite Complex of Southern Brazil, A Review. Gondwana Research, 1(3/4), 383-391.

Basei, M.A.S., Siga Jr, O., Reis Neto, J.M. dos, Passarelli, C.R., Prazeres, H.J., Kaulfuss, G., Sato, K. & Lima, P.S. de (1999) Paleoproterozoic Granulitic Belts of the Brazilian Southern Region (PR-SC). II South American Symposium on Isotope Geology. Cordoba, Argentine. Extended Abstracts. Actas, p.291-294.

Fornari, A. (1998) Geologia e Metalogênese da porção meridional do Cráton Luis Alves-SC. Campinas, 136p. (Tese de Doutoramento, Instituto de Geociências da Universidade de Campinas).

Harara, O. M. (2001) Mapeamento e Investigação Petrológica e Geocronológica dos litotipos da região do alto Rio Negro (PR-SC): Um exemplo de sucessivas e distintas atividades magmáticas durante o Neoproterozóico III. São Paulo, 206p. (Tese de Doutoramento, Instituto de Geociências da Universidade de São Paulo).

Hartmann, L. A., Santos, J. O. S., McNaughton, N. J. (2000) Ion microprobe (SHRIMP) dates complex granulite from Santa Catarina, southern Brazil. Anais da Academia Brasileira de Ciências, 72 (4), p.595-572.

Siga Jr. (1995) Domínios tectônicos do sudeste do Paraná e nordeste de Santa Catarina: Geocronologia e evolução Crustal. São Paulo, 212 p. (Tese de Doutorado, Instituto de Geociências da Universidade de São Paulo).

THE NAZARÉ PAULISTA-TYPE ANATECTIC GRANITE: MIXED SOURCES INFERRED BY ELEMENTAL GEOCHEMISTRY AND Sr-Nd ISOTOPES

Janasi, V.A. and Martins, L.

Instituto de Geociências, Universidade de São Paulo, SP, 05508-080, São Paulo-SP, Brazil. vajanasi@usp.br, lucemart@usp.br

Keywords: Granite, migmatite, crustal anatexis, Nd-Sr isotope geochemistry, Socorro-Guaxupé Nappe

INTRODUCTION

Research on the generation, extraction and migration of granitic melts in the continental crust has gained renewed interest in the geological literature in recent years, mostly with the introduction of new methodologies which allow a more precise determination of intensive and extensive parameters such P, T, t, fluid activities etc. More stimulating results have been obtained in studies in which the source areas of the granitic magmas are well characterized, either in anatectic terranes, where magmas and sources are directly associated (Watt & Harley, 1993; Barbero et al., 1995), or in regions such as the Himalayas, where continued studies over the last decades allowed the sources of the collisional leucogranites to be very well constrained (Harris et al., 1995).

The source identification typically makes use of a geochemical approach, with major and trace elements and radiogenic isotopes (especially Sr, Nd and Pb) yielding fundamental and complementary information (Inger & Harris, 1993; Harris et al., 1995) that can be confronted with experimental results (cf. Patiño Douce & Harris, 1998; Castro et al., 1999).

Crustal granites directly associated to migmatite terranes are abundant in extensive areas of the crystalline basement in Brazil. In the southernmost portion of the Socorro-Guaxupé Nappe (SGN) east of Atibaia (SP) (Fig. 1), three main types of anatectic granites closely associated to migmatites occur. In order of decreasing abundance, they are: the garnet-biotite Nazaré Paulista (NP) granite; the pink or grey biotite Quatro Cantos (QC) granite and white two-mica (2M) leucogranites.

This work uses elemental and isotope geochemistry as tools to identify the role of the main regional metamorphic units as potential sources for the different types of anatectic granites occurring in the Atibaia area.

THE COUNTRY ROCKS

Shown in Figure 1 is the southernmost portion of the SGN, a high-grade metamorphic terrane allochtonous over the SW portion of the São Francisco Craton in SE Brazil. The metamorphic units belong to the Piracaia Metamorphic Complex (Campos Neto et al., 1983), and locally three main units are recognized, from "base" to "top": (1) granitic to tonalitic biotite (± hornblende) gneisses; (2) banded garnet-biotite gneisses with centimeter to decimeter layers and variations towards more aluminous (sillimanite-bearing), and more calcic (with hornblende and andesine-labradorite plagioclase) gneisses, and frequent intercalations of hornblende gneisses, calc-silicate rocks wiht amphibolites, and (3) (± sillimanite)-garnet-muscovite-biotite schists (often with quartzite and quartz schist bands), that occasionaly grade into thin packages of micaceous quartzite (cf. Fig. 1).

On the basis of their chemistry, rocks from units 2 and 3 are identified as of dominantly metasedimentary origin. The sillimanite-bearing schists are invariably weathered, so it is hard to obtain samples suitable for chemical analysis; their derivation from pelite sediments is however undoubtful. The garnet-biotite gneisses are metagreywackes with different propotions of a pelitic component and possibly some contribution from associated basic volcanics now appearing as amphibolite layers. Rocks from unit 1 are of doubtful origin, and could include orthogneisses (from basement sequences or as early bodies locally intrusive into units 2 and 3) or strongly immature sediments. A peculiar feature of unit 1 gneisses are their strongly fractionated REE patterns and high Sr contents, reminescent of Archean TTG sequences.

THE ANATECTIC GRANITES

Under the name "Nazaré Paulista (NP) granite" are grouped several types of garnet-biotite granites, the most abundant product of crustal anatexis in the Atibaia region. Two main facies are present, both occurring as small bodies, no more than a hundred meters wide, sometimes crosscutting each other in the same outcrop. The grey facies is an equigranular garnet-biotite granite with M (mafic index)=5-8 strongly veined by a white, usually slightly coarser-grained, garnet leucogranite (M<4). The white facies is texturally similar to the latter veins, but forms independent bodies with pegmatitic pockets, and is chemically distinct. Monazite U-Pb dating of the grey facies resulted in an age of 624 ± 2 Ma (Janasi, 1999).

The QC anatectic biotite granites occur mostly to the north of the Nazaré Paulista granites, usually directly associated to the biotite gneisses from unit 1. The 2M leucogranites appear as small bodies southwest of the NP granites, surrounding the younger Atibaia granite (Figure 1), and mostly associated to the upper schist unit.

Compared to the experimental products of melting of crustal protoliths, the NP granites have an excess of quartz, plagioclase and mafic minerals, which appear to reflect a restite component. Melting temperatures, as inferred from zircon and monazite saturation thermometry, are within the range of muscovite dehydration-melting (~700-750°C) for the NP granites and the 2M granites; the lower values are shown by the NP garnet leucogranites. Higher temperatures, already within the biotite dehydration-melting field (>820°C), are obtained in the QC granites.

Relative to typical products of crustal anatexis such as the Himalayan leucogranites (Harris et al., 1995), the NP granites have lower Rb/Sr, higher La/Yb and lower phosphorous content. The QC granites have even higher Sr and La/Yb and can be modelled as products of melting of unit 1 biotite gneisses, which is suggestive that the latter could also be an important component in the Nazaré Paulista granites. Flatter REE patterns and low Sr contents thought to be typical of crustal leucogranites are only shown by the NP garnet leucogranites.

Sr-Nd ISOTOPE GEOCHEMISTRY

The $^{87}Sr/^{86}Sr_{625}$ of the anatectic granites are widely varied and increase from QC (0.7122-0.7128) to grey NP (0.7134-0.7187) to NP garnet leucogranite (0.7237-0.7245; data from Ragatki, 1998) to 2M granite (0.7327), pointing to sources with increasingly higher Rb/Sr ratios in this sequence (Fig. 2).

The εNd_{625} are strongly negative and less varied, and appear to reflect the geographic position of the samples rather than the petrographic type. Samples intrusive into the easternmost portion of the Piracaia Metamorphic Complex, near the Nazaré Paulista town (outcrops 41 and 51; cf. Figure 1) have $\varepsilon Nd_{625} = -12$ to -13, while those collected further west (outcrops 40 and 50) are more negative ($\varepsilon Nd_{625} \sim -16$). It is remarkable that the NP granite samples from the latter two outcrops show the lowest $^{87}Sr/^{86}Sr_{625}$, suggesting a (unusual) positive correlation between the Sr and Nd isotopes.

Also shown in Figure 2 are the fields of regional granulites and metasediments (from Janasi, 1999), and the Sr-Nd isotope compositions of metamorphic rocks from units 1 and 2 of the Piracaia Complex. The spread in $^{87}Sr/^{86}Sr_{625}$ is similar to that shown by the anatectic granites (0.7132-0.7275); the lowest value is shown by the unit 1 biotite gneiss. The εNd_{625} are on average less negative than in the granites (–8 to –13). Interestingly, samples spatially associated with granites showing $\varepsilon Nd_{625} \sim -13$ are the least negative (# 41 and 53), whereas samples with εNd_{625} overlapping those of the latter granites occur westwards, suggesting greater contribution from old sources in this direction.

IDENTIFICATION OF THE SOURCES

Elemental and isotope geochemistry data are consistent with the QC biotite granites deriving from unit 1 biotite gneisses, from which they must have inherited their high Sr and La/Yb and relatively low $^{87}Sr/^{86}Sr_{625}$. The NP garnet leucogranites and probably also the 2M leucogranites can derive mostly from the regional metasediment, as shown by the overlap in their Sr-Nd radiogenic signature, the high Rb/Sr and lower REE fractionation. The grey garnet-biotite NP granites cannot be derived solely from either of these sources; their chemical and isotopic character is intermediate between the QC biotite granites and the leucogranites, which is consistent with a mixed source involving a metasedimentary component similar to the regional garnet-biotite gneisses and a high-Sr, high-LREE component. Their εNd_{625}, which seem to become more negative westwards and are more negative than the country garnet-biotite gneisses in a given location, are suggestive that the latter component is or mostly derived from the erosion of old basement.

ACKNOWLEDGMENTS

Financial support: Fapesp, Proc. 97/2438-9 and 00/2509-8.

REFERENCES

Barbero, L.; Villaseca, C.; Rogers, G. & Brown, P.E. 1995. Geochimical and isotopic desequilibrium in crustal melting: An insight from the anatetic granitoids from Toledo, Spain. Journal of Geophysical Research, 100(B8): 15745-15765.

Campos Neto, M.C.; Basei, M.A.S.; Artur, A.C.; Silva, M.E.; Machado, R.; Dias Neto, C.M.; Fragoso Cesar, A.R. 1983. Geologia das Folhas Piracaia e Igaratá. In: 1ª Jornada sobre a Carta Geológica do Estado de São Paulo em 1:50.000. PRÓ-MINÉRIO, São Paulo, p. 61-78.

Castro, A.; Patiño Douce, A.E.; Corretgé, L.G.; De La Rosa, J.D.; El-Biad, M. & El-Hmidi, H. 1999. Origin of peraluminious granites and granodiorites, Iberian massif, Spain. An experimental test of granite petrogenesis. Contributions to Mineralogy & petrology, 135: 255-276.

Harris, N.B.W.; Ayres, M. Massey, J. 1995. Geochemistry of granitic melts produced during the incongruent melting of muscovite: Implications for the extraction of Himalayan leucogranite magmas. Journal of Geophysical Research, 100(B8): 15767-15777.

Inger, S. & Harris, N. 1993. Geochemical constraints on leucogranite magmatism in the Langtang Valley, Nepal Himalaya. Journal of Petrology 34 (2): 345-368.

Janasi, V.A. 1999. A idade dos granitos Nazaré Paulista e Pinhal e implicações para o metamorfismo da Nappe Socorro-Guaxupé (SP-MG). In: Simpósio de Geologia do Sudeste, 4, São Pedro-SP, Sociedade Brasileira de Geologia. Boletim de Resumos, p. 7.

Patiño Douce A. E. & Harris N. 1998. Experimental constraints on Himalayan anatexis. Journal of Petrology, 39 (4): 689-710.

Ragatki, D. 1998. Contribuição à geoquímica e geocronologia do Domínio São Roque e da nappe de Empurrão Socorro-Guaxupé na região de Igaratá e Piracaia, SP. Tese de Doutoramento, Instituto de Geociências, Universidade de São Paulo, 131pp.

Watt, G.R. & Harley, S. L. 1993. Accessory phase controls on the geochemistry of crustal melts and restites produced during water-undersaturated partial melting. Contributions to Mineralogy and Petrology 114: 550-566.

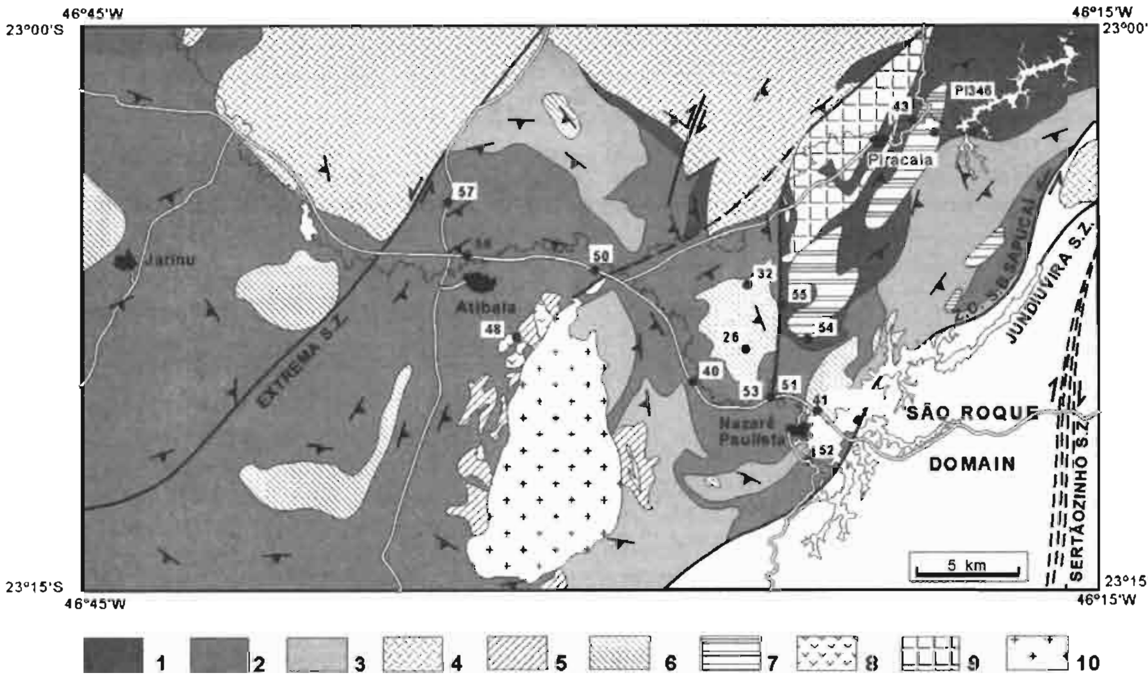

Figure 1. Simplified geologic map of the Atibaia region. 1, 2, 3 = Piracaia Metamorphic Complex (1= Bt gneiss; 2 = Grt-Bt gneiss; 3 = (Sil)-Grt-Bt-schist); 4 = high-K calc-alkaline granite; 5 = Ms-Bt (2M) leucogranite; 6 = Nazaré Paulista (NP) Grt-Bt granite ; 7 = Quatro Cantos Bt granite; 8 = Porphyritic tonalite-granodiorite; 9 = Piracaia monzodiorite; 10 = Atibaia granite. Numbers refer to sampling sites.

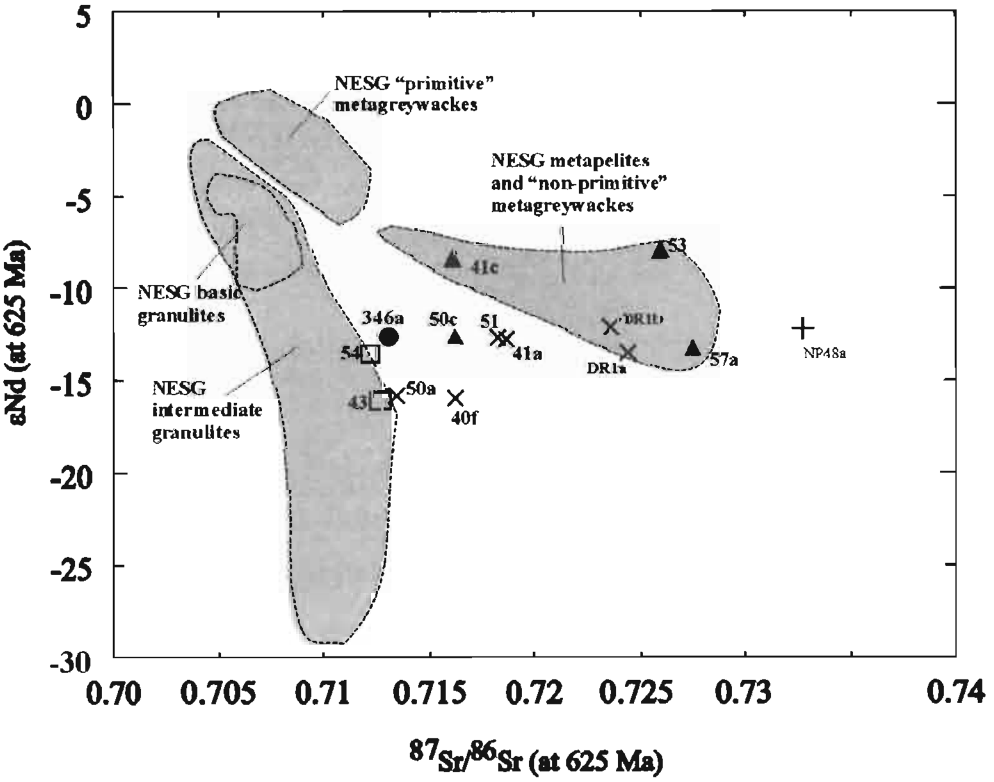

Figure 2. εNd x ^{87}Sr/^{86}Sr (calculated at 625 Ma) for crustal granites and metamorphic rocks from the Atibaia region. The fields of SGN granulites, metagreywackes and metapelites (from Janasi, 1999a) are also shown. Numbers refer to sampling sites (cf. Fig. 1).
Symbols: closed triangles, Grt-Bt gneiss (sample 50c is a calc-silicate rock); closed circle, Bt orthogneiss; open squares, QC bt granite; "x", NP Grt-Bt granite (samples DR1a, DR1b are Grt leucogranites analysed by Ragatki, 1998); "+", Ms-Bt granite.

MAFIC MAGMATISM ASSOCIATED WITH THE GOIÁS MAGMATIC ARC IN ANICUNS-GO, CENTRAL BRAZIL: NEW ID-TIMS AND SHRIMP U-Pb DATA

Laux, J.H.[1]; Pimentel, M.M.[1]; Dantas,E.L.[1]; Armstrong, R.[2] and Armele, A.[1]

1. Instituto de Geociências, Universidade de Brasília, Brasília-DF, 70910-900, Brazil.
lauxjh@unb.br, marcio@unb.br, elton@unb.br, alanarmele@bol.com.br
2. Research School of Earth Sciences, Australian National University, Canberra, Australia. richard.armstrong@anu.edu.au

Keywords: U-Pb, Goiás Magmatic Arc, Neoproterozoic, mafic magmatism

INTRODUCTION

The Anicuns-Itaberaí volcano-sedimentary sequence, in western Goiás, Brazil, has been correlated in the past with the Serra de Santa Rita Archean greenstone belt. More recent studies, however, suggest that these rocks are considerably younger and might belong to the Neoproterozoic Goiás Magmatic Arc (Pimentel et al. 2000a, b; Laux et al., 2001, 2002).

In this study, new ID-TIMS and SHRIMP U-Pb ages for mafic rocks from the Anicuns region demonstrate that volcano-sedimentary sequence is Neoproterozoic, and that mafic magmatism took place during at least two main episodes.

GEOLOGICAL SETTING

The Tocantins Province (TP) represents a large Brasiliano/Pan-African orogen developed between three major continental blocks: the Amazonian, São Francisco and Paranapanema cratons. The province comprises three important fold belts, known as the Paraguay Belt, in the southwest, the Araguaia Belt, in the NW, and the Brasília Belt which occupies large areas of the eastern part of the TP, along the western margin of the São Francisco Craton (for a review see Pimentel et al., 2000a). The westernmost part of the Brasília Belt is occupied by a large juvenile terrain known as the Goiás Magmatic Arc (Fig. 1) made of calc-alkaline orthogneisses and granitoid rocks, as well as island arc-type volcano-sedimentary sequences.

GEOLOGY OF THE ANICUNS REGION

In the Mossâmedes-Anicuns region (Figs. 1, 2), Barbosa (1987) recognized three distinct supracrustal sequences, and assigned different ages to them, based on field relationships and structural data: (i) the Anicuns-Itaberaí Sequence (AIS) was interpreted as the southern extension of the Serra de Santa Rita (Goiás Velho) greenstone belt, (ii) the Mossâmedes Sequence (Simões,

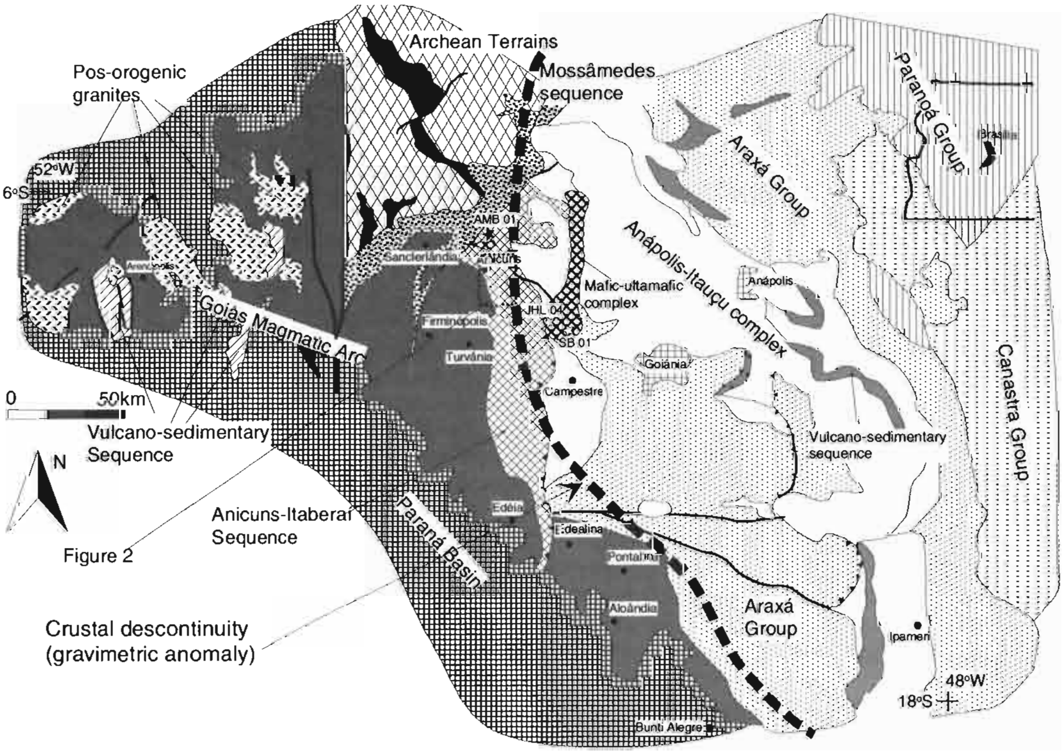

Figure 1. Location map showing the Goiás Magmatic Arc and the Anicuns-Itaberaí Sequence (Pimentel et al. 2000a).

1984), west/northwest of Anicuns, was assigned a Mesoproterozoic age, and interpreted as equivalent to the Araxá Group, and (iii) a younger detrital sequence (conglomerates, quartzites and schists) forming the Serra Dourada ridge, at the north. Nunes (1990) recognized two different N-S elongated sequences (Fig. 2). To the west is the Córrego da Boa Esperança Sequence (CBES), made of metapelites, andesitic/dacitic meta-tuffs, and iron formation and has been compared to the Araxá Group (Nunes, 1990). This sequence is separated from the AIS, in the east, by a NNW reverse fault. According to Nunes (1990), this sequence is formed by mafic/ultramafic metavolcanic rocks, metacherts, metarhytmites and marble lenses.

Both Nunes (1990) and Barbosa (1987) have suggested that the metavolcanic rocks in this region have calc-alkaline or calc-alkaline/tholeiitic nature, indicating a magmatic arc setting for their origin. Intrusive into the supracrustal sequences are three generations of granitic rocks, as well as mafic and mafic-ultramafic small bodies. The granitoid intrusions are represented by tonalites, granodiorites and granites, with subordinate quartz syenite, metamonzonites and metamonzodiorites.

The mafic/intermediate intrusions are collectively referred to as the Anicuns-Santa Bárbara Gabbro-Diorite Suite (Araújo, 1997). The Córrego Seco and Santa Bárbara intrusions (Fig. 2), investigated in this study, have been included in this plutonic suite.

The Americano do Brasil Mafic-Ultramafic Suite comprises small layered bodies known as Americano do Brasil, Mangabal I, Mangabal II, Adelândia, Fronteira do Norte, Palmeiras, and Serra do Gongomé exposed to the north of the area investigated. Mafic rocks are metagabbros, metagabbronorites, olivine gabbros and amphibolites, and ultramafic rocks include mainly metadunites, metaperidotites, metapyroxenites and hornblendites (Nilson, 1984; Candia & Girardi, 1985). The Serra do Gongomé and Americano do Brasil complexes have been dated at 637 ± 19 Ma and 610 ± 50 Ma, by Rb-Sr and Sm-Nd whole-rock isochrons (Winge, 1995; Gioia, 1997). The high initial Sr isotopic ratio for the Gongomé intrusion (0.7153) indicates interaction with older continental crust, whereas the positive ε_{Nd}(T) value (approximately +3.0) for the Americano do Brasil original magma indicates little or no contamination with older crust.

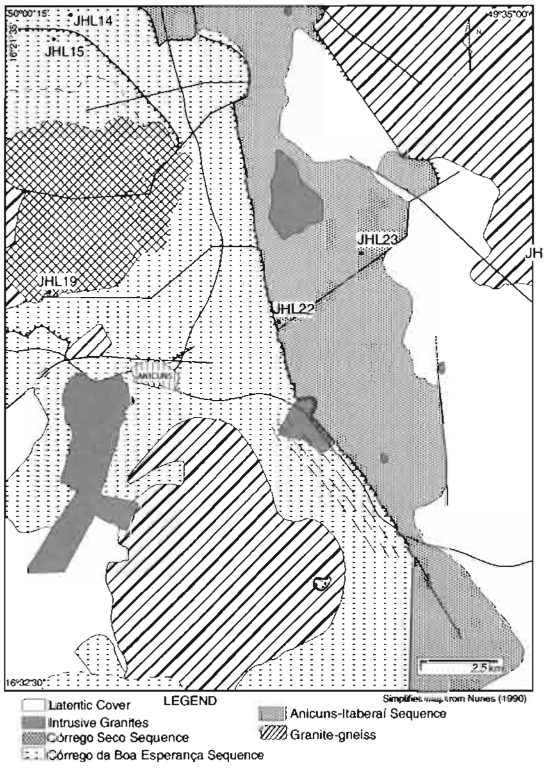

Figure 2. Sketch map of the Anicuns area showing sample location (Simplified from Nunes, 1990).

RESULTS

Eight new ID-TIMS and one new SHRIMP U-Pb results for mafic rocks of the Anicuns region are discussed in this work. Mafic rocks from the three distinct sequences recognized in the literature have been investigated. Three of them are within the Córrego da Boa Esperança Sequence [samples JHL-14, JHL-15 and AMB-01 (Figs. 1, 2)]. JHL-14 is an amphibole-garnet schist, most likely derived from a gabbro. CL images reveal that zircon grains in this rock present sector zoning typical of crystals formed from mafic magmas (Fig. 3b). The analyses yielded a concordia age of 886 ± 5 Ma (Fig. 3a), interpreted as the crystallization age (Laux et al., 2002). Sample JHL-15 consists of an amphibole schist, and the zircon crystals form yellow, long prisms. The U-Pb results produced an upper intercept age of 862 ± 5 Ma (Fig. 4a). Sample AMB-01 is a metadiorite with preserved igneous texture. The prismatic zircon grains analysed resulted in concordant to semi-concordant analytical points indicating the crystallization age of 856 ± 15 Ma.

Two samples within the Anicuns-Itaberaí Sequence were studied. Sample JHL-26B is a quartz diorite with preserved igneous texture, whereas JHL-23 is a coarse-grained amphibolite (metagabbro). Zircon grains JHL-26B are prismatic and brownish yellow, and produced the upper intercept age of 830 ± 9 Ma, interpreted as the igneous crystallization age. Prismatic, brownish, zircon grains from sample 5HL-23 form a discordia line with an upper intercept age of 815 ± 10 Ma, interpreted as indicative of the crystallization of the original mafic magma.

Four selected samples from the Anicuns-Santa Bárbara Gabbro-Diorite Suite were investigated (JHL-22C, JHL-19, JHL-04, SB-01 (Figs. 1, 2). Sample JHL-19 corresponds to a diorite belonging to the Córrego Seco Complex, intrusive into the Córrego da Boa Esperança Sequence. Zircon crystals are colorless, needle-shaped and yielded the age of 622 ± 6 Ma (Fig. 5d). Sample JHL-22C is an amphibolite intrusive into the Anicuns-Itaberaí Sequence, and presented the mean ^{206}Pb/^{238}U age of 630 ± 4 Ma (Fig. 5c), identical to the previous sample. Samples JHL-04 and SB-01 are from the Santa Bárbara de Goiás Complex (Silva & Nilson, 1990). Anorthosite

SB-01 with anhedral, colorless zircon crystals. One concordant analysis indicates the $^{206}Pb/^{238}U$ age of 594 ± 10 Ma. The other two points seem to have incorporated some inherited Pb. Discordia through the three points indicates a lower intercept age of 598 ± 8 Ma, interpreted as the crystallization age, and the upper intercept age of 1165 ± 97 Ma, indicative of Mesoproterozoic inheritance (Fig. 5a). Sample JHL-04 is a biotite tonalite with an upper intercept zircon age of 612 ± 6 Ma (Fig. 5c), representing the age of igneous crystallization of the original magma.

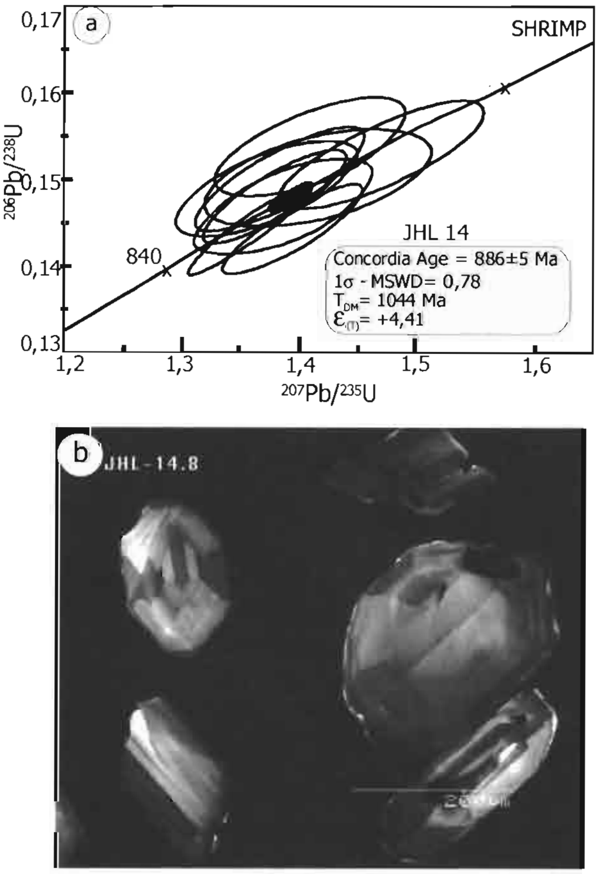

Figure 3. SHRIMP U-Pb age (a) and CL image (b), for Sample JHL-14.

CONCLUSIONS

The new U-Pb results presented here demonstrate that the mafic rocks belonging both the Anicuns-Itaberaí and Córrego da Boa Esperança sequences have the same ages.

The Anicuns-Santa Bárbara gabbro-diorite and Americano do Brasil suites are coeval, although they might not be genetically equivalent, as suggested by some authors (Nilson, 1984; Silva & Nilson, 1990).

All mafic rocks analysed present T_{DM} model ages of ca. 1.0 Ga, equivalent to model ages found for rocks of the Goiás Magmatic Arc. $\varepsilon_{Nd}(T)$ values are positive, indicative of the depleted nature of the mantle source (MORB-like). However, the lithological association found in the these supracrustal sequences, are not exactly similar to other island arc-like sequences of the Goiás Magmatic Arc in which felsic and intermediate volcanic products are abundant (e.g. the Arenópolis Sequence; Pimentel & Fuck 1986). The conspicuous presence of metacherts, marble, metapelites and the dominance of mafic metaigneous rocks suggests that these supracrustal sequences in the Anicuns region are equivalent to the Córrego Santo Antônio Unit, underlying the western part of the Arenópolis Sequence, which have been interpreted as an oceanic or fore-arc sequence.

The area of outcrop of the Anicuns-Itaberaí coincides with a regionally important gravimetric discontinuity (Fig.1) indicating that it marks an important crustal boundary, possibly separating juvenile rocks of the Goiás Magmatic Arc to the west, from rocks of the Anápolis-Itauçu Complex to the east, where older crustal components are obvious in the Nd isotopic compositions of the igneous rocks (Piuzana et al., 2003). This is suggested also by the initial isotopic compositions and inheritance patterns displayed by the mafic rocks around the Anicuns area. To the west of the gravimetric discontinuity, mafic rocks are pristine, and present positive $\varepsilon_{Nd}(T)$ values, whereas mafic rock associations towards the east display evidence of contamination of the original magmas with older crust. For instance, the Gongomé intrusion has very high initial Sr isotopic ratio (0.7153) (Winge, 1995), the Santa Bárbara de Goiás Complex have inherited zircon grains of possible mesoproterozoic age, and the Goianira-Trindade layered intrusion has a Sm-Nd isochron age of ca. 621 Ma and $\varepsilon_{Nd}(T)$ value of 0.0 (Pimentel, unpublished results).

ACKNOWLEDGEMENTS

We thank Simone M.C.L. Gióia and Sérgio L Junges for technical assistence, and Dr. Ariplinio A. Nílson for supplying sample AMB-01.

REFERENCES

Araújo, V.A. 1997. Programa de Levantamentos Básicos do Brasil, Folha SE.22-X-A-III – Itaberaí. GO, Escala 1:100.000. Texto Explicativo. CPRM, 112p.

Barbosa, P.A.R. 1987. Geologia e Recursos Minerais das Seqüências Supracrustais a Leste de Mossâmedes-GO. Dissertação de Mestrado, Univ. Brasília, 226 p.

Cândia, M.A.F. & Girardi, V.A.V. 1985. Geologia e petrologia dos complexos máfico-ultramáficos de Mangabal I e II, Sanclerlândia, Goiás. Rev. Bras. Geoc. 15(3): 221-230.

Gioia, S.M.C. 1997. Preparação da Metodologia Sm-Nd para Datação de Amostras Geológicas e sua Aplicação em Rochas das Áreas de Firminópolis, Fazenda Nova e Americano do Brasil. Dissertação de Mestrado, Univ. Brasília, 100p.

Laux, J.H., Pimentel, M.M., Dantas, E.L. 2001. Preliminary Nd isotopic data for the Anicuns-Itaberaí Sequence, associated orthogneisses, and granite intrusions, Goiás, Brazil. In: SSAGI, 3. Chile. CD-ROM.

Laux, J.H., Pimentel, M.M., Dantas, E.L., Armstrong, R. Armele, A. 2002. Idade do vulcanismo associado ao Grupo Araxá e Arco Margmático de Goiás na Região de Anicuns-GO. In: SBG Simp. Sobre Vulcanismo e Ambientes Associados, 2. Belém, Resumos, pg 42.

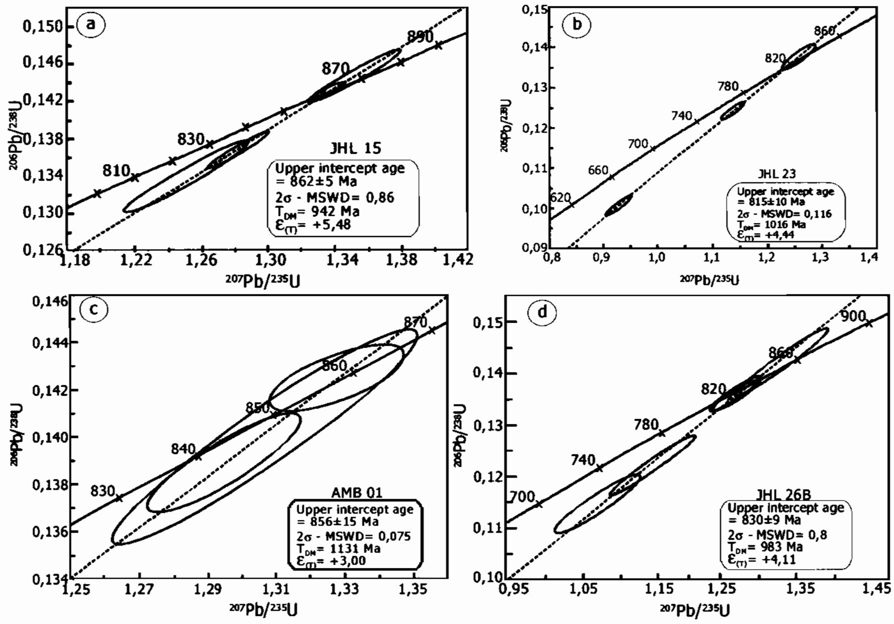

Figure 4. U-Pb concordia diagrams for the ca 800 Ma old samples.

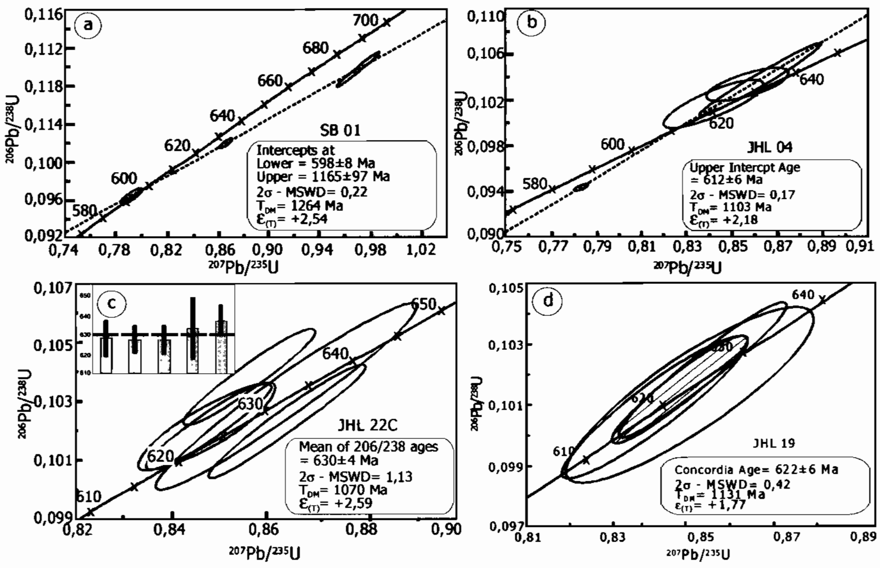

Figure 5. U-Pb concordia diagrams for the ca 600 Ma old samples.

Nilson, A.A. 1984. Complexo máfico-ultramáfico de Americano do Brasil, Goiás – Geoquímica das rochas e implicações petrogenéticas. In: SBG, Cong. Bras. Geol., 33. Anais...Rio de Janeiro. 9: 4204-4219.

Nunes, N.S.V. 1990. Geologia e Potencial Mineral da Região de Anicuns, Goiás. Dissertação de Mestrado. Univ. Brasília. 188p.

Pimentel, M.M. & Fuck, R.A. 1986. Geologia da Seqüência vulcano-sedimentar de Arenópolis. Rev. Bras. Geoc.. 16(2) 217-223.

Pimentel, M.M.; Fuck, R.A.; Jost, H.; Ferreira Filho, C.F.; Araújo, S.M. 2000a. Geology of the central part of the Tocantins Province: Implications for the geodynamic history of the Brasília belt. In: Cordani, U.G. (Editor), Tectonic Evolution of South America p.195-229.

Pimentel, M.M., Fuck, R.A., Gioia, D.M.C.L. 2000b. The neoproterozoic Goiás Magmatic Arc, Central Brazil: A review and new Sm-Nd isotopic data. Rev. Bras. Geoc., 30(1): 35-39.

Piuzana, D.; Pimentel, M.M.; Fuck, R.A.; Armstrong, R. 2003. Neoproterozoic magmatism and high-grade metamorphism in the Brasília Belt, central Brazil: regional implications of SHRIMP U-Pb and Sm-Nd geocronological studies. Precambrian Research. Prelo.

Silva, F.O. & Nilson, A.A. 1990. Caracterização do complexo gabro-anortosítico acamadado de Santa Bárbara de Goiás. In: SBG, Cong. Bras. Geol., 36. Anais...Natal. p. 1898-1912.

Simões, L.S. A. 1984. Geologia do Grupo Araxá na Região de Mossâmedes – Goiás, e as Ocorrências Minerais Associadas. Dissertação de Mestrado, Univ. Brasília. 219p.

Winge, M. 1995. Idade da supersuíte de Americano do Brasil. In: SBG-Núcleo Centro-oeste, Simp. Geol. Centro-Oeste, 5. Anais.... Goiânia p. 99-101.

NEW U-Pb DATA FOR ORTHOGNEISSES OF THE NEOPROTEROZOIC GOIÁS MAGMATIC ARC, CENTRAL BRAZIL

Laux, J.H.[1]; Pimentel, M.M.[1]; Dantas, E.L.[1]; Armstrong, R.[2] and Armele, A.[1]

1. Instituto de Geociências, Universidade de Brasília, Brasília-DF, 70910-900. lauxjh@unb.br, marcio@unb.br, elton@unb.br, alanarmele@bol.com.br
2. Research School of Earth Sciences, Australian National University, Canberra, Australia. richard.armstrong@anu.edu.au

Keywords: U-Pb geocronology, Goiás Magmatic Arc, orthogneiss

INTRODUCTION

Tonalitic to granitic orthogneisses underlie important areas in the Precambrian terrains between Bom Jardim de Goiás and Sanclerlândia, in western Goiás, central Brazil (Pimentel & Fuck, 1987; Pimentel et al., 2000a).

In several regional studies, these rocks were originally interpreted as part of Archean TTG terrains, however Nd, Pb and Sr isotopic data presented by Pimentel & Fuck (1992) for tonalitic/granodioritic rocks of the Arenópolis area demonstrated that they represent Neoproterozoic arc magmas, and were included in the Goiás Magmatic Arc.

In this study, new ID-TIMS and SHRIMP U-Pb ages for orthogneissic rocks from other areas of Goiás Magmatic Arc in western Goiás demonstrate that these Neoproterozoic rocks extend as far as the Anicuns region, comprising an extensive juvenile Neoproterozoic arc terrain.

GEOLOGICAL SETTING

The Tocantins Province (TP) represents a large Brasiliano/Pan-African orogen developed between three major continental blocks: the Amazonian, São Francisco and Paranapanema cratons. The province comprises three important fold belts, known as the Paraguay Belt, in the southwest, the Araguaia Belt, in the NW, and the Brasília Belt underlying large areas of the eastern part of the TP, along the western margin of the São Francisco Craton (for a review see Pimentel et al., 2000a). The westernmost part of the Brasília Belt is underlain by a large juvenile terrain known as the Goiás Magmatic Arc (Fig. 1) made of calc-alkaline orthogneisses and granitoid rocks, as well as island arc-type volcano-sedimentary sequences.

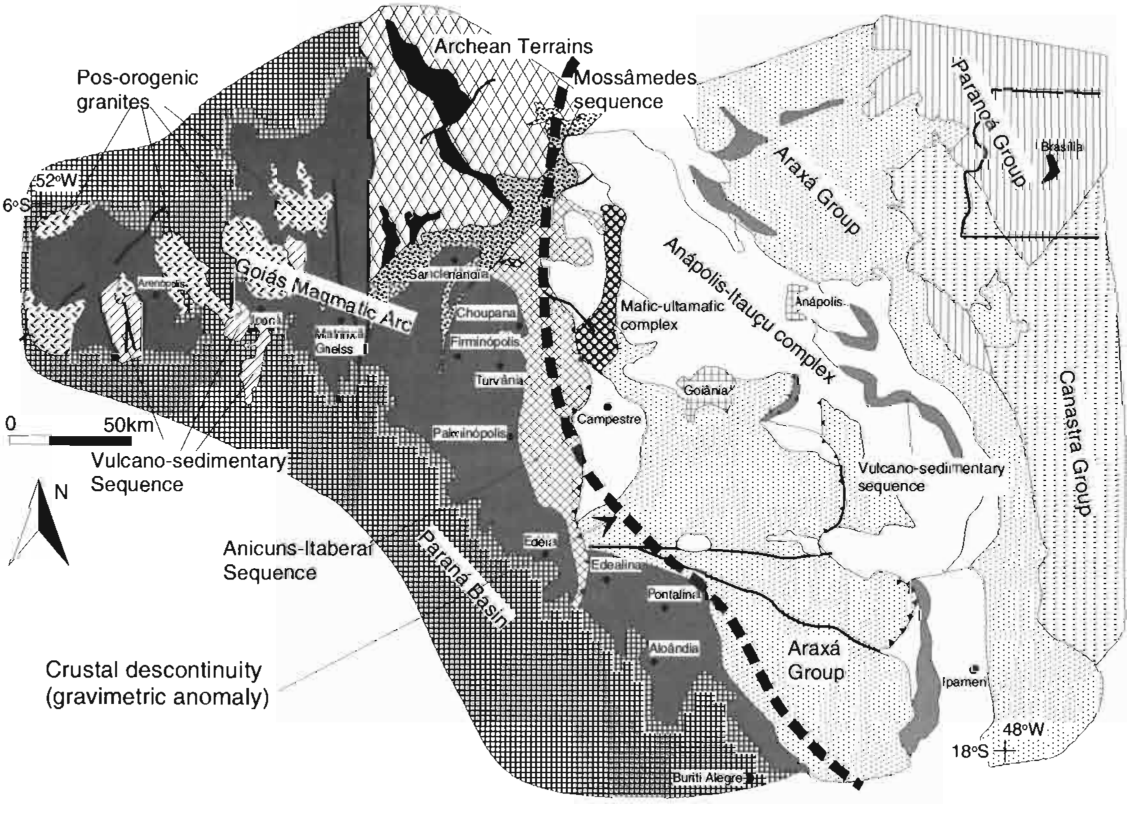

Figure 1. Schematic geological map showing the Goiás Magmatic Arc and sample location (Pimentel et al., 2000a).

The Arenópolis Arc underlies large areas in western and southwestern Goiás, extending from the vicinities of Bom Jardim de Goiás in the west, to Turvânia (Fig. 1). The supracrustal and orthogneissic units that make this section of juvenile Neoproterozoic continental crust are juxtaposed to each other along important NNE to NNW strike-slip faults.

GEOLOGY OF THE ORTHOGNEISSIC ROCKS

These are dominantly hornblende- and biotite-bearing metatonalites and metagranodiorites. They show mineral assemblages indicative of metamorphism under epidote amphibolite facies and commonly display relict igneous textures and structures. Major and trace element data suggest that the igneous protoliths were metaluminous, calcic- to calc-alkaline (Pimentel & Fuck, 1986, 1987). The Arenópolis, Sanclerlândia and Firminópolis gneisses are comparable to primitive M-type granitoids of intraoceanic island arcs, whereas the Matrinxã granodioritic rocks present characteristics of both I- and M-type rocks (Pimentel & Fuck, 1992, 1986, 1987; Rodrigues et al., 1999).

Tables 1 and 2 present a summary of isotopic and geochronological data for some of these orthogneisses. U-Pb, Sm-Nd and Rb-Sr isotopic determinations indicate ages between ca. 940 and 630 Ma. Initial $^{87}Sr/^{86}Sr$ ratios are low (<0.705) and $\varepsilon_{Nd}(T)$ values are positive indicating the juvenile character of the original magmas (Pimentel & Fuck, 1986, 1987; Rodrigues et al., 1999).

Hornblende-bearing granitoids exposed in the vicinities of Choupana and Turvânia, in the easternmost part of the Goiás Magmatic Arc, have T_{DM} model ages between ca. 0.94 and 1.13 Ga. A whole rock Sm-Nd isochron indicates the age of 863 ± 97 Ma and $\varepsilon_{Nd}(T)$ of +4.1, for the Choupana Granite, indicating the primitive nature of the protolith. To the south of Turvânia, however, orthogneisses have paleoproterozoic model ages (1.89 to 2.27 Ga), indicating the involvement of older sialic crust in between the neoproterozoic juvenile rocks. Examples of involvement of small blocks of older rocks in between the juvenile rock units have been described in previous studies in the Arenópolis Arc (Pimentel & Fuck, 1986, 1987; Rodrigues et al., 1999).

RESULTS

Six new conventional and U-Pb SHRIMP results for orthogneisses of the Goiás Magmatic Arc are presented in this study. These are the Matrinxã, Iporá, Firminópolis, Turvânia and Palminópolis gneisses and the Choupana granite (Fig. 1). Only the Palminópolis gneiss sample has been analysed by the SHRIMP method. The remaining samples have been investigated by the conventional U-Pb methodology at the Geochronology Laboratory of the Universidade de Brasília.

Zircon grains from the six samples form simple populations of well-formed, prismatic, pink crystals, without obvious core-overgrowth relationships, similar to the population from the Palminópolis gneiss, studied by cathodoluminescence, which present well-developed oscillatory zoning (Fig. 2).

Analyses of zircon grains from the Iporá gneiss yielded the upper intercept age of 804 ± 6 Ma (Fig. 3a) interpreted as the age of crystallization of the granitic protolith. Two concordant analyses for the Matrinxã gneiss indicate the age of 669 ± 3 Ma (Fig. 3b) also interepreted as indicative of the original crystallization of the protolith. The Choupana granite presented a pattern typical of inheritance, with a lower intercept at 662 ± 12, interpreted as the age of igneous crystallization, and an upper intercept at 1093 ± 25 Ma suggesting mesoproterozoic inheritance (Fig. 3c). Zircons from the Firminópolis gneiss indicate an upper intercept age of 634 ± 8 Ma (Fig. 3d). Similar upper intercept ages of 630±5 Ma (Fig. 3e) and 637±20 Ma (Fig. 3f) (Laux et al., 2002) are observed for the Turvânia and Palminópolis gneisses, suggesting that these rocks comprise a distinctively younger block in the eastern part of the Goiás Magmatic Arc.

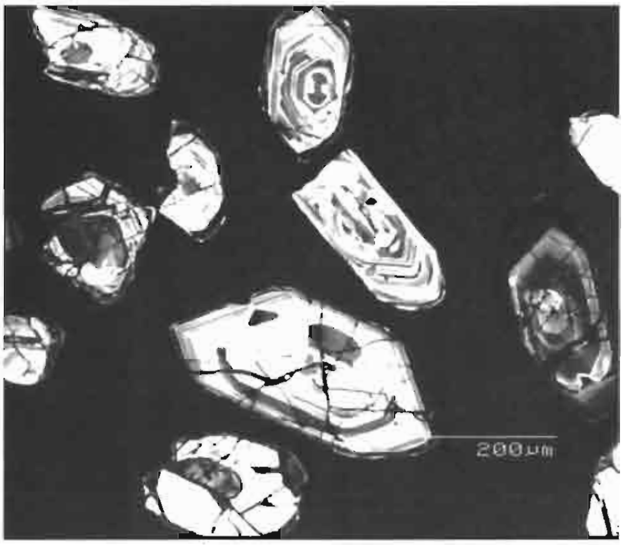

Figure 2. CL image of the zircon of Palminópolis Gneiss. $\varepsilon_{Nd}(T)$ for the samples investigated are dominantly positive (Choupana Granite - +2.86, Matrinxã Gneiss - +2.19, Iporá Gneiss - +0.36, Turvânia Gneiss - +0.35. Samples of the Firminópolis Gneiss 4.57, and Palminópolis Gneiss indicated negative $\varepsilon_{Nd}(T)$ values (-4.57 and -6.41, respectively), suggesting contribution from older sialic crust in this eastern area.

CONCLUSIONS

The new U-Pb ages indicate that the juvenile terranes of the Neoproterozoic Magmatic Arc in central Brazil underlie very large areas especially in the southwestern part of the Brasília Belt. Some localities the igneous activity seems to have involved older (Archaean-Paleoproterozoic) small continental blocks. The evolution of these arc terranes started in intraoceanic island arc settings at ca. 900 Ma, as indicated by the oldest of the tonalitic gneisses, the ca. 900 Ma old Arenópolis Gneiss. The new U-Pb data presented suggest two major periods of generation of calc-alkaline rocks: the older between ca. 900 and 800 Ma, and the younger at ca. 630 Ma.

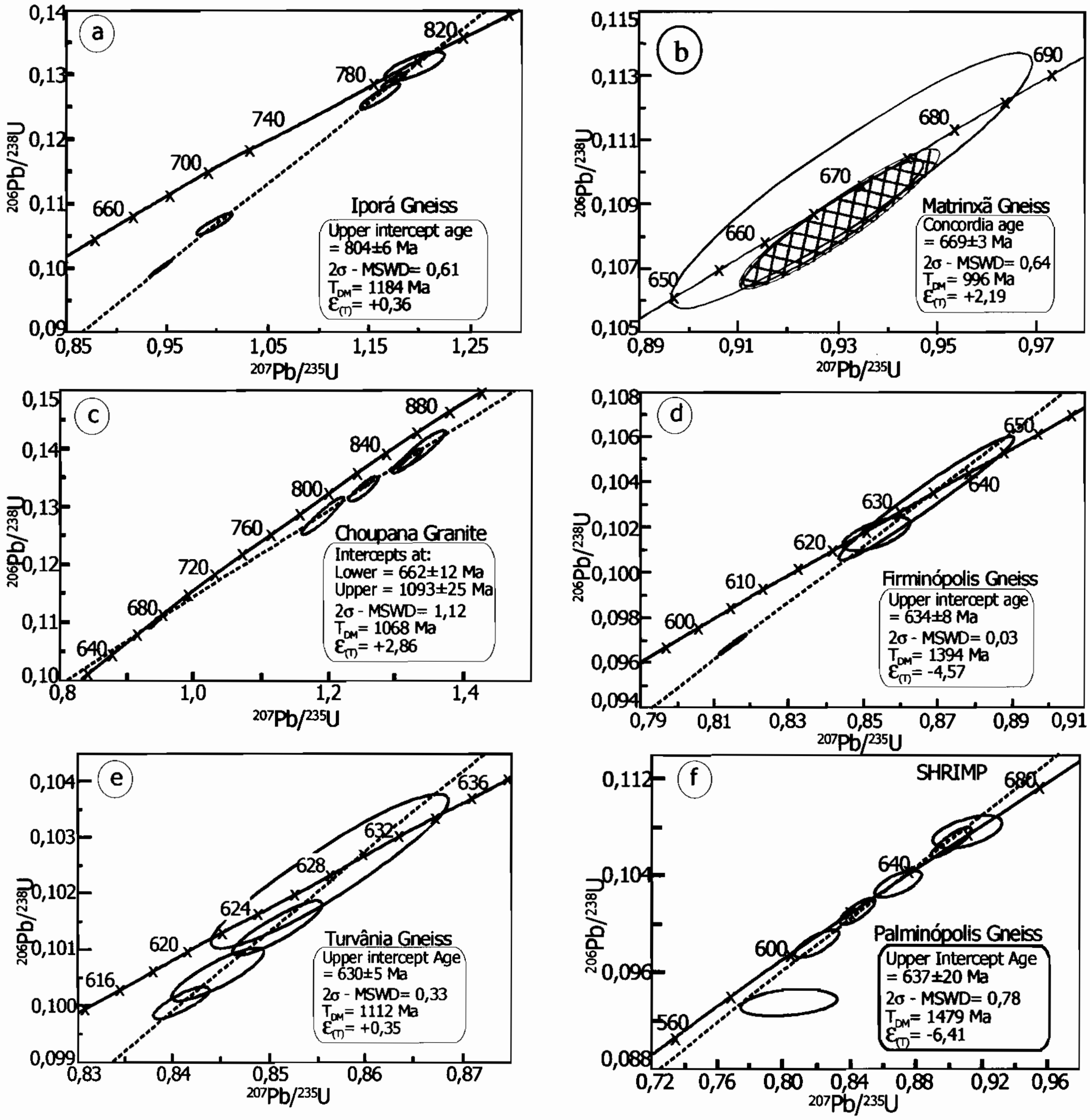

Figure 3. U-Pb concordia diagrams for the orthogneisses of the Goiás Magmatic Arc.

REFERENCES

Gioia, S.M.C. 1997. Preparação da Metodologia Sm-Nd para Datação de Amostras Geológicas e sua Aplicação em Rochas das Áreas de Firminópolis, Fazenda Nova e Americano do Brasil. Dissertação de Mestrado, Universidade de Brasília, 100p.

Laux, J.H., Pimentel, M.M., Dantas, E.L., Armstrong, R. Armele, A. 2002. O Arco Magmático de Goiás na região de Anicuns: Novos dados Sm-Nd e U-Pb. In: SBG, Congresso Brasileiro de Geologia. 41, Resumos, João Pessoa, pg 496.

Pimentel, M.M. & Fuck, R.A. 1986. Geologia da Seqüência vulcano-sedimentar de Arenópolis (GO). Revista Brasileira de Geociências 16(2): 217-223.

Pimentel, M.M. & Fuck, R.A. 1987. Origem e evolução das rochas metavulcânicas e metaplutônicas da região de Arenópolis (GO). Revista Brasileira de Geociências 17(1): 2-14.

Pimentel, M.M. & Fuck, R.A. 1992. Neoproterozoic crustal accretion in central Brazil. Geology. 20: 375-379.

Pimentel, M.M. & Fuck, R.A. 1994. Geocronologia Rb-Sr da porção sudeste do maciço de Goiás. Revista Brasileira de Geociências. 24(2): 104-111.

Pimentel, M.M., Heaman, L., Fuck, R.A. 1991. Zircon and sphene Pb-U geochronology of Upper Proterozoic volcanic-arc rock units from southwestern Goiás, central Brazil. Journal of South American Earth Science, 4: 329-339.

Pimentel, M.M.; Fuck, R.A.; Jost, H.; Ferreira Filho, C.F.; Araújo, S.M. 2000a. Geology of the central part of the Tocantins Province: Implications for the geodynamic history of the Brasília belt. In: Cordani, U.G. (Editor), Tectonic Evolution of South America p.195-229.

Pimentel, M.M., Fuck, R.A., Gioia, D.M.C.L. 2000b. The neoproterozoic Goiás Magmatic Arc, Central Brazil: A review and new Sm-Nd isotopic data. Revista Brasileira de Geociências, 30(1): 35-39.

Rodrigues, J.B., Gioia, S.M.L.C., Pimentel, M.M. 1999. Geocronologia e geoquímica de ortognaisses da região entre Iporá e Firminópolis: Implicações para a evolução do Arco Magmático de Goiás. Revista Brasileira de Geociências, 29(2): 207-216.

EVIDENCE FOR MULTIPLE SOURCES INFERRED FROM Sr AND Nd ISOTOPIC DATA FROM FELSIC ROCKS IN THE SANTA CLARA INTRUSIVE SUITE, RONDÔNIA, BRAZIL

Leite Júnior, W.B.[1]**; Bettencourt, J.S.**[2] **and Payolla, B.L.**[3]

1. Instituto de Geociências e Ciências Exatas, UNESP, Av. 24A, 1515, 13506-900, Rio Claro-SP, Brazil. wleite@rc.unesp.br
2. Instituto de Geociências, USP, Rua do Lago, 562, Cidade Universitária, 05422-970, São Paulo-SP, Brazil. jsbetten@usp.br
3. Centrais Elétricas do Norte do Brasil S/A, SQN 408, Bloco L, Apto 202, 70856-120, Brasília-DF, Brazil. bruno@eln.gov.br

Keywords: Sr isotopes, Nd isotopes, petrogenesis, rapakivi granite, Rondônia tin province

INTRODUCTION

The Proterozoic rapakivi granites of the Rondônia tin province have been intensively studied in the last three decades. The studies were initially undertaken owing to the important tin deposits spatially associated with some rapakivi granite plutons, and have contributed to understanding the metallogeny of the rapakivi granites in general. More recently these studies have also shown that the rapakivi granites provide important constraints on the tectonic models of the southwestern margin of the Amazonian craton (see e.g. Bettencourt et al., 1987, 1999). The Santa Clara Intrusive Suite (SCIS) is one of the three youngest rapakivi granite suites that are spatially related to Sn-polymetallic deposits, and have been mapped in semi-detailed scales (1:50,000 and 1:25,000) (Leite Júnior, 2002). In this paper, we present Sr and Nd isotopic data from rocks of early- and late-stage intrusions of the SCIS, and the results indicate the involvement of different source regions during magma genesis.

THE SANTA CLARA INTRUSIVE SUITE

The SCIS (1.08 - 1.07 Ga, U-Pb zircon ages) comprises at least one large batholith (Santa Clara massif) as well as smaller batholiths and stocks (Oriente Velho, Oriente Novo, Manteiga-Sul, Manteiga-Norte, Jararaca, Carmelo, Primavera and das Antas massifs) emplaced in to older medium- to high-grade metamorphic rocks (1.75 - 1.43 Ga). The SCIS is composed of several early- and late-stage intrusions, which are presently exposed in different configurations around each batholith or stock (Fig. 1).

The early-stage intrusions are dominant and have been divided into two subgroups: (1) dominant metaluminous to slightly peraluminous subgroup (SiO_2= 63.56 - 75.59%; A/CNK= 0.94 - 1.04) composed of coarse- to medium-grained porphyritic hornblende-biotite quartz-monzonite, and biotite (± hornblende) monzogranite and syenogranite, showing rapakivi textures; and (2) minor and local peraluminous subgroup (SiO_2= 73.17 - 73.73%; A/CNK= 1.05 - 1.07) composed of porphyritic biotite syenogranite and muscovite-biotite microsyenogranite. The volumetrically smaller late-stage intrusions are also divided into two subgroups: (1) metaluminous to peralkaline subgroup (SiO_2= 48.61 - 73.98%; A/CNK= 0.79 - 0.98) composed of hornblende alkali-feldspar syenite and microsyenite, biotite alkali-feldspar quartz-microsyenite, biotite (± sodic amphibole) alkali-feldspar microgranite, trachyandesite, trachyte, and minor basalt; and (2) peraluminous subgroup (SiO_2= 75.03 - 79.74%; A/CNK= 0.96 - 1.15) composed of biotite alkali-feldspar granite, alaskite, Li-mica alkali-feldspar granite, and rhyolite porphyry. The early- and late-stage granites exhibit geochemical characteristics of A-type and within-plate granites, whereas the dominant early-stage rocks also show rapakivi affinities (Leite Júnior, 2002).

ANALYTICAL PROCEDURES AND RESULTS

The preparation of rock powders was carried out at the Laboratory of Geochemistry of the University of São Paulo State (UNESP) at Rio Claro, São Paulo, Brazil. Seven whole-rock Rb-Sr analyses were realized at the Geochronological Research Center of University of São Paulo (USP), São Paulo, Brazil. Ten additional Rb-Sr analyses were obtained from studies done by Priem et al. (1971, 1989). Seven whole-rock Sm-Nd analyses were performed at the Laboratory of Isotopic Geology of the Institute of Precambrian Geology and Geochronology, Russian Academy of Sciences (IPGG RAS) at St. Petersburg, Russia, and other three at the Laboratory of Geochronology of the University of Brasilia (UnB) at Brasilia, Brazil.

The Rb-Sr data for samples of the early-stage granites reveal relatively low Rb/Sr ratios (1.26 to 4.21). The best-fit line through six analytical points for the metaluminous to slightly peraluminous granites (MSWD = 0.23) yields an isochron age of 1075±70 Ma (Fig. 2a), which agrees within uncertainties, with U-Pb zircon age of ca. 1082 Ma (cf. Bettencourt et al., 1999). The high initial $^{87}Sr/^{86}Sr$ ratio of ca. 0.709 indicates the involvement of older crustal components in the magma genesis. Crustal contribution is also suggested for one sample of the peraluminous granites (Sr_0 = 0.708). In contrast, the Rb-Sr data of the late-stage rocks show relatively high Rb/Sr ratios (9.01 to 123.72), reflecting their more evolved geochemical character. The best-fit line through three analytical points for the metaluminous to peralkaline rocks (MSWD = 0.53) indicates an isochron age of 1013±15 Ma and initial $^{87}Sr/^{86}Sr$ ratio of ca. 0.707 (Fig. 2b). A concordant age is defined by a regression line based on four analytical points for the late-stage nous granites (1015±75 Ma), despite the higher initial $^{87}Sr/^{86}Sr$ ratio of ca. 0.770 (Fig. 2c). Although this ratio is poorlydefined (MSWD = 62) due mainly to the strongly evolved geochemical character of these peraluminous granites, the high value favors crustal sources for the parent magma.

The Sm-Nd data reveal distinct isotopic compositions for the four subgroups of rocks investigated. The early-stage metaluminous to slightly peraluminous granites show T_{DM} model ages of 1.66 to 1.85 Ga, and negative ε_{Nd} (1.08 Ga) values between -4.5 and -2.9, suggesting that original magma is the product of re-melting of older continental crust. In contrast, a more negative ε_{Nd} (1.08 Ga) value of -6.2 for the early-stage peraluminous granites indicates a much less radiogenic sialic material was involved in their genesis. The late-stage rocks are more radiogenic than the early-stage rocks. The two samples of metaluminous to peralkaline rocks analyzed show T_{DM} model age of 1.34 and 1.47 Ga, but yielding positive ε_{Nd} (1.07 Ga) values of +1.1 and +2.3, suggesting a dominant mantle source for the parent magma. Inversely, the two samples of late-stage peraluminous granites show older T_{DM} model ages (1.69 and 1.75 Ga) and negative ε_{Nd} (1.07 Ga) values of -1.2 and -2.1, suggesting that the original magma was derived mainly from an older crustal source.

DISCUSSION AND CONCLUSION

In spite of the high uncertainties, the Rb-Sr isochron age for the early-stage metaluminous to slightly peraluminous granites is consistent with the U-Pb zircon age, and the Rb-Sr isochron ages for the late-stage rocks confirm the simultaneous emplacement of these intrusions, although these ages are circa 60 Ma younger than the U-Pb zircon age of ca. 1074 Ma (cf. Bettencourt et al., 1999; Leite Júnior, 2002). The initial $^{87}Sr/^{86}Sr$ ratios, although poorly defined for the late-stages rocks, are relatively high, suggesting that the original magmas are melts derived from older continental crust.

The Nd isotopic characteristics of the early- and late-stage intrusions are shown in ε_{Nd} vs. age diagram (Fig. 3). The time-integrated evolution of the early-stage granites is in close agreement with the evolution of the felsic basement rocks. In addition, the Nd isotopic compositions of the metaluminous to slightly peraluminous granites [ε_{Nd} (1.08 Ga) = -2.9 to -4.5] overlap with those 1.57 - 1.53 Ga granitic and charnockitic rocks at 1.08 Ga [ε_{Nd} (1.08 Ga) = -3.4 to -4.0], whereas the Nd isotopic signatures of the peraluminous granites are less radiogenic [ε_{Nd} (1.08 Ga) = -6.2], and support a contribution of older metapelitic rocks [ε_{Nd} (1.08 Ga) = -8.9 and -9.0] exposed in the area (cf. Payolla et al., 2002). The late-stage intrusions are more radiogenic than early-stage intrusion [ε_{Nd} (1.07 Ga) ≥ -2.1]. The late-stage peraluminous granites lie either within or just slightly above felsic basement rocks evolution line at 1.07 Ga, more precisely the Nd isotopic composition of one sample [ε_{Nd} (1.07 Ga) = -2.1] overlap with those 1.43 Ga fine-grained granitic and charnockitic rocks at 1.07 Ga [ε_{Nd} (1.07 Ga) = -2.0 to -3.0] (cf. Payolla et al., 2002). On the other hand, the Nd isotopic compositions of the metaluminous to peralkaline rocks [ε_{Nd} (1.07 Ga) = +1.1 and +2.3] lie between estimates for depleted mantle and 1.75-1.43 Ga felsic basement rocks at 1.07 Ga.

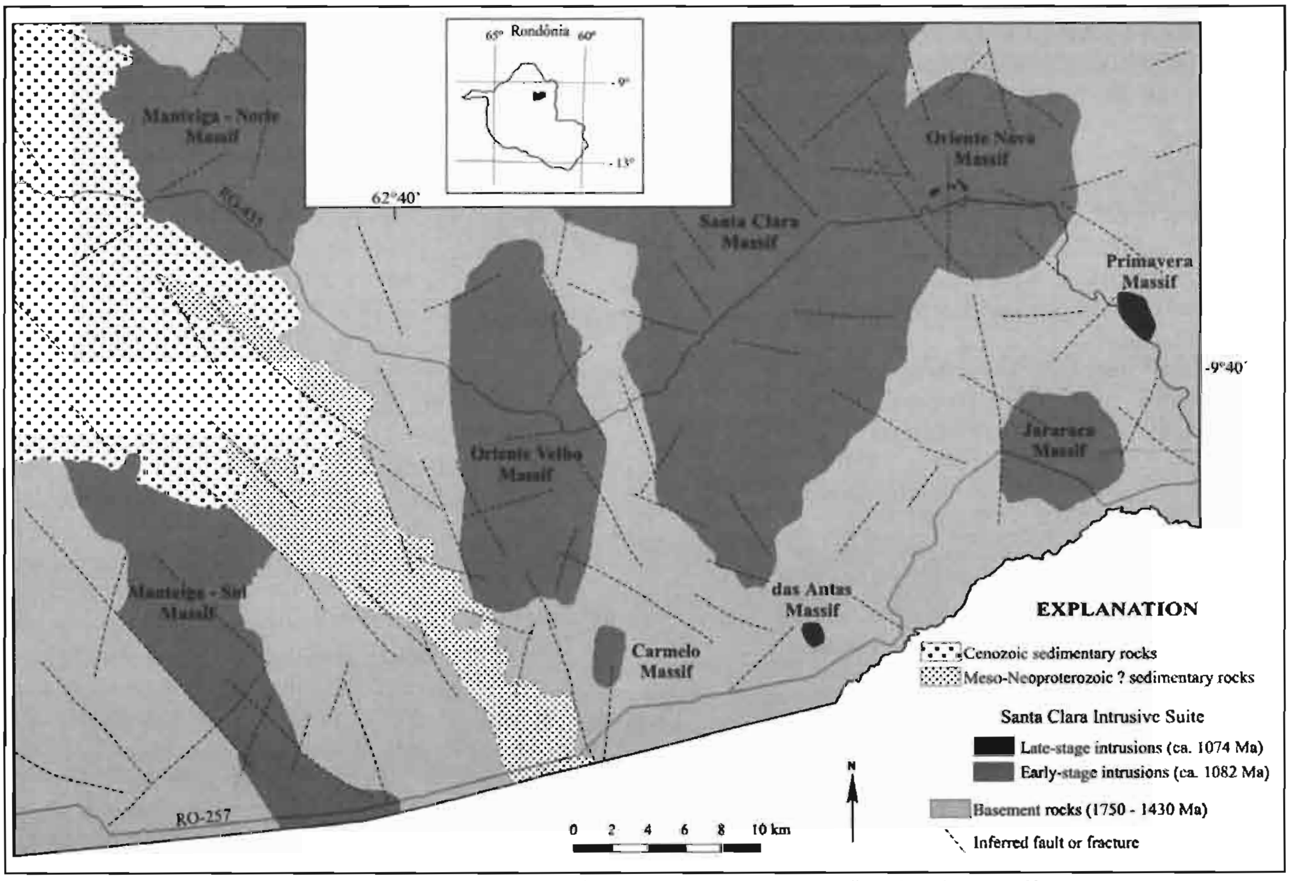

Figure 1 - Simplified geological map of the Santa Clara Intrusive Suite region (Modified after Leite Junior, 2002).

This study also suggests that the representatives of the younger episode are concentrated in the eastern part of the Goiás Magmatic Arc, forming a continuous gneissic block between Firminópolis and Palminópolis. Also in this block, the igneous protoliths of the gneissic rocks seem to have been more intensely contaminated with older sialic crust during ascent and crystallization, probably indicating proximity with the edge of the São Francisco continental plate.

ACKNOWLEDGEMENTS

We thank Simone M.C.L. Gióia and Sérgio L Junges for technical assistence.

Table 1. Summary of geochronological and isotopic data for orthogneisses from western Goiás. a. Zircon U-Pb age; b. whole-rock Rb-Sr isochron; c. Titanite U-Pb age; d. whole-rock Sm-Nd isochron age; 1. Pimentel et al., 1991; 2. Pimentel & Fuck, 1994; 3. Gioia, 1997.

Rock/Unit	Age (Ma)	$(^{87}Sr/^{86}Sr)_i$	T_{DM} (Ga)	$\varepsilon_{Nd}(T)$	Refer.
Arenópolis Gneiss	899±7 [a] 818±57[b] 637 [c]	0.7042	1.0-1.2	+1.9/+3.2	1,2
Matrinxã Gneiss	ca. 895[b]	0.7026	0.9	+ 6.0	2
Sanclerlândia Gneiss	ca. 940[b]	0.7025	0.9-1.0	+4.0/+6.0	2
Firminópolis Gneiss	628±65[d]		1.1-1.2	-1.7	3

Table 2. Summary of Sm-Nd isotopic data for some orthogneisses of the Goiás Magmatic Arc (Pimentel et al., 2000).

Sample	Sm (ppm)	Nd (ppm)	$^{147}Sm/^{144}Nd$	$^{143}Nd/^{144}Nd$ ($\pm 2\sigma$)	T_{DM}(Ga)
Choupana Granite-1	2.476	11.71	0.128	0.512426 (10)	1.09
Choupana Granite-4	1.787	7.452	0.145	0.512559 (20)	1.07
Choupana Granite-5	1.651	7.023	0.142	0.512540 (21)	1.06
Turvânia-1A	1.92	10.22	0.114	0.512395 (09)	0.99
Turvânia-1E	1.749	10.89	0.097	0.512320 (08)	0.94
Turvânia-2A	3.66	19.47	0.114	0.512342 (15)	1.07
Edéia-1C	7.786	35.93	0.130	0.511926 (08)	2.00
Edéia-2A	10.49	51.43	0.123	0.511818 (08)	2.04
Indianópolis-1A	18.85	99.56	0.114	0.511798 (09)	1.89
Palminópolis-1A	4.476	22.75	0.119	0.511626 (23)	2.27
Palminópolis -1B	5.700	31.32	0.110	0.511548 (09)	2.19
Palminópolis -2A	3.620	16.47	0.133	0.512504 (14)	0.98
Palminópolis -2B	6.903	47.32	0.088	0.512010 (13)	1.25
Aloândia-1	5.891	27.70	0.128	0.512219 (20)	1.45
Aloândia -2	3.771	18.68	0.122	0.512365 (12)	1.12

In conclusion, the Sr and Nd isotopic data for the early and late intrusions of the Santa Clara Intrusive Suite suggest different sources for the magmas of the four subgroups of rocks recognized in this suite. The early-stage intrusions seem to represent crustal anatectic melts, with the metaluminous to slightly peraluminous magmas originated mainly from re-melting of 1.57-1.53 Ga granitic and charnockitic rocks, whereas metapelitic rocks appear to be an important crustal component for the peraluminous magmas. The late-stage metaluminous to peralkaline rocks may be products of mantle-derived mafic magmas with minor crustal input, in contrast with the late-stage peraluminous magmas that may have originated from older crustal source with minor mantle input. It is interpreted that this source was the residue of the source from which the metaluminous to slightly peraluminous granites were previously extracted, although the 1.43 Ga fine-grained granitic and charnockitic rocks should not be ignored. Polymetallic (Sn, W, Nb, Ta, Zn, Cu, Pb) primary deposits are spatially and temporally associated with these late-stage peraluminous granites.

ACNOWLEDGMENTS

This study was supported by grants from FAPESP (PROC. Nº 2000/08033-5), and PADCT-FINEP 64.99.027.00). It is also a contribution to IGCP-426. Financial support: Finep/PADCTII, Fundunesp.

REFERENCES

Bettencourt, J.S.; Dall'Agnol, R.; Yokoi, O.Y.; Viglio, R.P.; Pinho, O.G.; Silva, R.F. 1987. The rondonian tin bearing anorogenic granites and associated mineralization. In: SGM, International Symposium on Granites and Associated Mineralization, 1, Salvador, Excursion Guide, p. 49-87.

Bettencourt, J.S.; Tosdal, R.M.; Leite Júnior, W.B.; Payolla, B.L. 1999. Mesoproterozoic rapakivi granites of the Rondônia Tin Province, southwestern border of the Amazonian craton, Brazil – I. Reconnaissance U-Pb geochronology and regional implications. Precambrian Research., 95:41-67.

Leite Júnior, W.B. 2002. A Suíte Intrusiva Santa Clara (RO) e a mineralização primária polimetálica (Sn, W, Nb, Ta, Zn, Cu and Pb) associada. IG-USP, São Paulo, Ph.D. Thesis, 305 p.

Payolla, B.L.; Bettencourt, J.S.; Kozuch, M.; Leite Júnior, W.B.; Fetter, A.H.; Van Schmus, W.R. 2002. Geological evolution of the basement rocks in the east-central part of the Rondônia Tin Province, SW Amazonian craton, Brazil: U-Pb and Sm-Nd isotopic constraints. Precambrian Research., 119:141-169.

Priem, H.N.A.; Boelrijk, N.A.I.M.; Hebeda, E.H.; Verdurmen, E.A.T.; Verschure, R.H.; Bon, E.H. 1971. Granitic complexes and associated tin mineralization of "Grenville" age in Rondônia, western Brazil. Geol. Soc. Amer. Bull., 82:1095-1102.

Priem, H.N.A.; Bon, E.H.; Verdurmen, E.A.T.; Bettencourt, J.S. 1989. Rb-Sr chronology of Precambrian crustal evolution in Rondônia (western margin Brazilian Craton). J. South America Earth Sci., 2:163-170.

Sm-Nd DATA IN GRANITIC AND MYLONITIC ROCKS IN THE SIERRAS PAMPEANAS OF CATAMARCA AND LA RIOJA, NORTHWESTERN ARGENTINA

López, J.P.[1]; Rodriguez Areal, M.M.[2]; Sales, A.[2] and Kawashita, K.[3]

1. Instituto Superior de Correlación Geológica, Universidad Nacional de Tucumán, Tucumán, Argentina. lopezjp00@yahoo.com.ar
2. Facultad de Bioquímica, Química y Farmacia, Universidad Nacional de Tucumán, Tucumán, Argentina.
adrivisci@hotmail.com, mrareal@unt.edu.ar
3. Universidade Federal de Rio Grande do Sul, Porto Alegre-RS, Brasil

Keywords: Sm-Nd metodology, Pampean Ranges, mylonitic rocks, combinated spike

GEOLOGIC SETTING

The study area is part of the Pampean Ranges in Northwestern Argentina, which is characterized by a peraluminous granitic basement of Lower Paleozoic age (Antinaco and Paimán Formation) related to subduction during the Famatinian orogeny. This granitic basement was affected by deformation that produced the TiPA Mylonitic Band (López & Toselli, 1993) of Upper Ordovician to Devonian (Ocloyic Phase, Salfity et al., 1984) age and followed by a new intrusive event during Devonian times (San Blas Granite).

In the Velasco Ranges three main petrologic units are identified: 1) Antinaco Formation which is composed of porphyritic monzogranites and granodiorites, with coarse matrix and large phenocrysts of K-feldspar of more than 10 cm 2) TiPA Mylonitic Band, of protomylonites, mylonites and mylonitic gneisses and schists with a strong mylonitic foliation, formed from Velasco Granite, distributed in bands of NNW direction, and 3) San Blas Granite, constituted by porphyritic monzogranites to granodiorites that appear in the north of the region, as circular structure, with depressed relief and which is also recognized in outcrops of the hillside W of the Velasco Range, near of the locality of Antinaco.

In the Copacabana Range it is possible to recognize outcrops of TiPa Band; non deformed granites and gabbroic bodies are recognized in their southern part.

The Paimán Range is constituted by granitic rocks of the Antinaco Formation, besides gabroic rocks and a thin band of mylonitic rocks on its eastern flank.

Sm-Nd METHODOLOGY

The method embraces the addition of a combined Sm/Nd spike and the chemical digestion using the HF/HNO_3 acid mixture in the proportion of 2:1.

The mixed spike used in this work was prepared from concentrated spike solutions of ^{149}Sm and ^{150}Nd. The concentrations calibrated with normal solutions were: [^{149}Sm] = 0.004722 μmols/g; [^{150}Nd] = 0.0033550 μmols/g. The error (1σ) in the ^{149}Sm/^{150}Nd ratio of 1.4075 was 0.25% and, hence the errors on ^{147}Sm/^{144}Nd determinations on samples were close to this value.

Samples weighing around 0.1 g were spiked according to the expected contents of Sm and Nd. These elements were separated in two stages; in the first, the rare earth elements (REE) were separated from other elements using a cation exchange column with AG50WX8 resin followed by separation of Sm and Nd using a teflon column with hydrogen di-ethylhexyl phosphate (HDEHP) supported by teflon powder and elution with 0.25 N HCl. The separated Sm and Nd were dried, then dissolved in 1μL H3PO4 and loaded on single Re filament and double (Ta-Re) filament arrangement, respectively. The Sm and Nd were analysed as Sm^+ and Nd^+ using a Micromass VG-354, equipped with a single collector, and a Finigan mat 262 multicollector instrument, respectively. All Sm-Nd procedures are described in detail by Sato et al. (1999). The Sm-Nd results obtained on 12 different rock types are presented in table 1.

DISCUSSION AND CONCLUDING REMARKS

Allowing for complexities introduced by two magmatic events, single dynamic metamorphism recognized in the area, and the known limitations to estimate the model ages by extrapolation and interception with the depleted mantle evolution curve for ^{143}Nd/^{144}Nd, the T_{DM} model ages presented in Table 1 show considerable spread. Usually, model ages used for interpretation of the origin of a given terrain exhibit variations between 10 to 20 % from average data. The ages of granitic rocks and mylonites of present work are in a large range comprised between 2490 and 1410 Ma indicating mixtures of different reservoirs and crustal source materials. The age pattern is very similar for those obtained for the Borborema Province granitoids of Brasiliano Cycle (Van Schumus et al. 1995; Cordani & Sato, 1999). The main difference resides in ε_{Nd} values. The $\varepsilon_{Nd}(0)$ of Pampean granitoids are less than -10, while for Brasiliano granitoids are ca. -20. Similar to Borborema granitoids the initial ε_{Nd} values calculated for 450 Ma (Ocloyic magmatic phase) are also moderately negative. These values, associated with initial ^{87}Sr/^{86}Sr values between 0.704 and 0.711 (Perez & Kawashita, 1992), revealed by some Pampean granitoids, suggest that reworking of previous crustal protoliths of Early Proterozoic ages occurred, although the participation of a juvenile component in their petrogenesis cannot be ruled out. In support of these ages and this interpretation, Höckenreimer et al. (2002) recently presented Sm-Nd data on garnets and rocks from same region indicating "early Devonian movement" and T_{DM} model ages between 2150-1800 Ma. SHRIMP U-Pb ages between 1.4 - 2.0 Ga obtained on nuclei of zircons separated from

Table 1. Sm-Nd data for rocks from Velasco (a), Paimán (b) and Copacabana (c) ranges. 1. Calculated with data normalized to $^{146}Nd/^{144}Nd = 0.7219$. The estimated internal error is ca. 25 ppm; 2. $f_{Sm/Nd} = 0.1967/(^{147}Sm/^{144}Nd)-1$; 3. Double-stage T_{DM} model ages (DePaolo et al., 1991).

No. Campo	Material	Sm (ppm)	Nd (ppm)	$^{147}Sm/^{144}Nd$	$^{143}Nd/^{144}Nd$ [1]	$f_{Sm/Nd}$ [2]	$T_{DePaolo}$ (Ma)	T_{DM} 2St [3]	$\varepsilon_{(0)}$	$\varepsilon_{(450Ma)}$
6498	grey porfirobl. Granite (a)	9.868	35.695	0.1672	0.512289	-0.15	2491	1437	-6.81	-5.11
6448	Pink Granite (a)	4.637	20.062	0.1398	0.512357	-0.29	1410	1230	-5.48	-2.21
6414	Schists (a)	2.423	9.257	0.1583	0.512212	-0.20	2292	1508	-8.31	-6.10
6281	Mylonite (a)	3.915	16.280	0.1454	0.512163	-0.26	1962	1523	-9.27	-6.32
6416	Catacl. Mylonite (a)	2.732	10.810	0.1528	0.512160	-0.22	2216	1558	-9.32	-6.81
6411	Pink Granite (a)	8.331	42.561	0.1184	0.512128	-0.40	1460	1461	-9.95	-5.45
5507	Granite (c)	8.616	38.931	0.1338	0.512143	-0.32	1714	1504	-9.66	-6.05
5508	Mylonite (c)	8.518	37.983	0.1356	0.512124	-0.31	1790	1537	-10.03	-6.52
5503	Amphibol (c)	7.805	36.295	0.1300	0.512209	-0.34	1516	1396	-8.37	-4.54
5426	Gneiss (c)	6.509	25.053	0.1571	0.512202	-0.20	2273	1517	-8.51	-6.23
5514	Gabbro (b)	4.952	19.357	0.1547	0.512322	-0.21	1857	1340	-6.16	-3.75
5512	Quartz (b)	5.345	21.939	0.1473	0.512315	-0.25	1666	1320	-6.30	-3.47

post-tectonic granites also suggested that Transamazonian protoliths and Pampean age materials were involved in their generation. The spread in model ages and difficulties for more realistic interpretations arise from the present scarcity of data, including Sm-Nd. Average Sm and Nd contents, 6.0 ppm and 25.1 ppm, respectively, are relatively close to those estimated for the average upper crust (Othman et al., 1984) but the $^{147}Sm/^{144}Nd$ ratios between 0.13 and 0.1672, almost certainly exclude the possibility that the Pampean granitoids were formed during a "single stage" event. The granitic rocks in this model usually exhibit ratios between 0.11-0.12 (*e.g.* De Paolo & Wasserburg, 1979; Jacobsen & Wasserburg, 1979). Thus, two stage model ages were also calculated using the proposal of De Paolo et al. (1991). These ages are more closely grouped at around 1450 Ma (see Fig. 2). Probably this age would be more realistic for the crust differentiation process, but a doubt remain if we take into account the 2.0 Ga inherited zircons mentioned previously. In conclusion: the classical interpretation of reworking of Early Proterozoic protolith seems more plausible.

ACKNOWLEDGEMENTS

One of the authors (M.M. Rodrigues Areal) is grateful to all staff of Geochronology Research Center – USP who introduced him to the Sm-Nd analytical work and also for fruitful discussion.

REFERENCES

Cordani, U.G. and Sato, K. (1999) Crustal evolution of the South American Platform, based on Nd isotopic systematics on granitoid rocks. Episodes, 22(3):167-173

DePaolo, D.J., and Wasserburg G.J. (1979). Sm-Nd age of the Stillwater complex and mantle evolution curve for neodymium. Geochim.Cosmochim. Acta 43, 999-1008.

De Paolo, D.J.(1981). Neodymium isotopes in the Colorado Front Range and crust-mantle evolution in the Proterozoic. Nature (Lond.).291: 193-196.

DePaolo, D.J.; Linn, A.M.; Schubert, G. (1991) The continental crust age distribution; methods o determining mantle separation aghes from Sm-Nd isotopic data and application to the Southwestern United States.J. Geophys. Res. B., Solid Earth and Planets. 96(2); 2071-2088.

Höckenreiner, M., Söllner, F. and Miller, H. (2002). The TiPA shear zone (NW-Argentina): evidence for early devonian movement verified by Sm-Nd dating of garnet and whole rock systems. SSAGI. Pucón. Chile.

Jacobsen and Wasserburg. (1979) The mean age of mantle and cristal reservoirs. J. Geophys. Res. 84 :7411-7427.

López, J.P. y Toselli, A.. (1993). La Faja Milonítica TiPA: faldeo oriental del Sistema de Famatina, Argentina. XII Cong. Geol. Argentino, Actas 3: 39-42.

Perez, W. A. and Kawashita, K. (1992) K-Ar and Rb-Sr geochronology of igneous rocks from the Sierra de Paimaán, nortwestern Argentina. Journ. Of South Amer. Earth Sci. 5 (3/4): 251-264.

Othman, D.; Polvé, M. And Allegre, C. (1984). Nd-Sr isotopic composition of granulites and constraints on the evolution of the lower continental crust. Nature, 307: 510-515.

Salfity, J.; Gorustovich, S. y Moya, M., (1984). Las fases diastróficas en los Andes del Norte Argentino. Intern. Simp. Central-Andean Tectonics and Relations with Natural Resources. Acad. Nac. Cs., Bolivia.

Sato, K.; Tassinari ,C.C.G.; Kawashita, K.and Petronilho, L. (1995) O método geocroniológico Sm-Nd no IG/USP e suas aplicações. Anais da Academia Brasileira de Ciencias, 67(3): 314-336.

Van Schmus, W.R.;Brito neves, B.B.; Hackspacher, P. and Babinski, M. (1995) U/Pb and Sm/Nd geochronologic studies of the eastern Borborema Province, Northeastern Brazil: initial conclusions. Joour. Of South Amer. Eart Sci. 8(3/4):267-288.

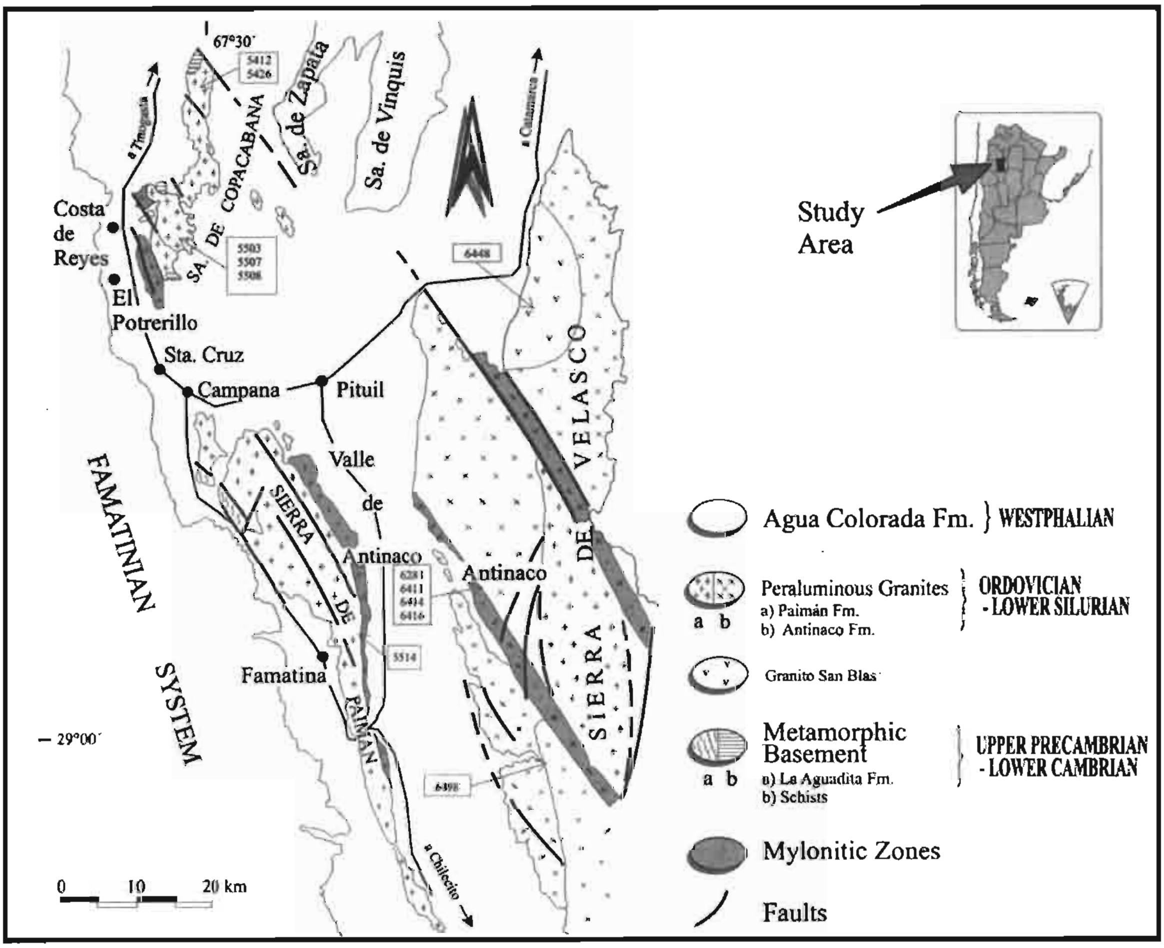

Figure 1: Samples Locations in Velasco, Paimán and Copacabana Ranges

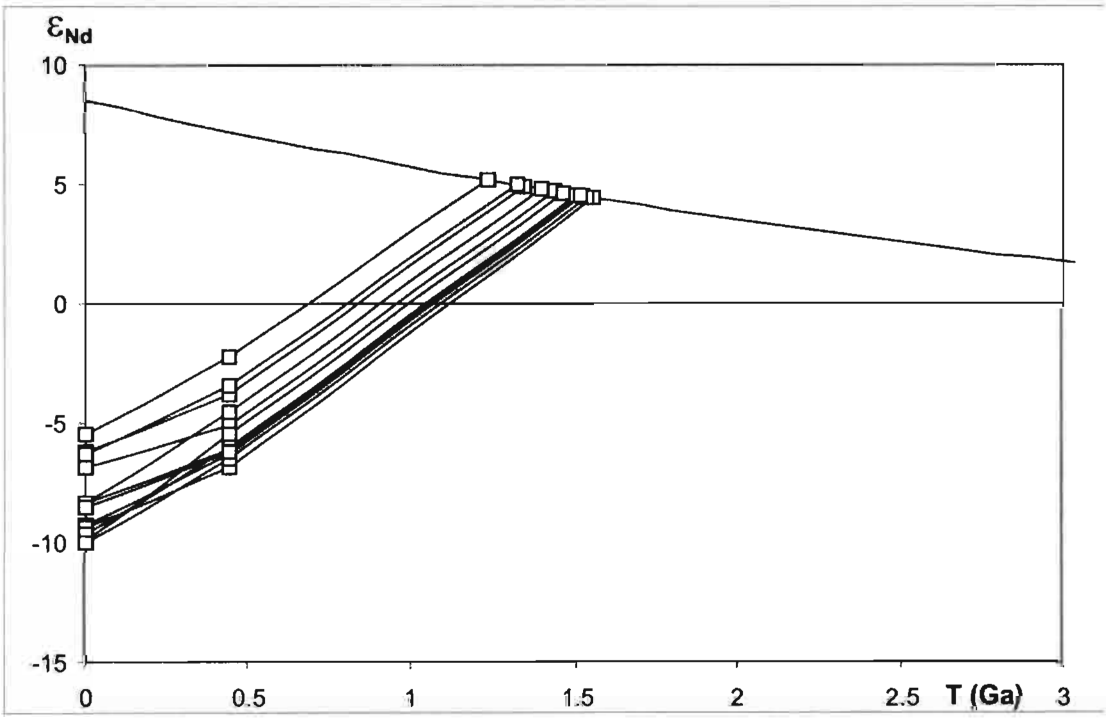

Figure 2 - Two stage model using the proposal of DePaolo et al. (1991)

Sr, Nd, AND Pb ISOTOPIC COMPOSITION OF CLINOPYROXENE AND TEMPERATURE AND AGE OF MINERAL EQUILIBRIA: LATE CRETACEOUS MANTLE XENOLITHS FROM THE CENTRAL ANDES

Lucassen, F.[1, 2]; Franz, G.[3]; Viramonte, J.[4] and Romer, R.L.[1]

1. GeoForschungsZentrum Potsdam, Telegrafenberg, 14473 Potsdam, Germany. Lucassen@gfz-potsdam.de
2. Freie Universität Berlin, FB Geowissenschaften, Malteserstr. 74-100, 12249 Berlin, Germany
3. Technische Universität Berlin, Inst. f. angewandte Geowissenschaften, FG Petrologie, Str. d. 17. Juni 135, 10653 Berlin. Germany
4. Universidad Nacional de Salta, Av. Bolivia 4650, 4400 Salta, Argentina

Keywords: Mantle xenolith, isotopic composition, evolution of the upper mantle, Central Andes

INTRODUCTION AND PETROLOGY

Mantle derived magmatism in W Argentina and Bolivia is bound to late Mesozoic extension, e.g. in the Salta Rift System (Fig. 1; Viramonte et al., 1999). The composition of these magmatic rocks indicates two different mantle sources, one comparable to a depleted mantle and a second comparable to old subcontinental mantel of the Brazilian Shield (Fig. 1; Lucassen et al., 2002). This study investigates chemical and isotopic composition of depleted mantle xenoliths from the Salta Rift/ Quebrada las Conchas (Fig.1), 26°S near the town of Cafayate in NW Argentina, which are hosted by small-volume basanitic dikes and sills within a continental rift basin (e.g. Viramonte et al., 1999; Lucassen et al., 2002). Mantle xenoliths and their host rocks are used to constrain the composition of the upper mantle before the onset of the Plateau formation in the Central Andes.

The occurrence of large xenoliths (ca. 4 – 20 cm), providing sufficient material for bulk methods of investigation as XRF, ICP-MS and TIMS, are restricted to few locations within the extended rift system. Most xenoliths are spinel lherzolite to harzburgite with variable amounts of olivine, clinopyroxene (cpx), orthopyroxene (opx) and spinel. Few samples are dunite. Carbonatization of these xenoliths occurred locally at the intrusion level, preserving clinopyroxene and spinel in a calcite matrix. Many samples show hydration of olivine along grain boundaries. Some large peridotite xenoliths show compositional layering or preferred orientation of the minerals. At the microscopic scale, all samples show well annealed metamorphic fabrics with straight grain boundaries, and 120° triple points are common. Optical zoning of the minerals is absent. Cpx of some samples shows small rims (10 -30 μm) of secondary low Al and Na cpx in palisade textures together with glass, considered to be typical of melting along grain boundaries during fast uplift of the xenoliths. Mineral assemblages of all samples selected for isotopic studies have been checked for compositional zoning by electron microprobe, which is absent however. The mineral assemblage appears to be in chemical equilibrium. Thermometric studies of cpx – opx indicate rather uniform temperatures between 1000 – 1100°C (12 samples). The peridotite xenoliths represent the uppermost mantle shallower than ca 70 km, outside the garnet stability field.

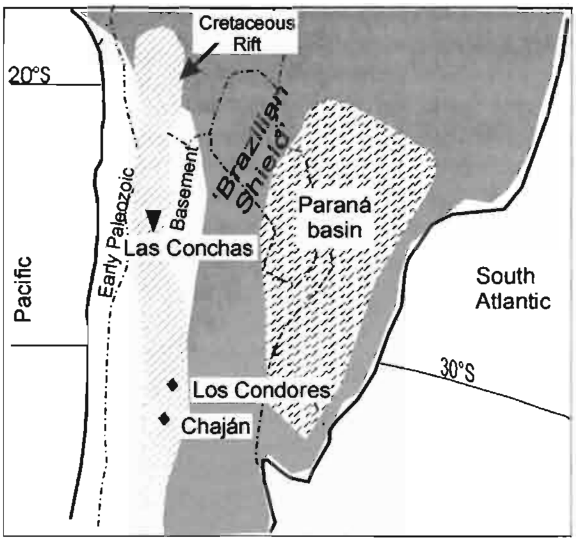

Figure 1. Distribution of the Cretaceous Rift, the Mesozoic Paraná volcanism, the Early Palaeozoic Basement, formed in a Palaeozoic mobile belt, and the Proterozoic Brazilian Shield. Sample locations of the xenoliths are in the Qda. Las Conchas. Occurrences of Cretaceous volcanic rocks with signatures of old subcontinental mantle at Los Condores and Chaján (ca 32-34°S) are also shown. Modified from Lucassen et al. (2002).

CHEMICAL AND ISOTOPIC COMPOSITION

Bulk rock compositions (XRF, 27 samples) are similar to other spinel peridotite xenoliths worldwide (Maaloe & Aoki, 1977) and Mg# varies between 89 – 92 at high Cr (1700 - 4000 ppm) and Ni (1700 – 2500 ppm) content. For Sr, Nd and Pb isotope measurement and REE analyses cpx (21 samples) has been separated (for analytical methods see: Lucassen et al., 2002). Cpx is the principal host of the respective elements in the peridotite because amphibole and phlogopite are absent. Selection and leaching avoids possible effects of alteration and accidental contamination during whole rock sample handling especially on the U-Th-Pb isotope system. Sr, U, Th, Pb, Sm and Nd element concentrations are variable in the cpx, whereas Rb is below detection limit. REE pattern of cpx are highly variable from mildly depleted to essentially flat patterns to prominent light REE enrichment (Fig. 2; La/Yb_N ratios between 0.4 – 110). Sr, Nd and Pb isotope ratios are corrected for in-situ decay to 100 Ma using the element concentrations from ICP-MS measurements. Sr and especially Nd isotope ratios show considerable variations (Fig. 3). Most samples scatter within the depleted mantle field (the main group, where the discussion is focused on), three samples have elevated Sr isotope ratios, two samples plot into the field of the crust or enriched mantle. $^{207}Pb/^{204}Pb$ and $^{206}Pb/^{204}Pb$ isotope ratios scatter from rather unradiogenic to radiogenic values (Fig. 4a). $^{208}Pb/^{204}Pb$ ratios (Pb from Th decay) of some xenoliths are high at given $^{206}Pb/^{204}Pb$ ratios (Fig. 4b).

Opx and cpx have been separated from selected samples in order to constrain the age of isotopic equilibration in the Sm-Nd system. Sm/Nd ratios in opx are slightly higher than in cpx. Ages from two point 'isochrons' of five samples vary between ca. 70–130 Ma. One sample yielded a late Palaeozoic age (ca. 300 Ma).

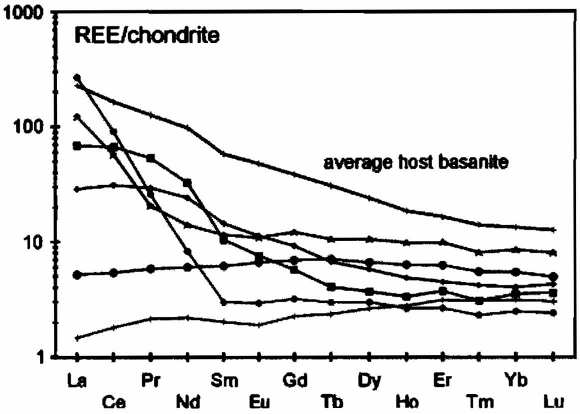

Figure 2. Representative REE pattern of cpx from peridotite xenoliths. Average host basanite from Lucassen et al. (2002).

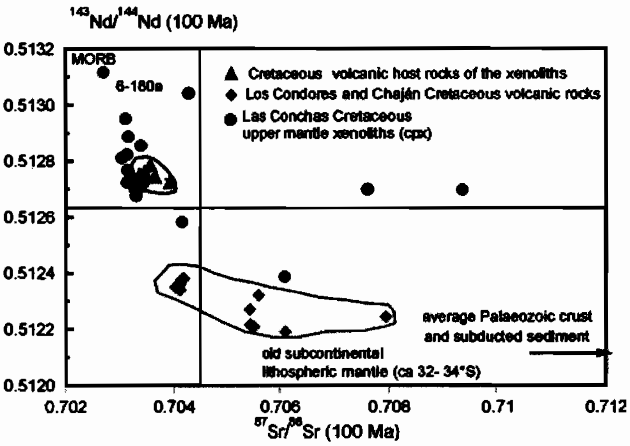

Figure 3. Nd- Sr isotope composition of cpx from peridotite xenoliths and regional important sources of Nd (references for MORB, average Palaeozoic crust and subducted sediment and volcanic rocks in Lucassen et al., 2002).

DISCUSSION – IMPLICATIONS FOR THE EVOLUTION OF THE UPPER MANTLE

Well equilibrated fabrics and the lack of chemical zoning in the minerals indicate chemical equilibrium between the minerals of the xenoliths. Temperatures of equilibration from cpx - opx thermometry are high (ca. 1000 – 1100°C). A precise age cannot be derived from the Sm-Nd systematics of opx – cpx pairs, due to the small differences in the Sm/Nd ratios. However, the data allow inferring a late Mesozoic age of the high-T metamorphism with possible Palaeozoic inheritance in the Sm-Nd system of one sample. A late Mesozoic age and high-T from mineral equilibrium are in good accordance with the high-T of metamorphism and Sm-Nd mineral isochron ages in lower crust felsic – mafic granulite xenoliths from the same location (ca. 900°C, 10 kbar; ca. 90 – 100 Ma; Lucassen et al., 1999). The peridotite xenoliths document the in-situ thermal condition of the upper mantle lithosphere in the Cretaceous. Lower crust and mantle lithosphere have been metamorphosed at high-T during the activity of the late Mesozoic rift. Older events of mineral formation i.e. core – rim textures and chemical zoning have not been found in the samples. Primary hydrous phases like phlogopite and amphibole are absent.

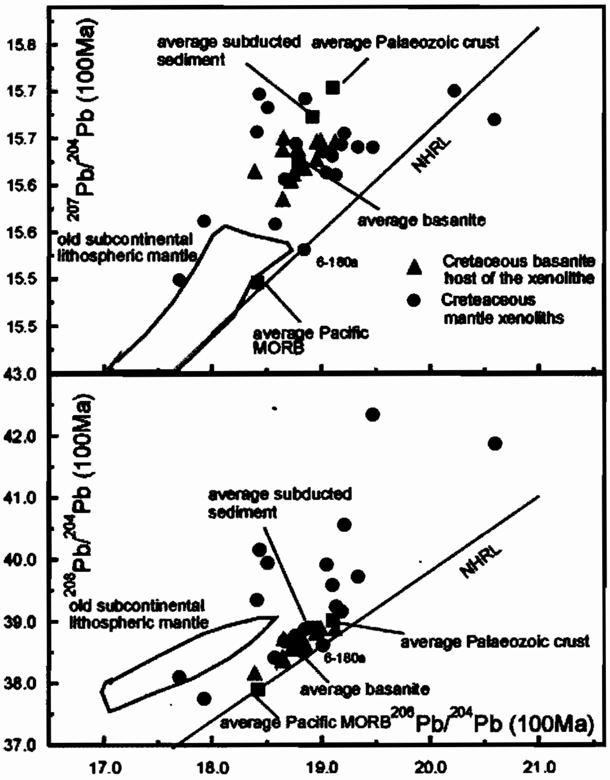

Figure 4. Pb isotope ratios of cpx from peridotite xenoliths and regionally important sources of Pb (references in Lucassen et al., 2002). Field of the subcontinental lithospheric mantle from Carlson et al. (1996) and Gibson et al., (1996).

Major element composition of the peridotite (whole rock) is considered typical for such rocks and varies in a relatively small range. The variation e.g. decreasing Al_2O_3 and CaO with increasing Mg# could be explained by increasing depletion by melt extraction. Variable REE pattern, trace element content and isotope ratios of the cpx however indicate a more complex evolution of the upper mantle lithosphere. There is no typical 'LREE depleted mantle' pattern and most of the variation within the LREE are variable degrees of enrichment. The HREE patterns are flat in most samples (Fig.2). The La/Yb ratio and Sr (Fig. 5a), REE content and the U/Pb ratios are positively correlated. Pb isotope ratios increase with Sr content (Fig. 5b) and La/Yb. ^{143}Nd/^{144}Nd ratios decrease with increasing Nd content (Fig. 6) and La/Yb ratios. ^{87}Sr/^{86}Sr ratios of the main group (0.703 – 0.704; 17 samples) show no correlation with the variable Sr content, but 4 samples with ^{87}Sr/^{86}Sr ratios > 0.705 show positive correlation with Sr content (Fig.7). Radiogenic growth since the Cretaceous is minor and the correlation between the isotope ratios and respective parent elements is weak. Variations in the Pb isotope ratios (^{207}Pb/^{204}Pb: ca. 15.5 – 15.7 and ^{206}Pb/^{204}Pb: ca. 17.5 - 20.5) and Nd isotope ratios (ca. 0.5124 -0.5138) indicate contributions of Pb and Nd from sources with long-term separate isotope evolutions. Principal regional sources are the Pacific MORB-type mantle, old subcontinental mantle of the Brazilian Shield and local continental crust as the contaminant in a subduction system (Figs. 3, 4). However, there is no clear affinity of a sample group to one of the sources or a uniform mixing relation between the sources.

Deviations of REE (and other trace elements) from the expected LREE depleted pattern in depleted mantle compositions are usually attributed to LREE enrichment during mantle metasomatism by percolating fluids or melts. In the investigated samples, Nd and Pb isotope ratios are correlated with increasing trace element contents of the cpx, whereas Sr isotope ratios are largely independent. Considering a isotopic composition close to depleted mantle as the starting condition (sample 6-180a; Figs. 3, 4; ^{206}Pb/^{204}Pb: 18.80, ^{207}Pb/^{204}Pb: 15.55, ^{208}Pb/^{204}Pb: 38.50, ^{143}Nd/^{144}Nd: 0.51312, ^{87}Sr/^{86}Sr: 0.70264, La/Yb$_N$: 0.9), a melt similar to the average basanite hosting the xenoliths could substitute the second endmember in the Nd – Sr isotope diagram (Fig. 3). However, the Pb isotope composition of the xenoliths does not indicate any systematic relation to the composition of the average basanite or other possible Pb source (Fig. 4). The REE patterns of the xenoliths do not show a gradual change from depleted to enriched patterns as expected from a reaction with varying volumes of compositional uniform magma under similar physical conditions (Fig. 2). These observations make a single and uniform process causing the observed variations in the peridotite unlikely.

Magmatism associated with the Cretaceous Rift is of minor volume in small isolated occurrences (Viramonte et al., 1999). The mainly alkaline rocks are derived from low degrees of melting in the mantle. If the magmatic activity is an expression of the degree of melting in the mantle and its regional distribution, most of the mantle volume beneath the Cretaceous Rift was unaffected by melting. Despite the chemical and isotopic equilibrium between the minerals on the handspecimen-scale, a larger scale equilibration of isotope composition and trace element distribution is unlikely without mayor melt extraction/percolation in the upper mantle. Therefore, inherited isotopic and trace element signatures could be preserved during the Cretaceous thermal overprint.

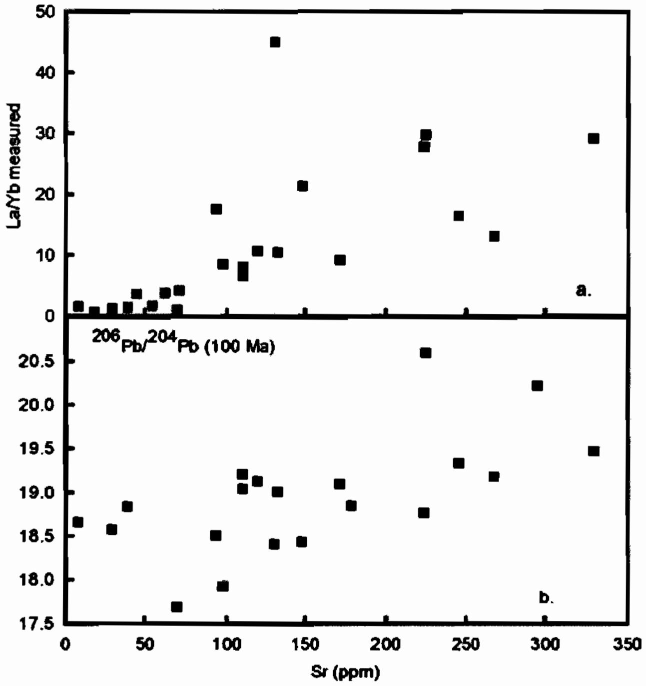

Figure 5 a, b. Variation of the (a) REE pattern (La/Yb ratio) and of the (b) ^{206}Pb/^{204}Pb with Sr content in cpx.

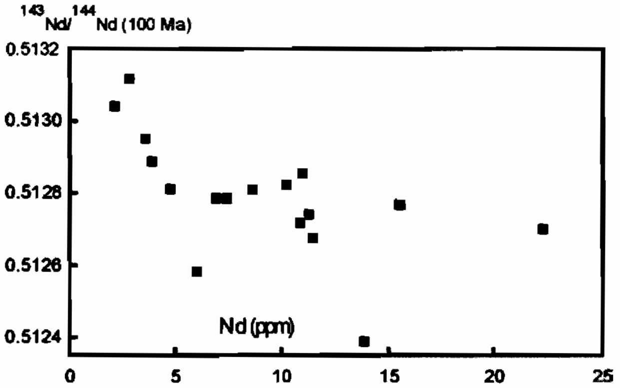

Figure 6. Variation of the ^{143}Nd/^{144}Nd ratios with Nd contents of cpx.

The western edge of Gondwana has long history as a sporadically active margin at least from the Early Palaeozoic onwards with major reworking of Proterozoic crust in a Palaeozoic mobile belt (Fig. 1). This and the isotopic and chemical composition of the xenoliths and mantle derived magmatic rocks are the basis of our working hypothesis for the evolution of the mantle in this section of the Central Andes. (1) The mantle at the leading edge of the continent has been modified by several timely distant systems of subducting oceanic plate – asthenospheric mantle wedge configurations. This resulted in a generally depleted mantle beneath the Palaeozoic orogens/magmatic arcs in contrast to the old subcontinental mantle beneath the Brazilian Shield or found in the Cretaceous magmatism between 32- 34°S

(Figs. 1, 3, 4). Most Early Palaeozoic to Mesozoic mantle-derived magmas (e.g. Lucassen et al., 2001) and the mantle xenoliths in the realm of the Palaeozoic mobile belt are from isotopically depleted mantle sources. (2) Compared with MORB mantle, this depleted mantle lithosphere is heterogeneous in isotope and trace element composition. The major heterogeneities occur in the Sm-Nd and U-Th-Pb isotope systems and trace elements (e.g. Sr and REE), whereas Sr isotope ratios are rather uniform (Figs. 3, 4, 7). The measured µ-ratios ($^{238}U/^{204}Pb$) in the cpx (ca. 1 – 300, the assumed mantle value is ca. 8) and the $^{147}Sm/^{144}Nd$ ratios (ca. 0.06 -0.25, the assumed mantle value is ca. 0.21) show considerable variations whereas Rb is below the detection limit or negligible compared with Sr content. If metasomatic processes in an ancient active mantle wedge occurred at large scale this could explain the observed differences. Assuming an average µ-ratio of 30 for a metasomatized depleted mantle, 200 Ma of separation (e.g. during lull of subduction) would be sufficient to cause substantial radiogenic growth in the U-Pb system (e.g. $^{206}Pb/^{204}Pb$ from 18 to 19 instead to 18.26 for a µ ratio of 8 of the depleted). A $^{147}Sm/^{144}Nd$ ratio of 0.1 would retard the radiogenic growth of $^{143}Nd/^{144}Nd$ compared with normal depleted mantle evolution (e,g from 0.5127 to 0.51283 instead to 0.51297 for a $^{147}Sm/^{144}Nd$ ratio of 0.21 of the depleted mantle). The uniform Sr isotope composition of the main group may result from generally anhydrous mantle without Rb bearing phases like phlogopite, whereas the few samples with high Sr-isotope ratios could be related to hydrous parts of the mantle. (3) Such modified mantle realms could be the source of xenoliths sampled by the host basanite or of melts modifying other parts of the mantle during ascent. The increase of La/Yb with increasing Sr (Fig. 5a) and the increase of the $^{206}Pb/^{204}Pb$ ratios with La/Yb (Fig. 5b) could reflect the varying amount of addition of such melts to an originally depleted peridotite. Small amounts of melt with high trace element content would change the trace element budget of a depleted peridotite dramatically, leaving the major element composition virtually unchanged. (4) Traces of melt/fluid infiltration such as possible hydrous phases or chemical zoning of minerals have been extinguished by Cretaceous high-T metamorphism.

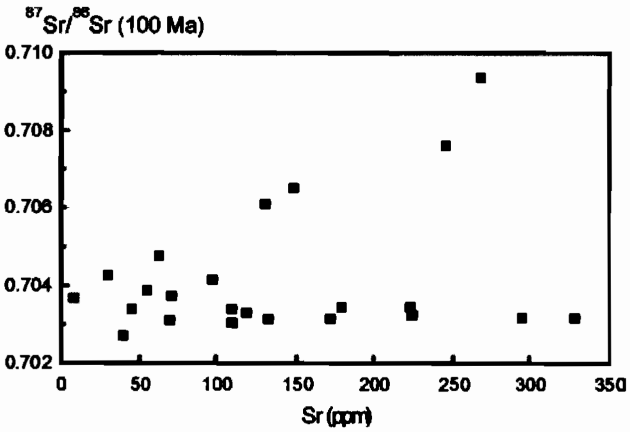

Figure 7. Variation of the $^{87}Sr/^{86}Sr$ ratios with Sr contents of cpx.

REFERENCES

Carlson, R.W., Esperança, S., Svisero, D.P., 1996. Chemical and Os isotopic study of Cretaceous potassic rocks from southern Brazil. Contributions to Mineralogy and Petrology 125: 393-405

Gibson, S.A., Thompson, R.N., Dickin, A.P., Leonardos, O.H., 1996. Erratum to 'High-Ti and low-Ti mafic potassic magmas: Key to plume-lithosphere interaction and continental flood-basalt genesis'. Earth and Planetary Science Letters 141: 325-341

Lucassen, F., Lewerenz, S., Franz, G., Viramonte, J., Mezger, K., 1999. Metamorphism, isotopic ages and composition of lower crustal granulite xenoliths from the Cretaceous Salta Rift, Argentina. Contributions to Mineralogy and Petrology 134, 325-341.

Lucassen, F., Becchio, R., Harmon, R., Kasemann, S., Franz, G., Trumbull, R., Wilke, H-G., Romer, R.L., Dulski, P., 2001. Composition and density model of the continental crust at an active continental margin- the Central Andes between 21°and 27°S. Tectonophysics 341, 195-223.

Lucassen, F., Escayola, M., Franz, G., Romer, R.L., Koch., K., 2002. Isotopic composition of Late Mesozoic basic and ultrabasic rocks from the Andes (23-32°S) - implications for the Andean mantle. Contributions to Mineralogy and Petrology 143, 336-349.

Maaloe S., Ken-ichiro, A., 1977. The major element composition of the upper mantle estimated from the composition of lherzolites. Contributions to Mineralogy and Petrology 63, 161 – 173.

Viramonte, J.G., Kay, S.M., Becchio, R., Escayola, M., Novitski, I., 1999. Cretaceous rift related magmatism in central-western South America. Journal of South American Earth Sciences 12: 109-121.

GEOCHEMICAL AND Sr-Nd-O ISOTOPIC FEATURES OF THE POÇOS DE CALDAS ALKALINE MASSIF (SP-MG, SE BRAZIL): RELATIONSHIPS WITH THE SERRA DO MAR ANALOGUES

Lustrino, M.[1-2]; Dallai, L.[2]; Giordano, R.[1]; Gomes, C.B.[3]; Melluso, L.[4]; Morbidelli, L.[1]; Ruberti, E.[3] and Tassinari, C.C.G.[3]

1. Dipartimento di Scienze della Terra, Università degli Studi di Roma La Sapienza, P.le A. Moro, 5, 00185 Rome, Italy. michele.lustrino@uniroma1.it
2. CNR – Istituto di Geologia Ambientale e Geoingegneria, Università degli Studi di Roma La Sapienza, P.le A. Moro, 5, 00185 Rome, Italy
3. Instituto de Geociências, Universidade de São Paulo, Rua do Lago, 562, Cidade Universitária, 05508-900, São Paulo, Brazil
4. Dipartimento di Scienze della Terra, Università degli Studi di Napoli Federico II, Via Mezzocannone, 8, 80134 Naples, Italy

Keywords: Alkaline, syenite, phonolite, geochemistry, petrology

INTRODUCTION

The Late Cretaceous Poços de Caldas intrusion, lying at the border between Minas Gerais and São Paulo States, extends for about 800 km^2. It is the largest known alkaline complex of Brazil and one of the largest of the world.

A study of the Poços de Caldas alkaline massif has been carried out during the last decade in the framework of a Brazilian-Italian scientific cooperation, in order to characterize the mineralogical and geochemical composition of the Cretaceous-Paleogene alkaline, alkaline-carbonatite and tholeiitic complexes of SE Brazil, Paraguay and Uruguay. The results of this study indicated that the Poços de Caldas can be considered as the westernmost occurrence of the Serra do Mar Province (Thompson et al., 1998), the latter extending from the Cabo Frio area (Atlantic Ocean, SE Brazil; Bennio et al., 2002) to the southeastern end of the Alto Paranaíba Igneous Province (APIP; SE Brazil; Araújo et al., 2001; D'Amelio et al., 2003).

GEOLOGICAL FRAMEWORK

The Poços de Caldas igneous complex forms a circular (ring) structure, about 28 km in diameter, emplaced between 78 and 76 Ma (Shea, 1992) mainly in the Guaxupé block, between the Paraná basin and São Francisco craton. The Guaxupé block separates the Brasília mobile belt from the Ribeira belt, where widespread alkaline-carbonatite and alkaline magmatism (with both potassic-ultrapotassic and sodic affinities) occurred during Late Cretaceous (Alto Paranaíba Province; 90-80 Ma; Gibson et al., 1995; Araújo et al., 2001), and Late Cretaceous to Paleogene (Serra do Mar Province; 80-54 Ma; Thompson et al., 1998), respectively.

The rock-types are potassic (K_2O/Na_2O generally >1) phonolites (~ 80% of outcrops) and nepheline syenites (~ 14%). Pyroclastic rocks (mainly breccias), mainly found at the western margin of the massif in the Vale do Quartel, are agglomerate blocks of tephrite with subordinate ankaramite, nephelinite and phonotephrite with sodic affinity ($K_2O/Na_2O < 1$; generally < 0.5). Tephrite, trachybasalt and basaltic trachyandesite dykes are present at the northwestern side of the complex. Mafic-ultramafic dykes of lamprophyric affinity occur within the Osamu Utsumi pit (Schorscher et al., 1991). Ultramafic lamprophyric (with alnöitic affinity) and silico-carbonatite dykes, intruding the Neoproterozoic quartz mangerites near the northern borders of the complex, are also present (Vlach et al., 1996). The presence of a carbonatite body at the Morro do Ferro mine was inferred by Waber (1992) through chemical balances on the Th-REE supergene mineralizations.

PETROGRAPHY AND MINERAL CHEMISTRY

Phonolites are holocrystalline, aphanitic, fine-grained, and sometimes show "tinguaitic" textures. Porphyritic textures are occasionally present, with pheno- and microphenocrysts of alkali feldspar (Or 93-60 wt%), nepheline (with kalsilite content up to 30 wt%), clinopyroxene (from diopside core with mg# = 0.84 to hedenbergite and aegirine-augite rims with mg# = 0.48 and Ae up to 80 mol%), sphene and rare opaques (mostly Ti-magnetite), set in a groundmass made up of the same minerals. Common pseudoleucite (intergrowth of alkali feldspar and nepheline) and rare analcime, believed to be late metasomatic modifications, occur as phenocryst-like phase. Accessory minerals allow to distinguish peralkaline phonolites [i.e., A.I.>1; A.I. = (Na+K)/Al], usually characterized by arfvedsonite, astrophyllite, eudialyte-eucolite, hainite, aenigmatite, sodalite, fluorite and other unidentified minerals (e.g., Atencio et al., 1999). Sphene and apatite are common accessories in the rare metalluminous rocks.

Nepheline syenites, phaneritic equivalent of the phonolites, in general contain less than 20 vol% of mafic minerals. Rarely, some eudyalite-rich variants (lujavrite) have up 28 vol% clinopyroxene (Ulbrich, 1993). Medium- to coarse-grained hypidiomorphic textures are prevailing, and foyaitic (trachytic s.l.) textures are occasionally present. The main mineral assemblages are made up of alkali feldspar (Or = 83-54 wt%), nepheline (kalsilite content 15-28 wt%), clinopyroxene (from augite with mg# =0.79 to aegirine with Ae up to 80 wt%) and occasional sodalite, amphibole (arfvedsonite) and biotite, the latter often appearing as substitution products of clinopyroxene or as poikilitic aggregates. Zircon is an ubiquitous accessory mineral. Similar to the phonolitic rocks; accessory phases of the prevailing agpaitic variants are eudialyte, hainite, rinkite, lamprophyllite and astrophyllite, that may have local importance (up to 14 vol.%, i.e. lujavrite and khibinite rocks; Ulbrich & Ulbrich, 2000). The prevailing accessories of the miaskite (metalluminous) variants are sphene, fluorite, magnetite, Ti-magnetite, ilmenite and sulphides.

Pyroclastic rocks are breccias, agglomerates, tuffites and surge deposits. Rounded to subangular blocks include ankaramite, basanite/tephrite and phonotephrite. The prevailing texture is aphanitic; the subordinate porphyritic rocks show diopsidic clinopyroxene (Wo 46-50, En 41-46) olivine (Fo 81-84), and Ti-magnetite pheno- and microphenocrysts set in a hypocrystalline groundmass made up of clinopyroxene, feldspar, biotite/phlogopite, opaques, altered olivine and analcime. Some analcime-like phenocrysts show leucite remnants at the core (Thompson et al., 1998). Variants rich in clinopyroxene megacrysts (up to 4 cm long) have been classified as ankaramites.

Dykes are usually phlogopite-rich rocks, having petrographic evidence of lamprophyric affinity (Schorscher et al., 1991; Waber et al., 1992). According to the TAS classification scheme some rock-types can be classified as basanites, trachybasalts and basaltic trachyandesites. The texture is porphyritic with mega-, macro-, pheno- and microphenocrysts of clinopyroxene (hedenbergitic core with diopside rims), phlogopite/biotite phenocrysts and olivine pseudomorphs (unaltered cores with Fo 80-75), set in a groundmass of hedenbergitic clinopyroxene, phlogopite, opaques and altered glass. In particular, ultramafic lamprophyre dykes of the Osamu Utsumi mine are characterized by high phlogopite and clinopyroxene contents (25-35 and 27-36 vol%, respectively) with some variants having up to 40-45 vol% groundmass carbonate, pointing to a carbonatitic affinity (e.g., Schorscher et al., 1991).

GEOCHEMISTRY

Over 150 samples were analyzed by XRF and 30 most representative samples were re-analyzed by ICP-MS techniques. TAS classification clearly evidences a bimodal distribution with clusters in the phonolite-tephriphonolite and the basanite/tephrite-phonotephrite fields.

K_2O/Na_2O ratio allows to distinguish a low to medium potassic affinity (K_2O/Na_2O mostly between 0.6 and 1.5) for the phonolite/nepheline syenite clan, versus the sodic affinity of the mafic blocks ($K_2O/Na_2O<1$). High-K compositions characterize the mafic-ultramafic lamprophyres (K_2O/Na_2O = 4.1-8.7). Blocks and dykes are distinguishable from the phonolite/nepheline syenite association also on the basis of their lower A.I. (0.61 to 0.92 for blocks/dykes and 0.89-1.38 for phonolite/nepheline syenite). The Poços de Caldas samples plot in the field of the corresponding types of Serra do Mar and Trindade-Martin Vaz islands. Only some phonolite/nepheline syenite plot to the right of the above mentioned field; these K-rich compositions can be considered the result of late stage K-metasomatism.

Major and trace element content of the Poços de Caldas products evidence an overall similarity with the correspondant rock-types of the Serra do Mar; the only exception are some K-rich phonolites and nepheline syenites that do not find any corresponding composition in the Serra do Mar products.

In primitive mantle-normalized incompatible element diagrams, phonolites and nepheline-syenites (both peralkaline and metaluminous) display parallel and overlapping patterns, similar to the analogues from Serra do Mar and Trindade-Martin Vaz. The basanite-phonotephrite-ankaramite association of Poços de Caldas shows more flattened patterns , similarly to that observed for the phonolite/nepheline-syenite association, overlaping the fields of the Serra do Mar and Trindade-Martin Vaz basic rocks. The Poços de Caldas lamprophyres show strong U, La, Nd, Eu, Y and HREE enrichment.

Sr-Nd ISOTOPES

The Poços de Caldas data set forms almost two distinct groups: the first (phonolite/nepheline syenites, phonotephrites and lamprophyres) clusters into an intermediate position between the Alto Paranaíba and Serra do Mar basic rock-types; on the other hand, the Poços de Caldas basanite-tephrite-ankaramite group plots in the field of the Serra do Mar and Trindade-Martin Vaz basic rocks. Two samples with highest $^{87}Sr/^{86}Sr$ values represent hydrothermal partially altered rocks, rather than contaminated magmas, considering all the geochemical parameters (e.g., Waber et al., 1992).

No systematic comparison between the Poços de Caldas rocks and the phonolite/nepheline syenite suite of the Serra do Mar province can be done due to the virtual absence of data on the latter outcrops. From the available Sr-Nd isotopic analyses a strong similarity between basanites (s.l.) and phonolite/nepheline-syenites (s.l.) of the Serra do Mar can be envisaged. This similarity is observed also among the rocks of Trindade-Martin Vaz, but not among those of Poços de Caldas. In the latter ones, samples of lamprophyric dykes show low $^{87}Sr/^{86}Sr_{78\ Ma}$ (0.70323), similar to the samples from Serra do Mar.

OXYGEN ISOTOPE COMPOSITION

Preliminary analyses on separate minerals have been performed via laser fluorination on clinopyroxenes from nepheline syenite (3), ankaramite (1), basaltic trachyandesite (1), tinguaite (1), phonolite (1) and lamprophyre (3). With the exception of two lamprophyres showing low $\delta^{18}O$ values (down to 2.88‰), the $\delta^{18}O_{SMOW}$ values of the analyzed clinopyroxenes are uniform ($\delta^{18}O = 5.54 \pm 0.16$‰). The extremely low $\delta^{18}O$ of the clinopyroxenes from lamprophyres are possibly related to high temperature isotopic exchange with meteoric/hydrothermal fluids that percolated along fractures or faults. Groundmass calcite of a basaltic trachyandesite breccia has been analyzed for oxygen and carbon isotopic ratios and the results ($\delta^{18}O$ = 23.32;

$\delta^{13}C_{PDB}$ = -1.75) are compatible with upper crustal provenance, excluding any primary (e.g., carbonatitic) origin of the carbonate.

CONCLUSIVE REMARKS

The Poços de Caldas massif is a composite alkaline complex. It was formed by multiple magmatic intrusions with phonolite/nepheline-syenite composition, and by basanite-tephrite-ankaramite volcanic rocks successively intruded by phonotephritic and lamprophyric dykes.

On geochemical basis a common origin of the Poços de Caldas complex and the Serra do Mar igneous provinces can be inferred. Similar major and trace elements contents of the Poços de Caldas and the Serra do Mar and Trindade-Martin Vaz rocks suggest a similar mantle source, as formerly proposed by Thompson et al. (1998). Lithospheric and sublithospheric mantle sources may have been mobilized by the Trindade mantle plume during the westward movement of the South American plate during the Cretaceous-Eocene. However, the Sr-Nd isotope data indicate that the phonolite/nepheline-syenite rocks from Poços de Caldas are more (Sr) and less (Nd) radiogenic when compared to the Serra do Mar and Trindade-Martin Vaz analogues. The mantle sources of the Poços de Caldas products are much more homogeneous in terms of oxygen isotopic ratios. The lower $\delta^{18}O$ of some lamprophyres can be related to meteoric/hydrothermal alteration during the late stages of consolidation of the magma.

REFERENCES

Araújo A.L.N., Carlson R.W., Gaspar J.C. and Bizzi L.A., 2001. Petrology of kamafugites and kimberlites from the Alto Paranaíba alkaline province, Minas Gerais, Brazil, Contrib. to Mineralogy and Petrolology 142, 163-177.

Atencio, D., Coutinho, J.M.V., Ulbrich, M.N.C. and Vlach, S.R.F., 1999. Hainite from Poços de Caldas, Minas Gerais, Brazil. The Canadian Mineralogist 37, 91-98.

Bennio L., Brotzu P., Gomes C.B., D'antonio M., Lustrino M., Melluso L., Morbidelli L. and Ruberti E., 2002. Petrological, geochemical and Sr-Nd isotopic features of alkaline rocks from the Arraial do Cabo Frio peninsula (Southeastern Brazil). Period. di Mineralogia 71, 137-158.

D'Amelio F., Ruberti E., Gomes C.B., Lustrino M., Melluso L., Morbidelli L. and Morra V., 2003. Clinopyroxene and perovskite partition coefficients in kamafugitic rocks. Proc. EGS-AGU-EUG Joint Assembly 2003, Nice, France.

Gibson, S.A., Thompson, R.N., Dickin, A.P. and Leonardos, O.H., 1995. High-Ti and low-Ti mafic potassic magmas: key to plume-lithosphere interactions and continental flood-basalt genesis. Earth and Planetary Sci. Let., 136, 149-165.

Schorscher, H.D., Garda, G.M., Shea, M.E. and Waber, N., 1991. Lamprophyre dykes from the Osamu Utsumi uranium mine, Poços de Caldas (MG), Brazil. International Symposium on Mafic Dykes, São Paulo, Extended Abstracts Volume, pp. 116-124.

Shea, M.E., 1992. Isotopic geochemical characterization of selected nepheline syenites and phonolites from the Poços de Caldas alkaline complex, Minas Gerais, Brazil. Journal of Geochemical Exploration 45, 173-214.

Thompson, R.N., Gibson, S.A., Mitchell, J.G., Dickin, A.P., Leonardos, O.H., Brod, J.A. and Greenwood, J.C., 1998. Migrating Cretaceous-Eocene magmatism in the Serra do Mar alkaline Province, SE Brazil: melts from the deflected Trindade mantle plume? J. Petrology 39, 1493-1526.

Ulbrich, H.H.G.J. and Ulbrich, M.N.C., 2000. The lujavrite and khibinite bodies in the Poços de Caldas alkaline massif, southeastern Brazil: a structural and petrographical study. Revista Brasileira de Geociências 30, 615-622.

Ulbrich, M.N.C., 1993. Mineralogy of nepheline syenites from the Poços de Caldas alkaline massif, SE Brazil: chemistry, X-ray data and microtextures of feldspars. Revista Brasileira de Geociências 23, 388-399.

Vlach S.R.F., Ulbrich, M.N.C. Ulbrich, H.H.G.J. and Garda, G.A.R., 1996. Rochas de afinidades alnoíticas e sílico-carbonatíticas periféricas ao maciço alcalino de Poços de Caldas (Mg-Sp). XXXIX Congresso Brasileiro de Geologia, Anais 2, 128-130.

Waber, N., 1992. The supergene thorium and rare-earth element deposit at Morro do Ferro, Poços de Caldas, Minas Gerais, Brazil. Journal of Geochemical Exploration 45, 113-157.

Waber, N., Schorscher, H.D. and Peters, Tj., 1992. Hydrothermal and supergene uranium mineralization at the Osamu Utsumi mine, Poços de Caldas, Minas Gerais, Brazil. Journal of Geochemical Exploration 45, 53-112.

EARLY CRETACEOUS MAGMATIC ACTIVITY IN SOUTHEAST URUGUAY: TRACE ELEMENT AND Sr-Nd ISOTOPIC CONSTRAINTS

Lustrino, M.[1,2]; Gomes, C.B.[3]; Melluso, L.[4]; Morbidelli, L.[1]; Muzio, R.[5]; Ruberti, E.[3] and Tassinari, C.C.G.[3]

1. Dipartimento di Scienze della Terra, Università degli Studi di Roma La Sapienza, P.le A. Moro, 5, 00185 Rome, Italy.
michele.lustrino@uniroma1.it
2. CNR – Istituto di Geologia Ambientale e Geoingegneria, Università degli Studi di Roma La Sapienza,
P.le A. Moro, 5, 00185 Rome, Italy
3. Instituto de Geociências, Universidade de São Paulo, Rua do Lago, 562, Cidade Universitária, 05508-900, São Paulo, Brazil
4. Dipartimento di Scienze della Terra, Università degli Studi di Napoli Federico II, Via Mezzocannone, 8, 80134 Naples, Italy
5. Facultad de Ciencias - Universidad de la República, Uruguay

Keywords: Subalkaline, Cretaceous, geochemistry, petrology

INTRODUCTION

During the early Cretaceous, in concomitance with the opening of the South Atlantic Ocean, the South American Plate was affected by a huge volcanic and plutonic event, with the formation of products with a wide chemical compositional spectrum. In this study we present major and trace element as well as Sr-Nd isotopic analyses for early Cretaceous (~132 Ma) basic to sialic rocks from SE Uruguay.

The description of the igneous products is divided into two parts. The first one deals with sialic volcanic rocks outcropping near São Miguel, Lascano, Rio Salamanca and Arequita areas, whereas the second part is devoted to the intrusive plug and ring dyke complex of the Valle Chico suite.

SIALIC ROCKS OF SÃO MIGUEL, LASCANO, RIO SALAMANCA AND AREQUITA

The mineral paragenesis of the sialic rocks is essentially anhydrous and is represented by plagioclase, alkali feldspar, quartz, iron oxides ± clinopyroxene, whereas the scarce basic rocks sampled consist of plagioclase (An=85-45%), clinopyroxene and, rarely, olivine. Alkali feldspars of the sialic rocks are sanidine, with orthoclase content ranging from 60 to 30%. Clinopyroxenes are essentially augites ($Wo_{42}En_{45}Fs_{13}$ to $Wo_{38}En_{15}Fs_{47}$). The Uruguayan sialic rocks can be classified as: rhyodacite, alkali rhyolite and quartz latite; the rarer basic rocks are hawaiite and olivine tholeiite. Compared to the sialic volcanic rocks of the Serra Geral Formation (Paraná Basin), the Uruguayan samples have a higher silica content, possibly related to some degree of alteration (silicitization) of the products.

Primitive mantle-normalized multielement diagrams evidence, for the sialic samples negative anomalies in Eu, Sr, Nb, P, Ti and, sometimes, in Ba, which can be related to fractional crystallization processes. The olivine tholeiite shows negative anomalies in Th, K and Ti, positive anomaly in Ba and is enriched in LREE, with an overall pattern resembling typical HIMU-OIBs. The sialic rocks of different localities can be distinguished on the basis of interelemental ratios (e.g., LILE/HFSE) such as Ti/Zr, Nb/Y, K/Ti and Rb/Nb.

The possibility of an origin from fractional crystallization process (in closed system) starting from a basaltic parental melt has been tested considering as parental magma the olivine tholeiite of Mariscala. The evolution of basaltic melts to rhyolite has been modelled with major elements mass balance after removal of about 86% of a gabbroic cumulate (pl+ol+cpx+mt+il). However, such a model cannot mimic the trace element concentration of sialic rocks. In particular, the HFSE (Nb, P, Hf) content of rhyolites is lower than those of the calculated liquid, whereas Rb and K are higher. Better results are obtained proposing a two-stage model: a first step is fractionation with evolution from basalt to quartz latite and then from quartz latite to rhyolite. However, also in this case, LILEs are higher whereas HFSEs and HREEs are lower in the rhyolites than in the calculated liquids.

The hypothesis which takes into account the origin by partial melting from basaltic (or granulitic) lithologies has been tested considering the composition of experimental liquids obtained starting from basic (basaltic to granulitic) compositions. A comparison with experimental melts has shown that the Uruguayan rocks have K_2O and FeO too high and Al_2O_3, CaO and Na_2O too low to be considered the product of anatexis of any basic source.

An origin related to AFC processes has been also tested. As parental liquids the olivine tholeiite of Mariscala has been chosen, whereas as crustal contaminant has been chosen a Proterozoic granite from Amazonas Craton. Trace element and isotopic evidences suggest that the combination of assimilation + fractional crystallization is the most viable process in order to explain the genesis of the volcanic rocks of the Arequita Formation. The highest LILE and HFSE concentration in quartz latites compared to rhyolites speak for the absence of genetic relationships between these two rock groups.

Open system processes are suggested also by the radiogenic Sr and unradiogenic Nd isotopic ratios of the Uruguayan rhyolites. Alkali rhyolites and quartz latites from Rio Salamanca and Arequita show the lowest $^{87}Sr/^{86}Sr$ (down to 0.70904) and the lowest $^{143}Nd/^{144}Nd$ (down to 0.511891) among the Uruguayan rocks. On the other hand, samples from Serra São Miguel and Lascano plot on a Sr-Nd isotopic space along a line in the enriched quadrant, with $^{87}Sr/^{86}Sr$ ranging from 0.71227 to 0.72391 and $^{143}Nd/^{144}Nd$ from 0.512287 to 0.511945. The olivine tholeiite show less radiogenic Sr and more radiogenic Nd. It is possible to propose a mechanism of fractional crystallization coupled with assimilation of crustal material which could be the upper crust in the case of Serra São Miguel and Lascano (samples shifted towards more radiogenic Sr) and the lower crust for Rio Salamanca and Arequita (samples with the lowest $^{87}Sr/^{86}Sr$).

IGNEOUS COMPLEX OF VALLE CHICO

The igneous complex of Valle Chico is made up of volcanic and plutonic rocks cropping out over an area of about 250 km^2; a dyke swarm cross-cuts the intrusive lithologies. The intrusive rocks are syenite (~9 %), quartz syenite (~9 %), quartz monzonite (~14 %), granite (~9 %) and alkali feldspar granite (~5 %). The volcanic rocks and the dykes are trachyte (~6%), quartz latite (~31 %) and alkali feldspar rhyolite (~17 %).

Textures of the syenites, quartz syenites, granites and alkali feldspar granites are hypidiomorphicic and, less commonly, autoallotriomorphic with large to mega-crystals (up to 4 cm in size) of perthitic and sometimes poikilitic alkali feldspar, occasionally in granophyric relation with quartz. Interstitial phases are quartz, rare plagioclase, amphibole, clinopyroxene, chloritized biotite, apatite, zircon and opaque minerals. Quartz monzonites are inequigranular, sometimes glomeroporphyritic with subhedral to anhedral plagioclase, sometimes with reaction rims. Interstitial phases are the same as above.

Among the volcanic and subvolcanic rocks, trachytes and alkali feldspar rhyolites are holo- to hypocrystalline with porphyricity index ranging from nearly 0 to 30%. Phenocrysts of alkali feldspar and quartz are common, while groundmass phases are quartz, alkali feldspar, chloritized biotite, apatite, opaque minerals and rare amphibole. Quartz latites are porthyritic to glomeroporphiritic rocks with sieved euhedral to anhedral plagioclase; plagioclase is pecilitic for the presence of opaques and clinopyroxenes. Groundmass phases are clinopyroxene, opaque minerals, quartz, apatite, plagioclase and alkali feldspar.

Alkali feldspar composition ranges from almost pure albite to Or_{48}, whereas plagioclase ranges from oligoclase to andesine. Clinopyroxene has low Na content and can be classified as Fe-augite to hedenbergite; only rarely Na-rich types (aegirine content up to 70%) have been found. Similarly rare is the presence of scarce pigeonite ($Wo_{12}En_{37}Fs_{51}$). Opaque minerals are ilmenite (Ilm > 95 %) and ulvospinel-magnetite s.s. (Ulv = 5-95 %). Amphiboles belong to calcic and sodic-calcic groups and are classified as richterite, katophorite, Fe-winchite, edenite and Fe-edenite.

Both plutonic and volcanic rocks show potassic character with K_2O content up to 8 wt%. TiO_2, Fe_2O_3, CaO, MgO and P_2O_5 of both plutonic and volcanic rocks are negatively correlated with D.I.

Primitive mantle-normalized multielemental plots show fractionated concentration of incompatible trace elements. All the plutonic rocks show strong negative peaks of Sr and Ti, together with negative peaks of Nb and Nd, and positive peaks of Rb and Pb; syenite and alkali feldspar granite show negative peaks also in Ba. Eu/Eu* negative anomalies range from 0.78 (quartz latite) to 0.09 (alkali feldspar rhyolite) The same geochemical features can be evidenced for the volcanic rocks as well. Quartz latite, trachyte, quartz trachyte and alkali feldspar rhyolite show negative anomalies in Sr, Ti and Eu, suggesting plagioclase and opaque minerals as the main fractionating phases. The amplitude of the negative anomalies grows from the less differentiated (quartz latite) to the most SiO_2-rich types (alkali feldspar rhyolite).

$^{87}Sr/^{86}Sr$ ranges from 0.7045 (quartz trachyte) to 0.7170 (alkali feldspar rhyolite) and $^{143}Nd/^{144}Nd$ ranges from 0.5117 (alkali feldspar granite) to 0.5121 (quartz trachyte). Also in this case, an active role of continental crust in the genesis of the volcanic and plutonic rocks of Valle Chico is evidenced by the Sr-Nd isotopic ratios.

Up to now the Valle Chico massif has been considered of alkaline affinity. However, on the basis of 1) the constant SiO_2 oversaturated character of the Valle Chico rocks, 2) the petrography and mineral chemistry (aegirine content of clinopyroxene mostly below 40% by weight; rare presence of pigeonite; amphibole belonging to the calcic or sodic-calcic groups) and 3) the chemical similarity with rhyolitic products of the Paraná-Etendeka CFB province, our results indicate that the most probable association for these igneous rocks can be ascribed to the tholeiitic or transitional series, rather than the alkaline one.

Major and trace element composition of the early Cretaceous volcanic and plutonic products of SE Uruguay evidence a close similarity, thus allowing to propose similar mantle sources variously contaminated by upper crustal material. This contamination is likely the effect of magma ponding at crustal levels and the contaminant can have either the composition of lower crustal lithologies (capable to shift the original isotopic ratios towards unradiogenic $^{143}Nd/^{144}Nd$ and moderately radiogenic $^{87}Sr/^{86}Sr$) or upper crustal lithologies (shifting the original isotopic ratios towards unradiogenic $^{143}Nd/^{144}Nd$ and strongly radiogenic $^{87}Sr/^{86}Sr$).

SUBDUCTION COMPONENTS IN THE GENESIS OF THE IGNEOUS ROCKS FROM THE SOUTH SHETLAND ARC, ANTARCTICA

Machado, A.[1]; Chemale Jr., F.[1]; Conceição, R.V.[1]; Kawashita, K.[1]; Morata, D.[2] and Van Schmus, W.R.[3]

1. Federal University of Rio Grande do Sul, Institute of Geosciences, Isotope Geology Laboratory, Av. Bento Gonçalves, 9500, Campus do Vale, Agronomia, 91501-970, Porto Alegre-RS, Brazil. adrianemachado@yahoo.com.br, farid.chemale@ufrgs.br, rommulo.conceicao@ufrgs.br
2. Department of Geology, University of Chile, Casilla 13518, Correo 21, Santiago, Chile. dmorata@cec.uchile.cl
3. Department of Geology, University of Kansas, Lawrence, KS, 66045, USA

Keywords: South Shetland Arc, subduction, melting, sediment

INTRODUCTION

Magmas emplaced in arcs were probably generated in the mantle wedge above subduction zones (Ringwood, 1974), but it is not even clear whether prior to the effects of subduction, the mantle wedge had MORB (Perfit et al., 1980), OIB (Morris & Hart, 1983) or some other chemical affinity. This uncertainty undermines assessment of the subducted material role in destructive plate margin magmas, and in turn limits discussion of whether recycled crust is subducted to greater depths, from where it might contribute to ocean island magmatism (White & Hofmann, 1982).

It is generally believed that slab-derived materials (melts and/or fluids, and sediments) are added to the mantle wedge from the subducting slab, and subsequently, these components induce the generation of island arc magma.

The slab-derived materials are frequently argued as melts and/or aqueous fluids derived by dehydration of the subducting slab, besides the oceanic sediment. This argument is based on the mobile and immobile element ratios in aqueous fluids, ratios of large ion lithophile elements (LILEs, such as Cs, Rb, Ba, Sr, light rare earth elements), high field strength elements (HFSEs, such as Nb, Zr, Hf, Y) (Ishikawa & Nakamura, 1994; Ryan et al., 1995) and isotope.

The South Shetland Islands arc (Fig. 1) provides an opportunity to compare and contrast the effects of melt and/or fluid, and sediment involvement in subduction zone. As the result of arc study, the rocks from South Shetland Islands are apparently uncontaminated by intra-crustal components and they should have largely evolved through simple fractional crystallization of a primitive island arc basalt precursor. These samples are similar in most aspects to typical island arc volcanic rocks which constitute the bulk of the database for subduction-related compositions.

In this abstract, Sr, Nd and Pb isotopic ratios, together with trace element compositions, are presented from samples from the South Shetland Islands. We use these data to discuss and investigate the chemical affinity of the mantle wedge and interactions between the subducting oceanic slab and mantle wedge. The samples used in this paper are from western Livingston Island (Byers Peninsula), south-eastern Greenwich Island (Fort Point), western Robert Island (Coppermine Peninsula), south-western King George Island (Fildes Peninsula) and north-eastern Ardley Island. The age of those rocks vary from 90 Ma to 45 Ma (Smellie et al., 1984, 1996).

ANALYTICAL PROCEDURES

Isotope determinations were carried out at the Isotope Geochemistry Laboratory of University of Kansas (UK), USA, and at the Isotope Geology Laboratory (IGL), Federal University of Rio Grande do Sul (UFRGS), Brazil.

Rock powders for Rb-Sr and Sm-Nd analyses were dissolved in Teflon bombs in a microwave furnace using an HF-HNO_3 mixture and 6N HCl with $^{87}Rb/^{84}Sr$ and $^{149}Sm/^{150}Nd$ spike (UK) and without spike (IGL). The Sr and REE were extracted using a standard AG-50W cation resin; Sm and Nd were extracted using HDEHP-coated Teflon powder.

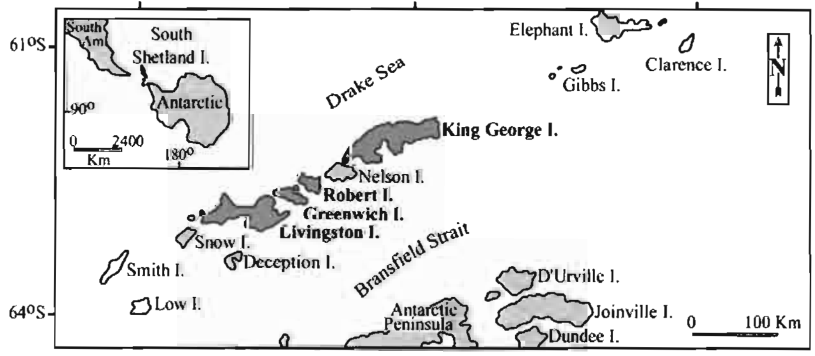

Figure 1. Location map of the South Shetland Islands.

Rb and Sr were loaded on a single Ta filament with H_3PO_4. Isotopic compositions were measured with a VG Sector multicollector mass spectrometer using dynamic mode (UK) and static mode (IGL). All analyses are adjusted for variations instrumental bias due to periodic adjustment of collector positions as monitored by measurements of our internal standard; on this basis our analyses of SRM987 is 0.710262 ± 0.000023 (n = 47, IGL), and 0.710253 ± 0.000024 (n = 12, UK).

Sm was loaded on a single Ta filament $H_3PO_4$and analyzed as Sm^+ in either static multicollector. Nd was loaded with phosphoric acid on a single Re filament having a thin layer of AGW-50 resin beads and analyzed as Nd^+ using dynamic mode at the UK and on triple Ta-Re-Ta filament using static mode at the IGL. We normally collect 100 ratios with a 1-volt ^{144}Nd beam. External precision based on repeated analyses of our internal standard is ± 20 ppm (1 standard deviation); all analyses are adjusted for instrumental bias due to periodic adjustment of collector positions as monitored by measurements of our internal standard; on this basis our analyses of La Jolla Nd average 0.51186 ± 0.000020 (UK) and 0.51185 ± 0.000029 (IGL). Sm-Nd ratios are corrected to within ± 0.5 percent, based on analytical uncertainties. ε Nd (t = crystallization age) values were calculated using the Ar-Ar ages or estimated ages based on the regional information.

During the course of the analyses Sr, Nd and Sm blanks were lesser than 1.5 ng, 500 pg and 100 pg, respectively.

For Pb method, an aliquot of 1 mL from the dissolved WR samples for Sr and REE analysis has been taken for Pb analysis. Pb was extracted with ion-exchange techniques, with AG-1 X 8, 200-400 mesh, anion resin. Isotopic analyses for Pb composition were carried out with VG Sector mass spectrometer of UK and IGL. Samples were loaded on single Re filaments with silica gel and H_3PO_4. Pb isotopic ratios were corrected to a fractionation factor of 0.13% amu based on sucessive determinations of NBS981 and NBS982 common Pb standards. External variations in isotopic ratios are normally 0.1% or lower, based on repeated analyses of NBS981 and NBS982 standards.

DISCUSSION

Trace element concentrations of the South Shetland samples are plotted in primitive mantle normalized diagrams on Figure 2. All of the South Shetland samples are enriched in Rb, Ba, K and Sr relative to primitive mantle, but they are depleted in Nb, Zr, Hf and Ti. All samples show positive Ba and Sr anomalies and pronounced negative Nb and Ti anomalies. On average, the rocks are depleted in HFSE, and enrichment in light and middle REE compared to primitive mantle.

In contrast to the LILE, the HFSE such as Zr and Nb are relatively insoluble in aqueous fluids. In island arc magmas, therefore, these elements are believed to be derived predominantly from the mantle wedge, and their relative concentrations reflect the composition of the mantle wedge beneath the arc (Keppler, 1996).

The mantle source underlying the Cretaceous-Tertiary South Shetland Islands arc appears to have been geochemically depleted, like MORB-type source, prior to metasomatism caused by subduction, because the samples show strong negative Nb and Ti anomalies. The stabilisation of Nb-rich phases in the mantle may explain the ubiquitous depletion of Nb in arc magmas (Woodhead et al., 1993). This is likely to be caused by a previous episode of melt extraction from the mantle source.

The $^{87}Sr/^{86}Sr$ ratios vary from 0.7033 to 0.7046. The $^{143}Nd/^{144}Nd$ ratios are between 0.5127 and 0.5129. εNd values vary from + 2.71 to + 7.30, which indicate asthenospheric mantle source for the analysed samples. The $^{208}Pb/^{204}Pb$ varies from 38.12 to 38.70, $^{207}Pb/^{204}Pb$ are between 15.49 and 15.68, and $^{206}Pb/^{204}Pb$ from 18.28 to 18.81.

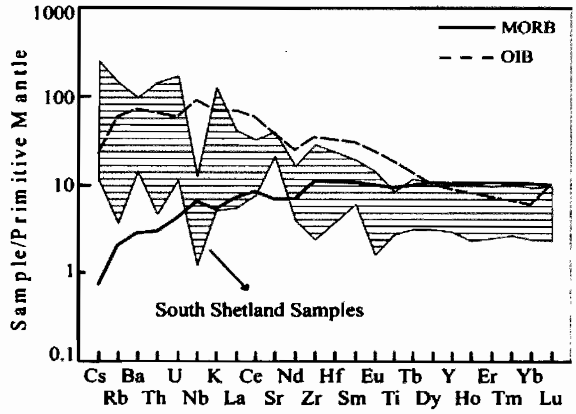

Figure 2. Primitive mantle normalised trace element diagram. Normalizing values from Taylor & McLennan, 1985.

The ε_{Nd} values of the samples (2.71 to 7.30) are all positive values. $^{87}Sr/^{86}Sr$ ratios values are typical for island arcs and indicate that there is no ancient continental crust involved in the South Shetland magmas.

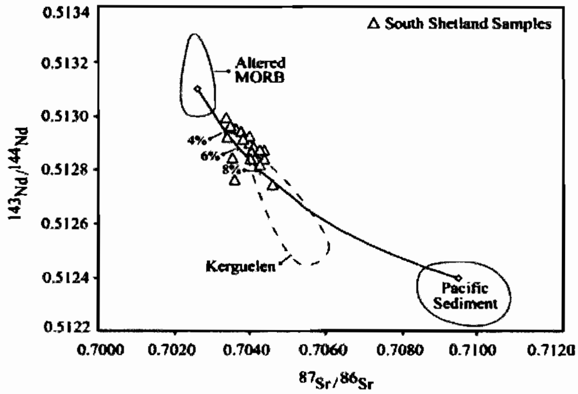

Figure 3. Estimation of the isotopic composition of the subduction component. The line is mixing between altered MORB and oceanic sediment. It indicates the bulk mixture between 4 wt % of oceanic sediment and 96 wt % of altered MORB. The isotope composition of altered MORB is from Cohen et al., 1980, and of oceanic sediment are from Othman, et al., 1989 and Kerguelen data are from http://georoc.mpch-mainz.gwdg.de/.

The $^{87}Sr/^{86}Sr$ ratios from South Shetland samples are lowest than Kerguelen data and the $^{143}Nd/^{144}Nd$ ratios are highest than those one (Fig. 3). These characteristics show that the South Shetland samples have isotope ratios similar to MORB, and not to OIB as Kerguelen does.

The Sr-Nd-Pb isotope systematics (Figs. 3, 4) show that the sediment is the main component with which the melt and/or fluid was in equilibrium. The isotope characteristics can be modelled reflecting three subduction components such as ≈ 96 wt % of melts and/or fluids from a MORB-type depleted manlte and the altered MORB plus ≈ 4% of oceanic sediment.

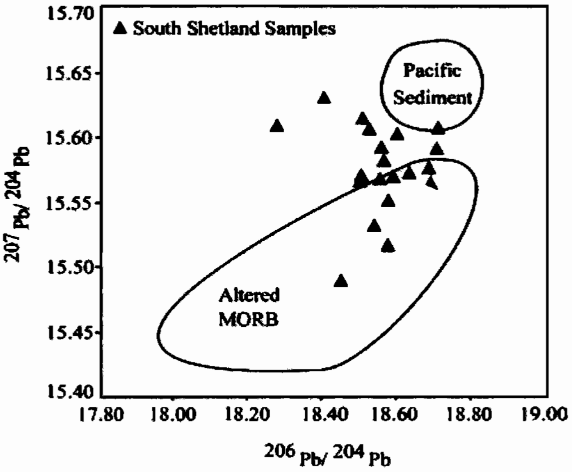

Figure 4. The ranges of altered MORB and ocenic sediment. Altered MORB data are from Cohen et al., 1980 and for oceanic sediment are from Othman, et al., 1989.

The exactly amount of fluid added is difficult to quantify due to uncertainties in the composition of subducted sediment, and it is not clear from the data whether this Pb isotope sedimentary signature would be carried in the fluid, or in a partial melt or a bulk addition. Some workers have argued that the fluid only carries the signature of the altered slab, and not that of the sediment (Turner et al., 1996).

On $^{206}Pb/^{204}Pb$ versus $^{207}Pb/^{204}Pb$ diagram (Fig. 4) it is possible to observe the ^{207}Pb enrichnment, which demonstrates the sediment involvement. It is not possible to demonstrate unequivocally whether the isotope systematics are best explained by variations from the melt and/or fluid composition or variations in sediment composition, or even a combination of both. Both processes are likely to have been active, and the question of their relative importance still remains open until we have more data.

CONCLUSION

The ε_{Nd} data presented here indicate that the isotope signature of rocks from the South Shetland Islands arc changes with time. This observation suggests that the amount of subduction component added to the wedge mantle varied with increasing the time.

Isotopic compositions of Sr, Nd and Pb are nearly similar to MORB-type depleted mantle in the South Shetland Archipelago region and the abundance ratios among HFSE are also identical to MORB, indicating that the mantle wedge under the South Shetland Islands was similar to MORB-type mantle prior to metasomatism caused by subduction.

The geochemical and isotopic characteristics of the rocks from the South Shetland islands need the involvement of sediment in their petrogenesis, and cannot be attibuted to melts and/or fluids variations in the mantle source alone.

REFERENCES

Cohen, R.S.; Evensen, N.M.; Hamilton, P.J., O'Nions, R.K., 1980. U-Pb, Sm-Nd and Rb-Sr systematics of mid-ocean ridge basalt glasses. Nature, 283, 149-153.

Ishikawa, T., Nakamura, E., 1994. Origin of the slab component in arc lavas from across-arc variation of B and Pb isotopes, Nature 370, 205-208.

Keppler, H., 1996. Constraints from partitioning experiments on the composition of subduction-zone fluids. Nature 380, 237-240.

Morris, J.D., Hart, S.R., 1983. Isotopic and incompatible element constraints on the genesis of island arc volcanics from Cold Bay and Amak Island, Aleutians, and implications for mantle structure. Geochim. Cosmochim. Acta 47, 2015-2030.

Othman,D., White, W.M., Patchett, J. , 1989. The geochemistry of marine sediments, island arc magma genesis, and crust-mantle recycling. Earth Planet. Sci. Lett., 94, 1-21.

Perfit, M.R., Gust, A.E., Bence, A.E., Arculus, R.J., Taylor, S.R., 1980. Chemical characteristics of island-arc basalt: implications for mantle sources. Chem. Geol. 30, 227-256.

Ringwood, A.E., 1974. The petrological evolution of island arc systems. J. Geol. Soc. London 130, 183-204.

Ryan, J.G., Morris, J., Tera, F., Leeman, W.P., Tsvetkov, A.W. P., 1995. Cross-arc geochemical variations in the Kurile arc as a function of slab depth. Science 270, 625-627.

Smellie, J.L., Pankhurst, R.J., Thomson, M.R.A., Davies, R.E.S., 1984. The geology of the South Shetland Islands: VI. Stratigraphy, geochemistry and evolution. British Antarctic Survey Reports 87, Cambridge, 83pp.

Smellie, J.L., Pallàs, R., Sàbat, F., Zheng, X., 1996. Age and correlation of volcanism in central Livingston Island, South Shetland Islands: K-Ar and geochemical constraints. J. South Am. Earth Sci., 9 (3/4), 265-272.

Taylor, S.R. and McLennan, S.M., 1985. The continental crust: Its composition and evolution. Blackwell, Oxford, 312 pp.

White, W.M., Hofmann, A.W., 1982. Sr and Nd isotope geochemistry of oceanic basalts and mantle evolution. Nature 296, 821-825.

Woodhead, J., Eggins, S., Gamble, J., 1993. High field strength and transition element systematics in island arc and back-arc basin basalts: evidence for multi-phase melt extraction and a depleted mantle wedge. Earth Planet. Sci. Lett. 114, 491-504.

Sr-Nd-Pb ISOTOPES AND GEOCHEMICAL DATA FROM THE WESTERN TRANS-MEXICAN VOLCANIC BELT: A CASE OF STUDY

Maldonado-Sánchez, G.[1,2] and Schaaf, P.[3]

1. Consejo de Recursos Minerales, Gregorio Gelati 40, Morelia, Mich., México.
2. Posgrado en Ciencias de la Tierra, Instituto de Geofísica, Cd. Universitaria, UNAM, México D.F. magma@ausi.com
3. Instituto de Geofísica, Cd. Universitaria, UNAM, México, D.F., México. pschaaf@tonatuih.igeofcu.unam.mx

Keywords: Geochemistry, isotopes, volcanic field, Mexico

THE TRANS-MEXICAN VOLCANIC BELT

The Transmexican Volcanic Belt (TVB) extends in a West-East direction for more than 1,000 km from the Pacific Coast to the Gulf of Mexico (Fig. 1). It is a late Miocene-Quaternary volcanic arc related to subduction of the Cocos plate beneath the North American plate (Nixon, 1982; Luhr, et al., 1985). However, the western part of the TVM is also influenced by the subduction of the Rivera plate (DeMets & Stein, 1991) and is dominated by a crustal block bound by three large rifts intersecting in form of a triple junction. These are the Colima, Tepic-Zacoalco and Chapala rifts (Fig. 2) and have been proposed as the continental boundaries of the Jalisco Block (JB). The rifts contain most of the Quaternary volcanic centers of the western TVB.

Figure 1. Tectonic framework of Mexico showing the four main plates. TVB = Transmexican Volcanic Belt; JB = Jalisco Block.

In the past years Luhr et al. (1985) related the complex tectonics of JB to an active rifting, but in recent works (Quintero-Legorreta et al., 1992; Rosas-Elguera et al., 1996; Ferrari et al., 1997), field studies have shown that the Plio-Quaternary tectonics is dominantly extensional. The rifts are ancient reactivated structures in response to plate boundary forces. Moreover, in this region there are alkaline (ocean-type) and calc-alkaline volcanism in close association since late Miocene (Wallace, et al., 1992; Moore et al., 1994). The calc-alkaline rocks are volumetrically predominant, most having been erupted from stratovolcanoes. The alkaline rocks are less voluminous and were erupted from scattered vents located along crustal fracture systems (Nelson & Carmichael, 1984; Nelson & Livieres, 1986).

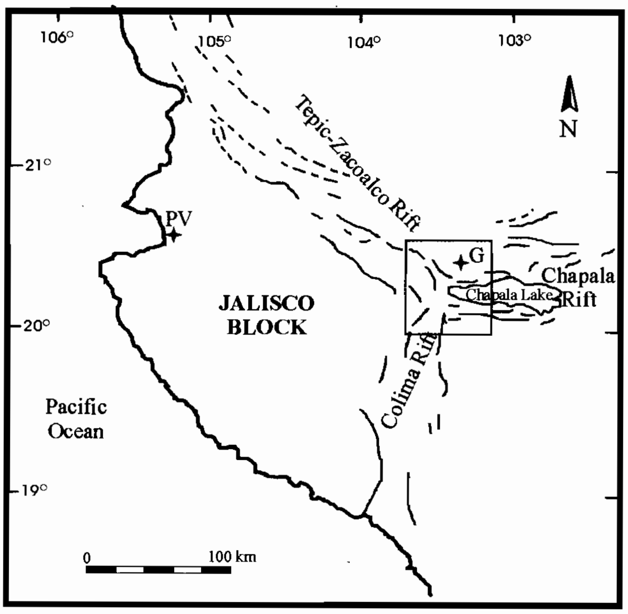

Figure 2. Map of western TVB and JB showing the three large structures. The stars show the localization of principal cities PV = Puerto Vallarta; G = Guadalajara. The open square is amplified in Fig. 3.

The paradox of the coexistence of two different magma sources in the TVB and JB has received the attention of several authors. In this work, we contribute to this topic and present new geochemical and isotopic data for a better understanding of this region.

ACATLAN VOLCANIC FIELD

The Tepic-Zacoalco rift (TZR) represents the northern boundary of JB. This is formed by several fault systems and was divided into two branches: the northern branch, which has two grabens developed at the boundary between JB and the North American plate, and the southern branch which consists of three half-grabens located inside the JB (Ferrari & Rosas-Elguera, 2000). The structures formed in the northern branch (average striking 125°) are the Ceboruco graben and Plan de Barrancas-Santa Rosa fault system. The structures in the southern branch with an average 125° trend are the

Amatlán de Cañas, Ameca and Zacoalco depressions, all parallel to the northern branch.

The Acatlán Volcanic Field (AVF) is located in the Zacoalco half-graben between two segments of faults (Fig. 3). The name was proposed by Rosas-Elguera et al. (1997) for a group of andesitic cones, lava flows, rhyolitic and dacitic domes developed along an accommodation zone. Rocks exposed in the AVF show a broad compositional variation in a small area and their ages range from 1.9 to 0.65 Ma.

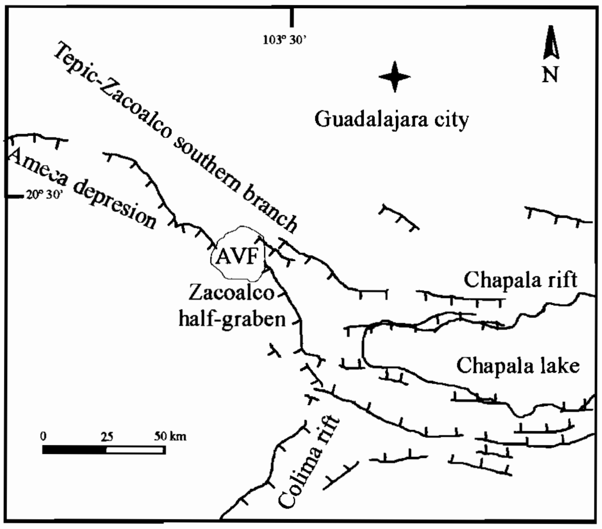

Figure 3. Location map for the Acatlan Volcanic Field (AVF) and structural setting (modified after Rosas-Elguera, et al., 1997).

The volcanic rocks from this area are mainly lavas but they also include cinder cones, domes, air-fall tuffs and pyroclastic flows. These rocks were erupted through fissures related to the main fault systems. The most well known unit is the Acatlan Ignimbrite, described by Wright & Walker (1981) as the type location for co-ignimbrite lag deposits. Black andesitic scoria and light pink to white rhyolitic pumice content in this unit shows evidence of mingling between a silicic and andesitic magma. This deposit was dated 0.66 ± 0.02 Ma (K-Ar method) by Rosas-Elguera et al., (1997). Normal faults striking 140° cut the Acatlan Ignimbrite.

Ten samples were chosen from the main units of the AVF for geochemical and radiogenic isotope analyses. Major and trace elements were analyzed by X-ray fluorescence spectrometry (XRF). Rare-earth elements (REE) were determined by Inductively Coupled Plasma-Mass Spectrometry (ICP-MS) and radiogenic isotopes were determined using a MAT 262 thermal ionization mass spectrometer (for Sr, Nd and Pb). The analyses were carried out at the Laboratorio Universitario de Geoquímica Isotópica (LUGIS), National University of Mexico (UNAM).

All samples were plotted on a total alkali vs. silica diagram (TAS; Le Maitre et al., 1989). The rock types cover a range from basaltic andesite, trachyandesite, trachydacite, dacite and rhyolite, (Fig. 4a) and display calc-alkaline affinity. In the AFM diagram, all samples plot within the calc-alkaline field (Fig. 4b).

Chondrite-normalized REE patterns are light REE enriched relative to heavy REE (Fig. 4c). Negative Eu anomalies are observed for rhyolitic and dacitic rocks but are absent in basaltic andesites and the black andesitic pumice of the Acatlan Ignimbrite, suggesting no interaction with plagioclase-bearing rocks from the continental crust. On the other hand, rhyolites show negative Ce anomaly in contrast to rhyolitic pumice and the younger rhyolites. Nevertheless enrichments of the large ion lithophile elements (LILE) with respect to the high field strength elements (HFSE), characteristic of magmas in convergent margins are observed. Such enrichments and depletions may be provided by metasomatizing fluids derived from the subducting slab. Moreover, the high light REE concentrations may be generated by the presence of olivine, but negative Ce anomaly and high REE concentrations may represent a complex crustal source.

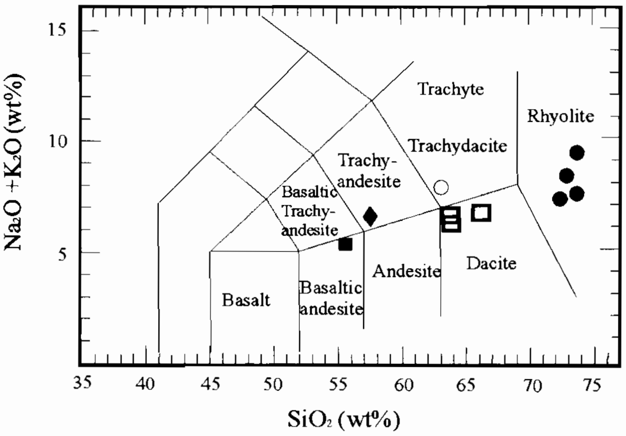

Figure 4a. Total alcalis versus silica for the rocks from AVF (after Le Maitre, et al., 1989).

● Rhyolite
☐ Dacite
■ Basaltic andesite
○ Trachydacite
◆ Trachyandesite

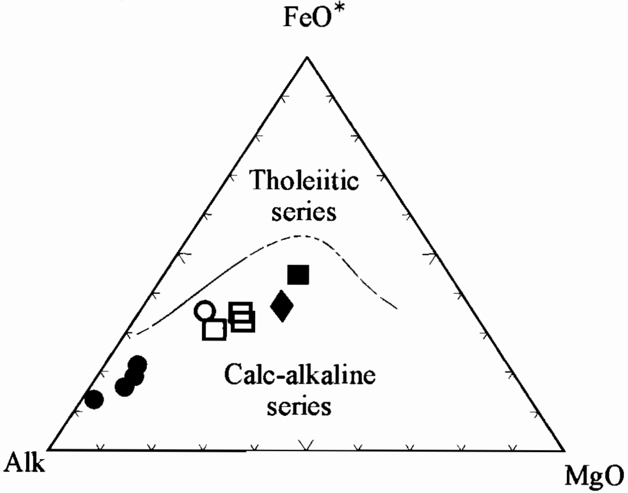

Figure 4b. AFM diagram for the rocks from the AVF (Irving and Baragar,1971).

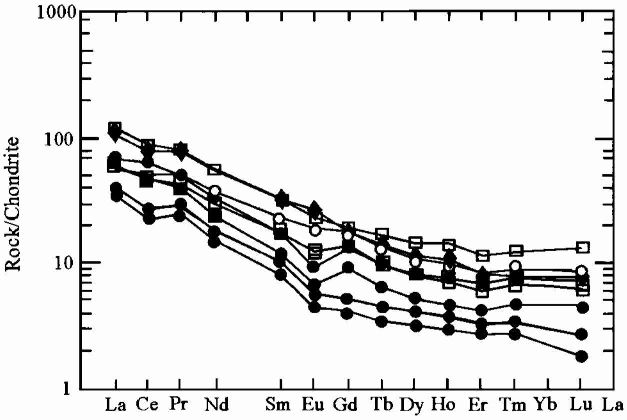

Figure 4c. REE concentrations from the AVF region normalized to condrite values of Nakamura (1974).

Isotopic ratios of the evolved AVF ranges as follows: $^{87}Sr/^{86}Sr$: 0.703612-0.704121, ε_{Nd}: + 2.3 to + 5.2, $^{206}Pb/^{204}Pb$: 18.61-18.75, $^{207}Pb/^{204}Pb$: 15.57-15.64, and $^{208}Pb/^{204}Pb$: 38.37-38.67. The isotopic ratio of the rhyolitic domes shows the highest $^{87}Sr/^{86}Sr$ while the lowest ratios are represented the oldest basaltic andesite flow. ε_{Nd} is the highest in the younger trachyandesite unit and lowest in a dacitic flow. All samples plot within the mantle array (Fig. 5). The $^{206}Pb/^{204}Pb$, $^{207}Pb/^{204}Pb$, and $^{208}Pb/^{204}Pb$ ratios are low in the trachyandesitic unit while high value is dacitic flow. Lead isotopes allow the identification of two reservoirs in the AVF: type-II enriched mantle and lower continental crust. The type-II enriched mantle (Zindler & Hart, 1986) is present in some dacites and rhyolitic rocks. However, the trachyandesites show influence of a lower continental crust reservoir.

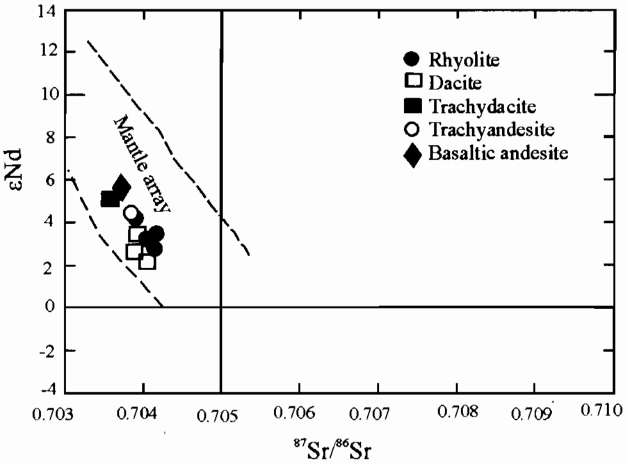

Figure 5. $^{87}Sr/^{86}Sr$ - εNd plot for the AVF rocks. Aproximate trace of Mantle-array is shown for easy reference using lines dashed.

On the basis of incompatible trace element concentrations and isotopic data, crustal assimilation and different sources of magmas for the AVF rocks are evidence. The rocks are related to subduction and magmas produced from partial melting have been influenced by upper crust continental rocks. Negative Eu anomalies and high $^{87}Sr/^{86}Sr$ ratios in rhyolitic rocks indicate assimilation and fractional crystallization of crustal rocks. In the case of younger rhyolitic unit there is no important crustal assimilation. On the other hand, data for basaltic andesite, trachyandesite, trachydacite and dacite suggest several magmatic sources. The high concentrations of incompatible trace elements in trachyandesite are unlikely the result of assimilation of crustal rocks because Eu anomalies are not present in the lava. Furthermore, isotopic signatures point to primitive sources.

The volcanic rocks from AVF are nearly contemporaneous but are not cogenetic. Their diversity is undoubtedly a consequence of the tectonic complexity in the region and of the mantle heterogeneity reflected in the variety of rock types. Extensional regime played an important role in this process. Until today, faults are affecting the area and cut Quaternary units.

REFERENCES

DeMets, C. and Stein, S., 1991, Present-day kinematics of the Rivera plate and implications for tectonics in Southwestern Mexico, Journal of Geophysical Research, v. 95, No. B13, p. 21,931-21,948.

Ferrari, L. and Rosas-Elguera, J., 2000, Late Miocene to Quaternary extension at the northern boundary of the Jalisco block, western Mexico: The Tepic-Zacoalco rift revised, in Delgado-Granados, H., Aguirre-Díaz, G. and Stock, J.M, eds., Cenozoic Tectonics and Volcanism of Mexico: Boulder, Colorado, Geological Society of America Special Paper 334, p. 41-63.

Ferrari, L., Nelson, S., Rosas-Elguera, J., Aguirre-Díaz, G. and Venegas-Salgado, S., 1997, Tectonics and volcanism of the western Mexican Volvanic Belt, in Aguirre-Díaz, G., Aranda-Gómez, J. J., Carrasco-Núñez, G. and Ferrari, L., eds., Magmatism and tectonics in the central and northwestern Mexico: a selection of the 1997 IAVCEI General Assembly excursions: Mexico, D.F., Universidad Nacional Autónoma de México, Instituto de Geología, Excursión 12, p. 85-129.

Irving, T. N. and Baragar, W. R. A., 1971, A guide to the chemical classification, Can. J. Earth Sci., v. 8, p. 523-548.

Le Maitre, R. W., Bateman, P., Dudek, A., Keller, J., Lameyre Le Bas, M. J., Sabine, P. A., Schmid, R., Sorensen, H., Streckeisen, A., Woolley, A. R. and Zanettin, B., 1989, A classification of igneous rocks and glossary of terms, Blackwell, Oxford.

Luhr, J. F., Nelson S. A., Allan, J. F., and Carmichael, I. S. E., 1985, Active rifting in southwestern Mexico: manifestations of an incipient eastward spreading-ridge jump, Geology, v. 13 p. 54-57.

Moore, G., Marone, C., Carmichael, I. S. E. and Renne, P., 1994, Basaltic volcanism and extension near the intersection of the Sierra Madre volcanic province and the Mexican Volcanic Belt, Geological Society of America Bulletin, v. 106, p. 383-394.

Nakamura, N., 1974, Determination of REE, Ba, Mg, Na and K in carbonaceous and ordinary chondrites, Geochimica et Cosmochimica Acta, v.38, p. 757-775.

Nelson, S. A. and Carmichael, I. S. E., 1984, Pleistocene to recent alkalic volcanism in the region of Sangangüey Volcano, Nayarit, Mexico: Contributions to Mineralogy and Petrology, v. 85, p. 321-335.

Nelson, S. A. and Livieres, R., 1986, Contemporaneous calc-alkaline and alkaline volcanism at Sanganguey Volcano, Nayarit, Mexico, Geological Society of America Bulletin, v. 97, p. 798-808.

Nixon, G. T., 1982, The relationship between Quaternary volcanism in central Mexico and the seismicity and structure of subducted ocean lithosphere, Geological Society of America Bulletin, v. 93, p. 514-523.

Quintero-Legorreta, O., Michaud, F., Bourgois, J. and Barrier, E., 1992, Evolución de la frontera septentrional del Bloque de Jalisco, México desde hace 17 Ma, Universidad Nacional Autónoma de México, Instituto de Geología, Revista, v. 10, p. 111-117.

Rosas-Elguera, J., Ferrari, L., Garduño-Monroy, V. H. and Urrutia-Fucugauchi, J., 1996, Continental boundaries of the Jalisco Block and their influence in the Pliocene-Quaternary kinematics of western Mexico, Geology, v. 24, p. 921-924.

Rosas-Elguera, J., Ferrari, L., López-Martínez, M. and Urrutia-Fucugauchi, J., 1997, Stratigraphy and tectonics of the Guadalajara region and triple-juntion area, Western, Mexico, International Geology Review, v. 39, p. 125-140.

Wallace, P., Carmichael, I. S. E., Righter, K. and Becker, T., 1992, Volcanism and tectonism in western Mexico: a contrast of style and substance, Geology, v. 20, p. 625-628.

Wright, V. J. and Walker, G. P. L., 1981, Eruption, transport and depositation of ingnimbrite: a case study from Mexico, Journal of Volcanology and Geothermal Research, no. 9, p. 111-131.

Zindler, A, and Hart, S.R., 1986, Chemical geodynamics, Ann. Review Earth Planetary Science, v. 14, p. 493-571.

LEAD ISOTOPES OF EARLY CRETACEOUS COASTAL DYKES OF PARANÁ MAGMATIC PROVINCE (FLORIANÓPOLIS SWARM): PRELIMINARY RESULTS

Marques, L.S.[1]; Babinski, M.[2] and Ruiz I.R.[2]

1. Instituto de Astronomia, Geofísica e Ciências Atmosféricas – Universidade de São Paulo, Rua do Matão, 1226, 05508-090, São Paulo-SP, Brasil. leila@iag.usp.br
2. Centro de Pesquisas Geocronológicas - Instituto de Geociências – Universidade de São Paulo, Rua do Lago, 562, 05508-080, São Paulo-SP, Brasil. babinski@usp.br

Keywords: Paraná Magmatic Province, dyke swarms, Florianópolis dykes, lithospheric mantle, lead isotopes

INTRODUCTION

The origin of large continental flood basalts is a intensively studied object in recent years, and there is not at all a consensus about the associated geodynamic process which caused the production of such large volumes of extrusive basic rocks. Specifically for the Paraná Magmatic Province (PMP), which preceded the opening of South Atlantic Ocean, there is presently an important debate about the causes of the magmatism, and consequently, about the involvement of asthenospheric and/or lithospheric mantle sources in the genesis of its rocks.

According to some interpretations (e.g. Gibson et al., 1995, 1999; Milner & Le Roex, 1996) the PMP basalt compositions reflect the participation of deep asthenosphere, since these models claim the igneous activity was triggered by the impact of Tristan da Cunha mantle plume beneath Western Gondwanaland. Conversely, an origin in heterogeneous lithospheric mantle is proposed (e.g. Peate and Hawkesworth, 1996; Piccirillo & Melfi, 1988; Comin-Chiaramonti et al., 1997; Marques et al., 1999), in order to explain the geochemical and isotope characteristics of low- and high-TiO_2 tholeiites, which also have different spatial distribution in the province. In this case, if the PMP magmatism was generated by the Tristan da Cunha plume, its participation was restricted to a heat source.

Very recently, Ernesto et al. (2002) ruled out the involvement of Tristan da Cunha mantle plume in the PMP tholeiitic genesis, proposing an alternative model compatible with geochemical, isotopic, paleomagnetic, and geoid anomaly data. According to those authors, the basaltic magmas were generated in the lithospheric mantle, due to small extension across an anomalously heated region, which remained over a thermal anomaly for about 50 Ma (from c.a. 180 to 130 Ma). This thermal anomaly is still present in the western African Plate, north of Walvis Ridge, and does not coincide with the Tristan da Cunha Island location.

Taking into account that the PMP dyke swarms (Ponta Grossa, Florianópolis and Santos-Rio de Janeiro) were emplaced after the main volcanic activity, they are crucial for obtaining information about the mantle sources involved in the late stages of the magmatism. Considering that Pb isotopes are essential for this kind of investigation, the aim of this study is to present preliminary lead isotopic data obtained on coastal dykes of Florianópolis Swarm to better constrain the mantle sources that participated in the magma generation. Additionally, an analytical procedure to measure Pb isotopic ratios of low concentration silicate rocks is presented, since they are very sensitive to contamination during sample preparation and/or lead chemical separation.

GEOLOGICAL OUTLINES

The Paraná Magmatic Province is mainly composed of continental flood tholeiites, and subordinate intrusive magmatism represented by sills and three dyke swarms (Ponta Grossa, Florianópolis, and Santos-Rio de Janeiro).

The volcanic and intrusive rocks are characterized by predominant tholeiitic basalts, which are divided in two groups: (1) LTi basalts, low in TiO_2 (< 2 wt %) and incompatible elements (e.g. P, Sr, Ba, Zr, Ta, Y and LREE) and (2) HTi basalts, high in TiO_2 (> 2 wt %) and incompatible elements. The HTi tholeiites dominate the northern PMP (north of latitude ~26°S), whereas the LTi ones prevail in the southern PMP (south of latitude ~26°S). Minor HTi and LTi rocks are also found in the southern and northern PMP, respectively.

Geochemical and isotopic data indicated significant differences between LTi tholeiites from southern and northern PMP, as well as between HTi basalts from those regions of PMP (Bellieni et al., 1984; Piccirillo & Melfi, 1988, Marques et al., 1989). The incompatible trace element distribution patterns normalized to primordial mantle, for tholeiites with initial $^{87}Sr/^{86}Sr$ lower than 0.7060, show that all southern and northern tholeiites have significant Ta negative anomalies, which are considered mantle source features.

The Florianópolis Dyke Swarm is located in Santa Catarina Island, comprising also the adjacent continental area. The dykes have thicknesses from 0.1 to 70 m, and are mainly cost-parallel (NE-SW trending), although a NW-SE trend is also found. Their $^{40}Ar/^{39}Ar$ radiometric ages vary from 129 to 119 Ma, and are concentrated in relatively narrow ranges of 129 - 126 Ma and 122 - 119 Ma (Raposo et al. 1998; Deckart et al. 1998). The paleomagnetic results also indicate that most Florianópolis dykes belong to the youngest magmatic episode.

Similarly to the Ponta Grossa and Santos - Rio de Janeiro Swarms, most of the Florianópolis dykes are of HTi-type (Comin-Chiaramonti et al. 1983; Piccirillo et al. 1990; Hawkesworth et al. 1992; Marques et al., 1993, Marques, 2001), corresponding to about 90% of the exposed basic rocks.

ANALYTICAL PROCEDURES

Eleven samples of Florianópolis dykes previously analyzed for major, minor and some trace elements (Cr, Ni, Rb, Ba, Sr, Y, Zr and Nb) by X-ray florescence, at University of Trieste (Italy), were selected (Marques et al., 1993; Marques, 2001 and unpublished data). Concentrations of rare earth and other incompatible trace elements (Ta, Th, U, and Hf) determined by instrumental neutron activation analysis are also available for those samples. The latter analyses were carried out at the Instituto de Pesquisas Energéticas e Nucleares (CNEN/SP, Brazil). Precision and accuracy are better than 3% for major and minor elements, and better than 10% for trace elements (Bellieni et al., 1983; Figueiredo & Marques, 1989; Marques, 2001).

Lead isotopic compositions were determined in the selected samples at the Centro de Pesquisas Geocronológicas of São Paulo University (Brazil). The sample preparation procedure employed was similar to that reported by Marques et al. (1999). The external surface of each sample was entirely removed, with especial care to eliminate sawed sections, which may provoke lead contamination in high levels. All the samples were hand broken in small fragments (diameters less than 0,5 cm), using a stainless steel mortar and pestle, then washed in distilled water, for several times until the washing solution is clean. Finally the sample is ultrasonically washed in ultrapure 0.25N HNO_3, for at least 3 times, and dried under ultraclean conditions. After that, rock fragments were powdered in a mechanical tungsten carbide crusher. In order to verify if the adopted sample preparation procedure introduces lead contamination, two basaltic rocks from the PMP, previously analyzed for Pb isotopes (418 and 980; Marques et al., 1999) were also chemically processed.

Complete sample dissolution was done using ultrapure HF, HNO_3, and HCl. The Pb separation was performed by ion-exchange chromatography method, using anionic resin and 0.6M HBr-HCl media. Lead was purified by repeating the elution in the ion-exchange chromatography column (Babinski et al., 1999). Several tests indicated that the lead purification process is necessary for obtaining reproducible results. After separation, lead was loaded on zone-refined rhenium filaments with phosphoric acid and silica gel.

The Pb isotopic ratios were measured on a VG354 mass spectrometer. The whole procedure analytical blanks were lower than 100 pg, which are negligible in comparison to the reported lead concentrations of PMP tholeiites. Replicate analyses of the SRM981 NBS standard was used for mass discrimination correction.

LEAD ISOTOPIC DETERMINATIONS IN REFERENCE GEOLOGICAL MATERIALS AND SOME PMP BASALTS

The described chemical procedure for lead isotopic analysis was applied to two USGS reference materials. The results for Pb isotopic ratios and the respective errors (2σ absolute standard deviations) of replicate analysis of the BCR-1 (4 aliquots) and AGV-1 (3 aliquots) geological standards were $^{206}Pb/^{204}Pb = 18.766 \pm 0.014$; $^{207}Pb/^{204}Pb = 15.636 \pm 0.011$; $^{208}Pb/^{204}Pb = 38.687 \pm 0.027$, and $^{206}Pb/^{204}Pb = 18.938 \pm 0.011$; $^{207}Pb/^{204}Pb = 15.651 \pm 0.011$; $^{208}Pb/^{204}Pb = 38.548 \pm 0.048$, respectively. Taking into account associated errors, the obtained results are in agreement to those reported in the literature (e.g. Woodhead and Hergt, 2000), showing the high accuracy and precision of the adopted methodology.

The sample preparation procedure, which is a very delicate step of lead analysis due to the possibility of contamination, is also appropriate. The determined lead isotopic compositions (Table 1) for the two analyzed basalts of PMP agree with those published (the absolute errors correspond to 2σ), since the relative deviations are lower than 0.2%.

Table 1. Lead isotopic compositions determined for PMP basalts in the present study (a) and published data (b).

Sample	$^{206}Pb/^{204}Pb$	$^{207}Pb/^{204}Pb$	$^{208}Pb/^{204}Pb$
418$^{(a)}$	18.430±0.008	15.624±0.007	38.585±0.016
418$^{(b)}$	18.387±0.006	15.609±0.007	38.520±0.024
980$^{(a)}$	17.922±0.004	15.534±0.004	38.432±0.013
980$^{(b)}$	17.918±0.006	15.547±0.007	38.437±0.024

LEAD ISOTOPES OF FLORIANÓPOLIS DYKES

The Florianópolis dykes which were selected for Pb isotopic determinations are of HTi-type ($TiO_2 > 3\%$) and according to De La Roche et al. (1980) they correspond to tholeiitic andesi-basalts (7 samples), lati-basalts (2 sample), and lati-andesites (1 sample). In addition, one LTi-type dyke was analyzed, which is a tholeiitic andesite ($SiO_2 = 55\%$). All investigated dykes have NE orientation, which is the dominant trend, corresponding to about 80% of the outcrops.

The tholeiitic andesite dyke has Pb isotopic compositions very similar to the LTi volcanics from southern PMP affected by low pressure crustal contamination ($^{87}Sr/^{86}Sr_i > 0.7060$).

On the other hand, the Pb isotopic ratios of HTi dykes show large variations ($^{206}Pb/^{204}Pb$: 17.747 - 19.441; $^{207}Pb/^{204}Pb$: 15.501 - 15.720; $^{208}Pb/^{204}Pb$: 38.222 - 39.482) and there is no systematic difference between the rocks that belong to the tholeiitic series (andesi-basalts and lati-andesite) and those of transitional nature (lati-basalts). The least radiogenic compositions ($^{206}Pb/^{204}Pb < 17.9$) are very similar to those of the HTi basalts from PMP, whereas the higher lead isotopic ratios, in general, coincides with those of the LTi from southern PMP. In addition, two andesi-basalts and a lati-basalt present very radiogenic lead ratios, mainly of $^{206}Pb/^{204}Pb$ (> 19.0), which are even higher than those of the LTi tholeiites from southern PMP, with $(^{87}Sr/^{86}Sr)_i > 0.7060$.

DISCUSSION

The data discussed here show that the LTi dyke of Florianópolis Swarm was affected by low pressure crustal contamination, since it has lead isotopic compositions and highly incompatible trace element ratios (e.g. La/Th, Th/Ta, Th/U) very similar to those of the LTi basalts from southern PMP, with $(^{87}Sr/^{86}Sr)_i > 0.7060$.

The Pb non-radiogenic compositions of the Florianópolis HTi dykes reinforce the interpretation that they are genetically related to the HTi basalts from southern PMP, as pointed out in previous geochemical studies (Marques, 2001).

The lead isotopic ratios of six HTi dykes of Florianópolis Swarm are comparable to or higher than those of the LTi basalts of southern PMP, with $(^{87}Sr/^{86}Sr)_i > 0.7060$. Although the lead isotopes may suggest a low pressure crustal contamination process, this interpretation is not compatible with the behavior of major (SiO_2), minor (K_2O) and trace elements (e.g. La, Th, Ta), as well as the incompatible trace element ratios (e.g. La/Th, La/Yb, Th/Ta) of those dykes. Alternatively, the very radiogenic lead isotopic compositions might be due to the involvement of a HIMU component in their genesis. However, additional isotopic data and further investigation is necessary to confirm this hypothesis.

The Pb isotopes and the geochemical data also rule out a significant participation of MORB and/or OIB (Tristan da Cunha) mantle components in the genesis of the dykes of Florianópolis Swarm. Therefore, the results contradict the classic plume model for the origin of PMP, which asserts that the basaltic compositions reflect the Tristan da Cunha plume component (e.g. Gibson et al., 1995, 1999). Moreover, considering that the Florianópolis Swarm represents the youngest magmatic episode of PMP, the data do not support some models of continental flood basalt generation (e.g. White & Mckenzie; 1989; Peate & Hawkesworth, 1996), which predicts a significant contribution of depleted mantle components (MORB-type) in the late stages of the magmatic activity.

ACKNOWLEDGEMENTS

Thanks are due to the Supervisão de Radioquímica do IPEN-CNEN/SP for the use of its facilities. This work was partially funded by FAPESP, PRONEX and PADCT-FINEP.

REFERENCES

Babinski, M.; Van Schmus, W.R.; Chemale Jr., F., 1999. Pb-Pb dating and Pb isotope geochemistry of Neoproterozoic carbonate rocks from the São Francisco basin, Brazil: implications for the mobility of Pb isotopes during tectonism and metamorfism. Chemical Geol., 160: 175-199.

Bellieni, G.; Brotzu, P.; Comin-Chiaramonti, P.; Ernesto, M.; Melfi, A. J.; Pacca, I.G.; Piccirillo, E.M.; Stolfa, D., 1983. Petrological and paleomagnetic data on the plateau basalts to rhyolite sequences of the Southern Paraná Basin (Brazil). Anais da Academia Brasileira de Ciências, 55: 355-383.

Bellieni, G.; Comin-Chiaramonti, P.; Marques, L.S.; Melfi, A. J.; Nardy, A. J. R.; Piccirillo, E. M.; Stolfa, D., 1984. High- and low-TiO2 flood basalts from the Paraná plateau (Brazil): petrology and geochemical aspects bearing on their mantle origin. Neues Jahrb. Mineral. Abh., 150: 273-306.

Comin-Chiaramonti, P.; Gomes, C.B.; Piccirillo, E.M.; Rivalenti, G., 1983. High TiO_2 dikes in the coastline of São Paulo and Rio de Janeiro States. Neues Jahrb. Mineral. Abh., 146: 133-150.

Comin-Chiaramonti, P.; Cundari, A.; Piccirillo, E.M.; Gomes, C.B.; Castorina, F.; Censi, P.; De Min, A.; Marzoli, A.; Speziale, S.; Velázquez, V.F., 1997. Potassic and sodic igneous rocks from Eastern Paraguay: their origin from the lithospheric mantle and genetic relationships with associated Paraná flood tholeiites. Journal of Petrology, 38(4): 495-528.

Deckart, K.; Féraud, G.; Marques, L.S.; Bertrand, H., 1998. New time constraints on dyke swarms related to the Paraná-Etendeka magmatic province, and subsequent South Atlantic opening, southeastern Brazil. Journal of Volcanology and Geothermal Research, 80: 67-83.

De La Roche, H.; Leterrier, P.; Grandclaude, P.; Marchal, M., 1980. A classification of volcanic and plutonic rocks using R1-R2 diagram and major-element analyses. Its relationships with current nomenclature. Chemical Geology, 29:183-210.

Figueiredo, A.M.G and Marques, L.S., 1989. Determination of rare earths and other trace elements in the Brazilian geological standards BB-1 and GB-1 by neutron activation analysis. Geochimica Brasiliensis, 3: 1-8.

Ernesto, M; Marques, L.S.; Piccirillo, E.M., Molina, E.C.; Ussami, N; Comin-Chiaramonti, P.; Bellieni, G., 2002. Paraná Magmatic Province - Tristan da Cunha plume system: fixed versus mobile plume, petrogenetic considerations and alternative heat sources. Journal of Volcanology and Geothermal Research, 118:15-36.

Gibson, S.A.; Thompson, R.N.; Dickin, A. P.; Leonardos, O. H., 1995. High-Ti and low-Ti mafic potassic magmas: key to plume-lithosphere interactions and continental flood-basalt genesis. Earth and Planetary Science Letters, 136: 149-165.

Gibson, S.A.; Thompson, R.N.; Leonardos, O.H.; Dickin, A.P.; Mitchell, J.G., 1999. The limited extent of plume-lithosphere interactions during continental flood-basalt genesis: geochemical evidence from Cretaceous magmatism in southern Brazil. Contributions to Mineralogy and Petrology, 137: 147-169.

Hawkesworth, C.J.; Gallager, K.; Kelley, S.; Mantovani, M.S.M.; Peate, D.; Regelous, M.; Rogers, N., 1992. Paraná magmatism and the opening of the South Atlantic. In: Storey, B., Alabaster, A., Pankhurst, R. (Eds.), Magmatism and the Causes of Continental Break-up. Geological Society Special Publication 68: 221-240, London.

Marques, L.S., 2001. Geoquímica dos diques toleíticos da costa sul-sudeste do Brasil: contribuição ao conhecimento da Província Magmática do Paraná. Tese de Livre Docência, IAG/USP, 86 p

Marques, L.S.; Piccirillo, E.M.; Melfi, A.J.; Comin-Chiaramonti, P.; Bellieni, G., 1989. Distribuição de terras raras e outros elementos traços em basaltos da Bacia do Paraná (Brasil Meridional). Geochimica Brasil., 3: 33-50.

Marques, L.S.; Bellieni, G.; De Min, A. and Piccirillo, E.M. , 1993. O enxame de diques da Ilha de Santa Catarina: resultados geoquímicos preliminares. IV Congresso Brasileiro de Geoquímica, Resumos: 3-4.

Marques, L.S.; Dupré, B.; Piccirillo, E.M., 1999. Mantle source compositions of the Paraná Magmatic Province: evidence from trace element and Sr - Nd - Pb isotope geochemistry. Journal of Geodynamics, 28: 439-459.

Milner, S. and Le Roex, A.P., 1996. Isotope characteristics of the Okenyenya igneous complex, northern Namibia: constraints on the composition of the early Tristan Plume and the origin of the EM1 mantle component. Earth and Planetary Science Letters, 141:277-291.

Peate, D.W. and Hawkesworth, C.J., 1996. Lithospheric to asthenospheric transition in low–Ti flood basalts from southern Paraná, Brazil. Chemical Geology, 127:1-24.

Piccirillo, E.M. and Melfi, A.J., 1988. The mesozoic flood volcanism of the Paraná Basin: petrogenetic and geophysical aspects. Instituto Astronômico e Geofísico - University of São Paulo, 600p., São Paulo.

Piccirillo, E.M.; Bellieni, G.; Cavazzini, G.; Comin-Chiaramonti, P.; Petrini, R.; Melfi, A.J.; Pinese, J.P.P.; Zantadeschi, P.; De Min, A., 1990. Lower cretaceous tholeiitic dyke swarms from the Ponta Grossa Arch (southeast Brazil): Petrology, Sr-Nd isotopes and genetic relatioships with the Paraná flood volcanics. Chemical Geology, 89: 19-48.

Raposo, M.I.B.; Ernesto, M.; Renne, P.R., 1998. Paleomagnetism and ^{40}Ar/^{39}Ar dating of the early Cretaceous Florianópolis dike swarm (Santa Catarina Island), Southern Brazil. Physics of the Earth and Planetary Interiors, 108: 275-290.

White, R. and MacKenzie, D.J., 1989. Magmatism at rift zones: the generation of volcanic continental margins and flood basalts. Journal of Geophysical Research, 94 (B6): 7685-7729.

Woodhead, J.D. and Hergt, J.M., 2000. Pb-isotope analyses of USGS reference materials. Geostandards Newsletters, 24 (1): 33-38.

U-Pb AND Rb-Sr DATING AND ISOTOPIC SIGNATURE OF THE CHARNOCKITIC ROCKS FROM VÁRZEA ALEGRE INTRUSIVE COMPLEX, ESPÍRITO SANTO, BRAZIL

Medeiros, S.R.[1]; Mendes, J.C.[2]; McReath, I.[3] and Wiedemann, C.M.[2]

1. IG/Universidade de Brasília. silviar@unb.br
2. Depto. de Geologia, IGEO/UFRJ. julio@geologia.ufrj.br, wiedeman@geologia.ufrj.br
3. IGEO/Universidade de São Paulo-SP. ianmcr@usp.br

Keywords: Charnockitic magmas, geochronology, isotope geology

INTRODUCTION

Hydrous and anhydrous magmatic rock associations have been studied by many authors around the world (e.g. Petersen, 1980; Hubbard & Whittley, 1979; Kaiyi et al., 1985; Janasi, 1992; Jordt-Evangelista, 1996). Many intrusive bodies containing charnockites, closely associated with rocks presenting an hydrous primary paragenesis occur in the central portion of the Espírito Santo State, SE Brazil (Pedrosa Soares & Wiedemann-Leonardos, 2000). A typical example is the Várzea Alegre Intrusive Complex (VAIC), related to the late- to post-tectonic Brasiliano magmatism in this region. The pluton has an almost circular shape with a gabbroic center surrounded by diorites and granite. An irregular charnockitic ring involves the inner structure. This paper highlights unpublished geochronological Rb-Sr and Sm-Nd isotopic data of the VAIC charnockitic rocks.

GEOLOGICAL SETTING

The Espírito Santo State is located in the northern portion of the Ribeira Belt, which is the continuation of the Neoproterozoic Araçuaí orogen (Pedrosa Soares & Wiedemann-Leonardos, 2000). In a late orogenic stage of the Brasiliano Cycle (535 - 490 Ma.), several complexly zoned plutons cut the enclosing high-grade gneisses, highlighting the post-collisional magmatism of this region (Wiedemann et al., 2002). According to Pedrosa Soares & Wiedemann-Leonardos (2000), the VAIC is included in the G5 suite, which is characterized by several diapirs with compositions varying from opx-gabbro to granite and corresponds to the latest magmatic event of the orogen. This suite comprises mataluminous, high-K calc-alkaline, I-type granitoids originated in the lowermost continental crust with important mantle contributions. The VAIC outcropps area of 150 km^2 and had geology, petrography and geochemistry studied (Mendes et al., 1997, 2001).

THE GEOLOGY OF THE VAIC

The Várzea Alegre pluton has an inversely zoned structure, with gabbros at the eroded center of the intrusion surrounded by diorites/quartz-diorites-monzodiorites and megaporphyritic granites. All these rocks are involved by a large ring of charnockitic rocks: opdalites, jotunites, opx-quartz diorites and quartz mangerites (Medeiros et al., 2000). The contact between the megaporphyritic granite and the gabbros/diorites is a mixed zone where contrasting lithotypes interfinger with each other. The charnockitic rocks have dark green color and megaporphyritic texture. Along the contacts with the enclosing rocks its foliation is well marked. Away from this region the rock becomes almost isotropic. When observed, the contacts with the enclosing rocks are sharp and parallel to the foliation. The border foliation and the schistosity of the gneisses are generally dipping toward the pluton. The contacts between the charnockitic outer ring and the magmatites of the inner domain are mainly interfingered, giving rise to locally intense mechanical mixing.

PETROGRAPHY AND GEOCHEMISTRY OF THE CHARNOCKITIC ROCKS

The charnockitic rocks consist essentially of plagioclase (An_{32-40}), perthitic ortoclase/mesoperthite, orthopyroxene, biotite, amphibole, ilmenite, magnetite, pyrite, apatite, zircon, rare allanite and hematite. Megacrysts of alkali feldspar and plagioclase, up to 6 cm, define a porphyritic texture. The matrix is medium to coarse grained and it may be finer-grained when compressed against and partially recrystallized around the megacrysts. Features of weak ductile deformation are observed in quartz and feldspar grains, as well as curved biotite and twining lamella of plagioclase. Opx may be partially replaced by biotite, amphibole and opaque minerals and is altered to chlorite and a brown secondary phase. Alkali felsdspar replaces plagioclase and the concentration of the perthitic lamella is very variable. Apatite and zircon appear as inclusions, single cristals or associated with mafic minerals.

The chemical composition of these rocks indicates SiO_2 values ranging from 54% to 65%. They are enriched in Ti, P, Zr, Ba and REE, relatively rich in K and Fe and they have low Mg, Al and V contents, when compared to granitoid rocks of similar silica contents (Mendes et al., 1997). A marked compatible behaviour is observed for Ca, Fe, Mg, Ti, P, Sr and V, in contrast to the incompatible behaviour of K, Na, Rb and Ba (Mendes et al., 1997); very high Al, Ca, Sr, K and Ba concentrations in some samples have been pointed by the authors as indicative of possible feldspar accumulation.

Table 1. Rb-Sr isotopic analytical results for the VAIC charnockitic rocks.

Sample	Rb (ppm)	Sr (ppm)	(^{87}Sr/^{86}Sr)$_0$	^{87}Rb/^{86}Sr	(^{87}Sr/^{86}Sr)i	ε (0)	ε (0.5 Ga)
VA-04	55.25	610.87	0.71074	0.2618	0.708875	88.57346	70.51839
VA-257	59.79	665.12	0.71074	0.2602	0.708886	88.57346	70.68035
VA-249B	54.20	675.20	0.71026	0.2324	0.708604	81.76011	66.67533
VA-249C	75.61	674.14	0.71198	0.3262	0.709656	106.1746	81.61543
VA-90	64.00	579.00	0.71080	0.3199	0.708521	89.42512	65.48923
VA-125	91.00	518.00	0.71223	0.5085	0.708607	109.7232	66.71384
VA-261	36.00	677.00	0.70963	0.1539	0.708534	72.81760	65.67343
VV-1751	82.70	591.90	0.71160	0.4000	0.708750	100.7807	68.74669
VV-1752	41.90	514.30	0.70980	0.2400	0.708090	75.23066	59.37111
VV-1756	54.90	545.40	0.71060	0.2900	0.708534	86.58623	65.67498
VV-1759	47.60	552.60	0.70960	0.2500	0.707819	72.39177	55.51760

Table 2. Sm-Nd isotopic results for the VAIC charnockitic rocks.

Samples	(^{143}Nd/^{144}Nd)i	(^{143}Nd/^{144}Nd)$_0$	^{147}Sm/^{144}Nd	T$_{DM}$ (Ga)	ε (0)	ε (0.5 Ga)
VA-90	0.511565	0.511922	0.1091	1.631	-13.967	-8.3805
VA-125	0.511539	0.511897	0.1094	1.672	-14.454	-8.8880
VA-261	0.511477	0.511839	0.1106	1.778	-15.586	-10.098
VA-257	0.511533	0.511889	0.1088	1.675	-14.611	-9.0059
VA-249	0.511621	0.511971	0.1068	1.527	-13.011	-7.2764
VA-04	0.511628	0.511955	0.0997	1.455	-13.323	-7.1347

Therefore, the charnockitic rocks from Várzea Alegre show metaluminous and high-K calc-alkalic character, with conspicous enrichment in LIL and HFS elements. These features indicate a mantle contribution associated to crustal melts in the genesis of the rocks. The geochemical behaviour suggests fractional crystallization and magma mixing as the main differentiation process during the evolution of the charnockitic suite (Mendes et al., 1997).

GEOCHRONOLOGICAL AND ISOTOPIC DATA

The Rb-Sr and Sm-Nd whole-rock isotopic data of the VAIC charnockitic rocks are presented in the tables 1 and 2. The analysis were carried out at the Laboratory of Geochronology of the University of São Paulo. Using the isotope dilution tecnique, single zircon U-Pb determinations for the charnockitic ring were obtained at the Laboratory of Geochronology of the University of Brasília.

The geochronological U-Pb in zircon method provided a concordia age of 498.6 ± 4.9 Ma for four zircon grains of the VAIC charnockitic rocks. This age interval agrees with the obtained result for the charnockites from the Aimorés Intrusive Massif , ca. 50 km west of Várzea Alegre (Melo, 2000).

The Rb-Sr data show high ^{87}Sr/^{86}Sr initial ratios and $\varepsilon_{Sr(0)}$ for the charnockitic lithotypes. Despite the observed variations in the total Sr contents, the similar calculated initial ratios values for the analyzed samples points to an homogeneous isotopic distribution during the evolution of the sequence. Such high ^{87}Sr/^{86}Sr initial ratios were preliminarly interpreted by Mendes et al. (1997) as a response to crustal contamination.

Such as verified to the Rb-Sr isotopes, the six samples ivestigated for Sm-Nd isotopes indicate a very similar ^{143}Nd/^{144}Nd ratios, as well as $\varepsilon_{Nd(0)}$. The low $\varepsilon_{Nd(0)}$ values, around -14.00, are in accordance with the high ^{87}Sr/^{86}Sr initial ratios. The T$_{DM}$ model ages for the VAIC charnockitic rocks range from 1.5 to 1.77 Ga. The average T_{CHUR} for these rocks is ca. 1.1 Ga. Medeiros et al. (2000) have considered such age interval as the most appopriate for the extraction of the parental magma from the mantle. As pointed by Mendes et al. (1997), the geochemical signature of the VAIC charnockitic rocks indicates participation of crustal and enriched mantle magmas for the generation of the rocks here studied. Having in mind such hypothesis, the T_{CHUR} age could be more realistic. Considering the crystallization age of ca. 500 Ma, a long lived crustal residence may be infered for the parental magma.

Plotting the analyzed samples in the 1/Sr x $^{87}Sr/^{86}Sr$ (0.5 Ga) diagram (Fig. 1), two groups can be separated. One of these could be related to samples evolved essentially by fractional crystallization, and the other may reflect mixing between a more radiogenic component with a less radiogenic one. The behaviour of the samples in the ε_{Nd}(0.5 Ga) x $^{87}Sr/^{86}Sr$ (0.5) diagram (Fig. 2) confirms this premise. An isochronic Rb-Sr age of 500 ± 12 Ma (Ri=0.70855) is indicated with selected samples from the mentioned diagrams.

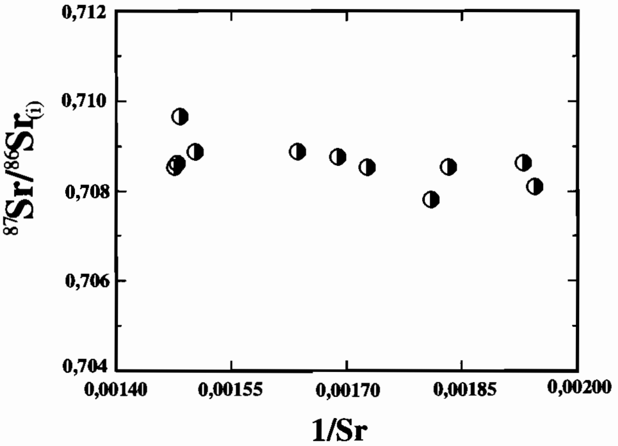

Figure 1. 1/Sr *versus* $^{87}Sr/^{86}Sr$ (0.5 Ga) diagram for the VAIC charnockitic rocks.

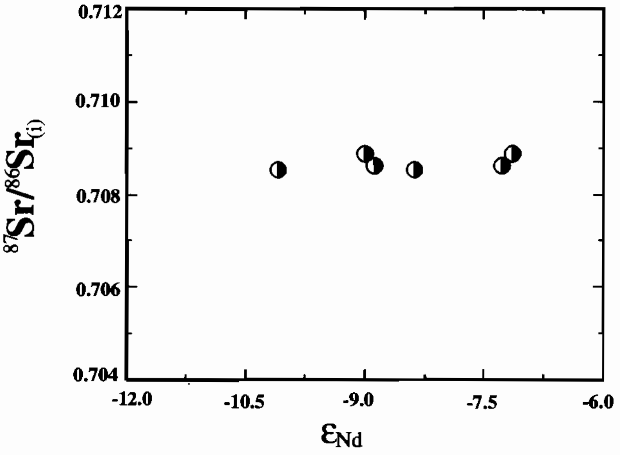

Figure 2. ε_{Nd} (0.5 Ga) *versus* $^{87}Sr/^{86}Sr$ (0.5 Ga) diagram for the VAIC charnockitic rocks.

DISCUSSION AND CONCLUSIONS

Mello (2000) found a lower concordia intercept age of 498.6 ±3 5.6Ma by conventional multigrain U-Pb zircon analysis, and U-Th-Pb ages in monazite between 562 and 468Ma for the Aimorés (MG) charnockite intrusion. High $(^{87}Sr/^{86}Sr)_i$ values at 500Ma associated with variable negative ε_{Nd} values attest either to an enriched mantle source or to a strong crustal influence on the petrogenesis of this intrusion.

The VAIC charnockitic rocks radiometric ages, U-Pb in zircons and whole rock Rb-Sr, of 498± 4.9 Ma and 500± 12 Ma respectivelly, can be surely considered as the crystallization age. This age is related to the post-tectonic magmatic activity in the central-north Ribeira Belt (Wiedemann et al., 2002). Mendes et al. (1997) pointed out the absence of solid state deformation in the VAIC charnockitic rocks. The young age obtained also corroborates this idea.

A whole rock Rb-Sr isochron age of 508 ± 12 Ma (Ri=0.7084) was obtained for the VAIC megaporphyritic granite (Medeiros et al., 2000). Therefore, the hypothesis of an early emplacement of the charnockitic outer shell (cf. Medeiros et al., 2000) is not accepted due to the age concordance between the lithotypes. This evidence indicates a possible simultaneous emplacement of the different magmas.

Possible combination of fractional crystallization and magma mixing process for the generation of the VAIC charnockitic rocks was suggested by Mendes et al. (1977). The Rb-Sr and Sm-Nd isotope interpretation described above agrees with this assumption.

Based on high $^{87}Sr/^{86}Sr$ initial ratios and incompatible elements anomalies detected in Brasiliano basic rocks, a sublithospheric enriched mantle has been proposed for this region (Ludka, 1998; Gimenez Filho et al., 2000). In spite of high $^{87}Sr/^{86}Sr$ initial ratios or $\varepsilon_{Sr(0)}$ and low $\varepsilon_{Nd(0)}$ values point to an exclusively crustal origin, the VAIC charnockitic rocks have conspicous enrichment in LIL and HFS elements which could indicate that the same enriched mantle contributed to the petrogenesis by interations with crustal melts (Mendes et al., 1999).

ACKNOWLEDGEMENTS

Part of the anaytical work was supported by FAPESP contracts 92/3467-9 and 95/4652-2, and PRONEX contract 41.96.0899.00. The authors thank the CNPq for Scholarships and Fellowships.

REFERENCES

Gimenez Filho, A.; Janasi, V.; Campanha, G.A.C.; Teixeira, W.; Júnior, L.E.T., 2000. U-Pb dating and Rb-Sr isotope geochemistry of the eastern portion of the Tês Córregos batholith, Ribeira fold belt, São Paulo. Rev. Bras. Geoc., 30(1): 45-50.

Hubbard, F.H. & Whitley, J.E., 1979. REE in charnockite and associated rocks, southwest Sweden. Lithos, 12: 1-11.

Janasi, V.A., 1992. Rochas sieníticas e mangerítico-charnoquíticas neoproterozóicas da região entre Caldas e Campestre (MG): aspectos petrológicos. Inst. of Geosciences, São Paulo University, Doctoral Dissert., 298p.

Jordt-Evangelista, H., 1996. Igneous charnockites in the southeastern transition zone between the São Francisco craton and the Costeiro mobile belt, Brazil. Rev. Bras. Geociências, 26 (2): 93-102.

Kaiyi, W.; Yuehua, Y.; Ruiying, Y. & Yifei, C., 1985. REE geochemistry of early precambrian charnockites and tonalitic-granodioritic gneisses of the Qianan region, eastern Hebei, north China. Precambrian Research, 27: 63-84.

Ludka, I. P.; Wiedemann, C. M. & Töpfner, C., 1998. On the origin of incompatible element enrichment in the Venda Nova pluton, Espírito Santo. Journal of South American Earth Sciences,11, 473-486.

Medeiros, S.R.; Wiedemann-Leonardos, C. & Mendes, J.C., 2000. Post-collisional multistage magmatism in the Ribeira Mobile Belt: geochemical and isotopic study of the Varzea Alegre Intrusive Complex, Espírito Santo, Brazil. Rev. Bras. Geoc., 30 (1): 30-34.

Medeiros, S.R.; Wiedemann, C. & Vriend, S., 2001. Evidence of mingling between contrasting magmas in a deep plutonic environment: the example of Várzea Alegre, in the Pan-Africa/Brasiliano Mobile Belt in Brazil. An. Acad. Bras. Ci., 73: 99-119.

Mello, F.M. 2000. Litogeoquímica e química mineral do Maciço Charnokítico Aimorés, MG. Unpublished Doctorate Thesis, Instituto de Geociências, Universidade de São Paulo, Brazil. 217 pp.

Mendes, J.C.; Mcreath, I.; Wiedemann, C.M. & Figueiredo, M.C.H., 1997. Charnoquitóides do Maciço de Várzea Alegre: um novo exemplo do magmatismo cálcio-alcalino de alto K no arco magmático do Espírito Santo. Rev. Bras. Geociências, 27 (1):13-24.

Mendes, J.C.; Wiedemann, C.M. & Mcreath, I., 1999. Conditions of formation of charnockitic magmatic rocks from the Várzea Alegre massif, State of Espírito Santo, southeastern Brazil. Rev. Bras. Geociências, 29 (1): 47-54.

Pedrosa Soares, A.C. & Wiedemann-Leonardos, C., 2000. Evolution of the Araçuaí Belt and its connection to the Ribeira Belt, eastern Brazil. In: Cordani, U. (ed.), Tectonic Evolution of South America. 31st IGC, pp. 265-285.

Petersen, J.S., 1980. Rare-earth element fractionation and petrogenetic modelling in charnockitic rocks, southwest Norway. Contrib. Mineral. Petrol., 73: 161-172.

Wiedemann, C.; Medeiros, S.R.; Ludka, I.P.; Mendes, J. C.; Costa De Moura, J., 2002. Architecture of late orogenic plutons in the Araçuaí-Ribeira fold belt, southeast Brazil. Gondwana Research, 5 (2): 381-399.

THE TRONADOR VOLCANIC COMPLEX: A PLEISTOCENE CALC-ALKALINE TO THOLEITIC ARC VOLCANISM IN THE SOUTHERN ANDES

Mella, M.[1]; Muñoz, J.[2]; Vergara, M.[3] and Stern, C.[4]

1. Departamento de Geología, Universidad de Chile, Casilla 13518, Correo 21, Santiago, Chile. mauromella@esfera.cl
2. Servicio Nacional de Geología y Minería, Oficina Técnica Puerto Varas, La Paz 406, Puerto Varas, Chile. jmunoz@sernageomin.cl
3. Departamento de Geología, Universidad de Chile, Casilla 13518, Correo 21, Santiago, Chile. mariover@cec.uchile.cl
4. Department of Geology, University of Colorado, USA. stern@colorado.edu

Keywords: Geochronology, geochemistry, petrogenesis, Southern Andean

INTRODUCTION

The partially eroded Pleistocene Tronador Volcanic Complex (TVC, 3,565 ma.s.l.) is located along the Chilean-Argentinean border at approximately 41°10'S and 72°45'W in the Southern Andean Volcanic Zone, behind the present day volcanic front at this latitude represented by Puyehue, Osorno and Calbuco volcanoes, among others. It covers more than 500 Km^2 and it is composed of two main volcanic units, the youngest Tronador stratovolcanoe and the basal Las Cauquenes sequence (Fig. 1). In addition, the Holocene Fonck postglacial monogenic cone is geographically located at the south of Tronador stratovolcanoe, but separated and possibly not directly related to the complex. Tronador stratovolcanoe itself is divided in tree main sub-units (Tronador I to III, Fig. 1). Subunits Tronador I and II are older than a volcanic caldera structure. The rocks of the TVC partially cover Palaeozoic-Mesozoic metamorphic rocks, and Cretaceous and Miocene granodioritic plutons. Volcanic units are partially covered by a summit glacial ice and a number of important glacial tongues spread into Chile and Argentine territories (Fig. 1).

General descriptions of the TVC have been presented by Larsson (1940), Ljungner (1930), Lliboutry (1956), Aguirre & Levi, (1964), Dessanti (1972), Greco (1975), Moreno & Parada (1976), and Gonzalez Bonorino (1976). Rabbasa & Evenson (1996) reported K-Ar ages of 1.32 and 1.39 Ma for lavas from the basal sequence and suggested a quaternary age for this volcanic complex.

In this contribution we present and discuss geochronological, geochemical and Sr and Nd isotopic composition for rocks from the TVC.

PETROGRAPHY

The TVC includes basalts to trachytes, but basalts and basaltic andesites are the predominant rock types. Also, pyroclastic, laharic and hyaloclastic flows are specially well represented in Tronador II and III. The Las Cauquenes Unit is conformed by porphyritic olivine-clinopyroxene basalts and basaltic andesites, with clinopyroxene and plagioclase phenocrysts in intersertal to intergranular groundmass. Tronador I is represented by columnar trachytic lavas, with porphyritic textures and plagioclase and hornblende in a glassy groundmass. This sub-unit interfinger with Tronador II sub-unit, which is conformed by pyroclastic, hydroclastic, laharic and glaciofluvial deposits with interbeded porphyritic and aphyric trachyandesitic, basaltic and basaltic andesitic lava flows. Tronador III includes trachytic basalts, trachitic basaltic andesites and trachyandesites interbeded with hyaloclastic and laharic flows. Lava flows from Tronador III sub-unit are mainly porphyritic with plagioclase, olivine, clinopyroxene phenocrysts in intergranular, intersectal or subophitic groundmass. In this sub-unit, one columnar basaltic lava flow and a laharic deposits expose along an old glacial valley, are porphyritic with megaphenocrysts of plagioclase and intergranular to intersertal palagonitic groundmass. The Fonck monogenic was building on top of Las Cauquenes Unit (Fig. 1) and the related lava flows is trachyandesitic in composition.

K-Ar GEOCHRONOLOGY

A new whole-rock K-Ar age of 1.3±0.3 Ma for a lava flow from Tronador I is in agreement with the previous data from Rabbasa & Evenson (1996) and confirms a maximum early pleistocene age for the older unit of the TVC. In this way, pliocene rocks may not be represented in the TVC, as was suggested by Lara et al. (2001). Other Ar-Ar dates for the younger rocks from Tronador III indicated ages between 0.34±0.040 and 0.53±0.11 Ma for the post-caldera activity, restricting the age from collapse at the 0.53 Ma. Younger Ar-Ar ages for TVC are older than the older ages known for active volcanoes along the present day volcanic front located to the west.

PETROCHEMISTRY

Major, trace and REE were measured for 17 selected samples from Tronador and Las Cauquenes units (Table 1). Normative nepheline is absent and normative quartz is rare. The basalts from the TVC are high alumina in composition and the Al_2O_3 contents are similar to the lavas from the present day volcanic front. In the alkalies-silica diagram (Peccerillo & Taylor, 1976), rocks are calc-alkaline basalts and basaltic andesites and high–K andesites. According to AFM diagram they are transitional to tholeitic. The tholeitic trend is confirmed in the FeO/MgO- SiO_2 diagram. In the Harker diagram, rocks show a rapid increase in K_2O and rapid decreasing in Al_2O_3, MgO and CaO with increasing SiO_2. Lava flows are enriched in K, Rb, Ba, and LREE (La, Ce, Pr and Nd) compared to lavas with similar SiO_2 content from the Osorno and Calbuco volcanoes along the present day volcanic front (Fig. 2).

La/Nb and Ba/La ratios are higher in Las Cauquenes Unit than in any sub-unit from Tronador stratovolcanoe. La/Nb and Ba/La ratios are similar to the lavas with same SiO_2 content from Osorno, Calbuco and Puyehue volcanoes. Although the REE pattern is relatively flat, the La/Yb ratios are higher than the rocks from the present day volcanic front (Fig. 2) and in cases comparable to those of lavas located to east of the volcanic front, in a back arc tectonic position.

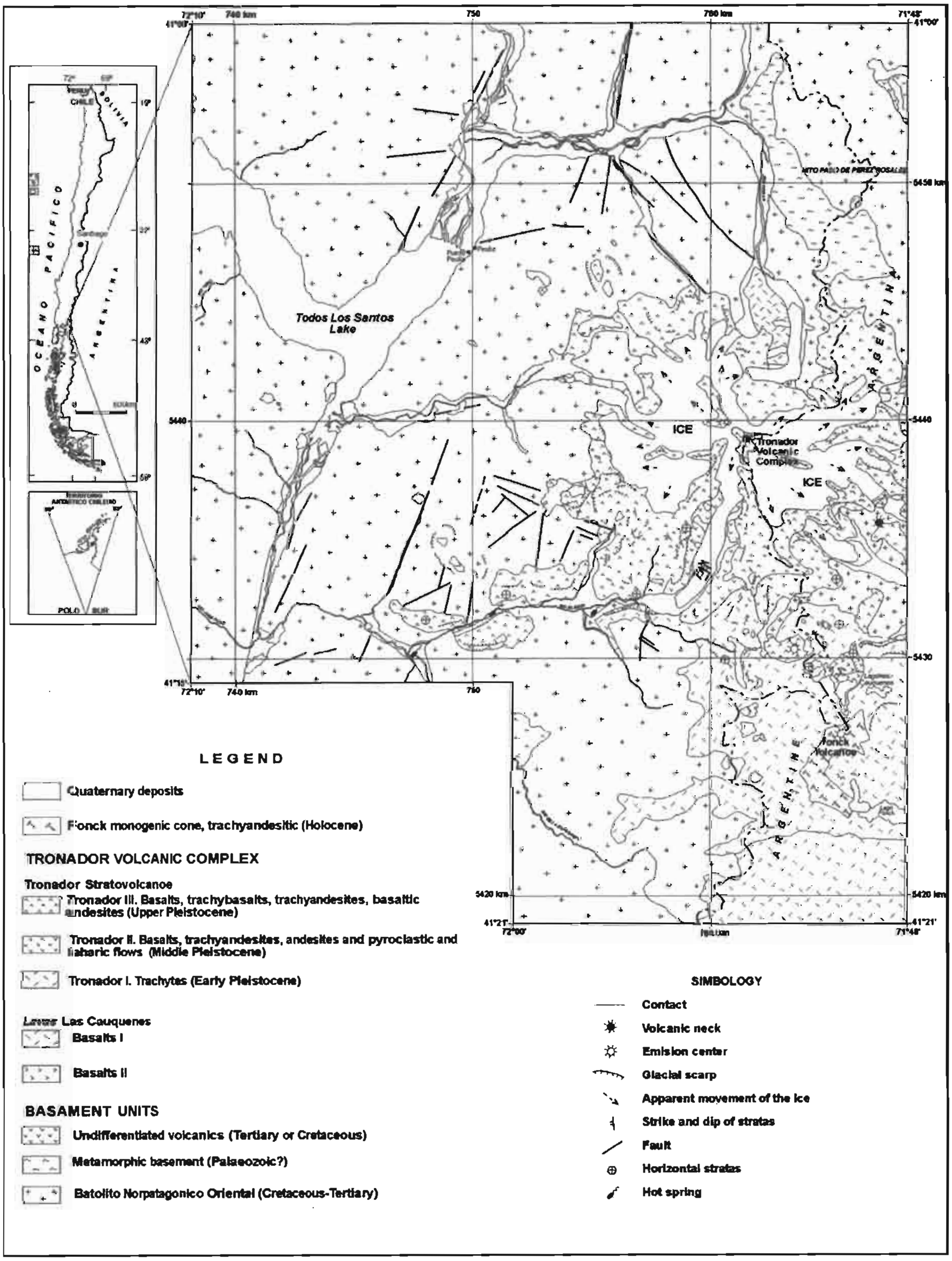

Figure 1. Geological Map of The Tronador Volcanic Complex

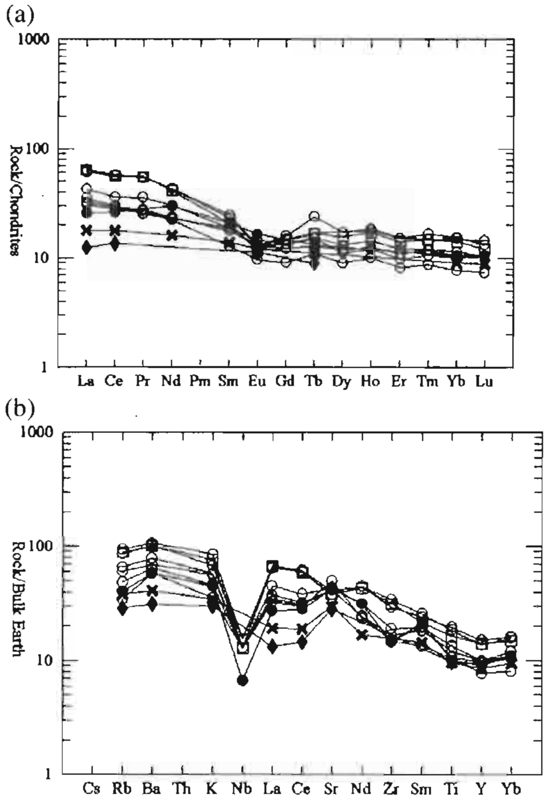

Figure 2. Spider diagram from illustrating trace element concentration from CVT basalt and Arc basalt (SVZ); (a) normalized to values of Chondrites from Sun et al. (1989); (b) normalized to values of bulk earth from Sun et al. (1979) after Hickey et al. (1986). △: Tronador I; □: Tronador II; ○: Tronador III; ●: Llaima volcano (Hichey, 1986); ♦: Calbuco 1 (López-Escobar et al., 1995), ✖: Osorno 3 (López-Escobar et al., 1992).

Lavas also evidence Nb negative anomaly and in cases minor Eu depletion. Sr isotopic composition for representative samples from the younger sub-units of Tronador and from the Fonck volcanoe are in the range 0.704107 and 0.704192. The lower value represents one basalt from Tronador III and the higher a trachyandesite from Fonck monogenic cone. Nd isotopic compositions are in the range 0.512773-0.512813 and the lower value is also representative of the Fonck monogenic cone. Sr and Nd isotopic compositions are in the range of the lavas from Osorno and Calbuco volcanoes along the present day volcanic front.

CONCLUSION

The TVC is an Early to Late Pleistocene partially eroded volcanic complex located to the east of the present day Late Pleistocene-Holocene volcanic front. Geochemical data support a calk-alkaline to tholeiitic trend and a transitional arc to back-arc composition. Sr and Nd isotopic compositions suggest a mantle source for parental magmas. In some basalts, minor Eu anomaly indicate plagioclase and high LREE and flat HREE suggest clinopyroxene cracking, respectively. Although not probe yet at this latitude, it is suggests that the partially eroded TVC could be part of the Pleistocene volcanic front located to the east of the Late Pleistocene-present day active volcanic front.

ACKNOWLEDGEMENTS

Carlos Pérez de Arce and Felipe Llona, both from the Laboratory of SERNAGEOMIN, are respectively acknowledged for the K-Ar ages and the chemical analysis. Sr and Nd isotopic compositions were carried out at the Isotopic Laboratory of the University of Colorado, USA. Publication sponsored by the Subdirección Nacional de Geología, Sernageomin-Chile.

REFERENCES

Aguirre, L. y Levi, B., 1964. Geología de la Cordillera de los Andes de las provincias de Cautín, Valdivia, Osorno y Llanquihue: Int. Investig. Geológicas, Bol. 17. Santiago.

Dessanti, R. N, 1972. Andes Patagónicos Septentrionales. Geología Regional Argentina (A. Leanza, ed.), Acad. Nacional Ciencias, p. 655-688. Córdoba.

Gonzalez Bonorino, F., 1976. Geología del río Manso. Fundación Bariloche, Departamento de Recursos Naturales y Energía (inédito).

Greco, R., 1974. Geología de la hoja 40 a, "Monte Tronador ". Fundación Bariloche (inédito).

Hichey, R., Frey, F., Gerlach, D., Lopez-Escobar, L., 1986, Multiple source for basaltic arc rocks from the southern volcanic zone of Andes (34°- 41°): Trace element and isotopic evidence for contribution from subducted oceanic crust, mantle and continental crust. J. Geophys. Res., Vol. 91, p. 5963 – 5983.

Lara, L.; Rodríguez, C., Moreno, H y Pérez de Arce, C. 2001. Geocronología K-Ar y Geoquímica del volcanismo Plioceno superior - Pleistoceno de los Andes del sur (39-42°S). Revista Geológica de Chile, Vol. 28, N°1, p. 67-90.

Larsson, W., 1940. Petrology of interglacial volcanic from the – andes of Northern Patagonia. Univ. Upsala, Geol. Inst. Bull., Vol. 28, p. 191-405.

Ljungner, E., 1931. Geologische Aufnahmes in der Patagonischer kordillera. Bull. Geol. Int. Upsala, Vol. 23, p. 203.

Lliboutry, L. 1956. Nieves y glaciales de Chile. Fundamentos de Glaciología. Universidad de Chile.

Lopez-Escobar L.; Kempton P.D.; Moreno H.; Parada M.A.; Hickey-Vargas R. and Frey F.A. 1995. Calbuco volcano and minor eruptive centers distributed along the Liquine-Ofqui fault zone, Chile (41°-42°S): contrasting origin of andesitic and basaltic magma in the Southern Volcanic Zone of the Andes. Contributions to Mineralogy and Petrology, Vol. 119, p. 345-361.

López-Escobar, L.; Parada, M.A.; Moreno, H.; Frey, F.A.; Hickey-Vargas, R.L. 1992. A contribution to the petrogenesis of Osorno and Calbuco volcanoes, Southern Andes (41°00'-41°30'S): comparative study. Revista Geológica de Chile, Vol. 19, No. 2, p. 211-226.

Moreno, H.; Parada, M.A., 1976. Esquema geológico de la cordillera de los Andes entre los paralelos 39°00' y 41°30'S. Congreso Geológico Chileno, No. 1, Actas, Vol. 1, p. A213-A225. Santiago.

Peccerillo, A.; Taylor, S.R. 1976. Geochemistry of Eocene calc-alkaline volcanic rocks from the Kastamonu area, Northern Turkey. Contributions to Mineralogy and Petrology, Vol. 58, No. 1, p. 63-81.

Rabassa, J.; Evenson, G. 1996. Reinterpretación de la estratigrafía glaciaria de la región de San Carlos de Bariloche (provincia de Río Negro, Argentina). Actas 13°

Congreso Geológico Argentino, Vol. 4, p. 327. Buenos Aires.

Sun, S.; Nesbit, R.W.; Sharaskin, A.Y., 1979. Geochemical characteristics of mid-ocean ridge basalts. Earth Planet. Sci. Lett., Vol. 35, p. 429-448.

Sun, S.; McDonough, W.F., 1989. Chemical and isotopic systematics of oceanic basalts: implications for mantle compositions and processes. Magmatism in the Ocean Basins (Saunders, A.D. and Norry, M.J., ed.). Geol. Soc. Am. Spec. Pub. No. 42, p. 313-345.

Table 1. Chemical composition of lavas from TVC.

	Tronador I	**Tronador II**		**Tronador III**										**Las Cauquenes**			
	XM23	**XM01**	**XB22-1**	**XM07**	**XM09**	**XM10**	**XM14**	**XM13**	**XM20**	**XM21**	**XM22**	**XB29**	**XB32**	**XV1**	**XM17**	**XB18**	**XB14-1**
SiO_2	64.9	52.9	49.0	55.9	50.8	50.5	51.6	49.9	61.3	50.3	57.1	50.1	52.5	53.0	52.1	54.5	55.6
TiO_2	0.6	1.0	1.7	1.9	1.4	1.2	1.1	1.1	1.5	1.9	1.9	2.0	2.0	1.0	1.2	1.5	2.0
Al_2O_3	17.1	18.2	17.4	15.8	18.8	18.8	18.3	19.3	14.5	17.5	15.1	16.2	16.7	17.6	19.2	17.4	15.7
Fe_2O_3	1.4	2.5	4.2	2.4	4.5	2.9	2.7	2.4	2.5	2.9	1.7	6.5	4.8	3.1	3.6	4.3	2.7
FeO	3.0	6.8	8.3	8.1	6.0	7.5	6.5	7.8	6.1	8.6	8.4	6.5	6.5	6.0	5.7	5.1	8.1
MnO	0.2	0.2	0.2	0.2	0.2	0.2	0.2	0.2	0.2	0.2	0.2	0.2	0.2	0.2	0.2	0.2	0.2
MgO	1.2	5.4	5.4	2.9	5.0	5.7	6.7	6.2	1.5	4.4	2.4	4.6	3.4	5.4	4.6	3.8	2.8
CaO	3.4	9.2	9.1	6.1	9.1	9.0	9.0	9.3	4.4	9.5	6.0	9.7	7.8	9.6	8.8	8.0	5.8
Na_2O	5.4	3.1	3.2	4.0	3.2	3.1	3.2	3.1	4.0	3.2	3.9	2.8	3.6	3.1	3.3	3.7	3.8
K_2O	2.5	0.6	1.1	2.2	0.8	0.8	0.5	0.7	3.6	1.2	2.7	1.0	2.2	0.8	1.0	1.3	2.9
P_2O_5	0.3	0.2	0.4	0.5	0.3	0.2	0.2	0.2	0.5	0.3	0.6	0.4	0.4	0.2	0.2	0.3	0.5
LOI	1.2	0.7	0.3	1.0	0.7	1.0	0.9	0.7	0.2	0.7	0.4	2.0	0.9	0.6	0.4	1.3	1.1
Mg#	34.0	51.6	44.2	33.3	46.8	50.2	57.3	52.6	24.2	41.2	29.7	40.0	35.8	52.3	47.9	43.4	31.9
Q	13.8	3.4	0.0	5.5	0.6	0.0	0.4	0.0	12.4	0.0	6.6	2.0	2.0	2.9	2.0	5.2	4.7
Ne	0.0	0.0	0.0	0.0	0.0	0.0	0.0	0.0	0.0	0.0	0.0	0.0	0.0	0.0	0.0	0.0	0.0
K	20922	4851	9163	18664	6943	6727	4246	5529	30128	10223	22581	8140	18098	7022	7915	11137	24258
P	1109	748	1576	2387	1099	928	919	881	2018	1498	2770	1605	1674	835	832	1198	2206
Ti	3838	6161	10106	11232	8276	7469	6493	6655	9161	11376	11657	12063	12283	6037	7400	8713	11820
Rb	49	18	31	56	23	21	12	17	105	33	78	30	62	20	26	28	68
Ba	662	257	350	544	276	242	202	224	795	369	684	354	584	319	295	388	676
Sr	498	493	421	386	475	460	548	462	287	451	341	416	448	520	460	521	382
Zr	217	78	176	132	106	93	84	85	143	191	144	163	257	79	119	157	287
Nb	8	<	5	8	<	<	<	<	11	6	10	6	9	<	<	5	9
Y	28.3	16.8	31	48.3	22	21.7	16.9	21	50	30	54	33	44	16.7	17.2	20	30
Cr	159	166	45	75	52	51	153	74	118	99	128	67	47	107	108	100	116
Ni	34	37	45	11	37	45	52	58	26	57	36	37	18	26	28	21	12
Co	2	24	31	16	24	28	25	29	12	42	14	25	22	24	24	19	18
V	10	247	282	178	272	253	231	245	65	350	127	353	239	251	245	278	171
Pb	15	<	10	18	8	6	<	4	23	21	23	10	16	5	8	9	19
Sc	7	32	32	29	32	31	28	30	21	37	28	37	29	32	30	34	27
Cu	11	87	159	118	118	112	74	102	102	338	158	202	188	81	107	90	116
Zn	91	83	124	132	98	94	79	93	118	189	131	123	121	79	92	96	129
La	28.4	11.3	21	34	14	11.6	10.2	10.7	41	21	38	20	32	12.1	14.6	17.1	38
Ce	62.7	25	48	73	31	25.9	24	25	93	50	90	48	75	26.2	34	40.9	81
Pr	6.63	3	6.2	8.15	4	2.83	3	3.1	11.1	6	11.1	6.2	8.7	2.53	4	4.65	8.6
Nd	30	14.4	26	40.7	19	14.8	14	14.5	47	27	50	27	41	12.5	13.4	14.4	26
Sm	5.62	3.3	4.2	9.22	3.8	3.58	2.6	3.8	9.4	5	11.2	4.7	8.6	2.78	1.69	1.71	3.2
Eu	1.47	0.97	0.89	2.125	1	0.998	0.74	1.12	1.2	0.98	2.1	1	1.85	0.803	0.374	0.385	0.58
Gd	4.52	2.8	4	8.46	3.7	3.36	2.5	3.7	8.6	4.4	10.1	4.1	7.8	2.5	1.33	1.39	2.6
Tb	1.02	0.55	0.78	1.7	0.72	0.598	0.51	0.7	1.81	1.12	1.69	0.8	1.66	0.503	0.38	0.393	0.63
Dy	5.34	3.7	5.4	9.81	4.5	4.06	3.1	3.8	9.1	5.9	10.3	5.9	8.4	3.25	2.55	2.76	4.4
Ho	1.2	0.88	1.19	2.2	1	0.876	0.7	0.84	2.1	1.3	2.2	1.25	1.8	0.719	0.602	0.7	1.09
Er	3.21	2.1	3.2	5.63	2.7	2.47	1.84	2.2	5.7	3.4	6	3.4	5.1	1.85	1.75	1.81	3.1
Tm	0.452	0.3	0.44	0.7	0.36	0.351	0.26	0.32	0.69	0.44	0.78	0.5	0.6	0.249	0.239	0.232	0.43
Yb	3.26	1.88	3.1	5.31	2.5	2.29	1.69	2.2	5.3	3.3	6.1	3.4	4.8	1.7	1.56	1.7	3
Lu	0.478	0.31	0.41	0.804	0.35	0.357	0.25	0.35	0.78	0.49	0.84	0.45	0.7	0.278	0.222	0.261	0.41
Ba/Nb	82.75		70	6.55					72.27	61.5	68.4	59	64.89			77.6	75.11
Zr/Nb	27.13		35.2	1.59					13	31.83	14.4	27.17	28.56			31.4	31.89
La/Nb	3.55		4.22	4.25					3.73	3.5	3.8	3.33	3.56			3.42	4.22
La/Yb	8.71	6.01	6.77	6.4	5.6	5.07	6.04	4.86	7.74	6.36	6.23	5.88	6.67	7.12	9.36	10.06	12.67
La/Lu	59.41	36.45	51.22	42.29	40	32.49	40.8	30.57	52.56	42.86	45.24	44.44	45.71	43.53	65.77	65.52	92.68
La/Sm	5.05	3.42	5	3.69	3.68	3.24	3.92	2.82	4.36	4.2	3.39	4.26	3.72	4.35	8.64	10	11.88
Ba/La	23.31	22.74	16.67	16	19.71	20.86	19.8	20.93	19.39	17.57	18	17.7	18.25	26.36	20.21	22.69	17.79
Ba/Rb	13.51	14.28	11.29	9.71	12	11.52	16.83	13.18	7.57	11.18	8.77	11.8	9.42	15.95	11.35	13.86	9.94

AGE AND STRONTIUM-NEODYMIUM ISOTOPE GEOCHEMISTRY OF GRANITOIDS OF THE SIERRA NORTE-AMBARGASTA BATHOLITH, CENTRAL ARGENTINA

Millone, H.A.[1]; Tassinari, C.C.G.[2]; Lira, R.[3] and Poklepovic, M.F.[3]

1. Gerencia de Minería de Córdoba, Celso Barrios 1712, 5016 Córdoba, Argentina. hmillone@hotmail.com
2. Centro de Pesquisas Geocronológicas, Instituto de Geociências, Universidade de São Paulo, Brazil. ccgtassi@usp.br
3. CONICET, Museo de Mineralogía y Geología "Dr. A. Stelzner", V. Sarsfield 299, 5000 Córdoba, Argentina.
rlira@com.uncor.edu, fpoklepovic@com.uncor.edu

Keywords: Granitoids, Rb/Sr, Sm /Nd, Sierra Norte, Argentina

INTRODUCTION

The Sierra Norte-Ambargasta batholith (SNAB) is a complex magmatic body composed of distinct granitoid units. Regional geology and petrological studies on different lithologies of the extensive body have been undertaken by several geologists and researchers since late 1800, and afterwards mainly by Lucero Michaut (1969, 1979), Bonalumi (1988), Rapela et al. (1991), Lira et al. (1997), Miró et al. (1998), Candiani et al. (1999) and Ramos (1999).

Granitoid units and enclosing metasedimentary rocks mapped by Lira et al. (1997) were re-examined in the field and new outcrops and lithological contacts were traced (Fig. 1). Based on field, petrographic and geochemical data, representative samples were selected for Rb-Sr and Sm-Nd isotopic analysis, in order to investigate the age of the granitic units and the nature of their magmatic sources. Previous geochronological pattern, mostly information specifically related to studied units, are summarized below to better constrain the geological interpretation of the new isotopic data.

GEOLOGICAL SETTING

Lira et al. (1997) established the intrusive sequence in the central-western area of the batholith, according to which most primitive representatives were diorite to tonalite enclaves, hosted in the dominant granodiorite-monzogranite basement (GM unit). A composite dacitic to rhyolitic subvolcanic body of the same series (DR-rocks), intruded earlier GM unit. The whole series (GM-DR) were later intruded by a group of leucocratic granitoids, that included highly evolved miarolitic monzogranites, rhyolite porphyries and large syenogranitic aplites, all grouped originally as HESG.

Based on this sequence, additional field, whole-rock geochemistry and mineral chemistry work was carried out, including new observations and definitions. One of the latter is that a formational name is suggested for the epizonal miarolitic monzogranites (formerly MM, an integral unit of the HESG group) designed as Puesto de Los Caminos Formation (PDLC) which were separated from the syenogranitic aplites, which presently would conform the Cerro Baritina Formation (CB).

PDLC monzogranite epizonal bodies (2-20 km^2) intruded the GM-DR series. Five separate bodies of this formation have been identified along ~40 km. Sharp magmatic contacts between PDLC units and GM regional granitoids can be traced at the Potrerillos pluton and Aguada Vieja pluton. The Puesto de los Caminos pluton intruded rocks of the GM unit in its northern border and rhyolite (DR unit) porphyries in its southern and southwestern contact. Cerro Baritina Formation units are the latest youngest intrusions in the study area. These bodies normally occur in subhorizontal units with thicknesses ranging from 10 to 20 m, covering areas over 10 km^2; they are normally found intruding GM rocks but at Cerro Baritina locality sharp linear contacts between CB aplite and Puesto de la Loma body (PDLC Formation) have been observed. CB Formation aplite outcrops are spread along a 60 km NS strip.

Most petrographic and whole-rock major and trace element geochemistry data of referred units are interpreted in Lira et al. (1997).

ANALYTICAL METHODS

All isotopic analyses were carried out at the Centro de Pesquisas Geocronológicas, Instituto de Geociências, Universidade de São Paulo, Brazil. The Rb-Sr and Sm-Nd analyses were prepared by standard methods according to the analytical procedures described by Kawashita (1972, modified) and Sato et. al. (1995), involving HF-HNO_3 dissolution plus HCl cation exchange. No visible solid residues were observed after dissolution. Samples with incomplete dissolution were discarded. The Sr isotopic ratios were normalized to $^{86}Sr/^{88}Sr = 0.1194$; replicate analyses of $^{87}Sr/^{86}Sr$ for the NBS987 standard gave a mean value of 0.71028 ± 0.00006 (2σ), the blanks for Sr were 5ng. Nd ratios were normalized to a $^{146}Nd/^{144}Nd = 0.72190$. The averages of $^{143}Nd/^{144}Nd$ for La Jolla and BCR-1 standards were 0.511847 ± 0.00005 (2σ) and 0.512662 ± 0.00005 (2σ), respectively. The blanks were less than 0.03 ng. Sr and Nd isotopic analyses were carried out on a multicollector VG 354 Micromass and Finnigan-MAT 262 mass spectrometers. The isotopic data were regressed using the program of Ludwig (1999), and, in the isochrons with large MSWD value, age calculations were based on Model 2. The ages were calculated using the decay constants established in Steiger and Jäger (1977); for ^{87}Rb was 1.42×10^{-11} yr^{-1}; for $^{147}Sm = 6.54 \times 10^{-12}$ yr^{-1}.

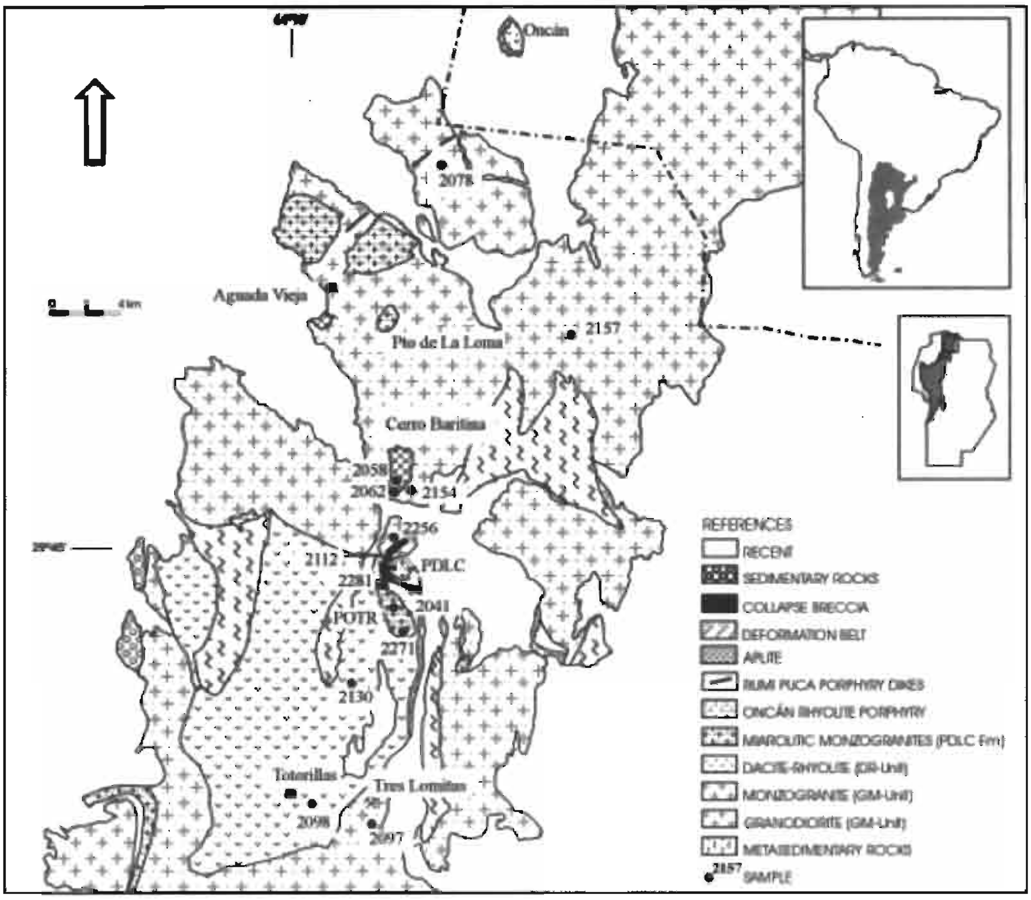

Figure 1. Location and simplified geological map of the SNAB studied granitoids (modified after Lira et al., 1997).

ISOTOPIC DATA

Rb-Sr isotope ratios are listed in table 1. These data were used to compute ages (Figs. 2, 3, 4) and to interpret magma sources of studied granitoids. Rocks of the granodiorite-monzogranite units (GM) have been previously dated in different regions of the batholith and indistinctly referred to as "granites" by González and Toselli (1974), "granites or leucocratic granites" by Castellote (1982, 1985), "granodiorites" by Rapela et al. (1998) and "Tres Lomitas granodiorite" by Koukharsky et al. (1999).

Table 1. Rb and Sr isotopic ratios of SNAB granitoids. Grd: granodiorite; Mgrn: monzogranite; Dac: dacite; Rhy: rhyolite.

Sample/Rock	Rb	Sr	$^{87}Rb/^{86}Sr$	Erro	$^{87}Sr/^{86}Sr$	Erro
GM-2097	124.0	227.6	1.579	0.036	0.72043	0.00002
GM-2256	108.2	253.2	1.238	0.010	0.71848	0.00002
GM-2157	198.1	147.6	3.897	0.045	0.74087	0.00007
GM-2078	115.7	231.6	1.448	0.009	0.71892	0.00008
GM-2154	158.3	157.5	2.916	0.006	0.73216	0.00008
DR-2130	157.7	171.4	2.669	0.058	0.73100	0.00005
DR-2112	152.8	117.4	3.776	0.012	0.73850	0.00008
DR-2098	131.4	174.4	2.185	0.012	0.72472	0.00002
PDLC-2271	200.3	31.1	18.901	0.154	0.84949	0.00021
PDLC-2041	157.8	31.5	14.655	0.119	0.81794	0.00009
PDLC-2281	137.6	86.8	4.602	0.031	0.74285	0.00011

Rocks of granitic composition have been linked to less evolved granodiorites by fractional crystallization processes (Lira et al., 1997). Selected samples were used for Rb-Sr dating which yielded an isochronic age of 627 ± 27 Ma (4 points, MSWD= 1.9); with $^{87}Sr/^{86}Sr$ initial ratio of 0.7061 ± 0.0009 (Fig. 2). This is the oldest age known for Sierra Norte, only comparable to data obtained by Gonzalez et al. (1985) who got an age of 606 Ma in Chuña Huasi. Nevertheless, Castellote (1985) dated a tonalite from Aguada Vieja, Sierra de Ambargasta, with an age of 628 ± 30 Ma, which is in close agreement with our data.

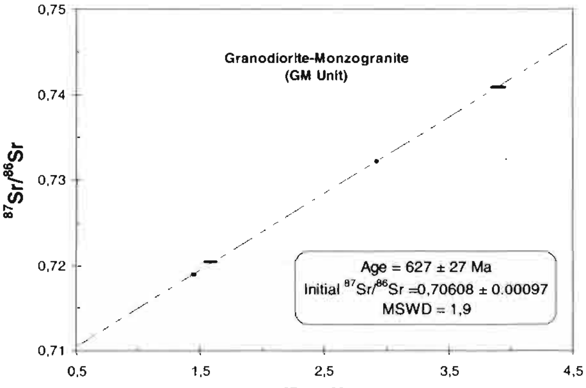

Figure 2. Rb-Sr isochrone for granodiorite-monzogranite regional rocks.

Dacite-Rhyolite (DR) rocks of Lira et al. (1997) compare well to those described as "dacites" by Castellote et al. (1985) which ages resulted 499 ± 20 and 523 ± 15 Ma. Rocks of the same body collected nearby Totorillas were sampled by Söllner et al. (2000) who defined them as rhyodacites of 557 ± 4 Ma using U-Pb in zircons. Rhyolite rocks (DR) of the Cerro de los Burros pluton yielded a new Rb-Sr age of 607 ± 7 Ma (2 points isochron), with $^{87}Sr/^{86}Sr$ initial ratio of 0,7058 ± 0,0003 (Fig. 3).

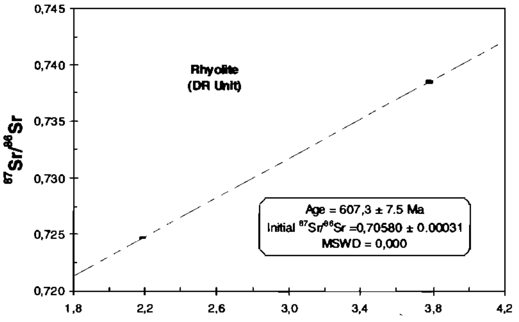

Figure 3. Rb-Sr isochronic age for rhyolites of the Cerro de los Burros subvolcanic pluton.

The analytical point related to one dacite sample is not colinear with the rhyolite analytical points, which could indicated that some subvolcanic pulses are not cogenetic. This age is the oldest up to the present for this porphyry intrusion, and is considered coherent with the age of the deeper GM rocks which were interpreted to be part of the same series. It is important to observe that both GM rocks and the rhyolite have the same Sr initial ratios, within analytical errors, which suggest the same sources.

Puesto de Los Caminos (PDLC) monzogranites (formerly part of HESG of Lira et al., 1997) could have likely been dated previously in more than one occasion mistaken for regional monzogranites, because PDLC units were not recognized prior to 1997 as plutons that intrude regional GM-DR series. This fact could have led to the publication of very different ages even in closely spaced outcrops. Three selected samples from the monzogranite PDLC yielded Rb-Sr isochron age of 523 ± 4 Ma (MSWD= 0.018), and an $^{87}Sr/^{86}Sr$ initial ratio of 0.7085 ± 0.0004 (Fig. 4).

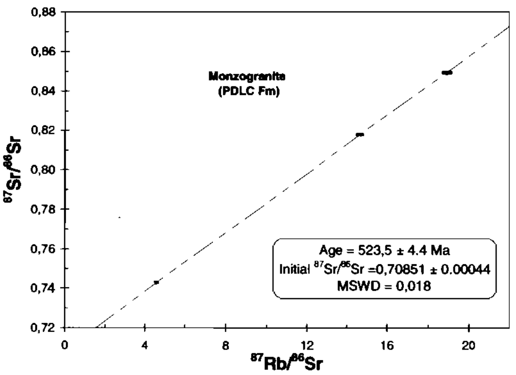

Figure 4. Rb-Sr isochrone for epizonal miarolitic monzogranites of the Puesto de Los Caminos Formation.

SOURCE OF MAGMAS: Sr AND Nd ISOTOPIC EVIDENCES

In order to evaluate the magma sources and potential magma-mixing process in the origin of the granitoids of the SNAB, Nd isotopic analysis from selected samples were used in conjunction with Sr data (Table 2).

Table 2. Nd-Sm isotope data and computed ratios for selected samples of representative granitoid units of the SNAB.

Sample #	**GM-2157 (Mgrn)**	**DR-2112 (Rhy)**	**PDLC-228 (Mgrn)**	**PDLC-227 (Mgrn)**
Sm	5.01	7.16	7.15	5.32
Nd (ppm)	20.71	33.96	35.19	19.65
$^{147}Sm/^{144}Nd$	0.1462	0,1275	0.1229	0.1638
$^{143}Nd/^{144}Nd$	0.512115	0.512060	0.512120	0.512232
ε_0	-10.20	-11.28	-10.10	-7.92
$f_{Sm/Nd}$	-0.26	-0.35	-0.38	-0.17
T_1	627.0	627.0	523.0	523.0
$\varepsilon_{(T1)}$	-6.16	-5.74	-5.18	-5.73
$\varepsilon_{(T2)}$	-10.20	-11.28	-10.10	-7.92

All SNAB granitoid units of this study have negative ε_{Nd} values and high Sr initial ratios (>0,706), which indicate crustal rocks as the main sources for the granitoids. The monzogranite and rhyolite of the GM-DR series have ε_{Nd} values, calculated to 627 Ma, of –6.16 and –5.74, and Sr initial ratios of 0.7060 and 0.7058, respectively. No significant difference in the Sr and Nd isotopic composition was perceptible between subvolcanic and plutonic rocks, suggesting that these rocks are comagmatic. The monzogranites of PDLC group contain more radiogenic Sr, with $^{87}Sr/^{86}Sr$ initial ratio of 0.70851 and slightly less negative ε_{Nd} values, calculated to 523 Ma, in a range from – 5.18 to – 5.73.

DISCUSSION AND CONCLUSIONS

Field setting and whole rock geochemistry sustain the existence of a magmatic arc intrusive sequence in the central-western sector of the extended Sierra Norte-Ambargasta batholith. Sr and Nd isotope geochemistry have yielded new information relative to melt sources and new age data on granitoids which field relationships are well established.

Major components of the magmatic arc basement of the region are granodiorites and fractionated monzogranites (GM unit) which yielded a Rb-Sr isochron age of 627 ± 27 Ma. This isochron is the oldest age even found for the batholith, being considerably older than recent SHRIMP data on zircon of Rapela et al. (1998) who obtained ages of 532 ±2.9 to 533.9 ±3.8 Ma for granodiorites of the GM unit.

Dacite-rhyolite subvolcanic rocks of the DR unit were interpreted as a differentiation product of deeper GM coarser grained granitoids. Its main representative unit is the Cerro de los Burros Formation which yielded an isochrone age of 607 ± 7 Ma, also the oldest measured up to present for these porphyries. This age is again older than U/Pb results from zircons published by Söllner et al. (2000), but in agreement with older parental granodiorite-monzogranite (GM) rocks.

Concerning dating of leucocratic highly evolved rocks of the PDLC Formation, these are the first reported ages for unequivocally identified intrusive units. We interpret that PDLC monzogranites (523 ± 4 Ma) represent the latest intrusions of the Pampean Orogeny during postcollisional stages. Nevertheless, the fact that some CB aplites have been found intruding PDLC monzogranites, is indicative of younger ages.

Interpretation of available Sr and Nd isotope data suggest that SNAB rocks are genetically linked to partial melting of crustal rocks and a possible subordinated mantelic contribution, always showing a sialic input in the source and spatially related to a subduction zone.

REFERENCES

Bonalumi, A.A., 1988. Características petrológicas y geoquímicas de los granitoides asociados a la mineralización de manganeso en el norte de la provincia de Córdoba y sur de Santiago del Estero, República Argentina. V Congreso Geológico Chileno 2: 47-61.

Candiani, J.C., Stuart-Smith, P. Gaido, F., Carignano, C., Miró, R., and López, H., 1999. Hoja Geológica 3163-I, Jesús María, Provincia de Córdoba. 1:250000. Boletín N° 314. 82 p., appendix and map. Subsecretría de Minería. SEGEMAR. Buenos Aires.

Castellote, P., 1982. La Formación La Clemira y edad de su metamorfismo (Sierra de Ambargasta, provincia de Santiago del Estero). Acta Geológica Lilloana 14 (1): 71-76.

Castellote, P., 1985. Algunas observaciones geológicas en la Sierra de Ambargasta y Sumampa (Provincia de Santiago del Estero). Acta Geológica Lilloana 16 (2): 259-269.

González, R.R., Cabrera, M.A., Bortolotti, P., Castellote, P., Cuenya, M.P., Omil, D.M., Moyano, R.O., and Ojeda, J.R., 1985. La actividad eruptiva en Sierras Pampeanas. Esquematización geográfica y temporal. Acta Geológica Lilloana 16 (2): 289-318.

González, R. R., and Toselli, A. J., 1974. Radiometric dating of igneous rocks from Sierras Pampeanas, Argentina. Revista Brasileira de Geociencias, 4: 137-141.

Kawashita, K., 1972. O método Rb-Sr em rochas sedimentares. Aplicação para as Bacias do Paraná e Amazonas. Unpublished PhD Thesis, Institute of Geoscience, University of São Paulo, 111p.

Koukharsky, M., Munizaga, F., Leal, P., Correa, M.J., and Brodtkorb, M.K., 1999. New K/Ar ages in the Ambargasta and Norte de Córdoba Ranges, Argentina. II South American Symposium on Isotope Geology (E. Linares, M.G. Lopez de Luchi, H.A. Ostera, and H.O. Panarello, eds). IGRM, SEGEMAR, Anales XXXIV: 76-77. Villa Carlos Paz, Córdoba, Argentina.

Lira, R., Millone, H.A., Kirschbaum, A.M., and Moreno, R.S., 1997. Calc-Alkaline Arc Granitoid Activity in the Sierra Norte-Ambargasta Ranges, Central Argentina. Journal of South American Earth Sciences 10 (2): 157-177.

Lucero, H.N., 1969. Descripción geológica de las hojas 16h, Pozo Grande y 17h, Chuña Huasi, Provincias de Córdoba y Santiago del Estero. Dirección Nacional de Geología y Minería, Buenos Aires, Boletín 107, 39 p., 4 pl., 10 fig.

Lucero Michaut, H.N., 1979. Sierras Pampeanas del norte de Córdoba, sur de Santiago del Estero, borde oriental de Catamarca y ángulo sudeste de Tucumán. Segundo Simposio de Geología Regional Argentina 1, Academia Nacional de Ciencias, Córdoba, 293-348.

Ludwig, K.R., 1999. Isoplot/Ex. Berkeley Geochronological Center. Special Publication 1, 41p.

Miró, R., 1998. Hoja Geológica 2963-III–Villa Ojo de Agua. IGRM-SEGEMAR. Versión Preliminar, 45 p.

Ramos, V.A., 1999. Ciclos orogénicos y evolución tectónica. En: Recursos Minerales de la República Argentina (E.O. Zappettini ed.). Instituto de Geología y Recursos Minerales SEGEMAR, Anales 35, Vol. I: 29-49.

Rapela, C.W., Pankhurst, R.J., and Bonalumi, A.A., 1991. Edad y geoquímica del pórfido granítico de Oncán, Sierra Norte de Córdoba, Sierras Pampeanas, Argentina. 6° Congreso Geológico Chileno, 19-22.

Rapela, C.W., Pankhurst, R.J., Casquet, C., Baldo, E., Saavedra, J., Galindo, C., and Fanning, C.M., 1998. The Pampean Orogeny of the southern proto-Andes: Cambrian continental collision in the Sierras de Córdoba. In: The Proto-Andean Margin of Gondwana. (Pankhurst, R.J and Rapela, C.W. eds.). Geological Society Special Publication N° 142: 181-217. Geological Society of London.

Sato, K., Tassinari, C.C.G., Kawashita, K. and Petronilho, L., 1995. O método geocrolonológico Sm-Nd no IGc – USP e suas aplicações. Anais da Academia Brasileira de Ciências, 67 (3): 313-336.

Söllner, F., Leal, P.R., Miller, H., and Brodtkorb, M.K., 2000. Edades U/Pb en circones de la riodacita de la Sierra de Ambargasta, provincia de Córdoba. En: Mineralogía y Metalogenia. (Schalamuk, I., Brodtkorb, M.K. and Etcheverry, R. eds.) INREMI, Publicación 6: 465-469. La Plata.

Steiger, R.H. and Jäger, E., 1977. Subcommission on geochronology: convention on the use of decay constants in geochronology and cosmochronology. Contributions to the geologic time scale. Studies in Geology, v. 6: 67-72. Michigan,USA.

Sr-Nd ISOTOPE DATA FOR THE ABANICO EAST FORMATION IN THE ANDEAN CORDILLERA OF CENTRAL CHILE (32°50'-33°50'S)

Muñoz, M.[1]; Vergara, M.[1]; Aguirre, L.[1]; Nyström, J. O.[2]; Montecinos, P.[1] and Fuentes, F.[1]

1. Dpto. Geología, Facultad de Ciencias Físicas y Matemáticas, Universidad de Chile, Casilla 13518, Correo 21, Santiago de Chile.
marmunoz@cec.uchile.cl, mariover@cec.uchile.cl
2. Swedish Museum of Natural History, SE 10405 Stockholm, Sweden. mi-jan@nrm.se

Keywords: Abanico, Oligocene, Sr-Nd Isotopes

GEOLOGICAL SETTING

Tertiary sequences in the Andean Cordillera form a discontinuous N-S trending belt that extends for *c.* 1500 km in northern and central Chile between 23° and 37°S. This belt crosses three tectonic segments of the Andes: one without Quaternary volcanic activity (28°-33°S) and the other two representing the end portions of the Central and Southern Volcanic Zones. The individual units forming the Tertiary belt vary in thickness from 2 to 6 km and consist of volcanic and volcaniclastic rocks deposited in continental basins (Vergara & Drake, 1979). Between 31° and 34°S, the oldest Tertiary volcanic unit is the Oligocene Abanico Formation. It is divided into two parts separated from each other by the N-S distributed Miocene Farellones Formation (Thiele, 1980).

The Oligocene units are known informally as Abanico West and Abanico East (AW and AE). The AW sequence crops out along the western foothills of the Andean Cordillera and shows broad open folds, whereas the tightly folded AE occurs in the High Andes. The former is dominated by volcanic rocks whereas volcaniclastic rocks predominate in the AE. Vergara & Drake (1979) suggested that both sequences were deposited simultaneously along the two flanks of a volcano-tectonic intermontane basin. According to other authors they were deposited in an intra-arc basin with the characteristics of an inverted hemi-rift (Godoy et al., 1999; Charrier et al., 2002).

The AW is composed of basic lavas, acid pyroclastic rocks and subordinate volcanoclastic sedimentary rocks in its type locality, the Cerro Abanico area (Vergara et al., 1993) situated in the western foothills of the Andes just east of Santiago (Fig. 1). Vergara et al. (1999) reported an age of 35-25 Ma for the formation ($^{40}Ar/^{39}Ar$ in plagioclase). The volcanic rocks have a tholeiitic chemical affinity and more primitive isotopic features than all the Mesozoic and Cenozoic volcanic rocks in the Andes of central Chile. Nyström et al. (1993) related the primitive features to eruption onto a thin continental crust. Furthermore, at Chacabuco at the end of Central Valley and in the Andean foothills (32°50'S) (Fig. 1), the coeval volcanic rocks have similar composition and isotopic signatures (Fuentes et al., 2002).

No type locality has been assigned to the AE and less is known about the chemistry of its volcanic rocks than for the AW. At Lo Valdés (33°50'S; Fig. 1), the AE is a *c.* 3000 m thick sequence of volcanic and volcaniclastic rocks, ash flows, airfall tuffs, basic lavas, and interbedded lacustrine sedimentary rocks (Thiele, 1980). An uncorformity and a hiatus separate the AE from the underlying Colimapu Formation that is Early Cretaceous in age (Charrier et al., 2002). At Portillo (32°50'; Fig. 1), the AE sequence is 4000 m thick and has been dated to 25.6 Ma (K-Ar whole rock; Rivano et al., 1993). The proportion of basic volcanic rocks is smaller here than at Lo Valdés. Two basaltic lava flows from Lo Valdés and three lavas from Portillo, one basaltic andesite and two andesites, have been sampled for Sr-Nd isotope analysis (Table 1).

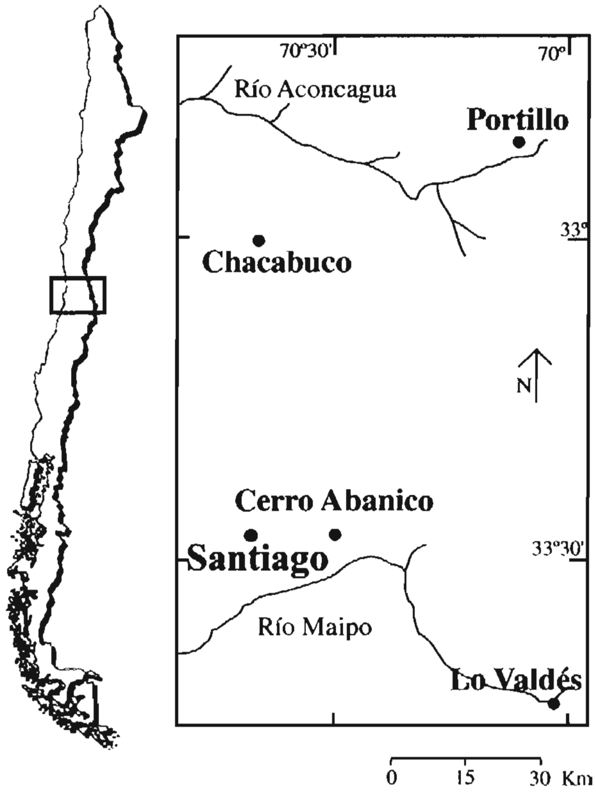

Figure 1. Sketch map showing the sampled areas.

Table 1. Sr and Nd isotope data for volcanic rocks of the Abanico units in the Andes of central Chile (see figure 1 for location).

Sample	Rock Type*	Sample Area	Age Ma	% SiO_2§	Rb ppm	Sr ppm	Sm ppm	Nd ppm	^{87}Sr/^{86}Sr	^{143}Nd/^{144}Nd	Initial ^{87}Sr/^{86}Sr	Initial ^{143}Nd/^{144}Nd	ε_{Nd}
ACO72	BA	Aconcagua	28†	56.3	63	459	9.25	37.6	0.70391	0.512800	0.70376	0.512773	+3.3
ACO83	A	Aconcagua	28†	61.5	38	419	7.25	30.6	0.70378	0.512846	0.70368	0.512820	+4.2
ACO41	A	Aconcagua	28†	61.9	40	619	5.45	24.2	0.70376	0.512816	0.70369	0.512791	+3.7
VAL159	B	Lo Valdés	28†	51.4	16	603	5.01	18.2	0.70372	0.512889	0.70369	0.512859	+5.0
VAL126	B	Lo Valdés	28†	52.8	13	571	5.11	18.7	0.70378	0.512845	0.70376	0.512815	+4.2
FF150	A	Chacabuco	28	54.1	36	333	8.68	32.3	0.70382	0.512907	0.70370	0.512877	+5.4
FF191	A	Chacabuco	28	49.0	5	454	2.62	9.1	0.70367	0.512943	0.70366	0.512911	+6.0
FF19	BA	Chacabuco	26	53.1	11	529	3.13	11.2	0.70368	0.512948	0.70365	0.512919	+6.1
MAP 25	A	C. Abanico	25†	58.8	48	364	6.48	28.0	0.70373	0.512918	0.70360	0.512895	+5.6
MAP23	B	C. Abanico	25†	51.2	24	505	5.15	19.9	0.70355	0.512923	0.70350	0.512897	+5.7
MAP19	BA	C. Abanico	25†	53.7	10	398	5.89	23.9	0.70357	0.512927	0.70355	0.512903	+5.8
MAP5	R. p	C. Abanico	25.4	71.1	35	218	7.10	31.0	0.70375	0.512916	0.70359	0.512893	+5.6

Isotopic ratios determined on a Finnegan MAT 261 multicollector mass spectrometer at the Swedish Museum of Natural History. Sr ratios were fractionation corrected to ^{86}Sr/^{87}Sr = 0.1194; eight determinations of the NBS 987 standard gave a mean of 0.710244 ± 0.000042 (2σ). Nd ratios (fractionation corrected to ^{146}Nd/^{144}Nd = 0.7219) are reported relative to a value of 0.511854 for the La Jolla standard; 14 runs of the standard gave a mean of 0.511753 ± 0.20%.

The Lo Valdés data were plotted in Nyström et al. (1993), corrected for a somewhat older age. The Cerro Abanico data are given in Nyström et al. (2003).

*B = Basalt, BA = Basalt andesite, A = Andesite, R = Rhyolite, and p = Pyroclastic rock

†Estimated age (no radiometric data available)

§Recalculated to 100% anhydrous

Sr AND Nd ISOTOPE RESULTS

The analyzed samples have low initial ^{87}Sr/^{86}Sr values, ranging between 0.70350 and 0.70376 and ε_{Nd} varies from 3.3 to 6.1 (Table 1). The ε_{Nd} *vs.* initial ^{87}Sr/^{86}Sr diagram (Fig. 2) including data for the AW at the latitudes of Portillo (Fuentes et al., 2002) and Lo Valdés (Nyström et al., 2003) shows that the lavas from the AE have higher ^{87}Sr/^{86}Sr initial ratios and lower ε_{Nd} values compared to those for the AW. A negative correlation between initial ^{87}Sr/^{86}Sr ratios and ppm Sr is shown by the lavas from both Abanico units (Fig. 3). The ε_{Nd} values are higher for the Lo Valdés rocks than for the Portillo samples, regardless of their SiO_2 content (Fig. 4, Table 1).

CONCLUSION

The differences in isotope ratios for the volcanic rocks of the two Abanico units, and the differences between the AE at Lo Valdés and Portillo, are consistent with eruption of more primitive magmas or less crustal contamination in the west than in the east.

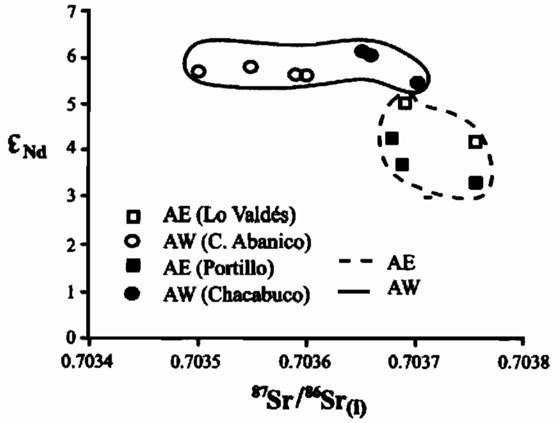

Figure 2. ε_{Nd} *vs.* initial ^{87}Sr/^{86}Sr ratios for volcanic rocks of the Abanico East (AE) and Abanico West (AW) sequences in the Andes of central Chile.

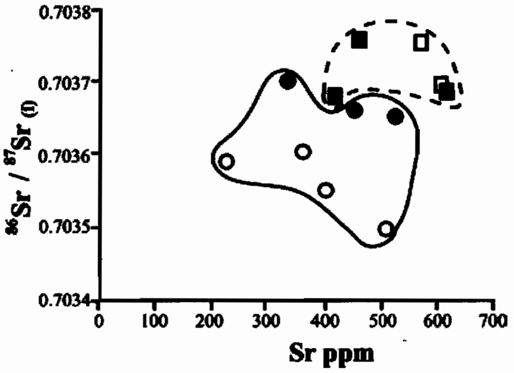

Figure 3. Initial $^{87}Sr/^{86}Sr$ ratios *vs.* ppm Sr for volcanic rocks of the Abanico units in the Andes of central Chile (see figure 2 for legend).

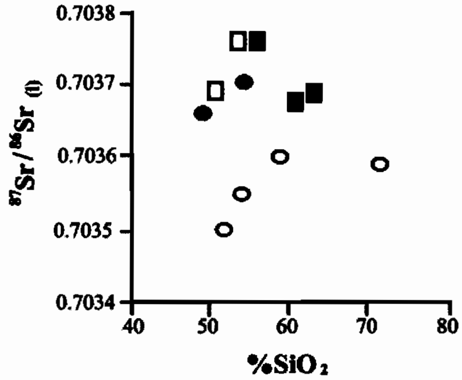

Figure 4. Initial $^{87}Sr/^{86}Sr$ ratios *vs.* percent SiO_2 for volcanic rocks of the Abanico units in the Andes of central Chile (see figure 2 for legend).

REFERENCES

Aguirre, L., 1960. Geología de los Andes de Chile Central, provincia de Aconcagua. Instituto de Investigaciones Geológicas, Santiago, Chile, Boletín N° 9, 70 p.

Charrier, R., Baeza, O., Elgueta, S., Flynn, J. J., Gans, P., Kay, S. M., Muñoz, N., Wyss, A. R. and Zurita, E., 2002. Evidence for Cenozoic extensional basin development and tectonic inversion south of the flat-slab segment, southern Central Andes, Chile (33°-36°S.L.). Journal of South American Earth Sciences, v. 15, p. 117-139.

Fuentes, F., Vergara, M., Aguirre, L. and Féraud, G., 2002. Relaciones de contacto de unidades volcánicas terciarias de los Andes de Chile central (33°S); una reinterpretación sobre la base de dataciones $^{40}Ar/^{39}Ar$. Revista Geológica de Chile, v. 29, N° 2 p. 207-225.

Godoy, E., Yáñez, G. and Vera, E., 1999. Inversion of an Oligocene volcano–tectonic basin and uplifting of its superimposed Miocene magmatic arc in the Chilean Central Andes: first seismic and gravity evidences. Tectonophysics, v. 306, p. 217–236.

Nyström, J. O., Parada, M. A. and Vergara, M., 1993. Sr-Nd isotope composition of Cretaceous to Miocene volcanic rocks in central Chile: a trend towards a MORB signature and a reversal with time. Second International Symposium on Andean Geodynamics, Oxford, Extended Abstracts Volume, p. 411-414.

Nyström, J. O., Vergara, M., Morata, D. and Levi, B., 2003. Tertiary volcanism during extension in the Andean Foothills of central Chile (33°15′–33°45′S). Geological Society of America (under revision).

Rivano, S., Sepúlveda, P., Boric, P. and Espiñeira, D., 1993. Hoja Quillota-Portillo. Servicio Nacional de Geología y Minería. Carta geológica N° 73, 201 p.

Thiele, R., 1980. Hoja Santiago. Carta Geológica de Chile N° 39, Instituto de Investigaciones Geológicas, 51 p. (with map).

Vergara, M. and Drake, R., 1979. Edades K/Ar en secuencias volcánicas continentales postneocomianas de Chile central; su depositación en cuencas intermontanas restringidas. Revista de la Asociación Geológica Argentina, v. 34, p. 42–52.

Vergara, M., Levi, B. and Villarroel, R., 1993. Geothermal-type alteration in burial metamorphosed volcanic pile, central Chile. Journal of Metamorphic Geology, v. 11, p. 449-454.

Vergara, M., Morata, D., Villarroel, R., Nyström, J. O. and Aguirre, L., 1999. $^{40}Ar/^{39}Ar$ ages, very low grade metamorphism and geochemistry of the volcanic rocks from "Cerro El Abanico", Santiago Andean Cordillera (33°30'S-70°30'-70°25'W). Fourth International Symposium on Andean Geodynamics, Georg August Universtät, Göttingen, Extended Abstracts Volume, p. 785-788.

^{40}Ar/^{39}Ar GEOCHRONOLOGY OF THE CABO MAGMATIC PROVINCE, PERNAMBUCO BASIN, NE BRAZIL

Nascimento, M.A.L.[1]; Vasconcelos, P.M.[2]; Souza, Z.S.[3]; Jardim de Sá, E.F.[3]; Carmo, I.O.[2] and Thiede, D.[2]

1. Programa de Pós-Graduação em Geodinâmica e Geofísica (PPGG/UFRN), PRH22-ANP,
Caixa Postal 1596, 59078-970, Natal-RN, Brazil. marcos@geologia.ufrn.br
2. Department of Earth Sciences, The University of Queensland; Brisbane Qld 4072, Australia. paulo@earth.uq.edu.au
3. Departamento de Geologia, PPGG/UFRN e PRH-22-ANP,
Caixa Postal 1596, 59078-970, Natal-RN, Brazil. zorano@geologia.ufrn.br, emanuel@ccet.ufrn.br

Keywords: ^{40}Ar/^{39}Ar geochronology, magmatic rocks, Pernambuco Basin, NE Brazil

INTRODUCTION

The Pernambuco Sub-Basin (PSB) corresponds to a thin belt of sedimentary and magmatic rocks belonging to the southern portion of the Cretaceous Pernambuco – Paraíba Basin. The continental component of the PSB is better known than its offshore counterpart (Lima Filho, 1998). Situated immediately south of Recife, the geologic limits of the PSB are the Pernambuco Lineament on the north, the Maragogi high on the south and the Pernambuco – Alagoas Massif on the west.

In its onshore portion (Lima Filho, 1998), the PSB is composed of a lowermost aptian to albian rift phase, characterized mainly by siliciclastic sediments of the Cabo Formation and the Cabo Magmatic Province (trachytes, rhyolites, basalts, ignimbrites, high level granite). These units stratigraphically underlie a calcareous sequence (the Estiva Formation) and a siliciclastic one (the Algodoais Formation), which comprise the drift phase of the basin (Lima Filho, 1998).

The available Rb-Sr (Long et al., 1986), K-Ar (Vandoros et al., 1966) and recent ^{40}Ar-^{39}Ar (Lima Filho & Szatmari, 2002) geochronologic data for the magmatic rocks of the CMP show ages in the range 111 Ma to 85 Ma (Albian to Santonian).

The ^{40}Ar-^{39}Ar data reported here (6 rhyolites, 3 trachytes, 1 basalt and 1 granite) provide new geochronological constraints for the magmatism in the PSB and suggest that the magmatic events in the Cabo Province are restricted to a much narrower time interval than previously proposed.

FIELD RELATIONS OF THE CABO MAGMATIC PROVINCE (CMP)

The CMP, first described by Sial (1976), is composed by a series of volcanic and subvolcanic rocks, including trachytes, rhyolites, basalts, ignimbrites and a high level granite pluton (the Cabo granite). Field observations show a close relationship between these rocks and the sedimentary sequences of the Cabo Formation. There is abundant evidence that the magmatic activity is synchronous with rift sedimentation (Lima & Pinho, 1997).

Trachyte flows, sills and NE-trending dykes, and rhyolite lopoliths, plugs and domes, are volumetrically the most important types of volcanic/subvolcanic bodies. The Cabo granite, ignimbrites of the Engenho Saco quarry, and small basalt flows and sills, are also present. Field exposures of the contacts between the magmatic rocks and the sedimentary country rocks are quite rare. Conglomeratic sandstones of the Cabo Formation, containing trachyte and rhyolite clasts, are intruded by similar rocks, suggesting different magmatic pulses in the CMP. Trachytic and rhyolitic fragments found within pyroclastic flows (ignimbrites) also point to successive volcanic events.

Even without exposed contacts, field relations indicate that the Cabo granite intruded the Cabo Formation and interlayered volcanic rocks. Shallow drill holes in the Suape area (Amaral & Menor 1989) suggest that the Cabo granite had been already uplifted during deposition of the Estiva carbonates. Furthermore, the siliciclastic sediments of the Algodoais Formation, containing abundant volcanic clasts, overlie the rift section (Cabo Formation + CMP rocks) in a clear unconformity. Therefore, dating of the CMP magmatic rocks will bracket a minimum (or very close) age for the syn-rift sedimentation (the Cabo Formation), as well as a maximum age for the beginning of the post-rift (drift) evolutionary phase of the basin.

ANALYTICAL PROCEDURES

All samples were irradiated (14 hours) together with Fish Canyon sanidine neutron flux standards in the Triga Reactor at the Oregon State University. After a two-month cooling period, each sample was incrementally heated under a continuous Ar-ion laser with a 2mm-diameter beam. The fraction of gas released was cleaned through a cryocooled cold-trap (T = -140 °C) and two C-50 SAES™ Zr-V-Fe getters and analysed for Ar isotopes in a MAP-215-50 mass spectrometer at the UQ-AGES (University of Queensland Argon Geochronology in Earth Sciences) laboratory. Automation and analytical procedures are described by Vasconcelos (1999) and Vasconcelos *et al.* (2002). Data corrections for mass discrimination, nucleogenic interferences and atmospheric contamination were used to calculate apparent ages for each degassing step. Although single crystals were analysed whenever possible, total rock samples were also analysed if the sample was sufficiently fine-grained (phenocrysts smaller than 50-100 μm). In some cases we analysed both phenocrysts and total rock grains for the same sample, in order to test the reproducibility of the results obtained from distinct Ar reservoirs. For the holocrystalline rocks, like the Cabo granite, K-feldspar, biotite, and amphibole crystals were analysed, allowing an insight of the cooling history of this intrusive rock. To ensure the accuracy of the results, single crystals of international standards Alder Creek sanidine (1.194 ± 0.007 Ma), GA 1550 biotite (98.8 ± 0.5 Ma) and HB3gr amphibole (1072 ± 11 Ma) (McDougall & Harrison, 1999) we also irradiated and analysed, following exactly the same procedures.

Given the large number of samples (11) and grains (51) analysed by the laser $^{40}Ar/^{39}Ar$ incremental heating technique in this study, the geochronological results are presented as probability density plots (ideograms), instead of illustrating simple individual incremental heating spectra. Although not shown here, most of the analyzed grains yield well defined plateau ages, using a plateau definition as a sequence of two or more steps corresponding to at least 50% of the total ^{39}Ar released, and whose age values are within two sigma from the mean value. If a sample reaches a well-defined plateau, it implies that the sample hosts its radiogenic and nucleogenic gas fractions in a tight crystallographic reservoir, that the reservoir has been closed during the history of the sample, and that contaminating hypogene phases are unlikely to be present. Sometimes a grain does not yield a plateau as defined above, despite the fact that the analytical results yield a well defined incremental heating spectrum with a "plateau-like segment". In these instances, we choose to visually estimate a plateau and calculate a "forced plateau age" for the significant steps.

$^{40}Ar/^{39}Ar$ GEOCHRONOLOGY RESULTS

RHYOLITES

Coarse to medium grained rhyolites from the Algodoais, Caeté and Pindoba plugs, contain quartz and feldspar (mainly sanidine) phenocrysts in a very fine grained groundmass. The ages obtained for the K-feldspar phenocrysts are shown in Figures 1A, 1B and 1C. Three sanidine grains from the Algodoais plug yield very well defined and concordant plateau ages (99.2±0.7, 101.2± 0.8, and 100.8±0.4 Ma), with a weighted mean age of 100.7±0.7 Ma. Only two of the three sanidine grains from the Caeté rhyolite yield well defined plateaus, with 102±3 and 101.6±1.3 Ma ages; the weighted mean age for all the steps from the three grains analysed for this sample was 102±3 Ma (Fig. 1B). Two out of three feldspar grains from the Pindoba rhyolite yield well defined and compatible plateau ages of 103.8±0.4 and 105.3±0.7 Ma; the weighted mean age for all steps from the three grains (104.4±0.8 Ma) is also within the 2-sigma confidence interval from the plateau ages. However, three whole rock samples from the same plug yield two plateau ages of 102.6±0.2 and 101.9±0.3 Ma; a third grain, which does not yield a plateau as defined in this study, also provides a well-defined "plateau-like" spectrum with a forced plateau age (8 steps, 100% of ^{39}Ar released) of 102.0±0.4 Ma. The weighted mean age for these whole rock grains, 101.1±1.1 Ma (Fig. 1D), is slightly younger than the age obtained for the phenocrysts from the same sample.

Fine grained rhyolites, represented by the Sítio dos Anjos, Usina Ipojuca and Mirador lopolith and plugs, were also dated. These lithologies also contain quartz and feldspar phenocrysts. Both phenocrysts and whole rock samples were analysed. Two of the three whole rock grains analysed for the Sítio dos Anjos lopolith yield well defined plateau ages of 102.2±0.5 and 102.8±0.3 Ma, with a weighted mean age of 102.4±0.7 Ma (Fig. 1E). A third grain analysed for this sample indicates the presence of an older contaminant and has been ignored. K-feldspar grains from the Ipojuca plug reveal some discrepancies in the plateau ages (103.1±0.6, 101.2±0.8, and 99.2±1.7 Ma). An ideogram for all analysed steps yields a weighted mean age of 101.4±1.4 Ma, considered as the best age estimate for this sample (Fig. 1F). Three whole rock fragments from the same sample yield a weighted mean age of 101±1 Ma (Fig. 1G), compatible with the age obtained for the feldspar phenocrysts. The Mirador plug, however, yield a weighted mean age of 102.9±0.8 Ma for three K-feldspar phenocrysts (Fig. 1H) (plateau ages of 102.7±0.4, 103.4±0.3, and 105.4± 0.5 Ma), whereas whole rock fragments for the same sample yield younger results (98.5±0.2, 96.7±0.8 and 98.2±0.8 Ma plateau or plateau-like ages), with a weighted mean age of 98.0±0.8 Ma for the 3 grains.

TRACHYTES

At least two types of trachytes are recognized based on field relationships and textural features; coarser grained, porphyritic types correspond mostly to sill-like intrusions, while fine grained ones occur as lava flows and dykes. A clast of fine to medium grained trachyte was sampled in conglomerates at the base of the Algodoais Formation. Three whole rock grains from this sample yield a weighted mean age of 102±2 Ma (Fig. 1I). A trachyte sample was also collected from a drill core of the 2-CP-1-PE well (known as the Cupe well). It is a fine gained, almost vitric trachyte, interlayered with the Cabo Formation sediments. Three whole rock grains analysed for this sample yield well defined and reproducible spectra, none of which defines a plateau age, despite their plateau-like appearance. The weighted mean age of all analysed steps (102.3±0.9 Ma, Fig. 1J) is a good estimate for this sample age. Another trachyte body, sampled at the Itapoama Beach, is a coarse grained, porphyritic unit, with abundant milimetric tabular K-feldspar phenocrysts. These feldspar phenocrysts yielded plateau ages of 103.2±0.4, 100.4±0.4, and 101.9±0.4 Ma. Whole rock fragments from the same sample yielded three extremely similar spectra; however, only one spectra yields a plateau age of 100.3±0.2 Ma; the other two yielded forced plateau ages of 100.6±0.3 and 100.8±0.3 Ma. The weighted mean age for all steps for the total rock sample is 99.4±0.7 Ma. The best estimate age for the Itapoama trachyte, considering all the analyzed grains, is 100.3±0.6 Ma (Fig. 1K).

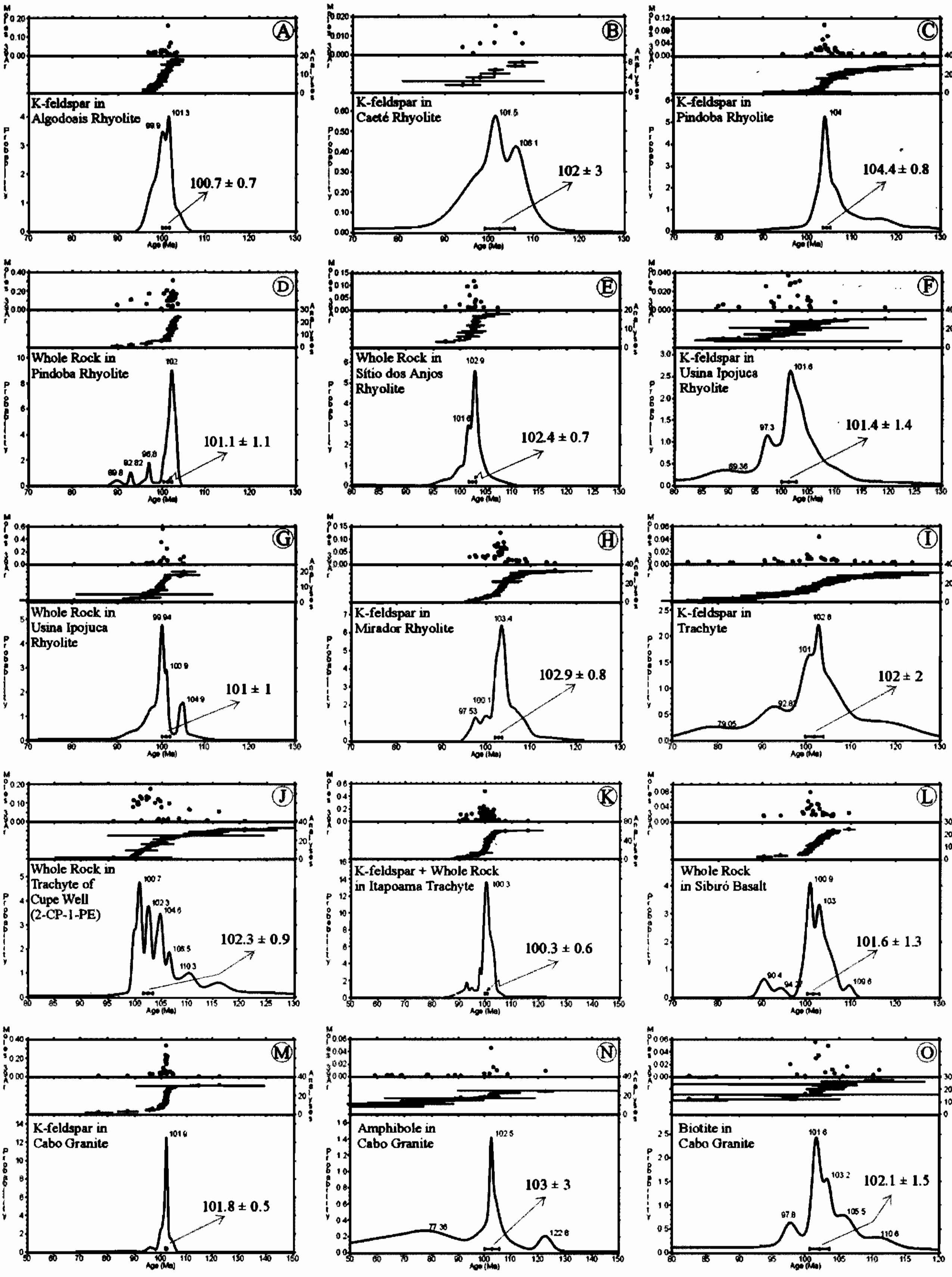

Figure 1. $^{40}Ar/^{39}Ar$ ideogram ages for whole rock and minerals of the Cabo Magmatic Province, NE Brazil.

BASALTS

Basalts in the CMP typically contain milimetric olivine and augite phenocrysts, plagioclase laths and small magnetite and biotite crystals, dispersed in a very fine grained to devitrified groundmass. Three grain analyzed for a representative unit, the Sibiró basalt, yield 3 similar spectra displaying slightly older results in the low temperature steps and younger results in the higher temperature; low K/Ca steps derived from the gas released from plagioclase phenocrysts. The best estimate age for the Sibiró basalt is 101.6±1.3 Ma (Fig. 1L).

CABO DE SANTO AGOSTINHO GRANITE

This hololeucocratic, medium grained, equigranular. high level granite is composed essentially of feldspar (oligoclase, orthoclase), quartz and accessory amphibole (riebeckite), apatite, zircon, allanite, magnetite and chloritized biotite. Miarolitic cavities are common, filled with carbonate, tourmaline and/or fluorite. The feldspar crystals are often altered to sericite and carbonate. Given the possibility of alteration-related Ar loss, we analyzed nine grains (3 feldspar, 3 biotite, and 3 amphibole single crystals) by the laser incremental heating technique. All 9 crystals yield well defined spectra, with reproducible plateau ages. The major difference between the 3 minerals is the amount of radiogenic ^{40}Ar obtained from each grain, which reflects in the absolute errors of the measured ages, with feldspar crystals providing the most precise ages and the amphibole crystals the least precise. The weighted mean ages for feldspar, amphibole, and biotite crystals are 101.8±0.5 Ma (Fig. 1M), 103±3 Ma (Fig. 1N) and 102.1±1.5 Ma (Fig. 1O). The absence of any statistically significant differences in the ages obtained for the 3 minerals, which are characterized by distinct closure temperatures, suggests that this granite underwent a relatively rapid cooling history during its emplacement at *ca.* 102 Ma.

DISCUSSION

The data reported here reveal that the emplacement of the Cabo Magmatic Province happened in a very short time interval, ranging from 104.4±0.8 to 100.3±0.6 Ma, with a predominance of results at 102±1 Ma. There is no significant age difference between the several magmatic centers described in the province. This age range is higher than that proposed by Vandoros et al. (1966) on the basis of conventional K-Ar dates, and compatible with Ar-AR results obtained by Lima Filho & Szatmari (2002), with one significant exception: the Cabo Granite. Lima Filho & Szatmari (2002) report a ^{40}Ar-^{39}Ar whole rock age of 111.2±1.3 Ma for this medium grained holocrystalline intrusive rock. The compatible and reproducible results obtained from 9 grains (3 feldspar, 3 biotite, and 3 amphibole single crystals) analyzed by the laser incremental heating method in this study suggest a much younger age (ca. 102±1 Ma), which may reflect a crustal contaminant in the whole rock age.

The laser incremental heating ^{40}Ar/^{39}Ar ages reported here are 8 to 14 Ma younger than the estimated ages for the P-260 to P-280 (approximately 116 to 112 Ma) palinozones recognized in the Cabo Formation sediments sampled at the Cupe well (Lima Filho, 1998). One possible explanation is that the Cabo Magmatic Province is *ca.* 10 million years younger than the host sedimentary sequence, a relation that would not hold for the lava flows and ignimbrites, apparently coeval with the intrusive bodies presently dated. Anyway, the Ar-Ar dates presented in this contribution set a minimum age for the Cabo Formation, and call attention to possible conflicts with the palynological age estimations.

The Algodoais Formation, on the other hand, must be younger than 100.3±0.6 Ma, the youngest result obtained for the magmatic units that intrude the Cabo Formation. The same holds true for the overlying Estiva Formation carbonates.

REFERENCES

Amaral, A.J.R. & Menor, E. A., 1979. A seqüência vulcano-sedimentar Cretácea na região de Suape (PE): interpretação faciológica e considerações metalogenéticas. Simp. Geol. do NE, 9, Natal, Atas, p. 251-269.

Lima Filho, M.F. 1998. Análise estratigráfica e estrutural da Bacia Pernambuco. Instituto de Geociências, Universidade de São Paulo, São Paulo, Tese de Doutorado, 139 p.

Lima Filho, M.F. & Szatmari, P. 2002. Ar-Ar geochronology of volcanic rocks of the Cabo Magmatic Province (CMP) – Pernambuco Basin. In: SBG/Núcleo Norte, Simp. sobre Vulcan. e Amb. Assoc., 2, Belém, Resumo, 59-59.

Lima, W.S. & Pinho, G.D.C. 1997. Petrographic characterization of the syn-rift volcanics from the Cabo Province, northeastern Brazil and its relations to the surronding sediments. In: IGCP Project 381 - South Atlantic Mesozoic Correlations, Rio de Janeiro, SAMC News, 7: 18-20.

Long, L.E.; Sial, A.N.; Ekvanil, H.E.; Borba, G.S. 1986. Origin of granite at Cabo de Santo Agostinho - Northeast Brazil. Contrib. Mineral. Petrol., 92: 341-350.

McDougall & Harrison, 1999. Geochronology and Thermochronology by the ^{40}Ar/^{39}Ar Method. 2nd ed., Oxford, Oxford University Press, 269p.

Sial, A.N. 1976. The magmatic province of Cabo de Santo Agostinho, Pernambuco: a Brazilian record of the ascencion plume activity in the past. In: Latin-Americ. Geol. Cong., 3, Acapulco, Procced, 105-105.

Vandoros, P.; Cordani, U.; Matzko, J.J. 1966. Idades absolutas das rochas ígneas da região do Cabo. In: SBG/Núcleo Sudeste, Cong. Bras. Geol., 20, Vitória, Anais, 1: 64-66.

Vasconcelos P.M. 1999. ^{40}Ar/^{39}Ar Geochronology of Supergene Processes in Ore Deposits. Rev. Econ. Geol. 12, 73-113.

Vasconcelos, P.M.; Onoe, A.T.; Kawashita, K.; Soares, A.J.; Teixeira, W. 2002. ^{40}Ar/^{39}Ar geochronology at the Instituto de Geociências, USP: instrumentation analytical procedures and calibration. Anais da Academia Brasileira de Ciências 74, 297-342.

MIGMATIZATION EVENT(S) IN THE CAMPO BELO METAMORPHIC COMPLEX

Oliveira, A.H.[1,2,3]; Kamber, B.S.[2]; Collerson, K.D.[2] and Carneiro, M.A.[3]

1. Conselho Nacional de Desenvolvimento Científico e Tecnológico (CNPq) - Fellow Process 200714/1– Brazil. arildo@earth.uq.edu.au
2. Advanced Centre at Queensland University Isotope Research Excellent (ACQUIRE), University of Queensland, QLD 4072 Brisbane, Australia. kamber@earth.uq.edu.au and k.collerson@mailbox.uq.edu.au
3. Depto. Geologia/Universidade Federal de Ouro Preto, Morro do Cruzeiro/SN, 35400.000 – Ouro Preto-MG, Brazil. mauricio@degeo.ufop.br

Keywords: Campo Belo Metamorphic Complex, Rb-Sr, Migmatization

INTRODUCTION

The geochronological history of the Campo Belo Metamorphic Complex is compatible with the evolution of the Bonfim and Belo Horizonte Metamorphic Complexes (Machado et al., 1992; Teixeira, 1993; Teixeira & Silva, 1993; Teixeira et al., 1996, 1998; Carneiro et al., 1998a; Pinese et al., 1997). Teixeira et al. (1998), dating zircons (ion probe U-Pb) from migmatites of the Campo Belo Complex, defined a polyphase Archean history. They proposed three major geological events in that area. The first took place at 3,205±17 Ma and marks the initiation of granitoid crust. A second period of intrusions occurred at 3,047±25 Ma and the third event is recorded at 2,839±17 Ma. The youngest date was considered to be the crystallization age of the neosome (migmatization event). Machado & Carneiro (1992) and Carneiro et al. (1998a, b) defined the Rio das Velhas orogeny (2,780-2,700 Ma) that is representing the most important event having affected the Campo Belo Complex. According to these authors, mafic-ultramafic intrusions were emplaced between ca. 2.75 and 2.66 Ga in association with distensional phases of the Rio das Velhas orogeny. Endo & Machado (1998) also defined discontinuities or distensional phases at the margins of the Rio das Velhas Greenstone Belt during this period. Teixeira et al. (1996) provided evidence that the latest major geological episode occurred at 2,650 Ma, during which the Rb-Sr and Pb-Pb systems were reset. Based on new Rb-Sr whole-rock dates for migmatites and amphibolite from Marilan quarry (3 migmatites), Fazenda Corumba quarry (3 migmatites) and Kinawa quarry (4 amphibolite) (Fig. 1, Table 1), this work discusses preliminary implications for the studied area in the Campo Belo Metamorphic Complex (Fig. 1).

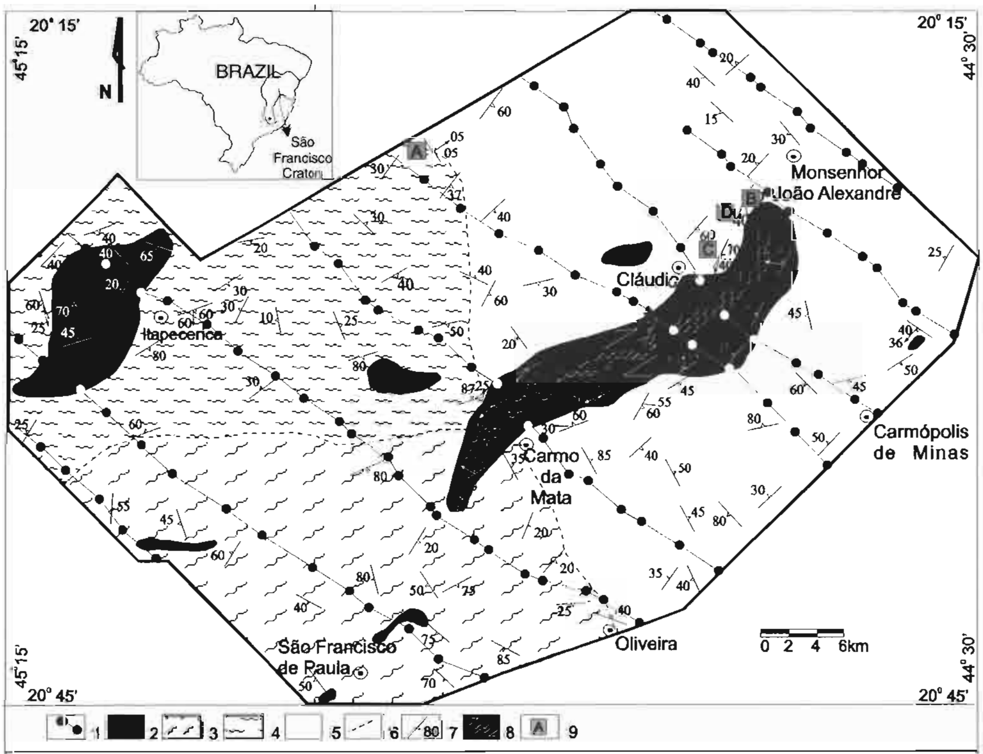

Figure 1 - Geological map of the studied area (modified from Oliveira and Carneiro 2001), showing the different lithologies units: 1) Fissure Mafic Unit; 2) Supracrustal Unit; 3) Candeias Unit; 4) Itapecerica Unit; 5) Claudio Unit; 6) Inferred Contact; 7) Foliation; 8) Claudio Shear Zone; and 9) Dimension stone quarry: A - Marilan; B - Fazenda Corumba quarry ; C - Kinawa quarry; and D - Corumba quarry.

Table 1. Rb-Sr isotopic data for whole rock from Campo Belo Metamorphic Complex. Coefficient of variation 1% (2σ) used for ^{87}Rb/^{86}Sr and 26ppm for ^{87}Sr/^{86}Sr. Migmatite/Marilan stone quarry (samples 2, 3 and 4); Migmatite/Fazenda Corumba stone quarry (samples 16, 17 and 18); Amphibolite/Kinawa Quarry (samples 25A, 25B, and 26) and Amphibolite/Corumba stone quarry (sample27)

Sample	Rb (ppm)	Sr (ppm)	^{87}Rb/^{86}Sr	Error (1%)	^{87}Sr/^{86}Sr	Error (26 ppm)
AO-2	187.20	104.10	5.20	0.0520	0.9034	0.0000026
AO-3	137.30	141.10	2.82	0.0282	0.8137	0.0000026
AO-4	134.30	155.10	2.51	0.0251	0.8017	0.0000026
AO-16	147.90	97.30	4.40	0.0440	0.8770	0.0000026
AO-17	107.00	208.10	1.49	0.0149	0.7612	0.0000026
AO-18	152.40	66.40	6.64	0.0664	0.9555	0.0000026
AO-25A	10.30	126.00	0.24	0.0024	0.7112	0.0000026
AO-25B	7.80	135.03	0.17	0.0017	0.7085	0.0000026
AO-26	47.00	138.30	0.98	0.0098	0.7403	0.0000026
AO-27	165.70	69.90	6.86	0.0686	0.9574	0.0000026

RESULTS

The Rb and Sr results were obtained at ACQUIRE (Advanced Centre of Queensland University Isotope Research Excellence). Sr-isotope ratios were obtained using TIMS (thermal ionization mass spectrometry) and Rb/Sr ratios from quadrupole ICP-MS (inductively coupled plasma mass spectrometry). Ages reported here were calculated using the Isoplot program (Ludwig, 1998). Experimental (2 sigma) errors used in the regression analyses were 1% for ^{87}Rb/^{86}Sr (based on standard reproducibility) and 26ppm for ^{87}Sr/^{86}Sr (external error based on NBS SRM 987 and EN-1 measurements over 6 years). Rb-Sr isotopic data for 3 migmatites from Marilan quarry, 3 migmatites from Fazenda Corumbá quarry and 3 amphibolites from Kinawa quarry are presented in Table 1 and are plotted on an isochron diagram shown in Figure 2. Data for 3 whole-rocks from Marilan quarry (Itapecerica Unit) yield a model I isochron equivalent to an age of 2609 ± 53Ma and an initial ^{87}Sr/^{86}Sr of 0.7072 ± 0.0024 (MSWD = 0.086) (Fig. 2, point A). Migmatites from Fazenda Corumbá quarry (Fig 1, point B, Claudio Unit) display a model I isochron equivalent to an age of 2603 ± 29 Ma and an initial ^{87}Sr/^{86}Sr of 0.70511 ± 0.00099 (MSWD = 0.21) (Fig. 2b). The population of three amphibolites from Kinawa quarry shows an age of 2694 ± 31 Ma and an initial ^{87}Sr/^{86}Sr of 0.70193 ± 0.00011 (MSWD = 0.00057) (Fig 2, point C, Cláudio Unit). The same amphibolites from Kinawa quarry when grouped with one amphibolite from Corumbá quarry display an age of 2570 ± 72 Ma with an initial ^{87}Sr/^{86}Sr of 0.7027 ± 0.0023 and MSWD of 18 (Fig. 2, point D). Field evidence presented by Oliveira & Carneiro (2001) indicates that the amphibolites which found, on the one hand in gneisses and on the other as boudins in migmatites, are cogenetic, possibly justifying using them for a single regression.

DISCUSSION/CONCLUSION

As reported by (Machado & Carneiro 1992; Teixeira et al. 1996, 1998; Carneiro et al. 1998a,b) the period of 2,612-2,593 Ma was associated with a Neoarchaean pulse of granite plutonism, representing the youngest generation of granites in southern part of the São Francisco Craton. These have four main implications for the interpretation of our data presented here:

1. What does the Rb-Sr method date in high-grade metamorphic terrains?
2. Are our results reflecting the reactivation of earlier discontinuities as recorded at the margins of Rio das Velhas Greenstone Belt (along the interpretation of Endo & Machado, 1998)?
3. Can the Rb/Sr data presented here be seen as evidence for a strong metamorphic event that affected the area around ~2,650-2,570 Ma as already reported by Teixeira et al. (1996)? However, the period ca. at 2.6 is considered to be associated with the Neoarchaean granitic pulse.
4. Thus, could the ca. 2.6-2.59 Ga granitoids be products of the migmatization event and record the same history as the migmatization period?

As illustrated by Collerson (1983) Rb-Sr systematics obtained for large whole rocks of multiply metamorphosed and deformed (including migmatisation) samples have the ability to still define the age of the protolith (known from zircon U-Pb dating). When smaller samples are used (e.g. neosomes, or biotite-rich palaeosomes), however, Rb/Sr data often date the time of migmatisation and not the time of protolith formation.

Teixeira (1993) interpreted, in the studied area, Rb-Sr ages for enderbites of ca. 2.566±53 Ga in terms of reworking (complete isotope resetting) without a detailed explanation of how whole-sale Sr-homogenisation could have occurred. Using our new data, including trace

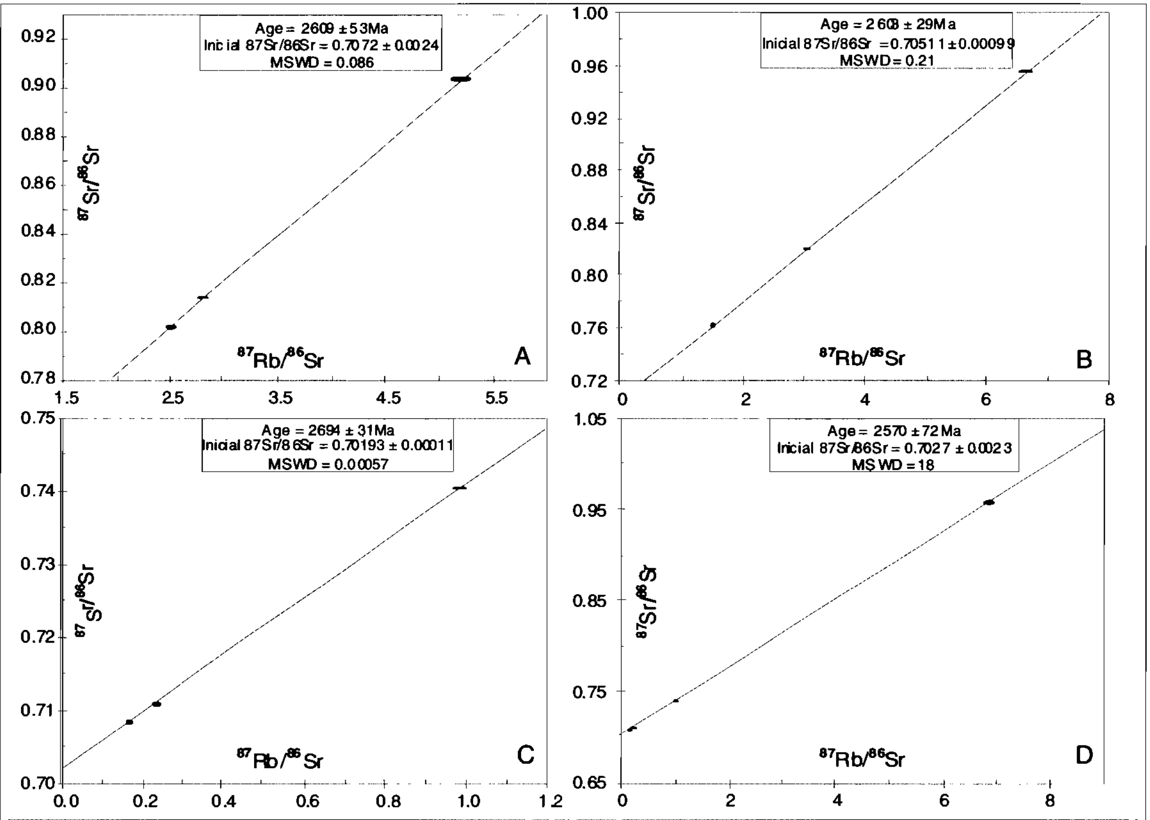

Figure 2 - Rb-Sr isochron diagram for the whole-rock samples of Campo Belo Metamorphic Complex. The Isoplot program (Ludwig, KR 1999) was used to calculate the model regression. A - Marilan quarry, B - Fazenda Corumba quarry, C - Kinawa quarry, and D - Kinawa and Corumba quarry.

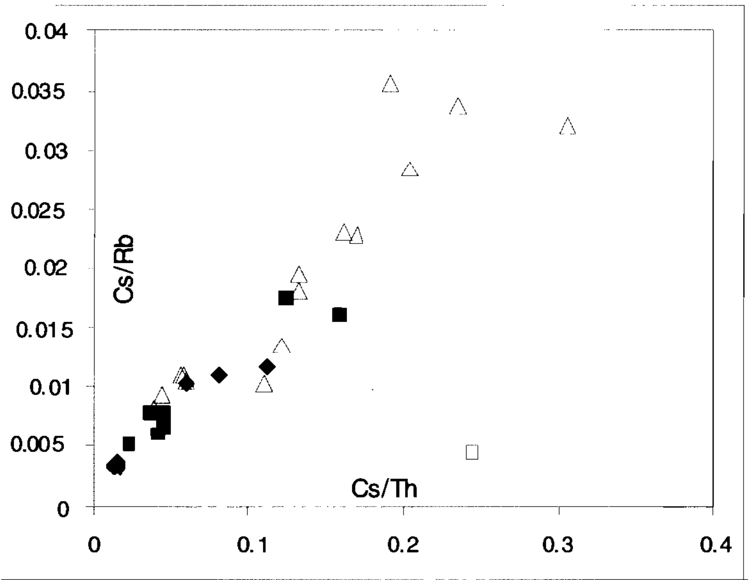

Figure 3 - Positive trend correlation between Cs/Rb vs vs Cs/Th from Claudio (open triangle), Itapecerica (solid square) and Candeias (solid diamond) Units.

element geochemistry for a wide variety of samples, we further test this hypothesis. From the outset, we selected homogenous large, fresh samples taken from quarry faces. Our data are, in general compatible with the earlier results of Teixeira (1993) but isochrons from different rock types have discernibly different initial $^{87}Sr/^{86}Sr$ isotope ratios. In the straightforward interpretation of these isochrons defining the time of protolith formation (rather than the age of migatization), the initial ratios would indicate a range of melt sources from mantle-like (amphibolites), intermediate (migmatites from Fazenda quarry) and crustal (Marilan quarry). However, if the Rb-Sr regression lines define the age of migmatization, the maximum protolith age can be estimated from the difference in initial Sr-isotope ratio of the regression and coeval mantle. Namely, in order for complete resetting to occur, it is necessary to homogenize Sr-isotopes on the scale of the quarry. Equilibration of this magnitude would also seriously affect the Rb/Sr ratios of different parts of the quarry. Indeed, based on our geochemical data we can point out that some elements were lost during the metamorphic event from most of our studied rocks from Candeias, Claudio and Itapecerica Units (Fig.1). In a plot of Cs/Rb vs Cs/Th (Fig. 3) a strong positive trend is displayed, which requires preferential element loss in the order Cs>Rb>Th. Hence, when compared with the average Upper Continental Crust (MacLennan, 2001) our rocks are depleted in Cs and Rb. The continental crust has a Cs/Rb ratio of about 0.036 (MacDonough et al., (1991), whereas our rocks have lower ratios. Sr was apparently not affected by element loss, as there is no obvious depletion in this element. The important conclusion from the trace element investigation is that the present Rb/Sr ratio of the quarry is certainly lower than the pre-migmatisation ratio. Hence, when calculating the crustal residence time prior to 2.57 Ga from the present-day Rb/Sr, we will obtain a maximum estimate. For the late Archaean mantle, we assume a $^{87}Sr/^{86}Sr$ of 0.7014 and use the difference with the initial recorded by the isochrons to estimate the maximum protolith age. For the Fazenda quarry we obtain a crustal prehistory of only ca. 70 Ma, while the samples from Marilan allow a prehistory of ca. 120 Ma. This can be interpreted to mean that the protoliths of these migmatites formed between 2670 and 2730 Ma, the period, which Machado & Carneiro (1992) defined as the Rio das Velhas orogeny (2,780-2,700 Ma). According to Machado & Carneiro (1992) this was a time when the study area was intruded by mafic magmas. Alternatively, the studied rocks were infiltrated during the 2.6 Ga migmatization event by unradiogenic (mantle) Sr, like that recorded by the amphibolite isochron initial ratio. In this case, it would be possible that our estimate for the crustal prehistory is too short. Clearly, this possibility needs to be tested with U-Pb zircons dates (work in progress). The combined data (trace element geochemistry, Sr-isotopes and U-Pb zircon ages) will yield a complete picture not only of timing but also of element mobility associated with migmatisation events.

REFERENCES

Carneiro, M.A., Carvalho Junior, I.M.d. and Teixeira, W., 1998a. Petrologia, Geoquímica e Geocronologia dos diques máficos do Complexo Metamorfico Bonfim Setentrional (Quadrílatero Ferrífero) e suas implicações na evolução crustal do Craton São Francisco Meridional. Revista Brasileira de Geociências, 28: 29-44.

Carneiro, M.A., Teixeira, W., Carvalho Junior, I.M. and Fernandes, R.A., 1998b. Ensialic tectonic of the Archaean Rio das Velhas Greenstone Belt:Nd and Pb isotopic evidence from the Bonfim Metamorphic Complex, Quadrílatero Ferrífero, Brazil. Rev. Bras. Geociências, 28: 71-82.

Collerson, K.D., 1983. The Archean gneiss complex of northern Labrador. 2. Mineral ages, secondary isochrons, and diffusion of strontium during polymetamorphism of the Uivak gneisses. Canadian J. of Earth Sci., 20(5): 707-718.

Endo, I. and Machado, N., 1998. The geologic architeture of the Quadrilátero Ferrífero (Minas Gerais, Brazil) after multiple transpressional and transtensional tectonic events., Int. Conf. Basement Tectonics, 14, Ouro Preto-MG, 126-127.

Ludwig, K.R., 1998. Isoplot/Ex (A geochronological Toolkit for Microsoft Excel). Barkeley Geochronology Center, Barkeley.

MacDonough, W.F., Sun, S.S., Ringwood, A.E., Jagoutz, E. and Hofmann, A.W., 1991. Potassium, rubidium, and cesium in the Earth and Moon and the evolution of the mantle of the Earth. Geochimica et Cosmochimica Acta, 56: 1001-1012.

Machado, N. and Carneiro, M.A., 1992. A major Archaean tectonothermal event in the São Francisco shield, Brazil: U/Pb evidence from the Quadrilátero Ferrífero, Minas Gerais. Canadian J. of Earth Sci., 29(11): 2341-2346.

Machado, N., Noce, C.M., Ladeira, E.A. and DeOliveira, O.B., 1992. U-Pb geochronology of Archean magmatism and Proterozoic metamorphism in the Quadrílatero Ferrífero, Southern São Francisco Craton, Brazil. Gological Society of America Bulletin, 104(9): 1221-1227.

MacLennan, S.M., 2001. Relationships between the trace element composition of sedimentary rocks and upper continental crust. Geochemistry, Geophysics and Geosystems.

Oliveira, A.H. and Carneiro, M.A., 2001. Campo Belo Metamorphic Complex: Tectonic evolution of an Archean sialic crust of the southern São Francisco Craton in Minas Gerais (Brazil). Anais da Academia Brasileira de Ciências, 73(3): 397-415.

Pinese, J.P.P., 1997. Geoquímica, geologia isotópica e aspectos petrológicos dos diques máficos pré-cambrianos da região de Lavras (MG), porção sul do Cráton São Francisco. Unpubl., PhD Thesis, São Paulo University, SP, 178 pp.

Teixeira, W., 1993. Avaliação do acervo de dados geocronológicos e isotópicos do Cráton São Francisco-Implicações tectônicas. In: SBG (Editor), I Simpósio sobre o Cráton São Francisco, Salvador, pp. 11-33.

Teixeira, W. and Silva, F.C., 1993. A evolução tectonotermal proterozóica do Cráton São Francisco, com base em interpretações geocronológocicas K-Ar. In: SBG (Ed.), 2 Simpósio Cráton São Francisco, Salvador, pp. 18-22.

Teixeira, W. et al., 1996. Pb, Sr and Nd isotope constraints on the Archaean evolution of gneissic-granitoid complexes in the southern São Francisco Craton, Brazil. Precambrian Research, 78(1-3): 151-164.

Teixeira, W., Cordani, U.G., Nutman, A.P. and Sato, K., 1998. Polyphase Archean evolution in the Campo Belo metamorphic complex, Southern São Francisco Craton, Brazil: SHRIMP U-Pb zircon evidence. Journal of South American Earth Sciences, 11(3): 279-289.

Nd-Sr ISOTOPIC AND GEOCHEMICAL CONSTRAINTS FOR THE ORIGIN OF THE SABANALARGA BATHOLITH, COLOMBIA

Ordóñez-Carmona O.[1]; Abad-Posada, A.M.[2]; Pimentel, M.M.[3] and Ángel-Cárdenas, P.[4]

1. Universidad Nacional de Colombia, sede Medellín. AA 1027. oordonez@unalmed.edu.co.
2. Universidad Nacional de Colombia, sede Medellín. AA 1027. amabadp@yahoo.com
3. Universidade de Brasília - Instituto de Geociências CEP 70910-900-Brasília, Brazil. marcio@unb.br
4. Integral S.A. patto@epm.net.co

Keywords: Sabanalarga Batholith, Colombian Andes

INTRODUCTION

The Colombian Andes are made of three ranges, formed in different tectonic settings. The Western Cordillera is made of rocks with oceanic affinity, the Central Cordillera comprises rocks of continental affinity represented by calc-alkaline batholiths and regional metamorphic rocks, and the Eastern Cordillera contains marine and continental sedimentary rocks deposited on a continental basement.

In this work, we present field and geochemical data for a sector of the Sabanalarga Batholith (Fig. 1), located west of Medellín near the Cauca river, between the Central and Western Colombian Cordilleras (Cauca-Romeral faults System). The data discussed in this study suggest that the intrusion in genetically related to the volcanic rocks of the Western Cordillera.

REGIONAL SETTING

The Sabanalarga Batholith is a N-S elongated intrusion underlying an area of ca. 410 km^2. It mostly includes hornblende diorite with local tonalite and gabbro (González et al., 1978). According to Álvarez (1983), this intrusion is located along an area which represents the boundary between rock units with continental affinity at the east and oceanic rocks to the west.

The Sabanalarga Batholith is intrusive into metamorphic rocks of Valdivia Group belonging to the Central Cordillera at the east, which is evidenced by the presence of hornfels in the country rocks (Hall et al., 1972); to the west, the Batholith is in tectonic contact with the volcano-sedimentary rocks of Cañasgordas Group belonging to the Western Cordillera (Álvarez, 1983).

Geochronological data obtained by the K-Ar method, yielded ages of 98 ± 3.5 Ma in hornblende (González & Londoño, 1998), 97 ± 10 Ma in biotite (González et al., 1978), and 91 ± 6 Ma in biotite (Göbel & Stibane, 1979). These ages are interpreted as minimum intrusion ages, and suggest that the Sabanalarga intrusion is coeval with Cretaceous magmatism in the Western Cordillera.

FIELD STUDIES

Field studies were carried out in the surroundings of Santafe de Antioquia, Liborina and Sabanalarga (Antioquia). In this area, the central and southern portions of the Sabanalarga Batholith are well exposed (Fig. 1).

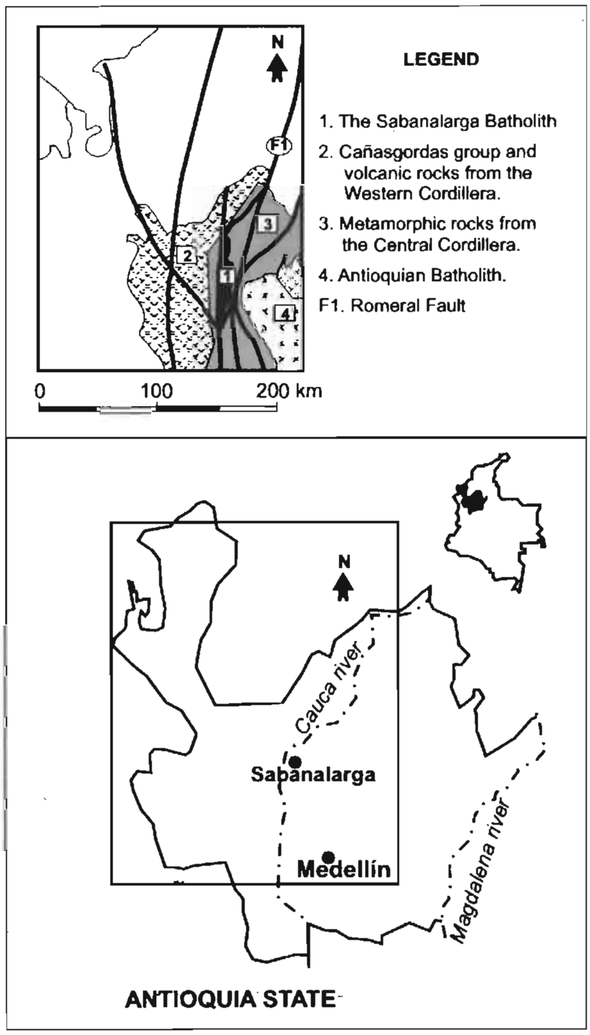

Figure 1. Localization and simplified geology of the Sabanalarga Batholith.

In the southern section, the batholith is dominated by rocks of intermediate to mafic composition, represented by hornblende diorites and gabbros. In the central portion, the batholith presents an interstratified structure characterized by the intercalation between felsic/intermediate facies (granodiorite and diorite) and intermediate/mafic facies (diorite and gabbro). The latter becomes progressively more important towards the north. In the section, the batholith is dominated by granodioritic rocks.

GEOCHEMISTRY AND Sr-Nd ISOTOPIC DATA

Geochemical and isotopic data were obtained in the laboratories of the Geosciences Institute of the University of Brasília-Brazil. The preliminary geochemical data indicate that the original magma is primitive, with a strong mantle input (Figs. 2, 3).

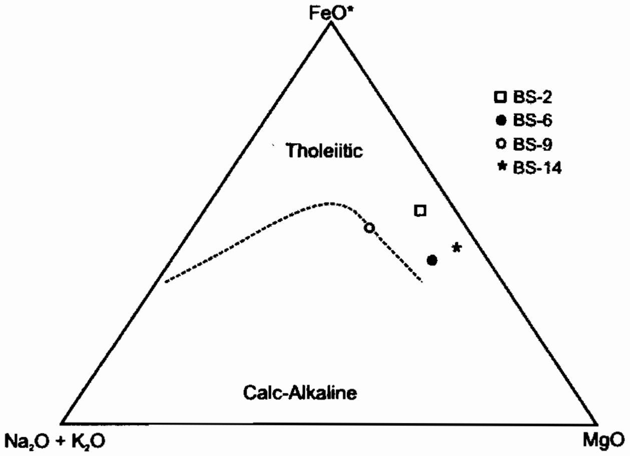

Figure 2. AFM diagram for the Sabanalarga Batholith (Irvine & Baragar, 1971).

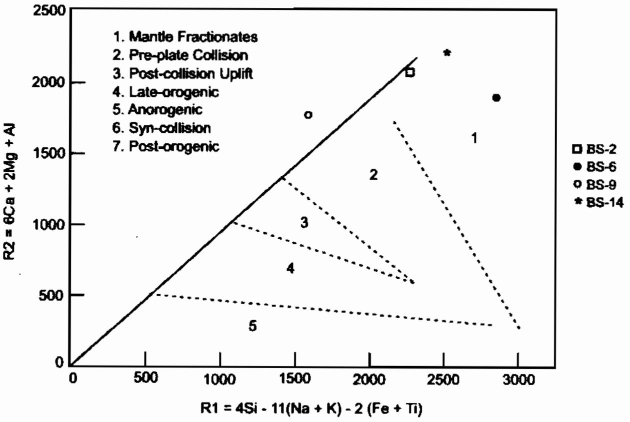

Figure 3. R1-R2 multicationic diagram for the tectonic setting (Batchelor & Bowden, 1985).

The Sr-Nd isotopic data are concordant with the primitive character of this magma, showing $\varepsilon_{Nd(100\ Ma)}$ values between +6.58 to +6:81 and $^{87}Sr/^{86}Sr_{(i)}$ values between 0.70469 to 0.70346, plotting in the depleted mantle quadrant of the ε_{Nd} x $^{87}Sr/^{86}Sr$ diagram (Fig. 4).

DISCUSSION

The Sabanalarga Batholith is an intrusive body well exposed in the vicinities of Sabanalarga town (northern sector of the batholith), where metamorphic rocks of the Central Cordillera had been transformed into hornfels (Hall et al., 1972). In the central sector (Liborina town), the batholith is found in tectonic contact with the metamorphic rocks of the Central Cordillera with no evident intrusive relationships (Abad-Posada, 2002). The same can be observed in the southern sector, where the intrusive is in tectonic contact with the adjacent units (Correa & Calle, 1988). This characteristic must be highlighted and considered as a very peculiar feature of this intrusion.

The geochemical and isotopic data presented here refer to samples from the southern and central part of the batholith, and therefore cannot be conclusive to all igneous rocks associated to this intrusion. Correa & Calle (1988) also presented geochemical data for the southern sector, which reveal the presence of rocks with tholeiitic and calc-alkaline affinity.

The field and geochemical data discussed above suggest that the Sabanalarga intrusion was emplaced into two mixed tectonic settings: one associated to magmatic arc activity, and the other, maybe related to the plume activity that originated the Caribbean-Colombia oceanic plateau characterized by Kerr et al. (1997). An alternative interpretation is that the Sabanalarga Batholith represents a composite intrusion made of several smaller bodies originated in different settings.

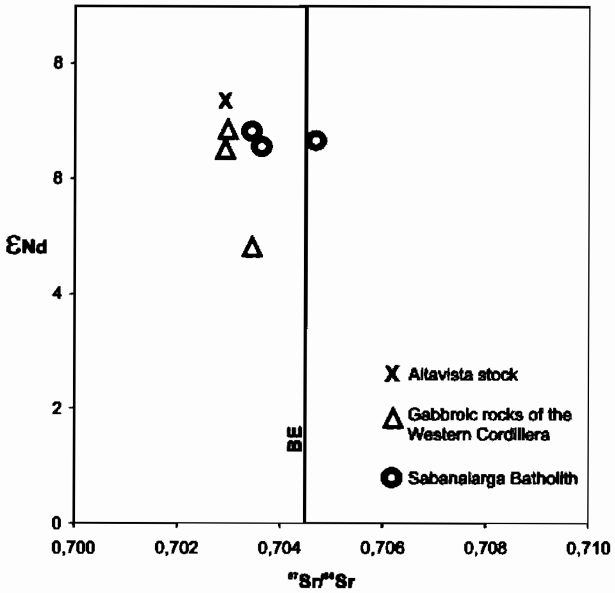

Figure 4. ε_{Nd} x $^{87}Sr/^{86}Sr$ diagram for the Sabanalarga Batholith and coeval rocks, calculated for 100 Ma.

REFERENCES

Abad-Posada A. M. (2002). Estudio de las milonitas asociadas a la Falla de Sabanalarga entre las quebradas Juan García y La Suecia. Liborina (Antioquia). Trabajo dirigido de grado. Universidad Nacional de Colombia. Medellín. 103: 60-66.

Álvarez J. (1983). Geología de la Cordillera Central y el Occidente Colombiano y petroquímica de los intrusivos granitoides Mesocenozoicos. Boletín Geológico de Ingeominas, 26(2): 1-175.

Correa V. C. F., Calle R. N. A. (1988) Geología, petrografía y petroquímica de la zona sur del Plutón de Sabanalarga Antioquia. Trabajo dirigido de grado. Universidad Nacional de Colombia. Medellín. 288.

Göbel V., Stibane F. (1979). Edad K-Ar en hornblenda de plutones tonalíticos, Cordillera Occidental, Colombia, S. A. Publicaciones Especiales de Geología, Univ. Nacional, Medellín, 17: 2.

González H., Londoño G. A. C. (1998). Edades K-Ar en algunos cuerpos plutónicos del graben Cauca-Patía y norte de la Cordillera Occidental. Geología Colombiana, 23: 117-131.

González H., Restrepo J. J., Toussaint J. F., Linares E. (1978). Edad radiométrica K/Ar del Batolito de Sabanalarga. Publicaciones Especiales de Geología, Univ. Nacional, Medellín, 8: 1-5.

Hall R. B., Álvarez A. J., Rico H. H. (1972). Geología de parte de los departamentos de Antioquia y Caldas (Sub-zona II-A). Boletín Geológico de Ingeominas, 20(1): 1-85.

Kerr A. C., Marriner G. F., Tarney J., Nivia A., Saunders A. D., Thirlwall M. F., Sinton C. W. (1997). Cretaceous basaltic terranes in Western Colombia: elemental, chronological and Sr-Nd isotopic constraints on petrogénesis. Journal of Petrology, 38(6): 677-702.

GEOCRONOLOGY AND ISOTOPE GEOLOGY OF THE PRECAMBRIAN TERRANES OF SOUTHEASTERN SÃO PAULO STATE, BRAZIL

Passarelli, C.R.; Prazeres Filho, H.J.; Siga Jr., O.; Basei, M.A.S. and Campos Neto, M.C.

Instituto de Geociências-Universidade de São Paulo, Rua do Lago, 562 Cidade Universitária
São Paulo-SP, 05508-900, Brazil. crpass@usp.br

Keywords: Neoproterozoic, U-Pb geochronology, tectonic domains, shear zone, gneiss-migmatitic rocks

Tectonic domains limited by significant shear zones compose the southeastern part of São Paulo State, and their interpretation is fundamental to the regional geotectonic picture (Fig.1). The present tectonic situation, where four major tectonic domains were defined (Fig.2), is the product of *collages* related to the formation of West Gondwanaland, which ended in the Neoproterozoic (Almeida et al., 2000).

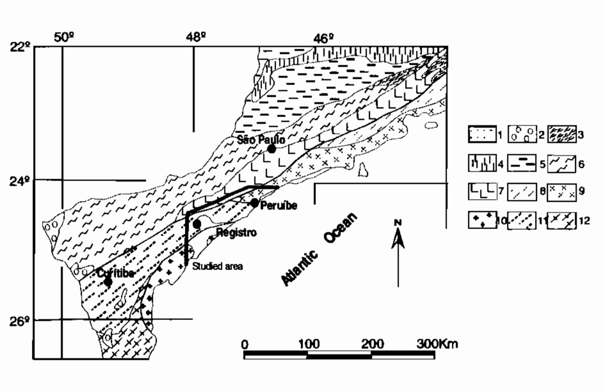

Figure 1. Outline of main tectonic domains of southeastern Brazil and localization of the studied area (mod. Campos Neto & Figueiredo, 1995; Basei et al., 1999). 1. Phanerozoic cover (Paraná Basin). 2. Neoproterozoic/Eo-Paleozoic Basins. 3. Juiz de Fora Infracrustal Terrane. 4. Alto Rio Grande Belt. 5. Socorro-Guaxupé Nappe. 6. Apiaí Folded Belt. 7. Embu Supracrustal Terrane. 8. Paraíba do Sul Terrane. 9. Serra do Mar Microplate. 10. Paranaguá Domain. 11. Curitiba Domain. 12. Luis Alves Terrane.

The Embu Domain occurs north of the Cubatão Shear Zone (CSZ), and it is mainly composed by metasedimentary rocks of medium to high metamorphic grade, locally migmatized, intruded by peraluminous granites which were controlled by E-NE shear zones (Cubatão - Itariri Shear System - CISS). Despite the analytical errors, the U-Pb monazite age of Sete Barras Granite (631 ± 23 Ma, Fig. 3A), is associated to the syn collisional stage of this sector of Ribeira Belt (RB) at around 620 Ma, (Janasi, 1999; Hackspacher et al., 2000) responsible for significant calc-alkaline magmatism. U-Pb (monazite) age of the Juquiá Granite (598 ± 8 Ma, Fig. 3B) dates the formation of these rocks from a crustal source and reflects the late collisional stage of this sector of RB which is characterized by lateral escape tectonics (NE-SW shear zones - formation of the CISS) and emplacement of granitic bodies. In addition, the Juquiá Granite has a model Nd T_{DM} age around 2.0 Ga.

The U-Pb zircon ages around 760 Ma (Figs. 3A and 3B) might reflect isotopic inheritance, but the possibility that represents the crystallization age of these granites and the monazite age (ca. 600 Ma) a later thermal event cannot be discarded. The peak of metamorphism in this domain at around 760 Ma was identified by Fernandes (1991), and reached high grade and anatexis. In addition, this phase was related to convergent tectonics (Vlach, 2001). Mylonitic orthogneisses of Embu Complex present a WR Rb-Sr isochron with an age of 770 Ma, and $(Sr^{87}/Sr^{86})i$ of 0.722 (Cordani et al., 2000), similar to the U-Pb zircon ages and $(Sr^{87}/Sr^{86})i$, found in this work (0.727). Nevertheless, the SHRIMP measurements reveal a very heterogeneous zircon population, with ages around 2,000, 800 e 660 Ma, indicating inherited, magmatic and metamorphic zircons respectively. The Nd and Sr isotopic data indicate that the granitic magmatism of this domain was produced from crustal source reworked in the Neoproterozoic.

The Mongaguá Domain is bounded to the northwest by CSZ, to the west by Itariri Shear Zone (ISZ) and to the east by the Atlantic Ocean (Fig. 2). It corresponds to undifferentiated migmatites of the Costeiro Complex (Gimenez Filho et al., 1987), to the Gneiss-migmatite Terrane of the Serra do Mar Microplate (Campos Neto & Figueiredo, 1995; Campos Neto, 2000), and to the Costeiro Granite Belt (Basei et al., 1999, 2000). The main rock type is gneiss-migmatite with granitic and dioritic compositions, in close association, and related granites. Passarelli (2001) defined three main groups of granite: the Itariri (IT), with gneiss migmatitic features, the Areado (A) with local gneissic features, and the Ribeirão do Óleo (RO) type with well-characterized magma mingling features. The main trend is E-NE, with the exception of the Itanhaém Gneiss (NW-SE structure and sub-horizontal dip).

For gneiss-migmatitic rocks conventional multicrystal zircon U-Pb dating provides an age of 612 ± 3 Ma (Fig. 4) interpreted as the crystallization age. Analyses of zircon indicate crustal inheritance in IT and RO Granites, and vague lower intercept U-Pb (zircon) ages around 580 and 620-630 Ma respectively (Passarelli, 2001). In this context, the A and RO granites are syn-kinematic to CISS since the ISZ movement conditioned the final phases of magmatic flow of IT Granite.

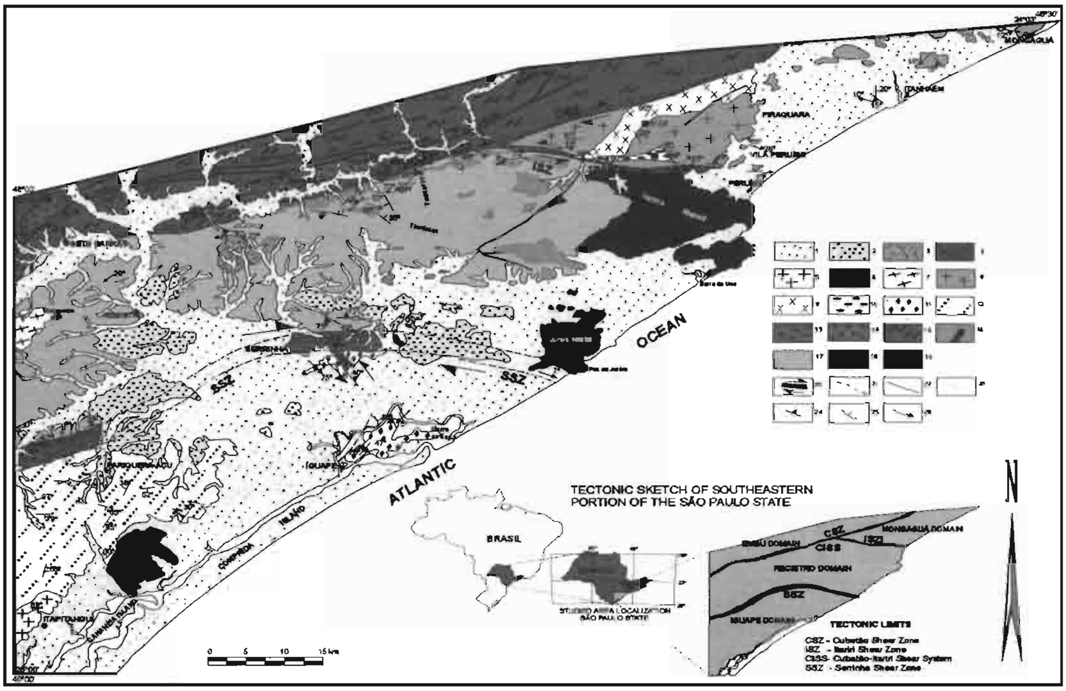

Figure 2. Geological map of southeastern São Paulo State. 1. Quaternary sediments. 2. Terciary sediments. 3. Juquiá Alkaline Complex (Cretaceous). 4.CISS and SSZ: mylonitic rocks (600-570 Ma). Serra do Mar Granitic Suite (c. 580 Ma): 5. Itapitangui; 6. Serra do Cordeiro 7. Serra do Votupoca. Mongaguá Domain: 8. Granite-gneiss-migmatitic Domain (c. 615-580 Ma). 9. Areado Granite (c. 610-580Ma). 10. Ribeirão do Óleo Granite (c.580 Ma). Iguape Domain: 11. Iguape Granite (c.600 Ma). 12. Iguape Metassediments (<2200 Ma). Embu Domain: 13. Juquiá Granite (c. 600 Ma). 14. Sete Barras Granite (c. 630 Ma). 15. Metassediments (<1600-1800 Ma). Registro Domain: 16. Granite-gneiss-migmatitic Domain (2100-580 Ma).17. Gneissic Domain (2200-580 Ma). 18. Itatins Complex (2200-580 Ma). 19.Juréia (> 750 Ma). 20. Transcurrent shear zones. 21. Infered Faults. 22. Lineaments. 23. Gradational geological contact. 24. Mylonitic foliation. 25. Principal foliation. 26. Mineral lineation.

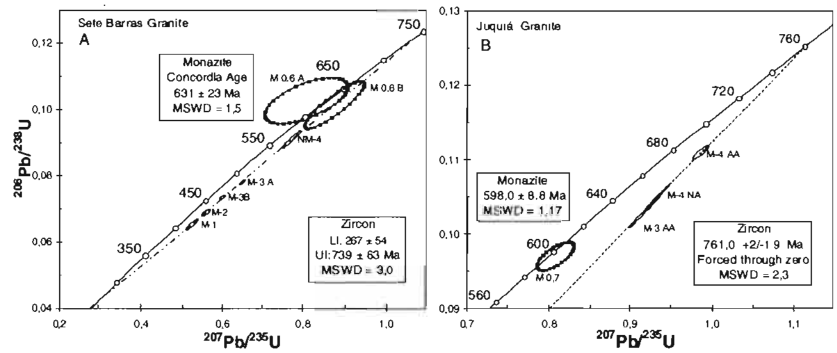

Figure 3. Concordia Diagram ^{207}Pb/^{235}U x ^{206}Pb/^{238}U (zircon and monazite). Embu Domain. A) Sete Barras Granite; B) Juquiá Granite

The similar TDM ages (1.7-1.8 Ga), negative ε_{Nd} values and (Sr^{87}/Sr^{86})i around 0,708, of the granitic and dioritic portions of the Mongaguá and Itanhaém rocks may indicate efficient mixing kinematics, as discussed by Perugini et al. (2002). The Sr and Nd isotopic compositions for the granites, demonstrate that differentiation of the different crustal sources from the mantle occurred during different paleoproterozoic events (1.7 Ga - RO and 2.2 Ga - IT).

The structural evidence provides a compressional setting to the generation and emplacement of the Mongaguá Domain rocks, and the recorded deformation is possibly related to the emplacement of these rocks and associated to the juxtaposition of the Mongaguá Domain to the others.

The Registro Domain, between the CISS and the Serrinha Shear Zone (SSZ) (Fig. 2) comprises granitic rocks with different degrees of assimilation by dioritic material and migmatitic features, and metasediments. Represents a paleoproterozoic domain (1.9–2.2 Ga) intensely affected in Neoproterozoic times (750 – 580 Ma), being correlated to Atuba Complex (Siga Jr. et al., 1995) of Curitiba Domain. The domain has a NW-SE structure, which swings to E or NE under the influence of the CISS.

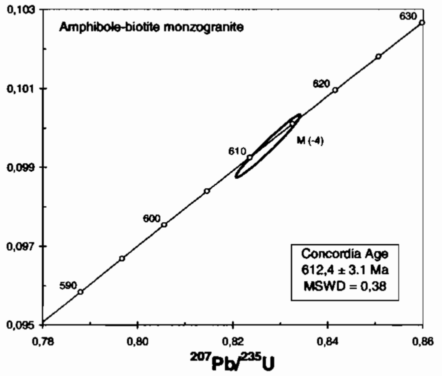

Figure 4. Concordia Diagram $^{207}Pb/^{235}U$ x $^{206}Pb/^{238}U$ (zircon) – Mongaguá Domain.

The migmatitic granites present evidence of extensional processes in the form of syn-plutonic dykes and enclave swarms. Mixing and mingling between the granitic and dioritic materials probably occurred between 2.2 and 1.9 Ga as shown by U-Pb (zircon) ages. The rocks were intensely affected by the Brasiliano tectono thermal event, as shown by the lower intercept U-Pb (zircon) ages of about 580 Ma in gneisses which have model Nd T_{DM} ages concentrated in the 2.7 - 2.9 Ga interval. The gneiss-migmatitic rocks present strongly discordant zircon U-Pb ages as a result of recrystallization during high grade metamorphism.

An upper intercept age of 1,894 ± 26 Ma was obtained in amphibole-biotite granodiorite (Fig. 5A) where ruptured syn-intrusive mafic dikes occur together with rounded enclaves. This result is interpreted as the minimum age for the crystallization of the granodiorite, and the mingling between granodioritic and dioritic magmas.

A record of paleoproterozoic and neoproterozoic ages is observed where hybrid rocks occur with gneissic and migmatitic features and with partially assimilated dioritic enclaves. An example is the mesocratic biotite-monzogranite with an upper intercept age of 2,197 ± 43 Ma interpreted as the probable age of crystallization of its protolith. The lower intercept age of 580 ± 23 Ma, in spite of being inaccurate, dates an important thermal / migmatitic event that caused neoformation of zircon crystals (Fig. 5**B**).

The mylonitic paragneiss from the Juréia Massif has a concordant U-Pb (monazite) age of 752 ± 4 Ma (Fig. 5C), that dates the amphibolite-grade metamorphism.

The Votupoca granite (Serra do Mar Suite, Kaul & Cordani, 1994) intruded into the gneiss-migmatites, has an age of 582 Ma (Passarelli, 2001).

Two distinct periods to mantle differentiation of the granitic rocks protolith are defined: 2.7-2.9 and 2.4 Ga.

The Sr and Nd isotopic compositions are clearly controlled by the hybridization degree of dioritic and granitic magmas. Where the mixing predominates both rocks present similar $(Sr^{87}/Sr^{86})i$ around 0.717 and negative εNd values. In some areas, the mixing was not so efficient, and the end members are isotopically different.

Rocks of the Iguape Domain, limited northwards by the SSZ and south-southeastwards by the Atlantic Ocean, include granites and metasediments with a dominantly NE structural orientation (Fig. 2). It is correlated to the Paranaguá Batolith (Basei et al., 1990) and Costeiro Granitic Belt (Basei et al., 1999, 2000).

The metasediments are mostly in low metamorphic grade, while the granites comprise three separate geochronological and geochemical groups. Protomylonitic granites of the Iguape massif have ages around 600 Ma (Fig. 6), and have geochemical signatures of volcanic arc or syncollision granites. The granites of the Paratiú - Cordeiro and Itapitangui hills are 580 Ma intraplate granites, similar to the Serra do Mar Granitic Suite (Kaul & Cordani, 1994). The SSZ has a dominantly E-W direction and dextral sense, but an important SE-oriented branch is sinistral.

Two distinct phases of mantle differentiation of the granitic rocks protolith are defined: 2.2 Ga and 1.8 Ga, and similar ε_{Nd} values that suggest similar crustal contributions to the generation of these rocks. $(Sr^{87}/Sr^{86})i$ between 0.711 and 0.714 corroborate this.

The studied rocks were originated and/or significantly affected by the Brasiliano Orogeny, and the oldest domains in the area (Embu and Registro) register an early thermo-metamorphic event at around 750 Ma.

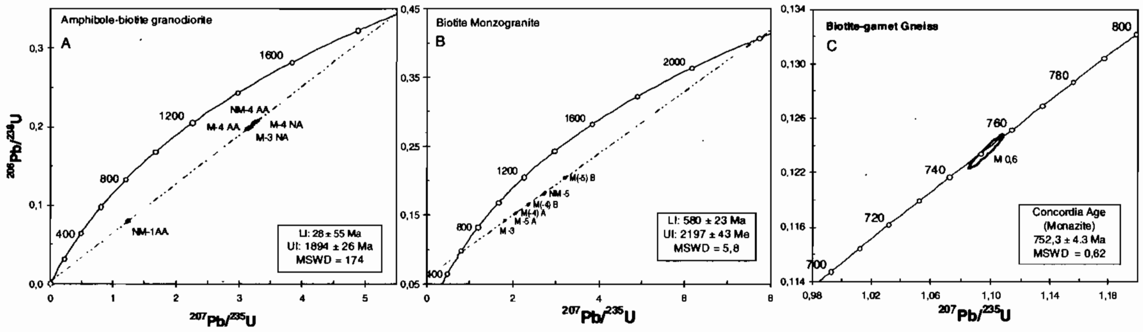

Figure 5. Concordia Diagram $^{207}Pb/^{235}U$x$^{206}Pb/^{238}U$ (zircon). A) Oliveira Barros; B) Serra Timirim; C) Juréia Massif–Registro Domain.

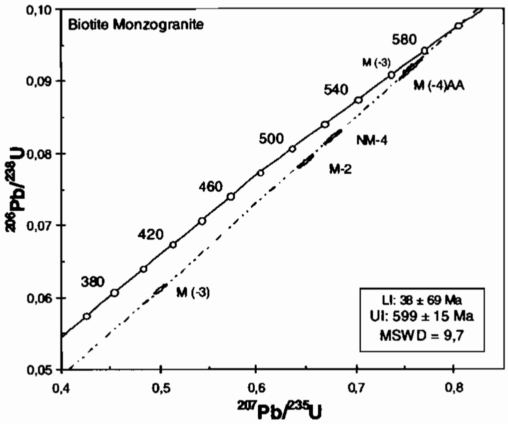

Figure 6. Concordia Diagram $^{207}Pb/^{235}U$ x $^{206}Pb/^{238}U$ (zircon) Morro do Espia – Iguape Domain.

It is likely that all these tectonic blocks were juxtaposed during a short time interval at the end of Neoproterozoic. The joining of the Registro and Embu Domains occurred at about 606 Ma along an E-W shear zone (Passarelli, 2001). The 598 Ma peraluminous granites (Embu Domain) may register the arrival of the Mongaguá Domain against the newly formed Registro-Embu Domain through E-W compression. The generation and emplacement of granite-gneiss migmatitic rocks of Mongaguá Domain (612 ± 3 Ma) might be associated to compressive regimes, possibly related to the juxtaposition kinematics of this domain to the others. The welding of the Iguape and Registro domains probably occurred between 580 and 570 Ma, as suggested by the U-Pb (monazite) age of the protomylonitic granites of the SSZ.

REFERENCES

Almeida, F.F.M.; Brito Neves, B.B.; Carneiro, C.D.R. (2000). The origin and evolution of the South Ameriacan Plataform. Earth Science Reviews, 50:77-111.

Basei, M.A.S.; Siga Jr., O.; Reis Neto, J.M. (1990). O Batólito Paranaguá. Proposição, idade, considerações petrogenéticas e implicações tectônicas. In: Cong. Bras. Geol., 36, Natal. Anais...Natal, SBG, v.4, p.1684-1699.

Basei, M.A.S.; Siga Jr., O.; Reis Neto, J.M.; Passarelli, C.R.; Prazeres, H.J.; Kaulfuss, G.; Sato, K.; Lima, P. S. de (1999). Paleoproterozoic granulitic belts of the Brazilian Southern Region (PR-SC). In: South-American Symposium on Isotope Geology, II. Cordoba, Extended Abstracts, p.291-294.

Basei, M.A.S.; Siga Jr., O.; Masquelin, H.; Harara, O.M.; Reis Neto, J.M.;Preciozzi, P. (2000). The Dom Feliciano Belt of Brazil and Uruguai and its foreland domain, the Rio de La Plata Craton: framework, tectonic evolution and correlation with similar provinces of southwestern Africa. In: Cordani, U.G.; Milani, E.J.; Thomas Filho, A.; Campos, D.A. Tectonic Evolution of South America, Rio de Janeiro, 2000, p: 311-334.

Campos Neto, M. C. (2000). Orogenic Systems from Southwestern Gondwana: an approach to Brasiliano-Pan African cycle and orogenic collage in southeastern Brazil. In: Cordani, U.G.; Milani, E.J.; Thomas Filho, A.; Campos, D.A. Tectonic Evolution of South America, Rio de Janeiro, 2000, p: 335-365.

Campos Neto, M.C.; Figueiredo, M.C.H. (1995). The Rio Doce Orogeny, southeastern Brazil. J S Am Earth Sci, 8(2): 143-162.

Cordani, U.G.; Coutinho, J.M.V.; Nutman A. (2000). Geochronological constraints for the age of the Embu Complex, São Paulo, Brazil. In: Cong. Bras. Geol., 39, Rio de Janeiro.

Fernandes, A.J. (1991). O Complexo Embu no E do estado de SP: contribuição ao conhecimento da litoestratigrafia e da evolução estrutural e metamórfica. MscThesis.São Paulo,IGc-USP,120p.

Gimenez Filho, A.; Albuquerque Filho, J.L.; Dantas, A.S.L. Fernandes, L.A.; Nagata, N.; Teixeira, A. L. (1987). Geologia da Folha Miracatu, S-SE do estado de São Paulo. In: Simp. Reg. Geol., 6.V. Rio Claro, 1987.Anais...Rio Claro,SBG v1, p.225-241.

Hackspacher, P.C.; Dantas, E.L.; Spoladore, A.; Fetter, A.H; Oliveira, M.A.F. de. (2000). Evidence of Neoproterozoic Backarc Basin development in the Central Ribeira Belt, Southeastern Brazil: new geochronological and geochemical constraints from the São Roque–Açungui Groups. Rev. Bras. Geoc., 30(1):110-114.

Janasi, V.A. (1999).Petrogênese de granitos crustais na Nappe de Empurrão Socorro-Guaxupé (SP-MG):uma contribuição da geoquímica elemental e isotópica. Thesis S Paulo, IG–USP,304 p.

Kaul, P.F.T.; Cordani, U.G. (1994). Aspectos petrográficos, geoquímicos e geocronológicos dos maciços graníticos da Serra do Mar no leste do Paraná e vizinhanças. In: Cong. Bras. Geol., 38, Camboriú. Bol.Res.Exp. Camboriú, SBG, v.2, p.371-372.

Passarelli, C. R. (2001). Caracterização estrutural e geocronológica dos domínios tectônicos da porção sul-oriental do Estado de São Paulo. Ph Thesis.São Paulo, IGc-USP, 254p.

Perugini, D.; Poli, G.; Gatta, G.D. (2002). Analysis and simulation of magma mixing processes in 3D. Lithos, 65: 313-330.

Siga Jr., O.; Basei, M.A.S.; Reis Neto, J.M.; Machiavelli, A.; Harara, O.M. (1995). O Complexo Atuba: um cinturão Paleoproterozóico intensamente retrabalhado no Neoproterozóico. Boletim - IG-USP, Série Científica, 26: 69-98.

Vlach, S. (2001). Micropobe Monazite Constraints for an early (ca. 790 Ma) Brasiliano Orogeny: the Embu Terrane, Southeastern Brazil. In: South-American Symposium on Isotope Geology. Chile, 2001. Extended Abstracts.

SHRIMP U-Pb AND Sm-Nd AGES OF THE NIQUELÂNDIA LAYERED COMPLEX: MESO- (1.25 Ga) AND NEOPROTEROZOIC (0.80 Ga) EXTENSIONAL EVENTS IN CENTRAL BRAZIL

Pimentel, M.M.[1]; Armstrong, R.A.[2] and Ferreira Filho, C.F.[1]

1. Instituto de Geociências, Universidade de Brasília, Brasília-DF, 70910-900. Brazil. marcio@unb.br, cesarf@unb.br
2. Research School of Earth Sciences, Australian National University, Canberra, ACT 0200, Australia. richard.armstrong@anu.edu.au

Keywords: Niquelândia, Brasília Belt, Neoproterozoic rift, Mesoproterozoic, SHRIMP

INTRODUCTION

Three large layered mafic-ultramafic complexes forming a discontinuous 350-km long belt, limited at the east by a west-dipping mylonite zone, represent one of the most relevant and debated features of the geology of the Neoproterozoic Brasília Belt, in central Brazil. Due to their sizes and metallogenetic potential, the age and tectonic significance of these large complexes have been the subject of ongoing debate and controversy.

Different tectonic models range from those advocating that they are fragments of Archean or Paleoproterozoic oceanic crust (e.g. Danni et al., 1982; Moores, 2002) to ideas suggesting that they represent Meso- or Paleoproterozoic rift-related layered intrusions (e.g Ferreira Filho et al., 1994; Brito Neves et al., 1995; Correia et al., 1996). In both cases they have been interpreted as the exposure of older units within younger rocks of the Brasiliano/Pan-African orogenic belt. The intrusions are known, from south to north, as the Barro Alto, Niquelândia and Cana Brava complexes. They are bordered in the west by bimodal volcano-sedimentary sequences known as the Juscelândia, Indaianópolis and Palmeirópolis sequences, respectively, together with their plutonic counterparts including gabbros, leucogabbros, anorthosite and granite intrusions.

The original igneous stratigraphy of the complexes has been partially disrupted by intense deformation associated with high grade metamorphism, although preserved igneous textures and structures are not uncommon (Danni et al., 1982; Ferreira Filho et al., 1992). Despite intense tectonism, several geological similarities between the three separate bodies have been used to suggest that they originally constituted a single continuous magmatic structure (Ferreira Filho, 1998).

Detailed mapping and petrological studies supported by conventional and SHRIMP U-Pb and Sm-Nd geochronology, carried out over the last ten years, especially on rocks of the Niquelândia Complex, have pointed out the following major aspects of their igneous and metamorphic evolution:

(i) they have been metamorphosed at high grade at ca. 760-790 Ma ago (U-Pb zircon ages), from granulite facies conditions in the east, to amphibolite facies in the west (Ferreira Filho et al., 1998a, 1994);

(ii) the Niquelândia Complex is made of two distinct intrusions, which have been tectonically juxtaposed along a NNE fault zone. A similar interpretation has been suggested for the Barro Alto intrusion (Ferreira Filho, 1998).

Conventional and SHRIMP U-Pb, Rb-Sr, Sm-Nd and Re-Os ages for these intrusions have generated intense debate. Dates vary from ca. 2.0 Ga to 1.3 Ga (Fuck et al., 1989; Fuji, 1989; Ferreira Filho et al., 1994; Suita et al., 1994; Correia et al.. 1996, 1997, 1999; Ferreira Filho & Pimentel, 2000). Poorly constrained U-Pb and Re-Os ages ranging from ca. 1.6 and 2.0 Ga, have been used to suggest a Paleoproterozoic age for the Niquelândia and Barro Alto complexes (Ferreira Filho et al., 1994; Suita et al., 1994; Correia et al., 1996, 1997, 1999)

In this study, new U-Pb and Sm-Nd geochronological data are discussed and support the idea that the Niquelândia Complex is in fact made of two different intrusions. Contrary to what has been suggested previously, its eastern part represents a Neoproterozoic layered intrusion emplaced into and contaminated with older continental crust. The western part of the complex, on the other hand, represents a 1.25 Ga old rift-related layered intrusion. The data, in combination with isotopic data available in the literature, were used to support the discussion on alternative interpretations not only for the tectonic significance of the large layered complexes and evolution of the Brasília Belt, but also for the previous geochronological data.

THE NIQUELÂNDIA COMPLEX

The Niquelândia Complex displays the best exposed and studied stratigraphic sequence of the three large layered intrusions in central Brazil. The southern and eastern limits are marked by the W-dipping Rio Maranhão Thrust Zone. To the west the complex is in tectonic contact with the Indaianópolis volcano-sedimentary sequence (Danni et al. 1982).

Recent detailed field and petrological studies have demonstrated that the complex comprises two petrologically distinct magmatic systems (Ferreira Filho, 1994, 1998a). The eastern system has been considered to be older (Paleoproterozoic), based on the geochronological data mentioned above, and is called the Lower Series (LS; Ferreira Filho, 1994). The mafic-ultramafic rocks underlying the western part of the complex (Upper Series – US), have been thought to be Mesoproterozoic (ca. 1.35 Ga) based on Sm-Nd whole-rock isochron ages for leucogabbros and coarse-grained amphibolites (Ferreira Filho & Pimentel, 2000).

The Lower Series is divided into a lower mafic zone (LMZ) dominated by gabbronorite with minor pyroxenite, an ultramafic zone (UZ) made of dunite and pyroxenite, and an upper mafic zone (UMZ) dominated by gabbronorite. Rocks of the UMZ display a trend of progressive Fe enrichment in pyroxene, accompanied by a strong enrichment in incompatible trace elements, compatible with crystal fractionation and strong contamination of the original magma with country rocks; extreme contamination with sialic country rocks has generated facies of dioritic/gabbrodioritic compositions which underlie significant areas in the westernmost part of the UMZ. The US is formed by leuco-troctolite, anorthosite, gabbro and minor pyroxenite. Trace element data indicate a distinct parental magma for the US (Ferreira Filho et al., 1998a). Sm-Nd whole-rock isochrons indicate ages of ca. 1.35 Ga and $\varepsilon_{Nd}(T)$ values between +4.8 and +4.1, indicating the very depleted nature (low Sm/Nd) of the mantle source (Ferreira Filho & Pimentel, 2000).

The progressive amphibolite to granulite facies metamorphic event was characterized in detail by Ferreira Filho et al. (1992, 1998b). Rocks of the Niquelândia Complex show changes in texture and mineral assemblages in response to changing metamorphic grade. Three metamorphic zones are distinguished from west to east: amphibolite zone (pl + hbl ± cpx ± gt), amphibolite-granulite transition zone (pl + hbl + opx + cpx) and granulite zone (opx + cpx + pl). A nearly isobaric cooling trajectory followed peak metamorphism, suggests cooling in the absence of tectonic unroofing. A second and chronologically distinct tectonic event is then required to uplift and expose the high-grade terrains. These two metamorphic events seem to be indicated by the available geochronological data. The older event, at ca. 770-795 Ma is constrained by SHRIMP and conventional U-Pb analyses on metamorphic zircon grains (Ferreira Filho et al., 1994; Suita et al., 1994; Correia et al., 1996). This is considerably older than the ca. 630-610 Ma event, which is recorded throughout the Brasília Belt (Pimentel et al. 2000). A younger metamorphic event at ca. 610 Ma has also been indicated by rutile U-Pb and garnet Sm-Nd isotopic data (Ferreira Filho et al., 1994; Ferreira Filho & Pimentel, 2000) and is interpreted as coeval with the eastward thrust that uplifted the complex.

RESULTS

Two samples of the LS and one of the US were selected for the analytical work. Samples CF-03 (LS diorite) and CF-04 (US milonitic rock) yielded a large number of zircon grains, whereas Ni-376 (LS gabbronorite) did not produce any. The latter was, therefore, analysed by the Sm-Nd isochron method on igneous minerals concentrates. Zircon cores in sample CF-03 yielded mostly concordant analyses showing a wide range of $^{206}Pb/^{238}U$ ages, mostly between ca. 1.0 Ga to 1.9 Ga representing varied inheritance. On the other side, analyses of rims as well as zones with oscillatory zoning have produced only Neoproterozoic $^{206}Pb/^{238}U$ ages (Fig. 1a). These included analyses of the bright luminescent rims, of rims displaying oscillatory zoning as well as of a few crystal cores. All rims present high values of the Th/U ratio (between 0.29 and 0.67). The analyses yielded a concordia age of 797 ± 10 Ma (probability of concordance of 0.71), which is interpreted as the age of crystallization of quartz diorite CF-03, and therefore of the LS of the Niquelândia Complex.

Pure plagioclase and clinopyroxene concentrates were separated from the lower series gabbronorite Ni-376. Together with the whole-rock sample, these igneous mineral concentrates define a Sm-Nd mineral isochron indicating the age of 767 ± 38 Ma (2σ) and $\varepsilon_{Nd}(T)$ of –5.8 (Fig. 1b). Although this is considerably younger than the SHRIMP U-Pb age, both ages agree within analytical uncertainty, and the Sm-Nd mineral isochron age may still be interpreted as a minimum estimate for the igneous age. The negative $\varepsilon_{Nd}(T)$ value is compatible with contamination of the original magma with older crustal material, as already indicated by the petrological data of Ferreira Filho et a. (1998) and also by the inheritance pattern in the U-Pb analysis.

Five additional whole-rock samples of the LS were analysed and the resulting 6-point "errorchron" (MSWD = 58) indicate the age of ca. 1.90 Ga. The Paleoproterozoic age, however, is defined by one analytical point with high Sm/Nd ratio. The remaining samples, with lower Sm/Nd ratios, however, seem to form a linear array suggesting a Neoproterozoic age (ca. 0.73 Ga). This indicates that the regression line giving the Paleoproterozoic age may represent a mixing line and not a true isochron relationship. This is analogous to the Re-Os data available for these rocks (Correia et al., 1996), which might therefore also represent a mixing line. The U-Pb and Sm-Nd presented above, therefore, are compatible with a Neoproterozoic age for the lower series of the Niquelândia Complex. Previous suggestions of a Paleoproterozoic age for these rocks, based on SHRIMP U-Pb ages of zircon cores and a whole-rock Re-Os isochron, are not supported by the new data.

Cathodo-luminescence images reveal that zircon grains from mylonite sample CF-04 of the upper series of the complex typically show cores displaying sector zoning, surrounded by bright luminescent, homogeneous rims. The cores are interpreted as remanescent of the original upper series gabbroic rock. The rims display low Th/U ratios, common in metamorphic zircon and ten analyses on them yielded a concordia age of 765 ± 4 Ma. Analyses of cores fall along a poorly constrained and shallow discordia line, between ca. 0.76 Ga and 1.25 Ga. The upper intercept is better constrained by the mean $^{207}Pb/^{206}Pb$ ages of the most concordant analyses, indicating the age of 1248 ± 23 Ma, interpreted, therefore, as the best estimate for the crystallization of the gabbroic rocks of the upper series. The strongly positive values of $\varepsilon_{Nd}(T)$ values indicated by the Sm-Nd isochrons (+4.1 and +4.8) for these rocks, contrast with the negative value observed for lower series rocks, supporting the idea that the upper and lower series of the Niquelândia Complex represent two distinct complexes, formed by magmas derived from different sources, and probably emplaced in contrasting tectonic settings. The ca. 1.25 Ga old gabbros of the upper series are, therefore, primitive, derived from a strongly depleted mantle, whereas the ca. 0.8 Ga old lower series rocks are strongly contaminated with continental crust.

CONCLUSIONS

The new geochronological and isotopic data presented here, combined with re-interpretation of existing data in the literature shed new light on the age of the large mafic-ultramafic complexes in the central part of the Tocantins Province and on the tectonic evolution of the Brasília Belt. They demonstrate that they are neither part of the ca. 2.0-1.8 Ga intracontinental rift in northern Goiás and Tocantins as suggested by previous studies (Brito Neves et al., 1995;, Correia et al., 1997, 1999), nor represent Archean/Paleoproterozoic oceanic (Danni et al., 1982; Moores, 2002).

The new data demand, thus, that alternative tectonic models are brought to discussion. In summary, the sequence of events suggested by the geochronological data is:

- ca. 1.3-1.25 Ga – formation of a continental rift, possibly evolving to a very narrow ocean, giving rise to the Juscelândia, Indaianópolis and Palmeirópolis volcano-sedimentary sequences and their plutonic equivalents of the upper series of the Niquelândia and Barro Alto complexes;
- ca. 0.80 Ga – establishment of another continental rift, with the emplacement of mafic magmas forming the lower series of the Niquelândia Complex, and by analogy, of the Barro Alto and Cana Brava intrusions.
- ca. 0.76 Ga – high-grade metamorphism
- ca. 0.63 Ga – regional metamorphism probably caused by final ocean closure and continental collision between the São Francisco and Amazonian continents. The final tectonic ascent of the mafic-ultramafic complexes along the Rio Maranhão Thrust Zone may be attributed to this stage.

These Meso- and Neoproterozoic rifting events have not been described before in other parts of the Brasília Belt or even within the São Francisco Craton. Although equivalent Meso- and Neoproterozoic extensional events have been abundantly reported in other continents (e.g. Laurentia and Baltica), they are not common in the Precambrian terrains of South America. The ca. 0.8 Ga event is roughly coeval with the world-wide extensional event which marked the fragmentation of Rodinia. However, the precursor rift of the passive margin of the Brasília Belt is believed to have started at ca. 1.0 Ga, as indicated by mafic dyke swarms within the São Francisco Craton. Therefore 1.25 Ga old oceanic crust seems to be too old to represent the product of the rifting event which led to the deposition of the passive margin sequences in the Brasília Belt, and the 0.8 Ga event seems to be too young. Furthermore, the ca. 0.76 Ga high grade metamorphic event is not described in other parts of the Brasília Belt, except for an isolated Sm-Nd garnet age for a garnet schist of the Mara Rosa arc, to the west of Niquelândia (Junges et al. 2003). High grade rocks and garnet bearing supracrustal rocks within the sedimentary sequences of the Brasília Belt present considerably younger metamorphic ages, between ca. 650 and 610 Ma (Pimentel et al., 2000; Piuzana et al., 2003a).

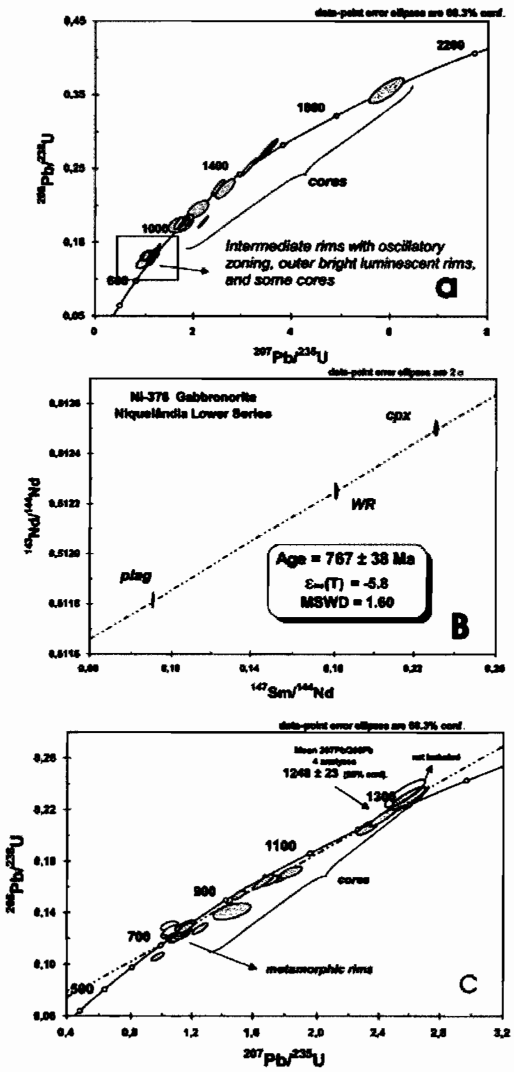

Figure 1. U-Pb data.

The mismatch between the sequence of events recorded for the Niquelândia Complex and that of the rest of the Brasília Belt, allied with the fact that the three large mafic-ultramafic complexes coincide with a regional gravimetric discontinuity typical of suture zones (Marangoni et al. 1995) suggest that they are part of an allochthonous block, formed away from the western margin of the São Francisco continent (Laurentia-Baltica?). This allochton was accreted to the western margin of the Brasília Belt during the Neoproterozoic, probably at ca. 0.76 Ga.

However, one might still argue that the time span between rifting (0.80 Ga) and metamorphism (ca. 0.76 Ga) is too short and may be difficult to reconcile with an allochtonous origin for the Niquelândia Lower Series. Thus, an autochthonous model in which the Niquelândia LS corresponds to a complex emplaced in a continental back arc setting, should also be considered, and both allochtonous and autochthonous models should be tested in future studies.

REFERENCES

Brito Neves,B.B, Sá, J.M., Nilson,A.A., Botelho,N.F. 1995. A tafrogênese estateriana nos blocos paleoproterozóicos da América do Sul e processos subseqüentes. Geonomos, 3(2):1-21.

Correia,C.T., Girardi,V.A.V., Lambert,D.D., Kinny,P.D., Reeves,S.J. 1996. 2 Ga U-Pb (SHRIMP II) and Re-Os ages for the Niquelândia Basic-Ultrabasic Layered Intrusion, central Goiás, Brazil. In: Cong. Bras. Geol., 39., Anais v. 6... Salvador, SBG, p. 187-189.

Correia,C.T., Girardi,V.A.V., Tassinari,C.C.G., Jost,H. 1997. Rb-Sr and Sm-Nd geoghronology of the Cana Brava layered mafic-ultramafic intrusion, Brazil, and considerations regarding its tectonic evolution. Rev. Bras. Geoc., 27(2):163-168.

Correia,C.T., Jost,H., Tassinari,C.C.G., Girardi,V.A.V., Kinny,P. 1999. Ectasian Mesoproterozoic U-Pb ages (SHRIMP-II) for the metavolcano-sedimentary sequences of Juscelândia and Indaianópolis and for high grade metamorphosed rocks of Barro Alto stratiform igneous complex, Goiás State, central Brazil. In: SAAGI - South Am Symp. On Isot. Geol., 2., Actas... SEGEMAR, Córdoba, p.31-33

Danni,J.C.M., Fuck,R.A., Leonardos Jr., O.H., 1982. Archean and Lower Proterozoic Units in Central Brazil. Geol. Rundschau, 71:291-317

Ferreira Filho, C.F. 1998. Geology and petrology of the large layered intrusions of central Brazil: implications for PGE mineralization. In: Platinum Symp., Rustemburg, South Africa, Extended Abst... p. 107-110.

Ferreira Filho,C.F., Kamo,S., Fuck,R.A., Krogh,T.E., Naldret,A.J. 1994. Zircon and rutile geochronology of the Niquelândia layered mafic and ultramafic intrusion, Brazil: constraints for the timing of magmatism and high grade metamorphism. Precambrian Res., 68:241-255.

Ferreira Filho, C.F, Moraes, R., Fawcett,J.J., Naldrett,A.J. 1998a. Amphibolite to granulite progressive metamorphism in the Niquelândia Complex, central Brazil: regional tectonic implications. J. South Am. Earth Sci., 11:35-50.Ferreira Filho 1998.

Ferreira Filho,C.F. & Pimentel,M.M. 2000 Sm-Nd isotope systematics and REE-Hf-Ta-Th data of troctolites and their amphibolitized equivalents of the Niquelândia Complex Upper Layered Series, central Brazil: further constraints for the timing of magmatism and high-grade metamorphism. Journal of South American Earth Sciences 13 (7): 647-659.

Fuck, R.A., Brito Neves, B.B., Cordani, U.G., Kawashita, K.. 1989. Geocronologia Rb-Sr no Complexo Barro Alto, Goiás: evidência de metamorfismo de alto grau e colisão continental há 1300 Ma no Brasil Central. Geochim. Brasiliensis 3(2), 125-140Fuck et al. 1989

Marangoni,Y., Assumpção,M., Fernandes,E.P. 1995. Gravimetria em Goiás, Brasil. Rev. Bras. Geofísica, 13(3):205-219.

Moores,E.M. 2002. Pre-1Ga (pre-Rodinian) ophiolites: their tectonic and environmental implications. Geol. Soc. Am. Bull, 114:80-95.

Piuzana,D., Pimentel,M.M., Fuck,R.A., Armstrong,R.A. 2003a. Neoproterozoic granulite facies metamorphism and contemporaneous granite magmatism in the Brasília Belt, central Brazil: regional implications of new SHRIMP U-Pb and Sm-Nd data . Precam Res. In press.

Piuzana,D., Pimentel,M.M., Fuck,R.A., Armstrong,R.A. 2003b. SHRIMP U-Pb and Sm-Nd data for the Araxá Group and associated magmatic rocks: constraints for the age of sedimentation and tectonic evolution of the southern Brasília Belt, central Brazil. Precamb. Res., in press.

Suita,M.T.F., Kamo,S., Kroght,T.E., Fyfe,W.S., Hartmann,L.A. 1994. U-Pb ages from the high-grade Barro Alto mafic-ultramafic complex (Goiás, central Brazil): middle Proterozoic continental mafic magmatism and upper Proterozoic continental collision. In: Intern. Confer. On Geochron. Cosmochr. and Isot. Geol. – ICOG, 8., Abstracts... Berkeley, USGS, p.309.

Sm-Nd ISOTOPIC CHARACTERIZATION OF METATONALITES FROM THE ITABUNA BELT, BAHIA BRASIL

Pinho, I.C.A.[1]; Barbosa J.S.F.[1] and Peucat J.J.[2]

1. CPGG - Centro de Pesquisa em Geofísica e Geologia-UFBA, Rua Caetano Moura 123, Federação, 40210-350, Salvador-BA, Brazil. ivana@cpgg.ufba.br, johildo@cpgg.ufba.br
2. Geosciences Rennes, UPR CNRS 4661, 35042 Rennes cedex, France. peucat@univ-rennes1.fr

Keywords: Geochronology, metatonalites, Paleoproterozoic, Bahia, Brazil

INTRODUCTION

The Archean to Paleoproterozoic granulitic region in the SSE of Bahia State is formed by two main geotectonic domains: the Jequié Block and the Itabuna Belt. Both are strongly deformed and have equilibrated at the granulite facies. These domains are kept apart by the Ipiaú Belt, which is metamorphosed at the amphibolite facies (Barbosa, 1986).

According to Barbosa & Sabaté (2000) the Jequié Block and the Itabuna Belt, both with protoliths of Archean age, collided during the Paleoproterozoic Transamazonian orogeny (Ledru et al., 1993), which involved a general NW-SE compression. This is identified by the presence of regional faults and transcurrent zones that contain kynematic indicators of a general sinistral movement. During the initial fase of this collision, ca. 2.4 Ga, a frontal ramp ductile tangential tectonism caused the thrusting of the Itabuna belt (Barbosa & Sabaté, 2000) above the Jequié block, thus generating recumbent folds with vergence towards the west. In the second episode of deformation, ca. 2.1–2.0 Ga (Ledru et al., 1993), these folds have been refolded in an aproximatetelly coaxial way, in association with the evolution of transcurrent zones.

According to Barbosa (1990, 1991) the Itabuna Belt, in the southern sector, is composed by three main lithological types: (i) basic granulites containing or not garnet (protoliths analogous to the basalt and/or tholeiitic gabbros) (ii) acid and intermediate granulites (protoliths of tonalite type, dacites and trondhjemites, calc-alcaline-low potassium rhyolite) and (iii) basic granulites bearing antiperthite (protoliths formed by monzonites and shoshonitic mangerites). Kinzigites, quartzites, banded iron formations, manganiferous formations, besides barite layers ocurr intercaleted in the granulites, mainly in those of intermediate and acid composition (Fig. 1).

GEOLOGICAL ASPECTS

The metatonalites in outcrop are generally fine to medium grained and invariably of dark grey at greenish grey color, when fresh. When altered they show a whitish color. In general, they are leuco to mesocratic, showing banding or foliation with attitude of N20° E and dips between 50° to 80° either towards SE or NW. These rocks present a xenoblastic to granoblastic texture, and are composed of: antiperthitic plagioclase, quartz, orthopyroxene, clinopyroxene, opaque minerals, zircon, and apatite. Biotite and hornblende are secondary, and have been formed during the retrometamorphism. Garnet is rarely present and in general appears when these plutonic rocks are next or enclosed in supracrustal, Al-rich rocks (Pinho, 2000).

Acording to lithogeochemical study of major, trace and ETR elements this rocks are calsified as true tonalites with SiO_2 values between 53 at 65.90%, and are predominantly calc-alcaline with low potassium content, therefore evidencing a trondhjemitic affinity (Pinho, 2000). The overall ETRL enriched and ETRP depleted pattern, the absence of Eu anomaly, and the Ce_N/Yb_N ratios between 6.21 and 22.41, indicate a moderate igneous fractionation.

RESULTS AND DISCUSSION

Three representative metatonalite samples (JF-142A, TD-06 and YJ-16) were taken to the isotopic study, which consisted of measurement of the Sm and Nd concentrations, along with the calculation of the respective isotopic ratios. Additionaly, in the sample JF-142A, the Rb-Sr ratio calculation and a geochronological zircon U-Pb SHRIMP analysis have been performed. The analytical work has been carried out in the Geochronology and Isotopic Geochemistry Laboratory of the Rennes University, France. The methodology is detailed in Peucat et al. (1999b). The U-Pb zircon analyses were performed using SHRIMP I at the Research School of Earth Sciences, Australian National University.

The Sm-Nd analyses revealed T_{DM} model ages varying between 2.52 and 2.82 Ga. The values of the $\varepsilon_{Nd\,(T=2.15\ Ga)}$ vary from -1.18 to -2.10 (Table 1). The JF-142A sample presented an $^{87}Sr/^{86}Sr$ initial ratio of 0,70549 and ε_{Sr} of 27.31 (Table 2).

U-Pb SHRIMP age is 2151 ± 22 Ma (Peucat, in personal comm.) is intrepreted as the crystallization age of the metatonalites, while the T_{DM} model ages could be considered as the timing of magma extraction from the mantle.

The positive ε_{Sr} and negative $\varepsilon_{Nd(T=2.15\ Ga)}$ are indicative of an enriched mantle source for this rock. However, the negative values of the $\varepsilon_{Nd(T=2.15\ Ga)}$ suggest a crustal contamination of the magma. This probably occured during the Transamazonian orogeny, and produced the older T_{DM} model ages.

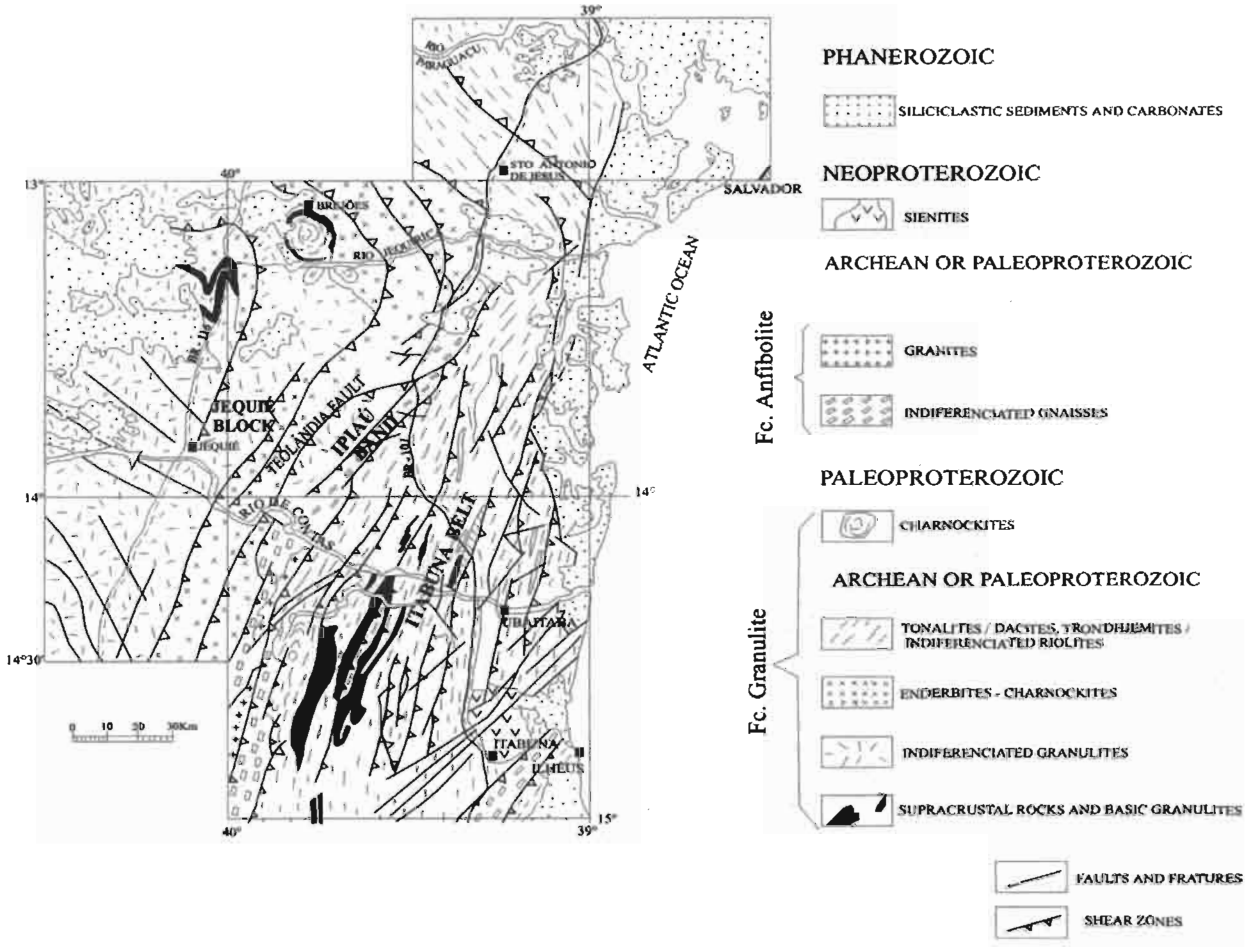

Figure 1. Geologic simplified map of the south-southwest granulitic region from the Bahia State (after Barbosa, 1991).

Table 1. Sm-Nd analytical dates of the metatonalites from the Ubaitaba region.

Sample	Sm (ppm)	Nd (ppm)	$^{147}Sm/^{144}Nd$	$^{143}Nd/^{144}Nd$	T_{DM} (Ga)	ε_{Nd} (2,15)
JF-142A	1.71	12.83	0.0806	0.510887	2.58	-2.10
TD-6	2.61	12.10	0.1304	0.511600	2.82	-1.95
YJ-16	3.30	25.06	0.0794	0.510917	2.52	-1.18

Table 2. Rb-Sr aAnalytical datum of the metatonalite from the Ubaitaba region.

Sample	Rb (ppm)	Sr (ppm)	$^{87}Rb/^{86}Sr$	$^{87}Sr/^{86}Sr$	ε_{Sr}(2,15)
JF-142A	17	990	0.0497	0.705428	27.31

ACKNOWLEDGEMENTS

Part of the anaytical work was supported by CAPES-COFECUB Project. M.L.S. Rosa and C. Leite to discussion and English revision.

REFERENCES

Barbosa, J.S.F, 1986. Constitution lithologique et metamorphique de la region granulitique du sud de Bahia Brésil. Tese Doutorado - Académie de Paris. Paris, Université Pierre et Marie Curie, 1986. 401 p., il., mapa anexo.

Barbosa, J.S.F. 1990. The granulites of the Jequié Complex and Atlantic Coast Mobile Belt, Southern Bahia, Brazil - An expression of archaen early proterozoic plate convergence. In: Vielzeuf, D.; Vidal, P. (ed.). Granulites and Crustal Evolution. s. l.: Kluwer Academic, p. 195-221., il.

Barbosa, J.S.F. 1991. Projeto Geologia e Metalogenia do Domínio da Costa Atlântica da Região Granulítica do Sul da Bahia - Brasil. Relatório final. Salvador: UFBA, Convênio SME-SGM-UFBA-PPPG p. 2-187, il.

Babosa, J.S.F. & Sabaté, P. 2000. Geological and Geochronological Features and The Paleoproterozoic Collision of The Four Archean Crustal Segments of The São Francisco Craton, Bahia, Brazil. 31 Congresso Internacional de Geologia. CD - ROM.

Babosa, J.S.F. & Sabaté, P. 2002. Geological Features and The Paleoproterozoic Collision of Four Archean Crustal Segments of The São Francisco Craton, Bahia, Brazil. A Synthesis. Anais da Academia Brasileira de Ciências 74 (2): 343-359.

Ledru, P.; Cocherie, A.; Barbosa, J.S.F.; Johan, V.; Onstott, T. 1993. Âge du Métamorphisme Granulitique dans le Craton du São Francisco (Brésil). Implications sur la Naturede l`Orogéne Transamazonien. C.R.Acad. Sci. Paris, 211:120-125.

Peucat, J.J., Ménot, R.P., Monnier O., Fanning C.M., 1999b The Terre Adélie basement in the Antarctica Shield: geological and isotopic evidence for a major 1.7 Ga thermal event: comparasion with Gawler Craton in south Australia. Precambrian Research 94, 205-224.

Pinho, I.C.A. 2000 Os Tonalitos/Trondhjemitos das regiões de Ipiaú-Ubaitaba-Ibicaraí-Itabuna, Bahia. Dissertação (Mestrado Geologia). Instituto de Geociências-UFBA, 193p.il.

U-Pb AND Sm-Nd DATA FROM TELES PIRES MAGMATIC PROVINCE, SOUTHWESTERN OF AMAZONIAN CRATON - MATO GROSSO-BRAZIL

Pinho, M.A.S.[1]; Chemale Jr., F.[2]; Schmus, R.W.[3]; Lima, E.F.[2] and Pinho, F.E.C.[1]

1. Universidade Federal do Mato Grosso - Departamento de Recursos Minerais - UFMT
2. Universidade Federal do Rio Grande do Sul - Instituto de Geociências - UFRGS
3. University of Kansas - KU

Keywords: Amazonian Craton, Teles Pires, piroclastic deposits, geochemistry

The Moriru region, situated in the SW Amazonian Craton (Fig. 1), Mato Grosso, Brazil, is composed of two main domains: 1) an area of undeformed bimodal volcanic rocks and 2) an area of deformed granitic-gneissic-migmatite rocks that also include a small occurrence of slightly deformed rhyolite. Pinho (2002) suggests that these rocks belongs to the Teles Pires Magmatism.

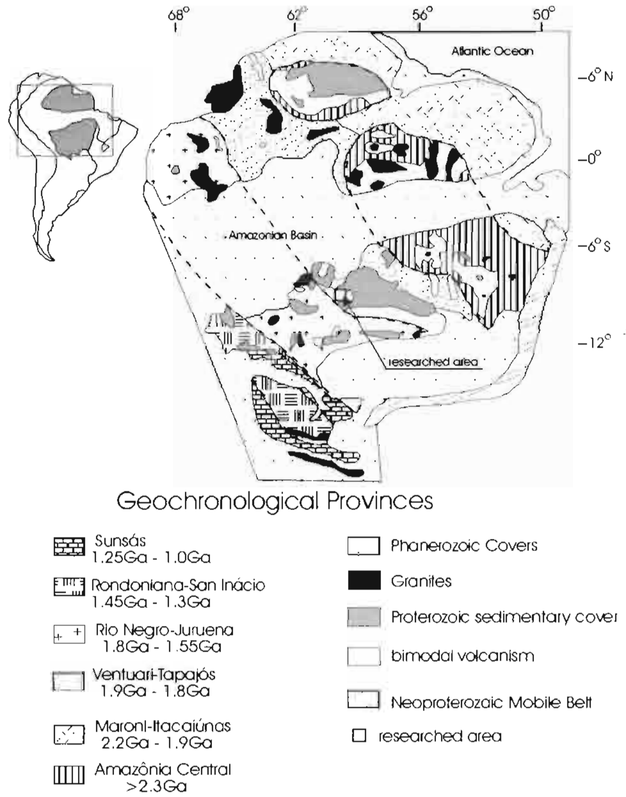

Figure 1. A Map of the Amazonian Craton of South America showing the main geochronology provinces defined by Tassinari & Macambira (1999).

The undeformed domain is composed of felsic to mafic flows and volcanoclastic sediments of the Teles Pires Magmatism (Fig. 2); the felsic flows are essentially explosive deposits classifyed as ignimbrites, however coherent flows occurs interlayed. The compositions of ignimbrites and associated felsic flows are rhyodacite to dacite. The mafic volcanics are phaneritic, fine grained, and are often strongly hydrothermally altered.

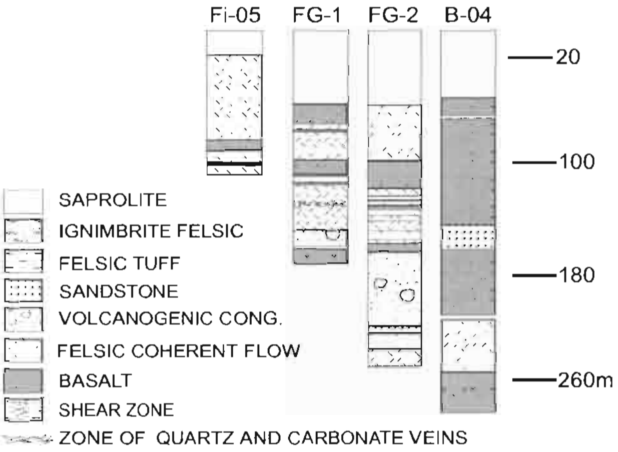

Figure 2. Graphic descriptions of rocks types in the drill cores from Moriru area (undeformed domain).

Unaltered samples have tholeiitic to transitional compositions (Fig. 3) and have within-plate petrologic and geochemical characteristics (Fig. 4).

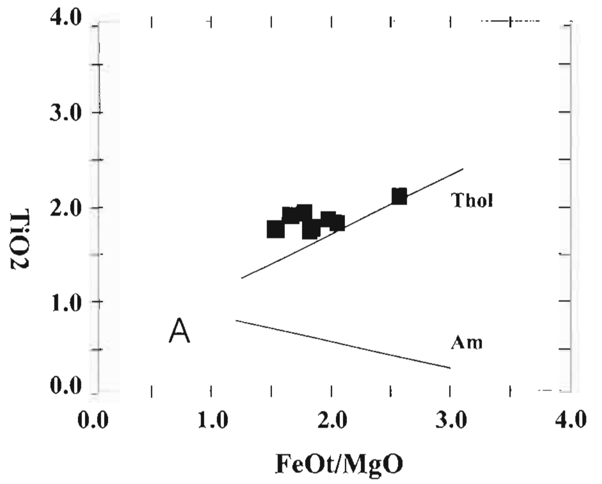

Figure 3. TiO_2 x FeO_t/MgO shows toleiitic afinities for mafic rocks.

The felsic volcanics are enriched in light REE, show a negative Eu anomaly, and are depleted in heavy REE. The trace elements indicate a post-collisional enviroment (Fig. 5).

U-Pb data on single zircon grains from the volcanic sequence yield ages between 1770 ± 8 Ma and 1797 ± 5 Ma (Fig. 6) $\varepsilon_{Nd}(t)$ range from -1.4 to +1.5 (t=1.75 Ga), and the T_{DM} model ages range from 2.02 to 2.16 Ga.

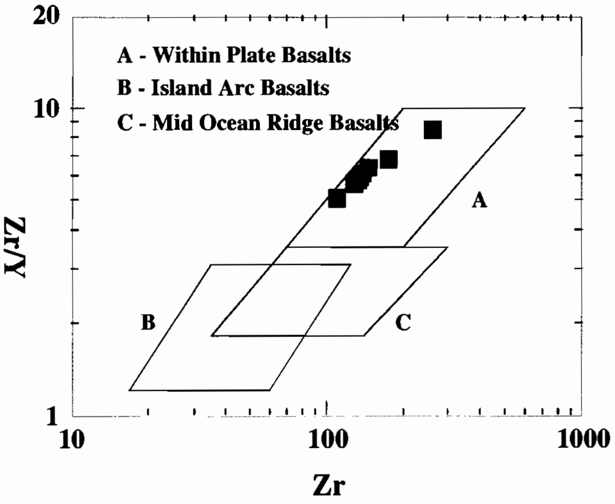

Figure 4. Zr/Y vs. Zr aplied for mafic volcanics from Moriru area plot the rocks into within-Plate environment.

Rocks from the deformed domain are calc-alkaline to transitional and have metaluminous to peraluminous compositions. The metaluminous granites are hornblende-monzogranites and the peraluminous rocks are biotite-granites and granodiorite. Both groups plot in post-tectonic fields of trace element diagrams.

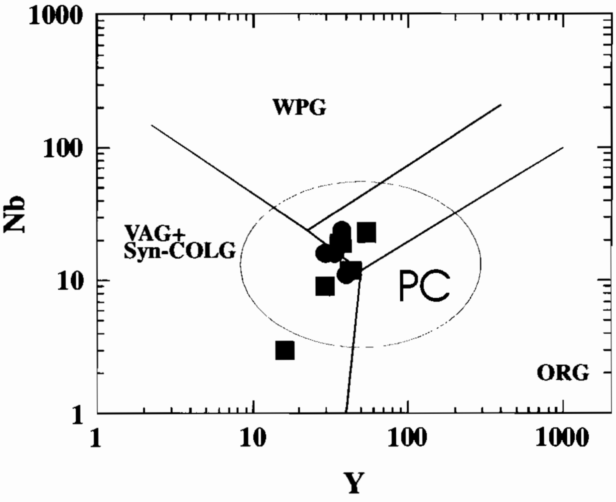

Figure 5. Nb vs Y diagram for felsic rocks from the region (fields from Pearce, 1996). Rocks from the study area plot into post-colisional fields.

U-Pb data on single zircon grains from the deformed granite-gneiss-migmatite domain range from 1662 ± 13 Ma (Fig. 7) to 1803 ± 6 Ma (Fig. 8), but most cluster about a mean of 1763 Ma (Fig. 9) (1759 ± 3 Ma to 1767± 2 Ma) (Fig. 6). $\varepsilon_{Nd}(t)$ values (t=1.75 Ga) vary from -3.4 to +3.0 (Fig. 7) and the T_{DM} model ages ranges from 1.94 to 2.28 Ga.

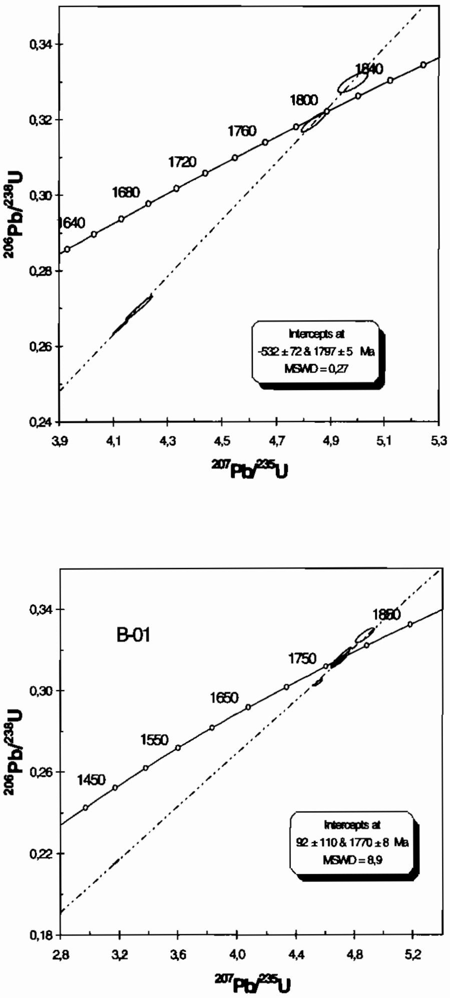

Figure 6. U-Pb concordia diagram for two representative felsic volcanics from undeformed domain.

The approximately 1775 Ma volcano-plutonic rocks in the area probably resulted from partial melting of slightly older continental lithosphere and may have formed during an extensional event about 1.78 to 1.76 Ga. The plutonic rocks seem to have a similar source and may be intrusive into the volcanic sequence, despite their more deformed nature. These ages are similar to those proposed for older parts of the 1.80 to 1.55 Ga Rio Negro-Juruena province and younger than 1.9 to 1.8 Ga, as proposed for the Ventuari-Tapajós province. Sm-Nd isotopic data are consistent with formation of these rocks from ca. 1.9 to 2.2 Ga continental lithosphere.

CONCLUSIONS

In the present paper we conclude that the Teles Pires Magmatic Province is composed of a bimodal volcano-plutonic association, with U-Pb ages 1,75 Ga in average, originated from remelting of a paleoproterozoic crust (T_{DM} = 2,0 - 1,95 Ga) during a post-colisional extentional event with some contribution of juvenil source.

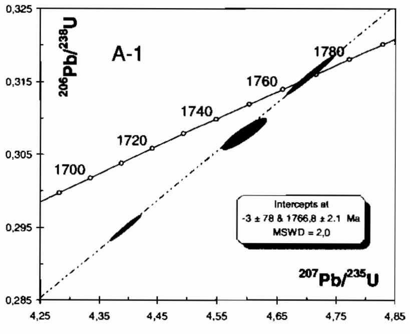

Figure 7. U-Pb concordia diagram showing younger granite into deformed domain.

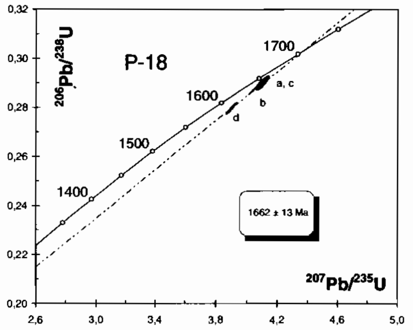

Figure 8. U-Pb concordia diagram showing oldest sample into the deformed domain.

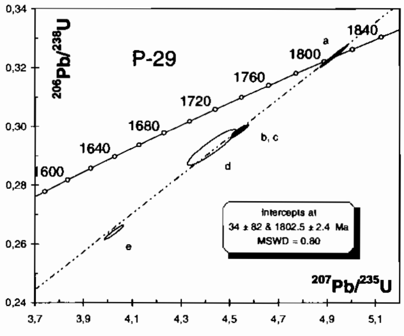

Figure 9. U-Pb concordia diagram showing a representative sample from deformed domain.

REFERENCES

Pearce, J.A., 1996. Sources and Settings of granitic rocks. Episodes, 19:120-125.

Pinho, M.A.S.B., 2001. Petrografia, geoquímica e geocronologia do Magmatismo bimodal paleoproterozóico ocorrente no norte do estado de Mato Grosso. Tese de Doutorado, curso de pós- graduação em geociências - UFRGs.

Pinho, M.A.S.B., 2002. Proposta de nova terminologia estratigráfica para rochas vulcano-plutônicas paleoproterozóicas do norte do estado de Mato Grosso, porção ocidental sul do cráton Amazônico. Revista Brasileira de Geociências. 32 (11): 153-156.

Tassinari, C.C.G. & Macambira, M.J.B., 1999. Geochronological Provinces of the amazonian Craton. Episodes, 22:174-182.

SHRIMP U-Pb DATA OF GRANULITES OF THE ANÁPOLIS-ITAUÇU COMPLEX: NEOPROTEROZOIC HIGH GRADE METAMORPHISM AND MAGMATISM IN THE SOUTHERN PART OF THE BRASILIA BELT, GOIÁS

Piuzana, D.[1]; Pimentel, M.M.[2]; Fuck, R.A.[2] and Armstrong, R.A.[3]

1. CPMTC - Instituto de Geociências, Universidade Federal de Minas Gerais, Belo Horizonte-MG, 31270-901, Brazil. danipiuzana@uol.com.br
2. Instituto de Geociências, Universidade de Brasília, Brasília-DF, 70910-900, Brazil. marcio@unb.br, rfuck@unb.br
3. Research School of Earth Sciences, The Australian National University, Canberra, ACT 0200, Australia. richard.armstrong@anu.edu.au

Keywords: U-Pb SHRIMP, Anápolis-Itauçu Complex, granulite, Brasília Belt

INTRODUCTION

The Tocantins Province (Almeida et al., 1981) in central Brazil is a Neoproterozoic orogenic zone developed between the Amazon and São Francisco cratons and possibly a third continental block, known as Parapanema Block, hidden under the sedimentary rocks of the Paraná Basin. The Tocantins Province comprises the eastward vergent Brasília Belt, adjacent to the São Francisco Craton (Marini et al., 1984), and the westward vergent Paraguay and Araguaia belts, developed on the eastern margin of the Amazon Craton.

In the northern part of the Brasília Belt the Barro Alto, Canabrava and Niquelândia mafic-ultramafic layered complexes are exposed. The isotopic data indicate that these Paleo- to Mesoproterozoic layered complexes were affected by high-grade metamorphism between ca. 740 and 790 Ma and were subsequently metamorphosed at lower grade at ca. 600 Ma (Ferreira Filho et al., 1994; Suíta et al., 1994; Correia et al., 1997, Ferreira Filho & Pimentel, 2000, Pimentel et al., 2001).

In the southern part of the Brasília Belt, in central Goiás, is the Anápolis-Itauçu granulite complex. It consists of a large complex of high-grade rocks and granites, exposed between metasediments of the Araxá Group, the main constituent of the internal zone of the Neoproterozoic Brasília Belt (Fuck et al., 1994). These granulites have traditionally been interpreted as the exposure of Archean sialic basement exposed as an inlier in the Brasília Belt (Danni et al., 1982, Marini et al., 1984; Lacerda Filho & Oliveira, 1995). However, this view has been challenged by Pimentel et al. (1999) and Fischel et al. (1999, 2001), based on reconnaissance Nd isotope studies. Sm-Nd data have indicated that the Nd isotopic signature and metamorphic ages of the Anápolis-Itauçu felsic granulites and intrusive granites are all very similar, with a large proportion of model ages in the interval between ca. 1.1 and 1.5 Ga (Fischel et al., 1998, 2001; Pimentel et al. 1999). This led Pimentel et al. (1999) and Fischel et al. (2001) to consider that, at least, part of the felsic granulites of the Anápolis-Itauçu Complex might represent high grade equivalents of the Araxá metasedimentary rocks, and that the granites represent the product of partial melting of these metasediments.

This work reports the results of regional SHRIMP U-Pb data in ortho- and paragranulites in order to assess (i) the age of crystallization of orthogranulites and intrusive granites in this area; (ii) the precise age of high grade metamorphism of rocks from the Anápolis-Itauçu Complex.

REGIONAL SETTING

The Anápolis-Itauçu Complex consists of: (i) orthogranulites, mainly represented by basic-ultrabasic intrusions, tonalite and granodiorite, as well as charnockitic and enderbitic bodies and (ii) paragranulites, mainly garnet- and sillimanite-bearing aluminous paragneiss with associated gondite, sillimanite quartzite, and diopside marble. Araújo et al. (1994) and Winge (1995) assume that these rocks were derived from pelitic or greywacke sediments, although Wolff (1991) argued that part of them are the result of recrystallization of leucosome material derived by partial melting of sedimentary protoliths.

The paragranulites are characterized by porphyroblastic garnet, plagioclase, sillimanite, quartz and orthopyroxene. These rocks have, in some localities, cordierite, sapphirine and spinel, with rutile and zircon as accessory minerals. Moraes et al. (2002) suggested that the mineral assemblages containing sapphirine and quartz in equilibrium are indicative of ultra-high temperature metamorphism, which may have reached ca. 1150° C and >10 kbar. Retrograde reactions textures in these rocks indicate near-isobaric cooling paths. The Anápolis-Itauçu granulites were intruded by a number of granite bodies which were deformed and metamorphosed under granulite facies conditions. SHRIMP U-Pb analyses on zircon show that granite ANA 1 is Neoproterozoic. In sample ANA 239, cores of zircon grains are Neoproterozoic, with concordant ages between 0.8 and 1.0 Ba (Fischel et al., 2001). Zircon crystals from sample ANA 30 indicate a more complex history. Most zircon grains are Neoproterozoic with significant differences between core and rim ages. Four of the analyzed grains are inherited (Fischel et al., 2001). One has a Paleoproterozoic core, probably inherited from the basement of the Brasília Belt. Samples ANA 30 and

ANA 239 are from the same granitic body, and their metamorphic ages are very similar. The zircon ages show that this granite intrusion contains inheritance from, at least, three distinct sources, with Paleoproterozoic and Mesoproterozoic age (1.7-1.5 Ba, in ANA 30) and Neoproterozoic ages varying between 1070 and 830 Ma (Fischel et al., 2001).

SHRIMP U-Pb DATA

ORTHOGRANULITE (ANA 318)

This is a medium-grained metatonalite which has been metamorphosed under granulite facies conditions. It contains zircon grains which show well developed euhedral to prismatic oscillatory zoning, typical of magmatic crystals. Rims with low luminescence are observed around the magmatic crystals. A subpopulation of zircon grains lacking oscillatory zoning was also identified, and probably represents metamorphic crystals.

Twelve analyses of the magmatic crystals yielded concordant results and indicate the concordia age of 759 ± 9 Ma (MSWD= 1.3) which is interpreted as the crystallization age of the igneous protolith. Analyses of the low luminescence rims and metamorphic grains show varied degrees of lead loss and yielded an upper intercept age of 638 ± 37 Ma (MSWD= 4) interpreted as indicative of the high grade metamorphic event.

Some analyses have older $^{206}Pb/^{238}U$ ages and indicate some degree of assimilation of older material by the original magma, a not unexpected result considering the Sm-Nd T_{DM} model age of 2.1 Ga and $\varepsilon_{Nd}(760)$ of -6.2 obtained for this sample (Fischel et al., 2001).

PARAGRANULITES (ANA 259 AND ANA 230)

Zircon grains in paragranulite ANA 259 (garnet-sillimanite-feldspar rock) are typically rounded detrital grains and are rimmed by metamorphic zircon overgrowths. Individual metamorphic crystals are also present. Rims have lower Th/U ratios, although some cores show equally low Th/U ratios. In such cases, ages of the cores are similar to those of the rims and both grew during the high-grade metamorphic event. The analyses produced a very complex age pattern most probably due to a combination of inheritance with recent and/or early Pb-loss. The best result for metamorphic zircon grains and rims is given by twenty-one concordant spot analyses indicating the concordia age of 639 ± 9 Ma (MSWD = 1.4), similar to that calculated for metamorphic overgrowths in orthogranulite ANA 318. This may be interpreted as the best estimate for the age of the high-grade metamorphism. Cores of detrital zircon grains which yielded concordant or nearly concordant analyses have $^{206}Pb/^{238}U$ ages between ca. 800 and 950 Ma. The younger cores represent, therefore, an upper age limit for the deposition of the original sediments, clearly indicating that the original sedimentary protolith is Neoproterozoic. Most zircon grains of garnet gneiss ANA 230 are metamorphic, and only a few of them show older cores (ages of ca. 815 Ma). Analyses of the metamorphic grains are concordant, however they display a rather large spread of $^{206}Pb/^{238}U$ ages. Therefore, we consider that the weighted mean $^{206}Pb/^{238}U$ age of 640 ± 8 Ma (MSWD = 0.68) for metamorphic zircon grains and rims represents the best estimate for the age of the high-grade event.

ULTRA-HIGH TEMPERATURE GRANULITE (ANA 279)

One sample of UHT granulite was investigated. This sample has a mineral assemblage typical of ultra-high temperature granulite with quartz, plagioclase, biotite, orthopyroxene, cordierite, garnet, spinel, sillimanite, sapphirine and rutile (Moraes et al. 2002). Twelve analyses in ten zircon grains were carried out, two in cores and ten in metamorphic grains or rims. Cores yielded $^{206}Pb/^{238}U$ ages of 1.18 and 0.68 Ga. Analyses of metamorphic zircon produced a coherent concordant population with a concordia age of 650 ± 10 Ma (MSWD= 1.3, 95% conf.). Despite the small number of zircon grains and cores of this sample, we observed that they are similar to those of samples ANA 230 and 259. Therefore, we deduce that the UHT granulite protolith is also of sedimentary origin and that it must be of Neoproterozoic age.

CONCLUSIONS

The new U-Pb data discussed in this study allow some relevant conclusions to be put forward regarding the nature and tectonic significance of the Anápolis-Itauçu granulites:

(i) Granitoids investigated are all Neoproterozoic, ranging in age from ca. 760 to 650 Ma. The older, pre-metamorphic, granitoid emplacement event is coeval with magmatic activity in the Goiás Magmatic Arc, further to the west. Contrasting with the Goiás Magmatic Arc rocks, however, this early magmatic event in the Anápolis-Itauçu Complex is not totally juvenile, and original magmas were emplaced into and contaminated with older (possibly Paleoproterozoic) continental crust;

(ii) Felsic granulites have detrital zircon populations which indicate Proterozoic sources, ranging in age from ca. 2.0 to 0.8 Ga. Therefore, the data show that the original sediments were deposited during the Neoproterozoic. Young sediment sources may be attributed to the Neoproterozoic Goiás Magmatic Arc (0.90 to 0.64 Ga) presently exposed to the west and southwest of the Anápolis-Itauçu Complex, and Paleoproterozoic sources are widely distributed to the east, constituting a large part of the São Francisco craton;

(iii) The peak of high grade metamorphism in the Anápolis-Itauçu Complex occurred between ca. 650-640 Ma, approximately 150-100 Ma later than the high-grade metamorphic event identified in the Barro Alto, Cana Brava and Niquelândia mafic-ultramafic layered complexes in the northern part of the Brasília Belt.

(iv) Voluminous granitic magmatism, presenting a general peraluminous nature, in the Anápolis-Itauçu Complex suggests important melt generation in the lower crust, concomitant with granulite-facies metamorphism. The granitoids have Sm-Nd isotopic patterns that are not much different from that observed for the felsic granulites, with T_{DM} model ages in the interval between ca. 1.37 and 2.15 Ga and ε_{Nd} (T) between -2.7 to -8.1, suggesting that the magmas are the product of remelted granulites and older sialic crust. This is also supported by the inheritance pattern observed in zircon grains from the granitoids.

The Anápolis-Itauçu Complex represents, therefore, the core of a metamorphic complex associated with the Brasiliano orogeny, and not the exposure of ancient sialic basement.

ACKNOWLEDGEMENTS

This work was supported by CNPq (grant 200520/01-6 to DP; grants 52.2269/95-8, 42.0081/99-2 to RAF) and FAP-DF (grant 193.000.068/96 to RAF). We thank Sérgio Junges for assistance in the Laboratory of Geochronology of Universidade de Brasília and Renato Moraes is thanked for supplying zircon concentrate of sample ANA 279.

REFERENCES

Almeida, F.F.M. DE; Hasui, Y.; Neves, B.B.B. & Fuck, R.A. - 1981 -Brazilian structural provinces: an introduction - Earth Sci. Rev. 17:291-317.

Araújo,V.A. 1994. Programa de levantamentos geológicos básicos do Brasil. Nerópolis – Folha SE.22-X-B-I. Estado de Goiás. Escala 1:100.000. Goiânia, DNPM/CPRM, 120p.

Correia, C.T., Tassinari, C.C.G., Lambert, D.D., Kinny, P.D. and Girardi, V.A.V. 1997. U-Pb (SHRIMP), Sm-Nd and Re-Os systematics of the Cana Brava, Niquelândia and Barro Alto layered intrusions in central Brazil, and constraints on the tectonic evolution. Actas, South-American Symposium on Isotope Geology, Campos do Jordão – SP, 1, 88-89.

Danni, J.C.M., Fuck, R.A. and Leonardos Jr., O.H. 1982. Archean and Lower Proterozoic Units in Central Brazil. Geol. Rundschau, 71, 291-317.

Ferreira Filho, C.F., Kamo, S., Fuck, R.A., Krogh, T.E. and Naldrett, A.J. 1994. Zircon and rutile geochronology of the Niquelandia layered mafic and ultramafic intrusion, Brazil: constraints for the timing of magmatism and high grade metamorphism. Precambrian Research 68, 241-255.

Ferreira Filho, C.F., Pimentel, M.M., 2000. Sm-Nd isotopic systematics and REE-Hf-Ta-Th data of troctolites and their amphibolitized equivalents of the Niquelândia Complex Upper layered Series, central Brazil: further constraints for the timing of magmatism and the high-grade metamorphism. Journal of South American Earth Sciences 13(7), 647-659.

Fischel, D.P.; Pimentel, M.M., Fuck, R.A. 1998. Idade de Metamorfismo de alto grau no Complexo Anápolis-Itauçu, determinada pelo método Sm-Nd. Revista Brasileira de Geociências, 28 (4): 543-544.

Fischel, D.P., Pimentel, M.M., Fuck, R.A., 1999. Preliminary Sm-Nd isotopic study of the Anápolis-Itauçu Complex, Araxá Group and associated granite intrusions, central Brazil: implications for the evolution of the Brasília Belt. Anais, South American Symposium on Isotope Geology, Córdoba, Argentina 2, 302-305.

Fischel, D.P.; Pimentel, M.M.; Fuck, R.A., Armstrong, R.A. 2001. U-Pb SHRIMP and Sm-Nd geochronology of the Anápolis-Itauçu Complex, Araxá Group and associated granite: Neoproterozoic high-grade metamorphism and magmatism in the central part of Brasília Belt. III South American Symposium on Isotope Geology. (SAAGI), Pucón, Chile.

Fuck, R.A., Pimentel, M.M. and D'el Rey Silva, L.J.H. 1994. Compartimentação tectônica da porção oriental da Província Tocantins. Actas, 38 ° Congresso Brasileiro de Geologia, Balneário Camboriú-SC, 1, pp. 215-216

Lacerda Filho,J.V. and Oliveira,C.C. 1995. Geologia da região centro-sul de Goiás. Boletim de Geociências do Centro-Oeste, 18(1/2), 3-19.

Marini, O.J., Fuck, R.A., Danni, J.C.M., Dardenne, M.A., Loguercio, S.O.C. and Ramalho, R. 1984. As faixas de dobramentos Brasilia, Uruaçu e Paraguai-Araguaia e o Maciço Mediano de Goiás. In Geologia do Brasil, ed. Schobbenhaus C., pp 251-303. Ministério das Minas e Energia - Departamento Nacional da Produção Mineral, Brasília, Brazil.

Moraes, R., Brown, M., Fuck, R.A., Camargo, M.A., Lima, T. M., 2002. Characterization and P-T Evolution of Melt-bearing Ultrahigh-temperature Granulites: an example from the Anápolis-Itauçu Complex of the Brasília Fold Belt, Brazil. Journal of Petrology 43(9):1673-1705.

Pimentel, M.M., Fuck, R.A. and Fischel, D.P. 1999. Estudo isotópico Sm-Nd regional da porção central da Faixa Brasília: implicações para idade e origem dos granulitos do Complexo Anápolis-Itauçu e sedimentos do Grupo Araxá. Revista Brasileira da Geociências, 29(2), 271-276.

Pimentel, M.M.; Fuck, R.A.; Jost, H.; Ferreira Filho, C.F. and Araújo, S.M. 2000. The basement of the Brasília Fold Belt and the Goiás Magmatic Arc. In: Tectonic Evolution of South America, p. 190-229. Cordani, U.G.; Milani, E.J.; Thomaz Filho, A., Campos, D.A. (eds) .Rio de Janeiro: 31st International Geological Congress, 2000.

Pimentel, M.M., Fuck, R.A., Piuzana, D., Moraes, R., Gioia, S.M.C.I., 2001. Isotopic evidence for two high grade metamorphic events in the Brasília Belt. Actas, South American Symposium on Isotope Geology, Pucón, Chile, 3, 205-208.

Suita,M.T.F., Kamo,S.L., Krogh,T.E., Fyfe,W.S. and Hartmman,L.A., 1994. U-Pb ages from the high-grade Barro Alto mafic-ultramafic complex (Goiás, central Brazil): middle Proterozoic continental magmatism and upper Proterozoic continental collision. In: Inter. Confer. On Geochron. and Isotope Geology, 8., Abstracts..., USGS, Berkeley, p.309.

Winge, M. 1995. Evolução dos terrenos granulíticos da Província Estrutural Tocantins, Brasil central. Unpublished Ph. D. thesis, Universidade de Brasília, Brasília, 600 pp.

Wolff, F. 1991. Caracterização petrográfica, litogeoquímica, química mineral e geotermometria de rochas de alto grau metamórfico do Complexo Anápolis-Itauçu, Goiás. Unpublished Master, Universidade Federal do Rio de Janeiro, Rio de Janeiro, 148 p.

SEDIMENTATION AGE OF THE ARAXÁ GROUP, SOUTHERN BRASÍLIA BELT, BASED ON U-Pb SHRIMP DATA FROM MICASCHIST, BONFINÓPOLIS AMPHIBOLITE AND INTRUSIVE TONALITE

Piuzana, D.[1]; Pimentel, M.M.[2]; Fuck, R.A.[2] and Armstrong, R.A.[3]

1. CPMTC - Instituto de Geociências, Universidade Federal de Minas Gerais, Belo Horizonte, MG, 31270-901, Brazil. danipiuzana@uol.com.br
2. Instituto de Geociências, Universidade de Brasília, Brasília-DF, 70910-900, Brazil. marcio@unb.br, rfuck@unb.br
3. Research School of Earth Sciences, The Australian National University, Canberra, ACT 0200, Australia. richard.armstrong@anu.edu.au

Keywords: SHRIMP U-Pb, Araxá Group, Bonfinópolis Amphibolite, Neoproterozoic, Brasília Belt

INTRODUCTION

The Brasília Belt extends for ca. 1000 km in the NS direction along the western margin of the São Francisco Craton, in central Brazil. It represents the central/eastern part of a large Neoproterozoic orogenic zone known as the Tocantins Province (Almeida et al., 1981), which resulted from the convergence and collision of three major continental blocks at the end of the Neoproterozoic (for a review see Pimentel et al., 2000b): the Amazon Craton, to the west, the São Francisco/Congo Craton, to the east, and the Paranapanema block, presently covered by Phanerozoic rocks of the Paraná Basin, to the south. It represents one of the best preserved and the most complete Neoproterozoic orogens in Brazil, comprising: (i) a large Neoproterozoic juvenile arc in the west (Goiás Magmatic Arc); (ii) a micro-continent (or allochthonous sialic terrain) formed by Archean rock units (the Crixás-Goiás granite-greenstones) and associated Proterozoic formations and (iii) a thick Meso-Neoproterozoic metasedimentary/sedimentary pile, formed by the Paranoá, Canastra, Araxá, Ibiá, Vazante, and Bambuí Groups, overlying mostly Paleoproterozoic and minor Archean basement (Fuck et al., 1994, 2001; Pimentel et al., 2000a, b). The age and tectonic significance of the different supracrustal rock units of the Brasília Belt have been the object of much controversy. A regional Nd isotopic investigation was carried out, which served to identify the possible major sources of the detrital sediments (Pimentel et al., 2001). The Araxá and Ibiá metapelites display a bimodal distribution of model ages, with an older group of T_{DM} values between ca. 1.8 and 2.3 Ga and a younger group with values between 1.0 and 1.3 Ga. The young model ages indicate contribution from Neoproterozoic juvenile source areas, such as the Goiás Magmatic Arc (Pimentel et al., 2001), suggesting that the Ibiá Group and part of the Araxá Group are younger than 900 Ma and were probably deposited in a marginal basin between the intraoceanic Goiás Arc and the continental passive margin (Dardenne, 2000; Pimentel et al., 2001).

In this study, detrital zircon grains from micaschist of the Araxá Group and associated magmatic rocks were dated with the SHRIMP U-Pb technique in order to better constrain: (i) the nature of possible sources of the Araxá sediments; (ii) the tectonic environment of deposition of the Araxá Group and its significance in the evolution of the Brasília Belt, and (iii) the upper age limit for the deposition of the original sediments.

REGIONAL SETTING

The Brasília Belt has been sub-divided into the southern and northern segments, based on their very distinct structural and tectonic characteristics. These are roughly separated from each other by the E-W Pirineus lineament, running for ca. 200 km in the central part of the belt (Marini et al., 1984; Fonseca & Dardenne, 1995; Araújo Filho, 2000). The central-southern segment of the Brasília Belt comprises mainly metasedimentary units included in the Araxá, Ibiá and Canastra groups. Metasedimentary rocks (schists and quartzites) of the Araxá Group surround the Anápolis-Itauçu Complex high-grade metamorphic complex.

In the Anápolis region, the Araxá Group comprises mostly micaschists, quartzites and carbonate-bearing schists. The most abundant rock types are garnet-feldspar-biotite-muscovite schist, kyanite-garnet-biotite-muscovite schist, garnet quartzite and chlorite-muscovite schist. Garnet crystals are involved commonly by biotite and muscovite, forming a protomylonitic foliation. Lithogeochemical data (REE) suggest that these rocks are representative of arkose to greywacke-type sediments with local carbonatic contributions (Lacerda Filho & Oliveira, 1995). Peraluminous granites intrusive into the Araxá Group are comon, although the field relationships between the meta-igneous rocks and metasediments are obscured by poor exposure of geological contacts. Small serpentinite and actinolite/talc schist bodies with podiform chromite, as well as amphibolite layers, are tectonically intercalated with the Araxá metasedimentary rocks and are very abundant in many localities. This association has been interpreted as an ophiolite *mélange*, emplaced over the São Francisco continental margin by the eastward nappes (Drake Jr., 1980; Strieder & Nilson, 1992).

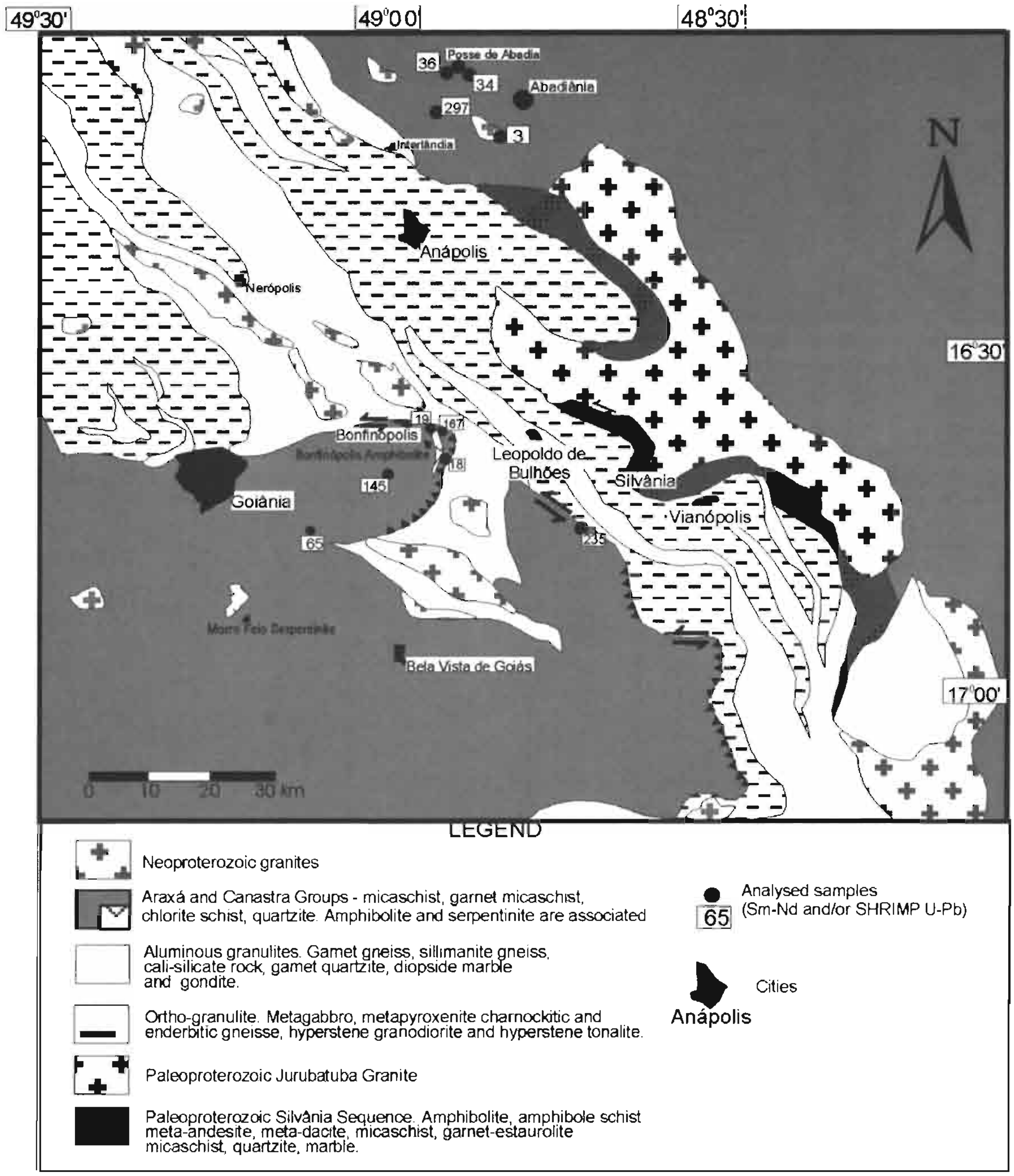

Figure 1. Geological sketch of the study area (after Lacerda & Oliveira, 1995).

In the northern part of the study area, the Araxá Group metasedimentary rocks are in tectonic contact with Anápolis-Itauçu granulites and with the Silvânia Volcano-Sedimentary Sequence (Fig. 1), through a N50-60W strike-slip shear zone. To the south, Araxá rocks show E-vergent nappes overlying the granulites and granites. Frontal ramps have N-S general direction and lateral ramps are mainly E-W and NW-SE. Kynematic indicators of the lateral ramps suggest left-handed movement.

SHRIMP U-Pb DATA

ANA 34: FELDSPAR-GARNET-BIOTITE SCHIST

Detrital zircon grains from sample ANA 34 (Fig. 1) show very well preserved prismatic shapes, suggesting erosion of local sources. Two distinct zircon populations were identified: grains with thick zoning, similar to crystals formed in mafic magmas and zircon grains with thin oscillatory zoning which follow the external prismatic habit of the mineral, typical of zircon from felsic igneous rocks. All grains have U-poor, very thin, metamorphic rims. A total of 42 analyses were carried out on 24 cores of zircon grains. Detrital zircon grains derived from mafic rocks have $^{207}Pb/^{206}Pb$ ages according to the following distribution: 626 to 644 Ma (4 grains), 670 Ma (3 grains), 729 to 760 Ma (5 grains), 1000 Ma (2 grains) and 2000 to 2200 Ma (2 grains), whereas zircon grains derived from felsic rocks present the following $^{207}Pb/^{206}Pb$ ages: 650 to 670 Ma (3 grains), 700 Ma (1grain), 800 to 840 Ma (3 grains).

ANA 18: KYANITE – GARNET – BIOTITE – MUSCOVITE SCHIST

Sample ANA 18 (Fig. 1) contains at least three distinct types of zircon grains: fragments of grains with structureless core and rim; igneous grains with metamorphic rims, and metamorphic grains. The zircon grains are smaller than those from ANA 34, with an average length of 100 µm. Most of them are anhedral, with rounded terminations. Contrary to what is observed in zircon grains from ANA 34, not every zircon grain from ANA 18 presents metamorphic overgrowth. Thirty-two analyses were carried out in 22 zircon grains. The youngest ages are from detrital metamorphic zircon grains and metamorphic rims, in which $^{206}Pb/^{238}U$ ages vary between 628 ± 12 and 734 ± 11 Ma. Twelve igneous cores were analyzed, indicating ages from Paleo- to Neoproterozoic. The youngest and most representative groups of ages were obtained in metamorphic rims and metamorphic zircon grains.

ANA 19: BONFINÓPOLIS AMPHIBOLITE

The amphibolite sample is from a strip of mafic rocks exposed close to the contact between Araxá micaschist and granulites of the Anápolis-Itauçu Complex (Fig. 1). Stratigraphic relationships between the amphibolite and Araxá supracrustals are not clear due to intense deformation, and it seems that the metabasic rocks are tectonically intercalated with the Araxá metasedimentary rocks.

Cathodoluminescence images show anhedral to subhedral zircon grains, which display a central area of zoned magmatic zircon surrounded by reworked brighter margins. Th-U values for these marginal areas do not show the typically low values found in metamorphic grains. There is some variation in the type and zoning in the cores and this may only reflect varying crystallization conditions of a single population, or it may indicate that at least some cores may be inherited. Sixteen analyses were carried out in eleven zircon grains. All analyses show U concentrations higher than Th, with U content varying between 99 and 412 ppm and Th between 49 and 407 ppm. The data show some discordance and scatter, and the preferred age is calculated with a regression through all data points, which indicates an upper intercept age of 838 ± 20 Ma (MSWD= 1.17), which is interpreted as the crystallization age of the original basaltic rock. A Sm-Nd isochron was calculated for six whole-rock samples from ANA 19 outcrop. The limited spread of Sm-Nd and strong scatter of analytical data (MSWD= 31) hampered the calculation of meaningful isochron age and uncertainty. Nevertheless, the six data points align about a regression line with slope indicating the age of ca. 0.9 Ga. More relevant than the Sm-Nd age is the strongly positive ε_{Nd}= +5.2 value revealed by the regression, indicating that the parental basaltic magma originated from a depleted, probably MORB-type, mantle source (Fischel et al., 1999, 2001). This concurs with lithogeochemistry data from Oliveira (1994) which display striking similarities with low-K tholeiites, suggesting origin in a mid-ocean ridge environment.

ANA 3: INTRUSIVE TONALITE

Zircon grains from ANA 3 tonalite (Fig. 1) are anhedral to subhedral, with round to prismatic zoned cores and bright and structureless rims showing low Th/U values, typical of metamorphic overgrowths.

Eighteen zircon grains of ANA 3 were analyzed. Seventeen analyses were performed in cores and one analysis in a rim. The analyses yielded a concordia age of 638 ± 11 Ma (95% conf., prob. of concordance= 0.122) interpreted here as the best estimate for the crystallization age of the original tonalitic magma. Therefore, the emplacement of this tonalite at ca. 638 Ma into Araxá metasediments should represent a minimum age for the deposition of the original sediments.

CONCLUSIONS

The SHRIMP U-Pb ages of detrital zircon grains of the Araxá Group reinforce the bimodal character of T_{DM} model ages in metasedimentary rocks observed in previous studies (Fischel et al., 2001; Pimentel et al. 2001). This pattern strengthens the hypothesis that the original sediments were accumulated in a basin which was receiving sediments from, at least, two sources. Young sediment sources are attributed to the Neoproterozoic Goiás Magmatic Arc (0.93 to 0.64 Ga), presently exposed to the west and southwest of the study area, whereas the older sources, Paleoproterozoic in age, are widely distributed to the east, constituting large part of the São Francisco Craton basement.

The $^{207}Pb/^{206}Pb$ ages obtained for micaschists ANA 34 and ANA 18 suggest that Paleoproterozoic mafic rocks contributed with detrital material during the sedimentation of the former Araxá basin in this region. However, Neoproterozoic zircon grains are much more frequent, indicating that young mafic and felsic sources were the main contributors to the sedimentation of the Araxá basin. This is compatible with the young T_{DM} model ages (1.18-1.37 Ga) of ANA 34, 36 and 297, from outcrops near Posse de Abadia (Fig. 1) (Fischel et al., 2001).

The best estimate for the maximum age of deposition of the Araxá sediments in this area is given by the youngest reasonably coherent group of concordant analysis, whose $^{206}Pb/^{207}Pb$ ages are around 640-650 Ma.

Internal features of Paleoproterozoic zircon grains in ANA34 indicate that they were probably derived from mafic rocks, which are common in nearby volcano-sedimentary associations, such as the Silvânia Sequence.

Tonalite ANA 3, intrusive into the Araxá metasedimentary rocks, presents ~~a~~ crystallization age of ca. 638 Ma, representing the minimum depositional age of the original sediments. Neoproterozoic detrital zircon grains are more abundant than Paleoproterozoic grains. The maximum age of deposition is given by a $^{206}Pb/^{238}U$ age group at ca. 643 Ma, comprising metamorphic rims and metamorphic grains in sample ANA18. These minerals indicate that the sources of the former sediments included metamorphic rocks. The age of these metamorphic minerals is identical to that of the high-grade metamorphism recorded in the Anápolis-Itauçu Complex, whose rocks, then, may have been part of the sediment source (Piuzana et al., 2003). Alternatively, metamorphic rocks in the Goiás Arc could have also provided that material. In any case, this observation implies that young metamorphic rocks have been uplifted, exposed and eroded, providing sediment for at least part of what is presently mapped as the Araxá Group. This means necessarily that the sediments of the Araxá basin in the Anápolis region were deposited and metamorphosed within a very short time interval of possibly only a few million years.

The age and depleted mantle-type affiliation of the Bonfinópolis amphibolite suggest that it is part of the ophiolitic *mélange* identified in association with the metasedimentary rocks of the Araxá Group near Posse de Abadia (Strieder & Nilson, 1992) or to the south of Goiânia (Morro Feio Serpentinite) (Fig. 1). Therefore, the crystallization age of the amphibolite at ca. 830 Ma is a marker of the extensional stage which may represent the so called Araxá Oceanic Expansion (Dardenne, 2000) or the Goiás Ocean (Pimentel et al., 2001).

ACKNOWLEDGEMENTS

This work was supported by CNPq (grant 200520/01-6 to DP; grants 52.2269/95-8, 42.0081/99-2 to RAF) and FAP-DF (grant 193.000.068/96 to RAF). We thank Sérgio Junges for assistance in the Laboratory of Geochronology of Universidade de Brasília.

REFERENCES

Almeida, F.F.M., Hasui Y., Neves, B.B.B., and Fuck, R.A., 1981. Brazilian structural provinces: an introduction. Earth-Sci Review 17, 1-29.

Araújo Filho, J.O., 2000. The Pireneus Syntaxis: an example of the intersection of two Brasiliano fold-thrust belts in central Brazil and its implications for the tectonic evolution of western Gondwana. Rev. Bras. Geociências 30(1):144-148

Dardenne, M.A., 2000. The Brasília Fold Belt. In: Tectonic Evolution of South America, p. 231-263. Cordani, U.G.; Milani, E.J.; Thomaz Filho, A., Campos, D.A. (eds) Rio de Janeiro: 31st International Geological Congress, 2000.

Drake Jr., A.A., 1980. The Serra de Caldas Window, Goiás. USGS Prof. Paper. 1119 A-B, 1-11.

Fischel, D.P., Pimentel, M.M., and Fuck, R.A., 1999. Preliminary Sm-Nd isotopic study of the Anápolis-Itauçu Complex, Araxá Group and associated granite intrusions, central Brazil: implications for the evolution of the Brasília Belt. Actas, II South American Symposium on the Isotope Geology, Córdoba, Argentina, 2, 302-305.

Fischel, D.P.; Pimentel, M.M.; Fuck, R.A., Armstrong, R.A. 2001. U-Pb SHRIMP and Sm-Nd geochronology of the Anápolis-Itauçu Complex, Araxá Group and associated granite: neoproterozoic high-grade metamorphism and magmatism in the central part of Brasília Belt. III South American Symposium on Isotope Geology. (SAAGI), Pucón, Chile.

Fonseca, M.A. and Dardenne, M.A., 1995. Estilos estruturais e a compartimentação tectônica do segmento setentrional da Faixa Brasília. Anais 5° Simp. Nac. Est. Tect., Gramado, SBG, 36-38.

Fuck, R.A., Jardim de Sá, E.F., Pimentel,M.M., Dardenne, M.A. and Soares, A.C.P., 1993. As faixas de dobramentos marginais do Cráton do São Francisco: síntese dos conhecimentos. In: Dominguez, J.M.L. and Misi, A. (eds.), O Cráton de São Francisco, SBG, CNPq, Salvador, pp.161-185.

Fuck, R.A., Pimentel, M.M. and D'el Rey Silva, L.J.H., 1994. Compartimentação tectônica da porção oriental da Província Tocantins. Actas, 38° Congresso Brasileiro de Geologia, Balneário Camboriú, SC, 1, pp. 215-216

Fuck, R.A., Dantas, E.L., Pimentel, M.M., Junges, S.L., and Moraes, R., 2001. Nd isotopes, U-Pb single grain and SHRIMP zircon ages from basement rocks from Tocantins Province. Actas, III South American Symposium on the Isotope Geology, Pucón, Chile, 3, 141-144.

Lacerda Filho, J.V. and Oliveira, C.C. 1995. Geologia da região centro-sul de Goiás. Boletim de Geociências do Centro-Oeste, 18(1/2), 3-19.

Marini, O.J., Fuck, R.A., Danni, J.C.M., Dardenne, M.A., Loguercio, S.O.C., Ramalho, R., 1984. Geologia do Brasil, Brasília, Ministério das Minas e Energia Departamento Nacional da Produção Mineral, Brazil, pp 251-303.

Oliveira, C.C. 1994. Programa de levantamentos geológicos básicos do Brasil. Leopoldo de Bulhões – Folha SE.22-X-B-V. Estado de Goiás. Escala 1:100.000. Goiânia, DNPM/CPRM, 172 pp.

Pimentel, M.M., Fuck, R.A., Gioia, S.M.C.L., 2000a. The Neoproterozoic Goiás Magmatic Arc, Central Brazil: A review and new Sm-Nd isotopic data. Revista Brasileira de Geociências, 30(1), 035-039.

Pimentel, M.M., Fuck, R.A., Jost, H., Ferreira Filho, C.F., Araújo, S.M., 2000b. The basement of the Brasília Fold Belt and the Goiás Magmatic Arc. In: Tectonic Evolution of South America, p. 190-229. Cordani, U.G.; Milani, E.J.; Thomaz Filho, A., Campos, D.A. (eds) .Rio de Janeiro: 31st International Geological Congress, 2000.

Pimentel, M.M., Dardenne, M.A., Fuck, R.A., Viana, M.G., Junges, S.L., Seer, H.J., Fischel, D.P., Dantas, E., 2001. Nd isotopes and the provenance of sediments of the Neoproterozoic Brasília Belt, central Brazil. Journal of South American Earth Sciences 14, 571-585.

Piuzana, D., Pimentel, M.M. , Fuck, R.A., Armstrong, R. 2003. Neoproterozoic Magmatism and High Grade Metamorphism in the Brasília Belt, central Brazil: regional implications of SHRIMP U-Pb and Sm-Nd geochronological studies. Precambrian Research, in press.

Strieder, A. J., and Nilson, A. A., 1992. Mélange ofiolítica nos metassedimentos do Grupo Araxá de Abadiânia (GO) e implicações tectônicas regionais. Revista Brasileira de Geociências 22, 204-215.

U-Pb ZIRCON AGES OF POST-OROGENETIC GRANITIC MAGMATISM IN APIAÍ FOLDED BELT (PARANÁ STATE, SOUTHERN BRAZIL): PETROLOGICAL AND GEOTECTONIC SIGNIFICANCE

Prazeres Filho, H.J.; Basei, M.A.S.; Passarelli, C.R.; Harara, O.M.M. and Siga Jr., O.

Instituto de Geociências, Universidade de São Paulo, Rua do Lago 562-Cid.Universitária, São Paulo-SP,
05508-900, Brazil. prazeres@usp.br

Keywords: U-Pb geochronology, post to non-orogenic granitic magmatism, Apiaí Folded Belt

The Apiaí Folded Belt (AFB) is a domain of the southern portion of Ribeira Belt, and in Paraná and São Paulo States, southern Brazil, is composed of metavulcano-sedimentary rocks, of low to medium metamorphic grade, grouped in the Açungui Supergroup (Fiori, 1993; Campanha & Sadowski, 1999). The Neoproterozoic granitic rocks represented by the Cunhaporanga, Três Córregos and Agudos Grandes batholiths intrude the supracrustal rocks and both are affected by latter granitic stocks. In this paper, it's presented new lithochemical and geochronological data for Morro Grande (MG) and Serra do Carambeí (SC) granites (Figs. 1, 2).

The neoproterozoic Cunhaporanga, Três Córregos and Agudos Grandes batholiths are calc-alkaline, metaluminous, I-type and magmatic arc-related granites. It is mostly represented by hornblende biotite monzogranites to granodiorites with U-Pb zircon ages ranging between 630 and 600 Ma (Gimenez Filho et al., 2000; Guimarães, 2000; Prazeres Filho, 2000; Prazeres Filho et al., 2001; Janasi et al., 2001).

The Morro Grande granite (MG) (Chiodi Filho et al., 1987; Prazeres Filho, 2000) covers an area of approximately 70 km^2 (Fig. 2). It is intruded into the metavolcano-sedimentary rocks of Votuverava Formation developing thermal aureole with metamorphic assemblages in the albite-epidote hornfels facies. The studied portion of MG is constituted by leucocratic, porphyritic, isotropic, light grey biotite monzo to sienogranites, with idiomorphic K-feldspar fenocrystals of up to 3 cm in a matrix with K-feldspar, plagioclase, quartz and biotite. The accessory minerals are zircon, apatite, titanite, fluorite and opaques.

The Serra do Carambeí granite (SC) (Fuck et al., 1967; Guimarães, 2000) is intruded into the Cunhaporanga batholith, covering an area of approximately 22 km^2. It is composed of a red, inequigranular, medium to coarse-grained biotite alkali-feldspar granite. Presents xenomorphic texture with crystals of quartz, mesopertite and interstitial biotite. The accessory minerals are zircon, apatite, fluorite and opaques.

The MG (SiO_2= 71%) and SC (SiO_2= 77%) are weakly peraluminous rocks, with low CaO (0.14 to 1.68%), Al_2O_3 (12.11 to 12.,88%), Sr (<5 to 110 ppm) and Ba (<10 to 571 ppm) and high Y (149 to 43) for SC in relation to MG. In the chondrite normalized REE patterns (Nakamura, 1977) for these rocks, it is noticed a different behavior of REE for the two granites. The SCG is depleted in LREE and enriched in HREE with La_N= 46 and Yb_N= 58, against La_N= 150 and Yb_N= 20 of the MG. The SC compared to MG presents a strong negative anomaly of Eu with Eu/Eu*=0.005, against Eu/Eu* = 0.25 of the MG (Fig. 3).

Conventional multi-grain U-Pb (zircon) dating of the crystallization age of the two granitic stocks was obtained in 3 and 4 zircon fractions, respectively of biotite sienogranite from MG and of biotite alkali-feldspar granite from SC. The zircon grains in both granites are prismatics with a ratio length/width ~ 2:1, rich in inclusions and fractures. Opaque crystals just happen in SC granite (see Fig. 4).

The U-Pb data presented in the figure 4 indicate an upper intercept age of 564±3 Ma (MSWD=0.55) for MG granite and of 569±2 Ma (MSWD= 1.5) for the SC granite. Both ages are interpreted to be the time of crystallization and emplacement of these rocks. The zircon fractions yield a very discordant result caused by lead loss, possibly due to metamictization, evidenced by the opacity of the zircon crystals and by the high U content (up to 1000 ppm - SC granite).

The MG and SC granites mineralogical characteristics (presence of the fluorite), petrographic features (xenomorphic textures) and lithochemical behavior, such as the low CaO, Ba and Sr, the high Y, Hf and Zr contents, as well as the negative anomalies of Eu, are suggestive of A-type rocks formed in a post to non-orogenetic setting. The Joaquim Murtinho, Cerne and Piedade granites, in the State of Paraná (Figs. 1, 2), also could be formed in similar setting.

The lithochemical differences between the MG and SC granites should reflect different sources or different petrological histories to granitic rocks produced in same geotectonic setting.

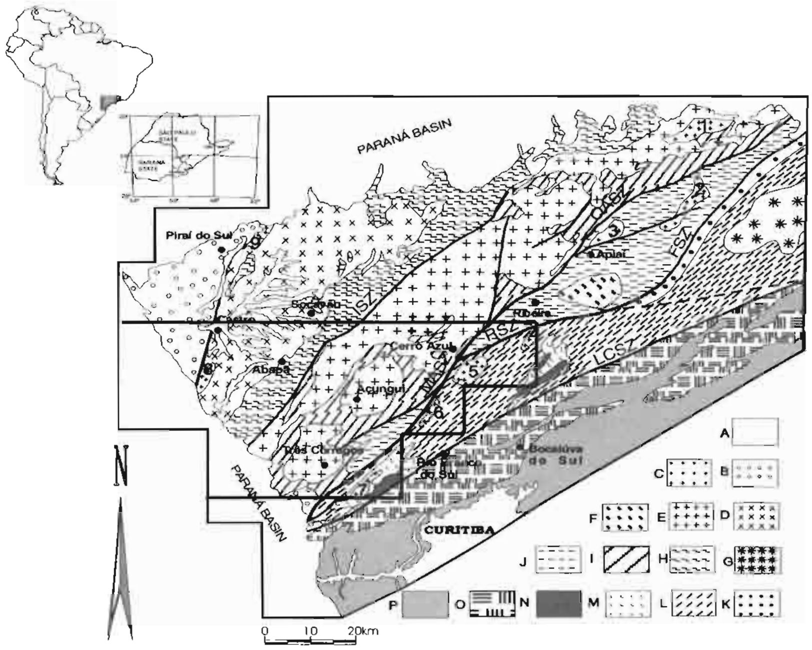

Figure 1. Geological sketch of part of the Ribeira Fold Belt in parts of the states of Paraná and São Paulo, Brazil, with location of studied area.(Mod. Campanha et al. 1987; Siga Jr, 1995; Basei et al. 1997; Campos Neto, 2000. A) Fanerozoic Cover, B) Neoproterozoic III/Eopaleozoic Basin; Apiaí Folded Belt: C) Granitic Stocks : 1- Capão Bonito, 2- Espírito Santo, 3- Apiaí, 4- Varginha, 5- Morro Grande, 6- Piedade, 7- Cerne, 8- Serra do Carambeí, 9- Joaquim Murtinho. Arc Related Neoproterozoic Calc-Alkaline Granitic Batoliths : D) Cunhaporanga; E) Três Córregos; F) Itaoca; G) Agudos Grandes. Açungui Super Group : H) Itaiacoca Group; I) Água Clara Formation; J) Lageado Subgroup ; K) Iporanga Formation ; L) Votuverava Formation ; M) Perau/Betara Formation; N) Granitic Basement Nuclei. Curitiba Microplate - O) Capirú Formation; P) Atuba Complex.

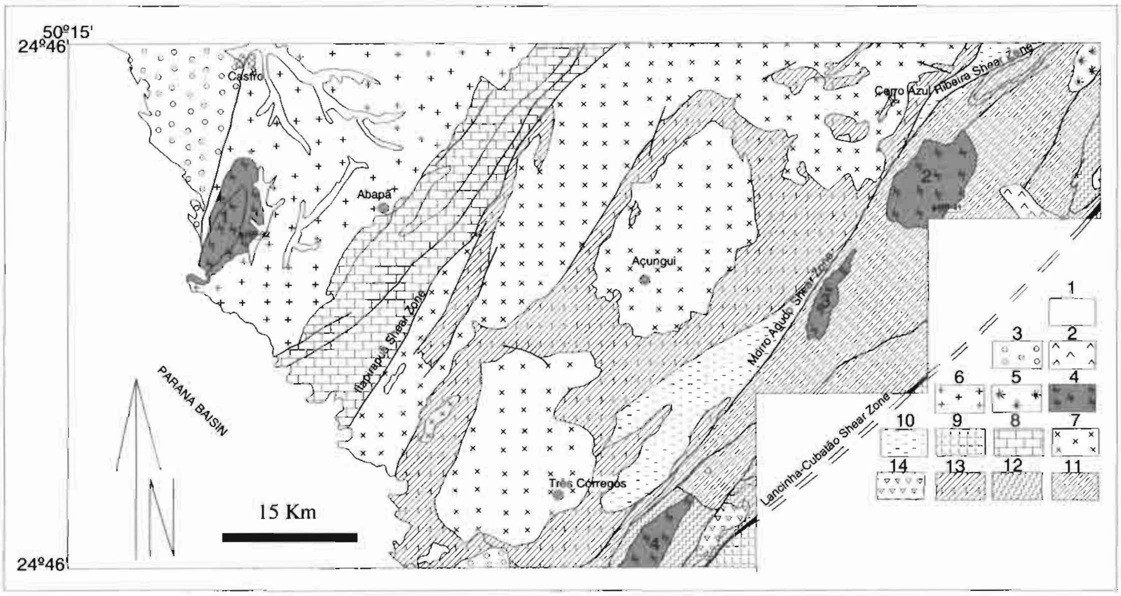

Figure 2. Detailed geological map of studied area. (Mod. Fiori, 1990; Prazeres Filho et al. 1998; Guimarães, 2000). Fanerozoic Units : 1) Recent deposits and Parana Basin, Alkaline rocks; Eocambrian/Neoproterozoic Units: Castro Group; Neoproterozoic Units: 4) Post to non- orogenic granites – 1, Serra do Carambeí, 2) Morro Grande, 3) Piedade, 4) Cerne; 5) Sin to late- orogenic granites: Varginha; Arc related granites: 6) Cunhaporanga Batholith and 7) Três Córregos Batholith; Metavulcanic-sedimentar sequences: 8) Itaiacoca, 9) Capirú, 10) Ribeira; Mesoproterozoic Units: Metavulcanic-sedimentar sequences: 11) Votuvera, 12) Perau, 13) Água Clara; Mesoproterozoic/ Paleoproterozoic Units: 14) Granitic nuclei.

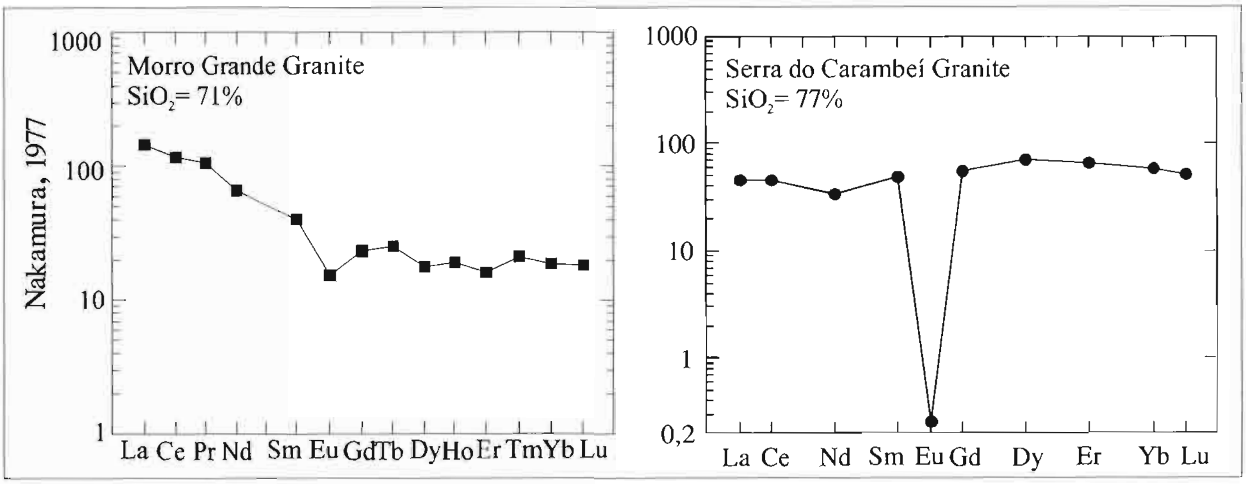

Figure 3. Nakamura normalized REE diagrams.

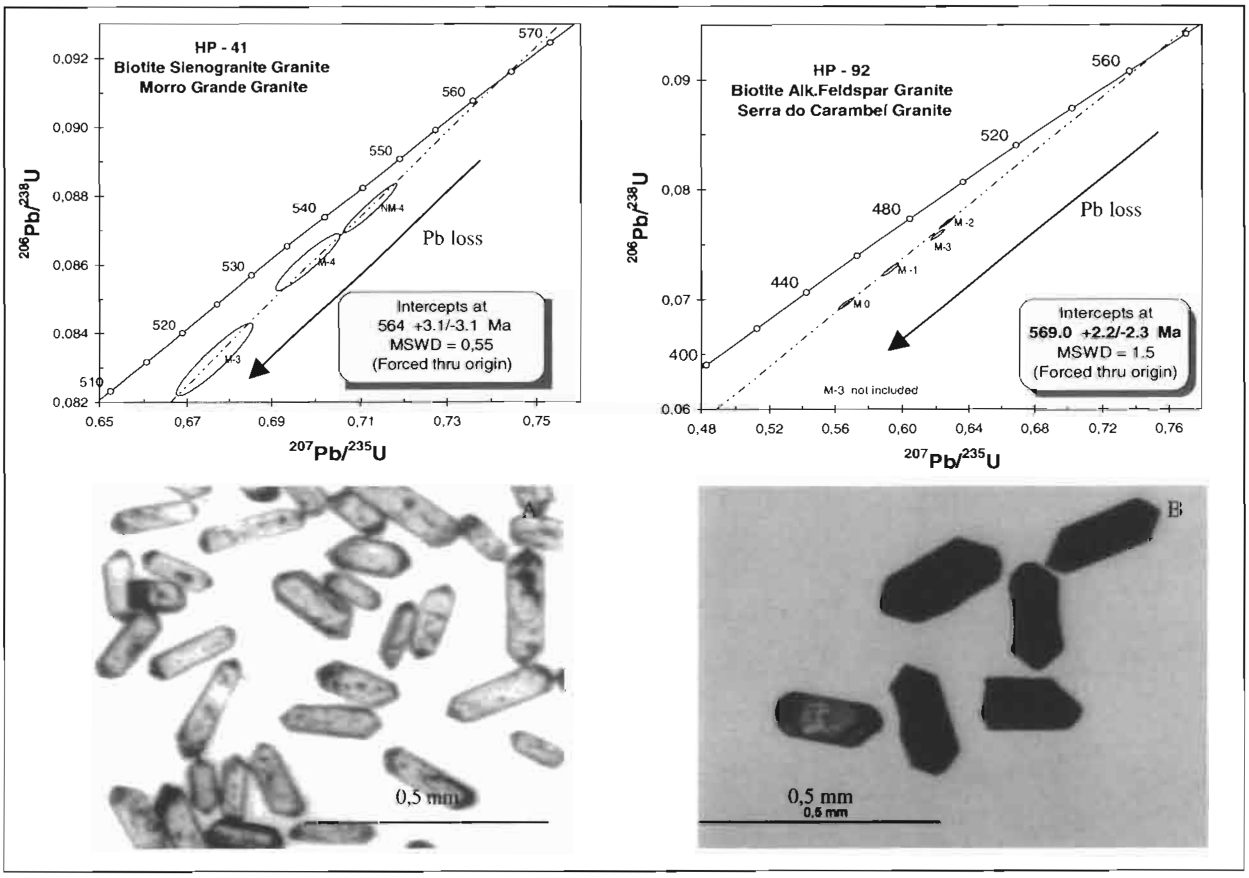

Figure 4. U-Pb Concordia diagrams for zircon grains from biotite sienogranite (MG, sample HP-41) and biotite alkali-feldspar (SC, sample HP-92). And photomicrograph of zircon from: A) Morro Grande Granite and B) Serra do Carambeí Granite.

The 564 and 569 Ma ages obtained in this work are younger than other granitic stocks from AFB, correlated to the MG and SC, for example, the Apiaí Granite, with U-Pb zircon age of 605±3 Ma (Hackspacker et al., 2000) and the Varginha Granite, with U-Pb zircon age of 603±23 Ma (Basei et al., submitted). However, the ages of MG and SC are similar to the U-Pb zircon ages of 580±3 Ma of the Capão Bonito Granite (Leite, 2003) and of 564±8 Ma of the Serra da Bateia Granite (Janasi et al., 2001) and they constrain main period of the late to post-non-orogenic transition in the AFB.

ACKNOWLEDGEMENTS

To FAPESP (grant 01/00962-0) and to Centro de Pesquisas Geocronológicas, IG-USP and Laboratório de Química and ICP, IG-USP.

REFERENCES

Basei, M.A.S.; Siga Jr, O.; Kaulfuss, G.A.; Cordeiro, H.; Nutman, A.; Sato, K.; Prazeres Filho, H.J.; Passarelli, C.R.; Harara, O.M.M.; Reis Neto, J.M. (submited) Magmatismo básico mesoproterozóico no Vale do Ribeira-implicações na idade de deposição das sequencias metavulcano-sedimentares Perau e Votuverava, PR, Brasil.

Campanha, G.A.C. & Sadowski, G.R. 1999. Tectonics of the southern portion of the Ribeira Belt (Apiaí) Domain. Precam. Research, 98:31-51.

Campos Neto, M. C. (2000). Orogenic Systems from Southwestern Gondwana: na approach to Brasiliano-Pan African cycle and orogenic collage in southeastern Brazil. In: Cordani, U.G.; Milani, E.J.; Thomas Filho, A.; Campos, D.A.. Tectonic Evolution of South America, Rio de Janeiro, 2000, p: 335-365.

Chiodi Filho, C.; Moretzshon, J.S.; Santos, J.F.; Soares, P.C. 1987. Aspectos Geológicos e metalogenéticos dos Granitos Morro Grande, Piedade e Varginha-Vale do Ribeira-Paraná.In: SIMP. SUL BRAS. DE GEOL, 3. Curitiba, 1987. Anais...Curitiba, SBG. v. 2, p. 515-542.

Fiori, A. 1993. Considerações sobre a estratigrafia do Grupo Açungui (Proterozóico Superior), Paraná, S-Brasil. Bol. IG-USP, Série Científica, 24: 1-19.

Fiori, A.P. 1990. Tectônica e estratigrafia do Grupo Açungui a norte de Curitiba. Tese de Livre Docência. São Paulo, IG-USP, 246p

Fuck, R.A.; Marini, O.J.; Trein, E. 1967. Contribuição ao estudo das rochas graníticas do Estado do Paraná. Bol. Paran. Geoc; 23/25:183-221

Gimenez F.°, A.G.; Janasi, V. A ; Campanha, G. A C.; Teixeira, W.; Trevizoli Jr., L.E. 2000. U-Pb dating and Rb-Sr isotope geochemistry of the Eastern portion of the Três Córregos Batolith Ribeira Fold Belt, São Paulo, Brazil. Rev. Bras. Geoc. 30(1): 45-50.

Guimarães, G. B. 2000. As rochas granitóides do Complexo Granítico Cunhaporanga, PR: aspectos geológicos, geofísicos, geoquímicos e mineralógicos. Tese de Doutoramento (inédita). São Paulo, IG-USP, 230p.

Hackspacher, P.C.; Dantas, E.L.; Spoladore, A.; Fetter, A.H.; Oliveira, M.A.F. 2000. Evidence for Neoproterozoic back arc basin development in the central Ribeira Belt, southeastern Brazil: new geochronological and geochemical constraints from the São Roque-Açungui Groups. Revista Brasileira de Geociências, 30(1):110-114.

Janasi, V.A.; Leite, R.J.; van Schmus, W.R. 2001. U-Pb chronostratigraphy of the granitic magmatism in the Agudos Grandes Batholith (west of São Paulo) – implications for the evolution of the Ribeira Belt. Journal of South American Earth Sciences 14:363-376

Leite R.J. 2003. Petrogenese e geocronologia U-Pb do magmatismo granítico tardi a pós-orogênico no Batólito Agudos Grandes – SP. Thesis IGc/USP. 218p.

Nakamura, N. 1977. Determination of REE, Ba, Fe, Mg, Na and K in carbonaceous and ordinary chondrites. Geochemica at Cosmochimica Acta, 38:757-775.

Prazeres Filho, H.J. 2000. Litogeoquímica, Geocronologia (U-Pb) e Geologia Isotópica dos Complexos Graníticos Cunhaporanga e Três Córregos, Estado do Paraná. Dissertação de Mestrado-IGc-USP, 180p.

Prazeres Filho, H.J.; Basei, M.A.S.; Harara, O.M.; Passarelli, C.R.; Siga Jr.,O.; Reis Neto, J.M.; Sato, K. 2001. The Alto Ribeira Magmatic Arc (Paraná State-Southern Brazil): Geochemical and Isotopic Evidences of Magmatic Focus Migration and Its Tectonic Implications. In: III Simpósio Sul-Americano de Geologia Isotópica, Pucon, Chile. Extend Abstract p.213-216

Prazeres Filho, H.J.; Guimarães, G.B.; Basei, M.A.S.; Siga JR., O.; Reis Neto, J.M.; Campanha, G.AC. Sallun Filho, W. 1998. Mapa Geológico 1:50.000 da porção centro-sul da Faixa Itaiacoca, PR. In: Cong.Bras.Geol., 40, Belo Horizonte, 1998. Anais... Belo Horizonte, SBG, p.36.

PUNTA DEL ESTE TERRANE: MESOPROTEROZOIC BASEMENT AND NEOPROTEROZOIC COVER

Preciozzi, F.[1]; Basei, M.A.S.[2]; Peel, E.[1]; Sánchez Bettucci, L.[1]; Cordani, U.[2] and Oyhantcabal, P.[1]

1. Depto. de Geología, Facultad de Ciencias. Iguá 4225, CP 11400 Montevideo, Uruguay.
fepre@fcien.edu.uy, elena@fcien.edu.uy, leda@fcien.edu.uy, oyhantca@fcien.edu.uy
2. Instituto de Geociências, Universidade de São Paulo-SP, Brasil. baseimas@usp.br, ucordani@usp.br

Keywords: Mesoproterozoic, Punta del Este Terrane, geochronology

Eastern basement of Uruguay consists of Meso and Neoproterozoic rocks. Mesoproterozoic basement had been deformed by pre-Brasiliano and Brasiliano events. Regional variations in this basement and in the Neoproterozoic cover show equivalent deformation styles and intensities.

Models proposed for tectonic evolution have been scarce and confusing. Specially, the ones that concern the moment of collision and/or juxtaposition of blocks.

The Punta del Este Terrane (PET) is composed of gneisses and migmatites formed between 1000 Ma to 900 Ma (Preciozzi et al., 2001). These rocks had been strongly reworked during Brasiliano and Rio Doce orogenesis (ca. 900-500 Ma). This crustal segment represents a high grade metamorphic terrane, which is correlated to some gneissic complexes southwest of Africa. Particularly, it is correlated to Kibaran-Namaqua Belt in Namibia.

U-Pb ages between 1000 Ma and 900 Ma, obtained in zircons from tonalitic granitoids, are interpreted as indicative of their crystalizations (Fig. 1). Besides, anatectic fluids related to migmatite leucosomes yielded ages of ca. 520 to 540 Ma. This denotes that superimposed metamorphic conditions during Brasiliano orogenesis reached, at least, lower anphibolite facies.

PET basement gneisses present Sm-Nd model ages (T_{DM}) between 2.4 to 1.8 Ga, showing long crustal residence, corroborated by the very negative ε_{Nd} values of –1.3 and –14.3. During Brazilian orogenesy they were affected by deformation processes and anatexis.

Metasedimentary PET cover occurs near La Paloma and Rocha towns. It is represented by a siliciclastic metasedimentary succession corresponding to the Rocha formation. In La Pedrera town recognized three sedimentary facies were (1-3): (1) sandstones and pelites; (2) green pelites; and (3) rhytmites. The transition from facies (1) to facies (3) shows the passage from fluvial environment with tidal influence to tidal flat with predominance of subtidal deposits (Pazos & Sánchez, 1999). Rocha Formation may correlate with the supracrustal Gariep Group. Rocha-Gariep basin closure and following deformation would have been occurred ca. 545 to 570 Ma.

Cerros de Aguirre formation (Campal & Gancio, 1993) represents a volcaniclastic sequence, of Vendian age, with an intermediate to acidic composition. This formation had suffered compression generating open folds with axial orientation N30°-40°E and local development of axial plane cleavage.

Isotrop granitoids represent the most important magmatic manifestation that affected PET. These granitoides of calcalkaline character includes José Ignacio and Santa Teresa plutons among others. Using Rb/Sr mineral isochron, ages of 611 – 590 Ma for José Ignacio pluton and of 550 – 537 Ma for Santa Teresa pluton were obtained.

REFERENCES

Campal, N & Gancio, F. 1993. Asociación Volcánitas – Piroclastitas de los Cerros de Aguirre (Departamento de Rocha): una Nueva Formación y sus implicancias en la Evolución del Ciclo Brasiliano en el Uruguay. In: 1° Simposio Internacional del Neoproterozoico – Cámbrico de la Cuenca del Plata, 2: 133-139, La Pedrera, Uruguay.

Pazos, P. & Sánchez Bettucci, L. 1999. Rasgos mareales en la sucesión neoproterozoica de la Pedrera, Grupo Rocha, Uruguay. XIV Congreso Geológico Argentino, Actas I pp.71, Salta.

Preciozzi, F.; Peel, E.; Muzio, R.; Ledesma, J. & Guerequiz, R. 2001. Dom Feliciano Belt and Punta del Este Terrane: Geochronological Features. Actas III SSAGI, Pucón, Chile. CD-ROM.

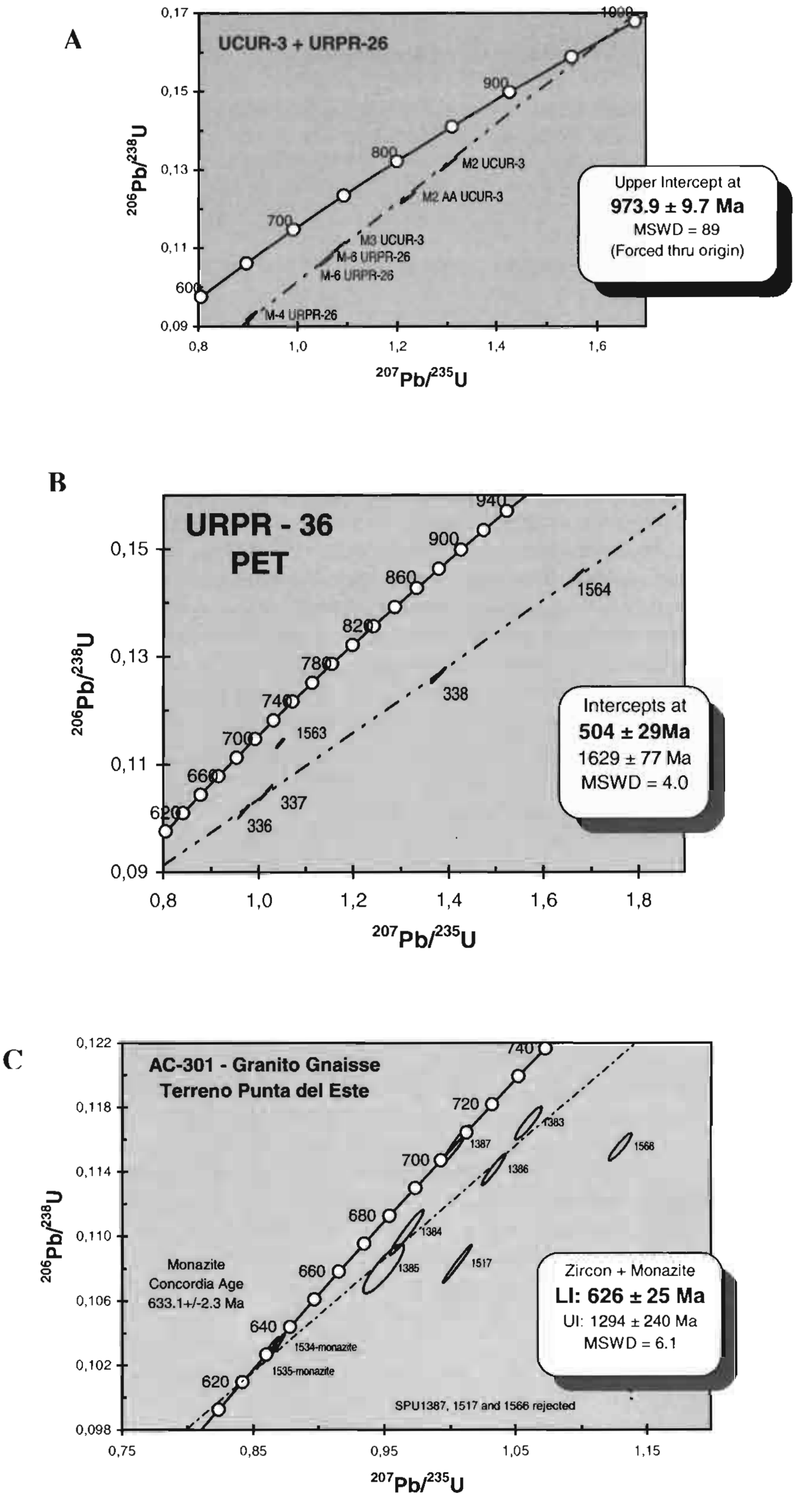

Figure. 1. U-Pb concordia of Punta del Este Terrane samples (A) UCUR3 & URPR26; (B) URPR36; (C) AC301.

Sr AND Nd ISOTOPIC SIGNATURES OF MANTLE AND CRUSTAL XENOLITHS FROM MERCADERES, NORTHERN VOLCANIC ZONE, COLOMBIA

Rodrigues A.[1]; Koester E.[2]; Mallmann G.[3]; Conceição R.V.[2,4]; Kawashita K.[2] and Weber M.B.I.[1]

1. Universidad Nacional de Colombia, UNC – Colombia. zafiromerca@hotmail.com, mweber@perseus.unlmed.edu.co
2. Laboratório de Geologia Isotópica, IG, UFRGS, C.P. 15001, Porto Alegre-RS, Brazil. koester@ufrgs.br
3. Programa de Pós-graduação em Geociências, IG, UFRGS, Brazil. guilherme.mallmann@ufrgs.br
4. Departamento de Geologia, IG, UFRGS – Brazil. rommulo.conceicao@ufrgs.br

Keywords: Mantle xenoliths, Sr and Nd isotopes, garnet and spinel peridotites and pyroxenites, crustal xenoltiths

INTRODUCTION

Mantle and crustal xenoliths have been described in the Andean region associated with alkaline magmatism related to the subduction of Nazca and Antartic Plate beneath the South American Plate. Crustal xenoliths present in these areas are mainly granulites, hornblendites, pyroxenites and gneisses and represent the lower crustal rocks (*e.g.* Selverstone & Stern, 1983; Weber et al., 2002). Mantle xenoliths, representing the lower and the upper lithospheric mantle have also been described, spinel peridotite generally being predominant (*e.g.* Gobernador Gregores, Lote 17 - Gorring & Kay, 2000; Laurora et al., 2001) whereas garnet peridotites are restricted to a few localities (*e.g.* Pali Aike, Stern et al., 1999; Weber, 1998).

Information on crustal lithologies is important for providing mineralogical and geochemical data, which are a powerful tool to the understating of crustal growth models. Mantle lithologies are also important, and their mineralogy, chemistry, geophysics and petrology will support the development of mantle models. These models include the knowledge of pressure-temperature mineral phase stabilities, the source characterization of mantle-derived magmas and the understanding of metasomatic processes, all of which still need to be studied and constrained (*e.g.* metasomatism process in Gobernador Gregores (Lote 17), Gorring & Kay, 2000 & Laurora et al., 2001).

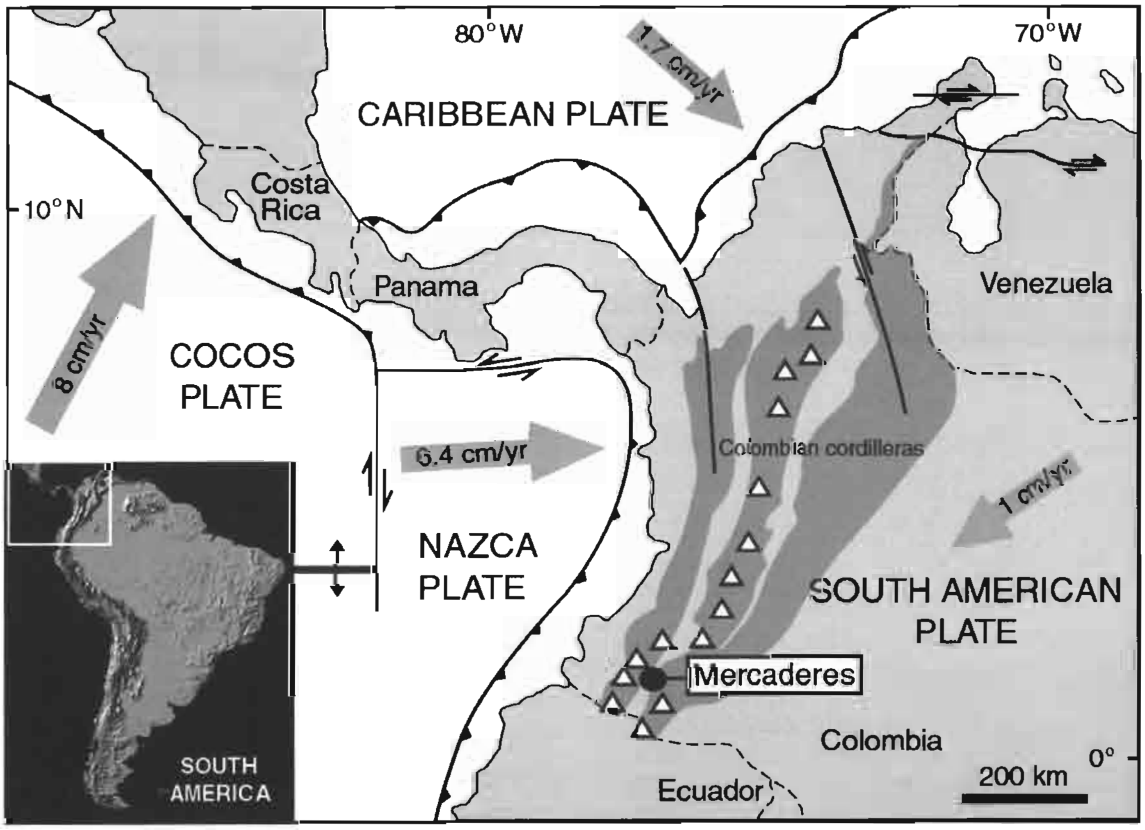

Figure 1. Main tectonic geological framework of the Colombian Andes, showing the convergence of the Nazca Plate beneath the South American Plate. Triangles represent the active volcanoes related to the Northern Volcanic Zone (NVZ) and the location of the Mercaderes area (Modified from González et al., 1988).

The Mercaderes area in SW Colombia, located in the Northern Volcanic Zone (NVZ) (Thorpe, 1982) is characterized by late Cenozoic volcanic activity, where the Mercaderes Tableland comprises young volcanic and volcano-sedimentary flows. On the southeastern part of this tableland lies the Granatífera Tuff, which is possibly a small, partially eroded tuff cone or tuff ring, containing xenoliths of both crustal (*e.g.* diorite, granulite, hornblendite) and mantle (*e.g.* garnet peridotite, garnet websterite) origin (Weber et al., 2002), providing a key area to improve the understanding of the crustal and particularly the mantle evolution model in the NVZ, especially since the garnet peridotites-pyroxenites are predominant in this area.

New Sr and Nd isotopic data are presented here, which help constrain the processes and mechanisms of the mantle in the Mercaderes area. This data provides an important tool that, combined with field, petrographic and geochemical whole-rock and mineral data, will support new discussions regarding mantle and crustal models.

GEOLOGICAL SETTING

The Granatífera Tuff in the Mercaderes area, Colombia (NVZ), is host to three main xenoliths groups: mantle, lower crustal and upper crustal xenoliths (Weber, 1998).

Mantle xenoliths are mainly represented by garnet-bearing rocks, ranging from peridotites to websterites. Garnet-free mantle xenoliths are also present, but less abundant, represented by pyroxenites and spinel peridotites. Spinel peridotites formed at low pressures (16 kbar, 1065°C) whereas garnet peridotites, formed at high pressures and temperatures (~30 kbar, ~1200°C). Two conditions were described, i) a sub-oceanic geotherm (29-35 kbar, 1250-1295°C) and ii) a sub-continental geotherm (> 38 kbar, 1140-1175°C).

Lower crustal xenoliths comprise a variety of pyribolites, hornblendites, amphibolites, granulites, pyroxenites and gneisses, showing a metamorphic amphibolite to granulite facies transition. Pressure and temperatures for these xenoliths range from: i) 730-830°C at 9 to 14 kbar (amphibolites), and ii) 950-1050°C at 13 to 15 kbar for all other rocks.

Upper crustal rocks are represented by diorites and volcanic rock fragments and bombs with andesitic, dacitic and lamprophiric characteristics.

Thus, garnet-bearing xenoliths represent deeper fragments (around 90 km) and spinel peridotite xenoliths are fragments of upper lithospheric mantle, as suggested by Weber (1998). Most other metamorphic fragments represent lower crustal material. Upper crustal rocks represent at least two magmas (andesitc & lamprophiric) that interact possibly during crustal growth, due to the subduction of the Nazca Plate.

Sr AND Nd ISOTOPIC GEOLOGY

Samples for radiogenic isotope analyses (twelve xenoliths) were spiked (mixed ^{87}Rb-^{84}Sr, ^{149}Sm/^{150}Nd) and processed using standard dissolution procedures using HF, HNO_3 and HCl in teflon vial, warmed on a hot plate until complete dissolution. Column procedures use cationic AG50W-X8 resin (200-400 mesh) in order to separate the Rb, Sr and REE, followed by Sm and Nd separation using anionic LN-B50-A resin (100-150 μm). Each sample was dried to a solid and then loaded with 0.25 N H_3PO_4 on appropriate filament, single Ta for Rb, Sr and Sm and triple, Ta-Re-Ta for Nd. The samples were analyzes in a VG Sector 54 thermal ionisation mass spectrometer at the Laboratório de Geologia Isotópica (Universidade Federal do Rio Grande do Sul) in a static mode. Nd and Sr ratios were normalised to ^{86}Sr/^{88}Sr = 0.1194, and ^{146}Nd/^{144}Nd = 0.72190 respectively. Measurements for the NIST standard NBS-987 gave ^{87}Sr/^{86}Sr = 0.710260 ± 0.000014, and for the La Jolla values of ^{143}Nd/^{144}Nd = 0.5118590 ± 0.000010. Total blanks averaged <750 pg for Nd and <150 pg for Sm, Rb and Sr.

Sr and Nd isotopic data performed on whole-rock are illustrated in Figure 2. Mantle xenoltihs have low Rb (<0.9 ppm), Sr (<96 ppm), Sm (<3.2 ppm) and Nd (3.3 ppm) values. Five garnet-peridotites and two websterites represent mantle samples, with ^{87}Sr/^{86}Sr ratios between 0.7029 and 0.7044 and ^{143}Nd/^{144}Nd between 0.5127 and 0.5134. Three lower crustal xenoliths (hornblendite, granulite, and pyroxenite) yield Rb values lower than 6.1 ppm, Sr lower than 713 ppm, Sm lower than 12 ppm and Nd lower than 65 ppm, with ^{87}Sr/^{86}Sr ratios between 0.7044 and 0.7054 and ^{143}Nd/^{144}Nd for the same xenoliths between 0.5128 and 0.5130. An upper crustal diorite sample shows the highest Rb and Sr of the analysed suite, with values of 68 and 1262 ppm respectively. Sm and Nd values for this xenolith are 8 and 39 ppm, and the ^{87}Sr/^{86}Sr ratios are 0.749 and ^{143}Nd/^{144}Nd ratios 0.5128. Two volcanic samples (one andesite and one lamprophyric rock) show Rb values lower than 18 ppm, Sr lower than 561 ppm, Sm lower than 4.5 ppm and Nd lower than 18.8 ppm, having ^{87}Sr/^{86}Sr values of 0.7045 and 0.7059 and ^{143}Nd/^{144}Nd of 0.5125 and 0.5128.

The Mercaderes garnet-peridotite mantle samples plot within the oceanic basalt field (OIB) in the ^{87}Sr/^{86}Sr versus ^{143}Nd/^{144}Nd diagram. The MORB-field is also shown and all data plot outside this field towards Bulk Silicate Earth (BSE) values, or more radiogenic Sr isotopic compositions. Only one sample has a distinct signature, with higher Nd values compared to other garnet peridotites. One spinel peridotite plots in the MORB-field related isotopic composition, while another sample plots away from MORB, this high radiogenic Sr probably related to the presence of high amounts of CaO (20 %) within this sample. Thus, a MORB signature is suggested for spinel peridotites, while an OIB signature is evidenced by the garnet-peridotites.

Lower crustal xenoliths show more radiogenic Sr compositions compared to mantle xenoliths. Neverthless, all samples plot near the crustal xenolith-field discriminated by Weber et al. (2002), and as suggested therein, show that the lower crust under Mercaderes area is isotopically heterogeneous.

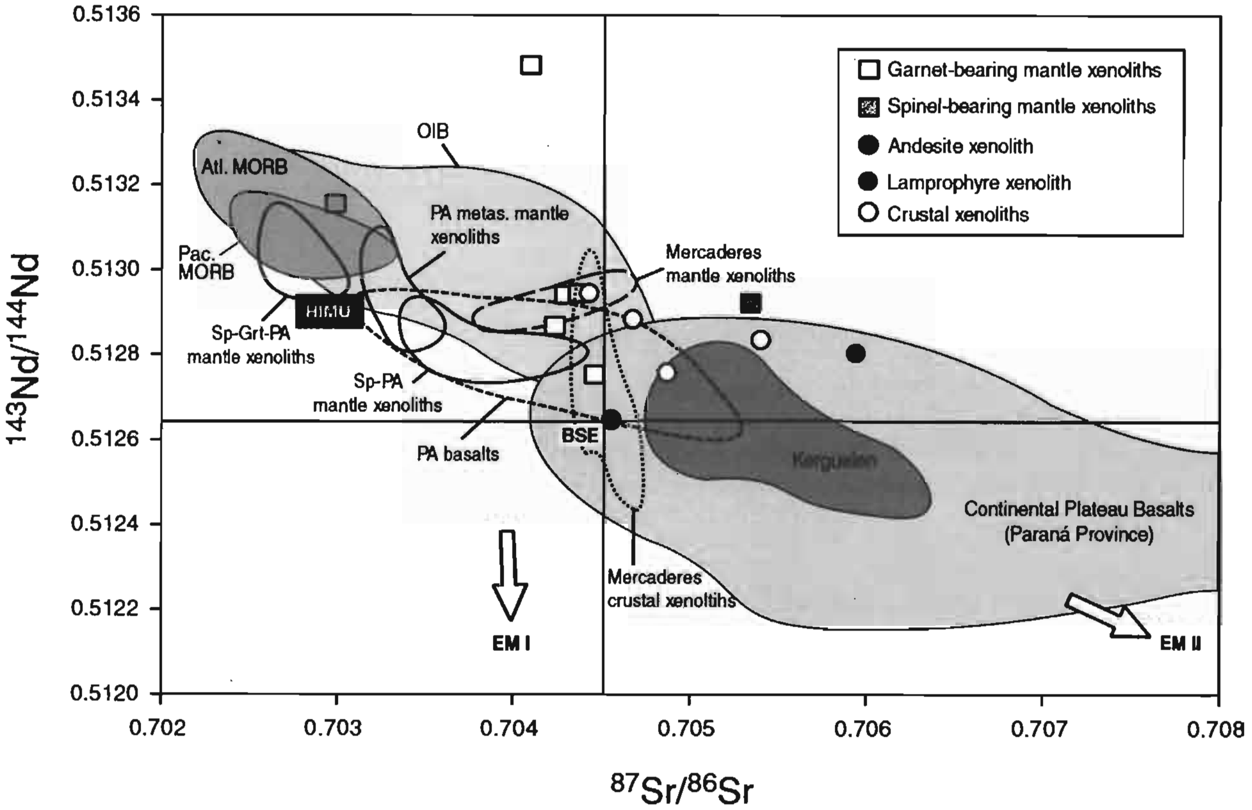

Figure 2. Sr and Nd isotopic variations for mantle and crustal xenoltihs from the Mercaderes area, Colombia. Fields compiled in the "http://georoc.mpch-mainz.gwdg.de/".OIB field includes Hawaii, La Palma, Azores, St.Helena, Easter and Ascencion Islands. PA = Pali Aike (Stern et al., 1999); Mercaderes fields from Weber et al. (2002).

Volcanic rocks have more evolved radiogenic Sr than garnet and spinel mantle xenoliths. Nevertheless they show different values: the andesitic rock plots within the NVZ volcanic field, whereas the lamprophyric sample shows the most radiogenic Sr composition of the whole suite, and plots outside the NVZ field.

ε_{Nd} (t=0) values for mantle xenoliths range from 2.4 to 16.5 and confirm the depleted isotopic composition of this material. Also, crustal xenoliths have positive ε_{Nd} (t=0) values, ranging from 2.4 to 6.0, suggesting the presence of orthoderived material in the lower crust, whereas for volcanic rocks ε_{Nd} (t=0) are 0.3 and 3.2. The higher value is given by a lamprophyric sample.

Sm/Nd model ages (T_{DM}-De Paolo, 1981), for crustal xenoliths indicate an extraction age varying from 0.3 to 0.4 Ga, which suggest crustal growth in this area at this time. However, for lamprophyre and andesite xenoliths T_{DM} provide ages of 0.6 to 0.7 Ga, older than the lower crustal xenoliths, suggesting distinct events of mantle extraction.

DISCUSSION

Mantle and crustal xenoliths in the Granatífera Tuff in Colombia have provided some approach to add knowledge to the discussion of the lithospheric mantle and also the crustal evolution of this area. Sm/Nd and Rb/Sr isotopic systematics integrated with field relationships, geochemistry and pressure-temperature data suggest the importance of garnet-bearing mantle xenoliths providing evidence of two distinct reservoirs. A main isotopic source for garnet peridotites, with OIB isotopic signature and high P-T conditions, showing a "sub-continental geothermal gradient", reflect the tectonic environment of this area, where a convergent tectonic setting is characterised by subduction of the Nazca Plate under the South American plate. On the other hand, garnet peridotite xenoliths with different pressure temperature conditions, representing a "sub-oceanic geothermal gradient", show similar Sr/Sr ratios, but distinct Nd/Nd isotopic signature. This enrichment in radiogenic Nd, suggests a different isotopic reservoir, maybe related to a process of chromatographic isotopic separation due to Nd increase, without disturbance in Sr values. Spinel peridotite shows low P-T conditions, a MORB signature and a similar "sub-oceanic geothermal gradient".

The lower crust comprises heterogeneous material, recorded by isotopic distinct signatures, formed during the 0.3-0.4 Ga. No similar age has been reported for rocks outcropping in the area.

The evolution of intermediate magmas as result of deeper mantle melt, and the signature similar to the BSE-"continental plateau basalts" suggest a different mantle source for these rocks.

The high amount of garnet-bearing mantle xenoliths is evidence of the importance of this material in the

Mercaderes area. Mantle xenoliths in Mercaderes were compared with the main garnetiferous mantle xenolith occurrence in the Andes, the Pali Aike region. Both areas show garnet and spinel mantle xenoliths, but isotopic signatures are quite distinct. Garnet-bearing mantle xenoliths of Pali Aike are more undepleted compared to the Mercaderes garnet peridotites, whereas Pali Aike spinel peridotites are Sr-enriched in comparison to similar rocks in Mercaderes. Pressure and temperature for garnet and spinel mantle xenoliths in Pali Aike area, also show distinct patterns, with temperatures around 970-1160°C and pressures between 19 to 24 kbar (Stern et al., 1999). Thus, regarding the lithosphere mantle evolution, these two regions present a MORB-like signature, but an OIB-like is suggested in the Mercaderes area.

The Mercaderes area in the NVZ represents an important mantle occurrence of garnet peridotites. Two distinct isotopic signatures were recognised, which agrees with field evidence, petrographic and P-T data. Together with crustal and lamprophyric rocks, these data show the importance of this area in the understanding of mantle-crustal evolution, since no other area in the Andean region shows similar characteristics. Thus, the mantle xenoliths in this area represent at least various different geologic events, showing a MORB and OIB signature, but also the importance of continental crust during its evolution.

ACKNOWLEDGEMENTS

We gratefully acknowledge Farid Chemale Junior for his support and constructive comments on various aspects of field and laboratory studies. This work was funded by PROSUL-CNPq (project AC-74).

REFERENCES

De Paolo, D.J., 1981. Neodymium isotopes in the Colorado Front Range and implications for crust formation and mantle evolution in the Proterozoic: Nature 291: 193-197.

González, H.; Nuñez, A.; Paris, G. 1988. Memoria explicativa del Mapa Geologico de Colombia. Ingeominas, 71p.

Gorring, M.L.; Kay, S.M. 2000. Carbonatite metasomatized peridotite xenoliths from southern Patagonia: Implications for lithospheric process and Neogene plateau magmatism. Contributions to Mineralogy and Petrology, 140:55-72.

Laurora, A., Mazzucchelli, M., Rivalenti, G., Vannucci, R., Zanetti, A., Barbieri, M.A., Cingolani, C.A., 2001. Metasomatism and melting in carbonated peridotite xenoliths from the mantle wedge: the Gobernador Gregores case (southern Patagonia): Journal of Petrology, 42(1): 69-87.

Selvertsone, J.; Stern, C.R. 1983. Petrochemistry and recristalization history of granulite xenoliths from the Pali-Aike volcanica field, Chile. American Mineralogist, 68:1102-112.

Stern, C.R.; Killian, R.; Olker, B.; Hauri, E.H.; Kyser, T.K. 1999. Evidence from mantle evolution for relatively thin (<100 km) contiental lithosphere below the Phanerozoic crust of souhternmost South America. Lithos, 48:217-235.

Thorpe, R.S. 1982. Andesites: orogenic andesites and related rocks. John Wiley & Sons, Chichester, 724 p.

Weber, M.B.I. 1998. The Mercaderes-Rio Mayo xenoliths, Colombia: Their bearing on mantle and crustal processes in the Northern Andes. PhD. Thesis, University of Leicester, UK, 277 p.

Weber, M.B.I.; Tarney, J.; Kempton, P.D.; Kent, R.W. 2002. Crustal make-up of northern Andes: evidence based on deep crustal xenolith suite, Mercaderes, SW Colombia. Tectonophysics, 345(1-4):49-82.

Pb-Pb ZIRCON AGE (EVAPORATION) OF BLUE COLOURED SODALITE-SYENITE ORE IN THE SOUTH BAHIA ALKALINE PROVINCE (NE BRAZIL)

Rosa, M.L.S.[1,2]; Conceição, H.[1,2]; Macambira, M.J.B.[3]; Marinho, M.M.[2,4]; Marques, L.S.[5]; Scheller, T.[3]; Rios, D.C.[2]; Peixoto, A.A.[2]; Cunha, M.P.[2] and Menezes, R.C.L.[2]

1. Pesquisadora CNPq – IGEO – UFBA, Rua Caetano Moura 123, 40201-340, Salvador-BA, Brazil. lourdes@cpgg.ufba.br
2. Grupo de Petrologia Aplicada. herbet@cpgg.ufba.br, debora@cpgg.ufba.br, mpcunha@ufba.br, menezesrita@hotmail.com, aap@cpgg.ufba.br
3. Laboratório de Geologia Isotópica, UFPA, CP 1611, 66075-900, Belém-PA, Brazil. moamac@ufpa.br, tscheller@ufpa.br
4. Companhia Baiana de Pesquisa Mineral, 4ª Avenida 460, 41760-300, Salvador-BA, Brazil. cbpmdt@cbpm.com.br
5. Instituto Astronômico e Geofísico-USP, Caixa Postal 3386, 01060-970, São Paulo-SP, Brazil. leila@iag.usp.br

Keywords: Sodalite-syenite, Pb-Pb, zircon, Bahia, Brazil

INTRODUCTION

The South Bahia Alkaline Province (SBAP) is the only place in Brazil were occurences of blue colored sodalite-syenite ore have been identified (Fig. 1). These syenites represent the most important dimension stone of Brazil.

The SBAP covers an area of about 6,500 km^2 been composed by twenty NE-SW elongated silica sub-saturated alkaline massifs. At this province, the sodalite-syenites consist of small stocks, less than 4 km^2, that intrude alkaline bodies and are always associated to nepheline-syenites. The alkaline massifs intrude an Archaean to Paleoproterozoic granulitic-migmatitic-anorthositic terrain at the tectonic interface between the São Francisco Craton and Araçuaí mobile belt.

The available geochronological data (Rb-Sr, K-Ar, U-Pb) for the SBAP alkaline massifs are very heterogeneous, ranging from 500 Ma to 740 Ma (Cordani et al., 1974; Martins & Santos, 1993; Teixeira et al., 1997, Côrrea Gomes & Oliveira, 2002). These data must reflect the crystallization ages and late metamorphic events related to Araçuaí Orogen.

At 1960 these sodalite-syenite start to be exploited as dimension stones, therefore only now $^{207}Pb/^{206}Pb$ zircon evaporation analyses have been performed. In this paper we will present for the first time the results of a geochronological investigation at two mineralized sites which are located at the Floresta Azul Alkaline Complex and Itarantim Syenitic Massif.

ANALYTICAL PROCEDURES

The ages of these blue syenites were investigated by single zircon Pb-evaporation technique developed by Köber (1986, 1987). The data were obtained at the Laboratory for Isotope Geology, Pará Federal University (Pará-Iso), Brazil, on a Finnigan MAT 262 thermal ionization mass spectrometer. The ages were calculated with 2σ error and common Pb values consider only those blocks in which the $^{204}Pb/^{206}Pb$ ratio were lower than 0.0004. For more details see Rosa et al. (2003).

FLORESTA AZUL ALKALINE COMPLEX (FAAC)

This complex cover an area of about 200 km^2 and intruded the granulitic rocks from Itabuna Belt. It is formed of two intrusions: granitic (East) and syenitic (South). The sample was colected in the south part in a quarry mainly composed by green coloured biotite-nepheline-syenite rocks. The blue coloured sodalite-syenites occur as sub-vertical bands with about 5 m of thickness (Cunha, 2003).

ITARANTIM SYENITIC MASSIF (ISM)

This massif cover an area of about 220 km^2 and intruded the archean and paleoproterozoic gneissic-granulitic basement rocks. The ISM is composed by aegirine-nepheline-syenites and sodalite-syenite alkaline dykes. The samples were colected in a 3 m wide dyke. At the sampled site, rocks are medium- to coarsed-grained and sodalite represents up to 40% in volume.

RESULTS AND DISCUSSION

Sample 2098 (UTM 415328-8345604), corresponding to a blue coloured biotite sodalyte-syenite, was selected at the FAAC site (Fig. 1). This is a coarsed grained rock with centimetric (up to 3 cm) zircon crystals. Only a single zircon population was identified at this sample, which correspond to brown rediish long prismatic habit crystals, ranging in size from 1 to 2 cm. Some fractures and inclusions have been observed.

The minnimum crystallization age obtained for this rock was 706 ± 12 Ma. The age of the alkali-feldspar syenites, which are the country rocks for them, is 688 ± 10 Ma (Côrrea Gomes & Oliveira, 2002) allowing us to consider them as contemporaneous rocks.

Two samples from ISM 2034 (UTM 379141-8251337) and 2035 (UTM 379146-8251340), which are sodalite-syenites, have been selected for geochronological analyses (Fig. 1). This single population analysed crystals were dark to light brow zircons, with sizes ranging from 0.2 to 0.5 mm, translucid and without observed inclusions.

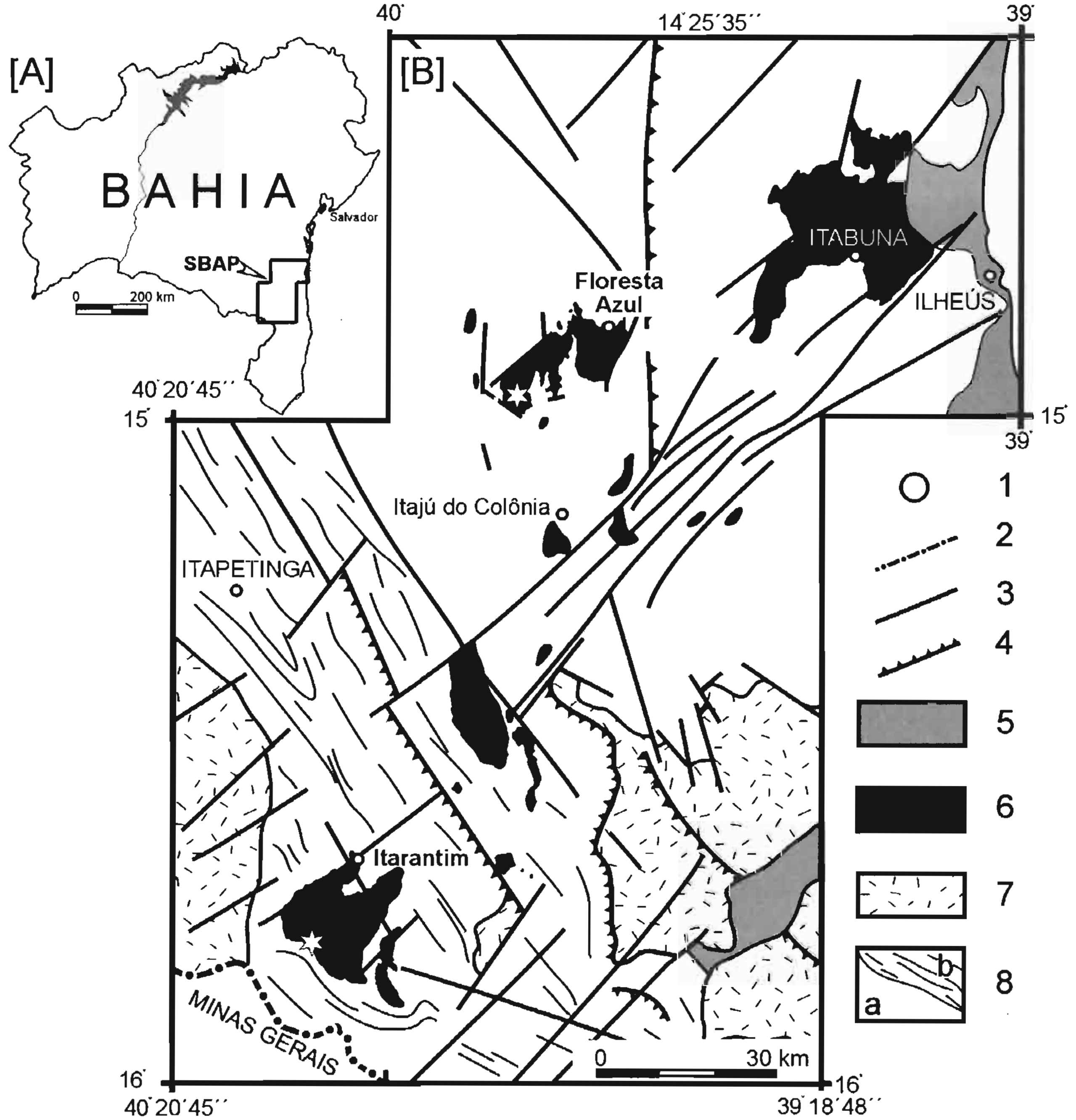

Figura 1. Location map of South Bahia Alkaline Province (SBAP) in the Bahia State [A]. Sketch map of SBAP [B]. City [1], State border [2], faults and fractures [3], overthrust fault [4], covers [5], neoproterozoic alkaline massifs [6], mesoproterozoic metasediments [7], archaean-paleoproterozoic rocks [8a= granulites and 8b= gneisses]. ☆ Localization of the samples.

They result in 720 ± 9 Ma and 732 ± 24 Ma ages. These ages are superposed to the ones obtained for their country rocks, which are aged at 727 ± 30 Ma (Rb-Sr on whole rock; Rosa et al., 2002). This suggests that the ore and country rocks were formed at the same time.

FINAL REMARKS

The data obtained with this work indicate that the Floresta Azul Alkaline Complex (706 ± 2 Ma) and the Itarantim Syenitic Massif (720 ± 9 and 732 ± 24 Ma) have similar ages, considering the errors involved. They superpose the ages obtained for the country rocks. These evidences reinforce the hypothesis that the blue coloured sodalite syenites generation can be related to special conditions, which occur during the final stages of the crystalization process and seems to vigorate at some of the syenitic massifs from the South Bahia Alkaline Province.

Moreover, these new ages are of great importance for the understanding of the regional tectonic context, showing that the alkaline magmatism emplacement has no correlation with the Araçuaí Collision (625 to 570 Ma; Cordani et al., 1974; Pedrosa Soares et al., 2001).

ACKNOWLEDGMENTS

This work was supported by CNPq (Process: 301392/00-5 and 303581-03-4) and Companhia Baiana de Pesquisa Mineral. This is contribution number 143 of GPA-CPGG-IGEO-UFBA.

REFERENCES

Cordani, U.G.; Bernat, M.; Teixeira, W. and Kawashita H. 1974. Idades radiométricas das rochas alcalinas do sul do Estado da Bahia. In: SBG, Cong. Bras. Geol., 27, Porto Alegre, Anais, 6:253-259.

Corrêa Gomes, L.C. and Oliveira, E.P. 2002. Dados Sm-Nd, Ar-Ar e Pb-Pb dos corpos plutônicos do Sudeste da Bahia, Brasil: implicações para o entendimento da evolução tectônica do limite Orógeno Araçuaí/ Cráton do São Francisco. Rev. Bras. Geociências, 32(2):185-196.

Cunha, M.P. 2003. Litogeoquímica dos sítios mineralizados em sodalita-sienitos azul do Maciço de Potiraguá e Complexo Alcalino Floresta Azul Vitória. Instituto de Geociências, Universidade Federal da Bahia, Salvador, Dissertação de Mestrado, 86 p.

Köber, B. 1986. Whole-grain evaporation for ^{207}Pb/^{206}Pb age ivestigations on single zircons using a double filament thermal ion source. Contrib. Mineral. Petrol., 93:482:490.

Köber, B. 1987. Single grain evaporation combined with Pb emitter bedding ^{207}Pb/^{206}Pb ivestigations using thermal ion mass spectrometry and implications to zircolonogy. Contrib. Mineral. Petrol., 96:63:71.

Martins, A.A.M. and Santos, R.A. 1993. Ibicaraí, Folha SD.24-Y-B-V, escala 1:100.000. Programa de Levantamentos Geológicos Básico do Brasil. MME-SMM-DNPM, Brasília, 192p.

Pedrosa-Soares, A.C.; Noce C.M.; Wiedmann. C.M and Pinto C.P. 2001. The Araçuaí-West-Congo Orogen in Brazil: an overview of a confined orogen formed during Gondowanaland assembly. Precambrian Research, 110:307-323.

Rosa, M.L.S.; Conceição, H.; Macambira, M.J.B.; Marinho, M.M.. and Marques, L.S. 2002. Geochronology of the South Bahia Alkaline Province (NE Brazil). Geochimica et Cosmochimica Acta, 66:A648.

Rosa, M.L.S.; Conceição, H.; Macambira, M.J.B.; Marinho, M.M. and Marques, L.S. 2003. Idade Pb-Pb em zircão, aspectos petrográficos e litogeoquímicos do Complexo Alcalino Floresta Azul, Sul do Estado da Bahia. Rev. Bras. Geociências, 33(1).

Teixeira, W.; Kamo, S.L. and Arcanjo J.B.A. 1997. U-Pb zircon and baddeleyte age and tectonic interpretation of the Itabuna alkaline suite, São Francisco Craton, Brazil. Journal South America. Earth Sciences, 10:91-98.

Rb-Sr AND Sm-Nd ISOTOPE GEOCHEMISTRY OF GRANITOIDS FROM ESPERANÇA GRANITIC COMPLEX, PARAÍBA STATE, BORBOREMA PROVINCE, NORTHEAST BRAZIL

Sampaio, M.A.[1]; Guimarães, I.P.[2]; Almeida, C.N.[3] and Carmona, L.C.M.[4]

1. CPRM-RE e PG-UFPE. angelicasampaio@bol.com.br
2. DGEO-UFPE. ignez@npd.ufpe.br
3 . DCR - CNPq - UFPB
4. PG-UFPE. kichick@bol.com.br

Keywords: Granitoids, Neoproterozoic, Borborema Province, Brasiliano Orogeny

INTRODUCTION

The Neoproterozoic evolution of Borborema Province, Northeast Brazil, was characterized by an intense granitic magmatism, associated with a network of continental-scale transcurrent ductile shear zone (Vauchez et al., 1995). Van Schmus et al. (1995, 1997) using U-Pb and Sm-Nd data, subdivided the Borborema Province in three tectonic domains: Northern, Central and Southern, which have shown contrasting isotopic characteristics The Central Tectonic Domain (CTD), region located betwen the continental shear zones Patos and Pernambuco, had affected by at least three thermotectonic events: Paleoproterozoic event (Transamazonian Orogeny, 2.2 to 1.8 G. a), Mesoproterozoic event (Cariris Velhos Orogeny, 1.0 to 0.9 G.a.) and Neoproterozoic event (Brasiliano Orogeny, 0.85 to 0.58 G. a), this last event was responsible for the intense magmatism which characterized Borborema Province.

Santos (1996, 1999) subdivided the Borborema Province in tectono-stratigraphic terrains, with distinctive stratigraphic, structural and petrologic features. The Central Tectonic Domain (CTD) was separated in five parts: West Gneissic Terrain (WGT), Piancó-Alto Brígida Terrain (PABT), Alto Pajeú Terrain (APT), Alto Moxotó Terrain (AMT), Rio Capibaribe Terrain (RCT). In the Alto Pajeú Terrain (APT), the magmatism was related at least to two orogenies (Cariris Velhos and Brasiliano events). The first event is characterized by low-angle structures, associated with low angle kinematics, wherever the last event is characterized for shearing structures, associated to an transcurrent kinematics.

Almeida et al. (1967) recognized four types of granitoids: Conceição type (granodiorites and tonalites, medium to fine grained), Itaporanga type (granodiorites with large phenocrystals of K-feldspar), Itapetim type (biotite fine grained granites, associated to Itaporanga type) and Catingueira type (peralkaline granites, syenites and quartz-syenites. Sial (1986) identified four granitoids types in the Piancó-Alto Brígida Terrain: calcalkalic (Conceição type), potassic-calcalkalic (Itaporanga type), peralkalic (Catingueira type) and trondhjemitic affinities (Serrita type).

Taking in consideration the crystallization age and geochemical characteristics, using U-Pb zircon and Sm-Nd data, Guimarães et al. (1999) divided the CTD granitoids into five groups: calc-alkaline granitoids (including the Conceição type and some Itaporanga type granitoids), which are examples the Tabira, Itapetim and Timbaúba Complexes; high-K metaluminous calc-alkaline granitoids (Itaporanga type granitoids), including the Fazenda Nova, Campina Grande and Esperança Complexes; syenites, quartz-syenites and syenogranites of shoshonitic affinities, including Bom Jardim, Toritama and Pajeú Complexes; monzogranites, syenogranites and syenites, including the Solidão, the east part of Teixeira, Queimadas, Triunfo and Serra Branca Complexes; and biotite syenogranites coarse to medium grained, equigranular to slightly porphiritic (Prata Complex, Pereiro, Serra do Velho Zuza, Serra da Engabelada and Serrote Santo Antônio plutons).

GEOLOGIC SETTING, GEOCHEMICAL AND MINERAL CHEMISTRY CHARACTERIZATION

The Esperança Complex comprises late tectonic Neoproterozoic intrusions, occupying an area of 580 km^2 intruded in ortogneisses of Mesoproterozoic ages of the Alto Pajeú Terrain (APT), Central Tectonic Domain (CTD) of Borborema Province. The emplacement of the Esperança Complex was controlled by transcurrent-extensional shear zones: Remígio-Pocinhos (Patos Lineament segment) in north and São Sebastião de Lagoa de Roça in the south.

Petrographic data suggest that the Esperança Complex comprises at least three intrusions, denominated north, south and west intrusions (Fig. 1).

The north intrusion comprises porphyritic to equigranulate fine grained biotite amphibole syeno and monzogranites; the south intrusion comprises coarse grained, porphyritic biotite amphibole syeno and monzogranites. The west intrusion comprises coarse-grained biotite amphibole monzogranites to quartz-monzonites. Biotite clots and syn-plutonic dykes of granodioritic to tonalitic composition occur in all intrusions. Dykes of pegmatites and late leucocratic alkali-feldspar granite are frequently recorded cutting the north intrusion.

Several textural features, mafic clots, sin-plutonic dykes of granodioritic to tonalitic composition, and rapakivi and anti-rapakivi texture, suggest coeval relationships between distinct granitic magmas, possibly implying processes of magma mixing and commingling.

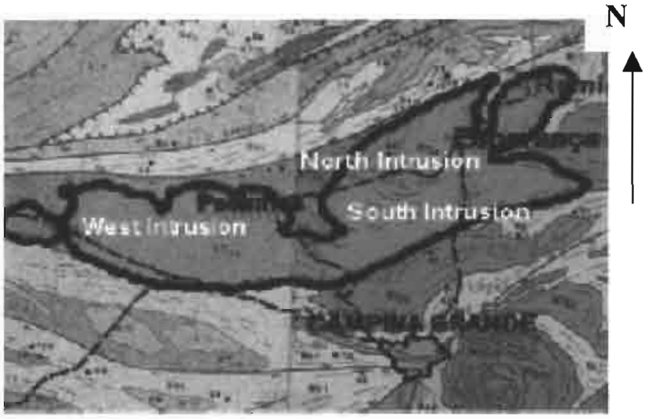

Figure 1. Geological sketching of Esperança Granitic Complex, PB. Modified from: Geological Map of Paraíba State, 2001, CPRM. Escale: 1/250.000.

The granitoids of the Esperança Complex are metaluminous to slightly peraluminous, and high-K calc-alkaline.

REE patterns normalized to chondrite values, display two distinct patterns: the pattern of the North Intrusion have $(Ce/Yb)_N$ ratios ranging from 16.6 to 24.4 and lack of the significant Eu anomalies. The granitoids of the south intrusion have REE pattern less fractionated, with $(Ce/Yb)_N$ ratios ranging from 8.4 to 16.6 and strong Eu negative anomalies, similar to those patterns recorded in A-type granites. Spiderdiagrams normalized to the primitive mantle are characterized by troughs at Nb, Sr and Ti.

Compositions of feldspars, biotites and amphiboles from the Esperança Complex granitoids also divided the complex in three distinct intrusions: the plagioclase of the north intrusion are slightly Ca-richer (oligoclase-andesine) compared to the plagioclase of the South and East intrusion (oligoclase composition). Biotites from the Esperança Complex divided their granitoids into three distinct groups: biotites from south intrusion show Fe# [100Fe/ (Fe+Mg)] values ranging from 64 to 66, FeO/MgO ratios ranging from 3.14 to 3.39 and Al^{IV} values ranging from 2.3 to 2.4; biotites from the north intrusion have Fe# ranging 36 to 53, FeO/MgO ratios ranging 1.6 to 2.0 and Al^{IV} values ranging 2.2 to 2.3. Biotites from the west intrusion are Fe-enriched, shown Fe# values ranging 68 to 73, FeO/MgO ratios ranging 3.8 to 4.7 and AlIV values ranging 2.46 to 2.53. In the discriminant diagrams to magmatic suites for biotite mineral chemistry (Abdel-Rahman, 1994), the biotites from granitoids of the north and south intrusions plotted within the calc-alkaline field, while the biotites from the west intrusion plotted within the peraluminous field.

Amphiboles from the all intrusions of Esperança Granitic Complex are calcic (Leake, 1997), with compositions ranging from Fe-edenite to Fe-pargasite. Fe# values of the amphiboles analyzed from the granitoids of the Esperança Complex define three distinct fields: 59 to 61 (north intrusion); 67 to 75 (south intrusion) and 70 to 72 (west intrusion), reflecting crystallization under different fO_2 conditions.

U-Pb ZIRCON GEOCHRONOLOGICAL DATA

U-Pb zircon data were obtained from three multicrystal magnetic fractions from the porphyritic granites from the south intrusion (ESP-01), at the Isotope Geochemistry Laboratory, University of Kansas. The analyzed zircon population comprises euhedral internally clear pink zircon grains without any inclusions. The zircon grains were abraded for 2h and then washed with HNO_3. The upper Concordia intercept defines an age of 581 ± 7 Ma (MSWD = 1.2) when forced to zero (Fig. 2).

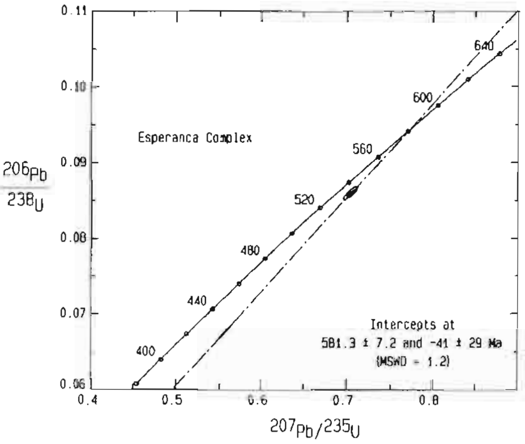

Figure 2. Concordia diagram for granitoids of Esperança Granitic Complex, PB.

Rb-Sr AND Sm-Nd ISOTOPIC DATA

Rb-Sr and Sm-Nd isotopic data of granitoids from the north and south intrusions of the Esperança Complex, were obtained at the Isotope Geochemistry Laboratory, University of Kansas. No isotopic data are available for the west intrusion. The results are showed in Tables 1 and 2.

The granitoids of the Esperança Complex show $\varepsilon_{Sr\,(580Ma)}$ ranging from 8.2 to 62.3 and exhibited initial rates Sr^{87}/Sr^{86} always less to 0.708, suggesting represent I-type granites (Chappell & White, 1974).

Sm-Nd data show distinct isotopic signatures, to the north and south intrusions granitoids. Both intrusions exhibited ε_{Nd} initials values strongly negative, suggesting crustal contribution in the source.

The granitoids of the north intrusion have $\varepsilon_{Nd(0)}$ values ranging –16.53 to –15.08, and T_{DM} model ages ranging from 1.82 to 2.1 Ga, suggesting a Paleoproterozoic source. The South Intrusion granitoids show $\varepsilon_{Nd\,(t)}$ values ranging from –7.19 to –6.02 and T_{DM} model ages ranging from 1.50 to 1.57 Ga, suggesting mixture of Paleoproterozoic crust with juvenile Mesoproterozoic (Cariris Velhos) or Neoproterozoic material (Brasiliano).

The Esperança Complex granitoids of the northintrusion, plotted in the ε_{Sr} initial vs ε_{Nd} initial diagram (Harmon et al., 1984), show isotopic composition similar to those recorded in the lower crust (Fig. 3). The sample analysed from the south intrusion plotted within the I-type granitoid field.

Table 1. Isotopic analysis obtained for Rb-Sr Method for the granitoids of Esperança Granitic Complex (PB State) (N) = North Intrusion; (S) = South Intrusion.

Samples	Rb (ppm)	Sr (ppm)	Rb^{87}/Sr^{86}	Sr^{87}/Sr^{86}hoje	$Sr^{87}/Sr^{86}i$ (580Ma)	ε_{Sr} i (580Ma)
ESP-03A (N)	148.0	1194.0	0.35698	0.70896	0.705997	30.888
ESP-08A (N)	125.0	989.0	0.36400	0.70938	0.706359	36.031
ESP-08B (N)	230.0	1010.0	0.65584	0.70869	0.703247	8.184
ESP-12 (N)	85.0	838.0	0.29212	0.71063	0.708206	62.274
PX-01 (S)	164.2	283.4	1. 66865	0.72092	0.707070	46.134

Table 2. Isotopic analysis obtained for Sm-Nd Method for the granitoids of Esperança Granitic Complex (PB State). (N) = North Intrusion; (S) = South Intrusion.

Samples	Sm (ppm)	Nd (ppm)	Sm^{147}/Nd^{144}	Nd^{143}/Nd^{144} today	$Nd^{143}/Nd^{144}i$	$\varepsilon_{Nd(0)}$	$\varepsilon_{Nd(t)}$ (±580 Ma)	T_{DM} (Ma)
ESP-03A (N)	5.9632	45.5536	0.07914	0.511401	0.511100	-24.13	-15.45	1822.4
ESP-08A (N)	4.3378	31.3306	0.08371	0.511437	0.511119	-23.42	-15.08	1843.0
ESP-12 (N)	4.6832	27.2022	0.10409	0.511440	0.511045	-23.37	-16.53	2155.4
ESP-01 (S)	6.9140	39.0374	0.10708	0.511930	0.511523	-13.82	-7.19	1568.2
PX-01 (S)	8.1498	45.2183	0.10897	0.511997	0.511583	-12.50	-6.02	1503.5

CONCLUSIONS

Isotopic and geocronological data suggest that the Esperança Complex constitutes a post-collision multiple source intrusion, constituted by at least two distinct sources: 1) Paleoproterozoic lower crust (north intrusion) and 2) a mixture between Paleoproterozoic lower crust and juvenile Mesoproterozoic material (Cariris Velhos) or Neoproterozoic material (Brasiliano) (south intrusion).

Mineral chemistry of the essential minerals and whole-rock geochemistry allowed identifying three distinct intrusions: south, north and west intrusions.

In all of the three intrusions mixing processes between granite, and granodiorite to quartz diorite magmas were recorded. The Fe# values of the mafic mineral phases point out that the west, north and south intrusions were crystallized under distinct degree of oxidation. The degree of oxidation in a magma is a function of dissolved water content, and the amount of water in granitic magma may depend on the tectonic setting. Because all three intrusions have approximately the same crystallization age, the differences in redox state recorded in the Esperança Complex granitoids may reflect distinct source rocks.

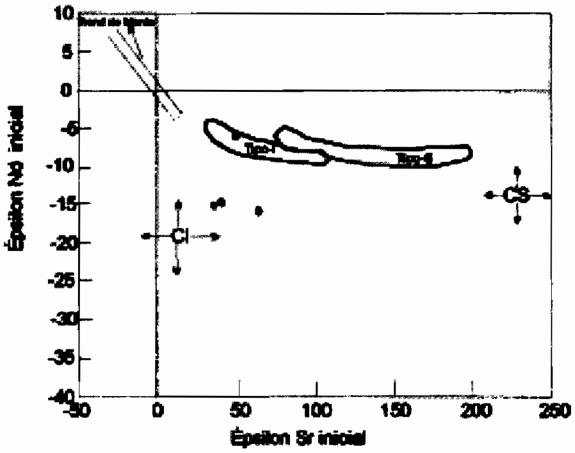

Figure 3. Discriminant diagram for I-type and S-type granites, using initial ε_{Sr} vs initial ε_{Nd} values, to Esperança Granitic Complex granitoids. CI = Lower Crust, CS: Upper Crust. (Harmon et al., 1984)

ACKNOWLEDGEMENTS

The authors wish to thank CNPq for support extended through grant 141597/2000-3; to Prof. W. R. Van Schmus - the Isotope Geochemistry Laboratory of the Kansas University, to Prof. Márcio Pimentel University of Brasília, for making available the Rb-Sr data. Maria Angélica Sampaio wishes to thank GEREMI-CPRM-Recife, for financial support to cover her expenses during the Symposium.

REFERENCES

Abdel-Rahman, A.F.M. 1994. Nature of biotites from alkaline, calc-alkaline and peraluminous magmas. *J. Petrol.*, 35(2): 525-541.

Almeida,F.F., Leonardos, O.H. & Valença, J. 1967. Review on granitic rocks of Northeast South America. Recife, IUGS/UNESCO, 41 p.

Chappell, B. W. & White, A.J.R. 1974. Two contrasting granite types. Pacific Geology, 8: 173-174.

Guimarães, I. P., Silva Filho, A F., Almeida, C. N., Melo, E. B., Melo, S. C., Araújo, J.M.M. & Sales, A. 1999. Sm-Nd isotope geochemistry and U/Pb in zircon ages of the Brasiliano granitoids from the Pajeú Paraíba Terrain, Borborema Province, Northeast Brazil. *II South American Symposium on Isotope Geology, Córdoba, Argentina.* ACTAS: 203-205

Harmon, R.S., Halliday, A.N., Clayburn, J.A.P. & Stephens, W.E. 1984. Chemical and isotopic systematics of the Caledonian intrusion of Scotland and Northern England: a guide to magma source region and magma-crust interaction. *Phil. Trans. R. Soc. London*, 310:709-742.

Leake, B.E. 1997. Nomenclature of amphiboles: Report of the Subcommittee on Amphiboles of the International Mineralogical Association, Commission on New Minerals and Mineral Names. *Am.Mineral.*, 82:1019-1037.

Santos, E.J. 1996. Ensaio preliminar sobre Terrenos e Tectônica Acrescionária na Província Borborema. In: SBG, Congresso Brasileiro de Geologia, Resumos, 6: 47-50.

Santos, E.J. 1998. Programa Levantamentos Geológicos Básicos do Brasil: Carta Geológica. Escala 1:250.000 (Folha SC.24-X-A- Belém do São Francisco). Brasília, CPRM.

Sial, A N. 1986. Granite-types in Northeast Brazil: current knowledge. Revista Brasileira de Geociências, 16 (1): 54-72.

Vauchez, A., Neves, S.P., Caby, R., Corsini, M., Egydio Silva, M., Arthaud, M.H. & Amaro, V. 1995. The Borborema shear zone system. Journal of South America Earth Sciences, 8: 247-266.

Van Schmus, W.R., Brito Neves, B.B., Hackspacher, P.C. & Babinski, M. 1995. U/Pb and Sm/Nd geochronological studies of the eastern Borborema Province, NE Brazil: initial conclusions. Journal of South America Earth Sciences, 8: 267-288.

Van Schmus, W.R., Brito Neves, B.B., Hackspacher, P.C., Babinski, M., Fetter, A. & Dantas, E.L. 1997. Application of U/Pb and Sm-Nd geochronology to understanding the geotectonic history of the Borborema Province, NE Brazil, and its implications for the evolution of West Gondwana. South America Symposium on Isotope Geology, Campos do Jordão, São Paulo, Brazil. Extended Abstracts, p. 27-29.

CAMPANERO UNIT: A PROBABLE PALEOPROTEROZOIC BASEMENT AND ITS CORRELATION TO OTHER UNITS OF SOUTHEASTERN URUGUAY

Sanchez Bettucci, L.[1]; Preciozzi, F.[1]; Basei, M.A.S.[2]; Oyhantçabal, P.[1]; Peel, E.[1] and Loureiro, J.[1]

1. Depto. de Geología, Facultad de Ciencias. Iguá 4225, CP 11400 Montevideo – Uruguay. leda@fcien.edu.uy, fepre@fcien.edu.uy, oyhantca@fcien.edu.uy, elena@fcien.edu.uy, judith@fcien.edu.uy
2. Instituto de Geociências, Universidade de São Paulo, SP, Brasil. baseimas@usp.br

Keywords: Paleoproterozoic, Campanero Unit, Carapé Complexe, geochronology

The basement of the supracrustal metamorphic belts of Uruguay is composed by batholiths formed in the margins of preexisting continental crust during the accretion picks and crustal recycling. The emplacement ages would correspond to inferred subduction periods that preceded juxtaposition of blocks and/or continental collision. Using this inference as a starting point, it is a way to recognize the paleoeffort regime in ancient arcs, where the rising of magma is controled by deformation and it is governed by the characteristic deformation partition of orogenes. The magmatic structures yield keys to reconstruct tectonic and geologic history. A detailed reinterpretation of gneissic structures of southeastern rocks of Uruguay suggests that, in spite of the presence of solid state deformation superimposed, there exist magmatic structures related to the emplacement (Sánchez Bettucci, 1998). In the southeasternmost point of the Dom Feliciano Belt it has been recognized a group of granitoids with variable deformation grade (Campanero Unit), which is intruded by a neoproterozoic calcalkaline granitoid suite corresponding to the Carapé Complex (Sánchez Bettucci, 1998).

On the other hand, the pretectonic granitoids grouped as Campanero Unit are represented by heterogeneous bodies that share the effects of deformation. These granitoids have variable texture from gneissic to mylonitic. Their characteristic feature is an outstanding mylonitic foliation that generated recrystalization (blastesis). Several facies use to show biotite bands (schlieren) (Sánchez Bettucci, 1998). U-P studies made on the Campanero Unit have yielded paleoproterozoic ages (Fig. 1).

Above this basement are developed in tectonic contact the Lavalleja Group. This group is represented by a neoproterozoic volcano-sedimentary sequence which was separated into three formations (Minas, Fuente del Puma and Zanja del Tigre) (Sánchez Bettucci, 1998; Sánchez Bettucci et al., 2001). U-Pb ages (obtained from rutile) from a metabasalt yielded a possible crystalization age of ca. 670 Ma and a metamorphic age of ca. 630 Ma (Fig. 2).

On the other hand, Carapé Complex intruded Campanero Unit basement and Lavalleja Group. This complex constitutes an example of poli-intrusive felsic magmatism that was syn-tardi to post orogenic separated (Sánchez Bettucci, 1998; Sánchez Bettucci et al., 2003). Isotopic studies made over the post-orogenic granitic body produced an U-Pb (zircon) age of 572 ± 14 Ma (fig. 3).

REFERENCES

Sánchez Bettucci, L. 1998. Evolución Tectónica del Cinturón Dom Feliciano en la Región Minas-Piriápolis, Uruguay. Tesis de Doctorado, UBA, 347 pp.

Sánchez Bettucci, L.; Cosarinsky, M. & Ramos, V. 2001. Tectonic Setting of the Late Proterozoic Lavalleja Group (Dom Feliciano Belt), Uruguay. Gondwana Research, V. 4, N°. 3, pp. 395-407.

Sánchez Bettucci, L.; Oyhantçabal, P.; Page, S. & Ramos, V. 2003. Gondwana Research, V. 6, N°. 1, pp. 89-105.

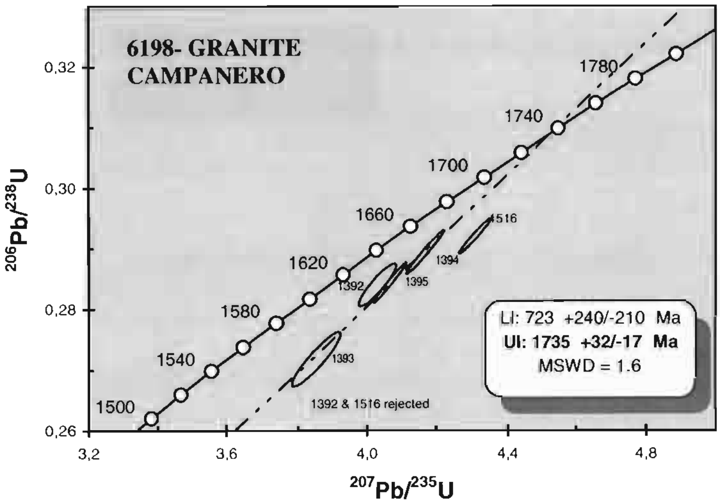

Figure 1. U-Pb concordia diagram of sample 6198 from biotite-amphibole mylonitic granite of the Campanero Unit.

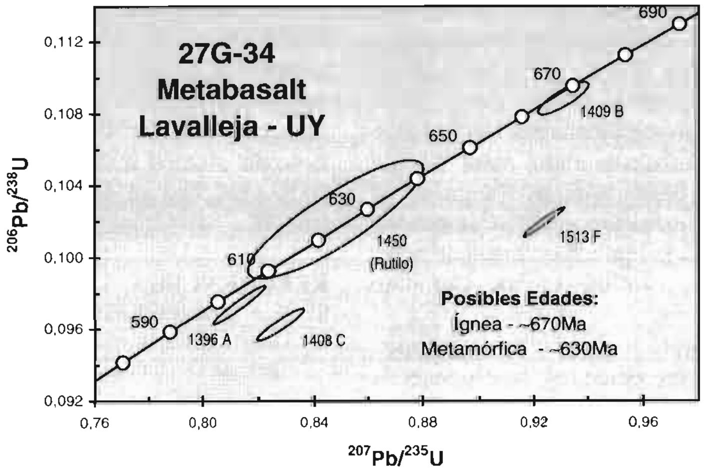

Figure 2. U-Pb concordia diagram of sample 27G-34 from metabasalt (Lavalleja, Uruguay)

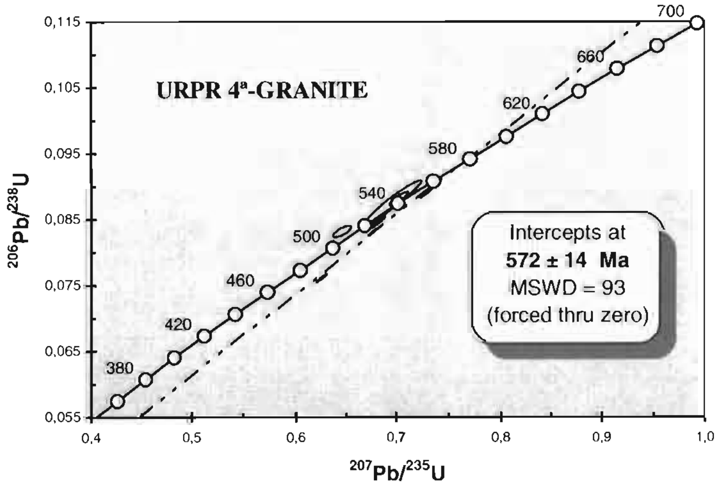

Figure 3. U-Pb concordia diagram of sample URPR 4Afrom biotite-amphibole granite, Carapé Granitic Complex.

^{226}Ra/^{238}U AND ^{228}Ra/^{232}Th ACTIVITY RATIOS OF CAMEROON VOLCANIC LINE: INVESTIGATION OF SECULAR RADIOACTIVE DISEQUILIBRIUM IN THE ^{238}U AND ^{232}Th DECAY SERIES

Santos, R.N.[1] **and Marques, L.S.**[2]

1. Pontifícia Universidade Católica de São Paulo, FMFT - CCET - PUC/SP - Rua Marques de Paranaguá, 111, Consolação, CEP 01303-050, São Paulo-SP, Brasil. rosana@pucsp.br
2. Instituto de Astronomia, Geofísica e Ciências Atmosféricas - Universidade de São Paulo - Rua do Matão, 1226, Cidade Universitária, CEP 05508-090, São Paulo-SP, Brasil. leila@iag.usp.br

Keywords: ^{238}U, ^{228}Th and ^{226}Ra specific activities, analytical techniques, Cameroon Mount, radioactive disequilibrium

INTRODUCTION

The natural radioactive series, headed by ^{238}U, ^{235}U, and ^{232}Th, are composed of nuclides with different chemical and physical properties, with half-lives varying from less than 1 second up to trillions of years. The measurement of the specific activities of the ^{238}U decay chain members allows to quantify the degree of chemical fractionation of radioisotopes, which compose that series, during the igneous processes. During the volcanic rock genesis, that involves partial melting of mantle and/or crustal sources, and fractional crystallization, the condition of secular radioactive equilibrium is disturbed, since the different decay products present distinct geochemical characteristics (Allègre & Condomines, 1976; Condomines et al., 1988). Therefore, in the time interval between system closure, and it secular radioactive equilibrium, is possible to obtain information about the extent of chemical fractionation and rock ages.

In the investigation of the radioactive disequilibria in ^{238}U series it should be considered magmatic processes do not provoke fractionation between ^{234}U and ^{238}U isotopes. Taking into account that equilibrium between ^{234}Th and ^{238}U is quickly attained (approximately 180 days), the radioactive equilibrium between those uranium isotopes is a very common characteristic in volcanic rocks, if subsequent alteration processes do not occur (Hémond et al., 1994). Conversely, due to their chemical characteristics and half-lives, ^{238}U, ^{230}Th, ^{226}Ra, and ^{210}Pb radioisotopes are frequently used in geochemical and geochronological studies. After the system is closed, ^{230}Th and ^{238}U only reach secular equilibrium in about 450,000 years. ^{226}Ra is essentially in equilibrium with its parent ^{230}Th in approximately 8,000 years, while ^{210}Pb reaches more than 95% of equilibrium with ^{226}Ra in hundreds of years. It is necessary, however, to emphasize the differences between ^{230}Th and ^{238}U activities are only observable in rocks with ages less than 300,000 years, due to experimental uncertainties. Therefore, the radioactive disequilibria of ^{238}U series can only be applied to petrogenetic and geochronological studies of volcanic rocks of the recent Quaternary.

The use of the radioactive disequilibria of ^{232}Th series to study magmatic systems is much more limited, since all decay products reach the condition of secular equilibrium in about 40 years. Taking into account the time interval involved in the process of magma generation, and its transport to the surface, which is, in general, between 30 and 8,000 years, ^{228}Ra and ^{232}Th are very frequently in secular radioactive equilibrium.

This work presents the results of a systematic investigation on the condition of radioactive disequilibrium in the ^{238}U and ^{232}Th decay series in volcanic rocks of Cameroon Mount and of the Bambouto Volcanic Complex (Foumbat area), both belonging to the Cameroon Volcanic Line. These rocks have never been the subjects of previous studies about radioactive disequilibria, except a basanite analysed by Chabaux & Allègre (1994), which eruption occurred in 1982. In order to identify and quantify disequilibria in those series, ^{238}U and ^{232}Th concentrations were determined by epithermal neutron activation, whereas ^{238}U, ^{226}Ra, ^{228}Ra, and ^{228}Th specific activities were obtained by natural gamma ray spectrometry. These analyses allowed the calculation of (^{226}Ra/^{238}U), (^{228}Th/^{228}Ra), and (^{228}Ra/^{232}Th) activity ratios, which were used to constrain the elapsed time since the crystallization of each analysed rock, as well as to obtain information about the processes involved in the magma genesis.

GEOLOGICAL SETTING AND SAMPLING

The Cameroon Volcanic Line (CVL) is located in the western area of Republic of Cameroon (Africa), extending as a succession of volcanic islands until reaching the continent, where it is represented by high mounts, hills and plateaus. The CVL 1,600 km long, beginning in Pagalu Island, across the Golf of Guinea, and ending in the Mandara Mount, inside the African continent, where it extends for 900 km. This intraplate magmatism has been continuous since Late Cretaceous, and several extrusive episodes were identified. Cameroon, Santa Isabel, and Fernando Poo volcanoes are still active (Fitton & Dunlop, 1985). Recently, the CVL has been the subject of geological, geochemical, and isotopic detailed studies (Fitton & Dunlop, 1985; Fitton, 1987; Halliday et al., 1988).

In the continental region, the recent magmatism is mostly concentrated on an area of about 5,000 km^2, which has an elongated shape in NE direction, comprising the Cameroon Mount. It is mainly composed of basalts and basanites, which are accompanied by subordinate differentiated lavas (trachytes and phonolites; Marzolli et al., 2000) and by some pyroclastic material

(Fitton, 1987). Fitton & Dunlop (1985) obtained a K-Ar age of 9 Ma for the Cameroon Mount oldest basalts, whereas Piper & Richardson (1972) attributed the whole building formation to the Brunhes time (age less than 0.72 Ma). In the hillsides of the volcano, as well as in its periphery, more than 100 small eruption centres were found, which are frequently controlled by parallel fissures to larger length axis of the mount (i.e. SW-NE direction).

Bambouto Volcanic Complex, also belonging to CVL, is composed by a sequence of basic lavas (mainly basalts), and intermediate (trachytes and phonolites) rocks, cut by younger dykes, which are the result of recent Quaternary magmatic events. Each basaltic flow may be more than 50 m thick, while the dyke thicknesses vary from few meters to 30 m approximately (Marzolli et al., 2000). Quaternary volcanic rock flows were registered in the surrounding area of Foumbat city, located about 50 km east of Bambouto Mountain.

Twenty-two rocks were collected in the continental part of CVL, and fifteen come from outcrops, which occur along the road that goes to Cameroon Mount's top. It is necessary to throw into relief one of those samples (MC1959) belongs to a historical flow, whose eruption took place in 1959. The remaining is from Foumbat area, and the sampling of each studied area was mainly focused on the recent magmatism. It is also important to emphasize that none of the samples presents any sign of intemperic alteration processes.

ANALYTICAL PROCEDURES

Samples were analyzed by X-ray fluorescence, neutron activation, and gamma spectrometry. The samples were crushed (diameter inferior to 0.5 mm), washed with distilled water, and dried in a furnace (50°C). Aliquots of approximately 50 g were powdered (150 mesh) in a mechanical agate mortar, and homogenized. This material was used in X-ray fluorescence, and neutron activation analyses. The remaining crushed rocks were used in the analyses by natural gamma spectrometry.

X-RAY FLUORESCENCE

Bulk-rock analyses for major and minor elements were performed by X-ray fluorescence, using Phillips PW 1404 spectrometer, at University of Trieste (Italy), following the procedures described in Bellieni et al. (1983). Analytical precision is 3% for the determination of major and minor element oxides.

INSTRUMENTAL NEUTRON ACTIVATION ANALYSIS

This methodology was used for the determination of ^{238}U and ^{232}Th activities, and consequently of their concentrations, since natural gamma ray spectrometry does not allow to determine both radionuclides directly.

For activation aliquots of international geological standards (GS-N and BE-N) were used, which were irradiated together with the samples, in the IEA-R1 reactor at IPEN/CNEN-SP. The mass of each aliquot varied around 100 mg. The epithermal neutron irradiation periods were of 24 hours, under a total flow of 10^{12} n.cm^{-2}.s^{-1}. For the measurements of the induced gamma ray activity, detectors of hyper pure germanium were used (HPGe), which have 20% of efficiency, and resolution of 2.0 keV for the ^{60}Co peak of 1332.49 keV. Two series of measurements were made, and the duration of each counting was on the average of 2 hours. The U determination was done about 6 days after the end of the irradiation, through the 277 keV peak of ^{239}Np. The Th concentrations were obtained in a second counting, which was carried out approximately 20 days after the irradiation, through ^{233}Pa radioisotope, whose peak has energy of 312 keV. The errors of those determinations were calculated by the reproducibility of BCR-1 standard, being of 4.9% for the uranium, and 4.4% for thorium (Marques, 2001).

NATURAL GAMMA RAY SPECTROMETRY

For analyses by natural gamma ray spectrometry, amounts between 110 g and 250 g of crushed rock, were put into plastic boxes, which were sealed, and left rest by a minimum period of 45 days before the measurements, in order to ^{238}U series achieves radioactive equilibrium from ^{226}Ra to ^{210}Pb. The samples were submitted to counting using a hyper pure germanium (HPGe) detector with 70% of efficiency, and resolution of 2.0 keV for the ^{60}Co peak of 1332.49 keV.

For the determination of the radioisotope activities existing in each sample, secondary activity standards of uranium (61.500 ± 0.086 Bq), and thorium (21.98 ± 0.11 Bq), in secular radioactive equilibrium, were employed. The activities of ^{234}Th, ^{214}Pb, and ^{214}Bi radioisotopes, as well as those of ^{228}Ac, ^{212}Pb, ^{212}Bi, and ^{208}Tl, belonging to the ^{238}U and ^{232}Th series, respectively, were determined by the comparison between the areas of their total absorption peaks observed in the spectrum of the samples, and secondary activity standards. The radioactive background was subtracted, which was determined through the counting of powdered quartz in the same geometry condition. The measurement time was of 48 hours, and they only considered radionuclides, whose counting exceeded the detection limit, which was of 0.3 µg/g for uranium, and 0.8 µg/g for thorium (Santos et al., 2000). Errors of the gamma activities of the analysed nuclides are mainly related to the uncertainty in the determination of the peak areas of the in the spectra of the samples and of the standards.

Specific ^{238}U activity was calculated by the peaks of ^{235}U (185.7 keV), and of ^{234}Th, which is in supposed secular radioactive equilibrium with ^{238}U. It was considered as the best estimative of ^{238}U activity, the average of the two determinations weighted in accordance with the inverse of their variances (Santos et al., 2000; Ribeiro et al., 2001). The ^{226}Ra specific activity was obtained by the average of ^{214}Pb and ^{214}Bi activities, weighted by the inverse of their variances. In a similar way, ^{228}Ra and ^{228}Th specific activities were estimated by the averages of activities of their decay products (^{228}Ac; ^{212}Pb, ^{212}Bi, and ^{208}Tl, respectively), weighted by the inverse of their variances.

As described in Santos et al. (2000), the application of this methodology in the analysis of ten aliquots of one sample provided results with very good reproducibility levels, as indicated by the relative precisions, which were of 3% for the ^{226}Ra, and of 8% for ^{228}Ra and ^{228}Th. These relative precision values were used for the calculation of associated errors of each activity determination.

Disequilibria in uranium series are evidenced when ^{238}U and ^{226}Ra isotope activities are statistically different. In the case of thorium series, the existence of radioactive disequilibria is indicated by the difference between ^{228}Ra and ^{228}Th activities.

RESULTS AND DISCUSSION

The total alkali-silica (TAS; Le Bas et al., 1986), and R1-R2 (De La Roche et al., 1980) diagrams were used for the classification and chemical nomenclature of the analysed rocks, where the alkaline nature of the samples was evidenced, except one corresponding to a tholeiitic basalt, collected in Cameroon Mount. Almost all analysed samples, including MC1959, are basic rocks ($45\% < SiO_2 < 52\%$), which do not show significant geochemical differences even if their geographical location is taken into account. The investigated rocks can be divided in two main groups, being one of them composed by alkaline basalts and trachy-basalts, while the other is represented by basanites and tephrites. The only one acid rock (alkaline rhyolite; $SiO_2 = 73\%$), which detaches from both groups, comes from the Foumbat area. MC1959 sample, whose age is known, is a tephrite.

The U and Th concentrations of the alkaline rocks, determined by neutron activation analysis, varied from 1.09 ± 0.04 µg/g to 3.6 ± 0.1 µg/g, and from 4.4 ± 0.2 µg/g to 9.3 ± 0.4 µg/g, respectively. Consequently, ^{238}U and ^{232}Th specific activities varied from 0.0135 ± 0.0005 Bq/g to 0.045 ± 0.001 Bq/g, and from 0.0179 ± 0.0008 Bq/g to 0,038 ± 0,002 Bq/g, respectively. The alkaline rhyolite has a thorium concentration of 20.5 ± 0.9 µg/g (0.083 ± 0.004 Bq/g), which is much bigger than those of the other samples. On the other hand, the tholeiite basalt presents ^{238}U and ^{232}Th specific activities of 0.0057 ± 0.0002 Bq/g, and 0.0077 ± 0.0003 Bq/g, respectively.

Although the determination of ^{238}U concentrations by ^{234}Th and ^{235}U activities, by means of natural gamma spectrometry, is possible, the errors relative to those determinations were relatively high, mainly due to the low uranium contents in analysed samples. Therefore, the ^{238}U specific activities obtained by neutron activation were preferred. The radium specific activity, calculated by the ^{214}Pb and ^{214}Bi activities, varied from 0.0016 ± 0.0001 Bq/g to 0.0301 ± 0.0009 Bq/g.

The equilibrium of ^{238}U series is noticed when (^{226}Ra/^{238}U) activity ratio is equal to the unit. In the analysed alkaline rocks, two groups, whose activity ratios indicate disequilibria, were individualized. The first one, corresponding to basanites and tephrites, presents activity ratios that vary from 1.11 ± 0.06 to 1.61 ± 0.08, indicating enrichment of radium relative to uranium during the genesis of those rocks. The second one, much less expressive, composed of alkaline basalts and trachy-basalts, presents ratios that vary from 0.75 ± 0.04 to 0.88 ± 0.04, indicating depletion of radium in relation to uranium. The tholeiitic basalt has (^{226}Ra/^{238}U) equal to 0.28 ± 0.02, which is very different of the other rocks. In summary, all those rocks probably have ages lower than 300,000 years. In them, there are three ones from Foumbat area, and ten samples from Cameroon Mount, including MC1959 rock, which has approximately 43 years in age. Considering the analytical uncertainties, nine samples are in radioactive equilibrium, which are mainly represented by alkaline basalts and trachy-basalts, as well as by the alkaline rhyolite.

In the case of ^{232}Th series, ^{228}Ra and ^{228}Th specific activities were obtained by natural gamma ray spectrometry, whereas ^{232}Th were determined by neutron activation analysis. The (^{228}Th/^{228}Ra), and (^{228}Ra/^{232}Th) activity ratios varied from 0.9 ± 0.1 to 1.1 ± 0.1. These results show that all investigated radioisotopes of the analysed samples are in secular radioactive equilibrium, indicating the rock systems are closed for more than 40 years.

ACKNOWLEDGEMENTS

We are grateful to R. U. Ubangoh and E.M Piccirillo, who kindly donated the samples for this study. Thanks are due to A. de Min, who performed the XRF analysis, F. B. Ribeiro, for valuable comments, and to S. H. A. Nicolai for the analyses by neutron activation. We also acknowledge the Supervisão de Radioquímica of the IPEN/CNEN-SP for permitting the use of its facilities. This research was supported by PADCT-FINEP, CNPq, and FAPESP.

REFERENCES

Allègre, C. J. & Condomines, M., 1976. Fine chronology of volcanic processes using ^{238}U-^{230}Th systematics. Earth and Planetary Science Letters, 28: 395-406.

Bellieni, G.; Brotzu, P.; Comin-Chiaramonti, P.; Ernesto, M.; Melfi, A. J.; Pacca, I. G.; Piccirillo, E. M.; Stolfa, D., 1983. Petrological and paleomagmatic data on the plateau basalts to rhyolite sequences of the southern Paraná basin (Brazil). An. Acad. Bras. Ciên. 55: 355-383.

Chabaux, F. & Allègre, C. J., 1994. ^{238}U-^{230}Th-^{226}Ra disequilibria in volcanics: A new insight into melting conditions. Earth and Planetary Science Letters, 126: 61-74.

Condomines, M.; Hemond CH.; Allègre, C. J., 1988. U-Th-Ra radioactive disequilibria and magmatic processes. Earth Planetary Science Letters, 90: 243-262.

De La Roche, H.; Leterrier, P.; Grandclaude, P.; Marchal, M., 1980. A classification of volcanic and plutonic rocksusing R1-R2 diagram and major-element analyses. Its relationships with current nomenclature. Chemical Geology, 29: 183-210.

Fitton, J. G., 1987. The Cameroon Line West Africa: a comparison between oceanic and continental alkaline volcanism, alkaline igneous rocks. Geological Society Special Publication, 30: 273-291.

Fitton, J. G. & Dunlop, H. M., 1985. The Cameroon Line, West Africa, and its bearing on the origin of oceanic and continental alkali-basalt. Earth and Planetary Science Letters, 72: 23-38.

Halliday, A. N.; Dickson, A. P.; Fallick, A. E.; Fitton, J. G., 1988. Mantle dynamics: a Nd, Sr and O isotopic study of the Cameroon Line Volcanic Chain. Journal of Petrology, 29: 181-211.

Hémond, C.; Hofmann, A. W.; Heusser, G.; Condomines, M.; Raczek, I.; Rhodes, J. M., 1994. U-Th-Ra systematics in Kilauea and Mauna Loa basalts, Hawaii. Chemical Geology, 116: 163-180.

Le Bas, M.J.; Le Maitre, R. W.; Streckeisen, A.; Zanettin, B., 1986. A chemical classification of volcanic rocks based on the total alkali-silica diagram. Journal of Petrology, 27: 745-750.

Marques, L. S., 2001. Geoquímica dos diques toleíticos da costa sul-sudeste do Brasil: contribuição ao conhecimento da Província Magmática do Paraná. Unpublished Thesis, IAG/USP, 86 p.

Marzolli, A.; Piccirillo, E. M.; Renne, P. R.; Bellieni, G.; Iacumin, M.; Nyobe, J. B.; Tongwa, A. T., 2000. The Cameroon Volcanic Line reviseted: Petrogenesis of continental basaltic magmas from lithospheric and asthenospheric mantle sources. Journal of Petrology, 41: 87-109.

Piper, J. D. A. & Richardson, A., 1972. The paleomagmatism of the Gulf of Guinea Volcanic Province, West Africa. Geophysical Journal Royal Astronomy Society, 29: 147-171.

Ribeiro, F. B.; Roque, A.; Boggiani, P. C.; Flexor, J. M., 2001. Uranium and thorium series disequilibrium in quaternary carbonate deposits from the Serra da Bodoquena and Pantanal do Miranda, Mato Grosso do Sul state, Central Brazil. Applied Radiation and Isotopes, 54(1): 153-173.

Santos, R. N. dos; Marques, L. S.; Ribeiro, F. B., 2000. Estudo do equilíbrio radioativo das séries do ^{238}U e ^{232}Th em rochas vulcânicas das Ilhas da Trindade e Martin Vaz. Geochimica Brasiliensis, 14(1): 135-153.

Sr-Nd-Pb ISOTOPIC MODIFICATIONS IN MANTLE XENOLITHS FROM CERRO REDONDO, PATAGONIA ARGENTINA: MANTLE METASOMATISM VERSUS HOST BASALT INFILTRATIONS

Schilling, M.[1]; Mallmann, G.[2]; Koester, E.[3]; Conceição, R.V.[3,4] and Kawashita, K.[3]

1. Facultad de Ciencias Físicas y Matemáticas, Departamento de Geología, Universidad de Chile, Chile. mschilling@esfera.cl
2. Programa de Pós-graduação em Geociências, CNPq, IG, UFRGS, Brazil. guilherme.mallmann@ufrgs.br
3. Laboratório de Geologia Isotópica, IG, UFRGS, Brazil. koester@ufrgs.br
4. Departamento de Geologia, IG, UFRGS, Brazil. rommulo.conceicao@ufrgs.br

Keywords: Subcontinental lithospheric mantle, South America, isotope geology, metasomatism, infiltration

INTRODUCTION

Ultramafic mantle xenoliths are commonly found in alkaline basalts from many regions in the world and are generally used to obtain petrographic and geochemical information about the mantle. In Patagonia (Argentina) the Pliocene-Holocene alkaline basic magmatism, that extends east from the Andes around 40° and 52° S, includes several peridotite xenoliths (Fig. 1).

The Cerro Redondo occurrence (Schilling, 2002) is located around 50 km south of Gobernador Gregores (49°07'S, 70°08'W), in the Santa Cruz province, Argentina. This volcanic body lies within the basaltic plateau known as Meseta Central and is located in the southwestern corner of the Deseado Massif, around 250 km behind the volcanic gap that exist between the Southern Volcanic Zone (SVZ) and the Austral Volcanic Zone (AVZ). This gap is attributed to the Chile ridge subduction (Ramos & Kay, 1992).

The importance of the Cerro Redondo xenoliths consists in its proximity to Gobernador Gregores (Lote17) locality, interpreted as a carbonate metasomatized xenolith suite, although different interpretations on the origin of metasomatic processes were proposed by Gorring & Kay (2000) (asthenospheric source) and Laurora et al. (2001) (subducted slab source).

The host basalt and six whole-rock samples of xenoliths from Cerro Redondo were studied in this work by Rb-Sr, Sm-Nd and Pb-Pb isotopic systems, in order to characterize them petrologically and investigate any influence interactions between host basalt and mantle xenoliths.

GEOLOGY, PETROGRAPHY AND GEOCHEMISTRY

Cerro Redondo, described in detail by Schilling (2002), is an alkaline basalt volcanic body erupted during the Pliocene-Pleistocene presenting subvertical columnar jointing and some pyroclastic bombs and including many mantle xenoliths that correspond to anhydrous spinel lherzolites and harzburgites. It is one of the many ancient eruptive centers of the basaltic lavas of the Meseta Central region exposed as volcanic necks and characterized by sharp dome form (Fig. 2).

The host basalt has porphyritic texture with olivine and pyroxene xenocrysts. Groundmass have intergranular texture with microlites of sanidine, andesine, olivine,

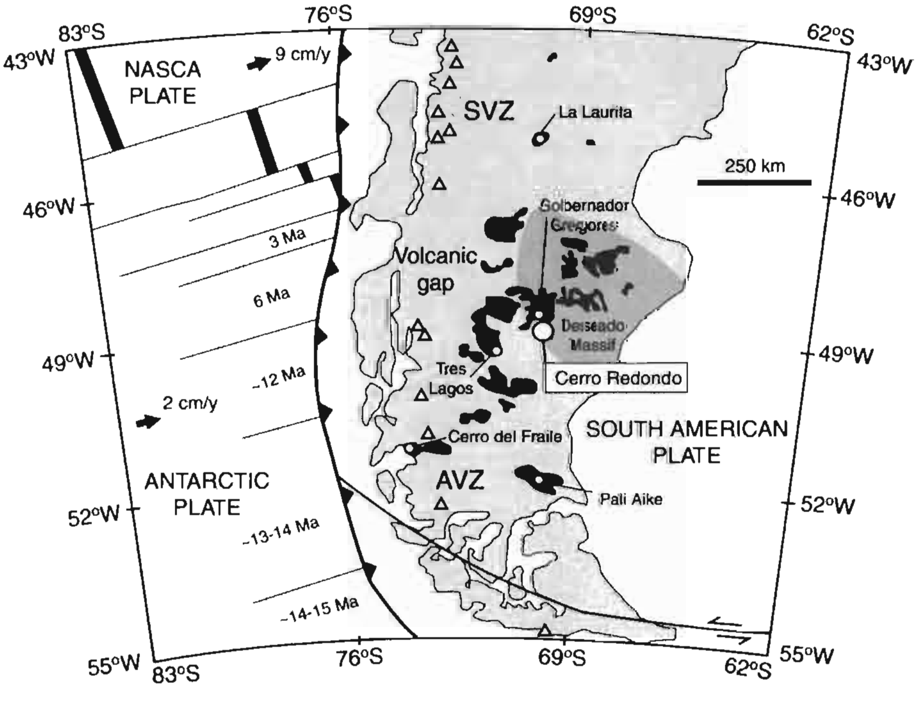

Figure 1. Southern South America continent showing mantle xenolith occurrences (circles), including Cerro Redondo, tectonic setting and distribution of Neogene Plateau lavas of southern Patagonia (black). Volcanic centers (triangle). SVZ - Southern Volcanic Zone, AVZ - Austral Volcanic Zone (after Gorring & Kay, 2000).

clinopyroxene, opaque minerals, apatite and glass. Some nepheline aggregate bands occur near xenolith contact and around some pyroxene crystals of the basalt.

The ultramafic mantle xenoliths are very fresh and disseminated in the basalt. They have subspherical or oval shapes, ranging in size from 2 to 30 cm in diameter (the longest axes), although there are samples that have polygonal and faceted shapes (Fig. 3). The xenoliths have protogranular textures, according to Mercier & Nicolas (1975), and are dominantly lherzolites (except sample X14-1F, harzburgite). The basalt-xenoliths boundaries are very sharp and no reaction rims between the basalt and the inclusions were observed macroscopically, although microscopic-scale reactions are widespread (Fig. 4). Some ultramafic xenoliths have a reddish color given by the alteration of olivine crystals to iddingsite.

Figure 2. Cerro Redondo (hill) outcrop.

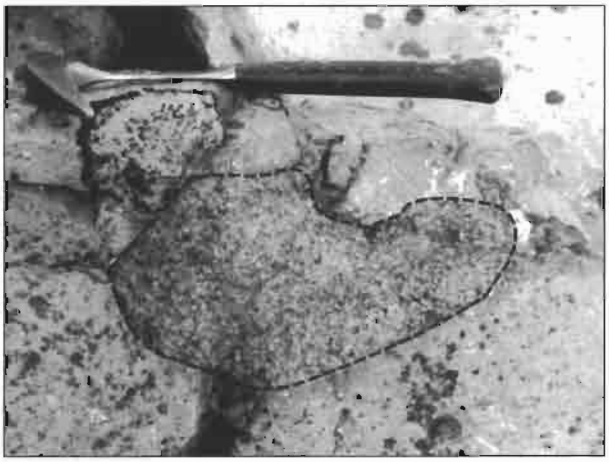

Figure 3. Example of peridotite xenolith from Cerro Redondo included in alkaline basalt.

Major, trace and REE geochemistry indicates that the host basalt is a trachybasalt with Mg# 44 [100MgO/(MgO+FeO^t)], LREE high content (140 times chondritic value for La), relative depleted in HREE (8 times chondritic value for Lu) and with enrichment of incompatible trace elements.

Ultramafic xenoliths can be separated into two groups according to petrographical and geochemical characteristics. Group I (samples X-14-1B, X-14-1C and X-14-1G) is characterized by strong development of reaction textures as exsolution lamellae and reaction rims (see sample X-14-1B photomicrographs in the Fig. 4). This group has the lowest Mg# 82-84 and except for sample X-14-1G, they show TiO_2-Na_2O-K_2O-P_2O_5 enrichment and REE and trace element patterns similar to those of the host basalt.

Group II (samples X-14-1D, X-14-1E and X-14-1F) is almost free of reaction textures, has Mg# up to 84, flat REE pattern, similar to chondrites (except sample X-14-1F, concave pattern caused by lower concentrations of Eu and Gd), and no enrichment in incompatible trace elements.

Thermobarometric estimative, presented by Schilling (2002), based on several pyroxene thermobarometers indicates stability of these xenoliths between 815° to 1226°C and pressures near 1 to 2 GPa.

Sr, Nd AND Pb ISOTOPES

Samples for radiogenic isotope analyses were spiked with mixed ^{87}Rb-^{84}Sr, ^{149}Sm-^{150}Nd tracer and processed using standard dissolution procedures with HF, HNO_3 and HCl in Teflon vial and warmed in hot plate until complete material dissolution. Column procedures use cationic AG-50W-X8 (200-400 mesh) resin in order to separate de Rb, Sr and REE, followed by Sm and Nd separation using anionic LN-B50-A (100-200μm) resin. Pb was separated using anionic A8-B500-F-CL (200-400 mesh) resin in a HBr solution. Each sample was dried to a solid and then loaded with 0.25N H_3PO_4 (Rb, Sr, Sm and Nd), plus silica gel for Pb, on appropriated filament (single Ta for Rb, Sr, Sm, Pb, and triple Ta-Re-Ta for Nd). The samples were analyzed in a multi-collector VG Sector 54 thermal ionization mass spectrometer at the Laboratório de Geologia Isotópica (Universidade Federal do Rio Grande do Sul) in static mode. Nd and Sr ratios were normalized to $^{87}Sr/^{86}Sr = 0.1194$ and $^{146}Nd/^{144}Nd = 0.7219$, respectively. Measurements for NIST standard NBS-987 gave $^{87}Sr/^{86}Sr = 0.710260 \pm 0.000014$, for La Jolla $^{143}Nd/^{144}Nd = 0.511859 \pm 0.000010$ and for Pb NBS-981 and NBS-982 was obtained variation less than 0.01%/a.m.u. Total blanks average were <150 pg for Sr and Sm, <750 pg for Nd, and <200 pg for Pb.

The $^{87}Sr/^{86}Sr$ measured ratio for the basalt was 0.70447. For the ultramafic xenoliths the values range from 0.70442 to 0.70519. These values plotted against Sr content, measured by isotope dilution, show a strong correlation of xenolith ratios to the host basalt ratios, as demonstrated by two-end members mixing model curves (Fig. 4), that tend to equalize the isotopic xenolith characteristics to the host basalt isotopic composition.

The $^{143}Nd/^{144}Nd$ measured ratio for the basalt was 0.51279. For the ultramafic xenoliths the values ranged from 0.51279 to 0.51297. Similar influence of the basalt into the xenolith was observed when plotted these ratios against Nd contents in the two-end members mixing model curves (Fig. 4).

Sm-Nd T_{DM} model ages (De Paolo, 1981) yield values close to 0.44 Ga for host basalt and sample X-14-1B, and between 0.59 to 0.64 Ga for the other mantle

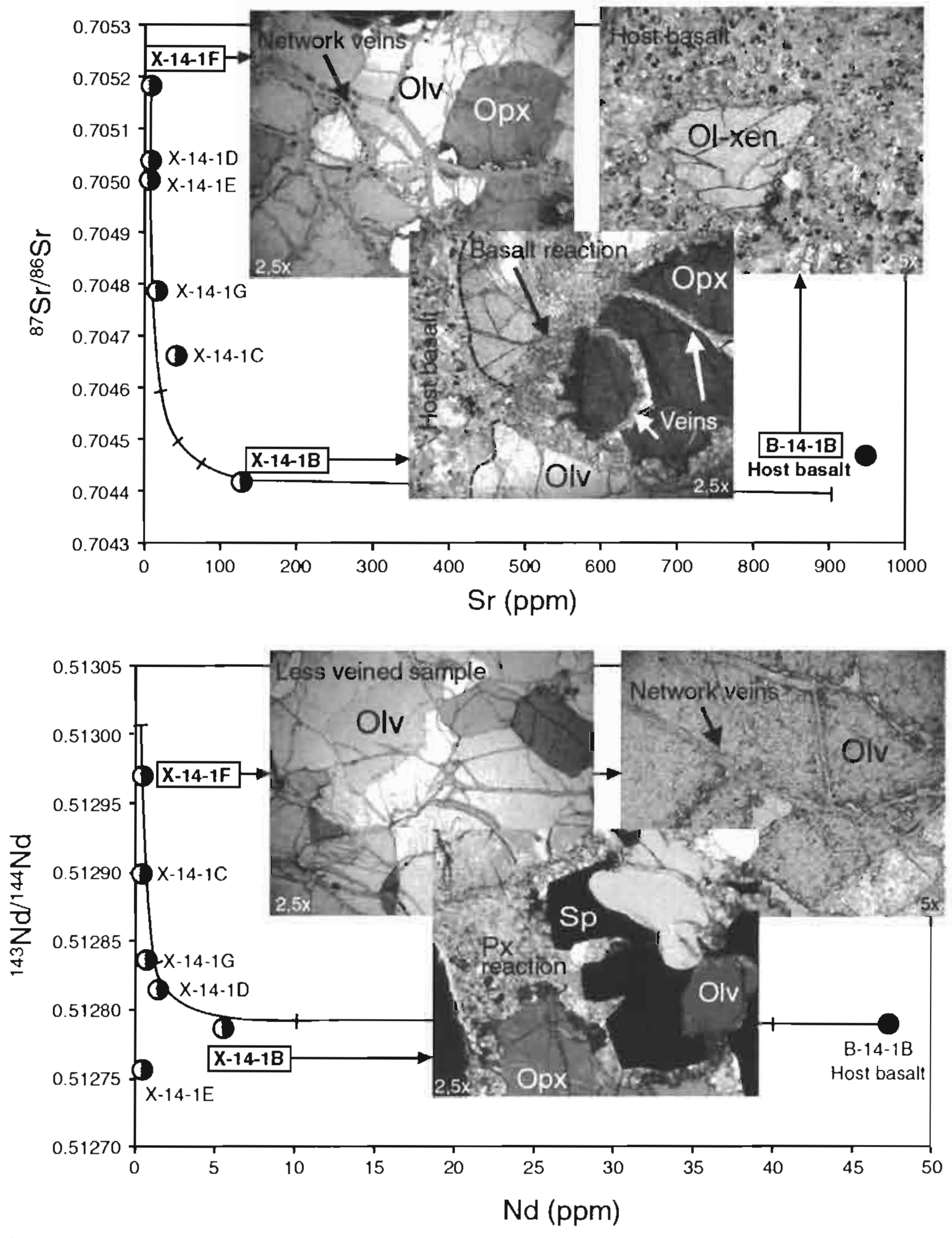

Figure 4. $^{87}Sr/^{86}Sr$ against Sr (ppm) and $^{143}Nd/^{144}Nd$ against Nd (ppm) two-end members mixing model curves showing influence of host basalt in the isotope ratios of ultramafic mantle xenoliths. Mixing models using as extreme values the basalt composition and the less modified mantle xenolith. Photomicrographs illustrate the main petrographic characteristics of mantle xenoliths and host basalt.

xenoliths. These values could be interpreted as a main mantle generation event if we assume that this alkaline magmatism is derived from an asthenospheric source.

The $^{206}Pb/^{204}Pb$ ratios for mantle xenoliths range from 17.987 to 18.401, $^{207}Pb/^{204}Pb$ ratios from 15.555 to 15.608 and $^{208}Pb/^{204}Pb$ ratios from 37.959 to 38.577. Invariably the sample X-14-1F yields the lowest and sample X-14-1B the highest Pb isotope ratios, suggesting the same Sr-Nd influence of the host basalt in the Pb isotopic system of the mantle xenoliths.

In spite of the strong influence of the host basalt in the major, minor, trace, REE and Sr, Nd and Pb isotopic compositions of the mantle xenoliths, the less modified samples seems to be X-14-1F, X-14-1E and X-14-1D, in this order.

In the $^{87}Sr/^{86}Sr$ versus $^{143}Nd/^{144}Nd$ covariation isotopic diagram (Fig. 5), decoupling of the Nd-Sr systems is evidenced by the increasing of the $^{87}Sr/^{86}Sr$ ratios without important modifications in $^{143}Nd/^{144}Nd$. This feature, also observed in many other works, has been interpreted as a consequence of chromatographic effects in the mantle (Navon & Stolper, 1987).

In the $^{206}Pb/^{204}Pb$ versus $^{87}Sr/^{86}Sr$, $^{143}Nd/^{144}Nd$ and $^{207}Pb/^{204}Pb$ diagrams (Fig. 5), samples without host basalt isotopic influence plot close to the Kerguelen OIB-type or in the normal OIB field.

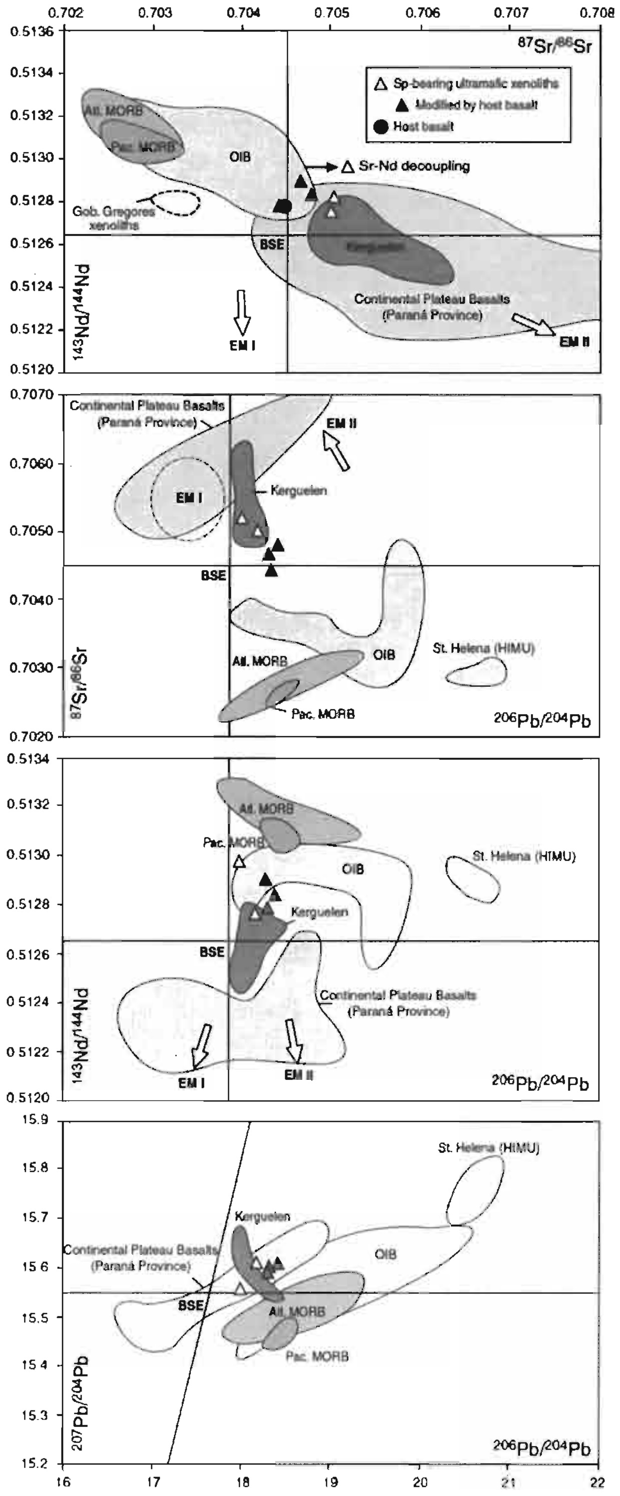

Figure 5. Isotopic covariation diagrams plotting the samples from Cerro Redondo. Fields compiled in the "http://georoc.mpch-mainz.gwdg.de/". OIB draw using Hawaii, La Palma, Azores, St. Helena, Easter and Ascencion Islands.

CONCLUDING REMARKS

Cerro Redondo ultramafic mantle xenoliths present a strong influence of the host basalt, causing modification in the major, trace, REE elements and Sr, Nd and Pb isotopic composition. Thus, only three samples can be used to estimate the composition of the subcontinental lithospheric mantle beneath the South American plate (X-14-1F, X-14-1E and X-14-1D) and clarify the mantle processes recorded there.

The influence of basalt isotopic composition into the mantle xenoliths seems to have relation to the dimension of these ones and quantity of veins. The modifications in the isotopic systems are accompanied by major, trace and REE disturbances as demonstrated prior by Ciuffi et al. (2002) in the xenoliths from Tres Lagos and Cerro Desconocido (Patagonia).

The xenolith samples less affected by host basalt present an event that seems to be related to a depleted mantle undergone to an event of metasomatism in which some kind of decoupling of the Sr-Nd system has occurred. This decoupling is characterized by an increasing in the Sr ratios and preserving the Nd ones, indicating probably an effect of chromatographic processes in the mantle beneath Patagonia region, although the origins of these metasomatic processes need clarification.

ACKNOWLEDGEMENTS

We thank to F. Hervé, C.A. Cingolani and D. Morata for our introduction in the "mantle kingdom", to G. Rivalenti for fruitfully discussions and to F. Chemale Jr. for analytical helps. This work was funded by PROSUL-CNPq (Project AC-74). Sampling of Cerro Redondo was supported by Y. Orihashi and financed by the Japanese government and the Institute of Technology of Tokyo.

REFERENCES

Ciuffi, S., Rivalenti, G., Vannucci, R., Zanetti, A., Mazzucchelli, M., Cingolani, C.A., 2002. Geochemical variations in the host basalts-derived glasses infiltrating mantle xenoliths: CD-ROM XV Congreso Geológico Argentino, El Calafate.

De Paolo, D.J., 1981. Neodymium isotopes in the Colorado Front Range and implications for crust formation and mantle evolution in the Proterozoic: Nature 291: 193-197.

Gorring, M.L., Kay, S.M., 2000. Carbonatite metasomatized peridotite xenoliths from southern Patagonia: implications for lithospheric processes and Neogene plateau magmatism: Contributions to Mineralogy and Petrology 140: 55-72.

Laurora, A., Mazzucchelli, M., Rivalenti, G., Vannucci, R., Zanetti, A., Barbieri, M.A., Cingolani, C.A., 2001. Metasomatism and melting in carbonated peridotite xenoliths from the mantle wedge: the Gobernador Gregores case (southern Patagonia): Journal of Petrology 42(1):69-87.

Mercier, J-C, C. & Nicolas, A., 1975. Textures and fabrics of upper mantle peridotites as illustrated by basalts xenoliths: Journal of Petrology 16(2): 454-487.

Navon, O. & Stolper, E., 1987. Geochemical consequences of melt percolation: the upper mantle as a chromatographic column: Journal of Geology 95: 285-307.

Ramos, V.A. & Kay, S.M., 1992. Southern Patagonian plateau basalts and deformation: back-arc testimony of ridge collision: Tectonophysics 205: 261-281.

Schilling, M., 2002. Estudio petrogáfico y geoquímico de enclaves ultramáficos incluídos em basalto alcalino Plioceno-pleistoceno de Cerro Redondo (49°07'S-70°08'W), em la provincia de Santa Cruz, Patagonia Argentina: Memoria, Universidad de Chile, 84p. (unpub.).

THE GEOCHRONOLOGY OF THE SETUVA NUCLEUS: POLYCYCLIC TERRAINS EXPOSED TO UPPER CRUSTAL LEVELS DURING THE NEOPROTEROZOIC

Siga Jr., O.[1]; Kaulfuss, G.A.[1]; Sato, K.[1]; Basei, M.A.S.[1]; Vasconcelos, P.M.[2]; Harara, O.M.[1] and Cury, L.F.[1]

1. Instituto de Geociências-USP. Rua do Lago 562. Cid. Universitária-SP, 05508-080. osigajr@usp.br
2. University of Queensland. Steele Building. Brisbane Qld 4072 - Australia

Keywords: U-Pb (zircon), polycyclic terrain, Setuva, archean nucleus

INTRODUCTION

The Precambrian terrains of the eastern Paraná and southern São Paulo States are largely represented by an expressive sequence of metasedimentary/metavolcano-sedimentary rocks (the Apiaí Fold Belt), limited to the south-southeast by gneissic-migmatitic rocks from the Atuba Complex. Conspicuous granitic magmatism stands out in the Apiaí Fold Belt context, as well as terrains considered as basement rocks, represented by the Tigre, Betara and Setuva nuclei, the latter object of this study (Fig. 1).

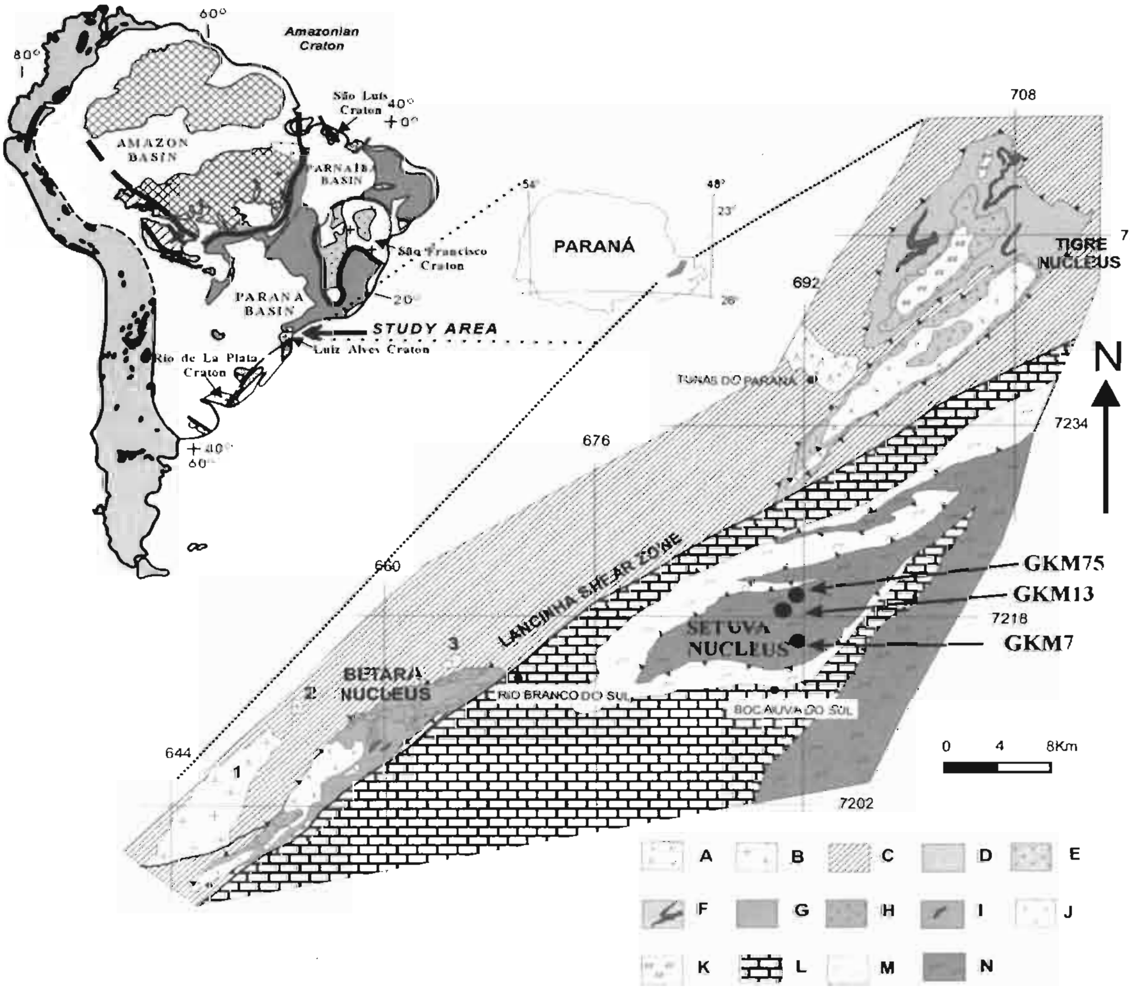

Figure 1. Geologic sketch map (after Kaulfuss, 2001) and sample location.

[Mesozoic]: Tunas alkaline Complex - (A) syenite, alkali syenite and volcanic breccia; [Neoproterzoic]: Late tectonic granitoids - (B) 1 Cerne granite, 2 Cerne syenite, 3 Rio Abaixo granite; [Mesoproterozoic]: Açungui Group - (C) Metavolcano-sedimentary sequences; [Mesoproterozoic / Paleoproterozoic]: Perau Complex - (D) schists and dolomite marble, (E) quartzites, (F) metabasic rocks; Betara Formation - (G) mica schist and phyllites, (H) quartzites, (I) metabasic rocks; [Upper Paleoproterozoic]: Folded granitoids - (J) syenogranite; [Paleoproterozoic / Archean]: (K) monzonites, granodiorites, quartz-monzonites, quartz-granodiortes; [Neoproterozoic]: Capiru Formation - (L) meta-calc-dolomite, metaritimite, phyllites and quartzites, (M) schists, phyllites and quartzites; [Neoproterozoic / Paleoproterozoic \ Archean]: Atuba Complex - (N) gneisses and migmatites, folded granitoids and amphibolites.

The main objective of this paper is to present an isotopic study (zircon U-Pb, whole-rock Sm-Nd, and biotite K-Ar and Ar-Ar methods) of the Setuva Nucleus, aiming at the correlation with other similar segments in Paraná and São Paulo, and to better understand the tectonic scenario of south-southeastern Brazil.

GEOLOGIC CHARACTERISTICS

The Setuva Nucleus is represented by allochthonous terrains, exposed within metasedimentary sequences (dolomitic marbles, phyllites, quartzites and schists) of the Capirú Formation. It occurs south of the Lancinha Shear Zone, and is elongated, sigmoidal, predominantly trending NE-SW. It is represented by protomylonitic to mylonitic rocks, predominating gneissic-migmatitic lithotypes in its southern portion and syeno- to monzogranites in its central-northern portion.

The gneissic-migmatitic lithotypes are strongly weathered and are characterized by centimeter- to millimeter-sized banding, formed by alternating quartz-feldspatic and reddish to ochre levels, the latter containing quartz, feldspar, micas and possibly amphiboles. Quartz-feldspatic injections of various dimensions and forms occur both concordant and discordant with the gneissic-migmatitic banding.

In Setuva's central-northern sector, proto- to mylonitic, rosy-gray syenogranitic rocks predominate, with abundant sub-millimeter to centimeter-sized, oval-shaped K-feldspar porphyroclasts. They contain K-feldspar, quartz, plagioclase and biotite, and additional chlorite and sericite/muscovite.

Proto- to mylonitic rocks of granodioritic to monzogranitic composition were also individualized in Setuva's western and northern sectors. In general, they are fine-grained and are composed of millimeter- to centimeter-sized K-feldspar porphyroclasts, quartz, plagioclase and biotite.

The structural pattern observed in the Setuva Nucleus is similar to the described for the Apiaí Belt, which is related to a low-angle tectonics, with kinematic indicators suggesting transport from NW to SE (in the direction of the Atuba Complex). These surfaces were affected by important transcurrent shear systems (such as the Lancinha Shear Zone) and wide associated folds, responsible for structuring and compartimentation of these terrains (Fiori, 1992; Silva et al., 1998; Yamato, 1999).

GEOCHRONOLOGIC STUDY

The geochronologic studies (U-Pb, Sm-Nd, and K-Ar/Ar-Ar) refer to three outcrops that represent proto- to mylonitic gneissic-migmatitic rocks (southern sector), protomylonitic syenogranites (central sector), and mylonitic syenogranites (northern sector).

The protomylonitic syenogranites (Setuva's central sector) contain elongated, prismatic zircon crystals, translucent to the transmitted light, presenting a few inclusions (Fig. 2). U-Pb analytical data, when plotted in the concordia diagram, cluster close to the upper intercept, yielding 2140 +/- 8 Ma (Fig. 3). Such value, related to the Transamazonian cycle, is interpreted as the time of zircon crystallization and consequently formation of the syenogranitic rocks. Sm-Nd analyses (T_{DM}) carried out for these lithotypes yielded an Archean model age of 2948 ± 16 Ma, interpreted as the time of mantle derivation of the syenogranite crustal protoliths. Additionally, K-Ar and Ar-Ar analyses carried out in biotites developped along low-angle Sc planes indicated ages of 586 ± 15 Ma and 585 ± 1 Ma respectively (Fig. 4). Such values indicate emplacement according to isotherms of temperatures lower than 300°C during the Neoproterozoic.

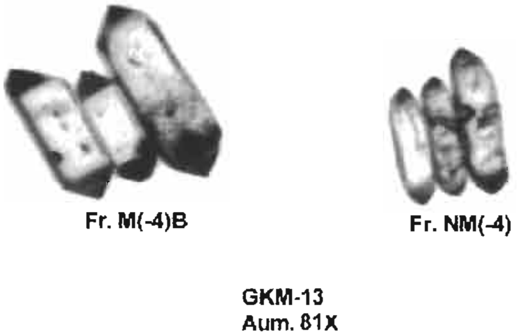

Figure 2. Transmitted light image from GKM-13 sample.

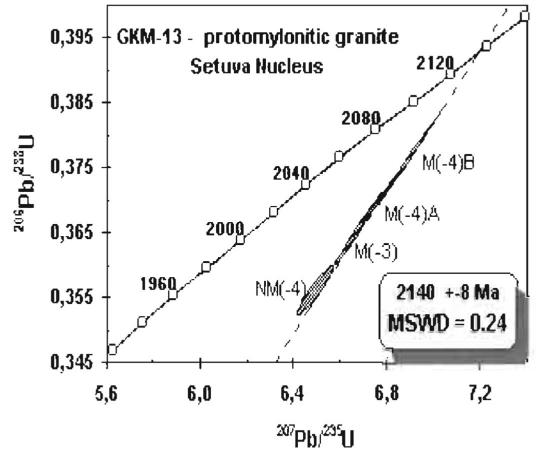

Figure 3. U-Pb Concordia diagram for GKM-13 zircon sample.

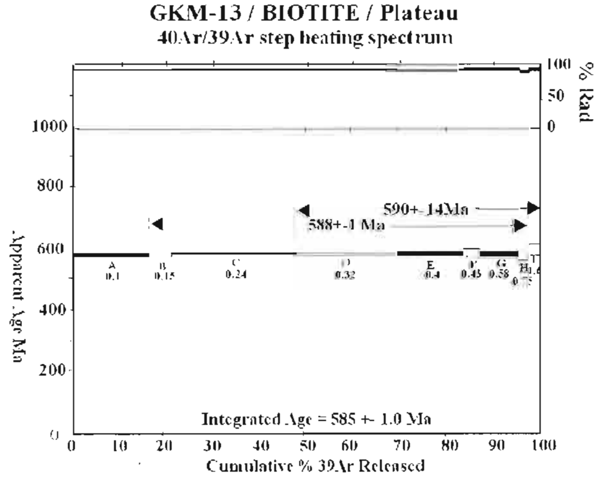

Figure 4. Ar-Ar diagram.

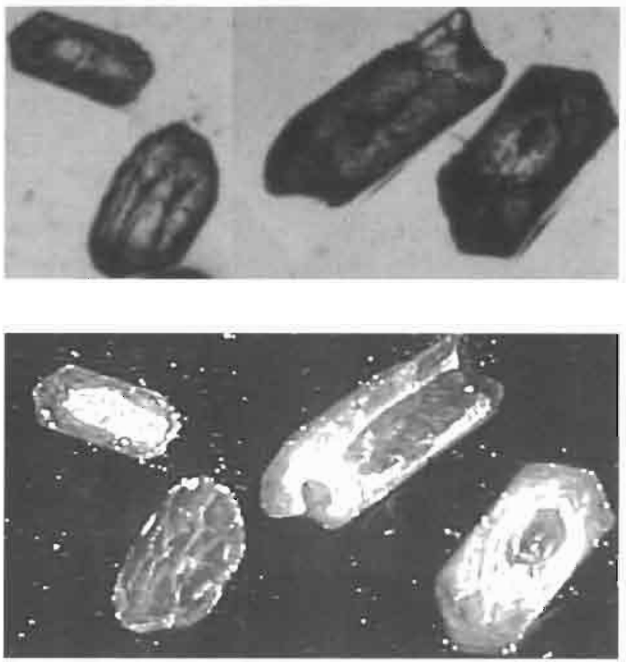

Figure 5. a -Tramsmitted light image (above) and b - cathodeluminescence image (below) from GKM 75 sample.

The zircon crystal that occur in mylonitic syenogranites of Setuva's northern portion are rosy, turbid, inclusion-rich, and fractured (Fig. 5a). Cathodeluminescence reveals bright nuclei surrounded by darker overgrowths (Fig. 5b). Possibly due to Pb losses, the analytical data, when plotted in the concordia diagram, yield ages devoid of geological meaning, both at the upper and lower intercepts (2400Ma and 480 Ma, Fig. 6).

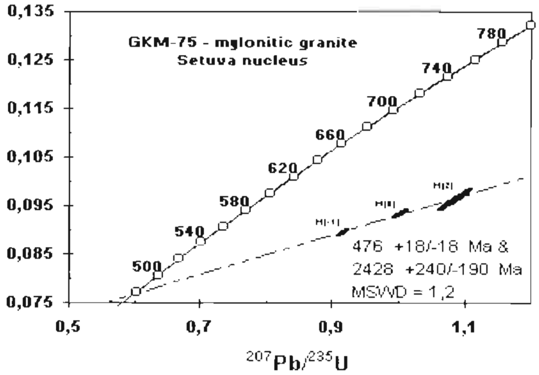

Figure 6. U-Pb Concordia diagram for GKM 75 sample.

These zircons, when analyzed with the single zircon Pb evaporation technique, show great isotopic complexity, with nuclei and overgrowth zones yielding Archean (3000 Ma and 2640 Ma) and Paleoproterozoic (2100 Ma) ages (Figs. 7a, b).

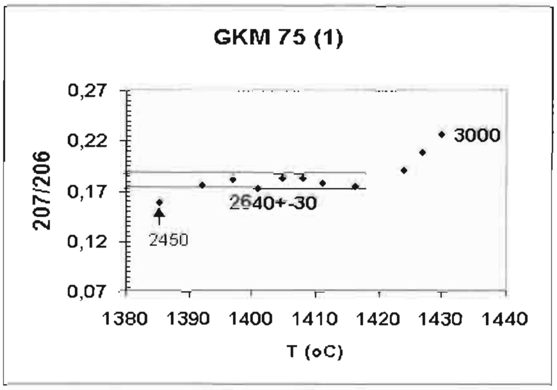

Figure 7a. Lead evaporation by step heating.

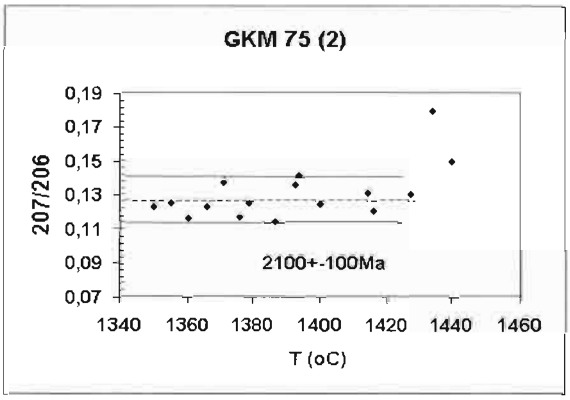

Figure 7b. Lead evaporation by step heating.

Regarding the gneissic-migmatitic rocks of Setuva's southern portion, U-Pb studies were carried out in zircons from thin-banded lithotypes (mesosome), from leucocratic levels intercalated concordant with banding (leucosome), and aplitic veins that are sometimes concordant, sometimes discordant with the general structuring. The zircons of the three lithotypes are very similar under the stereoscope, characterized by turbid elongated, biterminated prismatic crystals, showing aspect, usually containing fractures and inclusions (Fig. 8). In cathodeluminescence images, a central portion surrounded by dark, concentric overgrowths stand is better defined at the crystal terminations.

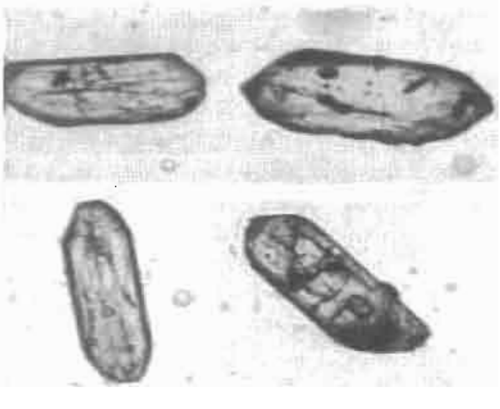

Figure 8. Transmitted light image from GKM 7 sample.

The analytical data, when plotted in the concordia diagram, reveal different isotopic heritages. The analytical results for the mesosome plot relatively close to the upper intercept, whereas those for leucosome and aplitic veins cluster closer to the lower intercept of the concordia curve. These data, when plotted together in the concordia diagram, are well aligned and distributed, indicating the age of 3175 ± 24 Ma for the upper intercept and a relatively young age of 513 ± 35 Ma for the lower intercept (Fig. 9).

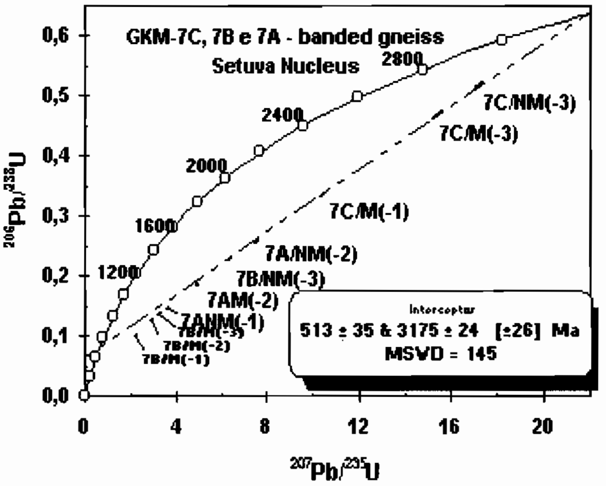

Figure 9. U-Pb concordia diagram for GKM7 sample.

Additional analyses were carried out for the mesosome, using the single zircon Pb evaporation technique, yielding steps of 3100 ± 50 Ma and 3150 ± 50 Ma (Figs. 10a, b), similar to the concordia diagram upper intercept. Sm-Nd model ages (T_{DM}) obtained for mesosome and aplitic veins, respectively 2866 ± 100 Ma and 2811 ± 100 Ma, are a little lower than the ones obtained for the zircons. Because the rocks are intensely weathered, these values may lack geological meaning, due to possible modifications in Sm/Nd ratios.

FINAL CONSIDERATIONS

The geological-geochronological study of gneissic-migmatitic, syenogranitic and monzo- to granodioritic terrains belonging to the Setuva Nucleus reveal a complex, polycyclic tectonic scenario. The U-Pb isotopic pattern in zircons characterizes the formation of gneissic-migmatitic rocks during the Archean (3175 ± 24 Ma), and the proto- to mylonitic syenogranitic lithotypes (central and northern portions) during the Archean (~2600 Ma) and Paleoproterozoic (2140 ± 8 Ma). In general, the analyzed zircons show overgrowths of doubtful Neoproterozoic ages, obtained by the application of the K–Ar and Ar–Ar methods in biotites (585 ± 1 Ma). Such isotopic pattern is very similar to the observed for the Atuba Complex gneissic-migmatitic terrains located south of Setuva. The Betara and Tigre Nuclei are relatively distinct from Setuva, once these are predominantly constituted by proto- to mylonitic granitoids (granodiorites, quartz monzonites and quartz monzodiorites) formed in the Archean (2600 Ma) and Paleoproterozoic (2200 Ma), intensely tectonized during the Neoproterozoic. In these terrains proto- to mylonitic syenogranites also stand out, associated with the Statherian Taphrogenesis (1750 Ma).

The geochronological pattern allied with the structural pattern suggests that the emplacement, largely controlled by shearing, at upper crustal levels occurred during the Neoproterozoic. The initial, low-angle tectonics, with kinematic indicators suggesting transport from NW to SE, in direction to the Atuba Complex, associated with transcurrent shear systems and later folding, should be responsible for the allochthony of these terrains and consequent emplacement at upper crustal levels.

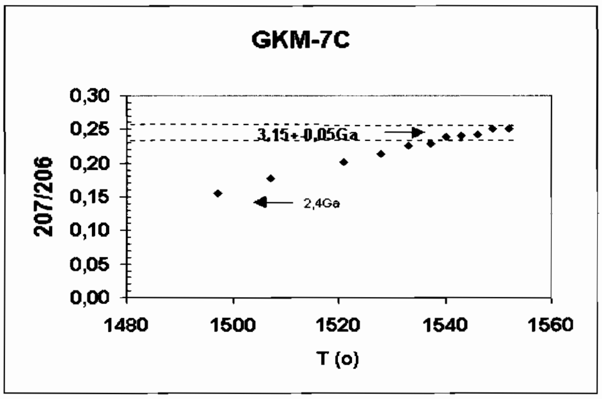

Figure 10a. Lead evaporation using step heating technique.

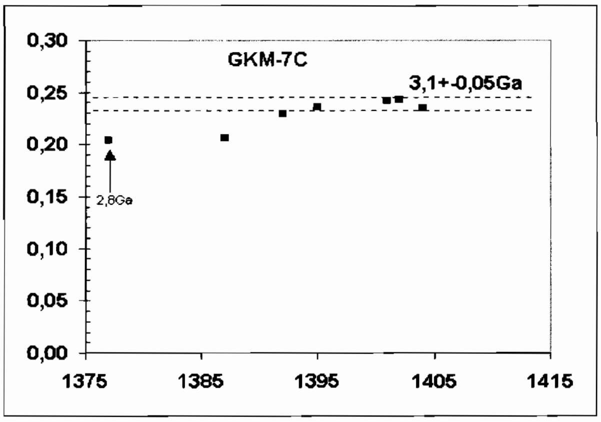

Figure 10b. Lead evaporation using step heating method.

REFERENCES

Kaulfuss, G.A. 2001. Geocronologia dos Núcleos de Embasamento Setuva, Betara e Tigre, norte de Curitiba – Paraná. M.Sc. Dissertation, IG-USP, 115 p.

Yamato, A.A. 1999. Mapeamento Geológico de parte da Folha Boaiúva do Sul (SG-22-X-D-1-2), escala 1:50.000. M.Sc. Dissertation, IG-USP, 108 p.

Silva, P.C.S.; Yamato, A.A.; Vasconcelos, C.S.; Lopes Junior, I. 1998. Projeto Folha Curitiba (SG-22-X-D-1): Relatório Final. CPRM, 91 p.

Fiori, A.P. 1992. Tectônica e Estratigrafia do Grupo Açungui, PR. Boletim IG-USP, Série Científica, V.3, p.55-74.

CONTRASTING ZIRCON GROWTH PATTERNS IN NEOPROTEROZOIC GRANITES OF SOUTHERN BRAZIL REVEALED BY SHRIMP U–Pb ANALYSES AND SEM IMAGING: CONSEQUENCES FOR THE DISCRIMINATION OF EMPLACEMENT AND INHERITANCE AGES

Silva, L.C.[1]; McNaughton, N.J.[2]; Hartmann, L.A.[3] and Fletcher, I.R.[2]

1. Serviço Geológico do Brasil-CPRM,Pesquisador Associado IG/UnB, Brasília-DF, Brazil. luizcarlos@aneel.gov.br
2. School of Earth and Geographical Sciences, UWA, Perth, Australia. nmcnaugh@geol.uwa.edu.au , ifletcher@geol.uwa.edu.au
3. IG/UFRGS, Porto Alegre-RS, Brazil. leo.hartman@ufrgs.br

Keywords: SHRIMP, Florianópolis Batholith, inherited zircons

INTRODUCTION

The Florianópolis Batholith is a major component of northern portion of the Neoproterozoic (Brasiliano Cycle) Dom Feliciano Belt/Pelotas Orogen in Santa Catarina state, southern Brazil. It is exposed over an area of about 12,000 km^2 (200 km long and about 60 km wide), along the Atlantic Ocean coast, extending continuously from 26° 45' S to 28° 45' S.

Despite of recent U-Pb studies (Silva et al., 2002a; Basei, 2000), many uncertainties persist regarding the relationships between magma generation and tectonic evolution within the batholith. We explore these chronological problems by means of the combined use of the U–Pb SHRIMP analyses and backscattered electron (BSE) and cathodoluminescence (CL) imaging of zircons from four critical plutons: Paulo Lopes (Sample 1), Valsungana II (Sample 2), Guabiruba (Sample 3) and Tabuleiro (Sample 4).

A complete version of this abstract, including Sm-Nd data, analytical tables, concordia diagrams, SEM images and analytical procedures may be found elsewhere (Silva et al., 2003).

No previous SHRIMP U-Pb zircon ages were available for the targeted plutons. The Paulo Lopes Suite yielded an imprecise Pb-Pb single crystal zircon evaporation age of 642 ± 46 Ma (Silva et al., 1997) and a U-Pb crystallization age of 644± 20 Ma (Basei, 2000). Basei (2000) obtained a conventional U-Pb crystallisation age of 638 ± 32 Ma for an early phase of the Valsungana Suite, distinct from the Valsungana II Granite dated herein (sample 2). Finally, a facies from the Guabiruba Granite yielded an imprecise age of 573 ± 44 (Basei, 2000).

SAMPLE 1 - PAULO LOPES GRANITE

Zircons from this sample are morphologically simple, composed of euhedral long-prismatic grains with typical magmatic length:width ratios of 3:1. They are mostly homogeneous, without core/rim separation, with Th/U ratios between 0.2-0.8, typical of felsic magmatic rocks. Forty three analyses were performed on 35 zircons. Most analyses fall in a single cluster of 38 concordant spots (filled error boxes in Fig. 1), with a weighted mean $^{206}Pb/^{238}U$ age of 626 ± 8 Ma (2σ) and with no scatter beyond that attributed to analytical error (mean χ^2 = 1.01). This date is more consistent than the *ca.* 640 Ma previously obtained (Silva et al., 1997; Basei, 2000) and is interpreted as the best estimate of the crystallization age of the magma. Because the granite was emplaced during, or shortly before, the peak of collisional deformation, the date also provides an estimate for the age of syn-collisional strike-slip related transpressive tectonics within the batholith.

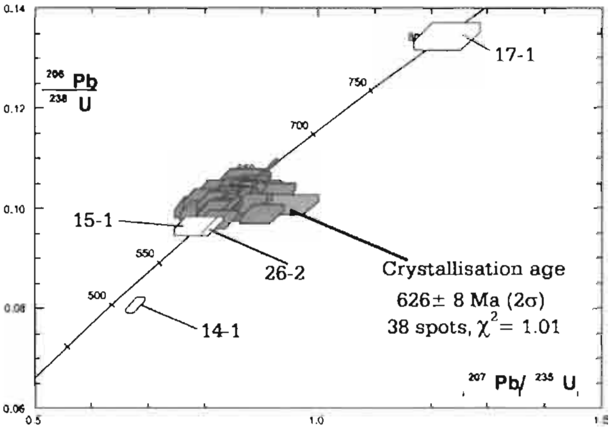

Figure 1. Concordia plot for zircon data from sample 1.

One crystal (spot 26.1) shows an oscillatory zoned, magmatic textured, high U, euhedral rim, with magmatic Th/U ratio, which consists of a smooth, scalloped overgrowth that truncates the oscillatory-zoned igneous core. These internally irregular overgrowths are relatively brighter patches in BSE and darker in CL images and are caused by metamictisation. The metamict margin, with high U contents and a relatively low $^{206}Pb/^{238}U$ apparent age of 593 ± 11 Ma (blank error boxes on Fig. 1), is interpreted to be new zircon associated with a post-magmatic melt-precipitated phase, possibly ascribed to post-crystallization granitic intrusions; the data were excluded from the age calculation. Spot 15-1 was also discarded on the basis of its low age (possibly due to radiogenic Pb loss). Spot 2-1 from a xenocryst yielded an age of *ca.* 1491 Ma and spot 17-1, from an inherited core, an age of *ca.* 812 Ma. These two analyses were also disregarded in the age calculation.

Some analyses obtained on discrete crystals, cores and overgrowths were rejected on the basis of their high discordance.

SAMPLE 2 - VALSUNGANA II GRANITE

The zircon population is composed of euhedral long-prismatic forms with typical magmatic length:width ratios between 2:1 and 3:1. Twenty five analyses were performed on seventeen crystals. Sixteen analyses from discrete homogeneous magmatic textured crystals and from complex crystals with magmatic textured cores and overgrowths rims were pooled as a single population, with no excess scatter (mean χ^2 = 0.90) (Fig. 2). With few exceptions in high-U metamict domains (spots 29-1 and 7-1), the Th/U ratios are typically magmatic (0.2-0.8). This group yielded a weighted mean $^{206}Pb/^{238}U$ date of 593 ± 16 Ma (shaded error boxes in Fig. 2), which is interpreted as the crystallization age for the granite.

As the overgrowths, like the cores, have the same isotopic and morphological magmatic signature and roughly equivalent dates the overgrowths are interpreted as a late-magmatic melt-precipitated zircon phase as suggested also by magmatic halos around inclusions. Some analyses (blank error boxes in Fig. 2), obtained on discrete crystals, cores and overgrowths were rejected on the basis of their high discordance.

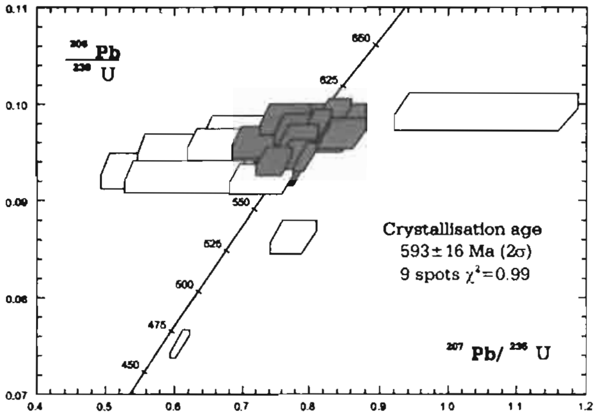

Figure 2. Concordia plot for zircon data from sample 2.

SAMPLE 3 – GUABIRUBA GRANITE

The zircon population is composed mostly of euhedral long-prismatic forms with typical length:width ratios of 3:1, interpreted as magmatic. Fourty two analyses were performed on thirty two crystals. Despite the homogeneity and simplicity of the external morphlogy of the zircons, the U-Pb data indicate a complex evolution, the results showing a large (70 m.y.), continuous age spread from *ca.* 660 Ma to *ca.* 590 Ma.

One major group of 19 spots were obtained on discrete, euhedral, oscillatory zoned magmatic grains, with magmatic Th/U ratios between 0.1 and 0.8 with few of them presenting ratios slightly higher (1.3). Overgrowth rims around inherited magmatic cores also present magmatic Th/U ratios for normal U-contents (Spot 4.1). Metamict domains also presenting high Th contents (up to ~750 ppm) and are recognized by highly BSE-luminescent, CL-dark luminescence domains which are accompanied by frequent fracturing in radial or concentric patterns, due to expansion by metamictisation. (spot 4.3). These high-luminescence BSE domains may also be seen as discordant irregular rims of smooth scalloped overgrowths that truncates and corrodes inherited cores. Some crystals show halos around mineral inclusions, seen as bright areas in BSE. The group represents a single data population, with no excess scatter in $^{206}Pb/^{238}U$ (mean χ^2 = 0.85) and an age of 610 ± 6 Ma (light grey error boxes on Fig. 3). As the date was obtained on discrete unzoned crystals and on new zircon overgrowths on corroded inherited cores (see below), we interpret the 610 ± 6 Ma $^{206}Pb/^{238}U$ date as the age of crystallization of the granite.

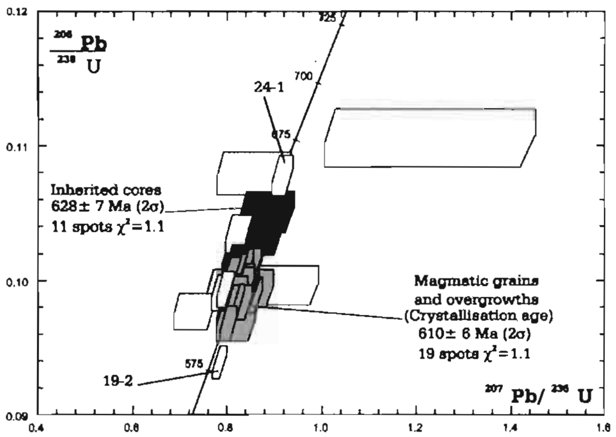

Figure 3. Concordia plot for zircon data from sample 3.

With the exception of spot 19-2 which has experienced recent Pb-loss, and spot 24-1, morphologically distinct, all the others discarded spots (blank error boxes on Fig. 3) were disregarded on the basis of their high discordance.

Eleven spots obtained from magmatic-textured, partly resorbed (corroded) inherited cores and on discrete unzoned grains represent a single U-Pb data population (dark grey error boxes on Fig. 3) with no significant excess scatter (mean χ^2 = 1.1), and furnish a $^{206}Pb/^{238}U$ date of 628 ± 7 Ma. This apparent age coincides within error with the age of the early syn-collisional granitic magmatism, dated at *ca.* 630 Ma (Sample 1). Accordingly, despite uncertainty regarding the source(s), nature and provenance(s) of the inherited cores, it is interpreted as a mean age of crystallization.

SAMPLE 4 - TABULEIRO SUITE

The morphology of the zircons is fairly homogeneous. The great majority of the grains are euhedral, with low aspect ratios (~2:1) and with well preserved fine-scale magmatic, oscillatory-zoned textures in both the rims and cores. Twenty three spots were analyzed on 21 zircons (Fig. 4). Like sample 3, results from sample 4 show a large continuous spread along concordia (from *ca.* 630 Ma to *ca.* 570 Ma).

A group of 6 analyses obtained from discrete, unzoned, magmatic-textured, euhedral grains and on magmatic- textured (oscillatory-zoned) melt-precipitated rim overgrowths forms a single data cluster with mean $\chi^2 = 0.7$ and an apparent $^{206}Pb/^{238}U$ age of 597 ± 9 Ma (light grey error boxes in Fig. 4). Most of these domains have normal (magmatic) U and Th contents and Th/U ratios between 0.2 and 0.7, and the result is interpreted as the crystallization age of the pluton. Only spot 22.1 shows an abnormal enriched U content (1105 ppm) and has bright domains in BSE (and dark in CL) typical of metamict domains. It also has high Th contents (277 ppm) but a normal Th/U ratio (0.25). With the exception of analysis 26-1 (Fig. 4), which has been omitted because it represents a mixed core/rim domain, all the other discarded analyses were rejected on the basis of their highly discordant results (blank error boxes in Fig. 4).

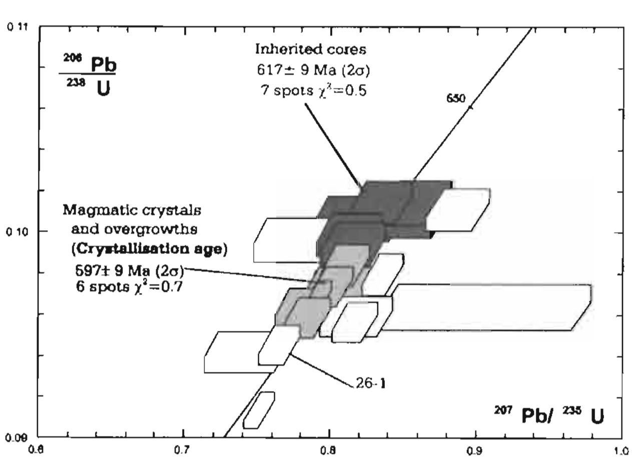

Figure 4. Concordia plot for zircon data from sample 4.

Seven spots obtained from magmatic-textured, partly resorbed (corroded) inherited cores and discrete unzoned grains (spots 9-1 and 9-2) form a single data population (mean $\chi^2 = 1.1$) with a mean $^{206}Pb/^{238}U$ date of 617 ± 9 Ma dark grey error boxes in Fig. 4). As with sample 3, this apparent age coincides within error with the age of the early syn-collisional granitic magmatism, dated at ca. 630 Ma (Sample 1) and it is interpreted as the crystallization age of an early, short-lived, rapidly recycled granitic source, although this source cannot be identified.

As observed in several crystals from the other analyzed samples, some domains show late-magmatic halos around mineral inclusions seen as light areas in BSE. In some crystals, this process caused the formation of paired bright/dark (in BSE), which are complementarily dark/bright in CL, similar to patterns previously ascribed to solid-state diffusion process by Vavra et al. (1996) and Hartmann et al. (1997). As the ages of these domains coincide within error with the age obtained for the "normal" zones, this textural pattern may not be related to a diffusion process or, if it is, the process must not have caused any important disturbance on the U-Th-Pb systems, *i.e.*, the age.

DISCUSSION AND CONCLUSIONS

In addition to the tectonic/magmatic repartition of the granitic phases within the batholith, this investigation is also a case study on the growing importance of spatially-resolved U–Pb SHRIMP systematics for the acquisition of reliable ages on inherited and melt-precipitated complex mixed zircon populations. The complex and varied internal structures of the analyzed zircon populations could lead to mixed ages and erroneous conclusions, in the absence of prior BSE/CL imaging. Further, we believe that conventional U–Pb dating of these samples would result in a complete spread of results between the two geological ages, possibly leading to erroneous conclusions. Even using SHRIMP systematics, the observation of only a small number of BSE/CL images may lead to equivocal conclusions. In a first approach to these data, Silva (1999) and Hartmann et al. (2000) overestimated the influence of the diffusion halos around mineral inclusions and the paired bright/dark (in BSE) zoning (diffusion bands?) on zircon U-Th-Pb systems. In light of similar patterns ascribed to solid-state hydrothermally-controlled diffusion process by Vavra et al. (1996), Gebauer et al. (1997) and Hartmann et al. (1997), these features led Silva (1999) and Hartmann et al. (2000) to interpret the younger melt-precipitated overgrowths as hydrothermally altered domains, and accordingly, their apparent ages were considered as the age of a post-magmatic overprinting process. The resorbed inherited cores, in turn, were interpreted as pristine magmatic populations, and their apparent ages as the crystallization ages of the plutons. Based on the study of a larger number of BSE/CL images of the Brasiliano granites, and on similar morphologic patterns described in many crustal-derived granitoids elsewhere (*e.g.* Williams, 1998) we believe the present reassessment has delineated the correct evolution of the U-Pb-Th systems and, consequently, ages of inheritance and melt-precipitation were properly discriminated and measured.

On the other hand, interpretations of the new ages as well as previous U–Pb data contradict the usual linear temporal partition between pre- syn- post-collisional and post-tectonic batholithic magmatism. Different tectono-magmatic stages were reached in different domains of the Florianópolis Batholith at the same time, giving rise to the unusual coarsely synchronous accretion from of *ca.* 610 Ma post-tectonic I-Caledonian (Guabiruba Suite); *ca.* 600 Ma post-tectonic A-type (Tabuleiro Suite); *ca.* 590 Ma strike-slip related (Valsungana II Granite). The apparently erratic magmatic evolution is also evident from other U-Pb studies. Silva et al. (2002b) dated an expanded calc-alkaline post tectonic suite (Maruim Suite) ranging in ages from *ca.* 610 Ma to *ca.* 580 Ma, whereas (Basei, 2000) obtained an age of *ca.* 650 Ma for a post-tectonic intrusion (Faxinal Syenite). This evolution implies important short-distance lateral changes in the stress field, giving rise to simultaneous transpressive and transtensive large scale magma generation. The peculiar pattern, uncommon in magmatic arcs within the Mantiqueira Province or elsewhere, emphasizes the necessity for more detailed geological mapping of the batholith magmatic phases to delineate a better constrained tectono-magmatic evolution.

REFERENCES

Basei, M.A.S. 2000. Geologia e modelagem geotectônica dos terrenos pré-cambrianos das regiões sul e oriental brasileira e uruguaia: possíveis correlações com províncias similares do sudoeste africano. (Tese de Livre Docência). Universidade de São Paulo, São Paulo. 123 p.

Gebauer, D., Schertl, H.-P., Brix, M., and Schreyer, W. 1997. 35 Ma old ultrahigh-pressure metamorphism and evidence for very rapid exhumation in the Dora Maira Massif, Western Alps. Lithos 41: 5-24.

Hartmann, L.A., Takehara, L., Leite, J.D., McNaughton, N.J., and Vasconcellos, M.A.Z., 1997. Fracture sealing in zircon as evaluated by electron microprobe analyses and back-scattered electron imaging. Chem. Geol. 141: 67-72.

Hartmann, L. A.; Leite, J. A. D.; Silva, L. C., Remus, M.V.D., McNaughton, N.J., Groves, D.I., Fletcher, I.F., Santos, J.O.S., Vasconcellos, M. A. A. 2000. Advances in SHRIMP geochronology and their impact on understanding the tectonic and metallogenic evolution of southern Brazil. Australian Journal Earth Science 47: 829-844.

Silva, L.C. 1999. Geocronologia U–Pb SHRIMP e Sm–Nd na Província Mantiqueira meridional, no Cinturão Saldania (África do Sul) e a evolução do Ciclo Brasiliano/Pan-Africano. (Tese de Doutorado). Universidade Federal do Rio Grande do Sul-UFRGS. Porto Alegre, 243p.

Silva, L.C. da, Macambira, M.J.B., Hartmann, L.A., Chemale Jr., F., 1997. Pb-Pb zircon evaporation age and petrology of the strike-slip-related Paulo Lopes granite, Southern Brazilian Granitic Province. In: South American Symposium on Isotope Geology, Campos do Jordão, 1997. Extended Abstracts, p. 309-311.

Silva, L.C. da, , Hartmann, McNaughton, N.J.,L.A., Fletcher, I., 2002a. The Neoproterozoic Mantiqueira Province and its African connections: a zircon-based U–Pb geochronologic subdivision for the Basiliano/Pan-African systems of orogens. Precambrian Research (Submitted).

Silva, L.C., Armstrong, R., Pimentel, M.M, Scandolara, J., Ramgrab, G.,Wildner, W., Angelim, L.A.A.,Vasconcelos, A.M., Rizzoto, G.,Quadros, M.L.E.S., Sander, A., Rosa, A.L.Z. 2002b. Reavaliação da evolução geológica em terrenos pré-cambrianos brasileiros com base me novos dados U-Pb SHRIMP, Parte III: Províncias Borborema, Mantiqueira Meridional e Rio Negro-Juruena. Rev. Bras. Geoc. (Submitted).

Silva, L.C, McNaughton, N.J. Hartmann, L.A., Fletcher, I.R. 2003. Contrasting zircon growth patterns in Neoproterozoic granites in southern Brazil revealed by shrimp U–Pb analysis and SEM imaging: consequences for the discrimination of emplacement and inheritance ages. International Geology Review (Submitted).

Vavra, G., Schmid, R., and Gebauer, D. 1999. Internal morphology, habit and U-Th-Pb microanalysis of amphibolite-to-granulite facies zircons: geochronology of the Ivrea Zone (Southern Alps). Contributions to Mineralogy and Petrology 134: 380-404.

Williams, I.S. 1998. U-Th-Pb geochronology by ion microprobe. In: McKibben,M.A., Shanks III,W.C., Ridley,W.I. (eds.) Applications of microanalytical techniques to understanding mineralizing processes. Reviews in Economic Geology, Society of Economic Geology 7: 1-35.

^{40}Ar/^{39}Ar GEOCHRONOLOGY OF MESOZOIC AND CENOZOIC MAGMATISM IN NE BRAZIL

Souza, Z.S.[1]; Vasconcelos, P.M.[2]; Nascimento, M.A.L.[3]; Silveira, F.V.[3]; Paiva, H.S.[4]; Dias, L.G.S.[4]; Thiede, D.[2] and Carmo, I.O.[2]

1. Departamento de Geologia e Programa de Pós-Graduação em Geodinâmica e Geofísica (PPGG)/UFRN; Caixa Postal 1596, 59078-970 Natal-RN, Brazil. zorano@geologia.ufrn.br, galindo@geologia.ufrn.br
2. Department of Earth Sciences, The University of Queensland; Brisbane Qld 4072, Australia. paulo@earth.uq.edu.au
3. PPGG/UFRN; Caixa Postal 1596, 59078-970 Natal-RN, Brazil. marcos@geologia.ufrn.br, silveira@geologia.ufrn.br
4. Curso de Geologia / UFRN, Bolsista de IC/ANP-PRH22; Caixa Postal 1639, 59078-970 Natal-RN, Brazil

Keywords: ^{40}Ar/^{39}Ar geochronology, volcanic and subvolcanic rocks, NE Brazil

INTRODUCTION

Mesozoic and Cenozoic magmatism and volcanism in the Borborema Province, Northeastern Brazil, reflect mantle thermal anomalies associated with the break-up of Gondwanaland and, possibly, the migration of the South American Platform over the Santa Helena plume (Cordani, 1970; Chang et al., 1992). To understand the fundamental mechanisms leading to the Borborema Province Mesozoic and Cenozoic magmatism, it is necessary to determine exact ages of magma emplacement, the chemical and isotopic characteristics of the magma sources, and the extent of crustal contamination in these magmas. To achieve these goals, we have comprehensively sampled the magmatic bodies in this region and are in the process of obtaining detailed isotopic and trace element data for these samples. We will present here some preliminary ^{40}Ar/^{39}Ar results for the magmatic events, discuss the possible reasons for the discrepancy between these results and previous dates, and discuss the advantages of the ^{40}Ar/^{39}Ar method as a geochronological tool in the study of these magmatic events.

ADVANTAGES OF ^{40}Ar/^{39}Ar GEOCHRONOLOGY

One of the major difficulties in providing accurate and precise age constraints for the Mesozoic and Cenozoic magmatic rocks from the Borborema Province is their advanced stages of weathering, the low K contents of some units, the presence of wall-rock contamination, and the possible presence of excess Ar. Previous K-Ar dating provides useful age constraints; however, the absolute ages of the magmatic events are not precisely determined by this method given the limitations of the method in addressing the complicating factors listed above.

Contrary to the K-Ar technique, where K and Ar are determined in different aliquots of the sample, in the ^{40}Ar/^{39}Ar method K and Ar contents are determined from the same aliquot, mineral grain, or crystallographic site in a sample. The main advantages of the application of the ^{40}Ar/^{39}Ar method are: i) the fine-scale resolution of the method, which allows the age determination of very fine-grained phases (0.5-1 mm grains of Cenozoic rocks can be dated); ii) the multiple-step analysis of single grains, which enables the determination of the Ar retention history for a mineral, the presence of excess/inherited Ar, and the possibility of K and/or Ar loss; iii) the crystallochemical information obtained by the analyses of ^{40}Ar, ^{39}Ar, ^{38}Ar, ^{37}Ar, and ^{36}Ar from the same gas aliquot.

METHODOLOGY

All samples were irradiated (for 14 hours) together with Fish Canyon sanidine neutron flux standards in the Triga Reactor at the Oregon State University. After a two-month cooling period, each sample was step-heated under a continuous Ar-ion laser with a 2mm-diameter beam. The fraction of gas released was cleaned through a cryocooled cold-trap (T=-140 °C) and two C-50 SAES™ Zr-V-Fe getters and analyzed for Ar isotopes in a MAP-215-50 mass spectrometer at the UQ-AGES (University of Queensland Argon Geochronology in Earth Sciences) laboratory. Automation and analytical procedures are described in Vasconcelos (1999) and Vasconcelos et al. (2002). Data corrected for mass discrimination, nucleogenic interferences, and atmospheric contamination were used to calculate apparent ages for each degassing step. Although single crystals are preferred to analyze, we also analyzed total rock samples if the grain sizes were sufficiently small (phenocrysts smaller than 50-100 μm).

In this study, we define an age plateau as a sequence of two or more steps corresponding to at least 50% of the total ^{39}Ar released, and whose age values are within two sigma from the mean value. If a sample reaches a well-defined plateau, it implies that the sample hosts its radiogenic and nucleogenic gas fractions in a tight crystallographic reservoir, that the reservoir has been closed during the history of the sample, and that contaminating hypogene phases are unlikely to be present.

OCCURRENCE OF MAGMATIC ROCKS IN NE BRAZIL

Northeastern Brazil comprises a widespread geotectonic unit of the South American platform, the Borborema Province. In this province, there are a great number of volcanic and hypabyssal rocks, with ages ranging from Cretaceous to Tertiary. They occur as dykes, sills, small flows, volcanic conduits and plugs (Sial, 1976; Almeida et al., 1988). These rocks preceded or succeeded the implantation of the Cretaceous rifts in this province (e.g., the Rio do Peixe interior basin and the Potiguar-Ceará and Pernambuco-Paraíba coastal basins) and they probably contributed to the processes of regional uplifting and re-heating. A recent compilation of geochronological data by Mizusaki et al. (2002) identifies three distinct magmatic events.

The oldest one, the so-called Rio Ceará Mirim Magmatism, yields a K-Ar age peak around 130 Ma. It is represented by several tholeiitic diabase dykes, oriented predominantly in an E-W direction, that outcrop mainly in the southeast portion of the Potiguar basin, with minor occurrences in the oriental part of the Parnaíba basin. Recent $^{40}Ar/^{39}Ar$ dates (Araújo et al., 2001) of plagioclase crystals from diabase dykes from João Câmara, Açu and Lajes (RN) yield plateau ages of 136 ± 4 Ma, 127 ± 1.3 Ma e 110.7 ± 1.3 Ma, respectively.

For the second event, Almeida et al. (1988) report K-Ar ages between 105 e 95 Ma for alkalic and calc-alkalic rocks from the Pernambuco Basin and, possibly, the Itapororoca region (eastern Paraíba state). They occur as dykes, plugs, small flows, sills and laccoliths, crosscutting cretaceous clastic sequences of the Cabo Formation in the Pernambuco Basin (Amaral & Menor, 1979; Sial, 1976). Recent whole rock $^{40}Ar/^{39}Ar$ analyses of basalts, trachytes, rhyolites and ignimbrites from this basin yield ages between 111 and 100 Ma (Lima Filho & Szatmari, 2002). Slightly younger K-Ar dates (80.4 ± 2 Ma) are cited for the Cuó basaltic flows from Açu (RN) (Sial et al., 1981). Based on compilation of available K-Ar data, Mizusaki et al. (2002) places the peak of the Cuó magmatism at ca. 90 Ma. However, Araújo et al. (2001) interpret an $^{40}Ar/^{39}Ar$ integrated age of 98.3 ± 0.8 Ma and a compatible weighted mean average age of 99 ± 2 Ma as the best estimate for this magmatic event, placing this magmatism temporally very close to the one found in the Pernambuco Basin.

The youngest magmatic event in the Borborema province is related to Tertiary volcanic rocks of the Macau-Queimadas and Mecejana-Fernando de Noronha alignment (Almeida et al., 1988). The K-Ar whole-rock data compiled by Mizusaki et al. (2002) is consistent with two groups, one with ages ranging between 12.3 ± 1 and 1.81 ± 0.13 Ma (peak around 7 Ma in Fernando de Noronha), and the other one with ages ranging between 45 ± 1 and 12.5 ± 1.0 Ma (peak around 30 Ma). For Mecejana phonolites, Vandoros & Oliveira (1968) furnished K-Ar ages of 28.6 ± 0.6 Ma and 26.6 ± 0.8 Ma, whereas Cordani (1970) obtained 27.8 ± 0.8 Ma. A Rb-Sr isochron of phonolites from Mecejana gave an age of 36 ± 2 Ma (Nascimento et al., 1981, in Almeida et al., 1988). A recent $^{40}Ar/^{39}Ar$ date for whole rock basalt sample from Serrote Preto (Cerro Corá/RN) yield a plateau age of 24.2 ± 0.3 Ma (Moraes Neto et al., 2002), estimated by these authors as the best age for this sample. Araújo et al. (2001), however, interpret an integrated age of 29.7 ± 0.6 Ma as the best estimate for the Cerro Corá magmatism. Basalts from the Cabugi neck (Lajes/RN) yield a plateau age of 23.7 ± 1.2 Ma (Araújo et al., 2001).

In this report we present new $^{40}Ar/^{39}Ar$ data of basalts from Cabugi neck (130 km western of Natal) and Cuó flow (4 km eastern of Açu and 190 km western of Natal), as well as one diabase dyke from Pedro Avelino (15 km north of Cabugi neck). We will provide detailed interpretation of the $^{40}Ar/^{39}Ar$ results, and discuss the pitfalls of $^{40}Ar/^{39}Ar$ geochronology interpretation. Appropriate interpretation of the $^{40}Ar/^{39}Ar$ results may contribute to a better understanding of the processes of regional uplifting and brittle tectonics associated to the magmatic events in the Borborema Province and may aid in directing future studies.

SAMPLE LOCATION AND TEXTURAL DESCRIPTION

One of the sampling sites was the central gabbroic zone a thick (40 m) diabase dyke (100° Az). This dyke crosscuts high grade gneisses of the Precambrian crystalline basement and shows a net variation to a fine grained border in the contact with the basement.

The other sampled site, the basaltic rocks from the Cuó magmatism, constitute small flows of olivine basalts outcropping in the interface between the crystalline basement and the sedimentary rocks of the Potiguar Basin, in this case the sandstone of the Açu Formation. The top of the flow is 52 m high, is slightly inclined toward north and probably constitutes a sill into this formation.

The third sampled site, the Cabugi body, is topographically very expressive in the region, forming a hill that reaches a 650 m height, surrounded by the 150 Lajes plain. It corresponds to a volcanic neck intrusive into the Precambrian gneissic rocks. In the Cabugi neck, Souza et al. (2002) distinguish three textural/stratigraphic facies. The oldest one is a medium to coarse-grained basalt (basalt$_1$), which forms the major part of the body and predominates in the NW, W and SW borders of the neck. The youngest one outcrops in the NE border, presenting fine grained texture and abundant xenoliths of peridotite, crystalline basement rocks (gneiss, granite, pegmatite) and basalt$_1$, and frequent xenocrysts of olivine, clinopyroxene, brown spinel, quartz and oligoclase. There are also several dykes of microgabbros (20-30° Az) crosscutting basalt$_1$ or, otherwise, found as inclusions in basalt$_2$. In this study, we analyzed one sample of basalt$_2$.

$^{40}Ar/^{39}Ar$ GEOCHRONOLOGY RESULTS

DIABASE DYKE

Two amphibole grains analyzed yield well-defined spectra with plateau ages of 133 ± 3 and 132.2 ± 1 Ma, and compatible integrated ages of 134.8 ± 1.3 and 132.8 ± 1.1 Ma (Fig. 1). An ideogram plotted for this sample yields a most probable peak of 132.1 Ma and a weighted mean average age of 133 ± 3 Ma for all the steps obtained for the two grains (Fig. 1). The best estimate age for this sample is the plateau age of 132.2 ± 1 Ma, given the size of the grain analyzed, the volume of ^{39}Ar contained, and the reproducibility of the steps defining the plateau. As the amphibole grains are derived from some process of uralitization of augite grains, this date is considered as a cooling age for the diabase dyke.

CUÓ BASALTIC FLOW

The Cuó basalts are fine to medium grained and show abundant, frequently serpentinized, olivine phenocrysts, sometimes in glomeroporphyritic aggregates. They have intergranular short augite grains, plagioclase laths and magnetite. Six total rock fragments (grains 2442-01/02/03 and 2512-01/02/03) analyzed by the incremental heating method yield the spectra illustrated in Figures 2a and b. An ideogram representing all the steps analyzed yield two high probability peaks, one at 99.2 Ma and another at 93.1 Ma and a weighted mean average age of 96.4 ± 0.9 Ma (Fig. 2c). This weighted mean average also corresponds, within 2 sigma, to the integrated age for each of the grains analyzed (96.4 ± 0.3, 96.3 ± 0.3, and 96.8 ± 0.3 Ma for grains 2442-01/02/03 and 95.0 ± 0.3, 95.5 ± 0.3 and 96.0 ± 0.3 Ma for grains 2512-01/02/03). Careful inspection of the incremental-heating spectra reveals a very similar pattern for the six grains, where the low temperature steps suggest a high K/Ca phase which yields higher apparent ages, while the high temperature steps are derived from a low K/Ca phase recording lower apparent ages. Because the older results are associated with the low temperature, K-rich, steps, and the younger ones are associated with the Ca-rich plagioclase phenocrysts, it is unlikely that the two peaks correspond to ages associated with the crystallization of the phenocrysts (which should be older, and recorded in the plagioclase crystals) and the extrusion of the basalt (which should be younger, and recorded in the glass). Because the feldspar ages are younger, it is also unlikely that the two-age pattern is related to excess Ar in the phenocrysts, either. A possible explanation for the pattern obtained is some degree of alteration and K loss from the glass matrix in this sample, leading to older results for the low temperature steps. If this interpretation is correct, the higher temperature steps, yielding a most probable peak at 93.1 ± 0.8 Ma, and related to the gas reservoirs represented by the unaltered feldspar phenocrysts, would be the best estimate for the age of this sample.

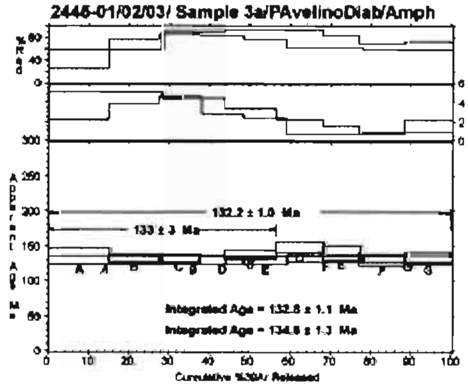

Figure 1. ^{40}Ar/^{39}Ar plateau ages for amphibole of a diabase dyke south of Pedro Avelino/RN (NE Brazil).

BASALT FROM CABUGI NECK

Two of the three total rock grains analyzed for this sample yield plateau ages of 24.8 ± 0.4 and 24.6 ± 0.6 Ma (Fig. 3). The integrated ages obtained for the two grains yielding plateaus are also indistinguishable at the 2-sigma confidence level (24.2 ± 0.3 and 24.1 ± 0.3 Ma). The third grain does not yield a plateau age, but the spectrum yielded by this grain is compatible with that obtained for the other two grains. However, this grain yields some steps recording slightly older results, possibly associated with recoil or excess Ar; and its integrated age, 25.0 ± 0.2 Ma, is also slightly older than that obtained for the other two grains. An ideogram plotted for this sample yields a wide peak, with most probable age at 24.14 Ma and a weighted mean average age of 24.6 ± 0.8 Ma (Fig. 3). The three incremental heating spectra show that the earlier steps, associated with plateau ages of 24.8 ± 0.4 and 24.6 ± 0.6 Ma are associated with fractions of gas released from K-rich reservoirs in the sample, while the higher temperature steps, which yield dates slightly different from the lower temperature steps, are associated with Ca-rich reservoirs, probably plagioclase crystals. The best age estimate for this sample is 24.6 ± 0.8 Ma.

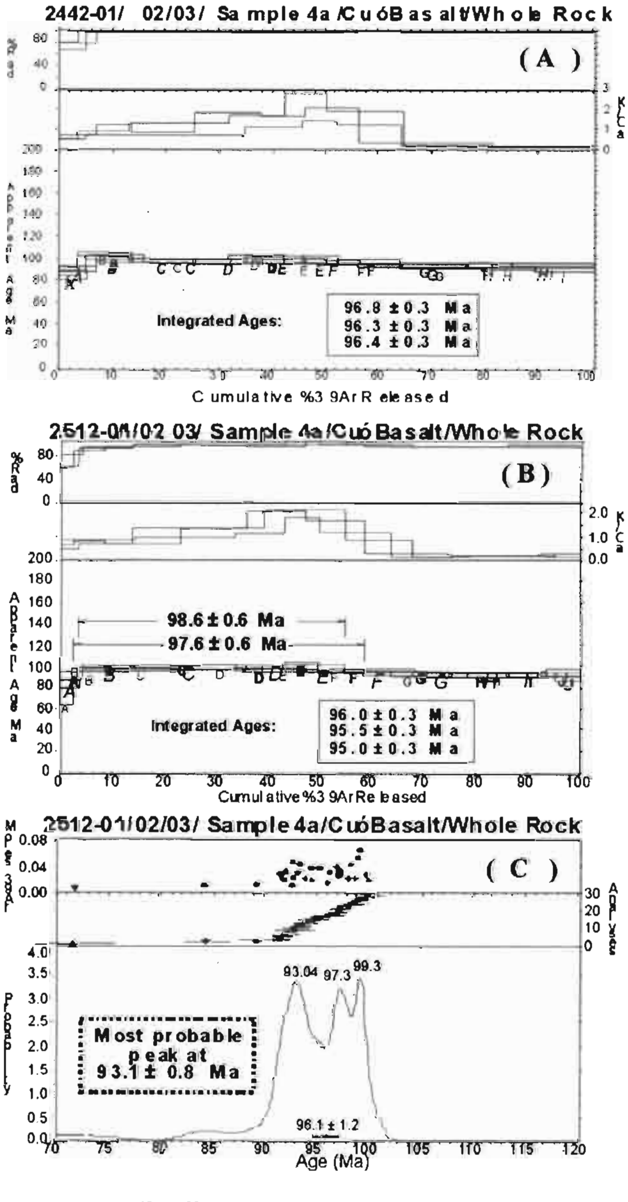

Figure 2. ^{40}Ar/^{39}Ar plateau (A, B) and ideogram ages for olivine basalt of the Cuó magmatism (Açu/RN, NE Brazil).

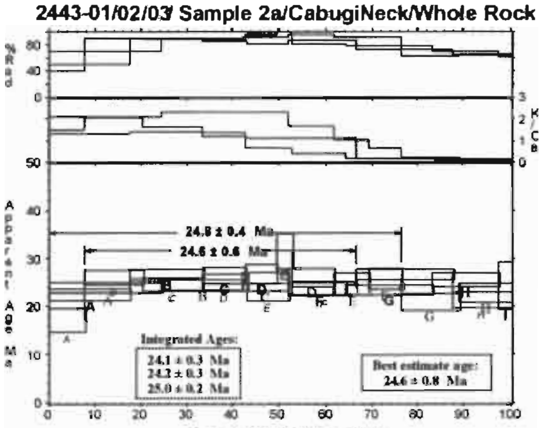

Figure 3. $^{40}Ar/^{39}Ar$ plateau ages basalt of the cabugi neck (Lajes/RN, NE Brazil).

GEOLOGICAL IMPLICATIONS

The $^{40}Ar/^{39}Ar$ geochronological data reported here confirm some previous results (i.e., our plateau age for the Cabugi basalt is compatible with the 23.7 ± 1.2 Ma plateau age obtained by Araújo et al., 2001), and also very close to the 25 ± 1 Ma age estimate for basalt of the Serrote Preto hill (Cerro Corá/RN) reported by Morais Neto et al. (2002). However, the age of 98.3 ± 0.8 or 99 ± 2 Ma determined for the Cuó magmatism by Araújo et al. (2001) is significantly different from our estimate of 93.1 ± 0.8 Ma for this magmatic event.

Based on the results presented here, results from the literature, and also the results presented by Nascimento et al. (this symposium), we identify four distinct Meso-Cenozoic magmatic events in the Borborema Province:

(1) The Rio Ceará Mirim dyke swarm magmatism, ranging from ca. 145 to 110 Ma (Araújo et al., 2001). Our plateau age of 132.2 ± 1 Ma represents one of the phases, possibly the main phase (Misuzaki et al., 2002), of this magmatic event.

(2) The Cabo Magmatic Province, with $^{40}Ar/^{39}Ar$ plateau ages ranging from 104.4 ± 0.8 to 98.3 ± 3 Ma, with a major peak at ca. 102 ± 1 Ma (Nascimento et al., 2003, this symposium).

(3) The Cuó Magmatism, with a most probable age of 93.1 ± 0.8 Ma.

(4) The alkaline basalt (Macau Magmatism), represented in this study by the Cabugi neck, with a best age estimate of 24.6 ± 0.8 Ma. These dates corroborate previous results (Araújo et al., 2001; Moraes Neto et al., 2002).

These magmatic events preceded or succeeded the implantation of Cretaceous rifts in this province. They likely contributed to the uplift and regional denudation related to the generation of sediments that filled continental and marginal basins; they probably enhanced the maturation and (re)mobilization of organic materials in sedimentary basins, being directly related to the generation of oil reservoirs in these basins; and they are possibly associated with tectonic reactivations that may have generated structural traps in these sedimentary basins.

Further $^{40}Ar/^{39}Ar$ geochronology is necessary to completely determine the spatial and temporal distribution of the magmatic centers in the Borborema Province and to answer an important question related to the genesis of the Meso-Cenozoic magmatic provinces in northeastern Brazil: are the magmatic centers indeed aligned in a north-south direction and related to a hot spot, as previously proposed by Almeida et al. (1988), Chang et al. (1992), and Mizusaki et al. (2002) based on K-Ar ages?

REFERENCES

Almeida, F.F.M.; Dal Ré Carneiro, C.; Machado Jr., D.L.; Dehira, L.K., 1988. Magmatismo pós-Paleozóico no nordeste oriental do Brasil. Rev. Bras. Geoc. 18: 451-462.

Amaral, A.J.R. & Menor, E. A., 1979. A seqüência vulcano-sedimentar Cretácea na região de Suape (PE): interpretação faciológica e considerações metalogenéticas. Simp. Geol. do NE, 9, Natal, Atas, p. 251-269.

Araújo, M.G.S.; Brito Neves, B.B.; Archanjo, C.J., 2001. Idades $^{40}Ar/^{39}Ar$ do magmatismo básico Meso-Cenozóico da Província Borborema Oriental, nordeste do Brasil. Simp. Geol. do NE, 19, Natal, Resumos, p. 260-261.

Chang, H.K.; Kowsmann, R.O.; Figueiredo, A.M.F.; Bender, A.A., 1992. Tectonics and stratigraphy of the east Brazil rift system: an overview. Tectnophysics, 213: 97-138.

Cordani, U.G., 1970. Idade do vulcanismo do Oceano Atlântico Sul. Boletim IAG / USP, 1: 9-75.

Gorini, M.A.; Bryan, G.M., 1976. The tectonic fabric of the Equatorial Atlantic and adjoining continental margins: Gulf of Guinea to Northeastern Brazil. An. Acad. Bras. Ciênc., 48: 101-119.

Lima Filho, M.F.; Szatmari, P. 2002. Ar-Ar geochronology of volcanic rocks of the Cabo Magmatic Province (CMP) – Pernambuco Basin. Simp. Vulcan. e Amb. Assoc., 2, Belém, Resumos, p. 59-59.

Mizusaki, A.M.P.; Thomaz-Filho, A.; Milani, E.J.; Césero, P., 2002. Mesozoic and Cenozoic igneous activity and its tectonic control in northeastern Brazil. J. South Amer. Earth Sci., 15: 183-198.

Moraes Neto, J.M.; Menezes, M.R.F.; Szatmari, P.; York, D., 2002. Datação Ar/Ar do plug basáltico "Serrote Preto" e seu significado para a cronologia da Formação Serra do Martins. Congr. Bras. Geol., 41, João Pessoa, Anais, p. 499-500.

Nascimento, M.A.L.; Vasconelos, P.M.; Souza, Z.S.; Sá, E.F.J.; Thied, D.; Carmo, I. 2003. $^{40}Ar/^{39}Ar$ Geochronology of the Cabo Magmatic Province, Pernambuco Basin, NE Brazil. (this symposium.)

Sial, A.N., 1976. The post-Paleozoic volcanism of north-east Brazil and its tectonic significance. An. Acad. Bras. Ciênc., 48: 299-311.

Sial, A.N.; Long, L.E.; Pessoa, D.A.R.; Kawashita, K., 1981. Potassium-argon ages and strontium isotope geochemistry of Mesozoic and Tertiary basaltic rocks, Northeastern Brazil. An. Acad. Bras. Ciênc, 53: 115-122.

Souza, Z.S.; Paiva, H.S.; Silveira, F.V., 2002. O edifício vulcânico Cabugi, Terciário do Rio Grande do Norte. Simp. Vulcan. e Amb. Assoc., 2, Belém, Resumos, p. 105-105.

Vandoros, P.; Oliveira, M.A.F., 1968. Sobre o Fonólito de Mecejana, Ceará. An. Acad. Bras. Ciênc, 40: 203-206.

Vasconcelos P.M. (1999) $^{40}Ar/^{39}Ar$ Geochronology of Supergene Processes in Ore Deposits. Rev. Econ. Geol. 12, 73-113.

Vasconcelos, P.M.; Onoe, A.T.; Kawashita, K.; Soares, A.J.; Teixeira, W. 2002. $^{40}Ar/^{39}Ar$ geochronology at the Instituto de Geociências, USP: instrumentation analytical procedures and calibration. An. Acad. Bras. Ciênc, 74: 297-342.

Nd-Sr ISOTOPIC COMPOSITION OF MICROGRANULAR ENCLAVES OF THE BREJINHO BATHOLITH, ALTO PAJEÚ TERRANE, BORBOREMA PROVINCE, NE BRAZIL

Torres, H.H.F.[1]; Sial, A.N.[2]; Santos, E.J.[3] and Silva Filho, M.A.[1]

1. CPRM Geological Survey of Brazil, Recife Branch, Pernambuco-PE, Brazil. geremipe@fisepe.pe.gov.br
2. NEG-LABISE, Department of Geology, UFPE, Universidade Federal de Pernambuco. Recife-PE, Brazil. ans@ufpe.br
3. Department of Geology. UFPE - Universidade Federal de Pernambuco. Recife-PE, Brazil. edilton@ufpe.br

Keywords: Nd-Sr isotopes, mafic enclaves, lithospheric mantle, tectonostratigrafic terranes

INTRODUCTION

The microgranular enclaves of intermediate to mafic composition are common in granitoid rocks, especially in calc-alkaline suites, being considered, in general, as products of incomplete mixing between coeval magmas of acid and mafic composition from different origins. They can also be interpreted as: a - refractory residue of mafic rocks remnants of an igneous protolith which was partially melted to yield the host granitoid magma (restite model), or b -together with the granitoids, originated by differentiation of a parental mafic magma constituting the "autoliths". In this case, these last two interpretations are less likely, in agreement with isotopic, petrographic, chemical and field constraints, so that the enclaves and the granitoids hosts are considered as representatives of two coexisting magmas, but with different composition and origin (Torres, 2001).

Among other investigation lines, the isotopic composition of mafic enclaves and granitoid hosts constitute one of the main tools for the interpretation of the genesis and evolution of granitoids plutons. It allows assessing the genetic relationships between the granitoids and the enclosed enclaves, making possible the understanding of the relative role of crustal and mantelic sources in the magmatism, and also the type(s) of source(s) involved.

Nevertheless, the study of the isotopic composition of these rocks not always lead to conclusive interpretations. So, frequently, the enclaves do not retain their primary isotopic signatures; being these, at least partially, acquired from the interaction with crustal melts in the lodging place, still in the lower crust, contamination with crustal rocks or mixing in the site of the emplacement, not representing original liquids.

Enclaves and the hosts granitoids originated from different magmas may show similar isotopic signature, if the mafic magma has been extracted from the enriched mantle or an almost complete isotopic equilibrium has been reached. In the case of the Brejinho batholith, the most prominent isotopic features are the overlap of the isotopic Nd values and the presence of Sr isotopic contrasts between the enclaves and the granitoids (all with negative ε_{Ndi} and positive ε_{Sri}).

Data for pristine mafic rocks are not available. Therefore, conflicting interpretations have been considered with relationship to type of mantle involved in the generation of the mafic magma (Guimarães & Da Silva Filho, 2000; Torres, 2001). The aim of this paper is to demonstrate the limitation of the use of these data for the resolution of this problem.

Addicionally, geochemical and Nd isotope data of the enclaves from several high-K calc-alkaline granitoids of the Borborema Province (BP) also related to the Brasiliano/Pan-African Cycle, have been used by some authors (Mariano et al., 2000) with the objective of contesting the widespread use of the tectonostratigraphyc terrane model in this province, proposed by Santos (1996). The present work suggests that the characteristics of the mantle source of the mafics enclaves of the Brejinho granitoid (and of other granitoids also located in the Alto Pajeú Terraine; APT), they oppose to the great part of BP mantle, unequivocally enriched, according to those authors.

GEOLOGICAL FRAMEWORK AND MAIN CHARACTERISTIC

The Brejinho batholith (also called Itapetim Granitics Complex; Guimarães & Da Silva Filho, 2000) is located in the central northern sector of the State of Pernambuco. It is inserted in the APT (Santos, 1996) which is part of the Transversal Zone Domain (TZD) of the BP. It is of Neoproterozoic age (638± 4.9 Ma–concordia U-Pb in zircon - Guimarães & Da Silva Filho, 2000), therefore related to the Brasiliano/Pan-African Cycle, being treated as a syn-transcorrent body that intrude orthogneisses and metasediments of the Cariris Velhos Cycle (ca. 1.0 Ga). It is constituted by porphyritic monzogranites and granodiorites, and contains quartz-diorites/diorites enclaves and sin-plutonics dikes, specially in the central portion (Central Zone of Mixing and Mingling). All the types have similar mineralogical composition, with quartz, oligoclase, ±KF, biotite, ±amphibole and titanite, differing in the modal proportion. It is a metaluminous granitoid, with peraluminous tendency, magmatic epidote-bearing, belonging to the high-K calc-alkaline series, with K_2O/Na_2O <1, some enrichment in Rb, K, and LREE (Torres, 2001).

The Nd isotope signature and the high MgO, CaO and compatible elements (Cr up to 300ppm) content regardless of the fractionation and the interaction with felsic melts indicate that the diorites are derived from a parental magma extracted from the upper mantle. To consider them as originated from a crustal source (Guimarães & Da Silva Filho, 2000), would demand high degree parcial melt and extremely high temperature, and a smaller LREE/HREE ratio, not supported by the patterns presented by these elements (Torres, 2001). The granitoids also present relatively high values of MgO, CaO, Cr (up to 216ppm) and ε_{Nd} close to CHUR, suggesting an origin from basic crust with participation of mantle-derived material. The values of $\delta^{18}O$, the peraluminous tendency and correlation with experiments accomplished by Patiño Douce (1995) they indicate participation of sedimentary component in the source (Guimarães & Da Silva Filho, 2000; Torres, 2001).

Nd AND Sr ISOTOPE DATA

The Sm/Nd model ages (T_{DM}) of granitoids are between 1.3 and 1.45Ga and $\varepsilon_{Nd\ 600}$ of –2.4 to –6.4. The values for the enclaves are also between the above interval (Torres, 2001). One granitoid sample located close to the contact with the regional rocks, presents T_{DM} 1.8Ga, interpreted as reflecting assimilation processes with these gneisses which display T_{DM} ca. 2.0Ga (Guimarães & Da Silva Filho, 2000) suggesting that these processes are restricted to the most external portion of the batholith.

The ε_{Sri} values (data of Guimarães & Da Silva Filho, 2000) are variable: 68 for a dioritic enclave, 61 for a hybrid type, 74 for a granodiorite and 110 for a monzogranite.

DISCUSSION ON POSSIBLE SOURCES

The variation in the the isotopic Sr_i values points to the fact that the system must have caught a sufficiently fast cold, not allowing to attain a complete isotope equilibrium. This hypothesis is also supported by the small fraction of the mafic rocks (enclaves) and by size enclaves, almost always smaller than 1.5m, that could lead to the accomplishing of a thermal equilibria before the chemical equilibria (Pin, 1992). The trends of geochemical variation (Torres, 2001) corroborate this behavior, showing that the system has been developed from an incomplete mixture of different magmas (fact corroborated by petrographyc and field data, and by the suggestion of a $\varepsilon_{Nd}/\varepsilon_{Sr}$ mixing trend, obtained by Guimarães & Da Silva Filho, 2000). The hybridization process was incipient and limited in volume, since the characteristics of each one of the suites are relatively well preserved (Torres, 2001). The time of coexistence between the felsic and mafic magma, besides the development of chilled margins in the enclaves (commingling evidence), they act as a strong barrier against isotopic and element equilibria (Fourcade & Javoy, 1992).

On the other hand, the overlap of Nd isotopic values between the enclaves and the granitoid differ clearly of the behavior presented by the Sr isotopes and geochemical variation diagrams, suggesting a near-complete equilibria. Experiments by Baker (1989) and Lesher (1990) indicate that isotopic homogènization through liquid-state diffusion (in spite of the diffusion, by itself, would not be enough to allow a complete mixing), is faster than the chemical equilibration, and that the velocity of Nd isotopes equilibrium are more slowly than the one of Sr, so that, it is very difficult that Nd isotopic equilibrium should occur. These observations suggest that the Nd isotopic signature is primary, implicating that the mafic magma has been extracted from an enriched mantle (Torres, 2001) without great isotopic contrast with the crustals melts.

Besides, the apparent mixing trend obtained by Guimarães & Da Silva Filho (2000) very shallow and flat, is not consistent with a model involving a depleted mantle and old crust as final members (Pin & Duthou, 1990).

However, another hypothesis should be considered. A sedimentary component contributed to the formation of the granitic melt (probably metagreywackes-biotite gneiss; Guimarães & Da Silva Filho, 2000 and Torres, 2001). The Sr isotopic variation in the system, could be attributed to a more heterogeneous source in terms of Rb/Sr that Sm/Nd, as commonly observed in sediments, or to the great mobility of Sr during the anatexis, inhibiting the Sr isotopic homogenization (Pin & Duthou, 1990; Pin,1992).

The presence of samples with lower ε_{Sr} and higher ε_{Nd}, they are, suggestive that some re-equilibrium process has operated. So, the primary Nd isotope signature in the enclaves, which could reflect a depleted mantle source (as proposed by Guimarães & Da Silva Filho, 2000) or CHUR, would have been erased through mixing (liquid-state diffusion) with the felsic magma.

Finally, the fact that the parental magma of the diorites is mantle-derived, and all the enclaves have Nd and Sr crustal isotopic signature, leads to two interpretations: (a) none of them was exempt of assimilation or equilibrium, even if in an incipient way, being derived from a depleted re-homogenized source or, (b) enriched-mantle source.

REGIONAL IMPLICATIONS

The subdivision of BP in tectono-stratigrafic terranes (Santos, 1996) was recently contested (Mariano et al., 2000), based in the study of diorites enclaves of the various high-K calc-alkaline associations which have a widespread distribution in this province. These authors argue that the very restricted isotopic and geochemical variation of the diorites, is not concordant with the Santos' model (1996) indicating that an enriched continental lithosphere (characterized by high LREE/HREE ratios, enrichment in LILE and ε_{Nd600} between -7 and -16 and T_{DM} of 1.8 to 2.0 Ga) permeates great part of the province, since the Transamazonic Cycle.

On the other hand, the characteristics of the mantle involved in the generation of the mafic enclaves of the Brejinho batholith (isotopic signature of uncertain source, €Nd with values less negative, smaller LREE/HREE ratios and smaller LILE enrichment) they suggest origin from a different source. T_{DM} also present significant differences, varying from 1.3 to 1.5 Ga in Brejinho and in the granitoids Riacho do Icó, Conceição das Creoulas e Tavares, all located in APT (see revision in Torres, 2001).

Additionally, two granitoids, included in Mariano et al. (2000) study, Serra da Lagoinha e Caruaru/Arcoverde, are inserted, respectively, in the Piancó/Alto Brígida and Rio Capibaribe terraines, both also belonging to TZD. The first one is juxtaposed to the APT by the NW side, and the second is separated from APT, at SE, by the Alto Moxotó terrane, in which, to the moment, Brasilian granitoids are scarce or not known.

These constraints suggest to the fact that these crustal segments do not have the same lithospheric mantle, pointing that they constitute different terranes in the TZD.

CONCLUSIONS

The available isotopic data of the enclaves for the Brejinho batholith don't allow unequivocal conclusions concerning the type of mantle envolved. It can be concluded that the source of the enclaves was the lithospheric mantle and they do not constitute residues of partial melt related to generation of felsic magmas, considered that the magma progenitor represents the magmatic end-member, juvenile, extracted from the mantle during the Brasiliano/Pan african event.

On the contrary to the enriched characteristics of the mantle considered as source of most enclaves of other high-K calc-alkaline associations of BP, the isotopic and geochemical data of the underlying mantle to APT, implies in considering this and other crustal segment of the TZD, as amalgamates terrains, testifying favorably to the model of Santos (1996), at least in this domain.

ACKNOWLEDGMENTS

We are grateful to Ignez P. Guimarães and A. F. da Silva Filho, for utilization of isotopic data, to Márcio M. Pimentel for the discussion about the isotopic constraints of the Brejinho batholith and to constructive criticism by an anonymous reviewer.

REFERENCES

Baker, D. R., 1989. Tracer versus trace element diffusion : diffusional decoupling of Sr concentration from Sr isotopic composition. Geoch. Cosmoch. Acta 53: 3015-3023.

Fourcade, S. & Javoy, M., 1992. Sr-Nd-O isotopic feature of mafic microgranular enclaves and host granitoids from the Pyrinees, France: Evidence for their hybrid nature and inference on their origin. . In : J. Didier and B. Barbarin (Editors), Enclaves and Granites Petrology. Developments in Petrology 13, Elsevier, Amsterdam. p. 345-366.

Guimarães, I. P. & Da Silva Filho, A. F., 2000. Evidence of multiple source involved in the genesis of the neoproterozoic Itapetim granitcs complex, NE, Brazil, based on geochemical and isotopic data. J. South Amer. Earth Science . 13: 561-586.

Lesher, C. E., 1990. Decoupling of chemical and isotopic exchange during magma mixing. Nature, 344 : 235-237.

Mariano, G., Neves, S. P., Guimarães, I. P. & Da Silva Filho, A. F., 2000. High-K calc-alkaline diorites of the Borborema Province, northeastern Brazil: geochemistry of the lithospheric mantle and implications for the terrane concept. In: SBG, XVIII Simp. Geolog. do NE, Recife, Resumos, Bol.16, p.99.

Patiño Douce, A. E., 1995. Experimental generation of hybrid silicic melts by reaction of high-Al basalt with metamorphic rocks. J. of Geoph. Res. 100 (8B) : 15623-15639.

Pin, C. & Duthou, J. L., 1990. Sources of Hercynian granitoids from the French Massif Central: Inferences from Nd isotopes and consequences for crustal evolution. Chemical Geol. 83 : 281-296

Pin, C., 1992. Sr-Nd isotopic study of igneous and metasedimentary enclaves in some Hercynian granitoids from the Massif Central, France. In : J. Didier and B. Barbarin (Editors), Enclaves and Granites Petrology. Developments in Petrology 13, Elsevier, Amsterdam. p. 333-343.

Santos, E. J., 1996. Ensaio preliminar sobre terrenos e tectônica acrescionária na Província Borborema. In: SBG, XXIX Congr. Brasil.Geolog., Salvador, Anais, 6 : 47-50.

Torres, H. H. F. 2001. Petrologia e geoquímica do batólito calcioalcalino de alto-K de Brejinho, Zona Transversal, Província Borborema, NE doBrasil. Centro de Tecnologia e Geociências, Universidade Federal de Pernambuco. PhD thesis. 185p.

GEOCHEMICAL AND Sr, Nd, AND Pb ISOTOPE SIGNATURES OF PHONOLITES AND NEPHELINE SYENITES FROM THE POÇOS DE CALDAS ALKALINE MASSIF, SOUTHEASTERN BRAZIL

Ulbrich, H.G.J.[1]; Demaiffe, D.[2]; Vlach, S.R.F.[1] and Ulbrich, M.N.C.[1]

1. Instituto de Geociências, Universidade de São Paulo, São Paulo-SP, Brazil. hulbrich@usp.br
2. Laboratoire de Geochimie Isotopique, Université Libre de Bruselles, Belgium. ddemaif@ulb.ac.be

Keywords: Sr, Nd, and Pb isotope signatures, geochemistry, phonolites and nepheline syenites, Poços de Caldas

INTRODUCTION

The large Poços de Caldas alkaline massif (PC) crops out as a subcircular structure over 800 km^2 in the states of Minas Gerais and São Paulo, southeastern Brazil (Ellert, 1959; Ulbrich & Ulbrich, 1992). The main rock types are phonolites and nepheline syenites, emplaced mainly at about 79-80 Ma ago (Ulbrich et al., 2002). It is the site of U, Th, and Zr mineralization, a corollary of widespread hydrothermal alteration that lasted to around 76 Ma (Shea, 1992).

Some Sr and Nd isotopic data for regional phonolites and nepheline syenites within the massif were already presented by Shea (1992).

We report here new Rb-Sr and Sm-Nd data as well as the first Pb-Pb data for several selected samples of phonolites and nepheline syenites and draw some preliminary petrological inferences from the results.

GEOLOGY AND PETROGRAPHY

The Poços de Caldas massif is mainly constituted by subvolcanic phonolites (tinguaites), nepheline syenites (NeS), and mostly altered volcanic phonolites, in part enclosing the overlying eolian Botucatu sandstones and some Serra Geral diabases (Ellert et al., 1959; Ulbrich & Ulbrich, 1992). Related mafic and ultramafic rocks with pyroxene, analcime and olivine as the main minerals, are seen as fragments of lava flows, agglomerates, lapilli, and tuffs, within its western border, at the Vale do Quartel (VQ).

Other minor ultramafic occurrences appear in the Osamu Utsumi open pit (mainly lamprophyres), within the district, and intruding metamorphic country rocks, close to the massif's northeastern limit (lamprophyres and associated silico-carbonatitic rocks at the Minas Pedras quarry, MP).

The NeS are mineralogically monotonous, with more K-feldspar than nepheline and lesser proportions of Na-pyroxenes, together with an assorted number of accessory rare silicates, some of which present as rock-forming minerals (*e.g.*, eudyalite in lujavrites and khibinites), constantly accompanied by late and post-magmatic phases (late aegirine, cancrinite, natrolite, fluorite, and rare minerals), a clear indication of the activity of late fluids rich in F, Fe, Na, CO_2, and rare metals. These rocks are in most cases clearly intrusive into tinguaites, appearing as discrete bodies, each characterized by a dominant petrographic facies, defined by structure, texture, and mineralogy.

The accessory mineralogy, eudialyte in particular, can be used in the field to separate agpaitic NeS (with agpaitic index over 1.1 and larger amounts of Zr, REE, Ti, U, Th, *etc.*) from intermediate and miaskitic varieties (*cf.* Ulbrich & Ulbrich, 1992).

The largest body of NeS is the Pedreira intermediate-miaskitic type, with an outcrop surface over 80 km^2, while other types are present as much smaller bodies.

GEOCHEMICAL BACKGROUND

All the NeS present rather similar whole rock chemistry for most major and minor components (own data), with the following mean values (wt. %): SiO_2: 53.55, Al_2O_3: 19.58, TiO_2: 0.52, MnO: 0.30, MgO: 0.22, CaO: 1.63, Na_2O: 7.74, K_2O: 8.31, and P_2O_5: 0.05. The larger variations are seen for K_2O and Na_2O, which are negatively correlated, and to a greater extent for $Fe_2O_3^T$ varying from 3-5 wt. % in most rocks to up to 11.2 wt. % in the mesocratic lujaurites. Usually the molar ratio Na_2O/K_2O is over 1; the agpaitic indices range from 0.98 to as high as 1.33.

The trace element contents (own data), on the other hand, present a wide range, especially within the agpaitic types, as shown (in ppm): Ba 16 to 1200, Rb 92-614, Sr 410-6360, Ta ~2-273, Nb 127-1000, Hf 7.7-82.40, Zr 383-4450, Y 8-125, Th 18.70-124, U 2.78-30.60, V 30-286, Pb 0-77, Zn 101-514, La 75.60-1080, Ce 81-1450, Yb 0.93-13.40, Lu 0.12-2.00. Ni, Co, Cu, and Cr are below detection limits. This is a common feature of most large massifs with significant amounts of agpaitic rocks (*e.g.*, Khibina and Lovozero; *cf.* Kramm & Kogarko, 1994).

The tinguaites show a similar spread of values for major, minor and trace element contents, with less enrichment. Chemical data of tinguaites plot closely to those of less differentiated NeS, while more agpaitic NeS show very high abundances in trace elements, possibly indicating a post-magmatic enrichment related to fluid activity.

Chondrite-normalized REE diagrams for NeS and tinguaites show a distinct concave pattern, significantly enriched in LREE, with no Eu anomaly, La/Yb ratios varying from about 50 to up to 100.

ISOTOPE Sr-Nd-Pb DATA

Isotopic Sr-Nd-Pb data were obtained for 18 assorted Poços de Caldas rocks (10 NeS and 8 tinguaites) representatives of the main petrographic facies within the massif.

The new Sr, Nd, and Pb isotopic analyses were made at the Laboratoire de Geochimie Isotopique of the Université Libre de Bruxelles. Errors are quoted at the 95% confidence level. Previous Sr-Nd data presented for the mafic-ultramaphic samples from VQ (Thompson et al., 1998) and MP (Vlach et al., 1998) are also considered for comparison purposes. All presented initial ratios were computed for a 80 Ma reference age.

^{87}Rb/^{86}Sr and ^{87}Sr/^{87}Sr measured values plot close to a 80 Ma reference line with an initial (^{87}Sr/^{87}Sr)$_{80}$ ratio about 0.70515 (Figure 1). The data do not fit a real isochron due to inherited ^{87}Sr/^{86}Sr contrasts in the magmas, or late to post-magmatic isotopic reequilibration, or both. (^{87}Sr/^{87}Sr)$_{80}$ values range from 0.70475 to 0.70552 and there is no significant difference among NeS and tinguaites.

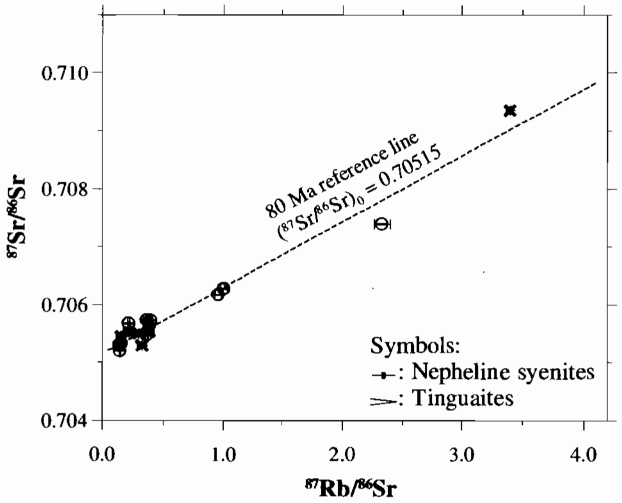

Figure 1. ^{87}Sr/^{87}Sr vs ^{87}Rb/^{86}Sr diagram for the Poços de Caldas NeS and tinguaites. Error bars at 2σ.

The (^{143}Nd/^{144}Nd)$_{80}$ ratios show a significant range from 0.51233 to 0.51239; three NeS stand out as the more evolved rocks (Fig. 2). The VQ and MP ultramafic rocks are clearly more primitive than the NeS and tinguaites as shown by the respective initial ratio. With the exception of one VQ sample, the ultramafic rocks present also higher Sm/Nd ratios, reflecting its less fractionated REE pattern. Depleted mantle model ages (DePaolo, 1981) of the felsic rocks vary within 650-750 Ma and give an almost normal distribution with a mean of 692 ± 54 Ma (2σ), while VQ and MP samples range between 630-810 and 580-640 Ma, respectively (Fig. 3).

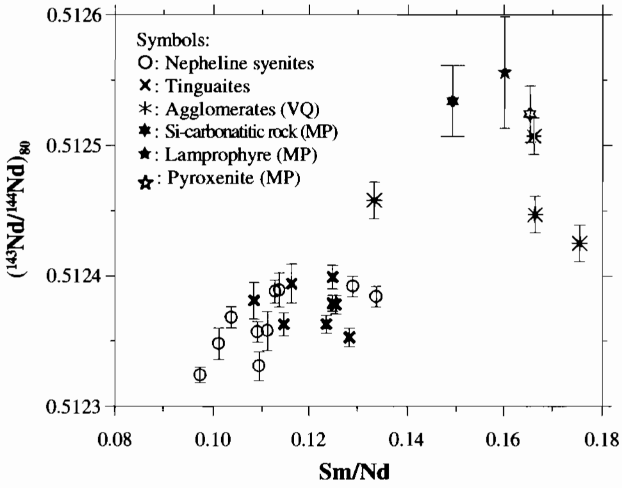

Figure 2. (^{143}Nd/^{144}Nd)$_{80}$ vs Sm/Nd plot for the Poços de Caldas NeS, tinguaites and associated VQ and MP ultramafic rocks. Error bars at 2σ.

The correlation among (^{87}Sr/^{87}Sr)$_{80}$ and (^{143}Nd/^{144}Nd)$_{80}$ ratios is depicted in Figure 4. The felsic PC rocks plot to the right of and below the Bulk Earth (BSE) value (at 80 Ma); they have similar Sr but more primitive Nd isotopic characteristics than the EMI reference reservoir, and plot at the lower limit of the OIB field (*cf.* Zindler & Hart, 1986). The Sr isotope variations in the ultramafic rocks cover the same range as the felsic samples, with the exception of the silico-carbonatitic rock from MP and one of the agglomerates from VQ. Sr and Nd isotope data for the Lovozero and Khibina massifs, emplaced at about 370 Ma in the Kola Alkaline Province (Kramm & Kogarko, 1994), are also represented for comparative purposes, showing that PC rocks have similar Nd, but greatly evolved Sr isotopic characteristics; the PC rocks plot to the right of, and Lovozero and Khibina to the left of the BSE (at their crystallization ages).

The (^{206}Pb/^{204}Pb)$_{80}$, (^{207}Pb/^{204}Pb)$_{80}$, and (^{208}Pb/^{204}Pb)$_{80}$ isotopic ratios of the NeS and tinguaite rocks are similar and range between 17.9-18.3, 15.43-15.48, and 38.10-38.55, respectively. With the exception of two NeS and one tinguaite samples, (^{208}Pb/^{204}Pb)$_{80}$ and (^{207}Pb/^{204}Pb)$_{80}$ have a good positive correlation with (^{206}Pb/^{204}Pb)$_{80}$. In the (^{207}Pb/^{204}Pb)$_{80}$ vs (^{206}Pb/^{204}Pb)$_{80}$ diagram (Fig. 5) the data array plots close to the NHRL (Northern Hemisphere Reference Line, *e.g.*, Zindler & Hart, 1986) and define a *ca.* 2.2 Ga reference line, which probably represents some kind of a mixing array. The cited tinguaite and one of the NeS plot close to the Geochron In Figure 6, a plot of (^{87}Sr/^{87}Sr)$_{80}$ against (^{206}Pb/^{204}Pb)$_{80}$, the data cluster relatively close to the EMI reference reservoir.

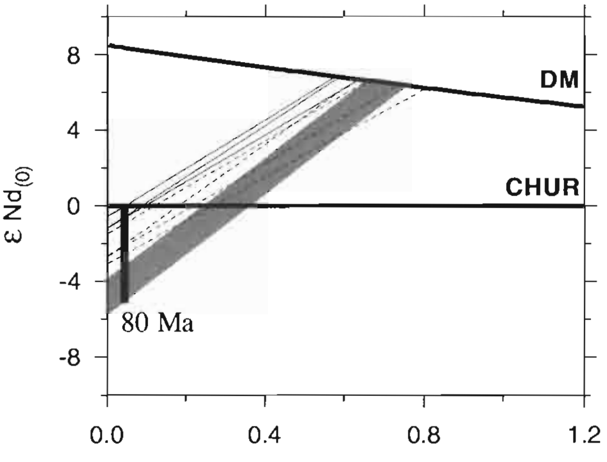

Figure 3. Isotope evolution of ε_{Nd} against time for NeS and tinguaites (dark area), VQ (dashed lines) and MP (solid lines) rocks from the Poços de Caldas Massif.

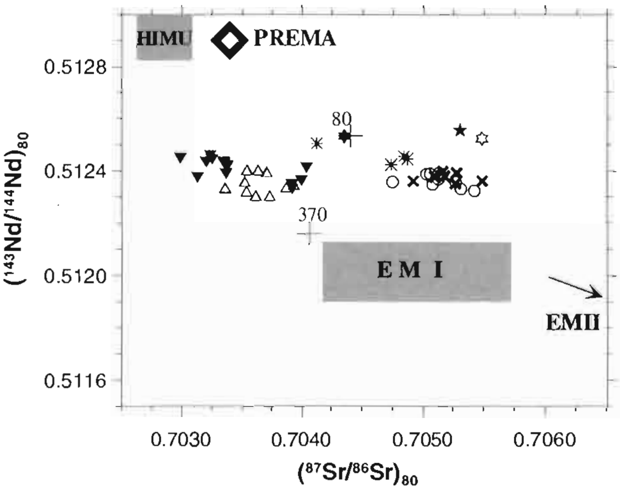

Figure 4. Sr-Nd isotope correlation diagram for the Poços de Caldas felsic and ultramafic rocks, showing also the present day compositions of typical mantle reservoirs. Symbols as for Figure 2. Inverted filled triangles: Khibina; normal triangles: Lovozero. Crosses are Bulk Earth compositions for the indicated ages.

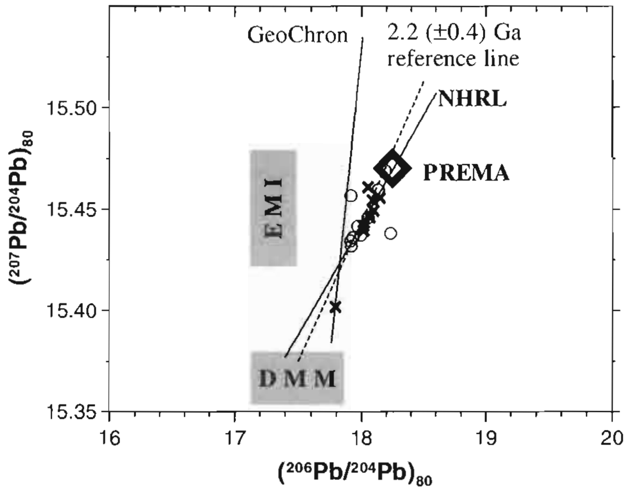

Figure 5. $(^{207}Pb/^{204}Pb)_{80}$ vs $(^{206}Pb/^{204}Pb)_{80}$ diagram showing the distribution of the NeS and tinguaites from Poços de Caldas and the present day compositions of some mantle reservoirs. Symbols as for Figure 2.

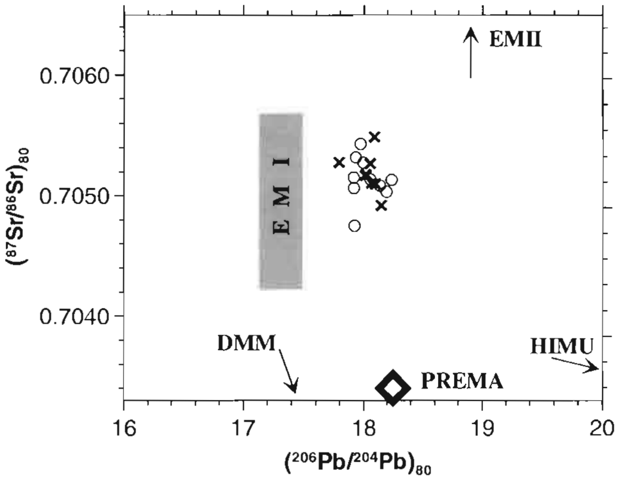

Figure 6. $(^{87}Sr/^{87}Sr)_{80}$ vs $(^{206}Pb/^{204}Pb)_{80}$ diagram showing the distribution of the Poços de Caldas NeS and tinguaites. Symbols and reservoirs as in previous figures.

PRELIMINARY DISCUSSION

The original NeS-phonolite magmas are clearly representative of end-member liquids collected in the undersaturated "low temperature valley" of the residual nepheline-kalsilite-quartz phase diagram, the data clustering around the minimum temperatures for a H_2O pressure of about 1 kbar. The absence of compatible elements (Cu, Ni, Cr and Co below d.l.) and the very low contents of MgO in almost all NeS and tinguaites strongly suggest extreme differentiation. The REE patterns are compatible with removal of clinopyroxene, titanite and/or apatite.

Three main hypotheses may account for the observed geochemical patterns: (1), a "wehrlitic" fractionation scheme trough the removal of clinopyroxene and Mg-olivine from parental ultrabasic nephelinite-like magmas; (2), low degree of partial melting of a similar alkaline ultrabasic protolith; and (3), low degree of fractional melting of an enriched mantle source followed by melt collection and homogeneization during ascent (*e.g.*, Kramm & Kogarko, 1994; Draper & Green, 1997). This latter possibility is less likely, on account of the absence of those incompatible elements and the low MgO values.

Our Sr-Nd isotope data, as well as those presented by Shea (1992) indicate contrasted sources for the VQ, MP, and the felsic rocks; the MP rocks are the most primitive in terms of the Nd isotopes. The data for NeS and tinguaites depict also some significant variations, considered at least in part as inherited features, each body of NeS and tinguaite presenting similar but proper isotope characteristics, in agreement with the petrographic and geochemical evidence (*e.g.*, Ulbrich and Ulbrich, 1992). Other variations could be acquired later during magma evolution and some of them may be related to localized felsic-ultramafic magma mixing phenomena. It is worth noting that most miaskitic NeS (the Pedreira syenites) and also some of the tinguaites contain augitic-bearing ultramafic enclaves and/or augite xenocrysts.

The isotope initial compositions of the felsic rocks do not support simple mixing relations between two or more of the typical mantle reference reservoirs in order to constrain the isotope compositions of their sources. A simple DMM-PREMA mixing relation, as suggested by the initial Pb composition variations in Figure 5, does not agree well with the observed Sr-Nd and Pb-Sr isotope initial ratios.

The enrichment in alcalies and trace elements in the NeS and tinguaites indicates that the magma generation event must have collected these elements from very large masses of mantle rocks, probably trough a preceding metasomatic episode, creating an enriched mantle source for later melting (*e.g.*, Kramm and Kogarko, 1994).

In any case, it appears that the main NeS and tinguaite bodies crystallized from discrete magma batches rather than being derived by crystal fractionation from the same parental magma.

REFERENCES

Draper D.S. and Green T.H., 1997. P-T phase relations of silicic, alkaline, aluminous mantle-xenolith glasses under anhydrous and C-O-H fluid-saturated conditions. Journal of Petrology, 38: 1187-1224.

DePaolo, D. J., 1981. Neodymium isotopes in the Colorado Front Range and crust-mantle evolution in the Proterozoic. Nature, 291:193-196.

Ellert R., 1959. Contribuição à geologia do maciço alcalino de Poços de Caldas. Boletim da Faculdade de Filosofia Ciências Letras, Universidade de São Paulo, 237, Geologia 18: 5-63.

Kramm, U. and Kogarko, L.N.,1994. Nd and Sr isotope signatures of the Khibina and Lovozero agpaitic centres, Kola Alkaline Province, Russia. Lithos, 32:225-242.

Shea, M.E., 1992. Isotopic geochemical characteristics of selected nepheline syenites and phonolites from the Poços de Caldas alkaline complex, Minas Gerais, Brazil. Journal of Geochemical Exploration, 54:173-214.

Thompson R.N., Gibson S.A., Mitchell J.G., Dickin A.P., Leonardos O., Brod A.J. and Greenwood J.C., 1998. Migrating Cretaceous-Eocene magmatism in the Serra do Mar alkaline province, SE Brazil: melts from the deflected Trindade mantle plume? Journal of Petrology, 39:1493-1526.

Ulbrich H.H.G.J. and Ulbrich M.N.C., 1992. O maciço alcalino de Poços de Caldas, MG-SP: características petrográficas e estruturais. XXXVII Congresso Brasileiro Geologia, São Paulo, SBG, Roteiro de Excursões, 1-64.

Ulbrich, H.H.G.J.; Vlach., S.R.F.; Ulbrich, M.N.C. and Kawashita, K., 2002. Penecontemporaneous syenitic-phonolitic and basic-ultrabasic-carbonatitic rocks at the Poços de Caldas alkaline massif, SE Brazil: geological and geochronological evidence. Revista Brasileira de Geociências, 32: 15-26.

Vlach, S.R.F.; Ulbrich, M.N.C. and Ulbrich, H.H.G. ,1998. Isótopos radiogênicos (Sr, Nd) e estáveis (C,O) de rochas máfico-ultramáficas potássicas da região de Poços de Caldas (MG-SP): inferências sobre a natureza do manto litosférico mesozóico. Anais do XL Congresso Brasileiro de Geologia, Belo Horizonte, SBG. p. 475.

Zindler A. and Hart S., 1986, Chemical Geodynamics. Annual Review Earth Planetary Sciences, 14: 493-571.

PHLOGOPITE FROM CARBONATITIC VEINS ASSOCIATED WITH THE POÇOS DE CALDAS ALKALINE MASSIF, SE BRAZIL: MINERALOGY AND $^{40}Ar/^{39}Ar$ DATING BY THE LASER STEP HEATING METHOD

Vlach, S.R.F.[1]; Vilalva, F.C.J.[1]; Ulbrich, M.N.C.[1]; Ulbrich, H.H.G.J.[1] and Vasconcelos, P.M.[2]

1. Instituto de Geociências, Universidade de São Paulo, São Paulo-SP, Brazil. srfvlach@usp.br
2. Department of Earth Science, University of Queensland, Brisbane, Australia. paulo@earth.uq.edu.au

Keywords: Phlogopite, mineralogy, $^{40}Ar/^{39}Ar$ dating, ultramafic rocks, Poços de Caldas

INTRODUCTION

A large number of geochronological data (mainly K-Ar and Rb-Sr) are known for the alkaline rocks of the Poços de Caldas alkaline massif, states of São Paulo and Minas Gerais (*e.g.*, Thompson et al., 1998; Ulbrich et al., 2002), mostly from older publications. In part, the data are incompatible with geological relationships or their precision is very low, and no consensus has been reached about the best age and age interval for the emplacement of the main felsic alkaline and related ultramafic magmatic events in that district. High precision and well-constrained age determinations are needed to solve the problem.

Ultramafic rocks closely related to the main felsic Poços de Caldas magmatism crop out near the northern contact of the massif, intruding Neoproterozoic basement rocks. They comprise ultramafic lamprophyric types and silico-carbonatitic rocks with associated late carbonatitic veins.

We present in this report mineralogical data and incremental laser step-heating $^{39}Ar/^{40}Ar$ ages for a phlogopite of one of those late hydrothermal veins. The results suggest a minimum age of about 84 Ma for the phlogopite crystallization and vein formation. Possible meanings of this result are addressed in the light of the existing geological and geochronological data for the alkaline and related rocks within the Poços de Caldas massif.

GENERAL GEOLOGY AND PETROGRAPHY

The ultramafic rocks appeared in the April, 1996, mining front, as a number of sub-vertical to steeply dipping dikes up to 2m wide and a somewhat larger breccia zone (up to 15–20m), in the Minas Pedras quarry (UTM coordinates: 7592573N 331954E). They cross cut highly deformed and partially migmatitic Neoproterozoic quartz-mangerites and are closely associated with larger phonolitic dikes doubtlessly related to the Poços de Caldas felsic magmatism.

The main lithotypes are an aphanitic silico-carbonatitic rock (up to 40 % vol. carbonate), massive or with flow structure, a massive fine grained phlogopite-rich rock with abundant carbonate ocelli and pseudomorphosed macrocrysts after olivine and/or pyroxene (now phlogopite-pyroxene-amphibole-ilmenite aggregates), and a laminated medium-grained facies with alternating phlogopite-rich and carbonate-rich layers. The breccia facies contains fragments of the country rocks and silico-carbonatitic, phlogopite-rich material in variable amounts. Preliminary petrographic, chemical, and isotopic characterizations of these rocks were presented by Vlach et al. (1996, 1998) and Ulbrich et al. (1998).

The massive varieties may be somewhat younger than the phonolites, as they contain cm-sized, partially fenitized, enclaves of the latter, but these features could also be due to the very contrasting viscosities of such magmas and their emplacement could be roughly coeval.

Several late, hydrothermal, carbonatitic veins (5-20 cm wide) cut all these rocks. Some of them are made up of almost pure calcite, others contain calcite + fluorite, calcite + phlogopite + fluorite, calcite + phlogopite + magnetite + apatite, calcite + phlogopite + fluorite ± albite. Occasionally they present thorite, REE-fluorcarbonates, and other rare accessory minerals.

ANALYTICAL METHODS

Clean euhedral phlogopite crystals (*ca.* 1-2 mm diameter on basal sections) from a selected calcite + phlogopite + fluorite vein were carefully handpicked under a stereomicroscope for X-ray diffratometry (XRD), electron microprobe (EPMA), and isotopic studies at the laboratories of the Instituto de Geociências of University of São Paulo.

A XRD powder pattern was obtained in the 5-65° 2θ interval for the $CuK\alpha$ radiation; pure quartz was added as an internal standard. About 40 reflections were chosen for cell refinement with the LCLSQ software (Burnham, 1962). The EPMA work included electron back-scattered imaging (BSE) and chemical quantitative spot analysis (WDS). The analytical conditions were 15 keV, 20 nA and 1 (BSE) or 5 (WDS) μm for the beam accelerating voltage, current, and diameter, respectively. Minerals and synthetic compounds were used as chemical standards. Matrix effects in quantitative analysis were corrected with a PROZA procedure.

$^{40}Ar/^{39}Ar$ dating analyses by the laser step heating method were made at the Centro de Pesquisas Geocronológicas on three phlogopite grains, previously washed with pure alcohol. Analytical procedures and data treatment are described in Vasconcelos et al. (2002).

MINERAL DATA

In petrographic thin sections, the phlogopite crystals from the studied carbonatitic vein are very clean. They do not present any kind of alteration or inclusions, and show a weak pleochroic scheme in pale yellow (α) to orange (β ≈ γ). They present a distinct zoning pattern, with euhedral cores surrounded by also euhedral discrete rims with somewhat less intense pleochroic colours.

The computed cell parameters, in Angstroms, for the studied phlogopite are $a_0 = 5.3489$ (1), $b_0 = 9.2560$ (3), $c_0 = 20.2460$ (7), β angle 94.730° (1), with a cell volume = 998.96 (1) $Å^3$. These results are compatible with a $2M_1$ structural polytype.

BSE imaging of phlogopite grains shows that the crystal rims have low back-scaterred coefficients and that both cores and rims present a very weak recurrent compositional zoning. Representative WDS analytical data for core and rims appear in Table 1.

Table 1. Representative chemical phlogopite analyses (WDS). c = core, r = rim, bd = below detection limit.

Spot	4, c	2, r		4, c	2, r
Oxides			***Cations***		
SiO_2	42.63	43.75	Si	6.356	6.463
TiO_2	1.55	1.10	Ti	0.174	0.123
Al_2O_3	9.10	8.80	Al	1.596	1.531
Cr_2O_3	bd	bd	Fe^{II}	1.372	1.088
FeO	10.92	8.81	Cr	0.000	0.000
MnO	1.58	1.43	Mn	0.199	0.178
MgO	18.01	19.30	Mg	4.000	4.250
NiO	0.04	bd	Ni	0.000	0.000
ZnO	0.10	0.10	Zn	0.010	0.010
CaO	bd	bd	Ca	0.000	0.000
BaO	0.04	0.06	Ba	0.002	0.004
Na_2O	0.35	0.34	Na	0.101	0.098
K_2O	9.94	10.08	K	1.889	1.900
F	4.78	4.86			
Cl	bd	bd	Sum	15.669	15.635
(O=F)	2.01	2.05			
Sum	96.89	96.49	mg#	74.46	79.62

The phlogopite from the carbonatitic vein has more than 6 Si c.p.f.u. and low Al contents. All Al cations are in tetrahedral sites. Ti and Ba contents are relatively low, F contents and mg# numbers are in the range 4.4 – 5.1 wt. % and 74.4 (core) and 79.7 (rims), respectively.

The compositional variations depict a slightly inverse and recurrent zoning pattern in the studied crystal, and its core is somewhat richer in Ti, Al, Fe, and Mn and poorer in Mg, Ba, and F than the rims. The main chemical variations within core, intermediate zones and rims are illustrated in Figures 1A, B, and C) for that single crystal. In general, Al_2O_3 shows a negative correlation with mg# in all those zones, a positive one with FeO^T and TiO_2 in the core and intermediate zones and a slightly negative one in crystal rims.

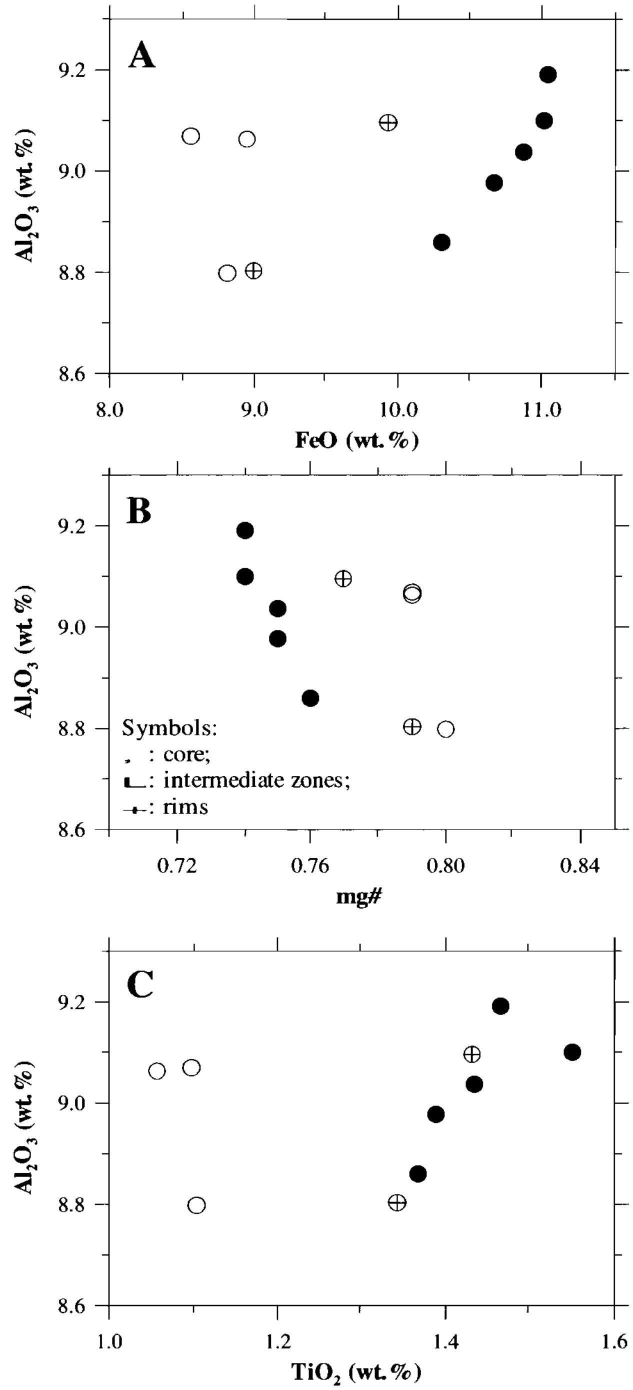

Figure 1 (A,B,C). Variation diagrams showing the main chemical trends for a single phlogopite crystal. mg# = $Mg/(Mg+Fe^{II})$, cation ratio.

$^{40}Ar/^{39}Ar$ DATING RESULTS

The dating results for the three analysed phlogopite grains are presented in Table 2. All crystals gave well-defined plateau and also integrated ages. Apparent ages for grains 1 and 2 are very concordant, in the 83.7 – 84.3 Ma range, while grain 3 yields a somewhat younger but close result, about 83.1 – 83.5 Ma.

Table 2. $^{39}Ar/^{40}Ar$ dating results for vein phlogopite.

Grain	Plateau age (Ma)	Dev. ±2σ	Step N	Integrated age (Ma)	Dev. ±2σ
1	83.8	0.2	4	84.1	0.1
	84.0	0.2	3		
2	84.3	0.2	5	84.3	0.1
3	83.5	0.2	2	83.1	0.1

The step heating ^{39}Ar release pattern from the grain 1 phlogopite, presenting two close and good plateau ages, is reproduced in Figure 2.

A summary including all data is presented in the ideogram displayed in Figure 3, which depicts a somewhat higher probability age peak at about 84.3 Ma and a minor one at 83.5 Ma. A value of 83.9 ± 0.3 (2σ), the weighted average of all measurements, is considered here as the best estimate for the age of the Ar isotopic system closure within the studied phlogopite.

DISCUSSION

Our results put some additional constraints on the geochronology of the Poços de Caldas alkaline massif and associated rocks, and also pinpoint the need for more geologically constrained geochronological work to elucidate the main age patterns within the massif.

In a recent review based on geological, paleomagnetic data, and all published ages for the Poços the Caldas rocks, Ulbrich et al. (2002) suggest a value of about 79 Ma as the best mean age for the emplacement of the main nepheline syenites and phonolites in the district. The authors suggest also a short time interval of about 1-2 Ma for the whole felsic magmatism.

Previous dating of Poços de Caldas ultramafic rocks comprise two older K-Ar results for from *ankaratrites* (*ca.* 89 and 78 Ma, whole rock, *cf.* Amaral et al., 1967) and two $^{40}Ar/^{39}Ar$ ages (75.7 ± 0.3 and 76.2 ± 0.8 Ma) for phlogopite from a fresh lamprophyric dike cutting across hydrothermally altered nepheline syenites and phonolites, the so-called "potassic rocks", in the Osamu Utsumi open pit uranium mine (Shea, 1992). A Rb-Sr isochron presented by Shea for these felsic hydrothermalized rocks gave a similar value of 76 (±1) Ma. Ulbrich et al. (2002) report also an age of 79 (±3) Ma obtained for thorite grains from another carbonatitic vein of the Minas Pedras quarry, with the Th-U-total Pb dating method by the electron microprobe.

The contrasting results obtained for the ultramafic rocks from Osamu Utsumi and Minas Pedras need some additional discussion, since there is no clear geological argument indicating one or more ultramafic rock emplacement events in the massif. There is always the possibility that one of the $^{40}Ar/^{39}Ar$ ages, or both, reflect either Ar excess or loss in the phlogopite system, although the ^{39}Ar release patterns in our data, or in those presented by Shea (1992), do not suggest significant disturbance. This question can only be correctly addressed with independent new high-precision age determinations.

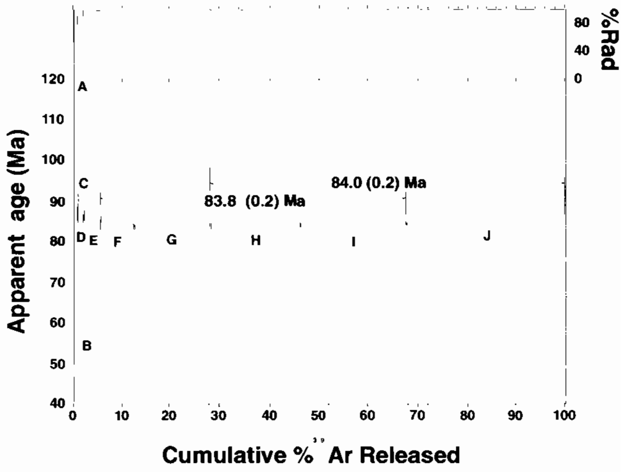

Figure 2. Step heating incremental ^{39}Ar release pattern plotted against apparent ages for the vein phlogopite (grain 1).

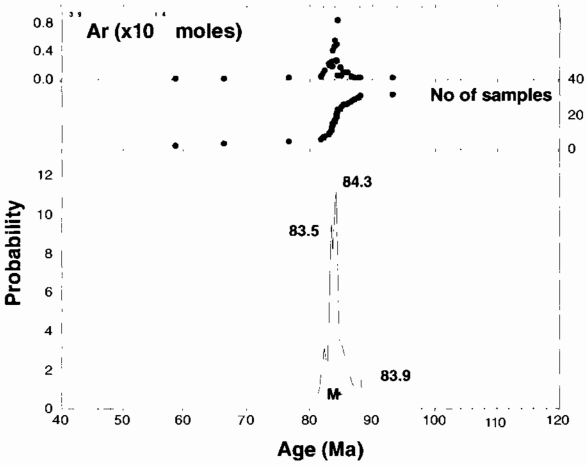

Figure 3. Ideogram showing the apparent age distributions against probability for vein phlogopite (grains 1, 2, and 3). M is the weighted average.

With these remarks in mind, the following conclusions can be reached with the data at hand:

1. Both dating results may be very close to the real phlogopite crystallization age and, therefore, of the age of vein and dike formation. In the Minas Pedras case, the phlogopite crystallized under a low-temperature hydrothermal environment, possibly not much higher than *ca.* 300-350° C, the closure temperature for the $^{40}Ar/^{39}Ar$ system and so the apparent ages should be very close to the real crystallization ages. The phlogopite in the Osamu Utsumi dike formed at a high magmatic temperature, and the measured ages will approach real ages only if the cooling down to *ca.* 300° C was fast. If this were the case, then at least two main episodes of carbonatitic-related ultramafic magmatism did occur.

The geological evidence at the Minas Pedras quarry suggests that at least some of the ultramafic rocks crystallized at the same time as the felsic phonolitic dikes. Similarly, the phlogopite-bearing rock in the Osamu Utsumi pit dated by Shea (1992) is at least coeval with the main hydrothermal event that followed the emplacement of the nepheline syenites and phonolites. If these figures are meaningful, then the Minas Pedras and Osamu Utsumi $^{40}Ar/^{39}Ar$ ages could date the beginning and the end of the magmatism in the district, in a minimum interval of about 8 Ma.

A mean age around 80 Ma for the felsic magmatism peak (Ulbrich et al., 2002), constrained by paleomagnetic data, which was considered also as a minimum reference age by Thompson et al. (1998) for the whole massif, is in this context still a good reference value, until high-precision ages will be available.

2. Despite its fresh aspect, another possibility is that the the ultramafic dike from the Osamu Utsumi open pit may have been subjected to late resetting at around 76 Ma, as hydrothermal alteration is widespread in the internal parts of the Poços de Caldas Massif. In this case, considering whole rock the Rb/Sr data, a minimum interval for the whole magmatism of about 5 Ma would fit better the available geocrhonological data.

ACKNOWLEDGEMENTS

We thank Fundação da Amparo à Pesquisa do Estado de São Paulo for continuous microprobe laboratory support, Flávio Carvalho and Artur T. Onoe for analytical support with XRD and $^{40}Ar/^{39}Ar$ facilities. FCJV thanks Conselho Nacional de Pesquisa for an undergraduate studentship.

REFERENCES

Amaral, G.; Bushee, J.; Cordani, U.G.; Kawashita, K. and Reynolds, J.H., 1967. Potassium-argon ages of alkaline rocks from southern Brazil. Geochimica et Cosmochimica Acta, 31:117-142.

Burnham, C.W., 1962. Lattice constants refinement. Carnegie Institute of Washington Yearbook, 61:132-135.

Shea, M.E., 1992. Isotopic geochemical characteristics of selected nepheline syenites and phonolites from the Poços de Caldas alkaline complex, Minas Gerais, Brazil. Journal of Geochemical Exploration, 54:173-214.

Thompson, R.N.; Gibson, S.A.; Mitchell, J.G.; Dickin, A.P.; Leonardos, O.H.; Brod, J.A. and Greenwod, J.C., 1998. Migrating Cretaceous-Eocene magmatism in the Serra do Mar alkaline province, SE Brazil: melts from the deflected Trindade mantle plume? Journal of Petrology, 39:1493-1526.

Ulbrich, H.H.G.J.; Vlach., S.R.F.; Ulbrich, M.N.C. and Kawashita, K., 2002. Penecontemporaneous syenitic-phonolitic and basic-ultrabasic-carbonatitic rocks at the Poços de Caldas alkaline massif, SE Brazil: geological and geochronological evidence. Revista Brasileira de Geociências, 32: 15-26.

Ulbrich, M.N.C.; Vlach., S.R.F. and Ulbrich, H.H.G.J., 1998. Geoquímica dos diques de rochas máfico-ultramáficas potássicas periféricos ao Maciço de Poços de Caldas (MG-SP). Anais do XL Congresso Brasileiro de Geologia, Belo Horizonte, SBG. p. 469.

Vasconcelos, P.M.; Onoe, A.T.; Kawashita, K; Soares, A.J. and Teixeira, W., 2002. $^{40}Ar/^{39}Ar$ geochronology at the Instituto de Geociências, USP: instrumentation, analytical procedures, and calibration. Anais da Academia Brasileira de Ciências, 74:297-342.

Vlach, S.R.F.; Ulbrich, M.N.C.; Ulbrich, H.H.G.J. and Gualda, G.A.R., 1996. Rochas de afinidades alnoíticas e sílico-carbonatíticas periféricas ao Maciço Alcalino Poços de Caldas (MG-SP). Anais do XXXIX Congresso Brasileiro de Geologia, Salvador. SBG. 2:128-130.

Vlach, S.R.F.; Ulbrich, M.N.C. and Ulbrich, H.H.G., 1998. Isótopos radiogênicos (Sr, Nd) e estáveis (C,O) de rochas máfico-ultramáficas potássicas da região de Poços de Caldas (MG-SP): inferências sobre a natureza do manto litosférico mesozóico. Anais do XL Congresso Brasileiro de Geologia, Belo Horizonte. SBG. p. 475.

U-Pb (ZIRCON) AGES OF METABASIC ROCKS OF THE ÁGUA CLARA FORMATION IN THE ARAÇAIBA REGION – SÃO PAULO (BRAZIL): PRELIMINARY DATA

Weber, W.[1]; Siga Jr., O.[1]; Sato, K.[1]; Basei, M.A.S.[1] and Reis Neto, J.M.[2]

1. CNPQ Scholarship - Instituto de Geociências, Universidade de São Paulo, Programa Geoquímica e Geotectônica, Rua do Lago 562, São Paulo-SP, Brasil, 05508-080. wweber@usp.br
2. Universidade Federal do Paraná – DEGEO – UFPR. jmreis@setuva.ufpr.br

Keywords: Metabasic rocks, Água Clara Formation, U-Pb ages

INTRODUCTION

The bibliography related to the Precambrian units of eastern Paraná and southeastern São Paulo states is extensive, and encompasses more than a hundred published papers and reports. The resulting scenario is confusing and fragmented, characterized by an immense proliferation of terms, many of them informal and applicable only locally, thus contradicting stratigraphic norms. One of these units, object of this study, is the Água Clara Formation defined by Marini et al. (1967), which is a pile of impure calcareous rocks outcropping northwest of Rio Branco do Sul - Paraná.

The main objective of this work is to present U-Pb isotopic data obtained from zircons of metabasic rocks and subordinate acid and associated rocks of the Água Clara Formation in the Araçaíba region, São Paulo (Fig. 1).

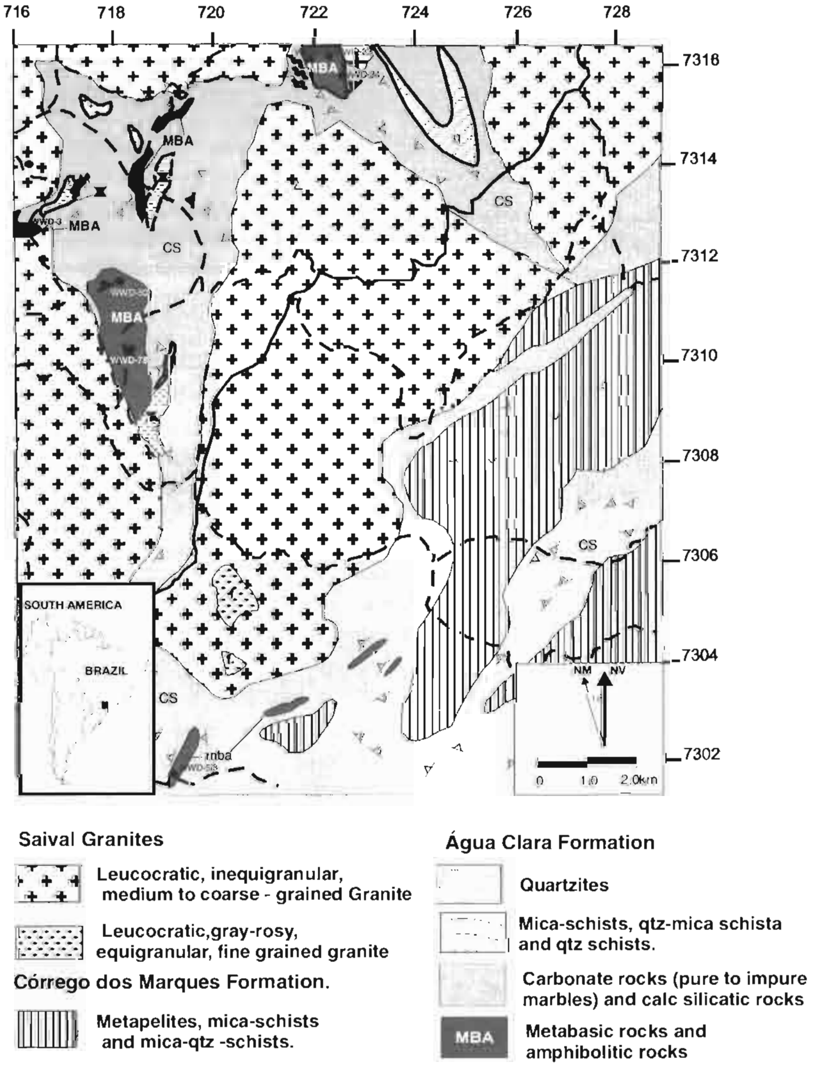

Figure 1 - Simplified geological map of Araçaiba Region

The Água Clara Formation is predominantly constituted by a sequence of carbonate rocks (pure to impure marbles), calc-silicate rocks, calcschists, micaschists, amphibole schists, quartzites, garnet-chlorite-biotite schists, metacherts, basic and intermediate metatuffs, metabasites, amphibolites and cornubianites.

The metabasic rocks have in general expressive dimensions reaching kilometers in length, and are hundreds of meters wide. They are greenish gray, fine- to medium-grained, and usually present nematoblastic texture. More isotropic terms also occur, showing granoblastic texture. They are composed of pyroxenes (diopside or augite), amphiboles (actinolite and hornblende), and plagioclases (andesine/oligoclase). The most common accessories are apatite, magnetite, epidote, titanite, and rare zircon.

In thin section, preserved ophitic and subophitic textures are observed, indicating a probable igneous origin.

The geochemical data suggest compositions similar to enriched midoceanic ridge basalts (E-MORB) tending to oceanic island basalts (OIB).

The subalkaline, tholeiitic characteristics, similar to E-MOR basalts tending to OI basalts, suggest distension or back-arc environments as the geotectonic settings for the basic magmatism.

GEOCHRONOLOGICAL DATA (U-Pb IN ZIRCONS)

Three analytic techniques (conventional, single-zircon filament evaporation and SHRIMP) were involved in the U-Pb isotopic study of zircons from metabasic rocks labeled WWD-03 in the field (vicinity of Araçaiba). Firstly, the zircon populations were selected by splitting, using a FRANTZ electromagnetic separator, and secondly by hand picking under the stereoscope.

Each zircon population is characterized by a specific crystal form (relatively well formed, oval-shaped, or with diffuse terminations), transparency, and presence of fractures and inclusions.

SHRIMP analytical data (rims and nuclei) for five zircons yielded a straight line in the Tera-Wasserbourg diagram (Fig. 2), characterizing for the upper intercept ages of 1593 ± 70 Ma, and for the lower intercept, 586 ± 24 Ma. Two points fall in intermediate positions between these values.

Cathodoluminescence images reveal overgrowths in practically all the studied zircons. The closest point to the upper intercept (oldest age) corresponds to the analysis of a more internal crystal portion, whereas the other analyses correspond to the more external portions, characterized by overgrowths and oscillatory zoning. The data suggest the Mesoproterozoic (1593 ± 70 Ma) as the time of zircon crystallization. The Neoproterozoic (586 ± 24 Ma) values correspond to the overgrowth zones, probably coeval with metamorphic processes, or processes related to the emplacement of the Três Córregos granitic batholith.

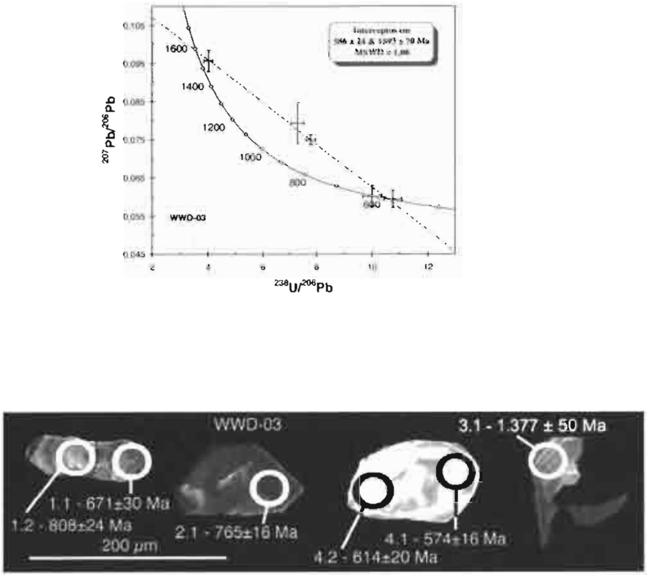

Figure 2. Tera-Wasserbourg diagram and cathodoluminiscence from zircons of WWD-03 sample.

The isotopic data obtained using the conventional technique for four populations from sample WWD-03 are aligned along the discordia, intercepting the concordia curve at 1561 ± 18 Ma (upper intercept) and at 751 ± 15 Ma (lower intercept). The intermediate positions of three analytical points in the discordia (Fig. 3) indicate partial Pb losses, probably associated with the Neoproterozoic tectonics. The sole point plotting close to the lower intercept is located left of the concordia curve, revealing isotopic disequilibrium, possibly related to incomplete crystal digestion. Therefore the age of 751 ± 15 Ma obtained for this intercept must be dealt with care, once it may lack geological significance. Anyway, these zircons crystallized during the Mesoproterozoic at 1561 ± 18 Ma, with Pb losses associated with the Neoproterozoic tectonics imprinted in these lithotypes. Using the single-zircon filament evaporation technique, for a zircon of the same sample (WWD-03) a step corresponding to an age of *ca.* 1461±51 Ma is observed (Fig. 4), characterizing once more crystallization events related to the Mesoproterozoic. It is worth mentioning that in this case such technique is not effective regarding zircon rims, due to the amount of common Pb present and relatively fast ignition of the rims.

Another outcrop of metabasic rocks occurs in the vicinity of Taquari-Mirim (field number WWD-32). Four zircon fractions of sample WWD-32 were analyzed, using the conventional technique. Two fractions - 32a and 32d – are composed of translucent, badly shaped zircon crystals with weakly defined edges, free of inclusions and fractures. In the concordia diagram both fractions plot in the upper intercept. Other two fractions, 32b and 32c, are composed of transparent, colorless, relatively well-formed prismatic zircon crystals with defined edges, usually having inclusions and/or fractures. The size of the prisms differs in fractions 32b and 32c, being shorter in the former (2:1) than in the latter (~3:1). Both sets plot in the lower intercept, practically on the concordia curve.

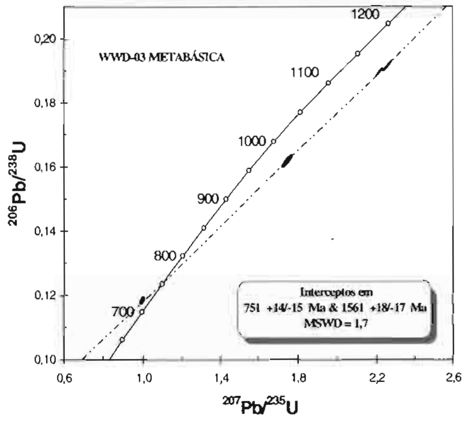

Figure 3. Concordia diagram using the conventional technique for four populations from sample WWD-03.

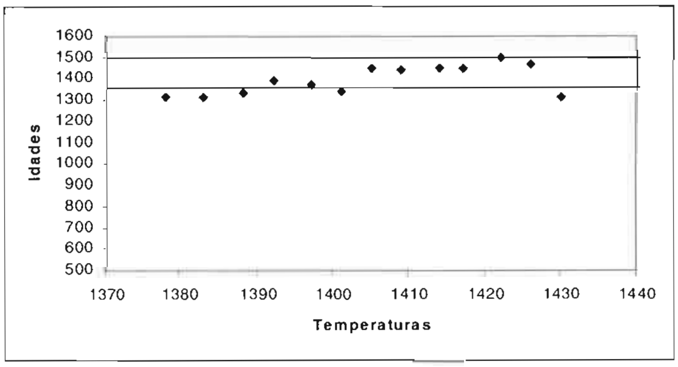

Figure 4. Single-zircon filament evaporation technique, for a zircon of the same sample (WWD-03) a step corresponding to an age of *ca.* 1461±51 Ma.

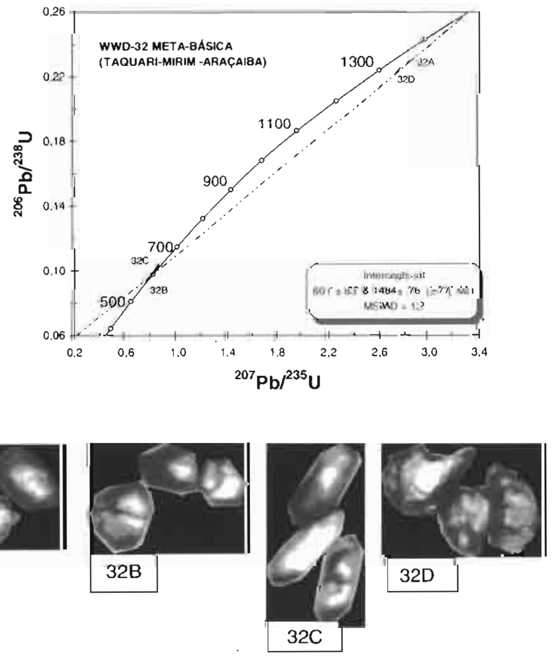

Figure 5. Concordia Diagram using the conventional technique for four populations from sample WWD-32.

The best-fitting discordia yielded the age of 1484 ± 76 Ma for the upper intercept and 601 ± 83 Ma for the lower intercept (figure 5).

FINAL CONSIDERATIONS

The geochemical characteristics (subalkaline tholeiitic basalts) indicate an extensional environment for the emplacement of the metabasic and amphibolitic lithotypes, suggesting a relationship with the opening of an oceanic basin.

The geochronologic and geochemical characteristics and structural patterns described for the Água Clara Formation metabasic lithotypes (probably sills and/or dikes) suggest volcanism periods with associated sedimentation related to the Mesoproterozoic, with ages close to 1500 Ma. Therefore such era represents an important mark in the evolution (sedimentation/ volcanism) of the Apiaí Domain. The Neoproterozoic values obtained refer to zircon recrystallization and neoformation processes (affecting metabasics/ amphibolites), emplacement of rocks of granitic/acid volcanic nature and regional cooling of the Água Clara Formation.

REFERENCES

Frascá, M. H. B. O.; Campanha, G. A. C.; Figueiredo, M. C. H.; Sadowski, G. R. –1996 – Geoquímica de metabasitos do alto e médio Vale do Ribeira, São Paulo e Paraná. Bol. IG-USP, Publ. Especial, 18: 129-131, 1996

Maniesi, V. 1997. Petrologia das rocha anfibolíticas das regiões de Adrianópolis, Campo Largo e Rio Branco do Sul/PR. Rio Claro. 215p. (Tese de Doutorado, IGCE-Cp. de Rio Claro-UNESP).

Marini, O.J.; Trein; E.; Fuck, R.A. 1967. O Grupo Açungui no estado do Paraná. In: Bigarella, J.J.; Salamuni, R.; Pinto, V.M. "Geologia do Pré-Devoniano e Intrusivas Subsequentes da porção oriental do estado do Paraná". Bol. Paran. Geoc., 23-25: 43-104.

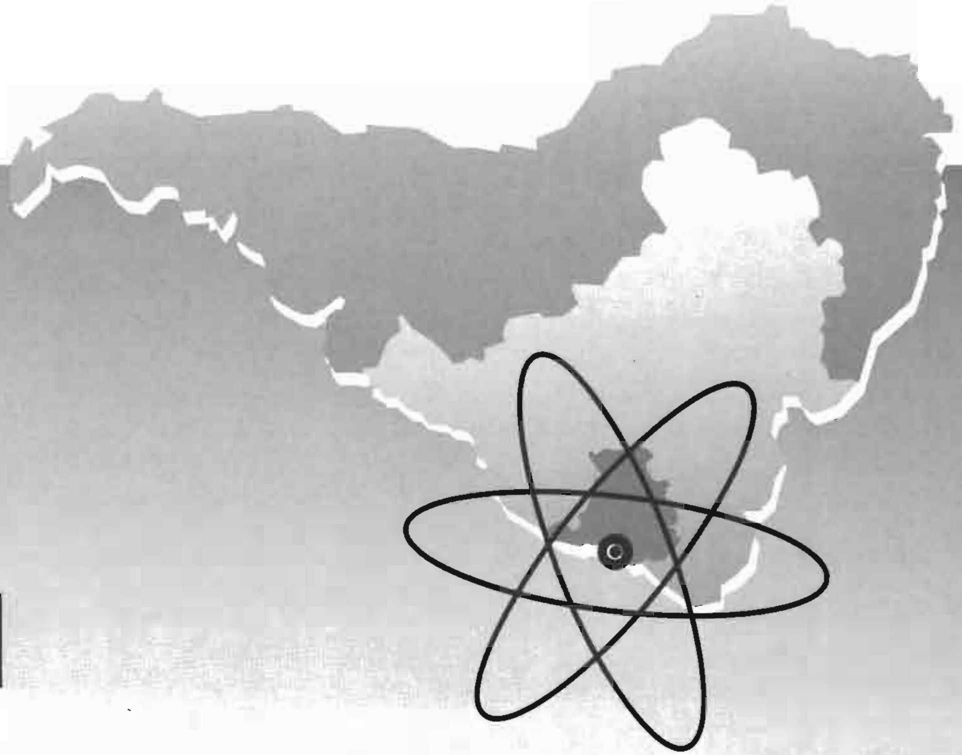

Metallogenesis and Mineral Exploration

Sn-POLYMETALLIC DEPOSITS FROM RONDÔNIA TIN PROVINCE AND ITU RAPAKIVI PROVINCE, BRAZIL: FLUID INCLUSIONS AND STABLE-ISOTOPE CONSTRAINTS

Bettencourt, J.S.[1]; Leite Júnior, W.B.[2]; Goraieb, C.L.[3]; Sparrenberger, I.[1]; Bello, R.M.S.[1] and Payolla, B.L.[4]

1. Instituto de Geociências, Universidade de São Paulo, São Paulo-SP, Brazil. jsbetten@usp.br ; sparrenb@usp.br ; rosabell@usp.br
2. Instituto de Geociências e Ciências Exatas, Universidade Estadual Paulista, Rio Claro-SP, Brazil. wleite@rc.unesp.br
3. Digeo/Instituto de Pesquisas Tecnológicas, São Paulo-SP, Brazil. cgoraieb@ipt.br
4. Eletronorte S/A, Brasília, Distrito Federal-DF, Brazil. bruno@eln.gov.br

Keywords: Rondônia tin province, rapakivi-granites, metallogeny, (Sn-W)-deposits

INTRODUCTION

Proterozoic rapakivi granites from Brazil range in age from 1.88 Ga to 0.59 Ga, and are to be found in anorogenic tectonic settings of the Amazonian craton (1.88 - 1.00 Ga) and Tocantins Province (1.77 - 1.55 Ga), and in post-orogenic tectonic settings as those of the Mantiqueira Province (ca. 0.59 Ga) (Dall'Agnol et al., 1999). Important Sn-polymetallic deposits are spatially and temporally associated with some of them. The Rondônia and Pitinga provinces situated in the Amazonian craton are responsible for major Brazilian tin production with a total output of ~500.000 t/Sn in-concentrate.

Despite the progress achieved in the last few years, the magmatic-metallogenetic history of the rapakivi granites from Brazil is far from being fully understood. Many fundamental questions still require answers before serious attempts to elucidate their origin, evolution, and relation with associated mineral deposits can be satisfactorily undertaken. The aim of this work is to give an overview of the present knowledge regarding the metallogeny of selected Sn-polymetallic deposits from Rondônia Tin Province (Amazonian craton) and Itu Rapakivi Province (Mantiqueira Province).

RONDÔNIA TIN PROVINCE (RTP)

According to Bettencourt et al. (1999), seven anorogenic rapakivi granite suites have been distinguished in the RTP (Fig. 1), showing ages between 1.60 Ga and 0.97 Ga.

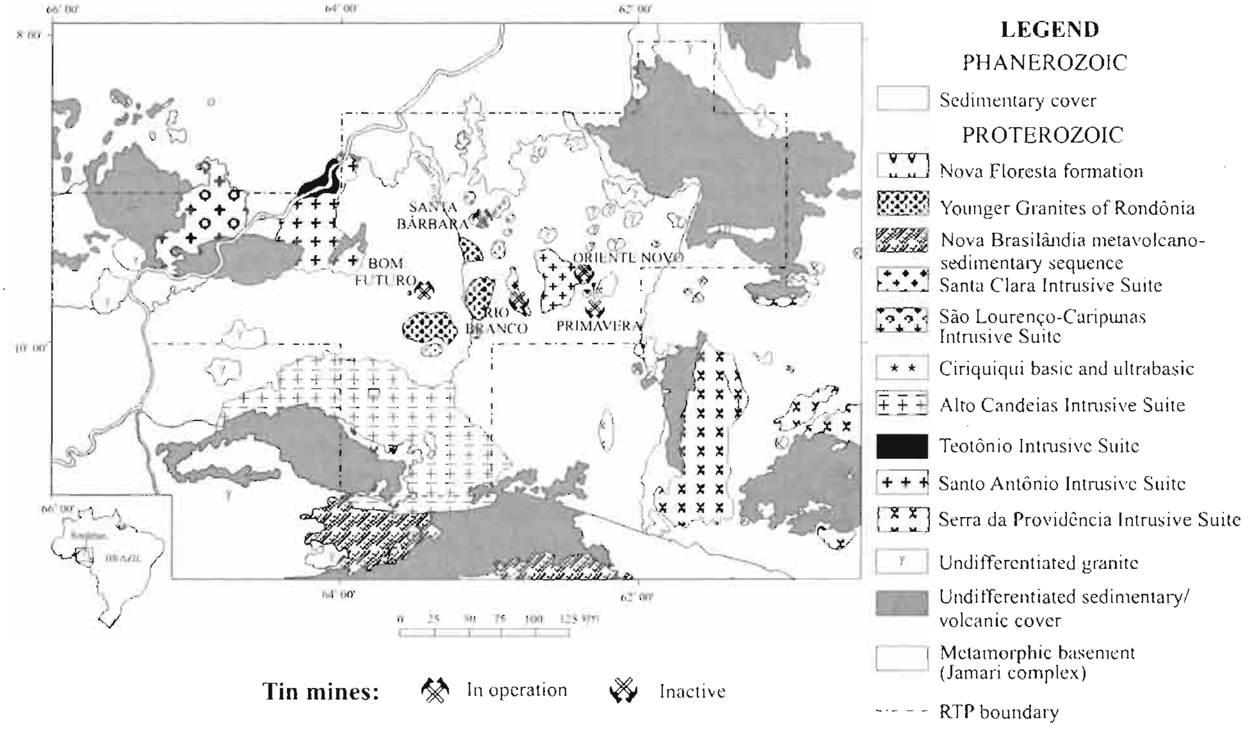

Figure 1. Simplified geological map of the Rondônia Tin Province (RTP) and adjacent areas (after Bettencourt et al., 1999).

Important Sn-polymetallic deposits are associated with at least the three youngest suites: the São Lourenço-Caripunas Intrusive Suite (ca. 1.31 Ga), the Santa Clara Intrusive Suite (1.08 – 1.07 Ga), and the Younger Granites of Rondônia (0.99 – 0.97 Ga). Detailed studies in the Santa Clara Intrusive Suite and Younger Granites of Rondônia have shown that both suites have petrographic, geochemical and metallogenetic similarities (Leite Júnior et al., 2000). These suites are composed of several early, and late-stage intrusions. The early-stage intrusions are dominant in area, exhibit a metaluminous to slightly peraluminous character, and are formed mainly by biotite (± hornblende) monzogranite and syenogranite, showing rapakivi textures. The late-stage intrusions are volumetrically smaller and comprise two compositional rock groups: (1) a metaluminous to peralkaline group composed mainly of hornblende (± pyroxene; ± biotite) alkali-feldspar syenite and microsyenite, trachyandesite and trachyte, as well as biotite (± sodic amphibole) alkali-feldspar microgranite and rhyolite; (2) a peraluminous group formed by biotite alkali-feldspar granite, alaskite, Li-mica (± topaz) alkali-feldspar granite and topaz-bearing rhyolite porphyry (ongonite). The Sn (W, Nb, Ta, Zn, Cu, Pb) deposits are closely associated with these late-stage peraluminous rocks in both suites, such as: Primavera (Sn, Pb), Oriente Novo (Sn, W, Nb, Ta), and Rio Branco (Sn, W, Zn, Cu, Pb) in the Santa Clara Intrusive Suite, and Potosi (Sn, W, Zn, Cu, Pb), Santa Bárbara (Sn, W), and Bom Futuro (Sn, W, Zn, Cu, Pb) in the Younger Granites of Rondônia.

In the first suite, the Sn-polymetallic greisen and vein-type deposits are spatially and temporally associated with biotite-alkali feldspar granite and alaskite, as well as with Li-mica-alkali feldspar granite and rhyolite porphyry (Leite Júnior & Bettencourt, 1995; Leite Júnior, 2002). Major styles of Sn (W, Nb, Ta) mineralization in the Oriente Novo massif can be divided from the oldest to youngest, into three groups: (1) stockwork vein/veinlets of greisen with cassiterite, and of quartz with cassiterite and wolframite hosted within older porphyritic biotite syenogranite; (2) disseminated cassiterite and columbite-tantalite in the Li-mica alkali-feldspar granite with greisen pods with cassiterite; and, (3) sub-parallel vein/veinlets of greisen bearing cassiterite and of quartz with cassiterite and wolframite, having a general strike of N30-50E, and dipping 50-80 SE. The stockwork mineralization is interpreted to be genetically related to the biotite-alkali feldspar granite and alaskite, whereas the disseminated and sub-parallel vein/veinlets mineralization system, to the Li-mica-alkali feldspar granite and rhyolite porphyry. Both were formed by similar magmatic aqueous-carbonic fluid with minor meteoric hydrothermal water input. Effervescence and greisenization are the principal processes responsible for Sn and W mineralization. Oxygen isotope geothermometry coupled with fluid-inclusion data suggest that mineralization took place between 370 – 240°C, at 2.4 to 1.0 kbar. The $\delta^{18}O_{H2O}$ = (+7.4 to + 8.4 ‰) is consistent with an origin as magmatic fluid that equilibrated with a granitic magma (T=700-650°C). However the δD_{H2O} of the fluids (-91 to -112 ‰) indicates mixing with meteoric water, with temperature decrease and vapor decompression.

In the Younger Granites of Rondônia, the Santa Bárbara deposit occurs in a 500 x 150 m zone and shows two principal structural types, both hosted by peraluminous siderophyllite-albite-microcline granite: horizontal and lensoid cassiterite-bearing topaz-siderophyllite-quartz greisen bodies, up to 40 m thick, and stockworks of cassiterite-bearing topaz-siderophyllite-quartz greisen veins, and/or of quartz veins and veinlets with cassiterite (± wolframite). Oxygen-isotope geothermometry indicates crystallization temperatures, calculated from the oxygen isotopic composition of mineral pairs, of quartz-pods (570°C), bedded-greisen (495°C), and greisen-vein (416°C), consistently higher by 46 to 170°C than fluid inclusion trapping temperatures. The calculated isotopic composition of water in equilibrium with host metasomatites ($\delta^{18}O_{H2O}$ = 3.8 to 10.4‰) is consistent with a magmatic origin for the fluids, exception made to late muscovite ($\delta^{18}O_{H2O}$ = -8.1‰ at 300°C), and late-quartz ($\delta^{18}O_{H2O}$ = -8.2‰ at 250°C) which suggest mixture with meteoric waters (Sparrenberger & Bettencourt, 2002a, b). Fluid inclusion studies in greisen and quartz veins, from the Bom Futuro deposit, indicate that cassiterite was formed by effervescence processes of an aqueous carbonic fluid characterized by low salinity and density, at homogenization temperatures between 420 and 320°C, and lithostatic pressure of approximately 1 kbar (Souza & Botelho, 2002).

ITU RAPAKIVI PROVINCE (IRP)

The batholiths and stocks of the IRP (Fig. 2) are composed mainly of subalkaline biotite syenogranite and monzogranite, with minor granodiorite, quartz syenite, quartz monzonite, tonalite, quartz diorite, and topaz-bearing granite sometimes spatially associated to mineral deposit as in Itu complex (W), and Correas massif (Sn, W, Zn, Cu, Pb) (Wernick et al., 1997; Goraieb, 2001). The Correas deposit comprises lode/stringer, pods, stockworks (exocontact), and their greisen border encompassing mica-topaz-quartz greisen and mica greisen, accompanied by breccia. The most abundant ore minerals are cassiterite and wolframite, followed by pyrite, sphalerite, and chalcopyrite. Successive phases of fluid evolution are mainly depicted from trapping of heterogeneous fluid inclusions as a result of partial mixing of magmatic and meteoric fluids, in the two-phase subsolvus region of the fluid system under variable pressure. A typical magmatic fluid, partly mixed with meteoric fluids (CO_2 ± CH_4, H_2O, NaCl, KCl, $FeCl_2$; $\delta^{18}O_{quartz}$ = 9.9 to 10.9‰; $\delta^{18}O_{H2O}$ = 4.13 to 6.95‰; $\delta^{18}O_{mica}$ = 4.7 to 5.2‰) was involved in the genesis of this deposit.

The depositional temperatures are in the range of 330 to 460°C, and 210 to 440°C (at pressure conditions from 0.8 to 2.6 kbar) obtained from quartz-cassiterite/quartz-wolframite pair and fluid inclusions, respectively.

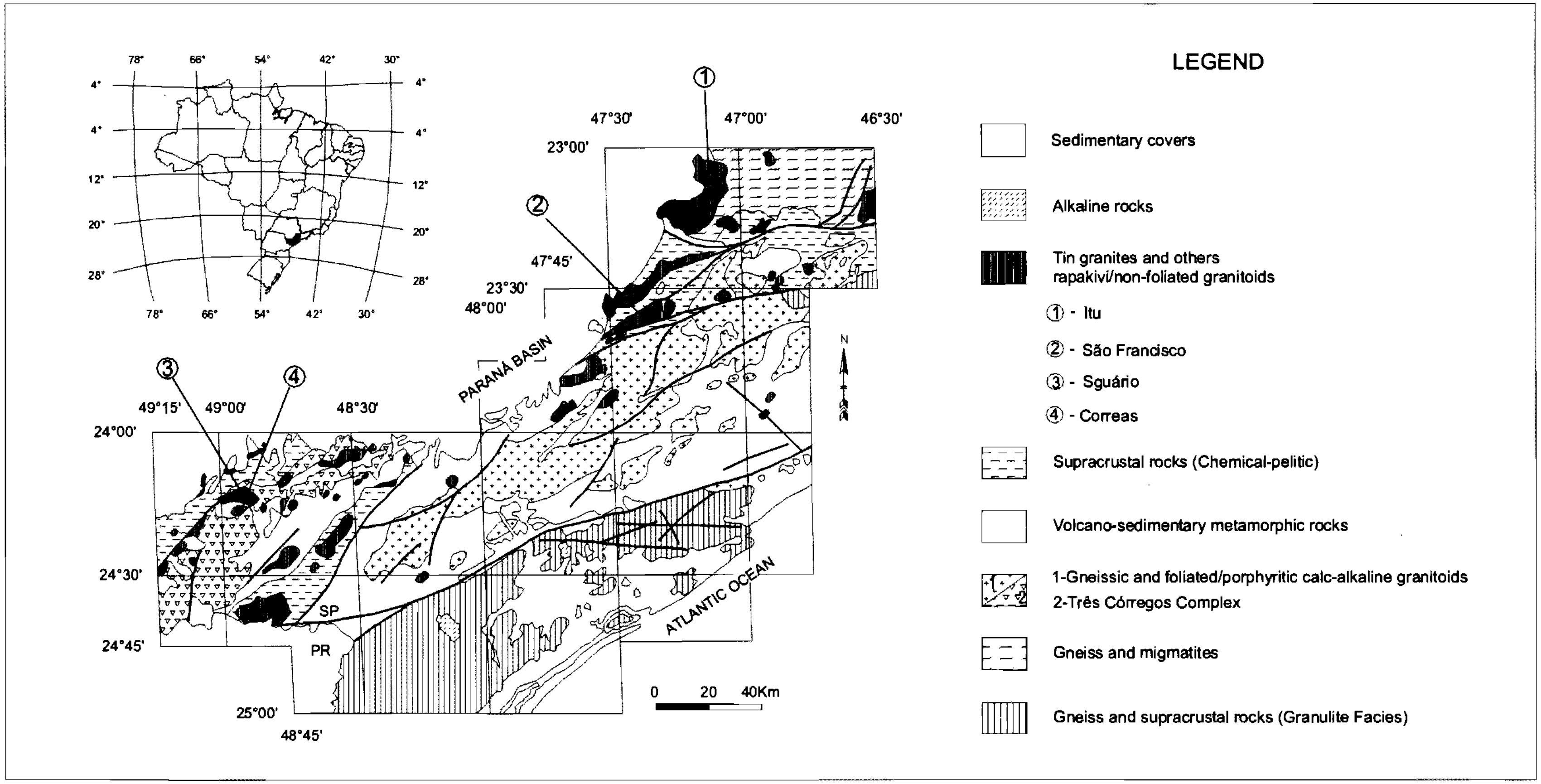

Fig. 2. Simplified geological map of the Ribeira Folf Belt (southeastern part of the State of São Paulo, Brazil) showing the main rapakivi granite massifs (after Goraieb, 2001)

DISCUSSION AND CONCLUSIONS

The tectonic settings are of importance for the formation of the mineralized granites: 1- post-collisional setting (e.g. IRP), and 2- anorogenic setting (e.g. RTP). All the tin-bearing granites are Neoproterozoic in age (1.31 to 0.59 Ga). In the (RTP), the intrusions that hosts rare-metal mineralization are highly evolved A-type, P-poor reduced peraluminous granites, whereas in the Correas massif (IRP) they are slightly peraluminous A-type transitional or mixed I-A-type granites. In both provinces the rare-metal mineralization is closely related to strongly fractionated peraluminous granites characterized by high values of SiO_2, FeO/FeO+MgO and Ga/Al ratios, F, Li, Rb, Ga, Sn, Ta, Nb, U, and Th, and low Mg, Ti, Ba, Sr, Eu. These studied granites show similarities and geochemical features to those of rare-metal peraluminous granites (Pollard, 1989).

The Correas and Oriente Novo deposits show the predominance of two fluids, which could be derived from a common late-stage parental magmatic hydrothermal fluid phase, which was separated into two immiscible fluids involving mixture-immiscibility and progressive decrease in temperatures. The data suggest that the mineralization in these deposits occurred at temperatures variable from 240 to 400°C under peak fluid pressures between 0.8 to 2.6 kbar. In the Santa Bárbara a quasi-continuous fluid evolution is depicted from an initial immiscible closed system (T=390 to 400°C), which changed into a immiscible system (T=350-370°C). The overall evolution of the fluid system, accompanied by immiscibility at lower temperatures, is represented by primary fluid inclusions from bedded greisen (T=350-370°C, at P~200 bar), and topaz-siderite-quartz greisen (T=350-370°C, at P variable from 200 to 250 bar. These suggest peak-fluid pressures during hydrothermal activities, at the post-magmatic late-stage of the deposit, between hydrostatic and near hydrostatic. The late fluid-type is either low-salinity or high-salinity low-temperature Ca-enriched solutions.

A typical magmatic fluid partly mixed with meteoric water is largely confirmed, in all deposits, by oxygen and hydrogen stable isotope studies. Hydrofracturing, boiling, immiscibility and greisenization, and loss of CO_2 (CH_4) with falling temperature, are the principal processes responsible for Sn-W deposition.

ACKNOWLEDGMENTS

This study was supported by grants from FAPESP (Proc. 2000/08033-5), and PADCT-FINEP (64.99.027.00). It is also a contribution to IGCP-426.

REFERENCES

Bettencourt, J.S., Tosdal, R.M., Leite Júnior, W.B., Payolla, B.L., 1999. Mesoproterozoic rapakivi granites of Rondônia Tin Province, southwestern border of the Amazonian craton, Brazil-I. Reconnaissance U-Pb geochronology and regional implications. Precambrian Research 95, 41-67.

Dall'Agnol, R., Costi, H.T., Leite, A.A.S., Magalhães, M.S., Teixeira, N.P., 1999. Rapakivi granites from Brazil and adjacent areas. Precambrian Research 95, 9-39.

Goraieb, C.L., 2001. Contribuição à genese do depósito primário polimetálico (Sn, W, Zn, Cu, Pb) Correas, Ribeirão Branco (SP). Ph. D. thesis, Institute of Geosciences. University of São Paulo, São Paulo, SP, Brazil.

Leite Júnior, W.B., 2002. A Suíte Intrusiva Santa Clara (RO) e a mineralização primária polimetálica (Sn, W, Nb, Ta, Zn, Cu e Pb) associada. Ph. D. thesis, Institute of Geosciences, University of São Paulo, São Paulo, SP, Brazil.

Leite Júnior, W.B., Payolla, B.L., Bettencourt, J.S., 2000. Petrogenese of two Grenvillian tin-bearing rapakivi suites in the Rondônia Tin Province, SW Amazonian craton, Brazil In: IUGS/SBG, Inter. Geol. Cong., 31, Rio de Janeiro, Abstracts CD-ROM.

Pollard, P.J., 1989. Geochemistry of granites associated with Tantalum and Niobium mineralization. In: Moller, P., Cerný, P. And Saupé, F. (eds). Lanthanides, Tantalum and Niobium. Springer-Verlag, Berlin, 145-168.

Souza, V.S., Botelho, N.F., 2002. Geology of the Bom Futuro tin deposit (State of Rondônia) and fluid composition in vein and greisen systems. In: Klein, E.L., Vasquez, M.L., Costa, L.T.R., (eds.) Contribuições à geologia da Amazônia, Belém: S.B.G.-Núcleo Norte, V. 3, pp. 199-214.

Sparrenberger, I., Bettencourt, J.S., 2002a. O Maciço granítico Santa Bárbara, Província Estanífera de Rondônia – Parte I. Caracterização petrográfica e Geoquímica. Anais XLI Cong. Bras. de Geol., João Pessoa, S.B.G., p. 475.

Sparrenberger, I., Bettencourt, J.S., 2002b. O Maciço granítico Santa Bárbara, Província Estanífera de Rondônia – Parte II. A mineralização Estanífera em greisens acamadados. Anais XLI Cong. Bras. de Geol., João Pessoa, S.B.G., p. 475.

Taylor, R.P., 1992. Petrological and geochemical characteristics of the Pleasant Ridge zinnwaldite-topaz granite, southern New Brunswick, and comparisons with other topaz- bearing felsic rocks. Canadian Mineralogist, 30, 895-922.

Wernick, E., Galembeck, T.M.B., Godoy, A.M., Hörmann, P.K., 1997. Geochemical variability of the Rapakivi Itu Province, State of São Paulo, SE Brazil. Anais da Academia Brasileira de Ciências, 69 (3), 395-413.

Pb-Pb ANALYSES ON PYRITE ASSOCIATED TO VEIN- AND PHYLLIC ALTERATIONS IN THE LAVRAS DO SUL GOLD MINING DISTRICT, RS - BRAZIL

Bongiolo, E.M.[1]; Conceição, R.V.[2] and Mexias, A.S.[2]

1. Programa de Pós-graduação em Geociências, PPGGeo, IG, UFRGS. embongiolo@netscape.net
2. Instituto de Geociências, UFRGS. rommulo.conceicao@ufrgs.br, andre.mexias@ufrgs.br

Keywords: Pb isotopes, gold, hydrothermal alteration, pyrite

INTRODUCTION

The Lavras do Sul Gold Mining District includes nineteen old mining prospects presently inactive, hosted by granitic rocks from the Lavras do Sul Intrusive Complex (LSIC) (Gastal & Lafon, 1998) and volcanogenic rocks from Hilário Formation (HF) (Ribeiro & Fantinel, 1978) (Fig. 1).

The LSIC contains a granodiorite Central Zone, partly assimilated by an alkaline magma (perthite granite – Border Zone), which generated hybrid rocks (syeno and monzogranites) in a Transitional Zone (Nardi, 1984). The HF is mainly related to basic and intermediate volcanogenic rocks.

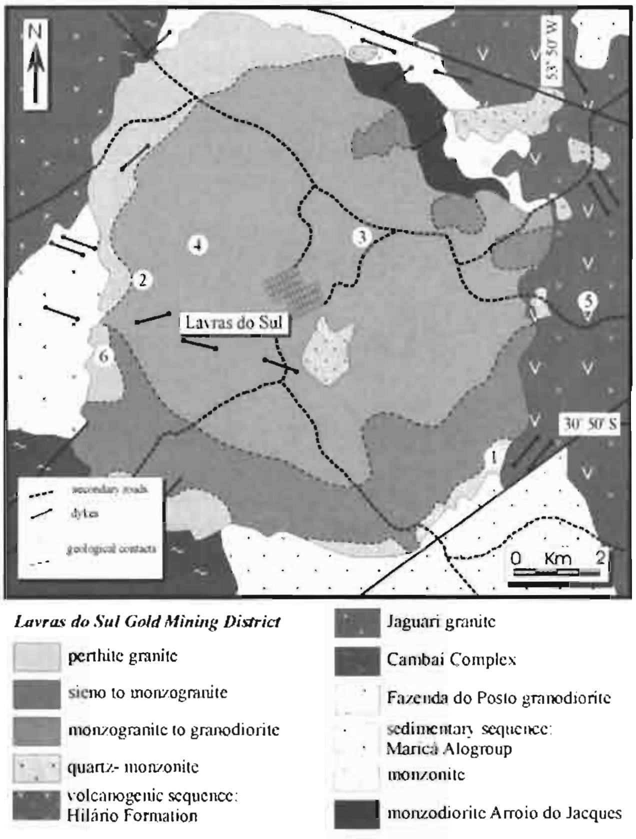

Figure 1. Lavras do Sul geological map (after Gastal & Lafon, 1998). The samples were collected in four of the local mines, named Valdo Teixeira (1), Caneleira (2), Cerrito (3), and Olaria (4). The Cerro Rico (5) and Bloco do Butiá (6) mines are also shown for data comparison (Remus et al., 2000).

The hydrothermal event is associated to vein (vein-veinlets, breccias and stockworks), phyllic and propylitic alteration, besides argillic and potassic alterations (Mexias et al., 1990a) in the volcanogenic rocks.

The major mineralization is N40°W to E-W quartz vein-type, while some calcite and dolomite veins occur at volcanogenic rocks. Some prospects show disseminated ore related to hydrothermal alteration haloes not associated to veins. The mineralized zones have 0.4 to 5 ppm Au content into the sulfide structure (pyrite and chalcopyrite).

The objective of this study is to add new lead isotope data in sulfide (pyrite) associated to the mineralization at Lavras do Sul Gold Mining District. These data were also compared with previous analyses made by Remus et al. (2000).

SAMPLING AND METHODS

Five samples of pyrite grains were analyzed for Pb isotope composition in four mines of the Lavras do Sul Gold Mining District: Valdo Teixeira (VT), Cerrito (Cer), Olaria (Ola), and Caneleira (Can) (Fig. 1). Two of them (VT-E, and Ola) were selected from quartz-pyrite veins while three samples are from the disseminated phyllic alteration (pyrite + white mica) around the veins. The samples VT (E and B) and Can-DB are from mines hosted by the perthite granite, while Ola and Cer samples are from granodiorite rocks.

Four samples analyzed by Remus et al. (2000) in pyrite grains from Bloco do Butiá and Cerro Rico (volcanogenic rocks) mines ores were also used for comparison.

The samples were processed according to the following steps: (1) the single grains (<1mm to 3mm) were handpicked and the concentrates (2) were put for one hour in a hot Teflon® capsule (60-80°C) within HCl (1:1); (3) the samples were cleaned in deionized water and (4) dried completely; (5) treated with hot (60-80°C) HF (40%, 10 ml) until evaporation to dryness and; (6) repeat the steps 1 and 2.

Samples for radiogenic isotope analyses were processed using standard dissolution procedures with aqua regia in Teflon® vial and warmed in hot plate until complete material dissolution. Pb was separated using anionic A8-B500-F-CL (200-400 mesh) resin in 0,6M HBr solution. Each sample was dried to a solid and then loaded with 0.25N H_3PO_4 plus silica gel on Ta filament.

The samples were run in a multi-collector VG Sector 54 thermal ionisation mass spectrometer at Laboratório de Geologia Isotópica (Universidade Federal do Rio Grande do Sul-Brazil) in a static mode. Measurements for the NIST standard NBS-981 and NBS-982 were obtained and variations are less than 0.01%/a.m.u. Total blanks average were <200 pg for Pb.

RESULTS AND DISCUSSION

The lead isotope data in pyrites from the studied mines are listed in Table 1. The lead isotope compositions range from 15.492-15.732 for $^{207}Pb/^{204}Pb$, from 17.122-17.420 for $^{206}Pb/^{204}Pb$ and from 37.252-37.862 for $^{208}Pb/^{204}Pb$.

Table 1. Lead isotope data from Lavras do Sul Gold Mining District. The samples were collected from Valdo Teixeira (VT-E and B), Caneleira (Can), Olaria (Ola) and Cerrito (Cer) mines. The analyses were made using the Faraday method.

Sample	$^{206}Pb/^{204}Pb$	error	$^{207}Pb/^{204}Pb$	error	$^{208}Pb/^{204}Pb$	error
VT-E	17.309	0.017	15.499	0.017	37.278	0.015
VT-B	17.283	0.008	15.498	0.008	37.280	0.008
Can-DB	17.175	0.009	15.492	0.012	37.252	0.015
Ola	17.420	0.297	15.732	0.302	37.862	0.302
Cer	17.122	0.147	15.551	0.150	37.411	0.151

The Pb isotope compositions of the investigated samples, in addition to the analysis made by Remus et al. (2000), were plotted in general $^{207}Pb/^{204}Pb$ vs. $^{206}Pb/^{204}Pb$ diagram (Fig. 2). The Can, VT-B, VT-E and Remus et al. (2000) samples clustered in a narrow area of the diagram. These samples have $^{206}Pb/^{204}Pb$ ratios between 17.122-17.421 and $^{207}Pb/^{204}Pb$ between 15.467-15.732. Few dispersions are observed in the Cer data ($^{206}Pb/^{204}Pb$= 17.122; $^{207}Pb/^{204}Pb$= 15.551), while the most disperse result is related to the Ola ($^{206}Pb/^{204}Pb$= 17.420; $^{207}Pb/^{204}Pb$= 15.732) analysis.

The showed Pb compositional dispersions are much more evident in relation to the $^{207}Pb/^{204}Pb$ ratio (Fig. 2), which could be related to different μ values in the source and evolution of the Pb at Olaria mine. A similar secondary and discordant linear array formed by the Cer and Ola lead compositions was showed by Ho et al. (1994), who attributed this behavior to the error associated with the uncertainty in the mass spectrometric analysis (fractionation and/or ^{204}Pb error; Richards, 1986). Alternative explanations for such data dispersions could be a remobilization of previous high U-Th/Pb source (Wagner and Schneider, 2002) or successive hydrothermal events at the same site (Marcoux et al., 2002).

When previous whole rock, feldspars and pyrite Pb isotopic data (Remus et al., 2000) from Lavras do Sul granitic and volcanogenic rocks are plotted in an uranogenic diagram, they are disposed in a straight line suggesting an association of all these rocks and mineralization to a 594 Ma event. Some samples from this study plot in the same line, which was defined based on U-Pb zircon SHRIMP data to granitic rocks (Remus et al., 2000). In this way, the authors proposed a genetic link between the ore formation and the granitic-volcanogenic association. It is important to observe that the Pb compositional range from the whole rock and feldspar are more radiogenic than the pyrite samples, as shown in their mean values (Fig. 2). However, the volcanic-plutonic event and the hydrothermal activity could be better linked if the whole rock and mineral Pb data were clustered in a narrow compositional interval.

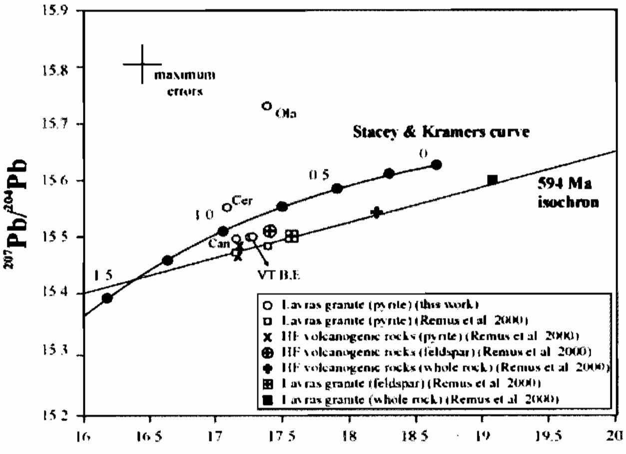

Figure 2. General $^{207}Pb/^{204}Pb$ vs. $^{206}Pb/^{204}Pb$ plots of pyrite lead isotope compositions from the studied mines. Pyrite data and mean lead compositions for whole rock and feldspar samples analyzed by Remus et al. (2000), are plotted in the 594 Ma isochron for the LSIC granitic rocks. Stacey & Kramers (1975) Pb growth curve is shown for reference.

Even if the Ola (D) sample is considered to be the best estimate of the initial (primitive) Pb composition, due to its position in the diagram, it is known that the least Pb composition in pyrite grains can be very heterogeneous (Ho et al., 1994), hence it is better to use galena samples for that purpose.

When plotted in the plumbotectonics (version II) model diagram (Zartman & Doe, 1981), the Ola and Cer samples have $^{207}Pb/^{204}Pb$ vs. $^{206}Pb/^{204}Pb$ (Fig. 3a) compositions that are related to upper crust (UC) isotopic evolution. The other samples are related to the orogene (O) mixing curve, within contributions from both upper crust and mantle (M). The $^{208}Pb/^{204}Pb$ vs. $^{206}Pb/^{204}Pb$ diagram show that all samples cluster between the orogene (O) and lower crust (LC) compositional curves, (Fig. 3b) but with higher $^{208}Pb/^{206}Pb$ contents to Ola sample.

From these results, we believe that the proposition of more than one hydrothermal event could be made, mainly because the heterogeneous ore (sulfide) lead isotope compositions. The various source contributions for the sulfide lead can argue for that assumption. The addition of more analysis can provide new advances in the local mineralization understanding.

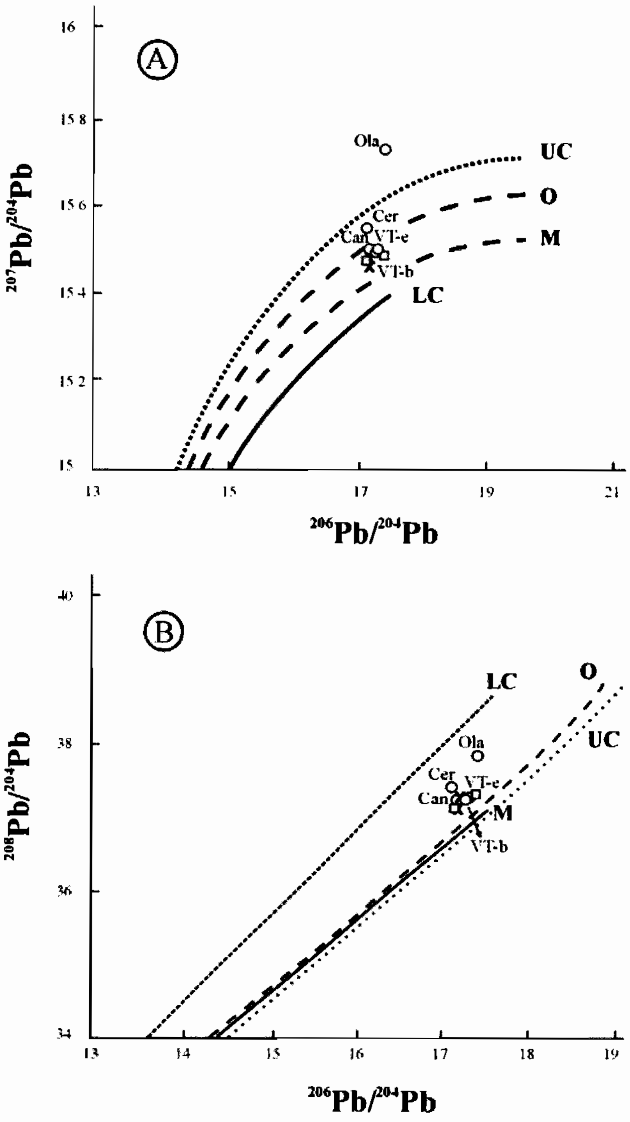

Figure 3. A and B. Lead isotope evolution curves generated by the plumbotectonics model (version II) for mantle (M), orogene (O), upper crust (UC) and lower crust (LC) proposed by Zartman & Doe (1981). Legends as in figure 2.

REFERENCES

Fouquet, Y. and Marcoux, E. 1995. Lead isotope systematics in Pacific hydrothermal sulfide deposits. J. Geophys. Res. 100(B4): 6025-6040.

Gastal, M. C. P. and Lafon, J. M. 2001. Novas idades ^{207}Pb/^{206}Pb e geoquímica isotópica Nd-Sr para granitóides shoshoníticos e alcalinos das regiões de Lavras do Sul e Taquarembó, RS. In: Congresso Brasileiro de Geoquímica, 8, 2001, Curitiba. Resumos... Curitiba, p. 50.

Ho, S. E., McNaughton, N. J. and Groves, D. I. 1994. Criteria for determining initial lead isotopic compositions of pyrite in Archean lode-gold deposits: a case study at Victory, Kambalda, Western Australia. Chemical Geology, 111: 57-84.

Marcoux, E., Grancea, L., Lupulescu, M. and Milési, J. P. 2002. Lead isotope signatures of epithermal and porphyry-type ore deposits from the Romanian Carpathian Mountains. Mineralium Deposita 37(2): 173-184.

Mexias, A. S.; Formoso, M. L. L.; Meunier, A. and Beaufort, D. 1990a. O Sistema Hidrotermal Fóssil de Volta Grande – Lavras do Sul/RS. Parte I – Petrografia do Hidrotermalismo. Geochimica Brasiliensis, 4(2): 139-157.

Nardi, L. S. V. 1984. Geochemistry and Petrology of the Lavras Granite Complex, RS, Brazil. London. 268 f. Ph.D. These, Department of Geology, University of London.

Remus, M. V. D., Hartmann, L. A., McNaughton, N. J., Groves, D. I. and Reischl, J. L. 2000. Distal magmatic-hydrothermal origin for the Camaqua Cu (Au-Ag) and Santa Maria Pb, Zn (Cu-Ag) deposits, southern Brazil. Gondwana Research 3(2): 155-174.

Ribeiro, M. and Fantinel, L. M. 1978. Associações Petrotectônicas do Escudo Sul-rio-grandense: I – Tabulação e distribuição das associações petrotectônicas no Rio Grande do Sul. Iheringia Série Geologia 5, p.19-54.

Richards, J. R. 1986. Lead isotopic signatures: further examination of comparisons between South Africa and Western Australia. Trans. Geol. Soc. S. Afr., 89:285-304.

Stacey, J. S. And Kramers, J. D. 1975. Approximation of terrestrial lead isotope evolution by a two-stage model. Earth and Planetary Science Letters, 26: 207-221.

Wagner, T. And Schneider, J. 2002. Lead isotope systematics of vein-type antimony mineralization, Rheinisches Schiefergebirge, Germany: a case history of complex reaction and remobilization processes. Mineralium Deposita, 37(2): 185-197.

Zartman, R. E. And Doe, B. R. 1981. Plumbotectonics – the model. In: R. E. Zartman and S. R. Taylor (Editors), Evolution of the Upper Mantle. Tectonophysics, 75: 135-162.

PRELIMINARY Sm-Nd AND Pb-Pb ISOTOPIC DATA OF THE Fe-Cu-Au-BEARING SERROTE DA LAJE COMPLEX, ARAPIRACA, ALAGOAS, BRAZIL

Brito, R.S.C.[1]; Amorim, J.L.*; Macambira, M.J.B.[2]; Leal, E.D.[3]; Pimentel, M.M.[4], Silva Filho, M.A.[1]; Torres, H.H.F.[1]; Gioia, S.M.L.[4] and Junges, S.L.[4]

1. CPRM - Geological Survey of Brazil - SUREG-RE, Recife-PE, Brazil. rscdebrito@bol.com.br
2. Centro de Geociências, Universidade Federal do Pará, Belém-DF, 66075-110, Brasil, moamac@ufpa.br
3. CVRD Companhia Vale do Rio Doce, emanoel@cvrd.com.br
4. Instituto de Geociências, Universidade de Brasília, Brasília-DF, 70910900, Brasil. marcio@unb.br
**Post-morten*

Keywords: Serrote da Laje, Sm-Nd isotopes, Pb-Pb isotopes, Cu-Au deposit, Arapiraca-Brazil

INTRODUCTION

Magnetic iron ore-hosted copper deposit occurs in layered mafic-ultramafic intrusions in the low Rio São Francisco River valley, in the States of Bahia, Sergipe and Alagoas in Northeastern Brazil. They are nested in metavolcano-sedimentary sequences, which are considered as part of the South Alagoas Zone, Amorim (1995). Two layered mafic-ultramafic complexes are recognized in this part of the Sergipano Belt: the Canindé and the Serrote da Laje complexes.

The age of the Serrote da Laje is uncertain, but it is roughly inferred to be older than 1,400 Ma, which was obtained via Rb-Sr dating of the younger Bela Aurora-type granites (Amorim et al., 1990).

This study is an exercise geared to assess the age relationships between the Serrote da Laje Complex and its metasedimentary host rocks using the Sm-Nd and Pb-Pb systematics. The preliminary age determinations of the deformed and polimetamorphosed rocks of this fragment of the South Alagoas Zone also aim to contribute to the understanding of the geological history of this part of the Borborema Province.

GEOLOGICAL SETTING

The Serrote da Lage Complex is a layered intrusion, lying within the South Alagoas Zone of the Sergipano Belt, as an intrusive body into the Rio Coruripe Domain of Jaramataia Group, (Amorim et al., 1995). The Jaramataia Group is a 120 km long bow-shaped folded belt, which crops out between the cities of Belo Monte and Igaci in the central part of the State of Alagoas, Brazil. It consists of plutonic, volcanic and sedimentary rocks, which were metamorphosed under the greenschist to granulite facies conditions (Fig. 1).

THE SERROTE DA LAGE COMPLEX

The Serrote da Lage Complex crops out between the cities of Craíbas and Arapiraca in the State of Alagoas (Fig. 1). It is composed of a sequence of gabbro, norite, hyperstenite and magnetite, hosted by clastic and chemical sediments (Horbach & Marimon, 1988).

The differentiates are mingled with fine- to medium-grained gabbroic rocks, which were interpreted as younger crosscutting diabase and gabbro (Fig. 2). The complex is highly deformed and recrystallized within the granulite facies condicions, which has produced a metamorphic paragenesis composed of hypersthene, sillimanite, cordierite and garnet. The sequence was later intruded by granite and pegmatite dykes. The granulites have been retrometamorphosed within the greenschist facies conditions in zones of britle deformation, which exhibit biotite, chlorite, talc and carbonate.

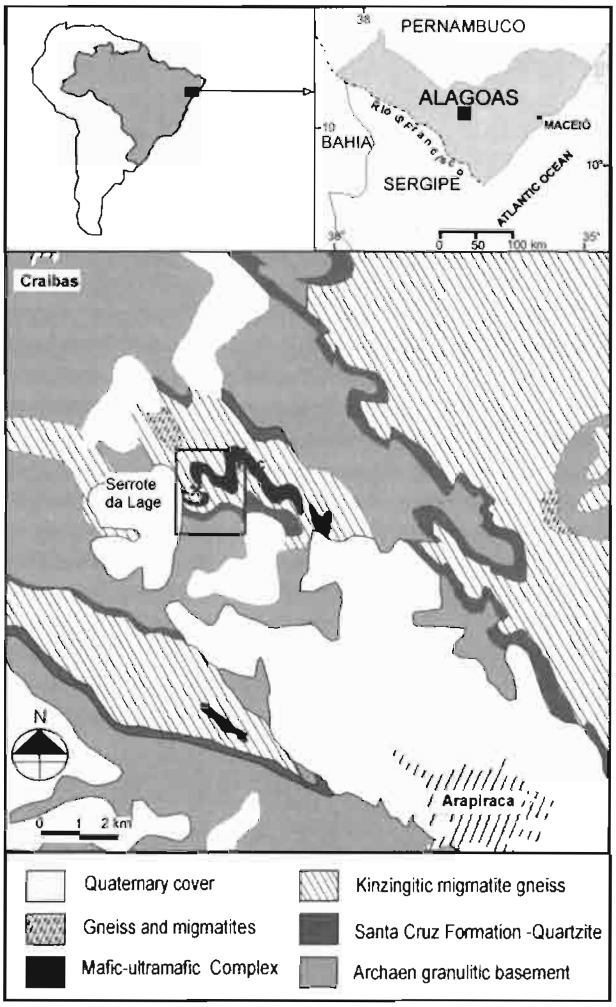

Figure 1. Geologic map of the Arapiraca and Craíbas area. (After Amorim , 1995).

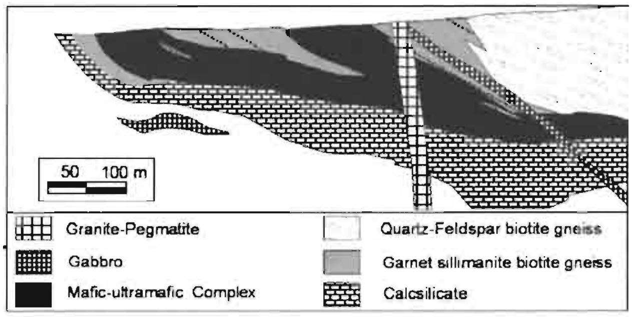

Figure 2. Geological section of the Serrote da Laje Complex (After Leal, 2002).

The Serrote da Lage Complex hosts a copper ore deposit, confined to the iron-rich differentiates which was evaluated by CVRD as large as 74 million tons of ore, bearing 0,62% Cu. An epigenetic gold mineralization, related to fractured zones of the copper ores, is also observed and the ore-grade is of the order of 0.17 ppm Au, (Figueiredo & Xavier, 1992).

GEOCHRONOLOGY

A reconnaissance isotopic research exercise was carried out in this complex in order to tentatively assess the age relationships between the mafic-ultramafic rocks and their host lythological units of the Rio Coruripe Domain. The meta igneous rocks of the Cu-Au deposits were studied via the Sm-Nd method and the enclosing metasedimentary rocks were indirectly dated through the Pb-Pb zircon evaporation method on detrital grains.

Sm-Nd SYSTEMATICS

The Sm-Nd isotopic study was carried out on nine samples of drill cores, which were kindly provided by CVRD – Companhia Vale do Rio Doce. Sampling aimed to cover the lythological spectra from leucocratic to ultramafic in order to obtain a whole-rock isochron. This procedure also aimed to distinguish, from the isotopic point of view, rocks that might have generated from different types of magma within the complex.

Sm and Nd were separated by standard ion-exchange techniques. Sr and Nd isotopic analyses were performed at the Geochronology Laboratory of the University of Brasília in static mode using a multi-collector Finnigan MAT-262 mass spectrometer. Total blanks were: Sr = 0.2 ng, and Nd < 0.2ng. 2σ uncertainties for the $^{87}Sr/^{86}Sr$ and $^{143}Nd/^{144}Nd$ ratios are smaller than 0.01% and 0.005%, respectively. Analytical procedures are those reported by (Gioia & Pimentel, 2000)

Decay constants are those recommended by Steiger and Jäger (1977), and ages are reported at the 95% confidence interval. Analysis of the NBS-987 Sr standard gave values between 0.71024 and 0.71029, and the LaJolla Nd standard yielded values between 0.511830 and 0.511848.

Samples taken from different drill holes are listed in Table 1. The rock specimens are metamorphic rocks, which still preserve some primary features, such as cumulus textures, rhythmic layering, and typical diabasic textures.

Table 1. Mineralogical composition of the samples. Opx - hyperstene; Pl - plagioclase; Cpx - diopside; Hb – hornblende; Gr - garnet; Bt - biotite; Cd - cordierite; Cl - chlorite; Qz - quartz; Mt - magnetite; Sulf - sulphide.

Sample Id	Rock Type	Mineralogy										
		Opx	Cpx	Pl	Hb	Gr	Bt	Cd	Cl	Qz	Mt	Sulf
FD37-25.20	Diabase		x	x	x						x	x
FD48-24	Meta leucogabbro		x	x	x	x	x				x	x
FD37-38	Meta gabbro		x	x	x	x	x				x	x
FD02-40.80	Meta norite	x		x	x	x	x	x		x	x	x
FD02-67-40	Meta norite	x		x	x	x	x	x		x	x	x
FD51-4.5	Magnetite chloritite	x					x	x	x		x	x
FD46-66-35	Metadunite	x					x		x		x	x
FD46-66-90	Meta- magnetitite	x			x						x	x

Table 2 displays the results of the Sm-Nd isotopic analyses. The samples exhibit $^{143}Nd/^{144}Nd$ expressed as ε_{Nd} values from -6.36 to -31.08. The data unfortunately did not yield sufficient spreading to produce reliable isochronic ages for the mafic-ultramafic differentiates. Nevertheless three groups of samples with distinct T_{DM} model ages could be distinguished.

The first correspond to the intrusive diabase, which yielded a Mesoproterozoic T_{DM} model age of 1.49 Ga. The second consists of the gabbroic rocks that yielded Lowerproterozoic T_{DM} ages, from 2.32 to 2.34 Ga. The third group comprises the noritoid and metamorphosed magnetite-hyperstenites that produced Archaean Sm-Nd model ages as old as 2.71-2.86 Ga.

Table 2. Sm-Nd data for the Serrote da Laje Complex.

Sample	Sm ppm	Nd ppm	$^{147}Sm/^{144}Nd$	$^{143}Nd/^{144}Nd$ (± 2σ)	ε(o)	T_{DM} (Ga)
FD 37-25.20	11.620	50.31	0.1396	0.512312±06	-6.36	1.489
FD 48-24(2)	6.709	32.01	0.1267	0.511711±06	-18.08	2.322
FD 37-38	5.921	28.59	0.1252	0.511677±06	-18.75	2.343
FD 02-40.80	2.729	12.366	0.1334	0.511618±09	-19.90	2.708
FD 02-67-40	3.007	13.130	0.1385	0.511634±06	-19.58	2.864
FD 51-4.5	0.361	1.513	0.1442	0.511465±16	-22.89	-
FD 46-66,35	0.490	3.158	0.0937	0.511045±13	-31.08	-
FD 46-90	0,151	0,385	0,2405	0,512692±16	+1,04	

Pb-Pb SYSTEMATICS

A sample from the enclosing biotite gneiss (metarkose) was collected 2 meter below the mineralized noritoids. Detrital zircon grains were investigated in order to assess upper limit for the age of deposition of the original sediment.

The zircon crystals separated from this sample were dated via Pb evaporation zircon method (*cf.* Kober, 1987) at Pará-Iso Laboratories (UFPa). Data are presented at 2σ level . The Pb corrections have been done according to basis of the Pb double stage evolution model (*cf.* Stacey & Kramers, 1975) Analyses were carried out using a Finnigan MAT 262 spectrometer.

Fifteen zircon crystals were separated from the original sample. They are interpreted as detrital grains, which have been classified into two morphological groups. The first displays corroded, round and dirty surfaces, which exhibit elongated prismatic-like shapes, yellow to brownish colors, rare concentric zoning, scarce metamictization and moderate to strong fracturing. The second group corresponds to brownish, corroded, round and sometimes weakly fractured pyramidal-shaped zircon crystals, some of them exhibiting metamictization.

Only five, out these fifteen analyzed zircon crystals, yielded reliable data for age determinations. Three crystals from the first group could be aligned in a plateau and $^{207}Pb/^{206}Pb$ ratios have given a mean age value of 1778 ± 23 Ma (Table 3). Two zircons of the second group produced similar age values yielding an averaged value of 1417 ± 14 Ma (Table 3). This preliminary data suggests, therefore, that the Serrote da Laje is younger than *ca.*1.4 Ga.

DISCUSSION

Sm-Nd method has been proved to be a valuable tool to date layered intrusions. Whole-rock Sm-Nd isochronic ages are usually obtained from coeval differentiates of fresh unmetamorphosed mafic-ultramafic series. Nevertheless the reliability of whole rock Sm-Nd dating is often challenged due to assimilation of older sialic contaminants by parent magmas during ascent.

Considering the 1.4 Ga as the maximum age for emplacement of the Serrote da Laje intrusion, the ε_{Nd} (t=1.4 Ga) values for the individual samples investigated must be smaller than approximately -7.5 (Table 2). This demonstrates that, regardeless of the time of intrusion, the original magma has been contaminated with older sialic crust (Fig. 3). Contamination with continental material is also suggested by low Sm/Nd ratios presented by most o the rock samples. The effect of this contamination would be more severe for the ultramafic differentiates which contains less neodymium and are more sensitive to assimilation of Nd from older external sources.

The preliminary Pb-Pb data from detrital zircons provided two groups of ages. The younger may be considered as the maximum age for the metarkose and it can be "correlated" to the 1,412 Ma Rb-Sr age of the granitic gneisses from Pedreira Triunfo site (Bela Aurora-type). Furthermore, this age is also the maximum age of the Serrote da Laje intrusion, which intrudes into the metasediments. These indirect dating of the Serrote da Laje and arkose should only be considered in the case that the Sm-Nd and Pb-Pb systems have both remained closed during the Brasiliano orogeny. Sm-Nd T_{DM} and Pb-Pb ages together, when considered as related to undisturbed isotopic systems would thus indicate that the Serrote da Laje Complex and the sediments are younger than 1,417 Ma (Fig. 3).

CONCLUSIONS

Sm-Nd and Pb-Pb ages reported here can not be related to the crystallization of the Serrote da Laje Complex. Sm-Nd method was able to discriminate the three groups of rocks that could either be coeval or represent three different magmatic events. Sm-Nd data also show that these rocks display different degrees of contamination with older sources. The Pb-Pb zircon evaporation younger ages were interpreted as the minimum age of the zircons so far analysed and this might be the possible maximum age of the metarkose. Pb-Pb dating indicate that Serrote da Laje Complex and metarkose are both younger than 1, 412 Ma and this is partially in agreement with the Rb-Sr age for the Bela Aurora-type granites. The older Pb-Pb zircon age is here considered an important data as it registered the possible presence of Paleoproterozoic crust in this part of the Southern Alagoas Zone during the metarkose deposition. Additional geocronological investigation is now being carried out by the Geological Survey of Brazil in this area, which will certainly help to constrain the age of the Serrote da Laje Complex.

Table 3. Pb-Pb data for 5 zircon crystals from a sample of metarkose.

Zircon	T(C°)	Ratios	$^{204}Pb/^{206}Pb$	2σ	$^{208}Pb/^{206}Pb$	2σ	$^{207}Pb/^{206}Pb$	2σ	$(^{207}Pb/^{206}Pb)c$	2σ	Age (Ma)	2σ
F037/10	1450	34/34	0.000118	4	0.02835	47	0.11042	57	0.10846	59	1774	10
F037/11	1500	8/8	0.000089	20	0.03892	51	0.11071	76	0.10951	81	1791	14
F037/14	1450	4/4	0.000080	2	0.07436	433	0.10883	33	0.10774	33	1762	6
F037/17	1450	36/36	0.000330	33	0.01273	153	0.09388	55	0.08955	69	1416	15
F037/13	1500	6/6	0.000000	0	0.02637	121	0.09031	255	0.09031	255	1432	54

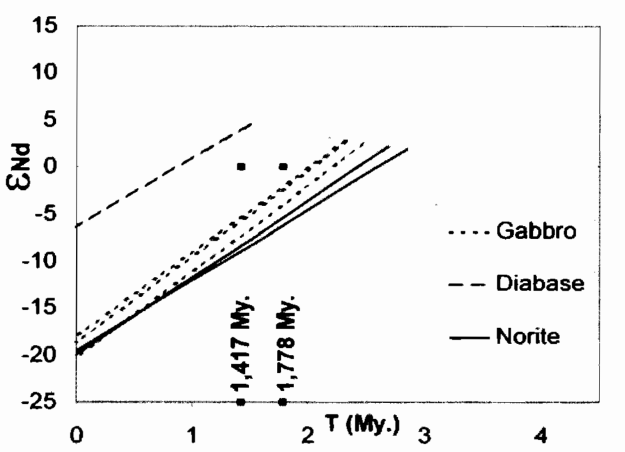

Figure 3. Nd evolution diagram displaying the two Pb-Pb evaporation zircon ages.

FINAL REMARK

The authors wish to pay a *post-morten* tribute to late Jânio Leite de Amorim who gave an outstanding contribution to the knowledge of the geology of Alagoas.

ACKNOWLEDGMENTS

The authors wish to thank M.A. Galarza for the precious help during the Pb-Pb zircon evaporation analyses at Para-Iso laboratory.

REFERENCES

Amorim, J.L.; Mendonça, J.C.G.S.; Torres, H.H.F., 1990. Dados geocronológicos relativos a Faixa Sergipana e do seu embasamento na Região de Arapiraca, Alagoas. XXXVI Congr. Bras de Geol. Natal, SBG, Boletim de Resumos, pp. 320-321.

Amorim, J.L., 1995. Programa Levantamentos Geológicos Básicos do Brasil. Arapiraca, Folha SC.24-X-D-V. Estado de Alagoas. Escala 1:100.000, Brasília, CPRM.

Leal, E.D., 2002. Relatório final de avaliação de reservas do projeto Serrote da Laje. Relatório interno COMPANHIA VALE DO RIO DOCE. Arapiraca, Alagoas.

Figueiredo, B.R., & Xavier, R.P., 1992. A mineralização de ouro no depósito de Serrote da Laje, Alagoas. XXXVII Congr. Bras. de Geol., São Paulo, Boletim de resumos expandidos, p. 241-243.

Gioia S.M.C.L. & Pimentel M.M., 2000. The Sm-Nd isotopic method in the geochronology Laboratory of the University of Brasília. Anais da Academia Brasileira de Ciências, v.72, p. 219-245.

Horbach, R. & Marimon, M.P.C., 1988. O depósito de Cobre de Serrote da Laje. Anais do XXXV Cogr. Brás. de Geol., Belém, Pará, V.1, p. 1-15.

Kober B., 1987. Single grain evaporation combined with Pb emitter bedding 207Pb/206Pb investigations using thermal ion mass spectrometry and implications to zircon chronology. Contributions to Mineralogy and Petrology, 96, p. 63-71.

Stacey J.S. & Kramers J.D., 1975. Approximation of terrestrial lead isotope evolution by a two stage model. Earth and Planetary Science Letters, 26, p. 207-221.

Steiger, R.H & Jäger, E. 1977. Subcomission on Geochronology: convention on the use of decay constants in geochronology and cosmochronology. A.A.P.G. Studies in Geology. 67-71.

GONDWANIC MAGMATISM AND MINERALIZATION IN EL ARRIERO ALTERATION ZONE, LA HUERTA RANGE, PROVINCE OF SAN JUAN, ARGENTINA

Castro de Machuca, B.[1,2,3]; Conte-Grand, A.[1,2]; Meissl, E.[1,2]; Pontoriero, S.[1] and Sumay, C.[1,2]

1. INGEO, FCEFN, Universidad Nacional de San Juan, Argentina. bcastro@unsj-cuim.edu.ar
2. Departamentos de Geología y de Geofísica, FCEFN, Universidad Nacional de San Juan, Argentina
3. Consejo Nacional de Investigaciones Científicas y Técnicas (CONICET)

Keywords: El Arriero Dacite, K-Ar date, Gondwanic magmatic-metallogenic cycle

INTRODUCTION

The K-Ar method on biotite is used to date a porphyritic dacite rock collected from El Arriero hydrothermal alteration zone, La Huerta range, province of San Juan, Argentina.

La Huerta range, located at approximately 145 km east of San Juan city (Fig. 1), is an old well-known mining district due to its polymetallic lead-zinc-silver and gold deposits.

As Ramos et al. (1988), Cardó and Castro de Machuca (1999) and Castro de Machuca et al. (1999, 2000) point out, it is clear that hydrothermal alteration and ore deposition are directly related and genetically associated to magmatic activity in the area. Magmatism is shown by several acid to mesosilicic volcanic and subvolcanic bodies amongst which is El Arriero Dacite (EAD). Alteration and metallic mineralization are parts of the same process.

Potassium-argon ages on volcanic and subvolcanic rocks from La Huerta range vary from 259±13 Ma to 246±8 Ma (Fig. 1). The ages showed in figure 1 indicate almost continuous magmatism in the area. This age range is coincident with the gondwanic magmatic cycle that affects the whole Pampean Ranges System.

K-Ar dating by Ramos et al. (1988) on a small rhyolite intrusion (El Temblor Rhyolite) and a volcanic acidic breccia (Cerro Blanco district) points out an age of 256±8 Ma and 246±8 Ma respectively. More recently, Castro de Machuca et al. (1998, 2001) obtain similar ages from a porphyritic andesite (PMV: 259±13 Ma) and from a basalt (BMV: 255±13 Ma) in the Marayes Viejo area. All cases were dated by means of the K-Ar whole-rock method.

The absolute age here presented (259±8 Ma) agrees with those previously reported, and permits assigning the porphyritic dacite of El Arriero to the Gondwanic magmatic-metallogenic cycle.

REGIONAL SETTING

La Huerta range is part of a much larger area of crystalline basement rocks called Western Pampean Ranges. It consists predominantly of Upper Proterozoic-Lower Paleozoic rocks that have been subjected to medium-high grade metamorphism (high-amphibolite to lower-granulite facies). Biotite-garnet gneisses, biotite-sillimanite-garnet gneisses, forsteritic marbles and amphibolites are intruded by plutonic rocks assigned to the Middle Ordovician magmatic arc (Famatinian magmatic arc) which are dominant along the eastern flank of the range. Amongst them metatonalites, metadiorites and metagabbros prevail.

Few small andesitic to rhyolitic intrusions and associated rhyolite dykes, are scattered throughout the igneous-metamorphic basement. The most important igneous outcrops are indicated in figure 1.

Since Upper Paleozoic time, the crystalline basement has behaved as a rigid element related to faulting. From the town of Marayes to the central part of La Huerta range, the structural setting is characterized by fault bounded blocks forming steps culminating at the Valle Fértil megafracture. The N30°-35°W trending megafracture is exposed along the western flank of the hill (Baldis et al., 1990).

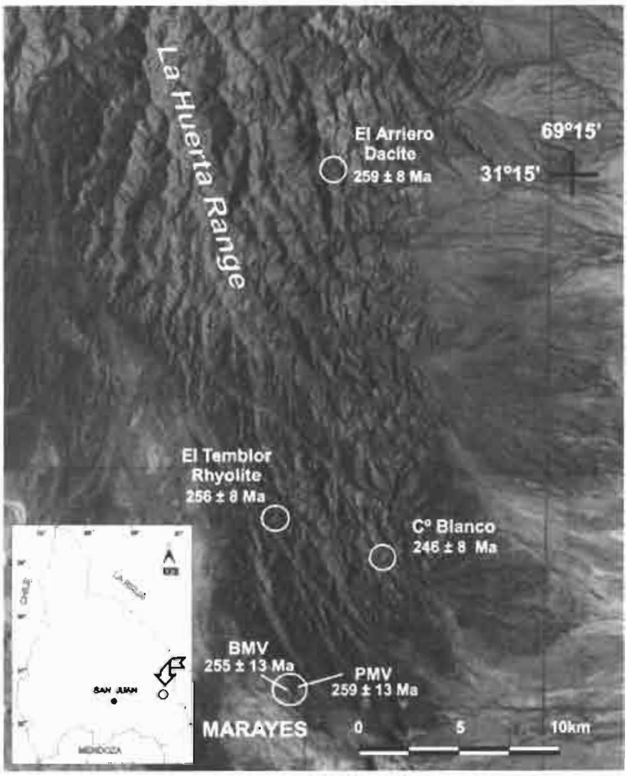

Figure 1. Location map and satellital image of southern La Huerta range showing the main igneous outcrops and the K-Ar ages.

LOCAL GEOLOGY - EL ARRIERO DACITE

El Arriero hydrothermal alteration zone lies on the eastern slope of La Huerta range, at 31°16'26" S latitude and 67°20'14" W longitude. It is located in El Arriero creek 12 km upstream from the discharging mouth of Santo Domingo main creek. The zone is about 1000 m long and 800 m wide, in average, and it is reachable only by trekking or horseback riding. No previous study has been done on the area, excepting those carried out by Cardó (1990) and Cardó & Pérez (1995).

Local basement made up of metatonalites with mafic microgranular enclaves, is intruded by the small irregular-shaped body of porphyritic dacite. A striking feature of the EAD is its alignment according to a NE-SW trend. The EAD is emplaced along an anular (ring) fracture surrounding by a tectonic breccia that forms a narrow rim at the contact of the igneous body and the enclosing sequence. Contacts are sharp. Clasts within the breccia are composed entirely of basement country rocks, suggesting that the roof of the magma chamber was not far above the present level of exposure. The breccia has abundant sulfide mineralization disseminated and/or in quartz/calcite veinlets.

The EAD exhibits rare xenoliths of basement rocks and isolated mafic microgranular enclaves. It is medium to light-pinkish gray, and shows a seriated porphyritic texture. It contains euhedral to subhedral plagioclase phenocrysts which conform 25% of the rock, and lesser amounts of quartz, hornblende and biotite in a fine-grained groundmass composed of the same minerals.

In thin section (Fig. 2), plagioclase (oligoclase) phenocrysts show notorious zoning and polysynthetic twinning. Sieve texture and corroded cores are common. Subhedral to euhedral, randomly oriented, brown-orange biotite phenocrysts of pseudohexagonal habit, compose approximately 5% of the rock. Brownish-green hornblende phenocrysts ranging from 8 to 10% are prismatic and strongly pleochroic. Rounded and embayed quartz phenocrysts are scarce (up to 3% of the rock).

The groundmass consists of fine-grained recrystallized quartz, altered plagioclase and small proportion of kaolinized alkali feldspar. Accessory minerals include apatite, sphene, zircon and opaques.

The EAD is altered and mineralized. It has moderate to strong silicification. Mafic minerals are variably altered to chlorite±calcite±epidote±quartz, with minor magnetite and sphene. Plagioclase is commonly altered to sericite and clay minerals. Propylitic alteration affecting the country rock, the tectonic breccia and the EAD is dominant, but quartz-sericite alteration also occurs. Weak potassic alteration (green biotite pseudomorphous after hornblende) is present in places. However, no clear alteration zoning directly associated with EAD has been identified.

The EAD is high in sulfides (>5% volume). Disseminated pyrite and lesser chalcopyrite±pyrrothite are the main ore minerals. Magnetite and native gold are also present. The igneous outcrop is cut by narrow (up to 0,60 m wide) quartz-pyrite veins which strike approximately N-S, extending not further than 30 m (Cardó & Pérez, 1995). The low density of veins and lack of pervasive alteration suggest that the EAD did not contribute much ore mineralization to the system.

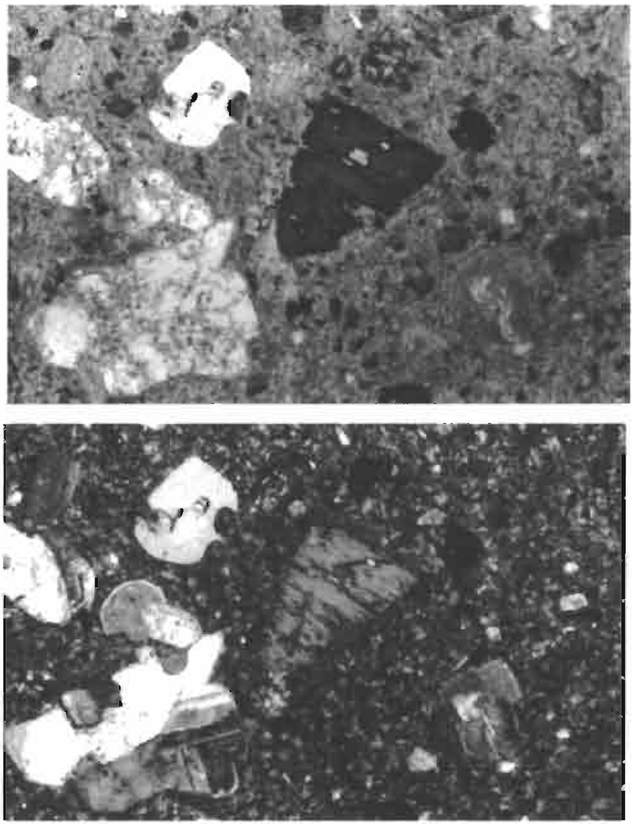

Figure 2: Phenocrysts of twinned plagioclase (some of them in clots), quartz, biotite and opaques, in a fine-grained groundmass of plagioclase±quartz. (X2,5-PPL and XPL)

K-Ar RADIOMETRIC DATING

Two samples of the EAD were analyzed at the Geochronology Laboratory of SERNAGEOMIN in Santiago, Chile. An attempt was made to select the freshest sample, but it still contains a small proportion of secondary alteration products. Biotite in dated sample (Arr s/n P96Arr) is a mixture of slightly chloritized of magmatic (dominant) and secondary (hydrothermal) ones. The former has been reseated to the temperature of formation of the later.

Analytical results are listed in Table 1.

Table 1. Analytical results obtained by the K-Ar method on biotite in El Arriero Dacite

Sample	Material	^{40}Ar rad. (nl/g)	%^{40}Ar atm.	%K	Isotopic age±error (Ma)
Arr s/n P96Arr	Biotite	34.781	11	3.206	259±8

The EAD is considered broadly contemporaneous with the stage of alteration and pyrite-copper mineralization. A slight decrease in the real age of the intrusion is explained as a consequence of ^{40}Ar loss attributed to the hydrothermal alteration (Faure, 1986).

DISCUSSION AND CONCLUSIONS

Since magmatic biotite in the dated sample is slightly altered (chloritized), and secondary biotite is also present, it is uncertain that this age is exactly that of the EAD intrusion. Nevertheless, the EAD is considered as a syn-mineralization igneous body, spatially and temporally associated with depositation of disseminated and/or veinlet ore mineralization and, thus, the obtained age could represents that of the magmatic-hydrothermal-mineralizing event. The intrusion was immediately followed by hydrothermal fluids derived from deeper zones, causing the depositation of ore minerals.

Further and more detailed radiometric data on specific alteration minerals, could help us to confirm the genetic relationship between El Arriero Dacite and the alteration-mineralization process.

The available K-Ar radiometric dating obtained for El Arriero Dacite, is consistent and shows no significant difference in ages respecting the previous dated volcanic and subvolcanic rocks in La Huerta range.

The absolute age of 259±8 Ma presented in this work, corresponds to the Middle Permian (Guadalupian), and confirms the presence of another component of the Gondwanic magmatic cycle in the Western Pampean Ranges.

ACKNOWLEDGMENTS

The authors would like to thank CICITCA-Universidad Nacional de San Juan for supporting this research.

REFERENCES

Baldis, B., R. Martínez, R. Villegas, E. Pereyra y A. Pérez, 1990. Estructura, provincialismo geológico y unidades tectonoestratigráficas de San Juan. En: Geología y Recursos Naturales de la Provincia de San Juan. 11° Congreso Geológico Argentino, Relatorio: 186-211, San Juan.

Cardo, R., 1990. Prospección de la sierra de La Huerta, provincia de San Juan. Secretaría de Minería de la Nación, Delegación San Juan, Informe inédito, 36pp.

Cardó, R. y L. Pérez, 1995.Síntesis de recursos metalíferos de la sierra de La Huerta, provincia de San Juan, Argentina. V Congreso Nacional de Geología Económica: 23-36, San Juan.

Cardo, R. y B. Castro de Machuca, 1999.Mineralizaciones metalíferas en la sierra de La Huerta, San Juan. *En* E. O. Zappettini (Ed.): Recursos Minerales de la República Argentina, vol. 1: 865-876 IGRM-SEGEMAR, Buenos Aires.

Castro de Machuca, B., C. Sumay, A. Conte-Grand y E. Meissl, 1998. Nueva evidencia de magmatismo neopaleozoico en las Sierras Pampeanas Occidentales: el Pórfido Marayes Viejo, provincia de San Juan, República Argentina. X Congreso Latinoamericano de Geología y VI Congreso Nacional de Geología Económica, II: 331-336, Buenos Aires.

Castro de Machuca, B., C. Sumay, A. Conte-Grand, E. Meissl y S. Pontoriero, 1999. Manifestación de la metalogénesis gondwánica en el área de Marayes Viejo, Sierras Pampeanas Occidentales, San Juan. XIV Congreso Geológico Argentino, Actas II: 312-315, Salta, Argentina.

Castro de Machuca, B., C. Sumay, E. Meissl, S. Pontoriero y A. Conte-Grand, 2000. Alteración hidrotermal y mineralización en el área del cerro El Temblor, sierra de La Huerta, provincia de San Juan. *En* I. Schalamuk, M. Brodtkorb y R. Etcheverry (Eds.): Mineralogía y Metalogenia. Publicación N° 6 INREMI: 80-86. La Plata. Buenos Aires.

Castro de Machuca, B., Sumay, C., Bruno, N., Meissl, E. y Conte-Grand, A., 2001. Geotectonic significance of the Marayes Viejo basalt based on K-Ar age dating, Western Pampean ranges, San Juan province, Argentina. III South American Symposium on Isotope Geology, Pucón, Chile, 5 pp. CD-ROM edition.

Faure, G., 1986. Principles of Isotope Geology, 2nd Ed., John Wiley & Sons, United States of America, 589 pp.

Ramos, V., F. Munizaga y G. Marín, 1988. Las riolitas neopaleozoicas de la sierra de La Huerta (provincia de San Juan): evidencias de una metalogénesis aurífera gondwánica en Sierras Pampeanas. III Congreso Nacional de Geología Económica, I: 149-159, Olavarría, Buenos Aires.

Pb ISOTOPIC CONSTRAINTS ON THE MINERALIZATION FROM THE VAZANTE GROUP, MINAS GERAIS, BRAZIL

Cunha, I.A.[1]; Babinski, M.[2] and Misi, A.[1]

1. Grupo de Pesquisa de Metalogênese, CPGG-CPG em Geologia. iona@cpgg.ufba.br, misi@ufba.br
2. Universidade de São Paulo, Instituto de Geociências, Centro de Pesquisas Geocronológicas. babinski@usp.br

Keywords: Vazante Group, Minas Gerais, Brazil, Pb isotopes

INTRODUCTION

The Morro Agudo and Vazante deposits are situated in the Vazante-Paracatu region, to the NW part of Minas Gerais, and represent the largest zinc district from Brazil. Other important deposits, such as the Ambrósia and Fagundes, besides several small occurrences are recorded in this district. The Morro Agudo and the Vazante mines are responsible for almost all the zinc concentrate production and by the whole lead production of the country (Oliveira, 1998).

The mineralizations are hosted by metapelitic-dolomitic sequences of the Vazante Group (Dardenne, 2000), and present many common characteristics and some contrasting features, being the most significant the willemitic nature of the ore, that distinguishes the Vazante deposit from the other deposits of the Vazante-Paracatu region (Bettencourt et al., 2001).

The Vazante-Paracatu deposits have been initially compared with Mississipi Valley Type (MVT) (Amaral, 1968; Rigobello et al., 1988; Iyer et al., 1992), Sedimentary Exhalative (SEDEX) (Misi et al., 1996; Freitas-Silva & Dardenne, 1997) and Irish type (Hitzman, 1997; Cunha et al., 2000; Misi et al., 2000; Dardenne, 2000; Monteiro, 2002). The Vazante deposit is classified as "Vazante Type" (Monteiro, 2002), because of the willemitic nature of the ore, differently of the other deposits from these zone.

Because the lead isotopic ratios are "fingerprints" from the galena-bearing mineral occurrences (Doe & Stacey, 1974), this technique can be used in genetic classification of the ore deposits and can provide important application for the economic appraisal of a deposit.

This paper relates the results of the lead isotope analyses in galenas of the Pb-Zn deposits of Morro Agudo, Vazante, Fagundes and Ambrósia, in the Vazante-Paracatu region, with the objective of helping in the establishment of a genetic model and to constrain the age of mineralization.

REGIONAL GEOLOGY

The Vazante-Paracatu region lies in the external part of the Brasília Fold Belt (BFB), which extends for more than 1000 km along the N-S direction, parallel to the western margin of the São Francisco Craton (CSF) (Fig. 1). The BFB represents an unstable tectonic unit that suffered successive reactivations of the old continental structures, and had its main evolution during the Brasiliano orogeny (~600 Ma), with a history of deformation and metamorphism (Marini et al., 1981).

The mineralizations are hosted in dolomitic rocks of the Vazant group (Dardenne, 2000), which represents one of the metasedimentary sequences of the southern segment of the BFB, involved in a complex imbricate system of nappes and thrusts, indicating vergences towards NE and tectonic transport towards SE, and marked by regional sinistral transcurrente shear zones (Dardenne, 2000). In the NW part of the State of Minas Gerais, the metasediments of the Vazante Group cover a 250 km long region, with general NS orientation (Fig.1). The Vazante Group (Dardenne, 2000) is divided into seven formations from base to top: Santo Antônio do Bonito, Rocinha, Lagamar, Serra do Garrote, Serra do Poço Verde, Morro do calcário and Serra da Lapa. The basal formations Santo Antônio do Bonito and Rocinha, are predominantly pelitic and contain large phosphate concentrations. The Lagamar formation represents a psammo-pelitic unit. The Serra do Garrote formation consists of a thick sequence, locally of slate, and rhythmic carbonaceous with pyrite. The Serra do Poço Verde is a dominantly dolomitic sequence divided into four members from the base to the top: Morro do Pinheiro Inferior Member, Morro do Pinheiro Superior Member, Pamplona Inferior Member, Pamplona Middle Member. The Morro do Calcário formation is composed by stromatolitic dolomites associated with dolarenite and dolorudite. The Pb-Zn mineralizations are hosted in this two, predominantly dolomitic later formations. The Serra da Lapa formation is composed by rhythmic carbonaceous phyllite, sericite-chlorite phyllite and carbonate bearing metasiltstone.

The Morro Agudo deposit is hosted by a sequence of breccias, dolarenite and the dolarenitic breccia of the Morro do Calcário formation. Interfingered or above the dolarenite occur a finely laminated clay-dolomitic sequence, constituted by dolomites and clay layers. The mineralization is limited by a normal fault (N10W/75SW), and all the orebodies are located to the west side of the fault zone. The orebodies are known in the mine as the G, H, I, J, K, L, M and N bodies, composed of sphalerite, galena, pyrite, and barite. The G, H and I orebodies are associated with dolomitic breccias, forming discontinuous and isolated levels of ore, with open-space filling textures and cementing brecciated structures. The J, K and L orebodies are stratabound and associated with dolarenites and dolarenitic breccias. The mineralization is an open-space filling and cementing oolitic dolostone beds with brecciated structures. The M orebody is hosted by dolarenite, made of sphalerite, galena and pyrite, which occurs filling open-spaces and veins. The N orebody is hosted by dolarenites intercaleted with the clay dolomitic sequence. The N orebody is stratiform, consists of venular alternate laminations of chert, galena, sphalerite and pyrite and shows sedimentary features indicating a syngenetic to syn-diagenetic formation (Cunha, 1999). Cunha (1999) reported a clear zonality of sulfur isotopic data in these different orebodies with a decreasing trend of $\delta^{34}S$ values from the fault zone towards the west, implying a possible feeder zone associated with the fault system. This is supported by temperature and salinity zonality of primary fluid inclusions in sphalerites from the same section (Cunha, 1999).

The Vazante deposit is associated with the Vazante fault zone (N50E/60NW), characterized by complex shear zones with irregular or anastomosed geometry (Monteiro, 2002). The mineralization styles are veins and anastomosed podiform bodies, composed by willemite, associated with hematite, siderite, zincite and dolomite. Metric bodies of metabasites occur tectonically imbricated by the sequences of the Pamplona and Morro do Pinheiro Members, along the fault zone of Vazante (Monteiro, 2002).

The Fagundes deposit is hosted in dolomites with stromatolitic chaotic structures of the Pamplona Upper Member, at the contact with the Serra do Velosinho Member (Monteiro, 2002). The mineralizated zones are stratigraphically analogous to the Morro Agudo deposit and above the Vazante zones. The mineralization is stratabound, characterized by strong hydrothermal alteration, such as silicification and dolomitization, composed by sphalerite, galena and pyrite associated with baroque dolomite, hosted by silicificated and brecciated dolomites. This deposit is characterized by later veins and breccias ore types, reflecting several intermediate stages of mobilization.

The Ambrósia deposit is controlled by a high angle fault zone (N30°), and is hosted by brecciated dolomite, which is imbricated with black shales and slates. The mineralization, composed of pyrite, marcasite, sphalerite, and minor galena, occur in brecciated comb-veins and veinlet infillings. (Monteiro, 2002). In this deposit the epigenetic style of mineralization predominates.

RESULTS AND DISCUSSION

Lead isotopic ratios were determinated in 41 samples of galenas: 29 from Morro agudo, 3 from Vazante, 6 from Fagundes and 3 from Ambrósia. The galenas were collected from samples coming from the different types of ore at the Vazante-Paracatu region, and the results are shown in the figures 2 and 3.

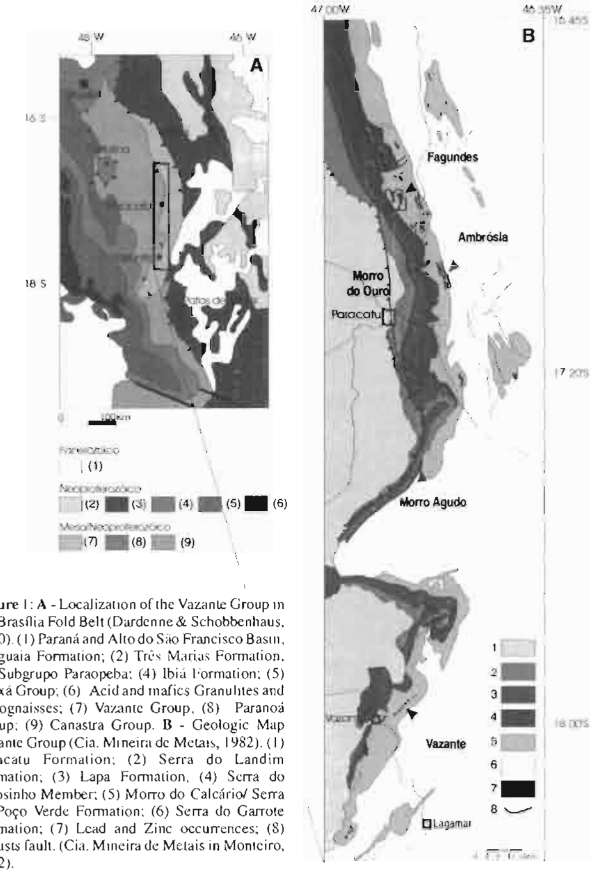

Figure 1: **A** - Localization of the Vazante Group in the Brasília Fold Belt (Dardenne & Schobbenhaus, 2000). (1) Paraná and Alto do São Francisco Basin, Araguaia Formation; (2) Três Marias Formation, (3) Subgrupo Paraopeba; (4) Ibiá Formation; (5) Araxá Group; (6) Acid and mafics Granulites and orthognaisses; (7) Vazante Group, (8) Paranoá Group; (9) Canastra Group. **B** - Geologic Map Vazante Group (Cia. Mineira de Metais, 1982). (1) Paracatu Formation; (2) Serra do Landim Formation; (3) Lapa Formation, (4) Serra do Velosinho Member; (5) Morro do Calcário/ Serra do Poço Verde Formation; (6) Serra do Garrote Formation; (7) Lead and Zinc occurrences; (8) Thrusts fault. (Cia. Mineira de Metais in Monteiro, 2002).

Pb ISOTOPIC COMPOSITION OF GALENA IN THE MORRO AGUDO DEPOSIT

The results for 29 galenas samples from the Morro Agudo deposit, display two separate populations (types I and II), indicating important difference in Pb composition according to the mineralization type (Fig. 2). The majority of the galenas contain lead whose $^{206}Pb/^{204}Pb$, $^{207}Pb/^{204}Pb$ and $^{208}Pb/^{204}Pb$ ratios had a small variation (17.588-17.839, 15.608-15.789, 36.998-37.558, respectively). The type I population is represented by isotopic ratios of the stratiform mineralization (N orebody). This is generally slightly less radiogenic than other orebodies in the mine. The type II population is constituited by isotopic ratios of other types of ore (open-space filling, veins, cementing brecciated structures) represented by the orebodies G, H, I, J, K, L and M. This population plots scattered along an apparent linear trend, and there is no distinction beteween the isotopic characteristics of the various types of mineralization.

According to Large et al. (1983), the slope of the steep linear trend, cannot be used to define an isochron; more probably it represents the result of mixing of Pb from at least two sources with different μ values.

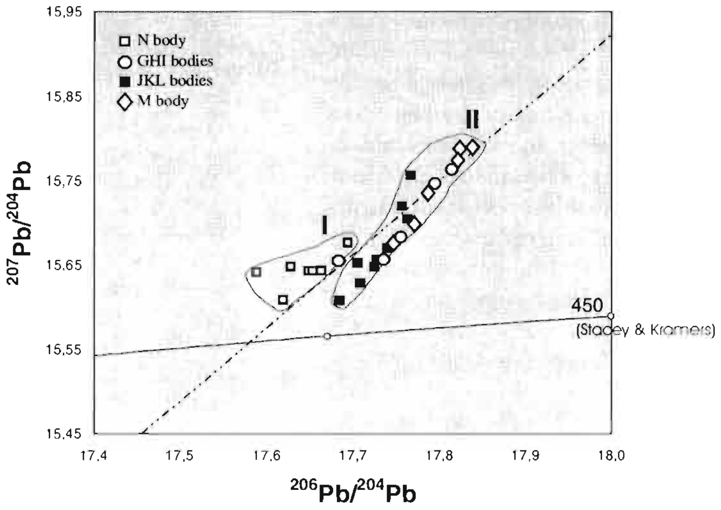

Figure 2 - Plot of Lead isotope data from the Morro Agudo deposit.

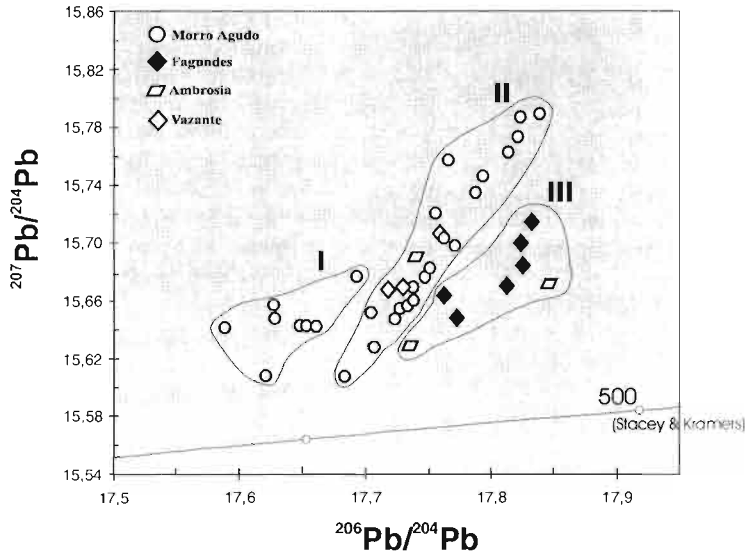

Figure 3-Plot of lead isotopes data from the Vazante-Paracatu region.

Pb ISOTOPE COMPOSITION OF GALENA IN THE VAZANTE, FAGUNDES AND AMBRÓSIA DEPOSITS

The figure 3 shows the whole Pb data from the Morro Agudo, Vazante, Fagundes and Ambrósia deposits, in which one additional population (III) can be identified. The majority of the galenas contain lead whose $^{206}Pb/^{204}Pb$, $^{207}Pb/^{204}Pb$ and $^{208}Pb/^{204}Pb$ ratios vary a little (17.718-17.846, 15.629-15.714, 37.170-37.475, respectively). The isotopic ratios of the Vazante deposit show many analogous to the Morro Agudo deposit, falling inside the same trend where the J, K, L, G, H, I and M orebodies are (field II), indicating a similar source of Pb.

The population III is characterized by isotopic ratios of the Fagundes and Ambrósia deposits. These are slightly more radiogenic that those of the Morro Agudo and Vazante deposits. Based on isotopic and fluid inclusion studies, Monteiro (2002) suggested clastic radiogenic sources for these deposits. This could explain the radiogenic values of the concerned galena.

The model ages based on Stacey & Kramers (1975) range from 716 to 929 Ma. However, the isotopic ratios plot above of the evolution curve of Stacey & Kramers, indicating that this ages lack any geologic significance.

The Pb of all the deposits has derivated from an early source with relatively high U/Pb and Th/Pb ratios. Taking the $^{207}Pb/^{204}Pb$ and $^{208}Pb/^{204}Pb$ ratios as an indicative parameter of the source, their isotope data plotted above of the evolution curve of Stacey & Kramers, clearly indicate a crustal source.

The N orebody shows sedimentary features indicating a syngenetic to syn-diagenetic formation (Cunha, 1999), differently from the other orebodies and deposits, which are typically epigenetic. The diversity of signatures could be explained by different lengths of time or periods of interaction of the hydrothermal solution with the source and the host rock.

The Pb isotopic compositions of hydrothermal titanite of the metabasite from the Vazante Group obtained by Babinski et al. (2003, this volume) are uniform and do not present a large variation. The obtained results are in agreement with the Pb isotopic ratios reported for galenas from the Pb-Zn deposits of Morro Agudo, Vazante, Ambrósia e Fagundes, indicating that the hydrothermal fluids responsible for the mineralizations might have affected the metabasic rocks.

ACKNOWLEDGMENTS

We are grateful to Companhia Mineira de Metais for continuous support and Prof. Dr. João Batista Teixeira by revision in this paper.

REFERENCES

Amaral, G., 1968b. Geologia e depósitos de minério na região de Vazante, Estado de Minas Gerais. Dep. de Eng. de Minas, Escola Politécnica, USP, Tese de doutoramento. 133p.

Dardenne, M.A., 2000. The Brasília Fold Belt. In: Cordani, U.G.; Thomaz Filho, A.; Campos, D.A. (eds). Tectonic evolution o South-American.Rio de Janeiro, 231-263 (international Geological Congress, 31).

Iyer, S.S., Hoefs, J.,& Krouse, H.R., 1992. Sulfur and lead isotope geochemistry of galenas from the Bambuí Group, Minas Gerais, Brazil--implications for ore genesis: Econ. Geol., v. 87, p. 437-443.

Large, D.; Schaeffer, R. & Höhndorf, A., 1983. lead isotope data from selected galena occurrences in the North Eifel and North Sauerland, Germany. Mineral. Deposita, 18, p. 235-243.

Marini, O.J.; Fuck, R.A.; Danni, J.C.; Dardenne, M.A., 1981. A evolução geotectônica da Faixa de Brasília e de seu embasamento. In: COM/SBG, Simpósio sobre o Crátion do São Francisco e suas Faixas Marginais, p. 100-115.

Misi, A.; Iyer, S.S.S.; Kyle, J.R.; Coelho, C.E.S.; Tassinari, C.G.G.; Franca-Rocha, W.J.S.; Gomes, A.S.R.; Cunha, I.A.; Toulkeridis, T.; Sanches, A.L., 2000 A metallogenic evolution model for the lead-zinc deposits of the Meso and neoproterozoic Sedimentary Basin of the São Francisco Craton, Bahia and Minas Gerais, Brazil. Ver.Bras.Geociências, 30(2):302-305.

Monteiro, L.V.S., 2002. Modelamento Metalogenético dos depósitos de Zn de Vazante, Fagundes e Ambrósia, associados ao Grupo Vazante, Minas Gerais. Tese de Doutorado, Universidade de São Paulo, Instituto de Geociência, 319p.

Oliveira, T.F., 1998. As Minas de Vazante e de Morro Agudo. In: CPGG-UFBA/ADIMB, workshop Depósitos Minerais Brasileiros de Metais Base, p.48-57.

Rigobello, A.E.; Branquinho, J.A.; Dantas, M.G.S.; Oliveira, T.F.; Neves Filho, W., 1988. Mina de zinco de Vazante. In: Schobbenhaus, C.; Coelho, C.E.S.(cords) Principais Depósitos Minerais do Brasil. DNPM, 3:101-110.

Hitzman, M. W., 1997a . Sediment Hosted Zn-Pb and Au Deposits in the Proterozoic Paracatu Vazante Fold Belt, Minas Gerais, Brasil. In: Geol. Society of America, Abstract with Programs.

Stacey & Kramers. 1975 – Aproximation of terrestrial lead isotope evolution by a two-stage model. Earth Planet. Sci. Lett.,26:207-221.

^{40}Ar/^{39}Ar MUSCOVITE AGES FROM HYDROTHERMALLY ALTERED DOLOSTONE HOSTING THE Pb-Ag CABOCLO DEPOSIT, BAHIA, BRAZIL

Cunha, I.A.[1]; Vasconcelos, P.[2]; Babinski, M.[3]; Misi, A.[1] and Franca-Rocha, W.J.S.[4]

1.Grupo de Pesquisa de Metalogênese, Centro de Pesquisa em Geofísica e Geologia e Curso de Pós-Graduação em Geologia,Universidade Federal da Bahia. iona@cpgg.ufba.br, misi@ufba.br
3. Centro de Pesquisas Geocronológicas, Instituto de Geociências, Universidade de São Paulo. babinski@usp.br
4. Universidade Estadual de Feira de Santana, Bahia, Brasil. wrocha@uefs.br

Keywords: Chapada Diamantina, Bahia, Caboclo Formation, Ar-Ar isotope dating

INTRODUCTION

The Caboclo Deposit lies in the northern border of the Chapada Diamantina, in the state of Bahia, Brazil (Fig. 1). It consists of galena mineralizations with associated silver, hosted by dolomitic rocks of the Caboclo Formation. The deposits have been studied by the Geological Survey of Bahia (CBPM) and by the Geological Survey of Brazil (CPRM) (Conceição Filho et al., 1984; Neves et al., 1980, respectively). Reserves of about 1 million tons grading 2% Pb and 5g/t Ag were estimated by CBPM geologists. The existence of a stratigraphical control of the orebody and a singenetic relationship were highlighted by Conceição Filho et al. (1986) who suggested a Sabkha model for the genesis of the deposit.

Franca-Rocha & Misi (1992a) and Misi et al. (1999) performed detailed geological and geochemical studies in the area, including stable isotope determinations (C, O, S) of host rocks and sulfides. The age of mineralization has been estimated to be Mesoprotereozoic (~1.2 Ga) by sulfur isotope variation of sulfides and sufates (Misi et al. 1999).

Franca-Rocha & Misi (1992b) described the orebodies as partially massive zone with gangue minerals, characterizing a hydrothermal paragenesis and an ore-hosting control by faults zones, all features suggesting that the deposit was originated by a sedimentary exhalative process (SEDEX).

This work presents ^{40}Ar/^{39}Ar ages of muscovite from the hydrothermally altered dolostone hosting the Pb-Ag deposits of the Caboclo Formation.

GEOLOGICAL SETTING

The Chapada Diamantina in the eastern part of the São Francisco Craton is formed by dominantly siliciclastic units and minor carbonate facies of the Chapada Diamantina Group. This is an approximately 2000 m Mesoproterozoic sedimentary pile composed of three formations: Tombador (fluvial and eolic quartzites and conglomerates), Caboclo (mainly pelites with subordinate carbonate lenses at the base, hosting the sulfide mineralization) and Morro do Chapéu (fluvial and eolic, with marine incursions in the upper section). Babinski et al. (1993) dated the pelites of the Caboclo Formation using Pb-Pb isochron ages at 1.14±0.14 Ga. This age was interpreted as the minimum time of deposition of the Caboclo Formation's uppermost limestones, being coherent with the interval from 1.0 to 1.2 Ga, previously obtained by other authors (Brito Neves et al, 1980).

THE Pb (Ag), Cu SULFIDE DEPOSITS

The Caboclo deposit is hosted by dolostone occurring in the basal portion of the marine Caboclo Formation and controlled by normal faults aligned N40E. Franca-Rocha (1995) and Misi et al. (1999) demonstrated that the Caboclo mineralization is mainly stratabound and formed by medium- to fine grained galena with minor chalcopyrite within dolarenite and/or dololutite. Quartz-veins with coarse-grained galena are also present, suggesting remobilization of the primary mineralization. According to these authors, mineralization forms a 'zebra-type' structure, in which clear bands, composed of quartz and feldspar, alternate with dark bands containing muscovite, biotite, K-feldspar, plagioclase, quartz, tourmaline and baroque dolomite. Galena is associated with the dark bands, forming small lenses and veinlets.

The gradual obliteration of the primary textures in the dolostone, the presence of an anomalous mineral association within the mineralized zone, and an ubiquitous association with normal faults, strongly suggest the overprinting of an extensive process of alteration originated by the percolation of hydrothermal fluids (Franca-Rocha, 1995).

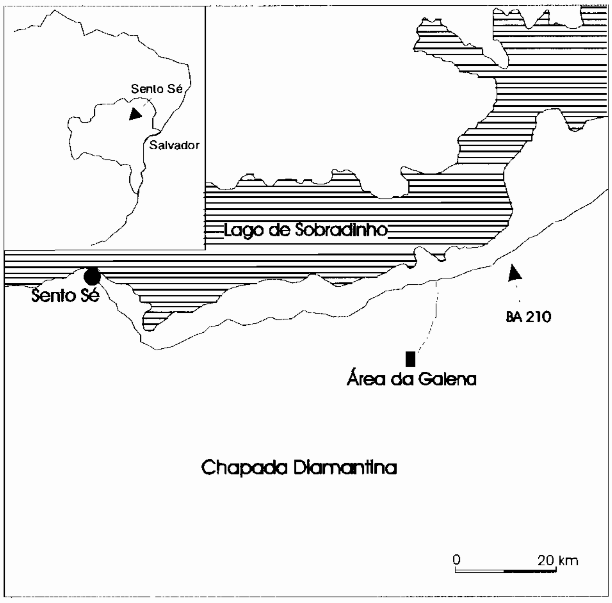

Figure 1. Location map of the studied area

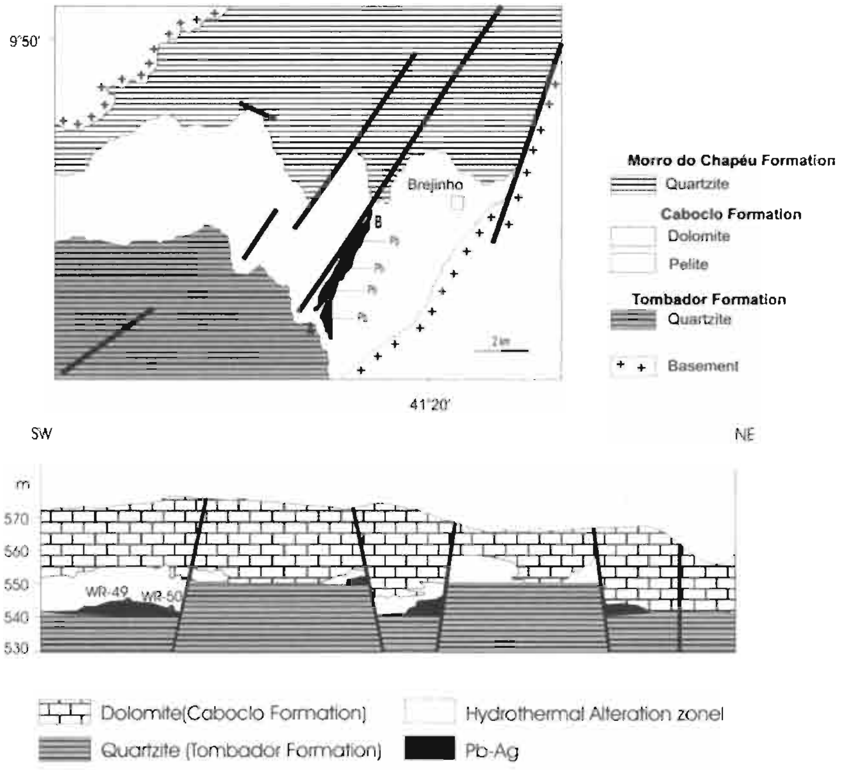

Figure 2. Geological Map (a) and Geological Section (b) of the Caboclo area.

RESULTS AND DISCUSSION

Three muscovite samples from the hydrothermal alteration zone, which are spatially associated with the sulfide mineralization, were selected for ^{40}Ar-^{39}Ar dating. The analyses were carried out at the Geochronology Research Center (CPGeo) of the University of São Paulo, following the procedures described by Vasconcelos et al. (2002).

Three muscovite grains from each sample were analyzed. All the muscovite grains yielded very well defined plateau ages and very close to the integrated ages for the same grains. Most of the plateaux are flat indicating absence of phases or domains with older ages inside the analyzed minerals.

The weighted average ages obtained from the grains in each sample are: 529 ± 3 Ma, 526 ± 4 Ma and 503 ± 3 Ma, being an appropriate age estimative for each sample. The difference of 26 Ma obtained among the samples probably represents the cooling time of the system, common in hydrothermal mineralization processes. Therefore, it is safe to suggest that the obtained ages represent the crystallization ages for these grains, and consequently, for the samples from the alteration area.

REFERENCES

Babinski, M.; Van Schmus, W, R.; Chemale Jr., F., Brito Neves, B. B.; Rocha, A. J. D., 1993. Idade isocrônica Pb-Pb em rochas carbonáticas da Formação Caboclo, em Morro do Chapéu, Ba. In: Anais do II Simpósio do CSF, pp.221-223.

Brito Neves, B. B.; Cordani, U. G.; Torquato, J. R. F., 1980. Evolução geocronológica do pré-cambriano do Estado da Bahia. In: Geologia e recursos minerais do Estado da Bahia. Textos básicos, v.3, pp. 1-104.

Conceição Filho, V. M.; Monteiro, M. D.; Carvalho, M. P., 1984. Projeto Borda Norte da Chapada Diamantina Fase II. Sinopse dos Resultados. Rel. Int. CBPM, 35p.

Conceição Filho, V. M.; Silva, R. W. S.; Lima, O. A. L., 1986. Controle estratigráfico das mineralizações de Cu, Pb e Ag nos metassedimentos da borda Norte da Chapada Diamantina-Bahia. In: XXXIV Cong. Bras. de Geologia, v.5, pp. 2105-2121.

Franca-Rocha, W. J. S. & Misi, A., 1992a. Evidências de alteração hidrotermal associada a mineralização de Pb e Ag na Formação Caboclo. In: Anais do I Simpósio Regional de Geologia Bahia-Sergipe, pp. 145-149.

Franca-Rocha, W. J. S. & Misi, A., 1992b. Mineralizações de sulfetos do tipo sedimentar-exalativo na formação Caboclo (Prot. Médio)-BA. In: Boletim de Resumos do XXXVII Cong. Bras. de Geologia, V.1, pp. 254-256.

Franca-Rocha, W. J. S. 1995. Origem das Mineralizações Sulfetadas nos sedimentos Mesoproterozoicos da Borda Norte da Chapada Diamantina - BA. Dissertação de Mestrado. Instituto de Geociências - UFBA. 130 p.

Misi, A.; Iyer, S.S.; Tassinari, C.C.G; Kyle, Jr.; Coelho, C.E.S.; Franca-Rocha, W..J.S.; Gomes, A.S.R.; Cunha, I.A., and Carvalho, I.G. 1999. Geological and isotopic constraints on the metallogenic evolution of the proterozoic sediment-hosted Pb-Zn (Ag) deposits of Brazil. Gondwana research, V.2, No. 1, pp. 47-65.

Neves, J. P.; Santana, A. C.; Silva, J. F.; Casé, M. G.; Bruni, D. C., 1980. Projeto Caboclo. Rel. Final, CPRM, 108p.

Vasconcelos, P.M.; Onoe, A.T.; Kawashita, K.; Soares, A.J. & Teixeira, W. 2002. 40Ar/39Ar Geochronology at the Instituto de Geociências, USP: Instrumentation, Analytical Produceres, and Calibration. Anais da Academia Brasileira de Ciências, 74(2):297-342.

ISOTOPIC DIFFERENTIATION IN VOLCANIC-EPITHERMAL SURFACE SULFUR DEPOSITS OF NORTHERN CHILE: $\delta^{34}S < 0$ ‰ IN "FERTILE" SYSTEMS (Au-Ag-Cu ORE DEPOSITS BELOW), VERSUS $\delta^{34}S \geq 0$ ‰ FOR "BARREN" SYSTEMS

Frutos, J.[1] **and Cisternas, M.E.**[2]

1. Servicio Nacional de Geología y Minería, Chile. jfrutos@sernageomin.cl
2. Instituto Geología Económica Aplicada, U. de Concepción. mcistern@udec.cl

Keywords: S Isotopes ($\delta^{34}S$), exploration, volcanic-epithermal systems

EXTENDED SUMMARY

Sulfur associated to hydrothermal systems, including sub-surface highly sulfured epithermal Au-Ag bearing ore systems of the Andean chain, comes essentially from magma fluids (H_2S, SO_2) of the calc-alkaline magmas produced by the subduction mechanism. In that form the mineralized sulfurate hydrothermal systems (Cu-Au-Mo porphyries, hydrothermal veins, Au-Ag epithermal systems and polymetalic skarns) are generated in the active borders, corresponding to the "oxided" magma systems of the magnetite series.

On another hand it is recognized (Oyarzún & Frutos, 1973; Frutos, 1975, 1978; Westra & Keith, 1981) that Sn-W porphyry systems belong to a "reduced" type of magmatism (illmenite series) of deep generation, in the inner part of the active border, with a less relative amount of S and higher relative contents of F than the magmas of the magnetite series (Fig. 1).

Magma-oxidation degree plays an important role on the geochemical evolution of sulfur, as it can be seen on the diagram of figure 2 (Hedenquist et al., 1994) which correlates oxide-reduction potential (redox R_h = log f H_2/H_2O) and temperature. Fields of stability of involved minerals allow to estimate the composition of the corresponding fluids.

The redox state at high temperature is initially controlled by the SO_2-H_2S relationship on gases associated to the evolving processes of magmatism–volcanism. As vapor begins to react with the host rock though fractures, and open-space structures through which it circulates at temperatures < 400°C, the S-bearing minerals begin to form and, consequently, the oxide-reduction potentials are controlled by the coexistence of the line alunite – pyrite . As the cooling of the systems continues, the acid dissociation and lixiviation of the host-rock increased. The subsequent rise of saline liquids containing metals follows a similar chemical line (for example, the isomolar coexistence line of HAu $(SH)_2$ and $AuCl_2$ on figure 2).

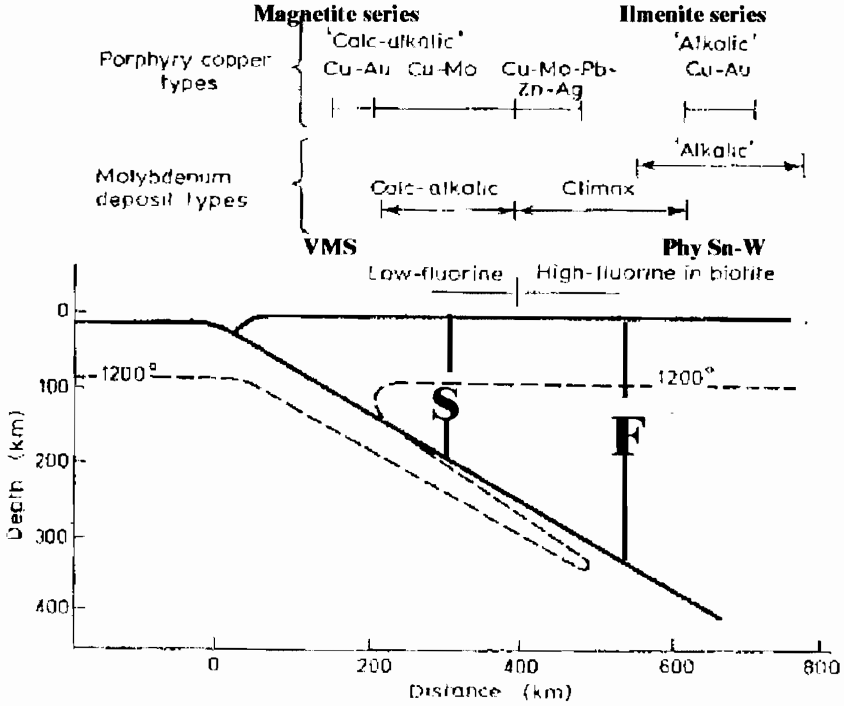

Figure 1. Tectonic-metallogenic schematic relationships between the magma types and the corresponding location of the porphyry-type ore deposits. After Oyarzún & Frutos, 1973; Frutos, 1975, 1978; Westra & Keith, 1981.

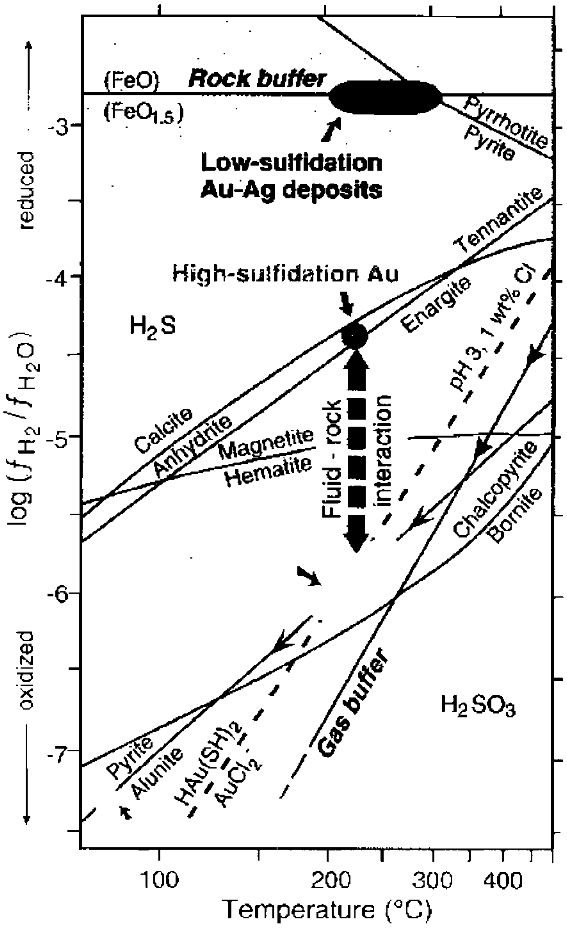

Figure 2. Correlation between the oxide-reduction potential (redox $R_h = \log f\ H_2/H_2O$) and temperature, indicating the fields of stability of the involved minerals and the composition of the corresponding fluids (Hedenquist et al., 1996).

This geochemical thermodynamic behavior of the fluids suggests that chloride complexes domain the Au transport under acid conditions (pH < 3) in the field of pyrite – alunite stability (high sulfidation Au-Ag deposits). Solubility of Au as $HAu(SH)_2$ is predominant for the redox conditions and lower temperatures typical of the Au – Ag low sulfidation systems.

DIFFERENTIATION IN THE SULFUR ISOTOPES RATIO AND THE RELATIONSHIP WITH Au-Ag ORE EPITHERMAL SYSTEMS

The characteristic of variable contents of oxygen of the calco-alkaline magmas leads to an important differentiation in relation to the different possibilities of producing sulfurate mineralized systems (Cu-Au-Mo porphyries, epithermal systems, surface sulfur volcanic ore deposits, etc.).

It appears a good correlation between "fertile" magmas (genetically related to the genesis of associated mineral deposits) with their extreme oxidation nature.

From this it is derived the generation in depth of sulfurate acid fluids (from the magmatic gases as: SO_2, H_2S, HCl) in which the H_2SO_4 will be rich in the ^{34}S sulfur isotope due to the chemical affinity recognized in isotopic measurements of these paragenesis (values of $\delta^{34}S > +1.6$ for the potassium alteration facies, and > +6 for the quartz-sericitic alteration facies) that so establishes it. In such mineral $\delta^{34}S$ values > + 10 ‰ are normally expected for the associated alunite and anhydrite. In consequence , the remanent SO_2 and H_2S, not used to produce these sulfurate phases, will be necessarily ^{34}S depleted, and, when finally, at the surface oxidation conditions, the exceeding S builds native S on the "roof" of the system, this will be necessarily "light" from the isotopic point of view ($\delta^{34}S < -7$ ‰) .

On the other hand, it must be noted that biogenic sulfur, which always shows a light nature from the isotopic point of view ($\delta^{34}S < -7$ ‰), doesn't justify (at the hydrothermal–epithermal process realms of the essentially volcanic geological environment) the former values as derived by geochemical contamination with the biogenic sulfur. It must be added to this the fact that the S of the sulfur mines without metal deposits underneath, in general presents S isotopic values similar to those of the magmas ($\delta^{34}S = 0$ ‰) . In this way, the finding of a "light S" isotopic characteristic in the surface native sulfur ore deposits and geothermal fields, could only be explained, and be compatible, with the formation of magmatic-hydrothermal sulfurate phases in depth (alunite and/or anhydrite), associated to highly oxidized magmas.

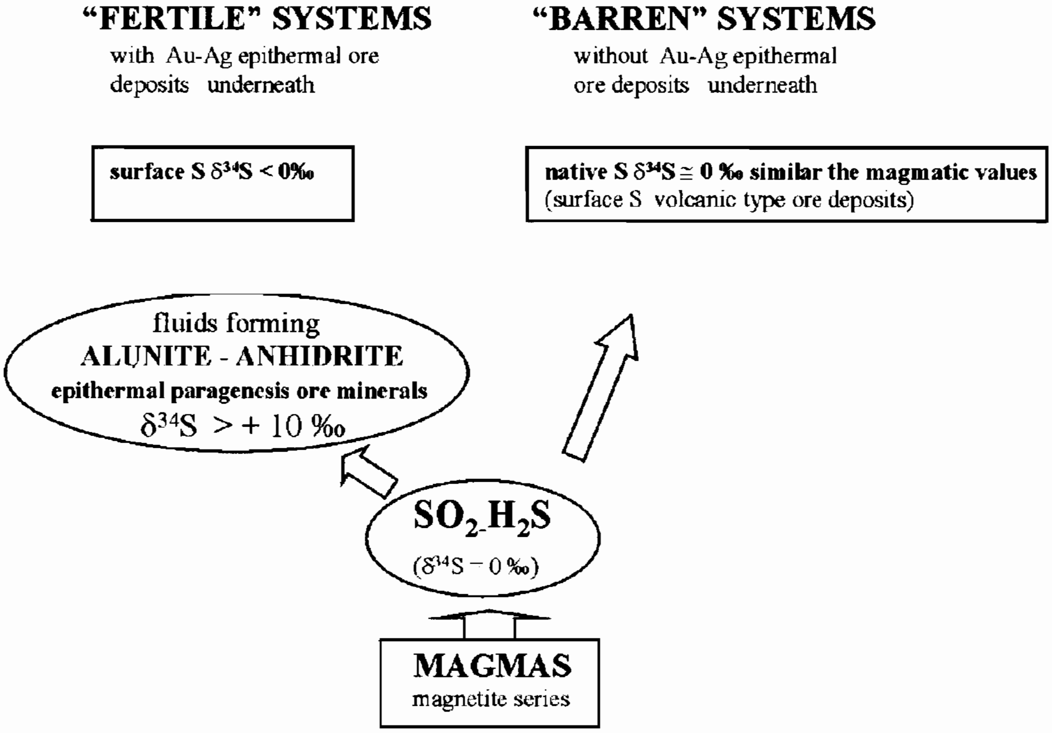

Figure 3. Model for "fertile" and "barren" systems.

If it wasn't like that, that is to say, not existing precipitation of sulfates in depth (and in consequence not existing a development of associated epithermal sulfurate mineralization) the isotopic ratio in the exceeding surface native S should show similar values to the magmatic ones ($\delta^{34}S \cong 0$ ‰).

CONCLUSIONS AND ECONOMIC GEOLOGY EXPLORATORY APPLICATIONS

These isotopic considerations allow to discriminate between probable "fertile" or "barren" systems.

In spite of the fact that this idea doesn't allow to confirm on the existence of an economic deposit under a native sulfur surface crust, anyhow it could represent an important exploratory criteria.

As a test mode, isotopic analysis have been made of the native S located in the "roof" higher parts of the Torito, Purén and La Coipa auriferous epithermal deposits, located in the Upper Cenozoic volcanic belt of Copiapó, in the northern Chile Andes.

The isotopic values found in each of the deposits are the following: La Coipa: $\delta^{34}S = -1.5$ ‰; Torito: $\delta^{34}S = -10.8$ ‰ and -4.7‰; Purén: $\delta^{34}S = -7.3$ ‰ and -2.9 ‰.

REFERENCES

Frutos, J. (1975) Porphyry copper type mineralization and Geosynclinal tectonic evolution in the Chilean Andes. An. Soc. Geol. Belgique. Vol. 98. Fasc. 1. pp.5-15.

Frutos, J. (1978) World Survey of Molybdenum Deposits. In International Molybdenum Encyclopaedia. Ed. Alexander Sutulov. Santiago Chile. pp. 427 – 439, T. I.

Hedenquist, J. W., Isawa, E., Arribas, A., White, N.C. (1996) Epithermal gold deposits: Styles, characteristics, and exploration. Resource Geology Special Publication N° 1, Tokyo, Japan.

Oyarzún, J. & Frutos, J. (1973) Porphyry coppers and tinbearing porphyries. A discussion of genetic models. Physics of the Earth and Planetary Interiors, 9 (1974), pp. 259-263. Elsevier.

Westra, G. & Keith, S. M. (1981) Classification and Genesis of Stockwork Molybdenum deposits. Ec. Geol. 76. pp. 844-873.

NEW TIMEFRAME FOR EL TENIENTE Cu-Mo GIANT PORPHYRY DEPOSIT: U-Pb, ^{40}Ar/^{39}Ar, Re-Os AND FISSION TRACK DATING

Maksaev, V.[1]; Munizaga, F.[1]; McWilliams, M.[2]; Mathur, R.[3]; Ruiz, J.[4]; Fanning, M.C.[5] and Zentilli, M.[6]

1. Departamento de Geología, Universidad de Chile, Casilla 13518, Correo 21, Santiago, Chile. vmaksaev@cec.uchile.cl, fmunizag@cec.uchile.cl
2. Department of Geological and Environmental Sciences, Stanford University, Stanford, CA 94305-2115. mcwilliams@stanford.edu
3. Geology Department, Juniata College, 1700 Moore Street, Huntington, PA 16652. mathur@juniata.edu
4. Department of Geosciences, University of Arizona, Gould-Simpson Building, 1040E. Fourth St., Tucson, AZ 85721-0077. jruiz@geo.arizona.edu
5. Research School of Earth Sciences, Australian National University, Canberra, ACT 0200, Australia. mark.fanning@anu.edu.au
6. Department of Earth Sciences, Dalhousie University, Halifax, Nova Scotia, Canada, B3H 3J5. marcos.zentilli@dal.ca

Keywords: Porphyry copper, geochronology, hydrothermal, El Teniente, Chile

INTRODUCTION

The timing and duration of hydrothermal activity are among the most fundamental questions regarding the genesis of porphyry copper deposits. We used a combination of SHRIMP U-Pb, Re-Os, ^{40}Ar/^{39}Ar and fission track dating methods to resolve the geochronology of mineralizing events and the duration of the hydrothermal activity of the El Teniente supergiant porphyry Cu-Mo deposit in the Chilean Andes. We show that multiple short-lived overprinting mineralization events within a single orebody related to a succession of felsic intrusions formed this enormous porphyry copper deposit.

GEOLOGY

The El Teniente Cu-Mo deposit is located ~70 km southeast of Santiago, in central Chile (Fig. 1). It is the youngest porphyry deposit in the Chilean Andes and the largest intrusion-related Cu-Mo orebody in the world, containing more than 75 Mt Cu in hypogene ores exceeding 0.65% Cu and, and more than 1.4 Mt Mo in ores exceeding 0.019% Mo. The orebody is 2700 m long by 1000 to 1700 wide with a vertical extent of about 1800m; current underground ore extraction is 98,000 t per day at 1.2% Cu and 0.026% Mo (Skewes et al., 2002). El Teniente deposit occurs within an arc-related Upper Miocene – Pliocene volcanic-plutonic complex on the western slopes of the Andes in the forearc of the northernmost section of the currently active Andean Southern Volcanic Zone that extends from 33° to 46°S. Approximately 80% of the Cu and Mo at El Teniente occur within a stockwork of mineralized veins and hydrothermal breccias within altered basalts, diabases, andesites and gabbros. Most of the primary characteristics of these host rocks are completely destroyed within the orebody by strong potassic alteration (biotite) and locally superposed chloritic and sericitic alterations.

Whole rock K-Ar ages outside the orebody from 10.9 ± 0.4 to 6.6 ± 0.4 Ma (Cuadra 1986) indicate the Upper Miocene age of the country rocks, and a concurrent new apatite fission track age of 8.9 ± 2.8 Ma for a sill some 5 km W of the mine.

Figure 1. Location map of El Teniente Cu-Mo deposit.

The remaining metal occurs in relatively small altered felsic apophyses and dikes with potassic (biotite, K-feldspar) alteration, locally with phyllic overprint (quartz-sericite). These include a number of quartz diorite to tonalite stocks occur aligned N-S in the eastern section of the deposit; the largest is the Sewell Quartz Diorite in the southeastern section of the orebody with 1 km of diameter, and other separate quartz-diorite to tonalite minor porphyritic stocks or apophyses to the north of the Sewell stock, referred as "Central Diorite" and "Northern Diorite" in the mine. These separate intrusions were customarily correlated with the Sewell Quartz Diorite (i.e. Cuadra, 1986) and our new U-Pb geochronological data confirmed this age correspondence.

A small stock of grey porphyritic quartz diorite (referred as "A" Porphyry) intrudes the Sewell Quartz-diorite and adjacent biotitized "andesites" in the southeastern section of El Teniente orebody; it contains abundant inclusions equigranular quartz-diorite inclusions from the Sewell Quartz-diorite and is surrounded by richly-mineralized hydrothermal breccias with an anhydrite matrix.

In the northern section of the orebody the Teniente Dacite Porphyry forms a vertical dike-like intrusion that extends N-S for 1.5 km with an average width of some 200 m. A number of dacite dikes 2 to 15 m thick also occur within the El Teniente orebody (referred as latite in the mine), some of them forming ring dikes and others following the main NE and NW structural orientations within the orebody. Most dacite dikes show only scarce pyrite veins, but some contain veins with the sulfide association typical of latest stage mineralization of El Teniente (chalcopyrite, molybdenite, tennantite-tetrahedrite, sphalerite, galena, and pyrite; Cuadra, 1986). It appears that a succession of dacite dikes was emplaced within a short period of time during late stages of evolution of El Teniente. In the center of the orebody is the large Braden Breccia Pipe which is a funnel-shaped diatreme vent with 1200 m in diameter at the surface, tapering to about 600 m at 1,800 m depth; this pipe is surrounded by a discontinuous rim of hydrothermal breccia with tourmaline and sulfide matrix (Cuadra, 1986).

GEOCHRONOLOGY

Zircon SHRIMP U-Pb dating of four samples from quartz diorite stocks of the eastern section of El Teniente orebody suggests crystallization between 6.46 ± 0.11 and 6.11 ± 0.13 Ma ($\pm 2\sigma$), but the samples yield bimodal U-Pb age distributions suggestive of partial Pb-loss between 5.67 ± 0.19 and 5.48 ± 0.19 Ma. These crystallization and Pb loss ages are similar to molybdenite Re-Os dates of 6.30 ± 0.03 and 5.60 ± 0.02 Ma from two hydrothermal breccias hosted by quartz diorite porphyritic intrusive rocks in the southeast section of the orebody. The data suggest that hydrothermal ore deposition was active during crystallization of these intrusions and also some 0.44 to 0.97 m.y. later. The time lag is significantly larger than the uncertainty of the U-Pb and Re-Os age analyses, demonstrating that hydrothermal mineralization was superimposed upon crystallized eastern quartz diorite plutons. Lead-loss in the zircons appears to be related to hydrothermal leaching during later circulation of hot fluids. The zircon crystals have mottled surfaces and some thin zircon overgrowths with notably higher U and Th content that substantiate the effect of hydrothermal activity (e.g. Rubin et al., 1989; Corfu & Davis, 1991). This is consistent with recent investigations suggesting that fluid circulation and related metasomatism may partly reset the U-Pb zircon geochronometer (i.e. Geisler et al., 2001, Cocherie et al., 2002, Kaulina, 2002). ^{40}Ar/^{39}Ar plateau ages at 5.63 ± 0.12 and 5.47 ± 0.12 Ma from magmatic biotite in unmineralized quartz diorite to the southeast of the El Teniente orebody suggests that a separate intrusion caused this hydrothermal mineralizing event and could be the heat source for the younger event inferred from U-Pb and Re-Os dating. Furthermore, coarse biotite from a hydrothermal breccia with anhydrite and sulfides matrix from the easternmost section of the orebody yielded a ^{40}Ar/^{39}Ar plateau age of 5.69 ± 0.08 Ma, this breccia is the same that produced a molybdenite Re-Os age of 6.30 ± 0.03 Ma.

Zircons from the Teniente Dacite porphyry from the northern section of the El Teniente orebody yielded an U-Pb age of 5.28 ± 0.10 Ma with unimodal age distribution indicating a simple cooling history, in contrast to the eastern quartz diorite stocks. This U-Pb date is slightly younger than the 5.67 ± 0.19 to 5.48 ± 0.19 Ma age range inferred for an overprint that affected intrusions in the eastern section of El Teniente, and also is younger than the molybdenite Re-Os age of 5.60 ± 0.02 Ma, suggesting that the eastern intrusions were affected by an earlier event unrelated to the Teniente Dacite porphyry. Coarse hydrothermal biotite from a vein within quartz diorite in the southeast section of the orebody yielded a plateau ^{40}Ar/^{39}Ar age of 5.06 ± 0.12 Ma and biotite from the "A" porphyry an age of 4.93 ± 0.12 Ma that may reflect hydrothermal activity driven by a 5.28 ± 0.10 Ma dacite porphyry. The crystallization age for the Teniente Dacite porphyry is older than published biotite K-Ar ages that range from 4.77 ± 0.18 to 4.6 ± 0.3 Ma, but these latter ages may reflect potassic alteration overprint (Clark et al., 1983, Cuadra, 1986). The Teniente Dacite Porphyry has long been regarded as the main mineralizing intrusion at El Teniente, because the main concentration of hypogene bornite-bearing veins and the disseminated bornite associated with pervasive potassic alteration occurs within this porphyry and host mafic rocks peripheral to the felsic intrusion. In addition, the bornite/chalcopyrite ratio decrease steadily away from the porphyry, coupled with a similar reduction on the intensity of biotite alteration of the host rocks (Cuadra, 1986, Howell & Molloy, 1960; Camus, 1975; Ip, 1987).

A set of discontinuous mineralized dacite ring dikes encircles the Braden diatreme breccia pipe in the center of El Teniente. Zircons from one dike yielded a U-Pb age of 4.82 ± 0.09 Ma with unimodal age distribution, in excellent agreement with molybdenite Re-Os ages from veins hosted by the Teniente Dacite porphyry (4.87 ± 0.03 Ma from a quartz-molybdenite vein with minor chalcopyrite and 4.78 ± 0.03 Ma from a vein with intergrowth molybdenite and chalcopyrite with sericitic alteration halo). This agreement suggests that ore deposition was related to subsequent injection of dacite magma and was superimposed on the Teniente Dacite porphyry. The cataclysmic explosion that created the diatreme at the center of El Teniente occurred during the same event suggested by a sericite ^{40}Ar/^{39}Ar plateau age of 4.75 ± 0.12 Ma from bleached clasts from altered sections of the Braden diatreme breccia pipe. We conclude that the large breccia does not postdate mineralization as previously interpreted (Sillitoe, 1985), but was a single synmineralization event that produced sudden decompression of the porphyry system the effect of which controlled ore deposition and further hydrothermal circulation on its shattered margins.

In contrast, a molybdenite vein containing minor chalcopyrite and a sericitic halo hosted by the Teniente Dacite porphyry yielded a molybdenite Re-Os age of 4.42 ± 0.02 Ma, identical to two molybdenite Re-Os determinations from molybdenite-bearing quartz veins with chalcopyrite in the northernmost quartz diorite stocks. The younger molybdenite ages represent a late ore deposition event that may be temporally related to youngest dacite injections, as an altered but largely unmineralized dacite stock underlies the northern section of the Braden breccia pipe with sericite ^{40}Ar/^{39}Ar plateau ages from 4.56 ± 0.12 to 4.46 ± 0.10 Ma. An apatite fission track age of 4.2 ± 2.8 Ma from the Teniente Dacite porphyry suggests that the porphyry system cooled under the apatite fission track closure temperature (~100ºC) shortly after. This is consistent with an ^{40}Ar/^{39}Ar age of 3.85 ± 0.18 Ma obtained for hornblende from a post-mineralization andesite dike at El Teniente that marks the end of magmatism within the deposit.

Duration of hydrothermal systems is a fundamental metallogenic question, particularly for supergiant deposits. Detailed ^{40}Ar/^{39}Ar step-heating dating of hydrothermal biotite and sericite at El Teniente yielded 37 plateau ages ranging from 4.81 ± 0.10 to 4.37 ± 0.10 Ma. Biotite ^{40}Ar/^{39}Ar ages are generally older than sericite ages. The mica ages record only the most recent hydrothermal activity lasting at least 0.44 ± 0.10 m.y., but this interval contains Mo deposition events at 4.8 and 4.4 Ma. We conclude that individual hydrothermal pulses lasted less than 0.44 ± 0.10 m.y. The concentration of the mica ages within such a short time span (4.81 to 4.37 Ma) from samples collected from different sections and levels of the large deposit, and their coincidence with published K-Ar ages (Clark et al., 1983, Cuadra, 1986) indicates that extensive high-temperature hydrothermal circulation took place during this period, probably related to the emplacement of successive dacite magmas and the interrelated cataclysmic explosion of the Braden Breccia. This later heating obliterated the K-Ar record of older thermal events at El Teniente identified by other isotopic systems with higher closure temperatures.

Estimating a cooling rate at El Teniente is made difficult by successive thermal overprinting, but the agreement of U-Pb zircon ages and Re-Os molybdenite dates suggests that ore deposition occurred immediately after the felsic intrusions crystallized, implying very fast cooling. Comparing the 4.82 ± 0.09 Ma zircon U-Pb age of a mineralized dacite dike with the 4.74 ± 0.10 Ma ^{40}Ar/^{39}Ar plateau age of coarse hydrothermal biotite at El Teniente, we conclude that cooling from about 800ºC (zircon U-Pb closure temperature) to 300ºC (biotite ^{40}Ar/^{39}Ar closure temperature) within ~80.000 years, leading to cooling rates in excess of 1000ºC/Ma. This is faster than, but in the order of rates estimated by Ballard et al. (2001) for distinct intrusions at Chuquicamata PCD. The high cooling rates we infer for El Teniente agree with model calculations of Cathles et al. (1997 and references therein) for kilometer-scale shallow-level intrusions.

DISCUSSION

Our new geochronological data suggest that El Teniente was generated by at least five superposed mineralizing events. Each was linked to short-lived hydrothermal events on the order of a few hundred thousand years at about 6.3, 5.6, 5.3, 4.8 and 4.4 Ma that correlate with the crystallization of felsic intrusions. This interpretation agrees with a multistage evolution proposed by Skewes & Stern (1995), but contradicts a recent model that minimizes the mineralizing role of felsic intrusions at El Teniente (Skewes et al., 2002). Hydrothermal overprinting and overlapping mineralizing events also have been resolved by geochronological studies at the enormous Chuquicamata (Ballard et al., 2001; Reynolds et al., 1998; Ossandon et al., 2001), Rio Blanco-Los Bronces (Serrano et al., 1996) and La Escondida deposits (Padilla et al., 2001), and from crosscutting relations between dikes and veins at Bingham (Redmond et al., 2002). It would appear that superimposed mineralizing events within a single orebody may be required to generate supergiant Cu-Mo PCDs. Overprinting appears to be the principal control on deposit size rather than possible Cu-richer hydrothermal fluids (e.g. Clark, 1993). Large-scale tectonic and local structural control are certainly important in focusing magma injection and hydrothermal fluid flow, but repeated ore deposition associated with felsic magmas in epizonal levels appears to produce supergiant Cu-Mo deposits.

Our study employed four different isotopic systems and has resolved at least five superimposed but short-lived mineralization events at El Teniente that correlate with crystallization of felsic intrusions. These multiple superposed thermal stages were not apparent from the previously available geochronologic data. Overprinted mineralizations appear to produce rich Cu grades and extraordinary tonnage at El Teniente. Other supergiant PCDs also revealed superposed events, indicating that overprinting is probably required to form these large porphyry copper deposits.

ACKNOWLEDGEMENTS

CONYCYT, Chile, through Fondecyt 1000932 grant to V. Maksaev and F. Munizaga (Universidad de Chile) supported this project. CODELCO-Chile financed the U-Pb dating. Special thanks to Francisco Camus (Exploration Manager) and to Jorge Skarmeta and Miguel Herve. We are particularly indebted to Patricio Zúñiga (El Teniente, Geology Manager) for granting access to the mine and drillcores. The assistance, guide, and helpful explanations at the mine by the geologists Alejandra Arévalo, Ricardo Floody, Jose Seguel, Andres Brzovic, Oscar Quezada, and other personnel of CODELCO El Teniente Division are truly appreciated, yet the interpretation of the data remain the sole responsibility of the authors. SHRIMP U-Pb analyses were done at the Australian National University, the ^{40}Ar/^{39}Ar step heating analyses at Stanford University, the Re-Os analyses at the Arizona University, and the fission track dates at Dalhousie University.

REFERENCES

Ballard, J.R., Michael-Palin, J., Williams, I.S., Campbell, I.H., and Faunes, A., 2001. Two ages of porphyry intrusion resolved for the super-giant Chuquicamata copper deposit of northern Chile by ELA-ICP-MS and SHRIMP: Geology, v. 29, no. 5, p. 383-386.

Camus, F., 1975. Geology of El Teniente orebody with emphasis on wall rock alteration: Economic Geology, v. 70, p. 1342–1372.

Cathles, L.M., Erendi, A.H.J., Thayer, J.B., and Barrie, T., 1997. How long can a hydrothermal system be sustained by a single intrusion event?: Economic Geology, v. 92, p. 766-771.

Clark, A.H.; Farrar, E.; Camus, F. and Quirt, G.S., 1983. K-Ar data for El Teniente porphyry copper deposit, central Chile: Economic Geology, v. 78, p. 1003 – 1006.

Clark, A.H., 1993. Are outsize porphyry copper deposits either anatomically or environmentally distinctive?: Society of Economic Geologists Special Publication, no. 2, p. 213-283.

Cocherie, A., Rossi, P., Fanning, C.M., and Deloule, E., 2002. Accretion and splitting within the Permian Pangea recorded by episodic metamorphic zircon growth, *in* Goldschmidt Conference Abstracts, Geochemica et Cosmochimica Acta, v. 66, Special Supplement, no. S1, p. A146.

Corfu, F. and Davis, D.W., 1991. Comment on "Archean hydrothermal zircon in the Abitibi greenstone belt: constraints on the timing of gold mineralization" by J.C. Claoué-Long, R.W. King and R. Kerrich. Earth and Planetary Science Letters, v. 104, p. 545-552.

Cuadra, P., 1986. Geocronología K-Ar del yacimiento El Teniente y áreas adyacentes: Revista Geológica de Chile, no. 27, pp. 3–26.

Geisler, T., Ulonska, M., Schleicher, H., Pidgeon, R.T., and Van Bronswijk, W., 2001. Leaching and differential recrystallization of metamict zircon under experimental hydrothermal conditions: Contributions to Mineralogy and Petrology, v. 141, p. 53-65.

Howell, F.H. and Molloy, J.S., 1960. Geology of the Braden orebody, Chile, South America: Economic Geology, v. 55, p. 863-905.

Ip, L., 1987. Estudio de inclusiones fluidas en vetillas tempranas del sector noroeste del yacimiento "El Teniente": Comunicaciones, no. 38, p. 27-45.

Kaulina, T.V., 2002. Metasomatic alteration of zircons from potassic granites, *in* Goldschmidt Conference Abstracts, Geochemica et Cosmochimica Acta, v. 66, Special Supplement, no. S1, p. A387.

Ossandon, G., Fréraut, R., Gustafson, L.B., Lindsay, D.D. and Zentilli, M., 2001. Geology of the Chuquicamata Mine: A Progress Report: Economic Geology, v. 96, p. 249-270.

Padilla, R., Titley, S.R. and Pimentel, F., 2001. Geology of the Escondida Porphyry Copper Deposit, Antofagasta Region, Chile: Economic Geology, v. 96, p. 307-324.

Redmond, P.B., Einaudi, M.T., and Landtwing, M.R., 2002. Cyclical P-T-X evolution of magmatic-hydrothermal fluids in the Bingham porphyry Cu-Au-Mo deposit, Utah: Geological Society of America Abstracts with Programs, v. 34, no. 6, p.187.

Reynolds, P., Ravenhurst, C., Zentilli, M., and Lindsay, D., 1998. High-precision 40Ar/39Ar dating of two consecutive hydrothermal events in the Chuquicamata porphyry copper system, Chile: Chemical Geology, v. 148, p. 45-60.

Rubin, J.N., Henry, Ch.D. and Price, J.G., 1989. Hydrothermal zircons and zircon overgrowths, Sierra Blanca Peaks, Texas. American Mineralogist, v. 74, p. 865-869.

Serrano, L., Vargas, R., Stambuk, V., Aguilar, C., Galeb, M., Holgrem, C., Contreras, A., Godoy, S., Vela, I., Skewes, A., and Stern, C.R., 1996: Society of Economic Geologists, Special Publication, no. 5, p. 119-130.

Sillitoe, R.H., 1985. Ore-Related Breccias in Volcanoplutonic Arcs: Economic Geology, v. 80, p. 1467-1514.

Skewes, M.A. and Stern, Ch.R., 1995. Genesis of the Giant Late Miocene to Pliocene Copper Deposits of Central Chile in the Context of Andean Magmatic and Tectonic Evolution: International Geology Review, v. 37, p. 893-909.

Skewes, M.A., Arevalo, A., Floody, R., Zúñiga, P., and Stern, Ch.R., 2002. The Giant El Teniente Breccia Deposit: Hypogene Copper Distribution and Emplacement. Society of Economic Geologists Special Publication, no. 9, p. 299-332.

Re-Os AND Sm-Nd ISOTOPE SETTING CONSTRAINTS ON THE ORIGIN OF CHROMITITES, IPUEIRA-MEDRADO SILL, BAHIA, BRAZIL

Marques, J.C.[1]; Carlson, R.W.[2]; Ferreira Filho, C.F.[3] and Pimentel, M.M.[3]

1. Instituto de Geociências, Universidade Federal do Rio Grande do Sul, R. Bento Gonçalves 9500, Porto Alegre-RS, 91509-900, Brazil. juliana.marques@ufrgs.br
2. Department of Terrestrial Magnetism, Carnegie Institution of Washington, 5241 Broad Branch Road, Washington, DC 20015, USA. carlson@dtm.ciw.edu
3. Instituto de Geociências, Universidade de Brasília, Campus Universitário, Asa Norte, Brasília-DF, 70910-900, Brazil. cesarf@unb.br, marcio@unb.br

Keywords: Os and Nd isotopes, crustal contamination, chromite deposit

INTRODUCTION

The chromite deposit of the Ipueira-Medrado sill is concentrated in a single thick (8 m) chromitite, which sets severe constraints for the origin of chromitites. The sill is part of a Paleoproterozoic swarm of mafic-ultramafic intrusions known as the Jacurici Complex (Fig. 1). The complex is located in northeastern Brazil, spatially related to two other Paleoproterozoic mafic-ultramafic complexes, and is considered to be emplaced in granulite-gneiss terranes of the Caraíba granulite complex (Barbosa et al., 1996) or possibly in the Serrinha block, an Archean middle grade, gneiss-migmatitic and granite-greenstone belt terrane (Teixeira et al., 2000).

GEOLOGY OF THE SILL

The Ipueira-Medrado sill is a single intrusion tectonically disrupted into two segments that crop out on the limbs of a synform. It is up to 300 m thick and is conformable with footwall quartz-feldspathic gneiss and with hanging-wall rocks, including olivine-bearing marble, calc-silicate rocks, and metachert (Deus & Viana, 1982). Shearing is restricted to the margins of the sill and fault zones. Primary igneous textures and minerals are largely preserved and fresh samples are obtained from drill cores.

The Ipueira-Medrado sill consists mainly of ultramafic rocks (80%) and was subdivided by Marques & Ferreira Filho (2003) in three main zones from the base to the top: the Marginal Zone; the Ultramafic Zone; and the Mafic Zone (Fig. 2). The Marginal Zone is 5 to 20 m thick and is composed mainly by sheared gabbros. The Ultramafic Zone is subdivided in three subunits: the Lower Ultramafic Unit (LUU); the Main Chromitite Layer (MCL); and the Upper Ultramafic Unit (UUU). The LUU is the thickest (100 to 180 m thick) and consists mainly of dunite interlayered with harburgite. The MCL is 5 to 8 m thick and has three sublayers. The lower sublayer is a massive chromitite (0.5 to 1 m thick), the intermediate sublayer is a chain-textured chromitite (0.3 to 0.5 m thick) characterized by fine-grained aggregates of chromite surrounding larger orthopyroxene crystals, and the upper sublayer consists of massive chromitite (4 to 6 m thick). The UUU is up to 50 m thick and consists mainly of harzburgite with subordinate interlayered dunite. This unit is characterized by abundant intercumulus amphibole (hornblende-tschermakite to Mg-

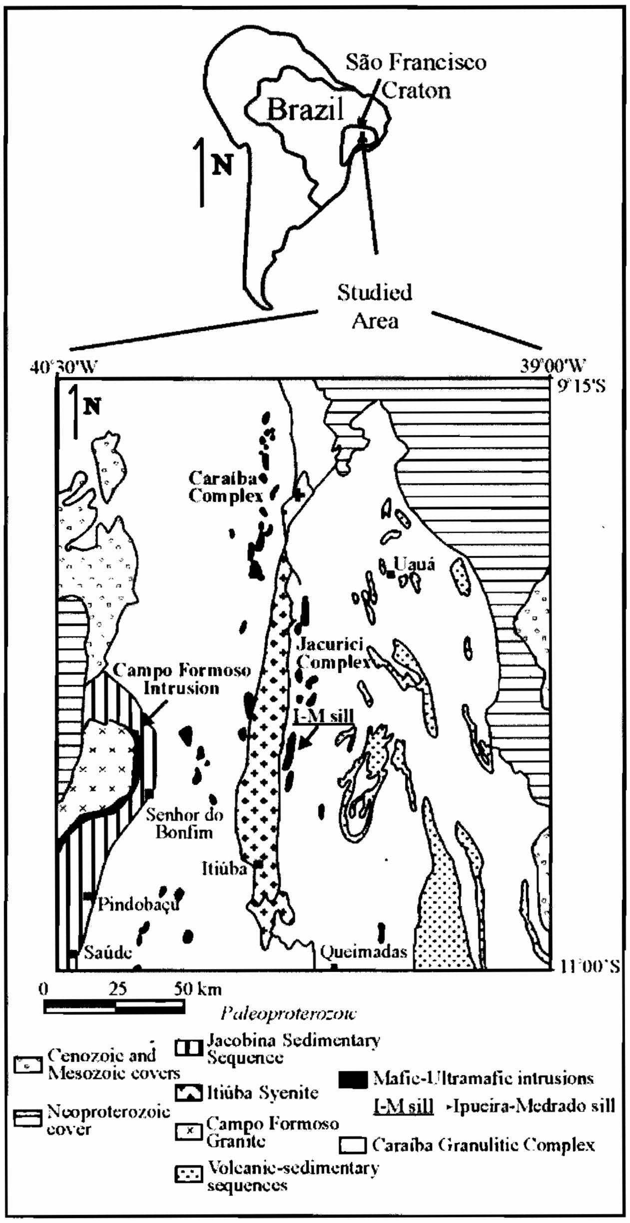

Figure 1. Geological setting of the Jacurici Complex (after Marinho et al., 1986). The arrow indicates the location of the Ipueira-Medrado sill.

hornblende) that occurs as large oikocrysts and is suggested to result from crustal contamination (Marques & Ferreira Filho, 2003). The amount of orthopyroxene increases with stratigraphy grading to an orthopyroxenite at the top. The Mafic Zone is up to 40 m thick and constitutes the upper part of the sill. It consists of norite with variable proportions of orthopyroxene and plagioclase. When partially metamorphosed, the mineral assemblage indicates amphibolite facies conditions of metamorphism.

The magmatic evolution of the sill was evaluated through the compositional variation of olivine and orthopyroxene in harzburgite samples throughout the stratigraphy (Marques & Ferreira Filho, 2003). Two magmatic regimes were identified. The first is expressed in the interval of the LUU and is characterized by a slow upward increase in MgO/FeO intensified immediately below the MCL (Fo and En up to 90) (Fig. 2). The second is located above the MCL and is characterized by rapid evolution toward more Fe-rich compositions (Fo decreasing to 84 and En to 82) (Fig. 2). The first regime was interpreted as an open magmatic system with concomitant injections of fresh magma and extrusion of fractionated magma, while the second was considered as a result of crystallization under a closed magmatic system. The MCL is interpreted to have formed at the transition from these two regimes, which appears to be important in instigating chromite crystallization.

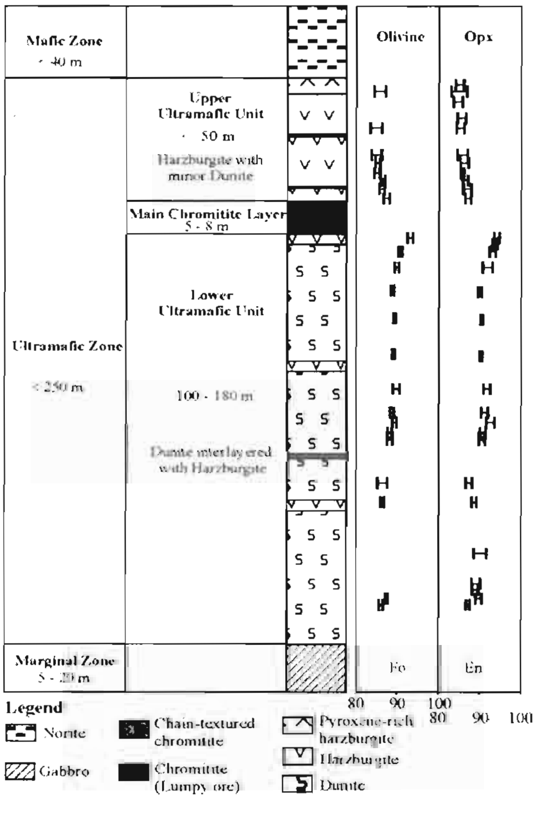

Figure 2. Generalized stratigraphic section of the Ipueira-Medrado sill and generalized stratigraphic variation of olivine and orthopyroxene (Opx) compositions from harzburgite samples throughout the sill. Data from Marques & Ferreira Filho (2003). Fo = forsterite, En = enstatite.

SAMPLING AND ANALYTICAL METHODS

Twelve whole-rock silicate samples were analyzed for Sm-Nd isotopic composition at the Laboratório de Geocronologia of the Instituto de Geociências of the Universidade de Brasília. Eleven samples, five from silicate rocks and six from chromitites, were analyzed for Re-Os isotopes at the Department of Terrestrial Magnetism of the Carnegie Institution of Washington. For chromitites, six analyses were performed from chromite mineral separates and one sample was repeated for whole rock. All samples were taken from one representative drill core from the south part of the Ipueira-Medrado sill. Details about sampling and analytical procedures, and complete data set can be found in Marques et al. (2003).

RESULTS

Sm-Nd SYSTEMATICS

The main characteristics from Sm-Nd isotopic compositions are the low Sm (<1.5 ppm) and Nd (< 6 ppm) contents, the small range in Sm/Nd ratios, the variable Archean Nd (CHUR) model ages and the negative ε_{Nd}. The data show considerable scatter in a Sm-Nd isochron diagram. Nevertheless, when the samples are separated into two groups (amphibole-free samples and samples containing ~25% amphibole), two almost parallel isochrons were obtained, both with very low MSWD and relatively low age uncertainty despite the small range in the Sm/Nd ratios and small number of samples. The ages yielded by both isochrons overlap the 2038 ± 19 Ma zircon age reported by Oliveira & Lafon (1995), which is from now on considered as the crystallization age of the sill.

When the ε_{Nd} is calculated for each sample using the 2038 Ma zircon age, the results are very interesting. The amphibole-free group is clearly distinguished from the amphibole-rich samples. The mean ε_{Nd} for the first one is -4.4, whereas for the second the mean is -6.5 (Fig. 3). These ε_{Nd} values are consistent with the initial ε_{Nd} obtained from the isochrons.

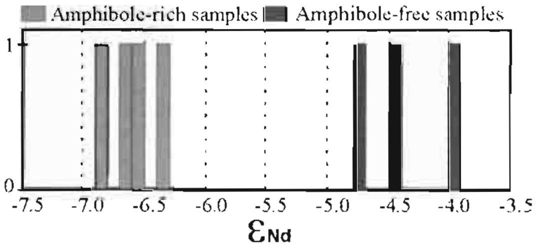

Figure 3. Histogram of the initial ε_{Nd} calculated for an intrusion age of 2038 Ma, showing differences between amphibole-free and amphibole-rich samples. Data from Marques et al. (2003).

Re-Os SYSTEMATICS

The harzburgite and pyroxenite samples have extremely low Re concentrations and calculated initial $^{187}Os/^{188}Os$ too high when compared to the sub- to near chondritic initial Os isotopic compositions from chromites. The silicate samples are believed to have lost Re during serpentinization. The chromite mineral separates and chromitite whole-rock have very low Re concentrations (near blank levels) and high Os concentrations. The low $^{187}Re/^{188}Os$ values preclude a Re-Os isochron.

The percent deviation of the sample's Os isotopic composition from that of a chondritic reservoir at the time of crystallization (γ_{Os}, Walker et al., 1989) is negative for chromitites from the LUU and MCL ($\gamma_{Os(2038)}$ = -4.6 to -3.2) whereas those from the UUU are slightly positive ($\gamma_{Os(2038)}$ = +1.4 to +3.3). This up-stratigraphy increase in γ_{Os} values can be observed even inside the MCL (Fig. 4).

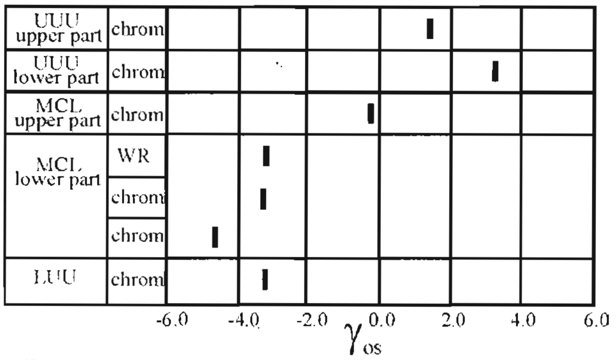

Figure 4. Chromitites γ_{Os} distribution through the Ipueira-Medrado sill. UUU = Upper ultramafic unit, LUU = Lower ultramafic unit, MCL = Main chromitite layer, chrom = chromite, WR = whole rock. Data from Marques et al. (2003).

DISCUSSION

The lower ε_{Nd} for amphibole-rich samples and for both marginal gabbro from the base of the sill and the norites from the top of the sill (up to –9.5, Marques et al. 2003) is consistent with the suggestion that these samples have larger crustal contribution than the rest of the sill. However, even the amphibole-free samples have strongly negative ε_{Nd} indicating that all parental magmas of the sill had experienced crustal contamination or the uncontaminated parental magma was derived from a source that can generate primary magmas with negative γ_{Os} and ε_{Nd}.

The cumulates from Ipueira-Medrado sill display a fairly wide range of initial Nd and Os isotopic compositions. The distribution of these initial isotopic compositions is suggestive of a magma composition evolving through combined fractional crystallization and crustal assimilation. The variation of Nd and Os isotopic composition in a magma undergoing crustal contamination is strongly dependent on the Nd and Os concentration assumed for both the parental magmas and the crustal component. The parental magma composition of the Ipueira-Medrado sill was assessed indirectly using the Ce, Sm and Yb concentrations from five harzburgite samples and the orthopyroxene and olivine partitioning coefficients (Marques et al., 2003). The composition obtained is very similar to that from the B1/U type magma from the Bushveld Complex and one of the parental magmas calculated for the Stillwater Complex (Fig. 5). Assuming this, the Nd concentration in the parental magma of the sill is constrained to be ~20 times chondritic. This high concentration makes the Nd isotopic composition of the magma relatively insensitive to changes caused by crustal contamination. Modeled variations in the Nd and Os isotopic compositions are shown in Fig. 6. If the parental magma started with a ε_{Nd}=+4 (MORB-like mantle at 2.0 Ga), almost 50% of Archean crust assimilation would be required to produce ε_{Nd}=-4, the average of amphibole-free samples. If a more mafic crustal component were used, more crust assimilation would be needed. Also, the higher Os concentration in mafic crust would cause γ_{Os} to rise and the isotopic signature of the sill (negative ε_{Nd} and near chondritic γ_{Os}) would not be achieved. Assuming a lower Nd concentration in the parental magma is also problematic, as the Nd concentration would not rise sufficiently quickly with fractionation/contamination to produce the magma REE abundances shown in Fig. 5.

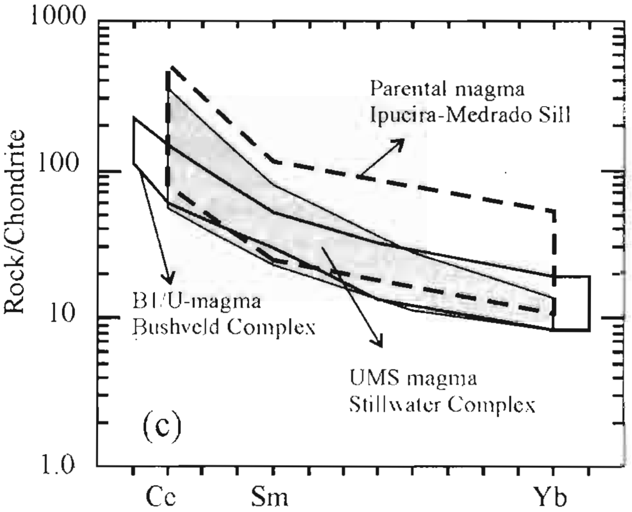

Figure 5. Best estimate of the chondrite-normalized REE (Ce, Sm an Yb) pattern of the parental magma of the Ipueira-Medrado sill (Marques et al., 2003). B1/U type magma from Bushveld Complex (Harmer & Sharpe, 1985) and calculated parental magma for the Stillwater Ultramafic series (UMS; Lambert & Simmons, 1987) are shown for comparison. Normalization values from Anders & Grevesse (1989).

A convecting mantle source would require enormous amounts of crustal contamination and cannot account for the negative γ_{Os} of some chromitites. If instead of assuming a convecting mantle source, we assume a primary magma generated from Archean subcontinental lithospheric mantle, the primary magma may have started with ε_{Nd}=-4 and γ_{Os}=-4.6. An old and enriched subcontinental lithospheric mantle seems to be the only terrestrial reservoir that combines negative γ_{Os} and ε_{Nd}. Partial melts of this source would be Mg rich with high concentrations of both Cr and Os, and incompatible elements such as LREE. Crustal contamination acting on this primary magma takes ε_{Nd} from -4 to -7 and γ_{Os} from -4 to zero with as little as 30% assimilation (Fig. 6).

Amphibole-rich harzburgite are scarce and chromite separates have negative γ_{Os} in the LUU, whereas in the UUU amphibole is abundant and the γ_{Os} from chromite separates are positive. The MCL is an interval that represents not only a change in the dynamic of the

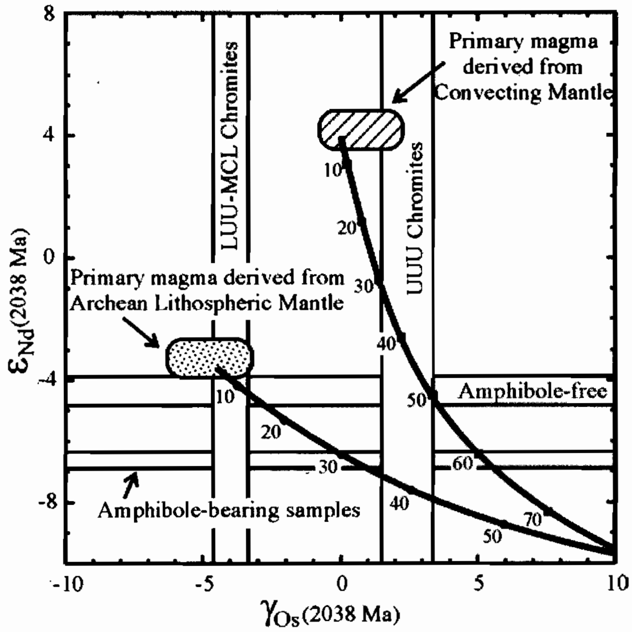

Figure 6. ε_{Nd}(2038Ma) versus γ_{Os}(2038Ma) isotopic variation in magmas undergoing crustal contamination. Primary magma from the convecting mantle assumes [Nd] = 30 ppm, [Os] = 1 ppb, $\varepsilon_{Nd} = +4$, $\gamma_{Os} = 0$ mixing with a crust with [Nd] = 50 ppm, [Os] = 0.02 ppb, $\varepsilon_{Nd} = -15$, $\gamma_{Os} = 210$. Lithospheric mantle source mixing calculation assumes a primary magma with the same Nd and Os concentrations as that from the convecting mantle but $\varepsilon_{Nd} = -3.6$ and $\gamma_{Os} = -4.4$. The crustal end member for this mixing curve has [Nd] = 50 ppm, [Os] = 0.1 ppb, $\varepsilon_{Nd} = -15$ and $\gamma_{Os} = 130$. The Nd concentration of both primary melts is dictated by the REE modeling of the parental magma of the sill, the Os concentration is in the range expected for a high-Mg magma (e.g. Shirey & Walker, 1998). Isotopic compositions of the primary magmas are within the range expected for 2 Ga ocean ridge basalt or for late-Archean Re-depleted but LIL-metasomatized mantle evolved to 2 Ga. Assumed crustal compositions have Nd concentration at the high end and ε_{Nd} (for an Archean crustal rock at 2 Ga) at the low end of the range observed for crustal rocks order to enhance the decrease in ε_{Nd} of the mixing curves so that they pass through the data observed for the sill. Crustal Os concentrations and isotopic compositions are within the range seen for estimates of the composition of the lower continental crust (e.g. Saal et al., 1998). The curves are calculated assuming simple binary mixing between crustal and primary magma endmembers. Marks along curves denote 10% increments in the amount of crust added. Bars show Nd and Os isotopic ranges for various sample groups from the Ipueira-Medrado sill. Diagram from Marques et al. (2003).

magma chamber from an open to a closed system, but also an important change in the parental magma composition with the role of crustal contamination increasing exactly at this time, when the magmatic system was probably most dynamic. Crustal contamination has possibly triggered the chromitite crystallization. Assimilation of SiO_2 enlarges the chromite crystallization field (Irvine 1977) and also can cause drop in temperature and increase in fO_2, thus favoring the crystallization of chromitites.

REFERENCES

Anders, E. & Grevesse, N. (1989) Abundances of the elements: meteoric and solar. Geochimica et Cosmochimica Acta 53, 197-214.

Barbosa, J. S. F., Sabaté, P. & Dominguez, J. M. L. (1996) O Estado da Bahia na Plataforma Sul-americana, suas subdivisões, critérios de empilhamento estratigráfico das coberturas plataformais e ciclos geotectônicos. In: Barbosa, J. S. F. & Dominguez, J. M. L. (eds.) Geologia da Bahia: Texto Explicativo para o Mapa Geológico ao Milionésimo. Salvador: SICM/SGRM 2: 39-61.

Harmer, R. E & Sharpe, M. R. (1985) Field relations and strontium isotope systematics of the eastern Bushveld Complex. Economic Geology 80, 813-837.

Irvine, T. N. (1977) Origin of chromitite layers in the Muskox intrusion and other layered intrusions: a new interpretation. Geology 5, 273-277.

Lambert, D. D. & Simmons, E. C. (1987) Magma evolution in the Stillwater Complex, Montana: I. Rare-Earth element evidence for the formation of the ultramafic series. American Journal of Science 287, 1-32.

Marinho, M. M., Rocha, G. F, Deus, P. B. & Viana, J. S. (1986) Geologia e potencial cromitífero do Vale do Jacurici-Bahia. 34th Congresso Brasileiro de Geologia, Goiânia, Anais 5, 2074-2088.

Marques, J.C. & Ferreira Filho, C.F. (2003) The chromite deposit of the Ipueira-Medrado Sill, São Francisco Craton, Bahia, Brazil. Economic Geology 98(1) In press.

Marques, J.C., Ferreira Filho, C.F, Carlson, R.W. & Pimentel, M.M. (2003) Re-Os and Sm-Nd isotope and trace element constraints on the origin of the chromite deposit of the Ipueira-Medrado Sill, Bahia, Brazil. Journal of Petrology 44 In press.

Oliveira, E. P. & Lafon, J. M. (1995) Idade dos complexos máfico-ultramáficos mineralizados de Caraíba e Medrado, Bahia, por evaporação de Pb em zircão. 5th Congresso Brasileiro de Geoquímica, Niterói, Anais (digital) iso-15.

Saal, A.E., Rudnick, R.L., Ravizza, G.E. & Hart, S.R. (1998) Re-Os isotope evidence for the composition, formation and age of the lower continental crust, Nature 393, 58-61.

Shirey, S.B. & Walker, R.J. (1998) The Re-Os isotope system in cosmochemistry and high-temperature geochemistry, Ann. Rev. Earth Planetary Science 26, 423-500

Teixeira, W., Sabaté, P., Barbosa, J., Noce, C. M & Carneiro, M. A. (2000) Archean and Paleoproterozoic tectonic evolution of the São Francisco Craton, Brazil. In: Cordani, U. G., Milani, E. J., Thomaz Filho, A. & Campos, D. A. (eds.) Tectonic Evolution of South America, International Geological Congress. Rio de Janeiro: CPRM. pp. 101-137.

Walker, R. J., Carlson, R. W., Shirey, S. B. & Boyd, F. R. (1989) Os, Sr, Nd and Pb isotope systematics of southern African peridotite xenoliths: Implications for the chemical evolution of subcontinental mantle. Geochimica et Cosmochimica Acta 53, 1583-1595.

TECTONIC SETTING AND PRELIMINARY AGE OF HYDROTHERMAL SYSTEMS IN LOW GRADE METASEDIMENTARY SEQUENCES, SIERRA NORTE DE CÓRDOBA, ARGENTINA

Millone, H.A[1]; O'Leary, M.S.[2]; Tassinari, C.C.G.[3] and Lira, R.[2]

1. Gerencia de Minería de Córdoba, Celso Barrios 1712, 5016 Córdoba, Argentina. hmillone@hotmail.com
2. CONICET, Museo de Mineralogía y Geología Dr. A. Stelzner, V. Sarsfield 299, 5000 Córdoba, Argentina. soleary@com.uncor.edu, rlira@com.uncor.edu
3. Centro de Pesquisas Geocronológicas, Instituto de Geociências, Universidade de São Paulo, Brazil. ccgtassi@usp.br

Keywords: Pb-Pb, mesothermal, orogenic, Sierra Norte, Argentina

INTRODUCTION

Alteration-mineralization systems hosted in low grade metasedimentary sequences in the Sierra Norte ranges, Córdoba, Argentina, were identified by Lira et al. (1995). Field and geochemical studies were performed during mining exploration tasks (Lira et al., 1997a) and subsequent work was oriented toward the investigation of genetic conditions of ore-bearing paragenesis (O'Leary et al, 2001; Millone et al, 2002).

This contribution deals with the Pb-isotopic composition of galenas associated with other sulfides in quartz-veins. Isotopic data were treated according to Zartman & Doe (1981) and Stacey & Kramers (1975) models with the aim of establishing lead sources and the age of mineralization, respectively.

REGIONAL GEOLOGY

The study area is located in the central-western portion of the Sierra Norte-Ambargasta batholith (SNAB), which is mainly composed of magmatic arc I-type calcalkaline granitoids of Neoproterozoic to Eopaleozoic ages, intruded in low grade metasedimentary sequences of probable Neoproterozic to Early Cambrian age. Dominant magmatic rocks are granodiorites and monzogranites which were intruded by a subvolcanic pluton of dacitic-rhyolitic composition. The whole sequence was afterwards intruded by small highly evolved subalkaline monzogranites and frequent rhyolite dikes. Latest intrusions correspond to thick syenogranitic aplites (Lira et al., 1997b). Neoproterozoic to Lower Cambrian ages have been registered for different plutonic and subvolcanic representative units (Rapela et al., 1998; Söllner et al., 2000; Millone et al., 2003).

Enclosing metasedimentary rocks occur as kilometer-sized roof-pendants that are well exposed in the western ranges of Sierra Norte. Main outcrops are known as Rodeíto, La Cañada-Nispo, El Tío-La Graciela, Agua del Río, La Salamanca (west of San Francisco del Chañar), San Jerónimo, and a few smaller ones. Some of them (for instance, Rodeíto, Agua del Río) are associated to structures of meridian strike.

LOCAL GEOLOGY

Galena-bearing assemblages are present in a ~6 km^2 north-south elongated low grade metasedimentary roof-pendant that outcrops in the vicinities of Rodeíto locality (29°45'35" - 29°47'29S; 64°07'27" - 64°08'59"W). This outcrop is composed of phyllites (N40°E, near vertical dip) interbedded with metagreywackes (quartzites). Several rhyolite dikes (N-S to NE-SO) were intruded into the metasedimentary sequence roughly along regional schistosity. Both metamorphic rocks and dikes host a remarkably well-developed network system of ore-bearing quartz-rich veinlets.

METASEDIMENTARY HOST ROCKS

The mineralized network was preferentially hosted by the multiple fractured metapsammitic facies. Veins and veinlets are 1 to 12 mm thick, though some can be as thick as 5 cm; drusy quartz growth and limonite boxworks are present. Some veins show thin selvages composed of fine grained aggregates of biotite and sericite.

The most representative mineral assemblages present in network veins are (after abbreviations of Kretz, 1983): Qtz-Chl, Qtz-Ep-Chl ± Bt ± Musc, Qtz-Cal-Chl ± Ms ± Ep, and Qtz-Kfs-Chl-Ep ± Plag. Two main quartz-textures were recognized: a) Fine-grained anhedral mosaic (5-20 μm); b) Comb texture (100 μm to 2 mm), prismatic crystals subparallel to vein walls, occasionally alternating with sericitized K-feldspar intergrown with plagioclase. Ore-bearing vein assemblages include: a) Galena, chalcopyrite, pyrite and minor bornite, partially transformed into malachite, goethite and hematite; b) Chalcopyrite and pyrite, with secondary assemblages of covellite, digenite, malachite, goethite and hematite; c) Sphalerite and galena partially altered to goethite and hematite; d) Sphalerite, chalcopyrite, galena and minor pyrite, with secondary association of covellite, digenite, malachite, goethite and hematite. Grain size of sulfides range from 0.1 to 5 mm, though sometimes cm-sized grains are present. Observed textures are intergrowths of chalcopyrite with bornite, chalcopyrite exsolutions in sphalerite and concentric replacement textures of Cpy→Dig→Cov→Goe. Pyrite is generally idiomorphic and frequently occurs as pseudomorphic replacements of hematite or goethite, sometimes associated to malachite, showing lattice textures.

Homogenization temperatures (Tht) obtained from fluid inclusion microthermometry in quartz from Qtz-Chl veins (Millone et al., 2000), fall in the range 300-400°C and estimated salinity range from 2.6 to 13.5 eq. wt % NaCl (n= 5, $\overline{X}$= 7.5).

Preliminary $\delta^{18}O$ data for the Qtz-Chl pair in equilibrium yielded temperatures in the range 600-

650°C; these formation temperatures are ~200-250°C higher than fluid inclusion Tht. These values, concurrently with the lack of boiling evidences, suggest that a "pressure correction" would be applicable to the mineralizing system (Millone et al., 2000).

Mean and maximum contents of 77 chemical analyses of representative network veinlets in metapsammitic rocks (Lira et al., 1997a; Millone et al., 2002) are summarized below (values in ppm, except for Au in ppb): Au (6.8, 38.0); Ag (2.3, 47.7); Cu (290.9, 5475.0); Pb (372.1, 14667.0); Zn (423.8, 19220.0); Mo (2.0, 51.0); As (23.3, 468.0); Cd (1.7, 22.0); Sb (2.8, 42.0) and Bi (0.4, 13.0). Mineralogical data and geochemical correlation among analyzed elements indicate an Ag-Cu-Pb-Zn-(Au)-(As) principal association.

RHYOLITE DIKES

Rodeíto metasedimentary roof-pendant is the country rock of several rhyolitic dike intrusions of submeridian strike. These bodies outcrop for hundreds of meters and have variable thickness (3 to >25 m). They have been classed into two categories, those of southern and central-western Rodeíto, which are characterized below.

Southern zone: 2 m thick dike crosscut by subhorizontal veins of drusy quartz up to 0.5 m thick. Observed sulfides include galena grains partially rimmed by covellite, small bornite grains with sporadically exsolved chalcopyrite and chalcopyrite with lamellar intergrowths of covellite included in pyrite; specular hematite is also present. Fluid inclusion Tht´s cover the range 290-335°C and estimated salinity vary between 5.2 and 11.0 eq.wt. % NaCl (n= 7, $\bar{X}$= 8.4).

Central-western zone: 25 m thick dike, crosscut by two main vein systems: a) Subhorizontal quartz veins with polyhedral mosaic texture, some with jig-saw borders (up to 1 cm grain size), associated to chlorite and grey chalcocite altered to covellite-malachite and pyrite partially oxidized to goethite-hematite. This vein type hosts Cu-mineralization (~ 2.5 % Cu) and Ag, Au and Zn anomalies. Tht in quartz (O´Leary et al., 2001) are within the range 190-351°C (n= 37, $\bar{X}$= 289°C) and salinity vary from 0.5 to 4 eq. wt. % NaCl (n= 10, $\bar{X}$= 2.1). b) Quartz veins (N310° strike and 35° NE dip) that carry oxydized pyrite (goethite), bornite associated with chalcocite-covellite and minor chalcopyrite replaced by covellite. This vein type is anomalous in gold (up to 550 ppb). Fluid inclusion thermometry yielded Tht in the range 155- 366°C (n= 36, $\bar{X}$= 259°C) and estimated salinity vary from 0.6 to 8.5 eq. wt. % NaCl (n= 17, $\bar{X}$= 6.3) (O´Leary et al., 2001).

Thirty three analyzed samples of mineralized rhyolitic porphyries yielded the following results (same units as in metamorphites): Au (24.4, 550.0); Ag (4.8, 85.3); Cu (983.4, 24157.0); Pb (280.9, 1067.0); Zn (344.7, 2508.0); Mo (4.4, 9.0); As (27.6, 191.0); Cd (1.0, 6.0); Sb (1.0, 6.0) and Bi (9.1, 199.0). Geochemical correlation show an association characterized by Ag – Au – Cu – Pb - (Zn) – Bi – As.

METHODOLOGY

Galena grains from vein quartz hosted in metagreywackes were handpicked under stereoscopic microscope (samples # 24032, 24082, 20105 and 24389); an additional galena sample was collected from quartz veins that cut a rhyolitic dike from the southern zone of Rodeíto (sample # 24078). Pb isotopic analyses were carried out at the Centro de Pesquisas Geocronológicas, Universidade de São Paulo, Brazil.

The Pb isotopic analyses on galenas included the use of HCl+HNO3 for washing and HCl for dissolution. Only in impure samples (galena + others sulfides) the Pb was extracted by HCl and HBr in an AG1-X8 (200-400#) column. The Pb isotopic analysis were carried out on a multicollector VG 354 Micromass mass spectrometer. The procedural blank for Pb was 70 pg. Pb isotope ratios were corrected relative to the values of the NBS981 standard, by 1.0024 for ^{206}Pb/^{204}Pb, 1.0038 for ^{207}Pb/^{204}Pb and 1.0051 for ^{208}Pb/^{204}Pb. The analytical error for these isotopic ratios was 0.15-0.48%, 0.13-1.07% and 0.104-0.45%, respectively. The isotopic data were regressed using the program of Ludwig (1999). The ages were calculated using the decay constants established in Steiger & Jäger (1977); for ^{235}U and ^{238}U the decay constants were 9.8485 x 10^{-10} yr^{-1} and 1.55125x10^{-10} yr^{-1}.

ISOTOPE RATIOS

Measured ratios are listed in table 1 and plotted in the Stacey & Kramers (1975) two-stage model diagram (Fig. 1).

Table 1. Lead isotope ratios of galenas from Rodeíto. Sample 24078 is located in a rhyolite dike, remainder are hosted by low grade metasedimentary rocks.

Sample #	24078	24032	24082	24105	24389
^{206}Pb/^{204}Pb	18.048	18.028	18.004	18.006	18.030
Error (1 σ)	0.023	0.051	0.030	0.447	0.010
^{207}Pb/^{204}Pb	15.642	15.634	15.597	15.589	15.609
Error (1 σ)	0.023	0.053	0.030	0.464	0.010
^{208}Pb/^{204}Pb	38.024	37.955	37.854	37.844	37.917
Error (1 σ)	0.024	0.056	0.031	0.476	0.010
T (Ma)	514.9	515.0	460.6	444.6	466.2
μ	9.964	9.935	9.771	9.737	9.821

From figure 1 an age of 433 Ma can be depicted from the intersection of the isochrone with the modeled curve. Ages computed according to the two-stage Pb-Pb evolution model of Stacey & Kramers (1975) would be within the range 445-515 Ma. Despite the fact that these are model ages, the age of the mineralizing event could be preliminarily assigned to the Eopalaeozoic, most likely to the Upper Ordovician-Lower Silurian.

The possible Pb sources were examined through the use of the plumbotectonic diagrams of Zartman & Doe (1981) who established different evolutionary models of Pb isotopes dependent on the reservoir.

In the diagram of figure 2a ($^{207}Pb/^{204}Pb$ *vs.* $^{206}Pb/^{204}Pb$), analyzed data are distributed along a trend drawn oblique to modeled curves, which suggest an heterogeneous source for Pb. Data points are located between the "Upper Crust" and "Orogen" curves, though closer to the orogenic reservoir. Similarly, in the case of the diagram of figure 2b ($^{208}Pb/^{204}Pb$ *vs.* $^{206}Pb/^{204}Pb$), data points plot close to the "Orogen" curve, between it and the curve representative of "Lower Crust".

On the other hand, computed µ values for galena ($^{238}U/^{204}Pb$) range from 9.7 to 9.9 (Table 1). These values suggest that Pb was predominantly derived from rocks with high U/Pb ratios, typical of the upper crust. In this sense, Pb isotopic data suggest an heterogeneous source for Pb, composed of rocks with high U/Pb and Th/Pb ratios.

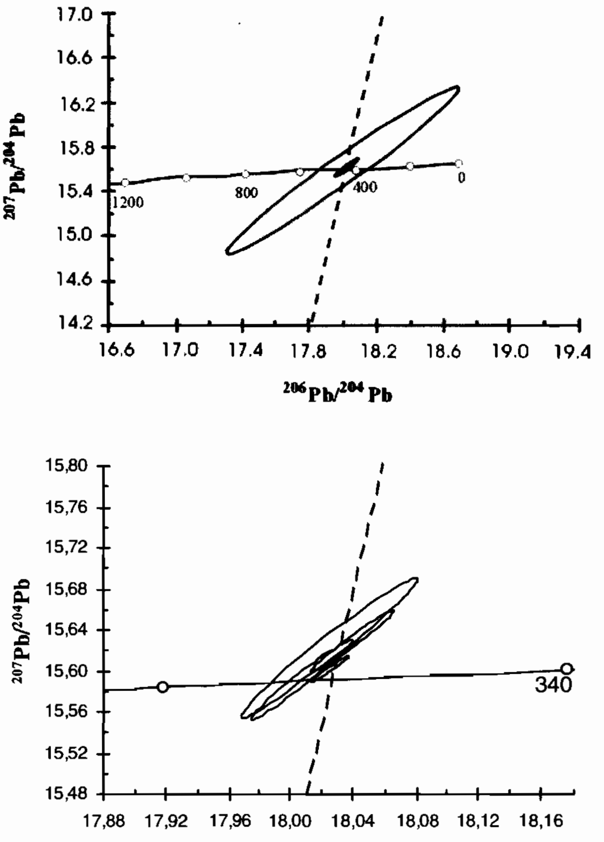

Figure 1. (a) Pb/Pb isotopic data for galenas of Rodeíto plotted in the "two-stage" Pb-Pb evolution model of Stacey & Kramers (1975). Intersection of the isochrone with the modeled curve indicates an age of 433 Ma. Data point error ellipses are 68.3 % confident. (b) Enlargement of figure 1 at the intersection zone.

DISCUSSION AND CONCLUSIONS

If the origin of fluids involved in Rodeíto mineralization are considered to be of metamorphic remobilization (Millone et al., 2000, 2002), the system might be classified as mesothermal following the scheme of Nesbitt (1988). Groves et al. (1998) proposed to designate this type of deposits as "orogenic gold deposits" considering that the tectonic setting was the unique feature common for the whole group. These deposits are associated with regional metamorphic terranes of all ages. Ore is formed during compressional or transpressional stages, where hydrated sediments and/or volcanic rocks are subducted facing continental margins. Heat derived from subduction increases the thermal gradient within the accretional prism, initiating hydrothermal fluid migration channeled along megastructures through long distances (Groves et al., 1998).

Rodeíto hydrothermal system gathers some of the typical parameters of these deposits, such as the host rock type, the mineral paragenesis, the textural features of the veins and the structural relationships.

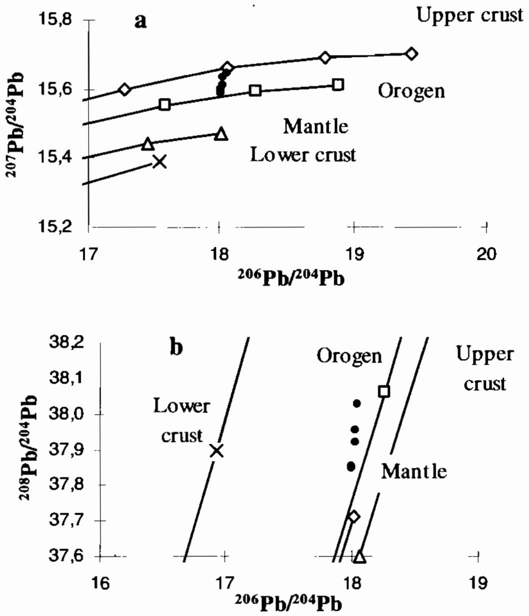

Figure 2. (a-b) Galenas from Rodeíto plotted in plumbotectonic diagrams (Zartman & Doe,1981).

Preliminary oxygen isotope geothermometric calculations using the Qtz-Chl pair yielded formational temperatures of 600 - 650 °C (Millone et al., 2000), which are higher than those strictly characteristic of phanerozoic mesothermal deposits, but are still possible (Groves et al., 1998). Fluid salinity varies from 13.5 to 0.5 eq. wt. % NaCl (Millone et al., 2000; O'Leary et al., 2001), which is too low for expected purely magmatic fluids. $\delta^{18}O_{H2O}$ computed at 600° varies between 9.8‰ (from quartz) and 8.5‰ (from chlorite); δD_{H2O} computed from chlorite at 600° varies from -56.2‰ to ~-26‰, depending on the equation used. These values suggest that the isotopic composition of water involved in Rodeíto mineral deposition could be of metamorphic origin (Millone et al., 2000).

Lead isotope data presented in this contribution show a crustal source possibly formed by mixing of crustal and successively recycled orogenic rocks, which is in line with the proposed metallogenetic model. On the other hand, there are important facts that do not rigorously meet typical features of the orogenic model, among them, the relatively high contents of Ag, Cu, Pb and Zn and the erratic distribution of Au in the system, as well as the apparent absence of nearly ubiquitous carbonic fluids (CO_2, CH_4) as indicated by fluid inclusion microthermometry.

It has been stated that Rodeíto Pb-isotope signature in plumbotectonic plots favors a mesothermal or orogenic origin in the sense of Groves et al. (1998). The common fact that thermal events linked to subduction could extend over periods greater than 100 Ma, makes it difficult to unequivocally assign the mineralizing event (430 to 515 Ma) to the ultimate stages of the Pampean cycle or to any specifical evolutionary stage of the Famatinian orogeny.

Compared to other geological units related to this ore deposit type in Argentina, to our knowledge, no other Middle Cambrian to Lower Silurian ages have been registered within the Sierras Pampeanas system. Ore deposits that keep some analogies with Rodeíto are those located in the Ordovician sequences of Sierra de Rinconada, in the Puna high plateau, Jujuy province (Rodriguez et al., 2001) and those of Incahuasi mine in Catamarca province (González, 1999). Most outstanding similarities are the characteristics of host rocks and the ages attributed to mineralization which span the Ordovician-Silurian boundary, coincident with the Ocloyic orogeny.

In relationship to worldwide occurrences of phanerozoic orogenic deposits, Rodeíto shares common features with the Bendigo-Ballarat district, in central Victoria, Australia (Bierlein & Crowe, 2000); most remarkable comparable parameters are the isotopic composition of mineralizing fluids, the structures of vein systems, the possible age and lithology of host rocks, the age of mineralization and the age of associated magmatic rocks.

REFERENCES

Bierlein, F.P. and Crowe, D.E., 2000. Phanerozoic orogenic lode gold deposits. SEG Reviews 13: 103-139.

González, O.E., 1999. Mina Incahuasi, Catamarca. In: Recursos Minerales de la República Argentina (E.O. Zappettini, ed.), Instituto de Geología y Recursos Minerales SEGEMAR, Anales 35:515-520, Buenos Aires.

Groves, D.I., Goldfarb, R.J., Gebre-Mariam, M., Hagemann, S.G. and Robert, F., 1998. Orogenic gold deposits: A proposed classification in the context of their crustal distribution and relationship to other gold deposit types. Ore Geology Reviews 13:7-27.

Kretz, R., 1983. Symbols for rock-forming minerals. American Mineralogist 68: 277-279.

Lira, R., Moreno, R.S. and Millone, H.A., 1995. Sistemas de alteración porfíricos con sulfuros de cobre y molibdeno en el basamento eopaleozoico de la Sierra Norte de Córdoba, Argentina. V Congreso Nacional de Geología Económica, San Juan, Argentina: 426-430.

Lira, R., Martínez, V. and Millone, H.A., 1997a. Sierra Norte Project Córdoba province, Geology and Geochemistry. BHP World Minerals, unpublished report, 78 p, 4 appendixes, 36 maps.

Lira, R., Millone, H.A., Kirschbaum, A.M. and Moreno, R.S., 1997b. Calc-Alkaline Arc Granitoid Activity in the Sierra Norte-Ambargasta Ranges, Central Argentina. Journal of South American Earth Sciences 10 (2): 157-177.

Ludwig, K.R., 1999. Isoplot/Ex. Berkeley Geochronological Center. Special Publication 1, 41p.

Millone, H.A., Lira, R., Gómez, G.M. and Ripley, E.M., 2000. Metamorphic and magmatic fluid sources for sulfide-bearing vein assemblages at Sierra Norte ranges, Sierras Pampeanas, Argentina. 31° International Geological Congress, Rio de Janeiro, Brazil, Abstract (CD).

Millone, H.A., Lira. R. and O'Leary, M.S., 2002. Geoquímica de elementos metalíferos de los sistemas de alteración-mineralización de la Sierra Norte central, Córdoba, Argentina. In: Cabaleri, N., Cingolani, C.A., Linares, E., López de Luchi, M.G., Ostera, H.A. y Panarello, H.O. (eds.) Actas del XV Congreso Geológico Argentino (I): 412-415.

Millone, H., Tassinari, C.C.G., Lira, R. and Poklepovic, M.F., 2003. New ages and strontium- neodymium isotope geochemistry of granitoids of the Sierra Norte-Ambargasta batholith, central Argentina (this volume).

Nesbitt, B.E., 1988. Gold deposit continuum: A genetic model for lode Au mineralization in the continental crust. Geology 16:1044–1048.

O'Leary, M.S., Millone, H.A. and Lira, R., 2001. Fluid Inclusions In Sulfide Bearing Auriferous Quartz Veins From Rhyolite Dikes, Sierra Norte, Argentina. XVI ECROFI, Portugal. Abstracts, p. 345.

Rapela, C.W., Pankhurst, R.J., Casquet, C., Baldo, E., Saavedra, J., Galindo, C and Fanning, C.M., 1998. The Pampean Orogeny of the southern proto-Andes: Cambrian continental collision in the Sierras de Córdoba. In: The Protoandean Margin of Gondwana (Pankhurst, R.J and Rapela, C.W., eds). Geological Society of London Special Publication N° 142:181-217.

Rodriguez, G.A., de Azevedo, F.I.Jr., Coira, B. and Brodie, C., 2001. Mineralizaciones auríferas en sedimentitas ordovícicas de la sierra de Rinconada (Jujuy-Argentina): implicancias para la exploración minera. Revista Geológica de Chile 28 (1): 47-66.

Steiger, R.H. and Jäger, E., 1977. Subcommission on geochronology: convention on the use of decay constants in geochronology and cosmochronology. Contributions to the geologic time scale. Studies in Geology, v. 6: 67-72. Michigan, USA.

Stacey, J.S. and Kramers, J.D., 1975. Approximation of terrestrial lead isotope evolution by a two-stage model. Earth and Planetary Science Letters 26: 207-221.

Zartman, R.E. and Doe, B.R., 1981. Plumbotectonics – the model. In: Evolution of the Upper Mantle (R.E. Zartman and Taylor, S.R. eds.). Tectonophysics 75: 135-162.

SULFUR, CARBON, OXYGEN AND STRONTIUM ISOTOPIC EVIDENCES FOR THE GENESIS OF THE HYDROTHERMAL ZINC NON-SULFIDE AND SULFIDE MINERALIZATIONS IN THE VAZANTE, AMBRÓSIA AND FAGUNDES DEPOSITS, MG, BRAZIL

Monteiro, L.V.S.[1]; Bettencourt, J.S.[1]; Bello, R.M.S.[1]; Juliani, C.[1]; Tassinari, C.C.G.[1]; Oliveira, T.F.[2] and Pérez-Aguillar, A.[1]

1. Instituto de Geociências, USP, Rua do Lago, 562, São Paulo, SP, Brazil, 05508-900. lenavsm@zipmail.com.br
2. Companhia Mineira de Metais, Minas Gerais, Brazil

Keywords: Stable isotopes, strontium isotope, carbonate-hosted Zn deposits, willemite, metallogenesis

INTRODUCTION

The Vazante-Paracatu region (Fig. 1), situated in the northwest part of Minas Gerais State, is host to the most important zinc district known in Brazil. Within this region, which extends up to 250 Km long in N-S direction, various zinc deposits are described, such as, Vazante, Morro Agudo, Ambrósia and Fagundes, and several zinc occurrences. The deposits are hosted by metapelitic-dolomitic sequences of the Vazante Group (Dardenne et al., 1998) and have contrasting geological characteristics.

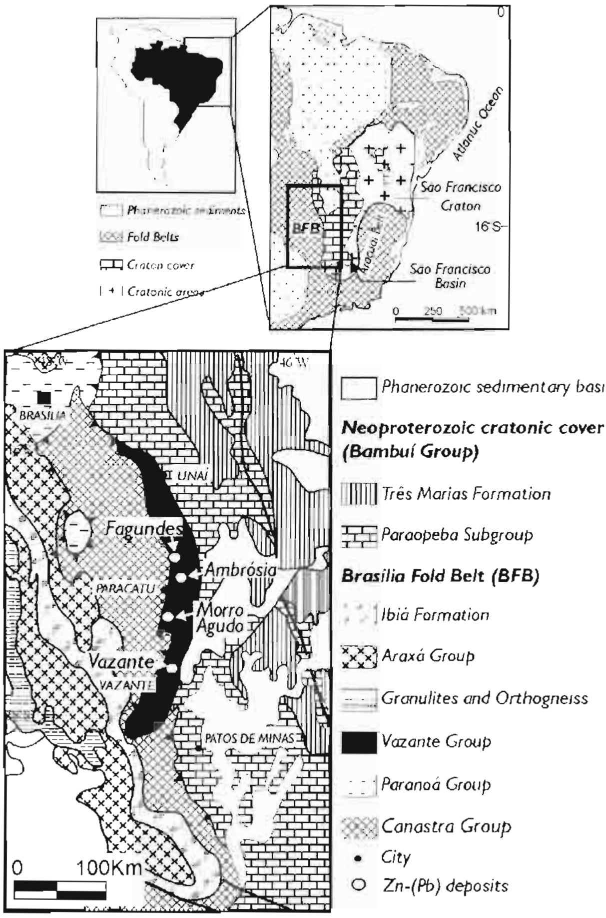

Figure 1. Geological setting of the Vazante-Group (Dardenne & Schobbenhaus, 2001).

The Vazante deposit is known as the major example of a new deposit class, named as carbonate-hosted willemite deposits or non-sulfide zinc deposits (Hitzman, 2001). The Vazante main ore is made of willemite (Zn_2SiO_4), dolomite, quartz, siderite, hematite, barite, franklinite, zincite, magnetite and Zn-chlorite (Monteiro, 1997). Small sulfide bodies composed mainly by Cd-rich sphalerite and galena occur tectonically imbricate with the willemitic ore and with the intensely hydrothermalized host rocks within the Vazante Fault.

The zinc ore from Morro Agudo, Fagundes and Ambrósia, however, are composed mainly of sphalerite, galena, pyrite, marcasite, dolomite and quartz. The mineralization styles in Fagundes deposit are late diagenetic, related with open space filling, and epigenetic, characterized by a late fissural stage. In Ambrósia deposit the predominant mineralization style is epigenetic. Several stages of mobilization of preexisting ore, related to ductile-brittle and brittle deformation, are common in both deposits (Monteiro, 2002).

These distinct mineralization episodes share a common evolutionary history related to diagenesis and deformation of the Vazante Group, during the Neoproterozoic.

The present paper aims to document isotopic variations related to well-constrained paragenetic sequence and to profile the geochemical processes associated with the genesis of non-sulfide and sulfide zinc deposits of the Vazante-Paracatu region.

SULFUR ISOTOPES

In Vazante deposit, sulfides show a narrow range of $\delta^{34}S$ values between +11.8‰ and +14.4‰ (Monteiro, 1997). This is a distinct sulfur isotopic signature in relation to sulfides from the other deposits in the district, such as Ambrósia ($\delta^{34}S$ = –5.4‰ to +22.2‰) and Fagundes ($\delta^{34}S$ = +14.8‰ to +36.3‰), which display a remarkable wide sulfur isotopic variation and a complex isotopic distribution related to the textural and paragenetic evolution of each deposit.

In Fagundes, early colloform sulfides are ^{34}S-enriched (up to +36.3‰), whereas mobilized sulfides and late epigenetic sulfides display lower $\delta^{34}S$ values ($\delta^{34}S$ = +14.8‰).

In Ambrósia, where the epigenetic style of mineralization is predominant, the same tendency of isotopically lighter values toward the late sulfide phases is observed ($\delta^{34}S$ = +12.2‰ to -5.4‰).

In these deposits, a relationship between $\delta^{34}S$ values and minor elements in sphalerite is also observed. The Fagundes early sphalerite is characterized by the highest $\delta^{34}S$ values, low average iron content (0.42 %) and low Zn/Cd ratio (= 140). The decrease in $\delta^{34}S$ values in late sphalerite is accompanied by slight increase of average iron content (0.56 %) and in Zn/Cd ratio (= 226). Sphalerite associated with epigenetic mineralization of Ambrósia is ^{34}S-depleted, iron-rich (until 1.57%) and has the highest Zn/Cd ratio (=1510).

In the Morro Agudo deposit, Cunha (1999) and Misi et al. (1999) described a wide range of sulfur isotopic values ($\delta^{34}S$ = -8.7‰ to +40.0‰), which are related to the deposit geometry and morphology. The highest values have a spatial relationship with deeper ore levels and with a fault zone considered as a feeder zone for mineralizing fluids.

OXYGEN AND CARBON ISOTOPES

Previous studies on the Vazante hydrothermal carbonates indicate that the gangue carbonates related with sulfide ore bodies and with willemitic ore reflect two different covariant trends. The first is characterized by ^{18}O-enrichment accompanied by ^{13}C-depletion. The trend related with the willemitic ore is characterized by decrease of $\delta^{18}O$ and $\delta^{13}C$ values (Monteiro, 1997; Monteiro et al., 1999).

The carbon and oxygen signature of the gangue carbonate related to Vazante sulfide ore ($\delta^{18}O$ = +21.58‰ to +31.85‰; $\delta^{13}C$ = -5.94‰ to +1.66‰) are quite different of those of Fagundes ($\delta^{18}O$ = +12.4‰ to +19.9‰; $\delta^{13}C$ = -2.3‰ to –0.2‰) and Ambrósia ($\delta^{18}O$ = +15.1‰ to +20.3‰; $\delta^{13}C$ = -2.3‰ to + 0.3‰) sulfide-rich deposits (Fig. 2).

In the $\delta^{18}O$ vs. $\delta^{13}C$ space (Fig. 2), the fields of hydrothermal gangue carbonates from Fagundes and Ambrósia are partially overlain by the carbonate field associated with the Vazante carbonates. However, the Fagundes and Ambrósia carbonates show, in general, lower $\delta^{18}O$ and $\delta^{13}C$ values than those of the gangue carbonates of the willemitic ore ($\delta^{18}O$ = +20.4‰ to +17.43‰; $\delta^{13}C$ = 0.29‰ to +0.86‰).

The individualization of the carbonate generations permit also the characterization of two evolutionary tendencies related to Ambrósia and Fagundes deposits.

The first tendency is referred to carbonates from early hydrothermal alteration, main mineralization and late epigenetic fissural mineralization. This trend is characterized by decrease of $\delta^{18}O$ and $\delta^{13}C$ values accompanying the evolution of each deposit. The lowest $\delta^{13}C$ values are related to late fissural stages.

The second tendency is associated to mobilization of the Fagundes and Ambrósia ore and post-mineralization pervasive alteration of Fagundes. This trend is characterized by decrease of $\delta^{18}O$ values, without significant $\delta^{13}C$ variation.

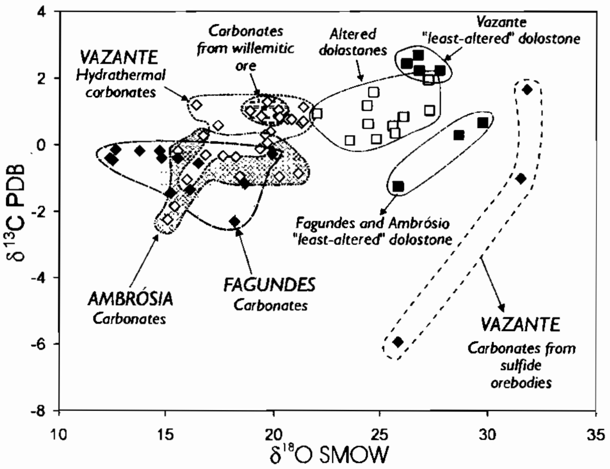

Figure 2. C and O isotopic compositions of host rocks and hydrothermal carbonates.

STRONTIUM ISOTOPES

The least-altered host dolostones exhibit $^{87}Sr/^{86}Sr$ ratios between 0.709764 and 0.71582. These signatures are more radiogenic than that relative to the best preserved dolostone of the Vazante Group ($^{87}Sr/^{86}Sr$ = 0.706144) reported by Azmy et al. (2001). This could reflect ^{87}Sr increase due to the radioactive decay of ^{87}Rb after the deposition. Calculated initial ratios for 750 Ma ($^{87}Sr/^{86}Sr_0$ = 0.705273 to 0.710458) however, are imprecise due to elevated errors in analytic measurement of Rb and Sr concentrations and to the uncertainties concerning the Vazante Group age and the nature of the system (closed or opened) during the post-depositional diagenetic process.

The altered dolostones (Fig. 3) have more radiogenic signatures ($^{87}Sr/^{86}Sr$ = 0.711126 to 0.7500399), and show, in Vazante and Ambrósia, positive correlation between $^{87}Sr/^{86}Sr$ values and Mn/Sr ratios, indicating that the more radiogenic ratios are related with the progressive hydrothermal alteration.

In all deposits, the strontium isotopic compositions in hydrothermal carbonates (siderite and dolomite) and sphalerite show a clear relationship with the paragenetic evolution of each deposit (Fig. 3).

In Vazante deposit, least-mylonitized sphalerite are less radiogenic ($^{87}Sr/^{86}Sr$ = 0.715380) than sphalerite strongly mobilized/mylonitized ($^{87}Sr/^{86}Sr$ = 0.729736). Seemingly siderite, related to the willemitic ore, is more radiogenic than sphalerite ($^{87}Sr/^{86}Sr$ = 0.721904 to 0.722250). In Fagundes, hydrothermal mineral phases are progressively more radiogenic. Dolomite associated with early colloform sphalerite has $^{87}Sr/^{86}Sr$ ratios of 0.713871, whereas late sphalerite shows $^{87}Sr/^{86}Sr$ ratios of 0.722737. Ore minerals from the epigenetic veins from Ambrósia deposit display the highest $^{87}Sr/^{86}Sr$ ratios (0.742125 to 0.53835). These strongly radiogenic signatures, however, define a narrow interval of strontium composition.

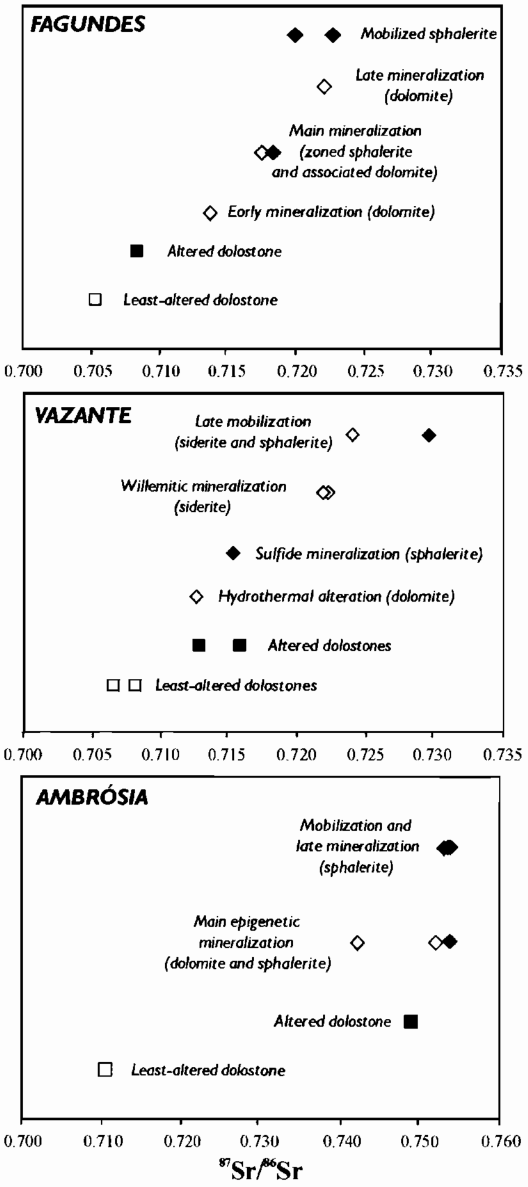

Figure 3. Sr isotopic compositions for host rocks and hydrothermal minerals.

FLUID INCLUSIONS

Fluid inclusion studies on sphalerite, quartz and dolomite from Vazante, Fagundes and Ambrósia deposits permitted the characterization of three aqueous fluid types:

(1) H_2O-NaCl-$CaCl_2$, high-temperature (> 250°C) and moderate salinity (~ 15 wt. % NaCl equiv.) fluid. This fluid type predominates in sphalerite from the early mineralization stages of the Fagundes deposit, but is also identified in quartz and sphalerite from Vazante and Ambrósia.

(2) H_2O-NaCl-$CaCl_2$-$FeCl_2$, moderate-temperature (140 - 190°C) and high salinity (> 23 wt. % NaCl equiv.) fluid, which fluid is associated mainly with the late mineralization stage of Fagundes and Ambrósia.

(3) H_2O-NaCl-$CaCl_2$, moderate to low temperature (~ 150 - 90°C) and low salinity (< 5 wt. % NaCl equiv.) fluid. This fluid type is present in mineral phases from all deposits, mainly in mineral phases formed after the main mineralization stage.

Variations of salinity and eutectic temperatures in primary fluid inclusions in the same mineral, mainly in zoned sphalerite, besides the relationship between homogenization temperature and salinity indicate progressive mixing between fluids (1) and (2), mainly in Fagundes and Ambrósia deposits. Primary fluid inclusions in late mobilized phases and secondary fluid inclusions in early minerals with moderate to low temperature and low salinity also suggest late mixing with meteoric waters (3).

DISCUSSION

SULFUR SOURCE

The Vazante sulfides display $\delta^{34}S$ values that are similar to those reported by Azmy et al. (2001) for trace sulfate trapped in carbonate from the host dolostones ($\delta^{34}S_{sulfate}$ = +8.5‰ to +16.9‰), which represent the best record of the sulfur isotopic composition of the sulfate seawater contemporary with the carbonate deposition. This could suggest that the sulfur source related to Vazante sulfide ore bodies is associated to thermochemical sulfate reduction, without significant fractionation. The main sulfur source could be related to the reduced sulfur content transported by the metalliferous oxidized fluids. The lowest Zn/Cd ratios (= 64 to 98) in Vazante sphalerite, however, could indicate that this metalliferous fluid had low reduced sulfur content (ΣS_{red}), which according to Schwartz (2000) may shift the total Cd distribution coefficient [K_t(ZnS, Cd)] to higher values, and hence favor the formation of Cd-rich sphalerite. Thus, the metalliferous fluid could represent a minimum reduced sulfur reservoir. This could be a important factor for the establishment of high fO_2/fS_2 conditions, which are necessary for the willemite stability (Monteiro, 1987).

The relationship between sulfur isotopic variations and the paragenetic sequences in Fagundes and Ambrósia deposits is systematic. The relation between $\delta^{34}S$ values and minor element contents in sphalerite, besides the evidences supported by fluid inclusions, suggest that mixing processes involving two distinct sulfur sources may be important for the genesis of the sulfide-rich deposits of the district.

The predominance of highest $\delta^{34}S$ values in the early sulfides, such as in Fagundes, and their relation with feeder zones in Morro Agudo (Misi et al., 1999), could suggest that the ^{34}S-enriched sulfur species were transported by the early high-temperature (>250 °C), moderate salinity (~ 15 wt. % NaCl), metalliferous mineralizing fluid.

Light sulfur was predominant during the epigenetic stages of mineralization, but possibly was also important for the late-diagenetic mineralization stages, judging from the Fagundes zoned sulfides, which exhibit lower $\delta^{34}S$ values than early phases. This isotopically light sulfur could be derived from bacteriogenic sulfate reduction in cold or distal parts of the system.

The predominance of lowest $\delta^{34}S$ values in epigenetic stages of mineralization may result from expulsion of moderate temperature, highly saline basinal fluids from the Vazante basin, related with Brasiliano compressive events. Alternatively, reduced shales that cover the host dolostones in Fagundes, Ambrósia and Morro Agudo deposits, might be mobilized by descending fluids, representing a potential sulfur source.

FLUID EVOLUTION

The $\delta^{18}O$ and $\delta^{13}C$ covariant trends related to sulfide and willemitic ore from the Vazante deposit were interpreted, based on the models of Zheng & Hoefs (1993), as related to fluid-rock interaction and fluid mixing, respectively (Monteiro, 1997, 1999). In the first case, the involved fluid is ^{18}O-enriched and has isotopic characteristics compatible with metamorphic or diagenetically ^{18}O-enriched fluids. In the second case, the covariant trend may be due to mixing between this metalliferous fluid with meteoric water.

The carbon and oxygen isotopic variations in hydrothermal carbonates from Fagundes and Ambrósia are partially overlaid by the field of Vazante carbonates and could also suggest the predominance of mixing processes.

The two identified trends related to Fagundes and Ambrósia may represent evolutionary tendencies related to mixing between the three fluid types identified by the fluid inclusion studies.

The relationship between isotopic variations and paragenetic evolution indicate that the fluids related to Ambrósia epigenetic mineralization are ^{13}C-depleted, suggesting interaction with organic matter. This carbon signature overlap the highest salinity and $^{87}Sr/^{86}Sr$ values for the late mineralization stage, suggesting predominance of radiogenic fluids, derived probably from reduced shale units, in the last stages. This basinal fluid was responsible for transport of isotopically light sulfur and subordinately of metals into the system.

The ^{18}O-impoverishment tendency observed mainly in mobilized and in post-mineralization carbonates could be related to the predominance of ^{18}O depleted, low salinity, meteoric waters during the final evolution of the hydrothermal system.

CONCLUSION

Fluid inclusion and isotopic studies indicate a common long-term evolutionary history of the hydrothermal systems, related to late-diagenesis and epigenetic events, for the genesis of both non-sulfide and sulfide zinc deposits of the Vazante-Paracatu district. The clear relationship between fluid composition, as traced by fluid inclusion and O, C and Sr isotopes, and paragenetic evolution of each deposit strongly suggest that progressive mixing processes were important for the genesis of these deposits.

In sulfide zinc deposits the influence of high salinity, strongly radiogenic basinal fluids is of great importance for ore genesis, mainly by its possible role in reduced sulfur supply.

The low-sulfidizing capacity of the Vazante willemitic system might be related to the scarcity of sulfur supply from upper shale units. The genesis of the sulfide ore from the Vazante deposit involves the interaction of oxidized ascending metalliferous fluids, of limited content of reduced sulfur, and the host dolostones.

The willemitic mineralization is coeval with the Vazante Fault development, which favors the overall mixture of metal-bearing and meteoric fluids channeled to the fault zone. This mixture process between low reduced sulfur-bearing fluids ($\sum S_{red}$) and oxidizing meteoric fluids favors the Vazante willemitic mineralization.

ACKNOWLEDGMENTS

This paper is part of the Doctorate thesis of the first author. We are grateful to Companhia Mineira de Metais for continuous support and hospitality at the mine. Special thanks are due to the Luiz Paulo B. Ribeiro, Solange L.de Souza, Ivone and Helen Sonoki (CPGeo, IGc-USP). The financial support was provided by FAPESP (Doctorate Scholarship 98/0412-5).

REFERENCES

Azmy, K.; Veizer, J.; Misi, A.; Oliveira, T.F. de; Sanches, A.L.; Dardenne, M.A., 2001. Dolomitization and isotope stratigraphy of the Vazante Formation, São Francisco Basin, Brazil. Precambrian Res., 112:303 - 329.

Cunha, I. de A., 1999. Estudos de inclusões fluidas e de isótopos de enxofre dos corpos de minério de Morro Agudo, Minas Gerais. Master Thesis, UFBa, 105p.

Dardenne, M.A.; Schobbenhaus, C. S., 2001. Metalogênese do Brasil. Brasília, Editora Universidade de Brasília/CNPq. 392 p.

Dardenne, M.A.; Freitas-Silva, F.H.; Souza, J.C.F.; Campos, J.E.G., 1998. Evolução tectono-sedimentar do Grupo Vazante no contexto da Faixa de Dobramentos Brasília. In: Congr. Bras. Geol., 40., Belo Horizonte, 1998., Resumos, SBG, p. 26.

Hitzman, M. W., 2001. Zinc oxide and zinc silicate deposits – a new look. In: GSA, Abstr. Programs, v. 33, p. A336.

Misi, A.; Iyer, S. S.; Kyle, J. R.; Coelho, C. E. S.; Franca-Rocha, W. J. S.; Gomes, A. S. R.; Cunha, I. de A.; Carvalho, I. G., 1999. Geological and isotopic constraints on the metallogenic evolution of the Proterozoic sediment-hosted Pb-Zn (Ag) deposits of Brazil. Gond. Res., 2: 47-65.

Monteiro, L.V.S., 1997. Contribuição à gênese das mineralizações de zinco da Mina de Vazante, MG. Master Thesis, IGc-USP, 159p.

Monteiro, L.V.S. 2002. Modelamento metalogenético dos depósitos de zinco de Vazante, Fagundes e Ambrósia, associados ao Grupo Vazante, Minas Gerais. Doctorate Thesis, IGc-USP, 317 p. il.

Monteiro, L.V.S.; Bettencourt, J.S.; Spiro, B; Graça, R.; Oliveira, T.F., 1999. The Vazante Zinc Mine, Mg, Brazil: Constraints on Fluid Evolution and Willemitic Mineralization. Exploration and Mining Geology, 8:21-42.

Schwartz, M.O., 2000. Cadmium in Zinc Deposits: Economic Geology of a Polluting Element. Intern. Geol. Rev,. 42: 445-469.

Zheng, Y-F. & Hoefs, J., 1993. Theoretical modeling on mixing processes and application to Pb-Zn deposits in the Harz Mountains, Germany. Mineral Deposita, 28:79 - 89.

U-Pb SHRIMP AGE OF THE CARAÍBA, MEDRADO AND S. JOSÉ DO JACUÍPE MAFIC-ULTRAMAFIC COMPLEXES, PALEOPROTEROZOIC ITABUNA-SALVADOR-CURAÇÁ OROGEN, SÃO FRANCISCO CRATON, BRAZIL

Oliveira, E.P.[1]; McNaughton, N.[2]; Armstrong, R.[3] and Fletcher, I.[2]

1. Instituto de Geociências, UNICAMP, 13083-970 Campinas, Brazil. elson@ige.unicamp.br
2. Centre for Global Metallogeny, School of Earth and Geographical Sciences, UWA, Crawley, WA 6009, Australia. mcn@iinet.net.au, ifletche@geol.uwa.edu.au
3. Research School of Earth Sciences, ANU, Canberra, ACT 0200, Australia. richard.armstrong@anu.edu.au

Keywords: U-Pb SHRIMP geochronology, mafic-ultramafic complexes, Itabuna-Salvador-Curaçá Orogen

INTRODUCTION

Several mafic-ultramafic complexes have been mapped in the northern segment of the Itabuna-Salvador-Curaçá Orogen (NISCO), some of which are currently mined for copper sulphide (Caraíba) and chromite (Medrado, Campo Formoso and Santa Luz). Information about their age are relevant for understanding the timing of mineralisation and their relative importance in the regional geologic evolution.

Here we report U-Pb ages on zircons extracted from noritic rocks of the Caraíba hypersthenite-norite complex, Medrado peridotite-norite sill, and the São José do Jacuípe layered gabbronorite-peridotite Suite, and comment on their regional significance.

GEOLOGIC SETTING

CARAÍBA HYPERSTHENITE-NORITE COMPLEX

This complex crops out in the Curaçá high-grade terrane and is made up of dykes, breccias and lensoid bodies of hypersthenite and norite with occasional peridotite and amphibolite enclaves (Oliveira & Tarney, 1995). Copper sulphides and magnetite are more concentrated in hypersthenite than in norite. The timing of emplacement of the Caraíba complex has been a matter of debate. On one hand, Silva (1985) argued that the mafic-ultramafic bodies intruded a supracrustal sequence and were later deformed during three main high-temperature deformation phases associated with granitic intrusions. On the other, Oliveira & Tarney (1995) presented field relations indicating that the Caraíba hypersthenite-norite complex was emplaced into rocks previously deformed at amphibolite facies conditions. Presently, we acknowledge that the Caraíba body was later reworked under the granulite facies conditions, and retrogressed to amphibolite facies during the two last ductile deformation phases of Silva (1985).

MEDRADO PERIDOTITE-NORITE COMPLEX

The Medrado mafic-ultramafic complex has a sill-like structure and occurs intruded in granulite grade metagranitoids and metasupracrustal rocks (marble, diopsidite and gneiss) (Deus & Viana, 1982; Mello et al., 1986; Marinho et al. 1986).

On the basis of regional geologic mapping, Marinho et al. (1986) recognized that the supracrustal sequence has a gneissic banding S1 parallel to So, as the result of D1 deformation. This sequence was intruded by the granodioritic orthogneiss G1 that also shows the metamorphic banding S1. Centimetric-thick mafic dykes crosscut S1 and are intruded by a granitic-granodioritic orthogneiss G2 with a prominent S2 metamorphic banding. G3 granites, the Itiúba Syenite, and associated pegmatites, intrude these rocks, all of them displaying a gneissic S3 fabric. With the exception of the G3 intrusions, which were metamorphosed under amphibolite facies conditions, all rocks have mineral parageneses indicative of granulite facies metamorphism.

SÃO JOSÉ DO JACUÍPE GABBRONORITE-PERIDOTITE SUITE

This suite occurs as dismembered bodies on the southern portion of NISCO, between the towns of Capela do Alto Alegre and Baixa Grande. According to Melo et al. (1991) it is composed mostly of norite and gabbronorite, and less often peridotite, ferrogabbro and pyroxenites. The gabbroic rocks were metamorphosed under the granulite facies, and were intruded by syntectonic granitoids. Primary igneous layering is observed in leucogabbro. Melo et al. (1991) suggested that rocks of the São José do Jacuípe suite are remnants of an oceanic crust formed during fragmentation of the Serrinha and Mairi blocks in the Archaean.

SAMPLING SITES

For U-Pb geochronology, one norite sample from each complex was collected. In Caraíba, sample PO-29.2 comes from the northern wall of the deepest bench of the mine open-pit. This rock is part of a breccia of hypersthenite and norite; it is aphyric, weakly foliated, medium- to coarse-grained and composed of plagioclase, hypersthene, and accessory apatite, zircon, biotite, magnetite and sulphide. Zircons are elongate to round in shape, always have smooth edges, and are pink to brown without visible inclusions. In back-scattered electron (BSE) images, the elongate zircons often show oscillatory zoning, whereas the round ones either show sector zoning or no zoning.

In Medrado, norite sample Gb-Medra consists of drill-core chips from borehole SSM-18/67. The rock is coarse-grained equigranular, aphyric, weakly foliated, and composed of plagioclase, amphibole, pyroxene relicts and accessory zircon and apatite. Zircons are mostly round to elongate, pink to brown grains with poorly developed oscillatory and sector zoning on BSE images.

A leucogabbro sample (3.4) of the São José do Jacuípe Suite was collected on the outskirt of Aroeira village. The rock is coarse-grained, aphyric and shows primary igneous layering marked by intercalation of dark, amphibole-rich layers with light, plagioclase-rich layers. Foliated mafic dykes of the Aroeira dyke swarm and granitoids crosscut the leucogabbro. Zircon population is made up of several generations, with cores of various shapes, sizes and proportions. They are generally zoned with compositional, concentric zoning. Some discrete grains, also variably zoned, show metamorphic rounding and recrystallisation.

U-Pb SHRIMP GEOCHRONOLOGY

Ion microprobe analyses of the Caraíba and Medrado zircons were carried out using SHRIMP II at the School of Applied Geology, Curtin University of Technology, Perth, based on the operation procedure described by Compston et al (1984) and operation conditions described by Smith et al. (1998). Zircons from the São José do Jacuípe leucogabbro were analysed using SHRIMP-RG at the School of Earth Sciences, Australian National University (Canberra), following the procedures of Williams & Claesson (1987) and Compston et al. (1992). The age-populations reported here are for data between 95% and 105% concordance. Pooled ages are quoted at the 95% confidence level and 1σ or 2σ error.

A total of 19 analyses were obtained on 19 zircons from the Medrado norite, 26 analyses on 20 zircons from the Caraíba norite and 22 analyses on 18 zircons from the São José do Jacuípe leucogabbro. The resulting ages are listed in Table 1.

Table 1: U-Pb SHRIMP results.

	Igneous crystallization (Ma)	**Metamorphism (Ma)**
Caraíba	2580 ± 10	2103 ± 23
Medrado	2085 ± 5	
S.J.Jacuípe	2583 ± 8	2082 ± 17

Fourteen zircon grains from the Medrado sample yielded a $^{207}Pb/^{206}Pb$ concordia age of 2085±5 Ma. No significant age difference was observed between elongate and round zircons. No older age population was found.

The Caraíba norite, on the other hand, yielded two main $^{207}Pb/^{206}Pb$ concordia ages, at 2580±10 Ma and 2103±23 Ma. Because the latter zircon population has Th/U ratios below 0.1, which is generally regarded as typical for metamorphic zircons (e.g. Rubatto & Gebauer, 2000), this younger age is interpreted to be the time of regional high-grade metamorphism that affected the Caraíba norite. The older age is derived from zircon cores, and we interpret it as the crystallisation age of the igneous protolith.

The São José do Jacuípe leucogabbro also give two concordant clusters. Eight analyses of cores and discrete grains representing the oldest grains were combined to give a $^{207}Pb/^{206}Pb$ concordia age of 2583±8 Ma, whereas 4 analyses of overgrowths give a weighted mean $^{207}Pb/^{206}Pb$ age of 2082±17 Ma.

DISCUSSION

The age results presented here have several implications for the geologic evolution of the Itabuna-Salvador-Curaçá orogen. Debate about the metallogenic contrast between the copper sulphide-bearing mafic-ultramafic bodies of the Curaçá high-grade terrane and the chromite-rich mafic-ultramafic bodies of the Jacurici terrane is long-standing. Mandetta (1982) and Silva (1985) suggested that the two main mineralised mafic-ultramafic bodies, viz. Caraíba in the Curaçá and Medrado in the Jacurici terranes, were derived from a common parental magma through fractional crystallization. In this model, the Jacurici chromiferous bodies fractionated first and the cupriferous Curaçá later. Our new geochronological data, viz. 2580 Ma for the Caraíba norite and 2085 Ma for the Medrado norite, show that these igneous complexes and their mineralisation are sufficiently different in age that it is almost impossible that they are co-genetic. The interpretation of the São José do Jacuípe age is more complex. Rocks of this suite are tectonically dismembered and are intruded by gray- and pink granitoids. Some of these granitoids entrain gabbronorite xenoliths that are generally interpreted as belonging to the São José do Jacuípe suite (Melo et al., 1991; Kosin et al., 2003). While in some places this assumption is valid, especially where the younger granitoids clearly crosscut the mafic rocks, in others may be not. This is particularly true for a TTG enderbite of the Caraíba Complex that contains gabbronorite xenoliths and was dated by Silva et al. (1997) at 2.69 Ga (U-Pb SHRIMP). This age and field relations indicate that the Sao José do Jacuípe suite should be older than 2.7 Ga (cf. Kosin et al., 2003). Our age of 2583 Ma is 100 Ma younger and supports the suggestion that more than one intrusion of mafic-ultramafic rocks with different ages might have taken place. Another interesting conclusion of our data is the regional occurrence of igneous bodies ca. 2.58 Ga old (e.g. Caraíba and S. José Jacuípe). Similar ages were reported for mafic dykes of the Uauá Block (Oliveira et al., 1999), protoliths of several granulites from NISCO (Silva et al., 1997), basement of the Rio Itapicuru greenstone belt (Chauvet et al. 1997) and as depleted mantle model ages in the Rio Capim sequence as well as in mafic dykes of the Uauá dyke swarm (Oliveira et al., 1998; 1999). Therefore, the ca. 2600 Ma is a crust-forming event of regional significance and coincides with the end of the Jequié orogenic cycle (2800-2600 Ma, cf. Ledru et al., 1994).

ACKNOWLEDGMENTS

The São Paulo State Foundation for Research Support (FAPESP) and the Brazilian National Research Council (CNPq) provided research grants for this project (FAPESP 99/05760-4; CNPq 300.845/91-0).

REFERENCES

Chauvet, A., Guerrot, C., Alves da Silva, F.C., Faure M., 1997. Géochronologie $^{207}Pb/^{206}Pb$ et $^{40}Ar/^{39}Ar$ des granites paléoprotérozoiques de la ceinture de roches vertes du Rio Iapicuru (Bahia, Brésil). Comptes Rendus de l'Academie des Sciences Paris II , 324: 293-300.Compston, W., Williams, I.S., Kirschvink, J.L., Zhang, Z., Guogan, M.A., 1992. Zircon U-Pb ages for the Early Cambrian time-scale. J. Geol. Soc. London, 149: 171-184.

Deus, P.B., Viana, J.S., 1982. Jacurici chromite district. ISAP – International Symposium on Archean and Early Proterozoic Geological Evolution, Abstract and Excursion, SME-Ba, pp. 97-107.

Kosin, M., Melo, R.C., Souza, J.D., Oliveira, E.P., Carvalho, M.J., leite, C.M.M.., 2003. Geologia do segmento norte do Orógeno Itabuna-Salvador-Curaçá e guia de excursão. Revista Brasileira de Geociências, 33 (in press).

Ledru, P., Cocherie, A., Barbosa, J., Johan, V., Onstott, T., 1994. Ages du métamorphisme granulitique dans le craton du São Francisco (Brésil). Implications sur la nature de l'orogène transamazonien. Comptes Rendus de l'Academie des Sciences Paris, 318, série II, p. 251-257.

Mandetta, P., 1982. Aspectos geológicos e petrogenéticos das associações máfico-ultramáficas da região de Caraíba, vale do Curaçá/BA. Dissertação de Mestrado. Instituto de Geociências, UFBa.

Marinho, M.M., Rocha, G. M.F., Deus, P.B., Viana, J.S., 1986. Geologia e potencial cromitífero do vale do Jacurici-Bahia. XXXIV Congresso Brasileiro de Geologia, Goiânia, V.5: 2074-2088.

Mello, C.H.M.P., Durão, G., Viana, J.S., Carvalho, C.J.C., 1986. Depósitos de cromita das Fazendas Medrado e Ipueira, município de Senhor do Bonfim, Bahia. In: Schobbenhaus, C. and Coelho, C.E.S. (coords) Principais Depósitos Minerais do Brasil, vol. II, DNPM, Brasília, p. 215-234.

Melo, R.C., Silva, L.C., Fernandes, P.C., 1991. Estratigrafia. In: R.C. MELO (org.) Pintadas – Folha SC.24-Y-D-V. Programa de Levantamentos Geológicos Básicos do Brasil, CPRM, p. 23-47.

Oliveira, E.P., Tarney, J., 1995. Genesis of the copper-rich Caraíba norite-hypersthenite complex, Brazil. Mineralium Deposita, 30: 351-373.

Oliveira, E.P., Lafon, J-M., Souza, Z.S., 1998. A Paleoproterozoic age for the Rio Capim volcano-plutonic sequence, Bahia, Brazil: whole-rock Pb-Pb, Pb-evaporation and U-Pb constraints. Anais XL Congresso Brasileiro de Geologia, SBG, p. 14.

Oliveira, E.P., Lafon, J-M., Souza, Z.S., 1999. Archaean-Proterozoic transition in the Uauá Block, NE São Francisco Craton, Brazil: U-Pb, Pb-Pb and Nd isotope constraints. First International Symposium on Tectonics of the Brazilian Geological Society, Lençóis-BA, 12-15 May. Abstract Volume, p. 38-40.

Rubatto, D., Gebauer, D., 2000. Use of cathodoluminescence for U-Pb zircon dating by ion microprobe: some examples from the Western Alps. In: Pagel, M., Barbin, V., Blanc, P., Ohnenstetter, D. (eds) Cathodoluminescence in Geosciences. Springer Verlag, pp. 373-400.

Silva, L.J.H.D., 1985. Geologia e controle estrutural do depósito cuprífero de Caraíba, Vale do Curaçá - Bahia. IN: P.V.S.V.Sá & F.B. Duarte (orgs.) Geologia e Recursos Minerais do Estado da Bahia. Textos Básicos, Vol.6°: 51-136.

Silva, L.C., McNaughton, N.J., Melo, R.C., Fletcher, I.R., 1997. U-Pb SHRIMP ages in the Itabuna-Caraíba TTG high-grade complex: the first window beyond the Paleoproterozoic overprinting of the eastern Jequié craton, NE Brazil. Proceedings 2nd International Symposium on Granites and Associated Mineralizations. Sociedade Brasileira de Geologia, Salvador-Bahia, p. 282-283.

Williams, I.S. & Claesson, S., 1987. Isotopic evidence for the provenance and Caledonian metamorphism of high grade paragneisses from the Seve Nappes, Scandianavian Calledonides: ion microprobe zircon U-Th-Pb. Contrib. Mineral. Petr.,97:205-217.

OXYGEN ISOTOPE HALOES IN OCEANIC MESOPROTEROZOIC PALEO-HYDROTHERMAL SYSTEMS FROM THE SERRA DO ITABERABA GROUP, SÃO PAULO, BRAZIL, AND ITS POTENTIAL APPLICATION TO MINERAL EXPLORATION

Pérez-Aguilar, A.; Juliani, C.; Monteiro, L.V.S. and Bettencourt, J.S.

Instituto de Geociências – USP, Rua do Lago, 562, São Paulo-SP, 05508-900, Barzil. aperez@usp.br, juliani@usp.br, lenavsm@zipmail.com.b1, jsbetten@usp.br

Keywords: Paleo-hydrothermal system, stable isotopes, oxygen isotope haloes, base metals, gold

Mesoproterozoic (Juliani et al., 2000) paleo-hydrothermal oceanic systems are present northeast of São Paulo city making part of the Serra do Itaberaba Group (SIG) (Juliani, 1993; Juliani & Beljavkis,1995).

In the SIG, the basal Morro da Pedra Preta Fm. is a metamophosed volcano-sedimentary sequence, composed mainly of N-MORB type metabasites and schists. Overlying is the Nhangucu Formation, with iron-manganesifeous schists, andalusite-rich schists, and lenses of meta-calcpelites and marbles. The Pirucaia Formation, with quartzites and quartz-rich schists, is a marginal facies of the Nhangucu Formation. These sequences are strongly deformed and were affected by two medium-grade and a low-grade metamorphic events during Mesoproterozoic and Neoproterozic orogenic events (Juliani, 1993; Juliani & Beljavskis, 1995).

The Morro da Pedra Preta Fm. was mostly deposited in an extensional regime, but also, together with the Nhanguçu Formation, during the subsequent installation of a back-arc basin, in a compressive regime (Juliani, 1993).

The paleo-hydrothermal systems developed during the installation of the back-arc basin, in the compressive regime, associated to intrusions with compositions varying from intermediate to felsic composition, and to which they are genetically linked (Juliani et al., 1992; Pérez-Aguilar, 1996, 2001).

Rocks constituted by cummingtonite and/or anthophillyte are the metamorphic product of variable hydrothermalized basic and intermediate/felsic protoliths, corresponding to pre-metamorphic propylitic hydrothermal alteration zones (Hemley & Jones, 1964; Meyer & Hemley, 1967; Rose, 1970; Pirajno, 1992).

These rocks formed by cummingtonite/anthophillyte are distributed in the interface between the Morro da Pedra Preta Fm. and the Nhanguçu Formation and are interpreted as formed by paleo-hydrothermal oceanic systems (Pérez-Aguilar et al., 2000; Pérez-Aguilar, 2001).

Surrounding intensely deformed intrusions of andesites/rhyodacites, due to tectonic transpositions, there is a zoned sequence of lithotypes that show a complete gradation between unaltered to strongly altered rocks, represented by groups of unaltered rocks, weakly altered rocks (typically with small amounts of metamorphic cordierite and/or cummingtonite), transitional rocks (where characteristically two ore three different metamorphic amphiboles coexist), moderately altered rocks (typically, in the metamorphic assemblage, all the hornblende was substituted by cummingtonite; also small amounts of cordierite and garnet may be present), and strongly altered rocks. Strongly altered rocks have a mineral association with cummingtonite and/or anthophillite + magnesian cordierite ± almandinic garnet ± quartz ± magnetite ± ilmenite ± rutile ± staurolite ± biotite ± chlorita. (Pérez-Aguilar, 1996, 2001).

Associated to these rocks are also observed layers of carbonatized rocks (constituted essentially by carbonate + epidote + actinolite + diopside), that typically occur under intermediate to felsic intrusions, marundites (rocks with corindon ± margarite ± muscovite ± rutile ± plagioclase ± tourmaline), hornblende-garnet amphibolites and meta-chloritites, that include, as an extreme cation lixiviation process, cummingtonite-garnet-chlorite schists. All of the above mentioned rocks are the metamorphic product of different types of hydrothermal alteration processes also present in the Morro da Pedra Preta Fm. Algoma type BIFs, sulfide-rich metapelites that were formed, at least, partially, by mineralizing pre-metamorphic processes, and extensive zones of rocks mineralized in gold are also present.

WHOLE-ROCK ISOTOPE DATA

The whole-rock oxygen isotope ratios are reported in values compared with the Standard Mean Ocean Water value (SMOW).

In the group of not altered and altered igneous metabasites, $\delta^{18}O$ values vary from 5.9‰ to 16.9‰. In the group of not altered and altered pyroclastic metabasites, genetically associated to igneous metabasites, these values range from 8.3‰ to 10.1‰, in altered meta-intermediate igneous rocks from 14.1‰ to 17.6‰, and in most meta-intermediate volcaniclastic rocks from 15.3‰ to 17.8‰. Finally, in meta-chloritites, formed after the alteration of igneous basic rocks, $\delta^{18}O$ values range from 9.0‰ to 10.6‰. A characteristic that can be observed in the groups of igneous metabasites, pyroclastic rocks, and meta-intermediate igneous rocks, are well-defined trends of increasing values of $\delta^{18}O$ with progressive intensity in alteration process.

Meanwhile, the meta-chloritites, that are the product of a more intense cation lixiviation process, show relative lower values of $\delta^{18}O$ (9.0‰ to 10.6‰), if compared with $\delta^{18}O$ values observed in strongly altered igneous rocks (11.8‰ to 16.9‰).

Regional zoning in the $\delta^{18}O$ values are present in the Kuroko type volcanogenic sulfide deposits, showing a progressive enrichment of theses values in the wallrocks around the mineralized zone (Cathles, 1993; Barrett & MacLean, 1994), as observed in $\delta^{18}O$ values obtained for the groups of igneous metabasites, pyroclastic rocks, and meta-intermediate igneous rocks here studied, and a progressive decreasing of them in direction to the mineralized zone (Vásquez et al., 1998; Gemmel et al., 1998; Cartwright, 1999), represented, in this case, by $\delta^{18}O$ data from meta-chloritites. These regional zoning produce concentric alteration haloes, characterized by positive anomalies of $\delta^{18}O$ in the rocks that regionally surround mineralized zone, and negative anomalies of $\delta^{18}O$ in the rocks near mineralized zones.

Decreasing values of $\delta^{18}O$ of rocks near mineralized zone would be produced by intense seawater circulation, typically with $\delta^{18}O$ close to 0‰, near hot intrusive bodies. In this situation, the thermal anomaly associated to intrusions would reduce the isotopic fractionation factor between rocks and seawater, producing isotopic anomalies in which the fluids become isotopically heavier and altered rocks isotopically more light (Cathles, 1983).

Regional enrichments of the $\delta^{18}O$ values of altered rocks can be produced by the circulation of hot fluids towards the colder parts of the system, in distal portions related to intrusions. In this situation, the isotopic fractionation factor between rocks and water increase very much so fluids become istopically light and altered rocks isotopically heavy (Cathles, 1983; Green et al. 1983; Cathles, 1993)

The values of $\delta^{18}O$ obtained for most of the meta-intermediate volcaniclastic rocks (15.3‰ to 17.8‰) are much higher as those observed in not altered intermediate rocks, in which values can vary from 6.0 to 10‰ (Paradis et al., 1993). The narrow interval of $\delta^{18}O$ values may indicate that these rocks achieved a relative isotopic homogenization due to hydrothermal alteration, independent of how strong was metasomatic event that affected them. This was probably due to the high porosity, permeability and relative abundance of volcanic glass that can be present in volcaniclastic material (Staudigel et al., 1995).

CONCLUSIONS

Isotopic data obtained in the igneous metabasites, meta-intermediate igneous rocks and in the pyroclastic rocks, indicate that original hydrothermal systems isotopic signatures were, at least, partially preserved, indicating that the different superimposed metamorphic events were not responsible, in these samples, for an homogenizations of isotopic values.

The high anomalies of positive $\delta^{18}O$ values are possible due to the long lifetime of hydrothermal system, caused by the discharge of hot fluids, that came from more deeper parts of the system, towards distal parts, so as observed in discharges responsible for the formation for the white smokers in actual back-arc basins.

Comparing the $\delta^{18}O$ values obtained for meta-chloritites with those of associated altered rocks, it is possible to infer higher fluid temperatures in alteration process, and consequently, relative lower $\delta^{18}O$ values, indicating a regional distribution nearer to mineralization zone.

In this context, the zones of the black smokers may correspond to the metaleferous meta-sediments, especially those sulfide-rich, that are present in the interface between the Morro da Pedra Preta and Nhangucu Fms, and where, potentially, gold and base metal deposits could be found.

ACKNOWLEDGEMENTS

The senior author would like to sincerely thank FAPESP for the grants number 98-15170-7.

REFERENCES

Barrett, T.J. & MacLean, W.H., 1994. Mass changes in hydrothermal alteration zones associated with VHMS deposits in Noranda area. Exploration and Mining Geology, 3, 131-160.

Cartwright, I., 1999. Regional isotope zonation at Broken Hill, New South Wales, Australia: large scale fluid flow and implications for Pb-Zn-Ag mineralizations. Economic Geology, 94, 357-374.

Cathles, L.M., 1993. An analysis of the hydrothermal system responsible for massive sulfide deposition in the Hokuroku basin of Japan. Economic Geology Monograph, 5, 439-487.

Cathles, L.M., 1993. Oxygen isotope alteration in the Noranda Mining District, Abitibi Greenstone Belt, Quebec. Economic Geology, 88, 1483-1511.

Gemmell, J.B.; Large, R.R.; Zaw, K., 1998. Palaeozoic volcanic-hosted massive sulphide deposits. Journal of Australian Geology & Geophysics, 17(4), 129-137.

Green, G.E.; Ohomoto, H.; Date, J.; Takahashi, T., 1983. Whole-rock oxygen isotope distribution in the Fukazawa-Kosaka area, Hokuroku district, Japan and its potential application to mineral exploration. Economic Geology Monograph, 5, 395-511.

Hemley, J. & Jones, W.R. (1964) Chemical aspects of hydrothermal alteration with emphasis on hydrogen metasomatism. Economic Geology, 59, 538-569.

Juliani, C. & Beljavskis, P., 1995. Revisão da litoestratigrafia da faixa São Roque/Serra do Itaberaba (SP). Revista do Instituto Geológico. 16(1/2), 33-58.

Juliani, C., 1993. Geologia, petrogênese e aspectos metalogenéticos dos grupos Serra do Itaberaba e São Roque na região das serras do Itaberaba e da Pedra Branca, NE da cidade de São Paulo. Tese de Doutoramento, Instituto de Geociências, Universidade de São Paulo, 2 vol., 803 p., 5 mapas.

Juliani, C.; Hackspacher, P.C.; Dantas, E.L. 2000. Serra do Itaberaba Group: a mesoproterozoic volcano-sedimentary unit at São Paulo State, Brazil. In: International Geological Congress, 31, IUGS/CPRM, Rio de Janeiro, Brazil. Special Symposia and General Symposia Abstracts Volume. [CDROM].

Juliani, C.; S Schorscher, H.D.; Pérez Aguilar, A.; Beljavskis, P., 1992. Cordierita-granada-cummingtonita anfibolitos no Grupo Serra do Itaberaba (SP): evidência de alterações hidrotermais metassomáticas pré-metamórficas. In: Jornadas

Científicas do Instituto de Geociências da USP, 2, São Paulo. Boletim IGUSP, Publicação Especial, 12:59-61.

Meyer, C. & Hemley, J.J. (1967) Wall rock alteration. In: Barnes, H.L. (Ed.) Geochemistry of hydrothermal ore deposits, 1st ed. New York, Holt Rinehart & Winston, 166-235.

Paradis, S.; Taylor, B.E.; Watkinson, D.H.; Jonasson, I.R., 1993. Oxygen isotope zonation and alteration in the Northern Noranda District, Quebec: Evidence for hydrothermal fluid flow. Economic Geology, 88, 1512-1525.

Pérez-Aguilar (1996) Geologia, petrografia e gênese dos granada-cordierita-cummingtonita/antofilita anfibolitos e rochas associadas do Grupo Serra do Itaberaba, SP. Dissertação de Mestrado, Instituto de Geociências, Universidade de São Paulo.São Paulo, 1v., 168p., 2 mapas

Pérez-Aguilar (2001) Petrologia e litoquímica de rochas de paleossistemas hidrotermais oceânicos mesoproterozóicos da seqüência metavulcanossedimentar do Grupo Serra do Itaberaba, SP. Tese de Doutoramento, Instituto de Geociências, Universidade de São Paulo, 223p.

Pérez-Aguilar, A.; Juliani, C.; Martin, M.A.B., 2000. Mesoproterozoic paleo-hydrothermal system in the Morro da Pedra preta formation, Serra do Itaberaba Group, São Paulo State, Brazil. Revista Brasileira de Geociências, 30(3), 413-416.

Pirajno, F., 1992. Hidrothermal mineral deposits. Principles and fundamental concepts for the exploration geologist. Springer-Verlag. Berlin Heidelberg, 709p.

Rose, A.W. (1970) Zonal relations of wall rock alteration and sulfide distribution at porphyry copper deposit. Economic Geology, 65, 920-936.

Staudigel, H.; Davies, G.R.; Hart, S,R.; Marchant, K.M.; Smith, B.M., 1995. Large scale isotopic Sr, Nd and o isotopic anatomy of altered oceanic crust: DSDP/ODP sites 417/418. Earth and Planetary Science Letters, 130, 169-185.

Vásquez, R.; Vennemann, T.W.; Kesler, S.E.; Russell, N. (1998) Carbon and oxygen isotope halos in the host limestone El Mochito Zn-Pb-(Ag) skarn massive sulfide-oxide deposit, Honduras. Economic Geology, 93, 15-31.

AGES AND SOURCES OF THE GOLD MINERALIZATIONS FROM MARMATO MINING DISTRICT, NW COLOMBIA, BASED ON RADIOGENIC ISOTOPIC EVIDENCES

Pinzon, F.D. and Tassinari, C.C.G.

Centro de Pesquisas Geocronológicas do Instituto de Geociências da Universidade de São Paulo

Keywords: Geochronology, Marmato District, gold, metallogenesis, Andes

INTRODUCTION

The Andean Cordillera, in Colombia, is composed of three ridges, with N-S trends, named Oriental, Central and Occidental. Geologically, the Colombian Andes, is divided in two different domains by the Cauca-Romeral Shear Zone; the first one, which includes the oriental and central ridges at the eastern side, is composed of precambrian and paleozoic continental basement, intruded by several mesozoic and cenozoic granitic plutons, and covered by sedimentary sequences. The second domain, that includes the occidental ridge, was formed by successive accretions of allochthonous terranes, which show oceanic affinities (Etayo et. al. 1986 and Toussaint & Restrepo 1989). These terranes were intruded by several sub-volcanic intrusions, which form the Combia Formation, and one of them, is the Miocene Marmato Stock, that is the host - rock of the epithermal Au-Ag Marmato mineralizations (Restrepo et. al. 1981).

The Marmato Mining District is located at the Setentrional Andes of Colombia, in the Caldas State, at 50 km from N-NW of Manizales capital city. The mineralizations are divided in three different levels: the first one near the surface is named Echandia, the intermediary is the Cien Pesos Sector and the deepest is the Marmato Bajo Sector.

In order to characterize the age and sources of the mineralizations of Marmato Minig District, Sr-Sr, Pb-Pb, Sm-Nd and K-Ar isotopic analyses were carried out on ore and gangue minerals at the Geochronological Research Center of University of São Paulo. The sample selection, for isotopic analyses, was made based on petrographic and mineralogical characteristics, that included analyses using thin sections and polished sections, beyond analized sections on the back scatter electron microscope.

GEOLOGICAL SETTING

The Marmato Mining District is located within the Calima Terrain (Toussaint & Restrepo, 1991), which is bounded by the Cauca and Romeral Faults. The oldest exposed rocks in the area belong to metasedimentary Arquia Complex, with Cretaceous metamorphic ages, and are represented by graphite-schists metamorphosed within low amphibolite facies and by chlorite-schists metamorphosed within greenschist metamorphic conditions (Rosseti et al., 1999). The Miocene sedimentary rocks of the Amagá Formation overly the metamorphic basement. and are composed of sandstones, shales and conglomerates. The youngest stratigraphic unit in the Marmato area is the Combia Formation, which is characterized by volcanoclastic unit. Pyroclastic rocks include clasts of basalt and andesites. Mafic lavas with subordinate tuffaceous intercalations also occur. Associate with the Combia Formation appear some sub-volcanic bodies, with andesitic and dacitic compositions, with ages ranging from 9 Ma to 6 Ma (Restrepo et. al., 1981).

One of these bodies is the Marmato Stock, which is the host-rock of the Marmato Au-Ag mineralizations. This stock is composed of porphyritic volcanic rocks with dacitic and andesitic compositions. The porphyritic andesites outcrop in the border of the stock, while the porphyritic dacites appear in the central part of the body. The andesite, which occur at Echandia sector (Plata Fria Mine), is composed of plagioclase phenocrystals (andesine) hydrothermaly alterated to sericite and carbonate, hornblende, and partially chloritized biotite, within a fine matrix composed of plagioclase, chlorite, magnetite, apatite and epidote. The porphyry-dacite, which is the host-rock of the most of the auriferous quartz veins in the area, presents a mineralogical composition with plagioclase phenocrystals hydrothermaly alterated to sericite, carbonate and epidote, quartz, hornblende and chloritized biotite, calcite and oxides. All these phenocrystals are immerse in a fine matrix composed of plagioclase, quartz, sericite and carbonates.

Within the Marmato Mining District the main structural features are related to sub-vertical faults, like Obispo Fault, with N25E trend, and distentional veins with N, NE and NW trends.

The porphyritic dacites contain abundant ore veins. The epithermal with low-sulphidation epithermal mineralization styles occur as distentional veins, stockwork structures and narrow brecciated zones with quartz veinlets. In general the ore veins are (no longer than 250 m) in length and 2 m thick. These veins present lateral zonation with pyrite in the border and sphalerite in the central zone. In the Echandia sector the ore consists of variable amount of pyrite, sphalerite and galena. Accessory and trace minerals include chalcopyrite, arsenopyrite, pyrrotite, argentite and gold electrum. In the Marmato Bajo the ore minerals are: pyrite, pyrrotite, sphalerite, arsenopyrite, chalcopyrite, gold, galena and marcassite (López-Rendon, 1991; Bedoya, 1998).

The volcanic unit is extensively affected by hydrothermal alteration, and two main alteration styles are depicted (sericitization and propylitization), silicification, argillization and albitization are also observed in some places.

Fluid inclusions study, in Marmato Mining District, were documented by Bedoya (1998) and Rossetti & Colombo (1999). In general, the fluid inclusion microthermometric results indicate homogenization temperature values, of the primary fluid inclusions in quartz, around 300°C and the salinity values are low to moderate, varying from 1,6 to 8,1 wt.% NaCl eq.

RESULTS AND DISCUSSION

Fifty five samples of ore, gangue and host rocks of the Marmato Mining District were investigated for their Pb, Sr and Nd isotopic compositions. In addition, one sample of hydrothermal altered plagioclase was analyzed by K-Ar method in order to determine the age of the mineralization episode. All isotopic analyses were carried out at the Geochronological Research Center of University of São Paulo.

AGE OF THE ORE DEPOSITION

A sample of sericitized plagioclase from altered host rock was dated by K-Ar method and yielded an precise age of 5.6 ± 0.6 Ma, which is interpreted as the time of ore deposition. This age is in close agreement with the Cauca-Romeral Fault System reactivation, which occurred at 5.6 ± 0.4 Ma and it is slightly younger than the cooling age of 6.7 ± 0.06 Ma, both ages were obtained by Ar-Ar technique on biotite from the Marmato Stock (Vinasco, 2001). In this way, we can consider that the mineralization is related to distensional tectonic regime, that allows the left reactivation of the Cauca - Romeral shear zone, and the formation of pull-apart basins in the Cauca - Patia depression, related with the accretion of the Panama magmatic arc into NW margin of South America.

SOURCES OF THE MINERALIZING FLUIDS

The host porphyry andesitic-dacitic rocks, dated at 6.7 ± 0.1 Ma (Vinasco, 2001), have $^{87}Sr/^{86}Sr$ initial ratios between 0.70440 and 0.70460 and ε_{Nd} values from from + 2.2 and + 3.2. These results allow us to consider a subduction-related mantle magma as their main magmatic source, produced during the subduction of the Nazca Plate beneath South American Continent.

The $^{87}Sr/^{86}Sr$ and the ε_{Nd} values obtained on sulphides from the gold quartz veins, which occur at the shallow and intermediary levels of Echandia and Cien Pesos sectors, range from 0.70500 to 0.71210 and from - 1.11 to + 2.40 respectively, while for the deepest mineralizations, which appear in the Marmato Bajo sector, the ε_{Nd} values of the sulphides are between + 1.25 and + 3.28 and the $^{87}Sr/^{86}Sr$ ratios of calcite and pyrite fall between 0.70444 and 0.70930. The highest $^{87}Sr/^{86}Sr$ ratio was from the pyrite from Mina La Mona in Cien Pesos sector. Concerning Sr isotopic compositions, all analyzed sulphides are more radiogenic than the carbonates, which are less radiogenic and very homogeneous, and have $^{87}Sr/^{86}Sr$ ratios around 0.70445. These values overlap the Sr isotopic compositions measured on samples from the host porphyritic dacite. Based on Sr isotopic data we can interprete that the carbonatic fluids have been subjected to a restrict ed hydrothermal circulation, within the host igneous body, without important admixture from the regional metassedimentary units. On the other hand, the more radiogenic sulphide-bearing fluids, seem to have circulated not only within the Marmato Stock, but also through some other older crustal rocks.

The present-day $^{87}Sr/^{86}Sr$ ratios and ε_{Nd} values of the metasediments of the Arquia Group are variable, ranging from 0.70431 to 0.73511 and from -12,91 to +10 respectively. The less radiogenic Sr isotopic compositions and the positive ε_{Nd} values are related to the amphibolitic schists, and the more radiogenic Sr isotopic compositions and the strong negative ε_{Nd} values are related to the quartz-biotite schists and graphite schists. The Sr and Nd isotopic compositions of the mafic and ultramafic rocks are close to Sr and Nd isotopic compositions obtained for amphibolitic schists, yielding, 0.70396 – 0.7068 for $^{87}Sr/^{86}Sr$ ratios and + 4.45 to + 10.32 for ε_{Nd} values.

The comparison of the Sr and Nd isotopic compositions from are mineral phases, gangue minerals, and of the whole-rocks from the metaedimentary sequences, indicates that the shallow level mineralizations from Echandia and Cien Pesos sectors were characterized by a more radiogenic meteoric fluids with significant crustal contributions derived mainly from the different kinds of metassediments of the Arquia Complex. In contrast the porphyritic rocks are more important sources for the deeper mineralizations of the Marmato Bajo sector, where the hydrothermal fluids seem to be a mix of meteoric and magmatic waters.

The $^{206}Pb/^{204}Pb$, $^{207}Pb/^{204}Pb$ and $^{208}Pb/^{204}Pb$ ratios of sulphides from all mineralizations fall between 18.970 - 19.258; 15.605 - 15.726 and 38.813 - 39208 respectively. The Pb isotopic compositions show that sulphides have radiogenic values, which is typical of crustal sources for Pb. The dacitic and andesitic porphyry rocks of the Marmato Stock display Pb isotopic compositions for $^{206}Pb/^{204}Pb$; $^{207}Pb/^{204}Pb$ and $^{208}Pb/^{204}Pb$, between 18.964 - 19.028; 15.561 - 15.570 and 38.640 - 38.745 respectively. The metassediments of the Arquia Group yielded Pb isotopic ratios of 18.948 - 19.652; 15.564 - 15.702 and 38.640 - 38.885 for $^{206}Pb/^{204}Pb$; $^{207}Pb/^{204}Pb$ and $^{208}Pb/^{204}Pb$. The average Pb isotopic composition for ore-minerals is more radiogenic than the Marmato Stock and a little less radiogenic than the metasediments. In the uranogenic diagram of the Plumbotectonic model of Zartman and Doe (1981), the analytical points related to sulphides plot above the orogenic growth curve and, some samples form a cluster between the Marmato Stock and the graphite schists, and others sulphides are more radiogenic, suggesting that the ores include Pb from upper crustal rocks, more radiogenic than the graphite schists and amphibolitic schists of the Arquia Complex fields (Fig. 1). The only compositions that could be more radiogenic than the part of ore fluids (superficial veins of Echandia sector and intermediary level veins of the Cien Pesos sector), in the area, are the biotite-quartz schists. So we can consider that Pb data indicate derivation of the ore fluids from country rocks, mainly from the Marmato

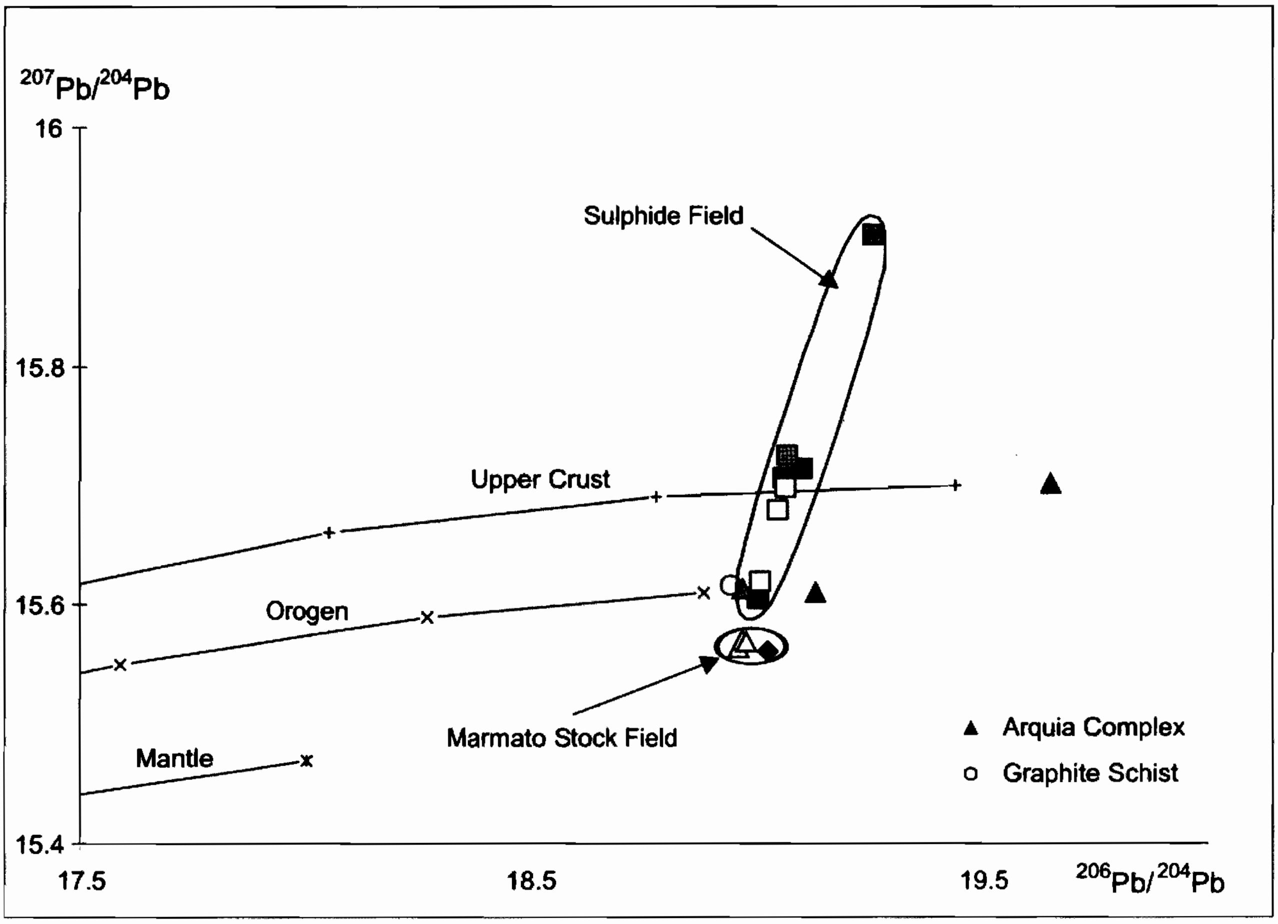

Figure 1. Uranogenic diagram with sulphide field and regional rocks in relation to Plumbotectonic curves (Zartman & Doe, 1981).

Stock with a minor contribution from the graphite schists and biotite-quartz-schists of the Arquia metamorphic Complex.

Based on previous geochronological data (Ordoñez, 2001, Vinasco, 2001, Sierra et. al., 2000, Restrepo et. al. 1981), and on our new isotopic results, the geological and metallogenetic evolution of the Marmato Mining District area, can be summarized as follows:

- 33 - 25 Ma: Magmatic activities of the Piedrancha-Farallones Arc.
- 22 Ma: Development of the back-arc basin, related to Piedrancha-Farallones Arc and beggining of Amagá Formation sedimentation.
- 12 Ma: Collision of the Panamá-Choco Arc against Sout America Continent. Reactivation of the Cauca-Romeral Shear Zone (CRSZ) and development of the pull apart basins.
- 11 Ma: Calc-alkaline and tholeiitic magmatism related to Combia formation, related to pull apart basins.
- 6,3 Ma: Marmato Stock magmatic crystallization, associated with Combia Formation. Beggining of the hydrothermal activities, related to CRSZ reactivation and fracturation of the Marmato Stock.
- 5,6 Ma: Last reactivation of the CRSZ, last magmatic activities of the Marmato Stock and main mineralization episode.
- 5.0 Ma: End of Combia Formation, magmatic activities.
- 3.1 - 3.7 Ma: Closure of the link between Pacific and Caribean Oceans through the collision of the Panamá-Choco Arc against South America.

The results of our study have implications in the mineral exploration programs in the area, because it was demonstrated that the igneous rocks of the Marmato stock are not exclusive sources for the Marmato ores, and that the sulphide deposition involved also ore-forming solutions from the graphite schists of the Arquia Complex, becoming these metasediments as potential target for gold mineralizations.

REFERENCES

Bedoya, O. G. 1998. Geology, hidrothermal alteration, paragenetic sequence and fluid inclusion analysis of La Maruja Level, Marmato District, Caldas Department, Colombia. Thesis of Master of Science, Colorado State University, Fort Collins Colorado, EU, 165p.

Etayo F. et al. 1986. Mapa de Terrenos geológicos de Colombia. Publicación Geológica Especial, Ingeominas, No 14. 235 p

Lopez-Rendon J. E. 1991. Geología, mineralogía y aspectos genéticos de las minas La Maria y Aguaceral, distrito minero de Marmato, Departamento de Caldas. Revista Universidad EAFIT, 8: 93-107.

Ordoñez C. O. 2001. Caracterização isotópica Rb-Sr e Sm-Nd dos principais eventos magmáticos nos Andes Colombianos. Tese de Doutorado, Instituto de Geociências, Universidade de Brasilia, Brasilia, 197p.

Restrepo J., Toussaint J., González H. 1981. Edades Miopliocénicas del Magmatismo asociado a la Formação Combia, Depto. Antioquia y Caldas. Geología Norandina, 3.

Rossetti P. e Colombo F. 1999. Adularia-sericite gold deposit of Marmato (Caldas, Colombia): field and petrographical data. Special Publication, Fractures, Fluids Flow and Mineralization, Geol. Society of London, 155:167-182.

Sierra G., Silva J., Correa L. 2000. Stratigraphic base level fluctuations and sandstone petrographic characterization as an indicator of the evolution of the late Oligocene-Late Miocene Amaga Formation. Papers, Stratigraphy and Sedimentology Research Group, EAFIT University, 35p.

Toussaint J. F. e Restrepo J. J. 1989. Acreciones sucesivas en Colombia: Un nuevo modelo de evolución geológica. V Congreso Colombiano de Geología, Bucaramanga, Tomo I: 127-146.

Toussaint J. e Restrepo J. 1991. El magmatismo en el marco de la evolución geotectónica de Colombia. Simposío sobre magmatismo andino y su marco tectónico, Manizalez, Mem. 1: 135-150.

Vinasco C.J. 2001. A utilização da metodologia ^{40}Ar / ^{39}Ar para o estudo de reativações tectônicas em zonas de cisalhamento. Paradigma: O Falhamento de Romeral nos Andes Centrais da Colômbia. Dissertação (Mestrado) – Instituto de Geociências, USP. São Paulo, 85 p.

Zartman R. E. e Doe B.R. 1981. Plumbotectonic-The Model. Tectonophysics, 75:135-162.

THE PLATINUM-BEARING BELT OF THE URALS, RUSSIA: Rb-Sr, Sm-Nd AND GEOCHEMICAL CONSTRAINTS

Ronkin, Y.L.; Ivanov, K.S.; Shmelev, V.R. and Lepikhina, O.P.

Institute of Geology and Geochemistry of Urals Branch of Russian Academy Sciences, Pochtovy per. 7, Ekaterinburg, Russia.
ronkin@igg.e-burg.su

Keywords: Platinum, geochemical, Urals, Russia

INTRODUCTION

In accordance with the current ideas the Platinum-bearing Belt of the Urals (PBU) is a gigantic chain with an extension from Cispolar to Middle Urals, almost 1000 km length, made up of the complicated zonal complexes, formed mainly by the association of ultrabasites (dunites, clinopyroxenites), olivine and two-pyroxene gabbro (Fig. 1). The Western part of PBU is marked by even more extensive in submeridional direction ophiolitic belt, related in its turn to the zone of the Main Uralian deep Fault (MUF). For all this, the Northern part of PBU is practically bordered with zone of MUF; here the rocks of the platinum-bearing association are located exactly in the MUF and surrounded by ophiolites (Shmelev & Puchkov 1988). It is quite obvious that the details of inner structure and the peculiarities of the majority of the Belt's massifs have been studied thoroughly enough, but the aspects of the nature of PBU itself, its age, geodynamical position, the place and role in geological history and in the Urals structure are still the source intense discussion (Efimov et al., 1993; Ivanov, 1994; Fershtater & Puchkarev, 1992).

According to one of the ideas (Efimov, 1993), the complexes composing PBU should be considered in the first approximation as allochthonous fragments of some deep zone, but not as monolithic moulds formed in magma chambers constitute the upper crust. The model suggested assumes the incorporation into the ancient structure of PBU blocks of metavolcanites in low pressure granulitic facies (two-pyroxene "hornfels"), isofacial with gabbro-ultrabasite blocks, that points to the bottoms of Paleozoic crust, as the places where it occurred the earliest from the reliably reconstructed stages of tectono-metamorphic evolution of this deep zone. It is supposed that just here it took place a long period of relative rest of the gigantic deformed hot and solid gabbro-ultrabasite mass of mantle nature. For this in PBU massifs in solid form two plutonic complexes "have been boiled": the first one presents itself a product of hot-tectonic and chemical mixture of platinum-bearing dunites and olivine-clinopyroxene-anorthite gabbro of problematic genesis; the second one is composed by orthomagmatic gabbro-norites. Platinum, titanomagnetite and copper sulphide ore concentrations are related exclusively to the first complex, the second one is ore-free.

In conformity with the other opinion (Fershtater & Puchkarev, 1992) as the complexes, composing PBU, should be taken a volcano-plutonic association (which volcanic members are destroyed by erosion) of the Upper Ordovician age formed "at the stage of stabilization of oceanic structure - before the laying down of the Tagil trough zone with its island-arc geodynamical regime".

GEOLOGICAL POSITION

The Chistop mafic-ultramafic massif (CUM) is presented in the plan (Fig. 1) by the Southern part of gabbroids of the large, compound-outlined complex, the Northern end of which is the Yalpig Nyor gabbroid massif. To the South-West from CUM it is observed the Salatim belt of serpentinites marking the MUF zone. The West contact of the CUM has a submeridional extension and, according to geophysical data, it has dip of 60° Eastward. On geochemical parameters enclosing rocks of the western contact are comparable with ophiolite formations of over-subduction type and presented by metamorphosed diabases and basaltoids with interbeds of tuffs and jaspoids, having Upper Ordovician age. In the section in the direction from West to East basaltoids are being changed by a stripe of diabases of a dike complex, which are located in direct contact with the massif's rocks; the level of metamorphism in this direction is increasing accordingly from the green-slated one to amphibolites, and the initial substratum is being transformed into gneiss-like stripped amphibole-plagioclase and amphibole-pyroxene-plagioclase blastomylonites with areas of thin-grained hornfels of the same content, which display signs of folded deformation. The massif's eastern contact has more complicated configuration (Fig. 1) and on geophysical data - relatively more slope fall in the eastern direction as well. In the northern part in close contact with gabbroids there is a huge body of Petropavlov massif of diorites, quartz diorites and plagiogranodiorites. To the East and South of diorites (close to contact) it is being traced a series of continuously differentiated Silurian volcanites of andesite-basalt content, which are a component part of island-arc section of Tagil zone of the Urals. Its contact with volcanites is a tectonic one and only in the very southern part where they are changing into a series of rocks of ophiolite-basalt content (Shemur suite, the age O_2-S_1), the late ones, related to ophiolites (Petrov, 1994) come into hornfels of gneiss-like stripped structure.

The Kumba (KUM) massif (Efimov et al., 1993) consist at least as four main structural-material units: (1) in the north - the block of mountain Kumba combined mainly by olivine-anorthite gabbro, containing rare isolated lenslike bodies of olivine pyroxenites; (2) in an middle part of a file - the extensive field combined gabbro-norites and their products of metamorphism; (3) in the extreme West of a file - the small block of the Gladkaya Sopka combined by dunite, pyroxenites and in very small degree of tylaite; (4) at last, the extended and powerful hot tectonic suture of very difficult structure which separating gabbro-norite a field from the block of the Gladkaya Sopka.

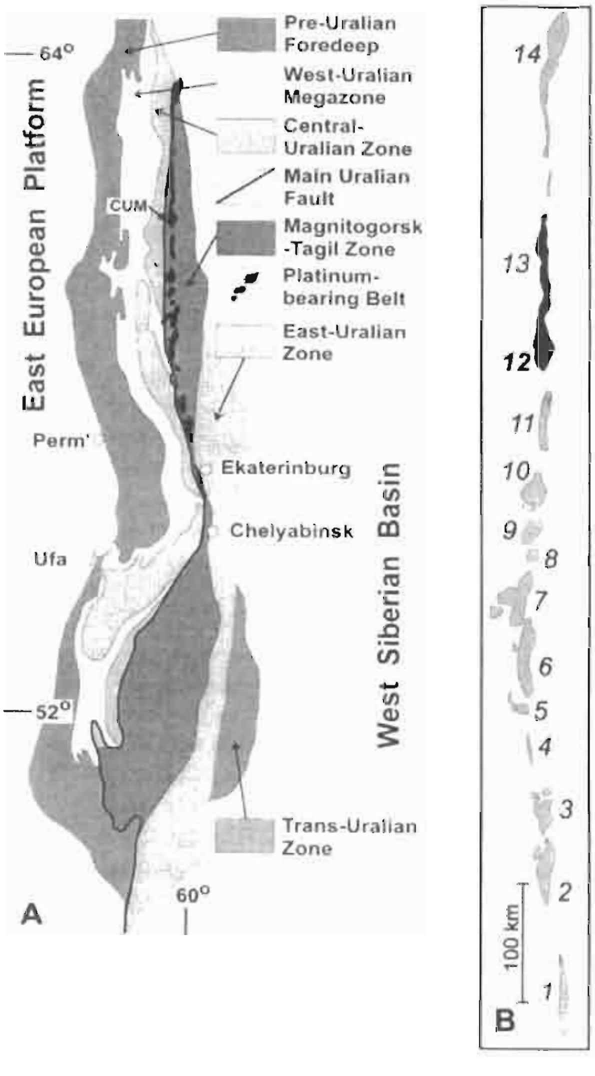

Figure 1. A - Sketch map of zonation of the Urals (modified after Ivanov et al., 1975). B - complexes of Platinum-bearing Belt of the Urals (after Efimov et al., 1993): 1-Revda; 2-Tagil; 3-Barancha; 4-Arbat; 5-Kachkanar; 6-Pavda; 7-Kytlym; 8-Knyaspa; 9-Kumba; 10-Denezhin Kamen; 11-Pomur; 12-Chistop; 13-Yalpig Nyor; 14-Khorasyur.

PETROCHEMICAL CHARACTERISTICS

On the content of the majority of petrogenic and small elements (titanium, vanadium, chrome, nickel and other) gabbroids of the Belt's massifs display an evident similarity with tholeiites of the island-arcs (Fig. 2). For all of its petrographical variability the rocks of PBU have a clear petrological relationship (Fig. 3) with gabbroid and ultrabasic xenoliths in basalts of island arcs, and as well with the rocks of gabbro-ultrabasite complexes of the North American Pacific ocean shore (Alaska, California), of Olyutor zone of Koryakia and of the other regions, for which is being established a relationship with the associating island-arc volcanic complexes (Batanova & Astrakhansev, 1992; Burns, 1985).

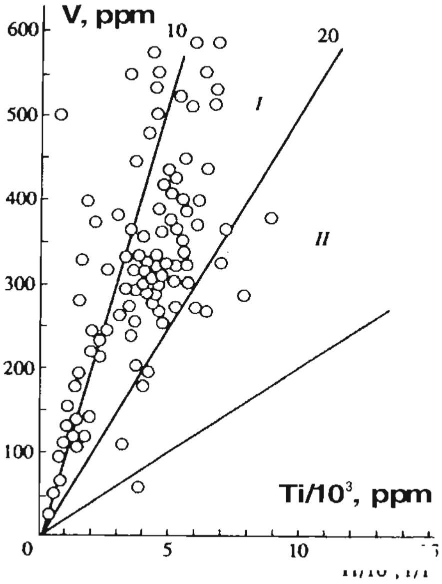

Figure 2. V-Ti/10^3 diagram (Shervais, 1982) for rocks of the gabbro-ultrabasite association of PBU of the Northern and Cispolar Urals. The areas are marked: I - of tholeiites of island arcs, II - of basalts of oceanic bottom.

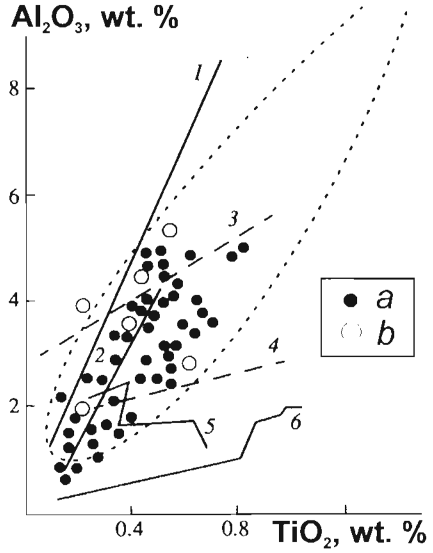

Figure 3. Al_2O_3-TiO_2 diagram for clinopyroxenes from rocks of PBU. a-clinopyroxenes of Khorasyur, Chshekur'ya, Yalping Nyor and Chistop massifs; b-clinopyroxenes of other massifs of PBU (Efimov et al., 1993). Dotted line shows the area of components for gabbroid and ultrabasic xenoliths from basalts of Aleutian and Antillian island arcs. 1-6 - trends of the content in gabbro-ultrabasite complexes (Batanova & Astrakhansev, 1992; Burns, 1985): 1-the belts of Bode-Range (Alaska), 2-massifs of Olyutor zone (Koryakia), 3-ophiolitic massifs of Bay of Island, 4-Semail (Oman) ophiolitic massif, 5 - Bushveld massif, 6 - Skaergaard massif.

In comparison with them the rocks of ophiolites and of the interbedded intrusions are characterized by different, more slope trends of variations of mineral content. The results of studying of platinum mineralization also testify to (Volchenko et al., 1992) the island-arc nature of PBU complexes.

SAMPLES RESEARCHED

CUM

For Rb-Sr and Sm-Nd isotope-geochronological studying there have been used relatively unchanged sample of bipyroxene gabbro, collected from the left shore of the river Ushma (Northern part of CUM) and the extracted from gabbro mineral components (only for Sm-Nd dating): plagioclase, orthopyroxene and the mixed fraction containing clinopyroxene and amphibole.

Plagioclase is changing on the content in the range of An_{43-94}. Variations of FeO content in plagioclase make up about 0.12-0.35%. Visually observing zonality, as a rule, is straight, (edges and small grains have more sodic content), nevertheless in relatively small individuals it is observed a reversed type of zonality.

Orthopyroxene. If gabbroids of the Western and Eastern massif's parts are isolated on alumina content at petrochemical diagrams, then on the rest of components they form overlapping areas of contents. Features of zonal structure are weakly expressed.

Clinopyroxene in olivine-clinopyroxenite-gabbro is presented in the row by a series of contents from diopside to augite which ferruginousness is changing accordingly in the range of 14-33%. At the diagrams in the coordinates ferruginousness is the content of the main petrogenic oxides; at the increasing of ferruginousness one can observe the appropriate decreasing of alumina and titanium content and the increasing of natrium content. Al_2O_3-TiO_2 dependence for clinopyroxenes of UPB is given in Fig. 3. Most clearly zonality is observed in titanium, which content in every case has clear tendency to the decreasing in the edges of huge grains correlated in the majority of cases with the decrease of ferruginousness.

Amphibole is mainly presented both by the rims around pyroxenes, olivine and magnetite and by ingrowths and areas of replacement; side by side with these one can meet isolated grains without signs of reactional relationship, and more rarely - poikiloblastic separations. In the majority of cases amphibole is related to aluminiferous (8.7-15.0% Al_2O_3) type; considerable variations of sodium oxide (0.65-3.10%) and titanium (0.05-2.32%) are determined; the content of K_2O usually does not exceed 0.8%.

KUM

The sample gabbro-norite (and minerals plagioclase, clinopyroxene, orthopyroxene and biotite separated from whole rock) from middle part of massif was analyzed. The gabbro-norites represents a more uniform type of rocks composed of basic plagioclase (An_{50-70}), clino- and orthopyroxene and magnetite. Biotite and quartz may be present in small amounts. The plagioclase often shows a normal zoning and the pyroxenes show a poikilitic and an exsolution texture.

ANALYTICAL TECHNIQUES

Rb, Sr, Sm and Nd concentrations and their isotope ratios were determined by isotope dilution with the finish on a modern variable multicollector precision mass spectrometer Finnigan MAT-262. Precision at the 2σ level was approximately 0.5% for the ratios of $^{87}Rb/^{86}Sr$ and $^{147}Sm/^{144}Nd$. Uncertainties of the measured isotope ratios $^{87}Sr/^{86}Sr$ and $^{143}Nd/^{144}Nd$ were better than 0.02-0.03% and 0.002% respectively.

ISOTOPE RESULTS AND THEIR INTEPRETATION

CUM

The obtained isotope results on the whole contents of gabbro and of their mineral fractions of plagioclase, orthopyroxene and mixture of clinopyroxene and amphibole form at the plot with coordinates $^{147}Sm/^{144}Nd$-$^{143}Nd/^{144}Nd$ a regression line (Fig. 4) which slope corresponds to the age 419±12 Ma and $\epsilon^{t}_{CHUR}=+6.1$, with MSWD=1.71 that affirms strict isochron dependence.

KUM

A four point (plagioclase, clinopyroxene, orthopyroxene, whole rock) Sm-Nd mineral isochron (MSWD=0.44) age 423±18 Ma ($\epsilon^{t}_{CHUR}=+5.9$) is in good accordance with one U-Pb zircon age are obtained in the paper (Bosh et. al., 1997).

The obtained age of homogenization of Sm-Nd isotope system on the mineral level is interpreted as the time of "closing" of Sm-Nd isotope system in minerals and in the whole content, being, in fact, a minimum estimation of the time of formation of the studied Chistop massif's bipyroxene gabbro and gabbro-norite of Kumba .

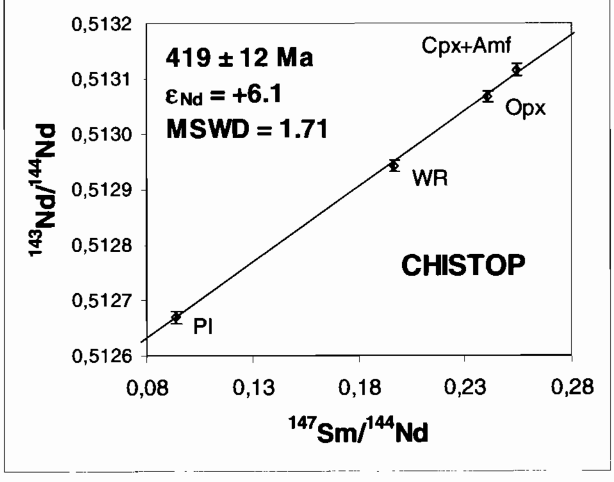

Figure 4. Sm-Nd evolution diagram for gabbro of Chistop complex of Platinum-bearing Belt of the Urals. WR-whole rock; Pl-plagioclase; OPX-orthopyroxene; CPX+AMF-mixed fraction containing clinopyroxene and amphibole.

Consideration in coordinates $\in^{t}_{UR}$-$\in^{t}_{CHUR}$ of Sr and Nd isotope contents corrected to the decay after the time of formation of CUM makes it possible to note the fact that figurative points for the studied formations are locating in II quadrant $\in^{t}_{UR}$-$\in^{t}_{CHUR}$ of correlation diagram and going along the line of Mantle Array, coming through isotope contents of the DM and CHUR.

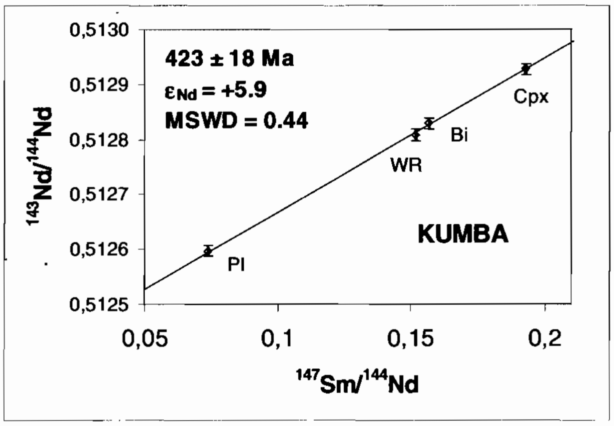

Figure 5. Sm-Nd isochron plot for gabbro-norite of Kumba massif of Platinum-bearing Belt of the Urals. WR-whole rock; Pl-plagioclase; OPX-orthopyroxene; CPX-clinopyroxene, Bt-biotite.

Sm-Nd model age calculation on the whole content of CUM's two-pyroxene gabbro and KUM gabbro-norite relatively a model depleted reservoir is being complicated by the value of ratio $^{147}Sm/^{144}Nd=0.1963\pm0.0009$, that makes it difficult to estimate the time of protolith separation for the studied kinds from the trend of the DM evolution (De Paolo, 1988).

CONCLUSION

Two PBU massifs taking place more than in 100 kms from each other have the similar ages.

The obtained Rb-Sr and Sm-Nd isotope systematics for bipyroxenic gabbro of the CUM and gabbro-norite of the KUM of PBU testifies to the belonging of the studied substance mainly to the mantle trend and in combination with the available data does not contradict to the hypothesis of its island-arc nature.

REFERENCES

Batanova, V.G. & O.B. Astrakhantsev 1992. Tectonic position and genesis of zonal mafic-ultramafic plutons of Northern Olyutor zone (Koryakia). Geotectonika. 2: 87-103.

Bosh, D., Krasnobayev, A.A., Efimov A.A., Savelieva, G.N., Franqoise B. 1997. Early Silurian ages for the gabbroic section of the mafic-ultramafic zone from the Urals Platinum Belt. EUG9. Strasbourg. Abstracts. Terra Nova Vol.9,. 122.

Burns, L.E. 1985. The Border Ranges ultramafic and mafic complex, South-central Alaska: cumulate fractionates of island-arc volcanics. Canadian Journ. Earth. Sci., 22(7): 1020-1038.

DePaolo, D.J., 1988. Neodymium isotope geochemistry: An introduction. Springer-Verlag Berlin: 187 pp.

Efimov, A.A., Efimova, A.A., & V.I. Maegov 1993. Tectonics of the Platinum-bearing Belt of the Urals: Correlation of complexes and Mechanism of Substantial-Formation. Geotectonika. 3: 34-46.

Fershtater, G.B. & E.V., Pushkarev 1992. Nepheline-contained tylaites in dunite-clinopyroxene-gabbro association of the Platinum-bearing Belt of the Urals. Bulletin of Russ. Acad. Sci. 4: 74-84.

Ivanov, O.K. 1994. Concentric-zonal ultramafic massifs of folded belts (on example of the Urals). Ph.D. thesis. Leningrad. 218 pp.

Ivanov, S.N., Perfil'ev, A.S., Efimov, A.A., Smirnov, G.A., Necheukhin, V.M., & G.B. Fershtater 1975. Fundamental features of the structure and evolution of the Urals. Am. Jour. Sci., 254A: 107-136.

Pearce, J.A., Lippard, S.J., & S. Roberts 1984. Characteristics and tectonic significance of supra-subduction zone ophiolites. In: Marginal basin geology. Oxford: Blackwel, 16: 77-94.

Petrov, G.A. 1994. Geology of complexes of North part of Zone Main Uralian Fault. Ph.D. thesis. Ekaterinburg. 273 pp.

Shervais, J.W. 1982. Ti-V plots and the petrogenesis of modern and ophiolitic lavas. Earth and Planet. Sci. Letters. 59: 101-118.

Shmelev, V.R. & V.N. Puchkov 1988. Gabbro-ultramafic association of Cispolar Urals. In: Formational separation, genesis and metallogenia of ultramafics. Ekaterinburg. 113-124.

Volchenko, Y.A., Koroteev, V.A., & K.K. Zoloev 1993. Efficiency of Platinum-bearing Belt of the Urals. Yearbook of IGG. Ekaterinburg. 89-92.

ISOTOPE-GEOCHEMICAL AND STRUCTURAL CHARACTERISTICS OF THE LOCATION OF LARGE IRON-ORE SKARN-MAGNETITE DEPOSITS: THE URALS, RUSSIA

Ronkin, Y.L.; Poltavets, Y.A. and Lepikhina, O.P.

Institute Geology and Geochemistry of Urals Branch of Russian Academy Sciences, Pochtovy per.7, Ekaterinburg, Russia.
ronkin@igg.e-burg.su

Keywords: Isotope, geochemical, iron, Urals

INTRODUCTION

The Urals folded system, extending for about 2500 km (~1500 mi) from its northern boundary at the Arctic Ocean to its southern limits at the Caspian Sea and separating the ancient Archean and Proterozoic crystalline basement of the East European craton from the Paleozoic terranes of Western Siberia and Kazakhstan, is one of the biggest metallogenic province of the world (Fig. 1).

Modern ideas about Urals folded (UFS) system development allow conditionally to consider UFS evolution in the content of some huge metallogenic megacycle (Koroteev et al., 1989; Necheukhin, 1991), which is characterized by a series of geodynamic and geotectonic regimes in the range of absolute chronology from Proterozoic to Phanerozoic inclusively. For this, as often as not, a model, (Necheukhin 1991; Prokin et al. 1993) is being taken as the tectonic basement of the UFS metallogenic analysis. According to this model the UFS appearance is the result of riftogenic extension of the ancient paleocraton, initially presented itself a segment of lithosphere with the crust of continental type. Further Urals folded system evolution is correlated with Paleozoic activization of the processes of riftogenic extension which brought to a full extension of paleocraton and to the formation of paleo-oceanic structure in the result of which development there have been formed proper Paleozoic formations of the UFS, which are genetically connected with the majority of iron-bearing ore geochemical systems.

REGULARITIES OF DISPLACEMENT IRON-ORE BEARING ORE-GEOCHEMICAL URALS SYSTEMS

Modern views of the iron-ore bearing ore-geochemical Urals systems allow to consider the processes of ore-formation, wall-rock alteration and endogenic geochemical halos in close connection with magmatism, which in its turn is closely related to iron-ore bearing magmatic rocks. Such systems possess a great vertical spreading and, in fact envelope practically all genetical types of iron-ore deposits, late-magmatic, metasomatic (proper skarn-magnetite) and volcanogenic-sedimentary ores, which are being formed in different stages of iron-ore bearing ore-geochemical Urals systems evolution. In structural relation iron-ore deposits of skarn formation are placed mainly in eugeosyncline part of the UFS (Fig. 1) and located in the shape of linear-stretched ore-bearing zones. In the limits of ore-productive zones the deposits are situated discretely, in the form of separate ore nodes or ore areas, presenting themselves separate structure-tectonic blocks, limited, as a rule, by faults of deep location. Inner structure of such blocks in connection with their differentiating mobility is different, as well as the appropriate peculiarities of magmatic activity are not identical. The character of magnetite mineralization (morphological peculiarities, composition and structure intensity and the scales of skarn-ore zones) are predetermined considerably by a specific character of its position in volcano-plutonic structure, by the level of a deep shear, at which the deposits are taken out and also by the dependence upon the depth of formation of fluid-magmatic center, feeding this ore-magmatic system. However it is not very much known about the degree of influence of these parameters upon the regularities of the deposits formation and their emplacement, as well as doubtful is the treatment by different researchers of the time and place of manifestation of iron-ore-bearing magmatism in an appropriate tectono-magmatic megacycle, including sequential change of geodynamic and geotectonic regimes.

SKARN-MAGNETITE DEPOSITS

Four types of skarn-magnetite deposits (SMD) are distinguished, in dependence on the distance from intrusive massifs and composition of wall-rock metasomatites. The scales of the magnetite deposits vary proportionally to the rock volumes of the parent volcano-plutonic complexes, their alkalinity, chemical differentiation of the volcanic and intrusive comagmatites, and chlorine abundances in metasomatites. The volcano-plutonic complexes containing economic skarn-magnetite ores were found to be higher in iron content in intrusive rocks and lower in co-magmatic volcanics.

KACHAR DEPOSIT

The huge (more than 2000 mln tons of ore) Kachar (position 19 in Fig. 1) SMD, formed in the island arc environment, is associated with the alkaline andesite-basalt-gabbro-diorite and is related to Valer'ayanov volcano-plutonic belt in the Tyumen'-Kustanai zone. Kachar deposit (KD) is situated among carboniferous sedimentary-volcanogenic rocks overlapped by a cover of the platform of Mezozoic-Kainozoic deposits. It is related to the South-West framing of Koskul ring structure presenting itself a volcano-tectonic depression.

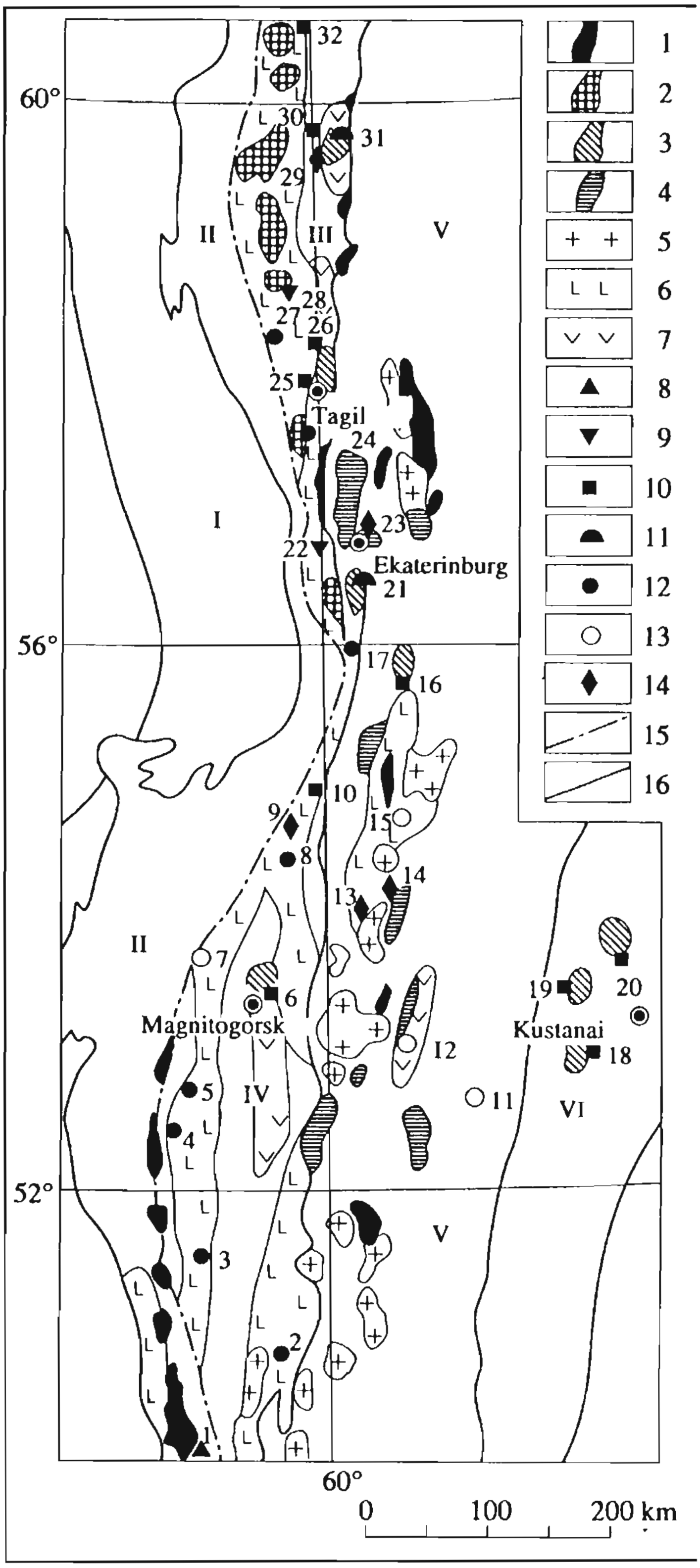

Ultrabasites (1); zonal dunite-clinopyroxenite-gabbro massifs (2); Gabbro-diorite, syenite-diorite-gabbro, gabbro-granite complexes, with which the skarn-magnetite deposits are associated (3); tonalite-granodiorite massifs (4); granites (5); oceanic and island-are volcanics (6); andesitoids and trahyrhyolite-basaltoid volcanics of the superimposed volcano-plutonic complexes (7); ore deposits (8 - 14): chromium (8), titanomagnetite (9), skarn-magnetite (10), copper-skarn (11), massive sulfide (12), copper-porphyry and porphyry-copper-molibdenum (13), gold (14); Main Uralian Fault (collisional suture) (15); boundaries of the present-day structural zones of the I order: PreUralian (foreland) (I); Central Uralian (marginal uplift) (II); Tagil (Tagil trough) (III); Magnitogorsk (Magnitogorsk trough) (IV); Urals-Tobol (uplift) (V); Tuymen'-Kustanai (trough) (VI). Ore deposits: Kempirsai group (I); Letneye (2); Gai (3); Bakr-Tau (4); Tubin (5); Magnitogorsk (6); Salavat (7); Uchalin (8); Murtykty (9); Kruglogor (10); Batalin (11); Novonikolaev (12); Svetlin (13); Kochkar (14); Birgil'din (15); Techen (16); Mauk (17); Sokolov (18); Kachar (19); Aleshin (20); Gumeshev (21); Pervoural'sk (22); Berezov (23); Levikhin (24); Vysokogorsk (25); Goroblagodatnoye (26); Kabansk (27); Kachkanarsk (28); Vorontsov (29); Auerbakh (30); Tur'in group (31); Pokrov (32).

Figure 1. Sketch map of distribution of some endogenous ore deposits in the Urals (after Prokin et al., 1993).

The deposit is characterized by a presence of seven blocks moved away in the process of evolution in horizontal and vertical directions. In four of them: Glubokoye, North-Eastern, Northern and Southern blocks sedimentary-volcanic sequence is being stratificated into four suites: Sarbai, Sokolov, Andreev and Koskul'. In the limits of the rest three blocks there are unstratificated (funnel and extrusive) rocks of paleovolcanic construction. All the sequence of rocks from East to West and from the bottom is limited by the regional shift-overthrust of a large amplitude, which separates the lower block from the rest ones.

MAGNITOGORSK DEPOSIT

The big (more than 500-1000 mln tons of ore) Magnitogorsk SMD (position 6 in Fig. 1), formed in the environment of the active continental margin, is associated with productive Magnitogorsk volcano-plutonic centrum. The composition of the ore-bearing volcano-plutonic complexes varies from granites and rhyolites to gabbro-diorites and andesite-basalts. In accordance with the available ideas (Fershtater et al. 1984) Magnitogorsk group of plutonic massifs contains stock-like Magnitogorsk and Kuibasov massifs and bed-like Mosov massif, which is probably a huge apophysis of common gabbro-granitic plutonic intrusive.

SAMPLING

For isotopic-geochronological studies there have been used relatively unchanged samples of rocks on the whole (with the extraction of mineral compounding for Sm-Nd dating), collected from different outcrops and bore-holes of the corresponding ore-association formations of Magnitogorsk ore field: gabbro, syeno-diorites, grano-syenites, granites of proper Magnitogorsk massif; gabbro, quartz diorites, granites of Kuibas massif; gabbro, syeno-diorites, syenites, granites of Mosov massif.

In the boundaries of KD there have been investigated: dacite porphyries composing extrusive dome, located in the limits of the North-Eastern blocks of Kachar ore-field; apatites from enclosing volcanites; apatites and magmatites extracted from the ore substance of the deposit's central part of KD.

ANALYTICAL PROCEDURES

Rb, Sr, Sm and Nd concentrations and their isotope ratios were determined by isotope dilution finishing with a modern variable multicollector precision mass spectrometer Finnigan-Mat 262. Precision at the 2σ level was approximately 0.5% for the ratios of $^{87}Rb/^{86}Sr$ and $^{147}Sm/^{144}Nd$. Uncertainties of the measured isotope ratios $^{87}Sr/^{86}Sr$ and $^{143}Nd/^{144}Nd$ were better than 0.02-0.03% and 0.002% respectively.

ISOTOPE RESULTS AND INTERPRETATION

ORE-ENCLOSING ORE FORMATIONS OF KD

In coordinates $^{87}Rb/^{86}Sr$-$^{87}Sr/^{86}Sr$ the position of figurative points of dacite porphyries composing extrusive dome located in the limits of the North-Eastern blocks of Kachar ore field are approximated by linear dependence (MSWD=2.75) determining Rb-Sr isotope age 315±24 (95% conf. limits) Ma. Close age meaning testifying to synchronousness (in the limits of the observing analytical uncertainties) magmatism and ore-formation is fixed by Sm-Nd isotope system of apatite and two magnetites separated from the ore substance of the central part of the deposit.

The obtained data on initial isotope characteristics of Sr ($^{87}Sr/^{86}Sr_i$=0.70443±0.00012) and Nd (ϵ^t_{CHUR} = +5.9) on the one hand testifies to a considerable role of mantle substance in KD formation. On the other hand relatively «kept up» isotope content of lead of sulphide phase in impregnated magnetite ore characterized by the weighted-mean values of isotope lead $^{206}Pb/^{204}Pb$=18.41±0.05 and $^{207}Pb/^{204}Pb$ =15.52±0.03 proves relative participation of intercrustal magmatism products (Fig. 2).

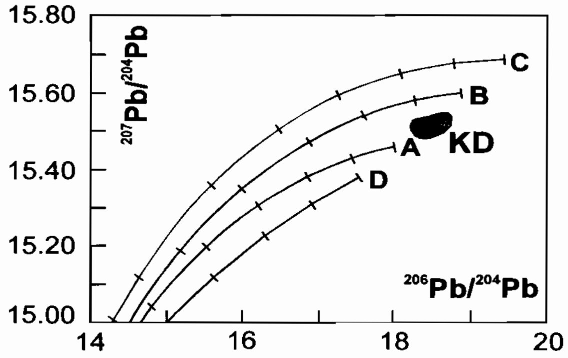

Figure 2. Lead-isotope characteristics for sulphide phase of KD and lead-isotope evolution curves gene rated by plumbotectonics model (Zartman & Doe, 1981) for the mantle (A), orogene (B), upper (C) and lower crust (D). Tick marks along each curve indicate progressively older time in 0.4 Ba increments.

ORE-ASSOCIATING FORMATION OF MAGNITOGORSK ORE FIELD

Consideration of the experimentally obtained data in coordinates $^{87}Rb/^{86}Sr$-$^{87}Sr/^{86}Sr$ gives way to a linear approximation which is characterized by the mean square weighted deviations (MSWD) 1.54 and makes it possible to calculate the age of Magnitogorsk massifs formation equal to 330±4 Ma. For the whole rocks contents of Kuibas and Mosov massifs analogical calculations determine the age meaning 329±17 and 336±17 Ma at the meaning of MSWD equal to 0.71 and 1.85 respectively.

The obtained isotope data on the whole content of gabbros and their mineral fractions form at the plot with coordinates $^{147}Sm/^{144}Nd$-$^{143}Nd/^{144}Nd$ regression lines, which slope corresponds to the age of 336±18 and 325±55 Ma with the MSWD equal to 0.16 and 0.84 accordingly, that affirms strict isochron dependences. The calculated and coincided in the limits of uncertainties the ages are interpreted as the time of «closing» of Sm-Nd isotope system in minerals and whole contents, being, in fact, a minimum estimation of time formation of the studied gabbros of Mosov massif.

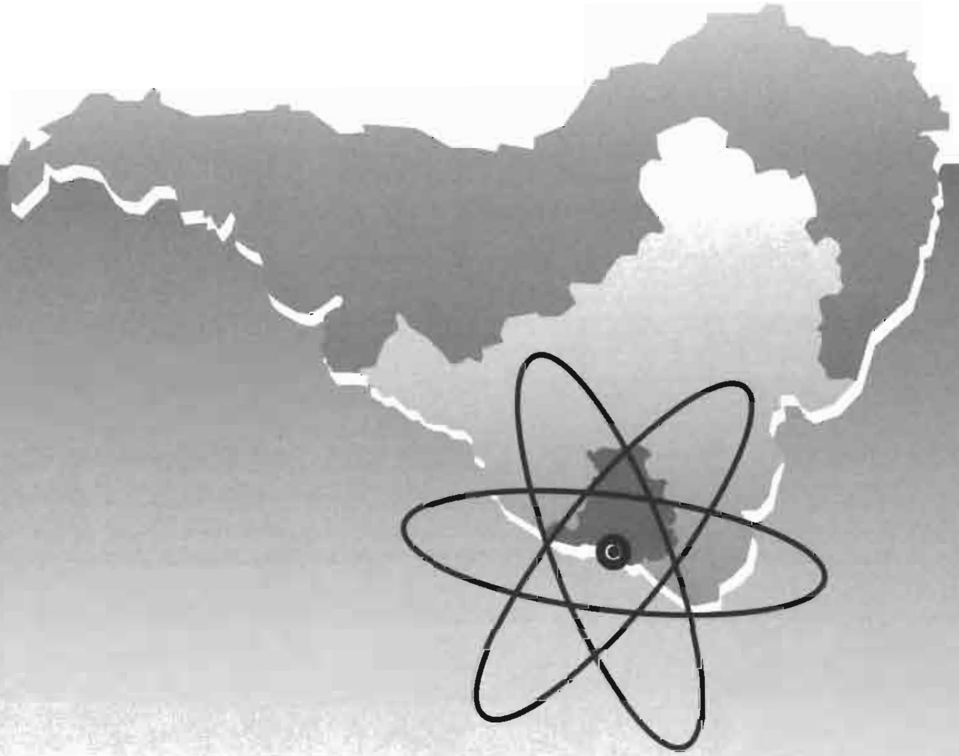

Oil Exploration

NOBLE GAS ISOTOPES AS PROXY FOR UNDERSTANDING OF PROCESSES IN PETROLEUM SYSTEMS: APPLICATION IN THE SOLIMÕES BASIN, BRAZIL

Santos Neto, E.V.[1]; Prinzhofer, A.[2]; Battani, A.[2]; Wanderley Filho, J.R.[3] and Cunha, P.R.C.[3]

1. PETROBRAS R&D Center, Av. Hum, Quadra 7, Rio de Janeiro (RJ) 21949-900, Brazil. eugenio@cenpes.petrobras.com.br
2. IFP, 1&4, Avenue de Bois-Préau, 92852 Rueil-Malmaison Cedex, France. alain.prinzhofer@ifp.fr, Anne.BATTANI@ifp.fr
3. PETROBRAS/UN-BSOL/ATEX, Manaus (AM), Brazil. jwand@petrobras.com.br, pcunha@petrobras.com.br

Keywords: Noble gas, isotopes, petroleum exploration, advances, Brazil

INTRODUCTION

Recent gas geochemistry developments use concentrations and $\delta^{13}C$ of hydrocarbons (C_1-C_4) as interpretative tools to study the origin of the gases, *i.e.*, proportions of thermogenic *versus* biogenic hydrocarbons, degrees of thermal maturity and of biodegradation of gases, as well as direction and relative distances of secondary migration (Prinzhofer et al., 2000).

Not just hydrocarbons but also noble gases (helium, neon, argon, krypton and xenon) have proven to be very useful as geochemical tracers of crustal fluids. Especially, when trying to determine physical processes responsible for gas migration in the subsurface (Zaikowski & Spangler, 1990; Ballentine et al., 1991, 1996, 2001; Battani et al., 2000; Prinzhofer & Battani, 2002). This is due to the fact that noble gases are chemically inert and therefore they behave as fossil or conservative natural tracers, as is the case of ^{3}He, ^{20}Ne, ^{36}Ar, ^{38}Ar, ^{84}Kr, and the main part of ^{136}Xe. On the other hand, some isotopes, mainly ^{4}He and $^{40}Ar^{*}$, are produced through time by radioactive decay, and may be used as chronological tools, keeping in mind that they provide a relative chronology rather than an absolute one.

In order to check the effectiveness of noble gases as a potential exploratory tool, the Solimões Basin was chosen because it has a relatively well-known petroleum system and plenty of geochemical data. This basin covers an area of about 600,000 km^2 in northern Brazil, being 450,000 km^2 represented by subcroping Paleozoic rocks (Fig. 1). It was filled up by two first order sedimentary sequences that reach up to 4,000 m. One is represented by Paleozoic sediments intruded by Mesozoic diabase sills, and the other by Cretaceous and Tertiary siliciclastic sediments (Eiras et al., 1994). Devonian marine black shales (Jandiatuba Formation) represent the source rocks in the basin, and it is conspicuous the relationship between the magmatic intrusions (Triassic-Jurassic) and thermal maturation of hydrocarbons (Mosmann et al., 1987; Rodrigues et al., 1990). Recent study has shown that igneous intrusions represent a complex chapter in the geological evolution of the basin, and contributed for primary cracking of kerogen and for the secondary cracking of hydrocarbons within reservoirs (Bender et al., 2001). Carboniferous sandstones (Juruá Formation) and evaporites (Carauari Formation) are the reservoirs and seals, respectively. The petroleum system that has been explored successfully in the Solimões Basin is known as Jandiatuba-Juruá (!); (Eiras, 1998).

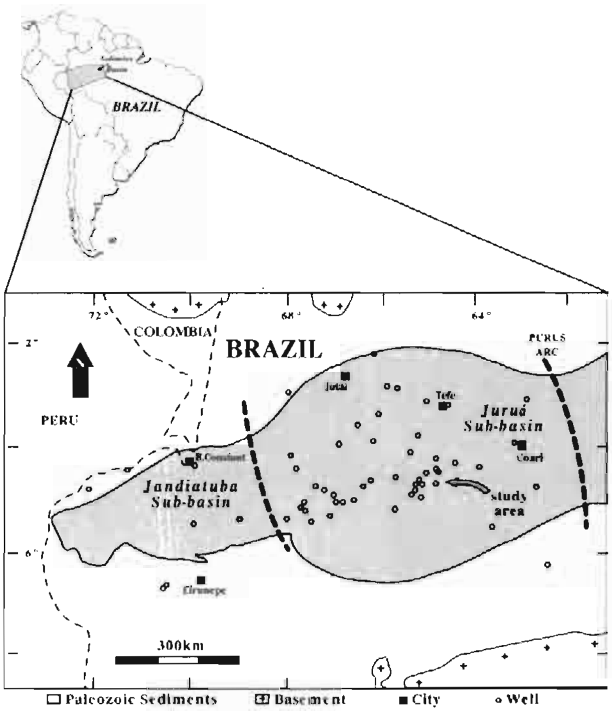

Figure 1. Location map of the Solimões Basin.

Sampling of noble gases is more elaborate than gas sampling for conventional gas geochemistry analyses (hydrocarbon concentrations and $\delta^{13}C$), as atmospheric contamination may occur and could severely affect the original noble gas signature of the sample. This is the case for argon, which has a concentration of about 1% in the atmosphere, while helium can be lost very easily from the sample, due to its small molecular size and high diffusion rate.

The analytical protocol for noble gas analyses has been developed accordingly and uses stainless steel sampling tubes with two valves, one in each of the two ends. Valves are closed one after the other once the tube has been flushed by the wellhead producing gas for several minutes.

Noble gas concentrations and isotopic ratios were measured using a VG5400 mass spectrometer that was especially devoted for these analyses at the IFP gas geochemistry lab. For more details about sampling and analytical methods of noble gases see elsewhere (Battani, 1999).

The main objective of this study is to discuss the use of noble gases as a potential tool for the understanding of secondary migration, residence time and leakage processes in petroleum accumulations using the Solimões Basin, northern Brazil, as the case study.

DISCUSSION OF RESULTS

All the gas samples in this study have shown values of $^3He/^4He$ ranging 0.015Ra to 0.023Ra indicating a relative enrichment in ^4He. Ra is the atmospheric $^3He/^4He$ ratio in air, equal to 1.41×10^{-6}. This is a compelling evidence of no significant mantle contribution and that the origin of helium was derived mainly from radioactive decay in the continental basement and/or sediments.

However, there is a discernible decrease of $^3He/^4He$ ratios along the studied petroleum accumulation trend, from SW to NE (Fig. 2). Such variation is interpreted as a product of fractionation processes due to the secondary migration, because ^3He migrates slightly faster than ^4He. Previous study, using concentrations and carbon isotopic compositions of hydrocarbons suggested the same direction for the secondary migration in the area (Santos Neto et al., 1999).

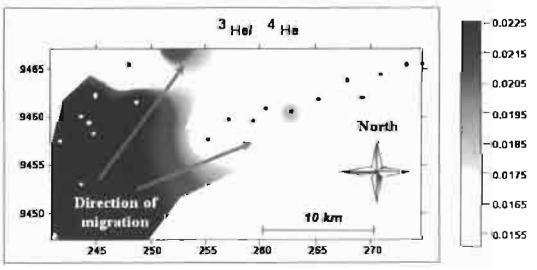

Figure 2. Isovalues of $^3He/^4He$ in the studied area. The increase of this ratio toward NE can be correlated with the direction of secondary migration.

The regression line between the nucleogenic-radiogenic isotopes $^{21}Ne^*$ and ^4He is excellent and crosses the origin, suggesting that the homogenization of these gases occurred before the hydrocarbon gas phase migrate to reservoir (Fig. 3a). Nevertheless, there is a shift in the relationship between the radiogenic isotopes ^4He and $^{40}Ar^*$ that is interpreted as a product of a partial leakage from reservoirs because of the enrichment of the heavier molecules in the residue (Fig. 3b). In fact, the ratios $^4He/^{40}Ar^*$ in the studied gases A-B are very close to the average production ratio of sediments on continental crust (4.93, Ballentine et al., 1991), and, therefore, strongly suggest absence of fractionation of these gases. Estimations, based on a simple distillation law, gave a range between 0 and 38% for the hydrocarbon loss (Fig. 3b). The diffusion factors considered in the above calculation are for ^4He and ^{40}Ar 3 and 1.4 time the diffusion factor of hydrocarbons, respectively.

Comparing nucleogenic and fossil parts of a same isotope it seems that straight correlations occur crossing the origin, but with different slopes for A-B and C-D accumulations (Fig. 4a). Thus, it is corroborating the hypothesis that a post-genetic physical fractionation is occurring.

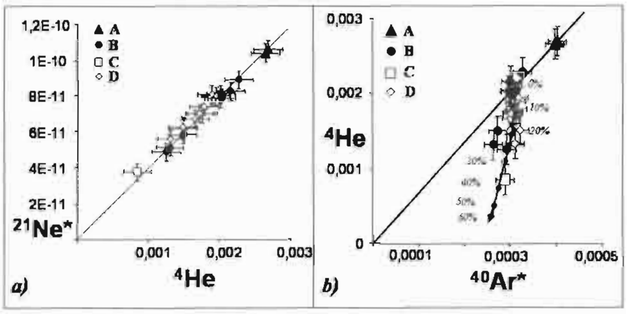

Figure 3. Excellent linear correlation between the concentrations of radiogenic-nucleogenic isotopes of helium and neon suggesting a homogenization of these isotopes before the entering of hydrocarbons in the reservoirs (a); ^4He *versus* ^{40}Ar concentrations. Notice the shift of the last from the average crustal production ratio line, suggesting anenrichment of the heavier molecule in the residue (b).

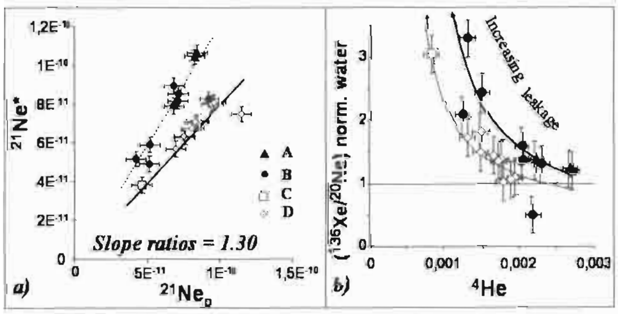

Figure 4. Cross correlation of the nucleogenic and fossil parts of the same isotope that suggests differences in the residence time in the A-B and C-D fields (a), associated fractionation of the fossil isotopes make strengthen the interpretation of leakage from the respective reservoirs.

A good correlation was identified between radiogenic isotopes, ^4He for example, and fossil gases. The curves correlating these isotopes converge asymptotically to ratios of fossil isotopes close to the concentrations found in water, for higher ^4He concentrations. Moreover, for some ratios involving high mass contrast ($^{136}Xe/^{20}Ne$ *versus* ^4He) there are different trends in different groups of petroleum fields (Fig. 4b). These correlations suggest a clear link between fossil and produced isotopes, implying physical fractionations independent of radiogenic genesis, and occurring after or during the generation of radiogenic isotopes.

CONCLUSIONS

The results obtained in this study suggest that noble gases are a promising tool for the understanding of processes in petroleum systems. However, more research is needed for the strengthening of this technique.

During this stage of development it is necessary to obtain a complete integration of noble gas results with the available geological, geophysical and geochemical data for the best interpretation.

In the case of the Solimões Basin, it was possible to assess the following conclusions:

- Helium in the studied petroleum accumulations is derived from radioactive decay (^{4}He-enriched), with no significant mantle contribution.
- Variations in ^{3}He/^{4}He ratio suggest fractionation due to the secondary migration along the trend SW-NE.
- Residence time of noble gases in the accumulation C-D is 30% smaller than the accumulation A-B.
- The hydrocarbon loss inferred for the study area varies from 0 (fluids in A-B) to about 38% (fluids in C-D).

ACKNOWLEDGEMENTS

To PETROBRAS for the authorization to publish part of the results of this research, and to Jarbas V.P. Guzzo for the critical review.

REFERENCES

Ballentine, C.J., O'Nions, R.K., Oxburgh, E.R., Horvath, Deak, J., 1991. Rare gas constraints on hydrocarbon accumulation, crustal degassing and groundwater flow in the Pannonian Basin. Earth and Planet. Sci. Letters, 105, p. 229-246.

Ballentine, C.J., O'Nions, Colemann, D., 1996. A Magnus opus: Helium, neon, and argon isotopes in a North Sea oilfield. Geochimica and Cosmochimica Acta, vol. 60, p. 831-849.

Ballentine, C.J., Schoell, M., Colemann, D., Cain, B.A., 2001. 300-Myr-old magmatic CO2 in natural gas reservoirs of the West Texas Permian Basin. Nature, vol. 409, p. 327-331.

Battani, A., 1999. Utilisation des gaz rares He, Ne et Ar pour l'exploration pétrolière: example des accumulations du Pakistan et de Macuspana (Mexique). Ph.D. dissertation, Paris University, 156 p.

Battani, A., Sarda P., Prinzhofer, A., 2000. Basin scale natural gas source, migration and trapping traced by noble gases and major elements: the Pakistan Indus Basin. Earth and Planet. Sci. Letters, 181, p. 229-249.

Bender, A.A., Eiras, J.F., Wanderley Filho, J.R., 2001. Modelagem 3D de um sistema petrolífero controlado por intrusões ígneas: Bacia do Solimões. III Seminário de Interpretação Exploratória, Natal (RN), 2-5 Outubro, 2001, Resumos Expandidos.

Eiras, J.F., 1998. Tectônica, sedimentação e sistemas petrolíferos da Bacia do Solimões, Estado do Amazonas, Search, Special Edition About Brazil, Chapter 2, p. 23-31.

Eiras, J.F., Becker, C.R., Souza, E.M., Gonzaga, F.G., Silva, J.G.f., Daniel, L.M.F., Matsuda, N.S., Feijó, F.J., 1994. Bacia do Solimões. Boletim de Geociências da PETROBRAS, 8(1), 14-45.

Mosmann, R., Falkenhein, F.U.H., Gonçalves, A., Nepomuceno Filho, F., 1987. Oil and gas potential of the Amazon Paleozoic Basin: In: Halbouty, M.T. (ed.), 1987, Future Petroleum Provinces of the World, AAPG Memoir 40, p. 207-241.

Prinzhofer, A., Battani, A., 2002. Tracing petroleum systems with noble gases: a new challenge for oil and gas geochemistry. 8th Latin-American Congress on Organic Geochemistry, Cartagena de Indias, Colombia, October 20-24,2002, Rangel A., Gonçalves, F.T.T., Parra, P., Hernández, C.S. (eds.), p. 2002-204.

Prinzhofer, A., Mello, M.R., Takaki, T., 2000. Geochemical characterization of natural gas: a physical multivariable approach and its applications in maturity and migration estimates. A.A.P.G. Bull., vol. 84, n° 8, p. 1152-1172.

Rodrigues, R., Triguis, J.A., Araújo, C.V., Brazil, I.R., 1990. Geoquímica e faciologia orgânica dos sedimentos da Bacia do Solimões. PETROBRAS/CENPES/DEPEX, Internal Report, 115 p.

Santos Neto, E.V., Prinzhofer, A., Pereira, I.E.M., Takaki, T., 1999. Helio em gases da Bacia do Solimões. Internal Report, November, 1999.

Zaikowski, A, Spangler, R.R., 1990. Noble gas and methane partitioning from ground water: an aid to natural gas exploration and reservoir evaluation. Geology, 18:72-74.

GEOCHEMICAL AND THERMAL EFFECTS OF BASIC INTRUSIVE ROCKS ON SEDIMENTS FROM THE IRATI FORMATION – NORTHEWESTERN PARANÁ BASIN

Santos, R.V.[1]; Dantas, E.[1]; Alvarenga, C.J. S.[1]; Bedran, F.[1]; Reis, W.[1]; Guimarães, E.M.[1]; Oliveira, C.G.[1]; Marques-Toigo, M.[2]; Mendonça Filho, J.G.[2]; Reis, C.W.D.[1] and Medeiros, S.R.[1]

1. Universidade de Brasília – Instituto de Geociências. rventura@unb.br
2. Universidade Federal do Rio Grande do Sul

Keywords: Irati Formation, Nd isotopes, REE

INTRODUCTION

The Paraná basin is an important sedimentary sequence from central and south Brazil that extends to Uruguay, Paraguay and Argentina. This basin has two important oil source horizons that have been extensively studied. The lower horizon is characterized by organic-rich sediments related to the Ponta Grossa Formation (Devonian), while the upper horizon is related to organic-bearing shales of the Irati Formation (Upper Permian, Araújo, 2001).

The Irati Formation has an average thickness of 40 m and extends over an area of 4 millions km^2 (South America and Africa). This unit is related to the Kazanian (Upper Permian, Daemon & Quadros, 1970) and made of organic-matter-rich shales and limestones. The presence of organic-rich rocks has made this unit very attractive for oil prospecting, mainly during the early geological studies in the basin (early 50's).

Evidence of gas is well known in the Paraná basin and is believed to be related to the thermal breaking down of the organic matter within rocks from the Irati and the Ponta Grossa Formations. An important heat source is the cretaceous basaltic igneous volcanism that extends over a large area of the basin. Even considering that the Irati Formation organic-rich rocks are one of the most important gas source in the basin, there are only limited data about the thermal evolution of theses rocks.

This study aims to better understand the thermal and geochemical interactions between basaltic magma and the Irati Formation sedimentary rocks. Particularly, it is focussed on the heating transfer mechanism (advection or diffusion) across the contact between a basaltic sill and sediments from the Irati Formation, which may lead to quite distinct thermal and geochemical evolution of the host rocks.

SAMPLING AND RESULTS

Samples were collected from a limestone mine quarry located on the northwestern part of the Paraná basin (Perolândia, GO). The sampling was performed across the upper and lower contacts between a 50m thick basic intrusive sill and black shales and limestones from the Irati Formation. After crushing, they were analyzed for Nd isotopes (Gioia & Pimentel, 2000) as well as major and trace elements (including REE) in the laboratories of the Geosciences Institute of the University of Brasília.

RESULTS AND DISCUSSIONS

Figure 1 shows the Nd isotopic composition across the contact between the sill and the host rock. While the basic sill has T_{DM} model ages around 1.2 Ga and ε_{Nd} (0) values of -4, the sedimentary host rock presents T_{DM} model ages ranging from 1.45 to 1.87 Ga and strongly negative ε_{Nd} (0) values (-11 to -14). Even samples of black shales a few centimeters from the sill present no signs of interaction with the basic magmatism, thus preserving its original sedimentary isotopic signature. In other words, there is no isotope exchange between the sill and the host rock.

Variations in the T_{DM} model ages and Nd concentration in the sediments could be related to fractionation process during sedimentary transport or mixing of different source areas of the sediments.

REE have been largely used to study the magmatic evolution of igneous rocks in terms of fractionation and contamination from the host rock. It has also been applied to understand source areas of sediments, thus giving further support to the Nd isotope interpretations. In the present study we have used REE to evaluate possible geochemical interactions between the sill and host rock. Figures 2 and 3 show the REE patterns of samples across sill-host rock upper and lower contact, respectively, in which is clear the sharp difference between the basic rocks and the sediments. For instance, the basic rock is enriched in LREE and displays no Eu anomaly. This sharp difference indicates that there was no geochemical interaction between the magma and the host rock, both on the upper as well as the lower part of the sill.

The REE patterns of the sediments are very similar and characteristic of the average crustal values. Except for one sample, the patterns display a slight negative Eu anomaly and are generally parallel to each other, thus reflecting dilution effect intrinsic to sedimentary rocks.

The absence of significant mass exchange between the sill and the host rock suggest that the mechanism of heat exchange was mostly controlled by thermal diffusion. It is also possible to anticipate that the mineralogical changes in the host rock induced by the thermal effect of the intrusion probably occurred under closed system conditions. The conclusion above also allows modeling the temperature variations with time across the contact by assuming a hot sheet with infinite lateral extend that is emplaced in a country rock with

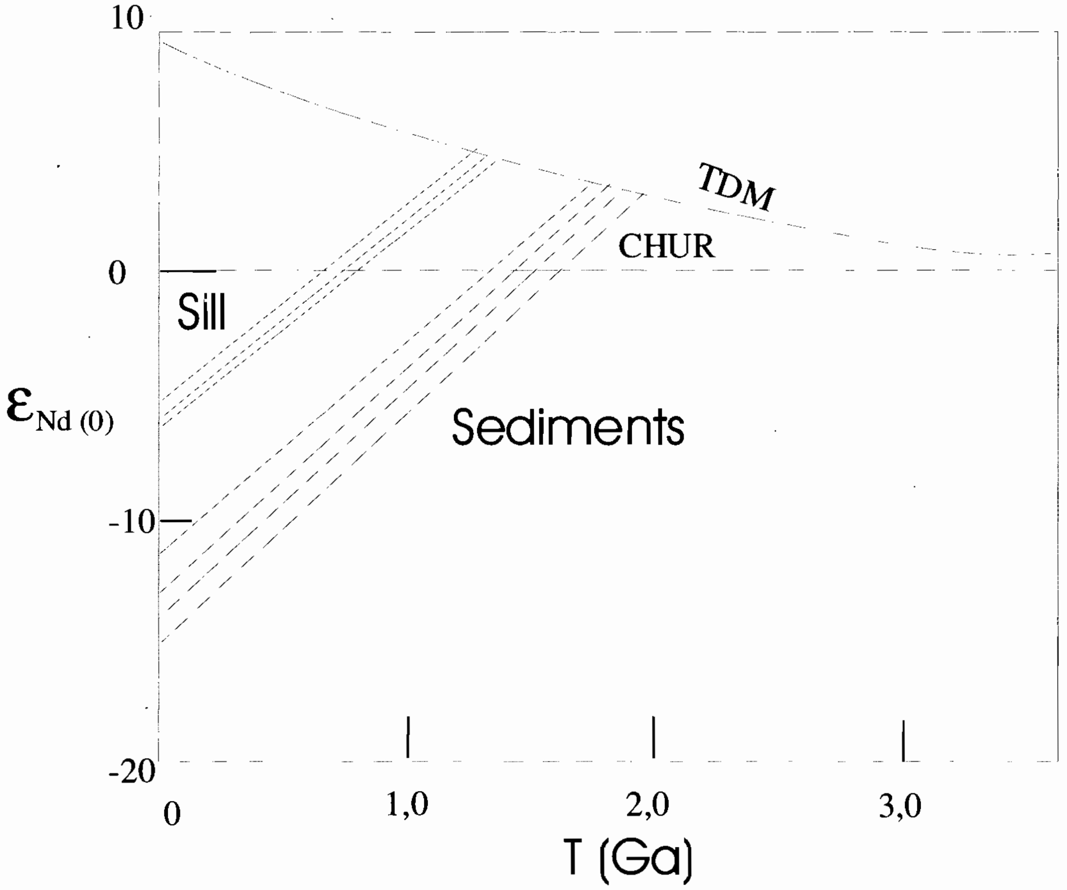

Figure 1. Nd isotope evolution of the sill and the host from the Perolândia quarry.

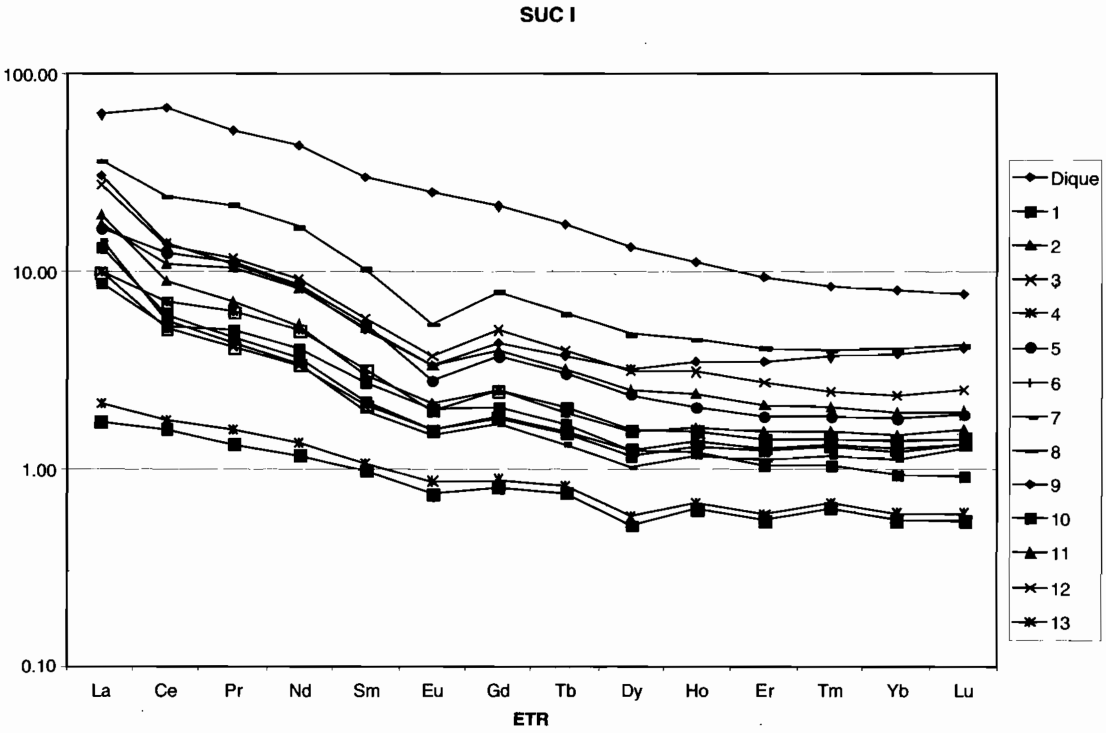

Figure 2. ETR patterns of the basic sill and sediments of the Irati Formation.
The numbers indicate increasing distance from the contact.

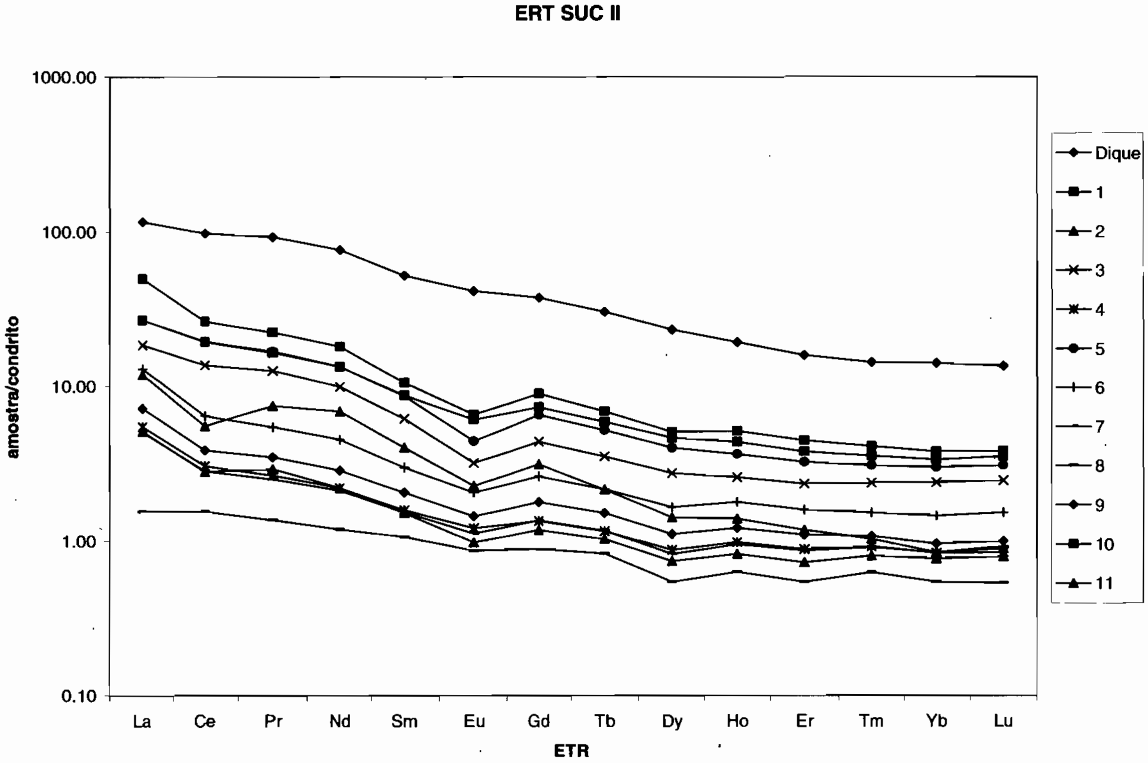

Figure 3..ETR patterns of the basic sill and sediments of the Irati Formation.
The numbers indicate increasing distance from the contact.

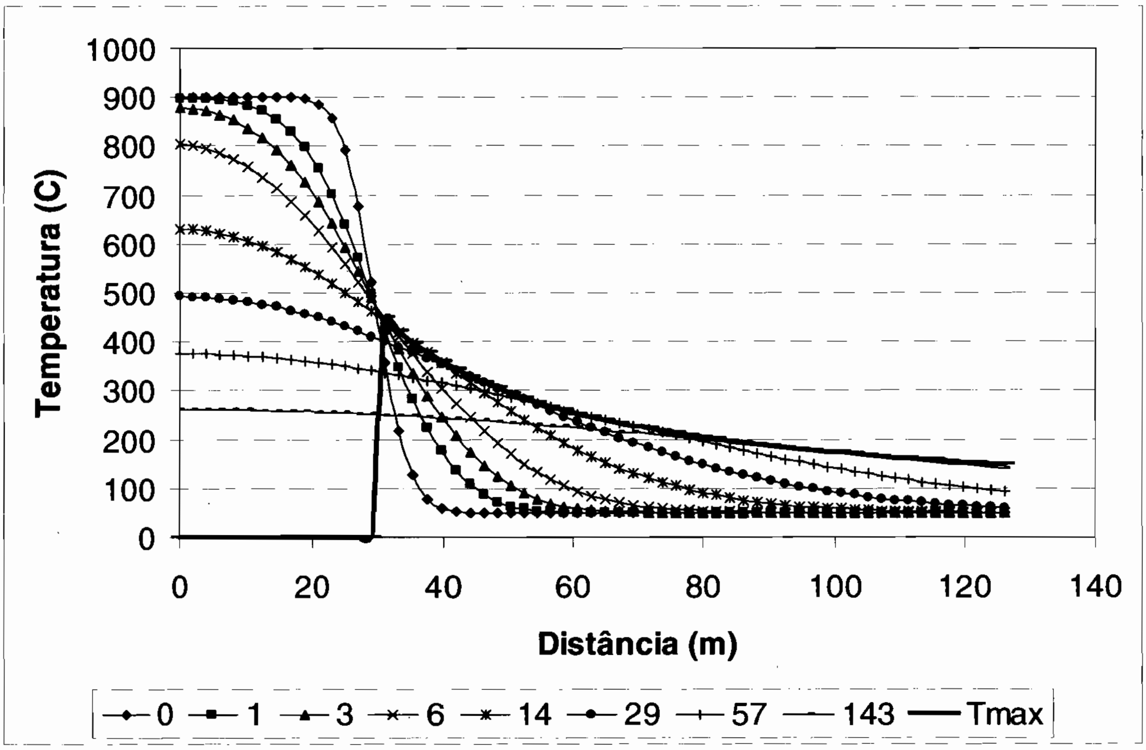

Figure 4. Modeling of the thermal evolution of the country rock assuming an infinite slab with 60m thick. The numbers at the bottom of the diagram represent the temperature in years and the maximum temperature. The model was performed using the following parameters: sill initial temperature = 900°C; country rock initial temperature = 50; and thermal diffusion coefficient = 1.0 10^{-6} m^2/s.

uniform initial temperature (Wickham & Oxburgh, 1987). A possible scenario for this modeling is presented in figure 4, which also shows the maximum temperature variations expected around the sill under the established conditions.

CONCLUSIONS

The mechanisms of heat transfer and geochemical exchange between a sill and the host rock may depend on the characteristics of the magma. In the present example we have shown that basaltic intrusion and the host rock have limited geochemical interaction, probably because this kind of magma is usually poor in volatiles. Taking into account that there was no mass transfer, we conclude that the exchange occurred mostly by thermal diffusion, which will facilitated modeling the mineralogical and organic matter on the host rock.

REFERENCES

Araújo, L.M. 2001. Análise da expressão estratigráfica dos parâmetros de geoquímica orgânica e inorgânica nas sequências deposicionais Irati. Tese de Doutorado, Instituto de Geociências, Universidade Federal do Rio Grande do Sul, 2 volumes, 307p.

Daemon, R. F. and Quadros, L.P. 1970. Bioestratigrafia do Neopaleozóico da bacia do Paraná. Anais... 24 Congresso Brasileiro de Geologia, Brasília, 1970. Sociedade Brasileira de Geologia (SBG), 359-412.

Gioia, S.M.C.L. and Pimentel, M.M. 2000. The Sm-Nd isotopic method in the Geochronology Laboratory of the University of Brasília. An. Acad. Bras. Cienc., 72(2):219-245.

Wickham, S.M. and Oxburgh, E.R. 1987. Low-pressure regional metamorphism in the Pyrenees and its implications for the thermal evolution of rifted continental crust. Phil. Trans. R. Soc. Lond., A 321:219-242.

Epsilon (ϵ) values, calculated by way of comparison of initial ratios of isotopes $(^{87}Sr/^{86}Sr)_i$ and $(^{143}Nd/^{144}Nd)_i$ (in its turn obtained in the result of isochron dating) with the same-named ratios, characterizing model reservoirs CHUR and UR 330, 329 and 336 Ma ago, are determined by the values: ϵ^{t}_{UR}= -15.3 for Magnitogorsk; ϵ^{t}_{UR}= -16.0 for Kuibas; ϵ^{t}_{UR}= -10.9 and ϵ^{t}_{CHUR}= +5.8 for Mosov massifs respectively. Consideration in coordinates ϵ^{t}_{UR}-ϵ^{t}_{CHUR} of Sr and Nd isotope contents corrected.

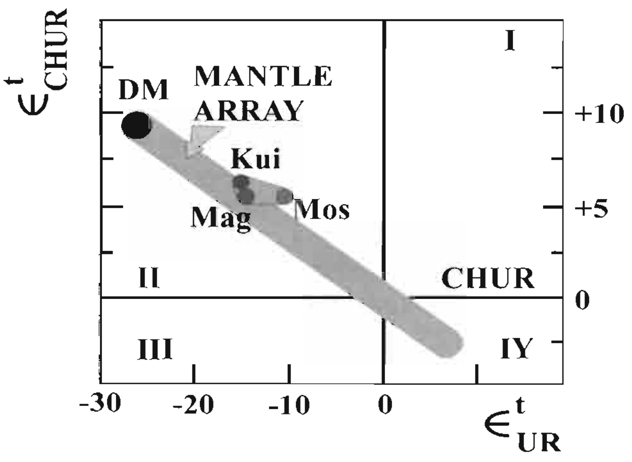

Figure 3. ϵ^{t}_{UR} vs. ϵ^{t}_{CHUR} variation for Magnitogorsk (Mag), Kuibas (Kui) and Mosov (Mos) massifs. to the decay after the time of formation of Magnitogorsk, Kuibas and Mosov massifs, makes it possible to note the fact that figurative points for the studied formations are located in II quadrant ϵ^{t}_{UR} - ϵ^{t}_{CHUR} of correlation diagram (Fig. 3) and going along the line of Mantle Array, coming through isotope contents of the Depleted Mantle (DM) and CHUR.

Sm-Nd model datings of the whole contents of Mosov massif's four gabbro relatively to model depleted reservoir, are characterized by a range of Nd-model ages of T_{DM} from 0.68 to 0.80 Ma, and allow to estimate «crust-formation» ages (DePaolo, 1988), which reflect different times of protolith separation for the studied kinds from the trend of evolution of the depleted source.

CONCLUSION

Thus the obtained Rb-Sr and Sm-Nd isotope systematics for magmatic series conjugated with large Magnitogorsk iron-ore deposit testifies to their mantle nature, while Sr-Nd-Pb isotope data for ore minerals and for synchronous in time the associating magmatism of the huge Kachar iron-ore deposit permit with a certain degree of validity to make a conclusion about the participation, as minimum, of two different-deep fluid-magmatic sources in the ore-forming process.

REFERENCES

DePaolo, D.J. 1988. Neodymium isotope geochemistry: An introduction. Springer-Verlag Berlin: 187 p.

Fershtater, G.B., Malakhova, L.V., Borodina, N.S., Rapoport M.C. & V.N. Smirnov 1984. Eugeosyncline gabbro granites series. Nauka, Moscow, 264 p.

Koroteev, V.A., Necheukhin V.M. & V.A. Prokin 1989. Model for metallogenic evolution of geosynclinal fold system of Uralian type. 28th Int. Geol. Congress. Abstracts of Papers. Washington. 2: 213-214.

Necheukhin V.M. 1991. Geodynamic regimes of the ore-formation in the development of geosynclinal-folded systems of the Urals type. Geodynamic and metallogenic of the Urals. Nauka. Ekaterinburg. 27-29.

Prokin, V.A., Sazonov V.N. & Yu. A. Poltavets 1993. Evolution of the endogenous ore deposits of the Urals within the context of the plate tectonics. Geology of Ore Deposits, 35(2): 135-143.

Zartman, R.E. & B.R. Doe 1981. Plumbotectonics-the model. Tectonophysics, 75: 135-162.

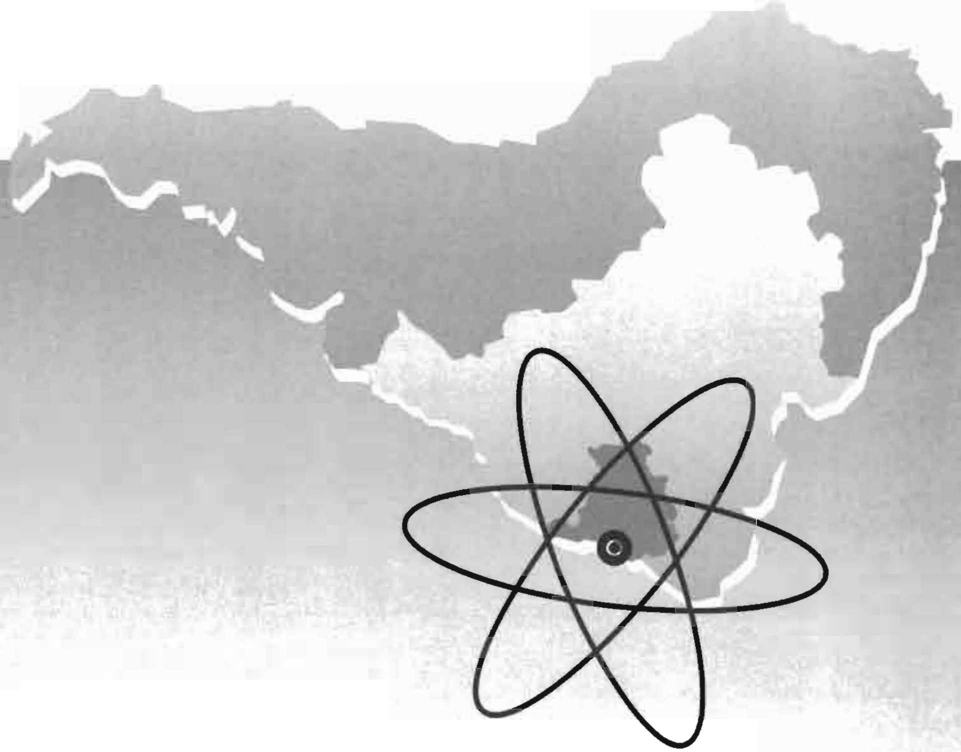

Sponsors Notes

SILICON ISOTOPE RATIO MEASUREMENTS WITH HIGH RESOLUTION, COLLISION CELL, MULTI-COLLECTOR ICPMS

Palacz, Z.; Goldsmith, S.; Meffan-Main, S. and Turner, P.

Micromass U.K. Ltd, Atlas Park, Simonsway, Manchester, M22 5PP, UK

Silicon is one of the most common elements in the earth. The isotopic composition of Silicon is believed to be uniform within the earth, except there is evidence of biological fractionation of Silicon at the per mil level in marine diatoms. Isotopic measurement of Silicon has been restricted to SiF in gas source mass spectrometers, however preparation involves the lengthy and dangerous procedure of fluorination. Measurement by ICP is possible, but it is restricted by the removal of interferences from NN,NO,NNH, commonly generated in acids and from the atmosphere.

These backgrounds can be eliminated by using a combination of collision cell and high resolution methods. Using He in the collision cell, the ^{28}Si background can be reduced to only 1-2mv, even with the use of a quartz torch. NNH and NO interferences, can be partially resolved by narrowing the source slit of the spectrometer, or completely resolved by using modified collector slits on the Faraday cups. The multi-collector simultaneously measures all isotopes of silicon, thereby reducing uncertainty due to ion beam instability. Reproducibilities for the ^{30}Si/^{28}Si ratio at the 0.02% level are obtainable following appropriate mass fractionation corrections, which makes this method of analysis a significant alternative to fluorination techniques.

AUTHORS INDEX

GOVERNO DA BAHIA
SECRETARIA DA INDÚSTRIA, COMÉRCIO E MINERAÇÃO

30 anos
companhia baiana de pesquisa mineral
Descobrindo as riquezas da Bahia

IRD
Institut de recherche pour le développement

CNPq
Conselho Nacional de Desenvolvimento Científico e Tecnológico

VIRTUTE SPIRITUS
UNIVERSIDADE FEDERAL DA BAHIA - UFBA
Grupo de Petrologia Aplicada a Pesquisa Mineral

CAPES

fapesb
Fundação de Amparo à Pesquisa do Estado da Bahia

BR
PETROBRAS

CPRM
Serviço Geológico do Brasil

Thermo Finnigan

SCIENTIFIC INSTRUMENTS CO.
SINC DO BRASIL
INSTRUMENTAÇÃO CIENTÍFICA LTDA.

micromass
The Mass Spectrometry People

MCMXVI

SOCIEDADE BRASILEIRA DE GEOLOGIA
DESDE 1946
Núcleo Bahia-Sergipe

GEOSOL